PROTECTION AND RESTORATION OF THE ENVIRONMENT XIV

INTERNATIONAL CONFERENCE

PROTECTION AND RESTORATION OF THE ENVIRONMENT XIV

BOOK OF PROCEEDINGS

EDITORS:

N. Theodossiou
C. Christodoulatos
A. Koutsospyros
D. Karpouzos
Z. Mallios

THESSALONIKI, JULY 2018

International Confernece Protection and Restoration of the Environment XIV
Proceedings (MEMORY STICK)

ISBN: 978-960-99922-4-4

PREFACE

"Protection and Restoration of the Environment" is a well-known series of international conferences, organized jointly by one American and one Greek University every two years, in Greece. It started in 1992, in Thessaloniki. In 2018, the fourteenth Conference of the series has taken place in Thessaloniki for one more time. It was jointly organized by: a) the Stevens Center for Environmental Engineering of the Stevens Institute of Technology, USA and b) the Division of Hydraulics and Environmental Engineering, and the Environment Council of the Aristotle University of Thessaloniki, Greece.

Thessaloniki is an inspiring place for an environmental conference: It is a large city, facing many environmental problems, but, at the same time, it is situated in the middle of an area of undisputable beauty (including Chalkidiki and Mount Olympus), which exhibits the environmental quality that we have to preserve for future generations.

Moreover, Thessaloniki is located in a rather small distance from Stagira, the birthplace of Aristotle and from Mount Athos. Aristotle contributed decisively to the formation of scientific thought, while Mount Athos represents the spirit and the moral discipline, which are indispensable for protection and restoration of the environment.

The conference was timely, as well. It served as a reminder that protection of the environment is not a luxury that could be temporarily disregarded under the pressure of financial crisis, but a basic prerequisite for viable future.

Participation has been very encouraging. Almost 150 papers have been selected for oral or poster presentation, covering a wide range of topics, which reflect the interdisciplinary nature of environmental challenges. They have been classified in the following sessions:

- Climate change impacts and adaptation measures
- Cultural and social issues
- Environmental education
- Environmental hydrology
- Environmental law and economics
- Ground water resources management
- Protection and restoration of coastal zone and open sea waters
- Protection and restoration of ecosystems
- River and open channel hydraulics
- Soft and renewable energy sources
- Solid waste management
- Sustainable architecture, planning and development - Built environment

- Sustainable architecture, planning and development - Urban environment
- Water and wastewater treatment and management
- Water resources management and contamination control

The conference hosted also a special session on Supporting Sustainable Development Goals Implementation using research, organized by the Sustainable Development Solutions Network (SDSN).

The editors would like to thank:

The authors of the papers, for contributing and sharing their own expertise.

The members of the organizing and the scientific committee, for their eager help.

The reviewers, for ensuring high scientific standards for the presentations.

The sponsors of the conference for their financial support.

All conference participants, for their active involvement in the exchange of knowledge, which is the essence of a conference.

The editors

CONFERENCE COMMITTEES

CONFERENCE CHAIRMEN

Christodoulatos C., Stevens Institute of Technology, USA
Karpouzos D., School of Agriculture, A.U.Th., Greece
Koutsospyros M, University of New Haven, USA
Mallios Z., Dept. of Civil Engineering, A.U.Th., Greece
Theodossiou N., Dept. of Civil Engineering, A.U.Th., Greece

ORGANIZING COMMITTEE

Christodoulatos C., Stevens Institute of Technology, USA
Fotopoulou E., Dept. of Civil Engineering, A.U.Th., Greece
Hatzigiannakis E., Hellenic Agricultural Organization, Greece
Karpouzos D., School of Agriculture, A.U.Th., Greece
Katsifarakis K.L. Dept. of Civil Engineering, A.U.Th., Greece.
Koutsospyros M., University of New Haven, USA
Mallios Z., Dept. of Civil Engineering, A.U.Th., Greece
Manakou V., Dept. of Civil Engineering, A.U.Th., Greece
Papageorgiou A., Dept. of Civil Engineering, A.U.Th., Greece
Petala M., Dept. of Civil Engineering, A.U.Th., Greece
Raptou E., Dept. of Agricultural Development, Democritus University of Thrace, Greece
Theodossiou N., Dept. of Civil Engineering, A.U.Th., Greece
Tsiridis V., Dept. of Civil Engineering, A.U.Th., Greece
Vasileiou E., Dept. of Civil Engineering, A.U.Th., Greece
Zafirakou A., Dept. of Civil Engineering, A.U.Th., Greece

SCIENTIFIC COMMITTEE

Anagnostopoulos P., Dept. of Civil Engineering, A.U.Th., Greece

Antonopoulos V., School of Agriculture, A.U.Th., Greece

Arampatzis G., Hellenic Agricultural Organization, Greece

Baltas E., School of Civil Engineering, National Technical University of Athens, Greece.

Benavente J., Faculta de Sciencias, Universidad de Granada, Spain

Bikas D. Dept. of Civil Engineering, A.U.Th., Greece

Boccia L., University of Naples Federico II, Italy

Braida W., Center for Environmental Systems, Stevens Institute of Technology, USA

Chintiroglou Ch., Department of Biology, A.U.Th., Greece

Darakas E., Dept. of Civil Engineering, A.U.Th., Greece

Dermatas D., School of Civil Engineering, National Technical University of Athens, Greece

Dermisi S., University of Washington, USA.

Diamadopoulos E., Dept. of Environmental Engineering, Technical University of Crete

Doveri M., Institute of Geosciences and Earth Resources, National Research Council, Italy

Droege P., Liechtenstein Institute for Strategic Development, Liechtenstein

Efthimiou G., TEI of Sterea Ellada, Greece

Fatta-Kasinos D., Nireas International Water Research Center, University of Cyprus, Cyprus

Georgiou P., School of Agriculture, A.U.Th., Greece

Goyal Manish, Indian Institute of Technology, Guwahati, India.

Kalavrouziotis I., Hellenic Open University, Greece

Kanakoudis V., Dept. of Civil Engineering, University of Thessaly, Greece

Karambas Th., Dept. of Civil Engineering, A.U.Th., Greece

Karatzas G., Dept. of Environmental Engineering, Technical University of Crete

Karatzas K., Dept. of Mechanical Eng., A.U.Th., Greece

Katopodes N., Dept. of Civil and Environ. Engineering, University of Michigan, USA

Kehagia F., Dept. of Civil Engineering, A.U.Th., Greece

Kolokytha E., Dept. of Civil Engineering, A.U.Th., Greece

Korfiatis G., Stevens Institute of Technology, USA

Kougias I., European Commission, DG JRC, Directorate for Energy, Transport and Climate, Italy

Koundouri Ph., Athens University of Economics and Business, Greece

Koutsoyiannis D., School of Civil Engineering, National Technical University of Athens, Greece

Koveos D., School of Agriculture, A.U.Th., Greece

Krestenitis I., Dept. of Civil Engineering, A.U.Th., Greece

Kungolos A.G., Dept. of Civil Engineering, A.U.Th., Greece

Larabi A., Universite Mohammed V de Rabat, Morocco

Latinopoulos D., Dept. of Spatial Planning and Development, A.U.Th., Greece

Latinopoulos P., Dept. of Civil Engineering, A.U.Th., Greece

Laudonia S., University of Naples Federico II, Italy

Liakopoulos A., Dept. of Civil Engineering, University of Thessaly, Greece

Lo Porto A., Institute of Water Research, National Research Council, Italy

Loukas A., Dept. of Civil Engineering, University of Thessaly, Greece

Loukogeorgaki E., Dept. of Civil Engineering, A.U.Th., Greece

Lyberatos G., School of Chemical Engineering, National Technical University of Athens, Greece

Mamassis N., School of Civil Engineering, National Technical University of Athens, Greece

de Marsily G., Université Paris VI- École des Mines-Académie des Sciences, France

Masciopinto C., Water Research Institute, CNR-IRSA, Italy

Melas D, Dept. of Physics, A.U.Th., Greece

Meng X., Center for Environmental Systems, Stevens Institute of Technology, USA

Miracapillo C., Dr, Switzerland

Moussiopoulos N., Dept. of Mechanical Eng., A.U.Th., Greece

Moustaka M., Dept. of Biology, A.U.Th., Greece

Moutsopoulos K.N., Dept. of Environmental Engineering, Democritus University of Thrace, Greece

Mylopoulos I., Dept. of Civil Engineering, A.U.Th., Greece

Nikolaou K., Organization for the Master Plan and Envir. Protection of Thessaloniki, Greece

Panagopoulos A., Hellenic Agricultural Organization, Greece

Papamichail D., School of Agriculture, A.U.Th., Greece

Papanikolaou P., School of Civil Engineering, National Technical University of Athens, Greece

Prinos P., Dept. of Civil Engineering, A.U.Th., Greece

Psilovikos A., School of Agricultural Sciences, University of Thessaly, Greece

Rangel B., Dept. of Civil Engineering, University of Porto, Portugal

Rao M.C., Dept. of Civil Engineering, National Institute of Technology Jamshedpur, India.

Ripa N., University of Vitterbo, Italy

Robesku D., Faculty of Engineering, University Polytechnica of Bucharest, Romania

Sapountzis M., School of Forestry, A.U.Th., Greece

Scarlatos P.D., Chair & Professor Dept. of Civil, Environmental and Geomatics Engineering, Florida Atlantic University, USA

Sidiropoulos E., Dept. of Rural and Surveying Engineering, A.U.Th., Greece

Skanavis C., Dept. of Environmental Studies, University of the Aegean

Tsakiris G., School of Rural and Surveying Eng, National Technical University of Athens, Greece

Tsalikidis I., School of Agriculture, A.U.Th., Greece

Tsihrintzis V.A., School of Rural, Surveying Eng, National Technical University of Athens, Greece

Tsikaloudaki K., Dept. of Civil Engineering, A.U.Th., Greece

Tsilingiridis G., Dept. of Mechanical Eng., A.U.Th., Greece

Tsitsoni, Th. Dept. of Forestry and Natural Environment, A.U.Th., Greece

Vafeiadis M., Dept. of Civil Engineering, A.U.Th., Greece

REVIEWERS

Karpouzos D., School of Agriculture, A.U.Th., Greece

Konstaninou Z., Department of Spatial Planning and Development, A.U.Th, Greece

Korfiatis G., Stevens Institute of Technology, USA

Kosmopoulos P., K-eco Projects

Kougias I., European Commission, DG JRC, Directorate for Energy, Transport and Climate, Italy

Kouloussis N., School of Agriculture, A.U.Th., Greece

Koutsospyros M, University of New Haven, USA

Kungolos A.G., Department of Civil Engineering, A.U.Th., Greece

Latinopoulos D., Department of Spatial Planning and Development, A.U.Th., Greece.

Latinopoulos P., Department of Civil Engineering, A.U.Th., Greece

Loukas A., Department of Civil Engineering, University of Thessaly, Greece

Loukogeorgaki E., Department of Civil Engineering, A.U.Th., Greece

Lyberatos G., School of Chemical Engineering, National Technical University of Athens, Greece

Makris Ch. Department of Civil Engineering, A.U.Th., Greece

Malea P., School of Biology, A.U.Th., Greece

Mallios Z., Department of Civil Engineering, A.U.Th., Greece

Mamassis N., School of Civil Engineering, National Technical University of Athens, Greece

Mavridou S., Thessaloniki Water Supply and Sewerage Company, S.A.

Moussiopoulos N., Department of Mechanical Eng., A.U.Th., Greece

Moustaka M., School of Biology, A.U.Th., Greece

Nikolaidou E., Hydromanagement LTD Greece

Papadopoulos A.I., School of Biology, A.U.Th., Greece

Papakostas K., Department of Civil Engineering, A.U.Th., Greece

Papastergiadou E., Department of Biology, University of Patras, Greece

Papatheodorou E.M., School of Biology, A.U.Th., Greece

Patsialis Th., Department of Civil Engineering, A.U.Th., Greece

Petala M., Department of Civil Engineering, A.U.Th., Greece

Pisinaras V., Hellenic Agricultural Organisation, Greece

Prinos P., Department of Civil Engineering, A.U.Th., Greece

Ramos E., aUnuversity of Valencia

Raptou E., Department of Agricultural Development, Democritus University of Thrace, Greece

Ripa M. N., Dept. of Agricultural and Forestry Sciences (D.A.F.N.E.), Tuscia University, Italy

Samaras A.G., Department of Civil Engineering, A.U.Th., Greece

Sapountzis M., Department of Forestry and Natural Environment, A.U.Th., Greece

Siarkos I., Department of Civil Engineering, A.U.Th., Greece

Sofiadis I., School of Geology, A.U.Th., Greece

Stefanidou M., Department of Civil Engineering, A.U.Th., Greece

Theodossiou N., Department of Civil Engineering, A.U.Th., Greece

Thoidou E., Department of Spatial Planning and Development, A.U.Th., Greece

Tsan-Liang Su, Stevens Institute of Technology, USA

Tsikaloudaki K., Department of Civil Engineering, A.U.Th., Greece

Tsilingiridis G., Department of Mechanical Eng., A.U.Th., Greece

Tsiridis V., Department of Civil Engineering, A.U.Th., Greece

Vafeiadis M., Department of Civil Engineering, A.U.Th., Greece

Vagiona D., Department of Spatial Planning and Development, A.U.Th., Greece

Valyrakis M., Water Engineering Lab, University of Glasgow, UK

Zafeiriou E., Dept. of Agricultural Development, Democritus University of Thrace, Greece

Zafirakou A., Department of Civil Engineering, A.U.Th., Greece



Table of Contents



Water resources management and contamination control

CLIMATE CHANGE EFFECTS ON THE AVAILABILITY OF WATER RESOURCES OF LAKE KARLA WATERSHED FOR IRRIGATION AND VOLOS CITY URBAN WATER USE

A. Alamanos[*] N. Mylopoulos, L. Vasiliades and A. Loukas

Laboratory of Hydrology and Aquatic Systems Analysis, Dept. of Civil Engineering, University of Thessaly (UTH), GR- 38334 Volos, Thessaly, Greece

[*]Corresponding author: e-mail: alamanos@civ.uth.gr, tel: +302421074153

Abstract

Climate change and its potential impacts on water resources may have a large impact on water resources and subsequent water resources management practices. Changes on future climate will likely affect the fundamental drivers of the hydrological cycle, rainfall and temperature. The Representative Concentration Pathways (RCPs), which simulate future projections of GHG emissions and atmospheric concentrations, are used to model future changes in these variables. The RCPs include a stringent mitigation scenario, one intermediate scenario and one scenario with very high GHG emissions until year 2100. Subsequent changes in rainfall and temperature are used to examine climate change effects on two study areas; an agricultural watershed and an urban city, in Thessaly, Greece. Lake Karla Watershed, a typical Mediterranean agricultural area with dry climate, and the neighboring city of Volos are examined. The Water Evaluation And Planning (WEAP) modeling system is used to simulate the water availability for historical and future periods and for various water uses. More specifically, the water balance is simulated under the three extreme climate change scenarios and current operational management practices. The two study areas are modeled separately in the Baseline Scenario. In the future, when the new reservoir of the technical Lake Karla will operate, 50 new drilling wells will also be used for the coverage of the urban water demand of Volos city. Thus, the two areas are connected and modeled as an integrated system in the future scenarios. Finally, a management scenario of irrigation and urban losses reduction is suggested and simulated (for the current and for the future conditions) under the climate change scenarios. The results of the water balances indicate the vulnerability of the study areas, especially of the agricultural watershed, under the climate change, and the alteration the of current water resources management practices is deemed necessary.

Keywords: water resources management, Water Evaluation And Planning system (WEAP), Lake Karla Watershed, Volos city, climate change.

1. INTRODUCTION

Climate models project a reduction in annual precipitation and an increment in temperature, which may sharpen water scarcity phenomena. Climate change has multiple and growing impacts on urban and agricultural activities (Feilberg and Mark, 2016). These impacts have serious potential consequences for every domain that is connected directly or indirectly with water resources (Molle and Berkoff, 2009). The impacts of climate change on water resources availability are among the most widely discussed environmental issues in the last decades (IPCC, 2014, OECD, 2015, IWA, 2015). In line with this, water resources management must consider long-term planning, and one of its main aspects, is the changing climate (Russo, et al., 2014, Mourato et al., 2015). This paper proposes a water demand management under climate change scenarios. Water demand management, opposed to augmenting supply is increasingly proposed as a way of mitigating water-scarcity problems (Gleick, 2003). A neglected area in the field of climate change studies is the combination of different water uses, as the majority of the previous works has only focused on a specific water use. A rural watershed and a city are examined in this paper, combining thus the agricultural and the urban water use, in terms of simulation and modeling, under management and climate change scenarios. The selected study areas are Lake Karla Watershed and the neighboring city of Volos, in Thessaly (Central Greece). Industrial water uses of the watershed and Volos Municipality, as well as the animal husbandry of Lake Karla watershed have been taken into account, to complement agricultural and urban water demands which are the most important water uses. Furthermore, the existing practices are examined and new policies are investigated to strengthen the management's adaptation plans to new climate conditions, especially in agricultural watersheds.

2. STUDY AREA

Lake Karla Watershed is a representative agricultural watershed with limited water resources. The climate of the wider area of Karla is characterized as Mediterranean with dry and hot summers and cold and humid winters, with a mean annual precipitation of 451.13 mm and a mean annual temperature of 15.2 °C (Hydromentor, 2015). The intense irrigation of water demanding crops increased the pumping, with catastrophic results to the ecosystem, and especially to the aquifer (Sidiropoulos, 2014). The water demand of the watershed is covered by the surface network Local Administration of Land Reclamation (LALR) of Pinios River and mainly from the groundwater aquifer. The lake was drained in 1962, for flood protection and for more agricultural land, but the planned works were not constructed, creating thus, a number of environmental problems which led to the reconstitution of the lake. To date all the reconstitution works have been completed and refilling the lake with water from Pinios River continues to target the highest level, so the operation of irrigation can start. The new reservoir's operation is already delayed, causing further environmental problems (Stamou, 2015).

Volos is the capital of the prefecture of Magnesia (Central Greece), in the South-East boarder of Lake Karla watershed (Fig. 1), with a population of approximately 144,450 inhabitants. Volos occupies an area of 387.1 km^2. Its climate is characterized as Mediterranean with an average annual temperature of 16.4°C and 504 mm of annual rainfall. The Municipal Water Utility of Volos is responsible for the city's water supply, as well as the Industrial Area (Fafoutis, 2008). The water needs are covered by 5 springs and 40 wells, and the water is collected in 8 reservoirs. The city faces water problems, especially during summer, mainly due to the losses, which are estimated to be above the 40% of the total supplied water, according to the Water Utility databases (Mylopoulos et al., 2017). Furthermore, major environmental issues arose the last decades, such as, the systematically pumping and the deterioration of the aquifer (Mylopoulos and Mentes, 2005).

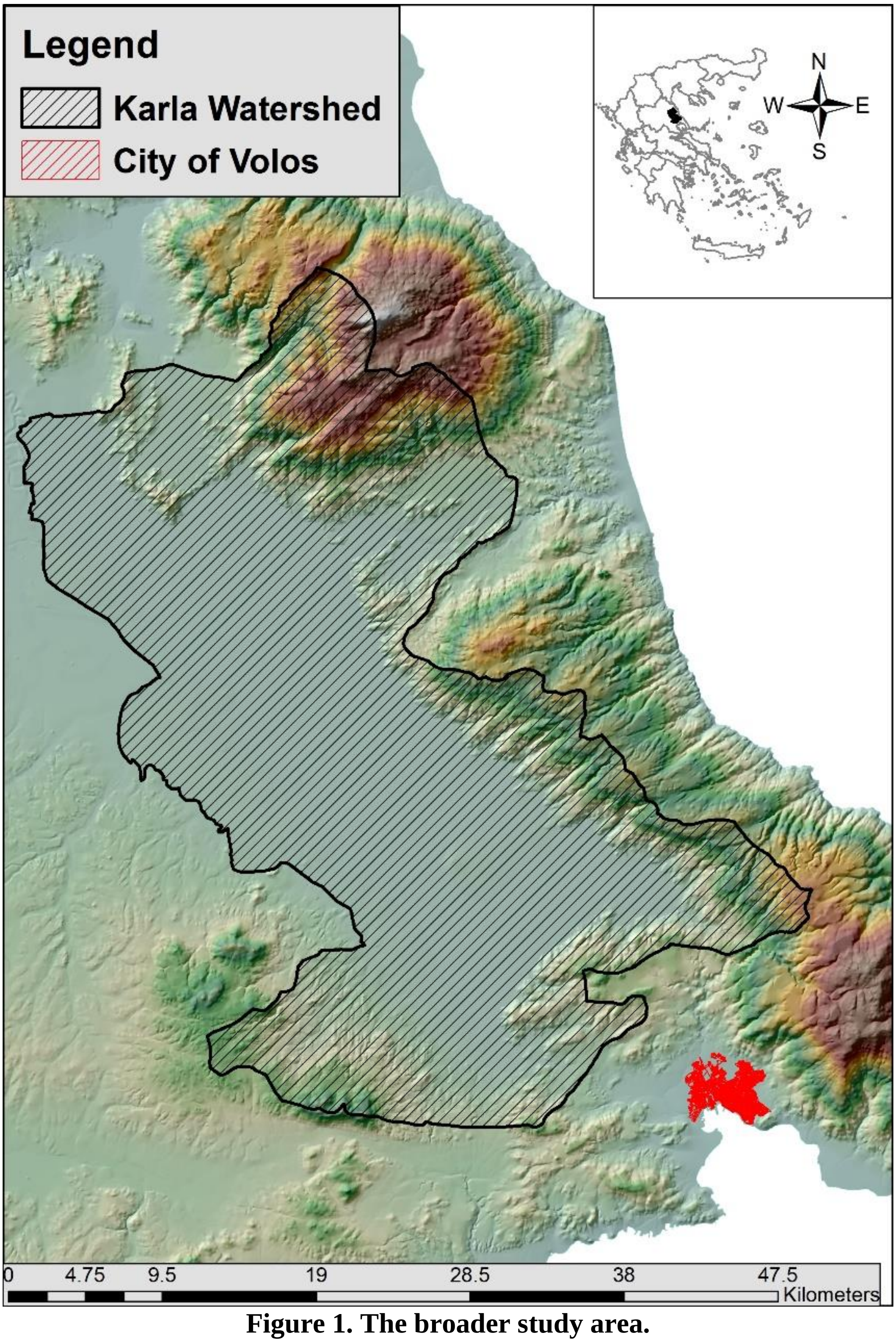


Figure 1. The broader study area.

When the Lake Karla reservoir will operate, significantly less water will be pumped from the groundwater aquifer. Karla watershed's area is 1663 km^2 now, but after the completion of the reservoir works its area will be 1171 km^2 due to the new irrigation areas that will be serviced from the reservoir's surface water (Loukas et al., 2008). The complementary works that accompany the reconstruction of the lake include the opening of 50 new wells to meet the water needs of the city of Volos and the surrounding settlements, with 2.9 hm^3 of water annually (Ministry of Environment, 2004). These wells will be distributed in the area of Stefanovikio up to Rizomylos, to 15 km^2 (Sidiropoulos et al., 2009). Of these 50 wells, the 10 are already operating on behalf of the Municipal Water Utility of Volos, but they will be replaced from the new ones (Water Utility of Volos, 2011).

3. METHODOLOGY

The methodology is focused on simulation of water supply sources, and water demand and the subsequent water balance estimation. Irrigation water needs were calculated with the software CROPWAT (FAO, 2015) and the urban water demand was calculated with a simple MS Excel model, given the quarterly consumption. The software WEAP (Water Evaluation And Planning system) (weap21.org), was used for the simulation of the water balance. The nodes of the system were schematized in WEAP. Figure 2 presents the positions of the supply sources, demand sites (nodes) and the linkage connections among the nodes.

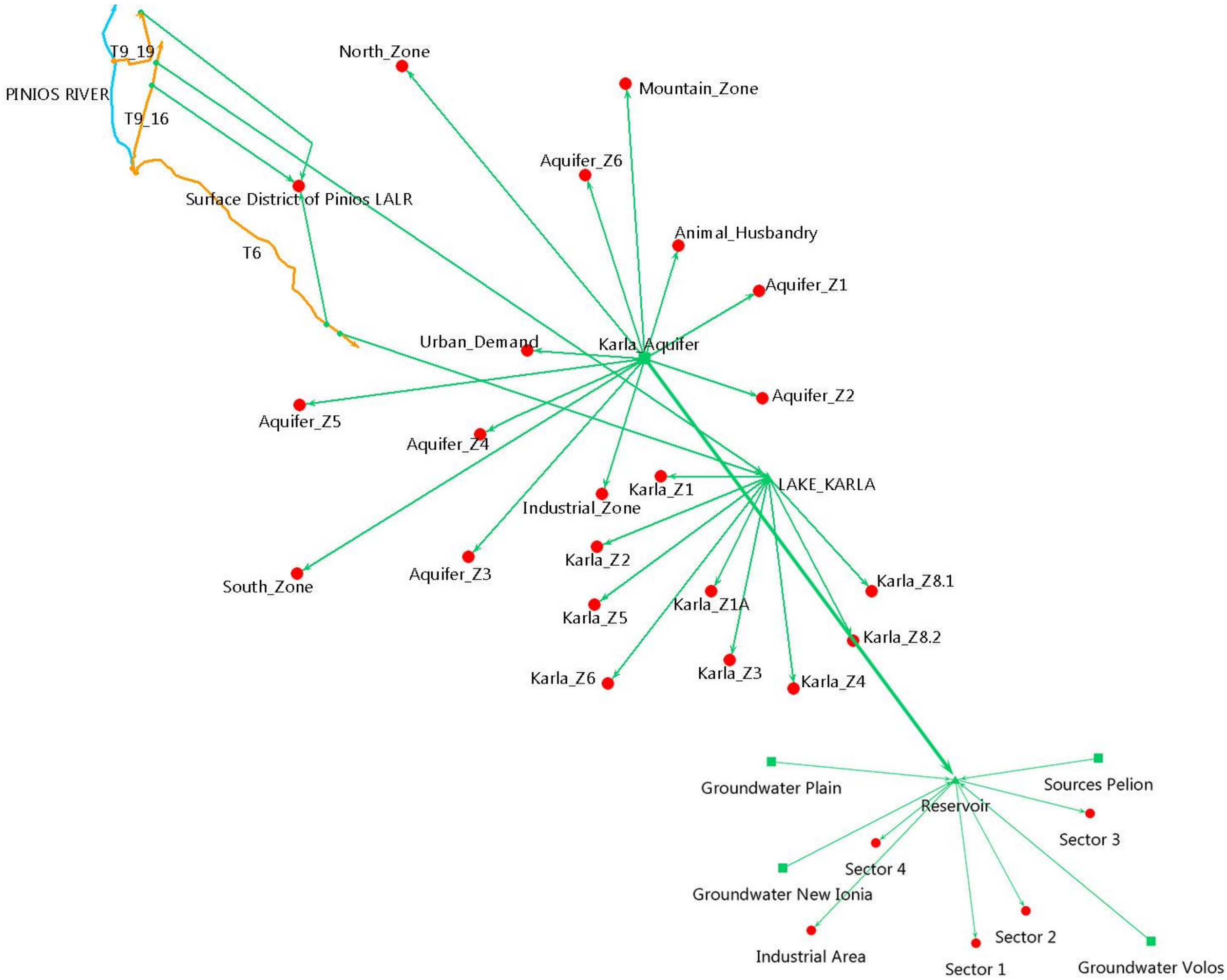


Figure 2. Water resources management system implementation for Lake Karla watershed and Volos city

For higher precision and spatial integration of the results, the watershed was divided into different zones (the demand nodes in Figure 2): North, South, Mountain, Surface Network of Pinios LALR, five (5) zones for the aquifer and nine (9) zones for the reservoir future serviced areas. The separation was based on common physical characteristics (e.g. soil) and common areas of administrative boundaries (Alamanos et al., 2016, 2017). For the analysis' needs the city of Volos was divided into five (5) main sectors (Fig. 2 and 3); sectors 1, 2, 3 and 4 cover the urban area, while the fifth sector covers the Industrial Area (Vagiona et al., 2005, Vagiona and Mylopoulos, 2009, Mylopoulos et al., 2017).

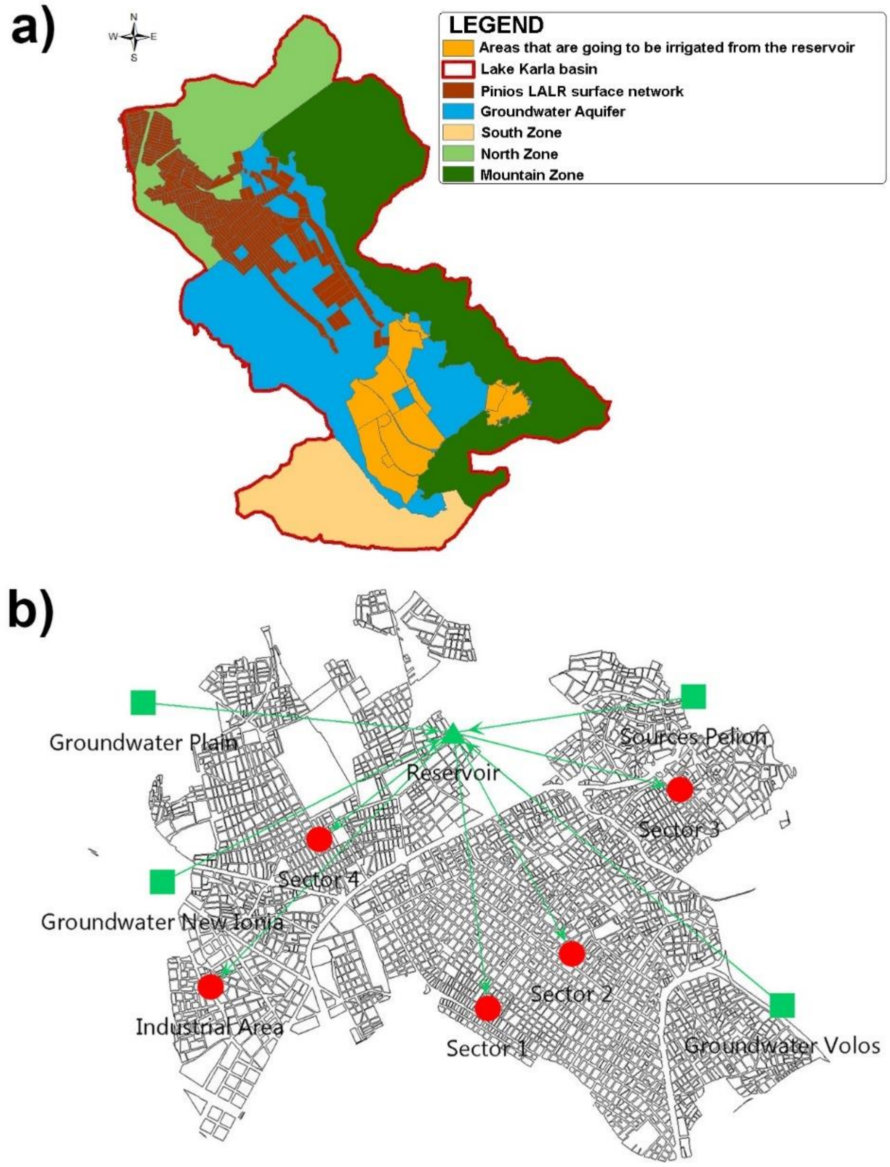


Figure 3. a) Lake Karla watershed divided into irrigation zones b) Volos city divided into sectors

Four management scenarios were developed to better reflect technical (engineering) measures on the efficient water use, as well as the future situation, and three climate change scenarios were developed to examine their effect on the water balance, for each management scenario:

Scenario 1: *The current situation, the BAU scenario*. The Karla reservoir is not active yet and the main supply sources are the groundwater aquifer and the river Pinios. The reservoir is expected to operate, but until then, the already overexploited aquifer is giving water to all the areas around the lake (Sidiropoulos, 2014). In the city of Volos the supply sources for the coverage of the urban water needs are the 5 springs (from Mountain Pelion) and the 40 wells (from the groundwater of the plain of Karla Watershed, from Nea Ionia and from the groundwater of Volos) (Mylopoulos et al., 2017).

Scenario 1a: *Reducing water losses on Scenario 1*. There are high evaporation losses in the open irrigation channels of Pinios LALR surface network, especially during summer months, where the water needs increase. There are also considerable leakages which aggravate water loss. The lack of maintenance, leads to big water losses, too. This scenario was simulated by using a higher coefficient for transfer efficiency equal to 0.75 instead of 0.4 used in the baseline scenario (for the surface network) and 0.9 instead of 0.8 for the pipeline network (Hydromentor 2015, Alamanos et al., 2016,

2017). Practically, this can be achieved by cleaning (from plants and rubbish) and maintaining the irrigation network. The losses of the network of Volos are estimated to be above the 40% of the total supplied water, and they can also be further reduced (Mylopoulos et al., 2017). In this scenario the losses are considered to be 30% of the total supplied water.

Scenario 2: *The future situation of Karla reservoir and new wells operation*. The main difference, compared to Scenario 1, is that the new irrigation areas that will be served from the reservoir, in the baseline scenario were served by the underlying aquifer (Sidiropoulos, 2014) and the extra water supply from the wells of Karla watershed will feed Volos (Ministry of Environment, 2004, Sidiropoulos et al., 2009). Thus, this connection of the two areas is taken into account, providing the overall results of the Volos' water balance.

Scenario 2a: *Reducing water losses on Scenario 2*, with the same way that it was achieved in Scenario 1a.

All the above management scenarios were examined under three climate change scenarios using the Representative Concentration Pathways (RCPs) as proposed by the IPCC in its 5th Assessment Report (AR5) in 2014 (IPCC, 2014). For the development of these scenarios, the results of the program CORDEX (cordex.org) were used for the RCP scenarios (Moss et al., 2008). Three RCPs are examined (namely the RCP2.6, RCP4.5 and the RCP8.5) that are consistent with a wide range of possible changes in future anthropogenic greenhouse gas (GHG) emissions. Their historic (baseline) period was from 1960 until 1990. Changes of precipitation (P) and temperature (T) are based on the ensemble mean of the 10 simulations of the RCMs based on five (5) different GCMs. The forecast period is from 2006 until 2100 and the grid resolution is 0.11 degrees, about 10x10 km^2. For the data's statistical adjustment (correction) on the existing ones, the D-test was implemented, according to the Equation (1). Thus, P and T have been downscaled by truncating their historical time series by the monthly change of the RCMs' results between the historical base period 1960-2005 and the future periods (divided to 30year-periods until 2100) (Loukas, et al. 2008).

$$PC = [(RCPav - Hav) / Hav] \cdot 100 \quad (1)$$

where: RCPav is the studied variable's average from the RCPs, of all the available RCMs, Hav is the studied variable's average from the historic period 1950-2005, PC is the percentage of change of the studied variables. The final P and T outputs (which will be used in the scenarios) are the estimated future time series and used to develop three representative climate change scenarios. The observed meteorological values are referring to time series of 1960-2009 (present period) for Lake Karla watershed and for Volos is the period 2007-2012. The developed scenarios are:

- The Mild (Conservative) Scenario, where annual temperature is increased by 6.39% and precipitation is decreased by 3.82%
- The Middle (Average) Scenario, where T is increased by 8.30% and P is decreased by 7.57%
- The Worst (Extreme) Scenario, where T is increased by 8.86% and P is decreased by 10.56%

These scenarios caused an increased agricultural water demand and also an increased urban water demand. The new water demand of the city of Volos was calculated using the demand elasticities on P and T (Mylopoulos, 2015). The elasticities express the percentage that the studied variables affect the water consumption.

The water supply from river Pinios, from Karla reservoir, from the aquifers and from Pelion springs, are considered to be the same (as designed in the studies of their operation). Also, the results of the study of Vasiliades and Loukas (2013) shows that the climate change does not affect the natural aquifer of Lake Karla, in contrast to human exploitation which is quite intense and requires immediate reassessment of water demands, before the situation becomes irreversible. The crop distribution can change only after managerial measures that will take into account the climate change, but on behalf of the farmers there cannot be such a prediction (as long as the consequences are not noticeable). So the crop distribution will be considered stable in the climate change scenarios.

4. RESULTS AND DISCUSSION

The results of the simulation procedure described above, regarding the annual water balance, are showing below (Table 1 and Figure 4). The results show that the water balance of Lake Karla Watershed is negative, under every scenario, and this illustrates the reality of the watershed, meaning its excessive irrigation water overexploitation and degradation of water resources. The water balance of Lake Karla Watershed and of Volos, under the climate change scenarios becomes much more negative. In Scenario 2 the Lake Karla Watershed is negative again, but less negative than in the BAU scenario 1 (by 33.6%). This shows the importance and the need of the immediate operation of the reservoir.

Table 1. The water balance for Lake Karla Watershed (LKW), under every management and climate change scenario

Management Scenarios	**Water Balance (hm^3)**			
	Lake Karla Watershed (L.K.W.)	LKW - milder climate change scenario	LKW - middle climate change scenario	LKW - worst climate change scenario
Scenario 1	-186.9	-211.68	-225.94	-235.67
Scenario 1a	-87.6	-103.78	-113.19	-127.92
Scenario 2	-124.1	-145.10	-158.51	-171.96
Scenario 2a	-25.1	-36.33	-48.81	-55.14

The only complete study that examines the water balance of this watershed under climate change is the research program “Hydromentor” (2015). The differences between the meteorological changes are between 2.19% and 7.06%. Thus, the water balances of Lake Karla Watershed under the studied climate change scenarios are a little bit more extreme, compared with Hydromentor’s results, as presented in Tzabiras et al. (2016).

The major difference between these studies is the primary data used for the climate scenarios development; the current study used the results from 10 simulations of the RCMs based on five (5) different GCMs referring to the RCPs, while Tzabiras et al. (2016) used one GCM’s results referring to the SRES scenarios.

The effort for a more representative illustration of the different possible futures, lead us to the use of more meteorological models, which gives a wider uncertainty. Also in our study, eleven different crops of the watershed were taken into account, while Tzabiras et al. (2016) used four main crops, due to insufficient data. This fact also increases the uncertainties in the calculation of the irrigation water requirements and thus, the water balance. The results also show the big uncertainty that accompanies the climate change, and the difficulty to have accurate results, which is also a reality, as it depends on the predictions.

The water balance of the city of Volos is slightly negative in the current situation, but with a 10% losses reduction, becomes positive, showing thus, the big effect that proper network maintenance can have on the coverage of the water needs. Volos’ water balance in Scenario 2 becomes positive, almost as much as the extra water supply of the new wells from Karla. Of course, not all this water amount is going to be used as an extra supply, but there will be a supply management. Lake Karla Watershed is obviously much more vulnerable under climate change.

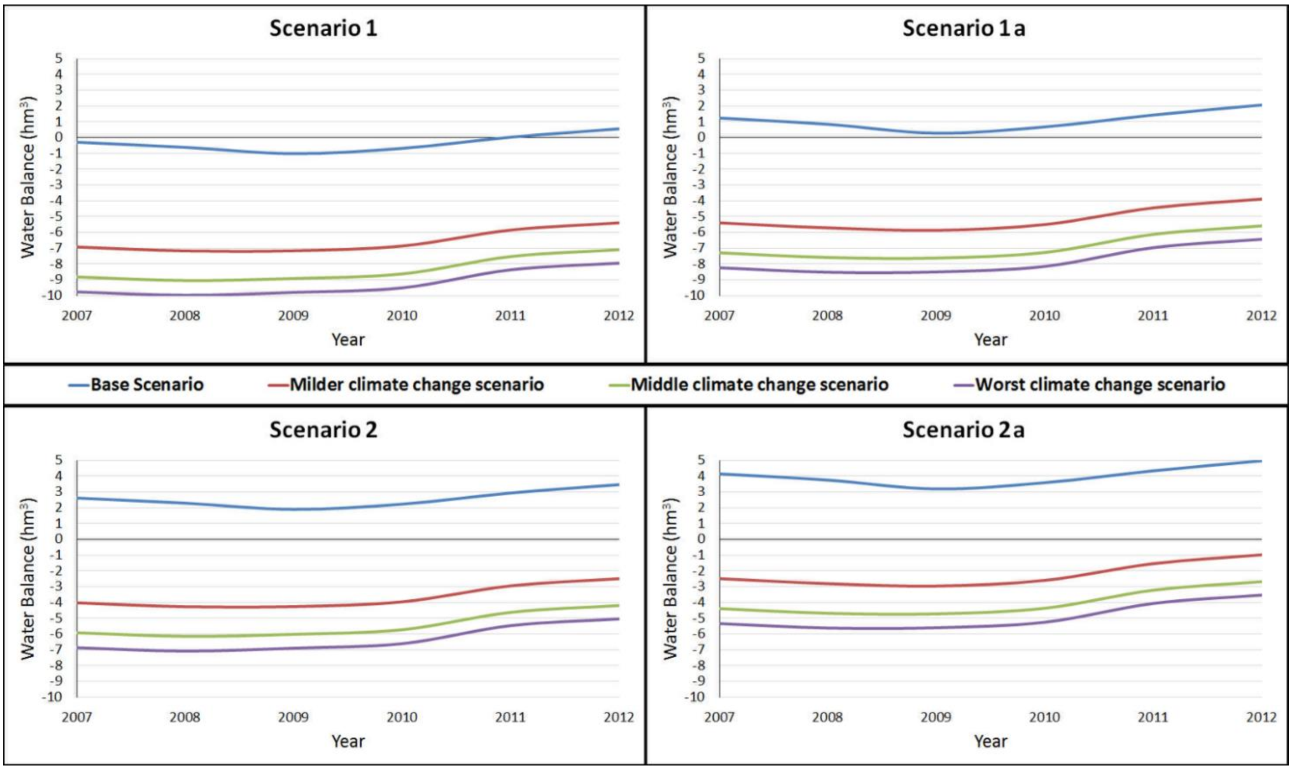


Figure 4. The water balance for Volos city, under every management and climate change scenario

5. CONCLUSIONS

This paper has investigated the water availability in an agricultural watershed and a city, as a system, under management and climate change scenarios. The current study was not specifically designed to provide a new methodological framework, but it could be the basis for a better understanding of the situation and a starting point for the authorities to turn to a more sustainable water demand management. This work has proved once more that the agricultural areas, where the managerial control is not as strict as the urban areas, are more vulnerable. Also, another important finding is that the demand management has a bigger effect on the water balance, than the climate change, on the watershed. This can be justified from the fact that the management Scenario 1a results a change of 53.11% and Scenario 2 results a change of 33.70% on Scenario's 1 water balance, while the worst climate change scenario results a change of 26.03%. On the other hand, in the city we observe the opposite. However, Scenarios 1a, 2 and 2a result a positive water balance in Volos and in that case the extra amount of water has to be preserved with a temporary pause of the operation of some of the wells. Our investigations into this area are still in progress and seem likely to confirm these finding. The continuation of the research includes the examination of more demand management scenarios, technical, economic, social measures, and different water pricing policies.

Acknowledgements

The authors would like to thank: Associate Prof. P. Zanis for providing immediate access to the climate models results from the project 'Application for Regional Climate Data Extraction' http://meteo.geo.auth.gr:3838/#tab-6186-7 elaborated in Aristotle University of Thessaloniki; A. Tsikerdekis, post-doctoral researcher in the same project, for his helpful advice on various technical issues; A. Barcio and V. Ragazzi, under the Erasmus Internship of which the research topic was conceived; Dr. G. Papaioannou for his assistance in the improvement of the maps and the figures.

References

1. Alamanos A., S. Xenarios, N. Mylopoulos, P. Stalnacke (2016) 'Hydro-economic modeling and management with limited data: the case of Lake Karla Basin, Greece', **European Water Journal**, 54, pp. 3-18.
2. Alamanos A., C. Fafoutis, G. Papaioannou and N. Mylopoulos (2017) 'Extension of an integrated hydroeconomic model of Lake Karla watershed, under management, climate and pricing scenario analysis' **Sixth International Conference on Environmental Management, Engineering, Planning and Economics (CEMEPE)**, June 25-30, 2017 Thessaloniki, Greece.
3. Fafoutis C. (2008) 'Integrated approach to water demand management in the residential sector - costing according to the full value'. **PhD Thesis, University of Thessaly, Department of Civil Engineering**, Volos.
4. FAO (2015), **Cropwat**, http://www.fao.org/nr/water/infores_databases_cropwat.html
5. Feilberg M. and O. Mark (2016) 'Integrated Urban Water Management: Improve Efficient Water Management and Climate Change Resilience in Cities', **Sustainable Water Management in Urban Environments**, Springer International Publishing Switzerland 2016, pp. 1–32.
6. Gleick P.H. (2003) 'Global freshwater resources: Soft-path solutions for the 21st century', **Science**, 302, pp. 1524–1528.
7. Hydromentor (2015) '**Development of an integrated monitoring system and management of quantity and quality of water resources in agricultural basins under climate change conditions. Application in the basin of Lake Karla**' Research Program.
8. Intergovernmental Panel on Climate Change, Synthesis Report (2014) 'Contribution of Working Groups I, II and III to the Fifth Assessment Report of the Intergovernmental Panel on Climate Change [Core Writing Team, R.K. Pachauri and L.A. Meyer (eds.)]. **IPCC**, Geneva, Switzerland, 151 pp.
9. International Water Association (IWA) (2015) 'Cities of the future – water security for cities through integrated design and water centric decision making', **http://www.iwa-network.org/projects2/cities-of-the-future.** Last day accessed 23 Nov 2015.
10. Loukas A., L. Vasiliades and J. Tzabiras (2008) 'Climate Change Impacts on Drought Severity', **Advances in Geosciences**, 17, pp. 23-29.
11. Ministry of Environment (2004) '**Study of the supplementary works for the water supply of the area of Volos'**, Athens, October 2004, pp. 72.
12. Molle F. and J. Berkoff (2009) 'Cities vs. agriculture: A review of intersectoral water re-allocation', **Natural Resources Forum**, 33, pp. 6–18.
13. Moss R., M. Babiker, S. Brinkman, E, Calvo, T. Carter, J. Edmonds, I. Elgizouli, S. Emori, L. Erda, K. Hibbard, R. Jones, M. Kainuma, J. Kelleher, J.F. Lamarque, M. Manning, B. Matthews, J. Meehl, L. Meyer, J. Mitchell, N. Nakicenovic, B. O'Neill, R. Pichs, K. Riahi, S. Rose, P. Runci, R. Stouffer, D. van Vuuren, J. Weyant, T. Wilbanks, J.P. van Ypersele and M. Zurek (2008) 'Towards New Scenarios for Analysis of Emissions, Climate Change, Impacts, and Response Strategies', Geneva: **Intergovernmental Panel on Climate Change**, **2008**.
14. Mourato S., M. Moreira and J. Corte-Real (2015) 'Water Resources Impact Assessment Under Climate Change Scenarios in Mediterranean Watersheds', **Water Resources Management**, 29, pp. 2377–2391.
15. Mylopoulos N. (2015) 'Assessment of urban water full cost under the conditions of an economic crisis', **European Water Journal**, 49, pp. 89-105.
16. Mylopoulos N. and A. Mentes (2005) 'A sustainable framework for water resources management in an urban watershed: the case of Volos, Greece', **Urban Water Journal**, 2 (1), pp. 13-22.

17. Mylopoulos N., C. Fafoutis, S. Sfyris and A. Alamanos (2017) 'Impact of water pricing policy and climate change on future water demand in Volos, Greece' **European Water Journal**, 58, pp. 473-479.

18. Organizations for Economic Co-operation and Development (OECD) (2015) 'Programme on Water Governance' **http://www.oecd.org/env/watergovernanceprogramme.htm.** Last day accessed 23 Nov 2015.

19. Russo T., K. Alfredo and J. Fisher (2014) 'Sustainable Water Management in Urban, Agricultural, and Natural Systems' **Water** Vol 6, pp. 3934 – 3956.

20. Sidiropoulos P. (2014) 'Groundwater Resources Management under Uncertainty: The value of information on environmentally degraded aquifers', **PhD Thesis, University of Thessaly, Department of Civil Engineering**, Volos.

21. Sidiropoulos P., N. Mylopoulos, A. Loukas (2009) 'Simulation of the impact of the new wells on Karla's aquifer', **Common Conference: 11th of the Greek Hydro-technical Union (EYE), 7th of the Greek Committee of Water Resources Management (ΕΕΔΥΠ)**, Volos, Greece.

22. Stamou M. (2015) 'Evaluation of the Environmental of the delay of Lake Karla reconstruction', **Msc thesis, University of Thessaly, Department of Economics,** Volos**.**

23. Tzabiras J., L. Vasiliades, P. Sidiropoulos, A. Loukas and N. Mylopoulos (2016) 'Evaluation of Water Resources Management Strategies to Overturn Climate Change Impacts on Lake Karla Watershed', **Water Resources Management,** 30, pp. 5819–5844.

24. Vagiona D. and N. Mylopoulos (2009) 'Water Price Elasticity And Public Acceptability On Conservation Options In The City Of Volos – Greece' **International Journal of Sustainable Development and Planning**, Vol 4, 4, pp. 322–332.

25. Vagiona D., N. Mylopoulos and C. Fafoutis (2005) 'Water demand management aspects in the residential sector. The city of Volos case, Greece' **Proc. 6th International Conference EWRA**, Menton, France, 2005.

26. Vasiliades L. and A. Loukas (2013) 'An Operational Drought Monitoring System Using Spatial Interpolation Methods for Pinios River Basin, Greece' **13th International Conference on Environmental Science and Technology (CEST 2013)**, 5-7 September 2013, Athens, Greece.

27. Water Evaluation And Planning System (WEAP), **Stockholm Environment Institute (SEI) -** weap21.org.

28. Water Utility of Volos (2011) 'The existing water supply situation in the new municipality Volos', **Directorate Planning and Development, Planning and Development Department.**

29. WCRP (2017) '**Coordinated Regional Climate Downscaling Experiment**' (cordex.org).

DEVELOPING AN INTEGRATED SURFACE WATER-GROUNDWATER MODELING SYSTEM FOR UPPER ANTHEMOUNTAS BASIN, GREECE

I. Siarkos, S. Sevastas*, D. Botsis and N. Theodossiou

School of Civil Engineering, Aristotle University of Thessaloniki, GR54124 Thessaloniki, Greece

*Corresponding author: e-mail: sevastas@civil.auth.gr, tel : +302310326576

Abstract

The need of integrated surface water-groundwater management is well recognized, since this type of management can provide a comprehensive and coherent understanding of the water cycle on catchment-level, leading to the proper and efficient use of water. Moreover, integrated water resources management (IWRM) is strictly imposed by the European Union Framework Directive 2000/60/EC and all relevant European and national legislation. An important role towards the successful implementation of IWRM plays the application of numerical modeling, through the coupling of hydrological models with groundwater flow models. Model coupling, even though it is a complex procedure including a number of conceptual and computational challenges, is widely used in modern IWRM. In this perspective, the present study investigates the interaction between surface water and groundwater on catchment-level by developing an integrated modeling system consisting of a hydrological and a groundwater model. The hydrological model was constructed within the framework of the widely used software Soil and Water Assessment Tool (SWAT), while the groundwater model was formed applying the MODFLOW code, which has evolved into the worldwide standard computer program used in groundwater modeling. The aforementioned models were interlinked and applied for the combined simulation of hydrological processes and groundwater flow in Upper Anthemountas basin. Moreover, a sensitivity analysis was performed in the case of groundwater flow model in order to investigate the impact of various model parameters (e.g. hydraulic conductivity, storativity, wells pumping rates, boundary conditions) on the model results (hydraulic head), which will be helpful in the case of a future calibration of the model.

Keywords: integrated water resources management; hydrological modeling; groundwater modeling; surface water-groundwater interactions; Upper Anthemountas basin

1. INTRODUCTION

In various parts of the world, both surface water and groundwater resources are considered important for the sustainability of local society and ecosystems, since they preserve life and cover the various water needs (Shanafield et al., 2012; Simpson et al., 2013; Wu et al., 2015). For the better management of water resources in those regions, which is based on the principles of integrated water resources management (IWRS), a complete understanding and a thorough investigation of the integrated surface water-groundwater system are required (Spanoudaki et al., 2005; Cho et al., 2009; Wu et al., 2015). To accomplish this task, numerical modeling is usually implemented, through the coupling of hydrological models with groundwater flow models. In this way, a spatially and temporally detailed description of both the hydrological processes on basin level and groundwater flow is achieved (Sophocleous and Perkins, 2000; Barthel, 2006; Wu et al., 2014; Wu et al., 2015).

Even though numerical modeling is widely used in modern IWRM, the integration between hydrological and groundwater flow models is considered to be a complex procedure, since the interaction between the two regimes is influenced by a number of factors, such as subsurface hydraulic properties, surface water and groundwater flow patterns, topography, and type of land use (Sophocleous, 2002; Barthel, 2006; Chao et al., 2009). Taking the aforementioned factors into consideration, it is important that the model system is able to investigate the hydrologic effects in conjunction with the proper study of surface water-groundwater interaction. Moreover, with regard to groundwater flow study, it is essential to simulate the spatial occurrence and distribution of return flow (Kim et al., 2008). The combined use of SWAT - MODFLOW models is able to successfully address these issues (Sophocleous and Perkins, 2000; Kim et al., 2008).

Within this context, in the present study an integrated modeling system applying the widely used computer codes, SWAT and MODFLOW, and consisting of a hydrological and a groundwater model was developed, in order to investigate surface water-groundwater interactions in the Upper Anthemountas basin. The governing equations solved by SWAT and MODFLOW can be found in Winchell et al. (2013) and McDonald and Harbaugh (1988) respectively. Regarding the simulation of hydrological processes, a model developed in a previous study (Sevastas et al., 2017a) was used, while concerning the groundwater flow simulation, a transient model was formed. This model was based on both the aforementioned hydrological model and a calibrated steady-state model already developed for the reference area (Sevastas et al., 2017b). The key point of the whole procedure is that the outputs of the hydrological model in terms of water percolation are introduced as inputs to the groundwater flow model, providing the aquifer recharge deriving from precipitation. Furthermore, a sensitivity analysis regarding the groundwater flow model was conducted in order to: a) gain insight into model behavior and b) identify those model parameters (e.g. hydraulic conductivity, storativity, wells pumping rates, boundary conditions) that affect most the model results and, therefore, should be taken seriously into account during a future model calibration (Carrera et al., 2010; Siarkos and Latinopoulos, 2016).

2. STUDY AREA

The Upper Anthemountas sub-basin, being the eastern part of the entire Anthemountas basin, is located in Halkidiki Peninsula, Greece, south east of the city of Thessaloniki (Figure 1). The basin covers an area of approximately 110 km^2, and is bordered to the west by the Lower Anthemountas basin and to the south by the Nea Moudania basin. The climate of the study area is typically Mediterranean with relatively low annual precipitation (470 mm) and high temperatures during summer (Latinopoulos, 2001; Sevastas et al., 2017a, 2017b).

The Upper Anthemountas basin is a typical rural area dominated by complex cultivation patterns (wheat, corn, cotton, alfalfa and olive trees) and mixed forest (mainly various types of oaks along with Platanus and Chestnuts trees). Water demand in the region is confined mainly to drinking and irrigation, and is met respectively through few public supply wells and a large number of privately owned irrigation wells. Moreover, there are few wells for both livestock and industrial purposes, as shown in Figure 1. Currently water needs in the region are exclusively covered by a semi-confined aquifer system, consisting of successive water-bearing layers without regular geometric growth, separated by lenses of semi-permeable or impermeable materials. From hydrological point of view, the catchment consists of a dense well-formed stream network. Most time of the year, surface flow of the river is very limited due to low precipitation and to the fact that some upper geological layers are comprised of semi-permeable soils. As a result, the river appears to have surface outflows only for a short time after intense rainfall (Latinopoulos, 2001; Sevastas et al., 2017a, 2017b).

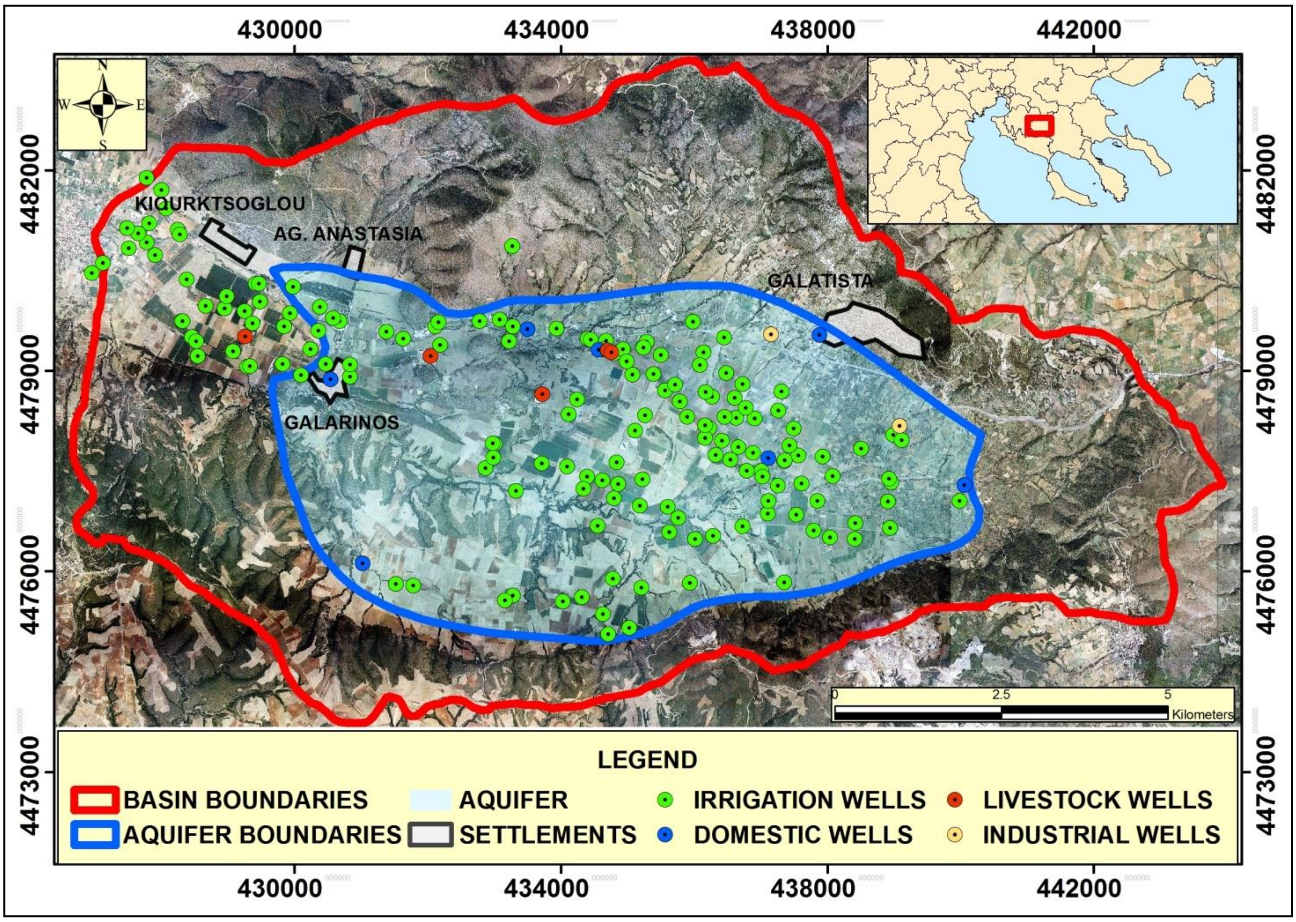


Figure 1. Boundaries of the Upper Anthemountas basin and the aquifer under study, along with the location of the operating wells per water use

3. HYDROLOGICAL MODELING

For the purposes of the present study, a hydrological model previously developed by Sevastas et al., (2017a) was adopted and kept intact. In short, the vital input data used in this model are classified into four major categories: i) topography (elevation), ii) land cover, iii) soil, and iv) climate data. Specifically, a topographic map was created by digitizing contours from twenty three connected Hellenic Military Geographical Service (HMGS) map sheets that cover the entire basin, with a scale of 1:5000. The map was then transformed into a Digital Elevation Model (DEM) in order to delineate the watershed. Multiple field inspections were performed in the study area so as to update the available CORINE2000 land use map and produce a more accurate land cover status of the reference area. A soil map was produced by collecting and analyzing thirty two soil samples from all over the study area. Figure 2 depicts all input spatial layers imported to the model. In addition, a ten year weather dataset (2002 to 2011) was applied for the simulation, containing precipitation and temperature values, obtained from the National Agricultural Research Foundation (NAGREF) climate station, which is located 15 kilometers away from the center of the basin. An in-depth description regarding all the aforementioned essential input data is fully presented in Sevastas et al. (2017a).

The model was run for a 10-year period, from 01/01/2002 to 31/12/2011, with a 2-year warm up period (years 2002 and 2003) in order to define the initial conditions. Model outputs concerning precipitation, evapotranspiration, recharge and surface runoff, were obtained on a monthly step for eight years (2004 to 2011) and are presented in Figure 3. According to this figure, poor values of surface runoff were generated. However, this is consistent with the fact that surface outflows in the

basin emerge only for a short period of time and, mainly, after intense rainfall events. It should be mentioned that the recharge values estimated were introduced as inputs to the groundwater model.

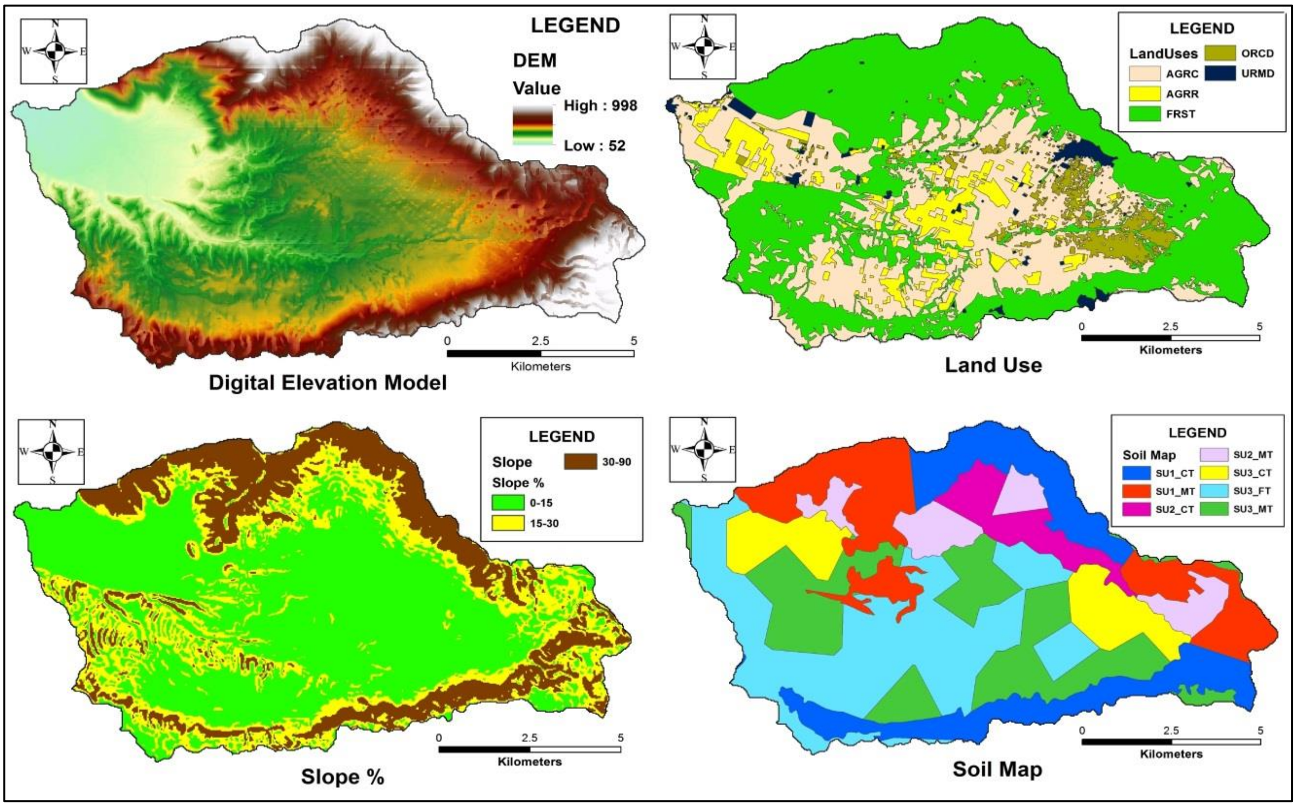


Figure 2: Input layers of the hydrological model adopted in this study (Sevastas et al., 2017a)

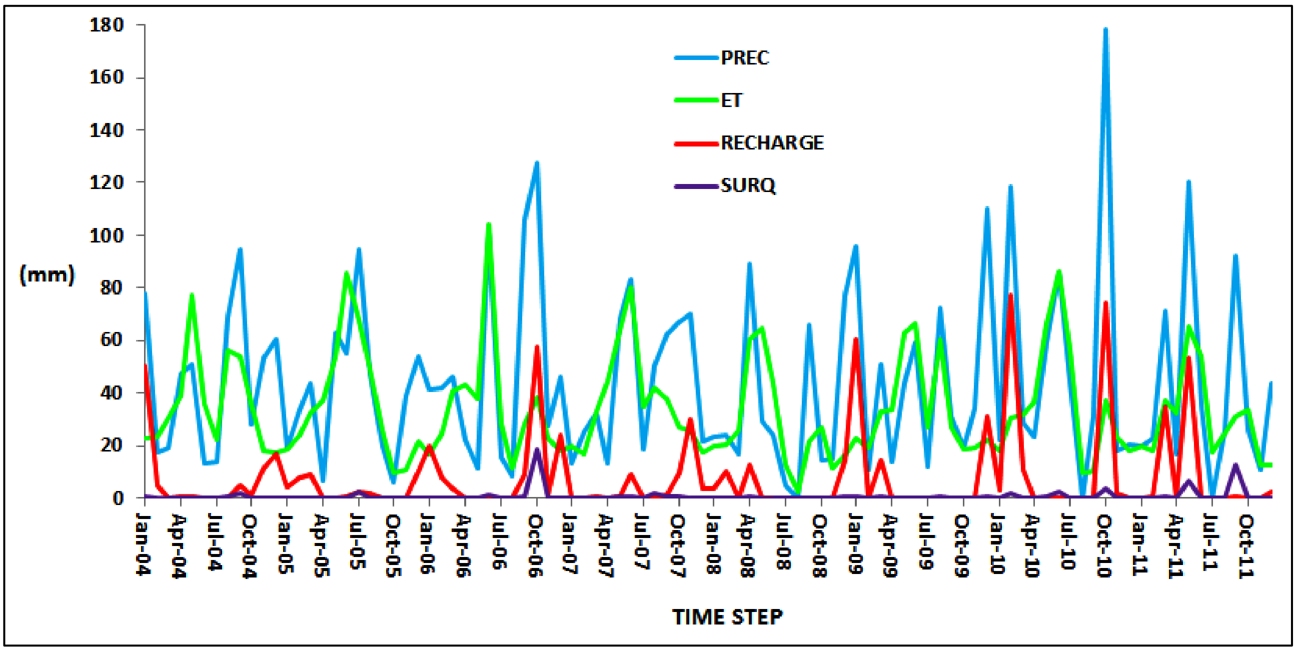


Figure 3: SWAT model results in Upper Anthemountas basin for years 2004 to 2011, in terms of precipitation (PREC), evapotranspiration (ET), recharge and surface runoff (SURQ)

4. GROUNDWATER MODELING

4.1 Conceptual model development

A prerequisite for the development of the transient model is the development of the conceptual model of the aquifer under study (Latinopoulos and Siarkos, 2014). In the present study, the conceptual model formed by Sevastas et al. (2014) and improved in Sevastas et al. (2017b) was used, while making certain modifications related to the nature of the problem under study (transient simulation). These modifications were necessary since in the previous studies only steady-state simulations were conducted, and they include:

- Determination of the aquifer's storativity which was based on values derived by previous research conducted in the study area (Latinopoulos, 2001). According to this study, storativity values range between $4.3*10^{-4}$ and $6.2*10^{-2}$. Since no reliable number of pumping tests exist and since they are not properly distributed, thereby making it difficult to assign different storativity zones by applying the Thiessen Polygon method (Sevastas et al., 2014), it was assumed that storativity: a) remains constant throughout the whole study area and b) is equal to the mean value ($3.1*10^{-2}$) of the aforementioned value range.

- Re-estimation of the equivalent pumping rate of irrigation wells, which is based on the total amount of water used for irrigation purposes and the total number of irrigation wells existing in the study area, since they operate only during the pumping/irrigation period (May-September, 5-month irrigation period). With regard to the other well categories, i.e. domestic, livestock and industrial wells, no re-calculation is required since it was considered that they operate during the whole year, as it is in the case of the steady-state simulation. Furthermore, what is worth mentioning is that for the calculation of the irrigation wells pumping rates, the total amount of irrigation water defined during the calibration procedure of the steady-state model developed by Sevastas et al., (2017b), was taken into consideration.

Re-calculation of the amount of water returning to the aquifer as irrigation return flow, based on the total amount of irrigation water defined during the calibration procedure of the steady-state model and assuming that 15% of irrigation water returns into the aquifer.

4.2 Transient model development

The groundwater flow simulation procedure involved the development of a transient model based on the hydrological model described in Section 3 and a calibrated steady-state model developed in a previous study (Sevastas et al., 2017b). As already mentioned, the outputs of the hydrological model as far as the percolation values are concerned were introduced as inputs to the transient model to obtain the aquifer recharge values resulting from precipitation. On the other hand, the values of various parameters as they were set in the steady-state model (e.g. boundary conditions) or they were adjusted during its calibration procedure (e.g. hydraulic conductivity), were assigned to the transient model. With regard to other model parameters, such as storativity, irrigation wells pumping rates and irrigation return flow, their values were based on the description made in Section 4.1. Furthermore, the results of the steady-state model with regard to the hydraulic head distribution were introduced as initial conditions to the transient model. Finally, the spatial discretization of the model was kept identical to the steady-state one (Sevastas et al., 2017b), while an 8-year simulation period was considered (2004-2011, equal to the simulation period of the hydrological model), which was divided into 96 monthly stress periods. The purpose of this simulation is twofold: a) to get a generic image of aquifer's behaviour under certain recharge and discharge conditions, as well as of the temporal variation of groundwater levels and b) to examine how the coupling between the hydrological and the groundwater flow models works at an initial stage. Due to the aforementioned reasons, no calibration of the transient model was performed.

The results of the transient simulation are expressed as water table contours maps and hydraulic head evolution chart, along with mass water balances for the model domain. First of all, Figure 4 depicts

the difference in hydraulic head distribution between the beginning (2004) and the end (2011) of the simulation period. It is observed that in most parts of the region, with an exception of a part located north-east of the study area (at a close distance to the eastern boundary), groundwater levels decrease (hydraulic head at the beginning of simulation is higher than in the end).

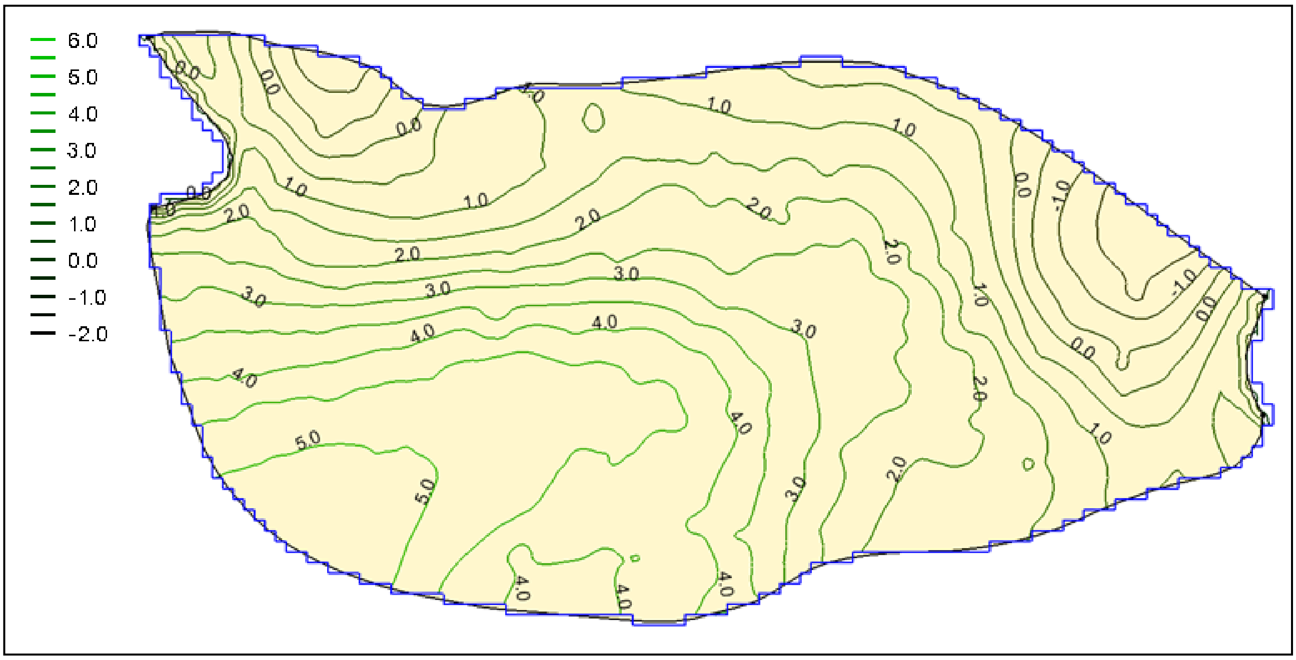


Figure 4. Difference (in m) in hydraulic head distribution between the beginning (2004) and the end (2011) of the simulation period.

Moreover, in Figure 5 the time variation of the hydraulic head (mean values) is illustrated. What is worth mentioning is that hydraulic head follows a downward trend on annual base from the beginning of the simulation (Jan-2004) until the end of the year 2009 (Dec-2009), and an upward trend from this point until the end of the simulation period (Dec-2011). This is wholly attributed to the fact that aquifer's recharge values in years 2010 and 2011 are presented rather high in relation to previous years as clearly displayed in Figure 3. Moreover, it should be noted that the largest hydraulic head decline occurs during the irrigation period (May-September), when the irrigation wells are fully operational leading to substantial increase of aquifer discharge.

Finally, Figure 6 shows the monthly distribution of the mean values of the water balance components of the Upper Anthemountas aquifer. In this figure, the term "Recharge" refers to the water inflow into the aquifer system, while "CHB" (Constant Head Boundaries) and "Wells" correspond to the outflow from the system. Inflow to the system is also observed through the eastern aquifer boundary, but in rather low quantities that cannot be depicted in the diagram. The main conclusion stemming from this figure is that the water outflow is higher than the water inflow during the pumping season (May-September), whereas the reverse occurs during the non-pumping season (October-April).

5. SENSITIVITY ANALYSIS

After the development and application of the hydrological and groundwater flow models, as well as their coupling procedure, a sensitivity analysis in the case of the transient groundwater flow model was performed. The analysis aims to investigate the influence of the model's input parameters upon the results of the model, i.e. hydraulic head distribution, and identify those parameters that are most sensitive and should be taken seriously into account during a future model calibration procedure. The model parameters that were considered during the sensitivity analysis were hydraulic conductivity, storativity, irrigation wells pumping rates, and boundary conditions, omitting aquifer's recharge since it derives from the hydrological model. The procedure was implemented by modifying only one input

parameter at a time while keeping the others constant (Don et al. 2005; Siarkos and Latinopoulos, 2016).

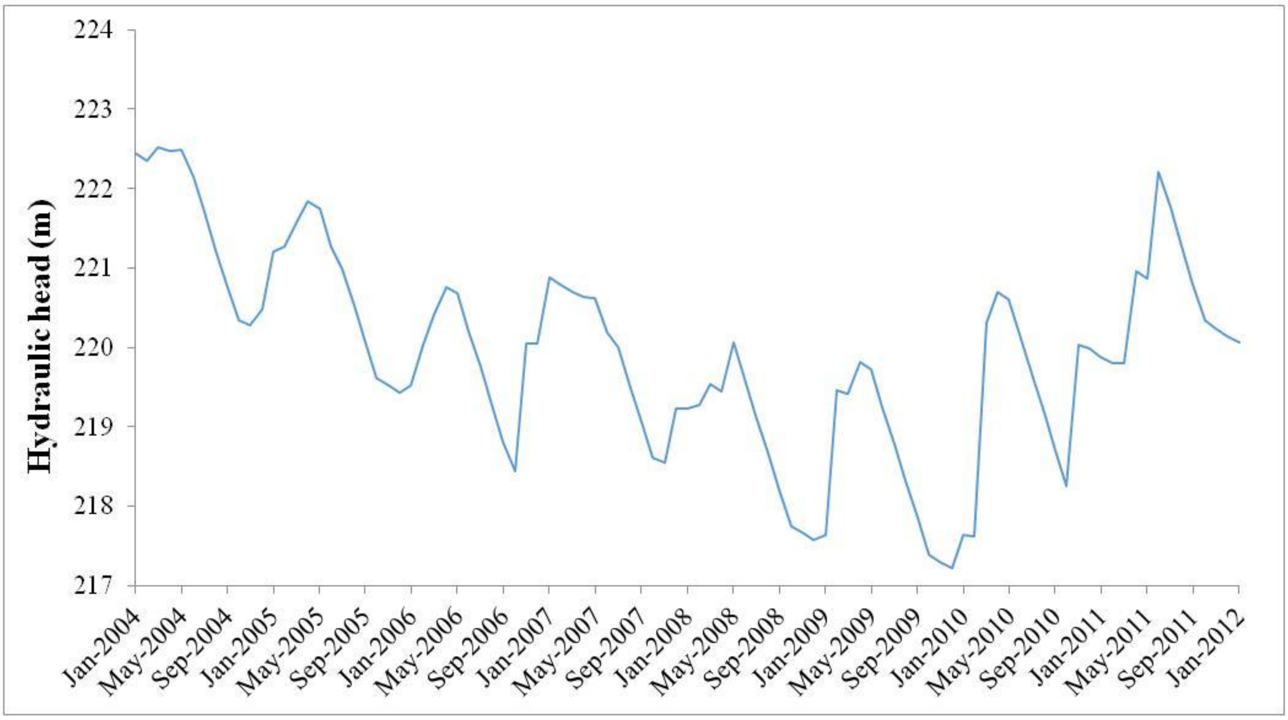


Figure 5. Time variation of hydraulic head (mean values) in the study area.

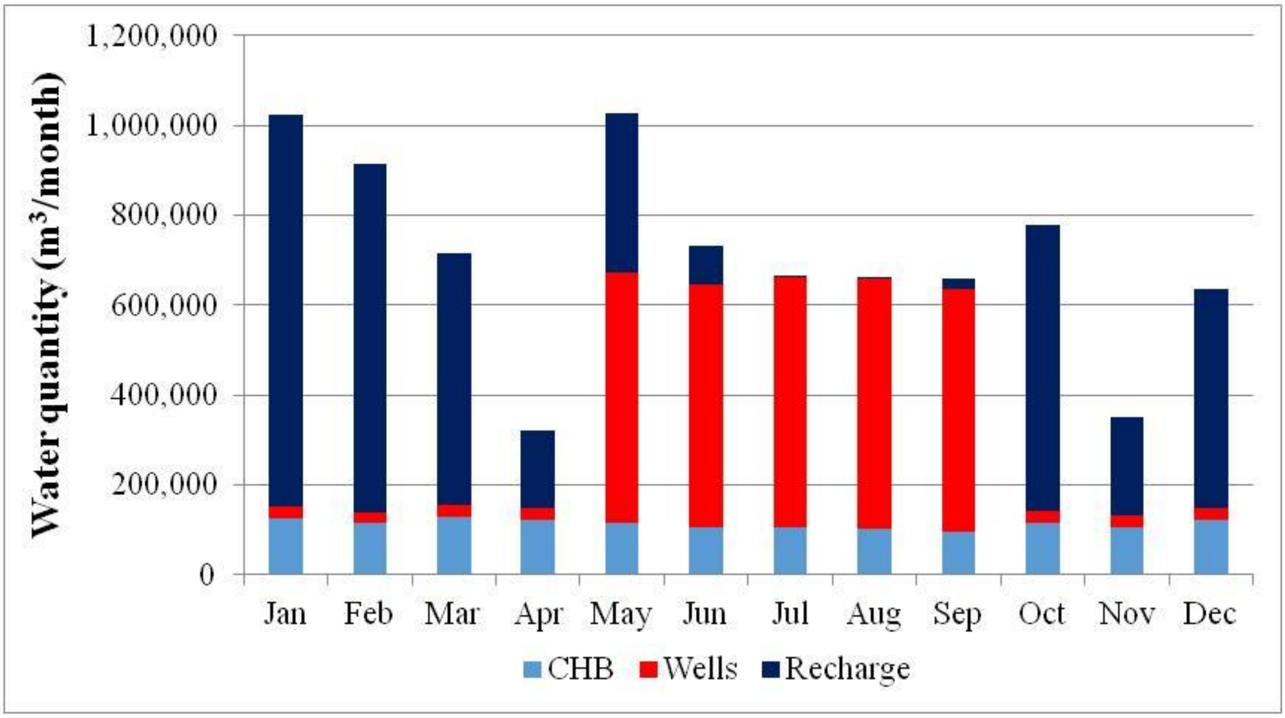


Figure 6. Monthly distribution of the water balance components (mean values) of the aquifer under study.

Figure 7 presents the influence of the model parameters examined through the sensitivity analyis on the hydraulic head (mean value) at the end of the simulation period (2011). The whole procedure includes the estimation of the hydraulic head variation due to the modification of the parameters examined for ±5, ±10, ±15 and ±20%. Based on Figure 7, the parameter of major influence on the hydraulic head is the eastern boundary of the aquifer. With regard to the other parameters, pumping rates of irrigation wells has remarkable influence on the hydraulic head values, while storativity is

the parameter which is characterized by the smallest effect. Finally, it should be noted that increase of the hydraulic head values assigned to both aquifer boundaries, as well as of the aquifer storativity, results in groundwater levels increase in the study area. Higher increase is observed in the case of modifying aquifer boundaries. On the contrary, increase of aquifer's hydraulic conductivity and irrigation wells pumping rates leads to hydraulic head decline.

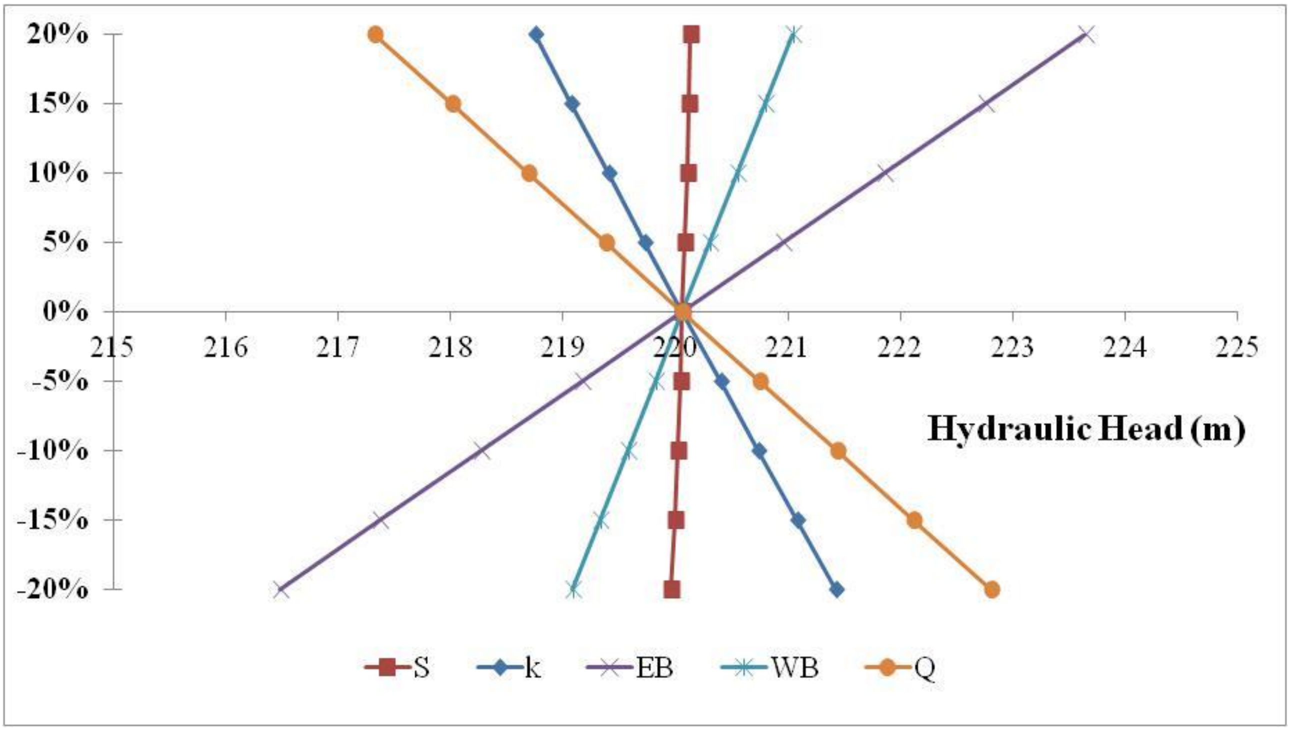


Figure 7. Influence of the various model parameters (S - storativity, k - hydraulic conductivity, EB - Eastern Boundary, WB - Western Boundary, Q - pumping rates) on the hydraulic head (mean values) at the end of the simulation period (2011).

6. CONCLUSIONS

In the present study, surface water-groundwater interactions in the Upper Anthemountas basin were investigated through the development of an integrated modeling system consisting of a hydrological and a groundwater flow model. In the first case, a hydrological model developed in a previous study was adopted, while, in the second case, a transient groundwater flow model, based on a previously developed steady-state model, was built. The two models were applied for a 8-year time period (2004-2011), while their connection was established through the introduction of the hydrological model outputs, in terms of aquifer recharge, as inputs to the groundwater model. Finally, a sensitivity analysis in the case of the groundwater model was carried out as an initial stage for a future model calibration.

Regarding the results of the hydrological processes simulation, poor values of surface runoff were produced, which is consistent with the fact that surface outflows in the basin emerge only for a short period of time. Moreover, high recharge values were observed beyond the year 2010 in relation to previous years, a fact which greatly affects the results of the groundwater flow model. Concerning the groundwater model, the results indicate that, in general, groundwater levels decrease over time in the study area mainly due to groundwater abstraction for irrigation purposes. The major decline of hydraulic head is observed during the irrigation period (May-September), when irrigation wells start operating. Finally, as far as the sensitivity analysis is concerned, results reveal that aquifer's eastern boundary is the most sensitive parameter considerably affecting the hydraulic head values in the study area. Irrigation wells pumping rates is the second most sensitive parameter, while storativity appears to have minimum influence on the model.

For future research, calibration of both the hydrological and the groundwater flow models has to be conducted in order to improve the integrated modeling system and develop a reliable projection and management tool for the area under study. In this case and as far as the groundwater flow model is concerned, great caution regarding the definition of the aquifer's boundary conditions and more specifically the determination of the hydraulic head values assigned to them has to be given, since they greatly affect model results.

References

1. Barthel R. (2006) 'Common problematic aspects of coupling hydrological models with groundwater flow models on the river catchment scale', **Advances in Geosciences**, Vol. 9, pp. 63-71.
2. Carrera J., J.J. Hidalgo, L.J. Slooten and E. Vázquez-Suñé (2010) 'Computational and conceptual issues in the calibration of seawater intrusion models', **Hydrogeology Journal**, Vol. 18, pp. 131-145.
3. Cho J., V.A. Barone and S. Mostaghimi (2009) 'Simulation of land use impacts on groundwater levels and streamflow in a Virginia watershed', **Agricultural Water Management**, Vol. 96, pp. 1-11.
4. Don N.C., H. Araki, H. Yamanishi and K. Koga (2005) 'Simulation of groundwater flow and environmental effects resulting from pumping', **Environmental Geology**, Vol. 47, pp. 361-374.
5. Kim N.W., I.M. Chung, Y.S. Won and J.G. Arnold (2008) 'Development and application of the integrated SWAT – MODFLOW model', **Journal of Hydrology**, Vol. 356, pp. 1-16.
6. Latinopoulos D. and I. Siarkos (2014) 'Modelling the groundwater flow to assess the long-term economic cost of irrigation water: application in the Moudania basin, Greece', In: Giannino M. (ed.), **Drinking Water and Water Management: New Research**, Nova Publishers, New York, pp. 249-274.
7. Latinopoulos P. (2001) **'Investigation and exploitation of the water resources in the basin of Upper Anthemountas (in Greek)'**, Research Project, Final Report prepared for: Municipality of Anthemountas, Aristotle University of Thessaloniki, Greece.
8. McDonald M.G. and A.W. Harbaugh (1988) **'A modular three-dimensional finite-difference ground-water flow model'**, U.S. Geological Survey, Techniques of Water-Resources Investigation, Book 6, Reston, VA, 586 pp.
9. Sevastas S., I. Siarkos, N. Theodossiou and I. Ifadis (2014) 'Simulating groundwater flow in Upper Anthemountas basin in Chalkidiki applying Modflow and Geographic Information System', Proc. of Int. Conf. **10th International Hydrogeological Congress**, Thessaloniki, Greece, 8-10 October, 2010.
10. Sevastas S., I. Siarkos, N. Theodossiou, I. Ifadis and K. Kaffas (2017a) 'Comparing hydrological models built upon open access and/or measured data in a GIS environment', Proc. of Int. Conf. **6th International CEMEPE & SECOTOX Conference**, Thessaloniki, Greece, 25-30 June, 2017.
11. Sevastas S., I. Siarkos, N. Theodossiou and I. Ifadis (2017b) 'Establishing wellhead protection areas and managing point and non-point pollution sources to support groundwater protection in the aquifer of Upper Anthemountas, Greece', **Water Utility Journal**, Vol. 16, pp. 81-95.
12. Shanafield M., P.G. Cook, P. Brunner, J. McCallum and C.T. Simmons (2012) 'Aquifer response to surface water transience in disconnected streams', **Water Resources Research**, Vol. 48, W11510.

13. Siarkos I. and P. Latinopoulos (2016) ‘Modeling seawater intrusion in overexploited aquifers in the absence of sufficient data: application to the aquifer of Nea Moudania, northern Greece’, **Hydrogeology Journal**, Vol. 24(8), pp. 2123-2141.
14. Simpson S.C., T. Meixner and J.F. Hogan (2013) ‘The role of flood size and duration on streamflow and riparian groundwater composition in a semi-arid basin’, **Journal of Hydrology**, Vol. 488, pp. 126-135.
15. Sophocleous M. (2002) ‘Interactions between groundwater and surface water: the state of the science’, **Hydrogeology Journal**, Vol. 10, pp. 52-67.
16. Sophocleous M. and S.P. Perkins (2000) ‘Methodology and application of combined watershed and ground-water models in Kansas’, **Journal of Hydrology**, Vol. 236, pp. 185-201.
17. Spanoudaki K., A. Nanou, A.I. Stamou, G. Christodoulou, T. Sparks, B. Bockelmann and R.A. Falconer (2005) ‘Integrated surface water-groundwater modelling’, **Global NEST**, Vol. 7(3), pp. 281-295.
18. Winchell M., R. Srinivasan, M. Di Luzio and M. Arnold (2013) **‘ArcSWAT interface for SWAT2012: User’s guide’**, Texas Agrilife Research and USDA Agricultural Research Service, Temple, Texas 76502, USA.
19. Wu B., Y. Zheng, Y. Tian, X. Wu, F. Han, J. Liu and C. Zheng (2014) ‘Systematic assessment of the uncertainty in integrated surface water-groundwater modeling based on the probabilistic collocation method’, **Water Resources Research**, Vol. 50, pp. 5848-5865.
20. Wu B., Y. Zheng, X. Wu, Y. Tian, F. Han, J. Liu and C. Zheng (2015) ‘Optimizing water resources management in large river basins with integrated surface water-groundwater modeling: A surrogate-based approach’, **Water Resources Research**, Vol. 51, pp. 2153-2173.

COMPARISON OF STOCHASTIC AND MACHINE LEARNING MODELS IN STREAMFLOW FORECASTING

D. Botsis[a]*, P. Latinopoulos[a] and K. Diamantaras[b]

[a]School of Civil Engineering, Aristotle University of Thessaloniki, GR- 54124 Thessaloniki, Macedonia, Greece,
[b]Information Technology Department, A.T.E.I. of Thessaloniki, GR-57400 Sindos, Greece

*Corresponding author: e-mail: jimbotsis@civil.auth.gr, tel : +306973822431

Abstract

One of the fundamental issues of hydrology is the rainfall-runoff relationship and streamflow forecasting that plays an important role in water balance. Up-to-date a large number of models have been developed to simulate the relationship of rainfall-runoff and forecasting the streamflow. In the present study a comparison between stochastic and machine learning methods is performed with respect to their forecasting capabilities and their performance and reliability in short term streamflow forecasting is evaluated. For this purpose, five popular methods were employed, two stochastic methods and three machine learning models, specifically Auto Regressive Moving Average (ARMA), Auto Regressive Integrated Moving Average (ARIMA), Multilayer Feed-Forward Artificial Neural Network (MFNN), Bayesian Neural Networks (BNN) and Ensemble methods (Boosting). The daily rainfall and streamflow data of two mountainous watersheds were used as a case study for developing the rainfall-runoff models. The performance and reliability of the models were evaluated through three different criteria: correlation coefficient, root mean square error and mean absolute error. Each criterion is represented by an efficiency indicator, estimated from the comparison of predicted values and the measured targets that have been initially placed. The objective of this paper is to illustrate the effectiveness of stochastic and machine learning models in streamflow forecasting. Our results show that both the stochastic and machine learning models can successfully approximate the rainfall-runoff relationship and efficiently estimate the resulting streamflow. The results from the individual methods do not differ dramatically and by and large all models have good performance and provide accurate predictions, but the best performing model is BNN.

Keywords: streamflow forecasting; ARMA; ARIMA; artificial neural networks, Bayesian neural networks; boosting

1. INTRODUCTION

Streamflow forecasting is very significant for watershed management. Planning and development of many water management applications require reliable streamflow predictions. Water management includes treatment and supply of drinking water, flood control works, water resources management, hydropower generation, construction of complex hydraulic works, optimal environmental operations, etc (Wang et al., 2009; Guo et al., 2011; Huang et al, 2014). A widespread technique used by many researchers for hydrologic time-series modeling is stochastic hydrology, including autoregressive moving average (ARMA) and autoregressive integrated moving average (ARIMA) models (Valipour et al., 2012, 2013). The key feature of these models is the assumed linearity of the relationship between inputs and outputs. However, in real terms the relationship between rainfall and runoff is nonlinear and, in addition, has a large degree of uncertainty.

Machine learning methods are an alternative and complementary set of techniques to traditional models. Since the early nineties extensive research has been devoted in the science of hydrology to investigating the potential of Artificial Neural Networks (ANN) as computational tools that simulate the nonlinear relationship of complex hydrological phenomena. Artificial neural networks have been successfully used in hydrology-related areas, such as streamflow forecasting, groundwater modeling, watershed management and rainfall-runoff simulation (ASCE Task Committee, 2000). In the last decades many non-linear data-driven models, such as multilayer feed-forward Artificial Neural Network (MFNN) (Zealand et al., 1999; Sahoo and Ray, 2006; Botsis and Latinopoulos, 2010; Botsis et al., 2011), Bayesian Neural Networks (BNN) (Khan and Coulibaly, 2006; Humphrey et al., 2016), and Ensemble methods (Boosting) (Erdal and Karakurt, 2012), have been proposed for rainfall-runoff simulation and streamflow forecasting.

The present study aims to compare ARMA and ARIMA models with machine learning methods, based on streamflow forecasting. The autoregressive and machine learning models were programmed in MATLAB software environment. The models were applied on data from two mountainous catchments in Greece: 1) Venetikos river watershed with total area 491.9 m^2 and 2) Kalarrytikos river watershed with total area 103.7 m^2.

2. SIMULATION MODELS

2.1 ARMA and ARIMA models

The ARMA(p,q) is one of the most common methods in time series analysis and the assumed model follows equation (1).

$$y_t = \sum_{i=1}^{p} \varphi_i \cdot y_{t-i} - \sum_{i=1}^{q} \theta_i \cdot \varepsilon_{t-i} + \varepsilon_t \qquad (1)$$

where y is the output (streamflow) at time t, p is the order of autoregressive model, q is the order of moving average model, φ is the vector of autoregressive parameters, θ is the vector of moving average parameters and ε_t is white noise (Wei, 2006). The ARIMA(p,d,q) model is defined by the expression (2).

$$y_t = \sum_{i=1}^{p} \varphi_i \cdot y_{t-i} + \sum_{i=1}^{d} \gamma_i \cdot x_{t-i} - \sum_{i=1}^{q} \theta_i \cdot \varepsilon_{t-i} + \xi_t \qquad (2)$$

where d is the differentiation order in the regular or nonregular part of the stationary series and γ_i is the weight parameter of the exogenous input x_t (rainfall). It should be noted that in equation (2) when d = 0, the ARIMA model becomes ARMA (Wei, 2006).

2.2 Artificial Neural Networks

The most common neural network used in hydrology applications is the multilayer feed-forward network, trained with the back-propagation algorithm (ASCE Task Committee, 2000). The back-propagation algorithm, introduced by Rumelhart et al (1986), is essentially a gradient-descent technique that minimizes the network error function (Haykin, 1999, ASCE Task Committee, 2000). The neural network employed in this investigation is the multilayer feed-forward model, trained with back-propagation. For streamflow forecasting, a network with one hidden layer was trained. More specifically, the networks were designed with thirteen inputs for the first watershed and seven inputs for the second watershed, h neurons in the hidden layer (testing 2, 3, 4, 7, 8, 10, 20 and 50 neurons) and one neuron in the output layer (the architecture of the neural network is shown in Figure 1).

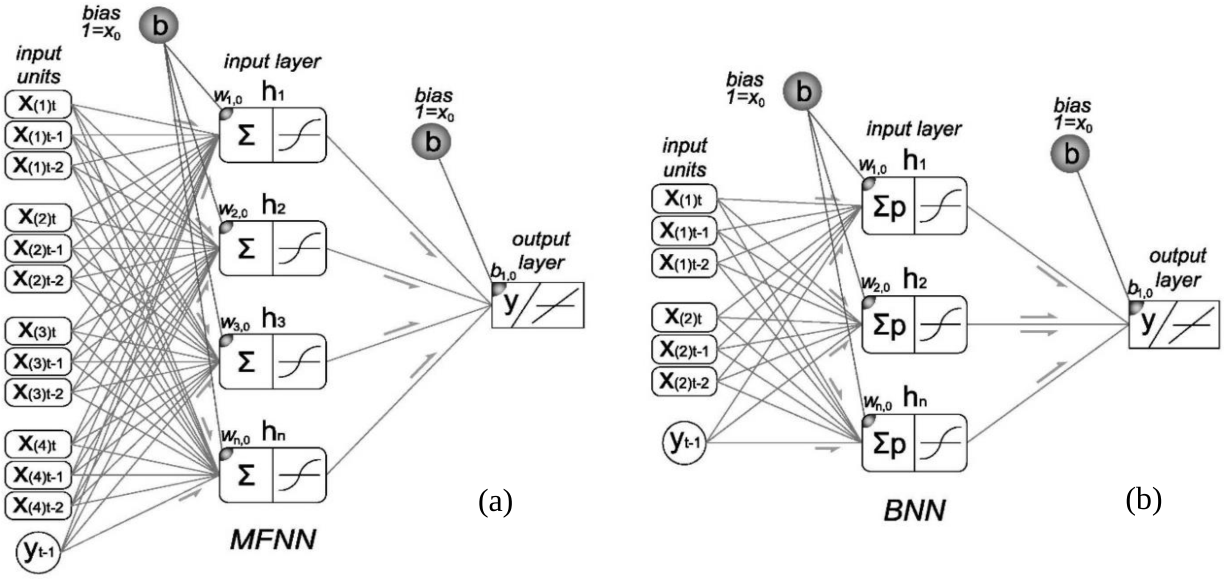


Figure 1. (a) Architecture of Multilayer Feed-forward Neural Network (MFNN) for Ventetikos watershed and (b) architecture of Bayesian Neural Network (BNN) for Kalarrytikos watershed.

The Levenberg-Marquardt version of Back-Propagation was selected as the learning algorithm, because it is faster and more reliable than any other back-propagation flavors (Jeong and Kim, 2005). The computation of the local gradient for each neuron of the neural network requires knowledge of the derivative of the transfer function associated with that neuron. For this derivative to exist, the function should be continuous. In basic terms, differentiability is the only requirement that a transfer function has to satisfy (Haykin, 1999). The transfer function should be differentiable, as most training algorithms in multilayer networks are based on optimization methods that use first- and second-order derivatives. In this study the hyperbolic tangent function (expression 3) is used, which is continuous, differentiable, and monotonically increasing.

$$g(x) = \frac{1-e^{-x}}{1+e^{-x}} \tag{3}$$

The output layer provides a linear activation function, so the output range is between -∞ and ∞. For the early stopping of the training process the cross validation method was used, which sets an acceptable error level for training and stops training when the mean square error reaches a minimum in the validation phase.

2.3 Bayesian Neural Networks

When the neural network learning process is implemented in the Bayesian framework, the weights w of the neural network are considered random variables (Foresee and Hagan, 1997). According to Bayes theorem, the posterior probability distribution p(w│D) conditioned on the data set D is given by the expression 4.

$$p(w|D) = \frac{p(D|w)p(w)}{p(D)} \tag{4}$$

where p(D│w) is the data likelihood function, p(w) is the prior weight distribution, p(D) is a normalizing factor known as the marginal distribution, which ensures that the total probability is equal to unity (Bishop, 2005). The Bayesian Neural Network (BNN) employed here is a two-layer feed-forward network trained with the Bayesian regularization back-propagation algorithm. More specifically the networks were designed with thirteen inputs for the first watershed and seven inputs for the second watershed, h neurons in the hidden layer (testing 2, 3, 4, 7, 8, 10, 20 and 50 neurons)

and one neuron in the output layer (see Figure 1). The activation function used is the hyperbolic tangent.

2.4 Boosting algorithm

Boosting algorithms for regression (Freund, 1995; Freund and Schapire, 1995) can reduce the error rate, when a small number of big errors contribute a significant part of the mean squared error. Avnimelech and Intrator (1999) proposed a boosting algorithm for forecasting optimization and in this study one of the Boosting algorithms proposed by Avnimelech and Intrator was used.

The proposed boosting algorithm consists of three estimators trained in a hierarchical fashion. All learners have the same BNN architecture described in Figure 1 with variable number of neurons in the hidden layer. The first learner (L1) is trained and then simulated with the original data set (I,T). Next, the errors (symbolized with "err"), which are the absolute value of differences between targets T and outputs values y, were calculated. Then the γ parameter is used for error evaluation and for forming the training data sets of the next two learners. After experimental tests it was found that the optimum value of γ is 0.01.

The next stage separates small and large errors based on the parameter γ. In particular, errors that are larger than γ (errors> γ) are classified as "bad" while the errors that are smaller or equal to γ (errors$\leq\gamma$) are classified as "good". The training data set of the second learner (L2) comprises 50% of patterns whose errors are larger than γ (classified as "bad") and the remaining 50% consists of patterns whose errors are smaller or equal than γ (classified as "good"). The input data set of second learner are symbolized with I2 and the corresponding target data set with T2.

The second learner (L2) was trained and simulated with the data set I2, T2 and the final output was symbolized with y2. The errors (symbolized with "err2") are the absolute values of differences between targets T and outputs values y2. In the next stage the inputs and the targets of the third learner are configured by selecting patterns that satisfy the following conditions: (1) the absolute value of the error of the first learner (err) is larger than γ and the absolute value of the error of the second learner (err2) is smaller or equal than γ, or (2) the reverse, that is the absolute value of the error of the first learner (err) is smaller or equal than γ and the absolute value of the error of the second learner (err2) is larger than γ or (3) the absolute value of the error of the first learner (err) is larger than γ and the absolute value of the error of the second learner (err2) is larger than γ and the product of errors (err*err2) is smaller than zero. The input data set of the third learner was symbolized with I3 and the corresponding target data set with T3 and the final output is the median of the three sequential learner outputs (y, y1, y3). Figure 2 shows the overall model and the flow diagram of the simulation process of Boosting algorithm. The proposed boosting algorithm was tested using sixteen different learner configurations (see Table 3)

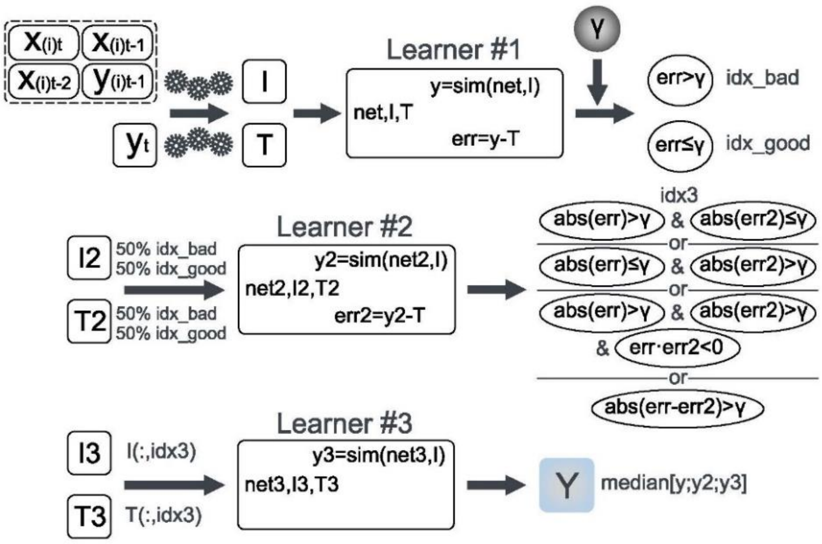


Figure 2. Architecture of Boosting algorithm.

3. EVALUATION OF PERFORMANCE

Four different evaluation criteria were used to measure the performance and reliability of the models. Each criterion is represented by an efficiency indicator, estimated from the comparison of predicted values and the measured targets.

The root mean square error (RMSE) is a measure of the differences between values predicted by a model or an estimator and the values actually observed (expression 5).

$$RMSE = \sqrt{\frac{1}{N}\sum_{i=1}^{N}(x_i - y_i)^2} \quad (5)$$

The mean absolute error (MAE) describes the average magnitude of the errors, without considering their direction, i.e. a linear term that expresses that all the differences (errors) are weighted equally (Anctil et al., 2008). The average absolute error is the average of the absolute values of differences between prediction and actual observation of the sample of all the data under consideration (expression 6).

$$MAE = \frac{1}{N}\sum_{i=1}^{N}|x_i - y_i| \quad (6)$$

The correlation coefficient (R-value) is a measure of the linear regression between the predicted values and the targets of models (expression 7).

$$R = \frac{\sum_{i=1}^{N}(x_i - x)(y_i - y)}{\sqrt{\sum_{i=1}^{N}(x_i - x)}\sqrt{\sum_{i=1}^{N}(y_i - y)}} \quad (7)$$

Finally, the Nash–Sutcliffe (NSE) efficiency coefficient was employed to estimate the accuracy of the models (expression 8).

$$NSE = 1 - \frac{\sum_{i=1}^{N}(x_i - y_i)^2}{\sum_{i=1}^{N}(x_i - \bar{x})^2}) \quad (8)$$

In all equations above N is the number of samples, xi and yi are the target and predicted values for i=1,….,n, and x and y are the mean values of the target and predicted data set, respectively.

A better agreement between target and predicted values is expressed by an R-value as close to unity as possible. At the same time, RMSE, MAE and NS values close to zero show that predictions from the models are more precise.

4. DATA PREPARATION

For the Venetikos river watershed there are four rain gauging stations and one river stage gauging station, placed on a bridge (Trikomo) at the exit of the watershed. Time series of daily precipitation data were obtained for each rain gauging station, while time series of daily discharges were obtained from Trikomo gauging station for a time period from 1/10/1996-30/9/2010. For the Kalarrytikos river watershed the precipitation data were obtained from two meteorological stations and the river stage data were obtained from the gauging in the Kipina bridge. The period for the precipitation and river stage record is 1/10/1995-30/9/2010.

For the machine learning models the input data is the precipitation at times t, t-1 and t-2 as well as the streamflow at time t-1 (t corresponds to days). For ARMA and ARIMA the same step was followed, with the large history t-i in some cases. In all models the target is the streamflow at time t.

The data are normalized in the range 0 to +1 and a regression analysis was carried out with the measured data. After training the models, their outputs were denormalized and their corresponding denormalized predicted data were obtained. The values of evaluation criteria were calculated from denormalized data.

For the ANN models the data are randomly divided into three sets: training, testing, and validation. While 70% of the data are used for training, 15% are used for validation and the rest 15% are used for testing. An important concept in BNN is that, since the evidence can be evaluated using the training data, Bayesian methods are able to deal with the issue of model complexity, without the need to use cross-validation method (separation of training, validation and testing data). The BNN automatically embodies Occam's razor that penalizes over complex models and for this reason is too difficult to get overfitting (Bishop, 2005). However each model or learner for ANN, BNN and Boosting algorithm was executed 10 times and the average root mean square error and average correlation coefficient were calculated in order to avoid either a very good or a very bad simulation. For the ARMA and ARIMA models the 70% of the data were used for training and the 30% of data were used for testing.

5. RESULTS

Numerical values of the RMSE, R, MAE and NSE performance indexes for the 5 different models (ANN, BNN, Boosting algorithm, ARMA, ARIMA) are shown in Tables 1, 2, 3, 4 and 5. From the simulation results of ANN (Table 1) it is easily noticed that the architectures 7–10–1 for Venetikos river and 7–20–1 for Kalarrytikos river were superior to all others. Respectively, from the simulation results of BNN (Table 2) it is concluded that the architecture with 50 neurons in the hidden layer for both watersheds was the best. For the Boosting algorithm, the values of the evaluation criteria indicate that the best model has 50 hidden neurons for first estimator, 35 hidden neurons for the second one and 15 hidden neurons for the third one for both watersheds. Finally, the best stochastic models are the ARMA(3,3) and ARIMA(3,3,2) for the Venetikos river and ARMA(2,3) and ARIMA(3,3,3) for the Kalarrytikos river. By comparing the models with each other, it turns out that the best, for both watersheds, is the BNN. However, it should be noted that all machine learning and stochastic models responded fairly well to the simulations and the differences between them are very small.

Table 1: Indicators of ANN models performance

ANN architecture	**Venetikos (13 inputs units)**				**Kalarrytikos (7 inputs units)**			
	RMSE	**R**	**MAE**	**NSE**	**RMSE**	**R**	**MAE**	**NSE**
13 or 7 – 2 -1	0.12322	0.96802	0.06174	0.93589	0.10018	0.92084	0.05277	0.84762
13 or 7 – 3 -1	0.13132	0.96303	0.06145	0.92536	0.09999	0.92123	0.05245	0.84818
13 or 7 – 4 -1	0.12355	0.96755	0.06094	0.93551	0.09916	0.92258	0.05151	0.85069
13 or 7 – 7 -1	0.12435	0.96800	0.06412	0.93446	0.09904	0.92265	0.05127	0.85104
13 or 7 – 8 -1	0.12287	0.96816	0.06301	0.93615	0.09854	0.92365	0.05140	0.85255
13 or 7 – 10 -1	0.12036	0.96927	0.06009	0.93880	0.09912	0.92303	0.05219	0.85081
13 or 7 – 20 -1	0.12854	0.96675	0.07018	0.92950	0.09847	0.92359	0.04982	0.85277
13 or 7 – 50 -1	0.12453	0.96751	0.06183	0.93435	0.09870	0.92412	0.05160	0.85200

Table 2: Indicators of BNN models performance

BNN architecture	Venetikos (13 inputs units)				Kalarrytikos (7 inputs units)			
	RMSE	R	MAE	NSE	RMSE	R	MAE	NSE
13 or 7 – 2 -1	0.11225	0.97305	0.05671	0.94680	0.09893	0.92272	0.05061	0.85141
13 or 7 – 3 -1	0.10994	0.97416	0.05583	0.94895	0.09798	0.92424	0.04994	0.85423
13 or 7 – 4 -1	0.09695	0.97567	0.05479	0.95191	0.09725	0.92543	0.04972	0.85641
13 or 7 – 7 -1	0.09914	0.97902	0.05197	0.95850	0.09430	0.93004	0.04853	0.86497
13 or 7 – 8 -1	0.09800	0.97953	0.05180	0.95947	0.09382	0.93077	0.04833	0.86634
13 or 7 – 10 -1	0.09379	0.98126	0.05017	0.96286	0.09164	0.93406	0.04759	0.87247
13 or 7 – 20 -1	0.08087	0.98610	0.04514	0.97241	0.08663	0.94130	0.04525	0.88605
13 or 7 – 50 -1	0.05690	0.99316	0.03382	0.98633	0.07465	0.95676	0.04024	0.91538

Table 3: Indicators of Boosting algorithm models performance

Neurons in hidden layer			Venetikos (13 inputs units)				Kalarrytikos (7 inputs units)			
L1	L2	L3	RMSE	R	MAE	NSE	RMSE	R	MAE	NSE
2	4	8	0.10373	0.97703	0.05339	0.95459	0.09637	0.92683	0.04921	0.85899
3	7	12	0.09630	0.98024	0.05074	0.96086	0.09391	0.93067	0.04798	0.86609
4	9	15	0.09186	0.98204	0.04929	0.96438	0.09222	0.93322	0.04736	0.87087
5	10	7	0.09657	0.98013	0.05099	0.96064	0.09434	0.92999	0.04831	0.86487
7	3	9	0.09875	0.97921	0.05185	0.95884	0.09475	0.92937	0.04831	0.86369
7	12	22	0.08464	0.98477	0.04597	0.96976	0.09104	0.93495	0.04688	0.87411
8	4	2	0.10340	0.97718	0.05356	0.95487	0.09635	0.92688	0.04946	0.85905
8	11	6	0.09441	0.98102	0.05034	0.96238	0.09285	0.93227	0.04781	0.86909
10	6	3	0.09885	0.97917	0.05200	0.95875	0.09437	0.92995	0.04836	0.86477
12	5	10	0.09205	0.98196	0.04956	0.96424	0.09249	0.93282	0.04769	0.87010
14	7	5	0.09370	0.98131	0.04985	0.96294	0.09287	0.93223	0.04770	0.86903
15	25	40	0.06893	0.98993	0.03894	0.97995	0.08674	0.94111	0.04474	0.88565
16	10	8	0.08830	0.98342	0.04799	0.96710	0.09111	0.93486	0.04681	0.87395
20	10	30	0.07728	0.98732	0.04242	0.97479	0.08597	0.94223	0.04469	0.88776
25	30	15	0.07258	0.98882	0.04124	0.97775	0.08435	0.94444	0.04394	0.89195
50	35	15	0.06018	0.99234	0.03599	0.98470	0.08088	0.94904	0.04154	0.90064

Table 4: Indicators of ARMA models performance

ARMA(p,q)	Venetikos				Kalarrytikos			
	RMSE	R	MAE	NSE	RMSE	R	MAE	NSE
(1,1)	0.17024	0.93846	0.07128	0.87769	0.12764	0.87267	0.05680	0.75263
(1,2)	0.16836	0.93925	0.07272	0.88038	0.12446	0.87675	0.05844	0.76480
(1,3)	0.16730	0.93974	0.07361	0.88188	0.12402	0.87715	0.05902	0.76647
(2,1)	0.17008	0.93866	0.07067	0.87791	0.12781	0.87350	0.05596	0.75198
(2,2)	0.16606	0.94031	0.07434	0.88363	0.12351	0.87754	0.05998	0.76838
(2,3)	0.16604	0.94031	0.07434	0.88365	0.12319	0.87781	0.06083	0.76957
(3,1)	0.16608	0.94029	0.07435	0.88359	0.12363	0.87725	0.06009	0.76794
(3,2)	0.16604	0.94030	0.07433	0.88365	0.12331	0.87776	0.06045	0.76914
(3,3)	0.16603	0.94032	0.07437	0.88366	0.12349	0.87755	0.06009	0.76846

Table 5: Indicators of ARIMA models performance

ARIMA(p,d,q)	Venetikos				Kalarrytikos			
	RMSE	R	MAE	NSE	RMSE	R	MAE	NSE
(1,1,1)	0.16580	0.94119	0.07188	0.88399	0.12475	0.87845	0.05505	0.76373
(1,1,2)	0.16531	0.94134	0.07252	0.88468	0.12302	0.88029	0.05655	0.77024
(1,1,3)	0.16469	0.94159	0.07340	0.88553	0.12275	0.88043	0.05689	0.77121
(1,2,1)	0.16543	0.94132	0.07221	0.88451	0.12455	0.87879	0.05499	0.76449
(1,2,2)	0.16518	0.94139	0.07252	0.88485	0.12301	0.88031	0.05656	0.77025
(1,2,3)	0.16466	0.94160	0.07340	0.88558	0.12270	0.88040	0.05728	0.77143
(1,3,1)	0.16524	0.94141	0.07241	0.88477	0.12447	0.87889	0.05522	0.76476
(1,3,2)	0.16484	0.94154	0.07299	0.88532	0.12285	0.88051	0.05680	0.77084
(1,3,3)	0.16449	0.94169	0.07360	0.88581	0.12256	0.88060	0.05753	0.77195
(2,1,1)	0.16566	0.94120	0.07223	0.88419	0.12388	0.87699	0.05944	0.76699
(2,1,2)	0.16477	0.94147	0.07316	0.88542	0.12286	0.88032	0.05671	0.77081
(2,1,3)	0.16451	0.94165	0.07346	0.88578	0.12275	0.88042	0.05690	0.77122
(2,2,1)	0.16541	0.94134	0.07213	0.88453	0.12437	0.87951	0.05489	0.76513
(2,2,2)	0.16335	0.94224	0.07438	0.88740	0.12194	0.88066	0.05967	0.77423
(2,2,3)	0.16334	0.94225	0.07437	0.88741	0.12165	0.88095	0.06025	0.77532
(2,3,1)	0.16518	0.94145	0.07234	0.88485	0.12219	0.87984	0.06036	0.77331
(2,3,2)	0.16320	0.94236	0.07446	0.88759	0.12184	0.88089	0.05962	0.77462
(2,3,3)	0.16319	0.94237	0.07449	0.88761	0.12162	0.88102	0.06022	0.77542
(3,1,1)	0.16496	0.94138	0.07296	0.88516	0.12312	0.88021	0.05629	0.76985
(3,1,2)	0.16464	0.94151	0.07340	0.88560	0.12275	0.88019	0.05721	0.77124
(3,1,3)	0.16434	0.94171	0.07366	0.88602	0.12264	0.88037	0.05723	0.77164
(3,2,1)	0.16327	0.94231	0.07434	0.88750	0.12196	0.88060	0.05967	0.77417
(3,2,2)	0.16327	0.94230	0.07435	0.88750	0.12194	0.88065	0.05969	0.77424
(3,2,3)	0.16327	0.94230	0.07434	0.88750	0.12162	0.88099	0.06023	0.77543
(3,3,1)	0.16317	0.94240	0.07449	0.88763	0.12193	0.88066	0.05966	0.77428
(3,3,2)	0.16317	0.94239	0.07449	0.88764	0.12166	0.88107	0.06009	0.77526
(3,3,3)	0.16318	0.94237	0.07452	0.88763	0.12162	0.88104	0.06025	0.77542

The comparison of the prediction values against the observed data is presented in Figure 3 for Venetikos river and in Figure 4 for Kalarrytikos river. The targets of the model are represented with blue continues line and the prediction values of models are represented with different lines (colors and shape). More specifically the ANN model is represented with red dashed line, the BNN model

with green dashed-dotted line, the Boosting model with purple dashed (large dashes) line, the ARMA model with light blue dashed (small dashes) line and the ARIMA model with orange dotted line. The very good performance of all models in both watersheds and for both the regular runoff and peak flows is evident from these figures. Moreover, the models successfully predicted the extreme peak streamflows which appeared at the time series. The successful prediction of extreme events is very important for the streamflow prediction because they are the cause of floods.

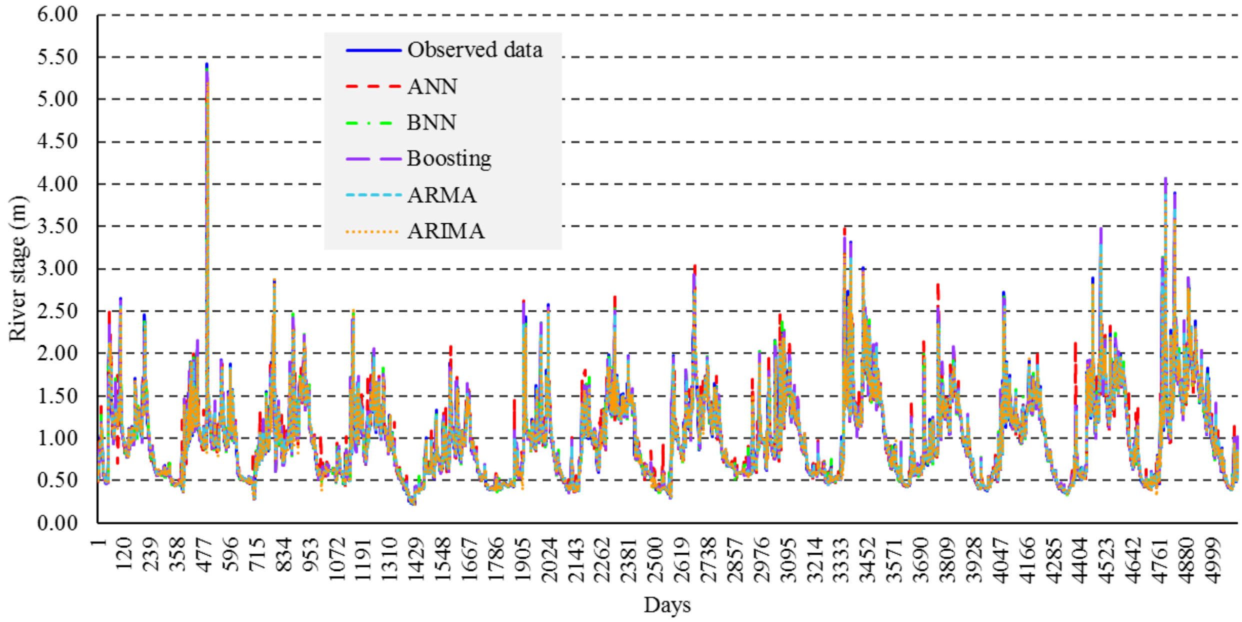


Figure 3. Predicted streamflow compared with corresponding flows in Venetikos river.

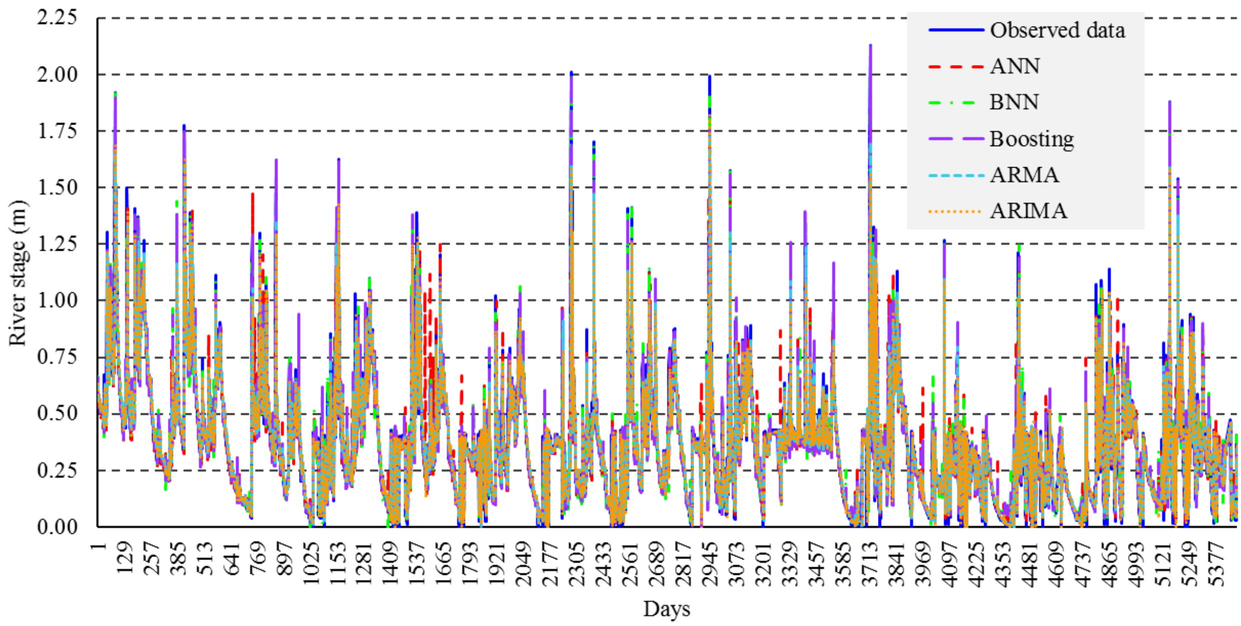


Figure 4. Predicted streamflow compared with corresponding flows in Kalarrytikos river.

6. CONCLUSIONS

In this study the application of three machine learning and two stochastic models for the streamflow prediction in two mountainous watersheds was investigated. Results show that the BNN model performed better than the other models, yet with very small differences. It is clear from the diagrams of Figures 3 and 4 that the results of all models were satisfactory and the predicted values in all cases

were very close to the observed data. Therefore, the most important conclusion that emerges from this study is that there is no model that stands out for its very good or very poor prediction.

Consequently, both machine learning and stochastic models can be useful tools in simulating the relationship of rainfall-runoff and in predicting watershed discharge.

The generalization capability of the machine learning and stochastic models is the biggest open question in streamflow forecasting problem. Also it has been realized that the development of effective forecasting models requires an exemplary combination of well measured data and input parameters, which describe very well the variables of physical phenomena. In several cases, the available data, combined with the particularities of each prediction method, can differentiate the hierarchical classification of the models based on their performance.

References

1. Anctil, F., N. Lauzon and M. Filion (2008) ‘Added gains of soil moisture content observations for streamflow predictions using neural networks’, **Journal of Hydrology**, Vol 359, p.p. 225-234.
2. ASCE Task Committee (2000) ‘Artificial neural network in hydrology’, **Journal of Hydrologic Engineering**, Vol 5 (2), pp. 124-144.
3. Avnimelech R. and N. Intrator, ‘Boosting regression estimators’, **Neural Computation**, Vol 11(2), p.p. 499-520, MIT Press.
4. Bishop C.M. (2005) ‘Neural networks for pattern recognition’, Clarendon Press, Oxford University Press.
5. Botsis D. and P. Latinopoulos (2010) ‘Rainfall-runoff modeling and peak flow forecasting using hydrologic and neural network modeling’. Proc. of Int. Conf. Protection and Restoration of the Environment X, Corfu, Greece, 2010.
6. Botsis D., P. Latinopoulos and K. Diamantaras (2011) ‘Rainfall-runoff modeling using support vector regression and artificial neural networks’. Proc. of 12th Int. Conf. on environmantal science and technology (CEST2011), Rhodes, Greece, 2011.
7. Erdal H.I. and O. Karakurt (2012) ‘Advancing monthly streamflow prediction accuracy of CART models using ensemble learning paradigms’, **Journal of Hydrology**, Vol 477, pp. 119-128.
8. Foresee, F.D. and M.T. Hagan (1997) ‘Gauss-Newton approximation to Bayesian learning’, in Proc. IEEE International Conference on Neural Networks, pp. 1930-1935.
9. Guo J., J. Zhou, H. Qin, Q. Zou and Q. Li (2011) ‘Monthly streamflow forecasting based on improved support vector machine model’, **Expert Systems with Applications**, Vol 38 (10), pp. 13073-13081.
10. Haykin S. (1999) ‘Neural Networks: A Comprehensive Foundation’, Macmillan, New York.
11. Huang S., J. Chang, Q. Huang and Y. Chen (2014) ‘Monthly streamflow prediction using modified EMD-based support vector machine’**, Journal of Hydrology**, Vol 511, pp. 764-775.
12. Humphrey G.B., M.S. Gibbs, G.C. Dandy and H.R. Maier (2016) ‘A hybrid approach to monthly streamflow forecasting: Integrating hydrological model outputs into a Bayesian artificial neural network’, **Journal of Hydrology**, Vol 540, pp. 623-640.
13. Jeong, D. and Y. Kim (2005) ‘Rainfall-runoff models using artificial neural networks for ensemble streamflow prediction’, **Hydrological Processes**, Vol 19, p.p. 3819–3835.
14. Khan M.S. and P. Coulibaly (2006) ‘Bayesian neural network for rainfall-runoff modeling’, **Water resources research**, Vol 42 (7), W07409 doi:10.1029/2005WR003971.

15. Rumelhart D.E., G.E. Hinton and Williams R.J. (1986) ‘Learning internal representation by error propagation. Parallel distributed processing: Explorations in the microstructure of cognition’, Rumelhart D.E. and J.L. McClelland, eds., Vol. 1, MIT Press, Cambridge, Mass., 318–362.
16. Sahoo G.B. and C. Ray (2006) ‘Flow forecasting for a Hawaii stream using rating curves and neural networks’, **Journal of Hydrology**, Vol 317, pp. 63-80.
17. Valipour, M., M.E. Banihabib and S.M.R. Behbahani (2012) ‘Parameters estimate of autoregressive moving average and autoregressive integrated moving average models and compare their ability for inflow forecasting’, **Journal of Mathematics and Statistics**, Vol 8, pp. 330-338.
18. Valipour, M., M.E. Banihabib and S.M.R. Behbahani (2013) ‘Comparison of the ARMA, ARIMA, and the autoregressive artificial neural network models in forecasting the monthly inflow of Dez dam reservoir’, **Journal of Hydrology**, Vol 476, pp. 433–441.
19. Wang W.C., K.W. Chau, C.T. Cheng and L. Qiu (2009) ‘A comparison of performance of several artificial intelligence methods for forecasting monthly discharge time series’, **Journal of Hydrology**, Vol 374(3-4), pp. 294-306.
20. Wei W.W.S. (2006) ‘Time Series Analysis, Univariate and Multivariate Methods’, second edition, Pearson Addison Wesley.
21. Zealand C.M., D.H. Burn and S.P. Simonovic, (1999) ‘Short term streamflow forecasting using artificial neural networks’, **Journal of Hydrology**, Vol 214, pp. 32-48.

APPLICATION OF MODIFIED METAHEURISTIC METHODS TO IDENTIFY CRITICAL AREAS IN WATER SUPPLY NETWORKS

D. Karakatsanis*, N. Theodossiou

Division of Hydraulics and Environmental Engineering, Dept. of Civil Engineering, Aristotle University of Thessaloniki, GR- 54124 Thessaloniki, Macedonia, Greece

*Corresponding author: E-mail: dkarakat@civil.auth.gr, Tel +30 2310995660

Abstract

Recently, metaheuristic methods have actively been used to minimize the cost of water supply networks. The algorithms of these methods search for optimal solutions using local searching strategies, thus skipping the exhaustive search analysis. Brute-force searching methods are also used and are typical for limited system sizes. However, brute-force is not commonly used in real-world problems due to time limitations and scaling problems. though metaheuristic search is more common for these case, they also have some limitations. Sufficiently large water supply networks or very small size of the mesh are typical cases that make computational time very long so that these methods never find the optimal solution. In this paper we try to overcome these limitations by applying a modified metaheuristic method in order to identify critical clusters of water pipe networks.

Keywords: metaheuristic; water supply networks; harmony search algorithm; pipe networks; water management

1. INTRODUCTION

In recent years, many metaheuristic methods have been used to optimize hydraulic networks. The vast majority of these methods implement novel bio-inspired strategies and use local searching in order to find optimal solutions (minimize cost, maximize benefit etc). Water supply networks must be computed in each step of these algorithms, thus leading to critical computational limitations as the network size scales up. An alternative approach can be achieved by using metaheuristic methods in order to find network communities. This way, the original problem is reduced to a community detection problem. The members of each community are characterized by some similar properties even ifthey are not directly connected with each other. For example, the Harmony Search Algorithm can be modified to detect pipes with some critical cost or similar water velocity. These pipes are treated as belonging to a community and are organized in a new cluster (subnetwork or subset of pipes with the same properties) of the supply water network. These clusters result in a similar-property network. If the property is the cost, then for example we can find the cluster whose members have the critical cost. By applying thie technique we reduce the original network to a cluster cost network. In our approach the pipes out of the cluster are ignored. Having reduce the original network of pipes to a clustered network where pipes with similar properties are grouped together one can overcome the aforementioned computational limitations. Furthermore, this new approach allows the study of dependencies between the members of the network associated with the question property. The topology is dependent on the question property. Thus, a family of clusters (cost, velocity, energy, chloride etc) can be created in order to simplify the original network.

2. OPTIMIZATION PIPE NETWORKS WITH HARMONY SEARCH ALGORITH – CLASSIC APPROACH

2.1 Harmony Search Algorithm (HSA)

The Harmony Search Algorithm (HAS) was inspired by the improvisation process that a skilled musician follows when playing in a music band. While performing the musician has one of the following choices:

- To play the famous tune, the melody that characterizes the music piece. This specific melody is called "theme" in music. Obviously, every member of the band knows the theme and can play it by heart. In other words, all musicians have this melody in their minds, stored in their memory.
- A common choice a musician has is to play something similar to the theme. Quite often, musicians try to enrich a music piece by slightly changing or adjusting pitches of the memorized theme. This way, the musicians are free to explore the theme and listeners hear its new versions. Tasteless iterations of the same tune are avoided.
- Other choice is to start an improvisation. This choice, which is very common in Jazz and folk music, gives the musician the freedom to play random tunes, sometimes notes with very small (or no) relation to the performed piece. The talent and the imagination of the performer, is used to express new music worlds and refreshes the music material with new themes.

The Harmony Search Algorithm is a stochastic meta-heuristic method based on the sequential production of possible solutions. It belongs to the category of "neighborhood meta-heuristics" that produces one possible solution per iteration. This process is completely different from that of the population methods that produce a number of possible solutions during every iteration (e.g. genetic algorithms). Every possible solution consists of a set of values of the decision variables of the function that needs to be optimized. Each one of these sets of values is called a "Harmony". During the optimization process, a number of "harmonies" equal to the "Harmony Memory Size" are stored in the "Harmony Memory" (HM), a database that includes the produced set of solutions. Every component of the new harmony chosen from HM, is likely to be pitch-adjusted, thus providing neighboring values for some of the harmonies chosen from HM. The third choice is to select a totally random value from the possible value range. Randomization occurs with very small probability and increases the diversity of the solutions.

2.2 Optimization water pipe networks with HSA

In the classic network cost optimization approach with metaheuristic methods, the costs can be considered as a function of the length and the diameter of the pipelines. However, in this paper, we consider an objective function that includes the diameter and the length of the corresponding pipeline. The objective function is shown in Equation 1

$$F = \sum Li * Di \qquad (1)$$

where Li is the length and Di is the diameter of the corresponding pipeline. The constraints are shown in equation 2

$$V_{min} \le V_i \le V_{max}$$

$$\sum Q_i = 0$$

$$D_i \ge 0 \qquad (2)$$

where:

- vi the flow velocity for pipe i that must be between a minimum and a maximum
- Qi water flow rate for node i

The HSA works as follows: First, a number of possible solutions is stored are in the "Harmony Memory" (HM). Every solution is one-dimensional array vector filled with Di values. During the optimization process, the algorithm creates new a solution called "New Harmony". If the "New Harmony" has good evaluation in the objective function, then it replaces the west vector of "Harmony Memory" (HM).

When the network structure is not tree-like, but has loops, a water distribution software must be used. In this paper we developed a MatLab script that connects HSA with EPANET. The linking between EPANET and MatLab is described in Chapter 4. The full optimization process is presented in Figure 1.

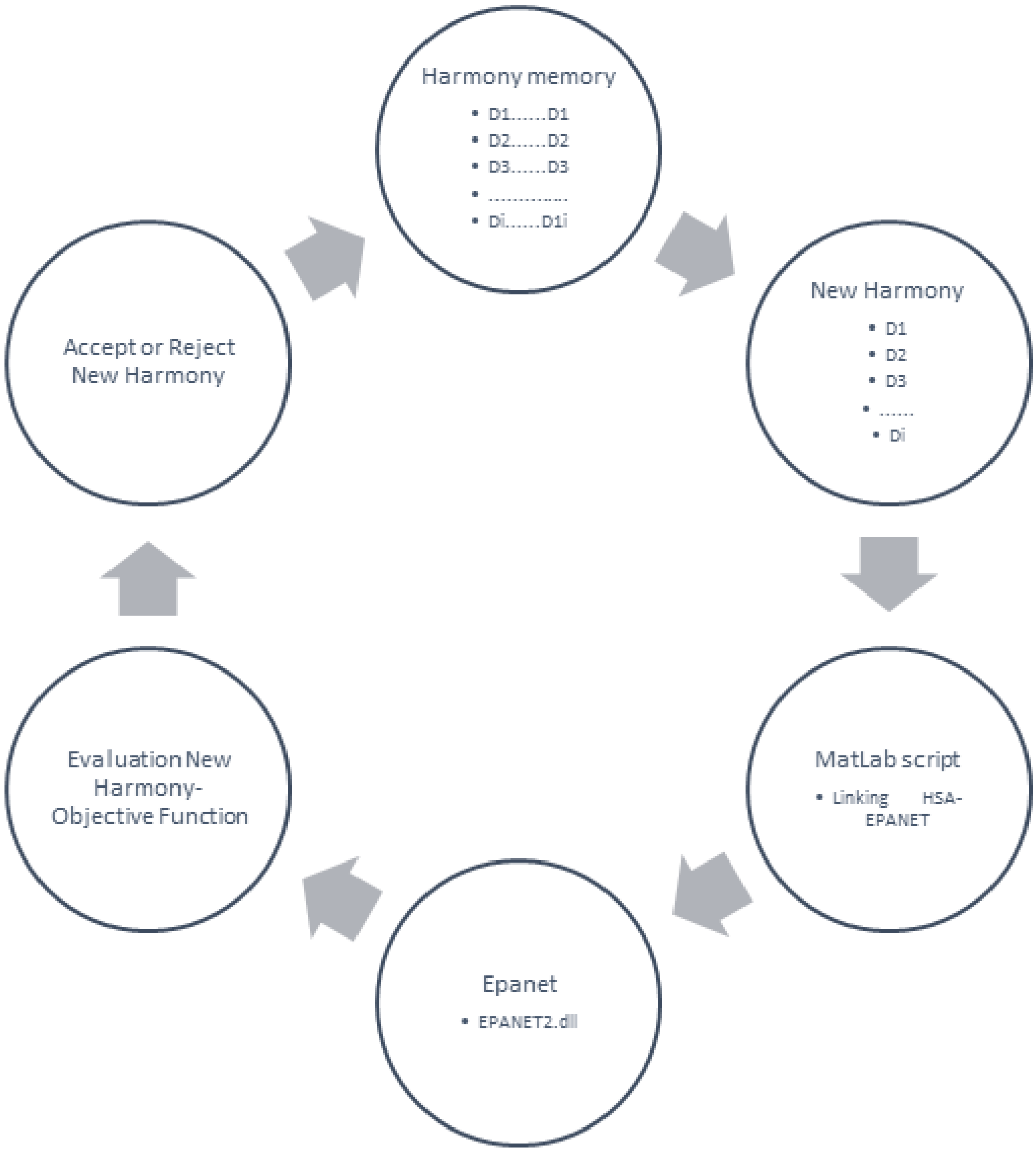


Figure 1: The optimization progress

3. LINKING MATLAB-EPANET

EPANET is a water distribution system modeling software package developed by the United States Environmental Protection Agency's (EPA) Water Supply and Water Resources Division. EPANET is freeware but not open source software. In order to use it in a loop progress a linking software must

be developed. The EPANET Programmer's Toolkit is a library (DLL, dylib, or .so) of API functions that allows developers to customize EPANET's computational engine for their own specific needs. The functions can be incorporated into applications written in any language that can call functions from a C library, like native C/C++, MatLab, Python, Visual Basic, etc. Here we use MatLab script to call the necessary functions.

loading `'epanet2.dll'` code is:

- `loadlibrary('epanet2.dll','epanet2.h')`

the most frequently used functions EPANET TOOL KIT are:

- Open the EPANET toolkit and hydraulics solver

```
calllib('epanet2','ENopen','input2.inp','report2.rpt','');
```

where 'input2.inp' is the initial water network

- Setting the values (diameters) to the network

```
calllib('epanet2','ENsetlinkvalue', index ,paramcode ,value)
```

paramcode get values from Table 1

Table 1: Values for the "calllib" function

EN_DIAMETER	0	Diameter
EN_LENGTH	1	Length
EN_ROUGHNESS	2	Roughness coeff.
EN_MINORLOSS	3	Minor loss coeff.
EN_INITSTATUS	4	Initial link status (0 = closed, 1 = open)
EN_INITSETTING	5	Roughness for pipes, initial speed for pumps, initial setting for valves
EN_KBULK	6	Bulk reaction coeff.
EN_KWALL	7	Wall reaction coeff.
EN_STATUS	11	Actual link status (0 = closed, 1 = open)
EN_SETTING	12	Roughness for pipes, actual speed for pumps, actual setting for valves

- Analyzing the pipe network

```
calllib('epanet2','ENsolveH');

calllib('epanet2','ENsolveQ');

calllib('epanet2','ENreport');
```

The original water supply network is included in the file 'input2.inp'. Calling: ENsetlinkvalue function we set the Harmony Memory vectors (Di) and calculate the network calling: ENsolveQ function. The objective function is the Equation 1.

4. CASE STUDY

The case study we choose to present in this paper is a network with loop and branch network topology. It is a Gravity-driven water flow network with a central tank. The branch (tree-like) parts represent the pipeline system connecting different cities, while the loop parts at the periphery of the network represent the water supply network around small cities.

Each destination node of a branch part has “q” flow rate demand. For each network member the head loss is estimated from the Equation 3.

$$hi = \frac{8fiLi}{\pi^2 gDi^4} \quad (3)$$

The pipes are made by PVC and the maximum pressure design is 10 Atm. Table 2 presents the available diameters and the costs, while figure 2 shows the cost function power fitting.

Table 2: Classes of pipe diameters

ID	D(mm)	Euro/m	ID	D(mm)	Euro/m
1	100	73	10	400	205
2	125	81	11	450	241
3	150	88	12	500	279
4	175	95	13	550	320
5	200	103	14	600	356
6	225	112	15	650	415
7	250	123	16	700	467
8	300	144	17	750	517
9	350	173	18	800	592

According to Mandry’s model the function that relates the cost with the internal diameter, reads:

$$\delta = AD^V \quad (4)$$

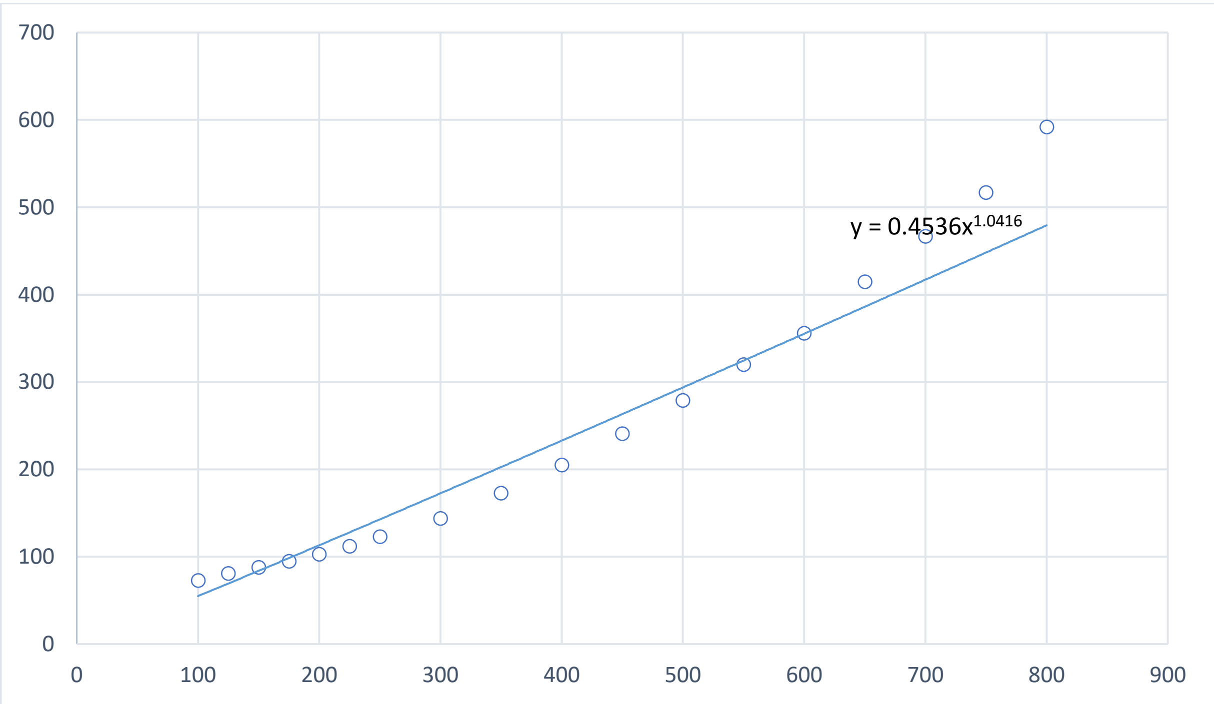


Figure 2: Cost function

Figure 3 illustrates the pipeline network and Figure 4 the water flow of the network.

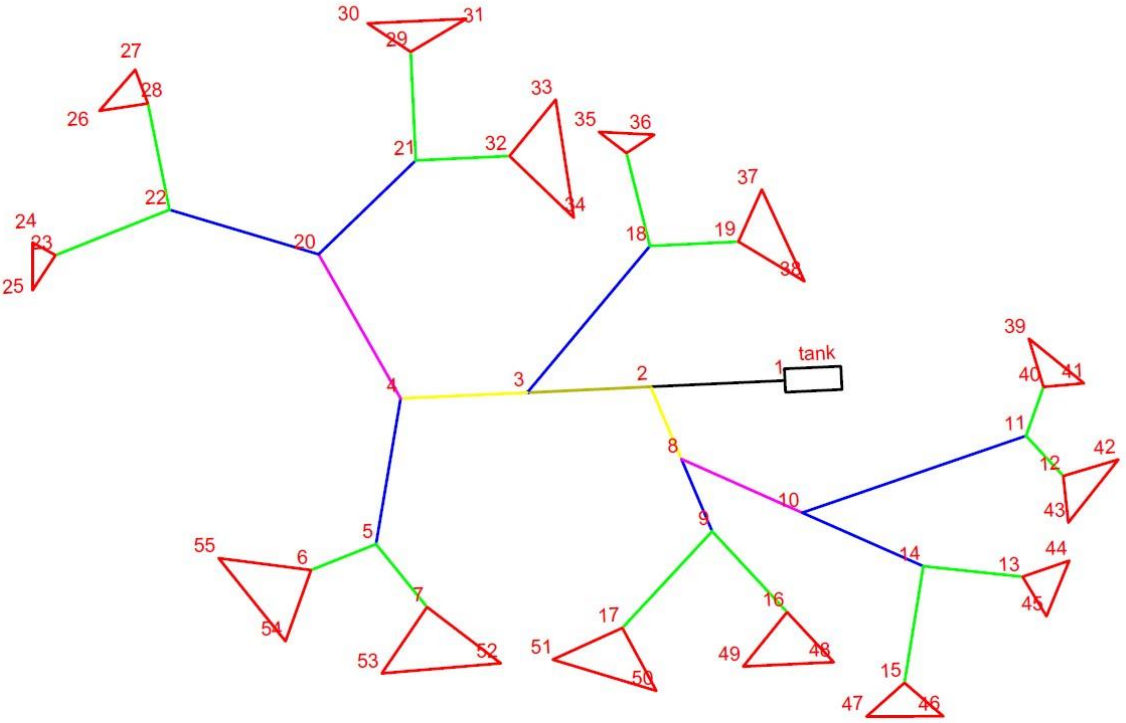


Figure 3: The water supply network with tank

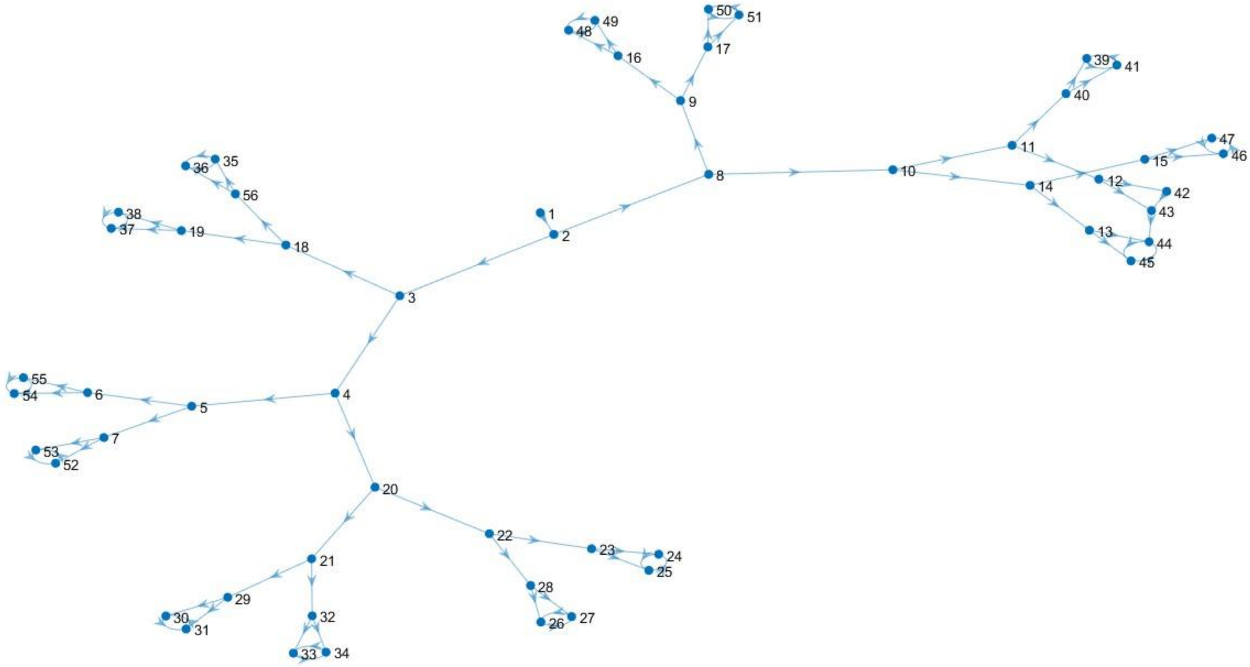


Figure 4: The water flow network

5. MODIFICATION OF HAS

In order to simplify large water supply systems, the algorithm described in Fig. 1 is modified. Gravity factors are defined using a) Equation 4 for all the pipes and b) the network betweenness centrality for all the nodes. This way, the objective function includes the centrality of the nodes of the pipeline network. The most central nodes receive a high weight factor as they are more indispensable for the network. Otherwise the algorithm prefers nodes of low centrality because they are connected to low-cost (Eq 4) pipes. The weights of the link are not constant but change as the algorithm evolves. This is due to the change in diameter and the cost. Figure 5 presents the network betweenness centrality.

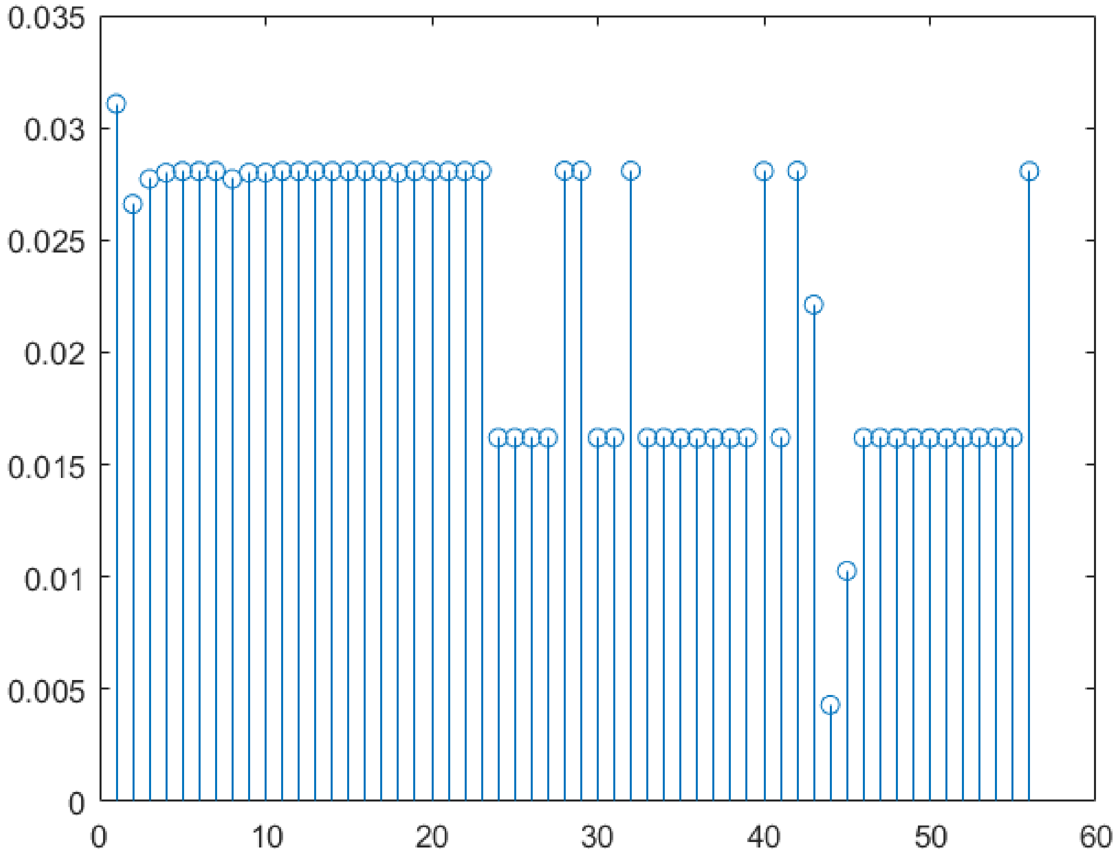


Figure 5 presents the network betweenness centrality

Figure 5 shows that the high centrality nodes are the nodes with the highest water supply and therefore the most critical for the network. Thus, if two pipes have about the same length and same supply, the algorithm will prioritize the critical centrality pipeline. Figure 6 presents the network's gravity factors.

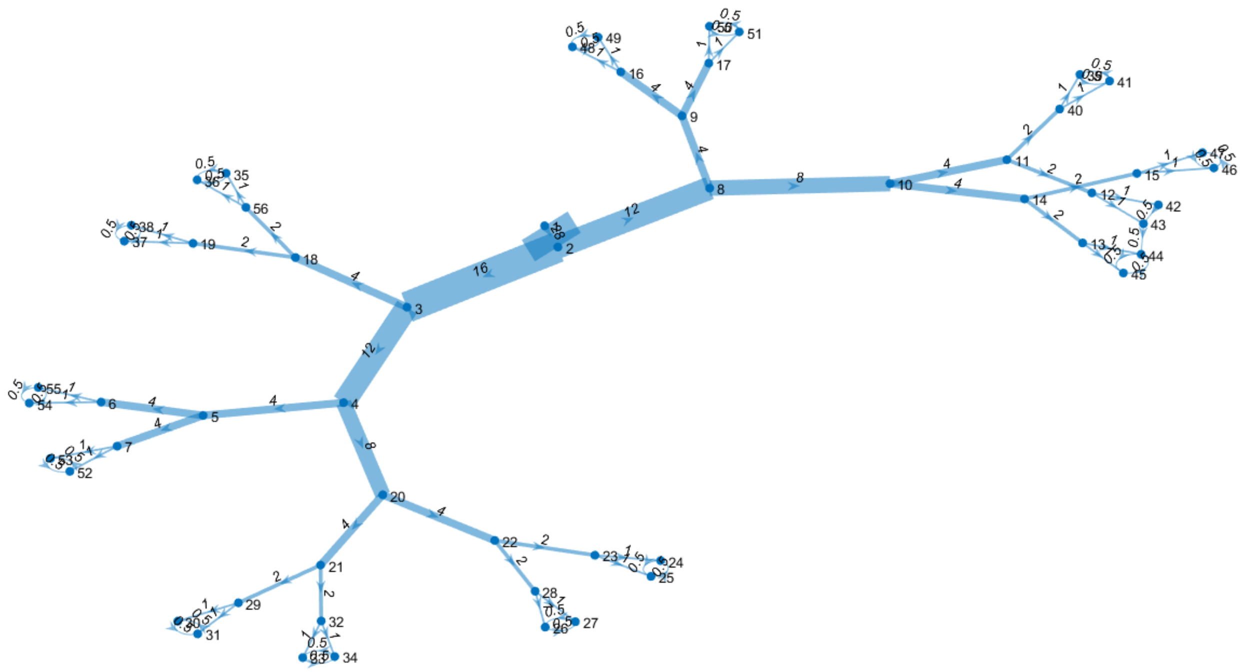


Figure 6: Gravity factors of the network

6. RESULTS

Figures 7,8,9 presents three implementations of the algorithm for different parameters of the HSA. In conclusion, HSA algorithm always locates as critical areas the ones having large cross sections. This happens because there are no alternative routes for the water and the factors of length and cross section of the pipelines have a significant contribution to the total cost. The color of the nodes represents the community that belong the pipes connecting them to the other nodes.

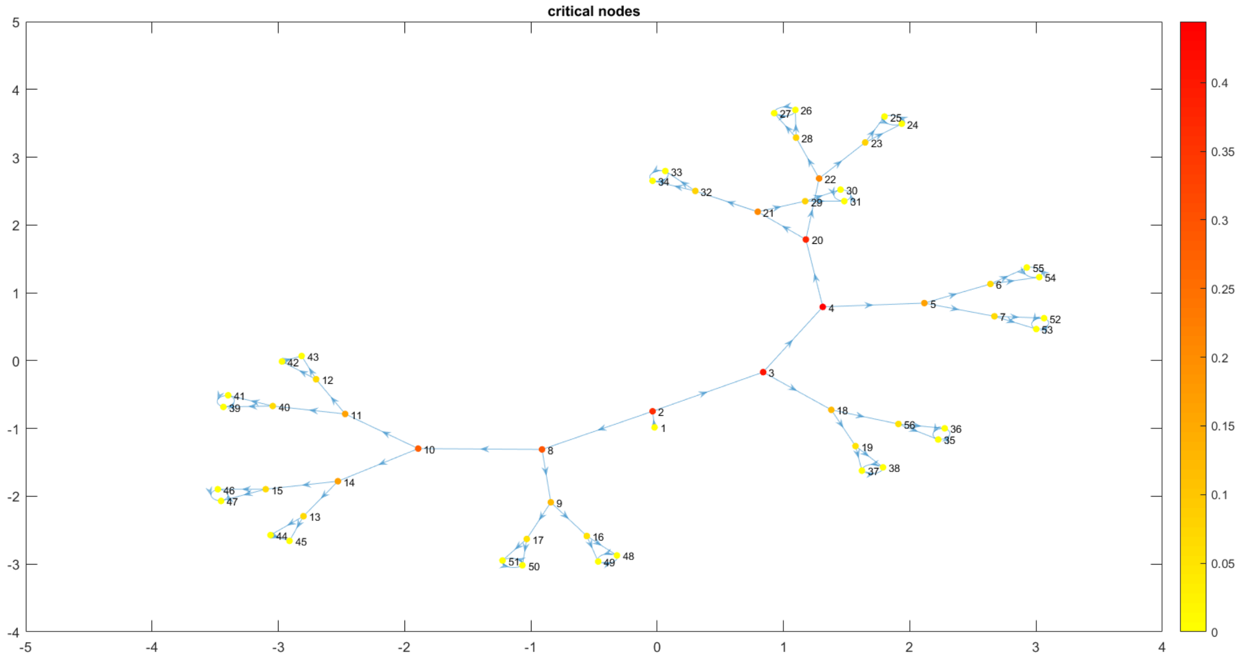


Figure 7: Critical nodes with HSA parameters (HM:30, HMCR:0.7, PAR:0.1,IN:1000)

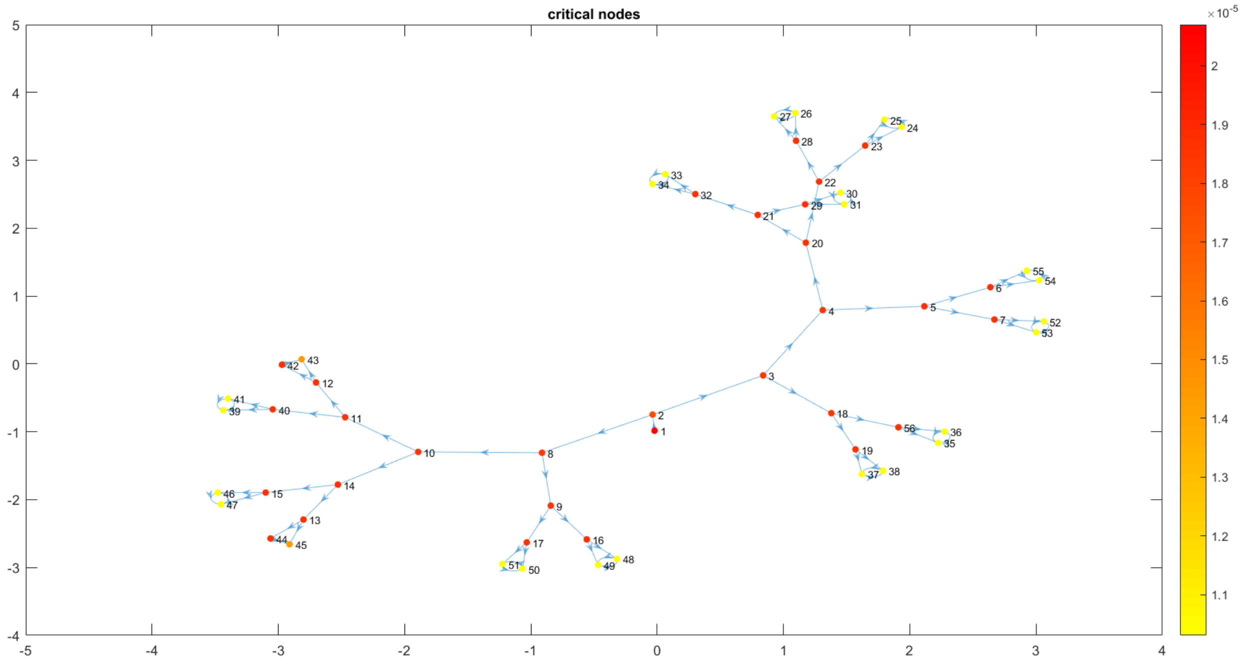


Figure 8: Critical nodes with HSA parameters (HM:70, HMCR:0.9, PAR:0.05,IN:1000)

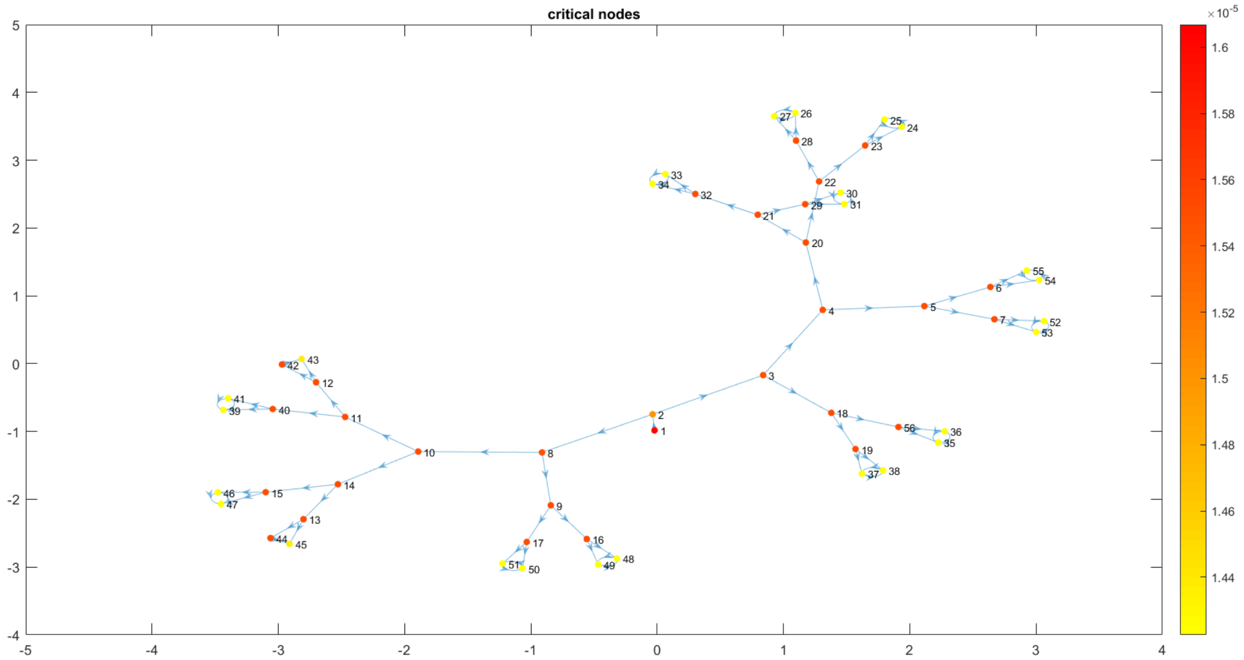


Figure 9: Critical nodes with HSA parameters (HM:50, HMCR:0.5, PAR:0.2, IN:1000)

7. CONCLUSIONS

The modification of the HSA simplifies the big water supply networks, since a large number of pipes can be ignored. This method approaches the minimum network construction cost as accurately as the full-network optimization, but in less computational time. The case study network is simplified as shown above (fig. 7, 8, 9) and the minimum cost is close to the full-network optimum cost. Checking the betweenness centrality of the network lets us know the important cost members which are absolutely necessary for the network. The cost of these members is as much as the cost of the full network. In order to estimate the cost of the full network we used method as shown on Fig 1.

References

1. Degertekin, S. O. (2012). Improved harmony search algorithms for sizing optimization of truss structures. ***Computers & Structures***, 92, 229-241.
2. Dorigo, M., Maniezzo, V., & Colorni, A. (1996). Ant system: optimization by a colony of cooperating agents. Systems, **Man, and Cybernetics, Part B: Cybernetics, IEEE Transactions on**, 26(1), 29-41.
3. Eberhart, R. C., & Kennedy, J. (1995). A new optimizer using particle swarm theory. In **Proceedings of the sixth international symposium on micro machine and human science** (Vol. 1, pp. 39-43).
4. Fesanghary, M., Mahdavi, M., Minary-Jolandan, M., &Alizadeh, Y. (2008). Hybridizing harmony search algorithm with sequential quadratic programming for engineering optimization problems. ***Computer methods in applied mechanics and engineering***, 197(33), 3080-3091.
5. Geem, Z. W., Kim, J. H., & Loganathan, G. V. (2001). A new heuristic optimization algorithm: harmony search. ***Simulation***, *76*(2), 60-68.
6. Geem, Z. W., Kim, J. H., & Loganathan, G. V. (2002). Harmony search optimization: application to pipe network design**. *International journal of modelling & simulation*,** *22*(2), 125-133.
7. Holland, J. H. (1973). Genetic algorithms and the optimal allocation of trials. **SIAM *Journal on Computing***, 2(2), 88-105.

8. Gholizadeh, S., & Barzegar, A. (2013). Shape optimization of structures for frequency constraints by sequential harmony search algorithm. ***Engineering Optimization***, 45(6), 627-646.
9. Kaveh, A., &Talatahari, S. (2009). Particle swarm optimizer, ant colony strategy and harmony search scheme hybridized for optimization of truss structures. ***Computers & Structures***, 87(5), 267-283.
10. Kirkpatrick, S., Gelatt, C. D., & Vecchi, M. P. (1983). Optimization by Simulated Annealing. ***Science***, 220(4598), 671-680.
11. Kougias, I., and Theodosiou, N. (2010). A new music-inspired harmony based optimization algorithm: Theory and applications. In Proceedings of: **International Conference on Protection and Restoration of the Environment X**, Corfu.
12. Kougias, I., Katsifarakis, L., & Theodossiou, N. (2012). Medley Multiobjective Harmony Search Algorithm: Application on a water resources management problem. ***European Water***, 39, 71-52.
13. Kougias, I., &Theodossiou, N. (2013). Multiobjective pump scheduling optimization using harmony search algorithm (HSA) and polyphonic HSA. ***Water Resources Management***, *27*(5), 1249-1261.
14. Lee, K. S., & Geem, Z. W. (2004). A new structural optimization method based on the harmony search algorithm. ***Computers & Structures***, *82*(9), 781-798.
15. Lee, K. S., Geem, Z. W., Lee, S. H., & Bae, K. W. (2005). The harmony search heuristic algorithm for discrete structural optimization. ***Engineering Optimization***, 37(7), 663-684.
16. Mahdavi, M., Fesanghary, M., & Damangir, E. (2007). An improved harmony search algorithm for solving optimization problems. ***Applied Mathematics and Computation***, 188(2), 1567-1579.
17. Maheri, M. R. & Narimani, M.M (2014). An enhanced harmony search algorithm for optimum design of side sway steel frames. ***Computers & Structures***, 136 (2014): 78-89.
18. Saka, M. P. (2009). Optimum design of steel sway frames to BS5950 using harmony search algorithm. ***Journal of ConstructionalSteel Research,*** 65(1), 36-43.
19. Xenakis, I. (1992). Formalized music: thought and mathematics in composition (No. 6). PendragonPress

HORIZONTAL CONVECTION INDUCED BY ABSORPTION OF SOLAR RADIATION

V.C. Papaioannou* and P.E. Prinos

Hydraulics Laboratory Dept. of Civil Engineering, A.U.Th, GR- 54006, Thessaloniki, Macedonia, Greece

*Corresponding author: e-mail: vaspapa@civil.auth.gr, tel : +302310995856

Abstract

In the present study, the formation and development of horizontal convective currents between open water and a shaded area are investigated numerically. Differential solar heating can result from shading aquatic canopy, producing a temperature difference between the shaded and illuminated region. The unsteady two-dimensional Navier-Stokes (NS) equations are used in conjunction with the energy equation, where the latter accounts for the absorption of radiation through an additional source term. The Boussinesq approximation is applied for taking into account the density difference due to temperature difference in the buoyancy term. Two radiation models are being implemented, one based on Beer's law and the other on the Radiative Transfer Equation (RTE). Both models divide the incoming radiation into three bands, each having a specific absorption coefficient. The RTE incorporates the emission and scattering processes, besides the absorption term, while Beer's law model uses only the absorption term. The effect of Grashof number (Gr), ranging from 10^7 to 10^9, on the characteristics of the convective currents are examined. The numerical results for the current velocity and water temperature profile are presented and compared against available experimental data.

Keywords: horizontal convection, absorption, radiation, Beer's law, Radiative Transfer.

1. INTRODUCTION

The horizontal convection is quite significant in various geophysical systems. This phenomenon has been studied in the field, in lake systems, from several scientists because of its importance in the transport of nutrients and other chemicals that determine, to a large extent, the ecosystem of an area. In lake systems the part of the water body with aquatic vegetation, near the shore, presents very low absorption of solar radiation, compared with the net water area [Lightbody et al., 2008] resulting in the development of convective currents.

The laboratory study and analysis of convective currents has focused on (a) small scale reservoir with horizontal and inclined section [Coates and Patterson, 1993; Lei and Patterson, 2002], (b) in the presence of aquatic vegetation in part of the reservoir, with either a horizontal or sloping bed [Zhang and Nepf, 2009] and (c) the effect of Rayleigh number (laminar and turbulent horizontal convection).

In the field, the morning heating and afternoon cooling (daily cycle) of water generates convective currents. The daily difference in temperature results in convective flow, where the speed reaches the 3 cm/s in the morning hours and 11 cm/s at noon [Monismith et al., 1990].

The computational simulation of convective currents has several advantages, compared with the laboratory investigation, in the use of different boundary conditions, changing radiation and heat supply in general, and simulation in real conditions. Most computational studies focus on low

Rayleigh numbers, [Mullarney et al., 2004] and recently with use of direct numerical simulation turbulent convective currents for Rayleigh number up to $3*10^{11}$ [Shishkina, 2017] and 10^{12} [Griffiths et al., 2013] have been simulated.

The effect of solar radiation and heat supply from the external environment in the water volume is taken into account through a source term in the equation of energy (temperature). The numerical calculation of radiation attenuation in water depends on (a) the three-band model of radiation [Hattori et al., 2014], (b) the law of Lambert-Beer for the attenuation of radiation in water [Tsakiri and Prinos, 2015] and (c) the discrete radiation model [Siegel and Spuckler, 1994] that is further analyzed in other papers [Kaluri and Dattarajan, 2010].

This paper focuses on the numerical simulation of convective currents due to solar radiation. An evaluation of the radiation models is investigated, through the necessary comparison with corresponding available experimental data [Coates and Patterson, 1993]. In addition, the effect of Grashof number (Gr), ranging from 10^7 to 10^9, on the characteristics of the currents is investigated.

2. COMPUTATIONAL MODELLING

2.1 Governing equations

The two-dimensional Navier-Stokes equations (1), (2) and (3) are solved in conjunction with the energy equation (4) for unsteady, incompressible flow. The Boussinesq approximation is used, which treats the density as constant in all equations, apart from the buoyancy term of the momentum equation, in which it varies due to temperature difference.

$$\frac{\partial u}{\partial x}+\frac{\partial v}{\partial y}=0 \tag{1}$$

$$\frac{\partial u}{\partial t}+u\frac{\partial u}{\partial x}+v\frac{\partial u}{\partial y}=-\frac{1}{\rho_o}\frac{\partial p}{\partial x}+\nu\left(\frac{\partial^2 u}{\partial x^2}+\frac{\partial^2 u}{\partial y^2}\right) \tag{2}$$

$$\frac{\partial v}{\partial t}+u\frac{\partial v}{\partial x}+v\frac{\partial v}{\partial y}=-\frac{1}{\rho_o}\frac{\partial p}{\partial y}+\nu\left(\frac{\partial^2 v}{\partial x^2}+\frac{\partial^2 v}{\partial y^2}\right)+ga\left(T-T_o\right) \tag{3}$$

$$\frac{\partial T}{\partial t}+u\frac{\partial T}{\partial x}+v\frac{\partial T}{\partial y}=\kappa\left(\frac{\partial^2 T}{\partial x^2}+\frac{\partial^2 T}{\partial y^2}\right)+S_h \tag{4}$$

where u and v are the horizontal and vertical velocity components, T is the temperature, p = 101,325 Pa is the pressure (incorporating the hydrostatic pressure), g = 9.81 m/sec^2 is the acceleration due to gravity, and ν = 0.000001051 m^2/sec, ρ_o = 998.2 kg/m^3, a = 0.000207 K^{-1} and κ = 1.4924E-07 m^2/sec are the kinematic viscosity, density, coefficient of thermal expansion and thermal diffusivity of the fluid at the temperature T_o = 294.55 K or 21.4 ^{o}C. The source term S_h in Equation (4) is an internal heating source, which represents the absorption of radiation by the fluid and is added in the energy equation only in the open region of the tank. In the opaque region, it is assumed that the water does not absorb any radiation. This internal heating source generates horizontal temperature gradients between the open water and the shaded region and these gradients induce circulation.

2.2 Computational Domain-Case Studies

The computational domain includes a rectangular reservoir of height h = 0.3m and total length L = 0.6m = (l + l_E), where l is the length of the opaque area and l_E the length of the transparent area where solar radiation penetrates water. The walls of the reservoir are considered to be adiabatic and the wall properties are shown in Figure 1.

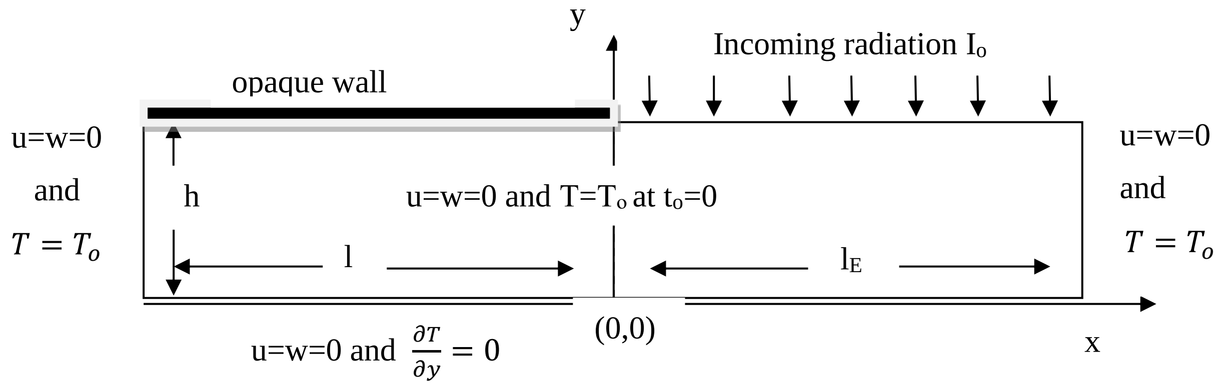


Figure 1. Computational domain and boundary conditions.

The case studies are based on the experiments of Coates and Patterson [1993]. The surface radiation intensity is equal to I_0 [W/m^2] which varies, as shown in Table 1, and hence the Grashof number varies from 6.79*10^7 to 1.19*10^9. In the same table, the characteristic times t_c, t_E and t_v which indicate the times of the three characteristic regimes (inertial, energy limited and viscous) are shown together with the scale velocity u_E in the energy-limited regime.

Table 1. Case studies and characteristic parameters.

Case Studies (CS)	Incoming Radiation I_o (W/m^2)	Grashof number (Gr)	t_c (sec)	t_E (sec)	t_v (sec)	u_E (mm/sec)
1	20	6.79*10^7	3.9	209	2040	1.43
2	127.5 (C.P. 1993)	4.33*10^8	1.6	113	2040	2.65
3	350	1.19*10^9	0.9	81	2040	3.71

2.3 The solar radiation model

The Fluent 15.0.7 CFD code, which uses a control volume technique, is applied for the numerical computations. The computational domain is divided into discrete control volume on which the governing equations are integrated. For the mesh generation, the Gambit program is used. The segregated solution method is used and the velocity-pressure coupling is achieved with the SIMPLE algorithm. For the discretization of the governing equations, the PRESTO scheme is used for the pressure and the Second Order Upwind scheme is used for the momentum and the energy [ANSYS Inc., 2013]. User Defined Functions (UDF), based on C++ code, is used for introducing the extra source term S_h. The RTE model is already included in the FLUENT's radiation panel. Two different radiation models are considered in this work, one based on Beer's law and the other based on the Radiative Transfer Equation [Modest M., 2013].

2.4 Beer's Law

According to Beer's Law the radiation intensity, decreases with increasing water depth and the source term is given by Equation (5).

$$S_h = \frac{1}{\rho \cdot C_P} \sum_{i=1}^{N} n_i \, I_i \, e^{-n_i (h-y)} \tag{5}$$

where N=number of bands, I_i is the surface radiation intensity, η_i is the extinction coefficient, h is the water depth and y is the distance from the tank bottom. In order to compute the I_i intensities the blackbody radiation distribution must be taken into account. The lamps used in the experiments are

mostly of 3200 ºK color temperature generating a surface radiation heat flux I_o, which is divided into i intensities based on the distribution of the spectral radiance as given in figure 2.

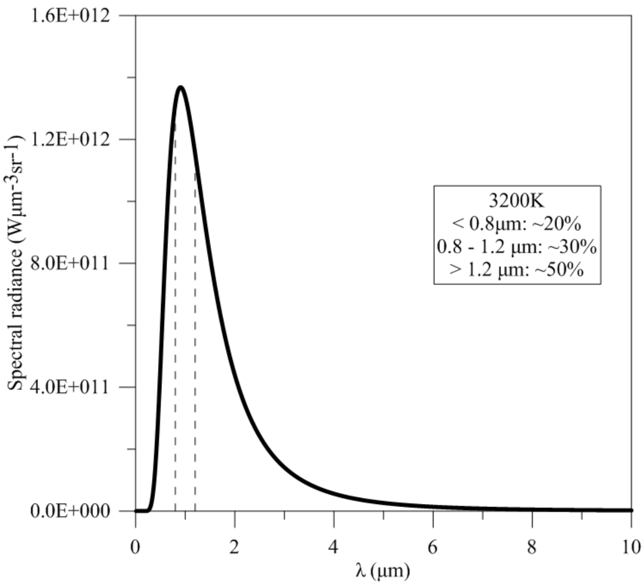


Figure 2. Spectral radiance distribution for the color temperature of 3200 K.

In fact, the extinction coefficient for the water depends on the wavelength of the radiation and the turbidity of the water. In an analysis of 1-m deep solar pond, Rabl and Nielsen [1975] developed four-band model to quantify the variation of the intensity of the solar radiation. They concluded that the absorption of the radiation passing a water column cannot be described by a single exponential, because different wavelengths differ widely in their absorption coefficients. Coates and Patterson [1993] developed a three-band model based on their temperature measurements in a 300-mm water column and found that it accurately reproduced the observed data. Hattori and Patterson [2014] divided the entire spectrum of the attenuation coefficient into N=50 wavebands of equal radiation intensity and found that the variation between the N=50 waveband solution and the three-band model solution is marginal. However, it is not uncommon to some limnological applications, that the absorption coefficient is assumed to be characterized by a single bulk extinction coefficient [Tsakiri and Prinos, 2016].

A three-waveband attenuation model is implemented in this paper, where the n_i coefficients were experimentally derived [Coates and Patterson, 1993], as shown in table 2. The thermistors were located at fixed depths in order to obtain a good temperature profile. The temperatures were measured after one hour of uniform surface heating of the tank to ensure that the deeper water was sufficiently heated.

The absorption of light decreases with decreasing wavelength and reaches a minimum absorption for blue [Hale and Querry, 1973] and then increases again in the ultraviolet (UV) region. According to Wetzel [2001], about 53% of the total light energy is transformed into heat and absorbed in the first meter of water.

Table 2. Three-band model characteristics [Coates and Patterson, 1993]

Band	Wavelength (nm)	Percentage total surface energy	Experimental n_i (m^{-1})
1	< 800	~20%	145
2	800-1200	~30%	15
3	> 1200	~50%	2.5

2.5 Radiative Transfer Equation

The discrete ordinates (DO) radiation model solves the Radiative transfer equation (RTE) for finite number of discrete solid angles, each associated with a vector direction $\vec{s}$ fixed in the global Cartesian system (x, y, z). It transforms the RTE equation into a transport equation for radiation intensity in the spatial coordinates (x, y, z). The DO model solves for as many transport equation a there are directions $\vec{s}$ [Chui and Raithby, 1993]. The last term in Equation 4, using this model, is given by

$$S_h = -\nabla \cdot q_r \cdot \left(\frac{1}{\rho_o C_p} \right) = -a_\lambda \left(4\pi I_{b\lambda} - \int_0^{4\pi} I_\lambda \left(\vec{r}, \vec{s} \right) d\Omega \right) \cdot \left(\frac{1}{\rho_o C_p} \right) \tag{6}$$

where λ is the wavelength, α_λ is the spectral absorption coefficient, $I_{b\lambda}$ is the blackbody intensity given by the Planck function. The intensity I_λ at the position $\vec{r}$ in the direction $\vec{s}$ is obtained by solving the RTE:

$$\nabla \cdot \left(I_\lambda \left(\vec{r}, \vec{s} \right) \vec{s} \right) + \left(a_\lambda + \sigma_s \right) I_\lambda \left(\vec{r}, \vec{s} \right) = a_\lambda n^2 I_{b\lambda} + \frac{\sigma_s}{4\pi} \int_0^{4\pi} I_\lambda \left(\vec{r}, \vec{s}' \right) \Phi \left(\vec{s}, \vec{s}' \right) d\Omega' \tag{7}$$

where n is the refractive index, σ_s is the scattering coefficient, $\vec{s}'$ is the scattering direction vector, Ω is the solid angle and Φ is the phase function. Equation (7) is the generalized equation for absorbing, emitting and scattering medium. In the present study scattering is ignored, as the experimental studies on scattering of radiation in pure water, indicate that the scattering phase function Φ is highly forward in nature [Kullenberg, 1968]. The scattered energy propagates in the direction of the beam. As suggested by Cengel and Ozisik [1984] scattering can be neglected, since all non-absorbed energy propagates in its original direction. Thus the additional source term in Equation 6 takes a much simpler form:

$$S_h = \left(\frac{1}{\rho_o C_p} \right) \cdot \sum_{i=1}^{N} \left(4 \cdot n_i \cdot \sigma \cdot T^4 - n_i \cdot G_i \right) \tag{8}$$

where G_i (W/m^2) is the incident radiation of each band and σ is the Stefan-Boltzmann constant. Both models are presented in figure 3, where the two radiation models are uniformly applied to the surface of the laboratory tank [Coates and Patterson, 1993]. The numerical results are in an excellent agreement with the experimental data. There is a slight difference between the two models on the top and bottom of the tank. This is due to the additional emission term of the RTE model.

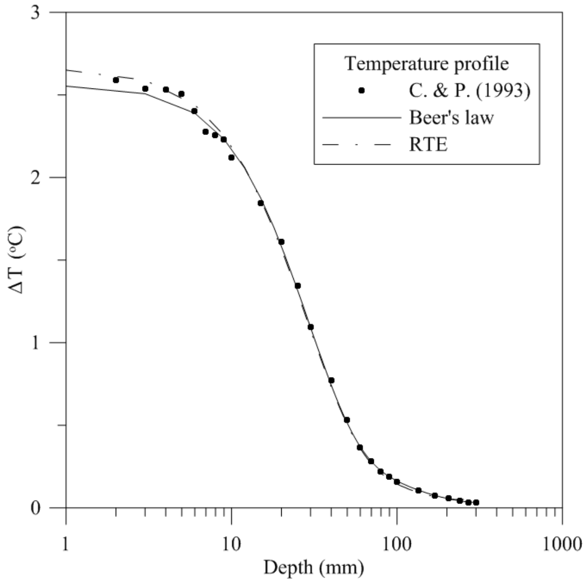
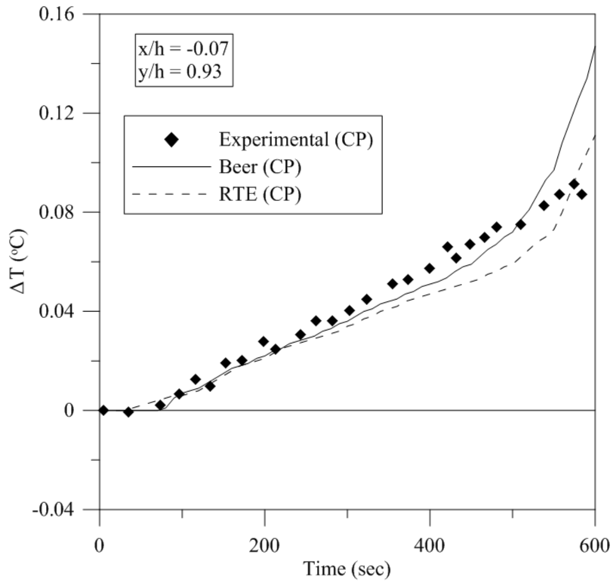


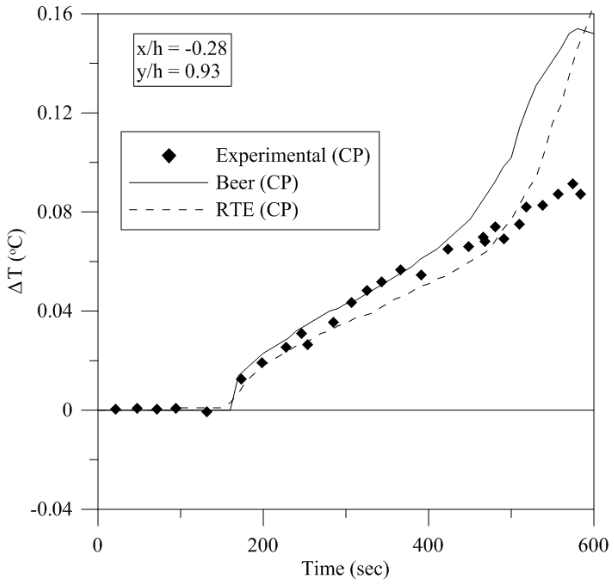
Figure 3. Temperature increase with water depth after one hour of uniform heating.

3. ANALYSIS OF RESULTS

In this section, numerical results from both radiation models (Beer's law and DO model) are presented and compared against experimental measurements and empirical relationships [Coates and Patterson, 1993]. In addition, numerical results are presented which show the effect of the Gr number on characteristics of the convective currents. For the three Gr numbers, ranging from 10^7 to 10^9, temperature increase and maximum velocity are presented.

Figure 4 shows the variation of temperature increase with time at four selected locations, within the shaded area, for Gr number equal to $4.33*10^8$ for which experimental data [Coates and Patterson, 1993] are also available. All locations are at a distance 20 mm from the top surface (y/h=0.93) and at various distances from the light/dark interface (x/h=-0.07, -0.28, -0.50, -0.72).





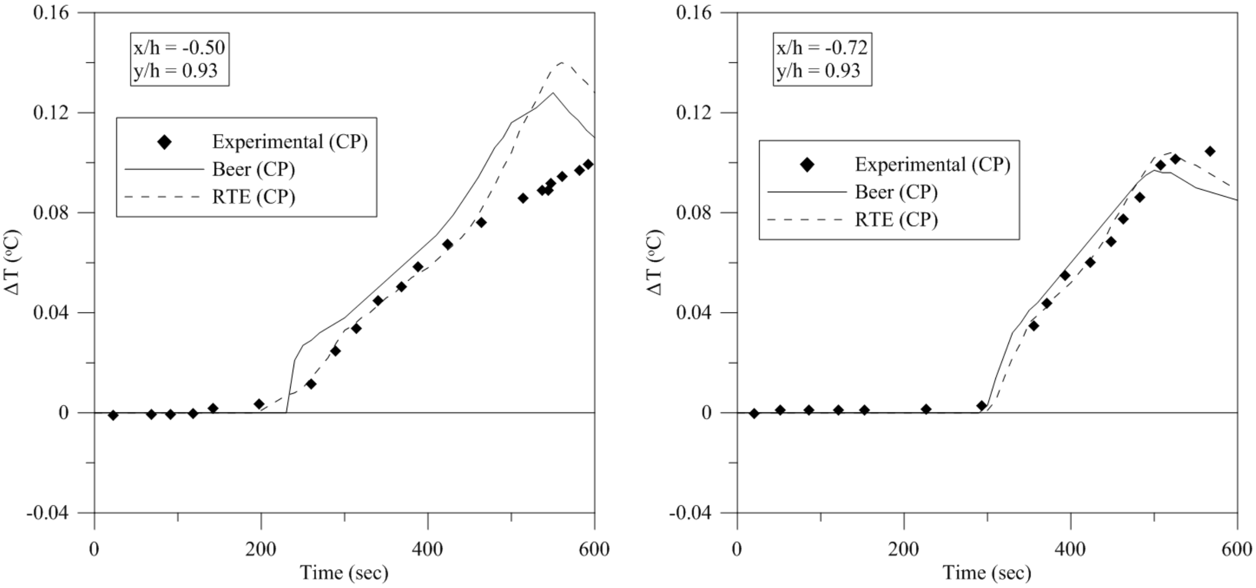


Figure 4. Temperature increase versus time.

At all locations the experimental measurements indicate that, after some time, the temperature increases gradually with a maximum increase of 0.12~0.14 °C after 600 s at the two locations near the shaded/open interface while, at the two remote locations, this increase is 0.09~0.11 °C after 600 s. The two models produce similar variations with temperature increase very close to the experimental for a time of 500 s. The RTE model produces results closer to the experimental especially at the locations x/h=-0.50 and -0.72. After 500 s both models compute much higher increased temperature that that of the experiments due to the side wall effects.

Figure 5 and 6 show the effect of Gr number on the dimensionless temperature increase at a location (x/h=-0.07) for t=200 s and 400 s. Both radiation models present the same behavior. As the Gr number increases the convective current becomes larger in width and its temperature increases with increasing Gr number.

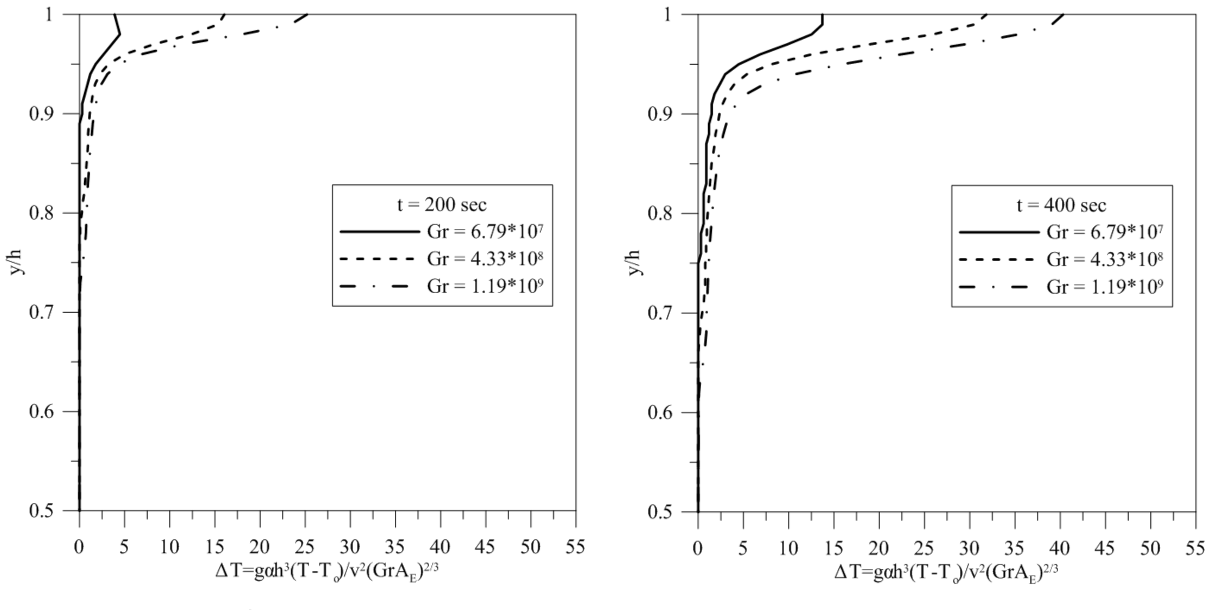


Figure 5. Variation of dimensionless temperature increase with depth at 20 mm (x/h= -0.07) from the light/dark interface (Beer's law model).

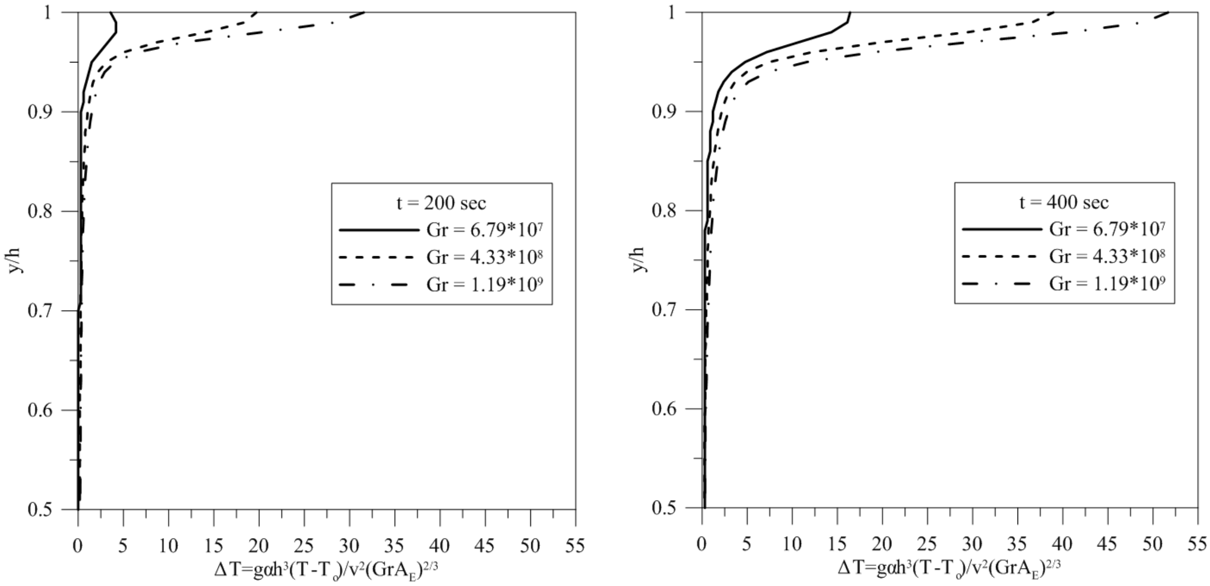


Figure 6. Variation of dimensionless temperature increase with depth at 20 mm (x/h= -0.07) from the light/dark interface (RTE model).

In the inertial regime, the velocity is expected to be linear with respect to $t^{0.5}$ and the data of figure 7 show that the maximum velocities for each case do fall well on a straight line. This confirms that the early stage of the flow is indeed inertial. The maximum horizontal velocities for all case studies are plotted against $(Gr\nu^3 t/h^4)^{0.5}$. In general, the Beer's law model produces velocities higher than those of the RTE model at all times. The figure 7 shows the straight line produced by the experimental results of Coates and Patterson [1993] which is in very good agreement with the numerical results of the Beer's law model. The velocities of the RTE model are slightly lower and the straight line, produced by these data, is slightly different.

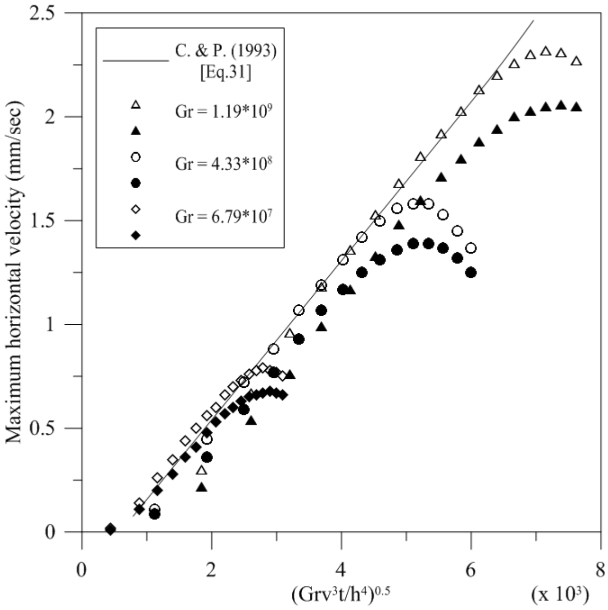


Figure 7. Variation of dimensionless maximum velocity with time. (The open and solid symbols refer to Beer's law and RTE model respectively).

In figure 8 the maximum velocity, made dimensionless with the scale velocity u_E, is plotted against time after the inertial period. The time scales t_E, calculated in Table 1 are lower than those of the simulations but of the same order of magnitude. This is in accordance with the computation of the

maximum velocity which is lower than the scale velocity u_E. In the energy-limited regime the two radiation models produce similar results with the Beer's law model to show higher velocities than those of the RTE model. The effect of Gr on the starting time of this regime, as well as on the velocity magnitude, is very clear. The experimental results, for Gr equal to $4.33*10^8$ also show velocities lower than the scale velocity as well as lower than the computed ones.

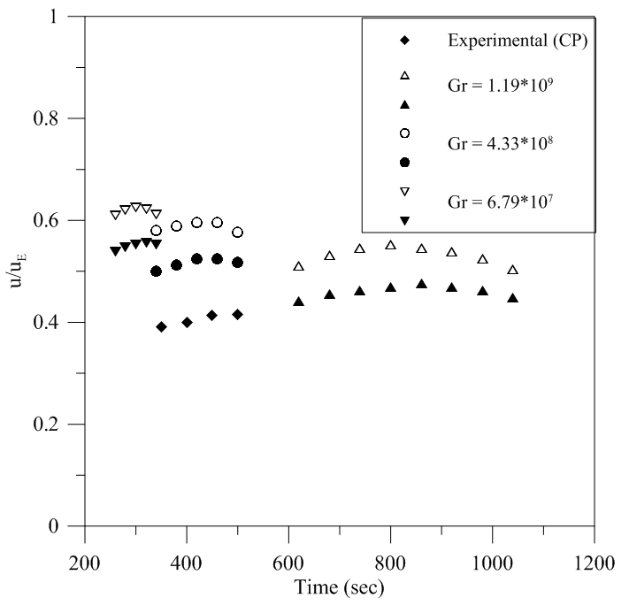


Figure 8. The maximum velocity, scaled against the expected constant velocity u_E versus time. (The open and solid symbols refer to Beer's law and RTE model respectively).

4. CONCLUSIONS

An extended work was performed to assess the effectiveness of two radiation models (Beer's law and RTE model) in predicting the development of convective currents due to differential heating. Also, the effect of Gr number on the characteristics of the convective currents was investigated. The following conclusions can be derived:

a) Both modes adequately reproduce the temperature profile, when uniform heating is introduced on the surface of the tank.

b) The numerical temporal evolution of temperature increase at various locations along the shaded area was compared with available experimental measurements [Coates and Patterson, 1993] for $Gr=4.33*10^8$. The comparison indicates a satisfactory agreement between experimental and computational results for time up to 500 s. The RTE model gives better predictions than the Beer's law model, especially in the region far from the light/dark interface.

c) The investigation of the effect of Gr on characteristics of the convective currents indicates that the width and the temperature of the current increase with increasing Gr number.

d) The variation of the maximum velocity, at the light/dark interface, with time indicates that, initially, the velocity increases linearly with $t^{0.5}$ (inertial regime) and becomes constant afterwards (energy limited regime). The constant maximum velocity is less, but of the same order of magnitude, than the scale velocity and its value depends on the Gr number.

References

1. Lightbody A. F., Avener M. E., and Nepf H. M. (2008). Observations of short-circuiting flow path within a free-surface wetland in Augusta, Georgia, U.S.A. **Limnology and Oceanography**, 53 (3), 1040-1053.

2. Coates, M. J., and Patterson, J. C. (1993). Unsteady natural convection in a cavity with non-uniform absorption of radiation, **J. Fluid Mech.**, vol. 256, pp. 133-161.
3. Lei C., and Patterson J. (2002). Natural convection in a reservoir sidearm subject to solar radiation: experimental observations**, Experiments in Fluids**, 32 (5), 590-599.
4. Zhang X., and Nepf H. M. (2009). Thermally driven exchange flow between open water and aquatic canopy. **Journal of Fluid Mechanics**, 632, 227-243.
5. Monismith S., Imberger J., and Morison M. L. (1990). Convective motions in the sidearm of a small reservoir. **Limnology and Oceanography**, 35, 1676-1702.
6. Mullarney J. C., Griffiths R. W., and Hughes G. O. (2004). Convection driven by differential heating at a horizontal boundary. **Journal of Fluid Mechanics**, 516, 181-209.
7. Shishkina O. (2017). Mean flow structure in horizontal convection. **Journal of Fluid Mechanics**, 812, 525-540.
8. Griffiths R. W., Hughes G. O., and Gayen B. (2013). Horizontal convection dynamics: insights from transient adjustment. **Journal of Fluid Mechanics**, 726, 559-595.
9. Hattori T., Patterson J. C., and Lei C. (2014). Study of unsteady natural convection induced by absorption of radiation model based on a three-wave-band attenuation model. **Journal of Physics: Conference Series**, 530, 012036.
10. Tsakiri M., and Prinos P. (2015). Numerical simulation of thermally driven exchange flow between open water and aquatic canopies. **E-proceedings of the 36th IAHR World Congress** 28 June - 3 July, The Hague, the Netherlands.
11. Siegel R., and Spuckler C. M. (1994). Effect of refractive index and diffuse or specular boundaries on a radiating isothermal layer. **Journal of Heat Transfer**, 116, 787-790.
12. Kaluri R. S., and Dattarajan S. (2010). Numerical simulation of direct absorption of solar radiation by a liquid. **Tech. rep.**, Siemens Corporate Research & Technologies.
13. ANSYS Inc. (2013). **ANSYS Fluent 15.0 User's Guide**, ANSYS Inc., USA.
14. Modest, F. M. (2013). **Radiative Heat Transfer (Third Edition)**, Academic Press, Boston, doi.org /10.1016/ B978-0-12-386944-9.50037-6.
15. Rabl, A., and Nielson, C. (1975). Solar ponds for space heating, **Sol. Energy**, 17, l-12.
16. Tsakiri, M., and Prinos, P. (2016). Microscopic numerical simulation of convective currents in aquatic canopies, **Procedia Engineering**, vol. 162(C), pp. 611-618.
17. Halle G. M., and Querry M. R. (1973). Optical constants of water in the 200nm to 200μm wavelength region. **Appl. Optics 12**, 555-563.
18. Wetzel, R. G. (2001). Light in inland water, **In Limnology, 3rd ed.** Academic Press.
19. Chui, E. H., and Raithby, G. D. (1993). Computation of Radiant Heat Transfer on a Non-Orthogonal Mesh Using the Finite-Volume Method. *Numerical Heat Transfer, Part B*, 23:269-288.
20. Kullenberg, G. (1968). Scattering of light by Sargasso Sea water. **DeepSea Res.**, 15, 423–432.
21. Cengel, Y.A., and Ozisik, M.N. (1984). Solar radiation absorption in solar ponds, **Sol. Energy**, vol. 33:6, pp 581-591.

SUPPORTING INTEGRATED WATER RESOURCES MANAGEMENT ON THE ESTABLISHMENT OF THE MAXIMUM WATER LEVEL IN LAKE VEGORITIDA

Ch. Doulgeris* and A. Argyroudi

Soil and Water Resources Institute-Dept. of Land Reclamation, Hellenic Agricultural Organisation, 57400, Sindos, Greece

*Corresponding author: e-mail: chdoulgeris@gmail.com, tel : +302310798790

Abstract

Water is a key element in sustaining any environmental and socio-economic balance. With the current context of rapid changes on hydrological and socio-economic patterns, water resources management is facing a special challenge, which is no other than dealing with competing claims of various stakeholders on water, or in other words, with water resource dilemmas, such as the determination of the maximum water level in Lake Vegoritida (Northern Greece). The lake's water level has undergone great changes, throughout the last decades, caused by severe water abstraction directly from the lake and its catchment. Along with the water level changes, it is not only the natural environmental conditions that have adapted to a new status, but also the social and economic ones. Nowadays, a discussion about the decision for the maximum water level in Lake Vegoritida becomes a source of conflict among stakeholders who have different claims and interests around the lake. In this paper, an outlining process is followed that includes the identification of stakeholders and the issues related to lake's water level, as well as the effects of alternative proposed scenarios of maximum water level on the natural and socio-economic environment. The engagement of the identified stakeholders in a management and decision-making process should be taken into account by the competent authorities towards the establishment of an environmentally sustainable, socially equitable and economically efficient maximum water level in Lake Vegoritida.

Keywords: lake level management; environmental aspects; socio-economic aspects; stakeholders; IWRM

1. INTRODUCTION

Despite the immense technological progress, societies still depend on the capacity of ecosystems to produce goods and services which sustain social and economic development. Water is a key element in sustaining any environmental and socio-economic balance. With the current context of rapid changes on hydrological and socio-economic patterns, water resources management is facing the special challenge to deal with competing claims of various stakeholders on water. Stakeholders hold strong but divergent values and perceptions about what is at stake and a situation of complexity is created through the way all interdependent, conflicting human activities adapt with changes on the natural environment.

As the economy and society are dynamic and the natural environment is also subject to change, the perspective of Integrated Water Resources Management (IWRM) is lately highly embraced by communities and researchers in the need to be capable of adapting to new economic, social and environmental conditions and to changing human values (GWP, 2004). Special focus is nowadays

given in socio-hydrology, with a basic statement of the International Association of Hydrological Sciences (IAHS) that co-evolution of hydrological and connected systems (including society) needs to be recognized and modelled with a suitable approach, in order to predict their reaction to change (Montanari et al., 2013). Usable science, as produced in a form that can be used by stakeholders in their management and decision-making roles, becomes meaningful through building ongoing relationships with stakeholders and ensuring their two-way communication (Meadow et al., 2015). A recent example in literature of this successful exchange of knowledge between researchers and research users has been explicit in the case of Upper Santa Cruz River basin in Arizona, where a hydrological model has been used as a vehicle to link stakeholder engagement with groundwater management (Eden et al., 2016).

Lake Vegoritida, one of the largest and deepest lakes in Greece, is just another example of a natural system whose management cannot be separated from the public, as the decision for maximum water level immediately becomes a source of conflict among stakeholders who have different claims and income around the lake. The lake’s water level has undergone great changes caused by severe water abstraction directly from the lake and its catchment; water level was around 525 m a.m.s.l in early 80’s and dropped down to 509 m in late 90’s whereas has partially recovered to around 518-519 m during the last decade. Researchers have studied the energy and water budget of the lake (Gianniou & Antonopoulos, 2007), or shown the inter-relations between the abiotic and biotic features of the lake (Antonopoulos and Gianniou, 2003; Pirini et al, 2011; Stefanidis, 2012). Gianniou & Antonopoulos (2014) have shown that significant changes on concentrations of phosphorus and dissolved oxygen have been caused due to water depth and volume alterations during the years 1981-1983. Recently, an assessment of the environmentally minimum water level for Lake Vegoritida reconciles the protection of lake ecosystems and the availability of water volume to meet the economic activities (Doulgeris et al., 2017). Nowadays, that the severe water abstraction directly from the lake has been ceased, the arising management question is ‘What would be the best maximum water level of Lake Vegoritida’ for both nature and society?

This paper supports the idea of IWRM towards the establishment of a maximum water level in Lake Vegoritida as a means to promote the coordinated management of water in a way that economic and social activities may be carried out in an equitable manner without compromising the sustainability of the lake’s ecosystem. The paper is an outlining process that includes (a) the identification of stakeholders and the issues that arise through a potential establishment of a maximum water level and (b) proposals of alternative scenarios of water level, considered as potential decisions of maximum water level, as a means to raise a constructive discussion associated with the effects of these scenarios on the dynamics between the natural and social environment. Furthermore, the perspective of engaging all levels of stakeholders in a process of establishing a maximum water level in Lake Vegoritida is discussed as a future potential approach in managing the lake’s water level.

2. THE ADAPTIVE SYSTEM OF LAKE VEGORITIDA

Lake Vegoritida is located in the water district of Western Macedonia in Northern Greece.The hydrological catchment of the lake covers an area of 2,145 km^2 and is drained by the streams Sklithro, Amyntas and Pentavryso (or Soulou) and the Lakes Zazari, Cheimaditida and Petron. Key inflows in Lake Vegoritida are the excess of surface water from Lake Petron, which is transferred to Vegoritida through a tunnel, and runoff of Pentavryso subcatchment.

Lake Vegoritida has undergone great changes on its natural environment in the last decades as a result of its water level alteration. Based on water level recordings from the 1980s’ and afterwards (Fig. 1), the water level dropped from 525 m to 510 m a.m.s.l. circa in the early 2000s’, mainly due to water abstraction by the Public Power Corporation (D.E.H.). During this period the lake has lost 45% of its volume and 29% of its surface area. Ever since the abstraction ceased, the water level is rising and nowadays varies around to 518.5 m. It should be mentioned that the water level recordings between 40’s and 60’s show that the water level was varying around 540 m a.m.s.l.



Figure 1. Water level (a.m.s.l.) fluctuation in Lake Vegoritida for the period 1980-2015.

The shrinking lake had revealed some extraordinary fertile land, which was perceived as an excellent opportunity of extra income for the local farmers. As it is shown in Fig. 2, part of the agricultural land is now flooded because of the lake level rising at 518 m, which is now a threat to the farmers. Meanwhile, if the water level exceeds the level of 519 m, the sewage treatment infrastructure, which was built during the period of low water level, will be inundated. On the other side, fishery and the tourist business, which are also part of the local community, seem pleased with a restoring lake. As far as the Public Power Corporation is concerned, it appears that it no longer has any stake on the lake as no more lake water is abstracted to supply a number of thermo-electrical and hydro-electrical power stations. Nowadays, water demands for the operation of these power stations are covered by water transfer from the neighboring hydrological catchment of Aliakmonas River.

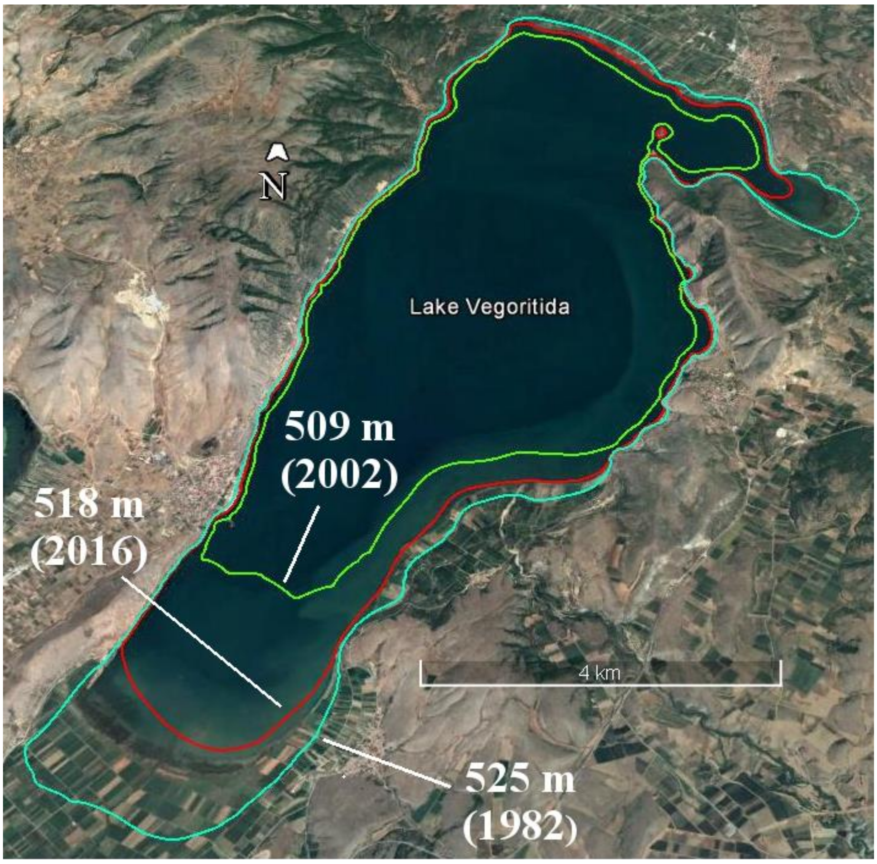


Figure 2. Coastline of Lake Vegoritida for various water levels (a.m.s.l.)

3. THE STAKEHOLDERS AROUND LAKE VEGORITIDA

To outline how stakeholders around Lake Vegoritida have constructed and defended their stakes, two distinct processes were involved. The first process includes the identification of stakeholders and the issues that emerge through a potential establishment of a maximum water level by creating the 'real picture' of the stakeholders' system and their interdependencies in regard with past experiences on the lake's water level fluctuation. The second process is an effort of the authors to create the 'conceptual picture' by proposing three different scenarios of water level, viewed as potential decisions of maximum water level, and exploring their effects on the dynamics between the natural and social environment.

3.1 Analysis of stakeholders and issues related to the maximum water level

Venn diagram (Fig. 3) was used to illustrate the extent to which stakeholders interact or overlap with each other and the importance of each, in regard to the issue of determining a maximum water level in Lake Vegoritida. Large circles represent powerful organisations, overlapping circles represent interacting organisations and a small circle within a larger circle represents a component of that organisation. Farmers and sewage treatment beneficiaries are directly concerned with a potential flooding of their properties, whereas fishermen, recreation business are favored by the lake expanding. The Organization for the Protection of Lake Vegoritida (OPLV) is a community group that has emerged with the aim to prevent the loss of the lake's water, as well as the degradation of its ecosystem. OPLV and farmers are key stakeholders and their efforts may affect authorities towards the determination of the maximum water level of the lake. Academics, researchers, consultants and the public have an indirect involvement and influence on the water level determination, as their livelihoods are not directly affected by a decision for a maximum water level; however, their input in knowledge is essential. Governmental bodies (e.g. Water Directorate), policy makers and local authorities are important in the process of establishing and maintaining the maximum water level, due to their power of legitimizing any decision.



Figure 3. Identification, importance and interaction of the stakeholders who may be directly or indirectly involved in the process of determining a maximum water level in Lake Vegoritida.

A rich picture (Fig. 4), as a mind-mapping tool, presents the plethora of natural, socio-economic and institutional themes that need to be considered in the process of determining a maximum water level in Lake Vegoritida. These themes represent possible issues that may emerge as components of the natural and human environment around the lake and mapping the themes, in regard with the determination of maximum water level, allows a better understanding of reality as well as of the interdependencies that are created. Once a maximum water level is determined (central circle as a starting point), emergent themes appear in a clear sequence of dependencies where a number of activities, for example the economic, will be 're-arranged', depending on the water level.

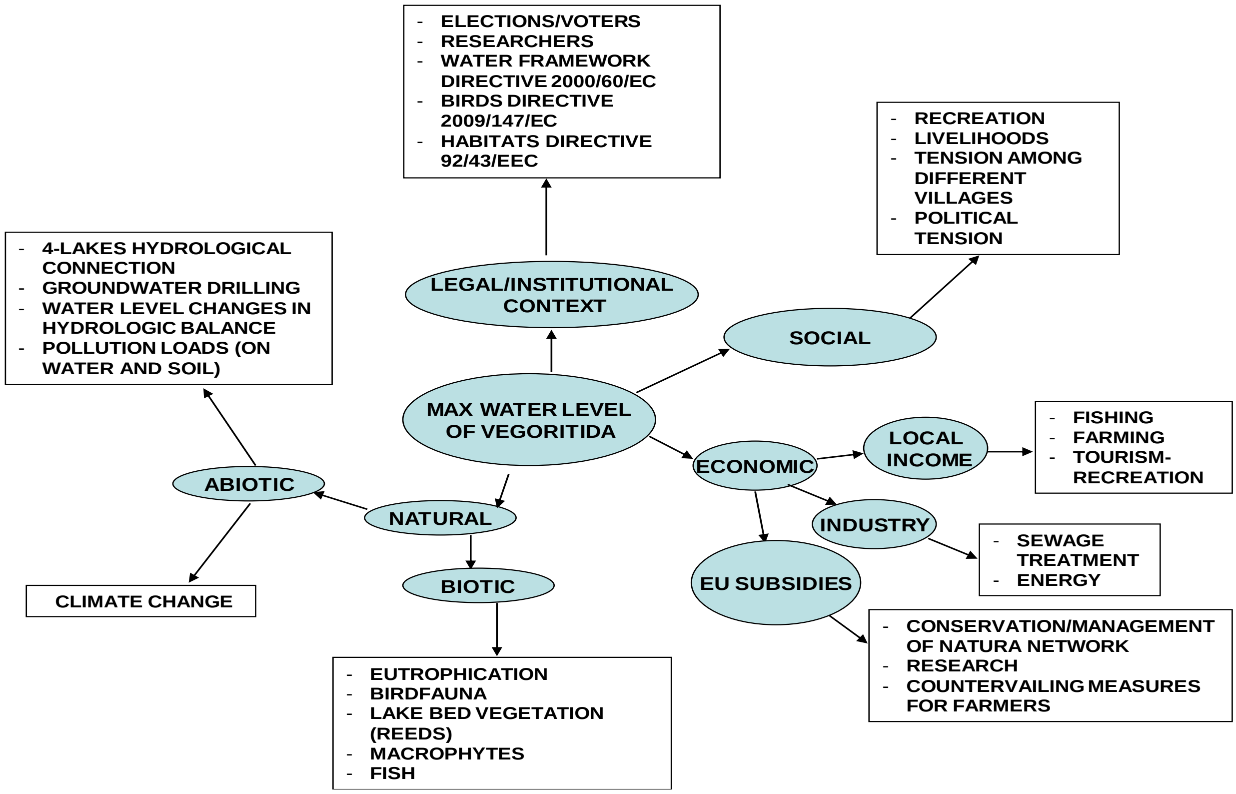


Figure 4. A rich picture of the issues that are related to the determination of a maximum water level in Lake Vegoritida

3.2 Dynamics of maximum water level scenarios

The identification and visualisation of alternative water level scenarios and their consequent effects can be a useful tool for clarifying options among stakeholders with apparently diverging perspectives on the maximum water level. Alternative proposed scenarios of a maximum water level may also promote a collective learning process by bridging knowledge among scenarists and scenario users and a meaningful discussion on the pros and cons of different scenarios while accounting for uncertainties (e.g. rainfall patterns) and possible social and environmental consequences of current watershed management.

Three scenarios of maximum water level for Lake Vegoritida are examined: Scenario 1 refers to a maximum water level of 518 m, which is the recorded water level in the present time period (2016-2017). Scenario 2 refers to a maximum water level of 509 m, which is the water level experienced in late 90's. Scenario 3 refers to a maximum water level of 525 m, which has been experienced in early 80's. In Table 1 are given the positively and negatively affected stakeholders and associated issues arising at each scenario of maximum water level. If there was only one view of reality we would be able to show the benefits and drawbacks of each scenario. However, in a system of stakeholders what is beneficial for one group of stakeholders might be a threat to another and vice versa.

Table 1. Positively and negatively affected stakeholders and issues arising at each scenario of maximum water level in Lake Vegoritida

	Scenario 1	**Scenario 2**	**Scenario 3**
Water Level, a.m.s.l. (m)	518	509	525
Stored Volume (10^6 m^3)	1,068	825	1,557
Surface Area (km^2)	44	38	54
Positively affected Stakeholders	Local community OPLV, Fishermen Tourists, Birdwatchers, Recreation business Farmers who benefit from an improved irrigation status	Farmers Local residents whose income significantly comes from farming Local Authorities	Local community OPLV, Fishermen Tourists, Birdwatchers, Recreation business Farmers who benefit from an improved irrigation status
Negatively affected Stakeholders	Local residents whose income significantly comes from farming Local Authorities	Local community OPLV, Fishermen Tourists, Birdwatchers, Recreation business	Farmers Local residents whose income significantly comes from farming Local Authorities Sewage treatment beneficiaries
Issues of interest			
Lake restoration	Not affected	Affected	Back to older state, unknown effects
Water quality	Affected	Affected	Unknown effects, probably deteriorated if sewage treatment no longer works
Available irrigation water	Currently ongoing	Will decrease	Will increase
Ecosystem functions	Have been restored	Habitat loss (birds, fish) Macrophytes will be re-arranged Loss of bird populations	Bird habitats flooded Fish spawning habitats flooded Macrophytes will be re-arranged New ecosystem balance
Business activities (farming, fishing)	Farmers have lost land, fish production and quality improved	'Farmland' will be revealed, unknown fishing production projections	More 'farmland' will be lost
Recreation activities (swimming, hunting, birdwatching)	Not affected	Will be affected due to ecosystem degradation	Possibly will be improved
Sewage treatment operations	Not affected	Not affected	Sewage treatment plant will no longer work
Social conflicts	Currently existing between farmers and OPLV -fishers, but conflicts have been almost at halt, after decision of Minister of Environment	Conflicts for claiming new property rights on revealed land among farmers of different villages, conflicts between farmers and OPLV-fishers. Local Authorities will need to take sides	Conflicts among sewage treatment beneficiaries, farmers against fishers, OPLV. Local Authorities will need to take sides

According to Table 1, three different ways of viewing Lake Vegoritida are outlined.

Scenario 1: There has been enough tension accumulating between stakeholders, whose income comes from tourism, fishing and recreation, and farmers who have been seeing their land being inundated. It has not been until the Ministry of Environment had put a halt to this tension, through an immediate intervention for stabilizing the water level at 518 m. Currently, the lake has been restoring at a great extent, although water quality is still poor. Local community is pleased with the lake's restoration, even a group of farmers who are foreseeing an improved irrigation status.

Scenario 2: This is a water level scenario that benefits a portion of the local community; the farmers who will regain their land as well as local authorities who will benefit from the farmers voting support. However, this scenario reflects not only a completely degraded ecosystem and its functions (as already experienced in the past), but also unresolved conflicts among local authorities, environmental groups for the protection of the lake, and other people whose income comes from the tourist and fishing business. An additional conflict among farmers emerges, as farmers from different villages claim 'property rights' of the revealing land. The potential of a deterioration of the lake's water quality is prominent for this scenario, as non-point and point pollution loads will outflow to a lake with a decreased water volume.

Scenario 3: Although this is a very optimistic scenario for groups of stakeholders with great environmental concerns for the lake, as well as fisheries and recreation business, an increase of the lake's water at 525 m means that the sewage treatment, as well as other public or private infrastructure that has been constructed over time will be inundated. It also remains unknown how the ecosystem will respond to such a change, as the expanding of the lake will flood existing habitats for birds and fish that have been re-adapted during the last decade. In such a case, any water level raise should take place gradually and under careful monitoring of the natural environment.

3.3 Establishing a maximum water level in Lake Vegoritida under IWRM

According to the second principle of the Dublin Statement on water and sustainable development (1992), on which IWRM is based, water development and management should be based on a participatory approach, involving users, planners and policy-makers at all levels. The participatory approach raises the importance of decision making at the lowest appropriate level, with public consultation and involvement of users in the planning and implementation of water projects in the context of IWRM.

Establishing the maximum water level of Lake Vegoritida, under an IWRM perspective, needs therefore to be seen in the context of a participatory management process. The objectives of such a management approach are related to the direct engagement of stakeholders in deciding about the maximum water level of Lake Vegoritida. These objectives are:

- To engage (rather than just inform) stakeholders in a participatory planning process, about the maximum water level (*Each stakeholder, from locals to authorities, business and scientists, has to propose a maximum water level*)
- To bring together scientific knowledge and experiences of the local people, so as to initiate processes of dialogue and learning from the stakeholders. (*What have we learnt from water level fluctuations all these years?*)
- To view scientists as 'stakeholders' and local people as 'water experts' (*What kind of knowledge can we make most of it and how, in order to decide for a maximum water level?)*
- To create the enabling institutional environment for establishing a water level, through strengthening capacity of networks, rather than persons (*Who has the responsibility/power for making and implementing the decision? And in what way/extent have existing institutions corresponded to the overall changes of the lake over time?*)

The use of the proposed three water level scenarios could be seen not only as a vehicle for stakeholders to recall their personal past experiences of the lake's water level, but also as a new guide

to imagine potential future water level projections and their responses, throughout a participatory management process.

4. DISCUSSION AND CONCLUSIONS

Lake Vegoritida is an interesting system to be studied under the umbrella of IWRM. The above review of the current situation brings on surface some dilemmas that stem from the diverging interests that various stakeholders have in regard with the lake's water level. The lake has been restoring throughout the last two decades, since water abstraction from D.E.H. has ceased. It now remains that farmers demand back their 'flooded' land, while other stakeholders who earn income from the lake (fishers, recreation business) or not (conservationists, local inhabitants) are opposed to that. However, apart from the dilemma of "Flooded farmland vs. Restoring lake", the present paper has revealed some other dilemmas that lie in the reality of the stakeholders around and beyond Lake Vegoritida. These include the following:

According to the Habitats Directive 92/43/EE, once special areas for conservation are designated, EU countries must introduce appropriate conservation objectives and measures. They must do everything possible to guarantee the conservation of habitats in these areas; avoid their deterioration and any significant disturbance to species. EU countries must also encourage the proper management of landscape features essential for the migration, dispersal and genetic exchange of wild species, undertake surveillance of both habitats and species. Therefore, a dilemma is formed as 'Is the lake seen as part of an EU protected area, that has to fulfill certain requirements, or as a distinct part owned only by stakeholders who use its water?'

Nature, economy and society constitute a system through which all water resources should be studied and managed. In an attempt to skip the sense of conflict behind opposing activities of stakeholders (such as farming and fishing), one can see that all kind of activities are part of the area's economy and culture, and people in the area have been adapting their economic activities and livelihoods along with nature changes throughout the years. Therefore, a new dilemma is 'Is the lake viewed only as part of nature, or part of economy vs. is the lake part of a system (nature, economy, society)? At this point of shaping a systemic view of the lake, the dimension of time is important, as both the historicity and the sustainability related to the use of water in the basin should be taken in account.

Humans have always been adapting water management and practice to natural hydrologic variability. However, it remains uncertain whether or not practices and activities designed with historical climate variability will be able to cope with future variability caused by atmospheric warming (de Loë & Kreutzwiser, 2010). Climate change projections in the Mediterranean come along with intensifying human demands on water (surface and groundwater abstraction for irrigation, building infrastructure, water pollution, population increase).

Finally, local authorities and decision makers have dealt with strong political tensions, due to the lake's water fluctuation associated with people's income. Is the lake management a means for politicians to exchange water services for votes and political support or a means for equity in water governance?

Once the issues at stake have been identified and dilemmas have been clearly articulated, the three potential scenarios proposed in this paper bring an answer to the question 'At which state of the lake do we want to move?'

The three scenarios form a conceptual route for a concrete visualisation of the lake's future and reveal the potential of embedding local know-how into future management strategies. Scenarios 2 and 3 have been experienced in the past, and their consequences may be seen as lessons learnt from stakeholders. Engaging stakeholders in discussions and analyses of these past experiences can reveal what kind of information is necessary to better prepare for future changes of water level, their costs, and period of adaptation. Their involvement is also fundamental because they not only represent the end users, but they also play a key role in implementing successful new management practices and

effective local actions (Re, 2015). Moreover, by integrating local and scientific knowledge is a process that can direct scientists towards new research questions that are relevant to stakeholders' needs. A thoughtful design of stakeholder engagement process, elaborated by water scientists can finally be seen as a powerful tool towards aiding water governance organisations in adaptive decision making.

Usually, established water governance organizations and their key members take the initiative to change the existing institutions (policies, laws and administration) on the basis of identified needs, often based on their own interests. However, existing laws and procedures for sharing of water resources among the different users may not be adequate in terms of present circumstances. The extent and the character of an observed gap between declared rules and rules-in-use is a good indicator for institutional change (Bandaragoda, 2000). Papageorgiou and Vogiatzakis (2006) have pointed the need in Greece for greater realisation of integrated conservation which necessitates reforms in the political culture, in terms of being more open and cooperative, and the setting up of a process to facilitate public dialogue. The change in political culture could be enhanced following policy reforms related mainly to sectoral legal frameworks and administrative structures as well as a stronger overall political commitment.

In the case of Lake Vegoritida, every meter of water level has to be translated into 'human behavior', in the process of reaching any optimal management state. This is due to the fact that networks of relationships and the activities of the people that form them around the lake are so well embedded in patterns of water use that imply difficulties in any long-term changes. In this work, the objectives of establishing a maximum water level of Lake Vegoritida are outlined under the umbrella of IWRM, and in particular under the potential engagement of all identified stakeholders in a participatory management and decision-making process. Even if the water level remains as in current, the authors suggest that whether this is the determined maximum water level or not, it has to be legitimized under a change in the management paradigm with which the water of Lake Vegoritida has been managed until now. Past experience of various water levels (empirical knowledge) during the last 30 years and the existing research background (scientific knowledge) constitute a great opportunity on which a change in the management process should be based. However, changes in water management procedures should be supported by institutional reforms, even if that means accommodating the principle of justice and equity in the process. Any water level scenario should be filtered through a holistic approach- in that integrating all environmental, social and economic dilemmas of the stakeholders, so that decision-making is participatory and finally enjoy a wide public acceptance and unproblematic implementation.

References

1. Antonopoulos V. and S. Gianniou (2003) 'Simulation of water temperature and dissolved oxygen distribution in Lake Vegoritis, Greece', **Ecological Modelling**, 160, pp. 39-53.
2. Antonopoulos V. and S. Gianniou (2014) 'Primary production and phosphorus modelling in Lake Vegoritis, Greece', **Advances in Oceanography and Limnology**, 5, pp. 18-40.
3. Bandaragoda, J. (2000), 'A framework for institutional analysis for water resources management in a river basin context', **Working Paper 5**. Colombo, Sri Lanka: International Water Management Institute.
4. Doulgeris C., P. Georgiou, A. Apostolakis, D. Papadimos, D. Zervas, O. Petriki, D. Bobori, D. Papamichail, V. Antonopoulos, C. Farcas and P. Stålnacke (2017), 'Assessment of the environmentally minimum lake level based on hydromorphological features', **European Water,** 58, pp. 197-202.
5. Eden S., B. Megdal, E. Shamir, K. Chief and M. Lacroix (2016), 'Opening the Black Box: Using a Hydrological Model to Link Stakeholder Engagement with Groundwater Management', **Water**, 8(5), pp. 216.

6. Gianniou S. and V. Antonopoulos (2007), 'Evaporation and energy budget in Lake Vegoritis, Greece', **Journal of Hydrology**, 345(3), pp. 212-223.
7. Global Water Partnership (2004), 'Catalyzing Change', **A handbook for developing IWRM and water efficiency strategies**, United Nations.
8. De Loë C. and D. Kreutzwiser (2000), 'Climate Variability, Climate Change and Water Resource Management in the Great Lakes', **Climatic Change**, 45, pp. 163-179.
9. Meadow M., B. Ferguson, Z. Guido, A. Horangic and G. Owen (2015), 'Moving toward the Deliberate Coproduction of Climate Science Knowledge', **Weather, Climate, and Society,** 7(2), pp. 179-191.
10. Montanari A., G. Young, G. Savenije, D. Hughes, T. Wagener, L. Ren, D. Koutsoyiannis, C. Cudennec, E. Toth, S. Grimaldi, G. Blöschl, M. Sivapalan, K. Beven, H. Gupta, M. Hipsey, B. Schaefli, B. Arheimer, E. Boegh, J. Schymanski, G. Di Baldassarre, B. Yu, P. Hubert, Y. Huang, A. Schumann, A. Post, V. Srinivasan, C. Harman, S. Thompson, M. Rogger, A. Viglione, H. McMillan, G. Characklis, Z. Pang and V. Belyaev (2013), 'Panta Rhei-Everything Flows: Change in hydrology and society-The IAHS Scientific Decade 2013-2022', **Hydrological Sciences Journal**, 58(6) pp. 1256-1275.
11. Papageorgiou K. and I. Vogiatzakis (2006), 'Nature protection in Greece: an appraisal of the factors shaping integrative conservation and policy effectiveness', **Environmental Science and Policy**, 9, pp. 476-486.
12. Pirini C., V. Karagiannakidou and S. Charitonidis (2011), 'Abundance, diversity and distribution of macrophyte communities in neighboring lakes of different trophic states and morphology in north-central Greece', **Archives of Biological Sciences,** 63, pp. 763-774.
13. Re Viviana (2015), 'Incorporating the social dimension into hydrogeochemical investigations for rural development: the Bir Al-Nas approach for socio-hydrogeology'. **Hydrogeology Journal,** 23, pp. 1293-1304.
14. Stefanidis K. (2012), 'Ecological Assessment of lakes of Northwestern Greece with emphasis on the associations between aquatic macrophytes, zooplankton and water quality', University of Patras, Postdoctoral Thesis, pp. 272.

RAINWATER HARVESTING AS AN ALTERNATIVE SOURCE TO CONFRONT WATER SCARCITY WORLDWIDE – CURRENT SITUATION AND PERSPECTIVES

S. Yannopoulos, I. Giannopoulou and M. Kaiafa-Saropoulou*

Faculty of Engineering, School of Rural and Surveying Engineering, Aristotle University of Thessaloniki, GR- 54124 Thessaloniki, Greece

[*] Corresponding author: e-mail: minakasar@gmail.com

Abstract

Earth's arid and semi-arid regions were always faced water scarcity problems due to the lack of precipitation and its unpredictability. However, there is global pressure on available water resources, which not only has demographic, economic and social causes, but also is connected with climate change. Rainwater harvesting (RWH) is an alternative source of water applied since antiquity. The practice is still in use in many areas throughout the world as it is adopted by many countries as a viable decentralized water source. Rainwater collection, protection and re-use are a viable process that can both significantly increase available water resources and reduce flood risks. The degree of its modern implementation varies greatly across the world, often with systems that do not maximize potential benefits. In recent decades, many countries are supporting updated implementation of such practice so as to confront the water demand increase, which is related to the climatic, environmental and societal changes. According to the current literature, RWH process belongs to a wider context called Sustainable Drainage Systems (SuDs). It can be applied additionally and designed appropriately so as to reduce frequency, peak and volume of urban runoff. The above thoughts motivate interest in considering the current situation and the perspective to further grow this method worldwide. In the present paper, the current situation of rainwater harvesting as an alternative water source to confront water scarcity around the world is studied. In particular, the paper presents: (a) the causes of water shortage; (b) a brief historical overview of the temporal evolution of the RWH; (c) the causes of the renewal of interest in the RWH technique; and (d) incentives for the spreading of the RWH method in various countries worldwide.

Keywords: Rainwater harvesting, alternative water source, water shortage, arid and semi-arid areas

1. INTRODUCTION

Water is an essential and irreplaceable element for the existence of all living beings and the ensuring of the continuance of life on earth. Access to clean and affordable water is one of the fundamental human rights, as water is the good that plays an important role in health, social and economic development of a country, food production and environment.

Arid and semi-arid regions of the earth were always facing water scarcity problems due to the lack of rainfall and its erratic pattern in spatial and temporal scales. Moreover worldwide, available water resources undergo pressures, due to demographic, economic and social causes, the environmental degradation and the impacts of climate change.

In this way, the population increase, the urbanization expansion and also the intensity of the industrialization and the irrigated agriculture rise water requirements and, consequently, provoke greater pressure on water resources. Between 2011 and 2050, the world's population is expected to

grow by about 33%, while the population that will be living in urban areas is estimated to grow by 72% (UNDESA, 2011). In general, rapid urbanization and improving living standards of urban population contribute to increase of the overall demand for water in cities. By 2030, almost half of the world's population will be living in areas of high water stress (UN Water, 2007).

By 2025, water withdrawals are predicted to increase by 50% in developing countries and 18% in developed countries (WWAP, 2006), while nearly 1.8 billion people will be living in areas under severe water stress and the meeting of the water requirements for different uses (agriculture, industry, domestic purposes, energy and the environment, etc.) will be in the threshold (UN Water 2007). Furthermore, it has to be noted that existing water resources are threatened by the sources' pollution, which affects the inland and coastal aquatic ecosystems. Also, climate change due to global warming can strongly affect the availability of water resources in a small or a wider region.

OECD Members enjoy high levels of access to networked systems of water supply and sanitation. However, OECD (2009) strongly doubts whether its Members will be able to face the major water and sanitation challenges even in urban areas due to the major investments required to repair and replace ageing infrastructure and the cost associated with meeting more stringent environmental requirements. For this reason, it recommends research on alternative sources in terms of water supply. In particular, it recommends RWH, grey and reclaimed water as alternative water sources.

Regarding the physical alternatives to realize sustainable management of freshwater, there are two solutions. The first one is to find alternative or additional water resources by using conventional centralized systems, while the second is the limited use of available water resources in a more efficient way. Till today, much attention has been paid to the first case. Due to the difficulty of developing new freshwater resources, rainwater harvesting, water reclamation and reuse are important additional water resources. Moreover, collection, protection and re-use of rainwater are a viable process that can significantly increase available water resources and also reduce flood risks. Harvested rainwater is an alternative source of water in many parts around the world.

The purpose of this paper is to investigate the current situation for rainwater harvesting as a tool to confront water scarcity, as well as the prospects for the spreading of the method in the various countries of the world.

2. BRIEF OUTLINE OF THE HISTORY OF RAINWATER HARVESTING (RWH)

RWH is a very old traditional and sustainable practice that has been adopted in many regions of the world as a water supply method both for potable and non-potable purposes. In many parts of the world, archaeological findings confirm that ways and means of collecting and storing rainwater for supplying water to human use, livestock farming and irrigation had been devised since antiquity. At that time the method of rain collection was very simple, while the use of water was immediate without any treatment. Probably, the first water collection system was a cavity either in a low permeability soil or in the rock in which the runoff was captured from the upstream surfaces.

People in ancient communities, which were situated in arid and semiarid regions without an access to springs, lakes, perennial rivers or other water sources had to cleverly manage the available water resources, which were unfortunately deficient (Evenari *et al.*, 1961). Rainwater was the main source of water for potable and non-potable use, thus rainwater harvesting was extremely important for their survival.

RWH was practiced about 4500 years ago by the people of the city Ur in the region of Sumer (southern Mesopotamia, in modern-day Iraq) and later by Nabateans and other people of the Middle East (Sivanappan, 2006). The concept of RWH must have been applied in China 6000 years ago (TWDB, 2005). However, archaeological evidence in the Edom Mountains in southern Jordan indicates the existence of water collection systems even 9000 years ago for agricultural purposes. Evenari *et al.* (1961) described water collection systems in the Negev desert of Israel, which were probably constructed about 4000 years ago (ca. 2000 BC), or more.

During prehistoric times (ca. 3200-1100BC), large stone conduits with branches were used to supply collected water to cisterns in different Minoan cities (Knossos, Phaistos, Tylissos, Zakros, etc.) (Yannopoulos *et al*., 2017). Archaeological evidences show that in the Palace of Knossos owned a sophisticated rainwater collection and storage system, which had been in use as early as 1700 BC. Probably, this might be the first example of RWH in a building.

The cistern construction technology of the Minoans and Mycenaeans was improved by the ancient Greeks during Archaic (c. 800-479 BC), Classical (478-323 BC), and Hellenistic (323-30 BC) periods. Specifically, during Hellenistic era, in several Greek cities rainwater was harvested through open spaces on the roofs, yards and other open spaces into covered cisterns for storage and future use, so as to meet their daily water needs (Yannopoulos *et al*., 2017). Numerous cisterns have been found in private or public buildings, quadrilateral, circular or bottle shaped. They were flat, pitched or vaulted roofed, while many of them were multi sectioned for water's filtration.

Afterwards, Roman private and public buildings included cisterns, usually under paved courtyards, in order to collect rainwater and increase the water available from the city's aqueducts. Their similarities with the rainwater tanks found in Minoan and Mycenaeans palaces or in Classical/Hellenistic buildings, in their form and technical characteristics, and generally in the whole technology related to their construction are more than obvious. The rectangular open space, called *compluvium*, which was gathering the rainwater falling on the surrounding roof into a basin placed below (*Impluvium*), so as to be available for household use, was a main architectural feature of Roman villas and houses.

Collection and storage of rainwater in earthen tanks for domestic and agricultural uses was also very common in India, where simple stone-rubble structures for impounding rainwater date back to the third millennium BC. In China, the history of rainwater harvesting dates back to 4,000 years. The RWH and management in the country included cisterns, roof open spaces, soil or rock pits, ditches and micro-dams (Akpinar-Ferrand and Cecunjanin, 2014). There are, also, several archaeological findings that suggest that RWH was common in many areas of the world, including Egypt, Thailand, Mexico, Pakistan, Ethiopia, Jordan, Korea, Sardinia, etc.

3. REVIVAL OF INTEREST FOR RAINWATER HARVESTING

As Fidelibus and Bainbridge (1995) reported, "like many great solutions to environmental problems rainfall catchments ("water harvesting methods") are a reinterpretation of ancient techniques developed in the Middle East and Americas, but forgotten by modern science and technology". However, the increasing urbanization affected RWH practice which was reduced or even almost abandoned because of: (a) the available technical means during the industrial era, which made the water transfer from remote areas possible, through long and complex systems; (b) the ability to withdraw water form deep aquifers, so as to ensure the supply of large quantities of water, for industry and urban water demands; (c) the ability to manage large quantities of water and supply it constantly and safely via organized networks.

During the 20th century, and specifically before 1950, very few activities had taken place on the research and implementation of water collection techniques. In particular, farmers in Australia had already begun collecting water for domestic use and livestock after World War I. During the World War II, there has been some water harvesting activities on islands with high rainfall, as e.g. in Antiqua (Prinz and Malik, 2003).

Interest in water harvesting, both at the research and application level, was renewed partly due to the successful reconstruction of the water collection system for irrigation (1958 and 1959) by Evenari and his colleagues in the Negev desert of Israel. Pacey and Cullis (1986) consider that the work of Evenari *et al*. (1961) was of great significance due to the runoff farming models applied, the completeness of the research they made and the historical sources of the models they used. Modern water harvesting research was started in the 1950's by H. J. Geddes, Professor of the University of

Sydney in Australia, who, according to Myers (1961), gave the first definition of water harvesting, in his attempt to differentiate "the collection end economic storage of farm runoff for irrigation" from "normal farm water conservation to provide water for livestock or household purposes" in the context of a project of the University of Sydney.

In the U.S.A. water harvesting begun during the 1940's and was generalized in the early 1950's when several small catchments were built from small sheets of steel and concrete to provide drinking water to animals and wildlife. Lauritzen in the 1950's had pioneered an innovative technique of constructing catchments and reservoirs, that required the evaluation and use of plastic and artificial rubber membranes.

In 1955, an important movement in research interest took place, when–cooperative studies on the collection of water for the livestock between the U.S. Department of Agriculture and the Utah Agricultural Experiment Station started by using the soil itself as a catchment surface and by treating it with waterproofing and stabilizing materials. In these studies, various soil cover materials were evaluated, such as plastic vinyl films and polyethylene-butyl rubber sheets, asphalt-coated jute fabrics, and chemical sealants (Lauritzen, 1960). Of these materials, plastic butyl films, when not under tension, exhibited excellent wear resistance from exposure to solar radiation, and their installation was relatively simple. However, many of these high cost structures, which were used only by public authorities on public lands, failed within 5-10 years mainly due to strong winds, which caused extensive damages. In 1960's, systematic studies were initiated by various organizations (governmental, private, and universities) in the U.S.A., as well as in other arid or semiarid countries that concerned both the development and the assessment of new methods and materials to be used for the construction of water collection systems at low installation costs and the improvement of system reliability (Frasier and Myers, 1983).

Further incentives for investigating the possibilities of water collection to improve plant production were provided due to the widespread droughts that occurred in the 1970's and 1980's in Africa and their effects on crops. Much of the experience with rainwater harvesting was gained in Israel, U.S.A. and Australia. However, this experience has limited relevance to resource-poor areas in the semi-arid regions of Africa and Asia (Critchley and Siegert, 1991).

Moreover, interest in collecting and storing water for irrigation purposes was enhanced due to the improvements of the earthmoving machinery and sealing soil materials, which were reducing the cost and difficulty of preparing catchment for collecting water and they were improving the efficiency of the collection system. In general, since the 1950's series of experiments developed the variety and sophistication of the water harvesting technology.

In recent years, many countries have renewed their attention in water collection techniques, which are regarded as a viable decentralized water source. The renewal of interest is also related to the role that decentralized water collection systems can play to mitigate flood risks, etc. and because the decentralized multi-purpose rainwater harvesting systems constitute useful infrastructures to mitigate other water related disasters, such as sudden water break and fire events, especially in highly developed urban areas. Nowadays, the art of collecting rainwater has received renewed attention and interest in many countries of the world as a viable decentralized water source e.g. Germany, Italy, Spain, France etc. in Europe; India, China, Malaysia, Japan etc. in Asia; Kenya, Ethiopia, Syria, etc. in Africa; in several states of U.S.A. (Nevada, Utah, etc.), Canada in North America; Brazil in South America; and Australia and New Zealand (Yannopoulos *et al*., 2017).

In the framework of the present study, RWH means the method by which rainfall that falls upon a surface catchment area (roof, sidewalks, parking lots, landscape areas, etc.) is collected and routed to a storage facility for direct or future use (domestic and agricultural use). It is noted that RWH does not reduce the demand, but it can reduce the water abstraction needs.

4. EXAMPLES OF RWH AND UTILIZATION AROUND THE WORLD

In recent decades, the interest in rainwater harvesting for both developing and developed countries (including several EU Member States) is growing. Notably, researches and applications have been carried out at various levels on: (a) the use and management of RWH; (b) the quality of harvested rainwater; and (c) hydrological or economic data for RWH.

In several countries, both governments and local / regional authorities have promoted measures to install and use RWH systems, mostly under a legal framework, with financial incentives (subsidies, reductions or tax refunds, etc.). For example, some form of RWH is mandatory for buildings and houses in various cities and states of India (New Delhi, Indore, Chennai, Rajastan, etc.), Catalonia in Spain, Flanders in Belgium, in new buildings of some states of U.S.A. (Tucson, Arizona, New Mexico, etc.), in many Caribbean islands, in Germany (Hessen, Baden-Württemberg, Saarland, Bremen, Thuringen, Hamburg, etc.) The same is true in some Australian States, such as South Australia, New South Wales and Queensland, where regulations stipulate a new rainwater collection system or alternative water source.

Meanwhile, manuals were developed about designing, constructing and managing of rainwater harvesting systems e.g. in the U.K., Malaysia, Japan, India, Canada, etc. In U.S.A. rainwater harvesting is not regulated by the federal government but rather it is up to individual States to regulate the collection and use of rainwater. Some States including Georgia, North Carolina, Texas, etc., have published manuals that provide information on the types of processing systems and components needed for meeting specific water quality objectives. In addition, at municipal level, several major cities, such as Los Angeles, San Francisco, Tucson, and Portland have issued guidelines and/or policy documents on treatment and permitting requirements for rainwater collection systems (USEPA, 2013).

To the best of our knowledge, there is neither European nor national regulations on the definition of quality standards for rainwater uses within the European Union. In several countries of the European Union, such as France (Décret du 2 Juillet 2008), the United Kingdom (BS 815, 2009), some standards have been proposed, which are merely guidelines (directives) focusing on domestic uses of rainwater. In Spain, there is the Royal Decree 1620/2007 which establishes quality standards for possible uses for recycled water (Llopart-Mascaró *et al*., 2010). However, there is a lot of interest for rainwater harvesting in many European countries including Germany, France, Spain, Italy, Cyprus, Malta, United Kingdom, Austria, Belgium, Denmark, Portugal, etc.

RWH is not restricted in simple small-scale roof collection systems, but it is extended to: (a) larger systems usually used for providing water for schools, stadiums, airports, etc.; (b) collection systems for high rise buildings in urbanized areas; (c) land surface catchment systems, and stormwater collection systems to prevent water sources' pollution from roads, industrial sites, and agriculture. Large-scale RWH systems exist: (a) in Germany, such as in Berlin the DaimlerChrysler Potsdamer Platz and the building complex at Belss-Luedecke-Strasse; in Darmstadt the Technical University; in Frankfurt the Airport, etc.; (b) in the U.K., such as in London the Millennium Dome, the Museum, the Velodrome, etc.; in Manchester the Honda Dealership; in Bristol the Imperial Tobacco Head; (c) in Singapore the Changi Airport; (d) in Japan, such as in Sumida city the Ryogoku Kokugikan Sumo-wrestling Arena, the Town Hall, etc.; in Tokyo the Rojison, the Sky Tower, etc.

In developed countries including Japan, Singapore, Belgium, France, Germany, U.S.A., etc. RWH is mainly used to supplement conventional systems for non-drinking water use, while in Australia the collected water has also potable use. In developing countries, such as Bangladesh, Botswana, India, Kenya, etc. RWH is mainly used to address water shortages for both potable and non-potable use (Lade and Oloke, 2015).

In several Latin American countries, such as Argentina, Brazil, Costa Rica, Chile, Mexico and Peru, the RWH practice from roofs for domestic consumption is applied, while in the semi-arid areas of

Argentina, Brazil and Venezuela, runoff collection from roads in drainage ditches and street gutters is used, from which water is then transferred to cultivated areas for irrigation (Ringler *et al*., 2000).

In Australian cities, RWH is popular. In urban areas, RWH systems are used to complement the main water system, whereas many rural and peri-urban communities completely rely on this. 30% of rural Australians use RWH while in the capital cities the 7% use it. About 13% of all Australian households ($2.6x10^6$ people) use RWH systems as a primary source of drinking water (Coombes, 2006). Local authorities throughout Australia encourage the use of RWH systems in urban areas to supplement main water supplies and to manage urban stormwater runoff. For this reason, the Australian, State and local governments, adopted a wide range of policies including (subsidies and grants) so as to provide the installation of rainwater tanks in houses. These incentives vary from State to State, depending on the size of the water reservoir and the purpose of using the collected water. In South Australia, almost 50% of the population lives in houses equipped with a rainwater tank. RWH is mandatory for new homes in Queensland (CMHC, 2013).

In the USA, rainwater harvesting has become an increasingly common practice. Since 2004, it is estimated that about 100,000 residential RWH systems were in use in the USA and its territories (TWDB, 2005). Some States and Territories (Hawaii, Kentucky, New Mexico, North Carolina, Ohio, Oregon, Texas, Utah, Washington, etc.) consider RWH as a serious practice for protecting water resources and also, for increasing available volume of water for potable use. However, even though the major use of harvested rainwater is for landscape watering, flushing toilets, etc. there are a number of systems that serve indoor uses as well. It is worth mentioning, that with proper design and appropriate treatment, harvested rainwater is considered as a safe and dependable source of water for potable uses, particularly in remote communities (Krishna, 2007).

In Bermuda, rooftop RWH is compulsory by law for all buildings and constitutes the primary source of water for domestic supply. Public Health Act regulates the details for the maintenance and conservation of the catchments, tanks, gutters, pipes, vents, and screens in order to be maintained in good situation (Lo and Gould, 2015).

In Canada, most of RWH systems are for residential use in rural areas, where there is no access to central public water supply systems. In cities, most cases relate to buildings that have been certified according to one of the green building rating systems, in which the reuse of rainwater and the reduction of runoff were taken into account (E.A., 2010). Since 2010 National Plumbing Code is in force which permits the use of rainwater for toilet and urinal flushing, as well as subsurface irrigation. In addition, it permits the use of rainwater, both for all indoor and outdoor, depending on the level of treatment. RWH is mandatory for new homes in Queensland (CMHC, 2013). In Ontario, several municipalities recognize RWH as an important tool of confronting water resources management problems. The City of Toronto and the Regional Municipality of Waterloo have been active in promoting the technology through stormwater and green building policies (TRCA, 2010).

In Mexico, RWH can make a significant contribution to reduce the water supply shortage that occurs in large areas of the country. In Guanajuato city of Central Mexico a project was conducted to harvest rainwater using the roof areas of the houses in a community with an average annual rainfall of 455.3 mm and water storage tanks of a 2.5 m^3 capacity were installed in roofs of 74 m^2. Both in the City and in rural areas hundreds of catchment systems have already been installed (Lizárraga-Mendiola *et al*., 2015).

In Brazil, there is no legislation to cover the RWH at the federal level. Since 2007, NBR-15227 is in force, which has normative character and regulates the use of rainwater for non-potable purposes in urban areas. However, there are various cities and municipalities with laws that regulate the catchment and storage of rainwater for non-potable uses. Since 2002, the city of Sao Paulo is pioneer as it implemented the first law regulating these aspects. Thence, other major cities including Rio de Janeiro, Curitiba, Paraiba, among others, have been implementing similar regulations. Due to the large number of different laws and regulations in force in the different parts of the country it is

difficult to assess the extent to which Brazil is implementing RWH as an alternative to the municipal water supply systems (da Costa *et al*., 2017).

In African countries rainwater collection systems are increasingly adopted. However, despite the rapid expansion of these systems progress is slow, because of: (a) the low rainfall and its seasonal nature, (b) the small number and size of impervious roofs, (c) the high cost of constructing catchment systems in relation to typical household incomes, (d) the lack of cement and pure graded sand in some parts of Africa, and (e) the lack of sufficient water for construction industry, which burden the total cost. However, RWH systems are increasingly expanding in Africa with works in Botswana, Mali, Malawi, South Africa, Namibia, Zimbabwe, Tanzania, etc. (UN-HABITAT, 2005).

The effort to develop rainwater collection systems in Africa is led by Kenya, which has a very long tradition in these systems through the centuries. Since late 1970s, interest in RWH has rapidly grown. In different parts of the country, many RWH projects have been carried out, each one with their own designs and implementation strategies, in an effort to provide long-term solutions to water resource problems (UN-HABITAT, 2005). In the middle of the 20th century, the Government began to build rock catchment systems that served communities in the semi-arid area of Kitui district (Lo and Gould, 2015). The variety of geographic and climatic conditions in the country has enabled the development of a very wide range of RWH technologies for water supply, agriculture and livestock. In Nairobi, there are several manufacturers of water tank from plastic, metal and other materials. These tanks are sold everywhere in East Africa and beyond (Lo and Gould, 2015). In many parts of Kenya, the United Nations Development Program and the World Bank consider rainwater storage tanks as an essential part of their programs on water supply and sanitation (Liu *et al*., 2016). It is noted, although it is not mandatory for institutional buildings to dispose RWH facilities, many of them especially in the rural areas have those facilities. In 1994, the Kenya Rainwater Association was established, which is the first national RWH association in Africa. Since then, tens of thousands of rainwater collection systems have been built in Kenya by a wide range of organizations, as a result millions of people are benefiting from these systems (Lo and Gould, 2015).

Japan is one of the developed countries in Asia, which has a strong international exchange of experience on the use of RWH. Since the mid-80s, Tokyo and other Japanese cities, as well as most municipalities and organizations of the country, have given particular importance to RWH so as to safe water supplies to deal with emergencies, floods, rehabilitation of the natural hydrological cycle and exploration of alternative water sources for non-potable use (König, 2001). Moreover, the abnormal drought of 1994 and the Great Hanshin-Awaji Earthquake of 1995 highlighted the importance of securing water supplies from the viewpoint of disaster preparedness. A large number of municipalities re-evaluated the importance of RWH and tried to identify alternative water resources, as a means to prevent urban flooding and to secure emergency water for disaster responses. The issue was regulated by ordinance and guidelines according to the local conditions (Furumai *et al*., 2008). According to the survey of the Association for Rainwater Storage and Infiltration Technology held in April 2011, 208 Municipalities are implementing subsidy programs for establishment of facilities for storing or filtration systems of rainwater and of these, 179 provide subsidies for installation of rainwater tank. In April 2014, the Japanese Diet passed the Act to Advance the Utilization of Rainwater, which went into force the May 2015. Under this Act, Municipalities are obliged to do their best effort to define and work toward rainwater utilization targets, while the national government is required to grant financial support for subsidy programs. These arrangements are expected to provide a national mobilization to promote technical rainwater use (JFS, 2014). On March 10, 2015 Japanese government, based on the above Act, approved the wider usage of RWH systems in newly constructed buildings by the state government or incorporated administrative agencies, aiming for a 100% installation rate (JFS, 2015).

In China, the growing interest for the RWH initiated in 1980s due to the widespread droughts of that decade, which was followed by serious shortages of drinking water and crop failures (Li, 2003). RWH practice and utilization is applied mainly in areas with the following types of water scarcity (Liu *et al*., 2016): (a) In water deficient areas with a lack of water resources, such as Gansu and central

Ningxia. (b) In areas with seasonal water deficit, such as Fujian, Guizhou and other hilly areas. (c) In areas with water deficit, but also with difficulty in exploitation, such as the southwest mountainous areas of the country. (d) In water deficient areas with poor water quality, e.g. brackish water, fluoride water, high-arsenic water, etc. In these areas, authorities have constructed water cellars, tanks, ponds and other miniature water conservancy projects as an effective solution to the problem of water shortage. Unfortunately, there are still problems of water deficit. Seventeen provinces in the country have adopted the RWH practice by building 5,600,000 tanks with a total capacity of $1.8x10^9$ m^3 supplying water about $15x10^6$ people and supplemental irrigation of $1.2x10^6$ ha of land (Lo and Gould, 2015). RWH systems are also applied in provinces of Northwestern China (Ningxia Region, Shanxi Shaanxi and the Inner Mongolia Region) as well as in Southwest and Southeast provinces of the country (Guangxi Region and Guizhou Province). The implementation of rainwater collection has a significant impact on the development of China's semi-arid rural areas and has practically solved the drinking water problems of populations living in semi-arid mountainous areas of the country (Li, 2003).

In India, RWH was revived in the 1960s in response to declining groundwater availability caused by the rapid expansion of irrigation pumping. Many Indian's cities have insufficient water supplies to meet their needs. Urban development makes it both difficult and expensive to build dams, pipelines and canals commonly used nowadays in order to supply water to cities. RWH was supporting agriculture for many years in India, while there is a demand in urban areas for novel methods for decentralized water supply systems. Since 2000 onwards, the legislation on RWH has been changed in the various States and federal regions of the country and it is compulsory for the new buildings. The rooftop RWH systems are mandatory for new buildings in 18 of the 28 States and 4 of the 7 Federal Regions of the country (MARWAS AG, 2010).

Germany has developed new and sophisticated RWH systems and techniques and is considered as one of the leading countries in the world in this field. In particular, Germany has more than $1.5x10^6$ integrated rainwater systems not only in homes for toilet use, but also for car washes and garden irrigation and also, in service water demanding industries (Herrmann and Schmida, 1999). According to the Environmental Agency (E.A., 2010), 35% of new buildings in the country are equipped with a RWH system, and such new systems are installed every year from 50,000 (Nolde, 2007) to 80,000 (Partzsch, 2009). As Partzsch (2009) pointed out, in 2005, every third new building in Germany was supplied with a rainwater storage tank. In Germany, the promotion of RWH in households became widespread since the 1980s (Nolde, 2007).

In the U.K., the modern RWH systems have been introduced relatively recently (E.A., 2010), since the interest in RWH research, technology, development and utilization has yet to mature, although several initiatives are in place to promote RWH (Ward, 2007). The Code for Sustainable Homes, which is in force in England, Northern Ireland and Wales, is supporting and encourages the promotion of RWH systems installation in new houses. In particular, owners of new homes are encouraged to save money and water resources by installing RWH systems for toilets, washing clothes, garden watering and car washing. According to UKRHA (2006), approximately 100,000 RWH systems already exist in the U.K. and approximately 4,000 systems per year are installed, which are commonly internally plumbed to supply toilet flushing as well as garden irrigation.

In France, the interest in RWH for indoor and outdoor uses has increased and it constitutes serious issue even in the urban areas. As Gerolin *et al.* (2013) pointed out "rainwater harvesting (RWH) has known a revival of interest since the establishment in 2006 of a national tax credit for households implementing a rainwater collection system". Since 2008, a decree (French Government Order of 21 August 2008) concerning RWH is in force. In reality, it is about regulations, which define better management of the use of rainwater and the precise technical requirements to be met by the components of the collection systems supplying both outdoor and indoor uses. Specifically, the regulations prohibit the use of harvested rainwater for drinking, showering or bathing, but they allow its use for toilet flushing, cleaning the ground and under certain conditions, washing clothes (Vialle

et al., 2015). In France, according to a survey conducted in 2009, 15% of the population has a RWH system in urban areas (Belmeziti *et al*., 2013).

Belgium has national legislation that supports RWH, which stipulates that all new constructions must have a rainwater collection system, the water of which can be used for washing the toilet and for external water uses. In Flanders, it is estimated that 10% of current household water consumption comes from RWH, which could be increased to 25% by 2025. It is estimated that households account for 72% of the total rainwater use in Flanders. (Campling *et al*., 2008).

In Portugal, the ERSAR (Water and Waste Services Regulation) guidelines allow the use of RWH only for non-potable use and, in particular, for irrigation purposes. ANQIP (National Association for the Quality of Building Installations), a nonprofit organization promoting water sustainability at building level, published in 2012 a technical document (ETA 0701, 2012) describing the procedures to be taken into account regarding installation of rainwater collection systems in Portuguese buildings (Silva *et al*., 2015).

In Malta a significant proportion of 35.4% of households are currently using RWH, of which 33.6% collect it in underground cisterns and a small percentage of 1.8% in plastic containers. Since 2004, the exploitation of RWH in new constructions is regulated by plan of the MEPA (Malta Environment and Planning Authority), which regulates the creation of water collecting surfaces on roofs, the possible size and capacity of the tanks etc. (Reitano, 2011).

5. CONCLUSIONS

One of the biggest challenges of the 21st century is tacking the growing water shortages worldwide. The continued increasing demand for water from various competing users (domestic, agriculture, industry, environment use, etc.) and also, urbanization, climate change, water pollution, etc. exert pressures on the existing water resources. For these reasons, many countries are facing water shortage. In general, the strategy, that they followed, was constructing of large-scale projects (dams, pipelines of long length, pump stations, etc.). Nevertheless their construction has not been proven to be able to meet water needs of the different users, while at the same time has significant social, economic and environmental impacts, and requires significant investment. So, searching for alternative water sources (grey water, desalination and RWH) has attracted worldwide interest. Rainwater harvesting is seen as a more promising alternative or supplementary water resource due to minimal environmental impact, the low treatment needs in comparison with other alternative water sources, the benefits from flood mitigation, and many more.

RWH is not a new technique, since it has been a very old traditional practice, which has been adopted in many regions of the world and is dated back several hundred years. In antiquity, the main uses of harvested rainwater were for domestic, irrigation and livestock purposes. Nevertheless, RWH, which was a worldwide technology, was neglected over the past 150 years due to the new technologies which enable us to store, pump from deep groundwater and transport huge volumes of water (ground and surface) via dams, pump stations and long length pipelines.

The literature reveals the interest and use of RWH systems, on a global basis, is increasing continually about from the beginning of the second half of the previous century onwards. As Yannopoulos *et al.* (2017) state: “Worldwide, rainwater harvesting has retrieved its importance as a valuable water resource, alternative or supplementary, in conjunction with more conventional water supply technologies. If rainwater harvesting is practiced more widely, many water shortages, actual or potential, can be alleviated.”

Nowadays, many countries all over the world consider RWH as a viable decentralized water source. However, a significant push to extend this technique is needed. Specifically, significant efforts are still needed in research, investments, information, education of the public on the importance of rainwater harvesting, economic incentives (subsidies and tax exemptions), suitable legislation and regulations.

Until today, two approaches have been applied concerning the extension of RWH, namely either voluntary via incentive based programs or mandated regulations. In several countries the government subsidies and rebate programs can be particularly effective in promoting RWH implementation. In contrary to regulations that require compliance, subsidies target individuals with an appreciation for RWH and provide an incentive for them to pursue adoption of this practice.

References

1. Akpinar Ferrand E. and F. Cecunjanin (2014) Potential of rainwater harvesting in a thirsty world: a survey of ancient and traditional rainwater harvesting applications, **Geography Compass**, 8(6), pp. 395–413.
2. Belmeziti A., O. Coutard and B. de Gouvello (2013) "A New Methodology for Evaluating Potential for Potable Water Savings (PPWS) by Using Rainwater Harvesting at the Urban Level: The Case of the Municipality of Colombes (Paris Region)", **Water**, 5, pp. 312-326.
3. Campling P., L. De Nocker, W. Schiettecatte, A.I. Iacovides, T. Dworak, M.A. Arenas, C.C. Pozo, O. Le Mat, V. Mattheiß and F. Kervarec (2008) "**Assessment of the Risks and Impacts of Four Alternative Water Supply Options",** European Commission – DG Environment.
4. CMHC (Canada Mortgage and Housing Corporation) (2013) "**Collecting and Using Rainwater at Home: A Guide for Homeowners**", CMHC, Canada.
5. Coombes P. (2006) "**Guidance on the Use of Rainwater Harvesting Systems for Rain Harvesting**", Available at: http://rainharvesting.com.au/wp-content/uploads/media_ Research_Assoc_Prof_Peter_Coomber_Expert_Report_for_Guidance_of_Rainwater_Harvesting_Systems_2006.pdf (accessed January 20, 2017).
6. Critchley W. and W.K. Siegert (1991) "**Water Harvesting: A Manual for the Design and Construction of Water Harvesting Schemes for Plant Production**", AGL/MICS/17/91, Food and Agriculture Organization of the United Nations (FAO), Rome, Italy.
7. da Costa Pacheco P.R., Y. Dumit Gómez, I. Ferreira de Oliveira and L.C. Girard Teixeira (2017) "A view of the legislative scenario for rainwater harvesting in Brazil", **Journal of Cleaner Poduction**, 141, pp. 290-294.
8. E.A. (Environmental Agency) (2010) "**Harvesting Rainwater for Domestic Uses: An Information Guide**", Environment Agency, Bristol, U.K.
9. Evenari M. L., L. Shanan, N. Tadmor and Y. Aharoni. (1961) "Ancient agriculture in the Negev", **Science**, 133, pp. 979-996.
10. Fidelibus M. W. and D.A. Bainbridge (1995) "**Microcatchment Water Harvesting for Desert Revegetation**", SERG Restoration Bulletin 5, San Diego State University, San Diego, CA.
11. Frasier G. W. and L. E. Myers (1983) "**Handbook of Water Harvesting**", U.S. Department of Agriculture, Agriculture Handbook No. 600.
12. Furumai H., J. Kim, M. Imbe and H. Okui (2008) Recent application of rainwater storage and harvesting in Japan, **3rd IWA International Rainwater Harvesting and Management Workshop as a part of IWA-Viena World Water Congress & Exhibition**, 7pp., Vienna, Austria.
13. Gerolin A., N. Le Nouveau and B. de Gouvello (2013) Rainwater harvesting for stormwater management: example-based typology and current approaches for evaluation to question French practices, 8ème International Conference, Novatech, 10 pp., Lyon, France.
14. Haque M.M., A. Rahman and B. Samali (2016) "Evaluation of climate change impacts on rainwater harvesting", **Journal of Cleaner Productions**, 137, pp. 60-69.

15. Herrmann T. and U. Schmida (1999) "Rainwater Utilisation in Germany: efficiency, dimensioning, hydraulic and environmental aspects", **Urban Water**, 1, pp. 307-316.

16. JFS (Japan for Sustainability) **(**August 24, 2014) "**Let's Use Rainwater! Recent Trends in Rainwater Use in Japan**". Available at: http://www.japanfs.org/en/news/archives/news_id035023.html (accessed January 20, 2017).

17. JFS (Japan for Sustainability) (May 25, 2015) "**Cabinet of Japan Decide to Make Full Use of Rainwater in Newly Constructed Buildings**",. Available at**:** http://www.japanfs.org/en/news/archives/news_id035257.html (accessed January 20, 2017).

18. König K. (2001) "**The Rainwater Technology Handbook**" (1st ed.), Wilo-Brain.

19. Krishna, H.J. (2007) Development of Alternative Water Resources in the USA: Progress with Rainwater Harvesting, 13th International Rainwater Catchment Systems Conference on Rainwater and Urban Design, 8pp., Sydney, Australia.

20. Lade O. and D. Oloke (2015) "Modelling Rainwater System Harvesting in Ibadan, Nigeria: Application to a Residential Apartment", **American Journal of Civil Engineering and Architecture**, 3(3), pp. 86-100.

21. Lauritzen C.W. (1960) "Ground Covers for Collecting Precipitation", **Farm & Home Science**, 21(3), **Utah Science**, 21(3), Article 1, pp.66-67.

22. Li X.-Y. (2003) "Rainwater harvesting for agricultural production in the semiarid loess region of China Food", **Agriculture and Environment**, 1(3&4), pp. 282-285.

23. Lizárraga-Mendiola L., G. Vázquez-Rodríguez, A. Blanco-Piñón, Y. Rangel-Martínez and M. González-Sandoval (2015) "Estimating the Rainwater Potential per Household in an Urban Area: Case Study in Central Mexico", **Water**, 7, pp. 4622-4637.

24. Llopart-Mascaró A., R. Ruiz, M. Martínez, P. Malgrat, M. Rusiñol, A. Gil, J. Suárez, J. Puertas, H. del Rio, M. Paraira and P. Rubio (2010) Analysis of rainwater quality: Towards sustainable rainwater management in urban environments -Sostaqua Project, **NOVATECH 2010**.

25. Liu, L.-S., L.-G. Liu, L.-X. Wu, L.-P. Wu and W.J. Huo (2016) "**Problems and countermeasures on the safety of rainwater harvesting for drinking in China**", MATEC Web of Conferences 68, ICIEA 2016.

26. Lo A.G. and J. Gould (2015) Chapter 7. Rainwater Harvesting: Global Overview, in: **Rainwater Harvesting for Agriculture and Water Supply**, Q. Zhu, J. Gould, Y.-H. Li and C.-X. Ma (eds.), Springer, pp. 213-233.

27. MARWAS AG (2010) "**Water & Water Treatment in India. Market Opportunities for Swiss Companies**", Osec, Zurich, Switzerland.

28. Myers L. E. (1961) "Waterproofing soil to collect precipitation", **Journal of Soil and Water Conservation**, 16(6), pp. 281-282.

29. Nolde E. (2007) "Possibilities of rainwater utilisation in densely populated areas including precipitation runoffs from traffic surfaces", **Desalination**, 215, pp. 1-11.

30. OECD (2009) "**Alternative Ways of Providing Water Emerging Options and Their Policy Implications**", Advance copy for 5th World Water Forum. Available at www.oecd.org/env/resources/42349741.pdf (accessed May 15, 2016).

31. Pacey A. and A. Cullis (1989) "**Rainwater Harvesting: The collection of rainfall and runoff in rural areas**", Intermediate Technology Publications, London, U.K.

32. Partzsch L. (2009) "Smart regulation for water innovation - the case of decentralized rainwater technology", **Journal of Cleaner Production**, 17, pp. 985-991.

33. Prinz D. and A.H. Malik (2003) "**Runoff farming**", WCA, InfoNET

34. Reitano R. (2011) "Water Harvesting and Water Collection Systems in Mediterranean Area. The Case of Malta", **Procedia Engineering**, 21, pp. 81-88.

35. Ringler C., W. Mark, M.W. Rosegrant and M.S. Paisner (2000) "**Irrigation and Water Resources in Latin America and the Caribbean: Challenges and Strategies**", International Food Policy Research Institute. Washington, D.C. U.S.A.. EPTD Discussion Paper No. 64.

36. Silva C.M., V. Sousa and N.V. Carvalho (2015) "Evaluation of rainwater harvesting in Portugal: Application to single-family residences", **Resources, Conservation and Recycling**, 94, pp. 21-34.

37. Sivanappan R. K. (2006) Rain Water Harvesting, Conservation and Management Strategies for Urban and Rural Sectors, **National Seminar on Rainwater Harvesting and Water Management**, pp. 1-5, Nagpur, India.

38. TRCA (Toronto and Region Conservation Authority) (2010) "**Performance Evaluation of Rainwater Harvesting Systems, Toronto, Ontario. Sustainable Technologies Evaluation Program (STEP)",** Final Report 2010 (revised June 2011). Available at: www.sustainabletechnologies.ca (accessed January 20, 2017).

39. TWDB (Texas Water Development Board) (2005) "**The Texas Manual on Rainwater Harvesting**" (3rd. ed.), Texas Water Development Board, Austin, Texas, USA.

40. UKRHA (United Kingdom Rainwater Harvesting Association) (2006) "**Enhanced Capital Allowance Scheme as it Applies to Rainwater Harvesting Systems**", The U.K. Rainwater Harvesting Association, Industry Fact Sheet No 3.

41. UNDESA (United Nations Department of Economic and Social Affairs) (2011) "**World Urbanization Prospects: The 2011 Revision**", United Nations.

42. UN-HABITAT (2005) "**Rainwater Harvesting and Utilisation**", Blue Drop Series, Book 2: Beneficiaries & Capacity Builders, UN-HABITAT, Mtwapa, Kenya.

43. UN Water (2007) "**Coping with water scarcity: challenge of the twenty-first century**", Prepared for World Water Day 2007. Available at: http://www.unwater.org/wwd07/downloads/documents/escarcity.pdf (accessed March 23, 2007).

44. USEPA (2013) **Rainwater Harvesting: Conservation, Credit, Codes, and Cost Literature Review and Case Studies**", U.S. Environmental Protection Agency (EPA), Office of Water, Office of Wetlands, Oceans, and Watersheds. EPA-841-R-13-002.

45. Vialle C., G. Busset, L. Tanfin, M. Montrejaud-Vignoles, M.-C. Huau and C. Sablayrolles (2015) "Environmental analysis of a domestic rainwater harvesting system: A case study in France", **Resources, Conservation and Recycling**, 102, pp. 178–184.

46. Ward S.L. (2007) "**Rainwater Harvesting in the UK - Current Practice and Future Trends**", Young Scientists Workshop, Amsterdam, Netherlands, April 1, 2007.

47. WWAP (World Water Assessment Program) (2006) "**The State of the Resource, World Water Development Report 2, Chapter 4**". United Nations Educational, Scientific and Cultural Organization, Paris.

48. Yannopoulos S., G. Antoniou, M. Kaiafa-Saropoulou and A. N. Angelakis (2017) "Historical development of rainwater harvesting and use in Hellas: a preliminary review", **Water Science & Technology: Water Supply**, 17(4), pp. 1022-1034.

MULTIOBJECTIVE OPTIMIZATION RAIN GARDENS USING HARMONY SEARCH ALGORITHM

D. Karakatsanis * and A. Basdeki

Division of Hydraulics and Environmental Engineering, Dept. of Civil Engineering, A.U.Th, GR-54124Thessaloniki, Macedonia, Greece

*Corresponding authors: e-mail: diamontkarakat@gmail.com

Abstract

The use of ecological rainwater management method and rain gardens in urban areas aims at: 1) reduction of total rain water runoff and of its peak and 2) reduction of property damage and activity disruption due to insufficient sewer network capacity. Rain Gardens cannot substitute by sewer networks, but they can be used as integral parts of sewer systems in a cost-efficient way. In this paper we apply and modify the Harmony Search Algorithm (HSA) in order to optimize the multi-objective problem of rain gardens. A Matlab script that estimates Pareto front is developed for this purpose. The HSA modification includes a gravity-factors system for every objective function. In conclusion the Pareto front is calculated at four different sets of gravity factors.

Keywords: Rain garden, Optimization, Urban rainwater management, Harmony search algorithm, Metaheuristic methods

1. INTRODUCTION

The typical way to deal with rainwater in urban areas is construction of sewer networks, to achieve its quick transfer away of the urban setting to sewage treatment facilities, exactly as it is done for domestic sewage. Whenever, though, rain intensity and duration exceeds a certain threshold, sewer networks fail to carry the required load and rainwater flows or stagnates on street surfaces, covers sidewalks or, even worse, inundates shops and houses.

Integrated rainwater management combines the aforementioned classical approach with low impact techniques (or sustainable management methods), such as rain gardens and green roofs. This type of management is advantageous from the environmental aspect and could be prove more cost efficient than sewer network upgrading.

These techniques promote an ecological growth pattern. The sustainable rainwater management facilities are not substitutes to sewer networks, but they should operate in a complementary way with the latter. These networks may fail to fully protect all parts of urban areas during heavy rain event, as a result the use of street surfaces and sidewalks by pedestrians, due to water accumulating ,is a challenging task and renders the car driving unsafe.

2. DESCRIPTION OF RAIN GARDENS

Rain gardens can be constructed in many kinds of sites, such as pre-existing green spaces, stream areas, squares, parking spaces, house yards, open spaces of building blocks, school and church yards, along streets, etc.

A typical rain garden includes the following:

a) Ponding area: It is a natural or artificial ground depression. In rather flat areas it is constructed by excavating soil from the ground surface. In sloping ground it is formed by soil excavation combined with building of an earth berm at the down slope side, using excavation material. Surfaces with large slope are not that suitable for rain garden construction.

The bottom of the rain garden is usually covered by a mulch layer, before constructing the top soil layer. If water infiltration rate in the underlying strata is small, a gravel layer could be constructed on the bottom of the ponding area. A perforated underdrain pipe could be used for the same reason.

b) Inflow structure, that directs rainwater from dounspouts or impermeable areas (streets, sidewalks) to the ponding area

c) Overflow structure that allows water to exit the rain garden when the ponding are is full. This structure is necessary in order to reduce erosion risk and to direct ouflowing water towards the desired place (usually the sewer network).

3. HARMONY SEARCH ALGORITHM

3.1 Relationship between music and mathematics

The relationship between music and mathematics has been close since the ancient times. Mathematicians tried to interpret the governing rules of mathematics using the art of music. On the other hand, composers tried to use mathematics in order to deeply understand music.

During recent times, since the Baroque period, this bond has been strengthened. Sometimes as a conscious effort by musicians-composers and sometimes as part of a rumored and almost mystical relationship, mathematics and music came closer. Iannis Xenakis represents a special example. His deep knowledge both in mathematics and music is illustrated in his work on the use of mathematical functions to compose music (1992) distinguishing him among the most eminent music figures of the 20th century.

3.2 Analysis of Harmony Search Algorithm (HSA)

3.2.1 The basic elements of the algorithm

The Harmony Search Algorithm is a stochastic meta-heuristic method based on the sequential production of possible solutions. It belongs to the category of “neighborhood meta-heuristics” that produce one possible solution (called “harmony”) in each iteration. Every possible solution consists of a set of values of the decision variables of the function that needs to be optimized. During the optimization process, a number of “harmonies” equal to the “Harmony Memory Size” are stored in the “Harmony Memory” (HM), a database that includes the produced set of solutions. The optimization process is completed as soon as the predefined total number of iterations has been achieved (Geem, 2001).

3.2.2 Characteristics of the Harmony Search Algorithm

Following the definition of the decision variables, the Harmony Memory matrix is formulated. Harmony Memory is m×n matrix, where m is the Harmony Memory Size and n, the number of decision variables included in the objective function. Then, the algorithm begins producing and evaluating new “Harmonies” through the application of HSA’s basic mechanisms:

1. Harmony Memory Consideration uses variables’ values already stored in the Harmony Memory. This mechanism ensures that good solutions located during the optimization process will contribute to the formation of even better solutions.
2. Some of the solutions selected by the Harmony Memory Consideration mechanism will be slightly altered. This is the second mechanism of the algorithm named Pitch Adjustment and it is performed by selecting a neighboring values of the decision variables

3. The third mechanism is Improvisation, which introduces new, random elements to the solutions. The probability of introducing such random values is (100-HMCR)%. In this way the variability of solutions is enriched.

After the creation of a new "Harmony", its performance is evaluated according to the corresponding value of the objective function. If this performance is better than that of the worst "Harmony" stored in the Harmony Memory, it replaces it. This procedure is repeated until the ending criterion, is reached.

4. OPTIMIZATION OF RAIN GARDENS

A typical cross section of a rain garden is presented in figure 4.1, consisting of two layers of different granulometry soil materials with height d1 and d2 respectively. The free water surface in the garden has height h, while at the bottom of the cross section there is a collecting pipe with cross section D. There are two objective functions-goals for the cross section optimization. The first objective function is defined as the sum of the thickness of each soil layer, which for economic reasons should be minimum. The second objective function results from the maximization of the flow rate that can be filtered in the cross section. Water infiltration from the rain garden surface to the deeper layers is calculated using the Darcy law (equation 4.1)

$$q = AK\frac{h}{L} \tag{4.1}$$

Where:

q: infiltration flow rate per cross section meter

A: area of infiltration surface

K: equivalent conductivity for the two soil layers

h: hydraulic load equal to the depth of the two layers plus the depth of the free surface

L: flow length equal to the depth sum of the two layers.

Since the flow is vertical to the soil layers, the equivalent conductivity for the two soil layers with conductivity K1 and K2 is resulting from the equation 4.2

$$K = \frac{d_1+d_2}{\frac{d1}{K1}+\frac{d2}{K2}} \tag{4.2}$$

Therefore, the two objective functions of the problem are the equations 4.3

$$\begin{cases} V1 = d1 + d2 \rightarrow MIN \quad (4.3.1) \\ V2 = A\dfrac{d_1 + d_2}{\dfrac{d1}{K1} + \dfrac{d2}{K2}}\dfrac{d1 + d2 + h1}{d1 + d2} \rightarrow MAX \quad (4.3.2) \end{cases}$$

For this specific multi-objective problem the two values of thickness and the type of soil layers are considered as decision variables. Therefore, the decision variables are the following four: d1, d2, K1, K2. The soil conductivity values are obtained considering the 7 soil classes shown at Table 4.

Table 4: Soil classes-Conductivity

Soil Texture	Conductivity (m/s)
Gravel	3×10^{-2}
Coarsesand	6×10^{-3}
Mediumsand	5×10^{-4}
Finesand	2×10^{-4}
Silt, loess	2×10^{-5}
Till	2×10^{-6}
Clay	4.7×10^{-9}

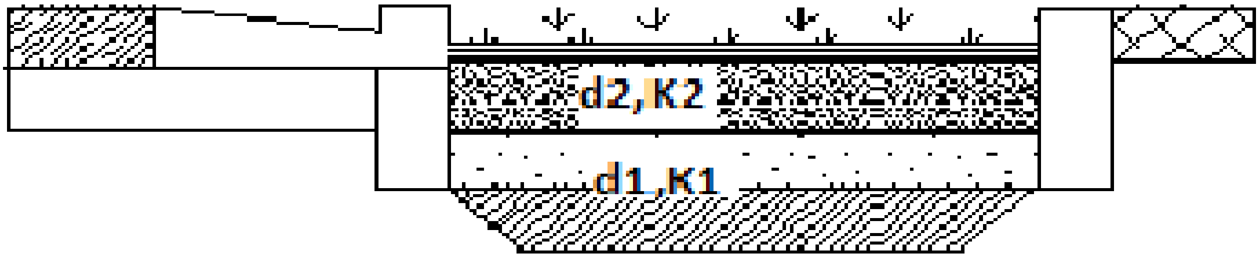


Figure 4.1: Cross section of a typical rain garden

In order to solve the problem and find the Pareto front we modify the typical algorithm of the Harmony Search so that we can solve the multi-objective problem. Since one objective function is minimized and the other one is maximized, we cannot compose the objective functions in one. Pareto front is a curve where every solution has equivalent performance for both objective functions. Therefore, the Pareto solutions cannot dominate one another. Finding the Pareto front (non-dominant solutions) is a quite complex process and the simplest way to deal with is to consider gravity factors for each objective function. Figure 4.1 presents the modification of the Harmony Search Algorithm along with gravity factors for the objective functions. Two possibilities-gravity factors are defined in this modification. The algorithm examines the objective function V1 with possibility p1 and function V2 with possibility 1-p1.

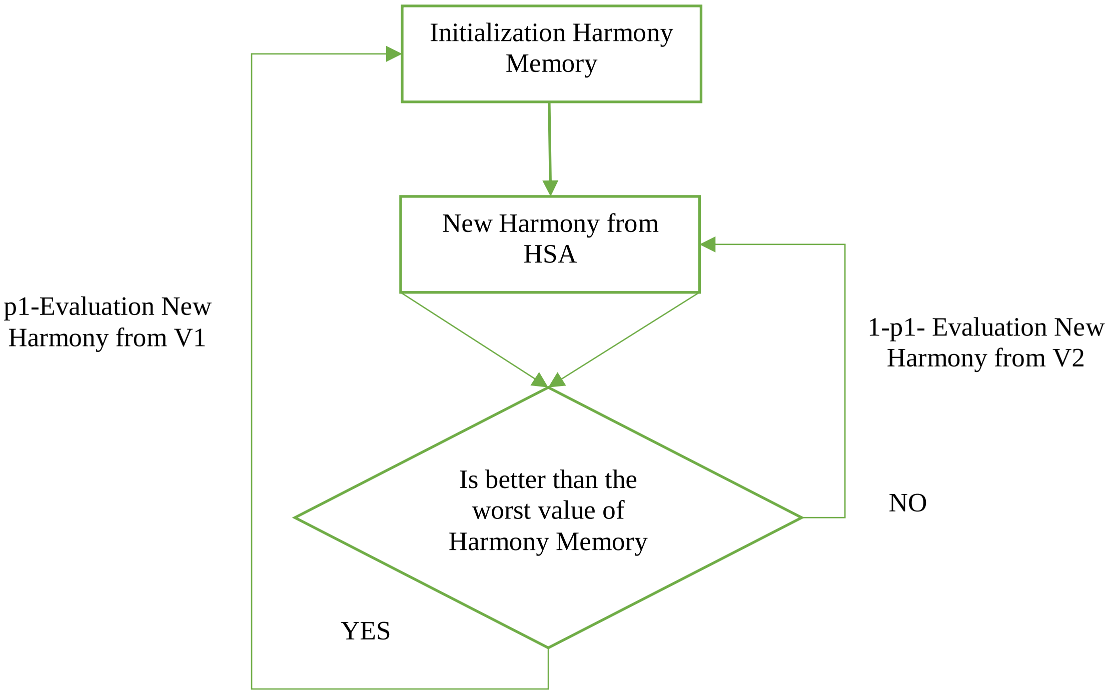


Figure 4.2: Application of Matlab programming language

The process is organized in Matlab programming language with various values of possibility p1 in order to find the Pareto front. A part of the code which presents the examination with gravity factors of the two objective functions is presented in Figure 4.2.

```
 ans1=NewHarmony(3,1).*NewHarmony(4,1)*(0.25+NewHarmony(1,1)+NewHarmony(2,1))/(NewHarmony(1,1).*NewHarmony(4,1)-
 ans2=NewHarmony(1,1)+NewHarmony(2,1);
[pas1,w1]=min(VHM1);
[pas2,w2]=max(VHM2);
if rand>0.5
 if ans1>pas1
  HM(:,w1)=NewHarmony;
  VHM1(w1)=ans1;
 end
else
   if ans2<pas2
  HM(:,w2)=NewHarmony;
  VHM2(w2)=ans2;
 end
```

Figure 4.3: The process in Matlab language

5. RESULTS AND CONCLUSIONS

The results for various values of gravity factors in objective functions are presented in Figure 5.1.

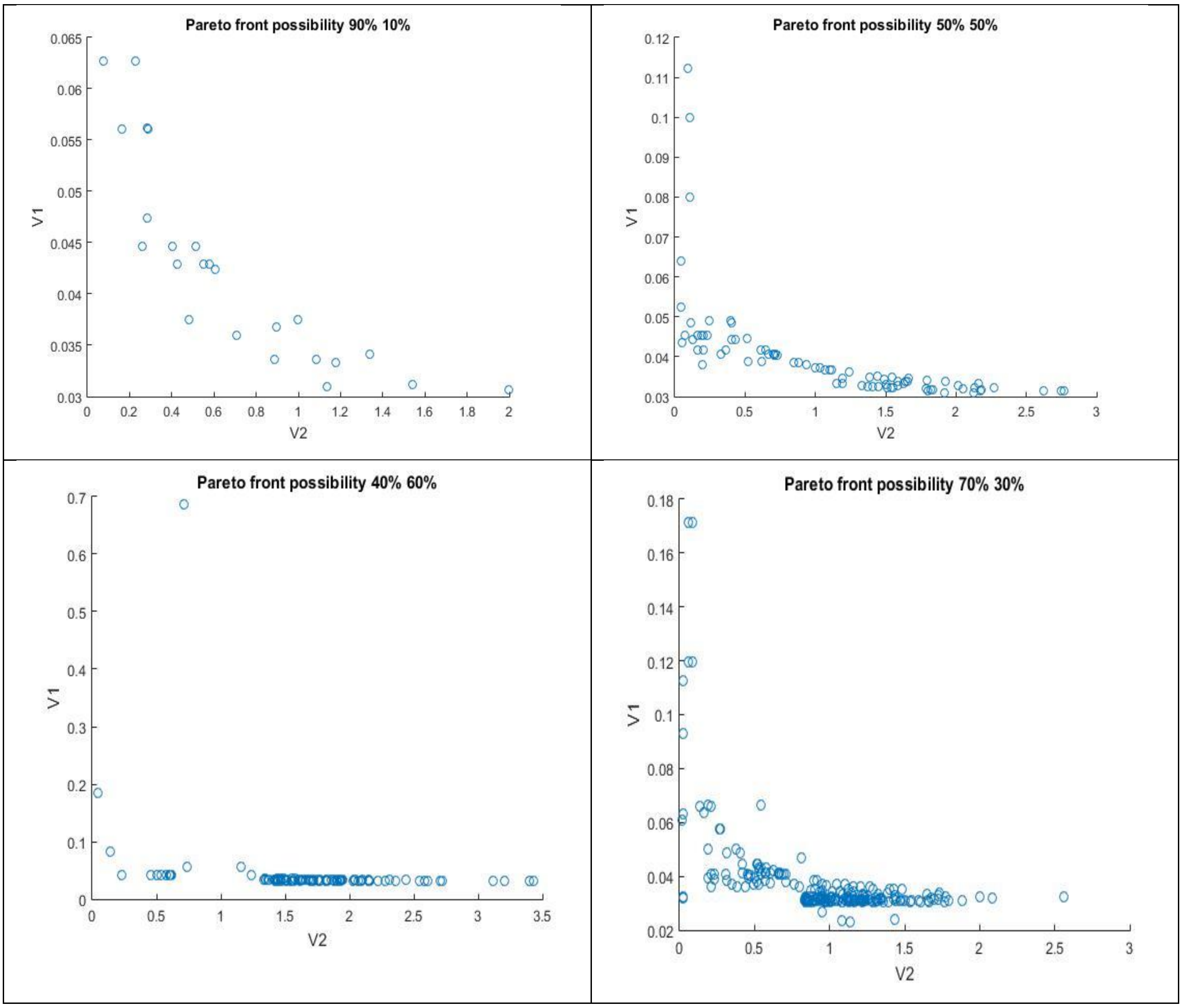


Figure 5.1: The results for various values of gravity factors

Conclusions:

- The p1 must be at least 50% in order to calculate the Pareto front. If p1 is less than 50%, then the algorithm cannot estimate the curve accurately. The best approach of the Pareto front appears when the p1 is between 60%-90%. Just a few values of Pareto fronts can be detected out of this range.
- In most cases the algorithm selects low values for depths d1 and d2 but high conductivity values. At the most Pareto solutions the depth values range from 1 to 1.5 meter. On the other hand the algorithm selects only high-conductivity soil classes. The solutions with low-conductivity soil classes or high-value depths are always in the shadow of the front.

References

1. Degertekin, S. O. (2012). Improved harmony search algorithms for sizing optimization of truss structures. ***Computers & Structures,*** 92, 229-241.
2. Dorigo, M., Maniezzo, V., &Colorni, A. (1996). Ant system: optimization by a colony of cooperating agents. Systems, Man, and Cybernetics, Part B: Cybernetics, IEEE Transactions on, 26(1), 29-41.
3. Eberhart, R. C., & Kennedy, J. (1995). A new optimizer using particle swarm theory. In Proceedings of the sixth international symposium on micro machine and human science (Vol. 1, pp. 39-43).
4. Fesanghary, M., Mahdavi, M., Minary-Jolandan, M., &Alizadeh, Y. (2008). Hybridizing harmony search algorithm with sequential quadratic programming for engineering optimization problems. **Computer methods in applied mechanics and engineering,** 197(33), 3080-3091.
5. Geem, Z. W., Kim, J. H., &Loganathan, G. V. (2001). A new heuristic optimization algorithm: harmony search. *Simulation*, *76*(2), 60-68.
6. Geem, Z. W., Kim, J. H., &Loganathan, G. V. (2002). Harmony search optimization: application to pipe network design. **International journal of modelling & simulation,** *22*(2), 125-133.
7. Holland, J. H. (1973). Genetic algorithms and the optimal allocation of trials. SIAM *Journal on Computing*, 2(2), 88-105.
8. Gholizadeh, S., &Barzegar, A. (2013). Shape optimization of structures for frequency constraints by sequential harmony search algorithm**. *Engineering Optimization,*** 45(6), 627-646.
9. Kaveh, A., &Talatahari, S. (2009). Particle swarm optimizer, ant colony strategy and harmony search scheme hybridized for optimization of truss structures. *Computers & Structures*, 87(5), 267-283.
10. Kirkpatrick, S., Gelatt, C. D., &Vecchi, M. P. (1983). Optimization by Simulated Annealing. *Science,* 220(4598), 671-680.
11. Kougias, I., and Theodosiou, N. (2010). A new music-inspired harmony based optimization algorithm: Theory and applications. In Proceedings of: International Conference on Protection and Restoration of the Environment X, Corfu.
12. Kougias, I., Katsifarakis, L., &Theodossiou, N. (2012). Medley Multiobjective Harmony Search Algorithm: Application on a water resources management problem. *European Water,* 39, 71-52.
13. Kougias, I., &Theodossiou, N. (2013). Multiobjective pump scheduling optimization using harmony search algorithm (HSA) and polyphonic HSA. **Water Resources Management,** *27*(5), 1249-1261.
14. Lee, K. S., &Geem, Z. W. (2004). A new structural optimization method based on the harmony search algorithm. **Computers & Structures**, *82*(9), 781-798.

15. Lee, K. S., Geem, Z. W., Lee, S. H., & Bae, K. W. (2005). The harmony search heuristic algorithm for discrete structural optimization. **Engineering Optimization**, 37(7), 663-684.

16. Mahdavi, M., Fesanghary, M., &Damangir, E. (2007). An improved harmony search algorithm for solving optimization problems. **Applied Mathematics and Computation**, 188(2), 1567-1579.

17. Maheri, M. R. &Narimani, M.M (2014). An enhanced harmony search algorithm for optimum design of side sway steel frames. **Computers & Structures**, 136 (2014): 78-89.

18. Saka, M. P. (2009). Optimum design of steel sway frames to BS5950 using harmony search algorithm. **Journal of ConstructionalSteel Research**, 65(1), 36-43.

19. Xenakis, I. (1992). Formalized music: thought and mathematics in composition (No. 6). PendragonPress

20. Basdeki, A.,Katsifarakis, L. and Katsifarakis, K.L., 2016. Rain gardens as integral parts of urban sewage systems-A case study in Thessaloniki, Greece, **Int. Conf. on Efficient & Sustainable Water Systems Management toward Worth Living Development, 2nd EWaS** *2016, Procedia Engineering*, 162, 426–432.

21. Katsifarakis, K.L. et al.,**Guide for integrated rain water management**,Final Report, Aristotle University of Thessaloniki, 2013 (in Greek).

22. Katsifarakis,K.L.,Vafeiadis,M. and Theodossiou, N., 2015.Sustainable Drainage and Urban Landscape Upgrading Using rain gardens. Site Selection in Thessaloniki, Greece,**Agriculture and Agricultural Science Procedia**, 338-347.

23. Sebti, A., Bennis, S. and Fuamba, M., 2016. Optimization of the restructuring cost of an urban drainage network.**Urban Water Journal**, 13(2), 119-132.

24. NY State Stormwater Management Design Manual (Chapter 9), available from:http://www.dec.ny.gov/docs/water_pdf/swdmredevelop.pdf[Accessed November 10, 2016].

25. Basdeki, A., Katsifarakis, L. and Katsifarakis, K.L., 2017, Design, calculations and performance evaluation of rain gardens in an urban neighborhood of Thessaloniki,Greece, Desalination and water Treatment Journal.

26. Trowsdale, S.A. and R. Simcock, R., 2011. Urbanstormwater treatment using bioretention.*Journal of Hydrology*, 397(3-4), 167-174.

ESTIMATION OF WATER FOOTPRINT FOR A HOTEL UNIT

A.E. Chatzi* and N.P. Theodossiou

Division of Hydraulics and Environmental Engineering,Dept. of Civil Engineering, A.U.Th,GR-54124 Thessaloniki, Macedonia, Greece

*Corresponding author : e-mail: annaxatz28@gmail.com

Abstract
Some of the most important issues concerning water resources are reduction of extreme consumption and protection of their quality. As time passes, researchers are trying to determine more effectively water consumption and pollutant burden which ends up in water resources in order to manage and protect them more appropriately. The constantly increasing water demand has currently led to global problems of pollution and water scarcity. However, the necessity of improving water management has led to the development and application of methods which aim to the extinction or at least the limitation of these phenomena. A recent perception of simultaneously estimating water consumption and water pollution is the concept of the water footprint, which was first introduced by Hoekstra in 2003. The water footprint concept comprises the efforts to identify freshwater consumption, not only through direct but also through indirect use. It forms a volumetric measurement of water consumption and water pollution while it also constitutes the base for local assessment of environmental, social and economic impacts. In this paper, the water footprint of the hotel unit 'Pantelidis' in the town of Ptolemaida, Greece, is analysed. Moreover, solutions that could reduce this footprint and make this industry more environmentally viable, in terms of water use, are being investigated.

Keywords: Water footprint, Water scarcity, Water pollution, Water consumption, Water resources management

1. INTRODUCTION

In this paper the water footprint of a hotel unit is analysed. At first, indicators about water use worldwide and the problems arising from the irrational and incorrect use of it, are presented. Then, having introduced the concept of the water footprint, reference is made to the hotel on which the methodology is applied. With the gathered information, the methodology, which has been applied primarily to agriculture so far, is adjusted to a service of the tertiary sector, such as a hotel unit. After the presentation of the results, the methods that are capable of converting the unit that is being investigated to an environmentally friendly one, in relation to the management of freshwater resources are suggested.

Water is a finite and unequally distributed natural resource. In the last century, the rise of living standards of people, especially in the western world, was based on the industrial development. This rise of living standards has led to an increase in demand for clean, potable water, while at the same time created more sources of pollution. Urbanization, the concentration of large numbers of people in specific urban areas, led to the depletion of their own natural resources and intensified the need of transporting clean water from other distant regions, and thus, to the expansion of the problem. All these activities, the new approaches in land exploitation, the new standards of life and the new habits, had a series of effects in this finite resource, making it even more rare.

Table 1: Water consumption in households per person and per day in European and other counties (litres per day per person) [https://www.watersave.gr/files/PDF/1415ekp.pdf]

Country	Consumption (Litres/day/person)	Country	Consumption (Litres/day/person)
Belgium	108	Austria	131
France	147	Sweden	199
Germany	146	Switzerland	264
Denmark	194	Spain	158
Finland	156	Hungary	150
Britain	132	Greece	130
Italy	220	USA	300
Luxembourg	171	Africa	20-50
Netherlands	159	Palestine	20-30
Norway	175	Israel	170

Table 2: Water consumption in households in Greece [https://www.watersave.gr/files/PDF/1415ekp.pdf]

Use	Litres	Large water bottles
Toilet	9 / time	6
Shower	15 / minute	100
Full bath	150	10
Washing the hands and face	30 / 2 minutes	20
Washing machine	150 / time	100
Dishwasher	50 / time	33
Washing fruits and vegetables	15 / minute	10
Washing dishes by hand	150 / day	100

The rapid population growth has as a consequence an increase in the needs for food supplies. The increasing demand of water for food production, industry usage, and maintenance of urban and rural populations has led to a growing shortage of fresh water (quantitative degradation) in many parts of the world. In many areas, groundwater is pumped at a rate that exceeds the corresponding replenishment, in a completely unsustainable manner. Likewise, the use of fertilizers and chemicals to improve soil quality, as well as the removal and the deposition of waste, degrades the quality of water supplies. Increasingly, therefore, natural resources are deficient both in quantity or quality.

Because of the rapid population growth on Earth, mass consumption, and misuse of natural resources, the availability of drinking water cannot cover the needs of modern societies and is constantly decreasing. For this reason, water is a strategic commodity throughout the world and has already begun to be the cause for many political conflicts. Today an estimated 40% of people living on Earth haven’t got enough water even for hygiene. More than 2,2 million people died in 2000 from diseases related to the consumption of contaminated water.

Water is consumed in various ways, and then a large percentage of the used water returns to nature, significantly damaged by industrial or agricultural waste (fertilizers, pesticides etc.), sewage, waste materials, and leachate from illicit or legitimate waste disposal areas. Around 90% of sewage and 70% of industrial waste water ends up in the environment without water purification [Bouguerra, 2005]. Tourism has a great impact on local environmental systems. A sector, directly stressed from the tourist activities, is that of water resources. The seasonality of the tourist activities is undoubtedly the most important factor that affects water recourses. The sharp increase in population in one place for a certain time-period causes even greater increase in water consumption, since during holidays, a reduction of the sense of water preservation from tourists, has been observed. This can result not only in the enlargement of water problems during the touristic season, but also to more general problems of water scarcity throughout the year, which affect the permanent population as well. Today it is commonly accepted that the models of the water resources management followed so far, has not led to the desired results, either due to defects of the models or, because of their misuse. The challenge now is not only to meet the demand and increase the supply of water, but also to manage and reduce the demand. New approaches refer to rational management of a finite social good, participatory consultation, reduced consumption, protection from pollution, and reuse [Bouguerra, 2005].

More and more, governments, companies and communities are worried about future availability and sustainability of water resources. The water footprint is a methodological tool for the rational management of water resources, since, estimating the water footprint of a product can shape the potentials of new policies in water resource management [Hoekstra, 2015].

2. INTRODUCTION TO WATER FOOTPRINT

A relatively new concept in the simultaneous estimation of water consumption and water pollution is the water footprint concept that was first introduced by Hoekstra (2003). Chapagain and Hoekstra (2003, 2004) have shown that the visualization of water uses, hidden behind production processes, can help in the understanding of the global freshwater consumption and to quantify its impact. In a next stage, better and more rational management of the freshwater resources of the planet will be possible, thus reducing the negative impacts of current practices mentioned in the previous chapter.

The water footprint can be identified as a volumetric index of the various types and quantities of water which are used in the production chain of goods and is not just limited to the traditional concept of water withdrawals. The water footprint consists of three components [Hoekstra et al, 2011]:

- The blue water footprint refers to the consumption of surface and groundwater resources within the production chain of a product.
- The green water footprint refers to the rainwater stored as territorial moisture.
- The grey water footprint, an indicator for pollution, is defined as the volume of water resources required for the assimilation of the polluting load from the water body.

2.1 Analysis of the three components of the water footprint

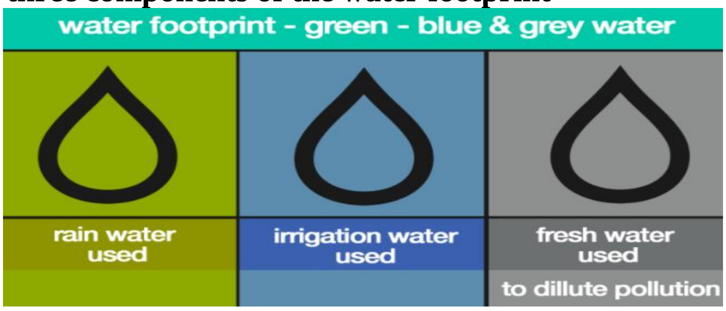


Figure 1: Illustration of the three components of the water footprint [Hoekstra et al, 2011]

2.1.1 Green water footprint

The green component refers to the rain which does not outflow on the surface nor replenishes the groundwater. The volume of rain refers to the part which is stored in the ground or remains temporarily on top of the soil or vegetation. Ultimately, this volume of water evaporates or is transferred through plants into the atmosphere. A definition that could be given for the green water footprint is the following: the green water footprint is the volume of rainwater consumed in the manufacturing process of a product.

It is clear that the volume of green water footprint depends directly on the season to which we refer. The volume of rainwater during the summer months is significantly smaller than that during the winter months. It would be appropriate to mention that the volume of rain that reaches the earth is not equal to the volume of rainwater consumed during the production process because, the water volume vaporized and driven straight into the atmosphere must be removed. The contribution of the green water footprint in irrigation procedures, whether they relate to agricultural or to garden watering for aesthetic purposes, is particularly important. This consumption of green water in irrigation is calculated from a set of empirical formulas and crop models, taking into account the evapotranspiration that varies depending on the climate, the soil, the type and characteristics of the irrigated area.

Green water footprint calculation: $W.F.green = CWU_g / Y$ (1)

where CWUg : green water (rainfall) (m^3/acre)

Y : crop yield (ton/acre)

2.1.2 Blue water footprint

The blue component is the amount of surface or underground water consumed in a manufacturing process of a product. This water is obtained by pumping water. Cases in which this water volume is assumed to be consumed are the following:

- Pumped water evaporates
- It is finally integrated into the product
- It does not return in the same catchment area from which it was pumped
- It does not return at the same time during which it was abstracted

Through the blue footprint it is possible to estimate the amount of water available from water resources for consumption over a specific time-period. The blue footprint represents a measurable quantity, on the basis of which human actions can be regulated in order to balance the ecosystem. There is of course a limit to the amount of water pumped from the surface as well as from underground, as these waters with their flows contribute to a significant part to the water balance of the aquatic system.

Blue water footprint calculation

$W.F.blue = CWU_b / Y$ (2)

where: CWUb : blue water (irrigation) (m^3/acre)

Y : crop yield (ton/acre)

$CWU_b = \Sigma u_b$ (3)

where: u_b : Blue monthly water use (mm/month)

$u_b = \max(0, PET_c - P_{eff}) = I_r$ (4)

where: PETC : evapotranspiration (mm/month)

Peff : beneficial rainfall (mm/month

Ir : crop irrigation requirements

$$Ir = PETC - Peff + GW + SM + L \quad (5)$$

where: PETC : evapotranspiration requirements
Peff : beneficial rainfall
GW : groundwater contribution
SM : water stored in the root
L : Salt leaching factor

2.1.3 Grey water footprint

The grey component refers to the volume of freshwater that is required for the assimilation of the polluting load caused by the manufacturing process of a product. The consumption of this water volume continues to dilute the pollutants, until they become safe according to the water quality standards of the region. The grey water footprint is an indicator of pollution of water expressed in freshwater volume.

The grey water footprint depends on the quality of the waste resulting at the end of its own management process. The ideal scenario is undoubtedly the zero outflow to the environment (zero grey). The most popular methods serving the above-mentioned purpose are the following two [Hoekstra et al, 2011]:

- Water recycling (reuse water on-site to serve the same purpose)
- Water reuse (reuse water to serve another purpose)

Grey water footprint calculation

The grey water footprint can be estimated through the application of the following equations.

$$L_{crit} = R * (c_{max} - c_{nat}) \quad (6)$$

where: Critical load (Lcrit) : the maximum pollution load that fully consumes the assimilation capacity of the water body (mass/time)
R: runoff water body (mass/time)
Cmax: maximum acceptable concentration of pollutants – quality limit (mg/l)
Cnat: the physical concentration of pollutants without the influence of the human factor (mass/volume)

$$WF_{proc,grey} = \frac{L}{c_{max} - c_{nat}} = \frac{Effl \times c_{effl} - Abstr \times c_{act}}{c_{max} - c_{nat}} \quad (7)$$

where: L: the polluting load resulting from the production process (mass/time)

Effl: outflow volume
Ceffl: concentration of pollutants in waste water (mass/volume)
Abstr: volume of water that is eliminated
Cact: concentration of pollutants in water intake

2.2 Total water footprint

The sum of the above three components is the total water footprint, which we wish to minimize

$$W.F. = W.F.green + W.F.blue + W.F.grey \quad (8)$$

2.3 Water footprint in Greece

The largest water related problem is, as expected, in the agricultural sector. This fact is justified by the estimations of the water footprint of Greece. Particularly unfavorable is the country's position regarding the water consumption. With an average annual consumption of 2,389 cubic meters per inhabitant, we have the second largest water footprint after the USA and twice the international average (1,24 m^3/year/inhabitant). Our large water footprint is due to increased water use for agriculture (85%), to the losses of the obsolete irrigation and water supply networks of the country, and to the overall mismanagement of water resources.

3. PRESENTATION OF THE HOTEL UNIT "PANTELIDIS"

The next section presents the profile of the hotel unit, in which the implementation of the water footprint methodology was assessed. The hotel complex "PANTELIDIS ' operates since 1989. It is located in the prefecture of Kozani. The area where the business is located, has an altitude of about 640 meters and the surrounding areas are characterized as farming. There is no water source near the hotel except for the aquifer, which lies at a depth of more than 40 meters.

3.1 Description of hotel unit

The hotel is located within an area of 45 hectares, 2 km from Ptolemaida. It's a classic 4 stars hotel. It has a total of 88 rooms, with 188 beds while the average occupancy is estimated to 60%. The following table shows the capacity of the hotel.

Table 3: The capacity of the hotel (room type, number of rooms, number of beds)

Type of room	Number of rooms	Number of beds
Double	82	164
Quadruple	6	24
Total	**88**	**188**

3.2 Swimming pool

The hotel features an outdoor swimming pool with a total area of 660,75 m^2. Its capacity is estimated at about 1000 m^3. The pool is filled in May and every day approximately 200 liters are removed and replenished. The pool is emptied in September.

3.3 Garden

The surrounding area is characterized by extensive planting, flowerbeds with various kinds of plants and lawns. The planting area is estimated at 3,371 m^2. Besides the lawn, the following species of trees and shrubs, which surround the hotel garden, can be found: plane trees, lindens, leilant.





Figures 2-3: The hotel's pool - Grass and trees in the restaurant

The area's rainfall is enough to meet the needs of plants. It should be noted that these species do not require large quantities of rainfall for their preservation. At the summer season when the temperature is high and the sunshine intense, an irrigation system is applied.

4. WATER FOOTPRINT CALCULATION OF THE HOTEL UNIT

The hotel's activities that require water are listed below, as well as the way the people in charge secure and store the water volume. Then, by categorizing these activities and with the help of some surveys already carried out, the water consumption per person and thus the water footprint of the business under investigation is calculated. The hotel ensures the freshwater volume required for the water needs, through a borehole. The pumped water is directed through special filters in order to be ready for any use by customers and staff. In order to apply the water footprint assessment methodology, water consumption is categorized in the following:

- Residence water footprint
- Activities water footprint
- Food water footprint

4.1 Residences water footprint

Refers to the fresh water consumed by customers to cover the majority of their needs. The following table shows the average daily water consumption per resident in a four-star hotel.

Table 4: Percentage of water consumption and per resident water consumption in liters/day per category of activities in hotels [Gössling et al., 2011]

Activity	Water consumption
Garden watering	50% (465 l.)
Cleanliness	5% (47 l.)
Visitor's hygiene	20% (186 l.)
Washing machines	5% (47 l.)
Restaurants	5% (47 l.)
Swimming pool	15% (140 l.)

The pool, the garden and the restaurants will be examined in the next category. According to the table above, the water footprint of the hotel is 280 liters per person. As the owners referred, the average occupancy is estimated to 60%. Considering that the rooms accommodate 188 beds, the average number of individuals served daily by the unit is 113.

Therefore the water requirements are 113 * 280 = 31.640 litres/day.

The above water footprint ranks in blue, because it is acquired from the aquifer through pumping.

4.2 Activities water footprint

Refers to water that is consumed for the operation of the swimming pool and for the irrigation of the garden.

4.2.1 Swimming pool

The duration of operation of the swimming pool is 5 months (May-September). It is filled with 1000 m^3 and daily 200 liters of water are removed and replenished. However, the consumption of this water will be split evenly on every day of the year.

Therefore: (1000 * 1000) + (153 * 200) = 1.030.600 liters/year

1,030,600/365 = 2.823,56 liters/day

The above water footprint ranks in blue, because it is acquired from the aquifer through pumping.

4.2.2 Garden

The calculation of the requirements and, thus, the blue and green water footprint resulting from the irrigation of the hotel garden was performed taking into consideration, the averages of the following three parameters: average monthly temperature, average monthly temperature difference, average monthly rainfall for the period between July 2009 and October 2017. Knowing the geographical coordinates, the extraterrestrial solar radiation was estimated. In general, the calculation of the water footprint ends up in water volume per product unit. If, for example, corn production was under examination, then the performance of cultivation should be taken into consideration. However, in this case the grass from which emerges no fruit is investigated. Thus, there is no connection with the performance of cultivation and it is simply reduced to water per day. Therefore, from the garden irrigation, the green water footprint was estimated to 348,95 liters/day and the corresponding blue, to 486,73 liters/day. It should be noted that the grey water footprint of garden irrigation is equal to zero, as no fertilizers and chemicals are being used, which would contribute to the pollution of local water resources.

4.3 Food water footprint

It refers to the water consumed by the customers of the hotel, both for the production of the products that make up the diet and for the direct consumption of water by themselves. Reference is also made to the volume of fresh water consumed in the restaurants.

4.3.1 Restaurant

Table 4 shows that the daily water consumption in the restaurant equals to 47 liters per day per resident. It has also been calculated that on average 113 people per day are served.

Therefore 113 * 47 = 5311 litres/day.

The above water footprint ranks in blue, because it is acquired from the aquifer through pumping.

4.3.2 Direct water consumption

The amount of direct water consumption varies and depends on many parameters. However, studies have resulted to an estimation of 3.18 liters/person as the average daily amount of total water consumed for drinking.

Therefore 113 * 3,18= 359,34 liters/day. The above water footprint is also ranked in the blue category.

4.3.3 Indirect water consumption

It refers to the food that is consumed by the customers of the unit and either contain water or water was used for their production. The daily diet of an average human being is estimated according to the following diagram.

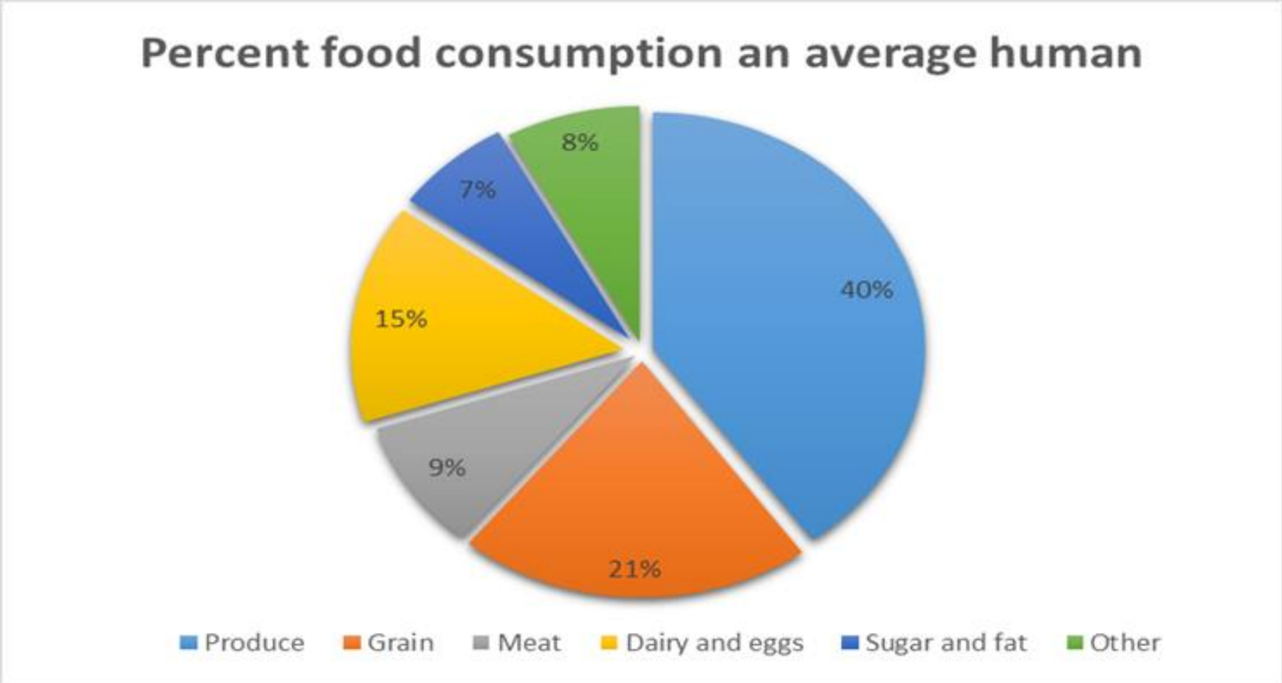


Figure 4: Percent food consumption of an average man [https://www.nationalgeographic.com/what-the-world-eats/]

The official water footprint website (http://temp.waterfootprint.org/?page=files/productgallery) has formed a product catalog which lists the liters needed to produce one kilogram of each product. The percentages corresponding to blue, green and grey water footprint are indicated respectively. On the basis of data reported and the diagram of figure 5, the following table configuration was formed, which expresses the water footprint of an average human food – customer of the hotel unit.

Table 5: Water footprint of each food that composes a daily diet of an average human

Produce	40%	Grams	litre/kilo	Total water footprint	Green water footprint	Blue water footprint	Grey water footprint
Starchy roots	9%	174	287	49,94	32,96 (66%)	5,49 (11%)	11,49 (23%)
Vegetables	20%	372	237	88,16	49,37 (56%)	10,58 (12%)	28,21 (32%)
Fruits	11%	203	822	166,87	113,47 (68%)	26,7 (16%)	26,7 (16%)
Grain	**21%**	**Grams**	**litre/kilo**	**Total water footprint**	**Green water footprint**	**Blue water footprint**	**Grey water footprint**
Rice	8%	148	2497	369,56	251,3 (68%)	73,91 (20%)	44,35 (12%)
Wheat	10%	179	1608	287,83	201,48 (70%)	54,69 (19%)	31,66 (11%)
Maize	2%	48	1222	58,66	45.17 (77%)	4,11 (7%)	9,39 (16%)
Other cereal	1%	28	1223	34,24	23,97 (70%)	6,51 (19%)	3,77 (11%)
Meat	**9%**	**Grams**	**litre/kilo**	**Total water footprint**	**Green water footprint**	**Blue water footprint**	**Grey water footprint**
Seafood	3%	52	-	-	-	-	-
Poultry	2%	39	4325	168,68	138,31 (82%)	11,81 (7%)	18,55 (11%)
Pork	2%	42	5988	251,50	206,23 (82%)	20,12 (8%)	25,15 (10%)
Beef	1%	26	5989	155,71	146,37 (94%)	6,23 (4%)	3,11 (2%)
Other meat	1%	14	5990	83,86	78,83 (94%)	5,03 (6%)	0

Table 6: Water footprint of each food that composes a daily diet of an average human

Dairy and eggs	15%	Grams	litre/kilo	Total water footprint	Green water footprint	Blue water footprint	Grey water footprint
Milk	13%	247	1020	251,94	214,15 (85%)	20,16 (8%)	17,64 (7%)
Eggs	1%	24	196	4,704	3,72 (79%)	0,33 (7%)	0,612 (13%)
Animal fats	1%	9	5553	49,977	42,48 (85%)	3,99 (8%)	3,5 (7%)
Sugar and fat	**7%**	**Grams**	**litre/kilo**	**Total water footprint**	**Green water footprint**	**Blue water footprint**	**Grey water footprint**
Sugar and sweeteners	4%	66	920	60,72	59,51 (98%)	0,61 (1%)	0,61 (1%)
Vegetables oils	2%	32	3015	96,48	79,11 (82%)	16,4 (17%)	2,9 (3%)
Other oils	1%	19	2854	54,226	41,75 (77%)	3,8 (7%)	8,77 (16%
Other	**8%**	**Grams**	**litre/kilo**	**Total water footprint**	**Green water footprint**	**Blue water footprint**	**Grey water footprint**
Alcoholic beverages	5%	102	436	44,472	31,13 (70%)	7,12 (16%)	6,23 (14%)
Miscellaneous	2%	22	528	11,616	11,12 (96%)	0,12 (1%)	0,35 (3%)
Pulses	1%	19	11397	216,543	216,54 (95%)	6,5 (3%)	4,33 (2%)

The sum of the columns of the above two tables resulted in the following results of the total green, blue and grey water footprint of the human diet

- Green water footprint: 1.976,176 liters/day/person
- Blue water footprint: 284,189 liters/day/person
- Grey water footprint: 247,298 liters/day/person

Considering the fact that 113 people are serviced daily:

- Green water footprint: 223.307,888 liters/day
- Blue water footprint: 32.113,357 liters/day
- Grey water footprint: 27.944,674 liters/day

Table 7: Aggregated results of green, blue and grey water footprint of the hotel unit

	Green (liters/day)	Blue (liters/day)	Grey (liters/day)
Accommodation	0	31640	0
Swimming pool	0	2823,56	0
Garden	348,95	486,73	0
Restaurant	0	5311	0
Direct water consumption	0	359,34	0
Indirect water consumption	223.307,888	32.113,357	27.944,674
Total	**223.656,838**	**72.733,987**	**27.944,674**

W.F. = W.F.green +W.F.blue +W.F.grey = 324.335 liters/day

5. PROPOSALS TO IMPROVE THE MANAGEMENT OF WATER RESOURCES OF THE HOTEL UNIT

At this point a simple report – summary of provisions and techniques for saving water in hotels is made. The application of these proposals is expected to reduce the water footprint of the unit [Meras, 2014; Chatzi, 2018]

- Biological cleaning installation..
- Sensors in all taps for automatic closure. (An open tap consumes 9 liters of water per minute).
- Installation of water consumption meters around the building, so the slightest leak can be immediately repaired. One drop per second costs over 4 liters a day or else 1500 liters per year.
- Water saving devices (hippo bags). The replacement of all hotel's cisterns with new technology is a highly expensive process. That is why there are special bags placed inside the muffler, saving significant amounts of water. Even placing a bottle inside the muffler does the same job and is estimated to save approximately a 10% water.
- Collecting rainwater for watering the garden and cleaning the unit's facilities.
- Replacement of showers and water spray taps with air rates. The water runs with air rates, so as to reduce the consumption of water.
- Replacement of bathtubs with showers. Use of ecological and biodegradable detergents, in order to recycle water from the kitchen, showers and washbasins for irrigation (grey water).
- Adoption of an optional linen change process in guest rooms. Changing of the towels and bed linen is only made on the suggestion of the tenant. This process has shown that it is particularly acceptable to the tenants and highly efficient in saving water resources.
- Recycling poll water.
- Inform visitors about water saving effort through a prospectus, mounted in every room.

References

1. Anon (2011), What world eats, Available: https://www.nationalgeographic.com/what-the-world-eats/
2. Bouguerra M.L. (2005) **Une economie au service de l' homme: L' eau sous la menace des pollutions et des marches**, pp 249-279.
3. Champagain, A.K. and Hoekstra A.Y. (2004), Water footprints of nations. **Value of Water Research Report Series 16**, the Netherlands: UNESCO-IHE.
4. Champagain, A.K. and Hoekstra, A.Y. (2003), Virtual water flows between nations in relation to trade in livestock and livestock products. **Value of Water Research Report Series No. 13**. Delft, the Netherlands: UNESCO-IHE.
5. Chatzi, A. (2018), Assessment of the water footprint of the hotel unit "Pantelidis" in Ptolemaida, Diploma thesis, Aristotle University of Thessaloniki, Thessaloniki
6. Gossling, S., Garrod, B, Aall, C. (2011), Food management in tourism: Reducing tourism's carbon footprint, **Tourism management** 32 (3), 534-543.
7. Hoekstra A. (2015), The Water Footprint: The Relation Between Human Consumption and Water Use. In book: M. Antonelli and F. Greco-The water we eat. Combining Virtual Water and Water Footprints, **Springer water**, p.35-48

8. Hoekstra, A.Y. (2003), Virtual water trade: In: International Expert Meeting on Virtual Water Trade, Delft, The Netherlands, 12-13 Dec. 2002, **Value of Water Research Report Series No.12**, UNESCO-IHE, Delft, The Netherlands.

9. Hoekstra, A.Y., Chapagain, A.K., Aldaya, M.M., Mekonnen, M.M. (2011), The water footprint assessment manual: Setting the global standard. **London: Earthscan**. p 203.

10. http://temp.waterfootprint.org/?page=files/productgallery

11. Meras V. (2014), Improvement of water resource management in urban hotels, Diploma Thesis, Aristotle University of Thessaloniki, Thessaloniki

12. Michalis Hadjikakou, Jonathan Chenoweth et al, (2013), The electronic journal: Journal of Environmental Management, **Estimating the direct and indirect water use of tourism in the eastern Mediterranean**, pp 548-556.

13. Ogunjimi A. (2017) The Average Consumption of Water Per Day, Available at: https://www.livestrong.com/article/338496-the-average-consumption-of-water-per-day/

SEDIMENT TRANSPORT CASE STUDY: NESTOS RIVER

[1]S. M. Bagiouk*,[2]K. C. Anagnopoulos,[2]S. S. Bagiouk, [2]A. E. Agiou, [1]A. S. Bagiouk

[1]Division of Hydraulics and Environmental Engineering, Dept. of Civil Engineering, Aristotle University of Thessaloniki, 54124 Thessaloniki, Greece,

[2]Department of Civil Engineering, Democritus University of Thrace, 67131, Xanthi, Greece

*Corresponding author: [1]E-mail: smpagiou@civil.auth.gr, Tel +30 2310 995893, +30 6944189218

Abstract

In the current paper are presented the results of a survey conducted in specific sections of the Nestos river pointing out some of the basic features of the river behavior, in order to create a real data base available to everyone who is interested in further study and research. It consists of two sections; the first one is the calculation of suspended sediment and the second one the calculation of trolling matter. Specifically, in the first part the flow rate and sediment transport were calculated, where it was observed that the increase of flow rate resulted in the increase of sediment transport, which is fully verified by the results of the research and it is concluded that the initiative assumptions were correct. Moreover, in the second part, the transportation of the trolling matter on the field was initially measured and then the same data were reevaluated using the Meyer-Peter and Müller equation, which is one of the most reliable equations concerning the evaluation of trolling matter transport. In the end, after a comparison of the results relative convergence was observed and the results are reliable for use, expressing the basic characteristics of the Nestos river.

Keywords: Suspended sediment, trolling matter, flow rate, Nestos river, Meyer-Peter and Müller equation

1. INTRODUCTION

As load transport materials are characterized solids that are transported by water or deposited.They are presented in the form of suspended, bottom or floating materials[5]. The suspended solids, which are usually the bulk of the load transport material, are in static or dynamic balance with water and are kept suspended by turbulence [2]. The bottom materials move on the bed or on the ground by sliding, rolling or bouncing(trolling matter)[2]. The floating materials have usually organic origin, such as e.g. aquatic plants, tree parts etc.and constitute 2 to 5% of the suspended materials.a Many times, however, they prevent dams operation. Measurements [1] of load transport material are a prerequisite in order to estimate the accumulation of sludge in riverbed and along the banks of rivers, sediment deposition in natural and artificial lakes, the delta formed at the estuary of a river to the sea, quantity of harmful substances (e.g. heavy metals that affect water quality) and finally the erosion of a catchment area due to heavy rain and surface runoff [10]and for the application of appropriate measures against corrosion. The delimitation between floating and bottom load transport materials depends on the instantly state of transport such as the velocity of water[2]. For suspended material in rivers with high velocity of water is sufficient the sampling in a single spot near the water surface in the middle of the river. Generally, the determination of the amount of suspended materials is based on the float rate [kg/s], float rate per width unit of the river[kg/(s·m)], floating load [t],the concentration[g/m^3] or content[ppm] or density [kg/m^3]of suspended materials[3].For the bottom or trolling materials, similar definitions apply, concerning the determination of the quantity of bed load

transport [kg/s], the bed load transport per width unit [kg/(s · m)] and the transport load of this bed[t] [3]. The bed load material transport is taken per unit of width, if the weight of the 'captured' materials is divided by the time of measurement and the width of the opening (of the gabion). The measurements of the bed load transport are difficult due to the discontinuous movement of the bottom materials in the form of sandblasts [1]. Such measurements are mostly made only on large rivers.

This paper describes the process of measuring the bed or sediment load transport of international importance Nestos River and concerns the load of the bottom materials(or trolling matter) and the load in suspension. These are the basis for the calculation of the quantity of sediments, in specific time, which are transferred to the estuary of the river[7] to the sea, which constitutes a Wetland of International importance and part of the National Park.

2. MEASUREMENTS OF SUSPENDED LOAD TRANSPORT

Nestos River is one of the five largest rivers in Greece[7] and delineates the borders between Macedonia and Thrace as well as the prefectures of Kavala and Xanthi. Five measurements were performed between 17 – 30 of July 2015 in five different sections of the river in order to estimate the suspended load transport[11]. These measurements took place in cross sectionsof the river which are approximately 2 km from the village Kyrnos.

Measurements include the following sub – tasks:

- Section selection and its division in subsections. In each section, separately, the depth of the river and the flow rate were measured with a special rotational speed measuring instrument(current meter, VALEPORT model BFM001).
- Water sampling (1.5L volume) from each section. Laboratory processing of each sample to find the net weight of sediment.
- Estimation of surfaces of already separated sections.
- Finding water flow in each subsection of the cross – section and estimation of suspended load transport throughout the cross – section, with the following equations [6]:

$$Q_i = V_{mi} A_i \tag{2.1}$$

$$C_s = \frac{\sum C_i Q_i}{\sum Q_i} \tag{2.2}$$

$$m_s = C_s \sum Q_i \tag{2.3}$$

Where:

V_{mi}: average flow velocity in part i of the cross - section [m/s]

A_i:area of part i of cross – section [m^2]

Q_i: flow rate of part I of the cross – section [m^3/s]

C_i:concentration of suspended matter in the part i of the cross – section [kg/m^3]

C_s:concentration of suspended matter in the entire cross – section [kg/m^3]

m_s: total suspended load transport matter in the cross – section [kg/s]

Below it is presented in detail the procedure[12] followed for the five measurements.It was typicallychosen to be presented only the measurement process of the first measurement with the stages, calculations and laboratory tests that took part.The remaining four measurements did not show any difference in how they were applied and tested as they followed exactly the same procedure and sequence of actions.

2.1 Procedure of the first measurement

The first measurement was performed on Tuesday 17 – 07 – 2015 and took place at a total cross – section width of 18 m. Figure 1 shows the cross – section of Nestos river, where the first measurement was made. The results of the flow rate measurements at a characteristic point of the cross – section is shown in Table 1.

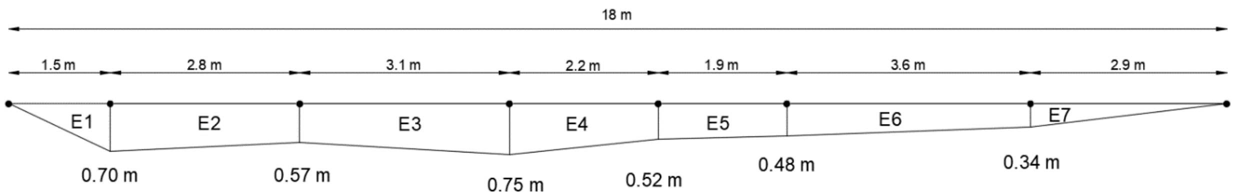


Figure 1: Graphic representation of the cross – section (1st measurement)

Table 1. Depth and flow velocity at a characteristic point of the cross – section (1st measurement)

Measurement	Depth [cm]	Velocity [m/s]
1	75	0.778

2.2 Cross section area measurement

The cross – sectional area in which the first measurement was made is estimated by measuring the surface width of the cross – section divided into subsections. In each section correspond two trapezoids or a trapezoid and a triangle, which are on either side of each measurement position (Figure 1). The sum of the areas of subsections constitutes the total area of cross – section[2].

The measurements of all individual trapezoids and triangles givethe following results (Table 2):

Table 2. Area of individual trapezoids and triangles of cross – section (1st measurement)

Measurement	A/A trapezoid or triangle	E [m^2]
1	1	0.53
	2	1.78
	3	2.05
	4	1.40
	5	0.95
	6	1.48
	7	0.49

2.3 Laboratory test on the water sample of the first measurement

The test was performed on a sample of water taken from the cross – section, located about 2km from the village of Kyrnos with coordinates LL 40.99 – 24.75.

The sample content in sediments was calculated with special retention filters. The retention filters were weigh twice. The first weighing gave the filter weight and the second the weight of the suspended material.

The test took place at the laboratory of the Environmental Engineering Department of DUTH. The test results are summarized in Table 3

Table 3. Weight of suspended matter from the sample of the 1st measurement

Sample	Filter weight before retention [g]	Filter weight after retention [g]	Weight of suspended matter inside water bottle of 1lt [g]
1	0.09293	0.09344	0.00102

2.4 Calculation of suspended load transport from the 1st measurement

In Table 4 below, it is shown in detail the calculation of the flow through the cross – section considered. The same Table gives the concentration of suspended materials.

Table 4. Flow estimate (1st measurement)

Position	V_m	A	Q	C_s
	[m/s]	[m^2]	[m^3/s]	[g/lt]
1	0.778	8.68	6.753	0.00102

The suspended load transport of the entire cross – section is calculated[6] according to equation 2.3:

$m_s = C_s * \sum Q_i$=0.0069 kg/s=6.9 g/s

The suspended load transport per unit of river width is:

0.0069/18 = 0.000383 kg/s·m

3. PARTICLE SIZE ANALYSIS

In the bed of Nestos River[7], during the five measurements the load transport sediment was trapped with a special landing net, with a specific square opening (7.5cm*7.5cm) at the back of which a net for collecting sediments is attached.

The device was placed parallel to the stream for a period of one to five (1-5) minutes. Each sample drained at a temperature of 105^{o}Cand then, in the laboratory of Hydraulic Sector of the Civil Engineering Department of DUTH was performed the particle size analysis with sieves.

Table 5 below shows the particle analysis[4] of bed load transport samples of the first measurement, which is representative of all other measurements, while in Figure 2 is given the particle size curve of the first measure. The particle curves of the samples of other measurements employ identical form[10].

Table 5. Particle size analysis of 1st sample (1st measurement)

Particle size analysis with sieves						
Date:17/07/2015			Overall ground weight: 172.81g			
α/α	Sieve number	Loop size	Retained ground weight	Retained percentage	Cumulative retained percentage	Percentage thinner
		[mm]	[g]	[%]	[%]	[%]
1	-	1.5	126	73	73	27
2	-	1	40.90	23.6	96.6	3.4
3	35	0.5	5.80	3.34	99.94	0.06
4	60	0.25	0.09	0.05	99.99	0.01
5	120	0.125	0.02	0.01	100	0.00
6	230	0.063	0.00	-	-	-

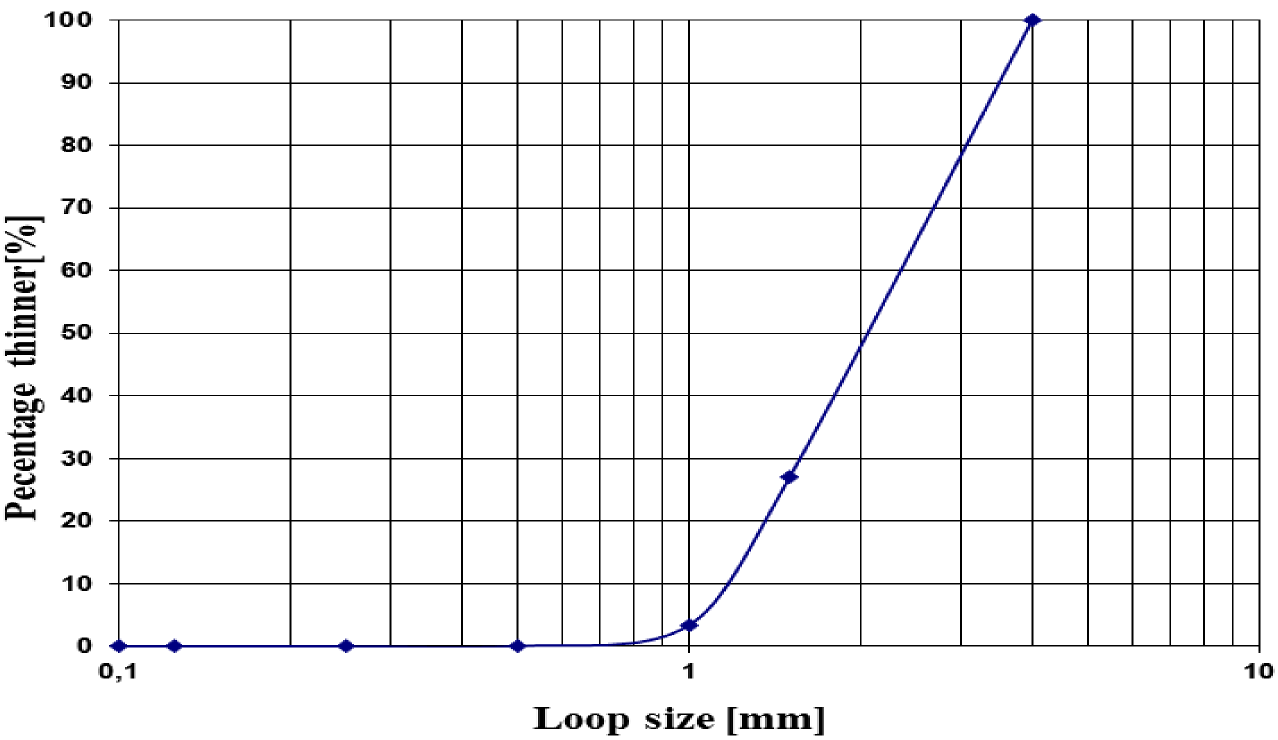


Figure 2. Particle size curve of 1st sample

4. MEASUREMENTS AND CALCULATIONS OF LOAD TRANSPORT BED

4.1 Equation of Meyer – Peter and Müller

For the calculation of load transport rate of the river (due to sliding) a semi – imperial equation exist that applies to certain values of hydraulic parameters of sediments. In the present paper Meyer – Peter and Müller equation (1949) was used, which has a very good position between equations for estimating the load bed [13]. This can be written:

or $$m_G = \frac{8}{g}\frac{\rho_F}{\rho_F - \rho_w}\sqrt{\frac{1}{\rho_w}}\left(\tau_0 - \tau_{cr}\right) \qquad (4.1)$$

The introduction of the hydraulic radius Rs into equation (4.1) was made to take indirect account of the roughness of the side walls of the open duct [4]. The Qs/Q ratio is often taken equal to 0.8 approximately or 1 in square conductors. The introduction of the Ir friction gradient was made, because only one part of the available energy is consumed to move the weighed matter [5].

4.2 Calculation of K_{st} factor and his calibrated value

In order calculate K_{st}, all known parameters of the current test were replaced in formula (4.1), according to the Meyer-Peter and Müller method [13]. Hence, having only the unknown size of the K_{st} , the corresponding K_{st} was calculated each time. After the same procedure was followed for all measurements, all the values of K_{st} factor were gathered and presented in table 6 and also their average value.

Table 6.Values of $K_{st} m^{1/3}/s$

Measurement	1	2	3	4	5
K_{st}	15.03	19.18	18.31	13.62	15.52
Average	16.33				

4.3 First measurement of load transport bed

In this project, as it was mentioned before, a specific metal collector was used with a square opening 7.5cm x 7.5cm at the back of which a net for collecting sediments and trolling matter is attached. The device was placed parallel to the stream for a period of one to five (1-5) minutes. The overall mass of the captured matter of the sample during the first measurement was 172.81g or 0.17281kg.

For the measurement of sediment transport rate of the bed (table 7), the 0.17281 kg of sediment were divided with the width of the opening of the device (0.075 m)and the time of collection (61 s).

$m_G = 0.17281/(0.075 \times 61) = 0.03777$ kg/(m·s)

Table 7. Measured sediment transport rate (1st measurement)

Sample mass	m=	0.17281 kg	
Collector's width	b=	7.5 cm	0.075 m
Collection time	t=	1.02 min	61 s
Sediment transport rate	m_G=	0.03777 kg/(m·s)	

4.4 Calculation of sediment transport rate for the data of the first measurement

The Meyer-Peter και Müller type in combination with Einstein and Barbarossa method, is now applied in the data of the measurement in order to calculate the sediment transport rate of the bed (table 8)[13].It is also noted that factor K_{st} is taken equal to 16.33 $m^{1/3}/s$, exactly as it was calculated from calibration procedure[2].

Table 8. Data of first measurement and sediment transport rate calculation

Overall bed width	$b=$	18m
Depth of flow	$h=$	0.482m
Average velocity	$V_m=$	0.778 m/s
Bottom inclination	$I=$	0.005
K_{st} factor	$K_{st}=$	$16.33m^{1/3}/s$
Characteristic particle diameter	$d_{90}=$	0.00355m
Interstitial particle diameter	$d_{50}=$	0.0021 m
Density of sample of suspended load	$\rho_F=$	2650 kg/m^3
Gravity factor	$g=$	9.81 m/s^2
Water density	$\rho_w=$	1000 kg/m^3
Wet section	$A=b\times h=$	$8.68m^2$
Wet wall perimeter	$U_W=2\times h=$	0.964 m
Wet bed perimeter	$U_s=b=$	18m
Average particle diameter	$d_m=d_{50}=$	0.0021 m
Calculation		
$\rho'=(\rho_F-\rho_W)/\rho_F=$	1.65	
$K_r=$	$66.57m^{1/3}/s$	
$I_r=$	6.075×10^{-4}	
$R_s=$	0.453 m	
Sediment transport rate $m_G= 47.92 \times 10^{-3}$ **kg/(m·s)**		

After the same procedure was followed for the rest of the measurements, it was observed that there is convergence in a great level between measured and calculated sediment transport rate of the bed in most cases.

5. DISCUSSION AND CONCLUSIONS

In order to provide some clear conclusions from the measurements and the calculations, which are referred previously, a centralized statement [9] is made through two tables. Table 9 includes the flow rate, concentration of suspended sediment and suspended sediment transport rate in every of the five specific sections, as they emerged from the measurements, while table 10 includes the measured and calculated sediment transport rate for each of the five sections.

Table 9.Flow rate, concentration and transport rate of suspended sediment

Measure	Date	Flow rate [m^3/s]	Concentration [g/lt]	Suspended sediment transport rate [g/s]	Suspended sediment transport rate [kg/(m·s)]
1	17.07.2015	6.753	0.00102	6.9	0.000383
2	21.07.2015	2.418	0.00146	3.5	0.000304
3	24.07.2015	11.022	0.00112	12.34	0.000494
4	27.07.2015	9.284	0.00106	9.84	0.000502
5	30.07.2015	9.01	0.00114	10.27	0.000642

It is observed that the highest value of flow rate was measured during the third measurement, which completely corresponds to the highest value of suspended sediment transport rate. Furthermore, the lowest value of flow rate (second measurement) matches with the lowest value of suspended sediment transport rate.

In the following table the measured and calculated sediment transport rate are presented during the five measures in some sections of Nestos River.

Table 10.Calculated and measured sediment transport rate

Measure	Date	Measured sediment transport rate [kg/(m·s)]	Calculated sediment transport rate [kg/(m·s)]
1	17.07.2015	0.03777	0.04792
2	21.07.2015	0.02658	0.004071
3	24.07.2015	0.05832	0.04691
4	27.07.2015	0.0854	0.1068
5	30.07.2015	0.10021	0.1225

As it is occurred from table 10, there is a relative deviation between the sediment transport rate that was measured and the one that was calculated during the second measurement. This deviation was probably the result of a random incident or a mistake in this specific measurement. As far as the rest of the measurements are concerned, the deviations between measured and calculated sediment transport rate of the section of Nestos River are under reasonable bounds.In conclusion, in the first stage, in which there was calculation of the flow rate and sediment transport rate, the increase of the flow rate resulted to the increase of sediment transport rate, which is a fact that can be fully confirmed from the rest of the outcomes. Furthermore, we can conclude that the initial assumptions were correct [2]. In the second stage the trolling matter transport rate was measured in the field and afterwards with the same data there was again calculated the same rate but this time using the Meyer-Peter and Müller equation [13], which is one of the most famous and reliable equations concerning the

evaluation of trolling matter transport rate. Thus, there was a comparison of the results [8] and it was observed that there is a sufficient convergence between them. Finally, it became clear that these results are reliable for further use, they express the basic features of Nestos River[5] and they constitute a reliable data base for the future. It is worth to mention that is necessary, in order to avoid mistakes and for more representative results of this kind of measurements, to have a more adequate number of measurements, from which some extreme rates should not be taken under consideration or, differently, lower importance to be given to them [9].

The creation of a real archive of measurements and data forms the basic purpose of this project as the only goal is the possibility of using them for further study and research. Moreover, the potential comparison and evaluation of new calculations, measurements and results and finally the designation of the behavior and basic features of Nestos River.

References

1. Weiming Wu, 2007. **Computational River Dynamics**. CRCPress
2. Sakkas I.,1994 G.: **"Technical Hydrology: Vol. I, Surface Waters Hydrology "** Ekdosis Aivazi , Xanthi.
3. Soulis I .,1999: **"Open Duct Hydraulics"**, Ekdosis Aivazi, Xanthi.
4. Tsakiris G., 1995: **"Water Resources: I. Technical Hydrology",** Simmetria Publications, Athens.
5. Chongas X, 1993: **"River Engineering"**, Ion Publications, Athens.
6. Chrysanthou B., 1996: **"River Hydraulics and Technical Works Notes"**, Department of Civil Engineering, DUTH, Xanthi.
7. https://el.wikipedia.org/wiki/ (accessed October 21st, 2017)
8. Yu, K.K. and Woo, H.S. (1990) Comparative Evaluation of Some Selected Sediment Transport Formulas**. KSCE Journal of Korean Society of Civil Engineers**, 10, 67-75.
9. Walter Hans Graf ,1984 .**Hydraulics of Sediment Transport**. Water resources publications.
10. Wilbert Lick, 2008. **Sediment and Contaminant Transport in Surface Waters**. CRC Press
11. Ellen Wohl,2014. **Rivers in the Landscape: Science and Management**. Wiley-Blackwell
12. Andre Robert, 2003. **River Processes: An Introduction to Fluvial Dynamics**.Taylor & Francis
13. https://en.wikipedia.org/wiki/Sediment_transport (accessed October 9th, 2017)

ASSESSMENT OF IRRIGATION WATER QUALITY IN ANTHEMOUNTAS BASIN, CENTRAL MACEDONIA, GREECE

Hatzigiannakis, E., Tziritis, E., Ilias, A., Arampatzis, G., Doulgeris, C., Pisinaras, V. Panagopoulos, A.

Soil and Water Resources Institute,
Hellenic Agricultural Organization-DG Research,
GR- 57400 Sindos, Macedonia, Greece

*Corresponding author: e-mail: tziritis@gmail.com, tel : +302310798790

Abstract

This research focuses on the assessment of irrigation water quality in a cultivated basin (Anthemountas Basin) of central Macedonia, Greece. Specifically, it was performed a risk assessment of soil salinization or alkalization due to irrigation water quality, as well as an assessment of the anticipated adverse effects and the potential toxicity in crops due to the presence of harmful substances in irrigation water. In this context, 45 samples from irrigation boreholes were analyzed for assessing electrical Conductivity (ECw), pH, Sodium Adsorption Ratio (SAR), Na, Ca, Mg, Cl and B. Results revealed that regarding ECw, 71% of boreholes appeared to have values below 0.7mS/cm, hence characterized as of negligible risk, and 29% of the boreholes had values between 0.78-1.1mS/cm, hence characterized as of small to medium risk. In respect to crop toxicity due to the concertation of specific ions at soils, the risk due to sodium (Na) and Chlorides (Cl) appears to be low; however, the risk due to boron (B) appears to be significant in a few cases accounting for concentrations up to 2.87 mg/L in irrigation water. The pH values are within the acceptable range of irrigation waters and the probability of irrigation system clogging due to salinization effects appears to be low to negligible. Nevertheless, agricultural practices including the management of irrigation water resources should be frequently monitored and managed rationally in order to maintain an optimal quality status of water reserves and soils, hence contributing significantly to the sustainable agriculture. Towards this direction, specific suggestions are given taken into account the specific conditions and characteristics of the area.

Keywords: Irrigation water quality; salinization; alkalization; crop toxicity; Anthemountas basin

1. INTRODUCTION

Water used for irrigation can vary greatly in quality depending upon type and quantity of dissolved salts; salts are present in irrigation water in relatively small but significant amounts. They originate from dissolution or weathering of the rocks and soil, including dissolution of lime, gypsum and other slowly dissolved soil minerals (Singh, 2018). These salts are carried with the water to wherever it is used. In the case of irrigation, the salts are applied with the water and remain behind in the soil as water evaporates or is used by the crop.

The suitability of a water for irrigation is determined not only by the total amount of salt present but also by the kind of salt. Various soil and cropping problems develop as the total salt content increases, and special management practices may be required to maintain acceptable crop yields. Water quality or suitability for use is judged on the potential severity of problems that can be expected to develop during long-term use.

The problems that result vary both in kind and degree, and are modified by soil, climate and crop, as well as by the skill and knowledge of the water user. As a result, there is no set limit on water quality; rather, its suitability for use is determined by the conditions of use which affect the accumulation of the water constituents and which may restrict crop yield. The soil problems most commonly encountered and used as a basis to evaluate water quality are those related to salinity, water infiltration rate, toxicity and a group of other miscellaneous problems.

While the salinity tolerance of crops varies among species, all crops are negatively affected at some point by increasing salinity levels of irrigation water (Western Fertilizer Handbook, 1995; Ayers and Westcot, 1976; Buckman and Brady, 1967; Miller and Donahue, 1995; Pereira and Marques, 2017). Use of salty irrigation water may lead to two major problems in crop production; salinity hazard and sodium hazard (McFarland et al., 2002). When irrigation water is used by plants or evaporates from the soil surface, salts contained in the water are left behind and can accumulate in the soil. These salts create a salinity hazard because they compete with plants for water. Even if a saline soil is water saturated, plant roots may be unable to absorb the water, and plants will show signs of drought stress. Foliar applications of salty water often cause marginal leaf burn and, in severe cases, can lead to defoliation and significant yield loss (McFarland et al., 2002). Higher electrical conductivity and salinity in irrigation water cause an increase in soil solution osmotic pressure (United States Laboratory Staff (USSLS), 1954). Excess soluble salts in the root zone restrict plant roots from withdrawing water from the surrounding soil, effectively reducing the plant available water (Western Fertilizer Handbook, 1995; Bauder, 2001; Bauder and Brock, 2001; Hanson et al., 1999; United States Development Agency (USDA) Natural Resources Conservation Service, 2002).

The aim of the present study focuses on the assessment of irrigation water quality in a cultivated basin (Anthemountas Basin) of central Macedonia, Greece. Specifically, it seeks to perform a risk assessment of soil salinization due to irrigation water quality, as well as an assessment of the anticipated adverse effects and the potential toxicity in crops due to the presence of harmful substances in irrigation water.

2. STUDY AREA DESCRIPTION

Anthemountas River basin is located in central Macedonia, Greece. It is the northwest part of the Chalkidiki peninsula and covers 318 Km2 approximately (fig. 1). It consists of two main sub basins, namely Basilika (208 Km2) which occupies the lower parts and Galatista (110 Km^2), which is situated topographically higher.

A dense well-formed stream network drains the area while the geological features include a large variety of different sediments combined with various geological formations. The hydrogeology, consequently, presents complex features (Fikos et al., 2005). The sedimentary formations are the hosts of confined and unconfined porous aquifers with variable morphological characteristics. Fissured rock aquifers are developed in the crystalline and metamorphic rocks, whereas a karstic aquifer is located in the carbonate rocks (Kazakis et al., 2016). A detailed description of these aquifers' characteristics can be found in previous studies (Kazakis et al., 2015).

The main crops of the area include weed (70%), followed (30%) by corn, cotton and vegetables. The irrigation water is solely based upon the abstraction of groundwater resources by private boreholes. The dominant irrigation method is drip irrigation accounting for the 85% of cotton, corn and vegetables, followed by springler irrigation which accounts for 15% of the same crops, respectively. Regarding weed crops, they are mainly rain-fed, and is rare episodes of extended drought, they are irrigated once or twice by springler irrigation.

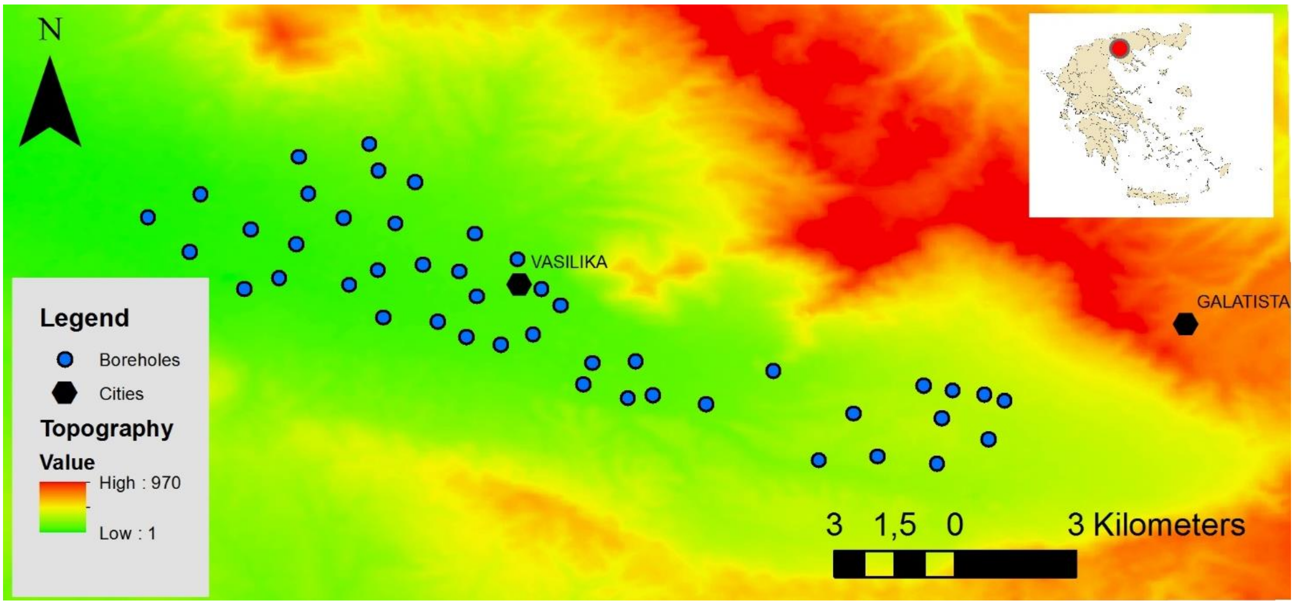


Figure 1: Study area and borehole sites

3. MATERIALS AND METHODS

Totally 180 samples were collected from 45 irrigation boreholes of Anthemountas basin (fig. 1) during 4 sampling campaigns (May 2010; August 2010; November 2010; January 2011), practically covering an entire hydrological year. Samples were collected in 500ml polyethylene bottles; prior to sampling, boreholes were operating for sufficient time (10 min) and bottles were rinsed three times with borehole water. Electrical Conductivity (EC) and pH were measured in situ by portable means; the collected battles were stored in refrigerators (≈4C^{o}) and transported in the laboratory for further analysis. Specifically, samples were analyzed for the following parameters (the analytical methods in brackets):

- Na (Flame Photometer)
- Cl (Volumetrically)
- B (UV-Vis in 420nm)
- Ca, Mg (Atomic Adsorption AAS-flame)
- Sodium Adsorption Ratio - SAR (calculated)

4. RESULTS

Based on the measured values for all periods, the pH is slightly alkaline (median=7.7) ranging from 7.2 to 8.4. In respect to EC, irrigation water is not saline in general; however, few samples appear to have values up to 1.28 mS/cm). Calcium (Ca) is the dominant cation (median=52.7 mg/L), with values ranging from 1.1 to 142.5 mg/L, followed by Sodium (Na) ad Magnesium with median values of 37.7 and 24.6 mg/L, respectively. Chlorides (Cl) range from 7.1 to 187 mg/L (median=42.6) and Boron (B) from 0 to 3.2 mg/L (median=0.08). Based on these values, the calculation of Sodium Adsorption Ration (SAR) as defined by Reeve et al. (1954), gave values that ranged from 0.16 to 238, with a median of 0.64

Table 1: Basic statistics parameters of irrigation water samples for all periods. Standard deviation refers to average values

Variable	Minimum	Average	Median	Maximum	StDev
pH	7.20	7.5	7.7	8.40	0.25
EC (mS/cm)	0.30	0.63	0.64	1.28	0.16
Na (mg/L)	7.77	24.2	24.60	108.20	16.61
Ca (mg/L)	1.10	48.4	52.70	142.50	26.64
Mg (mg/L)	3.50	34.8	37.70	239	26.64
Cl (mg/L)	7.10	40.2	42.60	187	25.07
B (mg/L)	0.00	0.08	0.08	3.20	0.44
SAR	0.16	0.63	0.64	2.38	0.42

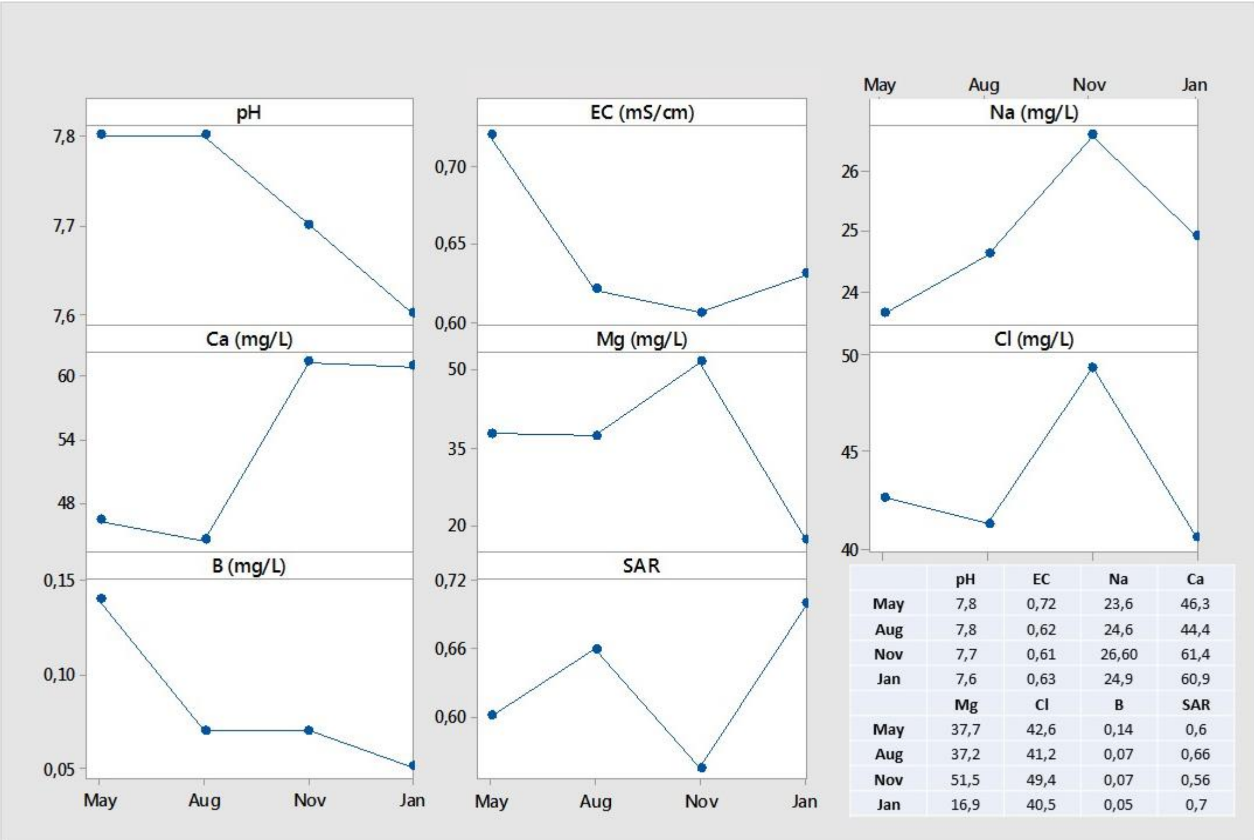


Figure 2: Temporal variations of the measured parameters in irrigation water

In respect to the temporal variations of the measured parameters during the 4 sampling periods (fig.2), it is evident that the values fluctuate according to the dominant hydrological conditions (wet and dry hydrological period), the followed irrigation practices, and secondary hydrogeological/ hydrogeochemical process triggered by water recharge/abstraction.

Specifically, the pH slightly decreases from the dry (May, Aug) to the wet (Nov, Jan) hydrological periods, a general trend which is also followed by Boron. Variations of Chlorides and Sodium are minor and practically their values are constant or slightly modified during the four sampling periods. Similarly, Calcium remains constant during the dry periods and increases during the wet, during which it remains practically stable. The same trend is also followed by Magnesium; however, a sharp decrease is identified from November to January. The EC values are progressively decreasing from

May to November, with a slight increase during January. Finally, the SAR values appear a slight increase during the dry hydrological periods as expected, and eventually decrease towards the wet period (Nov); nevertheless, a significant increase is observed from Nov to Jan, corresponding to an increase of 20% for its value.

5. DISCUSSION

Regarding salinity risk assessment for the entire hydrological year, the collected samples may be classified into two groups according to Ayers ad Westcot (1985): a) no risk (EC<0.7 mS/cm) and, b) low to medium risk (0.7<EC<3 mS/cm). No sample of high risk (EC>3 mS/cm) was identified. The first group contains 32 samples (71%), whilst the second one 13 (29%).

The infiltration of water in soils is chiefly dependent on the overall salinity of the irrigation water, expressed by the SAR (fig.3) and EC values. Based on their compilation, the samples may be classified in two groups: a) 0<SAR<3 and EC<0.7, corresponding to negligible risk (29% of samples), and b) 0<SAR<3 and 0.7<EC<3, corresponding to low-medium risk (71% of samples). The use of irrigation waters belonging to group "a" does not hider any risk for plots; whilst, for the second (b) group, attention is needed in order to monitor regularly the SAR values or decrease of infiltration capacity.

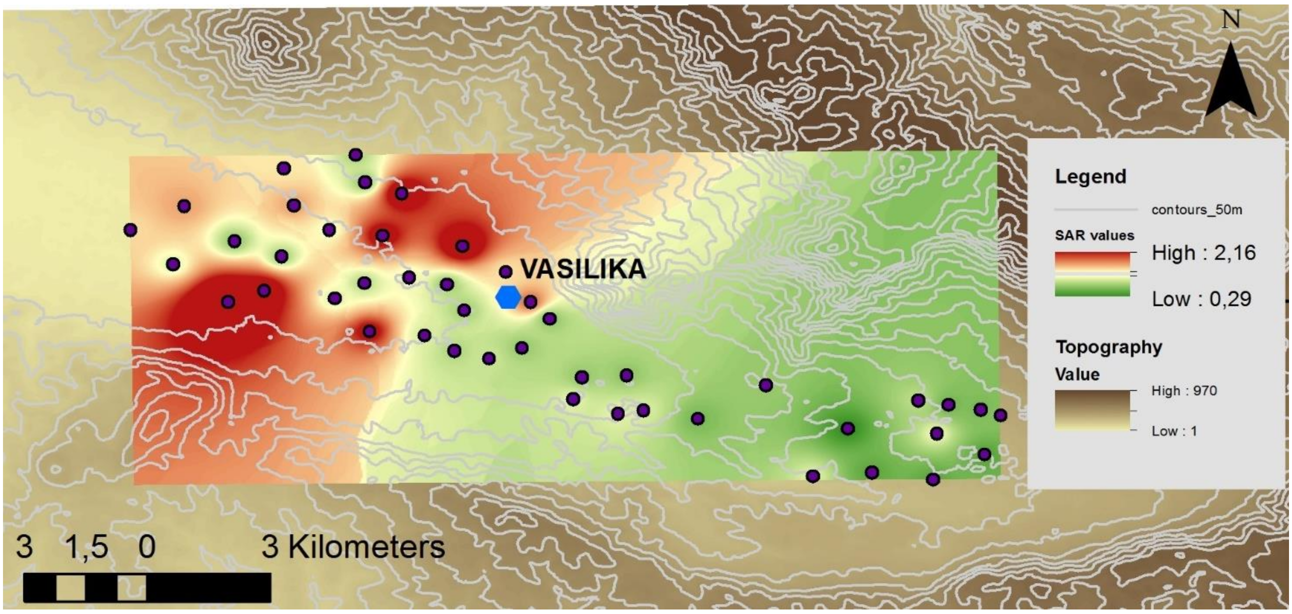


Figure 3: Spatial interpolation (IDW algorithm) of SAR values in the study area

Regarding the toxicity of other parameters to crops, there is negligible risk from sodium and chlorides, apart from few boreholes (2 and 1, respectively) whose sample impose low to medium risk. In respect to Boron, most of its values are low, thus toxicity risk is negligible; however, few values mainly at the northwestern part are elevated (up to 2.87 mg/L), denoting a significant impact to crops, especially to boron sensitive crops such as the vegetables and vineyards. The elevated values of Boron to groundwater are likely to be attributed to geogenic factors related to the hydrothermal activity (Tziritis et al., 2016) of the wider area. In respect to pH values, they do not have impact to crops when considered individually, but jointly with other parameters. However, none of the samples appear to have pH values which may under circumstances cause adverse effects to crops.

Accumulation of salts in soils is a relatively slow process, triggered mainly by two factors: a) salts contained in the irrigation water which are accumulated in the upper soil horizon, and b) by salts which are contained in a low-depth phreatic aquifer and are accumulated through hyporheic transport or evaporation as the soil horizons. A supplementary factor is also the application of fertilizers, but their impact is temporary. Nevertheless, when their use is excessive, fertilizers may cause salinization impacts. In order to sufficiently manage irrigation water and minimize salinization risk, a frequent

monitoring scheme of critical parameters should be established. In this context, parameters such as EC, SAR, ESP and pH should be closely monitored jointly with other critical external conditions (such as precipitation), in order to deliver optimal irrigation practices intended to maximize environmental protection and yield.

6. CONCLUSIONS

Totally 45 samples from irrigation boreholes were analyzed for assessing electrical Conductivity (ECw), pH, Sodium Adsorption Ratio (SAR), Na, Ca, Mg, Cl and B. Results revealed that regarding ECw, 71% of boreholes appeared to have values below 0.7mS/cm, hence characterized as of negligible risk, and 29% of the boreholes had values between 0.78-1.1mS/cm, hence characterized as of small to medium risk. The temporal variations of ECw, probably reflect the impact of fertilization; hence, elevated values of May are attributed as the direct impact of accumulated solids due to prior fertilization practices.

Regarding crop toxicity, the risk due to sodium (Na) and chlorides (Cl) appears to be low. The observed temporal variations are attributed to precipitation events during September, which subsequently trigger soil leaching of solutes that slowly (depending on the infiltration conditions) reach the uppermost aquifer with a time-lag following a relative dilution, probably in January. Additionally, the risk due to boron (B) appears to be significant in a few cases accounting for concentrations up to 2.87 mg/L in irrigation water. The temporal variations of boron values should be probably attributed to changes in the hydrogeological conditions. Differentiation in recharge rate that directly influence groundwater level, seem to chiefly impact boron leaching from the subsurface strata. The pH values are within the acceptable range of irrigation waters and the probability of irrigation system clogging due to salinization effects appears to be low to negligible. Nevertheless, agricultural practices including the management of irrigation water resources should be frequently monitored and managed rationally in order to maintain an optimal quality status of water reserves and soils, hence contributing significantly to the sustainable agriculture.

REFERENCES

1. Ayers, R.S. and D.W. Westcot. 1976. **Water Quality for Agriculture**. FAO Irrigation and Drainage Paper No, 29 (Rev 1), Food and Agriculture Organization of the United Nations.
2. Ayers, R.S., and Westcot, D.W., 1985. Water quality for agriculture. F.A.O. **Irrigation and Drainage** Paper 29:99-104, Rev.1.
3. Bauder, J. W. and T.A. Brock. 2001. "Irrigation water quality, soil amendment, and crop effects on sodium leaching." **Arid Land Research and Management**. 15:101-113.
4. Bauder, J.W. 2001. **"Interpretation of chemical analysis of irrigation water and water considered for land spreading."** Personal communication. Montana State University, Bozeman, Montana.
5. Buckman, H.O. and N.C. Brady. 1967. **The nature and properties of soils**. The MacMillan Company, New York, New York
6. Fikos, I., Ziankas,m G., Rizopoulou, A., Famellos, S. (2005) water balance estimation in Anthemountas river basin and correlation with underground water level. **Global nest Journal** 7(3):354-359
7. Geogenic Cr oxidation on the surface of mafic minerals and the hydrogeological conditions influencing hexavalent chromium concentrations in groundwater, **Science of the Total Environment**, 514, 224-238.
8. Hanson, B., S.R. Grattan and A. Fulton. 1999. **"Agricultural Salinity and Drainage."** University of California Irrigation Program. University of California, Davis.

9. Kazakis, N., Kantirais, N., Kaprara, M., Mitrakas, M., Vargemezis, G., Voudouris, K., Chatzipetros, A., Kalaitzidou, K., Filippidis, A. (2016) Potential toxic elemets (PTES) in ground and sprig waters, soils and sediments: an interdisciplinary study in the Anthemountas basin, N. Greece. **Bulletin of the geological Society of Greece**, vol.L, P.2171-2181

10. Kazakis, N., Kantiranis, N., Voudouris, K.S., Mitrakas, M., Kaprara, E. and Pavlou, A., 2015.

11. McFarland, M., Lemon, R., and Stichler, C., (2002). **Irrigation water quality: Critical Salt Levels for Peanuts, Cotton, Corn and Grain Sorghum**, Texas Cooperative Extension, Texas.

12. Pereira, H., Marques, R.C. (2017). An analytical review of irrigation efficienvy measured using deterministic and stochastic methods. **Agricultural Water Management** 185:28-35

13. Reeve, R. C.; Bower, C. A.; Brooks, R. H.; Gschwend, F. B. (1954). "A comparison of the effects of exchangeable sodium and potassium upon the physical condition of soils". **Soil Science Society of America Journal**. 18 (2): 130

14. Singh, A. (2018). Managing the salinization and drainage problems of irrigated areas through remote sensing ad GIS techniques. **Ecological Indicators** 89:584-589

15. Tziritis, E., Tzamos, E., Vogiatzis, P., Matzari, C., Kantiranis, N., Filippidis, A., Theodosiou, N., Fytianos, K. (2016) Quality assessment and hydrogeochemical status of potable water resources in a suburban area of northern Greece (Thermi Municipality, central Macedonia). **Desalination and Water Treatment** 57:11462-11471

16. United States Development Agency Natural Resources Conservation Service. 2002. Soil Conservationists. **Salinity Management Guide - Salt Management**. Available at http:// www.launionsweb.org/salinity.htm. 2002

17. United States Saline Laboratory Staff. (USSLS), (1954). **Diagnosis and Improving of Saline and Alkali Soils.** United States Department of Agriculture, Washington: USA.

18. Western Fertilizer Handbook. 1995. **Produced by the Soil Improvement Committee of the California Fertilizer Association. Interstate Publishers**, Inc., Sacramento, California, 1995.

GIS-BASED MULTI-CRITERIA DESIGN OF A HYDROMETRIC SYSTEM IN THE ATTICA REGION

E. Theochari[1], E. Feloni*[1], A. Bournas[1], D. Karpouzos[2], E. Baltas[1]

[1]Department of Water Resources and Environmental Engineering, School of Civil Engineering, National Technical University of Athens, 5 Iroon Polytechniou, 157 80, Athens, Greece
[2]Department of Hydraulics, Soil Science and Agricultural Engineering, School of Agriculture, Aristotle University of Thessaloniki, University Campus, 54124 Thessaloniki, Greece

*Corresponding author: e-mail: feloni@central.ntua.gr, tel : +302107722413

Abstract
The lack of adequate hydrological data affects the ability to model, predict and take measures for catastrophic events, such as floods and droughts, which have obvious negative impacts on public health and socio-economic aspects. The collection of stream flow and stage-gauge measurements that are accurate and representative for a watershed is necessary; however, it is difficult to decide for an optimum stage-gauge station location. This research work presents a methodological framework based on Geographical Information Systems (GIS) techniques and multi-criteria decision-making (MCDM) for the optimal design of a Hydrometric Station Network. The implementation was held in seven basins in Attica region, namely Sarandapotamos, Giannoula, Eschatia, Erassinos, Rafina, Haradros and Rapendossa. These basins face an existing flood hazard, especially in the residential areas. In the context of the optimal network design, different criteria, such as morphology, land cover, network density, and general guidelines of the World Meteorological Organization (WMO) were taken into consideration. The criteria weights were estimated with the use of Analytic Hierarchy Process (AHP) and the final results, based on the Weighted Linear Combination (WLC), indicated the optimal hydrometric stations locations for each basin. Furthermore, a sensitivity analysis on factors weights was performed and presented indicatively for Eschatia basin.

Keywords: hydrometric station network; river monitoring; floods; GIS; MCDM

1. INTRODUCTION

The collection of stream flow data that are accurate and representative of water resources is considered necessary, since the lack of adequate hydrological data affects the ability to model, predict and plan for catastrophic events such as floods and droughts which have obvious negative impacts on public health and socio-economic aspects (Hong et al, 2016). The monitoring of the components of the hydrological cycle including rainfall, groundwater characteristics, as well as water quality and flow characteristics of surface waters is called Hydrometry (Boiten, 2008). The most widely used monitoring tools to measure the river flow are the stream gauge stations. In order to correctly acquire these measurements, a hydrometric station networks should be applied. The objective of setting a hydrometric station network is to address all concerns in order to provide timely, quantitative and comparable information, as well as, to design a comprehensive, comprehensible and effective network that provides coverage in all river basins where flow data are required (Hong et al, 2016). The extend and number of the hydrometric stations depends on the specific purpose of recording the stream flow, such as the hydrological study of a region, the floods prevention and the proper technical works design. The need to monitor river flow is also in line with the objectives of the European policies, and particularly with the Directive 2007/60/EC (EU, 2007) on the assessment and

management of flood risks. The configuration of this directive resulted as a need after devastating flooding that struck Europe during the period 1998-2002. Since the hydrological and flood regime in Europe varies, because of the high variability of the relief and the climate among different regions, severe floods have been observed not only in residential areas but also in rural, cultivated land.

More specifically in Greece, due to the high spatial variability of hydroclimatic conditions and the complex topography, flood events are one of the most frequent natural disasters. Particularly for the Attica region, despite the dry climate, extreme rainfalls occurring in small time scales, show a rise compared to other regions of the country, leading to an increasing number of flash-flood events. Floods in Attica has cost more lives (182 people) during the last century (1887-2011) while the cost in human lives due to flooding for the whole country during the same period has been 284 people (Karagiorgos et al, 2012). It is a fact that flood risk is exacerbated by the extreme interference of the anthropogenic environment into the natural characteristics of a basin, thus often leading to the production of insoluble flood-related problems in order to management them (Diakakis, 2012; 2014). The lack of stage gauge stations is one of the most decisive factors in the context of an integrated system for the river monitoring and the civil protection warning in case of an emergency.

This study presents a method using Geographical Information Systems (GIS) with the aim of designing an optimal Hydrometric Station Network according to a set of proposed geomorphological, technical and spatial criteria. A basic application of optimization in network design is to maximize information with respect to minimizing cost (Mishra and Coulibaly, 2009). With respect to this scope, the minimum number of station per watershed in combination with the optimal site selection are the main objectives of the procedure. The proposed methodology is implemented in seven watersheds of Attica. The entire procedure is treated as a multi-criteria decision-making (MCDM) problem with the scope of the best position determination, using the pairwise comparisons of the Analytic Hierarchy Process (AHP) developed by Saaty (1977) as a way to estimate the factors weights and the Weighted Linear Combination (WLC) to estimate the final scores (FS).

2. STUDY AREA AND DATA USED

Seven watersheds in Attica region were selected for the implementation of the proposed method, as they have an extensive natural hydrographic network, they morphologically diverse and face severe flood problems after intense rainfall and most of them are ungauged. There watersheds are depicted in Figure 1. Regarding the data used in the present study, seven layers were initially created:

(i) Digital Elevation Model (DEM) for the Attica region obtained by the National Cadastre & Mapping Agency of Greece. The DEM has a pixel size of 5x5m, its geometric accuracy RMSE is z ≤ 2,00m and the absolute accuracy ≤ 3,92 m for a 95% confidence level. This raster layer has been used for the slope raster, flow accumulation raster and the river network extraction, with the aid of the Surface and Hydrology Toolsets of ArcToolbox (ESRI, 2010). Additionally, the layer of watershed has been created using this DEM. Finally, a layer produced after this procedure is the confluence of stream branches.

(ii) Historic floods of the region. This layer is a combination of freely available data from the Ministry of Environment and Energy and from geocoded data that correspond to the Fire Service operations in flooded properties the last 15 years.

(iii) Land cover map from CORINE Land Cover (2012), for the extraction of the margins of settlements.

(iv) The basemap of National Cadastre & Mapping Agency of Greece (Fig.1) for the evaluation of the GIS-based river network extraction.

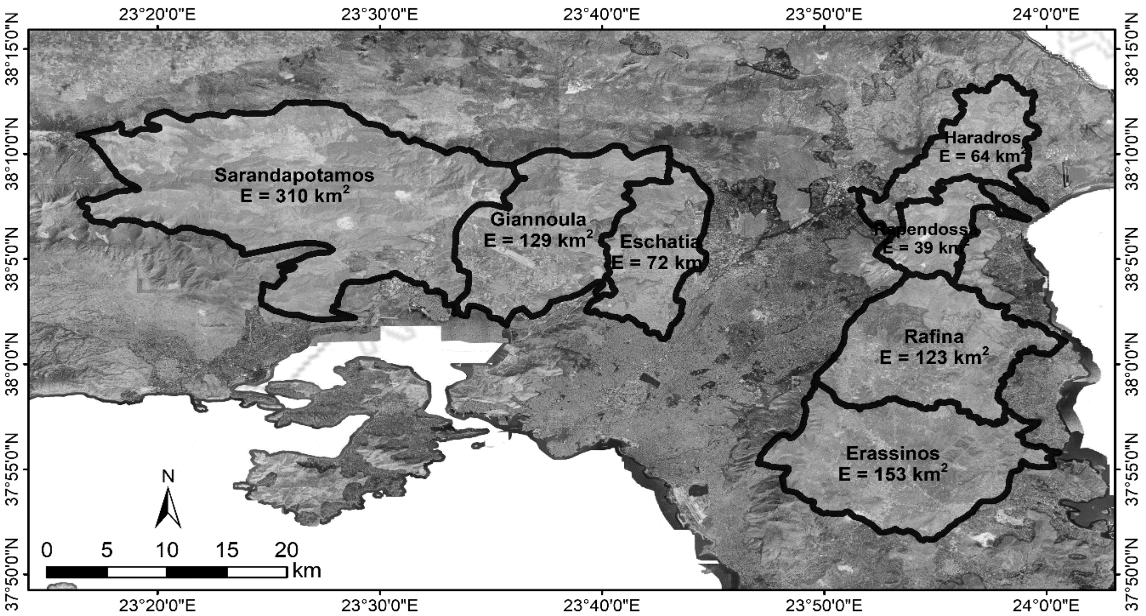


Figure 1: Study areas in Attica (Basemap ©National Cadastre & Mapping Agency of Greece).

3. METHODOLOGY

The aim of this study is the optimal positioning of a Hydrometric Station Network as a proposed methodology implemented in seven basins in Attica region. The methodology followed concerns a multi-criteria GIS-based decision analysis. Generally, decision problems that include geographic data are referred to as geographic or spatial decision problems (Malczewski 1999; 2004). These problems often require that a large number of feasible alternatives must be evaluated on the basis of multiple criteria. Consequently, many real-world spatial problems can lead to multi-criteria decision-making (MCDM) based on the geographic information system (GIS). The problem addressed in this study is a *spatial* decision problem as it includes a large number of geographic data and is also based on GIS techniques for its solution. For this purpose, multi-criteria decisions were made, following the methodology of the Analytical Hierarchy Process (AHP). In this framework, Multi-Criteria Decision Analysis (MCDA) aims to develop standardized procedures that help decision-makers (i.e., station network designers) to solve various problems (i.e., site selection) by linking factors (i.e., geomorphological, technical, etc.) associated with the problem. MCDA is a process that combines and transforms geographic data (inputs) into a resulting decision (output), it defines a relationship between "input maps" and "output maps". Geographic information can be defined as georeferenced data processed in a form that is meaningful to the recipient. Data in the GIS are usually organized as separate thematic maps referred to as ‘layers’. Firstly, the general problems as well as the individual objectives are identified, criteria and alternatives are then identified. Criteria may be factors and constraints related to the spatial problem. The second step of the analysis is related to the criteria values standardization and constraints determination. Then, decision-makers should select the method of composing the criteria and determining the relevant weights, in order to produce the final results and any alternatives. Finally, the proposed solutions are based on the evaluation of alternative options (Drobne and Lisec, 2009). There are many ways in which decision criteria can be combined into MCDA. The Weighted Linear Combination (WLC) and its variants require an aggregation of the weighted criteria. The Analytical Hierarchy Process (AHP) is used in WLC in the stage of factors’ weights estimation. AHP was proposed by Saaty (1977) and is based on the principle that, for making a decision, decision maker's experience and knowledge is as important as the available data. This technique was first developed with a variety of analytical resources, while the use of GIS techniques

was first introduced by Rao et al. (1991). AHP method implementation is divided into the following steps:

(i) Deconstruction of the problem studied in a hierarchical (or network) model, made up of its basic components, allowing for pairwise comparisons.
(ii) Comparative assessment of each component - criterion.
(iii) Composition of the evaluated criteria in order to produce the final results.
(iv) Optimal position determination.

The application of the method therefore includes two general phases, the structure of the hierarchy and the stage of evaluation of the individual criteria. The current application, which is based on the idea of pairwise comparisons of different criteria according to the subjective (personal, empirical, bibliographic, field research, etc.) view of the researcher, determines the relative significance by comparing the criteria per two of them. These pairwise comparisons are based on the fundamental comparison scale introduced by Saaty (1977) (Tab. 1).

Table 1: Scale for pairwise comparison (Data adopted by Saaty, 1977).

Numerical value	Description of importance
1	equal
2	equal to moderate
3	moderate
4	moderate to strong
5	strong
6	strong to very strong
7	very strong
8	very strong to extremely strong
9	extremely strong

In Saaty's technique, weights come from a series of operations of a matrix of comparable pairs among the criteria. The comparisons concern the relative relevance of the two criteria related to the determination of suitability for the intended objective. To assess the weight of each criterion, the following procedure is followed:

1. Column values of each matrix of comparable pairs are assumed.
2. Division of each matrix element with the sum of its column previously found.
3. Calculation of the average of the data for each matrix sequence that occurred in the previous step

The resulting averages are the weights of the criteria (Drobne and Lisec, 2009). A check follows in the consistency of the comparison of the criteria and the severity factors that have emerged. The consistency ratio (Eq. 1) should not overcome the value of 10% in order to consider the hierarchy and the comparison between the primary factors and to accept the resulting weighting factors. Saaty suggests that weights should be reassessed by changing uterine elements if the limit of CR ≤ 0.10 does not apply. The consistency ratio is calculated as:

$$CR = \frac{CI}{RI} \tag{1}$$

A further procedure is the standardization of the criteria by categorizing each of them into a single grading scale (eg., between 0-1). This step aims to create comparable sizes for each criterion is order

to result in a final score (FS) of the same scale. Voogd (1983) reviewed a variety of standardization processes, usually using minimum and maximum values as scaling points. The simplest way to perform this standardization is by using a linear transformation as shown in Eq.2a when the maximum value of the criterion corresponds to the best case and Eq.2b when it corresponds to the worst case.

$$x_i = \frac{(FV_i - FV_{min})}{(FV_{max} - FV_{min})} \cdot SR \quad (2a)$$

$$x_i = 1 - \frac{(FV_i - FV_{min})}{(FV_{max} - FV_{min})} \cdot SR \quad (2b)$$

The last step of the method involves creating and calculating the required level of information regarding the suitability of the areas for the optimal positioning of a Hydrometric Station Network in specific basins. Therefore, the suitability map should be developed. The WLC is incorporated into the GIS environment through Raster Calculator (Map Algebra Toolset) and the FS is calculated then as follows:

$$FS = \sum w_i x_i \quad (3)$$

In cases where the Boolean constraints also apply, the process can be modified by multiplying the FS value with the product of constraints (c_i):

$$FS' = \sum w_i x_i \cdot \prod c_i \quad (4)$$

The scores are calculated for all alternatives and the appropriate number of sites (i.e., these with the highest FS) is all selected. The final number of stations per watershed was defined according to the World Meteorological Organization (WMO, 2010) guidelines for the Hydrometric Station Network density (Tab. 2).

Table 2: Density of Hydrometric Station Network (2010).

Type	**Density**
Coastal	1 station *per* 2750km^2
Mountainous	1 station *per* 1000km^2
Hilly	1 station *per* 1875km^2
Plains	1 station *per* 1875km^2
Small islands (area<500km^2)	1 station *per* 1985km^2
Polar, arid	1 station *per* 20000km^2

For the implementation of the MCDM in the hydrometric station design, different criteria were selected. The ideal gauge site satisfies the following criteria, many of which are defined in WMO (2010):

I. The general course of the stream is straight for about 10 times the stream width, upstream and downstream from the gauge site.
II. The total flow is confined to one channel at all stages and no flow bypasses the site as subsurface flow.
III. The stream-bed is not subject to scour and fill and is relatively free of aquatic vegetation.
IV. Banks are permanent, high enough to contain floods, and are free of brush.
V. Upstream of the station location, a pool is formed in order to ensure a recording of stage at extremely low flow, and to avoid high velocities at the stream ward end of stage recorder intakes, transducers, or manometer orifice during periods of high flow. The sensitivity of the control should be such that any significant change in discharge should result in a measurable change in stage.

VI. The gauge site should be far enough upstream from the confluence with another stream or from tidal effect to avoid any variable influence from another stream or the tide which may affect the stage recording.

VII. The site should be readily accessible for ease in installation and operation of the gauging station.

According to the aforementioned criteria, in the present study the following were taken into account:

1. The density of stations according to WMO guidelines,
2. Distance from settlements,
3. Distance from the flood-prone area,
4. Topographic slopes,
5. Distance from confluence with another stream.

For the estimation of the criteria' weights, the QGIS plug-in Easy-AHP tool (https://plugins.qgis.org/plugins/EasyAHP/) was used, which includes the Pairwise Comparison and Weighted Linear Combination (WLC) analysis. As the tool operates in a GIS environment, it is capable for land use, agricultural, disaster management, environmental resources and relevant applications. The user-friendly interface makes the analysis easier by dividing operations to different steps. According to the relevant significance of design criteria, slopes (C1) is the most important and then the criteria of distance from confluence (C2), distance from settlements (C3) and distance from flood-prone areas (C3) follow (Tab. 3). Accordingly, other spatial characteristics were considered as constraints (c_i). Table 4 summarizes the way that the eight factors were involved in the procedure.

Table 3: Pairwise comparison matrix and AHP results.

	Criteria				**AHP Indicators**		**Weights**	
	C1	C2	C3	C4				
C1	1	3.03	4	7.042			C1	0.529
C2	0.33	1	3.03	8.0	λ	4.148	C2	0.303
C3	0.25	0.33	1	2	CI	0.049	C3	0.112
C4	0.142	0.125	0.5	1	CR	0.054	C4	0.056

Table 4: Criteria and GIS-procedure.

Factor ***(criterion/constraint)***	**Standardizatio n procedure**	**Constraints**	**Remarks**
1. Surface Slope	2b	-	Technical Criterion of maximum importance
2. Distance from settlements	2b	Boolean Map '1' (buffer 500m) ; '0' (d<500)	Mosaic with "Euclidean distance"raster Flow accumulation layer for the upstream-downsteam identification
3. Distance from floods	2b	Boolean Map '1' (buffer 1000m) ; '0' (d<1000)	Based on the historic floods Mosaic with "Euclidean distance"raster layer Flow accumulation layer for the upstream-downsteam identification
4. Distance from confluence from another stream	2a	Boolean Map '1' (buffer 250m) ; '0' (d<250)	Technical Criterion Point Feauture class of confluence sites Mosaic with "Euclidean distance"raster layer
7. Elevation (station density)	Definition of station number	-	It is performed for the final selection of stations. The number of stations per zone is based on the values of Tab. 3.4 and positions of maximum score are finally selected for each basin.
8. River	-	Boolean Map '1' (in channel) ; '0' (out of channel)	-

4. RESULTS AND DISCUSSION

The implementation of the WLC per watershed provides different FS per grid along the mainstream of the hydrographic network. Final scores vary significantly, and as a more representative way to group the results, Fig. 2 shows the frequency (i.e., the normalised number of cells per basin) of FS in five clusters. It should be noted that as the FS increases the number of cells decreases, as expected, but some exceptions can also be found.

- For Sarandapotamos basin, 7.8% of possible locations meet a final score of 90% or more. The majority of the optimum proposed locations are seen in the western part.
- For Erassinos basin, which is the only watershed with low slopes, a high number of locations meet the applied criteria.
- For Eschatia basin, only three locations can be characterized as satisfactory for a stage gauge station installation (i.e., FS>90%). These positions marginally meet the proximity constraints. Giannoula basin is also a complicated case as the topography of the watershed leads to low or moderate values of FS. Only 15 locations are indicated as proper for a stage gauge installation according to the methodology followed.
- Haradros and Rapendossa basins are areas with historic floods and for this reason. For these basins, the locations of two and one stations are proposed correspondingly. Erassinos generally appears higher scores for longer distance along the mainstream, but, after the MCDM application, only about 7% of this reaches a FS at least equal to 90%. The corresponding percentage for Rapendossa basin is 3.7%.
- Rafina basin appears a total of 296 locations with a score equal or lower to 60%. Instead, the optimum proposed locations are only 6 with a score higher than 90%. For this basin, an evaluation of the existing network was held and this indicated that two in three stations are in positions of high score.

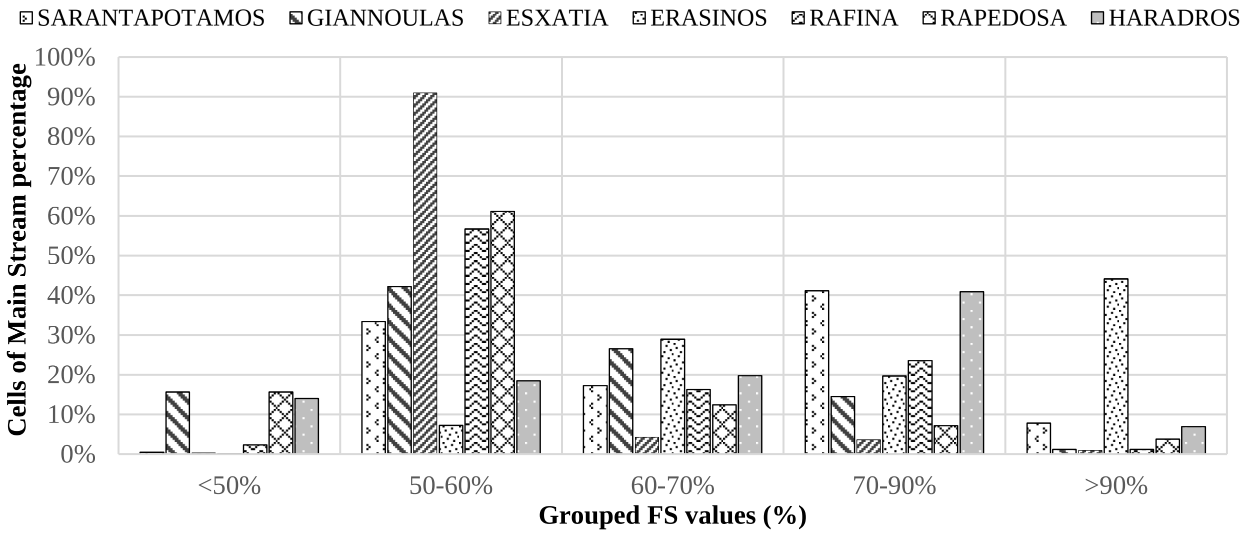


Figure 2: Grouped FS distribution per basin.

Among the positions that reach a FS>90%, these of highest score are selected as the optimal positions (Fig. 3). Concerning the number of stations, which is one in most of the basins, the number derives from the WMO guidelines (Tab. 2). Sarandapotamos basin is an exception, as the current design considers a number of two stations because of the basin's extent. Another exception is Haradros basin, were the installation of two hydrometric stations is also proposed, due to the frequent flash-flooding and the complexity of the basin. Finally, for Vravrona basin, where the archaeological site of Vravrona is located at the plain, the proposed location is upstream enough, in order to operate as an alarming indicator in case of flood occurrence. It should be noted that the installation strategy for a

hydrometric network may differ based on the network design purpose. For instance, when focusing on flood warning purposes, as in this study, a hydrometric station should be placed upstream critical locations, such as settlement, while for water management purposes a hydrometric station should always be installed on or near basin's exit points to allow for rainfall-runoff studies.

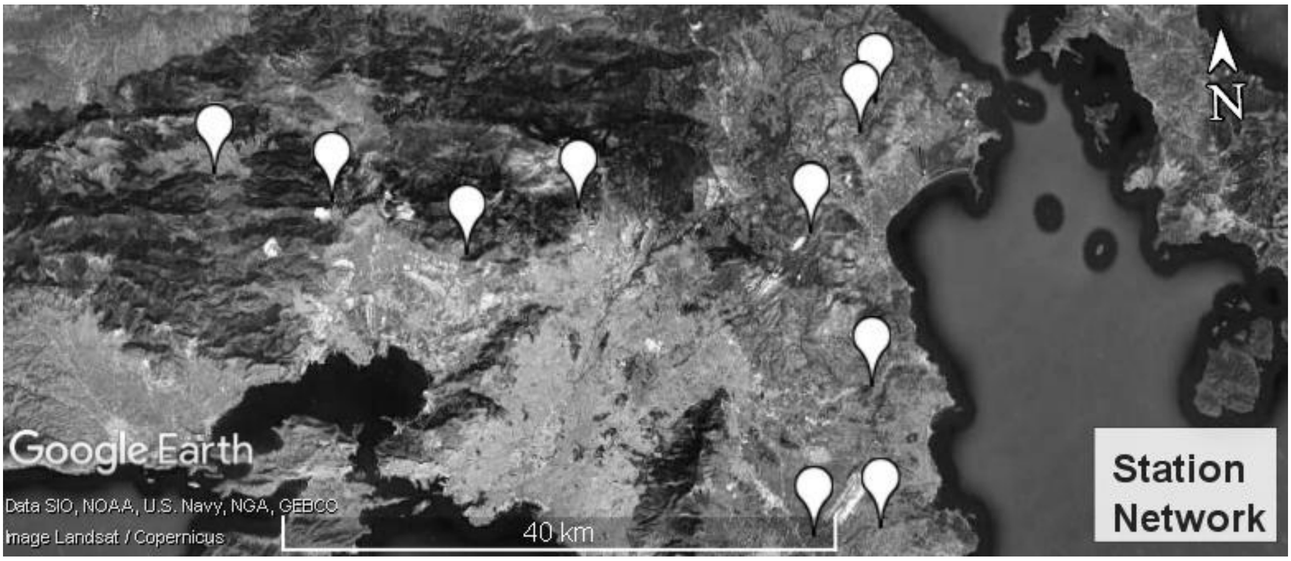


Figure 3: Optimum recommended positioning sites for hydrometric stations at seven study basins

After the proposed AHP procedure, a once-at-a-time sensitivity analysis was conducted by performing an alteration of ± 5% on the weights of slope and flood distance criterion. These criteria are the one of highest importance and the one of lowest importance, correspondingly. The alteration in weights was performed separately and this change is added linearly in the other three criteria each time, in order to quantify the criterion influence in the final results.

Indicatively, Figure 4 depicts two locations in Eschatia basin where the alterations affected significantly the FS values.

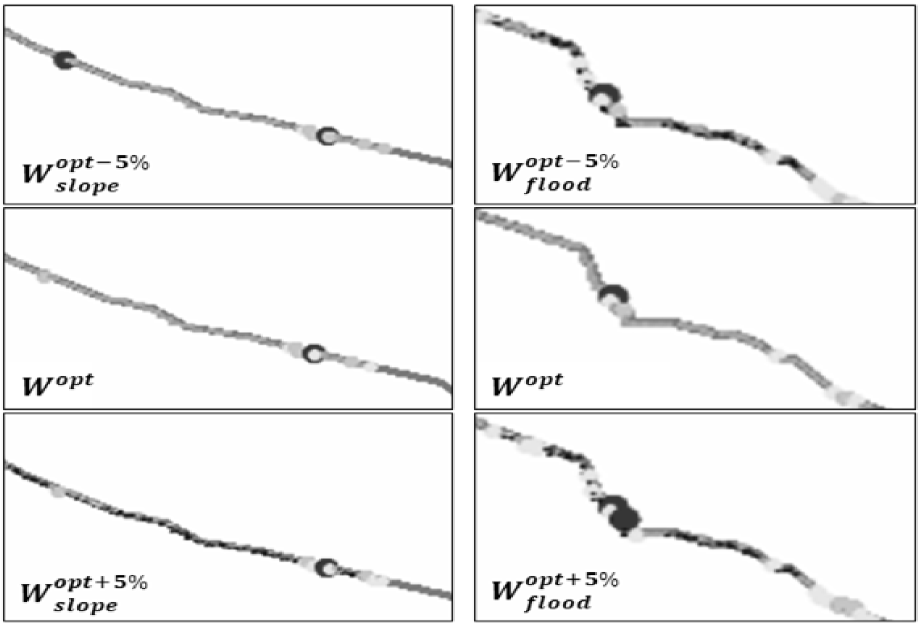


Figure 4: Sensitivity analysis results by altering weights for stream slopes criteria (left panel) and distance from floodplains (right panel). The case of Eschatia basin.

More specifically, in this figure one can compare the middle maps (left panel for the slope criterion and right panel for flood distance criterion) with the upper and lower one. The middle named 'W^{opt}' correspond to FS values as resulted according to the proposed WLC, while the upper named '$W^{opt-5\%}$' (for a decrease of 5% in the criterion weight) and the lower one named '$W^{opt+5\%}$' (for an increase of 5%). In the case where the weight of slopes was reduced by 5%, it is observed that two new proper (FS>90%) locations were obtained; an expected result, as the resilience of the slope criterion increased. Points of FS higher that 90% are marked with a dark circle. When the weight of slopes increased by 5%, then the corresponding number of proposed locations was reduced compared to the original ones (middle map) and the FS of the most locations decreases. In the case of a 5% reduction in the weight of the flood criterion, the proposed locations meet a lower FS. When the flood weight increased by 5%, a new extra optimal location emerged. In the case of the 5% weight increase, new proposed locations are appeared as linearly the weight of the other three criteria are decreased.

5. CONCLUSIONS AND FUTURE RESEARCH

In this research work, a methodology was developed for the optimal design of hydrometric stations network in seven basins of Attica using GIS methods. The methodology was based on multi-criteria analysis and particularly on the Analytical Hierarchy Process (AHP), which was implemented for four criteria. These criteria concern the distance from settlements, the distance of river junctions along the mainstream, the location of historic floods, and the slope along the mainstream. Several constraints to the above criteria were implied, such as securing that the positions are located upstream of settlements and historically flooded areas as well as being deployed in areas of mild slope and away from river junctions. In addition, a sensitivity analysis was performed to evaluate the weight factor of each criterion in the final score. Finally using GIS-based methods for the MCDM process, the proposed hydrometric station positions for all seven basins were defined. The proposed positions have been found to be appropriate for actual station installation. It should be noted however that when designing an optimal hydrometric network station, one must choose between flood prevention and early warning systems, as in this study, where upstream locations of settlements are ideal, and water management purposes, where the exit point of a basins should be sought after for rainfall-runoff studies.

Specific conclusions of this study are summarized as follows:

- By setting a value of FS at least 90% as a satisfactory value, a large number of proposed hydrometric site positions was derived.
- The basin containing the most satisfactory station locations is the Erassinos basin, with a total of 644 suggested locations, while this with the less satisfactory station locations is the Eschatia basin, with only three satisfactory locations.
- From the sensitivity analysis performed for the Basin of Eschatia, it was observed that the most sensitive criterion is the slope along the mainstream.

This study added a variety of findings and, in this framework, some suggestions for future research are proposed.

- The use of remote sensing data in similar applications for larger catchment areas is recommended. In this case, there is no error of the digitization of the stream or of the DEM-based process for the automatic extraction, since the actual position of the stream can be detected by remote sensing applications.
- A more detailed sensitivity analysis may be performed, in order to better evaluate the impact of each criterion in the whole process.

- A different set of rules or new criteria can also be examined, based on the actual hydrometric network purpose such as in cases of water resources management and rainfall-runoff studies where the basin's outlet is an ideal location.

REFERENCES

1. Boiten W., (2008), **Hydrometry**, Taylor and Francis
2. CORINE Land Cover (2012). 'Land cover dataset for 2012.' <https://land.copernicus.eu/pan-european/corine-land-cover/clc-2012> (Aug. 12, 2017)
3. Diakakis M., S. Mavroulis and G. Deligiannakis (2012) 'Floods in Greece, a statistical and spatial approach', **Natural hazards** Vol 62(2), pp.485–500.
4. Diakakis, M. (2014) 'An Inventory of Flood Events in Athens, Greece, during the Last 130 Years. Seasonality and Spatial Distribution', **Journal of Flood Risk Management**, Vol 7(4), pp. 332–343
5. Drobne, S., and A. Lisec (2009) 'Multi-Attribute Decision Analysis in GIS: Weighted Linear Combination and Ordered Weighted Averaging', **Informatica**, 33(4), PAGE
6. ESRI R. (2010) 'Arc GIS Desktop: Release 10', **Environmental Systems Research Institute**, 2010
7. EU (2007) Directive 2007/60/EC of the European Parliament and of the Council of 23 October 2007 on the assessment and management of flood risk.
8. Hong N. T., P. T. T. Truc, N. D. Liem, and N. K. Loi (2016) 'Optimal Selection of Number and Location of Meteo-Hydrological Monitoring Networks on Vu Gia–Thu Bon River Basin using GIS', **International Journal on Advanced Science, Engineering and Information Technology**, Vol 6(3), pp. 324-328.
9. Karagiorgos, K., M. Chiari, and J. Hübl (2012) 'Flood hazard assessment validation based on the Flood Risk Directive 2007/60/EC–a case study in Rafina (Attica, Greece) catchment' Proc. Int. Conf. **12th Congress INTERPRAEVENT**, eds. G. Koboltschnig, J. Hübl and J. Braun.Grenoble, France, 2012.
10. Malczewski, J. (1999) '**GIS and multicriteria decision analysis',** John Wiley & Sons.
11. Malczewski, J. (2004) 'GIS-based land-use suitability analysis: a critical overview', **Progress in planning,** Vol 62(1), 3–65.
12. Mishra, A. K., and P. Coulibaly (2009) 'Developments in Hydrometric Network Design: A Review', **Rev. Geophys**, Vol 47, p.p. 1-24
13. Rao M. S. V. C., S. V. C. Sastry, P. D. Yadar, K. Kharod, S. K. Pathan, P. S. Dhinwa, K. L. Majumdar, D. Sampat Kumar, V. N. Patkar and V. K. Phatak, (1991) 'A weighted index model for urban suitability assessment—a GIS approach', **Bombay Metropolitan Regional Development Authority**, Bombay.
14. Saaty T. L. (1977) 'A Scaling Method for Priorities in Hierarchical Structures. **Journal of Mathematical Psychology**, Vol. 15(3), pp. 234–281
15. Voogd, H. (1983) '**Multicriteria evaluation for urban and regional planning**', London: Pion.
16. WMO) (World Meteorological Organization Manual on Stream Gauging-Volumn 1: Fieldwork, Geneva, Switzerland: **World Meteorological Organization**, 2010.



Sustainable architecture, planning and development - Built environment

LIFE CYCLE ASSESSMENT OF MODERN AND TRADITIONAL MASONRY MORTARS FOR SUSTAINABLE CONSTRUCTION

A. Liapis*, A. Karozou, A. Batsios, M. Stefanidou

Laboratory of Building Materials, Dept. of Civil Engineering, A.U.Th, GR- 54124 Thessaloniki, Macedonia, Greece

*Corresponding author: e-mail: aliapisk@civil.auth.gr, tel : +302310995699

Abstract

Sustainability in construction has become even more essential over the past few decades, mainly due to natural resources overexploitation, as well as an increasing rate at construction-related emissions that contribute to major environmental issues, such as climate change. The rising demands in affordable housing and in the utilization of environmentally efficient alternatives, led to the revival of traditional building materials in modern construction. Clay and traditional materials in general, are considered sustainable materials mainly because of the harvesting method that makes them easy to produce. At the same time, these materials are being used in conservation and restoration of historic buildings, not only for their compatibility with the existing structure, but also for their economic and environmental benefits. For this paper, an effort is conducted to assess the environmental and financial benefits of three of the most common traditional building materials used in the production of masonry mortars: clay, lime and pozzolan. A cement-based mortar is also assessed, as a reference mixture. The environmental assessment is conducted according to the Life Cycle Assessment methodology, a comprehensive tool that is used extensively in construction applications. Along with the environmental assessment, a cost estimation of the different scenarios presents their financial profile and the potential for implementation in the construction industry. The results of the study document the sustainability of the traditional materials and clarify, in a quantitative way, the importance of the utilization of traditional materials in masonry mortars, leading to benefits for both modern construction and conservation and restoration projects.

Keywords: Sustainability, traditional building materials, masonry mortar, life cycle assessment

1. INTRODUCTION

The concept of sustainability, as it was defined by Brundtland in the much renowned report "Our common future" [World Commission on Environment and Development, 1987] considers three areas of interest: environment, economy and society. These areas don't exist separately, but they need to be regarded as a threefold system. Naturally, same rules apply in the field of constructions diachronically: during the design of a construction project, the designer is first interested in the needs and requirements of the people that will use the project, the society where the project will be placed in. The cost is also an important factor that will determine the feasibility of the construction and use of the project. However, these two areas will not result to a sustainable application, if the project doesn't consider the impact that the construction will have to the environment, not only in terms of raw materials and fossil fuel consumption during the construction, but also due to emissions and wastes throughout its life cycle. This environmental impact is the main subject of this study, along with an estimation of costs, in an effort to approach sustainable thinking as much as possible. Due to the complexity of the societal assessment, it is kept out of this study's scope. These for-mentioned

values seem to be valid for ancient masons and they were consistent ethic rules that the masons were following in their building technology [Papayianni et.al, 2007].

The materials that are assessed are utilized here in masonry mortars for traditional and modern constructions. Traditional constructions include mainly restoration and renovation works in structures of important cultural value. However, the sustainable thinking in constructions has led to the revival of traditional building materials in modern structures. Clay, and earthen materials in general, have been connected to human societies for centuries, from monumental structures and simple dwellings to modern constructions of high performance and eco-efficiency [Pacheco Torgal and Jalali, 2012]. The reason for that is the numerous advantages of these materials: lower embodied energy, reduced CO_2 emissions during production, maximum use of locally sourced materials, provision of good sound and thermal insulation, fireproof abilities, healthy living conditions. Under the light of sustainability, earthen structures have been reconsidered and efforts are made for them to be restored and revitalized with proper materials and techniques. On the other hand, there is a revival of the interest on building with earth all over the world (i.e. France, Germany), due to the constructional, economic and environmental benefits.

Moreover, the combination of lime with natural pozzolans rendered mortars of adequate resistance and they formed a type of lime-pozzolan concrete. Many monumental structures of those historic periods were constructed with this concrete, mentioned by many writers as “Roman cement”. Up to 19th century this lime-pozzolan concrete was the dominant material [Papayianni, 1994]. Under the prism of sustainability, the understanding of the diachronic principles of constructions could contribute to maximizing the effectiveness of the contemporary building materials and minimizing their cost and environmental footprint.

2. MATERIALS AND METHODS

The materials considered for this study are all coming from industries mainly located in Northern Greece. Regionality holds an important part in the sustainable design of constructions, not only for the reduction of emissions and costs due to shorter distance transportations, or the more accurate monitoring of depletion of natural resources [Van den Heede & De Belie, 2012], but also for boosting local economies by supporting local businesses. In Table 1, there is an overview of the distances from the suppliers to the construction site, which for this study, is set at the Laboratory of Building Materials, in Aristotle University of Thessaloniki.

Table 1. Distances from materials’ suppliers to construction site.

Material	Supplier	Distance (km)
Cement	Cement industry in Northern Greece	12.1
Clay	Traditional building materials’ supplier in Northern Greece	22.6
Lime (hydrated)	Lime industry in Northern Greece	17.8
Pozzolana	Traditional building materials’ supplier in Northern Greece	22.6
River Sand	Traditional building materials’ supplier in Northern Greece	22.6

In Table 2, the composition of the studied mixtures is being shown. The mixture design is based in common practice as well as the existing experience of the Laboratory of Building Materials in

traditional and modern mortars. The workability achieved was according the regulations for structural mortars based on EN196-1 [CEN, 2016] and EN1015-3 [CEN, 1999]. The cement mortar is coded as CEM, the clay mortar as CLM and the lime-pozzolana mortar as LPM.

Table 2. Mixtures for masonry mortars.

Material	Quantity (kg/m^3)		
	CEM	CLM	LPM
Cement CEM I 32.5N	470.5	-	-
Clay	-	398.5	55.1
Lime, hydrated [$Ca(OH)_2$]	-	-	183.5
Pozzolana	-	-	128.5
River Sand (0-4 mm)	1411.5	996.3	1101
Water	235.3	239.1	249.6

Regarding the environmental impact of the mixtures implementation, it is calculated using the Life Cycle Assessment (LCA) methodology. The methodology is being used since the late 1960's, gaining constantly momentum in industrial, agricultural and other applications, where the environmental burden of the production of goods and services is under study. In late 1990's and early 2000's the International Organization for Standardization published the standards 14040 [ISO, 2006a] - 14044 [ISO, 2006b], where the LCA methodology is described and conducted by four main steps: goal and scope definition, inventory analysis, impact assessment and finally interpretation of the results.

For the goal and scope definition, the aim of the study must be clearly stated. This is also the stage where the boundaries, spatial and temporal, need to be set, along with all the assumptions being made for the assessment, including the functional unit. The step of inventory analysis includes the detailed recording of all the inputs (e.g. materials, energy, transportation, labor, land occupation etc.) and outputs (products, by-products, emissions to air and/or wastes to water and soil) that participate in the production phase of the studied product. The impact assessment step is the heart of the LCA. It is the stage where all the recorded inputs and outputs are related to certain categories of environmental impact categories, such as climate change, eutrophication, acidification, natural resources' depletion etc. The correlation is accomplished by multiplying the inventory analysis results with factors (characterization factors) according to each one's contribution to the environmental issue that is under study. The interpretation of the results is the stage where the assessment is evaluated in terms of fulfilling its goal, and the discussion of the outcome sets the frame for further study. This step is not strictly placed at the end of the assessment, since it can play a monitoring part throughout the whole assessment, evaluating each of the other steps.

3. LIFE CYCLE ASSESSMENT AND COST ESTIMATION

The calculations and the results of the environmental assessment are presented below, following the four steps of the LCA methodology:

3.1 Goal and scope definition

The goal of this assessment is to measure and compare the environmental impact of the production and implementation of three different masonry mortars. The first mortar, which is the reference mixture, is a cement mortar, and is used in modern structures. The second mortar has clay as a binder and is used in modern structures as well as in restoration works. The third mortar is a combination of lime, pozzolana and clay and is used mainly in restoration works and traditional construction. As the

study is about masonry mortars, the functional unit, instead of being a unit regarding volume of mortar mixture (e.g. 1 m^3 of mortar), is set as 1 m^2 of constructed masonry, which, in the writers' opinion is easier to comprehend by a wider audience. For the construction of the 1 m^2 of brick wall, 80 solid bricks are being used, with dimensions of 20x10x5 cm (width, depth, height), and the mortar is to be applied in joints of 1 cm thick. Regarding the boundaries of the assessment, they are characterized as "cradle to gate", which means that the LCA includes the stages of raw material extraction, processing, building materials production, mortar mixing and construction of 1 m^2 of masonry. The stages of use of the construction and its final disposal or recycling after its lifetime has ended, are not considered, because they require data that go beyond the frame of this study.

3.2 Inventory analysis

As it is mentioned in a previous section, the materials (inputs) that are considered for this study are all coming from industries located in the Northern Greece area. The same thing applies also for energy consumption, meaning that, for instance, the electricity mix (sum of electricity that comes from various sources, such as lignite combustion, renewable sources, etc) that was considered is that of the Greek Electricity Industry. To be consistent with that choice, all the emissions and wastes (outputs) had to come from Greek industries as well. However, this proved to be very difficult, because Greek industries either don't have detailed measurements, or if they do, they are not always eager to share such sensitive data. After repeated communication with some of the largest industries of Greece, and the use of literature referring to Greek reality, this obstacle was surpassed. For the few cases, where data was impossible to acquire, the Ecoinvent [Frischknecht et.al., 2005] database was used, which is a much renowned tool for LCA.

More specifically, the emissions for the cement production are a combination of data acquired by Greek cement industries and from the Ecoinvent database, mainly for procedures regarding fuel combustion. For clay, the data regarding materials and energy consumption along with emissions and wastes refer to Greek industries, as they were recorded and presented by [Koroneos & Dompros, 2007]. For the hydrated lime, data where acquired from an industry near the city of Thessaloniki, Greece, with the addition of data regarding energy consumption taken from literature [Moropoulou et.al., 2006], that refer also to Greek industries. The emissions from the extraction of pozzolana and aggregates (sand) are taken from Greek industries. Regarding the bricks, the Ecoinvent database has been used, because a) the emission data are similar to [Koroneos & Dompros, 2007] and b) the bricks are the same for all three scenarios, both in quantity and quality, so they don't really contribute to the variation of the results.
The cost estimation is conducted alongside the environmental assessment, using data from the Greek market, as it was recorded in the second half of 2016, and the first half of 2017.

3.3 Impact assessment

The input and output data that were collected for the inventory analysis step, will now be related to environmental impact categories. The main category that has been chosen for this study is the contribution of the walls' construction to climate change, through their Global Warming Potential (GWP). Each recorded emission that contributes to the impact category is assigned with a Characterization factor, which expresses the magnitude of the contribution compared to the contribution of CO_2. This way, all emissions are expressed in the same unit (kg of equivalent CO_2 per m^2 of constructed wall - kg CO_2 eq/m^2) and can by summarized into one single result. For this study, the assessment is based on the Characterization factors that are proposed by the Intergovernmental Panel on Climate Change (IPCC) [IPCC, 2013], for a 100-year time frame. The results can be seen in Table 3, where they are sorted in three categories: materials, which includes all processes up to the production of bricks and the materials used on site to produce the mortar mixture, transportation, which refers to the transportation of the bricks and mortars' materials to construction site and energy which refers to the energy consumed (electricity) for mixing the mortar on site.

Table 3. Global Warming Potential of the studied scenarios

	CEM	**CLM**	**LPM**
Unit	kg CO_2 eq/m^2	kg CO_2 eq/m^2	kg CO_2 eq/m^2
Materials	47.7	38.8	42.1
Transportation	1.1	1.1	1.1
Energy	0.1	0.1	0.1
Total	48.9	40.0	43.3

Despite GWP, the assessed constructions have a contribution to other environmental impact categories, as well. Some of them (abiotic depletion, acidification, eutrophication and ozone layer depletion) are presented in Figure 1. The abiotic depletion impact category refers to the depletion of natural resources due to extraction of minerals and fossil fuels, and it is expressed in kg of equivalent Antimony (Sb) per m^2 of wall. Acidification refers to the impact of acidifying substances to ecosystems as well as constructions, and it is expressed in kg equivalent SO_2 per m^2 wall. Eutrophication includes the environmental impacts caused by the emission of macro-nutrients in excessive levels, into air, water and soil. It is expressed in kg equivalent PO_4 per m^2 wall. The last category includes the impacts of increased UV-B radiation, due to ozone layer depletion, that affects the health of ecosystems. The same rules as GWP apply in the assessment of all these impact categories, with the Characterization factors following the CML impact assessment method [Guinee, 2002]. For the calculations, the LCA software SimaPro [Goedkoop et.al., 2004] was also implemented.

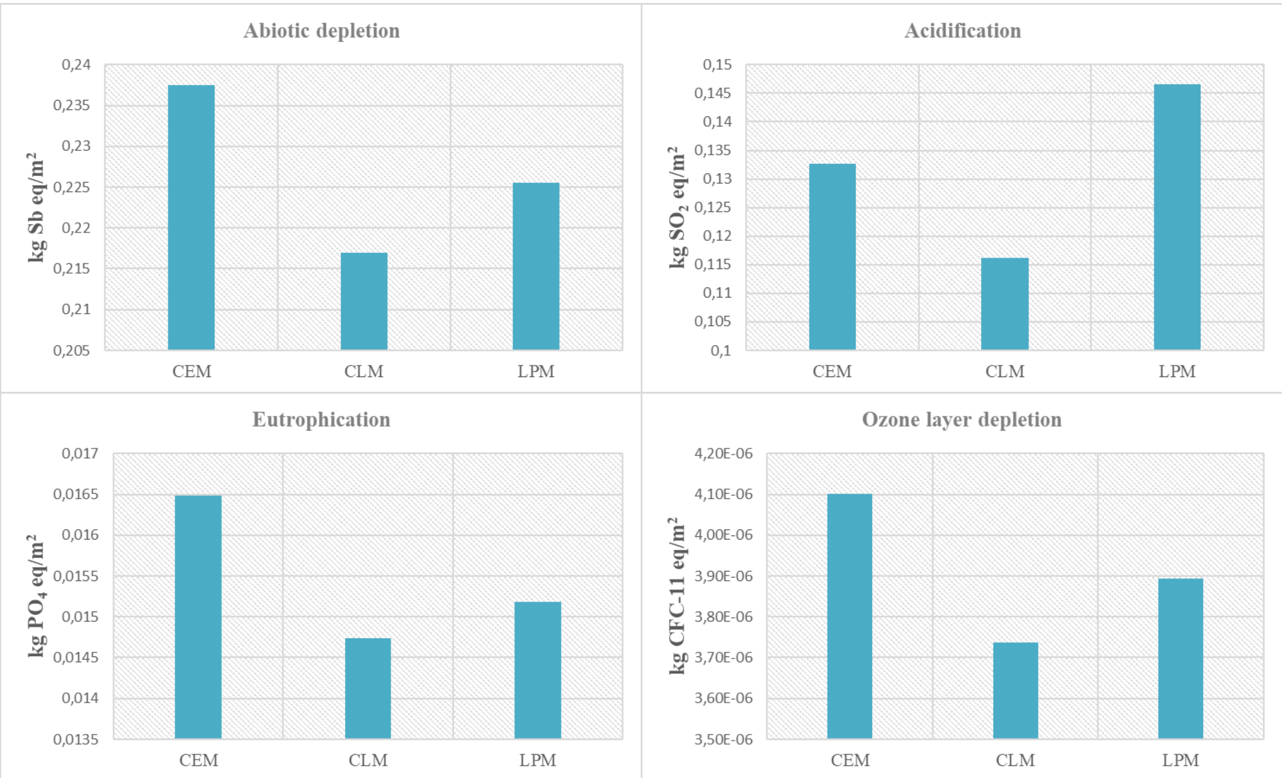


Figure 1. Four impact categories for the construction of 1 m^2 of brick wall, for the three studied mortars.

For the cost estimation, results are shown in Table 4. For each scenario, the cost has been analyzed into three categories: "materials", which includes the costs for the purchase of the bricks and the mortars' constituents, "transportation", which includes the costs for the transportation of the bricks and the mortars' constituents at the construction site, and "construction", which includes the energy costs for preparing the mortars along with the personnel costs for the construction of the 1 m^2 wall.

Table 4. Cost estimation of the studied scenarios

	CEM	CLM	LPM
Unit	€/m^2	€/m^2	€/m^2
Materials	9	8,21	8,26
Transportation	0,36	0,35	0,35
Construction	4,01	4,01	4,01
Total	13,37	12,57	12,62

3.4 Interpretation of the results

The Life Cycle Assessment of the three different scenarios gives an interesting scope for the environmental evaluation of the utilized building materials. Regarding the Global Warming Potential impact category, the construction with cement mortar gives the highest environmental burden, something that was expected considering the intensiveness of emission production during cement manufacturing. The construction with clay mortar has the lowest burden, with lime-pozzolana mortar being somewhere in the middle of the three. This is also expected, because other than some energy consumption for drying and mixing/sorting, clay requires minimum industrial processing to be ready to use. Whatever the distribution of total burden may be, between the three scenarios, the common feature among them is that the materials' production is dominating over the other stages.

The same conclusions apply also for the assessment of the other three environmental impact categories (abiotic depletion, eutrophication, ozone layer depletion). The clay-mortar construction shows the lowest contribution to these environmental issues, with lime-pozzolana following and the reference cement mortar construction giving the higher environmental burden. However, the construction that utilizes the lime-pozzolana mortar contributes most in acidification, mainly due to higher SO_2 emissions during lime production.

Clay shows also a slight advantage over lime-pozzolana when considering costs. Of course, the differences between the three scenarios are minimum for such a small scale (1 m^2 of constructed wall), but the trend can be identified more clearly over larger constructions, where the choice for the most efficient solution will be of great importance. As in LCA, the importance of materials in the overall cost is also very distinct here.

4. DISCUSSION AND CONCLUSIONS

Sustainability in constructions is a diachronic principle which ancient masons followed unremittingly. Nowadays, cement prevails in construction technology and it seems to be an energy and emissions intensive material. This paper proves in a quantitative way the relation between traditional binders and cement in terms of environmental impact and cost. Clay shows the best performance both in environmental and economical assessment. Comparing to the reference mortar (cement) it improves the environmental profile of the studied construction by a rate of 18%, regarding the contribution of the process to climate change, and it is by 6% more cost efficient. In the other environmental impact categories, clay mortar shows a better performance as well, in various rates. The lime-pozzolana mortar is also more environmental and economical efficient than the reference mortar (11% and 5.6% respectively), while in the other environmental impact categories it shows variances, with the

category of acidification being the one where the lime-pozzolana mortar contributes the most of the three scenarios.

For this paper the boundaries of the assessment have been characterized as 'cradle to gate' and the considered phases are extraction of the raw materials, production of building materials and construction. However, it would be useful to consider the whole life of the project, meaning the stages of use and final disposal or recycling, in the framework of future research, where data of durability properties will be utilized. Overall cost is also very distinct here. Moreover, there is an evident need for the composition of national, or even regional environmental databases for the stage of Inventory Analysis, to have more comprehensive results. Academic and industrial research should work for this purpose, within, of course, a national regulative frame.

Acknowledgements
Part of the research was developed within a scholarship, funded by the Act "Support of research manpower, through the development of PhD research", coming from resources of the OP "Human Resources Development, Education and Lifelong Learning", 2014-2020 with support from the European Social Fund and the Greek Government. Also, Author Karozou A. would like to thank the General Secretariat for Research and Technology (GSRT) and the Hellenic Foundation for Research and Innovation (HFRI) for founding the research through the scholarship foundation program for PhD candidates.

References

1. World Commission on Environment and Development. (1987) **'Our common future'**, Oxford: Oxford University Press.
2. Papayianni I., Stefanidou M. (2007) 'Durability Aspects of ancient mortars of the archaeological site of Olynthos', **Journal of Cultural Heritage**, Vol. 8, pp. 193-196.
3. F. Pacheco-Torgal and S. Jalali (2012) 'Earth construction: Lessons from the past for future eco-efficient construction', **Construction and Building Materials**, Vol. 29, pp. 512–519.
4. Papayianni I.(1994) "**Durability lessons from the study of old mortars and concretes"** P.K. Mehta Symposium on Durability of Concrete, May, Nice, France pp.145-153.
5. Van Den Heede P. and N. De Belie (2012) 'Environmental impact and life cycle assessment (LCA) of traditional and 'green' concretes: Literature review and theoretical calculations', **Cement and Concrete Composites**, Vol. 34(4), pp. 431-442.
6. CEN (2016) Methods of testing cement - Part 1: Determination of strength, EN 196-1. European Committee for Standardization (CEN), Brussels.
7. CEN (1999) Methods of test for mortar for masonry - Part 3: Determination of consistence of fresh mortar (by flow table), EN 1015-3. European Committee for Standardization (CEN), Brussels.
8. ISO (2006a) Environmental management – life cycle assessment – principles and framework, ISO 14040. International Organization for Standardization (ISO), Geneva.
9. ISO (2006b) Environmental management – life cycle assessment – requirements and guidelines, ISO 14044. International Organization for Standardization (ISO), Geneva.
10. Frischknecht R., N. Jungbluth, H.-J. Althaus, G. Doka, R. Dones, T. Heck, S. Hellweg, R. Hischier, T. Nemecek, G. Rebitzer and M. Spielmann (2005) 'The ecoinvent database: Overview and methodological framework', **International Journal of Life Cycle Assessment**, Vol. 10, pp. 3–9.
11. Koroneos C. and A. Dompros (2007) 'Environmental assessment of brick production in Greece', **Building and Environment**, Vol. 42, pp. 2114-2123.

12. Moropoulou A., C. Koroneos, M. Karoglou, E. Aggelakopoulou, A. Bakolas, and A. Dompros (2006) Life Cycle Analysis of Mortars and Its Environmental Impact, **Materials Research Society Symposia Proceedings**, Vol. 895, pp. 145-150.
13. Intergovernmental Panel on Climate Change, & IPCC. (2013) '**IPCC Fifth Assessment Report (AR5)'**, WMO, IPCC Secretariat.
14. Guinée, J. B. (2002) '**Handbook on life cycle assessment: Operation guide to the ISO standards'**, Dordrecht: Kluwer.
15. Goedkoop M., M. Oele and S. Effting, (2004) **'SimaPro 6 Database Manual—Methods library'**, v. 2.0, PRé Consultants.

HAZARD ASSESSMENT AND VULNERABILITY REDUCTION IN THE MEDITERRANEAN LANDSCAPE: THE CASE OF CRAPOLLA ARCHEOLOGICAL SITE IN THE SORRENTO-AMALFI PENINSULA, ITALY

L. Boccia*, A. Capolupo, M. Rigillo, V. Russo

University of Naples Federico II, Department of Architecture, Via Forno Vecchio,12- 80134, Naples (NA), Italy

*Corresponding author: e-mail: lorenzo.boccia@unina.it , tel : +39 0812539151

Abstract

The Crapolla Fiord, near to the Amalfi Coast, thanks to its special landscape, can be classified as an example of a Mediterranean landscape, with exceptional cultural and natural scenic values, resulting from its outstanding nature and historical evolution. The area hosts the archaeological site of the San Pietro Abbey, built before the 12th century, and the so-called "monazeni", vernacular constructions used by local fishermen for boat sheltering. At present, the site has been just interested by a deep research experience leaded by the Department of Architecture (DiARC) of the University Federico II. The study, committed by the local Municipality of Massa Lubrense involved a range of specialized knowhow represented by four different departments of the University of Naples Federico II, including an important archaeological survey campaign. As part of the study, the analysis of the surface-water hydrology has carried out at local scale, by the aim of assessing hazard potential for the site conservation. The current land cover is bare soil on a specific rocky substratum, although traces of terraces dating from the time of the Abbey activity are still recognizable. Taking into account the site exposure (South), its land use, as well as the scenario of further climate change - consistent with the A1B like scenario (IPCC, 2014) - the increase of site vulnerability is expected. Starting by these assumptions, the study evaluates the hydrology hazard potential in estimating the variations in flow rates at secondary auctions, comparing current Land Cover and the one at the time of Abbey activity,. Due to both the reduced infiltration capacity and the local climate specific, the increase of hazard potential is expected, as well as the rise of the site vulnerability, and the intensification of the values exposed in terms of losses potential (the immaterial value of the cultural asset) and hence the increase in overall site risk. The study quantifies the hazard potential and demonstrates that the introduction of small interventions aimed at regenerating vegetation and/ or at increasing infiltration capacity, would be justified and sustainable.

Keywords: Risk assessment, Cultural heritage, Climate change impact

1. INTRODUCTION

World Cultural Heritage has been object of dedicated policies of conservation since 1972, when the UNESCO underlined the importance to preserve it and forward it to future generations, enhancing the ethical involvement of each State and each citizen [World Heritage Convention (WHC), Paris, 16 November 1972]. Therefore, the most important, and largely widespread, factors treating cultural and environmental heritage have been investigated by scientists, in order to identify which initiatives have to be undertaken to safeguard those vestiges. To meet that purpose, the key factors to be shifted through are the climate change risk, and, in particular the water cycle [Cassar, 2005; Sabbioni et al.,

2008; 2009]. Indeed, the water cycle rules all the aspects related to the climate changes, such as flood and drought, rainfall extreme events and heat waves, which strongly affect the human settlement and tourism. Moreover, as shown by a research conducted by the Centre for Sustainability Heritage, University College London, in cooperation with the Institute of the climate and atmosphere sciences of the National Research Centre (CNR), “Southern Europe appears to be more vulnerable, although the North Sea coast has a high exposure to flooding” [Sabbioni et al., 2009]. Consequently, climate changes will have a great influence on Italian territory and, in particular, on Campania Region (Southern Italy), characterized by a mild climate. Rainfall events drastically increase the run-off, eroding the mountainside, from top to bottom [Campania Region, 2014]. The lack of vegetation, caused by the several forest fires, occurred in the summer period, exacerbates the erosion process [Campania Region, 2014]. Nevertheless, the Amalfi coast area is not extraneous at extreme rainfall events, like that one occurred on 25th of October 1954, when 500 mm of rain fall occurred in 4 hours causing life losses (318 people dead) and huge damages to the built environment [Caneva et al., 2007].

The detecting of some proper actions for conserving the huge cultural heritage and the great beauty of Campania Region landscape, should be a priority for the Italian Government and the citizens. Therefore, a correct management plan should be provided for considering the natural hazard potential Natural hazard is here intended according to the United Nations definition (2004) as the probability that a harmful occurrence happens. The vulnerability concept is closely linked to the natural hazard notion, since it is related to its consequences, pondered in terms of damages and loses (Fuchs et al., 2007). A synthetic definition of vulnerability was given in the glossary of IPPC 2014: “The propensity or predisposition to be adversely affected. Vulnerability encompasses a variety of concepts and elements including sensitivity or susceptibility to harm and lack of capacity to cope and adapt”. Wilson et al., (2005) specify the main components of vulnerability. Wilson et al., (2005) described the vulnerability as the combination of three elements: exposure, defined as the probability that a damaging event occurred in a specific time, the impact, pinpointed as the consequences of a specific harmful process on some peculiar features, and the intensity, indicated as the magnitude, the duration and the frequency of a particular element. Hence, the need to forecast the risk potential starts in order to properly evaluate hazard potential and its consequences. Further, natural hazard assessment is largely influenced by the scale adopted for the analysis of the slope morphology and surface. So that the scale of the study should be always adapted to the object under investigation [Capolupo et al., 2015b].

The essential baseline for the morphological analysis is the Digital Elevation Model (DEM), as shown by Florinsky, (1998). Therefore, the DEM resolution is an essential factor to be considered to improve the hazard analysis: the highest the resolution is, the most accurate the natural hazard assessment is. Several techniques have been introduced to generate more and more precise DEM over the years, such photogrammetry or Laser Image Detection And Ranging (LIDAR).

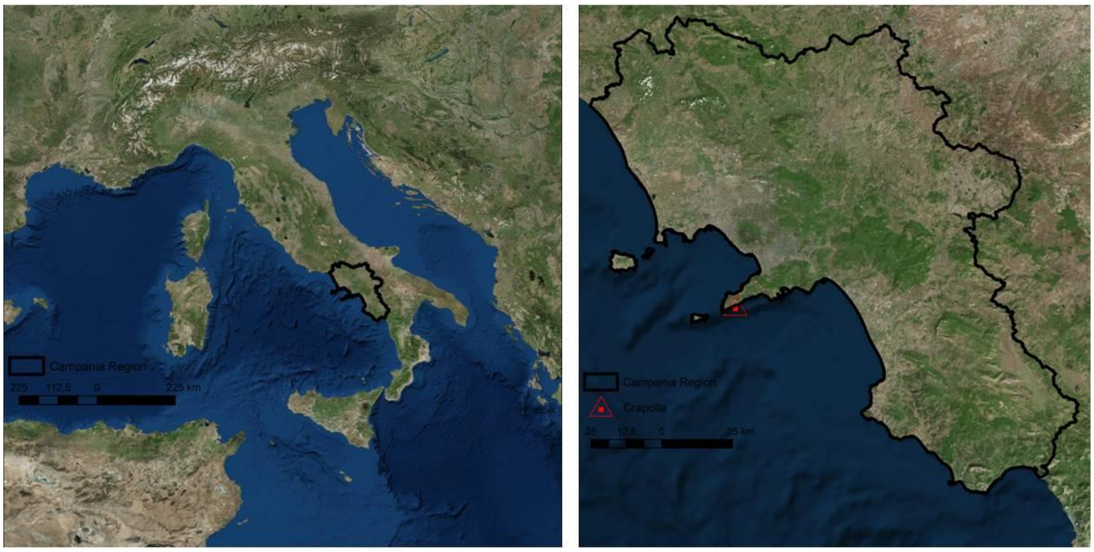
The current paper aims at evaluating the potential natural hazard that could occur in the area of the Fiord of Crapolla located in the Amalfi Coast, Campania Region). This area is worldwide famous for its outstanding landscape and for the presence of historic and cultural goods, potentially subjected to such as extreme rainfall events and land abandonment. Hence, an empirical analysis of the vulnerability has also been introduced.

2. MATERIAL AND METHOD

2.1 Study area

The study has done in the Fiord of Crapolla, an inlet of Sorrento Peninsula. Sorrento Coast is a promontory, interposes between the Gulf of Naples and the Gulf of Salerno, in Campania Region (Southern Italy) (Figure 1). The Peninsula of Sorrento covers an area of 121,14 km^2 and it includes nine municipalities. Although differences in terms of vegetation between the bottom part, characterized by the typical Mediterranean greenwood and scrublands, and the upper part, typified by the temperate forest [Caneva and Cancellieri, 2007; Pindozzi et al., 2016] have found out. The two

sides of promontory have many characteristics in common, such as the presence of terraced landscapes, featuring the local agricultural economy. Although, the area is distinguished by the Mediterranean mild climate, the rainfall events are quite plentiful with not so rare catastrophic showers, as that one above mentioned occurred on 25th of October 1954.



a b

Figure 1: Area under investigation location: 1a) Campania Region location in Italy; 1b) Location of Crapolla Fiord in Campania Region

The Fiord of Crapolla is inhabited since the Roman period, as testified by the archaeological ruins of storage rooms and of other proofs found out on its territory. Its reputation has not been slackened off over the years, indeed, an Abbey, which belonged to the Benedectine Order, was built before 12th century [Russo, 2014]. Unfortunately, the Abbey have been continuously pillaged and destroyed and therefore, just few ruins have been survived (Figure 2). Moreover, that area have been intensely inhabited over the last past years, as testified by the presence of some terraced landscapes, which shape the slope from the top till the bottom [Caneva and Cancellieri, 2007]. Those terraces are subjected to a quick downfall because of the abandonment of agricultural practise on their steps, due to the difficulty of accessing and their inadequate competitiveness in terms of production efficiency [Capolupo et al., under review; Capolupo et al., 2017; Capolupo et al., 2018b; Capolupo et al., 2018c]. Therefore, the terraces are already weakly recognized on the slope morphology (Figure 2).



Figure 2: Details of the study area

2.2 Data Sources

In order to meet the purpose of the research, the dataset refers to two data sources: the rainfall information, provided by Italian National Hydrographic Service in the "Hydrological Annals", and the landform mapping, provided by the Digital Surface Model (DSM) and Digital Terrain Model

(DTM), both commissioned by the Department of Territorial Information System (SIT) of the "Città Metropolitana di Napoli".

The "Hydrological Annals" reports the hourly rainfall data for each year from 1928 until the end of 1990s. Those events are classified in five categories according to the duration of 1, 3, 6, 12 and 24 hours. The weather stations (Figure 3) useful for the investigations have been selected considering two criteria: the distance between the weather stations and the study area and amount of available data. As first, the stations located less than 20 Km and included in the areas territorial compatible with the site under investigation (Figure 4) have been picked. Subsequently, they have been chosen according to the continuity of the series of data. The weather stations used in the consecutive steps are reported in Table 1.

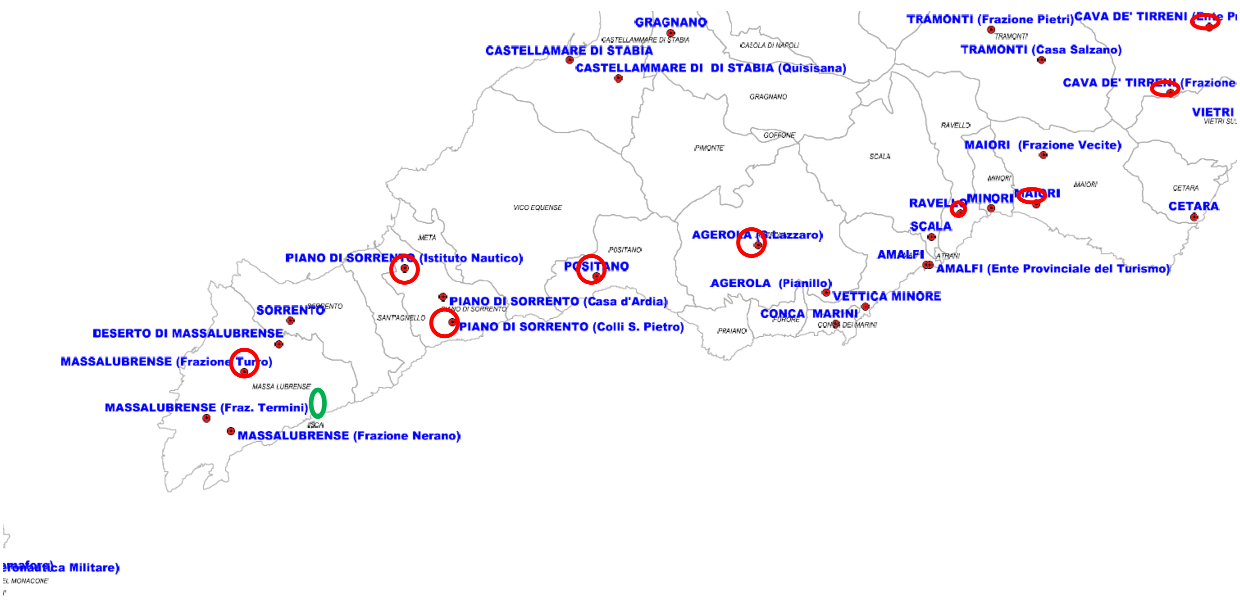


Figure 3: Weather stations close to the study area, identified in the picture with a green circle

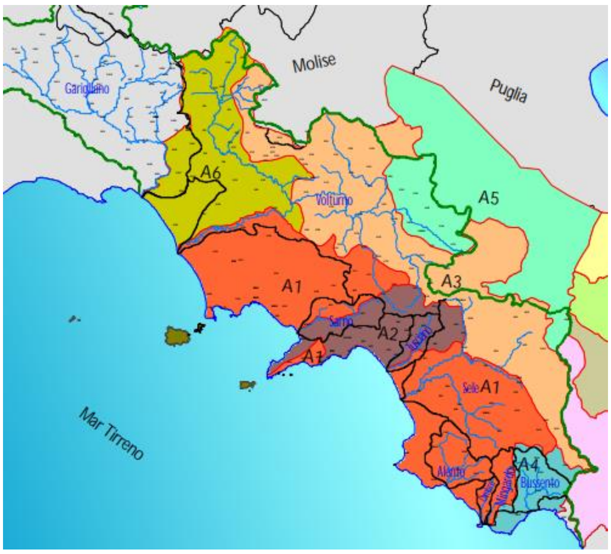


Figure 4 : Wheatear homogeneous areas

The DSM and DTM was obtained by a LIDAR survey in 2009 – 2012. Their resolution was equal to 1 m^2 and the altitudinal range accuracy was of 0.15 m. They have been scanned using 4 points/m^2. Since their raster cells could show some small imperfections, commonly called "pits", which can

create discontinuities in the hydro-graphic scenes, both DTM and DSM have been pre-processed with the ArcGIS' hydrology tool (version 10.1) for filling the holes [Infascelli et al., 2013].

Table 1: The wheatear stations useful for the analysis

Weather station	Quota	Distance from the study area (km)	Period of available data	Number of useful data
Piano di Sorrento San Pietro	309	5	1957-1996	28
Piano di Sorrento Ist. Nautico	122	5.5	1950-1998	28
Massa Lubrense Fraz Turro	250	4	1977-1999	19
Positano	195	10	1928-1943	11
Agerola San Lazzaro	683	16	1928-1966	19
Ravello	315	21	1928-1995	30
Maiori	60	23	1928-1985	34
Cava de Tirreni – Badia	367	23	1955-1984	23
Cava de Tirreni – Ente Turismo	199	21	1956-1996	21

2.3 Rainfall event identification

The rainfall event has been determined using the Gumbel theory, that is considered the most largely widespread procedure for meteorological purposes [Nadarajah & Kotz, 2004]. Actually, this approach is not able to describe the meteorological catastrophic events, like that one occurred in 1954. However, it defines the meteorological probability curves for a specific return period for each class of rainfall data of each selected weather station. It was applied in the current research because the rainfall events considered have relatively short return period (T).

Therefore, the average (μ) and the Deviation Standard (DS) have been computed for each class of information of each weather station. This step was essential since it allows to calculate the parameters needed to describe the Gumbel probability distribution (α and u). The equation of the two parameters are described in Equations 1 and 2, respectively:

$$\alpha = \frac{\pi}{\mathrm{DS} x \sqrt{6}} \tag{1}$$

$$\mathrm{u} = \mu - 0.45 \text{ x DS} \tag{2}$$

Therefore, the rainfall intensity (h) has been computed for each data class of each weather station using Equation 3. Subsequently, the results of each station have been averaged.

$$\mathrm{h_{ij}}(\mathrm{T} = 100) = \mathrm{u_{ij}} - \frac{1}{\alpha_{ij}} \text{x} \ln[-\ln(1 - \frac{1}{\mathrm{T}})] \tag{3}$$

where i is referred to the weather station considered and j to the data class considered.

Considering the limited extension of the mountainside (about 1500 m) and the difference in altitude (about 500 m), a return period less than 1 hour was preferred for the current analysis. Therefore, it was realistic to focus the attention on a return period equal to 0.5 hour. Consequently, the rain intensity on T = 30 minutes was estimated using the formula of Bell (Equation 4) [Bell, 1969] and not spatializing the rainfall events extracted from the weather stations.

h30'(T=100)= h1h(T=100)*(0,54*300,25-0,50) (4)

2.4 Potential hazard assessment

Combining the identification of vegetated areas and the slope analysis allows to identify the flow directions and, consequently, the water accumulated in two different points: the former corresponding to the Fiord of Crapolla and the latter, related to the Abbey of Saint Peter at Crapolla. The vegetated areas have been detected by subtracting the DSM and DTM, while the surface flow direction have been carried out using the eight-direction flow model (D8), implemented in ArcGis (vers. 10.1), since Wolock et al., (1995) and Beaujouan et al., (2001) showed that this approach was suitable for shaping the micro-rill network at field scale. This procedure has been described more in details in Capolupo et al., [2014; 2015a; 2018a]. An outlet has been located on the rill corresponding to the Fiord of Crapolla and another on the micro-rill in the vicinity of the Abbey. Therefore, two basins have been identified.

Thus, the flow rate has been calculated for both conditions by applying Equation 5:

$$Q = A \text{ x } I \text{ x } C \qquad (5)$$

where A is the basin area, I is the rain intensity and C is the coefficient of run-off, which was defined considering the texture and the type of soil. The most vegetated and cultivated areas were characterized by a sandy loam soil, while the zone close to the Abbey is mainly rocky. Therefore, according to the indication of the American Society of Civil Engineers, C was assumed equal to 0.8 for T = 100 and 0.5 for T = 1 for the rocky zone and, equal to 0.2 (T=100) and 0.15 (T=1) for the sandy loam soil.

3. RESULTS

3.1 Rainfall event

The rain intensity, considering a return period equal to 100 years (T=100), related to all the weather stations suitable for the research, is reported in Table 2. The weather station of Massa Lubrense has been the closest one to the site under investigation. It shows a very high value of rainfall, comparing to the other stations. Indeed, for the examined cases (1h, 3h, 6h, 12h and 24h) the rainfall intensity is equal to 130 mm, 139 mm, 142 mm, 151 mm and 158 mm, respectively; on the contrary, the station of Ravello has a value equal to 54 mm, 81 mm, 124 mm, 153 mm and 180 mm, respectively; the rainfall intensity is equal to 76 mm, 104 mm, 125 mm, 140 mm and 156 mm, respectively; the station of Piano Sorrento (S. Pietro) is equal to 69 mm, 83 mm, 96 mm, 129 mm and 151 mm, respectively. That situation depends on the discontinuity of the available data and on the presence of an exceptional event occurred in 1992, that has a great influence on the final result. Therefore, that information is not reliable and it was preferred to assume that the rain intensity varies between 70 and 130 mm in 1 hour, considering a return period equal to 100 years.

Table 2 : Rain Intensity considering (T=100)

Weather stations	Rainfall intensity (h) in 1h (T=100) (mm)	Rainfall intensity (h) in 3 h (T=100) (mm)	Rainfall intensity (h) in 6 h (T=100) (mm)	Rainfall intensity (h) in 12 h (T=100) (mm)	Rainfall intensity (h) in 24 h (T=100) (mm)
Ravello	54	81	124	153	180
Piano Sorrento (Istituto Nautico)	76	104	125	140	156
Piano Sorrento (S. Pietro)	69	83	96	129	151
Massa Lubrense	130	139	142	151	158

Because of that variability of data, the rain intensity in 30 minutes was obtained using the Bell's equation. The results, for each weather station, are shown in Table 3. Therefore, the intensity of rain is equal to 60 and 23 mm in 30 minutes, respectively taking into consideration a return period of 100 and 1 year.

Table 3 : Rain Intensity in 30 minutes (T=100)

Weather stations	Rain intensity (h) in 30' (T=100) (mm)
Ravello	41
Piano Sorrento (Istituto Nautico)	58
Piano Sorrento (S. Pietro)	52
Massa Lubrense	99

3.2 Potential hazard assessment

Figure 5 shows the vegetation distribution overall the study area, obtained from the subtraction of DSM from DTM. The vegetation is rare around the archaeological ruins of the Abbey, while it is a little bit more prominent along the steep mountainside. That situation is also visible in Figure 2, where the site under investigation is depicted. That information is essential because it affects the flow directions and, consequently, the flow accumulation in some specific zones.

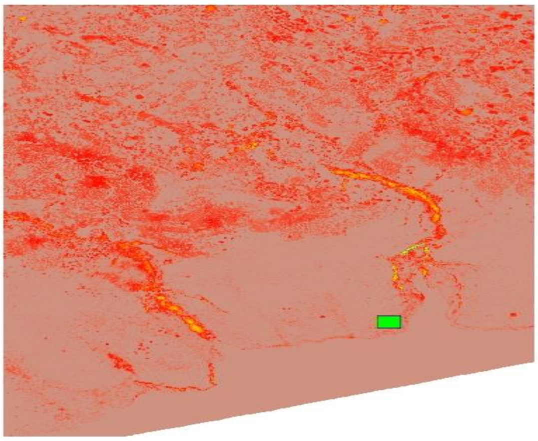
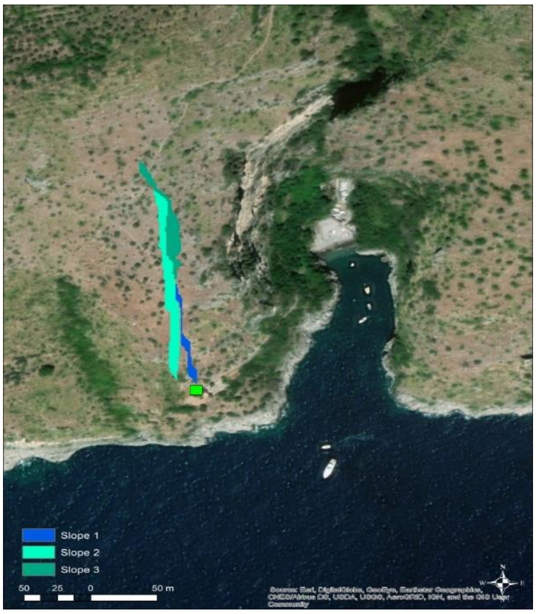


Figure 5: Vegetated zone in Crapolla Fiord. The green square symbolizes the Abbey

Thus, combining it with the information related to the slope aspect, the identification of the basins is carried out (Figure 6). Figure 5a shows the micro-basins in a close proximity of the Abbey, while

Figure 5b portrays the basin in the vicinity of the Fiord. The maximum flow rate is equal to 0.04 and 8.3 m^3/s for the micro-basins (Figure 6a) and the basin (Figure 6b) respectively, taking into account a rainfall event of 60 mm in 30 minutes (T=100); on the contrary, considering a rainfall event of 23 mm in 30 minutes (T=1), the flow rate is equal to 0.02 and 2.4 m^3/s, respectively.





a b

Figure 6: Micro - basins identified in the study area at slope (7a) and Fiord (7b) scale

4. DISCUSSION AND CONCLUSION

The current research activity intends to assess the potential hazard and to consider the vulnerability in an archaeological site of invaluable price in terms of cultural heritage and landscape. It is characterized by the presence of the archaeological ruins of an ancient Abbey on the mountainside and on some characteristics, called "monazeni" fishing houses in the inlet (Figure 2) [Russo, 2014]. Moreover, the steep mountain shows barely visible signs of old terraces, currently abandoned (Figure 2) [Russo, 2014].

The analysis has been carried out at two different levels: at basin scale, to evaluate the potential hazard to which is subjected the Fiord, and at mountainside scale, to analyse the damages suffered by the Abbey. The starting stages of the procedure were the same for both levels. They concern the identification of the rainfall events and, consequently, the flow rate, weighing on the Abbey and on the Fiord, respectively. The rain intensity was computed for each weather station separately. As mentioned above, the meteorological station of Massa Lubrense, the closest to the study area, shows an anomalous value of rainfall in 1 hour (130 mm), because of the presence of an extreme rainfall events (1992). Therefore, the rain event in 30 minutes was calculated using the Bell's equation and not spatializing the meteorological data (Table 3). The rain intensity, on a period of 30 minutes, was of 60 and 23 mm, considering a return time of 100 and 1 year, respectively. Those results and the size of the basins, identified at the two considered levels, were set up in eq. 5 and the flow rate was evaluated (Figure 6). Figure 6a describes the situation at slope aspect scale, while the Figure 6b depicts the flow rate which damage the Fiord in case of the occurrence of the determined rain event. As expected, the two flow rates are completely different, since the final result is strongly affected by the coefficient of run-off and the basin size: the bigger the basin area is, the higher the flow rate is, and consequently, the potential hazard. Hence, the potential hazard related to the archaeological ruins is smaller than that one of the Fiord. Nevertheless, both flow rates show a value suitable for damaging the Abbey and completely destroying the inlet and the fishing houses located in that zone (Figure 2).

Not only the potential hazard but also the vulnerability assumes a different significance at the two levels, since affected by the exposed value [Wilson et al., 2005]. The vulnerability includes the value of "intangible assets", as the historical landmark and the archaeological ruins, the infrastructures for improving the accessibility, like, for instance, paths and stairways, and, finally, the human lives that could be damaged. Even if the vulnerability assumes a different value at the two levels, it is pretty high in both cases and consequently, some actions are required to mitigate the potential hazard. Fragmenting the flow directions to minimize the flow rates looks a possible solution for reducing the potential hazard. Clearly, the initiatives suggested for meeting the purpose are essentially different at the two analysed scales. At Abbey scale, the actions should be focused on building a gutter at the sides of the ladder, since it is the main direction that guide the flow on the archaeological ruins. On the contrary, at mountainside level, it is necessary to preserve the vegetated and cultivated areas in order to not change the permeability of the soil, which influence the coefficient of run-off. Indeed, a change of soil from sandy loam to rocky will increase the run-off coefficient from 0.2 to 0.8 and consequently, the flow rate will rise till 33 m^3/s for T=100 and to 8 m^3/s for T=1. Hence, the idea of recovering the old terraced landscapes, currently barely visible on the ground, was born. Indeed, that action is twofold: the potential hazard is minimized, as first, and the original landscape heritage in the inlet is safeguarded, secondly.

References

1. IPCC, (2014): Annex II: Glossary [Mach, K.J., S. Planton and C. von Stechow (eds.)]. In: Climate Change 2014: Synthesis Report. Contribution of Working Groups I, II and III to the Fifth Assessment Report of the Intergovernmental Panel on Climate Change [Core Writing Team, R.K. Pachauri and L.A. Meyer (eds.)]. IPCC, Geneva, Switzerland, pp. 117-130.
2. Convention for the Protection of the World Cultural and Natural Heritage (Paris, 16 November 1972) (WHC), entered into force 17 December 1975.
3. Cassar M. (2005) Climate change and the historic environment. Centre for Sustainable Heritage, University College, London
4. Sabbioni, C., Cassar, M., Brimblecombe, P., and R. A. Lefevre (2008). Vulnerability of Cultural Heritage to Climate Change, Report for E. FERNANDEZ-GALIANO, **Council of Europe European and Mediterranean Major Hazards Agreement (EUR-OPA)**, 6 November 2008.
5. Sabbioni, C., Cassar, M., Brimblecombe, P., and R. A. Lefevre, (2009). Vulnerability of cultural heritage to climate change. *Pollution Atmospherique*, *202*, 157-169.
6. Regione Campania, Piano Regionale Triennale 2014-2016 per la Programmazione delle Attività di Previsione, Prevenzione e Lotta Attiva Contro gli Incendi Boschivi available at http://burc.regione.campania.it Carta pp.149-150, accessed 20.10.2016
7. Caneva, G., Cancellieri, L., Zivkovic, L., Grilli, R., Lombardozzi, V., and G.Salerno (2007). *Il paesaggio naturale ed il paesaggio culturale*.
8. International Strategy for Disaster Reduction. (2004). *Living with risk: a global review of disaster reduction initiatives* (Vol. 1). United Nations Publications.
9. Fuchs, S., Heiss, K., and J. Hübl (2007). Towards an empirical vulnerability function for use in debris flow risk assessment. **Natural Hazards and Earth System Science,** *7*(5), 495-506.
10. Wilson, K., Pressey, R. L., Newton, A., Burgman, M., Possingham, H., and C.Weston, (2005). Measuring and incorporating vulnerability into conservation planning. *Environmental management, 35*(5), 527-543.
11. Capolupo, A., Kooistra, L., Berendonk, C., Boccia, L., and J.Suomalainen (2015b). ″Estimating plant traits of grasslands from UAV-acquired hyperspectral images: A comparison of statistical approaches″. **ISPRS International Journal of Geo-Information**, 4(4), 2792-2820.

12. Florinsky I. V. (1998). Combined analysis of digital terrain models and remotely sensed data in landscape investigations. **Prog. Phys. Geogr**. 22, 28.

13. Pindozzi, S., Cervelli, E., Capolupo, A., Okello, C., and L. Boccia (2016). Using historical maps to analyze two hundred years of land cover changes: case study of Sorrento peninsula (south Italy). **Cartography and Geographic Information Science**, *43*(3), 250-265.

14. V. Russo (2014). Landscape as Architecture. Identity and Conservation of Crapolla Cultural Site, V. Russo (ed.), Nardini, Firenze 2014.

15. Capolupo, A., Cervelli, E., Pindozzi, S., and L.Boccia (2017). Assessing volumetric and geomorphologic changes of terraces in Amalfi Coast using photogrammetric technique. **In: "Biosystems Engineering addressing the human challenges of the 21st century".** Bari: Università degli Studi di Bari Aldo Moro, ISBN: 978-88-6629-020-9, Bari - Italy, July 5-8, 2017

16. Capolupo, A., Kooistra, L. and L.Boccia (2018b). Geomorphological change detection and historical evolution analysis of terraced landscapes, an old irreversible agricultural practice: the case study of Minori, in Campania Region. Geophysical Research Abstracts, In Vol. 20, EGU2018-18700, 2018, **EGU General Assembly 2018**. Vienna – Austria, 8-13 April, 2018.

17. Capolupo, A., Rigillo, M. and L. Boccia (2018c). Photogrammetric technique for analysing the anthropization process in coastal areas: the case study of Minori. "**Il Monitoraggio Costiero Mediterraneo: problematiche e tecniche di misura**" (Edition VII), Livorno - Italy, June 19-21, 2018.

18. Infascelli R, Faugno S, Pindozzi S, Boccia L, and P. Merot (2013). Testing different topographic indexes to predict wetlands distribution. Procedia Environmental Sciences. 00, 000–000

19. Nadarajah, S., & Kotz, S., 2004. The beta Gumbel distribution. Mathematical Problems in engineering, 2004(4), 323-332.

20. Bell, F. C. (1969). Generalized rainfall-duration-frequency relationships, **J. Hydraul. Eng**., 95(HY1), 311-327.

21. Wolock D. M., and G. J. McCabe (1995). Comparison of single and multiple flow direction algorithms for computing topographic parameters in TOPMODEL. Water Resour Res 31, 1315-1324.

22. Beaujouan V, Durand P, L. Ruiz (2001). Modelling the effect of the spatial distribution of agricultural practices on nitrogen fluxes in rural catchments. **Ecol Model** 137, 93–105.

23. Capolupo, A., Kooistra, L. and L.Boccia, (under review). A novel approach for detecting agricultural terraced landscapes from historical and contemporaneous photogrammetric aerial photos. **International Journal of Applied Earth Observation and Geoinformation**.

24. Capolupo, A., Pindozzi, S., Okello, C., and L.Boccia (2014). ″Indirect field technology for detecting areas object of illegal spills harmful to human health: application of drones, photogrammetry and hydrological models″. **Geospatial Health**, 8(3), 699-707.

25. Capolupo, A., Pindozzi, S., Okello, C., Fiorentino, N., and L. Boccia (2015a). ″Photogrammetry for environmental monitoring: The use of drones and hydrological models for detection of soil contaminated by copper″. **Science of the Total Environment**, 514, 298-306.

26. Capolupo, A., Nasta, P., Palladino, M., Cervelli, E., Boccia, L., and N. Romano (2018a). Assessing the ability of hybrid poplar for in-situ phytoextraction of cadmium by using UAV – photogrammetry and 3D flow simulator. **International Journal of Remote Sensing (TRES)**. DOI: 10.1080/01431161.2017.1422876.

TERRACED LANDSCAPES LOCATED IN AREAS OF GREAT VALUE FOR TOURISTIC PURPOSES AS AN IRREVERSIBLE PRACTICE

A. Capolupo and L. Boccia*

University of Naples Federico II, Department of Architecture,Via Forno Vecchio,12- 80134, Naples (NA), Italy

*Corresponding author: e-mail: lorenzo.boccia@unina.it , tel : +39 0812539151

Abstract

Since Neolithic, terraced landscapes have been an essential element for moulding mountain or steep slope into habitable arable areas. Over the last decades, they have been subjected to a quick abandonment because of their inadequate economic competitiveness causing a gap in their maintenance and, consequently, incrementing the hydrogeological instability of those areas. Minori is a small municipality (256 ha), protected by UNESCO, located in Amalfi Coast. That area is well known not only for the beauty of its territory but also for some catastrophic raining events, like in 1954 when a rain shower of 500 mm topped up to 24 hours. The current research work intends to analyse the landscape changes in Minori over sixty year period (1956 - 2017) for assessing the new values taken on the land use and the agricultural sites. A detailed orthophoto and a high resolution Digital Elevation Model (DEM) of the study area have been reconstructed using the historical photogrammetric photos of 1954, acquired by the Italian Military Geographic Institute (IGM), and the aerial photogrammetric pictures of 2017, obtained by an own flight. DEM and orthophoto have been reconstructed applying Agisoft Photoscan Professional. The resolution of the generated DEM is equal to 0.48 and 0.1 m for 1956 and 2017, respectively. The orthophoto resolution is of 0.24 and 0.07 for 1956 and 2017, respectively. Comparing the generated products of the two periods, it is pointed out that terraces extension has not been amended, while the amount of human constructions have increased of about 800%. To give a first idea of the most vulnerable areas to be investigated more in depth through simulation procedures, a first proposal of an expeditious index of vulnerability (EVI) has been introduced and tested. It is based on the ratio between the amount of surface occupied by buildings and the amount of areas subjected to a debris flow event. The increase of the vulnerability, exposure values and probability of accident occurring involve a risk rise.

Keywords: Agricultural terraces, Risk assessment, Aerial photogrammetry, Historical series

1. INTRODUCTION

Terraced landscapes are largely widespread in all Mediterranean area since Neolithic time. They have been built to exploit the great fertility of the slope of the mountain, making them arable and habitable. Indeed, that geomorphological element is recognized as the most significant human activity that affected and transformed the Earth Surface. Unfortunately, over the last few years, they have been quickly abandoned because of their scarce competitiveness in term of agriculture production [Tarolli et al., 2014]. This caused a lack of maintenance of their retaining walls and, consequently, the boost of hydrological instability, soil erosion, loss of agricultural lands and debris flow. Therefore, editing a proper management plan to preserve the terraced landscapes looks essential and priority in all the world, according also to the European Common Agricultural Policy (CAP). The situation becomes more complex when the considered area is included in the UNESCO World Heritage List, like Amalfi

Coast (year 1997 n. 830). Since 1972, UNESCO have pushed their members to preserve and conserve all the sites, involved in the World Heritage List, for present and future generation ["World Natural and Cultural Heritage", Paris, 16 November 1972]. Nevertheless, UNESCO does not provide any models or indications regarding the management plans to be developed [Gullino et al., 2015]. Consequently, the necessity to define and implement a proper risk management program is still alive. It should be edited considering the natural hazard to be opposed. As underlined by Fuchs et al., (2007), natural hazard is a physical event which cause a catastrophic event in a defined time and space, damaging the human being and their environment. More in general, the natural hazard has been defined by United Nations (2004) as the "probability of the occurrence of a potential damaging phenomenon". The debris flow, triggered by rainfall, is recognized as the most common hazard for terraced landscapes and, therefore, it needs a particular attention.

The vulnerability concept is directly connected to the natural hazard. It is defined as the probability to be damaged following the occurrence of a determined event [Birkmann, 2006]. Nevertheless, [Wilson et al., 2005] extended that definition, involving the three dimensions of vulnerability: exposure, intensity and impact. It is expressed by an index which varies between 0 and 1, where 1 is associated to a complete destruction while 0 is related to ability of the people, buildings and infrastructures to not be damaged. Even if several indices have been developed and tested for investigating the vulnerability of buildings and infrastructures, just few indicators have been introduced to assess the vulnerability of the landscape. Nevertheless, each of them requires a laborious and expensive procedure to evaluate the vulnerability in particular at detailed scale. Hence the need to develop an expeditious indicator for assessing the vulnerability of the areas subjected to a debris flow at detailed scale on terraces.

To fill that gap of knowledge, the information related to terraces position and status at detailed scale are necessary. Capolupo et al., (in review) developed a novel approach for detecting terraced landscapes at detailed scale, going beyond the limits of the traditional approaches. It was based on the combination of photogrammetry and object-oriented analysis (OBIA) technique. The former is an essential tool for generating high resolution Digital Elevation Models (DEMs) and orthophotos able to describe the morphological surface of the Earth [Capolupo et al., 2015a; Capolupo et al., 2015b; Capolupo et al., 2018a]. The latter, was preferred to the pixel oriented classification procedure because it is able to take advantages of both spectral signature and morphological contribution.

The new abilities of territorial analysis and terraced landscapes detection constitute the presuppositions to estimate the vulnerability at detailed scale. Indeed, the current research activity aimed to introduce a first proposal of a morphological Expeditious Indicator of Vulnerability (EVI) able to identify the most vulnerable areas, which need an analysis more in depth through simulation procedures.

2. MATERIAL AND METHOD

2.1 Study area

The research activity was conducted in Minori (40° 39' 00" N, 14° 37' 35" E), the most ancient municipality of Amalfi Coast, in Salerno province (Southern Italy). Its territory extends over 2.56 km^2 and, as underlined by Caneva and Cancellieri, (2007), it is well-known overall the world for several aspects: the uniqueness of its landscape, modelled by human activities since 950 – 1025 AC, the great variety of vegetation, the cultural heritage of great value, dating from Roman period, the high quality farming products, such as chestnuts, lemons and grapes. Although the first two points are getting prevalent in the last few years attracting more and more tourists, the agricultural was and is the main source of income [Caneva and Cancellieri, 2007; Pindozzi et al., 2016]. Indeed, the terraced landscapes construction started during the Middles Ages to increase the soil permeability and reduce the slope gradients of mountains in order to make that area arable and habitable [Tarolli et al., 2014]. Unfortunately, just traditional agricultural techniques can be adopted on terraced landscapes because of their structures and locations. This involves that agriculture sector of that area

is not competitive anymore and, consequently, their abandonment has been getting more frequent, focusing the local economy on the tourism branch. The climate is mainly Mediterranean in the lower part of the municipality, while in the upper part, it is essentially temperate [Caneva and Cancellieri, 2007]. Usually, the annual rainfall average is higher than 1000 mm, even if the area has been subjected to some catastrophic events, like the showers of more than 500 mm fallen in about four hours on the 25^{th} of October 1954. Those events cannot be described using the Gumbel distribution, the most widely applied for describing the meteorological problems, but by the Two Component Extreme Value (TCEV) [Rossi and Villani, 1994].

2.2 Field data and photogrammetric aerial photos collection

The data sources of the current research activity involves:

- the panchromatic historical series of the 13th of April 1956;
- the RGB photogrammetric aerial photos of the 13th of March 2017;
- the multispectral photogrammetric aerial photos of the 13th of March 2017;
- 162 Ground Control Points (GCPs).

The panchromatic historical series is composed by the three different frames (197-V-1811; 197-V-1812; 197-V-1813) acquired at the quotas of 3900 m. They have been scanned using a photogrammetric scanner by the Italian Military Geographical Institute (IGM). Their format is equal to 230 x 230 mm.

The RGB and the multispectral photogrammetric aerial photos were instead acquired by an own flight campaign, conducted under clear sky conditions at the altitude of 1000 m, using a Piper PA 18 Super CUB-I-CGAO & I-NIKI (VFR). That airplane was chosen because of the presence of a trapdoor located at the bottom of the chassis, where the cameras were placed. A Reflex Nikon D800e, characterized by 36.3 Mp and a pixel size of 0.00487 mm, was used to acquire the RGB images. A lens of 50 mm was mounted on it in order to adapt the final resolution to the size of the object under investigation. Also an external Global Position System (GPS) was employed on the camera in order to georeference the acquired pictures and to optimize the following metric reconstruction. A specific external circuit, composed by Arduino components, was designed and built by the Landscape and Rural Planning research unit (LARP) of the University of Naples Federico II to remotely control the shutter camera. The Tetracam ADC Snap, characterized by 1.3 Mp and a pixel size of 0.005 mm, was instead chosen to capture the multispectral photos. Its range of acquisition is comprised between 520 and 920 nm, corresponding to Red, Green and Near Infrared bands. Its internal timer was adequately set to control the camera shutter and to acquire the image at a specific instant.

As suggested by Nex and Remondino, (2014), the GCPs were acquired to improve the accuracy of the final metric reconstruction. Therefore, three field data campaigns were performed the 25^{th}, 27^{th} of January 2016 and the 27^{th} of April 2017 and 162 GCPs were acquired using a Differential Global Position System (DGPS) Sokkia GRX1 in ETRF2000 Epoch 2008. Two different sub-datasets were randomly generated extracting the GCPs from the original data source, as suggested by Höhle and Höhle, (2009): the former was employed for the metric reconstruction; the latter for the accuracy assessment.

2.3 Scene metric reconstruction and terraces classification

Each block of images has been separately processed in order to obtain the photogrammetric outcomes from each of them. Before starting the metric reconstruction, two preliminary steps (quality check of the photogrammetric pictures and the image orientation) were performed on the historical and on the recent datasets in order to improve the final outcomes. In addition, also the laboratory camera calibration was carried out for the RGB contemporaneous dataset using Agisoft Photoscan Lens software (Agisoft LLC, St. Petersburg, Russia). That phase could not be applied on the historical series and on the multispectral images since, in the first case, the interior parameters of the camera

were unknown while, in the second case, the dataset would be subjected to a specific procedure applying PixelWrench2 software (Tetracam, inc, Chatsworth, Cal.).

The quality check was performed selecting the photos to be utilized during the reconstruction stage through their visual inspection. The results of that phase were essentially different for the three data sources: no defects were detected on the historical series; on the other hand, the 3% of RGB and multispectral pictures were blurry, and, consequently, they were removed and not took into account during the following procedures. That step has not affected the final results of the reconstruction procedure because these frames had been acquired during the phase to achieve the flight quotas and the first waypoints. Thus, the image orientation phase, consisting in the extraction of tie points and pictures alignment, started in Agisoft Photoscan Professional environment (Agisoft LLC, St. Petersburg, Russia). The deformation of the images blocks was minimized importing the subdataset of GCPs suitable for the metric reconstruction in that environment. Two Digital Elevation Models (DEMs) were extracted from the historical series and from the contemporaneous RGB dataset; on the contrary, three orthophotos were generated from each data sources. All the details regarding the photogrammetric process have been reported in Capolupo et al., (2014, 2015a, 2017).

Before starting the classification phase to identify and classify the terraces, the small discontinuities in the two DEMs were removed applying ArcGis Hydrological tool of ESRI ArcGis Software, version 10.1 (Redlands, CA., USA) as reported in Infascelli et al., (2013). Moreover, all the obtained photogrammetric rasters were purified from the sea and the border areas, since they were characterized by a high error in terms of elevation caused by the lack of GCPs in that zones.

The photogrammetric results were subsequently processed in eCognition Developer 9 software (TRIMBLE Germany Gmbh) in order to generate a binary map, in which the terraced and not terraced landscapes were distinguished. An OBIA approach was preferred to the common pixel oriented classification technique in order to exploit the advantages of multispectral images and DEM. That procedure involved two different stages: the former, related to the segmentation phase, while, the latter, regarding the construction of a proper classification model. Two different segmentation algorithms, the "multiresolution segmentation" and the "spectral difference segmentation" were performed to fit the size of the generated objects to the real - world elements under investigations [Benz et al., 2004]. The second algorithm was applied only on the blocks of contemporaneous images since the spectral signature was not available for the historical series. The parameters of the two algorithms were set iteratively adapting them to the complexity and the heterogeneity of the study area, as described in Capolupo et al., (in review). A specific tree-level hierarchical structure, based on a proper rule – set, was built enhancing the contribution of each layer suitable for the terraces detection. The weighs attributed to each layer and the indices chosen for optimizing the classification have been reported and described in Capolupo et al., (in review). All the objects included in the terraces class were, subsequently, merged and exported as a single layer.

The accuracy assessment phase was composed by two different aspects: the error analysis of the photogrammetric products and of the detected terraced landscapes. The former was obtained developing a specific code in R environment, which was based on the statistical approach reported by Höhle and Höhle (2009). It considers the calculation of residuals between the estimated and measured points. Therefore, the coefficient of determination (R^2) and the Mean Error was examined to analyse their spatial trend. On the contrary, the accuracy of the generated binary map was expressed in terms of the percentage of terraced landscape correctly classified. It was assessed by comparing the final outcome with thirty validation data, manually selected during an interpretation phase of the generated orthophotos.

2.4 Landslide event and vulnerability indicator

The terraced landscapes largely widespread in the area under investigation have been subjected to a quick abandonment because of their scarce competitiveness (Tarolli et al., 2014). This caused a lack of maintenance of their retaining walls, which, consequently, are exposed to a high hazard for slope failures, easily triggered by the particular climate conditions of Minori, prone to heavy showers, like

the event of the 25th of October 1954. The effects on the cultivations, buildings and safety of people depends on the intensity and prevalence of the phenomenon. Catastrophic rainfall entail the landslides of all the mountain slope, damaging the floodplain and destroying all the buildings. No actions could be taken to prevent that situation. On the contrary, the landslide of a small piece of terrace damages a defined area. That kind of incidents are more common, as shown by the bibliography [Crosta et al., 2003; Del Ventisette et al., 2012], and, consequently, they are more interesting to investigate.

In particular, the morphological characteristics of Giampilieri area in Messina Province are similar to that ones of Minori. Therefore, the seven debris flows occurred in Giampilieri on 1th of October 2009, described by Del Ventisette et al., (2012), could be similar to the landslides could verify in the area under investigation. In that case, they observed that the landslides volume of the seven debris flows was comprised between 817 and 13507 m^3.

In the current study, an hypothetical debris flow, which characteristics are similar to that ones of the incident occurred in Giampilieri, was supposed and its effects were investigated. Its volume was assumed equal to 1000 m^3, corresponding to an area of 20 x 30 m^2 with a depth of 1.5 m.

The pre-processed photogrammetric DEMs were separately processed in order to detect the slope direction for each cell using the Surface Tool of ArcGis software. Therefore, for each direction a travel distance (L) of the debris flow was computed using the Equation 1, introduced by Rickenmann (1999):

$$L = 1.9 \times V^{0.16} \times H^{0.83} \tag{1}$$

where V is the volume and H is the total fall height. Crosta et al., (2003) showed the efficiency of the Equation 1 for describing the debris flow on terraced slopes.

The comparison between the travel distance and the length of the mountain slope gives an idea of the debris flow hazard potential. Indeed, if L is smaller than the length of the mountain slope, the underlying area will not be not reached by any debris and, consequently, it is not damaged. On the contrary, if L is bigger than the other parameter, the underlying zones will be reached by the landslides and the damages will be proportional to the travel distance and the speed of the flow. The bigger the travel distance (L), the more vulnerable the underlying zone is. Therefore, on one hand the travel distance is an empirical indicator of the debris flow hazard potential, as underlined by Rickenmann (1999), on the other hand it allows to detect the vulnerable areas to be analyse more in depth. Examining the bibliography [Crosta et al., 2003; Del Ventisette et al., 2012] and the geometry of terraced landscapes, the overall conclusion is that the surface mainly interested by the debris flow on the flat at the basis of the terraced landscapes is of the order of 25 m. Each identified zone is characterize by a vulnerability value depending on the amount of buildings, historical ruins and the quantity of people which live in that area. To be able to define an univocal vulnerability value adapted to each area requires a laborious work based on the knowledge of each territorial element and the exact trend of the debris flow through an expensive simulation process.

The assessment of the house volume (m^3) in the detected vulnerable areas could be a first expeditious indicator of the vulnerability value for each identified areas. Such justification shall demonstrate the acronym Expeditious Vulnerability Index (EVI) (Equation 2). That index allows to minimize the simulations by limiting them just to the areas managed by a high value of EVI.

$$EVI = \Sigma\, V_{bi} / A_V \tag{2}$$

where V_{bi} is the volume of each building included in that area and A_v is the area of the vulnerable zone in question. EVI is expressed in term of percentage. Each building was detected by manually interpreting the obtained orthophoto. The volume of each of them was calculated by multiplying the surface occupied and its height.

3. RESULTS

3.1 Scene metric reconstruction and terraces classification

Each block of images were separately processed to generate the photogrammetric outcomes. A high resolution orthophoto was generated from the three data sources: block of 1956, RGB pictures of 2017 and multispectral photos of 2017. Their resolution (GSD) was equal to 240 mm, 7 mm and 15 mm, respectively. Instead, the DEMs were obtained only from the dataset of 1956 and the RGB pictures of 2017. Their resolution was equal to 480 mm and 10 mm, respectively. Comparing the two orthophotos show that the buildings have boosted of 800% in the last 60 years. The consecutive procedure has led to generate a binary map, where the non terraced landscapes were distinguished from the terraced landscapes, shown in Figure 1. The accuracy assessment of the two final binary maps (Figure 1) was equal to 93% and 98% for the historical and the contemporaneous series, since three points have not been recognized in the first one and just one in the second one. The not recognized terraces have been marked with the yellow dots in Figure 1.

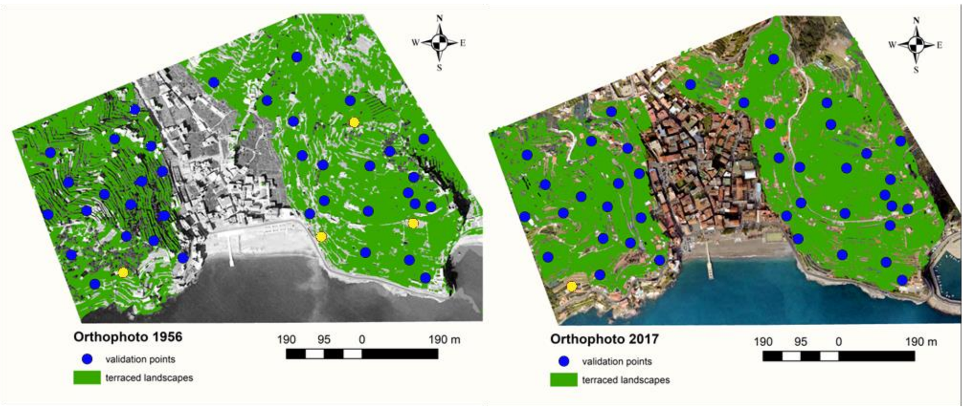


Figure 1: Validation of terraced landscapes for the dataset of 1956 and 2017, respectively. The blue points are correctly recognized; while, the yellow points are not recognized

3.2 Vulnerability indicator

Nine slopes, corresponding to nine directions of flow have been identified on the two sides of the mountains which go downs towards the municipality of Minori (Figure 2). For each of them the travel distance have been computed and compared with the length of the considered slope in order to identify the vulnerable areas. The results are reported in Table 1.

Table 4: Travel distance for each slope and the length of each of them

Slopes ID	*Colour corresponding to the slopes in Figure 2*	*Length of each slope (m)*	*Travel Distance (L)(m)*	*Difference between the length of the slope and L (m)*
1	Red	222	1425	1203
2	Yellow	361	941	579
3	Green	288	751	463
4	Blue	310	933	623
5	Black	205	2768	2563
6	White	329	1305	977
7	Orange	118	4102	3984
8	Purple	269	74	-195
9	Pink	303	861	557

The travel distance (L) (Equation 1) of the slope number 8 (the purple area in Figure 2) is smaller than the length of the slopes, as shown in Table 1. Indeed, the difference between the length and the travel distance is -195 m. Therefore, a landslide generated at the top of that slope is not dangerous because the debris will not reach the underlying portion of municipality. Consequently, there is no reason to investigate the vulnerability of that area more in depth. On the contrary, the highest debris flow hazard potential is traced in the numbers 1, 5, 7 with a value of 1203 m, 2563 m and 3984 m, respectively. The values identified was the same for both data sources.

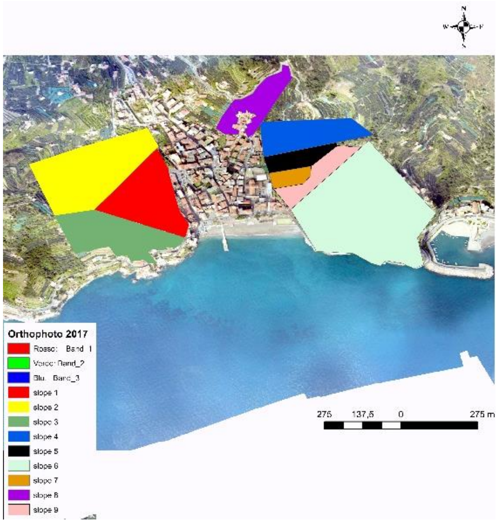


Figure 2: Slope direction

Eight vulnerable areas with a thickness of 25 m have been inspected in correspondence of slopes 1, 2, 3, 4, 5, 6, 7, 9. In each of them, EVI have been computed and shown in Figure 3, where the colour at each areas was assigned according to the vulnerability significance: green to the lowest value, orange to the medium rate and red to the highest one. The higher the EVI, the more vulnerable the area is. For the contemporaneous dataset, the highest value was detected for the slope number 5 with the value of 75%, followed by the number 1 and 7 with the value of 45% and 44%, respectively. The highest value of the dataset of 1956 (45%) has been identified in slope number 1. That slope shows the same value for both periods since the area has not been subjected to any changes. On the contrary, the remaining areas show a substantially lower value: the zones number 5 and 7 equal to 0%, the number 6 equal to 1%, the number 4 equal to 5%, the numbers 9, 3 and 2 equal to 15%, 18% and 22% respectively.

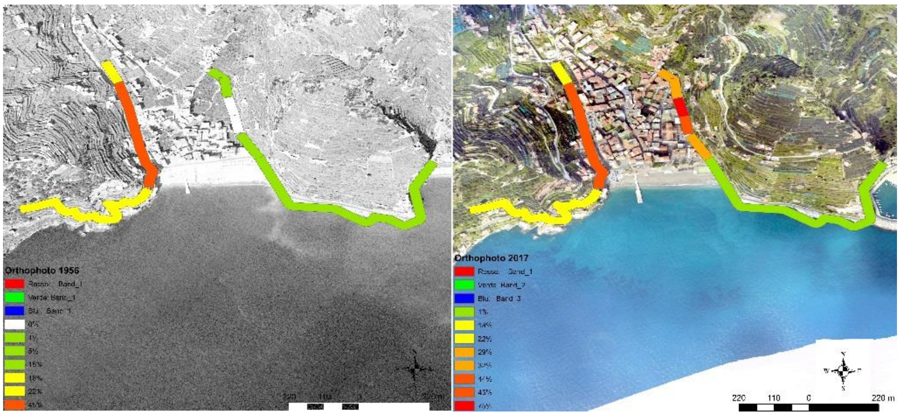


Figure 3: Expeditious Index of Vulnerability for dataset of 1956 and 2017, respectively

4. DISCUSSION AND CONCLUSIONS

The current paper was intended to develop an easy and quick methodology to detect and investigate the vulnerable areas subjected to a debris flow caused on terraced landscapes slope. Indeed, in the last few years, the abandonment of terraces is becoming a problem more and more evident due to their scarce competitiveness. This phenomenon, in conjunction with the lack of knowledge related to their position and conservation status (Capolupo et al., in review), caused a lack of maintenance of those areas. Consequently, the possibility of occurrence of debris flows, triggered by rainfall, is more and more frequent, damaging the underlying areas [Crosta et al., 2003; Del Ventisette et al., 2012]. In addition, those events are more recurring in Amalfi Coast because of difficult meteorological situation, characterized by the occurrence of catastrophic event, like that one of the 25th of October 1954, when more than 500 mm fell in about four hours. That situation cannot be described using Gumbel distribution [Rossi and Villani, 1994]. Analysing the status of Amalfi Coast terraces is even more interesting since they have been included in the UNESCO World Heritage List (year 1997 n. 830). Preserving them is perfectly in line with UNESCO policy, expressed in the "World Cultural and Natural Heritage" convention of 1972, in which is underlined that all the historical sites to be protected and brought to the future generations. Therefore, Minori, the most ancient municipality of Amalfi Coast, has been chosen as the study area of the current research activity.

The experiment was mainly composed by two steps. First of all, the position of terraced landscapes in the area under investigation have been detected using the combination of aerial photogrammetry and OBIA approach, as suggested in Capolupo et al., (in review). The generated binary maps show a high accuracy equal to 93% and 98% for the historical and contemporaneous datasets (Figure 1). The different result related to the accuracy assessment depends on the different resolution and the lack of multispectral information for the data of 1956. Both results are satisfying since they are suitable for describing complexity of territory at detailed scale. Moreover, the approach is really innovative and it allows to go beyond the limits of the traditional methods. Moreover, that technique can be applied at detailed scale. Moreover, it is based on an objectively classification approach and not an image interpretation. Comparing both orthophotos (Figure 1), it is also possible to point out that Minori has been subjected to an anthropization process: the amount of buildings have increased of about 800% [Capolupo et al., 2018b; Capolupo et al., 20148c], while the extension of terraces has not changed. That observation has been also confirmed by the results reported in Figure 2 and Table 1, related to the length of the slopes and the travel distance of an hypothetical debris flow caused by a small portion of terraces with a volume of 1000 m^3. Those components have the same values both for the historical and the contemporaneous series. Nevertheless, the EVI, an expeditious indicator of the vulnerability, shows different values for the two investigated periods because of the anthropization process of the municipality of Minori (Figure 3). Figure 3 underlines that the vulnerability of each area has been subjected to an enormous rise.

The methodology introduced in the present paper looks promising because it allows to quickly identify the priority areas to be investigated more in depth through the simulations of debris flow. Indeed, the amount of buildings underlying the terraces is just one of the indicator to be considered to define the most vulnerable areas, since, first of all, the travel distance of debris flow and the length of the slopes of the mountains have to be investigated. Therefore, the EVI indicator looks an important tool for the landscape planners.

Acknowledgement
It was financially supported by UniNA and Compagnia di San Paolo, in the frame of Programme STAR, and by I.Z.S.Me/C.I.R.AM "Campania trasparente".

References

1. Tarolli P., Preti F. and Romano N. (2014) "Terraced landscapes: From an old best practice to a potential hazard for soil degradation due to land abandonment". **Anthropocene**, 6, 10-25.
2. Capolupo A., Kooistra L. and Boccia L. (in review) "A novel approach for detecting agricultural terraced landscapes from historical and contemporaneous photogrammetric aerial photos". **International Journal of Applied Earth Observation and Geoinformation**.
3. Gullino P., Beccaro G. L. and Larcher F. (2015) "Assessing and monitoring the sustainability in rural world heritage sites". **Sustainability**, 7(10), 14186-14210.
4. Fuchs S., Heiss K. and Hübl J. (2007) "Towards an empirical vulnerability function for use in debris flow risk assessment**". Natural Hazards and Earth System Science**, 7(5), 495-506.
5. United Nations: International Strategy for Disaster Reduction. (2004**). Living with risk: a global review of disaster reduction initiatives (Vol. 1)**. United Nations Publications.
6. Birkmann J. (2006) "Measuring vulnerability to natural hazards: towards disaster resilient societies" (No. Sirsi) (i9789280811353).
7. Wilson K., Pressey R. L., Newton A., Burgman M., Possingham H. and Weston C. (2005) "Measuring and incorporating vulnerability into conservation planning". **Environmental management**, 35(5), 527-543.
8. Capolupo A., Pindozzi S., Okello C., Fiorentino N., and Boccia L. (2015a) ″Photogrammetry for environmental monitoring: The use of drones and hydrological models for detection of soil contaminated by copper″. **Science of the Total Environment**, 514, 298-306.
9. Capolupo A., Kooistra L., Berendonk C., Boccia L., and Suomalainen J. (2015b) ″Estimating plant traits of grasslands from UAV-acquired hyperspectral images: A comparison of statistical approaches″. **ISPRS International Journal of Geo-Information**, 4(4), 2792-2820.
10. Capolupo A., Nasta P., Palladino M., Cervelli E., Boccia L. and Romano N (2018a) "Assessing the ability of hybrid poplar for in-situ phytoextraction of cadmium by using UAV – photogrammetry and 3D flow simulator". **International Journal of Remote Sensing (TRES)**. DOI: 10.1080/01431161.2017.1422876.
11. Caneva G., Cancellieri L., Zivkovic L., Grilli R., Lombardozzi V. and Salerno G. (2007) **"Il paesaggio naturale ed il paesaggio culturale".**
12. Pindozzi S., Cervelli E., Capolupo A., Okello C. and Boccia L. (2016) "Using historical maps to analyze two hundred years of land cover changes: case study of Sorrento peninsula (south Italy)". **Cartography and Geographic Information Science**, 43(3), 250-265.
13. Rossi F., and Villani P. (1994) "A project for regional analysis of floods in Italy". **In Coping with floods** (pp. 193-217). Springer, Dordrecht.
14. Nex F. and Remondino F. (2014) "UAV for 3D mapping applications: a review". **Applied Geomatics,** 6(1), 1-15. doi 10.1007/S12518-013-0120-x.
15. Höhle, J. and Höhle, M. (2009) "Accuracy assessment of digital elevation models by means of robust statistical methods". **ISPRS Journal of Photogrammetry and Remote Sensing**, 64(4), 398-406. DOI: 10.1016/j.isprsjprs.2009.02.003
16. Capolupo A., Pindozzi S., Okello C. and Boccia L. (2014) ″Indirect field technology for detecting areas object of illegal spills harmful to human health: application of drones, photogrammetry and hydrological models″. **Geospatial Health**, 8(3), 699-707.
17. Capolupo A., Cervelli E., Pindozzi S. and Boccia L. (2017) "Assessing volumetric and geomorphologic changes of terraces in Amalfi Coast using photogrammetric technique". **In: Biosystems Engineering addressing the human challenges of the 21st century.**

Bari:Università degli Studi di Bari Aldo Moro, ISBN: 978-88-6629-020-9, Bari - Italy, July 5-8, 2017

18. Infascelli R., Faugno S., Pindozzi S., Boccia L. and Merot. P. (2013) "Testing different topographic indexes to predict wetlands distribution". **Procedia Environmental Sciences**. 19, 733-746. Journel AG, Huijbregts CJ. Mining Geostatistics. Academic Press, New York, NY. 1978; pp 600.
19. Benz U.C., Hofmann P., Willhauck G., Lingenfelder I., Heynen M. (2004) "Multiresolution, object-oriented fuzzy analysis of remote sensing data for GIS-ready information". **ISPRS J. Photogr. Remote Sens**. 58, 239e258.
20. Crosta G. B., Dal Negro P. and Frattini P. (2003) "Soil slips and debris flows on terraced slopes". **Natural Hazards and Earth System Science**, 3(1/2), 31-42.
21. Del Ventisette C., Garfagnoli F., Ciampalini A., Battistini A., Gigli G., Moretti S. and Casagli N. (2012) "An integrated approach to the study of catastrophic debris-flows: geological hazard and human influence". **Natural Hazards and Earth System Sciences,** 12(9), 2907.
22. Rickenmann D. (1999) "Empirical relationships for debris flows". **Natural hazards**, 19(1), 47-77.
23. Capolupo A., Kooistra L., and Boccia L. (2018b) "Geomorphological change detection and historical evolution analysis of terraced landscapes, an old irreversible agricultural practice: the case study of Minori, in Campania Region". **Geophysical Research Abstracts**, In Vol. 20, EGU2018-18700, 2018, EGU General Assembly 2018. Vienna – Austria, 8-13 April, 2018.
24. Capolupo A., Rigillo M. and Boccia L. (2018c) "Photogrammetric technique for analysing the anthropization process in coastal areas: the case study of Minori". Conference on **Il Monitoraggio Costiero Mediterraneo: problematiche e tecniche di misura** (Edition VII), Livorno - Italy, June 19-21, 2018.

PRELIMINARY INVESTIGATION OF THERMAL EFFECT IN STREET CANYONS

M.K. Stefanidou, E.S. Bekri, P.C. Yannopoulos*

Environmental Engineering Laboratory, Department of Civil Engineering,University of Patras, 265 04 Patras, Greece

*Corresponding author: e-mail: yannopp@upatras.gr, tel : +302610996527

Abstract

Modern cities suffer from degraded air quality caused among others by the nature and the characteristics of the urban infrastructure and the contemporary building types and construction styles. Street canyons, created by continuous building alongside narrow or medium width streets, are quite common in many cities. They have a negative effect on urban air quality and thermal comfort conditions of city inhabitants. The aim of the present work is to simulate and predict flow fields at street canyons, as well as to assess the resultant heat fluxes. It analyses the aforementioned phenomenon under four scenarios changing the sources of heat fluxes. For this purpose a computational fluid dynamic model is used. Based on the results, the most adverse effect is found at about the middle of the building height, when considering as source of heat flux the building face, where the maximum temperature near the building is found. The temperature at the intermediate places of the city canyon remains, as expected, at lower levels than the temperature close to the heat sources. It is of note that the warm air near the building faces will deteriorate the comfortable interior room climatic conditions.

Keywords: street canyons, thermal effect, CFD, heat fluxes, room comfort

1. INTRODUCTION

Air quality in urban areas is an important issue for the citizens' health (Schwela, 2000). Many factors affect urban air quality such as the shape and the size of the buildings, as well as the orientation and the width of the main and secondary road network. In most modern cities, the structure of the buildings has been developed into various patterns of urban grids which resulted to the formulation of the so-called street canyons. Urban street canyon is a principal structure that characterizes the form of a whole city. It is built by continuous buildings on both sides of a narrow street (Zakaria et al, 2015).

In recent years, the impact of street canyons on the quality of residents' life, including their effect, firstly, on the energy potential accumulated in the city, secondly, on the energy performance of buildings and, thirdly, on the diffusion of air pollutants, has gained an increased scientific interest. Several studies have focused on the environmental effect to the building urban areas (De Lieto Vollaro et al, 2013; Memon et al, 2009) and more precisely to the indirect effect on the energy efficiency due to urban thermal field variations (De Lieto Vollaro et al, 2015a, b). The variation of the urban fabric caused by the rapid urbanization of cities leads to the flow and thermal field with a direct effect on the city environment.

Computational fluid dynamics (CFD) may be used to analyze the thermal flow field condition around the buildings in order to investigate the temperature effects inside and above urban canyons (Li et al, 2012; Battista and Mauri, 2016), considering an idealized two-dimensional model.

To the best of our knowledge, there have been few studies that investigate the flow temperature field of street canyons due to the thermal effects in calm conditions.

The present work studies numerically the heat transfer by buoyancy within and above a street canyon, which is caused by the solar heating of road and building surfaces in a calm atmosphere.

2. MATERIALS AND METHODS

2.1 Model description

In order to conduct the computational fluid dynamics (CFD) simulation, the ANSYS® Fluent 19 software has been used, based on a two-dimensional model, as shown in the schematic representation in Figure 1. The geometry of the model was prepared using the software ANSYS® Design Modeler. More specifically, the street canyon is simulated as a 0.4 m wide slot, having 1 m high side walls, which was placed 0.20 m above the road in order to allow air inlet. In this way, the air entered by the cross roads is simulated in the present two-dimensional model. The simulated canyon is placed in a wider test computational space of total dimensions of 6 m wide and 4.60 m high. The test space has two inlets of 0.20 m at the side walls near the bottom to allow the entrance of 20°C ambient air and other two outlets near the top of side walls to allow exit of the air. The temperature of the ambient air was set to 20°C. The duration of the numerical experiment was approximately two minutes so that to prevent air recirculation and stratification. In this sense the phenomenon may be considered quasi steady-state.

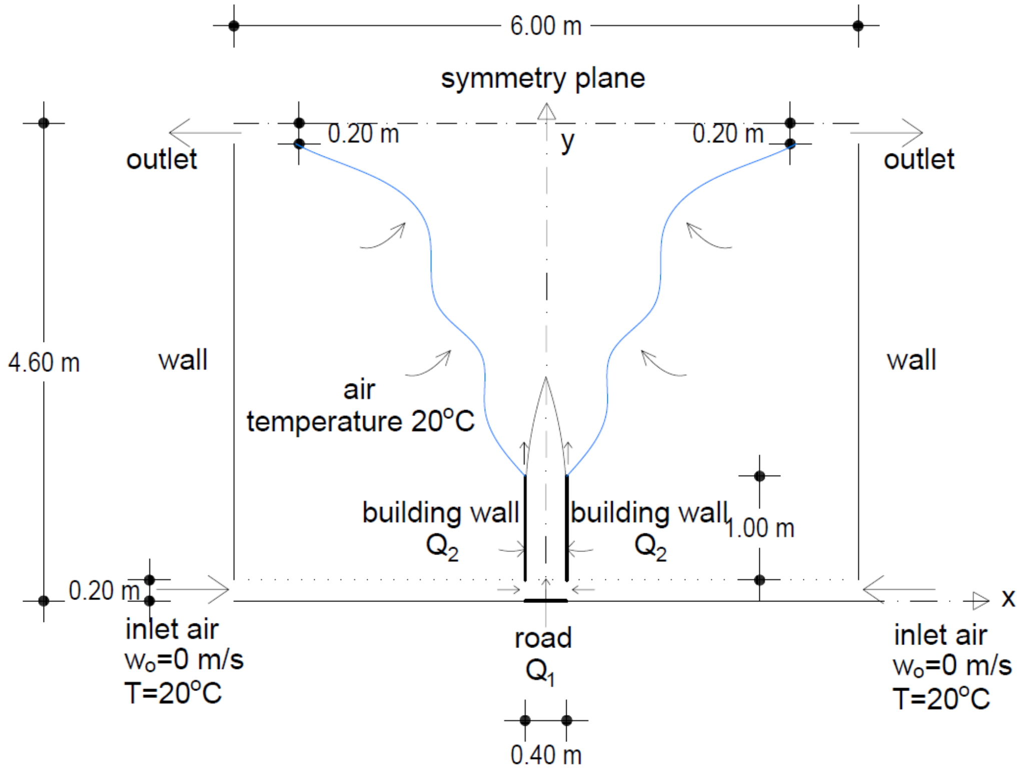


Figure 1: Configuration of the 2D flow field due to heat fluxes coming from road and building walls within and above a street canyon, simulated in an ample computational domain.

Our study analyses the aforementioned phenomenon of a street canyon under four scenarios concerning the sources of heat fluxes: Scenario I- road heat flux; Scenario II- building walls heat fluxes; Scenario III- road and left building wall heat fluxes; and Scenario IV- road and building walls heat fluxes.

2.2 Model set-up

The model domain was discretized using rectangular cells. For greater accuracy, the mesh has been refined in the focused area that includes the road and the walls of the buildings up to the top of the computational domain.

The software was set-up by using 2D double precision, to reduce the error of numerical calculation, pressure-based version and the unsteady Reynolds-Averaged Navier–Stokes (RANS) equations have been solved in combination with the standard k-ε turbulence model.

The governing equations of the phenomenon are RANS equations with a Boussinesq assumption for buoyancy effects:

Continuity equation

$$\frac{\partial w}{\partial y}+\frac{\partial u}{\partial x}=0 \tag{1}$$

y-momentum equation

$$\frac{\partial w}{\partial t}+\frac{\partial\left(w^2+w'^2\right)}{\partial y}+\frac{\partial\left(wu+w'u'\right)}{\partial x}=ga\left(T-T_0\right)-\frac{\partial p}{\rho_0\partial y}+\nu\left(\frac{\partial^2 w}{\partial y^2}+\frac{\partial^2 w}{\partial x^2}\right) \tag{2}$$

x- momentum equation

$$\frac{\partial u}{\partial t}+\frac{\partial\left(wu+w'u'\right)}{\partial y}+\frac{\partial\left(u^2+u'^2\right)}{\partial x}=-\frac{\partial p}{\rho_0\partial x}+\nu\left(\frac{\partial^2 u}{\partial y^2}+\frac{\partial^2 u}{\partial x^2}\right) \tag{3}$$

Energy equation

$$\frac{\partial T}{\partial t}+\frac{\partial\left(wT+w'T'\right)}{\partial y}+\frac{\partial\left(uT+u'T'\right)}{\partial x}=\kappa\left(\frac{\partial^2 T}{\partial y^2}+\frac{\partial^2 T}{\partial x^2}\right)+\frac{J}{\rho_0 C_p} \tag{4}$$

where w is the axial mean velocity component, u is the transverse mean velocity component, w' and u' are their corresponding fluctuations due to turbulence, g is the gravity acceleration, p is the pressure, $\rho=\rho_0-a\rho_0\left(T-T_0\right)$ is the local density of air, ρ_0 and T_0 are the reference density and temperature, a is the thermal expansion coefficient, κ is the thermal diffusivity of air, C_p is the isobaric heat capacity, J is the rate per unit volume heat production, w'^2, $w'T'$, $u'T'$ are the local mean axial velocity and tracer fluxes due to turbulence fluctuations of w, u and T.

The following boundary conditions were assigned: No-slip velocity on the road surface, building walls and on the bottom and side boundaries of the domain, while symmetry conditions are assigned on the top boundary. The temperature of air entered the computational domain was set to 20°C. A 300 W/m^2 heat flux is considered to come out from the road during the midday hours for Scenarios I, III and IV, in combination with a 100 W/m^2 heat flux coming out from the left building wall for Scenario III and from both side walls of the canyon for Scenario IV. No heat flux is considered to come out from the canyon side walls for Scenario I, from the road for Scenario II or from the right building wall for Scenario III. Initially, zero velocity value was assigned at the entire computational domain.

3. RESULTS AND DISCUSION

3.1 Axial velocity and temperature on the canyon centreline

The axial velocity and temperatures of the simulated canyon calculated on its centreline are shown in Figure 2 for the four simulated scenarios. Paying attention on the Figure 2(a), it is observed that the velocities inside the city canyon are linearly increased with the height from the road surface until $y = 0.3h$ taking values from 0 to 0.20 m/s for Scenarios I, III and IV, while Scenario II has given somewhat greater values (0 to 0.26 m/s). This increase is a result of the accelerating air masses due to the thermal buoyant forces. In the centreline region from $y = 0.3h$ and up to the top of the buildings ($y = 1.2h$) the axial velocities are decreased up to values in the range (0.12 – 0.15 m/s) mainly due to the friction effects of the building walls. In the free space above the city canyon, due to thermal buoyancy, the centreline axial velocities are increased up to a value of 0.3 m/s for Scenario I and up to 0.44 m/s for Scenario II, while for Scenarios III and IV the values reach 0.4 m/s.

The heat sources of Scenario III are non symmetrical; thus, the centreline axial velocities vary in the range (0.3 – 0.4 m/s) in the region above the height $y = 2h$ and up to $y = 4h$, while Scenarios I and IV give approximately constant axial velocities in this region. This behaviour is characteristic in two-dimensional plume flows (Yannopoulos, 2006). In further heights the centreline axial velocities are decreasing as the flow is approaching to the ceiling of the computational space.

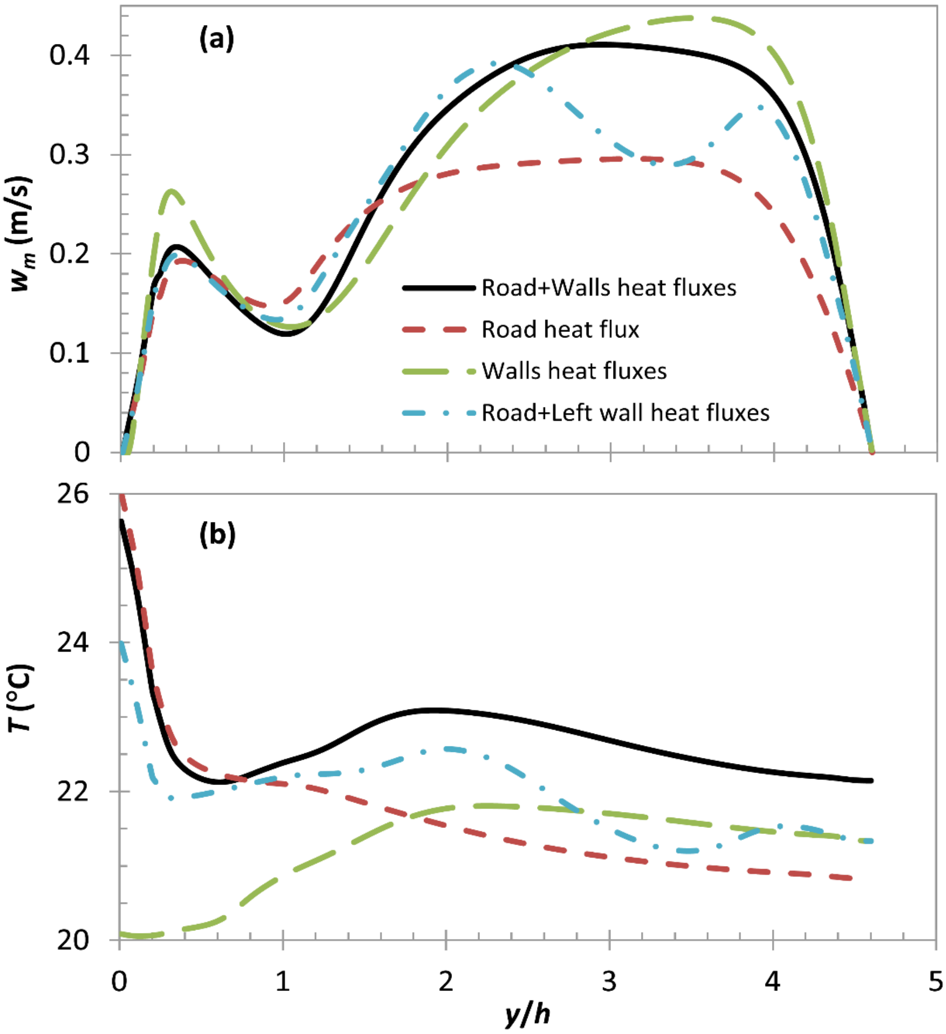


Figure 2: Variation with height of: (a) axial velocities; and (b) temperatures, for Scenarios I, II, III and IV simulated.

The variation of the air temperature along the city canyon centreline is shown in Figure 2(b). The temperature starts from 24 – 26°C at the road heat source (Scenarios I, III and IV) and from 20°C (ambient air temperature), when the heat source is only at the side walls. For Scenarios I, III and IV, the temperature is decreasing with about the same rate and reach the value of 22°C at the height region from $y = 0.4h$ up to $y = 0.8h$, while for Scenario II the temperature is increasing due to the wall thermal influence. This is also evident if paying attention on the temperature variation in further heights for Scenarios III and IV, which show a temperature increase from $y \approx 0.4h$ up to $y = 2h$, due to wall thermal plumes, while there is a gradual decrease for Scenario I, which has only a road heat source. In the height $y \approx 2h$ the temperature takes a maximum value of 23°C, 22.5°C and 21.8°C for Scenarios IV, III and II, correspondingly. Above this height there is a gradual decrease of temperature for Scenarios I, II and IV of symmetrical heat sources.

3.2 Transverse profiles of axial velocity and temperature

The transverse profiles of axial velocity at several heights above the road of the city canyon are shown in Figure 3 for the four scenarios simulated. The velocity profiles are shown in Figures 3(a), (b) and (d) for Scenarios I, II and IV of symmetrical heat sources, correspondingly. Therefore, the velocity profiles are symmetrical as expected, while the profiles of Scenario III, which has non symmetrical heat sources, are non symmetrical as well. The maximum value of axial velocity near the building is found at about the half building height ($y \approx 0.7h$) for Scenarios II, III and IV and is varied in the range

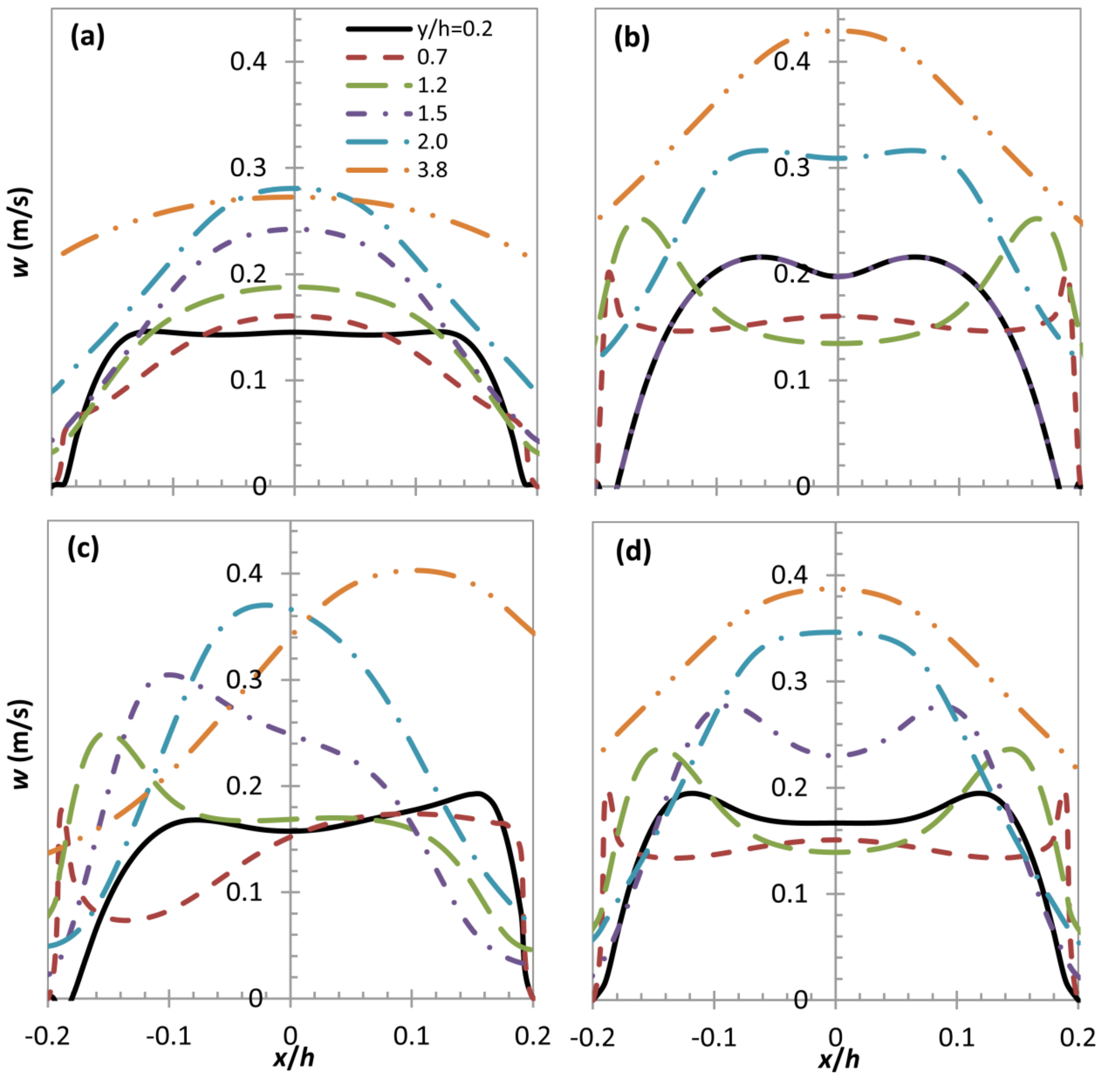


Figure 3: Transverse profiles at several heights of axial velocities for the simulated: (a) Scenario I; (b) Scenario II; (c) Scenario III; and (d) Scenario IV.

(0.17 – 0.2 m/s). The maximum axial velocity calculated is 0.44 m/s which is in the range of velocities measured in a calm atmosphere.

The transverse profiles of temperature at several heights above the road of the city canyon are shown in Figure 4 for the four scenarios simulated. The temperature profiles are shown in Figures 4(a), (b) and (d) for Scenarios I, II and IV of symmetrical heat sources, correspondingly. Therefore, the temperature profiles are symmetrical as expected, while the profiles of Scenario III, which has non symmetrical heat sources, are non symmetrical as well. The maximum value of temperature near the building is found at about the half building height ($y \approx 0.7h$) for Scenarios II, III and IV and is varied in the range (27 – 28°C or a bit higher). As expected, the temperature at the intermediate places of the city canyon is kept at lower levels than the temperature near the heat sources. It is interesting to note that the warm air near the building faces will deteriorate the comfortable interior room climatic conditions. The most adverse effect is found at about the middle of the building height for Scenarios II, III and IV, which assume that the building face is a source of heat flux.

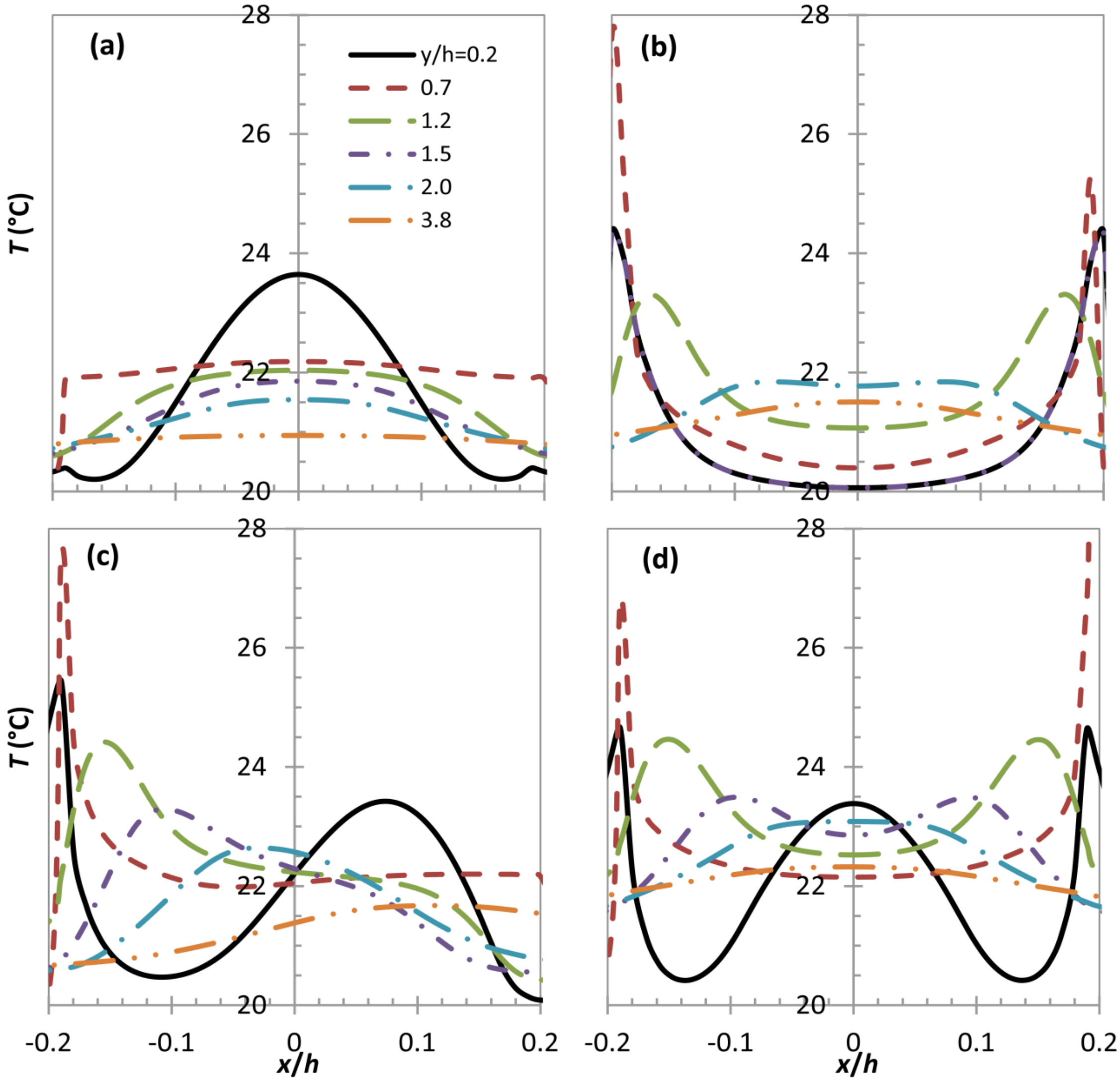


Figure 4: Transverse profiles at several heights of temperatures for the simulated: (a) Scenario I; (b) Scenario II; (c) Scenario III; and (d) Scenario IV.

4. CONCLUSIONS

For the four scenarios examined numerically regarding the thermal effects in a city street canyon due to heat fluxes originated from either the road (300 W/m^2) or/and the side building faces (100 W/m^2), the following conclusions are drawn:

- The axial velocities increase linearly initially up to about 0.3*h* taking values from 0 to 0.26 m/s and then decrease to 0.12 – 0.15 m/s up to the top of the buildings. The axial velocities near the faces of the buildings take values up to 0.20 m/s.
- The temperature at the street canyon centerline is about 24 – 26°C near the heat flux sources and initially starts decreasing linearly up to about 0.3*h* taking values around 22°C and then is kept nearly constant up to the top of the buildings. Near the faces of the buildings, when heat sources are considered, the temperature reaches 28°C or may be higher in the lower half of the building height that may affect adversely the comfort of room climatic conditions.

Over the buildings height, the air velocities are increasing up to a maximum value of 0.44 m/s, which characterizes a calm atmosphere. The temperature remains also at a level of 21 – 23°C.

References

1. Battista G. and L. Mauri (2016) 'Numerical study of buoyant flows in street canyon caused by ground and building heating', 71st Conference of the **Italian thermal Machines Engineering Association**, AT12016, 14-16 September, Turin.
2. De Lieto Vollaro A., Galli G. and A. Vallati (2015a) 'CFD Analysis of Convective Heat Transfer Coefficient on External Surfaces of Buildings', **Sustainability**, Vol. 7, pp. 9088-9099.
3. De Lieto Vollaro A., Galli G., Vallati A. and R. Romagnoli (2015b) 'Analysis of thermal field within an urban canyon with variable thermophysical characteristics of the building's walls', **Journal of Physics: Conference Series**, 655, 012056.
4. De Lieto Vollaro R., Vallati A. and S. Bottillo (2013) 'Differents Methods to Estimate the Mean Radiant Temperature in an Urban Canyon', **Advanced Materials Research**, 650, pp. 647-651.
5. Li L., Yang L., Zhanh L.J. and Y. Jiang (2012) 'Numerical Study on the Impact of Ground Heating and Ambient Wind Speed on Flow Fields in Street Canyons', **Advances in Atmospheric Sciences**, 29(6), pp 1227-1237.
6. Memon R.A., Leung D.Y.C. and C. Liu (2009) 'An investigation of urban heat island intensity (UHII) as an indicator of urban heating', **Atmospheric Research**, Vol. 94 pp. 491–500.
7. Schwela D. (2000) 'Air Pollution and Health in Urban Areas', **Reviews on Environmental Health**, Volume 15, Issue 1-2, pp. 13–42.
8. Yannopoulos P. (2006) 'An improved integral model for plane and round turbulent buoyant jets', **J. Fluid Mech**, Vol. 547, pp. 267-296.
9. Zakaria M., Abu Bakar M., Ridhwan J., Mohd and M. Hanafi (2014) 'CFD analysis of flow, pollutant dispersion and thermal effect in street canyons', **Journal of Engineering and Technology**, Vol.5 No.1, pp. 99-120.

IMPACT OF THE TUMULUS ON THE STABILITY OF MICROCLIMATE IN UNDERGROUND HERITAGE STRUCTURES

V.Th. Kyriakou* and V.P. Panoskaltsis

Department of Civil Engineering, Demokritos University of Thrace, University Campus Xanthi-Kimmeria, Xanthi, 67100, GREECE

*Corresponding author, e-mail: vanta.kiriakou@gmail.com, tel: +30 6945380388

Abstract

After having scientific documentation of the variations of temperature and relative humidity inside three Macedonian tombs excavated in the area of Pella and Agios Athanasios, comparative analysis of the data was conducted. The analysis of the hydrothermal behavior of these underground chambers showed that the tumulus protected the tombs and their treasures against the deterioration processes.

The tumuli over tombs in north Greece named “Macedonian tombs” were constructed in ancient times as “far seen signs” of important persons’ burials. Structurally, the tumulus is a big mass of artificial earth, covering monumental tombs which are dated between the 4th and 2nd century B.C. Its construction is the artificial packing of different layers of earth, with different consistency. These layers created a perfect drainage system. This way, the rain water was directed to the periphery of the cone-shaped tumulus and not inside the tombs. Because of the thermal inertia of the surrounding soil, fluctuations of temperature were of less width inside the tombs than outside. The tombs were preserved under stable microclimatic conditions in a very good state.

This study shows that the tumulus is a very important technical achievement for its era, not only due to its great mass -sometimes 12 m. high, but due to its construction and the impact to the protection of the underneath tombs, which are significant heritage structures. Other factors that affected the microclimate stability inside the tombs were the volume of the interior space, the rate of exposure to the external climate and the protection measures after the excavation. Estimations according to the analysis are presented in this paper.

Keywords: Microclimate, Hydrothermal performance, Heritage structures, Macedonian tombs, Tumulus

1. INTRODUCTION

An important feature of the Macedonian tombs is their artificial sedimentation with soil, in the shape of a conical tomb, the reason for its creation may have been local religious beliefs and burial customs. [Gossel, 1980] The result was that these monumental graves remained completely unseen, destined exclusively to the dead and the goddesses, according to the metaphysical beliefs of the ancient Macedonians.

Although up to now more than 100 tombs have been excavated throughout Macedonia, archaeological interest has been traced to the importance of the Macedonian tombs revealed and no systematic research has been done on the tumulus itself, the way it was constructed and the significance of existence and preserving it.

References are only made to archaeological announcements, but they are always fragmentary and short. Manolis Andronikos, the archaeologist who supervised the excavation of the royal tombs of Vergina, wrote that the tumulus is a "monument of a significant burial", meaning that the artificial embankment is a "monument" itself. At the same time, he noticed that it is not a simple build-up of soil but has a specific structure.

P. Harisis wrote in 1978 his first technical essay, titled "Rules for the Construction of Burial Tumuli", where he tried to analyze the tumulus as a geometric solid and to explain its static structure [Harisis, 1978].

During the last decade, archaeologists who excavated Macedonian tombs have made simple references to the construction of the tumuli. There have been designed depictions of the stratigraphic sections, but no further research has been done on the structure and the reason for the existence of the tumulus. It is still treated as a mass of soil, which should be removed during the excavation in order to reveal the hidden treasure.

The present work is a first attempt to decode this huge technical work, not only in terms of its construction, but mainly in terms of its operation in relation to the tombs underneath. The 3-year study of Macedonian tombs in the area of Pella and Agios Athanasios, with continuous measurements of the microclimatic conditions in these monuments, revealed the direct correlation of the volume of the tumulus with the hydrothermal conditions in the tombs and the subsequent damage to their building materials.

2. THE TUMULUS

2.1 Origin - Geographical location

The practice of building mounds as burial marks has a long-standing presence in the area of the Balkan Peninsula. Tombs clusters have been identified in ancient Thrace as well as in ancient Illyria. In Greece, the most representative example is the necropolis in Vergina, with tombs dating back to 1000-700 B.C. until the 2nd century B.C. Some interaction between the three areas must be considered certain and expected. It is very difficult to determine when, under what conditions and from which geographic area it began and how the practice of mound building was adopted by Macedonia [Gurova, 1999]. Apart from the Balkan region, similar burial monuments have been studied all over the world, concerning their hydrothermal performance. In the international literature, we can find references to the Etruscan tombs in Tarquinia - Italy, the massive burial tombs in Turkey, the graves of Japan emperors, the tombs in Valley of the Kings - Egypt.

2.2 Reasons for constructing the tumulus in the ancient era

According to Homer, the tumulus is a "far seen sign" (the sign that appears from a distance) and according to Manolis Andronikos it is the "tombstone" of a significant burial. It is not yet confirmed whether tombstones were placed at the top of the tumulus, although it was enough to mark the site of burial. Apart from the operation of the sign, there were definitely and practical reasons that led to the construction of the artificial tumulus. These reasons are:

1. to protect the grave and valuable burial offerings from the tomb thieves, and

2. to protect the structural materials of the tomb from deterioration due to environmental conditions.

Therefore, with the construction of the tumulus, the ancient technicians aimed to protect the burial of desecration and the tomb from deterioration.

2.3 The tumulus as a technical project

The tumulus must be considered as a technical achievement for that era, taking into account the huge quantities of soil that had to be transported and spread, with the use of transport means, lifting machines and the laborious work of hundreds of people. Ancient builders knew very well the characteristics of the soil and its layering. Observations on how the tumulus was built, lead to the

conclusion that it is not just a random build-up of soil but it is a properly designed work with structural consistency to withstand time and stratification to ensure water runoff to its periphery so as little as possible water retention and minimal inflow to the grave. (Fig.1)

This is accomplished by alternating successive layers of chopped and coarse material. The condensed fine-grained layer has a low degree of water permeability; therefore it does not allow rain water to penetrate deep so that it concentrates on its upper surface. The layer of coarse material allows the free flow of water, which before it would penetrate into the lower layers, flows, due to the slope, to the perimeter of the tumulus, away from the tomb [Harisis, 1978]. In addition, the volume of accumulated soil with its high heat capacity ensures temperature stability and relative humidity inside the monument, since it isolates it from the climate conditions.

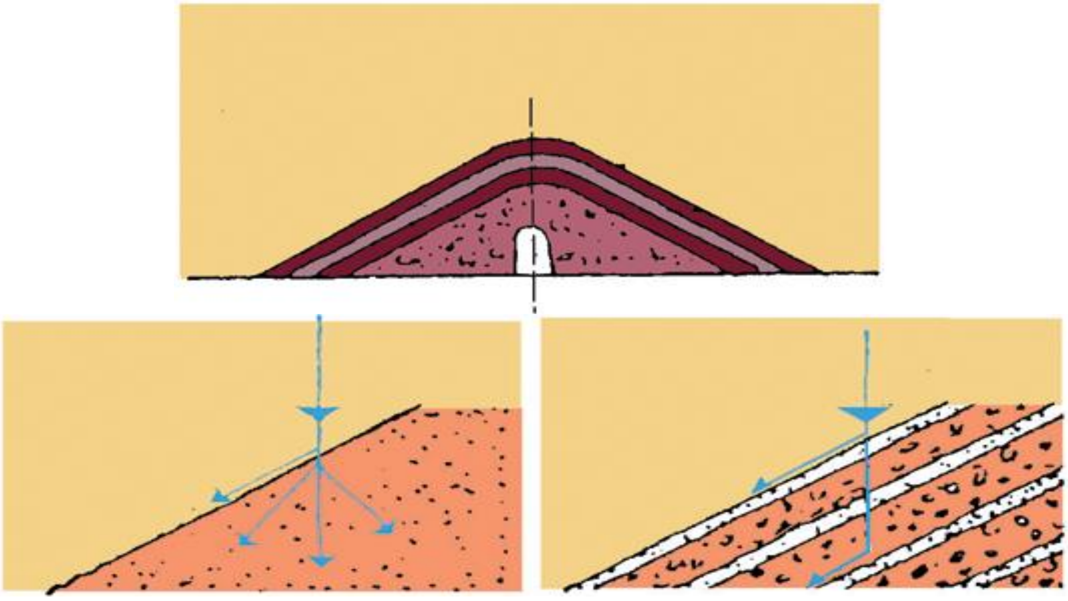


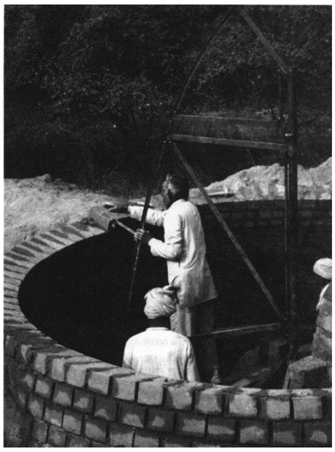
Figure 1: Representation of the water fluxes due to the different construction layers of the tumulus [Harisis, P., 1978. Computer coloring by authors]

2.4 Discussion about how the tumulus was constructed

The excavation process which has been applied and continues to be the accepted method of exploration in the tombs of the Macedonian tombs, led to the complete demolition of the tumulus, often without being previously designed. Until now, as far as is known from the literature, detailed research on the layering of the tumulus has not been mentioned. Technically, the way that the tumulus was built remains unknown. No evidence has been found of the methods of construction. Evidently, certain tools and machines were used for the elevation of the soil, the layering, the condensation of the layers, the achievement of the geometry of the conical shape as a one.

2.4.1 The example of modern constructions

The technology of our times is far from that of our ancient ancestors. But there are some elements in practical methodology that are so basic, that they may not have changed much since antiquity. If we observe the construction of circular buildings today, beyond the image of modern materials and machinery, we can see that it is based on reference to the center of the base circle and the vertical axon. (Fig.2a) A crane machine is placed at the center point and the construction is raised parametrically, from the bottom to the top. The rationale is very simple and leads to the question: was the tumulus built in a similar way?

Figures 2-3: Circular modern buildings [Photo by authors] - Traditional circular clay buildings [Pearlmutter, D., 1992]

2.4.2 The example of traditional circular clay buildings

Corresponding building styles can be found in traditional architecture, with dome construction. A central vertical guide serves as a reference (Fig.2b) while its horizontal stem ensures proper layering [Pearlmutter, 1992].

2.4.3 An example from the excavation of a Phrygian tumulus

The only example of a detailed excavation of a tumulus has been reported in the case of the Tomb in Gordion, Phrygia, where the excavation reveals the existence of a wooden vertical guide in the center of the tumulus [Young, 1981].

2.5 Hydrothermal behavior and water-proofing

An underground construction is influenced by seasonal cycles but not by daily ones. The hydro-thermal evolution within this interior is related to the following factors:

1. The thermal energy transferred through the soil to the building elements (floor, walls, roof) and then through the building elements to the air of the interior. This thermal energy is associated with daytime and seasonal cycles.

2. Water exchanges at all concentration stages, in a similar way between soil and indoor air. These latter, moreover, are in close connection with the exchanges of thermal energy [Massari, 1993]. In literature, there are reports of methods of waterproofing tombs, not only to the ancient Macedonians. Characteristic is the case of the Tomb in Gordion, Phrygia, where a layer of clay carefully compressed and polished over the wooden grave was able to keep its shape even after the tomb roof collapsed [Young, 1981] The use of this material is attributed to the intention of waterproofing the tomb, but also to the static reinforcement of the roof (Fig.3).

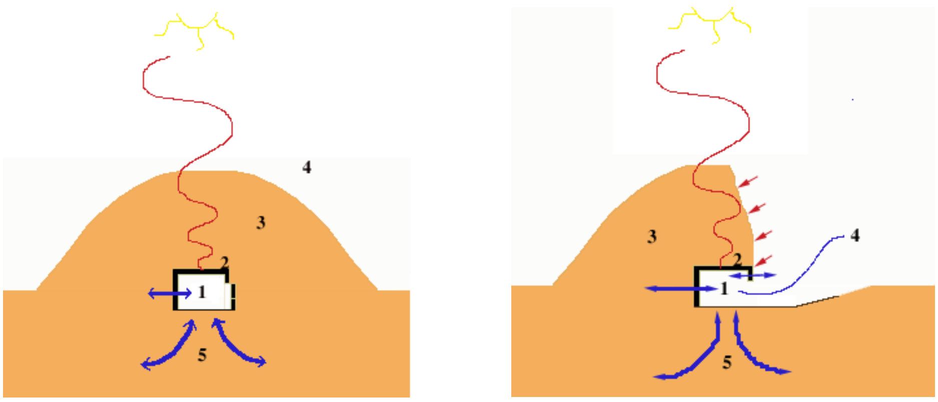
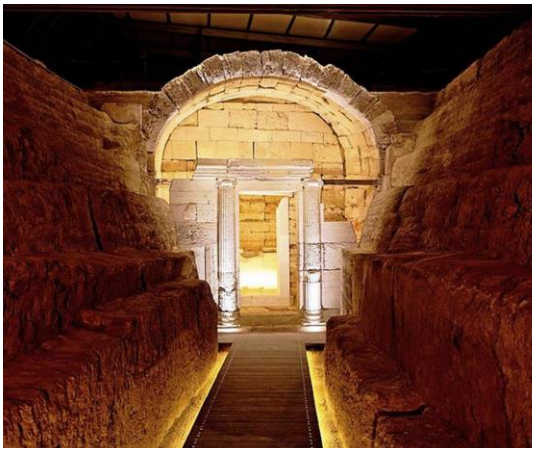


Figure 4: Exchanges of air and humidity between interior and the surroundings. [Authors]

Observations on the layering of the tumuli in various Macedonian tombs are presented. The construction with alternating layers is evident in the vertical slopes of the excavated tumuli. In the tomb of Agios Athanasios, there was observed the existence of a layer of solid clay just above the arc-like roof of the tomb. The same layer of clay was also found above the roof-arch in the tomb of Langada. (Fig.4)

Figures 5 - 6: Macedonian tombs in Agios Athanasios and Langada

3. THE RESEARCH

3.1 Location and climate conditions

The monuments studied are located geographically at the plain of Thessaloniki, NW from the present bay of Thermaikos gulf. The local climatic conditions present the characteristics of the Mediterranean climate. The air temperature during the year shows a simple fluctuation, with a maximum in July and a minimum in January. Rains usually fall late in autumn and spring. Thus, in the winter and spring months there is excess water and high humidity, while in the summer there happens a very intense evaporation.

3.2 Tombs of Pella

Sixteen burial tombs are located in the area of Pella. [Chrysostomou, 1987, 1994] Two of them were the subject of this research.

A. The tumulus D', at the eastern cemetery of Pella has a diameter of 60m and a height of 9 m. A two-chamber burial structure with a Doric facade was found at the south part of the tumulus, at a depth of 4.30 counting from the top. The tomb dates back to the end of the 4th century B.C.

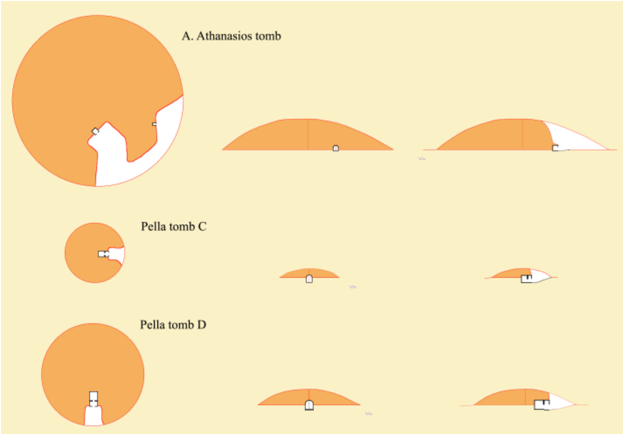
B. The tumulus C' of the cemetery of Pella, located south of the road of Thessaloniki - Giannitsa, 3.3 km away from it. Tomb dimensions: 5m height and a diameter of 35m. A two-chamber burial building with Ionic facade and "road" (dromos) was found, under the 5m tumulus. The orientation of the facade is towards the east. The tomb dates back to the beginning of the 3rd century B.C.

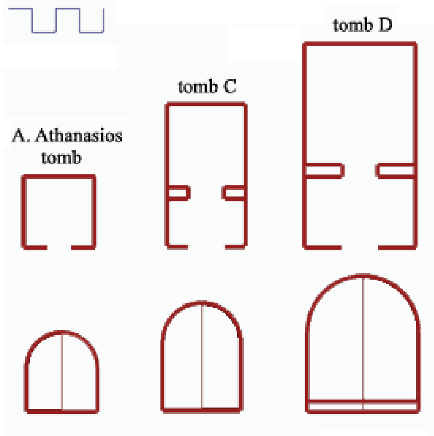
3.3 Tombs of Agios Athanasios, Thessaloniki

The cemetery at Agios Athanasios is related to the settlement in the neighboring tumulus Topsin, on the east bank of Axios river, where there are indications of habitation from the Neolithic to the late Hellenistic period, which likelihood can be identified with the ancient city Halastra. The big tumulus is 100m in diameter and 18m height [Tsimbidou, 1993, 1994]. After an excavation survey in the tumulus, two important tombs were found:

- a monumental box-shaped tomb, having internal dimensions of 2.00 x 1.45m and a height of about 1.50 m. It dates back to the late 4th or early 3rd century B.C.

- a Macedonian tomb with a painted facade. It is dated in the 4th century B.C. It is characterized by frescoes on the façade, an important example of painting in Macedonia.





Figures 7 - 8 : Horizontal and vertical cross-sections of three tumuli [Authors] - Comparative sections of four tumuli [Authors]

3.4 Recording the microclimate in the tombs

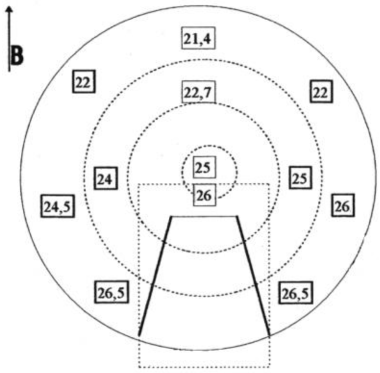
The precise hydrothermal state of the structure had to be studied after recording of the surface temperatures on the interior walls in contact with the soil, the façade wall exposed to the external climate, as well as in the air of the interior space. In particular, changes in the thermal status of the monuments were recorded on a daily and annual basis, with reference to the horizontal direction (façade-antechamber-chamber) and the vertical direction (floor - middle level - arch). Recordings were made in two ways (Fig.6) :

1. Instantaneous recordings once a month, all over the inner surface of the monuments and on the facade, with a simple temperature display.

2. Continuous electronic recording with sensor placement at specific points of the walls, with an hourly step.







Figures 9 – 10 - 11: Electronic data were obtained inside the tomb D and on the surface of the tumulus [Source: Authors]

4. DIAGRAMS – OBSERVATIONS

Observations on the recordings in the four monuments over three years, led to stating the following:

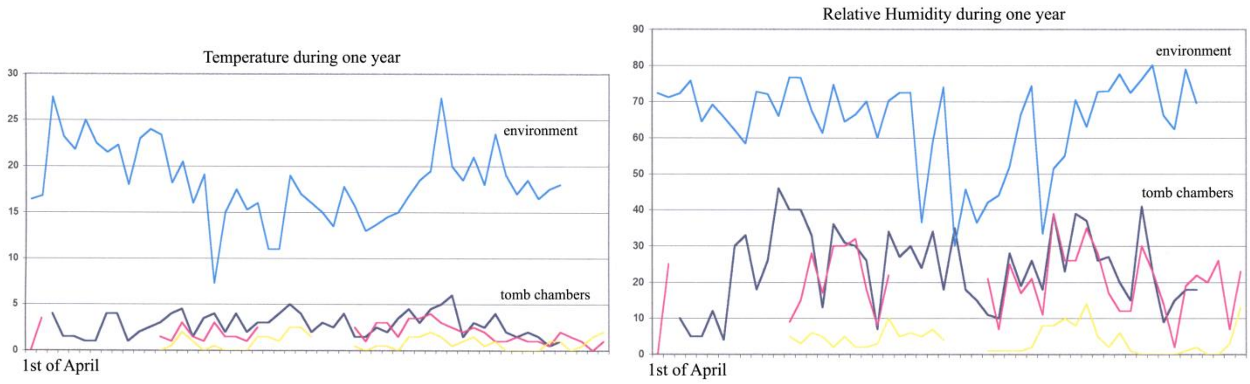
1. All tombs present reduced range of temperature and relative humidity in their interior space and phase delay in relation to external environmental conditions, due to the increased heat capacity of their construction materials and the embankment of the tumulus.

2. The most stable state of the microclimate prevails in the Doric tomb of Pella. Compared to the rest of the tombs, it is the largest in size and is covered by the second in size tumulus. The revelation of his structural body has only been made at the level of the facade.

3. The second tentacle of stability is the Ionic tomb of Pella. It is the second in dimensions and is covered by the smallest tumulus. The revelation of his structural body has only been made at the level of the face.

4. The third is the Macedonian tomb of Agios Athanasios. It is the third largest in size and is covered by the largest tumulus. A large part of the building structure was exposed to the environment, since, due to the poor static view of the arched state, a large part of the tumulus was disembarked over it. Thus, in addition to the facade, most of the roof remained unprotected. To protect it was made a wooden enclosure with sheets and nylon, which later was strengthened with double entry and stylized, with obvious results in the reduction of the range of fluctuations.

5. The box-shaped tomb has the smallest size and is covered by the largest tumulus. It shows the greatest instability of environmental conditions. The revelation of his structural body has been made only at the level of the facade.



Figures 12 - 13: Diagrams of temperature and relative humidity. Relationship between the three tombs and the environment [Authors]

5. CALCULATIONS

Calculations have been done with the use of the software WUFI pro, on moisture transfer and moisture content in the building elements. Equations - The Calculation Model

5.1 Moisture Transfer

In porous building materials the predominant moisture transport mechanisms are vapor diffusion, surface diffusion and capillary conduction. Other transport phenomena, for example seepage flow through gravitation in non-saturated pore spaces or migration of water molecules due to electric fields or osmotic pressures, cannot yet be computed in a satisfactory way. However, since they only play a major part in exceptional cases, they are not further considered here. Convection effects, for example moist interior air permeating building components because of pressure differentials between the interior and the exterior side, are ignored as well. Since airtightness is an essential property of a building wall, air convection is in practice only found in unplanned cases of defective parts or inappropriate building components. It is therefore difficult to quantify beforehand and could also only be realistically determined by three-dimensional fluid dynamical simulation programs. The driving force for surface diffusion is therefore relative humidity and not vapor pressure. Thus under the boundary conditions, vapor diffusion and surface diffusion go in opposite directions. Surface diffusion must therefore be regarded as a type of liquid transport, not a type of vapor transport in the gas phase.

5.2 Hygrothermal Material Properties

In general, the following material properties are necessary for the non-steady computation of the temperature fields:

bulk density ρ of the dry material, specific heat capacity c, thermal conductivity λ

The hygric properties that need to be known for all (i.e. also for non-hygroscopic) materials are:

- Water vapor diffusion resistance factor μ (μ-value)
- Porosity ε (as a measure of the maximum possible water content wmax)

If the behavior of hygroscopic, capillary active materials is to be simulated correctly, the moisture storage function and the moisture-dependent liquid transport coefficients are also needed.

5.3 Climate Conditions and Surface Transfer

Through its surfaces, every building component is undergoing hygrothermal interaction with its surroundings. The surroundings are affecting the component and the component is affecting its surroundings, for example by releasing stored heat or by sorption of indoor air humidity. Basically, three types of boundary conditions must be distinguished: the exterior ambient conditions above and below the ground and the indoor conditions. In all three cases, different surface transfer conditions have to be employed, due to the different exchange processes involving convection and radiation or conduction and diffusion.

5.4 Hygrothermal conditions below ground

Below ground, the variations of the exterior air temperature only propagate strongly damped. A study show that at a depth of 1m below the surface the damping eliminates all daily variations. Furthermore, there is a phase shift of several weeks with respect to the air temperature which is most noticeable in spring and in autumn. The humidity in the ground usually lies between 99% and 100% RH if vegetation is present, since plants cannot extract moisture from the ground at lower humidities. This also applies to substrate layers in planted roofs, although at different temperature levels.

5.5 Equations - The Calculation Model

A number of hygrothermal simulation models which provide reliable results has been developed in different countries. The following description discusses the model which forms the basis for the PC program WUFI (**W**ärme- **U**nd **F**euchtetransport **I**nstationär) [Künzel, 1994]. In this model the non-steady heat and moisture transport processes in building components are described by the following coupled differential equations:

$$\frac{\partial H}{\partial \vartheta}\frac{\partial \vartheta}{\partial t} = \frac{\partial}{\partial x}\left(\lambda\frac{\partial \vartheta}{\partial x}\right) + h_v\frac{\partial}{\partial x}\left(\frac{\delta}{\mu}\frac{\partial p}{\partial x}\right) \quad \textbf{Heat transport} \qquad (1)$$

$$\rho_w\frac{\partial u}{\partial \varphi}\frac{\partial \varphi}{\partial t} = \frac{\partial}{\partial x}\left(\rho_w D_w\frac{\partial u}{\partial \varphi}\frac{\partial \varphi}{\partial x}\right) + \frac{\partial}{\partial x}\left(\frac{\delta}{\mu}\frac{\partial p}{\partial x}\right) \quad \textbf{Moisture transport} \qquad (2)$$

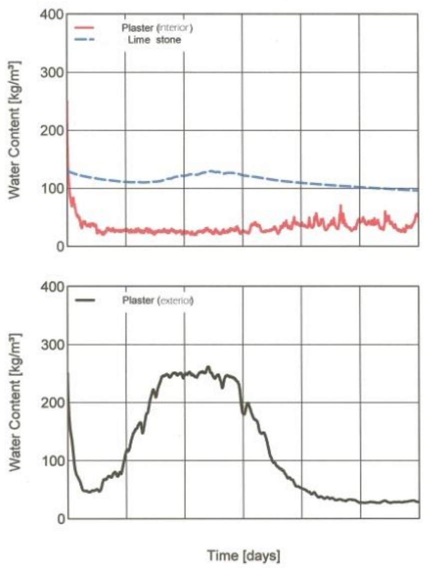
D_W [m²/s] : Liquid transport coefficient
H[J/m³] : Enthalpy of moist building material
h_v [J/kg] : Evaporation enthalpy of water
p [Pa] : Water vapor partial pressure
u [m³/m³] : Water content
δ [kg/msPa] : Water vapor diffusion coefficient in air
[°C] : Temperature
λ [W/mK] : Heat conductivity of moist material

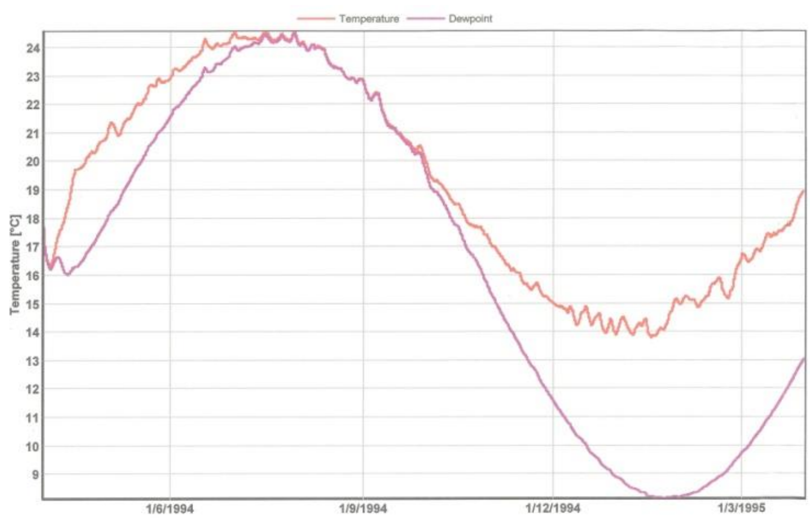
μ [-] : Vapor diffusion resistance factor of dry material
ρ_w [kg/m³] : Density of water
φ [-] : Relative humidity

6. DISCUSSION

6.1 Exposure to the external environment, evaporation, condensation and water content

Periods with open entrance to the tomb, cause great intensity of the phenomenon of evaporation, especially during the midday and afternoon hours. It is characteristic that the excavation and opening of the tombs took place between April and June, precisely during the less appropriate period of the year. For the parts of the structure that have been excavated, the condensation conditions are different. Thus, condensation may occur on the internal surfaces of the exposed walls or within their mass. This phenomenon may occur during winter or at night in the summer and if the relative humidity of the indoor air is high.





Figures 14 - 15: Water content in three different layers of the facade during one year - Temperature and dew point inside the stone mass, in one year period [Authors]

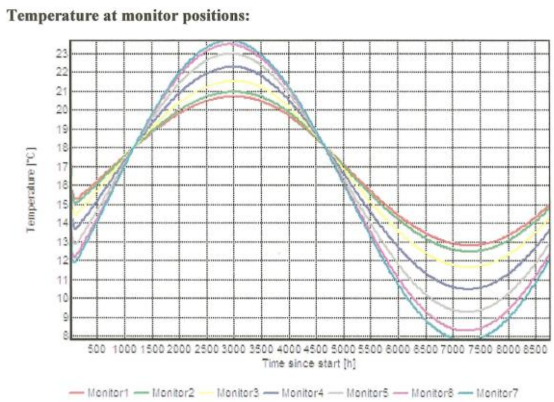


Figure 16: Temperature inside the stone mass of the facade during one year, at different positions of a cross section [Authors]

6.2 The type of the shelter

The construction of a closed shelter aimed to reduce to a greater extent the air exchanges and the better guarding of the monument, but not a complete protection from the weather changes, due to the absence of thermal insulation.

6.3 Human interventions

Generally, the relative humidity increase, happened in the indoor air of the monuments due to human presence, as well as due to the movement of air layers, resulting in evaporation from interior walls. Air currents may be caused by a rise in pressure in front of the entrance of the tomb. When it becomes greater than the pressure inside, it causes air to move out, due to a pressure difference.

6.4 Excavation period

An important outcome seems to be the diagrams showing the total water content in three different hypothetic excavation periods. The opening of the tomb is supposed to have started in case 1 at the 1st of April, in case 2 at the 1st of September and in case 3 at the 1st of January.

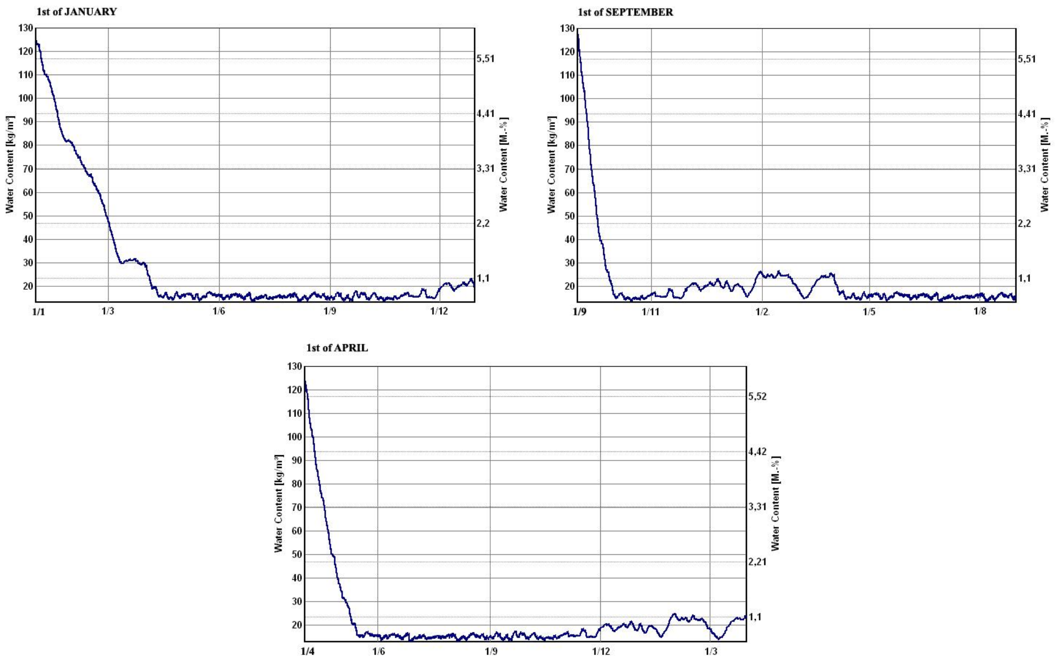


Figure 17: The water content in the tomb's façade, in relation to the excavation period. Comparison between April, September and January [Authors]

The comparison between the three situations gives the following results: the building component of the tomb's façade, that is mainly exposed after the excavation to the outdoor climatic conditions, is getting dry immediately. The drying period is one month during April and September, in cases 1 and 2. The drying period is more extended in case 3, when the hypothetic excavation begins in January. The building component of the tomb's façade is getting dry after three months. (Fig. 10)

7. CONCLUSIONS

The tumulus must be subject of great attention and thorough investigation. The disturbance of the constructional balance of the tumulus as a natural solid shape with internal retaining forces, as well as the exposure of the slopes of the excavation to the devastating effect of the environment (rains, winds, solar radiation, wetting-drying procedures), are serious risks for future gradual collapse and total loss.

The materials of Macedonian tombs easily absorb moisture due to their porous composition and easily dry by evaporation to the environment. Generally, they are subjected to an annual cycle of wetting-drying. The same cycle is created on a daily basis to the parts of the tomb that remain exposed to changes in climatic conditions and have a higher intensity over specific periods of time, mainly during summer and less during winter. Evaporation is especially favored during the summer and only in

special conditions until late autumn. The phenomenon of condensation mainly takes place in spring, but it can occur occasionally in winter under special conditions. Generally the greatest intensity of the phenomena occurs in the exposed parts of the walls. Deterioration of wall paintings occurs mainly during the evaporation phase. Reconsidering the prevailing practices regarding excavation activity on tumuli, in connection with the final formation of the microclimate in the tombs, one can draw conclusions about the human interventions that lead to the deterioration of the monuments.
Simulation of the opening of the tomb in three different hypothetic excavation periods, leads to a drying period of one month during April and September and three months when the excavation begins in January. So the most dangerous period is between April and September. Late autumn, and winter is the best time for excavation activity. In the future, the excavation process should be planned according to the dehumidification of the building components, in order to protect the important wall paintings.

References

1. Accardo, G. - Cacace, C. - Rinaldi, R., "La Tomba dei Rilievi in Cervetery: Applicazione della Metodologia Climatica"
2. Gossel, B., 1980 "Makedonische Kammergraber", Doctoral thesis, Berlin
3. Harisis P., 1978 "Rules for the Construction of Tumuli of Burials" publication of the EHS - Hepiros Studies Company (in Greek)
4. Gurova, N., 1999 «Kimerios Vosporos. The big Tumuli», **Journal Corpus – Archaeology and History of Cultures**, Vol.7, p.48-59
5. Pearlmutter, D., 1992 "The Thermal Performance of Vaulted Roofs in Hot Arid Zones" **3rd International Conference Energy and Building in Mediterranean Area**, p.295-302, April 8-10, Thessaloniki, Greece
6. Young, S.R., 1981 "Three great early Tumuli", The Gordion Excavations. Final Reports. Volume I. The University Museum, Pennsylvania
7. Massari, G., Massari, I., 1993 "Damp Buildings, Old and New", Rome
8. Chrysostomou, P., 1994 «Excavation research of Macedonian Tombs at Pella during 1994» **Archaeological Works at Macedonia and Thrace**, No 8, 1994**,** p.53 (in Greek)
9. Chrysostomou, P., 1987 «New tumuli in the land of Pella» Archaeological Works at Macedonia and Thrace, n. 1, 1987, σελ.147-157 (in Greek)
10. Tsimbidou, M., 1993 «Burial tumulus at Agios Athanasios in Thessaloniki: Complete of the research», **Archaeological Works at Macedonia and Thrace**, n. 7, 1993, σελ.251-259 (in Greek)
11. Tsimbidou, M., 1994 «Agios Athanasios 1994. The chronicle of a reveal», **Archaeological Works at Macedonia and Thrace**, n. 8, 1994, p. 231 (in Greek)
12. Künzel H.M., 1994 Verfahren zur ein- und zweidimensionalen Berechnung des gekoppelten Wärme- und Feuchtetransports in Bauteilen mit einfachen Kennwerten; Dissertation Universität Stuttgart

COMPARING ENVIRONMENTAL IMPACTS OF TWO OFFICE SEATING UNITS VIA LIFE CYCLE ASSESSMENT

Merve Mermertas[1], Koray Ozsoy[2], Thomas P. Gloria[3], Fatos Germirli Babuna*[1]

[1]Environmental Engineering Department, Istanbul Technical University, Maslak 34469, Istanbul, Turkey

[2]Koleksiyon Furniture Ltd. , Istanbul, Turkey

[3]Division of Continuing Education, Harvard University, Cambridge, United Kingdom

*Corresponding author: e-mail: germirliba@itu.edu.tr, tel: +9053240903555

Abstract

This study aims to compare the environmental impacts of two office-seating units via life cycle assessment (LCA) methodology. The system boundary covers raw material extraction and pre-processing, transportation, manufacturing, distribution and usage and end of life stages. Therefore, the results are obtained on the whole life cycle. The evaluated impact categories are as follows: Global warming potential (GWP), acidification potential (AP), eutrophication potential (EP) and photochemical ozone creation potential (smog) (POCP). This study is a pioneering one conducted on the Turkish furniture industry. For both of the seating units under investigation raw material extraction and pre-processing stage have the highest share in all impact categories. Considerable differences in impacts are observed for the two seating units evaluated.

Keywords: environmental impact; life cycle assessment; furniture; office seating; sustainability

1. INTRODUCTION

Life cycle assessment (LCA) is the most commonly used tool to find out the environmental impacts of services, products and processes in a holistic point of view. While indicating the environmental burdens of various products, it grounds a very beneficial platform for comparing the products designated to fulfil the same function, and/or improving diverse stages of production/transportation/end of life to achieve sustainability.

Up to now inadequate number of LCA studies are conducted in Turkey by considering the site specific issues (Atmaca, 2016; Atilgan and Azapagic, 2016; Ozkan et. al., 2017; Gunkaya et. al., 2016; Demirel and Erkayaoglu, 2016).

The furniture industry is one of the emerging sectors in Turkey. The firms range from large scale that manufacture by automated mass-production techniques to small workshops. The large ones mainly produce for exporting the goods to different parts of the world. An accelerating trend in exports is observed in the last decade reaching to US $ 2,2 billion in 2015 (MoE, 2016).

One can find LCA studies concerning the furniture industry in literature (Iritani et. al., 2015; Cordella and Hidalgo 2016; Kouchaki-Penchah et. al., 2016; Piekarski et. al., 2017; González-García et. al., 2012; Mirabella et. al., 2014). However, Turkish furniture industry is not studied through LCA methodology based on country specific data.

In this context, the objective this study is to compare the environmental impacts of two office-seating units through LCA approach. A cradle to grave scope covering the whole life cycle is adopted. Inventory data is collected from a large scale Turkish furniture manufacturer.

2. MATERIALS AND METHODS

The scope of LCA is from cradle to grave. Therefore, the system boundary covers raw material extraction and pre-processing, transportation, manufacturing, distribution and usage and end of life stages.

The following assumption is made about the end of life stage: 80 % of the product (by mass) is sent to a landfill area and the rest is directed to incineration.

The functional unit is one unit of seating to be used by one individual, maintained for a 10 year period of time.

Global warming potential (GWP), acidification potential (AP), eutrophication potential (EP), photochemical ozone creation potential (smog) (POCP) and ozone depletion potential (ODP) are the investigated impact categories.

Data is collected for 12 consecutive months from the actual furniture manufacturing plant. Fabric manufacturing and the distribution are not take place in Turkey.

The LCA study analysis is realized by following the Product Category Rule (PCR) (BIFMA PCR for Seating: UNCPC 3811) (NSF, 2018), in accordance with ISO 14040 series standards (ISO, 2006).

GaBi DB Version 6.115 software system is used for modelling. TRACI 2.1 Impact Categories are adopted.

The energy is allocated by considering the total annual amount of energy consumed in the facility during manufacturing of the seating units and the total number of seating units produced.

During the packaging of the final product 50 staples are assumed to be used.

The company has no data on the type of trucks used for the transportation of some materials. Therefore, 18.4 payload capacity trucks are assumed to be used for this type of transportation.

Cargo aircrafts are used for transportation to US and Europe. A road transportation of 32 km’s (by trucks) is considered for reaching the end of life facilities (as given in US EPA Waste Reduction WARM Model) (US EPA 2018).

3. PRODUCTION OF THE SEATING UNITS AND PRODUCT SPECIFICATIONS

The investigated office seating units are illustrated in Figure 1. The production flowcharts are given in Figure 2.

Seating unit A has a length of 745 mm and a height of 1127 to 1247 mm. On the other hand, product B has a length of 728 mm and a height of 1120 mm. Both of the units are covered with fabric.



(A) (B)

Figure 1: Office seating units A and B

Quite a similar manufacturing scheme is applied for both of the seating units. As the first step, the polyurethane rigid foam base of seating units A and B is subjected to manual sanding to get a smooth surface for fixing the upholstery. The cut fabric is sewed and cladded on the foam base. Cut and shaped sheet iron are used for various parts of the seating unit such as legs and accessories. Painting is applied on legs of seating unit B. Parts are get together in montage step and the packaging is applied.



(A)



(B)

Figure 2: Production flowcharts of A and B

For both of the products cardboard, polypropylene and polyethylene are the used materials for packaging. The packaging materials are easily separable. Most of the packaging materials are collected, sorted and recycled.

The wastes arising from the manufacturing of seating unit A and B is textile scraps, packaging materials and scraps of iron. Apart from these paint wastes are also generated during the production of seating unit B. All these wastes are sent to recycling facilities.

4. RESULTS

4.1 Life Cycle Inventory (LCI)

The data collected per one seating for both of the seating units are presented in Table 1, 2 and 3.

Table 1: Raw materials for seating unit A and B

Main Materials	Mass (kg)	Mass Percentage (%)
Polyurethane :	7,000	55,10%
Fabric :	0,480	3,78%
Mechanisim / Aluminium :	1,200	9,45%
Gas Cylinder Mechanism :	0,800	6,30%
Furniture Leg :	2,000	15,74%
Wheel :	1,225	9,64%
TOTAL Weight :	**12,705**	**100%**

(A)

Main Materials	Mass (kg)	Mass Percentage (%)
Polyurethane Seat :	8,686	41,70%
Fabric :	2,628	12,62%
Mechanism :	1,917	9,20%
Interlining Fabric :	0,412	1,98%
Fiber :	0,144	0,69%
Furniture Leg :	7,041	33,81%
TOTAL Weight :	**20,828**	**100%**

(B)

Table 2: Auxiliary materials for seating unit A and B

Ancillary Materials	Mass (kg)	Mass Percentage (%)
Fastener :	0,080	32,65%
Adhesive :	0,100	40,82%
Zipper :	0,060	24,49%
Cursor in Zipper :	0,004	1,63%
Label :	0,001	0,41%
TOTAL Weight :	**0,245**	**100%**

(A)

Ancillary Materials	Mass (kg)	Mass Percentage (%)
Steel joint bar :	0,016	4,10%
Adhesive :	0,100	25,64%
Zipper :	0,066	16,92%
Cursor in Zipper :	0,016	4,10%
Label :	0,001	0,26%
Nylon :	0,066	16,92%
Wedge :	0,020	5,13%
Sheep wool yarn :	0,001	0,26%
Paint :	0,104	26,67%
TOTAL Weight :	**0,39**	**100%**

(B)

Table 3: Packaging materials for seating unit A and B

Packaging Materials	Mass (kg)	Mass Percentage (%)
Cardboard :	3,250	91,37%
Nylon Packaging Bag :	0,195	5,48%
Plastic Packaging Rope :	0,112	3,15%
TOTAL Weight :	**3,557**	**100%**

(A)

Packaging Materials	Mass (kg)	Mass Percentage (%)
Cardboard :	4,045	96,20%
Nylon Packaging Bag :	0,048	1,14%
Plastic Packaging Rope :	0,112	2,66%
TOTAL Weight :	**4,205**	**100%**

(B)

4.2 Environmental Impacts

The obtained environmental impacts of seating unit A and B are summarized in Table 4. The resource use for both of the products are given in Table 5.

Table 4: Environmental impacts of seating unit A and B

Impact Category	Global Warming Potential [GWP]	Acidification Potential [AP]	Eutrophication Potential [EP]	Photochemical Ozone Creation Potential (Smog) [POCP]
Unit	kg CO_2 Eq.	kg SO_2 Eq.	kg N Eq.	kg O_3 Eq.
Raw Material	80,67	0,387	0,0512	4,026
Transportation	2,37	0,008	0,0006	0,212
Manufacturing	9,78	0,025	0,0054	0,440
Distribution & Usage	5,02	0,015	0,0012	0,286
End of Life	8,80	0,005	0,0020	0,080
TOTAL	**106,64**	**0,440**	**0,0604**	**5,044**

(A)

Impact Category	Global Warming Potential [GWP]	Acidification Potential [AP]	Eutrophication Potential [EP]	Photochemical Ozone Creation Potential (Smog) [POCP]
Unit	kg CO_2 Eq.	kg SO_2 Eq.	kg N Eq.	kg O_3 Eq.
Raw Material	90,200	0,645	0,101	5,860
Transportation	8,180	0,029	0,002	0,829
Manufacturing	10,000	0,039	0,007	0,522
Distribution & Usage	7,010	0,048	0,003	1,010
End of Life	13,700	0,001	0,004	0,090
TOTAL	**129,090**	**0,761**	**0,117**	**8,310**

(B)

Table 5: Resource use for seating unit A and B

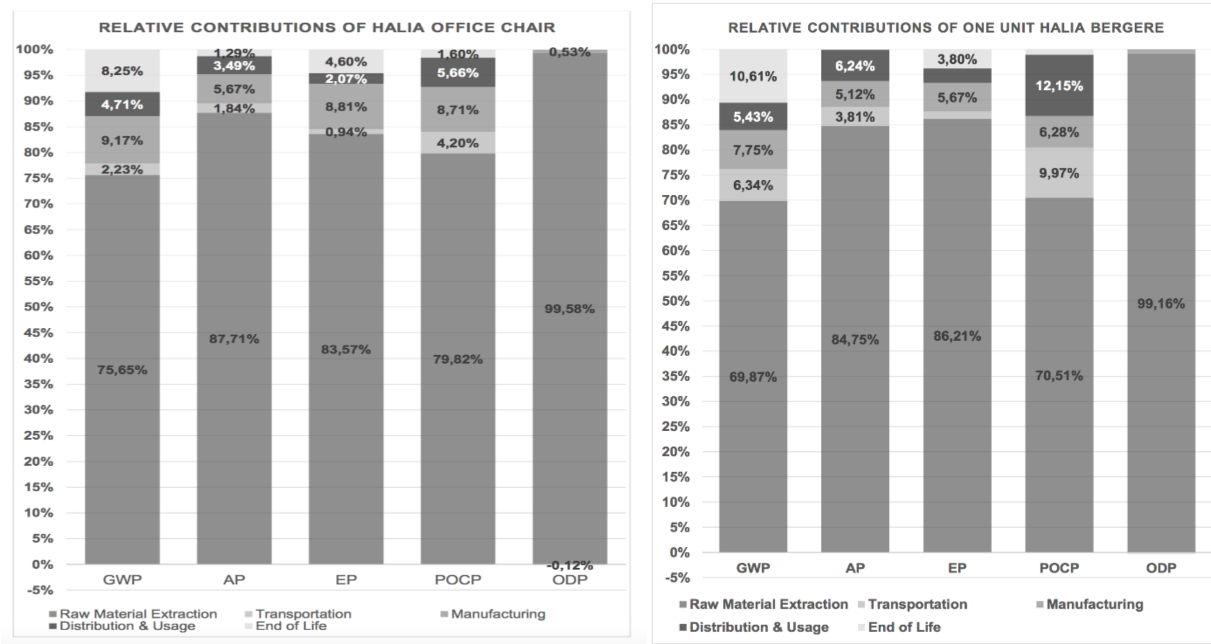
Parameter	Unit	Product
Primary Energy from Nonrenewable Resources (net cal, value)	[MJ]	1,52
Primary Energy from Renewable Resources (net cal, value)	[MJ]	0,425
Primary Energy demand from Ren, and Non Ren, Resources (net cal, value)	[MJ]	1,95
Total Freshwater Use	[kg]	553

(A)

Parameter	Unit	Product
Primary Energy from Nonrenewable Resources (net cal, value)	[MJ]	1760
Primary Energy from Renewable Resources (net cal, value)	[MJ]	412
Primary Energy demand from Renewable and Nonrenewable Resources (net cal, value)	[MJ]	2172
Total Freshwater Use	[kg]	154000

(B)

The relative contribution of various phases in life cycle for both of the products are presented in Figure 3.



(A) (B)

Figure 3: Contribution of various phases for seating unit A and B

5. DISCUSSION AND CONCLUSIONS

All the environmental impacts are higher for the seating B. This elevation can be as much as 94 % in EP, 73 % in AP, 65 % in POCP and 22 % in GWP. This result indicates the importance of product design.

For both of the seating units, raw material extraction and pre-processing stage is the highest contributor to all impact categories. The used aluminum for the mechanic parts and leg, rigid polyurethane foam and the textile are the main contributors to this stage in seating A. The impacts arise from transportation stage is due to cargo aircraft usage. For both of seating units, impacts due to distribution and usage stage are generated because of sending paper wastes to landfills. Waste cardboard, nylon and paper used in packaging are the contributors of manufacturing process. While the highest impact is generated from sending the obsolete seating units to landfills.

ACKNOWLEDGMENT

The authors would like to sincerely thank Koleksiyon Ltd. for their valuable contribution. The prominence of this study is supported by Koleksiyon Ltd's decision to publish all findings transparently in the public domain.

References

1. Atmaca, A. (2016) Life cycle assessment and cost analysis of residential buildings in south east of Turkey: part 1—review and methodology, **The International Journal of Life Cycle Assessment**, 21:831–846, 2016.
2. B. Atilgan and A. Azapagic. (2016) Renewable electricity in Turkey: Life cycle environmental impacts, **Renewable Energy**, 89, 649-657, 2016.
3. E. Ozkan, N. Elginoz and F. Germirli Babuna. (2017) Life cycle assessment of a printed circuit board manufacturing plant in Turkey, **Environmental Science and Pollution Research**, DOI: 10.1007/s11356-017-0280-z, 2017.
4. Gunkaya, Z, Ozdemir, A, Ozkan, A and Banar, M (2016) Environmental Performance of Electricity Generation Based on Resources: A Life Cycle Assessment Case Study in Turkey, Sustainability, 8(11), Number: 1097, DOI: 10.3390/su811109
5. Demirel, N.; Erkayaoglu, (2016) M. Sustainability Comparison of Mining Industries by Life Cycle Assessment for Turkey and European Union, 16th International Symposium on Environmental Issues and Waste Management in Energy and Mineral Production (SWEMP) / International Symposium on Computer Applications (CAMI), Istanbul, Turkey.
6. MoE, (2016) Ministry of Economy, Republic of Turkey, Industry– Furniture. https://www.economy.gov.tr/portal/content/conn/UCM/uuid/dDocName:EK-021146
7. D. R. Iritani, D.A.L.Silva, Y.M.B.Saavedra, P.F.F.Grael, A.R.Ometto, (2015) Sustainable strategies analysis through Life Cycle Assessment: a case study in a furniture industry. **Journal of Cleaner Production**, 96(1), Pages 308-318.
8. Mauro Cordella, Carme Hidalgo. (2016) Analysis of key environmental areas in the design and labelling of furniture products: Application of a screening approach based on a literature review of LCA studies. **Sustainable Production and Consumption**, 8, 64-77.
9. H. Kouchaki-Penchah, M. Sharifi, H. Mousazadeh, H. Zarea Hosseinabadi. Life cycle assessment of medium-density fiberboard manufacturing process in Islamic Republic of Iran. **Journal of Cleaner Production**, 112:351-358, DOI10.1016/j.jclepro.2015.07.049, 2016.
10. C. M. Piekarski, A. Carlos de Francisco, Antonio Carlos de Francisco Leila Mendes da Luz, Diogo Aparecido Lopes SilvaDiogo Aparecido Lopes Silva (2017). Life cycle assessment of medium-density fiberboard (MDF) manufacturing process in Brazil. **Sci Total Environ**. 1;575:103-111. doi: 10.1016/j.scitotenv.2016.10.007, 2017.
11. .I. González-García, García Lozano R, Moreira MT, Gabarrell X, Rieradevall i Pons J, Feijoo G, Murphy RJ (2012).Eco-innovation of a wooden childhood furniture set: an example of environmental solutions in the wood sector. Sci Total Environ. 426:318-326. doi: 10.1016/j.scitotenv.2012.03.077, 2012.
12. Nadia Mirabella, Valentina Castellani, Serenella Sala. (2014) LCA for assessing environmental benefit of eco-design strategies and forest wood short supply chain: a furniture case study. **The International Journal of Life Cycle Assessment**, 19:1536-1550, DOI 10.1007/s11367-014-0757-7, 2014
13. NSF, 2019. International, National Center for Sustainability Standard (valid through September 30, 2019) . Product Category Rule for Environmental Product Declarations. BIFMA PCR for Seating: UNCPC 3811 Version. https://www.nsf.org/newsroom_pdf/seating_pcr-new.pdf
14. ISO 14040 (2006) Environmental management -- Life cycle assessment -- Principles and framework. https://www.iso.org/standard/37456.html
15. US EPA (2018) Waste Reduction WARM Model. https://www.epa.gov/warm

REGENERATION AND PLACE-MAKING THROUGH HERITAGE: A CASE STUDY FROM A HISTORIC BUILDING IN NORTHERN GREECE

S.M. Bagiouk[1], E. Sofianou[2]*, A.S. Bagiouk[3], S.S. Bagiouk[4]

[1,3]Division of Hydraulics and Environmental Engineering,
[2]Division of Transport and Project Management,
Dept. of Civil Engineering, Aristotle University of Thessaloniki, GR- 54124 Thessaloniki, Macedonia, Greece,
[4]Dept. of Civil Engineering, Democritus University of Thrace, GR - 67131 Xanthi, Greece

*Corresponding author: e-mail: sofianou@civil.auth.gr

Abstract
Cities are entering a new era underpinned by theoretical notions concerning their role as nodes in a global competitive network. Urban areas of historical value are spatial structures that express the evolution of the local society and its identity. Urban building stock with its connotative meanings is an important part of the city as historical and cultural evidence. Within this framework, urban regeneration is encouraged by local authorities to attract people. Rapid transformation of urban buildings of historical significance, urban area revival and aesthetic investments are some of the regeneration strategies towards revenue-generating potential and more sustainable urban forms.

Contemporary urban regeneration projects aim to plan creative spaces by reintegrating historic complexes and buildings in the city and by creating distinctive urban areas with various functions and a sense-of-place. Placemaking is an inherently collaborative and inclusive planning approach compared to the envisaged planning model. As a concept it refers to the process of place production with the aim to advance the living quality of a space. People are attracted to places which can become focal points of economic, social activity and attractiveness including various functions.

This paper faces an important challenge in the field of urban heritage regeneration towards the sustainable city. The paper focuses on a listed building of the rich historical building stock of Thessaloniki in Northern Greece, the Branch of the 1st Secondary School (former Josef Modiano Mansion). In particular, through this case study, the paper explores a series of issues associated with the rehabilitation of abandoned historical buildings and their reintegration in the modern city through placemaking strategies. The ultimate goal is to propose new aspects of urban building upgrade through new creative uses and introduce a community based regeneration methodology.

Keywords: Urban regeneration; cultural heritage; place-making; historical buildings; sustainable city

1. INTRODUCTION

Heritage is one of the important elements which create character, identity and image of the city concerning the past, present and future. Built cultural heritage is a dominant component and an important means of historical, economic and social development. However, technology, demographic and economic changes and lack of systematic assessment methodologies for adequate consideration of the divergence between sustainable urban development and the protection of cultural heritage, have put pressures on the built urban assets. Viable strategies combined with architectural intervention and

conservation methods of built heritage are needed for the reintegration of such assets in the city and the improvement of living conditions and microclimate.

Today there is an increasing interest towards more sustainable city forms and local community participation in policy making. When a person or group links a space to their own personal experiences, cultural values and social meanings, it is transformed into a place for them (Hunziker, *et al.*, 2007). The increased participation of citizens is important for the integration of cultural assets into urban development strategies. Within this framework the notion of placemaking tends to be used to refer to a specific approach to 'revitalising, planning, designing and managing public spaces' (Stewart, 2010). Placemaking is the process of place production and a collective process of space arrangement with the aim to advance the usage and living quality of a space.

Thessaloniki in Northern Greece presents rich built heritage however, large part of the urban building stock remains untapped. In the present paper, the aim is to explore the potentials of heritage revival of the Branch of 1st Secondary School through social participation and placemaking. Using empirical data from the area and through structured planning methods are investigated the factors that hinder or promote sustainable development planning strategies. The aim is to develop a holistic methodology to cover the gap between sustainable development and reuse of historical built resources and to assess local communities' performance concerning sustainable strategies for urban regeneration through creativity and placemaking strategies.

2. LINKS BETWEEN SUSTAINABLE DEVELOPMENT AND CULTURAL HERITAGE WITHIN THE URBAN CONTEXT

2.1 Built heritage and urban regeneration

For a city to be sustainable, economic and social benefits need to be maximized in order to enhance living standards as far as the city target is sustainable in terms of environmental limitations and socioeconomic equity (Mori & Yamashita, 2015). One of sustainable development's principals is the protection and promotion of heritage and conservation of identity. Each place has a meaning, mostly defined by the environment and human activity. Urban areas of historical significance are spatial structures that express the evolution of local society and its cultural identity. These areas consist of tangible (urban and architectural elements, open air spaces, buildings and landmarks) and intangible elements (functions, activities, memories, traditions). They are an integral part of a broader natural or manmade context and the two must be considered as inseparable.

Heritage is referenced in the international agenda for sustainability and for its role in defining the distinctiveness of cities and improving their competitiveness. And vice versa urban competitiveness regards culture as capital, so it is important to consider heritage as an essential resource of the urban ecosystem. Sustainability in the redevelopment of historic city centers is innovative and necessary as it contributes to the objectives of environmental reevaluation, economic and social regeneration and durable development in the sense of protection of environmental resources for future generations (Minetto, *et al.*, 2011).

Built heritage conservation carries benefits in many areas of the urban environment (Vicente, *et al.*, 2015), however, the protection and reintegration of architectural heritage into modern urban landscape is a complex procedure with many aspects. The continuous degradation of the urban environment and the emerging problems caused during the last decades, are the major menace of historic centers and monuments.

The term regeneration includes the sense of transformation, i.e. of a place with specific or mixed uses (residential, commercial, educational), that through time and mainly due to lack of political initiatives, shows signs of degradation (social, economic and environmental and can affect specific or wider areas of the city). Upgrading the built environment, social fabric and urban spaces, contributes to

increasing their adoption as places for public congregation and activity, consequently increasing social interaction and cohesion between citizens (Elnokaly & Elseragy, 2011).

2.2 New culture-based urban models

National governments and European institutions increasingly recognize the value of cultural heritage (Tweed & Sutherland, 2007). In modern economies appears the 'cultural turn' in the positioning and marketing of towns and cities, as a response to the profound implications for how cities work and survive (Rodwell, 2013). Cultural resources, amenities, facilities etc, are considered nowadays as strategic tools for the new economy. The ability of cities to integrate the conservation of urban resources and to monitor impacts of development requires the recognition of heritage values (e.g. historic, social, economic) and heritage-designated attributes (tangible and intangible).

Urban conservation is now considered as a dynamic process within an urban system aimed at enhancing cultural values and managing change (United Nations, 2015). Urban regeneration aims to renew areas in decline (Bassett, 2013), and this decline could be in the form of physical, social and/or economic functions in the urban fabric (Chohan & Ki, 2005). Heritage is a catalyst for sustainable urban regeneration and a comprehensive policy for identity conservation by involving the community as a partner. Integrating the heritage conservation in the process of urban regeneration can lead a way to sustainable development (Chohan & Ki, 2005).

Cultural infrastructures can become social spaces for interconnection and knowledge of local identity. Safeguarding and promoting culture at the local level is a way to develop endogenous resources and create conditions for sustainable revenue generation (United Nations, 2015). Furthermore, there are many different sites of historical significance and attraction (i.e. archaeological sites, museums, architecture and art landmarks, local tradition activities, festivals), that could be included in programmes linking history, humanity and tourism.

3. PLACEMAKING AS A MEANS OF URBAN REGENERATION

3.1 The notion of placemaking

The link between heritage as a consumable experience and urban regeneration as an economic development activity is potentially attractive, widely exploited, can be assumed to be self-evidently symbiotic but conceals the different motivations and aspirations of different stakeholders (Pendlebury, 2002). The instrumental use of heritage in regeneration is a global phenomenon, often linked into both strategies seeking to develop so-called cultural industries and a process of 'place-making', a term variously used by urban designers in establishing attractive physical locales as part of the backdrop of successful social space and, more critically, to be synonymous with place-branding (Pendlebury & Porfyriou, 2017).

Culture and creativity have increasingly been incorporated into urban strategies aimed at supporting the economic vitality of city-regions, and especially the ability of cities to compete for resources in the context of globalization and intensified inter-urban competition (Evans, 2009). Placemaking can trace its roots back to the seminal works of urban thinkers who, beginning in the 1960s, espoused a new way to understand, design and program public spaces by putting people and communities ahead of efficiency and aesthetics (Silberberg, *et al.*, 2013). Urban author and visionary Jane Jacobs (as cited in Baeker & Millier, 2013) sums up much of the logic of creative placemaking with the phrase: "New ideas need old buildings".

More recently introduced is the term "creative placemaking" which is decidedly 21st century-esque (Salzman & Yerace, 2017). Creative placemaking is a skill that identifies and catalyzes local leadership, funding, and other resources. As a bottom-up approach empowers and engages people in ways that traditional planning processes do not and draws on the assets and skills of a community, rather than on relying solely on professional "experts" (Project for Public Spaces, 2012). Initiatives

that are used to shape the social and physical character of a place, including contexts like health, transport or education, has become increasingly popular (Oakley, 2015).

3.2 Urban heritage regeneration through placemaking

Cities are the places where different people and cultures mix and creativity is the lever for new ideas, artefacts and institutions. In the long history of human settlement, public places have reflected the needs and cultures of community; the public realm has long been the connective tissue that binds communities together (Silberberg *et al*., 2013). For cities seeking to enhance their competitive position, the use of heritage as a driver for economic growth is now an established feature of the policy agenda. In addition to generating income and employment, their tendency to cluster within rundown inner city districts often provides opportunities for area revitalization and regeneration (Bayliss, 2007).

Placemaking is the process of creating quality places that people want to live, work, play and learn in (Wyckoff, 2014). Successful placemaking initiatives create places active, interesting, visually attractive, often with public art and creative activities, people-friendly, safe, and walkable with mixed uses. Placemaking serves livability and social cohesion through heightened public safety, local identity and environmental protection initiatives. It results in a place where the community feels ownership and engagement, and where design serves function.

Placemaking embodies the common sense approach that guided how most historic places were created, as people worked together over decades to create buildings, streets and public spaces that would fulfill social, economic and political needs in their communities. Placemaking helps expand the impact of preservation projects, as preserving historical places protects them from physical destruction, but also, by embracing a community-oriented vision that draws upon local knowledge and assets, preservationists can create places of long-lasting value (Project for Public Spaces, 2010).

The placemaking process is defined by the recognition that when it comes to public spaces, the community is the expert and follows that strong local partnerships are essential to the process of creating dynamic, healthy public spaces that serve citizens. Many creative placemaking efforts address specific neighborhoods, including downtowns and residential and industrial areas that offer under-utilized private and public capacity ripe for human ingenuity (Markusen & Gadwa, 2010).

Placemaking projects celebrate history and distinctive culture, add layers of meanings and create a common vision for the community (Redaelli, 2018). They also generate economic returns in multiple ways as cultural investments help a locality capture a higher share of local expenditures from income. Furthermore, instead of traveling elsewhere for entertainment and culture, residents spend more on local venues, money that re-circulates at a higher rate in the local economy. Another potential benefit is the higher project value, as uniqueness of a place and innovative mixed-use project design may establish premium value. As well as enhanced branding and market recognition feature as new opportunities than the outcomes of budgeted marketing activities (Hardy, 2016).

Creative placemaking animates public and private spaces, rejuvenates structures and streetscapes, improves local businesses viability and public safety, and brings diverse people together to celebrate, inspire, and be inspired (Markusen & Gadwa, 2010). As far as it concerns the building stock, the physical atmosphere of historic buildings contributes to placemaking at the site scale. Retaining original features of the buildings serves as a physical reminder of what the building once was, making the space unique in comparison to newly constructed spaces (Chan, 2011).

Restoration and rehabilitation of traditional buildings can favor the accommodation of various uses. By using vacant and underutilized land, buildings and infrastructure, investments increase their contribution to the public good and private sector productivity. Sales, income and property tax revenues paid to local governments, rise enabling better maintenance and additions to public infrastructure. Also, additional jobs and incomes are generated in construction, retail businesses, and arts and cultural production (Markusen & Gadwa, 2010).

4. REGENERATION OF INNER-CITY AREAS: THE CASE OF THE 1ST SECONDARY SCHOOL BRANCH (FORMER JOSEF MODIANO MANSION)

Thessaloniki is a 2300-year-old city and a contemporary metropolitan center of Northern Greece. Thessaloniki started to grow as a commercial and geopolitical node of multicultural character. The city's traditional structure lost its oriental character and gradually became Europeanized. Today, the metropolitan area of Thessaloniki looks like a puzzle of varied uses and a mixture of irregular elements. However, within the densely built centre can still be found unique tangible and intangible cultural resources. There are numerous historic monuments many of them still untapped, traditional buildings representing folk architecture, modern landmarks and open air spaces of significant value. There are also exquisite neoclassical buildings, most of them built as residences of the wealthy society during the late 19th century.

The study area provides opportunities for urban revival as a significant historical and cultural asset within the modern urban fabric. It is a place of traditions, cultures, specific activities, which can be preserved and enhanced, through actions for sustainability. The neoclassical buildings found in the dense urban fabric of this central study area are the main architectural assets that may be regenerated and rehabilitated towards sustainable patterns. The majority of them are characterized by small, usually two-storey residences often with a private open space. In some cases the streets are very narrow prohibiting physical solar access and ventilation. Some buildings have been restored and house municipal facilities and services, for instance, educational buildings, or they are used for recreation, leisure and service facilities. The reuse of buildings is a solution to avoid constructing new buildings in the constricted urban built space. Furthermore, the building-monument may be involved in a perpetual dialogue with the space and the visitor.

4.1 Aims of the present research

As mentioned above, the paper focuses on a historical building, which for many years remained abandoned. The case study building is located in the eastern extend of Thessaloniki's city centre, an area with rich historical and architectural assets. The building's restoration project was conducted by Angelos Vacalopoulos' architectural firm for the Region of Central Macedonia. The architects and planners of the team were: A. Vacalopoulos, St. Koukopoulos, A. Mitropoulos, G. Papadimitriou, A. Stergiannis. S. Bagiouk and Z. Al Saayyah, associate architects and A. Manousi-Vacalopoulou and K. Stylianidis, engineers – consultants. Especially in the second phase of the restoration project and more specifically, the internal décor restoration study – which was a great task for this project – the team joined St. Papanikolaou, A. Fostiridou and D. Kapizonis, conservators of antiquities and works of art.

Part of this project conducted by Vacalopoulos and Associates Architectural firm in the early 2000's is analysed below, giving a sign of the extended survey and sustainable methods of regeneration proposed, which can be adapted in other building rehabilitation cases. The information provided in this paper, as well as the underlying material (plans and photographs) are from the personal archive of A. Vacalopoulos and S. Bagiouk. Within this framework, the present paper focuses on this project to provide guidelines for other rehabilitation projects for cultural or educational uses and help local communities create a dialogue with the buildings and their history.

4.2 Brief historical overview of the case study building

Based on the technical report of the building's current situation analysis, conducted by Angelos Vacalopoulos, Samir Bagiouk and Zahi Al Saayyah, in 1899, in the location Tzanlik of the eastern side, Josef Isaak Modiano bought an area of 3.040sq.m. at 48 'Allatini Degirmeni' (Allatini Mill) street, today 5 Vas. Olgas avenue. At the beginning, Modiano built a sericulture mill and later his residence to house his family coming from Italy. Modiano and Allatini family created the most important commercial Houses of Thessaloniki, including cereal, silk, cocoon, textile commerce etc.

After his death the building became property of this family. His son Jiomtov Josef Modiano, bought his mother's and sister's shares. In 1931 sold his share to at commerce man Jacob I. Molho, which past after his death in 1940 to his wife and daughters. The rest 70% which remained at the Modiano family, was obtained after the World War II by the close relatives of the Modiano family.

Later on, the property was committed by the Greek State and more specifically, its' operation was managed by the Exchangeable Holdings Service. At this time it housed 22 families and individuals. In the period 1946-58 at the residence lived 15 families and 6 more at the factory. In 1960, part of the property was transferred to the Ministry of Education and Religion in order to operate as the Branch of the 1st Secondary School. In 1984, the Departmental Fund (successor of the School Building Organisation) bought 18% and the for joint State's share (Exchangeable Holdings Service, Land Registry, School Building Organisation), became 90,7% of the total property.

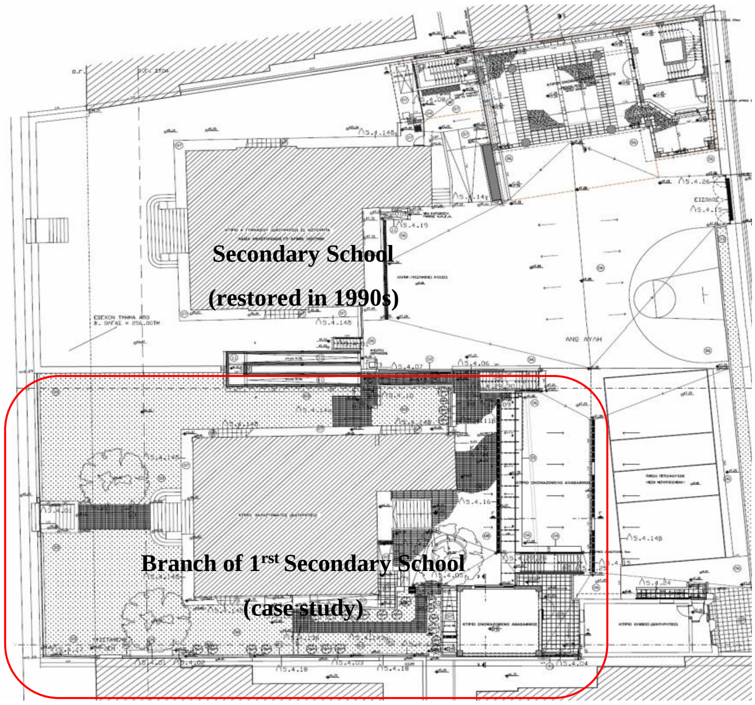
4.3 Main tasks of the building regeneration project

The plot is located in a densely built area, dual-aspect between the Vas. Olgas and Spartis streets, covering a total area of 3484,41 sq.m. The study building is listed and it houses educational uses. At the west side of the plot the former 1st Male Secondary School was restored in 1990 and today it operates a Secondary School, the small building (part of the former silk mill), gymnasium hall, and the Branch of the school, abandoned building since 1978 and in bad condition. The buildings and their surrounding space, were listed as protected by the Ministry of Environment.

The higher level from the Vas. Olgas part, the high pines, the old hoardings constitute with the buildings, an exquisite ensemble for the area's environment with a strong historical identity, as an important pole of attraction. The building extends on three levels and despite the damages, large parts of its' structure and form was preserved. Within the framework of the building's regeneration and rehabilitation with educational uses, the regeneration project focused on the reinforcement of the bearing structure, its' functional reintegration into the modern city and highlighting of its rich architectural mouldings, which were of historical significance.

The study focuses on the restoration of the Branch and its rehabilitation as an educational building. The study's goal is to investigate the potentials created after the building's regeneration and the dialogue created between the 100 year-old construction and the local society. The presented methodology's main aim was to serve as a tool for guiding urban planning and intervention, with particular importance from the building rehabilitation point of view for buildings in urban and historical centres, and also in the definition of maintenance priorities. There was no standard model, but general principles and major steps, so this methodology needs to be adapted in different urban characteristics and features. It intended to present an important contribution to urban strategies in the extent of rehabilitation of the buildings of old historical city centres, with the sense of creativeness and culture.

At the first stage, an analytical survey of the current situation about the building and the wider area was conducted, using mostly historical testimonies and plans, and on site survey. The preliminary report was the main product of this stage including the technical reports and plans of the current situation, the building's condition and a risk assessment. Through this analysis, a qualitative and quantitative characterization of several elements and aspects of the building were recorded (second stage). These two initial stages were the basis of the process, in order to acknowledge all variables and sensibilities involved.



Picture 1: Topographic plan of the plot and its' buildings (Vacalopoulos et al., 2000).

The main aim of the project was the regeneration of this cultural asset and reintegration into the urban fabric, as a node of social expression and interaction. The third stage proposes uses focused mainly on educational but also, on other cultural and leisure activities with respect to the building and the wider area. All the information, observed and recorded for the building and the neighborhood in the formed database, is a tool to promote the development of future rehabilitation projects, in point interventions or in a larger scale (city block projects).



Picture 2: The building before its restoration (Vacalopoulos et al., 2000).

According to the needs of contemporary planning based on creativity and placemaking, vacant buildings are proposed to house uses connected to education and arts in order to create a dialogue between the building and the local society. Taking into consideration creativity principals and the building's history, typology, size and structure of spaces, its main phases and the surrounding area's characteristics, was proposed the reconstruction and rehabilitation of the building as a multifunctional educational space with respect to its historical character. The main aim was to promote a regenerated space for education and creativity.

Among the main uses proposed by the project are classrooms, creative spaces for educational needs, and potentials of education through new technologies. Among the project's main goals were the restoration and highlighting of the rich architectural décor, the reconstruction through environmental planning methods and the provision for people with special needs. The ultimate goal was to reintegrate this historical building into the urban fabric and create a space of education accessible to the local community and getting in touch with the local history.



Picture 3: The building after the restoration programme (authors' archive).



Picture 4: Aspect from the first floor's interior (authors' archive).



Picture 5: Restoration of the magnificent ceilings was a main goal of the project (authors' archive).

According to the building's restructuring programme, the proposed uses by floor include:

- 1st floor: Principal's office, educational offices, parent's association office, auxiliary spaces.
- Ground floor (main educational spaces): four classrooms, teacher's office, central and secondary staircases.
- Underground level (main educational spaces): classrooms of informatics, classroom of technology, teacher's office, pupils' space, storage, staircases.

Special attention was paid to the restoration of the building's décor as an element of historical and architectural significance. The damage of the floors and the collapse of parts of the roof causing detachment of parts of the ceilings, were key elements of the restoration programme. In addition, interventions of environmental character were another important goal of the project. The ensure of enough solar access and physical ventilation was obtained through detailed planning and choice of adequate materials and frames.

5. FURTHER DISCUSSION AND CONCLUSIONS

Creative placemaking is a geographically targeted urban revitalization strategy (Forman & Creighton, 2012). Evidence has demonstrated that creative placemaking has resulted in a wide range of positive outcomes, including strengthening networks and building social capital and community capacity, among others (Baeker & Millier, 2013). Building on uniqueness of place and community practices is a strong predictor of success (Markusen & Gadwa, 2010).

Governments have developed programs to fund arts, education, turn vacant properties into community cultural centers, and stimulate interest in local heritage and culture (Kratke, 2011). Thessaloniki's urban fabric and the structure of buildings demand skills on appropriate traditional refurbishment and restoration methods that are crucial for upgrading the area. Moreover, the city's rich cultural built heritage should prioritize the marriage of building regeneration with local community and economy. The restoration and rehabilitation of historic buildings is not only an important end in its own right. Each building can provide a stimulus and focal point for regeneration schemes creating more jobs.

The regeneration of the Secondary School Branch (of educational and creativity uses), was an innovative project. The main aim of the project was to create a space of education and interaction with respect to the building's history and typology, as well as to local identity. As an example of inner-city regeneration using sustainable planning methods, the main scope was to promote the city's tradition and citizen participation and to create a local and regional node of heritage.

The architects and planners created a new space for education enhancing the architectural character of the building and bringing together local community with its' history. The project puts heritage at the heart of placemaking as it shows that this historic building provides a focal point for vibrant development by finding a long-term use within the context of a successful commercial and community development. The visitors can move in a space that is their everyday life environment and act as researchers, collaborators, and facilitators. People of all ages can use this new space and develop educational activities or other artistic activities.

The surrounding space of the building was upgraded and became a beautiful garden and an open air space within the dense urban fabric. Moreover, the revival of the space provides now a sense of safety to the neighbors, as it has wed out any 'intruders', who entered into the abandoned building and with the new lighting of its open space, especially at night.

Also, the secure rehabilitation of the building through the reconstruction and reinforcement of the load-bearing structure is an important benefit. The building was vacant for many years, becoming a dark hole for the neighborhood. After its' restoration the building opened its doors to the public, enhancing the building's history and architectural character. All the interventions were formed to integrate to the building's current structure with respect to its historical character and according to the legal framework of listed buildings' protection.

Furthermore, retaining original features of the buildings serves as a physical reminder of what the building once was, making the space unique in comparison to newly constructed spaces. In this case, the past comes alive for kids in the new classrooms, as they get in touch with the building's and the city's history on a daily basis. The form of the suggested revival project is designed to be implemented in various heritage regeneration cases. The project's results demonstrate the power of regeneration projects to bring communities together with their heritage and identity through educational uses.

The aim of this paper is to highlight the benefits of this regeneration project, as a paradigm for new aspects of building upgrade through creative uses and introduces a community based regeneration example through strengthening public participation and increasing local residents' sense of belonging. The investigation of this project shows the way in which place-based cultural policy paradigms are based on a conceptual shift in the regeneration of vacant and abandoned buildings and the establishment of uses for the public promoting arts, education, cultural activities.

References

1. Baeker, G., & Millier, L. (2013). Creative Placemaking. **Municipal World,** (February), 9–10.
2. Bassett, S. M. (2013). The Role of Spatial Justice in the Regeneration of Urban Spaces. **Rijkuniversiteit Groningen**, (May).
3. Bayliss, D. (2007). The Rise of the Creative City: Culture and Creativity in Copenhagen. **European Planning Studies,** 15(7), 889–903. http://doi.org/10.1080/09654310701356183
4. Chan, R. C. (2011). Old Buildings, New Ideas : Historic Preservation and Creative Industry Development as Complementary Urban Revitalization Strategies. University of Pennsylvania.
5. Chohan, A. Y., & Ki, P. W. (2005). Heritage Conservation a tool for Sustainable Urban Regeneration : A Case study of Kaohsiung and Tainan , Taiwan. **In 4th ISoCaRP Congress.**
6. Elnokaly, A., & Elseragy, A. (2011). Sustainable Urban Regeneration of Historic City Centres – Lessons Learnt. In World Sustainable Building Conference. Helsinki. Retrieved from http://eprints.lincoln.ac.uk/8490/1/SB2011-2 **historic Regeneration V3**.pdf
7. Evans, G. (2009). Creative Cities, Creative Spaces and Urban Policy. Urban Studies (Vol. 46). http://doi.org/10.1177/0042098009103853
8. Forman, B., & Creighton, T. (2012). Building vibrancy : Creative placemaking strategies for gateway city growth and renewal. The Massachusetts Institute for a New Commonwealth. Massachusetts: Massachussets Institute.
9. Hardy, J. (2016). Growing Value through Creative Placemaking. Urban Land. Retrieved from https://urbanland.uli.org/industry-sectors/growing-value-creative-placemaking/
10. Hunziker, M., Buchecker, M., & Hartig, T. (2007). Space and Place - Two Aspects of the Human-landscape Relationship. In F. Kienast, O. Wildi, & S. Gosh (Eds.), A Changing World - Challenges for Landscape Research (pp. 47–62). **Dordrecht: Springer Netherlands.** http://doi.org/10.1007/978-1-4020-4436-6
11. Kratke, S. (2011). The creative capital of cities: Interactive knowledge, creation and the urbanization economies of innovation. Chichester: Wiley-Blackwell.
12. Markusen, A., & Gadwa, A. (2010). Creative Placemaking. City Design Initiative. Washington. Retrieved from http://www.planning.ri.gov/documents/comp/CreativePlacemaking.pdf
13. Minetto, F., Pirlone, F., & Tomasoni, L. (2011). Proposal of a methodological approach for sustainable regeneration in the historical centers of the Mediterranean Basin. **Procedia Engineering,** 21, 1015–1022. http://doi.org/10.1016/j.proeng.2011.11.2107
14. Mori, K., & Yamashita, T. (2015). Methodological framework of sustainability assessment in City Sustainability Index (CSI): A concept of constraint and maximisation indicators. Habitat International, 45(P1), 10–14. http://doi.org/10.1016/j.habitatint.2014.06.013
15. Oakley, K. (2015). Creating Space: A re-evaluation of the role of culture in regeneration. Leeds.
16. Pendlebury, J. (2002). Conservation and regeneration: Complementary or conflicting processes? The case of grainger town, Newcastle upon Tyne. Planning Practice and Research, 17(2), 145–158. http://doi.org/10.1080/02697450220145913
17. Pendlebury, J., & Porfyriou, H. (2017). Heritage, urban regeneration and place-making. Journal of Urban Design, 22(4), 429–432. http://doi.org/10.1080/13574809.2017.1326712
18. Project for Public Spaces (2010). Placemaking meets preservation. Retrieved from https://www.pps.org/article/placemaking-meets-preservation

19. Project for Public Spaces (2012). Placemaking and the Future of Cities (Draft), 35. Retrieved from http://www.pps.org/reference/placemaking-and-the-future-of-cities/

20. Rodwell, D. (2013). Heritage as a driver for creative cities. In D. Wiktor-Mach & P. Radwanski (Eds.), The idea of creative city/The urban policy debate (pp. 11–26). Cracow: European Scientific Institute.

21. Salzman, R., & Yerace, M. (2017). Toward understanding creative placemaking in a socio-political context. **City, Culture and Society,** (February). http://doi.org/10.1016/j.ccs.2017.10.004

22. Silberberg, S., Lorah, K., Disbrow, R., & Muessig, A. (2013). Places in the Making: How placemaking builds places and communities, 63.

23. Stewart, A. (2010). Place-making and Communities: A review of concepts, indicators, policy and practice. **Forest Research, Edinburgh.**

24. Tweed, C., & Sutherland, M. (2007). Built cultural heritage and sustainable urban development. Landscape and Urban Planning, 83(1), 62–69. http://doi.org/10.1016/j.landurbplan.2007.05.008

25. United Nations. (2015). (H3)**Urban Culture and Heritage. Habitat III,** 2015(May), 0–8.

26. Vacalopoulos, A., Koukopoulos, S., Mitropoulos, A., Bagiouk, S., Saajach, Z., & Kotroni, T. (2000). Restoration of First Secondary School Branch project. (A. (consultant) Manousi-Vacalopoulou, Ed.). **Technical report,** Thessaloniki.

27. Vicente, R., Ferreira, T. M., & Mendes da Silva, J. A. R. (2015). Supporting urban regeneration and building refurbishment. Strategies for building appraisal and inspection of old building stock in city centres. **Journal of Cultural Heritage,** 16(1), 1–14. http://doi.org/10.1016/j.culher.2014.03.004



Environmental education

RAISING AWARENESS ON CLIMATE CHANGE THROUGH HUMOR

L. Topaltsis, V. Plaka* and C. Skanavis

Research Center of Environmental Communication and Education, Dept. of Environment, University of the Aegean, GR- 81100 Mytilene, Lesvos, Greece

*Corresponding author: e-mail: plaka@env.aegean.gr, tel: +302251036234

Abstract

Environmental awareness, for issues like climate change, is on top of the list with the concerns, humanity is facing. We are being exposed to a gigantic number of environmental messages but still we haven't reached the optimum level of environmental sensitivity.

Most of the climate change awareness campaigns use fearful stimuli such as scary titles, and images of catastrophes and uncertain futures. That kind of campaigns create emotions like fear, anxiety and worry to the public. That's an explanation why lots of people ignore climate change and deny its importance. According to various researches, humor can boost successfully educational and communication processes at stake. Participants being confronted with pleasant approaches have responded positively to the new information and their intention to retain longer their behavioral change has been recorded.

Through a quality process, this study aims to study the importance of humor, and how it can be used in climate change awareness campaigns in a way that will influence public's attitudes and behavior, so that a positive response will be created.

Keywords: Climate change, Humor, Environmental awareness, Environmental communication

1. INTRODUCTION

Climate change and global warming are a growing problem in the world at this present time and the future as well (IPCC, 2007). The first legally binding national commitment to greenhouse gas (GHG) emissions reduction was through the Kyoto Protocol, adopted in 1997 and entered into force in 2005 (O'Neill and Nicholson-Cole, 2009). However, in 2007, the Intergovernmental Panel on Climate Change suggests that actions are quickly needed to reduce global climate change (IPCC, 2007). The human cause of global climate change has been identified as increasing levels of greenhouse gases: for example, carbon dioxide (CO2) emitted by burning fossil fuels for transport and heating; and methane emitted by cattle raised for the meat industry (Parant et al., 2017). Within the European Union (EU), a target has been set to reduce greenhouse gases by at least 20% by 2020 compared with the 1990 level (European Commission, 2011). The Intergovernmental Panel on Climate Change stated in its most recent report that warming of the climate system is "unequivocal (IPCC, 2007). Impacts of climate change are projected to be many and varied, ranging from changes in ecosystems (e.g., LeemansandEickhout, 2004), to impacts on human systems such as water resources (Arnell, 1999), to potential forced human migrations (e.g.,Barnett andAdger,2003), to widespread acidification of the oceans (e.g., Caldeira and Wickett, 2003), to insurance and reinsurance difficulties (e.g., Munich Re, 2004). Both mitigation and adaptation are needed to appropriately manage the challenge of climate change (O'Neill and Nicholson-Cole, 2009) and global efforts have so far tended to concentrate on the mitigation of GHG emissions (O'Neill and Nicholson-Cole, 2009).

Nowadays, many environmental campaigns appear to be based on the presumption that people need more information to behave pro-environmentally (Howell, 2014). In recent years, governments, nongovernmental organizations, and individuals have all been involved in creating "climate change communications" aimed at changing public attitudes and behavior related to climate change. These include leaflets and flyers, billboard, press and television advertisements, movies, and publications of many kinds are disseminated to the population (Parant et al. 2017).

Also, there is a growing consensus that we must engage publics in scientific dialogue (House of Lords, 2000). Scientists are increasingly expected to become prominent actors in communicating science to the lay public (Bentley and Kyvik, 2011; Dudo, 2012; Trench and Miller, 2012).One of the reasons this need arises is based on the fact that scientific knowledge is at the core of many of the issues that society faces today (Poliakoff and Webb, 2007). However, the approach in terms of "information-deficit" has been widely criticized as being inadequate to promote behavioral change (Kellstedt, Zahran and Vedlitz, 2008; Ockwell, Whitmarsh, and O'Neill, 2009; Schultz, 2002).Organizations such as Futerra (2005) and the Institute for Public Policy Research (Ereaut and Segnit, 2006), and academics such as Kloeckner (2011),Pooley and O'Connor (2000), and Moser (2007) advise that environmental messages should appeal to the emotions rather than simply providing factual information, to be more engaging.

1.1 Fear is no productive

Climate change communications frequently use disaster framing to create a fear appeal intended to motivate mitigation action (Howell, 2014). Fear appeals in climate change are prevalent in the public domain, with the language of alarmism appearing in many guises (O'Neill and Nicholson-Cole, 2009). The literature that does exist suggests that using fearful representations of climate change may be counterproductive (Moser and Dilling, 2004). Current climate change discourses are often characterized by fear and catastrophe narratives (Doulton and Brown, 2009; Hulme, 2008).

For example, the U.K. government talks of "dangerous climate change" (Conference on Dangerous Climate Change, 2005), the media of a "climate of fear" (Bonnici, 2007) and NGOs of "climate chaos" (Stop Climate Chaos,a U.K. coalition for action on climate change). Even so, Ereaut and Segnit (2006) state that the alarmist climate repertoire is characterized by an inflated or extreme lexicon, with an urgent tone: It is a terrible, immense, and apocalyptic problem, beyond human control. They find alarmist climate messages employ narratives of doom, death, judgment, and heaven and hell (Ereaut and Segnit, 2006). Fear is also strongly apparent in the kinds of imagery used in association with climate change more broadly (O'Neill and Nicholson-Cole, 2009). The U.K. Green Party used an image of a catastrophically flooded and drowned "British Isle [sic]" to campaign in the 2005 national elections (Wootton, 2005). Images of polar bears stranded on ice floes have become iconic of climate change (O'Neill, 2008), and those depicting human struggle are evident in the famine and water shortages depicted in the climate campaign literature of charity Christian Aid (2008).

The mediation of fear messages is illustrated in Hulme (2007). The researcher conducted a study into the coverage of the IPCC Working Group I report in 10 major U.K. national newspapers. Only one newspaper did not run a story on the IPCC report. The other nine, all ran articles introducing the adjectives catastrophic, shocking, terrifying, or devastating. Yet none of these words were present in the original IPCC document. Weingart, Engels, and Pansegray (2000) offer some explanation that newsworthiness increases if identifiable events can be linked to a threat to human life, and in order to do this levels of alarm are often magnified (Joffe, 1999). Accordingly, some authors report that climate change is most commonly communicated in the media in the context of dramatic climaterelated events (e.g., Carvalho and Burgess, 2005).

Furthermore, in their research O'Neill and Nicholson-Cole (2009) argued that "fearful" and "shocking" representations of climate change are "likely to distance or disengage individuals from climate change, tending to render them feeling helpless and overwhelmed when they try to comprehend their own relationship with the issue". However, they can also act to distance and

disempower individuals in terms of their sense of personal engagement with the issue (O'Neill and Nicholson-Cole, 2009). This research has shown that dramatic, sensational, fearful, shocking, and other climate change representations of a similar ilk can successfully capture people's attention to the issue of climate change and drive a general sense of the importance of the issue.

Although shocking, catastrophic, and large-scale representations of the impacts of climate change may well act as an initial hook for people's attention and concern, they clearly do not motivate a sense of personal engagement with the issue and indeed may act to trigger barriers to engagement such as denial and others (Lorenzoni et al., 2007; O'Neill and Nicholson-Cole, 2009). All of these which presented here certainly demonstrate that on a standalone basis fear, shock, or sensationalism may promote verbal expressions and general feelings of concern but that they overwhelmingly have a "negative" impact on active engagement with climate change (O'Neill and Nicholson-Cole, 2009).

The "wicked" nature of climate change makes it, for many people, an impersonal and distant issue (Lorenzoni et al., 2006). A further consequence of long-term reliance on fear appeals, as stated by Hastings et al. (2004), is that it is possible that a law of diminishing returns may exist. If this exists, fear approaches need to be made more intense as time goes by because of repeated exposure to threatening information in order to produce the same impact on individuals.Linville and Fischer's (1991) "finite pool of worry" effect is also worthy of note here.

An ill-considered fear approach may damage (or further damage) the reputation of the communicating organization and the ability of that organization to attempt further engagement approaches. This is key when considering the need for sustained and consistent messages to communicate climate risks (Futerra, 2005). The continued use of fear messages can lead to one of two psychological functions. The first is to control the external danger, the second to control the internal fear (Moser and Dilling, 2004). If the external danger—in this case, the impacts of climate change—cannot be controlled (or is not perceived to be controllable), then individuals will attempt to control the internal fear. These internal fear controls, such as issue denial and apathy, can represent barriers to meaningful engagement.

Lorenzoni et al. (2007) divide the barriers to engagement with climate change, into two types, individual-level and social-level barriers. Of particular consequence for this discussion of fear appeals are the barriers acting individually to inhibit engagement with climate change. Although hoping that climate change would not affect them, three participants in the imagery study specifically noted that thinking about climate change made them feel so scared and depressed that they purposefully did not think about it. Fear appeals may act to increase this response, leading to denial of the problem and disengagement with the whole issue in an attempt to avoid the discomfort of contending with it (O'Neill and Nicholson-Cole, 2009).

1.2 Humor versus fear

Using humor in environmental communication can help communicators avoid overwhelming audiences with feelings of fear, helplessness, and guilt, which may otherwise discourage them from taking action against climate change (O'Neill and Nicholson-Cole, 2009). Similarly, Howell (2014) states that fear appeals about climate change need to be combined with discussion of how to avoid the threat in order not to trigger maladaptive defensive responses. Fear appeals need to be combined with high-efficacy messages (useful information about how to avoid the threat) in order not to trigger maladaptive defensive responses (Lewis, Watson and White, 2010; Moser, 2007). However, O'Neill and Nicholson-Cole (2009) found that fear-based climate change representations do not motivate personal engagement with the issue, while Spence and Pidgeon (2010) found that positive framing produced attitudes toward climate change mitigation that were significantly more positive than those produced by loss frames. Morton, Rabinovich, Marshall, and Bretschneider (2011) found that positive framing combined with higher uncertainty about outcomes increased individuals' intentions to mitigate climate change, compared with negative framing.

In a meta-analysis on the use of fear appeal in health prevention, Peters, Ruiter, and Kok (2013) confirm the link between threat and efficacy in initiating positive behaviors. However, they underline that “a potent efficacyenhancing element” is required in the intervention to increase positive outcomes (Peters et al., 2013; Parant et al., 2017). In a binding communication paradigm, it is possible to reduce the potential drawbacks from fear appeals when the preparatory act includes solutions for the issue at hand (Parant et al., 2017). Even if movies are able to present information and have been shown to engage their audience emotionally, our data suggest that fear appeal-based movies could be inefficient if not accompanied by concrete solutions (Parant et al., 2017).

2. METHODOLOGY

Through a qualityassessment process, this study aims to emphasize the importance of humor, and point out how it can be used in climate change awareness campaigns, in a way that will influence public’s attitudes and behavior to a positive response. Also, this study examines if stand-up comedy is a successful alternative way to communicate about climate change through raising environmental awareness.

3. HUMOR: ANALTERNATIVE WAY IN CLIMATE CHANGE COMMUNICATION

Although the definitions of humor vary, there is widespread agreement among scholars that humor involves the communication of multiple, incongruous meanings that are amusing in some manner (Martin, 2007). Humor is not a common tool scientists use to communicate, but there are nevertheless several examples of comedy in scientific academia (Pinto et al, 2015). Humor is sometimes argued to be an effective way of communicating science (Bultitude, 2011). Also, it requires a coordinated network of responses involved in generating expectations and associations, perceiving incongruities, and revising these expectations, resulting in affective and expressive responses of mirth and laughter (Robert et al., 2011).

In evaluating over 40 years of research on humor and education, general conclusions about the effects of instructional humor as well as directions for future research can be reached (Banas et al., 2011). The use of humor is a prevalent communication behavior in pedagogical settings and serves different purposes. On Banas et al. (2011) research, the clearest findings regarding humor and education concern the use of humor to create learning environment. The use of positive, nonaggressive humor has been associated with a more interesting and relaxed learning environment, higher instructor evaluations, greater perceived motivation to learn, and enjoyment of the course. Conversely, the use of negative or aggressive humor aimed at students has been associated with many of the opposite outcomes, including a more anxious and uncomfortable learning environment, lower evaluations of instructors, increased student distraction and less enjoyment of class (Banas et al., 2011).

3.1 Satire

Satire uses humor as a weapon, attacking ideas, behaviors, institutions, or individuals by encouraging us to laugh at them (Bore and Reid, 2014). It may be gentle or hostile, clear-cut or ambiguous, aimed at “us” or “them” - or it may oscillate between different approaches, remaining flexible and surprising (Bore and Reid, 2014).

First, satire can facilitate audience reflection, investigation, and action (Bore and Reid, 2014). Second, the use of humor can help audiences manage feelings of fear, helplessness, and guilt, which may otherwise prevent them from taking action (Bore and Reid, 2014). However, as Herr (2007) notes, a key critical dilemma associated with theatrical satire is the belief that “the presence of human actors on stage fosters sympathy”. While such sympathy can help the satirist by encouraging audience members to recognize themselves in the characters’ portrayed, it also undermines “the possibility of sardonic detachment.” Herr suggests that this conundrum is often resolved “by tempering the

bitterness of the attack.” He describes it as “instructing through laughter rather than punishing through scorn”.

As Spicer (2011) notes, “Satire is a slippery customer. It weaves in and out of reality and makes itself accessible enough for the instantaneous laughter while it is just tricky enough not to be pinned down. Also, Bore and Reid (2014) claim that the first key benefit associated with the use of satire on climate change communication is that the satirical mode can promote active engagement with climate change by encouraging reflection, investigation, and action. The second significant benefit associated with the use of satire on climate change communication is that a humorous tone can help promoting a positive engagement with climate change (Bore and Reid, 2014).

While satire can encourage positive engagement with climate change, communicators need to take measures to avoid confining their engagement with climate change issues to the realm of humor, so that they can make productive proposals to climate change debates (Bore and Reid, 2014).While the distinction between the realm of humor and the realm of seriousness is analytical and it is clearly possible to make fun of climate change while remaining committed to taking action against it, it is important that the use of humorous distance does not discourage citizens’ action (Bore and Reid, 2014). Nisbet and Scheufele (2009) have called for further research “on the potential for using this style of humor [satire] as a tool for public engagement on science”. They believe that satire could be developed as a tool to make science more accessible for nonelite audiences, particularly young people.

3.2 Stand-Up Comedy

Among the different genres of humour, stand-up comedy is one of its most recent forms and can be described as a performer standing on a stage and speaking to an audience with main purpose making people laugh (Pinto et al, 2015). However, some comedians can seek a reaction that is not necessarily laughter, but instead invites the audience to think about certain issues (McCarron and Savin-Baden, 2008). The performances are composed of a succession of funny stories, one-liners or short jokes, and anecdotes, in which each “bit” usually has a set-up (that establishes the context of the joke and introduces necessary background of information to prepare the audience for the punchline, which is the joke about that subject (Greenbaum, 1999; Schwarz, 2010).

The application of stand-up comedy to science communication is still uncommon but has been gaining momentum in recent years in the United States of America and the United Kingdom (Pinto et al, 2015). Probably the most well-known example is the US former scientist Brian Malow (self-proclaimed Earth’s Premier Science Comedian), who develops several activities as a science communicator, not only acting in comedy clubs, conferences and other venues, but also teaching other scientists to better express themselves through the use of comedy (Malow, 2010; Pilcher, 2010). Other examples include US biologist Tim Lee (Chang, 2009), with performances that are usually a parody of science seminars, and the UK mathematician Matt Parker, who does stand-up comedy in clubs, science and comedy festivals, as well as presentations about mathematics in schools (Parker, 2013). Other professional comedians such as Ricky Gervais and Tim Minchin have also adopted themes concerning science in recent years, which is indicative that this humor format has the potential to be used in science communication (Gunderson, 2006; Chang, 2009; Pilcher, 2010).

In their research with students, Robert et al. (2011) investigated neural activation underlying humor specifically as it applies to a naturalistic, dynamic social interaction, addressing the puzzling lack of evidence for mesolimbic responses using such dynamic stimuli. The study examined the neural activation associated with watching stand-up comedians, specifically contrasting high- and low-amusing skits of the same comedians, as selected based on prating made by a sample of raters from the same student population. Although stand-up comedy is certainly still a performance art, it simulates the joke-telling experience in everyday life, where one person surrounded by others captures the attention of the group and delivers the necessary cognitive structure and elements to produce a mirth response and receive the social capital that comes with it(Robert et al., 2011). This may be the case because when instructors enact successful humor, their students enjoy their

educational experiences and learn more (Booth-Butterfield and Wanzer, 2010; Chesebro and Wanzer, 2006).

4. DISCUSSIONAND CONCLUSIONS

Global issues, like climate change is a growing problem, which concerns everyone about a sustainable future. But communication and education about climate change are on the topic last years, such as directly and interactive tools. Developing ways of communicating complex messages and implementing science-policy interface mechanisms are not ends in themselves. Collating, interpreting and disseminating information on climate impacts has as a long-term goal to wisely use scientific information in policy and decision-making in order to plan and manage communities accordingly (Skanavis et al., 2018).

Through humor in environmental communication, communicators avoid overwhelming audiences with feelings of fear, helplessness, and guilt, which may otherwise discourage them from taking action against climate change (O'Neill and Nicholson-Cole, 2009). The reward is a central mechanism of humor, motivating a process of debugging inferential errors in our comprehension of the world that is essential for smooth cognitive functioning (Hurley, Dennett, and Adams, 2011). Humor can thus serve as a means of assessing the shared underlying knowledge, attitudes, and preferences of others and "works, in a sense, as a mind reading spot-check, 'pinging' various minds in the environment and discovering those which are most compatible" (Flamson and Barrett, 2008). This confirms that climate change communicators need humor as a good vehicle for awareness.

Professional comedians have adopted themes concerning science in recent years, which is indicative that this humor format has the potential to be used in science communication (Gunderson, 2006; Chang, 2009; Pilcher, 2010). Comedians can seek a reaction that is not necessarily laughter, but instead invites the audience to think about certain issues (McCarron and Savin-Baden, 2008). The application of stand-up comedy to science communication is still uncommon but has been gaining momentum in recent years in the United States of America and the United Kingdom (Pinto et al, 2015).

Although stand-up comedy is certainly still a performance art, it simulates the joke-telling experience in everyday life, where one person surrounded by others captures the attention of the group and delivers the necessary cognitive structure and elements to produce a mirth response and receive the social capital that comes with it (Robert et al., 2011). This may be the case because when instructors enact successful humor, their students enjoy their educational experiences and learn more (Booth-Butterfield and Wanzer, 2010; Chesebro and Wanzer, 2006). The use of humor is a prevalent communication behavior in pedagogical settings and serves different purposes (Banas et al., 2011).

The clearest findings regarding humor and education concern the use of humor to create a learning environment. The use of positive, nonaggressive humor has been associated with a more interesting and relaxed learning environment, higher instructor evaluations, greater perceived motivation to learn, and enjoyment of the course (Banas et al., 2011). Specifically, instructor's humor increases student performance on exams, especially on knowledge and comprehension items (Hackathorn, Garczynski, Blankmeyer, Tennial, and Solomon, 2011), recall of information (Garner, 2006), and final examination scores (Ziv, 1988). Humor, therefore, guarantees or makes highly likely that specific, hidden knowledge was necessary to produce the humorous utterance, and that the same knowledge is present in anyone who understands the humor (Flamson and Barrett, 2008). Similarly, Martin (2007) argued that the positive emotions aroused by instructional humor may become associated with learning.

References

1. Arnell N. W. (1999). Climate change and global water resources. **Global Environmental Change**, Vol 9, S31-S49.

2. Banas J. A., Dunbar N., Rodriguez D. and Liu S. J. (2011). A Review of Humor in Educational Settings: Four Decades of Research. **Communication Education**, Vol 60 (1), pp. 115-144.

3. Barnett J. and Adger W. (2003). Climate dangers and atoll countries. **Climatic Change**, Vol 61, pp. 321-337.

4. Bentley P. and Kyvik S. (2011). Academic staff and public communication: A survey of popular science publishing across 13 countries. **Public Understanding of Science**, Vol 20(1), pp. 48-63.

5. Bonnici T. (2007). Climate of fear: Stark warning. **The Sun**, pp. 26.

6. Booth-Butterfield M. and Wanzer M. B. (2010). Humor and communication in instructional Contexts: Goal-oriented communication. In D. L. Fassett and J. T. Warren (Eds.). **The SAGE handbook of communication and instruction**, pp. 221-239, Los Angeles: Sage.

7. Bore I. L. K. and Reid G. (2014). Laughing in the Face of Climate Change? Satire as a Device for Engaging Audiences in Public Debate. **Science Communication**, Vol 36 (4), pp. 454-478.

8. Bultitude K. (2011). The why and how of science communication. In: Rosulek P (ed.) **Science Communication**. Pilsen: European Commission, pp. 1-18.

9. Caldeira K. and Wickett M. E. (2003). Anthropogenic carbon and ocean pH: The coming centuries may see more ocean acidification than the past 300 million years. **Nature**, Vol 425, pp. 365.

10. Carvalho A. and Burgess J. (2005). Cultural circuits of climate change: An analysis of representations of "dangerous" climate change in the UK broadsheet press 1985-2003. **Risk Analysis**, Vol 25, pp. 1457-1469.

11. Chang K. (2009). Did you hear the one about the former scientist?. **The New York Times**, 14 December. Available at: http://www.nytimes.com/2009/12/15/science/15comic.html/

12. Chesebro J. L. and Wanzer M. B. (2006). Instructional message variables. In T. P. Mottet, V. P. Richmond and J. C. McCroskey (Eds.). **Handbook of instructional communication: Rhetorical and relational perspectives**, pp. 89-116, Boston: Allyn and Bacon.

13. Christian Aid. (2008). **The issues: climate change**, Retrieved August 14, 2008, from http://www.christianaid.org.uk/issues/climatechange/index.aspx

14. Doulton H. and Brown K. (2009). Ten years to prevent catastrophe? Discourses of climate change and international development in the UK press. **Global Environmental Change**, Vol 19, pp. 191-202.

15. Dudo A. (2012). Toward a model of scientists' public communication activity: The case of biomedical researchers. **Science Communication**, Vol 29, pp. 413-434.

16. Ereaut G. and Segnit N. (2006). **Warm words: How are we telling the climate story and can we tell it better?** London, England: Institute for Public Policy Research.

17. European Commission. (2011). **A roadmap for moving to a competitive low carbon economy in 2050** (Article No. 52011DC112). Retrieved from http://eur-lex. europa.eu/legal-content/EN/ALL/?uri=CELEX:52011DC0112

18. Flamson, T. and Barrett H. C. (2008). The encryption theory of humor: A knowledge-based mechanism of honest signaling. **Journal of Evolutionary Psychology**, Vol 6, pp. 261-281.

19. Flamson, T. and Barrett H. C. (2008). The encryption theory of humor: A knowledge-based mechanism of honest signaling. **Journal of Evolutionary Psychology**, Vol 6, pp. 261-281.

20. Futerra. (2005). **The rules of the game: Principles of climate change communication**. London, England: Futerra.

21. Garner R. L. (2006). Humor in pedagogy: How ha-ha can lead to aha!. **College Teaching**, Vol 54, pp. 177-180.
22. Greenbaum A. (1999). Stand-up comedy as rhetorical argument: An investigation of comic culture. **Humor**, Vol 12(1), pp. 33-46.
23. Gunderson L. (2006). Science plays come of age. **The Scientist**, 28 July. Available at: http://www.the-scientist. com/?articles.view/articleNo/24219/title/Science-plays-come-of-age/
24. Hackathorn J., Garczynski A. M., Blankmeyer K., Tennial R. D. and Solomon E. D. (2011). All kidding aside: Humor increases learning at knowledge and comprehension levels. **Journal of the Scholarship of Teaching and Learning**, Vol 11, pp. 116-123.
25. Hastings G., Stead M. and Webb J. (2004). Fear appeals in social marketing: Strategic and ethical reasons for concern. **Psychology and Marketing**, Vol 21, pp. 961-986.
26. Hauke R. (2015). Why did the proton cross the road? Humour and science communication. **Public Understanding of Science**, Vol 24 (7), pp. 768-775.
27. Herr C. J. (2007). Satire in modern and contemporary theater. In R. Quintero (Ed.). **A companion to satire**, pp. 460-475, Malden, MA: Blackwell.
28. House of Lords. (2000). **Science and society: Third report**. London, England: Her Majesty's Stationery Office.
29. Howell R. A. (2014). Investigating the Long-Term Impacts of Climate Change Communications on Individuals' Attitudes and Behavior. **Environment and Behavior**, Vol 46(1), pp. 70-101.
30. Hulme M. (2007). Newspaper scare headlines can be counter-productive. **Nature**, Vol 445, pp. 818.
31. HulmeM. (2008). The conquering of climate: Discourses of fear and their dissolution. **Geographical Journal**, Vol 174, pp. 5-16.
32. Hurley M. M., Dennett D. C. and Adams R. B. Jr. (2011). **Inside jokes: Using humor to reverse-engineer the mind**, Cambridge, MA: MIT Press.
33. Intergovernmental Panel on Climate Change. (2007). **Climate change 2007— Summary for policymakers: Working Group II report: Impacts, adaptation and vulnerability**, Available from http://www.ipcc.ch
34. Intergovernmental Panel on Climate Change. (2007). **Climate change 2007: Synthesis report. Summary for policymakers. Cambridge**, UK: Cambridge University Press.
35. Joffe H. (1999). **Risk and "the other."** Cambridge, UK: Cambridge University Press.
36. Kellstedt P. M., Zahran S. and Vedlitz A. (2008). Personal efficacy, the information environment, and attitudes toward global warming and climate change in the United States. **Risk Analysis**, Vol 28, pp. 113-126.
37. Kloeckner C. A. (2011). Towards a psychology of climate change. In W. L. Filho (Ed.). **The economic, social and political elements of climate change**, pp.153-173, Berlin, Germany: Springer-Verlag.
38. Leemans R. and Eickhout B. (2004). Another reason for concern: Regional and global impacts on ecosystems for different levels of climate change. **Global Environmental Change**, Vol 14, pp. 219-228.
39. Lewis I. M., Watson B. and White K. M. (2010). Response efficacy: The key to minimizing rejection and maximising acceptance of emotion-based anti-speeding messages. **Accident Analysis and Prevention**, Vol 42, pp. 459-467.

40. Linville P. W. and Fischer G. W. (1991). Preferences for separating and combining events: A social application of prospect theory and the mental accounting model. **Journal of Personality and Social Psychology**, Vol 60, pp. 5-23.

41. Lorenzoni I., Jones M. and Turnpenny J. (2006). Climate change, human genetics and postnormality in the UK. **Futures**, Vol 39, pp. 65-82.

42. Lorenzoni I., Nicholson-Cole S. A. and Whitmarsh L. (2007). Barriers perceived to engaging with climate change among the UK public and their policy implications. **Global Environmental Change**, Vol 17, pp. 445-459.

43. Malow B. (2010). **About Brian. Brian Malow: Earth's Premier Science Comedian**. Available at: http://www. sciencecomedian.com/

44. Martin R.A. (2007). **The psychology of humor: An integrative approach**, Oxford: Elsevier Academic Press.

45. McCarron K. and Savin-Baden M. (2008). Compering and comparing: Stand-up comedy and pedagogy. **Innovations in Education and Teaching International**, Vol 4 (4), pp. 355-363.

46. Morton T. A., Rabinovich A., Marshall D. and Bretschneider P. (2011). The future that may (or may not) come: How framing changes responses to uncertainty in climate change communications. **Global Environmental Change**, Vol 21, pp. 103-109.

47. Moser S. C. (2007). More bad news: The risk of neglecting emotional response to climate change information. In S. C. Moser and L. Dilling (Eds.). **Creating a climate for change: Communicating climate change and facilitating social change**, pp.64-80, New York, NY: Cambridge University Press.

48. Moser S. C. and Dilling L. (2004). Making climate hot. **Environment**, Vol 34, pp. 32-46.

49. Munich Re. (2004). **Megacities-megarisks**. London:Author.

50. Nisbet M. C. and Scheufele D. A. (2009). What's next for science communication? Promising directions and lingering distractions. **American Journal of Botany**, Vol 96, pp. 1767-1778.

51. O'Neill S. and Nicholson-Cole S. (2009). "Fear won't do it": Promoting positive engagement with climate change through visual and iconic representations. **Science Communication**, Vol 30 (3), pp. 355-379.

52. O'Neill S. J. (2008). An iconic approach to communicating climate change. **Unpublished PhD thesis**, School of Environmental Sciences, University of East Anglia, UK. Accessed 9 December 2009 from: www.cru.uea.ac.uk/~saffron

53. Ockwell D., WhitmarshL. and O'Neill S. (2009). Reorienting climate change communication for effective mitigation: Forcing people to be green or fostering grass-roots engagement?. **Science** Communication, Vol. 30, pp. 305-327.

54. Parant A., Pascual A., Jugel M., Kerroume M., Felonneau M. L. and Guéguen N. (2017). Raising Students Awareness to Climate Change: An Illustration With Binding Communication. **Environment and Behavior**, Vol 49 (3), pp. 339-353.

55. Parker M. (2013). Matt Parker. **Matt Parker: Stand-up Mathematician**. Available at: http://www.standupmaths.com/

56. Peters G. J. Y., Ruiter R. A. and Kok G. (2013). Threatening communication: A critical re-analysis and a revised meta-analytic test of fear appeal theory. **Health Psychology Review**, 7(Suppl. 1), S8-S31.

57. Pilcher H. (2010). Communication: A better class of heckle. **Nature**, Vol 467, pp. 530.

58. Pinto B., MarçalD. and Vaz S. G. (2015). Communicating through humour: A project of stand-up comedy about science. **Public Understanding of Science**, Vol 24(7), pp. 776-793.
59. Poliakoff E and Webb TL (2007). What factors predict scientists' intentions to participate in public engagement of science activities?. **Science Communication**, Vol 29, pp. 242-263.
60. Pooley J. A. and O'Connor M. (2000). Environmental education and attitudes: Emotions and beliefs are what is needed. **Environment and Behavior**, Vol 32, pp. 711-723.
61. Robert G., Franklin Jr., Reginald B. and Adams Jr. (2011). The reward of a good joke: neural correlates of viewing dynamic displays of stand-up comedy. **Cogn Affect BehavNeurosci**, Vol 11, pp. 508-515.
62. Schultz P. W. (2002). Knowledge, information and household recycling: Examining the knowledge deficit model of behavior change. In T. Dietz and P. Stern (Eds.). **New tools for environmental protection: Education, information, and voluntary measures**, pp. 67-82, Washington, DC: National Academies Press.
63. Schwarz J. (2010). **Linguistic Aspects of Verbal Humor in Stand-up Comedy**. Göttingen: Sierke-Verlag.
64. Skanavis C., K. Antonopoulos, V. Plaka, S.P. Pollaki, E.Tsagaki-Rekleitou, G. Koresi and Ch. Oursouzidou. (2018). Linaria Port: An Interactive Tool for Climate Change Awareness in Greece. In **Second World Symposium on Climate Change Communication**. Graz, Austria.
65. Spence A. and Pidgeon N. F. (2010). Framing and communicating climate change: The effects of distance and outcome frame manipulations. **Global Environmental Change**, Vol 20, pp. 656-667.
66. Spicer R. N. (2011). Before and after The Daily Show: Freedom and consequences in political satire. In T. Goodnow (Ed.). **The Daily Show and rhetoric: Arguments, issues, and strategies**, pp. 19-41, Lanham, MD: Lexington.
67. Trench B. and Miller S. (2012). Policies and practices in supporting scientists' public communication through training. **Science and Public Policy**, Vol 39, pp. 722-731.
68. Weingart P., Engels A. and Pansegray P. (2000). Risks of communication: Discourses on climate change in science, politics and the mass media. **Public Understanding of Science**, Vol 9, pp. 261-283.
69. Wootton M. (2005). **Green Party 2005 election communication: National campaign**, Northampton, UK: Centreweb.
70. Ziv A. (1988). Teaching and learning with humor: Experiment and replication. **Journal of Experimental Education**, Vol 57, pp. 5-15.

EARLY CHILDHOOD ENVIRONMENTAL CAMP IN A GREEK PORT

G. Koresi, V. Plaka* and C. Skanavis

Research Center of Environmental Education and Communication, Dept. of Environment, University of the Aegean, GR-81100 Mytilene, Lesvos, Greece

*Corresponding author: e-mail: plaka@env.aegean.gr, tel: +302251036234

Abstract

In Greece, the Port of Skyros Island has established an environmental campaign in its area, which is running for the last three years. The name of the above campaign is "SKYROS Project". It is a cooperative project between the University of the Aegean and the Skyros Port Fund. Since 2015, every summer, academic students and researchers of the Research Center of Environmental Education and Communication of the Department of the Environment of the University of the Aegean are visiting the Island of Skyros in the spectrum of their internship requirements. The environmental communication tasks of SKYROS Project include a variety of different environmental actions. One of them is the Environmental Kids' Camp, in which children 6 to 13 years old are participating in environmental education programs. They are being educated in a specially designed area, on how to take care, respect and protect the environment. The ultimate goal is to create environmentally active citizens with a responsible behavior. So, the main object of this research is to create a program complementary to the one already existing, based on environmental education guidelines for early childhood. For the first time, this summer of 2018, the research team of SKYROS Project will attempt to involve kids of early childhood age as well.

This program provides the opportunities for young children of locals and tourists to participate in a variety of eco-social interactions, including playing and exploring the outdoors. Based on a quality assessment process, this paper will present the benefits of environmental education in early childhood in outdoors places, like a port. The extension of the environmental camp would be based on the Guidelines for Excellence of the North American Association of Environmental Education. The overall goal of these guidelines is to chart an appropriate and positive process whereby educators can start young children on their journey towards becoming an environmentally responsive youth and later on adults. Environmental education in early childhood is a holistic concept that encompasses knowledge of the natural world strengthening this way environmental literacy for all.

Keywords: Environmental education, Environmental camp, Early childhood, Outdoor activities, Environmental responsible behavior

1. INTRODUCTION

Environmental Education (EE) was born in the middle of the previous century amid a generalized concern that was developed within the modern environmental movement (Flogaitis et al, 2005). According to the definition, given by UNESCO (1978) at the Conference in Tbilisi, EE is the process of shaping a global population, which should be informed, interested in the environment and its issues, and have the knowledge, skills, attitude and will to work, alone and collectively, on solving the current environmental issues and preventing the appearance of new ones.

The Tbilisi Declaration identified that humans and the environment were interdependent on each other and governments should consider both the needs of the present and the needs of the future generations in their policies. It emphasized that for significant change to happen, countries had to engage on environmental education for people of all ages both in formal and informal settings in order to handle the problems affecting the quality of this planet (Croft, 2017).

The main purpose of environmental education is to give every individual the opportunity to express a positive environmental attitude and responsibility towards the environment they live (Sabo, 2010). Environmental education is a way to reach an understanding of the relationship between humanity and the living environment. Young children are active and inquisitive (NAAEE, 2000). The curiosity that is a common stake of children is the way to make them interested to explore nature and learn about life in general. Everything is worth exploration for them and all their senses are involved in the understanding of how the environment is built. Children from early age are interested to connect with others and experience both indoors and outdoors environments. Outdoors Environmental Education (OEE) is one of the most successful ways to lure children towards building a solid succeeding environmental literacy (Okur-Berberoglu et al, 2014).

1.1 Environmental education in coastal areas

To sustainably manage coastal areas and conserve coastal biodiversity, the participation of local residents and other stakeholders is indispensable (Sakurai et al, 2017). Sustainable management of coastal biodiversity as well as conservation of coastal and marine areas were declared as important goals for the Aichi Targets, which all countries and stakeholders need to pursue (Sakurai et al, 2017). Researchers in various fields have tested and explained factors that affect people's willingness to behave in an environmentally friendly manner (Zanetell and Knuth, 2004; Sakurai et al, 2015).

Previous studies have identified that people's sense of place could affect their willingness to conserve the coastal area (Sakurai et al, 2017). Several studies have suggested that sense of place can include place attachment, which is the strength of the bond between a person and place. The place meaning, is the symbolic meaning people attribute to a place (Halpenny, 2010). Although sense of place has been discussed and acknowledged by many researchers as an important concept, affecting people's willingness to take care of a place, conceptualizing and quantitatively identifying this framework has been challenging (Stedman, 2002).

Environmental education is a field that aims to encourage people to adopt more sustainable lifestyles through 1) acquiring awareness, 2) developing knowledge, 3) acquiring attitudes, 4) acquiring skills, and 5) encouraging participation (Jacobson, 2009). One of the most important goals of environmental education is to understand the relationship between current and future generations (specifically, the importance of protecting the natural environment and resources for future generations), which could be regarded as directly connected to two environmental education aims: acquiring awareness and positive attitudes (NAAEE, 2009; Japanese Society of Environmental Education, 2012).

The importance of developing conservationist attitudes with regard to future generations can also be explained in the context of a major environmental worldview (Sakurai et al, 2017). The stewardship worldview assumes that we (human beings) are borrowing the earth's natural capital from future generations, and therefore, we have an ethical responsibility to leave the earth in a healty condition for the generations to come (Miller and Spoolman, 2015).

1.2 Environmental Education at the Port of Skyros Island: Daily Environmental Kid’s Camp

In Greece, Linaria Port of Skyros Island is famous for the innovative approaches enacted by the specific Port Authority. Since 2015, a worldwide environmental campaign, under the brand name “SKYROS Project”, has launched there, presenting an innovative cooperation with the University of the Aegean and the Skyros Port Authority. University students, locals and visitors become the decision makers for environmental issues taking in their hands environmental planning and management of the specific port area (Skanavis et al, 2018). However, this approach in terms of “information-deficit” has been widely criticized as being inadequate to promote behavioral change

(Ockwell et al, 2009 Skanavis & Kounani 2017). To tackle such concern, the SKYROS Project, taking off in 2015, established at Linaria port an interactive lab which included the port as a way of promoting environmental issues awareness through hands on experience (Skanavis et al, 2018). Significant environmental actions that were implemented were an Environmental Kid's Camp, Tourist Observatory, Maritime Tourism Observatory and a Summer Academy for Environmental Educators (Plaka et al, 2017). This project was recognized at national and international competitions as one that excels on environmental awareness (Plaka et al, 2017 and Antonopoulos et al, 2017a).

2. METHODOLOGY

2.1 Study Area

Skyros Island belongs to a complex of islands, which is called Sporades. The importance of this island is considered huge not only because it is placed in the center of the Aegean Sea, but also because it connects many destinations (Antonopoulos et al, 2017a). In Linaria, the Port Authority Administration has adopted an environmental and sustainable agenda. Delivered at the port, a series of innovative environmental education projects that could promote environmentally responsible behavior for both visitors and residents (Antonopoulos et al, 2017b) proved to be a breakthrough in the promotion of responsible environmental behaviors. This port has been distinguished as a unique one for the whole country (Antonopoulos et al, 2015). Furthermore Linaria as a community has been characterized as an environmentally sustainable one (Antonopoulos et al, 2016).

The last six years, this small port constantly implements interesting ideas, such as the construction of seadromes, the use of electric scooters, the PV panels, a gas station and the cooperation of the Port Authority of Skyros with the University of the Aegean's Department of Environment, known as SKYROS Project. These actions have attracted the interest and respect of travelers from around the world (Antonopoulos et al, 2016). Environmental actions at no cost for users, gradually formed conscious citizens at the island and encouraged visitors to become environmentally sensitive (Plaka et al, 2017). United Nations during the Climate Change Summit of 2016, recognized the Linaria Port as "the blue port with a shade of green" (Skanavis et al, 2018).

2.2 Planning and implementation

The Environmental Kids' Camp has been offered every summer for the last four years. The ages of the participants range between 6-13 years old. This coming summer, pre-school children (ages 3-6) will be welcomed. Environmental education in early childhood is a holistic concept that encompasses knowledge of the natural world, strengthening appropriate code of ethics and promoting environmental literacy for all.

This paper is based on a qualitative study, presenting the benefits of environmental education at early childhood in outdoors places, like a port. Having a high quality educational program tailored to the participants' interests and being inspired by familiar surroundings is very important for practicing theory in real time conditions (Skanavis et al., 2018). The objectives of the summer environmental camp at Skyros Island were related to the dissemination of environmental education to children and to the promotion of their responsible environmental behavior through theory and hands on experience in an outdoors set up (Skanavis and Kounani 2017).

The environmental camp set up is based on the "Guidelines for Excellence" of the North American Association of Environmental Education (NAAEE 2017). The main goal behind the specific quidelines is to chart an appropriate and positive process whereby educators can start young children on their journey towards becoming an environmentally responsive youth and later on adults.

This research focuses on the part of preschool kids environmental education through their interaction with a port. The plan for this program is to use procedures, which will be easy to comprehend from participating kids of very young ages (3-6 years old). An environmental awareness approach may be best handled through interaction with nature, excursions and camps (Sabo, 2010). Early childhood environmental educators need to create a climate in which children are motivated to learn about and

explore the environment and practice their developed skills with procedures based on a basic understanding of the goals, theory, practice, and history of the field of environmental education (NAAEE, 2000).

3. THE MAGNITUDE OF ENVIRONMENTAL EDUCATION IN EARLY CHILDHOOD

Environmental education is becoming an increasingly important learning area in early childhood education (Pearson & Degotardi, 2009). The approach to environmental education for early childhood learners is less about organization of graduated achievements and more about free discovery on each child's own terms (NAAEE 2000). The preschoolers get their first exposure to the worldwide profile of the environmental issues, and the destructive potential of individuals to nature (Sabo, 2010).

Wilson (2012) outlines how the early childhood years are fundamental in developing ‘’ environmental attitudes and a commitment to caring for the Earth’’. The natural world can give children instant responses to their curiosity through all of their senses as they touch, taste, smell, see and hear what is going around them. Early Childhood Environmental (ECE) programs are expected to foster the physical, mental, and social- emotional development of children, and, increasingly, to address an array of the threats to children's health and wellness (Cooper, 2015). In early childhood, it is important to concentrate on building a foundation that will allow for positive examination of issues and appropriate action later in life (NAAEE 2000). Children are the future guardians of earth. Thus, studies on children's environment from children's perspective are vital because the environment shapes children's attitude and behavior as children and later on as adults (Mustapa et al, 2015).

3.1 The relationship between young children and nature

The task of environmental education for young children is to forge the bond between children and nature (NAAEE, 2000). Connection to nature during childhood has a significant impact on attitude and behavior towards nature in later life (Mustapa et al, 2015). Research by Fjortoft (2001, 2004) found young children playing in a natural environment had a greater increase in gross motor skill development, motor fitness, balance, and coordination than their peers in a traditional playground setting (Ernst and Tornabene, 2012). Freeman and Tranter (2011) also categorized the experience in nature in three types: direct, indirect and observing without contact (Mustapa et al, 2015).

Providing high-quality early childhood programs, and allowing children to follow their curiosities about their word and what nature has to offer, can bring incredible richness to their lives (NAAEE 2000). Direct experiences in nature encourage connection and increase children's affinity towards nature (Mustapa et al, 2015). Children, who participated in a nature camp with and without environmental education showed an increase in their affinity towards nature, ecological beliefs and environmental behavior (Collado et al, 2013).

Experience in nature increases their score on eco-affinity, eco-awareness and environmental knowledge (Larson et al, 2009). They are learning how to explore and use tools of exploration such as magnifying glasses and pop sickle sticks (NAAEE, 2000). Moreover, time spent in nature is found to be an indicator on environmental attitudes (Mustapa et al, 2015). Children are watching plants and animals change through their life cycles, and learn how to respect the natural world and living things (NAAEE, 2000). Experience in nature for prolonged time has been found to be an indicator on positive environmental attitude resulted from the connection and the empathy feelings associated with it (Stern et al, 2008). The interest and curiosity that young children typically show for plants, animals, water, clouds, rocks, and other natural phenomena are the basis for environmental educators' work (NAAEE, 2000).

Indirect experience in nature is also associated positively to children's affinity and environmental attitude and behavior. Children involved in an environmental club showed positive attitudes toward the natural environment compared to children who had not joined the club (Mcallister et al, 2012). Children who respect the environment feel an emotional attachment to the natural world, and deeply understand the link between themselves and nature. They will eventually become environmentally

literate citizens (NAAEE, 2000). Children with lack of experience and exposure to nature will see themselves separated from the natural world (Mustapa et al, 2015).

3.2 The role of play

As a natural and compelling activity, play promotes cognitive, physical, social, and emotional well being, offering the necessary conditions for children to thrive and learn (Bento and Dias, 2017). Wood and Attfield (2005) argue: Play cannot be easily defined or categorized because it is always context dependent, and the contexts can vary. There are many different forms of play including: role play, imaginative play, socio-dramatic play, heuristic play, constructive play, fantasy play, free-flow play, structured play, rough and tumble play, all of which involve a wide range of activities and behaviors and result in varied learning and developmental outcomes (Mackenzie and Edwards, 2013).

Through play, the child can experiment, solve problems, think creatively, cooperate with others, etc., gaining a deeper knowledge about his/her self and the world (Bento and Dias, 2017). This way of thinking about play has contributed on the learning and teaching approaches of environmental education at early childhood because it allows the value of experience (including values and action) and engagement with the sources behind the theoretical knowledge (Mackenzie and Edwards, 2013). From an early age, the possibility to experience during the unstructured play, in which the child can decide what to do, with whom and how, promotes positive self-esteem, autonomy, and confidence (Bento and Dias, 2017). Children communicate with peers and develop friendship when playing in the natural environment. They learn social skills such as manners, how to behave and interact with peers, confidence and work ethics (Laaksoharju et al., 2012).

Play and exploration promote physical development, are soothing and reduce stress, and help to restore attention. An enjoyable task has a tremendous potential for promoting creativity, helping children construct an understanding of their world, and facilitates learning in many different areas (NAAEE, 2000). Play and experience in nature, highly contributes to children's cognitive, physical and social development, restores positive emotion, develops sense of place, empathy and care for nature, as well as, associates positively with environmental attitude and behavior (Mustapa et al, 2015).

3.3 Play in outdoors places

The outdoors can be described as an open and constantly changing environment, where it is possible to experience freedom, gross and boisterous movements, and contact with natural elements (Bento and Dias, 2017). Outdoor play provides learning opportunities for infants and toddlers that they cannot get elsewhere (NAAEE, 2000). While playing outside, children benefit from being exposed to sunlight, natural elements, and open air, which contributes to bones development, stronger immune system and physical activity (Bento and Dias, 2017).

Early-learner programs provide opportunities for young children to participate in a variety of social interactions, including play and exploration in the outdoors that allow them to grow as contributing members of their community (NAAEE, 2000). The need to be physically active from an early age is particularly relevant if we consider the concerning growth of children's obesity and overweight (Bento and Dias, 2017). Nutrition is improved since children who get engaged into grow food are more likely to eat fruits and vegetables (Bell and Dyment, 2008). Gardens that support children's engagement with vegetables and fruits and increase frequency of consumption are associated with acceptance of diverse tastes (Cabalda et al, 2011) as a positive strategy to support healthy eating (Meinen et al 2012). Thus, it is important to understand benefits of the nature and environment on children's developmental needs in order to create an environment that meets the quality standards (Mustapa et al, 2015).

Because injuries can take place in outdoor play areas, safety is a major consideration (NAAEE, 2000). Three basic safety rules are as follows:

1. Provide soft, level surfaces with good drainage. Grass is best for toddling and crawling; wood, mulch, or rubber mats work well under “fall zones.”
2. Eliminate possibilities for entrapment.
3. Provide watchful maintenance for items dangerous for babies to put in their mouths. Remove items that are a choking hazard.

Through outdoor play and the exploration of natural elements, it is possible to promote education in its broadest sense. Activities related to playing with soil and water can serve as examples of learning opportunities in which concepts related to mathematics, science or language were promoted in an integrated way (Bento and Dias, 2017).

3.4 Places and spaces

Early childhood environmental education programs provide places and spaces, both indoors and out, that are safe, enticing, comfortable, and enhance learning and development across all learning domains; and provide opportunities for development across social, emotional, physical, and cognitive development domain. Helping children to look more closely, listening more carefully, and understanding the natural world in rich and varied ways by providing opportunities for children to marvel in the beauty of nature are important reasons to invest in outdoors environmental education (NAAEE, 2000).

Today’s society often neglects the importance of risk in children’s learning agenda and developmental approaches (Bento and Dias, 2017). The integration of natural components throughout places and spaces is essential if learning opportunities and development are to be maximized (NAAEE, 2000). A culture of fear lead us to underestimate what children are capable to do, creating an even more “dangerous” learning environment, where children do not have the possibility to learn, by experience, how to stay safe (Bento and Dias, 2017). In the outdoor environment, opportunities to exceed personal limits often emerge in situations like climbing up a tree or using a tool (Bento and Dias, 2017).

In risky play, the adult should interpret the signs of the child, giving the necessary support or space that he or she needs. From experts experience and relevant studies in this area, it is possible to state that risky play promotes important skills related to persistence, entrepreneurship, self-knowledge and problem solving. During outdoor play, children should have the opportunity to experiment moments of failure and success, learning by trial and error. If we try to prevent all risky situations, children will not know how to deal with unpredictable environments and will lack the necessary confidence to overcome challenges in an autonomous way (Bento and Dias, 2017).

To develop quality outdoor practices, that can have a positive impact ion children’s health and development, it is fundamental to promote conditions for adults to feel comfortable and motivated during the time the children spent outside. Often educators are concerned about keeping children together outdoors in order to keep them safe, away from streets, and to prevent them from getting lost (NAAEE, 2000). It is important not to forget that most families just want the best for their children and it is the job of professionals to help them achieve this goal (Bento and Dias, 2017).

4. DISCUSSION AND CONCLUSSIONS

Environmental education often begins close to home, encouraging learners to understand and forge connections with their immediate surroundings. The environmental awareness, knowledge, and skills needed for this localized learning provide a foundation for moving out into larger systems, broader issues, and a more sophisticated comprehension of causes, connections, and consequences (NAAEE, 2000). Young individuals should experience the power, fragility, interconnectedness and awe of nature, so they can become environmental stewards of the future (Plaka and Skanavis, 2016).

Linaria is characterized as an environmentally sustainable small port community (Antonopoulos et al, 2016). Through various case studies, research has identified that people's sense of place could play an important role in motivating place-protective behavior (Halpenny, 2010; Tonge et al, 2014; Sakurai et al, 2016). Environmental Education in a port which has adopted a sustainable agenda

strengthens the above mentioned feeling. The action of Environmental Camp of SKYROS Project at the Port of Skyros Island is internationally unique (Plaka et al, 2017). The variety of free environmental actions which are being held at this port, gradually transform participating kids to conscious citizens (Plaka et al, 2017). In order to achieve a satisfying deepening in environmental education, it is necessary to connect it to all three forms of education (Aposotolopoulou et al, 2016) something that been done successfully at Linaria Port.

Most environmental education, outreach, and communication programs are designed to help people understand their impact on future generations and how we need to take care of resources so that future generations can use them as well (Jacobson, 2009; NAAEE, 2009; Japanese Society of Environmental Education, 2012). However, there has not been much systematic and scientific research to understand what actually affects people's attitudes regarding future generations (Sakurai et al, 2017). This could be an interesting quantitative assessment project about an environmental education program at a port.

Youth must be educated, in and out the classrooms, in how to take care, respect and protect the environment. Promoting sustainable development should be a priority in the school system's educational agenda. The way to reach this state of excellence is through environmental education from an early age. Early learning programs provide children with opportunities to develop curiosity, ask their own questions, and be able to develop reasoning and problem-solving skills (NAAEE, 2000). Young people, by all available means, must learn to care for the planet, be familiar with nature and be a part of an environmentally active community (Plaka and Skanavis., 2016).

Connection to nature during childhood has a significant impact on attitude and behavior towards nature in later life (Mustapa et al, 2015). Providing high-quality early childhood programs, and allowing children to follow their curiosities about their word and what nature has to offer, can bring incredible richness to their lives. In early childhood, it is important to concentrate on building a foundation that will allow for positive examination of issues and appropriate action later on in life. Children are the future guardians of earth. Thus, studies on children's environmental perceptions from the children's perspectives are vital because the environment shapes children's attitude and behavior (Mustapa et al, 2015). The integration with natural components throughout places and spaces is essential if learning opportunities and development potential are to be maximized (NAAEE, 2000).

Nevertheless, the ultimate goal of Environmental Education is the development of an environmentally literate citizenry (NAAEE, 2000). As Skanavis et al. (2005) indicate "our youth is the most precious asset. Supporting their environmental conscious, would later on enable them to actively participate in the environmental decision making. As children explore their environment, they begin to develop understandings of how the world works (NAAEE, 2000). When environmentally educated young individuals grow up, as residents they would willingly participate in a societal movement, especially when they observe that their way of life is endangered" (Nastoulas et al, 2017).

References

1. Antonopoulos K, C. Skanavis and V. Plaka. (2015). 'Exploiting futher potential of Linaria Port-Skyros: From vision to realization' (in Greek). In **Proceedings of the First Hellenic Conference on Tourist Port, Marinas**, eds. Athens, Greece, Laboratory of Harbour Works, N.T.U.A pp. 101-111.

2. Antonopoulos K., V. Plaka and C. Skanavis. (2016). 'Linaria port, Skyros: An environmentally friendly port community for leisure crafts'. Proc. of Int. Conf. **Protection and Restoration of the Environmental island,** Greece, 2016.

3. Antonopoulos K., V. Plaka, A. Barbakonstanti, D. Dimitriadou and C. Skanavis. (2017b). 'THE BLUE PORT WITH A SHADE OF GREEN: The case study of Skyros Island'. Proc. Int.Conf. **Proceedings of the 7th Health and Environment, Innovation Arabia Conference**, Dubai, Unated Arab Emirates, pp. 175-187.

4. Antonopoulos K., V.Plaka and C. Skanavis. (2017a). 'INNOVATIVE IMPLEMENTS TO COLLECT INFORMATION: EFFECTIVENESS AND SAFETY IN LINARIA PORT, SKYROS'. In **Seventh Hellenic Conference Management and Improvement of Coastal Zones**. Athens, Greece.

5. Apostolopoulou S., G. Grigoroglou, M. Karamperis, C. Skanavis and A. Kounani. (2016). 'Environmental Summer Camp in a Greek Island'. In **Thirteenth Int. Conf. Protection and Restoration of the Environment**, Mykonos Island, Greece.

6. Bell, Anne C., and Janet E. Dyment. (2008). 'Grounds for movement: green school grounds as sites for promoting physical activity'. **Health Educ. Res.** (2008), Vol. 23(6), pp. 952-962.

7. Bento G. and G. Dias. (2017). 'The importance of outdoor play for young children's healthy development'. **Porto Biomedical Journal,** Vol. 2(5), pp. 157-160.

8. Cabalda A., P. Rayco-Solon, J.A. Solon and F. Solon. (2011). 'Home gardening is associated with Filipino preschool children's dietary diversity'. **J Am Diet Assoc**, Vol 111 pp.711-715.

9. Collado S., H. Staats and J. A. Corraliza. (2013). 'Experiencing nature in children's summer camps: Affective, cognitive and behavioural consequences'. **Journal of Environmental Psychology**, 33, pp. 37–44.

10. Cooper A. (2015). 'Nature and Outdoor Learning Environment: The Forgotten Resource in Early Childhood Education'. **National Wildlife Federation,** Vol. 3(1), pp. 85.

11. Croft A. (2017). 'Learning the change toward education for sustainability in early childhood education'. New Zealand Tertiary College.

12. Cutter-Mackenzie A. and S. Edwards. (2013). 'Toward a Model of Early Chilhood Environmental Education: Foregrounding, Developing, and Connecting Knowledge Through Play- Based Learning'. **The Journal of Environmental Education**, Vol 44(3), pp. 195-213.

13. Ernst J. and L. Tornabene. (2012). 'Preservice early childhood educators' perceptions of outdoor settings as learning environments'. **Environmental Education Research,** 18(5), pp. 643 664.

14. Fjortoft I. (2001). 'The natural environment as a playground for children: The impact of play activities in pre-primary school children'. **Early Childhood Education Journal**, Vol. 29(2), pp. 111–7.

15. Fjortoft I. (2004). 'Landscapes as playscape: The effects of natural environments on children's play and motor development'. **Children, Youth and Environments**, Vol. 14(2), pp. 21–44.

16. Flogaitis E., M. Daskolia and E. Agelidou. (2005). 'Kindergarten Teachers' Conceptions of Environmental Education'. **Early Childhood Education Journal**, Vol. 33(3) pp. 125-136.

17. Freeman C. and P. Tranter. (2011). 'Children & Their Urban Environment'. Earthscan.

18. Halpenny E.A. (2010). 'Pro-environmental behaviours and park visitors: the effect of place attachment'. **J. Environ Psychol**, 30, pp. 409–421.

19. Japanese Society of Environmental Education. (2012). Environmental Education**. Kyoiku-Shuppan**, Tokyo, Japan (in Japanese).

20. Laaksoharju T., E. Rappe and T. Kaivola. (2012). 'Garden affordances for social learning, play, and for building nature–child relationship'. **Urban Forestry & Urban Greening**, Vol. 11(2), pp. 195–203.

21. Larson L.R., G. T. Green, and S. B. Castleberry. (2009). 'Construction and Validation of an Instrument to Measure Environmental Orientations in a Diverse Group of Children'. **Environment and Behavior**, Vol 43(1), pp. 72–89.

22. Jacobson S.K. (2009). ‘Communication Skills for Conservation Professionals’. **Island Press**, Washington, D.C.
23. Mcallister C., J. Lewis and S. Murphy. (2012). ‘The green grass grew all around: rethinking urban natural spaces with children in mind’. **Children Youth and Environments**, Vol. 22, pp. 164–193.
24. Meinen A, B. Friese and W. Wright. (2012). ‘Youth gardens increase healthy behaviors in young children’, **J Hunger Environ Nutr**, Vol. 7, pp. 192-204.
25. Mille, G.T. and S.E. Spoolman. (2015). ‘Living in the Environment’. Eighteenth eds. Cengage Leaning, Connecticut.
26. Mustapa N.D., Z. Maliki and A. Hamzah. (2015). ‘Repositioning Children’s Developmental Needs in Space Planning: A Review of Connection to Nature’. **Procedia- Social and Behavioral Sciences,** Vol. 170, pp. 330-339.
27. Nastoulas I., K. Marini and C. Skanavis ‘Middle School Students’ Environmental Literacy Assessment in Thessaloniki Greece’ In. **Proceedings of the 7th Health and Environment, Innovation Arabia Conference** pp. 198-209. Dubai, Unated Arab Emirates.
28. North American Association for Environmental Education (NAAEE). (2009). ‘Environmental Education Materials: Guidelines for Excellence. North American Association for Environmental Education’. Washington, DC.
29. North American Association for Environmental Education (NAAEE). (2017). ‘Professional Development of Environmental Educators: Guidelines for Excellence’. Washington.
30. Ockwell D, WhitmarshL,O’Neill S. (2009). ‘Reorienting Climate Change Communication for Effective Mitigation:Forcing People to be Green or Fostering Grass-Roots Engagement?’. **Science Communication**, Vol. 30(3), pp. 305-327
31. Okur-Berberoglu E., Ozdilek H.G., Yalcin- Ozdilek S., Eryaman M. Y. (2014). ‘The Short Term Effectiveness of an Outdoor Environmental Education on Environmental Awareness and Sensitivity of In-service Teachers’. **International Electronic Journal of Environmental Education**, 5 (1), 1-20.
32. Pearson E. and Degotardi S. (2009). ‘Education for sustainable development in early childhood education: A global solution to local concerns’. **International Journal of Early Childhood**, 419, pp. 97–111.
33. Plaka V., Tsagaki-Rekleitou E. and Skanavis C. (2017). ‘Creation of an environmental educational kit: the port as an interactive tool’. In **Seventh Hellenic Conference Management and Improvement of Coastal Zones**. Athens, Greece.
34. Sabo H.M. (2010). ‘Why from early environmental education’. **US- China Foreign Language,** Vol. 8(12), pp. 57-61.
35. Said I. (2012). ‘Affordances of Nearby Forest and Orchard on Children ’ s Performances’. Procedia - Social and Behavioral Sciences, Vol. 38, pp. 195–203.
36. Sakurai R., H. Kobori, M. Nakamura and T. Kikuchi. (2016). ‘Influence of residents' social interactions in and affections toward their community on their willingness to participate in greening activities’. **Environ. Sci.** Vol. 29 (3), pp. 137–146.
37. Sakurai R., T. Ota and T. Uehara. (2017). ‘Sense of place and attitudes towards future generations for conservation of coastal areas in the Satoumi of Japan’. **Biological Conservation,** Vol. 209, pp. 332-340.

38. Sakurai, R., H. Kobori, M. Nakamura, and T. Kikuchi. (2015). 'Factors influencing public participation in conservation activities in urban areas: a case study in Yokohama' Japan. Biol. Conserv. 184, pp. 424–430.

39. Skanavis C. and A. Kounani. (2017). 'Children Communicating on Climate Change: The Case of a Summer Camp at a Greek Island.Leal-Filho W', eds. Manolas E, Azul AM, Azeiteirou, Elsevier, Amsterdam, Handbook of Climate Change Communication.

40. Skanavis C., K. Antonopoulos, V. Plaka, S.P. Pollaki, E.Tsagaki-Rekleitou, G. Koresi and Ch. Oursouzidou. (2018). Linaria Port: An Interactive Tool for Climate Change Awareness in Greece. In **Second World Symposium on Climate Change Communication**. Graz, Austria.

41. Stedman R.C. (2002). 'Toward a social psychology of place: predicting behavior from place based cognitions, attitude, and identity'. Environ. Behav. 23 (5), 561–581.

42. Stern M.J., R.B. Powell and N.M. Ardoin. (2008). 'What Difference Does It Make? Assessing Outcomes From Participation in a Residential Environmental Education Program'. **The Journal of Environmental Education**, Vol. 39(4), pp. 31–43.

43. Tonge J., M.M. Ryan, S.S. Moore, L.E. Beckley. (2014), 'The effect of place attachment on pro-environment behavioral intentions of visitors to coastal natural area tourist destinations', J. Travel Res. 1–14.

44. UNESCO. (1978). 'The Tbilisi Declaration Intergovernmental Conference on Environmental Education'. 14 - 26 October.

45. Wilson R. (2012). 'Nature and young children: Encouraging creative play and learning in natural environments., New York, NY: Routledge.

46. Wood E. and J. Attfield. (2005). 'Play, learning and the early childhood curriculum 2nd ed.'. London, UK: Sage.

IN SEARCH FOR AN ISLAND TO HOST AN ECOVILLAGE

M. Ganiaris, F. Zouridaki, V. Plaka*, C. Skanavis, K. Antonopoulos and M. Avgerinos

Research Center of Environmental Education and Communication, Dept. of Environment, University of the Aegean, GR- 81100 Mytilene, Lesvos, Greece

*Corresponding author: e-mail: plaka@env.aegean.gr, tel : +302251036234

Abstract

Creativity has come to be viewed as a source of competitive advantage in social life, emerging from a set of financial and social concerns affecting daily routine in our days. This research proposes the operation of an ecovillage, where responsible environmental behaviors will be enforced through "creative tourism". Researchers show that creative tourism makes available to visitors the chance to develop their creative skills through active participation in learning experiences.

The proposed Ecovillage in Skyros Island, Greece, will be accessible to families who wish to spend their vacation time in environmentally inspired set ups and use the opportunity to personally contribute to environmental protection as well as expose their children to ways to actively object to environmental issues of concern. Also, it refers to groups of people who don't have to be physically at work, like digital nomads, who choose as living set up an environmental awareness type of community. Specifically this study attempts to assess all activities, educational and empirical, which will be offered to visitors/residents of an "ecovillage". A complete search of related literature guides the tasks and services that would be offered to those spending their vacation time at the proposed ecovillage. In detail the participants would be active operators of the sustainable living structure and their needs will be based on the concepts of environmental conservation and protection in order to minimize the consequences that affect irreversibly nature and human life. Through their daily involvement at this chosen vacation format, environmental awareness will be accomplished in a successful manner. For the young ones the ecovillage will hold a daily environmental camp tailored to the needs of the participant children.

Keywords: Ecovillages, Circular economy, Creative tourism, Environmental education

1. INTRODUCTION

Such factors as globalization of trade, accelerated environmental degradation, the rise of information technology, and the changes that have resulted from these, have radically altered our perception of space and place [Putnam, 2000]. The ecovillage movement is a worldwide phenomenon that has arisen in response to the effects of the modern lifestyle on both our social and ecological environments. The ecovillage, a term that came into common usage in the early 1990s, is a specific form of intentional community [Global Ecovillage Network, 2002]. "An ecovillage is an intentional or traditional community using local participatory processes to holistically integrate ecological, economic, social, and cultural dimensions of sustainability in order to regenerate social and natural environments". At the core of an ecovillage lies the intention of its inhabitants to design their own pathway into the future [GEN, 2015].

The search for a sustainable lifestyle, combined with the reduction and the solution of environmental problems is a field of research of scientific community and an aim to be reached for governments and

societies. The adoption of responsible environmental behavior of all stakeholders (society, individuals, organizations, governments, etc.) is one of the key solutions [Andriopoulos et al, 2017]. The ecovillage, with their principles and values, is an example of responsible environmental behavior, a remarkable issue for scientific research. At the same time there has been an increasing sense of the breakdown of community principles as modern life has become even more segmented. This has resulted in feelings of isolation and disconnectedness, and further withdrawal from traditional forms of political and social participation [Putnam, 2000].

1.1 What is an Ecovillage

Ecovillages aim at “helping our society to get closer to nature again and to develop new ways of living together on the land in a genuinely more sustainable way” [Kovasna, 2012]. Furthermore they are known for aspects as “ecological sustainability through such practices as generating solar energy, raising animals, and growing their own food” [Meijering, 2012]. Theseare done through the ecovillage promotion concept, which is seen as an innovation offering solutions to problems related to the distribution of resources, climate change, and the social life in the region. Ecovillages are presented as “an alternative to the individualistic, consumerist, and commoditized systems many cities represent” [Kovasna, 2012]. Besides ecological sustainability, the communities also strive for communal sustainability, which refers to sharing one’s life with other people and practicing a common ideology together [Meijering, 2012].

Based on a review of literature, there are ten basic features of the Ecovillages [Kanaley, 2000; Gaia Education, 2009; Kasper, 2008; Joseph & Bates, 2003; Sevier, 2008; Jackson, 2004; Jackson & Svensson, 2002], which are essential for a successful ecovillage application. One of the most familiar and straightforward ways of aligning people’s behavior with community goals is to establish rules. Every ecovillage has a specific set of policies that govern everyday life in its premises.

Such communities have developed over time an astonishing array of internal democratic governance systems and low impact/high quality lifestyles. They have been proven to successfully empower, sustain and promote truly sustainable ways of living, both in rural and urban settings [GEN, 2015]. Together, they aim to build a world living within its own means, and a world at peace with itself.They know that innovation, creativity and the wise use of modern technology and resources, when combined with traditional heritage and wisdom, can massively contribute to addressing global issues of poverty and environmental destruction [GEN, 2015].

Some of the most important aspects of ecovillage planning involve identifying zones for agriculture, commerce, and high and low density building clusters [Kasper, 2008]. Clustering buildings (including workspaces, residences, and community buildings) is a way to minimize a community’s physical footprint, while maximizing privacy, opportunities for work, and social interaction. The human home, however, remains an important aspect of the physical environment, and one in which prospective residents and people curious about ecovillages seem to be most interested. One of the most striking features among all of the communities is the architectural diversity. The latter approach to construction focuses on minimizing site disturbance and waste, while maximizing energy efficiency. Characterized by their uses of high tech insulation, wall building techniques, window glass, and heating and cooling systems, “green homes” tend to resemble more conventional residences. Ecovillages are also thoughtfully organized to promote social interaction, another important means of reinforcing an alternative way of thinking [Kasper, 2008].

In a recent review of ecotourism research, Weaver and Lawton [2007] maintain that ecotourism satisfies three “core criteria” namely, (1) attractions should be predominantly nature-based, (2) visitor interactions with those attractions should be focused on learning or education, and (3) experience and product management should follow principles and practices associated with ecological, socio-cultural and economic sustainability. In a similar fashion, Donohue and Needham [2006] identify six “key tenets” of ecotourism: (1) nature-based, (2) preservation/ conservation, (3) education, (4) sustainability, (5) distribution of benefits and (6) ethics/responsibility/awareness.

Opportunities for visitor participation in habitat restoration and other environmental conservation activities are also important [Walter, 2009]. Members of Global Ecovillage Network (GEN) have recently coined the phrase, “ecovillage tourism” to denote “a new type of green travel, whereby people visit ecological communities around the world to experience low-impact living and community”. GEN has formally designated some sites devoted to these activities as “living and learning centers” [GEN, 2015].

According to Kasper [2008] and Zeppel [2006], the principles that should govern Ecovillage based tourism are mainly characterized with the following features:

- They are sustainable settlements that integrate the tourism services into the activities necessary to reachtheir main goals.
- The agricultural activities are necessarily environmentally friendly.
- The tourism activities are considered to be an economic option to provide financial support and employment facilities for the villagers.
- Tourists can pay a certain accommodation fee, or contribute to the villagers by means of physical participation in the village works to substitute the accommodation fee.
- They can offer the customers with the accommodation, meal-drink and bed facilities as well as introduction and practical application of production activities, civil and garden works, harvesting, traditional handicrafts, preparation of specific regional foods, animal care and similar Ecovillage activities.

Furthermore, if the idea of well-being is to be introduced as the overarching objective in society, the more open-minded next generation of adults would be the easiest segment of the population to start with [Grinde, 2009]. As children gather together at kindergartens, schools and youth clubs, promoting a focus on well-being this may not just be beneficial to achieving a higher level of well-being, but also socio-economically efficient in reducing social costs and the economic waste of creating maladjusted citizens. Thus, caring for the development of children’s emotional wellbeing is an important cross-cutting issue for any national wellbeing strategy [Grinde,2009]. Children’s contact with their parents in workplaces is more frequent than what can be expected in urban environments. Ecovillages, many times with car-free environments, encourage smaller children to move freely around in the settlement, from home to workplaces and other social venues.

1.2 Circular Economy and Ecovillages

It is in this context,that a new approach to sustainability, the ‘Circular Economy’, is being examined. This economy is emerging as a possible strategy, that companies of all sizes might adopt in order to deal with the environmental challenges. However, as the circular economy concept is relatively new in its conceptualization and implementation, there may also be tensions and limitations inherent in its appropriation and application [Murray et al, 2015]. Greyson [2007] claims that Kenneth Boulding [1966] was the originator of the term when he wrote: “man must find his place in a cyclical ecological system which is capable of continuous reproduction of material form even though it cannot escape having inputs of energy”. More recently, Mathews and Tan [2011] suggested that “the goal of the eco-initiatives is to eventually establish a so-called circular economy, or what is otherwise known as a ‘closed-loop’ economy”, while Yang and Feng [2008] called the Circular Economy an “abbreviation of Closed Materials Cycle Economy or Resources Circulated Economy”.

The term linear economy was brought into popular use by those writing on the Circular Economy and related concepts [Murray et al, 2015]. The word circular has a second, inferred, descriptive meaning, which relates to the concept of the cycle. There are two cycles of particular importance here: the biogeochemical cycles and the idea of recycling of products. Recycling has been a significant part of sustainable practice for many years, and it is fundamental to the Circular Economy. The circular economy is ultimately linked to resource cycling. These ideas are further developed in industrial symbiosis, where firms use each other’s waste as resources, and in the service economy, where work

is done to slow down cycles of use, in order to delay waste output. The model character of the planned village consists of the comprehensive attempt to integrate all spheres of life (home life, work, provision, free time) as part of an ecological circular economy.

The Circular Economy represents the most recent attempt to conceptualize the integration of economic activity and environmental wellbeing in a sustainable way. These include an absence of the social dimension inherent in sustainable development that limits its ethical dimensions, and some unintended consequences. This leads us to propose a revised definition of the Circular Economy as “an economic model wherein planning, resourcing, procurement, production and reprocessing are designed and managed, as both process and output, to maximize ecosystem functioning and human well-being” [Murray et al, 2015].

1.3 Creative Tourism and Ecovillage

At the same time, creativity has been seen as a source of competitive advantage in social life, evolving from a series of economic and social problems that affect daily routine nowadays. The cyclical economy, a necessary perception, comes to revitalize creativity by promoting new environmental actions. Researchers have been shown that creative tourism is “tourism which offers visitors the opportunity to develop their creative potential through active participation in learning experiences which are characteristic of the holiday destination where they are undertaken” [Richards & Raymond, 2000].

Lifestyle travel is a phenomenon that illustrates a de-differentiation of everyday life and tourist experiences, a process that Uriely [2005] identifies as characteristic of tourism in late modernity. In this consideration local people may become more environmentally aware because of their participation in ecotourism in the connection with the activities of visitors. Ecotourism guides also teach visitors about local plants, wildlife, forest, history and cultural attractions [Uriely, 2005]. Tourism brings together very diverse people and nationalities that influence the process of cultural development in a destination. This brings new ideas that combined with innovation can become a unique asset to the destination [OECD, 2014].

2. PROPOSING ACASE STUDY OF AN ECOVILLAGE

Without any doubt the road to sustainable development goes through environmental protection and sustainable management of local natural resources [Andriopoulos et al, 2017]. The aim of this research is to propose a geographical location to establish an ecovillage, in which all the principles of an ecovillage will be established while adhering to the concepts of circular economy and creative tourism. The proposed location in a Greek island, Skyros Island, with environmental infrastructures and influences, where our research center has set up a satellite unit.

2.1 Choosing the Right Location

In Greece there are more than 2.500 islands, of which only 227 are inhabited [European Union, 2015]. In the heart of the Aegean Sea, Skyros Island is unique about its environmental characteristics.The island of Skyros has been chosen as a study area, due to its remarkable characteristics [Andriopoulos et al., 2017].This proposed Ecovillage Project at Skyros Island will be assessed. This project will be based on preset criteria and principles. The visitors will be accommodated in tents, in a specially designed area in Acherounes Village (Figure 1). The locals who until a few years ago lived in perfect harmony with the natural environment, can provide a great baseline, while at the same time they have the opportunity to find new pathways towards sustainable development, preserving this way the unique natural environment of the island [Andriopoulos et al, 2017]. So, the Skyros Ecovillage Project proposes the operation of an ecovillage where responsible environmental behavior will be imposed through "creative tourism". In other words, these two concepts, creative tourism and the circular economy in the context of ecovillage are the ones this research aims to incorporate.

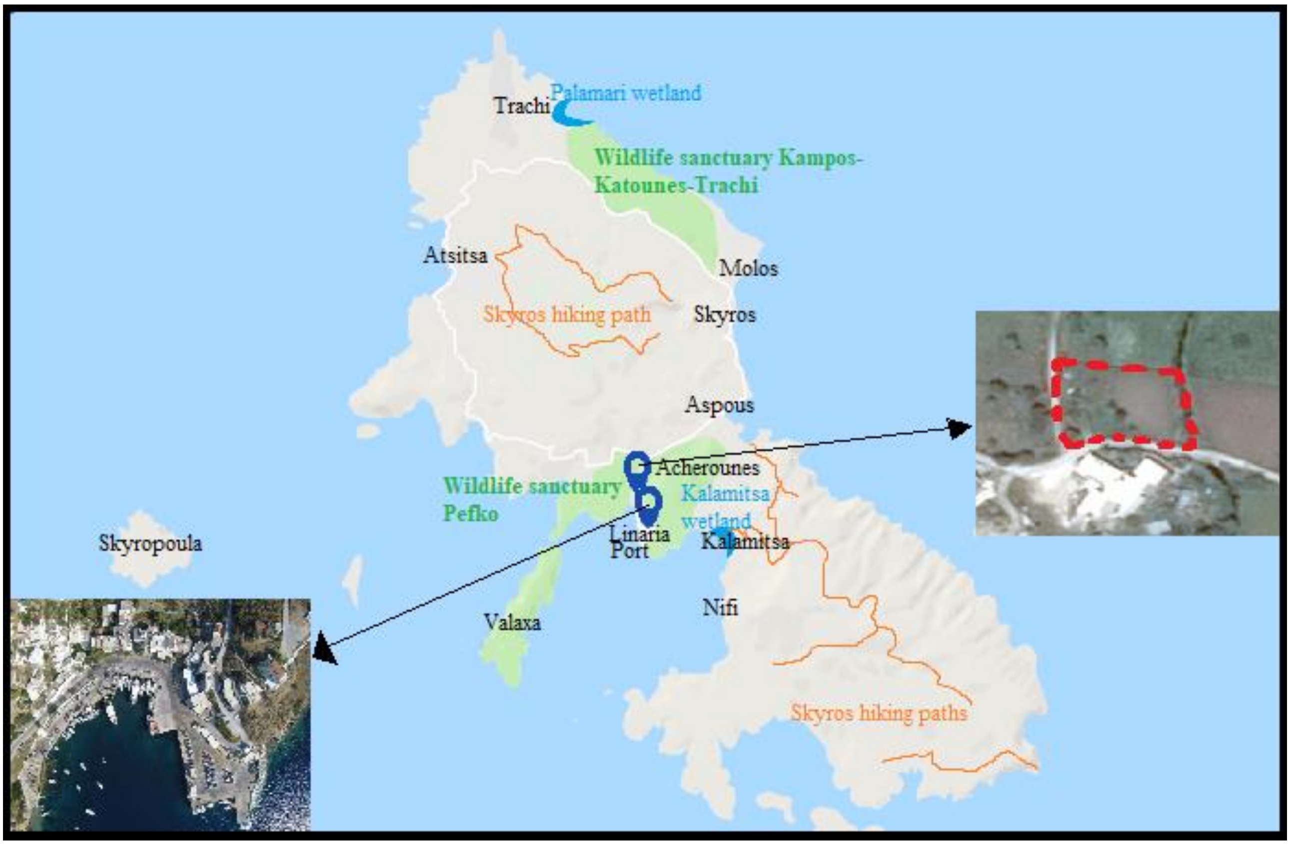


Figure 1: Skyros Island: Linaria Port and Location of Ecovillage Project (Source: Google maps)

Skyros Island (Figure 1) has well defined hiking paths and is known for a unique wildlife sanctuary. At its Port, named Linaria, the well-known "SKYROS Project" is involved with various environmental actions. The island's morphology and biodiversity have raised interest from the scientific community. The Hellenic Ornithological Society organizes actions for the protection of rare birds on the island and many Universities have been coming to Skyros to perform specific ecological research. In 2015, the University of the Aegean initiated the collaboration with the Skyros Port Authorityon running an environmental campaign under the brand name "SKYROS Project".

The Authority of Linaria Port has implemented a new sustainable agenda, since 2010. In a short time the port of Skyros, Linaria Port, has succeeded to attract tremendous publicity and has been recorded as the fuller and friendliest public port of Greece [Antonopoulos et al., 2015], with the arrivals reaching an increase of 975%. Linaria Port serves as an interactive lab. University students, locals and visitorsare trainedtobecome the decision makers for environmental issues taking initiatives on environmental planning and management of the specific port area. This state of art educational approach has secured the success of SKYROS Project [Antonopoulos et al. 2017a]. The above Project is a paradigmatic cooperation of two public sectors, the Research Center of Environmental Communication and Education of the Department of Environment of University of the Aegean with the Skyros Port Authority. The enthusiastic students through their daily environmental investment in the area led the way to a permanently established remote training site that invests into environmental research and education practices [Antonopoulos et al, 2017b]. Worthwhile accomplishments include the establishment of the tourism observatory anda marine one, both located at Linaria Port of Skyros Island. Also a free of charge kids' camp was established at the same port.

2.2 Design the Appropriate Environmental Activities

Without any doubt the road to sustainable development goes through environmental protection and sustainable management of local natural resources. Skyros Island due to its unique environmental

characteristics is considered to be the ideal place for such activities, in which families will be come together.

Skyros is one of the richest Islands in biodiversity of Aegean Sea with special ecological importance. Especially the southern part of the island, Mount Kohilas, the surrounding islands and the remaining wetlands of the island are important regions for birds especially migratory while have been recorded important species of bats in the area. Also, the island is the natural habitat of "*Equuscaballus skyriano*". It's an old breed of semi-savage horses, with roots in the Classic period, or even the Prehistoric period, the origin of which can be lost in the depths of the Geological centuries. The unique, world-wide, small horse of the breed of *Equus caballus* lives in the natural environment of Skyros, in the area of the "Mountain" which is in the south-east part of the island [Andriopoulos et al., 2017]. There are farms, where the visitors are able to work in and care or feed these endangered species.

The southern part of Skyros is a unique area of biodiversity observation for the visitors. There are safety pathways, where families will be able to walk in the area around Mount Kohilas (the highest mountain on the island with 792m altitude), which is included in the European Natura 2000 network and where the Bantam breed Skyros horse (race *Equus caballus*), one of the rare breeds horses in the world, is living today. In this area there are many kinds of rare and endemic plants, some of which have been included in the Red Book of Rare and Threatened Species of Greek Flora. In the same area there are maple clusters, an important habitat for local biodiversity unique in the Aegean region, especially for birds that nest and shelter there. In the Island, is also living a native kind of lizard, while the Mediterranean seal *Monachus monachus* is frequently found in caves of the island. Finally, there are several important species of flora and a significant number of endemic and endangered plant species [Andiopoulos et al., 2017].

The accommodation, in Acherounes Village will be provided by the SKYROS Project. There, while the kids staying in will participate in environmental actions designed for the young ones, the adults will be involved is a variety of environmental activities.These will include but not limited to getting their hands dirty in collecting trash, growing organic food, recycling and reusing materials and the conservation of energy. Skyros Ecovillage Project would provide a shining example of sustainable development approach.

This Ecovillage Project attempts to assess all activities, educational and empirical, which will be offered to visitors/residents at Skyros Island. A complete search of related literature guides the tasks and services that would be offered to those spending their vacation time at the proposed ecovillage. In detail the participants would be active operators of the sustainable living structure and their needs will be based on the concepts of environmental conservation and protection in order to minimize the consequences that affect irreversibly nature and human life. Through their daily involvement at this chosen vacation format, environmental awareness will be accomplished in a successful manner.

Outdoor environments can enhance mental health of participating students, contribute to students' intellectual and emotional development, support their environmental awareness and can give them opportunities to play and get involved in creative activities as well as connect directly with nature [Plaka & Skanavis, 2016]. Children who participated in Ecovillage Project have the opportunity to join in Daily Environmental Camp in Linaria port, an action of Skyros Project. Since 2015, the Environmental Camp for children offers to the local community's children and the visitors a high quality educational program tailored to the participants' interests, being inspired by the familiar port surrounding. The objectives of the summer environmental camp at Skyros Island are focusing on the dissemination of environmental education to children and to the promotion of their responsible environmental behavior through practicing theory in real time conditions and hands on experience in an outdoors set up [Skanavis & Kounani 2017]. A research group of SKYROS Project, specifically handling educational approaches for the young, has created this well-prepared educational program [Skanavis et al., 2018], based on the North American Association for Environmental Educators'

(NAAEE) Guidelines for Excellence [NAAEE, 2017] and the basic principles of Environmental Education [UNESCO, 1978].
A characteristic day for the adults (Table 1) and for the children (Table 2) at the ecovillage includes:

Table 1: A characteristic day for the adults at the ecovillage

08.00 – 10.00	Daily workout and hiking in NATURA area, Daily workout and farming.
10.00 – 13.00	Participation in Summer Academy of Environmental Educators, in which they will educate to communicate the environmental protection message.
13.00 – 15.00	Break for lunch with organic food.
15.00 – 19.00	Training seminar for cleaner beaches, participation in environmentally friendly sea sports like scuba diving in beaches of Skyros Island, seminars on cultivation organic food, biodiversity observation.
19.00 – 20.00	Break for diner with organic food.
20.00 – 22.30	Outdoors cinema (environmental films and documentaries), outdoor mental activities

Table 2: A characteristic day for the children at the ecovillage

08.00 – 10.00	Daily workout and hiking in NATURA area, Daily workout and farming.
10.00 – 13.00	Participation in Daily Environmental Camp of Skyros Port, in which they will educated to communicate the environmental protection message and will be environmental active future citizens. Topics: Biodiversity Conservation, Climate Change, Sea Pollution, Clean Water, etc.
13.00 – 15.00	Break for lunch with organic food.
15.00 – 19.00	Training seminar for cleaner beaches, participation in environmentally friendly sea sports like scuba diving in beaches of Skyros Island, seminars on cultivation organic food, biodiversity observation.
19.00 – 20.00	Break for diner with organic food.
20.00 – 22.30	Outdoors cinema (environmental films and documentaries), outdoor mental activities

3. DISCUSSION AND CONCLUSION

The Skyros Ecovillage Project is a proposal for establishing a vacationing site for those interested to actively participate in the environmental protection and sustainable living. This Project will be an action of Skyros Project, of Skyros Port Fund and University of the Aegean, as a prerequisite to be part of an economic funding. Then, this Ecovillage Project will serve as a meeting point for local families, members of scientific groups andvisitors of the island interested in getting involved in environmental protection activities in real time conditions. The local community, which until a few years ago lived in perfect harmony with the natural environment, can provide in a great impulse in the preservation of the uniqueness of the natural environment of Skyros Island [Andriopoulos et al, 2017].

In a holistic approach, families who experience the ecovillage lifestyle will be communicating this experience to others who are in search for a new sustainable way of living. Contemporary tourists are more in demand of selecting their holiday destinations and activities. Therefore, "destinations are increasingly facing a challenge to develop new — place/product combinations which are competitive, unique and attractive for special interest or niche markets that want specific products and

environmental experiences" [Fernandes, 2011]. This is especially important for small and distant destinations with poor tourism resources, because when applying creative thinking, an interesting tourism product can be developed in any environment [OECD, 2014].

The adoption of responsible environmental behavior of all stakeholders (individuals, organizations etc.) is one of the key solutions for all modern societies and governments. The ecovillages with their principles and values are examples of responsible environmental behavior, a remarkable issue for scientific research. The philosophy behind the understanding of life and society, through the four dimensions (social, ecological, spiritual, economic) which are basic principles-values of ecovillages, can form the fundamental core of responsible environmental behavior as a response to environmental problems and distortions of local communities [Andriopoulos et al, 2017].

The successful relationship with nature is not just a pleasant task, but it is an essential component of the human wellbeing general goal [Plaka & Skanavis, 2016]. It is of paramount importance to understand children's perspectives, since the young ones both now and in the future will influence and be influenced by environmental issues in many ways [Skanavis & Manolas, 2015]. The concept is to begin at early childhood, the environmental awareness. We are suiting for a more open-minded generation of adults, who by participating in this Project, would useit as a tool to connecting people and also kids to a common vision. This is a way to promote a new sustainable lifestyle.

References

1. Putnam, R. D. (2000). Bowling alone: The collapse and revival of American community.
2. Global Ecovillage Network. (2002). http://gaia.org/ (accessed January 10th, 2018).
3. Global Ecovillage Network (GEN). (2015). GEN Ecovillage Transition Strategy 2015-2020 https://ecovillage.org/(accessed January 7th, 2018).
4. Andriopoulos C., E. Avgerinos, and C. Skanavis. (2017). Is an Ecovillage Type of Living Arrangement a Promising Pathway to Responsible Environmental Behavior?
5. Kovasna, A. (2012). **'Collaborative Research: Examples and Lessons from a Baltic Sea Project'**,eds. M.Andreas and F.Wagner, Munich, Germany, 2012.
6. Meijering, L., (2012). **'Ideals and Practices of European Ecovillages'**, eds. M.Andreas and F.Wagner, Munich, Germany, 2012.
7. Kanaley, D. (2000). Ecovillages; A Sustainable Lifestyle, **A Report For Byron Shire Council**, Australia, Mullumbimby.
8. Gaia Education. (2009). Ecovillage Design Education Curriculum, Scotland, Findhorn, http://gaia.org/global-ecovillage-network/ecovillage/
9. Kasper, D. V. S. (2008). "Redefining Community in the Ecovillage", **Human Ecology Review**, Vol. 15, No. 1, pp.12-24.
10. Joseph, L. and Bates, A. (2003). "What is an Ecovillage", **Communities Magazine**, Issue 117, pp. 1-3.
11. Sevier, L. (2008). "Ecovillages: A Model Life", Ecologist, May 2008, pp. 36-41.
12. Jackson, R. (2004). "The Ecovillage Movement", **Permaculture Magazine**, No. 40, pp. 25-30.
13. Jackson, H. and Svensson, K. (2002). Ecovillage Living: Restoring the Earth and Her People, UK, Devon.
14. Weaver D. B. and Lawton, L. J. (2007). Progress in tourism management. Twenty years on: the state of contemporary ecotourism research. Tourism Management, 28,1168e1179.

15. Walter, P. (2009). Local knowledge and adult learning in environmental adult education: community-based ecotourism in southern Thailand. **International Journal of Lifelong Education**, 28(4), 513e532.
16. Zeppel, H. (2006). Indigenous Ecoturism: Sustainable Development and Management, Trowbridge.
17. Grinde, B. (2009). An evolutionary perspective on the importance of community relations for quality of life. **The Scientific World Journal**, 9, 588–605.
18. Murray, A., K. Skene, K. Haynes (2015), The Circular Economy: An Interdisciplinary Exploration of the Concept and Application in a Global Context.
19. Greyson, J. (2007). An economic instrument for zero waste, economic growth and sustainability. **Journal of Cleaner Production**, 15(13– 14), 1382–1390. doi: 10.1016/j.jclepro.2006.07.019.
20. Mathews, J. A., & Tan, H. (2011). Progress towards a circular economy in China: The drivers (and inhibitors) of eco-industrial initiative. **Journal of Industrial Ecology**, 15, 435–457.
21. Yang, S. and Feng, N. (2008). A case study of industrial symbiosis: Nanning Sugar Co., Ltd. in China. Resources. **Conservation and Recycling**, 52, 813–820.
22. Richards, G. and C.Raymond (2000) “Creative tourism”. **ATLAS NEWS**, 23, 16-20.
23. Uriely N. (2005). **“Theories of Modern and Postmodern Tourism”**, Annals of Tourism Research, 24 (1997), pp. 982-984.
24. OECD, 2014. “Tourism and the Creative Economy” OECD Studies on Tourism, **OECD Publishing**, 2014, http://dx.doi.org/10.1787/9789264207875-en
25. European Union. 2015. European countries - Greece. http://europa.eu/about-eu/countries/member-countries/greece/index_el.htm(accessed August 1st, 2015).
26. Antonopoulos K, C. Skanavisand V. Plaka. (2015). ‘Exploiting futher potential of Linaria Port-Skyros: From vision to realization’ (in greek) In. **Proceedings of the First Hellenic Conference on Tourist Port, Marinas**, eds. Athens, Greece, Laboratory of HarbourWorks, N.T.U.A pp. 101-111.
27. Antonopoulos K., V. Plaka, A .Barbakonstanti, D. Dimitriadou and C. Skanavis. (2017a). ‘THE BLUE PORT WITH A SHADE OF GREEN: The case study of Skyros Island’, Proc. Int.Conf. **Proceedings of the 7th Health and Environment, Innovation Arabia Conference**, pp. 175-187. Dubai, United Arab Emirates.
28. Antonopoulos K., Margariti A, Marini K, Skanavis C. (2017b). The case of the port of Linaria-Skyros, Greece: the human factor as the main dimension of impression and other findings in the GUESTBOOK tourists’ evaluation. **Journal of Psychology Research** (in submission process).
29. Plaka V. and Skanavis C. (2016). The feasibility of school gardens as an educational approach in Greece: a survey of Greek schools. **International Journal of Innovation and Sustainable Development** 10(2):141-159.
30. Boulding K. (1966). The Economics of the Coming Spaceship Earth. Jarett H. (ed), MD: Resources for the Future/ Johns Hopkins University Press, Baltimore, **Environmental Quality in a Growing Economy**.
31. Skanavis C. and Kounani A. (2017). Children Communicating on Climate Change: The Case of a Summer Camp at a Greek Island. Leal-Filho W, Manolas E, Azul AM, Azeiteiro U (ed) Elsevier, Amsterdam, **Handbook of Climate Change Communication** (In Press)
32. Skanavis C., Antonopoulos K., Plaka V., Pollaki S.P., Tsagaki-Rekleitou E., Koresi G. and Oursouzidou Ch. (2018). Linaria Port: An Interactive Tool for Climate Change Awareness in Greece. In **Second World Symposium on Climate Change Communication**. Graz, Austria.

33. North American Association for Environmental Education (NAAEE). (2017). Professional Development of Environmental Educators: Guidelines for Excellence, Washington.

34. UNESCO. (1977). **Final Report**: Intergovernmental Conference on Environmental Education. UNEP: Tbilisi.

35. Fernandes, C. (2011). "Cultural planning and creative tourism in an emerging tourist destination", **International Journal of Management Cases**, 13, no. 3 (2011): 630.

36. Skanavis C. and Manolas E. (2015). School Gardens and Ecovillages: Innovative Civic Ecology Educational Approaches at Schools and Universities. Transformative Approaches to Sustainable Development at Universities. World Sustainability Series, **Springer International Publishing Switzerland** doi: 10.1007/978-3-319-08837-2_37.

AUGMENTED REALITY PROVES TO BE A BREAKTHROUGH IN ENVIRONMENTAL EDUCATION

P. Theodorou*, P. Kydonakis, M. Botzori and C. Skanavis

Research Center of Environmental Communication and Education, Greece

*Corresponding author: e-mail: ptheod@env.aegean.gr

Abstract

This paper deals with the implementation of augmented reality technology as a means of communicating environmental issues and boosting environmental education for 241 school students in the 4th, 5th, 6th classes of two primary schools in Athens, during the course of Computer Science. Specifically, an early version of two augmented reality applications for android mobile devices were designed and deployed. Two activities combining this technology were designed in order to address environmental learning goals concerning climate change concepts and fundamental aid in the understanding of renewable energy resources. The study assessed whether the students liked the applications and the rate of knowledge change, driven by pre-post questionnaires, which were given both at the start and at the end of the implementation. The results showed that the implementation of Augmented Reality applications for environmental educational concepts have a significant supplemental learning effect as a mobile-assisted learning tool. Finally, the paper concludes with future guidelines in the field of other environmental issues of great importance.

Keywords: augmented reality; environmental education; mobile education; climate change; renewable energy sources

1. INTRODUCTION

Today, we increasingly live between the analogue and the digital, the physical and the virtual world. The emerging digital systems offer new dimensions and innovative ways to challenge the transformation of experiences and the creation of new opportunities for interactivity.

Many emerging technologies have been explored and proposed in an effort to optimise teaching methods and enhance learning experience. Augmented Reality is a relatively new technology promising a great tool for communicating concepts and ideas about environmental issues. Although AR applications for education have been implemented, their impact on learning is just beginning to be explored (Medicherla et al, 2010).

2. BACKGROUND - LITERATURE REVIEW

2.1 Environment / Environmental communication

Environmental communication has many branches and has become an increasingly important area of study (Alison, 2015). Both citizens, corporations and civil servants, journalists and environmental groups are seeking to influence decisions that have a direct impact on the planet. (Cox, 2012).

With the development of environmental studies, educational and professional opportunities, which recall the role of human communication and the affairs in environmental issues, have been created (Pedelty, 2015).

Steve Depoe (1997), argued that environmental communication is the combination of "relationships between our speech and our experiences from our natural environment".

Environmental communication is of great importance to environmental issues as it is "a pragmatic and structured way to understand the environment and our relationship to the natural world" (Cox and Pezzullo, 2015). Essentially, environmental communication is much more than the discussion of the different social, cultural, political, economic, and linguistic settings of the environment, but it is the deep understanding of the environment as well as the building of strong relationships with the natural world, which is the focus of environmental science (Platonova, 2016).

2.1.1 Climate change education

Teachers, considering the complex nature of climate change education, are required to simplify the complexity that lies at the science core in order to provide a more reachable way. In addition, it should be ensured that the simplifications remain faithful to the science, while not overwhelming the students (Oversby, 2015).

2.1.2 Energy - Communication

The advent of several new approaches that are emerging in the field of renewable energy education and communication are due to the globally recognized need for education and training in this field (Kandapal et al, 2014; Jennings, 2009). The creation of responsible energy consumers in the future will contribute to the promotion of environmental awareness (Liarakou et al., 2009). Education may be an important factor in the instillation of the youth and in the empowerment of their morality in order to understand and solve energy-related environmental problems (Jennings et al, 2001). For the acquisition of knowledge and the formation of basic values except for school and family, media and technology are the most important influences today (Halder et al, 2011).

2.2 Augmented reality

Augmented Reality can be defined as something that combines real and virtual objects in the same space. It is also interactive in real-time and it is registered in three-dimensions (Azuma, 1997).

Computer interfaces can be represented as a continuum between real and virtual environment (Milgram et al, 1994). Starting from left to right and moving away from reality, there is an increase in virtual content (Figure 1). Augmented Reality can be seen as a "mixed reality" state in which computer-generated content is laid on top of the real world to augment the world with additional information.



Figure 1. Reality-Virtuality Continuum (Milgram et al, 1994)

Virtual objects used in Augmented Reality can be any computer-generated data like text, images, video, audio, 2-dimensional or 3-dimensional models and animations. Unlike Virtual Reality, AR supplements reality rather than replaces it (Bower et. al, 2013).

2.3 Mobile augmented reality

Over the last decade, technology has massively evolved. While the main concept of AR has not changed, the ways in which it can be accessed have been advanced. In recent years, Augmented

Reality applications tend to run on mobile or wearable devices. A Smartphone consists of all hardware requirements of augmented reality. This means that the hardware required to implement an AR application is wearable (Craig, 2013).

The technological demands for a mobile AR application consist of the following characteristics: the **input**, either a camera or sensors such as gyroscope or accelerometer, the **processing**, to specify the type of information that is going to be displayed in the screen and the **display**, either a monitor, a handheld device, eyeglass or Head Mounted Displays (HMD) (Chatzopoulos et al, 2017).

2.4 Augmented reality types (How it works)

Munnerley et al (2012), refer to two main types of mobile AR applications: artefact-based (or marker-based) and geolocated (or location-based).

Artefact-based AR is based on image recognition. Virtual objects are assigned to identify visual markers or objects, such as QR codes or bar codes (Figure 2). Though, recent technological advances have enabled the use of any kind of image within the AR technology (FitzGerald et al, 2013).

Additionally, the markers can be located by the device camera. Once a marker is detected, the application displays a three-dimensional model, animation or video on the screen. The orientation of the AR object depends on the position of the marker. When you are moving the marker, the displayed model or animation is transformed accordingly. This technique allows the use of virtual objects, such as 3D models and other media displayed together with real world scenery (Figure 3) (Otilia Pasareti et al, 2011).

Figure 2. AR Marker (QR code)



Figure 3. Marker-based AR Application

Geolocated AR don’t need markers, instead, they use Global Positioning Systems (GPS) and other position detectors (digital compass, velocity meter, or accelerometer), which are integrated in the mobile device. They are usually used for displaying directions, locating nearby businesses, and other mobile navigation applications (FitzGerald et al, 2013).

2.5 Augmented Reality in education

Several researchers (eg Billinghurst & Duenser, 2012; Johnson, Adams & Cummins, 2012; Chen & Tsai, 2012; Dede, 2009; Dunleavy, Dede, & Mitchell, 2009; Squire & Jan, 2007; Squire & Klopfer, 2007; Kaufmann & Schmalstieg, 2003; Shelton, 2002) argued that AR technology in education could be identified as the most exciting and interesting teaching method. This technology has been used in many lessons, some of which are mathematics in geometric courses, 3D imaging of cells in biology

(Fugger et al) and molecular structure exhibiting in chemistry (Asai, 2005). In that way each issue has the potential to include more color and be more interactive for participants (Pasareti et al, 2011).

AR allows students to challenge the limitations they have enables students to access inaccessible positions by giving them the possibility to have a different viewpoint. AR combines both pedagogical and technological additions to teaching and learning (FitzGerald et al, 2013).

AR has more advantages compared to the traditional teaching methods. One of these advantages is that it activates many senses such as touch, hearing, and vision at the same time. In this way, students have an active participation in learning and teaching (Kaufmann, 2003).

Additionally, AR allows access to learning content in three-dimensional perspectives. 3D offers the possibility of ubiquitous learning and makes learners more cooperative. It gives users a sense of presence and immediacy with the object of exploration. It does something that is invisible to be visible (Wu et al, 2013).

More recently, researchers (Azuma et al, 2011; Martin et al, 2011) have turned their attention to the AR applications on mobile devices such as mobile phones (Lin et al, 2013). According to the Horizon 2013 report **(**Johnson et al, 2013**)**, in iTunes, educational mobile applications (including Enhanced Reality) targeting children was the second popular category of entertainment and business applications (Shuler et al, 2012).

This combination of a mobile device and an application allows to digital objects to superimposed within real-world environments and bridges contexts for formal and informal learning (Wu et al, 2013). The concern about AR is that learning may not be driven by pedagogy but most of the advantages and weaknesses of AR tools (FitzGerald et al, 2013).

3. METHODOLOGY

3.1 Sample

The study was conducted in two primary schools of Athens city in Greece, during the course of Computer Science. Both selected schools had a medium socio-economic background. These schools were chosen because one of the researchers worked there as a teacher at the same period, so the access was easier. This study involved in total 241 students in the 4th, 5th, 6th classes, including 122 (50.6%) girls and 119 (49.4%) boys. In the 4^{th} grade females were 51.9% and males 48.1%. In the 5^{th} grade, the sample consisted of 45.8% females and 54.2% males. Finally, in the 6^{th} grade the sample consisted of 54.5% females and 45.5% males. The students were in the age group of 9 to 12 years of age.

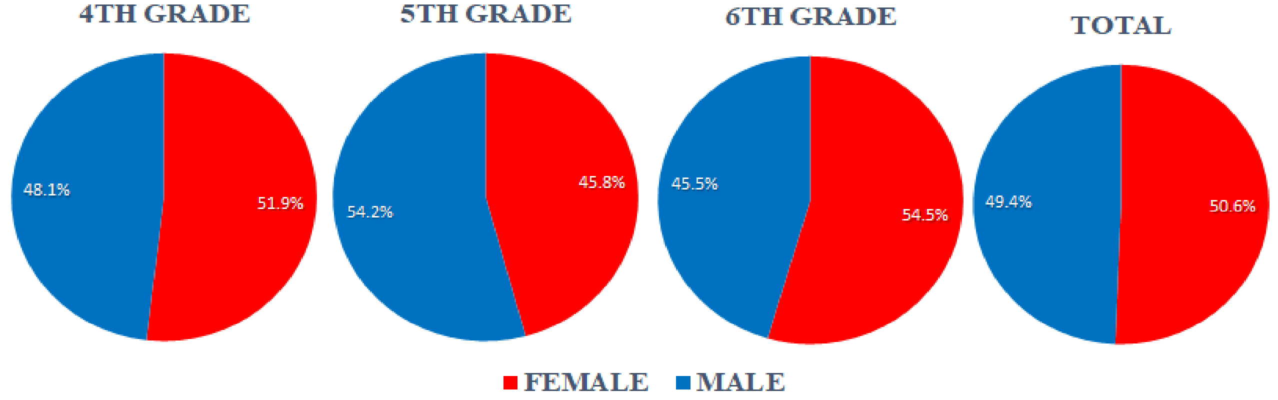


Figure 4. Gender of 4th, 5th and 6th grade

3.2 Questionnaires

The particular implementation lasted two teaching hours depending on the level of the class and/or the perceived attention that students showed during the elaboration of the implementation. The role

of the teacher was directive and accommodative. Specifically, a pre test questionnaire was given to the students to examine their former knowledge on climate change and renewable energy sources.

This pre-test consisted of thirteen multiple choice text-based questions, as it can be seen in the following table, where nine of them were concerned environmental topics and four of them are related to their experience with AR application. Afterwards, the same questionnaire was given for the second time. Moreover, the results were not announced to the students, unless they requested their evaluation. The statistical analysis is conducted with the tool of Excel 2016 of Microsoft Office.

Table 1: Questionnaires

No:	Questions:	Answers:
1	Do you think that the average temperature of the earth has increased?	❑ Yes ❑ No
2	Do levels of sea-level rise because of the overheated Land?	❑ Yes ❑ No
3	The more trees we have, the more oxygen and less carbon dioxide (CO_2) is produced.	❑ Correct ❑ Wrong
4	Recycling helps in the reduction of carbon dioxide (CO_2).	❑ Very ❑ Little ❑ No
5	Do human activities affect the rates of carbon dioxide (CO_2) in the atmosphere?	❑ Very ❑ Little ❑ Not
6	Can LED lamps help in the conserving of energy?	❑ Yes ❑ No
7	Geothermal energy comes from a renewable energy source.	❑ Correct ❑ Wrong
8	Wind power converts the energy to electricity.	❑ Correct ❑ Wrong
9	What are the main fossil fuels that are used to produce energy? (You can select MORE THAN ONE answer)	❑ Carbon ❑ Gas ❑ Diesel fuel ❑ Water
10	Did you like the application?	❑ Yes ❑ No
11	Do you think that the application has helped you implement to understand better the environmental issues?	❑ Yes ❑ No
12	Do you think that the audio narrative makes is more interesting?	❑ Yes ❑ No
13	Would you like to have other courses with this application?	❑ Yes ❑ No

***Pre and post questionnaire were the same.**

3.3 Application design and development

This study demonstrates the teaching and understanding of environmental education concepts of great difficulty, such as Energy Sources (Renewable and Nonrenewable-fossil fuels) and Climate Change (causes, effects and solutions). Specifically, it explains these concepts with the use of Augmented Reality technology.

Both Augmented Reality applications were designed and developed to be deployed on an Android mobile device. For the development of the applications two tools were used, Unity3D and Vuforia. Unity3D is a game engine or a game authoring instrument that is used to develop both 3D and 2D games and deploy them across different platforms. For the creation of Augmented Reality applications, the system needs an external SDK. Vuforia is an external SDK that enables Unity3D developers to create Augmented Reality applications on mobile devices using as targets, images or QR codes that can detected and tracked. (Diaz et al, 2016).

The user activates the application and points the camera to the image target. The application then captures the target and recognizes it. If the recognized image matches the image target, specified 3D models will be loaded and displayed on the screen. The movement of the target is being tracked by the camera and adjusts the size of the image according to the movement (Parvathy et al, 2016).

In the case of our applications we choose to use QR codes as image targets. These applications require only a smart mobile device with a camera, and the image targets printed on a piece of paper. In both applications, three-dimensional animated models and sound were used.

The focus of the script was the students. Students are divided into groups and learn to use AR on their own. Students should explore and achieve results through team effort not being benefited from the presence of the teacher in the classroom. The applications had a duration of about two minutes each.

For the first application were used two image targets (Figure 5).

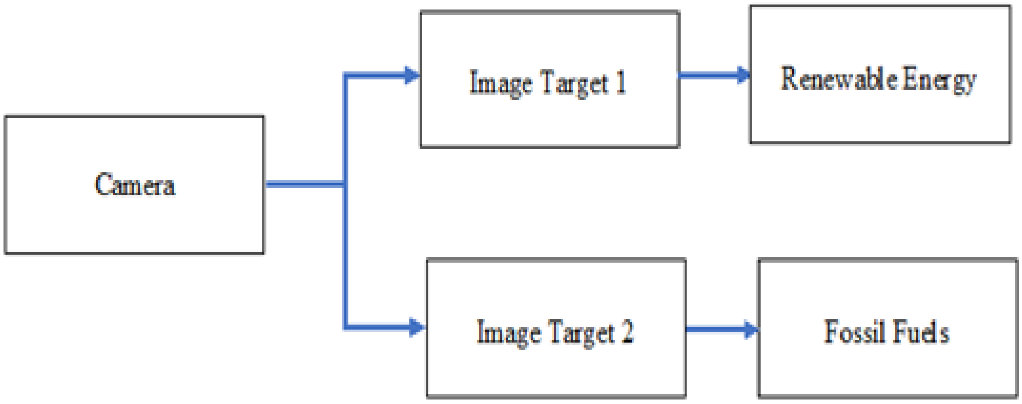


Figure 5. Energy Source application workflow

The first image target presents the renewable energy sources, such as solar power, geothermal power and wind power, while the second presents the fossil fuels (coal, oil and natural gas). The result is shown in Figure 7.

For the second application were used only one image target (Figure 6).



Figure 6. Climate Change application workflow

The second application deals with the phenomenon of climate change. At first, we present the causes of temperature increase, such as deforestation and burning fossil fuels that increase CO2 emissions, then we show the impact of the above, such as ice melting, sea level rise and desertification. Finally, we propose various practices to reduce the progress of climate change such as recycling, energy saving and reduce car usage. A screenshot is shown in Figure 8.

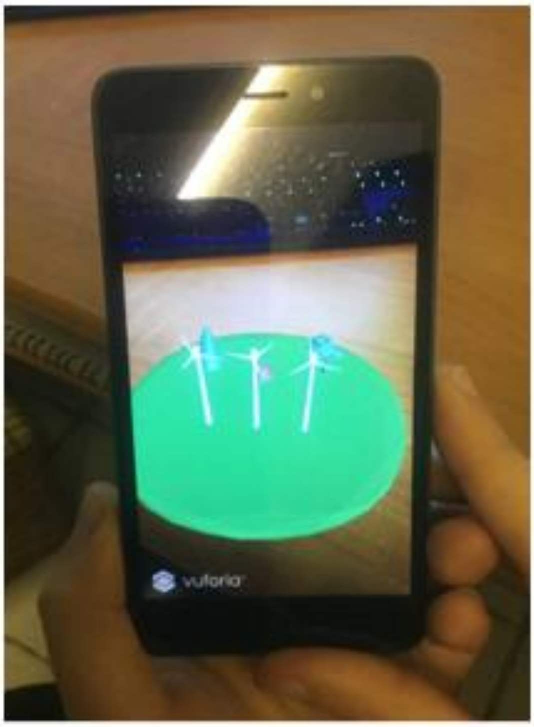


Figure 7. Wind Power

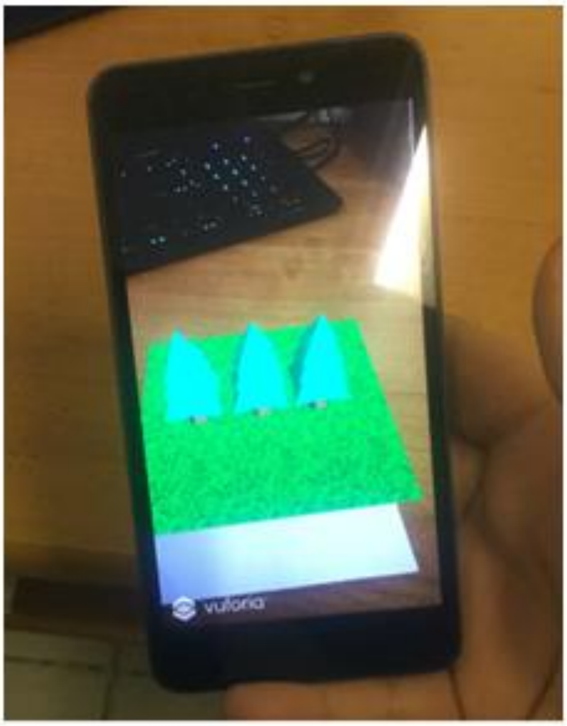


Figure 8. Climate Deforestation

Both applications are tested on Android smartphone Xiaomi Redmi 4A with Qualcomm Snapdragon 425 Quad-core 1.4 GHz.

4. RESULTS

This study correlated on the supplemental learning effect of AR-based learning tools in a course teaching environmental concepts as climate change and renewable energy resources.

The results recorded after the conduction of the questionnaires are divided into two categories. The first concerns the level of change of knowledge by the students and the second concerns the students' opinion about the learning experience with the AR application. Tables 2 and 3 show the comparison between the grade obtained by the students when they performed the pre-test and the post-test. Pre-test scores will represent students' learning outcomes before, and post-test scores will represent students' learning outcomes after using the AR applications.

The results showed that the change of knowledge for the 4th grade was 29.5%, the change for the 5th grade was 25.6% and the change for the 6th grade was 21.7%. The next factor that is examined is the change of learning experience that was 38% for the 4th grade, 32.3% for the 5th grade and 26.9% for the 6th grade.

Table 2: The results of questions about knowledge change

4TH GRADE				5TH GRADE				6TH GRADE			
Q.	BEFORE	AFTER	CHANGE	Q.	BEFORE	AFTER	CHANGE	Q.	BEFORE	AFTER	CHANGE
1	15.8	42.2	26.4	1	23.5	49.5	26	1	17.6	49.5	31.9
2	20.4	48.2	27.8	2	22.9	40.8	17.9	2	15.9	40.8	24.9
3	17.1	46.8	29.7	3	23.2	49.5	26.3	3	23.6	49.3	25.7
4	16.4	42.2	25.8	4	18.3	48.2	29.9	4	28.3	38.2	9.9
5	19.1	42.9	23.8	5	15.6	49.5	33.9	5	22.5	39.5	17
6	15.1	47.2	32.1	6	22.4	49.7	27.3	6	22.4	49.7	27.3
7	13.2	42.2	29	7	24.3	42.1	17.8	7	24.3	42.1	17.8
8	7.2	48.2	41	8	20.4	41.4	21	8	20.4	41.4	21
9	16.4	46.2	29.8	9	16.4	46.3	29.9	9	16.4	36.2	19.8
Total	**15.6%**	**45.1%**	**29.5%**	**Total**	**20.8%**	**46.3%**	**25.6%**	**Total**	**21.3%**	**43.0%**	**21.7%**

Table 3. The results of questions about learning experience

4TH GRADE				5TH GRADE				6TH GRADE			
Q.	BEFORE	AFTER	CHANGE	Q.	BEFORE	AFTER	CHANGE	Q.	BEFORE	AFTER	CHANGE
10	23.7	47.5	23.8	10	33.6	40.8	7.2	10	23.6	40.8	17.2
11	9.9	45.3	35.4	11	12.4	53	40.6	11	9.9	53	43.1
12	9.9	55.1	45.2	12	11.9	53.1	41.2	12	12.3	23.1	10.8
13	9.9	57.3	47.4	13	12.7	53	40.3	13	14.6	51.2	36.6
Total	**13.4%**	**51.3%**	**38.0%**	**Total**	**17.7%**	**50.0%**	**32.3%**	**Total**	**15.1%**	**42.0%**	**26.9%**

5. DISCUSSION AND CONCLUSIONS

Due to the widespread Internet access and the increased use of laptops, Augmented Reality (AR) is a phenomenon that over time has seen an increase in mobile devices (FitzGerald et al, 2013). This study attempted to demonstrate the state of the art in innovative means of technology such as Augmented Reality were effective in teaching environmental issues.

Our results verify that the cognitive performance of students in primary schools is reinforced by the AR tool according to the study. In addition, students opposed to the tool of AR are receptive and have a positive attitude as they enjoy the exploration experience.

In total, the change of knowledge for all grades was 25.6%, while the change of learning experience was 32.4% on average of all grades. The best rate was achieved on learning experience with 32.4% total change, which can be said that was expected based on previous studies.

The future objective is to conduct an experimental test involving more students and include other environmental topics. Furthermore, we want to observe how this AR tool compares with other learning software beyond traditional teaching methods. Finally, one difficulty we faced was that in primary schools is forbidden to use mobile phones.

References

1. Anderson, A. (2015) ‘Reflections on Environmental Communication and the Challenges of a New Research Agenda’, **Environmental Communication,** Vol 9. No. 3, pp. 379-383
2. Asai, K., Kobayashi, H., Kondo, T. (2005) ‘Augmented instructions - a fusion of augmented reality and printed learning materials’, **Fifth IEEE International Conference on Advanced Learning Technologies (ICALT'05)**, pp. 213-215, Kaohsiung, Taiwan
3. Azuma, R. (1997) ‘A Survey of Augmented Reality’, **Presence: Teleoperators and Virtual Environments**, Vol. 6. No. 4, 1997, pp. 355-385.
4. Azuma, R., Billinghurst, M., & Klinker, G. (2011) ‘Special Section on Mobile Augmented Reality’, **Computers & Graphics**, Vol 35(4), pp. vii-viii

5. Billinghurst, M. and A. Duenser (2012) ‘Augmented Reality in the classroom’, **Computer**, 45(7), pp. 56-63
6. Bower, M., Howe, C., McCredie, N., Robinson, A. and D. Grover (2013) ‘Augmented reality in Education: Cases, places, and potentials’, **2013 IEEE 63rd Annual Conference International Council for Education Media (ICEM)**, Singapore, Singapore pp. 1-11
7. Chatzopoulos, D., Bermejo, C, Huang, Z., Hui, Z. (2017) ‘Mobile Augmented Reality Survey: From where we are to where we go’, **IEEE Access**, Vol. 5, pp. 6917-6950
8. Chen C-M and Y-N Tsai (2012) ‘Interactive augmented reality system for enhancing library instruction in elementary schools’, **Computers & Education**, Vol. 59 No. 2, pp. 638-652
9. Cox, R. and P.C. Pezzullo (2015) ‘**Environmental communication and the public sphere (4th ed.)**’, SAGE Publications
10. Cox, R. (2012) ‘**Environmental communication and the public sphere (3th ed.)**’, SAGE Publications
11. Craig, B. A. (2013) ‘**Understanding Augmented Reality: Concepts and Applications**’, Morgan Kaufmann, pp. 209-220
12. Dede, C. (2009) ‘Immersive interfaces for engagement and learning’, **Science**, Vol 323(5910), pp. 66-69
13. Depoe, S. (1997) ‘Environmental studies in mass communication’, **Critical Studies in Mass Communication**, Vol. 14, pp. 368–372
14. Diaz, C., Hincapié Montoya, M. and Moreno Lopez, G. (2015) ‘How the Type of Content in Educative Augmented Reality Application Affects the Learning Experience’, **Procedia Computer Science**, Vol. 75, pp. 205-212
15. Dunleavy, M., Dede, C. and Mitchell, R. (2009) ‘Affordances and limitations of immersive participatory Augmented Reality simulations for teaching and learning’. **Journal of Science Education and Technolog**y, Vol 18(1), pp. 7-22
16. FitzGerald, E., Ferguson, R., Adams, A., Gaved, M., Mor, Y., Thomas, R. (2013) ‘Augmented reality and mobile learning: The state of the art’ **International Journal of Mobile and Blended Learning** Vol 5(4), pp. 43-58
17. Fugger T., Hornung N. and F. Koller, ‘**The herbarium:An interactive augmented book of trees’**
18. Halder, P., Nuutinen, S., Pietarinen, J., Pelkonen, P. (2011) ‘Bioenergy and the youth: analyzing the role of school, home, and media from future policy perspectives’, **Journal of Applied Energy,** Vol 88 No 4, pp. 1233-1240
19. Jennings, P., & C., Lund (2001) ‘Renewable energy education for sustainable development’, **Journal of Renewable Energy**, Vol. 22, pp. 113
20. Jennings, P. (2009) ‘New directions in renewable energy education’, **Renewable Energy**, Vol. 34(2), pp. 435-439
21. Johnson, L., Adams Becker, S., Cummins, M., Estrada, V., Freeman, A., H. Ludgate (2013) ‘**NMC Horizon Report: K-12 Edition**’. The New Media Consortium, Austin, Texas
22. Johnson, L., Adams Becker, S., and M. Cummins (2012) ‘**NMC Horizon Report:K-12 Edition**’, The New Media Consortium, Austin, Texas
23. Kandpal T. C. and L. Broman (2014) ‘Renewable energy education: A global status review’, **Renewable and Sustainable Energy Reviews**, Vol. 34, pp. 300-324

24. Kaufmann, H., and D. Schmalstieg (2003) 'Mathematics and geometry education with collaborative augmented reality', **Computers & Graphics**, Vol 27(3), pp. 339-345.
25. Kaufmann, H. (2003) 'Collaborative augmented reality in education', Institute of Software Technology and Interactive Systems, Vienna University of Technology
26. Liarakou, G., Gavrilakis, C. and E., Flouri (2009) 'Secondary school teachers' knowledge and attitudes towards renewable energy sources', **Science Education and Technology**, Vol. 18(2), pp. 120-192
27. Lin, T.J., Duh, H.B.L., Li, N., Wang, H.Y., Tsai, C.C. (2013) 'An investigation of learners' collaborative knowledge construction performances and behavioral patterns in an augmented reality simulation system', **Computers & Education**, Vol. 68, pp. 314–321
28. Martin, S., Diaz, G., Sancristobal, E., Gil, R., Castro, M., & Peire, J. (2011) 'New technology trends in education: Seven years of forecastsand convergence', **Computers & Education**, Vol .57 No. 3, pp. 1893-1906
29. Medicherla, S. P. & Chang, G. and P. Morreale (2010) 'Visualization for increased understanding and learning using augmented reality' **MIR '10 Proceedings of the international conference on Multimedia information retrieval**, pp. 441-444
30. Milgram, P., Takemura, H., Utsumi, A. and F. Kishino (1994) 'Augmented Reality: A class of displays on the reality-virtuality continuum', **In Proceedings of Telemanipulator and Telepresence Technologies**, pp. 2351–2334
31. Munnerley, D., Bacon, M., Wilson, A., Steele, J., Hedberg, J., & Fitzgerald, R. (2012) 'Confronting an augmented reality', **Research in Learning Technology**, Vol. 20, pp. 1–10
32. Oversby, J. (2015) 'Teachers' Learning about Climate Change Education', **Procedia - Social and Behavioral Sciences**, Vol. 167, pp. 23-27
33. Parvathy, K.R., McLain, M.L., Bijlani, K., Jayakrishnan R. and R.R. Bhavani (2016) 'Augmented Reality Simulation to Visualize Global Warming and Its Consequences', **Emerging Research in Computing, Information, Communication and Applications**, pp. 69-78, India
34. Pasaréti, O., Hajdin, H., Matusaka, T., Jambori, A., Molnar, I., and M. Tucsányi-Szabó (2011), 'Augmented Reality in education' **INFODIDACT 2011 Informatika Szakmódszertani Konferencia**
35. Pedelty, M. (2015) 'Environmental communication and the public sphere', **Environmental Communication**, Vol. 9(1), pp.139-142
36. Platonova, M. (2016) 'Applying Emotive Rhetorical Strategy to Environmental Communication in English and Latvian', **Procedia - Social and Behavioral Sciences**, Vol. 236, pp. 107-113
37. Shuler, C., Levine, Z. and J. Ree (2012) 'iLearn II: an analysis of the education category of Apple's app store'. **Joan Ganz Cooney Center at Sesame Workshop**
38. Squire, K. and M. Jan (2007) 'Mad City Mystery: Developing scientific argumentation skills with a place-based augmented reality game on handheld computers', **Journal of Science Education and Technology**, Vol 16(1), pp. 5-29
39. Squire, K. and E. Klopfer (2007) 'Augmented reality simulations on handheld computers', **Journal of the Learning Sciences**, Vol 16, pp. 371-413
40. Wu, H.-K., Lee, S. W.-Y., Chang, H.-Y. and J.-C. Liang (2013) 'Current status, opportunities and challenges of augmented reality in education', **Computers & Education**, 62, 41-49

RECYCLING AND EDUCATION THROUGH DIGITAL STORYTELLING IN THE AGE GROUP "8-12" IN GREECE

P. Theodorou*, K.C. Vratsanou, E. Moriki, M. Botzori, M. Karamperis and C. Skanavis

Research Center of Environmental Communication and Education, Greece

*Corresponding author: e-mail: ptheod@env.aegean.gr

Abstract
In this study, primary school students were assessed on their environmental knowledge on recycling, upcycling, their attitudes and willingness to change behavior, after their exposure to digital social stories. Specifically, we propose the creation and the application of particular teaching interventions in classes of primary school of Greece. This implementation concerns the use of a web tool, Pixton, to educate students on the process of recycling, reusing and reducing. Specific digital stories with recycling content were created by the participant students under given guidelines, developing their own stories. In order to conduct the survey, 689 students participated from both urban and rural regions. The results have shown that the implementation with Pixton tool has influenced the level of knowledge, attitude and willingness to change behavior of the students.

Keywords: Recycling, Digital storytelling, Environmental attitude, Willingness to change behavior, Education awareness, Learner-generated comics

1. INTRODUCTION

The most effective way to reduce waste is to not create it in the first place. A lot of materials and energy is required in order to make a new product. As a result, reduction and reuse are the most effective ways you can save natural resources, protect the environment and save money (EPA, 2018). These three concepts, in combination, could make society adopt a greener, environmentally friendly behavior (EPA, 2018).

According to several studies affective factors, such as emotional affinity, empathy, and sympathy are of greatest importance in the procedure of predicting pro-environmental behaviors (Allen & Ferrand, 1999; Geller, 1995; Kals, 1999; Mayer & Frantz, 2004). The emotional status seems to be the key factor for the children's attitude toward environment, but the investigation about the reasons behind environmental behavior of children surfaced supplementary outcomes. Another stated factor that influences pro environmental behavior is the connection to nature (Cheng & Monroe, 2010). Additionally, being environmentally educated from an early age has the consequence that people, by all available means, learn to care for the planet, be familiar with nature and be part of an environmentally active community (Plaka & Skanavis, 2016). Briefly, the more experiences individuals have in their childhood, including school and family activities, the more likely it is to have an environmentally friendly behavior when they grow up (Plaka & Skanavis, 2016).

Recent years have seen the need to transform environmental education from passive knowledge into active action through the expression and the communication of students' own ideas with the use of activities like storytelling, photography and environmental drama (Tsevreni, 2011). Each of these activities has been recorded as helping children understand better reality, become active members of the community they belong to and develop decision making skills (Tserveni, 2011).

Children should be encouraged to be involved, by expressing and communicating their experiences, ideas and emotions about their environment and their everyday life (Barratt et al., 2007). The aim of this study is to examine how environmental concepts of Recycling, Reducing and Re-using can be transmitted and transmigrated through the expression and the communication of students' own ideas. Taking the above into consideration, in this research, an attempt was made to comprehend the impact on students' knowledge, attitude and willingness to change behavior using a lecture in recycling concept and DST (Digital Storytelling).

The fundamental issues of this study are briefly presented including the concepts of environmental education and in particular the related concerns based on Recycling, Reducing and Re-using. Subsequently, Digital Storytelling and the Pixton tool are described. The results from this research, showed that after class implementation based on addressed tools, students were more aware of recycling and upcycling. This in turn affected significantly their opinions and later on their attitudes and willingness to change behavior towards the mentioned practices.

2. BACKGROUND AND LITERATURE REVIEW

2.1 Environmental Education (EE)

Environmental education is considered to be the best way to create citizens with environmental conscientiousness (Nicolae, 2005), but it is also directly linked to environmental protection behavior as well as greener life choices (Schauer, 2006).

Environmental Education programs influence positively students' environmental beliefs, attitudes and behavior (Ballantyna et al., 2001), (Dresner & Gill, 1994). Particularly, educational interventions in field trips and other school-based programs with the aid of technology indoors affected the environmental knowledge and attitudes of students and in some cases their behavior (Rickinson, 2001). However, Rickinson (2001) supports "The field of EE research lacks evidence that EE promotes long-term behavioral changes".

Environmental education can be defined as the process through which the knowledge and experience of environmental problems are the keys to the creation of environmentally sensible people with perceived environmental behavior and with an ultimate goal for a positive attitude towards the physical world, its preservation and its protection (Rakotomamonjy et al., 2014). In other words, it is considered to be the most powerful tool to make young people think and act greener and more environmentally friendly (Schauer, 2006).

Especially, environmental education referring to the children/students, shapes the citizens of the future. In this way, our society is improving by people who are more environmentally aware with a deep respect for the environment **(**Varga et al., 2007), (Cheong, 2005).

2.2 Recycling, Reducing and Re-using

One of the most extended environmental problems humanity is confronted with is solid wastes. The strongest and most successful solution is recycling (Jekria & Daud, 2015). According to the United States Environmental Protection Agency, recycling is the procedure of collection and selection of materials that otherwise would be considered garbage and turn them into new products after being processed (EPA, 2018).

The more people that are involved in recycling, the more willing they are to be engaged in these practices (Barr, 2007). Some of the benefits of the recycling for the society as total and earth as well, include the decrease of contamination from poisonous gasses, the protection of regular assets and vitality, the incitement of financial and innovative advancement and the safeguarding of assets (Prestin & Pearce, 2010).

2.3 Digital storytelling

Fletcher and Cambre (2009) have found that digital storytelling can be a dynamic classroom practice when used "as a pedagogical tool that brings the creator/student and the viewer together in a dialogue around nature based on representation, meaning, and authority embedded in imagery and narrative".

According to Robin B. R. (2016. p.18) Digital Storytelling:

"…consolidates the craft of recounting stories with advanced media, including a mixture of content, pictures, recorded sound portrayal, music and video. These multimedia elements are blended together using computer software, to tell a story revolving around a specific theme or topic and containing a particular point of view. Most digital stories have the short length between 2 and 10 minutes, and are saved in a digital format that can be viewed on a computer or other device capable of playing video files…"

2.4 The tool of Pixton

Pixton belongs to the category of learner-centered tools, shifting the focus from teaching to learning (Azman et al ,2016). That means that Pixton gives all its priorities to personalized, differentiated and empowered learning. Opportunities provided to students focus on sharing comics, collaboration on projects with other students and commenting on each other's work, contributing to a high value involvement (Anderson, 2008).

Pixton is accessible through web browser and from smartphones, tablets, and computers. There are three different types of user accounts, Pixton for Fun, Pixton for School, and Pixton for Business. Pixton for Fun offers limited options to users, such as the ability to share and remix content with others. Additional options are only available to users who sign up to Pixton for School. Pixton for School allows teachers to create classroom and individual accounts, in order to assign activities to students and rate them at the end (Pixton, 2018).

Pixton can be integrated into the classroom and across the curriculum over different educational modules and subject areas such as Computer and Technology, History and Social Studies, Science, World Languages, Fine and Performing Arts, Mathematics, Special Education, Economics and Health Education (Pixton Lesson Plans, 2018).

3. METHODOLOGY

In the context of the survey, students were given lectures on recycling in combination with comics created by them through the Pixton app. In particular, the students received a pre-assessment questionnaire to assess their existing knowledge, behavior and attitude in relation to recycling.

Afterwards, researchers delivered a short lecture based on a PowerPoint 2016 presentation in order to impart concepts about recycling like the practice of reusing something for its original purpose (conventional reuse) or fulfilling a different function (creative reuse or repurpose).

In addition, the presentation included visual means (multimedia) explaining recycling, reusing and reducing concepts. Then, students, following specific instructions, developed their own storyboards and T-chart using the Pixton tool. Afterwards, participants were given the same questionnaire as a post-test, with the exception of the four questions concerning willingness to change behavior. After implementation, the students continued their course in the respective disciplines.

3.1 Sample

The selected schools had all an average common socio-economic background. The reason the particular schools were chosen, was based on the provision that there was parental consent.

In the 3rd grade, the respective students were 113 (17%) from urban areas; female 45% and male 55%. In the 4th grade, the sample consisted of 133 (19%) students from urban areas; female 47% and

male 53%. In the 5th grade, the sample consisted of 120 (18%) children from urban areas; female 46% and male 54%. Finally, in the 6th grade the sample consisted of 110 (16%) children from urban areas; female 45% and male 55%.

Concerning rural areas, in the 3rd grade, the respective students were 37 (5%); female 51% and male 49%. In the 4th grade, the sample consisted of 36 (5%) children; female 58% and male 42%. In the 5th grade, the sample consisted of 54 (8%) children; female 52% and male 48%. Finally, in the 6th grade the sample consisted of 86 (12%) children; female 56% and male 44%. The students were in the age group of 9 to 12 years of age. In total, 689 students took part in this study, 355 (52%) female and 334 (48%) male.



Figure 1 & 2: Total students of urban and rural region - Gender of urban and rural schools

3.2 Questionnaire

The questionnaires regarding recycling were consisted of 22 questions. The study took place during autumn of 2017. This survey had to be fulfilled within 2 or 3 teaching hours of 45-min school time period. External variables causing delays had to do with attention span of students and their level of understanding related issues as well as bureaucratic obstacles on the permission given to enter the classroom. Questionnaires were anonymous. Knowledge, attitude and willingness to change behavior were assessed by this survey. There were 8 questions on the knowledge of respondents and 4 questions that were associated with attitude. Furthermore, there were 6 questions that were dealing with the willingness to change behavior regarding recycling concepts. A pre and post questionnaire was given to the students. The two questionnaires were identical, concerning the parts of knowledge and attitude. The parts with enquiries of willingness to change behavior were altered to the post questionnaire. Moreover, the results were not announced to the students, unless they requested them for their own assessment.

3.3 Learning tool (Pixton) and activities

The implementation of the above activity is achieved with Pixton web software. At this stage, students were invited to create a timeline that reflected the lifetime of an object of their everyday life depending on the material that was made from. Once the scheduled timetable had been completed, students were asked to create an illustrated story of a character (student) presenting 3 different activities mentioned in the above practices (reusing – recycling – reducing) to be implemented at school (eg. material recycling, use of reusable utensils, water conservation, electricity, etc.). In the evaluation phase students were asked to create a mind map with Pixton that illustrated a variety of activities of 3R's that they could perform in their daily lives. This would show whether the students have achieved the objectives set out from the beginning and acquired the new knowledge from the activities that preceded them. In this activity, students learned how to find useful information on the Internet. This tool helps them to successfully use the creation of alternative and more attractive representations of teaching material by teachers who have no specialized knowledge about painting or comic design (Lazarinis et al., 2015).

Table 1: Questionnaire

QstN	Type	Topic
Q1	Profile	Gender
Q2	Profile	Age
Q3	Profile	Class
Q4	Profile	Where are you from?
Q5	Willingness	I am not willing to separate my family's trash so that I can recycle
Q6	Willingness	I am willing to go from house to house and ask people if they recycle
Q7	Attitude	It makes me happy when people recycle used plastic bottles paper and aluminum cans
Q8	Attitude	It troubles me when I think how much things people are throwing away that could be recycled
Q9	Attitude	I have asked my family to recycle things we use
Q10	Knowledge	In comparison with normal paper the recycled paper
Q11	Knowledge	Where do most trashes go after they are thrown in garbage trucks?
Q12	Knowledge	The main problem with landfills is that
Q13	Knowledge	Pre-recycle means that
Q14	Knowledge	Objects that cannot be recycled and used again are
Q15	Knowledge	How important is recycling for the conservation of natural resources
Q16	Knowledge	How important is recycling as a component of solid waste management
Q17	Willingness	Do you recycle at your house?
Q18	Attitude	In the future you are going to
Q19	Knowledge	I recycle to preserve natural resources
Q20	Willingness	I recycle for charitable purposes
Q21	Willingness	I recycle so that I can make money
Q22	Willingness	I recycle because it seems like the right thing to do

Below, the scenario is described:

A. In the first activity the students create a timeline that will display the maximum lifetime of every object-material that we throw in trash (from least to bigger). Each panel should include description with the estimated decomposition lifetime, an appropriate picture and include an appropriate description for each object-material.

B. In the second activity the students create a storyboard that present a student and depicts three activities; each one will also refer to a different practice, which can be implemented at school. One will refer to reducing, one to recycling and one to reuse. The activity was identified, by including

appropriate description, a dialogue that describes the activity and a corresponding image for each table.

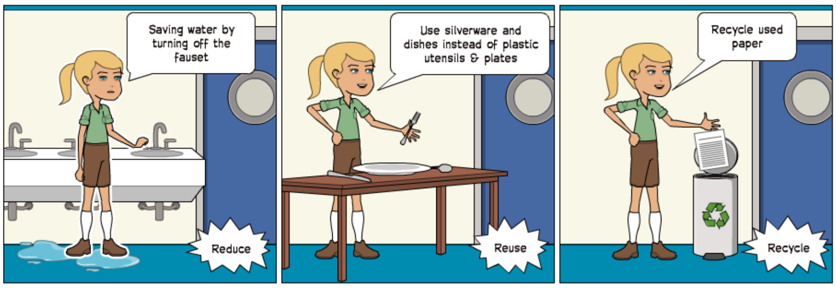


Figure 3: Second activity – Storyboard

C. In the third activity the students create, a mind map that illustrates a variety of activities for reducing, reusing and recycling. Each panel should include a title, an appropriate picture and a detailed description.

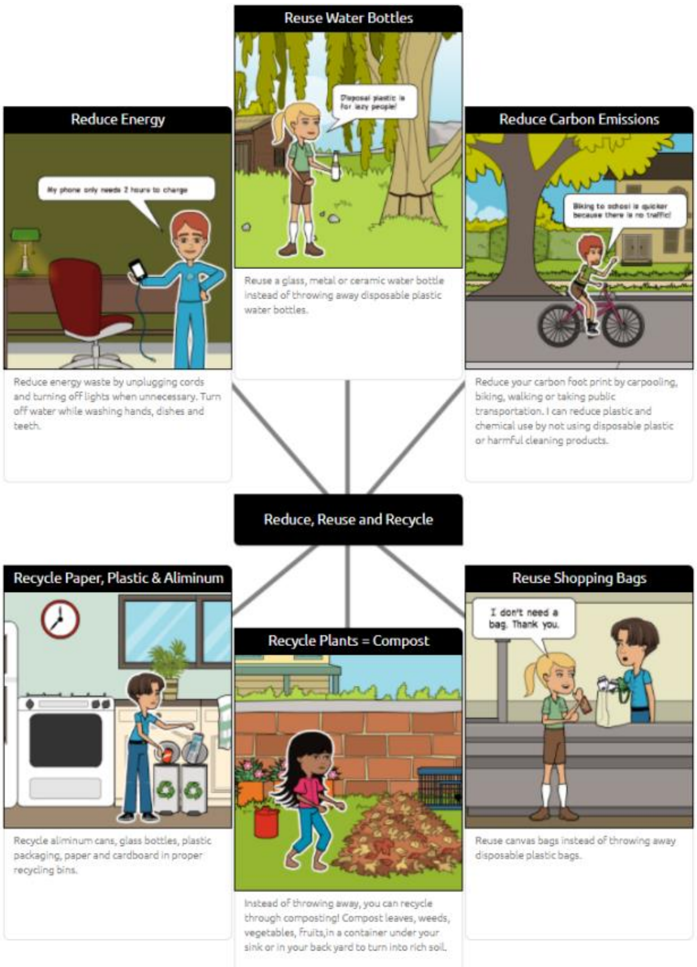


Figure 4: Third activity - Mind Map

4. RESULTS

Regarding total result of urban and rural region concerning knowledge, the change for the 3rd grade was 48.9%, the change for the 4th grade was 56.8%, the change for the 6th grade was 65.5% and the change for the 6th grade was 74.1%. The category of attitude gave us results such as 57.7% for the 3rd grade, 56.6% for the 4th grade, 56.9% for the 6th grade and 59% for the 6th grade. For all these

questions concerning willingness to change behavior, it was recorded that the change was 59.3% for the 3rd grade, 51.3% for the 4th grade, 52.9% for the 5th grade and 54.6% for the 6th grade.

Specifically, from the questions concerning knowledge in urban region, the change for the 3rd grade was 39.2%, for the 4th grade, 46.1%, for the 5th grade 39.4% and for the 6th grade was 54.6%. The change of attitude category in urban was 47.6% for the 3rd grade, 45.3% for the 4th grade, 36.8% for the 5th grade and 44.4% for the 6th grade. The category willingness to change behavior of the participants in urban region was 46.8% for the 3rd grade, 45.3% for the 4th grade, 42.4% for the 5th grade and 40.7% for the 6th grade.

Particularly, for all the questions concerning knowledge in rural region, 10% was the change for the 3rd grade, 10.6% for the 4th grade, 24.8% for the 5th grade and 19.2% for the 6th grade. The change of attitude category in rural region was 11% for the 3rd grade, 11.3% for the 4th grade, 25.1% for the 5th grade and 14.6% for the 6th grade. The change in the willingness to change behavior of the participants in rural areas was 9.6% for the 3rd grade, 5% for the 4th grade, 12.7% for the 5th grade and 13.8% for the 6th grade.

In urban, in 3rd, 4th, 5th and 6th grade, the willingness to change behavior was 53.8%, 31.9%, 47.4% and 51.4%. Whereas, in rural the 3rd, 5th and 6th grade had a change of 17.8%, 7.3%, 21.1% and in the 4th grade the change was 4%.

The most remarkable observations concern the questions with the greatest differences in the percentages, being the 13th and 14th questions. In particular, in the 6th grade of the urban region, it was recorded that in total, there was the biggest change of 64% and in the 14th question, there was also the biggest change of 64.6% compared to other school classes of the urban and rural regions. In attitude category of the urban and rural region, the 3rd grade has increased a level of 57.7%, respectively in fourth grade, the increment percentage was 56.6%, in the fifth grade was 56.9% and in the sixth 59%. As for the question 8 that delineates also attitude, there were observed larger changes on average in all classes of urban, from 25.5% to 45.5%, except at 5th grade of the urban area that the students' answers showed a 15.7% increase after the intervention.

Notably, in question 8 at rural region in the 3rd grade the change was 15.1%, in the 4th grade 9.2%, in 5th grade (bigger of other classes) 30.3% and in the 6th grade 13.1%. It was remarkable that in the sixth grade of primary school concerning question 18 of the attitudes group, there was the highest success rate of 64%. Of course, there is an exception at the fourth grade of rural areas whose environmental attitude was improved only by 11.2%.

Another noticeable question was 22. The change in urban areas was from 32.5% to 49.1%, whereas in the rural areas the change was from 4% to 39.5%. Taking into consideration the questions concerning willingness to change behavior, it is observed that there is a stable total change in all the grades of urban and rural areas from 47.2% to 140.1%.

Table 2: Total changes in 3rd 4th 5th and 6th grade of Urban Region

URBAN	3RD GRADE			4TH GRADE			5TH GRADE			6TH GRADE		
	BEFORE	AFTER	CHANGE	BEFORE	AFTER	CHANGE	BEFORE	AFTER	CHANGE	BEFORE	AFTER	CHANGE
Knowledge	47.82	87.69	39.26	37.21	83.39	46.18	48.49	89.63	39.44	27.21	81.81	54.60
Attitude	40.88	88.53	47.65	40.45	85.77	45.32	46.28	79.73	36.85	30.25	74.73	44.48
Williness	45.32	91.05	46.88	40.45	85.77	45.32	47.62	88.42	42.40	46.65	87.43	40.78

Table 3: Total changes in 3rd 4th 5th and 6th grade of Rural Region

RURAL	3RD GRADE			4TH GRADE			5TH GRADE			6TH GRADE		
	BEFORE	AFTER	CHANGE	BEFORE	AFTER	CHANGE	BEFORE	AFTER	CHANGE	BEFORE	AFTER	CHANGE
Knowledge	5.05	14.15	10.02	3.52	14.21	10.68	2.53	26.98	24.83	1.56	21.13	19.25
Attitude	7.22	18.25	11.02	7.57	18.92	11.35	5.25	28.77	25.17	4.80	19.40	14.60
Williness	5.26	18.04	9.65	11.98	18.02	5.03	17.57	29.76	12.78	9.21	23.03	13.81

Table 4: Total changes in 3rd 4th 6th and 6th grade of Urban and Rural Region

TOTAL	3RD GRADE			4TH GRADE			5TH GRADE			6TH GRADE		
	BEFORE	AFTER	CHANGE	BEFORE	AFTER	CHANGE	BEFORE	AFTER	CHANGE	BEFORE	AFTER	CHANGE
Knowledge	52.86	101.83	48.97	40.73	97.59	56.86	51.01	116.60	65.59	28.77	102.94	74.17
Attitude	49.10	106.77	57.67	48.02	104.68	56.66	51.53	108.49	56.96	35.05	94.12	59.07
Williness	50.58	109.90	59.32	52.43	103.78	51.35	65.18	118.17	52.99	55.86	110.46	54.60

5. DISCUSSION

Understand what shapes the children's attitude toward the environment is of vital importance if one wishes to administer the necessary skills to face the environmental problems of our society in their adulthood (Cheng & Monroe, 2010). In Greece, formal environmental education in the mandatory part of the school system (primary and secondary) has not fully reached the desired results on a responsible environmental behavior of participating students (Karamperis et al., 2016).

The formulation of environmental knowledge, attitude and behavior from young ages play a crucial role in recycling and reusing campaigns, especially when complex solutions are applied. In order to succeed a satisfying deepening in environmental education, it is necessary to associate it to all three forms of education (formal, non formal, in formal) from an early age (Plaka & Skanavis, 2016). While there are numerous technical policies and solutions for transmitting environmental concepts like recycling, changing the behavior of individuals from an early age will be the most critical component of the process (Vaughter, 2016). This paper's results are in alignment with results from prior research projects.

The results strongly suggest that the production of digital stories can improve students' knowledge, attitude and willingness to change behavior about recycling. This confers to the main goal of environmental education that aims to ameliorate the knowledge of people on the subject, restructure the assertive attitude towards the environment within a contiguous positive behavior (Jensen & Schnack, 1997). In particular, the total results regarding knowledge showed that the proportions were modified before and after the implementation. Comparatively, it is recorded the total knowledge of urban and rural region the 3rd grade was increased in a level of 48.9%, respectively in fourth, the growth percentage was 56.8%, in the fifth grade was 65.5% and in the sixth 74.1%.

In fact, the national Greek curriculum shows that environmental education is being taught only up to the fourth grade of primary school. After this grade, scattered topics are concluded in biology, geography, physics and chemistry subjects. Students also amply demonstrated that educational, digital comics could assist them to understand difficult technical and scientific content. These findings align with prior claims that comics were able to assist students' comprehension (Mallia, 2007) (Recine, 2013) (Yıldırım, 2013).

A remarkable observation with recorded big changes in the percentages concerns question 5 that represents the willingness of the respondents to change their behavior. In these questions there was a difference between classes, depending on the region. This asserts the few studies that have been conducted into the impact of environmental education on children and youth which show that the level of environmental awareness is relatively low and the willingness to change behavior differs depending on the region, type of area (urban/rural) and school (Domka, 2001).

In sum, DST is time-consuming and some educators believe that it is an effort that is tedious (Theodorou et al., 2017). That is, because it may take students several attempts at creating digital stories before they demonstrate proficiency in technology and knowledge on the topic (Dogan & Robin, 2017). As with all new instructional methods, students will need time to learn using DST (Dogan & Robin, 2017). During the research, relative inefficiencies were identified concerning mostly technical problems. Another barrier that appeared in this particular research was the slow internet connection that caused problems to the speed and the quality of the process. In addition, the

hours that primary school teachers offered were limited and that created difficulties in the overall completion of the process.

6. CONCLUSION

Future implications of this study would involve the improvement of the particular programs in order to stabilize the role that students can acquire as dominants and leaders of environmental knowledge, attitude, as well as the appropriate behavior in both family and community through educational constructivist methods such as the applications of DST.

Although there are no similar surveys on the use of DST in the environmental education in Greek primary schools, it is clear from our results that DST can be a very useful tool in the field of environmental education, and more specifically in the teaching process of recycling concepts. The findings of the research could be a starting point for a series of studies that would further analyze the use of DST in other environmental issues in education. It's also very important to mention that the use of DST in the classrooms gives students the opportunity to become familiar with technology and to include it more easily into the learning process.

From the above, it can be seen that, this research provides us with a lot of interesting and enlightening data while presenting the possibilities for far-reaching research as well as the systematic use of DST for environmental education. Having already shown the positive results that can arise from the use of digital tools such as Pixton in environmental education, a next step would be to explore the effects of using other similar tools such as WebQuest with the content of environmental education.

References

1. Anderson T. (2008). **'Towards and theory of online learning'**. Athabasca University.
2. Azman F., S. Zaibon, and N. Shiratuddin. (2016). 'Pedagogical analysis of comic authoring systems for educational digital storytelling'. **Journal of Theoretical and Applied Information Technology**, 89(2), pp. 461-469
3. Allen, J. and J. Ferrand. (1999). 'Environmental locus of control, sympathy, and proenvironmental behavior'. **Environment and Behavior**, 31, pp.338-353.
4. Ballantyna, R., Fien, J. and J. Packer. (2001). 'Intergenerational influence environmental education: A quantitative analysis'. **Australian Journal of Environmental Education**, 17, pp. 1-7.
5. Barr S. (2007). 'Factors influencing environmental attitudes and behaviors: A U.K. case study of household waste management'. **Environment and Behavior**, 39(4), pp. 435-473.
6. Barrat H.E., Barrat R. and W. Scott. (2007). 'Engaging children: research issues around participation and environmental learning'. **Environmental Education Research,**13(4). pp. 529-544.
7. Cheong I.P.A. (2005). 'Educating pre-service teachers for a sustainable environment'. **Asia-Pacific Journal of Teacher Education**, Vol 33(1), pp. 97-110.
8. Dogan B. and R.B. Robin. (2017). **'Climate Change Education From Critical Thinking to Critical Action'.** Institute for the Advanced Study of Sustainability.
9. Dresner M. and M. Gill. (1994). 'Environmental education at summer nature camp'. T**he Journal of Environmental Education**, 25(3), pp. 35-41.
10. Fletcher C. and C. Cambre. (2009). 'Digital storytelling and implicated scholarship in the classroom'. **Journal of Canadian Studies**, 43(1), pp. 109-130.
11. Geller, E. (1995). 'Actively caring for the environment: An integration of behaviorism and humanism'. **Environment and Behavior,** 27, pp.184-195.

12. https://www.epa.gov/education/what-environmental-education (accessed January 7th, 2018).
13. https://www.researchgate.net/publication/322245683_Children_Communicating_on_Climate_Change_The_Case_of_a_Summer_Camp_at_a_Greek_Island (accessed Febuary 27th, 2018).
14. Jekria N. and S. Daud . (2016). ‘Environmental Concern and Recycling Behaviour’. **Procedia Economics and Finance**, 35, pp. 667-673.
15. Jensen B. and K. Schnack. (1997). ‘The action competence approach in environmental education’. **Environmental Education Research**, 12(3–4), pp. 471–486.
16. Cheng J.C.H and M.C. Monroe. (2010). ‘Connection to Nature: Children’s Affective Attitude Toward Nature Environment and Behavior’. **Environment and Behavior**,44,pp.31-49.
17. Kals E., D. Schumacher, and L. Montada. (1999). ‘Emotional affinity toward nature as a motivational basis to protect nature’. **Environment and Behavior**, 31, pp. 178-202.
18. Karamperis M., S. Apostolopoulou, G. Grigoroglou, C. Skanavis and A. Kounani. (2016). Environmental Summer Camp in a Greek Island, **International Conference on Protection and Restoration of the Environment**, pp. 1024-1030, Mykonos Island, Greece.
19. Lazarinis F., A. Mazaraki, V.S. Verykios and C. Panagiotakopoulos. (2015). E-comics in teaching: Evaluating and using comic strip creator tools for educational purposes. **International Conference on Computer Science & Education**, pp. 1023-1041, Cambridge, United Kingdom.
20. Mayer F. and C. Frantz. (2004). ‘The connectedness to nature scale: A measure of individuals feeling in community with nature’. **Journal of Environmental Psychology**, 24, pp. 503-515.
21. Mallia G. (2007). ‘Learning from the sequence: The use of comics in instruction’. **Imagetext: Interdisciplinary Comics Studies**, 3(3), pp. 1-10.
22. Nicolae L. (2005). ‘Council of Europe Plenary Session: Youth Education for Sustainable Development’.
23. Plaka V. and C. Skanavis. (2016). ‘The feasibility of school gardens as an educational approach in Greece: a survey of Greek schools’. **International Journal of Innovation and Sustainable Development,** 10(2), pp. 141.
24. Plaka V. and C. Skanavis. (2016). ‘The feasibility of school gardens as an educational approach in Greece: a survey of Greek schools’. **International Journal of Innovation and Sustainable Development**, 10(2), pp. 141.
25. Prestin A. and E.K Pearce. (2010). ‘We care a lot: Formative research for a social marketing campaign to promote school-based recycling’. **Resources, Conservation and Recycling**, 54, pp.1017-1026.
26. Rakotomamonjy S. N., J. P. G. Jones, J. H. Razafimanahaka, B. Ramamonjisoa and S. J. Williams. (2015). ‘The effects of environmental education on children's and parents' knowledge and attitudes towards lemurs in rural Madagascar’. **Animal Conservation**, 18(2), pp. 157–166.
27. Rickinson M. (2001). ‘Learners and Learning in Environmental Education: A critical review of the evidence’. **Environmental Education Research,** 7(3), pp. 207-320.
28. Recine D. (2013). ‘Comics aren’t Just For Fun Anymore: The Practical Use of Comics by TESOL Professionals’. University of Wisconsin River Falls.
29. Bernard R. (2016). ‘The Power of Digital Storytelling to Support Teaching and Learning’. **Digital Education Review**, 30, pp. 17-29.
30. Schauer T. (2006). ‘EU Strategies and the Role of Education for Sustainable Development’. Vienna: The Club of Rome – European Support Centre.
31. Skanavis C. (2004). **‘Environment and Community’.** Kalidoskopio, Athens.

32. Tserveni I. (2011). 'Towards an environmental education without scientific knowledge: an attempt to create an action model based on children's experiences, emotions and perceptions about their environment'. **Environmental Education Research**,17(1), pp. 53-67.

33. Theodorou V., K. Vratsanou, H. Nastoulas, E.S. Kalogirou and C. Skanavis. (2017). Climate change Education through DST in the age group "10-13" in Greece. **World Symposium On Climate Change Communication.**

34. Varga A., M.F. Koszo, M. Mayer and W. Sleurs. (2007). 'Developing teacher competences for education for sustainable development through reflection: The environment and school initiatives approach'. **Journal of Education for Teaching**, 33(2), pp. 241-256.

35. Vaughter P. (2016). 'Climate Change Education From Critical Thinking to Critical Action'. **United Nations University Institute for the Advanced Study of Sustainability**, 4, pp. 4.

36. Yıldırım A.H. (2013). 'Using graphic novels in the classroom'. **Journal of Language and Literature Education**, 8, pp. 118-131.

SOCIAL EXPERIMENT IN THE ENVIRONMENTAL FIELD OF EDUCATION

[1]S. M. Bagiouk*, [2]S. S. Bagiouk, [2]A. E. Agiou, [1]A. S. Bagiouk

[1]Division of Hydraulics and Environmental Engineering, Dept. of Civil Engineering, Aristotle University of Thessaloniki, 54124 Thessaloniki, Greece,
[2]Department of Civil Engineering, Democritus University of Thrace, 67131, Xanthi, Greece

*Corresponding author: [1]E-mail: smpagiou@civil.auth.gr, Tel +30 2310 995893, +30 6944189218

Abstract
Climate change that has taken place over the last few decades requires a different approach of the environment. For this reason, a different philosophy and behavior of citizens is needed, characterized by respect and proper use of the environment, stimuli acquired mainly through education. The aim of this paper is to identify the problems and the dissuasive trends as well as to highlight actions and motivations for environmental awareness and activation, in order to show and build an innovative and efficient model of education and mobilization. This research was carried out using the "questionnaire" method, as well as the statistical analysis and the statistical sample came from students of secondary and tertiary education in Northern Greece. In particular, it focused on the active population of society so as to have on the one hand the necessary maturity required for the problems to be taken into account and on the other hand the potential for immediate activation.

Keywords: Environment, Education, Innovation, Action, Questionnaire

1. INTRODUCTION

The **education** comes from the **verb educate**, which means raise, form, edify. It is the process of acquiring knowledge, developing skills and competencies, and forming values. As far as Environmental Education is concerned, it is the education about the environment that places it as an area of our daily life and contributes to the development of knowledge, attitudes, abilities and action for its preservation, protection and restoration. Its aim is to raise awareness of environmental issues and on these issues by social groups and citizens. The definitions for Environmental Education are varied and have been given from time to time by various operators and environmentalists. The first definition of Environmental Education was given by the International Union for the Conservation of Nature organization in 1970 [17], although along the way the most acceptable definition was given by UNESCO in 1977 [17] in Tbilisi of the former Soviet Union. All the definitions that have been expressed and formulated have as a common denominator the responsible and harmonious relationship between the man and the environment. Environmental education is governed by three dimensions [17], [Figure 1]. The Education around the Environment on the accumulation of knowledge about the biophysical dimensions of the environment, the Education in the Environment that highlights the beneficial effect of the person's contact with nature and finally the Education for the Environment which introduces the notion of citizen responsibility for the fate of the environment in which two trends have been formed, the technocratic, which claims that technology has the potential to provide solutions to environmental issues, and the ecocentric, which considers that science and technology can not by themselves provide solutions. These three dimensions are not only not contradictory, but instead complement one another, and in combination they all define the modern concept of Environmental Education, that is, an Education that meets the needs of modern times and

builds a constructive relationship between the man and the nature. In general, **Environmental Education (EE)** has been progressively developed since the 1960s in America and Europe [13] with the aim of raising environmental sensitization of citizens and the prospect of opposing the widespread perception that considers man as the sovereign of the nature. Particularly important was the first international working meeting in Carson City, Nevada, USA, [6] in 1970, on EE where the term ‘’Environmental Education’’ was introduced in international vocabulary. At the Stockholm Conference (1972), the role of EE is recognized for environmental protection and the results of the conference include the establishment of the United Nations Environment Program (UNEP) and the expansion of new ministries of the environment worldwide [3]. During the 1980s, the new notion of 'Sustainable Development' is changing the environmental data [13]. Specifically, it is introduced in 1987 with the publication of the Brundtland report by the World Commission on Environment and Development and it is adopted by the Rio International Conference [15] on Environment and Development in 1992 and by the Thessaloniki Conference (1997) [9] [10]. Sustainable Development is a development that meets today's needs without limiting the potential of future generations to cover their own needs. UNESCO (2005) declares an Implementation Plan [16] that concerns Education for Sustainable Development in the Decade of Education (2005-2015) so that its principles and characteristics can be reformed. Today Education for Sustainable Development is considered to be a stage of Environmental Education as Environmental Education evolves continuously with the sole purpose of shaping responsible citizens actively involved in socio-environmental issues. The present paper aims at the emergence of an innovative model of education that puts the trainee rather than the trainer in the centre, free of using rote memory as a learning technique, but instead linked to modern educational techniques that focus on practice rather than theory. The paper was based on the "questionnaire" method introduced to secondary and tertiary education students in Northern Greece and on the results and conclusions that resulted, in bibliographic research as well as in interviews with secondary and tertiary teachers.

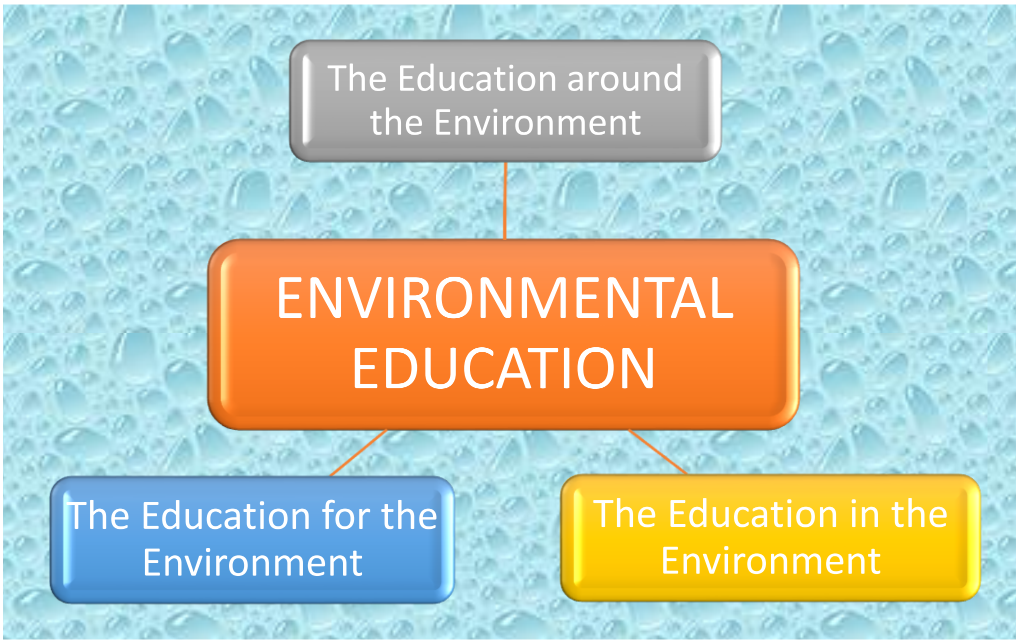


Figure 1: The three dimensions that govern Environmental Education

2. THE SURVEY

2.1 The aim

The survey put young people in the lead as pupils and students constitute and represent the active population and the future of the country. The aim of this research is to put the trainee in focus and to formulate the trainers' stimuli, pulse, needs, crisis and suggestions. This endeavor does not follow and does not identify with traditional education but opposes and conflicts with it. It does not

marginalize the pupil's - student's needs, requirements and necessities as he embraces and assimilates them [8]. It does not begin in order to end up with the trainee as a conservative package of education and knowledge which while it is referring to him and it is determined for him not only does not give him the maximum weight required to reform the education system but does not even take his or her opinion into account for this equation. Instead, the innovative education model proposed is started by the trainee so as to end up with him. Today's era sets a different approach to the environment more timely than ever, which couldn't not start from the classrooms. Thus this innovative model of education sets its foundation in the first stages of education but with its heart beating at secondary education, since should children have built the appropriate environmental background in previous classes, they will be able with the appropriate maturity to apply what they were taught, to take initiatives and to coordinate and take the lead in more actions [14] in their future life, such as in higher education, in which they may continue. It will also contribute to the creation of radical change concepts body that will reschedule organizational structures, build an environmentally responsible and active citizen, a person in direct contact with the environment, promote a new concept and philosophy for the environment, and emphasize the position and the role of the man in this [12]. It will also emphasize the need to face the ecological crisis and the demands of the ecological movement in order to create conditions that will prevent the emergence of similar crises in the future. Hence, the aim of this paper is the education model [7] proposed to constitute the vehicle for challenging and introducing changes in traditional education through the use of innovative approaches to reality, the opening of the school to life, the resolution of real problems and the learner's active participation [5] in the learning process with modern educational methods and techniques.

2.2 The method

The survey was carried out with the help of a questionnaire, which was distributed to pupils of secondary education and to students of higher education, schools and universities of Northern Greece respectively. No specific place or school or university was selected so that the sample would be more representative and reliable. In particular, 368 questionnaires were distributed and 309 completed in October-November 2016. The data after being collected were put for statistical analysis and for conclusions. The questionnaire was formed in full association with the objectives, the research goals, the age, the stimuli and the psychology of the participants on the basis of the relevant literature[3][7][1]. In all questions the children were asked to answer on a five-level scale where 1 was identified with "not at all" and 5 with "very strong" as well as optionally with the addition of a comment or a detailed answer. In particular, it included questions in which respondents identify problems and deterrents and assess the impact of each individually on the concept of environmental consciousness [2]. The questionnaire was also enriched with questions about the emergence of solutions, proposals and actions to achieve an environmentally friendly behavior, environmental sensitization and activation [14]. At the end of the questionnaire, there are questions about the socio-demographic details of the person completing it, which relate to gender, age, class or year, and the type of study respectively, as well as the place of origin and the activities the person maintains.

2.3 The sample of the survey

The young people's view, coming from the answers given by pupils and students to the specific questionnaire adapted to the psychology of age, knowledge, stimuli, experiences and the other characteristics that govern them [1], was imprinted, analyzed and expressed with statistical accuracy, with observations and fruitful conclusions. Specifically, 78% of the pupils and 83% of the students answer that the environmental education learning techniques and how they are taught are not attractive and do not cause interest. Then 68% of the boys as well as 76% of the girls paint as the main disincentive of the environmental process, the non-active attitude of the state combined with a simple theoretical approach to the environmental crisis as dissatisfaction to inertia, procrastination, distraction from actions, social events, the promotion of environmental awareness and radical changes to the curriculum that has never been applied, was developed. Another analgesic factor that was determined by almost the entire sample with 92% was the predominant position of memorization and

rote memory. Questions related to the offer and activity so far have shown that students with artistic activities and students of social sciences (psychology, special education, etc.) have developed to a greater extent the feeling of volunteering. It has also been recorded that children from rural areas in relation to children living in urban centers as well as those engaged in sports directly related to nature and to environment, have shown greater interest in recycling and similar actions. Moreover, the age factor was considered at many points crucial as the 19-year-olds (19) seemed to be more mature and more aware of the importance of the problems faced and studied by environmental education. While in the process of identifying problems and dissuasive trends pupils of theoretical direction and students of theoretical sciences showed greater ability and intent to identify them, but in the process of highlighting actions and proposals they came second since students of positive direction and students of natural science and Polytechnical Universities have shown greater readiness, willingness and ability to propose solutions, organize and coordinate actions as well as to work on innovative programs. Some of their suggestions were the use of models and software as well as the wider use of technology and the internet, such as the use of the latter as a mechanism for promoting and raising awareness and developing broader partnerships. In the question of what are the main components for finding solutions and developing actions, the dominant responses were motivation and dialogue as they were not selected only by the small percentage of 7%, while in the question of whether the institution of the group, by using learning methods centered in this, would help the educational process, 86% responded positively. Finally, in the crucial and all-important question whether it is feasible and profitable to make radical changes in environmental education and education in general, almost the whole sample with the percentage touching the absolute and specifically with the overwhelming percentage of 98% answered "Yes", [Figure 2].

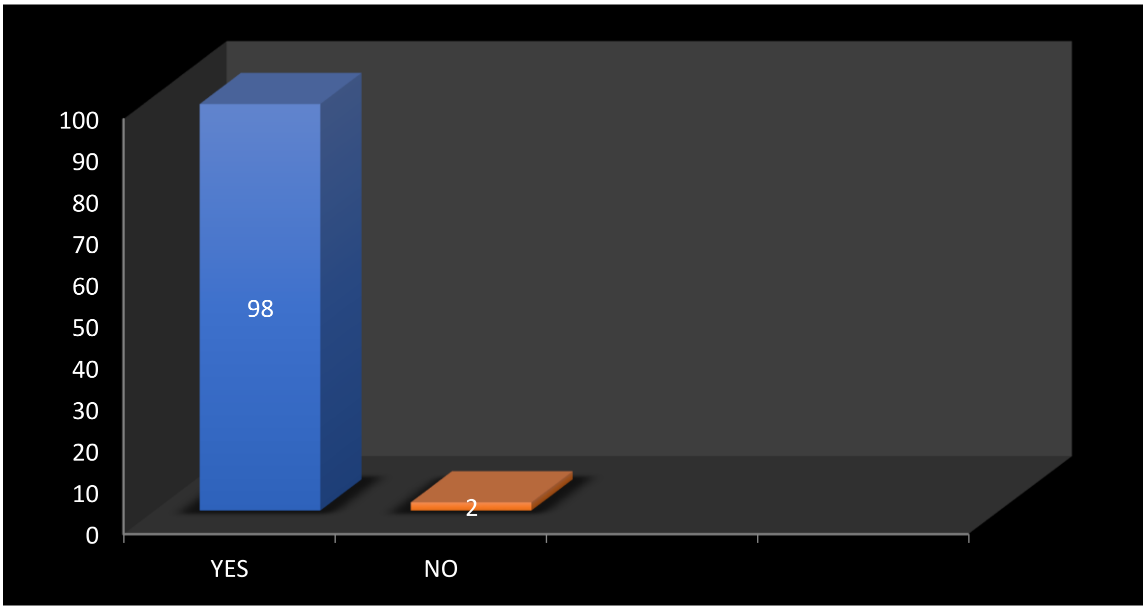


Figure 2: The statistical representation of the sample according to whether they want changes in the form of the current Educational System.

Analytically, young people are looking for new learning techniques and methods, learner-centered, focusing on example, experiment, application, and more generally on the practical part [4]. In those that provide appreciable motivation to the apprentice and not to the techniques being a consequence of existing traditional education that puts the focus on sterile memorization and rote memory. An experiential education that in addition to the essential and necessary knowledge will provide the student with the power of discernment as well as the necessary tools that will shield him for tomorrow. The sample of the survey as far as the teachers views is concerned, that were elicited through the interviews, harmonizes and moves in a very large part of it in the same context while it opposes to very few individual views that were adopted and supported by the teacher-centered method.

3. INNOVATIVE TECHNIQUES OF AN EXEMPLAR EDUCATION SYSTEM

3.1 The model

Taking into account the sample of research, ie the results and conclusions that have been reached, bibliographic research [2], interviews with secondary and tertiary educators, psychology and the needs of youth [1] as well as the technological and scientific evolution of the era, a study and research was carried out to build an innovative model of education that promotes learning techniques tailored to the occasional learning level of each era starting from primary or even pre-primary education and ending with tertiary education and its extensions.

A model of education not moving within traditional education [10] but introducing a new form of learning that will be experiential and more effective [12]. A learner-centered learning with high interactivity, communication and participation that pulls the learner out of the background and puts him at the forefront giving him a leading role [5]. An education that hears and respects his voice and his opinion [8], which allows him to experience and even lapse into errors without, of course, affecting the respect and dignity of each individual as the error will be an opportunity for improvement and the starting point for a set of actions that will evolve him and complete him as a person and personality.

The instructor's monologue is replaced by the discussion and the direct and universal participation of apprentices with new radical methods and innovative education techniques aimed at utilizing all the senses so that new knowledge can be easily and more efficiently engraved in memory. For example, if the knowledge ends up to the trainee visually and verbally, then since people use two sensory organs, there are now two "ways" to retrieve this information from their memory in the near future.

Through this the trainee is not trying to acquire a conservative and impersonal knowledge package but to acquire and build a philosophy of thinking that will accompany him to the environmental problems and dilemmas and to his everyday life in society. More simply, a way of thinking and acting that perceives situations and stimuli him correctly and through specific stages and a large scale of practical knowledge and skills not only leads him to a solution but to a range of solutions through which the student may choose the best [11].

This process, ie algorithmic thinking and action [Figure 3], which is proposed in the current education model for the learner, follows a sequence of things and events starting from the perception and diagnosis of a problematic situation. Then create scenarios and set goals. Afterwards, the trainee continues collecting, organizing and coordinating information and data in order to arrive at a range of possible solutions. Having the right knowledge base he defines the criteria for choosing an appropriate solution and chooses the most appropriate. By completing this logic, the trainee creates an action plan based on the best solution and achieves his purpose. Of course, at the end of each such act, he enters the evaluation process with the goal of self-improvement and the achievement of better results in the future.

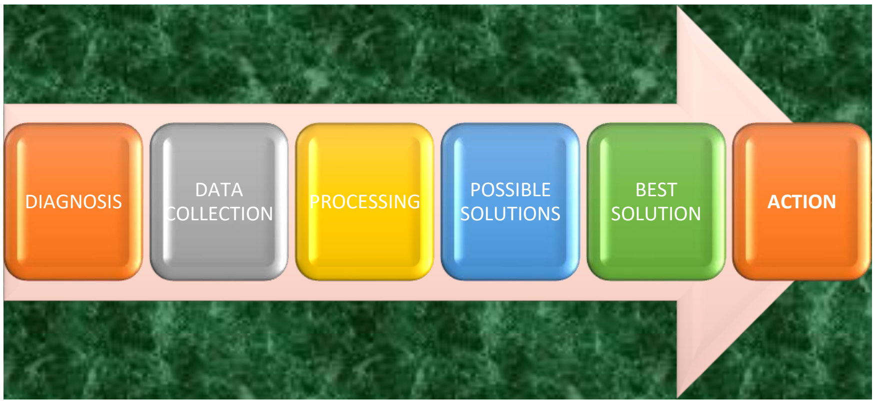


Figure 3: Algorithmic thinking

3.2 The trainer's role

The trainer's role is of crucial importance as he is the one who will apply these techniques and methods, educate young people and try to lead them to their original goals [11]. In the context proposed, the role of the trainer does not endorse the dominant role adopted in traditional education [10] but introduces a new aspect that makes him co-star with the learner, having as his sole concern the active involvement of the young and his goals achievement. In particular, he is the one that will provide the knowledge, stimulate the learner's interest and introduce him / her into the educational process with the element of challenge, not by leaving him as a mere observer and passive recipient [5] [1]. In this model, the trainer's duties do not only not decrease but instead increase as we speak of a much more demanding process. . Specifically, the trainer is asked to effectively organize and plan the teaching before practicing it and additionally while he is supervising the work of the students, providing support and guidance, encouraging and puzzling the young. Even to provide, if necessary, feedback on the young, to lead him to consciously work, to keep children at a desired pace, to identify the advantages and disadvantages of their work and to control the process. He also links teaching with pre-existing knowledge, provides a wealth of sources of knowledge, aims at high interactivity, communication and feedback, teamwork, research, cooperation, uses participatory strategies [4] [11], constitutes a role model, spares time to propose alternative solutions for the best result, to give the appropriate instructions and to advise thoroughly. Finally, to ensure everyone's involvement and the right approach to the problem concerned. It is understood that all of these methods are not only teacher-centered and do not follow the beaten track but instead collide frontally with traditional education. Thus, the trainer simply acquires a coordinating, organizational and counseling role, that is, more limited, giving space and time to the apprentice with the sole aim of his spiritual shielding as well as his independence.

3.3 Techniques - Methods

Techniques and methods [4][14] designed to frame this innovative environmental education model place the learner in the center and all the rest around him. They aim at applying and acting to meaningful understanding rather than sterile memorization and rote memory. They relieve the trainee from a passive receiver and place emphasis on high interactivity, collaboration, technology, science advances, and effective strategies [5]. Below, a range of techniques, methods and teachings are presented that could be used for more efficient and up-to-date education [11]. For a better illustration of the concept, the content and the correlation of the techniques and methods were grouped together. This, in any case, does not imply that techniques that are not placed in the same group are strange to each other and that when applied one another cannot work complementarily. They all adopt features that make them attractive, appropriate and efficient, but a number of criteria highlight which one or which ones are the most appropriate.

Group 1

- Problem Solving
- Decision-making Method

Group 2

- Debate
- Avalanche
- Brainstorming
- Questions and discussion inspired by Socrates method (maieutics) [18]

Group 3

- The Jigsaw Method

- Teams, Expert Groups
- Games, Role playing
- Project Method, Interdisciplinary teaching
- Case study
- Dramatization

Group 4

- Experiment
- Models-Modeling -Using software in teaching
- Multimedia presentation

Group 5

- Learning Stations
- Educational Visits, Theater-Cinema

Group 6

- Demonstration
- Description and explanation
- Concept maps - Virtual representation
- Fairy tale

The choice of the appropriate method depends on the age, the stimuli, the knowledge and the background [1] of the learners, the goals and the strategies [11] of the teaching, the content and the objectives set for the environmental education, the trainer's judgment, the time available and infrastructure.

4. CONCLUSIONS – DISCUSSION

Based on the findings of the research in which the apprentice starred, the weaknesses, concerns and dissuasive tendencies in environmental education were perceived and his intentions, needs, attitudes and perceptions were clarified. In addition, solutions and suggestions for action and mobilization were expressed, but most important the main request of young people for radical changes in teaching, methods and learning techniques was expressed and depicted [11] [4]. As a result of all this, an innovative model of education that respects the apprentice is designed and characterized as a learner-centered model which focuses on application, motivation, action, inspired and based on efficient strategies [14]. Subsequently, on this model a range of methods and techniques was presented distinguished by high interactivity, participation, use of groups, dialogue, actions and use of technology. In the effort to choose the most appropriate one at a time, the question of which is the best is also addressed. The answer is that there is no good or bad method, because in each individual case some method will be seen as the most suitable. For example in preschool and small classes of elementary education and environmental education, is singled out and recommended by group 6 the teaching through fairy tale, games and multimedia, while in larger classes of primary schools through Learning Stations, Experiment and Project Method. Moreover, for the first classes of the secondary education, the Decision Making Method, the Jigsaw Method, Dramatization and the Method with questions and discussion inspired by Socrates method (maieutics) [18] stand out. While in larger classes that children have developed a good level of maturity and knowledge, methods of the second group can be approached, such as Debate, Interdisciplinary Teaching, Brainstorming and Avalanche.

Finally, the Problem Solving, Expert Groups, Case Study and the use of modeling (modeling) and software, which is a basic tool in scientific research, are particularly recommended in higher education, especially when the representation and study with the use of real objects seems impossible. Such an integrated and innovative model of education offers many opportunities and resources to young children and, at the same time, good coordination and good organization makes it capable of approaching in an alternative and efficient way Environmental Education, Environmental awareness and Ecological education so as to provide the best strong results for the environment as well as for the whole society.

References

1. Dietz, T., Stern, P.C. and Guagnano, G. A. (1998). ΄Social structural and social psychological bases of environmental concern΄. **Environment and Behavior**, 30 (4), 450–471.
2. Flogaiti E. (1993). **'Environmental Education',** Ellinikes Panepistimiakes Ekdoseis (Greek Academic Publications).
3. Flogaiti, E. (2006). **'Education for the Environment and Sustainability'**. Ellinika Grammata.
4. Georgopoulos A., Tsaliki E. (1993). **'Environmental Education (Principles, Philosophy, Methodology, Games and Exercises)'**, Gutenberg.
5. Hart, R. (2011). **'The children participate',** (assiduity K. Tamoutseli), Epikentro.
6. IUCN. (1970). International Working Meeting on Environmental Education in the School Curriculum. Carson City, Nevada, USA.
7. Kousouris Th., Athanasakis A. (1994). **'Environment, Ecology, Education'**, Savalas.
8. Maloney, M.P. and Ward, M. (1973). 'Ecology: Let's hear from the people'. **American Psychologist**, 28 (7): 583-586.
9. Manual for Environmental Education. (1992). Ministry of National Education and Religious Affairs - U.N.E.S.C.O. , Athens.
10. Papadimitriou B. (2006). **'Environmental education in the school. A timeless view'**, G.Dardanos Publications.
11. Pressley, M., Harris, K.R., & Marks, M.B. (1992). 'But good strategy instructors are constractivists'. **Educational Psychology Review**, 4, 3-31.
12. Shallcross,T.,Robinson,J.,Pace,P.,Tamoutseli,D. (2004). 'The role of Students'voices and their Influence on Adults in Creating more sustainable Environments in three schools'. **Improving Schools**,Vol10: 72-85.
13. Skanavis, K. (2004). **'Environment and Society: A Relationship in Continuous Evolution'**, Kaleidoscope Publications.
14. Steg, L., Perlaviviute, G., Werff, E. and Lurvink J. (2012). ΄ The Significance of Hedonic Values for Environmentally Relevant Attitudes, Preferences and Actions΄. **Environment and Behavior**, 46 (2): 163-192.
15. UN. (1992). Report of the United Nations Conference on Environment and Development, Rio de Janeiro: UN editions.
16. UNESCO. (2005). UN Decade of Education for Sustainable Development 2005-2014: International Implementation Scheme – Draft, Paris.
17. https://el.wikipedia.org/wiki/ Environmental education (accessed September 5th ,2017).
18. http://old.primedu.uoa.gr/sciedu/new_ant/new_ergal.htm (accessed October 1st , 2016).



Sustainable architecture, planning and development - Urban environment

SUSTAINABLE URBAN PLANNING AND ENVIRONMENTAL IMPACTS: FROM THEORY TO PRACTICE THROUGH INTERNATIONAL CASE STUDIES

E.K. Oikonomou* and K. Kalkopoulou

Department of Transportation and Hydraulic Engineering, Faculty of Rural & Surveying Engineering, Aristotle University of Thessaloniki, 54124 Thessaloniki, Hellas

*Corresponding author: e-mail: eoikonom@topo.auth.gr, tel: +30 2310 994360

Abstract

It is widely recognized that there is a strong relation between planning, sustainable development and environmental management: planning is an essentially collective, public interest activity, which operates to secure the efficient and effective development and use of land (in the public interest), and today a planning system should aim at guiding policy formulation and decision making towards the goal of sustainable development. In most developed countries, the planning system is seen as a key instrument in the delivery of sustainable development. Effective use of resources and materials, energy efficiency, sustainable water resources management, atmospheric conditions and climate factors and effective waste management towards a cycle economy reflect some crucial parameters that can be related to planning in the 21st century.

In the present paper, examples of how sustainable planning strategies are implemented in several urban areas internationally, are presented and conclusions are reached towards the target of sustainable communities and high quality of life in urban areas. Furthermore, it is examined whether and how the new Hellenic planning framework, as described by the Law 4447/2016, is capable of establishing a stronger connection between future planning projects and sustainable development in communities and urban areas. Special focus is placed on Local Spatial Plans, which reflect the new key instrument for sustainable planning of Hellenic municipalities, while only predictions can be made, as the new planning framework has not yet been implemented in practice: the technical requirements of the new planning projects have just been enacted in June 2017 (Ministerial Decision 27016/2017). Therefore, assumptions can be made, based on similar planning projects' experience, on the efficiency of the new tool in promoting sustainable urban planning, diminishing the urban 'footprint' of Hellenic municipalities and dealing successfully with bureaucratic processes in planning projects until their final approval by the necessary Presidential Decree. It is predicted that Local Spatial Plans of the new Law 4447/2016 will be more effective in protecting ecologically sensitive areas, promoting more effective waste management and sustainable transport mobility; however, they will demand a great effort and extended time to be finally, approved by a Presidential Decree.

Keywords: Sustainable urban planning, General Local Plans, Local Spatial Plans, The Law 4447/2016

1. INTRODUCTION

Planning, as a system or an essentially collective, public interest activity, is regarded as a key issue towards sustainable development, for many reasons: in most developed countries development plans may include specific 'green' measures; secondly, environmental subjects may be placed at the front

of the plans, affecting the strategic options of the plans in other issues; and thirdly, development plans may use sustainability criteria in all of their proposed development policies. Thus, land-use planning is expected to meet the most critical objectives of sustainable development, such as economic competitiveness, urban regeneration, rural diversification, sustainable transport and mobility schemes, social inclusion, health and safety, and creation of sustainable communities. In order to meet such targets, the planning system may: develop policies related to renewable energy supply and use; promote sustainable transport by reducing traffic volumes, especially in cities, and encouraging cycling and walking; develop waste management practices based on the implementation of recycling and waste minimization methods; protect habitat, ecologically sensitive areas and wildlife sites, as well as cities' green space; and, finally, protect surface and ground water bodies, as well as minimize air pollution, especially in cities and industrial areas [1]. As a result of this, General Local Plans, as planning projects at municipality level, aim at promoting sustainable economic development, encouraging and supporting of regeneration and social justice, and maintaining and enhancing of the natural heritage and built environment quality [2]. General Local Plans influence economic development and environmental protection by four main means: they offer inspiration, commitment, guidance and control [3]. However, planning entails a participative democratic political system in order to be considered as an effective tool for the conservation of resources and the control of pollution and therefore, a necessary condition for the achievement of sustainable development [4].

Simultaneously, the notion of sustainable communities is in the center of planning attention, followed by the ideas and values of democracy, public participation, social and ecological harmony, and social cohesion [2]. And sustainable communities include the flexibility to adapt to new conditions, in order to cover the economic and social needs of their members, as well as enhance a high-quality environment [5]. Therefore, sustainable communities are based on: professionals that support with their knowledge all other community members; community problems identification by all members' participation; solutions to problems deriving from community members; introduction of sustainability issues and indices to all community activities; public participation and consultations at all levels of decision-making; and finally, social and cultural development by contribution of all community members [6]. Major sustainability criteria for such communities and urban areas refer to issues of local governance, urban design, innovation and competitiveness, consumption patterns, resources management, global change impacts, urban transport and mobility, public space, spatial development, etc. [7]. Especially for cities in developed and high-industrialized countries, the environmental targets are set towards: minimization of per capita energy consumption and air emissions; minimization of impacts to natural resources and ecosystems; use of renewable resources, replacing fossil fuels; minimization of use of toxic substances and materials with substantial ecological footprint; and urban design enhancing high quality of life through citizens' health protection [8]. For this reason, the idea of urban ecology has also been developed since the 1990s, which regards urban areas as ecosystems, concentrating its efforts in assessing the urban environment and its biodiversity, in order to ensure better quality of life and high standards for their citizens [9]. Eco-cities show major emphasis on their structure, by copying the structure of the nature, while they include mostly two strategic goals: sustainable urban mobility and urban biodiversity conservation [10].

2. PLANNING PARADIGMS TOWARDS SUSTAINABLE COMMUNITIES

Following the trend of the 1980s and 1990s, related to the strong relation between planning and environmental sustainability through the urban environment, many examples can be found in European cities:

- In Berlin, Block 103 is mentioned as an example of successful urban and social regeneration by transforming old buildings, occupied by several citizens (squatters), to modern ecological buildings, using new materials for energy efficiency, and showing emphasis on water resources consumption and green space available. After the regeneration project, the squatters were offered the opportunity to own the apartments they occupied. In Berlin, in the area Mitte another

regeneration project took place in the 2000s, as an effort to make the capital of Germany cleaner, 'greener' and 'friendlier' [11].

- In Manchester and Glasgow, major urban regeneration projects took place in the city centers (roads "Crown" and "Merchant City" in Glasgow and "Hulme" and "Whitworth" in Manchester), by enhancing housing activities in the city centers, as well as cultural projects e.g. the Museum of Science and Industry in Manchester and Glasgow Royal Concert Hall, as an effort to 'revive' the central urban areas [12]. The 'Manchester 2020' plan involved an effort to change and ameliorate the urban environment, by: conservation, restoration and protection of the natural environment, farmland and assets critical to public health and safety; conservation, restoration and protection of cultural and historic resources; redevelopment of commercial centers and areas with mixed land-uses; concentration of development around transportation nodes and major transportation corridors; and expansion of housing opportunities and design choices in several housing types. The plan also set a number of specific goals and targets e.g. for less 'greenhouse' gases emissions, less energy consumed, less traffic loads in urban areas, more green space in urban areas, introduction of renewable energy resources and more jobs related to environmental protection and management [2].
- In Parma, plastic wastes are transformed into building material and in Rimini, an eco-station was created for waste management by former drug addicts. The Oeiras project, a successful program in the metropolitan area of Lisbon, reduced the amount of wastes disposed in the landfill, offering also the inhabitants the possibility to produce a high-quality fertilizer for their gardens [11].
- In many European cities programs for minimization of the use of vehicles in the city centers were implemented: Naples and Perugia historic centers are no more accessible by vehicles; Amsterdam is the capital city of the bicycle; in Copenhagen and Münster approximately 35% of all trips are done by bicycles; in Zurich and La Rochelle bicycles are offered for free to inhabitants and visitors; in many European cities the trams are important factors of the transport systems; in Heidelberg, Freiburg, Basil there are areas of low noise; and in many Danish cities, in Paris, Barcelona, Maastricht programs for road accidents minimization were implemented, as well as, efforts to enhance the social bonds of the citizens [11].

Almere and Milton Keynes are two cities in the Netherlands and Britain, both designed in the 1970s, for a population of around 200,000 inhabitants; however, they are mentioned as a typical example of how urban planning affects urban mobility, which is related to major environmental impacts. The different philosophy in urban design between the two cities led to five times more use of the bicycle in Almere, although the average trip distances in both cities are almost the same (around 7 km), while local trips are 20% more in Almere, reflecting the notion of its inhabitants to support local markets. On the other hand, for this average trip of around 7 km in both cities, the time needed is 30% more in Milton Keynes, which reflects worse traffic conditions than in Almere, with negative impacts in energy (fuel) consumption for transport and air pollution [2].

Table 1: Basic urban transport characteristics for Almere and Milton Keynes, both designed for a population of around 200,000 inhabitants

Basic urban transport characteristics	Almere	Milton Keynes
Percentage of trips by private vehicles (%)	43.1 %	65.7 %
Percentage of trips by bicycle (%)	27.5 %	5.8 %
Average distance travelled per trip (km)	6.85 km	7.18 km
Average trip duration (minutes)	11.0 min.	14.5 min.
Percentage of local trips	74 %	60 %

- In Swansea, after the industrial decline of the second half of the 20th century, the urban regeneration project led to: the Enterprise Zone in 1981, the first and largest in Britain, which contributed to physical and economic inner city regeneration; the Maritime Quarter redevelopment comprising the old docklands of the city offered physical and economic benefits to the waterfront; and promotion of housing in the city center by expanding the residential function in inner city area, bringing back people to the center [13].
- In Greenpoint-Williamsburg of Brooklyn, New York, one of the poorest and degrades urban area of the city, a program of environmental benefit was implemented, in cooperation with the Municipality and local people; the aim was environmental monitoring by local people, in order to reveal pollution sources and environmental problems, so as to be dealt successfully, early as discovered. This program enhanced social cohesion and the development of trust and cooperation between the local people [2].
- In Singapore and Hong-Kong an excellent public transport system was developed, especially by using modern electric trains and small, flexible buses. Apart for pedestrianization schemes and many new bicycle routes, Singapore imposed taxes on citizens for their private vehicles. Finally, a major parameter in Singapore was also the use of technology in planning, e.g. by enforcing e-commerce, while the government was committed to offer innovative and transparent policies and guarantee for security in the urban area and political stability. Singapore is now considered as a 'smart' city for the effective transport system.
- In Frankfurt, the major business and economic European center. a roadmap for a 100% renewable energy supply was set in 2008, defining the main strategies and instruments to achieve this goal by 2050. This master plan for 100% climate protection involves 50% reduction of energy consumption, which will be achieved by energy savings and energy efficiency. Energy will be produced 50% in Frankfurt and the rest in the Region of Rhine-Main. Another strategic plan of the city in 2010 is related to noise reduction, by new green belts with bicycle lanes only, upgrade of rail infrastructure and the use of new materials in road construction. During the period 1990-2010, water consumption by households and small enterprises was reduced by 14% and the surface of green space and recreational areas was increased by 16.5% [14].

Curitiba, the 7th in size city of Brazil, is well known for its public urban transport generated in the 1980s, its integrated urban planning and the less number of accidents per 1,000 vehicles in Brazil. City expansion to cover vast housing needs was followed by commercial activities and several other services developed in new urban areas, while major pedestrianization schemes were implemented in the city center, together with a renovation program of historic buildings. The result was not only to make the city center accessible, eco-friendly and attractive to citizens, but also to attract various cultural activities too. The urban public transport system serves more than 1,9 million inhabitants daily, by the use of 2,160 buses. Bus lanes and traffic management succeeded in cutting down economic expenses; consequently, it was realistic to implement an economic transport policy, which was in favor of many inhabitants with low annual income. The bicycle network includes more than 120 km of bike lanes, mostly leading also to parks and recreational sites (Figure 1). In urban planning, the period 1960-1980 was characterized by successful cooperation between the central government and local stakeholders, while flexibility in solving quickly urban problems and public participation in decision-making were in the center of its attention. Nowadays, Curitiba is believed to be the ecological capital of Brazil with 28 parks and forest areas in the city, with an average surface of 52 m^2 per inhabitant. Ecoville is famous for its high buildings surrounded by dense green space in between them (Figure 2). The mobilization of local people in environmental management issues was catalytic in enhancing green space, in waste management issues, such as recycling of several waste streams as well as organic wastes (Figure 3). Social issues were also dealt with success: social housing was constructed for citizens with very low income; the 'Lighthouses of Knowledge' project in the 1990s constructed 50 small buildings in the city, offering books and internet access to citizens, as well as organizing several cultural activities (Figure 4); 40 special social centers offer for free food

and education to homeless children, while industries, which reflect a major economic activity in Curitiba, cooperate in the project for homeless children, offering them the opportunity to work in some special jobs like gardening or even office work; and two small buildings, located in two major road corridors, . The industrial activities in the city area diminished their environmental impacts by: using heat produced as by-product for heating purposes of communities; re-using and recycling of wastes; and implementing the basic principles of industrial ecology. The example of Curitiba is strongly related to a multi-level successful cooperation between the municipality, several stakeholders and local people [15].




Figures 1 and 2: Bicycle lanes in Curitiba of the 120 km network and the area Ecoville with high buildings and much green space in between them




Figures 3 and 4: Effective urban waste management and a 'Lighthouse of Knowledge' building

- Ljubljana, the capital city of Slovenia, is also famous for its environmental performance. The surface of green space in the city represents approximately the 2/3 of the total urban area, which reflects an index of 560 m^2 per inhabitant, including parks, forest areas, farmland and protected natural areas, as a result of a rehabilitation program of brownfields. "Natura 2000" protected areas represent more than 20% of the surface of the urban area. The bicycle lane network, a network to rent a bicycle, a monthly card for public transport system that offers a transfer trip for free for the first 90 minutes and a small number of electric vehicles reduced traffic loads in the city center, as well as air pollution. In 2007 an ecologic zone in the city center was introduced, where vehicles are not allowed to enter, and in 2013 it was expanded. The last decade there is a major program for public buildings, in order to reduce energy consumption mostly in schools, nurseries and in sport centers. In the city center, the urban waste disposal network is underground and a program for waste minimization was implemented; as a result of this, the annual average amount of waste disposed per capita was diminished by 52 kilos in three years, from 2009 to 2012. A major strategic goal is also set: to inform citizens and professionals on innovative projects, activities,

competitions, issues and problems, which are related to the environment, so as to participate in decision-making or expand their professions [16].

- In Vancouver, the Canadian city with the smallest footprint in per capita CO_2 emissions of all cities in North America, the Greenest City Action Plan aims at a strong local economy, inclusive and vibrant neighborhoods, and an internationally recognized city that meets the needs of future generations. An important role is identified in local people, governmental institutions and private stakeholders, which need to cooperate effectively to take initiative and action to make change possible. In the economic sector, 'green' professions are enhanced, as well as 'green' economy in general, including 'green' technology, products, construction, urban transportation, waste management, etc. A good example is the Olympic Village, which was constructed in 2010 for the Winter Olympic Games and used methods for energy efficiency and reduction of energy consumption produced by fossil fuels, while today the area is used as a residential area, mixed with commercial land-uses, services and recreational parks. In the transport sector, walking and cycling were increased from 18% to 22% of total trips, while with the Program 'Share the Road', in four neighborhoods for some hours every day, vehicles were not allowed to enter and roads were transformed to playgrounds. In waste management, the 'zero-waste' production was set, including waste minimization, recycling and reuse, and the Vancouver Tool Library was invented, in order to share several tools for do-it-yourself and gardening. Finally, the Program 'Our Welcoming Community' aims at social inclusion of any vulnerable citizens or groups, so as to help them and support them with their problems [17].

In Hellas, the example of the village Anavra should be mentioned as a vey interesting example of building sustainable communities. Anavra, a small mountainous village in Thessaly Region, Regional Department of Magnesia, seemed to be a typical Hellenic mountainous village, difficult to access, with poor infrastructure in terms of road, social aspects, and environmental management, and its economy was based on livestock farming. In the 1990s a major change took place, by implementing a scheme of redevelopment in terms of infrastructure projects and economic activities, as well as environmental protection: all livestock farms were transferred to three new livestock parks, well-organized, with freshwater installation and waste management techniques; pasture areas were made accessible by new roads and water infrastructure; organic farming was set as an important target in the primary sector; seminars and education programs were organized for the farmers; the road network was reconstructed, as well as the water supply network, and a sanitary landfill was constructed in 1994; regeneration of public space took place by several projects for pedestrian roads, parks, car parking and appropriate lighting; new buildings were constructed for the kindergarten, the primary school, the athletic center and housing for the teachers to cove their needs for free; a folklore museum was opened, a community library was organized and a cultural center was built to support several events, conferences, etc.; energy is produced by anaerobic digestion of livestock wastes, which is used to heat water from a central boiler and heat all houses in the village; the Environmental – Cultural Park was established in the natural environment nearby. Sustainable economic activities provide jobs for all citizens and zero unemployment is identified, when in Hellas unemployment rates are more than 25% the last years of the economic crisis. Anavra community was funded by some economic resources deriving from a private investment of a wind-energy park, located in the mountainous next to the village and this is how it was possible to support such development and social projects. Apart from funding, there was a Mayor with a vision, looking for the change and local people who were happy to participate in this project. Now the "miracle" of Anavra is fading away: since 2011 Anavra has been part of the Municipality of Almyros, with 43 settlements and 18,614 inhabitants (census 2011); thus, the economic resources from the wind farm are now available to the whole municipality and not the Anavra community only.

3. PLANNING PROSPECTS IN HELLAS: IS IT POSSIBLE TO MAKE IT HAPPEN?

3.1 The past experience

Sustainable communities, ‘smart’ cities and many other titles are given to efforts to make urban areas sustainable in terms of energy, transport, waste management, social inclusion, economic development, etc. In European cities, as well as many other cities all over the world, many examples can be found towards these goals and targets, while local authorities and citizens offer their commitment to ameliorate the quality of life in urban areas and leave a better world to future generations. However, in Hellas, many cities are still one or two steps backwards and very few examples can be found, describing environmental planning activities. This may be explained by looking briefly at the history and experience of planning in Hellas.

Although town planning legislation in Hellas has existed since 1923 (a Decree about Town Plans), it took 60 years to establish technical requirements for urban and local planning projects at the level of each community administrative boundaries (Law 1337/1983 “On the Extension of Cities and Towns, Urban Development and Associated Arrangements”), while in the 1980s the Urban Reconstruction Operation was responsible for many Community Local Plans and many urban plans all over the Hellenic Territory, aiming at covering future housing needs in many settlements and controlling unauthorized urban sprawl [18]. It is worth mentioning that the Law 1337/1983 dealt only with urban areas, areas within their town limits, and there was no provision for rural areas, all areas in-between urban areas; thus, there was no control of land-uses leading to conflicts in land-use patterns, which were defined according to private investments.

It is not until the late 1990s that the Law 2508/1997 “Sustainable Urban Development of Cities and Towns of Greece and Associated Arrangements” and the Law 2742/1999 “Regional Spatial Planning and Sustainable Development”, try to keep up with European planning policies, covering spatial development at urban, regional and national level and completing the institutional framework of the contemporary planning system in Hellas [19]. The Law 2508/1997 regulates spatial planning at the municipality level (General Local Plans, GLPs), which involves many settlements and their in-between rural areas. It is an important law, bringing together environmental issues, sustainable development and planning at a local level, as it clarifies that: GLPs are obligatory for all municipalities and so land-use maps are produced, for the Hellenic territory; regeneration and rehabilitation schemes of declining urban areas are in the center of attention of planning; there are specific implementation mechanisms (urban planning studies) that are part of the whole planning process; and, each GLP deals with the definition not only of land-use patterns within urban areas of all of its towns, but also of the whole area of the municipality (urban and suburban land, agricultural land, forests, etc.). Finally, UPSs are conducted in order to implement GLPs’ proposals, defining new building areas, new streets, open green space and space for social facilities, building regulations, etc. and the whole planning process is terminated by the Implementation Plan, which is officially recorded in the appropriate Land Registration Office. The Law 2742/1999 provides with all necessary regulations in relation to the targets and the principles of planning [20]. It is the first legislative document introducing the environmental dimension in planning and this is proved by: firstly, the adoption of the concept of sustainability, as perceived in the European Union, in regional planning; and, secondly, there is an extensive reference on the protection of nature (article 15) and on the necessary requirements in order to create managing authorities of the protected areas.

Planning in practice suffers from many deficiencies: it takes 5-10 years for the approval of a GLP by the competent public authorities and 10-20 years for the approval of urban planning studies by Presidential Decrees, as the State Court interferes in the approval process; public participation is generally weak; bureaucracy and excessive regulation, as well as too many petitions for annulment of administrative acts and administrative judges in Hellas, producing too many norms and principles in spatial planning and a failure in successful decentralization of spatial planning responsibilities, as discussed by Oikonomou (2013) [21]. Therefore, some new legal framework has been established

since 2014, making changes in the "heart" of the planning system in Hellas, in an effort to tackle the deficiencies recognized by many authorities and practitioners.

3.2 The new legal framework

The Law 4269/2014 "Spatial and urban planning reform – Sustainable development." was enacted in the 28th June 2014: in Part A the new planning system and its tools are described, as well as the basic processes for planning at all levels; and in Part B the new categorization of land uses is set, by changing completely the old Presidential Decree for land uses of 1987. The latter was very useful and important because since 1987 many new economic activities and land uses have risen, as well as activities related to environmental management and protection, such as wastes recycling, composting, etc. or renewable energy resources infrastructure, complex touristic development, technology parks and industrial activities related to innovation, etc. However, there was not enough time for ministerial decisions to be enacted in order to define some necessary details and technical requirements of the new planning tools and projects, since elections took place in Hellas in January 2015 and the new government elected abolished this law.

The Law 4447/2016 "Spatial planning – Sustainable development and other provisions." was enacted in the 23rd December 2016, replacing the abolished Law 4269/2014, at least the Part A, because the issue of a new framework for up-to-date land uses is not included in the new legislation. Its most important aspects are briefly mentioned below: in Part A all new definitions are described, as well as the major parameters of the new planning system; Part B is related to Strategic Spatial Planning (SSP), by describing the tools of Special Planning Frameworks and Regional Planning Frameworks; Part C is dedicated to Regulatory Spatial Planning and refers to the Local Spatial Plans (LSP), the Special Spatial Plans (SpSP) and Urban Implementation Plans; and several other provisions are mentioned in the rest of the Law e.g. aspects of waste management and recycling issues (green points).

The Law 4447/2016 is important as it introduces a completely new planning system with novel planning tools, especially at municipality level with Local Spatial Plans and Urban Implementation Plans, as well as Special Spatial Plans aimed at spatial development mostly of public parcels of large areas for touristic or other exploitation and development. The past planning system with General Local Plans and Urban Planning Studies needed an average period of 15 – 30 years in order to be approved and implemented; however, the Law 4447/2016 defines that Local Spatial Plans include all aspects of the abolished General Local Plans, but also the regulatory framework of the Urban Planning Studies as well and this is the reason why the planning projects are approved by Presidential Decrees. More specifically, Local Spatial Plans define all land uses in the municipality area and in detail in every town and settlement of the municipality, while they also define land use patterns in each town area, as well as possible urban expansions to cover housing needs or specific future economic activities. They also define the building regulations that are enacted in each urban area, within its town limits. Thus, the new planning framework sets a target of planning at municipality and town level simultaneously and this way, it seems that new planning proposals will be easier implemented in less time than in the past. Planning projects of all levels are also followed by environmental appraisal by Strategic Environmental Assessment, as described by the Ministerial Decision 107017/2006. Two Ministerial Decisions 27016/2017 "Technical requirements of the Local Spatial Plans" and 27022/2017 "Technical requirements of the Special Spatial Plans" define the details of these planning tools. The technical requirements are quite detailed, however, there are questions to be answered when the first planning projects will be assessed and implemented. The Ministry of Environment and Energy is currently seeking for funding, in order to commence Local Spatial Plans in municipalities in all Hellenic Regions and a possible solution could be to exploit EU funding of the Programming period 2014-2020. When the first pilot Local Spatial Plans begin, planners and all teams participating in the problems will face up difficulties and problems related to technical and procedural issues mostly.

4. DISCUSSION AND CONCLUSIONS

After presenting successful planning examples of cities all over the world, towards sustainable urban development and commenting on the immaturity of the planning system in Hellas, since the early 1980s, some conclusions may be reached related to the new planning framework that has been enacted since 2016, which seems to be some steps forward than the planning framework of the past, offering an opportunity to propose, approve and implement planning projects of several levels quicker than before. It could also be criticized that the new planning system, in terms of technical requirements, is in favor of the use of modern tools, such as Geographic Information Systems, digital spatial data available, etc. More specifically, the strengths of the new planning system can be summarized as follows:

It offers the idea to municipalities of “one stop shop”, meaning that with just one planning project (Local Spatial Plan) the municipality will be able to set all necessary planning and building regulations, measures to protect the natural, cultural and built environment, proposals to enhance sustainable economic development and social inclusion. Municipalities will have the opportunity to plan starting from a more strategic level to a more detailed level, solving problems arising from the implementation General Local Plans approved from 2000 up until now, as well as several environmental issues, such as waste management, water resources management flood risk minimization programs, etc.

- The technical requirements of the Local Spatial Plans imply the use of modern tools and technology aspects e.g. the use of Geographic Information Systems, satellite spatial data and satellite images, data from the operating cadastral offices related to the properties of all land parcels, data from the operating Forest Cadastre to define officially forest areas in the municipality, etc.
- By using digital spatial data and Geographic Information Systems, Local Spatial Plans will be more flexible, easier to organize and present the necessary and available data in maps and the aftermath, after their final approval by a Presidential Decree, will be related to the fact that the LSP will be a valuable tool for the municipalities to be used for land uses monitoring in the future, etc. Consequently, LSPs will add value to the municipalities and they will be used as a valuable tool from several municipal authorities for many purposes. They may well contribute to implement e-governance at local level, with all advantages related to the establishment of transparency and democracy through participatory in decision-making.
- It is also an excellent opportunity to organize effectively all data used in the LSP in appropriate data bases and for this reason, all data will be assessed for its quality and reliability, consequently, there will be references for the data used, affecting positively the quality of the LSP. Thus, the GIS will be able to support municipal authorities even after the LSP is approved.
- LSPs, as being approved by Presidential Decrees, will have the opportunity to change any other plan of the past, “correcting” it, in favor of environmental protection and generally, local communities. It is underlined that urban legislation in Hellas seems to be a “labyrinth”, since the 1980s, as many important issues defined in laws, ministerial decisions, etc. have been “blocked” by the State Court several years after they have been enacted. By this way, it was impossible for many planning projects to be implemented by local authorities. Such deficiencies may be dealt with successfully by LSPs because before being approved by Presidential Decrees, they will be examined by the Law Department of the State Court, controlling whether all proposals are compatible with every piece of urban legislation.

Although the new legislative framework reflects a major “step” forward for planning in Hellas, there are some questions still waiting for an answer:

- First of all, digital spatial data in Hellas is still missing: only a small percentage of Hellenic territory is covered by the cadastre, the forest cadastre; especially in rural territories cadastre is

more missing, because emphasis was shown in urban areas; and much other spatial data, such as town limits, "Natura 2000" area limits, etc. exist in digital form, but their reliability is doubtful, while this is the most important parameter. It is easy to have access to a polyline in its digital form, but it is very difficult to find a "reliable" digital polyline. Consequently, LSPs will have to struggle with this issue, unless they stay "inactive" until the projects of cadastre and forest cadastre are finished. However, this could not be the proper solution; on the other hand, data used in LSPs has to be reliable also because such studies are approved by Presidential Decrees and mistakes are not "forbidden".

- Secondly, the total time needed from the beginning of a LSP Study to the final approval by Presidential Decree is estimated in at least 10 years, taking into consideration the past experience of the Urban Planning Studies, as the planning process is almost the same. Approval by Presidential Decree means that at the end of the whole process of planning, the outcome as well as some other crucial parameters e.g. the results of public consultations and participation are submitted to the Ministry of Environment and Energy; then the whole process is checked and the proposed plan is finally examined by the Law Department of the State Court – all proposed plans of all Hellenic municipalities will have to pass this final legal control, which will result in great delays.
- Thirdly, delays in time needed for the final approval of LSPs by Presidential Decree may bring more delays and the need to change some planning proposals of the LSPs. For example, the Special Framework of Spatial Planning and Sustainable Development for Tourism was enacted for the first time in Hellas in 2008 and in 2013 a new Framework was enacted in order to include complex and major investments in tourism. However, sometime in 2015 the State Court decided that the Special Framework of 2013 was not compatible with Hellenic Constitution and few months later the same decision affected the Framework of 2008; Hellas has no more a strategic plan for tourism! And GLPs needed to alter many of the proposals each time there was a new decision of the State Court related to the Framework of Tourism. This is an example of how more delays may be introduced in the whole planning process.
- Finally, and most important, it is not at all obvious how such LSP Studies may introduce sustainable criteria in environmental management, economic development and social inclusion or how they can enhance initiatives and projects like the ones described in paragraph 2. Past experience has shown that municipalities and local people are willing in promoting their own interests, while many times environmental protection is regarded as an obstacle to their targets. Although LSPs will be approved by Presidential Decrees, this does not guarantee that the plans will include such proposals in order to promote "smart" cities, sustainable communities, etc., but they only guarantee that the plans will be 100% compatible with all urban legislation in action.

To sum up with, there are many reasons to be optimistic about the new legal framework for planning and the new planning system that is introduced. New procedures need to be implemented and public participation should be enhanced in order to succeed in producing the best possible plans for local people. However, it would be of great benefit to planning, if all legislation related to spatial and urban planning could be simplified and if more tools related to e-governance were introduced in the new planning process.

References

1. Selman P.H. (1996). '**Local Sustainability: managing and planning ecologically sound places.**' Paul Chapman Publishing.
2. Smith M., Whitelegg J. and N. Williams. (1998). '**Greening the Built Environment.'** Earthscan Publications Ltd.
3. Davidson F. (1996). 'Planning for performance: requirements for sustainable development.'. **Habitat International**, vol. 20, no. 3, pp. 445-462.

4. Blowers A. (1992). ‘Sustainable Urban Development: the Political Prospects.’ in: **Sustainable Development and Urban Form**, (ed. M.J. Breheny), Pion Limited.
5. Roseland M. (2000). ‘Sustainable community development: integrating environmental, economic, and social objectives.’ **Progress in Planning**, vol. 54, pp. 73-132.
6. Hautekeur G. (2005). ‘Community development in Europe.’. **Community Development Journal** vol. 40, no. 4, pp. 385-398.
7. McCormick K., Anderberg S., Coenen L. and L. Neij. (2013). ’Advancing sustainable urban transformation.’. **Journal of Cleaner Production** vol. 50, pp. 1-11.
8. Jepson E. and M. Edwards. (2010). ‘How Possible is Sustainable Urban Development? An Analysis of Planners' Perceptions about New Urbanism, Smart Growth and the Ecological City.’. **Planning Practice & Research,** vol. 25, no. 4, pp. 417-437.
9. White R.R. (2002). ‘**Building the Ecological City.**’ UK: Woodhead Publishing.
10. Register R. (2002). ‘**Ecocities. Building Cities in Balance with Nature**’ Berkeley: Berkeley Hills Books.
11. Mega V. (2000). ‘Cities inventing the civilization of sustainability: an odyssey in the urban archipelago of the European Union.’. **Cities**, vol. 17, no. 3, pp. 227-236.
12. Seo J-K. (2002). ‘Re-urbanisation in Regenerated Areas of Manchester and Glasgow’. **Cities**, vol. 19, no. 2, pp. 113-121.
13. Tallon A.R., Bromley R.D.F. and C.J. Thomas. (2005). ‘City profile Swansea’. **Cities**, vol. 22, no. 1, pp. 67-76.
14. https://frankfurt-greencity.de (assessed February 2nd 2018).
15. Macedo J. (2004). ‘City profile Curitiba.’. **Cities**, vol. 21, no. 6, pp. 537-549.
16. Nastran M. and H. Regina. (2016). ‘Advancing urban ecosystem governance in Ljubljana.’. **Environmental Science & Policy**, vol. 62, pp. 123-126.
17. Holden M. and A. Scerri. (2013). ‘More than this: Liveable Melbourne meets liveable Vancouver.’ **Cities**, vol. 31, pp. 444-453.
18. Serraos K., Gianniris E. and M. Zifou. ‘**The Greek spatial and urban planning system in the European context.**’ Available at: http://courses.arch.ntua.gr/106909.html (accessed February 2nd 2018).
19. Yiannakou A. and A. Tasopoulou. (2012). ‘Sustainable development, planning integration and spatial plans in Greece: from the institutional framework to planning practice.’. Proc. **26th Annual Congress of the Association of European Schools of Planning,** eds. M. Blamir et al., Ankara, Turkey.
20. Christofilopoulos D.G. (2002). ‘**Cultural Environment – Spatial Planning and Sustainable Development.**’, Economy & Law, P.N. Sakkoulas (in Greek).
21. Oikonomou E.K. (2013). ‘Planning for performance in Greece: the challenges and opportunities ahead for development and environmental protection’. Proc. **4th Int. Conf. Environmental Management, Engineering, Planning and Economics (CEMEPE 2013) and SECOTOX Conf.**, eds. A. Kungolos, K. Aravossis, A. Karagiannidis, P. Samaras and K.W. Schramm, Mykonos Island, Hellas, pp. 994-999.

A NOVEL METHOD FOR STRATEGIC ENVIRONMENTAL ASSESSMENT OF PLANNING PROJECTS: THE CASE STUDY OF THE GENERAL LOCAL PLAN OF GJIROKASTRA MUNICIPALITY, ALBANIA

E.K. Oikonomou* and K. Kalkopoulou

Department of Transportation and Hydraulic Engineering, Faculty of Rural & Surveying Engineering, Aristotle University of Thessaloniki, 54124 Thessaloniki, Greece

*Corresponding author: e-mail: eoikonom@topo.auth.gr , tel: +30 2310 994360

Abstract

The planning system is Albania is currently under reform, while in many municipalities General Local Plans (GLPs) are conducted, with the aim of environmental protection of ecologically sensitive areas, housing needs definition, new technical infrastructure identification, future development action prediction and new building regulations' formulation for urban areas. Within the planning process, there is an effort to enhance public participation, through specific procedures with public hearings and specialists' meetings, promoting publicity and thus, transparency. As part of the planning process, Strategic Environmental Assessment (SEA) studies are also conducted as necessary environmental appraisal studies of the strategic proposals of the GLPs. Such planning and environmental projects include several difficulties related to: lack of experience from public authorities; possible weak public participation and consultation; and expectations from municipalities that may not be met, etc.

A novel method for strategic impact assessment is described in the present paper, reflecting a three-level assessment with the aid of the tool of matrices, which are used in the first step of impact identification, then in the second step of impact prediction and then in the last step of impact evaluation. The purposes of the implemented method are: to be effective in strategic impacts assessment of the GLPs' proposals; to be easy to be used in several SEA studies for GLPs and not just one specific study; to be comprehensive to the public authorities in Albania, which probably do not have much experience in such environmental studies; and finally, to be simple and comprehensive as well, for stakeholders and local people, so as to participate in public hearings and affect positively the process of environmental appraisal of planning projects. The findings of a case study of the SEA Study of the GLP of Gjirokastra Municipality are presented, showing great results and success in the implementation of the tool of matrices in the three-level impact assessment.

Keywords: Strategic environmental assessment, General Local Plan, Matrix, Identification-prediction-evaluation

1. INTRODUCTION

Strategic Environmental Assessment is an impact assessment tool, a systematic process for evaluating environmental consequences of proposed policies, plans and programs – PPPs. SEAs are implemented in PPPs, and their results affect Environmental Impact Assessment studies (EIAs) at the project level [Arce R. and N. Gullón N. (2000)]. According to the definition for SEA, provided by Therivel et al. (1992), it refers to "the formalized, systematic and comprehensive process of evaluating the environmental effects of a PPP and its alternatives, including the preparation of a written report on the findings of that evaluation, and using the findings in publicly accountable

decision-making" [Therivel R., Wilson E., Thompson, S., Heany, D. D. and Pritchard (1992)]. The international regulatory framework for SEA is set by the European Directive 2001/42/EC and the Kyiv SEA Protocol. The former defines a general framework for the environmental assessment of proposed plans and programs prepared for agriculture, forestry, fisheries, energy, industry, transport, waste management, water management, tourism, town and and land use planning, precluding proposed policies, even if they set the framework for lower tiers, as well as excluding plans and programs related to issues of national defense and civil emergencies [Directive 2001/42/EC of June 2001]. It is underlined that the SEA Directive involves general requirements that do not pose restrictions to the Member States, but it leaves space for them to formulate their own procedures in terms of scoping, screening, public participation and consultation, etc. [Risse N., Crowley M., Vincke P. and J.-P. Waaub (2003)] The Kyiv SEA Protocol to the Convention of Environmental Impact Assessment in a transboundary context, prepared by the United Nations Economic Commission for Europe in 2003, is similar to the European Directive, but also includes environmental assessment of proposed policies and legislation proposals; it also shows more emphasis on health issues, impacts of proposed PPPs on human health [United Nations Economic Commission for Europe (2003]. The tool of SEA has also been implemented by several international organizations e.g. the UN Development Program, the UN Environment Program, the USAID, the World Bank, the OECD Development Assistance Committee, etc., in order to offer financial assistance to initiatives deriving from strategic policies, plans and programs that are environmentally evaluated in terms of their possible impacts [Chaker A., El-Fadl K., Chamas, L. and B. Hatjian (2006)].

The main steps on SEA studies involve: screening, by determining the need for SEA, usually from a mandatory list; identifying the necessity and goals of the PPP examined, as well as its relation with other PPPs in force; setting objectives and targets, and establishing indicators; describing the major parameters and aspects of the PPP that are predicted to provoke the most significant environmental impacts; setting the environmental baseline and describing the environmental parameters that are expected to be mostly affected by the proposed PPP; identifying, predicting and evaluating impacts of the proposals and comparing alternative options; seeking mitigation measures to tackle the impacts and describing the necessary monitoring system to be established; organizing public participation and consultations; conducting the final report on SEA; and decision-making on both SEA and PPP examined. These steps are described in the SEA Directive and are included in all relative legislation of Member States, more or less, with minor modifications, as also in Hellas and Albania. Specific issues that are mostly procedural and bureaucratic are considered of less importance and not further discussed for this reason. The SEA process (Figure 1), as described in Hellenic Ministerial Decision 107017/2006, involves the following steps: the competent authority (CA), responsible to prepare a SEA study for the proposed Plan or Program, submits the SEA preliminary report to the responsible for approval authority (RAA); RAA organizes consultation and public participation process; CA organizes one public presentation of the SEA preliminary report and makes it publicly available for 45 days; the findings of the consultation and participation process are taken into consideration for the approval of the SEA by the RAA, otherwise CA is asked to alter the SEA and possibly the proposed Plan, according to these findings and resubmit it to RAA for the final approval. Planning projects and SEA studies are either approved by the Ministry of Environment and Energy or by the Decentralized Authority: in many cases bureaucratic problems arise when the planning project is municipal e.g. a General Local Plan, approved by the Decentralized Authority, while its SEA study is approved by the Ministry because within the municipal boundaries there is a "Natura 2000" protected area.

A similar SEA process exists in Albania. First of all, Albania is part of the Stabilization and Association Process, announced for five Eastern European countries at the Zagreb Summit in 2000, while in order to become an EU Member State, the criteria established in the Copenhagen European Council in June 1993 must be met. Since then, Albania has adopted much European legislation in its national legislation, while the National Plan for European Integration was synchronized with the National Strategy for Development and Integration 2014-2020. Albania has introduced policies through legislation for sustainable waste, wastewater and water management, sustainable planning at

national and municipal level, environmental impact assessment of projects, strategic environmental assessment of plans and programs, and protection of ecologically sensitive areas and nature. SEA was introduced in February 2013 by the Law 91/2013 (on SEA), while EIA was introduced in July 2011 by the Law 10440/2011 (on EIA) and planning projects at municipal level supported the reform of Albania by the Law 107/2014 (on development of the territory). The Albanian SEA process is considered to be simpler and more clarified than the Hellenic one: the competent authority (CA) sends a notification to the Ministry (the one and only responsible for approval authority), including some general information on the proposed plan, the environmental parameters expected to be affected, as well as the need to conduct a SEA study; the Ministry approves the commencement of the process and informs the public about it by a preliminary declaration within 30 days; the CA organizes a preliminary public hearing and consultations with regional authorities in case of a municipal plan, in order to conclude of people's and authorities' opinions related to the most crucial environmental parameters, the opportunities for sustainable environmental management, the environmental factors that may be affected by the proposed plan, etc.; the CA prepares the preliminary SEA report and makes it available for a public hearing as well as consultations with regional authorities; the final SEA report is prepared and the total SEA (SEA report and a report with all opinions of stakeholders, public authorities and institutions participated in the consultations) are submitted to the Ministry for the final approval (environmental declaration).

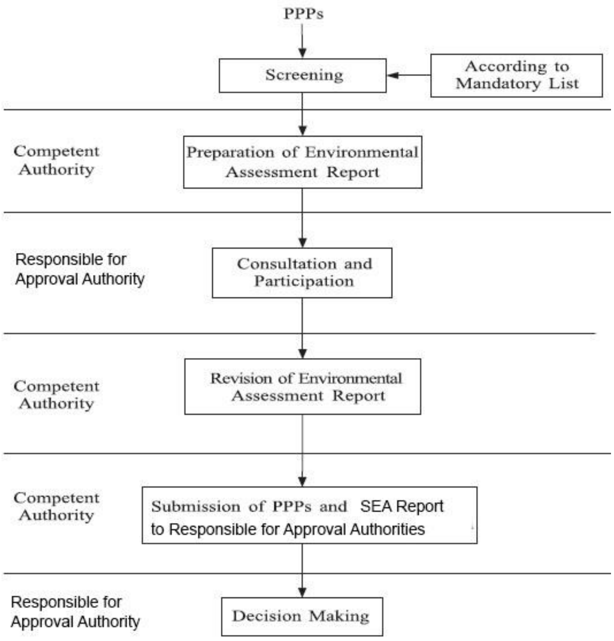


Figure 1: The SEA process, as described in the Hellenic Ministerial Decision 107017/2006

2. COMMENTS ON STRATEGIC ENVIRONMENTAL ASSESSMENT

First of all, the necessity for SEA is based on two major aspects: it counteracts some of the limitations of EIAs, such as additive effects of many small projects (cumulative impacts), indirect impacts and synergistic impacts deriving from different projects in the same geographical area; and it may promote sustainable development by introducing early in strategic planning decision-making process sustainability criteria or more generally, environmental parameters and issues to be dealt with [Therivel R. and Partidario (1996)]. Consequently, its major advantages refer to: taking into consideration environmental issues and aspects while forming strategic action through PPPs; the capability of dealing with cumulative and synergistic impacts, not able to be dealt with by EIA at a project level; promotion of PPPs alternatives; and incorporation of environmental and sustainability aspects in strategic decision-making [Therivel R. (2004)]. What is underlined by Noble (2000) is characteristic: EIA is reactive as it reacts or assesses a particular option, a specific project, while SEA is proactive, by examining alternative options and focusing on alternatives, opportunities, regions and

sectors [Noble B.F. (2000)]. In its worldwide implementation the last 20 years, SEA may be organized in several different ways: firstly, SEA may be introduced as EIA-based, following the requirements of Environmental Impact Assessment (EIA) legislation (uses similar tools for impact assessment); secondly, the SEA process runs parallel but independently from the planning process; thirdly, SEA is part of the planning process; and finally, the SEA framework is defined by the planning process, according to its level of requirements. However, what is really important, reflects the following issues: if SEA is sustainability-led, using sustainability criteria to assess possible significant environmental impacts of proposed PPPs; the extent to which SEA will be accepted, adopted and implemented; the effectiveness in public participation, as a means of increasing transparency of planning and decision-making; the objectivity of the SEA process; and its effectiveness in shaping public decision-making [United Nations Economic Commission for Europe (2003)].

Apart from strategic impact identification and evaluation, the importance of public participation in the SEA process is widely recognized: it can provide valuable information on the proposed PPP and the SEA study, and contribute to identify weaknesses in the study; it can show how groups and stakeholders are affected by the impacts identified by the SEAs; it may reduce the danger of later delays by protest actions against proposed projects and actions; it may help in viable suggestions for mitigation measures and alternative scenarios; it may contribute positively to public awareness, by making citizens more interested in public affairs and more environmentally responsible; and it may reduce time needed for public participation in EIAs, at the project level [Seht von H. (1999)]. However, it is also underlined that: political systems are traditionally based on closed and limited participation procedures; and public participation depends on pluralistic and democratic structures in several countries that are implemented. It is also believed that the SEA Directive requires that the public is involved too late in the decision-making process when alternatives and preferences have already been defined [Kornov L. (1997)].

SEA has also disadvantages, related to the fact that it adds extra cost and time needed for plans and programs approval, and deals with much complexity, as there is an interaction and relevance between many plans and programs between them, which must also be taken into consideration. It is also believed that SEA has generally focused on impact assessment and its proactive role in strategic decision-making, thus leaving implementation of SEA (follow-up) aside [Gachechiladze-Bozhesku M. and T.B. Fischer (2012)]. This may be due to: lack of legislated requirements for SEA follow-up; non-suitable existing monitoring systems that cannot contribute to SEA follow-up; vague follow-up goals as described in the monitoring program of the SEA study; costs of implementing a monitoring program or unavailability of skills or resources, etc.

It should be underlined that it is not easy to conclude on the quality and effectiveness of SEA, implemented in many countries the last 20 years or more. Firstly, quality refers to all SEA process, including the assessment methods, the institutional arrangements, the whole procedure with public participation and consultations: thus, the quality of information used in SEA, analysis and synthesis of different opinions of stakeholders, technical validity and credibility affect the idea of quality. Secondly, effectiveness refers to the output of the quality of the SEA and to the SEA follow-up, which are related to the achievement of the environmental goals set by the SEA, the realization of the impacts predicted and evaluated, the successful implementation of mitigation measures, the effectiveness of the SEA monitoring system and the influence of SEA on the project-level EIAs that are related to the PPPs examined by the SEAs [Gachechiladze-Bozhesku M. and T.B. Fischer (2012)]. Van Doren et al. (2013) refer to the quality of SEA as "procedural effectiveness" and to the effectiveness of SEA as "substantial effectiveness", while criteria are set in order to evaluate the substantial effectiveness of SEA: acquaintance (planners consult the SEA), consideration (SEA is the reason to review and develop further the PPPs), consent (proposed PPPs are altered according to the SEA results), formal conformity (the PPPs become environmentally friendlier due to the SEAs), behavioral conformity (the PPPs affect follow-up tiers e.g. other plans and programs or projects) and final conformity (environmental protection, proved by several environmental indicators and quality standards) [Van Doren D., Driessen P.P.J., Schijf B. and H.A.C. Runhaar (2013)]. The general factors

influencing the success of SEA are summarized by Zhang et al. (2013), who found that the communication and interaction between several stakeholders are important factors for SEA implementation, as communication is responsible for acceptance of the SEA and also values its results. PPPs are sometimes vague and abstract, limiting communication and coordination, while affecting transparency too. Other important factors include: resources related to available time and money, factors that affect both participation and the quality of the assessment; timing and organization e.g. planning and SEA may be interacting and parallel or SEA may be adapted to existing planning procedures; and political will and trust between stakeholders and other participants that affects also transparency and implementation of SEA. The results, related to how several scientists and stakeholders regard SEA, are also interesting: some planners see SEA as "more of the same"; developers regard SEA as one more administrative obstacle; environmentalists may see it as a bureaucratic process with no practical influence on the proposed PPP; and SEA practitioners have a weak understanding of strategic decision making [Zhang J., Christensen P. and L. Kornov (2013)]. On the contrary, Noble's research on SEA studies reached the conclusion that many of them are labelled as "SEA", but they are in fact non-strategic assessments, as they are not focused on alternative options, they do not examine broader visions, goals and objectives, but they rather assess impacts of predetermined options [Noble B.F. (2000)].

Chaker et al. (2006) examined the SEA systems in 12 developed countries all over the world in terms of legislation, responsible authorities, screening, scoping, types of impacts considered, public participation, alternatives and mitigation of impacts. It was concluded that a SEA system should draw special attention to: early consideration of significant impacts, including synergistic and cumulative impacts (this is an opportunity for SEA, while EIA is difficult to identify, predict and evaluate such impacts of proposed projects); formulation of better alternative scenarios of the proposed PPPs; public participation and effective stakeholder involvement for transparency and effectiveness of the SEA; and finally, the efficiency of strategic decision-making [Risse N., Crowley M., Vincke P. and J.-P. Waaub (2003)]. However, the methodologies/tools used for impact assessment were not examined and compared between the different SEA systems, although the use of such tools is considered to be important. Von Seht underlines correctly that the closer the policy, plan or program is to the following project stage, the more detailed the environmental assessment of the SEA should be and at the end, at the project level, EIA should include the most detailed assessment [Noble B.F. (2000)]. As a result of this, it is obvious that the more detailed the environmental assessment is in a SEA, the more detailed will be the mitigation measures of the expected impacts, as well as the environmental indices for the monitoring program.

In Hellas, experience on SEA, as implemented in National, Regional and Municipal Plans, in Sectorial Plans for Industry, Tourism, Fisheries, Renewable Energy, in the Regional Operational Programs 2007-2013 and 2014-2020, necessary for the EU Funds, and in several private planning projects, shows that in terms of the impacts assessment methods used, there is not much variety: in many SEA studies the methodology is similar to the one used in the Handbook on SEA for Cohesion Policy [Helander E. and G. Lawrence (2006)]. The tool of matrix is used for impacts assessment and therefore, simple matrices are used, together with the symbols proposed in the above-mentioned handbook, usually one matrix per environmental factor, followed by the necessary text that presents arguments about the characterization of environmental impacts. The assessment is done in one level; there is only qualitative evaluation of impacts, while the steps of impacts identification and prediction are not included, as proposed in methodologies for EIA studies [Glasson J., Therivel R. and A. Chadwick (2012)]. It should be underlined that no specific technique for impact assessment is proposed by the Ministerial Decision 107017/2006.

3. THE SEA OF THE GENERAL LOCAL PLAN OF GJIROKASTRA MUNICIPALITY

3.1 The area of study and the proposed General Local Plan

Gjirokastra Municipality is located in the southwest part of Albania, including an area of 469 km^2, with a population of around 29,000 inhabitants. The city of Gjirokastra (20,000 inhabitants), known

as the “city of stone”, is built in the eastern side of the Mount Gjerë and its old part of the city has been in UNESCO World Heritage since 2005 for the famous old castle – the biggest in Albania, with the Museum of Weapons inside – and the traditional buildings. The city was built in the 4th century and was named Argyrokastro (Hellenic name) in 1336, while in 1417 it was conquered by the Ottoman army. The characteristics of old traditional houses – some of them newly restored (e.g. the house where the famous writer Ismail Kadare was born) – with the fortress look, the streets of cobblestone, the National Folk Festival (in the house of dicator Enver Hoxha was born), the Ethnographic Museum, the Old Bazaar, the archaeological park of Antigone (ancient town found by King Pyrrus of Epirus in 295 B.C. with a 4 km fortification around it), 14 km away from Gjirokastra, the many Byzantine churches in the municipality (the oldest and most beautiful St Mary in the village of Labove e Kryqit), the ancient theater of Hadrianopolis with a capacity of 4,000 seats and the ancient settlement of Paleokaster are some major parameters for tourism attraction, bringing a special color in the area. Gjirokastra, located between the lowlands of Western Albania and the highlands of Central Albania, is characterized by a Mediterranean climate, with warm summer (average high temperature 34^{o}C in August) and heavy rainfall during the period November – February (total 1.800 mm annually). The natural environment of the municipality is characterized by: the River Drino and its small productive valley, tributary of the River Aoos, with source in Epirus Region of Hellas, total length of 85 km and basin size of 1,320 km^2, contributing to a small productive valley with opportunities for irrigation; the strict protected area of Kardhiq (Natura 2000); the natural monument of Zheji (proposed as a Natura 2000 area); and the natural park Rrëzomë of 1,400 Ha with important biodiversity.




Figures 2 - 3: Part of the old traditional urban area of Gjirokastra and part of the castle [photos by co-authors]

The General Local Plan of Gjirokastra Municipality was conducted in three phases: the first phase was the analysis of existing situation, covering all aspects of population and demographic issues, cultural aspects, urban characteristics and land-uses in all settlements, all parameters of the natural environment, covering issues in geology, water, wastewater and waste management, natural protected areas and characteristics of flora and fauna, climate conditions, etc., current technical infrastructure, landscape and morphology of the area, economic issues for professional activities and investments, environmental and other problems, sources of pollution, etc.; the second phase included the proposals for the territorial strategy, proposals for every system (natural, water, urban, infrastructural and agricultural) together with SWOT analysis, the vision of the strategy, the strategic objectives and the priority axes for each strategic objective, and finally, the action plan for all proposed projects with emphasis on priority projects and pilot projects; the third phase of the General Local Plan involved detailed land-use patterns for all settlements and all municipal territory, detailed proposals on building regulations in every settlement and the action plan of the second phase in its final form. It is worth noticing that the SEA was conducted simultaneously with the third phase of the General Local Plan, assessing the impacts of the strategic proposals of the second phase (objectives and priority axes).





Figures 4 - 5: River Drino in the summer and old traditional bridge [photos by co-authors]

3.2 The three-level impact assessment of the SEA

It was chosen to assess environmental impacts of the GLP's proposals by a three-level impact assessment, using the simple tool of matrix, in variations, in order to identify, predict and evaluate the environmental impacts. The notion of this three-level impact assessment derives from EIA international literature and not EIA practice – as it is concluded EIA studies do not include such a detailed assessment. The methodology is detailed but simple to present, easy to explain, both to public authorities, regional institutes and authorities as well as to the Ministry, responsible for the approval of the SEA. The methodology was also proved to be satisfactory in terms of scientific cooperation between all members of the SEA study, as it offered clarification to many issues related to expected impacts and their significance. As proposed by the Hellenic and Albanian SEA legislation (and the Directive 2001/42EC), the impacts are examined in the fields of soil, air, climatic factors, water, biodiversity, wastes, noise, material assets, cultural heritage and landscape.

The first step of this impact assessment methodology is identification of potential impacts of the General Local Plan on the environment. Therefore, the following simple matric is formed with all proposed priority axes (PA) in the first column and all environmental parameters examined in the next columns. If a significant effect between a priority axis and an environmental parameter is identified, the symbol "√" is used, otherwise, if no effect is identified, the symbol "X" is used (Table 1). The simple matrix, is further explained and justified in the SEA study of Gjirokastra Municipality General Local Plan by helpful text with arguments on how an effect may be expected or not between each priority axis and all the environmental parameters examined – however, it is not possible to include these arguments in this paper. It is worth noticing that these arguments have been accepted by all authorities and stakeholders, participating in the SEA process, either in the consultation stages or in the final approval stage.

The second step of this impact assessment methodology is prediction of potential impacts of the GLP on the environment: for this reason, the same simple matrix is used, as follows, by using colours, instead of symbols, with two variations of green expressing a positive impact, yellow and red a negative impact and grey expresses that there is no impact identified (Table 2). In Table 2 it is worth noticing that in some cases, inside a cell, two different colours may be seen e.g. in PA 11 "Use of Renewable Energy Resources" it is believed that it may have negative impacts on water if small hydropower stations may be constructed in the future and if they do not operate with sustainable criteria in terms of water management; the same PA is believed to have very negative impacts on landscape if wind farms may be constructed in the future next to several traditional settlements or in the top of mountainous areas, depending on their visibility to many people; however, some people find wind farms "attractive" because they are a symbol of "green" energy.

Table 1: The simple matrix used for environmental impact identification

	Soil	**Air**	**Climatic factors**	**Water**	**Biodiversity**	**Wastes**	**Noise**	**Material Assets**	**Cultural Heritage**	**Landscape**
Strategic Objectiv 1: Strengthening the key position of the Municipality as a southern gateway of Albania, while strengthening the role of Gjirokastra as a regional tourism center.										
PA 1: Improve and strengthen the national transport infrastructure	√	√	√	X	√	X	√	√	√	√
PA 2: Monitoring system of land-use changes in Gjirokastra Region	X	X	X	X	X	X	X	X	X	X
Strategic Objectiv 2: Protecting and promoting the cultural environment of the Municipality and its cultural heritage.										
PA 3: Promotion of archaeological / cultural monuments and traditional buildings of the Municipality.	X	√	X	X	X	X	√	√	√	√
PA 4: Strengthening the tourist activity and development of alternative forms of tourism.	√	√	X	√	X	√	√	√	√	√
Strategic Objectiv 3: Economic revitalization of the area led by the principles of sustainable development, through the expansion of production base and balanced development of the three production sectors.										
PA 5: Strengthening tertiary activities in Gjirokastra (additional public services, trade, tourism) in order to create new jobs.	X	X	X	√	X	√	√	√	√	√
PA 6: Enforcement of the secondary production sector.	X	X	X	√	X	√	√	√	√	X
PA 7: Strengthening local economy through employment opportunities in the primary sector.	√	X	X	√	X	X	X	X	√	X
Strategic Objectiv 4: Protection and sustainable management of the natural environment by emphasizing and promoting the strong points of the Municipality.										
PA 8: Protection and sustainable management of natural resources.	√	X	X	X	√	√	X	√	X	√
PA 9: Protection and sustainable management of water resources.	√	X	X	√	√	X	X	√	X	√
PA 10: Protection of cultivated land and agricultural space.	√	X	X	√	X	√	X	√	X	√
PA 11: Use of Renewable Energy Resources.	√	√	√	√	√	X	√	√	X	√
Strategic Objectiv 5: Improving the quality of life of the inhabitants by completing the technical infrastructure and creating a high level of social infrastructure.										
PA 12: Improvement of urban public utility networks (water supply, sewage, energy, waste management) in the city and other settlements,	√	√	X	√	√	√	X	√	X	X
PA 13: Improving social infrastructure (education and health).	X	X	X	X	X	X	X	√	X	X
PA 14: Urban renovation and planning in settlements.	√	√	√	√	X	X	√	√	√	√
PA 15: Improving mobility and public transport at the municipal level.	X	√	√	X	X	X	√	√	√	√
PA 16: E-government and the improvement of electronic infrastructure.	X	√	X	X	X	√	√	√	√	X
PA 17: Strengthening the role of the University.	√	X	X	√	X	√	X	√	√	√

Table 2: The simple matrix used for environmental impact prediction

	Soil	Air	Climatic factors	Water	Biodiversity	Wastes	Noise	Material Assets	Cultural Heritage	Landscape
Strategic Objectiv 1: Strengthening the key position of the Municipality as a southern gateway of Albania, while strengthening the role of Gjirokastra as a regional tourism center.										
PA 1: Improve and strengthen the national transport infrastructure										
PA 2: Monitoring system of land-use changes in Gjirokastra Region										
Strategic Objectiv 2: Protecting and promoting the cultural environment of the Municipality and its cultural heritage.										
PA 3: Promotion of archaeological / cultural monuments and traditional buildings of the Municipality.										
PA 4: Strengthening the tourist activity and development of alternative forms of tourism.										
Strategic Objectiv 3: Economic revitalization of the area led by the principles of sustainable development, through the expansion of production base and balanced development of the three production sectors.										
PA 5: Strengthening tertiary activities in Gjirokastra (additional public services, trade, tourism) in order to create new jobs.										
PA 6: Enforcement of the secondary production sector.										
PA 7: Strengthening local economy through employment opportunities in the primary sector.										
Strategic Objectiv 4: Protection and sustainable management of the natural environment by emphasizing and promoting the strong points of the Municipality.										
PA 8: Protection and sustainable management of natural resources.										
PA 9: Protection and sustainable management of water resources.										
PA 10: Protection of cultivated land and agricultural space.										
PA 11: Use of Renewable Energy Resources.										
Strategic Objectiv 5: Improving the quality of life of the inhabitants by completing the technical infrastructure and creating a high level of social infrastructure.										
PA 12: Improvement of urban public utility networks (water supply, sewage, energy, waste management) in the city and other settlements.										
PA 13: Improving social infrastructure (education and health).										
PA 14: Urban renovation and planning in settlements.										
PA 15: Improving mobility and public transport at the municipal level.										
PA 16: E-government and the improvement of electronic infrastructure.										
PA 17: Strengthening the role of the University.										

Consequently, in order to deal with the vague character of the GLP and its impact on the SEA study, scenarios can be developed in some cases and inside a cell, two different colours may be used to express these two different scenarios. Another example may be the development of the primary

sector: it may cause negative impacts on soil, if many agrochemicals are used to increase production, but if organic farming is developed, then impacts on soil may be positive.

Finally, the third step of this impact assessment methodology is evaluation of potential impacts of the General Local Plan on the environment: for this reason, many simple matrices are used, as follows, one matrix for each environmental parameter, by using the symbols (enriched) of the Handbook on SEA for Cohesion Policy 2007-2013 [Helander E. and G. Lawrence (2006)]. These symbols are presented in Table 3:

Table 3: Assessment Legend (third step – evaluation)

Impact character	Symbols	Explanation
Probability	!!	Very probable
	!	Probable
	0	Not probable
Scale	++	Large-scale positive
	+	Positive
	0	Neutral
	–	Negative
	– –	Large-scale negative
Frequency/Duration	>>	Frequent to constant / Long-term to permanent
	>	Occasional / Short-term
	0	Not viable
Reversibility	IR	Irreversible
	R*	Reversible under mitigation measures
	R	Reversible
Transboundary dimension	TR	Possible transboundary effect
	0	Not transboundary effect
Uncertainty	?	Possible impacts depend on implementation of the GLP
Sequence	P	Primary impact
	S	Secondary impact
Interoperability	C	Cummulative impact
	SI	Synergistic impact
	0	Not influence with other parameters / impacts

As it is not possible to present all matrices used in the third step of this impact assessment methodology, let us refer to an example, the matrix of the environmental parameter of water. In the first left column of the matrix, all priority axes that are identified and predicted to have a negative or positive impact on water are presented and then the characteristics of these impacts are described by using the symbols of Table 3. Each simple matrix for each environmental parameter, as the one presented in Table 4, is followed by arguments presenting and explaining the character of impacts expected. It should be underlined that reversibility of possible impact is only examined for negative impacts; when there is uncertainty, then this impact character affects also “scale”, by using both “negative” and “positive” symbols.

4. CONCLUSIONS

A novel approach of three-level impact assessment is presented, as used in SEA study of Gjirokastra Municipality GLP. This new methodology is believed to offer specific advantages in the SEA process, for all stakeholders:

- First of all, it made it easier for all participants in the SEA study (group of scientists preparing the draft and final report) to organize better impact assessment, by making for themselves the process of impact assessment clearer and more specific. It was also easier for them to communicate, cooperate and discuss some issues with the planners working on the GLP project of Gjirokastra Municipality.

Table 4: The evaluation of impacts of the General Local Plan of Gjirokastra Municipality on water

	Impact character							
Priority Axes with negative or positive impacts on water, according to the findings of Table 1 and Table 2.	Probability	Scale	Frequency/ Duration	Reversibility	Transboundary dimension	Uncertainty	Sequence	Interoperability
PA 9: Protection and sustainable management of water resources.	!!	++	>>				P	
PA 10: Protection of cultivated land and agricultural space.	!!	++	>>				S	
PA 12: Improvement of urban public utility networks (water supply, sewage, energy, waste management) in the city and other settlements.	!!	++	>>				P	
PA 14: Urban renovation and planning in settlements.	!!	+	>>				P	
PA 17: Strengthening the role of the University.	!	+	>>				S	
PA 4: Strengthening the tourist activity and development of alternative forms of tourism.	!!	–	>>	R	0		P	0
PA 5: Strengthening tertiary activities in Gjirokastra (additional public services, trade, tourism) in order to create new jobs.	!!	–	>>	R	0		P	0
PA 6: Enforcement of the secondary production sector.	!!	–	>>	R	0		P	0
PA 7: Strengthening local economy through employment opportunities in the primary sector.	!!	–	>>	R	0		P	C
PA 11: Use of Renewable Energy Resources.	!	+/–	>>	R/IR	0	?	P	0

- Secondly, as a more detailed impact assessment methodology, it seems that it helped local authorities, regional authorities, local people, any stakeholders participating in the consultation phase, to understand in depth how a SEA assesses impacts of a GLP in a strategic level. This was very useful, because in Albania there is not much experience in SEA studies and it had to be clear that SEA does not deal with projects and details but evaluates impacts in a strategic level, proposing mitigation measures at a “parallel” strategic level, as well as a monitoring system with more vague and strategic indicators.
- Thirdly, the results of the consultations and opinions of public authorities and stakeholders showed that only minor revisions were made to the draft SEA report, the final SEA report was

accepted by the Ministry without any comments and the environmental declaration (the official acceptance of the SEA by the Ministry) was issued in less than five months from the beginning of the SEA process.

In conclusion, the three-level impact assessment methodology, as presented, is proposed to be the best available technique to identify, predict and evaluate environmental impacts of GLPs at municipal level, as advantages are identified for all parties of the SEA process (scientists preparing the SEA reports, public authorities, local people, stakeholders, regional authorities, ministry, etc.).

References

1. Arce R. and N. Gullón N. (2000) ‘The application of Strategic Environmental Assessment to sustainable assessment of infrastructure development.’ **Environmental Impact Assessment Review**, Vol. 20, pp. 393-402.
2. Therivel R., Wilson E., Thompson, S., Heany, D. D. and Pritchard (1992) ‘**Strategic Environmental Assessment**’, Earthscan Publications Ltd.
3. Directive 2001/42/EC of June 2001 on ‘the assessment of the effects of certain plans and programs on the environment.’, **Official Journal of the European Communities**, L 197, p. 30.
4. Risse N., Crowley M., Vincke P. and J.-P. Waaub (2003) ‘Implementing the European SEA Directive: the Member States’ margin of discretion.’, **Environmental Impact Assessment Review**, Vol. 23, pp. 453-470.
5. United Nations Economic Commission for Europe (2003) ‘**Protocol on Strategic Environmental Assessment to the Convention on Environmental Impact Assessment in a Transboundary Context’**. Available at: www.unece.org (accessed February 12th 2018).
6. Chaker A., El-Fadl K., Chamas, L. and B. Hatjian (2006) ‘A review of strategic environmental assessment in 12 selected countries.’**, Environmental Impact Assessment Review**, Vol. 26, pp. 15-56.
7. Therivel R. and Partidario (1996) ‘**The practice of Strategic Environmental Assessment**.’, Earthscan Publications Ltd.
8. Therivel R. (2004) ‘**Strategic Environmental Assessment in Action’**, 1st ed. Earthscan.
9. Noble B.F. (2000) ‘Strategic Environmental Assessment: what is it? And what makes it strategic?’, **Journal of Environmental Assessment Policy and Management**, Vol. 2, No. 2, pp. 203-224.
10. Seht von H. (1999) ‘Requirements of a Comprehensive Strategic Environmental Assessment System.**’ Landscape and Urban Planning**, Vol. 45, pp. 1-14.
11. Kornov L. (1997) ‘Strategic Environmental Assessment.’ **European Environment**, Vol. 7, pp. 175-180.
12. Gachechiladze-Bozhesku M. and T.B. Fischer (2012) ‘Benefits of and barriers to SEA follow-up – Theory and practice.’, **Environmental Impact Assessment Review**, Vol. 34, pp. 22-30.
13. Noble B.F. (2003) ‘Auditing Strategic Environmental Assessment practice in Canada.’, **Journal of Environmental Assessment Policy and Management**, Vol. 5, No. 2, pp. 127-147.
14. Van Doren D., Driessen P.P.J., Schijf B. and H.A.C. Runhaar (2013) ‘Evaluating the substantive effectiveness of SEA: towards a better understanding.’ **Environmental Impact Assessment Review**, Vol. 38, pp. 120-130.
15. Zhang J., Christensen P. and L. Kornov (2013) ‘Review of the critical factors for SEA implementation.’**, Environmental Impact Assessment Review**, Vol. 38, pp. 88-98.
16. Helander E. and G. Lawrence (2006) **‘Handbook on SEA for Cohesion Policy 2007-2013**.’ Available at: www.ec.europa.eu (accessed February 12th 2018).
17. Glasson J., Therivel R. and A. Chadwick (2012) **‘Introduction to Environmental Impact Assessment.’**, 4th edition, Routledge.

ANALYSIS AND MODELLING OF BIOLOGICAL WEATHER DATA IN THESSALONIKI, GREECE

Th. Kassandros[1], A. Tsiamis[1], A. Damialis[2,3], D. Vokou[3], N. Katsifarakis[1], K. Karatzas*[1]

[1] Environmental Informatics Research Group, Department of Mechanical Engineering, Aristotle University, Thessaloniki, Greece,
[2] Chair and Institute of Environmental Medicine, UNIKA-T, Technical University of Munich, Augsburg, Germany,
[3] Department of Ecology, School of Biology, Aristotle University, Thessaloniki, Greece

*Corresponding author: e-mail: kkara@auth.gr, Tel +30 2310 994176

Abstract
We study the levels and the profile of aeroallergens (pollen and fungal spores), which constitute biological weather parameters affecting health and quality of life, in the city of Thessaloniki, Greece. We employ a data-driven approach with the aim to investigate the relationships between aeroallergen parameters as well as meteorological conditions that may dictate biological weather patterns and levels. A number of computational experiments are performed to assess the ability and performance of various statistical and machine learning methods including linear regression, artificial neural networks, decision trees and ensemble-based approaches. Results suggest that it is possible to properly describe the behaviour of the aeroallergens and thus to operationally forecast their levels. The latter is expected to have a direct positive impact of the quality of life of aeroallergen sufferers in the area of study.

Keywords: Aeroallergens, Computational intelligence, Regression

1. INTRODUCTION

Allergies are caused by the interaction between the human immune system and various exogenous (environmental) parameters. When the latter consist of airborne biological agents (like pollen and fungal spores) they are called aeroallergens and are affecting more than 20% of the population in Europe [Bousquet et al., 2007, Eder et al., 2006]. Important allergenic plants are grass and birch which affect about 65% and 30% of all hay fever sufferers in Europe, respectively. In the Southern parts of the continent, the second most-important allergenic plant after grass is olive, with up to 70% of allergy patients sensitive to it, this being also true for the Thessaloniki area [Gioulekas et al. 2004]. Fungal spores have also been found to generate allergic reactions in Thessaloniki, Greece [Gioulekas et al., 2004]. It is therefore evident that allergic rhinitis (hay fever) as well as other allergic manifestations depend on aeroallergen levels and have an impact on the overall Quality of Life (QoL). For this reason, the analysis and modelling of biological weather data (i.e. data describing the meteorological, air pollution and aeroallergen levels in the atmosphere as described in Klein et al., 2011) contributes to the understanding and improvement of the QoL of sensitive parts of the population. In the rest of the paper we present the biological weather data and the methods and tools employed in their analysis and modelling (chapters 2 and 3). Results follow in chapter 4, and we then draw our conclusions and state future research directions (chapter 5).

2. MATERIALS

2.1 Area of study

The Greater Thessaloniki Area (GTA) is the largest urban agglomeration in Northern Greece with more than 1,000,000 inhabitants. Traffic and industrial activities constitute the main sources of air pollution. The city of Thessaloniki is located in the inmost part of the Thermaikos Bay, bounded to the North by the Hortiatis Mountain. Residential areas are found in the periphery of the city and an industrial zone is situated to its north-west side. The climate of the area is Mediterranean with hot and dry summers and mild winters.

2.2 Biological weather data

2.2.1 Pollen Data and associated meteorological data

Airborne pollen in Thessaloniki is monitored with the aid of a 7-day recording Burkard volumetric trap. The trap is placed on the roof of a University building in the city centre approximately 30m above ground level. The measurements are based on the trapping of air particles on an appropriate tape surface. Once every week dedicated personnel collects the sampling tape, brings it to the Lab, and with the aid of a microscope the pollen grains are identified and counted (categorized per taxon). The pollen types addressed in this paper are Cupressaceae, Oleaceae and Poaceae while the study period covers years 1987–2016 with a time resolution of one day. The overall procedure is described in detail in Damialis et al., 2010, and is characteristic of pollen measurements in many countries. On this basis, the collection of pollen concentration data is characterized by a 7-day cycle. Therefore, in order to build operational models, this cycle should be taken into consideration.

Meteorological data associated with pollen counts come from the International Thessaloniki Airport monitoring station, made freely available via the www.wunderground.com and consist of daily minimum, maximum and mean of the following parameters: temperature (in ^{o}C), pressure (in hPa) wind speed (in m/s), wind direction (in degrees) and relative humidity. The aforementioned data are considered to represent the mean meteorological conditions of the GTA and are rendered as appropriate to be included in the analysis of pollen data. Descriptive statistics of the meteorological data, accompanied by relevant pollen data (i.e. a total of 16 parameters), are presented in Table 1.

2.2.2 Fungal Spore Data and associated meteorological data

Airborne fungal spores in Thessaloniki are monitored by the same Burkard volumetric trap located on the roof of a 30m university building, in the centre of Thessaloniki. The study period covers years 1987–2004 (with the exception of years 2001-2002). Counts are expressed as mean daily spore concentrations (number of spores per m3 of air), as described in [Damialis et al., 2015]. In this study we chose the three spore types summing up the largest percentage of the overall yearly concentrations, namely Alternaria, Cladosporium and Ustilago.

As fungal spores were available for a different time period in comparison to pollen, we wanted to make use of meteorological data that actually matched the spore count period. For this reason we included in the analysis meteorological data which were recorded by the station operating within the central Aristotle University campus and consist of minimum temperature (in ^{o}C), relative humidity, solar radiation and rainfall daily (in mm). Descriptive statistics of the meteorological data, accompanied by relevant spore data (i.e. a total of 7 parameters), are presented in Table 2.

Table 1: Descriptive Statistics for 13 meteorological parameters and 3 Pollen taxa

Parameter	min	max	mean	std
Meantemp	-4.00	34.00	15.92	8.07
Meanpressure	989.53	1036.44	1016.07	6.69
Meanwindspd	0.00	52.00	8.80	6.14
Meanwdird	-1.00	360.00	221.51	90.50
Meanhumidity	30.00	100.00	65.80	13.95
Maxtemp	-2.00	44.00	20.51	8.99
Mintemp	-10.00	27.00	11.29	7.53
Maxhumidity	36.00	100.00	83.07	12.03
Minhumidity	6.00	96.00	44.61	17.24
Maxpressure	995.00	1040.00	1018.29	6.49
Minpressure	982.00	1036.00	1013.91	7.00
Maxwspd	0.00	224.00	23.54	12.95
Minwspd	0.00	41.00	0.97	3.58
Cupressaceae	0.00	2626.98	11.36	76.72
Oleaceae	0.00	452.07	2.21	10.35
Poaceae	0.00	76.34	1.51	4.52

Table 2: Descriptive Statistics for 4 meteorological parameters and 3 Fungal Spore types

Parameter	mean	max	min	std
RelativeHumidity	0.68	1.00	0.20	0.14
Rainfall	1.13	60.70	0.00	3.94
SolarRadiation	359.00	884.00	4.00	210.25
MinTemperature	11.41	26.20	-8.20	7.18
Alternaria	*28.39*	*561.00*	*0.00*	*44.52*
Cladosporium	*203.48*	*11991.00*	*0.00*	*429.70*
Ustilago	*22.46*	*2094.00*	*0.00*	*69.36*

3. METHODS

3.1 Correlation analysis

The first step of our analysis aimed at the identification of relationships between parameters of the pollen as well as of the spore's data spaces. For this reason, the Pearson correlation coefficient was employed, as a relative measure of association, calculated according to the following formulae:

$$r = \frac{\sum_{i=1}^{n}(x_i-\overline{x})(y_i-\overline{y})}{\sqrt{\sum_{i=1}^{n}(x_i-\overline{x})^2}\sqrt{\sum_{i=1}^{n}(y_i-\overline{y})^2}} \quad (1)$$

Here x_i andy_i represent the two parameters studied for association while n is the number of available data records. Results are presented and discussed in the relevant sections of this paper.

3.2 Further data association analysis

In a next step, we aimed at identifying inter-dependencies among data parameters which are not well depicted by the (linear in its nature) Pearson correlation coefficient. For this reason, we applied the Self-Organizing Maps (SOMs) method, which makes use of the Artificial Neural Networks main constituents, i.e. neurons. SOMs are composed of lattice-oriented neurons which aim to represent multidimensional data sets via their weights, in a topological manner. As the neural network is exposed to data points, the latter are represented via winning neurons causing the network topology to adjust and eventually form clusters on the basis of a similarity criterion (usually the Euclidian distance within the initial data space). The method is agnostic of the structure or of the content of the data and can deal with missing values. Neurons are arranged grids (usually 2-D but also 3-D). Eventually similar neurons are topologically grouped in similar areas of the constructed "maps" [Kohonen et al., 1997].

3.3 Features

Both datasets presented here where handled in a similar manner in terms of modelling. Due to the way that data are collected (daily values made available every 7 days) and taking into account that persistence is a main characteristic of aeroallergen as already indicated by Voukantsis et al., 2010, a lag of up to 7 days has been chosen to be applied in our study. We therefore indicate as d_0 (zero day) the day for which we aim to develop a model for any one of the three pollen taxa studied. Then, we indicate as d_1(lag1 day) the day before, and so on. As a result and for each one of the three pollen taxa, we generate a total of $13\sum_{i=0}^{i=7} d_i$(meteo)+7(target pollen taxa)+2(other pollen taxa) = 113 features for their concentration levels. Similarly, and for each one of the three spore type, we generate a total of s and $4\sum_{i=0}^{i=7} d_i$ (meteo)+7(target taxa)+2(other taxa) = 41 features for the modelling of their concentration levels. Due to the large number of features, we additionally aimed to identify which of those are the most important in terms of their ability to lead to improved model results in either nowcasting or forecasting mode. Among the many methods available, we chose to make use of a Computational Intelligence algorithm in order to rank the features according to their "modelling" effectiveness. More specifically, we employed the Random Forest [Breiman, 2001] method, which consists of a population of decision trees. At each node of each tree, a condition is applied based on a single feature that actually splits the tree in two. The optimal condition by which the split is made locally at each node is called impurity, and for regression problems this is the variance, the average of which can be calculated for all nodes and trees involved in the modelling procedure. This means that when each tree is trained, there is a criterion which may be used to calculate how much each feature contributes to the decrease of its impurity. This is the feature importance measure included in the Python data mining Random Forest implementation used in this paper (available at http://scikit-learn.org). In all regressors the dataset was split in a training and a testing set with a ratio=3/4 for fungal spores and a ratio=2/3 for pollen taxa on the basis of preliminary computational experiments and in order to avoid over fitting.

3.4 Modelling algorithms

Modelling focused of three pollen taxa (namely Cupressaceae, Oleaceae and Poaceae) and three fungal spore types (Alternaria, Cladosporium, Ustilago). Each parameter served as a target parameter and all other data available served as the initial feature space. Modelling focused on the nowcasting of the parameter of interest (i.e. estimation of its level based on features from the same day) as well as on forecasting (i.e. making the same estimation but now using features from previous days). The following algorithms were used in both modelling approaches.

3.5 Linear Regression

Linear Regression is the oldest and most frequent technique for regression. The relationships between the features and the target parameter are modelled using linear predictor functions. The model is

developed using the least square approach, in order to minimize the mean squared error between the predicted values and data.

3.6 Random Forest

Random forests consist of a population of trees (forest) which are trained and then used as an ensemble, i.e. each tree via weighted voting contributes to the final result. In random forests each tree in the ensemble is built from a sample drawn with replacement from the training set. In addition, when splitting a node during the construction of the tree, the split that is chosen is no longer the best split among all features. Instead, the split that is picked is the best split among a random subset of the features. Because of this randomness, the bias of the forest usually slightly increases (with respect to the bias of a single non-random tree) but, due to averaging, its variance also decreases, usually more than compensating for the increase in bias, hence yielding an overall better model.

3.7 Neural Networks

In the current work a Multi-Layer Perceptron (MLP) is used as described in Voukantsis et al., 2010. A MLP network consists of at least 3 hidden layers. Each node is a neuron that takes as input the weighted sum of all neurons from the previous layer. Then the neuron uses an activation function, usually the sigmoid, to produce a signal in the range of (-1,1), which is then used to produce the signal for the neurons of the next layer. The goal of the training is to adjust the weights of each neuron to accomplish the minimization of the error between training and predicted values, using a technique called back propagation.

4. RESULTS

4.1 Correlation Coefficient and SOMs

In Tables 3 and 4 the Pearson correlation coefficient between the target variables and all the available ones, are presented. Concerning pollen, the highest correlation is observed between Oleaceae and Poaceae (0.46). In addition, both Oleaceae and Poaceae demonstrate a loose correlation to temperature. On the other hand, Cupressaceae doesn't seem to correlate with any of the available features. Within the fungal spores dataset, the highest correlation is observed between Cladosporium and Alternaria (0.59). In addition, those two spore types correlate strongly to minimum temperature and solar radiation. Ustilago correlates loosely to minimum temperature, solar radiation and Clasosporium.

Table 3: Correlation Coefficient Matrix for Pollen taxa

	Meantemp	Meanpressure	Meanwindspd	Meanwdird	Humidity	Maxtemp	Mintemp	Maxhumidityy
Cupressaceae	-0.08	-0.05	0.04	-0.01	0.02	-0.08	-0.09	0.04
Oleaceae	0.09	-0.06	-0.03	0	-0.05	0.1	0.08	-0.01
Poaceae	0.22	-0.07	-0.02	0	-0.14	0.23	0.2	-0.1
	Minhumidity	Maxpressure	Minpressure	Maxwspd	Minwspd	Cupressaceae	Oleaceae	Poaceae
Cupressaceae	-0.01	-0.03	-0.06	0.06	0	1	0.01	0
Oleaceae	-0.08	-0.07	-0.05	0.01	-0.04	0.01	1	0.46
Poaceae	-0.15	-0.09	-0.06	0.04	-0.05	0	0.46	1

The SOMs created for the pollen taxa (and their associated meteorological parameters) are presented in Fig. 1. Overall, it is evident that Oleaceae and Poaceae demonstrate a similar pattern. They show a relationship to mild and high temperatures, verifying that their flowering occurs in late spring and summer periods. Logically, they both indicate a repellent behaviour concerning humidity. Cupressaceae seems to be related with low atmospheric pressure, high wind speed and northerly winds in terms of wind direction. This suggests that possibly the specific pollen taxa enter the city centre during winter periods as reported by Galan et al., 1998, for the Cypresae pollen season in Spain, transferred from the northern part of the GTA (where some tree areas exist).

Concerning Fungal Spores, Alternaria and Cladosporium seem to be related with each other. Also, solar radiation and minimum temperature seems to influence all the studied spore types.

Table 4: Correlation Coefficient Matrix for Fungal Spores

	RelativeHumidity	Rainfall	SolarRadiation	MinTemperature	Alternaria	Cladosporium	Ustilago
Alternaria	-0.18	-0.07	0.39	0.54	1.00	0.59	0.23
Cladosporium	-0.13	-0.03	0.31	0.38	0.59	1.00	0.27
Ustilago	-0.08	-0.03	0.17	0.19	0.23	0.27	1.00

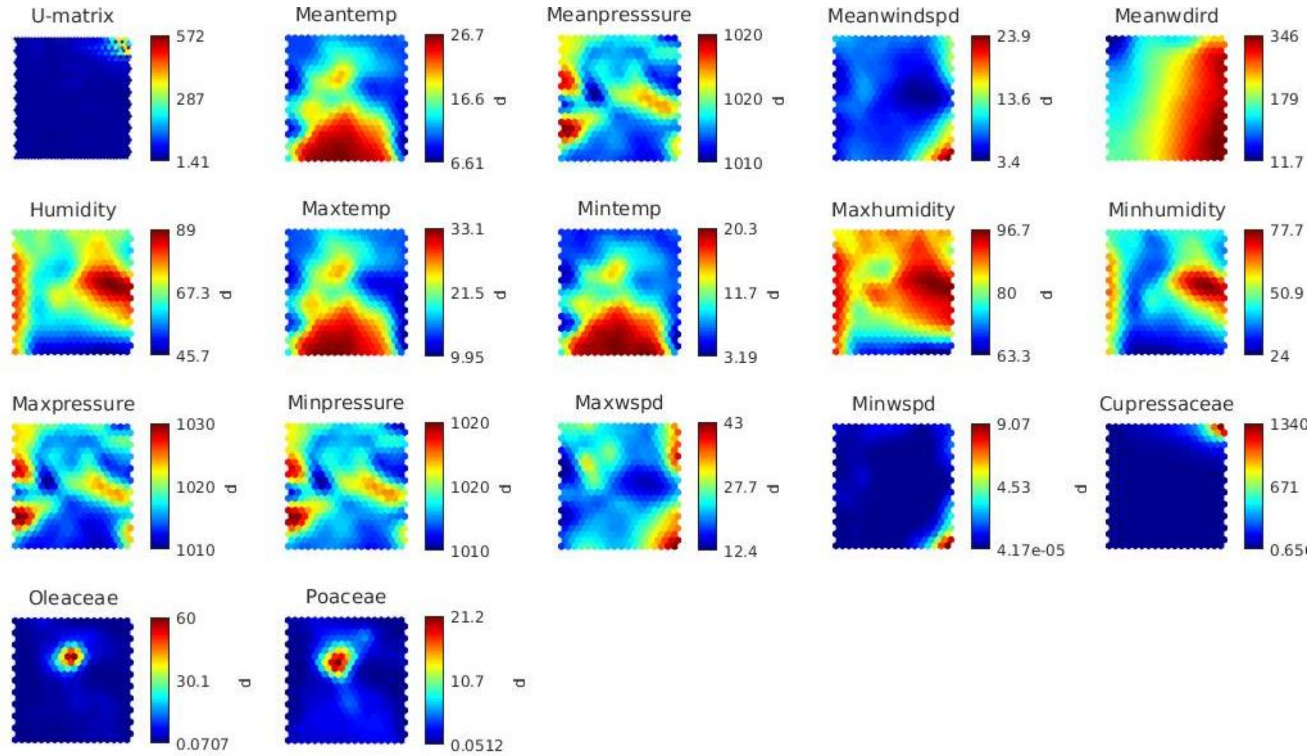


Figure 1: SOM for Pollen taxa and related meteorological parameters

4.2 Variable Importance

The procedure for evaluating the importance of the features described in section 3.3, was implemented for both pollen and fungal spore analysis. The most important features were found to be the lagged values of the target aero-allergen. These results confirm the persistence of the phenomenon. Also, in relevance with the results of section 4.2, other aeroallergens within the studied datasets were found to contribute importantly.

4.3 Predictive Models

In this section the prediction of the daily pollen and spore concentrations is approached in a twofold manner: on the basis of the results already presented in previous sections, various models where developed and applied using different set of features in a series of computational experiments.

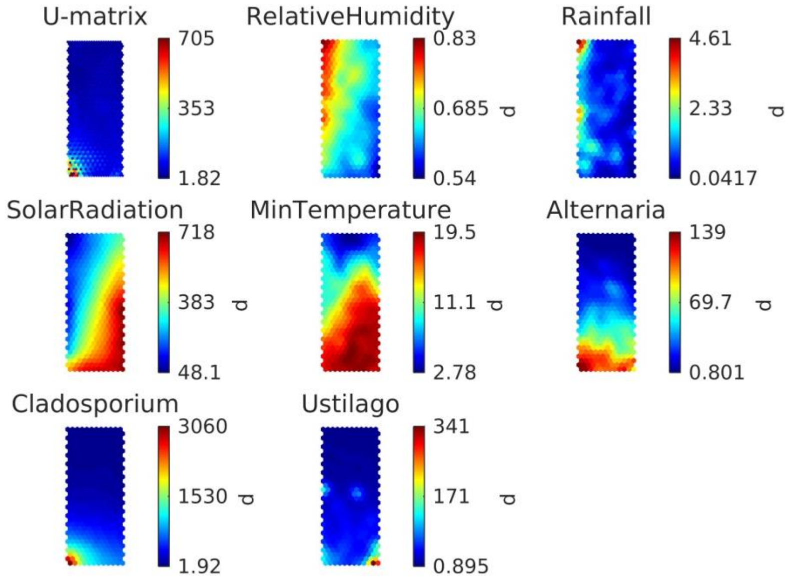


Figure 2: SOM for Fungal Spores and related meteorological parameters

4.4.1 Nowcasting

When referring to nowcasting we should take into account that all features are considered to be available, including the ones of day being modelled, with the exception of the target parameter. On the basis of computational experiments, it was decided to use a set of features which includes the meteorological data from lag0 to lag1, the target pollen taxa or spore type of lag1 and all the other available taxa/types of lag0. An indicative set of worst and best performance model is presented in Figure 3. The negative values that appear in the graphs in both linear regression and ANN models result from the effort made by the models to depict the actual values as well as the fluctuations of aeroallergen measurements. Since aeroallergen concentration cannot take negative values, those results should be interpreted as very low concentrations (or zeros for simplicity). The Pearson correlation coefficient as well as the mean absolute error between modelled and actual values is presented in Figure 4.

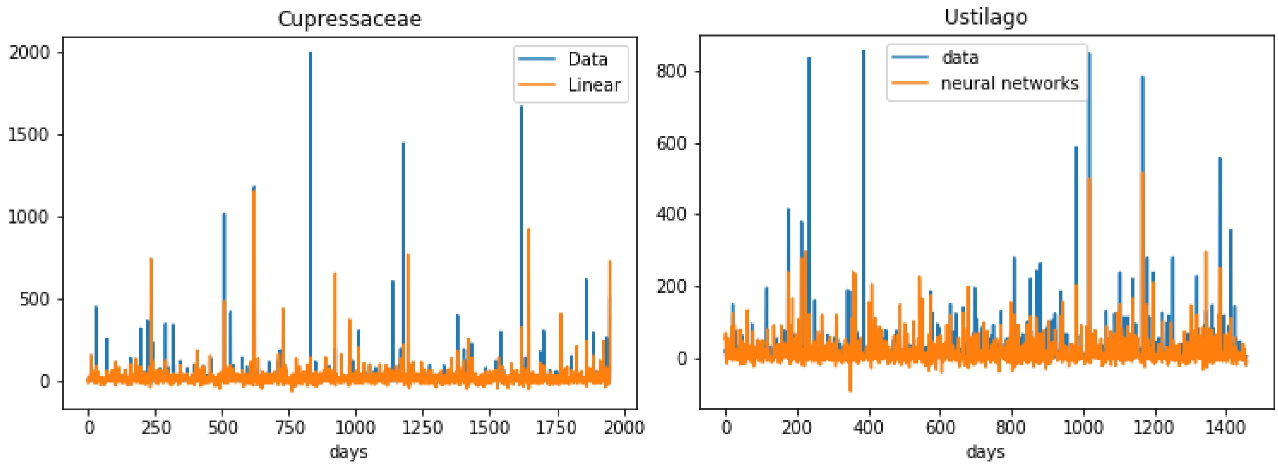


Figure 3: A representative example for the best (left) and worst (right) nowcasting outcome among models developed and tested. Model algorithm and aeroallergen type are indicated in the graph. Values are in pollen/spores per cubic meter

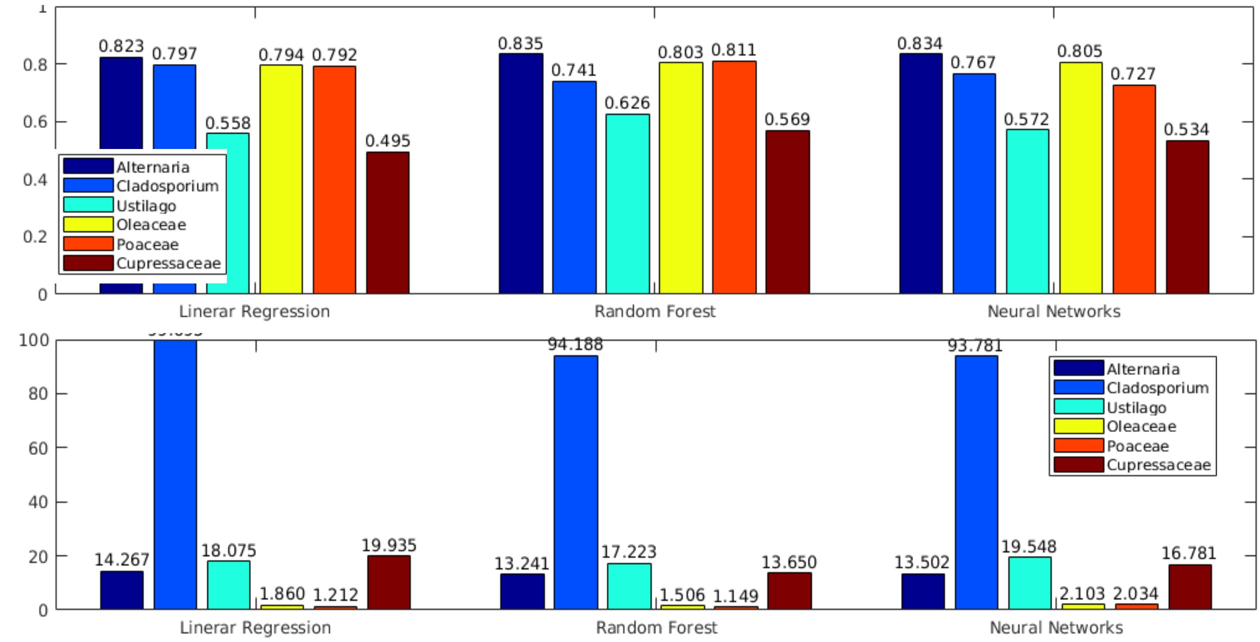


Figure 4: Comparison of the Pearson Correlation Coefficient (up) and the mean absolute error (down) between the different models used for nowcasting

4.4.2 Forecasting

When referring to forecasting we should take into account that only features which are already known at the day of the forecast are used.

Models for the forecasting of Pollen taxa: The set of features includes the meteorological data from -1day to -2day and the target pollen taxa or spore type of -1day.

Models for the forecasting of Fungal Spore type: The set of used features includes the meteorological data from -1day to -7day the target pollen taxa or spore type from -1day to -7day.

An indicative set of worst and best performance model is presented in Figure 5. The Pearson correlation coefficient as well as the mean absolute error between modelled and actual values are presented in Figure 6.

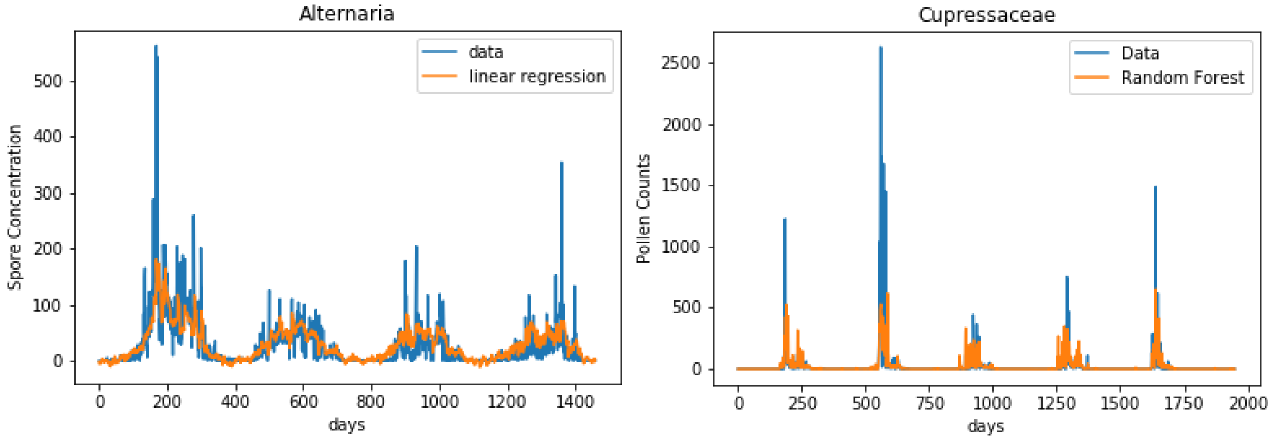


Figure 5: A representative example for the best (left) and worst (right) forecasting outcome among models developed and tested. Model algorithm and aeroallergen type are indicated in the graph. Values are in pollen/spores per cubic meter

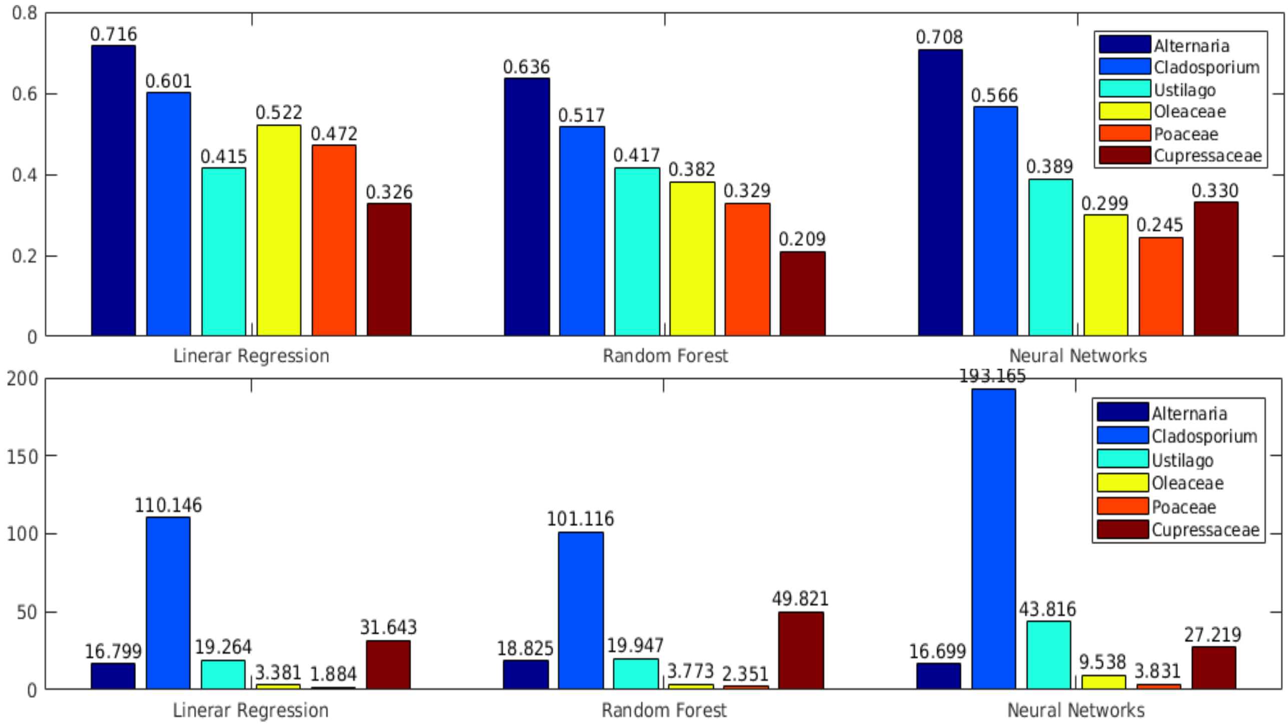


Figure 6: Comparison of the Pearson Correlation Coefficient (up) and the mean absolute error (down) between the different models used for forecasting

5. DISCUSSION AND CONCLUSION

The analysis of the correlation and the dependencies between pollen data and meteorological conditions as well as fungal spores and meteorological conditions suggests that there are specific inter-relationships which may be identified, both in terms of aeroallergen as well as in terms of meteorology. The use of the SOMs method provides with additional insights, that allow for the identification of behavioural patterns of the aeroallergens under study like in the case of the possible winter appearance of Cypresae originating from the northern part of the GTA,

Concerning the modelling approach, it is evident that both pollen as well as spores models demonstrate a high correlation coefficient for nowcasting, regardless of the modelling approach used, with r values ranging from approx. 0.5 for Cypressacaeae up to more than 0.83 for Alternaria. The mean absolute error varies considerably, with Cladosporium demonstrating the highest values, and thus jeopardising the good correlation coefficient achieved in terms of practical model implementation.

In the case of forecasting, pick values are harder to depict, this being the main reason for lower correlation coefficient values. For this reason and in the case of the three pollen taxa included in this study the 7-day ahead forecast achieves a low correlation coefficient that surpasses 0.5 only in the case of Oleaceae for a linear regression model. On the contrary, Voukantsis et al. in 2010 have reaches a correlation coefficient of 0.75 with similar models, yet with differences in the feature space, including more meteorological parameters. When coming to fungal spore forecasting 7-day ahead, the correlation coefficient is much better, ranging from 0.41 for Ustilago to 0.71 for Alternaria, accompanied by low mean absoluter error values. This indicates that our approach is capable of supporting operational spore level forecasting for the GTA regardless of the low dimensionality of the feature space used.

A general pattern that can be seen in all models, depending on the regression approach, is that random forests are more effective for nowcasting, while linear regression for forecasting. But for a more reliable result, a validation method (i.e. k-fold cross-validation) should take place.

Future research should include the investigation and use of a feature space of higher dimension, complemented by a more advanced and sophisticated method for feature identification, prioritisation and selection. In addition, we should develop models focusing on specific aeroallergen periods, which is still an open issue for Fungal spores, but have already been suggested for pollen [Pfaar et al. 2017].

References

1. Bousquet J., Dahl R., Khaltaev N. (2007), Global alliance against chronic respiratory diseases, **Allergy,** 62 (3), pp. 216-223
2. Eder W., Ege M.j., von Mutius E. (2006), The asthma epidemic, **N. Engl. J. Med**., 355, pp. 2226-2235
3. Gioulekas D, Papakosta D, Damialis A, Spieksma F, Giouleka P, Patakas D. (2004), 'Allergenic pollen records (15 years) and sensitization in patients with respiratory allergy in Thessaloniki, Greece', **Allergy,** 59, pp. 174–184
4. Gioulekas, D., Damialis, A., Papakosta, D., Spieksma, F. T. M., Giouleka, P. and Patakas, D. (2004), 'Allergenic fungi spore records (15 years) and sensitization in patients with respiratory allergy in Thessaloniki-Greece.', **J. Investig. Allergol. Clin. Immunol.**, 14, pp. 225–231.
5. Klein Th., Kukkonen J., Dahl Å., Bossioli E., Baklanov A., Fahre Vik A., Agnew P., Karatzas, K., and Sofiev M. (2011) 'Interactions of physical, chemical and biological weather calling for an integrated assessment, forecasting and communication of air quality', **Ambio,** 41(8), 851-864
6. Dimitris Voukantsis, Kostas D. Karatzas, Athanasios Damialis, and Despoina Vokou 'Forecasting Airborne Pollen Concentration of Poaceae (Grass) and Oleaceae (Olive), using Artificial Neural Networks and Genetic Algorithms, in Thessaloniki, Greece', **The 2010 International Joint Conference on Neural Networks (IJCNN)**, Barcelona, Spain.
7. Athanasios Damialis, Despoina Vokou, Dimitrios Gioulekas, John M. Halley (2015), 'Long-term trends in airborne fungal-spore concentrations: a comparison with pollen, Fungal Ecology', **Fungal Ecology**,13, pp. 150-156.
8. Kohonen, T., (1997). **'Self-Organizing Maps, 2nd edition.'** Springer-Verlag Berlin Heidelberg, Germany
9. Voukantsis D., Niska H., Karatzas K., Riga M., Damialis A. and Vokou D. (2010), 'Forecasting daily pollen concentrations using data-driven modeling methods in Thessaloniki, Greece', **Atmospheric Environment,** 44(39), pp. 5101-5111
10. Breiman, L. (2001), 'Random Forests.', **Machine Learning**, 45(1), pp. 5-32
11. Carmen Galán,Maria José Fuillerat,Paul Comtois,Eugenio,Domínguez,(1998),'A predictive study of cupressaceae pollen season onset, severity, maximum value and maximum value date, '**Aerobiologia,** 14, pp. 195.
12. Pfaar O, Bastl K, Berger U, Buters J, Calderon MA, Clot B, Darsow U, Demoly P, Durham SR, Galán C, Gehrig R, Gerth van Wijk R, Jacobsen L, Klimek L, Sofiev M, Thibaudon M, Bergmann KC. (2017) 'Defining pollen exposure times for clinical trials of allergen immunotherapy for pollen-induced rhinoconjunctivitis – an EAACI Position Paper'. **Allergy**, 72, pp.713–722.

PM_{10} LEVELS OF THE CITY AND A SUBURB OF PATRAS, GREECE, DURING THE PERIOD 2013-2015

A. A. Bloutsos and P. C. Yannopoulos*

Environmental Engineering Laboratory, Department of Civil Engineering, University of Patras, 265 04 Patras, Greece

*Corresponding author: E-mail: yannopp@upatras.gr, Tel +30 2610 996527, Fax: +30 2610 996573

Abstract

The present work deals with the concentration levels of air-borne particulate matter of diameter less than 10 μm (PM_{10}) of the area of the city of Patras and of the University of Patras Campus during the period of 2013 - 2015. The stationary air pollution monitoring station of the Environmental Engineering Laboratory (EEL) of the Civil Engineering Department of the University of Patras is operating continuously since 2012. The sampling site is in a suburb. Additional PM_{10} data are obtained from the "Greek National Monitoring Network of Atmospheric Pollution (GNMNAP)" for two air quality stations, which are installed in Patras downtown and have operated intermittently since 2001.

The monthly variation of PM_{10} concentration for the time period 2013 -2015 is presented at each station. Calculating Spearman's correlation factor, the correlation among stations' measurements is significant at 0.01 or 0.05 levels, but there is no correlation between EEL's data and warm or cold period. On the contrary, there is rather strong correlation between downtown data and warm or cold period. In addition, the monthly average values of a typical year are presented for both stations. Finally, the yearly variations of mean monthly values are shown and the influence of warm or cold period is examined.

The aim of this project is to derive implications from the PM_{10} levels of the air of both the University of Patras Campus and the city of Patras. The statistical analysis of such a program of continuous measurements of air quality may provide a cost-effective strategy for air quality monitoring.

Keywords: Air pollution, air quality, PM_{10}, suburban concentration, suburban

1. INTRODUCTION

The airborne particulate matter (PM) is one of the most significant air pollutants [1, 2]. They consist of a mixture of solid particles and liquid droplets that are suspended in air with a wide range in size and chemical composition. Human health is affected mainly by the "inhalable particles" of a diameter less than 10μm (PM_{10}), and more specifically by the "fine particles" of diameter less than 2.5μm ($PM_{2.5}$). PM is originated by anthropogenic combustion and non-combustion sources as well as by natural sources, like sea salt emissions, re-suspended dust and transported Saharan dust [3].

The existence of particle pollution affects both health and the environment. Health effects of short or long term exposure to PM may be the appearance or aggravation of cardiovascular and respiratory diseases. The correlation between PM and mortality is also significant. The environmental impact may be assessed by the temporary occurrences of PM that affect visibility, climate and vegetation. In addition, building materials do not remain unaffected due to exposure to particulate pollution [1, 3, 4]. Air quality standards by European Environment Agency (EEA) [2] and US Environmental

Protection Agency (US-EPA) [4] and Guidelines by World Health Organization (WHO) [1], which are given in Table 1, are continuously updated according to the progress of research data.

Table 1 Air Quality Standards and Guidelines for PM_{10}

	Annual Mean (μg m^{-3})	Daily Mean (μg m^{-3})
European Union (EEA)	40	50[1]
US Environmental Protection Agency (US-EPA)	-	150[2]
World Health Organization (WHO) Guidelines	20	50[3]

[1] Not to be exceeded on more than 35 days per year

[2] Not to be exceeded more than once per year on average over 3 years

[3] 99th percentile (3 exceedances permitted per year)

There are several studies regarding PM_{10} measurements in Patras area, which give also mean monthly values for time intervals of the period from January 2004 up to April 2014. More precisely, the following intervals have been covered: January – December 2004 [13], December 2005 – March 2006 [14], 2008 – 2011 [15], 2009 and 2010 PM_{10} episodes [16], July 2012 [17], Winter periods of 2012 and 2013 [18] and January 2012 – April 2014 [19]. Exempting the four studies [14, 17, 18, 19], which have conducted their own PM_{10} mass concentration measurements, all the rest studies have used the PM_{10} data monitored by the Department of Environment & Planning of the Region of Western Greece.

The University of Patras Campus (UPC) occupies an area of 2.66 km^2, 12 km NNE of the city center, adjacent to Rion and at the foot of Panachaicon Mountain. It has 23 Departments with a total population of 30,000 approximately, including the University Hospital of Patras, where extensive infrastructure works, sports facilities, agricultural and other significant activities take place (Pappas, 2011). The present study deals with the presentation of PM_{10} concentrations measured by the Environmental Engineering Laboratory (EEL) of the Civil Engineering Department of the University of Patras during the period 01/01/2013 - 31/12/2015. The monthly average values, as well as the average values of the cold and warm period have been calculated and used herein. Several pertinent characteristics of PM_{10} are compared to the corresponding measurements available by the Department of Environment & Planning of the Region of Western Greece and useful implications are drawn.

2. MATERIALS AND METHODS

2.1 Description of sampling area

The position of the air quality monitoring EEL station is shown in Figure 1. It is located at the western parking lot of the Building of the Department of Civil Engineering (geographical longitude 21º47΄22΄΄, geographical latitude 38º17΄22΄΄ and 60.60 m altitude above sea level). At this area the inclination is 4-5% toward NW. Apart from asphalt-covered streets, the major area consists of natural soil with low vegetation, bushes, and sporadic trees, mainly pine and olive trees. The EEL station is settled at a distance more than 15 m W from the 3-storey building of the Civil Engineering Department, while all other buildings are even further away. The old National Road and the new National Road Korinthos – Patras (E65) are 0.7 km far N, approximately. At the same direction and at a distance 2.2 km, the local ferry port of Rion – Antirrion is located. The Patras By-Pass (E55) is

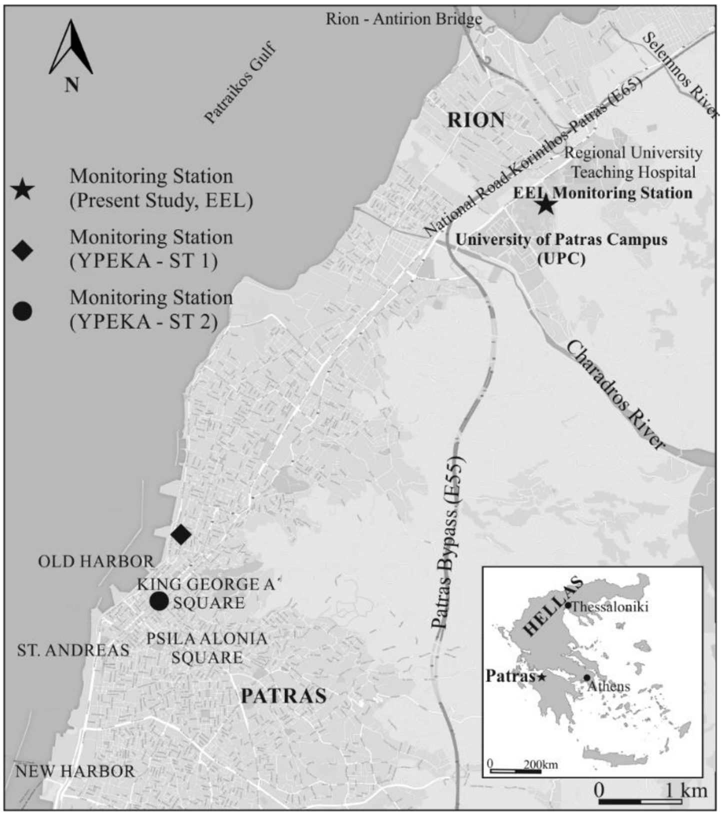


Figure 1: General view of Patras area and air quality monitoring locations

1.2 km SE away from the EEL station. The University Hospital of Patras is located 1.5 km NE it. Also, more than 2 km toward NE, there is a limited number of industrial activities of moderate size. The EEL station is free from nearby objects of any kind from the NE to SE wind sectors (i.e., for an angle of at least 247.5°). The EEL air pollution originates from classic sources of a suburban- rural area, augmented by emissions due to central heating during winter and additional emissions from aforementioned activities and a cement factory operating 2-3 km NE of the UPC. The Station is classified as “Suburban – background station”. More details about the location of the monitoring EEL station are given in the literature [6].

At Patras downtown, the Department of Environment & Planning of the Region of Western Greece is responsible for the operation of two air quality stations (ST 1 and ST 2, Figure 1) that have been installed and operated since 2001 in the frame of integration of “Greek National Monitoring Network of Atmospheric Pollution (GNMNAP)” [7]. The city is settled at the foot of Panachaicon Mountain extending mainly along the seashore of the NE Patraikos Gulf. Until July of 2014, the center was affected by the traffic load directed to the New Port through the city as the latter was not connected to the National Road. Since then, the traffic load due to heavy vehicles and cars is reduced, decongesting downtown Patras. A general view of Patras downtown and suburban areas is shown in Figure 1. Location of ST 1 is at Drosopoulou Sq., 180 m E of the nearest shoreline (harbor docks). ST 1 is characterized as an urban traffic oriented station. Location of ST 2 is at the E corner of King George A´ Sq. [11], 400 m SE of the nearest shoreline (harbor docks). Both monitoring stations are characterized as urban traffic oriented stations [11]. More details about the city of Patras and these two locations are given in the literature [7, 8, 9].

2.2 Sampling Equipment

The EEL station includes an automatic analyzer of PM_{10} (model Grimm 180) based on the 90° scattering light measurement principle. The analyzer provides data records of mean values every five minutes. At the roof of the station, a weathering station is located. Downtown Patras, the air quality monitoring stations (ST 1 and ST 2) are equipped with continuous operation beta-attenuation

analyzers (FH 62 I-R, Thermo Electron Corp., USA) for PM_{10} measurements. More details about this sampling equipment are given in the literature [6, 7, 10].

3. RESULTS AND DISCUSSION

In Figure 2, PM_{10} monthly average concentrations (Sites EEL, ST 1, ST 2) for the specific monitoring period are presented. The monthly PM_{10} concentrations at location of EEL station (suburban area) ranged from 5.7 to 24.7 μg m^{-3} with an average value of 13.7±3.9 μg m^{-3}. From GNMNAP's database [11], the monthly PM_{10} concentrations at locations of ST 1 and ST 2 (urban-traffic) ranged from 26.3 to 51.8 μg m^{-3} and from 29.6 to 58.5 μg m^{-3}, respectively, with corresponding mean values 40.4±7.7 μg m^{-3} and 39.5±7.6 μg m^{-3} (Table 2). It must be noticed that the data completion at EEL station, ST 1 and ST 2 is 100.0%, 27.8% and 100.0%, respectively. As expected, the concentrations at the suburban monitoring EEL station found less than those at urban-traffic areas (ST 1 and ST 2). It is noticed that PM_{10} concentrations at EEL station were 62.7% and 65.4% lower than those at ST 1 and ST 2, respectively. At cold period (October - March), EEL's levels were 67.0% and 68.1% lower than those at ST 1 and ST 2, respectively. Also, at warm period (April – September) EEL station's levels were 59.8% and 62.5% lower than those at ST 1 and ST 2, respectively. Additionally, the average ratio of PM_{10} concentrations of warm over cold period is 1.05, 0.79 and 0.88 for EEL, ST 1 and ST 2, respectively, indicating that the influence of cold or warm period at EEL station (suburban area) is weaker compared to stations ST 1 and ST 2. It must be noticed that the latter results obtained from ST 2 for warm and cold periods are indicative but not representative due to low percentage of recorded data completion.

The values of the Spearman's correlation factor *r* among stations measurements were calculated using SPSS® statistical software (IBM SPSS Statistics 24) with 0.01 or 0.05 significance levels. There is no correlation between EEL station's data and warm or cold period, while there is rather strong correlation between downtown data and warm or cold period (Table 3a).

From the daily PM_{10} concentrations recorded at Locations EEL, ST 1 and ST 2 the monthly variations of a typical year is calculated and shown in Figure 3. It is obvious that the variation of EEL's PM_{10} concentration is shifted down in comparison to corresponding variations of monitoring stations ST 1 and ST 2.

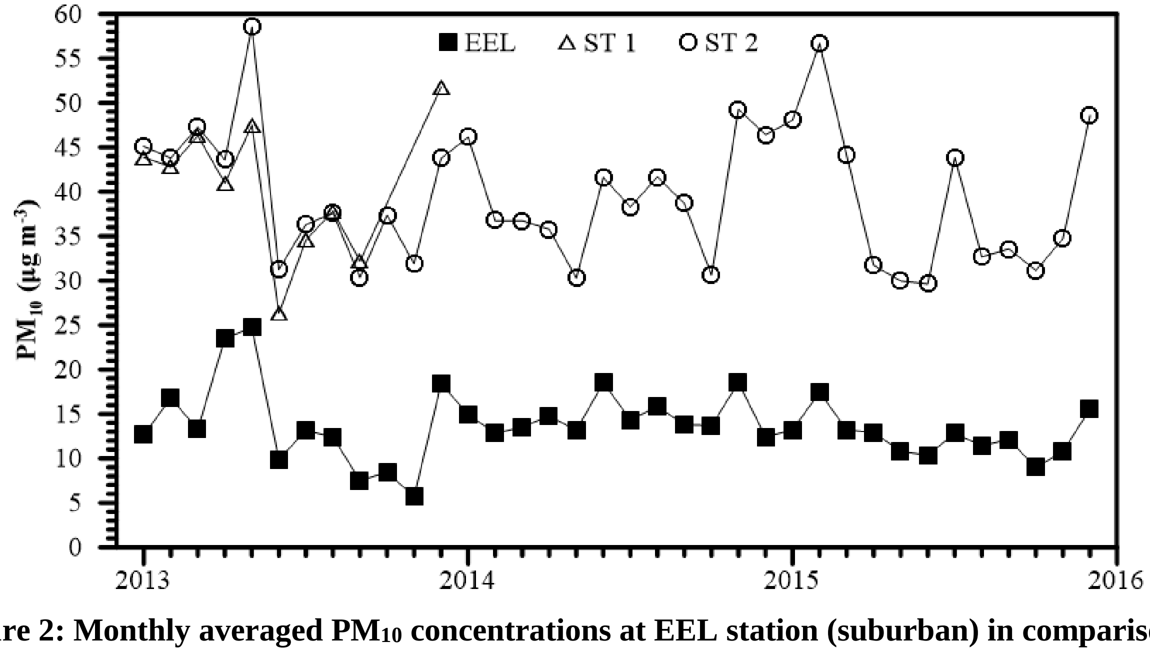


Figure 2: Monthly averaged PM_{10} concentrations at EEL station (suburban) in comparison to the corresponding PM_{10} concentrations at Locations of ST 1 and ST 2 (urban-traffic) during 2013-2015

Table 2: Statistical analysis of monthly PM_{10} concentrations (μg m^{-3}) during 2013-2015 at the monitoring stations EEL, ST 1 and ST 2 plus supplementary data

PM_{10}	Month	Cold Period	Warm Period	Distance from shoreline (m)	Elevation above sea (m)
Monitoring EEL Station, University of Patras Campus (geographical longitude 21º47΄22΄΄; geographical latitude 38º17΄22΄΄)					
Range (μg m^{-3})	5.7 – 24.7	5.7 – 18.5	7.5 – 24.7	1900	61
Average (μg m^{-3})	13.7	13.3	14.0		
St. Dev. (μg m^{-3})	3.9	3.4	4.4		
Completion (%)	100.0	100.0	100.0		
Monitoring ST 1 Station, Drosopoulou Sq. (geographical longitude 21º44΄18.35΄΄; geographical latitude 38º15΄11.15΄΄)					
Range (μg m^{-3})	26.3 – 51.8	42.8-51.8	26.3-47.5	180	16
Average (μg m^{-3})	40.4	46.2	36.6		
St. Dev. (μg m^{-3})	7.7	4.0	7.3		
Completion (%)	27.8	22.2	33.3		
Monitoring ST 2 Station, King George A΄ Sq. (geographical longitude 21º44΄09.23΄΄; geographical latitude 38º14΄45.51)					
Range (μg m^{-3})	29.6 – 58.5	30.6 – 56.7	29.6 – 58.5	400	19
Average (μg m^{-3})	39.5	42.1	37.0		
St. Dev. (μg m^{-3})	7.6	7.3	7.2		
Completion (%)	100.0	100.0	100.0		

Table 3: Spearman's correlation factor *r* for (a) monthly data during 2013 – 2015, and (b) monthly data of a typical year, among monitoring stations EEL, ST 1 and ST 2

(a)	EEL	ST 1	ST 2	Warm/Cold Period
EEL	1.000	0.745[1]	0.643[2]	0.048
ST 1		1.000	0.867[2]	0.640[1]
ST 2			1.000	0.401[1]
Warm/Cold Period				1.000

(b)	EEL	ST 1	ST 2
EEL	1.000	0.624	0.608[1]
ST 1		1.000	0.794[2]
ST 2			1.000

[1] Correlation is significant at the 0.05 level   [2] Correlation is significant at the 0.01 level

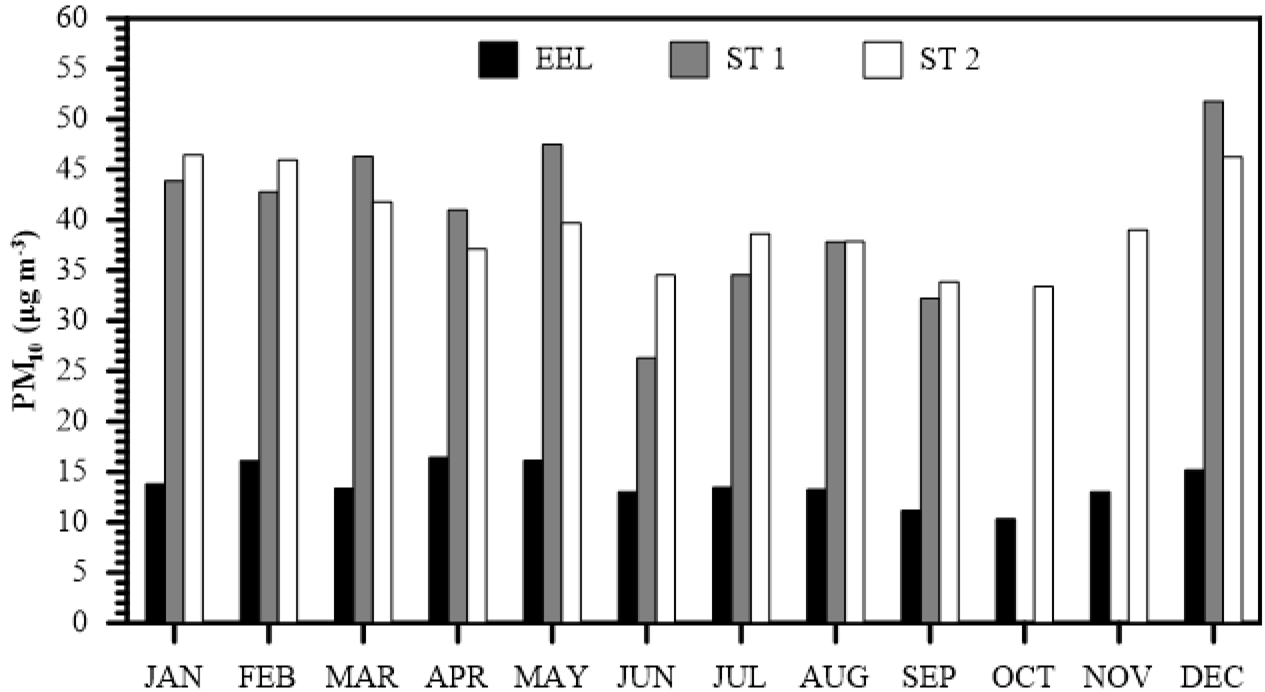


Figure 3: Monthly variations of PM_{10} concentrations at EEL (suburban) in comparison to the corresponding PM_{10} concentrations at Locations of ST 1 and ST 2 (urban-traffic) during 2013 - 2015

It is noticed that PM_{10} range during a typical year is much less significant at EEL station compared to the corresponding range at downtown monitoring stations. Except that, the variation is similar at the monitoring stations; higher PM_{10} levels are recorded during cold and at early warm period where increased demands on heating purposes [11] and Saharan dust effects [12] occurred. Table 3b shows Spearman's correlation factor among EEL, ST 1 and ST 2 for monthly data of a typical year. There is strong correlation (at 0.05 significance level) between EEL and ST 2. Analogous correlation is found between EEL and ST 1, but the rather low percentage of completion of ST 2 data prevents safe conclusions.

In Figure 4, PM_{10} yearly average concentrations from monthly values (Sites EEL, ST 1, ST 2) for the specific monitoring period are presented. The monthly PM_{10} levels at EEL location (suburban area) ranged from 5.7 to 24.7 μg m^{-3} (2013), 12.4 to 18.5 μg m^{-3} (2014) and 9.0 to 17.4 μg m^{-3} (2015). The yearly average PM_{10} concentrations were 13.9±6.0 μg m^{-3}, 14.7±2.0 μg m^{-3} and 12.5±2.3 μg m^{-3}, correspondingly. From GNMNAP's database [11], during 2013, PM_{10} levels at ST 1 location (urban-traffic) ranged from 26.3 to 51.8 μg m^{-3}. During the warm period of 2013 monthly values ranged from 26.3 to 47.5 μg m^{-3}, while at cold period ranged from 42.8 to 51.8 μg m^{-3}. The corresponding mean values were 40.4±7.7 μg m^{-3}, 36.6±7.3 μg m^{-3} and 46.2±4.0 μg m^{-3}. No data are available during 2014 - 2015 at GNMNAP's database for ST 1. The monthly PM_{10} concentrations at ST 2 location (suburban area) ranged from 30.4 to 58.5 μg m^{-3} (2013), 30.3 to 49.3 μg m^{-3} (2014) and 29.6 to 56.7 μg m^{-3} (2015). The yearly average PM_{10} concentrations were 40.6±8.1 μg m^{-3}, 39.4±6.0 μg m^{-3} and 38.7±9.1 μg m^{-3}, correspondingly, showing a slight reduction.

Table 4 summarizes statistical results for PM_{10} annual values during 2013 – 2015. Additionally, relative results are presented separately for both warm and cold period for each year. It is clearly shown that the air quality at the UPC suburban area and the entire area is rather insignificantly affected by seasonal factors that influence PM_{10} concentration levels. On the other hand, the increased concentrations that appear at downtown area during the cold period show that central heating sources also contribute to PM_{10} levels. Annual PM_{10} concentration levels at UPC are below the EEA's and US-EPA's Limits and also the stricter WHO's Guidelines (Table 1). On the other hand, the air quality

at Patras downtown seems rather aggravated by PM_{10} concentrations during 2013 - 2015. At that period, the annual PM_{10} levels at UPC remained practically constant, while the corresponding levels in Patras downtown show a somewhat decrease, as it is deduced by ST 1's data. Cold's period PM_{10} levels were higher than warm's period.

Table 4: Statistical analysis of annual PM_{10} concentrations (μg m^{-3}) during 2013-2015 at the monitoring stations EEL, ST 1 and ST 2

	Period	Range (μg m^{-3})	Average ± St. Dev (μg m^{-3})	Completion (%)
		Monitoring EEL Station, University of Patras Campus		
2013	Year	5.7 – 24.7	13.9 ± 6.0	100.0
	Warm	7.5 – 24.7	15.2 ± 7.2	100.0
	Cold	5.7 – 18.4	12.5 ± 4.8	100.0
2014	Year	12.4 – 18.5	14.7 ± 2.0	100.0
	Warm	13.2 – 18.5	15.1 ± 1.9	100.0
	Cold	12.4 – 18.5	14.3 ± 2.2	100.0
2015	Year	9.0 – 17.4	12.5 ± 2.3	100.0
	Warm	10.4 – 12.9	11.7 ± 1.0	100.0
	Cold	9.0 – 17.4	13.2 ± 3.1	100.0
		Monitoring ST 1 Station, Drosopoulou Sq.		
2013	Year	26.3 – 51.8	40.4 ± 7.7	83.3
	Warm	26.3 – 47.5	36.6 ± 7.3	100.0
	Cold	42.8 – 51.8	46.2 ± 4.0	66.7
2014	Year	n/a	n/a	n/a
	Warm	n/a	n/a	n/a
	Cold	n/a	n/a	n/a
2015	Year	n/a	n/a	n/a
	Warm	n/a	n/a	n/a
	Cold	n/a	n/a	n/a
		Monitoring ST 2 Station, King George A΄ Sq.		
2013	Year	30.4 – 58.5	40.6 ± 8.1	100.0
	Warm	30.4 – 58.5	39.6 ± 10.4	100.0
	Cold	31.9 – 47.3	41.5 ± 5.8	100.0
2014	Year	30.3 – 49.3	39.4 ± 6.0	100.0
	Warm	30.3 – 41.7	37.7 ± 4.3	100.0
	Cold	30.6 – 49.3	41.0 ± 7.3	100.0
2015	Year	29.6 – 56.7	38.7 ± 9.1	100.0
	Warm	29.6 – 43.9	33.6 ± 5.3	100.0
	Cold	31.2 – 56.7	43.9 ± 9.5	100.0

n/a: Not available data

4. CONCLUSIONS

Analyzing PM_{10} concentrations for three monitoring stations in major Patras area during a three years period, we may conclude that Patras air quality depends on the city's activities. Low annual levels of concentrations occur at the suburban area, below the limit values of EEA and US-EPA, as well as the WHO guidelines, while higher PM_{10} concentrations are recorded at Patras downtown. Continuous maintenance of GNMNAP's monitoring stations is great importance as the poor data completion of ST 1 prevents safe conclusions. Relocation and redesign of the GNMNAP's stations may be

necessary, especially for the monitoring station ST 1, as its values are overlapped by the other station (ST 2) at the city center, while there are other more critical areas of Patras needing air pollution monitoring.

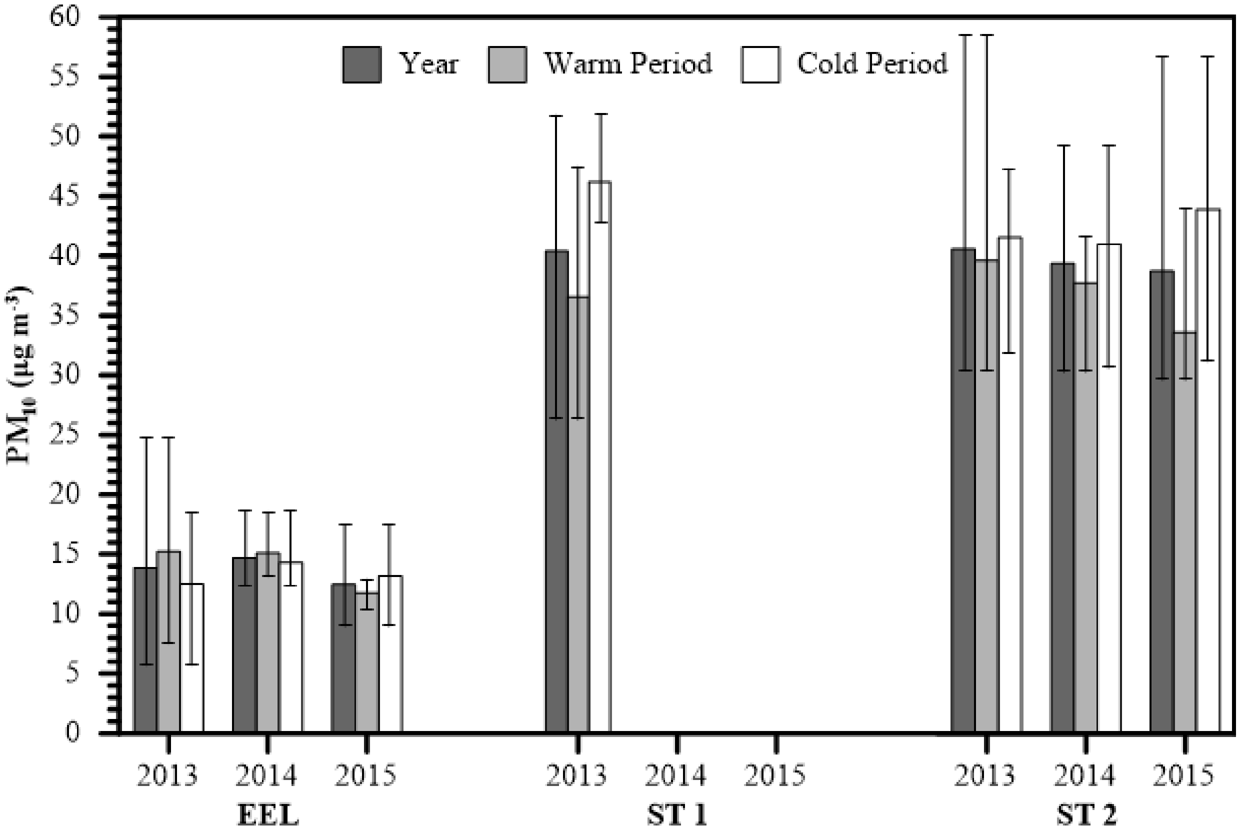


Figure 4: Yearly variations of mean monthly PM_{10} concentrations at EEL (suburban) in comparison to the corresponding PM_{10} concentrations at Locations of ST 1 and ST 2 (urban-traffic) for warm and cold period during 2013 - 2015

References

1. World Health Organization (2006). "**Air Quality Guidelines - Global Update 2005**", ISBN 92 890 2192 6.
2. European Environment Agency (2012). "**Air Quality in Europe – 2012 Report**", ISBN 978 92 9213 328 3 doi:10.2800/55823
3. European Environmental Agency (2013). "**Air Pollution Fact Sheet 2013. European Union**", (EU-27).
4. US-EPA (2009*). "***Integrated Science Assessment for Particulate Matter**", EPA/600/R-08/139F
5. Pappas V. (2011). "The master plan of the University of Patras Campus", **Chorographies** 2 (1): 13-20, ISSN 1792 3913 (in Greek)
6. Yannopoulos, P.C. and Bloutsos, A. A. (2014). "**Monitoring Air Pollution in the University of Patras Campus, Greece, and Data Evaluation for the period 2012-2013**". LAP Lambert Academic Publishing - ISBN: 978-3-659-64074-2
7. http://www.ypeka.gr (accessed November 1st, 2017, in Greek)
8. Yannopoulos, P.C. (2008). "Long-term assessment of airborne particulate concentrations in Patras, Greece", **Fresenius Environmental Bulletin**, 17 (5), pp. 608-616.

9. Yannopoulos, P.C. and Skokaki, G. N. (2003). "Particulate and sulfur dioxide concentration measurements in Patras, Greece", **Air and Waste Management Association**, 53, 957-970.
10. Bloutsos A.A. and Yannopoulos P.C. (2017). "Monitoring Particulate Pollution in the University of Patras Campus, Greece". In: Karacostas T., Bais A., Nastos P. (eds) **Perspectives on Atmospheric Sciences. Springer Atmospheric Sciences**. Springer, Cham. ISBN 978-3-319-35095-0
11. Yannopoulos P.C. (2014). "A cost-effective methodology for spatial concentration distributions of urban air pollutants", **Water, Air, & Soil Pollution**, 225:1989 (doi: 10.1007/s11270-014-1989-7).
12. Bloutsos, A. A. and Yannopoulos, P. C. (2014). Atmospheric pollution at the University of Patras Campus during fire events. **Proceedings of the 12th International Conference on Meteorology, Climatology and Atmospheric Physics** (COMECAP 2014), 28-31 May, Heraklion of Crete Island, Greece.
13. Pikridas, M., Tasoglou, A., Florou, K. and Pandis, S. N. (2013). "Characterization of the origin of fine particulate matter in a medium size urban area in the Mediterranean". **Atmospheric Environment**, 80, 264–274.
14. Maraziotis, E., Sarotis, L., Marazioti, C. and Marazioti, P. (2008). "Statistical analysis of inhalable (MP10) and fine particles (PM2.5) concentrations in urban region of Patras, Greece". **Global NEST J.**, 10, 123–131.
15. Karagiannidis, A., Poupkou, A., Giannaros, T., Giannaros, C., Melas, D. and Argiriou, A. (2015). "The Air Quality of a Mediterranean Urban Environment Area and Its Relation to Major Meteorological Parameters". **Water Air Soil Pollut**, 226:2239 (doi: 10.1007/s11270-014-2239-8).
16. Matthaios, V. N., Triantafyllou, A. G. and Koutrakis, P. (2017). "PM_{10} episodes in Greece: Local sources versus long-range transport—observations and model simulations". **J. Air Waste Manage. Assoc.**, 67(1):105–126 (doi: 10.1080/10962247.2016.1231146).
17. Tsiflikiotou, M. (2014). "**Spatial distribution of summertime particulate matter and its composition in Greece**". Master Thesis in Chemical Engineering, Energy & Environment, University of Patras, Patras, Greece.
18. Valavanidis, A., Vlachogianni, T., Loridas, S. and Fiotakis, C. (2015). "Atmospheric Pollution in Urban Areas of Greece and Economic Crisis. Trends in air quality and atmospheric pollution data, research and adverse health effects".
19. http://www.chem.uoa.gr/wp-content/uploads/epistimonika_themata/atmosph_pollut_greece.pdf
20. (accessed April 12, 2018).
21. Manousakas, M.-I. G. (2014). "**Study of the effect of anthropogenic and natural sources in the concentration of Airborne Particulate Matter PM10 and PM2.5 in urban and industrial areas**". Ph.D. Thesis, Department of Chemistry, University of Patras, Patras (in Greek).

SATELLITE DATA AS INDICATOR OF FOREST DIEBACK: THE STUDY CASE OF THE PINEWOOD FOREST OF CASTELPORZIANO (CENTRAL ITALY)

F. Recanatesi[*1], C. Giuliani[2], B. Cucca[1] and M.N. Ripa[1]

[1] Department of Agricultural and Forestry Sciences (D.A.F.N.E.) University of Tuscia, Viterbo (Italy),

[2] PhD student in Landscape and Environment. Sapienza University, Rome (Italy)

[*]Corresponding author: e-mail: fabio.rec@unitus.it

Abstract

Mapping forest health condition, especially in protected areas, is a major concern for forest planning, biodiversity assessment and for understanding the potential impacts of antropic activities on natural ecosystems. In this context, at wide scale, remote sensing of satellite data is one of the most important data sources for monitoring health state of forest stand. Till now, many satellites and sensors with different resolutions suitable for variety of land cover monitoring tasks have been launched. Within all these sensors, those with high temporal and spatial resolution play an important role especially in mediterranean environment where high landscape fragmentation and spatial distribution of stand forest represent a limiting factor in vegetation analysis.

The current work deals with the use of the Sentinel-2 images to produce long-term monitoring system based on the Normalized Difference Vegetation Index (NDVI). The study area is represented by the pinewood forest of Castelporziano, a protected area located in the metropolitan area of Rome (Central Italy), recently involved in a quick decline of vegetative condition due to a scolytidae (*Tomycus destruens* Mill.) pest propagation.

Keywords: Remote sensing, NDVI, Sentinel-2, GIS, Mediterranean pinewood, Insect infestation

1. INTRODUCTION

Landscape fragmentation characterizes Mediterranean regions and causes an increase in environmental vulnerability, especially due to the antropic activities. As a consequence, many protected areas located in urban or peri-urban environments today are highly vulnerable towards landscaping changes that, in most cases, cause a decline of environmental quality and cultural heritage. In this context, monitoring forest health is a key indicator of environmental ecological conditions and, in particularly, for those performing an essential role in maintaining the ecological balance in vulnerable territories.

Indeed, forestry ecosystems play a significant social, economic and environmental impact and nowadays they are considered a source of ecosystems services especially in peri-urban territory characterized by high population density.

In this topic, the availability of high-frequency remote sensing time series represents an efficient tool in monitoring the evolution of an ecosystem to be assessed at different temporal and spatial scales.

Among modern methods to monitor terrestrial ecosystems, remote sensing of multispectral satellite images is of primary importance thanks to its capability of providing synoptic information over wide areas with high acquisition frequency [Frampton et al., 2013; Sheeren et al., 2016; Topaloglu et al.,

2016; Lia et al., 2017]. For this reason, scientists working in this field have developed vegetation indices (VI) for qualitatively and quantitatively evaluating vegetative cover using multi-spectral data. In fact, over forty vegetation indices have been developed during recent decades, amongst which the Normalized Difference Vegetation Index (NDVI) is the most widely used in monitoring the health conditions of forest surfaces [Bannari et al., 1995]. In fact, the degree of vigor in forest vegetation cover can be classified according to its spectral response, which in the red (630-690 nm) is strongly correlated with chlorophyll concentration, while the spectral response in near infrared (760-900 nm) is correlated by the leaf area index and green vegetation density. Thanks to these properties, NDVI can be utilized as an indicator of possible vegetation stress, particularly that due to water shortage or pest diffusion [Maselli 2004; Gooshbor et al., 2016].

In the present research, we have developed a monitoring system to map crown dieback of a coastal pinewood forest located in a protected area in the metropolitan area of Rome and that, in 2016, declined by a sudden diffusion of bark beetle (*Tomicus destruens* Mill.). To achieve this goal, we used a time series data set from 2015 to 2017, which is offered by Sentinel-2 satellite, provided by the European Space Agency (ESA) and processed according to NDVI index in a Geographic Information Systems (GIS) environment. Due to its high fragmentation, the pinewood stand has been previously determined, at the scale of forest unit, using a supervised classification of multispectral images and data fields.

In order to correlate the various levels of NDVI decrease in risk classes, a campaign of field surveys was carried out in 2017 to correlate data acquired to vegetative vigor of pinewood.

The results of this research allowed us to separate with high precision the pinewood canopy by the rest of the forest and, in this way, to diachronically analyze the vegetative vigor by using NDVI index in an accurate way.

2. MATERIAL AND METHODS

The study area is represented by the pinewood forest of Castelporziano, a State Nature Reserve located in a peri-urban area of the municipality of Rome, figure 1. Castelporziano has a total surface area of 6.000 ha and its land use is characterized mainly by forest and to a lesser extent by agricultural activities.

This territory is the last remnant of the ancient Mediterranean coastal forest, in which the predominant species are broadleaf oaks (4.000 ha) and pinewood (900 ha) mainly characterized by *Pinus pinea* L. In particular, the pinewood forest of Castelporziano, with numerous trees aging over one hundred years or more, is the last remaining example today of mature pinewood forest along the Tyrrhenian coast after the recent fire, which occurred in August 2017, causing huge damage to the neighboring ancient pinewood forest of Castelfusano. For these reason, the territory of Castelporziano can be considered as a unique environment in terms of natural and cultural values [Recanatesi et al., 2013; Recanatesi 2014]. Furthermore, it is listed in the Habitat Directive with two Sites of Community Importance (SCI) and the whole territory is classified as a Special Protection Area (SPA).
In October 2016, the ongoing environmental monitoring program in the Castelporziano pinewood forest, carried out by remote sensing of multispectral Sentinel-2 images, allowed the detection of a diffuse crown dieback in several areas due to a sudden infestation of *Tomicus destruens* Woll,.

Before applying NDVI index, a preliminary classification of pinewood canopy, at forest unit scale, was required. Indeed, Castelporziano pinewood forest, at unit forest scale, especially along the shore, presents an heterogeneous distribution on the territory and, often, consociated with other species or, in other cases, with mediterranean macchia.

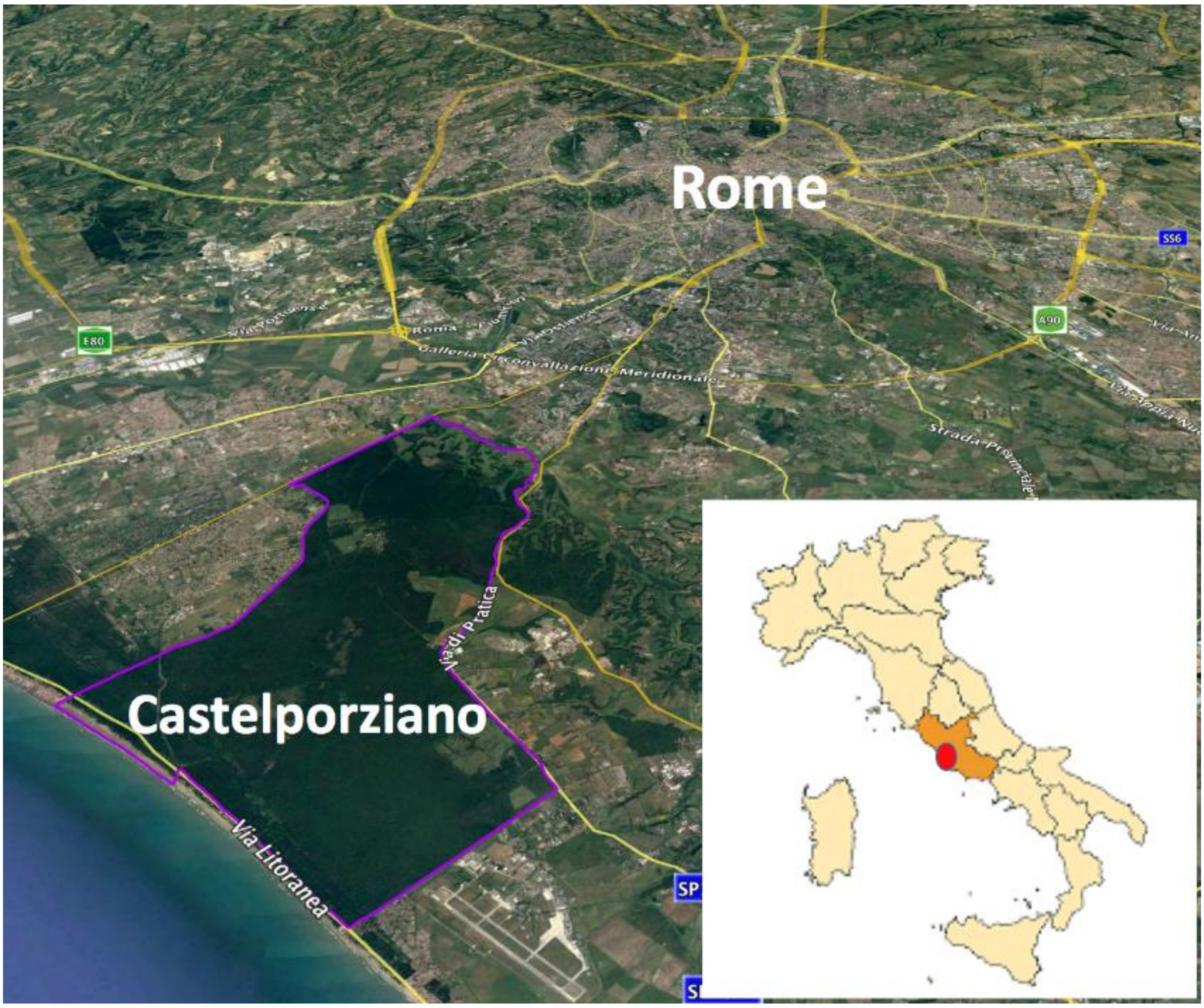


Figure 1: Nature State Reserve of Castelporziano (41°42’50’’N - 12°24’03’’E) and the metropolitan area of Roma

Referring to resolution satellite data used, these characteristics represent a limiting factor in monitoring NDVI difference at unit forest scale. For this reason, using Quickbird satellite multispectral images (year 2002; 0.7m resolution) and Maximum Likelihood algorithm, a supervised classification of pinewood forest was conducted using over 150 points of training set derived by aerial photo interpretation and field investigations. Figure 2 shows an example of classification for a forest unit where pinewood canopy is classified and separated by other land cover stands.

Once defined the canopy layer of pinewood forest for Castelporziano, a series of georeferenced Sentinel-2 images (06/21/2015; 06/08/2016; 06/06/2017), provided by the ESA, were analyzed to map forest decline using NDVI index.

The Pinewood forest was assumed to be relatively healthy in 2015 and therefore the data relating to this period served as reference in this research. According to Richter’s atmospheric correction method (Richter et al., 2011), the selected images were corrected with the Sentinel Application Platform (SNAP) program running in Sen2Core. This performs the atmospheric, terrain and cirrus correction of Top-Of- Atmosphere Level 1C input data. Geometric distortion of the analyzed images was corrected with the rectified 10 m Digital Terrain Model (D.T.M.) provided by the Italian Ministry of Environment.

The forest inventory data were acquired from the Mediterranean Ecosystem Observatory Office of Castelporziano in a GIS resource. This data base contained spatial information of individual stands, topographic features, species composition and biophysical information such as tree age, basal area and site index for each forest stand. In the present research all land use except pinewood forest were treated as non-forest and were excluded in the following analysis.

Using the NDVI image in 2015 as a reference, the 2016 and 2017 NDVI images were normalized by means of histogram match. The differential NDVI (ΔNDVI) could then be calculated as:

$$\Delta NDVI_{(t-t_{+1})} = \frac{NDVI_{(t+1)} - NDVI_{(t)}}{NDVI_{(t)}} \tag{1}$$

The histograms of the 2016 and 2017 NDVI images are characterized by an approximately standard Gaussian distribution, centered at approximately ΔNDVI = 0. In accordance with the interpretation used by Wang (Wang at al., 2007; Wang et al., 2008), negative ΔNDVI in the left tail of the histogram reveals pinewood crown dieback and tree mortality attributed from loss of leaf moisture content. Positive ΔNDVI, in the right tail, of the histogram represents crown recovery of the pinewood. To create a map of the risk, a field survey was carried out in summer 2017 to define the risk classes based on ΔNDVI percentage values. To this aim, according with the methodology proposed by Ogaya [Ogaya et al., 2015] a conspicuous number of pine trees with different ΔNDVI was examined so as to classify them in different thresholds of decline as reported in Table 1. In this phase we visually determined the percentage of dead vegetative apices for sampled trees and stand canopy density.

Once the risk classes had been defined and validated in the field, a preliminary analysis was conducted to correlate the risk classes to dendrometric variables, such as volume and age. To do this we matched map risk class information with volume and age layers detected at the scale of forest parcel. No environmental variable, such as slope, aspect or elevation, was considered in this study because the territory analyzed is mainly flat, being located in a coastal area.

Table 1: Risk classes and relative Δ NDVI (2015-2017) percentage value

Risk classes	Δ NDVI
Strong Recovery	from +5 to +20%
Neutral Recovery	from -5% to just less than +5%
Low Decline	from -5% to just less than -15%
Medium Decline	from -15% to just less than -25%
High Decline	from -25% to just less than -45%
Dead Plants	-100%

3. RESULTS

The supervised classification of Quickbird images performed for the determination of pinewood canopy has resulted very efficient. Through a check carried out with over 70 control points, a Kappa Index of Agreement (KIA) of 85% was found.

In the observation period 2015-2017, based on the classes risk reported in Table 1, in terms of pinewood decline four levels of forest change were identified from the ΔNDVI images: low decline, medium decline, high decline and dead plants respectively with 10, 17, 21 and 5% of the whole surfaced analyzed, the remaining surface (47%) was classified as strong recovery or, weak recovery. In figure 3 the risk assessment of the whole territory is reported and an example of methodology used is shown in the different steps: unit forest, the pinewood canopy layer extracted by supervised classification, the NDVI index applied to determine the risk classes calculated as difference for the observed period.



Figure 2: Pinewood forest canopy. From the top to bottom: Unit Forest pinewood (green dashed line); canopy cover derived by supervised classification of Quickbird images; Corresponding cells of the Sentinel-2



Figure 3: On the left: Castelporziano Nature Reserve zoning of the pinewood according to the identified risk classes shown in Table 1. On the right, an example of the methodology used: Forest Unit; Pinewood canopy layer; NDVI index for 2015, 16 and 17 with the classification in risk classes

To determine/find out the effect of biological variables on the pinewood decline, we compared the occurrence rate for the class “high decline” (ΔNDVI from -25% to just less than -45%) with volume and age. For the latter, the correlation occurred just for that forest units in which the age was known. Nonetheless, from the results obtained and considering the observed parameter, it emerges that a strong correlation exists between age and pinewood decline (R^2=0.6), as shown in figure 4. On the contrary, only a weak correlation was observed between volume and pinewood decline (R^2=0.3), as shown in figure 5. Regarding the role played by volume in causing pinewood decline, it was observed that a significant increase in decline occurred starting from 350 m^3/ha.

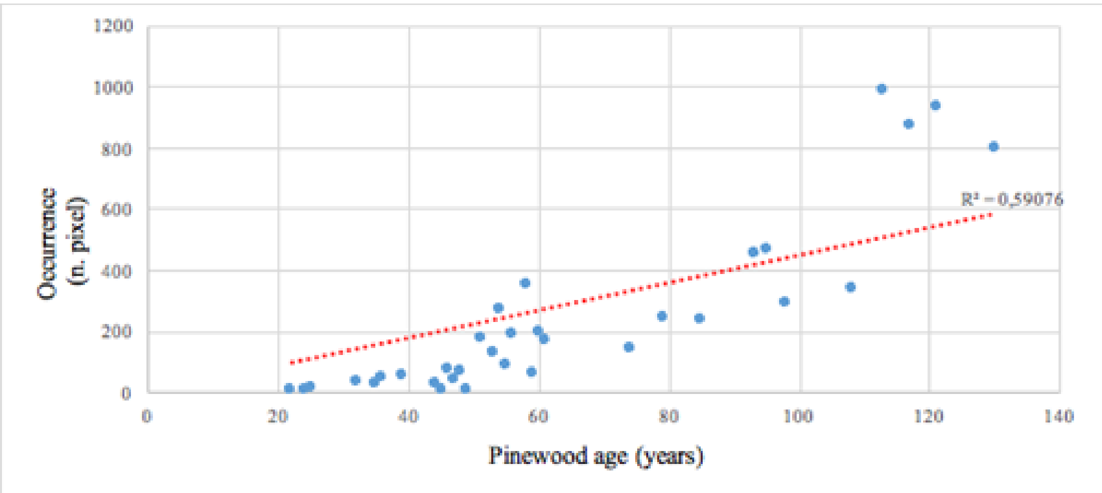


Figure 4: Comparison between pinewood age (years) and occurrence of the risk class - high decline

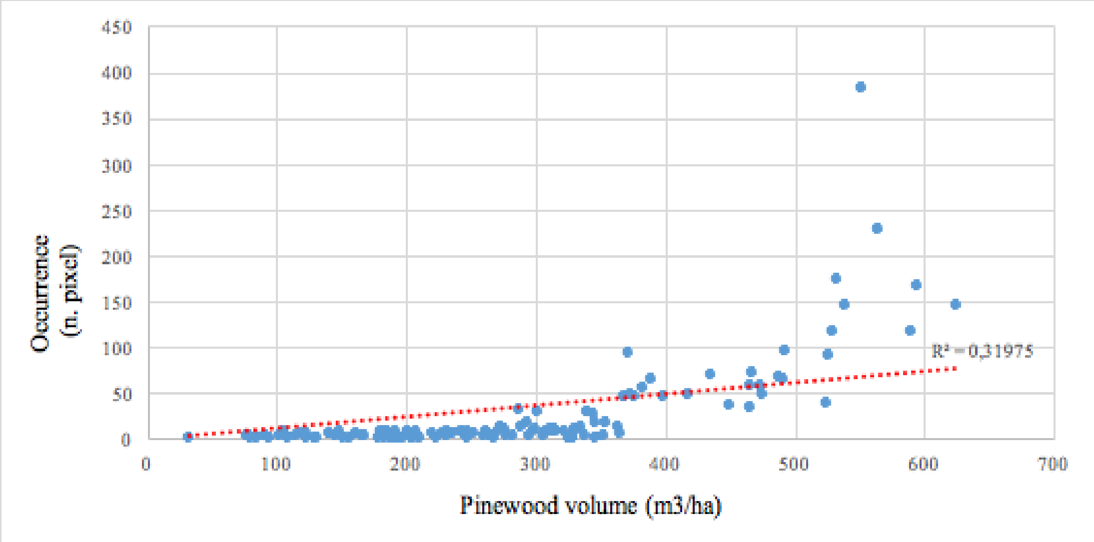


Figure 5: Comparison between pinewood volume (m³/ha) and occurrence of the risk class - high decline

4. DISCUSSION AND CONCLUSIONS

The high resolution classification concerning the canopy of Castelporziano pinewood today represents, in the medium and long term, a strategic tool in monitoring vegetation health condition by remote sensing data and Sentinel-2 multi-spectral images used in the environmental monitoring of the protected area of Castelporziano and has be proven to be both accurate and efficient in monitoring the health conditions of vegetation, by application of the NDVI index.

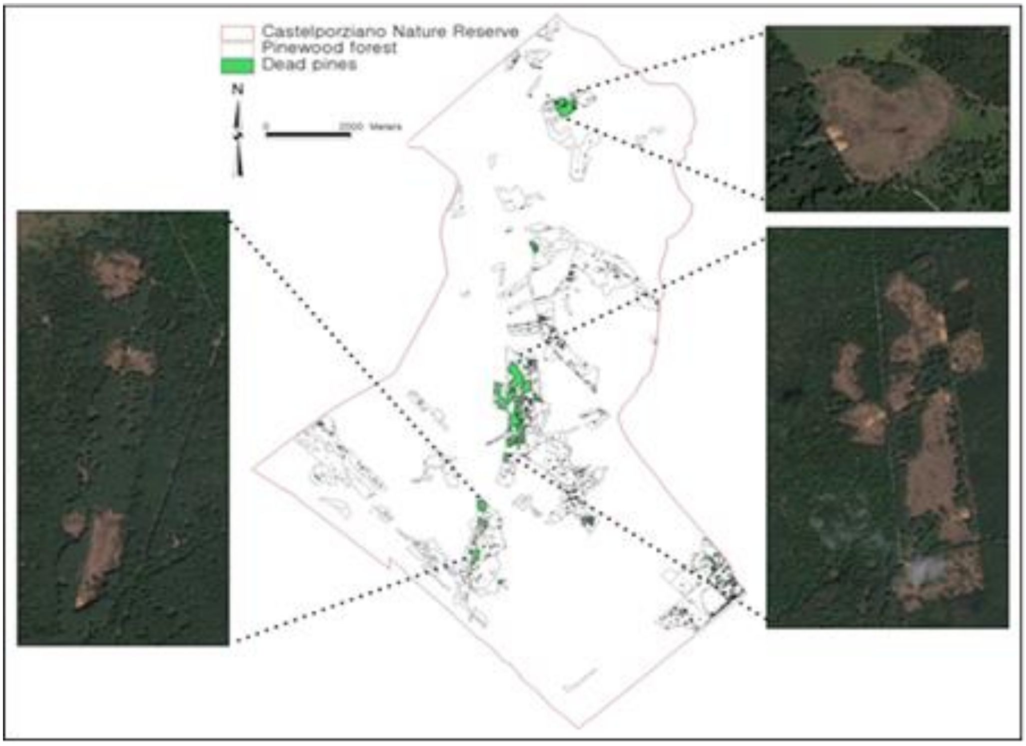


Figure 6: Pinewood forest of Castelporziano and Dead pines detected by NDVI index. Photo images shows the consequent forest thinning action occurred in April 2017

The calibration of the NDVI values in risk classes allowed us to zone the whole territory in terms of pinewood crown decline rate and consequently to plan efficacious measures to mitigate the spread of Tomicus in Castelporziano. In this way, from the first observation of Tomicus in the pinewood of

Castelporziano, which occurred in October 2016, a program of forest harvesting was promptly planned to mitigate the diffusion of pest in the rest of the Castelporziano pinewood. Thus, in just four months, almost 60 ha were subjected to forest thinning and, by 2018, another 100 ha will have been thinned as shown in figure 6 that shows the areas of decline detected by the NDVI index application and the consequent forest thinning measures already implemented.

References

1. Bannari A., Morin D., Bonn F. (1995). A review of vegetation indices. **Remote Sensing Reviews**, Vol. 13, pp. 95-120
2. Frampton W. J., Dash J., Watmough G., Milton E. J. (2013). Evaluating the capabilities of Sentinel-2 for quantitative estimation of biophysical variables in vegetation. **Journal of Photogrammetry and Remote Sensing** 82 (2013) 83–92
3. Gooshbor L., Pir Bavaghar M., Amanollahi J., Ghobari H. (2016). Monitoring Infestations of Oak Forests by Tortrix viridana (Lepidoptera: Tortricidae) using Remote Sensing. **Plant Protect**. **Sci.** Vol. 52, 2016, No. 4: 270–276, doi: 10.17221/185/2015-PPS
4. Lia F., Songa G., Liujunb Z., Yanana Z., Dia L. (2017). Urban vegetation phenology analysis using high spatio-temporal NDVI time series. **Urban Forestry & Urban Greening**. Vol.25, pp.43–57
5. Maselli F. (2004). Monitoring forest conditions in a protected Mediterranean coastal area by the analysis of multiyear NDVI data**. Remote Sensing of Environment**. Vol.89, pp. 423–433
6. Ogaya R., Barbeta A., Başnou C., Peñuelas J. (2015). Satellite data as indicators of tree biomass growth and forest dieback in a Mediterranean holm oak forest. **Annals of Forest Science**, Vol.72, pp.135–144
7. Recanatesi F., Tolli M., Ripa M.N., Pelorosso R., Gobattoni F., Leone A. (2013). Detection of Landscape patterns in airborne LIDAR data in the Nature reserve of Castelporziano (Rome). **Journal of Agricultural Engineering**. Vol.XLIV, pp. 472-477
8. Recanatesi F. (2014). Variations in land-use/land-cover changes (LULCCs) in a peri-urban Mediterranean nature reserve: the estate of Castelporziano (Central Italy). **Rend. Fis. Acc. Lincei** DOI 10.1007/s12210-014-0358-1
9. Richter, R., Wang, X., Bachmann, M., and Schlaepfer, D., "Correction of cirrus effects in Sentinel-2 type of imagery", **Int. J. Remote Sensing,** Vol.32, 2931-2941 (2011).
10. Sheeren D., Fauvel M., Josipovic´ V., Lopes M., Planque C., Willm J., Dejoux J. F. (2016). Tree Species Classification in Temperate Forests Using Formosat-2 Satellite Image Time Series. 8, 734; **doi:10.3390/rs8090734**
11. Topaloglu R. H., Sertel N., Musaoglu N. (2016). Assessment of classification accuracies of sentinel - 2 and Landsat (for land cover/use mapping. The International Archives of the Photogrammetry, **Remote Sensing and Spatial Information Sciences**, Volume XLI-B8, 2016 XXIII ISPRS Congress, 12–19 July 2016, Prague, Czech Republic
12. Wang C., Lu Z., Haithcoat T.L. (2007). Detection forest dynamics responding to oack dieback in the Mark Twain National forest, Missouri. **Forest Ecology and Management**. 240, pp70-78.
13. Wang C., He H. S., Kabrick J. M. (2008). A remote sensing-assisted risk rating study to predict oak decline and recovery in the Missouri Ozark. **GIScience & Remote Sensing**. Vol.45, n.4, pp.406-425.

SURFACE TEMPERATURES AND THERMAL COMFORT CONDITIONS IN NORTHERN GREECE

P. Kosmopoulos[1], A. Kantzioura[1]. K. Michalopoulou[1]

[1]K-eco Projects

[*]Corresponding author: e-mail: pkosmos@env.duth.gr

Abstract

This paper aims, through research and field measurements in open urban spaces, to study the behavior and effect of coating materials to the urban microclimate and to draw conclusions regarding the factors that affect the thermal comfort conditions.

The study attempts to benchmark the effect of design parameters of outdoor urban spaces to the microclimate and the comfort conditions. Two urban areas in different urban centers, Thessaloniki and Kastoria in Northern Greece, are investigated. Considering the analysis of the design parameters and the effects of design interventions to the microclimate, it focuses on thermal indices expressing the conditions of thermal comfort of the users of urban spaces.

Keywords: Thermal comfort, PMV, Urban Open Spaces

1. INTRODUCTION

The covering and construction materials in the contemporary cities and the urban geometrical characteristics affect the microclimatic conditions inside the urban centers (Lau et al, 2011). The radiant balance of the urban space, the convective heat exchange between the ground and the surfaces, the air flowing above the urban area and the heat generated within the city (Mihalakakou et al, 2002), (Santamouris et al, 1999) increase the air temperature in the city. The city has the capacity to modify local climate, and even creats environmental conditions that could be regarded as urban microclimate (Gago et al, 2013), (Giridharan et al, 2004). The urban microclimate affects the thermal comfort conditions in the city.

In the present study two central open areas, a crossway and a square, are selected. The study areas are located in Northern Greece, Thessaloniki and Kastoria. A number of experimental procedures were carried out, in order to measure the surface temperature of asphalt, concrete and stones and to evaluate by using appropriate software the thermal comfort conditions in the study areas. Also, alternative proposals for upgrading are suggested.

2. METHODOLOGY

The field surveys involve surface temperature measurements by a thermal camera and microclimatic monitoring with portable mini-weather stations.

The study areas are located in North Greece, Thessaloniki and Kastoria. The measurements took place during the summer period.

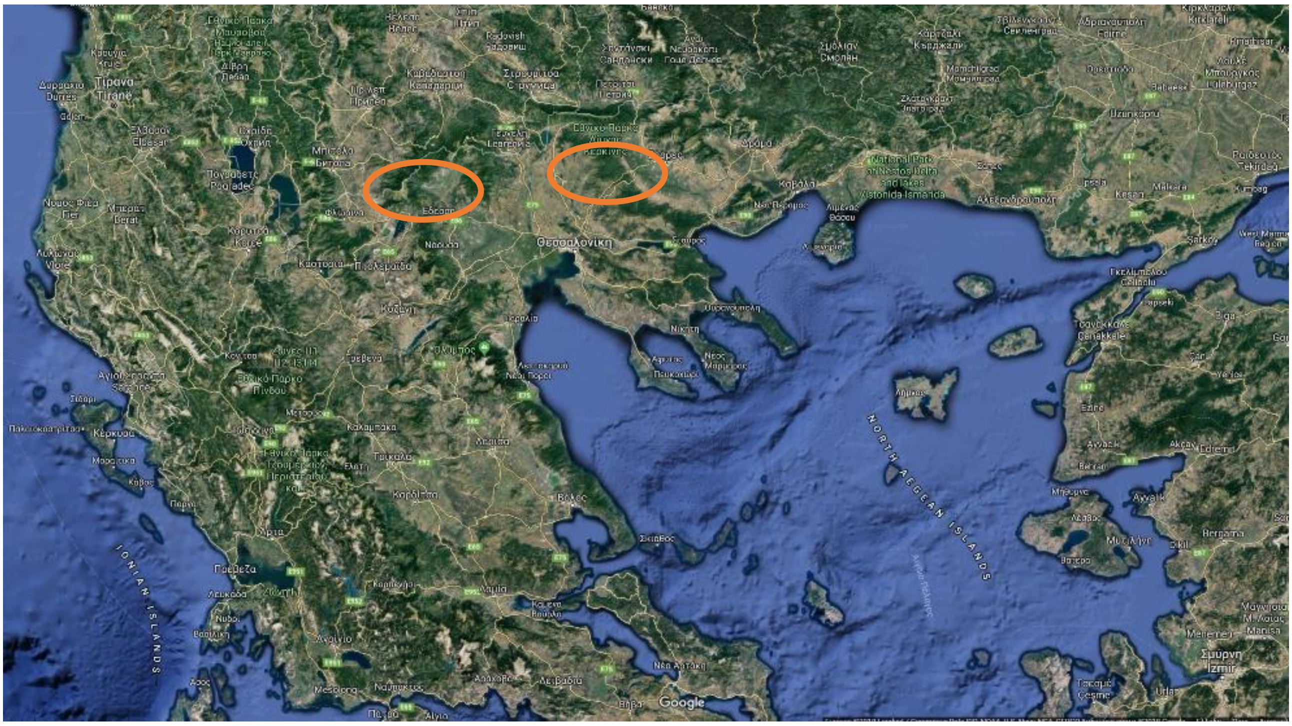


Figure 1: The two Urban Centers in North Greece

The area in Thessaloniki is a central crossway, Metropoleos and Agias Sofias Street (Figure 2), and it consists of high building blocks (Table 1). Data from different measurement points along the streets, from different heights and orientation were collected.

Table 1. Geometric Characteristics of streets, Thessaoloniki

Orientation	Av. Height H (m)	Str Length, L (m)	Av Str Width, W (m)	H/W
West	23	60	12.5	1.8
North	21	70	14	1.4
East	21	100	14	1.5
South	18	50	14	1.3

The area in Kastoria is the Dolcho Square, which occupies an area of about 1075m^2. The height of the surrounding buildings is 3, 6 and 9m. The width of the northern road is about 8m, of the southern road is 6m, of the west side 9 m and of the east side 7-20m. On the other hand, the park is covered by stone plates and there are a few trees.

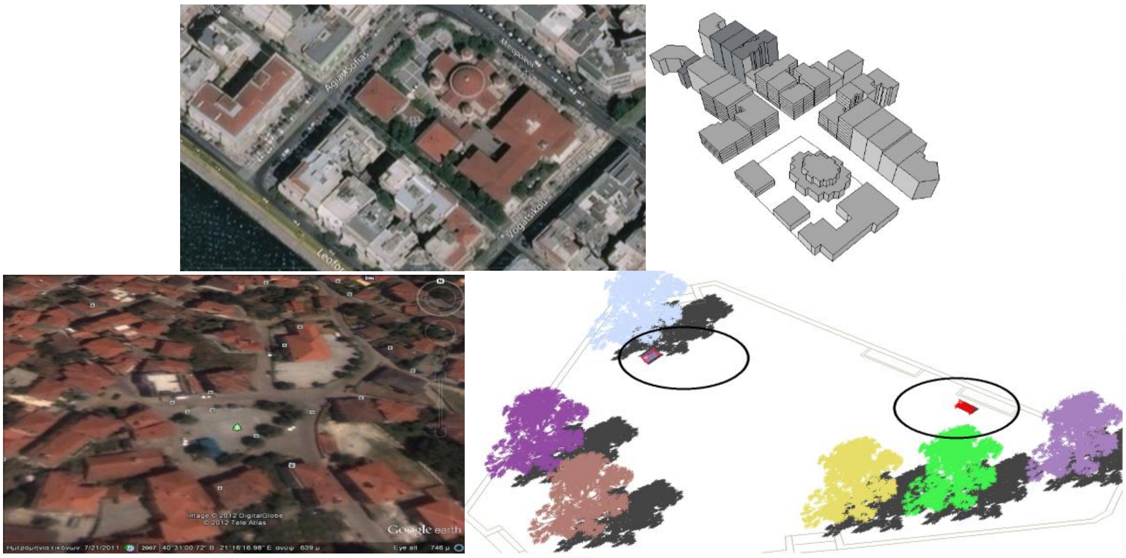


Figure 2: Study areas in Urban the Centers, Norh Greece

3. ANALYSIS

3.1 The crossway

In the crossway the horizontal surface temperatures of asphalt were measured by a thermal camera. In Figure 3, both the observed and the simulated horizontal surface temperature for the crossway are presented, with the use of an ENVI-met model. The average deviation percentage between field measurement data and simulation result data, is about 5-8% for every street. The simulation model calculates greater horizontal Tsurf than the measured values.

The Envi-met model were used to simulate the microclimatic conditions and the surface temperatures. The calculated values were close to measured data. The accuracy of the calculated data permit the simulation of the thermal comfort conditions.

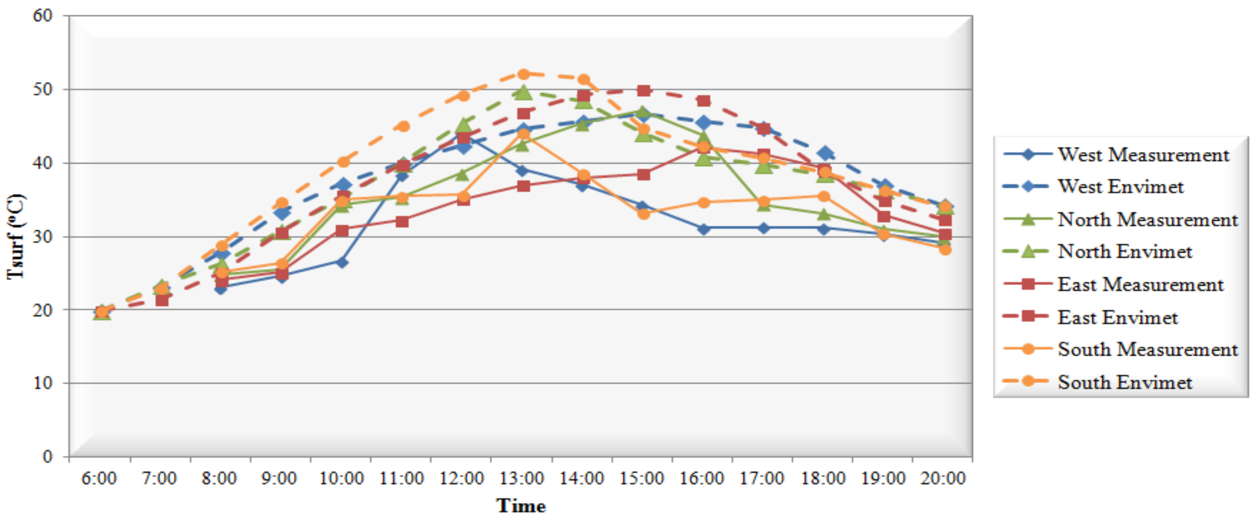
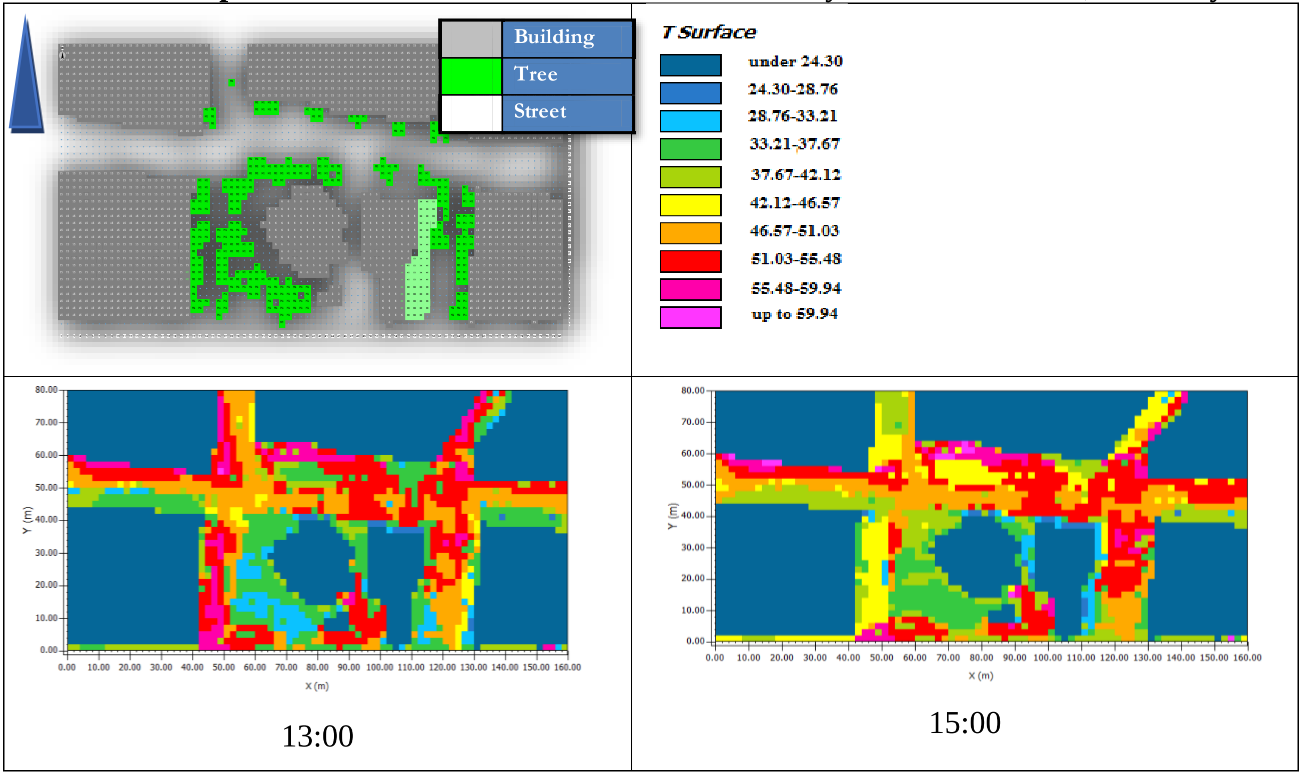


Figure 3: Horizontal surface temperatures in the crossway

According to the ENVI-met simulation results, the maximum horizontal surface temperature is observed at 13:00 pm at the streets located on the North-South axis, while at 15:00 pm at the East-West axis. The maximum calculated temperature approximates 52.20°C, in South Street (Figure 4).

In Table 2 the temperature fluctuations of horizontal surfaces at 13:00 and 15:00pm, according to the simulation model are presented.

Table 2: Temperature fluctuation of horizontal surfaces by simulation model, crossway



The Figure 4 we present a comparison of the variation of thermal comfort index PMV with the temperature variation of the Tsurf. The index PMV is increasing from 8:00am until midday. The increasing of surface temperature is continuing for two more hours. The decreasing of index PMV (reinstatement of thermal comfort) begins two hours earlier than the decreasing of Tsurf (except of the south orientated road).

So, while the feeling of thermal comfort is gradually restored, the surface temperature of the materials remains in high levels. The maximum PMV is approximately 2.5 and displayed at 13:00 to 16:00pm.

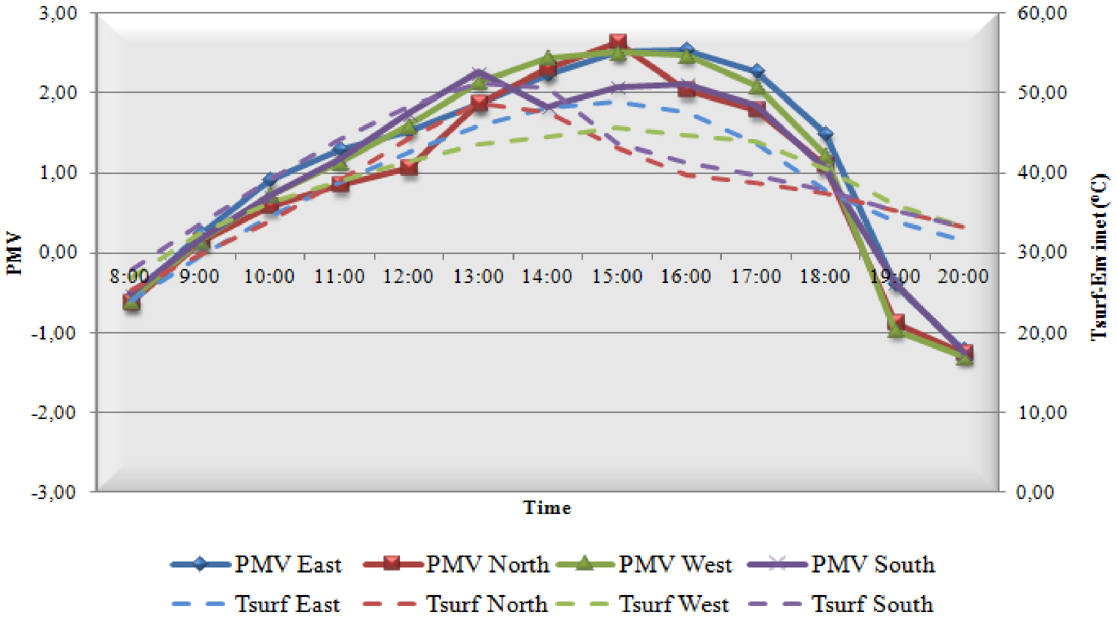


Figure 4. The PMV index and the Tsurf, in each of the four differently orientated streets of the crossway

3.2 The Square

In Figure 5, the surface temperatures of the covered materials in the square is presented.

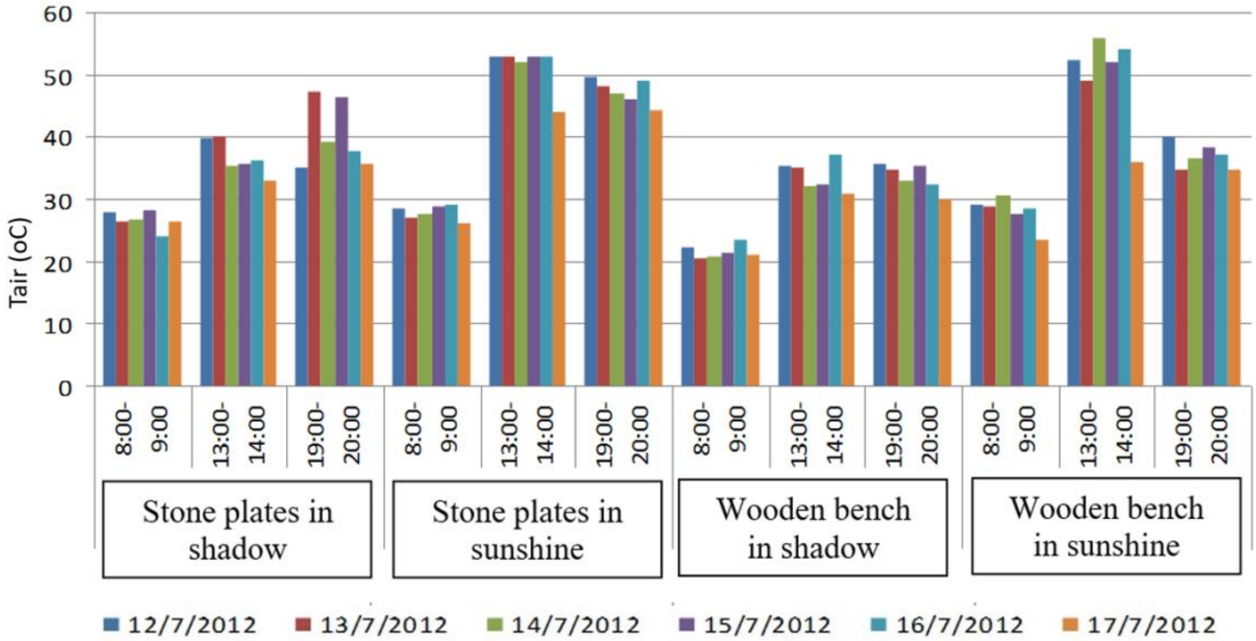


Figure 5: Surface Temperatures of covering and other materials

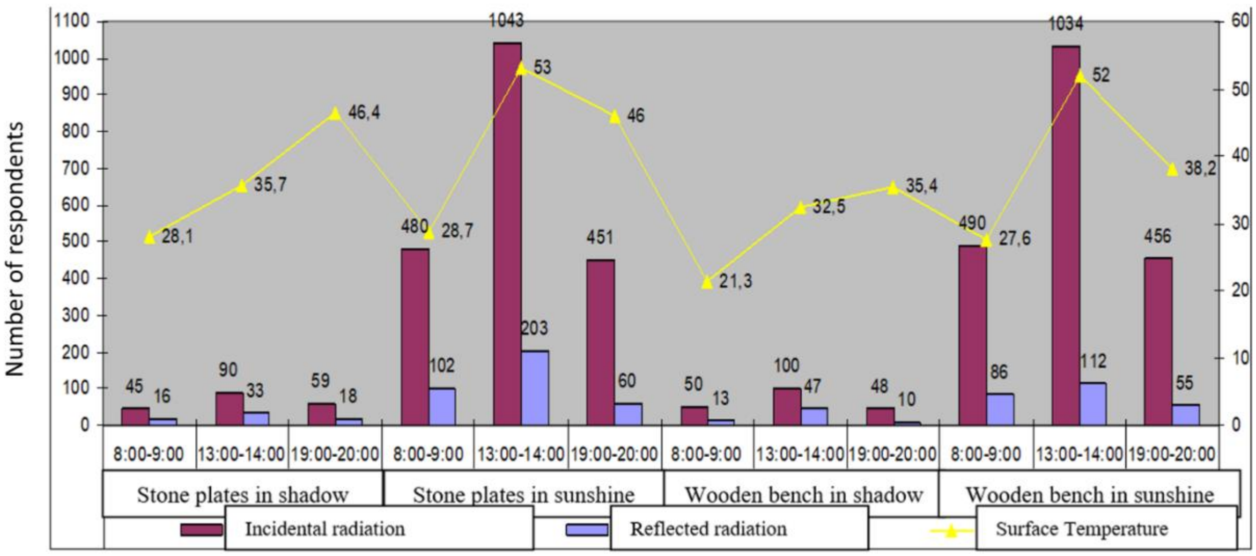


Figure 6: Surface Temperature, Air Temperature (Tair), Black Ball Temperature

In Figure 7 the surface temperatures of covering materials in Square and the Tair over specific materials on height of 1.20 to 1.50m are observed (Kosmopoulos, 2017). The Pv studio, Weather data analysis and Ecotect analysis are used in order to simulate the conditions.

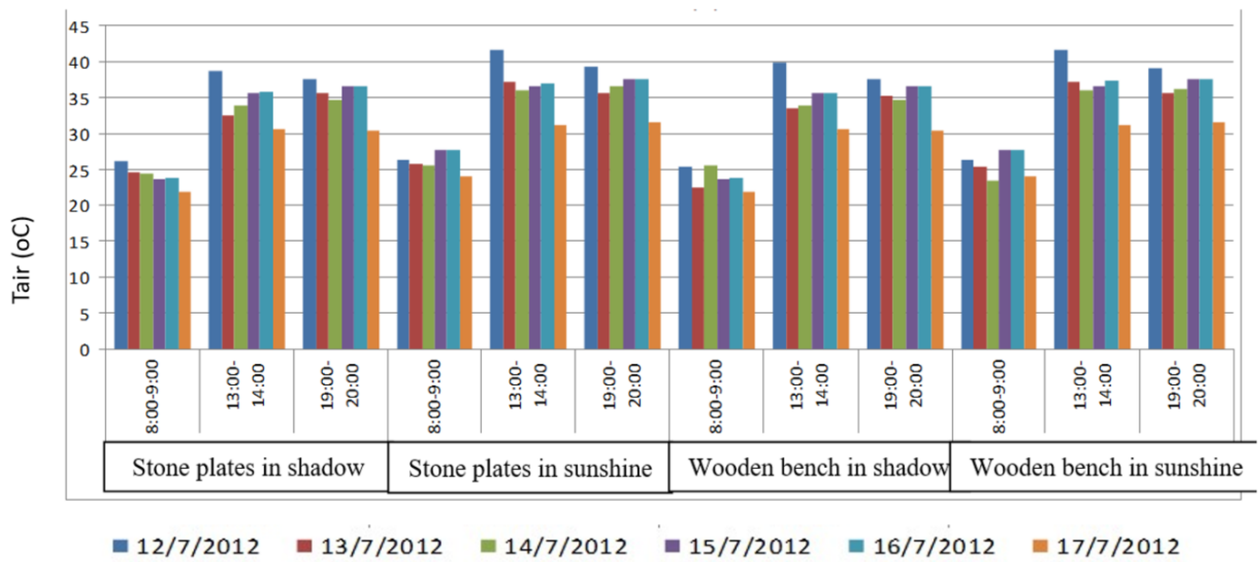


Figure 7: Surface Temperature, Black Ball Temperature

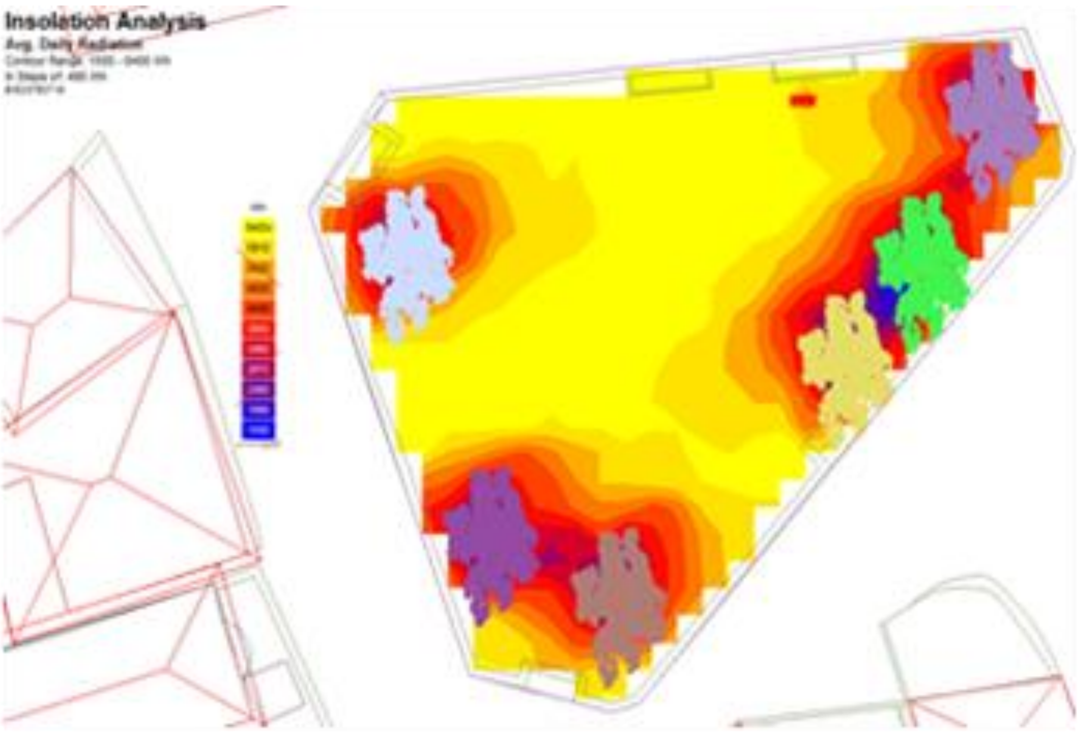


Figure 8: Direct and Diffuse Radiation at the open space.

In the questionnaires gathered, the thermal comfort conditions during morning, noon and afternoon time are investigated. A five-point scale has been used (very cold, cold, neutral, hot, very hot) in order to study the subjective comfort conditions. In Figure 9 the comfort conditions of Doltso Square are observed, during 12-17 July.

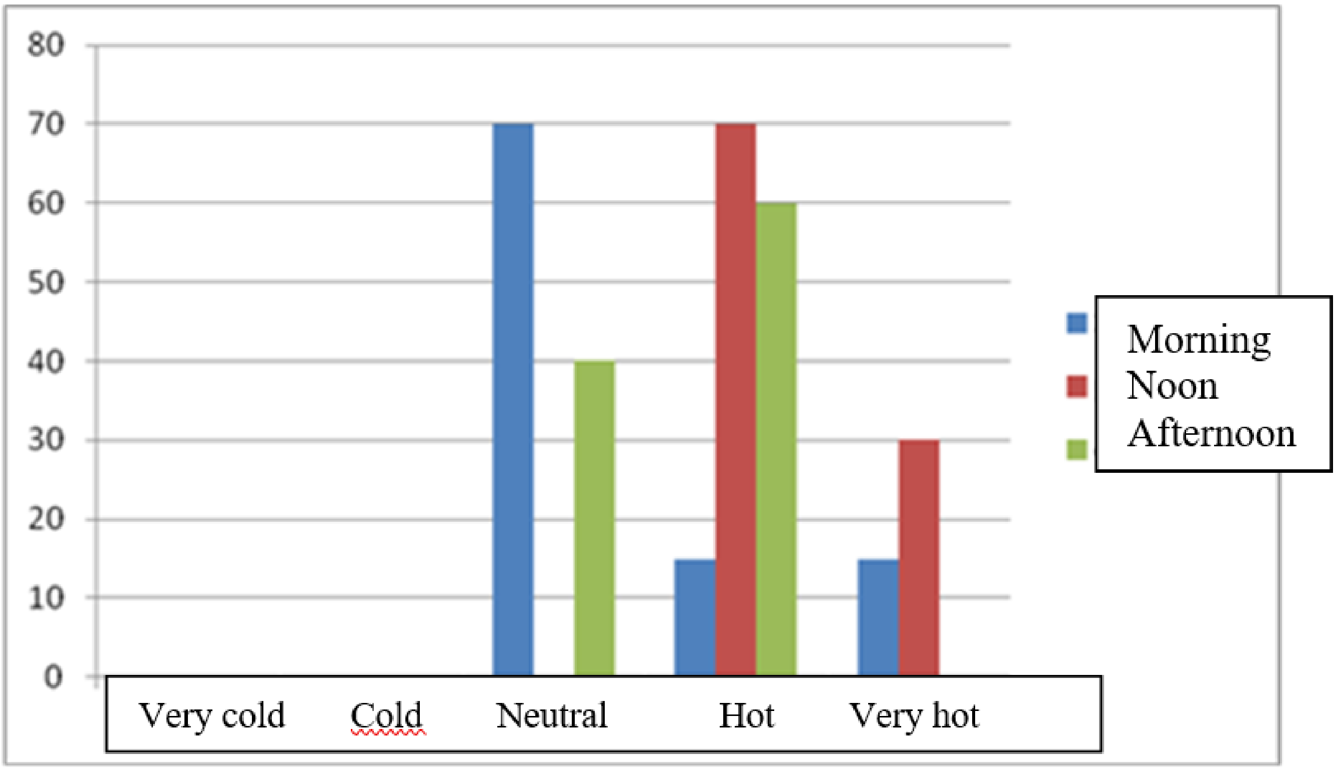


Figure 9: Subjective comfort conditions in square, 42 persons

4. DISCUSSION AND CONCLUSIONS

In this paper, we have presented data gatered from two central areas in two cities in Northern Greece. Although different measuring approaches have been used, very useful conclysions have been extracted regarding the thermal comfort conditions at the height of 1,20 to 1,50 m from the ground, which affect the persons that are walking or are sitted.

Unfortunately, most of the open spaces of Hellenic cities, have been covered with “hot” materials and also suffer from lack of green (trees, grass tec) Thus, we may cloncluded our remarks as follows:

After the analysis of Surface temperatures, air temperature, black ball temperature and the existing thermal comfort conditions intervention, proposals for the upgrading of the comfort conditions are wing.

The replacement of the asphalt (tar) with perforated cement blocks over natural grass, and/or simply grass areas, and specific kinds of trees planted around the study area were analyzed. The improvement of the sensation of thermal comfort is presented in Table 3.

Table 3: Tmrt thermal index before and after the interventions

EXISTING MATERIALS	Tmrt	PROPOSED MATERIALS	Tmrt
White cement stone plates 	65,9	Perforated stones 	63,4
Stone plaques 	65,2	Grass-Planted areas 	63,8
White marble 	68,3	Grass or perforated cement plaques at the parking places 	64,5
Tar 	66,3	Large trees 	62,4

By comparing all the data gathered, it has been concluded that the replacement of the usually used in Greece open spaces materials (asphalt, concrete, stones) with perforated materials or grass, and the plantation of specific kinds of trees, improves largely the thermal comfort conditions of the urban microclimate.

This research project has studied in two urban centers the thermal comfort conditions in open spaces with on site measurements, questionnaires and the use of software. The covered open areas by asphalt, concrete and stones is characterized by high temperatures that lead to the degradation of urban microclimate and the deterioration of thermal comfort conditions. The paper has led to conclusions and proposals towards the improvement of thermal conditions in urban centers and the optimization of urban environment.

References

1. Gago E.J., Roldan J., Pacheco- Torres R., Ordóñez J., The city and urban heat islands: A review of strategies to mitigate adverse effects, **Renewable and Sustainable Energy Reviews**, Volume 25, (2013), pp.749–758
2. Giridharan R, Ganesan S, Lau S.S.Y., Day time urban heat island effect in high- rise and high-density residential developments in Hong Kong. **Energy and Building**, Volume 36, (2004), pp. 525–34.
3. Kosmopoulos P., Michalopoulou K., 2017, Comfort Conditions and microclimate in open urban areas, **University Studio Press**, Thessaloniki

4. Lau, S. S. Y., Yang, F., Tai, J., Wu, X. L., & Wang, J., (2011), The study of summer-time heat island, built form and fabric in a densely built urban environment in compact Chinese cities: Hong Kong, Guangzhou. **International Journal of Sustainable Development**, Vol. 14(1-2), pp. 30-48

5. Mihalakakou, P., Flocas, H.A., Santamouris, M., Helmis, C.G., (2002), Application of neural networks to the simulation of the heat island over Athens, Greece, using synoptic types as a predictor. **Journal of Applied Meteorology**, Vol. 41 5, pp. 519–527.

6. Santamouris, M., Mihalakakou, G., Papanikolaou, N., Assimakopoulos, D.N., (1999), A neural network approach for modeling the heat island phenomenon in urban areas during the summer period. **Geophysical Research Letters**, Vol. 26 3, pp. 337–340.

INVESTIGATION OF THERMAL COMFORT CONDITIONS IN URBAN CENTERS OF NORTHERN GREECE

P. Kosmopoulos[1], A. Kantzioura [2], A. Moumtzakis[2]

[1]K-eco Projects co, f. Director of the Laboratory of Environmental and Energy Design of Buildings and Settlements, DUTH,

[2]Laboratory of Environmental and Energy Design of Buildings and Settlements, Democritus University of Thrace, Department of Environmental Engineering, Xanthi, Greece

*Corresponding author: E-mail: pkosmos@env.duth.gr

Abstract

This study investigates the thermal comfort conditions during the summer period in a central area of Northern Greece, Thessaloniki. In the study area takes place a large number of financial and social activities of the inhabitants.

A number of in situ experimental procedures were carried out. Surface temperatures, microclimatic data and urban morphology data were gathered. Also, simulation models have been used to calculate the outdoor thermal comfort sensation. The thermal comfort indices which have been used is the Predicted Mean Vote, (PMV) which provides the average response of a large sample of individuals, the Predicted Percentage Dissatisfied, (PPD) which provides the percentage of people in a large sample who do not feel comfortable in a space, and the Standard Effective Temperature, (SET).

Keywords: Thermal comfort, PMV - PET - SET

1. INTRODUCTION

The covering and construction materials in contemporary cities and the urban geometrical characteristics affect the microclimatic conditions inside the urban centers (Lau et al, 2011). The thermal comfort and energy efficiency of cities are largely determined by urban climatology, which in turn is influenced by the thermo-electric mechanisms of the structured environment and especially by atmospheric transport phenomena (Steemers, 2003). The most important parameters determining the degree of environmental stress as well as the energy losses of the built environment are the geometry of the buildings - open spaces, the vegetation rate, the building materials and ventilation of the urban spaces, as it results from the thermomechanical behavior of the surrounding atmosphere in relation to the urban terrain (Santamouris et al, 2001).

The high UHI has a strong negative effect on thermal comfort of humans. In addition, higher temperatures in urban sections have led to an increase in peak and total energy demand (Golden, 2004), (Oxizidis and Papadopoulos 2013). Strategies which include items such as shading, increased cooling from tree shading and building ventilation, as well as permeable pavements and higher reflecting surface materials could improve the thermal comfort sensation. Results from this and other similar studies, should nonetheless be utilized to determine the ideal and sustainable urban design for outdoor human comfort and heat mitigation (Hedquist and Brazel, 2014).

2. CLIMATE ANALYSIS IN THESSALONIKI

The climate in the region of Thessaloniki can be considered as Mediterranean, with a strong continental influence in the different seasons. The temperature has the highest average in July and the lowest in January, the annual temperature range is close to 20 ° C, while in the cold season very cold air masses blow over and often frost the liquid. The average annual air temperature is around 16 ° C, the lowest average temperature (January) around 6 ° C while the highest (July) around 26 - 26,50 ° C. The annual rainfall is around 500 mm. Snow is not a rare phenomenon. The winds are different in seasons: in the winter prevail North winds from the valley of Axios (Vardaris), and less the western ones, in the spring the more frequent are the southwest, in the summer the northern and southwest dominate while in September the Southwest is diminished and in November the northern and the western dominate again at the region.

3. METHODOLOGY

The research is concluded by 3 different measurement and analysed cycles.

During the first, a number of experimental procedures were carried out in order to investigate the effect of urban planning on microclimatic conditions. The study area is located in the urban center of Thessaloniki, Greece (Figure 1) in the crossway Metropoleos and Agias Sofias Street, and it consists of high building blocks. Data from different measurement points along the streets, from different heights and orientation were collected. The data gathered investigate the variation of Surface Temperature (Tsurf) on a 24 hours basis and Air Temperature (Tair). The measurements took place during summer. The field surveys involve surface temperature measurements by a thermal camera and microclimatic monitoring with portable mini-weather stations. The geometric characteristics of the streets and the observations for the measurement points are given in Table 1.



Figure 1: Study area in Urban Center of Thessaloniki, Greece

Table 1: Geometric Characteristics of streets

Orientation	Av. Height H (m)	Str Length, L (m)	Av Str Width, W (m)	H/W
West	23	60	12.5	1.8
North	21	70	14	1.4
East	21	100	14	1.5
South	18	50	14	1.3

Also, a simulation model ENVI-met is used in order to investigate the thermal comfort conditions in the study area. The gathered data for temperatures of vertical and horizontal surfaces and microclimatic data (Air temperature, Wind Speed, Wind Direction) from Masurement Points located in different places along the streets and on different heights is used (Kosmopoulos and Kantzioura, 2014). The simulation results were compared with measurement data and the deviation was about 8%, which is regarded satisfactory.

During the second cycle, 28 points examined in Aristotelous' square, in order to analyze the buildings and the existing vegetation at the level of annual shading. Data collection have been made with a specialized instrument in the study area while measurement system analysis lead and modeling data using appropriate software (Solar Pathfinder - SketchUp). Measurements took place during the day, when the less traffic volume prevailed, to achieve an accurate representation of the obstacle mask. Humidity, wind speed, and temperature measurements were also performed to analyze and simulate the characteristics of the area. The data analyzed by software (RayMAN) to extract thermal comfort indicators (Matzarakis et al, 2007).

The paper refers to two open spaces in urban centers, in a city at Northern Greece. In these areas a large number of social and commercial activities take place. So, the study of the thermal comfort conditions is a very interesting subject. The size of the two areas is about 500 square meters but the two open spaces have different geometric characteristics. The one is a square and the second a crossway.

We consider that the choice of these indexes describes optimal the conditions in the two open spaces, which are characterized by different geometrical characteristics.

4. ANALYSIS

4.1 Central crossway

According the Vertical surface temperatures, the road located on the North-South axis appears different thermal behavior according to the orientation of each side of the road. The vertical surfaces of buildings' façade on west side develop high temperature during morning time, while on east side at the afternoon. Greater Tsurf is observed at west side. On West-East axis road, the maximum surface temperature is observed mainly during evening hours. The orientation of each side of the road doesn't affect the thermal behavior of the surfaces, as observed in the North-South axis (Kantzioura and Kosmopoulos, 2016).

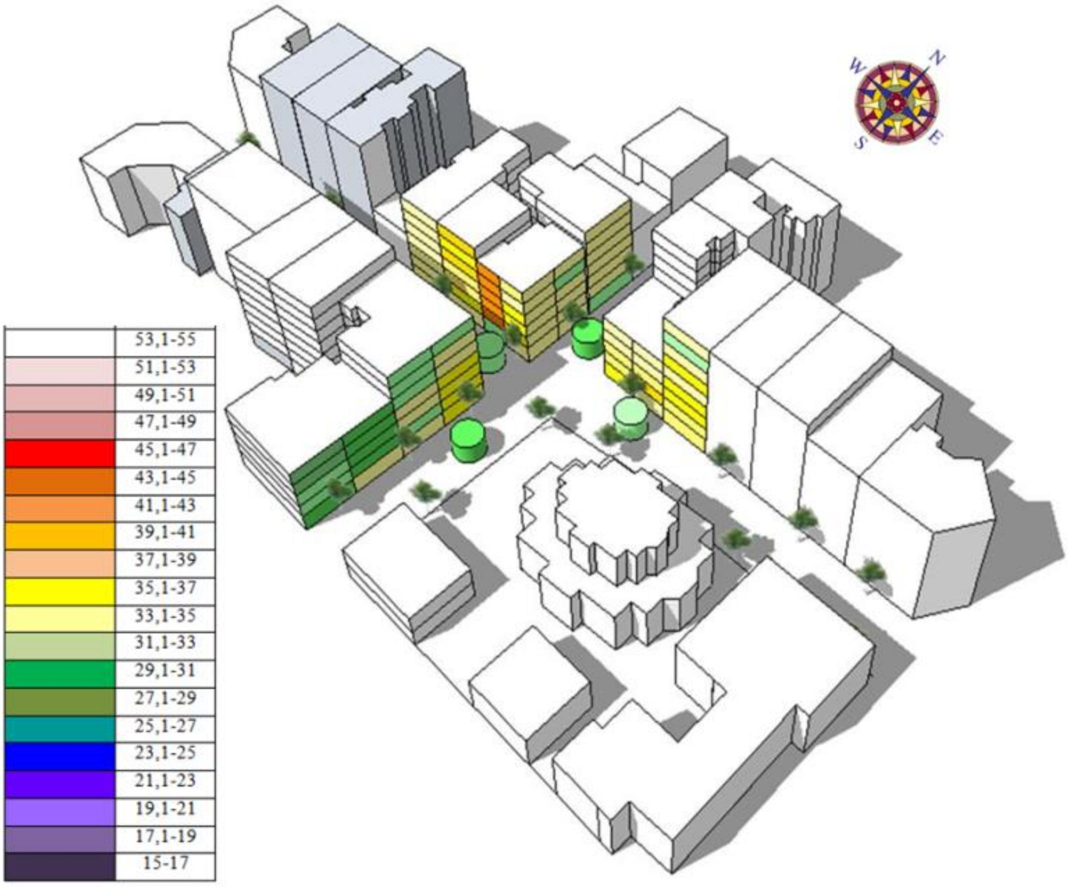


Figure 2: Temperature varation of vertical surfaces

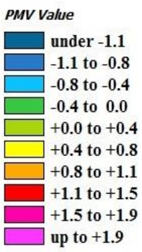
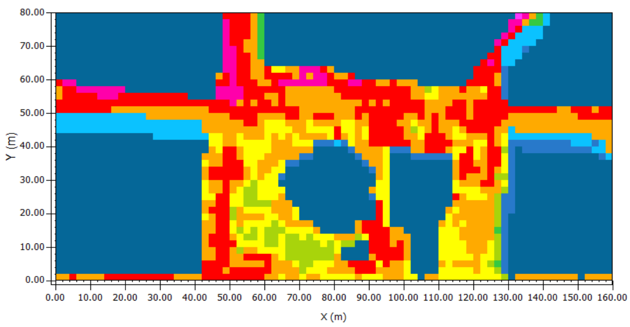
In order to investigate the Thermal comfort conditions in the central crossawy, the index PMV is calculated on pedestrian's level, on 1.20-1.50m height. The 1.5m height is considered as representative pedestrian's level of adults and children, seating and passing passengers (Kosmopoulos, 2017).

The simulation model and the corresponding measurement data is referred in 21 July, the day of the maximum Tair in 24h basis in Thessaloniki, according to the Technical Guidelines of the Technical Chamber of Greece (TOTEE).

The simulation time step is 1h, from 6:00 a.m. to 20: 00pm. The start time of the simulation model was set 2 hours earlier than the first in situ measurement (8:00 a.m.), in order to achieve the optimal predictive accuracy.

The thermal comfort scale used is from -3 to +3 (Very Cold, Cool, Slightly Cool, Comfort, Slightly Warn, Hot, Very Hot).

Table 2: Depiction of Thermal comfort index at 12:00pm

 	 12:00

In Figure 3, the PMV index and the Tair on pedestrian's level, for each of the different orientated streets are observed.

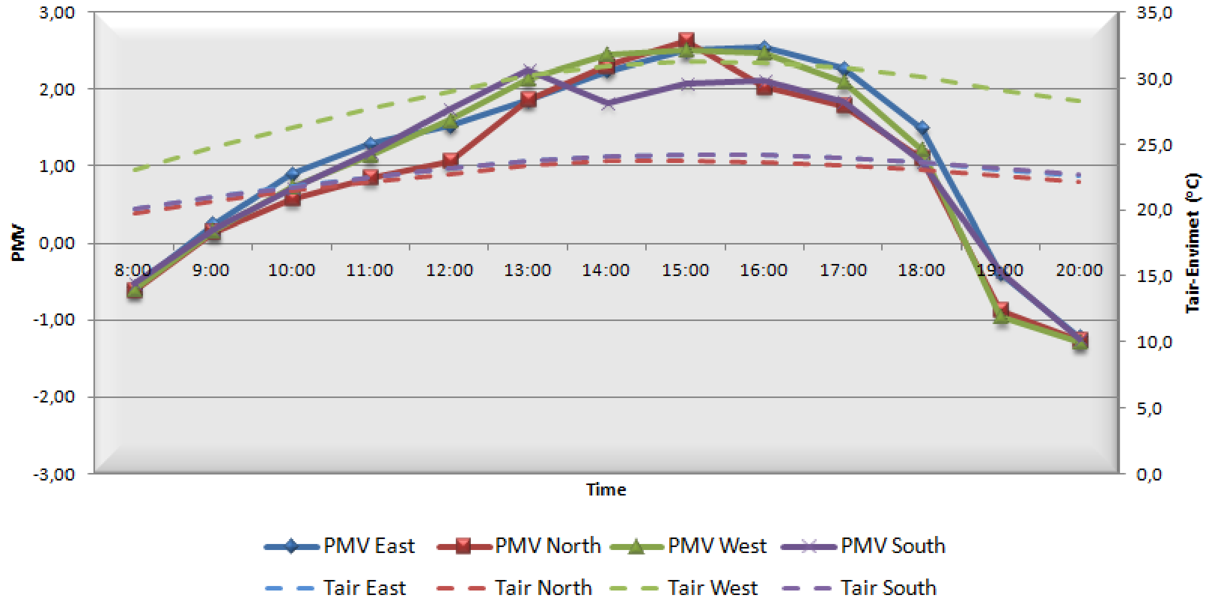


Figure 3: The PMV index and the Tair, in each of the four different orientated streets, on pedestrian's level.

The feeling of thermal comfort starts from "comfort" in the morning (8:00 to 10:00) and gradually deteriorates in "very hot" at 14:00 pm-16: 00pm. In the afternoons, the PMV decreases gradually and restored the sensation of "comfort". The index PMV and the Tair have the same fluctuation during the day, especially in west oriented urban canyon.

Increasing of Tair followed by an increase of thermal comfort index PMV, as well as decreasing of Tair leads to a decrease in the PMV (Figure 4).

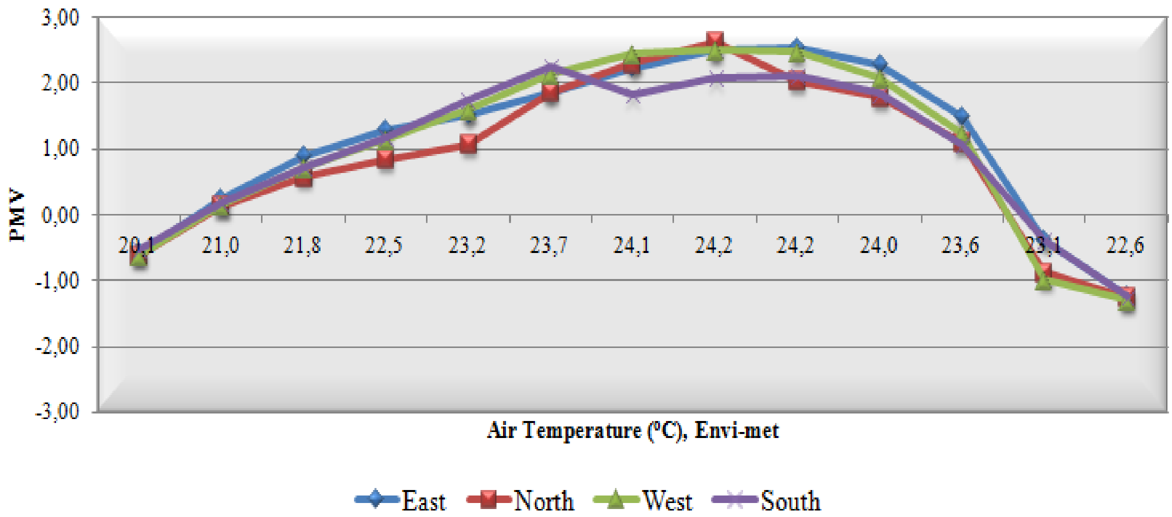


Figure 4: Fluctuation of index PMV and Tair

The Figure 5 comparing the variation of thermal comfort index PMV with the temperature variation of the horizontal surfaces Tsurf. The index PMV is increasing from 8:00am until midday. The increasing of surface temperature is continuing for two more hours (Figure 5). The decreasing of index PMV (reinstatement of thermal comfort) begins two hours earlier than the decreasing of

horizontal surface temperature (except of the south orientated road). The maximum PMV is approximately 2.5 and displayed at 13:00 to 16:00pm.

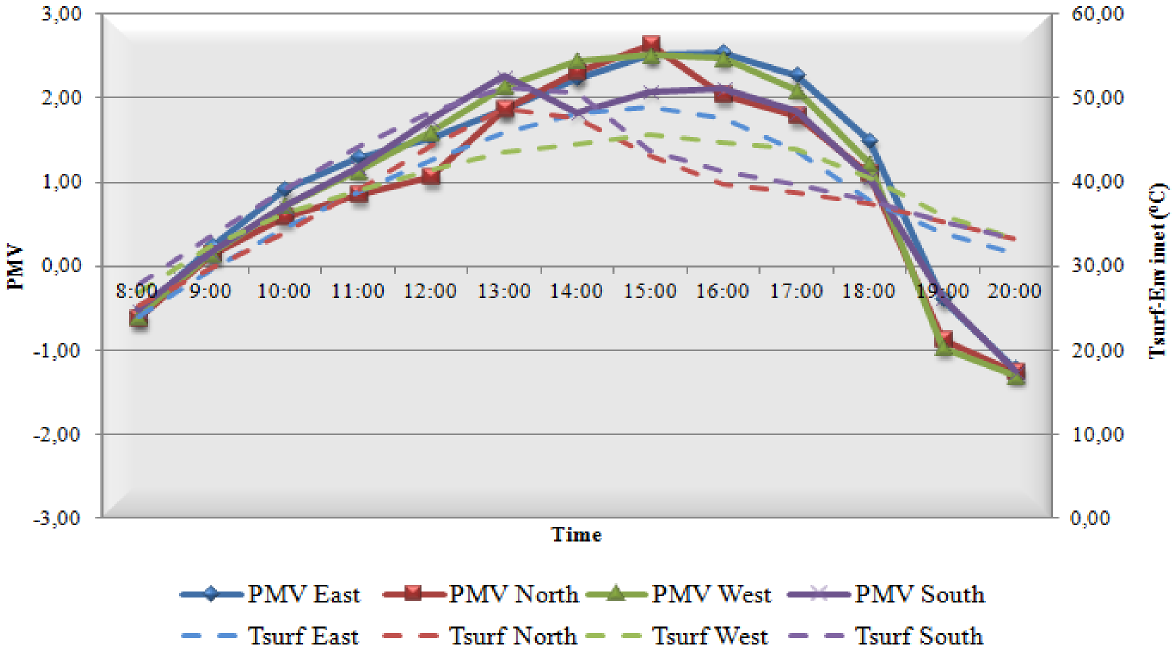


Figure 5: The PMV index and the Horizontal Tsurf, in each of the four differently orientated streets

In Figure 6, the correlation coefficient p between the thermal comfort PMV, the air temperature at pedestian's level and surface temperature of the horizontal surfaces is calculated. The correlation between the PMV and Tair is about 0.7, and between the PMV and Tsurf is about 0.8-0.9.

It is concluded that there is satisfactory correlation and the thermal comfort conditions are affected by the air temperature and the horizontal surface temperature.

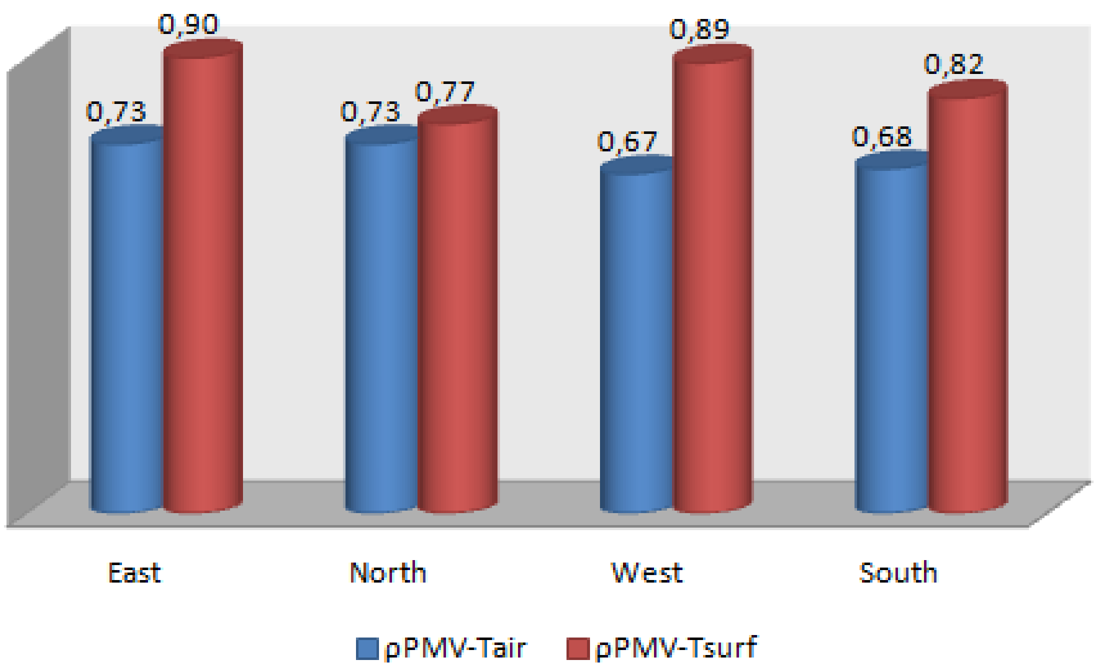


Figure 6: Correlation coefficient between PMV and Tair, and between PMV and Tsurf.

4.2 central square

The square's area comprises to the left and right large high-rise buildings that shade a large part of the open space during the day, resulting in the drop-in temperature values at single points.

Table 3: Annual rate of shadow at the square.

MONTH	PERCENTAGE% UNSHADED AREA	SOLAR RADIATION, KW/m2/day
JANUARY	39,97%	0,71
FEBRUARY	50,23%	1,46
MARCH	58,96%	2,35
APRIL	65,07%	3,19
MAY	67,78%	4,08
JUNE	69,50%	4,93
JULY	68,40%	4,82
AUGUST	65,11%	4,06
SEPTEMBER	59,60%	2,84
OCTOBER	51,72%	1,64
NOVEMBER	42,77%	0,84
DECEMBER	35,59%	0,54

The results of the shading models presented in Table 3 show the difference in energy load and solar input rate generated during the year in the square area. It is observed that there is an increase of the solar load and expansion of the solar space during the summer period (Fig.7). The requirements for shading in the summer affect the levels of thermal comfort, resulting in the adaptation of the planning strategies. The vegetation in the space and reaching levels of thermal comfort is a powerful planning tool aimed at the decisive intervention of the engineer in the field. An important factor is also the materials of the square, the main part of which is made of granite, asphalt and marble resulting in the high density of the material, which works in relation to the large area of coverage as a large heat storage in the summer (Kosmopoulos, 2008).

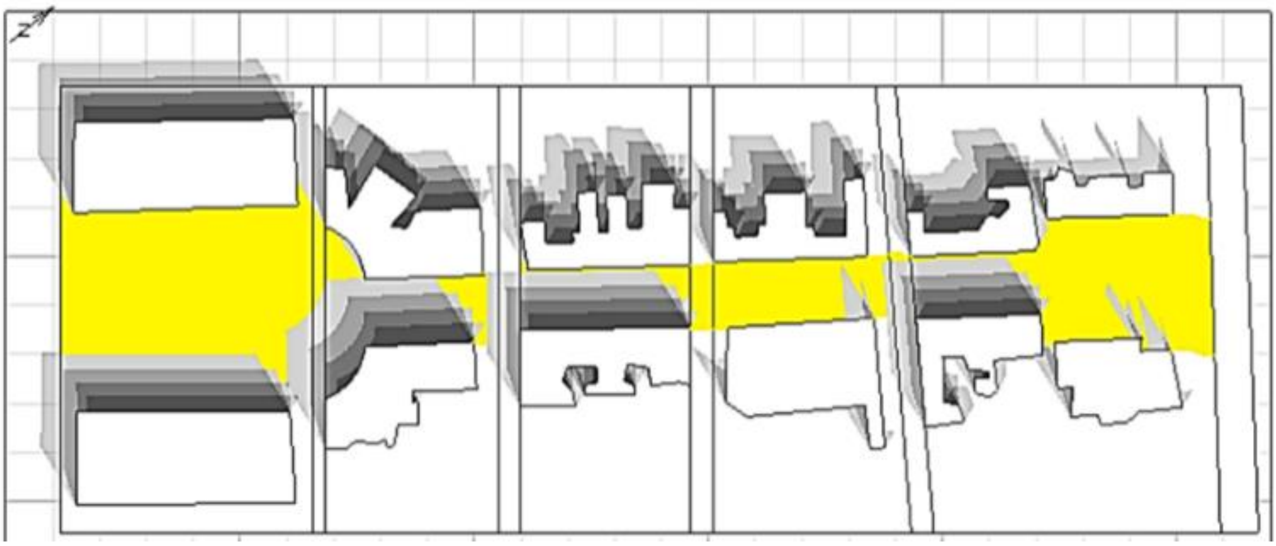


Figure 7: 21/6, shading model in summer season.

An important element on the record of data in the study area is the dynamic movement of the wind and the pressure around the Aristotle square which is under consideration. The wind analysis represents graphically (Fig. 8,9) those points that develop high velocities between the obstacles in the space as well as in the hidden places where the wind remains stationary. The modeling of velocity

and wind direction in the Aristotle square area uses a wind speed model of 3 m/s for average values as well as 7.5 m/s, which is the average of maximum values. The models were reviewed for the summer of 1 June - 31 August.

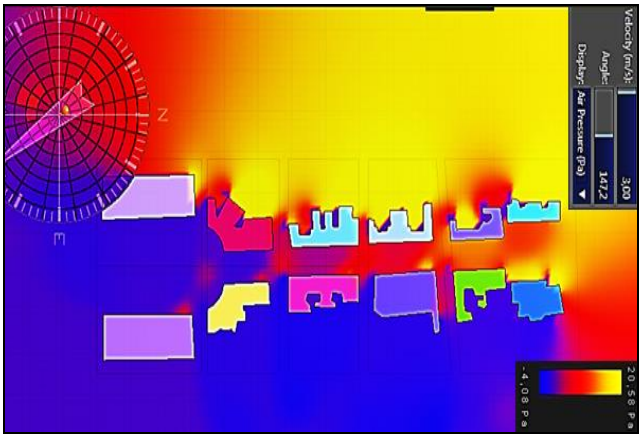


Figure 8: North Wind 3m/s.

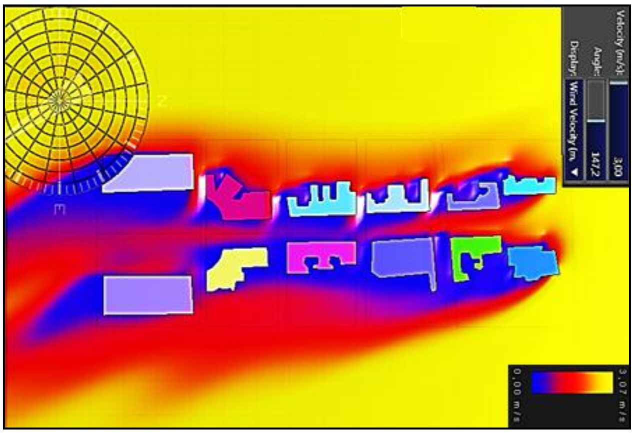


Figure 9: Pressure of N. Wind.

The wind movement is a key factor in creating thermal comfort which is used to increase comfort levels when high outdoor temperatures prevail during the summer period. In order to achieve upgrade levels, changes to the direction and reduction of the speed in specific parts of the study area should be considered. The graphical of wind velocity gradient as shown in Figures 8 and 59 is an important information that explains the way in which the square's behaviorand the thermal comfier conditions will improve.

Modeling of trees in the field of study was carried out in order to analyze the behavior of the area during the day. Trees which have been recorded are evergreens, bitter oranges, and coconut trees. The ave height of the bitter oranges is about 6 meters long and the average height of the palm trees at 9-12 meters (Moumtzakis, 2013).

Table 4: Length of shadow related to the type of vegetation.

Month - Hour	Type of vegetation	Height	Length of shadow
21 June - 09:00	Bitter orange	5.569 m	6.644 m
21 June - 12:30	Bitter orange	5.569 m	1.834 m
21 June - 15:00	Bitter orange	5.569 m	5.305 m
21 June - 18:00	Bitter orange	5.569 m	15.469 m
21 June - 09:00	Palm tree	11.735 m	14.959 m
21 June - 12:30	Palm tree	11.735 m	7.253 m
21 June - 15:00	Palm tree	11.735 m	11.300 m
21 June - 18:00	Palm tree	11.735 m	33.529 m

The RAYMAN software evaluates the comfort conditions in the study area, analyzes the input data and informs the user of the thermal indices prevailing at the reference point. The indicators are PET that examines the human energy balance (Matzarakis et al, 2007), PMV, which is the average vote of a set of people expressing their reaction to thermal sensation under different environmental conditions, on a scale ranging from -3 to +3, and SET which provides a reasonable basis for measuring the equivalence of any combination of environmental factors, clothing, and metabolic rate (Guodong et al, 2003).

The research based on the work of two basic scenarios. The first scenario estimates at the existing situation while the following scenario attempts to improve the conditions that exist by adding vegetation components to the site. The inputs are a) temperature b) humidity c) wind speed d) activity data and clothing. The temperature factor analyzed in two phases 1) in the set of maximum averages

and 2) in the average set, thus an unfavorable scenario can be evaluated, while in the second case a regular one can be studied.

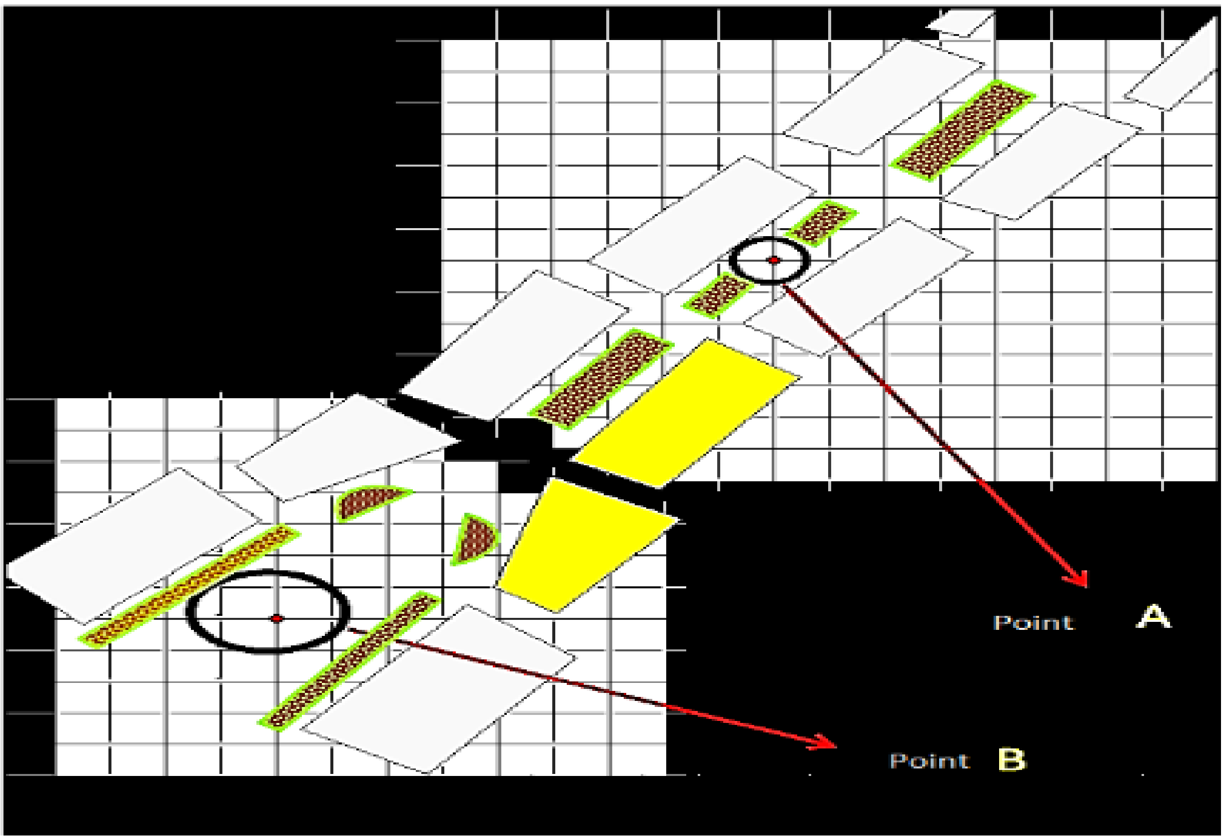


Figure 10: Simulation models. 1st scenario, with vegetation in the present situation

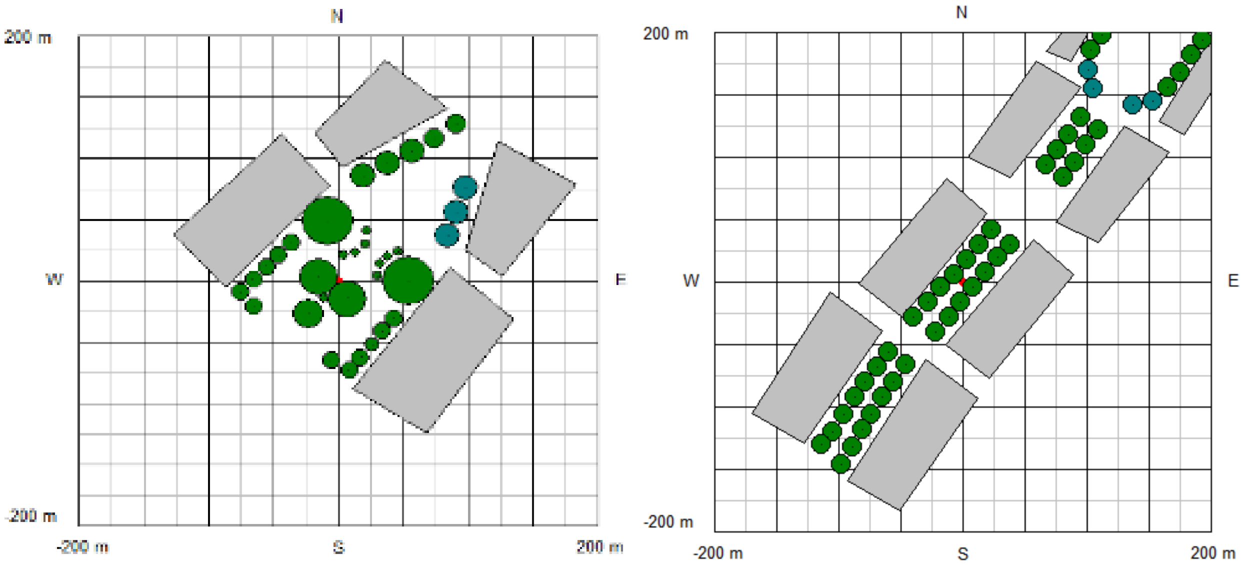


Figure 11: Thermal comfort indicator points. 2nd scenario with vegetation in the summer

Analyzing the results of a survey (Table 5), observed a significant reduction in thermal comfort indicators. The intervention - outdoor upgrade is effective during the summer months.

Table 5: Thermal Comfort Indices

CURRENT SITUATION			BIOCLIMATIC DESIGN		
SUMMER UNPLEASANT SCENARIO CENTRAL PART			SUMMER UNPLEASANT SCENARIO CENTRAL PART		
PMV	**PET**	**SET**	**PMV**	**PET**	**SET**
2,9	**35,2**	**27,6**	**1,9**	**28,7**	**21,2**
Hot	Hot	Warm	Warm	Warm	Slightly cool
SUMMER MILD SCENARIO-CENTRAL PART			SUMMER MILD SCENARIO-CENTRAL PART		
PMV	**PET**	**SET**	**PMV**	**PET**	**SET**
1,0	**26,6**	**19,1**	**-0,1**	**20,8**	**12,4**
Slightly warm	Slightly warm	Slightly cool	Comfortable	Comfortable	Cold
SUMMER UNPLEASANT SCENARIO SOUTH PART			SUMMER UNPLEASANT SCENARIO SOUTH PART		
PMV	**PET**	**SET**	**PMV**	**PET**	**SET**
3,2	**36,6**	**28,9**	**2,2**	**30,9**	**26**
Very Hot	Hot	Slightly warm	Warm	Warm	Slightly warm
SUMMER MILD SCENARIO-SOUTH PART			SUMMER MILD SCENARIO SOUTH PART		
PMV	**PET**	**SET**	**PMV**	**PET**	**SET**
1,2	**28**	**20,4**	**0,3**	**22,3**	**14,8**
Slightly warm	Slightly warm	Slightly cool	Comfortable	Slightly cool	Cool

5. CONCLUSIONS

The urban geometry and vegetation influences the surface temperatures, the microclimatic parameters in the urban centers and configures the conditions inside the urban canyons.

The present study indicates that the thermal behavior of buildings' envelope is affected by the urban geometry, the measurement height, the orientation, the position of the measurement points along the street. Also concluded, that there is a correlation between the surface temperatures and air temperatures on pedestrian's level. This correlation affects the microclimatic conditions and the thermal comfort sensation in outdoor spaces.

The present study should help effectively in improving the urban microclimatic conditions and in energy efficiency design of buildings, according to the specificities of each position in the built environment.

References

1. Hedquist, B.C., Brazel, A.J., (2014), Seasonal variability of temperatures and outdoor human comfort inPhoenix, Arizona, U.S.A., **Building and Environment**, 72, pp. 377-388.
2. Golden J.S., (2004), The built environment induced urban heat island in rapidly urbanizing arid regions: a sustainable urban engineering complexity, **Environ Sci**, 1 (4), pp. 321–349
3. Guodong, Y., Changzhi, Y., Youming, C., Yuguo, 2003, ''A new approach for measuring predicted mean vote (PMV) and standard effective temperature (SET*)'', **Building and Environment**, 38, pp.33 – 44.
4. Kantzioura A., Kosmopoulos P., Research on how buildings and covering materials affect microclimate conditions: Case study the center of Thessaloniki, **13th International Conference**

on Protection and Restoration of the Environment, Mykonos island, Greece, 3rd to 8th of July, 2016

5. Kosmopoulos P., Kantzioura, A., 2014, Effects of urban development in microclimatic conditions in Thessaloniki, **Global Nest Journal**, 16 (5), pp. 840-855.
6. Kosmopoulos P., Michalopoulou K., 2017, Comfort Conditions and Microclimate in open urban areas, **University Studio Press**, Thessaloniki
7. Kosmopoulos, P., 2008, Buildings Energy And The Environment, **University Studio Press**, Thessaloniki, GR.
8. Lau, S. S. Y., Yang, F., Tai, J., Wu, X. L., & Wang, J., (2011), The study of summer-time heat island, built form and fabric in a densely built urban environment in compact Chinese cities: Hong Kong, Guangzhou. **International Journal of Sustainable Development**, Vol. 14(1-2), pp. 30-48
9. Matzarakis, A., Rutz, F., and Mayer, H., 2007, ‘’Modelling radiation fluxes in simple and complex environments — application of the RayMan model’’, **Int J Biometeorol**, 51, pp. 323 – 334,.
10. Moumtzakis, A., 2013, “Integrated Environmental Design of Energetically Autonomous Building’’, **MSc. Thesis**, Democritus University of Thrace, Xanthi, Greece.
11. Oxizidis, S., Papadopoulos, A., (2013), Performance of radiant cooling surfaces with respect to energy consumption and thermal comfort, **Energy and Buildings**, Volume 57, pp. 199-209
12. Santamouris, M., Papanikolaou, N., livada, I.Koronakis, I., Georgakis, Argiriou, A., and Assimakopoulos, D.N., 2001, “On the impact of urban climate on the energy consumption of buildings’’, **Solar Energy**, 70(3), pp. 201–216.
13. Steemers, K., 2003, “Energy and the city: density, buildings and transport’’, **Energy and Buildings**, 35, pp. 3-14.
14. Solar Pathfinder Manual. http://www.solarpathfinder.com (8 Νοεμβρίου 2014).



Cultural and social issues

REFUGEE CRISIS: GREEK RESIDENTS' ATTITUDES TOWARDS WASTE MANAGEMENT IN THEIR REGION

A. Kounani[*], C. Skanavis

Department of Environment, University of the Aegean, University Hill, 81100, Mytilene, Greece

*Corresponding author: E-mail: kounani@env.aegean.gr, Tel +30 2321047710

Abstract

Todays' refugee crisis is considered an unceasing challenge of the current century, since the mass exodus of people from their own country has exponentially increased. The consequences of this worldwide phenomenon are much bigger than the actual issue itself. Migrants and refugees flocking into Europe from the Middle East, South Asia and Africa, have presented European leaders and policymakers with a heavy task since the debt crisis. Syria is presenting the biggest humanitarian and refugee crisis of recent years, a continuing cause of suffering for millions of people. This massive immigration is known as the "Middle East Refugee Crisis", and obviously it has affected all the neighboring to Syria, countries including Greece. Refugee movements in such astonishing numbers are prospective to produce rampant, quotidian effects on social, environmental and political sector of the receiving and hosting regions' local community.

The purpose of the present research was to explore the knowledge, awareness and attitudes towards waste management and "special waste" management of residents in Lesvos Island, a migrant receiving community. As "special waste" are considered the life jackets, rubber dinghies and fiberglass boats. In the spring of 2017, a questionnaire-based survey was administered on Lesvos Island. Furthermore, the findings revealed the locals' total environmental awareness as well as their perceptions towards refugee crisis that Greece is being confronted with. The issue of waste management is vital in receiving and hosting regions, since the settlement of refugees in regions that don't have the capacity to absorb the pressure of huge influxes is expected to cause social instability and pose a threat to national security.

Keywords: Syrian Refugee Crisis; Waste Management; Environmental Awareness; Special Wastes; Lesvos; Greece

1. INTRODUCTION

Living in a world where nearly 20 individuals are forcibly displaced every minute as an outcome of environmental disasters, persecutions or conflicts, every human being on this planet is witnessing the highest refugee movement ever recorded. According to UNHCR an unprecedented 65.6 million people around the world have been forced to leave home at the end of 2016, while almost the 22.5 million are refugees, over half of, whom are under the age of 18 (UNHCR 2018).

Today, undeniably, migration is being exploded in a number of ways: in coverage, in politics and as an area of academic inquiry. In 2015, Global Risk Reports have recognized water as the most significant challenge globally, and the principal economic and societal jeopardy for the years to come. Although the world as a whole has plentiful freshwater resources, seasonal scarcity as well as spatial discrepancy of freshwater, aggravated by climate change, is developing as a critical peril for numerous areas worldwide (Zhang 2015).

One of the foremost phenomena challenging the countries influenced by immigration are refugee camps where huge numbers of displaced people settle down at places that were not prepared for such enormous influx (Braun et al. 2016). Host countries, due to the spontaneous nature of migration, often lack the means to plan effective camp constructions. Despite the fact, both refugees and the host populations could benefit from a strategic plan of infrastructure and social services by UNHCR or the non-governmental organizations (Braun et al. 2016; Perouse de Montclos and Kagwanja 2009). Furthermore, the particular numbers of dwellings, people who live in them, the size of the camp and the conditions of the surrounding areas need to be estimated. It is quite obvious that large camps accelerate land degradation (Braun et al. 2016).

Evidently, whenever refugees settle in a specific area, it is proven that they will affect the social, environmental and political sector of the hosting region. Due to lack of appropriate planning and anticipation for such an intense increase of people arriving, specifically when the hosting nation does not have sustainable and integrated management plans, the problems that are caused are unaffordable (Kherfan 2016).

The aim of the research was to explore the knowledge, awareness and attitudes towards waste management and “special waste” management of residents in Lesvos Island, a migrant receiving community. The findings revealed the locals’ total environmental awareness as well as their perceptions towards refugee crisis that Greece is being confronted with.

2. THE SYRIAN CIVIL WAR

In early 2006, Syria and The Fertile Crescent experienced the worst 3-year drought ever recorded there. The drought exacerbated existing water and agricultural insecurity and caused massive agricultural failures and livestock mortality. The most significant consequence was the migration of as many as 1.5 million people from rural farming areas to the peripheries of urban centers. Government agricultural policy is prominent among the many factors that shaped Syria’s vulnerability to drought. De Chatel (2014) explains how the 2006-2010 droughts in Syria led to the uprising increase of emigrants that followed the years after. She particularly argues that it was not the drought per se that generated a conflict and produced millions of refugees but the government’s failure to respond to humanitarian needs affected by environmental reasons (Kelley et al. 2015).

With poor governance and unsustainable agricultural and environmental policies, the drought led to environmentally-induced migration from rural Syria to urban. Subsequently, the greater population density in cities and the increased unemployment contributed to people’s frustration with the governmental and political unrest being at state. In 2011 this unrest was further triggered by the Arab Spring, which led to the Syrian civil war (Kelley et al. 2015). Pro-democracy protests, all-over the country, stood against President Bashar Al Assad’s, who was characterized by authoritarianism, political corruption and human rights violation. Protesters were armed with the help of opposition militias who were fighting against governmental forces. At 2012 the conflict has erupted in a full-grown civil war between the pro government ones against the ones opposing to it (Holliday 2013). This ongoing war causes massive migration of people from Syria and the surrounding countries to Europe (Skanavis and Kounani 2016).

3. THE IMPACTS OF REFUGEE CRISIS IN GREECE

Greece has faced immense challenges under the pressure of the ongoing “European refugee crisis”. Still covering from the 2008 financial crisis, Greece was not prepared to deal with such a massive migration flow (Skanavis and Kounani 2016). The Greek islands close to the Turkish borders were affected the hardest by the refugee crisis and while the political and humanitarian challenges of the migration flow were immense and gained precedence in the global media, the environmental challenges were over looked.

Many of refugees made their way through Turkey to Greece, and eventually to other European countries. According to the UNHCR, since 2014 more than one million refugees have crossed over the Aegean Sea from Turkey to Greece in order to reach European soil (UNHCR 2017a). Greece became a major migration route and while most of the people arriving in Greece were from Syria, the country saw also an unprecedented number of migrants from other countries such as Afghanistan and Iraq, as well as smaller numbers from countries such as Eritrea, Somalia and Sudan (UNHCR 2015). In 2015, and the years before, the refugees and migrants traveled through the Greek islands and quickly continued their journey to Athens and onwards to other European countries. But as the Balkan countries built fences and closed their borders, refugees got stranded, at the borders and in all of Greek mainland. With an unambiguous departure date many of the refugees in Greece today are trapped (Skanavis and Kounani 2016). Greek islands in particular were intended as transition routes, but have now become migrant host communities. For instance, on the island of Lesvos just 8 to 10 km off the Turkish coast, the local population saw unprecedented numbers of migrants arriving in 2015 and early 2016. While the numbers of sea arrivals have decreased and people have been transferred further on to mainland Greece, there are still an estimated 5,000 migrants and refugees residing on the island (UNHCR 2017b). This is a nearly 6% increase of Lesvos' local population of 86,436 residents, a percentage which takes its toll on an island community (Hellenic Statistical Authority 2014)

The environmental effects of mass migration movements on host environments are alike to those of overpopulation (Lee 1995). On the Greek islands in particular, these impacts included pressure on water and energy demand, soil destruction, air pollution, deforestation and increased waste production. Especially, the enormous amounts of waste from the life jackets and rubber dinghies that the migrants used to cross the sea pose a massive challenge to the Greek islands. However, with inadequate landfill capacity and no facilities in Greece to recycle these materials from the life jackets in particular, the islands are not only being confronted with the challenges of refugees but also the ever increasing amounts of waste (Skanavis and Kounani 2016).

To conclude with, the refugees' footprint can be summarized as: pressure on water and energy demand, soil destruction, air pollution, deforestation, waste production. However, every refugee crisis is unique and needs to be observed and managed as an individual condition (UNHCR 2011). Therefore, overpopulation of Greek islands is projected that it causes significant environmental degradation. Greece was not well organized to deal with the refugee flow while being in a harsh economic crisis (Skanavis and Kounani 2016).

4. THE CASE OF LESVOS ISLAND

The island of Lesvos, located in the North-Eastern Aegean Sea, has a coastline of 370 km and is separated from the Asia Minor coast, to which it is geologically related, by two shallow channels ranging from 6 to 14 miles (10 to 23 km) wide, the Muselim (north) and the Mitilini (east), which join at the apex of the triangular island, forming the entrance to the Turkish Gulf of Edremit (Encyclopaedia Britannica 2017).

The Municipality of the island of Lesvos consists of 13 sections and 190 villages with a total population of 85,412 residents (Hellenic Statistical Authority, cited in Skanavis and Kounani 2016).

4.1 Municipal solid waste (MSW) production and environmental management of Lesvos Island

According to receiving data from the "Service of Planning Department, Cleanliness, Recycling, Waste Collection" of the Municipality of Lesvos the amounts of MSW on the island is about 100 tones/day in winter and ranges from 120-130 tones / day in the tourist season. Specifically, the amount of unsorted waste and the recyclables in years 2013 to 2016 are depicted in Table 1.

Table 1. The amount of produced solid wastes

Year	Total Amount of Municipal Solid Waste (tones/year)	Total Amount of Recyclables (tones/year)	Total amount of Produced waste (tones/year)
2013	33,228.93	-	33,228.93
2014	37,146.39	1,285	38,431.39
2015	36,322.14	2.186	38,508.14
2016	38,056.71	2,844	40,900.71
2017	39,108.72	3,322.1	42,430.82

(Municipality of Lesvos 2018)

The responsibility of uploading, disposal and recovery of wastes is placed on the Municipal Waste Management and Environmental Development Company of Lesvos. Sorting, compression, and sale of recyclables is occurred in a private center, the Recycling Sorting in Moria area, run by the company "Sea-Lesvos Foundries Recycling SA" (Skanavis and Kounani 2016).

4.2 Management of "special wastes"

The major waste problem the island of Lesvos is being confronted with, due to refugees' inflows, is the disposal of plastic from their life jackets and inflatable crafts, which remain behind upon their arrival to the island. Plans have been proposed in order to deal with the issue. Moreover, landfill capacity is not adequate for the unexpected inflow of people in the islands where refugees arrive. The volume of lifejackets and boats collected until December 2017 was about 20,000 cubic meters. This type of waste has been collected and transferred to 3 municipal stations, in an effort to find a way to recycle it. The materials, though, the life jackets are made from, cannot be recycled in Greece (Skanavis and Kounani 2016).

5. METHODOLOGY

In May 2017, a questionnaire-based research was conducted in order to evaluate Lesvians' attitudes towards the waste management of their region, the management of "special" waste, as well as their awareness towards environmental issues.

5.1 Research area

The research area was the island of Lesvos.

5.2 Research instruments

The implementation of the questionnaire was on a door-to-door basis. The questions, the total numbers of which were 35, were derived from other research projects and were divided into 4 groups. The first group of 6 questions inquired demographics information. The second group of 6 questions provided data towards the perceptions of the participants on general environmental issues. The third group of 18 questions supplied information according to the knowledge, perceptions and willingness to behave towards the MSW management and the management of the "special" wastes produced by the refugees. The final group of 5 questions provided data towards their perceptions on refugee crisis Greece is confronting

For the statistical analysis of the received data, SPSS was used.

5.3 Research sample

The research sample was composed of the inhabitants of Lesvos Islands, the total number of whom were 140. The sample was a random selection of residents of the specific island, during the summer months of 2017. The age of the participants and their gender are presented in Figures 1 and 2.

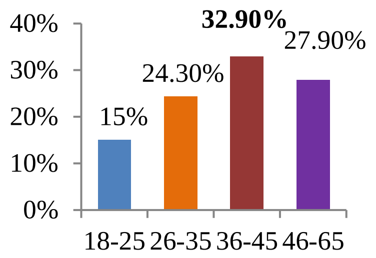


Figure 1. Inhabitants of Lesvos age groups

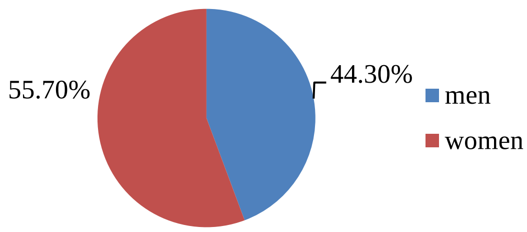


Figure 2. Inhabitants' gender

The marital status of the participants and their number of children are shown in Figures 3 and 4.

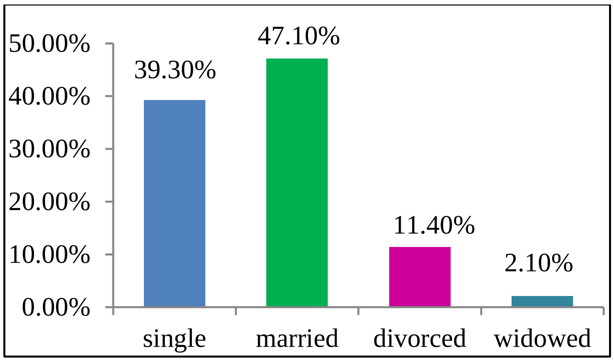


Figure 3. Marital status of Lesvos inhabitants

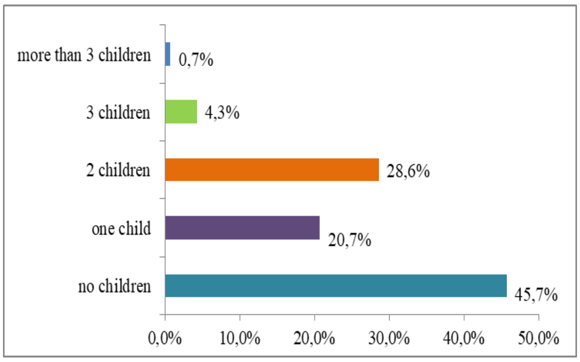


Figure 4. Participants' number of children

Their educational level and professional condition is presented in Figures 5 and 6.

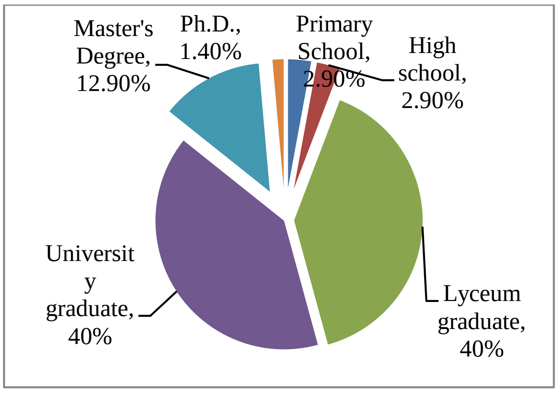


Figure 5. Educational level of Lesvos' residents

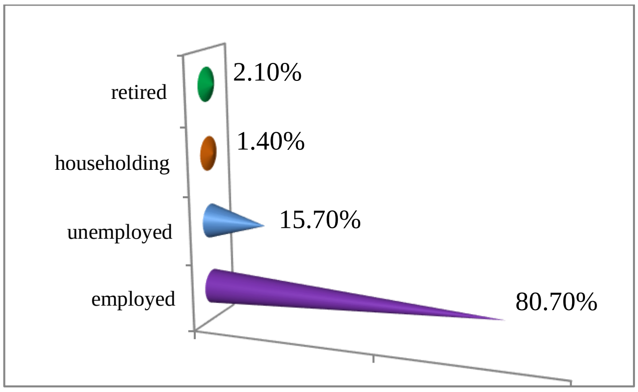


Figure 6. Professional condition of Lesvos' participants

6. RESULTS

The questions of the questionnaire were divided into four groups. The results are presented in a similar way.

6.1 Participants' Total Environmental Awareness

First of all, most of the participants (87.1 %) considered themselves as environmentally aware individuals, while the 10.7% were apathetic and the 2.1% weren't aware. Moreover, the 92.9% appeared to worry about the environment of their region, whilst the 5.7% were not perturbing and the 1.4% had no worries.

At the same time, Lesvians' aspects about the weightiness of the following environmental challenges for Greece, on a scale of 1 (not serious at all) to 5 (extremely serious) are depicted in Table 2.

Table 2. Lesvos residents' aspects about the weightiness of the following environmental challenges for Greece, on a scale of 1 (not serious at all) to 5 (extremely serious)

	N	Mean	SD	Min	Max
Environmental- Climate Refugees	140	4.11	1.09	1	5
Water pollution	140	4.02	0.96	1	5
Increase in Municipal Solid Waste Production	140	4.00	0.94	1	5
Deforestation	140	3.85	1.09	1	5
Climate change	140	3.83	1.17	1	5
Air pollution	140	3.78	1.00	1	5
Ozone depletion	140	3.52	1.20	1	5
Endangered species	140	3.32	1.26	1	5
Valid N (listwise)	140				

(N= sample size, Mean= mean, SD= standard deviation, Min=Minimum, Max= maximum)

6.2 Lesvos residents' Attitude towards Waste Management and management of "special" wastes

Concerning the management of MSW, the residents' of Lesvos Island were asked some questions in order to be assessed for their knowledge on the particular issue. Most of them (90%) appeared to be aware of "who collects the MSW of their region", while the 80.7% were knowledgeable "where the collected waste is taken for final disposal", and the 72.1% knew about "the bad effects of ill-treated solid waste".

In the sequel they were asked some questions in order to be assessed about their attitudes towards the waste management. So, most of them appeared to worry (94.3%) about whether the final disposal of MSW is environmentally secure.

Regarding Lesvian participants' perceptions on the issue of "special" waste that their region is being confronted with, are presented in Table 3.

Table 3. Lesvos residents' attitudes towards "special" waste issue [On a scale of 1 (strongly disagree) to 5 (strongly agree), they agree with the following statements]

	N	Mean	SD	Min	Max
Inadequate "special" waste collection and disposal influences tourism	140	4.42	0.86	1	5
Inadequate "special" waste collection and disposal influences public health	140	4.26	0.77	1	5
The management of "special" waste is urgent	140	4.25	0,67	2	5
Recycling infrastructure is needed to solve the "special" waste problem	140	4.23	0.80	1	5
Worry about the collection and disposal of "special" waste	140	3.92	0.88	1	5
The solution in refugees' crisis will solve the problem of "special" waste	140	3.86	1.20	1	5
Using the process of combustion could solve the problem of "special" waste	140	2.54	1.26	1	5
Valid N (listwise)	140				

(N= sample size, Mean= mean, SD= standard deviation, Min=Minimum, Max= maximum)

Finally in Figure 7 are shown Lesvians' points of view towards the municipality's way of waste collection in their region.

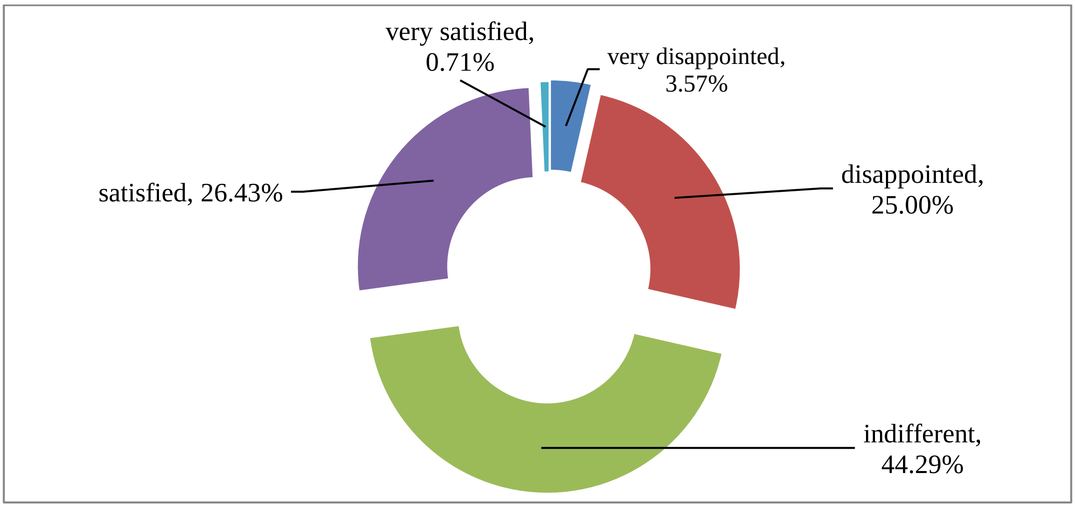


Figure7. The extend of Lesvians' satisfaction towards the waste collection of their region

Finally, the residents of Lesvos appeared to have the willingness "to participate in protests" in a percent 54.3 %, "to inform the mass media for the condition in MSW management of their region" in a 38.6%, "to support an NGO in order to put pressure on local authorities and government" in a portion of 30.7 %, "to pay for waste management" in a percent 18.6 %, "to do nothing" in a percent 17.1% and "to move to another Greek region due to the environmental degradation" in a small quota (5.7%).

6.3 Residents' Attitude towards the refugees' mass arrivals in their region

Firstly Lesvos' inhabitants were asked in what extent they worry about the refugee crisis and their perceptions are depicted in Figure 8.

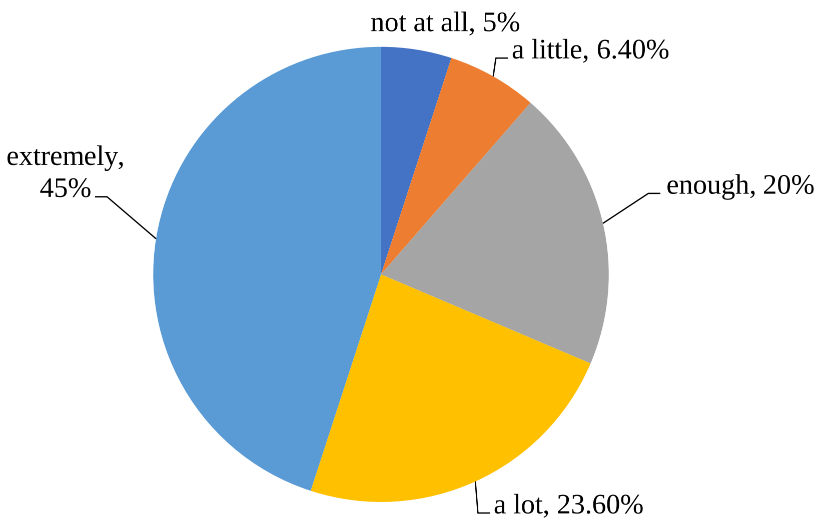


Figure 8. The extend of Lesvians' worry towards refugee crisis

Concerning Lesvians' options towards the refugees' mass arrivals in Greece are depicted in Table 4 and their perception towards the way Greece dealt with refugee crisis.

Table 4. Lesvos residents' perception towards refugees mass arrivals [On a scale of 1 (strongly disagree) to 5 (strongly agree), how much do you agree with the following statements]

	N	Mean	SD	Min	Max
Inadequacy of the state mechanisms causes environmental pressure	140	4.3357	0.7158	2	5
Mass refugees influx causes environmental pressure in receiving regions	140	4.1714	0.8562	1	5
Refugees' arrivals could cause conflicts between the inhabitants of receiving region and refugees, due to the competition in natural resources	140	4.1357	0.7885	1	5
Valid N (list wise)	140				

(N= sample size, Mean= mean, SD= standard deviation, Min=Minimum, Max= maximum)

Table 5. Lesvians' perception towards the way Greece dealt with refugee crisis [On a scale of 1 (strongly disagree) to 5 (strongly agree), how much do you agree with the following statements]

	N	Mean	SD	Min	Max
Due to the economic crisis, Greece hasn't had the appropriate infrastructure to deal with the consequences of refugees inflows.	140	4.1286	1.137	1	5
Greece was ready to deal with refugees influxes	140	1.5643	1.0051	1	5
The way in which the refugee crisis has been addressed in Greece, is satisfactory	140	1.7643	0.9642	1	5
Valid N (list wise)	140				

(N= sample size, Mean= mean, SD= standard deviation, Min=Minimum, Max= maximum)

Regarding Lesvians' perceptions on how it would be more appropriate to address the refugee issue the 48% answered through "repatriation of refugees", while the 51.4% said "the resettlement in other European areas". Finally, only a portion of 8.6%, proposed as a solution " the resettlement of refugees in other Greek areas".

7. DISCUSSION

Studying the results of the conducted research it is preferable to deal with each group of questions separately in order to acquire a holistic perception of the issue at stake.

7.1 Total Environmental Awareness

Most of Lesvos' dwellers (87, 1%) considered themselves as environmentally aware and appeared to worry about the natural environment of their region. This increased proportion of environmentally aware citizens is most likely due to the fact that the Department of Environment of the University of the Aegean is based at Lesvos Island, which means that locals are more often, environmentally confronted, with generated information. Furthermore, concerning the general environmental issues (Table 3), as they reside in an area that is the receiving point of refugees' mass inflows, it appears that "Environmental-Climate Refugees" were the most serious environmental challenge that Greece is facing (mean= 4.11).

7.2 Attitude towards waste management and management of "special wastes"

Locals of the island (90%) appeared to be aware who collects the MSW in their region, and 80.7% of them even knew the place the collected MSW are being transferred to for their final disposal. Moreover, a percentage of 72.1 the inhabitants were mindful of the negative effects of ill-treated solid waste. And the vast majority appeared to worry about the environmental security of the MSW's final disposal.

Referring to the management of "special wastes", as it is depicted in Table 3, the citizens worried about the collection and disposal of "special" wastes since they believed that the inadequate collection and disposal would influence tourism and public health. These reactions are justified, since inadequate waste collection results in indiscriminate waste disposal in any available land and into surface water bodies, causing water and soil pollution with series of environmental and human health

risks (Onu et al 2014). Furthermore, surveys on tourism sector have revealed that it can be seriously influenced by the poor solid waste disposal, although it is also a generator of solid wastes as well (Bashir and Goswami, 2016). This way the locals perception that the “special waste” management issue is an urgent one for Lesvos connecting it with the refugee crisis issue, finds grounds to be supported.

7.3 Residents’ Attitude towards the refugees’ mass arrivals in their region

As the literature refers, poor host countries’ fear of letting refugees put further strain on the already scarce resources of theirs and cause instability in the country, making them to want to only offer impermanent settlement in refugee camps as an alternative of letting them integrate (Dyrholm and Lindholm Mikkelsen 2013). The integration of refugees is contingent on the tolerance of host communities. Where the activities of refugees threaten the social system of the host population, peaceful coexistence is likely to be a problematic one (Miledzi Agblorti and Awusabo-Asare 2011).

The findings of the specific research revealed the same situation in Lesvos Island. So, Lesbians appeared to worry “extremely” (45%) and “a lot” (23, 6%), while at the same time, they strongly agreed that mass refugees influxes could cause environmental pressure in receiving and hosting regions (M=4.17) and the inadequacy of the state mechanisms could contribute negatively in that pressure (Mean=4.33). Also, the inhabitants maintained that refugees’ mass arrivals could cause conflicts among locals and refugees due to the competition in natural resources.

On the issue of how Greece has tackled the refugee crisis, the locals of Lesvos expressed that Greece was not ready to deal with refugees’ influxes, while at the same time it was facing an economic crisis that hasn’t been handled in a satisfactory way. Finally almost half of them proposed as a solution “the repatriation of refugees” and the transfer and resettlement of refugees in other European countries.

8. CONCLUSIONS

Syrian war has all the characteristics to be considered as a climate induced war, since the impacts of climate change had caused environmental and economic instability, facts that in the sequel posed social and political instability and triggered conflicts. Syrian refugees undoubtedly should be considered as environmental refugees, though they are supposedly individuals that fled from their homes for the fear of war. In the matter of fact, the environmental degradation of the region caused by war, would end being in such extent, that they will not be able to return to their homeland after the war’ s ending, as they won’t have access to healthy natural resources.

Greece, the main transit point for refugees who arrive on European shores, is among the countries that are less financially able to handle the influx. The Greek economy is still reeling from the economic crisis and the massive austerity measures required by the three international bailouts from 2010 onwards. There are fears that unabated refugee flow and its impact on the economy create the risk of adding xenophobic elements in the country. Initially the locals have welcomed the refugees with open arms. However, later on they have begun to dislike having an international community for which too many resources are being spent for helping out refugees, while ignoring the economic plight of Greece, which the refugee crisis has intensified.

The displaced people who are not resettled and rehabilitated in a sustainable way, after the degradation they cause to the region, they will soon become environmental refugees, not only trying to find a safer place to go on in life, but are also in search for a place to secure their survival, based on basic human rights like food, water and sanitation availability. The same environmental problems will become a nightmare for the residents of Lesvos due to the intense environmental impact.

The current migrant situation in Europe and Greece in particular, is referred to as the “European refugee crisis”. Europe is awed by the massive flow of migrants and refugees crossing its borders and hasn’t responded in a satisfactory way. Having in mind climate change and the massive numbers of migrants expected to be mobilized by the impacts of climate change, it is obvious that measures to

deal with the migration flows are needed. At the governmental level the migration crisis will be dealt with through border control, security measures, and integration policies as appropriate to the specific laws and interest of the country. However, what is frequently ignored is the environment. Therefore, there is a necessity for measures to confront the environmental impacts in a localized manner and to build environmental resilience in zones prone to climate migration.

Acknowledgments
We would like to express our appreciation to Mrs. Georgia Bletsa, Head of Service of Planning Department, Cleanliness, Recycling, and Waste Collection of the Municipality of Lesvos for the supplied data.

References

1. Bashir S. and S. Goswami (2016) 'Tourism induced Challenges in Municipal Solid Waste Management in Hill Towns: Case of Pahalgam', **Procedia Environmental Sciences**, 35, pp. 77 – 89.
2. Braun A., Lang S. and V. Hochschild (2016) 'Impact of Refugee Camps on Their Environment A Case Study Using Multi-Temporal SAR Data', **Journal of Geography, Environment and Earth Science International**, 4(2), pp.1-17.
3. Dyrholm L. and L.M. Lindholm Mikkelsen (2013) 'Finding global solutions: Alternatives to long-term encampment of refugees, 1st master module on Global Studies', ROSKILDE UNIVERSITE, p. 64velopment Review 69 (1), p.160. doi:10.2307/1972177.
4. de Chatel F (2014) 'The role of drought and climate change in the Syrian uprising: Untangling the triggers of the revolution'. **Middle East Stud**, 50(4), pp. 521–535.
5. Encyclopedia Britannica, 2017, https://www.britannica.com
6. Hellenic Statistical Authority, 2014.Amendment of Decision No 6519 / 31.07.2012 (Government Gazette 2230 / B / 31.07.2012)"Results of Population-Housing Census 2011 related In the Legal Population (citizens) of the Country"
7. Holliday J (2013) 'The Assad Regime: From Counterinsurgency to civil war', MIDDLE EAST SECURITY REPORT 8. Institute for the Study of War, Washington, 42 Available at: http://www.understandingwar.org/sites/default/files/TheAssadRegime-web.pdf [Accessed: 20th February 2018]
8. Kelley C.P., Mohtadi S., Cane M.A., Seager R., and Y. Kushnir (2015) 'Climate Change in the Fertile Crescent and Implications of the Recent Syrian Drought', **Proceedings of the National Academy of Sciences**, 112 (11), pp.3241–46. doi:10.1073/pnas.1421533112.
9. Kherfan R.A. (2016) 'What are the most pressing environmental concerns of refugee camps in conflict-zones?, American University of Beirut, Faculty of Health Sciences, Department of Environmental Health, p.14. DOI: 10.13140/RG.2.1.3245.4162
10. Kreibaum M. (2016) 'Their Suffering, Our Burden? How Congolese Refugees Affect the Ugandan Population', **World Development**, 78, pp.262–287
11. Lee S. (1995) 'When Refugees Stream: Environmental and Political Implications of Population Displacement', In Environmental Impact of Sudden Population Displacements - Expert Consultation on Priority Policy Issues and Humanitarian Aid. ECHO/CRED/UCL.
12. Miledzi Agblorti S.K. and K. Awusabo-Asare (2011) 'Refugee-Host Interaction in the Krisan Refugee Settlement in Ghanam Ghana', **Journal of Geography**, l (3), pp.35-59
13. Mynicipality of Lesvos, (2018). Waste production in Lesvos Island, Data provided by email.

14. Onu B., Surendran S.S, T. Price (2014) 'Impact of Inadequate Urban Planning on Municipal Solid Waste Management in the Niger Delta Region of Nigeria', **Journal of Sustainable Development**, 7(6), pp.27-45. doi:10.5539/jsd.v7n6p27.
15. Perouse de Montclos M. and P. Kagwanja (2009) 'Refugee Camps or Cities? The socio-economic dynamics of the Dadaab and Kakuma Camps in Northern Kenya'**, Journal of Refugee Studies**, 13(2), pp. 205–222. DOI: 10.1093/jrs/13.2.205
16. Skanavis C., and A. Kounani (2016) 'The Environmental Impacts of the Refugees' Settlements at Lesvos Island', **13th International Conference on Protection and Restoration of the Environment**, Mykonos island, Greece, 3rd to 8th of July 2016, pp.996-1003.
17. UNHCR (2011) 'Convention and Protocol Relating to the Status of Refugees'. Published by: UNHCR, Communications and Public Information Service, P.O. Box 2500 1211, Geneva, Switzerland.
18. The United Nations Refugee Agency (UNHCR) (2015) 'The Sea Route to Europe : The Mediterranean Passage in the Age of Refugees'.
19. http://www.unhcr.org/protection/operations/5592bd059/sea-route-europe-mediterranean-passage-age-refugees.html.
20. UNHCR (2017a) Operational portal: refugee situation (Mediterranean situation: Greece), Source: http://data2.unhcr.org/en/situations/mediterranean?id=58&country=83&region=43 Access: 16-12-2017
21. UNHCR (2017b) Europe Refugee Emergency Daily map indicating capacity and occupancy (Governmental figures) (Greece), Sourcehttps://data2.unhcr.org/en/documents/download/54465 Access: 16-12-2017
22. UNHCR (2018) Figures at a glance, http://www.unhcr.org/figures-at-a-glance.html
23. Zhang H. (2015), Sino-Indian water disputes: the coming water wars?, **WIREs Water**, 3, pp. 155–166. doi: 10.1002/wat2.1123

DEVELOPMENT AND EVALUATION OF A SMART APPLICATION FOR SUSTAINABLE CROP PRODUCTION - CASE STUDY: COTTON (GOSSYPIUM SPP)

D. Arampatzis*, C. Costopoulou, A. Efthymiou

Informatics Laboratory, Department of Agricultural Economics and Rural Development, Agricultural University of Athens, 118 55 Athens, Greece

*Corresponding author: e-mail: arampatzis.d@hotmail.com, tel : +30 210 5294183

Abstract

The constant evolution of current technologies widens the horizons of practices concerning a number of different environmental sectors. Thus, nowadays it can be possible to implement “smart applications” in micro - managing and improving cultivations to verify the successful outcome of the crops produce. The current environmental situation (climate change, extreme weather conditions, destruction of ecosystems, etc.) calls for the implementation of such methods, in order to protect and insure a framework for sustainable environmental development. The purpose of this paper is to review the present situation of mobile applications which are associated with field crops such as cotton (*Gossypium spp*) and possibly expand the used methodology in other species, in order to provide adaptable plants in the wider spectrum of sustainable production. An application named ‘Cotton Diseases’ was developed via App Inventor 2 an open - source web application, provided by Massachusetts Institute of Technology (MIT), to provide educational and scientific content on cotton diseases and parasites. Whereas, an evaluation was conducted through questionnaires directed to students of Agriculture University of Athens and agriculturalists for the usage of said application. Finally, the research provided a number of conclusions, as well as suggestions to better bridge the gap between technology and environment for a common purpose.

Keywords: Mobile application, Agricultural sector, Environmental sustainability, Technology, Cotton

1. INTRODUCTION

The global increase of population, the stronger demands for food, the climate change and the struggle to maintain or increase the number of crop yields leads to discover new ways to cover the existence needs. Researches show that one out of nine people suffers from chronic hunger and 12.9% of the population in developing countries is undernourished (World Bank, 2012). Thus, technology could be one of the solutions to meet the needs as well as to improve the environmental sustainability.

On the other hand, the widespread use of smartphones, tablets and plethora of existing mobile applications have brought significant changes in the everyday life of people in various sectors. The term ‘mobile application’ or ‘mobile app’ refers to a type of application software designed to run on a mobile device, such as a smartphone or tablet. Mobile apps frequently serve to provide users with similar services to those accessed on PCs. They are generally small, individual software units with limited function. The diversity of mobile apps is the most important asset which explains their popularity and enormous usage. Users are able to communicate, entertain, and get informed about topics of interest such as work, education, lifestyle and scientific context. Mobile apps are particularly easy to use as they are accessible for all ages and regardless of the educational level. An additional

advantage is the technological features of the mobile devices (e.g. smartphones, tablets), such as easy internet access, geographic positioning system (GPS) which supports specialized navigation services and the ability to storage large amount of data base.

Initially, mobile apps were designed to fulfill users' daily needs, such as email, weather, and calendar. In recent years, rapid technological development has contributed to the development of apps with specialized content (Arampatzis, 2017). For instance, mobile apps cover the entire productive spectrum of an enterprise or organization and provide general and specialized information in the scientific field. Agriculture is one of the most important sectors for both the economy and the environmental sustainable development worldwide. However, the development of agricultural mobile apps is still in its infancy. Already existing agricultural mobile apps (about 1,300 apps) mostly offer agricultural news, agricultural activities, management of irrigation systems, management of crop sensors, productions of yield forecasting and registration of soil types and are related to the needs of the farmers and agricultural businesses (Ntaliani et al., 2008; Karetsos et al., 2014; Costopoulou et al., 2016).Moreover, there is a small number of agricultural mobile apps related to the environmental impact of agricultural practices.

Bridging the gap between intelligent technology and agriculture, could be achieved through the deployment of specific applications regarding traditional cultivation of each country. In particular, Greek agricultural history is linked to the cultivation of cotton. Cotton products are widely used, both in the industry (e.g. textile, fiber, feed) and have an important place in the economy. The largest cotton production comes from India, China, the USA and Pakistan. Greece holds the 13th place in the world cotton production and the 7th place in the world cotton exports (World Cotton Production and Exports, 2018). In this light, the objective of this paper is two-fold: firstly, to investigate the current situation of mobile apps for cotton production and its diseases and natural enemies; and secondly, to develop a pilot mobile app for cotton diseases and natural enemies for agricultural educational purpose. The structure of the paper is as follows: Section 2 provides an overview of mobile apps for sustainable production on field crops such as cotton (Gossypium). Section 3 describes the modeling and the development of a mobile app entailed ‘Cotton Diseases’ app. In addition, the results of a questionnaire survey conducted for evaluating the proposed app are presented. The participants in the survey were students by the Agricultural University of Athens and agriculturalists. The last section provides the conclusions and possible directions for a better relationship between mobile apps, agriculture and environment in the future.

2. A SURVEY ON COTTON MOBILE APPS

Mobile technology is a sector with the fastest growth and high rates of increase worldwide. This rising digital culture consist of developers, software platforms and thousands of users. Innovations in this technology are expanding not only for what can be done with mobile apps but also making these apps more accessible to a larger number of users. Mobile apps are accessible through distribution platforms, known as app stores and the most known are Apple App Store, Google Play Store and Windows Phone Store. Moreover, in 2016, consumers downloaded 149.3 billion mobile apps and it is predicted that in 2021, 203.6 billion more mobile apps will be downloaded (Statista, 2016). In addition mobile apps show a noteworthy prospect of innovation in the agricultural sector and may bridge the gap between technology and the environment. Prospects are auspicious, as they can boost farm income, ensure optimal quality characteristics in the production, and use lower inputs during the growing season and agricultural practices. According to the World Bank the benefits of these apps in the development of the agricultural sector could be achieved through the following ways:

- Provision of better access to information: By providing to producers immediate access to valid information relating to weather, pests and diseases, better environmental management as well as to market information and increased demand.

- Provision of better access to agricultural extension services: Valid information and counseling for good agricultural practices can be given.
- Provision of better connection with the market and networks: Helping producers, suppliers and buyers be more efficient and less manipulated.

In order to identify mobile apps regarding cotton production, in Apple App Store, Google Play Store and Windows Phone Store, a survey based on particular characteristics has been carried out (Costopoulou et al., 2016). The characteristics are as follows:

Logo: the graphic mark of app;

Title: the name of app;

Category: the agricultural topic or task covered by the app;

Language: available languages;

Geographical coverage: the country or countries in which the app can be used;

Date: the release date of the app or the date the app has been updated;

Cost: the cost for acquiring the app (e.g. free, subscription or one-off payment);

Rating: evaluation of the app from the users;

Support: operating system and devices that support the app.

The survey has been conducted during November 2016 till January 2017. Twenty six mobile apps have been identified, and have been described according to the aforementioned characteristics. The analysis of the survey per characteristic has shown the following results:

Category: Agricultural information on variety topics (8%), weather forecast(8%), tools and GIS (8%), calculators (4%), agricultural management(42%), productivity(11%), education (19%) (Figure 1a).

Language: 70% of the apps support only the English language, 22% of the apps support two languages i.e. English and a second language, and 8% support more than two languages.

Geographical coverage: 33% of the apps have limited geographic coverage and 67% have global geographical coverage

Date: 30% of the apps were released in 2016, 22% of the apps in 2015, 26% of the apps in 2014 and 22% of the apps were released between 2010 and 2013.

Cost: 94% of apps were purchased free and 4% of apps required payment for download.

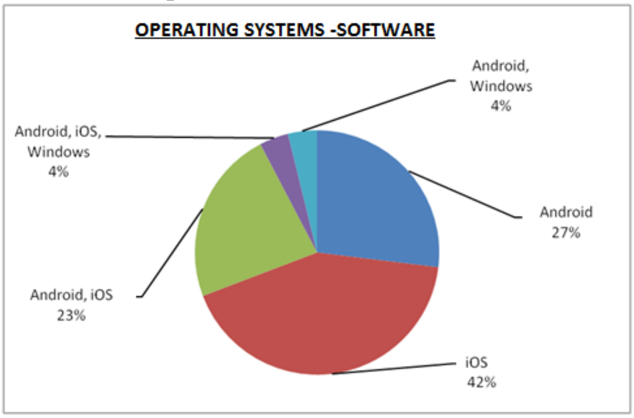
Rating: The rating was fairly low.

Support: 42% of the apps are supported by iOS, 27% are used by Android, 23% of the apps are supported by Android and iOS, 4% for Android, iOS and Windows and 4% for Android and Window (Figure 1b).

3. THE COTTON DISEASE MOBILE APP

This section presents the development and the evaluation of the proposed mobile app for cotton diseases. In particular, the deployment of this app has been chosen for the following reasons: Firstly, cotton is one of the traditional cultivations of Greek agriculture. Greece is the main cotton producer country of the European Union (Papakosta, 2013). In particular, cotton is produced mainly in two Member States on around 300.000 ha. **Greece** is the main cotton grower, with 80% of European cotton area, followed by **Spain** with a share of 20%. Also, cotton production can be considered as a pillar of economic growth for Greek agriculture. Secondly, the cultivation of cotton is characterized

as a demanding cultivation because of the agricultural techniques that are used, such as fertilization, pesticides, irrigation and herbicides. Third, the quality criteria for cotton fibers are very strict and Greek production manage to fulfill them. Finally, Greek cotton producers as well as agriculturalist students need specific knowledge, such as valid information about various practices for different diseases and parasites of cotton to intend a sustainable production and eco-friendly practices.



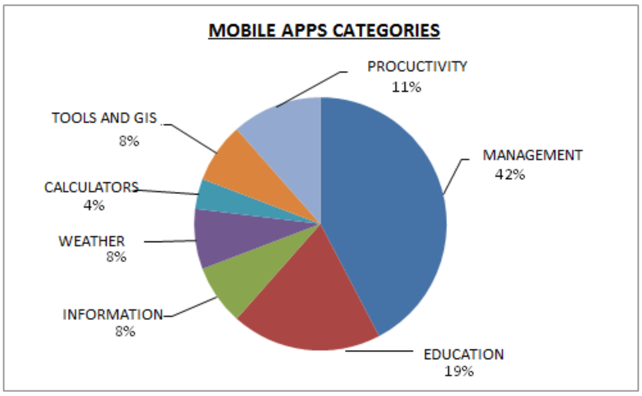


Figure 1: a) Mobile apps categories, b) Mobile apps operating systems

3.1 App development

The proposed app entitled 'Cotton Diseases' app has been developed for the Android operating system (OS) for smartphones. It uses App Invertor 2, an open - source web application, provided by Massachusetts Institute of Technology (MIT) that creates software applications for the Android OS. It uses a graphical interface, which allows users to drag-and-drop visual objects to create an application that can run on Android devices. The decision of using Android OS is based on the rationale that this OS has greater freedom in its development program. The development was based on the "drag-and-drop building blocks" system (Figure 2), which signifies that the assignments were already made and the user could transfer them to specific blocks (Pokress and Veiga, 2013).

The key functionality of the app includes a front screen comprising three options (buttons) namely bacterial disease, fungal diseases and natural enemies, such as *Heliocoverpa armigera*, *Pectinofora gossypiella* (Ioannou, 1988). Touching on the first option certified content about a bacterial disease as well as images of the symptoms is revealed. The second option provides data and information about fungal diseases and images with the symptoms (Figure 3), and the last option information about different parasites, which are the most dangerous for Greek cotton production. The 'Cotton Diseases' app provides educational and certified content (in Greek) on cotton diseases and parasites and is directed mainly to Greek cotton producers and students. It could be purchased free of charge through Google Play and is able only for Android devices.

3.2 App evaluation

A questionnaire survey has been conducted in order to evaluate the proposed app. The survey has been conducted during February 2017 and the sample consists of 59 participants. 36 participants were students of the Agricultural University of Athens and 23 participants were agriculturalists (Table 1). The initial version of the questionnaire was pre-testes by two volunteers so as to be checked for its clarity. The online version of the questionnaire is based on the Google Forms and includes 18 questions about demographic characteristics, the usage of agricultural mobile apps and the benefits of "Cotton_Diseases" app during the yield practices. Indicative examples of questions are "Did you find the app useful for recognizing any symptom?" or "Would you like to use this agriculture app or any other?"

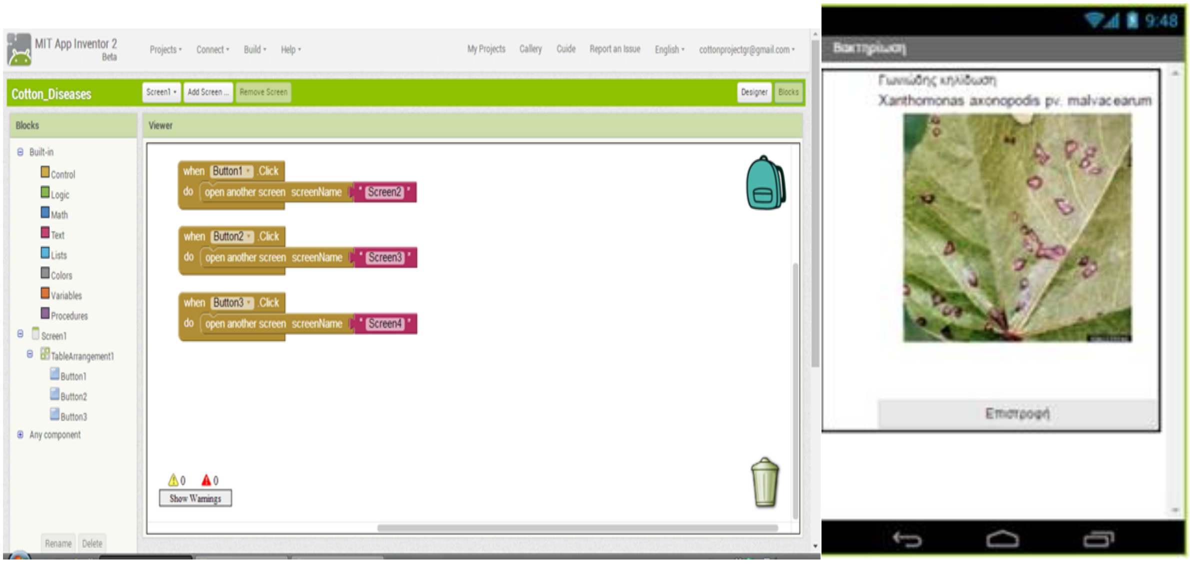


Figure 2 & 3: A screen of 'Cotton Diseases' App Inventor 2 - A screen of cotton symptoms

Table 1: Sample Demographics

Profile of Respondents	Frequency	Percentage (%)
Gender		
Male	36	61
Female	23	39
Age (yrs.)		
18-25	36	61
26-35	10	17
36-45	6	10
46-55	7	12
Educational level		
AUA students	36	61
Producers	23	39

The evaluation of the app was divided into two parts, namely the evaluation by the students referring to the participants of the age group 18-25 years old, and the evaluation by the agriculturalists referring to the participants of the age group of 26-35, 36-45 and >45 years old. The evaluations is as follows.

3.2.1 Evaluation of the app by students

The analysis results shows that most of the students use smartphone (56%) and 44% use both smartphone and tablet. None of the participants uses a tablet only. As far as students' mobile device software is concerned, 50% of them are Android based, 33% are iOS based and 17% are running Windows. All of the participants use mobile apps mainly for social networking (facebook, whatsapp, viber, instagram, twitter, snapchat) as well as for games and educational applications. For the ease of use of the 'Cotton Diseases' app, 11% of the responders found it difficult to moderate, 47% somewhat easy, while 42% very easy to use. Regarding the ease of finding information, 3% answered that it was a bit easy, 8% moderate, 53% fairly easy and 36% very easy. For the information structure, 0% found the organization chaotic, 2.8% almost chaotic, 2.8% said the organization was moderate, 13.9% considered the organization good, 50% fairly organized and 30.5% organized. The screen switching was characterized by 8% of the students as modest, 39% as helpful and 53% as very helpful. 84% of the students answered that they would use the app and 16% would not. 56% responded that they would pay for the app while 44% responded negatively. Considering 'Cotton Diseases' app in general terms, 5.6% rated it moderate, 16.7% good, 41.7% satisfactory, and 36% fully satisfactory. 83.3% would suggest applying to other users, while 16.7% would not suggest it. Regarding improvements

to the ‘Cotton Diseases’ app, 33% suggests improved information, 39% improvements in images, and 28% do not consider the need for further improvements.

3.2.2 Evaluation of the app by producers

According to the educational level of the producers, 39% of them are graduates of high school, 18% have higher education (IEK etc), 22% holds university degree, 21% hold a postgraduate or a PhD. 39% of the responders has only a smartphone and 61% have both devices (smartphone and tablet). 52% of the producers holds Android mobile device, 26% iOS mobile device and 22% Windows mobile device. Furthermore, 91% use daily various types of mobile apps and 9% does not have any apps in their mobile devices. Concerning the type of the apps that they already use, 61% of the responders use informative apps, 17% games, 13% social networking apps, 4% educator and 5% other type. For the ease of use of the app, 9% found the difficulty level to be moderate, 43% somewhat easy, while 48% very easy to use.Regarding the finding of information, 22% answered that it was a bit easy, 48% fairly easy and 30% very easy.As for the information structure, none of the found the organization chaotic, 13% said the organization was moderate, 9% considered the organization good, 52% fairly organized and 26% organized.Regarding the question of whether the texts presented are informative, 9% responded almost not as well as little informative, 22% responded moderately, 52% found it quite explanatory and 17% very informative.74% responded that they would pay for the app while 26% responded negatively.Considering ‘Cotton Diseases’ app in general terms, 4% rated it moderate, 18% good, 52% satisfactory, and 26% fully satisfactory. 96% of the participants would suggest this app to other users, while 4% of them would not suggest it. 30% of the responders believes that the provided information could be improved, 22% the provided images, 5% the switching of monitors can be improved and 43% do not suggest any changes neither for information, images or switching of monitors. It is worth noting that all of the producers willing to use the app during the growing season.

4. CONCLUSIONS

Recent technological advances, new mobile products and the strong demand of the agricultural stakeholders as well as consumers has resulted in the notable need to develop agricultural mobile apps to support various kinds of services, such as weather forecasting, eco-friendly managements and to insure easy access to valid agricultural information, communication between producers etc. It has been observed that in the mobile agricultural app market, the number of displayed apps is around 1.300, which reflects a small number in relation to the importance of agriculture in global environmental issues, such as climate change, as well as in the economy and business sectors. For this study, twenty six mobile apps regarding cotton production were studied based on their technological characteristics and their provided content. The majority of the selected apps are free of charge to download, 96% and 4% were on payment. iOS is the main platform among the publishers for mobile agricultural apps (42%), closely followed by Android (27%). In addition, Windows platform offers a few mobile agricultural apps. However must be mentioned that 31% of the selected apps could be purchased by all the platforms. In addition, most apps' primary language is English. As far as the usage of agricultural mobile apps by Greek producers and students, the results show that a very small amount of people take advantage of the technology and more specifically from the mobile apps. The explanation of this phenomenon could be the absence of agricultural apps with Greek content, poor explanatory information or scientific advices for the Greek environmental conditions, lack of awareness of the app beneficial outcomes in the agricultural practices, and minor usage of apps by important stakeholders. It is noteworthy, that in the age group above 45 years old, technology does not have an important factor in their daily life; participants in that age group did not own any technological product, such as smartphones or tablets. The advantages of agricultural mobile apps may be important but the development of these kind of apps presents a lot of challenges, described as follows:

- For the development of mobile agricultural applications, the contribution of stakeholders from different sectors is important, such as producers, agronomists, agriculturalists, programmers, mathematicians and meteorologists.
- The development of agricultural mobile apps should provide information on crop cultivation techniques and its needs, aiming at economic and predominantly environmental sustainability.
- Agricultural mobile apps should be developed for different geographic locations, as each area is characterized by different soil and climate conditions. In plants with high requirements in cultivation techniques, the development of agricultural apps is necessary for low risk management.
- Seminars could be organized to inform the producers for the benefits of the apps usage and universities should include specialized lectures for students.
- Agricultural stakeholders should be appropriate informed, educated and persuade producers to use agricultural mobile apps.

References

1. Arampatzis, D. (2017). '**Developmentand evaluation of a mobile application for cotton diseases and pests**'. MSc Thesis, Agricultural University of Athens. (in Greek).
2. Costopoulou C., M. Ntaliani, S. Karetsos. (2016). '**Studying Mobile Apps for Agriculture**. IOSR Journal of Mobile Computing & Application 3(6), Issue 6 (Nov. - Dec. 2016), pp. 44-49.
3. Ioannou D. (1988). '**Cotton: Enemies, Diseases, Weed**'. Stamoulis Edition, Athens. (in Greek).
4. Karetsos S., C. Costopoulou and A.Sideridis. (2014). '**Developing a smartphone app for m-government in agriculture**'. Journal of Agricultural Informatics, 5(1),2014, pp. 1-8, 2014.
5. Ntaliani, M., C. Costopoulou, S. Karetsos. (2008). '**Mobile government: A challenge for agriculture**'. Government Information Quarterly, 25(4), pp. 699-716.
6. Papakosta-Tasopoulou D. (2013). '**Industrial Crops**'. Athens: Modern Education Edition. (in Greek).
7. Pokress, S. C., Veiga, J. J. D. (2013). **MIT App Inventor: Enabling personal mobile computing**. arXiv preprint arXiv: 1310.2830.
8. Statista. (2016). Available: https://www.statista.com/statistics/271644/worldwide-free-and-paid-mobile-app-store-downloads/ [Accessed: 26-01-2018] .
9. World Bank. (2012). Mobile applications for agriculture and rural development. Washington, D.C.:WorldBankGroup.http://documents.worldbank.org/curated/en/167301467999716265/Mobile-applications-for-agriculture-and-rural-development [Accessed: 24-01-2018] .
10. World Cotton Production and Exports. (2018). World Cotton Production http://www.cottoninc.com/corporate/Market-Data/MonthlyEconomicLetter/pdfs/English-pdf-chartsand-tables/World-Cotton-Production-Bales.pdf

EXPLORING PUBLIC PREFERENCES AND PRIORITIES FOR CONTROLLING INVASIVE MOSQUITO SPECIES: THE IMPLEMENTATION OF A WEB SURVEY IN GREEK HOUSEHOLDS FOR THE CASE OF THE ASIAN TIGER MOSQUITO

K. Bithas[a], D. Latinopoulos[b,*], A. Kolimenakis[a], C. Richardson[a], K. Lagouvardos[c] and A. Michaelakis[d]

[a] University Research Institute of Urban Environment and Human Resources, Panteion University,
[b] School of Spatial Planning and Development, Aristotle University of Thessaloniki, Greece,
[c] National Observatory of Athens/Institute for Environmental Research, Athens, Greece,
[d] Benaki Phytopathological Institute, Department of Entomology and Agricultural Zoology, 14561, Kifissia, Greece

*Corresponding Author: email: dlatinop@plandevel.auth.gr, tel. +302310994248

Abstract

The introduction of invasive mosquito species in the Mediterranean area along with intense urbanization poses new challenges for both scientists and policy makers. The last decade has seen the wide spread of the invasive Asian tiger mosquito *Aedes albopictus* in various urban ecosystems of Greece. Compared to native species, Asian tiger mosquitoes are accompanied by greater risks of infectious diseases, higher nuisance levels, and increased expenses for their confrontation. Consequently, future decisions on mosquito control should take these risks into consideration. Public perceptions and preferences regarding these risks are crucial in order to make decisions more responsive to citizens' needs and thus more effective. The aim of this paper is to investigate various socio-economic aspects of the Asian tiger mosquito problem, through a web-based questionnaire. The survey was conducted nationwide, aiming to record (a) the impact of invasive mosquito species in Greek households, (b) associated costs and perceived risks, and (c) priorities and policy directions in mosquito control. The results indicate that citizens are highly concerned with the health risks associated with the new mosquito species and consider public prevention strategies highly important for the confrontation of the problem. The spatial patterns of these results are further investigated aiming to identify regions with different levels of risk and/or policy priorities.

Keywords: urban ecosystems; Asian tiger mosquito; web survey; infectious diseases; citizens' preferences

1. INTRODUCTION

In recent years, concern has arisen over the threatened increase in mosquito-borne diseases in the Mediterranean region as new sanitary and environmental risks emerge, including the appearance of chikungunya, dengue and West Nile viruses, calling for the adoption of specific measures and strategies by both policy makers and scientists. These public health challenges are associated particularly with the presence of the Asian tiger mosquito (*Aedes albopictus*), an invasive mosquito species implicated in the transmission of a wide range of human pathogens. The first presence of the Asian tiger mosquito in Greece (in north-western prefectures) is dated back to 2003 [Samanidou-Voyadjoglou et al., 2005], and it was confirmed for the first time in Athens (Attica Region) in 2008

[Koliopoulos et al., 2008]. The mosquito problem in Greece, as in other parts of Europe, has recently intensified and is favoured by both the geographic position and climatic conditions of Greece.

The invasive mosquito species (IMS) problem can affect the economy and society in various ways, through impacts on human and animal health, as well as on various services and activities. These impacts generate certain economic costs related to control strategies, public health expenses, illness treatments, productivity losses, information and awareness campaigns, and economic losses in tourism and other sectors. Economic impacts can be direct or indirect. Direct economic impacts are represented by the net increase in spending as a result of the appearance of IMS and include, for example, control-and-surveillance programmes, private expenditures and direct medical costs. These are the most clearly defined impacts as they can be expressed explicitly and immediately in monetary values. Indirect impacts include effects on residents' quality of life, impacts on public health, costs associated with new research and management services (in both the public and private sectors of the economy), effects on tourism, and so on. Indirect effects are often difficult to evaluate as they cannot be expressed easily in monetary terms. Various valuation techniques are usually applied, such as stated preference methods (e.g. the contingent valuation method, choice experiment method, etc).

Studies conducted in Europe and the USA have examined the socioeconomic benefits and costs associated with the overall mosquito problem [e.g. John et al., 1992; von Hirsch and Becker, 2009; Dickinson and Paskewitz, 2012; Halasa et al., 2014; Brown et al., 2015; Bellini et al., 2014; Kolimenakis et al., 2016; Bithas et al., 2018]. Most of these studies conclude that the perceived benefits that arise from the reduction of nuisance levels and health threats exceed the costs of prevention and control strategies against various mosquito species. Some of these studies have focused on the assessment of the non-market benefits of mosquito control programs [e.g. John et al., 1992; von Hirsch and Becker, 2009; Dickinson and Paskewitz, 2012; Halasa et al., 2014; Bithas et al., 2018]. The present study aims to enrich the existing literature by investigating: (a) the impact of invasive mosquito species on Greek households, at the national level, (b) the associated costs and the perceived risks, (c) the priorities and policy directions in mosquito control from a citizen's perspective, and (d) the spatial variation in these results.

2. METHODS

The implementation of a web questionnaire followed a process of surveys and evaluations [Kolimenakis et al., 2016; Bithas et al., 2018] aiming to elicit citizens' preferences for mosquito control strategies as well as to evaluate the effectiveness level of prevention programs in Greece. The present study was designed to address qualitative dimensions not previously recorded in the surveying processes and to extend the sampling of answers at the national level, using a web questionnaire in order to save costs. For this purpose collaboration was established with a web meteorological platform of high visiting frequency (www.meteo.gr) in order to increase the geographical dispersion of the sample. It should be noted that the specific web platform had already implemented a real time monitoring application for the identification of mosquito presence, covering the whole of Greece.

The questionnaire was specifically designed to elicit citizens' opinions regarding certain socio-economic aspects of the mosquito problem. The overall aim was to examine and then to validate at the national level a set of parameters related to private prevention costs for IMS and to investigate individual preferences between various mosquito control programs. The questionnaire contained an introductory page explaining the purpose of the study and some general information about the Asian tiger mosquito and its associated health risks. The first questions focused on the respondents' knowledge of the Asian tiger mosquito. The next questions concerned: (a) the current perceived level of nuisance during the day and separately at night (rated using a 5-point Likert scale), (b) the portion of the year (months) with significant mosquito nuisance, (c) the monthly household expenditure for private prevention measures, and (d) the main reasons for taking individual prevention measures (i.e. they had to choose between health risk reduction and nuisance reduction). Subsequently, participants were asked about the importance of taking further public measures for mosquito control (using a 5-

point Likert scale) and further questions were included to identify the main targets of future public control measures/programs. The final section of the questionnaire focused on participants' demographics (age, residence area, family status).

For the purpose of our survey, a special banner appeared on the home page of the host web platform from which visitors followed a link to the web survey. The banner appeared randomly to visitors, but a selection bias could arise due to (i) the non-representative nature of the internet population in general and users of *meteo* in particular, and (ii) self-selection of participants - the `volunteer effect' [Eysenbach, 2004] which was possibly related to their interest in mosquito control. The survey took place in September and October 2016 with a total of 1,204 responses from all over the country. The regional distribution of the final sample is presented in Table 1. This distribution is quite representative of the population (see Table 1) but it is also a first indicator of regional differences in people's attitudes and experience of mosquito-associated problems.

Table 1. Sample distribution per region

	Sample		Population[1]	
	Frequency	Percent	Residents	Percent
Attica	664	55.1%	3,827,624	35.39%
Central Greece	43	3.6%	547,390	5.06%
Central Macedonia	131	10.9%	1,881,869	17.40%
Crete	57	4.7%	623,065	5.76%
Eastern Macedonia and Thrace	49	4.1%	608,182	5.62%
Epirus	35	2.9%	336,856	3.11%
Ionian Islands	33	2.7%	207,855	1.92%
North Aegean	12	1.0%	199,231	1.84%
Peloponnese	49	4.1%	577,903	5.34%
South Aegean	26	2.2%	308,975	2.86%
Thessaly	60	5.0%	732,762	6.78%
Western Greece	38	3.1%	679,796	6.29%
Western Macedonia	7	0.6%	283,689	2.62%

[1] Data from population census in Greece, conducted by the Hellenic Statistical Authority (2011)

3. RESULTS

Most of the respondents to the web questionnaire (89.5%) already knew of the Asian tiger mosquito and health risks before the survey. About 66% of the respondents reported that the Asian tiger mosquito is established in their residence area. Regional differences in this response are relatively small (ranging from 55% to 71%) and are not significantly correlated with the actual detection of this mosquito species over Greece [Badieritakis et al., 2018]. Therefore, public perception cannot safely be used as an indicator of the presence of *Aedes albopictus* in an area.

In contrast to the study of Bithas et al. (2018), which reported a higher nuisance during the night than the day in the region of Attica, we found that nationally night nuisance levels are almost identical with the daytime levels, with a mean value of 3.6 on the 5-point Likert scale (indicating a nuisance level between average and high). Figure 1 presents the distribution of the perceived nuisance level at night, as well as the regional variation of the mean nuisance value. Figure 2 presents the corresponding perceived nuisance levels during the day, which can be taken as an indication of the nuisance caused by the Asian tiger mosquito (which, unlike native mosquitoes, causes biting nuisance b). According to these results it can be concluded that respondents living in the regions of Eastern Macedonia and Thrace, Peloponnese, Central Greece and Western Greece experience a higher daytime biting nuisance which can be attributed to the presence of the Asian tiger mosquito.

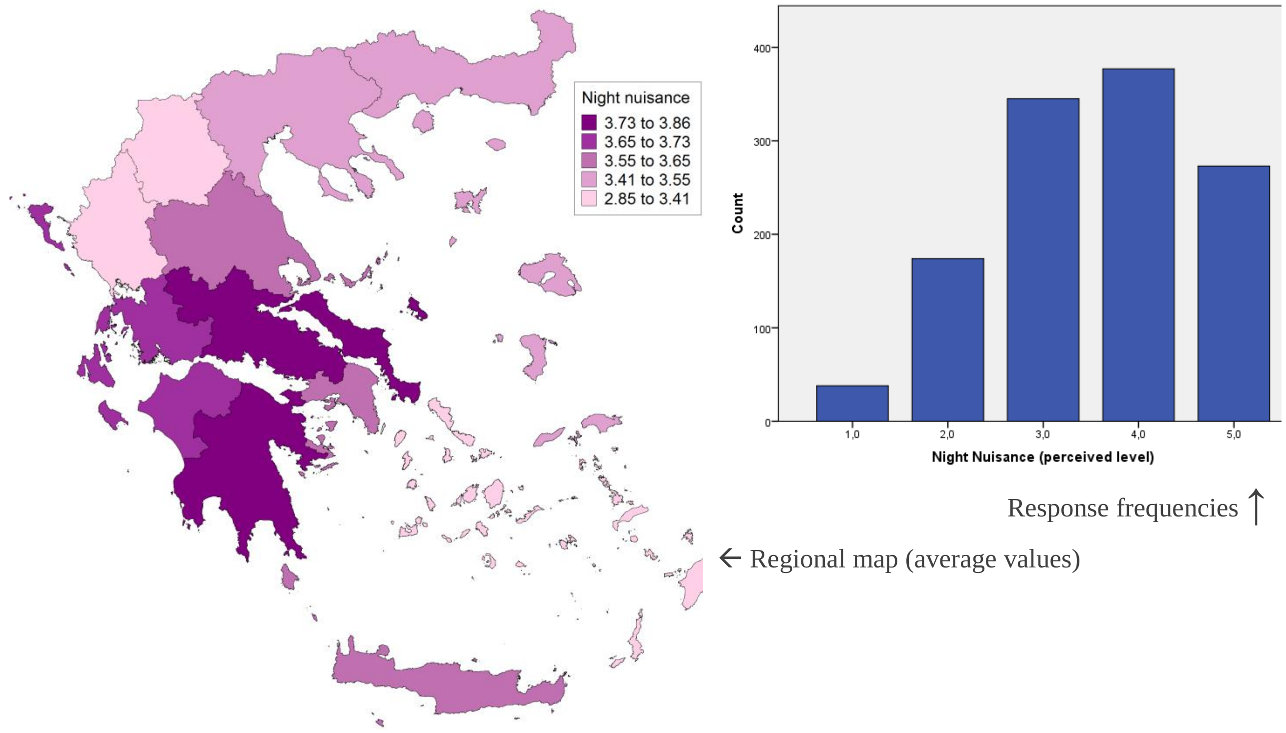


Figure 1. Nighttime nuisance *(Likert scale 1-5: 1= no nuisance, 5= intolerable nuisance)*: mean nuisance by region and distribution of individual responses

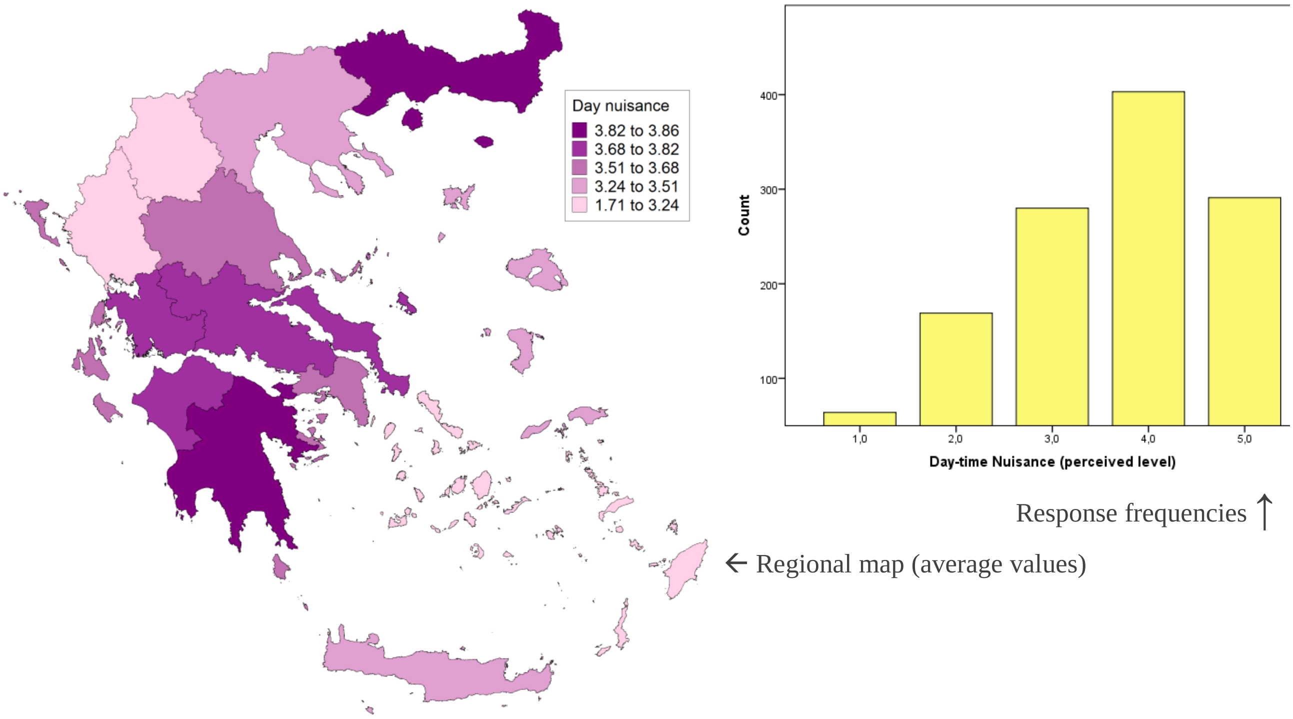


Figure 2. Daytime nuisance *(Likert scale 1-5: 1= no nuisance, 5= intolerable nuisance)*: mean nuisance by region and distribution of individual responses.

As shown in Figure 3, the average "nuisance period" according to the survey respondents follows an approximately normal distribution and lasts 5.7 months on average approximately. The regional variation of this period is depicted in the corresponding thematic map (Figure 3), revealing a longer nuisance period in South and South-eastern regions.

Concerning the private prevention costs, it was found that households are paying on average 17.6 € per month when mosquitoes are active. This estimate is much higher than that found by Bithas et al. (2018) in the Attica Region (6.6 €/month). This difference may be attributed to the self-selection of participants, which is likely to be related to their interest in mosquito control, which in turn may depend on the nuisance level. Therefore, these results are likely to be overestimates, but can be used in order to explore the regional variation in prevention costs. In order to do so, we estimated the annual prevention costs by multiplying the monthly costs by the nuisance period. The average annual cost in our sample was found to be 100.1€/household. Significant spatial variations were observed in these estimates (Figure 4), as annual costs ranged from below 80€ in some regions (e.g. Thessaly and the North Aegean) to over 125€ in others (e.g. Eastern Macedonia and Thrace, and Central Greece). This variation may be an indirect indicator of the magnitude of the mosquito problem, which is strongly associated with the nuisance conditions in each area. It should be also noted that this revealed behavior concerning prevention can be used as a proxy of individuals' potential benefits from improved control measures in each region.

Figure 5 shows which of health and nuisance appears to be the respondents' main reason for taking individual prevention measures. Nuisance seems to be the main reason in about 73% of respondents, while health risks are stated as the main reason in only 27% of the sample. It should be also noted that: (1) nuisance was considered more important than health risks in all regions, and that (2) the two regions where health risks appear to be more related with individual prevention strategies (costs) are those of Central Greece and Western Greece. This result partly contradicts the findings of Bithas et al., (2018), who found health to be the main prevention priority for citizens of the Athens metropolitan area, but on the other hand is in accordance with the findings of most of the recent literature. However, as will be seen below, when expenses are viewed from the point of view of a public good, citizens are more concerned with the threats to health than with nuisance.

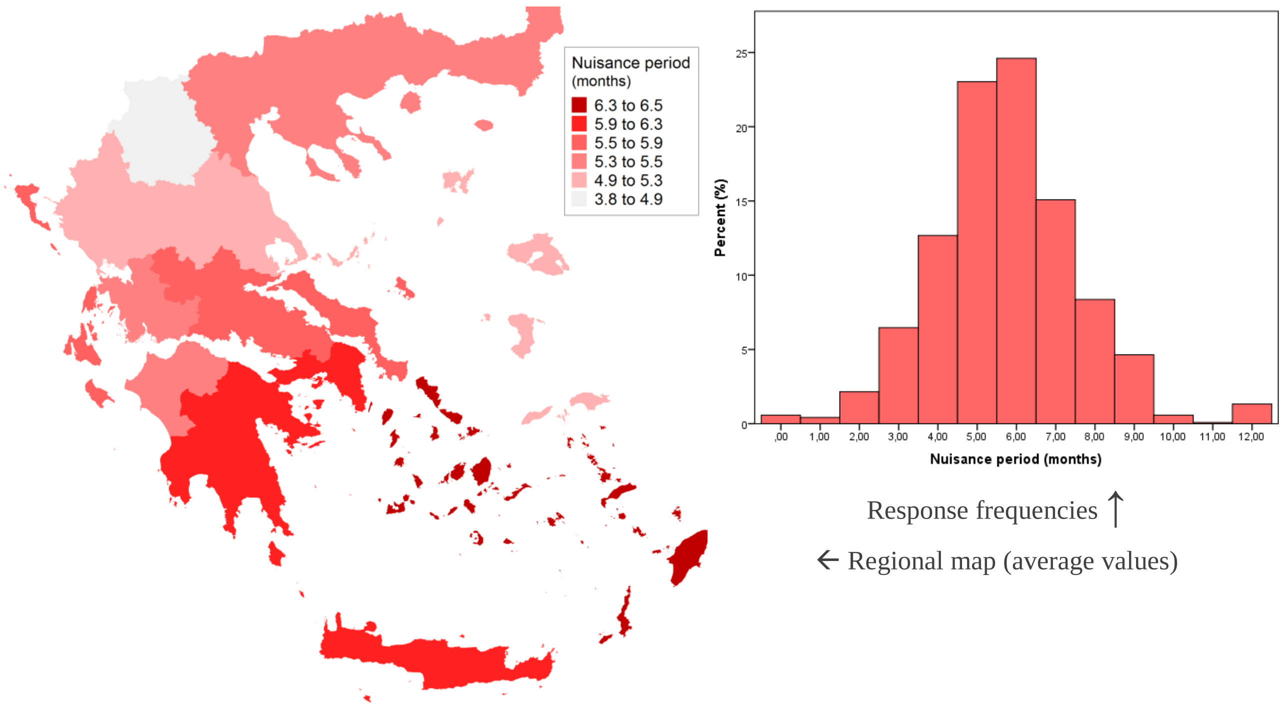


Figure 3. Nuisance period (months): mean values by region and distribution of individual responses.

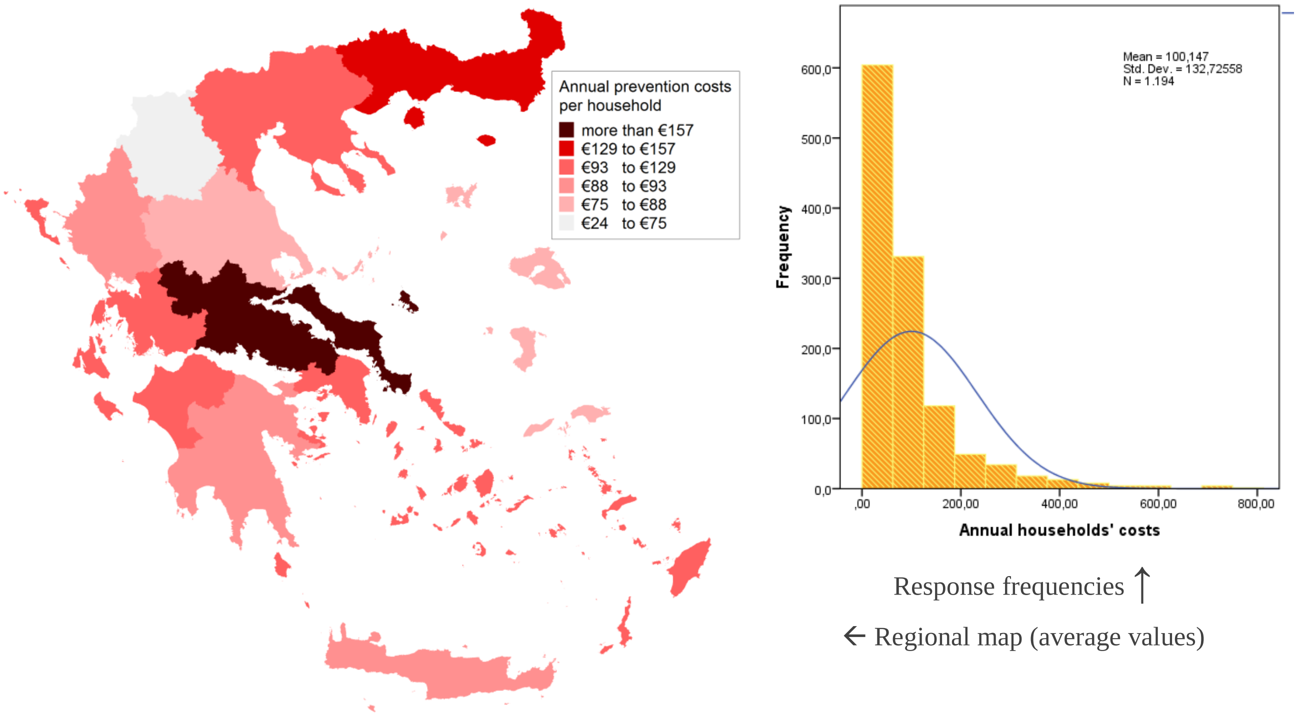


Figure 4. Annual prevention costs (€/year/household): mean by region and distribution of individual responses.

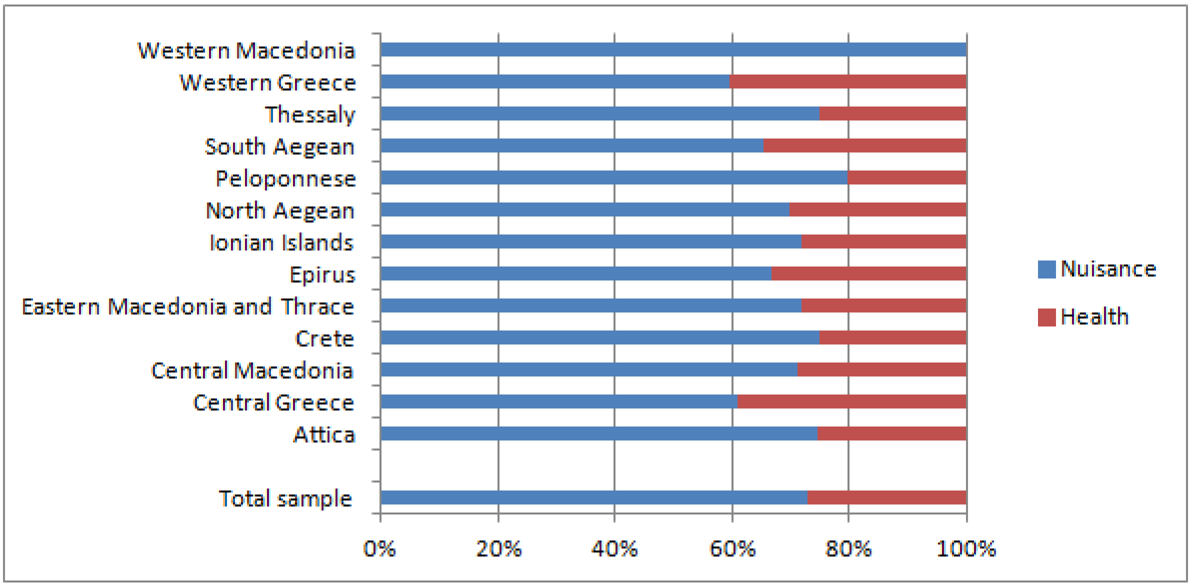


Figure 5. Main reason for taking individual prevention measures, by region.

Finally, the web survey attempted to gather information regarding the preferences of individuals for the various mosquito control programs, and particularly about the importance of taking further public measures for mosquito control, as well as about the main targets of future public control measures and programs. Overall, 83% of the survey respondents believed that the current prevention and control measures are insufficient or inadequate for dealing with the mosquito problems and therefore there is scope for further measures to be taken. Concerning the main targets of these measures (Table 2), health impacts were considered to be more important than nuisance impacts, confirming the findings of previous surveys in Greece [Kolimenakis et al., 2016; Bithas et al., 2018]. Furthermore, as in those two studies, transmission of disease from invasive species was considered to be a serious threat. On the other hand, nuisance levels and the financial burden on households for mosquito control were also rated highly, thus constituting them as important additional decision factors.

Finally, an important finding of this survey was that citizens seem to be aware of the environmental consequences of mosquito control measures. In particular, 74% of the sample stated their disagreement with measures that may potentially affect the physical environment and the ecosystems.

Table 2. Individuals' rating of the objectives of mosquito control programs (web survey results)

	Reduction of mosquito-borne disease risks		**Reduction of nuisance**		**Low cost to households**
	From native species[1]	From invasive species[2]	From native species[3]	From invasive species[4]	From future control programs
Highly important	73.2%	76.7%	47.1%	39.5%	26.8%
Important	19.1%	15.9%	32.3%	25.3%	17.8%
Neutral	5.4%	5.6%	15.7%	20.2%	26.5%
Less important	1.6%	1.2%	4.0%	10.3%	17.4%
Non important	0.7%	0.6%	0.9%	4.7%	11.6%

[1] for example: malaria, West Nile Virus
[2] for example: chikungunya, dengue, Zika Virus
[3] Nighttime nuisance
[4] Daytime nuisance

4. DISCUSSION AND CONCLUSIONS

The present paper aims to provide an overview of citizens' perceptions and attitudes towards the problem of invasive mosquitoes, as well as towards the future targets of mosquito control programs. In this framework a web based survey was designed and implemented at the national level in Greece. The results show that nuisance from mosquitoes: (a) is significant all over the country, although showing some regional differences, thus indicating areas of higher priority for future policy actions; (b) is similar for both invasive and native species; and (c) is the main reason for taking individual prevention measures. The cost of individual prevention measures was estimated to be quite high (about 100€/household/year), which could be the result of the selection bias (i.e. the volunteer effect) due to the survey mode (web). However, regional variation in this cost may be an indirect indicator of the magnitude of the mosquito problem, which is strongly associated with the nuisance conditions in each area. Furthermore, this revealed behavior concerning prevention can be used as a proxy of individuals' potential benefits from future improved control programs in each region.

One of the most important findings of the present study is that citizens perceive the protection from mosquito-borne diseases as an important public good which should be funded by public expenses. The results of our study indicate that, on the one hand, citizens are more willing to incur personal expenses against daily nuisance from mosquito species and, on the other hand, they are willing to pay for an improved control program against disease threats when implemented by public authorities. Therefore, to a certain extent, citizens seem to transfer the responsibility of health related protective measures onto experts and public health practitioners. This might imply that they feel rather insecure with regard to the efficiency of their personal measures against the various mosquito-associated diseases. However, similar a case in the Mediterranean [Carrieri et al., 2011] indicates that citizens' participation is also highly important especially in the monitoring and control of invasive mosquito species. Regarding the Greek case, a certain lack of information from public authorities may increase both the insecurity and lack of awareness of citizens concerning the particular problem. However, there are recent ongoing initiatives funded by the EU (LIFE CONOPS) which enhance public information and lead to collaboration between the scientific community, public authorities and citizens. It should be noted that citizens' participation in many cases is stimulated by the appearance of disease outbreaks as in the case of the 2007 Chikungunya outbreak in the Italia Region of Emilia Romagna. In any case the level of citizens' participation in public policy decisions might also be associated with socio-cultural traits and might differ if examined in diverse contexts and countries.

Another important outcome of the present study is the examination of citizens' perception of the ecosystemic threats associated with mosquito control, an issue not well examined so far in the recent bibliography. While citizens appear to be sensitive to the environmental consequences associated with the mosquito abatement methods, they also seem to have difficulty in identifying the environmental consequences of mosquito control methods. This raises the complexity of the issue at hand when trying to discern the possible level of citizens' participation in public decision making for similar problems. The fact that climate change trends may worsen the mosquito problem and increase the risks of transmitting new diseases (e.g. Zika virus), making the prevention and control methods even more sophisticated, increases even more the complexity of citizens' participation and the associated dilemmas (e.g. human health versus environmental consequences). The interrelation of a wide set of parameters and multiple public decisions associated with the problem of invasive mosquitoes renders necessary the examination of the ecosystemic dimension of the particular issue from a rather holistic point of view.

Funding
Part of this research was co-financed by the European Union (EU Environmental Funding Programme LIFE+ Environment Policy and Governance) and Greek national funds through the LIFE CONOPS project 'Development & demonstration of management plans against the climate change enhanced invasive mosquitoes in S. Europe' (LIFE12 ENV/GR/000466).

References

1. Samanidou-Voyadjoglou A., E. Patsoula, G. Spanakos and N.C. Vakalis (2005) 'Confirmation of *Aedes albopictus* (Skuse) (Diptera: Culicidae) in Greece', **European Mosquito Bulletin**, 19, pp. 10-12.
2. Koliopoulos G., I. Lytra, A. Michaelakis, E. Kioulos, A. Giatropoulos and N. Emmanuel (2008) 'Asian tiger mosquito. First record in Athens', **Agriculture Crop and Animal Husbandry**, 9, pp. 68-73 [in Greek].
3. John K.H., R.G. Walsh and C.G. Moore (1992) 'Comparison of alternative nonmarket valuation methods for an economic assessment of a public program', **Ecological Economics**, 5 (2), pp. 179-196.
4. von Hirsch H. and B. Becker (2009) 'Cost-benefit analysis of mosquito control operations based on microbial control agents in the upper Rhine valley (Germany)' **European Mosquito Bulletin**, 27, 47-55.
5. Dickinson K. and S. Paskewitz (2012) 'Willingness to pay for mosquito control: how important is West Nile virus risk compared to the nuisance of mosquitoes?' **Vector Borne and Zoonotic Diseases**, 12, pp. 886–892.
6. Halasa Y.A., D.S. Shepard, D.M. Fonseca, A. Farajollahi, S. Healy, R. Gaugler, K. Barlett-Healy, D.A. Strickman and G.G. Clark (2014) 'Quantifying the impact of mosquitoes on quality of life and enjoyment of yard and porch activities in New Jersey', **PloS One**, 9(3), e89221.
7. Brown Z., K. Dickinson and S. Paskewitz (2015) 'A generalized latent class logit model of discontinuous preferences in repeated discrete choice data: an application to mosquito control in Madison, Wisconsin', **2015 AAEA & WAEA Joint Annual Meeting**, July 26-28, San Francisco, California.
8. Bellini R., M. Calzolari, A. Mattivi, M. Tamba, P. Angelini, P. Bonilauri, A. Albieri et al. (2014) 'The experience of West Nile virus integrated surveillance system in the Emilia-Romagna region: five years of implementation, Italy, 2009 to 2013', **Euro Surveill**,19, no. 44.
9. Kolimenakis A., K. Bithas, C. Richardson, D. Latinopoulos, A. Baka, A. Vakali, C. Hadjichristodoulou, S. Mourelatos, S. Kalaitzopoulou, S. Gewehr, A. Michaelakis and G. Koliopoulous (2016) 'Economic appraisal of the public control and prevention strategy against

the 2010 West Nile Virus outbreak in Central Macedonia, Greece', **Public Health**, 131, pp. 63-70.

10. Bithas K., D. Latinopoulos, A. Kolimenakis and C. Richardson (2018) 'Social benefits from controlling invasive Asian tiger and native mosquitoes: a stated preference study in Athens, Greece', **Ecological Economics**, 145, pp. 46-56.
11. Eysenbach G. (2004) 'Improving the quality of Web surveys: the Checklist for Reporting Results of Internet E-Surveys (CHERRIES)', **Journal of Medical Internet research**, 6(3).
12. Badieritakis, E., D. Papachristos, D. Latinopoulos, D. Stefopoulou, A. Kolimenakis, K. Bithas, E. Patsoula, S. Beleri, D. Maselou, G. Balatsos and A. Michaelakis (2018) '*Aedes albopictus* (Skuse, 1895) (Diptera: Culicidae) in Greece: 13 years of living with the Asian tiger mosquito', **Parasitology Research**, 117 (2), pp. 453-460.
13. Carrieri M., A. Albieri, P. Angelini, F. Baldacchini, C. Venturelli, S.M. Zeo and R. Bellini (2011). Surveillance of the chikungunya vector *Aedes albopictus* (Skuse) in Emilia-Romagna (northern Italy): organizational and technical aspects of a large scale monitoring system. **Journal of Vector Ecology**, 36(1), 108-116.

ENVIRONMENTAL CHALLENGES TO ACHIEVE THE SDG (11) FOR SUSTAINABLE CITIES - CASE STUDY: TRIKALA, GREECE

M.E Chatzi*, E. Kolokytha

Department of Civil Engineering, Aristotle University of Thessaloniki, 54124, Thessaloniki, Greece

*Corresponding author: e-mail: mmchatzi@hotmail.com

Abstract

Nowadays, over half the world's population lives in urban areas, whereas in Europe, by 2020, it is estimated by the EEA, that almost 80% of EU citizens will be living in cities. This unprecedented urban growth has brought enormous challenges concerning clean water, pollution, greenhouse gas emissions, ecosystem degradation, waste management, security from extreme natural events, health issues and many others.

This paper introduces the concept of urban sustainability and explores the characteristics of the Sustainable Development Goal (SDG) 11, concerning sustainable cities and communities. Measuring sustainability is a complex issue and in the case of a city, is mainly depending on local conditions, as each city operates within a specific ecosystem and a socio-cultural context. Urban sustainability of the city of Trikala, in Greece is tested by analyzing major domains such as water resources, energy sector, transportation systems, waste management, urban green spaces and air quality, whereas, given that cities are hubs for social and human development as well, the cultural heritage is also taken into account. The DPSIR model is used as an analytical framework, through the use of indicators, for the assessment of the current situation. In parallel, a survey to more than 300 citizens of the city of Trikala was conducted in order to identify priorities and values, as well as what is considered most important when it comes to decision making, in order to make life in the city more sustainable. Finally, a number of conclusions and suggestions derived, on the changes that could be made and the actions that should be taken, in order for Trikala to strive for sustainable development.

Keywords: SDGs, sustainable cities, sustainable development, environmental protection, Trikala

1. INTRODUCTION

The SDGs, also known as Global Goals, build on the success of the Millennium Development Goals (MDGs) (UN, 2018) and aim to go further to end all forms of poverty, while being unique in that they call for action by all countries, poor, rich and middle-income to promote prosperity while protecting the planet. They recognize that ending poverty must go hand-in-hand with strategies that build economic growth and addresses a range of social needs including education, health, social protection, and job opportunities, while tackling climate change and environmental protection. While they are not legally binding, governments are expected to take ownership and establish national frameworks for the achievement of the 17 Goals. Countries have the primary responsibility for follow-up and review of the progress made in implementing the Goals, which will require quality, accessible and timely data collection Cities are hubs for ideas, commerce, culture, science, productivity, social development and much more (UN, 2018).

Measuring sustainability is a complex issue and in the case of a city, is mainly depending on local conditions, as each city operates within a specific ecosystem and a socio-cultural context. A

sustainable city is considered to be a place where achievements in social, economic and environmental development are robust, provide security and ensures the well -being of its citizens. The question of how to promote sustainable cities and indeed sustainable urbanization though, cannot be isolated from the global economy and the way it affects the relationships between people, environment and development (OECD, 2003).

This paper, explores the characteristics of the Sustainable Development Goal (SDG) 11, concerning sustainable cities and communities, by applying the DPSIR framework, using indicators of sustainable development, in the small city of Trikala in order to identify potential changes which should be encouraged towards urban sustainability to promote sustainable development and environmental protection. Remarkable findings from a citizens' survey coupled with data analysis from relevant agencies lead to interesting conclusions.

2. THE AREA UNDER STUDY

Trikala is a city in northwestern Thessaly (Figure 1), Greece. Based on Hellenic Statistical Authority (2011) census data, the Municipality of Trikkai counts 608,485 km^2 of land and 81,355 permanent residents, with a population density of 133.7 inhabitants per km^2. The Trikala Municipal Area, which is also the urban center of the city of Trikala, has an area of 70,100 km^2 and 62,154 inhabitants, with a population density of 886.6 inhabitants per km^2, making it the most densely populated area of the Municipality (Strategic Planning of Municipality of Trikala, 2014-2019).



Figure 1: The city of Trikala, Greece

3. METHODOLOGY AND DATA

The DPSIR framework is a systems-thinking framework that assumes cause-effect relationships between interacting components of social, economic, and environmental systems. According to this framework, social and economic developments or (D)rivers, exert pressure (P) on the environment and, as a consequence, the state (S) of the environment changes, as ie. in the provision of adequate conditions for basic needs such as health, resource availability, and/or biodiversity. In turn, (I)mpacts are the ways in which changes in state influence human well-being. Whereas (R)esponses generally refer to efforts to address changes in state, as prioritized by impacts and provide action to correct or improve the situation (EEA, 2009, Kristensen 2004).

Sustainable development indicators should reflect all elements of the causal chain that link human activities to their environmental impacts and the responses of the society to these impacts (CIDA, 2012). The DPSIR framework is useful in describing the relationships between the origins and consequences of environmental problems; however, in order to understand their dynamics, it is also useful to focus on the links between DPSIR elements (WWF, 2015).

The application of DPSIR in this case, for the assessment of sustainability issues in Trikala city, is coupled with the aggregated impacts of local responses on drivers, pressures and states being evaluated by the answers of the surveys' respondents. In this study, indicators of all categories were selectively used, as shown below (Table 1).

Table 1: Major domains and selected indicators for the area under study

SDGs 11: Sustainable cities and communities		
Trikala	Water	Water Balance
		Consumption - Pricing
		Water Reserves
		Future Problems
		Natural Hazards
	Urban Green	Area of urban / peri-urban parks
		Average distance from city center
		Flora & fauna
		Maintenance costs
	Solid Waste	Solid Waste Management
		Recycling
		Hazardous Waste Management
		Urban Wastewater Quality
	Energy	Electricity Use (per capita)
		Use of Renewable Energy Sources
		City Current Consumption
		Innovations & participation in European programs
	Transportation	Road Safety
		Cycle Paths Length
		Pedestrian walkways
		Air Quality
		Public Transportation Fleet
	Culture	Cultural Points per 10.000 citizens
		Maintenance costs
		Citizen Participation

Data to support the indicators were collected from relevant agencies, such as the Technical Service, the Department of Greening and Gardening, the Department of Urban Applications, the company Urban KTEL SA, as well as the Municipal Water Supply and Sewerage Company and the Traffic Department of Trikala. Furthermore, data from the city's strategic planning report (2014 – 2019) were also taken into consideration, as well as other related studies on the matter.

3.1 Water resources & sanitation

In order to determine the current conditions of the city, a number of indicators were used, concerning the water resources and sanitation of the city with respect to climate change, imprudent water use, the possibility of water scarcity in the future and possible flood risks. Water resources, according to the DPSIR model, are part of the pressures and state, its poor management constitutes an impact and its proper management is part of the responses.

The area of the Municipality of Trikkai belongs to the catchment area of Pinios (Figure 2).

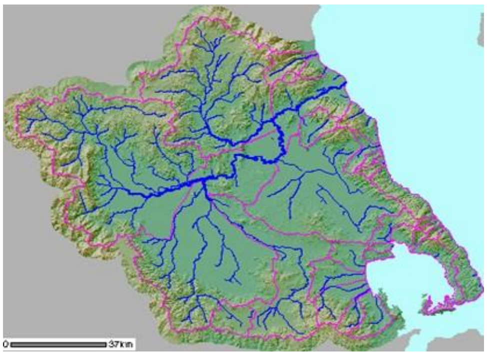


Figure 2: Thessaly: Pinios river basin

The water quality characteristics of the rivers are good, plus there is aquatic and riparian vegetation developments on their banks. The water table in most flat areas is generally quite high, during the winter it reaches approx. 3 meters. Within the urban fabric of the city, there are no floods that can pose a risk of damage or disasters/human lives, however during the summer months, short-range rainwater projects are being carried out mainly in drains, to protect. The water supply of the Municipality comes from groundwater

is pumped through 56 boreholes. After the chlorination process, the water is led to the water supply network. Based on official data, the total water supply network covering the needs of the Municipality is about 767km.

Frequent checks are conducted to monitor network conditions and consumption, especially during periods of water scarcity. According to data analyzed, there is a significant decrease on water consumption of the city of Trikala, in the past ten years due to public awareness on rational water use, and the effectiveness of existing pricing policy ($1m^3$ = 0,49 euros). The quality of the drinking water of the city of Trikala is controlled by the Municipal Water Quality Laboratory where daily chemical and microbiological analyzes are carried out according to the European Specifications. The drainage structures of the city of Trikala include a pipeline network of approximately 200km before reaching the waste water treatment plant.

3.2 Energy sector

The energy sector is part of both pressures and state, according to the DPSIR model, while its efficiency is part of the responses. The relationship between the driving forces and the pressure from economic activities is a function of the eco-efficiency of the technology, with less pressure coming from more driving forces, if eco-efficiency is improving. Monitoring energy use, electricity consumption and use of renewable energy sources, are of major importance when it comes to sustainability and striving to achieve a “green” status in city. By participating in innovative research programs, in an effort to reduce power consumption, the municipality has completed a study to upgrade the lighting system of municipal streets, by replacing it with new LED technology, whereas, a Smart Lighting System is implemented in order to monitor and manage it. It is estimated that more than 60% of energy will be saved. In order to reduce CO_2 emissions, the municipality has decided to proceed to an energy upgrading of municipal buildings by linking them to the natural gas network. The final link list includes a total of 64 buildings, with a total heat output of 16,823,700 (kcal/h). According to data from the Municipal Council, approximately 250 connections for photovoltaic roofs of up to 10Kw and about 30 photovoltaic connections by farmers up to 100KW have been activated. Apart from photovoltaic installations, no other power plants such as urban turbines and wind turbines are used in the area, and there is no record of the use of either open or closed circuit geothermal systems.

3.3 Transportation systems

A sustainable city is also defined by green, accessible and safe transportation, road safety, extensive pedestrian areas and cycle tracks that insure air quality and easy mobility for its citizens. Such indicators will provide a plethora of information that could also determine essential planning changes and proper management to the local administration. The transportation system is a part of drivers, pressure and state, according to DPSIR model, while its efficiency and management is part of the responses.

The main road network of the city of Trikala is radial. For the most part, the road network is a one-way street. The main existing roads (those that receive the largest volume of traffic) are two-way. The pedestrian roads are concentrated mainly in the center of the city, however they are not organized and continuous, while the area in use is not officially recorded by the municipality. Due to its geography, the city provides the possibility of easy bicycle travel. The total length of the city's bicycle paths is estimated to be 14.5 km long, relatively continuous in the city center. With regard to air quality, the Municipality of Trikala, in collaboration with Space Hellas and Cisco, will set up an environmental monitoring system. Using special environmental measurement devices for the collection of particulate and noise emissions, it will assess the quality of the atmosphere in order to review the impact on public health. The private company "Urban KTEL Trikalon SA" carries out daily local trips to the city of Trikala and to the local communities of the Municipality, with a fleet of 17 petrol running buses.

3.4 Waste management

The volume and type of waste is directly related to the living standards of a city, and their method of managing, depositing and processing controls the correctness and efficiency of practices based on the envisaged regulations at national and European level, while reflecting attitudes of citizens towards in the current situation. When it comes to waste management, sustainability can be achieved through proper hazardous waste management, recycling, urban waste water quality control and drafting a management plan for solid waste.

It is estimated that the per capita production of municipal solid waste in the municipality of Trikala amounts to 336.77 kg per capita/year. The collection, transport and disposal of waste is the responsibility of the Department of Waste Management of the Operational Project Directorate, which uses 21 fitting waste trucks. When it comes to recycling, according to data provided, from 2010 up to today, there is generally a significant reduction in waste. Between 2010-2011 there was a decrease of 5,43%, a decrease of 8,32% in 2011-2012, a decrease of 2,98% in 2012-2013 and finally, between 2013-2014 an increase of +2,15%. These percentages relate to municipal waste and entering the Recycling Sorting Centers.

3.5 Urban green spaces

Proper management of green areas within a city is not only about large areas, but also about tree-stands, small parks and free spaces. It can effectively change the way of life of the inhabitants providing a range of health benefits by improving the quality of life of those who live in densely built areas and influencing positively the quality of the air. Environmental benefits include reducing the temperature during the summer, absorbing the flowing water after severe weather events, increase percolation of surface water into the ground and improving the aesthetics of the landscape, as well as supporting the biodiversity and carbon capture. Economic benefits include regeneration and attracting new services. Measuring, managing and protecting the urban green spaces, is part of DPSIR pressures, state, impact and response.

The city is considered to be one of the most "green" in the country. This fact mainly is due to the existence of the river of Lethaios that crosses Trikala from side to side. The total area of the cultivated green area of the Trikala Municipal Unity is approx.530 acres. This area includes neighborhood tree trunks, small squares and large green areas near the riverbanks, as well as the recorded urban parks. From time to time, the municipality has proceeded to plantings to the whole extent of the city. According to the World Health Organization and SDGs 11.7, which promotes safe and universal access to public and green spaces for all, urban centers must provide 9 m^2 to each resident within 15 minutes of their residence (Pafi et. al, 2016). Based on the data above and the population of the city of Trikala, it is estimated that approximately 8.10 m^2 corresponds to each inhabitant of the city. For the management of the green areas in the city, the municipality has a staff of 40 people.

3.6 Cultural heritage

The cultural heritage of a city provides its foundation, identity and character, while often constitute a pole of attraction for visitors, thus driving the local economy. The concept of sustainability does not limit itself strictly to the environment, ecology, energy or water, but it is a wider concept, which incorporates civilization and culture. For this reason, an urban sustainability research could not exclude the investigation of indicators that review the citizens' perception and reaction to culture as part of their reality and life. Cultural identity and heritage is part of DPSIR drivers and pressures and lack of management is part of impacts.

There are many different places of significant historical importance throughout the city. From the first “hospital” of the Hellenistic period and the Ottoman built Castle that was erected over the ancient citadel, to the Ottoman Mosque and the historical - Matsopoulos Industrial Park that housed the first roller mill ever built in Greece, to the newly founded Research Center – Tsitsanis Museum that resides in the formerly used prisons in honor of the city’s music artists. All venues are managed by either the Municipality or the Ephorate of Antiquities of Trikala and are used by the local community as venues

for cultural events, conferences, exhibitions, concerts and school trips. The execution of the projects are carried out following a tendering procedure (by auction) and are funded by the European Regional Development Fund.

4. THE SURVEY

About 307 questionnaires were collected altogether from the city's citizens, representing a 5 per thousand of the city's population. Sampling was performed by the *random sampling method*, where there is a known probability that each unit is selected as the unit of the sample.

Through 26 questions, concerning urban green, water, energy, transport, recycling and cultural issues of the city were formulated. The objective was to evaluate the citizens' view and ability to identify priorities and values, as well as what is considered most important when it comes to decision making, in order to make life in the city more sustainable.

For the output of the results, the process of encoding the questionnaire elements is followed in a table, which assigns each question to the questionnaire in a variable. Variables receive different values. This creates a data file where variables and attributes are defined and which results in a series of commands. Processing took place on two levels. Initially, a descriptive statistical analysis was presented, showing the frequency distributions of the variables as well as the central phase indicators, followed by inductive statistical analysis to check empirically the existence or not of statistically significant variations in the fluctuation of the averages of the research variables and to check the research questions that have been formulated. Because the 62 research variables are categorical, either as dependent or as independent, the appropriate statistical criterion for the above test is the x^2 Test. At the same time, the Monte Carlo simulation was used because the sample (307) is greater than 250 to overcome the limitation of the x^2 Test application. SPSS was used for the analysis of the findings.

The "identity" of the survey comprises of 42.7% men and 57.3% women. The 28.3% were citizens between 18-25 years olds followed by a 44% belonging to the 26 - 40 age group, 25% are between 41 – 65 years old and 2.6% are over 65. In terms of education, 52.8% are university graduates, 17% hold postgraduate degrees (MSc / MA/PhD), 25% are high school graduates, and the rest 5,2% were priests, military men etc. Responses were taken from all neighborhood areas within the city to allow for an objective representation of the sample.

Transportation systems

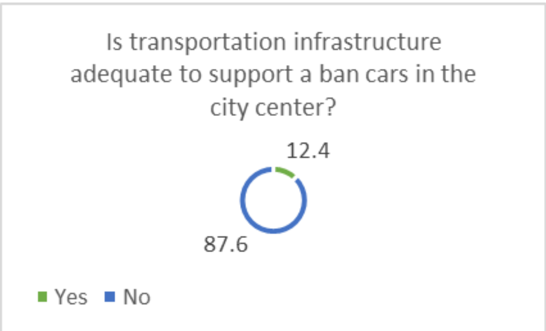


Figure 3: Infrastructure adequacy

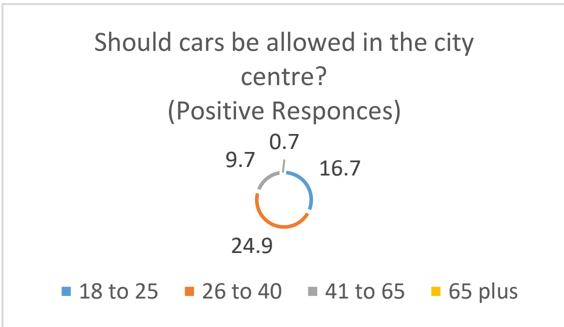


Figure 4: Prohibit the moving of cars in the city center

According to the results of the survey, 88% (Figure 3) of the respondents claim that current infrastructure is inadequate to support a ban on cars in the city center, whereas, most young people (Figure 4), would prefer for the city center to be accessible only by foot. More than half of the respondents (62%) choose to move with a car or motorcycle to and from their workplace, while the option of more environmentally friendly transportation means, such as bicycle, public transportation and walking, are of low preference, despite the fact most distances are not long. Furthermore, the

survey showed that the citizens of Trikala do not feel safe either by walking (36%) or by using the bicycle (68%), although data on deaths and accidents, provided by the Hellenic Department of Traffic Police, are reported to be lower in the last 5 – 8 years.

Waste management /Recycling

More than 50% of the respondents tend to recycle mostly paper (28%) and plastic (30.3%) given that those are most commonly used, whereas those who do so, do it frequently (Figure 5). Furthermore, the survey showed that citizens seem fairly satisfied (74,3%) by the recycling methods provided (Figure 6).

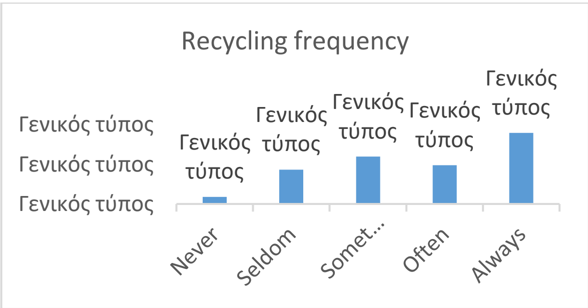


Figure 5:
Recycling frequency of all materials

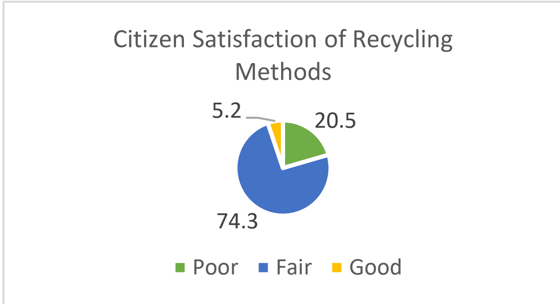


Figure 6:
Satisfaction of recycling methods used

Water issues

The city's water quality is checked daily by appropriate tests on the basis of European criteria and its quality is found excellent, so, as expected, 85% of citizens use tap water provided by the Water Supply Network. However, a high 15% prefer to drink bottled water on a permanent basis. The relationship between trust of tap water and bottle water showed a statistically significant difference.

The majority of the respondents are aware of the global water scarcity problem and almost 60% are willing to change their water habits even though at the moment the city does not face intensive water issues. They do keep using water, for purposes other than the usual household standard use (60%) though, such as car washing and gardening (Figure 7).

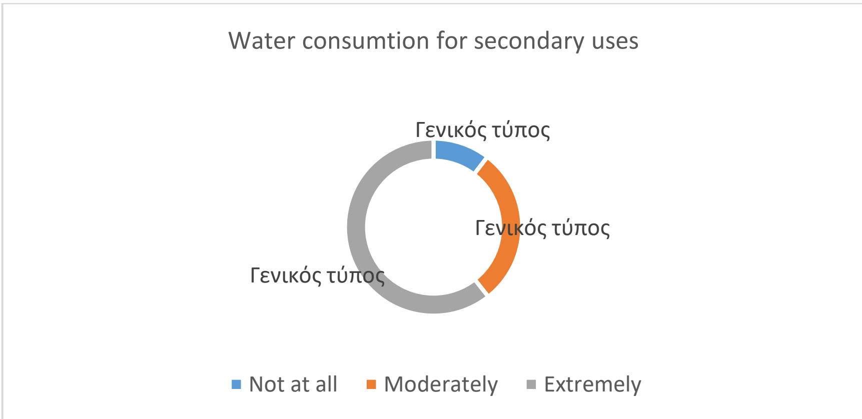


Figure 7:
Non-household water consumption frequency

Cultural heritage

Almost 71% or the respondents are willing to financially contribute to promote and preserve their cultural heritage.WTP shown in figure 8 reveals that 4 out of 10 can give up to 20 euros per year, which indicates the important role the culture plays in their quest of a sustainable city.

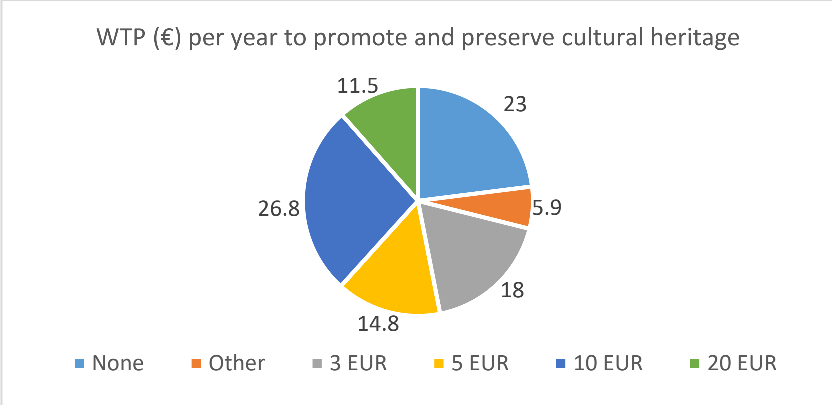


Figure 8: Willingness to contribute financially in order to support the local cultural identity

Urban green spaces

Despite living in a smaller city, with it being closer to nature, citizens, seemed to value and make use of organized green sites such as urban parks for both walks and sports, as well as other activities, most of them regularly (45% do so once a week) as seen in figure 9 whereas most of them are women (57,3%).

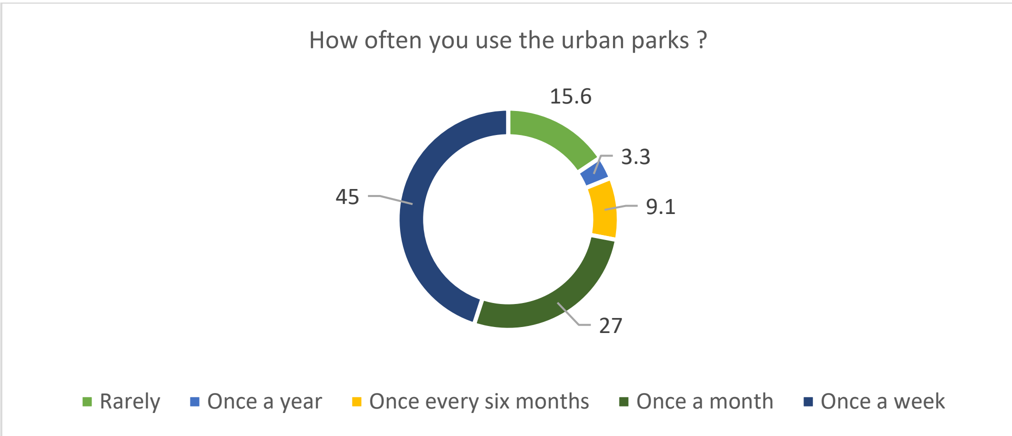


Figure 9: Use frequency of urban parks in Trikala

Energy

The survey showed that most people (90%) do not use Renewable Energy Sources for electricity purposes in their homes (Figure 10), however half of them are willing to use conservation methods to reduce energy consumption and they welcome the municipality's efforts in promoting such innovative methods.

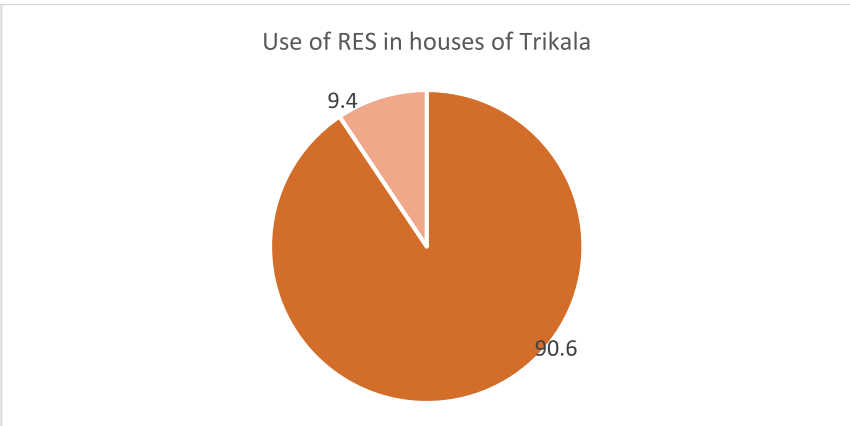


Figure 10: Current use of RES in the cities' housing

5. CONCLUSION-DISCUSSION

According to the combined results through the analysis of data and the respondents' answers, Trikala city has the potential to become a sustainable city, but there is still much to be done.

The structure of the agencies and services of the public sector are inadequately organized, which made data collection particularly difficult. The fragmentation of competences into different agencies and the lack of synergies between competent bodies, which is essential for achieving sustainable management in the context of sustainability, reveal the extent of the problem.

In transportation, lack of security and respect towards cyclists, prevent aspiring cyclists to move around, despite the limited, but existing, bicycle path network.

The lack of organized pedestrian areas does not affect those who choose to move on foot, however, there is a strong sense of insecurity, due to the increased use of cars in the city center.

As far as water resources and sanitation is concerned, water quality and water resources management are satisfactory, although there is quite a significant percentage of respondents who use bottled water on a permanent basis. People seems to be aware of the global water problem and claim to be ready to accept water conservation measures and change the way they think and act, even though there is a large percentage of those who keep using water in an unscrupulous way.

When it comes to recycling there seems to be a good management plan at hand by the authorities, which is confirmed by the citizens satisfaction of the means used. On their part, numbers showed that citizens have embraced the idea and practice of recycling avidly.

Innovation and technological advances, capable to improve life as a whole are improving the current situation and lead the way to implement sophisticated technology to facilitate changes when it comes to the energy sector and the decrease of the ecological footprint.

Changes that could possibly improve the well-being of the city's inhabitants and could be implemented are:

Importance should be given to official data recordings that can lead to the creation of data platforms accessible to operators and citizens both, by making use of their network and capabilities.

Link bicycle routes to urban and suburban parks inside and outside the city for safe and easy access for all.

Redesigning and shaping the flowerbeds and small squares with emphasis put on using suitable species that can limit the phenomenon of the urban heat island, will act as windbreakers during the winter, improve the air quality and ameliorate the overall aesthetics.

Promoting green and sustainable practices in their home, might interest citizens in taking part in national and union financial programs that will improve their lifestyle, when it comes to energy.

Developing alternative forms of tourism, such as ecotourism, agrotourism or religious tourism that could probably attract global interest, making the city an attractive destination for everyone.

Setting up an information platform online for the many places of historical and cultural importance, such as sights, museums, churches etc. of the area, using the power of the internet to attract visitors.

These changes are targeted to better the municipality's resource management, in order to provide social benefits (better organized green spaces, recycling etc.), improve the quality of life of the citizens (clean air, organized transportation and sense of security), decrease the environmental impact (waste management, energy efficiency), boost the local economy by promoting the comparative advantages of the city and strengthen their cultural identity and heritage. The major responsibility in implementing those changes lays on the municipality, according to the citizens input – as presented in the survey conducted – however it is of upmost importance to support groundbreaking initiatives

and provide means in communicating and disseminating the benefits to the local community in order to strive for essential sustainability.

References

1. CIDA, 2012. Indicators for Sustainability: **How Cities Are Monitoring and Evaluating Their Success.** The Canadian International Development Agency, Ottawa, Canada.
2. Kristensen, P., 2004. **The DPSIR Framework.** Paper presented at the 27-29 September 2004 workshop on a comprehensive / detailed assessment of the vulnerability of water resources to environmental change in Africa using river basin approach, UNEP Headquarters, Nairobi, Kenya.
3. Piante C., Ody D.,2015. **Blue Growth in the Mediterranean Sea: the Challenge of Good Environmental Status**. MedTrends Project. WWF-France. Pages 14-15.
Pafi M., Siragusa A., Ferri S., Halkia M., **Measuring the Accessibility of Urban**
4. **Green Areas**. A comparison of the Green ESM with other datasets in four European cities; EUR 28068 EN;
5. Science for Environment Policy (2015) **Indicators for sustainable cities**. In-depth Report 12. Produced for the European Commission DG Environment by the Science Communication Unit, UWE, Bristol **Urban green spaces and health**. Copenhagen: WHO Regional Office for Europe, 2016.
6. Organization for Economic Co-operation and Development (2003) **Environmental Indicators: Development Measurement and Use**, Reference Paper, OECD, Paris
7. Hellenic Department of Traffic Police - 23/10/2017
8. https://www.eea.europa.eu/publications/signals-2009 (accessed March 15th 2018)
9. http://trikalacity.gr/wp-content/uploads/2016/03/stratigikos-sxediasmos.pdf(accessed March 6th 2018).
10. https://sustainabledevelopment.un.org/sdg11 (accessed February 2nd 2018)
11. http://www.un.org/sustainabledevelopment/development-agenda/ (accessed February 23rd 2018)

INVESTIGATING STAKEHOLDERS PRIORITIES FOR TRANSDISCIPLINARY COASTAL & MARINE MANAGEMENT: THE CASE OF THERMAIKOS GULF

Z.I. Konstantinou* and D. Latinopoulos

School of Spatial Planning and Development, Faculty of Engineering, Aristotle University of Thessaloniki,GR- 54124 Thessaloniki, Greece

*Corresponding author: e-mail: zkon@civil.auth.gr, tel.: +306977960420

Abstract

Aim of this work is to investigate institutional stakeholders' priorities, regarding transdisciplinary coastal and marine management in Thermaikos Gulf. The targeted coastal and marine area is shared by four Greek regional units, hosting a variety of human activities such as intense urban development, agriculture and husbandry, industry, mussel-culture, fisheries, tourism, etc. There are more than 90 entities which have some kind of jurisdiction or stake in the management of the coastal and marine area of the Gulf, the majority being sectoral public administration agencies. To cover their range of opinions, we developed and distributed a questionnaire focused in identifying the most important management issues in the area, as well as the main reasons behind the possible management failures until know. To test the questionnaire, we contacted a series of interviews with selected representatives of key management authorities, assisting also to acquire a deeper understanding of the current management regime in the area. Through the results we will: a) attempt a preliminary evaluation of stakeholders' willingness to participate in Science-Policy-Society collaboration processes; b) identify the management issue(s) with the highest importance for the local stakeholders and c) investigate deeper the relationship between key local socio-ecological problems and the current institutional and legal status regarding coastal and marine management.

Keywords: stakeholders' engagement, integrated coastal and marine management, transdisciplinary approaches, Thermaikos Gulf

1. INTRODUCTION

Coastal and marine environments are paramount to the socio-economic performance and well-being of societies. Under the current global social-ecological conditions and especially in countries as Greece, phasing extreme financial challenges, coastal and marine resources become even more important for prosperity and more prompt to overexploitation and mismanagement. To remediate or even try to prevent poor coastal and marine management decisions, knowledge-based, participative and transdisciplinary management is necessary [Tett *et al.*, 2011]. This type of management requires an organised Science-Policy-Society integration and the use of novel scientific tools [Cornell *et al.*, 2013]. One of the greatest challenges in such an approach is to design a process, which will include a wide range of stakeholders, at different times and with different levels of involvement. In this process, stakeholders' priorities and concerns should be placed in the centre of any management attempt and their collective knowledge should be utilised alongside scientific findings. Involving stakeholders in coastal and marine management assists greatly with the effective implementation of relevant plans [Buanes *et al.*, 2005], hand-by-hand with the development of a sound legislative basis, which is another essential prerequisite for efficient management [McKenna *et al.*, 2008]. In order to determine stakeholders' priorities related to Integrated Coastal Management (ICM) and Marine

Spatial Planning (MSP), especially in areas where participative processes are not yet well accustomed practices, interviewing and questioning key institutional stakeholders is a commonly adopted technique [Villares *et al.*, 2006; Fletcher *et al.*, 2007]. Such approaches will be the base to support further and more complex participative processes of Science-Policy-Society integration, as is the co-development of integrated tools to support management [Voinov *et al.*, 2016].

Thermaikos Gulf is a large coastal and marine area in Northern Greece, shared by four Regional Units (Thessaloniki, Imathia, Pieria and Chalkidiki) and hosting a variety of intense human activities, such as urban development, agriculture and husbandry, industry, mussel-culture, fisheries, tourism, etc. The coastal area also hosts the second largest city of Greece (Thessaloniki), as well as a Ramsar wetland of international importance (Axios Delta).

2. METHODOLOGY

To investigate the stakeholders' priorities, regarding transdisciplinary coastal and marine management in Thermaikos Gulf, a questionnaire was developed, comprising of four parts, targeted in collecting information relevant to the subject. It was accompanied by an introductory part which explained the overall research goals, i.e. (a) the identification of the most important management issues for the area, (b) the development of management procedures and tools that will support efficient resource management, as well as (c) the development of robust social-ecological policies. The first part of the questionnaire was devoted to general information, information on the entity that each respondent represents as well as on their specific jurisdiction or stakes in the coastal and marine area of the gulf. The second part attempted to investigate the knowledge of respondents regarding the European and Greek legislation on ICM and MSP, as well as their opinion on the coherence and effectiveness of this legislation and the manner in which the existing environmental legislation affects their work and responsibilities.

The third part of the questionnaire aimed in determining the stakeholders' priorities regarding the coastal and marine management of the area of Thermaikos gulf. Eleven key and known management issues were preselected so that the respondents could evaluate their importance for the area in a 5-point Likert-type scale ranging from 1, not important, to 5, very important (respondents could also declare that they have no knowledge regarding the importance of the issue). The following issues were explored: a) Management of point and non-point land inputs/Pollution; b) Fisheries management, including fleets, fish stocks, etc.; c) Management of coastal/marine tourism activities; d) Management of port and other navigation activities; e) Management of urban and peri-urban development at the coastal zone; f) Management of aquaculture activities; g) Management of the protected areas; h) Management of existing or potential conflicts between tourism and other activities (o.a.); i) Management of existing or potential conflicts between fisheries and o.a.; j) Management of existing or potential conflicts between port activities and o.a.; k) Management of existing or potential conflicts between aquaculture and o.a. Participant were also informed that the list was not exhaustive, so they could determine other management issues as well. The next question aimed to determine the stakeholders' opinions on the nature of the impact of the aforementioned management issues (including the ones they may have suggested) to the social-ecological system of Thermaikos gulf. The respondents could select one or more impacts (economic, social, environmental, on lawful operation) but they could also declare that they have no knowledge on the issue or that they do not consider it of sufficient importance.

By the same rationale, the following question aimed to determine their opinion about the causal factors of these issues. The respondents could select between the following options: a) lack of knowledge/technology/infrastructure; b) lack of adequate legal framework; c) inability to implement the existing legal framework (caused by institutional deficiencies, lack of resources, etc.); d) lack of political will; and e) overexploitation of available resources/illegal activity. They could once again declare lack of personal knowledge or insufficient importance of the issue. For both questions the respondents were given space and opportunity to declare additional impacts and causal factors, should they

consider something was missing. Finally, the last set of questions aimed to determine the top stakeholders' priority for the area, thus asked for the selection of the issue that was considered as the most crucial and urgent for Thermaikos gulf. Since the area is large and with spatial variability, the respondents were asked to determine in which areas did they believe that their selected issue was more prominent (see also Figure 6), as well as to determine more specific environmental, social and economic impacts of this issue.

The final part of the questionnaire asked for personal information, on a volunteer basis, and investigated the respondents interest to participate to potential future efforts of collaboration between the research team and the area's stakeholders.

The stakeholders' pool targeted for this study was selected aiming to capture the opinions of representatives working in public, semi-public or private entities with varying levels of jurisdiction, responsibilities or stakes in the coastal and marine area of Thermaikos gulf [Konstantinou *et al.*, 2017]. The selection included representatives of various ministry directorates with direct jurisdiction on the selected area; departments of the two branches of regional government (elected and de-centralised) with either environmental responsibilities or responsibilities in the fields of fisheries, aquaculture, tourism, etc; coastal municipalities; organisations (e.g. Thessaloniki's Water and Waste Company and Thessaloniki's Port Authority); environmental NGO's; as well as major research and education institutes which have conducted studies in Thermaikos gulf.

In order to initially test the way that the questionnaire was perceived by respondents and then to adjust any parts which may not be clear, 9 interviews (10 planned, 9 executed) with selected respondents were conducted. The interviewees were selected in a way to represent: the regional level of governance (covering all the Regional Units), the national level of governance (Ministry of the Environment), the NGOs and the research institutes. The interviews allowed for deeper understanding of the governance regime in the area, as well as for the identification of further representatives of authorities with relevant responsibilities in Thermaikos gulf. As a result of these interviews, the language used in the questionnaire was slightly modified, to facilitate clarity. The questionnaires were distributed to the identified authorities through e-mail. During two and a half months, the questionnaire was repeatedly sent to the selected respondents, at least once a week (maximum 3 times a week), while when possible phone calls were also made.

3. RESULTS

3.1 General information

A total of 97 authorities, organisations and key stakeholders were contacted repeatedly, during a period of 75 days. Among them, 66 were governance and management authorities, on local, regional or national level of jurisdiction, 4 were research and education bodies, 14 were environmental NGOs and 13 were private or semi-private organisations, such as professional associations, semi-private management authorities, etc. 20 responses were collected in total, 9 of them through face-to-face interviews and 11 through e-questionnaires. 17 of these responses corresponded to personnel of public authorities (25.75% response rate), 1 response was collected from professionals in research and education (25% response rate), 1 from an NGO representative (7.1% response rate) and 1 from a representative of a private association (7.7% response rate). The 9 initial interviews were contacted during the first 10 days of the study, while the rest of the responses where provided during the remaining period of time, after multiple contacts. It should be noted that all the responders were higher education graduates, with the majority of them holding an MSc qualification (55%), while 30% of them also hold a PhD, mainly in environmental related fields. Regarding the spatial distribution of responders, based on the area where they are active, 35% of them are active at the Regional level (Region of Central Macedonia), 30% are active in the Regional Unit (R.U.) of Thessaloniki, 15% in the R.U. of Pieria, 10% in the R.U. of Imathia, while only one person is active specifically in the R.U. of Chalkidiki. Finally, 10% of the interviewees are active at the national level.

More than half of the responders identified themselves as personnel of public authorities with management jurisdiction in the area of interest, in and around Thermaikos gulf, while 20% were identified as personnel of authorities with other jurisdiction in the area. A single respondent identified himself as working in research (although at the moment is also leading an organisation with very crucial management responsibilities for the area) and a single respondent identified himself as working in the tourism sector (although working for a regional level public authority). Finally, out of the four responders which identified themselves as working in another sector, one was identified as NGO personnel, one as private organisation personnel while two of them were identified as working for authorities of the regional government.

3.2 EU and Greek legal framework regarding ICM and MSP

The evaluation of the legal framework knowledge, understanding and use, took place through different clusters of questions. The participants were asked to determine their level of knowledge regarding the EU and Greek legislation related, directly or indirectly, to ICM or MSP. The majority of the respondents claimed no, little or medium level knowledge of the respective legal framework (80% regarding the EU legislation and 75% regarding the Greek legislation; Figure 1). Only one respondent declared to have excellent knowledge of the EU legal framework, while two respondents declared to have excellent knowledge of the Greek legal framework regarding the relevant topics.

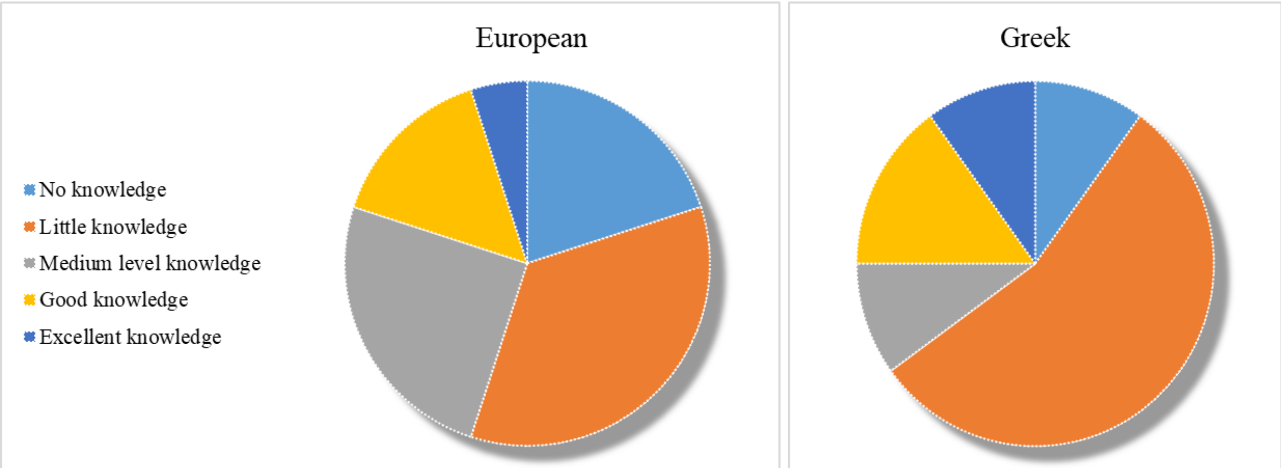


Figure 2: Self-evaluation of the knowledge of the legal framework regarding ICM and MSP.

Regarding the efficiency of the EU and Greek legal framework to create and regulate the conditions for ICM and MSP, 40% of the respondents declared that the European legislation presents medium efficiency, 25% declared no knowledge to support an evaluation, while the rest of the respondents were divided between “full efficiency” and “no efficiency”, with the latter being supported by fewer respondents (Figure 2). Regarding the Greek legal framework on ICM and MSP, 35% of the respondents declared medium efficiency, 25% little efficiency and the rest were divided equally between “no efficiency” and “sufficient efficiency”. No respondent declared either “no knowledge” or full efficiency” of the legal framework.

When asked to evaluate the level of support that the Greek environmental legal framework provides to their everyday activity (related to the coastal and marine management of Thermaikos gulf), 40% of the respondents declared that the existing framework provides medium support on their activity, 10% declared that their activity is fully supported by the existing legal framework, while the rest were equally divided between “little support” and “good support”. It should be mentioned that no respondent declared that the existing environmental framework does not provide any support for their activity

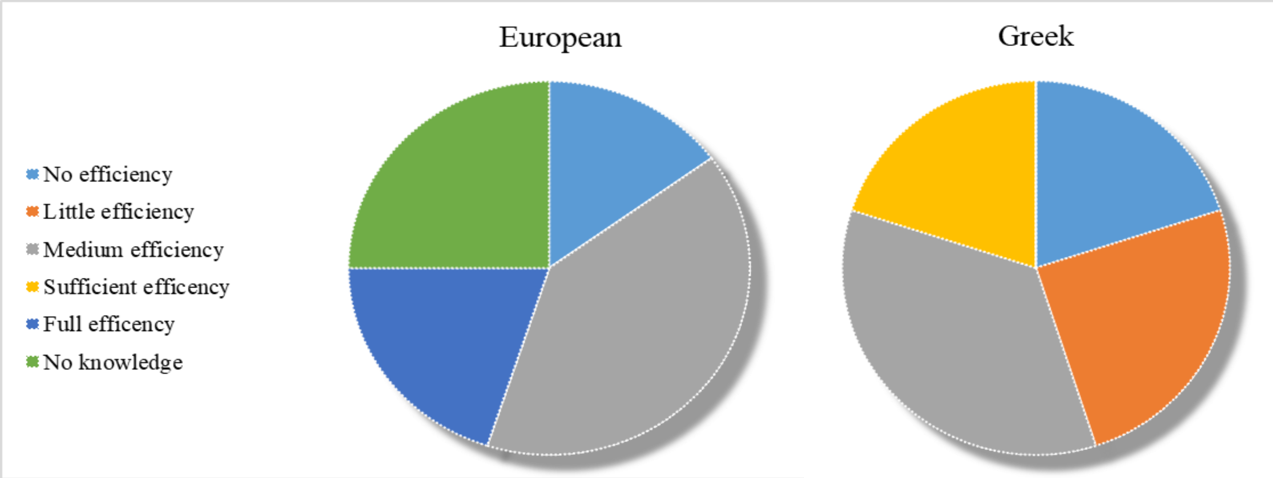


Figure 3: Evaluation of the efficiency of the legal framework

3.3 Evaluation of management issues

The evaluation of the selected management issues is presented in Figure 3. As shown, all issues are perceived as very important. However, the Land input management and the associated pollution of the coastal and marine waters, is evaluated by the majority of respondents as very important. Other issues that come forward as important/very important are the Protected area's management and the Management of urban and peri-urban development. The Management of aquaculture activities in the area is also conceived in a spectrum from medium to very important, with some respondents to comment that they are reluctant to characterise it as very important for the gulf due to the localised character of the activity. From Figure 3 it is also obvious that the existing or potential conflicts between activities are conceived as less important compared to the rest of the management issues.

As the respondents were able to also determine other management issues of importance, a number of suggestions were received. Nevertheless, in their majority these issues were directly linked to the defined management issues, if only more thematically or spatially determined. The only proposed issue that could be considered completely autonomous, was the Management of Marine Litter, linked only indirectly with the management of tourism activities.

The identification of the nature of impacts (environmental, social, economic, impacts on lawful operation) in either local or regional level is presented in Figure 4, which demonstrates that stakeholders' perception varies sufficiently depending on the issue at hand. The issue of Land input management, and thus pollution, is perceived by all the respondents as having an impact in the environmental state of the gulf, but only half of the respondents believe that this degradation causes economic impacts and even less that it causes impacts in the social coherency or in the lawful operation of society. Issues such as the Management of urban/peri-urban development and the Protected area management, although also perceived as mainly having environmental impacts, are almost equally perceived as having economic impacts as well, while in both cases either impacts on lawful operation or in social coherency are considered significant from a considerable number of respondents. It is mainly in the Management of human activities (fisheries, tourism, navigation, aquaculture) that the environmental, social and economic impacts are equally identified as important, while the Management of conflicts is perceived as mainly having economic and social impacts and not so much environmental ones.

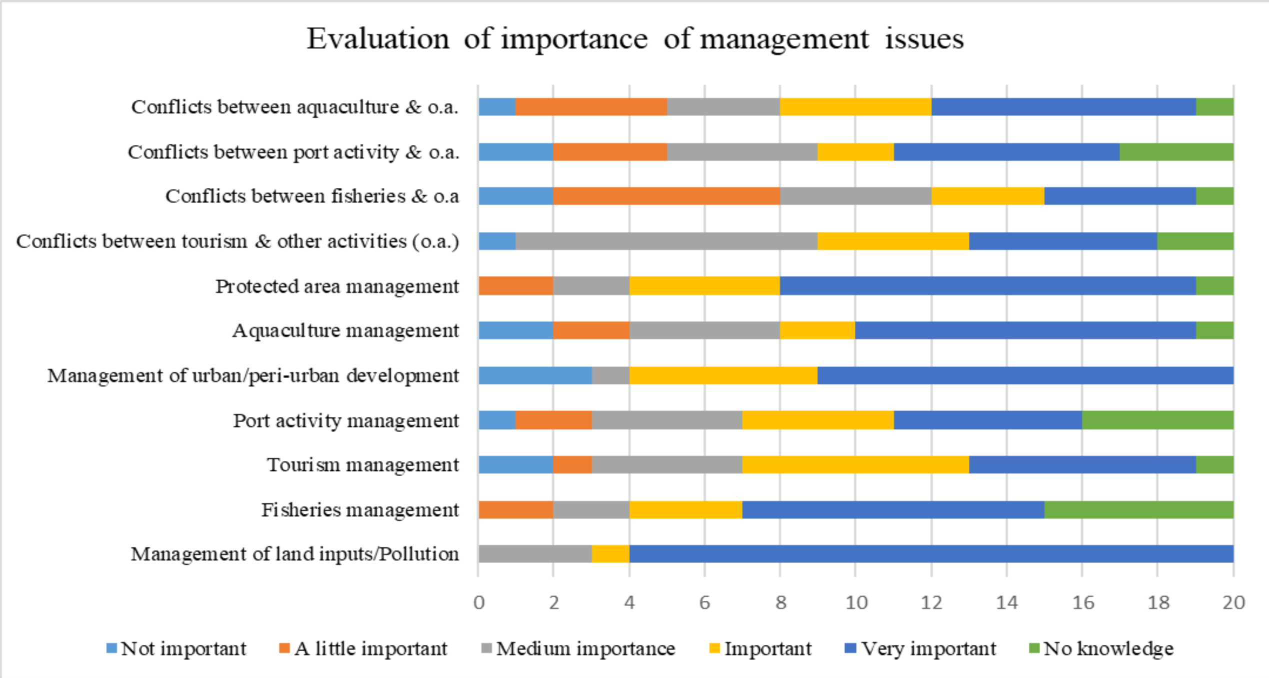


Figure 4: Evaluation of the importance of the pre-selected coastal and marine management issues for the case of Thermaikos gulf.

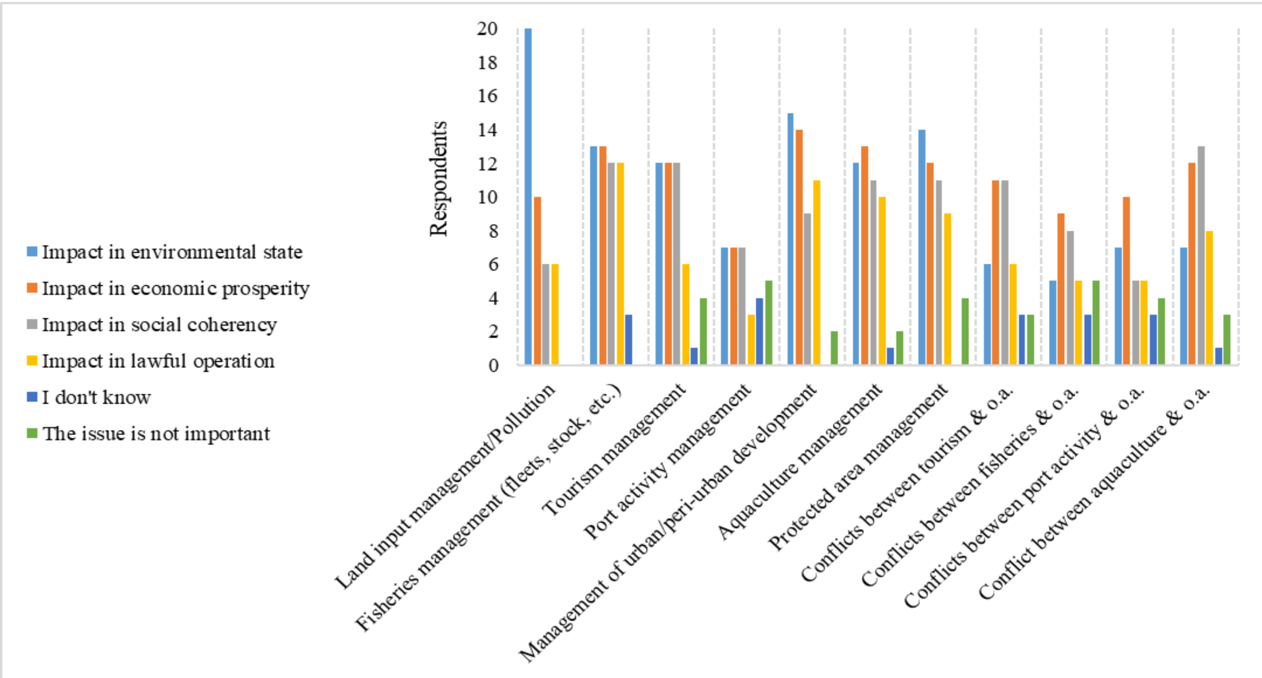


Figure 5: Identification of the nature of impacts of the selected management issues for the case of Thermaikos gulf

The identification of the causal factors of the management issues, as perceived from the stakeholders, is very crucial in better understanding the nature of these issues and in identifying management actions, procedures and tools to remediate them. The responding stakeholders perceive that, with the exception of the Protected area management, the major causal factor for all the management issues is the inability to implement the existing legal framework, due to institutional deficiencies, lack of resources, etc. Regarding the Protected area management, the lack of adequate legal framework is perceived as a more important causal factor, but the inability for implementation is still the second more important one. The potential lack of knowledge, technology and infrastructure is perceived as significant regarding the Land input management, while it is considered a rather secondary causal

factor for most issues. Lack of political will (to identify and implement solutions) is considered as a high ranking causal factor for the issues of Land input management, Tourism management, Management of urban/peri-urban development and Protected area management, while the overexploitation of resources/illegal activity is perceived as an important causal factor for Aquaculture management, Management of urban/peri-urban development, Tourism management, Fisheries management and Land input management.

When the respondents were asked to identify the sole most important management issue in Thermaikos gulf, 55% choose Land input management, while 25% declared the Management of urban/peri-urban activity. The respondents were additionally asked to determine the importance of the most important management issue on a spatial level. According to their answers, the areas of the Gulf of Thessaloniki and the Axios-Loudias-Aliakmonas estuaries, were determined as the areas of highest interest (Figure 6).

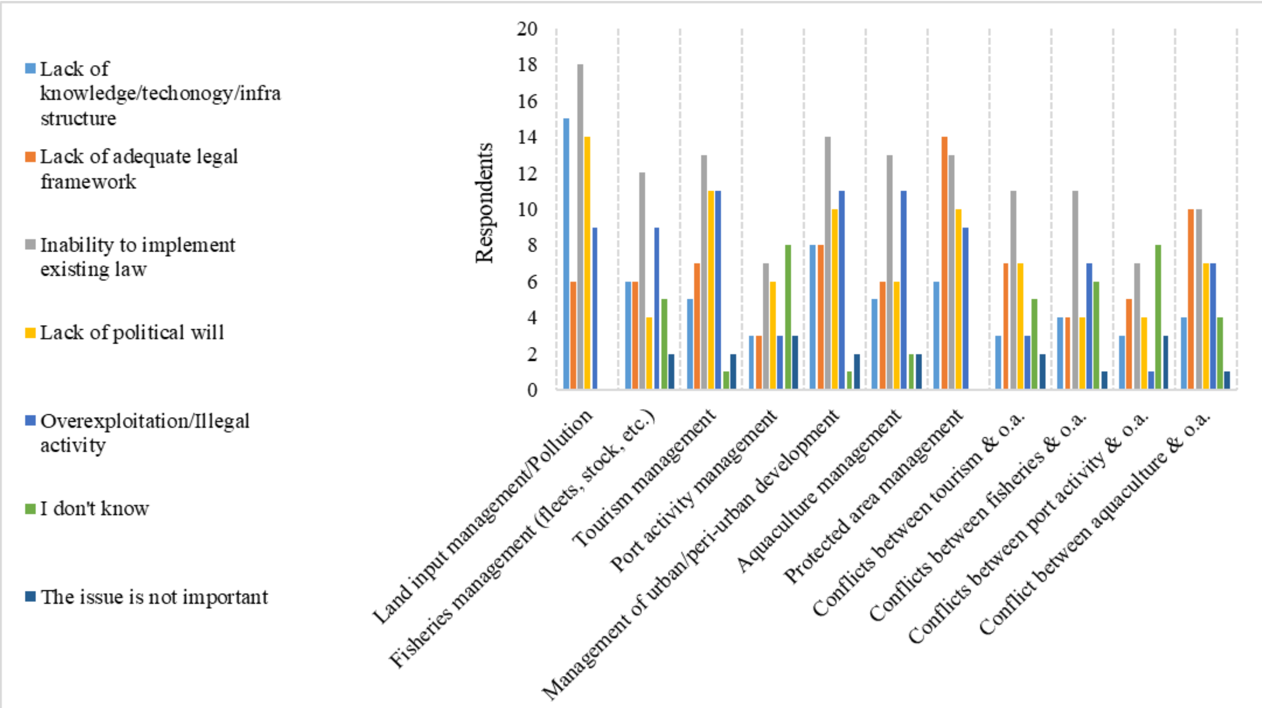


Figure 6: Identification of causal factors for the selected management issues in the case of Thermaikos gulf.

4. DISCUSSION

The most important finding of this paper is connected to the willingness of Greek stakeholders to participate to Science-Policy-Society collaboration efforts. Only 20% of the intended targets replied to the survey. Answering an e-questionnaire is probably the less engaging, less time-consuming and less personal way to participate in such efforts. Nevertheless, only a small portion of the invited stakeholders choose to participate and this participation was provoked after numerous reminders and, in some cases, phone calls. In at least 20 cases, stakeholders where contacted in a personal level, based either in previous collaborations or the interference of a common acquaintance, acting as a liaison between the researcher and the potential respondent, and still the stakeholders did not engage to the survey (besides the fact that many of them declared that they will).

Additionally, numerous stakeholders which were contacted in the framework of this survey, believed firmly that they didn't have the adequate background or jurisdiction to answer the survey. Authorities with environmental responsibilities or responsibilities connected to productive activities (fisheries, aquaculture, tourism, etc.) claimed, through email or phone calls, that they don't perceive their field of expertise as relevant to the research, proposing at the same time individuals in other organisations

as potential respondents. When informed that the proposed organisations were also contacted, but that their input would still be useful, most of them declared unavailability or unwillingness to respond. Similar considerations where expressed also from interviewees and respondents; some of them also insisted in not declaring themselves as "representatives" of their authority or organisation but only as "personnel, providing an educated opinion".



Figure 7: Coastal and marine areas of Thermaikos gulf, identified from the responders as the most crucial regarding the Land input management in connection to pollution.

These behaviours are indicators of the infantile level that Science-Policy-Society collaboration efforts are in Greece [Koutrakis *et al.*, 2010; Apostolopoulou *et al.*, 2012; Konstantinou *et al.*, 2013]. In other words, many stakeholders do not perceive science as a means which can provide tangible, efficient solutions for persistent social-ecological problems and thus are reluctant to invest their time in this procedure. Even for the case of stakeholders who believe in the capacity of such efforts to produce results, considerable doubts have been expressed as to whether such solutions can find their way to implementation in policy development and governance, thus again making their engagement futile or treat them purely as "scientific exercises" which in the end will benefit science, but neither policy or society [Glenn *et al.*, 2012]. At the same time, the structure of the governance, with multiple authorities holding fragments of jurisdiction, creates a public regime where responsibility is an elusive concept and in which authorities are invested only in the small part of their jurisdiction, ignoring thus what happens beyond their circle of influence. As a result, the concept of integrated (and transdisciplinary) management of the environment and its resources becomes impossible to approach: jurisdiction and authority is divided to everyone and thus to no-one, resulting in ineffective national, regional and local administrative structures, weak enforcement, and no policy integration [Trumbic, 2008].

The obstacles in approaching a more integrated and transdisciplinary approach in coastal and marine management are also evident in the limited knowledge of EU and Greek legislation regarding ICM and MSP, as also identified in other previous studies [Koutrakis *et al.*, 2010]. The low percentage of institutional stakeholders having a good or excellent knowledge of the specific EU legal provisions, but also of the much wider way in which European legislation is ratified into different Greek laws and legal documents, is indicative of the lack of central integrated management mentality in Greek governance. Each sectoral jurisdiction is focused in the part of the legislation, which is absolutely necessary to know in order to take specific decisions; outside this spectrum the responsibility is transferred to other authorities and no knowledge is required. At the same time, this specific legal

framework isn't perceived even indirectly connected to approaches as ICM or MSP. Nevertheless, when asked to evaluate the environmental related legal framework which they work with, the respondents were much more confident to provide opinion and to comment on it with specificity. They underlined the fragmentation of jurisdiction, gaps and overlaps, as well as the absence of clear legal guidelines for specific issues (e.g. protected area management/Natura 2000 sites). On the other hand, they also comment that the existing legal framework, even if not perfect, is the only existing tool to achieve some level of (social-ecological) management (mainly in terms of managing productive activities).

The stakeholders' priorities are revealed clearly through the results. Namely, the issue of Land inputs management, and thus the pollution caused in the coastal and marine areas of the gulf, is definitely a leading priority for the majority of the respondents. The evaluation of different management issues as of high importance for the area, reveals their general concerns, as well as an understanding that when discussing social-ecological management, especially in coastal and marine areas, a certain level of interconnection between different policy issues is to be expected. It is interesting to observe, that the respondents seem to view the management of productive activities as issues with various impacts for the area (environmental, social, economic, legal). On the contrary, Land inputs management was mainly considered as an environmental issue, despite the fact that these inputs are mainly anthropogenic, have an impact on a number of other activities (aquaculture, tourism, etc.) and can be the product of illegal activity (e.g. unregulated waste disposal and agricultural inputs).

Finally, another interesting observation on the results of this survey is related to the most prominent causal factor of the identified management issues, which is the inability to implement the existing legal framework due to a number of institutional deficiencies. Again, it is necessary to underline that the majority of respondents are institutional stakeholders, thus they represent the bodies which should or could implement the existing legal framework to enable better environmental management. The identification of institutional deficiencies as major causal factor of inadequate management, even when referring to lack of resources (human and financial) is a strong indicator pointing towards the need for re-thinking and re-structuring of the legal framework (including the governing structures which implement it). Re-structuring of the legal and institutional brunches of the management process could have a positive output to at least two other important causal factors, according to the survey: the lack of adequate legal framework and the overexploitation of resources/illegal activities, which are, in a way, different expressions of the same problem.

5. CONCLUSIONS

The Greek stakeholders' reluctance to participate on a quite simplified, impersonal and preliminary effort for Science-Policy-Society interface is a discouraging, yet expected result. Even in societies where such efforts are more accustomed and better integrated in the social structure, engagement can be a challenging task [Fletcher *et al.*, 2007]. Nevertheless, this output is also an indicator that corrective actions need to be taken in order for such processes to be more meaningful and successful in the future. Part of these actions should target the increase of trust in the claim that science can provide knowledge-based, efficient and ethical tools to support fair and sustainable policy development and governance [Glenn *et al.*, 2012].

Although through a limited, yet varying sample, the stakeholders' priorities regarding the coastal and marine management of Thermaikos gulf are clear and coherent: the most important issue is Land input management in association with pollution. This issue is highly complicated and challenging, as well as spatially varying in the gulf. Our goal, through the next steps of this research, is to develop transdisciplinary processes and tools which will make its management more efficient and successful. These tools will aim: a) to increase the knowledge (scientific and other) on the issue and b) to identify and propose solutions for the institutional deficiencies. To achieve that in detail, the focus of future work should be placed in those areas which were identified as more affected by the management issue.

ACKNOWLEDGEMENTS

This work is realised as part of a post-doctoral grand, funded from the Greek State Scholarships Foundation, under the framework of the action "Post-doctoral Researchers Support" (MIS: 5001552) of the operational programme "Human Resources Development, Education and Life Long Learning" – NSRF 2014-2020.

References

1. Tett, P., Mette, A., Sandburg, A. & Bailly, D. (2011) '**The Systems Approach**', in *Sustaining Coastal Zone Systems* (eds. Tett, P., Sandburg, A. & Mette, A.) Dunedin Academic Press,Edinburgh, Scotland., 2011.
2. Cornell, S., Berkhout, F., Tuinstra, W., Tàbara, J. D., Jäger, J., Chabay, I., de Wit, B., Langlais, R., Mills, D., Moll, P., Otto, I. M., Petersen, A., Pohl, C. & van Kerkhoff, L. (2013) 'Opening up knowledge systems for better responses to global environmental change', **Environmental Science and Policy**, 28**,** 60–70.
3. Buanes, A., Jentoft, S., Maurstad, A., Søreng, S. U. & Runar Karlsen, G. (2005) 'Stakeholder participation in Norwegian coastal zone planning', **Ocean and Coastal Management**, 48**,** 658–669.
4. McKenna, J., Cooper, A. & O'Hagan, A. M. (2008) 'Managing by principle: A critical analysis of the European principles of Integrated Coastal Zone Management (ICZM)', **Marine Policy**, 32**,** 941–955.
5. Villares, M., Roca, E., Serra, J. & Montori, C. (2006) 'Social Perception as a Tool for Beach Planning: a Case Study on the Catalan Coast', **Journal of Coastal Research**, 118–123.
6. Fletcher, S. & Pike, K. (2007) 'Coastal management in the Solent: The stakeholder perspective', **Marine Policy**, 31**,** 638–644.
7. Voinov, A., Kolagani, N., McCall, M. K., Glynn, P. D., Kragt, M. E., Ostermann, F. O., Pierce, S. A. & Ramu, P. (2016) 'Modelling with stakeholders - Next generation', **Environmental Modelling and Software**, 77**,** 196–220.
8. Konstantinou, Z. I. & Latinopoulos, D. (2017) 'Trandisciplinary ICM and MSP in thermaikos gulf', in **13th International MEDCOAST Congress on Coastal and Marine Sciences, Engineering, Management and Conservation, MEDCOAST 2017**, 1**,** 2017.
9. Koutrakis, E. T., Sapounidis, A., Marzetti, S., Giuliani, V., Martino, S., Fabiano, M., Marin, V., Paoli, C., Roccatagliata, E., Salmona, P., Rey-Valette, H., Roussel, S., Povh, D. & MalváRez, C. G. (2010) 'Public stakeholders' perception of ICZM and coastal erosion in the mediterranean', **Coastal Management**, 38**,** 354–377.
10. Apostolopoulou, E., Drakou, E. G. & Pediaditi, K. (2012) 'Participation in the management of Greek Natura 2000 sites: Evidence from a cross-level analysis', **Journal of Environmental Management**, 113**,** 308–318.
11. Konstantinou, Z. I. & Krestenitis, Y. N. (2013) '**An Overview of the Implementation of SAF Methodology Regarding the Stakeholder Response, in the Mussel-Farming Area of Chalastra, Thermaikos Gulf**', *Global Challenges in Integrated Coastal Zone Management* 2013.
12. Glenn, H., Tingley, D., Sánchez Maroño, S., Holm, D., Kell, L., Padda, G., Runar Edvardsson, I., Asmundsson, J., Conides, A., Kapiris, K., Bezabih, M., Wattage, P. & Kuikka, S. (2012) 'Trust in the fisheries scientific community', **Marine Policy**, 36**,** 54–72.
13. Trumbic, I. (2008) 'New protocol on Integrated Coastal Zone Management', **Environmental Policy and Law**, 38**,** 145–153.



Solid waste management

LIFE CYCLE ASSESSMENT OF MUNICIPAL SOLID WASTE MANAGEMENT PRACTICES IN CENTRAL MACEDONIA

M. Batsioula1, G. Banias2*, Ch. Achillas2,3, M. Lampridi2, and D. Bochtis2

[1]International Hellenic University, School of Economics and Business Administration, GR-57001 Thermi, Greece
[2]Centre for Research and Technology-Hellas, Institute for Bio-economy and Agritechnology, GR-57001Thermi, Greece
[3]Technological Educational Institute of Central Macedonia, Department of Logistics, GR-60100 Katerini, Greece

[*]Corresponding author: e-mail: g.banias@certh.gr, tel : +302311257650

Abstract
The continuously expanding amounts of waste produced in the EU constitute a major concern at a European level. Municipal waste management represents one of the most critical problems that need to be addressed in Greece, because of the lack of available funds due to the financial crisis. To date, several illegal landfills still pollute the environment, with Greece being penalized by the European Court of Justice for several cases since 2005. On this basis, the development of an optimal waste management strategy, exploiting all available technologies and taking into account all waste streams is more than critical at a national level. In this work, we focus on the Life Cycle Assessment (LCA) of different scenarios of municipal solid waste management practices in an effort to estimate quantitively their environmental impacts. The work is conducted for the Region of Central Macedonia, Greece.

Keywords: waste management; municipal solid waste; life cycle analysis; Region of Central Macedonia.

1. INTRODUCTION

The world population is constantly growing and lifestyles and trends are changing rapidly. Increasing quantities of municipal waste is a key issue in modern cities worldwide, and one of the major challenges for municipalities is the collection, recycling, treatment and disposal of solid waste (Cherubini, Bargigli and Ulgiati, 2009). In European Union, Waste Framework Directive (2008/98/EC) and Landfill Directive (1999/31/EC), it is set the regulatory framework within which member states should adopt more environmental options, based on the “Waste Hierarchy” concept, which includes the ideas of reduce, reuse, recycling/compost and energy recovery from waste, thereby aiming at waste prevention and landfill minimization.

Consequently, there has been a growing interest in sustainable management of MSW, which covers generation, collection, transfer, sorting, treatment, recovery and disposal of waste. On this basis, it has been done much research on integrated solid waste management systems, which include various options like materials recycling, biological treatment of biodegradable fractions, composting or thermal treatments with energy recovery. Several publications have appeared evaluating several MSW management strategies at local, regional and national level. Different practices on waste management have been reviewed for countries such as: Germany, Denmark, Greece and other European countries (Bassi et al., 2017; Gentil et al., 2009), for regions: Lombardia, Italy (Rigamonti

et al., 2013), for cities: Niš, Serbia (Milutinović et al., 2017), Porto, Portugal (Herva, Neto and Roca, 2014), Naples, Italy (Hornsby et al., 2017).

However, limited amount of publications can be found in the literature that discuss the issue of municipal waste management in Greece, despite the fact that Waste Framework Directive is poorly implemented, with the country being penalized by the European Court of Justice since 2005. Trends and patterns of solid waste generation and waste composition (Papachristou et al., 2009), challenges of waste management (Erkut et al., 2008), dynamics, comparison and evaluation of waste policies and treatment methods (Koroneos and Nanaki, 2012; Karagiannidis et al., 2013; Minoglou and Komilis, 2013; Koufodimos and Samaras, 2002) have been reviewed for the city of Thessaloniki. Nevertheless, most of the previous studies do not take into account the revised Regional Waste Management Plan (RWMP) for the Region of Central Macedonia (RCM).

On this basis, the development of an optimal waste management strategy is more than urgent in the area. The current study focuses on the environmental impacts caused by the existing waste management system in the RCM and the comparison of alternative scenarios regarding MSW management in the RCM. LCA is adopted to benchmark the alternative practices on the basis of specific environmental indicators that were considered important for the environment and human health.

2. MATERIALS AND METHODS

2.1 Municipal solid waste management in the Region of Central Macedonia

Greece consists of 13 administrative regions, which are further subdivided into 54 prefectures. This paper is focused on the management of municipal waste in the RCM, which is located in North Greece and consists of the central part of the geographical region of Macedonia. The region has the largest surface area (18.811km^2) among all regions, and it is divided into seven prefectures: Thessaloniki, Imathia, Pella, Kilkis, Pieria, Serres and Chalkidiki. Additionally, it is the second most populous region after Attica, with intense urbanization and a high density of inhabitation, especially in Thessaloniki and its metropolitan area, which is the capital of the region.

In the Region of Central Macedonia 842.490 tons/year of waste generated in 2014, according to up-to-date Regional Waste Management Plan (RWMP) (RWMP,2016), from which 82% ended up to Sanitary Landfills. In general, the composition of MSW depends on the socioeconomic conditions and the various consumption patterns in the RCM. However, within the context of this study, a typical average composition of the waste is used, in accordance with the data available in RWMP (Batsioula, 2018). The fractions of MSW included in the study are: (i) total amount of household organics, (ii) paper, (iii) plastic, (iv) metals, (v) glass, (vi) wood, (vii) other recoverable such as batteries and household appliances, as well as other unclassified materials including also hazardous waste like textiles, inks, medicine. The composition of total municipal waste in the RCM is illustrated in Figure 1.

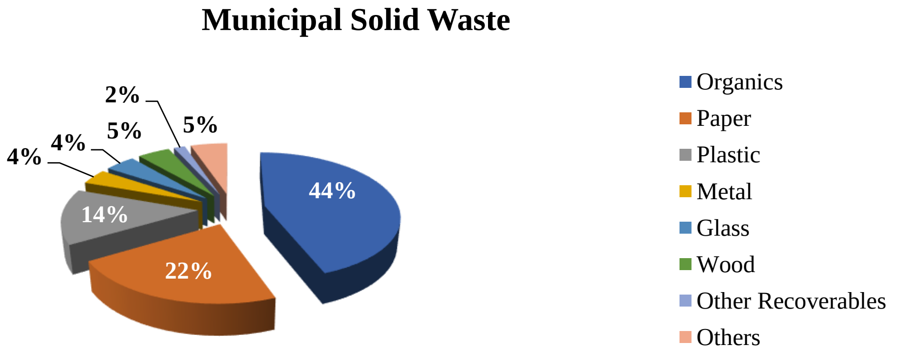


Figure 1: Typical composition of total MSW in Region of Central Macedonia (RWMP, 2016).

According to the RWMP, except for sorting at the source of packaging waste and some other streams such as batteries and Waste Electrical & Electronic Equipment (WEEE), all municipal waste of the RCM is disposed to landfills. More specifically, 82% of MSW are disposed directly to landfills, whereas only 12% are sorted at the source. RCM still has not implemented a MSW system which includes advanced waste treatment methods. RCM’s waste management policy involves mainly the collection and disposal of waste in the landfill. The current situation in the prefectures of the region is such that initially, municipal waste, that are temporarily storaged into bins or containers, are collected by a public company using waste collection vehicles and then transported in Waste Transfer Stations (WTSs). At the same time, waste streams such as paper, glass and packaging waste, are separately collected in special bins and collection vehicles transport them in Material Recycling Facilities (MRFs) (RWMP, 2016).

With respect to bio-waste, no separate collection program is implemented in the RCM, with the exception of diversion in rural areas for the purpose of animal feeding and on-site composting, as well as pilot composting programs and programs for the collection of cooking oil and grease waste in some schools of the region, that send it in a recycling company which converts it into an alternative fuel, biodiesel. Also, WEEE in almost all municipalities, are collected by private companies and led to processing plants. Moreover, bulky waste is collected by the Municipalities' Cleanup Department. In the majority of the municipalities of RCM, after the collection, it is sent mainly direct or after shredding disposal in landfills or dispatch to private companies. Similarly, management of garden waste includes segregation and disposal in landfills, since in most of the municipalities of RCM there is not organized system for collection and management of green waste (RWMP, 2016).

2.2 LCA method

The goal of this study is to analyze and compare different MSW management strategies that can be implemented in the RCM from an environmental point of view. Therefore, different treatment methods were investigated and alternative MSW management systems were compared (Batsioula, 2018). More specifically, three (3) alternative scenarios have been compared regarding the management of MSW generated in the RCM. Each scenarios consists of the storage and collection of MSW in bins, both mixed bins and those for separately sorting of recyclable fractions at the source, the gathering of municipal waste and their transport by collection vehicles to the WTS. Besides that, the alternatives include the main treatment available in each scenario such as the mechanical separation of the waste, recycling or composting, and the final disposal of the residues of those processes in a landfill site. The LCA methodology was used in order to choose the optimal MSW management system. The application of LCA was carried out with the use of SimaPro software, which enables the evaluation of environmental impacts for all alternatives for the waste management by using specific environmental impact indicators that will be further analyzed in the following sections.

Within the framework of this study, the functional unit is defined equal to the reference flow. More specifically, this is the whole amount of municipal solid waste generated in the RCM over a period of one year (842.490 ton). The choice to use the entire amount of waste produced as a functional unit may limit the ability to draw general conclusions for regions and municipalities. However, it was considered more relevant than to select a standard unit like 1 ton of waste, since the current study attempts to define the situation as it is in the RCM.

The system under study is defined as an integrated waste management system for 842.490 tons of MW. Its boundaries involve the final stage of the life cycle of the waste generated in the RCM. More specifically, the system boundaries include all processes from the moment the waste is collected until it leaves the system either as an emission or as a secondary raw material, biogas or energy (Figure 2). MW enters the system after been discarded either as mixed waste or as source-segregated streams which are separately collected. The system covers waste collection from bins, transport, mechanical separation, when is available, recycling or other waste treatment, and finally disposal in a landfill. Also, within the system boundaries, besides the main treatment of MSW, the required fuels for the

transport, as well as energy for both the operation and construction of all required facilities are included.

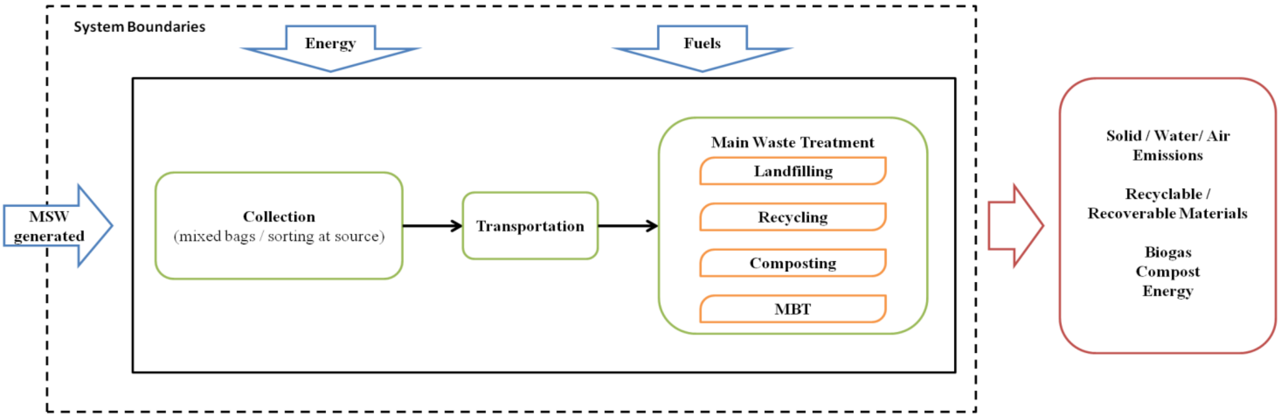


Figure 2: Schematic Flowchart of System's Boundaries (Batsioula, 2018).

2.3 Scenarios description

With the intention to examine and outline the benefits and drawbacks of the techniques used on municipal solid waste management, diverse MSW strategies have been analyzed. The differentiation of the proposed strategies is based on the variations of the waste flows in comparison to the different waste control methods, such as landfill, recycling, composting and others. With the core of conventional waste treatment methods and the final disposal in landfills, the different proposed strategies focuse on reuse and recycling most of MSW, as well as on energy recovery are following:

- Scenario 0: the main treatment of this scenario is landfilling without energy recovery,
- Scenario I: the main treatment of this scenario is landfill with energy recovery, and except for landfilling includes small percentages of recycling of some MSW fractions,
- Scenario II: the main waste treatment of this scenario is recycling and material recovery, thus it incorporates the future targets that must be completed according to the European Directive.

Scenario 0: represents the most common until recently waste treatment method in Greece, landfilling. It assumes that the all the municipal waste generated is collected and transferred to WTS. Then, without a process of separation of the produced waste, MSW are disposed to regional landfill sites, where they are disposed without energy recovery to take place (Figure 3).



Figure 3: Mass balance flow chart for Scenario 0 in the RCM (Batsioula, 2018).

Scenario I: models the basic scenario that corresponds to the present situation in the RCM. Figure 4 illustrates the flowchart of Scenario I. 694.873 tons (82%) of municipal waste are sent to landfills, whereas only 147.617 tons (18%) of waste are separated collected as shown in Table 1. According to RWMP and the existing recycling facilities, recyclable waste fractions in the amount of 103.213 tons (12% of the total waste amount) are recycled, around 5% of the waste sorted at the source are composted at home facilities, and 1% is sent for reuse.

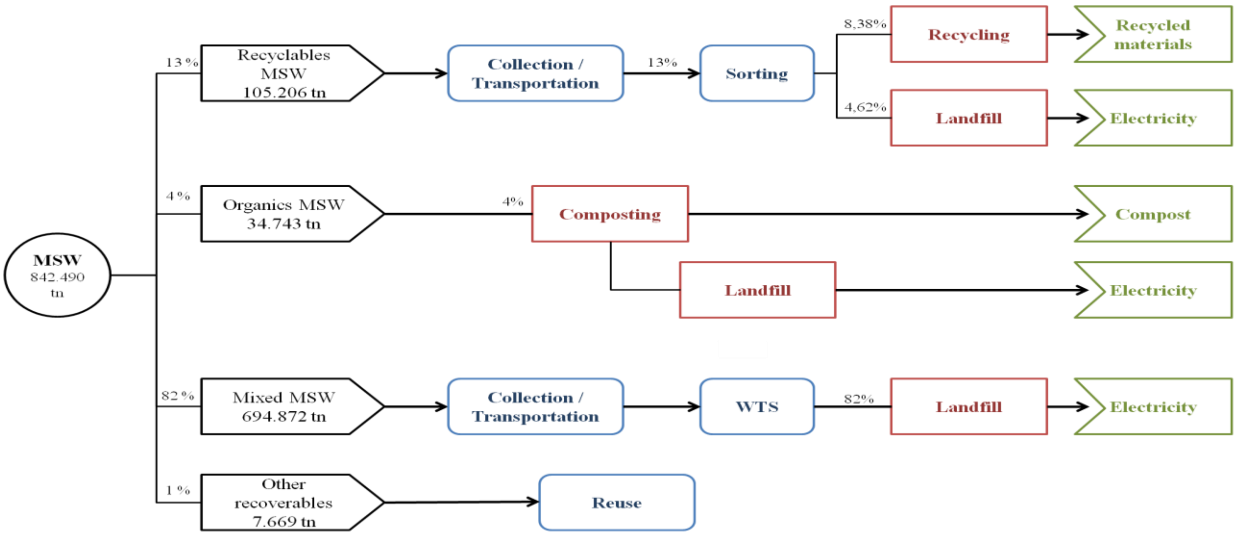


Figure 4: Mass balance flow chart for Scenario I in the RCM (Batsioula, 2018).

Table 1: Current waste management system in RCM (Scenario I) (RWMP, 2016).

MSW Fraction	Total amount generated	Mixed collection (tons / % of the total)		Sorting at the source (tons / % of the total)	
Organics	373.224	338.481	91%	34.743	9%
Paper	187.033	270.011	72%	103.213	28%
Plastic	117.107				
Metal	32.857				
Glass	36.227				
Wood	38.753	36.760	95%	1.993	5%
Other recoverables	13.480	5.811	43%	7.669	57%
Others	43.809	43.809	100%	0	0%
Total MSW	**842.490**	**694.872**	**82%**	**147.618**	**18%**

Scenario II: describes the future waste management plan for 2020 as it is defined by the reviewed RWMP. This scenario emphasizes on reuse and recycling of all fractions of waste generated in RCM, while minimizing the amounts of waste that are sent directly to landfill sites. Particularly, according to the RWMP, 74% of the total municipal waste must be recovered whereas only 26% of the aggregate MSW quantities should be disposed in the regional landfill sites (Table 2). Figure 5 illustrates the flowchart of Scenario II.

Table 2: Future waste management system in the RCM (Scenario II) (RWMP, 2016).

MSW Fraction	MSW generated	Sorting at source (tons / % of the total)		Mixed collection			
				Recovery at WTP (tons / % of the total)		Landfilling (tons / % of the total)	
Organics	373.224	149.290	40%	149.290	40%	74.644	20%
Paper	187.033	110.323	59%	18.729	10%	57.981	31%
Plastic	117.107	79.617	68%	11.727	10%	25.763	22%
Metal	32.857	25.293	77%	4.935	15%	2.629	8%
Glass	36.227	27.362	76%	1.983	5%	6.883	19%
Wood	38.753	19.377	50%	11.626	30%	7.751	20%
Other recoverables	13.480	9.436	70%	674	5%	3.370	25%
Others	43.809	0	0%	0	0%	43.809	100%
Total MSW	**842.490**	**420.698**	**50%**	**198.964**	**24%**	**222.830**	**26%**

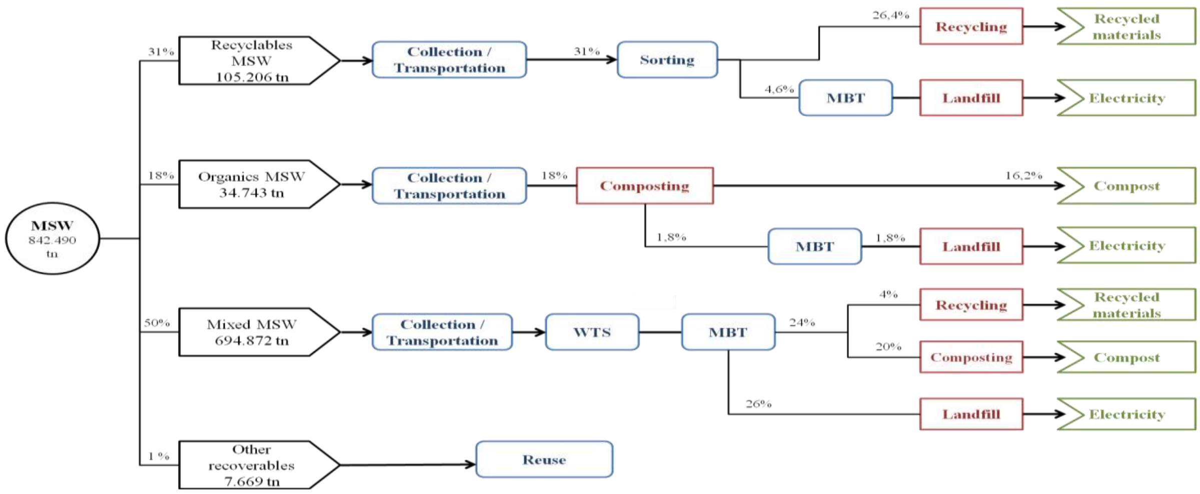


Figure 5: Mass balance flow chart for Scenario II in the RCM (Batsioula, 2018).

2.4 Life cycle inventory

In the LCA, an inventory was created for the proposed alternative scenarios. The selected inventory was based on those available in the Ecoinvent database v2.2. Due to the complexity that an integrated MSW management system has, several reasonable assumptions are required in order to simplify complex calculations and overcome the problem of lack of data, so as to comply with the requirements of the SimaPro software and result in a proper comparison between the different scenarios. The summary of the main assumptions, as well as the major data used in the modeling of the alternatives are the following:

- In order to export valid results, and given the lack of information regarding the management practices, waste treatment techniques included in the SimaPro software was performed.
- The collection type is assumed curb collection and consists of the gathering of municipal waste in bins from various locations in the municipalities of the RCM. Besides that, closed-body vehicles also are considered as part of the collection system. The type of the collection vehicles that is assumed to be used is "*Transport, municipal waste collection, lorry 21t"*, as appeared in Ecoinvent database. Nevertheless, only the environmental impacts from waste transportation with collection vehicles and not those of raw material and manufacture of bins are taken into consideration.
- Due to software restrictions, the environmental impacts of the energy (biogas collection, as well as electricity generation and consumption during the operation phase for mechanical separation and energy recovery when is available) are not taken into consideration. Similarly, the construction of new facilities, in Scenario II, is not taken into consideration as well.
- Since the quantities of WEEE that are separately collected and sent for reuse are small (< 1% of the total MSW generated), and due to lack of information regarding their treatment, it is assumed that WEEE amounts are sent for recycling.
- Transport to the various waste management facilities was entered on the software according to the following assumptions. Initially, the required total distance for waste collection is comprised of the distance between the capital city of each prefecture and the final management point. Also, the distance calculations are made on the basis of the assumption that empty-collection vehicles returns are also included. Besides that, regarding the new waste facilities that are established in Scenario II, the required distance for transportation are calculated based on data provided by RWMP.

2.5 Life cycle assessment

Life Cycle Assessment data was mainly compiled from the SimaPro (Ecoinvent) databases, from the bibliography, as well as from the inventory of current waste management system in RCM as described

in the latest RWMP. For the Life Cycle Impact Assessment, which based on the outcomes of the inventory, both Eco-indicator 99 and CML 2001 methods were utilized.

According to CML 2001 Method, the emissions from the alternative scenarios studied are classified to the following impact categories: Abiotic Depletion Potential (ADP, kg Sb eq), Global Warming Potential (GWP, kg CO_2 eq), Human Toxicity Potential (HTP, kg 1,4-DCB eq), Acidification Potential (AP, kg SO_2 eq), Eutrophication Potential (EP, kg PO_4 eq), Ozone Layer Depletion Potential (OLD, kg CFC-11 eq), Photochemical Ozone Creation Potential (POCP, kg C_2H_4). On the other side, Eco-indicator 99 is a damage-oriented method which classifies the various impact categories and the damages caused into three damage categories: Damage to Human Health, Damage Ecosystem Quality and Damage to Resources.

3. RESULTS AND DISCUSSION

The environmental burdens of each practice were calculated with both selected Methods (CML 2001, Eco-indicator 99) and graphically, presented in Figures 6 and 7 respectively. Taking into consideration CML 2001 methodology's results from Figure 6, it is obvious that an integrated waste management system can minimize significantly the environmental impacts caused by municipal waste generated. Application of sustainable practices and treatment methods such as sorting at the source, recycling and composting lead to the reduction of waste disposal.

In accordance to the results of life cycle impact assessment, Scenario 0, and its main waste treatment method, landfilling, results the worst performance for all the indicators analyzed. This high level of environmental burdens in all of the impact categories, compared with the other management systems, is due to the lack of reuse and the disposal of all waste generated in sanitary landfills. Besides that, findings show that the Scenario II contributes to savings in many impact indicators. The replacement of primary products with products which come from the waste treatment recompenses the impacts caused by the actual process of the treatment, thus Scenario II which corporate high rates of recycling and composting is advantageous to most of the impact categories.

However, the status in cases of global warming and eutrophication indicators is different. Global warming potential has positive values for all Scenarios. Scenario 0 has the higher contribution for global warming because of the very low level of separate collection. As a result, all waste sent to landfills and many CO_2 and CH_4 emissions are released. On the other hand, Scenarios I and II results positive values for GWP_{100} indicator, which are associated with the CO_2 and CH_4 emissions emitted in the landfill and are not captured by the landfill gas control system. Moreover, all alternatives have positive sign of Eutrophication indicator, as they are leachable from landfill, although they are treated in wastewater facilities, releasing NO_3^- and NH_3. Thus, in all three alternative management systems, those emissions represent the biggest contribution to eutrophication. Even in Scenario II, which has generally the most beneficial performance, this indicator shows positive value.

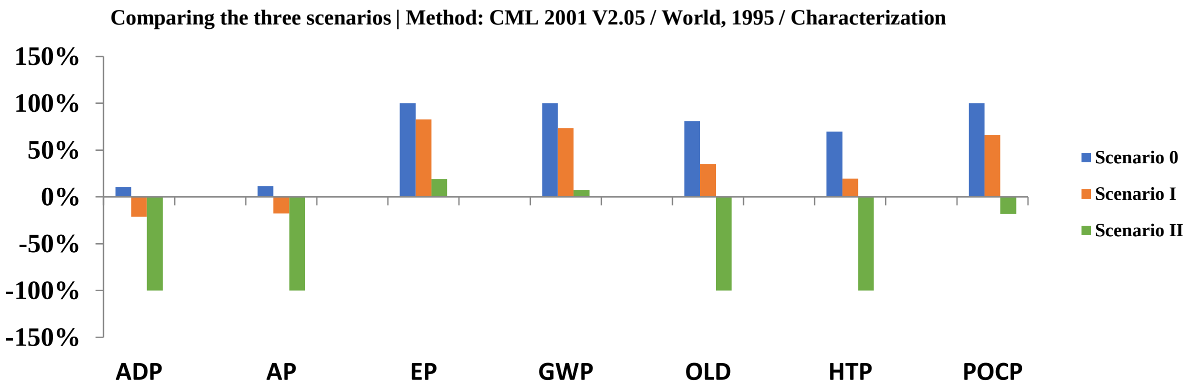


Figure 6: Comparison of the proposed scenarios for the seven categories of impact (CML 2001).

With respect to the results from Eco-indicator 99 methodology is concerned, from the single score that is illustrated in Figure 7 - It is clear that Scenario 0 is the worst waste management system that can be implemented in the RCM. Its environmental burden is significant, according to both methodologies used. Similarly with CML 2001, results for Eco-indicator 99 methodology indicates that the main impacts caused by landfilling treatment process and the huge amount of waste that is disposed (Scenarios 0 and I). Furthermore, the environmental benefits that derive from the replacement of primary products with recycled ones are significant (Scenario II). As Figure 7 illustrates, savings of the resources are more advantageous when high rates of sorting collection, recycling and composting are implemented.

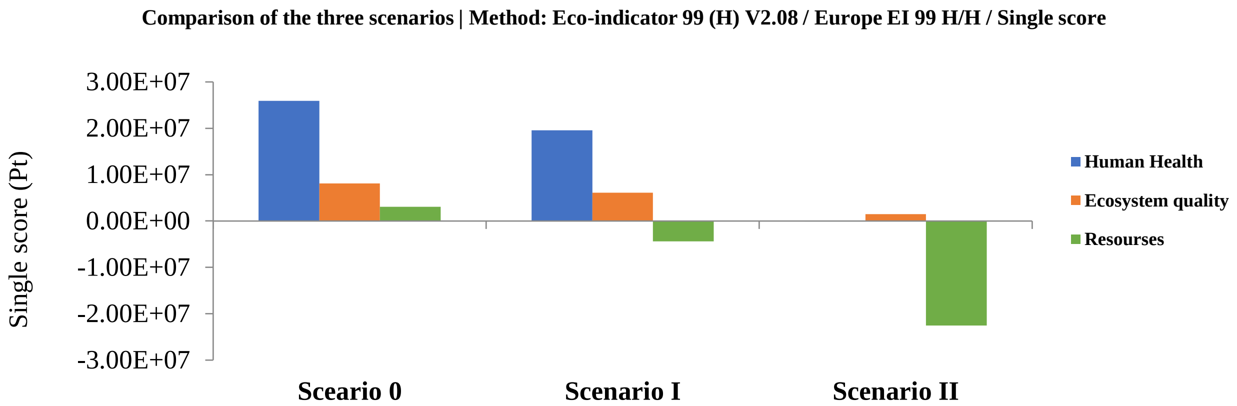


Figure 7: Comparison of the proposed scenarios (Single score of Eco-indicator 99 methodology).

Overall, taking into consideration the final results of the two methods (Table 3, Figure 8), it becomes clear that Scenario II is the best waste management practice, due to high environmental benefits derived from the recycling of waste streams, as well as the small environmental burden from waste disposal, because of the comparatively less amounts of waste sent to landfill sites. On the other hand, landfilling of municipal waste, as it has already be mentioned in the literature, is thought to be the worst method from the treatment of waste generated. That is because of the significant impacts this process has both to the environment and human health. As a final consideration on the results, the uncertainty of such studies is a significant factor that should be taken under consideration. However, due to lack of time, the analysis of uncertainty does not included in the scope of this study, and thus will not be presented.

Table 3: Final normalized results of CML 2001 and Eco-indicator 99 methodologies.

CML 2001

	ADP	AP	EP	GWP_{100}	ODP	HTP	POCP
Scenario 0	1,72E-06	9,83E-07	1,67E-05	9,96E-06	1,21E-08	6,01E-06	1,24E-06
Scenario I	-3,4E-06	-5,3E-07	1,39E-05	7,32E-06	5,27E-09	1,69E-06	8,22E-07
Scenario II	-1,6E-05	-4,6E-06	3,2E-06	7,43E-07	-1,5E-08	-8,6E-06	-2,2E-07

Eco-indicator 99

	Human Health	Ecosystem Quality	Resources
Scenario 0	8,63E+04	2,02E+04	1,03E+04
Scenario I	6,53E+04	1,52E+04	-1,45E+04
Scenario II	-3,95E+02	3,79E+03	-7,51E+04

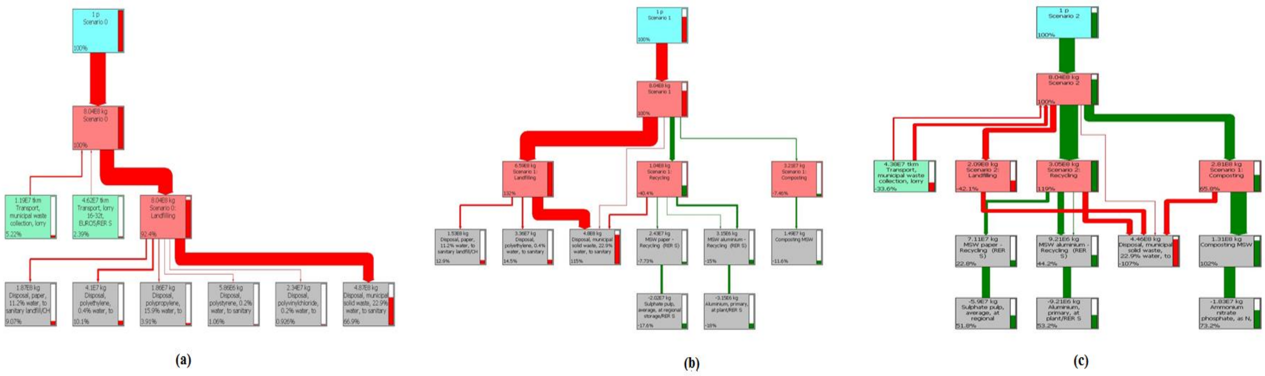


Figure 8: Network chart flow for: (a) Scenario 0, (b) Scenario I and (c) Scenario II, which refers to single score as resulted from Eco-indicator 99 method.

4. CONCLUSION

The aim of this study was the development and application of a life cycle methodological framework in order to compare the different management practices and select the optimal and most sustainable integrated waste management system from an environmental point of view. According to all indicators examined, waste management practices that involve either wholly or partial disposal in landfill sites have the worst performance. The parameters that contribute to these negative results are the large quantities of untreated municipal waste that are disposed in landfill and the low rates of landfill gas collection. It should be highlighted that the alternative management practice of municipal waste, which combines the recycling of metals, glass, plastics and paper, with the composting of organic fractions of MSW after the separately collection at source, is the best solution. And that is because, in this scenario the rate of untreated waste which is sent to landfill sites is significantly low, and at the same time the material recovery offers many environmental benefits. However, it should not be forgotten that alternative waste treatment methods such as recycling do have negative environmental impacts, and these loads do not overshadow the environmental benefits of material recovery.

Taking into consideration the results of the LCA analysis, it has been found that the implementation of an integrated waste management system is important to the sustainable management of municipal waste. Nevertheless, this system may not be effective if there is no efficient sorting of waste streams at the source. Overall, a significant percentage of municipal waste can be treated in various ways, recycled or reused before disposed in a landfill site, thus minimizing environmental impacts of the continuously expanding amounts of waste produced nowadays.

References

1. Andreasi Bassi, S., Christensen, T. and Damgaard, A. (2017). Environmental performance of household waste management in Europe - An example of 7 countries. **Waste Management**, 69, 545-557.

2. Batsioula M. (2018). Environmental impact assessment of municipal solid waste management. Master dissertation. International Hellenic University, School of Economics and Business Administration.

3. Cherubini, F., Bargigli, S. and Ulgiati, S. (2009). Life cycle assessment (LCA) of waste management strategies: Landfilling, sorting plant and incineration. **Energy**, 34(12), 2116-2123.

4. Council Directive 1999/31/EC of 26 April 1999 on the landfill of waste, **Official Journal of the European Union**, L 182, 1–19.

5. Directive 2008/98/EC on waste and repealing certain Directives, **Official Journal of the European Union**, L 312, 22.11.2008, p. 3–30.

6. Erkut, E., Karagiannidis, A., Perkoulidis, G. and Tjandra, S. (2008). A multicriteria facility location model for municipal solid waste management in North Greece. **European Journal of Operational Research**, 187(3), 1402-1421.
7. Gentil, E., Clavreul, J. and Christensen, T. (2009). Global warming factor of municipal solid waste management in Europe. **Waste Management & Research**, 27(9), 850-860.
8. Herva, M., Neto, B. and Roca, E. (2014). Environmental assessment of the integrated municipal solid waste management system in Porto. **Journal of Cleaner Production**, 70, 183-193.
9. Hornsby, C., Ripa, M., Vassillo, C. and Ulgiati, S. (2017). A roadmap towards integrated assessment and participatory strategies in support of decision-making processes. The case of urban waste management. **Journal of Cleaner Production**, 142, 157-172.
10. Karagiannidis, A., Kontogianni, S. and Logothetis, D. (2013). Classification and categorization of treatment methods for ash generated by municipal solid waste incineration: A case for the 2 greater metropolitan regions of Greece. **Waste Management**, 33(2), 363-372.
11. Koroneos, C. and Nanaki, E. (2012). Integrated solid waste management and energy production - a life cycle assessment approach: the case study of the city of Thessaloniki. **Journal of Cleaner Production**, 27, 141-150.
12. Koufodimos, G. and Samaras, Z. (2002). Waste management options in southern Europe using field and experimental data. **Waste Management**, 22(1), 47-59.
13. Milutinović, B., Stefanović, G., Đekić, P., Mijailović, I. and Tomić, M. (2017). Environmental assessment of waste management scenarios with energy recovery using life cycle assessment and multi-criteria analysis. **Energy**, 137, 917-926.
14. Minoglou, M. and Komilis, D. (2013). Optimizing the treatment and disposal of municipal solid wastes using mathematical programming - A case study in a Greek region. **Resources, Conservation and Recycling**, 80, 46-57.
15. Papachristou, E., Hadjianghelou, H., Darakas, E., Alivanis, K., Belou, A., Ioannidou, D., Paraskevopoulou, E., Poulios, K., Koukourikou, A., Kosmidou, N. and Sortikos, K. (2009). Perspectives for integrated municipal solid waste management in Thessaloniki, Greece. **Waste Management**, 29 (3), 1158-1162.
16. Regional Waste Management Plan (RWMP) of Central Macedonia (2016). Solid Waste Management Association of Central Macedonia (FODSA), Thessaloniki, url: https://fodsakm.gr/site/wp-content/uploads/2017/02/PESDA_KM-1.pdf (In Greek)
17. Rigamonti, L., Falbo, A. and Grosso, M. (2013). Improving integrated waste management at the regional level: The case of Lombardia. **Waste Management & Research**, 31(9), 946-953.

INNOVATIVE BIOGEOCHEMICAL SOIL COVER TO MITIGATE LANDFILL GAS EMISSIONS

K. R. Reddy[1],*, D.G. Grubb[2] and G. Kumar[1]

[1]University of Illinois at Chicago, Department of Civil & Materials Engineering, 842 West Taylor Street, Chicago, IL 60607, USA [2]Phoenix Services, LLC, 148 West State Street, Suite 301, Kennett Square, PA 19348, USA

*Corresponding author: e-mail: kreddy@uic.edu, tel : +13129964755

Abstract
The municipal solid waste (MSW) in landfills undergoes anaerobic decomposition to produce landfill gas (LFG), which predominantly consists of methane (CH_4) and carbon dioxide (CO_2). Fugitive LFG emissions which are otherwise not targeted by gas collection system escape into the atmosphere, forming one of the largest anthropogenic sources of CH_4 and CO_2 emissions in the United States. The landfill cover soil plays an important role in mitigating the LFG emissions by microbial oxidation of CH_4 to CO_2 thereby reducing the CH_4 emissions to atmosphere. Several researchers have investigated the addition of organic amendments to the cover soils in order to enhance microbial oxidation of CH_4 in landfill covers. In recent years, biochar as an organic amendment has shown promise in enhanced microbial oxidation due to its inert/stable chemical nature to degradation, high surface area, high internal porosity, and high moisture holding capacity. However, in all these efforts there is no regard given to the CO_2 that still escapes into the atmosphere in undesirable amounts. Steel slag, a product from steel making industry, due to its high alkaline buffering capacity, high carbonation potential, and its unique cementitious properties has found numerous applications in civil and environmental engineering. But, until now there has been no study on the potential use of steel slag in landfill covers to sequester the CO_2 emissions. Ongoing research study, funded by the U.S. National Science Foundation, explores the use of BOF steel slag in conjunction with biochar amended cover soil so as to first convert CH_4 to CO_2 by microbial oxidation and thereafter sequester the resulting CO_2 from CH_4 oxidation and the prevailing CO_2 from anaerobic decomposition together by steel slag, thereby significantly mitigating the LFG emissions from landfills. In this paper, a review on the current applications and carbon sequestration mechanisms of BOF steel slag is presented. Finally, the proposed concept of the biogeochemical soil cover for mitigation of LFG emissions and some of the results from a preliminary investigation indicating the CO_2 sequestration potential by steel slag are discussed.

Keywords: MSW landfills, landfill cover; landfill gas; bio-geochemistry; BOF steel slag; biochar; carbonation

1. INTRODUCTION

The global greenhouse gas (GHG) emissions including the methane (CH_4) and carbon dioxide (CO_2) have been rapidly increasing due to population growth and the corresponding energy and resource consumption across the globe. This has contributed significantly to global climate change. Although landfilling of waste is considered an unsustainable option, it still remains the primary waste management technique in the US and many other countries. According to United States Environmental Protection Agency (USEPA) out of the 258 million metric tons of MSW generated in 2014, about 136 million metric tons of MSW was landfilled (USEPA 2016). The MSW placed in

landfills undergoes anaerobic decomposition producing the landfill gas (LFG) which predominantly consists of CH_4 and CO_2. MSW landfills are regarded one of the largest anthropogenic sources of CH_4 and CO_2 emissions into the atmosphere in U.S. In this regard, the U.S. regulations mandate the installation of active gas extraction systems to substantially minimize the emission of LFG and other non-methane organic compounds into the atmosphere. However, fugitive emissions persist as they are otherwise not targeted by the gas extraction systems.

Several researchers have demonstrated the limited oxidation of CH_4 into CO_2 in the soil naturally due to methanotrophic bacteria in the landfill cover soils (Whalen et al. 1990; Hilger et al. 2000). In order to enhance the microbial oxidation of CH_4 in landfill cover, biocovers were introduced that involved amending the cover soil with organic material to promote the microbial growth. Several organic amendments such as compost, manure, biosolids, and digested sludge which could be used to enhance microbial activity, had several limitations. Compost or sewage sludge, if it is not substantially degraded, can undergo anaerobic decomposition producing CH_4 and CO_2 itself, thus exacerbating emissions.

Recent lab-scale investigations and field pilot tests have demonstrated that biochar shows good performance as an organic amendment for enhanced microbial oxidation of CH_4 in landfill covers (Yargicoglu and Reddy, 2017a, b, 2018). Biochar is a solid byproduct derived from gasification or pyrolysis of biomass under anoxic or low oxygen conditions (Reddy et al., 2014). Biochar with its high porosity and large specific surface provides favorable environment for the methanotrophs to proliferate and thrive in the cover soil thereby facilitating the CH_4 oxidation (Yargicoglu et al., 2015). Although the biochar-amended soil cover system mitigates the CH_4 emissions into the atmosphere, it can only oxidize CH_4 into CO_2, leading to continued emission of CO_2 into the atmosphere in undesirable amounts. Hence, it is desirable to develop a cover system that can minimize both the CH_4 and CO_2 emissions into the atmosphere.

Mineral sequestration of CO_2 by carbonation using steel slag is proposed to be an effective approach to substantially alleviate CO_2 emissions into the atmosphere (Huijgen et al., 2005, 2006). Steel slag is a product generated during the steel making process. There are several studies in the literature that have investigated the potential use of steel slag for CO_2 sequestration. Most of the studies focused on CO_2 sequestration for slag pre-treatment (for pH reduction) in civil engineering applications such as its use as aggregates in concrete, base layer in roadways and pavements, railroad ballasts thereby preserving the virgin materials. There are a few studies that investigated the utilization of steel slag in landfill covers as hydraulic barrier material. However, there has been no study on the use of steel slag in landfill cover systems specifically for CO_2 sequestration. This paper discusses steel slag and its unique characteristics that aid in CO_2 sequestration. Thereafter, the geochemistry of mineral sequestration of CO_2 by carbonation is presented. A review of typical applications of steel slag leveraging the process of carbonation is also presented. Finally, the paper proposes the concept of zero emission from landfills to investigate the use of biochar and steel slag amendments to soil in the landfill cover system to sequentially mitigate both CH_4 and CO_2 emissions from landfills.

2. STEEL SLAG

Steel is one of the most used materials on earth. The global annual steel production in the year 2016 reached 1.63 billion metric tons and 78.5 million metric tons of which was produced in U.S. (World Steel Association, 2017). Steel slag is a product obtained from the iron and steel making process. It originates as a molten liquid melt while impurities are being separated from molten steel and is a complex solution of silicates and oxides that solidifies upon cooling. The amount of steel slag produced depends on both the feed and the type of furnace used, but typically 0.2 ton of steel slag is produced per ton of steel. The steel making industries in U.S. generate approximately 10-15 million tons of steel slag every year (Yildirim and Prezzi, 2011).

There are three principal types of slag based on the type of furnace used for steel production namely, (i) Basic Oxygen Furnace (BOF) Slag, (ii) Electric Arc Furnace (EAF) Slag, and (iii) Ladle Furnace

(LF) Slag. A detailed explanation of the production process in each of the furnaces and the typical chemical composition of different slag types can be found in Shi (2004), Pan et al. (2016) and National Slag Association, (2013). The composition of furnace charges, grades of steel produced, rate of slag cooling and furnace operating practices also influence the composition and properties of steel slag. The typical composition of steel slag mainly comprises of calcium silicates, calcium aluminoferrites, and fused oxides of calcium, iron, magnesium, manganese and trace heavy metals. There also exists approximately 10 to 15% free lime in steel slag based on the operating conditions employed for steel making and the steel making process. The pH of the fresh steel slag is usually similar to lime products or up to 12.5.

The steel slag generated at the steel plants is initially stockpiled at the plant and eventually sent to slag disposal sites, if there is no use or market for it. In this regard, several researchers have studied the use of steel slag in order to reduce its disposal in landfills and also preserve the natural resources. Steel slag exhibits some unique characteristics that make it suitable for its use in many civil and environmental applications. Moist or wet steel slag has a high affinity for atmospheric CO_2. The lime, Portlandite and several Ca silicates in steel slag undergo dissolution in the presence of moisture to react with CO_2 and precipitate as carbonates. This results in increased physical stability, strength and compressibility characteristics due to the binding nature of the carbonate precipitates. A detailed explanation on the carbonation mechanisms and some of the important factors influencing the process is discussed in the following section.

3. CARBONATION IN STEEL SLAG

The fundamental mechanism behind the carbonation of steel slag is to allow for the reaction between cations (Ca^{2+}, Mg^{2+}) in the presence of moisture and CO_2 to form thermodynamically stable and insoluble carbonates. BOF steel slags are ideal minerals for carbon sequestration as they are low-cost, with high CaO content (Pan et al. 2016). Various studies have demonstrated that the accelerated carbonation of steel slag is an effective technique to stabilize the alkaline mineral while simultaneously fixing the CO_2 (Pan et al. 2016; Olajire 2013).

Carbonation of alkaline solid wastes (e.g. steel slag) may occur in two ways: (a) direct carbonation (one step process), and (b) indirect carbonation (two or more step process). Moreover, the direct carbonation could be classified as dry or aqueous based on the liquid-to-solid ratio. The direct reaction of gaseous CO_2 with solid mineral or alkaline waste is the most straight forward mineral carbonation route. However, the reaction rate of dry carbonation is very slow and carbonate conversion is low. The dry carbonation of Ca silicate minerals can be generalized as in Eq. 1.

$$\text{Ca-silicate}_{(s)} + CO_{2(g)} \rightarrow CaCO_{3(s)} + SiO_{2(s)} \qquad (1)$$

Aqueous carbonation is faster and results in higher carbonate formation than dry carbonation. Direct aqueous carbonation involves three coexistent mechanisms based on the minerals available. First, dissolution of lime and portlandite takes place to readily produce Ca^{2+} ions as shown in Eq. 2 and 3. Then, carbon dioxide dissolves in water resulting in an acidic environment and CO_3^{2-} ions species as shown in Eq. 4.

$$CaO + H_2O \rightarrow Ca(OH)_2 \qquad (2)$$

$$Ca(OH)_2 \rightarrow Ca^{+} + 2OH^{-} \qquad (3)$$

$$CO_{2(g)} + H_2O_{(l)} \rightarrow H_2CO_{3(aq)} \rightarrow 2H^{+}_{(aq)} + CO_3^{2-}{}_{(aq)} \qquad (4)$$

Ca^{2+} leaches from the mineral matrix (larnite), facilitated by the protons present as shown in Eq. 5.

$$\text{(Ca)-silicates}_{(s)} + 2H^{+}_{(aq)} \rightarrow Ca^{2+}_{(aq)} + SiO_{2(s)} + H_2O_{(l)} \qquad (5)$$

Finally, calcium carbonate precipitates as shown in Eq. 6

$$(Ca)\text{-silicates}_{(s)} + CO_3^{2-}{}_{(aq)} \rightarrow CaCO_{3(s)} \quad (6)$$

Hence, the fundamental mechanism of direct carbonation reaction in steel slag involves (1) the leaching of alkaline mineral metal from the mineral matrix (predominantly Ca), (2) dissolution of gaseous CO_2 into aqueous phase followed by conversion of carbonic acid to carbonate ions, and (3) consequent precipitation of stable carbonates from Ca silicates (Pan et al. 2016). A schematic of the direct carbonation is shown in Fig. 1.

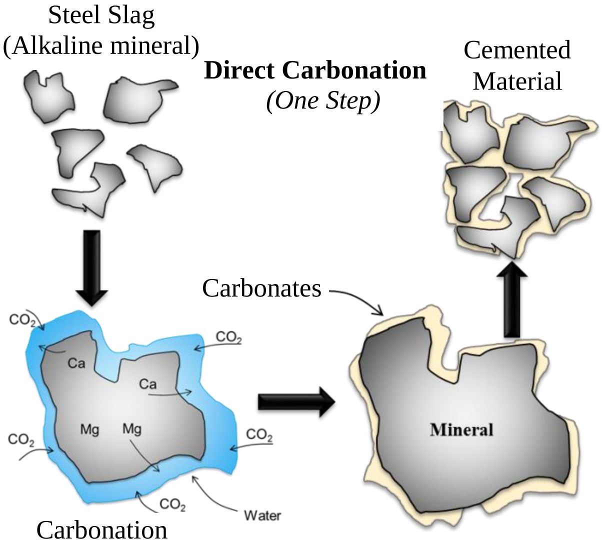


Figure 1: Direct Carbonation

Indirect carbonation is the process where reactive alkaline earth metal is first extracted from the steel slag using chemical extractants (e.g. acetic acid) and subsequently carbonated which is given by the chemical reactions in equations 7 and 8 below. This method is usually employed in commercial manufacturing of carbonates.

$$CaSiO_{3(s)} + 2\,CH_3COOH_{(aq)} \rightarrow Ca^{2+}{}_{(aq)} + 2\,CH_3COO^-{}_{(aq)} + SiO_{2(s)} + H_2O_{(aq)} \quad (7)$$

$$Ca^{2+}{}_{(aq)} + 2\,CH_3COO^-{}_{(aq)} + CO_{2\,(g)} + H_2O_{(aq)} \rightarrow CaCO_{3\,(s)} + 2\,CH_3COOH_{(aq)} \quad (8)$$

The mechanism of carbonation in steel slag can vary based on the composition of steel slag. A detailed explanation on each of the carbonation approaches is presented by Pan et al. (2016) and Olajire (2013). In this study, the concept that is of relevance is the direct carbonation of steel slag to realize CO_2 sequestration by forming stable and insoluble carbonates. The various advantages/benefits of carbonation of steel slag and its application in civil and environmental engineering is discussed briefly in the following section.

4. BENEFICIAL USES AND APPLICATIONS OF STEEL SLAG

BOF steel slag has been predominantly used as a construction material in asphalt paving, unpaved roads, agricultural lime, acid mine drainage remediation, manufacture of cement all of which can be ascribed towards its enhanced mechanical and pozzolanic properties resulting from carbonation. In addition to its use as a construction material, several researchers assessed the use of steel slag for environmental remediation applications, especially phosphorous removal (e.g., Drizo et al., 2006). BOF steel slag has been used as base and subbase layers in pavements in addition to its use as coarse aggregates in surface layers of pavements, mainly due to its high strength, high binding capacity with

high abrasion and high frictional resistance. Due to their high density, strength, rough texture and durability, they can be processed as high-quality aggregates, comparable with natural aggregates.

Relevant to this study is the work of Herrmann et al. (2010), who investigated the potential use of EAF slag and Ladle slag (LS) as a barrier material in landfill cover. Surprisingly, these slags possessed very low hydraulic conductivity. Field investigation using ten lysimeters confirmed that the leachate collected at the base of the cover is well below the regulatory criterion and can potentially be used as a barrier material in landfill covers.

Diener et al. (2010) studied the stability of steel slag (mixture of EAF and LS) by performing long term laboratory tests to understand the leaching behavior, acid neutralization capacity and mineralogy of steel slag using multivariate data analysis. The researchers investigated the effect of CO_2 content in the atmosphere, relative humidity, aging time, temperature and water quality on the accelerated aging in steel slag. It was observed that the aging time and the CO_2 content in the atmosphere were the prime factors that had a significant effect on long term stability of steel slag. Mineralogical changes during the aging process showed the formation of calcite which was confirmed using XRD. A review on several other applications of steel slag can be found in Pan et al. (2016), Olajire (2013) and Yi et al. (2012).

In all of the literature on applications of steel slag, it has been used as a construction material or as a hydraulic barrier material in the final cover in landfills. However, to date, there has been no study on the use of steel slag for the sequestration of CO_2 emissions from the MSW landfills. This study proposes to utilize the carbonation and other mechanisms associated with CO_2 sequestration in steel slag and thereby mitigate the CO_2 emissions released into the atmosphere from the landfills. A new concept of "Zero Emissions Cover System" is proposed as detailed in the following section.

5. BIOGEOCHEMICAL SOIL COVER SYSTEM

There are several studies in the literature that have looked at the potential use of steel slag in carbon sequestration using the carbonation process. However, there has been no investigation on the use of steel slag as a cover soil amendment in landfills to sequester CO_2 emissions. A new research project funded by the U.S. National Science Foundation is currently in progress to fully explore the fundamentals and practical aspects of an innovative, low-cost landfill cover system consisting of steel slag in combination with biochar which can mitigate the CH_4 and CO_2 emissions from MSW landfills. In a previous investigation at UIC, biochar-amended soil cover was conceived and developed as an effective sustainable biocover for CH_4 oxidation. A systematic and comprehensive study was performed involving material characterization, batch tests, and lab-scale column experiments to investigate the adsorption and transport mechanisms associated with biochar amended cover soil systems. Microbial characterization was also performed to identify the specific methanotrophs that were involved in CH_4 oxidation. A full-scale field demonstration was also implemented to evaluate the performance of biochar-amended soil cover at a landfill exposed to variable environmental conditions. This research work advanced the knowledge on the fundamental processes and system variables responsible for enhancing the methanotrophic activity by providing a favorable environment for the methanotrophs to proliferate and thrive in the cover system. Unfortunately, such a biocover system can only microbially oxidize CH_4 into CO_2, leading to continued emission of CO_2 into the atmosphere.

It is essential to develop a cover system that can minimize both the CH_4 and CO_2 emissions into the atmosphere. It is hypothesized herein that biochar and steel slag amended soil cover systems can eliminate both CH_4 and CO_2 emissions via biochar-aided methanotrophic oxidation of CH_4 into CO_2 and subsequent or simultaneous slag-aided carbonation/sequestration of all of CO_2, thus ideally eliminating the LFG emissions from the landfills. This concept of "Zero Emissions Cover" is a transformative approach to substantially mitigate, if not eliminate, the carbon footprint associated with LFG emissions. The concept of biochar and steel slag amended soil cover system to achieve zero emissions is shown schematically in Fig.2. As shown in Fig.2, the proposed biogeochemical

cover system also has the potential to mitigate hydrogen sulfide (H_2S) if present in the landfill gas, due to co-disposal of construction and demolition (C&D) waste with MSW.

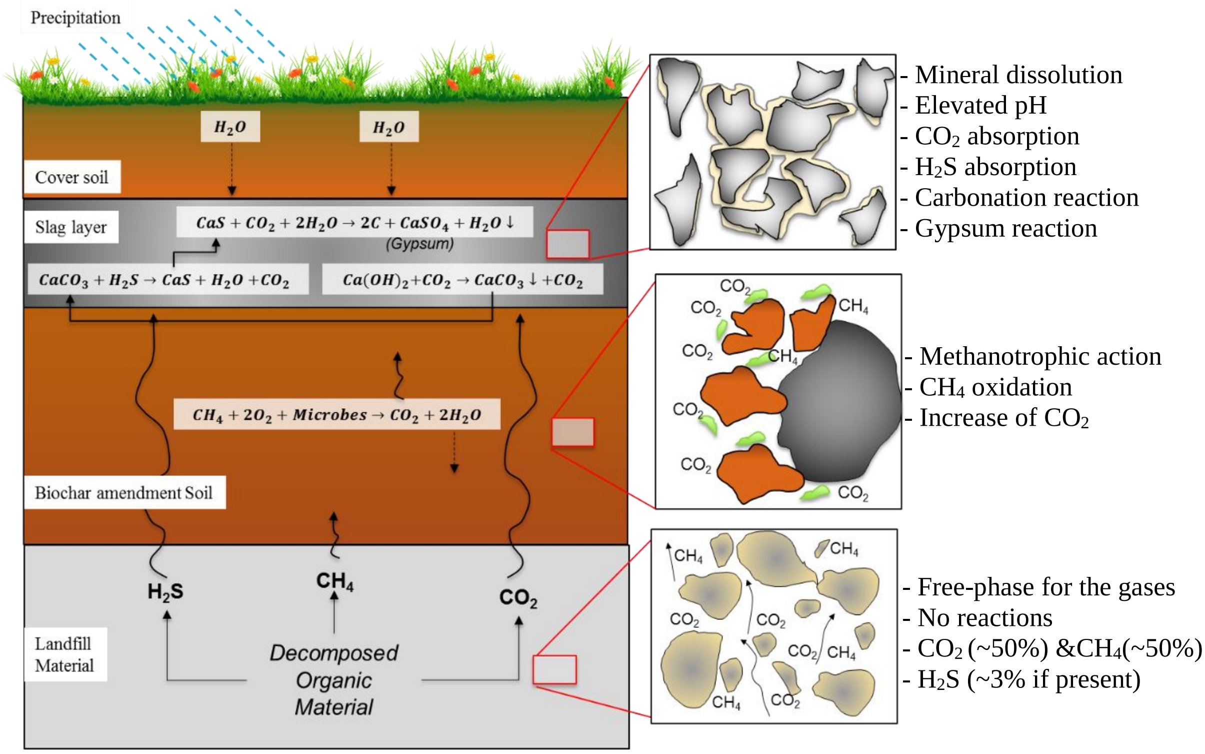


Figure 2: Concept of Biochar Steel Slag amended Soil Cover System for Zero Emissions

The combination of steel slag and biochar with their inherently distinct properties has several characteristics that are highly desirable in a landfill cover system. These include: (a) preferential adsorption of CH_4 by biochar thereby increasing its bioavailability for oxidation; (b) strong alkaline buffering capacity of steel slag which results in CO_2 absorption, and (c) increased physical stability, strength and compressibility characteristics due to the pozzolanic nature and angularity of steel slag. In addition, biochar and steel slag fines are very inexpensive, sustainable and practical to employ in field. Although there are numerous benefits identified with the use of these materials, it is of utmost importance to delineate the complex fundamental coupled biogeochemical processes that dictate the transport, adsorption, microbial oxidation, and carbonation of LFG. Moreover, it is important to assess the influence of various factors – including moisture, pH, LFG composition, loading rates, flow rates, particle size, steel slag and biochar source and composition, and several others – on the fundamental processes that occur in the proposed “zero emissions” cover system.

6. PRELIMINARY INVESTIGATION

In order to evaluate the potential for carbonation in steel slag, a preliminary experimental study was conducted at UIC to examine the ability of steel slag to sequester CO_2 at normal atmospheric conditions. A BOF steel slag sample was obtained from the Indiana Harbor East (IHE) steel plant, the cover soil from Zion Landfill, IL, and the biochar produced from gasification of wood pellets (which was used in a previous biochar study at UIC). The soil, biochar and steel slag were first characterized for their physical and geotechnical properties following relevant ASTM standards and the results are shown in Table 1.

A series of batch tests were conducted using these samples individually as well as in combinations of these materials in different proportions. The combinations of materials tested were: soil and biochar (S/BC); soil and slag (S/SL); slag and biochar (SL/BC); soil, biochar and 10% of slag by weight (S/BC/SL 10%); soil, biochar and 5% of slag by weight (S/BC/SL 5%); and soil, biochar and 2% of slag by weight (S/BC/SL 2%). The biochar content was 10% by weight in all of these combinations.

The samples were prepared in glass 125 ml vials at the same moisture content of 10% by weight and analyzed at room temperature. All the samples were tested in triplicate to ensure repeatability. The samples were injected with 12 ml of synthetic landfill gas mixture (50% CH_4 – 50% CO_2) and analyzed using a Gas Chromatograph (SRI 9300B) immediately after the injection of gas into the vial (Time 0) and after 24 hours from the injection (Time 24) according to the headspace sampling methodology. The preliminary investigation based on these batch tests showed complete depletion of CO_2 in all steel slag containing samples after 24 hours. Fig. 3 summarizes the results obtained the preliminary batch tests.

Table 1: Properties of Cover Soil, Biochar and Slag

Properties	Cover Soil	Biochar	Steel Slag
Organic Content (%)	3.10	63.7	0
Organic Carbon Content (%)	0.52	32.0	0
pH	5.3	8.7	12.3
Specific Gravity	2.65	0.81	3.04
Atterberg Limits:			
Liquid Limit (%)	31	Non-Plastic	Non-Plastic
Plastic Limit (%)	19		
Plasticity Index (%)	12		
Grain Size Distribution:			
Gravel (%)	0.0	67.8	15.78
Sand (%)	8.35	31.4	76.42
Fines (%)	91.6	0.0	7.8
Hydraulic Conductivity (cm/s)	$4.3x10^{-9}$	$1.2x10^{-2}$	$3.9x10^{-4}$

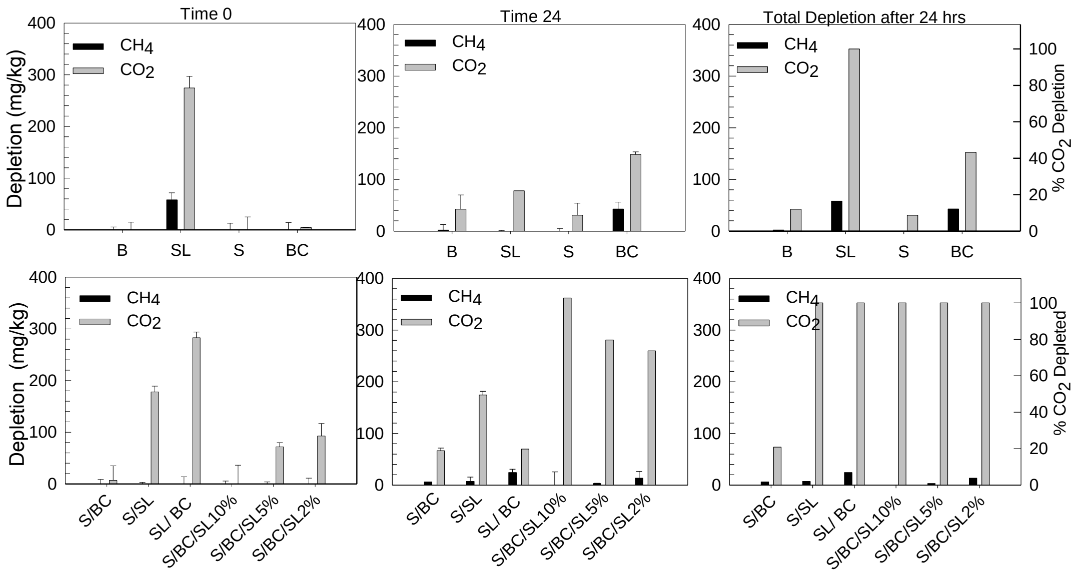


Figure 3: CO_2 and CH_4 Uptake in Samples with Soil (S), Biochar (BC) and Slag (SL) (B-Blank, S-Soil, BC-Biochar, SL-Steel Slag)

These preliminary results (SL/series results) clearly demonstrate that the CO_2 sequestration by slag can be rapid and substantial under normal landfill conditions. In addition, the CH_4 depletion in samples containing biochar and slag was observed (SL/BC data), indicating the removal of CH_4. However, the relative contributions of microbial oxidation or adsorption have not been established.

Therefore, there is still a need for extensive analysis of the carbonation potential of steel slag under various conditions including moisture, temperature, CO_2 loading, and particle size. It is also essential to investigate the effects of highly alkaline pH on the growth and activity of methanotrophs in cover soil and biochar. Some methanotrophs are found to be sensitive to pH, while others such as extremophile methanotrophs are shown to be resilient to high pH conditions (Trotsenko and Khmelenina, 2002; Saari et al., 2004; Roadcap et al., 2006). In addition, the individual mechanisms, reaction kinetics and interdependency of the microbial oxidation and carbonation must be quantified. All of these aspects are being investigated in our ongoing study.

7. ONGOING RESEARCH

It is anticipated that this innovative, low-cost, feasible and sustainable cover system will help in realizing the overarching goal of eliminating the LFG emissions from landfill into the atmosphere. In order to achieve this goal sequentially or simultaneously, it is essential to investigate the fundamental coupled biogeochemical processes involved in CO_2 sequestration by BOF steel slag and biochar/steel slag amended soils and optimize the cover system to achieve maximum CH_4 oxidation in biochar and at the same time maximize the CO_2 sequestration in steel slag. Fundamental questions that need to be addressed include: interactive geochemical changes due to the presence of slag and biochar together; survival and growth of methanotrophs; carbonation mechanisms and moisture and porewater composition impacts; clogging of pores and long-term permeability of the materials, among others.

In the ongoing research, we are focused on quantifying the physical, chemical and geotechnical characteristics of different types of slag including their leachability and surface characteristics. Thereafter, a detailed experimental investigation involving bench-scale testing and column experiments will be performed to identify the extent of carbonation in steel slag under varying environmental conditions including moisture, LFG composition, particle size, slag types among others. One of the important aspects of the conceptualized biochar-slag amended cover system is to determine the synergistic effects of having both biochar and steel slag in the cover system. It is essential to determine the extent of carbonation, microbial oxidation and the microbial activity in the cover system. Furthermore, long term column tests using large columns simulating typical landfill cover systems will be carried out to assess the simultaneous interactions of transport, adsorption, oxidation and carbonation for various simulated biochar, soil and steel slag cover systems under the influence of transient and dynamic changes in gas flow and environmental conditions. Microbial analysis of the selected tested samples will be to ensure there is adequate biological activity in the cover system for microbial oxidation of methane. Additional analysis involving the quantification of the extent of carbonation and the mineralogy of the carbonated samples will be performed using appropriate methods (SEM and XRD). Finally, based on the observations from the large-scale column experiments, few selected profiles will be tested for their performance at a landfill under realistic gas production and environmental conditions.

Acknowledgements
This project is funded by the U.S. National Science Foundation (CMMI # 1724773), which is gratefully acknowledged.

References

1. Herrmann, I., Andreas, L., Diener, S., and Lind, L. (2010). 'Steel slag used in landfill cover liners: laboratory and field tests'. **Waste Management & Research**, Vol. 28(12), 1114-1121
2. Hilger, H. A., Cranford, D. F., and Barlaz, M. A. (2000). 'Methane oxidation and microbial exopolymer production in landfill cover soil.' **Soil Biology and Biochemistry**, Vol. 32(4), 457-467.
3. Huijgen, W. J., Witkamp, G. J., and Comans, R. N. (2005). 'Mineral CO2 sequestration by steel slag carbonation'. **Environmental Science & Technology**, Vol. 39(24), 9676-9682.

4. Huijgen, W. J., and Comans, R. N. (2006). 'Carbonation of steel slag for CO2 sequestration: leaching of products and reaction mechanisms'. **Environmental Science & Technology**, Vol. 40(8), 2790-2796

5. National Slag Association (NSA). (2013). http://www.nationalslag.org/steel-furnace-slag

6. Olajire, A. A. (2013). 'A review of mineral carbonation technology in sequestration of CO_2.' **Journal of Petroleum Science and Engineering**, Vol. 109, 364-392

7. Pan, S. Y., Adhikari, R., Chen, Y. H., Li, P., and Chiang, P. C. (2016). 'Integrated and innovative steel slag utilization for iron reclamation, green material production and CO_2 fixation via accelerated carbonation'. **Journal of Cleaner Production**, Vol. 137, 617-631

8. Reddy, K.R., Yargicoglu, E.N., Yue, D., and Yaghoubi, P. (2014). 'Enhanced microbial methane oxidation in landfill cover soil amended with biochar.' **Journal of Geotechnical and Geoenvironmental Engineering**, ASCE, Vol. 140(9), 04014047

9. Roadcap, G. S., Sanford, R. A., Jin, Q., Pardinas, J. R., and Bethke, C. M. (2006). 'Extremely alkaline (pH> 12) ground water hosts diverse microbial community.' **Groundwater**, Vol. 44(4), 511-517.

10. Saari, A., Rinnan, R., and Martikainen, P. J. (2004). 'Methane oxidation in boreal forest soils: kinetics and sensitivity to pH and ammonium'. **Soil Biology and Biochemistry**, Vol. 36(7), 1037-1046

11. Shi, C. (2004). 'Steel slag—its production, processing, characteristics, and cementitious properties.' **Journal of Materials in Civil Engineering**, Vol. 16(3), 230-236.

12. Trotsenko, Y. A., and Khmelenina, V. N. (2002). 'Biology of extremophilic and extremotolerant methanotrophs'. **Archives of Microbiology**, Vol. 177(2), 123-131

13. Whalen, S. C., Reeburgh, W. S., and Sandbeck, K. A. (1990). 'Rapid methane oxidation in a landfill cover soil.' **Applied and Environmental Microbiology**, Vol. 56(11), 3405-3411.

14. Yargicoglu, E., Sadasivam, B.Y., Reddy, K.R. and Spokas, K. (2015). 'Physical and chemical characterization of waste wood derived biochars.' **Waste Management**, Vol. 36(2), 256-268

15. Yargicoglu, E.Y., and Reddy, K.R. (2017a). 'Microbial abundance and activity in biochar-amended landfill cover soils: Evidences from large-scale column and field experiments' **Journal of Environmental Engineering**, Vol. 143(9), 04017058

16. Yargicoglu, E.Y., and Reddy, K.R. (2017b). 'Effects of biochar and wood pellets amendments added to landfill cover soil on microbial methane oxidation: A laboratory column study' **Journal of Environmental Management**, Vol. 193, 19-31

17. Yargicoglu, E.Y., and Reddy, K.R. (2018) 'Biochar-amended soil cover for microbial methane oxidation: Effect of biochar amendment ratio and cover profile.' **Journal of Geotechnical and Geoenvironmental Engineering**, ASCE, Vol. 144(3): 04017123

18. Yi, H., Xu, G., Cheng, H., Wang, J., Wan, Y., and Chen, H. (2012). 'An overview of utilization of steel slag'. **Procedia Environmental Sciences**, Vol. 16, 791-801

19. Yildirim, I. Z., and Prezzi, M. (2011). 'Chemical, mineralogical, and morphological properties of steel slag.' **Advances in Civil Engineering**, Article ID 463638, 13 p.

20. USEPA (2016). '**Advancing Sustainable Materials Management**', 2014 Fact Sheet

21. World Steel Association (2017). '**World Steel in Figures 2017**', Retrieved from https://www.worldsteel.org/en/dam/jcr:0474d208-9108-4927-ace8-4ac5445c5df8/World+Steel+in+Figures+2017.pdf (Accessed on January 18, 2018)

CO_2 SEQUESTRATION USING BOF SLAG: APPLICATION IN LANDFILL COVER

K. R. Reddy[1,*], G. Kumar[1], A. Gopakumar[1], R.K. Rai[1] and D.G. Grubb[2]

[1]University of Illinois at Chicago, Department of Civil & Materials Engineering, 842 West Taylor Street, Chicago, IL 60607, USA [2]Phoenix Services, LLC, 148 West State Street, Suite 301, Kennett Square, PA 19348, USA

[*]Corresponding author: e-mail: kreddy@uic.edu, tel : +13129964755

Abstract

Fugitive methane (CH_4) and carbon dioxide (CO_2) emissions at municipal solid waste (MSW) landfills constitute one of the major anthropogenic sources of greenhouse gas (GHG) emissions to the atmosphere. In recent years, biocovers involving the addition of organic-rich amendments to landfill cover soils is proposed to promote microbial oxidation of CH_4 to CO_2. However, most of the organic amendments used have limitations. Biochar, a solid byproduct obtained from gasification of biomass under anoxic or low oxygen conditions, has characteristics that are favorable for enhanced microbial oxidation in landfill covers. Recent investigations have shown the significant potential of biochar-amended cover soils in mitigating the CH_4 emissions from MSW landfills. Although the CH_4 emissions are mitigated, there is still considerable amount of CO_2 that is emitted to the atmosphere as a result of microbial oxidation of CH_4 in landfill covers as well as the CO_2 derived from MSW decomposition. Basic oxygen furnace (BOF) slag is a product of steel making has great potential for CO_2 sequestration due to its strong alkaline buffering and high carbonation capacity. In an ongoing project, funded by the U.S. National Science Foundation, the potential use of BOF slag in landfill covers along with biochar-amended soils to mitigate both CH_4 and CO_2 emissions is being investigated. This paper presents the initial results from this study and it includes detailed physical and chemical and leachability characteristics of BOF slag, and a series of batch tests conducted on BOF slag to determine its CH_4 and CO_2 uptake capacity. The effect of moisture content on the carbonation capacity of BOF slag was also evaluated by conducting batch tests at different moisture contents. In addition, small column experiments were conducted to evaluate the gas migration, transport parameters and the CO_2 sequestration potential of BOF slag under simulated landfill gas conditions. The result from the batch and column tests show a significant uptake of CO_2 by BOF slag for the tested conditions and demonstrates excellent potential for its use in a landfill cover system.

Keywords: CO_2 sequestration; BOF slag; biochar; carbonation; MSW landfills; landfill cover; landfill gas

1. INTRODUCTION

Global climate change and the rapidly increasing global population are currently some of the major concerns of the modern world. This has led to depletion of natural resources and increased generation of waste. In the U.S., landfills are the most dominant method of managing MSW. The MSW in landfills undergoes anaerobic decomposition to generate landfill gas that predominantly consists of methane (CH_4) and carbon dioxide (CO_2). The landfill gas (LFG) emissions are estimated to be one of the largest sources of greenhouse gas emissions into the atmosphere.

According to Resource Conservation and Recovery Act (RCRA) Subtitle D regulations, all new landfills are required to have active gas extraction systems to collect the LFG and prevent it from

releasing into the atmosphere. In addition, a final cover with specific design requirements is made essential to minimize the infiltration into the waste as well as limit the escape of landfill gas into the atmosphere. However, the gas collection systems do not perform with 100 percent efficiency due to the limited radius of influence of each extraction well. Thus, there are always some fugitive emissions that cannot be targeted by the gas extraction systems. While serving the intended purpose, landfill covers also aid in reducing the fugitive emissions of LFG into the atmosphere to a certain extent by microbial oxidation of CH_4 to CO_2 in the presence of methanotrophs that naturally exist in the soil cover. But, the proliferation of these methanotrophs is limited and is not very effective in oxidizing large amounts of CH_4 emissions from the landfills.

In this regard, alternative covers called biocovers, involving the addition of organic amendments to the soil have gained great attention in the recent past. The addition of organic rich matter such as compost, digested sludge, biosolids, and peat moss enhances the microbial activity by providing the nutrients and microbial inoculums to the soil. But, the use of these materials has some limitations. For example, compost, dewatered sludge and biosolids like materials may themselves undergo anaerobic degradation adding to the already existing CH_4 and CO_2 emissions rather than reducing these emissions. Biochar is a promising material as an organic amendment in soil cover because of its unique characteristics (Reddy et al., 2014). Biochar is a solid byproduct derived from gasification or pyrolysis under low oxygen conditions. Biochar exhibits high internal porosity and high specific surface area which provides favorable conditions for microbial colonization and proliferation (Yargicoglu et al., 2015). In addition, it consists of stable organic carbon and doesn't undergo any degradation. Recently, an extensive investigation involving lab-scale testing and field demonstration of the efficacy of biochar-amended soil cover system was performed (Sadasivam and Reddy, 2015; Yargicoglu and Reddy, 2017a, b, 2018). These studies confirmed the use of biochar as a potential organic amendment to mitigate CH_4 emissions from landfills quite successfully. However, one of the major limitations of the biochar amended soil cover system is that it does not address the fate of CO_2 which continues to be emitted into the atmosphere in undesirable amounts. In order to alleviate the problems from GHG emissions it is desirable to mitigate the CO_2 emissions as well.

The current study focuses on an innovative concept to mitigate both CH_4 and CO_2 emissions from MSW landfills by leveraging BOF slag. BOF slag is a product of the steel making process and it is known to possess unique characteristics suitable for CO_2 sequestration. Several different types of steel slag are obtained based on the steel type and steel making process (Shi, 2004). Currently, the coarser (larger aggregate sized) BOF slag material is utilized in asphalt paving due to its strong rutting resistance and durability, while the BOF slag fines are still largely stockpiled at steel plants. The BOF slag which has high alkaline buffering capacity can react with CO_2 in the presence of moisture to sequester CO_2 in the form of stable and insoluble carbonates. This process is generally known as the carbonation process.

In this study, a series of batch experiments were performed to estimate the carbonation capacity of a BOF slag. In addition, the effect of varying moisture contents on the carbonation capacity of the BOF slag was also studied. Furthermore, small column experiments were performed to evaluate the carbonation capacity of BOF slag under a continuous supply of simulated LFG emission conditions. The rate of carbonation and the breakthrough time are estimated based on the column experiments. The results show a substantial carbonation capacity of BOF slag and favor its use as a potential amendment in landfill cover system to mitigate CO_2 emissions.

2. MATERIALS AND METHODS

2.1 Steel Slag Characterization

Basic Oxygen Furnace (BOF) slag is produced when molten iron from blast furnace mixes with the fluxing agents (calcium oxide and dolomite) in the presence of 10-20% scrap steel melt and 99% pure oxygen blown at supersonic speed (National Slag Association 2013). According to U.S. Geological Survey, every year almost 15-20 million tons of ferrous slag and about 10-15 million tons of steel

slag is produced. The BOF slag was collected from the Phoenix Services LLC facility at the Indiana Harbor East Steel Mill. BOF slag contains minerals that contain divalent cations of calcium, magnesium and iron that carbonate with time in the open environment. The mineral carbonation reaction of metal oxides (MO) can be simplified as:

$$MO + CO_2 \rightarrow MCO_3 + Heat$$

The mineral carbonation also results in the production of thermodynamically more stable products (carbonates). The natural mineral carbonation process could be accelerated and technologically viable in the presence of moisture and abundant availability of the minerals such as in BOF slag. The calcium silicates (and other silicates and aluminates) in the presence of moisture contributes to CO_2 sequestration (Huijgen et al., 2005) by the following chemical reactions.

$$CO_{2(g)} + H_2O_{(l)} \rightarrow 2H^+{}_{(aq)} + CO_3^{2-}{}_{(aq)}$$

$$CaSiO_{3(s)} + 2H^+{}_{(aq)} \rightarrow Ca^{2+}{}_{(aq)} + SiO_{2(s)} + H_2O_{(l)}$$

$$Ca^{2+}{}_{(aq)} + CO_3^{2-}{}_{(aq)} \rightarrow CaCO_{3(s)} \downarrow$$

In order to put BOF slag for beneficial use efficiently in a landfill cover system, it is necessary to understand its chemical, physical and geotechnical properties. Hence, a detailed characterization of the BOF slag was performed.

The elemental and mineralogical composition of the BOF slag was evaluated by XRF and quantitative XRD analysis (Grubb, 2017). In order to evaluate the potential toxicity of the use of BOF slag from leaching of toxic metals, both Toxicity Characteristic Leaching Procedure (TCLP) and Synthetic Precipitation Leaching Procedure (SPLP) leaching tests were conducted as per the laboratory procedures established by United States Environmental Protection Agency (USEPA) under SW-846 (Grubb, 2017). **Table 1** provides the mineralogy of BOF slag used in this study. The TCLP and SPLP leaching test results of BOF slag are summarized in **Table 2**. Further, the basic chemical characteristics of the BOF slag were determined by measurement of pH, redox potential and electrical conductivity. The BOF slag used consisted majorly of oxides of calcium and iron. The leaching test results as shown in **Table 2** shows that the constituents leached from the material are within the regulatory limits.

The results indicated that the BOF slag was highly alkaline with pH in the range of 11.7-12.1. This is due to the presence of basic oxides like CaO, MgO and FeO in BOF slag. The specific gravity of the BOF slag was found to be 3.04 which is within the reported range of 3.0-3.46 in literature (Malasavage et al. (2012). The samples were analyzed for their particle size distribution (ASTM D422) and classified as poorly-graded sand. The hydraulic conductivity of the material was tested as per ASTM D2434 with a rigid wall permeameter. The hydraulic conductivity was evaluated to be in the order of 10^{-4} cm/s. The sample was also tested for its moisture retention capacity using the procedure described in Kinney et al. (2012). The physical, chemical and geotechnical properties of the BOF slag are shown in **Table 3**.

Table 1: Typical Mineral Composition of BOF Slag

Mineral	Mineral Formula	Percent Weight
Larnite	Ca_2SiO_4	20.6
Srebrodolskite	$Ca_2Fe_2O_5$	10.4
Iron Magnesium Oxide	FeO.76MgO.24O	6.7
Brownmillerite	$Ca_4Al_2Fe_2O_{10}$	5.8
Wuestite	FeO	5.4
Lime	CaO	4.1
Portlandite	$Ca(OH)_2$	6.5
Periclase	MgO	3.1
Magnetite	Fe_3O_4	3.0
Mayenite	$Ca_{12}Al_{14}O_{33}$	2.7
Quartz	SiO_2	0.5
Iron	Fe	0.3
Amorphous Material		31.1
Total		100.0

Table 2: Results from TCLP and SPLP Leaching Tests

Constituent	Symbol	RCRA Allowable Limit (mg/L)	TCLP Result (mg/L)	SPLP Result (mg/L)
Aluminum	Al		0.62	0.16
Antimony	Sb		<0.00031	<0.00016
Arsenic	As	5	0.00087	0.00029
Barium	Ba	100	0.14	0.12
Beryllium	Be		<0.00025	<0.00013
Boron	B		0.12	0.027
Cadmium	Cd	1	<0.00028	<0.00015
Calcium	Ca		2300	800
Chromium	Cr	5	0.011	0.002
Cobalt	Co		0.0034	0.0013
Copper	Cu		<0.005	<0.0025
Iron	Fe		0.031	0.011
Lead	Pb	5	<0.00041	<0.00020
Magnesium	Mg		0.077	<0.050
Manganese	Mn		0.005	0.00072
Mercury	Hg	0.2	<0.00005	<0.00005
Nickel	Ni		0.036	0.013
Potassium	K		0.76	0.66
Selenium	Se	1	0.0047	0.0019
Silver	Ag	5	<0.00025	<0.00013
Sodium	Na		6.4	4.8
Thallium	Tl		<0.00025	<0.00013
Vanadium	V		0.0058	0.00078
Zinc	Zn		0.035	0.024

Table 3: Physical, Chemical and Geotechnical Properties of Soil, BOF Slag and Biochar

Properties	Method	Soil	BOF Slag	Biochar
Physical				
Color	Visual	Brown, Brownish-grey, Grey	Grey	Black
Odor	Visual	Trace odor	Odorless	Odorless
Chemical				
Redox Potential (mV)	ASTM D4972-01	-37.7	-317.9	-6.3
Conductivity (μS/cm)	ASTM D4972-01	0.5	0.2	0.8
pH	ASTM D4972-01	7.04	11.7	6.5
Geotechnical				
Water Holding Capacity (w/w)	Kinney et.al. (2012)	45.93	40.54	51.55
Organic Content (%)	ASTM D2974-14	4.47	NA	96.71
Specific Gravity	ASTM D854-14	2.65	3.04	0.65
Atterberg Limits: Liquid Limit (%) Plastic Limit (%) Plasticity Index (%)	ASTM D4318-10	35.0 20.34 14.66	Non-Plastic	Non-Plastic
Grain Size Distribution: Gravel (%) Sand (%) Fines (%)	ASTM D422-63	12 7 81	0 90.5 9.5	45 54 1
Classification		CL	SP type	SP Type
Hydraulic Conductivity (cm/s)	ASTM D2434-68	2.75×10^{-8} @ 2.11 g/cc	4.2×10^{-4} @ 1.32 g/cc	2×10^{-4} @ 1.15 g/cc

2.2 Batch Tests

The BOF slag was evaluated for its CO_2 sequestration capacity by conducting a series of batch experiments. The batch tests were conducted to evaluate the effect of moisture conditions as moisture is an essential component in the carbonation process. In addition, these experiments were aimed at determining if there is any optimum moisture content for maximum amount of carbonation to occur in BOF slag. Since, the landfill covers predominantly remain under unsaturated conditions most of its lifetime, the water content range is selected such that lower limit is zero and the higher limit is the water holding capacity of the material. Also, all the tests were conducted under atmospheric temperature and pressure.

The BOF slag sample was dried at 100-110°C for 24 hours before it was used to conduct batch tests. The batch tests were conducted at 0%, 10%, 20%, 30% and 40% moisture content. To obtain the

required water content, 1 g of the dried sample was mixed with 0g, 0.1g, 0.2g, 0.3g and 0.4g of distilled water separately and transferred to five separate 125 ml glass vials. Each vial was then purged completely with a synthetic landfill gas mix containing 50% CH_4 and 50% CO_2 by volume and closed with rubber septa and secured tightly with a metal crimp cap. For each of the water contents evaluated, the tests were conducted in triplicates. The samples were shaken vigorously before sampling the gas from their headspace. Gas samples were taken and analyzed using a gas chromatograph (SRI 9300 GC) equipped with a thermal conductivity detector (TCD) and CTR-1 column capable of separating N_2 and O_2 for simultaneous analysis of CO_2, CH_4, O_2 and N_2. Each 1ml of gas sample withdrawn from the vial was then reduced to 0.5ml sample volume before injection into the GC. This ensured the sample volume was within the acceptable limit for the GC and in equilibrium with the atmospheric pressure. A 3-point calibration curve was constructed for the GC using standard gas mixtures of 5%, 25%, and 50% methane.

2.3 Column Experiments

After the batch tests, long term column experiments were conducted to study the cumulative carbonation (CO_2 uptake) capacity of the BOF slag with continuous flow of the synthetic landfill gas (50% CH_4 and 50% CO_2) through the BOF slag packed in a small glass column with inlet and outlet ports. A schematic of the column experimental setup is shown in **Figure 2**.

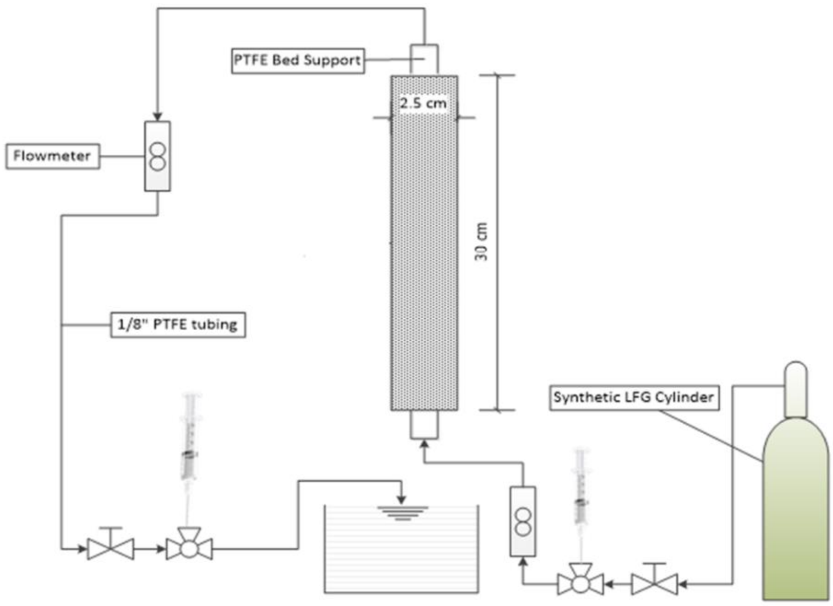


Figure 2: Schematic of Column Experimental Test Setup

An acrylic glass column of 30 cm height and 2.5 cm inner diameter was used. The column was filled with the BOF slag at 10% moisture up to its full length in two layers of 15 cm each with light tamping. It was secured with bed support mesh screen, end connections and screw caps at both ends. PTFE tubing was used to connect all components in the setup. Flow meters were installed at both ends of the column to control the influent gas flow rates and monitor the effluent flow rates. Gas samples were collected from both influent and effluent sampling ports at different time intervals until the breakthrough condition (where the inlet and outlet concentration of the gas becomes equal) was established.

3. RESULTS AND DISCUSSION

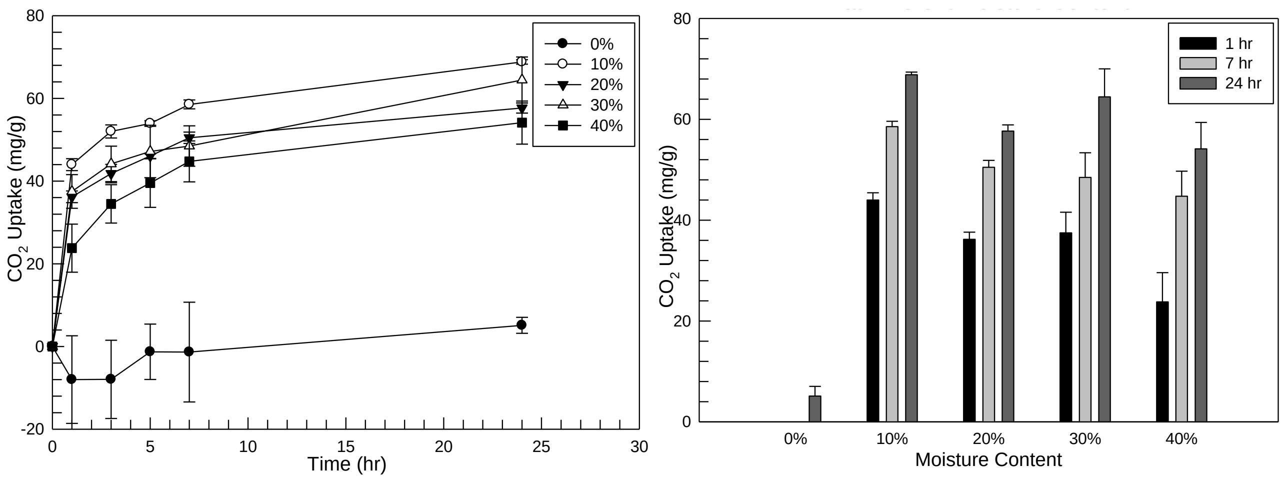
3.1 Composition and Properties of BOF Slag

The chemical, physical and geotechnical properties of the BOF slag are favorable for its use in a landfill cover. The hydraulic conductivity of the BOF slag is in the order of 10^{-4} cm/s which is

comparable with the hydraulic conductivity of biochar (10^{-4} cm/s). Due to the high hydraulic conductivity, the BOF slag and the biochar materials tested may not qualify as a barrier material. However, these materials could be used as individual thin layers in the cover soil or mixed with the cover soil for use in the landfill cover system. One of the characteristics that is unique to BOF slag is its high pH. The results from TCLP and SPLP confirmed that BOF slag is not a material of concern from the environmental risk standpoint as the results were found to be well within the regulatory limits (**Table 1)**. Hence, the BOF slag is not hazardous and can be used as a cover material in landfills. The water holding capacity of BOF slag (40%) was comparable to that of the typical cover soil material (46%) indicating that the impacts of evaporative losses from landfill cover soils (such as desiccation cracking) could be minimum. BOF slag will not cause an additional odor since it does not contain any biodegradable material or sulfur and is characteristically odorless. Malasavage et al. (2012) conducted isotropically consolidated undrained triaxial shear tests on steel slag fines and reported a friction angle of 45.7° and cohesion of 48 kPa, while studying its geotechnical performance as synthetic fill materials. These high shear strength parameters of steel slag can as well enhance slope stability of a landfill cover. Additionally, the high specific gravity of BOF slag could also act as a factor that enhances the slope stability and reduces loss of material due to erosion.

3.2 Effect of Moisture Content on Carbonation of BOF Slag

Most of the previous studies that discuss the use of BOF slag for CO_2 sequestration focus on its industrial applications and involves carbonation of BOF slag under slurry conditions. This condition rarely exists in a landfill cover. The batch tests conducted at low moisture contents below saturation levels showed that substantial carbonation does takes place at moisture levels below saturation water content (**Figure 3**).



(a) **(b)**

Figure 3: Carbon Dioxide uptake by BOF Slag for Different Initial Moisture Contents

The results from the batch tests showed carbonation in the range of 53-68 mg of CO_2 per gram of BOF slag in 24 hours, with the maximum uptake of 68 mg/g. **Figure 3a** shows that the amount of CO_2 sequestered increased with time. However, the CO_2 uptake curve shows two distinct regions with different slopes indicating an initial rapid carbonation for a short period of time. The initial rapid carbonation could be due to the readily available free-lime and portlandite ($Ca(OH)_2$) in fine particles. The region of slow rate of carbonation for the rest of the time period could be from the lime diffusing out of larger particles. It could also be attributed to the limited access of CO_2 to the minerals due to the formation of carbonate precipitates over the mineral surface. A negligible amount of carbonation was observed in the absence of water as shown in **Figure 3b.** In addition, it was observed that there was no specific trend in the CO_2 sequestration with the moisture content and the CO_2 uptake was rather high and similar for all the moisture contents tested. This indicates that even moisture content

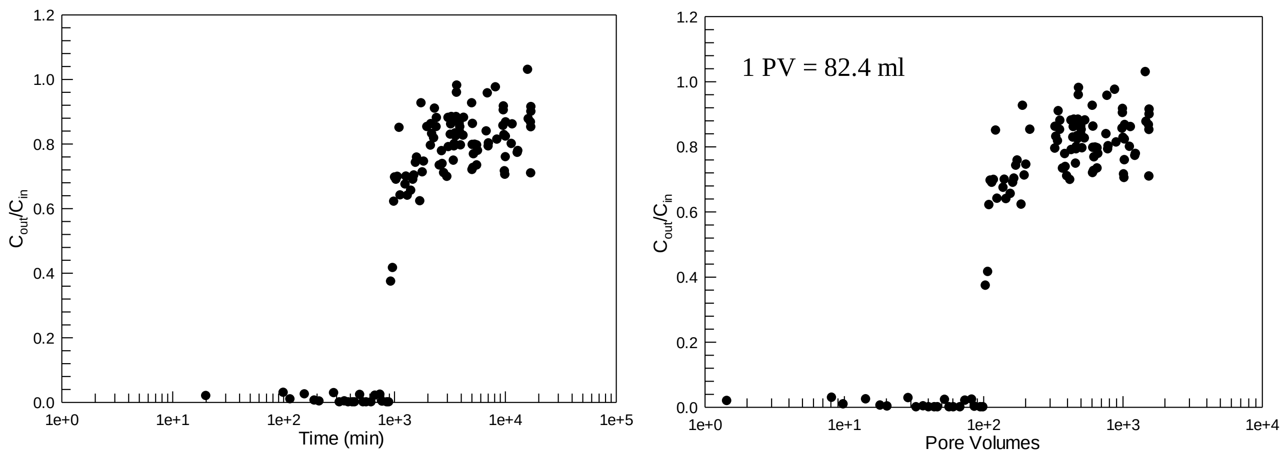
as low as 10% could lead to substantial carbonation and is not significantly affected by the amount of moisture available in the system.

3.3 Gas Transport and CO_2 Uptake Capacity of BOF Slag

The breakthrough curve for CO_2 uptake with respect to time and pore volume of simulated LFG is shown in **Figure 4**. The breakthrough was obtained between 800-1,500 min and $C_{out} \geq C_{in}$ was achieved after 18,000 min. The cumulative uptake of CO_2 in the column test after 24 hours was in the same range as that of the 24 hour uptake in batch tests (see **Figure 5)**. The breakthrough curve was also plotted with respect to pore volume of gas for better understanding of CO_2 uptake in a large scale application. Accordingly, the breakthrough curve was obtained between 100-350 pore volumes (PV) of simulated LFG and the equilibrium was achieved at around 1,900 PV of gas. For the initial 100 PV the CO_2 was completely removed by the BOF slag. The breakthrough was achieved at around 100 PV after which the CO_2 uptake diminished rapidly, until a plateau was achieved at 350 PV where C_{out}/C_{in} was around 0.81. The curve maintained this ratio until there was no more uptake after 1,800 PV of CO_2 flow through the system.

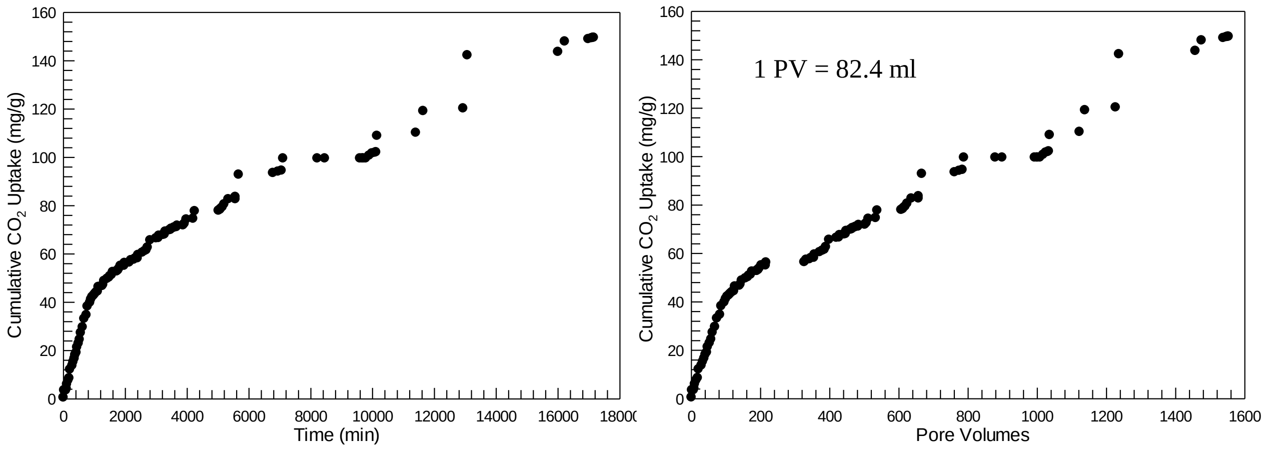
The initial reaction is attributed to the chemical reaction between the available free-lime and Portlandite in the material (which was ~4% and 6.5% respectively, see **Table 2**) with the CO_2 in the presence of moisture. After the exhaustion of the free lime, the reaction with other minerals such as calcium silicates (Ca_2SiO_4) could have been the source of continued uptake until the breakthrough. The adsorption and reaction with the interstitial minerals and other less reactive oxides and silicates that release calcium and/or portlandite could have led to the decent in the further reaction with CO_2 thus leading to the completion of the breakthrough curve. The lower reaction rates could also be attributed to the exhaustion of the limited moisture available in the system which was not replenished. Moisture plays a vital role in the carbonation reaction. It helps in dissolution of gas as well as interstitial CaO. Hence, the availability of persistent moisture on an actual landfill site could have higher capacity to capture more CO_2 during its lifetime. Also, the spreading of BOF slag over a larger area could generate more surface area allowing more interaction between gas and moisture leading to higher CO_2 sequestration.

In addition, a crust of carbonate precipitates was observed around the BOF slag material inside the glass column surface during the experiments which almost certainly limited mass transfer and reaction rates.



(a) **(b)**

Figure 4: Breakthrough Curve of Carbon Dioxide in Small Column Experiment with respect to (a) Time and (b) Pore Volumes



(a) **(b)**

Figure 5: Cumulative Uptake of Carbon Dioxide in Small Column Experiment with respect to (a) Time and (b) Pore Volumes

4. SUMMARY AND CONCLUSIONS

BOF slag has been extensively investigated for its potential use in different civil and environmental applications with the aim of preserving the natural resources and aim of mitigating the global CO_2 emissions (Motz and Geiseler, 2001) These studies have been useful in reducing the use of natural resources by replacing it with steel slag in various forms, alleviating the amount of steel slag stockpiling at the steel plants. There have been recent efforts at the potential use of steel slag in landfills, but as a drainage material in the landfill covers. This study explores the use of BOF slag to mitigate the CO_2 emissions from MSW landfills by leveraging the mineral carbonation process of BOF slag. In this regard, a series of batch tests were conducted to evaluate the amount of CO_2 that can be sequestered by the BOF slag. Furthermore, the carbonation and CO_2 sequestration under varying moisture contents was conducted to evaluate the effect of moisture content on the carbonation capacity of the BOF slag. Small column experiments simulating the flow of landfill gas through BOF slag were conducted with the optimum moisture content as derived from the batch test results.

Following conclusions could be drawn from this study.

- The BOF slag was found to have characteristics suitable for its use in a landfill cover based on the physical, chemical and technical characterization performed. The BOF slag used was classified as non-hazardous based on the TCLP and SPLP test results.
- The results from the batch tests showed that the carbonation capacity (CO2 uptake) of the BOF slag was about 68 mg/g within 24 hours. It was also observed that, for the range of moisture content tested, the CO2 uptake in 24 hours from the batch tests was comparable to the cumulative uptake of CO2 in column test.
- The cumulative uptake of CO2 from the column experiments is a conservative estimate since there was an exhaustion of the moisture available in the system for carbonation reaction over the course of the column test. The limited moisture availability in a continuous gas flow system could hinder the maximum possible carbonation of the BOF slag used in the column.
- Further studies are being performed to analyze the carbonation mechanism and evaluate the effects of various system parameters on carbonation capacity of BOF slag, including field landfill gas flow and environmental conditions.

Acknowledgements
This project is funded by the U.S. National Science Foundation (CMMI # 1724773), which is gratefully acknowledged.

References
1. Grubb, D.G. (2017). Personal Communication.
2. Huijgen, W. J., Witkamp, G. J., and Comans, R. N. (2005). 'Mineral CO_2 sequestration by steel slag carbonation.' **Environmental Science & Technology**, Vol. 39(24), 9676-9682
3. Kasina, M., Kowalski, P. R., and Michalik, M. (2015). 'Mineral carbonation of metallurgical slags.' **Mineralogia**, Vol. 45(1-2), 27-45
4. Kinney, T. J., Masiello, C. A., Dugan, B., Hockaday, W. C., Dean, M. R., Zygourakis, K., and Barnes, R. T. (2012). 'Hydrologic properties of biochars produced at different temperatures.' **Biomass and Bioenergy**, Vol. 41, 34-43
5. Malasavage, N. E., Jagupilla, S., Grubb, D. G., Wazne, M., and Coon, W. P. (2012). 'Geotechnical performance of dredged material—steel slag fines blends: laboratory and field evaluation.' **Journal of Geotechnical and Geoenvironmental Engineering**, Vol. 138(8), 981-991
6. Motz, H., and Geiseler, J. (2001). 'Products of steel slags an opportunity to save natural resources.' **Waste Management**, Vol. 21(3), 285-293.
7. National Slag Association (NSA). (2013). http://www.nationalslag.org/steel-furnace-slag
8. Reddy, K.R., Yargicoglu, E.N., Yue, D., and Yaghoubi, P. (2014). 'Enhanced microbial methane oxidation in landfill cover soil amended with biochar.' **Journal of Geotechnical and Geoenvironmental Engineering**, ASCE, Vol. 140(9), 04014047
9. Sadasivam, B.Y., and Reddy, K.R. (2015). 'Engineering properties of waste-wood derived biochars and biochar-amended soils.' **International Journal of Geotechnical Engineering**, Vol. 9(5):521-535
10. Shi, C. (2004). 'Steel slag—its production, processing, characteristics, and cementitious properties.' **Journal of Materials in Civil Engineering**, Vol. 16(3), 230-236.
11. U.S. Geological Survey. (2015). '**Mineral Commodity Summaries**' Retrieved from https://minerals.usgs.gov/minerals/pubs/commodity/iron_&_steel_slag/
12. Yargicoglu, E., Sadasivam, B.Y., Reddy, K.R. and Spokas, K. (2015). 'Physical and chemical characterization of waste wood derived biochars.' **Waste Management**, Vol. 36(2), 256-268
13. Yargicoglu, E.Y., and Reddy, K.R. (2017a). 'Microbial abundance and activity in biochar-amended landfill cover soils: Evidences from large-scale column and field experiments' **Journal of Environmental Engineering**, Vol. 143(9), 04017058
14. Yargicoglu, E.Y., and Reddy, K.R. (2017b). 'Effects of biochar and wood pellets amendments added to landfill cover soil on microbial methane oxidation: A laboratory column study' **Journal of Environmental Management**, Vol. 193, 19-31
15. Yargicoglu, E.Y., and Reddy, K.R. (2018) 'Biochar-amended soil cover for microbial methane oxidation: Effect of biochar amendment ratio and cover profile.' **Journal of Geotechnical and Geoenvironmental Engineering**, ASCE, Vol. 144(3): 04017123

RECYCLING OF CRT FUNNEL GLASS: A REVIEW OF ITS UTILIZATION IN INTERLOCKING CONCRETE BLOCKS

G. Perkoulidis* and N. Moussiopoulos

Laboratory of Heat Transfer and Environmental Engineering, Dept. of Mechanical Engineering, A.U.Th, GR- 54124 Thessaloniki, Macedonia, Greece

*Corresponding author: e-mail: gperk@auth.gr, tel : +302310996060

Abstract

CRT monitors are evacuated glass envelopes containing an electron gun and a fluorescent screen and when they are dismantled, glass is separated into: (a) nonhazardous panel and (b) funnel with lead (Pb). The utilization of cathode-ray tube funnel glass has been promoted as a substitute for sand, while recent studies were focused on the mechanical and durability properties of concrete containing such glass as aggregate. Future products such as precast concrete structural interlocking blocks could contain cathode-ray tube funnel glass aggregate and in case their lead content is high, then they could be classified as hazardous waste.

The aim of the present manuscript was to review the methods of cathode-ray tube glass recycling and to evaluate the potential risks for the utilization of funnel glass in interlocking concrete blocks. The critical evaluation of published literature data will help the development of new product methods through recycling.

Keywords: cathode-ray tube; funnel glass; waste recycling; concrete block

1. INTORDUCTION

Electrical and electronic equipment (EEE) falling within the scope of the Waste from Electrical and Electronic Equipment (WEEE) Directive was currently classified under 10 “product - oriented” categories (European Commission, 2017): 1) large household appliances, 2) small household appliances, 3) Information Technology (IT) and telecommunications equipment, 4) consumer equipment, 5) lighting equipment, 6) electrical and electronic tools, 7) toys, leisure and sports equipment, 8) medical devices, 9) monitoring and control instruments, 10) automatic dispensers. From 15 August 2018, EEE will be classified under 6 “collection - oriented” categories (European Commission, 2017): 1) temperature exchange equipment; 2) screens, monitors and equipment containing screens with a surface greater than 100 cm^2; 3) lamps; 4) large equipment (any external dimension greater than 50 cm); 5) small equipment (no external dimension greater than 50cm); 6) small IT and telecommunications equipment (no external dimension greater than 50cm). Old monitors will belong to “collection - oriented” category 2 from 15 August 2018, as has already been mentioned above.

The sections from CRTs were characterized by the neck, the funnel, and the face panel, as shown in Figure 1 (Musson et al., 2000).

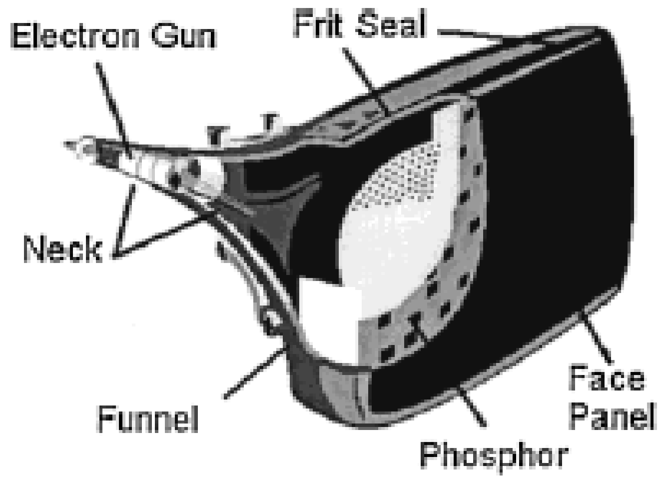


Figure 1. Funnel and other parts of a CRT (Mousson et al., 2000).

The most significant quantities of lead were obtained from the funnel portion of the CRTs at an average lead concentration of 75.3 mg/L, while the major source of lead in the funnel was the frit seal of color CRTs (Table 1).

Table 1. Lead content in various CRT glass components by mass (Microelectronics and Computer Technology Corporation, 1994, Musson et al., 2000).

Glass	Color CRT (%)	Monochrome CRT (%)	Glass	Color CRT (%)	Monochrome CRT (%)
Panel	0-3	0-3	Neck	30	30
Funnel	24	4	Frit	70	N/A

Leaded glass was used in cement mortar by using recycled beverage and CRT funnel glass as fine aggregate in dry-mixed concrete paving blocks (Ling and Poon, 2014; Yu et al., 2016; Lee et al., 2012; Ling and Poon, 2012a; Sikora et al., 2015). Some of the advantages of using large precast concrete block systems for retaining structures included (Elite precast concrete limited, 2017): (a) relatively low cost, (b) simple and quick to build, while dry laid ensured that structure could be loaded without waiting for concrete/mortar to set, (c) durable with low on-going maintenance costs and (d) re-usable structures that could be readily dismantled and reused elsewhere. Different organisations could be responsible for the design, manufacture, installation and maintenance of the retaining wall, such as (Elite precast concrete limited, 2017): (i) design – professionally qualified civil, structural or geotechnical engineer, (ii) third- party engineer to perform a design check, especially for road and rail infrastructure projects, (iii) a precast concrete manufacturer, (iv) a civil/building contractor or specialist earthworks sub-contractor and (v) an owner/operator of the infrastructure or storage facility. Walls formed from interlocking concrete blocks were, defined in BS 8002:2015 as gravity walls (Elite precast concrete limited, 2017): "Gravity retaining walls are earth retaining structures that depend primarily on their own self-weight (and that of any enclosed material) to support the retained ground and any structures or loads placed upon it".

From the other hand, precast concrete structural interlocking blocks that were imported from Netherlands to UK, contained high lead concentration, and in accordance with Parker (2014), that recycled glass aggregate had to be reclassified as hazardous waste. The suspect blocks had come into the UK from 2010 to 2014, and the Environment Agency stated that the producer had failed to provide evidence that it complied with environmental protection regulations. The producer had to demonstrate that the "processed substance" could be used in the same way as a non-waste, and could be stored and used with no worse environmental effects. Reclassifying the giant Legioblocks, which were dry-

stacked to form retaining walls, storage bays and firewalls, would had serious implications for those who had purchased them in good faith.

The aim of the present manuscript was to review the methods of cathode-ray tube glass recycling and to evaluate the potential risks for the utilization of funnel glass in interlocking concrete blocks. The critical evaluation of published literature data will help the development of new product methods through recycling.

2. METHODS AND MATERIALS

2.1 Utilization of CRT funnel glass

Cathode ray tube (CRT) funnel glass had been used for monitor displays for decades. It was classified as hazardous waste, which could not have been buried without treatment of contained lead (Lv et al., 2016). From the other hand, using recycled cathode ray tube funnel glass as a substitute for sand contributed to both reducing natural aggregate consumption and CRT funnel glass disposing (Liu et al., 2017).

Various studies had been carried out to solve the discarded CRT waste problem, particularly with methods to reuse leaded funnel glass as it contained a large amount of lead (Table 2).

Table 2. Studies for solving the CRT waste problem.

No	Recycled materials	Utilized as…	Final product	Source
1	CRT funnel glass	Substitute for sand	Concrete structures	[1]
2	CRT funnel glass and recycled beverage	Fine aggregate	Cement mortar	[2-6]
2	Recycled glass from CRT	Fine aggregate	Dry-mixed concrete paving blocks	[7]
3	CRT funnel glass	Raw material	Crystal	[3]
4	CRT funnel glass	Processed substance	Precast concrete structural interlocking blocks	[8]
5	Waste lead glass	Wollastonite synthesis	Wollastonite	[9]

[1]: Liu et al., 2017; [2]: Ling and Poon, 2014; [3]: Yu et al., 2016; [4]: Lee et al., 2012; [5]: Ling and Poon, 2012a; [6] Sikora et al., 2015; [7]: Ling and Poon, 2014; [8]: Parker, 2014; [9]: Erzat and Zhang, 2014.

Laboratory of Heat Transfer and Environmental Engineering (LHTEE), Mechanical Engineering Department, Aristotle University Thessaloniki, Greece, presented the benefits from using CRT glass in the ceramic industry (LIFE-CLAYGLASS) (Malamakis et al., 2016). The main objective of the project was to reduce the environmental impact in the structural ceramic industry by including CRT glass, as a flux, in the ceramic mass. During the industrial pilot test, six (6) different clay mixtures were used. Two different clay types, namely Segovia and Blanca, with two different CRT glass types (funnel and panel) and two possible glass percentages (5% and 10%). For each combination of clay and glass, 300 thousand bricks were produced in the industrial gas-fired oven of MORA, which was a brick manufacture with more than 50 years on the ceramic industry. The number was selected to produce one full batch of each type (Laboratory of Heat Transfer and Environmental Engineering, 2017). In the frame of LIFE-CLAYGLASS, a new stoneware production using recycled glass demonstrated which leaded to (Malamakis et al., 2016): (a) the commercial use of difficult-to-recycle glass that was land-filled, (b) reduced demand for natural resources in clay tile production, (c) energy savings of 10-15%, (d) a reduction of about 2,000 t of CO_2 emissions per year for a medium-size factory (brick production capacity of 300 t per day), (e) a reduction in the cost of producing clay tiles.

2.2 Precast concrete structural interlocking blocks

An example of precast concrete structural interlocking blocks was given by Elite precast concrete limited (2017), but without the use of CRT funnel glass (Figure 2). The design shear resistance, R_d, was calculated taking account the vertical design action, V_d, and the angle of interface friction, δ. At the interface between the base and the bottom layer of blocks, there were no interlocking 'nibs', so δ was based upon the friction angle between two concrete surfaces, ϕ; conc. For the block-block interfaces, the effect of the interlocking nibs was to increase the shear resistance. This might be expressed in terms of an enhanced friction angle along a smooth horizontal surface, ϕ; interlock. However, the interlocking shear resistance was limited to a maximum value, R_d; Max, based upon the characteristic shear strength of the concrete and the size and number of interlocking nib elements. The base layer shear resistance and the base layer shear resistance were given by equations (1) and (2).

$$R_d \text{ - base} = V_d \text{ - base.} \times \tan \phi \text{ conc;d:} \quad (1)$$

$$R_d - \text{Layer n} = (V_d - \text{layer n.} \times \tan \phi \text{ interlock ;d}) \leq R_d\text{; Max} \quad (2)$$

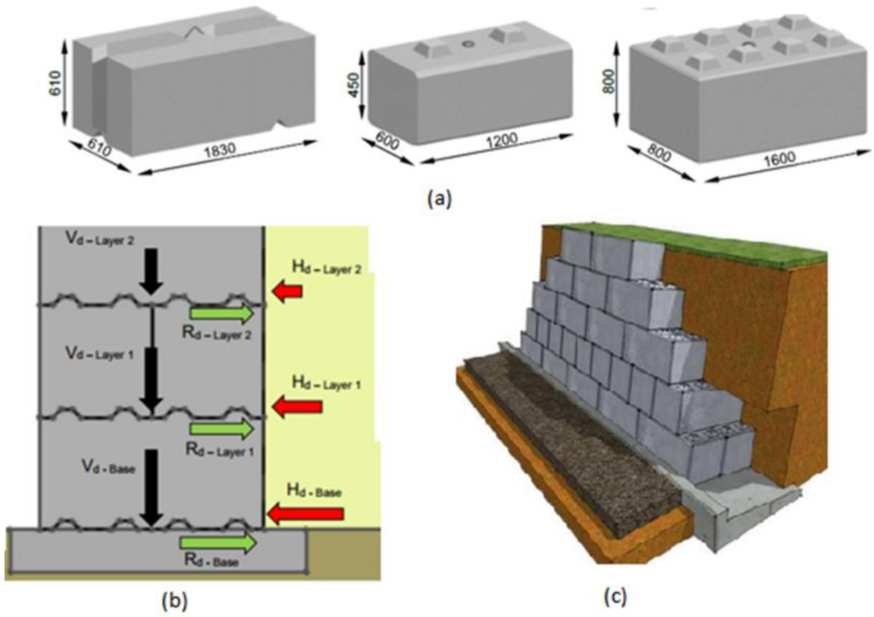


Figure 2. Standard block: (a) dimensions (mm), (b) sliding resistance, and (c) wall constructed with inclined front face (Elite precast concrete limited, 2017).

2.3 Use of CRT funnel glass in concrete blocks

In 2008, in collaboration with the Hong Kong Polytechnic University, the Environmental Protection Department (EPD) developed a recycling process for CRT recycling. Treated Funnel Glass (TFG) rendered as non-hazardous material according to the Toxicity Characteristic Leaching Procedure (TCLP) test results after an acid washing process [Nitric Acid 5% (w/w) solution to extract lead from the crushed glass surface for 3h], soaking tap water and rinsing (to remove the remaining acid)] (Ling and Poon, 2012b).

Ling and Poon (2014) studied the use of CRT funnel glass in concrete blocks prepared with different aggregate-to-cement (A/C) ratios. Their experimental results showed that due to the impermeable nature of TFG, the produced concrete blocks were more resistant to water penetration and had lower drying shrinkage. Based on the findings, they concluded that it was possible to utilize high percentages of TFG in concrete blocks if a proper A/C ratio and appropriate casting method were used. CRT funnel glass had been studied as a replacement for natural sand as fine aggregate in mortar or concrete by many researchers (Ling and Poon, 2012c, 2012b, 2013; Kim et al., 2009). Zhao et al.

(2013a) reported that the replacement of sand with CRT funnel glass had a positive effect on the fluidity of mortar, which was attributed to the smooth surface and low water absorption of CRT glass. On the contrary, Sua-iam and Makul (2013) found that the flowability of mortar decreased with the replacement ratio of CRT glass, which was associated with the poor geometry of CRT glass particles.

Ling and Poon (2011, 2012a) carried out experimental studies to demonstrate that it was feasible to use TFG (100%) as a fine aggregate to replace natural river sand to produce cement, mortar and concrete. However, the design concept to manufacture a dry mixed concrete block was in contrast to conventional wet-mixed concrete, which mainly adopted a low water-to-cement ratio and high compaction method. Therefore, it was expected that the change of these parameters could have a significant influence on the properties of concrete, particularly alkali-silica reaction (ASR) behavior and the potential risk of lead (Pb) leaching. No study has been done on the feasible use of TFG in dry-mixed concrete blocks, which were produced with very different aggregate-to-cement ratios and casting methods. Ling and Poon (2014) presented the work flow of recycling the TFG in pre-cast concrete blocks and the testing methods used to identify applicability, quality of product and impact on the environment (Figure 3).

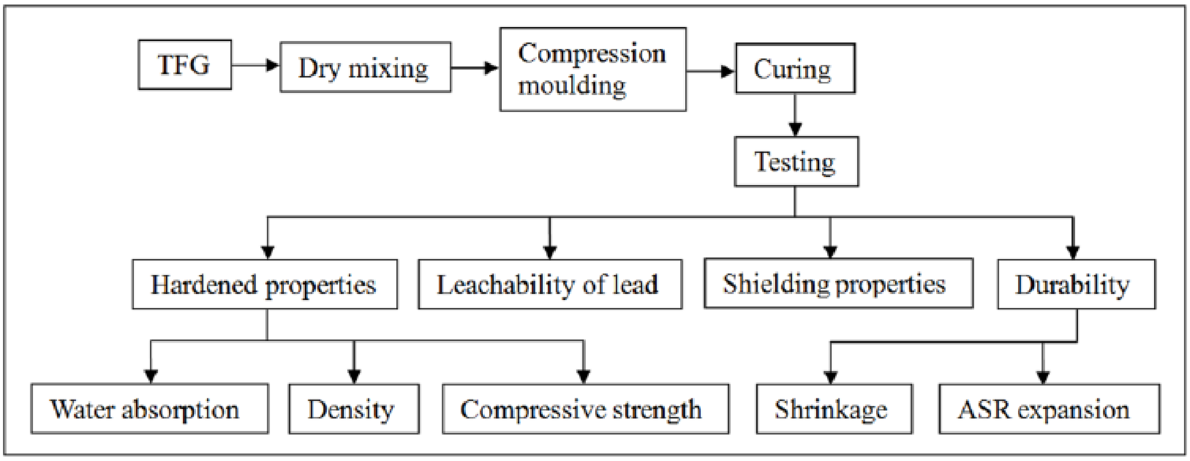


Figure 3. Work flow for moulded concrete block and testing methods (Ling and Poon, 2014).

In 2016, Meng et al. studied a variety of new methods in laboratory. They introduced several advanced methods such as high temperature separation and hydrometallurgical leaching. Bursi et al. (2017) found that chemical pretreatment was necessary for use of CRT glass in cementitious composites. Aim of their work was to investigate the effect of a mild chelating agent treatment based on nitrilotriacetic acid (NTA) on the reactivity of funnel glass to be used in cement mortars as supplementary cementing material (SCM) and as fine aggregate.

Yu et al. (2016) showed that crystal could be made from waste CRT funnel glass. The lead quantity in waste CRT glass and in lead crystal glass ($PbO \geq 24\%$) were almost the same, therefore, it was found a way to use of waste CRT funnel glass as the raw material of crystal products. In the process of producing crystal, the addition of lead oxide took place to increase the product material properties. The production of one ton of crystal glass products could reduce the use of 0.2 tons of lead oxide by using funnel glass.

3. RESULTS

The results of the chemical analyses from the literature review were the following (Table 3):

- A higher percentage of CRT glass (up to 100%) could be incorporated in the blocks if alternate block forming and compaction methods were used to reduce the fragmentation of the incorporated CRT glass. The experiment showed that the material was not dangerous (No. of test 1, Table 3).

- The addition of limestone powder in the CRT waste glass reduced Pb immobilization. TCLP test results were below the US EPA Pb limit of 5 mg/L. The experiment showed that the material was not dangerous (No. of test 2, Table 3).
- The Synthetic Precipitation Leaching Procedure (SPLP) analysis was used. A cross-linked biopolymer had a large impact on reducing the amount of lead that leached from the samples and ultimately yielded results in which up to 20% CRT can be substituted into the concrete and still be below the drinking water limits. The experiment showed that the material was not dangerous (No. of test 3, Table 3).
- Incorporating CRT glass in cement mortar successfully prevented the leaching of lead. Mortar mixes contained 0 - 100% of CRT glass, with a step change of 25%. The experiment showed that the material was not dangerous (No. of test 4, Table 3).
- Funnel glass were heated to 1,480 oC in an electric furnace for 1.5 h at a heating rate of 5 oC/min to produce cement clinker. The samples contained 10 -50 wt % of CRT funnel glass ground to less than 75 mm (No. of test 5, Table 3).
- Six mortar mixes were analyzed, which used from 0% to 100% CRT glass for replacing river sand. Also, fly ash (F) and ground granulated blast-furnace slag (GGBFS) were used as a mineral admixture (No. of test 6, Table 3).

Table 3. The results of the chemical analyses from the literature review.

No. of test	% of CRT funnel glass	Leaching Procedure	Treated funnel glass with…	Results	Source
1. Dry-mixed concrete paving blocks	**25% <**	**TCLP**	**Acid**	**Nonhazardous material**	**[1]**
2. Concrete	**40% <**	**TCLP**	**Limestone powder (5, 10 and 15% by weight)**	**Nonhazardous material**	**[2]**
3. Concrete	**20%<**	**SPLP, EPA Method 1312**	**Biopolymers**	**Nonhazardous material**	**[3-4]**
4. Cement mortar	**0 - 100%**	**TCLP**	**Acid**	**Nonhazardous material**	**[5]**
5. Cement clinker	**10 – 50%**	**X-ray techniques**	**Samples of cement raw material were heated to 1480 ºC in an electric furnace**	**Maximum PbO encapsulation in 10% funnel**	**[6]**
6. Use in the mortar as natural river sand fine aggregate replacement	**CRT glass as fine aggregate with natural river sand**	**-**	**CRT glass was utilized to replace river sand as fine aggregates in the mortar**	**Mortar with larger ASR expansion values than that of river sand**	**[7]**

[1]: Ling and Poon, 2014; [2]: Sua-iam and Makul, 2013; [3]: Romero et al., 2013; [4]: USEPA, 1994; [5]: Ling and Poon, 2011; [6]: Lairaksa et al., 2013; [7]: Hui and Sun, 2011.

4. CONCLUSIONS

In the case of concrete with the same A/C ratio, the water absorption shrinkage values decreased with the incorporation of TFG due to the near-zero porosity of TFG aggregate. The lead leaching behaviour of concrete blocks was greatly affected by the TFG content, A/C ratio and casting method. Decreasing the A/C ratio (with a higher cement content) maintained a high alkaline environment and a strong cement matrix to stabilize and solidify the TFG in the concrete blocks. In addition, using mechanical

compression only (without vigorous manual compaction) minimized the fragmentation of the TFG and hence reduced the risk of lead leaching from the broken TFG. Thus, the research results showed that it was feasible to utilize a high percentage of TFG in concrete blocks if a proper A/C ratio and appropriate casting method were used.

Pretreatment methods could effectively improve the lead leaching effect from the glass, but they had their disadvantages. The consumption of alkali, energy and operation costs were high. In the case of chemical pretreatment of funnel glass, the NTA treated glass became less soluble because of Pb depletion and the risk of pollution from leaching was reduced. Even though the NTA treatment decreased the pozzolanic activity of the glass, making it a filler material rather than SCM, NTA treatment allowed its use as fine aggregate in substitution of natural sand suppressing ASR reactions. Thus, this application was environmentally preferred since it reduced the costs of strong milling process.

The densities of concrete blocks made with TFG were higher than those of traditional control blocks, making it suitable for use as a shielding material for medical and diagnostic room construction as it was shown in the x-ray shielding experiment.

Finally, the recycling of CRT funnel glass seemed that had interest for many researchers; their results by various analyses showed that funnel glass could be characterized as nonhazardous material and that it could be utilized to produce dry-mixed concrete paving blocks, cement mortar and clinker. The only case, where negative comments were reported, it was the case where unknown composition of processed substance from CRT funnel glass, was utilized in interlocking concerned blocks.

As far as the possibility of utilizing CRT in dry-mixed concrete paving blocks in Greece, essays with known CRT funnel glass composition should be prepared, and then leaching procedures should be applied to assess their lead (Pb) leachability.

Aknowledgments

The authors would like to acknowledge the company Konstantinidis Bros S.A. for funding the presented research. Konstantinidis Bros S.A. was the first company in Northern Greece, which started the recycling of waste electrical and electronic equipment.

Acronyms

A/C: Aggregate-to-Cement ratio

ASR: Alkali-Silica Reaction

ASTM: American Society for Testing & Materials

C&D: Construction and Demolition

CRT: Cathode Ray Tube

EEE: Electrical and Electronic Equipment

EPD: Environmental Protection Department

IT: Information Technology

NTA: Nitrilotriacetic Acid

OPC: Ordinary Portland Cement

RCA: Recycled Coarse Aggregate

RFA: Recycled Fine Aggregate

SCM: Supplementary Cementing Material

TCLP: Toxicity Characteristic Leaching Procedure

TFG: Treated Funnel Glass

WEEE: Waste from Electrical and Electronic Equipment

References

1. Bursi E., Lancellotti I., Barbieri L., Saccani A. and M. C. Bignozzi (2017), 'CRT glass management: chemical pretreatment for use in cementitious composites', Proc. of **5th International Conference on Sustainable Solid Waste Management**, Athens, Greece, 21-24 June 2017.
2. Chen M.J., F.-S. Zhang and J.X. Zhu (2010), 'Effective utilization of waste cathode ray tube glass–crystalline silicotitanate synthesis', **Journal of Hazardous Materials**, 182(1–3), pp. 45–49.
3. Chen M.J., Zhang F.-S. and J.X. Zhu (2009a), 'Lead recovery and the feasibility of foam glass production from funnel glass of dismantled cathode ray tube through pyrovacuum process', **Journal of Hazardous Materials**, 116(2–3), pp. 1109–1113.
4. Chen M.J., Zhang F.-S. and J.X. Zhu (2009b), 'Detoxification of cathode ray tube glass by self-propagating process', **Journal of Hazardous Materials**, 165(1–3), pp. 980–986.
5. Elite precast concrete limited (2017), 'Reference guide for designing retaining walls using interlocking concrete blocks', Document No. **EPCL-2017-RWRG-01** – P01, June.
6. Erzat A. and F.-S. Zhang (2014), 'Detoxification effect of chlorination procedure on waste lead glass', The 8th International Conference on Waste Management and Technology (ICWMT) 2013, **Journal of Material Cycles and Waste Management**, 16, pp. 623–628.
7. European Commission (2017), 'Re-examination of the WEEE recovery targets, on the possible setting of separate targets for WEEE to be prepared for re-use and on the re-examination of the method for the calculation of the recovery targets set out in Article 11(6) of Directive 2012/19/EU on WEEE, Report from the Commission to the European Parliament and the Council, **COM(2017) 173 final**, Brussels, 18.4.2017.
8. Kim D., Quinlan M. and T. F. Yen (2009), 'Encapsulation of lead from hazardous CRT glass wastes using biopolymer cross-linked concrete systems', **Waste Management**, 29(1), pp. 321-328.
9. Laboratory of Heat Transfer and Environmental Engineering (2017), 'Sustainability Dimensions', **Annual Report**, Mechanical Engineering Department, Aristotle University Thessaloniki, Greece.
10. Lee C.-H. and C.-S. Hsi (2002), 'Recycling of scrap cathode ray tubes', **Journal of Environmental Science Technology**, 36(1), pp. 69–75.
11. Lee J.-S., Cho S.-J., Han B.-H., Seo Y.-C., Kim B.-S. and S. P. Heo (2012), 'Recycling of TV CRT Panel Glass by Incorporating to Cement and Clay Bricks as Aggregates', **Advances in Biomedical Engineering**, Vol 7, p. 257.
12. Ling T. C. and C. S. Poon (2011), 'Utilization of recycled glass derived from cathode ray tube glass as fine aggregate in cement mortar', **Journal of Hazardous Materials**, Vol 192, pp. 451-456.
13. Ling T. C. and C. S. Poon (2012a), 'Feasible use of recycled CRT funnel glass as heavyweight fine aggregate in barite concrete', **Journal of Cleaner Production**, Vol 33, pp. 42-49.
14. Ling T. C. and C. S. Poon (2012b), 'Development of a method for recycling of CRT funnel glass', **Environmental Technology**, Vol 22, pp. 2531-2537.
15. Ling T. C. and C. S. Poon (2012c), 'A comparative study on the feasible use of recycled beverage and CRT funnel glass as fine aggregate in cement mortar', **Journal of Cleaner Production**, Vol 29, pp. 46-52.

16. Ling T. C. and C. S. Poon (2014), 'Use of CRT funnel glass in concrete blocks prepared with different aggregate-to-cement ratios', **ICE- Green Materials**, 2(1), pp. 43-51.
17. Ling, T. C. and C. S. Poon (2013), 'Effects of particle size of treated CRT funnel glass on properties of cement mortar', **Materials and Structures,** 46(1-2), 25-34.
18. Liu T., W. Song, D. Zou and L. Li (2017), 'Dynamic mechanical analysis of cement mortar prepared with recycled cathode ray tube (CRT) glass as fine aggregate', **Journal of Cleaner Production**, 10.1016/j.jclepro.2017.11.057.
19. Lv, J., H. Yang and Z. Jin (2016), 'Feasibility of lead extraction from waste Cathode-Ray-Tubes (CRT) funnel glass through a lead smelting process', **Waste Management**, Vol 57, pp. 198-206.
20. Malamakis A., S. Kontogianni, G. Perkoulidis, N. Moussiopoulos, J. Velasco and A. Perez (2016), 'Environmental protection through utilization of recycled glass as fluxing agent in the structural ceramics industry', **4th International Conference on Sustainable Solid Waste Management**, CYPRUS 2016, 23 - 25 June, Limassol, Cyprus.
21. Microelectronics and Computer Technology Corporation (1994), Electronics Industry Environmental Road map, 1994.
22. Musson T., Y.-C. Jang, T. G. Townsend and I.-H. Chung (2000), 'Characterization of Lead Leachability from Cathode Ray Tubes Using the Toxicity Characteristic Leaching Procedure', **Environmental Science & Technology**, Vol 34, pp. 4376-4381.
23. Parker D. (2014), 'Fears emerge that imported Dutch precast concrete blocks could be hazardous waste', **New Civil Engineer** (https://www.newcivilengineer.com/fears-emerge-that-imported-dutch-precast-concrete-blocks-could-be-hazardous-waste/8672933.article, 25/12/2017).
24. Romero D., J. James, R. Mora and C. D. Hays (2013), 'Study on the mechanical and environmental properties of concrete containing cathode ray tube glass aggregate', **Waste Management**, Vol 33, 1659–1666.
25. Sikora P., E. Horszczaruk and T. Rucinska (2015), 'The effect of nanosilica and titanium dioxide on the mechanical and self-cleaning properties of waste-glass cement mortar', **Procedia Engineering**, Vol 108, 146-153.
26. Sua-iam, G. and N. Makul (2013), 'Use of limestone powder during incorporation of Pb-containing cathode ray tube waste in self-compacting concrete', **Journal of Environmental Management**, Vol 128, pp. 931-940.
27. U.S. EPA (1996), 'Test Methods for Evaluating Solid Waste', SW-846, 3rd ed., **Office of Solid Waste**, Washington, DC.
28. Yu M., L. Liu and J. Li (2016), An overall solution to cathode-ray tube (CRT) glass recycling, The Tenth International Conference on Waste Management and Technology (ICWMT), **Procedia Environmental Sciences**, Vol 31, 887 – 896.
29. Zhao H., C. S. Poon and T. C. Ling (2013a), Properties of mortar prepared with recycled cathode ray tube funnel glass sand at different mineral admixture, **Construction and Building Materials**, Vol 40, pp. 951-960.

A SYSTEM DYNAMICS MODEL FOR SMALL HOUSEHOLD APPLIANCES' WASTE MANAGEMENT: A CASE OF TURKEY

A.Kemal Konyalıoğlu* and İ.Bereketli Zafeirakopoulos

Department of Industrial Engineering, Galatasaray University, Istanbul, Turkey

*Corresponding author: e-mail: konyalioglua@itu.edu.tr

Abstract

Nowadays sustainability is one of the most important subjects in the developing world. Thanks to sustainability, waste management also gains more importance. Waste management is composed of many sub-areas in which liquid, gas or solid wastes are treated. The waste category that will be studied in this paper is waste of electric and electronic equipment (WEEE) under solid wastes. Turkey is a country whose household appliances sector is outstandingly large. Furthermore, many small household appliances are thrown away or destroyed due to end of life or quality issues. Most of those wastes do not go through any treatment process even if Turkey has collection and recovery targets for all WEEE categories. As they are not properly treated, the process to destroy without reusing or recycling them causes environmental damage.

The aim of this paper is to put forward a system dynamics model for increasing recovery options of waste of small household appliances in electric and electronic sector, which is not treated in an environmentally friendly way. The proposed model provides decrease in environmental damage.

In this model, Anylogic program will be used for the simulation of the proposed system dynamics model. Different scenarios will be conducted to give recommendations on how the whole system works in the case of Turkey.

Keywords: Waste management, System dynamics, WEEE, Sustainable supply chain management

1. INTRODUCTION

Waste management, which effects on sustainability in every aspect, is an important topic in the world. Sustainability can be taken into consideration in three main areas which include economic, social and environmental dimensions [Dyllick and Hockerts, 2002]. Waste management is particularly included in environmental sustainability. For pursuing a "sustainable" policy, each waste has an important topic to investigate and one of them is Waste of electric and electronic equipment (WEEE). As the number of households using electric and electronic equipment increases and technological improvements go further year by year, management of WEEE becomes more important. This equipment can be classified as large household appliances and small household appliances on which Turkey has recycling and recovery targets according to the WEEE Regulation which was published in 2008 (URL1). Furthermore, recovery and recycling targets are qualified based on the types of wastes which can be taken into consideration by collecting, economic and technical dimensions (Fischer, 2011).

In Turkey, electric and electronic sector is sharply growing thanks to technological improvements and needs. Thus, environmental perspective is dependently changing since production and consumption of this equipment causes an increase in pollution and decrease in resources. To avoid these damages, Turkish government and enterprises in Turkey developed regulations to enable reuse or recycling of the electric and electronic equipment. One of those fields is white good sector

including small household appliances. There are humble eco-design efforts for small household appliances in Turkey however unless there is a strict waste management policy those efforts will not be sufficient. To have a holistic environmental sustainability, not only production process but also recovery processes for end-of-life products are important. This can be perceived as a whole system or process because in the whole system, each detail matters from suppliers to the recycling facility. [Jie and Buekens, 2014].

The aim of the study is to recommend a system dynamics model for minimizing wastes of small household appliances in Turkey and maximizing recovery applications instead of disposing them. The study will also help to understand how environmental sustainability concept works in Turkey. There exists a lot of studies about wastes of electric and electronic equipment in Turkey but there are not many especially focusing on waste management of small household appliances by using a system dynamic model.

The study includes four main parts: introduction, background, methodology and modeling which includes system dynamics and waste management of small household appliances' model, and finally conclusion and future studies.

2. BACKGROUND

Building a system for waste management is seen as one of the most crucial parts in terms of environmental waste management. A waste management system mainly describes the management of all tasks including responsibilities, routines, actions, measures and resources building a system which intends to manage wastes and abides by regulations. Besides, waste management is an important part in terms of economy and society. All countries, which are currently developing or developed, produce many types of wastes.

Furthermore, choosing the option between reusing, recycling and waste energy utilization, collection and processing without discounting the lowest total (social) cost and deciding the value obtained by selling the collected materials, will be of social benefit. [Inghels et al., 2011]. Effective solid waste management systems, which must be sustainable in nature and economics, are needed to provide better human health and safety [Saxena et al, 2010].

The amount of wastes has been increasing because of growing population and increasing needs for raw materials in a range including usual wastes and wastes of electric and electronic equipment (WEEE) [Takiguchi, 2016]. WEEE can be defined as an electrically operated device that no longer satisfies the user or manufacturer for a specific purpose. (Sinha-Khetriwal et al, 2005). If WEEE is mismanaged; these wastes can clearly affect the environment and the human health. Environmental regulatory agencies; electronic equipment manufacturers, retailers and non-governmental organizations are quite concerned with the updated statistical data to which WEEE is produced, stored, recycled, or discarded [Jang, 2010]. With the rapid development and use of electronic devices, the WEEE problem is growing rapidly in all countries. WEEE wastes appear many times in developing or emerging countries which cannot have any important infrastructure to manage WEEE problems. [Safdar et al., 2015]. On the other hand, in developed countries, for example in EU countries, it is expected that the EU will reduce its long-term differences in the level of recycling by linking its minimum recycling targets. In the last 15 years, the EU Member States have been able to change their perception of waste management. In the mid-1990s, EU member states have been able to gain more wastes and recycled them. They have made a very good start, although they need to do more things [Fischer, 2011]. In addition to developed countries, not only managing WEEE or associated researches but also legal arrangements have sped up in recent years with its conduction by Special Wastes Management Department at Waste Management Department. Collection of e-waste in Turkey, transports, recoveries are carried out by companies which the Ministry of Environment and Urbanization approves. When the E-device category and tags are placed; compliance documents are also given for collection, separation and reusing by the same Ministry [Öztürk, 2015].

There are many models to suggest new options of how to manage wastes. One of them is system dynamics modeling.

3. METHODOLOGY AND MODELLING

3.1 System dynamics

As a definition, system dynamics makes possible to understand and improve system thinking and operations management systems. After all, as a first step, we have to deal with the real world in many steps. It is possible to define system dynamics by better understanding equations of a model, simulation to understand dynamic behaviors, evaluation of other alternatives, selection and implementation of a better method. [Forrester, 1994] In this case, Al-Khatib et al. (2016) suggested a more understandable and sophisticated simulation method for hospital waste management by using system dynamics model. Also, Lee et al. (2015) proposed a system dynamics approach based on functional dynamics to evaluate product-service systems. In the production area, system dynamics is again used by Greasley (2005) to provide a discrete-event simulation method. Botha et al.(2017), used system dynamics modeling to compare three inventory management methods for theoretical and actual, daily data set by comparing the parameters of stock target settings.

System dynamics model is not only used in production field. For example, in financial field, Nair and Rodrigues (2013) explained financial parameters during production expansion by using system dynamics. . On the other hand, in management area, Barnabè (2011) suggested a balanced scorecard method based on system dynamics to evaluate strategic decision making. In education field, Pedamallu (?) applied a system dynamics model to evaluate educational infrastructure based on the quality of primary school of a developing country. As well, in health area, Devi et al. (2010) studied system dynamics modeling for the waiting list of corneal transplants patients.

Aside from many areas, also about WEEE, system dynamics models can be proposed. For example, Ghisolfi et al. (2016) presented a system dynamics model to investigate legal bargaining power and incentives for the waste pickers of desktops and laptops measured by the volume of wastes.

Furthermore, to mention Anylogic simulation program, it can be said that Anylogic is a simulation program used for mainly discrete event, agent-based simulation and system dynamics. Also, by the program, some graphs resulting from the simulation can be obtained (URL4).

3.2 Model for the waste management of small household appliances

In this study, recycling and recovery targets and total number of small household appliances in Turkey will be used. The proposed model, given in Figure 1, aims to increase recovery options for decreasing environmental damage by decreasing CO_2 emission and increasing recovery options. The model runs without any error by using simulation software; Anylogic. According to GFK's press release (URL2), the number of small household appliances sold out in Turkey is estimated to 17, 3 million (2017).

The supply chain starts from suppliers, which provide raw materials for production. According to Lu (2011), a supply chain can basically be defined as a group of independent establishments which are connected to each other by products and services that are collectively adding value to transmit them for final consumer. In the model, three suppliers have been taken into consideration as representative. These three suppliers defined as stock variable, provide raw materials for production process. The production process which is in the model is hereby considered as a total amount of all small household appliances' companies in Turkey. As there is noeffective and real data, system dynamics model has been constructed by using the total sold small household appliances in Turkey and 2018 target. Besides, after the main distributor, there are 3 sub-distributors to reach end consumers. End consumers are assumed to change their products intentionally or at the end of life cycle in the model. The used products are collected in general waste collection centers or municipality waste collection centers. For attracting wastes and increasing social benefit, municipalities can apply a campaign or inform public to create awareness. In this case, small household appliances are collected to be recycled, incinerated or be thrown away.

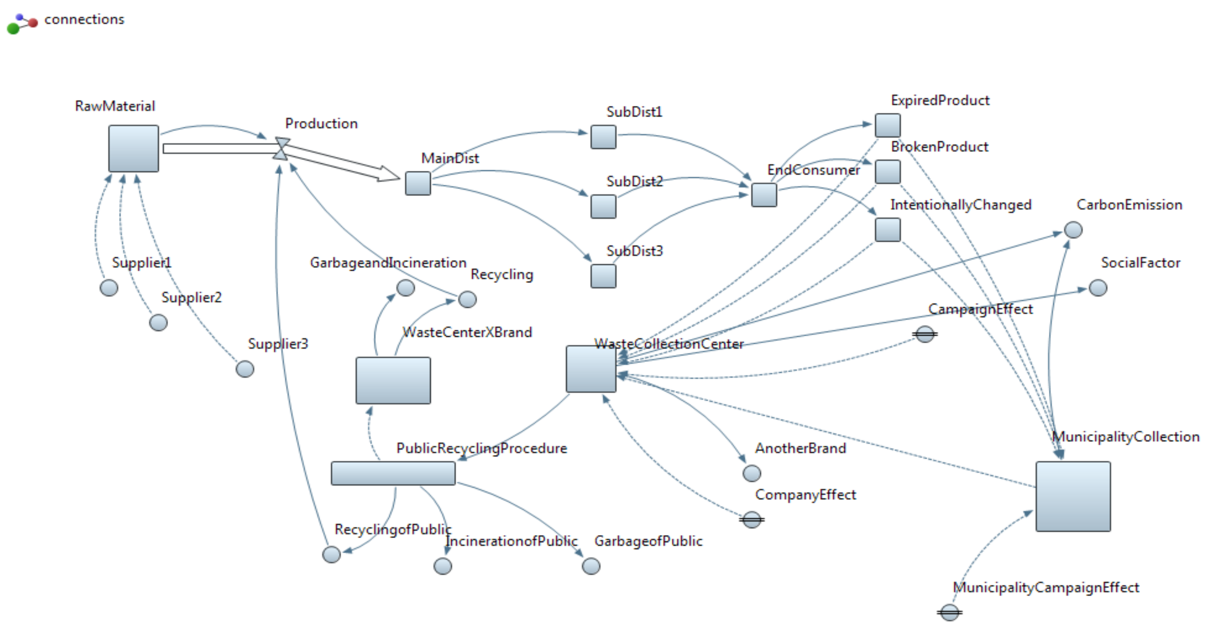


Figure 1: System dynamics model of small household appliances' waste management in Turkey

In Figure 2, the relationship between production and waste amount is given. The amount of production and waste is directly proportional. The decreasing point of production is explained as the raw material taken from suppliers is a dynamic variable. It seasonally changes according to the demand. Besides, as production increases, wastes also increase. Wastes thereby change and sometimes have different increasing and decreasing points. Model has been simulated for nearly 65 years and the result is in Figure 2.

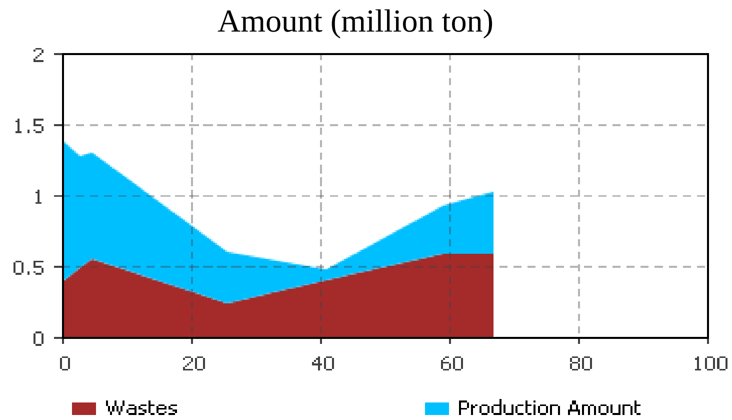


Figure 2: The relationship between wastes and production amounts

It is assumed that 50% of small household wastes in Turkey are going to be recycled by 2018 according to the recycling target of small household appliances which was published in the Official Gazette of Turkey in 2012 (URL3). All assumptions are based on this official target. Hence, in this model, 50% of total expired, broke-down and intentionally changed products go into recycling process. The proposed model has two main recycling collections' locations: a municipality collection center and a waste collection center. According to the official Gazette (2012), municipality collections have different targets from city to city.

Municipalities can use a campaign to increase public awareness for bringing expired, break-down of changed small household appliances to municipalities' recycling centers. In this model, it is used as a motivating and positive factor affecting municipality collection amounts.

Generally, all appliances are collected in waste collection centers in the model. The quantity of small household appliances gone into waste centers is assumed according to the target of 50% and proportionally, expired, broken or changed products are distributed accordingly. In Turkey, some electronic equipment companies have their own recycling centers. However, only one of these companies is put in the model as representative. Government or municipalities can sell the products to be recycled to electronic companies and these companies can use campaigns to attract appliances to their recycling centers. Companies can use these appliances in favor of their own companies or sell to public or governments after recycling or during recycling process. As indicated in the model, appliances recycled by government or companies can directly go into production processes. On the other hand, the rest of appliances which is not recycled, named as garbage, cannot be in the production process again. They can be incinerated or thrown away, not be reused. In this case, government and companies can make campaigns to create public awareness. In Turkey, some companies exchange old appliances with new ones, in order to recycle them.

Furthermore, it is obtained that Incineration-Garbage rate decrease while recycling amount increases as given in Figure 3. This relationship shows that as the amount of small household appliances thrown away or incinerated decreases due to the campaign effects and awareness.

In this model, there are three additional effects that are used. These effects are assumed constant numbers and while running the model, it is seen that they have a positive and enhancing effect on waste collection amount and recovery options.

These effects can be explained as:

1. Campaign Effect: This effect considers “bring the old one and take the new one” situation, which means consumers can pay a lower price for a new appliance. From the producers’ point of view, it means reaching governmental target by collecting appliances.
2. Company Effect: This effect includes the governmental effect that provides the company, government support if they encourage recycling and recycling centers.
3. Municipality Campaign Effect: Consumers sometimes do not prefer to bring their old small household appliances to companies or private recycling centers. In other words, they can bring their appliances to municipality recycling centers. Municipalities can provide public awareness by campaigns about environmental protection.

In the model, carbon emission and social factor are also accounted. The carbon emission has been affiliated by the number of appliances brought to waste collection center.

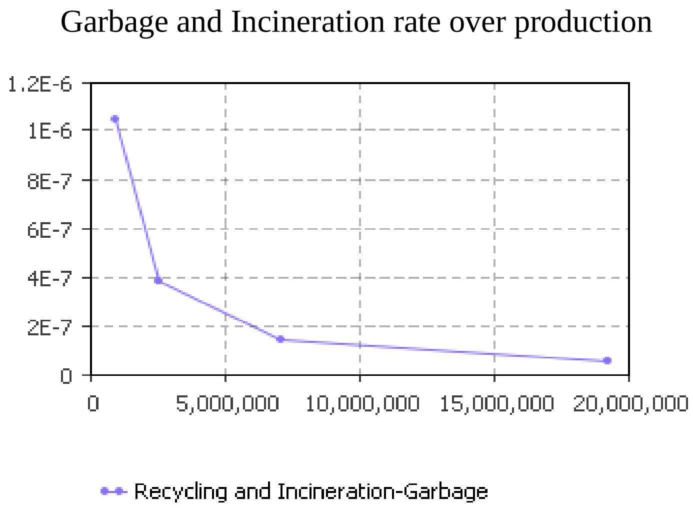


Figure 3: Relationship between recycling and Incineration-Garbage Rate

4. CONCLUSION AND FUTURE STUDIES

In this study, a system dynamics approach has been studied for small household appliances' waste management in Turkey. The model was run by using Anylogic simulation program. The study mainly shows that the proposed model can support a more effective and enhanced view about small household appliances' waste management. Developed and supported waste collection centers by municipalities, government or companies provide a more intensive and increased recovery option, while it decreases garbage and incineration rate. In the model, several factors have been considered in order that recycled products can be added to production line according to the target of Turkey. The real data of the proposed system is limitedly used, because of lack of data, but main future targets have been put in the model. The system dynamics model at this point suggests also that campaign effects and company effects are outstandingly important in order to bring wastes to waste centers and to inform public or increase public awareness about recycling. It has also been obtained that carbon emission decreases and social factor increases when the system works without any errors. The model also calculates how many of small household appliances in Turkey will be in process of recycling in order to reach the target of Turkey by 2018.

For future studies, the real data should be used for all variables mentioned in the model and if the data of companies can be obtained, the model can be revised.

References

1. Al-Khatib, I. A., Eleyan, D., & Garfield, J. (2016). A system dynamics approach for hospital waste management in a city in a developing country: the case of Nablus, Palestine. **Environmental monitoring and assessment**, 188(9), 503.
2. Barnabè, F. (2011). A "system dynamics-based balanced scorecard" to support strategic decision making. **International Journal of Productivity and Performance Management**, 60(5), 446-473. http://dx.doi.org/10.1108/17410401111140383.
3. Botha, A., Grobler, J., & Yadavalli, V. S. (2017). System dynamics comparison of three inventory management models in an automotive parts supply chain. **Journal of Transport and Supply Chain Management**, 11(1), 1-12.
4. Buekens, A., & Yang, J. (2014). Recycling of WEEE plastics: A review. **The Journal of Material Cycles and Waste Management**, 16(3), 415-434. doi:http://dx.doi.org/10.1007/s10163-014-0241-2
5. Devi, S. P., Rao, K. S., Krishnaswamy, S., & Wang, S. (2010). **System dynamics model for simulation of the dynamics of corneal transplants.** Opsearch, 47(4), 284-292. http://dx.doi.org/10.1007/s12597-010-0023-0
6. Dyllick, T., & Hockerts, K. (2002). Beyond the business case for corporate sustainability. **Business Strategy and the Environment**, 11(2), 130.
7. Fischer, C. (2011). The development and achievements of EU waste policy. **The Journal of Material Cycles and Waste Management**, 13(1), 2-9. doi:http://dx.doi.org/10.1007/s10163-010-0311-z
8. Forrester, J. W. (1994), **System dynamics, systems thinking, and soft OR. Syst. Dyn. Rev**., 10: 245–256. doi:10.1002/sdr.4260100211
9. Ghisolfi, V., Chaves, G. D. L. D., Siman, R. R., & Xavier, L. H. (2017). System dynamics applied to closed loop supply chains of desktops and laptops in Brazil: A perspective for social inclusion of waste pickers. **Waste Management**, 60, 14-31.

10. Greasley, A. (2005). Using system dynamics in a discrete-event simulation study of a manufacturing plant. **International Journal of Operations & Production Management**, 25(5), 534-548. Retrieved from http://160.75.22.2/docview/232358137?accountid=11638

11. Inghels, D., & Dullaert, W. (2011). An analysis of household waste management policy using system dynamics modelling. **Waste Management & Research**, 29(4), 351-370.

12. Jang, Y. C. (2010). Waste electrical and electronic equipment (WEEE) management in Korea: generation, collection, and recycling systems. **Journal of Material Cycles and Waste Management**, 12(4), 283-294.

13. Lee, S., Han, W., & Park, Y. (2015). Measuring the functional dynamics of product-service system: **A system dynamics approach. Computers & Industrial Engineering**, 80, 159. Retrieved from http://160.75.22.2/docview/1649225891?accountid=11638

14. Lu, D. (2011). **Fundamentals of supply chain management**. Bookboon.

15. Nair, G. K., & Raj Rodrigues, L. L. (2013). Dynamics of financial system: A system dynamics approach. **International Journal of Economics and Financial Issues**, 3(1), 14-n/a. Retrieved from http://160.75.22.2/docview/1266465919?accountid=11638

16. Öztürk, T. (2015). Generation and management of electrical–electronic waste (e-waste) in Turkey. **Journal of Material Cycles and Waste Management**, 17(3), 411-421.

17. Pedamallu, C., Ozdamar, L., Ganesh, L., Weber, G., & Kropat, E. (2010). **A system dynamics model for improving primary education enrollment in a developing country**. Organizacija, 43(3), 90. http://dx.doi.org/10.2478/v10051-010-0010-5

18. Safdar Shah Khan, Suleman A. Lodhi, Faiza Akhtar, (2015) "Sustainable WEEE management solution for developing countries applying human activity system modeling", **Management of Environmental Quality: An International Journal**, Vol. 26 Issue: 1, pp.84-102, https://doi.org/10.1108/MEQ-05-2014-0072

19. Saxena, S., Srivastava, R. K., & Samaddar, A. B. (2010). Towards sustainable municipal solid waste management in Allahabad City. **Management of Environmental Quality: An International Journal**, 21(3), 308-323.

20. Sinha-Khetriwal, D., Kraeuchi, P., & Schwaninger, M. (2005). A comparison of electronic waste recycling in Switzerland and in India. **Environmental Impact Assessment Review**, 25(5), 492-504.

21. Atık Yönetimi Eylem Planı: 2008-2012. (2008, May). Retrieved from: http://www.cygm.gov.tr/-cygm/files/eylemplan/atikeylemplani.pdf

22. Küçük Ev Aletleri Yeni Trendlerle Büyüyor. (2017, July 19). Retrieved from: http://www.gfk.com/en-gb/insights/press-release/kuecuek-ev-aletleri-yeni-trendlerle-bueyueyor/

23. Resmi Gazete-Official Gazette (2012, May 22) Retrieved from: http://www.resmigazete.gov.tr/-eskiler/2012/05/20120522-5.htm

24. Anylogic simulation (2017, May 3) Retrieved from: https://www.anylogic.com/

RAPID STABILIZATION OF MUNICIPAL SOLID WASTE IN BIOREACTOR LANDFILLS: PREDICTIVE PERFORMANCE USING COUPLED MODELING

G. Kumar and K. R. Reddy*

University of Illinois at Chicago, Department of Civil & Materials Engineering, 842 West Taylor Street, Chicago, IL 60607, USA

*Corresponding author: e-mail: kreddy@uic.edu, tel : +13129964755

Abstract

Municipal solid waste (MSW) landfills are one of the major and most preferred waste management options in the United States and many other countries across the globe. The waste in conventional MSW landfills undergoes very slow decomposition due to limited amount of moisture. In this regard, the bioreactor landfills have emerged as an effective waste management option, wherein leachate recirculation/injection is carried out to enhance the moisture levels within the waste thereby facilitating rapid waste decomposition and leading to early waste stabilization. However, in practice the performance of bioreactor landfills has remained inconclusive due to the lack of sound basis for effective design and operation of such landfills. This further stems from the fact that there is a limited understanding of the physical, chemical and biological processes and their coupled interactions on the MSW behavior in landfills. Hence, it becomes imperative to understand the influence of the coupled processes on the overall performance of bioreactor landfills. Several researchers have developed numerical models to simulate landfill systems but only a few models have considered the simultaneous interactions of hydraulic, mechanical, and biological processes in the landfill. In this study, newly developed numerical framework incorporating coupled thermo-hydro-bio-mechanical processes is presented. The numerical model has the ability to predict the spatial and temporal variation of waste temperatures, moisture distribution, gas generation, pore pressures, waste settlement, waste slope stability, and interface shear response in the landfill liner system. The numerical model has been validated with lab-scale and field-scale experiments and could be used to design and operate stable and effective bioreactor landfills.

Keywords: Solid waste management; bioreactor landfills; leachate recirculation; coupled processes; numerical modeling

1. INTRODUCTION

Landfilling of municipal solid waste, although being the least preferred option, is the most dominant method of managing waste in U.S. and many other countries across the globe. In the light of steady increase in the population and rapid urbanization, the amount of waste produced is also increasing considerably. According to United States Environmental Protection Agency (USEPA), about 254 million tons of MSW was produced in 2014 of which 136 million tons was landfilled (USEPA, 2016). The current practices for construction of traditional engineered landfills that just serve as waste containment systems are well established. This isolated system primarily contains the landfilled MSW in a relatively dry state and is designed with cover systems to prevent infiltration of water from the precipitation and with leachate collection and removal systems to remove any leachate accumulated over the bottom liner system. This in turn results in a very dry condition within MSW and consequently slow decomposition of the organic matter (biodegradable constituents) within the waste

due to the lack of adequate moisture. The slow decomposition of waste leads to several problems such as low gas generation rates, prolonged waste stabilization periods, increased post-closure monitoring requirements, increased leachate treatment and disposal costs, and a long-term liability of the land use with no beneficial purpose.

In recent years the idea of bioreactor landfills has gained wide attention because of its numerous benefits that can lead to sustainable waste management. A schematic of the operation of bioreactor landfill is shown in Fig. 1. The bioreactor landfill uses the concept of an anaerobic digester, wherein the favorable conditions for rapid biodegradation of organic matter within the waste are maintained to accelerate the waste stabilization. In the field, these favorable conditions are achieved by recirculation of leachate and other permitted liquids along with supplemental nutrients and/or inoculum of microbes, thus enhancing the moisture levels essential for rapid waste decomposition. Thus, bioreactor landfills offer several benefits such as rapid waste decomposition, increased gas generation rates, high settlement rates and early waste stabilization. In addition, there are other secondary benefits such as reduced post-closure monitoring cost, reduced leachate treatment and disposal costs, and landfill space reclamation. Several laboratory studies and field-scale pilot tests have been performed confirming the enhanced decomposition of MSW with leachate recirculation into the waste mass. Although the leachate recirculation seems to be a viable concept, there are no established design practices for leachate recirculation, mainly due to the inherent heterogeneity and anisotropy associated with the MSW. Unlike conventional landfills where leachate generation is limited, bioreactor landfills operate on leachate recirculation and if the leachate levels and pore pressures induced by recirculation are not properly managed, it may cause instability in landfill.

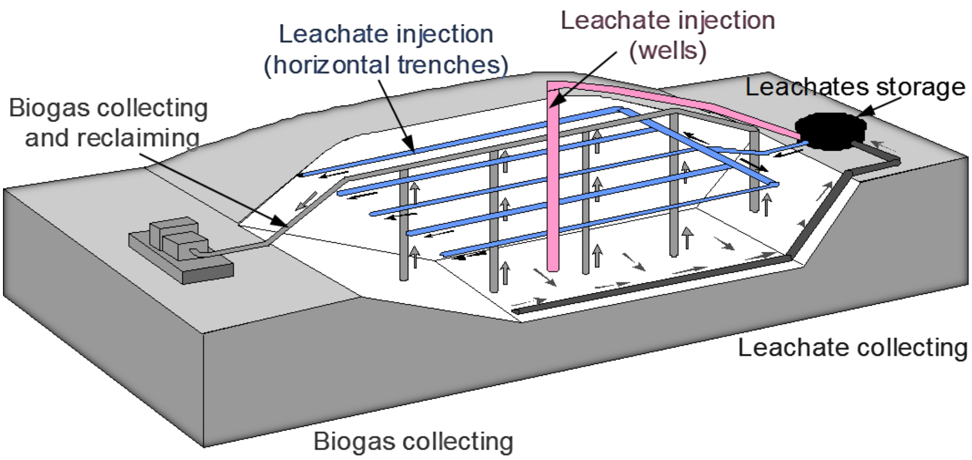


Figure 1: Schematic of Bioreactor Landfill and its Fundamental Operations

In this regard, several numerical modeling efforts were carried out, to investigate the effectiveness of different leachate recirculation systems (LRS) in various configurations for uniformly distributing the injected leachate while maintaining the stability of landfill slopes under pressurized leachate injections (see Reddy et al. 2017a). However, most of these studies neglected the effects of biodegradation and its consequent effects from settlement and gas generation on the fluid flow within the waste. The overall performance of a bioreactor landfill is influenced by several interdependent processes including the leachate flow and distribution, waste settlement due to the overburden stress and mass loss induced by waste decomposition, changes in the shear strength of the waste with degradation, and changes in temperature and heat generated from waste decomposition. Thus, there exists a complex system of simultaneously occurring and interdependent processes within the waste mass. There have also been several numerical investigations that looked at the coupled behavior of MSW accounting for the hydraulic, biochemical and mechanical behavior of MSW into a numerical model to simulate the coupled hydro-bio-mechanical response of MSW in landfills. But these models do not holistically assess the influence of the coupled processes on the performance of other engineered components of a landfill in terms of their stability and integrity within the landfill. In

addition, most of the studies did not account for the heat generation and thermal behavior within the landfill and furthermore, if they did incorporate the effects of heat generation on the transient temperature distribution its influence on the biodegradation of waste mass was not accounted.

In this study a mathematical framework is formulated that can holistically assess the overall performance of the landfill by accounting for the interdependency of hydraulic (fluid flow and pore fluid pressure distribution), mechanical (stress and deformation, waste settlement and slope stability), biological (waste decomposition and gas generation) and thermal (heat generation and temperature distribution) processes within the MSW. A brief review of literature on the attempts to model MSW behavior in bioreactor landfills is presented and some of the major challenges associated with numerical modeling of MSW behavior in such landfills are presented.

2. COUPLED PROCESSES IN MSW LANDFILLS

Municipal solid waste is a highly heterogeneous porous media with its properties (physical, mechanical and biological) varying spatially across the landfill due to inherent differences in waste composition. In addition, the rapid decomposition of the waste under leachate recirculation further exacerbates the situation by causing temporal changes in the waste properties. Thus, the overall performance of a bioreactor landfill is dictated by the combined effect of several interdependent system processes including hydraulic, mechanical, biochemical and thermal processes. A detailed explanation of each of the system processes and their interactions with one another is explained in this section. A schematic of the major system processes and their interactions within the MSW landfills is shown in Fig. 2.

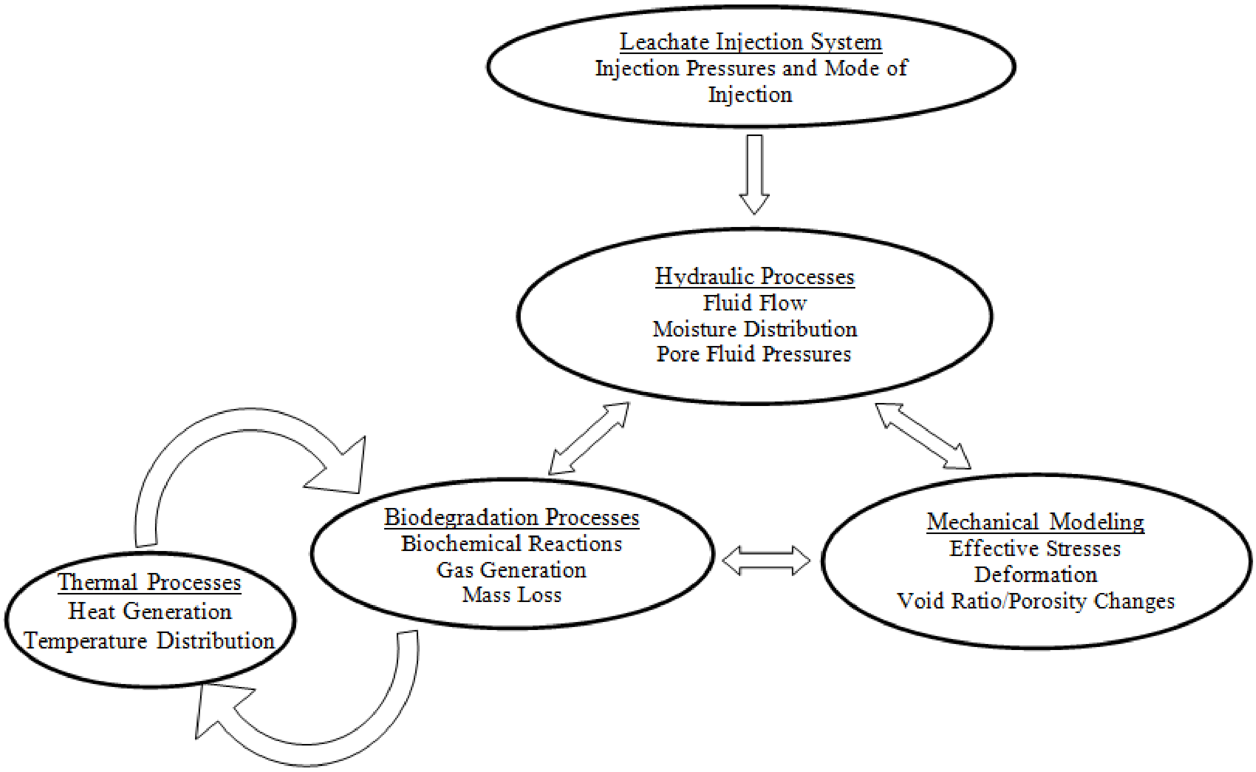


Figure 2: Major Processes and their Coupled Interactions in MSW Landfills

The hydraulic processes within the bioreactor landfills include the fluid flow (leachate flow) and the resulting distribution of moisture and pore-fluid pressures (liquid and gas phase). Due to the relatively low moisture availability in the MSW pore spaces, the fluid flow is generally and suitably assumed to follow unsaturated fluid flow behavior. Moreover, the decomposition of waste generates landfill gas (predominantly methane and carbon dioxide) leading to the gas flow and development of pore gas pressures within the MSW pore space that can have a great influence on the transient leachate

flow and distribution. Thus, a two-phase flow (essentially a multi-phase flow) behavior can be used to adequately simulate the unsaturated fluid flow within the waste mass.

The mechanical behavior of the waste is influenced by the overburden stress from the overlying waste layers and this differs spatially based on the landfill geometry and the spatially varying waste properties. The deformation and consequently the settlement of the waste is partially influenced by the mechanical properties of the waste (e.g. stiffness or modulus, strength parameters). However, the mechanical properties of the waste change temporally as the waste degrades and hence the settlement of the waste induced by overburden stress. In addition to this, a significant amount of the waste settlement is borne out of the mass loss (conversion of biodegradable solids to landfill gas) resulting from the periodic increase and decrease in void spaces within the waste. This contributes to the majority of the waste settlement in MSW landfills.

The biochemical behavior of the waste is mainly dependent on the waste composition. Typically, most of the readily degradable matter is found to be cellulosic and hemi-cellulosic in nature and it contributes the most to the total landfill gas production. A majority of the biodegradation takes place anaerobically due to oxygen deprived conditions within the waste mass. The major biochemical reactions leading to the landfill gas production are hydrolysis involving the breakdown of higher molecular weight organic compounds to easily degradable monomers, followed by acid production (typically acetic acid) by microbially aided acidogenesis through fermentative bacteria, and finally the generation of methane by methanogenic bacteria. In all of this, the leachate chemistry and the biochemical reaction kinetics dictate the generation of landfill gas. Moreover, the biodegradation process is influenced by many factors including, temperature, pH, and moisture among others.

The anaerobic biodegradation of organic matter in the MSW releases heat which influences the temperature within the waste mass. Furthermore, the resulting temperature in turn dictates the biodegradation of waste mass since the optimum degradation of waste occurs only at a certain temperature range. In addition, the overall spatial and temporal distributions of temperatures within the waste are influenced by the seasonal temperature changes as well. Thus, understanding the thermal behavior of MSW and incorporating its influence on the other system processes in a landfill plays a significant role in a better prediction of the overall performance of the landfill.

Each of the above-mentioned processes occur and interact simultaneously influencing the overall behavior of MSW. For example, the fluid flow (leachate and gas) within the MSW is dictated by the porosity, available moisture and the permeability of waste for the fluids. However, the decomposition of waste that occurs simultaneously as the fluid flows through the MSW causes the mass loss resulting in changes in the void spaces (porosity) and in turn influences the fluid flow thereafter. In addition, the increase in the void spaces can cause the waste to settle under the overburden stresses causing changes in the pore fluid pressures. Furthermore, the changing void space (void ratio) alters the moisture availability in MSW across the landfill, consequently influencing the biodegradation rates of MSW at different locations in the landfill. The temperature dependent heat generation constantly influences the biodegradation of MSW and thereby the other processes impacted by the biodegradation of waste. It is quite evident that the landfill system is a unique and complex multiphase system with several processes occurring simultaneously in a coupled manner. It is of utmost importance to understand the individual system processes and their coupled interactions accurately to have a good prediction on the performance of a landfill system thereby enabling safe and effective construction and operation of bioreactor landfills.

3. PREVIOUS INVESTIGATIONS ON BIOREACTOR LANDFILLS

Over the past few years a comprehensive research has been performed at the University of Illinois at Chicago (UIC) on bioreactor landfills involving field investigations, laboratory tests on MSW samples and numerical modeling of MSW behavior based on the characteristics of MSW as observed from the experimental studies. A list of all the previous studies on bioreactor landfills performed at UIC is shown in Table 1. A thorough field investigation was performed to determine the variation of

in-situ moisture and density variation with depth and leachate injection were monitored to characterize the field waste. In addition, geophysical testing was performed to determine other dynamic and mechanical properties of waste. Several laboratory investigations were performed which involved testing of field MSW samples from a leachate recirculation landfill for their geotechnical properties such as the compressibility, shear strength, hydraulic conductivity, specific gravity, unit weight and other crucial properties. These properties were further evaluated at different stages of waste degradation to determine the effect of degradation on waste properties. In addition, biochemical testing was performed on the field MSW samples to determine the biochemical properties of MSW. All of the tests performed on field MSW samples were also performed on synthetic waste to have a control on the degradation and thereby evaluate the variation in waste properties with time.

Table 1: Previous Research on Bioreactor Landfills at UIC

Research Type	Topic of the Study	Reference
Field Investigation	In-situ properties of MSW at a leachate recirculating landfill	Grellier et al. (2006, 2007)
	Geophysical testing for evaluating dynamic properties of MSW	Carpenter et al. (2013a,b)
	Field Monitoring and performance assessment of bioreactor landfill	Reddy et al. (2009a)
Laboratory Investigation	Laboratory testing of geotechnical properties (compressibility, shear strength, hydraulic conductivity, etc.) of field and synthetic waste samples	Reddy et al. (2009b,d,e); Reddy et al. (2009b); Reddy et al. (2011); Reddy et al. (2015a)
Numerical Modeling/ Simulation	Settlement modeling	Babu et al. (2010, 2011)
	Modeling single phase (liquid) fluid flow in bioreactor landfills to evaluate the moisture distribution by different leachate injection systems	Kulkarni and Reddy (2012); Reddy et al. (2013a,b); Reddy et al. (2014); Giri and Reddy (2014a); Reddy et al. (2015b,c)
	Slope stability under pressurized leachate injection	Giri and Reddy (2014b,c); Giri and Reddy (2015a)
	Modeling of coupled hydro-mechanical processes	Giri and Reddy (2015d)
	Modeling of coupled hydro-bio-mechanical processes	Reddy et al. (2017a,b); Reddy et al. (2018a,b)

Numerical modeling techniques are a great tool in simulating the coupled processes within MSW. It has been extensively used in order to understand the behavior of MSW and the influence it has on the performance of different components of a landfill. It is quite essential to maintain the integrity and stability of landfill components such as the liner and cover systems along with the stability of landfill slopes for a holistic assessment of the performance of a landfill system. In the recent years, a progressive modeling effort has been laid on trying to accurately simulate the different processes and their interactions. Most of the initial numerical studies on bioreactor landfills performed in this regard neglected the combined effects of different processes and mainly focused on the hydraulic aspects of bioreactor landfills (e.g. moisture and pore pressure distribution). Some of the studies evaluated the effectiveness of different subsurface leachate recirculation systems (horizontal trenches, vertical

injection wells, drainage blankets) in uniformly distributing the injected leachate (Kulkarni and Reddy 2012; Reddy et al. 2013a,b; Reddy et al. 2014; Giri and Reddy 2014a; Reddy et al. 2015b,c). Thereafter, the study was focused on evaluating the stability of landfill slopes under different injection pressures or flow rates (Giri and Reddy 2014b,c; Giri and Reddy 2015a). Design recommendations were developed based on these investigations suggesting the safe injection pressures and setback distance for locating the injection system from the landfill slope that needs to be followed.

Recently, there have also been efforts to incorporate the coupled interactions between hydraulic, mechanical and biological processes into the numerical model to predict the MSW behavior in landfills (Reddy et al. 2017a). These studies focused on simulating the coupled hydro-bio-mechanical processes to try and understand the complexity associated with the MSW behavior within the landfill and how it affects the holistic performance of a bioreactor landfill. In this regard a mathematical modeling framework that incorporates the coupled hydro-bio-mechanical processes and its impacts on the stability and integrity of the landfill system has been formulated. In particular, this mathematical framework integrates a two-phase flow hydraulic model, a 2-D plain strain mechanical model, and a first order decay biodegradation model. The entire mathematical framework is implemented in a commercial software named FLAC.

The two-phase flow model built-in FLAC simulates the saturated-unsaturated fluid flow based on the Darcy's law. The hydraulic conductivity of the fluids under unsaturated conditions is given by the relative permeability functions of the van Genuchten form (van Genuchten, 1980). The mechanical model for MSW involves the 2-D plain strain formulation of Mohr-Coulomb constitutive law to simulate the stress-strain behavior of MSW. The biodegradation of waste is simulated using the first order decay kinetics. The gas generation from waste degradation is similar to the USEPA's LandGEM model. However, the biodegradation model formulated in this study incorporates the effect of changing moisture as fluid flows through the MSW on the rate of biodegradation of waste. The extent of waste degradation at a location in the landfill is derived from the gas produced and the biochemical methane potential of the waste. Meanwhile as the biodegradation takes place the waste properties also change as per the correlations developed between the extent of degradation and the geotechnical properties of the waste from previous experimental investigations on field MSW samples, thus simulating a transient coupled hydro-bio-mechanical behavior of MSW. A detailed explanation of the entire numerical framework and simulations performed using the abovementioned numerical framework is presented in Reddy et al. (2017b). Some of the results obtained from these numerical simulations performed using the numerical framework is presented in this study.

Fig. 3a shows the comparison of the variation of surface settlement with time for a conventional and bioreactor landfill. It can be observed that total settlement in both the cases is the same due to the same amount of waste and its composition in both conventional and bioreactor landfill simulation. However, the time it takes for attaining the total settlement in a bioreactor landfill is significantly less than the conventional landfill. This is mainly because of the higher rates of biodegradation in bioreactor landfill due to the availability of moisture. Thus, the numerical model could simulate the different landfill settlement behavior with and without recirculation reasonably well. Likewise, three numerical simulations of a landfill with the same waste conditions and landfill geometry were carried out. However, each of the three simulations incorporated different system processes. The first simulation represented a bioreactor landfill (with leachate injection) but neglected the effect of biodegradation on the MSW behavior (coupled hydro-mechanical simulation). The second simulation represented a conventional landfill (with no leachate injection) and the third simulation represented a bioreactor landfill (with leachate injection) but incorporated the effect of biodegradation on MSW behavior. The three landfill models were evaluated for their slope stability under different simulated conditions. For the coupled hydro-mechanical simulation the factor of safety (FOS) against slope stability decreased continuously with increasing pore pressures from leachate injection (see Fig. 3b). For the coupled bio-mechanical simulation, there were no excess pore pressures as such in the system due to the absence of pressurized leachate injection. Thus, the FOS values almost remained constant over the entire simulation. However, for the coupled hydro-bio-mechanical simulation resulted in an

initial decrease in the FOS values until certain time where the effect of increasing pore pressures was dominant. Meanwhile the changes in the waste properties (increasing unit weight, increasing cohesive strength of waste) resulted in an overall increase in the slope stability as indicated by the increase in FOS values. In the long-term with substantial settlement and dissipated pore water pressures and limited changes in the waste properties the FOS values reached equilibrium. Hence, incorporating the effects of biodegradation along with other processes is essential for accurate prediction of the stability of a bioreactor landfill.

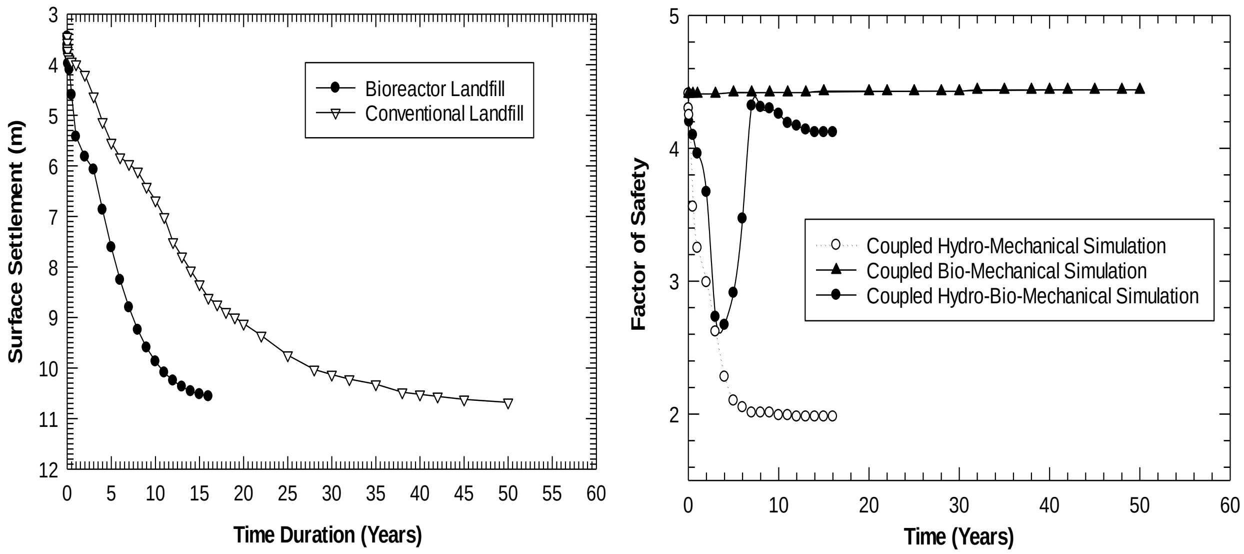


Fig. 3: (a) Variation of Surface Settlement in Conventional and Bioreactor Landfill; (b) Variation of Factor of Safety of Landfill Slope with Elapsed Time for coupled hydro-mechanical, coupled bio-mechanical and coupled hydro-bio-mechanical simulation

4. SUMMARY AND ONGOING RESEARCH

Bioreactor landfills are an attractive option for effective and efficient management of waste. They offer numerous advantages over the traditionally constructed and operated landfills in several aspects. Moreover, in the light of sustainable development, bioreactor landfills prove to be an ideal concept of waste management. However, there are no rigorous procedures or guidelines for safe design of such landfills. Unlike conventional landfills, the construction and operation of bioreactor landfills require adequate knowledge and accuracy on the required moisture levels within the landfill, the injection pressures and flow rates all of which depends on a good estimation of the properties of waste. One of the major concerns in leachate recirculating landfills is to ensure uniform distribution of moisture across the landfill space, which is hindered by the lack of understanding of the hydraulic behavior in MSW. In addition, the biodegradation of MSW makes the understanding of the landfill system quite complex due to the interdependency of the hydraulic flow, mechanical response and biodegradation on one another. Thus, understanding these individual processes and their interactions will aid in simulating this behavior mathematically thereby allowing us to design safe and effective bioreactor landfills.

Several researchers have performed numerous studies to numerically simulate the coupled processes and evaluate the performance of the landfill system. However, these studies do have some limitations from the simplification made in simulating the hydraulic, mechanical and biochemical processes. The current research at UIC is focused on addressing the research challenges pertaining to adequate mathematical description and accurate simulation of the biochemical reactions and their kinetics within the MSW. None of the existing coupled models account for the influence of heat generation and temperature distribution within the landfill on the biodegradation of MSW. Thus, numerical

modeling of temperature distribution and heat generation within the landfill is currently being carried out to have an accurate description of the biodegradation of MSW. In addition, accurate simulation of the mechanical response of the waste undergoing degradation is another important ongoing research topic at UIC. Understanding the mechanical behavior of waste has always been a challenging task and requires adequate experimental investigation to delineate the constitutive behavior and to formulate mathematical description that can simulate the experimental behavior. Finally, integration of all these different aspects into a comprehensive coupled model is crucial to predict overall performance of a bioreactor landfill.

Acknowledgements
This project is funded by the U.S. National Science Foundation (CMMI # 1537514), which is gratefully acknowledged

References

1. Carpenter, P.J., Reddy, K.R., and Thompson, M.D. (2013a) ‘Dynamic properties of municipal solid waste in a bioreactor cell at orchard hills landfill, Illinois, USA’ **7th International Conference on Case Histories in Geotechnical Engineering**, Wheeling, IL, USA
2. Carpenter, P.J., Reddy, K.R., and Thompson, M.D. (2013b). ‘Seismic imaging of a leachate recirculation landfill: Spatial changes in dynamic properties of municipal solid waste’ **Journal of Hazardous, Toxic, and Radioactive Waste**, Vol. 17(4), 331-41
3. Giri, R.K., and Reddy, K.R. (2014a). ‘Design charts for selecting minimum setback distance from side slope to horizontal trench system in bioreactor landfills’ **Geotechnical and Geological Engineering Journal**, Vol. 32(4), 1017-1027
4. Giri, R.K., and Reddy, K.R. (2014b). ‘Slope stability of bioreactor landfills during leachate injection: Effects of unsaturated hydraulic properties of municipal solid waste’ **International Journal of Geotechnical Engineering**, Vol. 8(2), 144-156
5. Giri, R.K., and Reddy, K.R. (2014c). ‘Slope stability of bioreactor landfills during leachate injection: Effects of heterogeneous and anisotropic municipal solid waste’ **Waste Management & Research**, Vol. 32(3), 186-197
6. Giri, R.K., and Reddy, K.R. (2015a). ‘Slope stability of bioreactor landfills during leachate injection: Effects of geometric configurations of horizontal trench systems’ **Geomechanics and Geoengineering**, Vol. 10(2), 126-138
7. Grellier, S., Reddy, K., Gangathulasi, J., Adib, R., and Peters, C. (2006). ‘Electrical resistivity tomography imaging of leachate recirculation in orchard hills landfill’ **SWANA Conference**, Charlotte, 7p.
8. Grellier, S., Reddy, K.R., Gangathulasi, J., Adib, R., and Peters, C. (2007). ‘US MSW and its biodegradation in a bioreactor landfill’ Sardinia 2007, **11th International Waste Management and Landfill Symposium**, S. Margherita di Pula, Cagliari, Italy, 10p
9. Kulkarni, H.S., and Reddy, K.R. (2012). ‘Moisture distribution in bioreactor landfills: A review’ **Indian Geotechnical Journal**, Vol. 42(3), 125-149
10. Reddy, K.R., Gangathulasi, J., Parakalla, N., Bogner, J., Carpenter, P., and Lagier, T. (2009a). ‘Field monitoring and performance assessment of Orchard Hills bioreactor landfill’ **NSF Engineering Research and Innovation Conference**, Honolulu, HI, 13p
11. Reddy, K.R., Hettiarachchi, H., Gangathulasi, J., Parakalla, N., Bogner, J.E., and Lagier, T. (2009b). ‘Compressibility and shear strength of municipal solid waste under short-term leachate recirculation operations’ **Waste Management & Research**, Vol. 27(6), 578-587

12. Reddy, K.R., Hettiarachchi, H., Gangathulasi, J., Bogner, J.E., and Lagier, T. (2009c). 'Geotechnical properties of synthetic municipal solid waste' **International Journal of Geotechnical Engineering**, Vol. 3(3), 429-438
13. Reddy, K.R., Hettiarachchi, H., Parakalla, N., Gangathulasi, J., Bogner, J.E., and Lagier, T. (2009d). 'Hydraulic conductivity of MSW in landfills' **Journal of Environmental Engineering**, Vol. 135(8), 677-683
14. Reddy, K.R., Hettiarachchi, H., Parakalla, N.S., Gangathulasi, J., and Bogner, J.E. (2009e). 'Geotechnical properties of fresh municipal solid waste at Orchard Hills landfill, USA' **Waste Management Journal**, Vol. 29(2), 952-959
15. Reddy, K.R., Hettiarachchi, H., Gangathulasi, J., and Bogner, J.E. (2011). 'Geotechnical properties of municipal solid waste at different phases of degradation' **Waste Management**, Vol. 31(11), 2275-2286
16. Reddy, K.R., Hettiarachchi, H., Giri, R.K., and Gangathulasi, J. (2015a). 'Effects of degradation on geotechnical properties of municipal solid waste from Orchard Hills Landfill, USA' **International Journal of Geosynthetics and Ground Engineering**, Vol. 1(3), 1-14
17. Reddy, K.R., Kulkarni, H.S., and Khire, M.V. (2013a). 'Two-phase modeling of leachate recirculation using vertical wells in bioreactor landfills' **Journal of Hazardous, Toxic and Radioactive Waste**, Vol. 17(4), 272-284
18. Reddy, K.R., Kulkarni, H.S., Srivastava, A., and Sivakumar Babu, G.L. (2013b). 'Influence of spatial variation of hydraulic conductivity of municipal solid waste on performance of bioreactor landfills' **Journal of Geotechnical and Geoenvironmental Engineering**, Vol. 139(11), 1968–1972
19. Reddy, K.R., Giri, R.K., and Kulkarni, H.S. (2014). 'Design of drainage blankets for leachate recirculation in bioreactor landfills using two-phase flow modeling' **Computers and Geotechnics**, Vol. 62, 77-89
20. Reddy, K.R., Kulkarni, H.S., and Giri, R.K. (2015b). 'Design of horizontal trenches for leachate recirculation in bioreactor landfills using two-phase modeling' **International Journal of Environment and Waste Management**, Vol. 15(4), 347-376
21. Reddy, K.R., Kulkarni, H.S., and Giri, R.K. (2015c). 'Design of vertical wells for leachate recirculation in bioreactor landfills using two-phase modeling' **Journal of Solid Waste Technology and Management**, Vol. 41(2), 203-218
22. Reddy, K.R., Kulkarni, H.S., and Giri, R.K. (2015d). 'Modeling coupled hydro-mechanical behavior of landfilled waste in bioreactor landfills: Numerical formulation and validation' **Journal of Hazardous, Toxic and Radioactive Waste**, ASCE, Vol. 21(1), D4015004
23. Reddy, K.R., Kumar, G., and Giri, R.K. (2017a). 'Modeling coupled processes in municipal solid waste landfills: An overview with key engineering challenges' **International Journal of Geosynthetics and Ground Engineering**, Vol. 3(1), 6
24. Reddy, K.R., Kumar, G., and Giri, R.K. (2017b). 'Influence of dynamic coupled hydro-bio-mechanical processes on response of municipal solid waste and liner system in bioreactor landfills' **Waste Management**. Vol. 63, 143-160
25. Reddy, K.R., Kumar, G., and Giri, R.K. (2018a). 'System effects on bioreactor landfill performance based on coupled hydro-bio-mechanical modeling' **Journal of Hazardous, Toxic and Radioactive Waste**, ASCE, Vol. 22(1), 04017024
26. Reddy, K.R., Kumar, G., Giri, R.K. and Basha, B.M. (2018b). 'Reliability assessment of bioreactor landfills using Monte Carlo simulation and coupled hydro-bio-mechanical model' Waste Management, 72:329-338. (10.1016/j.wasman.2017.11.010)

27. Sivakumar Babu, G.L., Reddy, K.R., Chouskey, S.K., and Kulkarni, H.S. (2010). 'Prediction of long-term municipal solid waste landfill settlement using constitutive model' **Practice Periodical of Hazardous, Toxic, and Radioactive Waste Management**, Vol. 14(2), 139-150
28. Sivakumar Babu, G.L., Reddy, K.R., and Chouskey, S.K. (2011). 'Parametric study of MSW landfill settlement model' **Waste Management Journal**, Vol. 31(6), 1222-1231
29. USEPA (2016). '**Advancing Sustainable Materials Management: 2014 Fact Sheet**'

COLLECTION AND HANDLING OF SHIP WASTE AND CARGO RESIDUES IN GREECE: PRESENT AND FUTURE

Th. Giantsi*, S. Tsioupli, K. Flegkas, P. Koufos and J. Angelopoulos

Regulatory Authority for Ports, GR- 185 35 Gr. Lambraki 150, Piraeus, Greece

[*]Corresponding author: e-mail: thegiant@raports.gr

Abstract

Waste streams generated on board ships en route and during cargo operations are governed by the MARPOL 73/78 waste/residues UN Convention; their efficient delivery at shore and final disposal is a Member States obligation. In order to ensure availability and safe delivery to the Port Reception Facilities (PRF), the European Parliament and the European Council adopted the Directive 2000/59/EU on for ship-generated waste and cargo residues, taking into account International Maritime Organization (IMO) measures. The main difference between the MARPOL 73/78 Convention and the 2000/59/EU Directive is that the former focuses mainly on board operations, whereas the Directive regulates shore side activities. Implementation of the MARPOL 73/78 waste/residues Convention and of the Directive 2000/59/EU in Greece, was implemented by the Common Ministerial Decision 8111.1/41/2009; both Directive and Decision are currently under revision. A proposal for a new Directive has been published in January 2018.

The recent EU Regulation 2017/352 establishes a framework for the provision of port services and common rules on the financial transparency of European ports, affecting as well the ship waste handling sector. In Greece, the regulator that ensures application of the regulation in the domain of ports is the Regulatory Authority for Ports (RAL).

The main targets of this work include the presentation of a) the existing state of delivery and shore-side management procedure for ship waste in Greece, b) the service provision market challenges, c) the assessment of environmental friendly processes and d) the regulatory aspects.

Keywords: ship waste; cargo residues; ports; regulation; port reception facilities; MARPOL 73/78

1. INTRODUCTION

In the domain of the International Agreements, Conventions constitute documents are signed by Member States of International Organizations and then implemented within Member States through their adoption by National Legislative Frameworks. In the case of European Union (EU), an additional step can be required, involving the adoption of the Agreement by the EU legislative system itself. In Greece, us a member state of E.U., the hierarchical implementation steps include: International Convention, EU legal acts (such as Regulation, Directive, or Decision) and, finally, national legal acts as Law, or Presidential Decree or (Common) Ministerial Decision or combination of the above. In the case of ship waste legislation, the procedure is more complicated due to the fact that, the management of waste on board ships is under the conventions of International Maritime Organization (IMO), until their shore-side delivery, where other Conventions or Legislative acts are set in force.

Despite the focus of the European Union on the environmental issues, several waste management related issues are still unresolved, including different definitions for the same or similar terms, (e.g. definition of MARPOL, for residues/wastes versus the Directive's ship –generated waste) which

causes problems to the complicated procedure of the treatment and the disposal of all kinds of wastes in the EU. The lead time between transitions of measures from one legal system to another contributes to missing or newly added clauses and procedures, resulting to amendments and delays, rendering some measures obsolete. Implementation differences between Member States add additional complexity and confusion. The current standards set by the European Maritime Policy for the good environmental status of the marine waters are high, resulting to minimization of waste disposal.

In the case of Greece, an additional factor of complication for waste and cargo residue management is posed by the complexity of its National Port System: Due to the geomorphology of the country, where more than 3.000 islands exist and more than 1.000 registered port facilities operate, the adoption, implementation and surveillance of a system for the collection handling, treatment and final disposal of ship waste is a very difficult procedure, involving many stakeholders including local / municipal authorities, prefectures, ministries and one regulator, the Regulatory Authority for Ports.

In this paper a succinct description of the Greek Port System is presented, including the primary responsibilities of Regulatory Authority for Ports. The rapidly evolving International, European and National Legal frameworks, concerning the ship waste are also presented. The structure of the Greek Market at the field of ship waste handling is described and compared to other European practices. The European market of ship waste services faces new, regulatory challenges. The Greek State has the opportunity to legislate appropriately to the benefit of market stakeholders, service providers and end-users alike.

2. THE GOVERNANCE OF THE GREEK PORT SYSTEM

2.1 Greek Port System

As of 2018, more than 1.060 port facilities operated in Greece, managed by 97 Port Authorities (Giantsi, 2016). The role of Port Authorities is fulfilled by four different institutional frameworks i.e. Port Authorities S.A., as private enterprises, Public Port Funds, Public Port Offices, and Municipal Port Funds as public enterprises. Notwithstanding, a large number, approximately 240, of port facilities do not belong to any managing body.

With respect to their significance, Greek Ports are divided in four main categories: a) ports of *international significance* (16), b) Port of *national significance* (16), c) ports of *major interest* (25) and d) *local* ports (~1000). Categorization according to their major six uses include: a) *Commercial / Freight ports*, b) *Passenger ports*, c) *Tourist Ports*, d) *Fishing Ports*, e) *Multipurpose Ports*, and f) *Special Purpose Ports* (e.g. military ports, shipyards); this allocation is in Figure 1. The majority (42%) of the Greek Port Facilities is comprised by small fishing ports; 18% are multipurpose, 15% are commercial, 15% are Tourist. Only 5% are passenger ports, and the last 5% corresponds to special purpose ports.

Tourist ports are licensed and supervised by the Ministry of Tourism, while the rest categories by the Ministry of Maritime Affairs and Insular Policy. Furthermore, Tourist Ports are divided in 3 categories: Marinas, Shelters and Moorings.

25 Greek Ports have joined the *Trans European Transport Network* (TEN-T), 5 of which belonging to the *core network* and 20 to the *comprehensive network*. The allocation of these 25 ports is presented in Figure 2.

Due to the privatization of the biggest Greek Ports, (Piraeus and Thessaloniki) a new entity, (the Public Port Authority), subject to the Ministry of Maritime Affairs and Insular Policy, was established to take over the administrative responsibilities of the Greek State that cannot be delegated to private entities. At the same time, the *Regulatory Authority for Ports* was established, in order to regulate port services and oversee concession agreements, as an independent regulator, subject only to the Greek Parliament.

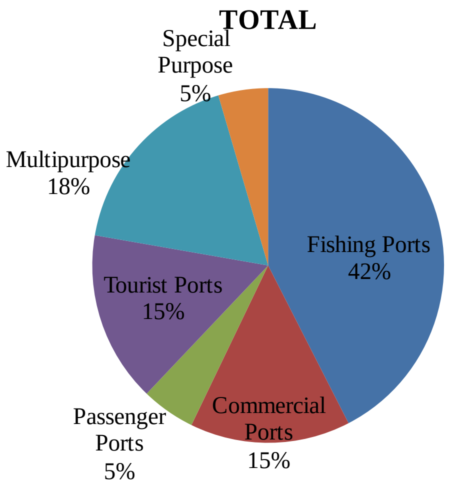


Figure 1: Distribution of Greek Ports per use

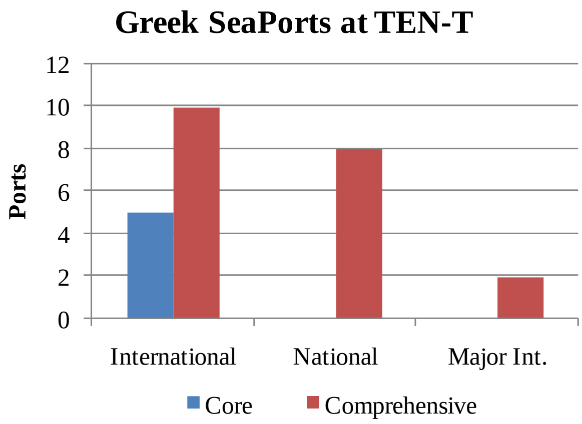


Figure 2: Distribution of TEN-T Greek Ports

2.2 The Regulatory Authority for Ports

The *Regulatory Authority for Ports* was initially established in May 2014 pursuant to the Laws of 4150/2013, 4254/2014 and 4258/2014 as an Independent Public Authority, subject to the Ministry of Shipping and the Aegean, with administrative and financial autonomy. Pursuant to the Law 4389/2016, (G.G., A' 94/27.05.2016) in May 2016 it was transformed into an Independent Authority, subject to the Greek Parliament. The mission of the Authority includes overseeing, regulating and catering for the legality of relations between public and private entities in the national port system. Emphasis is given to contractual compliance and the application of competition law in the port industry. Responsibilities of the Authority include:

- issuing of regulatory, directly enforceable regulatory and advisory decrees,
- overseeing the level of service, the compliance of stakeholders with competition law and the accomplishment of the financial objectives in ports under concession contracts,
- exercising of the contractual rights of the Hellenic Republic in ports under concession contracts,
- resolving differences between ports operators and port users,
- establishing of port charging methodologies,
- deciding for provisional measures in emergency situations and inspections, in cooperation with judicial bodies and
- advisory support to the Greek state with respect to the organization and legislative framework of the national port system, port services and port planning.

The Regulatory Authority for Ports supervises commercial methods and practices of port service providers and enforces regulatory measures, ensuring the unobstructed provision of port services to users, and access to port services.

The deliveries of Regulatory Authority for Ports, as an Independent Authority from May 2016 until today, includes the completion of 79 case requests and complaints with respect to port services, port infrastructure charges, port service contracts and dredging services.

The main arguments for the creation of the Regulatory Authority for Ports include: a) the need to monitor, control and enrich European experience with respect to *total concessions* of public ports and port authorities, b) the need to reduce uncertainty and enhance management consistency and continuity in the management, by monitoring of total concession contracts, sub-concessions of port infrastructure and the rendering of certain port services from the Greek State, c) the need to regulate

port access, charging and performance in relation to the required level of service for port service users, d) the need for specialized, multilevel knowledge (economic, technical and legal knowledge) and a focus on: i) the ex-ante regulation of the port services market, the advice on more specific issues for port services and the prevention of market failures without excessive interference, and ii) the ex-post investigation of competition issues deriving from breach of the legal and contractual obligations of port operators and port services market distortions.

Apart from Greece, rapid developments in the international and European port industry are taking place in the recent years, and the formation of alliances between international port terminal management companies (*global operators*), large shipping companies and logistics companies (*mega carriers*) are blurring the distinction between the port industry, shipping, transport and logistics, developing a so-called post-globalized framework (Angelopoulos et al,. 2018). This framework calls for novel aspects of regulation at a transnational, European and global level, and to this end the establishment and operation of institutions similar to the Regulatory Authority for Ports.

3. LEGISLATIVE FRAMEWORK

3.1 MARPOL73/78 Convention

In order to prevent the pollution from ships, IMO set in force the MARPOL 73/78 waste/residues UN Convention (IMO, 2017), in 1973 for the first time. A large number of amendments have been incorporated in the initial edition. New amendments are also expected to be set into force in the near future.

All waste streams generated on board ships during normal operations and during cargo operations are to be treated and final disposed under a clear procedure, according to the MARPOL Convention. Regulations for management of waste and residues are divided within six Annexes:

Annex I: Regulations for the Prevention of Pollution by Oil
Annex II: Regulations for the Control of Pollution by Noxious Liquid Substances in Bulk
Annex III: Regulations for the Prevention of Pollution by Harmful Substances Carried by Sea in Packaged Form
Annex IV: Regulations for the Prevention of Pollution by Sewage from Ships
Annex V :Regulations for the Prevention of Pollution by Garbage from Ships
Annex VI :Regulations for the Prevention of Air Pollution from Ships

According to MARPOL 73/78, garbage is categorized as follows:

a) Plastics, b) Food wastes, c) Domestic wastes (e.g., paper products, rags, glass, metal, bottles, crockery, etc.), d) Cooking oil, e) Incinerator Ashes, f) Operational wastes, g) Cargo residues, h) Animal Carcass(es), i) Fishing gear.

Efficient delivery of MARPOL wastes / residuals at shore, treatment and final disposal are obligations of Member States.

A so-called *Waste Reception and Handling Plan* is required by the managing bodies of the port. In order to ensure compliance with MARPOL, IMO published the Circular MEPC/834 *Consolidated Guidance for Port Reception Facility Providers and Users* (IMO, 2014).

3.2 European legislative framework

Traditionally, EU has been very sensitive with respect to environmental issues. A litany of Regulations, Directives and Decisions has been entered in force in order to ensure high environmental standards. The impact of the implementation of each legal act is always under examination, and when new legal acts are adopted, the old ones are amended or repealed and Member States are obliged to implement the new acts to their legislative system.

In order to reduce the discharges of ship-generated waste and cargo residues, the European Parliament and the European Council adopted the Directive 2000/59/EU (OJEC, L 332/28.12.2000)- currently

under revision-, in accordance with the MARPOL Convention. In order to facilitate Member State implementation of the Circular MEPC/834 and based on the experience gained from monitoring and assessing the implementation of Directive 2000/59/EC during the past 15 years, the Commission has decided to clarify some of the key provisions of the Directive via a Commission's Notice (2016/C 115/05) entitled *Guidelines for the interpretation of Directive 2000/59/EC*. (OJEC, 2000)

The Directive 2000/59/EU refers only to Annexes I, IV and V to MARPOL 73/78 waste and residues and applies to *"a) all ships, including fishing vessels and recreational craft, irrespective of their flag, calling at, or operating within, a port of a Member State, with the exception of any warship, naval auxiliary or other ship owned or operated by a State and used, for the time being, only on government noncommercial service; and (b) all ports of the Member States normally visited by ships falling under the scope of point (a)."*

Waste and residues from other Annexes are treated differently according to other EU directives and regulations. The obligation for the development of a *Waste Reception and Handling Plan* (WRH) is included within the Directive. Pursuant to the Directive, these WRH Plans are to be revised every three years.

A study has been conducted for the European Commission by ECORYS (2017), assessing the impact and challenges of the 2000/59/EU Directive implementation. Two main problems were identified, namely: a) waste discharged at sea and b) administrative burden.

The first problem was attributed to the significant difference between volumes of waste produced on board, and waste delivered at shore. A significant amount of *Ship Generated Wastes* (SGW) are being discharged at sea, under the permission of MARPOL and constitute a negative impact for the marine environment. Significant volumes of waste are believed to be discharged illegally, resulting also in a serious negative impact; finally, a non documented sufficiently yet volume of wastes is being treated on board. A review of present technologies and methods being used to reduce SGW, is presented by a study conducted by CE Delft, for the European Maritime Safety Agency (EMSA, 2017). To eliminate the discharge of waste at sea, several new measures are proposed. One of these measures includes the elimination of the direct and indirect cost of the delivery at shore, the treatment and the final disposal of the wastes. Increase of the waste treatment on ship is also another measure.

The marine environment is also protected with several other EU legislative acts:

a) the Directive 2008/98/EC, (OJEC, 2008), of the European Parliament and of the Council of 19 November 2008 on waste and repealing certain Directives b) the Directive 2008/56/EC, (OJEC, 2008a) of the European Parliament and of the Council of 17 June 2008 establishing a framework for community action in the field of marine environmental policy (Marine Strategy Framework Directive), c) the Regulation (EC) 1069/2009, (OJEC, 2009) of the European Parliament and the Council of 21 October 2009 laying down health rules as regards animal by-products and derived products not intended for human consumption and repealing Regulation (EC) 1774/2002, d) the Directive 2009/16/EC, of the European Parliament and the Council of 23 April 2009 on port state control and, finally, e) the Regulation (EU) 2017/352 (OJEC, 2017) of the European Parliament and of the Council of 15 February 2017 establishing a framework for the provision of port services and common rules on the financial transparency of ports.

The Regulation (EU) 2017/352 applies to seven port services, including the collection of ship-generated waste and cargo residues and applies also to all maritime ports of the Trans-European Transport Network (TEN-T), as listed in Annex II to Regulation (EU) 1315/2013, (OJEC, 2013). Regulation 2017/352 is dealing with the following issues: a) minimum requirements for the provision of port services, b) limitations on the number of providers, c) public service obligations and d) restrictions related to internal operators.

Finally, the Proposal for a Directive on port reception facilities for the delivery of waste from ships, repealing Directive 2000/59/EC and amending Directive 2009/16/EC, (OJEC, 2009) and Directive 2010/65/EU, (OJEC, 2010) is published in January 2018, (EC, 2018).

Another important parameter is that the procedures for reception, collection, storage, treatment and disposal should always conform to European Environmental Policy.

During the consultation for the revision of the Directive, four Policy Options were examined: 1) Baseline, 2) Minimum revision, 3) MARPOL alignment, 4) EUPRF regime for all discharges; and variant options 3b and 4b on Marine Litter. The 3b option was selected, targeting to: a) clarify the relationship with the MARPOL Convention, b) simplify the legislative framework and c) reduce administrative burden.

Key changes on the proposal for the new Directive include:
a) The Annexes I, II, IV, V and VI are included at the proposal (The Annexes II and VI were not included in Directive 2000/59/EU.)
b) Changes in definitions - terms, in accordance with IMO
c) Directive Annexes (forms) changes, in compliance with IMO forms
d) The new Directive shall apply to all ports and not just to the selected ones, based on criteria imposed by each Member State (e.g. magnitude of port facility)
e) Shipyard wastes are excluded from the Directive proposal
f) Inspection changes are proposed
g) Fees replaced by the cost recovery schemes

Changes a) and d) above may increase both administrative burden and the infrastructure cost.

3.3 Greek legal compliance

Implementation of Directive 2000/59/EU in Greece was conducted mainly by the Common Ministerial Decision 8111.1/41/2009 (G.G., 412 B/06.03.2009).

All major ports of the country (*international*, *national* and *of major interest*), including touristic ports, are required to have waste reception facilities, in order to collect waste and cargo residues produced by all kinds of ships normally using the port, including fishing vessels and recreational crafts. To achieve this objective, a WRH Plan must be developed by the Port managing bodies to ensure the effectiveness of the service provided. These Plans, according to the Directive 2000/59/EU can be regional, incorporating many Ports under the same Plan, distinguishing the involvement of each port and the availability of the reception facilities of each port. The duration of WRH Plans is set to three years; they are validated by the Ministry of Maritime Affair and Insular Policy, and evaluated by the Ministry of Environment and Energy. To maximize the quality of the services, the managing bodies of the Ports, in most cases, provide these services via private companies with expertise in the specific domain.

Wastes are divided in two categories: a) liquid and b) solid waste. Initially, service providers bid for each waste category separately and only one provider per port was permitted to operate per waste category. Before the publication of Regulation (EU) 2017/352, the Regulatory Authority for Ports issued 3/2017 advisory decree entitled *Providers in the Hellenic Ports for Waste Management*, in order to clarify the procedure.

Just before 2018, Law 4504/2017 (G.G., 184 A/29.11.2017) entered into force. In article 105, core principles and articles of Regulation (EU) 2017/352 with respect to waste management of ships and cargo residues are incorporated to the Greek legislation. Despite that Regulation (EU) 2017/352 applies only to TEN-T ports (with only 25 Greek Ports having the obligation to comply), signaling a policy choice focusing on environmental protection by imposing higher standards nationwide. Article 105 provides the procedure of port reception services and waste management, by opening the market imposing at least two providers per service for private managing bodies (total concession). One more important change can be observed in the new law: a 5-year duration of the WRH plans. The no. 3/2017 RAL advisory decree was in turn repealed, in order to be in conformity to the new Law 4504/2017.

Currently a proposal for the revision of the CMD 8111/49/2009 is under consultation. However, it is based on the Commission's Notice (2016/C 115/05) and not on the proposal of the new Directive.

Another significant issue seems to be the transmission of the waste from the port area to the inland facilities for treatment, where other legislative acts are in force and the waste by MARPOL's Annexes must follow the European List of Waste procedure.

4. SHIP WASTE DELIVERY AND RECEPTION IN GREECE

4.1 Waste Reception and Handling Plans

In most cases, WRH Plans in Greece are regional, incorporating neighboring smaller port facilities in the vicinity of the main port, even not managed by the same managing body. As a result, ships can deliver waste at many port facilities in Greece. 57 ports are obliged to develop WRH Plans (ports of: international importance, national importance, and major interest), including approximately 50 Tourist Ports (Marinas) and 60 private port terminals / facilities; a total of 167. Several of these facilities are incorporated in the same WRH Plan.

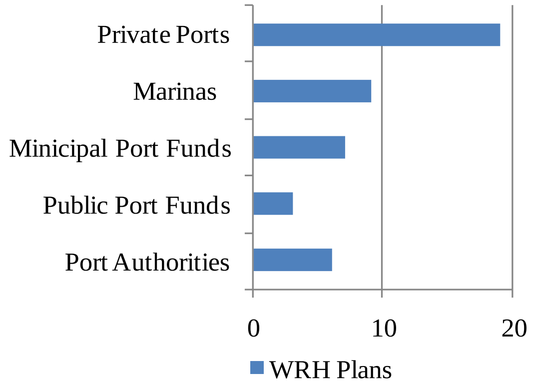


Figure 3: WRH Plans per managing body category

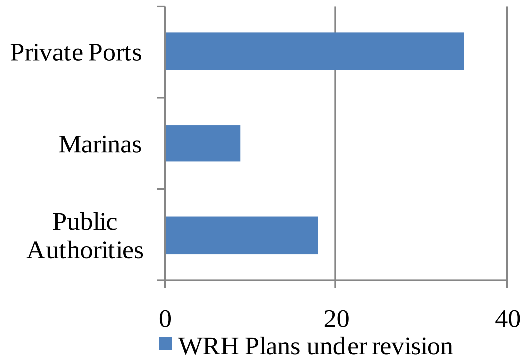


Figure 4: WRH Plans under revision per managing body category

As of 2018, 44 WRH Plans are in force and 62 are under revision in Greece. Figures 3 and 4 present WRH Plans per managing body type and under revision respectively. All Port Authorities and the majority of private ports / facilities have developed WRH Plans. Notwithstanding, several Port Funds have not complied with the law.

4.2 Port Reception Facilities

According to the proposal of the new Directive the definition of *port reception facilities*, (P.R.F.) is: *any facility, which is fixed, floating or mobile and capable of receiving the waste from ships*. In most cases all three types of facilities or combination of them are used for each Greek port. Quantities, required capacity and the quality are set in the WRH Plans. In most cases, shore-side facilities - especially for liquid waste, are situated within the port area and owned by the managing body of the port. In some Port Authorities (e.g. Piraeus Port Authority), construction and operation of P.R.F. has been assigned to a provider through a sub-concession.

Floating and mobile facilities can be either private or owned by the public managing body of the port. In both cases, mobile facilities must be licensed for the specific operation.

No obligation for separation of garbage is recognized within the Greek Legal system; therefore solid waste services providers, do not separate waste (mainly from Annex V), thus lowering national recycling indicators.

4.3 The market of waste reception services in Greece

The Greek system for the collection and handling of the ships waste is based on a bidding procedure. The lowest bidder and the managing body sign a sub-concession contract for a specific amount of

money estimated as the income from the provided services for a period no longer than 3 years. After the end of the contract, a new contest procedure and a revision of WRH Plan are conducted. It is a tough and long procedure. Due to the delays in the contest procedure, services can be provided by the incumbent provider under an expired WRH Plan. As RAL is the responsible authority for the resolution of the differences between port managing bodies and stakeholders, a lot of complaints arrive at RAL, during the contest procedure.

The Greek market appears to have the characteristics of an oligopoly: As of 2018, four major waste service providers are active; one is specialized in liquid waste, two in solid waste and one in both.

In contrary, most of European Ports have more than one provider collecting the waste for each MARPOL's Annex. In Table 1 the number of providers involved in the collection of waste at several European Ports is presented.

Table 1: Number of ship waste collection services Providers per MARPOL Annexes for selected European Ports[1].

PORT→ ANNEX↓	Rotterdam	Antwerp	LeHavre	Valencia	Trieste	Piraeus
I	17	16	6	2	5	1
II	13	12	4	-	-	1
III	-	-	-	-	-	1
IV	10	11	5	3	3	1
V	5	12	4	4	3	1
VI	-	9	2	-	3	1

Waste from Annex III, is subject to the ship's captain choice to be delivered at shore. Only the Port of Piraeus gives this option to clients. Although collection of Annex II and VI wastes is not included in the Directive 2000/59/EU, these services are provided by major European Ports.

5. EXPECTED IMPACTS FROM THE NEW LEGISLATION IN THE GREEK MARKET

The existing legal framework faces challenges both in Greece and the rest of EU Member States. An update of the existing legislative framework is a requirement; currently under consultation.

A new, amended Common Ministerial Decision is the next necessary step for the Greek legal system, incorporating, among others, the obligation to all ports to develop WRH Plans and receive waste from MARPOL's Annex VI; the current proposal for the new directive includes also waste from MARPOL's Annex II. The proposal of the new Directive is on the right direction, oriented to IMO principles, facilitating ships with respect to the shore-side waste delivery procedure. Alignment with MARPOL is expected to lead to reduction of administrative burden. On the other hand, the obligation to maintain reception facilities for all ports, is expected to increase administrative burden and infrastructure costs, to the benefit, however, of additional investments and creation of new jobs, not neglecting the environmental profit.

With respect to WRH Plans, the introduction of Annex II and Annex VI wastes will result to revision requirements; at the same time, expansion of their duration from 3 years to 5 years, will reduce administrative burden.

Finally, the proposed cost recovery systems, introducing an indirect and a direct fee for the reception and ship-side treatment of waste -excluding the cargo residues from this obligation-, is expected to increase volumes of shore-side waste deliveries.

[1]Data collected by the official port's websites, as of 12.2017

Two issues appear to persist in the Greek market: The current low levels of market competition, and the environmental target of recycling. Some entry barriers still remain. They strangle of competition and at the same time mitigate the environmental profits.

6. CONCLUSION

The procedures for reception, collection, storage, treatment and disposal of ship wastes and cargo residues are part of a robust industry in Greece; however, they have characteristics of an oligopoly. The proposed National and European legislative acts are expected to reinforce the sector, offering more jobs and better quality for the marine environment. Still they remain entry barriers in the Greek market.

Issues to be solved in Greece are the number of providers for waste collection services, the separation of garbage etc.

The decision of the E.U. to align the procedure with IMO principles is to the right direction.

Clarification of the terms, matching of the waste categories between MARPOL's Annexes and European List of Waste and simplification of the procedures are needed to empower the ship - waste management services.

Even those, in Greece more interventions are needed to strengthen competition in the market and to facilitate the waste management. The upcoming legislative acts, could transform the new challenges to the booster of the market and the Greek Market can benefit from them.

We are in a transitional period and based on the experience obtained, we expect a healthy and strong market in the near future at the waste reception and handling sector of port services.

References

1. Angelopoulos J., C. Chlomoudis and T. Styliadis (2017) 'Effect of Global Supply Chain Developments on the Governance of Port Regulation', in Pettit, S. & Beresford, A. (Eds.). **Port Management: Cases in Port Geography, Operations and Policy** (pp. 62-93), Kogan Page Publishers.
2. EMSA (2017) '**The Management of Ship-Generated Waste On-board Ships**', Delft, by CE Delft.
3. European Commission (EC) (2018) '**Proposal for a DIRECTIVE OF THE EUROPEAN PARLIAMENT AND OF THE COUNCIL on Port Reception Facilities for the Delivery of Waste from Ships, repealing Directive 2000/59/EC and amending Directive 2009/16/EC and Directive 2010/65/EU**', Strasburg
4. ECORYS (2017) '**Supporting Study for an Impact Assessment for the Revision of Directive 2000/59/EC on Port Reception Facilities**', Final Report, European Commission.
5. Giantsi Th. (2016) '**Effective Port Governance and Management. The Case of East-Central Greece**', Master Thesis, University of Piraeus.
6. Government Gazette, (G.G.) (2017) 184 A / 29.11.2017, Law 4504/2017.
7. G.G., (2016) 94 A/27.5.2016, Law 4389/2016.
8. G.G. (2009) 412 B / 6.3.2009, Common Ministerial Decision 8111.1/41/2009.
9. IMO (2017) MARPOL Consolidation Edition 2017
10. IMO (2014) MEPC/834 "Consolidated Guidance for Port Reception Facility Providers and Users".
11. Official Journal of the European Communities (OJEC) (2000) '**Directive 2000/59/EU on Port Reception Facilities (PRF) for ship-generated waste and cargo residues**'.

12. OJEC (2008) '**Directive 2008/56/EC of the European Parliament and of the Council of 17 June 2008 establishing a framework for community action in the field of marine environmental policy (Marine Strategy Framework Directive)**'.
13. OJEC (2008b) **'Directive 2008/98/EC of the European Parliament and of the Council of 19 November 2008 on waste and repealing certain Directives**'.
14. OJEC (2009) '**Regulation (EC) 1069/2009 of the European Parliament and the Council of 21 October 2009 laying down health rules as regards animal by-products and derived products not intended for human consumption and repealing Regulation (EC) 1774/2002**'.
15. OJEC (2009b) '**Directive 2009/16/EC of the European Parliament and the Council of 23 April 2009 on port state control**'.
16. OJEC (2017) '**Regulation (EU) 2017/352 of the European Parliament and of the Council of 15 February 2017 establishing a framework for the provision of port services and common rules on the financial transparency of ports'**.
17. OJEC (2016) '**Commission Notice (2016/C 115/05) Guidelines for the interpretation of Directive 2000/59/EC on port reception facilities for ship generated waste and cargo residues**'.
18. OJEC (2013) '**Regulation (EU) No 1315/2013 Of the European Parliament and of the Council, of 11 December 2013, guidelines for the development of the trans-European transport network and repealing Decision No 661/2010/EU**'.
19. OJEC (2010) **'Directive 2010/65/EU of the European Parliament and of the Council of 20 October 2010 on reporting formalities for ships arriving in and/or departing from ports of the Member States and repealing Directive 2002/6/EC.**

PASSIVE ACID MINE DRAINAGE REMEDIATION USING BOF STEEL SLAG AND SUGARCANE BAGASSE

T.S. Naidu[1]*, L.D. Van Dyk[1], C.M. Sheridan[1], and D.G. Grubb[2]

[1]Faculty of Engineering and Built Environment, Richard Ward Building, University of the Witwatersrand, 1 Jan Smuts Avenue, Johannesburg, RSA 2000,
[2]Phoenix Services LLC, 148 W. State Street, Suite 301, Kennett Square, PA 19348 USA

Corresponding author: *E-mail: tsnaidu@live.co.za, Phone: +27 827715880

Abstract
This research incorporates the use of two regionally available industrial byproducts produced close to the coal mining region in Eastern South Africa to treat acid mine drainage (AMD): steel slag and sugarcane bagasse, i.e., the shredded cane stalk residual after sugar extraction. Basic oxygen furnace (BOF) slag is regionally produced in Newcastle in large quantities and its high alkalinity makes it ideal for neutralizing acids. Kwa-Zulu Natal is home to the South African sugar industry and the high surface area, polysaccharide content and slow breakdown via acid hydrolysis of sugarcane bagasse makes it an ideal host media for sulfate reducing bacteria (SRB). Accordingly, this research explores the viability of remediating AMD in a two-step continuous process combining both materials. BOF slag eluate (generated from a recycle loop) contacted with raw AMD at an Eluate:AMD ratio of 20:1 was used to initially buffer the AMD solution (pH) and precipitate heavy metals in a sedimentation tank to avoid toxic shocking the SRBs in the sugarcane bagasse bioreactor. Overflow from the sedimentation tank was then passed through a packed bed containing sugarcane bagasse inoculated with SRBs as a polishing step to remove sulfate, precipitate metal sulfides and elevate pH to near neutral pH conditions based on a 16.46 h residence time. A portion of the effluent (95%) was recycled through a packed bed of BOF slag to create the eluate for pre-treatment of the raw AMD solution. The AMD used in these experiments was characterized by: pH 2.4; 388 mg/L Al, 4256 mg/L Fe, 426 mg/L Mg, 96 mg/L Mn, 418 mg/L Ca and 15995 mg/L SO_4^{2-}. Operation of the designed process at a laboratory scale treating 1 L/day, has confirmed the buffering of the AMD solution to a pH of between 7 and 8, and the removal of heavy metals and sulfate to levels of below 10 mg/L for Al, Fe, Mg, Mn and <200 mg/L for sulfate. The bench scale system is currently being scaled up for a pilot treatment system to be deployed in February 2018 near Emalahleni, South Africa, about 150 km due East of Johannesburg.

Keywords: BOF slag, Acid mine drainage (AMD), sugarcane bagasse, sulfate reducing bacteria (SRBs)

1. INTRODUCTION

Mining activity has been an important element in the development and advancement of the South African economy for over a century [Durand, 2012], with mineral extraction occurring at numerous industrial sites across the country. Although much wealth has been generated because of the gold, coal, iron ore and copper mining industries, mining activities have also resulted in detrimental ecological problems that have had adverse effects on both the environment and the population of South Africa. One such problem is that of Acid Mine Drainage (AMD) or Acid Rock Drainage (ARD) [Mccarthy et al. 2011].

AMD is formed when rocks and waste mine materials that contain sulfide components, oxidize on exposure to water or air [Naicker et al. 2003]. Pyrite, the main component that contributes to the formation of AMD, is found largely in both coal and gold mining sites, but it is also found in smaller quantities in other metal ores. Waters that have been contaminated with AMD are characterized by a low pH, high acidity and high concentrations of sulfates and metals [Feng et al. 2004]. Water scarcity issues (both surface and groundwater impacted by AMD) serve as a major motivation to address point and non-point sources of AMD in north and north-eastern South Africa (Gauteng, Mpumalanga and Limpopo), where polluted water is generated at multiples coal field sites in the volumes of tens of ML/day. Research into treatment and prevention methods is thus relevant in South Africa and other countries with similar socio-economic situations.

Fortuitously, two industrial by-products are regionally available in large volumes with the potential to passively remediate AMD: Basic Oxygen Furnace (BOF) Slag and sugarcane bagasse, i.e., the shredded cane stalk material remaining after sugar extraction [Ziemkiewicz 1998; Grubb et al. 2000; Ziemkiewicz et al 2003; Skousen & Ziemkiewicz 2005]. The BOF slag with 10-15 wt% lime/portlandite and various alkaline silicates and oxides, is able to generate highly alkaline solutions and can be used to buffer and elevate the pH of AMD [Roadcap et al. 2005; Riley & Mayes 2015]. As pH rises, a substantial portion of metals precipitate out of solution in the form of oxides, hydroxides and sulfates, lowering the metal content of the water and making the AMD solution more amenable to biological treatment by Sulfate Reducing Bacteria (SRB) cultures. SRB is able to reduce sulfates to sulfides via dissimilatory sulfate reduction (DSR), promoting more metal and sulfate removal by means of metal sulfide precipitation. SRB need a substrate to function and sugarcane bagasse has shown potential in this regard [Hussain & Qazi 2016; Grubb et al, in press]. If a process using the abovementioned methods and industrial by-products is optimized and implemented successfully, areas affected by AMD pollution could be restored and the water quality could be improved to acceptable grey water standards.

This paper reports on the research and the implementation of such a process at a laboratory scale which comprises of two main steps, neutralisation and sulfate reduction. It aims to incorporate slag and sugarcane bagasse to treat severely polluted mine drainage which is continuously produced from a mine in Mpumalanga, South Africa.

2. MATERIALS AND METHODS

2.1 Materials

Basic oxygen furnace (BOF) slag was sourced from Phoenix Slag Services based in Newcastle, Kwazulu Natal, South Africa. The sugarcane bagasse was collected from Illovo's sugar plant in Eston, Kwazulu Natal, South Africa. The bagasse was transported loosely in plastic bags and stored in a temperature controlled room at 25 °C before use in the process.

The acid mine drainage (AMD) was obtained from a mine tailings dam in Emalahleni, Mpumalanga, South Africa and was stored away from direct contact with sunlight before use. The elemental composition and other chemical and physical properties of the AMD as collected from the site are provided in Tables 1 and 2 respectively. This initial quality of water is typically what the treatment regime aims to remediate (the treatment facility is currently being upscaled to a pilot plant system to be constructed at site).

Table 1: Elemental composition of AMD

Element	Concentration (mg/L)	Element	Concentration (mg/L)
S	11182.500	Ga	2.160
Fe	7432.500	Hg	1.840
Ca	1395.000	Co	1.749
Mg	795.000	Ni	1.514
Y	219.300	Pb	1.156
Mn	133.200	Sr	0.941
Ir	48.900	Na	0.863
Li	37.800	Ag	0.803
Zn	13.800	V	0.627
Si	11.320	U	0.571
Te	10.560	Ge	0.499
Sn	10.080	Ti	0.243
Ce	8.240	Cd	0.199
Cu	5.980	W	0.171
Gd	4.300	Be	0.073
K	3.074	Eu	0.053

Table 2 shows that the sulfide content was 0.019 mg/L, which suggests an existing SRB presence within the dam, or unreacted sulfides present in the AMD. Concentrations measured at the time of commencement of experimentation differ to the concentrations obtained at time of collection, due precipitation that occurred because of the highly saturated nature of the AMD and the stagnant storage conditions. At the mine site, water is continuously recycle and pumped into the mine tailings dam, creating agitation that prevents precipitation. The performance of the treatment facility was assessed based on initial concentrations of the liquid entering the setup.

Table 2: Selected chemical and physical properties of AMD

Parameter	Value
Redox Potential (mV)	391
Dissolved Oxygen (mg/L)	2.5
Total Dissolved Solids	29112
Sulfide (mg/L)	0.019
Conductivity (mS/M)	1300
pH	2.38
Total Suspended Solids	290
Acidity (H^+)	362
Turbidity	54
Total Organic Carbon (TOC)	<0.1
Sulfate (mg/L)	20146
Hydroxypropyl cellulose	<1

2.2 Experimental setup and procedure

A laboratory scale AMD treatment facility was designed and constructed (Figure 1) to study the effectiveness of a process which combines the use of BOF slag and sugarcane bagasse to treat AMD. Results from initial test work (not discussed here) were used as a basis for the process configuration and control scheme, as well as the optimum process parameters and conditions.

The remediation setup (Figure 1) comprises of two pumps and a number of process vessels (an AMD feed tank, two slag vessels, a sedimentation vessel, primary and secondary DSR vessels, a water reservoir and an outlet storage tank) which were sealed and anaerobic. The sample points are numbered on the diagram. Movement of the liquid between tanks is achieved via gravity flow.

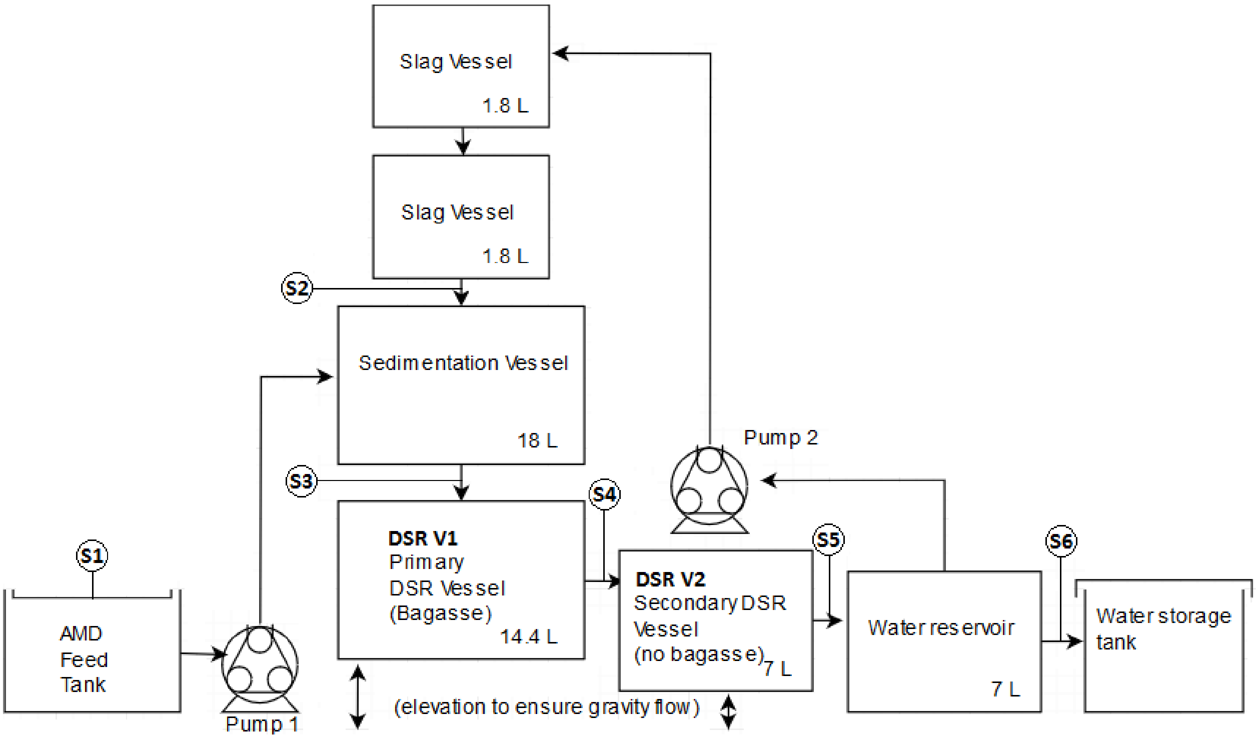


Figure 1 Laboratory scale passive AMD remediation setup

The setup was operated for 32 days in continuous mode by constantly filling the feed tank with AMD. Samples were taken at all sample points and analysed for pH, redox potential, sulfate, dissolved and precipitated iron, manganese, aluminium, calcium and magnesium.

Specifically, AMD was fed into a sedimentation vessel where it was mixed with an alkaline solution from the slag vessels. The pH of the mixture was controlled at 9 by adjusting the feed rate of the AMD versus of the BOF slag eluate addition rate. Metal oxides, hydroxides and sulfates precipitated out of solution and settled at the bottom of the vessel which was occasionally opened to remove sediment. The partially treated AMD solution then flowed to the primary DSR vessel (DSR V1). This vessel contained 600g of bagasse inoculated with SRB cultures. The AMD promoted hydrolysis of the bagasse to release sugars and organic acids which served as the substrate for the subsequent DSR by the SRBs with end products including precipitated metal sulfides or H_2S.

Preliminary experiments showed that DSR occurs faster when the liquid and bacteria are no longer in direct contact with the organic substrate and a secondary DSR vessel (DSR V2), not containing bagasse, was used for this purpose. Accordingly, effluent from DSR V2 served the dual purpose of being the treated water for potential release and feedstock for stripping alkalinity from the BOF slag vessels (at 17 mL/min). The BOF slag vessels contained 5 kg each of 10 mm minus BOF slag particles. In the slag vessels, water leaches hydroxides from the slag and become alkaline. This

alkaline solution is fed to the sedimentation vessel as previously mentioned. The remainder of water in the water reservoir flows to a water storage tank.

2.3 Analytical methods

The metal concentrations of aluminium, calcium, iron, magnesium and manganese were measured with an Agilent 2000 series atomic spectrometer. Redox potential and pH were measured using a combined pH and ORP meter. Sulfate was measured using turbidimetric spectrophotometric sulfate tests [Center for bioprocess engineering research, 2016; American Public Health Association , 1975]. Standard concentration solutions were used for each test to obtain relevant calibration equations.

3. RESULTS AND DISCUSSION

Samples were taken from the process sample points (S1-S6, Figure 1) every two days over the 32 day operational period. The samples were analyzed for pH, redox potential, sulfate, dissolved and precipitated iron, manganese, aluminium, calcium and magnesium. Sulfide analysis was done 4 times over this period on samples taken from the bagasse chamber to ensure DSR was occurring. A selection of the results is presented here to show the functioning and synergy between each section of the laboratory AMD treatment setup.

The purpose of the slag vessels is to house the slag and allow enough time for the water entering the vessels to gain sufficient alkalinity. Water exiting the water reservoir is either allowed to flow into a storage vessel or is recycled back into the system via the slag vessels, where a rise in pH and alkalinity occurs. This is essential for system performance as the pH of the slag vessel outlet stream will directly affect the pH of the sedimentation vessel. The largest proportion of metal and sulfate removal occurs in the sedimentation vessel (due to pH adjustment), which avoids toxic shocking the SRBs which then, in turn, remove sulfate.

It can be seen from Figure 2 that the pH of the recycled water increases from 7-8 to 11-12 and remains relatively constant over the 32-day period. The alkalinity and pH generation in the BOF slag vessels can generally be attributed to two processes: (i) the rapid hydration and dissociation of lime/portlandite, and (ii) the additional dissolution of Ca-silicate minerals (like rankinite, larnite and akermanite) [Gomes et al 2016]. The data from the BOF slag vessel inlet and outlet streams (Figure 2) confirms this as the pH increase occurs in conjunction with an increase in dissolved calcium in the liquid. The magnesium content also increases by 39.6 % over the slag vessel. The reactor ran for only 32 days (not including start up), and thus the slag was deemed insufficiently depleted to allow for the dissolution of casilicate minerals. The presence of other oxides within the slag does not affect the pH rise, as the data showed that there was no increase in concentrations of iron, aluminium or manganese. The outlet of the slag vessel entered the sedimentation vessel, along with untreated, raw AMD.

The Sample 3 location (sedimentation tank effluent) concentrations are shown in Figure 3. Sulfate concentrations varied between 70 and 340 mg/L, versus the AMD (S1) concentration of approximately 15995 mg/L. On average, the metals removal rate from the AMD was: Al (99.09%), Ca (78.06%), Fe (99.85%), Mg (96.33%) and Mn (94.77%). It should be noted that this decrease in concentration of contaminants is not only due to the induced precipitation of the metals due to higher pH conditions, but also in part due to the dilution factor between the AMD inlet and the recycle inlet.

Chemical precipitation commonly occurs in AMD, even without the onset of remediation [Lottermoser 2007], however the amount and rate of precipitation can increase with increasing pH [Plasari & Muhr 2007]. The increase in pH is connected with metal precipitation in the form of hydroxides [Balintova & Petrilakova 2011], oxyhydroxides or oxyhydroxysulfates [Lottermoser 2007]. Due to the large decrease in dissolved sulfate, the counter-ion consumed by the metal ions during precipitation, in conjunction with the hydroxyl groups, was probably sulfate.

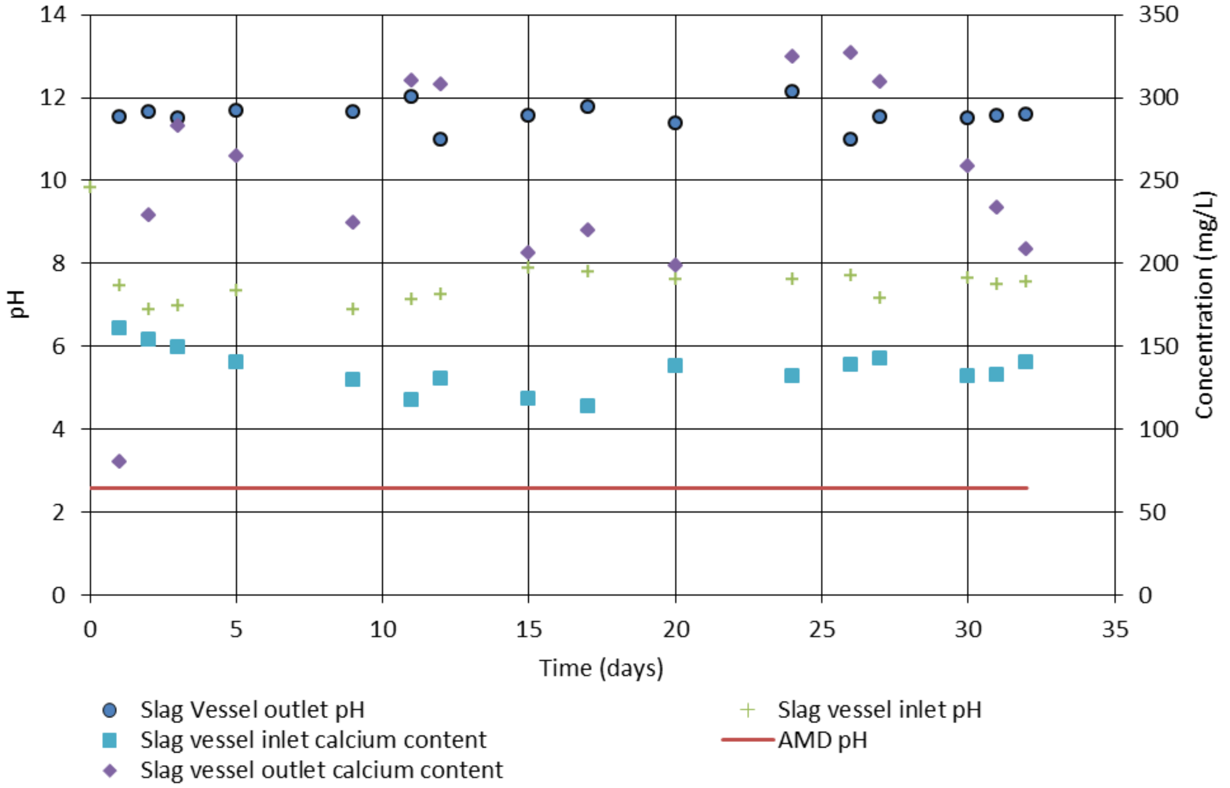


Figure 2: Calcium content and pH of slag vessel inlet and outlet over time

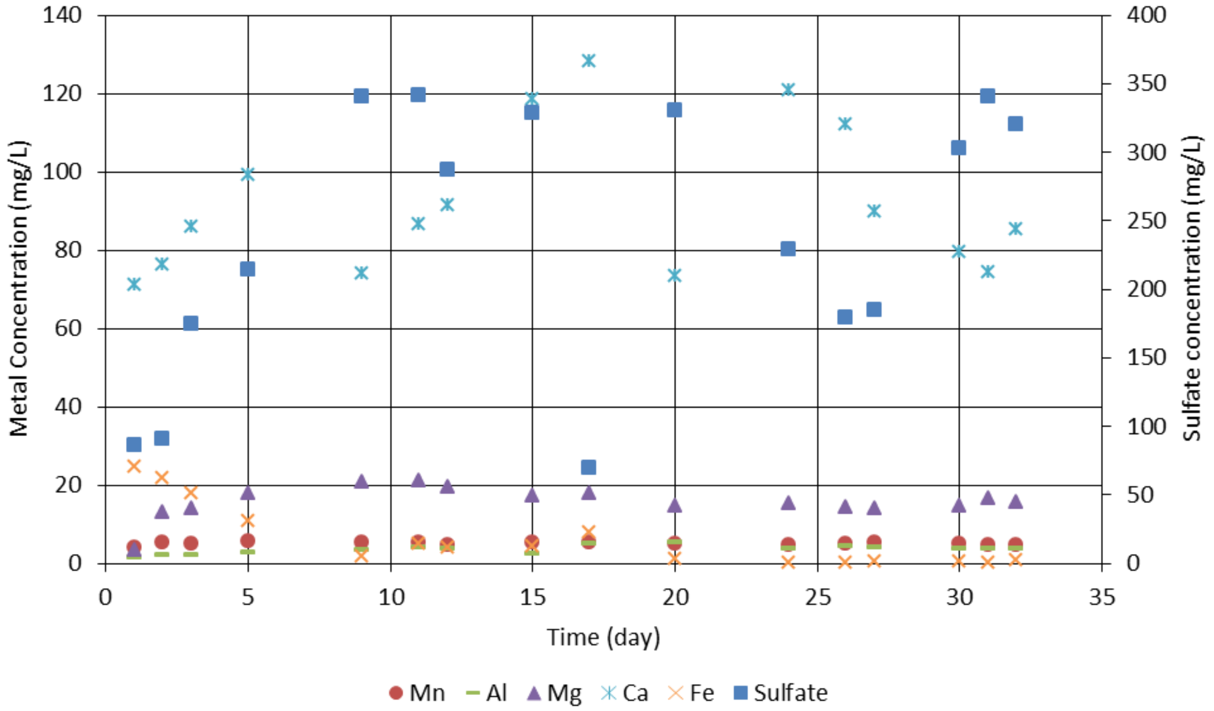


Figure 3: Metal and sulfate concentration in sedimentation vessel outlet

The water exiting the sedimentation vessel entered the primary DSR vessel (DSR V1) where DSR occurred under the action of SRB. The decrease in dissolved sulfate over this vessel is shown in Figure 4. On average a decreased of 36.25% in sulfate was achieved across this reactor. This is similar to findings in the preliminary experiments where a sulfate reduction of 33.6 % was achieved under similar conditions. Since SRB are sensitive to pH [Janyasuthiwong et al., 2016], it was initially

theorized that a fluctuation in pH as well as the high pH entering the DSR V1 may be inhibiting SRB performance. However, as shown in Figure 4, the pH exiting the vessel remained fairly constant, with an average pH of 7.2 – very close to the ideal pH for SRBs. The pH entering DSR V1 remained fairly constant at an average of 9.2.

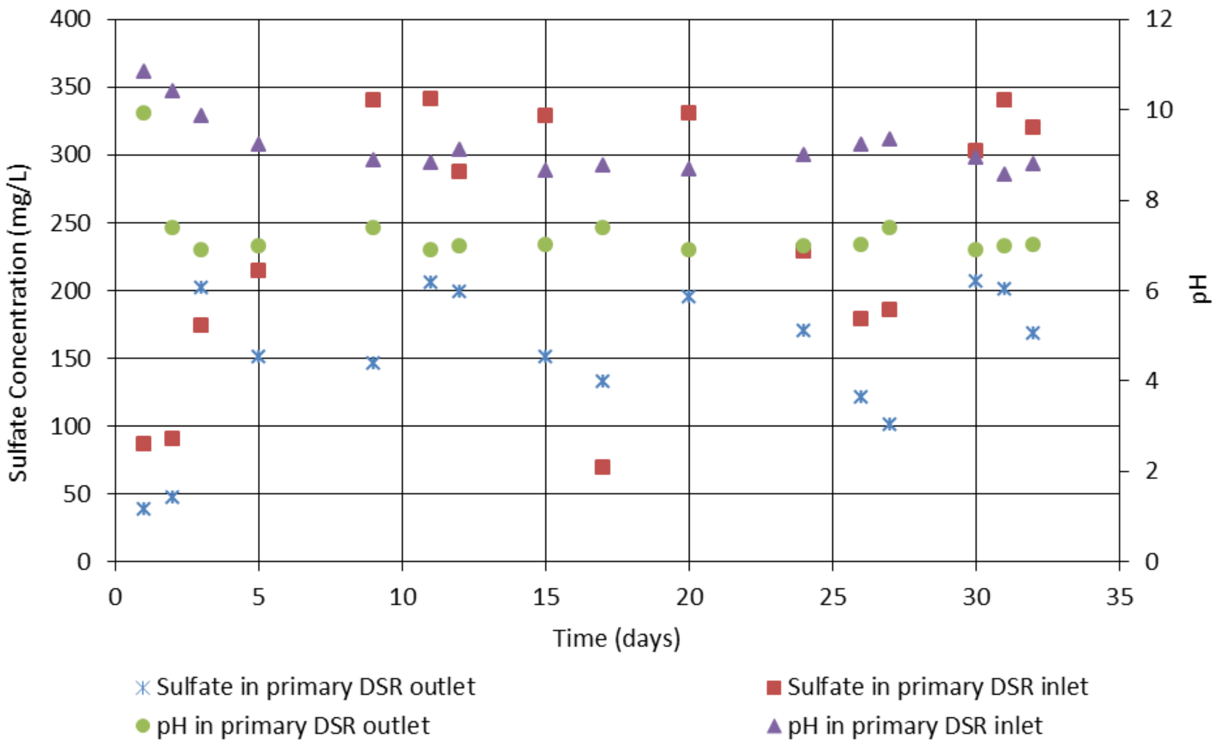


Figure 4: Sulfate concentration and pH in primary DSR (DSR V1) inlet and outlet

The difference in pH levels across DSR V1 could potentially confirm SRB functioning, as a drop in pH is most likely due to the breakdown and release of organic acids from the sugarcane bagasse (this breakdown is attributed to the SRB using the substrate). Another confirmation of SRB activity is the presence of sulfide, which was measured in the outlet and averaged at 12.47 mg/L. A 2% drop in manganese, an 84% drop in magnesium, a 6% drop in calcium and a 27% average drop in iron was measured over DSR V1.

There was also a large drop in the proportion of precipitated metals found in the liquid sample (S4), however, this may be due reactions within DSR V1 or through gravitational settling within the vessel. The metals likely precipitated out of the solution as metal sulfides and adhered to the surface of the bagasse.

The outlet of DSR V1 fed directly into the secondary DSR vessel (DSR V2) which did not contain sugarcane bagasse. Only manganese, magnesium and calcium decreased in concentration in DSR V2, with all other metals increasing in concentration. Sulfate decreased over DSR V2 on average by approximately 24.32 %, giving an average final concentration of 116 mg/L. The overall percentage change in concentrations for aluminium (from 388 mg/L to 6 mg/L), calcium (from 418 mg/L to 95 mg/L), iron (from 4256 mg/L to 18 mg/L), magnesium (426 mg/L to 5 mg/L), manganese (from 96 mg/L to 5 mg/L) and sulfate (from 15995 mg/L to 116 mg/L) over the entire process is shown in Figure 5.

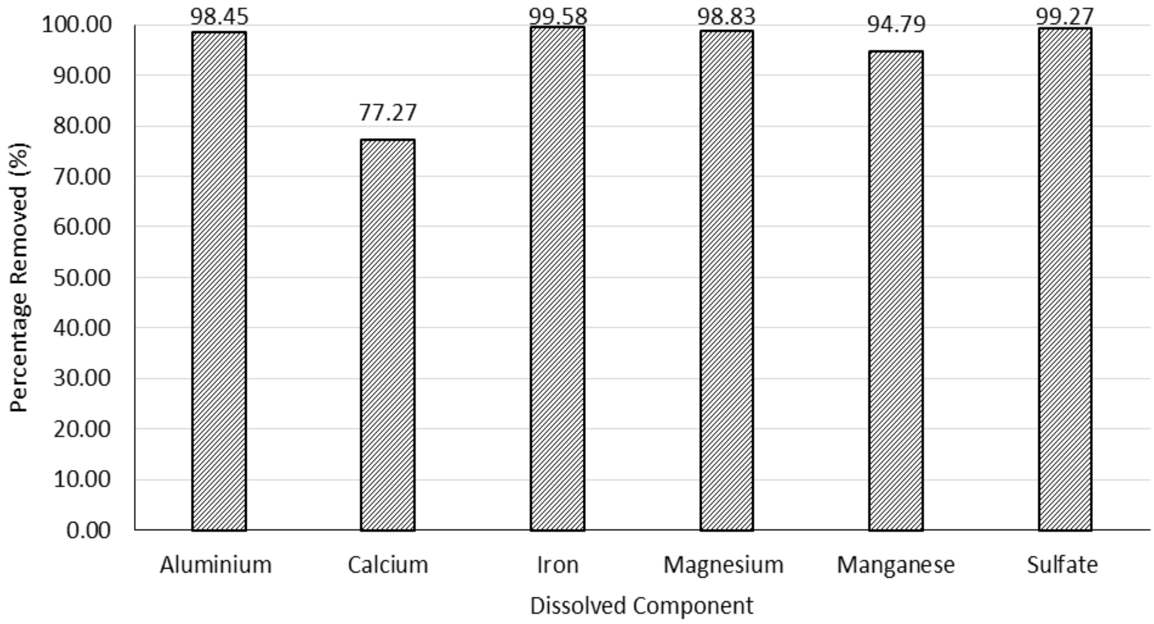


Figure 5: Concentration of metals and sulfates in inlet and outlet of entire system

A significant change in colour of the untreated AMD could also be observed (Figure 6) which could be attributed to the removal of metal and sulfate by the process. The initial pH of the system was 2.38 and a final pH of 7.66 was measured for the outlet. These conditions changed slightly after storage in the water reservoir due to exposure to oxygen, but the quality of the water remained fairly constant. Over the 32 day period, approximately 30 L of AMD was treated.

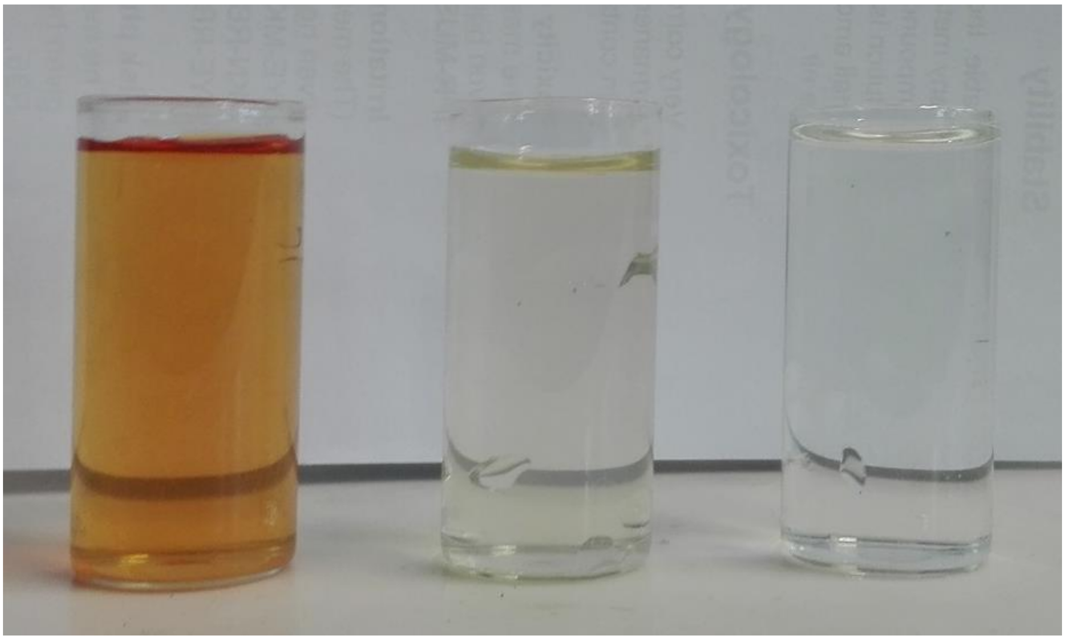


Figure 6: Image of untreated AMD (left), partially treated AMD exiting sedimentation vessel (middle) and remediated AMD (right) exiting secondary DSR vessel (DSR V2)

4. CONCLUSIONS AND RECOMMENDATIONS

The AMD was remediated to a pH of between 7 and 8, and heavy metals and sulfate to levels of below 10 mg/L for Al, Fe, Mg, Mn and <200 mg/L for sulfate. Thus, the system showed promising results. However, the recycle rate was high (95 %) due in part to lack of automated pH controls on the sedimentation tank which lead to very high pH. Future work will focus on lowering the pH of the

sedimentation tank into the 5-6 pH range which will also aid in optimizing the ability of the SRBs to achieve sulfate removal and metals precipitation.

ACKNOWLEDGEMENTS
The authors would like to thank Phoenix Slag Services, Illovo Sugar and our mining partner for their support. We would also like to thank the Water Research Commission (WRC) of South Africa for their financial contribution through project K5/2757.

References

1. Durand, J. (2012) 'The impact of gold mining on the Witwatersrand on the rivers and karst system of Gauteng and North West Province, South Africa' **Journal of African Earth Science**, 68, pp. 24-43
2. Mccarthy, T.S., Africa, S. & Africa, S. (2011) 'The impact of acid mine drainage in South Africa' **South African Journal of Science**, 107(5/6), pp.1–7.
3. Naicker, K., Cukrowska, E. & Mccarthy, T.S. (2003). 'Acid mine drainage arising from gold mining activity in Johannesburg', **South Africa and environs**. 122, pp.29–40.
4. Feng, D., Deventer, J.S.J. Van & Aldrich, C. (2004) 'Removal of pollutants from acid mine wastewater using metallurgical by-product slags' **Seperation and Purification Technology**. , 40(1), pp.61–67.
5. Ziemkiewicz, P. (1998) Steel Slag: Application for AMD control. **Conference on Hazardous Waste Research**, (304), pp.44–62.
6. Grubb, D.G., Landers, D.G. & Hernandez, M. (2000) 'Utilization of Sugarcane Bagasse to Treat Acid Mine Drainage' **GeoEng**, 355, pp.19–24.
7. Ziemkiewicz, P., Skousen, J., Simmons, J. (2003) 'Long-term performance of passive acid mine drainage treatment systems' **Mine Water and the Environment**, 22, pp. 118-129
8. Skousen, J.G., Ziemkiewicz, P. (2005) 'Performance of 116 passive treatment systems for acid mine drainage' **National Meeting of the American Society of Mining and Reclamation**. Breckenridge, Colorado, pp. 1100–1133
9. Roadcap, G., Kelly, W. & Bethke, C. (2005) 'Geochemistry of extremely alkaline (pH>12) ground water in slag-fill aquifer' **Groundwater**, 43, pp.806–816.
10. Riley, A.L. & Mayes, W.M. (2015) 'Long-term evolution of highly alkaline steel slag drainage waters' **Environmental Monitoring and Assessment** 187, pp. 1-16
11. Available at: http://dx.doi.org/10.1007/s10661-015-4693-1.
12. Hussain, A. & Qazi, J.I. (2016) 'Application of sugarcane bagasse for passive anaerobic biotreatment of sulphate rich wastewaters' **Applied Water Science**, 6(2), pp.205–211. Available at: http://link.springer.com/10.1007/s13201-014-0226-2.
13. Grubb, D.G. & Hernandez, M (In Press) 'Sugarcane Bagasse as a Microbial Host Media for the Passive Treatment of Acid Mine Drainage' **Journal of environmental engineering**
14. Center for bioprocess engineering research (2016). 'CeBER laboratory methods manual' CeBER
15. American Public Health Association (1975) '**Standard methods for the examination of water and wastewater'** 14th Editi., New York: APHA.
16. Gomes, H. I., Mayes, W. M., Rogerson, M., Stewart, D. I., Burke, I. T. (2016) 'Alkaline residues and the environment: a review of impacts, management practices and opportunities' **Journal of cleaner production**, 112, 3571-3582

17. Lottermoser, B. (2007) **'Mine Wastes: Characterization, Treatment and Environmental Impacts'** 2nd ed., Springer Science & Business Media.
18. Plasari, E. & Muhr, H. (2007) 'Developments in precipitation engineering for the process intensification in the environmental protection and other purification industrial activities' **Chemical Engineering Transactions**, 11, pp.65–70.
19. Balintova, M. & Petrilakova, A. (2011). 'Study of pH influence on selective precipitation of heavy metals from acid mine drainage' **Chemical Engineering Transactions**, 25, pp.345–350.
20. Janyasuthiwong, S. et al. (2016) 'Effect of pH on the Performance of Sulfate and Thiosulfate-Fed Sulfate Reducing Inverse Fluidized Bed Reactors' **Journal of environmental engineering**, 142(9).

USE OF SOLID WASTES IN CEMENT PRODUCTS- A REVIEW

S. D. Mavridou*

Division of Technical Works, Thessaloniki Water Supply & Sewerage Co. S.A (EYATH S.A.), GR- 54622 Thessaloniki, Macedonia, Greece

*Corresponding author: e-mail: smavridou@eyath.gr, tel : +30-2310-966933, +30 6979248470

Abstract

Waste management is a major concern towards sustainable development and natural resources savings. In particular, the objectives of worldwide environmental policy are to preserve, protect and improve the quality of the environment, to protect human health and to utilize natural resources prudently and rationally, by retrieving valuable secondary raw materials. Worldwide, researchers are examining the possible utilization of various materials such as End of Life (EOL) Tires, C&D (Construction and Demolition) Wastes and WEEE (Wastes from Electrical and Electronic Equipment), in many applications. Civil Engineering sector can utilize, under specific circumstances, many of those secondary materials for the production of new mixtures based on cement, asphalt or soil either as alternatives to natural aggregates or as additives to the mixtures. Moreover, legislation in force, concerning alternative management of wastes, makes these efforts more urgent, since all European Countries should comply with its demands as far as quantitative and chronicle targets are concerned.

Current paper monitors and evaluates technical knowhow on basic properties of cement products with EOL Tires, C&D Wastes and WEEE gained during the last 24 years worldwide. Properties discussed are workability, specific weight, air content and compressive strength. Laboratory experiments certify that addition of wastes in the production of cement mortars is possible, leading to mixtures with satisfactory characteristics as far as strength and durability is concerned. At the same time environmental protection is achieved by decreasing the huge amount of wastes generated and by increasing natural resources savings.

Keywords: Solid wastes, EOL Tires, C&D Wastes, WEEE, Cement products, Legislation, Strength, Recycling

1. INTRODUCTION

Economy growth depends strongly on the infrastructure of the cities mainly composed by buildings, roads and geotechnical projects either in the stage of construction or in the stage after the end of their life cycle. More frequently used building material is concrete. Given on the one hand that cement and aggregates- main constituents of concrete products- play an important role in mixtures properties since they occupy the larger volume of about >90% of total one and legislation in force on the other hand, alternative management of various wastes in civil engineering applications and especially for the production of cement based products is of crucial importance.

Huge amounts of wastes are generated annually worldwide. As a result, in force legislation demands alternative management of either solid or liquid wastes, so civil engineering applications can be the solution, since various wastes can be utilized for the production of green concrete products. Secondary materials such as tire rubber from EOL Tires, recycled aggregates from Construction and Demolition wastes and plastic particles from Waste Electrical and Electronic Equipment, after special treatment and in appropriate gradation and percentage, can be reused either as substitute for cement,

when performing pozzolana properties, leading to energy consumption savings, or as aggregates, since many of these wastes comply with specifications for their use as such.

So, current review includes brief information regarding up to date situation concerning quantities and law demands, as well as regarding the effect of wastes' addition in cement based products, while conclusion section focuses on suggestions for future/additional research.

2. LEGISLATION CONCERNING WASTE MANAGEMENT

2.1 End of Life Tires

Most of tires are derived from land based vehicles (eg cars, trucks) and are constituted by natural /synthetic rubber, carbon black, steel cord, polyester, nylon, steel bead wire and other chemicals. EOL Tires pose a major environmental issue, since their often illegal disposal affects negatively the environment and public health; discarded stockpiles can promote mosquitos development, fire hazards, while leaching effects can pollute surface and sub-surface water and soils.

Since 2000, landfilling of end-of-life tires is banned in all European countries as a result of the European Directive 1999/31/EC. As far as Greece is concerned, current relevant Presidential Decree 109/04 demands that by 31/7/2006, utilization of EOL Tires should be at least 65%, while recycling should come up to at least 10%. Ecoelastika is the only legislated system responsible for the collection and valorization of EOL Tires, aiming at their alternative management taking into account environmental and economic criteria and the law. Data related to EOL Tires amount as well as on their alternative management in Greece can be found on figures 1,2 and 3, respectively (http://ecoelastika.gr).

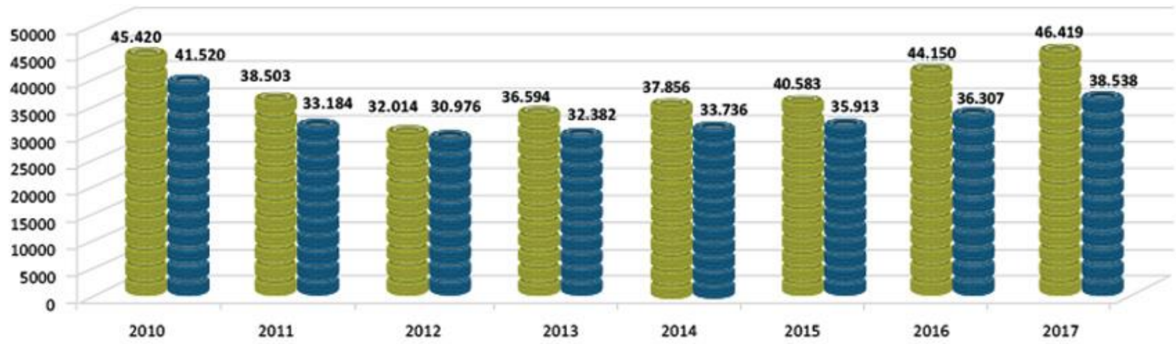


Figure 1: New tires (first green column) and collected (second blue column) EOL Tires in Greece

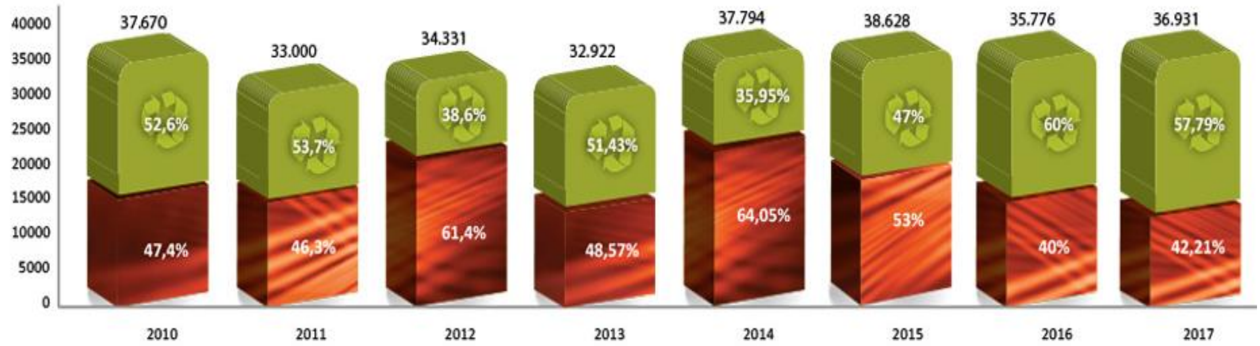


Figure 2: Energy recovery (in red) and recycling (in green) of EOL Tires in Greece

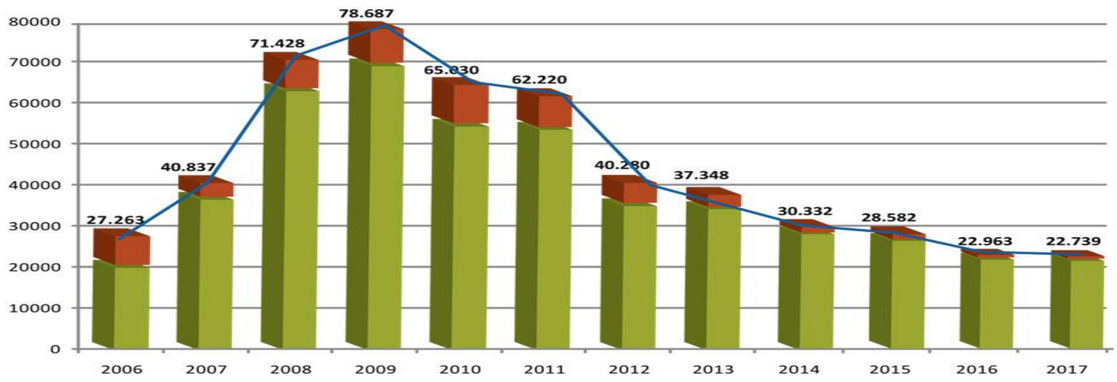


Figure 3: EOL Tires in Collective spaces (in red), in processing units (in green) and total quantity (blue line) in Greece

2.2 Construction and Demolition Wastes (C&DW)

Construction and demolition wastes (C&DW) is one of the most voluminous waste streams generated worldwide from activities such as the construction and/or total or partial demolition of buildings and civil infrastructure after their reach the end of their life cycle, road planning and maintenance actions. Especially for Europe, it accounts for approximately 25% - 30% of all waste generated in the EU and consists of materials such as concrete, bricks, wood, glass, metals, plastic, solvents, asbestos and excavated soil. There is a high potential for recycling and re-use of C&DW, since some of its components have a high resource value (eg concrete, bricks and metals). In particular, there is a re-use market for aggregates derived from C&DW waste in construction projects based on cement, asphalt and soil. Technology for the separation and recovery of construction and demolition waste is well established and easily accessible http://ec.europa.eu/environment/waste/studies/deliverables-/CDW_Greece_Factsheet_Final.pdf.

One of the objectives of the "Regulating issues of the Ministry of Environment, Energy and Climate Change" Directive (2008/98/EC) is to provide a framework so Member States shall take the necessary measures designed to achieve that by 2020 a minimum of 70% (by weight) of non-hazardous construction and demolition waste excluding naturally occurring material defined in category 17 05 04 in the List of Wastes shall be prepared for re-use, recycled or undergo other material recovery" (including backfilling operations using waste to substitute other materials).

Table 1: Quantities and % recycling of generated CDW in different EU member states in 2006

Country	RCD *	% Recycled	Country	RCD *	% Recycled
Denmark	5,27	94%	Malta	0,8	0%
Estonia	1,51	92%	Netherlands	23,9	98%
Finland	5,21	26%	Poland	38,19	28%
France	85,65	45%	Portugal	11,42	5%
Germany	72,40	86%	Romania	21,71	0%
Greece	11,04	5%	Slovakia	5,38	0%
Hungry	10,12	16%	Slovenia	2,00	53%
Ireland	2,54	80%	Spain	31,34	14%
Italy	46,31	0%	Sweden	10,23	0%
Letonia	2,32	46%	UK	99,10	75%
Lithuania	3,45	60%	EU-27	531,38	46%
Luxembourg	0,67	46%			

* million tones.

Source: http://ec.europa.eu/dgs/environment/index_en.htm

According to Table 1, the recycling rate for C&DW in *Denmark, Estonia, Germany, Ireland and the Netherlands* is very high >70%, so the 70% of 2020 EU recycling target is already exceeded. The

major part of the C&DW is mineral waste (concrete waste, bricks) which is currently used as aggregate in roads, parking areas or in embankments. However, there are other countries, including Greece, that recycle much smaller amounts of wastes.

The management of Construction and Demolition Waste in Greece faces several challenges and appears to be significantly underperforming, despite the existing quite rich legislative framework concerning the management of C&DW which is in place since 2010 with several new legislation, regulations and amendments following up since then. In particular, the legislative framework for waste management in Greece is defined by Law 4042/2012-"Penal protection of the environment", which complies with Directives 2008/98/EC and 2008/99/EC "Framework for waste generation and management". Further legislation, regulations and guidelines concerning C&DW in Greece includes mainly the Joint Ministerial Decision (JMD) 36259/1757/E103 of 2010 stipulating measures, conditions and programmes for the alternative management of excavation, construction and demolition waste (ECDW), Law 4030/2011 and especially article 40, which describes permit issuing provisions for C&DW treatment facilities in inactive quarries and the rules for accepting and managing CDW in these treatment facilities, Law 4067 of 2012, where Article 17 stipulates that for the construction of any building and the landscaping of the building surroundings, the provisions of the relevant legislation for alternative management of waste from excavation, construction and demolition waste should be applied, Circular 13 of the Ministry of Environment, Energy and Climate Change No. 4834 of 25 January 2013 with subject the 'Management of excess excavation materials from Public Works - Clarifications on the requirements of the JMD 36259/1757/E103/2010', exempting the management of excess materials from excavation activities during public works through the certified systems of alternative C&DW management, as long as the excess material is handled in sound environmental manner, Commission Decision 2011/753/EU establishing rules and calculation methods for verifying compliance with the targets set in Article 11(2) of Directive 2008/98/EC of the European Parliament and of the Council14.

Quantitative data concerning 2012, indicates that about 815 thousand tonnes of C& DW was generated, of which only 2.7 was recovered (including backfilling), while the rest was sent to landfills. C&DW generation is decreasing steadily since 2010, due to the significant slowdown in the construction sector; however, given that many building and infrastructure projects are reaching the end of their life cycle, these amounts are expected to be increased in the future.

Additionally, preliminary data for 2014, estimates that the actual C&DW recovery performance of Greece lies approximately between 12-15%. However, those data are relative, since large quantities of C&DW are illegally managed, through landfilling/ illegal deposit in natural sites preferably in remote locations which are difficult to be detected http://ec.europa.eu/environment/waste/studies/-deliverables/CDW_Greece_Factsheet_Final.pdf.

2.3 Waste of Electrical and Electronic Equipment (WEEE)

Waste of Electrical and Electronic Equipment (WEEE) is one the fastest growing waste streams in the EU, with approximately 9 million tonnes generated in 2005, and expected to grow to more than 12 million tonnes by 2020. Such wastes include Tv's, fridges, cell phones, cables electric switchboards, distribution boards, circuit breakers and disconnects, electricity meter, transformers etc. Main characteristic of some of those devices is their hazardous content, which if not properly managed, can cause severe environmental and health issues. This is also why this sort of waste should be separated collected.

The relevant Directive (WEEE Directive) is the European Community Directive 2012/19/EU on Waste Electrical and Electronic Equipment (WEEE) which followed Directive 2002/96/EC and is in accordance with RoHS Directive 2002/95/EC. The legislation requires heavy metals such as lead, mercury, cadmium, and hexavalent chromium and flame retardants such as polybrominated biphenyls (PBB) or polybrominated diphenyl ethers (PBDE) to be substituted by safer alternatives. From 15 August 2018 onwards the scope of the Directive is widened to include all EEE. The Directive aims to prevent or reduce the negative environmental effects resulting from the generation and

management of WEEE and from resource use. As reflected in the Directive's recital 6, its key purpose is to contribute to sustainable production and consumption by, as a first priority, the prevention of WEEE and, in addition, by the re-use, recycling and other forms of recovery of such wastes. The Directive thus incorporates the waste hierarchy as established in Article 4 of Directive 2008/98/EC on waste (http://ec.europa.eu/environment/waste/weee/index_en.htm).

The new WEEE Directive (2012/19/EU of the European Parliament and the Council of 4 July 2012 on waste electrical and electronic equipment) introduces a collection target of 45% of electronic equipment sold that will apply from 2016 and, as a second step from 2019, a target of 65% of equipment sold, or 85% of WEEE generated. The new collection targets agreed will ensure that around 10 million tons, or roughly 20kg per capita, will be separately collected from 2019 onwards. Article 11 (in combination with annex V) sets the recycling targets for the different product categories.

Regarding Greece, approximately 80 to 115 million tonnes of WEEE are estimated to be generated annually. Those wastes are classified of high priority, because of their hazardous content, of their continuously increase and of their negative effect on the environment.

The only legislated system for the proper management of all categories of WEEE is Recycling of Devices, which is responsible since 2004 (MD 105134/2004) and till 2018 (https://www.eoan.gr).

As far as quantitative targets set by legislation (JMD 23615/2014), a minimum of 50-55% of total WEEE shall be recycled and 70-75% shall be recovered. However, these percentages vary for different materials which are included in Annexes I, II and III of the law.

3. CEMENT PRODUCTS WITH WASTES

Studies on the use of secondary materials-from wastes- either as coarse or fine aggregates in concrete and cement mortars is possible, when such particles are used with the appropriate method and in the appropriate gradation and percentage. Main research has been focused on the production of new concrete mixtures with the use of various wastes, in order to examine the effect of their gradation to the mixtures properties, while only few studies include examination of this effect on cement mortars. Following, indicative laboratory results are briefly presented. These results examine the sole or combined use of EOL Tires, C& DW and Electrical and Electronic Equipment for the production of new cement based concrete and mortars.

3.1 Properties of cement products with EOL Tires in fresh and hardened state

Workability is defined as the mixture's property to be properly managed in fresh state. Addition of coarse rubber particles results in mixtures with increased workability, while addition of fines has an opposite effect (Khatib and Bayomy, 1999). However, addition of rubber particles even coarse ones in more than 40% per volume gives mixtures with zero workability, so the mixture is not at all workable. This fact is attributed to the high viscosity of aggregates, given the increased friction between tire rubber particles and the rest of the mixture as well as on the decreased mixtures' density. As far as cement mortars is concerned, according to Raghavan et al (1998), performance of mortars with tire rubber is better or similar to the one of reference mixture, while use of rubber particles as substitutes for fine ones at 100%, results in a decrease of workability up to 17% (Mavridou, 2010).

Specific weight of rubberized concrete (rubcrete) decreases by the increase of rubber substitute's percentage. This is mainly due to the lower specific weight of rubber compared to the one of natural aggregates, occupying, especially when used as fines, at the same time more volume (El-Dieb et al, 2001). According to Eldin and Senouci (1993) the decrease in specific weight comes up to 25% with fully substitution of coarse aggregates and to 10% when 33% of fines are replaced with rubber (Li et al, 1998). As far as cement mortars is concerned, use of tire rubber particles as substitute for cement causes decrease in specific weight of the mixture (42% for 50% substitution of cement by rubber

according to Benazzouk et al, 2007, while for 100% substitution of the sand the decrease comes up to 46% (Mavridou, 2010).

Air content: addition of rubber particles in concrete results in an increase of air content, even when air additive is not used (Siddique and Naik, 2004). Gradation of rubber particles plays a significant role on air content, since fine rubber particles leads to a higher increase of air content as compared to coarse ones for percentages of >20% (Khatib and Bayomy, 1999). This can be attributed to the trend of rubber particles to repel water and to include air in their tough surface. As far as cement mortars is concerned addition of tire rubber caused a negligible increase of 2% in air content.

Compressive strength: Addition of rubber particles in concrete may cause a significant decrease in compressive strength when added in high percentages >5% (Li et al, 2004; Turatsinze et al, 2005; Ganjian et al, 2009; Blessen and Gupta, 2016). However, regarding strength development, rubber seems to increase prime strength, while decreasing strength at 28 days and for addition of rubber particles more than 20 per volume (Khatib and Bayomy, 1999). Strength decrease can be attributed to three reasons: first of all, rubber is a material with increased elasticity compared to the rest of the mixture, so developed cracks are monitored peripheral to rubber particles leading to failure at a lower load. Secondly, rubber particles can act as voids, so mixture's structure is weaker. Finally, strength of concrete is mainly based in the shape, density and hardness of coarse aggregates, so when those are replaced with ones of lower hardness, a strength loss is the result (Mehta and Monteiro, 1993). In particular, factors such as percentage, gradation, way of mixing and surface of rubber particles may cause strength's loss, while this loss is higher when coarse aggregates are replaced (Topçu, 1995). Optimum percentage of rubber particles used is 50% and 25% per volume for fines and coarse ones, respectively (El-Dieb et al, 2001), while decrease comes up to 85% and 65%, with fully replacement of coarse and fines respectively (Eldin and Senouci, 1993).

Moreover, particles surface plays an important role on strength's development, since their surface is strongly related to the bonding between particles and the rest of the mixture, leading to increased strength (Nehdi and Khan, 2001). Many researchers examined ways of changing particles surface. Means for this change can be by rinsing with water, with saturated NaOH solution [rubber includes zink stearate which causes strength's loss, so by rinsing with NaOH, zink is removed and homogeneity is increased (Segre et al, 2002)]; with HNO_3 and H_2SO_4 solution, by the use of coupling agents, etc (Siddique and Naik, 2004).

According to Rostami et al, 1993, concrete with rinsed with water rubber particles shows improved strength by 16%, while the increase by the use of solvent can come up to 57%. Moreover, addition of latex can cause improvement of the bonding between rubber particles and the rest of the mixture, so strength is increased (Lee et al, 1998).

As far as cement mortars is concerned, 30% replacement of fines causes a decrease in strength up to 55-80%, for different water to cement ratios (Turatsinze et al, 2006, Mavridou 2010). Furthermore, mortars with rinsed rubber particles- either with water or NaOH causes an increase in strength up to 19%, while addition of latex and bitumen anionic emulsion increased strength ranging between 10 and 21%, respectively (Mavridou, 2010).

3.2 Properties of cement products with C& D Wastes in fresh and hardened state

Recycled aggregates (REC) can be used for the production of new concrete mixtures and cement mortars, respectively with quite satisfactory characteristics (Dapena et al, 2011). However, often, C&D Waste's composition is not steady, while there is no CE for those materials, so since they may generate from buildings of different age, different concrete category etc, the recycled C& DW at the output of the recycling process should comply with standards and must have technical criteria similar to that of the natural products in order to be used for construction activities.

Main problem of recycled aggregates (REC) is related to the increased water absorption (Poon et al, 2004), which is due to the cement paste attached in recycled aggregate's surface. This fact results in

decreased mechanical strength, since for specific w/c ratio, recycled aggregates absorb significant water content, so cement's hydration is limited.

Researches on **conventional concrete** with recycled aggregates lead to the following results:

- A decrease in workability, an increase in air voids, as well as a decrease in compressive strength has been monitored (Khatib 2005; Xiao et al, 2018). This decrease is influenced by recycled aggregates gradation and is higher for fine aggregates substitution by recycled ones (Evangelista and de Brito, 2007).
- However, concrete mixture with recycled coarse aggregates and conventional fines, can have a slightly higher compressive strength compared to conventional one by up to 5% (~47MPa), which indicate that the use, mainly of coarse aggregates, has potential and can lead to mixtures with satisfactory characteristics and similar to the ones of mixtures with natural aggregates. Moreover, such mixtures can be cost effective. In particular, when recycled coarse aggregates substituted natural ones of the same gradation, the price of concrete mixture came up to 55.05€/m3, while conventional mixture costs 55.65€ (Mavridou and Oikonomou, 2009). This difference in cost can be increased by the wider use of recycled aggregates in public and private construction projects, so secondary's material cost will be decreased.

As far as **self compacted concrete** is concerned, the optimum percentage of substitution of fines by recycled aggregates has been found to be 30% w/t of the aggregates (fine and coarse ones) while compressive strength of the mixture came up to 28.48MPa with a cost of 66.58€/m^3 (Mavridou et al, 2013).

Moreover, **light transmitting concrete** with recycled aggregates has also been examined. REC replaced natural aggregates. According to laboratory results, transparent concrete with plastic optical fibres and recycled aggregates show satisfactory characteristics, while compressive strength at 28 days can come up to 22MPa for percentage of optical fibres 1.04v/v (Mavridou et al, 2018).

Regarding cement mortars, recycled aggregate- recycled sand (RS) - can replace part of the fine aggregate fraction (Neno et al, 2014). However, due to the high demand of RS for water, as expected, mixtures are of worse mechanical strength and of lower workability (Westerholm et al, 2008). For replacement of standard sand by 50% of recycled sand, compressive strength is found to decrease by 47%. As far as workability is concerned, it can be improved by the addition of superplastisizer at a percentage of 1.25% for RS replacement of 50 and 75% of sand (Ferro et al, 2015). Another research of Behera et al, 2014, examined the effect of washed recycled sand in mortars properties. According to laboratory results, washing and sieving of the recycled aggregates can give mixtures with satisfactory and even equal to reference mixture's characteristics given that an additional amount (1%) of super plasticizer is added.

3.3 Properties of cement products with Wastes from Electrical and Electronic Equipment in fresh and hardened state

There are quite few studies on the use of WEEE in cement based products (Mahdi 2017; Vishwakarma and Ramachandran, 2018). However, preliminary studies include WEEE's use as alternative to conventional aggregates or as additives to the cement products.

An experimental study has been made on the utilization of E-waste particles as fine and coarse aggregates in concrete with a percentage replacement up to 30% by weight of cement on the strength criteria of M20 Concrete (design compressive strength of 20MPa). Addition of e-waste plastic was found to decrease mixtures' workability, density and compressive strength by increasing plastic percentage, while strength's value reached 44MPa for 10% addition of e- waste plastic. Moreover, in such mixtures, given the weak bonding between plastic aggregates and cement paste, the effect of water to cement ratio is not prominent. Furthermore, addition of plastics in concrete tends to make concrete ductile, hence increasing the ability of concrete to significantly deform before failure,

increasing mixtures' durability against harsh weather such as expansion and contraction, or freeze and thaw (Aswini Manjunath 2016).

Subramani and Pugal (2015) examined the suitability and advantages of the use of recycled plastics, and especially of Polyhydroxybutyrate (PHB) as coarse aggregates in concrete. Plastic has replaced coarse aggregates by 5-15% wt of the aggregates leading to mixtures with strength comparable to the one of the reference mixture (~25MPa). However, in percentages >20%, plastic was found to have detrimental effect on mixtures strength.

Another research of Lakshmi and Nagan (2010) for the replacement of up to 30% of coarse aggregates by e-waste ones lead to concrete with good strength gain for relatively low percentages (<4%) of plastic (~20MPa), while Prasanna and Rao (2014) found that compressive strength of concrete was optimum when coarse aggregate is replaced by 15% with E-Waste reaching a value of ~31 MPa. These differences in strength for various e-wastes percentages are attributed to raw materials properties- eg chemical composition, gradation-, to water to cement ratio as well as to the treatment method of e-waste.

The usage of e-waste to make Green Concrete can reduce the land-filled or disposal problems of the E-waste materials. Especially, plastics can be used to replace some of the aggregates in a concrete mixture, contributing mainly to reducing the unit weight of the concrete. This is useful in applications requiring non-bearing lightweight concrete, such as concrete panels used in facades.

3.4 Properties of cement products with the combined use of EOL Tires, C& D Wastes and WEEE in fresh and hardened state

Even though there are many studies on the sole use of wastes in cement based products, there is only little on the combined use of solid wastes. In Greece, recent laboratory experiments have been conducted on the combined use of such materials (both recycled aggregates and rubber tire, or recycled aggregates, rubber tire and plastic from EEE) for the production of cement mortars. First step was the examination of basic properties such as gradation curve, water absorption and sand equivalent of raw materials according to European Specifications. Following, cement mortars have been produced and examined as far as their properties in fresh and hardened state are concerned. Fresh state properties included workability, specific weight and air content, while in hardened state tests on specific weight, flexural and compressive strength and water absorption have been conducted. According to laboratory results, addition of recycled aggregates at percentage up to 40% w/t of the sand and tire rubber at a percentage of 2,5% w/t of the sand results in a decrease on the strength of the mixtures. Moreover, as expected, both recycled aggregates and tire rubber gave mixtures with decreased workability and strength (~25MPa). However, mixture including all three wastes resulted in compressive strength of more than 20MPa, value quite high for cement mortars.

4. CONCLUSIONS- FUTURE RESEARCH

Waste streams such as EOL Tires, C&D Wastes and WEEE pose a significant health and environmental concern if not recycled and/or discarded properly. Management issues of such wastes are relatively complicated; on the one hand the high availability of conventional raw materials, while on the other hand the recent legislation, which public organizations and construction involved people are not so familiar to, makes the problem more difficult to deal with.

All wastes may have many secondary uses; EOL Tires can be a low cost source of fuel in power plants, while they can be used in a variety of civil engineering projects such as embankments, backfill for walls, for the production of rubber-modified asphalt (resulting in reduced traffic noise), lightweight concrete, sports fields, ground cover in playgrounds etc. Their characteristics (light weighting, permeability, insulating properties, shock and noise absorbing) make them excellent materials for these uses. Furthermore, all waste streams are a resource that can be used as substitutes for natural aggregates, reducing resource depletion and lowering environmental costs associated with

natural resource exploitation. So, over the years, more and more researchers examine the possible use of these wastes in various applications and especially into concrete products.

This review summarizes the main advances in the use of EOL Tires, C&D Wastes and WEEE in concrete and cement mortars. The general findings monitored in current paper may vary from others, since any change in materials characteristics, proportions of the ingredients, mixing and curing procedure as well as use of admixtures or additives may lead to slightly different conclusions.

In general, and in most of the cases addition of wastes, especially in fine gradation and in relatively high percentage, in cement based products, may result in the production of mixtures with decreased workability, increased air content, decreased specific weight and compressive strength.

Modified with wastes cement products can be advantageous for special applications where the main request is not for mechanical properties. Such applications are in the production of sound barriers, of pedestrian and cement blocks, as lightweight concrete walls, in stabilized base layers in flexible pavements, building facades and architectural units as well as in structures exposed to aggressive environments where high resistance to chloride ions penetration is required.

The use of such wastes, even in small percentages, in concrete can have additionally numerous indirect benefits such as reduction in landfill cost, saving in energy, and protection of the environment from possible pollution effects, while at the same time, cement products with satisfactory characteristics are provided.

However, further researches should focus on the improvement of the bonding between the wastes and the rest of the mixtures, so as to give mixtures with both increased mechanical characteristics and improved durability performance. This improvement may be achieved by the use of appropriate chemicals/ additives, by cleaning secondary materials, by modifying their surface as well as by combining appropriate percentage and gradation of wastes included.

References

1. Presidential Decree No.109. (2004). '**Means and terms for alternative management of worn mobile tires**'. Program for their alternative management, 5th March 2004, Paper of Government of Hellenic Democracy, 1st Part.
2. http://ec.europa.eu/environment/waste/studies/deliverables/CDW_Greece_Factsheet_Final.pdf. (accessed April 3rd 2018).
3. Joint Ministerial Decision (JMD) 36259/1757/E103. (2010). 'Measures, terms and program for the alternative management of waste from excavation, construction and demolition (ECDW)'.
4. Directive 2012/19/EU of the European Parliament and of the Council of 4 July 2012 on waste electrical and electronic equipment (WEEE).
5. https://www.eoan.gr (accessed April 3rd 2018).
6. JMD 23615/2014, 'Measures, terms and conditions for the alternative management of waste materials of electrical and electronic equipment'.
7. Khatib Z.K. and F.M. Bayomy. (1999). 'Rubberized Portland cement concrete'. **ASCE Journal of Materials in Civil Engineering** 11 (3), pp.206-213.
8. Raghvan D., H. Huynh, C.F. Ferraris. (1998). 'Workability, mechanical properties and chemical stability of a recycled tire rubber-filled cementitious composite'. **Journal of Materials Science** 33 (7), pp.1745–1752.
9. Mavridou S. (2010). '**Utilization of recycled tire rubber form automobiles in special cement of asphalt based mortars and concrete**', Ph.D. thesis, Aristotle University of Thessaloniki, Greece.

10. El-Dieb A.S., M.M Abdel-Wahab and M.E. Abdel-Hameed. (2001). ‘Concrete using rubber tyre particles as aggregate’. In: Dhir, R.K. (Ed.), Proceedings of the **International Symposium organized by the Concrete Technology Unit**, University of Dundee, UK, pp.251-259.
11. Eldin N.N. and A.B. Senouci. (1993). “Rubber-tire particles as concrete aggregates”. **ASCE Journal of Materials in Civil Engineering** 5 (4), pp.478–496.
12. Li Z, Li F and Li JSL. (1998). ‘Properties of concrete incorporating rubber tyre particles’. **Magazine of Concrete Research**, Vol.50, No 4, Dec 1998, pp.297-304.
13. Benazzouk A, Douzane O, Langlet T, Mezreb K, Roucoult JM, Quéneudec M. (2007). ‘Physico-mechanical properties and water absorption of cement composite containing shredded rubber wastes’. **Cement & Concrete Composites**, 29, pp.732-740.
14. Siddique R., R.T. Naik. (2004). ‘Properties of concrete containing scrap-tire rubber-an overview’. **Waste Management** 24, pp.563-569.
15. Rostami H, Lepore J, Silverstraim T, Zundi I. (1993). ‘Use of recycled rubber tires in concrete’. In: Dhir, R.K. (Ed.), **Proceedings of the International Conference on Concrete 2000**, University of Dundee, Scotland, UK, pp.391–399.
16. Li G, Stubblefield MA, Garrick G, Eggers J, Abadie Ch, Huang B. (2004). ‘Development of waste tire modified concrete’. **Cement and Concrete Research** 34, pp.2283-2289.
17. Turatsinze A, Bonnet S, Granju J-L. (2005). ‘Mechanical characterization of cement-based mortar incorporating rubber aggregates from recycled worn tyres’. **Building and Environment** Vol.40, pp. 221-226.
18. Ganjian E, M. Khorami and A.A. Maghsoudi. (2009). ‘Scrap- tyre- rubber replacement for aggregate and filler in concrete’. **Construction and Building Materials,** 23, pp.1828-1836.
19. Blessen S. T. and Gupta R. Ch. (2016). ‘A comprehensive review on the applications of waste tire rubber in cement concrete’. **Renewable and Sustainable Energy Reviews**, 54, pp.1323-1333.
20. Mehta P K and Monteiro P J M. (1993). ‘**Concrete, Structures, Properties and Materials’**, 2nd Edition, Prentice-Hall, Englewood Cliffs, NJ.
21. Topçu IB. (1995). ‘The properties of rubberized concrete’. **Cement and Concrete Research** 25 (2), pp.304–310.
22. Nehdi M. and A. Kan. (2001). ‘Cementitious Composites Containing Recycled Tire Rubber: An overview of Engineering Properties and Potential Applications’. **Cement, Concrete and Aggregates**, CCAGDP, Vol.23, No1, pp. 3-10.
23. Lee HS, H. Lee, J.S. Moon and H.W. Jung. (1998). ‘Development of tire- added latex concrete’. **ACI Materials Journal**, 95, (4), pp.356-364.
24. Turatsinze A, J-L Granju and S. Bonnet. (2006). ‘Positive synergy between steel-fibres and rubber aggregates: Effect on the resistance of cement-based mortars to shrinkage cracking’. **Cement and Concrete Research**, 36, pp.1692-1697.
25. Shi-Cong, K. and Chi-Sun, P. (2009). ‘Properties of concrete prepared with crushed fine stone, furnace bottom ash and fine recycled aggregates as fine aggregates’. **Construction and Building Materials** 23, pp.2877–2886.
26. Dapena, E., P. Alaeyos, A. Lobet and D. Pérez. (2011). ‘Effect of recycled sand content on characteristics of mortars and concretes’. **Journal of Materials in Civil Engineering** 23, pp. 414-422.

27. Poon C.S, Z.H. Shui, L. Lam, H. Fok, S.C. Kou. (2004). 'Influence of moisture states of natural and recycled aggregates on the slump and compressive strength of concrete'. **Cement and Concrete Research**, 34 (1), pp. 31-36.
28. Khatib, J.M. (2005). 'Properties of concrete incorporating fine recycled aggregates'. **Cement and Concrete Research** 35, pp. 763–769.
29. Xiao J., Z. Ma, T. Sui, A. Akbarnezhad and Z. Duan. (2018). 'Mechanical properties of concrete mixed with recycled powder produced from construction and demolition waste'. **Journal of Cleaner Production**, 188, pp.720-731.
30. Evangelista, L. and J. de Brito. (2007). 'Mechanical behaviour of concrete made with fine recycled concrete aggregates'. **Cement and Concrete Composites** 29, pp. 397-401.
31. Mavridou, S. and N. Oikonomou. (2009). 'Experimental approach of using recycled aggregate from industrial processing in the production of new concrete'. Part II, Electronic Proceeding of the **16th Concrete Conference**. Paphos, Cyprus.
32. Mavridou S., N. Oikonomou and E. Kaisidou. (2013). 'Utilization of construction and demolition wastes (C&D W) for the production of new concrete mixtures'. In abstract Proceedings of the **CEMEPE/SECOTOX 2013 Conference**. Mykonos, Greece.
33. Mavridou S, A. Savva and N. Trochoutsou. (2018). 'Compressive strength in regular and high temperatures of light transmitting concrete with conventional and recycled aggregates'. **Proc. Pan-Hellenic Concrete Conference**. Technical Chamber of Greece, Athens, Greece.
34. Neno, C., J. de Brito and R. Veiga. (2014). 'Using fine recycled concrete aggregate for mortar production'. **Materials research** 17, pp.168-177.
35. Westerholm, M., B. Lagerblad, J. Silfwerbrand, E. Forssberg. (2008). 'Influence of fine aggregate characteristics on the rheological properties of mortars'. **Cement and Concrete Composites** 30, pp.274–282.
36. Ferro G.A, C. Spoto, J.M. Tulliani, L. Restuccia. (2015). 'Mortar made of recycled sand from C&D', in XXIII Italian Group of Fracture Meeting, **Procedia Engineering** 109, pp.240-247.
37. Behera M., S.K. Bhattacharyya, A.K. Minocha, R. Deoliya, S. Maiti. (2014). 'Recycled aggregate from C&D waste & its use in concrete- A breakthrough towards sustainability in construction sector: A review'. **Construction and Building Materials**, 68, pp.501-516.
38. Mahdi I. (2017). 'Environmental impacts and benefits of state-of-the-art technologies for E-waste management'. **Waste Management** 68, pp.458-474.
39. Vishwakarma V. and D. Ramachandran. (2018). 'Green concrete mix using solid waste and nanoparticles'. **Construction and Building Materials**, 162, pp.96-103.
40. Aswini Manjunath B.T. (2016). 'Partial replacement of e-plastic waste as coarse aggregate in concrete'. **Procedia Environmental Sciences**, Vol35, pp.731-739.
41. Subramani T. and V.K. Pugal. (2015). 'Experimental Study on plastic waste as a coarse aggregate for structural concrete'. **International Journal of Application or Innovation in Engineering & Management**, Vol 4 (5), ISSN 2319-4847.
42. Lakshmi R. and S. Nagan. (2010). 'Studies on concrete containing E plastic waste'. **Int. J. Environ. Sci**. 1 (3), pp. 270-281.
43. Prasanna K. and M. K. Rao. (2014). 'Strength variations in concrete by using E-waste as coarse aggregate'. IJEAR 4 (2), pp.82-84.

A WEB-BASED PLATFORM FOR LANDFILL LEACHATE ESTIMATION AND MANAGEMENT

M. Kotsikas and K. Poulios*

Regional Association of Solid Waste Management Agencies of Central Macedonia, GR- 54626 Thessaloniki, Macedonia, Greece

*Corresponding author: e-mail: kpoulios@civil.auth.gr, tel : +302310508800

Abstract
The water balance method was used to develop a landfill leachate management and monitoring software, on behalf of the Regional Association of Solid Waste Management Agencies of Central Macedonia (RAACM). The aim of the software is to monitor and estimate the leachate generation rate in each landfill operating in the region. It can be used retrospectively where no direct flow measurement is possible, and also as a design tool for future leachate management works under different scenarios. A web-based application was selected, since large spreadsheets can be error prone, and to overcome difficulties arising from the large geographical dispersion of the landfills. A monthly step is used for the estimation of the generation rate and the performance of each wastewater treatment plant (WWTP) is evaluated by modeling the hydrologic and hydraulic conditions in each landfill. The innovation of this software is that it estimates leachate generation for landfills that are in operation, when most of the existing tools (e.g. HELP) are for inactive sites.

During the development of the software, a group of assumptions were tested for their influence in the leachate generation rate. According to the results of water balance that was applied to Mavrorachi landfill for the period 2008-2017, separating the landfill in lifts results in leachate generation rates that differ up to 22% from those calculated without separating it. Nevertheless, other parameters, such as the precipitation distribution between different lifts, that are difficult to estimate or collect monthly, affect the calculation of leachate generation rate very little (1-5%).

Keywords: Sanitary landfill, Water balance, Leachate management, Environmental tools, Solid waste management

1. INTRODUCTION

Landfills still constitute an important part of any waste management system and will continue to do so in the foreseeable future, as final sinks for non recyclable or hazardous materials (Brunner, 2013; Kral & Brunner, 2014; Scharff, Hansen, & Thrane, 2014). Despite efforts to the contrary, in Greece an average of ca. 82% of Municipal Solid Waste (MSW) were still landfilled in 2016 (Brennan et al., 2016; EUROSTAT, 2018). One of the most significant environmental impacts of landfills, emanating *inter alia* from the long operational periods and even longer aftercare and final stabilization times, is leachate generation (Christensen, 2010; Scharff et al., 2013). When designing leachate management works, such as WWTPs, estimating and predicting accurately the leachate generation rate has many environmental and economic benefits. A large underestimation of landfill's leachate generation rate could result in many WWTP operation failures and severe environmental impacts. On the other hand overestimation of landfill's leachate generation rate results in oversized and unnecessary WWTPs with large investment and operating costs.

The RAACM operates ten active MSW landfills and two sites under aftercare, along with their corresponding WWTPs. Through the years the landfills continuously receive waste, so their capacity and the leachate generation rate are raised. Correspondingly, the leachate management works need upgrades which are designed by estimating the leachate generation rate.

In order to optimize the estimation, a platform is developed where landfill data are input, and through a complex algorithm that uses the water balance method the leachate generation rate is calculated. The water balance method used in its analytical form, as presented by (Tchobanoglous et al, 1993) separating the landfill in lifts. Available tools such as HELP (Schroeder et al, 1994) are less suited for use on landfills in operation (Athiniotou et al, 2012).

2. MATERIALS AND METHODS

2.1 Theoretical background

The most common method for estimating the leachate generation rate in landfills is the water balance method. This method takes into account all the water inflows in the landfill and subtracts the water losses (Figure 1). The most significant inflow parameters are the amount of precipitation that is infiltrated, the moisture from fresh MSW and leachate recirculation. The losses are due to landfill gas formation (a part is consumed during biodegradation and another escapes as vapor with landfill gas).

Another very important parameter is the field capacity of MSW, since it determines the amount of leachate generated from each lift and finally onto the Leachate Collection and Removal System (LCRS), as generally reported in the literature (Frikha et al, 2017), and demonstrated in this study.

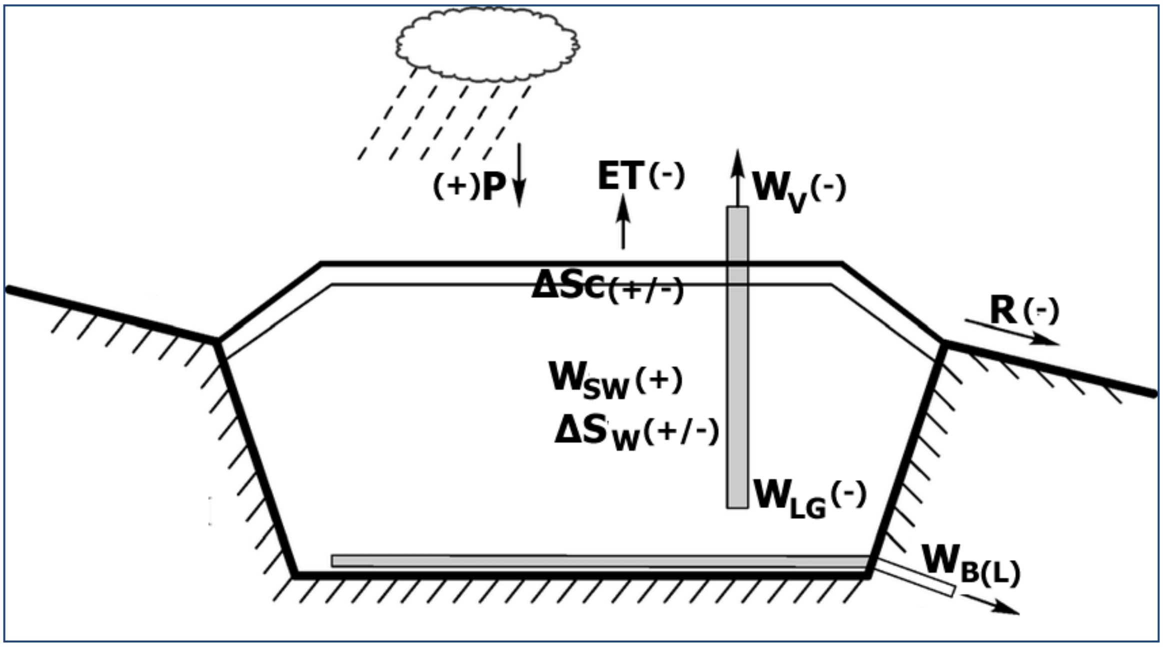


Figure 1: Water balance applied in a sanitary landfill

2.2 Infiltration

The infiltration is the amount of precipitation that falls on the landfill and passes through the daily cover. It can be estimated by the following equation:

$$PERSW = P - R - ET - \Delta S_w \quad (1)$$

Where:

PERSW = amount of water percolating through the unit area of landfill cover into compacted solid waste (mm)

P= amount of precipitation per unit area, (mm)

R= amount of runoff per unit area (mm)

ET= amount of water lost through evapotranspiration per unit area (mm)

ΔSLC = change in the amount of water held in storage in a unit volume of landfill cover (mm)

Precipitation (P): Precipitation can be estimated from data obtained from weather stations inside or near the landfill area. In case of weather stations not inside the landfill area, the data are adjusted according to the altitude difference.

Evapotranspiration (ET): Evaporation is the process where liquid water is converted to vapor and escapes from the evaporating surface. Transpiration consists of the vaporization of liquid water to the atmosphere via plant roots.

In order to estimate the ET from landfill cover the Potential ET (PET) is calculated. PET is considered as the amount of ET when there is excess of water in the landfill cover. The most widely used equations for estimating PET are Penman-Montheith and Thornthwaite's. The first is more accurate but needs more data such as mean temperature, wind speed, humidity and solar radiation. Thornthwaite's equation is simpler because it requires only the mean temperature as input. For the development of software the Thornthwaite's equation is used because it is the simplest one and the differences in the leachate generation estimation are small.

Mean temperature can be estimated from data obtained from weather stations inside or near the landfill area. In case of weather stations not inside the landfill area, the data are adjusted according to the altitude difference, as with precipitation.

Run-off (R): Run-off is the amount of precipitation that flows in the surface of landfill cover, is collected from the perimeter drainage trench and is not infiltrated inside the landfill body. Run-off is the most difficult parameter to estimate in active landfills because the hydraulic characteristics of surface area change dynamically. So, to calculate the water balance, in short time periods, ideally per month, the landfill must be divided into segments with common hydraulic characteristics.

Run-off is calculated as a percentage of the precipitation, according to the following equation:

$$R = C_R \cdot P \quad (2)$$

Where:

C_R = run-off co-efficient (dimensionless)

Run-off co-efficient is an empirical dimensionless constant with values between 0 (no run-off) and 1 (100% run-off). For landfill applications, the value of C_R depends on landfill cover's slope and soil composition.

Figure 2 presents a hypothetic and quite simple landfill state where A1 represents the part of landfill that has no waste in place yet, and A2 and A3 represents the parts that are filled with MSW. The slope of the bottom is towards A3. Each part has a different hydraulic behavior which is described as follows:

Part A1: Precipitation that falls on part A1 area flows directly onto the drainage layer of the (LCRS) and ends up to the lowest point of the landfill where leachate is collected. In this part there is no amount of precipitation that is drawn away to the perimeter drainage trench and run-off equals 0. Evapotranspiration also equals 0 because the water is quickly infiltrated through the drainage layer to the lowest point of the landfill.

Part A2: Precipitation that falls on part A2 flows at A1 area and run-off have the same behavior with Part A1. Evapotranspiration is normally calculated because precipitation falls in the cover of landfill where the infiltration is slow.

Part A3: Precipitation that falls on part A3 flows over the landfill cover to the perimeter drainage trench T. Both run-off and evapotranspiration are normally calculated. In this case part A3 is further

divided in two parts, one part where the cover has high slope and run-off co-efficient and one part where the cover has low slope and run-off.

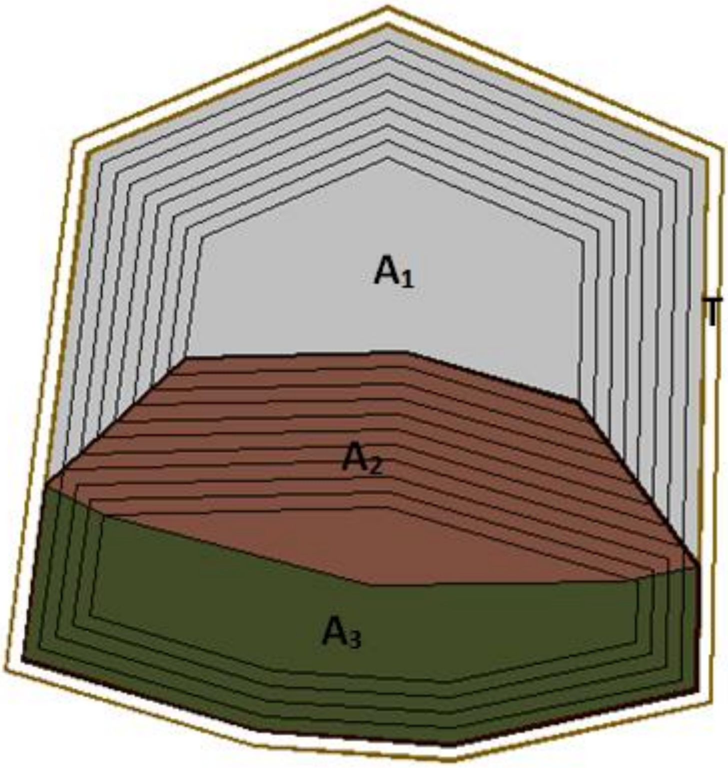


Figure 2: Hypothetic scenario of a landfill's operating state

2.3 Recirculation

Recirculation is the process where leachate is returned into the landfill body in order to keep the moisture of the MSW in a desired level to accelerate waste settlement, stabilize the waste mass and also accelerate the start of methanogenesis and gas generation. If there are no flow meters in the recirculation pumps of the WWTP a mass balance approach has to be used.

2.4 MSW moisture – field capacity

MSW moisture is one of the most important parameters of leachate generation. Moisture is related to the organic fraction that is contained in MSW. The amount of water that compacted MSW can retain is known as field capacity and depends on compaction due to overburden mass.

Field capacity can be estimated as percentage of the dry weight of the MSW in landfill from the following equation (Tchobanoglous & Kreith, 2002):

$$FC = 0.6 - 0.55 \cdot W / (5.44 + W) \qquad (3)$$

Where:

FC = field capacity of waste as fraction of dry weight (%)

W = the overburden weight at the mid height of the waste per surface unit (tn/m^2)

The amount of water the can be retain in waste is:

$$W_H = FC \cdot W_{dry} \qquad (4)$$

Where Wdry = dry waste weight (tn)

2.5 Leachate losses

There are two main processes in landfill that contribute to water losses: formation of landfill gas and escape as water vapor.

Formation of landfill gas. Leachate is consumed during the anaerobic decomposition of the organic constituents in MSW. The amount of water consumed by the decomposition reaction can be estimated per cubic meter of gas produced and is in the range from 0,192 to 0,24 kgr H_2O/m^3.

Water vapor. Landfill gas usually is saturated in water vapor. The quantity of water vapor escaping the landfill is determined by assuming the landfill gas is saturated with water vapor. The numerical value for the mass of water vapor contained per cubic meter of landfill gas at 32,2°C is about 0,0352kg H_2O/m^3 landfill gas.

Both leachate losses are calculated as fraction of the landfill gas produced. Landfill gas generation is estimated using LandGEM software methodology. Methane generation rate is calculated considering that the biodegradation process follows first order kinetics.

A M (tn) mass of MSW in landfill, produces landfill gas according to the equation:

$$Q_{CH4} = k \cdot L_0 \cdot M \cdot e^{-kt} \tag{5}$$

Where:

Q_{CH4} = methane generation rate per year (m^3/yr)

k = methane generation rate co-efficient (= 0,05yr^{-1})

L_0 = potential methane generation per MSW mass (=170m^3/tn)

t = time passed from the disposal of MSW (yr)

Landfill gas contains approximately 50% methane so it is easy to be calculated when methane generation is known.

2.6 Water balance algorithm

The water balance method is applied in each landfill lift separately in order to calculate the leachate generation. The step by step algorithm is described as follows:

Step 1. The infiltration rate is calculated from the landfill cover to the upper lift of wastes.

Step 2. Starting from the upper waste lift of landfill, the outflow is calculated with the following equation:

$$W_{bl} = W_{ar} + W_{sl} - S_w - W_g \tag{6}$$

where:

W_{bl} = outflow from the upper waster lift to lower (m^3)

W_{ar} = water entering from the upper of the lift (m^3) = PER_{sw}

W_{sl} = moisture of new waste disposed (m^3)

S_w = water that can be retained in the waste due to field capacity (m^3)

W_g = water losses due to gas formation

Step 3. Equation (5) is used to solve all lifts from upper to the bottom taking into account that:

$$W_{bl,i-1} = W_{ar,i} \tag{7}$$

Where i refers to the waste lift located bellow lift i-1.

Step 4. The leachate outflow from the last waste lift ($W_{bl,0}$), the lowest lift at the landfill is the leachate generation rate of the landfill that can be collected through the leachate collection system to WTP.

2.7 Software requirements and development

Since the RAACM owns and operates a large number of sites with a significant geographical dispersion, there is a need for many users to enter a lot of data from many different locations, in order to estimate leachate generation on site, for each site. Furthermore, large spreadsheets can be error prone and difficult to manage and maintain.

Therefore, software was developed to work as a web-based application, allowing remote access. Its goal is to serve as a management and decision support tool. All data is stored in a database which has been built using MySQL. The water balance calculation has been developed in PHP, a widely-used open source scripting language that is especially suited for web development and can be embedded into HTML.

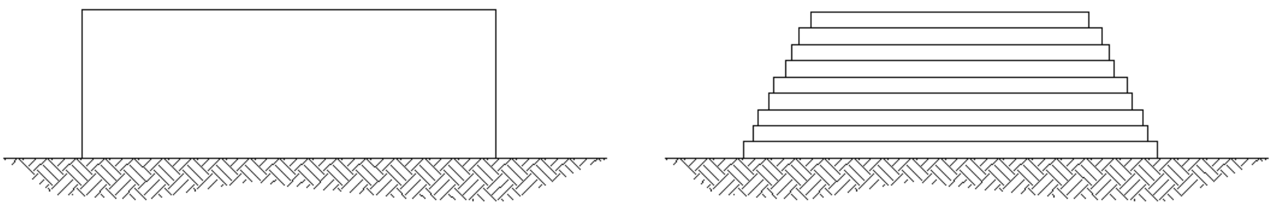
The front-end environment for entering data, results and diagram presentations, was developed with Javascript, CSS and HTML.

3. RESULTS AND DISCUSSION

3.1 Evaluation of assumptions

Many parameters or data that need to be input to the water balance can be difficult to measure or estimate. Their influence on the results is evaluated below.

Separating the landfill in lifts. When MSW is disposed in a landfill, they are placed in lifts. To calculate the water balance for each lift, many parameters need to be monitored (area, weight, MSW disposals etc). A more simplified assumption that is widely used in landfill design is to consider the landfill as a single rectangular mass (Figure 3).



Figures 3-4: Simplified shape of landfill - Shape of landfills with lifts

Rain distribution in each lift. When the rain is falling onto the landfill cover, each lift receives an amount of rainwater that is related with its exposed area. Although this reflects reality better, it is difficult to estimate the exposed area of each lift, especially when the landfill has many lifts and water balance is applied monthly. In this case, a simplifying assumption is to consider that all the rain is falling and infiltrated in the cover of the top most lift (Figure 4).

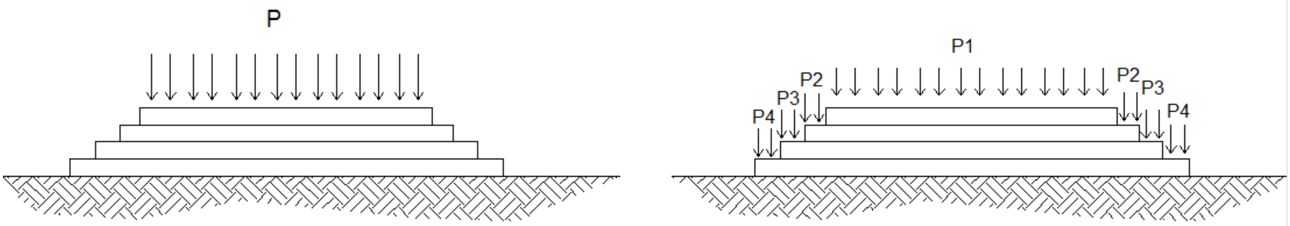


Figure 5-6: Rain falls only in the upper lift of landfill - Rain divided according to the exposed area of each lift

Conditions in the area where landfill's cells are in contact. Large landfills are often designed with multiple disposal sites (cells) to minimize the catchment area of the MSW disposal. When a cell is filled with MSW to capacity, a new cell opens to receive waste. The lifts, as they develop vertically, always lean to the old cell, so for some years they behave as one cell (Figure 5). In order to apply the water balance, two different assumptions can be considered, none of which reflects reality 100%.

Assumption 1. The water balance is applied separately for each cell, considering that there is no hydraulic connection between them. This assumption has two major problems: (a) the weight of one basin's lifts (e.g. TB3 in Figure 5) is not taken into account while the water balance is applied to the other cell (e.g. TA3 in Figure 5) and (b) it is considered that leachate produced in cell A does not leak into cell B.

Assumption 2. It is considered that there is no hydraulic separation between the cells and the new one is an extension of the old one, e.g. lift TB1 is actually the extension of lift TA1 (Figure 5). The main problem of that assumption is that when a new lift is placed, e.g. TB3, its area is increased and according to equation (3) the field capacity of the waste in lift TA3 (+TB3) is raised, affecting the leachate generation rate.

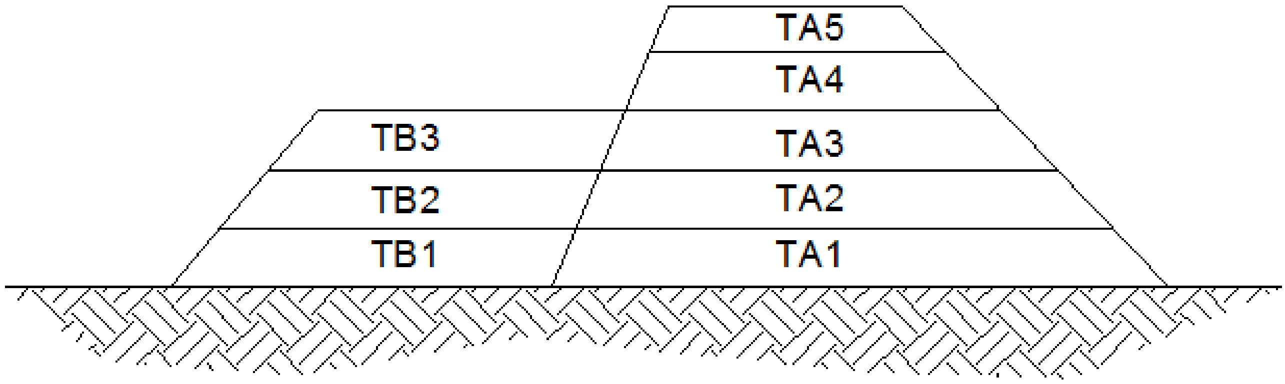


Figure 7: Typical landfill cross section with two waste disposal basins

3.2 Application results

The landfill at Mavrorachi is chosen to apply the water balance method and evaluate how the assumptions affect the leachate generation. Mavrorachi landfill is located in municipality of Lagadas and accepts the MSW from all the Prefecture of Thessaloniki, about 450.000 tn/yr. All available data is used for the years 2008 (opening date) to 2017.

The evaluation criterion that is chosen is the cumulative leachate generation and the mean leachate generation rate per year. The results of the evaluation for each of the assumptions is presenting below.

Separating landfill in lifts. Water balance was applied for the period 2008 – 2017. The mean leachate generation rate when the landfill's shape is simplified differs up to 22% (Table 1) from the scenario where the landfill is divided in horizontal lifts. The cumulative leachate generation has large differences in the beginning of operation but through the years it is stabilized around 3%. However, when a new waste disposal cell started to operate (2015), it affects the difference and raised it to 5-10% (Figure 6). The peak of approximately 80% difference in cumulative leachate generation happens because in the beginning of the operation of landfill the first lift was small (two month disposal), so the overburden weight of the second lift causes a high reduction of waste field capacity.

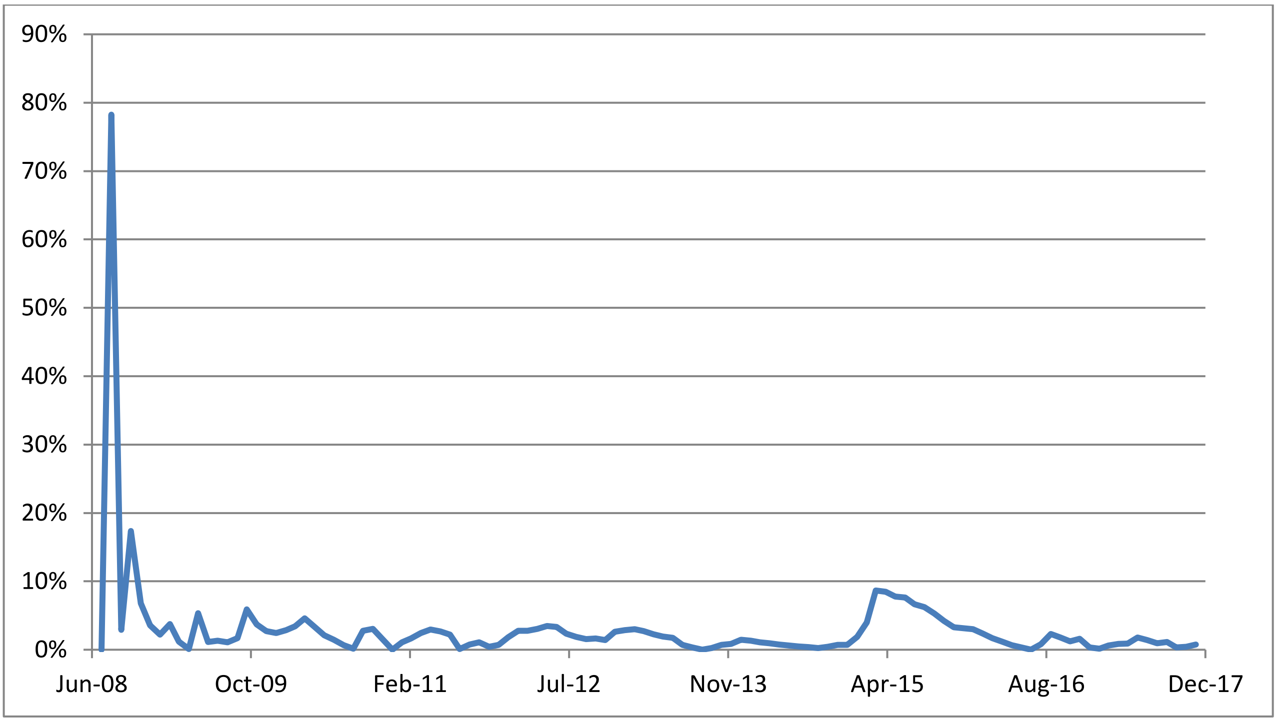


Figure 6: Difference in cumulative leachate generation when landfill lifts is not taken into account

Table 1: Comparison between dividing the landfill in lifts and not dividing

Year	Mean leachate generation rate (m^3/d)		Difference (%)
	Landfill with lifts	Landfill without lifts	
2008	173,1	179,4	3,64%
2009	288,1	295,5	2,57%
2010	298,9	299	0,03%
2011	202,6	198,4	2,07%
2012	222,2	245,6	10,53%
2013	281,7	240	14,80%
2014	250,2	250,3	0,04%
2015	374,3	324,7	13,25%
2016	347,3	372,2	7,17%
2017	253,5	309,3	22,01%

Rain distribution in each lift. Water balance applied for the period 2008 – 2013 because it was difficult and time consuming to estimate and collect data for the area of exposed in rain from each liftr of landfill. In this case the difference between simplified and analytic assumption where very small. The mean leachate generation rate difference in all these years where <3% (Table 2) and the cumulative leachate generation has a peak (6,72%) at the beginning of the operation of landfill but it stabilizes through the years around 1% (Figure 7).

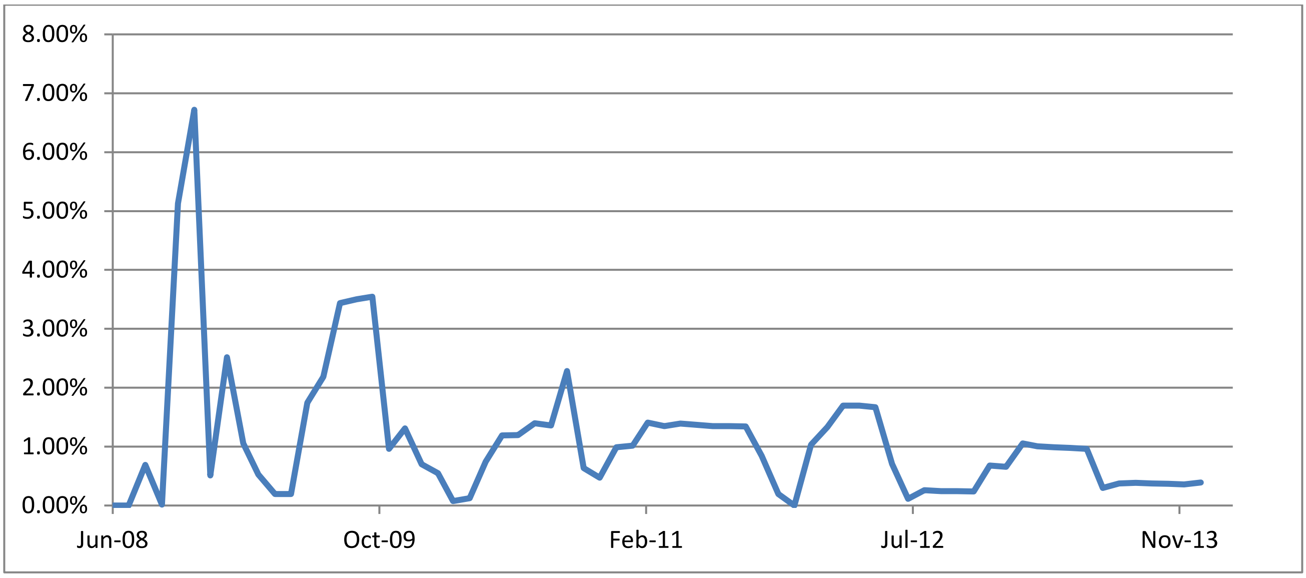


Figure 7: Difference in cumulative leachate generation when the rain is not distributed in each lift

Table 2: Comparison between simplified and analytical distribution of rain

Year	Mean leachate generation rate (m^3/d)		Difference (%)
	Simplified distribution	Rain distribution per lift	
2008	101,24	100,72	0,51%
2009	268,12	264,19	1,49%
2010	269,88	276,94	2,55%
2011	198,10	195,28	1,45%
2012	231,62	238,65	2,95%
2013	265,35	262,98	0,90%

Conditions in the area where landfill's cells are in contact. The time period when a new cell started to operate at the landfill was in 2015. So, the comparison period was 2015-2017 and the year 2018 added not using real data, but estimated data. As is shown to Table 3, for years 2015 – 2017 the difference between Assumption 1 and Assumption 2 in mean leachate generation rate is 3,55% - 13,78%. Moreover in year 2018, when estimated data are used the difference is raised to 29,64%. It is noteworthy that none of the assumptions reflects 100% reality.

Table 3: Comparison between simplified and analytical distribution of rain

Year	Mean leachate generation rate (m^3/d)		Difference (%)
	Assumption 1	Assumption 2	
2015	352,8	374,3	5,74%
2016	359,6	347,3	3,55%
2017	288,4	253,5	13,78%
2018	317,0	244,55	29,64%

4. CONCLUSIONS

In this paper the water balance method is presented as it is applied for the development of a web-based application to be used for monitoring multiple sites. Furthermore, the most significant assumptions' evaluation is presented concerning their influence in leachate generation rate. The results of the evaluation show that:

1. Simplifying the calculation of water balance and considering that landfill is a single rectangular mass has significant difference in estimation of leachate generation rate. So it is suggested to calculate water balance for each lift.
2. Distributing precipitation in each lift, proportional to the exposed area, only affects the leachate generation by a small percentage, so the error is negligible (<3%).
3. Water balance is difficult to be calculated in the situation where two or more waste disposal cells come in touch. There are two assumptions that can be made and each one has some disadvantages. The leachate generation is calculated for both assumptions and its difference reaches 29,64%.

Field capacity of MSW is the most significant parameter of water balance model. As shown in Figure 8, when the new waste disposal cell started to operate (Feb 2015), the total field capacity of the landfill is affected less and is more stable in assumption 1. So this is the assumption chosen for the software developed. There is a need for further study in this direction.

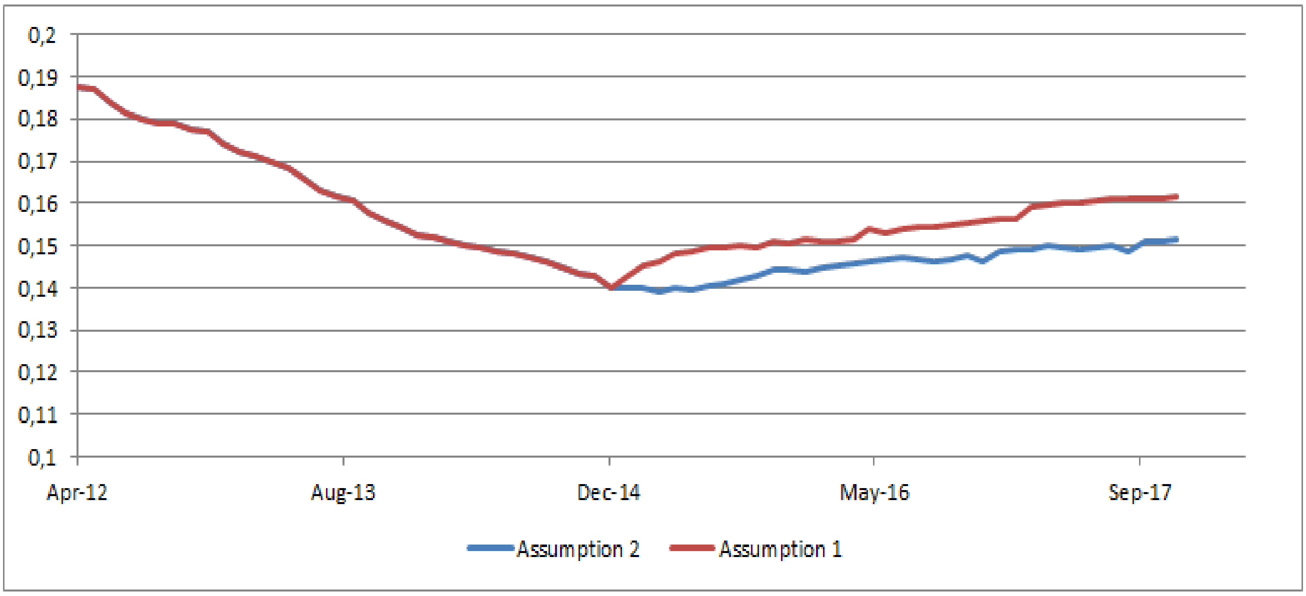


Figure 8: Holding capacity of MSW in landfill for two different assumptions

References

1. Brunner, P. H. (2013). Cycles, spirals and linear flows. **Waste Management and Research**, 31(10 SUPPL.), 1–2.
2. Kral, U., & Brunner, P. H. (2014). The incorporation of the "final sink" concept into a metric for sustainable resource management. **Sustainable Environment and Resources**, 24(6), 431–441.
3. Scharff, H., Hansen, J. B., & Thrane, J. (2014). Key Issue Paper The Role of Landfills in the Transition toward. **International Solid Waste Association**.
4. Brennan, R. B., Healy, M. G., Morrison, L., Hynes, S., Norton, D., & Clifford, E. (2016). Management of landfill leachate: The legacy of European Union Directives. **Waste Management**, 55, 355–363.

5. EUROSTAT. (2018). **Municipal waste generation and treatment**, by treatment method. Retrieved May 4, 2018, from http://ec.europa.eu/eurostat/web/waste/municipal-waste-generation-and-treatment-by-treatment-method
6. Christensen, T. H. (Ed.). (2010). **Solid Waste Technology & Management.** Chichester: John Wiley & Sons, Ltd.
7. Scharff, H., Crest, M., Lanner, D., Greedy, D., Kallassy, M., & Milke, M. (2013). Landfill Aftercare. **International Solid Waste Association**, 6.
8. Tchobanoglous, G., Theisen, H., & Vigil, S. (1993). **Integrated solid waste management**: engineering principles and management issues.. McGraw-Hill.
9. Schroeder P.R., Dozier T.S, Zappi P.A., McEnroe B.M., Sjostrom J.W. and Peyton R.L. (1994) **'Hydrologic Evaluation Of Landfill Performance (H.E.L.P.)** Model – Engineering Documentation for v.3', Environmental Laboratory - U.S. Army Corps of Engineers - Waterways Experiment Station.
10. Athiniotou A., Papaspyros I. and Komilis D. (2012) 'Modeling Leachate Generation From An Active Sanitary Landfill', Proceedings of the **4th WSWMA International Conference**.
11. Frikha, Y., Fellner, J., & Zairi, M. (2017). Leachate generation from landfill in a semi-arid climate: A qualitative and quantitative study from Sousse, Tunisia. **Waste Management and Research**, 35(9), 940–948. https://doi.org/10.1177/0734242X17715102
12. Tchobanoglous, G., & Kreith, F. (2002). **Handbook of Solid Waste Management**, 2nd edition, McGraw Hill.

Protection
and
Restoration
of the
Environment
XIV

Protection and restoration of coastal zone and open sea waters

SUSTAINABLE COASTAL ZONE MANAGEMENT OF STRYMONIKOS GULF – IMPLEMENTATION OF THE D.P.S. FRAMEWORK FOR COASTAL ACTIVITIES PRESSURES ANALYSIS

E. Yiannakopoulou and E.K. Oikonomou*

Department of Transportation and Hydraulic Engineering, Faculty of Rural & Surveying Engineering, Aristotle University of Thessaloniki, 54124 Thessaloniki, Hellas

*Corresponding author: e-mail: eoikonom@topo.auth.gr, tel: +30 2310 994360

Abstract
Sustainable management of coastal areas strives for the maximum long-term societal good, including environmental, economic, social and cultural considerations. Coastal zones, as ecologically sensitive areas, are considered as the main location of residential, economic, industrial and touristic development, due to their natural characteristics and the high aesthetic value of their landscape. However, they are vulnerable to pollution by large quantities of organic load, fertilizers and pesticides, urban and industrial wastewater, which eventually end up in the sea, through the aquatic recipients. The application of the D.P.S. (Driving Forces-Pressures-State) Framework, which is a subsystem of the D.P.S.I.R. Framework (Driving Forces – Pressures – State – Impacts – Response), is proposed to the coastal zone of Strymonikos Gulf. It focuses on the identification, assessment and evaluation of potential impacts of coastal activities, such as tourism, industry, agriculture, fishery, etc., by using the appropriate economic, environmental and social indicators, in the context of sustainable coastal zone management. As a result, it is obvious that there is a growing need for the application of such a framework in a coastal zone, which can be used to organize research that increases understanding about interaction between environmental and societal processes, in order to help understand and support as well, sustainable coastal zone management scenarios.

Keywords: D.P.S. framework, Evaluation, Coastal zone sustainable management, Strymonikos Gulf

1. INTRODUCTION

From a human history perspective, the characteristics of coastal zones have made them preferential sites for human occupation and, consequently, intense areas of development. A direct consequence of human occupation of these coastal areas is that coastal zones rank among the environments most affected by human presence and activities. The coastal area includes a wide range of economic activities. The main uses, located on coastal areas, are: urban settlements, tourism and recreation activities, industrial sites, fisheries, energy production industries, transportation infrastructure, agricultural activities and forestry. The concentration of significant economic activities on the coastal zone is responsible for: marine, freshwater and air pollution, degradation of sensitive marine and terrestrial ecosystems, loss of land resources, loss of historic resources, as well as noise and congestion. The fast expansion over the last decades of socio-economic activities on coastal and estuarine areas made management tasks much more complex. In recent years, there has been a growing concern to maintain a steady growth in economic activities and social development in estuarine areas, while preserving their natural features and ecological service [1]. The area of study is the coastal zone of Strymonikos Gulf, where human activities include mass tourism, house

construction, industries, fishing, aquaculture, agriculture and farming. These activities are not always practiced wisely, leading to increasing environmental problems, such as pollution and landscape deterioration. In this study, the application of the D.P.S. (Driving Forces-Pressures-State) framework is proposed, which is a subsystem of the D.P.S.I.R. framework (Driving Forces – Pressures – States – Impacts – Responses), to the coastal zone of Strymonikos Gulf. It focuses on the identification, assessment and evaluation of potential impacts of coastal activities, by using the appropriate economic, environmental and social indicators, in the context of sustainable coastal zone management.

2. SUSTAINABLE COASTAL ZONE MANAGEMENT

Coastal zones are recognized to be areas of high ecological and economic value. Coastal and marine ecosystems provide a wide range of services to human beings. These include provisioning services such as supply of food, fuel wood, energy resources and natural products; regulating services, such as shoreline stabilization, flood prevention, storm protection, climate regulation, nutrient regulation, detoxification of polluted waters, and waste disposal; cultural and amenity services such as culture, tourism, and recreation; and supporting services such as habitat provision, nutrient cycling, primary productivity, and soil formation. These services are of high value, not only to local communities living in the coastal zone, but also to national economies and global trade as well [2]. As a majority of human settlements and towns lie in or are close to the coastal zone, the intense demand on coastal resources to support economic activities provokes adverse effects on the coastal ecosystems. It is worth mentioning that more than half the world’s population today lives within 60 kilometers of the shoreline. While it is easy to take a biased view and support either economic development or ecological preservation, the challenge in sustainable development lies in fostering measured socio-economic growth, which does not compromise the ecological integrity and value of the area [3].

The concept of sustainable development acknowledges the principle that economic well-being, social justice and environmental objectives cannot be decoupled, but are inherently interdependent over the long run. Sustainable management of coastal areas strives for the maximum long-term societal good, including environmental, economic, social and cultural considerations. It strives to promote social equity through the fairer distribution of opportunities both within the present population, and between present and future generations. Within a sustainability framework, it is important, at a minimum, to ensure that the process of tradeoffs is disciplined such that economic, environmental and social objectives are all met at some “threshold level”, even in the short-run. Furthermore, since the coastal resource is finite in physical and spatial terms, certain short-term decisions may permanently destroy resources for the future. One of the goals of sustainable development must therefore be to ensure that present decisions do not foreclose future options, what is often recognized as intergenerational equity [4].

3. THE P.S.R. AND D.P.S.I.R. FRAMEWORKS

The Organization for Economic Cooperation and Development (OECD) created the ‘‘Pressure–State–Response’’ (P.S.R.) Model in 1993 to help model the cause and effect relationship between human activities and the environment [5]. The P.S.R. model considers that: human activities exert pressures on the environment and affect its quality and the quantity of natural resources (“state”); society responds to these changes through environmental, general economic and sectoral policies, and through changes in awareness and behavior (“societal response”). It highlights the cause-effect relationships between economic activities, environmental and selected social conditions, and helps decision-makers and the public to deal with environmental and economic issues as interconnected. It thus provides a means of selecting and organizing indicators in a way, which is useful for decision-makers and the public. The P.S.R. Model has the advantages of being one of the easiest frameworks to understand and use; and of being neutral in the sense that it shows which linkages exist, and not whether these have negative or positive impacts. This should however not obscure the view of more

complex relationships in environment-economy and environment-society interactions. Depending on the purpose for which the P.S.R. Model is used, it can be easily adjusted to account for greater details or for specific features. Examples of adjusted versions are the Driving force – State – Response (D.S.R.) model used by the U.N.C.S.D. in its work on sustainable development indicators, the framework used for O.E.C.D. sectoral indicators and the Driving force – Pressure – State – Impact – Response (D.P.S.I.R.) Model used by the European Environment Agency [6].

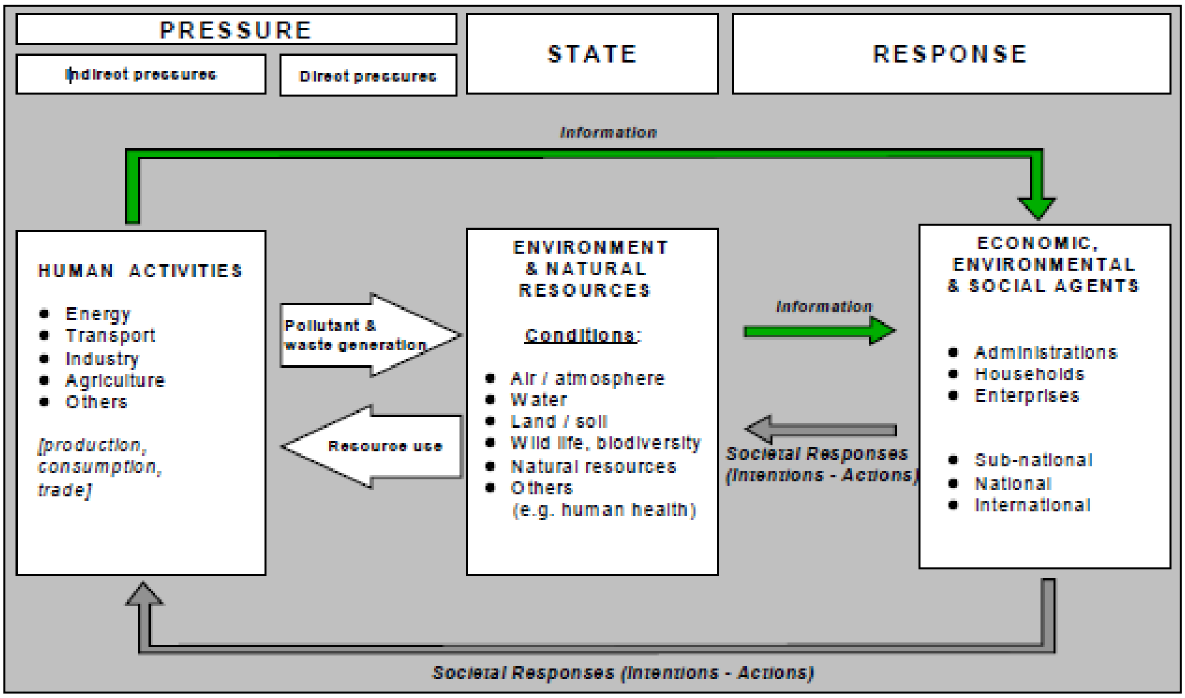


Figure 1: The Pressure – State – Response (P.S.R.) Model presented in a diagram

The D.P.S.I.R. (Driving forces – Pressures – States – Impacts – Responses) framework usually represents the systems analysis and the assessment of the relation between human activities and the environment. According to this systems analysis view, social and economic development (D) exert pressure on the environment (P) and, as a consequence, the state of the environment changes (S). This leads to impacts on e.g. human health, ecosystems and materials (I) that may elicit a societal response (R) that feeds back on the driving forces, on the pressures or on the state or impacts directly, through adaptation or curative action by mitigation measures. Indicators for Driving Forces describe the social, demographic and economic development in societies, and the corresponding changes in lifestyles, overall levels of consumption and production patterns. Pressure indicators describe developments in release of substances (emissions), physical and biological agents, the use of resources and the use of land by human activities. The pressures exerted by society are transported and transformed in a variety of natural processes to manifest themselves in changes in environmental conditions. State indicators give a description of the quantity and quality of physical, biological and chemical phenomena (such as atmospheric CO_2 concentrations) in a certain area. Impact indicators are used to describe changes in these conditions. It is the change in the availability of species that influences human use of the environment. In the strict definition, impacts are only those parameters that directly reflect changes in environmental use functions by humans. As humans are a part of the environment, impacts also include health impacts. Response indicators refer to responses by groups (and individuals) in society, as well as government attempts to prevent, compensate, ameliorate or adapt to changes in the state of the environment Examples of response indicators are the relative number of cars with catalytic converters and recycling rates of domestic waste [7]. The D.P.S.I.R. framework has increasingly become accepted and applied to different case studies, in order to aid problem solving that involves a range of coastal marine environments including estuaries, coastal lagoons and coastal areas. In many cases this framework has been complemented with use of

numerical models, which have been increasingly becoming indispensable tools in management decisions [1].

4. IMPLEMENTATION OF THE D.P.S. FRAMEWORK IN STRYMONIKOS GULF

4.1 The area of study

The area of study involves the coastal zone of Strymonikos Gulf, which is a semi-enclosed coastal water body in North Aegean Sea in Central Macedonia Region, Hellas, located in east of Thessaloniki, 50 km away. It is defined by an imaginary line that connects the capes of Eleftheras (Halkidiki) and St.Dimitriou (Kavala). The coastal zone is rich in natural resources, landscapes and cultural features. More specifically, the most significant environmental parameters of the area include Lake Volvi, Rentinas narrows, Strymonas and Rihios river estuary and Stratonikos mountain.



Figure 2: The area of study, the coastal zone of Strymonikos Gulf

Human activities in the area include mass tourism, house construction, industries, fishing, aquaculture, agriculture, farming, etc. These activities are not always practiced wisely and in harmony, leading to increasing environmental problems, such as pollution and landscape deterioration, which is expected to become by far more serious in the next decades [8].

Sustainable development is based on a balance between the components of economic prosperity, social justice and environmental conservation. Accordingly, the criteria that are chosen in the proposed methodology for the evaluation of all coastal activities of the Strymonikos Gulf, are economic, social and environmental. Then, those criteria are divided to sub-criteria, in order to reduce the complexity of activities pressures analysis. Criteria and sub-criteria used in the case study are presented in Table 1.

4.2 Implementation of the D.P.S. framework for Strymonikos Gulf activities pressures analysis

An economic, social and environmental pressures analysis is held for better understanding of the pressures of Strymonikos Gulf activities with the implementation of the D.P.S. (Driving forces – Pressure – State) framework, which is a subsystem of the D.P.S.I.R. framework. According to the framework, human activities are considered as Driving Forces. In the case study, the major economic activities of the Strymonikos Gulf are examined and more specifically, tourism, agriculture, farming,

industry, fisheries and aquaculture. The economic, social and environmental pressures analysis results are presented in Tables 2, 3 and 4.

Table 1: Proposed criteria and sub-criteria of Strymonikos Gulf activities pressures analysis

Criteria	Economic	Social	Environmental
Sub-criteria	Economic growth Land use Implementation cost	Reduction of unemployment Social acceptance Quality of life – Health Protection of cultural heritage	Surface- Underground water quantity Surface- Underground water quality Land quality Erosion Air quality Noise pollution Ecosystems –Biodiversity Climate change Natural resources consumption

Table 2: Implementation of the D.P.S. framework for economic pressures

DRIVING FORCES	PRESSURE	STATE
Tourism	Services and settlements production	Economic growth
Agriculture	Agricultural products	
Farming	Farming products	
Industry	Industry products	
Manufacturing units	Product production	
Fisheries	Fisheries products	
Aquaculture	Aquaculture products	
Tourism	Land demanding	Land use
Industry		
Agriculture		
Tourism	Accommodation and infrastructure	Implementation cost
Industry	Facilities	

Table 3: Implementation of the D.P.S. framework for social pressures

DRIVING FORCES	PRESSURE	STATE
Tourism	Jobs	Reduction of unemployment
Industry		
Agriculture		
Farming		
Manufacturing units		
Fisheries		
Aquaculture		
Tourism	Seasonal population increase, noise, pollution of the environment, Jobs	Social acceptance
Industry	Pollution of the environment, Jobs	
Tourism	Solid wastes - domestic wastes, working conditions, coastal landscape quality	Quality of life – Health
Agriculture	Solid wastes, working conditions, air pollution	
Industry	Industrial wastes, noise, working conditions, coastal landscape quality, air pollution	
Tourism	Uncontrollable development	Protection of cultural heritage

Table 4: Implementation of the D.P.S. framework for environmental pressures

DRIVING FORCES	PRESSURE	STATE
Agriculture	Water consumption, irrigations	Surface- Underground water quantity
Tourism	Water consumption	
Farming		
Industry		
Manufacturing units		
Tourism	Tourism facilities sewage	Surface- Underground water quality (eutrophication, salinization)
Agriculture	Pesticides, fertilizers and nutrients discharges, use of insecticides	
Farming	Liquid waste disposal, nitrogen and phosphorus discharges	
Industry	Industrial waste disposal, industrial emissions of nitrogen and phosphorus	
Manufacturing units	Wastewater, gas emissions	
Fisheries	Oil from intensive fishery	
Aquaculture	Wastewater	
Tourism	Solid wastes, απορρίμματα	Land quality
Agriculture	Agricultural waste, nutrient runoff through rain	
Industry	Industry waste	
Manufacturing units	Solid wastes	
Tourism	Facilities (hotels, restaurants)	Erosion
Farming	Overgrazing	
Agriculture	intensive agricultural uses	
Industry	Industrial facilities	
Agriculture	Agricultural emissions (use of chemicals)	Air quality
Tourism	Polluting gas emission	
Industry	Polluting gas emissions (CO_2, NO_x, SO_2), emissions of particulate matter - dust	
Transport	Engine exhaust gas (Polluting gas emission CO_2, NO_x, VOCs)	
Tourism	Entertainment and recreation centers	Noise pollution
Industry	Industrial noise from factories	
Transport	Great number of vehicles	
Agriculture	Losses of agricultural nutrients-use of fertilizers, pesticides, air pollution	Ecosystems – Biodiversity
Tourism	Building- service facilities for the tourists, population growth, tourism activities	
Industry	Building -waste disposal, air pollution	
Fisheries	Intensive fishery	
Aquaculture	Wastewater	
Industry	Greenhouse gas emissions	Climate change
Transport		

DRIVING FORCES	PRESSURE	STATE
Farming		
Tourism	Overexploitation of water	Natural resources consumption
Industry	Increased use of power, water and raw materials	
Agriculture	Overexploitation of water	
Tourism	Unregulated building (hotels, restaurants, refreshment rooms)-increased use of natural recourses-household waste, urban wastewater	Environmental quality
Industry	Building-solid waste	
Agriculture	Alternating agricultural landscapes	

4.3 Discussion

From the analysis presented in Tables 2, 3 and 4, it is possible to evaluate the economic, social and environmental pressures of the Strymonikos Gulf activities, in order to be used for the comparison of any future proposed coastal zone management plans.

Consequently, tourism development will introduce the new services and settlements (hotels, recreation settlements, commercial activities), which will attract tourists and will help with the economic growth of the area. The development of primary and secondary sector of production will increase the production of the corresponding products and therefore, the economic growth of Strymonikos Gulf. On the other hand, the development of agriculture and industry increases land demand, which leads to land-use conflicts. Both tourism accommodations with the necessary infrastructure, and industrial facilities lead to the increase of the implementation cost.

The development of Strymonikos Gulf economic activities leads to jobs creation and consequently, to the reduction of unemployment. However, tourism and industrial development, except for job creation, put pressure on the natural environment, which makes it difficult for people to approve any management plans of the area of study and accept severe environmental impacts. Also, the development of tourism, agricultural and industrial activities leads to pressures to the environment due to solid wastes, air emissions and noise, which cause the degradation of the quality of life and health of the people leaving in the coastal zone of Strymonikos Gulf. At the end, uncontrollable development of tourism may provoke impacts on their cultural heritage and archaeological sites.

According to Table 4, in agriculture and more specifically, in irrigation over-pumping of both surface and ground water and therefore, reduction of the water quantity may be a serious problem. Also, development of tourism, agriculture, industry and farming may increase greatly water demand. The development of agriculture influences the quality of both surface and ground water, through eutrophication (water acidification) and salinization. Whereas, farming influences the quality of water directly with wastewater disposal and indirectly, with nitrogen and phosphorus discharges into the coastal zone. The development of industry and manufacturing, also, influences water quality of Strymonikos Gulf, though waste disposal around industrial facilities and gas emissions (nitrogen and phosphorus). Tourism facilities, mostly from sewage, lead to water pollution and degradation of coastal water quality. Also, the coastal waters are polluted from intensive fisheries, due to oil residues dumping and from aquaculture, because of the wastewater, which is rich in nutrients.

Land quality is influenced by the solid waste disposal from industrial facilities and manufacturing units and by the agricultural waste and nitrates emissions, which run off to the soil through rain. Tourism development has a negative influence to land quality, because of possible uncontrolled waste disposal from tourists and solid waste from hotels and restaurants. Except from land quality, industrial facilities and infrastructures raise the possibility of erosion. Also, because of the construction of facilities for the tourists (hotels, restaurants, recreation, organized beaches), there is great possibility of coastal erosion. Furthermore, the intensive agricultural uses rise the sensitivity of coastal land to erosion.

Agriculture and more specifically, the use of chemicals (air sprays) cause atmosphere pollution. Also, chemical substances emissions from combustion, which takes place at industry facilities, as well as emissions of particulate matter and dust coming from industrial activities, constitute of important pressures that configure the state of the air quality. Tourism development pollutes the atmosphere as much from the tourists' facilities gas emissions as from the increase of traffic.

Tourism, also, can cause noise pollution because of the density of settlements, the entertainment and recreation centers and the great number of vehicles. Noise pollution is also caused by the industrial noise from factories.

Agricultural uses, because of the losses of agricultural nutrients play a very important role to the condition of biodiversity. Also, the overuse of pesticides and fertilizers in agriculture constitutes a threat to the biodiversity. A major threat to biodiversity and ecosystems is the development of tourism, because of service facilities for the tourists (hotels, restaurants, night clubs), seasonal population growth and tourism activities. Many changes in the state of biodiversity come from industrial development, due to industrial facilities construction, sewage and air pollution. Furthermore, intensive fisheries and aquaculture influence biodiversity as they reduce marine life.

Tourism and industrial development as well as the increase of transport leads to release to the atmosphere of great amounts of CO_2 (the most important greenhouse gas) as a result of the burning of fossil fuel such as carbon, oil and natural gas, and as a consequence to climate change. The second more important greenhouse gas is methane, which is produced mostly through farming, which also contributes to the climate change. The development of tourism and agriculture change the amount of natural recourses because of the overexploitation of water. The amount of natural resources is also changed by the increased use of power, water and raw materials from industrial facilities. The environmental quality is negatively influenced both from the development of tourism through facilities unregulated building (hotels, restaurants, refreshment rooms), household waste (plastic boxes, glass bottles, etc.) and increased use of natural recourses, and from the development of industry because of land clearing for factories construction and solid waste disposal. Agriculture, on the other hand has a positive influence to the quality of environment, because of alternating agricultural landscapes.

5. DISCUSSION AND CONCLUSIONS

Sustainable coastal zone management is a broad, multi-purpose effort, aimed at improving the quality of life of the communities dependent on estuarine resources and helping local decision makers to achieve sustainable development of estuarine areas, from the headwaters of coastal watersheds to the outer marine areas. As such, sustainable coastal zone management approaches are required, in order to combine all aspects of the human, physical and biological aspects of the coastal zone within a single management framework. It is imperative to address the ecological and socio-economic links in the management of dynamic systems, such as estuaries and coastal areas. As a result, it is obvious that there is a growing need for the application of such a framework in coastal zones, which can be used to organize research that increases understanding about interaction between environmental and societal processes, and help understand and support as well sustainable coastal zone management scenarios. In many cases the DPSIR framework has been used as a base for coastal zone environmental management allowing the linkage between environmental and economic models, making it possible to integrate the conservation functions (biodiversity and ecological) with socio-economic development [9]. Examples could be: EEA (1999) [10], Elliott (2002) [11], Picollo et al. (2003) [12], Cave et al. (2003) [13], among others. In this study, it is obvious the need for the application of the D.P.S. framework in coastal zones, in order to promote sustainable development taking into account environmental, social and economic factors. The D.P.S. framework could be easily applied to other catchment/coastal zone systems, which have experienced human interventions during past decades. This would help in the identification and assessment of socio-economic drivers, pressures, economic, social and environmental state, in the long term, thus providing a holistic and

comprehensive approach on issues, pertaining to environmental protection and the sustainable management of natural resources. Moreover, the ability to apply future scenarios enlarges the use of D.P.S. to a robust and reliable management tool. Natural scientists, stakeholders, and policy makers would all benefit from such integrated coastal activities pressures analysis.

References

1. Campuzano F., M. Mateus, Paulo Leitão, Pedro Leitão, V. Marín , L. Delgado, A. Tironi, J. Pierini, A. Sampaio, P. Almeida, R. Neves. (2011). 'Integrated coastal zone management in South America: A look at three contrasting systems.'. **Ocean & Coastal Management**, Elsevier Ltd.
2. UNEP. (2006). '**Marine and coastal ecosystems and human wellbeing: A synthesis report based on the findings of the Millennium Ecosystem Assessment'**, UNEP, pp.76.
3. Varghese K., Ganeshb L., Manic M., Anilkumara P., Murthyd R. & B. Subramaniamd. (2008). 'Identifying critical variables for coastal profiling in ICZM planning - A systems approach.'. **Ocean & Coastal Management**, vol.51, 2008, pp.73–94, Elsevier Science Ltd.
4. European Commission. (1999). '**Towards a European Integrated Coastal Zone Management (ICZM) Strategy: General Principles and Policy Options.**', A reflection paper, Directorates-General Environment, Nuclear Safety and Civil Protection, Fisheries & Regional Policies and Cohesion.
5. Bowen R. & C. Riley. (2003). Socio-economic indicators and integrated coastal management. **Ocean & Coastal Management**, vol.46, 2003, pp.299-312, Elsevier Science Ltd.
6. Organization for Economic Co-operation and Development. (2000). 'Towards Sustainable Development: Indicators to measure progress.'. Proc. of the **OECD Rome Conference**.
7. European Environment Agency. **(**2003). '**Environmental Indicators: Typology and Use in Reporting**.', Peder Gabrielsen and Peter Bosch, EEA, Technical report No 25, August 2003.
8. Koutrakis E., Lazaridou T. and M. D. Argyropoulou. (2003). 'Promoting integrated management in the Strymonikos coastal zone (Greece): a step-by-step process.'. **Coastal Management**, vol. 31, pp. 195–200.
9. Caeiro S., Mourão I., Costa M., Painho M., Ramos T. and S. Sousa. (2004). 'Application of the DPSIR model to the Sado Estuary in a GIS context – Social and Economical Pressures.' In **Seventh AGILE Conference on Geographic Information Science** 29 April-1May 2004, Heraklion, Greece Parallel Session 4.3- "Environmental / Social Modelling".
10. EEA. (1999b). '**State and Pressures of the Marine and Coastal Mediterranean Environment.**' Environmental Assessment Series. European Environment Agency, Copenhagen, Denmark.
11. Elliott M. (2002). 'The role of the DPSIR approach and conceptual models in marine environmental management: an example for offshore wind power.'. **Marine Pollution Bulletin** vol. 44, pp. 3-7.
12. Picollo A., Albertelli G., Bava, S. and S. Cappo. (2003). 'The Role of Geographic Information Systems (GIS) and of DPSIR Model in Ligurian Coastal Zone Management.' Proceedings of 5th **International Symposium on GIS and Computer Cartography for Coastal Zone Management.** GISIG/ICOOPS, Genoa, Italy, pp. 1 – 5.
13. Cave R.R., Ledoux L., Turner K., Jickells T., Andrews J.E. and H. Davies. (2003). 'The Humber catchment and its coastal area: from UK to European perspectives.'. **Science of The Total Environment**, vol. 314–316, pp. 31–52.

IMPLEMENTATION OF THE MULTICRITERIA METHOD AHP FOR THE EVALUATION OF STRYMONIKOS GULF MANAGEMENT SCENARIOS WITHIN THE CONTEXT OF INTEGRATED COASTAL ZONE MANAGEMENT

E. Yiannakopoulou and E.K. Oikonomou*

Department of Transportation and Hydraulic Engineering, Faculty of Rural & Surveying Engineering, Aristotle University of Thessaloniki, 54124 Thessaloniki, Hellas

*Corresponding author: e-mail: eoikonom@topo.auth.gr, tel: +30 2310 994360

Abstract

Integrated Coastal Zone Management contributes towards maximizing the environmental, economic and social benefits provided by coastal zones, while minimizing all potential negative impacts of activities upon each other. Coastal areas are of particular interest as they usually include a wide variety of habitats and ecosystems, as well as many important human/economic activities. Human coastal population increases continually and consequently, there is much stress from all settlements and economic activities to coastal zones. A proposed methodological approach for management plans evaluation, in the context of Integrated Coastal Zone Management, is described. Therefore, alternative management scenarios for the examined area of the coastal zone of Strymonikos Gulf, are presented. The selection of the prevailing alternative proposal is made through the process of multi-criteria analysis. More specifically, the method of Analytical Hierarchical Process is applied, so that the suggested alternative solutions are estimated and classified by using economic, ecological and social criteria, in order to contribute positively to Coastal Zone Integrated Management towards sustainability.

Keywords: Multicriteria analysis, AHP, Integrated Coastal Zone Management, Management plans evaluation

1. INTRODUCTION

Coastal ecosystems are one of the most productive natural systems in the world [1]. They provide a wide range of services to human beings: “provisioning services”, such as food supply, fuel wood and energy resources; “regulating services”, such as shoreline stabilization, flood prevention, storm protection, hydrological services and nutrient regulation; “cultural and amenity services”, such as culture, tourism and recreation; and finally, “supporting services”, such as habitat provision, nutrient cycling, primary productivity [2]. These services are of high ecological, social and economic value, not only to local communities living in the coastal zones, but also to national economies and global trade. Several threats on coastal systems are discussed in the scientific literature. The most important and crucial are industrialization and urbanization, sea-level-rise, increase of carbon dioxide and greenhouse gases, deposition of agricultural substances, fisheries and aquaculture development, etc. As a consequence, approximately 70% of the European coastal ecosystems are highly threatened, in relation to their biological productivity [3].

Integrated sustainable planning for coastal areas (including land-use, resources and pollution control management) is needed in order to resolve competition and conflict that occur frequently among residential, tourist, commercial, industrial, transportation, recreational and agricultural activities,

competing usually within limited space. Certain sectoral-oriented land-uses might coexist in a multiple land-use approach, while others might not or would have to be severely restricted from coastal areas. Integrated Coastal Zone Management's role is to sort out the appropriate land-use patterns and recommend the optimal mix, while meeting effectively environmental, economic and social criteria. A number of methods have been, for that reason, researched, tested and applied, in order to support decision makers. One of them is Analytical Hierarchical Process (AHP), which was selected by the authors, to resolve the problem of sustainable development of the coastal zone of Strymonikos Gulf, in the context of Integrated Coastal Zone Management.

Integrated Coastal Zone Management (ICZM) is also known under a variety of different names, such as Integrated Coastal Area Management (ICAM), Integrated Coastal Management (ICM) and Integrated Marine and Coastal Area Management (IMCAM). Although there are many different definitions of ICZM, the actual differences amongst them are minor. Most definitions recognize that ICZM is a dynamic, continuous and iterative process, designed to promote sustainable management of coastal zones. Most definitions also taken into consideration that the goals of ICZM have to be achieved within the constraints of physical, social, economic, and environmental conditions, as well as within the constraints of legal, financial and administrative systems and institutions [4].

It is also important to underline that in Greece, with a total shoreline of 16,500 km, respectively the 25% of the European shoreline, there are no specific instruments or methodologies for ICZM Programs, while the Special Framework for Spatial Planning & Sustainable Development of coastal areas and islands has never been enacted: after consultations had taken place, the project was withdrawn. Oikonomou and Kalkopoulou (2009) commented on the fact that only General Local Plans in Greece (planning projects at municipal level) contribute to ICZM. However, it is concluded that: the majority of these General Local Plans have been excluded from Strategic Environmental Assessment, mostly due to bureaucratic reasons (GLPs were introduced for the first time in 1997, while the Ministerial Decision 107017/2006 about Strategic Environmental Assessment was enacted almost 10 years later); by examining four GLPs in coastal areas all over Hellas, it was concluded that they do not show any special concern about coastal areas and marine space, but they define land-use patterns, as well as future infrastructure projects needed to support future economic activities, without any environmental appraisal [5].

2. INTEGRATED COASTAL ZONE MANAGEMENT

2.1 The necessity for ICZM

Almost all coastal and marine areas produce or support multiple products and services. Sectoral solutions usually “transfer” the problem between resources, products and services. Tourism will not flourish if the area loses its attraction to visitors; fisheries are usually on the receiving end of everyone else’s problems. Industry and energy facilities may degrade the environment for all other activities. There is, therefore, a need to bring sectoral activities together, in order to achieve a commonly acceptable coastal management framework. ICZM attempts to avoid this, by broad multiple-sector planning and integrated project development, by future-oriented resource analysis and by applying the test of sustainability to each development initiative.

Coastal zone management is also a critical issue in many countries with a high intensity of marine and coastal resource use. Managing complex systems, such as coastal areas, requires an integrated approach, capable of coordinating the implementation of all three major objectives/components of sustainable development (environmental, social and economic) and bringing together the multiple, interwoven, overlapping interests in the coastal area in a coordinated and rational manner, harnessing coastal resources for optimum social and economic benefit, for present and future generations as well, without prejudicing the resource base itself, while maintaining the security of ecological processes.

2.2 Designing an Integrated Coastal Zone Management program

Every country, evaluating the potential of an ICZM-type program, will have its own special approach to conservation of resources and will be facing its own distinct array of coastal issues. The particular form of any ICZM program will depend upon the national and regional issues it is meant to address. No two countries would be expected to have identical programs. While each country's program will be unique, there are several basic stages in the generation of an ICZM program that will be found to be common to all, in one form or another. These stages are presented briefly as follows:

- Stage A – Policy Formulation. Creation of a policy framework to establish goals, and to authorize and guide the ICZM program, accomplished by executive and legislative action.
- Stage B – Strategy Planning. Sometimes called Preliminary Planning, this is the stage at which the potential impacts of the ICZM policy action are explored, while expected benefits are evaluated, a wide array of data is accumulated and organized, a general strategy is created and recommendations are made for organization and administration of the ICZM program.
- Stage C – Program Development. Once the Strategy Plan is accepted by policy makers, development of the ICZM program can commence and a detailed Master Plan for its implementation may be proposed.
- Stage D – Implementation. Once the Master Plan is approved and budget and staff are authorized, the Implementation Stage may commence.

In practice, the above stages are not so discrete and linear as theory suggests. Instead, there will be feedback and revisions of earlier stages, as new facts and opportunities come to light in later stages. For example, there will certainly be the need for policy revision and strengthening, as a result of findings and recommendations from Stages B and C. Therefore, the whole program must be flexible and adaptable [6].

3. THE ANALYTIC HIERARCHY PROCESS

The Analytic Hierarchy Process (AHP) is one of the most popular Multicriteria Decision Making (MCDM) tools for formulating and analyzing decisions. The technique is employed for ranking a set of alternatives or for the selection of the best in a set of alternatives. The ranking/selection is done with respect to an overall goal, which is broken down into a set of criteria [7]. The AHP enables the decision maker to structure a complex problem in the form of a simple hierarchy and to evaluate a large number of quantitative and qualitative factors in a systematic manner, under conflicting multiple criteria [8]. AHP can deal with qualitative and quantitative factors of the decision-making process, and it is practical, systematic and terse. It determines the relative importance, or weight, of the alternatives in terms of each criterion involved in a given decision-making problem [9]. Application of AHP to a decision problem involves four steps: a) structuring of the decision problem into a hierarchical model; b) making pair-wise comparisons and obtaining the judgmental matrix; c) obtaining the local priorities and consistency of comparisons; and d) aggregation of weights across various levels to obtain the final weights of alternatives. The first two steps involve the decision maker’s opinion, whereas the last two are strictly computational.

The first step includes decomposition of the decision problem into elements, according to their common characteristics, and the formation of a hierarchical model, having different levels [10]. Each level in the hierarchy corresponds to the common characteristic of the elements in that level. The topmost level corresponds to the ‘focus’ of the problem. The intermediate levels correspond to criteria and sub-criteria, while the lowest level contains the ‘decision alternatives’ (Figure 1).

In the second step, the elements of a particular level are compared pair-wise, with respect to a specific element in the immediate upper level. A judgmental matrix is formed and used for computing the priorities of the corresponding elements. First, criteria are compared pair-wise with respect to the goal already set. A judgmental matrix, denoted as “A”, will be formed using the comparisons. Each entry

“a_{ij}” of the judgmental matrix is formed comparing the row element “*A*i” with the column element “*A*j”. Saaty (2000) suggests the use of a 9-point scale to transform the verbal judgements into numerical quantities, representing the values of a_{ij}.

In the third step, once the judgmental matrix of comparisons of criteria with respect to the goal is available, the local priorities of criteria are obtained and the consistency of the judgements is determined.

At last, in fourth step, the local priorities of elements of different levels are aggregated, in order to obtain final priorities of the alternative scenarios.

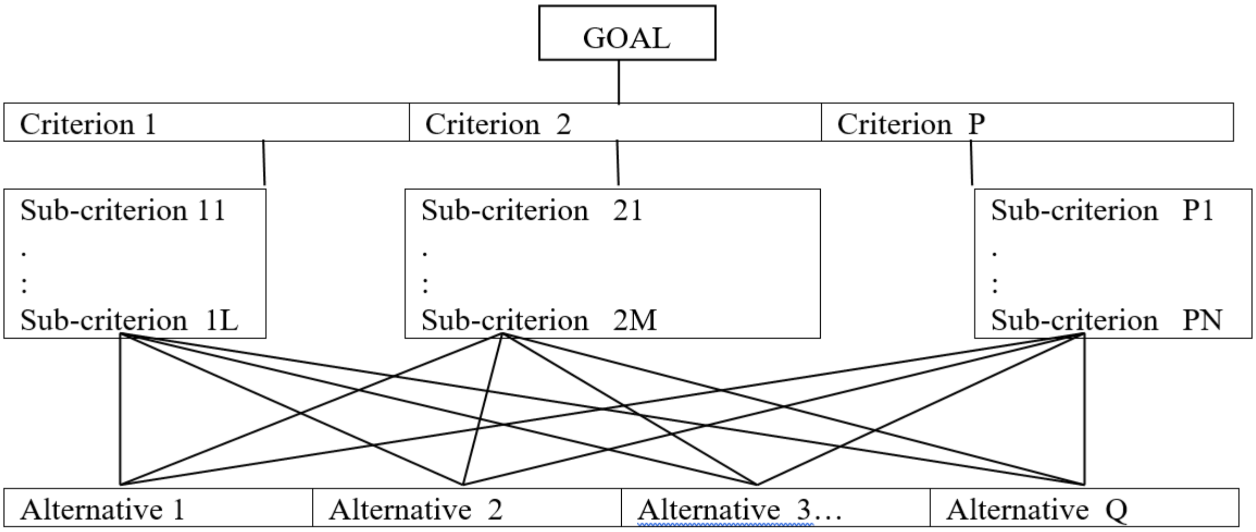


Figure 1: Hierarchic structure of a decision problem

Table 1: The fundamental scale used in AHP

Intensity of importance	Definition	Description
1	Equal importance	Elements *A*i and *A*j are equally important
3	Weak importance of *A*i over *A*j	Experience and Judgement slightly favour *A*i over *A*j
5	Essential or strong importance	Experience and Judgement strongly favour *A*i over *A*j
7	Demonstrated importance	*A*i is very strongly favored over *A*j
9	Absolute importance	The evidence favoring *A*i over *A*j is of the highest possible order of affirmation
2, 4, 6 , 8	Intermediate	When compromise is needed

4. IMPLEMENTATION OF AHP IN THE COASTAL ZONE OF STRYMONIKOS GULF

4.1 The area of study

The area of study includes the coastal zone of Strymonikos Gulf, which is a semi-enclosed coastal water body in the North Aegean Sea in Central Macedonia Region, Hellas, located in east of Thessaloniki, 50 km away. It is defined by an imaginary line that connects capes of Eleftheras (Halkidiki) and St.Dimitriou (Kavala). The coastline is 75 km long and communicates with North Aegean through an opening in its east side. Strymonikos Gulf belongs expands geographically to four Regional Departments: Kavala, Serres, Thessaloniki, and Halkidiki. The Kavala Regional

Department is part of the East Macedonia & Thrace Region, while the other three Regional Departments are part of the Region of Central Macedonia, Hellas.

The coastal zone of Strymonikos Gulf is rich in natural resources, landscapes and cultural elements. More specifically, the most significant environmental parameters of the area include Lake Volvi, Rentinas narrows (also known as the Valley of Macedonian Tembi), Strymonas and Rihios river estuary and Stratonikos mountain. For the purposes of this paper, the boundaries of the coastal zone of Strymonikos Gulf were defined, as shown in Figure 2, taking into account the morphology ant topography of the area, land-uses and the nearby watersheds. So, the area of study includes the sea area of Strymonikos Gulf and the land area of the coastal zone, which was defined based on the water bodies, the significant coastal ecosystems (Lake Volvi, Rentinas narrows, Strymonas river estuary and Stratonikos mountain, etc.) and in few cases the administrative boundaries (boundaries of the municipalities). In Figure 2, different colors represent different proposed land-use patters from General Local Plans, with the dark green representing forest areas, light green agricultural land, in blue color some industrial sites and in magenta color some touristic zones.



Figure 2: The area of study, the coastal zone of Strymonikos Gulf

4.2 Structuring of the decision problem into a hierarchical model

At this point, the decision problem is structured, according to the formation of the Analytical Hierarchical Process (AHP). So, at first, the decision problem is analyzed into a hierarchical model.

At the topmost level, the Focus of Goal is set, which in the case study refers to sustainable development of the coastal zone of the Strymonikos Gulf. The lowest level contains the alternative scenarios. It is obvious that we cannot compare the alternative scenarios to such a general and strategic goal. Therefore, the goal is analyzed into sub-goals (criteria), which are then analyzed based on the hierarchical model, in a way that can be used efficiently for the comparison of alternative scenarios. Sustainable development is based on the balance between the components of economic prosperity, social justice and environmental conservation. Accordingly, the criteria that are chosen, for the evaluation of the alternative scenarios, are economic, social and environmental. Then, those

criteria were divided to sub-criteria, in order to reduce the complexity of the problem dealt with. At last, the alternative development scenarios were defined for the area of study, which represent the lowest level of hierarchy. Three alternative scenarios were introduced, which are hypothetical and they are based on proposed by General Local Plans land-use patterns for each municipality.

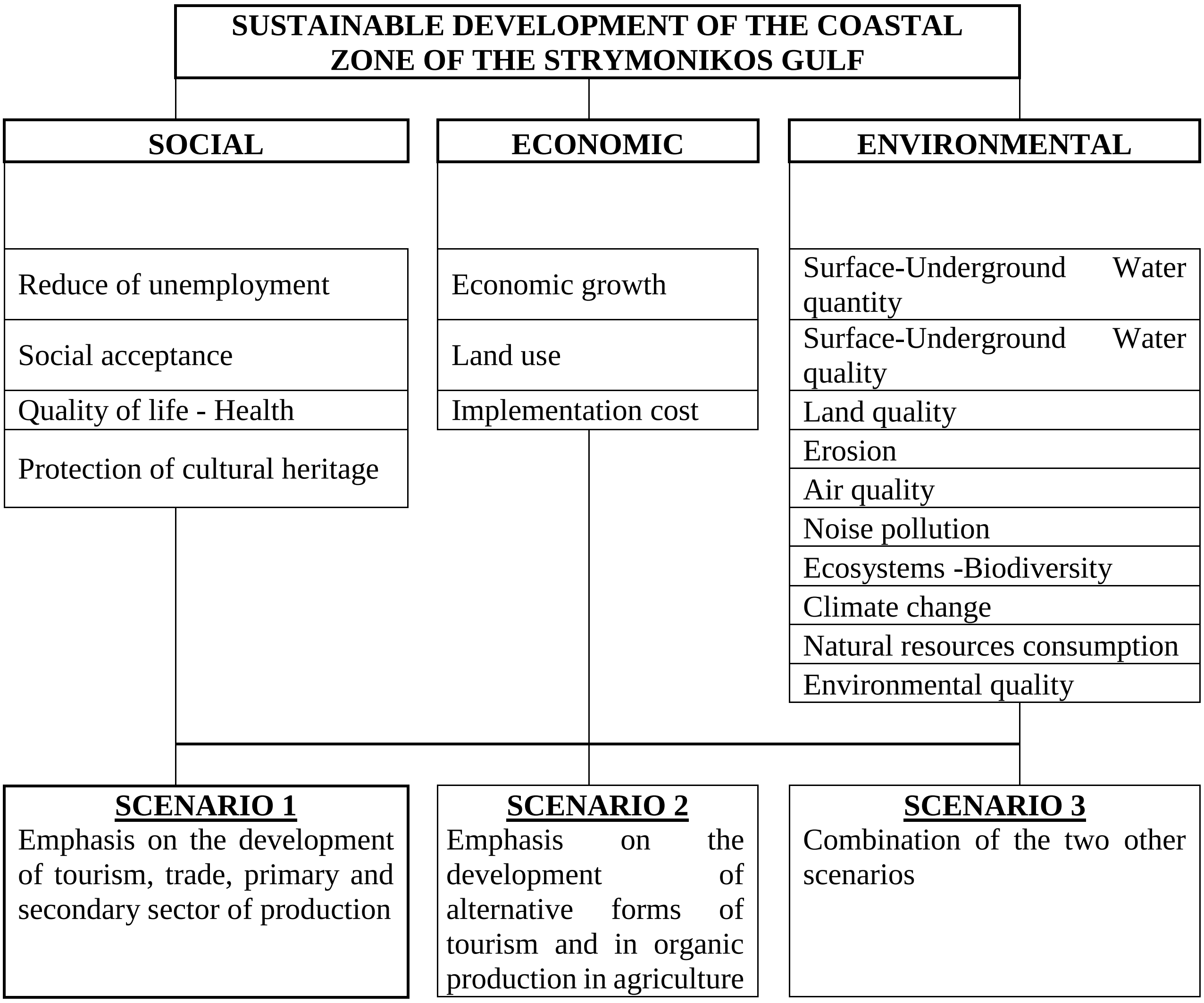


Figure 3: Hierarchical analysis of the decision problem

In the first proposed scenario, major parameters are: the development and growth of the primary sector of production in agricultural areas, with agricultural and farming settlements, houses for farmers and infrastructure networks; in forest areas the promotion of forest exploitation facilities and beekeeping is proposed; for the development of the secondary sector of production, the creation of industrial areas is proposed in three areas, north of the road to Vrasna, west of Olympiada and parallel to the Nea Madytos-Varvara road; in non-forest areas small industries related to the local forest, agricultural production and livestock farming, beekeeping, the production of local goods and also showrooms and selling places for the above products are proposed; the development of tourism and leisure activities is proposed in coastal areas and more specifically, in Asprovalta, Ofrynio beach and Karianni with the development of hotels up to 150 beds, tourism settlements, organized camping and shopping centers are proposed. Special tourism settlements (conference centers, athletic tourism centers, etc.) and swimming service settlements in Ofrynio beach and a tourism port in Asprovalta are also proposed. At the end, in protected areas light infrastructure settlements, such as guardhouses, scientific equipment, wooden sits, observatories, etc. are proposed. The use of ecosystems as fisheries and the function and maintenance of the current fish-capture settlements in Rihios River are also proposed. At the end, small units of aquaculture, agricultural products, sustainable farming units, as well as camping and outdoor sport grounds near Nea Apollonia and near Rentina are proposed.

In the second scenario, alternative forms of tourism are proposed in the municipality of Arethousa. In forest areas not-permanent settlements (wooden kiosks, pathways, observatories, etc.) for the development of exploring and archeological tourism are proposed. In non-forest areas agrotourism settlements up to 80 beds, other tourism settlements and eating and leisure spaces are proposed. An archeological route with a watercraft in Strymonas River, begging from the estuary and the seaport to the Amfipolis archeological site is also designed. In the primary sector, alternative forms of production in agricultural areas, such as biological production, are proposed. The integrated management of wastes and the biological production of honey are also proposed. In protected areas the same proposals with those of the first scenario are generally proposed, in addition to the lake Volvi biological aquiculture, biological aquiculture and biological holdings in small units at Rihios River and at forest areas beekeeping and production of biological honey.

The third scenario combines the proposals of the other two scenarios. So, it suggests a light development of primary and secondary sector of production, whereas it focuses on the integrated development of tourism and promoting alternative tourism in highlands. Therefore, it respects the environment and the sensitive ecosystems of the area of study.

4.3 Making pair-wise comparisons

Once the decision problem is analyzed into a hierarchical model, as shown in Figure 3, the pair-wise comparisons and the formation of the judgmental matrices should be made. So, at first, the criteria are evaluated with respect to the goal, next the sub-criteria with respect to the criteria and at the end, the alternative scenarios with respect to the sub-criteria, according to how much more important is one element to another. The evaluation is based on the fundamental scale of values of Saaty, as shown below:

$$P = \{1, 2, 3, 4, 5, 6, 7, 8, 9, 1/2, 1/3, 1/4, 1/5, 1/6, 1/7, 1/8, 1/9\} \quad (1)$$

where: 1 = equal importance, 3 = moderate importance, 5 = strong importance, 7 = very strong importance, 9 = extreme importance – 2, 4, 6, 8 = intermediate values. The reciprocals of the above judgments represent the reverse preferences of the decision maker.

4.3.1 Comparison of criteria (and sub-criteria) with respect to the goal

Primarily, the criteria are compared pair-wise, with respect to the upper goal, which in the case study is sustainable development of the coastal zone of the Strymonikos Gulf. It is assumed that the participation of criteria in the achievement of the upper goal is the same, so they were evaluated with number 1. Then, in the next level of hierarchy, sub-criteria are compared pair-wise, with respect to criteria, which are social, economic and environmental, the three aspects of sustainable development. The evaluation is made using the following question: “Of the two sub-criteria (row and column), which is more important with respect to the criterion set?”.

4.3.2 Comparison of alternative scenarios with respect to criteria

Next, in the lowest level of hierarchy, alternative scenarios are compared pair-wise, with respect to the sub-criteria in the immediate upper level. The evaluation is made using the following question: “Of the two alternative scenarios (row and column), which is more important with respect to the sub-criterion?”. The answer to the question in the case study is based on the opinion of the researcher. However, in a ‘real’ case study, ICZM Program, many researchers and generally, stakeholders may answer such question, supporting many and maybe different opinions and evaluations. In the following tables representative examples of judgmental matrices of scenarios with respect to some sub-criteria are shown:

Table 2: Judgmental matrix of scenarios with respect to sub-criterion "Social acceptance"

SOCIAL ACCEPTANCE	Scenario 1	Scenario 2	Scenario 3
Scenario 1	1	1	1/4
Scenario 2	1	1	1/4
Scenario 3	4	4	1

Table 3: Judgmental matrix of scenarios with respect to sub-criterion "Economic growth"

ECONOMIC GROWTH	Scenario 1	Scenario 2	Scenario 3
Scenario 1	1	4	2
Scenario 2	1/4	1	1/4
Scenario 3	1/2	4	1

Table 4: Judgmental matrix of scenarios with respect to sub-criterion "Water quantity"

WATER QUANTITY	Scenario 1	Scenario 2	Scenario 3
Scenario 1	1	1/3	1/2
Scenario 2	3	1	2
Scenario 3	2	1/2	1

4.4 Discussion

The final results of the comparison of alternative scenarios are obtained with the application of the two last steps of the Analytical Hierarchy Process method, which are strictly computational. The last two steps were calculated with a program that was made in a programming language called "Visual C# (sharp)". The purpose of the program is to reduce the large number of calculations that are needed for the estimation of the final results, which increase as the number of criteria and alternative scenarios increases and the whole process becomes an exhausting, for the decision maker, process. It is also useful in forming an ICZM Program, because throughout the process, more parameters, new assumptions, other proposals may be described. More specifically, through the program, at first the priorities of the alternative scenarios with respect to criteria, as shown in Figure 4, were calculated. and then, the final priorities of the alternative scenarios, as shown in Figure 5.

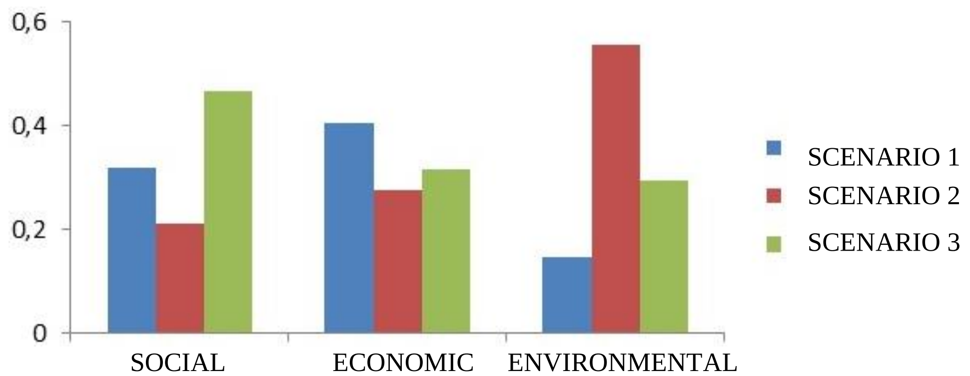


Figure 4: Priorities of alternative scenarios with respect to criteria

As shown in Figure 4, the first scenario is better than the other two with respect to economic criteria, the second scenario is better with respect to environmental criteria and the third one is better with respect to social criteria. The third scenario, which combines development and protection and

restoration of the environment, is better than the other two, with respect to social criteria. The first scenario, which focuses on the development and growth of all three sectors of production, is better than the other two, with respect to economic criteria, then, the third scenario, that proposes a more ‘light’ development, follows, whereas the second scenario, that provides alternative forms of tourism, comes last. As it is also expected, the second scenario is much better than the other two with respect to environmental criteria.

Finally, in Figure 5 the classification of the alternative scenarios is presented, as they came up from the software used, in the following order of preference, and their final results. The most applicable alternative scenario is the third one, which is a combination of the other two scenarios, with ‘light’ development of tourism and industry and promotion of the primary economic sector with emphasis on organic production. Then the second scenario comes, which emphasizes on the development of alternative forms of tourism and on organic production in agriculture, and the last one is the first scenario, which emphasizes greatly on economic development and growth of the area of study.

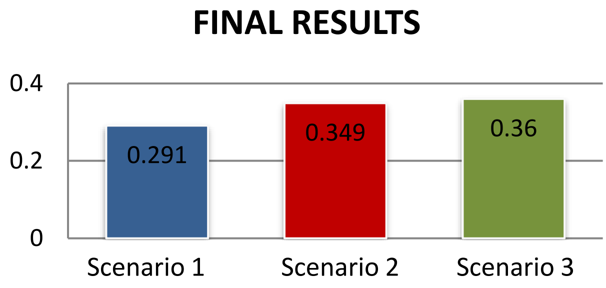


Figure 5: Final Results: Priorities of alternative scenarios with respect to the Goal

5. CONCLUSIONS

The problem of the evaluation and the selection of an alternative scenario, which adjusts sufficiently to the data and input parameters of each area of study, is a crucial matter, as well as the parameters that must be taken into consideration for sustainable development, which are many and multidimensional. In the case study presented, the use of AHP for the selection, between three, of the best management scenario in Strymonikos Gulf, was examined, in order to be objective, even though the evaluations are subjective. A research with questionnaire surveys in the area of study may be conducted, in order to determine the weight that local people and stakeholders attribute to the three dimensions of sustainable development, as it is not a fact that they have the same weight, as assumed in the case study and the model used.

In the case study the choice of the best alternative was investigated, from three alternative scenarios. Analytical Hierarchy Process may be also used for the ranking of the alternatives from the best one to the worst one, or even for the sorting of alternatives in pre-defined categories. This possibility is very important in practice. When a number of scientists cooperate for the solution of a coastal zone management problem, the alternative scenarios that will come up are many. This large number of data can be processed with Analytical Hierarchy Method, in order to have a ranking of alternatives, according to several criteria.

To summarize, it is concluded that the method presented, with its simplicity and its explicitness, and also with the many possibilities that offers to the user, is a valuable tool for a “good” decision making process and can be used efficiently for the purposes of Integrated Coastal Zone Management.

References

1. European Environment Agency. (2006). **‘The changing faces of Europe's coastal areas’**, EEA report No 6/2006, Copenhagen.
2. United Nations Environmental Program. (2006). **‘Marine and coastal ecosystems and human wellbeing: A synthesis report based on the findings of the Millennium Ecosystem Assessment’**, UNEP.
3. EUCC – The Coastal Union. (2006). Integrated coastal management – do we really have a choice?. **Coastline Special on Integrated Coastal Management**, vol. 15, no 2006-1/2.
4. Nandelstädt T. (2008). **‘Guiding the coast - Development of guidelines for ICZM in Germany’**, IKZM-Oder Berichte 44, Technical University Berlin, Germany, March 2008.
5. Oikonomou E.K. and K. Kalkopoulou. (2009). ‘The contribution of General Local Plans in Coastal Zone Management’. Proc of Conf. **Integrated Water Resources Management under Climate Change Conditions**, eds. A. Liakopoulos, V. Kanakoudis, E. Anastasiadou-Partheniou and V. Tsihritzis. Volos, Hellas (in Hellenic).
6. Clark J.R. (1996). ‘**Coastal Zone Management Handbook**’ Lewis Publishers, pp. 694.
7. Ramanathan R. (2006). Data envelopment analysis for weight derivation and aggregation in the AHP. **Computers & Operations Research**, vol.33, pp. 1289–1307, Elsevier Ltd.
8. Kubde R.A. and S.V. Bansod. (2012). ‘The Analytic Hierarchy Process Based Supplier Selection Approach for Collaborative Planning Forecasting and Replenishment Systems.’. **International Journal of Engineering Research & Technology**, vol. 1 (7), pp. 1-11.
9. Hongmei L., Fuijan N., Dong Q. and Y. Zhu. (2017). ‘Application of analytic hierarchy process in network level pavement maintenance decision-making.’. **International Journal of Pavement Research and Technology**, https://doi.org/10.1016/j.ijprt.2017.09.015.
10. Gunasekaran A., Jabbour C. & A. Jabbour. (2014). ‘Managing organizations for sustainable development in Emerging countries: an introduction.’. **International Journal of Sustainable Development & World Ecology**, vol. 21 (3), pp. 195-197.

MODELLING THE IMPACT OF CLIMATE CHANGE ON COASTAL FLOODING WITH THE USE OF A 2DH BOUSSINESQ MODEL

A.G. Samaras* and Th. V. Karambas

Department of Civil Engineering, Aristotle University of Thessaloniki, 54124, Thessaloniki, Greece

*Corresponding author: e-mail: asamaras@civil.auth.gr

Abstract

In the present work, an advanced numerical model based on the solution of the higher-order Boussinesq-type equations for breaking and non-breaking waves is applied in order to simulate the impact of climate change on coastal flooding. The model is tested against two-dimensional (cross-shore) experimental data by Roeber at al. (2010), and is afterwards applied to the area of the Bay of Thessaloniki (northwestern Aegean Sea, Greece) for representative scenarios of climate change-induced wave and storm surge events. Results highlight the model's capabilities and set the basis for a comprehensive evaluation of the use of advanced modelling tools for the design of coastal protection and adaptation measures against future climatic pressures.

Keywords: climate change, coastal flooding, numerical model, Boussinesq equations, wave modelling

1. INTRODUCTION

Climate change is expected to have significant effects on the intensity and frequency of occurrence of extreme weather events, consequently affecting sea levels, circulation patterns, currents and waves in oceans and seas around the world (Mentaschi et al., 2017; Vousdoukas et al., 2017). Moving from the open sea to the densely populated coastal zones, more frequent storm surges and higher waves will be experienced through a number of impacts such as beach/dune erosion and inundation of low-lying areas, leading to increased flooding risks and dictating the need for effectively designed coastal protection and adaptation measures (Wong et al., 2014). Numerical models are indispensable tools for the above purpose, as they allow the quantification of the above risk through the analysis of simulations for multiple scenarios of combinations of projected climatic pressures.

In the following, the impact of climate change on coastal flooding is modelled with the use of an advanced numerical model based on the solution of the higher-order Boussinesq-type equations. The theoretical background and structure of the model is presented in detail in Section 2; the model capabilities are validated through comparison with the experimental data by Roeber et al. (2010) in Section 3; model applications for the area of the Bay of Thessaloniki (northwestern Aegean Sea, Greece) are presented and discussed in Section 4, while Section 5 presents the conclusions drawn from this work.

2. COASTAL FLOODING MODELLING

Coastal flooding is modelled in this work using, in sequence, a storm surge model and an advanced nearshore wave propagation model. The first model estimates storm surge levels due to wind effects;

these are used as offshore boundary conditions for the second model, which estimates wave runup on beaches.

2.1 The storm surge model

The storm surge model is based on the depth-averaged wind-induced circulation equations, following Koutitas (1988):

$$\frac{\partial \zeta}{\partial t} + \frac{\partial(\mathrm{Uh})}{\partial x} + \frac{\partial(\mathrm{Vh})}{\partial y} = 0 \tag{1}$$

$$\frac{\partial U}{\partial t} + U\frac{\partial U}{\partial x} + V\frac{\partial U}{\partial y} + g\frac{\partial \zeta}{\partial x} = \frac{1}{h}\frac{\partial}{\partial x}\left(v_h h\frac{\partial U}{\partial x}\right) + \frac{1}{h}\frac{\partial}{\partial y}\left(v_h h\frac{\partial U}{\partial y}\right) + fV + \frac{\tau_{sx}}{\rho h} - \frac{\tau_{bx}}{\rho h} \tag{2}$$

$$\frac{\partial V}{\partial t} + U\frac{\partial V}{\partial x} + V\frac{\partial V}{\partial y} + g\frac{\partial \zeta}{\partial y} = \frac{1}{h}\frac{\partial}{\partial x}\left(v_h h\frac{\partial V}{\partial x}\right) + \frac{1}{h}\frac{\partial}{\partial y}\left(v_h h\frac{\partial V}{\partial y}\right) - fU + \frac{\tau_{sy}}{\rho h} - \frac{\tau_{by}}{\rho h} \tag{3}$$

where ζ is the water surface elevation above the mean water level, d is the still water depth, h is the total water depth ($h = d + \zeta$); U, V are the depth-averaged velocity components along the x- and y- directions respectively, g is the gravitational acceleration, v_h is the horizontal eddy viscosity coefficient, f is the Coriolis coefficient and ρ is the water density The terms τ_{sx}, τ_{sy} are the shear stress components at the water surface along the x- and y- directions respectively, which represent the vertical boundary condition, expressed as:

$$\tau_{sx} = \rho k W_x \sqrt{W_x^2 + W_y^2} \tag{4}$$

$$\tau_{sy} = \rho k W_y \sqrt{W_x^2 + W_y^2} \tag{5}$$

where k is the surface friction coefficient (in kg/m^3, typically of the order of 10^{-6}; here we assume $k = 10^{-6} \div 3 \cdot 10^{-6}$), and W_x, W_y are the wind speed components along the x- and y- directions (in m/s) respectively. The bed friction terms (τ_{bx}, τ_{by}) are also expressed by quadratic forms, following Karambas and Karathanassi (2004).

The horizontal eddy viscosity coefficient is expressed by the well-known Smagorinsky model, used for the representation of the damping by eddies smaller than the computational grid size, as:

$$\nu_h = \ell^2 \left[\left(\frac{\partial U}{\partial x}\right)^2 + \left(\frac{\partial V}{\partial y}\right)^2 + \frac{1}{2}\left(\frac{\partial U}{\partial y} + \frac{\partial V}{\partial x}\right)^2 \right]^{1/2} \tag{6}$$

where ℓ is the mixing length, approximated as equal to half the grid cell size Δx (Madsen et al., 1988).

Differential Equations 1, 2 and 3, are approximated by finite difference equations according to the explicit scheme developed by Koutitas (1988). Land in the model is represented as a total reflection boundary, where $U = 0$, $V = 0$ and $\partial\zeta/\partial n = 0$, n being the unit vector normal to the boundary.

2.2 The advanced nearshore wave propagation model

Over the years, the classical Boussinesq equations have been extended so as to be able to include higher order nonlinear terms, which can describe better the propagation of highly nonlinear waves in the shoaling zone. The linear dispersion characteristics of the equations have been improved as well, in order to describe nonlinear wave propagation from deeper waters (Zou, 1999).

Based on the aforementioned velocity profile, the following higher order Boussinesq-type equations for breaking and nonbreaking waves can be derived (Zou, 1999; Karambas and Koutitas, 2002; Karambas and Karathanassi, 2004):

$$\zeta_t + \nabla\left(h\mathbf{U}\right) = 0 \tag{1}$$

$$\mathbf{U}_t + \frac{1}{h}\nabla\mathbf{M_u} - \frac{1}{h}\mathbf{U}\nabla(\mathbf{U}h) + g\nabla\zeta + G = \frac{1}{2}h\nabla\left[\nabla\cdot\left(d\mathbf{U}_t\right)\right] - \frac{1}{6}h^2\nabla\left[\nabla\cdot\mathbf{U}_t\right] + \frac{1}{30}d^2\nabla\left[\nabla\cdot\left(\mathbf{U}_t + g\nabla\zeta\right)\right] + \frac{1}{30}\nabla\left[\nabla\cdot\left(d^2\mathbf{U}_t + gd^2\nabla\zeta\right)\right] - d\nabla(\delta\nabla\cdot\mathbf{U})_t - \frac{\boldsymbol{\tau}_b}{h} + \mathbf{E} \tag{2}$$

where $\mathbf{M_u}$ is defined as:

$$\mathbf{M_u} = \left(d+\zeta\right)\mathbf{u_o^2} + \delta\left(c^2 - \mathbf{u_o^2}\right) \tag{3}$$

and G as:

$$G = \frac{1}{3}\nabla\left\{d^2\left[\left(\nabla\cdot\mathbf{U}\right)^2 - \mathbf{U}\cdot\nabla^2\mathbf{U} - \frac{1}{10}\nabla^2\left(\mathbf{U}\cdot\mathbf{U}\right)\right]\right\} - \frac{1}{2}\zeta\nabla\left[\nabla\cdot\left(d\mathbf{U}_t\right)\right] \tag{4}$$

In Equations. 1 to 4 the subscript "t" denotes differentiation with respect to time, d = still water depth, $\mathbf{U}$ = horizontal velocity vector $\mathbf{U}$ = (U,V) with U and V being the depth-averaged horizontal velocities along the x- and y- directions respectively, ζ = surface elevation, h = total depth ($h = d + \zeta$), g = gravitational acceleration, $\boldsymbol{\tau_b} = (\tau_{bx}, \tau_{by})$ = bottom friction term (shear stress components approximated by the use of the quadratic law according to Ribberink, 1998), δ = roller thickness (determined geometrically according to Schäffer et al., 1993), $\mathbf{E}$ = eddy viscosity term (according to Chen et al, 1999), and $\mathbf{u_o}$ = bottom velocity vector $\mathbf{u_o} = (u_o, v_o)$ with u_o and v_o being the instantaneous bottom velocities along the x- and y- directions respectively.

The Boussinesq-type equations with the improved nonlinearity and linear dispersion characteristics in deeper water, are accurate to the third order $O(\varepsilon^2,\varepsilon\sigma^2,\sigma^4)$ (Zou, 1999); the nonlinearity and dispersion parameters are defined as $\varepsilon = A/d$ and $\sigma = d/L_0$ respectively, where A = characteristic wave amplitude and L_0 = characteristic wave length.

The numerical solution of the Boussinesq-type equations is based on the accurate higher-order numerical scheme of Wei and Kirby (1995), with the respective scheme consisting of the third-order in time explicit Adams–Bashford predictor step and fourth-order in time implicit Adams–Bashford corrector step (Press et al., 1992; Wei and Kirby, 1995).

Finally, regarding coastal flooding, the process is simulated using the "dry bed" boundary condition which, according to Militello et al (2004), can be written as the following set of pairs of conditions for any given grin point (i,j):

if $(d+\zeta)_{i,j} > h_{cr}$ and $(d+\zeta)_{i-1,j} \le h_{cr}$ and $U_{i,j} > 0 \rightarrow U_{i,j} = 0$
if $(d+\zeta)_{i,j} > h_{cr}$ and $(d+\zeta)_{i,j-1} \le h_{cr}$ and $V_{i,j} > 0 \rightarrow V_{i,j} = 0$

if $(d+\zeta)_{i,j} \le h_{cr}$ and $(d+\zeta)_{i-1,j} \le h_{cr} \rightarrow U_{i,j} = 0$
if $(d+\zeta)_{i,j} \le h_{cr}$ and $(d+\zeta)_{i,j-1} \le h_{cr} \rightarrow V_{i,j} = 0$

if $(d+\zeta)_{i,j} \le h_{cr}$ and $(d+\zeta)_{i-1,j} > h_{cr}$ and $U_{i,j} < 0 \rightarrow U_{i,j} = 0$
if $(d+\zeta)_{i,j} \le h_{cr}$ and $(d+\zeta)_{i,j-1} > h_{cr}$ and $V_{i,j} < 0 \rightarrow V_{i,j} = 0$

where ζ is the mean water surface elevation and h_{cr} is a terminal depth below which drying is assumed to occur (here this depth is set to h_{cr} = 0.001 m).

3. MODEL VALIDATION

The capability of the presented model in the representation of coastal flooding was validated through the comparison with the two-dimensional (cross-shore) experimental data by Roeber at al. (2010), who tested wave transformation over idealized fringing reefs, carrying out a series of experiments in two flumes at the O.H. Hinsdale Wave Research Laboratory of Oregon State University.

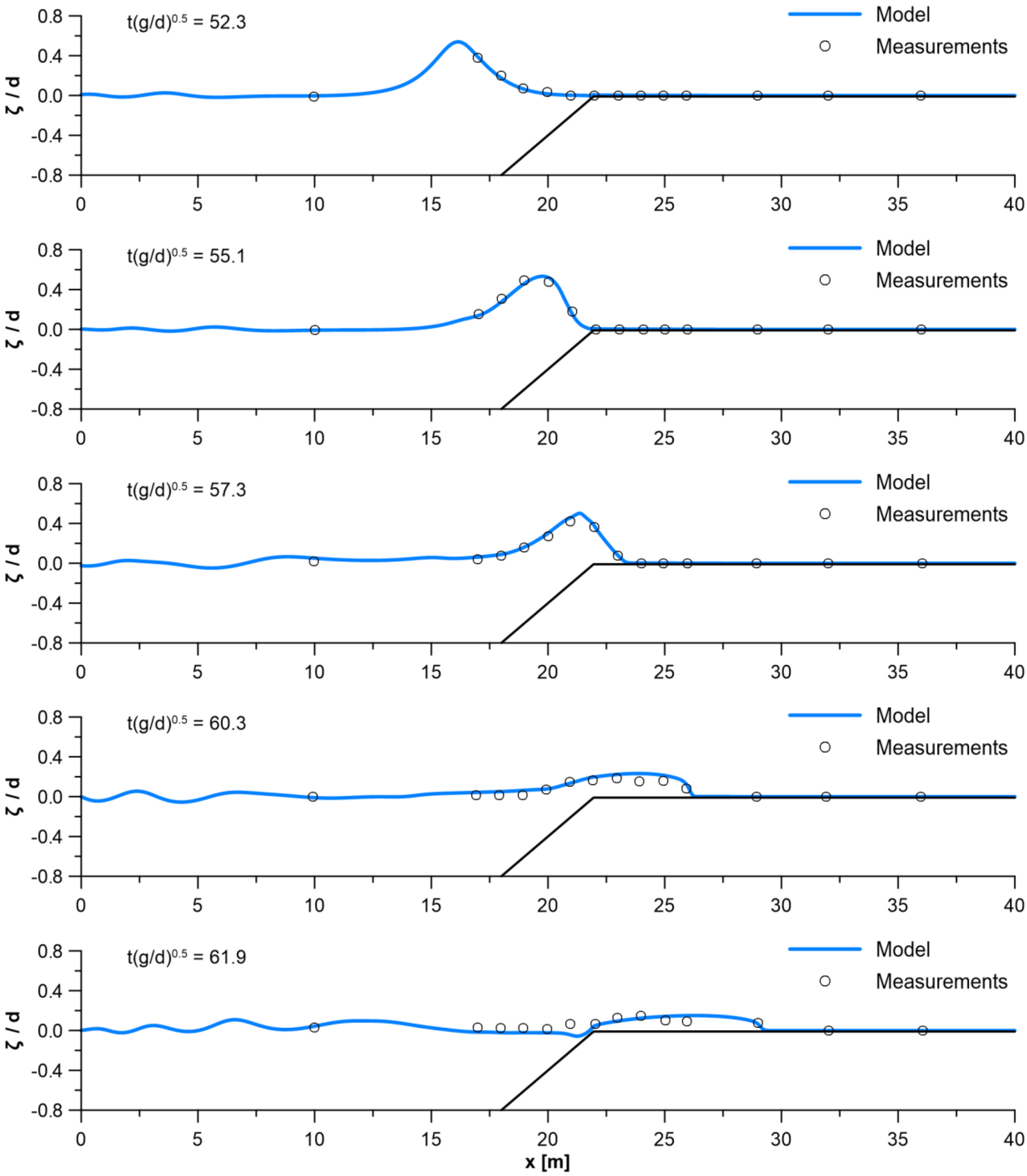


Figure 1: Surface profiles of solitary wave transformation over a dry reef flat with *A/d* = 0.5 and a 1:5 slope. Solid lines denote the results of the presented model and circles denote the measurements of Roeber et al. (2010)

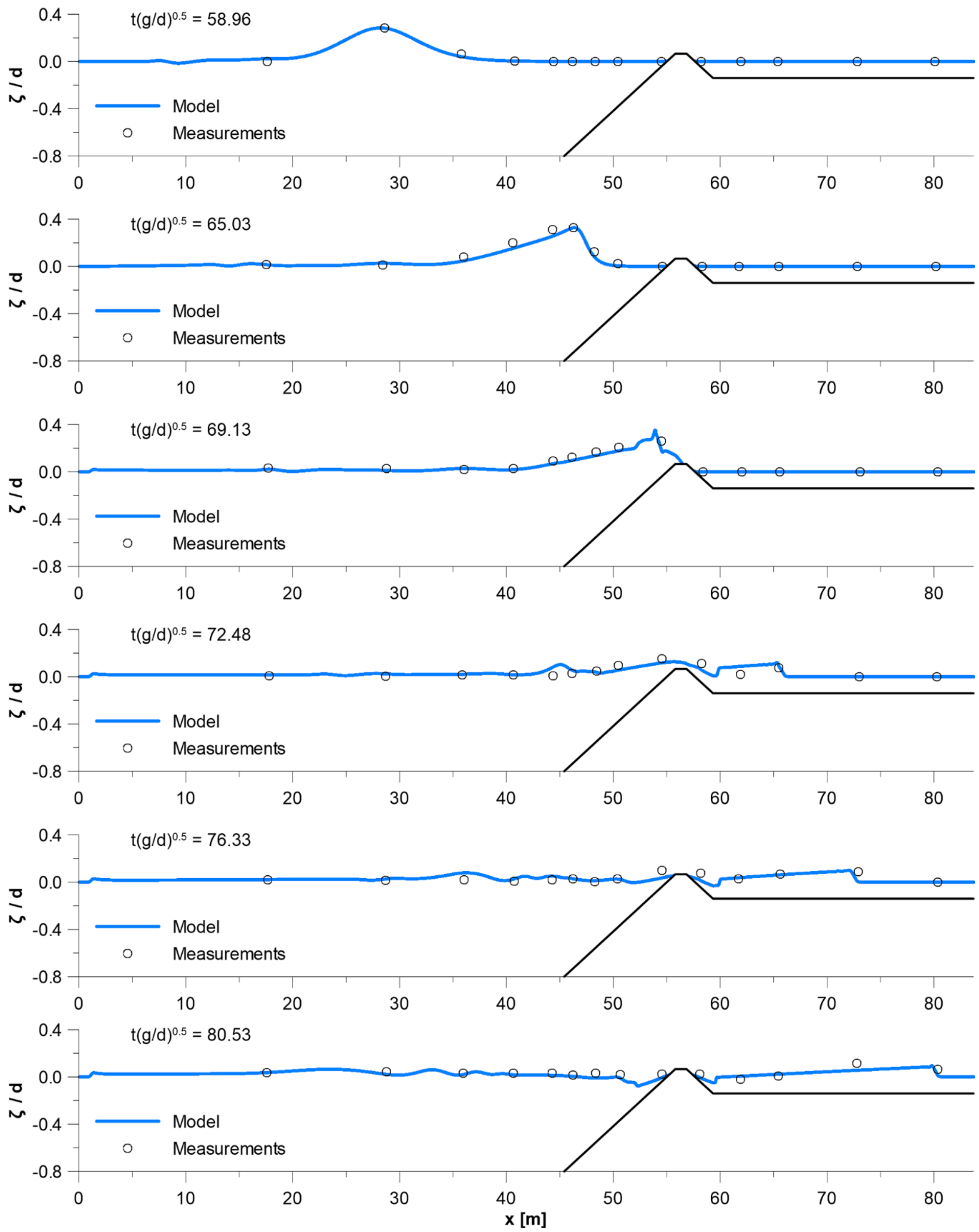


Figure 2: Surface profiles of solitary wave transformation over an exposed reef crest with A/d = 0.3 and a 1:12 slope. Solid lines denote the results of the presented model and circles denote the measurements of Roeber et al. (2010)

The experimental setup in the first – 48.8 m long, 2.16 m wide and 2.1 m high – flume, included a steep 1:5 slope starting at x = 17.0 m, followed by a reef flat up to the flume's rigid wall at x = 45.0 m (x being the direction along the flume). The test in this flume regarded a steep solitary wave of A = 0.5 m and a water depth of d = 1.0 m, resulting in A/d = 0.5 and an initially dry reef flat. Figure 1 shows the comparison between measurements and model results for this test, as a series of snapshots of surface profile evolution. Measured and computed data are in very good agreement at all transformation stages. The model successfully captures the wave's skewness as it propagates

across the toe of the slope, the formation of its steep front over the steep slope, and its eventual flow transition from sub- to super-critical as it surges over the reef flat.

The experimental setup in the second – 104.0 m long, 3.66 m wide and 4.57 m high – flume, included a fore reef slope of 1:12 starting at x = 25.9 m, a 0.2 m reef crest and a reef flat behind it up to the flume's rigid wall at x = 83.7 m (x being the direction along the flume). The test in this flume regarded a steep solitary wave of A = 0.75 m and a water depth of d = 2.5 m (A/d = 0.3), initially exposing the aforementioned reef crest by 0.06 m and submerging the reef flat with 0.14 m of water. Figure 2 shows the comparison between measurements and model results for this test, as a series of snapshots of surface profile evolution. Again, as for the first test, measured and computed data are in very good agreement at all transformation stages. The model successfully captures wave shoaling over the relatively gently slope, wave breaking on top of the reef crest, as well as the propagation of the wave bore (clearly identified by the bore front) over the reef flat.

4. MODEL APPLICATIONS

The presented model was applied to the area of the Bay of Thessaloniki, i.e. the northern part of Thermaikos Gulf, located in northwestern Aegean Sea, Greece. Figure 3 shows the geographic location and a satellite image of the study area.

The model domain was bounded to the south by the virtual East-West line connecting the Mikro Emvolo Cape to the western coast of the Bay (see Figures 4 and 5). The intermittently dry/wet area at the western part of the Bay (green dotted area in Figures 4 and 5) was modelled as a dry flat for the scenarios run in this work; this is justified by the consideration that the specific area – even when wet at highest tide – is covered by no more than a few centimetres of water. The domain also included the projected final geometry of the 6th pier of the Port of Thessaloniki (grey crossed area in Figures 4 and 5), while it should also be noted that the artificial coast of the Bay of Thessaloniki (Port of Thessaloniki and waterfront eastwards of the Port up to the Mikro Emvolo Cape) was modelled as a solid boundary (i.e. no flooding allowed).



Figure 3: Geographic location and satellite image of the study area (Google Earth, 2018; privately processed)

The model was run for a/two representative scenarios of climate change- induced wave and storm surge events. The first scenario (henceforth denoted by *S1*) regarded a southern wave of significant

wave height H_s = 1.58 m and peak period T_p = 4.60 sec. The second scenario (henceforth denoted by *S2*) regarded the same wave combined with a storm surge of height *SSH* = 0.50 m.

Figure 4 shows model results for scenario *S1*, indicating the flooded area at the western coast of the Bay of Thessaloniki; Figure 5 shows the respective results for scenario *S2*. The model performed satisfactorily in both cases, resulting in smooth flooding contours that follow the modelled topography. For scenario *S1* the flooded area mainly covers parts of the aforementioned dry flat (flooded area approximately equal to 2.5 km^2), while for scenario *S2* the flooding covers most of the dry flat and extends to the low-lying coastal areas of the Bay as well (flooded area approximately equal to 6.3 km^2).

5. CONCLUSIONS

Knowledge of the flooding extent is critical in relevant studies, as it allows the direct quantitative assessment of the impact of climate change on coastal areas, using the projected flooded area as the basis for the evaluation of the respective damage and adaptation costs (Hinkel et al., 2014). The use of advanced numerical models in the above context has certain advantages over estimates of the flooded area from simple superelevations of the water surface or from the spatial extension of cross-sectional run-up results, as such models are able to simulate the inundation over complex natural and/or artificial topographies, resulting in more accurate, case-specific results, suitable for detailed coastal flooding risk assessment and mitigation.

Following this rationale, this work presents a coastal flooding model consisting of a storm surge model and an advanced nearshore wave propagation model based on the solution of the

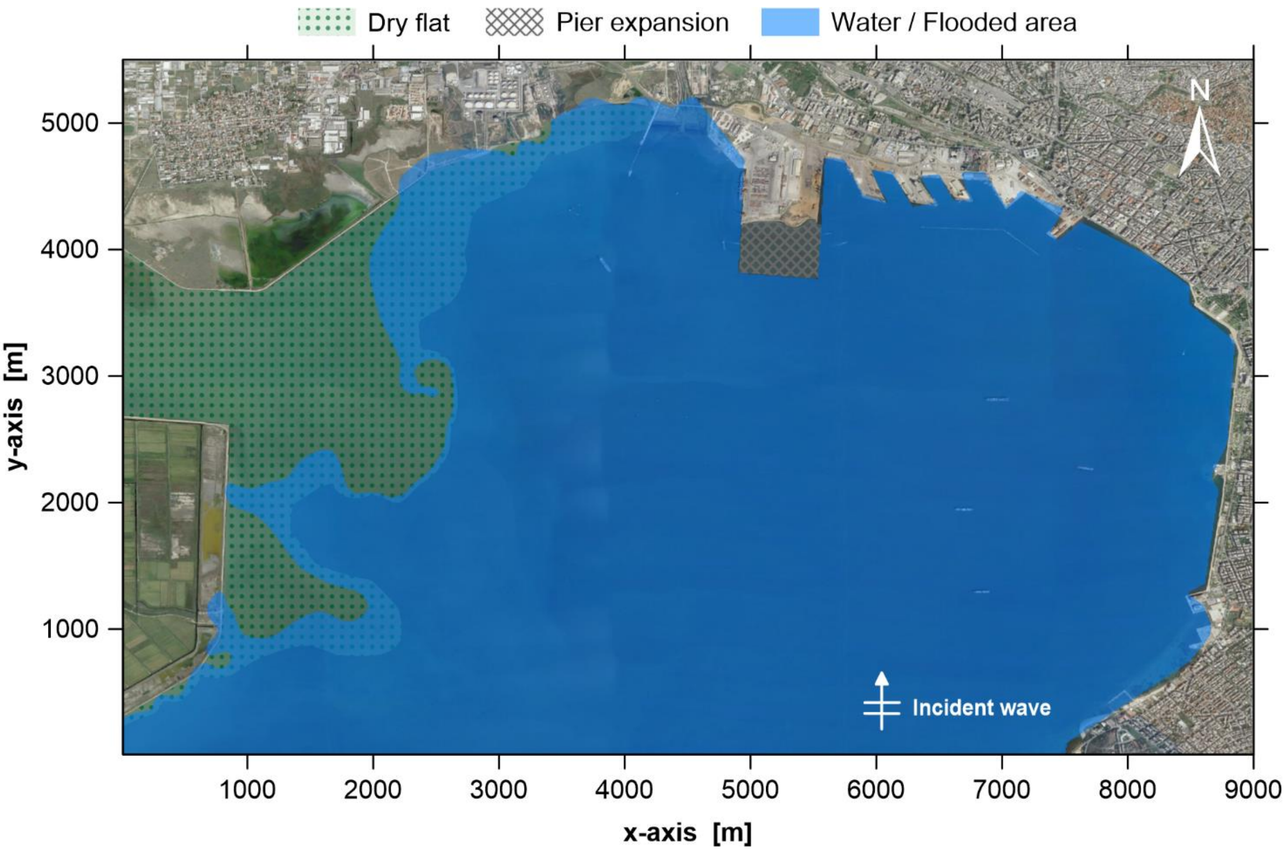


Figure 4: Model results indicating the flooded area for scenario *S1*

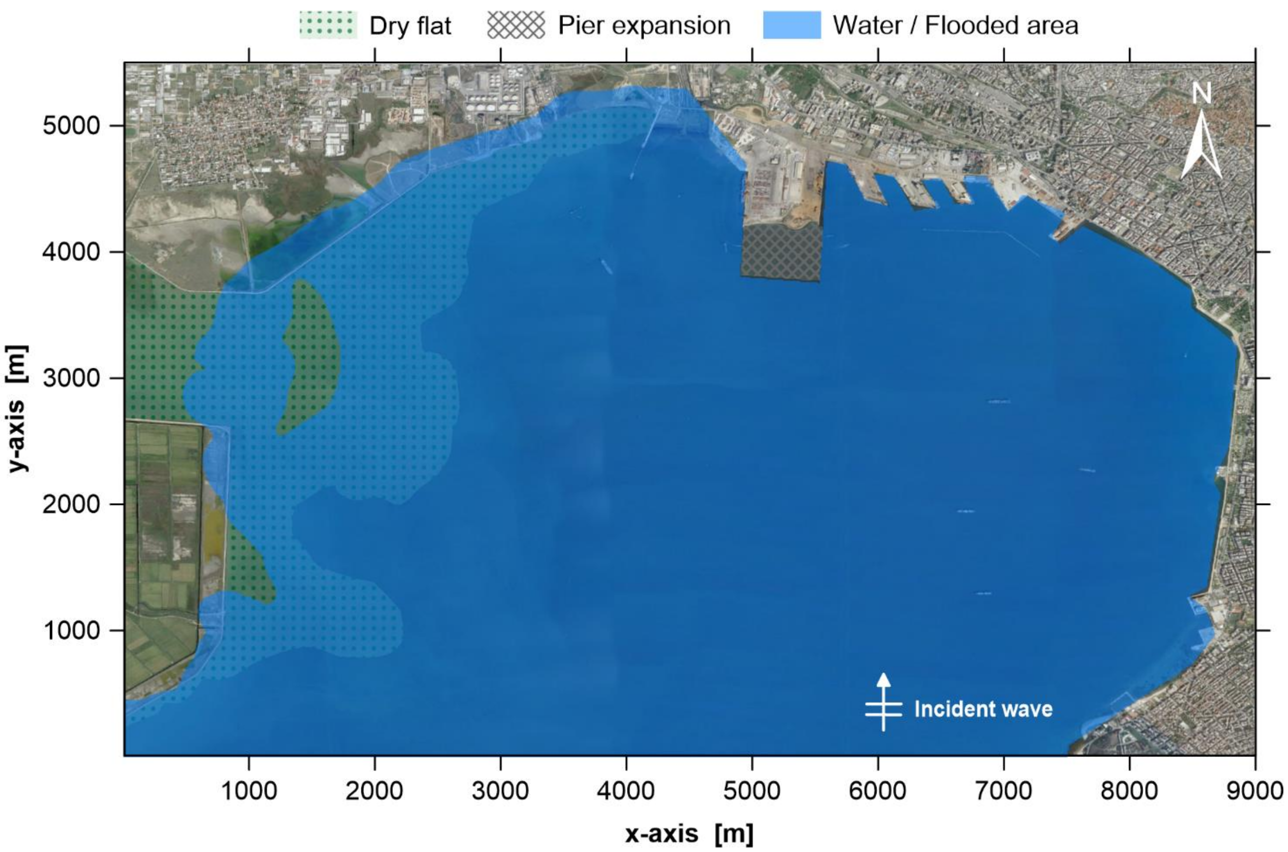


Figure 5: Model results indicating the flooded area for scenario S2

higher-order Boussinesq-type equations for breaking and non-breaking waves. The model was validated through the comparison with two-dimensional experimental data of wave transformation over idealized fringing reefs (Roeber et al., 2010), and was afterwards applied in order to simulate the effect of two representative scenarios of climate change- induced wave and storm surge events on coastal flooding for the area of the Bay of Thessaloniki, in Greece. The presented model performed well overall, highlighting its capabilities and setting the basis for a comprehensive evaluation of similar models' use in the above context.

References

1. Chen Q., R.A. Dalrymple, J.T. Kirby, A.B. Kennedy and M.C. Haller (1999) 'Boussinesq modeling of a rip current system', **Journal of Geophysical Research: Oceans**, Vol 104(C9), pp. 20617-20637.

2. Google Earth (2018) Image ©2018 TerraMetrics, Data SIO, NOAA, U.S. Navy, NGA, GEBCO.

3. Hinkel J., D. Lincke, A.T. Vafeidis, M. Perrette, R.J. Nicholls, R.S.J. Tol, B. Marzeion, X. Fettweis, C. Ionescu and A. Levermann (2014) 'Coastal flood damage and adaptation costs under 21st century sea-level rise', **Proceedings of the National Academy of Sciences of the United States of America**, Vol 111(9), pp. 3292-3297.

4. Karambas T.V. and E.K. Karathanassi (2004) 'Longshore sediment transport by nonlinear waves and currents', **Journal of Waterway, Port, Coastal and Ocean Engineering**, Vol 130(6), pp. 277-286.

5. Karambas T.V. and C. Koutitas (2002) 'Surf and swash zone morphology evolution induced by nonlinear waves', **Journal of Waterway, Port, Coastal and Ocean Engineering**, Vol 128(3), pp. 102-113.

6. Koutitas C.G. (1988), **'Mathematical models in coastal engineering'**, Pentech Press: London.

7. Mentaschi L., M.I. Vousdoukas, E. Voukouvalas, A. Dosio and L. Feyen (2017) 'Global changes of extreme coastal wave energy fluxes triggered by intensified teleconnection patterns', **Geophysical Research Letters**, Vol 44(5), pp. 2416-2426.
8. Militello A., C.W. Reed, A.K. Zundel and N.C. Kraus (2004), **'Two-Dimensional Depth-Averaged circulation model M2D: version 2.0, Report 1, Technical Documentation and User's Guide'**, Report ERDC/CHL TR-04-2, US Army Corps of Engineers, Engineering Research and Development Center: Washington, DC, USA.
9. Press H.W., S.A. Teukolsky, W.T. Vetterling and B.P. Flannery (1992), **'Numerical Recipes in Fortran 77'**, Cambridge University Press: Cambridge, UK.
10. Ribberink J.S. (1998) 'Bed-load transport for steady flows and unsteady oscillatory flows', **Coastal Engineering**, Vol 34(1–2), pp. 59-82.
11. Roeber V., K.F. Cheung and M.H. Kobayashi (2010) 'Shock-capturing Boussinesq-type model for nearshore wave processes', **Coastal Engineering**, Vol 57(4), pp. 407-423.
12. Schäffer H.A., P.A. Madsen and R. Deigaard (1993) 'A Boussinesq model for waves breaking in shallow water', **Coastal Engineering**, Vol 20(3–4), pp. 185-202.
13. THALIS - CCSEWACS 'Estimating the effects of climate change on sea level and wave climate of the Greek seas, coastal vulnerability and safety of coastal and marine structures', http://thalis-ccseawavs.web.auth.gr/en/ (accessed February 1st, 2018).
14. Vousdoukas M.I., L. Mentaschi, E. Voukouvalas, M. Verlaan and L. Feyen (2017) 'Extreme sea levels on the rise along Europe's coasts', **Earth's Future**, Vol 5(3), pp. 304-323.
15. Wei G. and J. Kirby (1995) 'Time-Dependent Numerical Code for Extended Boussinesq Equations', **Journal of Waterway, Port, Coastal, and Ocean Engineering**, Vol 121(5), pp. 251-261.
16. Wong P.P., I.J. Losada, J.-P. Gattuso, J. Hinkel, A. Khattabi, K.L. McInnes, Y. Saito and A. Sallenger. (2014), 'Coastal systems and low-lying areas', **Climate Change 2014: Impacts, Adaptation, and Vulnerability. Part A: Global and Sectoral Aspects. Contribution of Working Group II to the Fifth Assessment Report of the Intergovernmental Panel on Climate Change**, eds. C.B. Field et al., Cambridge University Press: Cambridge, UK and New York, NY, USA.
17. Zou Z.L. (1999) 'Higher order Boussinesq equations', **Ocean Engineering**, Vol 26(8), pp. 767-792.

ON THE INTEGRATED MODELLING OF WATERSHED-COAST SYSTEMS: CONSIDERATIONS FOR MORPHOLOGICAL MODELLING UNDER A CHANGING CLIMATE

A.G. Samaras*, Th.V. Karambas and C.G. Koutitas

Department of Civil Engineering, Aristotle University of Thessaloniki, 54124, Thessaloniki, Greece

*Corresponding author: e-mail: asamaras@civil.auth.gr

Abstract

The term Watershed-Coast Systems (WACS), coined by Samaras and Koutitas (2014a), refers to the entities consisting of watersheds of rivers/natural streams and the areas adjacent to their outlets where sediment delivery from the upstream is critical for the balance of the coastal sediment budget, thus playing a key role in long-term evolution of coastal morphology. In the present work, a concise critical review of the existing knowledge on the integrated modelling of WACS' morphodynamics is presented, along with considerations regarding the introduction of the impact of climate change in the above context. This work systemises the theoretical background of this emerging scientific field and highlights the major challenges ahead, setting the basis for a comprehensive evaluation of the methodological approaches used in relevant research with a clear focus on their applicability.

Keywords: Watershed-coast systems, integrated approaches, morphological modelling, climate change

1. INTRODUCTION

Climate change is an issue of major concern nowadays. Its impact on the natural and human environment is studied intensively, as the expected shift in climate will be significant in the next few decades (IPCC, 2013). Located at the land-sea interface, coastal areas are subject to a wide range of natural- and human- induced pressures. Inhabited by almost two thirds of the world's population, it goes without saying that the impact of climate change will extend from morphological implications (i.e. erosion, flooding) to significant socio-economic ones, threatening not only settlements and infrastructure, but human life as well. Moreover, the connection of coastal areas to upstream watersheds through water and sediment transport in estuaries extends the spatial scale of climate change effects in watersheds to coastal areas as well.

The term Watershed-Coast Systems (WACS), coined by Samaras and Koutitas (2014a), refers to the entities consisting of watersheds of rivers/natural streams and the areas adjacent to their outlets where sediment delivery from the upstream is critical for the balance of the coastal sediment budget, thus playing a key role in long-term evolution of coastal morphology. Given the fact that the connection of these two fields is self-evident, it is deduced that climate change will not only impact coasts through affecting sea levels, currents and waves but also through its effects in watersheds (Li and Fang, 2016) that will "travel" downstream contributing to a series of coastal processes, from the disturbance of the stability of estuaries to wide-scale morphodynamic changes.

The objective of this work is to provide with a concise overview of the theoretical background of coastal evolution modelling, leading through a critical review of its strengths and weaknesses to a comprehensive evaluation of: (a) the advances and gaps in the modelling of WACS; (b) the introduction of climate change in the above context; and (c) the major challenges ahead in this

emerging scientific field. Fundamental concepts of coastal evolution understanding and modelling are presented in Section 2; advances in the integrated modelling of WACS are presented in Section 3, including considerations for such modelling attempts under a changing climate; Section 4 presents the major challenges ahead towards the effective implementation of relevant methodological frameworks for watershed/coastal management and engineering purposes, while Section 5 summarises the conclusions drawn from this work.

2. COASTAL EVOLUTION: CONCEPTS AND MODELLING

The evolution of coastal morphology has been studied extensively over the years, starting from purely theoretical concepts for the systemisation of empirical knowledge and observational understanding, up to entire methodological frameworks for the implementation of modelling tools of varying types and complexity in order to simulate natural and human induced geomorphic processes at different scales in space and time.

The above are intermittently organized and presented in various review papers. However, not many of them are truly insightful, ending up being repetitive and overcomplicated due to: (a) the tendency to amass references rather than classify and highlight the most important of them, and (b) lack of focus of their review thesis. The above do not help in resolving a series of ambiguities on issues ranging from the terminology used for relevant geomorphic systems and processes, to the applicability of the proposed methodologies in order to effectively address "real-world" problems in watershed/coastal management and engineering.

This work aspires to set a new paradigm in relevant research, limiting the amount of excessive references and setting its focus on the dynamics of Watershed-Coast Systems (see Section 3). Furthermore, being the first step towards an extended critical review by the authors, in its present form it is intentionally self-constrained to the presentation and brief analysis of only a few works that – in the authors' view – stand out in literature.

2.1 The coastal tract concept

Building essentially on the fundamental "coastal sediment budget" concept, Cowell et al. (2003a), in a landmark work, devised and presented three related concepts: (a) the coastal tract; (b) the coastal-tract cascade; and (c) coastal-tract templating (see Figure 1). The coastal tract was defined by the authors as *"a spatially contiguous set of morphological units representative of a sediment-sharing coastal cell"*. Its composite nature implies that its actual form can vary geographically and, therefore, any individual coastal tract has meaning only in the context of analysing a specific problem, for a specific site, on an associated time-scale. The coastal-tract cascade was introduced as the means in order to separate low-order coastal change from morphodynamics on smaller space and time scales, with contiguous morphological units being associated with intermediate morphodynamic scales in the cascade hierarchy in the way presented in Figure 2b. Finally, coastal-tract templating was introduced as a protocol for the design of numerical modelling experiments (definition of boundary conditions and extent of coastal cell, data transformation, etc.), which would also be able to clarify significant processes for each such experiment.

Regardless of its limitation with respect to the study of WACS that are briefly analysed in Section 3, it is true that the coastal tract concept as a whole set the precedent for a series of studies on

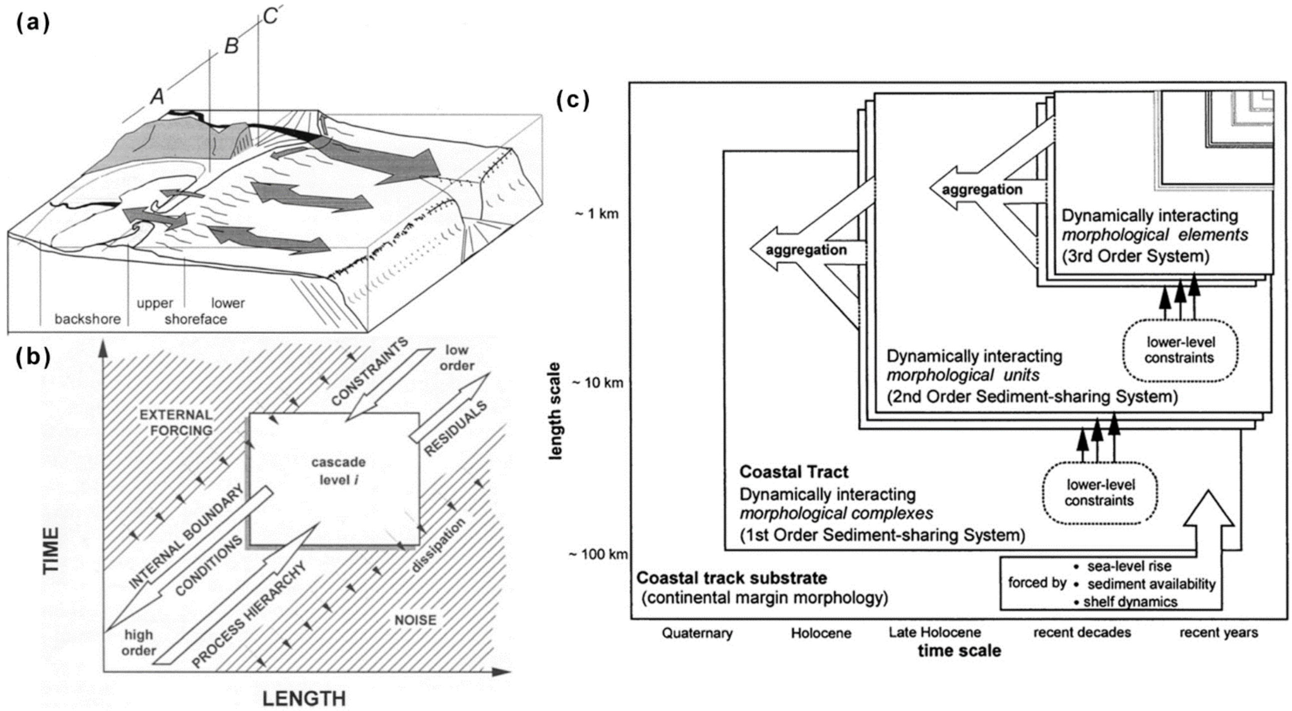


Figure 1: (a) Physical morphology encompassed by the coastal tract; (b) coastal-tract cascade; (c) nested systems of the coastal-tract cascade (figures adopted from Cowell et al., 2003a).

coastal evolution modelling, and "traces" of its constituent concepts can be identified in most of the studies that succeeded it.

2.2 The CSDMS approach

The Community Surface Dynamics Modeling System (CSDMS; Peckham et al., 2013) proposes a component-based approach to integrated modelling, aiming to simulate the full range of Earth-surface processes on time scales ranging from individual events to millions of years. This NSF-funded international and community-driven effort essentially works towards founding a new paradigm in the modelling of earth-surface dynamics, adopting a component-based software development framework and creating a suite of modular open-source numerical models that can be used to perform coupled simulations at various scales of interest in space and time.

Using CSDMS one could, ideally, simulate the entire water cycle and its effect on landscape evolution, by coupling climate, atmospheric, hydrological, terrestrial, ocean and coastal models, with the potential to represent all involved processes. However, it is even intuitively deduced that such a complicated task also involves a large number of problems and uncertainties. These range from mere computational issues (computational time, input/output models' interface, data formats' compatibility, etc.) to issues regarding the essence of attempting to couple models that come from different scientific disciplines, that are built to operate at different scales and that focus on different aspects of the natural world (see discussion in French et al., 2016). The limitations of the implementation of this approach regarding the subject of this work are briefly analysed in Section 3.

2.3 The iCOASST Project

The NERC-funded project iCOASST (integrating COASstal Sediment sysTems) focused on the simulation of decadal coastal morphodynamics, in order to achieve a breakthrough in the prediction of coastal behaviour under conditions of change. A number of conceptual and applied works that resulted from this project stand out in literature. However, special reference should be made to:

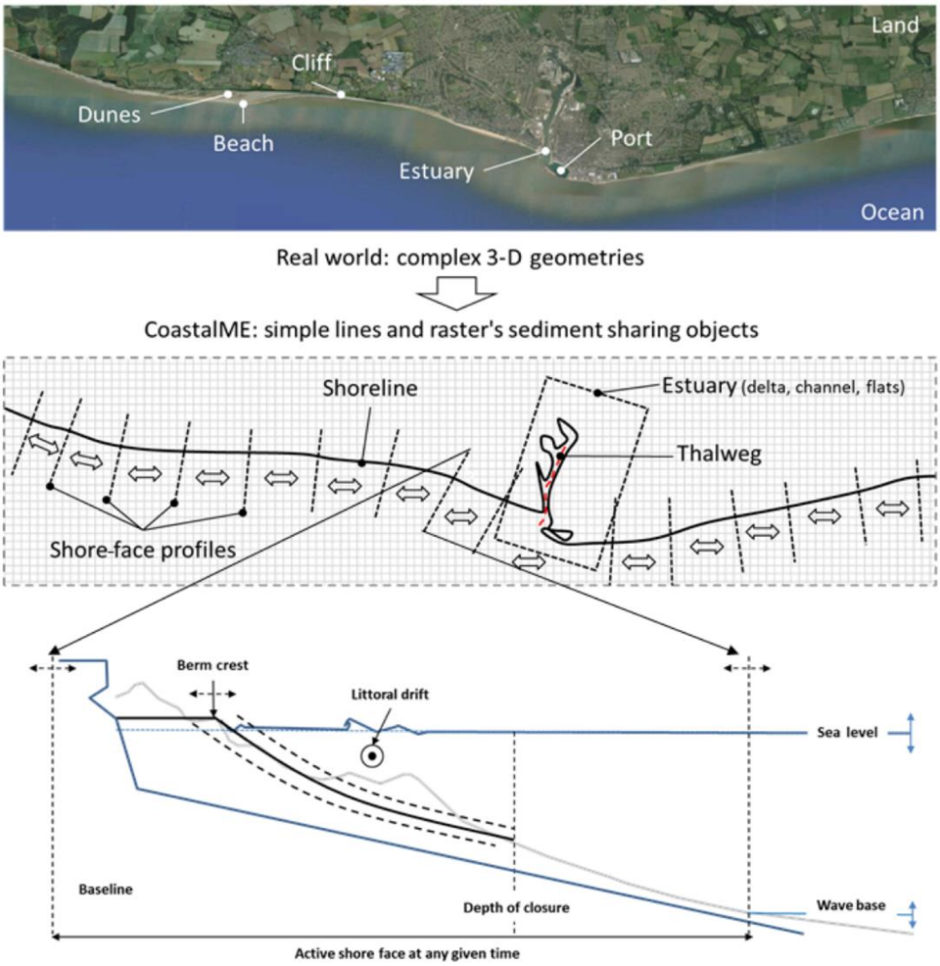


Figure 2: The modelling approach of CoastalME (adopted from Payo et al., 2016)

French et al. (2016), who provide with a thorough and insightful assessment of the appropriate complexity for the prediction of mesoscale coastal and estuarine behaviour; van Maanen et al. (2016), who presented a new framework for decadal coastal management, integrating a series of complimentary modelling approaches ranging from reduced complexity models to qualitative conceptual models; and Payo et al. (2017), who presented Coastal Modelling Environment version 1.0 (CoastalME), a framework for integrating landform-specific component models and applied it, as a proof-of-concept, for representative geomorphic systems.

The modelling approach of CoastalME is based on dynamically linking line and raster objects in order to simulate coastal evolution, and is schematically represented in Figure 2. The middle panel shows how a real-world geometry (top panel) is conceptualized as three distinct types of elements, namely: shorelines, shore-face profiles and estuaries. All three fundamental elements can share sediment among them, while the shore face (bottom panel) comprises both consolidated and non-consolidated material, the former adding to the drift material depending on sea level and wave energy constraints. Eventually, the large-scale coastal behaviour models integrated in CoastalME predict morphology evolution as the combined change in the aforementioned constituent elements.

3. ON THE INTEGRATED MODELLING OF WACS AND CLIMATE CHANGE IMPACT

3.1 The physical problem in question and the limitations to its study

Coastal morphology evolves as the combined result of both natural- and human- induced factors that cover a wide range of spatial and temporal scales of effect. Areas in the vicinity of river and natural stream mouths are of particular interest, as the direct connection with the upstream watershed extends the search for drivers of morphological evolution from the coastal area to the inland as well, especially

considering that the terrestrial field contributes approx. 90% of the sediment entering the global ocean (Syvitski et al., 2003).

However, despite the fact that the connection of the terrestrial field and the coastal field – as well as their behaviour as a spatiotemporal entity – is self-evident, literature lacks of references that study their dynamics concurrently and under the perception of an integrated morphodynamic system. The impact of watershed management (dams, regulation works, land use changes, etc.) on coastal dynamics has been studied to some extent, but this was mostly done either qualitatively, or identifying/surveying the impact without modelling the dynamics, or using data at the watershed outlet without them being subject to evaluation and further examination (e.g. Luan et al., 2016). The introduction of the impact of climate change imposes an additional challenge to be met, as climate pressures have to be added to the aforementioned system, affecting not only the dynamics in the watershed and the coast, but their interaction as well.

Samaras and Koutitas (2014) coined the term Watershed-Coast Systems (WACS), in order to describe the entities consisting of watersheds of rivers/natural streams and the areas adjacent to their outlets where sediment delivery from the upstream is critical for the balance of the coastal sediment budget. In this context, the physical problem in question under our changing climate can be divided into four basic components: (A) climate change; (B) watershed dynamics; (C) coastal dynamics; and (D) integration of the WACS (Figure 3). Components (B) and (C) have been extensively studied over the years; the last few decades so are (A) and, to a lesser extent, the impact of (A) on (B) and of (A) on (C). The most important component, though, the integration of the watershed-coast system (D) – which independently of (A) defines the essence of the WACS concept – has not been analysed to the extent one would expect to considering its importance for coastal evolution modelling.

The works presented in Section 2, as already mentioned, stand out in literature. Nevertheless, they do all present specific limitations regarding the integrated modelling of WACS. The two most essential limitations are briefly presented in the following; it is noted that, in the context of this work, they should be examined along with the issues listed in Section 4.

The first and most important limitation in many relevant approaches is the not-integrated study of the terrestrial and coastal fields as an entity; this applies to the coastal tract and iCOASST project

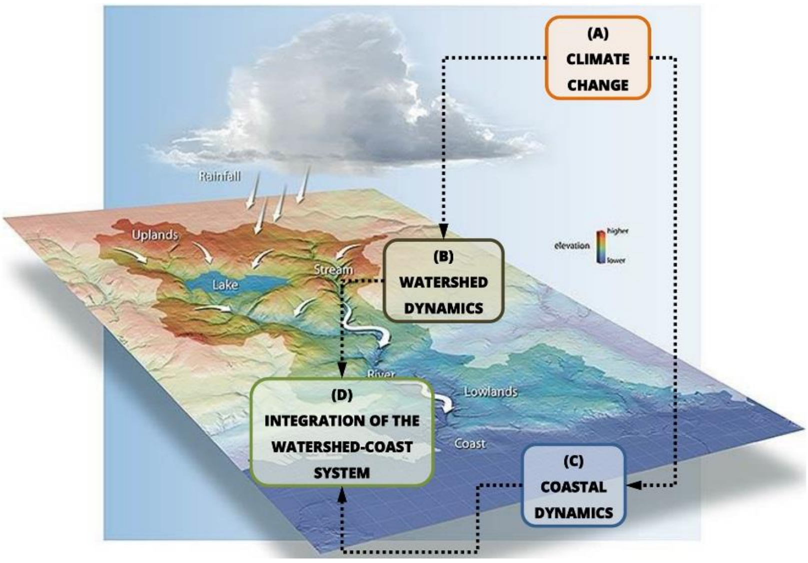


Figure 3: The physical problem in question (SWFWMD, 2014; privately processed).

approaches in the previous. Limiting the study of coastal morphology evolution at the outer (or at most the inner) estuary, i.e. using flow rate and sediment discharge as inputs from other individual studies, limits the capability of better understanding the dynamics of the system as it hinders the understanding of its evolution up to now, and therefore of its projected future behaviour. Given that,

historically, natural- and human- induced factors have combined to not only shape the Earth's surface but also affect and/or dictate changes in watersheds (e.g. from changes in cultivation practices, to technical interventions and up to population movements), it is counter-intuitive to leave watershed dynamics out of the study of coastal morphodynamics. As an example regarding the modelling of WACS under future climate scenarios, one should think about how accurate a projection about coastal morphology evolution could be if, let's say, the effect of increased drought in watershed dynamics (i.e. alteration of cultivation processes leading to a decrease in overland erosion resulting in subsequent decrease in sediment delivery to the coast) was not to be studied and taken into account for the definition of the morphodynamic system's forcings. This is one aspect of what component (D) in the previous is about.

The second limitation regards the scales in space and time at which relevant approaches have been successfully implemented, as well as how these scales relate to actual case-studies of importance for watershed/coastal management and engineering purposes. This is another aspect of what component (D) in the previous is about. This second limitation applies to the coastal tract approach, which is subject to the first limitation too, but also to the CSDMS approach which does study WACS as entities. Following the coastal tract approach, Cowell et al. (2003b) modelled coastal change for four case studies of actual contrasting continental margins around the world, limited however to time scales of 10^2 to 10^3 years. Following the CSDMS approach, Ashton et al. (2013) used the modelling system's capabilities to couple watershed and coastal dynamics, but only to simulate the evolution of an idealized WACS under scenarios of changes solely in climatic pressures and for over 10^3 years, a research attempt applicable to the study of the emergence of landforms rather than that of mesoscale coastal evolution.

3.2 Towards the integrated modelling of WACS for management and engineering purposes

Approaches that have attempted to overcome the basic limitations described in the previous have been presented by Samaras and Koutitas (2012) and Duong et al. (2016).

Samaras and Koutitas (2012) proposed an integrated approach to study the impact of watershed management on coastal morphology through numerical modelling. Its essence refers to a coupled-calibration approach of the models in the watershed and the coast, which incorporates three scenarios of data availability regarding the parameters of interest in both fields (overland sediment transport and coastal sediment transport and morphology). The specific approach is divided in three discrete stages, namely: (a) the stage of preliminary operations, (b) the stage referring to the preparation for the applications of the numerical models and (c) the stage comprising the final applications of the numerical models. Its flowchart is presented in Figure 4 and its detailed analysis in the original publication; it is essential to underline, though, the role of the sediment discharge at the watershed outlet (denoted by q_S in Figure 4) in the entire extent of the methodological approach, operating as the quantitative link between the models in the watershed and the coast during simulations. Samaras and Koutitas (2014a) presented the successful implementation of their approach for the study of a WACS in North Greece, where severe erosive phenomena in the vicinity of a small watershed outlet were attributed to extensive land-use changes in the watershed over a couple of decades' time. In a follow-up work (Samaras and Koutitas, 2014b), the authors presented a first attempt on the introduction of climate change in the integrated study of WACS, through the study of distinct scenarios that dictated changes in specific weather/climate characteristics, in accordance with basic IPCC projections.

This body of work as a whole (both conceptual and applied parts) does present certain advantages for the study of WACS, such as: (a1) its focus and applicability to scales suitable for

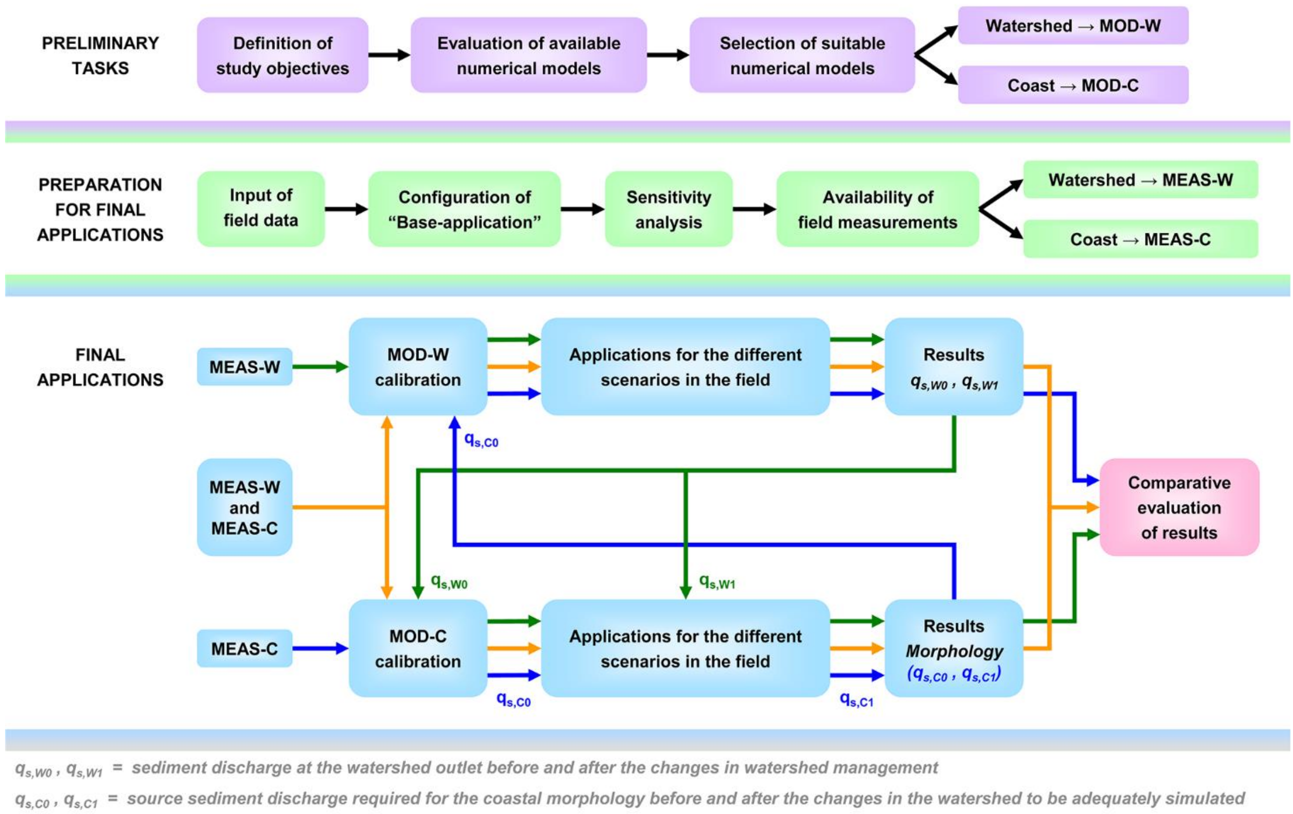


Figure 4: Flow chart of the methodological approach of Samaras and Koutitas (2012).

watershed/coastal management and engineering purposes; (a2) its applicability to data poor environments; (a3) its focus on the relative impact of changes in watershed management and climate pressures on coastal morphology evolution in order to study case-specific phenomena; and (a4) its flexibility in the study of climate change impact on WACS dynamics through a scenario-based approach, which allows for the simulation of multiple potential future states with limited computational effort. Nevertheless, there is still ground to cover, regarding: (b1) applications to WACS of varying characteristics and dynamics and (b2) the approach's connection to climate change models, as well as the general major challenges presented in the following section.

Building on the conceptual modelling framework set by Ruessink and Ranasinghe (2014) and Ranasinghe (2016), Duong et al. (2016) presented a thorough analysis on assessing climate change impacts on the morphological stability of small tidal inlets. The modelling framework presented in Figure 5 does retain the WACS approach discussed in the previous (proposing the concurrent modelling of both watershed and coastal dynamics; see also Figure 3), while it also formally defines the steps needed in order to incorporate climate change into the problem in question through ensemble modelling. Particularly regarding climate change impacts on coastal change, the authors suggest that they could be evaluated through the analysis of sets of "strategic snap-shot" (~ 1year) simulations for future forcings, which should be run for desired future times (e.g. 2050, 2100). Duong et al. (2017, 2018) applied this approach to three case study sites along the southwest coast of Sri Lanka, the first study perceiving them as data poor environments and the second one as the data rich environments they actually represented.

Again, this body of work does present certain advantages for the study of WACS. These include (a1) and (a2) described in the previous but also extend to: (a5) the incorporation of the study of climate change impacts through ensemble modelling; and (a6) the adaptation and testing of 2D coastal evolution modelling to the above framework. However, limitations do exist in this approach as well, regarding: (b3) the inherent difference between estuaries in general and small tidal inlets this approach refers and was applied to; (b4) the uncertainty regarding how "snap-shot" simulations

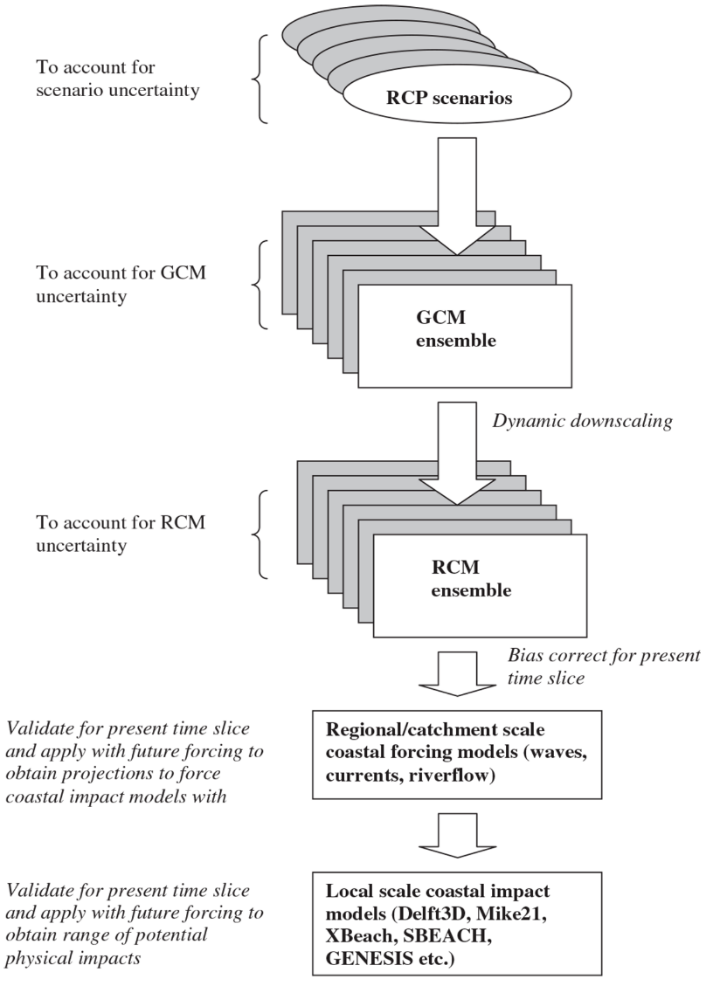


Figure 5: The modelling framework applied by Duong et al. (2016) in order to study climate change impact on the stability of small tidal inlet (figure adopted from Ranasinghe, 2016).

could actually be useful in the process of strategic planning in WACS; and (b5) the unclarity of how watershed modelling was actually applied in the three cases studies (Duong et al., 2017, 2018), since this aspect, according to the authors, was studied by previous researchers and not during studying the dynamics of the specific systems as entities. The general major challenges presented in the following section apply to this approach as well.

4. MAJOR CHALLENGES AHEAD

As seen from the previous, the integrated modelling of WACS has come a long way over the years, with several important research attempts laying the ground towards a better understanding of how watershed and coastal processes are intertwined into a web co-dependencies regarding coastal morphology evolution, how future climate change would affect such systems, and, eventually, how scientists could be able to describe the above through numerical modelling in order to plan climate change adaptation in coastal areas. Conclusively, major challenges ahead can be coded into the following issues, moving from general to specific ones:

(1) Setting the framework for resolving long-standing issues on the mutual understanding of essential processes in the study of WACS between different disciplines, which – although trivial in essence – are still hindering transcendence between scientific fields.

(2) Conceptualizing and defining what should be considered as a “satisfactory representation” of coastal change in the study of WACS (i.e. in terms of morphological features evolution/analysis and resolution in space and time).

(3) Integrating the concurrent study of climate change and watershed/coastal dynamics into a robust framework and a respective modelling system that will be suitable for management and engineering purposes (and will be properly tested in successfully doing so).

(4) Resolving the issue of identifying and adequately representing co-dependent processes in WACS whose temporal evolution varies interanually and/or over annual/decadal scales as, simply put, significant events won't happen at the same time or time frame in the terrestrial and the coastal fields (this applies to modelling WACS under climate change as well).

(5) Defining modelling parameters that can act as "quantitative links" between watershed and coastal processes that are co-dependent for the evolution of coastal morphology.

(6) Identifying the suitable complexity for riverine sediment input analysis, with regard to how this input to the coastal environment should be modelled.

The in-depth analysis of the above issues is understandably quite complicated and will be the subject of a future extended version of this work.

5. CONCLUSIONS

This work presents a concise critical review of the existing knowledge on the integrated modelling of Watershed-Coast Systems' (WACS) morphodynamics, along with considerations regarding the introduction of the impact of climate change in the above context. Through the theoretical background of conceptualizing and modelling coastal evolution, as well as the recent advances in the study of WACS under a changing climate (along with the analysis of their strengths and limitations), major challenges ahead are identified and coded into six main issues. These issues encompass the essence of the authors' view on how to move forward towards a better understanding and simulation of such systems in order to plan climate change adaptation in coastal areas.

References

1. Ashton A.D., E.W.H. Hutton, A.J. Kettner, F. Xing, J. Kallumadikal, J. Nienhuis and L. Giosan (2013) 'Progress in coupling models of coastline and fluvial dynamics', **Computers and Geosciences**, Vol 53, pp. 21-29.
2. Cowell P.J., M.J.F. Stive, A.W. Niedoroda, H.J. de Vriend, D.J.P. Swift, G.M. Kaminsky and M. Capobianco (2003a) 'The Coastal-Tract (Part 1): A Conceptual Approach to Aggregated Modeling of Low-Order Coastal Change', **Journal of Coastal Research**, Vol 19(4), pp. 812-827.
3. Cowell P.J., M.J.F. Stive, A.W. Niedoroda, D.J.P. Swift, H.J. de Vriend, M.C. Buijsman, R.J. Nicholls, P.S. Roy, G.M. Kaminsky, J. Cleveringa, C.W. Reed and P.L. de Boer (2003b) 'The Coastal-Tract (Part 2): Applications of Aggregated Modeling of Lower-Order Coastal Change', **Journal of Coastal Research**, Vol 19(4), pp. 828-848.
4. Duong T.M., R. Ranasinghe, M. Thatcher, S. Mahanama, Z.B. Wang, P.K. Dissanayake, M. Hemer, A. Luijendijk, J. Bamunawala, D. Roelvink and D. Walstra (2018) 'Assessing climate change impacts on the stability of small tidal inlets: Part 2 - Data rich environments', **Marine Geology**, Vol 395, pp. 65-81.
5. Duong T.M., R. Ranasinghe, D. Walstra and D. Roelvink (2016) 'Assessing climate change impacts on the stability of small tidal inlet systems: Why and how?', **Earth-Science Reviews**, Vol 154, pp. 369-380.
6. French J., A. Payo, B. Murray, J. Orford, M. Eliot and P. Cowell (2016) 'Appropriate complexity for the prediction of coastal and estuarine geomorphic behaviour at decadal to centennial scales', **Geomorphology**, Vol 256, pp. 3-16.

7. IPCC (2013) 'Summary for Policymakers', Climate Change 2013: The Physical Science Basis. Contribution of Working Group I to the Fifth Assessment Report of the Intergovernmental Panel on Climate Change, eds. Stocker T.F., et al., Cambridge University Press.
8. Li Z. and H. Fang (2016) 'Impacts of climate change on water erosion: A review', **Earth-Science Reviews**, Vol 163, pp. 94-117.
9. Luan H.L., P.X. Ding, Z.B. Wang, J.Z. Ge and S.L. Yang (2016) 'Decadal morphological evolution of the Yangtze Estuary in response to river input changes and estuarine engineering projects', **Geomorphology**, Vol 265, pp. 12-23.
10. Payo A., D. Favis-Mortlock, M. Dickson, J.W. Hall, M. Hurst, M.J.A. Walkden, I. Townend, M.C. Ives, R.J. Nicholls and M.A. Ellis (2017) 'Coastal Modelling Environment version 1.0: a framework for integrating landform-specific component models in order to simulate decadal to centennial morphological changes on complex coasts', **Geoscientific Model Development**, Vol 10(7), pp. 2715-2740.
11. Peckham S.D., E.W.H. Hutton and B. Norris (2013) 'A component-based approach to integrated modeling in the geosciences: The design of CSDMS', **Computers & Geosciences**, Vol 53, pp. 3-12.
12. Ranasinghe R. (2016) 'Assessing climate change impacts on open sandy coasts: A review', **Earth-Science Reviews**, Vol 160, pp. 320-332.
13. Ruessink B.G. and R. Ranasinghe (2014) 'Beaches', Coastal environments and Global change, eds. Masselink, G. and Gehrels, R., Wiley.
14. Samaras A.G. and C.G. Koutitas (2012) 'An integrated approach to quantify the impact of watershed management on coastal morphology', **Ocean and Coastal Management**, Vol 69, pp. 68-77.
15. Samaras, A.G. and C.G. Koutitas. (2014a) 'The impact of watershed management on coastal morphology: A case study using an integrated approach and numerical modeling', **Geomorphology**, Vol 211, pp. 52-63.
16. Samaras A.G. and C.G. Koutitas (2014b) 'Modeling the impact of climate change on sediment transport and morphology in coupled watershed-coast systems: A case study using an integrated approach', **International Journal of Sediment Research**, Vol 29(3), pp. 304-315.
17. SWFWMD - Southwest Florida Water Management District (2018) http://swfwmd.state.fl.us (accessed Feb 5th, 2018).
18. Syvitski J.P.M., S.D. Peckham, R. Hilberman and T. Mulder (2003) 'Predicting the terrestrial flux of sediment to the global ocean: A planetary perspective', **Sedimentary Geology**, Vol 162(1-2), pp. 5-24.
19. Van Maanen B., R.J. Nicholls, J.R. French, A. Barkwith, D. Bonaldo, H. Burningham, A. Brad Murray, A. Payo, J. Sutherland, G. Thornhill, I.H. Townend, M. van der Wegen and M.J.A. Walkden (2016) 'Simulating mesoscale coastal evolution for decadal coastal management: A new framework integrating multiple, complementary modelling approaches', **Geomorphology**, Vol 256, pp. 68-80.

ASSESSING THE RESILIENCE OF THE RIA FORMOSA BARRIER ISLAND SYSTEM: PRELIMINARY FINDINGS

K. Kombiadou*, A. Matias, A.R. Carrasco, S. Costas, O. Ferreira, T.A. Plomaritis and G. Vieira

Centre for Marine and Environmental Research (CIMA), University of Algarve, 8005-139, Faro, Portugal

*Corresponding author: e-mail: akompiadou@ualg.pt

Abstract

The aim of the present paper is to analyse the recent morphological evolution of the sandy barriers of Ria Formosa, a multi-inlet system located in South Portugal, to assess evolution regimes and related controlling factors and to identify resilience mechanisms in response to natural and artificial drivers of change. The data collected comprise aerial photographs and wave buoy and hindcast time-series, covering the period from the 1950s to 2014. The results show that the barriers have either been growing, or remaining stable. The growth patterns were either promoted by natural mechanisms, or triggered by stabilization works and supported by natural factors (e.g. longshore transport, shoal attachment). The presence of a broad marsh platform in the backbarrier was found to promote barrier stability, while the sustainance of transgressive barriers is advocated by frequent overwash, combined with low depths in the backbarrier lagoon and localised replenishment of sand. These long-term evolution regimes and their relation to artificial and natural factors show that the barriers of Ria Formosa have been resilient during the time-frame of the study, either absorbing disturbances (Armona and Tavira), or adapting to change while maintaining their functions (rest of the barriers).

Keywords: Geomorphology, remote sensing, multi-decadal analysis, ecological resilience

1. INTRODUCTION

Ria Formosa is a roughly triangularly-shaped multi-inlet barrier island system (Figure 1) in southern Portugal, with a total extension of around 55 km, and expanding at a maximum distance of 6 km from mainland (at Cape Santa Maria). At present, it consists of two peninsulas and five islands, developed along two flanks, while the connection between the tidal lagoon and the ocean is performed through six tidal inlets. The more energetic western flank is impacted by frequent (71% occurrence) waves originating from W-SW and the longer, eastern, flank is exposed to E-SE waves (23% occurrence) [Costa *et al.*, 2001]. The tidal regime is semi-diurnal, with average amplitudes of 1.3 and 2.8 m for neap and spring tides, respectively, while maximum spring tides can reach 3.5 m. The wave climate is moderate, with average annual offshore significant wave heights of 1.0 m and peak periods of 8.2 s [Costa *et al.*, 2001]. The area, declared a Natural Park, is of high ecological and socio-economic significance [Guimarães *et al.*, 2012]; it is the most important wetland in South Portugal, supporting a variety of diverse habitats and species (e.g. dunes, marshes, seagrasses, etc.), as well as various anthropogenic activities (e.g. fisheries, tourism, bivalve gathering, etc.). Still, the crucial importance of the sandy barriers themselves to the existence and persistence of the entire system and the supported habitats is often overlooked.

The aim of the present paper is to investigate the recent (past 60 years) long-term morphological evolution of the barriers of Ria Formosa in the presence of human interventions and natural processes

(i.e., storms), to identify the main drivers of change for each barrier and, based on those results, to gain insights on the major mechanisms promoting resilience.

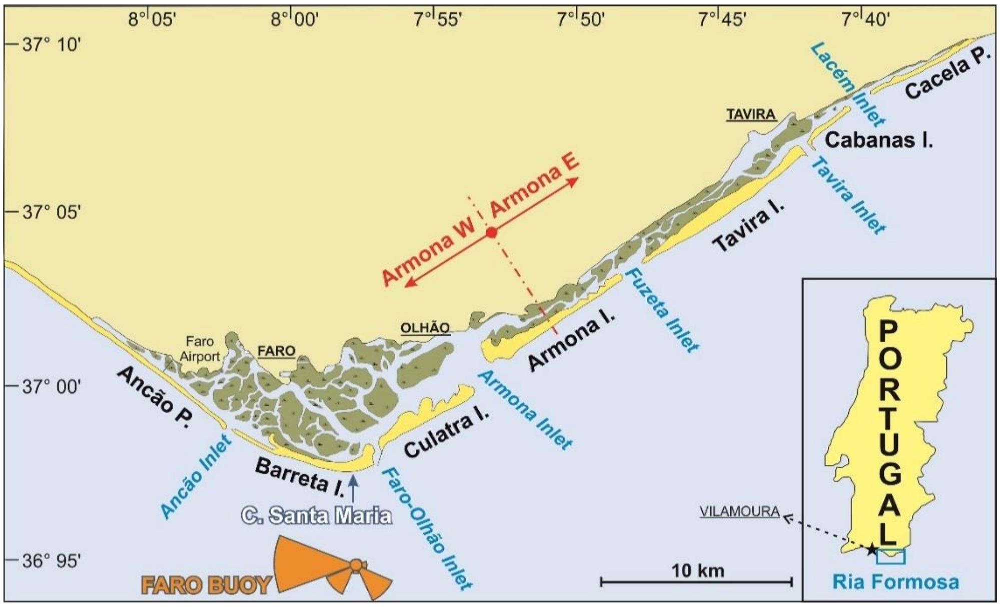


Figure 1: The Ria Formosa barrier island system; the location of the Faro buoy and the Santa Maria Cape are noted on the map, as well as the names of islands, peninsulas, inlets and the division of Armona to W and E.

2. DATA AND METHODS

The morphological evolution analysis was based on aerial photographic data that cover the period from 1947 to 2014. Aerial photographs were georeferenced using the orthophotography of 2002 (oldest available orthorectified photos) as the basis for a backwards-in-time process. The available flights, related characteristics of the rasters and the RMSE related with the georeferencing process are given in Table 1; the average Residual (Res.) RMSE refers to the error remaining after rectification, while the average Accumulated (Acc.) RMSE refers to the error that can cumulate due to the backwards-in-time georeferencing (assessed comparing each flight with the 2002 orthophotos). The average Res. RMSE ranges from 0.6±0.2 m for the most recent, high-resolution, flights, to 1.6±0.6 m for the oldest ones. The Acc. RMSE is also low, between 0.6 and 1.1 m for high-resolution flights and reaches 2 m for low-resolution aerial photographs.

To assess the barrier evolution, the wet-dry line was digitised, as a shoreline proxy in the ocean side and the limit of upper-mash vegetation, or the debris line (MHWL) was digitised, as a coastline proxy for the lagoon side. It is noted that the wet-dry line includes a high variability due to the tidal level and swash runup at the time of the flight. Weighted Linear Regression (WLR) analysis was performed on the entire dataset, using the Digital Shoreline Analysis Tool [Thieler *et al.*, 2009]. The uncertainty values used were taken equal to the total shoreline position error [Morton *et al.*, 2004], calculated from the rectification and digitizing errors. The former was defined as the total Acc. RMSE for each island and the latter was related to the image cell size [Jabaloy-Sánchez *et al.*, 2014].

In terms of forcing, significant wave heights from the Faro buoy were used; the insitu data cover the period from 1993 to 2014 and was complemented with hindcasting results (SIMAR; Spanish State Port Authority) for the period 1958-1992. The storm thresholds considered are 2.5 m for significant wave height and 6 hours for storm duration [after Oliveira *et al.*, 2018]. Only waves incident to the coast were taken into account for each flank (e.g. for E flank only waves from the SE sector: E to S).

Table 1: List of available rasters, including year, resolution, bands (1: BW, 3: RGB, 4: RGB+NIR), average Residual (Res.) RMSE and Accumulated (Acc.) RMSE. Datasets prior to 2001 are orthoimages.

Year	Resolution	Bands	Res. RMSE (m)	Acc. RMSE (m)	Year	Resolution	Bands	Res. RMSE (m)	Acc. RMSE (m)
2014	0.7m	4	-	-	**1989**	1:8000	3	1.0 ± 1.0	1.4
2009	0.5m	3	-	-	**1986**	1:8000	3	0.7 ± 0.4	1.1
2008	0.7m	4	-	-	**1985**	1:15000	1	1.2 ± 1.6	1.3
2005	3.5m	3	-	-	**1980**	variable	1	1.0 ± 1.9	1.6
2002	3.5m	3	-	-	**1976**	1:30000	1	1.1 ± 1.6	1.8
2001	1:8000	3	0.6 ± 0.2	0.6	**1972**	1:6000	1	0.8 ± 0.5	1.1
2000	1:8000	3	0.7 ± 0.6	0.8	**1969**	1:25000	1	1.1 ± 0.6	1.5
1999	1:8000	3	0.6 ± 0.2	0.8	**1958**	1:26000	1	1.1 ± 0.7	2.1
1996	1:8000	3	0.8 ± 1.0	1.0	**1952**	1:20000	1	1.1 ± 0.6	1.7
1989	1:10000	1	0.7 ± 0.2	1.2	**1947**	unknown	1	1.6 ± 0.6	2.0

3. RESULTS AND DISCUSSION

3.1 Linear regression analysis

The results of the long-term morphological analysis of the barriers are given in Figures 2 and 3 for the western (Ancão Peninsula and Barreta and Culatra Islands) and for the eastern (Armona, Tavira and Cabanas Islands and Cacela Peninsula) part of Ria Formosa, respectively. To show the main evolution patterns and to facilitate interpretation of WLR rates, indicative digitised shorelines (1950s, 1980s and 2014) are also presented. For Cabanas-Cacela 1996 is the last flight examined. Given that natural inlets are highly energetic environments, with temporal scales of change much smaller than the frame of study, the WLR rates presented and discussed focus mainly on the areas of the barrier not the directly affected by inlets.

The evolution of the Ancão Peninsula is dominated by longshore sediment transport and the eastward migration of the Ancão Inlet [Vila-Concejo *et al.*, 2002]. As seen in Figure 2a, the backbarrier is generaly stable, with low rates of -0.2 to +0.4 m/yr, while, in the oceanfront, retreating shoreline tendencies prevail in the western part and accretive in the eastern, ranging within ±0.8 m/yr. In the inlet-affected eastern part of the barrier the variability increases in both margins. In Barreta Island (Figure 2b), the beach is dominated by strong progradation, with rates that reach 6 m/yr in the Santa Maria Cape and range from +2.4 to +3.5 m/yr in the rest of the coast of the western flank. The southward expansion of the island (maximum shoreline progression of 350 m between 1952 and 2014 at the Cape) is due to the stabilisation of the Faro-Olhão (hereafter F-O) Inlet that enabled the entrapment and accumulation of longshore sediment drift. In the vicinity of the F-O Inlet, erosive tendencies that reach -1.0 m/yr are observed, possibly due to local flow conditions near the western

jetty. In the leeside, the coast is very stable, with near-zero rates, mainly due to the presence of a broad, mature marsh. The evolution of Culatra Island (Figure 2c) is dominated by the rapid eastward elongation of the island, also initiated by the stabilisation of the F-O Inlet. The stabilisation caused sediment starvation to the western shore, with recession rates of -0.5 to -2.0 m/yr, and a decrease in the tidal prism of the downdrift Armona Inlet [Pacheco *et al.*, 2010] that resulted to the attachment of the ebb delta shoals to Culatra and accretion of the eastern part of the island, with rates that reach 22 m/y. The island tip progressed eastwards by an average of 3.2 km between 1952 and 2014. The backbarrier area of the island is relatively stable, with low rates of ±0.5 m/yr in the western, oldest part and with slighly higher variability and erosive tendencies of, on average, -0.6 m/yr in the eastern, recently formed, part.

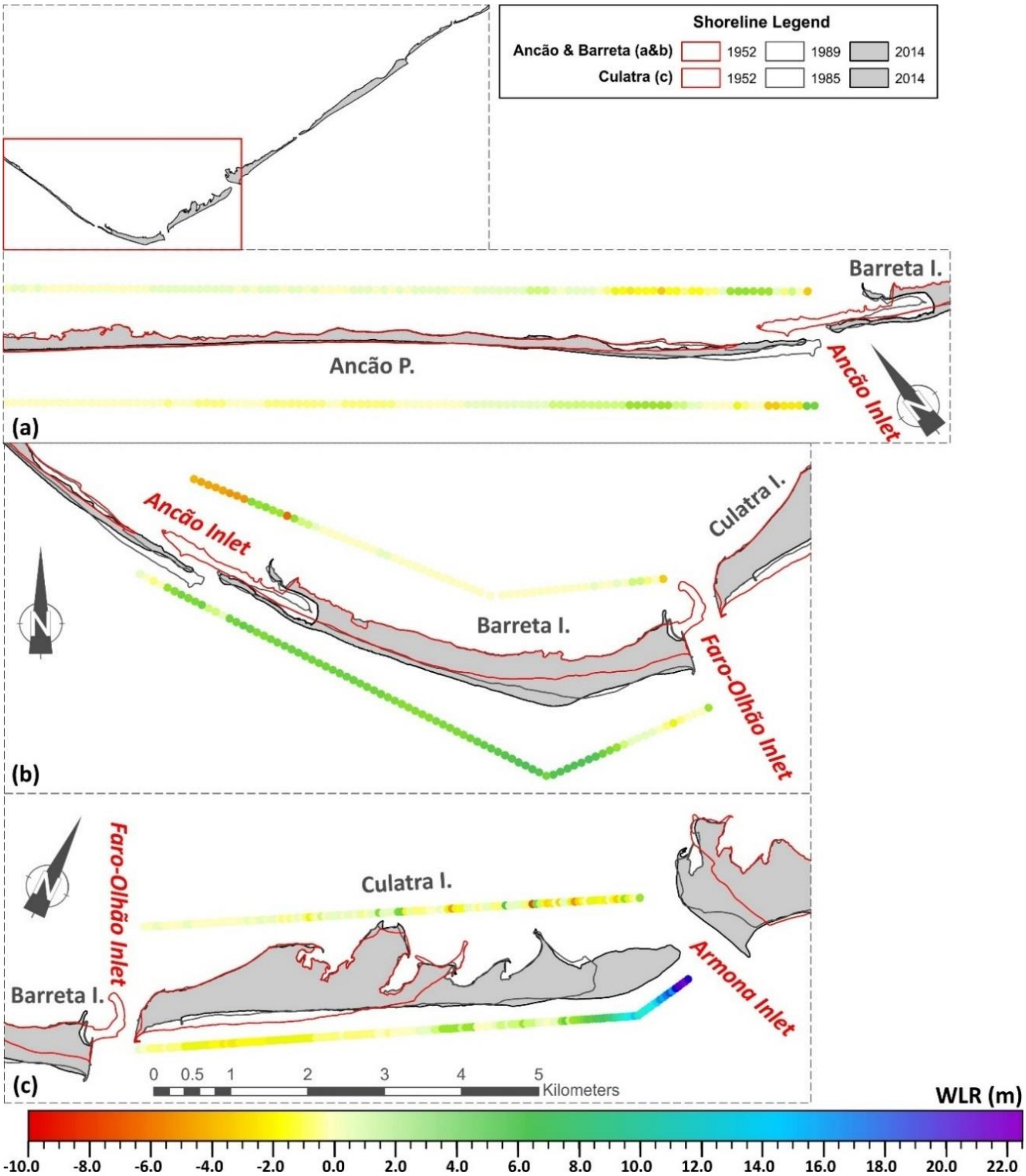


Figure 2: WLR values (in m/yr) for Ancão Peninsula (a) and Barreta (b) and Culatra (c) Islands, presented as coloured dots along the ocean and lagoon-side baselines (erosive rates: red-yellow; accretive rates: green-blue-purple, with reference to the horizontal colour-bar); indicative shorelines are presented and the location of the area is noted on the (top-left) map.

Armona Island (Figure 3a), also impacted by the reduction of the tidal prism in the updrift Armona Inlet, grows towards the NW near the inlet, with average shoreline progradation of 470 m during the study period, significantly lower than the one of Culatra. The related rates in the area are of the order of +5.5 to +15.5 m/yr. These accretive tendencies extend along the ocean side until the middle of the island, with decreasing rates towards the east (average of +0.6 m/yr) and turn erosive near the Fuzeta Inlet, ranging from -0.2 to -1.6 m/yr. The island has an extensive backbarrier and the lagoon-side coastline is stable, apart from the areas near the inlets, where rates can reach -6.8 and +9.6 m/yr. Tavira Island also possesses a mature and extensive marsh in the backbarrier and, thus, the rates in the related coastline are near-zero. In the ocean side, the shoreline is accreting near the Tavira Inlet (up to 3 km from the jetty, updrift), on average by 1.5 m/yr and by a maximum of +4.8 m/yr, and retreating in the central part, with an average rate of -0.8 m/yr. For Cabanas Island and Cacela Peninsula, hereafter referred to as C-C for brevity, the analysis extends only up to 1996, due to extensive nourishment in the area, implemented in 1997 (around $48 \cdot 10^4$ m^3) [Vila-Concejo *et al.*, 2002]. Thus, extending the analysis beyond this date would make it impossible to distinguish natural from artificial evolution. As shown in Figure 3c, the entire subsystem presents strong regressive behaviour. Maximum erosion trends are identified in the central part (2.5 to 6.5 km downdrift from the Tavira jetty) and range from -5 to -10 m/yr, with an average of -6.4 m/yr. Coastal retreat decreases towards the SW and NE parts of C-C, due to frequent small scale nourishment with dredged material from the channel (unrecorded) near the Tavira jetty, for the former, and the attachment to the mainland, for the latter. The backbarrier is also migrating landwards by an average of 3.3/yr and local maximum rates of 8.5 m/yr. The low depths of the backbarrier bay have enabled the transgression of C-C, through frequent overwashes [Matias *et al.*, 2008] that move sediment towards the mainland, thus allowing the barriers to shift their position landwards under storm waves.

3.2 Barrier morphological evolution trends

To analyse the evolution of the barriers in relation with the wave activity and human interventions, the total area of the barriers was calculated and is presented in Figure 4 for each flank, as change relative to the first available recording (1952), along with the average annual significant storm wave height and total annual storm duration. Significant interventions in the area are also noted in the timeline, along with breaching events in each flank.

In the west flank (Figure 4a&b), it can be noted that the evolution of Ancão and Barreta is highly interlinked, with the growth of one barrier to be largely followed by a reduction of the other. Ancão presents accretion in the period of 1952 to 1972, related with the eastward migration of the Inlet. In the same period, Barreta is growing southwards due to the stabilization of the downdrift F-O Inlet. The storms of 1973 caused the breaching of a second inlet in the peninsula [Vila-Concejo *et al.*, 2002], initiating losses for Ancão and corresponding gains for Barreta. From 1976, the inlet started an eastward migration cycle, reaching its eastmost position in 1996, which is reflected in the growth of Ancão and the reduction of Barreta barrier areas following 1985. The reduction in Ancão between 1972 and 1985 is attributed to the construction of the Vilamoura jetties, around 10 km west (updrift; location shown in embedded map of Figure 1) from the Peninsula, that reduced the longshore drift reaching Ancão [Ferreira *et al.*, 2006]. In June 1997, extensive coastal management work was performed in Ria Formosa, including the relocation of Ancão Inlet [Vila-Concejo *et al.*, 2002]. This is reflected in the evolution of Ancão and Barreta, with significant drop to the former and related increase to the latter that lasted up to 2002, where the inlet reached its westernmost point. Subsequently, a new eastward migration cycle started, coincident with beach nourishment projects in Ancão ($2.65 \cdot 10^6$ m^3 distributed in Ancão, Armona, Tavira and Cabanas) [Dias *et al.*, 2003] and in the updrift coastal zone (1998, 2004 & 2010) [Oliveira *et al.*, 2008] that increased sediment availability in the area and halted coastal retreat in Ancão. From 2002 onwards, Ancão and Barreta showed only small-scale changes (within ±5%). Taking into account that longshore sediment transport is directed eastwards and assuming that the sediment bypassing the F-O jetties is low, the summation of the area

of the two barriers (dashed blue line in Figure 4a) can reveal the direct impacts of the F-O stabilisation to the sediment balance of the western flank. The curve shows that the accumulation of sand initiated by the F-O jetties was intense up to 1972, reaching 18% in 20 years. The growth was slower up to the early 2000s, with a further increase of around 8% in 30 years, which appears to have stabilised; at present, the width of Barreta has reached the width of the jetty (grey-filled curve in Figure 2b) and accumulation is occurring as submerged sand banks in front of the island [Pacheco *et al.*, 2008].

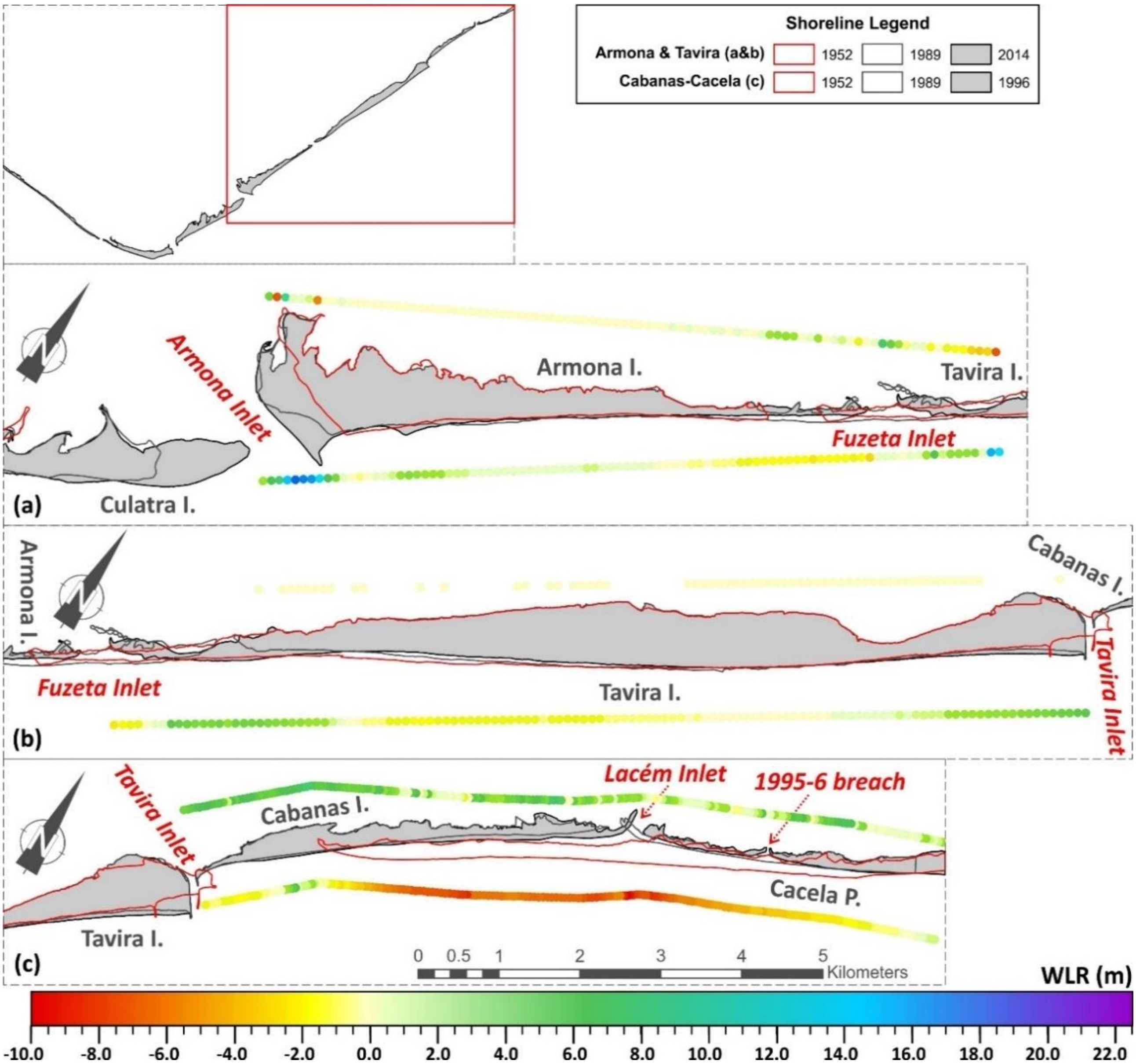


Figure 3: WLR values (in m/yr) for Armona (a) and Tavira (b) Islands and Cabanas Island-Cacela Peninsula (c), presented as coloured dots along the ocean and lagoon-side baselines (erosive rates: red-yellow; accretive rates: green-blue-purple, with reference to the horizontal colour-bar); indicative shorelines are presented and the location of the area is noted on the (top-left) map.

In the eastern flank, Culatra and Armona present a growing tendency almost throughout the study period. This growth is also attributed to the stabilisation of F-O that, as mentioned previously, induced the reduction of the tidal prism of the in-between Armona Inlet. The growth of Armona is also affected by the eastward migration of the Fuzeta Inlet, migration that also impacts the downdrift barrier of Tavira. To elucidate the evolution of the barriers and the 'net' contribution of the stabilisation works (F-O and Tavira jetties), Armona was split in two parts, W and E (see Figure 1 for location), which were added to each neighbouring barrier, assimilating, in this manner, the short-term, strong

morphological changes due to the Fuzeta Inlet movement. Thus, the joined barrier evolution of Culatra and west Armona (Culatra+Armona W in Figure 4c) and of east Armona and Tavira (Armona E+Tavira in Figure 4c) can be studied; given that the margins of these two groups correspond to stabilised inlets (F-O to the W and Tavira to the E), the ocean-side longshore gains and losses of the total area can be omitted. As shown by the evolution of Culatra and Armona W, the area is growing continuously throughout the study period, with a linear trend of $3.1 \cdot 10^4$ m^2/yr (R^2=0.97), reaching an increase of 40% in 2014, compared to 1952. Small-scale shifts to the relative change of the accumulated sand area are attributed to storm events (e.g. trend reduction between 1980-85, due to the intense wave activity of 1983). The evolution of Tavira shows reduction in total area, however, after the addition of Armona E the curve shows low variability, within ±5% (orange solid vs. dashed lines in Figure 4c); it, thus, becomes evident that the reducing trend in the area of Tavira is due to the migration of Fuzeta and not to storm impacts. The extension of the Tavira jetties in 1985 seems to invoke sediment accumulation that lasts up to 1997, after which, slightly decreasing trends are observed, most likely related to the highly energetic storms and to long-lasting events (Figure 4d). The beach nourishment of 1999-2000 in Tavira and Armona [Dias *et al.*, 2003] caused limited changes in the barrier area evolution. The C-C barriers present relative stability in total area, with the values to fluctuate between -10 and +7%, mainly due to storms and overwash events. The average roll-over of the system between 1947 and 1996 is of the order of 150 to 200 m in the west-central part and reduces to 80 m in the eastern part (east from the 1995-6 breach, see Figure 3).

3.3 Evolution regimes and resilience mechanisms

The main long-term barrier evolution trends for the period of 1952-1996 for C-C and 1952-2014 for the other barriers, identified in Ria Formosa, are summed-up in Figure 5 and the related major evolution regimes and corresponding drivers of change (artificial triggers and natural mechanisms that sustain these regimes) are summarised in Table 2. Human pressures such as intense occupation (e.g. Ancão and Culatra) and frequent dredging of backbarrier channels (e.g. Ancão and Tavira) to ensure navigability are not considered in the analysis, since they generate changes at shorter spatial-temporal scales and can be omitted for the ones considered in the study.

Apart from the presence of the Vilamoura jetties, inlet relocations and beach-dune nourishments that are the main artificial factors in the area, the evolution of the Ancão Peninsula is largely dominated by longshore sediment transport, promoting its elongation and the eastward migration of the Ancão Inlet. The stabilisation of F-O Inlet played a decisive role to the evolution of Barreta, Culatra and Armona W, generally promoting growth in all cases (apart from localised erosion in Culatra directly downdrift from the jetty). For Barreta, it caused strong southward accretion by trapping sediments from longshore drift and by changing local circulation patterns around the western jetty. For Culatra and Armona W, the mechanism boosting this growth (and the narrowing of the in-between inlet) was the increase of the tidal flow through F-O and the corresponding loss of hydraulic efficiency in Armona after the stabilisation. Excluding the changes due to the eastward migration of Fuzeta, Armona E and Tavira W are relatively stable, supported by broad backbarrier zones. The stabilisation of the Tavira Inlet induced accumulation immediately updrift (east Tavira) and lack of sediment to the downdrift Cabanas Island, contributing to the generic erosive trend at C-C. Losses in W Cabanas are replenished using dredged matter (unrecorded), sustaining a ‘forced’ stability of the area. C-C are at a transgressive state, fed by frequent overwash and the shallow depths of the backbarrier lagoon, while largely retaining the total barrier area.

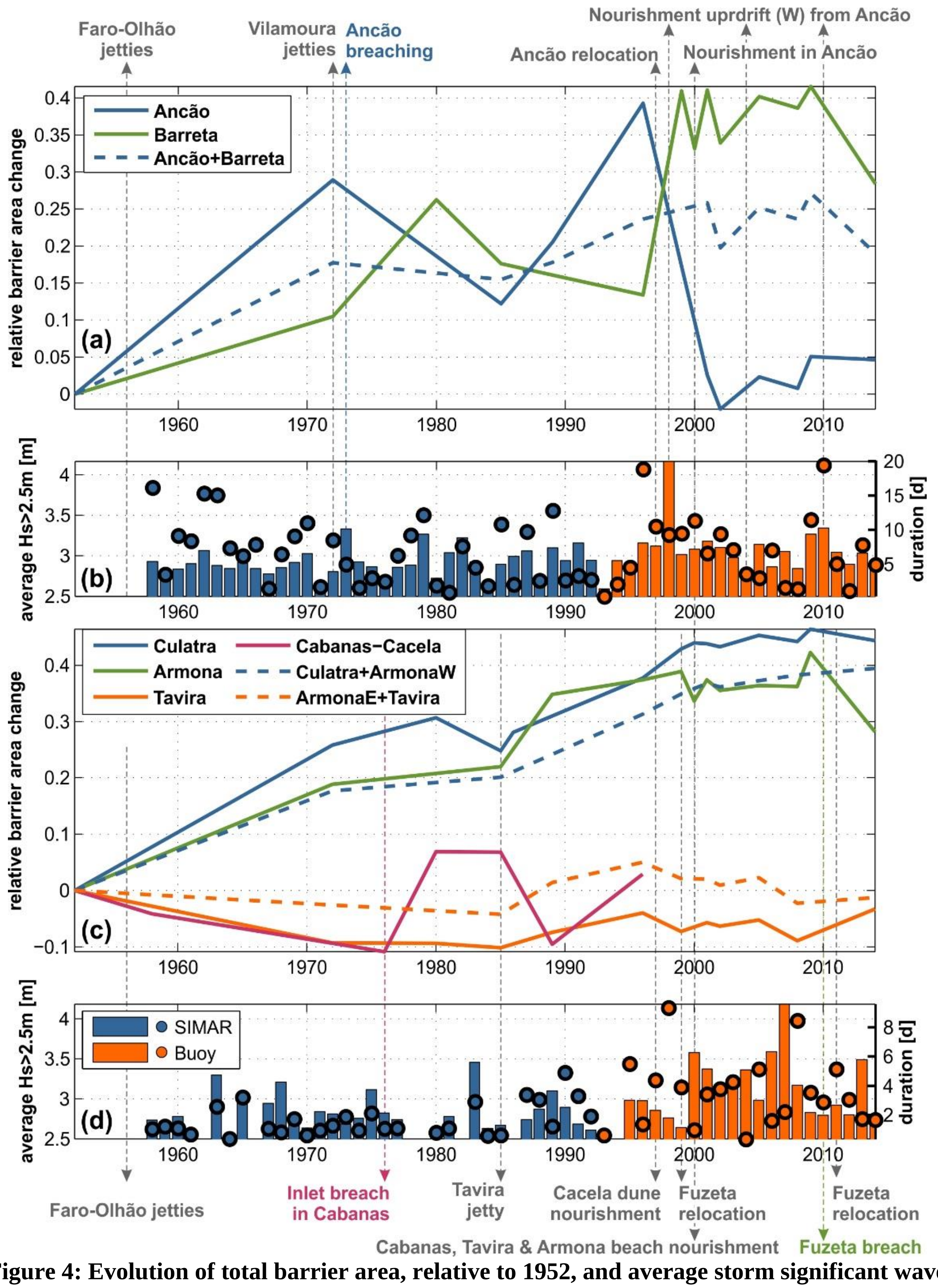


Figure 4: Evolution of total barrier area, relative to 1952, and average storm significant wave height for the western (a, b) and eastern flank (c, d). Wave data include average significant storm wave heights (bars, with reference to the left axis) and total annual storm duration (scatter-points, with reference to the right axis) at the location of the Faro buoy (Figure 1); data after 1993 are buoy records and older ones are SIMAR hindcasting data (Spanish State Port Authority). Human interventions (grey and black arrows: W from the area) and Inlet breaching events (arrows coloured as the related island) are noted.

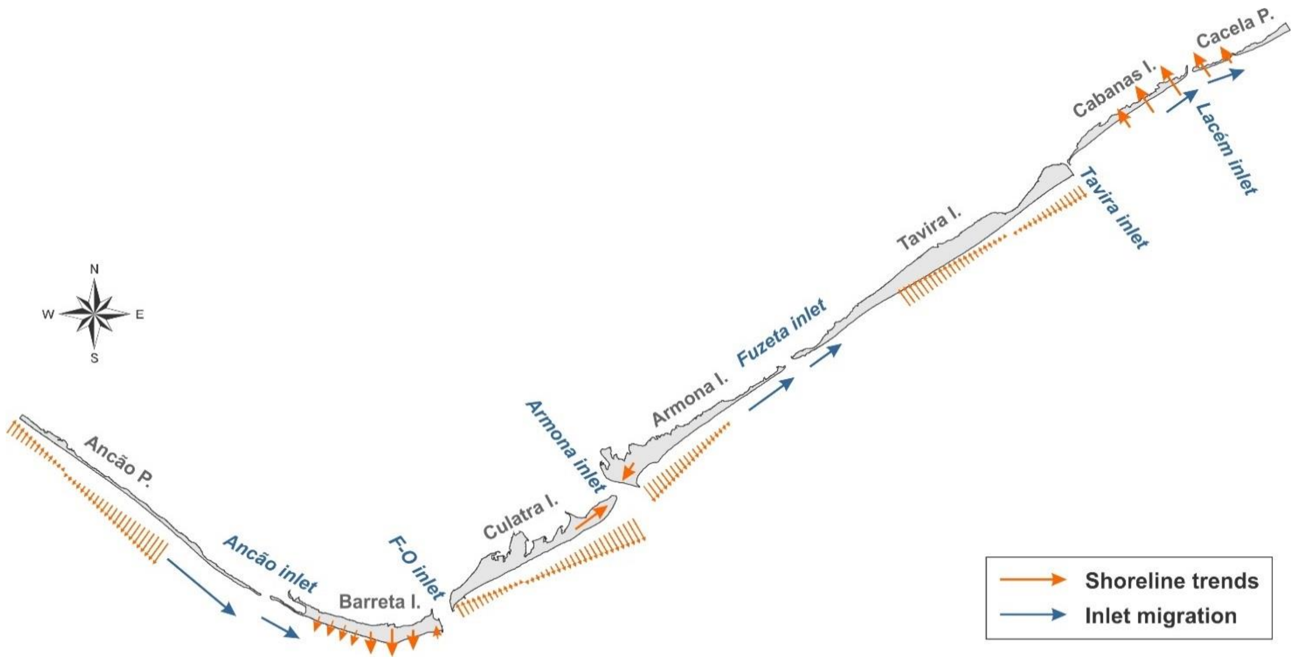


Figure 5: Schematic representation of the multi-decadal morphological response of the barriers of Ria Formosa. The major trends are noted as arrows (orange for shoreline and blue for Inlets) on the 2014 map.

The evolution regimes identified (Table 2) include: a) natural growth, limited by artificial factors (Ancão), b) artificially triggered growth, promoted by natural factors (Barreta, Culatra and Armona W), c) stability, promoted by natural (Armona E) and artificial factors (Tavira) and d) transgression triggered by artificial factors and supported by natural and artificial factors (C-C). Therefore, accepting the definition of ecological resilience as '*the capacity of a system to absorb disturbances or shocks, re-organize and adapt to change, while retaining its structure, identity and feedbacks*' [Folke, 2006], it can be deduced that the barriers of Ria Formosa appear resilient to natural (i.e., storms) and human disturbances. The barriers have either absorbed disturbances, remaining practically unchanged (Armona and Tavira), or adapted to the changing conditions while maintaining their main functions (rest of the barriers).

Table 2: Morphological evolution of barriers, related main artificial and natural drivers of change, triggering and/or supporting evolution, and resilience mechanisms (NR: Nourishment; LST: Longshore Sediment Transport; SBL: Shallow Backbarrier Lagoon).

Barrier	Evolution Regime		Limiting/Promoting Factors		Resilience Mechanism
	Growth	Position	Artificial	Natural	
Ancão	growing (SE)	stable	Vilamoura jetties, NR	LST	adaptation
Barreta	growing (S)	stable	F-O jetties	LST	adaptation
Culatra	growing (NE)	stable	F-O jetties	Armona ebb shoals	adaptation
Armona W	growing (SW)	stable	F-O jetties	Armona ebb shoals	adaptation
Armona E	stable	stable	-	broad backbarrier	absorption
Tavira	stable	stable	Tavira jetties	broad backbarrier	absorption
C-C	stable	retreating	Tavira jetties, NR	SBL, overwashes	adaptation

4. CONCLUSIONS

Raster datasets from the last 60 years (1947-2014) were used to define ocean and lagoon-side coastlines and to analyse the multi-decadal morphodynamic changes of the Ria Formosa barriers. With the exception of Cabanas-Cacela, the analysis showed overall low rates in the backbarrier coasts. In the ocean side, the shoreline in the Ancão Peninsula presents erosive tendencies in the west

part that turn accretive towards the east (-0.8 to +0.8 m/yr). In Barreta, there is a generalised tendency for shoreline progradation that peaks in the Santa Maria Cape (+6 m/yr) and extends to the rest of the west flank (+2.4 to +3.5 m/yr), while localised erosion is identified near the Faro-Olhão jetty. In Culatra, the shore downdrift from the jetty (up to 3.5 km from it) is receding (-0.5 to -2 m/yr), while strong accretion rates prevail in the rest of the island (maximum: +22 m/yr). The shoreline in Armona is accreting in the west part, with highest rates near the inlet (+5.5 to +15.5 m/yr), and showing limited erosive tendencies in the east part (-0.2 to -1.6 m/yr). The shore in east Tavira, and up to 3 km west from the jetty, is prograding (on average by +1.5 m/yr) and turns retreating in the central-western part (on average by -0.8 m/yr). In Cabanas-Cacela, both barriers are migrating landwards, with peak rates in the central part (ocean-side: -5 to -10 m/yr; lagoon-side: -3.3 to -8.5 m/yr).

Regarding existing morphological evolution regimes, the related promoting factors and the resilience of the barriers of Ria Formosa, the investigation showed:

1. The existence of two main barrier evolution patterns in the area: growth and stability.
2. The decisive contribution of jetty construction to the recent evolution of the majority of the barriers; barrier growth has been largely triggered by such interventions and, consequently, fuelled by natural processes (e.g. longshore sediment transport). For example, the stabilisation of the Faro-Olhão Inlet resulted to an increase in total barrier area of the west flank by 25% and of the affected barriers of the east flank by 40% (corresponding to an overall increase of the entire east flank by 8%), between 1952 and 2014.
3. The long-term resilience of the barriers to artificial (stabilisation works) and natural (storms) stressors is demonstrated through two main mechanisms: adapting to change (either growing, or transgressing landwards), or absorbing shocks while remaining stable in terms of position and area (observed in barriers with broad salt marsh platforms in the backbarrier).

The assessment of resilience indicators and the evaluation of future scenarios for barrier island evolution will be the next steps of the research.

ACKNOWLEDGEMENTS

The work was implemented in the framework of the EVREST project (PTDC/MAR-EST/1031/2014), funded by FCT, Portugal. A. Matias was supported by the contract IF/00354/2012, S. Costas by the contract IF/01047/2014 and A.-R. Carrasco by the grant SFRH/BPD/88485/2012, all funded by FCT.

References

1. Costa, M., Silva, R. & Vitorino, J. (2001) 'Contribuição para o Estudo do Clima de Agitação Marítima na Costa Portuguesa (in Portuguese)', in **2ªs Jornadas Portuguesas de Engenharia Costeira e Portuária, AIPCN/PIANC Secção Portugal**, 2001.
2. Guimarães, M. H. M. E., Cunha, A. H., Nzinga, R. L. & Marques, J. F. (2012) 'The distribution of seagrass (Zostera noltii) in the Ria Formosa lagoon system and the implications of clam farming on its conservation', **Journal for Nature Conservation**, 20**,** 30–40.
3. Thieler, E. R., Himmelstoss, E. A., Zichichi, J. L. & Ergul, A. (2009) '**The Digital Shoreline Analysis System (DSAS) version 4.0—an ArcGIS Extension for Calculating Shoreline Change**', 2009.
4. Morton, R. A., Miller, T. L. & Moore, L. J. (2004) 'National assessment of shoreline change: Part 1: Historical shoreline changes and associated coastal land loss along the US Gulf of Mexico', **U.S. Geological Survey Open-file Report 2004-1043**, 45.
5. Jabaloy-Sánchez, A., Lobo, F. J., Azor, A., Martín-Rosales, W., Pérez-Peña, J. V., Bárcenas, P., Macías, J., Fernández-Salas, L. M. & Vázquez-Vílchez, M. (2014) 'Six thousand years of coastline evolution in the Guadalfeo deltaic system (southern Iberian Peninsula)', **Geomorphology**, 206**,** 374–391.

6. Oliveira, T. C. A., Neves, M. G., Fidalgo, R. & Esteves, R. (2018) 'Variability of wave parameters and Hmax/Hs relationship under storm conditions offshore the Portuguese continental coast (under revision)', **Ocean Engineering**, 153**,** 10–22.
7. Vila-Concejo, A., Matias, A., Ferreira, Ó., Duarte, C. & Dias, J. M. A. (2002) 'Recent Evolution of the Natural Inlets of a Barrier Island System in Southern Portugal', **Journal of Coastal Research**, 36**,** 741–752.
8. Pacheco, A., Ferreira, Ó., Williams, J. J., Garel, E., Vila-Concejo, A. & Dias, J. A. (2010) 'Hydrodynamics and equilibrium of a multiple-inlet system', **Marine Geology**, 274**,** 32–42.
9. Matias, A., Ferreira, Ó., Vila-Concejo, A., Garcia, T. & Dias, J. A. (2008) 'Classification of washover dynamics in barrier islands', **Geomorphology**, 97**,** 655–674.
10. Ferreira, Ó., Garcia, T., Matias, A., Taborda, R. & Dias, J. A. (2006) 'An integrated method for the determination of set-back lines for coastal erosion hazards on sandy shores', **Continental Shelf Research**, 26**,** 1030–1044.
11. Dias, J. A., Ferreira, Ó., Matias, A., Vila-Concejo, A. & Sá-Pires, C. (2003) 'Evaluation of Soft Protection Techniques in Barrier Islands by Monitoring Programs: Case Studies from Ria Formosa (Algarve-Portugal)', **Journal of Coastal Research**, 117–131.
12. Oliveira, S., Catalão, J., Ferreira, Ó. & Alveirinho Dias, J. M. (2008) 'Evaluation of Cliff Retreat and Beach Nourishment in Southern Portugal Using Photogrammetric Techniques', **Journal of Coastal Research**, 4**,** 184–193.
13. Pacheco, A., Vila-Concejo, A., Ferreira, Ó. & Dias, J. A. (2008) 'Assessment of tidal inlet evolution and stability using sediment budget computations and hydraulic parameter analysis', **Marine Geology**, 247**,** 104–127.
14. Folke, C. (2006) 'Resilience: The emergence of a perspective for social–ecological systems analyses', **Global Environmental Change**, 16**,** 253–267.

EFFECTS OF CLIMATE CHANGE IN THE PORT OF TRELLEBORG AND PROTECTIVE MEASURES

A. S. Bagiouk[1]*, Th. V. Karambas[1], S. S. Bagiouk[2]

[1]Division of Hydraulics and Environmental Engineering, Dept. of Civil Engineering, Aristotle University of Thessaloniki, 54124 Thessaloniki, Greece,
[2]Department of Civil Engineering, Democritus University of Thrace, 67131, Xanthi, Greece

*Corresponding author:E-mail: mpagiouka@civil.auth.gr, Tel +30 2310 300918, +30 6979206060

Abstract
This paper refers to the effect of climate change on the rise of the sea level, particularly in the south-western Baltic region, at the port of Trelleborg. The port of Trelleborg from 1862 till present has changed and has expanded in terms of its area of activity and in terms of its size, being the second largest port in Sweden and the largest Ro-Ro Port in Scandinavia. Addressing climate change aims to deal with the upcoming ecological disruptions. Although the results of climate change are unknown, potential future climates based on natural principles and greenhouse gas emission scenarios can be projected. Satellite measurements show that the sea level is rising at a steady pace worldwide. In the case of this study, for the mean wave height it was assumed that there would be a greater increase due to the uncertainty about the direction of the waves in the prediction models and the maximum wave height was considered as high due to the more frequent occurrence of extreme phenomena than in the past. The WAVE-L model was used to study 7 possible solutions in order to protect the harbor from the rise of the sea level and to ensure resting conditions. The solutions focus on the number, position and length of floating breakwaters. The choice of the floating breakwater was made as it is a mild method of protection with environmentally friendly character and ability to move and rearrange. Finally, by comparing the individual results for mid and extreme waves, the optimal solution is chosen to adequately protect the port.

Keywords: Trelleborg Port, Climate change, Sea level

1. INTRODUCTION

In the coastal zone, the seaports and the transnational links are key types of infrastructure that support the global supply chain and provide regional economic activity, local transport services and jobs. The protection of coastal projects and ports is taken for granted during a prolonged period of climate stability. However over the last few years the forecasts for a new period of climate change and severe weather have been predominant and most of the existing projects are not ableto deal with them successfully. The port of Trelleborg belongs to the Baltic Sea segment, which is expected to show changes because of its geographic location. Over the past hundred years, the Baltic Sea level has been raised by 20 centimeters, which was a precursor to imminent disasters of coastal structures. This abstract aims at assessment of the evolution of the port over time, analyzing the impact of climate change on it and proposing solutions for its protection.

2. THE PORT OF TRELLEBORG

Trelleborg is a city in Sweden with 28,290 inhabitants according to a record made in 2010. It is the southernmost city in Sweden and it is one of the most important cities that have a port in Scandinavia

as well as across the Baltic Sea. The port has a very strategic location. The first link with Germany was opened in 1897. Later it was replaced by a railway to Sabnitz in 1909 as part of the Malmo - Berlin line. During the time of the German Democratic Republic, a larger line of coastal lines was opened for Travemünde (which can be said to be the "modern harbor" of the historically important Lubeck, initially as a line belonging to the Swedish national railways (SJ) since 1962. After the fall of the Berlin Wall in 1989, many new lines and routes were opened. The Trelleborg municipality created a ferry terminal for all services, known as the "Kontinentbron" or "the Continental Bridge." From 2015, the Shipping Lines and routes that are in operation are TT-line, Unity line and Stena line. Most of the ferry services are trucks, which makes the port of Trelleborg the largest in Sweden, regarding to goods by weight-criteria. In 2005, 11 million tonnes of merchandise passed through the port (along with nearly 2 million passengers). (TrelleborgsHamn AB).

3. CLIMATE CHANGE

Addressing climate change is the process of adapting to the real or expected climate and its impacts in order to deal with the imminent ecological disruptions and exploit the beneficial opportunities for social and environmental systems. Although the magnitude of the change is not known, possible future climates based on natural and greenhouse gas scenarios can be projected. It is notonly the climate change, but there are alsoother environmental or social changes that are expected to come to the fore in the course of years. The predicted climate change in the Baltic Sea region can be divided into immediate and indirect changes:

DIRECT CHANGES:

- The rise in temperature will be significant in the coming decades, with the biggest changes occurring in the winter and in the northeast part.
- Short-term temperature limits will change more than long-term averages.
- Extreme cold temperatures will be unusual, while hot summers are expected.
- Winter rains are projected to increase throughout the whole region.
- Scenarios and assumptions about summer rainfall are less likely, and most rainfall appears to be concentrated in the north and there may be minor changes or declines in the south part.
- Extreme rainfall is expected to be more frequent even in areas likely to experience a general reduction in average rainfall.
- Possible scenario is to exacerbate extreme precipitation for a long time (eg hours, days, weeks).
- In terms of wind speed, the majority of scenarios show an increase in average speed but with great uncertainty of relative prediction. Also the extreme wind conditions remain uncertain, but it is likely a slight upward trend in the south and a decline in the north.

INDIRECT CHANGES:

- Reduce of the amount of snow, the duration of snow cover and the appearance of sea ice.
- The average annual flow of the river is expected to be much increased in the northern parts of the basin. The total discharge of rivers in the Baltic Sea, is expected to increase, which can reduce and affect the salinity of the sea.
- General trends show increases in river flow in winter combined with lower and earlier peak flows during spring due to changes in snow cover.
- The waves of the Baltic Sea are changing as a result of large-scale atmospheric traffic. Some model simulations in the Baltic Sea show an increase in maximum wind speed and frequency of extreme events.

4. BALTIC SEA

Baltic Sea is a semi-enclosed sea characterized by complex coastline and bathymetry, by the presence of seasonal sea ice and by the high variability of wind fields in its various sub-basins. These factors

strongly affect the wave conditions in the sea area. Being aware of the wave climate is important as waves have a major impact on coastal and offshore activities such as coastal infrastructure, port operations, shipping, offshore platforms and people's safety. Changes in long-term wind and sea ice conditions may also cause changes at the waves' climate and can strongly affect the public and economic sectors. Future climate changes simulations generally provide higher wavelengths for the most areas except from the northern part.

Average waves show time and space changes over continual changes, while extreme waves show much greater variability depending on the simulations. Analyzing four scenarios of possible emissions of carbon dioxide, methane and nitrogen dioxide over a long term reaching the end of the 21st century across the Baltic Sea, it is concluded that significant changes were limited to some areas that were heterogeneously distributed in each scenario. Changes in the average annual wind speed through 30 years showed a decrease in all cases at the parts of the northern Baltic Sea and an increase at the most parts of the southern Baltic Sea. These changes in the wave fields result not only from the higher wind speeds but also from the possible shift to the western winds, which lead to different expansions and also to a different wave height and direction. However, the direction of the wind is a very important unpredictable and unstable parameter whose effects are controversial among the models and therefore it is a factor for which there are no reliable predictions. For this reason, this parameter should also be taken under account at the wave height which is used at our model. The port area of Trelleborg is located southwest in the Baltic Sea.

Previous and present wave conditions have been well explored over the last few decades by analyzing observations and numerical simulations. Among several other studies, wave velocity was analyzed in the south-western Baltic and northern Baltic. All surveys show the high time variability (seasonal and annual) due to the ice and wind variability. The maximum observed significant wave heights varies between 4.46 m in the south-west Baltic Sea and 7.7 m in the northern Baltic.

All the four climatic cases demonstrated a slight increase in wind speed in most areas, especially at the end of the 21st century, which was rarely above 5% of the reference values for the period 1961-1990. In preliminary analysis, changes in wind speed cannot be linearly transferred into wave changes, so in some scenarios the expected increase in significant wave height is often over 5%, sometimes reaching 15%. In addition, the decline in Baltic ice cover in the northern part of the sea caused larger wave changes. In particular, the average annual increase in wave height over the next 30 years is justified by the decline in ice.

The analysis of routine climatic changes in all the under consideration scenarios emphasized the increase in the average wave height of more than 5% for most of the Baltic Sea area. Of course, the significant wave height has increased, reaching more than 5% in the eastern Kattegat, along the coasts of Lithuania, Latvia and Estonia, and in the Gulf of Finland. In some parts of the Baltic Sea, especially to the east of the coast, there was a decrease not exceeding -5% compared to the reference values. These results are in agreement with those who pointed to changes on Estonian western coasts in a possible hypothetical change. For this region an increase of between 5% and 20% was found on the west coast and a decrease on the east coast.

The analysis of the variation of waves due to climate change over the decades over 140 years of simulations has shown different characteristics depending on the position of the Baltic study point and 3 spatial parameters of the distributions. The analysis over the decades has shown that the average annual wave height has increased beyond the confidence interval according to the reference period for all positions and the simulations at the end of the 21st century. The maximum annual wave height, the confidence interval of the reporting period was much broader, and the changes over the confidence interval beyond the confidence interval were well above 5% and occurred in some scenarios of climate change. This demonstrates the high degree of uncertainty of the changes in extreme waves.

Analysis of the wave direction change showed a change of frequencies to an increased wave frequency in the eastern directions, which is in line with the increase in frequencies of strong western winds as analyzed by the North Sea and a positive North Atlantic oscillation. Using the same

atmospheric data, it also showed a trend towards the western winds in the southwest Baltic Sea. Also, the trend towards the most western winds has also emerged in more modern studies. The effects of wave changes are quite significant as stereo transfer as demonstrated by Dreier et al. (2011). In addition to the limitation due to the use of only one model, temporal and spatial differences in wave height and wave direction indicate the uncertainties due to different scenarios of emission and original conditions, and therefore there is internal variability. However, the four situations of a potential future wave change in the climate field have shown an increase in wave height in the Baltic Sea. Changes in maximum extreme waves were smaller and more uncertain than in the mean. Changes in the direction of the waves indicated more (less) frequent waves that were directed east (west). Changes in wave directions may also explain the variations between small but homogeneous variations in wind velocity and larger but more heterogeneous wave height changes as the effects of waves growth are related to Baltic Sea composite bathymetry.

5. APPLICATION OF THE WAVE-L MODEL IN THE TRELLEBORG NEW PORT

The WAVE-L model is a linear wave transmission model applied to medium and small scale coastal areas. The equations that are solved are excessive and result from the replacement of the pressure and velocity distribution, from the linear wave ripples to the linearized Navier-Stokes equations and thus have the ability to describe the transmission of simple harmonic linear waves to any depth of mild tilt (combination of diffraction, diffraction, reflection and shallow).
The above described model has been applied to simulate wave propagation in the new Port of Trelleborg.

The time discretisation step is taken equal to: Δt = 0.025 sec (1)

The space discretisation steps are taken as: $\Delta x = \Delta y$ =2.5 m (2)

Thus the computational domain consists of 2600x1600 grids or an area 5500 m x 4000 m.
The rubble mound slopes (which reduce the wave reflection) are represented in the model by adopting the technique proposed by to Karambas and Bowers (1996). The values of the reflection coefficients Rs, are estimated using the formula proposed by Zanuttigh and van der Meer (2008):

$$Rs= \tanh(\alpha\xi bo) \tag{3}$$

where a and b are coefficients given by Zanuttigh and van der Meer (2008) (a=0.12, b=0.87) and ξ_o is the Iribarren number.
The wave conditions which were studied concern the port's response to an imminent change. Therefore, the wave height and wave conditions in the port were studied at an increase in the height of the waves due to climatic conditions. The two wave conditions are WC1 and WC2. The first is the average wave height while the second is the maximum. The WC2 case was made only for the most prevalent solutions between the results given by WC1 as average wave height is the basic design parameter. For each condition, significant wave height, peak period and incidence angle have been calculated by applying a SWAN model. The above characteristics are given in Tables 6.1 and 6.2.

The Trelleborg harbor as it is located in the southwest of the Baltic will face an imminent increase in the mean and extreme wave heights. The proliferation factor in the event of extreme events is from 5 to 10 and a predicted rise in the climatic conditions is estimated at 0.4 m as described in Chapter 2. The calculated current average wave height in this area without taking into account the climatic the change is 3.4 while the extreme height is 4.4m. For the model's requirements, an increase in the height of the waves of 15%, which means an average height of 3.91 m (increase of 0.51 m till 2100) and maximum height = 5.06 m, was considered. (an increase of 0.66 to 2100). For the mean wave height, it was assumed that there would be a larger increase due to the uncertainty that exists about the direction of the waves generally in the prediction models. For the maximum wave height, it was

thought to be equally large due to the more frequent occurrence of extreme phenomena than in the past, which makes its observation more important.

The basic solution the protection of the port was based on the use of floating breakwaters. This choice was made because the advantages of floating breakwaters are multiple, with respect to the following:

- The ecological advantage of seawater renewal, biological exchange, sediment transport under their structure and the development of marine ecosystems.
- The cost of classic fixed breakwaters increases rapidly depending on the depth of water, as opposed to floating breakwaters that offer a cheaper solution.
- Construction speed and construction period are much shorter than the fixed breakwater
- Possibility of future expansion and rearrangement since the position of floating waves can be easily changed. In a protection project based on a probabilistic scenario, the variability of the size and location of the project is very important as the waveguide factor can be introduced later and integrated into each solution without being bound.

In order to protect the construction from the stresses and to have calm conditions in the port, the following cases were specifically considered as possible solutions. The difference between the solutions is the quantity of the constructions and if they will be located near or far of the coast. The cases that have been studied are:

- EXISTING CASE: Response of an existing port without any intervention
- CASE 1: Port with two floating breakwaters (200m long) at a distance of 330m. from the entrance of the harbor.
- CASE 2: Port with two floating breakwaters (200m long) at a distance of 200m. from the entrance of the harbor.
- CASE 3: Harbor with a floating breakwater (200m long) at a distance of 330m. west of the harbor entrance.
- CASE 4: Port with a floating breakwater (200m long) at a distance of 200m. from the entrance of the harbor
- CASE 5: Harbor with a floating breakwater (360m long) at 1000m. west of the harbor entrance
- CASE 6: Port with a floating breakwater (360m long) at a distance of 700m. west of the harbor entrance
- CASE 7: Port with a floating breakwater (360m long) at a distance of 480m. west of the harbor entrance

Table 1: Wave characteristics for scenario WC1

Wind velocity (m/s)	Wave heightH_s (m)	Wave direction	T_p (sec)	T (sec)
20	**3.91**	**206.5**	**8.5**	**5.2**

Table 2: Wave characteristics for scenario WC2 (100yr)

Wind velocity (m/s)	Wave height Hs (m)	Wave direction	Tp (sec)	T (sec)
31.6	**5.06**	**202.9**	**10.3**	**5.7**

6. RESULTS

At the Figure 1 it is shown how the port will face the imminent rise of 15% of the wave height. The average height of the waves is estimated to reach 3.91m and it is obvious that the desired conditions do not exist.

The problem is intensified in the case of the occurrence of the hundred-year wave. Although this is an extreme ripple with a chance of recurrence once a hundred years, and planning will not be based on it, it should nevertheless be taken into account so that the consequences are not disastrous. Indeed, due to the instability of climatic conditions in recent years, which is going to be intensified due to the imminent climate change, the prediction of extreme phenomena and ripples becomes more important.

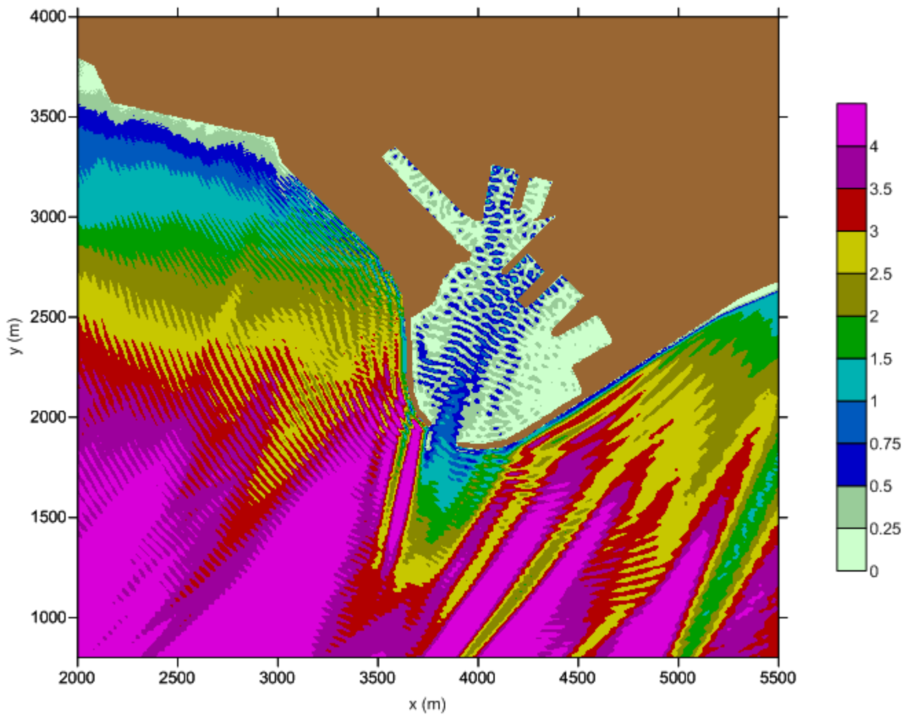


Figure 1: Wave height without any structural intervention in the existing structure, taking into account the factor of climate change

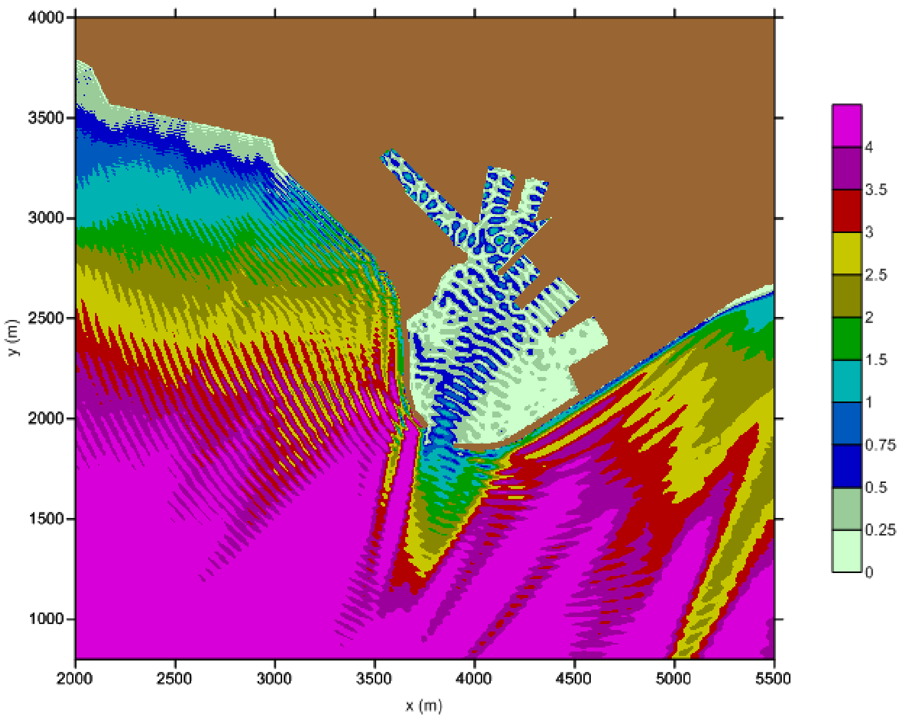


Figure 2: Wave height (hundred-year wave) without any structural intervention in the existing structure, taking into account the factor of climate change

From the results analysis for all scenarios it is clear that Case 5 and Case 6 are the best solutions. It means that installing a single breakwater westwards at a distance slightly further from the port entrance, between 700-1000 meters offers greater protection and maintains resting conditions. The most prevalent solutions will also be exported by their behavior in a hundred-year wave.

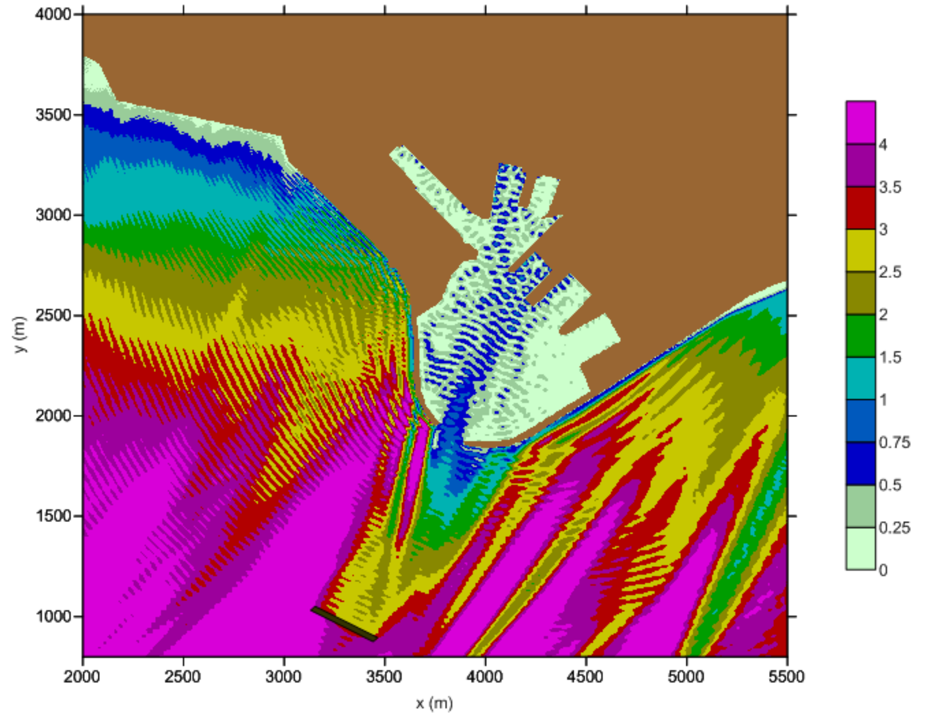


Figure 3: Wave height at the port with a floating breakwater (360m long) 1000m. west of the harbor entrance

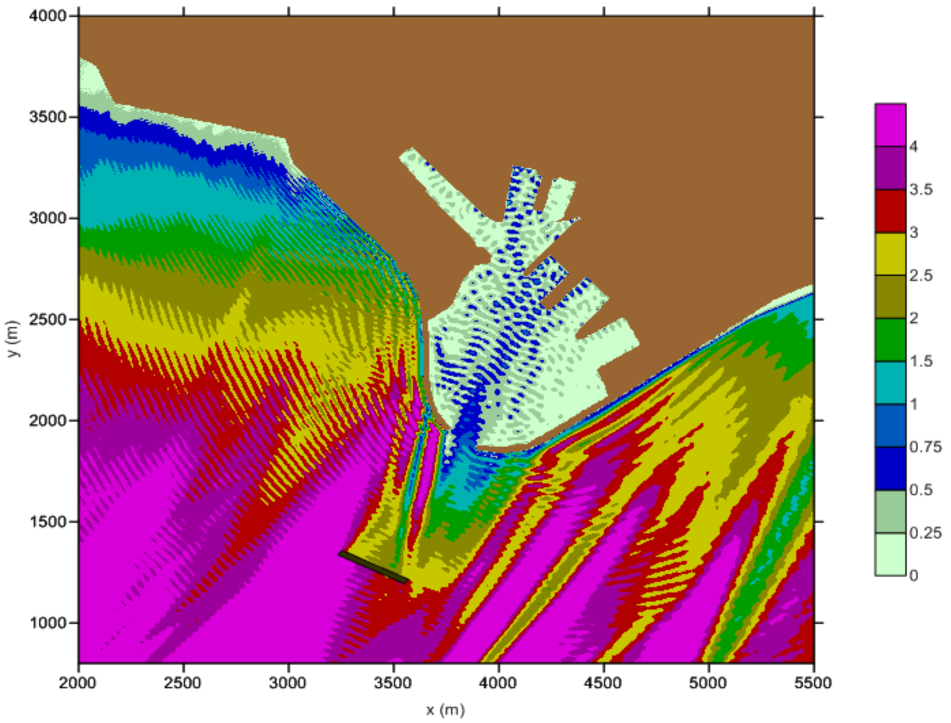


Figure 4: Wave Height at the port with a floating breakwater (360m long) 700m. west of the harbor entrance

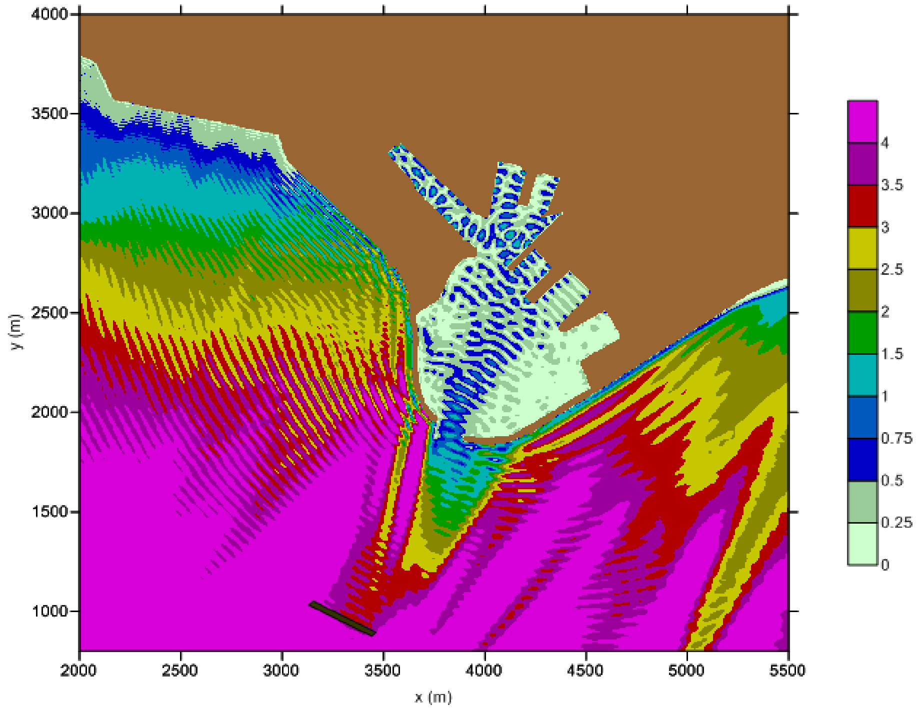


Figure 5: Wave height (hundred wave) at the port area with a floating breakwater (360m long) at 1000m. west of the harbor entrance

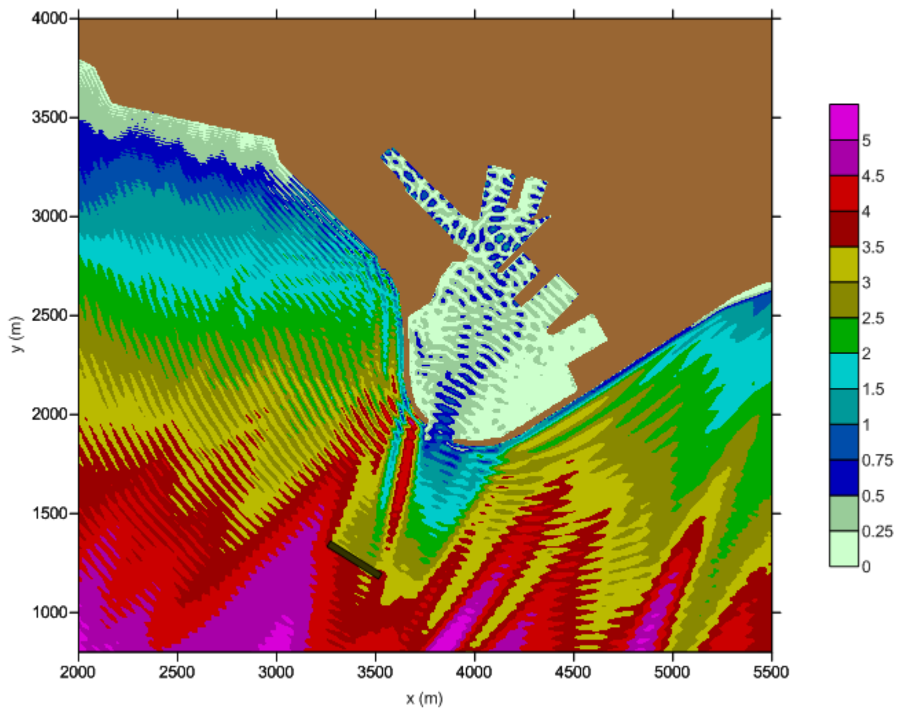


Figure 6: Wave height (hundred wave) at the port area with a floating breakwater (360m long) at 700m. west of the port entrance

Therefore, it is estimated that the case 6 responds best in both cases compared to case 5.

7. CONCLUSIONS

In this abstract through mathematical, hydrodynamic and morphodynamic simulation models, it is investigated the effectiveness of floating breakwaters as a means of protecting the port from elevation and the more frequent occurrence of extreme waves.

For this purpose, it was chosen a floating breakwater. The floating breakwater is a mild method of protecting coasts from erosion and it is increasingly used as an environmentally friendly alternative method. Their main advantages are the speed of their construction, the allowance of interventions to them, the ability to allow the renewing of the water and also the low cost compared to the conventional constructions.

A further advantage of the use of floating breakwater is their ability to move so as to be re-routed in the direction of the winds. This feature is necessary because the wind direction factor is important and unpredictable and cannot be accurately calculated by using computational models.

The possible proposed solutions varied in terms of their length and their distance from the shore where they be placed. As it is assumed from the results, the location of the breakwater installation is particularly important. Cases 1 and 2 using 200m length breakwaters in the distance of 330 meters and 200m respectively from the coast, gave similar results with Cases 3 and 4, which differ only in the doubling of the breakwaters. Cases 5, 6 and 7 are based on the use of a united breakwater with the length of 360 meters and they vary in their position, being in the distance of 1000m, 700m and 480m respectively from the coast.

The best results were observed in Case 5 and 6, showing that at a greater distance from the coast there is better port protection. Among these two main scenarios, the performance of the floating breakwaters at extreme wave height was examined. Case 6 gave the best results in both situations with small differences from Case 5. In conclusion, it is proposed to use a united breakwater at a distance varying between 700 and 1000 meters from the coast.

References

1. Baltadapt (2012). **Baltadapt Strategy for adaptation to climate change in the BalticSea region**. A proposal preparing the ground for political endorsement throughout theBaltic Sea region
2. Bank of Greece (2011). **Changes in sea level and impacts on coasts**. Athens (ingreek)
3. **European Environment Agency**. https://www.eea.europa.eu/ (accessed September27, 2017)
4. JochenHinkel et al. (2015), **'Sea-Level Rise Scenarios and Coastal RiskManagement',Nature Climate Change 5'**, no. 3
5. Karambas, Th. V. and Bowers E. C. (1996). **Representation of partial wave reflection and transmission for rubble mound coastal structures**, Hydrosoft 96, Malaysia.
6. KristerNordland (2015).**Real-time information in the port of Trelleborg WorkshopRostock**, 2015-01-22
7. M. Mokrech et al. (2014), '**An Integrated Approach for Assessing Flood Impacts dueto Future Climate and Socio-Economic Conditions and the Scope of Adaptation inEurope'**,Climatic Change 128, no. 3–4
8. Ralf Weisse et al. (2014), 'Changing Extreme Sea Levels along EuropeanCoasts'**,Coastal Engineering,** Coasts@Risks: THESEUS, a new wave in coastalprotection, 87
9. Robert E. Kopp et al. (2014), '**Probabilistic 21st and 22nd Century Sea-LevelProjections at a Global Network of Tide-Gauge Sites'**,Earth's Future 2, no. 8

10. S. Brown et al. (2011),‘**The Impacts and Economic Costs of Sea-Level Rise in Europeand the Costs and Benefits of Adaptation’**. Summary of Results from the EC RTDClimateCost Project, The ClimateCost Project, Technical Policy Briefing Note 2,Stockholm
11. TheophanisV. Karambas, EkateriniKriezi, **Simulation of wave propagation in the new Trelleborg port,** Thessaloniki
12. Trelleborg Marine Systems (2012). **Design Manual**. Trelleborg
13. Trelleborg Marine Systems (2012). **Port of the future**. Trelleborg
14. TrelleborgsHamn AB (2012). **150 years with the Port of Trelleborg**. Trelleborg
15. TrelleborgsHamn AB (2015). **The most efficient, friendliest and most environmental friendly port in the Baltic Sea.** Trelleborg
16. TrelleborgsHamnAB. **www.trelleborgshamn.se** (accessed September 2,2017)
17. Zanuttigh B. and J. W. van der Meer (2008). **Wave reflection from coastal structures in design conditions.** Coastal Engineering, Vol. 55, 771-779
18. Ü. Suursaar, T. Kullas, and R. Szava-Kovats (2009), ‘**Wind and Wave Storms, StormSurges and Sea Level Rise along the Estonian Coast of the Baltic Sea’**,WITTransactions on Ecology and Environment 127, 149–60

EVALUATION OF IMPACTS OF TORRENT CORRECTION WORKS AT FOURKA-HALKIDIKI IN THE COASTAL ZONE OF FOURKA BEACH

V. Pavlidis

Civil Engineer, Aristotle University of Thessaloniki (A.U.Th.)
Alexandrou Moraitidi 6, Kifissia,
GR- 54655 Thessaloniki, Macedonia, Greece

*Corresponding author: e-mail: vasileiospavlidis@gmail.com, tel : +306909701698

Abstract

The major characteristic of the torrent of Fourka-Halkidiki, one of the most devastating streams of Kassandra peninsula, is the intense flooding behaviour in conjunction with the production and transportation of huge, for its size, sand-composed debris. The formation of Fourka sandy beach, which is a tourist attraction pole, is mainly ought to the stereo-transportation of Fourka stream. The continuous, during the stage of increased supplies, accumulation of sand from Fourka stream combined with the sea-waving, drifting of sand towards the axis of Fourka (NW) → Poseidi (NE) form the shaping causes of Fourka beach. Until recently, in 2010, these two opposite-functioning phenomena (accumulation of sand from the Fourka stream and abduction of sand form the coastal sea sea-waving Fourka → Poseidi), were relatively balanced. After the devastating floods of 1990 and 2006 and the implemented stream correction works, the sand accumulations have been interrupted (practically eliminated) a fact that resulted to the destabilization of existing balance among each other and the shrinkage of coastal zone. In the present paper are recorded and evaluated the impacts of the implemented anti-flood correction works of Fourka's stream upon the movement of the produced sand and the destabilization of the coastal zone at Fourka beach.

Keywords: Fourka stream, stereo-transportation of Fourka stream and flood genesis, sand-accumulation of beaches, Fourka beach

1. INTRODUCTION

The Greek space is characterized by the vital presence of sea, the complicate-shaped coastline, the extensive or bay-shaped sandy beaches, interchanged by steep rocky parts and sea caves. The morphology of the Greek coastline with the sandy beaches and the combination of sea and sun constitute the major cause of the development of its summer tourism. A determinant element of the summer tourism is the geometry, the quantity, the rating and the quality of sandy beaches

The creation and stability of sandy beaches is ought to the balance of sand adduction (inputs) and sand abduction (outputs) mechanisms. Usually, it prevails a steady small-changeable but rapidly restored balance between the adduced and the abducted sand debris, with most common case small seasonal deviations of the coastline. These increasing-decreasing incidents are ought to an elevation-activation of sand adducing or abduction mechanisms. An increase of sandy coastline is recorded in cases of increased accumulations from flood-stereo-loads of streams and rivers, from increased marine waving of adducing sand or reduced carrying-away capacity. In opposition to this, a decrease is recorded due to intensification of the abduction mechanism or reduction of adducing sand. In both cases the equilibrium of inputs-outputs is disturbed positively or negatively with a respective increase

or decrease of the sandy coastline. Phenomena of steady shrinkage (Pefkofyto beach, Photo 1a) or expansion of sandy coastline (Glarokavos, Photo 1ab), are rarely observed.



α β

Photo 1ab: a) General view of beach shrinkage at Pefkofyto Kassandra and of transportation of sand to the area of Glarokavos bay, blocking its entrance. b) the sandy alluviums in the coastline area at Glarokavos Kassandra where, in order to maintain the opening of Glarokavos bay, continuous sand-takings are taking place.

The streams, by carrying out sandy debris materials, create qualitative sandy coasts in their delta space. Torrents, stream-rivers and rivers, with muddy air-transport, expand on one hand, but on the other they deteriorate the quality of their estuary beaches and consequently the provided tourist product. The most beautiful Greek beaches are met at discharge points of streams carrying out sandy debris or eroded sandy sea slopes. Such an example, are the sandy neo-genic formations at Kassandra and the de-flaky granites and gneiss at Sithonia (Photo 2a,b), whereas the clay formations at Kallikrateia-Moudania (Photo 2c) discharge sandy debris, but also encompasses plenty of clay sediment that was deposited from suspension, leading to the downgrading of the beaches.



α β γ

Photo 2abc: Views of a) eroded sandy-composed neogenic formations at Fourka-Kassandra stream, b) decomposed marble granites and gneiss at Sithona and c) the clay-composed neo-genic formations at Kallikrateia - Moudania.

2. STUDY AREA

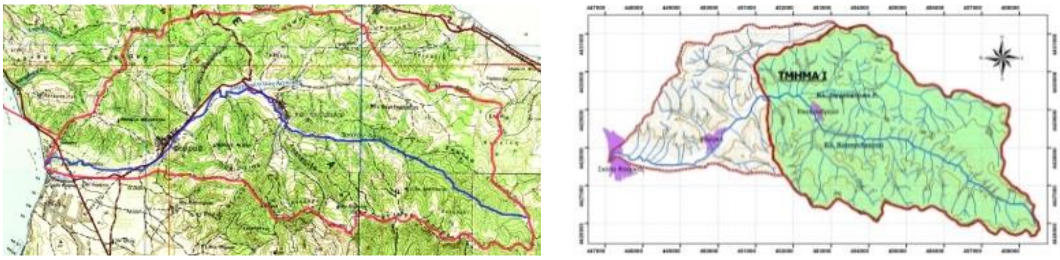
The research area is the coast and the torrent of Fourka. The location of Fourka's torrent watershed within the aquatic division of Central Macedonia, prefecture of Halkidiki, peninsula of Kassandra, is given in Fig. a,b,c.. Its watershed, the hydrographic network and the central bed with W, SW course discharging to Fourka beach, is given in Fig. 2a,b.

The Fourka's stream, the biggest and most disastrous stream at Kassandra peninsula, has a rich flooding background with main feature the production and movement of bulky, sandy stereo-transportation which has shaped the extensive sandy plain area of Kassandrinos - Fourka. Upon this area have occurred successive phenomena of erosions and alluviums of the sandy beds and slopes of the stream (Photo 3a,b) resulting to the thin-grained sandy stereo-transportation in the estuary of the Fourka Beach stream.



a b c

Fig. 1abc: The position of Fourka's torrent a) in the Central Macedonia, b) in the prefecture of Halkidiki and c) in the Kassandra peninsula.



a b

Fig. 2ab: Watershed and hydrographic network a) of Fourka's torrent and b) of its upper mountainous watershed, consisting of Kassandrino and Zografitiko Lako branches.



a



b

Photo 3ab: Views of intense slope erosions and b) depositions 2-8m high in the estuary bed of Fourka's torrent, associated with the expansion of the coast (Pavlidis Th. 1991).

To the formation of Fourka's coast, concurrently with the adduction of sand, it was also acting a coastal carrying-away marine waving of sand abduction with a SE direction. Until 1970, that agriculture was the main activity of local people, the ploughing of sandy fields resulted to the transportation of additional increased sand amounts towards Fourka Beach with a small positive equilibrium of the adduced sand. At the same time, the good quality sand of the stream's watershed

soils (Photo 4a) has led to their exploitation for construction use and cement preparation (Pavlidis Th. 1998).

A significant fact for the evolution of Fourka Beach were the arriving, during the flooding phenomena, huge amounts of sand resulting to the extensive expansion of the beach towards the sea. Eventually, until the arrival of new flooding sandy stereo-loads, the carrying-away marine mechanism has gradually eroded the alluvial seashore, bringing it back to its almost initial condition. The photo 4b provides the extensive, during the big flood on 2.3.4/12.1990, pushing forward per 170m of the alluvial discharge front of Fourka's stream towards the sea (Pavlidis Th. 1991).



a β

Photo 4ab: Views a) of the vulnerable sandy soils of Fourka's stream, b) of pushing forward per 170m to the seashore of Fourka during the flood of 1990.

By the abandonment of cultivations within the stream watershed and their coverage by compact protective natural vegetation the sand equilibrium at Fourka beach became marginally negative. After the recent works of layering gabions and gabion mattresses as a protective measure to the central bed, the adduction of sand into the Fourka beach has ceased, leading to the shrinkage of coastal zone and the deterioration of the beach. Until the completion of gabion's gaps takes place (Photo 5), in the coastal line - area of Fourka beach, it only functions the marine carrying-away mechanism, shrinking the sandy beach. The phenomenon will continue until the completion of all gabion gaps (Fig. 3) and the arrival of new sand loads to the beach. Therefore, this fact constitutes to the biggest threat for the tourism since the quality of the sandy beach is not as it used to be.



Photo 5: Views of gabions used for covering the central bed of Fourka's stream (Fig. 3) and the covering of gaps at the initial part downwards of Kassandrino.



Fig. 3. The coated with wire-constructions central bed of Fourka's stream.

3. MATERIALS AND METHODS

The research method in the present paper is as follows:

We looked up in local authorities and Services (Forest Office, Region of Central Macedonia, Municipality of Kassandra, I.G.M.R., etc.) for papers, projects, reports and accomplished or under

construction works of anti-flood stream correction, dealing with background information about the torrential environment of Fourka.

We approached and analyzed the factors of the torrential environment (climate, relief, geo-deposit, vegetation) as much as for the entire stream watershed, as well as for the upper mountainous watershed (Fig. 2a,b), downwards of which, has been implemented the major part of the correction works. The calculation was done according to the applied methods in the hydronomics science (kotoulas D. 2001, Pavlidis Th. 2007).

It was delimitated on map of Hellenic Military Geographical Service (HMGS), scale 1:50.000 and 1:5.000, the watershed of the stream and the upwards watershed of the corrected, with gabions and gabion mattresses, parts (Kassandrino-Fourka-Fourka beach) (Fig. 2b.)

We calculated the conditions of the torrential environment (morphometry-relief, climate, geology, vegetation). Specifically, we calculated the hypsometry of the watershed, the length of central bed, the average slope of bed and watershed, the density of the hydrographic network, the degree of round-shape form, the form of relief and the orographic coefficient of the stream watershed (Moulopoulos Chr. 1968, Tsakiris G. 1996, Kotoulas D. 2001, Pavlidis Th. 1998).

The maximum water-supplies, stereo-supplies and water-stereo-supplies of Fourka's stream (total and upper mountainous watershed Fig. 2a,b), were taken from the thesis of Pavlidis (Pavlidis V. 2012), with the maximum water-supply resulting from the equation of rational method (Equat. 1.1) and the maximum stereo-supply by the formula of Stiny-Hercheulidze (1.2)

Rational method: $maxQ_{100}=0,278*c*maxi_{100}*F$ 1.1

Stiny – Hercheulidze: $maxG_{100}=\{Pn*m/Yn*(100-Pn)\}*maxQ_{100}$ 1.2

The gathering time tc was calculated by the formula of Giandotti (Equat. 1.3):

$$t_c=[(4*F^{1/2})*(1,5Lk)] / [0,8*(Hm-Hmin)^{1/2}] \quad 1.3$$

Where: tc= time of gathering (hours)

$maxQ_{100}$, $maxG_{100}$=the maximum water-supply and stereo-supply (m^3/s),

F=surface of watershed (Km^2),

c=runoff coefficient,

$maxi_{100}$=average intensity of rain of maximum rainfall with a duration equal to tc,

Hm, Hmin=average and minimum altitude of stream (m),

Lk=length of central bed (Km),

Pn, m, Yn=coefficients of inclination Pn, torrentiality m, special gravity of debris Yn

From the report *«Study of immediate anti-flooding protection works in the area of the stream estuary Fourka-Kassandrino»*, conducted by Gaia S.A. Projects in 2008, there have been taken the details of the coated central bed of Fourka's stream (Fig. 3). By in situ research it was measured the average porous of the solid-stone-layer the average thickness of which was 1,40m.

The period 07.2009-06.2013, it was measured the alluvium of the coated bed (Photo 7b), the sandy debris of which originated from the upwards watershed (Fig. 2b). The deposited debris load was

considered as equal to the sum of alluvium of the upwards non-coated bed and the bulk of the gaps of the alluvial section of wire-made constructions. By the above alluvium it was resulted the average annual alluvium of the period and was estimated the completion time of the total coated bed so that the sand starts to flow towards the Fourka beach.

From the local people we gathered data of the loss of Fourka beach and the timeless changes after the flood of 1990 and after the full coverage of the bed with stone-layers. From the collected data we have approached the average annual abducted amount of sandy debris of the Fourka Beach and estimated the course of its degradation for the required period up to the full alluvial process of wire-layers by the stream's debris materials.

9. The research proceeded to the investigation of the activation potentials of the stream in respect of moving sand towards the Fourka coast, before the full alluvium of stone-layers, so that Fourka Beach is maintained at a tolerable level.

4. RESULTS

4.1 CONDITIONS OF TORRENTIAL ENVIRONMENT

The results of the morphological-hydrographic research for Fourkas stream, the watershed and the hydrographic network of which is given in Fig. 3, are shown in Table 1.

Table 1: Morphometric, hydrographic data of Fourka's stream and its upper watershed (Fig. 2a,b)

Size Symbol Unit	Upper watershed of Fourka	Fourka stream
1. Watershed surface F, Km2	25,30	36,94
2. Water-table perimeter Π, Km	24,01	31,61
3.Watershed hypsometry		
i) maximum elevation Hmax, m	350	350
ii) minimum elevation Hmin, m	65	0
iii) average elevation Hm, m	183	163
4. Watershed hydrography		
i) length of central bed Lκ, Km	8,96	14,45
ii) average slope of central bed JLK, (%)	2,51	2,01
iii) density of hydrographic network (D=SL/F) D,(Km/Km2)	3,28	3,22
5. Watershed relief		
i) average slope of watershed, JF=(Hd*ΣS*100)/F JF, (%)	26,34	26,64
ii) hypsometrical development ΔHi=Hi-Hmin		
α) maximum (ΔHmax=Hmax-Hmin) ΔHmax, m	285,0	350,0
β) average (ΔHm=Hm-Hmin) ΔHm, m	117,6	163,4
iii) degree of relief (Ah =ΔH/SLκ)		
α)maximum (Ahmax =ΔHmax/SLκ) Ahmax	34,46	26,53
β) average (Ahm =ΔHm/SLκ) Ahm	14,22	12,39
iv) round-formity degree		
α) Gravelius index (KF=Π/ΠF=0,282Π/F1/2) KF	1,35	1,47
β) watershed form index (Jf=F/S2F) Jf	0,33	0,28
γ) circularity index (RF=4πF/Π2) RF	0,55	0,46
v) horographic coefficient (CF=H2/1000F)		
α) maximum (CFmax=H2max/1000F) CFmax	4,84	3,32
β) average (CFm=H2m/1000F) CFm	1,32	0,72

The climate data of the stream were taken from the M.S. of Kassandria, a few kilometers away from the center of watershed. The results from the research are shown hereunder in Table 2.

Table 2: Average monthly and average annual air temperatures and rain heights at the M.S. of Kassandria-Halkidiki (period 1978-1990)

I	**F**	**M**	**A**	**M**	**J**	**J**	**A**	**S**	**O**	**N**	**D**	**Year**
Air temperatures ^oC												
7,38	7,92	10,31	14,16	18,85	24,04	26,11	25,59	22,37	17,57	11,82	9,02	16,3
Rain height mm												
60,5	60,4	54,6	40,1	32,3	20,5	20,5	22,1	24,6	77,4	92,3	96,5	601,7

By the results of the geology and vegetation of the under research area (Fig. 4b,c, Tab. 3, Photo 6), it arises that the neo-genic formation is the dominant one whereas the flat area around the central bed is dominated by the alluvial one (Fig. 4b). By Fig. 4c, Photo 6a,b and Table 3 it arises that the dominant species around the Fourka's stream are Aleppo Pine (P. halepensis) forests (59,4%) followed by the farming lands with 11,67km^2 (31,59%). The cultivated soils are vulnerable during the stage of ploughing (Photo 2a) and become an 'easy prey' to strong rainfalls resulting to the large transportation of sandy debris. Thus, it came out the alluvial-borne area downwards Kassandrino village and the sand seashore of Fourka beach. On the contrary, the abandoned fields that were firmed with natural herbaceous vegetation produce very small amounts of sand.



α β γ

Fig. 4abc: a) Hydrological map (the coated bed upwards of the watershed is colored green b) Geological map and c) Vegetation map of watershed of Fourka's stream.

Table 3: Vegetation forms grown in Fourka's stream watershed

Land use	Km^2	%	Land use	Km^2	%	Land use	Km^2	%
Olive orshards	2,36	6,40	Aleppo pine	21,94	59,40	Evergreens-Broadleaves	0,10	0,27
Farms	11,67	31,59	Bare-Barren Soils	0,49	1,33	Settlements	0,37	1.01
Total							36,94	100,00



α b

Photo 6ab: Forest a) evergreens-broadleaves and b) Aleppo pine (P. halepenesis)

4.2 STREAM HYDROLOGY, DEBRIS MATERIAL, ALLUVIAL DEVELOPMENT

The maximum water-supply, stereo-supply and the gathering time *tc*, of the upper and total watershed of Fourka's stream, are as follows (Tables 4, 5).

Table 4: Maximum water-supplies ($maxQ_{100}$) of the upper and total watershed of Fourka's stream (Fig. 4a) by the rational method ($maxQ_{100}=0,278*c*maxi_{100}*F$)

Watershed	Surface F, Km^2	c	$maxi_{100}$ (mm/h)	Maximum water-supply ($maxQ_{100}$) (m^3/s)
Upper	F_1 =25,30	0,453	20,89	66,56
Total	F =36,50	0,428	19,40	84,25

Table 5: Gathering times tc, maximum stereo-supplies ($maxG_{100}$) and water-stereo-supplies {$max(Q+G)_{100}$), of the upper and total watershed of Fourka's stream

Gathering times $tc=[4*(F)^{1/2}+1,5Lk]/0,8(Hm-Hmin)^{1/2}$, maximum stereo-supplies ($maxG_{100}$), and water-stereo-supplies [$max(Q+G)_{100}$], of the upper and total watershed of Fourka's stream

Watershed	F Km^2	H_m (m)	H_{min} (m)	L_k (km)	tc (h)	$maxQ_{100}$ (m^3/s)	Pn	m	Special gravity Yn (t/m^3)	($maxG_{100}$) (m^3/s)	$max(Q+G)_{100}$ (m^3/s)
Upper	25,30	183	65	8,96	3,862	66,56	20	1,01	2,34	7,18	73,74
Total	36,50	163	0,0	20,89	4,502	84,25	20	1,01	2,32	9,17	93,41

By the papers of Pavlidis Th. (Pavlidis Th. 1999a), Gaia S.A. Projects (2008) and Pavlidis V. (Pavlidis V. 2012) and the conducted plotting, the following data in respect of the coated bed, were acquired (Fig. 2ab and 3, Photo 5ab and 7ab):

Total length of coated plotted bed L=9.320m

Covered surface E=214.360m^2

Average thickness of bottom solid-stone-layering Tx = 1,40m

Total bulk of bottom layering (it refers only to the bottom and not the slope) V= E .Tx = 214.360 x 1,40 = 300.104m^3

Average porous stone-layer 32,80% (Pavlidis V. 2012)

Based on the above data, the porous state of the entire wire-stone-layer of the stream, amounts to:

ΣV_{porous}= 300.104m^3 x 0,328 = 98.434,11m^3

Based on the alluvium of a) **$E_{\varepsilon\pi.}$=6.840m^2** (Photo 9b), the coated bed downwards the confluence of the branches Kassandrino S. and the **$E_{\alpha\nu}$=16.250m^2** (Photo 9a) of the non-coated section of Kassandrino S. branch, it arises that the deposited debris for the under consideration 4-year period (01.07.2009 – 31.06.2013), have alluvial a total bulk amounting to:

Bulk of alluviums upwards of the non-coated alluvial bed:

$V_{non\text{-}coated} = E_{\alpha\nu}.x\ h_{non\text{-}coated}$ = 16,250 x 0,34= 5.525,00m^3

Bulk of alluviums in the coated alluvial surface:

$V_{coated} = E_{\varepsilon\pi}$ x h_{coated} = 6.840 x (0,32 x 1,40) = 3.064,32m^3

Total alluvial bulk of a 4-year period:

$\Sigma V=V_{\alpha\nu}+V_{\varepsilon\pi}$=5.525+3.064,32=**8.589,32m^3**

Therefore, the average arrived bulk during the 4-year period 01.07.2009 – 31.06.2013, from the watersheds of the branches Zografitiko S. and Kassandrino S., amounts to:

$Vm_{\text{(4-year period)}}$ = 8.589,32/4= 2.147,33m^3/year

This amount produced by a surface **F=25,30Km^2** (branches Kassandrinos S. And Zografitiko S.), conversed to an average annual deposited load of debris in this location, amounts to: **w=2.147,33/25,30=84,875m^3/Km/year.** This load corresponds to an average annual arrived (not produced) to the measuring location downgrading amount **w_T= 84,875mm/year**.



α β

Photo 7ab: Views of depositions a) of non-coated and b) coated bed. The non-coated bed upwards of the coated one was paved later in 2013-2014).

By the acceptance that the average annual amount of debris of w_T=84,875m^3/Km/year constitutes the average annual amount of the total surface F=36,50Km^2 of the stream's watershed, the average annual arriving and deposited amount of debris into the central bed of the stream, amounts to:

W = w_T x F = 84,875 x 36,50 = 3.097,93m^3/year

By the average annual adducing amount of debris of 2.654,65m^3/year and the total bulk of porous of the wirenet-stone-coated bed which was found to be equal to:

V_{porous}=98.434,11m^3

It arises that the full alluvium of the porous of wirenet-stone-coated central bed of the stream will take place at a time:

T= 98.434,11m^3 / 3.097,93m^3/year = 31,774= 31,8 years

5. CONCLUSIONS, PROPOSALS

Briefly, the results of the research, are as follows:

The Fourka's torrent is considered as the most dangerous stream in the Kassandra peninsula with a rich flooding background. Within the frames of providing anti-flood correction, the entire bed of the stream was paved from the point of Kassandrino up to Fourka Beach at a length **L=9.320m.** A major characteristic of the torrent is the big moving-out sand stereo-supply which contributes to the flooding riskiness of the stream and arriving to the discharge place of the stream that has shaped the Fourka's sandy Beach. A physical phenomenon which constitutes the main cause of the tourist development of the area.

The Fourka Beach is the functional print of two opposite acting mechanisms, one depositional (Fourka stream) and one carrying-away (coastal transporting with S, SE movement). Until the decrease of cultivated lands in 1970, which through the ploughing have provided great amounts of sand that were transported by the stream and deposited on Fourka Beach, the adduction of sand was much bigger than the abduction, with a slightly positive balance, resulting to a very slow but steady increase of the beach. After 1970 and mostly after the coating of the torrent's bed with gabions and

gabion mattresses, the porous of which are much bigger, than the biggest of the average transported sandy debris, has led to the discontinuance of sand movement towards the beach, a process which will last as much as the completion time of gaps of the layer of gabion mattresses. Due to this fact, for that time span in the beach will only act the abducting, carrying-away mechanism, leading to the downgrading of Fourka Beach.

During the 4-year period 01.07.2009 – 30.06.2013, the measured alluvium $\mathbf{V_{4\text{-year period}}=8.589,32m^3}$, after the bed coating, produces an average alluvium $\mathbf{W=2.147,33m^3/year}$. Based on this figure, the full alluvium of the porous of gabions will occur in 32 years. Therefore, only the carrying-away coastal mechanism will be function for this time span **and Fourka beach will be put into a steady downgrading process. As confirmation of the above stated, we report the recent significant loss of Fourka beach westwards of the stream junction.**

To encounter this problem the following are proposed:

The compulsory ploughing of the cultivated lands. This measure, aims at the increase of the produced and incoming, to the central stream bed, debris amount.

The stirring up of sandy beds and slopes of central beds of contributing branches particularly of those closer to Fourka Beach.

The disclosure – stirring up – broadening of slopes of the stream bed nearest to the stream estuary. The broadening, beyond the starting of sand flow towards the beach, will be aiming at the improvement of the anti-flood protection of the area.

The construction of sand-hold projections (Groynes) at the beach which will prevent the abduction of sand from Fourka Beach.

REFERENCES

1. Cadenas Lopez, 1993: ***«Torrent control and streambed stabilization»***, Food and Agriculture Organization of the United Nations, Italy
2. Chow, V.T. (ed.). (1964): *«Handbook of Hydrology»,* New York.
3. Gregory, K.J. and Walling, O. (1983): *«Drainage Basin. Form and Process. A. Geomorphological Approach»,* Fletcher and Son L TD, Norwich. U.K.
4. Horton, R.E. 1945: «Erosional development of streams and their drainage basins: Hydrological Approach to quatitative morphology», **Bull of the Geol. Soc. Am**., 56: 275-370.
5. Kirkby, M.J. and R.P.C. Morgan. 1980: *«Soil erosion»*, John Willey and Sons.
6. Murphy, J., Wallace, O. and Lane, L. (1977). Geomorphic Parameters: Predict Hydrographic Characteristics in the Southwest. **Water Res. BuI. Am. Water. Res. Ass**. vol. 13(1), pp. 25-38.
7. HMGS., I.G.M.R.: Maps of scale 1:50.000: Sheet *"Kassandreia "*
8. Gaia S.A. Projects 2008: «Study of immediate anti-flooding protection works in the area of the stream estuary Fourka-Kassandrino», Thessaloniki
9. Kotoulas D. 2001: «Mountainous Hydronomics, Vol. 1: 'Flowing waters'», Thessaloniki
10. Margaropoulos P. 1963: «The aquatic erosion and the torrential phenomenon». Athens
11. Margaropoulos P. 1964: «Rapport sur la classification des basins torrentiels», FAO/EFC/TORR/64/2.
12. Moulopoulos, Chr. 1968: *«Mountainous Hydronomics»,* Thessaloniki
13. Pavlidis, Th. 1991: «Analysis of the flood action mechanism of Fourka's stream and its correction system under the prism of the recent flood of December 1990» **Scient. Annals of School of Forestry and Nat. Environ**., Vol. ΛΛ/1, No. 24, pp. 664-720.

14. Pavlidis T.V., Emmanouloudis O. A., Rodriguez J.L., Filippidis E. I. "Analysis and Interpretation of the flood Activity Mechanism of the Fourka Chalkidiki Torrent", GREECE/SPAIN
15. Pavlidis Th. 1999a: «Study of utilizing the water dynamics and the debris material of Fourka's stream within the frames of managing the water and flood problems of Kassandreia Municipality, Halkidiki». Thessaloniki. Study implemented for Fourka's community.
16. Pavlidis Th. 1999b: «*Study of correction-delimitation of Fourka's stream*», Thessaloniki. Study implemented for Fourka's community.
17. Pavlidis, Th. 2007: *«Mountainous Hydronomics II».* Thessaloniki.
18. Pavlidis V. 2012: *«Stream corrections at coastal areas within the Greek space: The case of Fourka's stream, Halkidiki*». Thesis submitted to the Faculty of Civil Engineering, Aristotle University, Thessaloniki
19. Tsakiris G. 1995: 'Aquatic Resources, Technical Hydrology', Athens



Environmental hydrology

COMPARISON OF METEOROLOGICAL DROUGHT INDICES IN THESSALY WATER DEPARTMENT, GREECE

T. Karampatakis, L. Vasiliades* and A. Loukas

Laboratory of Hydrology and Aquatic Systems Analysis, Dept. of Civil Engineering, University of Thessaly (UTH), GR- 38334 Volos, Thessaly, Greece

*Corresponding author: e-mail: lvassil@civ.uth.gr, tel : +302421074115

Abstract

In an effort to capture various aspects of drought which contribute to the intensification of the phenomenon, many indices have been suggested, based on one or more hydro-climatic parameters. In this paper the behavior of four meteorological drought indices with different structure is discussed, analyzing the spatial and temporal characteristics of drought in the water department of Thessaly. More specifically the widely used indices: Standardized Precipitation Index (SPI), Standardized Precipitation-Evapotranspiration Index (SPEI), and two modified multivariate indices based on the Multivariate Standardized Drought Index (MSDI), are selected for a comparative regional drought analysis. The first multivariate index is derived combining probabilistically the hydro-climatic variables of precipitation and potential evapotranspiration, – while the second combining the indices SPI and SPEI. The monthly precipitation and temperature data, covering the hydrological period 1960-2002, were used for the calculation of the considered indices at time scales: 1, 3, 6, 9 and 12 months. In order to obtain equal amount of precipitation and temperature data, the lapse rate method is applied, forming 78 meteorological stations. A time-series analysis and a drought classification for all the stations are performed, presenting the main similarities/differences in the behavior of four indices. Additionally, a correlation analysis is conducted, displaying scatter plots and spatial patterns of correlation values for the possible combinations of the examined indices. SPI and SPEI seem to be the most appropriate indices for the detection of drought episodes in our region. Furthermore, it was ascertained that the indices SPI and SPEI are more strongly correlated in the mountainous regions where the influence of the potential evapotranspiration is not so noticeable.

Keywords: Standardized Precipitation Index (SPI), Standardized Precipitation-Evapotranspiration Index (SPEI), Multivariate Drought Indices; Drought Variability, Thessaly Water Department

1. INTRODUCTION

Several meteorological drought indices have been proposed based on the hydro-climatic variable of precipitation. An illustration of this classification is the Standardized Precipitation Index (SPI; McKee et al., 1993) which is acclaimed by an increasing number of scientists around the world and has been recommended by the World Meteorological Organization as the primary tool for monitoring meteorological droughts (WMO 2006). However, in some cases a single variable may not provide adequate information for the assessment of droughts because droughts constitute a complex process associated with multiple variables. Thus, apart from precipitation the parameter of temperature can be included in a meteorological drought assessment. This approach is great significance especially for studies related to climate change, as the indications of climate models for warmer climate conditions in the future can affect considerably the drought characteristics (intensity, duration, frequency, spatial extent) (Sheffield and Wood, 2008; Dai, 2013; Touma et al., 2015). The first attempt was made in 1965 when the Palmer Drought Severity Index (PDSI; Palmer, 1965) was

developed and its original purpose was to identify drought conditions in the crop-producing regions of the United States. Recently, Vicente-Serrano et al. (2010) proposed the Standardized Precipitation Evapotranspiration Index (SPEI; Vicente-Serrano et al., 2010) as an enhanced version of SPI, introducing a simplified mode of water balance concept (Precipitation minus Potential Evapotranspiration) in order to examine the effect of temperature on drought analysis. Finally, according to Hao and AghaKouchak (2013, 2014) it is pointed out that "no of the existing single indices is able to identify all aspects of meteorological, agricultural, and hydrological droughts". Consequently, a new multivariate approach based on the combination of several drought indices and variables should be conducted for an overall drought assessment. In this view, they suggested the Multivariate Standardized Drought Index (MSDI; Hao and AghaKouchak, 2013), which has the capacity to combine the drought information not only from different drought-related variables, but from different drought indices as well. The incorporation of different drought related variables and indices can lead to more reliable and timely findings for the drought characteristics (Hao and AghaKouchak 2013, 2014).

Main scope of this study is to examine the behaviour of four meteorological indices with different structure taking into account the drought-related variables of precipitation and potential evapotranspiration (PET). It should be mentioned that the selection of these indices was encouraged considering their multi-temporal nature and their similar probabilistic procedure. More specifically, the identification of drought events in the water department of Thessaly is attempted using the commonly used index SPI, the more recent index SPEI, and two produced multivariate indices motivated by the new promising index MSDI. It is highlighted that the first produced multivariate model is estimated through constructing the joint distribution function of two meteorological variables (precipitation and PET), while the second it is formed through constructing the joint distribution function of two meteorological drought indices (SPI and SPEI). The major aim of this multivariate synthesis is to extend the properties of MSDI concept, examining different combinations of climate variables-indices from the original index, purposing to obtain two effective meteorological drought measures, which can be used as supplementary tools in drought monitoring process. In order to assess the short and medium term drought conditions, the four indices were calculated at time scales: 1, 3, 6, 9, and 12 months.

2. STUDY AREA – DATABASE

The study area of this research is the water department of Thessaly, Greece. It is located in the central department of the mainland of Greece forming the greatest plain of the country which is also known for the intense agricultural activity. It is surrounded by large mountainous masses, among which Mount Olympus, rising to over than 2800 m, situated at the northern part of the plain. In the west, there is the Pindus mountain range which is approximately 230 km long and reaches a width of over 70 km. Mountains Kissavos and Pelion are located in the east. In the south, there is the Othrys mountain range. The total acreage of the region is 13377 km^2 while the average elevation is estimated at 500 m above sea level. As far as the climate of the area is concerned, two different areas can be distinguished namely the coastal (lowland) eastern side of Thessaly with a Mediterranean climate, which is characterized by warm and dry summers and cold and humid winters, – and the mountainous western side, with a typical continental climate with great temperature variations between summer and winter time. The average precipitation is relatively high in the west, more than 1850 mm, and decreases in the plain region by 400 mm. The main drainage basin of the hydrological department of Thessaly is the basin of the river Pinios which extends across an area of about 9500 km^2. Smaller tributaries are also included in the hydrological department.

The available precipitation and temperature data of the region were provided by the Laboratory of Hydrology and Aquatic Systems Analysis of the University of Thessaly (Department of Civil Engineering) and cover 42 hydrological years, from October 1960 to September 2002. Specifically,

the monthly precipitation data from 78 precipitation stations uniformly distributed over the water department of Thessaly (Figure 1) have been used for the calculation of SPI.

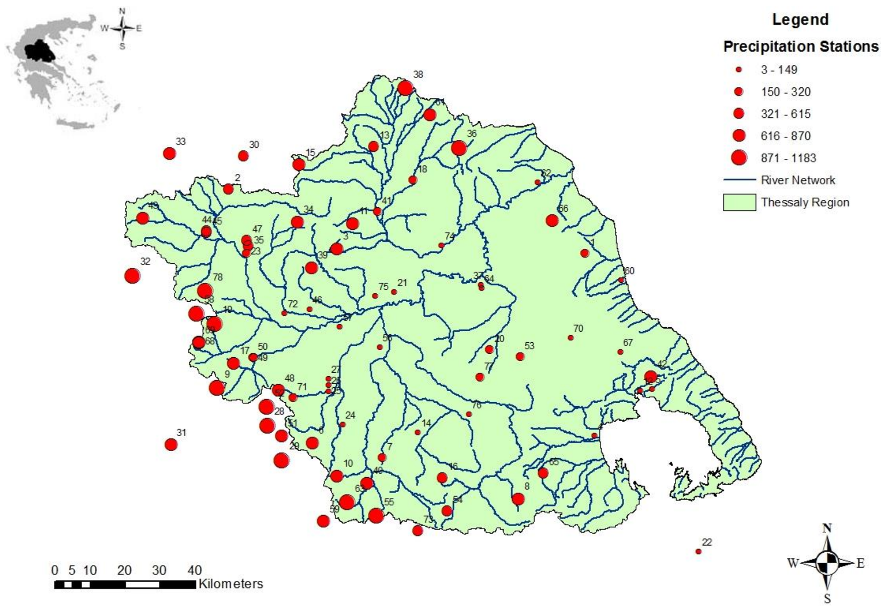


Figure 1: Location and elevation of precipitation stations of Thessaly Water Department

In this project except for precipitation data, the inclusion of temperature data at the same positions of precipitation stations must be considered for the estimation of PET and therefore of SPEI. Monthly temperature data can be derived using the temperature lapse rate method, as there is a limited number of meteorological stations at the desirable locations (locations of precipitation gauges). This method relied on the assumption that temperature decreases linearly with increasing altitude. Based on this assumption, a linear regression line can be fitted to the mean annual temperature data of the available meteorological stations of Thessaly (Figure 2).

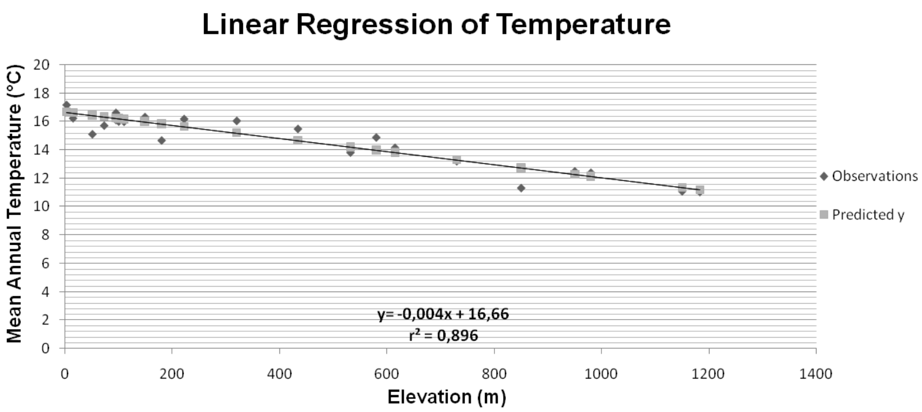


Figure 2: Linear regression of mean annual temperature for 26 meteorological stations in Thessaly

3. METHODOLOGY

The four examined meteorological drought indices of this study are differentiated in their structure, incorporating the drought related variables, precipitation and PET in a unique way, defining the different purpose of their formation on drought assessment. However they share some similar characteristics, as the statistical approach of SPEI and MSDI relied on the tenable advantages of SPI as analyzed by Hayes et al. (1999). Therefore, the four meteorological drought indices can be standardized into normal variables, presenting the dry and the wet events in a similar way ensuring

their interpretability over space and time. Positive values (above the average) of the indices depict the wet conditions while negative indications (below the average) represent the intensity of drought episodes. Furthermore they can be calculated at multiple time scales (1, 3, 6, 9, and 12 months), examining the drought evolution among the various hydrological subsystems. Finally, they are simple in their calculation, as in our case only precipitation and temperature data are required.

The computation of SPI (McKee et al., 1993) involves the accumulation of precipitation records for each station, considering a predefined time step (usually over n months), and their fitting to the gamma probability distribution which is then transformed into the standardized normal distribution with mean 0 and standard deviation 1. The gamma distribution is defined by its frequency or probability density function as:

$$g(x) = \frac{1}{\beta^{\alpha}\Gamma(\alpha)} x^{\alpha-1} e^{-\frac{x}{\beta}} \; for \;\; x > 0 \qquad (1)$$

where α and β stand for shape and scale parameters respectively, x describes the amount of precipitation, and $\Gamma(\alpha)$ is the gamma function.

Since the gamma distribution is undefined for x=0, a modified expression of the gamma cumulative probability can be applied, solving the problem with the possible zero values in our monthly precipitation data.

$$H(x) = q + (1-q)G(x) \qquad (2)$$

where q is the probability of no precipitation and $G(x)$ the cumulative probability of the incomplete gamma function.

The more recently proposed index SPEI (Vicente-Serrano et al., 2010) was developed based on the methodology of SPI, following similar computational processes. Therefore SPEI values can be derived, adapting the accumulated monthly (or weekly) water balance (Precipitation minus Potential Evapotranspiration), into a parametric statistical distribution, taking into account a fixed desired period (time scale).The three parameter Log-logistic has been used for the normalization of SPEI considering that it is possible to have negative values, as the applicability of the index is related with the identification of moisture deficit (Precipitation < PET).The probability density function of a three parameter Log-logistic distributed variable is expressed as:

$$f(x) = \frac{\beta}{\alpha}\left(\frac{x-\gamma}{\alpha}\right)^{\beta-1}\left(1+\left(\frac{x-\gamma}{\alpha}\right)^{\beta}\right)^{-2} \qquad (3)$$

where α, β and γ represent the scale, shape and origin parameters respectively, for the accumulated water balance x, in the range $(\gamma > x < \infty)$.The estimation of monthly PET series has been conducted using the Thornthwaite equation (Thornthwaite, 1948) as it only demands the temperature and the latitudinal coordinate of the location.

The nonparametric method as proposed by Hao and AghaKouchak (2014) has been selected in order to derive two multivariate models based on the available data (precipitation and temperature) of our study area. According to this multivariate approach, a nonparametric empirical method expressed by Weibull (Hirsch, 1981) or by Gringorten (Gringorten, 1963) plotting position formula, can be applied in order to obtain the empirical joint probability of drought-related variables (or indices). Hence, denoting the drought-related variables, precipitation and PET, as two random variables X and Y respectively at a specific time scale, the empirical joint probability of the variables (x_k, y_k) can be calculated as:

$$P(x_k, y_k) = \frac{m_k}{n+1} \quad \text{Weibull (Hirsch, 1981)} \qquad (4)$$

where n is the number of the observation, and m_k is the number of occurrences of the pair $(x_{i,} \, y_i)$ for $x_i \leq x_k$ and $y_i \leq y_{k,}(1 \leq i \leq n)$.

As the empirical joint probability of the drought-related variables, precipitation and PET, has been estimated, the multivariate standardized drought model MSDI(Pr-PET) is formed according to the following equation:

$$MSDI = \Phi^{-1}(P) \quad (5)$$

where φ is the standard normal distribution function. Following the same procedure as described by the equations (4) and (5) for the drought indices SPI and SPEI, the second multivariate standardized model MSDI(SPI-SPEI) is derived.

In this study, a correlation analysis, is performed among the indices: SPI, SPEI, MSDI(Pr-PET) and MSDI(SPI-SPEI), at time scales: 1, 3, 6, 9 and 12. Main purpose of this analysis is to conduct a more integrated comparison among the indices providing scatter plots with their possible combinations at all time scales. The Pearson correlation coefficient r has been used as a statistical measure in order to express the linear dependence among them. Furthermore, the Ordinary Kriging (OK) as an effective interpolation method (Best Linear Unbiased Estimator, BLUE) Isaaks and Srivastava (1989) has been selected, providing a spatial insight of these correlations in the water department of Thessaly, at all time scales. Ordinary Kriging, as a geostatistical technique, differs from other spatial interpolation methods such as IDW (Inverse Distance Weighting) method, considering not only the distance between the sample points and the prediction location, but also the spatial covariance structure (autocorrelation) of the sample points.

A general equation of Ordinary Kriging method can be determined as:

$$\hat{z}(x_0) = \frac{1}{2n}\sum_{i=1}^{n} \lambda_i \, z(x_\mathrm{i}) \quad (6)$$

where $\hat{z}(x_0)$ is the value to be estimated at location x_0, $z(x_\mathrm{i})$ is the measured value at station x_i, λ_i represents the weight of the measured value $z(x_\mathrm{i})$ at the i^{th} station, and n is the number of measured values.The spatial dependence (autocorrelation) of the sample points is determined by fitting an experimental semivariogram. An experimental semivariogram $\gamma(\mathrm{h})$ can be defined as half the average squared difference between two neighbouring points:$\mathrm{Z}(x_\mathrm{i})$, $\mathrm{Z}(x_\mathrm{i} + \mathrm{h})$, separated by the distance h (Goovaerts, 2000):

$$\hat{\gamma}(\mathrm{h}) = \frac{1}{2n} \sum_{i=1}^{n} [\mathrm{Z}(x_\mathrm{i}) - \mathrm{Z}(x_\mathrm{i} + \mathrm{h})]^2 \quad (7)$$

4. RESULTS AND DISCUSSION

The results from station-2 which is located in the northwest side of Thessaly (Figure 1), will be used indicatively for illustration purposes, analyzing the basic similarities/differences of SPI, SPEI, MSDI(Pr-PET) and MSDI(SPI-SPEI) series at the examined time scales (1, 3, 6, 9 and 12). It should be pointed out that it was considered appropriate a shorter period of time than the initial to be used, in order to achieve best clarification of the results. Thus, the presentation of the results is conducted during the hydrological period: October 1982 - September 2002. Concerning the results of station-2 (Figure 3), the monthly patterns of indices SPI, SPEI, MSDI(SPI-SPEI) seem to be quite similar at all time scales. Therefore, they can be characterized as 3 highly correlated indices, providing a similar behavior for the short and medium term drought conditions of the station. On the contrary, the MSDI(Pr-PET), differs significantly from the other indices and appears to be biased in negative values at all time scales. Regarding the results of the widely used indices SPI, SPEI, and the outcomes of the research of Loukas and Vasiliades (2004), which were based on the average SPI values for the period of time from 1960 to 1993 in Thessaly, the results of the index MSDI(Pr-PET) can be characterized as overrated and abnormal for the region, showing several prolonged drought episodes.

Examining the effectiveness of the measures SPI, SPEI and MSDI(SPI-SPEI) in detecting the extreme drought events (≤-2.0), of station-2, SPI and SPEI seem to be the more capable indices to capture these extreme conditions, while the multivariate model MSDI(SPI-SPEI) limited to identify only

severe drought episodes (-1.5 to -1.99), at all time scales. Specifically, at time scale (1), the most extreme drought episode has been determined by the SPEI index (mid of 90s). As the time scale increases (time scales: 3, 6, 9 and 12) and more smoothed patterns of temporal variability can be derived, the most extreme drought events have been identified by the SPI index (early of 90s). It is essential to underline once more, that the results above are suggestive and consequently the last indication about the indices SPI and SPEI is distinctive for station-2, and does not represent the results of the rest stations. For example, in stations where remarkable upward trends of temperature were recorded, the most severe drought episodes in longer time scales have been identified by the SPEI index.

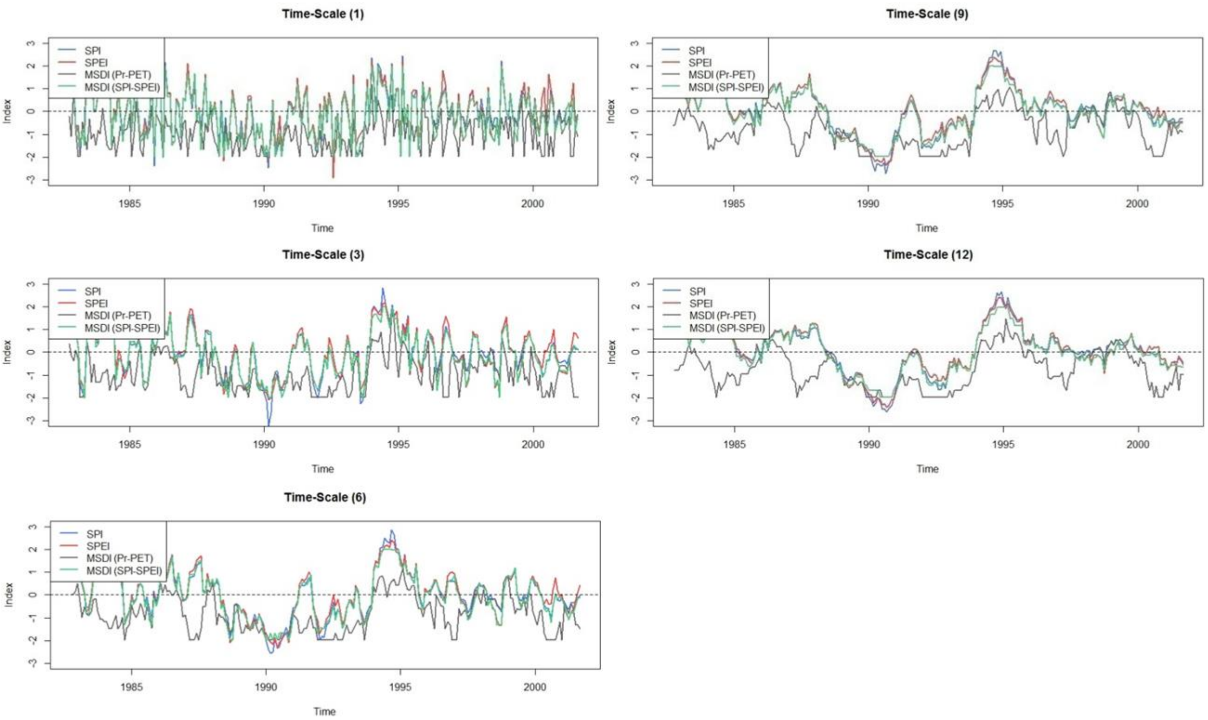


Figure 3: Station-2 (Direction:Northwest, Elevation:586m). Time-series plots of drought indices SPI (blue line), SPEI (red line), MSDI(Pr-PET) (grey line), MSDI(SPI-SPEI) (green line), for 20 hydrological years (October 1982-September2002), at time scales: 1, 3, 6, 9 and 12 months.

A drought classification for 42 hydrological years has been performed, taking into account the results of four indices, for all the stations, at all time scales. This classification involves the categories: Extreme Drought (≤-2.0), Severe Drought (-1.5 to -1.99), Moderate Drought (-1.0 to -1.49), Normal (-0.99 to 0.99), Moderately Wet (1.0 to 1.49), Severely Wet (1.5 to 1.99) and Extremely Wet (≥2.0) conditions. In Table 2 are provided suggestively, the percentages of drought and rainfall events as detected by the four examined indices, at all time scales, for the station-2. Analyzing the outcomes related to the drought episodes of station-2, the similar behavior of indices SPI and SPEI can be ascertained in this study for a second time. More specifically, the indices SPI and SPEI seem to have similar results in each of the three categories of drought (slightly more increased are the percentages of SPEI in the categories Moderate and Severe Drought, in most of the stations). In contrast, the MSDI(Pr-PET) differs significantly in the number of moderate and severe drought events compared to the other indices, accumulating higher rates in these categories. Moreover, it fails to detect extreme drought episodes at all time scales (similar behavior at all stations). Therefore, the choice of the variables of precipitation and PET for the formation of a competent drought index through a joint distribution concept, does not infer the desirable results. Finally, the MSDI(SPI-SPEI) index shows similar outcomes compared with SPEI index in the categories of Moderate Drought and Severe Drought. Furthermore, it should be highlighted that in this case as well, the weakness of the

multivariate model to capture the extreme drought conditions of the station is obvious (also 0 values at all stations in this category).

Table 2: Station-2 (Direction: Northwest, Elevation: 586m). Drought classification for 42 hydrological years (October 1960 - September 2002), providing the percentages of drought events for indices: SPI, SPEI, MSDI(Pr PET), MSDI(SPI-SPEI), at time scales:1, 3, 6, 9 and 12 months.

Time-Scale (1)				
	SPI%	SPEI%	MSDI(Pr-PET)%	MSDI(SPI-SPEI)%
Extremely Wet	2	2	0	0
Severely Wet	5	6	0	4
Moderately Wet	8	11	2	9
Normal	71	64	53	68
Moderate Drought	9	12	23	13
Severe Drought	4	4	22	6
Extreme Drought	1	1	0	0
Time-Scale (3)				
	SPI%	SPEI%	MSDI(Pr-PET)%	MSDI(SPI-SPEI)%
Extremely Wet	1	1	0	0
Severely Wet	7	8	0	4
Moderately Wet	6	7	1	9
Normal	71	66	55	70
Moderate Drought	8	12	22	11
Severe Drought	4	5	22	6
Extreme Drought	3	1	0	0
Time-Scale (6)				
	SPI%	SPEI%	MSDI(Pr-PET)%	MSDI(SPI-SPEI)%
Extremely Wet	3	2	0	0
Severely Wet	4	6	0	4
Moderately Wet	7	8	1	9
Normal	72	69	55	69
Moderate Drought	7	8	24	12
Severe Drought	4	5	20	6
Extreme Drought	3	2	0	0
Time-Scale (9)				
	SPI%	SPEI%	MSDI(Pr-PET)%	MSDI(SPI-SPEI)%
Extremely Wet	3	2	0	0
Severely Wet	5	6	0	4
Moderately Wet	6	7	1	9
Normal	72	69	55	69
Moderate Drought	7	10	25	13
Severe Drought	3	3	19	5
Extreme Drought	4	3	0	0
Time-Scale (12)				
	SPI%	SPEI%	MSDI(Pr-PET)%	MSDI(SPI-SPEI)%
Extremely Wet	3	2	0	0
Severely Wet	5	7	0	4
Moderately Wet	6	6	1	10
Normal	72	70	55	70
Moderate Drought	8	9	27	11
Severe Drought	2	3	17	5
Extreme Drought	4	3	0	0

In Figure 4, the scatter plots among the indices of station-2 (Northwest) are indicatively presented. Similar results have been observed at all time scales for the 78 stations of the region. According to the results of station-2, the standardized indices SPI and SPEI, appear significantly correlated at all time scales. Furthermore, it is observed that as the time scale increases, the correlation between the indices SPI and SPEI becomes stronger and therefore a perfect correlation can be accomplished. This is reasonable, as in longer time scales the effect of PET is limited considerably, while for the parameter of precipitation this is no true. Concerning the results of the MSDI(Pr-PET), the unconformity of the multivariate model with the other indices can be determined. Specifically, considerably lower correlation values (moderately to extremely low for most of the stations) compared to the other indices at all time scales, are presented for all the possible combinations of the model, indicating that the MSDI(Pr-PET) differs significantly from the indices SPI, SPEI and MSDI(SPI-SPEI). The small number of correlated observations as was observed for several stations, in each pair of MSDI(Pr-PET), can be explained by the tendency of model to approach many negative values as described in subsection 4.1. Finally, the MSDI(SPI-SPEI) appears to be notably correlated

with the indices SPI and SPEI, at all time scales. This can be explained by the fact that the multivariate model has been structured, combining the drought information of two strong interrelated indices (SPI and SPEI), ensuring highly correlated values for the pairs, MSDI(SPI-SPEI):SPI and MSDI(SPI-SPEI):SPEI.

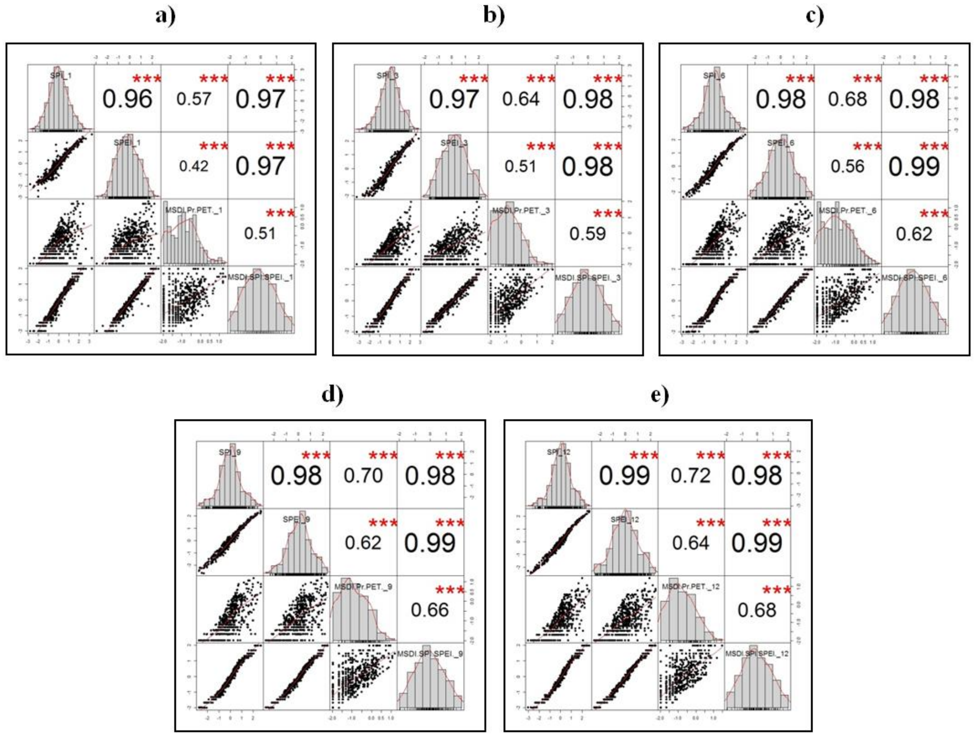


Figure 4: Cross correlation among the indices: SPI, ,SPEI, MSDI(Pr-PET), MSDI(SPI-SPEI) for time scales: (a) 1-month, (b) 3-month, (c) 6-month, (d) 9-month, and (e) 12-month

Subsequently, the spatiotemporal correlation distribution for each pair of the analyzed indices will be discussed. Figure 5a shows the spatial patterns of Thessaly between SPI and SPEI. The results suggest a strong correlation between these indices at all time scales ($r \geq 0.75$), as expected. A remarkable characteristic of these patterns is that the western region which is characterized as mountainous seems to be more correlated than the central and eastern sides (plain areas) where many stations with lower elevation are located (Figure 1). This can be explained by the fact that the effect of PET in mountainous regions compared to the plain areas is lower, signifying that the indices SPI and SPEI respond mainly to the fluctuations of precipitation, and therefore more correlated values can be obtained for them. Paulo et al. (2012) presented a similar behavior for both indices at time scales (9) and (12), comparing humid and semiarid environments in Portugal. Furthermore, it is important to reiterate again that the PET variability decreases in longer time scales. Hence, the most correlated patterns for these indices have been derived at time scales 6, 9, and 12, while in shorter time scales, weaker correlation values have been extracted, verifying the above claim. It should be noted that the correlations values at time scales: 9 and 12 compared to the 6-month timescale, appeared slightly lower. According to Vicente-Serrano et al. (2010) the correlation between the two indices may decrease in longer time scales when there are noticeable temporal trends in temperature. Regarding the results of the MSDI(SPI-SPEI):MSDI(Pr-PET), moderately to extremely low correlation values predominate in all maps, at all time scales ($r \leq 0.72$) (Figure 5b). The limited number of correlated observations between the two multivariate models can be explained by the fact, that the MSDI(SPI-SPEI) seems to be in accordance (similar patterns) with the widely used indices SPI and SPEI, while the second model which is based on the combination of two hydro-climatic variables (precipitation, PET) is differentiated considerably.

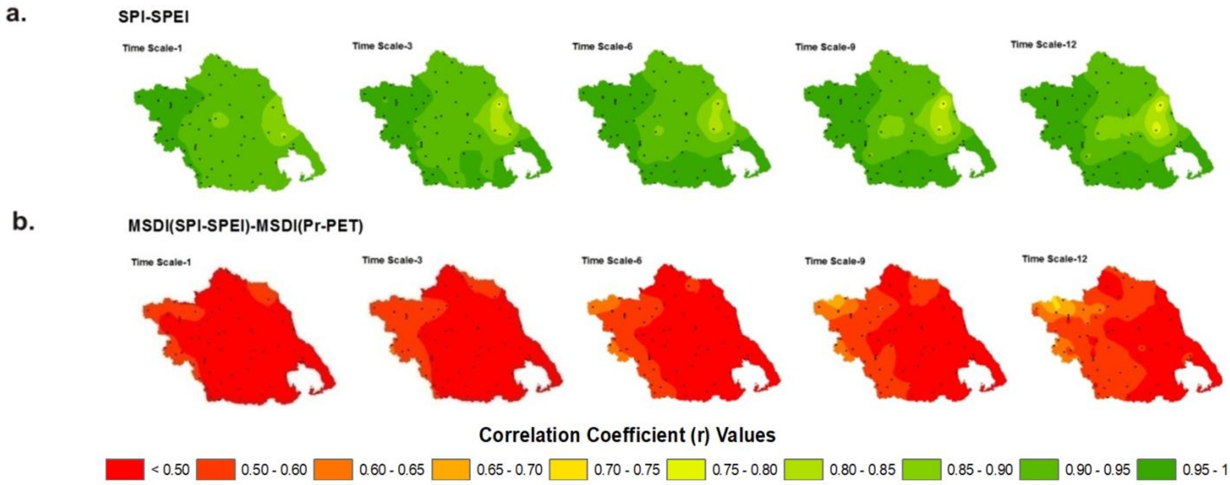


Figure 5: Spatial patterns of Thessaly, providing the correlation coefficient values between the indices: a) SPI-SPEI, b) MSDI(SPI-SPEI)-MSDI(Pr-PET), at all time scales (1, 3, 6, 9, 12 months)

However, it is notable to mention that the MSDI(SPI-SPEI) seems to response slightly better with the SPEI index, indicating more correlated values in northern and eastern regions. The highest correlated patterns for the two observed pairs have been detected at longer time scales (9-month and 12-month). Examining the correlation strength of the multivariate model MSDI(Pr-PET) with the indices SPI and SPEI, moderately to extremely low correlation values seem to prevail in both cases, at all time scales (a: $r \leq 0.72$, b: $r \leq 0.67$) for all the stations in the water department of Thessaly.

5. CONCLUSIONS

The main objective of this study was to examine the effectiveness of four meteorological drought indices with different structure, detecting the drought events in the water department of Thessaly. Specifically, the recommended index SPI, its increased version SPEI, and two multivariate models which combine probabilistically two hydro-climatic variables (precipitation and PET) and two drought indices (SPI and SPEI) respectively, have been used for the drought analysis of the area. The time-series analysis and the drought classification for each station showed that the indices SPI and SPEI represent the most suitable measures for the drought monitoring of the region, appearing similar patterns and similar rates in each category of drought events. Small differences between them have been identified in stations where significant increased temperature values were noted, strengthening the ability of SPEI index in the detection of the most severe drought events relative to SPI. Examining the results of the two multivariate models, the MSDI(Pr-PET) appeared to be biased in negative values, overestimating the number of moderate and severe drought episodes of the region compared to the other indices. On the other hand, the second multivariate model MSDI(SPI-SPEI) was found to be in consistency with the widely used indices SPI and SPEI, displaying similar patterns at all time scales. Furthermore, it was shown the weakness of the two produced multivariate indices to determine the extreme drought conditions of the region. A more comprehensive comparison among the indices was conducted examining their linear dependence, and providing the spatiotemporal distribution of correlation values, for all the possible combinations of the indices. The results suggested a strong correlation between SPI and SPEI at all time scales. Also the discordance of MSDI(Pr-PET) with the other indices was confirmed again presenting in several stations moderately to extremely low correlation values, while the second multivariate model appeared highly correlated with the interrelated indices SPI and SPEI. Moreover, it was observed that in mountainous areas (west side) where the effect of potential evapotranspiration it is not significant, the indices SPI and SPEI appeared to have more correlated coefficient values compared to the plain areas (central side). This means that the two indices in high-altitude regions respond mainly to the variations of precipitation. Additionally,

it should be noted that the weakest correlation values were presented at time scales: 1 and 3, indicating the importance of PET in the short term drought conditions.

References

1. Dai A. (2013). 'Increasing drought under global warming in observations and models'. **Nature Climate Change**, 3, pp. 52-58.
2. Goovaerts P. (2000). 'Geostatistical approaches for incorporating elevation into the spatial interpolation of rainfall'. **Journal of Hydrology**, 228(1), pp. 113-129.
3. Gringorten I.I. (1963). 'A plotting rule for extreme probability paper'. **Journal of Geophysical Research**, 68(3), pp. 813-814.
4. Hao Z. and A. AghaKouchak. (2013). 'Multivariate standardized drought index: a parametric multi-index model'. **Advances in Water Resources**, 57, pp. 12-18.
5. Hao Z. and A. AghaKouchak. (2014). 'A nonparametric multivariate multi-index drought monitoring framework'. **Journal of Hydrometeorology**, 15(1), pp. 89-101.
6. Hayes M.J., M.D. Svoboda, D.A. Wilhite, and O.V. Vanyarkho. (1999). 'Monitoring the 1996 drought using the standardized precipitation index'. **Bulletin of the American Meteorological Society**, 80, pp. 429-438.
7. Isaaks E.H. and R.M. Srivastava. (1989). 'An introduction to applied geostatisics'. **Oxford University Press**, New York.
8. Loukas A. and L. Vasiliades. (2004). 'Probabilistic analysis of drought spatiotemporal characteristics in Thessaly region, Greece'. **Natural Hazards and Earth System Science**, 4(5/6), pp. 719-731.
9. McKee T.B., N.J. Doesken and J. Kleist. (1993). 'The relationship of drought frequency and duration to time scales'. *Proceedings of the 8th Conference on Applied Climatology*, 17–22 January, Anaheim, CA, American Meterological Society, Boston, MA, pp. 179–184.
10. Palmer W.C. (1965). 'Meteorological drought'. **Weather Bureau Research Paper No 45**, US Department of Commerce, Washington, DC.
11. Paulo A., R. Rosa, and L. Pereira. (2012). 'Climate trends and behaviour of drought indices based on precipitation and evapotranspiration in Portugal'. **Natural Hazards and Earth Systems Sciences**, 12 pp. 1481-1491.
12. Shieffield J. and E.F. Wood. (2008). 'Projected changes in drought occurred under future global warming from multi-model, multi-scenario, IPCC AR4 simulations'. **Climate Dynamics**, 31, pp. 79-105.
13. Thornthwaite C.W. (1948). 'An approach toward a rational classification of climate'. **Geographical Review**, 38(1), pp.55-94.
14. Touma D., M. Ashfaq, M.A. Nayak, S.C. Kao, and N.S. Diffenbaugh. (2015). 'A multi-model and multi-index evaluation of drought characteristics in the 21st century'. **Journal of Hydrology**, 526, pp.196-207.
15. Vicente-Serrano S.M., S. Beguería and J.I. López-Moreno. (2010). 'A multiscalar drought index sensitive to global warming: The Standardized Precipitation Evapotranspiration Index'. **Journal of Climate**, 23(7), pp.1696-1718.
16. WMO. (2006). 'Drought monitoring and early warning: concepts, progress and future challenges'. **WMO-No. 1006**, World Meteorological Organization, Geneva, Switzerland.

RAINFALL TEMPORAL DISTRIBUTION IN THRACE BY MEANS OF AN UNSUPERVISED MACHINE LEARNING METHOD

K. Vantas, E. Sidiropoulos* and M. Vafeiadis

Faculty of Engineering Aristotle University of Thessaloniki, GR- 54124 Thessaloniki, Macedonia, Greece

*Corresponding author e-mail: nontas@topo.auth.gr

Abstract

An unsupervised method that utilizes a combination of statistical and machine learning techniques is presented in order to classify statistically independent rainstorm events and create a limited number of design hyetographs for the Water Division of Thrace in Greece. The whole process includes the necessary steps from importing raw precipitation time series data to producing the initially unknown optimal number of representative design hyetographs. These hyetographs can be used for stochastic simulation, water resources planning, water quality assessment and global change studying. The present type of analysis is applied for the first time on data from a Greek region and, in addition, it presents certain characteristics of a more general applicability. Namely, the method employed is fully unsupervised, as no empirical knowledge of local rainfalls is implicated or any arbitrary introduction of quartiles for grouping. Also, the critical time duration of no precipitation between rainstorm events is not defined in advance, as is the case in the pertinent literature.

Keywords: Rainfall temporal distribution; design hyetographs; unsupervised machine learning; hierarchical clustering; Principal Components Analysis

1. INTRODUCTION

Knowledge about the temporal distribution of rainfall is essential in current methods of water resources management such as drainage design, erosion control, water quality assessment and global change studies. A typical methodology includes the determination of total duration and height of rainfall and disaggregation of this height using a temporal pattern that represents the expected internal rainfall structure, the design hyetograph (DH). Veneciano and Villani (1999) provided categorization of methods for the production of design hyetographs, distinguishing four types. The first two methods are based on intensity-duration-frequency curves, the third method is based on standardized profiles derived from rainfall records and the last method relies on stochastic rainfall models via simulation. The first three methods are used more frequently.

Huff (1967) presented a probabilistic method, in which storm data are classified using the quartile where the maximum intensity occurs. More details about the development and utility of Huff's curves in disaggregation and stochastic simulation can be found in the literature (Bonta and Rao, 1987; Bonta and Shahalam, 2003; Bonta, 2004a, 2004b; Vandenberghe et al., 2010). A necessary step prior to the construction of Huff's curves is the extraction of individual rainstorm events from precipitation time series. Huff used a six-hour fixed Critical time Duration (CD) of no precipitation to separate these events, and many researchers followed the same approach (Loukas and Quick, 1996; Williams-Sether et al., 2004; Azli and Rao, 2010; Dolšak et al., 2016), although Bonta (2001) showed that CD has

seasonal variability. The determination of rainfall temporal distribution is dealt with in this paper by means of machine learning methods.

Applications of machine learning using hydro-meteorological data, in general, has been dealt within the literature, in terms of supervised methods trained on big datasets, such as infilling erosivity values (Vantas and Sidiropoulos, 2017) or to create more accurate models than widely used formulae, such as the flow velocity prediction (Kitsikoudis et al., 2015). The use of unsupervised methods in relation to the special issue of temporal distribution of rainfall is scarce. Self-organized maps have been applied to a small data-set to estimate design storms (Lin and Wu, 2007) and k-means clustering has been used to create a predefined number of rainfall patterns (Nojumuddin and Yusop, 2015).

This paper presents an original, controlled, fully reproducible, unsupervised method that produces automatically and objectively the optimal number of DHs using precipitation records. This method comprises of the following steps: a) Raw precipitation data is cleaned from noise and errors. b) CD is determined on the basis of a Poisson process hypothesis. c) A temporal model of CD is constructed with the above rainfall data. d) Unitless Cumulative Hyetographs (UCH) are compiled and Principal Components Analysis (PCA) is applied to the UCH's. e) Agglomerative hierarchical clustering is applied on the principal components (HCPC). f) The number of clusters is determined by repetitive statistical comparisons between the centers of the clusters already produced at the previous steps. g) Finally, a limited number of DHs is produced that represents the rainstorm records.

2. MATERIAL AND METHODS

2.1 Study area and Dataset

The study region, located to the north-east Greece (Fig 1.), extends to an area of 11,243 km^2 that covers the Water Division of Thrace. It is delimited by the boundaries of Greece, Bulgaria and Turkey on the north and east, by the Thracian Sea on the south and by the watershed of Nestos River on the west.

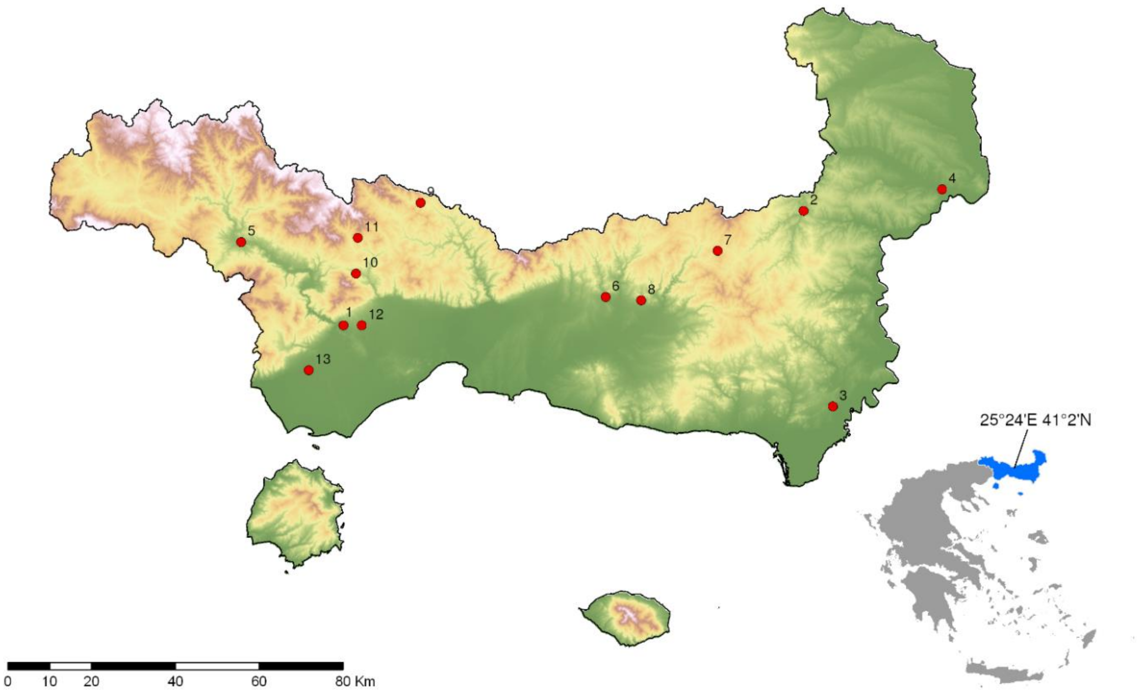


Figure 1: Location of the study area and the 13 meteorological stations from the Greek National Databank for Hydro-meteorological Information.

The climate is predominantly Mediterranean and annual rainfall ranges from 500 mm in coastal and insular areas to 1000 mm in the northern mountainous areas (Ministry of Environment and Energy, 2013). The data utilized in the analysis was taken from the Greek National Databank for Hydro-

meteorological Information (Vafeiadis et al., 1994) and came from 13 meteorological stations. The data coverage was 37%, on average (Table 1). The time series comprised a total of 413 years of pluviograph records with a time step of 30 minutes for the time period from 1956 to 1997. The time series rainfall records were checked for consistency and errors which were: a) There were repetitive values, where the same rainfall was recorded over a long-time period, and these were set to zero, b) there were records of aggregated values, where the time step was larger than 30 min, and these were removed, c) there were records where the time step was 5 min and these where aggregated to 30 min, d) probably due to the initial digitization of the pluviometers' bands, there were values near zero ≪ 0.01 mm) which were set to zero.

Table 1: Meteorological stations location, pluviograph records data coverage and duration.

	ID	Name	Lat (°)	Long (°)	Elevation (m)	Data Length (yr)	From	To	Data Coverage
1	200249	TOXOTES	41.09	24.79	75	41	1956	1997	62%
2	200259	MIKRO DEREIO	41.32	26.10	116	24	1973	1997	63%
3	200260	FERRES	40.90	26.17	43	35	1962	1997	56%
4	200263	DIDYMOTEIXO	41.35	26.50	25	41	1955	1996	62%
5	200311	PARANESTI	41.27	24.50	122	36	1960	1996	65%
6	500250	GRATINI	41.14	25.53	120	31	1965	1996	21%
7	500251	KECHROS	41.23	25.86	700	31	1965	1996	20%
8	500253	MIKRA KSIDIA	41.13	25.64	70	31	1965	1996	25%
9	500262	THERMES	41.35	25.01	440	31	1965	1996	21%
10	500265	GERAKAS	41.20	24.83	308	31	1965	1996	26%
11	500267	ORAIO	41.27	24.83	656	31	1965	1996	18%
12	500272	SEMELH	41.09	24.84	65	24	1968	1992	21%
13	500273	CHRYSOUPOLI	40.99	24.69	15	26	1966	1992	16%

2.2 Storm identification

A Poisson process hypothesis is assumed for the division of the precipitation time series to statistically-independent rainstorm events, in which: a) the events' interarrival times t_α that come from the same month are distributed exponentially, b) the events are separated by a monthly, constant, minimum Critical time Duration of no precipitation, CD, and c) there is a seasonal pattern for CD in the area of interest. The probability density function of t_α is (Restrepo-Posada and Eagleson, 1982):

$$f(t_a) = \omega \cdot e^{-\omega \cdot t_\alpha}, \quad t_a \geq 0 \quad (1)$$

where ω is the average storm arrival rate and:

$$t_a = t_r + t_b \quad (2)$$

where t_r is the storm duration and t_b is the dry time between rainstorms. The estimation of CD is based on an iterative procedure of statistical tests where inter-month data per station are used to ensure homogeneity (Koutsoyiannis and Xanthopoulos, 1990). In Algorithm 1, Appendix, a vector of test CD values is used to compute t_α values and $\widehat{\omega}$ is estimated from this sample of values. Then a non-parametric bootstrap method (Babu and Rao, 2004) that utilizes the one-sample Kolmogorov-Smirnov test (William, 1971) is applied to test the goodness-of-fit, only if the sample size is moderate to large (i.e. ≥ 50), because the data suffer from significant proportions of missing values. Finally, a

temporal, sinusoidal model for the Water Division's CD values per month is fitted (Equation 4, Algorithm 1).

2.3 Development of Unitless Cumulative Hyetographs and Principal Components Analysis

The rainstorms are extracted from the dataset using the monthly CD values obtained from the fitted model of Algorithm 1. The general approach given by Bonta (2004) is followed and only the events with duration greater than 3 hours and cumulative rainfall greater than 12.7 mm are used in the analysis. The hyetographs of the rainstorms that meet these criteria are transformed to unitless form in which a) the time expresses the percentage of the rainstorm duration and b) the cumulative rainfall expresses the percentage of total rainstorm height. Because the UCHs' vectors in this form have variable length, linear interpolation is applied to compute the unitless cumulative rainfall for every 1% of unitless time values. Finally, a matrix of UCHs, $\boldsymbol{U}$ is produced with the values of unitless cumulative rainfall, with every row representing the rainstorm and every column the unitless time values.

Because the time variables (i.e. the m columns of the $\boldsymbol{U}$ matrix) are highly correlated, Principal Component Analysis (PCA, Pearson, 1901) is applied to reduce the dimensionality of the data to a few dimensions. The number of dimensions to retain is determined using the proportion of total variance of the data explained (Jolliffe, 1986). In this analysis this level is set to 99.5%, to ensure that almost all the information from UCHs will be preserved.

2.4 Clustering Analysis

The Hopkins index, H (Lawson and Jurs, 1990), for clustering tendency is applied, because all the clustering algorithms can return clusters even if there was no structure in the $\boldsymbol{U}$ matrix. The computed value of H was 0.88, thus it indicates clustering tendency at the 90% confidence level (Han et al., 2011). The clustering method applied is Hierarchical Clustering on Principal Components (HCPC), using Ward's minimum variance criterion that minimizes the total within-cluster variance (Ward, 1963). This criterion was utilized because it is based on the minimum variance as is PCA (Husson et. al, 2010). The result is a tree-based representation of the UCHs.

The number of clusters is selected from the produced hierarchical tree using the top-down iterative Algorithm 2, Appendix. At each step of the iteration the dendrogram is cut into different groups of UCHs. The center of each group represents a different design hyetograph and these hyetographs, for all possible pairs, are tested if are drawn from the same distribution using the two-sample Kolmogorov-Smirnov test (William, 1971). Because of the multiple pairwise tests, the p-values that resulted are adjusted using the Benjamini and Hochberg method (Benjamini and Hochberg, 1995), which controls the false discovery rate. If any of the produced design hyetographs' p-values is not smaller than a predefined significance level α, the procedure stops and the optimal number of clusters is found. Silhouette analysis (Rousseeuw, 1987) was applied to validate the internal structure of clustering.

3. RESULTS

The relation between the p-values and CD-values was found to have a global maximum for every station and month, which is a desirable feature of Algorithm 1. The fitted monthly sinusoidal model of CD shows a temporal variation during summer months, with an average value of 9 hours, while for the rest of the year the same quantity averages 6.5 hours. Using the calculated CD-values a population of 1,622 out of 25,377 extracted rainstorms met the criteria of minimum duration and cumulative height. From PCA it is concluded that using only the first two dimensions explains 78.5% of total variance and the first 15 explains 99.5%. The application of Algorithm 2 identifies four clusters and some of their statistics are presented in Table 2. The percentiles' values of the DHs are given in Table 3. The first cluster has the highest variance in monthly occurrence, and the highest average value of maximum 30 min duration's intensity. In Figure 2 the clusters' 10th, 50th and 90th

percentiles are shown with the UCHs that belong to them and in Figure 3 the clusters' monthly occurrence.

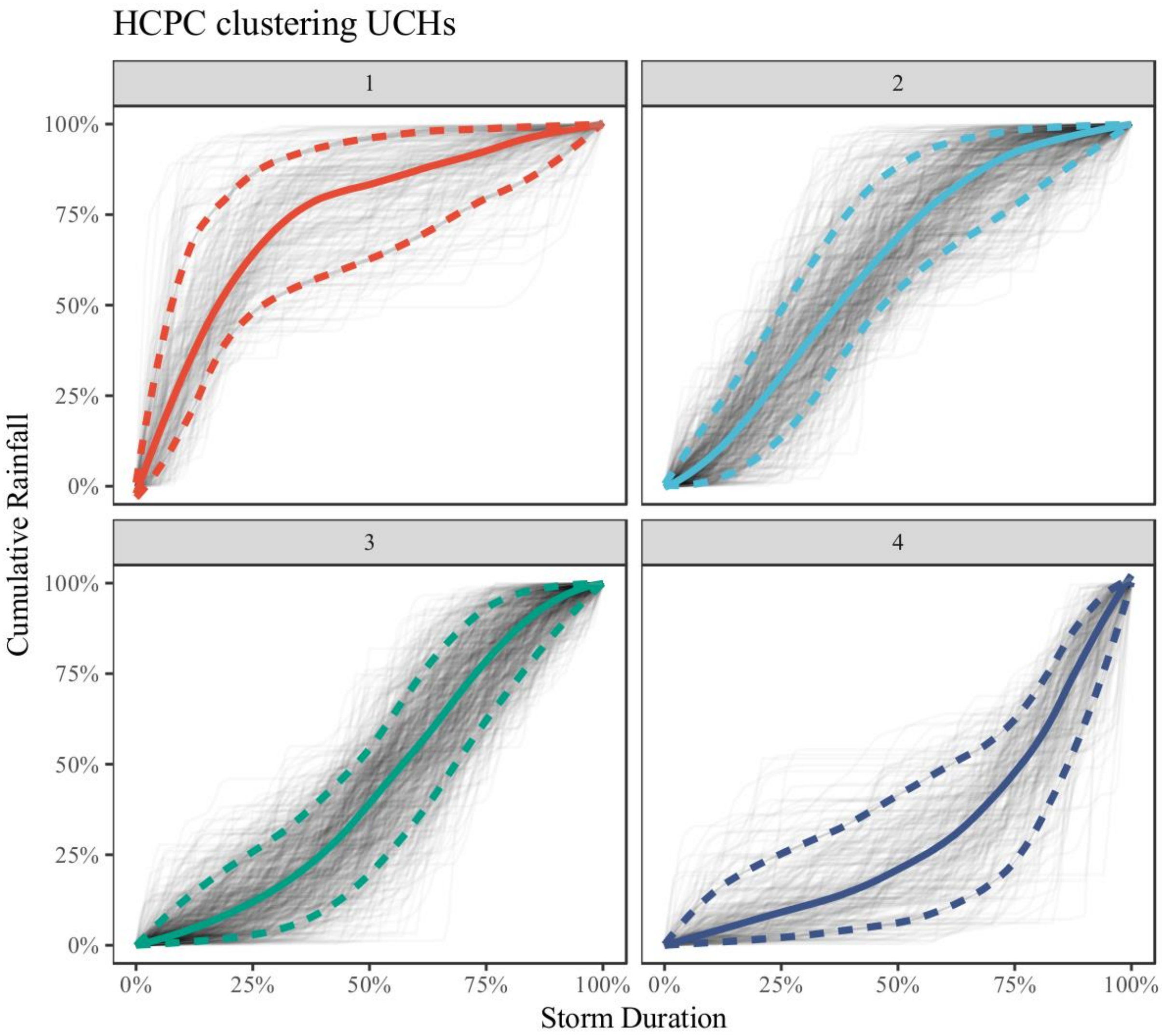


Figure 2: Results from Algorithm 2. At the top the 10th, 50th and 90th-percentiles dimensionless hyetographs curves derived from the four identified clusters. With grey lines are shown the UCHs of each cluster.

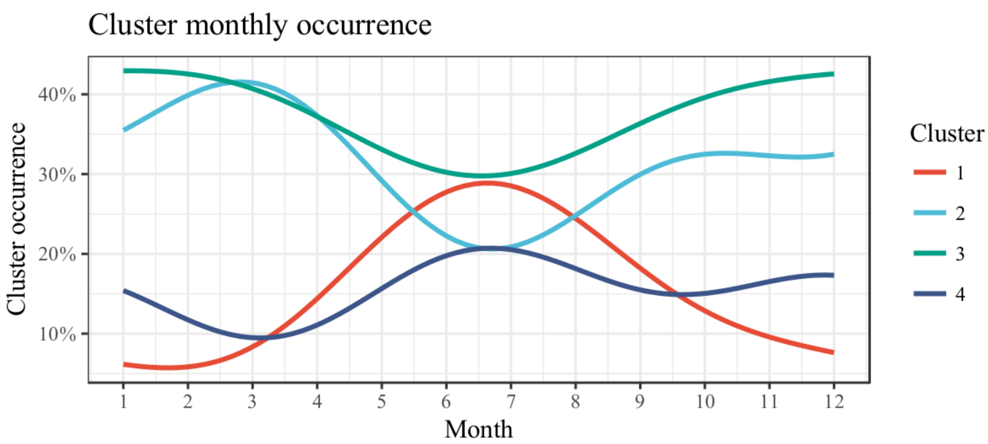


Figure 3: The plot presents the variability of clusters' monthly occurrence.

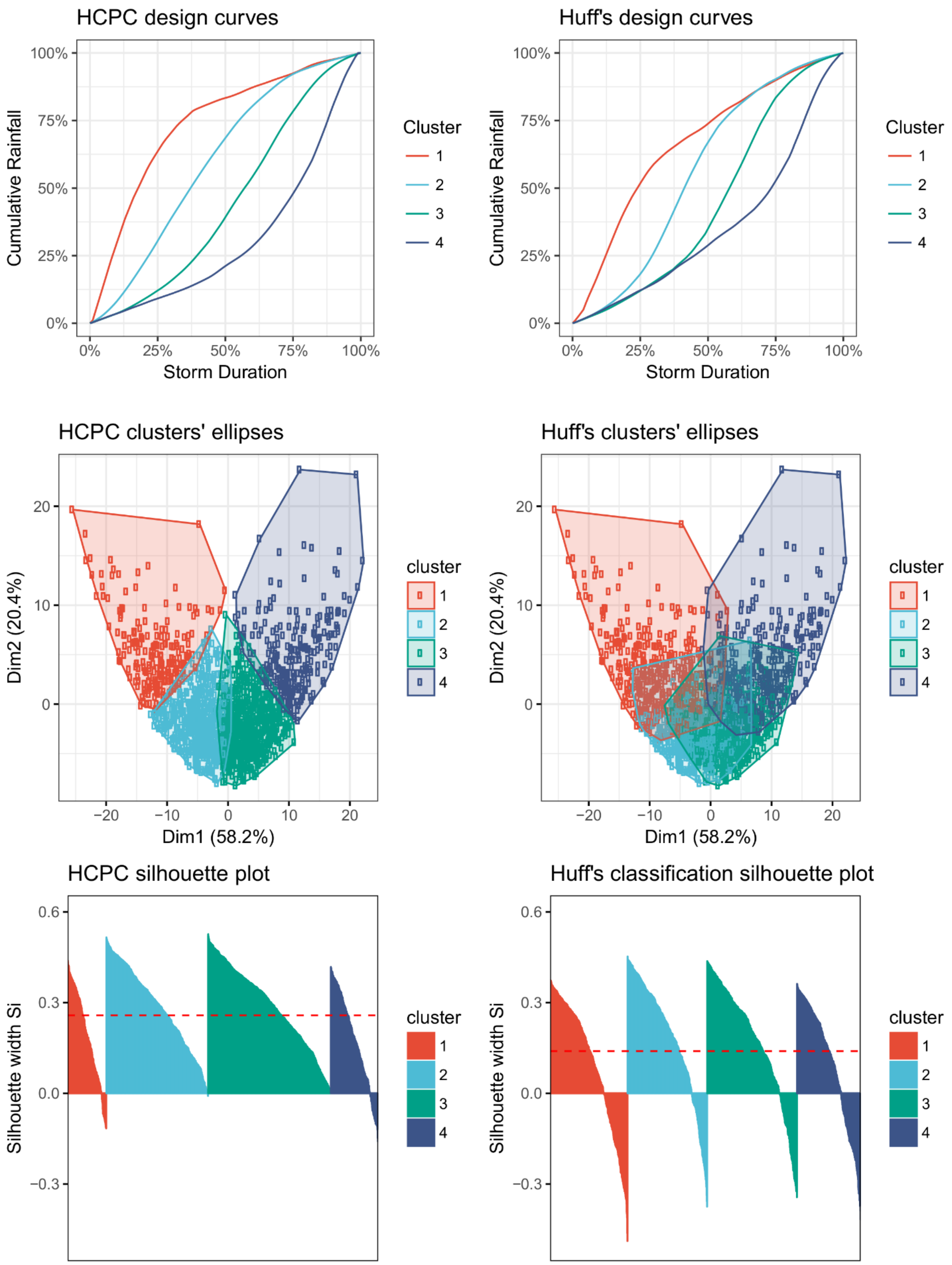


Figure 4: A comparison between the results from HCPC and Huff's quartiles clustering. At the top the derived dimensionless hyetographs curves are shown. In the middle the UCH's plots are shown using the first two principal components and ellipses around the clusters. At the bottom the silhouette plots are shown and with red, dashed line the average silhouette width of the clustering methods

Table 2: Average values of occurrence of clusters, duration, precipitation height and maximum 30 min duration's intensity of clusters' rainstorms.

Cluster	Occurrence (%)	Duration (hr)	Prec. (mm)	$I30_{max}$ (mm/hr)
1	12.50	16.25	16.5	20.1
2	32.80	18.75	19.4	13.0
3	39.50	19.5	19.5	12.4
4	15.20	16.5	18.5	16.8

After developing DHs for each station and for every month, correlation matrices were computed, utilizing Pearson's r coefficient (Helsel and Hirsch, 1992), using the respective UCHs per cluster. These matrices showed very high similarity between a) the DHs per station with $r \geq 0.98$ and b) the DHs per month with $r \geq 0.95$. A comparison among HCPC and Huff's curves is shown in Figure 4. Three pairs of the Huff's curves fail to reject the hypothesis that are drawn from the same distribution for both $\alpha = 0.05$ and $\alpha = 0.10$. HCPC results in the clear separation of UHCs, as its clusters ellipses are not overlapping and it creates clusters with better internal structure, as average sill width is almost two times better.

4. CONCLUSIONS

A temporal model of critical dry duration between rainstorms was introduced and implemented and a seasonal variability of rainfall patterns is simulated by the proposed method, in contrast to more simplified approaches of the literature. The unitless cumulative hyetographs produced were subjected to Principal Components Analysis in order to investigate if they can be compressed to a few dimensions, due to high correlation values, and it turned out that only a small number of them sufficiently explain almost all of the variability. Hierarchical Clustering on Principal Components was subsequently applied that yielded a small number of clusters. Clustering tendency and internal structure validation was appropriately investigated and documented. Finally, based on the clustering analysis four representative design hyetographs were produced. These hyetographs do not exist in Greece, especially in a way that covers the various Water Divisions. The proposed methodology may be utilized for the systematic production of such hyetographs, also based on intensity-duration-frequency curves. This method is fully unsupervised, as no prior empirical knowledge is used.

Table 3: Design Hyetographs

Storm	Cluster 1			Cluster 2			Cluster 3			Cluster 4		
duration (%)	10th	50th	90th	10th	50th	90th	10th	50th	90th	10th	50th	90th
0.0	0.0	0.0	0.0	0.0	0.0	0.0	0.0	0.0	0.0	0.0	0.0	0.0
5.0	3.9	15.7	38.4	0.4	3.1	10.0	0.4	1.7	6.6	0.4	1.9	8.1
10.0	15.0	31.4	63.5	1.6	8.1	19.2	0.8	3.6	12.4	0.8	3.7	14.3
15.0	29.8	44.9	73.0	3.9	14.9	28.5	1.3	6.0	17.3	1.1	5.5	18.7
20.0	41.8	55.7	80.4	8.0	22.4	38.2	2.0	8.9	21.8	1.6	7.4	22.2
25.0	47.8	64.5	86.8	13.5	30.5	48.6	2.9	12.0	26.0	2.2	9.2	25.3
30.0	52.0	71.4	89.6	20.7	38.9	58.6	4.2	15.7	30.2	2.7	10.9	28.2
35.0	55.8	76.7	92.2	29.9	46.7	67.6	6.2	20.1	35.1	3.5	12.7	31.0
40.0	57.5	80.0	93.7	39.5	54.5	76.9	9.6	25.5	41.1	4.3	14.9	33.8
45.0	60.3	81.8	95.2	47.5	61.8	83.5	13.8	31.6	47.3	5.2	17.6	37.7
50.0	62.7	83.5	96.2	54.0	68.7	88.2	19.6	39.2	54.2	6.1	21.1	41.7
55.0	65.2	85.3	96.9	60.0	75.1	92.2	26.9	47.1	63.4	7.7	24.4	45.0
60.0	68.7	87.4	97.8	64.7	80.4	94.5	34.4	54.2	73.3	10.1	28.3	49.4
65.0	71.8	89.1	98.3	69.0	84.9	96.0	43.4	62.4	80.9	13.0	33.6	52.6
70.0	76.0	90.8	98.5	72.8	89.1	97.4	53.1	71.0	87.8	16.9	40.3	56.4
75.0	79.5	92.5	98.7	77.6	92.3	98.3	62.2	78.5	93.3	22.8	47.7	62.3
80.0	82.0	94.8	99.1	82.1	94.3	98.9	70.7	85.4	96.3	32.4	56.1	70.8
85.0	85.5	96.6	99.3	86.7	96.0	99.3	79.0	91.3	98.1	46.2	67.0	81.3
90.0	89.5	97.7	99.5	91.2	97.5	99.5	86.9	95.5	99.1	60.2	81.1	91.7
95.0	94.6	98.8	99.7	95.6	98.8	99.8	94.0	98.3	99.6	78.0	92.7	98.3
100.0	100.0	100.0	100.0	100.0	100.0	100.0	100.0	100.0	100.0	100.0	100.0	100.0

APPENDIX

The analysis and the algorithms were implemented in the R language (R Core Team, 2018) using the packages: hydroscoper (Vantas, 2018), FactoMineR, (Lê et al., 2008) and factoextra (Kassambara and Mundt, 2017).

Algorithm 1: Temporal model of CD

Input: Stations' precipitation time series $\boldsymbol{P_i}$ where $i = 1, \ldots, k$; Critical durations test vector $\boldsymbol{CD} = [120, 180, \ldots, 1800]$ (min); Number of samples that are drawn for parametric bootstrapping $s = 50,000$;

for *station* $i \leftarrow 1$ *to* k **do**
- **for** *month* $m \leftarrow 1$ *to* 12 **do**
  - **for** *cd in* $\boldsymbol{CD}$ **do**
    - Compute the vector of interarrival times $\boldsymbol{t_\alpha}$ using inter-month data and n = length($\boldsymbol{t_\alpha}$);
    - **if** $n \geq 50$ **then**
      - Estimate the average storm arrival rate $\widehat{\omega}$ from $\boldsymbol{t_\alpha}$ using Maximum Likelihood Estimation;
      - Obtain the Kolmogorov–Smirnov's p-value for the original sample $\boldsymbol{t_a}$ and the estimated distribution;
      - Generate s samples of size n from the estimated distribution;
      - For each sample compute the one-sample Kolmogorov–Smirnov's p-value using the estimated distribution as theoretical;
      - Use the empirical non-parametric distribution of p-values to obtain the p-value for the original sample $\boldsymbol{t_\alpha}$;
  - Get minimum dry period duration $MDPD_{i,m}$ from $\boldsymbol{CD}[max(p - value)]$;

Use $MDPD$ values to fit the smooth sinusoidal model:

$$f(CD) = \theta_1 sin\left(\frac{2\pi}{12}m\right) + \theta_2 sin\left(\frac{4\pi}{12}m\right) + \theta_3 cos\left(\frac{2\pi}{12}m\right) + \theta_4 cos\left(\frac{4\pi}{12}m\right) \tag{4}$$

Result: Monthly values of CD for the area

Algorithm 2: Optimal number of clusters

Input: tree produced from HCPC algorithm; significance level $\alpha = 0.05$

while *all p-values* $< \alpha$ **do**
- moving down the tree cut into q different clusters $q = 1, ..., m$;
- calculate the mean values $\bar{x}_q$ of the UCHs that belong to cluster q;
- for all $\bar{x}_q$ obtain the Kolmogorov–Smirnov two sample test, p-values;
- adjust the obtained p-values using Benjamini and Hochberg method;

Result: optimal number of clusters q_{opt} and design hyetographs $\bar{x}_{opt}$

References

1. Azli, M. and Rao, A. R. (2010), 'Development of Huff curves for peninsular Malaysia', **Journal of Hydrology** 388(1-2), pp. 77-84.

2. Babu, G. J. and Rao, C. (2004), 'Goodness-of-fit tests when parameters are estimated', **Sankhya** 66(1), pp. 63-74.

3. Benjamini, Y. and Hochberg, Y. (1995), 'Controlling the false discovery rate: A practical and powerful approach to multiple testing', **Journal of the Royal Statistical Society**. Series B (Methodological) pp. 289-300.

4. Bonta, J. (2001), 'Characterizing and estimating spatial and temporal variability of times between storms', **Transactions of the ASAE** 44(6), pp. 1593-1601.

5. Bonta, J. (2004a), 'Development and utility of Huff curves for disaggregating precipitation amounts', **Applied Engineering in Agriculture** 20(5), pp. 641-643.
6. Bonta, J. (2004b), 'Stochastic simulation of storm occurrence, depth, duration, and within-storm intensities', **Transactions of the ASAE** 47(5), pp. 1573-1584.
7. Bonta, J. and Rao, A. (1987), 'Factors affecting development of Huff curves', **Transactions of the ASAE** 30(6), 1689-1693.
8. Bonta, J. and Shahalam, A. (2003), 'Cumulative storm rainfall distributions: Comparison of Huff curves', **Journal of Hydrology (New Zealand)** pp. 65-74.
9. Dolšak, D., Bezak, N. and Šraj, M. (2016), 'Temporal characteristics of rainfall events under three climate types in Slovenia', **Journal of Hydrology** 541, pp. 1395-1405.
10. Han, J., Pei, J. and Kamber, M. (2011), Data mining: Concepts and techniques, Elsevier.
11. Helsel, D. R. and Hirsch, R. M. (1992), Statistical methods in water resources, Vol. 49, Elsevier.
12. Huff, F. A. (1967), 'Time distribution of rainfall in heavy storms', **Water Resources Research** 3(4), pp. 1007-1019
13. Husson, F., Josse, J. and Pages, J. (2010), 'Principal component methods-hierarchical clustering partitional clustering: Why would we need to choose for visualizing data', Technical Report-Agrocampus.
14. Jolliffe, I. T. (1986), Principal component analysis and factor analysis, in 'Principal Component Analysis', Springer, pp. 115128.
15. Kassambara, A. and Mundt, F. (2017), factoextra: Extract and Visualize the Results of Multivariate Data Analyses. R package version 1.0.5.
16. Kitsikoudis, V., Sidiropoulos, E., Iliadis, L. and Hrissanthou, V. (2015), 'A machine learning approach for the mean flow velocity prediction in alluvial channels', **Water resources management** 29(12), pp. 4379-4395.
17. Koutsoyiannis, D. and Xanthopoulos, T. (1990), 'A dynamic model for short-scale rainfall disaggregation', **Hydrological Sciences Journal** 35(3), 303-322.
18. Lawson, R. G. and Jurs, P. C. (1990), 'New index for clustering tendency and its application to chemical problems', **Journal of Chemical Information and Computer Sciences** 30(1), pp. 36-41.
19. Lê, S., Josse, J. and Husson, F. (2008), 'FactoMineR: A package for multivariate analysis', Journal of Statistical Software 25(1), pp. 1-18.
20. Lin, G.-F. and Wu, M.-C. (2007), 'A SOM-based approach to estimating design hyetographs of
21. ungauged sites', **Journal of Hydrology** 339(3-4), pp. 216-226.
22. Loukas, A. and Quick, M. C. (1996), 'Spatial and temporal distribution of storm precipitation in
23. southwestern British Columbia', **Journal of hydrology** 174(1-2), pp. 37-56.
24. Ministry of Environment and Energy (2013), Management plan of Thracian Water Division, Technical report.
25. Nojumuddin, N. S. and Yusop, Z. (2015), 'Identification of rainfall patterns in Johor', **Applied**
26. **Mathematical Sciences** 9(38), pp. 1869-1888.
27. R Core Team (2018), R: A Language and Environment for Statistical Computing, R Foundation for Statistical Computing, Vienna, Austria.

28. Restrepo-Posada, P. J. and Eagleson, P. S. (1982), ‘Identification of independent rainstorms’, **Journal of Hydrology** 55(1), pp. 303-319.
29. Rousseeuw, P. J. (1987), ‘Silhouettes: A graphical aid to the interpretation and validation of cluster analysis’, **Journal of Computational and Applied Mathematics,** 20, pp. 53-65.
30. Vafeiadis, M., Tolikas, D. and Koutsoyiannis, D. (1994), HYDROSCOPE: The new Greek national database system for meteorological, hydrological and hydrogeological information, in ‘WIT Transactions on Ecology and the Environment’, pp. 1-8.
31. Vandenberghe, S., Verhoest, N., Buyse, E. and De Baets, B. (2010), ‘A stochastic design rainfall generator based on copulas and mass curves’, **Hydrology and Earth System Sciences** 14(12), pp. 2429-2442.
32. Vantas, K. (2018), ‘hydroscoper: R interface to the Greek National Data Bank for Hydrological and Meteorological Information’. **Journal of Open Source Software**, 3(23), 625.
33. Vantas, K. and Sidiropoulos, E. (2017), ‘Imputation of erosivity values under incomplete rainfall data by machine learning methods’, **European Water** 57, pp. 193-197.
34. Veneziano, D. and Villani, P. (1999), ‘Best linear unbiased design hyetograph’, **Water Resources Research** 35(9), pp. 2725-2738.
35. Ward, J. (1963), ‘Hierarchical grouping to optimize an objective function’, **Journal of the American Statistical Association,** 58(301), pp. 236-244.
36. William, J. C. (1971), Practical Nonparametric Statistics, John Wiley & Sons, New York.
37. Williams-Sether, T., Asquith, W. H., Thompson, D. B., Cleveland, T. G. and Fang, X. (2004), ‘Empirical, dimensionless, cumulative-rainfall hyetographs developed from 1959-86 storm data for selected small watersheds in Texas’, Technical report, US Geological Survey.

DEVELOPMENT AND QUANTIFICATION OF VISUAL ANALYTICS ALGORITHMS FOR INVESTIGATING EXTREME WEATHER EVENTS IN TIME-VARYING GEOGRAPHIC DATA

P. P. Giannopoulos* and K. Moustakas

Dept. of Electrical and Computer Engineering, University of Patras, Greece

*Corresponding author: e-mail: ece7756@upnet.gr, tel : +302610450612

Abstract
The large amount of measurement data from Greece's meteorological network requires visualization and processing to be more understandable and useful. In this paper we study measurements and forecasts of temperature and wind velocity for the geographical area of Greece and we produce useful depictions through an interactive application. We also include statistical processing on the wind data so that we can understand in which area of Greece there is a greater probability of extreme weather events occurring. In general, Visual Analytics may help the emerging area of Artificial Intelligence and Decision Support Systems. The data used in this work is obtained from the National Observatory of Athens through the site of meteo.gr.

Keywords: Measurements, Temperature, Wind Data, Extreme Weather Forecasts, Decision Support Systems

1. INTRODUCTION

1.1 Motivation

Nowadays, the amount of information that passes through our eyes in a daily basis, from the newspaper we read at breakfast, the emails we receive throughout the day, the data generated when we make a bank statement to receive or store money or the conversation we have, is enormous. For that reason, several scientific fields have been developed, such as Information Visualization and Visual Analytics, in order to make the information we receive more comprehensive and cohesive, and to make our lives simpler. The Information Visualization, the art of presenting the data in such a way that we can clearly understand and manage it, can help us understand the meaning behind that information in order to adopt and use it in everyday life.

On the other hand, Visual Analytics, which is an emerging field of Artificial Intelligence and Decision Support Systems, aims to support analytical reasoning through various interactive visual interfaces. The basic idea is the integration of the outstanding capabilities of humans in terms of visual information exploration and the enormous processing power of computers to form a powerful knowledge discovery environment.

1.2 Related work

A technique for classification of information visualization and optical data mining techniques have been proposed [Keim, Daniel A. "Information Visualization and Visual Data Mining], based on the type of data, the visualization method and the specific interaction and distortion of them. A new approach regarding the visualization of data mining from a large database has been described and evaluated [Keim, D.a., and H.-P. Kriegel, . Keim, D.a., E.e. Koutsofios, and S.c. North]. The basic idea of the visualization techniques used for that purpose is to present as much as possible information

on the screen at the same time, mapping every data value to a specific pixel and arranging the pixels sufficiently. The information visualization techniques are usually limited to only a few thousand objects. Fortunately, a description of new interaction techniques, that can manage millions of objects and the emerging hardware-oriented techniques and new animation methodologies such as stereovision and overlap count, have been given and evaluated [Fekete, J.-D., and C. Plaisant]. Also, recent researchers [Kandel, S., Heer, J., Plaisant, C., Kennedy, J., van Ham, F., Riche] have invented techniques, as well as visualization ones, that are pixel-based, in order to increase the density of the data, that can be displayed, without the loss of the possibility to display individual values.

As statistics data sets become increasingly large and complex, the users require more effective multi-dimensional visualization tools and faster interactive performance. This challenge demands improved fundamental methods for data model and visual exploration analysis. The potential to apply integrated infovis and geovis tools for analyzing multivariate statistics data over time represents another interesting research challenge. An attempt for summarization of those challenges has been done [Jern, M] through real time examples.

Weather conditions concern multiple aspects of human life, such as economy, security and social activities. For this reason, meteorological forecasts play an important role in society. Current weather forecasts are based on Numerical Weather Prediction (NWP) and create representations of atmospheric flow. Interactive visualizations of geospatial data [Diehl, A., L. Pelorosso, C. Delrieux, C. Saulo, J. Ruiz, M. E. Gröller, and S. Bruckner] have been widely used to facilitate analysis of NWP models. A system that provides geographical representation of the probability of fire and the identification of areas of the highest risk [Kalabokidis, Kostas & Nikos, Athanasis & Gagliardi, Fabrizio & Karayiannis, Fotis & Palaiologou, Palaiologos & Parastatidis, Savas & Vasilakos, Christos], based on a high-performance pilot application running on a server, has been developed.

1.3 Our contribution

We propose a visualization method of grid-based point data that describe weather conditions in different locations in the area of Greece. We also make a statistical analysis of the data so that we can make predictions of weather changes. Thus, we can make useful depictions of extreme weather conditions, such as high wind accelerations through interactive visualizations.

2. STATISTICAL ANALYSIS

Our goal was to implement a semitransparent visualization above a map so that we could find wind-based sensitive areas of Greece at a particular time. Those areas should tell us if the wind speed had changed enough so that we could determine whether an extreme weather condition event was occurring. A way to achieve this goal was to calculate from various timeframes the specific local pixel mean value from the group of wind speed values in the given timeframe. Then, we had to find the variance from the wind gust information we had about the specific pixel and the mean value we already calculated. In this way, we can clearly see which areas are most vulnerable from extreme weather conditions because the more the wind gust is away from the mean wind speed value the bigger the value of the final pixel will be. The computational procedure is as follows:

First, we calculate the mean wind speed, $\overline{u_j}$, at each pixel j

$$\overline{u_j} = \frac{1}{n}\sum_{i=1}^{n} u_i \tag{1}$$

where u_i is the wind speed at the time interval i, $i \in \{1,2,\ldots,n\}$. Then, we calculate the wind speed variance of the gust speed and as a last but important step, the standard deviation at each pixel j

$$Var(u_{gi}) = \frac{1}{n}\sum_{i=1}^{n}(u_{gi} - \bar{u_J})^2 \ (a) \qquad stdev(u_{gi}) = \sqrt{Var(u_{gi})} \ (b) \tag{2}$$

The standard deviation is used as the criterion revealing the most vulnerable regions.

3. ESTIMATING GRID VALUES FROM SCATTERED POINTS

3.1 Simple approach to grid approximation

The visualization of the data of interest would not be possible if we could not convert the input scattered points to an actual regular grid first. In order to do that, we needed to map the values of the input scatter point data to match the individual values of the grid covering the area of Greece. An algorithm that is easy to implement and understand is the Kriging Method [A Basic Understanding of Surfer Gridding Methods] which finds an approximate value of each grid point based on the corresponding neighboring scattered points. Every point from the scattered points has a weight that is been calculated based on the neighborhood area of the grid point. The flow diagram of the Kriging's Method algorithm can be seen in Figure 1. For example, in order to calculate the estimated value of the grid point based on its neighbors we use the relationship:

$$Z_A = \sum_{i=1}^{n} W_i Z_i \tag{3}$$

where Z_A is the estimated value, n is an arbitrary number of neighbors, W_i is the corresponding weight of the current neighbor and Z_i is the value of the current neighbor. The weights are calculated in a way that the sum of them equals to unity. For example, we use the following formula:

$$W_i = \frac{Z_i}{\sum_{j=1}^{n} Z_j} \tag{4}$$

3.2 Inverse Distance Weighting (IDW) and Kriging method's algorithm

The problem that occurs with the previous equation of the simple approach is that smaller distances of the neighbors from the current grid point do not affect the corresponding weight and thus the final estimation. Although, we always search for the closest neighbors from the grid point to find the neighborhood and we get reliable results, we can still use better techniques to increase the accuracy of the results. One of them is the Inverse Distance Weighting Method also called the Shepard method [Robert Weibel] and is the method we have used in this work. Inverse Distance Weighting considers the distance of the chosen neighboring points and calculates their weights. A simple approach of this method is to find the weights from the direct inverse distance:

$$W_i = \frac{1}{d_i} \tag{5}$$

where d_i is the distance of the current grid point from the i-th point of neighbors i.e. a hyperbolic weight allocation method. Also with the prior weighting calculation the estimation now changes to:

$$Z_A = \frac{\sum_i^n W_i Z_i}{\sum_i^n W_i} \tag{6}$$

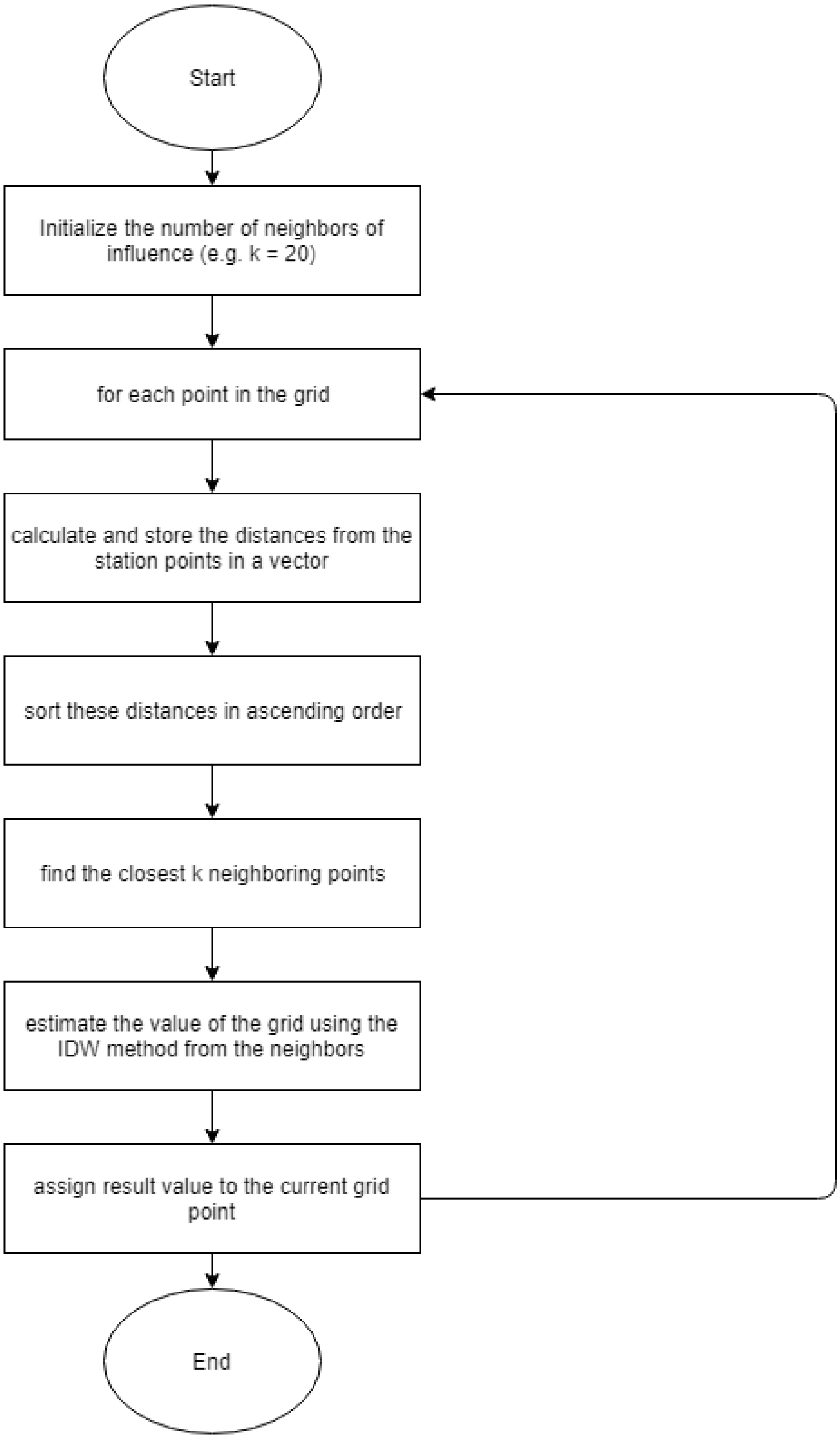


Figure 1: Flow diagram of the Kriging method

With the IDW simple equation we simply improved the distance correlation and the accuracy of the results. The IDW method allows for very fast calculations and different distances can be integrated in the equation. Also, with the usage of the distance-weighting exponent we can precisely control the influence of those distances. Using the IDW method we are not able to do a direction-dependent weighting. That means that spatially oriented relationships are ignored. There are also some undesirable artifacts that appear called «Bulls-eyes» as shown in Figure 2.

Those artifacts are circular areas of equal values around known data points. In order to improve the results and make the artifacts disappear we use a variation to the above equation using an exponent of the distance as a parameter:

$$W_i = \frac{1}{d_i^p} \tag{7}$$

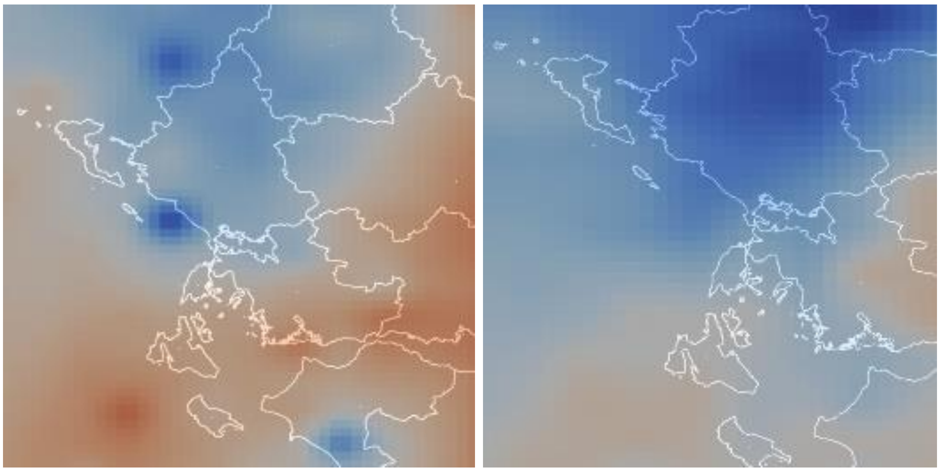


Figure 2: The undesirable artifacts, also called "Bulls-eyes" that we try to reduce using an exponent parameter p = 0.02 shown in the right image

4. COLOR MAP BASED VISUALIZATION

Finding the values that match the grid coordinates from a group of scattered points is only the first step that only requires some math computations and no visualization. In order to create the grid mesh and visualize it on the screen, we have to follow some rules in order to give meaning to the final visualization based on the variable we are currently working on (e.g. Temperature). A good way to fulfill that purpose is to create a color map that is basically a collection of colors that have been arranged in a "map" or array of colors so that each color corresponds to a specific value of our variable. There are three types of color maps: The Qualitative, the Sequential and the Diverging color map as shown in Figure 3. The Qualitative map is a collection of colors that cannot be related to each other. A usage of it could be in a map where we want to distinguish one country from the other based on its unique color. That type of color map has not been used in that particular work because the emphasis is focused on the values appeared in the several regions of Greece and not on the regions themselves. The Sequential color map is an important one because each color, when we look at the colors in the array, has a slight difference, in terms of hue, from the neighboring colors. A great example of a sequential color map is the Rainbow color map, which is widely used in many scientific fields that require visualization to present the results. Although, that type of color map is very important and gives a good sense of where our value belongs in the range of our variable and on the color map, the following type of color map gives more reliable results and the more colorful nature of it can be more aesthetically pleasing.

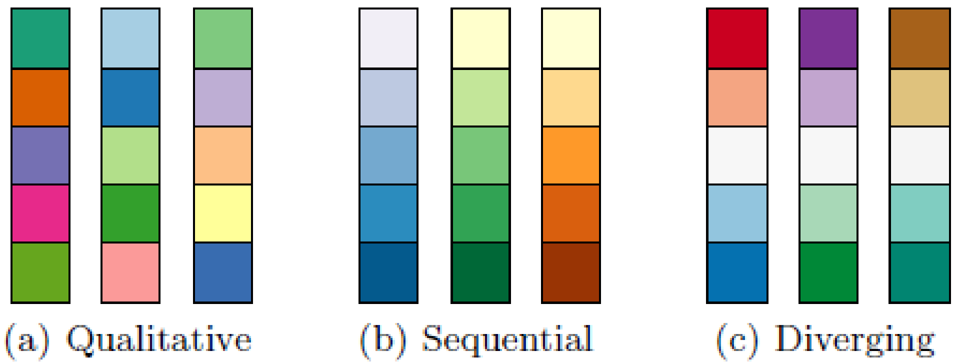


Figure 3: The different types of color maps: (a) Qualitative, (b) Sequential, (c) Diverging

The Diverging color map [Moreland, Kenneth] can have up to twice the perceptual resolution of the sequential color map without sacrificing the requirements of surface shading or losing viewers with dichromatic vision. To create a diverging colormap we need to choose 2 colors that will play the role of the extreme values of our scalar variable. Every color in between will be a combination of those two and the color in the middle of the color map, which is an unsaturated color (e.g. the white). In general, diverging color maps lack a natural ordering of the colors and because of that we have to choose the extreme colors in a way so that we can understand them naturally. For example, a common diverging color map is the cool to warm map, in which the endpoint colors are chosen so that they have a natural meaning. It has been proven from studies that people identify red and yellow as warm colors and blue or green as cool colors across subjects, contexts and cultures. When creating a diverging color map, we must ensure that it maintains a perceptual uniformity and therefore it must be true that the quantity

$$\frac{\Delta E\ \{c(x), c(x+\Delta x)\}}{\Delta x} \tag{8}$$

is constant for every *x*, where *ΔE* expresses a slight change in the visual color difference between two consecutive colors.

We use CIELAB color space for precise control of the color difference. Unfortunately, the three colors (e.g. red, white and blue) that the map passes through may not be in a line in CIELAB space.

That means we cannot use only a single interpolation method to find the colors of the diverging color map directly from the difference between the three basic colors of the colormap. Prosperously, we can ensure that the rate of change of the color difference between two consecutive colors is constant if

$$\lim_{\Delta x \to 0} \frac{\Delta E\{c(x), c(x+\Delta x)\}}{\Delta x} \tag{9}$$

is also constant.

We can resolve the above equation by applying the *ΔE* operation and splitting up the *c* function into its components ($\Delta E\{c_1, c_2\} = \|c_1 - c_2\| = \sqrt{\sum_i (c_{1i} - c_{2i})^2}$).

$$\lim_{\Delta x \to 0} \frac{\|c(x+\Delta x) - c(x)\|}{\Delta x} = \lim_{\Delta x \to 0} \left\| \frac{c(x+\Delta x) - c(x)}{\Delta x} \right\| =$$

$$= \lim_{\Delta x \to 0} \sqrt{\sum_i \left(\frac{c_i(x+\Delta x) - c_i(x)}{\Delta x} \right)^2} = \sqrt{\sum_i \left(\lim_{\Delta x \to 0} \frac{c_i(x+\Delta x) - c_i(x)}{\Delta x} \right)^2} \tag{10}$$

In the final form of the equation (10), we can notice that the limit is the definition of a derivative and by replacing the limit with a derivative, we get the following result:

$$\lim_{\Delta x \to 0} \frac{\|c(x+\Delta x) - c(x)\|}{\Delta x} = \sqrt{\sum_i \left(c'_i(x) \right)^2} = \|c'(x)\| \tag{11}$$

where $c'(x)$, the constant rate of change requirement, is declared as the piecewise derivative of $c(x)$ and the easiest way to ensure that the equation (11) is constant is to linearly interpolate in the CIELAB color space. To make the linear interpolation pass also from the middle color (e.g. white), a piecewise linear interpolation had to be implemented. That interpolation may cause undesirable artifacts in the color map also called Mach bands, that can be reduced by setting a “leveling off” of the luminance

as we approach the middle area. To preserve the properties of a diverging color map the chromaticity should also change more dramatically when we are working with that specific area.

The most suited color map for our work was the diverging color map so we chose to implement it and used it for every possible visualization.

5. IMPLEMENTATION

To test the results, we used temperature data as well as wind data from scattered points of meteorological stations across Greece. Without the Inverse Distance Method, the results were good, but they were lacking detailed estimation near specific areas because of the distance of each neighboring point that was not considered when calculating the corresponding weights. Using the Inverse Distance Method with exponent equal to 1 (p=1) we made a more detailed visualization also causing the "bulls-eyes" artifacts to appear. To reduce those artifacts, we simply chose the exponent to be equal to 0.02 (p=0.02) without loss in the quality.

For the temperature data, the cool to warm diverging color map was very well suited and helped a lot to distinguish higher values from lower ones. The usage of green and purple colors as endpoints for the description of the wind data also follows the same approach. The nature of green colors can interpret mild or lower values of the wind speed perfectly. In contrast, purple colors can describe more tense or higher values of the wind.

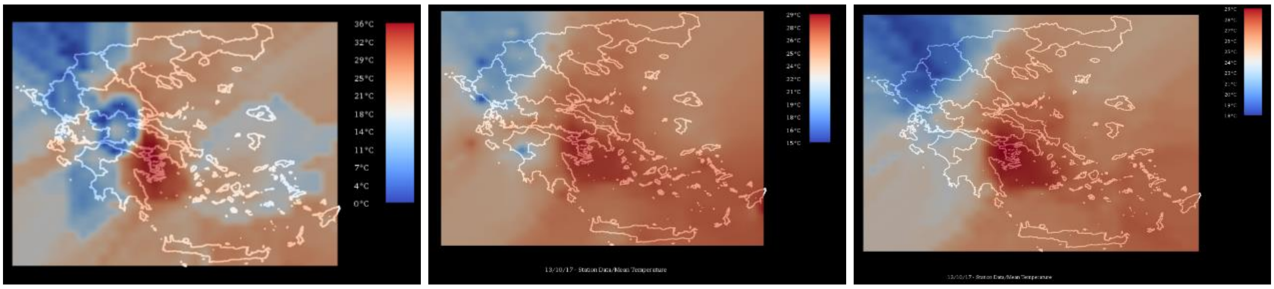
Another useful visualization which has been done in this work is the flow visualization of a vector field either with the arrows in the corresponding positions of each grid cell or with the streamlines that are tangent to each vector of the field. That kind of visualization is very useful for presenting wind speed data that has a vector form and the intention of motion of the wind that is taking place in certain regions of the map.

Beyond those visualizations, the interaction with the user is such so that zooming in specific area with updated values through proper local normalization is possible. Additional features also included in this work such as increasing the quality of the grid visualization using bilinear interpolation [Numerical Recipes in C].

6. RESULTS

Usually, in a GIS based application such as Virtual Fire [Kalabokidis, Kostas & Nikos, Athanasis & Gagliardi, Fabrizio & Karayiannis, Fotis & Palaiologou, Palaiologos & Parastatidis, Savas & Vasilakos, Christos], where meteorological data are needed for the visualization, greater accuracy can benefit the results and the decisions we make based on those. Our application, even though it is simple at its core, can produce good-quality images. It is also capable of providing control for increasing or decreasing the quality of the visualization grid as much as we want overall or at specific regions of the map.

The visualizations created with the temperature data is shown in Figure 4 and we can see how the method that takes into account the distance for the calculation of the weights affects the accuracy of the results. The user can interact with the grid by rotating it in 3D space holding the right mouse button and moving the mouse around. Also, it is possible to zoom in and extract more detailed information about a specific area. By looking at the colormap, the user can understand how each value matches the values in the Greece and make proper decisions. The same techniques apply for the visualization in Figure 5 where the data used as input is the wind data. The procedure is the same, with the only noticeable difference in the results and the color map used in the specific visualization. In Figure 6 we can see the visualization of the vector field and the corresponding streamlines for presenting the wind speed data in a better way using also a separate color map.



(a) (b) (c)

Figure 4: Grid Based Visualization of temperature data using (a) a simple neighboring approach, (b) a simple Inverse Distance Weighting Method, (c) variation of the simple Inverse Distance Weighting Method. Undesirable artifacts have been reduced in image (c) comparing to image (b)

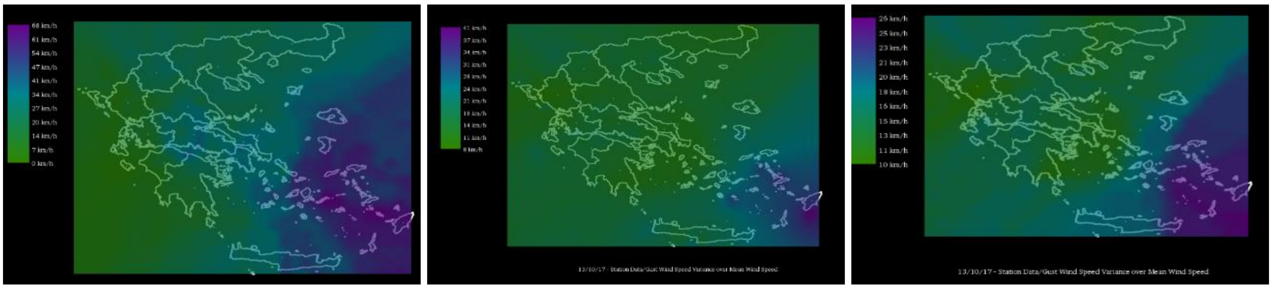


Figure 5: Visualization of Wind Speed Stand. Deviation Data based on multiple timeframes

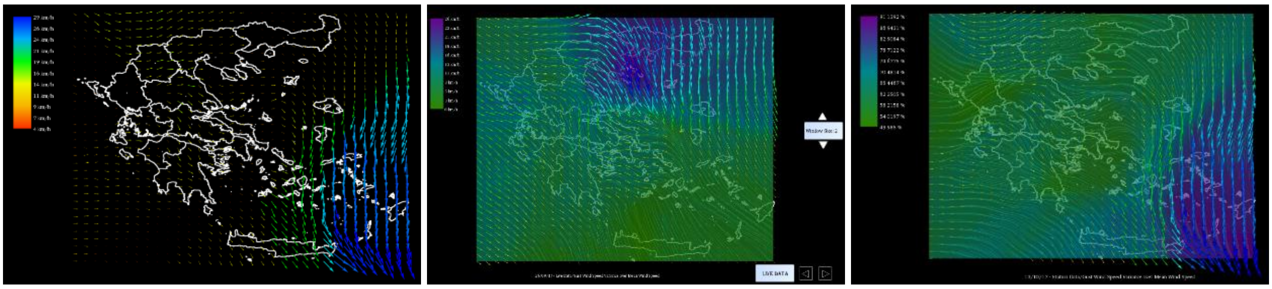


Figure 6: Visualization of vector field. Image (a) shows the arrows that represent the wind speed vectors in the vertices of each grid cell, image (b) shows the corresponding streamlines and the wind speed stand. deviation on the values of the grid, image (c) shows the wind speed stand. deviation in percentage

7. CONCLUSIONS AND FUTURE WORK

By using the values of meteorological data from Greece, we can predict the wind changes in a specific area of the map and the results are quite precise and reliable. Usually, typical weather models extract ready-to-use grids that describe a specific meteorological variable, but in our case, we needed data that should be taken in frequent periods (e.g. 10 minutes). If the sampling frequency of the weather data provided by the weather forecasts increases in the future, we can get more accurate results.

The present finding may be helpful to Artificial Intelligence and Decision Support Systems.

ACKNOWLEDGEMENTS

We would like to thank the PhD candidate Mr. Dimitar Stanev and the research associate Mr. Stavros Nousias for their help to improve the work. We acknowledge Mr. Lagouvardos, Research Director of the National Observatory of Athens, providing accessibility to the meteorological data of the Observatory stations.

References

1. Keim, Daniel A. "Information Visualization and Visual Data Mining." **IEEE Transactions on Visualization and Computer Graphics**. http://dl.acm.org/citation.cfm?id=614508 (accessed October 18, 2017).
2. Keim, D.a., and H.-P. Kriegel. "Visualization techniques for mining large databases: a comparison**." IEEE Transactions on Knowledge and Data Engineering 8**, no. 6 (1996): 923-38. doi:10.1109/69.553159.
3. Keim, D.a., E.e. Koutsofios, and S.c. North. "Visual exploration of large telecommunication data sets." **Proceedings User Interfaces to Data Intensive Systems**, 1999. doi:10.1109/uidis.1999.791458.
4. Fekete, J.-D., and C. Plaisant. "Interactive information visualization of a million items." **IEEE Symposium on Information Visualization**, 2002. INFOVIS 2002. doi:10.1109/infvis.2002.1173156.
5. Kandel, S., Heer, J., Plaisant, C., Kennedy, J., van Ham, F., Riche, N.H., Weaver, C., Lee, B., Brodbeck, D., Buono, P.: Research directions in data wrangling: visualizations and transformations for usable and credible data. **Inf. Vis**. 10(4), 271–288 (2011).
6. Jern, M. "Research Advances in Geovisualization and Remaining Challenges." **Ninth International Conference on Information Visualisation** (IV05). doi:10.1109/iv.2005.108.
7. Diehl, A., L. Pelorosso, C. Delrieux, C. Saulo, J. Ruiz, M. E. Gröller, and S. Bruckner. "Visual Analysis of Spatio-Temporal Data: Applications in Weather Forecasting." **Computer Graphics Forum 34**, no. 3 (2015): 381-90. doi:10.1111/cgf.12650.
8. Kalabokidis, Kostas & Nikos, Athanasis & Gagliardi, Fabrizio & Karayiannis, Fotis & Palaiologou, Palaiologos & Parastatidis, Savas & Vasilakos, Christos. (2013). Virtual Fire: A web-based GIS platform for forest fire control. **Ecological Informatics**. 16. 62–69. 10.1016/j.ecoinf.2013.04.007.
9. A Basic Understanding of Surfer Gridding Methods – Part 1. (n.d.). Retrieved from "https://support.goldensoftware.com/hc/en-us/articles/231348728-A-Basic-Understanding-of-Surfer-Gridding-Methods-Part-1"
10. Robert Weibel(Overall), Philipp Weckenbrock(Translation), Helmut Flitter (Specials), Samuel Wiesmann(Specials). (n.d.). Retrieved from
11. "http://www.gitta.info/ContiSpatVar/en/html/Interpolatio_learningObject2.xhtml
12. Moreland, Kenneth, "Diverging Color Maps for Scientific Visualization (Expanded)," Proceedings in ISVC '09, **Proceedings of the 5th International Symposium on Advances in Visual Computing: Part II**, Springer-Verlag, Belin, Heidelberg, Nov. 26, 2009, pp. 1-20.
13. Numerical Recipes in C, 1988–92 Cambridge University Press, ISBN 0-521-43108-5, pp. 123–128. "http://www.aip.de/groups/soe/local/numres/bookcpdf/c3-6.pdf"

DEVELOPING FLOOD ACTION PLANS ON THE ADMINISTRATIVE LEVEL OF FARMERS' ORGANIZATION

V. Pisinaras*, G. Arampatzis and A. Panagopoulos

Soil & Water Resources Institute, Hellenic Agricultural Organization - DEMETER, GR-57400 Sindos, Thessaloniki, Greece

*Corresponding author: e-mail: vpisinar@gmail.com

Abstract

Agriculture constitutes one of the most vulnerable sectors on floods impacts, the frequency and severity of which are expected to increase within the context of climate change. Despite the fact that floods' action plans are commonly developed on national or regional level, it is important for each water resources "key player" within a basin to compile local and case specific action plans in order to increase its adaptability to the corresponding impacts and sufficiently contribute to floods management in the basin. This necessity is also addressed by the business-oriented water management certification schemes (e.g. the European Water Stewardship Standard), according to which management of such incidents are of major importance.

Taking into account the above, this paper aims to introduce a simplified approach for the compilation of flood action plans in Farmers' Organization (F.ORs), which constitutes a common organizational scheme of agricultural production in the Mediterranean. The first step is to assess the risk of: a) river floods, based on flood risk assessment reports developed within the context of Floods Directive by EU and b) flash floods, based on surface runoff potential estimated by a simplified methodology incorporating spatially distributed runoff curve numbers, ground slope and precipitation. The second step is to propose practices and actions in order to: a) contribute to basin's flood risk reduction and b) mitigate the impact of flood incidents. The above mentioned methodologies are applied in the area of activity of a F.OR located in Crete Island, Greece.

Keywords: floods, droughts, agricultural water management, curve number, good agricultural practices

1. INTRODUCTION

Agriculture constitutes one of the production sectors that are fully exposed and impacted from disasters related to climate. According to FAO (2015): a) 25% of total damage and losses related to climate-induced disasters are absorbed by the agriculture sector and b) for the period 2003-2013, the economic loss in crop and livestock production resulted from medium to large scale climate-induced disasters in developing countries was estimated at USD 80 billion. This evidence indicate the high vulnerability of agricultural sector in climate conditions and indicate not only the economic, but also the social impact of such disasters. Among the several climate-induced disasters, floods and droughts are considered the most frequent and severe. Indicatively, it is mentioned that crop and livestock production losses occurred after floods and droughts in developing countries is estimated at 83%.

Considering the above, the well-organized and prompt response of agriculture sector in floods is of paramount importance in order to reduce the socio-economic impact of those disasters. One of the tools towards this way is the development of local and case specific flood action plans. The necessity of flood action plans has been identified by the European Commission as reflected in the relevant

Directives (2000/60/EC, 2007/60/EC). Moreover, business-oriented water management certification schemes (e.g. the European Water Stewardship Standard) according to which management of such incidents is of major importance, have also identified the necessity to develop such plans. Flooding is an issue of major concern for farmers both at field and farm level (Pivot and Martin, 2002; Posthumus et al, 2008).The present study aims to introduce an easily applied approach for the compilation of flood action plans in Farmers' Organization (F.ORs), which constitutes a common organizational scheme of agricultural production in the Mediterranean. So, it is applied for Public Services Company of Platanias Municipality, located in Crete Island, Greece. A set of practices and measures are proposed in order to increase its preparedness and response level to floods, while establishing communication channels with the competent authorities is necessary.

2. MATERIALS AND METHODS

2.1 Floods action plan development methodology

In this study, the methodological framework followed in order to establish the flood action plan is presented in Figure 1. Two are the main steps that each F.OR has to follow in order to compile it: a) identify the areas characterized by high flood risk and b) compile a flood management strategy by identifying actions, measures and practices that will lead to reduction of agricultural activity contribution to surface runoff and mitigation of the corresponding floods' impact. There are three types of floods, which can potentially affect the agricultural sector: river floods, flash floods and coastal floods. River floods occur when river water system capacity is exceeded and therefore river water is not able to be channeled through the river course. Flash floods are developed from localized, intense rainfalls and can occur anywhere in the basin, while coastal floods constitutes the result of increased sea level rise caused by storm surges driven by tropical storms or strong windstorms. According to Morris et al (2010), flood development consists of three major components: the sources, the pathway and the receptor. Flood sources are the extreme rainfall events and/or the sudden snow-cover melt, while pathway is considered as the land and the hydrological system which transfer the water to the receptor. Finally, flood receptor is the area where flooding occurs. Agricultural land can serve either as pathway or receptor.

With regard to river floods risk assessment, it can be based on reports, data and information developed within the context of Directive 2007/60/EC, since it requires heavy scientific effort, which cannot be maintained by a F.OR. Every EU Member State has to be conform to Directive 2007/60/EC on the assessment and management of flood risks and therefore useful information such as preliminary flood risk assessment reports and flood hazard and risk maps already produced for the most EU countries can be used to identify high agricultural areas of flood risk and hazard.

With regard to flash floods risk assessment, it can be estimated by a simplified GIS-based methodology (Figure 2), in which meteorological and physical factors are incorporated. The methodology is based on the spatial determination of easily estimated or calculated parameters, namely Curve Number (CN), ground's slope and rainfall. CN corresponds to an empirical parameter applied in hydrology for the prediction of direct runoff or infiltration from rainfall excess. The CN constitutes the fundamental parameter of the runoff curve number method, which was originally developed by USDA Soil Conservation Service (SCS) at 1954 in order to simulate direct runoff from agricultural fields for specific rainfall events and since then, SCS-CN method is considered as the most widely applied method for runoff estimation (Ajmal et al, 2015), while it has been integrated in a wide variety of hydrologic, erosion and water quality models (Mohammad & Adamowski 2015). CN is a function of soil type, land use and antecedent soil moisture conditions. Based on soil hydrologic group and land use, an extensive record of CN values have been estimated and proposed by NRCS (1986). The land use has been divided into three main categories including cultivated agricultural land, other agricultural land and urban areas. Based on these categories and taking into account the soil hydrologic group, the user can assign the appropriate CN in the study area.

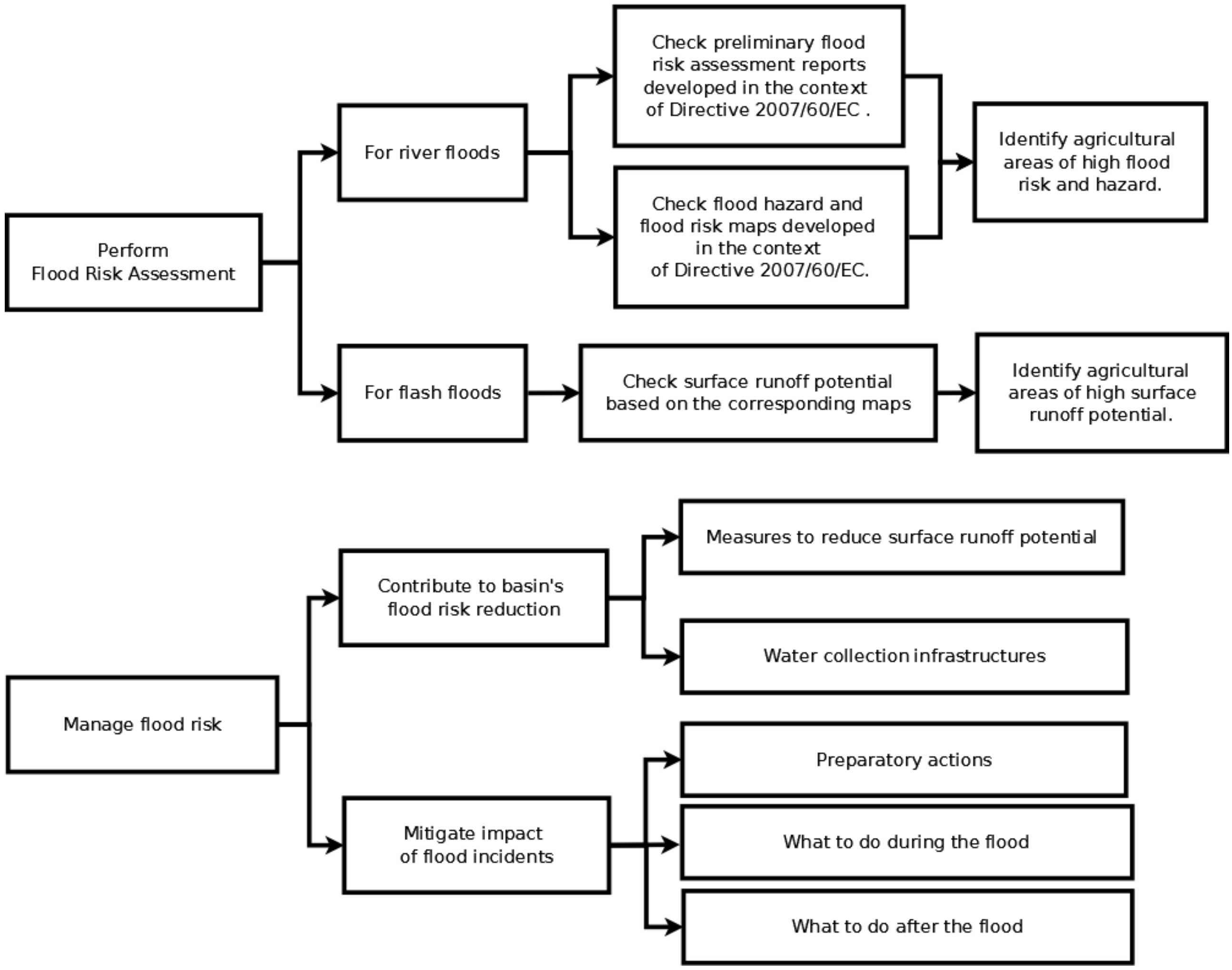


Figure 1: Diagram of floods action plan development methodology.

Slope is considered as one of the most influential parameters that can affect runoff. Slope gradient can be easily calculated in GIS software using a Digital Elevation Model (DEM) and it is expressed as degrees or percentage. ASTER GDEM (Tachikawa et al, 2011) is a product of NASA and METI and was used for the purposes of this study. Rainfall is considered as the major contributor to runoff due to the fact that it constitutes the water source of the runoff process. In fact it is not only the rainfall amount related to runoff, but also its intensity and duration. Nevertheless, in a simplistic way, the more precipitation that reach the ground, the more water is available for runoff. Therefore, in order to incorporate the rainfall component in the runoff risk assessment methodology the annual rainfall spatial distribution within the basin was produced by interpolation on meteorological station data with kriging algorithm. Since the variation range of the three components is significantly different (31-100 for CN, 0-5% for slope, 0-1,800 mm for precipitation), it was necessary to perform a standardization procedure in order to obtain a common variation scale. Therefore, linear increasing fuzzy membership functions were applied in the three components. The variation range of the produced spatial distribution maps is 0-1. After the standardization process, which can be easily applied in ArcGIS software, the three components are summed and as a results the runoff risk assessment map is produced with values ranging between 0 and 3. This range was classified into five categories, ranging from very low to very high runoff potential (Figure 2).

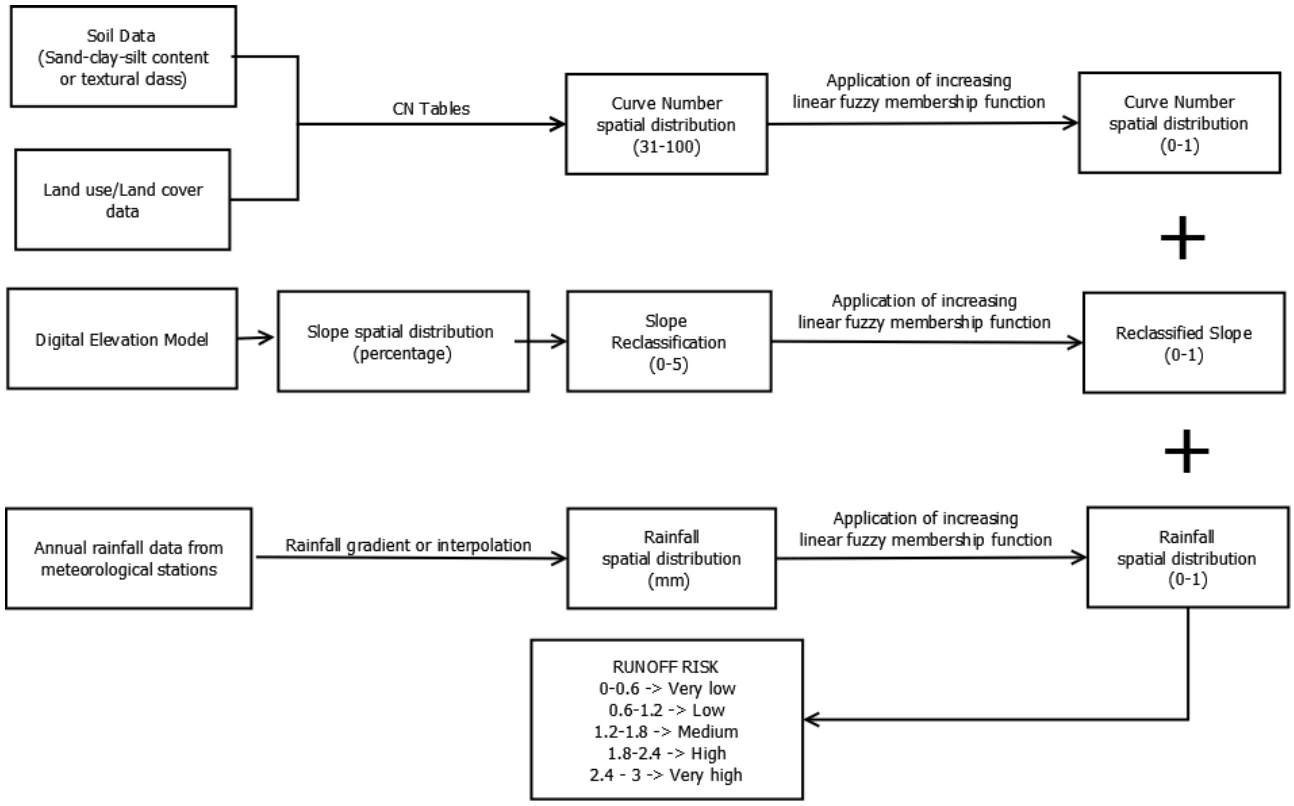


Figure 2: Diagram of flash floods risk assessment methodology.

Concerning flood risk management, actions, mechanisms and practices have to be identified in order to:

Reduce the contribution of farms that indicate high surface runoff potential. These actions, measures and practices are also contributing to the mitigation of flash floods impacts both in the farm and the basin scale. They can be divided into two major categories including: a) measures that are applied on farm and aim to reduce surface runoff potential and therefore flash flood risk and b) infrastructures in which surface runoff can be collected and therefore flash floods impact can be mitigated, while these infrastructures may also contribute to mitigate river floods.

Mitigate the impacts of river floods before their occurrence (i.e act in a preventive manner), during them and after them. The actions, mechanisms and practices identified in the basin's flood risk management plans (in case that it is existing) which are related to F.OR activities, have to be incorporated into the current flood risk management plan.

2.2 Study area

The above described methodology is applied for Public Services Company of Platanias Municipality, located in Crete Island, Greece. Apart from the other activities, supporting the agricultural sector is one of the main duties of the company. The agricultural activity is taking place in Tavronitis watershed the boundaries and location of which are presented in Figure 3. As illustrated in Figure 3, the upper half of the watershed is dominated by agricultural land, while olives constitute the main crop cultivated there. The watershed covers an area of about 140 km^2 while the elevation varies between 0 and more than 1400 m amsl. According to Kourgialas et al (2015), the average annual precipitation for the watershed is about 665 mm, while more than 95% of the total annual precipitation occurs between October and May (Chartzoulakis et al, 2001). The hydrogeological regime of the watershed consists of karstic formations (high to moderate permeability), alluvial deposits (variable permeability, miocene deposits (moderate to low permeability), granular non-alluvial deposits (small to very small permeability) and impermeable formations. According to Kourgialas et al (2015),

Tavronitis watershed indicate significant surface runoff potential which is mainly attributed to the impermeable formations existing at the semi-mountainous part of the watershed.

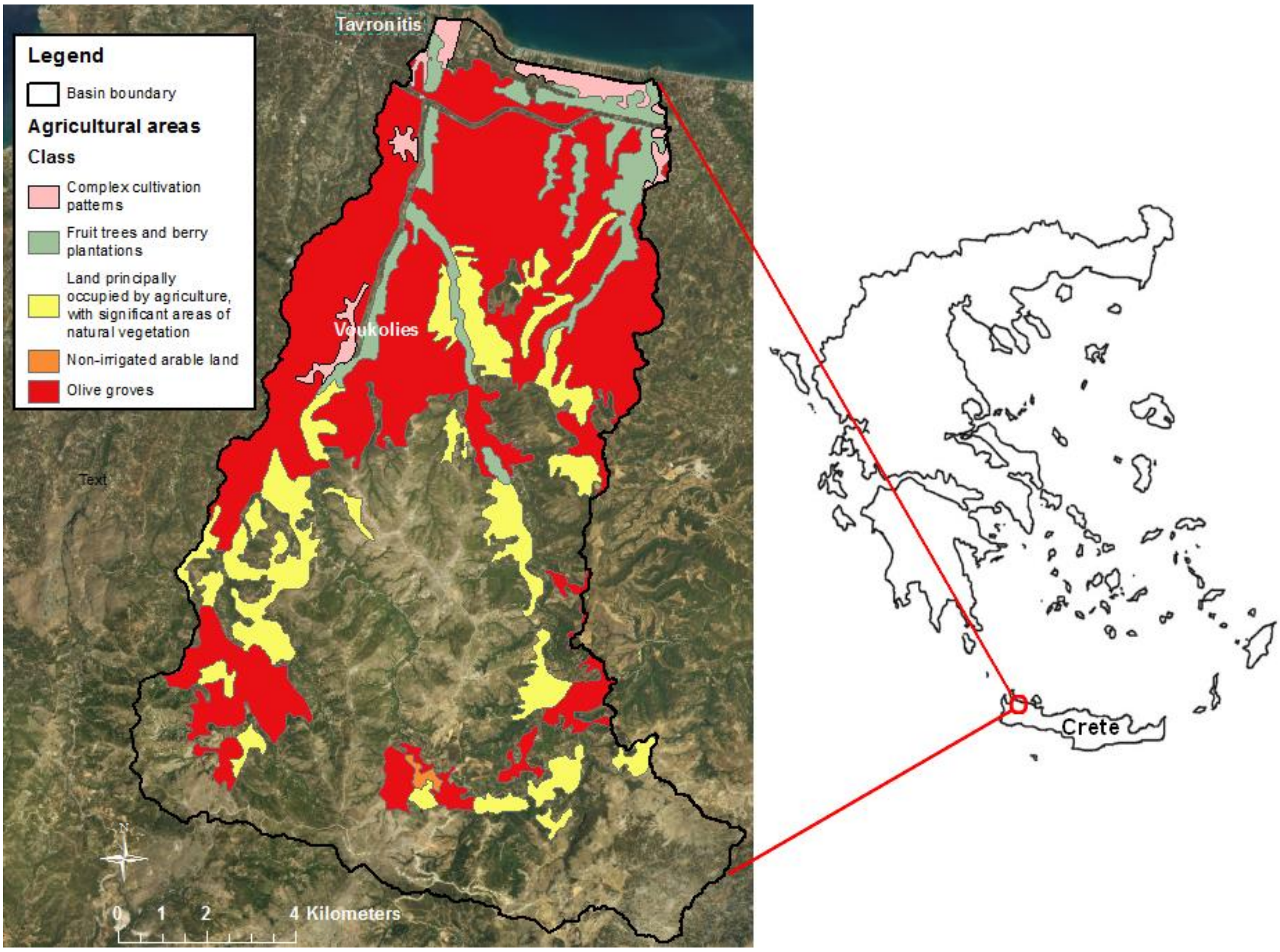


Figure 3: Location map and agricultural areas of Tavronitis watershed.

3. RESULTS AND DISCUSSION

3.1 Floods risk assessment

With regard to river floods risk assessment, it was based on the Preliminary Floods Risk Assessment report for Crete District (Hellenic Special Secretariat for Water 2012) as found on the website of the Hellenic Ministry of Environment and Energy (http://www.ypeka.gr/Default.aspx?tabid=252), as well as the corresponding flood risk and hazard maps (http://floods.ypeka.gr/) (Hellenic Special Secretariat for Water 2016). As presented in Figure 4, one high flood risk zone was identified, located in the northern half of Tavronitis basin, and mainly along Tavronitis main river courses. Moreover, four recorded historic flood events were identified in Tavronitis River basin, based on the Preliminary Floods Risk Assessment report, while several other flood events were found in the surrounding area. The major part of the high flood risk zone is covered by agricultural land, while two education facilities, one sport facility, two livestock farms and three water supply boreholes are included in the infrastructures that can potentially be affected by a river flood in Tavronitis basin. With regard to the population affected three settlements of less than 500 inhabitants each are identified. For recurrence periods of 50 and 100 years, potential flood impact is predicted to be low or very low. Even for recurrence interval of 1000 years, potential flood impact can be overall considered as low, except from the northern part of the basin in which a moderate impact zone is identified and Voukolies village in which a high impact zone is foreseen. According to the above, river floods risk for the agricultural sector in Tavronitis basin is not high and it is concentrated to specific areas which cover a small part of agricultural areas in the basin.

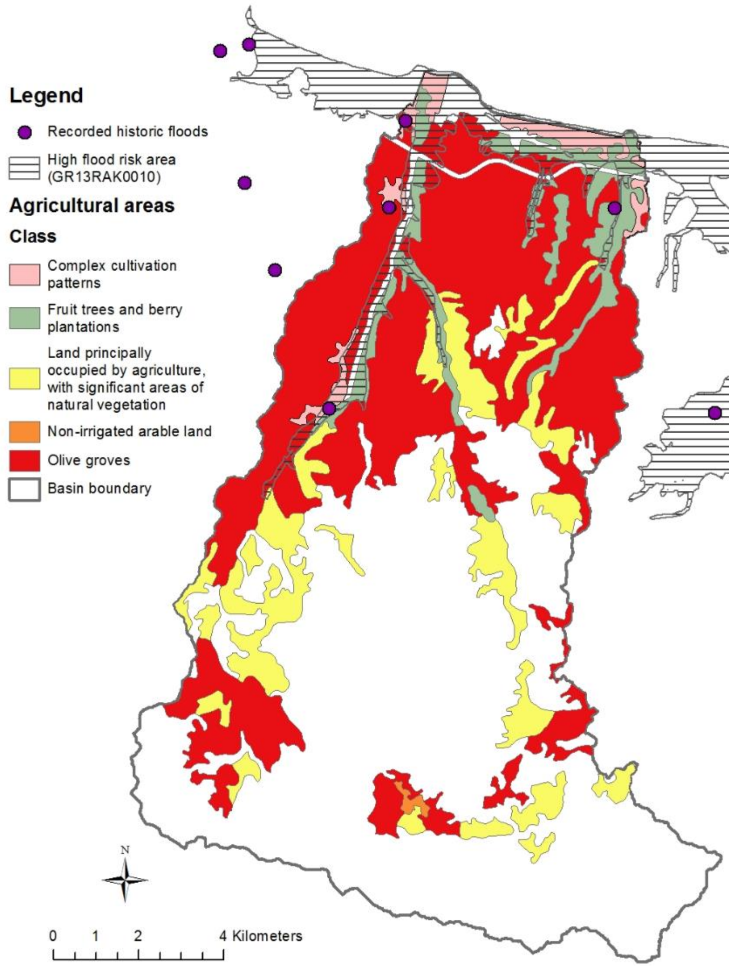


Figure 4: High flood risk areas and historic floods in Tavronitis basin, as identified in the Hellenic Preliminary Floods Risk Assessment report.

With regard to flash flood risk assessment, the results of surface runoff potential estimation are presented in Figure 5. The average runoff potential for all agricultural areas ranged from moderate to high. The lowest average runoff potential was calculated for fruit trees and berry plantations (1.59-moderate), while the highest runoff potential was calculated for land principally occupied by agriculture, with significant areas of natural vegetation (2.52-very high). Especially for olive groves, which constitute the dominant land cover for Tavronitis basin (32.34%), the average runoff potential was 2.06 and it is considered as high, while the corresponding range of variation was 0.88 (low) – 2.75 (very high), thus indicating a significant degree of runoff potential variation. Considering the above, it can be concluded that overall the contribution of the agriculture activity developed in Tavronitis basin to the development of flash floods is moderate to high, and this is mainly attributed to significant rainfalls experienced in the southern part of the basin and to the steep slopes of the topographic relief.

3.2 Floods risk management

3.2.1 Reducing farms contribution to floods

The actions presented below aim to contribute to surface runoff potential reduction and therefore to directly reduce the contribution of agricultural activity to flash floods. The direct reduction of flash floods may reduce (depending on the incident) the contribution of agricultural activity to river floods. A wide range of practices are proposed in the literature which aim to contribute to surface runoff reduction from crop covered land. The actions practices and measures presented below are chosen

from the pool of practices that are to be implemented in the context of the project as well as other actions applicable to the specific case of Tavronitis basin.

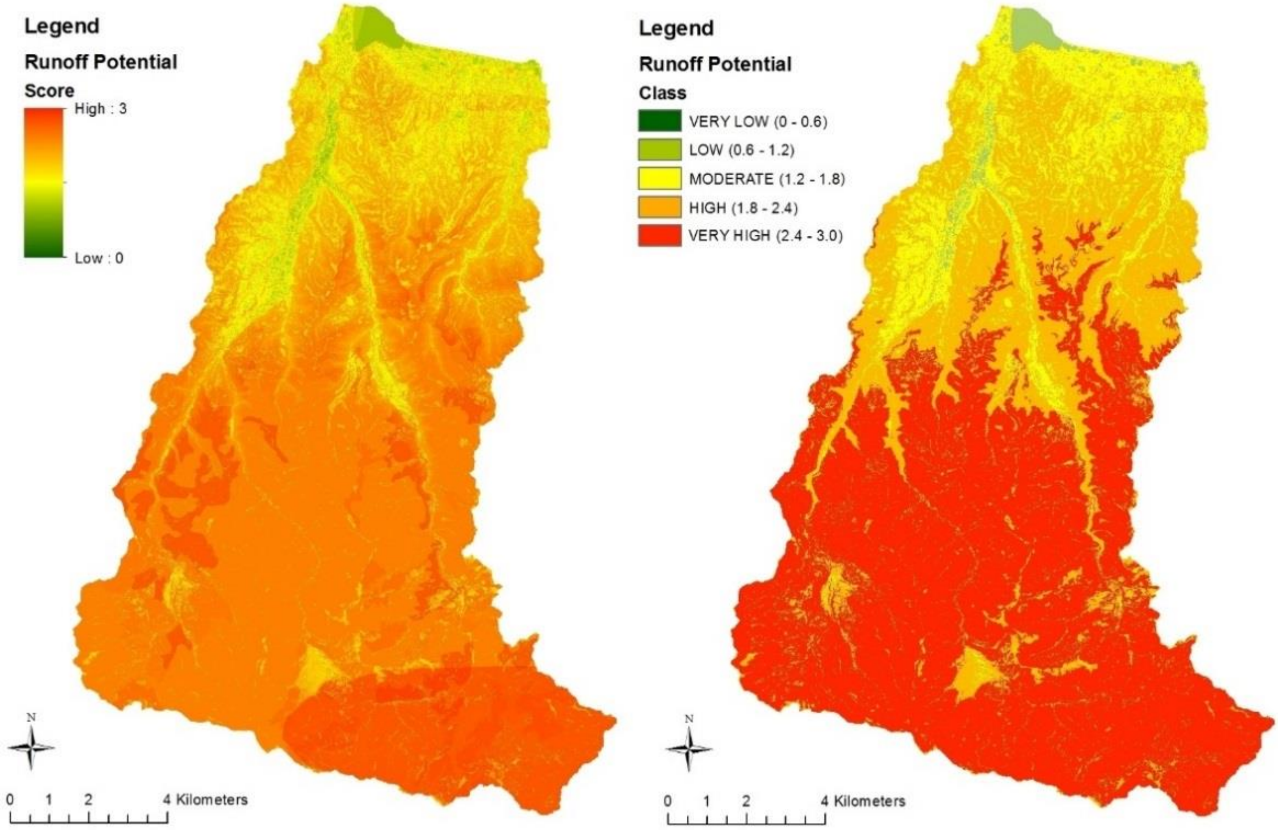


Figure 5: Spatial distribution of runoff potential score and classes in Platanias basin.

The practices implemented and tested within the context of LIFE AgroClimaWater project that directly or indirectly contribute to surface runoff potential reduction are the following:

No weed control: According to this practice, natural vegetation is preserved during the wet season. Therefore, soil is covered during the rainy season resulting in surface runoff potential decrease. This practice is similar to the establishment of cover crops.

No soil tillage: Despite the fact that this practice was incorporated with a view to reduce evaporation losses, according to Aina (1993) other benefits such as storm runoff reduction and improved infiltration capacity can be expected by its application.

Physical reduction of surface runoff: Surface runoff can be reduced by introducing physical materials along the contour lines.

Other practices and measures that are well known to be effective in reducing surface runoff potential from the farms are the following:

Conservation buffers: This practice includes the development and/or maintenance of small areas or strips of permanent vegetation. There are several versions of this practice applied such as riparian buffers, filter strips and grassed waterways.

Avoidance of vehicle movements and wheel ruts on wet soil.

Avoidance to the best possible degree, of heavy machinery use within the farm. Heavy machines are contributing to soil compaction, which reduces water infiltration capacity thus increasing surface runoff potential.

Water collection infrastructures can also contribute to flood impacts mitigation and serve as water saving infrastructures that will provide water during the peak water demand periods. The F.OR has to upgrade and maintain collaboration with the local authorities and mainly with the local Technical Services Division and the Water Directorate, Decentralized Administration of Crete in order to perform a feasibility study for the construction of water collection infrastructures and identify

potential funding tools such as the National Strategic Reference Framework (NSRF). With regard to Tavronitis basin, Kourgialas et al. (2015) applied a hydrologic model and indicated several possible locations for the construction of small hydraulic structures (dam and/or reservoir).

3.2.2 Actions before the flood

Two set of actions are proposed to be taken when a flood incident is expected to occur in order to ensure sufficient preparation for the flood. The first set of actions is related to actions that can be taken by the F.OR. The F.OR has to establish a communication channel with the local authorities in order to be informed when a flood event is expected to occur, which in our case are the Independent Civil Protection Offices and Fire Stations. Moreover, the F.OR can maintain a list of available member farmers' machinery that can be set at the disposal of the authorities to serve during the flood and/or alleviate its impacts. This list that is originally drawn and maintained by the F.OR administration, is notified to the Independent Civil Protection Office. As a second step, the F.OR has to establish a second communication channel with its farmers-members in order to inform them about the expected flood incident.

A second set of actions that can be applied by the farmers has to be established and communicated to them. This set includes practical directions easily understood and applied by the farms such as:

Avoid applying fertilizers and plant protection products prior to the flood, since the possibility for water bodies' pollution from runoff or leaching is high.
In case that electricity supply is available in the farm, the farmers has to be sure that it is turned off and secured.
In case that a groundwater pumping well or borehole exists in or near the farm, it has to be sealed properly in order to avoid runoff water entering through the annulus.
A list of the existing on-farm machinery and equipment has to be drawn.
The farmer has to be sure that potentially hazardous substances, such as fertilizers, plant protection products and fuels are not exposed in the farm. These should be securely stored in appropriate infrastructure at the field or removed to such a place off the farm.
The farmer has to secure or remove heavy/hazardous equipment and machinery from the farm.

3.2.3 Actions during the flood

A set of actions can be taken in order to ensure sufficient preparation for the flood. The F.OR has to get informed about the flood status. Therefore, the F.OR has to stay in touch with the local authorities (e.g. the Independent Civil Protection Office and Fire Station) and report the availability of F.OR member farmers' machinery to help in case this is needed. Information about flood status can be also retrieved by the local media. Moreover, it has to be clearly stated to the farmers that it is very critical to avoid being on the farm or any other exposed location during the flood, to find a safe place to stay and do move without any specific scope and finally to avoid using flooded bridges or river/creek passages.

3.2.4 Actions after the flood

The set of actions that could be taken after the flood can be divided into those that can be implemented by the F.OR and those that can be applied by the farmers. Concerning the F.OR actions, it has to get informed about the impacts of the flood and follow the directions of local Independent Civil Protection Office and Fire Station. Also the F.OR has to communicate with the local Department of Rural Economy and Veterinary Prefecture since it is responsible for providing information of farmers for the protection of agricultural properties according to the Preliminary Flood Risk Assessment report (Hellenic Special Water Secretariat 2012). As a next step, the F.OR has to communicate the information to the farmers and ask farmers if fertilizers of plant protection products have been applied in the farm before the flood and relay this information to the Water Directorate of the District.

With regard to the actions that can be applied by the farmers, the following are proposed:

Be careful when trying to approach your farm in order to avoid injury.

Compare the list of your equipment compiled before flood in order to identify damages or losses.
Check the overall status of your farm before and after the flood.
Stay in touch with the F.OR in order to guide you for the next steps.
In case that fertilizers of plant protection products have been applied in the farm before the flood, communicate this information to the FOR.
Report loss of any agrochemical, piece of equipment or machinery and any changes to the soil cover at your farm.
The most significant impacts of floods in a farm are deposition of sediment of productive land, agricultural soil erosion and soil nutrient losses. In order to mitigate the above mentioned impacts the following practices could be applied by the farmers:

Try to incorporate the sediment excess into the field by tillage. In case that this is not feasible the sediment has to be removed from the farm and disposed off in a designated site. By no means should this sediment be disposed off next to the course of a creek, torrent or river.
Try to rehabilitate soil erosion with appropriate tillage. In case that this is not feasible, try to fill the erosion gaps with material from other sites. Take all precautions to use appropriate soil for this purpose (adjacent site, consult an agronomist, etc).
Check the nutrient concentrations of the soil in the farm and properly adjust. Cover crops application has been found to significantly contribute to soil recovery after flooding.

4. CONCLUSIONS

Although a task of high scientific resources demand, usually organized in regional or national level, the results of the present study indicate that flood action plans can be compiled in smaller scales, such as this of Farmers Organization. This can be accomplished by:

gathering existing data from the relevant documents and maps developed in the context of Floods Directive by EU,
implementing simplified methodologies based on GIS technology and
gathering well-established measures and practices that can contribute to floods' risk management and impact mitigation.
It is expected that the compilation and implementation of such action plans can significantly contribute to floods impact preparedness and response level in the basin scale, since stakeholders and groups of water users are more actively involved in floods risk and impact management and mitigation, while the tailor-made action plans maximize the potential of action plans implementation.

With regard to application of the proposed methodology in Tavronitis basin, the results indicated that despite the fact that river floods risk and impact is mild, flash flood risk is high in a significant part of agricultural areas. A set of practices and measures easily applied are proposed in order to increase its preparedness and response level to floods, while establishing communication channels with the competent authorities is considered as necessary.

Acknowledgements
This work has been elaborated in the framework of the LIFE AgroClimaWater project (LIFE14 CCA/GR/000389) which is gratefully acknowledged.

References

1. Aina P.O. (1993) **'Rainfall runoff management techniques for erosion control and soil moisture conservation'**, FAO Soils Bulletin (FAO).
2. Ajmal, M., M. Waseem, J.H. Ahn and T.W.Kim (2015) 'Improved runoff estimation using event-based rainfall-runoff models', **Water Resources Management**, Vol 29(6), pp.1995-2010.

3. Chartzoulakis K.S., N.V. Paranychianakis and A.N. Angelakis. (2001) 'Water resources management in the island of Crete, Greece, with emphasis on the agricultural use', **Water Policy**, Vol 3(3), pp. 193-205.

4. FAO (2015) **'The impact of disasters on agriculture and food security'**, Food and Agriculture Organization.

5. Hellenic Special Secretariat for Water (2012) **'Preliminary Flood Risk Assessment'**, Hellenic Ministry of Environment, Energy & Climate Change.

6. Hellenic Special Secretariat for Water (2016) **'Flood risk management plan of Crete Water District basins'**. Hellenic Ministry of Environment & Energy.

7. Kourgialas N.N., G.P. Karatzas and G. Morianou (2015) 'Water management plan for olive orchards in a semi-mountainous area of Crete, Greece', **Global Nest Journal**, Vol 17(1), pp. 72-81.

8. Mohammad F.S. and J. Adamowski (2015) 'Interfacing the geographic information system, remote sensing, and the soil conservation service–curve number method to estimate curve number and runoff volume in the Asir region of Saudi Arabia', **Arabian Journal of Geosciences**, Vol 8(12), pp.11093-11105.

9. NRCS-USDA (1986) **'Urban hydrology for small watersheds'**, Technical Release 55 (TR-55) (Second ed.). Natural Resources Conservation Service, Conservation Engineering Division.

10. Pivot J.M. and P. Martin (2002) 'Farms adaptation to changes in flood risk: a management approach', **Journal of Hydrology**, Vol 267(1-2), pp.12-25.

11. Posthumus H., Hewett C.J.M., Morris J. and P.F. Quinn (2008) 'Agricultural land use and flood risk management: engaging with stakeholders in North Yorkshire', **Agricultural Water Management**, Vol 95(7), pp.787-798.

12. Tachikawa T., Kaku M., Iwasaki A., Gesch D.B., Oimoen M.J., Zhang Z., Danielson J.J., Krieger T., Curtis B., Haase J. and M. Abrams (2011) **'ASTER global digital elevation model version 2-summary of validation results'**. NASA.

MODERN MAPPING TECHNOLOGIES FOR MORPHOMETRY DYNAMICS OF KERKINI RESERVOIR

I. Tsolakidis[1*] and M. Vafiadis[2]

[1]Lake Kerkini Management Authority, GR-62055 Kerkini, Kato Poroia, Serres, Macedonia, Greece,
[2]Division of Hydraulics and Environmental Engineering, School of Civil Engineering, A.U.Th, GR-54124 Thessaloniki, Macedonia, Greece

[*]Corresponding author: e-mail: tsolakidisioannis@gmail.com, tel : +302327028004

Abstract
In a lake ecosystem environment or a reservoir system, the knowledge of some basic parameters, such as the morphometry of the lake, the basin and the distribution of physical, chemical and biological parameters is very crucial. The determination of these parameters is fundamental in the implementation of a management plan for the protection and restoration of lakes and reservoirs. This paper investigates modern mapping technologies such as GNSS/GPS and sonar systems, for the estimation of morphometric parameters, as the bottom relief, the hypsographic curves, the volume-heights tables and also the calculation of the deposition rate of sediments in a reservoir. The latter is a particularly critical problem in reservoirs where hydroelectric plants operate. At the same time, the paper examines a mapping method, alternative to traditional techniques, faster and significantly more economical, making a management plan viable. It is the method of satellite bathymetry, which is based on the extraction of depths, using information from the spectral bands, of a satellite image. For this purpose, the multi-spectral image of the Worldview-2 satellite is being used. In both mapping techniques (hydrography and satellite bathymetry), all the necessary reliability checks are implemented and the comparison between them, lead to conclusions about the use and applicability of each method. The Kerkini reservoir is the case study, where all these methods and techniques are applied. The aim of this paper is to describe and propose reliable mapping techniques that contribute to the efficient management of water systems such as the Kerkini reservoir.

Keywords: Morphometry, GNSS/GPS, satellite bathymetry, reservoir management

1. INTRODUCTION

In the guidance manuals for lake and reservoir restoration (Olem & Flock, 1990), the calculation of basic morphometric parameters such as depth, area, volume, shoreline length and other important elements, that can characterize the ecological value of the water body, is fundamental. The water quality variables and aquatic organisms (Stefanidis & Papastergiadou, 2012) are also of prime concern. Moreover, many researchers have highlighted the relationship between the morphometry and other variables, such as fish production, benthic communities, sedimentation, stratification, and other (Håkanson, 2005a; Håkanson, 2005b). In our case study, the Kerkini reservoir is a sensitive ecosystem whose overall status is characterized as "Incomplete" according to the River Basin Management Plan of the Eastern Macedonia Water Basin (EL11) (Antonaropoulos, 2017). In addition, no methods and techniques are described for optimal monitoring morphometry of the reservoir.

In the first part of the study, modern hydrographic techniques are used, such as the GNSS/GPS systems and a topographical precision single beam sonar, for the determination of a) lake morphometry and b) deposition rate of sediments, contributing to the overall assessment of ecological

status of the reservoir (Gąsiorowski, 2008). In the second part of the paper, the hydrographic method is compared to the alternative method of satellite bathymetry, using the Worldview-2 satellite image, with 2m spatial resolution and 8 spectral bands. The method of satellite bathymetry, investigates which bands of the image have the least water absorption, or in other words which bands are most suited for mapping the bottom (Philpot, 1989; Chang, 2011). For this purpose, two models are examined, a) the Stumpf algorithm and b) a model of multiple linear regression (Dierssen et al, 2003). The case study area for this work is the reservoir of lake Kerkini, at the Lake Kerkini National Park, located in the northern western part of the prefecture of Serres, in the Region of Central Macedonia, in Greece (Figure 1).



Figure 1. Location of Kerkini reservoir (https://www.google.gr/maps)

2. HYDROGRAPHY OF KERKINI RESERVOIR

2.1 Methodology

The hydrographic process involved four steps: a) preparing the measurements, b) collecting data, c) processing and finally d) analyzing the observations. During the first stage, the design of measurements, calibration and control of measuring instruments (GNSS/GPS system + sonar) was implemented. For this purpose, stainless steel structures were designed and constructed for both the stabilization of instruments on the vessel (Figure 2) and their calibration. After all the necessary tests, the hydrographic measurements were carried out.



Figure 2. Mounting pole with survey instruments on the surveying vessel

For the mapping of Kerkini reservoir, the RTK GNSS/GPS method was used (Figure 3), in conjunction with the depth measurements from echo sounder, while the contribution of the Network RTK method of Virtual Reference Station (VRS) was investigated. (Henning, 2008; El-mowafy, 2012; Mageed, 2013). The mapping datum of the project was the Greek Geodetic Reference System of 1987 (GGRS '87). The overall period of hydrographic measurements lasted from 29/05/2014 until 11/07/2014 (Figure 4).

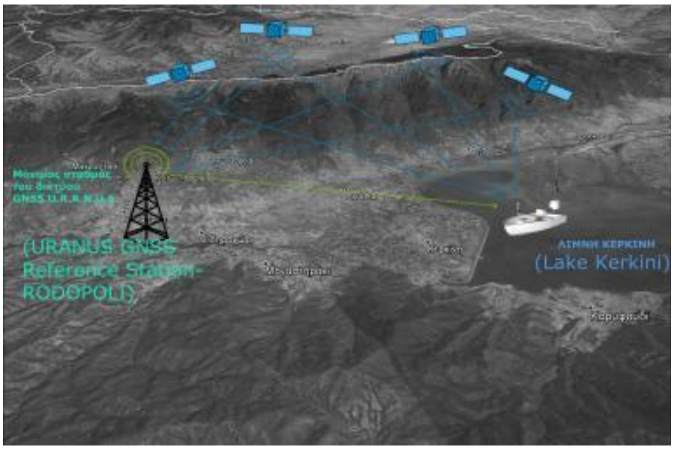


Figure 3. Schema of RTK measurements

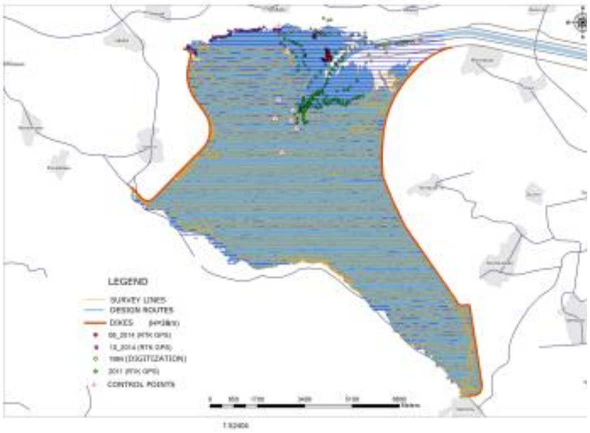


Figure 4. Final hydrographic and topographic measurements at Kerkini reservoir

The mapping statistics of the Lake Kerkini were as follows:

- 17 days of hydrography
- 3 days of additional topographic measurements
- Total Points: 87271
- Total route length: 445.58Km
- Average hydrographic speed of the vessel: 6.19Km/h
- Total working hours: 69h 14m 30sec

A quality assessment of the GNSS/GPS observations from hydrographic measurements was then followed. The last step was the "data cleaning" process and the selection of the interpolation method, for the creation of bathymetric model (Figure 5).

For the external accuracy control of the bathymetric model, ten (10) points were topographically measured with the RTK GNSS/GPS technique, well distributed in the revealed delta, during the lowest water level season. Their elevations were then compared, with the corresponding elevations of the model. After the completion of the external control, morphometric data were produced, such as the bottom relief, volumetric tables, hypsographic curves, etc. (Figures 5, 6).

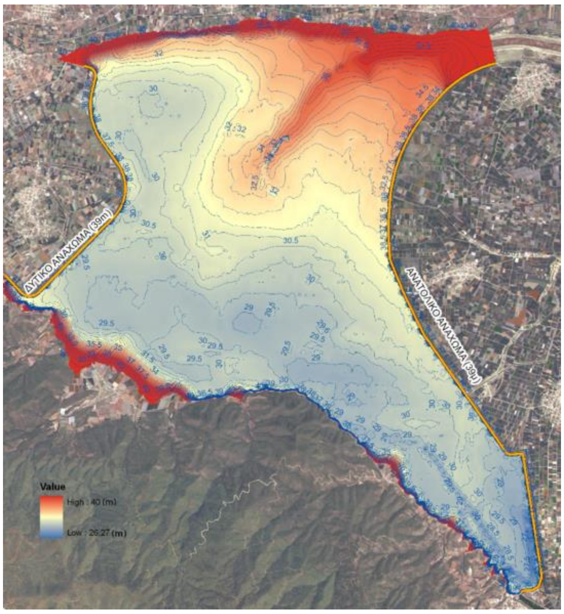


Figure 5. Bathymetry model of Kerkini reservoir with contour interval = 0.5m (pixel size=20x20m)

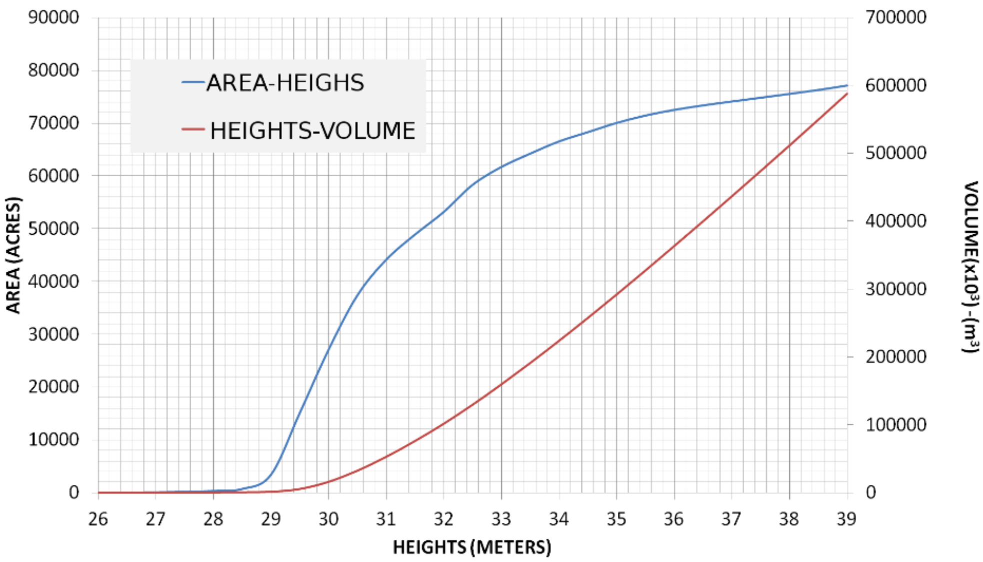


Figure 6. Hypsographic curves of Kerkini reservoir

2.2 Sedimentation rate

Another study, very significant for monitoring the reservoir storage and also for the smooth operation of hydroelectric plants at dams, was the determination of the deposition rate of sediments. It is noted that a hydroelectric plant is operating at a close distance from Kerkini Dam. In order to draw conclusions about the deposition rate at Kerkini reservoir, volumetric tables were used from earlier mapping projects of Kerkini in 1984 and older. Comparing the volumes, a decrease in the deposition rate of the reservoir was recorded, for the period of thirty years (1984-2014), equal to $683x10^3$ m^3/yr. Combining older data, from the early years of construction and operation of the reservoir in 1933 (Psilobikos et al, 1994), the decline trend of the deposition rate can be observed for over all these years, up to the last mapping in 2014 (Figure 7). It should be noted, however, that any calculations, such as volumes and changing rates of volumes, must be accompanied by their respective uncertainties, since the accuracy and specifications of the work and the instruments used in each mapping project are not always known (Dorst, 2004; Wilson L & Richards M, 2006; Czuba et al, 2012; Tsolakidis, 2017).

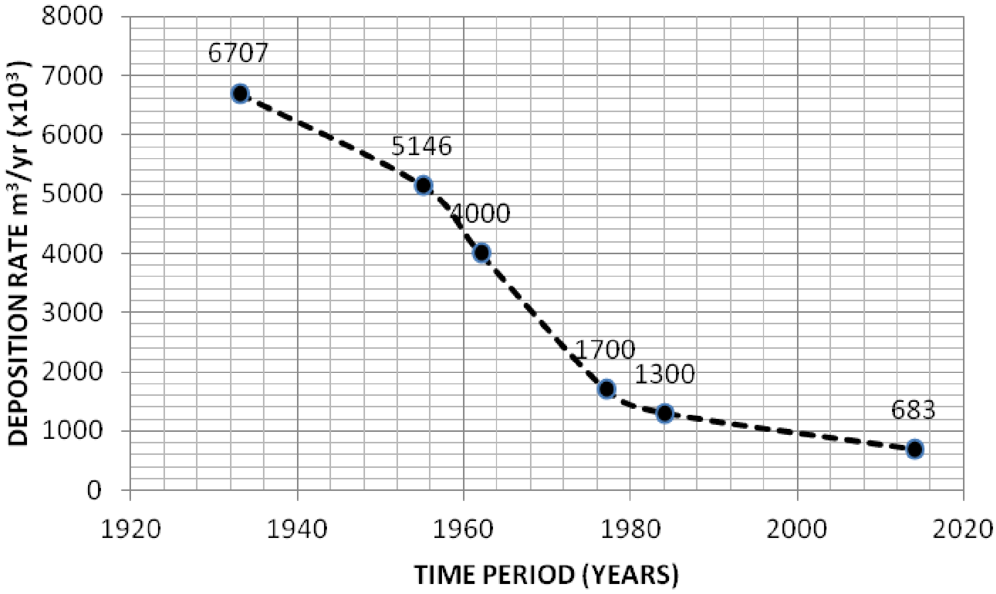


Figure 7.Deposition rate from 1933 to 2014 at Kerkini reservoir

3. SATELLITE BATHYMETRY OF LAKE KERKINI

3.1 Methodology

The next step was the implementation of satellite bathymetry for extracting the depths of Lake Kerkini. Satellite bathymetry is a more economical method for studying the morphology of water bodies, which under conditions, might replace more traditional techniques, due to increasing spatial and spectral resolution of new satellites. This method, which belongs to passive remote sensing methods, attempts to replace the calculation of scattering and absorption coefficients at each point with regression models using known depths and spectral values (Lyzenga, 1978; Stumpf & Pennock, 1989; Stumpf et al, 2003). Finally, two models were tested, a) the Stumpf linear model (Equation 1), which is suitable for low reflectance bottoms and b) the model of Multiple Linear Regression (Equation 2). The available captured date of the image used for satellite bathymetry, was 08/08/2014, few days after the completion of hydrographic measurements.

$$z = m_1 \times \left(\frac{ln\left(nR_w(\lambda_1)\right)}{ln\left(nR_w(\lambda_2)\right)} \right) - m_0 \qquad (1)$$

Where:

- z is the depth
- m_1, m_0 are the addition and offset to adapt the results of the algorithm to the depth, respectively

$R_w(\lambda_1)$, $R_w(\lambda_2)$ the values of the pixels in the bands λ_1 and λ_2, respectively

$$Z = a_0 + a_1 X_1 + a_2 X_2 + \ldots + a_n X_n \qquad (2)$$

Where:

- z is the depth
- $a_0, a_1, a_2, \ldots, a_n$ are the coefficients of the multiple regression
- $X_1, X_2, \ldots, X_n$ are the linearized values of the pixels of the satellite image, $\lambda_1, \lambda_2, \ldots, \lambda_n$, respectively

For practical reasons, the Stumpf model will be referred to as model 1 and the model of the multiple regression as model 2.

3.2 Worldview-2 satellite image processing

All the necessary calibrations and corrections (geometric, atmospheric etc) were performed on the Worldview-2 satellite image (Figure 8), in order to compute the water leaving radiance. The last step was to apply a mask to the image, so that only the "wet" pixels (lakes, rivers) remain. The resulting final image (Figure 9) was used to apply and evaluate the bathymetric models.

For the implementation of model 1, the Coastal and Yellow bands of the Worldview-2 final image (Figure 8) were used, while all the bands were involved in model 2. The coefficients of the linear regression were then calculated and the two models compared, based on the criterion of the largest R^2. The equation applied to the Worldview-2 image (Figure 9) was the one of multiple linear regression (Equation 3).



Figure 8. Multispectral image of Worldview-2 satellite before any correction (R=6,G=3,B=2)



Figure 9. Final image of "wet" pixels at Kerkini reservoir after all corrections (R=5,G=3,B=2)

$$Z = 83.694 - 6.4314X_1 - 2.7718X_2 + 4.7243X_3 - 5.3607X_4 - 6.4147X_5 + 2.7699X_6 - 1.0949X_7 - 2.0323X_8 \quad (3)$$

The last step was the accuracy control of the bathymetric model, obtained by the method of satellite bathymetry. For this purpose the difference image technique was applied (Williams, 2012). The result of satellite bathymetry was subtracted from the model that resulted from the hydrography. Then, based on the difference image (Figure 10), the difference diagram was calculated, according to specific depth ranges. From the study of the diagram of Figure 11, it appears that a percentage of 63.03% of the pixels of the two models have a difference ranging from 0 to 50cm.

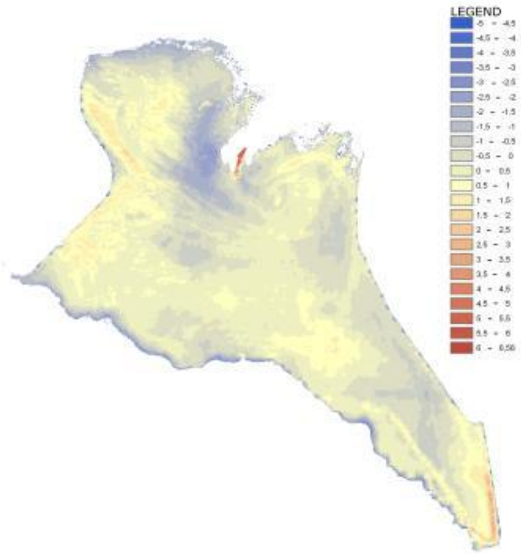


Figure 10. Difference image from hydrography and satellite bathymetry

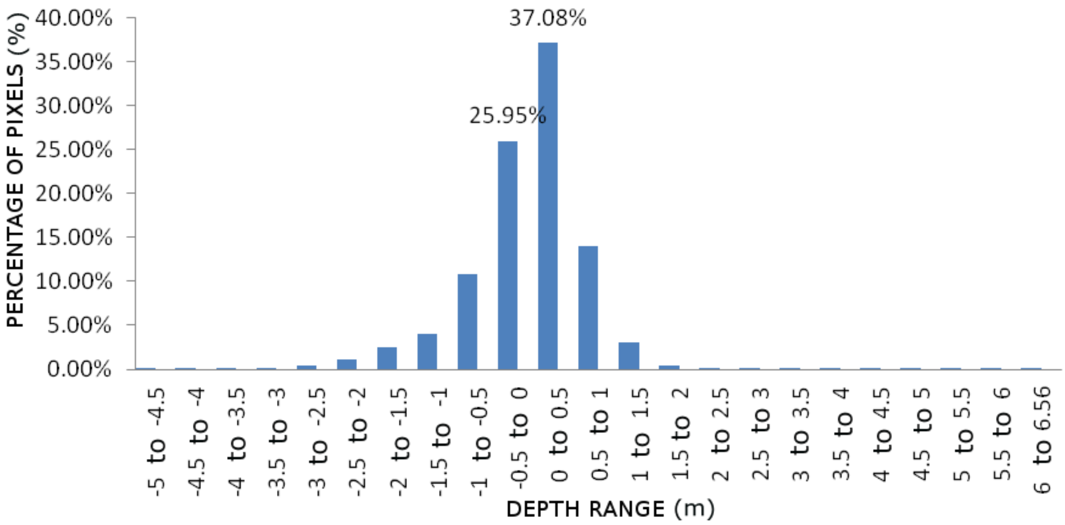


Figure 11. Percentage of pixels per depth range from difference image

4. DISCUSSION AND CONCLUSIONS

In this paper, the application of modern mapping technologies and methods (GNSS/GPS and sonar) for the extraction of reliable morphometric parameters of Kerkini reservoir, aiming to the efficient management of the water body was presented. In addition, it was investigated whether an alternative technique such as satellite bathymetry, could replace more traditional mapping techniques and reduce the final cost.

From the hydrographic results, it has been shown that the use of RTK GNSS/GPS and sonar systems is indicated, for an efficient and accurate mapping of large reservoirs. For Kerkini, it should be noted that any future mapping should follow modern methods (continuous semi automated) rather than classical ones (manual point by point). In addition, the applied system can provide satisfactory accuracy in calculating the bottom elevation. With the RTK GNSS/GPS method, this accuracy decreases as the vessel moves away from the permanent GNSS station. Using the network method of VRS, this problem is solved. Regarding the changing rate of the volume at the Kerkini reservoir, a continuous decrease in the deposition rate was observed until 2014. However, it is crucial to mention that in such applications, the knowledge of methods and accuracy of hydrographic projects is

prerequisite. The extraction of important morphometric data, such as volumetric tables etc, is based on their reliability. Comparison between volumes of different years, produced by different instruments and other specifications, should be carefully considered, taking into account relevant uncertainties, in order to draw safe conclusions.

With regard to satellite bathymetry, it has emerged that the model of multiple linear regression leads to better results than the Stumpf model. The most important band variables, from the Worldview-2 satellite, which contributed most to the depth extraction model, were Green and Red. However, the results in a bathymetric model and their interpretation are directly dependent upon the clarity of water and the atmospheric conditions that affect the image captured by the satellite. Concerning the comparison of the model of the satellite bathymetry with the hydrographic model, it was found that the majority of the pixels of the difference image (63.03%), had a difference ranging from 0 to 50cm. The precision tolerance of the satellite bathymetry, for 63.03% of the bottom pixels, has a mean value of ±25cm, if the hydrography is considered as a reference surface. For the other pixels, this value is increased.

In general, the adoption of a method, in the extraction of morphometric parameters, depends on the instruments and data available, the environmental and atmospheric conditions and the estimated budget. In low-budget cases, where the morphometry of a reservoir is selected to be studied with passive remote sensing methods, a distinction should be made between water status, turbidity and atmospheric factors, because they are all affecting the reliability of satellite bathymetry. In cases of low turbidity (typically<10 NTU), satellite bathymetry can be used with greater reliability, always in conjunction with on-site depth measurements, which will calibrate the bathymetry model. In addition, by using free data from Sentinel missions, with high temporal, spatial and spectral analysis, the total cost is dramatically reduced. In cases of high turbidity of reservoirs such as Kerkini, the method to be applied depends on the precision requirements of the application. For extracting bottom elevations and assessing the changing rate in volume, where the specifications on accuracy are strict, the hydrographic method is considered more appropriate. However, as shown in Figure 10, satellite bathymetry has yielded satisfactory results across the depth range of the lake. The average accuracy of ±25cm refers to both the low depths and the high ones. With a more appropriate date of image selection and at a period with less turbidity in the reservoir, the percentage of the difference pixels, ranging from 0 to 50cm, is estimated to increase over 85%, leading in more encouraging results about the use of the method.

Acknowledgments

We would like to thank the Lake Kerkini Management Authority, which provided us with the satellite image data and contributed to the implementation of hydrographic measurements. Also we are grateful, for all the help they provided to this project, to Professor Krestenitis Ioannis, School of Civil Engineering, AUTh, who provided us with the necessary topographic instruments and Professor Albanakis Konstantinos, School of Geology, AUTh, for his comments on the sedimentation process in lake Kerkini and satellite bathymetry models.

References

1. Antonaropoulos, P. (2017) ‘Review of River Basin Management Plan of Water District of Eastern Macedonia (EL11)’, (in Greek).
2. Chang, C.W. (2011) ‘Retrieval of Water Optical Properties From Eight-Spectral Band Worldview-2 Satellite Images’, **32nd Asian Conference on Remote Sensing 2011, ACRS 2011**.
3. Czuba, J. a. et al. (2012) ‘Changes in Sediment Volume in Alder Lake’, Nisqually River Basin , Washington, 1945 – 2011.
4. Dierssen, H.M. et al. (2003) ‘Ocean color remote sensing of seagrass and bathymetry in the Bahamas Banks by high resolution airborne imagery’, **Limnology and Oceanography**, 48(1_part_2), pp.444–455.

5. Dorst, L.L. (2004). ‘Survey plan improvement by detecting sea floor dynamics in archived echosounder surveys’, **International Hydrographic Review**, 5, pp.49–63.
6. El-mowafy, A. (2012) ‘Precise Real-Time Positioning Using Network RTK’, **Global Navigation Satellite Systems - Signal, Theory and Applications**, pp.161–188.
7. Gąsiorowski, M. (2008) ‘Deposition Rate of Lake Sediments Under Different Alternative Stable States’, **Geochronometria**, 32(1), pp.29–35. Available at:
8. http://www.degruyter.com/view/j/geochr.2008.32.issue--1/v10003-008-0020-y/v10003-008-0020-y.xml.
9. Håkanson, L. (2005a) ‘The importance of lake morphometry and catchment characteristics in limnology - Ranking based on statistical analyses’, **Hydrobiologia**, 541(1), pp.117–137.
10. Håkanson, L. (2005b) ‘The importance of lake morphometry for the structure and function of lakes’, **International Review of Hydrobiology**, 90(4), pp.433–461.
11. Henning, W. (2008) ‘National Geodetic Survey User Guidelines For Classical Real Time GNSS Positioning’, Tech. Report.
12. Lyzenga, D.R. (1978) ‘Passive remote sensing techniques for mapping water depth and bottom features’, **Applied optics**, 17(3), pp.379–383.
13. Mageed, K.M.A. (2013) ‘Accuracy evaluation between GPS Virtual Reference Station (VRS) and GPS Real Time Kinematic (RTK) techniques’, **World Applied Sciences Journal**, 24(9), pp.1154–1162.
14. Olem, H. & Flock, G. (1990) ‘The Lake and Reservoir Restoration Guidance Manual Second Edition Lake and Reservoir Restoration’, pp.1–35. Available at:
15. http://dx.doi.org/doi:10.7282/T3JD4WCD.
16. Philpot, W.D. (1989) ‘Bathymetric mapping with passive multispectral imagery’, **Appl. Opt.**, 28(8), pp.1569–1578. Available at: http://ao.osa.org/abstract.cfm?URI=ao-28-8-1569.
17. Psilovikos, A. et al. (1994) ‘Study of Environmental Impact Assessment of Strymonas River Protected Area Projects, Lake Kerkini, Streams of the Serres Plain’, Ministry of Environment and Waters, Directorate of Land Reclamation Works (D7), Department of Technical Support.
18. Stefanidis, K. & Papastergiadou, E. (2012) ‘Relationships between lake morphometry, water quality, and aquatic macrophytes, in greek lakes’, **Fresenius Environmental Bulletin**, 21(10 A), pp.3018–3026.
19. Stumpf, R.P. et al. (2003) ‘Determination of water depth with high-resolution satellite imagery over variable bottom types’, **Limnology and Oceanography,** 48(1_part_2), pp.547–556.
20. Stumpf, R.P. & Pennock, J.R. (1989) ‘Calibration of a general optical equation for remote sensing of suspended sediments in a moderately turbid estuary’ **Journal of Geophysical Research**, 94(C10), p.14363.
21. Tsolakidis, I., (2017) ‘Comparison of hydrographic and satellite bathymetry methods for geomorphology study of reservoirs: Case study of lake kerkini reservoir’, Phd Thesis, Aristotle University of Thessaloniki, (in Greek).
22. Williams, R.D. (2012) ‘DEMs of Difference’, **Geomorphological Techniques**, 2, pp.1–17.
23. Wilson L, G. & Richards M, J. (2006) ‘Procedural Documentation and Accuracy Assessment of Bathymetric Maps and Area / Capacity Tables for Small Reservoirs’,**U.S. Geological Survey Scientific Investigations Report 2006-5208**, 24p.

Protection
and
Restoration
of the
Environment
XIV

Ground water resources management

BUILDING GROUNDWATER CONCEPTUAL MODELS UNDER LIMITED INFORMATION SUPPLY: A CASE STUDY ON AXIOS DELTA, NORTH GREECE

L. Kapetas[1]*, N. Kazakis[1], T. Spachos[2], K. Voudouris[1]

[1]Lab. of Engineering Geology & Hydrogeology, Dept. of Geology, Aristotle University of Thessaloniki, Greece [2]Thessaloniki Water Supply & Sewerage Co. S.A.

*Corresponding author: E-mail: leonkapetas@gmail.com

Abstract

Poor hydrogeological conceptualisation can have adverse effects on the accurate representation of flow processes simulated by numerical models. This work explores the idea of conceptual model building in complex settings with limited spatiotemporal information supply. The case study of the eastern coastal aquifer in the Axios Delta area is examined, where ecological, irrigation and urban water supply demands exert pressure on local water resources. The water demands are covered by the exploitation of surface water and groundwater resulting in a decrease in river flow over the last decades and the salinization of Axios Delta area. The Delta is currently under the environmental responsibility of numerous agencies which have available data according to their specific activities. A detailed step-by-step data collection was performed including lithological profiles, water level measurements, river abstractions, climatological data, geological and geomorphological maps. In this context, a conceptual model accounting for surface-subsurface interactions, recharge processes and human interventions is developed to support hydrogeological modelling for evaluating risk of saltwater intrusion and long-term sustainability of the ecosystem under climate change scenarios. Further uncertainty is introduced by the complex nature of the deltaic deposits. Confidence in the conceptual model is discussed and how it propagates through to the simulation predictions. The numerical model will inform systematic monitoring recommendations on an ease-of-implementation basis to improve confidence. This can have implications on improving the understanding and overall resilience of the deltaic ecosystem resource as supported by international policies. The establishment of the hydrogeological conceptual model in this area could be the base of an integrated monitoring plan, which is essential for a rational water management in the coastal zone.

Keywords: Coastal zone; Conceptual modelling; Hydrogeological model; Uncertainty management; Saltwater intrusion; Climate change

1. INTRODUCTION

Numerical simulation modeling has become the standard methodology in industry and academia in the effort of analysing hydrological and hydrogeological processes. This has become possible thanks to advanced commercial/research simulation engines that are supported by affordable, significant computational power. It is critical that these computational models are based on a sound conceptual model (Anderson et al., 2015). Good conceptual understanding requires data that are obtained in strategically selected spatiotemporal scales. Only then computational models can become useful tools to test the conceptual model, be calibrated to a set of observations and finally used to make future predictions as, for instance, on the impact of anthropogenic activities, specific policies or those of climate change (Middelkoop et al., 2001). It can be conceived as a three-step iterative methodology: (i) information collection, (ii) conceptual model building, and finally (iii) computational model

construction, calibration and predictive simulations. There is an iteration between these three steps depending on the confidence to the results.

Though hydrological or hydrogeological applications can vary in scale or purpose, the framework remains broadly the same. For instance, flood modeling requires detailed terrain observations and hydrological inputs over a catchment scale (Komi et al., 2017). This information is used to conceptually understand the behavior of the catchment and supports models to understand the key factors contributing to flood risk. Models can then be used to predict the impact that hard or soft flood alleviation engineering measures can have (Roger Few, 2003). Other basin models exist that focus on water resources management and planning. In this case, the information required is not focused on extreme events, rather is meant to provide accurate water balance to inform decision making around usage and allocation (Berhe et al., 2013). With regards to the development of groundwater models, the conceptual model understanding requires knowledge on aquifer characteristics, such as geometry, type, boundary conditions and thickness, aquifer properties (i.e. hydraulic conductivity, storativity) and piezometric information as well as on recharge and discharge rates (Ye et al., 2010). Groundwater interactions with surface water features (lakes, rivers), or the sea for a coastal aquifer, define boundary conditions that influence subsurface flows.

The number of observations that are used for calibration of these models range across different spatial scales (rainfall, head) and extrapolation is always applied. The density of the information network will depend on the complexity of the study area, economics, as well as the spatial and temporal scale at which the problems is explored. Depending on the nature of the particular study, seasonal variability due to rainfall, exchange with surface water bodies or well abstractions is doomed less important and the impact of these processes on the model can be dampened (Sutanudjaja et al., 2011). On the other hand, when studying saltwater intrusion in a coastal aquifer or the mixing between waters of different salinity such information becomes critical. Furthermore, as variable density will affect flow dynamics, the computational model needs to account for mass transfer phenomena (Bear et al., 2013). Thus, geochemical information is also required.

The iterative process of information collection and use in conceptual model building and simulation model calibration is summarised in Figure 1. When there is sufficient confidence on the conceptual model, based on the agreement between the numerical model and the observations, then the iteration process is deemed complete.

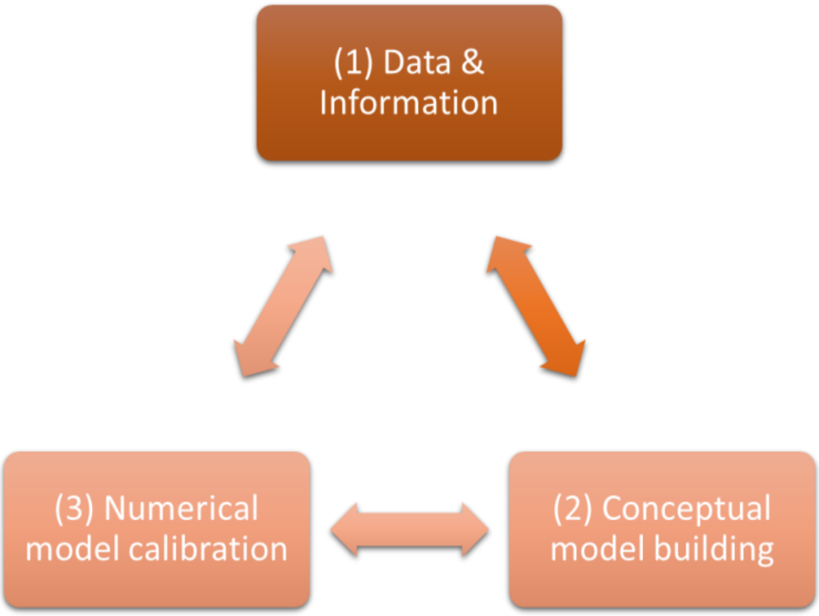


Figure 1. Iterative process of information collection, its use to construct a conceptual model and calibrate the numerical model.

The breadth of applications clearly demonstrates the need to work across different scales where catchments include different users and have physical complexity: decision-making regarding water allocation can be modelled on the regional scale but can have impacts on sensitive ecosystems and aquifers on a local scale. This is a well-known persisting challenge that policies for Integrated Water Resource Management (IWRM) aim to address (Ingold et al., 2016). How data are collected to supplement models and decision-making by stakeholders across different scales is the focus of this paper. This is explored for the case of Axios Delta and its coastal aquifer. It is intended to build a conceptual model using information collected by public and private organisations involved in a variety of sectors and activities. This conceptual model will serve as the basis for a numerical simulation model that will support the hydrogeological understanding of the aquifer. Recommendations are made for new information requirements that will increase the confidence of the conceptualisation and modeling response. Ultimately, this modeling tool will be used to produce recommendations for the protection of the aquifer from climate change and anthropogenic threats.

2. CASE STUDY AREA

2.1 Geography

The Axios River Delta is located on the coast of Northern Greece where Axios River discharges into the Mediterranean Sea in the Gulf of Thermaikos. The Delta is formed at the confluence of four rivers, namely Aliakmonas, Loudias, Axios and Gallikos from west to east. Aliakmonas contributes significant flows to the delta. Axios is a transboundary river shared between FYROM and Greece. Its catchment has an area of 24,437 Km^2, with about 12% of this area in the Greek territory. Though an agreement on river flow management and coordination was established between the two countries in 1959 (Global Water Partnership, 2012), no formal agreement is practically active today. Like Greece, FYROM makes abstractions from the river for agricultural use. This has resulted in uncertain flows reaching across the border depending on upstream abstractions requirements and climatic conditions. Within the Greek territory, most abstractions take place at the mouth of the river as water intensive rice paddy fields cover the largest part of the deltaic valley. Groundwater abstractions on its eastern part take place to cover urban demands, primarily during drought condition when the alternative major sources of water supply for the city of Thessaloniki are under pressure (EYATH, 2018). At the same time, quality of transboundary surface water and groundwater is moderate due to nitrate contamination, metal pollution, wastewater discharges and solid dumping (Karageorgis et al., 2005; Milovanovic, 2007).

Axios Delta comprises a National Park since 2009 (Axios-Loudias-Aliakmonas Management Authority, 2018), has significant biodiversity value and offers extensive ecosystem services supported by the ecological flow (Hadjicharalambous et al., 2015), i.e. maintaining the functions of this ecosystem depends on the supply of sufficient water quantity of good quality. It is critically important to consider the aquifer's regime in an Integrated Water Resource Management Plan especially when a strong interaction between groundwater and surface waters occurs.

Climate is transitional continental to Mediterranean on the Koppen-Geiger classification (Bear-ID Novatek, 2016; Kotinis-Zambakas et al., 1984). The mean annual precipitation is 443 mm, as calculated from a continuous rainfall record in the area (Chalastra Station, 1974-2004) (Grimpylakos et al., 2016) though recent years have seen higher precipitation.

2.2 Geology and Hydrogeology

The Axios catchment spans a range of geological formations and with complex geotectonical structure. The mountainous part of the catchment comprises of schists, gneiss, ultramafic rocks and granites as wells as carbonate rocks such as limestones and dolomites. Neogene and Quaternary sediments are located in lowlands of the basin. In this study we focused on the sedimentary formation in the boundaries of the model domain (Figure 2). Holocene deposits dominate in the study area consisting of coastal deposits (gravel and sand), red clay with calcareous concretionary bodies, while

in the base the conglomerates dominate. Sand accumulations occur along the Axios river bed. Coarse materials of pebbles and sand of small thickness occur in the northwestern part of the study area. In the northern west part Neogene formation of sand and loose conglomerates of great thickness in alternation with cohesive conglomerates and sandstones are placed. In the Northern east part of the study area the red clay series consisting of red to brick red silty clays with mica and calcareous concretionary bodies are located. The hydrogeological units can be distinguished based on the geological formations of the quaternary and Neogene porous aquifers (Figure 2). The area of interest is located in the quaternary formations and the aquifers are under unconfined and semi-confined conditions. Groundwater flow direction is from the Northern part to the coast, while a strong interaction occurs between the Rivers of Axios and Gallikos with the unconfined aquifer. The aquifer is recharged by Axios River during the entire hydrological year, while Gallikos River has seasonal flow recharging the aquifer during the winter period. However, the interaction between the Gallikos River and the upper aquifer is under consideration. The deeper aquifers are recharged from margins of the basin as well as the leaks of the upper aquifer.

2.3 Water Management

Water management for the protection of the Delta is addressed in the Integrated Water Management Plan for the catchment of Axios, along with plans for other catchments in the Central Macedonia Region (Ministry of Environment and Energy, 2014). The plan identifies as pressures to the broader Delta area (i) the relatively small extent (3.3%) of urbanisation, (ii) the diversion of flows from the River, (iii) the drainage of flows from Artzan and Amatobou to Axios River. With regard to the Delta, the second intervention is the most significant. As shown in Table 1, the total abstraction at the Axios Delta area amount to an annual 432,300,000 m^3. Agricultural activities at the eastern section are responsible for 50% of these extractions. Regarding the objectives set out in the Water Framework Directive 2000/60, according to the Management Plan, the area is deemed likely not to meet them. The key reasons are contamination from Loudias and the Deltaic Area (industrial/agro-industrial waste, cattle farming, agricultural waste).

With respect to subsurface water bodies, the Management Plan pulls current knowledge (up to 2014) of groundwater quality from different studies. A surface phreatic aquifer spreads across Axios Valley (from Axioupoli to the Delta area), with a variable depth. This system is fed through interaction with the surface and directly by the river. Well abstractions in the central part of the valley have caused a significant drop in the local water table which is now below sea level. This causes concerns for seawater intrusion. However, the surface irrigation of the rice fields in the delta area acts as a hydraulic barrier. The effectiveness of this mechanism is not clear (AUTH & YETOS consultants, 2010). In the same study, historical precipitation and flow conditions (potentially indicating a drought) have been analysed based on the Standardised Precipitation Index (SPI) and Standardised Runoff Index (SRI) (Angelidis et al., 2012). Significant water stress periods have been detected for four years between 1984-1992. An action plan is in place for drought emergencies and it includes strategic drought prevention/precautionary measures, operational measures (water uses prioritization), organisational and monitoring measures (European Commission - EuropeAid Co-operation Office, 2007). Operational measures include, among others, the increased use of groundwater, the protection of protected wetlands, the increased abstraction from rivers near discharge to the sea by relaxation of environmental flow regulation and the interruption of irrigation to water-demanding crops. In the aforementioned measures a trade-off is necessary for the case of Axios delta: the use of groundwater will affect the delta ecosystem. At the same time, the permitted abstraction from the delta region will affect the protected zone. Post-drought measures include water allocation to support ecosystem recovery. Droughts can also induce sea-water intrusion (Kouzana et al., 2009). Depending on the local geochemistry this process can be near to irreversible (Han et al., 2015) but this has not been recognised in the Management Plan (Ministry of Environment and Energy, 2014).

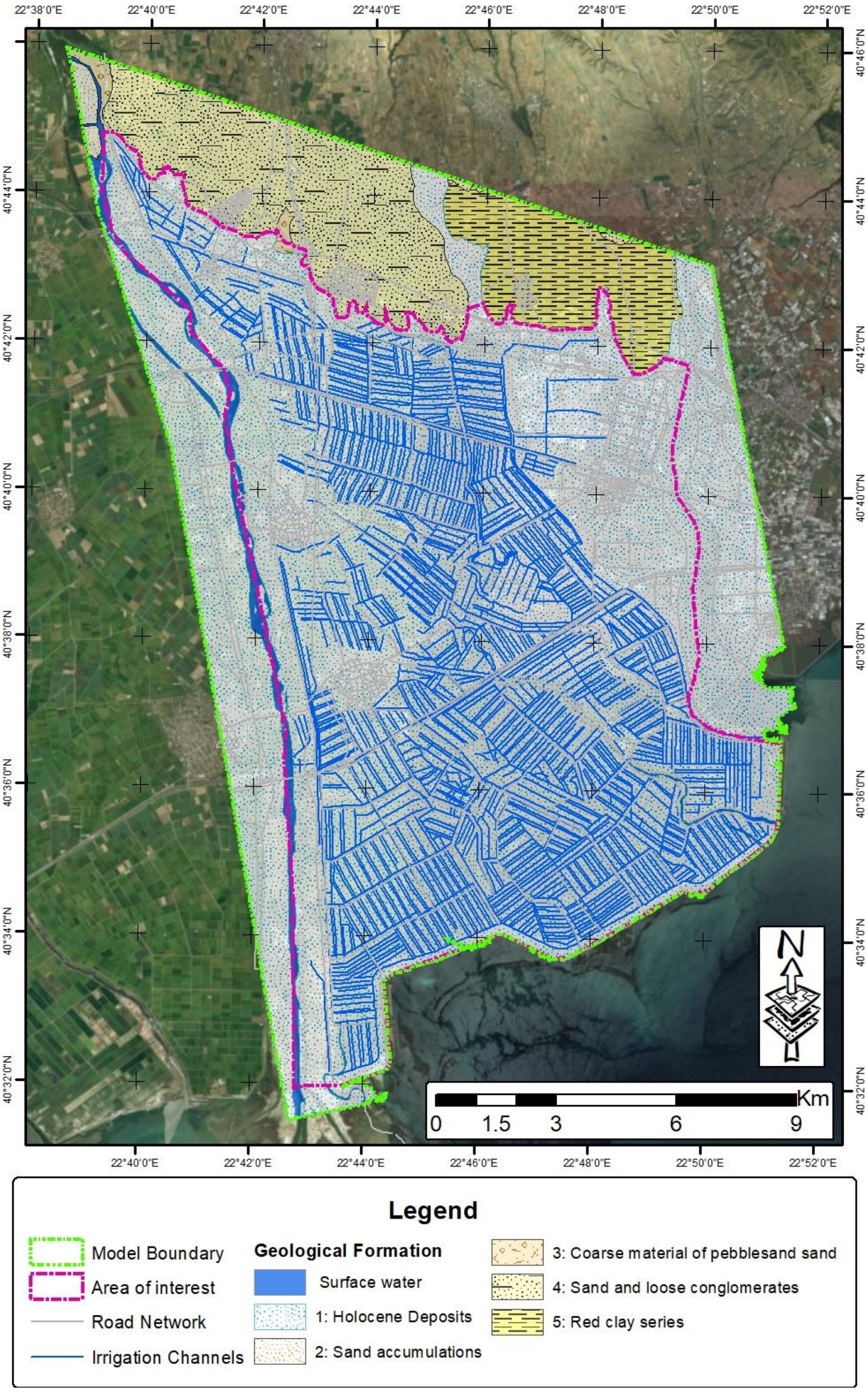


Figure 2. Conceptual model boundaries and hydrogeological units to be considered. Axios and Gallikos rivers form the west and east boundaries respectively.

3. CONCEPTUAL MODEL

Potential impacts of climate change to the regional climate may lead to: (i) changes of rainfall patterns both in terms of absolute total annual rainfall or seasonal variability with an increase of extreme events, (ii) temperature changes altering evapotranspiration patterns and irrigation requirements (iii) changes in river flows, and (iv) increased sea levels which can have a significant effect on the deltaic area and the coastal aquifer. Such climate change impacts are non-uniform across Europe. Projections have been attempted based on climate models and downscaling processes, while researchers have been attempting to provide impact envelopes for projections (Gampe et al., 2016; Kontogianni et al.,

2014; Marcos-Garcia et al., 2017; Masciopinto & Liso, 2016). These projections can inform scenario formulations of predictive simulations using hydrogeological flow/mass-transfer models.

At the same time, anthropogenic interactions with water resources, such as the excessive exploitation of groundwater in the central Axios valley, can further increase risks to the subsurface water systems. These risks combined make a risk analysis necessary for the subsurface system of Axios Delta and estuary; the conceptual model presented here is the first step for this analysis. This model will inform a hydrogeological flow/mass-transfer models.

Table 1. Average annual abstractions from Axios River at different locations in the wider Delta Area. (source: Ministry of Environment and Energy, 2015).

Location	Annual Volume ($10^3 m^3$/year)
Ag. Athanasios (east)	88,232
Nea Magnisia (east)	6,488
Chalastra-Kalochori (east)	119,949
Brahias	40,180
Koufalia	4,570
Malgara	74,343
Monastiri	65,901
Chalkidona	32,637
Delta Total =	432,300
Delta East =	214,669
Abstractions Ratio (East/Total)%	49.7

The biophysical processes which comprise the components of the subsurface-surface interactions are shown in Figure 3. Based on the hydrogeological information presented in Section 2, two aquifers are conceptualized at this stage. Their thickness is variable and there are potentially other local-scale aquifer units. However, due to lack of detailed information no further compartmentalization is considered. Axios and Gallikos Rivers form the west and east boundaries of the area were also considered. On the north of the modelled area, two hydrogeological units are conceptualized, namely sand and loose conglomerates and red clay series.

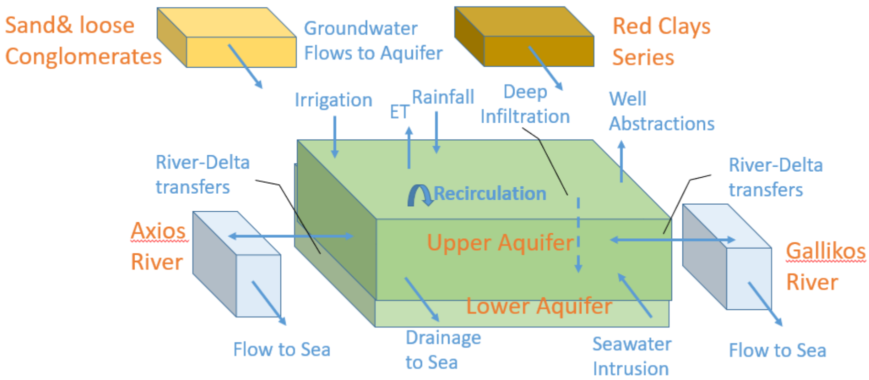


Figure 3. Water fluxes among various conceptual model components.

Moreover, as shown in Figure 2, the boundaries of the conceptual model are marginally narrower than the area of interest. The reason for this selection is that no information is currently available to support a wider domain definition. The processes taking place in the domain include: upper aquifer exchanges with Axios River (the direction of this flow is predominantly from Axios to the aquifer),

similar exchanges between the aquifer and Gallikos River, flows from the upper to the lower aquifer, groundwater flows from the Hydrogeological Units of sand and loose conglomerates and red clay series to the two aquifers, net deep-infiltration to the upper phreatic aquifer as a function of rainfall, irrigation, water recirculation and evapotranspiration, river discharges to the sea, aquifer groundwater discharge to the sea, well abstractions and seawater intrusion to the aquifers.The dynamics between the latter three processes will be the subject for further characterisation in the numerical model (not part of the present work).

4. DATA ANALYSIS

Existing data to carry out this analysis have been collected from literature and stakeholders active in the area. As data collection has been carried out for diverse purposes, and not for this particular investigation, the spatial and temporal resolution is not ideal. Some extrapolations/projections were carried out in this section and, whenever this was required, it has been reported. The ideal spatial and temporal resolutions are being discussed to provide a better understanding of uncertainty propagation when these are used as input to the numerical model.

(i) River water levels: as Axios and Gallikos rivers comprise the boundary conditions of the models, information regarding their water levels is necessary. For Axios river, these are obtained for a range of fluxes from 5 to 60 m^3/s which represent baseline to high flows at six locations along the lower half of the east boundary. The respective free water surface is also known. Relationships between topographic information and water surface will be used to calculate the boundary condition in the upper half of the boundary. This input is obtained from the hydrodynamic model of Axios River (Papadimos, 2015). Gallikos deltaic area in the downstream had been depleted in the past due to anthropogenic interventions. Currently, continuous flow has been restored due to the recovery of the river as well as due to water transfers from Aliakmonas River (channel transfer for Thessaloniki's water supply). Regular monitoring is proposed in the area to improve knowledge of this boundary condition.

(ii) River abstractions and irrigation: abstractions from Axios River are considered here in order to calculate the irrigation rates. Irrigation takes place between the months of May and October. Daily data were provided for the three main irrigation zones, namely Agios Athanasios, Chalastra and Nea Magnisia. These data are averaged on a daily basis for every month as seen in Table 2. These values can be uniformly distributed (as rice fields cover the whole area predominantly) to calculate irrigation rates per unit area.

(iii) Groundwater abstractions: groundwater abstractions within the model area are located in the east section. An abstraction annual average of about $60x10^6$ m^3/year and $6x10^6 m^3$/year is estimated for Axios and Gallikos basins respectively (Ministry of Environment and Energy, 2014). These extractions take place in the summer months; hence, a daily average needs to reflect the period between May and September.

(iv) Rainfall: a rainfall record is available for the last seven years. Table 3 presents total rainfall depths for the years that have a complete record. These observations serve for the calculation of deep infiltration, i.e. aquifer recharge.

(v) Evapotranspiration and Recirculation: rice cultivation requires flooding of the area during the summer months. For this reason, potential evapotranspiration (PET) rates are practically taking place. The recirculation of drained water via a pumped system suggests that there is increased time for PET to take place and, therefore, reduced deep percolation/infiltration occurs.

Groundwater levels and hydrochemistry: groundwater piezometric information exists for a number of wells primarily situated in the east part of the study area. These observations suggest the presence of an unconfined and a partially pressurized aquifer, as discussed in section 3. This inference is corroborated by the differing hydrochemistry of the two sets of observations (Nitrate and TDS levels).

Ideally, more observations would be required on the southern border to identify the saltwater-freshwater interface.

Table 2. Daily averaged abstraction flows (m3/s) from Axios River between 2010-2013 (source: GOEB).

Month	May	June	July	August	September	October
Daily Average (cumecs)	47	41	42	37	12	2

Table 3. Monthly rainfall depths (mm) for years with complete record between 2010-2017.

Month/Year	Jan	Feb	Mar	Apr	May	Jun	Jul	Aug	Sep	Oct	Nov	Dec	Total
2010	16	126	46	29	76	49	72	1	20	140	20	27	622
2012	24	27	45	45	110	29	1	15	59	34	111	60	561
2014	32	68	35	0	0	0	48	37	81	69	105	167	643
2015	45	40	111	19	11	93	4	36	69	101	33	0	562
2016	30	43	106	12	94	23	15	50	157	39	21	1	591

5. DISCUSSION AND CONCLUSIONS

This work provided a methodological understanding of the building process of a hydrogeological conceptual model under limited information supply. Hydrometric and hydrogeological data are not always collected in a suitable spatiotemporal scale. Yet, the production of a conceptual model to support the construction of a numerical model can still be feasible. The confidence to this conceptual model will then need to be established during numerical model calibration. On this basis, new observations can be requested in specific areas where simulation confidence is lower, i.e. recommended targeted observation points. In the case study, these are the interface between saltwater-freshwater and Gallikos river levels. Complementarily, piezometers on the north boundary with longer record could improve confidence.

It was shown that a compromise needs to be made with regard to model dimensions, i.e. the selection of boundaries. In cases where the available data do not provide sufficient information for a larger area, it is proposed that the selected area can be smaller than the area of interest. The boundary conditions of the model will play a major role in how the domain interacts with the area outside the model. This approach was followed for Axios River Delta and its aquifers. Trade-offs exist between (i) model domain size, (ii) expected simulation times (computational power), (iii) amount of collected information and (iv) confidence to simulation results. Model parsimony has been the key principle adopted. This model will support the construction of a hydrogeochemical model evaluating seawater intrusion in the subsurface water systems.

Water management can affect how the phenomenon plays out in an uncertain future. Climate change might alter hydrological patterns resulting in droughts and/or also cause sea level rise. The numerical model supported by this conceptual model can be a useful tool to test these scenarios and create a portfolio of effective management options; informed decision-making on water use and allocation can be part of a mitigation strategy of seawater intrusion. This evaluation is relevant for other coastal aquifers that are over-exploited and/or are likely to suffer similar impacts of climate change.

Acknowledgement

We thank the National Scholarship Foundation of Greece (IKY) for funding this research work. We also thank the local stakeholders (Institute for Geology and Mineral Exploration, GOEV, the Hellenic Agricultural Organisation, Land Reclamation Institute, Axios Delta National Park Authority) for sharing their data and knowledge on the area.

References

1. Anderson, M.P., Woessner, W.W., & Hunt, R.J. (2015). **Applied Groundwater Modeling: Simulation of Flow and Advective Transport**. Academic Press.
2. Angelidis, P., Maris, F., Kotsovinos, N., & Hrissanthou, V. (2012). Computation of Drought Index SPI with Alternative Distribution Functions. **Water Resources Management**: An International Journal, Published for the European Water Resources Association (EWRA), 26(9), 2453–2473.
3. AUTH & YETOS consultants (2010). Surface and Groundwater Quality Control in Macedonia-Thrace-Thessaly: Results for Axios River Basin. **Ministry of Agricultural Development** (in Greek).
4. Axios-Loudias-Aliakmonas Management Authority. (2018). **Protection status – Axios Delta National Park**. Retrieved January 8, 2018, from http://axiosdelta.gr/en/national-park/protection-status/
5. Bear, J., Cheng, A., Sorek, S., Ouazar, D., & Herrera, I. (2013). **Seawater Intrusion in Coastal Aquifers: Concepts, Methods and Practices**. Springer Science & Business Media.
6. Bear-ID Novatek (2016). **European climate zones and bio-climatic design requirements**. Horizon 2020. Retrieved from www.pvsite.eu
7. Berhe, F.T., Melesse, A.M., Hailu, D., & Sileshi, Y. (2013). MODSIM-based water allocation modeling of Awash River Basin, Ethiopia. **CATENA**, 109(Supplement C), 118–128. https://doi.org/10.1016/j.catena.2013.04.007
8. European Commission - EuropeAid Co-operation Office. (2007). Euro-Mediterranean Regional Programme for Local Water Management (MEDA Water) and Mediterranean Drought Preparedness and Mitigation Planning (MEDROPLAN).
9. EYATH (2018). **EYATH abstractions**. http://www.eyath.gr/ (accessed January 2018)
10. Gampe, D., Nikulin, G., & Ludwig, R. (2016). Using an ensemble of regional climate models to assess climate change impacts on water scarcity in European river basins. **Science of The Total Environment**, 573, 1503–1518. https://doi.org/10.1016/j.scitotenv.2016.08.053
11. Global Water Partnership (2012). **Vardar/Axios River basin** — TWRM-Med [Page]. Retrieved January 8, 2018, from http://www.twrm-med.net/southeastern-europe/transboundary-river-basin-management/shared-surface-water-bodies/new-river-basins/vardar-axios-river-basin
12. Grimpylakos, G., Karacostas, T.S., & Albanakis, K. (2016). Spatial and temporal distribution of rainfall and temperature in Macedonia, Greece, over a thirty year period, using GIS. **Bulletin of the Geological Society of Greece**, 47(3), 1458–1471. https://doi.org/10.12681/bgsg.10984
13. Hadjicharalambous, H., Dimaki, M., Zervas, D., Koutrakis, E., Poulis, G., Sapounidis, A., & Hatziiordanou, L. (2015). **Identification of ecological water requirements of the target habitat types and species that depend on water, in the Axios River Delta, the Aliakmonas River Delta and at the Coastal Lagoon Kitros**. Greek Biotope/Wetland Centre.Han, D., Post, V. E. A., & Song, X. (2015). Groundwater salinization processes and reversibility of seawater intrusion in coastal carbonate aquifers. **Journal of Hydrology**, 531, 1067–1080. https://doi.org/10.1016/j.jhydrol.2015.11.013
14. Ingold, K., Fischer, M., de Boer, C., & Mollinga, P. P. (2016). Water Management Across Borders, Scales and Sectors: Recent developments and future challenges in water policy analysis. **Environmental Policy and Governance**, 26(4), 223–228. https://doi.org/10.1002/eet.1713
15. Karageorgis, A.P., Skourtos, M.S., Kapsimalis, V. et al. (2005). An integrated approach to watershed management within the DPSIR framework: Axios River catchment & Thermaikos

Gulf. **Regional Environmental Change**, 5(2–3), 138–160. https://doi.org/10.1007/s10113-004-0078-7

16. Komi, K., Neal, J., Trigg, M.A., & Diekkrüger, B. (2017). Modelling of flood hazard extent in data sparse areas: a case study of the Oti River basin, West Africa. **Journal of Hydrology**: Regional Studies, 10(Supplement C), 122–132. https://doi.org/10.1016/j.ejrh.2017.03.001
17. Kontogianni, A., Tourkolias, C. H., Damigos, D., & Skourtos, M. (2014). Assessing sea level rise costs and adaptation benefits under uncertainty in Greece. **Environmental Science & Policy**, 37, 61–78. https://doi.org/10.1016/j.envsci.2013.08.006
18. Kotinis-Zambakas, S.R., Angouridakis, V.E., & Zambakas, J.D. (1984). A criterion for defining transitional zones between humid continental and mediterranean climates in the region of Greece. **Journal of Climatology**, 4(1), 99–104. https://doi.org/10.1002/joc.3370040108
19. Kouzana, L., Mammou, A.B., & Felfoul, M.S. (2009). Seawater intrusion and associated processes: Case of the Korba aquifer (Cap-Bon, Tunisia). **Comptes Rendus Geoscience**, 341(1), 21–35. https://doi.org/10.1016/j.crte.2008.09.008
20. Marcos-Garcia, P., Lopez-Nicolas, A., & Pulido-Velazquez, M. (2017). Combined use of relative drought indices to analyze climate change impact on meteorological and hydrological droughts in a Mediterranean basin. **Journal of Hydrology**, 554, 292–305. https://doi.org/10.1016/j.jhydrol.2017.09.028
21. Masciopinto, C., & Liso, I.S. (2016). Assessment of the impact of sea-level rise due to climate change on coastal groundwater discharge. **Science of The Total Environment**, 569–570, 672–680. https://doi.org/10.1016/j.scitotenv.2016.06.183
22. Middelkoop, H., Daamen, K., Gellens, D., et al. (2001). Impact of Climate Change on Hydrological Regimes and Water Resources Management in the Rhine Basin. **Climatic Change**, 49(1), 105–128. https://doi.org/10.1023/A:1010784727448
23. Milovanovic, M. (2007). Water quality assessment and determination of pollution sources along the Axios/Vardar River, Southeastern Europe. **Desalination,** 2007, 213(1), 159–173. https://doi.org/10.1016/j.desal.2006.06.022
24. Ministry of Environment and Energy (2014). **Management Plan for the River Catchments of Central Macedonia**.
25. Papadimos, D. (2015). **Setup and calibration of the two dimensional hydrodynamic models of the Axios delta, Aliakmonas delta and of Kitrous lagoon: part 1**. Greek Biotope Wetland Centre.
26. Roger Few (2003). Flooding, vulnerability and coping strategies: local responses to a global threat. **Progress in Development Studies**, 3(1), 43–58. https://doi.org/10.1191/1464993403ps049ra
27. Sutanudjaja, E.H., van Beek, L.P.H., de Jong, S.M., van Geer, F.C., & Bierkens, M.F.P. (2011). Large-scale groundwater modeling using global datasets: a test case for the Rhine-Meuse basin. **Hydrology and Earth System Sciences**, 15(9), 2913–2935. https://doi.org/10.5194/hess-15-2913-2011.
28. Ye, M., Pohlmann, K.F., Chapman, J.B., Pohll, G.M., & Reeves, D.M. (2010). A Model-Averaging Method for Assessing Groundwater Conceptual Model Uncertainty. **Ground Water**, 48(5), 716–728. https://doi.org/10.1111/j.1745-6584.2009.00633.x

INVESTIGATING GROUNDWATER FLOW AND SEAWATER INTRUSION IN NEA MOUDANIA AQUIFER UNDER VARIOUS MANAGEMENT SCENARIOS

I. Siarkos[1], M. Katirtzidou[1*], D. Latinopoulos[2] and P. Latinopoulos[1]

[1]School of Civil Engineering, Aristotle University of Thessaloniki, GR54124 Thessaloniki, Greece
[2]School of Spatial Planning and Development, Aristotle University of Thessaloniki, GR54124 Thessaloniki, Greece

[*]Corresponding author: e-mail: mkatir@civil.auth.gr, tel : +302310695475

Abstract

Many coastal areas all over the world face significant water availability issues due to population increase and numerous human activities (i.e., tourism development, commercial and agricultural activities) taking place in the interior of them. This problematic situation becomes even worse when groundwater resources constitute the sole source of freshwater. Moreover, coastal areas are threatened by seawater intrusion caused due to the substantial decline of groundwater levels. To this task, the implementation of various protective countermeasures, that should be carefully examined and evaluated, is often required in these regions. For this reason numerical modeling is usually applied, since it enables studying the spatial and temporal evolution of both hydraulic head and seawater encroachment under different management perspectives. Within this framework, the present study investigates the implementation of various management scenarios aiming at dealing with both groundwater drawdown and seawater intrusion in the coastal aquifer of Nea Moudania, Halkidiki, Greece, which faces both considerable decrease of groundwater levels and increased salinization due to seawater intrusion. All management scenarios are actually related to the reduction of pumping rates of the abstraction wells (irrigation and/or domestic wells) due to the implementation of pumping restriction measures or the exploitation of alternative water resources (i.e. use of surface water). The investigation and evaluation of the alternative scenarios are performed through the application of a calibrated transient groundwater flow-solute transport model already developed for the reference area, by studying the spatial and temporal evolution of both hydraulic head and chloride concentrations resulting from each scenario.

Keywords: groundwater drawdown; seawater intrusion; groundwater resources management; numerical modeling; Nea Moudania aquifer

1. INTRODUCTION

Over-exploitation of groundwater resources in coastal areas worldwide has evolved into a widespread environmental issue that in addition affects negatively the economy of these regions (Datta et al., 2009; Werner et al., 2013; Siarkos and Latinopoulos, 2016a). Not only does groundwater over-exploitation causes the intense decline of groundwater levels (quantitative degradation), but also has as direct effect the intrusion of seawater (qualitative degradation), which, in turn, results in reduction of the available and exploitable amounts of freshwater (Werner et al., 2013; Siarkos and Latinopoulos, 2016b; Siarkos et al., 2017). For this reason, application of preventive measures and development of management strategies regarding groundwater abstraction are considered to be of utmost importance (Papadopoulou, 2011; Siarkos et al., 2017).

The aforementioned management strategies in order to be effective and have positive results to the local groundwater reserves should be thoroughly investigated in conjunction with the proper study of the aquifer's behavior. To this task numerical modeling is usually implemented. In this way, not only does the aquifer's behavior under various stresses (i.e., recharge and discharge conditions) is examined, but also the comparison and evaluation of possible management scenarios are accomplished in terms of both hydraulic head and seawater encroachment evolution (Pliakas et al., 2005; Dausman et al., 2010; Pool and Carrera, 2010; Siarkos et al., 2017).

In this perspective, the present study investigates through numerical modeling the impact of various management scenarios on the quantitative and qualitative status of the aquifer of Nea Moudania, Halkidiki, Greece. These scenarios are related to the reduction of pumping rates of the abstraction wells and/or the suspension of their operation, which is one of the most well-known preventive countermeasures implemented in the effort of controlling seawater intrusion in coastal regions (Oude Essink, 2001; Pool and Carrera, 2010; Kallioras et al., 2013; Siarkos et al., 2017). More specifically, the management scenarios include: a) reduction of the pumping rates of irrigation wells in order to achieve a balance between aquifer inflows and outflows and, therefore, no further groundwater level decline occurs, b) suspension of the operation of certain wells located in the southern part of the aquifer, due to probable unsuitable drinking water quality (salinization), and c) construction and operation of a reservoir in a nearby basin (Olynthios river basin) and use of stored surface water in order to cover water needs of the Nea Moudania basin, thus reducing groundwater resources exploitation. To apply, compare and evaluate these alternative scenarios, a transient model involving the simulation of both groundwater flow and solute transport and developed in a previous study (Siarkos and Latinopoulos, 2016a), was used.

2. STUDY AREA

The hydrological basin of Nea Moudania is located in the south-western part of the Halkidiki Peninsula (south-east of Thessaloniki) and belongs to a wide region called "Kalamaria Plain". The basin occupies an area of about 127 km^2 with a mean soil elevation of 211 m above mean sea level and a mean soil slope of 1.8%. It is bordered to the south by Thermaikos Gulf and, therefore, there is hydraulic connection between groundwater and seawater in this part of the region (Latinopoulos, 2003; Siarkos and Latinopoulos, 2016a, 2016b). In Figure 1 both the location and boundaries of this basin are depicted, along with the two sub-regions of the basin: the hilly area in the north and the flat area in the south. The climate of the study area is semi-arid to humid, typically Mediterranean, and the average annual precipitation is 417 mm for the flat area and 504 mm for the hilly one (Latinopoulos, 2003).

The basin is an agricultural area that is intensively cultivated and irrigated, thus requiring high water quantities. Currently water needs in the region (irrigation, domestic and livestock needs) are exclusively covered by the Nea Moudania aquifer system, which is considered to be semiconfined, consisting of successive water-bearing layers separated by lenses of semi-permeable or impermeable materials. Intense agriculture and uncontrollable irrigation have led to over-exploitation of local groundwater resources, causing net deficit in the aquifer water balance and substantial decline of groundwater levels. As a consequence, phreatic conditions are encountered in several locations. Moreover, qualitative degradation of the aquifer is observed due to seawater intrusion caused by groundwater over-exploitation, especially for irrigation purposes (Siarkos and Latinopoulos, 2016a, 2016b). An in-depth description of the Nea Moudania basin and the subjacent aquifer is presented in Siarkos and Latinopoulos (2016a).

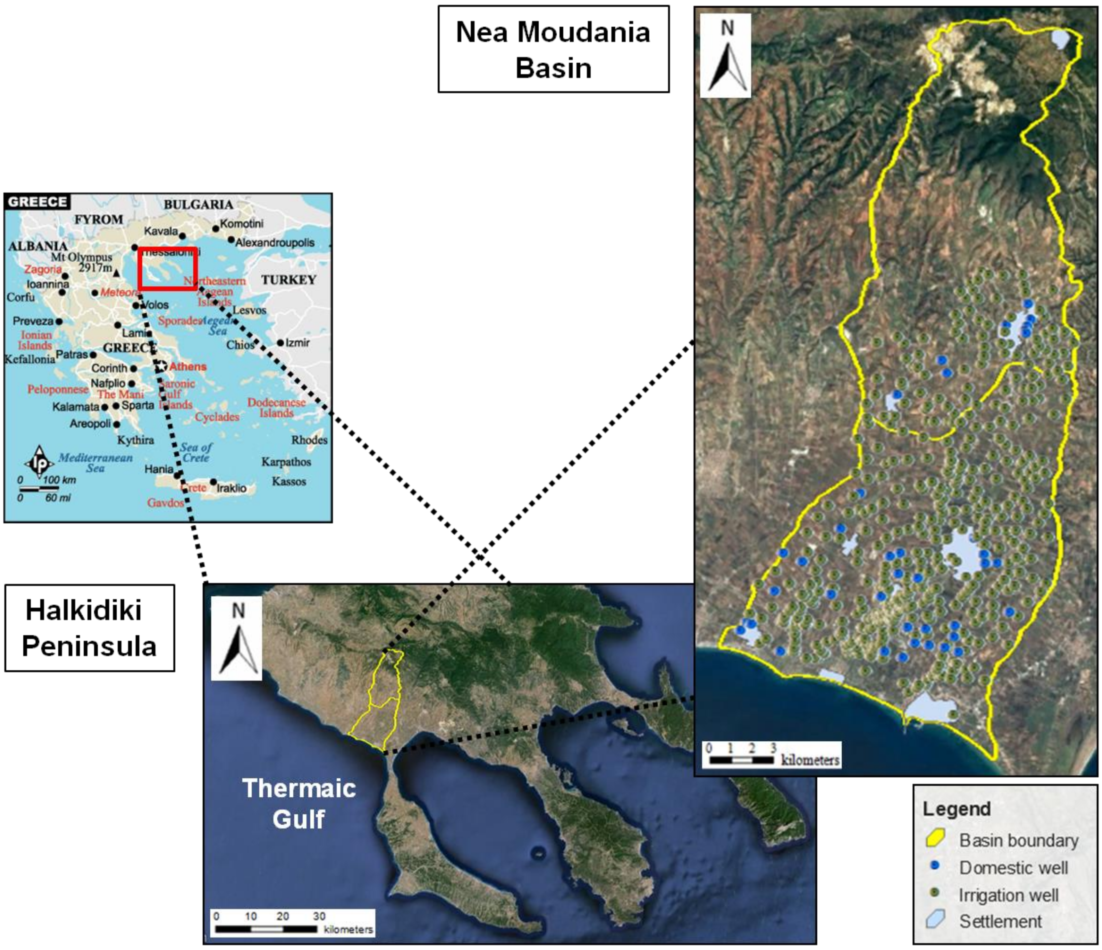


Figure 1. Location and boundaries of the Nea Moudania basin.

3. GROUNDWATER MODELING

As already mentioned, for the application and evaluation of various management scenarios a transient model, previously developed by Siarkos and Latinopoulos (2016a), was used. In this model the simulation of both groundwater flow and solute mass transport –chloride ions in particular– under transient conditions was performed by applying the SEAWAT code (Guo and Langevin, 2002). The SEAWAT design is based on the concept of combining two well-established and proven groundwater programs, MODFLOW (McDonald and Harbaugh, 1988) and MT3DMS (Zheng and Wang, 1999), into a single program that simulates variable-density groundwater flow and transport. The governing equations of variable-density flow problems can be found in Guo and Langevin (2002). The procedure followed for the development and application of the aforementioned model is thoroughly described in Siarkos and Latinopoulos (2016a). In the present study, since its scope is focused on the comparison and evaluation of the management scenarios, only the basic implementation steps of the proposed methodology are presented:

- Step 1: Development of three different models, i.e. a steady-state groundwater flow model by applying the MODFLOW code, a false transient groundwater flow and solute transport model and a transient groundwater flow and solute transport model by applying, in both cases, the SEAWAT code. Each of these models has its own specific objectives, while their connection constitutes the backbone of the whole procedure.

- Step 2: Calibration of the aforementioned models by properly adjusting the models parameters, i.e. aquifer hydraulic-hydrodynamic parameters, recharge and discharge components, boundary conditions, and applying a repetitive trial-and-error procedure between the false transient and the transient simulations.

- Step 3: Performing a sensitivity analysis in order to strengthen the proposed methodology by enhancing the calibration procedure and optimizing the adjustment of the various models parameters.

By applying the transient model under certain aquifer stresses, the temporal and spatial evolution of both hydraulic head and seawater encroachment can be investigated, producing a clear image of the aquifer's quantitative and qualitative status. In the study of Siarkos and Latinopoulos (2016a), the model was run for 33 years, and the projection of the two system variables, i.e. hydraulic head and chloride concentrations, was made until October 2034 (the end of the assumed simulation period). In this simulation, which will be henceforth called "Scenario 0", and during the projection time period (20 years), the pumping rates of the wells were assigned the values estimated during the calibration procedure, corresponding to current abstraction conditions (2014 - model validation year). In Figure 2, both hydraulic head and chloride concentrations distributions at the end of the simulation period are displayed. According to this figure it is expected that: a) high negative hydraulic head values will be observed in the southern and central part of the study area and b) the seawater front will penetrate at a considerable level towards the interior of the aquifer being at a maximum distance of 2.2 km from the coast.

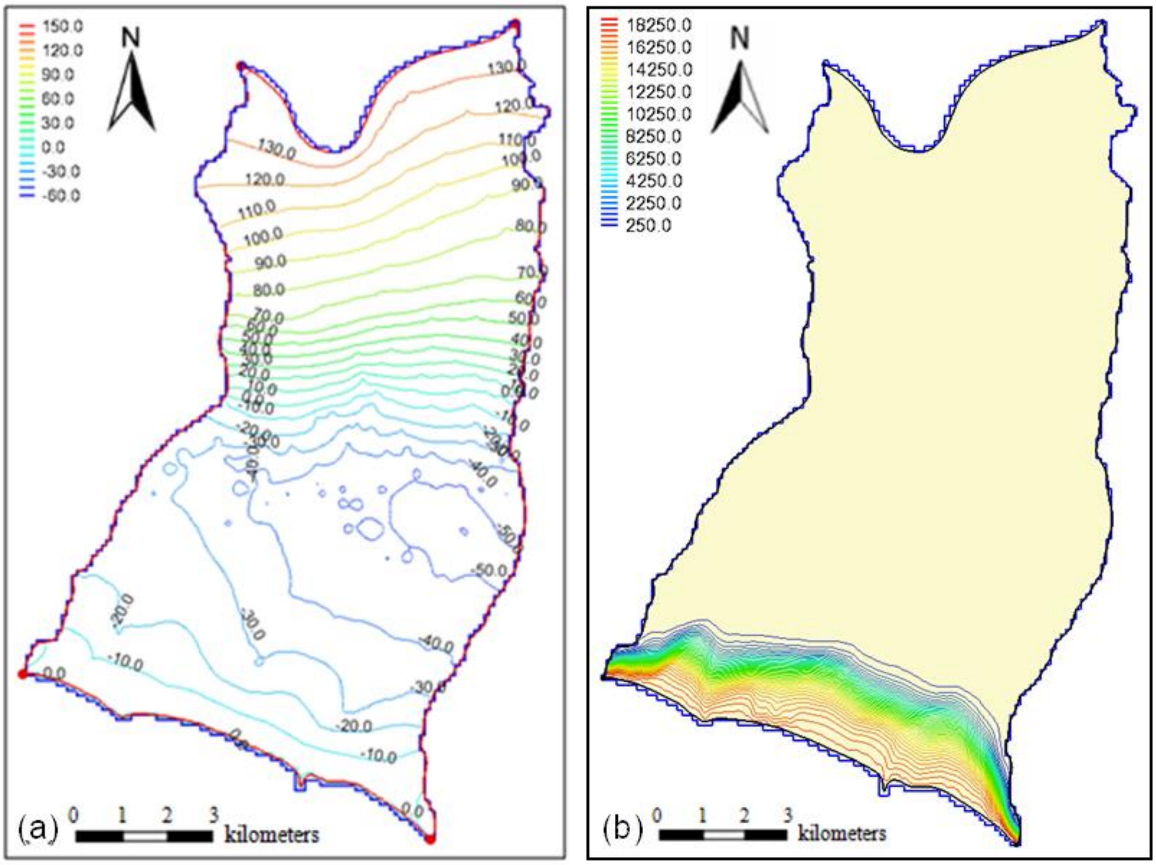


Figure 2. a) Hydraulic head (in m) distribution at the end of the simulation period (2034), b) chloride concentrations (in mg/L) distribution at the end of the simulation period (2034).

4. MANAGEMENT SCENARIOS

4.1 General issues

Based on the results of the transient model, maintaining the current groundwater exploitation conditions, i.e. the current well abstraction regime, will inevitably lead to further deterioration of both quantity and quality of local groundwater resources. This is translated to further groundwater levels decline, as well as to further expansion of the seawater wedge towards the interior of the aquifer. Therefore, in order to alleviate the existing problems, immediate preventive countermeasures should be taken. In the present study three alternative practices/scenarios, referring to the modification of the

abstraction status of the study area (reduction of the pumping rates and/or suspension of the operation of the wells) are examined, compared and evaluated applying the transient model mentioned in Section 3. In the following sections (4.2 - 4.4), a detailed description of the aforementioned scenarios is given by presenting the specific characteristics of every one of them. However, it is necessary beforehand to provide some general issues referring to the application procedure of the alternative scenarios:

- The reduction of the pumping rates and/or the suspension of the operation of the abstraction wells implies the decrease of the amount of groundwater extracted and, subsequently, of the amount of water returning to the aquifer, either as irrigation return flow or as water supply leakage. This decrease was taken into consideration in all cases.
- The hydraulic head values assigned to the northern aquifer boundary (time-variable general head boundary) in Scenarios 2 and 3 were the same as in Scenario 0 in order to achieve better comparison of the management scenarios (focused on the effect of abstraction wells) and avoid setting arbitrary hydraulic head values to the boundary. An exception was made in the case of Scenario 1, where the nature of the problem requires the modification of the hydraulic head in that boundary, which is analysed in detail in Section 4.2.
- The implementation period of Scenarios 1 and 2 was set equal to the one of Scenario 0 (2014 - 2034), while in Scenario 3 a 10-year implementation period was considered (2024 - 2034).

4.2 Scenario 1

In this scenario, the pumping rates of irrigation wells are reduced in order to achieve a balance between groundwater inflows and outflows and, therefore, maintain groundwater levels constant on an annual base through the 20-year implementation period. To determine the new well pumping rates a repetitive trial-and-error procedure was applied, modifying pumping rates in such a way that groundwater levels, both locally and regionally, remain stable on annual base. At this point, it should be noted that it is essential the hydraulic head at the northern boundary of the aquifer to be maintained at the level calculated at the initial time step of the implementation period (May 2014). Therefore, the hydraulic head values assigned to the northern aquifer boundary remain constant through the implementation period, not following the temporal evolution of the other scenarios, i.e. Scenarios 0, 2 and 3.

4.3 Scenario 2

According to Scenario 2, pumping is locally ceased by pausing the operation of certain wells located in the southern part of the reference area, due to probable unsuitable drinking water quality (salinization). The selection of these specific wells was based on their relative position with respect to the seawater wedge, as well as on the chloride concentration observed at the beginning of the implementation period of the scenario. If chloride concentrations exceed certain limits, that vary according to the use of the wells (water supply or irrigation wells), the wells operation is suspended, considering them as unsuitable for the respective use. More specifically, in the case of water supply wells, pumping is stopped when chloride concentration exceeds 250 mg/L (drinking water limit). On the other hand, the operation of irrigation wells is paused when electrical conductivity, which determines the suitability of water for irrigation purposes, exceeds the value of 5,000 μS/cm, which denotes the limit between sensitive and partially sensitive crops (Maas, 1984).

4.4 Scenario 3

Scenario 3 investigates the alternative of designing and constructing a reservoir in a nearby basin that will increase the study area’s water reserves by capturing the surface water runoff of the Olynthios River hydrological basin. The operation of the reservoir aims to serve: (a) the domestic water needs and (b) irrigation water requirements.

The Olynthios hydrologic basin covers 252 km^2. The dam is designed to be rockfill, with a clay core and a lateral spillway, with a height of 73 m and a volume of storage of 22.84 Mm^3 (Karamouzis et al., 2008). The reservoir inflows were calculated using the Thornthwaite and Mather model (McCabe and Markstrom, 2007) for the Olynthios catchment and the average monthly values (Demertzi, 2013) were imported in the model. Finally, the evaporation from the water surface of the reservoir was estimated using the DeBruin equation (DeBruin, 1978). The simulation of the reservoir operation was performed using the Water and Evaluation Planning (WEAP) software (Sieber and Purkev, 2005) with a monthly step and no return flows, while first and secondary priority of the water supply were assigned in the model to urban and agricultural demand sites, respectively (Katirtzidou and Latinopoulos, 2017). The reservoir begins operating as empty on May 2024, while urban water supply begins on November 2024 and agricultural water supply on May 2025. The reservoir water storage volume during the study period is presented in Figure 3. The stored water quantity marginally covers the annual water needs of the study area, while the higher and lower level is observed on April and September of each year respectively.

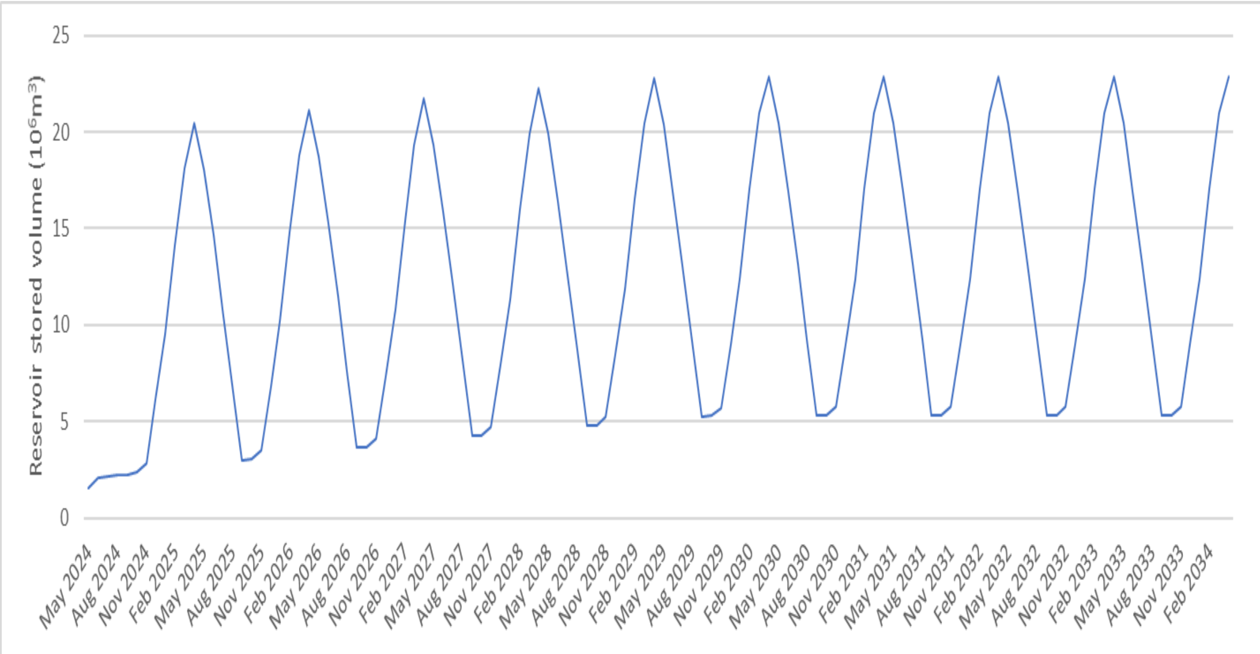


Figure 3. Reservoir storage volume.

5. APPLICATION AND EVALUATION OF MANAGEMENT SCENARIOS

In this section, the results of the application of the alternative scenarios are presented and evaluated. The results refer to the impact of the management scenarios on both groundwater levels and chloride concentrations in the study area, and are produced by applying the transient model and making necessary modifications according to the nature of each scenario. First of all, in Figure 4 the temporal evolution of the hydraulic head in a typical grid cell of the model through the whole simulation period (2001 - 2034) for all scenarios is presented. What is worth mentioning is the steep increase of the hydraulic head in the case of Scenario 3 when it is applied, which is attributed to the fact that all abstraction wells in the study area cease operating and, therefore, no groundwater is used anymore. With regard to the other scenarios, in Scenario 1 the hydraulic head remains constant on annual base which is consistent with the fact that the aquifer's water budget is balanced, while in Scenarios 0 and 3 the hydraulic head decreases over time, which is more intense in the case of Scenario 0, where no preventive measures were applied.

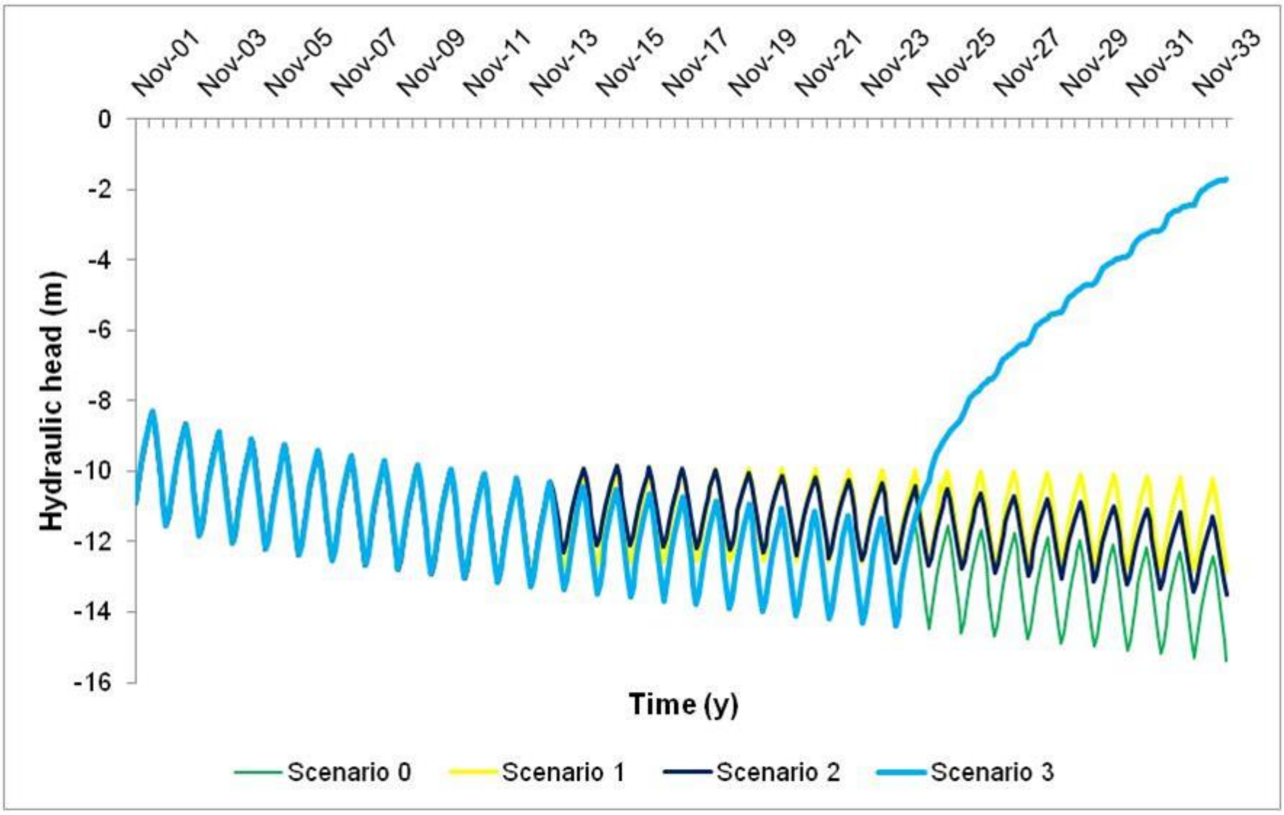


Figure 4. Hydraulic head evolution through the simulation period (2001 - 2034) for all scenarios.

Moreover, in Figure 5 the groundwater level in a certain aquifer section (section A-A') at the end of the simulation period (i.e. the year 2034) for all scenarios is illustrated. It is observed that the hydraulic head in Scenario 3 is higher than in other scenarios, even though its implementation period is shorter (10 years in Scenario 3 instead of 20 years in Scenarios 1 and 2). An increase in the hydraulic head of Scenario 1 is also observed, in relation with Scenario 0, but to a lesser extent than in the case of Scenario 3. In Scenario 2 only a slight increase of groundwater level occurs in the southern part of the aquifer at a near distance from the coastline (local effect). What is worth noting is that in all scenarios the hydraulic head is below the mean sea level (m.s.l.) in various parts of the study area (south and central parts), with the lowest values being observed in Scenarios 0 and 2. This is very important regarding seawater intrusion, since, as long as the hydraulic head is below the m.s.l., seawater will continue to infiltrate inland.

Finally, Figure 6 shows the location of the seawater front in terms of the 250 mg/L chloride concentration contour at the end of the simulation period (2034) for all scenarios, as well as its location at the beginning of the simulation (2001). It is worth mentioning that in all management scenarios, i.e. Scenarios 1, 2 and 3, the seawater front expands over time ending up very close to the position it occupies in the case of Scenario 0, where no protective measures were implemented. In other words, seawater intrusion is slightly affected by the countermeasures examined in this study.

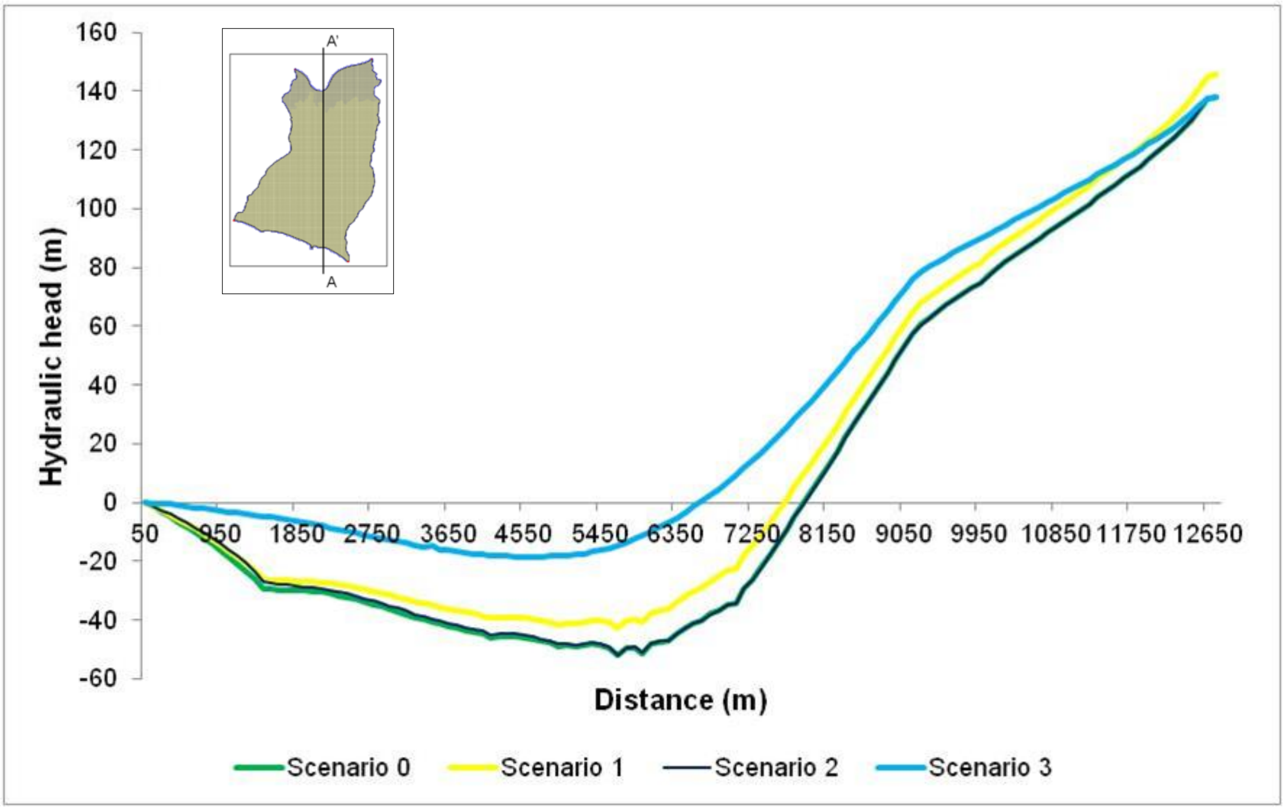


Figure 5. Groundwater levels at the end of the simulation period (2034) for all scenarios.

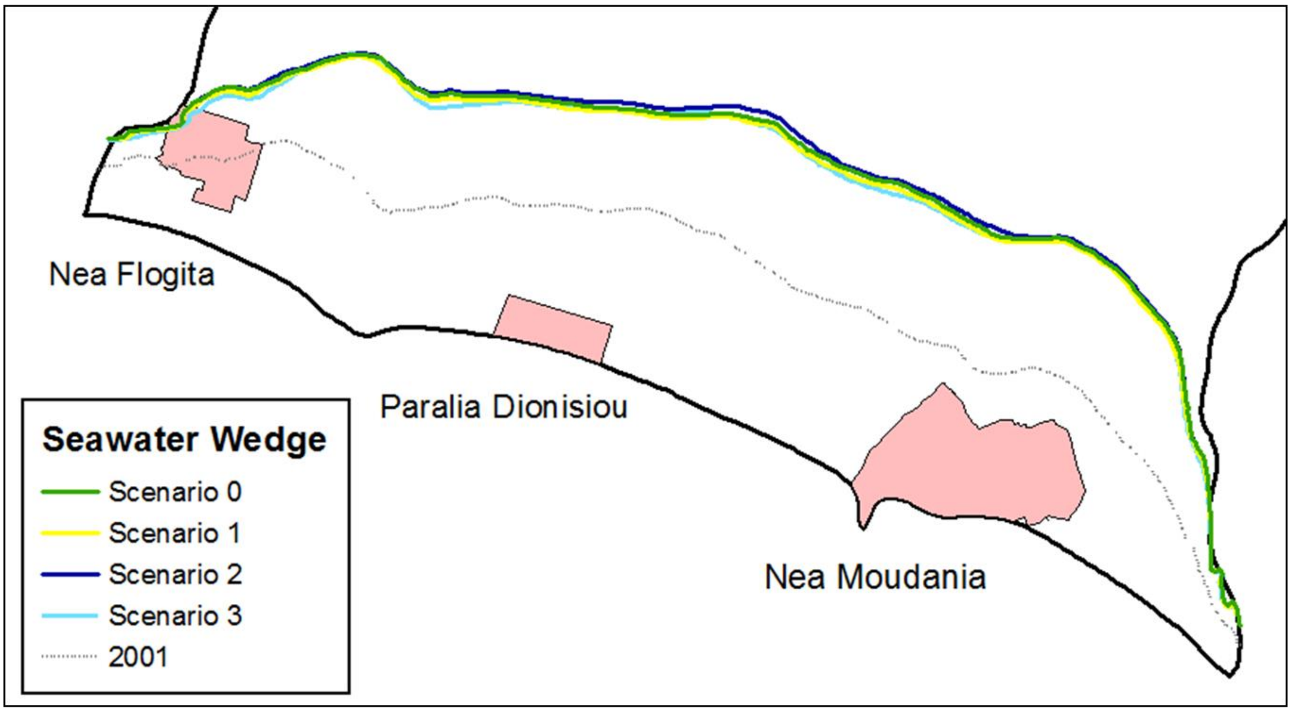


Figure 6. Location of the seawater front at the end of the simulation period (2034) for all scenarios, along with its location at the beginning of the simulation period (2001).

Based on the results presented above, with regard to hydraulic head Scenario 3 is the most effective one, since its application results in a considerable increase of groundwater levels throughout the study area. This is wholly attributed to the fact that the operation of all abstraction wells in the region is suspended, resulting in the substantial decrease of the aquifer discharge. Scenario 1 is the second most effective, also leading to the increase of groundwater levels all over the study area, while

Scenario 2 shows a rather poor performance, since its impact on groundwater levels is minor and limited only to the southern part of the region close to the coastline (local effect). Regarding seawater intrusion, no measure can be characterized as effective, since in all cases (Scenarios 1, 2 and 3) seawater intrusion occurs and seawater front expands, while the results are almost similar to those of Scenario 0, as if no preventive measures have been implemented.

6. CONCLUSIONS

In the present study, various management scenarios regarding groundwater abstraction were implemented, compared and evaluated in order to improve the quantitative and qualitative status of the Nea Moudania aquifer. These scenarios are related to the reduction of the pumping rates and/or the suspension of the operation of the abstraction wells in the study area. For the application of the management scenarios a previously developed transient groundwater flow and solute transport model was used. The evaluation of each scenario was based on the analysis of the results of the aforementioned model regarding both the hydraulic head and chloride concentrations evolution over time.

According to the results the case of constructing a reservoir in a nearby basin and providing the study area with supplementary surface water (Scenario 3) is considered to be the most effective solution, since it leads to the suspension of the operation of all abstraction wells in the study area, completely ceasing the groundwater exploitation. But, even though the application of this scenario results in considerable increase of groundwater levels, its impact, as far as the seawater intrusion is concerned, is minor, as of other scenarios as well, not intercepting the movement of seawater front inland. Therefore, it is concluded that in order to deal with seawater intrusion and avoid the expansion of seawater wedge in the reference area, other type of preventive measures, like the construction of injection and/or extraction barriers, have to be investigated and probably implemented.

References

1. Datta B., H. Vennalakanti and A. Dhar (2009) ‘Modeling and control of saltwater intrusion in a coastal aquifer of Andhra Pradesh, India’, **Journal of Hydro-environment Research**, Vol. 3, pp. 148-159.
2. Dausman A.M., J. Doherty, C.D. Langevin and J. Dixon (2010) ‘Hypothesis testing of buoyant plume migration using a highly parameterized variable-density groundwater model at a site in Florida, USA’, **Hydrogeology Journal**, Vol. 18(1), pp. 147-160.
3. DeBruin H.A.R. (1978) ‘A simple model for shallow lake evaporation’, **Journal of Applied Meteorology**, Vol. 17, pp. 1132-1134.
4. Demertzi K.A., D.M. Papamichail, P.E. Georgiou, D.N. Karamouzis and V.G. Aschonitis (2013) ‘Assessment of rural and highly seasonal tourist activity plus drought effects on reservoir operation in a semi-arid region of Greece using the WEAP model’, **Water International**, Vol. 39(1), pp. 23-34.
5. Guo W. and C.D. Langevin (2002) **‘User’s Guide to SEAWAT: a computer program of simulation of three-dimensional variable-density ground-water flow’**, U.S. Geological Survey, Techniques of Water-Resources Investigation, 6-A7.
6. Kallioras A., F. Pliakas, C. Schuth and R. Rausch (2013) ‘Methods to countermeasure the intrusion of seawater into coastal aquifer systems’, In: Sharma S.K. and R. Sanghi (eds.), **Wastewater Reuse and Management**, Springer Science & Business Media, Dordrecht, pp. 479-490.
7. Katirtzidou M. and P. Latinopoulos (2017) ‘Allocation of surface and subsurface water resources to competing uses under climate changing conditions: a case study in Halkidiki, Greece’, **Water Science and Technology: Water Supply**, doi: 10.2166/ws.2017.166.

8. Karamouzis D. et al. (2008) **‘Preliminary environmental impact assessment of dam and networks of Olynthios dam (in Greek)’**, Final Report, Supplemental research for water development plants in Chalkidiki–Olynthios dam, Thessaloniki, Greece.
9. Latinopoulos P. (2003) **‘Development of water resources management plan for water supply and irrigation (in Greek)’**, Research Project, Final Report prepared for: Municipality of Moudania, Department of Civil Engineering, Aristotle University of Thessaloniki, Greece.
10. Maas E.V. (1984) ‘Crop tolerance’, **California Agriculture**, Vol. 38, pp. 20-21.
11. McCabe G. and S. Markstrom (2007) **‘A monthly water-balance model driven by a graphical user interface’**, U.S. Department of the Interior, U.S. Geological Survey, Reston, VA, USA.
12. McDonald M.G. and A.W. Harbaugh (1988) **‘A modular three-dimensional finite-difference ground-water flow model’**, U.S. Geological Survey, Techniques of Water-Resources Investigation, Book 6, Reston, VA, 586 pp.
13. Oude Essink G.H.P. (2001) ‘Improving fresh groundwater supply - problems and solutions’, **Ocean & Coastal Management**, Vol. 44(5-6), pp. 429-449.
14. Papadopoulou M.P. (2011) ‘Optimization approaches for the control of seawater intrusion and its environmental impacts in coastal environment’, **Pacific Journal of Optimization**, Vol. 193, pp. 532-540.
15. Pliakas F., C. Petalas, I. Diamantis and A. Kallioras (2005) ‘Modeling of groundwater artificial recharge by reactivating an old stream bed’, **Water Resources Management**, Vol. 19(3), pp. 279-294.
16. Pool M. and J. Carrera (2010) ‘Dynamics of negative hydraulic barriers to prevent seawater intrusion’, **Hydrogeology Journal**, Vol. 18(1), pp. 95-105.
17. Siarkos I., D. Latinopoulos, Z. Mallios and P. Latinopoulos (2017) ‘A methodological framework to assess the environmental and economic effects of injection barriers against seawater intrusion’, **Journal of Environmental Management**, Vol. 193, pp. 532-540.
18. Siarkos I. and P. Latinopoulos (2016a) ‘Modeling seawater intrusion in overexploited aquifers in the absence of sufficient data: application to the aquifer of Nea Moudania, northern Greece’, **Hydrogeology Journal**, Vol. 24(8), pp. 2123-2141.
19. Siarkos I. and P. Latinopoulos (2016b) ‘Development of constant and variable density models to study groundwater flow and seawater intrusion in the aquifer of Nea Moudania, Greece’, **European Water**, Vol. 55, pp. 53-66.
20. Sieber J. and D. Purkey (2005) **‘WEAP - Water Evaluation and Planning System. User Guide for WEAP 21’**, SEI, Stockholm Environment Institute, Somerville, USA.
21. Werner A.D., M. Bakker, V.E.A. Post, A. Vandenbohede, C. Lu, B. Ataie-Ashtiani, C.T. Simmons and D.A. Barry (2013) ‘Seawater intrusion processes, investigation and management: recent advances and future challenges’, **Advances in Water Resources**, Vol. 51, pp. 3-26.
22. Zheng C. and P.P. Wang (1999) **‘MT3DMS: a modular three-dimensional multispecies transport model for simulation of advection, dispersion, and chemical reactions of contaminants in groundwater systems - documentation and user’s guide.’**, Contract report SERD-99-1, US Army Corps of Engineers, Washington, DC.

SPATIOTEMPORAL GEOSTATISTICAL MODELING OF AQUIFER LEVELS USING PHYSICALLY BASED TOOLS

E.A. Varouchakis*, P.G. Theodoridou and G.P. Karatzas

School of Environmental EngineeringTechnical University of Crete, Chania, Greece

*Corresponding author: e-mail: varuhaki@mred.tuc.gr, tel : +302821037803

Abstract

Spatiotemporal geostatistics is a significant tool for groundwater level modeling and resources management. Geostatistics is complementary to the physical models which are based on partial differential equations that govern the flow and transport of pollutants in the groundwater. However, physical models require significant amount of data for calibration (e.g., boundary conditions, estimation of the hydraulic conductivity statistics and spatial correlation). In the case of sparsely monitored areas the number of available data often does not support the use of physical models, which makes a statistical stochastic approach necessary. Researchers in the field of hydrology investigating the variability of aquifer properties are often involved in cases with scarce spatial and temporal data. In such cases, modeling of the groundwater level as a random field, which can be analyzed and estimated by means of geostatistics, is an alternative accessible option. Thus, it can be implemented with fewer measurements and is computationally less complex than the solution of partial differential equations. A recently developed non-separable physically based covariance function is appropriately modified employing tools of physical meaning to enhance the efficiency and reliability of spatiotemporal geostatistical modeling in groundwater applications. The proposed covariance function is mathematically valid (i.e., constitutes permissible models), and provides a useful tool to model scarce space-time groundwater level data. Herein, the efficiency of the proposed tools is tested using groundwater level data from an alluvial unconfined aquifer.

Keywords: non-separable covariance; space-time interpolation; space-time modelling, groundwater; sparse data

1. SPATIOTEMPORAL GEOSTATISTICAL MODELLING

Spatiotemporal geostatistical models provide a probabilistic framework for data analysis and predictions which is based on the joint spatial and temporal dependence between observations (Kyriakidis and Journel 1999, Fischer and Getis 2010). Initial approaches to spatiotemporal data modeling were based on separable covariance functions, obtained by combining separate spatial and temporal covariance models (Rodriguez-Iturbe and Mejia 1974, Rouhani and Myers 1990, Cressie 1993, Dimitrakopoulos and Luo 1994). The last two decades there is significant development of non-separable covariance functions. These models aim to improve spatiotemporal data modeling and prediction (Cressie and Huang 1999, De Iaco, Myers et al. 2001, Gneiting 2002, Kolovos, Christakos et al. 2004) by extracting in some case the covariance functions from physical laws such as differential equations and dynamic rules (Christakos and Hristopulos 1998, Christakos 2000, Gneiting 2002, Kolovos, Christakos et al. 2004).

The main goal of space-time analysis is to model multiple time series of data at spatial locations where a distinct time series is allocated. The time variable is considered as an additional dimension in geostatistical prediction. A spatiotemporal stochastic process can be represented by $Z(\mathbf{s},t)$ where

the variable of interest of random field Z is observed at N space-time coordinates $(\mathbf{s}_i, t_i), \ldots, (\mathbf{s}_N, t_N)$, while the optimal prediction of the variable in space and time is based on $Z(\mathbf{s}_i, t_i), \ldots, Z(\mathbf{s}_N, t_N)$ (Cressie and Huang 1999, Giraldo Henao 2009). S/TRF $Z(\mathbf{s},t)$ can be decomposed into a mean component $m_Z(\mathbf{s},t)$ modeling the presence of a correlated trend and a residual S/TRF component $Z'(\mathbf{s},t)$ modeling fluctuations around that trend in both space and time. The trend can be calculated either deterministically and the fluctuations using a stochastic framework such as space-time kriging (Christakos 1991, Kyriakidis and Journel 1999).

2. SPATIOTEMPORAL PREDICTION OF AQUIFER LEVEL

Mires basin of the Messara valley is a sparsely monitored basin located on the island of Crete, Greece. Since 1981 where a rapid increase of drip irrigation and increased pumping were started, only 10 wells were consistently monitored biannually until the year 2015. The basin is consistently overexploited and the result is a great drawdown of the water table; more than 35m since 1981. The water resources availability in the area, especially the groundwater, are encountering great shortage. The application of spatiotemporal geostatistics exploits the spatially short groundwater level dataset to identify the historic spatiotemporal behavior of the aquifer and to take useful information regarding the space-time data correlations for future predictions. Space-time geostatistical analysis considers the following steps: 1) space-time variogram calculation, 2) application of space-time kriging, STOK for prediction, 3) estimation of prediction accuracy.

STOK is a well-established method for space-time interpolation (Christakos, Bogaert et al. 2001, De Cesare, Myers et al. 2001). It is however complicated, as the kriging system of equations needs to be solved at the same time for spatial and temporal weights (Skøien and Blöschl 2007).

The primary concerns when modeling space–time structures, is to ensure that the chosen spatiotemporal dependence model is valid and appropriate for space-time analysis. First, the experimental spatiotemporal variogram is determined. Then it is modeled with theoretical spatiotemporal variogram functions to determine the space-time dependence parameters.

3. GEOSTATISTICAL TOOLS

Spartan covariance and variogram functions were introduced by Hristopulos (2003) and have been applied to various environmental data sets (Hristopulos 2003, Elogne, Hristopulos et al. 2008, Elogne and Hristopulos 2008, Hristopulos and Elogne 2009, Varouchakis and Hristopulos 2013, Varouchakis and Hristopulos 2017). Herein, this family of functions is modified appropriately to model hydro-geological data. The Spartan covariance functions in d=3 dimensions are expressed as follows:

$$C_z(\mathbf{h}) = \begin{cases} \dfrac{\eta_0\, e^{-h\beta_2}}{2\pi\sqrt{|\eta_1^2-4|}}\left[\dfrac{\sin(h\beta_1)}{h\beta_1}\right], & \text{for } |\eta_1|<2,\ \sigma_z^2 = \dfrac{\eta_0}{2\pi\sqrt{|\eta_1^2-4|}} \\ \dfrac{\eta_0\, e^{-h}}{8\pi}, & \text{for } \eta_1 = 2,\ \sigma_z^2 = \dfrac{\eta_0}{8\pi} \\ \dfrac{\eta_0\,(e^{-h\omega_1}-e^{-h\omega_2})}{4\pi(\omega_2-\omega_1)\,h\sqrt{|\eta_1^2-4|}}, & \text{for } \eta_1>2,\ \sigma_z^2 = \dfrac{\eta_0}{4\pi\sqrt{|\eta_1^2-4|}} \end{cases} . \quad (1)$$

In the above function, η_0 is the scale factor, η_1 is the rigidity coefficient, $\beta_1 = |2-\eta_1|^{1/2}/2$ is a dimensionless wavenumber, $\beta_2 = |2+\eta_1|^{1/2}/2$ and $\omega_{1,2} = \left(|\eta_1 \mp \Delta|/2\right)^{1/2}$, $\Delta = |\eta_1^2 - 4|^{1/2}$, are

dimensionless damping coefficients, ξ is a characteristic length, $\mathbf{h} = \mathbf{r}/\xi$ is the normalized lag vector, $h = |\mathbf{h}|$ is the separation distance norm and σ_z^2 is the variance. A covariance function that is permissible in *three* spatial dimensions is also permissible in two dimensions (Christakos 1991). Hence, (1) can be used in two dimensions. The exponential covariance is recovered for $\eta_1 = 2$, while for $|\eta_1| < 2$ the product of the exponential and hole-effect model is obtained.

The spatiotemporal Spartan function constitutes a new approach in the interdependence modeling of spatiotemporal data (Varouchakis and Hristopulos 2017). It forms a non-separable function, which is based on the spatial Spartan variogram family. The function is derived by substituting *h* with the following equation in its spatial form (1),

$\mathbf{h} = \sqrt{\mathbf{h}_r^2 + \alpha\, \mathbf{h}_\tau^2}, \quad \mathbf{h}_r = \frac{r}{\xi_r}, \quad \mathbf{h}_\tau = \frac{\tau}{\xi_\tau}$, where τ is the time step lag.

The scale factor η_0 that defines partly the variance of the variogram is expressed in terms of the average spatiotemporal hydraulic gradient ($\eta_0^{dh/dl}$) of the space-time groundwater level data set. The latter is applied to obtain a physical parameter in the function that determines the highest value (sill) of the measurement variable in terms of different spatial separation distances. A similar approach is common in developing physically based covariance structures by including a parameter that affects the spatial or temporal behavior of the measurement variable (Kolovos, Christakos et al. 2004).

Another new approach in the modeling of spatiotemporal data is the application of non-Euclidean distance metrics. In this study we apply the Manhattan metric, described by equation (2), to examine the effect of distance calculation on the data interdependence modelling and the prediction results:

Manhattan: $$d_1 = |x_i - x_j| + |y_i - y_j| \tag{2}$$

where, (x_i, y_i), (x_j, y_j), $i, j \in 1,..,n$, are the Cartesian coordinates of the ith and jth monitoring points (wells) at the corresponding study area and *n* is the number of wells.

Given a constant distance each time, the equation of locus of all points that equidistant from a given point (focus) is a concentric circle in case of Euclidean distance and a concentric rhombus in case of Manhattan distance, useful for grid-path data. Due to this special feature, the aforementioned distance has the potential to capture spatial hydrogeological discontinuities in terms of the separation distances between the measurements (Theodoridou, Varouchakis et al. 2017).

4. RESULTS AND DISCUSSION

Spatiotemporal geostatistical analysis of Mires basin groundwater level data was applied to identify the spatiotemporal behavior of the aquifer since 1981 and to undertake predictions based on the space-time data correlations using the proposed tools. The space-time experimental variogram is determined from the biannual groundwater level time series at the 10 sampling stations for the period 1981-2014. Validation of the estimates was performed for the wet and dry period of the year 2015.

The theoretical space-time variogram model fitting on the experimental space-time variogram obtained from the observed data is presented in Figure 1. The average spatiotemporal hydraulic gradient was calculated equal to *dh/dl*= 0.08m. The respective variogram parameters are $\sigma_z^2 = 46.60$ m^2, $\xi_r = 0.27$ (≈ 3km), $\xi_\tau = 0.94$ (≈ 12 months), $\eta_1 = 1.87$, $\alpha = 0.12$ and nugget variance $c = 3.83$ m^2. The nugget term was considered to improve the experimental variogram fit.

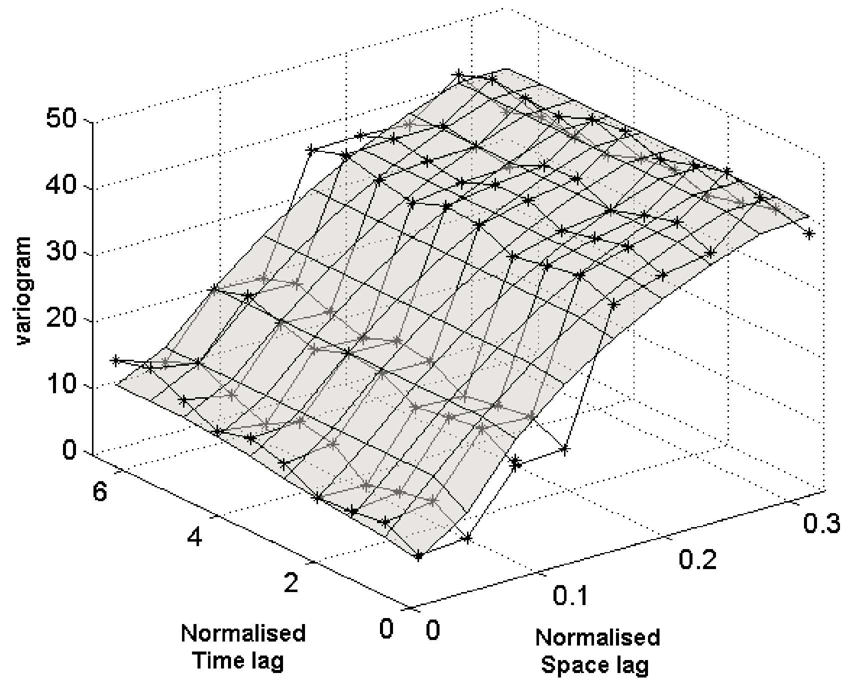


Figure 1. Space-time product-sum variogram fit using the Spartan structure.

The prediction involves STOK application to estimate the groundwater level at the specified locations and time during the wet and dry period of the year 2015. The validation results in terms of absolute estimation error (AE) are presented in the following table.

As it is presented in Table 1, STOK provides very good agreement with the reported values improved by 35% compared to previous work that involved the original space-time Spartan variogram and the Euclidean distance metric. The aquifer level map is then derived using STOK with the modified Spartan spatiotemporal variogram structure and the Manhattan distance metric for the wet and dry periods of the year 2015, the last period of available data and the most recent to date. The contour maps of groundwater level spatial variability in physical space are presented in Figures 2 and 3. The maps are constructed using estimates only at points inside the convex hull of the measurement locations.

Table1. Absolute Error (AE) of STOK estimates for the wet and dry period of the year 2015.

Well No	Wet period AE (m)	Dry Period AE (m)
G1	1.2	1.38
G2	1.02	1.29
G3	0.72	0.94
G4	1.21	1.34
G5	1.32	1.43
G6	1.04	1.24
G7	0.84	0.95
G8	0.95	0.99
G9	0.68	0.84
G10	0.73	0.96

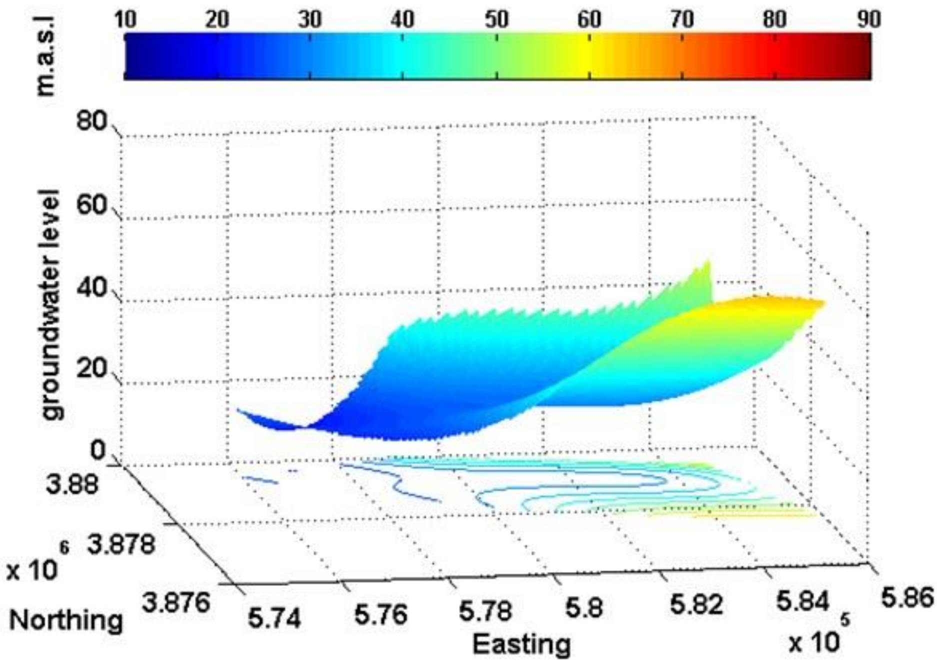


Figure 2. Map of estimated groundwater level (meters above sea level – m.a.s.l) in the Mires basin using STOK for the wet period of the year 2015.

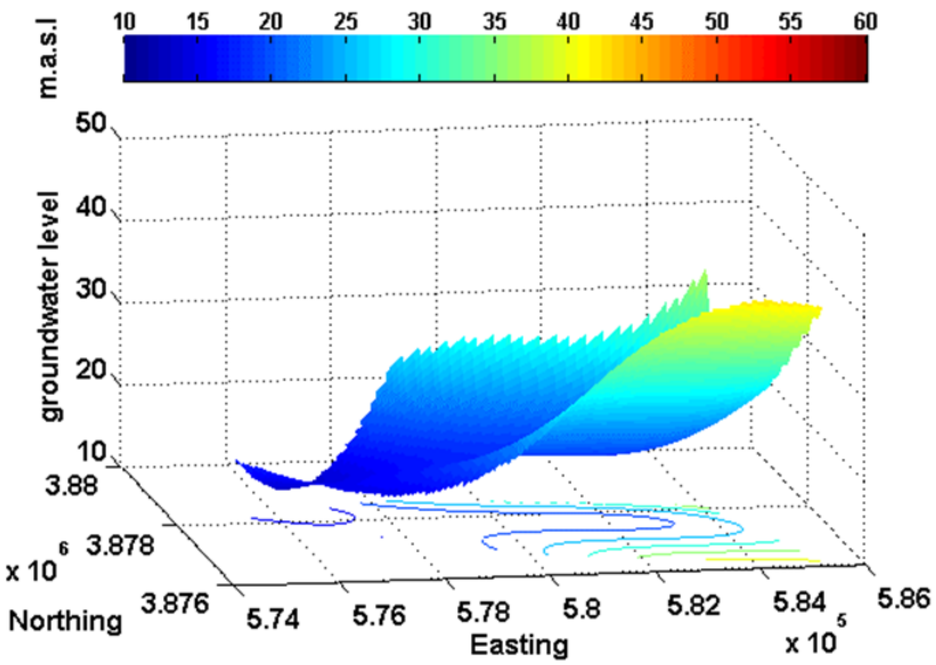


Figure 3. Map of estimated groundwater level (meters above sea level – m.a.s.l) in the Mires basin using STOK for the dry period of the year 2015.

The scope of this work was to employ two new tools of physical meaning in the variogram calculation of the available data and to test their efficiency to model the spatiotemporal response of the groundwater level variations in an aquifer. The model delivers an excellent variogram fit and very accurate estimates. The spatial correlation length is determined after the variogram fitting equal to

almost 3km and the temporal length equal to almost 12 months. The latter denotes that spatiotemporal prediction considers so the wet as the dry hydrological period of measurements. Therefore, leads to accurate results. Figures 2 and 3 present the spatial variability of the estimated groundwater level based on the space-time correlations of the data that consider the dynamic aquifer behavior.

5. CONCLUSIONS

Reliable space-time estimates are important for groundwater resources management. This work presented the space-time geostatistical analysis framework and examined the spatiotemporal modeling of groundwater level in a hydrological basin where the groundwater resources have been significantly depleted the past 35 years. The spatiotemporal approach employed the application of the Spartan variogram function involving the term of hydraulic gradient to approximate the scale parameter of the space-time variogram. This spatiotemporal structure fits very well the experimental space-time variogram of the groundwater level capturing the space-time correlations of the available data.

The Manhattan distance metric provides improved predictions. This may results from the physical characteristics of the aquifer. Moreover, Manhattan distance metric has the property to estimate the distance between two points of axes x and y accordingly to the axes orientation, while Euclidean does not have this special feature. Thus, Manhattan metric is preferred to estimate a distance between two locations when a geological barrier interferes (e.g. in a karstic aquifer, presence of faults). However, it is worth mentioning that the aforementioned approach is not necessarily the appropriate for each data set, but it depends on the characteristics of the system under study and on the scope of each study.

The STOK estimates presented accurately the groundwater level variability for the examined validation period and provided the spatial distribution of the aquifer level at ungauged locations for the wet and dry period of the year 2015. The examined approach is shown to provide a reliable alternative in spatiotemporal modeling of aquifer level. Another advantage is that it requires less data than a numerical model to represent the head field and in less computational time.

References

1. Christakos, G. (1991). '**Random field models in earth sciences**'. San Diego, Academic press.
2. Christakos, G. (2000). '**Modern Spatiotemporal Geostatistics**'. New York, Oxford University Press.
3. Christakos, G., P. Bogaert and M. L. Serre (2001). '**Temporal GIS: Advanced functions for field-based applications**'. Berlin, Springer Verlag.
4. Christakos, G. and D. T. Hristopulos (1998). '**Spatiotemporal environmental health modelling: A tractatus stochasticus**'. Boston, Kluwer.
5. Cressie, N. (1993). '**Statistics for spatial data (revised ed.)**'. New York, Wiley.
6. Cressie, N. and H. C. Huang (1999). "Classes of Nonseparable, Spatio-Temporal Stationary Covariance Functions." **Journal of the American Statistical Association**, 94(448), 1330-1340.
7. De Cesare, L. D., D. E. Myers and D. Posa (2001). "Estimating and modeling space-time correlation structures." **Statistics & Probability Letters**, 51(1), 9-14.
8. De Iaco, S., D. E. Myers and D. Posa (2001). "Space-time analysis using a general product-sum model." **Statistics & Probability Letters**, 52(1), 21-28.
9. Dimitrakopoulos, R. and X. Luo (1994). '**Spatiotemporal modeling: covariances and ordinary kriging systems**'. Dordrecht, Kluwer.

10. Elogne, S., D. Hristopulos and E. Varouchakis (2008). "An application of Spartan spatial random fields in environmental mapping: focus on automatic mapping capabilities." **Stochastic Environmental Research and Risk Assessment**, 22(5), 633-646.
11. Elogne, S. N. and D. T. Hristopulos (2008). Geostatistical applications of Spartan spatial random fields. '**geoENV VI - Geostatistics for environmental applications in series: Quantitative geology and geostatistics'**. A. Soares, M. J. Pereira and R. Dimitrakopoulos, Berlin, Gemany: Springer. **15:** 477-488.
12. Fischer, M. M. and A. Getis (2010). '**Handbook of applied spatial analysis: software tools, methods and applications'**. Berlin, Springer Verlag.
13. Giraldo Henao, R. (2009). '**Geostatistical analysis of functional data'** PhD, Universitat Politechnica de Catalunya.
14. Gneiting, T. (2002). "Nonseparable, stationary covariance functions for space-time data." **Journal of the American Statistical Association**, 97(458), 590-600.
15. Hristopulos, D. T. (2003). "Spartan Gibbs random field models for geostatistical applications." **SIAM Journal on Scientific Computing**, 24(6), 2125-2162.
16. Hristopulos, D. T. and S. N. Elogne (2009). "Computationally efficient spatial interpolators based on Spartan spatial random fields." **IEEE Transactions on Signal Processing**, 57(9), 3475-3487.
17. Kolovos, A., G. Christakos, D. T. Hristopulos and M. L. Serre (2004). "Methods for generating non-separable spatiotemporal covariance models with potential environmental applications." **Advances in Water Resources**, 27(8), 815-830.
18. Kyriakidis, P. and A. Journel (1999). "Geostatistical Space-Time Models: A Review." **Mathematical Geology**, 31(6), 651-684.
19. Rodriguez-Iturbe, I. and M. J. Mejia (1974). "The design of rainfall networks in time and space." **Water Resources Research**, 10(4), 713–728.
20. Rouhani, S. and D. Myers (1990). "Problems in space-time kriging of geohydrological data." **Mathematical Geology**, 22(5), 611-623.
21. Skøien, J. O. and G. Blöschl (2007). "Spatiotemporal topological kriging of runoff time series." **Water Resources Research**, 43(9).
22. Theodoridou, P. G., E. A. Varouchakis and G. P. Karatzas (2017). "Spatial analysis of groundwater levels using Fuzzy Logic and geostatistical tools." **Journal of Hydrology**, 555, 242-252.
23. Varouchakis, E. A. and D. T. Hristopulos (2013). "Improvement of groundwater level prediction in sparsely gauged basins using physical laws and local geographic features as auxiliary variables." **Advances in Water Resources**, 52(2013), 34-49.
24. Varouchakis, E. A. and D. T. Hristopulos (2017). "Comparison of spatiotemporal variogram functions based on a sparse dataset of groundwater level variations." **Spatial Statistics**, https://doi.org/10.1016/j.spasta.2017.1007.1003.

COST MINIMIZATION OF INTERMITTENT TRANSIENT GROUNDWATER PUMPING

Iraklis A. Nikoletos

Division of Hydraulics and Environmental Engineering, Dept. of Civil Engineering, A.U.Th, GR- 54124 Thessaloniki, Macedonia, Greece

Corresponding author: e-mail: irakniko@civil.auth.gr

Abstract

In this paper, consideration is being given to minimizing the pumping cost from a system of wells under transient groundwater flow conditions in a confined aquifer.

In particular, previous work has been extended to include cases of intermittent pumping in both infinite and semi-infinite aquifers, where the method of images applies.

The mathematical method used to find the minimum of the cost function was the Lagrange multipliers.

It has been proved analytically that at any time, the pumping cost is minimized when the hydraulic head level drawdowns at the locations of the wells are equal to each other.

Keywords: Optimization, method of images; Lagrange multipliers, pumping cost, groundwater management

1. INTRODUCTION

The cost of energy consumed for the pumping of water is one of the main problems of groundwater management. This energy can be divided in two categories. The first category includes the energy required to lift the water from the underground aquifer and the second one the energy needed to overcome friction in pipes, the local losses of the pumps as well as other parts of the distribution network used for transport of the water (Ahlfeld et al. 2011). The rapid advances in science have helped to develop simulation models that solve quite accurately various pumping problems in different types of aquifers. To make proper use of programs the user should be equipped with the necessary theoretical background, in order to be able to check the computational results. This is achieved through analytical solutions that justify, clarify and scientifically evaluate the results (Mahdavi 2015). Conclusions resulting from analytical solutions are inextricably linked to simulation models that lead to the realistic depiction of real situations and problems and contribute to their optimal management both economically and environmentally (e.g. Fowler et al. 2008; Saeedpanah et al. 2017; Shourian et al. 2017; Siarkos et al. 2017; Theodossiou 2004).

In this paper, analytical solutions taking into account transient flow (Katsifarakis et al, 2018) are extended to intermittent transient groundwater pumping.

2. FORMULATION OF THE OBJECTIVE COST FUNCTION

Energy consumption depends directly on the total flow rate pumped from a system of N wells. The cost function of the energy consumed at any time in any type of aquifer is given by the relationship.

$$K = A \cdot \sum_{J=1}^{N} Q_J(t)(s_J(t) + \delta_J) \qquad (1)$$

Where K is the pumping cost, Q_J is the flow rate of well J, $s_J(t)$ is the transient drawdown at point J at the time t and δ_J is the distance between the initial hydraulic head level at well J and the reference level. Since A is a constant coefficient, which is dependent on energy cost and with the assumption that the aquifer is horizontal namely $\delta_J = \delta$, the objective function that should be minimized is

$$K = \sum_{J=1}^{N} Q_J(t) s_J(t) \qquad (2)$$

2.1 Initial conditions - Constraints

We consider a system of N wells, which pump given total flow rates for K successive time periods.

For any well $m \in [1,N]$ just before pumping begins ($t_0 = 0$)

$$Q_m^{t_0} = 0, \; s(t_0, m) = 0 \qquad (3)$$

For any time period i the following constraint applies (i=1, 2, 3… K)

$$\sum_{m=1}^{N} Q_m^i = Q_T^i \qquad (4)$$

Where Q_T^i is the total pumped rate during time period i.

3. INFINITE AQUIFERS

In infinite confined aquifers the drawdown at a point m at a random moment t_k is given by the relationship (Latinopoulos 1996, Theis 1935):

$$s(t_k, m) = \sum_{i=1}^{K} \sum_{j=1}^{N} \frac{1}{4\pi T}(Q_j^i - Q_j^{i-1}) W\left(\frac{Sr_{mj}^2}{4T(t_k - t_{i-1})}\right) \qquad (5)$$

Where

$$W(u_{mj}) = W\left(\frac{Sr_{mj}^2}{4T(t_k - t_{i-1})}\right) = \int_{u_{mj}}^{\infty} \frac{e^{-y}}{y} dy \qquad (6)$$

is the well function, T is the aquifer's transmissivity, S the aquifer's storativity and r_{mj} the distance between well m and j. It is worth mentioning that $W(u_{mj})$ decreases while u_{mj} is increasing. Using the superposition principle (Bear 1979) the cost function at any time K-1 <t_k<K takes the form

$$K_{t_k} = \sum_{i=1}^{K} \sum_{j=1}^{N} (Q_j^i - Q_j^{i-1}) \sum_{z=1}^{N} \frac{1}{4\pi T}(Q_z^i - Q_z^{i-1}) W\left(\frac{Sr_{zj}^2}{4T(t_k - t_{i-1})}\right) \qquad (7)$$

3.1 Analytical solution of the optimization problem for infinite confined aquifer

To find possible critical points under constraints, the method of Lagrange' multipliers will be used. The function (7) is subject to K equality constraints, as many as the periods of different total pumped flow. Therefore, the function to be studied is the following:

$$L_{t_k} = K_{t_k} + \sum_{i=1}^{K} \lambda_i g_i \qquad (8)$$

So, the system of equations that we need to solve, in order to find a critical point is

$$\nabla L_{t_k} = \nabla K_{t_k} + \sum_{i=1}^{K} \lambda_i \nabla g_i = 0 \tag{9}$$

$$g_i = 0, \forall i = 1,2,3...,K \tag{10}$$

Where λ_i is every Lagrange multiplier for every constraint and g_i is the total pumping constraint for each time step,

$$g_i = \sum_{z=1}^{N} Q_z^i - Q_T^i = 0 \tag{11}$$

According to all these we shall calculate the first derivatives of L_{t_k} with respect to the decision variables, which are the flow rates Q_j^i.

For any $m \in [1, N]$ and for any $y \in [1, K-1]$

$$\begin{aligned}\frac{\partial L_{t_K}}{\partial Q_m^y} &= \sum_{j=1}^{N-1} \frac{1}{4\pi T}(Q_j^y - Q_j^{y-1}) W\left(\frac{Sr_{mj}^2}{4T(t_k - t_{y-1})}\right) + \\ &+ 2\frac{1}{4\pi T}(Q_m^y - Q_m^{y-1}) W\left(\frac{Sr_{mm}^2}{4T(t_k - t_{y-1})}\right) + \\ &+ \sum_{z=1}^{N-1} \frac{1}{4\pi T}(Q_z^y - Q_z^{y-1}) W\left(\frac{Sr_{mz}^2}{4T(t_k - t_{y-1})}\right) - \\ &- \sum_{j=1}^{N-1} \frac{1}{4\pi T}(Q_j^{y+1} - Q_j^y) W\left(\frac{Sr_{mj}^2}{4T(t_k - t_y)}\right) - \\ &- 2\frac{1}{4\pi T}(Q_m^{y+1} - Q_m^y) W\left(\frac{Sr_{mm}^2}{4T(t_k - t_{y-1})}\right) - \\ &- \sum_{z=1}^{N-1} \frac{1}{4\pi T}(Q_z^{y+1} - Q_z^y) W\left(\frac{Sr_{mz}^2}{4T(t_k - t_y)}\right) + \lambda_y\end{aligned} \tag{12}$$

$$\frac{\partial L_{t_K}}{\partial Q_m^y} = 2s_{m(t_k - t_{y-1})} - 2s_{m(t_k - t_y)} + \lambda_y = 0 \tag{13}$$

For the last time step y=K and for any $m \in [1, N]$

$$\frac{\partial L_{t_K}}{\partial Q_m^y} = 2s_{m(t_k - t_{y-1})} + \lambda_y = 0 \tag{14}$$

To complete the system, we use the K equations of (10)

The system consists of K x (N+1) equations with K x (N+1) unknowns

For y=1, 2… K-1 and for any $m \in [1, N]$ and $n \in [1, N]$

$$s_{m(t_k - t_{y-1})} - s_{m(t_k - t_y)} + \lambda_y = s_{n(t_k - t_{y-1})} - s_{n(t_k - t_y)} + \lambda_y \tag{15}$$

For y=K respectively

$$s_{m(t_k - t_{y-1})} + \lambda_y = s_{n(t_k - t_{y-1})} + \lambda_y \qquad (16)$$

Introducing the N equations of (16) to K x N equations of (15) results into

$$s_{m(t_k - t_{y-1})} = s_{n(t_k - t_{y-1})} \qquad (17)$$

Therefore, only one critical point exists, namely $P(Q_1^1, Q_2^1, ..., Q_K^N)$

Point P refers to a local extreme point or to a saddle point. To decide we shall calculate the quantity q, which is defined as:

$$q = \left[h_1^1, h_2^1, .., h_N^1, h_1^2, .., h_N^K\right] \mathrm{H} \begin{bmatrix} h_1^1 \\ h_2^1 \\ ... \\ h_N^K \end{bmatrix} \qquad (18)$$

Where $h_1^1, h_2^1, ..., h_N^K$ are real numbers verifying the following equality:

$$\begin{bmatrix} \frac{\partial g_1}{\partial Q_1^1} & \frac{\partial g_1}{\partial Q_2^1} & ... & \frac{\partial g_1}{\partial Q_N^1} & ... & \frac{\partial g_1}{\partial Q_N^K} \\ \frac{\partial g_2}{\partial Q_1^1} & \frac{\partial g_2}{\partial Q_2^1} & ... & ... & ... & ... \\ ... & ... & ... & ... & ... & ... \\ ... & ... & ... & ... & ... & ... \\ ... & ... & ... & ... & ... & ... \\ \frac{\partial g_K}{\partial Q_1^1} & \frac{\partial g_K}{\partial Q_2^1} & ... & \frac{\partial g_K}{\partial Q_N^1} & ... & \frac{\partial g_K}{\partial Q_N^K} \end{bmatrix} \begin{bmatrix} h_1^1 \\ h_2^1 \\ ... \\ h_N^1 \\ h_1^2 \\ ... \\ \\ h_N^K \end{bmatrix} = 0 \qquad (19)$$

And **H** the Hessian matrix with dimensions K*NxK*N whose elements have values

$a_{ij} = \frac{\partial^2 L_{t_k}}{\partial Q_j \partial Q_i}$ Where Q_j and Q_i are the flow rates arranged in time order.

(i.e. $\frac{\partial^2 L_{t_k}}{\partial (Q_1^1)^2} = W(\frac{Sr_{11}^2}{4Tt_k}) + W(\frac{Sr_{11}^2}{4T(t_k - t_1)})$)

After trivial calculations we conclude from eq. (19)

$$\begin{aligned} &h_1^1 + h_2^1 + ... + h_N^1 = 0 \\ &h_1^2 + h_2^2 + ... + h_N^2 = 0 \\ &... \\ &h_1^K + h_2^K + ... + h_N^K = 0 \end{aligned} \qquad (20)$$

And from eq. (18)

$$q=\sum_{j=1}^{N}h_j^1\sum_{z=1}^{N}h_z^1W(\frac{Sr_{zj}^2}{4Tt_k})+\sum_{j=1}^{N}h_j^1\sum_{z=1}^{N}(h_z^1-h_z^2)W(\frac{Sr_{zj}^2}{4T(t_k-t_1)})+\sum_{j=1}^{N}h_j^2\sum_{z=1}^{N}(h_z^2-h_z^1)W(\frac{Sr_{zj}^2}{4T(t_k-t_1)})+$$

$$+\sum_{j=1}^{N}h_j^2\sum_{z=1}^{N}(h_z^2-h_z^3)W(\frac{Sr_{zj}^2}{4T(t_k-t_2)})+\sum_{j=1}^{N}h_j^3\sum_{z=1}^{N}(h_z^3-h_z^2)W(\frac{Sr_{zj}^2}{4T(t_k-t_2)})+.... \tag{21}$$

$$+\sum_{j=1}^{N}h_j^K\sum_{z=1}^{N}(h_z^K-h_z^{K-1})W(\frac{Sr_{zj}^2}{4T(t_k-t_{K-1})})>0$$

We also take advantage of the properties $a_{ij}=a_{ji}$, $W(\frac{Sr_{ij}^2}{4T(t_k-t_y)})=W(\frac{Sr_{ji}^2}{4T(t_k-t_y)})$

and $W(\frac{Sr_{ii}^2}{4T(t_k-t_y)})=W(\frac{Sr_{jj}^2}{4T(t_k-t_y)})=W(\frac{Sr_o^2}{4T(t_k-t_y)})$

The quantity q is positive for the following reasons

1) $W(\frac{Sr_o^2}{4T(t_k-t_y)})-W(\frac{Sr_{zj}^2}{4T(t_k-t_y)})>0$ (Katsifarakis et al. 2017)

where r_o is the radius of each well

2) From eq. (20) $h_1^1+h_2^1+...+h_N^1=0 \Rightarrow (h_1^1+h_2^1+...+h_N^1)^2=0 \Rightarrow$
$(h_1^1)^2+(h_2^1)^2+...+(h_N^1)^2=-2h_1^1h_2^1-2h_1^1h_3^1-...-2h_{N-1}^1h_N^1>0$

The left-hand side of the last equation is positive as sum of squares. Hence, the right-hand side is positive. Applying this result to q

$$(-2h_1^1h_2^1-2h_1^1h_3^1-...-2h_{K-1}^1h_K^1)W(\frac{Sr_{zz}^2}{4T(t_k)})+(2h_1^1h_2^1W(\frac{Sr_{12}^2}{4T(t_k)})+2h_1^1h_3^1W(\frac{Sr_{13}^2}{4T(t_k)})+...+$$

$$+2h_{K-1}^1h_K^1W(\frac{Sr_{N-1,N}^2}{4T(t_k)}))>0$$

3) From eq. (20) for 2 consecutively time steps we get

$$h_1^i+h_2^i+...+h_N^i=h_1^{i+1}+h_2^{i+1}+...+h_N^{i+1} \Rightarrow h_1^i+h_2^i+...+h_N^i-h_1^{i+1}-h_2^{i+1}-...-h_N^{i+1}=0$$

$$(h_1^i+h_2^i+...+h_N^i-h_1^{i+1}-h_2^{i+1}-...-h_N^{i+1})^2=0 \Rightarrow$$

$$(h_1^i)^2+(h_2^i)^2+...+(h_N^i)^2+(h_1^{i+1})^2+(h_2^{i+1})^2+...+(h_N^{i+1})^2=-2h_1^ih_2^i-2h_1^ih_3^i-...-2h_{N-1}^ih_N^i+2h_1^ih_2^{i+1}+...$$

$$+2h_N^ih_N^{i+1}>0$$

$$(-2h_1^ih_2^i-2h_1^ih_3^i-...-2h_{N-1}^ih_N^i+2h_1^ih_2^{i+1}+...+2h_{N-1}^ih_N^{i+1})W(\frac{Sr_o^2}{4T(t_k-t_i)})+$$

$$(+2h_1^ih_2^iW(\frac{Sr_{12}^2}{4T(t_k-t_i)})+2h_1^ih_3^iW(\frac{Sr_{13}^2}{4T(t_k-t_i)})+...+2h_{N-1}^ih_N^iW(\frac{Sr_{N-1,N}^2}{4T(t_k-t_i)})-$$

$$-2h_1^ih_2^{i+1}W(\frac{Sr_{12}^2}{4T(t_k-t_i)})-...-2h_{N-1}^ih_N^{i+1}W(\frac{Sr_{N-1,N}^2}{4T(t_k-t_i)})>0$$

So, quantity q is positive for all non-zero matrices $\begin{pmatrix} h_1 \\ \ldots \\ h_{KN} \end{pmatrix}$ that verify equation (19).

For all these reasons we infer that P is a minimum of K_k, and since it is the only critical point it's the absolute minimum.

Thus, at any time, the pumping cost is minimized when the hydraulic head level drawdowns at the locations of the wells are equal to each other.

4. SEMI INFINITE AQUIFERS

In the following paragraphs, we work on the pumping cost minimization problem, described by equations (1) to (4), in semi-infinite aquifers, to which the method of images applies. We have studied two fields. The first one has a straight-line impermeable boundary and the second one has a straight-line rectilinear constant head boundary. The optimization procedure remains the same for both cases as in the infinite aquifers. The basic concept of method of images is that a boundary can be "removed" by adding a number of fictitious (or image) wells, symmetrical of the real ones with respect to it. The relationship between the flow rate of each real well and that of its image depends on the boundary condition along the "removed" boundary and guarantees its observance.

4.1 Flow fields with a straight-line impermeable boundary

The drawdown at the location of each well m at a random moment t_k is given by the relationship

$$s(t_k, m) = \sum_{i=1}^{K} \sum_{j=1}^{N} \frac{1}{4\pi T} (Q_j^i - Q_j^{i-1}) (W(\frac{Sr_{mj}^2}{4T(t_k - t_{i-1})}) + W(\frac{Sr_{mJ}^2}{4T(t_k - t_{i-1})})) \tag{22}$$

Hence the cost function at any time K-1 <t_k <K takes the form

$$K_{t_k} = \sum_{i=1}^{K} \sum_{j=1}^{N} (Q_j^i - Q_j^{i-1}) \sum_{z=1}^{N} \frac{1}{4\pi T} (Q_z^i - Q_z^{i-1}) (W(\frac{Sr_{zj}^2}{4T(t_k - t_{i-1})}) + W(\frac{Sr_{zJ}^2}{4T(t_k - t_{i-1})})) \tag{23}$$

As in the case of infinite aquifers we introduce the function

$$L_{t_k} = K_{t_k} + \sum_{i=1}^{K} \lambda_i g_i \tag{24}$$

For any $m \in [1, N]$ and for any $y \in [1, K-1]$

$$\frac{\partial L_{t_K}}{\partial Q_m^y} = \sum_{j=1}^{N-1} \frac{1}{4\pi T} (Q_j^y - Q_j^{y-1}) (W(\frac{Sr_{mj}^2}{4T(t_k - t_{y-1})}) + W(\frac{Sr_{mJ}^2}{4T(t_k - t_{y-1})})) +$$

$$+ 2 \frac{1}{4\pi T} (Q_m^y - Q_m^{y-1}) (W(\frac{Sr_{mm}^2}{4T(t_k - t_{y-1})}) + W(\frac{Sr_{mM}^2}{4T(t_k - t_{y-1})})) +$$

$$+ \sum_{z=1}^{N-1} \frac{1}{4\pi T} (Q_z^y - Q_z^{y-1}) (W(\frac{Sr_{mz}^2}{4T(t_k - t_{y-1})}) + W(\frac{Sr_{mZ}^2}{4T(t_k - t_{y-1})})) -$$

$$- \sum_{j=1}^{N-1} \frac{1}{4\pi T} (Q_j^{y+1} - Q_j^y) (W(\frac{Sr_{mj}^2}{4T(t_k - t_y)}) + W(\frac{Sr_{mJ}^2}{4T(t_k - t_y)})) -$$

$$-2\frac{1}{4\pi T}(Q_m^{y+1}-Q_m^y)(W(\frac{Sr_{mm}^2}{4T(t_k-t_{y-1})})+W(\frac{Sr_{mM}^2}{4T(t_k-t_y)}))-$$

$$-\sum_{z=1}^{N-1}\frac{1}{4\pi T}(Q_z^{y+1}-Q_z^y)(W(\frac{Sr_{mz}^2}{4T(t_k-t_y)})+W(\frac{Sr_{mZ}^2}{4T(t_k-t_y)})) \quad (25)$$

$$\frac{\partial L_{t_K}}{\partial Q_m^y}=2s_{m(t_k-t_{y-1})}-2s_{m(t_k-t_y)}+\lambda_y=0 \quad (26)$$

For the last time step y=K

$$\frac{\partial L_{t_K}}{\partial Q_m^y}=2s_{m(t_k-t_{y-1})}+\lambda_y=0 \quad (27)$$

As in the case of infinite aquifers, it results in

$$s_{m(t_k-t_{y-1})}=s_{n(t_k-t_{y-1})} \quad (28)$$

To verify that point P refers to the absolute minimum we follow the same procedure as in infinite aquifers. We just need to prove that the value $W(\frac{Sr_{zj}^2}{4T(t_k-t_{i-1})})+W(\frac{Sr_{zJ}^2}{4T(t_k-t_{i-1})})$ is positive.

It is obvious that the sum of two positive numbers gives a positive number.

Hence, minimization of pumping cost in the case of semi-infinite aquifers with a straight-line impermeable boundary results from equality of drawdowns at each time step.

4.2 Flow fields with a rectilinear constant head boundary

The drawdown at the location of each well m at a random moment t_k is given by the relationship

$$s(t_k,m)=\sum_{i=1}^{K}\sum_{j=1}^{N}\frac{1}{4\pi T}(Q_j^i-Q_j^{i-1})(W(\frac{Sr_{mj}^2}{4T(t_k-t_{i-1})})-W(\frac{Sr_{mJ}^2}{4T(t_k-t_{i-1})})) \quad (29)$$

Hence the cost function at any time K-1 <t_k <K takes the form

$$K_{t_k}=\sum_{i=1}^{K}\sum_{j=1}^{N}(Q_j^i-Q_j^{i-1})\sum_{z=1}^{N}\frac{1}{4\pi T}(Q_z^i-Q_z^{i-1})(W(\frac{Sr_{zj}^2}{4T(t_k-t_{i-1})})-W(\frac{Sr_{zJ}^2}{4T(t_k-t_{i-1})})) \quad (30)$$

The Lagrange function is

$$L_{t_k}=K_{t_k}+\sum_{i=1}^{K}\lambda_i g_i \quad (31)$$

For any $m\in[1,N]$ and for any $y\in[1,K-1]$

$$\frac{\partial L_{t_K}}{\partial Q_m^y}=\sum_{j=1}^{N-1}\frac{1}{4\pi T}(Q_j^y-Q_j^{y-1})(W(\frac{Sr_{mj}^2}{4T(t_k-t_{y-1})})-W(\frac{Sr_{mJ}^2}{4T(t_k-t_{y-1})}))+$$

$$+2\frac{1}{4\pi T}(Q_m^y-Q_m^{y-1})(W(\frac{Sr_{mm}^2}{4T(t_k-t_{y-1})})-W(\frac{Sr_{mJ}^2}{4T(t_k-t_{y-1})}))+$$

$$+\sum_{z=1}^{N-1}\frac{1}{4\pi T}(Q_z^{y}-Q_z^{y-1})(W(\frac{Sr_{mz}^2}{4T(t_k-t_{y-1})})-W(\frac{Sr_{mZ}^2}{4T(t_k-t_{y-1})}))$$

$$\sum_{j=1}^{N-1}\frac{1}{4\pi T}(Q_j^{y+1}-Q_j^{y})(W(\frac{Sr_{mj}^2}{4T(t_k-t_y)})-W(\frac{Sr_{mJ}^2}{4T(t_k-t_y)}))-$$

$$-2\frac{1}{4\pi T}(Q_m^{y+1}-Q_m^{y})(W(\frac{Sr_{mm}^2}{4T(t_k-t_{y-1})})-W(\frac{Sr_{mJ}^2}{4T(t_k-t_y)}))-$$

$$-\sum_{z=1}^{N-1}\frac{1}{4\pi T}(Q_z^{y+1}-Q_z^{y})(W(\frac{Sr_{mz}^2}{4T(t_k-t_y)})-W(\frac{Sr_{mZ}^2}{4T(t_k-t_y)})) \quad (32)$$

$$\frac{\partial L_{t_K}}{\partial Q_m^y}=2s_{m(t_k-t_{y-1})}-2s_{m(t_k-t_y)}+\lambda_y=0 \quad (33)$$

For the last time step y=K

$$\frac{\partial L_{t_K}}{\partial Q_m^y}=2s_{m(t_k-t_{y-1})}+\lambda_y=0 \quad (34)$$

As in the case of infinite aquifers, it results in

$$s_{m(t_k-t_{y-1})}=s_{n(t_k-t_{y-1})} \quad (35)$$

We just need to prove that the value $W(\frac{Sr_{zj}^2}{4T(t_k-t_{i-1})})-W(\frac{Sr_{zJ}^2}{4T(t_k-t_{i-1})})$ is positive.

The distance zj is smaller than the distance zJ so

$$r_{zj}^2<r_{zJ}^2 \Rightarrow \frac{Sr_{zj}^2}{4T(t_k-t_{i-1})}<\frac{Sr_{zJ}^2}{4T(t_k-t_{i-1})} \Rightarrow W(\frac{Sr_{zj}^2}{4T(t_k-t_{i-1})})>W(\frac{Sr_{zJ}^2}{4T(t_k-t_{i-1})})$$

Therefore, minimization of pumping cost in case of semi-infinite aquifers with a rectilinear constant head boundary results from equality of drawdowns of each time step. The results are shown to be related to the proofs by (Katsifrakis 2008) and (Katsifarakis and Tselepidou 2009) for steady state flow. This is something that is reasonable, if we consider that the steady state is achieved after successive time intervals.

5. CONCLUSIONS AND DISCUSSION

In this paper we have studied the minimization of pumping cost under transient groundwater flow conditions and in particular the case of intermittent pumping in both infinite and semi-infinite aquifers, where the method of images applies. The basic conclusion was that minimizing pumping cost at any time, and by extension of energy consumption, is achieved when drawdowns due to intermittent pumping of the total pumped flow rate of each time step are equal to each other. The next step of this study would be to investigate its applicability to a real field. The way of construction and the efficiency of the new system to reduce cost compared to existing systems is an issue of future research.

Acknowledgement
The author would like to thank Professor K. L. Katsifarakis for his spiritual, moral but mostly insightful support.

References

1. Ahlfeld, D.P., Laverty, M.M., 2011. Analytical solutions for minimization of energy use for groundwater pumping. **Water Resources. Research**. 47, W06508.
2. Bear J. (1979) **'Hydraulics of Groundwater'**, McGraw-Hill.
3. Fowler KP, Reese JP, Kees CE, Dennis JE Jr, Kelley CT, Miller CT, Audet C, Booker AJ, Couture G, Darwin RW, Farthing MW, Finkel DE, Gablonsky JM, Gray G, Kolda TG (2008) Comparison of derivative-free optimization methods for groundwater supply and hydraulic capture community problems. **Advances in Water Resources** 31(5):743–757
4. Siarkos I, Latinopoulos D., Mallios Z., Latinopoulos P. A methodological framework to assess the environmental and economic effects of injection barriers against seawater intrusion. **Journal of Environmental Management** Volume 193, 15 May 2017, Pages 532-540
5. Katsifarakis KL (2008) Groundwater pumping cost minimization-An analytical approach. **Water Resources Management** 22(8):1089–1099
6. Katsifarakis KL, Tselepidou K (2009) Pumping cost minimization in aquifers with regional flow and two zonesof different transmissivities**. Journal of Hydrology** 377(1-2):106–111
7. Katsifarakis, K.L., Nikoletos, I.A. & Stavridis, C. Minimization of Transient Groundwater Pumping Cost - Analytical and Practical Solutions **Water Resources Management** (2017).
8. Latinopoulos P. (1996) **'Hydraulics of groundwater'**, XARIS PUBL.
9. Mahdavi, A. Transient-State Analytical Solution for Groundwater Recharge in Anisotropic Sloping Aquifer. **Water Resources Management** (2015) 29: 3735.
10. Saeedpanah I, Golmohamadi Azar R (2017) New analytical expressions for two-dimensional aquifer adjoining with streams of varying water level. **Water Resources Management** 31(1):403–424
11. Shourian, M. & Davoudi, S.M.J. Optimum Pumping Well Placement and Capacity Design for a Groundwater Lowering System in Urban Areas with the Minimum Cost Objective **Water Resources Management** (2017) 31: 4207.
12. Theis CV (1935) The relation between lowering of the piezometric surface and the rate and duration of discharge of a well using ground water storage. **Trans. Am. Geophys. Un., 16th Annual meeting**, 519-524
13. Theodossiou, N.P., 2004. Application of non-linear simulation and optimization models in groundwater aquifer management. **Water Resources Management** 18, 125–141.

STUDY ON GROUNDWATER NITRATES IN THE NORTHWEST OF THE THESSALONIKI REGIONAL UNIT (GREECE)

A. Terzopoulos*

2nd General Lyceum of Oraiokastro, GR–57013, Oraiokastro, Thessaloniki, Greece

*Corresponding author: e-mail: terzopoulosalexandros@gmail.com, tel : +302310695778

Abstract

The present study deals with the issue of local high nitrate ion concentrations in the groundwater of the Greek region of Mygdonia. The specific phenomenon can be of great importance to Mygdonia due to health effects described in literature and a possible reduction of crop yield, a major concern for the regional agriculture-centred economy. Nitrate concentrations were measured in samples collected from a multitude of locations in all three settlements of the region. Concentrations exceeding the 50 mg/L EU limit were found in the majority of locations, especially around the area of the plains of Mygdonia (settlements Drymos and Lete). This result was followed by statistical analysis of past measurement data, which confirm chronically high levels in these locations as opposed to the more mountainous area where acceptable concentrations were observed. Furthermore, slight rising linear trends were calculated in locations of high nitrate concentrations and minimal negative trends in those of lower concentrations.

A phytotoxicity screening of species *Sorghum saccharatum* and *Sinapis alba* in the presence of high nitrate content water was also conducted, indicating a significant hindrance of early plant growth. Thus, crop cultivation may also be at risk due to nitrate presence in groundwater used for irrigation. Finally, probable causes are discussed and compared to previous studies, wherefrom an obvious pattern of correlation to agriculture and N-fertiliser application arises; the region-specific hydrogeological profile, however, also significantly raises the risk of groundwater contamination. Specific handling suggestions for facing the nitrate problem are discussed in this study.

Keywords: Groundwater nitrates, Mygdonia aquifer, Phytotoxicity, N-fertilisation effects, Nitrate vulnerability

1. INTRODUCTION

Mygdonia is a 99.03 km^2 rural region of the Thessaloniki regional unit (Greece), located about 15 km north of the city. Mygdonia has been recorded to experience a problem of high nitrate (NO_3^-) concentration in the region's drinking water supply for at least the last decade (see section 2.1). The issue has been principally associated with the arable plains of Mygdonia, which encompass the settlements of Lete, Drymos, and the eastern part of Melissochori. According to hydrogeological data of the respective Basin Management Plan [2012] compiled by the Ministry of Environment, Energy and Climate Change of the Hellenic Republic, the region of Mygdonia is located on top of the more extensive Mygdonia aquifer network (and corresponding groundwater body). Specifically the settlements of Mygdonia belong to the Koroneia subsystem (GR1000071), whose ecological status has been classified as "bad" (lowest possible classification) and the waters' chemical characteristics as "failing to achieve good" (*i.e.* the majority thereof has had various substances' concentrations in levels of potential threat to human health). In addition, data from the relevant municipal authorities indicate that drinking water supply in Mygdonia originates exclusively from drilled water wells

exploiting said groundwater. Thus, the issue of excessive nitrates in the region's water can be viewed as a specific case of nitrate accumulation in groundwater, a situation which has been repeatedly encountered in existing literature [Gardner and Vogel, 2005; Johnson and Kross, 1990; Power and Schepers, 1989; Strebel *et al.*, 1989; Zhang *et al.*, 1996].

Nitrates have been documented to negatively affect human health in numerous studies; according to extant analytic reviews thereof [Bruning-Fann and Kaneene, 1993; Parvizishad *et al.*, 2017; WHO, 2011], some common health risks arising from high nitrate consumption include infant ("blue baby syndrome") and adult methaemoglobinaemia, as well as thyroid gland dysfunctions. The exact correlation of nitrate intake and gastrointestinal tract tumours is still widely debated within existing literature. Yet, nitrates in drinking water are generally considered harmful to public health and acute toxicity results, such as methaemoglobinaemia, are observed when the concentration in drinking water exceeds 45–50 mg/L of NO_3^-. In response to this, many countries including all members of the European Community have set the "maximum admissible concentration" (*MAC*) of NO_3^- in drinking water to 50 mg/L [Council Directive 98/83/EC, 1998].

Besides the great concern for human health, nitrates have been associated with adverse effects on plant growth and potential reduction of crop yield [Chen *et al.*, 2004; Maynard *et al.*, 1976; Zhang *et al.*, 1996]. This would be a point of principal focus in Mygdonia, since the main economic activity of the region is agricultural. The 2010 agricultural utilisation data from the Greek Payment Authority of Common Agricultural Policy Aid Schemes ("*OPEKEPE*"), shows that 5014.71 ha (*i.e*. 50.64% of the total region area) are fully irrigated and used for crop farming. Thereof, the vast majority (90.28% of all farming area) is dedicated to the growing of cereals– mainly wheat, but also barley, oats, *etc*. Existing research has focused on either nitrate content in plants as a risk to human health [Maynard *et al.*, 1976] or the correlation of soil nitrate concentration and plant growth [Chen *et al.*, 2004]; the present study examines the correlation of phytotoxicity and high nitrate concentration waters, such as the ones that might be expected to be found in Mygdonia since water for irrigation is obtained from the same aquifers as with drinking water.

From what has been discussed so far, high nitrate concentration in groundwater is evidently a major issue and calls for further, case-specific, research on the possibly affected region of Mygdonia. To this purpose, the present study has been compiled; experimental evaluation of the concurrent situation in the drinking water of Mygdonia, statistical analysis of past data, the experimental testing of high nitrate waters' effect on plant toxicity, discussion of the results and aetiology combined with suggested measures comprise the total of the case study. The conclusions therefrom derived constitute an as complete as feasible region profile in relation to groundwater nitrates; this profile can be valuable in general as one additional reference case in related bibliography. Furthermore yet, it can serve as an instrument for policy makers and local authorities aiding the better handling of the issue, as well as a resource for public acknowledgement thereof.

2. MATERIALS AND METHODS

2.1 Measurement of nitrate concentration (NO_3^- mg/L) in the waters of Mygdonia & statistical analysis of past nitrate concentration data

For the quantification of nitrate levels, a total of 9 samples of drinking water were obtained, 3 from each settlement of the Mygdonia region (samples L1, L2, L3 from Lete; D1, D2, D3 from Drymos; M1, M2, M3 from Melissochori; refer to Table 1). The samples were collected in clean PET bottles from a multitude of outside faucets. After sampling was completed, all sample bottles were kept in an insulated cool box until the measurements were conducted ~45 min later.

Table 1: Information and labelling of the samples collected for assessment of nitrate concentration

Lete samples	*Sampling location*	*Drymos samples*	*Sampling location*	*Melissochori samples*	*Sampling location*
L1	Lete Comm. Hall	D1	Drymos Comm. Hall	M1	Cultural Association
L2	Local Fuel Station	D2	"Heroon" Region	M2	M/chori Comm. Hall
L3	"Skout" Region	D3	"Diskina" fountain	M3	Local Bakery

The procedure followed for the determination of nitrate concentration was the colourimetric dimethylphenol method for drinking water, using the TNTplus^{TM} 836 kit and HACH method 10206 as a reference method. LCK 339 cuvettes and 2,6-xylenol ("dimethylphenol") indicator were utilised, with a DR 3900 spectrophotometer employed for measurements. The process was repeated twice (25 Jan 2018 & 1 Mar 2018) 35 days apart, with a set of 10 drinking water samples from the same sources analysed using the same method.

Moreover, a statistical analysis of nitrate concentration measurements from the last ten years (2008–2017) was performed. Past measurement data were treated with respect to water supply source (*i.e.* water tank of each region), as per information provided by the Municipal Water Supply and Sewage Corporation of Oraiokastro ("*DEYAO*"). According thereto: a) water distribution in Melissochori originates from 3 disjoint water tanks ("*Papadam*", "*Bizynou-Toumpa*", and "*Stam Petra*", hereafter referred to as m(I), m(II) and m(III) respectively); b) water supply in Lete is achieved through 2 disjoint water tanks ("*Patoki*" and "*Vlahou*", hereafter referred to as ℓ(I) and ℓ(II)); c) water distribution in Drymos is comprised of multiple water tanks, which all do however originate from the same larger tank ("*Tsoukes*") and as such the settlement's supply network is uniform (thus, it will be treated as consisting of a single source, referred to as d). The value of nitrates (in mg/L) for each source in the respective date was calculated as the average of all available measurements from sample locations supplied by the corresponding source.

2.2 Experimental determination of phytotoxicity in high nitrate concentration waters

A phytotoxicity test was carried out in order to examine possible effects of high nitrate concentrations in waters from Mygdonia on the germination of seeds and plant growth. To this purpose, 2 different plant species (monocotyledon sorghum *Sorghum saccharatum* and dicotyledon white mustard *Sinapis alba*) were screened using a MicroBio Tests Phytotoxkit, in 3 repetitions each with reference soil and control water and further 3 repetitions each with reference soil and sample water. This process completely adheres to the ISO standard 18763:2016 for the "determination of the toxic effects of pollutants on germination and early growth of higher plants". Prior to the phytotoxicity testing, the water sample collected from the D2 location to be used in the test group plates was spiked with $NaNO_3$ to a final concentration of 300.0 mg/L of NO_3^-. The plates containing the seeds and the reference soil hydrated either with distilled water or sample water were kept in the incubator at a steady temperature of 25°C (±0,5°C) and in constant darkness for 72 hours. At the end of the exposure period, all plates were scanned. Afterwards, three different variables were measured:

i) Percentage of seed germination

For the ten seeds of each plate, the number of those which had germinated was recorded as a percentage. The average of the germination success for each group (control/test) was calculated, as well as the percent inhibition, which is given by the following formula:

$$I_g = \frac{\overline{g_c} - \overline{g_s}}{\overline{g_c}} \times 100\%$$

,where I_g is the seed germination success percent inhibition, $\overline{g_C}$ is mean control group germination success and $\overline{g_S}$ is mean test group germination success. The corresponding *p*-values were also calculated by Welch's unequal variances *t*-test (for a one-tailed hypothesis) using the statistical software *PSPP v. 1.0.1-g818227*.

ii) Root growth (length measurement)

Root length measurement was carried out with image analysis software *ImageJ v. 1.50i*. Mean root length *r* (in mm) for each plate was calculated from length measurements of the respective plate. For the estimation of percent inhibition of root growth (I_r) the group mean root lengths (referred to as $\overline{r_C}$ for a control group and $\overline{r_S}$ for a test group) were computed, as the average of each group's plates' *r* values. The formula

$$I_r = \frac{\overline{r_C} - \overline{r_S}}{\overline{r_C}} \times 100\%$$

was then used to obtain I_r values for each plant species. Subsequently, *p*-values for the totality of each group's root length data were calculated in PSPP by Welch's *t*-test for a one-tailed hypothesis. The results are discussed in section 3.2.

iii) Shoot growth (length measurement)

The identical procedure as with root length was adopted for the measurement of shoot length of individuals that exhibited any significant shoot growth; thus, mean shoot length values (*s*, in mm) were determined for each individual plate. The group mean shoot lengths ($\overline{s_C}$ for a control group and $\overline{s_S}$ for a test group, henceforth) were next calculated, as the average of each group's plates' *s* values. The respective percent inhibition of root growth (I_s) was given by the formula:

$$I_s = \frac{\overline{s_C} - \overline{s_S}}{\overline{s_C}} \times 100\%$$

Finally, *p*-values for each group's aggregate shoot length data were calculated by Welch's *t*-test for a one-tailed hypothesis; results are presented and discussed in section 3.2.

3. RESULTS

3.1. Experimental results of nitrate concentration measurement & past nitrate concentration data statistical analysis

Table 2: Results of NO_3^- measurements (expressed as NO_3^- mg·L^{-1})

Date	*Sampling location*								
	L1	L2	L3	D1	D2	D3	M1	M2	M3
25 Jan 2018	56.6	61.8	62.9	72.6	72.4	70.1	7.86	8.06	6.86
1 Mar 2018	59.0	56.8	57.8	60.7	61.3	71.5	7.21	7.41	7.11
Loc. Average	**57.8**	**59.3**	**60.4**	**66.7**	**66.9**	**70.8**	**7.54**	**7.74**	**6.99**

The results of the spectrophotometric measurements conducted (refer to section 2.1) are given in Table 2. Date and sampling location are noted, while the average of the measurements for each location has also been included. All locations in Lete and Drymos were found to have NO_3^- levels above the *MAC*, with notably high results observed in Drymos. In contrast, samples from Melissochori all had acceptable levels.

Following the experimental confirmation of the existence of a concurrent nitrate issue in Mygdonia, the past data collected in section 2.1 were statistically evaluated. The concentration values (in mg/L) for each water supply source were plotted against time for the 10-year interval of study (2008–2018). In the resulting graph, Figure 1, nitrate concentrations are represented as data points (circles) of a scatter plot, while a continuous straight line represents the linear trend for each supply source calculated with the least squares method. Linear regression was selected to examine the nitrate concentration statistical trend for all sources except m(II) as this particular data series was found to be highly irregular and non-linear with a Pearson correlation coefficient of $|r|$~0,05. The irregularity of m(II) values is consistent with –and could be caused by– the supply source using a multitude of water sources (*i.e.* different wells) which exhibit varying behaviour in relation to nitrates, leading to such scattered data.

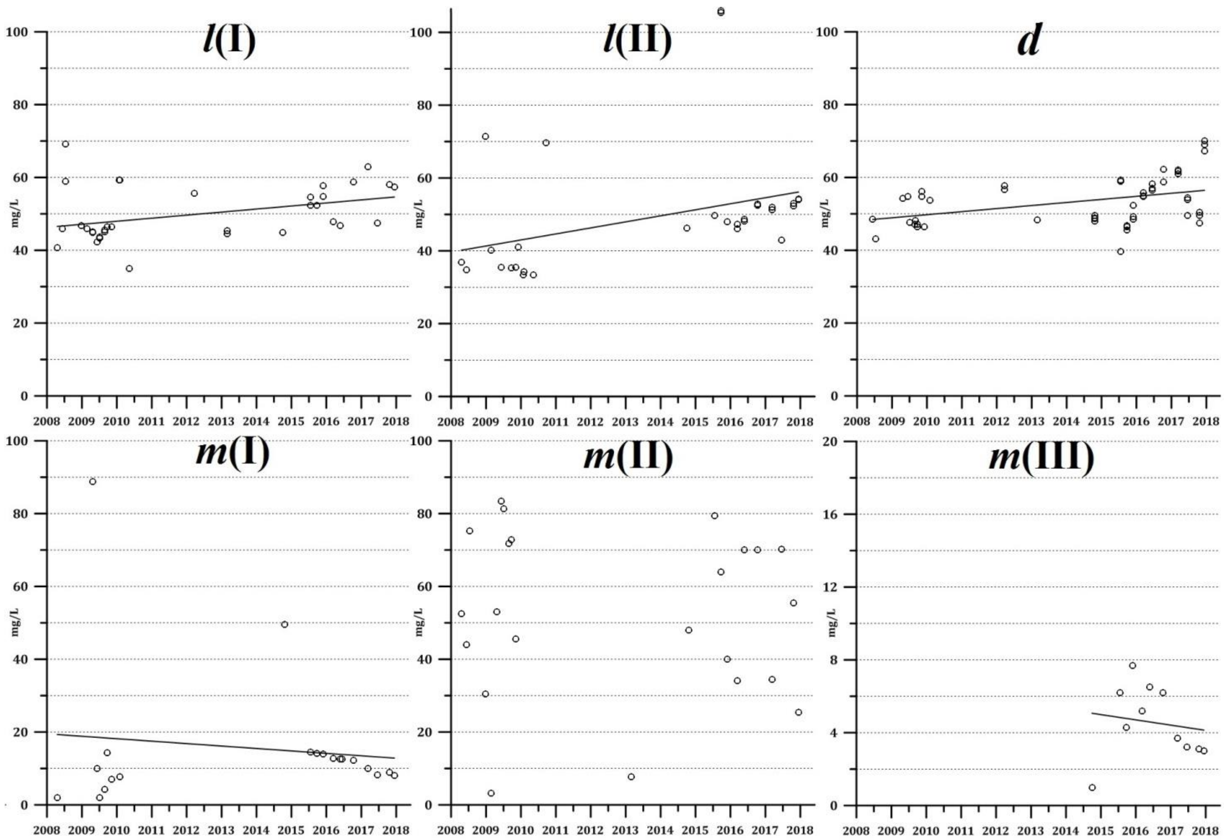


Figure 1: Scatter plots of the evolution of nitrate concentration with time in different supply sources of Mygdonia. Linear trends (in mg·L^{-1}·annum^{-1}) for each source were: ℓ(I) +0.84; ℓ(II) +1.68; d +0.84; m(I) -0.66; m(III) -0.84

The choice of linear regression for the other sources was decided upon as a simple statistical modelling of the concentrations, whose measurements can be approximately considered error-free and homoscedastic. In reality, nitrate concentration in drinking water is an issue stemming from complicated interrelations between many factors, some of which are discussed in section 3.3; therefore, a more realistic model for groundwater nitrates would require complex statistical relations and robust multivariable analysis [Strebel *et al.*, 1989]. Such a task, and corresponding multi-level research, is considered beyond the scope of the present study.

The sources' linear trends' rates of change (nitrate concentration in relation to time) were extracted from the respective line's gradient; both positive and negative trending rates were found (expressed as change of concentration units in respect to time units). It is notable that higher nitrate concentrations as well as mostly positive trends were consistently observed in the area of the plains of Mygdonia (Lete–Drymos–eastern Melissochori, the respective supply sources being ℓ(I), ℓ(II), d and m(II)), while minimal negative trends and acceptable nitrate concentration were associated with

mountainous regions (in western Melissochori; specifically in sources m(I) and m(III)). These correlations suggest that further causes lie behind the sub-regional situation of nitrate occurrence in each landform's vicinity; said causes can be attributed to differing geological composition, variable agricultural practice, water well construction details, *etc.*, more thoroughly discussed in section 3.3.

3.1 Results and discussion of experimental phytotoxicity assessment

When the twelve plates were examined after the 72 h incubation period, a visually obvious impediment of plant growth was observed in the test group plates, for both species. Yet, for the exact assessment of phytotoxicity, the three dependent variables were separately examined:

Table 3: Results of the phytotoxicity experiment: average germination success, average root length (in mm), average shoot length (in mm) and percent inhibition for each variable

Germination % and inhibition				***Root length (mm) and inhibition***				***Shoot length (mm) and inhibition***			
Sorghum sacch.		***Sinapis alba***		***Sorghum sacch.***		***Sinapis alba***		***Sorghum sacch.***		***Sinapis alba***	
$\overline{g_C}$	83.33%	$\overline{g_C}$	96.67%	$\overline{r_C}$	43.14	$\overline{r_C}$	53.92	$\overline{s_C}$	14.82	$\overline{s_C}$	22.09
$\overline{g_S}$	83.33%	$\overline{g_S}$	93.33%	$\overline{r_S}$	33.27	$\overline{r_S}$	37.58	$\overline{s_S}$	13.34	$\overline{s_S}$	21.05
I_g	0.00%	I_g	3.45%	I_r	22.88%	I_r	30.31%	I_s	9.94%	I_s	4.68%
p	0.5000	p	0.2592	p	0.0344	p	0.0017	p	0.3023	p	0.4117

i) Percentage of seed germination

No inhibition of seed germination was observed for *Sorghum saccharatum*, and only a small percentage (3.45%) for *Sinapis alba*. Both results are not considered statistically significant as $p>0.05$, therefore suggesting that high nitrate concentration plays no substantial role in negatively influencing the process of seed germination of the two examined species.

ii) Root growth (length measurement)

The obtained values show major inhibition of root growth for both species, the impediment being especially prevalent in the roots of dicotyledon *Sinapis alba*. The inhibition is statistically significant ($p<0.05$) for both plants, yet for *Sinapis alba* an extremely strong result was obtained. This is indicative of the sample water exhibiting unmistakable phytoxical effect.

iii) Shoot growth (length measurement)

Some inhibition was manifested for this variable, as well, though statistically insignificant as the *p*-values suggest. Shoot growth impediment was marginally more prominent in monocotyledon *Sorghum saccharatum*.

In total, the comparative examination of the phytoxicity test for the two plant species, returned the following findings in relation to the dependent variables: i) zero to minimal seed germination inhibition; ii) significant to strongly significant root growth for both species; iii) insignificant shoot growth inhibition. Nonetheless, it should be noted that in general, and also according to the directives of ISO 18763:2016 and relevant standards referenced therein, shoot development is of secondary use as a phytotoxicity indicator; germination success and root growth should be primarily referred to, instead. The implication for both species is that high nitrate concentration waters can pose a considerable factor of phytotoxicity, as the hindrance of early plant growth is a significant indication thereof. Existing literature confirms that nitrates in excess can have detrimental effects on plant development similar to the ones recorded, however previous research was conducted solely on examining effects of varying nitrate concentration soils and not the water used [Chen *et al.*, 2004].

As such, the assertion can be made that excessive nitrate is an environmental pollutant, affecting plant growth at least, in areas where its concentration in water has been steadily high. This potential phenomenon can then be applied in the region of Mygdonia, inferring plausible peril for agriculture and regional economic activities akin thereto, since the chronically high in nitrate water has been used for the irrigation of the mainly monocotyledonous crops (*e.g.* wheat) as shown in section 1.

3.2 Discussion on aetiology

The arable plains of Mygdonia, where above limits nitrate concentrations and positive trends were found, also comprise the chief area of the regional agricultural activity. Nitrate contamination of groundwater and resulting accumulation in agricultural land areas is a common phenomenon in previous studies, and has been most importantly linked to extensive use of nitrogen fertilisers (*N-fertilisers*) in crops therein grown [Ju *et al.*, 2004; Power and Schepers, 1989; Strebel *et al.*, 1989; Zhang *et al.*, 1996]. These fertilisers contain the essential plant nutrient N in a range of possible forms (nitrate salts, ammonium salts, urea, anhydrous ammonia, cyanamide salts, *etc.*); however their application in soil invariably leads to formation of some nitrates due to the natural process of nitrification [Tsitsias, 2000]. The aforementioned studies have consistently linked higher N-fertiliser application rates, especially so on irrigated land, to continuously lower crop N-uptake and nitrates leaching into groundwater, therefore being the principal cause of nitrate contamination. In addition, according to official documents "international literature suggests that [nitrate] concentrations above 10 mg/L are likely to be connected to anthropogenic pollution" [Special Secretariat for Water of the Ministry of Environment, Energy and Climate Change of the Hellenic Republic, 2012], as "the natural nitrate concentration in groundwater under aerobic conditions is a few milligrams per litre" [WHO, 2011].

Greek soils are generally quite poor in plant-available N, and as such the utilisation of N-fertilisers is almost universal and necessary for most crops [Stylianidis *et al.*, 2002; Tsitsias, 2000]. For wheat and related cereals, which constitute the main crop of Mygdonia, the following fertilisation scheme is most commonly adhered to in Greece, according to Tsitsias [2000]: a) an initial basal dressing of N-fertiliser (usually NH_4NO_3 or other nitrate salts) or binary NP-fertiliser ($NH_4H_2PO_4$, $(NH_4)_2HPO_4$ *etc.*) during sowing; b) a later topdressing and foliar application of straight N-fertiliser (most preferably urea $(NH_2)_2CO$), which is ideally administered in two doses. The total recommended N-input is 70–180 $kg \cdot ha^{-1}$ equally distributed between basal and topdressing. Actual application may not follow this amount or not be correctly distributed, which in combination with multiple factors of fertiliser loss (*e.g.* surface runoff) leads to an average N-uptake of crops in Greece in the order of 50–70%, in extreme cases getting as low as 20% [Stylianidis *et al.*, 2002; Tsitsias, 2000]. Thus, an excess of leftover N is expected in Greek soils, comparable to cases in international literature.

The specific qualitative geolithological characteristics of Mygdonia also indicate a natural vulnerability to nitrate accumulation; the following information pertaining to the region's strata was retrieved from the geological survey of Kockel *et al.* [1978] and lithostratigraphic analysis accompanying water well data provided by *DEYAO*. According to these sources, the Mygdonian underground is mainly composed of Quaternary sedimentary deposits (eluvial mantle, fluvial terraces, fans, *etc.*). In the eastern part of the region, where plains predominate the landscape, strata of granular characteristics (gravel, sand, sandy clay, gritstone, clay conglomerates, red clay series) are abundant and constitute the vast majority of the underground around Lete, Drymos and east of Melissochori. Some older Neogene deposits (red and silty clays) have also been detected in the vicinity of Lete. The common pattern in the plain areas is an initial thin surface layer of clay (thickness 5–40 m), followed by alternating granular layers as aforementioned.

The type of lithological formations described above is the most susceptible to nitrate leaching and contamination of groundwater, according to existing literature [Johnson and Kross, 1990; Power and Schepers, 1989; Strebel *et al.*, 1989; Tsitsias, 2000; Zhang *et al.*, 1999]. This could result due to the clay layers of limited thickness, interposed between hydraulically conductive sand–gravel layers, not being able to sufficiently mitigate nitrate-rich surface water from leaching to lower groundwater

levels of the aquifer [Durner, 1994; Pupisky and Shainberg, 1979; Strebel *et al.*, 1989]. This situation can be aggravated in seasons of intense precipitation, markedly so when combined with N-fertiliser application [Johnson and Kross, 1990; Ju *et al.*, 2004; Strebel *et al.*, 1989].

Specific to the region of the Koroneia basin subunit, the Greek Government under Joint Ministerial Decision № 20419/2522/2001 has recognised the Mygdonia unit along with others in the wider region of Thessaloniki as a "zone vulnerable to nitrate contamination from agricultural sources". The slight rising trends found in section 3.1 can therefore be paralleled to similar trends all over Europe or other parts of the world, where continuing rise of nitrates is observed in areas of agricultural activity and/or granular–sandy soil composition [Ju *et al.*, 2004; Strebel *et al.*, 1989; Zhang *et al.*, 1999]. The corresponding minute negative trends in the case of western Melissochori could signify a presumed break in the otherwise hydraulically connected –albeit variable– groundwater body of Mygdonia or a differentiated response of the local lithostratigraphy. Indeed, in the westernmost of the region the terrain becomes increasingly mountainous and the respective strata are differentiated. Therein, the older Melissochori-Cholomon Unit exhibits calcareous flysch deposits of alternating calcareous sandstone, phyllites and shale, dating to the Triassic–Middle Jurassic Era. Therefore, the aquifer is expected to be situated in such types of formations rather than granular layers. Whether this can affect the aquifer's response to nitrate contamination and the extent of such an effect has to be met with future hydrogeological investigation.

In general, while the lithological and hydrogeological features of a region considerably determine the risk of high nitrate levels in groundwater as has been hitherto discussed, the prevailing nitrate source appears to be anthropogenic activity mainly through the use of fertilisers, as per the first paragraphs of the section. Indeed, at least one multivariable statistical model for the description and prediction of groundwater NO_3^- concentration has been presented, wherein nitrate levels are directly correlated to land use; therein, significantly higher concentrations were predicted and observed in regions of agricultural activity [Gardner and Vogel, 2005] where N-fertiliser use is expected.

3.3 Suggested measures for lowering groundwater nitrate concentration

A measure of prime significance for dealing with the most probable cause of nitrate accumulation – excessive fertilisation, as per section 3.4– is the adoption of better N-fertiliser management practices, as has been repeatedly proposed in existing literature [Ju *et al.*, 2004; Power and Schepers, 1989; Zhang *et al.*, 1996, *etc.*]. Such course of action calls for monitoring of N-fertiliser input and crop productivity, change of fertilisation regime (more frequent administration and in smaller dosages), prevention of fertiliser application during rainy season, local government co-operation and incentive schemes; in cases where some or all of said measures were applied, nitrate levels reduction and increase of crop yield were accomplished [Power and Schepers, 1989; Zhang *et al.*, 1996]. Assertive action relating to economic policy has been proposed, as well [Ju *et al.*, 2004].

The necessity of analogous measures in Mygdonia is evident, considering that fertilisation control in Greece is minimal and bad farming practice is occasionally customary [Tsitsias, 2000]. While relative legislature has been passed (Joint Ministerial Decision № 16175/824/2006) setting the acceptable fertilisation level for wheat cultivation at 80–120 $kg \cdot ha^{-1}$ of N with variable incentives-penalties, nitrate levels remain higher than acceptable, as has been shown in sections 3.1 & 3.3. The existence of said legislature, however, counts in itself as a positive step in addressing the issue.

In a further attempt to increase the efficiency and plant N-uptake from fertilisers, the use of slow-release (otherwise known as *controlled-release*) N-fertilisers has been advocated [Tsitsias, 2000; Zhang *et al.*, 1996, *etc.*]. This type of fertilisers consist of granular particles which are either encapsulated in a protective, slowly-dissolving polymer or sulfur layer, or contain urea derivatives that have been treated to be insoluble in water, and as such less rapidly acting. Yet, their cost compared to regular fertilisers has discouraged farmers from utilising them broadly.

At least one study has also demonstrated the effectiveness of catch-crop treatment of cereal crops in substantially reducing the soil and drainage water nitrate content, as well as the extent of nitrate

leaching [Lewan, 1994]. Catch crops, such as Italian ryegrass (*Lolium multiflorum*) used in said study, are fast-growing annual crops let to grow between successive main crop sowings. The fact that the aforementioned study was conducted on sandy soils with cereals as the main crop indicates such a solution might be highly suitable to Mygdonia.

Further specialised suggestions involve construction of denitrification beds [Ghane *et al.*, 2014]. Such systems exploit the natural action of denitrifying anaerobic bacteria which are able to metabolise nitrate NO_3^- primarily to harmless nitrogen gas N_2 and secondarily nitrous oxide N_2O; their application has been proposed on a theoretical level in previous literature as well [Strebel *et al.*, 1989]. The particular setup of Ghane *et al.* [2014] performed notably well in raising subsurface water quality in relation to nitrates; comparable action can be suggested for the *in situ* or *ex situ* (in small scale water-treatment plants) remediation of nitrate-contaminated groundwater in Mygdonia.

Another possible suggestion by Johnson and Kross [1990] for the handling of high nitrate concentrations in drinking water obtained from wells in rural communities is the adoption of proper well construction techniques. As per the *DEYAO* data relating to extant water wells in Mygdonia basic construction conforms to the aforementioned instructions: wells have been so far drilled (rather than dug) and in all cases their depth is greater than the 30 m minimum suggested by Johnson and Kross (the range of depths being 140–260 m). Yet, a further, pivotal factor that should be considered is the correct application of insulation (grouting) on the upper well layers so as to prevent the migration of surface and subsurface water, which can hold the largest amount of nitrates from irrigation effluents, to lower levels of the well wherefrom drinking water is extracted [Johnson and Kross, 1990]. Cement grouting has been occasionally used in the water wells of Mygdonia, with great variation observed on the depth of application. Grouting of 40–90 m has been employed in some newer wells, while older wells have had a mere 4–20 m of upper layer insulation; swallow insulation is especially evident around the settlements of Drymos and Melissochori. The effectiveness of current insulation ought to be more thoroughly examined in future studies, with focus on the choice of the most appropriate material and grouting depth.

Lastly, the compiling of a more complete local groundwater body profile is required. Therein a comprehensive mapping of the aquifer in its present situation may be included, as well as specific determination of the water renewal rate and monitoring of water mass equilibria. Such data could be moreover used to assess whether blending water in the supply network of Mygdonia with other regions' water, as has been proposed for analogous cases by the World Health Organization [2011], is a viable strategy. It is worth noting that no singular course of action can guarantee the best achievable reduction of nitrate levels; a combination thereof should be considered.

4. CONCLUSIONS

The problem of higher than allowable NO_3^- concentrations in the drinking water of Mygdonia was attested both experimentally in early 2018 and throughout data from the past decade. In the plain regions (primarily surrounding Lete and Drymos) where the issue was the most prevalent, slight rising trends of the nitrate levels were moreover found by statistical analysis. In contrast, around Melissochori the acceptable nitrate levels observed were also accompanied by mostly negative trends of small magnitude. Underlying differences may include varying hydrogeological substrates, since the sandy soil of the plains makes the region much more vulnerable to groundwater nitrates than the flysch deposit of the more mountainous Melissochori. The aetiology of the problem has also been discussed focusing on human activity, *viz.* excessive N-fertiliser application since agriculture is the main economic activity of Mygdonia and N-fertilisation is widespread. The aforementioned lithostratigraphic factors have also been taken into consideration.

As part of the research on consequences from groundwater nitrates, notable phytotoxocity and inhibition of early plant growth was experimentally verified by testing on plant species *Sorghum saccharatum* and *Sinapis alba*. This indicates a possible cause of harm to crops, and an ensuing negative impact on regional economy. Therefore, as well as due to considerations of human and

animal health described in previous studies, an overview of proposed solutions from analogous cases in existing literature has been presented. Such measures should be adopted promptly, so as to ensure both remediation and future prevention of high nitrate concentrations in the groundwater and drinking water of Mygdonia.

ACKNOWLEDGEMENTS
The author wishes to express his utmost gratitude foremost to Dr M. Petala and also to Dr V. Tsiridis of the School of Civil Engineering of the Aristotle University of Thessaloniki for their helpful guidance and scientific advice. All experiments were conducted in the Laboratory of Environmental Engineering & Planning of the Aristotle University of Thessaloniki (School of Civil Engineering). The assistance of the Municipal Water Supply and Sewage Corporation of Oraiokastro ("*DEYAO*") in obtaining valuable data about regional water wells and past nitrate concentration measurements in Mygdonia is appreciated.

References

1. Special Secretariat for Water. (2012). **‘Management Plan of the River Basins of Central Macedonia River Basin District (GR10)’**. Ministry of Environment, Energy and Climate Change of the Hellenic Republic.
2. Gardner K.K. and R.M. Vogel. (2005). ‘Predicting ground water nitrate concentration from land use’, **Ground Water.** 43(3), pp. 343–352.
3. Johnson C.J. and B.C. Kross. (1990). ‘Continuing Importance of Nitrate Contamination of Groundwater and Wells in Rural Areas’. **American Journal of Industrial Medicine**, 18(4), pp. 449–456.
4. Power J.F. and J.S. Schepers. (1989). ‘Nitrate Contamination of Groundwater in North America’. **Agriculture, Ecosystems & Environment**, 26(3-4), pp. 165–187.
5. Strebel O., W. Duynisveld and J. Böttcher. (1989). ‘Nitrate Pollution of Groundwater in Western Europe’. **Agriculture, Ecosystems & Environment**, 26(3-4), pp. 189–214.
6. Zhang W.L., Z.X. Tian, N. Zhang and X.Q. Li. (1996). ‘Nitrate Pollution of Groundwater in Northern China’. **Agriculture, Ecosystems & Environment**, 59(3), pp. 223–231.
7. Bruning-Fann C.S. and J.B. Kaneene. (1993). ‘The Effects of Nitrate, Nitrite, and N-nitroso Compounds on Human Health: A Review’. **Veterinary & Human Toxicology**, 35(6), pp. 521–538.
8. Parvizishad M., A. Dalvand, A.H. Mahvi and F. Goodarzi. (2017). ‘A Review of Adverse Effects and Benefits of Nitrate and Nitrite in Drinking Water and Food on Human Health’. **Health Scope**, 6(3):e14164.
9. World Health Organization. (2011). **‘Nitrate and nitrite in drinking-water: Background document for development of WHO Guidelines for Drinking-water Quality’**. WHO.
10. Council of the European Union. (1998). ‘Council Directive 98/83/EC on the quality of water intended for human consumption’. **Official Journal of the European Communities**, № L 330, pp. 32–54.
11. Chen B.M., Z.H Wang, S.X. Li, G.X. Wang, H.X. Song and X.N. Wang. (2004). ‘Effects of nitrate supply on plant growth, nitrate accumulation, metabolic nitrate concentration and nitrate reductase activity in three leafy vegetables’. **Plant Science**, 167(3), pp. 635–643.
12. Maynard D.N., A.V. Barker, P.L. Minotti and N.H. Peck. (1976). ‘Nitrate Accumulation in Vegetables’. **Advances in Agronomy**, 28, pp. 71–118.
13. https://it.opekepe.gr/aggregate (accessed 1 Mar 2018).

14. ISO. (2016). 18763:2016(en): Soil quality- Determination of the toxic effects of pollutants on germination and early growth of higher plants. International Organization for Standardization, Geneva.
15. Ju, X., X. Liu, F. Zhang and M. Roelcke. (2004). 'Nitrogen Fertilization, Soil Nitrate Accumulation, and Policy Recommendations in Several Agricultural Regions of China'. **AMBIO**, 33(6), pp. 300–305.
16. Tsitsias K. (2000). **'Lipasmatologia'**. Technological Educational Institute of Larissa.
17. Stylianidis D.C., A.D. Simonis and G.D. Syrgiannidis. (2002). **'Nutrition-Fertilization of Deciduous Fruit Trees'.** Stamoulis Publications.
18. Kockel F., P. Antoniadis, K. Ioannidis and N. Lalehos. (1978) **'Geological Map of Greece'**. Institute of Geological and Mining Research of Greece.
19. Durner W. (1994). 'Hydraulic conductivity estimation for soils with heterogeneous pore structure'. **Water Resources Research**, 30(2), pp. 211–223.
20. Pupisky H. and I. Shainberg. (1979). 'Salt Effects on the Hydraulic Conductivity of a Sandy Soil'. **Soil Science Society of America Journal**, 43(3), pp. 429–433.
21. Lewan E. (1994). 'Effects of a catch crop on leaching of nitrogen from a sandy soil: Simulations and measurements'. **Plant and Soil**, 166(1), pp. 137–152.
22. Ghane E., N.R. Fausey and L.C. Brown. (2015). 'Modeling nitrate removal in a denitrification bed'. **Water Resources**, 71, pp. 294–305.

SIMULATION OF WATER FLOW IN THE UNSATURATED SOIL ZONE TO ASSESS IRRIGATION IN A MAIZE FIELD

Ch. Doulgeris[1], D. Voulanas[2]*, G. Arampatzis[1] and E. Hatzigiannakis[1]

[1]Soil and Water Resources Institute-Dept. of Land Reclamation, Hellenic Agricultural Organisation, GR 57400, Sindos, Greece

[2]Lab of Engineering Geology and Hydrogeology, Dept. of Geology, A.U.Th, GR 54124 Thessaloniki, Greece

[*]Corresponding author: e-mail: dvoulanas@yahoo.com tel: +306947511281

Abstract

Accurate estimation of the hydrological features in the unsaturated zone is mandatory for the effective planning of irrigation strategies. Irrigation scheduling depends on crop and soil type as well as climatic characteristics and is usually empirically conducted. This paper simulates the water flow in the unsaturated zone of an agricultural field located in the River Strymonas basin using the HYDRUS-1D model. The model is fed with meteorological data, soil data and soil moisture measurements derived by field experiments. After the calibration of the model, model results were used to evaluate the irrigation activities applied in the experimental field in terms of irrigation dose, irrigation interval and soil moisture variation for the cultivation period.

Keywords: Vadose zone simulation, HYDRUS-1D, Maize, Irrigation

1. INTRODUCTION

In agricultural areas where rain is insufficient during the cultivation period, irrigation consists of a significant consumption of water resources and thus needs to be optimized in order to economically secure the agricultural production and to environmentally protect water resources. Optimal planning of irrigation depends heavily on climatological factors, crop and soil type. Irrigation activities are usually scheduled and evaluated through empirical practices that quantify and predict the soil water balance and related characteristics under a cultivated crop. On the other hand, analytical and numerical models are continuously improving to study and evaluate water movement characteristics and related phenomena (Vereecken et al. 2015). Numerical modelling of vadose zone can simulate water fluxes within the soil-vegetation-atmosphere system to improve water use efficiency in agriculture, especially in case of water scarcity (Babajimopoulos et al. 1995; Babajimopoulos et al. 2007; Sutanto et al. 2012; Zheng et al. 2017).

HYDRUS-1D model can simulate one-dimensional variably saturated water flow, heat movement and transport of solutes involved in sequential first-order decay reactions by handling flexibly various boundary conditions (Šimůnek et al. 2008a). It has been applied in several case studies and at various climatological conditions to simulate, optimize and predict the water flow and solute transport in the soil vadose zone under field experiments and lab conditions (Hanson et al. 2008; Jellali et al. 2009; Ramos et al. 2011; Tafteh et al. 2012; Chang et al. 2015; Zheng et al. 2017).

This paper assesses the irrigation practices and estimates the groundwater recharge in an irrigated maize field located in the River Strymonas basin by simulating the water flow in the unsaturated soil zone. For that, the mixed form of Richards's equation is numerically solved by applying the HYDRUS model. Model results are evaluated both in terms of applied irrigation and soil moisture

measurements that have been conducted by the Institute of Soil and Water Resources (LRI, 2009; Arampatzis et al., 2010; 2014).

2. MATERIALS AND METHODS

2.1 Study Area and Available Data

Nigrita – Flampouro agricultural area (Fig.1) is located at the southern part of River Strymonas basin at an altitude of around 15 m a.m.s.l and a distance of 22 km from the sea. An irrigation network operates under pressure using five pumping stations and supplies 6300 hectares. The main crop types in the area are maize, cotton, alfalfa and industry tomato.

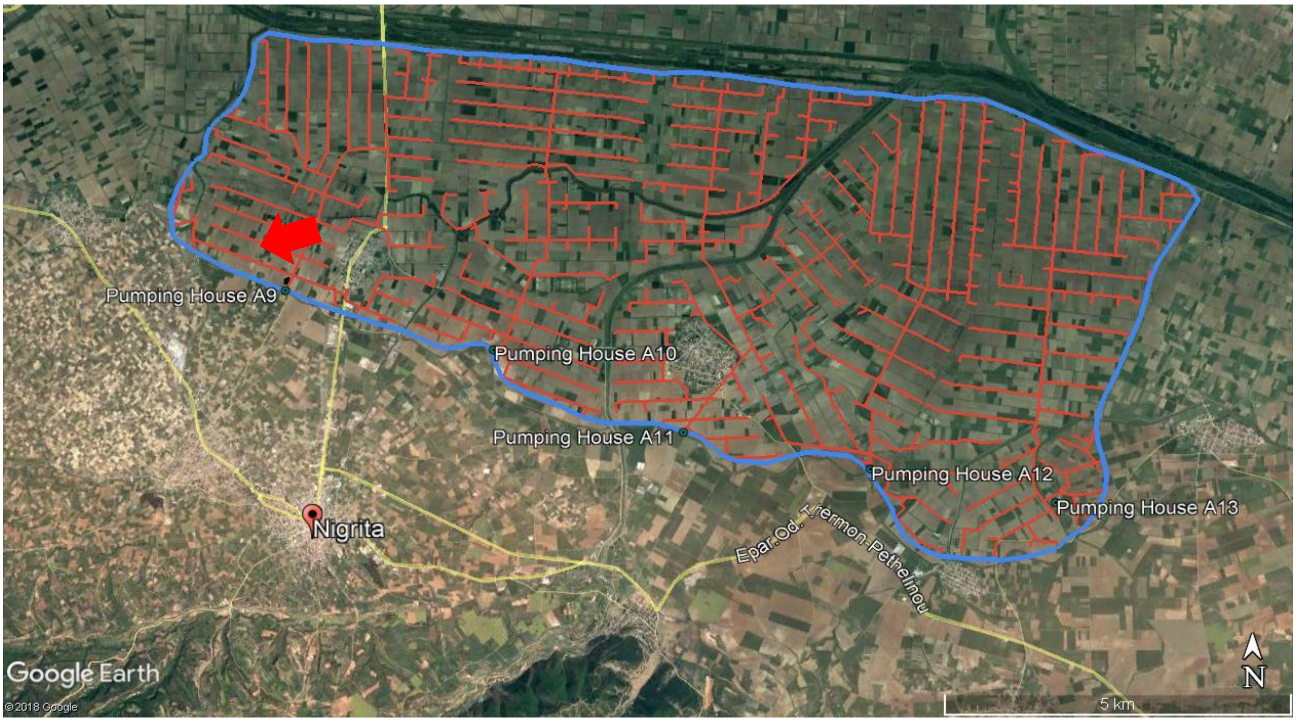


Figure 1: Nigrita - Flampouro agricultural area (outlined by the blue line) and the under study maize field (pointed with the red arrow); the reddish lines depict the underground distribution network

Data for the area were available from the project "Irrigation of crops with the use of meteorological stations at Strymonas basin" and include meteorological data, soil data and in situ soil moisture measurements (LRI, 2009). Meteorological data were recorded by an automatic meteorological station located close to the agricultural area. The recorded meteorological parameters are precipitation, temperature, relative humidity, wind speed and direction, sunshine duration and evaporation measured with a class An evaporation pan. Soil samples were analysed in the lab using the Bouyoucos method to determine the percentages of sand, silt and clay while the saturated hydraulic conductivity, Ks, was measured with a Guelph device in situ (Table 1). The hydraulics parameters in the soil column were determined by regression analysis based on the soil moisture characteristic curve and van Genuchten equation (Table 2).

Soil moisture measurements were taken by field experiments that conducted from late March to early August. A 10 cm diameter hole was dug up to 1 m depth and a DIVINER-2000 pipe was installed to take measurements of soil moisture every 10 cm at regular intervals. Also, two wells of 2 m depth were placed near the edge of the field to monitor the water table level. During the field experiments the water table was below the 2 m depth and was not recorded.

Table 1: Soil properties in the study area

Sand (%)	Silt (%)	Clay (%)	K_s (cm/day)
66.8	19.2	14.0	0.3

Table 2: Hydraulic and van Genuchten parameters in the soil column

θ_s	θ_r	a	n	m	Field Capacity	Wilting Point
cm^3 cm^{-3}	cm^3 cm^{-3}	1/m			cm^3 cm^{-3}	cm^3 cm^{-3}
0.37	0.16	2.59	1.67	0.4	0.345	0.16

2.2 HYDRUS model setup

The HYDRUS model (Šimůnek et al. 2008b) applies the Galerkin finite element method to discretise the soil profile in vertical one-dimension domain and simulate the unsaturated and transient water flow under the presence of a crop. A soil column of 1 m height was considered by placing a computational node every 1 cm. A variable time step was used; initial, minimum and maximum time steps were set up to 0.01, 0.001 and 0.01, respectively. Uniform soil moisture of 0.25 was used as the initial condition of the simulation considering the precipitation events prior to the simulation. The simulation period was from 1 April to 31 August 2008.

The water movement in the unsaturated soil zone is described with the mixed form of Richard's equation (Eq. 1):

$$\frac{\partial\theta}{\partial t} = \frac{\partial}{\partial z}\left[K(h)\left(\frac{\partial h}{\partial z} + 1\right)\right] - S(z,t) \qquad (1)$$

where θ is the volumetric water content (cm^3 cm^{-3}); h is the water pressure head (cm); t is time (day); z is the vertical coordinate (cm); K is the hydraulic conductivity (cm day^{-1}); and S is root water uptake (cm^3 cm^{-3} day^{-1}).

In this HYDRUS application, the soil-hydraulic functions of van Genuchten (1980), who used the statistical pore-size distribution model of Mualem (1976), are used to obtain a predictive equation for the unsaturated hydraulic conductivity function in terms of soil water retention parameters. The van Genuchten expressions are formulated as:

$$\theta(h) = \begin{cases} \theta_r + \frac{\theta s - \theta r}{(1+|ah|^n)^m} & h < 0 \\ \theta_s & h \geq 0 \end{cases} \qquad (2)$$

$$K(h) = K_s S_e^l \left[1 - \left(1 - S_e^{\frac{1}{m}}\right)^m\right]^2 \qquad (3)$$

$$S_e = \frac{\theta - \theta_r}{\theta_s - \theta_r} \qquad (4)$$

where θ_s is the saturated water content (cm^3 cm^{-3}); θ_r is the residual water content (cm^3 cm^{-3}); K_s is the saturated hydraulic conductivity (cm day^{-1}); S_e is the effective water content; and α, n, m are relative empirical parameters, where $m=1-1/n$ and l is the pore-connectivity parameter and is assumed to be about 0.5 as an average for many soils.

The boundary conditions in the soil column were set up in the HYDRUS environment. The upper boundary condition includes the inflow from precipitation and irrigation and the outflow from evaporation and is given by:

$$-K\left(\frac{\partial h}{\partial z}+1\right)=q_0(t) \qquad z=0 \tag{5}$$

where q_0 is the net inflow or outflow (mm/day).

The lower boundary condition is simulated as a free drainage condition, as the water table was not recorded in any of the two wells placed near the field, and is expressed as:

$$\frac{\partial h}{\partial z}=0 \qquad z=100\ cm \tag{6}$$

2.3 Evapotranspiration and irrigation

The reference evapotranspiration was calculated using the Penman-Monteith equation as recommended by FAO (Allen et al. 1998). Actual evaporation (E_a) is calculated by HYDRUS based on potential evaporation (E_p) and soil water content using Beer's Law (Ritchie 1972; Childs 1975). Potential evaporation is calculated using Eq. 7.

$$E_p=ET_0e^{-kLAI} \tag{7}$$

where ET_0 is the reference evapotranspiration (cm), k is the constant for the radiation extinction by canopy and LAI is the leaf area index adapted to the four crop growth stages by data obtained by Antonopoulos (2000).

Root growth was modelled using the Verhulst-Pearl logistic growth function (Eq. 8) supposing that 50% of the growth is reached at the middle of the growing season. The root growth coefficient is expressed as:

$$f_r(t)=\frac{L_0}{L_0+(L_m-L_0)e^{-rt}} \tag{8}$$

where L_0 is the initial value of the rooting depth at the beginning of the growing season, r is the growth rate, L_m is the maximum rooting depth and t is the time.

HYDRUS couples the aforementioned growth function with the root distribution model of Hoffman and van Genuchten (1983). The potential water uptake distribution function in the soil root zone, b(x), is given by:

$$b(x)=\begin{cases}\frac{1.66667}{L_R} & x>L-0.2L_R\\ \frac{2.0833}{L_R}\left(1-\frac{L-x}{L_R}\right) & x\in(L-L_R,L-0.2L_R)\\ 0 & x<L-L_R\end{cases} \tag{9}$$

where x is the soil coordinate measuring from the bottom of the soil column, L is the maximum length of soil column and L_R is the root depth. Therefore, the root depth, L_R, is the product of the maximum rooting depth, L_m, and the root growth coefficient, f_r (Šimůnek and Suarez, 1993a).

Actual transpiration (T_a) is considered equal to the root water uptake assuming that plants use a minor water quantity for tissue building. Actual transpiration was calculated using the Feddes water uptake reduction model (Feddes et al. 1976).

$$T_a=S(z,t)=a(h,z)\beta(z)T_p \tag{10}$$

where S is the water volume removed from the soil volume per time by plant water uptake, α is the root water uptake stress response function (-), $\beta(z)$ is the function of root water uptake distribution (cm^{-1}) and T_p is the potential transpiration (cm).

Irrigation is simulated within HYDRUS by triggering an irrigation event each time the pressure head at a selected computational node, which was arbitrarily selected at 10 cm below soil surface, drops below the value of -3950 cm. This pressure value was selected through a trial and error procedure and intended to replicate the irrigation practices followed in the field experiments in terms of the average irrigation dose and the irrigation date.

3. RESULTS

3.1 Model calibration

The calibration of the model was performed by using a set of parameters for saturated hydraulic conductivity (i.e. 0.3, 0.03 and 3 cm day^{-1}), saturated water content (i.e. 0.37, 0.42 and 0.47 cm^3 cm^{-3}) and irrigation dose, and by comparing graphically and statistically the modelled soil moisture with measurements and modelled irrigation doses with the experimental ones. Table 3 shows the final selected set of model parameters.

Table 3: Calibrated model parameters

θ_s	θ_r	*a*	*n*	*m = 1-1/n*	*l*	K_s
cm^3 cm^{-3}	cm^3 cm^{-3}	1/m				cm/day
0.42	0.16	2.59	1.67	0.4	0.5	0.3

Figure 2 compares the modelled and measured mean soil moisture in the soil column for the simulation period (1 April to 31 August 2008). Modelled soil moisture is considerably varied by increasing rapidly in the initial stage of the simulation due to precipitation events and then follows a gradual decline until the irrigation events begin. The soil moisture estimated by the model is comparable with the soil moisture measurements, especially in terms of the response of the model to irrigation and precipitation events. Considering the statistical criteria, the average mean error, root mean square error and the mean absolute error are 1.25, 4.65 and 3.62 cm^3 cm^{-3}, respectively, suggesting that the efficiency of the model is fairly good and model results are acceptable. A different model setup involving a non uniform soil profile is expected to increase model performance and it will be the focus of further research.

Figure 3 shows the irrigations doses and the date at which irrigation was applied in the field experiments and the corresponding ones simulated by the model. The total amount of irrigation water estimated by the model is 40.8 cm and is quite comparable with the total irrigation water applied in the field experiments, which was 40.5 cm. The interval among irrigation dates estimated by the model do not quite match with experiment data set, mainly because the irrigation module of HYDRUS does not allow using a variable value for the irrigation dose.

3.2 Soil water balance assessment

The soil water balance can be expressed by Eq 11.

$$P + I = \Delta S + E + T + D \tag{11}$$

where P is precipitation (cm); I is irrigation (cm); ΔS is the soil water change; E is evaporation (cm); T is transpiration (cm); D is deep percolation (cm) that recharges groundwater. Water balance parameters estimated by the model are shown in Figure 4 for each month and summarized in Table 4

for the simulation period. Crop evapotranspiration (E+T) is estimated to 67.2% of the total water inflow (*P+I*). The evapotranspiration is considerably higher than precipitation during the crop growing period, except for April, and thus sufficient irrigation water should be applied to fulfil the crop water requirements.

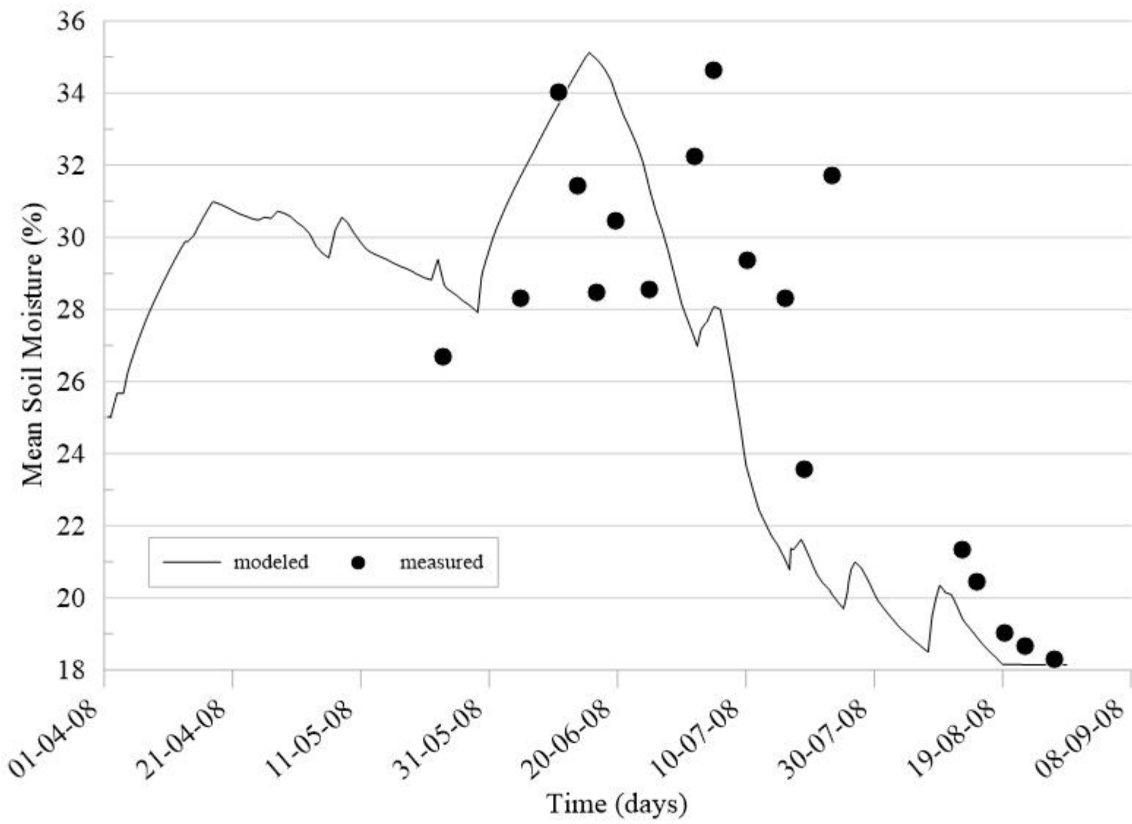


Figure 2: Soil moisture in soil column estimated by the model and field experiments

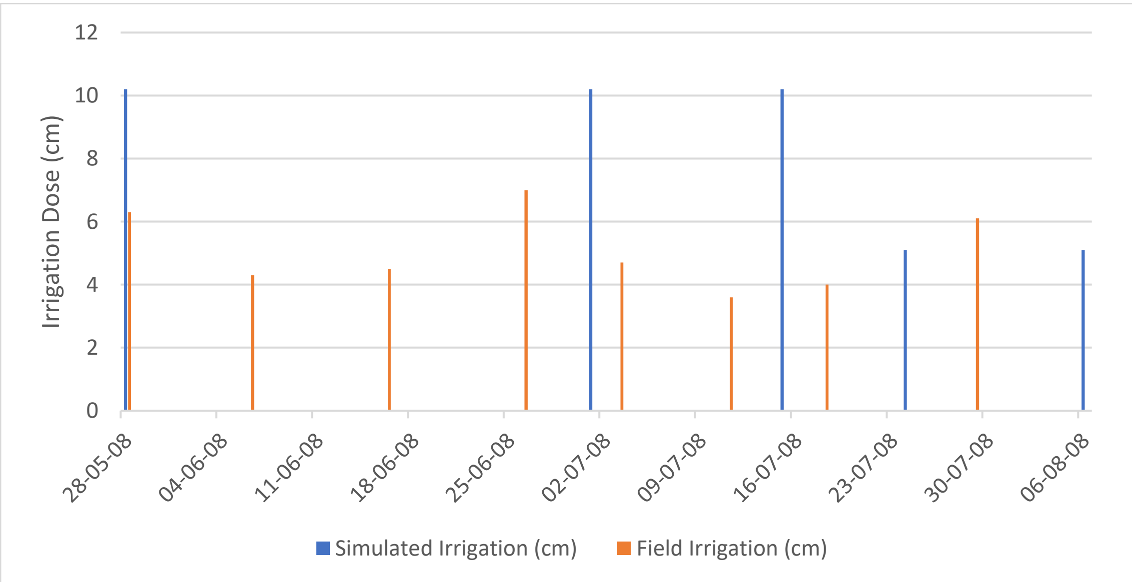


Figure 3: Irrigation doses applied in field experiments and simulated by the model

Table 4: Water balance parameters for the simulation period

P (cm)	*I (cm)*	*ΔS (cm)*	*ET (cm)*
14.66	40.8	-6.88	37.25

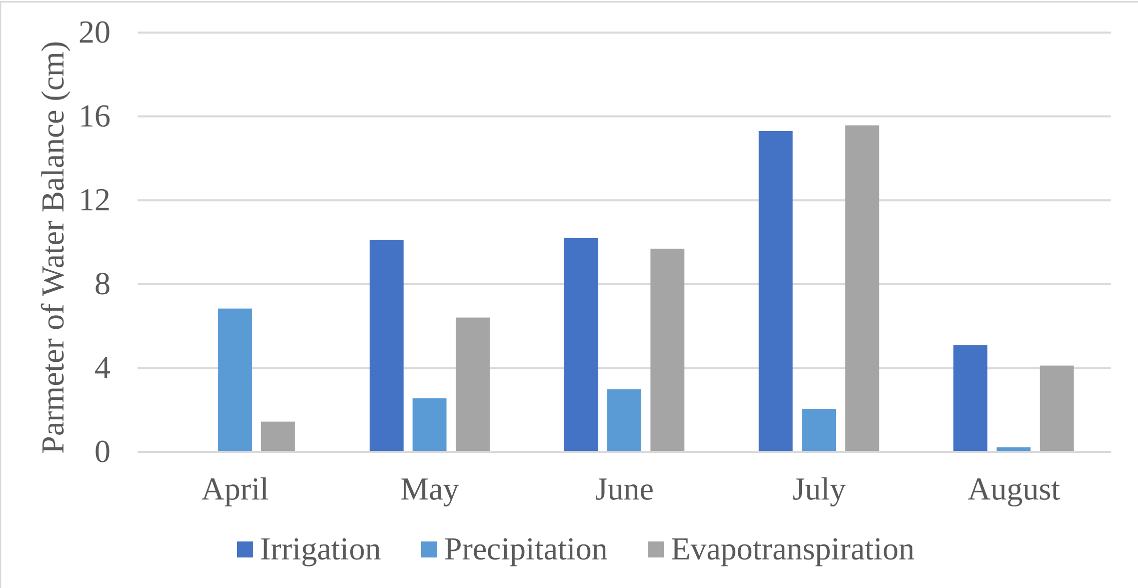


Figure 4: Monthly water balance parameters estimated by the model

4. CONCLUSIONS

Irrigated agriculture consumes a significant amount of available water resources in the summer period - when water availability is decreased in Greece - and thus irrigation water management is necessary both for the protection of environment and for the maintenance of agricultural income. This paper evaluates the irrigation activities applied in an experimental field located at an irrigation network of the River Strymonas basin. For that, the HYDRUS model was used to simulate the flow in the unsaturated soil zone of a maize field and to estimate the irrigation dose, the irrigation interval and the variation of soil moisture for the cultivation period. HYDRUS model was proved capable to simulate the soil water movement in the experimental field by providing useful information related to water balance parameters and assisting to irrigation water management in the area. Further development of this work will focus on modelling single irrigation events to find more efficient solutions for various soil types and crops in the area as well as the involvement of inverse modelling towards an efficient calibration of the model based on the soil moisture measured in situ at several depths as well as the average moisture in the soil profile.

References

1. Allen R., Pereira L.S., Raes D. and M. Smith. (1998). 'Crop evapotranspiration: guidelines for computing crop water requirements'. FAO Irrigation and Drainage Paper 56. **Food and Agriculture Organization of the United Nations**.
2. Antonopoulos V. Z. (2000). 'Modelling of soil water dynamics in an irrigated corn field using direct and pedotransfer functions for hydraulic properties'. **Irrigation and Drainage Systems**, 14, pp. 325–342.
3. Arampatzis G., Hatzigiannakis E., Evangelides C. and A. Panagopoulos. (2014). 'A handy irrigation management method through meteorological data. Case study in N. Greece'. **Global NEST Journal**, 16(2), pp. 219-228.
4. Arampatzis G., Hatzigiannakis E., Panoras A., Panagopoulos A., Evangelides C. and S. Stathaki. (2010). Irrigation water management though meteorological data. Case study in Nigrita area. **International Conference on Protection and Restoration of the Environment X**, Corfu, Greece.
5. Babajimopoulos C., Budina A. and D. Kalfountzos. (1995). 'SWBACROS: A model for the estimation of the water balance of a cropped soil'. **Environmental Software**, 10(3), pp. 211–220.

6. Babajimopoulos C., Panoras A., Georgoussis H., Arampatzis G., Hatzigiannakis E. and D. Papamichail. (2007). ‘Contribution to irrigation from shallow water table under field conditions’. **Agricultural Water Management**, 92(3), pp. 205–210.
7. Chang X., Zhao W., and F. Zeng. (2015). ‘Crop evapotranspiration-based irrigation management during the growing season in the arid region of northwestern China’. **Environmental Monitor Assess**, 187(11), pp. 1–15.
8. Childs S.W. (1975). ‘Model of soil salinity effects on crop growth’. **Soil Science Society America of Journal**, 39(4), pp. 617–622.
9. Feddes R.A., Kowalik P. and H. Zaradny. (1976). ‘Simulation of field water uptake by plants using a soil water dependent root extraction function’. **Journal of Hydrology**, 31(1), pp. 13–26.
10. Hanson B., Hopmans J.W. and J. Šimůnek. (2008). ‘Leaching with subsurface drip irrigation under saline, shallow groundwater conditions’. **Vadose Zone Journal**, 7(2), pp. 810–818.
11. Hoffman, G.J. and M.Th. van Genuchten. (1983). ‘Soil properties and efficient water use: water management for salinity control’. In: H.M. Taylor, W.R. Jordan and T.R. Sinclair (Editors), Limitations to Efficient Water Use in Crop Production. **American Society of Agronomy**, Madison, Wisconsin, pp. 393-417.
12. Jellali S., Diamantopoulos E., Kallali H., Bennaceur S., Anane M. and N. Jedidi. (2010). ‘Dynamic sorption of ammonium by sandy soil in fixed bed columns: Evaluation of equilibrium and non-equilibrium transport processes’. **Journal of Environmental Management**, 91(4), pp. 897–905.
13. LRI. (2009). ‘Irrigation of crops with the use of meteorological stations at Strymonas basin, Land Reclamation Institute’. **National Agricultural Research Foundation**, Sindos, Greece.
14. Mualem Y. (1976). ‘A new model for predicting the hydraulic conductivity of unsaturated porous media’. **Water Resources Research**, 12(3), pp. 513–522.
15. Ramos T.B, Simunek J., Goncalves M.C., Martins J.C., Prazeres A., Castanheira N.L., and L.S. Pereira. (2011). ‘Field evaluation of a multi- component solute transport model in soils irrigated with saline waters’, **Journal of Hydrology**, 407(1–4), pp. 129–144.
16. Ritchie J.T. (1972). ‘Model for predicting evaporation from a row crop with incomplete cover’, **Water Resources Research**, 8(5), pp. 1204–1213.
17. Šimůnek J., Sejna M., Saito H., Sakai M. and M.T.H. van Genuchten. (2008a). The HYDRUS-1D software package for simulating the one dimensional movement of water, heat, and multiple solutes in variably-saturated media version 4.0. Department of Environmental Sciences, University of California Riverside, California.
18. Šimůnek J., van Genuchten MTH and M. Sejna. (2008b). ‘Development and applications of the HYDRUS and STANMOD software packages and related codes’. **Vadose Zone Journal**, 7(9), pp. 587–600.
19. Šimůnek, J., and D. L. Suarez. (1993a). ‘Modeling of carbon dioxide transport and production in soil: 1. Model development’. **Water Resources. Research**, 29(2), pp. 487-497.
20. Sutanto S. J., Wenninger J., Coenders-Gerrits A. M. J. and S. Uhlenbrook. (2012). ‘Partitioning of evaporation into transpiration, soil evaporation and interception: a comparison between isotope measurements and a HYDRUS-1D model’. **Hydrology and Earth System Sciences**, 16, pp. 2605-2616.
21. Tafteh A. and A. R. Sepaskhah. (2012). ‘Application of HYDRUS-1D model for simulating water and nitrate leaching from continuous and alternate furrow irrigated rapeseed and maize fields’, **Agricultural Water Management**, 113, pp. 19-29.
22. van Genuchten MTH. (1980). ‘A closed-form equation for predicting the hydraulic conductivity of unsaturated soils’. **Soil Science Society America of Journal**, 44(44), pp. 892–898.
23. Verrecken M., Huisman J. A., Hendricks Franssen H. J., Bruggemann N., Bogena H. R., Kollet S., Javaux M., van der Kruk J. and J. Vanderborght. (2015). ‘Soil hydrology: Recent methodological advances, challenges, and perspectives’, **Water Resources Research**, 51, pp. 2616-2633.

24. Zheng, C., Lu, Y., Guo, X., Li, H., Sai, J., & Liu, X. (2017). 'Application of HYDRUS-1D model for research on irrigation infiltration characteristics in arid oasis of northwest China'. **Environmental Earth Sciences**, 76(23), pp. 785.



Climate change impacts and adaptation measures

LAND-USE CHANGE ROLE IN CLIMATE CHANGE MITIGATION GOALS ACHIEVEMENT

V. Jurevičienė*[1,2] and R. Dagiliūtė[1]

[1] Vytautas Magnus University, Faculty of Natural Sciences, Dept. of Environmental Sciences, LT - 44404 Kaunas, Lithuania

[2] State Forest Service, Dept. of National Forest Inventory, LT – 51327, Kaunas, Lithuania

*Corresponding author: e-mail: vkazanaviciute@gmail.com, tel : +37062761662

Abstract

Land use, land-use change and forestry (LULUCF) sector plays an important role in climate change mitigation and is a key element in Paris agreement. Long-term goal of carbon neutral economy in second half of this century depends on LULUCF ability to sequestrate greenhouse gases (GHGs) emissions in biomass and soil. With reference to the Paris Agreement, accounting rules of GHG emissions and removals in LULUCF sector has been heavily discussed recently in the European Union, seeking of trustworthy inclusion in the assessment of Union's GHG emission reduction target. Therefore, paper aims to analyze Lithuanian situation regarding LULUCF sector and total GHG balance from the climate change perspective. For this, changes in greenhouse gas emissions and removals in Lithuania have been studied during years 1990 - 2015. Lithuania's total GHG emission balance has changed significantly since 1990, with more than twice decreased emissions till 2015. LULUCF sector absorption was increasing since 1990 and was equal around 1/3 of total country emissions in 2015, removals were mainly composed of carbon sequestration in forest land. However, mainly the basic level of estimations (Tier1 methodological level) is applied currently for GHG absorption and emissions potential. Therefore, more exact emission factors and other possible determinants (biomass demand for energy purposes, energy efficiency, economic growth) of LULUFC potential should be analyzed in more detail in order to make corresponding and sound political decisions.

Keywords: Land-use change; GHG inventory; sequestration; emissions; removals; climate change mitigation; policy achievement

1. INTRODUCTION

Land use, land-use change and forestry (LULUCF) sector is an important contributor in climate change mitigation and greenhouse gas emission reduction, related to atmospheric GHG removals, regarding its ability to sequestrate carbon in biomass and soil (Garcia-Oliva, Masera, 2004), as well as substitution of biological products for fossil fuels or energy-intensive products (Smith et al., 2014; Sanchez, 2015). However, due to its high uncertainties, sector's contribution to the targets' achievement were under strong debates since the start of Kyoto Protocol commitments (1st KP Commitment period started in 2008) (Macintosh, 2011; Grassi, 2012). Sector's contribution depends on the accounting rules and is previously estimated to vary from 2 % of total EU GHG emissions in 1990 to 33 % of New Zealand's 1990 emission level (Grassi, 2012). Regarding more detailed understanding, forest carbon accounting for mitigation purposes is dependent on the definition of the reference baseline (McKechnie et al., 2014), since the reference level has to be applied. Study in Europe shows that forest harvesting for bioenergy use led to a slight decrease in the soil carbon equilibrium but significantly increased the mitigation effect through bioenergy use (Perez-Cruzado

et al., 2012). Due to the specific nature of the sector and high uncertainties as well as significant importance to cover other sectors' GHGs emissions, LULUCF accounting rules have been updated in 2011 before the second Kyoto Protocol Commitment period (UNFCCC, 2012). Kyoto Protocol has established the possibility to account credits from GHG sequestration in forestry and agricultural activities (Garcia-Oliva, Masera, 2004). Credits from afforestation and reforestation activities were proposed under the Clean Development Mechanism to cover part of the GHG emission reduction target under Kyoto Protocol commitment (UNFCCC, 2013). Furthermore, one of the latest policy changes in EU intends to include LULUCF sector into overall GHG emission reduction target after 2020 (post Kyoto). EU is taking a significant step forward to implement Paris agreement goals with the proposal of Effort Sharing Regulation (European Commission, 2016a) and the so called LULUCF regulation (European Commission, 2016b). Proposal of LULUCF regulation provides guidelines to include GHG emissions/removals from LULUCF sector and maintains similar rule as in Kyoto Protocol requirements: emissions from the sectors accounting categories should be covered with respective removals (European Commission, 2016b). Climate scientists state (Bötther, Graichen, 2015), that LULUCF inclusion into overall target would mean lower efforts from other sectors: after the removals from LULUCF are accounted (sequestration effect assessed), 40 % emission reduction target would actually mean only 35 %. In addition, other scientists claim that turnover to renewal energy sources and exceptionally biomass would also affect LULUCF climate change mitigation potential (Frank et al., 2016). Hence, these factors might be of importance to include for estimation of LULUCF potential in climate change mitigation target achievement altogether with land-use change induced carbon sequestration in pools.

2. MATERIALS AND METHODS

Methods used in this study consists of policy and GHG accounting changes analysis, total and sectoral (LULUCF) GHG emissions and removals analysis in 1990 - 2015 in the line with LULUCF role in climate change mitigation goals achievement.

Lithuanian GHG emissions and removals in land use, land-use change and forestry sector for 1990 - 2015 were estimated using 2006 IPCC Guidelines (IPCC, 2006O with several national carbon stock factors and default emission factors values. Activity data for LULUCF GHG estimation was obtained from various databases and data sources. Most of the data is obtained from National forest inventory measurements, which contains area estimates of different land uses and changes between land uses and growing stock volume change. Additional activity data of areas is collected from State Forest Cadastre (aerial data of forest land and newly afforested/reforested areas), data from National Paying agency (declared agricultural land areas), Geological Survey of Lithuania (areas of peat extraction lands), Statistics of Lithuania, etc. GHG emissions and removals were estimated for 5 main pools: biomass, dead wood and litter (forest land category), mineral and organic soils. In addition to the carbon stock changes in abovementioned pools, greenhouse gas emissions from biomass burnt in wildfires (forest land, cropland and grassland categories), emissions due to the drainage of organic soils and nitrogen oxide emissions due to the carbon loss in mineral soils were estimated for the whole-time series. Emissions and removals from other sectors were obtained from submitted for United Nations Framework Convention on Climate Change Secretariat on 14th April 2017 (Lithuania's National Inventory Report, 2017).

Statistical analysis was performed in order to estimate the most important categories under land use, land-use change and forestry sector and sector's impact to the overall country GHG emissions.

3. CLIMATE CHANGE AND LULUCF RELATED POLICY

Accounting rules of LULUCF has been at least slightly changed for each of the commitment period. Accounting in the terms of anthropogenic GHG emissions and removals means calculation of annual (or at the end of commitment period) GHG emissions and removals under certain conditions, for

instance, for Kyoto Protocol LULUCF categories it is either net-net accounting, gross-net accounting or business as usual (BAU) accounting. Net-net accounting means total GHG emissions/removals in reporting year minus the value of the reference year/period, meaning that for the accounting reported GHG emissions or removals shall be compared to the reference year/period GHG emissions or removals to evaluate the change (country's accomplishment). On the contrary, gross-net accounting is the total GHG emissions or removals change in the accounting period without comparison to the reference year/period value. BAU accounting is the most controversial and arguable way to account GHG emissions and removals in the accounting category (Macintosh, 2011; CAN Europe, 2016) – reported GHG emissions/removals are compared to the projected GHG emissions or removals in that category for that certain year or period (European Commission, 2016). Despite the changes in accounting rules between commitment periods, core "no debit" rule remains. "No debit" rule has been applied in the 2nd KP CP (UNFCCC, 2012) and maintained for post-Kyoto EU legislation in order to provide reliable and comparable country's GHG emissions/reductions data (European Commission, 2016), meaning that sector's emissions from sources shall not exceed corresponding sector's removals by sinks.

The commitment under the Kyoto Protocol, contained in Article 3, paragraph 1, requires each Annex I Party (Annex I parties - developed countries with targets to reduce emissions) to ensure that its total emissions over the commitment period do not exceed its allowable level of emissions, the so called Party's assigned amount (UNFCCC, 2008). LULUCF sector was not included in the GHG emission reduction target, however, the requirements for KP LULUCF sector was established. Under the rules set in the decisions of Conference of the Parties of the UNFCCC (15/CMP.1, 17/CMP.1, 2005) mandatory reporting of Kyoto Protocol Article 3.3 activities (afforestation/reforestation and deforestation, A/R/D) and optional reporting on article 3.4 activities (forest management (FM); grazing land management (GM); cropland management (CM)) was established, with the aim to use removal units (RMU's) for balancing assigned emission amount. Kyoto Protocol LULUCF accounting categories slightly differ from UNFCCC LULUCF reporting categories, due to its activity based nature, while LULUCF categories are land-based.

For the second commitment period under Kyoto Protocol reporting, accounting rules for KP LULUCF sector were slightly updated (6/CMP.9, 2013) to apply "no debit" rule and business as usual accounting for forest management category which became mandatory, however, only up to 3.5 % of total country's base year emissions could be used from accounted FM credits to RMU's – FM credits were „cap'ed". Forest management reference level is based on projection of GHG emission/reduction changes in 2013 – 2020 using the historical (1990 – 2009) data on forest resource use, management practice and most recent forest age class distribution as well as growing stock volume increment values. The EU's current 2020 greenhouse gas reduction target of -20% below 2005 emissions level does not include GHG emissions nor removals from LULUCF sector, due to the heated debate on how removals from LULUCF sector should be treated to transparently indicate its contribution to the overall target. At the same time, KP LULUCF sector is included in the EU Kyoto Protocol's targets (UN, 2012). After the long discussions between climate scientists, NGO's, politicians and other stakeholders, starting in 2014 (European Council, 2014), accounting rules to include LULUCF sector into EU's target achievement were agreed in negotiations between European Parliament and Commission in the end of 2017. Proposal for Regulation of LULUCF inclusion in EU target achievement (European Commission, 2016) sets rules of accounting of GHG emissions and removals from LULUCF categories until 2030. Changes from 2nd Kyoto Protocol commitment period cover changes from activity-based (KP LULUCF) to land-based (LULUCF) accounting, keeping the "no debit" rule for the accounted categories and "cap" for the forest management (forest land remaining forest land) category as in 2nd Kyoto Protocol commitment period. Adoption of the LULUCF regulation altogether with Effort Sharing regulation will provide EU member states both the possibility to cover GHG emissions from sectors with least mitigation potential with LULUCF credits and sets the requirement to keep LULUCF carbon stock in balance, compared to the historical level.

4. GHG EMISSIONS AND REMOVALS IN LITHUANIA

4.1 Land-use changes and LULUCF GHG removals

Land use matrix has significantly changed since 1990 after the collapse of Soviet Union, which resulted in abandonement of large agricultural areas (decreased cropland resulted in increasing grassland areas). Land-use change pattern has turned over after 2005, when application of Common Agricultural Policy measures started in Lithuania (Ministry of Agriculture, 2017). Forest land area is constantly increasing in Lithuania, both due to the human induced afforestattion/reforestation and natural forest expansion and has increased more than 3.5% since 1990 (State Forest Service, 2016). Currently forests in Lithuania cover 33.5% of total country area (State Forest Service, 2016) with agricultural land (cropland and grassland) covering another 50 % of total country area.

LULUCF sector has been a net sink of greenhouse gas emissions in Lithuania almost for the whole reporting period (1990 – 2015), except for the 1996 and 1997 when LULUCF was a net source of emissions (Figure 1). Emissions in 1996 and 1997 were the result of repetitive droughts and consequent pests (*Ips Typographus*) invasion which caused huge damages and death of spruce stands in Lithuania (Vasiliauskas, 2015). Greenhouse gas removals in LULUCF sector varies significantly during the inventory time period, depending presumably on climate related factors, economic situation, affecting land-use changes and biomass use for wood products. Three most important subcategories in LULUCF sector are forest land, cropland and grassland, covering most of the country territory – approx. 90 % of the total country area, with the increasing share of forest land subcategory harvested wood products (Figure 1). While forest land acts as a net carbon sink, sequestrating carbon in biomass, cropland has been acting as a net source of emissions due to intensive use of soils (mineral and organic). It should be noted, that changes in cropland and grassland GHG emission and removals depend directly on changes between those two categories – reduction of GHG emissions in cropland during 1990 – 2005 resulted from changes of cropland to grassland enhancing carbon sequestration in mineral soils.

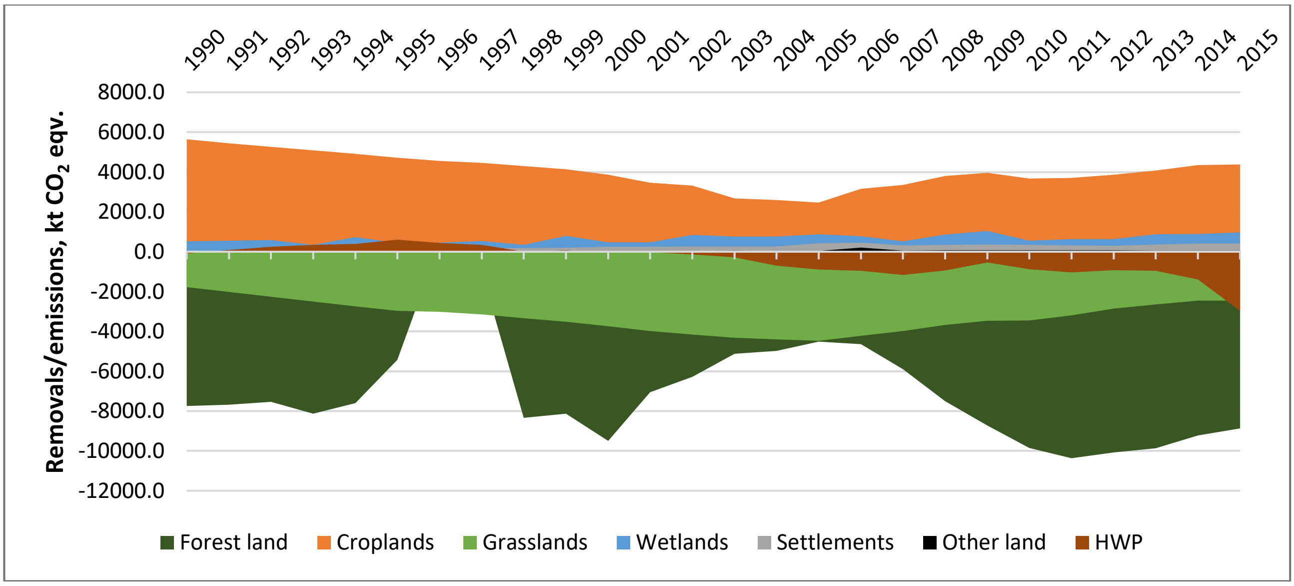


Figure 1. Total GHG emissions/removals in Lithuania during 1990 – 2015, kt CO_2 eqv. Data from Lithuania's National Inventory Report, 2017

4.2 Total Lithuania's GHG emissions and target achievement

Tendencies of greenhouse gas emissions and removals in all economic sectors of Lithuania and ratio between total GHG emissions and removals in LULUCF sector are presented in this part of the study. Figure 2 shows total Lithuania's GHG emissions trend during 1990 – 2015 and LULUCF potential to sequestrate GHG emissions in biomass and soil if no accounting rules are applied (total reported

country removals) and if 2nd Kyoto Protocol Commitment period accounting rules are applied (KP LULUCF accounted removals).

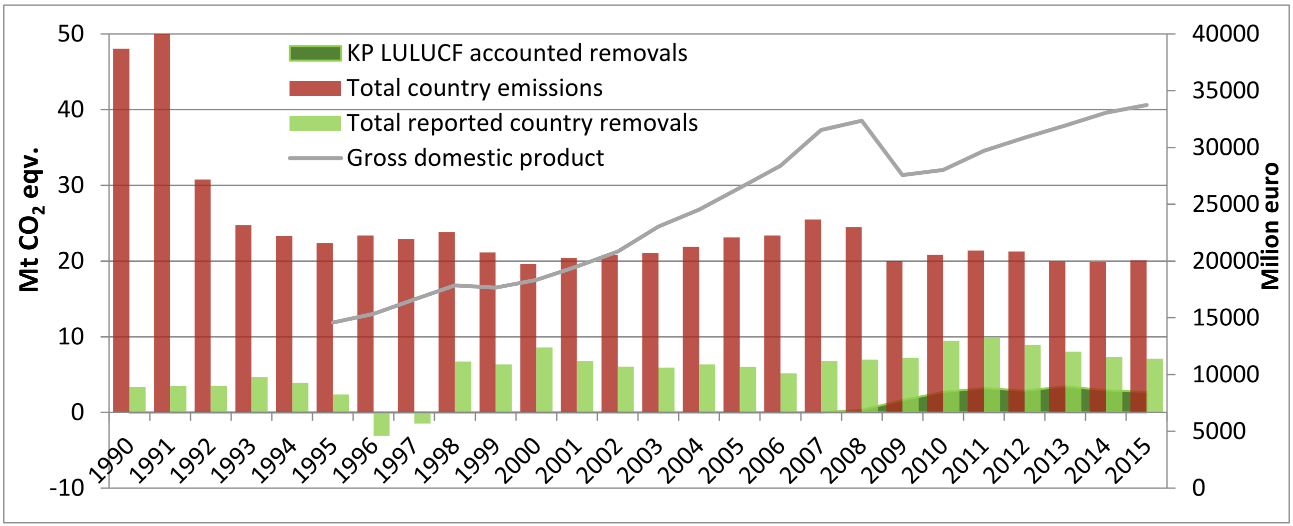


Figure 2. GHG removals by LULUCF sector in Lithuania during 1990 – 2015, kt CO_2 eqv. Gross domestic product at market prices values - chain linked volumes (2010), million euro Data from Lithuania's National Inventory Report, 2017

GHG emissions were significantly decreasing in Lithuania since 1990 and have reached half as its value in 2015 comparing to 1990. Lithuania has overachieved its target for 1st Kyoto Protocol commitment period – GHG emissions in 2012 were reduced more than 50% instead of required 8%. Increase in GHG emissions in overall Lithuanian GHG balance was observed during the economic upturn period until 2008, as it can be seen from Figure 2. LULUCF sector, due to its nature, is less dependent on economic situation, whereas its emissions and removals vary according to the natural conditions – removals in LULUCF sector drastically decreased in 1996 and 1997 due to the abovementioned adverse natural conditions (Figure 1, Figure 2). Total land use-related sector in Lithuania could absorb nearly 40% of net country's emissions in some years (without application of specific accounting rules), therefore LULUCF contribution to achieve Paris agreement commitment is of the most importance (Figure 2).

However, the picture of accounted GHG removals in Lithuania is significantly different if Kyoto Protocol 2nd commitment period accounting rules are applied. GHG removals would decrease more than half if estimated forest management reference level is applied (estimated in 2011, recalculated in 2013 and 2015, included under EU decision 529/2013/EU), comparing to the bare LULUCF removals. Forest management reference level for Lithuania is -5474 kt CO_2 eqv., taking into account technical recalculations which took place in 2013 and 2015. Accounted GHG removals from LULUCF sector under 2nd Kyoto Protocol commitment period could cover from 17 % (in 2013) to 14 % (in 2015) of total other sectors' emissions. LULUCF role in climate change mitigation target achievement increases with increasing emissions from other sectors, especially after 2020, when Lithuania's national target for non-ETS sectors (not taking part in EU emission trading system) is set to be –9%, comparing to 2005, which could be difficult to implement with economic growth.

5. DISCUSSION AND FUTURE OUTLOOK

As mentioned before, LULUCF sector is very complex and its total GHGs removals may depend not only on human-induced actions, but also natural circumstances, such as extreme climate events. However, despite its complexity and high uncertainty, sector's potential to participate in climate change mitigation is undeniable through its direct carbon sequestration and substitution effects (Nabuurs et al., 2017).

Changes in LULUCF sector's weight in total Lithuania's emissions and removals balance is related to both decreased emissions from other sectors - energy, industrial processes and product use, agriculture, waste and increased GHGs removals in LULUCF sector. There is a strong connection between LULUCF and agriculture sectors - with increasing cropland areas (since 2005) emissions from agriculture sector also increased and now plays an important role (nearly ¼ of total country's emissions in 2015) in the overall GHG emission balance in Lithuania, therefore complex measures to decrease GHGs emissions and enhance carbon sequestration in land-use related sectors are needed. Taking into account policy changes, enhanced carbon sequestration in LULUCF sector is of utmost importance, due to the need of keeping the "no debit" rule and possibility to cover part of other sectors' emissions with LULUCF credits. It should be highlighted, that forestry sector shall maintain good balance of carbon sequestration, sufficient wood supply for industry and biomass supply for energy purpose, keeping in mind EU's 27% renewable energy target until 2030 (COM, 2014). Lithuania has already exceeded EU renewable energy source (RES) target in 2016, reaching more than 25% of RES in total energy consumption (Ministry of Energy, 2017). In addition to the RES target, adopted climate change mitigation strategies (2030 climate and energy framework) in EU (COM, 2014) work proactive in enhancing the role of harvested wood products, as it may have a significant impact to climate change mitigation not only due to the sequestrated carbon locked in long-term wood based products (furniture, buildings, etc), but also due to the reduced use of less climate friendly materials (substitution effect) (Bottcher, Graichen, 2015). Harvested wood products pool should be considered for further incentivising in Lithuania also due to the significant role in Lithuanian economy, covering 4.7% of country's gross domestic product (State Forest Service, 2016). Energy efficiency target is also strongly related to renewable energy target and harvested wood products promotion; therefore, energy efficiency trends should be of importance in further LULUCF climate change mitigation potential evaluation.

LULUFC sector plays an important role in climate change mitigations policy. Depending on the accounting rules and applied emissions factors, national achievements might significantly differ. Therefore, more detail analysis including accurate emissions factors and other determinants of net emissions from this sector are needed.

References

1. Grassi, G., Elzen, M. G. J., Hof, A. F., Pilli, R., Federici, S. (2012). 'The role of the land use, land-use change and forestry sector in achieving Annex I reduction pledges', **Journal of Climatic change**, 115(3–4), pp 873-881. doi: 10.1007/s10584-012-0584-4

2. Macintosh, A. K. (2011). 'Are forest management reference levels incompatible with robust climate outcomes? A case study on Australia', **Journal of Carbon Management**, 2(6), pp. 691-707

3. UNFCCC (2012). Decision 2/CMP.7 Land use, land-use change and forestry. URL: http://unfccc.int/resource/docs/2011/cmp7/eng/10a01.pdf#page=11 (accessed September 6th, 2017)

4. Garcia-Oliva, F., Masera, O. R. (2004). 'Assessment and Measurement Issues related to Soil Carbon Sequestration in Land-Use, Land-Use Change and Forestry (LULUCF) Projects under the Kyoto Protocol', **Journal of Climatic Change**, 65(3), pp. 347-364

5. Smith, P., Clark, H., Dong, H., Elsiddig, E. A., Haberl, H., Harper, R., House, J., Jafari, M. et al. (2014). *Chapter 11 - Agriculture, forestry and other land use (AFOLU).* In: *Climate Change 2014: Mitigation of Climate Change. IPCC Working Group III Contribution to AR5.* Cambridge University Press

6. Sanchez, O. C. (2015). 'The climate effect of increased forest bioenergy use in Sweden: evaluation at different spatial and temporal scales'. Wiley Interdisciplinary Reviews: **Journal of Energy and Environment**, 5(2015), pp. 351-369

7. McKechnie, J., Colombo, S., MacLean, H. L. (2014). 'Forest carbon accounting methods and the consequences of forest bioenergy for national greenhouse gas emissions inventories. **Journal of Environmental Science and Policy**, 44, pp. 164-173

8. Perez-Cruzado, C., Mohren, G. M. J., Merino, A., Rodriguez-Soalleiro, R. (2012). 'Carbon balance for different management practices for fast growing tree species planted on former pastureland in southern Europe: a case study using the CO_2Fix model', **European Journal of Forest Research**, 131(6), pp. 1695–1716

9. UNFCCC (2013). Afforestation and Reforestation Projects under the Clean Development Mechanism: A Reference Manual. URL:

10. http://unfccc.int/resource/docs/publications/cdm_afforestation_bro_web.pdf, (accessed 20th March, 2018)

11. European Commission (2016a). Proposal for a Regulation of the European Parliament and of the Council on binding annual greenhouse gas emission reductions by Member States from 2021 to 2030 for a resilient Energy Union and to meet commitments under the Paris Agreement and amending Regulation No 525/2013 of the European Parliament and the Council on a mechanism for monitoring and reporting greenhouse gas emissions and other information relevant to climate change. COM (2016) 482 final, Brussels.

12. European Commission (2016b). Proposal for a Regulation of the European Parliament and of the Council on the inclusion of greenhouse gas emissions and removals from land-use, land-use change and forestry into the 2030 climate and energy framework and amending Regulation No 525/2013 of the European Parliament and the Council on a mechanism for monitoring and reporting greenhouse gas emissions and other information relevant to climate change. COM (2016) 479 final, Brussels.

13. Bottcher, H., Graichen, J. (2015). 'Impact on the EU 200 climate target of including LULUCF in the climate and energy policy framework. Report.' Öko-Institut e.V. URL: http://www.fern.org/sites/fern.org/files/Impact%20of%20including%20LULUCF%20in%202030_Final_corr.pdf

14. Frank, S., Bottcher, H., Gusti, M., Havlik, P., Klaasen, G., Kindermann, G., Obersteiner, M. (2016). 'Dynamics of the land use, land-use change and forestry sink in the European Union: the impacts of energy and climate targets for 2030', **Journal of Climatic change**, 138, pp. 253-266.

15. State Forest Service (2016). 'Lithuanian Statistical Yearbook of Forestry'. URL: http://www.amvmt.lt/index.php/leidiniai/misku-ukio-statistika/2016, (accessed 15th January, 2018)

16. IPCC (2006). 2006 IPCC Guidelines for National Greenhouse Gas Inventories, Prepared by the National Greenhouse Gas Inventories Programme, Eggleston H.S., Buendia L., Miwa K., Ngara T. and Tanabe K. (eds). Published: IGES, Japan

17. Lithuania's National Inventory Report (2017). Lithuania's GHG inventory submission under UNFCCC, Kyoto Protocol and Regulation No 525/2013of the European Parliament and of the Council of 21 May 2013 repealing Decision No 280/2004/EC. URL: http://unfccc.int/national_reports/annex_i_ghg_inventories/national_inventories_submissions/items/10116.php, (accessed 16th October, 2017)

18. UNFCCC (2008). 'Kyoto Protocol Reference Manual on Accounting of Emissions and Assigned Amount'. URL: https://unfccc.int/resource/docs/publications/08_unfccc_kp_ref_manual.pdf, (accessed 1st October, 2017)

19. UN (2012). Doha Amendment to the Kyoto Protocol. C.N.718.2012.TREATIES-XXVII.7.c (Depositary Notification). Adoption of the Amendment to the Protocol

20. European Council (2014). European Council (23/24 October 2014) conclusions. EUCO 169/14. URL: http://www.consilium.europa.eu/uedocs/cms_data/docs/pressdata/en/ec/145397.pdf, (accessed 17th November, 2017)

21. COM (2014). Communication from the Commission to the European Parliament, the Council, the European Economic and Social Committee and the Committee of the Regions. **A policy framework for climate and energy in the period from 2020 to 2030,** /* COM/2014/015 final */., Brussels.

22. CAN Europe: Climate Action Network (2016). NGO position on the post-2020 LULUCF Regulation. URL: http://www.fern.org/sites/fern.org/files/CAN%20Europe-LULUCF-Position_final.pdf, (accessed 15th December, 2017)

23. Ministry of Agriculture of the Republic of Lithuania (2017). Bendrosios žemės ūkio politikos įgyvendinimas Europoje bei Lietuvoje: tiesioginės išmokos. URL: https://www.zur.lt/wp-content/uploads/2017/09/BZUP-igyvendinimasES-LT1.pdf (accessed 24th January, 2018)

24. Vasiliauskas, V. (2015). Žievėgraužis tipografas pasiruošęs pulti eglynus, **Journal Mūsų girios**, 4, pp. 14-16. URL:

25. http://www.amvmt.lt/Images/Veikla/MSAT/Publikacijos/2015.04.%20%C5%BDiev%C4%97grau%C5%BEis%20tipografas%20pasiruo%C5%A1%C4%99s%20pulti%20eglynus.%20V.Vasiliauskas%20(pdf).pdf (accessed 21st November, 2017)

26. Nabuurs, G. J., Delacote, Ph., Elison, D., Hanewinkel, M., Hetemaki, L., Lindner, M. (2017). 'By 2050 the Mitigation Effects of EU Forests Could Nearly Double through Climate Smart Forestry'. **Journal of Forests**, 8(12), 484; doi:10.3390/f8120484

27. Ministry of Energy of the Republic of Lithuania (2017). Renewable energy resources, statistics.

28. URL:https://enmin.lrv.lt/lt/veiklos-sritys-3/atsinaujinantys-energijos-istekliai/statistika, (accessed 24th January, 2018)

CLIMATE CHANGE ADAPTATION STRATEGIES IN GREECE: RECENT DEVELOPMENTS AND TRENDS

E.D. Thoidou[2*] and D.N. Foutakis[2]

[1]School of Spatial Planning and Development Engineering, A.U.Th., GR- 54124 Thessaloniki, Macedonia, Greece,

[2]Civil Engineering and Surveying Engineering and Geoinformatics Department, Technological Institute of Central Macedonia, Serres, Greece

[*]Corresponding author: e-mail: thoidouel@plandevel.auth.gr , tel.: +302310995518

Abstract

In recent years, climate change policies have put special emphasis on climate adaptation strategies, alongside climate mitigation strategies, in an effort to address the inevitable impacts of climate change. Many European countries have proceeded with the elaboration of adaptation strategies at the national, regional and local levels, while many cities have prepared their adaptation strategies or have incorporated adaptation options into their spatial planning strategies. The sustainable development principles as well as the risk management approach have largely determined the character of these strategies. At the same time, of key importance are the spatial dimensions of climate adaptation strategies, since climate change impacts are territory-specific and are mostly addressed at the local and regional levels.

In Greece, climate change mitigation is included in the targets set by the country's strategy for sustainable development launched in 2002. Provision for the country's National Adaptation Strategy (NAS) was first made in line with its EU cohesion policy and climate policy commitments and has been ratified in 2016. Subsequently, the specifications of the regional plans for climate adaptation have been prepared by the competent ministry, in order to promote the elaboration of such plans.

This paper seeks to examine the above-mentioned developments in the field of climate change adaptation in Greece. It examines the character of the NAS as well as the emerging characteristics of the regional plans for climate adaptation, especially in relation to sustainable development principles and the risk-management approach. Particular emphasis is placed on the spatial dimensions of the plans which are considered critical for both the implementation of plans and their linking with spatial planning at the local and regional levels.

Keywords: Regional adaptation strategies, Climate adaptation strategies in Greece, Spatial planning

1. INTRODUCTION

Concern about climate change adaptation has accentuated in recent years, due to the fact that on the one hand the impact of climate change is becoming all the more evident and on the other hand prospects for climate change mitigation face significant constraints. Adaptation is defined as "The process of adjustment to actual or expected climate and its effects. In human systems, adaptation seeks to moderate or avoid harm or exploit beneficial opportunities. In some natural systems, human intervention may facilitate adjustment to expected climate and its effects" [IPCC, 2014]. These adjustments may have a behavioural, technological, regulatory, institutional, or financial character. Moreover, they may be proactive or reactive, with the majority of them being reactive, at least in Europe, where "implemented adaptation measures are more of reactive nature, that is to say they do

not anticipate climate change impacts, but rather react to those impacts once they manifest" [Venturini, Medri and Castellari, 2012, p. 28]. Adaptation strategies can be developed by various bodies that extend from the world community to individuals, and at various levels, from the global to the household. Two types of adaptation strategies can be discerned, namely collective and individual, with the latter being less efficient in addressing climate change impacts [Eikelboom and Janssen, 2013]. The inadequacies of individual reaction to climate change impacts raise the need for reinforcing collective reactions from the global to the local level. Adaptation strategy "for a country, region or municipality refers to a general plan of action for addressing the impacts of climate change, including climate variability and extremes. It may include a mix of policies and measures, selected to meet the overarching objective of reducing the country's vulnerability" [EEA, 2016a]. The characteristics of and challenges for climate adaptation strategies with respect to their spatial structure, particularly in Greece, are outlined below.

2. CLIMATE ADAPTATION STRATEGIES

Climate change, despite being a global phenomenon, has strong territorial dimensions which are reflected in the spatial dimensions of climate policies. This is much more true of climate adaptation policies due to the fact that they deal with climate change impacts that occur in certain territorial areas and are mainly addressed by territorial authorities. Climate adaptation policies are implemented from the local to the national and global level (Martins and Ferreira, 2011), with local areas facing the greater challenges. According to Aakre and Rübbelke [2010, p. 161], adaptation "requires many levels of decision-making (EU, national, regional, local)".

At the EU level, following the White Paper on adaptation [CEC, 2009], the EU Strategy on Adaptation to Climate Change was adopted in 2013 with the aim of enhancing "the preparedness and capacity to respond to the impacts of climate change at local, regional, national and EU levels, developing a coherent approach and improving coordination" [EC, 2013]. It is stated in the strategy that, "in view of the specific and wide ranging nature of climate change impacts, […] adaptation measures need to be taken at all levels, from local to regional and national levels" (ibid.). Some preliminary findings of the assessment of this strategy indicate that "it delivered its individual objectives, with progress recorded against each of the individual actions. At the same time "the need for an intensification and extension of the scope of action" is stressed [EC, 2017b].

In general all levels of adaptation strategies have distinct, albeit interconnected roles which are the first to reveal their spatial dimensions. Interconnections between the levels of adaptation strategies, either predefined or ad-hoc ones, are also representative of the spatial dimensions. At the national level climate adaptation commitments are made in relation to the supranational and transnational context (UN and EU). It is then, at the national level, that the adoption of global targets, guidelines and commitments is made, as it happens with climate mitigation. On the other hand, the local level is considered to be "the most important level for implementing national and regional adaptation strategies and related amendments to planning laws. This is due to local responsibilities for urban development and building permissions, but also to the fact that the population, in general, has more trust in local authorities" [Greiving and Fleischhauer, 2012, p. 37]. As for the regional level, it could be considered crucial in linking national and local levels, while at the same time specific adaptation strategies, which concern the relationship between urban and peri-urban space as well as between natural and human ecosystems, can be applied at this level. More particularly, these are defined as follows:

- A National Adaptation Strategy (NAS) "is a long term vision or general plan of action for addressing the impacts of climate change, including climate variability and extremes" [Swart et al. cited in Termeer, Biesbroek, and Van den Brink, 2012].
- A Regional Adaptation Strategy (RAS) is "the combination of possible measures that help develop from a current state of a region to one that better manages, adjusts to or copes with climate

change. The development of an adaptation strategy is an iterative, continuous learning process" [Eikelboom and Janssen, 2013, p. 2].

- A Local Adaptation Strategy (LAS) concerns local areas, usually cities or local territories with specific geomorphological characteristics (coastal, mountain etc.). Despite the fact that they are highly dependent on national adaptation strategies, local adaptation strategies have a long tradition that extends from the first Local Agenda 21 [Hamin and Gurran, 2011]. Several initiatives have given rise to local adaptation strategies since then. This is the case of the ICLEI (International Council for Local Environmental Initiatives) as well as of the Covenant of Mayors Initiative.

The overall characteristics of adaptation strategies, namely their status, content and structure, their interlinkages, as well as the way they address sustainability and promote their objectives, relate to their spatial dimensions.

With regard to the way the sustainable development dimension appears in each one of the three types/levels of adaptation strategies, a National Adaptation Strategy (NAS) should adopt the sustainability principle among its key objectives, which in turn characterizes adaptation strategies at all levels. Regional Adaptation Strategies (RAS) can be considered capable of addressing the relationship between environmental values and climate change impacts, which means that issues pertaining to territorial organization and environmental protection are given priority. Local Adaptation Strategies (LAS) are suitable for the implementation of sustainable solutions in practice such as green infrastructure.

Concerning the status of adaptation strategies, the question arises for all the three types/levels as to whether or not they constitute single and integrated policy domains. In other words, the question is whether they only set the overall context, e.g. in the form of a policy document [Hamin and Gurran, 2011] or whether they also have institutional and funding instruments at their disposal to promote adaptation.

The types of adaptation options are crucial. Among the various categorizations of adaptation responses the one suggested by the European Environment Agency (EEA) identifies three broad categories: "technological solutions — grey measures; ecosystem-based adaptation options — green measures; behavioural, managerial and policy approaches — soft measures". It is noted that "Green and soft measures specifically aim at decreasing the sensitivity and increasing the adaptive capacity of human and natural systems, basically, building resilience" [EEA, 2010]. It is then through the notion of resilience that a connection with sustainable development can be made.

A description of the structure of adaptation strategies can be found in the climate adapt platform of the EU [EEA, 2016b] as well as in the guidelines document on Regional Adaptation Strategies (RAS) conducted on behalf of the European Commission [Ribeiro et al., 2009]. This structure is closely related with the method and steps for their preparation and implementation. The climate adapt platform of the EU has prepared the climate adapt tool to assist various users in preparing their own strategies and plans at all levels. It suggests the following six steps: "Preparing the ground for adaptation; assessing the risks and vulnerabilities to climate change; identifying adaptation options; assessing adaptation options; implementation; monitoring and evaluation" [EEA, 2016b]. In the same direction the guidelines document on RAS identifies the following factors for a successful RAS: "Meaningful and sustained stakeholder engagement" (participation of public authorities, citizens and stakeholders); "Use and dissemination of appropriate information" (specification of information from the national and transnational level as well as collection of information at the local level); "Awareness Raising" (leaders make RAS widely known in close cooperation with stakeholders, aiming to increase resilience); "Monitoring, Evaluation & Review" (on the basis of the objectives set); and "Successful management of multilevel governance" (vertical coordination between the levels of governance and horizontal coordination between sectoral interests) [Ribeiro et al., 2009, pp. 17-18].

When it comes to the implementation stage, the issue arises as to which means are available for promoting climate adaptation strategy in practice. Both institutional and funding instruments should be utilized, however, the way these are embedded within overall governance and funding structures vary among countries. Three cases can be discerned:

- Identifying climate adaptation (and mitigation) as a distinct policy domain, possibly within the framework of a wider policy. In many countries climate adaptation strategies are translated to adaptation programmes within the context of environmental policy. For instance, in the case of England the legislative framework for climate change is being specified by particular programmes and actions [Carina and Keskitalo, 2010, pp. 103-105].
- Mainstreaming adaptation to various other policies of either a developmental or a regulatory character such as regional policy and regional spatial planning [Thoidou, 2017]. For example in Finland, which is a pioneer in developing a National Adaptation Strategy, "On the one hand, at the national level, the NAS predominantly concentrates on administrative sectors by mainstreaming adaptation. On the other hand, the lower levels of governance are pursuing their separate climate strategies that are based on voluntary initiatives with little input from the national level" [Juhola, 2010, p. 149].
- Emphasizing disaster risk reduction as a means of immediate response to the need to confront climate adaptation impacts. Following Greiving and Fleischhauer [2012, p. 37] "Issues which are related to climate change adaptation are in many cases communicated through disaster management, which is usually better established than spatial planning. Therefore, adaptation is at least indirectly addressed in those countries that do not yet have an adaptation strategy, such as Greece and Poland".

As regards the relationship between sectoral and spatial approaches, in most cases the former have a key role, as climate change has an indispensable impact on a variety of sectors. A great deal of work is being undertaken all over the world in order to analyse and forecast impacts as well as to identify solutions. Territorial specification of this work is then dependent on the specificities of each country's characteristics such as governance structure. At the same time the role of spatial planning in addressing climate change impacts, particularly at the initial stages of adaptation planning, has been accentuated [Greiving and Fleischhauer, 2012; Davoudi, Crawford and Mehmood, 2009]. Spatial planning can serve as a policy framework which is capable of coordinating various policies and actions on a territorial basis as well as planning future developments on a territorial basis [Thoidou, 2013]. On the other hand, adaptation reflects a climate-sensitive approach with a wider view to risk prevention and management that is important for spatial planning per se.

3. ADAPTATION STRATEGIES IN GREECE

Adaptation strategies in Greece are being developed at the national and the regional level. As in all countries, the first official documents on climate change in Greece in the early 2000s were dedicated to climate mitigation, in accordance with commitments made within the UN and the EU framework. The successive National Communications to the UN Framework Convention on Climate Change (UNFCCC) are the most representative documents in this respect. Even though they refer to the national level, they do include several references to particular territorial areas regarding climate adaptation, which could be considered to be a way of responding to the need for an adaptation policy with a spatial approach. It was only in 2016 that the study for NAS was ratified by law for a 10-year period, under the competence of the Ministry of Environment and Energy, following commitments made within the EU. The key objectives of NAS are the following (MEEN, 2016):

"(1) Systematizing and improving decision making process (short and long term) regarding adaptation (2) Linking adaptation with the promotion of a sustainable development pattern through regional/local action plans (3) Promoting adaptation policies and actions in all sectors of the Greek economy with an emphasis on the most vulnerable (4) Creation of a mechanism for monitoring,

evaluation and updating of adaptation policies and actions (5) Strengthening adaptive capacity of the Greek society through information and awareness raising actions".

The preparation of Regional Adaptation Action Plans (RAAPs) started in 2017 in accordance with provisions made by the above-mentioned law. Following the drafting of specifications by the competent ministry, the Plans for the 13 NUTS II regions of the country are being launched by the corresponding regional authorities. In RAAPs "the sectors and territorial areas of priority are identified and measures and actions for them are proposed with the aim of: avoiding impacts, reducing the intensity and extent of impacts, and restoration" [MEEN, 2017]. The evaluation of proposed measures and actions should be made against these aims, while the key objectives of the Plans are connected with those of NAS.

Both national and regional adaptation strategies refer to each other. In the NAS it is declared that due to its strategic role the feasibility and prioritization of specific measures and actions either on a sectoral or on a territorial basis is a task not for the NAS but rather for the 13 RAAPs, which should take into account the specificities of each region. In the same way NAS is considered to be the guiding framework for RAAPs [MEEN, 2017].

Local adaptation strategies are not in the official agenda. However a variety of adaptation options are being implemented at the local level, such as the bioclimatic upgrade of open public spaces in cities and the protection of biodiversity in protected areas. Many local authorities have undertaken action in the context of the EU climate adapt networks such as the Covenant of Mayors Initiative.

The dimension of sustainability in NAS is declared in the form of "a sustainable development pattern" that constitutes one of its key objectives. Sustainable development in RAAPs is not referred to as such, but it is included in specific themes such as that for "Fauna – Flora and Protected areas". It is noted that adaptation objectives should be linked to other objectives which pertain to sustainability such as green development and prudent use of water resources [MEEN, 2017].

Both NAS and RAAPs are in the form of a study. NAS was prepared by the Ministry in cooperation with the Climate Change Impacts Study Committee of the Bank of Greece and was exceptionally endorsed by law as a public strategy [EC, 2017a]. NAS is a strategic orientation document. Therefore, a question arises as to whether it follows the strategic planning approach, according to which emphasis should be placed on the process of setting the objectives and promoting implementation, above all by enhancing participatory procedures. RAAPs follow a rather different course: studies are commissioned by regional authorities and performed by experts, a process which is currently in progress.

As far as their content is concerned, all the above-mentioned three categories of adaptation options are included in the measures proposed by NAS. The emphasis placed on green infrastructure in the context of the ecosystems approach is perhaps the most innovative among them. Provision is also made for grey infrastructure and technological solutions. In RAAPs grey infrastructure has a key role, with the emphasis on climate-proof solutions being one of the innovations introduced, probably in accordance with NAS, while green infrastructure is less evident. Provision is also made for soft measures in both strategies. As far as the structure of the strategies is concerned, the main pillars of the NAS are the following: "Analysis of climate risk and vulnerability of the Greek territory; adaptation measures in fifteen sectors; instruments for the evaluation of adaptive investments and policies; instruments for mainstreaming of adaptation policy into wider policy domains; the international dimension; the enhancement of adaptive capacity; consultation with stakeholders; and monitoring and revision of adaptation policies" [MEEN, 2016, p. 93]. RAPPs consist of the following steps: "Analysis of objectives; overview of natural and human environment; evaluation of expected climatic changes and climate vulnerability of sectors and territorial areas; estimation of direct and long term impact of climate change in various environmental and socioeconomic domains; proposed measures for priority sectors and territorial areas; examination of mainstreaming of measures into other policies; examination of the compatibility of RAAP with other regional plans, examination of

the compatibility of RAAP with those of neighbouring regions; way of consultation; way of raising awareness; monitoring of implementation" [MEEN, 2017].

It is evident that both NAS and RAAPs follow the main steps suggested by the above-mentioned adaptation tools. As regards the participatory process which has a key role in shaping an adaptation strategy [Ribeiro et al., 2009], in the case of NAS it was confined to formal public consultation. This could be related to the fact that NAS was drafted by organizations which, despite their high scientific performance, do not have competencies in participatory governance. In the specifications' document for RAAPs, the role of participatory processes is stressed, at both preparation and implementation stages. This is not unrelated to the fact that adaptation strategy at the regional level falls under the competence of regional self-government which can enable participatory processes for drawing up the strategy. Finally, a shortcoming could be argued to be the fact that the role of the local level in adaptation planning is yet not so clear.

The characteristics of adaptation strategies are related to their institutional status. One question is whether and to what extent these strategies have a binding character and, furthermore, whether they constitute single policy domains with their own institutional and funding instruments. Some evidence can be drawn from the way the implementation of adaptation options is pursued. The following ways can be found in the chapter "Adaptation in practice" of the NAS document [MEEN, 2016, pp. 75, 85]:

- Adaptation policies should be mainstreamed into wider policy domains (prevention of natural disasters, policies for food, infrastructure, energy, transport, quality of life in cities, protection of biodiversity, and so on). Linking adaptation with mitigation efforts especially in the energy sector is also a way of promoting adaptation. Closely related with this is the introduction of the criterion of "climate-resilient investment" in all stages of approving and funding of any investment. It is argued that "In nowadays' recession and budgetary constraints an autonomous policy of adaptation investments could not be justified. 'Climate resilient investments' will be increasingly mainstreamed into individual sectoral policies. This entails deep transformations in the decision making on investments" [MEEN 2016, p. 74].
- Risk prevention and management is also very important, due to its long tradition in the country. The civil protection law (No 3013/2002) aims at "protecting life, health and properties against natural […], technological […] and other disasters which cause emergency situations at times of peace". In recent years civil protection has been developed within the Hyogo framework (2005-2015) and the Sendai framework (2015-2030).
- Other ways of promoting adaptation options include the transnational and transboundary dimension of adaptation, improving adaptive capacity through research, education and raising awareness, as well as consultation with stakeholders. In the same way, mainstreaming adaptation action into other policies, above all in the policy for natural disaster management, as well as establishing the criterion of "climate-resilient investment" are also foreseen with regard to the implementation of the measures proposed by RAAPs [MEEN, 2017].

In the NAS, the sectoral dimension is of major importance while a clear spatial dimension is not particularly evident. The action "land use regulation" is included in the section "Biodiversity and Ecosystems" under the logic of land protection and ecosystem services. References to the spatial planning context are made in relation to the need for mainstreaming adaptation into various polices as well as the need to link adaptation and mitigation policies. Particular reference is made to coastal zones and transnational - transboundary areas. The role of cities and consequently of urban planning with an emphasis on green infrastructure is stressed in the section "Built environment".

The spatial dimension is more evident in the RAAPs and particularly in the part relating to the evaluation of expected climatic changes and the climate vulnerability of sectors and territorial areas. Priorities and measures proposed by RAAPs are also specified on a territorial basis, along with the sectoral one, while coastal zones are particularly emphasized. Specific provision is made for the role

of spatial plans at all levels, from regional to local. As noted in the evaluation document of the whole adaptation policy of the country, “the RAAPs will propose ways to integrate adaptation into existing strategies, policies and plans, including urban and spatial (land/sea) policies and plans”, while projections and assessments about climate change impacts will be useful inputs for spatial planning [EC, 2017a, p. 16].

At the same time, from the view point of spatial policies, an awareness of climate adaptation can be observed, especially in the two parallel policy contexts that constitute regional policies in Greece, namely regional spatial planning and regional development policy with the latter having a significant influence in terms of funding [Thoidou, 2017]. However, as Cartalis et al. (2017) note, the potentialities offered by development programmes have not been fully exploited due to the fact that national spatial plans have not yet been updated to explicitly address the dimension of climate change adaptation.

In the context of the ongoing evaluation of the EU's Strategy for Adaptation to Climate Change a draft country fiche was prepared which assess the state of play within the country. As noted in this document “Despite the significant progress made in the last two years, there are still significant needs with regard to policy coordination, development and dissemination of good practice, and most importantly in terms of capacity building” [EC, 2017a, p. 5].

4. CONCLUSIONS

Having as its starting point recent developments in the field of climate change adaptation, this paper shortly presented adaptation strategies in Greece with a view to their spatial characteristics. The development of these strategies in the country is quite recent. National Adaptation Strategy was ratified in 2016 and Regional Adaptation Strategies are at the preparation stage in the form of RAAPs. A hierarchical structure with spatially differentiated roles of the two strategies can be observed. The spatial dimensions of both strategies are rather limited, especially in NAS which has adopted a sectoral approach. The local level seems to be a part of the regional level, without having a distinct role in the making of adaptation strategies and the same can be said about urban adaptation strategies. At the same time the role of spatial planning in promoting climate adaptation is widely acknowledged by both strategies. Hierarchical structure is reflected in the formal way participatory processes are applied, which does not strengthen adaptive capacity. This goes in tandem with shortcomings regarding the status and the strategic character of both strategies. As far as sustainable development is concerned, the provision made by NAS [MEEN, 2016] for “linking adaptation with the promotion of sustainable development through regional/local action plans” remains general and it is expected to be specified through RAAPs.

Innovative elements introduced by adaptation strategies have to do with their structure and the way they translate objectives into practice. Especially noteworthy is the emphasis placed on green infrastructure as well as the so-called climate resilient investments. Mainstreaming adaptation action into various policies as a means of promoting adaptation is stressed perhaps for the first time. At the same time, the risk management policy seems to keep its key role in dealing with climate change impacts, which indicates a reactive approach.

Overall, climate adaptation strategies at various territorial levels in Greece are at an initial stage, therefore there is not enough evidence to estimate their characteristics and performance. As concluded for the European level [ESPON CLIMATE, 2010, p. 77], “it appears that policy developments are evolving in an interactive fashion between the central and the regional government”. This entails a twofold challenge: on the one hand the elaboration of adaptation strategies at all levels in an interconnected way, and on the other hand the elaboration of these strategies in the context of a territorial governance approach that goes beyond formal competences and promotes an open participatory process at all levels, from national to local. Possible improvements of adaptation strategies in Greece may include an active role for the local and especially the urban level, as well as an accentuation of the role of spatial planning in climate adaptation action at all levels. Moreover,

citizen and stakeholder involvement in all types and levels of the adaptation process is crucial, in order that the prevailing top-down approach can be complemented by a bottom-up one.

References

1. Aakre S. and D.T.G. Rübbelke (2010) '**Adaptation to Climate Change in the European Union: Efficiency versus Equity Considerations**', Environmental Policy and Governance, Vol. 20, pp. 159–179.
2. Carina E. and H. Keskitalo (2010) **'Climate Change Adaptation in the United Kingdom: England and South-East England**', Developing Adaptation Policy and Practice in Europe: Multi-level Governance of Climate Change', ed. H. Keskitalo, Springer: Sweden.
3. Cartalis C., Coccossis H., Economou D., Santamouris M., Agathagellidis H. and H. Polydoras (2017) '**The impact of climate change on development'**, https://www.dianeosis.org/wp-content/uploads/2017/06/climate_change10.pdf (accessed 1-2-2018) (in Greek).
4. Commission of the European Communities (CEC) (2009) '**White Paper. Adapting to climate change: Towards a European framework for action'**, COM (2009) 147 final.
5. Davoudi S., Crawford J. and A. Mehmood (eds) (2009) '**Planning for climate change: strategies for mitigation and adaptation for spatial planners'**, Routledge.
6. Eikelboom T. and R. Janssen (2013) '**Interactive spatial tools for the design of regional adaptation strategies**', Journal of Environmental Management, Vol. 127, pp. S6-S14.
7. ESPON CLIMATE (2010) **'Climate Change and Territorial Effects on Regions and Local Economies'** Applied Version 22/03/2010, Applied Research Project 2013/1/4Revised Interim Report https://www.espon.eu/sites/default/files/attachments/Annex.pdf (accessed 1-2-2018).
8. European Commission (EC) (2013) '**An EU Strategy on adaptation to climate change'**, Brussels 16.4.2013, COM(2013) 216 final, http://eur-lex.europa.eu/legal-content/EN/TXT/PDF/?uri=CELEX:52013DC0216&from=EN (accessed 1-8-2015).
9. European Commission (EC) (2017a) '**Adaptation preparedness scoreboard: Draft country fiche for Greece'**, https://ec.europa.eu/clima/consultations/evaluation-eus-strategy-adaptation-climate-change_el (accessed 28-2-2018)
10. European Commission (EC) (2017b) **'Study to support the evaluation of the EU Adaptation Strategy (Summary)**', https://ec.europa.eu/clima/sites/clima/files/consultations/docs/0035/summary_interim_findings_en.pdf (accessed 10-5-2018).
11. European Environment Agency (EEA) (2010) '**The European Environment State and Outlook 2010: Adapting to Climate Change**', Publications Office of the European Union: Luxembourg.
12. European Environment Agency (EEA) (2016a) '**Glossary**', https://climate-adapt.eea.europa.eu/help/glossary/index_html/#linkAdaptationStrategy (accessed 10-5-2018).
13. European Environment Agency (EEA) (2016b) '**European Climate Adaptation Platform'** [online], http://climate-adapt.eea.europa.eu/knowledge/tools/adaptation-support-tool (accessed 15-2-2018).
14. Greiving S. and M. Fleischhauer (2012) '**National Climate Change Adaptation Strategies of European States from a Spatial Planning and Development Perspective'**, European Planning Studies, Vol. 20(1), pp. 27-48.
15. Hamin, E.M. and N. Gurran (2011) '**Local Actions, National Frameworks: A Dual-Scale Comparison of Climate Adaptation Planning on Two Continents'**, University of Massachusetts 34 Working paper, http://scholarworks.umass.edu (accessed 15-2-2018).

16. Intergovernmental Panel on Climate Change (IPCC) (2014) Annex II: '**Glossary**' [Mach, K.J., S. Planton and C. von Stechow (eds)]. In: Climate Change 2014: Synthesis Report. Contribution of Working Groups I, II and III to the Fifth Assessment Report of the Intergovernmental Panel on Climate Change [Core Writing Team, R.K. Pachauri and L.A. Meyer (eds)]. IPCC, Geneva, Switzerland, pp.117-13

17. Juhola S. (2010) '**Mainstreaming Climate Change Adaptation: The Case of Multi-Level Governance in Finland'**, Developing Adaptation Policy and Practice in Europe: Multi-level Governance of Climate Change', ed. H. Keskitalo, Springer: Sweden.

18. Martins R.D.A. and L.C. Ferreira (2011) '**Opportunities and constraints for local and subnational climate change policy in urban areas: insights from diverse contexts'**, International Journal of Global Environmental Issues, Vol.11 (1), pp. 37–53.

19. Ministry of Environment and Energy (MEEN) (2016) '**National Adaptation Strategy for Greece'** http://www.ypeka.gr/LinkClick.aspx?fileticket=crbjkiIcLlA%3d&tabid=303&language=el-GR (accessed 15-2-2018) (in Greek).

20. Ministry of Environment and Energy (MEEN) (2017) '**Specifications for Regional Adaptation Action Plans'**, Government Gazette B/873/16-3-2017 (in Greek).

21. Ribeiro M., Losenno C., Dworak T., Massey E., Swart R., Benzie M. and C. Laaser (2009) '**Design of guidelines for the elaboration of Regional Climate Change Adaptations Strategies**', Study for European Commission – DG Environment - Tender DG ENV. G.1/ETU/2008/0093r. Ecologic Institute: Vienna.

22. Termeer C., Biesbroek R. and M. Van den Brink (2012) '**Institutions for adaptation to climate change: comparing national adaptation strategies in Europe'**, European Political Science, Vol. 11(1), pp. 41-53.

23. Thoidou E. (2013) '**The climate challenge and EU cohesion policy: implications for regional policies**', International Journal of Innovation and Sustainable Development, Vol. 7(3), pp. 303-320.

24. Thoidou E. (2017) '**Climate adaptation strategies: cohesion policy 2014-2020 and prospects for Greek regions'**, Management of Environmental Quality: An International Journal, Vol. 28(3), pp. 350-367.

25. Venturini S., Medri, S. and Castellari, S. (2012) '**Overview of key climate change impacts, vulnerabilities and adaptation action in Europe'**, CMCC Research Papers RP0142 https://dx.doi.org/10.2139/ssrn.2195399 (accessed 15-2-2018).

SPATIAL ANALYSIS FOR VULNERABILITY ASSESSMENT OF URBAN COASTAL AREAS TO SEA LEVEL RISE

E.A. Stamatopoulou[*1], G. Ovakoglou[2], T.K. Alexandridis[2], I.A. Tsalikidis[3]

[1]Joint Master Programme in Landscape Architecture, Dept. of Architecture and Dept. of Agriculture, A.U.Th, GR-54124 Thessaloniki, Macedonia, Greece

[2]Laboratory of Remote Sensing, Spectroscopy and GIS, Faculty of Agriculture, A.U.Th GR- 54124 Thessaloniki, Macedonia, Greece

[3]Laboratory of Floriculture and Landscape Architecture, Faculty of Agriculture, A.U.Th GR- 54124 Thessaloniki, Macedonia, Greece

[*]Corresponding author: e-mail: amystamatopoulou@gmail.com, tel: +306945354313

Abstract

It is widely accepted that climate change poses a potential threat for urban environments, thus is one of the largest challenges for humanity nowadays. The most common effect of climate change is the Sea Level Rise (SLR), which develops in the long run and is directly connected to extreme weather conditions at the coastal zone level. Coastal zones are most affected by extreme weather phenomena caused by SLR. The understanding of the potentially dire impacts of climate change has resulted in the widespread use of the resilience concept. This study examines methods of spatial analysis that can introduce the variable of climate change to the landscape architecture analysis with the intention to enhance resilience in the design process. The study reports the results of the application of a methodology for the assessment of the vulnerability of coastal areas to SLR due to climate change. It also allows identifying critical areas to this phenomenon and providing a useful classification of the coastal areas in the selected study areas. Introducing Geographical Information System (GIS) techniques and spatial analysis, the study approaches a methodology of determining coastal zone vulnerability for Thermaikos and the Corinthian Gulf. Both case studies are vulnerable due to accelerated SLR, high erosion rate that threatens urban areas and protected ecosystems on the coastal zone. For the determination of the Coastal Vulnerability Index (CVI) geologic and physical variables were considered. The CVI is giving results towards an evaluation of the likelihood that physical changes may occur. The study attempts to introduce resilience on the coastal zone by identifying the most vulnerable areas to SLR and consider them as an indispensable support for landscape architecture projects and spatial intervention.

Keywords: Resilience, SLR, Coastal zone, Soft infrastructure, GIS, Spatial analysis, CVI

1. INTRODUCTION

The impact of climate change and its consequent phenomena are in the centre of the discussion regarding urban resilience. Climate is defined as long-term averages and variations in weather measured over a period of several decades. Its effects have already been quite observable on the environment through Sea Lever Rise (SLR), the melting of the Greenland ice sheet, the greenhouse effect, causing intense droughts and floods, mean temperature rise and extreme weather conditions. As the cities become vulnerable to climate change, their ability to adapt to expected or unexpected changes defines their resiliency [Vale and Campanella, 2005]. Spatial analysis is a means of recording the vulnerabilities or strengths of the environment and enables the understanding of space. The

Geographical Information System (GIS) techniques can relate spatial or geographic data with unrelated information, such as climate change effects, by using location as the key index variable.

It is common ground, that the first step to coastal protection against SLR is the spatial analysis and quantification of the coastal erosion that takes place. In order to produce such results, the study looks into literature for creating indices that can follow this principle.

Gornitz et al. (1991) argues that one of the most common worldwide methods of assessing coastal vulnerability is the Coastal Vulnerability Index (CVI). The study of Dwarakish et al. (2009) has been carried out with a view to calculate the Coastal Vulnerability Index (CVI), in order to identify the high and low vulnerable areas and area of inundation due to future SLR, as well as the land loss due to coastal erosion. The study of Doukakis (2005) has used CVI to map the relative vulnerability along the coastline of western Peloponnese. The CVI calculation used physical contributors in order to highlight the regions with maximum SLR effects and following, each CVI was computed on digitized maps for comparison reasons. Using percentiles the coastline was grouped based on the vulnerability extend.

This study uses the CVI in order to examine the coastal zone of two gulfs (Thermaikos and the Corinthian Gulf) where the coastline is of a different morphology (closed gulf) than the above mentioned studies. The study areas are characterized by densely populated coastlines, resulting in a high risk in case of a future SLR. The aim of the study is to figure out whether it is possible to extract results about CVI in areas other than linear coastlines and in small scale study areas. During this study both conventional and remotely sensed data were used.

1.1 Coastal Vulnerability

1.1.1 Characteristics of the coastal zone

The coastal zone is historically important, as the space where human activity has developed throughout the centuries. This theory is proved by the fact that two thirds of the planet's total population live within a distance of few kilometres from the coastline, given its socio-economic and ecological importance. Coastal ecosystems are highly productive, rich in biotopes of fauna and flora. Additionally, they work as a natural defence against the destructive forces of the sea.

However, the coastal zone faces pressures that alter its structure. These pressures can be distinguished in two types, natural and anthropogenic processes, which in many cases cause irreversible effects in the coastal landscapes. A noticeable natural process is the coastal erosion that can cause full or partial remodelling of the landscape and tidal waves. Anthropogenic factors are the unregulated urban development, loss of ecosystems and biodiversity, pollution, landscape degradation, depletion and pollution of water resources. The above mentioned are common characteristics at most of the coastal areas worldwide. Adding to these pressures, climate change causes short-term effects, as analysed following.

1.1.2 Climate change and coastal vulnerability

Climate change has several impacts on urban environments with SLR being the most crucial for the coastal zone. SLR develops over time due to thermal expansion, as causing the occurrence of extreme weather events in the coastal zone. It is indicative of the magnitude of the impact on urban environments, that 60% of the world's population lives within a distance of 60 kilometres from the coastline, while 11 of the largest cities in the world are in coastal low-altitude areas [Bergdoll and Nordenson, 2011].

SLR is a phenomenon that progresses over time, affects coastal, island regions, as well as areas adjacent to Delta Rivers and causes compulsory migration of the population. It will lead to an increase in the frequency of phenomena that are now characterized as extreme flooding. Krestenitis et al., (2015) pointed out that due to the higher water level, the frequency and intensity of floods due to heavy storms will increase dramatically.

In this context, coastal vulnerability is defined as the composition of the risk of a natural coastal system and the risk of the socio-economic system due to climate change [Doukakis, 2007]. The impacts of SLR on a natural coastal system depend on its vulnerability to these, its adaptation, as well as its strength. Adaptability and strength describe its physical stability in changes. In particular, the strength expresses the ability of the system to resist to a possible disturbance, while adaptability expresses the speed with which the system returns to its original condition. The ability of the coastal system to respond and adapt to extreme changes mitigates its vulnerability and develops its resiliency for the future.

2. METHODOLOGY

2.1 Variables

Complexity in the form and functions of coastal zones does not favour the development of a coastal vulnerability model with general application. Additionally, data used for the analysis of the variables of a coastal vulnerability model show high variability in different spatial scales. Hammar-Klose and Thieler (1999), argue that for a more comprehensive study of coastal vulnerability it is considered that large-scale variables (waves, tides, sea-level trends) should be mapped with relatively good accuracy, while small scale variables (geomorphology, coastal slope, shoreline change rate) should allow the perception of their effects on the coast.

Historic shoreline change, geomorphology, coastal slope, mean tidal range, mean significant wave height and global SLR are the six variables to the CVI calculation. The CVI allows these six variables to be related in a quantifiable manner that expresses the relative vulnerability of the coast to physical changes due to future sea level rise. The CVI calculation yields numerical data that cannot be equated directly with particular physical effects. However, it does highlight areas where the various effects of SLR may be the greatest. The six variables are classified into two groups, the Geologic variables and the Physical variables [Dwarakish et al., 2009].

The geologic variables include (a) historic shoreline change, (b) geomorphology and (c) coastal slope. The physical variables include (a) mean tidal range, (b) mean significant wave height and global SLR. Once each section of the coastline is assigned a vulnerability value for each specific data variable, the CVI is calculated as the square root of the product of the ranked variables divided by the total number of variables:

$$CVI=\sqrt[2]{\frac{abcdef}{6}} \quad (1)$$

where a: geomorphology, b: shoreline change rate (m / yr.), c: coastal slope (%), d: mean tidal range (m), e: mean significant wave height (m), f: global SLR (mm / yr.)

Actual variable values are assigned a vulnerability ranking based on value ranges, whereas the non-numerical geomorphology variable is ranked qualitatively according to the relative resistance of a given landform to erosion (Table 1).

2.1.1 Geomorphology

The geomorphology variable expresses the relative erodibility of different landform types. The ranking is on a linear scale from 1 to 5 in order of increasing vulnerability due to SLR. Data from Joint Research Centre (JRC) European Soil Data Centre (ESDAC) were used and in particular the soil erosion by water dataset (RUSLE2015). From this dataset the layer of soil erodibility (ERODI) was selected, which relates to the soil erodibility factor (K-factor).

Table 1: Ranges of vulnerability ranking for both study areas

a/a	Variable	Ranking of coastal vulnerability				
		Very low 1	**Low 2**	**Moderate 3**	**High 4**	**Very high 5**
a	Geomorphology	Rocky cliffed coasts	Medium cliffs, indented coasts	Low cliffs, lateritic plain	River deposits, alluvial plain	Coastal plain, beach mud flats
b	Shoreline erosion/accretion (m / yr.)	>+15	+5 to +15	-5 to +5	-15 to -5	<-15
c	Coastal Slope (%)	>0.6	0.5-0.6	0.4-0.5	0.3-0.4	<0.3
d	Mean tide range (m)	>4.0	3.0-4.0	2.0-3.0	1.0-2.0	<1.0
e	Mean significant wave height (m)	<0.7	0.7-1.4	1.4-2.1	2.1-2.8	>2.8
f	Mean sea level rise (mm / yr.)	<1.8	1.8-2.5	2.5-3.0	3.0-3.4	>3.4

2.1.2 Shoreline change rate
The value of this variable was retrieved from literature and the study of Doukakis (2007), since the available data is not detailed enough in order to provide accurate results in the study area's scale. The study shows that for a large number of coastal areas in Greece, an annual shoreline change rate is calculated slightly more than -1.0 m / yr. With a horizon of 50 (2050) or 100 years (2100), a mean rate was calculated resulting an annual rate of – 1.76 m / yr. (intensive erosion) and at - 0.14 m / yr. (low erosion).

2.1.3 Coastal slope
Determination of the regional coastal slope identifies the relative vulnerability of inundation and the potential rapidity of shoreline retreat [Dwarakish et al., 2009]. The coastal slope was calculated by defining a distance of 12 km perpendicular to the coastline, 6 km towards the sea and 6 km towards shore. The selection of the coastal zone distribution, as well as the classification of the slope was based on literature. The bathymetric data was retrieved from the EMODNET (Portal for Bathymetry-Bathymetry Viewing and Download Service), and DEM topography data was retrieved from curves interpolation digitized from 1: 100000 GIS maps. The two raster files were delimited within the study area and were then converted into joined slope data giving the total coastal slope.

2.1.4 Mean tidal range
Mean tidal range carries the information of the potential influence of storms on coastal evolution, and their impact relative to the tide range. In Greece generally, the literature [Doukakis, 2007] explains that tidal waves especially for small-scale study areas is negligible. This can be explained by the fact that a micro tidal coastline is essentially always ''near'' high tide and therefore always at the greatest risk of inundation from storms.

2.1.5 Mean significant wave height
Mean significant wave height information was retrieved from the COPERNICUS system and the MEDSEA_ANALYSIS_ dataset FORECAST_WAV_006_011, using the layer "Spectral layer significant wave height-mean significant wave height". Daily data was used from each last day of the month, for one year (systematic sampling), which we compiled to get the average maximum and minimum values in the study areas.

2.1.6 Mean sea level rise

A sea level rise would directly result in a corresponding higher shift to the zone of wave action on the beach**.** According to the projected SLR for Low Emissions (RCP2.6) of the European Environment Agency, a mean sea level rise is expected for the Thermaikos Gulf about 0.3-0.4mm / yr., while for the Corinthian Gulf, 4-0.5mm / yr.

2.2 Study areas

The study areas where CVI is calculated are Thermaikos (northern Greece) and the Corinthian Gulf (south-west Greece). Their selection was based on literature research [Doukakis, 2007], since they are considered areas with significant impacts from climate change.



Figure 1: The study areas of Thermaikos Gulf (left) and the Corinthian Gulf (right)

The intense erosion of the Corinthian Gulf coastline - nowadays - on the one hand and the hazard scenarios of the coastal zone of the Thermaikos Gulf on the other, both imply the threat of the coastal zone from human activities and increases vulnerability to SLR. As mentioned in the study of Doukakis (2007) the Thermaikos Gulf west area is particularly vulnerable. Thermaikos is considered the third most threatened Mediterranean region from SLR after the Nile Delta and the Gulf of Venice. At the same time, the Corinthian Gulf faces very significant erosion problems, setting the coastal zone particularly fertile for further study.

The two study areas have a high population density in their coastal zone and are strongly related to socioeconomic activities. At the same time, their location favours research, as different climatic conditions prevail, but also a different degree of exposure to natural phenomena, varied geomorphology and landscape. They also both consist of different ecosystems (delta river, long coastline), adding to variegated results.

2.3 Variables' ranking in buffer zones

The variables that were analysed in chapter 2 were assigned in polygons defined through buffer zones in the study area and thus CVI was calculated for these zones. Buffer zones are defined as areas of influence of the coastline. Each buffer zone is partitioned in polygons per 5 km in a straight line, taking into account their structure (small bays, estuaries, rivers) so that the polygon information is proportionally equal. Polygons with special coastline structure are assigned as one in order to retain the characteristics.

The 5km distance was set for this particular scale to provide the best possible variability of data, while pointing out the micro scale coastline qualities. Additionally, the detail of the available data is applied to the size of the polygons. The buffer zones for the two study areas were numerically separated as shown in Figure 2:

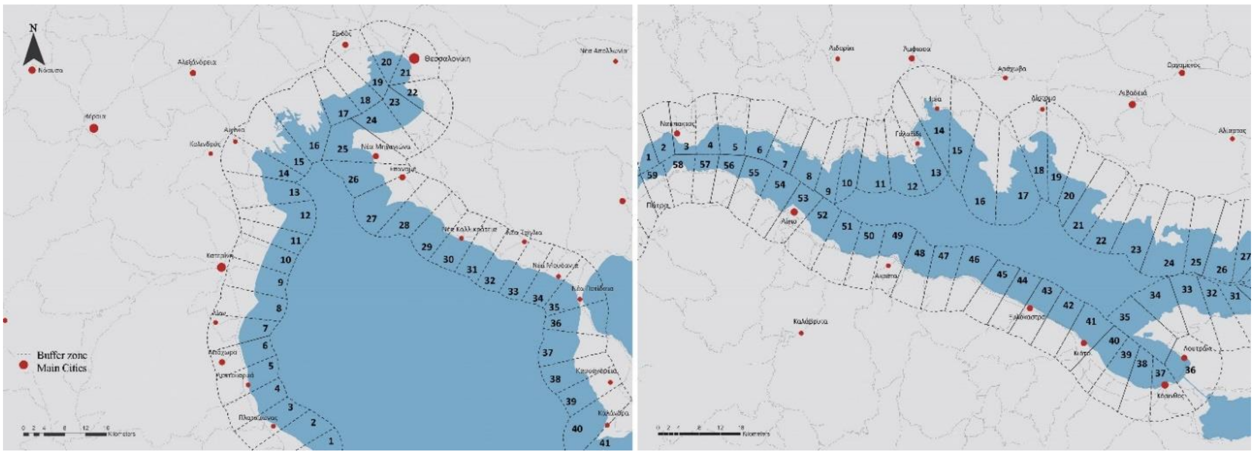


Figure 2: Thermaikos Gulf (left) and the Corinthian Gulf (right) with buffer zone and the numbered polygons used for the assignment of the values per variable

3. RESULTS

3.1 Variables' classification

Regarding geomorphology, no available data for coastal erosion models was retrieved. In order to extract relatively detailed results we used the model of soil erodibility factor that was quite detailed. The soil erodibility factor was used for the different erosion tendencies, with the results shown in Figure 3:

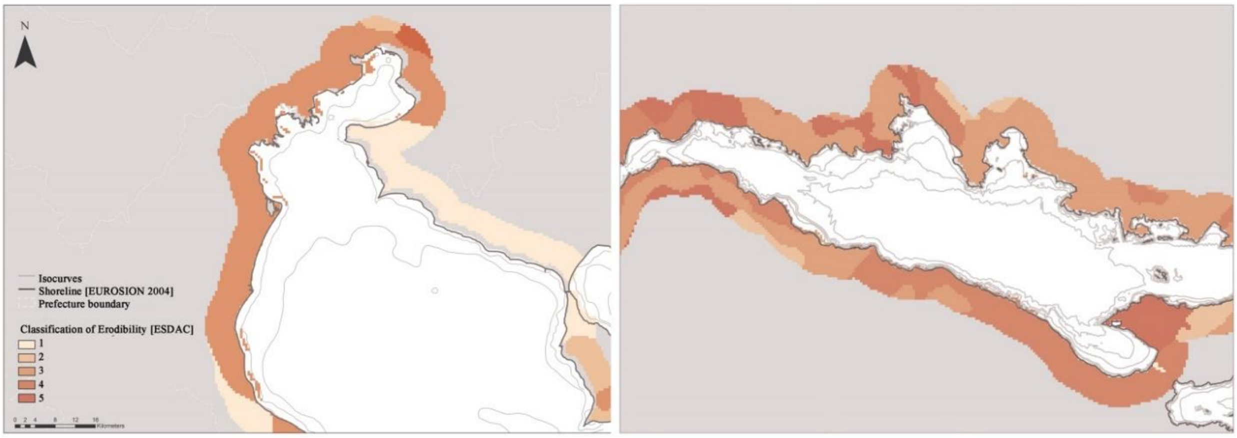


Figure 3: Thermaikos Gulf (left) and the Corinthian Gulf (right) erodibility classification

The shoreline change rate is calculated slightly more than -1.0 m / yr. [Doukakis, 2007] as explained in the Chapter 2.1.2; therefore both study areas belong to the class number 4. The calculation of coastal slope was retrieved with gradient values that have a maximum value for Thermaikos Gulf 0.33%, while for the Corinthian 1.78% (Figure 4).

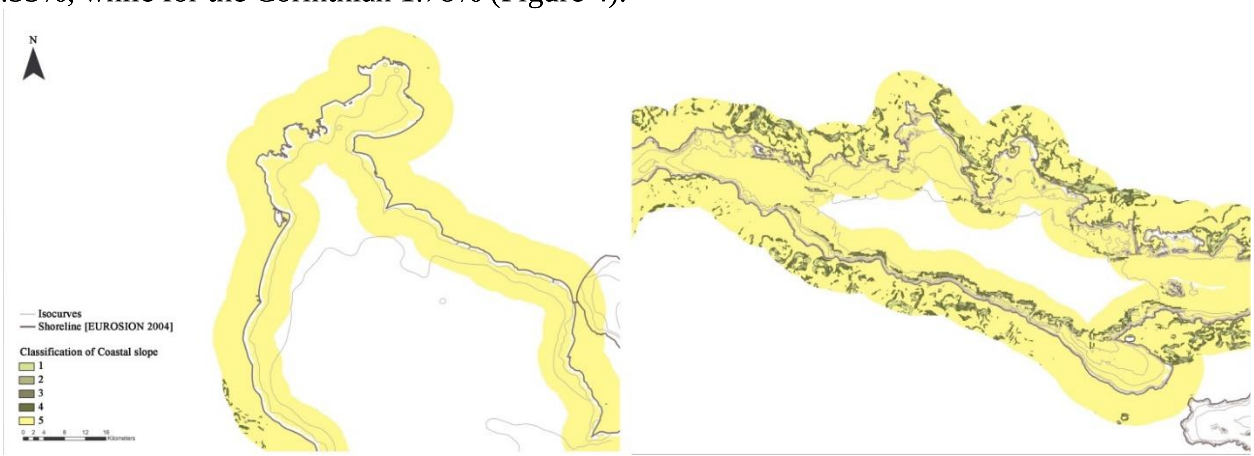


Figure 4: Thermaikos Gulf (left) and the Corinthian Gulf (right) coastal slope classification

The tide value in Greece reaches a maximum height of 0.3 m and is therefore included in the category 5 of very high vulnerability (mean tidal rate less than 1 m.) In the Corinthian Gulf, values for the mean significant wave height vary from 0.095 m up to 0.17 m and in Thermaikos Gulf from 0.157 m up to 0.59 m. The classification in the case of study areas is limited in the category of very low vulnerability, due to values less than 0.7 m. Value 5 is given in regions with average significant wave height greater than 2.8 m. As a result, the value for both study areas is defined as: 1- minimum vulnerability < 0.7 m. In both study areas, the mean sea level rise is classified as with very low vulnerability, since its values are less than 1.8 mm / yr., which is the least compared with the Dwarakish et al., (2009) study.

Providing a specific value for each polygon of the coastline, the CVI has been calculated using Eq. (1). The calculated CVI value for the Thermaikos Gulf varies from 6.20 to 8.62 and for the Corinthian Gulf from 6.67 to 9.04 (Figure 5). The classification was made on a 5-pronged scale to indicate differentiation within the study areas. Also, the distribution of values is made equally in 5 classes per study area rather than comparing the two study areas to each other. As a result, areas of minimum and very high vulnerability are related to the values of the area itself. The average coastal vulnerability value for the Thermaikos Gulf is 7.16 and for the Corinthian Gulf 7.53, while the standard deviation is 1.08 and 0.69 accordingly.

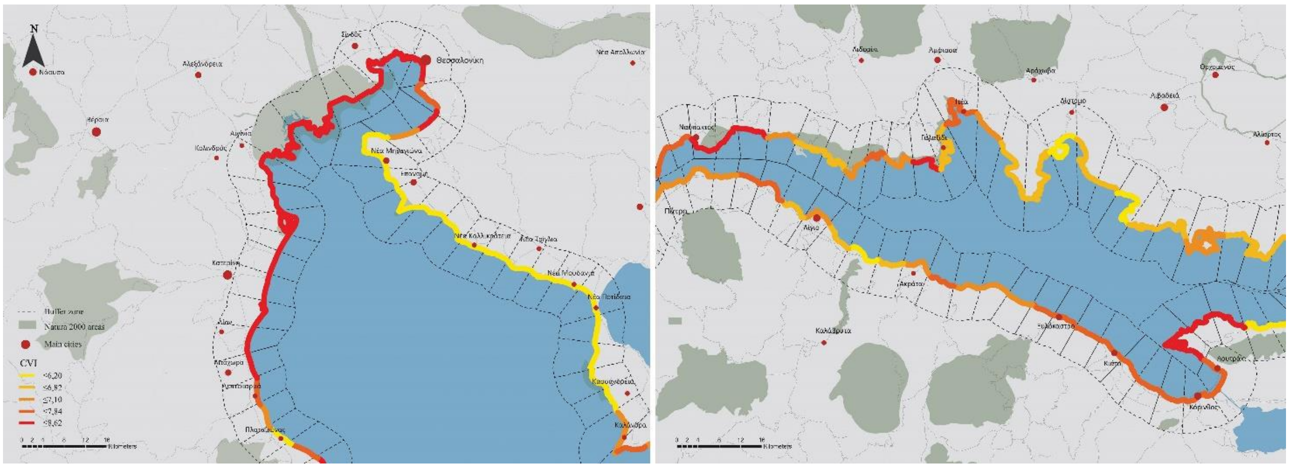


Figure 5: The visualisation of the CVI results for Thermaikos Gulf (left) and the Corinthian Gulf (right) added with the Natura areas and the main cities in the surrounding area

4. DISCUSSION

Regarding GIS and spatial analysis, this study attempted to highlight their valuable contribution in analysing landscapes, especially in cases of changes that are unable to be measured. Presenting various changes as concrete facts through numbers can make a decisive contribution to understanding these phenomena, while at the same time facilitating their transmission to the general public. Through a widen understanding the environmental issues can have a recognition that will inspire collaboration between designers / architects and the public. The coastal vulnerability index in its depiction is an understandable image for the public and gives the opportunity to open the discussion. Therefore, it is proposed to be researched further and in depth, in order to point out the necessary tools for coastal zone protection.

The present study was an attempt to combine a landscape architecture analysis and design process with the realistic impacts of climate change. The methodology though, faced several difficulties in providing an accurate result. The choice of the study areas led to a very large coastline with not much detailed data for variables as the shoreline change rate. The scale of the data was hard to apply to a length of several kilometres, since the available data could not depict the complexity of the coastline. Variables such as geomorphology are appropriate to be used in large scale study areas (Doukakis,

2007), yet the retrieved data did not include information on the coastal area itself providing relative results.

The CVI analysis should probably better be applied in specific coastline parts with higher interest (e.g. highly-densed or nature-protected areas). The land use could also be a variable in order to provide results on the risk level of the coastal areas, adding to the information on vulnerability and providing a social aspect on the final result. Compared to the Dwarakish study (2009) the results extracted give a relatively good response of the study areas in future SLR with lower vulnerability level. The study of Doukakis (2007) extracted higher CVI results for its areas of study in Western Peloponnese than the present study, giving an opportunity to re-examine the present results.

5. CONCLUSIONS

The CVI methodology can support spatial analysis for the coastal zone, providing useful results for landscape architecture projects, policy making and risk management. It can be considered a support for spatial intervention. Areas characterised with ‘high vulnerability’ should be set into priority for protection as a means of prevention from future challenges due to SLR. The scale of the study areas and the data available are crucial to the accuracy of the results and need to be clearly set from the research context. Greece is a country developed by the coast and methodologies as CVI should be able to support its future resilience practices to respond to climate change and SLR.

AKNOWLEDGEMENTS

We thank Konstantinos N. Topouzelis from the Department of Marine Sciences of the University of the Aegean for assistance with material of bathymetric data for this study.

References

1. Vale, J.L., Campanella, J.T. (2005). ‘**The Resilient City: How modern cities recover from disaster’**. Oxford University Press.
2. Gornitz, V.M., White, T.W., and Cushman, R.M. (1991). Vulnerability of the U.S. to future sea-level rise. **In Proceedings of Seventh Symposium on Coastal and Ocean Management.** Long Beach, CA, USA.
3. Doukakis, E. (2005). Coastal vulnerability and risk parameters. **European Water**, *11*(12), pp. 3-7.
4. Dwarakish, G. S., Vinay, S. A., Natesan, U., Asano, T., Kakinuma, T., Venkataramana, K., Jagedeesha Pai B., Babita, M. K. (2009). Coastal vulnerability assessment of the future sea level rise in Udupi coastal zone of Karnataka state, west coast of India. **Ocean & Coastal Management**, 52(9), pp. 467-478.
5. Bergdoll, B., & Nordenson, G. (2011). **’Rising currents: projects for New York’s waterfront’**. Museum of Modern Art.
6. Krestenitis, I., Kombiadou, K., Makris, C., Androulidakis, I., Karampas, T. (2015). **Changes of Sea Level.**
7. Thieler E. R., Hammar-Klose E. S. (1999). *National assessment of coastal vulnerability to Sea-* **Level** *Rise: preliminary results for the U.S. Atlantic coast***.** U.S. Geological Survey, Open-File Report 99–593.
8. Doukakis, E. (2007). Natural Disasters and Coastal Zone. **Conference of Preventing - Managing natural disasters. The Role of the Rural-Surveying Engineer**. Athens, Greece.

REFERENCE EVAPOTRANSPIRATION ASSESSMENT IN CHALKIDIKI REGION UNDER CLIMATE CHANGE USING FOUR EARTH SYSTEM MODELS

P. Koukouli*, P. Georgiou and D. Karpouzos

Dept. of Hydraulics, Soil Science and Agr. Engineering, School of Agriculture, A.U.Th, GR- 54124 Thessaloniki, Macedonia, Greece

*Corresponding author: e-mail: pkoukoul@agro.auth.gr, tel : +306973091293

Abstract

Reference evapotranspiration (ET_o) is an important component in water resources, agricultural and environmental modeling. Thus, the assessment of ET_o changes in response to future climate change has a great impact in agricultural sector. In this study, the effect of climate change on reference evapotranspiration in Northern Greece, was assessed. For this purpose, the climate change scenario RCP4.5 based on four Earth System Models (ESMs) CanESM2, GFDL-ESM2M, HadGEM2-ES and IPSL-CM5A-LR was used for the time period 2081-2100 and for the baseline period (1981-2000). The downscaling was performed using the weather generator ClimGen. Reference evapotranspiration was estimated with the use of the FAO Penman-Monteith equation. Results showed that mean annual reference evapotranspiration is projected to increase (from 6% up to 25%) in response to climate change during 2081-2100 according to the four ESMs. Regarding reference evapotranspiration of the irrigation period (May to September), the increase will be similar to annual, ranging from 5% to 27%. The results indicate that the development of adaptation strategies is necessary for the improvement of agricultural water management and the reduction of climate change impacts on agriculture.

Keywords: Climate change, Reference evapotranspiration, RCPs, Earth system models, ClimGen

1. INTRODUCTION

Climate change is considered a major problem worldwide and its impacts on different aspects of social activity and on the natural environment require careful assessment. Warming of the climate system in recent decades is unequivocal, as is now evident from observations of increases in global average air and ocean temperatures, widespread melting of snow and ice, and rising global sea level (IPCC, 2013). The Intergovernmental Panel on Climate Change (IPCC) Fifth Assessment Report (AR5) projects that the global mean temperature will increase by the late 21st century (2081-2100) relative to 1986-2005, by 1°C to 3.7°C according to RCPs scenarios (IPCC, 2013).

Climate warming observed over the past several decades is associated with changes on hydrological and meteorological systems such as: changing precipitation patterns, intensity and extremes, melting of snow and ice, increasing atmospheric water vapour, increasing evaporation, and changes in soil moisture and runoff. Evapotranspiration is affected by climate change through many processes beginning with the increasing concentration of greenhouse gases, followed by their impacts on large scale circulation and changes to the global distribution of energy and moisture. Other factors that can might affect ET under a changing climate include changing land cover patterns and the CO_2 fertilization effects that can limit the rate of plant transpiration under elevated levels of CO_2 (Guo et al., 2017).

Climate change impact studies are usually based on projections of future climate from General Circulation Models (GCMs) and recently Earth System Models (ESMs) which are converted into reference evapotranspiration (ET_o) using appropriate models. The assessment of ET_o changes is critical in understanding the impacts of anthropogenic climate change on the sector of agriculture. Climate projections show increases in evapotranspiration (ET) over the 21st century because the evaporative demand, or 'reference evaporation', is projected to increase almost everywhere. Changes in ET are controlled by changes in precipitation and radiative forcing, and the changes would, in turn, impact on the water balance of runoff, soil moisture, water in reservoirs, the groundwater table and the salinization of shallow aquifers (IPCC, 2008).

The objective of this study was to investigate the effect of climate change on reference evapotranspiration in Agios Mamas area in Greece for the end (2081-2100) of the running century. For this purpose, data was derived from four ESMs: CanESM2 (Arora et al., 2011), GFDL-ESM2M (Dunne et al., 2013), HadGEM2-ES (Martin et al., 2011) and IPSL-CM5A-LR (Dufresne, 2013) under RCP4.5 climate change scenario using as a baseline period 1981-2000. The selected models are the current generation of models used in IPCC AR5. The models performance has shown a good capability in representing the observed behavior in past climate (IPCC, 2013). Although these models can be considered a sufficient tool for future projections, no individual model clearly emerges as 'the best' overall. For this reason, a number of models with different grid resolutions, was selected for increasing the reliability of the future projections. Based on the data taken from the climate models, the downscaling of daily climate variables was performed with the use of the weather generator ClimGen (Stöckle and Nelson, 1999) for the generation of synthetic time series which depict the future change of the climate variables. Future reference evapotranspiration was estimated using the FAO Penman-Monteith equation for all climate models. The annual and irrigation period (May to September) ET_o for period 2081-2100 was compared with the baseline period for the assessment of climate change impacts according to the different climate models used.

2. MATERIALS AND METHODS

2.1 Study area and data

The impact of climate change on reference evapotranspiration was studied in Agios Mamas area in the prefecture of Chalkidiki in Northern Greece which is located between 40°15' latitude and 23°20' longitude (Figure 1). The climate in the Prefecture of Chalkidiki is mainly Mediterranean, with hot summers and cool winters. The study area is agricultural and meteorological data that were used to generate the climate change scenarios were provided by station. Furthermore, the station of Agios Mamas is located in low altitude and, therefore, describes better the irrigation area. The time series data used in this work were precipitation (mm), wind speed (m/s), actual sunshine duration (hrs), mean temperature (^oC), and relative humidity (%) for the baseline period 1981-2000 at daily time step.

2.2 RCP scenarios

In climate research, emission scenarios are used as input to climate models to make projections of possible future climate change. Emission scenarios provide plausible descriptions of how the future may evolve with respect to a range of variables including socio-economic change, technological change, energy and land use and emissions of greenhouse gases and air pollutants (van Vuuren et al., 2011).

The Representative Concentration Pathways scenarios (RCPs) are the product of an innovative collaboration between integrated assessment modelers, climate modelers, terrestrial ecosystem modelers and emission inventory experts. The four RCPs together span the range of year 2100 radiative forcing values found in the open literature, from 2.6 to 8.5W/m^2 (van Vuuren et al., 2011) and are supplemented with extensions (Extended Concentration Pathways, ECPs), which allow climate modeling experiments through the year 2300. The above scenarios are named after the

approximate radiative forcing (RCP2.6, RCP4.5, RCP6 and RCP8.5) relative to the pre-industrial period achieved either in the year 2100, or at stabilization after 2100 (van Vuuren et al., 2011). They include one mitigation scenario leading to a very low forcing level (RCP2.6), two medium stabilization scenarios (RCP4.5 and RCP6) and one very high baseline emission scenario (RCP8.5) (van Vuuren et al., 2011). According to the IPCC (2013) the atmospheric concentration of carbon dioxide (CO_2) in the year 2100 is predicted to reach 490 ppm, 650 ppm, 850 ppm and 1370 for pathways RCP2.6, RCP4.5, RCP6 and RCP8.5, respectively. In this study, the moderate scenario RCP4.5 is used for the assessment of reference evapotranspiration under climate change.

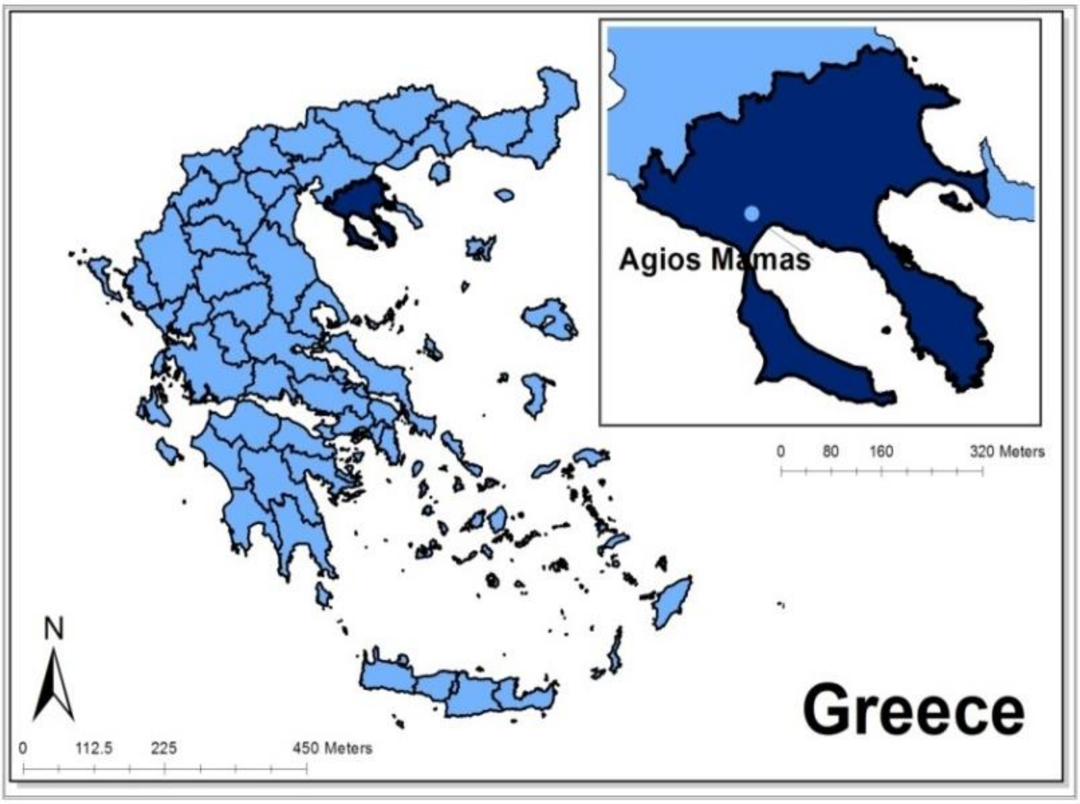


Figure 1: The location of Agios Mamas in Northern Greece

2.3 Climate models

Climate models are the primary tools for investigating the response of the climate system to various forcings, for making climate predictions on seasonal to decadal time scales and for making projections of future climate over the coming century and beyond (IPCC, 2013). Climate models have seen a number of improvements with developing improved physical process descriptions, introducing new model components and the improving model resolution. These models allow for policy-relevant calculations such as the carbon dioxide (CO_2) emissions compatible with a specified climate stabilization target (IPCC, 2013). Many models have been extended into Earth System Models (ESMs) by including the representation of biogeochemical cycles important to climate change. ESMs are the current state-of-the-art climate models and are the most comprehensive tools available for simulating past and future response of the climate system to external forcing, in which biogeochemical feedbacks play an important role (IPCC, 2013). Climate model simulations for the IPCC Fifth Assessment Report (AR5) are based on the fifth phase of the Coupled Model Intercomparison Project (CMIP5) which incorporates the latest versions of climate models, the Earth System Models, and focuses on the new scenarios RCPs.

In this study, CanESM2, GFDL-ESM2M, HadGEM2-ES and IPSL-CM5A-LR models under the newly developed RCPs were used for assessing climate change impact. CanESM2 is an Earth System Model developed at the Canadian Centre for Climate Modelling and Analysis (CCCma). The atmospheric component of CanESM2 uses the spectral transform method with T63 resolution in the

horizontal (2.81 long x 2.79 lat) and has 35 vertical levels and the ocean component has a horizontal resolution of 1.418 x 0.948 (long x lat) (Arora et al., 2011). GFDL-ESM2M is a global coupled climate-carbon Earth System Model developed at the National Oceanic and Atmospheric Administration (NOAA)/Geophysical Fluid Dynamics Laboratory (GFDL). The model, on land, includes a revised land model to simulate competitive vegetation distributions and functioning, including carbon cycling among vegetation, soil, and atmosphere and in the ocean, new biogeochemical algorithms including phytoplankton dynamics (Dunne et al., 2013). This model has an atmospheric horizontal resolution of 2.5 x 2.0 (long x lat) and its ocean component has a horizontal resolution of 1.0 x 1.0 (long x lat). The HadGEM2-ES of the Met Office Unified Model (MetUM) includes atmosphere, ocean and sea-ice components and an Earth-System (ES) component which includes dynamic vegetation, ocean biology and atmospheric chemistry (Martin et al., 2011). HadGEM2-ES has an atmospheric horizontal resolution of 1.875 x 1.25 (long x lat) that equates to about 140 km at mid-latitudes. The ocean component has a horizontal resolution of 1.0 x 1.0, with latitudinal resolution increasing smoothly from 30 N/S to 0.33 at equator. The IPSL-CM5A model developed at Institute Pierre Simon Laplace (IPSL) is an Earth System Model (ESM). This model includes an interactive carbon cycle, a representation of tropospheric and stratospheric chemistry, and a comprehensive representation of aerosols (Dufresne, 2013). IPSL-CM5A-LR is a low resolution version of IPSL-CM5A model with atmospheric horizontal resolution of 3.75 x 1.89 (long x lat).

2.4 Downscaling with weather generator - ClimGen

There is a great need to develop downscaling methods which establish relationships between local weather variables and the large-scale ESMs' outputs for climate change impact assessment. Stochastic weather generators are statistical models used to produce synthetic weather time series, which are expected to be statistically similar to the observed weather time series for a location of interest (Georgiou and Karpouzos, 2017; Koukouli et al., 2018). They are usually combined with hydrological and environmental models for water resources and environmental management and more often as downscaling tools to produce high-resolution climate change projections (Chen and Brissete, 2014). The weather generators compared to other statistical downscaling methods have the advantage of producing an ensemble of equiprobable realizations of climate change projections for analyzing risk-based environmental impacts (Chen and Brissete, 2014). ClimGen (Stöckle and Nelson, 1999) is a daily time step stochastic model that generates daily precipitation (mm), maximum and minimum temperature (^oC), solar radiation (MJ/m^2day), maximum and minimum relative humidity (%) and wind speed (m/s) data series which preserve the statistical characteristics of the historical weather data. The model requires inputs of daily series of these weather variables to calculate the parameters used in the generation process for any length of period at a location of interest. ClimGen has produced promising results for the generation of weather data for various climatic conditions (Stöckle and Nelson, 1999).

2.5 Estimation of reference evapotranspiration

Given the likelihood of future change in the global hydrological cycle, clear understanding of ET_o dynamics is vital for the assessment of impacts of future climate change on water and subsequent implications for the agricultural sector. Reference evapotranspiration (ET_o) is the evapotranspiration from a crop with specific characteristics and which is not short of water (McMahon et al., 2013). Among the methods available to estimate ET_o, the Food and Agricultural Organisation of the United Nations (FAO) recommends the use of the Penman-Monteith equation (Allen et al., 1998) which is known as FAO Penman-Monteith method, as it directly incorporates the relevant meteorological variables which control evapotranspiration. It is often referred to as a combinational method, as it combines the energy balance and mass transfer components of evapotranspiration, and takes into account vegetation-dependent processes such as aerodynamic and surface resistances (Guo et al., 2017). This method is the most reliable where sufficient meteorological data exist, but that in certain climatological environments and where empirical calibrations are robust, less data-intensive methods can also provide reliable approximations of ET_o (Kingston et al., 2009). The FAO Penman-Monteith

equation is based on temperature, net radiation, wind speed and relative humidity. Adopting the characteristics of a hypothetical reference crop (height=0.12 m, surface resistance=70 s/m and albedo=0.23), FAO Penman-Monteith equation is described as follows (Allen et al., 1998):

$$ET_o = \frac{0.408 \cdot \Delta \cdot \left(R_n - G\right) + \gamma \cdot \frac{900}{T_{mean} + 273} \cdot u_2 \cdot \left(e_s - e_a\right)}{\Delta + \gamma \cdot \left(1 + 0.34 \cdot u_2\right)} \tag{1}$$

where ET_o is the reference evapotranspiration, (mm/day), R_n is the net radiation (MJ/m^2day), G is the soil heat flux (MJ/m^2day), γ is the psychrometric constant ($kPa/^oC$), e_s is the saturation vapour pressure (kPa), e_a is the actual vapour pressure (kPa), Δ is the slope of the saturation vapour pressure - temperature curve ($kPa/^oC$), T_{mean} is the mean daily air temperature (^oC) and u_2 is the mean daily wind speed at 2 m (m/s).

3. RESULTS AND DISCUSSION

This study was focused on the impact of climate change on the reference evapotranspiration (ET_o) of Agios Mamas in Northern Greece. For this purpose, weather data from CanESM2, GFDL-ESM2M, HadGEM2-ES and IPSL-CM5A-LR Earth System Models under the climate change scenario RCP4.5 were used for the climate change period 2081-2100 and for the baseline period (1981-2000).

Based on the data derived from the four climate models, the downscaling of a 20-year data set (1981-2000) of daily climate variables including precipitation (Pr), maximum and minimum temperature (T_{max}, T_{min}), solar radiation (R_s), maximum and minimum relative humidity (RH_{max}, RH_{min}), and wind speed (u_2) performed using the weather generator ClimGen for the generation of synthetic time series which depict the future change of the climate variables. The change between the baseline period and the period of climate change 2081-2100 was calculated for the different climate variables. According to that change, the historic data series of the study area was perturbed. The perturbed time series then was used by ClimGen for the generation of an ensemble of synthetic time series of the weather variables which preserve the statistic characteristics of the historic time series. The generated and observed weather data series were compared in order to confirm the statistical consistency. Finally, this ensemble of synthetic time series of climate variables was used for the estimation of an ensemble of reference evapotranspiration (mean annual and irrigation period) time series of the study area.

First the change in temperature is analyzed since it is a critical variable for the estimation of evapotranspiration. In Table 1, the mean annual temperature and mean temperature during the irrigation period of Agios Mamas under RCP4.5, based on CanESM2, GFDL-ESM2M, HadGEM2-ES and IPSL-CM5A-LR models, for the period of climate change 2081-2100 and for the baseline period 1981-2000, are presented. The models' projections indicate that mean annual temperature will increase by the end of the 21st century.

The predicted increases during 2081-2100 will be by 3.04^{o}C (CanESM2), 1.08^{o}C (GFDL-ESM2M), 3.83^{o}C (HadGEM2-ES) and 3.39^{o}C (IPSL-CM5A-LR) compared to the baseline period 1981-2000. The rise in temperature of the irrigation period is projected to be by 3.89^{o}C (CanESM2), 1.69^{o}C (GFDL-ESM2M), 4.62^{o}C (HadGEM2-ES) and 3.29^{o}C (IPSL-CM5A-LR). The greatest rise, both in annual and irrigation period temperature, is projected by HadGEM2-ES model while the lowest by GFDL-ESM2M. It is observed that the increase in mean temperature during the irrigation period will be slightly greater compared to the annual, according to the climate models with the exception of IPSL-CM5A-LR.

Box plots of mean temperature change (^{o}C) under RCP4.5 projected by the four different climate models are shown in Figure 2 concerning a) annual and b) irrigation period temperature. The increase

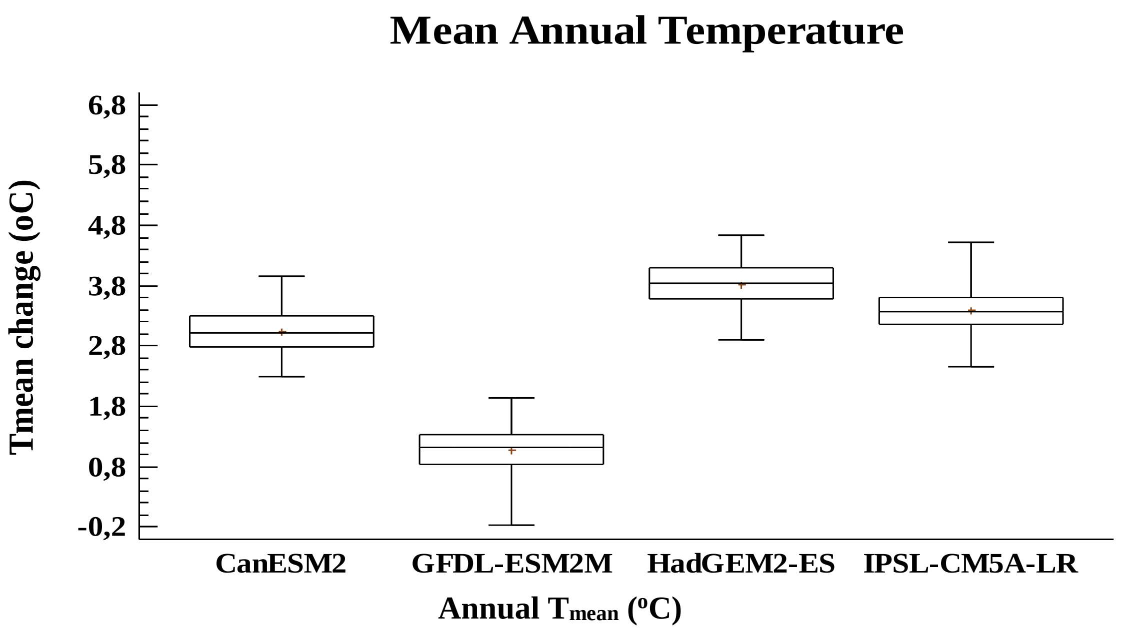
in mean annual and irrigation period temperature, projected by the models is obvious according to the box plots. HadGEM2-ES model has the greatest maximum and mean value among all models, indicating that the above model gives the highest increase in annual and irrigation period temperature. The lowest maximum and mean value is observed according to GFDL-ESM2M showing the lowest rise in annual and during the irrigation period temperature among the models used. According to the box plots analysis, the largest spread in distribution of the mean temperature is observed for GFDL-ESM2M climate model for both annual and irrigation period.

Table 1: Differences in mean annual and irrigation period temperature (ºC) of Agios Mamas according to CanESM2, GFDL-ESM2M, HadGEM2-ES and IPSL-CM5A-LR under RCP 4.5 during 2081-2100 in relation to 1981-2000

Mean Temperature (ºC)						
Historical		**RCP4.5 2081-2100**				
Ag. Mamas		**Climate Models**				
1981-2000		**CanESM2**	**GFDL-ESM2M**	**HadGEM2-ES**	**IPSL-CM5A-LR**	
Annual	**14.42**	**17.46**	**15.50**	**18.25**	**17.81**	
	ΔT_{mean}	3.04	1.08	3.83	3.39	
Irrigation period	**21.99**	**25.88**	**23.68**	**26.61**	**25.28**	
	ΔT_{mean}	3.89	1.69	4.62	3.29	

In Table 2, the mean annual and irrigation period reference evapotranspiration of the study area under RCP4.5 projected by the climate models CanESM2, GFDL-ESM2M, HadGEM2-ES and IPSL-CM5A-LR for the period of climate change 2081-2100 and for the baseline period (1981-2000), are depicted. It can be noted that all climate models predict an increase of mean annual reference evapotranspiration during the period 2081-2100 compared to the historical period. CanESM2 projects a rise in annual ET_o by 181 mm, GFDL-ESM2M 60 mm, HadGEM2-ES 262 mm and IPSL-CM5A-LR 195 mm. HadGEM2-ES gives the highest increase in annual ET_o of 25% while GFDL-ESM2M predicts the lowest increase of 6%. CanESM2 and IPSL-CM5A-LR give moderate values of ET_o increase of 17% and 18%, respectively. As regards to reference evapotranspiration of the irrigation period, the increase will be by 123 mm, 32 mm, 182 mm and 113 mm according to CanESM2, GFDL-ESM2M, HadGEM2-ES and IPSL-CM5A-LR models, respectively. HadGEM2-ES projects the highest increase in ET_o of the irrigation period of 27% whereas GFDL-ESM2M predicts the lowest increase of 5%. CanESM2 and IPSL-CM5A-LR models give moderate values of increase (18% and 17%).

In Figure 3 the box plots of a) annual and b) irrigation period reference evapotranspiration change (%) for climate change period in relation to baseline period based on the four climate models are presented. The greatest mean and maximum value is observed under HadGEM2-ES whereas the lowest under GFDL-ESM2M model for both annual and irrigation period. CanESM2 and IPSL-CM5A-LR have similar mean values indicating that the above models show similar rise in future annual and irrigation period reference evapotranspiration for 2081-2100 in relation to the historical period. All models show quite similar spread in the distribution of their values in mean annual ET_o. Additionally, regarding ET_o for the irrigation period, it can be noted that the largest spread in distribution is observed for GFDL-ESM2M and the lowest for HadGEM2-ES while the rest climate models show similar spread.



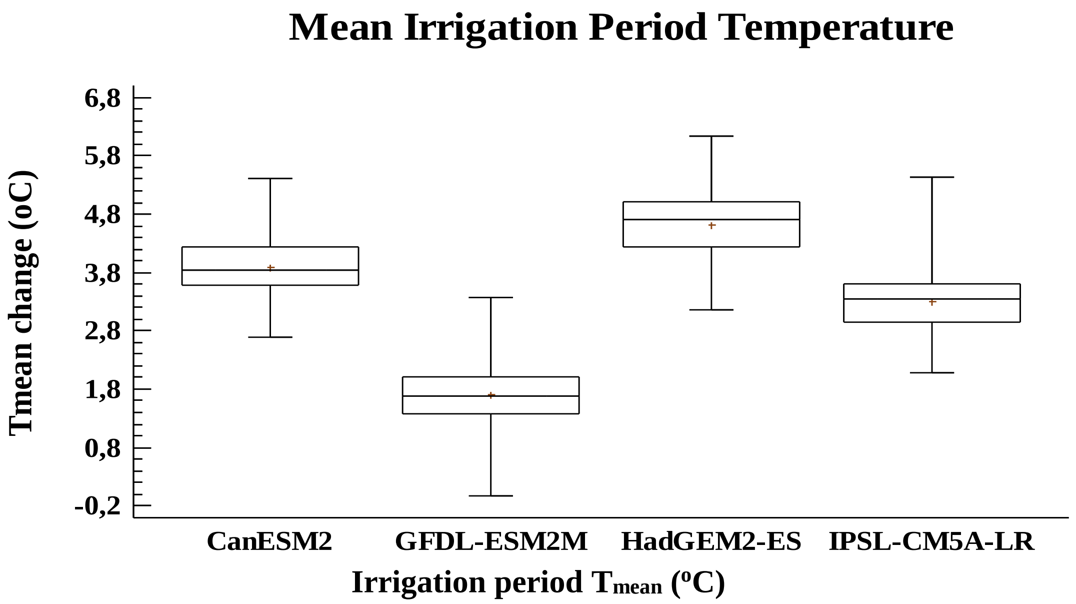
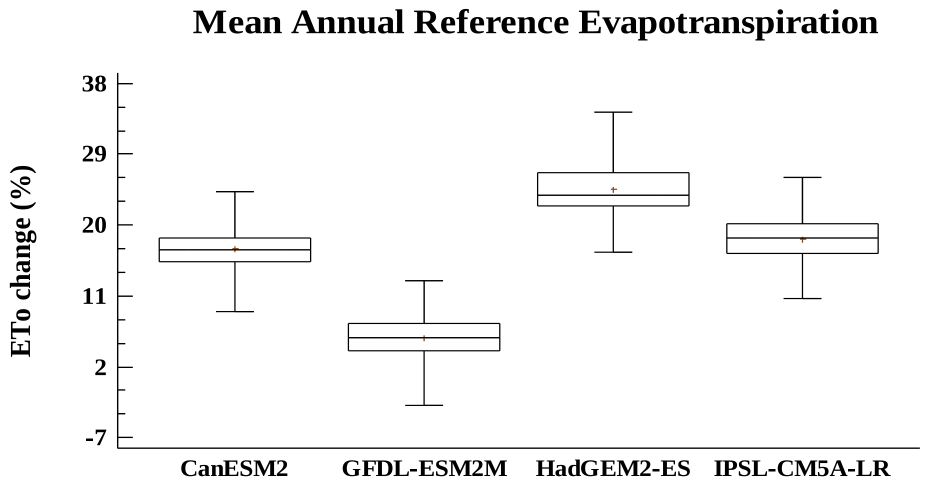


Figure 2: Box plots of mean a) annual and b) irrigation period temperature change (ºC) of Agios Mamas according to CanESM2, GFDL-ESM2M, HadGEM2-ES and IPSL-CM5A-LR under RCP 4.5 during 2081-2100 relative to 1981-2000

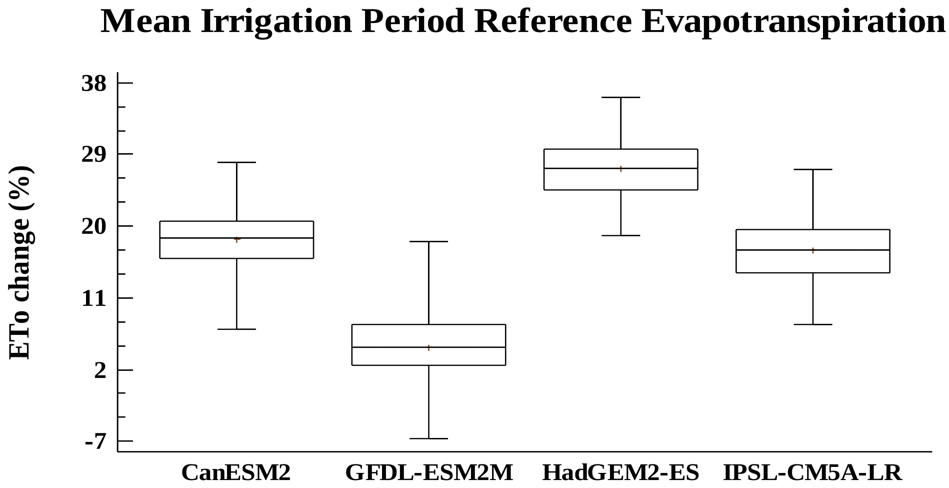
The box plots of reference evapotranspiration change (Figure 3) have similar pattern with those of temperature change (Figure 2) for both annual and irrigation period. The greatest increases are recorded for HadGEM2-ES while the lowest under GFDL-ESM2M for both ET_o and temperature. Additionally, CanESM2 and IPSL-CM5A-LR models show moderate values of increase in ET_o as well as in temperature. The above confirm that the rise in reference evapotranspiration is controlled by the increase of temperature in the future. With higher temperatures, the water-holding capacity of the atmosphere increases resulting in reference evaporation increase. Additionally, CO_2 enrichment of the atmosphere can increase plant growth, resulting in increased leaf area, and thus increased transpiration. There were differences in future projections of temperature and ET_o among the selected climate models, which seem to not be related only with the model resolution. Thus, a number of models with different spatial and meteorological characteristics should be used for increasing the reliability of the results.

Table 2: Differences in mean annual and irrigation period reference evapotranspiration (mm) of Agios Mamas according to CanESM2, GFDL-ESM2M, HadGEM2-ES and IPSL-CM5A-LR under RCP 4.5 during 2081-2100 in relation to 1981-2000

Mean Reference Evapotranspiration (mm)						
Historical Ag. Mamas 1981-2000		RCP4.5 2081-2100 Climate Models				
		CanESM2	GFDL-ESM2M	HadGEM2-ES	IPSL-CM5A-LR
Annual	**1066**	**1247**	**1126**	**1328**	**1261**
	ΔET_o	181	60	262	195
	%	17	6	25	18
Irrigation period	**666**	**789**	**698**	**848**	**779**
	ΔET_o	123	32	182	113
	%	18	5	27	17



a) Annual ET_o (%)



b) Irrigation period ET_o (%)

Figure 3: Box plots of a) annual and b) irrigation period reference evapotranspiration change (%) of Agios Mamas according to CanESM2, GFDL-ESM2M, HadGEM2-ES and IPSL-CM5A-LR under RCP 4.5 during 2081-2100 relative to 1981-2000

4. CONCLUSIONS

In this study, the effects of climate change on the reference evapotranspiration (ET_o) of Agios Mamas in Northern Greece for the end of the 21st century (2081-2100), were assessed. The climate change projections were done according to CanESM2, GFDL-ESM2M, HadGEM2-ES and IPSL-CM5A-LR Earth System Models under RCP4.5 climate change scenario. The results suggested that mean annual temperature is projected to increase in 2081-2100 compared to 1981-2000. The rise in mean annual temperature will, in turn impact on mean annual reference evapotranspiration which will increase from 6% to 25% considering the climate model used. During the irrigation period, the rise in temperature will be slightly greater compared to annual while the increase is projected to be similar regarding ET_o, ranging from 5% to 27%. There were differences in temperature and reference evapotranspiration increase among the four climate models showing great variation for the ensemble synthetic time series. This indicates that the use of a number of climate models is required in climate change studies for increasing the reliability of the future projections. The changes in reference evapotranspiration in response to the future climate change will have major impacts on the agricultural sector. As a result, the estimation of reference evapotranspiration in climate change research is critical in the development of adaptation strategies regarding irrigation planning and water resources management.

References

1. Allen R.G., L.S. Pereira, D. Raes and M. Smith. (1998). 'Crop evapotranspiration guidelines for computing crop water requirements'. **FAO Irrigation and Drainage Paper**, No. 56. Rome, Italy.
2. Arora V.K., J.F. Scinocca, G.J. Boer, J.R. Christian, K.L., Denman, G.M. Flato, V.V. Kharin, W.G. Lee and W.J. Merryfield. (2011). 'Carbon emission limits required to satisfy future representative concentration pathways of greenhouse gases'. **Geophysical Research Letters**, Vol. 38, L05805, doi:10.1029/2010GL046270.
3. Chen J. and F.P. Brissete. (2014). 'Comparison of five stochastic weather generators in simulating daily precipitation and temperature for the Loess Plateau of China'. **International Journal of Climatology**, Vol. 34, pp. 3089-3105.
4. Dufresne J.-L., M.-A. Foujols, S. Denvil, A. Caubel, O. Marti, O. Aumont, Y. Balkanski, S. Bekki, H. Bellenger, R. Benshila, S. Bony, L. Bopp, P. Braconnot, P. Brockmann, P. Cadule, F. Cheruy, F. Codron, A Cozic, D. Cugnet, N. de Noblet, J.-P. Duvel, C. Ethé, L. Fairhead, T. Fichefet, S. Flavoni, P. Friedlingstein, J.-Y Grandpeix, L. Guez, E. Guilyardi, D. Hauglustaine, F. Hourdin, A. Idelkadi, J. Ghattas, S. Joussaume, M. Kageyama, G. Krinner, S. Labetoulle, A. Lahellec, M.-P. Lefebvre, F. Lefevre, C. Levy, Z.X. Li, J. Lloyd, F. Lott, G. Madec, M. Mancip, M. Marchand, S. Masson, Y. Meurdesoif, J. Mignot, I. Musat, S. Parouty, J. Polcher, C. Rio, M. Schulz, D. Swingedouw, S. Szopa, C. Talandier, P. Terray, N. Viony and N. Vuichard. (2013). 'Climate change projections using the IPSL-CM5 Earth System Model: from CMIP3 to CMIP5'. **Climate Dynamics**, Vol. 40, pp. 2123-2165.
5. Dunne J.P., J.G. John, E. Shevliakova, R.J. Stouffer, J.P. Krasting, S.L. Malyshev, P.C.D. Milly, L.T. Sentman, A.J. Adcroft, W. Cooke, K.A. Dunne, S.M. Griffies, R.W. Hallberg, M.J. Harrison, H. Levy, A.T. Wittenberg, P.J. Phillips and N. Zadeh. (2013). 'GFDL's ESM2 Global Coupled Climate - Carbon Earth System Models. Part II: Carbon system formulation and baseline simulation characteristics'. **Journal of Climate**, Vol. 26, pp. 2247-2267.
6. Georgiou P.E. and D.K. Karpouzos. (2017). 'Optimal irrigation water management for adaptation to climate change'. **International Journal of Sustainable Agricultural Management and Informatics**, Vol. 3(4), pp. 271-285.
7. Guo D., S. Westra and H.R. Maier. (2017). 'Sensitivity of reference evapotranspiration to changes in climate variables for different Australian climatic zones'. **Hydrology and Earth System Sciences**, Vol. 421, pp. 2107-2126.

8. IPCC. (2008). Climate Change and Water. In B.C. Bates, Z.W. Kundzewicz, S. Wu and J.P. Palutikof (eds.), Technical paper if the Intergovernmental Panel on climate change. IPCC Secretariat, Geneva, Switzerland.

9. IPCC. (2013). Climate Change 2013: The physical science basis. In T.F. Stocker, D. Qin, G.-K. Plattner, M. Tignor, S.K. Allen, J. Boschung, A. Nauels, Y. Xia, V. Bex and P.M. Midgley (eds.), Contribution of Working Group I to the Fifth Assessment Report of the Intergovernmental Panel on Climate Change. Cambridge, United Kingdom and New York, NY, USA.

10. Kingston G., M.C. Todd, R.G. Taylor, J.R. Thompson and N.W. Amell. (2009). 'Uncertainty in the estimation of reference evapotranspiration under climate change'. **Geophysical Research Letters**, Vol. 36, L20403, doi:10.1029/ 2009GL040267.

11. Koukouli P., P. Georgiou and D. Karpouzos. (2018). 'Assessing the hydrological effect of climate change on water balance of a River Basin in Northern Greece'. **International Journal of Agricultural and Environmental Information Systems** (Accepted for publication-in press).

12. Martin G.M., N. Bellouin, W.J. Collins, I.D. Culverwell, P.R. Halloran, S.C. Hardiman, T.J. Hinton, C.D. Jones, R.E. McDonald, A.J. McLaren, F.M. O'Connor, M.J. Roberts, J.M. Rodriguez, S. Woodward, M.J. Best, M.E. Brooks, A.R. Brown, N. Butchart, C. Dearden, S.H. Derbyshire, I. Dharssi, M. Doutriaux-Boucher, J.M. Edwards, P. D. Falloon, N. Gedney, L.J. Gray, H.T. Hewitt, M. Hobson, M.R. Huddleston, J. Hughes, S. Ineson, W.J. Ingram, P.M. James, T.C. Johns, C.E. Johnson, A. Jones, C.P. Jones, M.M. Joshi, A.B. Keen, S. Liddicoat, A.P. Lock, A.V. Maidens, J.C. Manners, S.F. Milton, J.G.L. Rae, J.K. Ridley, A. Sellar, C.A. Senior, I.J. Totterdell, A. Verhoef, P.L. Vidale and A. Wiltshire. (2011). 'The HadGEM2 family of Met Office Unified Model climate configurations'. **Geoscientific Model Development**, Vol. 4, pp. 723-757.

13. McMahon T.A., M.C. Peel, L. Lowe, R. Srikanthan and T.R. McVicar. (2013). 'Estimating actual, potential reference crop and pan evaporationusing tandard meteorological data: a pragmatic synthesis'. **Hydrology and Earth System Sciences**, Vol. 17, pp. 1331-1363.

14. Stöckle C.O. and R.L. Nelson. (1999). ClimGen: A weather generator program. Biological Systems Engineering Department, Washington State University, Pullman, WA.

15. van Vuuren D.P., J. Edmonds, M. Kainuma, K. Riahi, A. Thomson, K. Hibbard, G.C. Hurtt, T. Kram, V. Krey, J.-F. Lamarque, T. Masui, M. Meinshausen, N. Nakicenovic, S.J. Smith and S.K. Rose. (2011). 'The representative concentration pathways: an overview'. **Climatic Change,** Vol. 109, pp. 5-31.

ASSESSING THE TEMPERATURE CHANGES OVER EUROPE FOR THE 21ST CENTURY USING A REGIONAL CLIMATE MODEL

I. Sofiadis[1]*, E. Katragkou[1], V. Pavlidis[1], S. Kartsios[1], K. Tsigaridis[2], M. Karypidou[1], D. Melas[3]

[1]Department of Meteorology and Climatology,
School of Geology, Aristotle University of Thessaloniki, 54124 Greece,
[2]NASA Goddard Institute for Space Studies, New York, NY 10025, USA
[3] Laboratory of Atmospheric Physics, School of Physics, Aristotle University of Thessaloniki, 54124 Greece

*Corresponding author: e-mail: sofiadis@geo.auth.gr

Abstract
In the framework of the 7th FP project REQUA-"Regional climate-air quality interactions", we assessed climate change for the 21st century over Europe. Five regional climate modelling systems from the Euro-CORDEX initiative were used, covering the time period from 1986 to 2100 with a spatial resolution of 50 Km. The selected future scenario was the Representative Concentration Pathway RCP8.5. The regional climate model simulations were forced by different Global Climate Models and compared to available observational data, to estimate the models' biases. The analysis highlights the ability of regional climate models to properly simulate the European climate as well as an expected average temperature increase for Europe until the end of the 21st century. Temperature trends are estimated to be higher in southern Europe mainly in the summer. Geospatial information on climate change is extremely useful for studies focusing on the impact of climate change on different sectors including protection of the environment, adaptation and mitigation policies.

Keywords: Climate models, Euro-CORDEX, Climate projections, Climate change

1. INTRODUCTION

Climate change has become one of the most urgent challenges for today's society**.** According to WMO (Weather Meteorological Organization), climate change refers to a statistically significant variation in either the mean state of the climate or in its variability, persisting for an extended period (typically decades or longer). Climate change may be due to natural internal processes or external forcings, or to persistent anthropogenic changes in the composition of the atmosphere or in land use.

Climate models (numerical representations of the climate system) play a catalytic role in studying and simulating climate. They solve extremely complex equations on a grid of spatial discrete points with various arithmetic methods (Neelin, 2010). In essence, the result of calculations for a field on a grid point refers to the mean value of the field in the grid box. Modern climatic models, thanks to the strengthening of supercomputers, incorporate in their equations many natural processes that take place between the elements of the climate system (IPCC, 2014).

Climate models are distinguished in global and regional depending on whether they cover the entire Earth or only a limited area. Global models are characterized by low spatial resolution (the horizontal distance between the grid points) and simulate only large scale spatial phenomena (Hong et al., 2014). The need for study of regional climate has led scientists to the dynamic downscaling of global models.

In dynamic downscaling, the grid with the highest spatial resolution is placed in the grid with lowest resolution and driven by it at its lateral boundaries (Laprise, 2008). Furthermore, regional climate models due to their higher spatial resolution (~11km at continental level), are capable of simulating natural processes with higher accuracy, as opposed to global models (Giorgi et al., 2015). However, there are natural processes characterized by a very small spatial scale (e.g convection) and their assessment through regional models is made using empirical formulas called parameterizations (IPCC, 2014).

The assessment of the future climate through climate models (climate projection) requires the choice of a climate scenario. According to IPCC, as climate scenario is called a plausible and often simplified representation of the future climate, based on an internally consistent set of climatological relationships that has been constructed for explicit use in investigating the potential consequences of anthropogenic climate change, often serving as input to impact models. The most pessimistic scenario of the newest version of IPCC scenarios is RCP8.5 which, among other things, estimates that the world's population will almost double and humanity will rely mainly on fossil fuels by the end of the 21st century (Riahi et al., 2007).

Because of the many uncertainties that arise from the different scenarios, the parameterizations, the model structures as well as the physical climate variability, there is a need for coordination to study the regional climate. Euro-CORDEX initiative (www.euro-cordex.net) includes a suite of experiments and provides the scientific community with a controlled framework for models' evaluation and regional climate projections.

Five regional climate models (CCLM4, RCA4, REMO2009, RACMO22E, ALADIN53) with different configurations and physical parameterizations are implemented in this work, all performed within the framework of Euro-CORDEX. The aim of this study is to evaluate the above regional climate models as to their credibility and to identify in which regions and to what extent is there a strong signal of the temperature change by the end of the century.

2. DATA&METHODOLOGY

Mean surface temperature is analyzed for the time period 1986-2100. The simulations cover the Euro-CORDEX domain (Figure 1) with a spatial resolution of 50 km. All simulations use the same Representation Concentration Scenario (RCP8.5) for the climate projection (2006-2099) but driven by different Global Circulation Model (GCM) (Table 1).

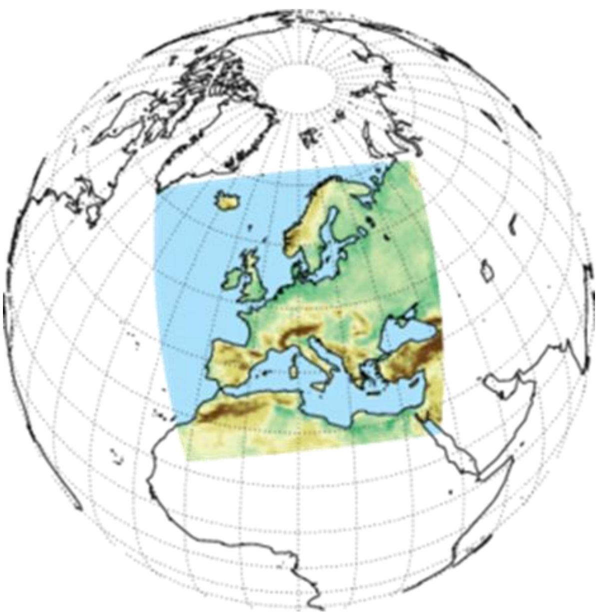


Figure 1: Euro-CORDEX domain.

Table 3: In the first column (left) are presented the Regional Climate Models (RCMs) used in this study. In the middle column are the Institutes where simulations performed and in the right column are the Global Circulation Models (GCMs) forcing the RCMs.

RCM	Institute	GCM
RCA4	Meteo-France/ National Center for Meteorological Research	CCCMa-CanESM2
REMO2009	Helmholtz-Zentrum Geesthacht, Climate Service Center, Max Planck Institute for Meteorology	MPI-M-MPI-ESM-MR
ALADIN53	Meteo-France/ National Center for Meteorological Research	CNRM-CERFACS-CNRM-CM5
RACMOE22	Royal Netherlands Meteorological Institute, De Bilt, The Netherlands	ICHEC-EC-EARTH
CCLM4	Climate Limited-area Modelling Community (CLM-Community)	MPI-M-MPI-ESM-LR

In order to evaluate models' simulations, we use E-OBS version 15.0 observational data set (www.ecad.eu) which are available on a 50km rotated pole grid in order to have almost equal areas over Europe. The RCM grid was interpolated to the EOBS grid, using the nearest neighbor method.

2.1 Methodology

The temporal analysis of surface temperature was carried out over three periods, corresponding to the IPCC 5th Report (AR5) reporting periods: 1986-2005, 2046-2065 and 2080-2099, considering 1986-2005 as reference period. Also, the spatial analysis was carried out in eight sub-areas (Figure 2), corresponding to the study areas of the PRUDENCE program.(Christensen et al., 2007).

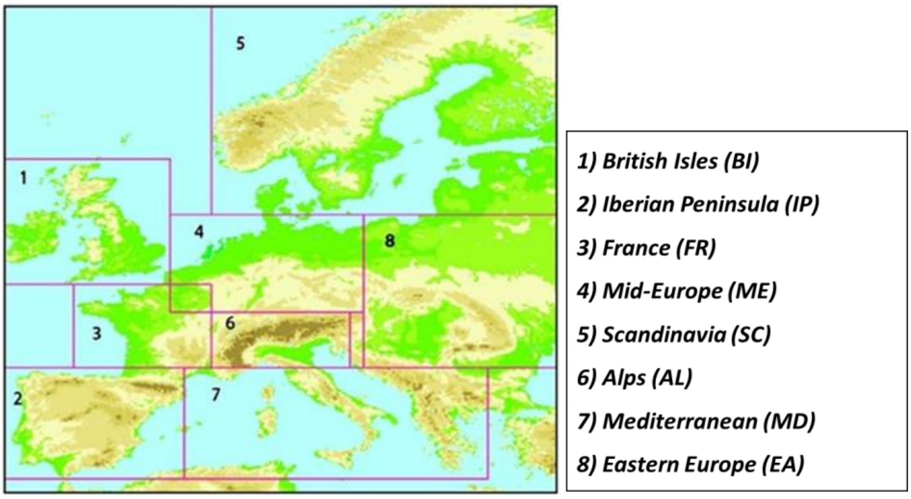


Figure 2: The PRUDENCE sub-areas.

The temperature field was averaged and analyzed on a seasonal base. The seasons were averaged from June to August (JJA) and December to February (DJF).

In order to test the statistical significance of differences between the two future periods and the reference period, we calculate the quantity t (paired t-test):

$$t= (x-y) / (\frac{s^2}{n}) \quad (1)$$

where x and y are the arithmetic means of the n=20 seasonal values, s is the standard deviation of the n values. Differences are deemed significantly different at the 95% level if t >2.03.

Mann-Kendall is a non-parametric test which used so as to test if there is monotonic trend of average seasonal anomalies of temperature of the period 2006-2099 comparing to reference period, at 95% significance level. (Mann, 1945).

3. RESULTS AND DISCUSSION

The mean winter (DJF) and summer (JJA) temperature bias (Models minus EOBS) for the period 1986-2005 is presented in Figure 2. Their evaluation with EOBS indicates the ability of models to reproduce the observed climatology. The ensemble mean of Euro-CORDEX models is systematically colder than EOBS over the whole European domain both in summer and winter. Specifically, in winter the bias is small and about the same for all areas (Table 2). In the summer, all areas are characterized by greater bias values, mainly Alps, Scandinavia and France (average bias is -1.8ºC, -1.6ºC and -1.5ºC respectively). Previous evaluation studies (Pavlidis 2015, Sofiadis 2017) have shown that these regional climate simulations systematically underestimate the surface temperature over the whole European domain in all seasons. According to Boberg and Christensen (2012), the uncertainties presented by climate models for the present climate are linked with future uncertainties, so it's very important to evaluate climate models and identify areas with large bias in order to better interpret climate projections.

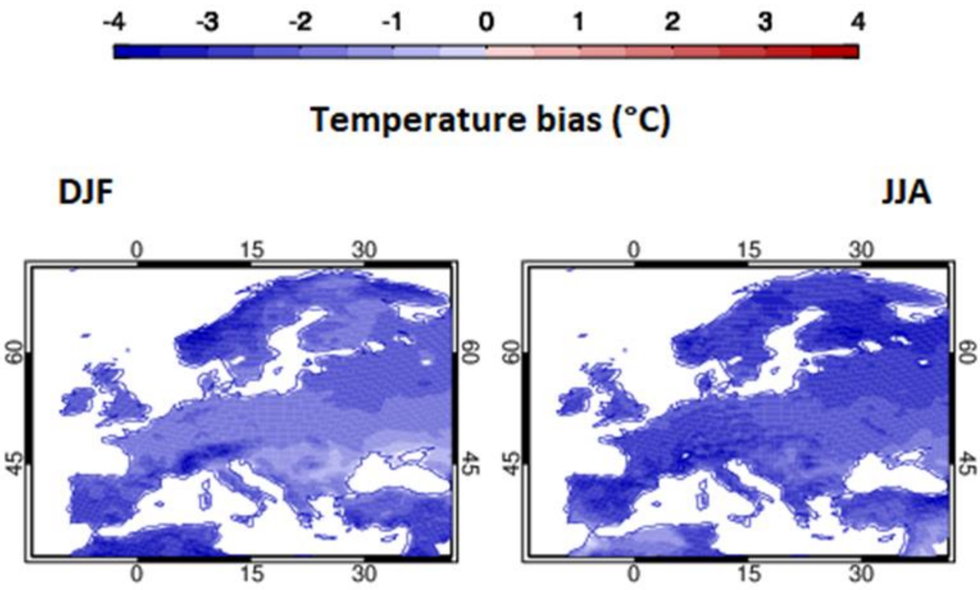


Figure 3: Temperature winter (left) and summer (right) bias (Ensemble mean of models minus EOBS) for the period 1986-2005. Units in degrees Celsius.

Then, the mean seasonal temperature anomalies over the period 2006–2100, relative to the period 1986–2005, have been calculated based on ensemble mean of Euro-CORDEX models output. The time series of mean seasonal temperature anomalies at Scandinavia and Mediterranean regions are shown in Figure 4. The temperature changes are evident, and the rates of change per decade for the other PRUDENCE sub-areas are indicated in Table 3. All trends are statistically significant at the 95% confidence level. The temperature trends typically vary from 0.26° to 0.53°C per decade in winter and from 0.39ºC to 0.65ºC in summer. The largest increases appear in regions of North-East Europe for the winter and in South Europe for the summer. Our findings are consistent with those of Sofiadis (2017), who presented recent warming trends and the respective models spread over these regions.

Table 2: Average temperature winter and summer bias (Ensemble mean of models minus EOBS) for the period 1986-2005. Units in degrees Celsius.

Subregions	Temperature Bias (°C)	
	Winter	Summer
AL	**-0.6**	**-1.8**
SC	**-0.5**	**-1.6**
IP	**-0.8**	**-1.2**
BI	**-0.2**	**-0.7**
FR	**-0.1**	**-1.5**
MD	**-0.1**	**-0.5**
EA	**-0.2**	**-0.6**
ME	**-0.1**	**-1.1**

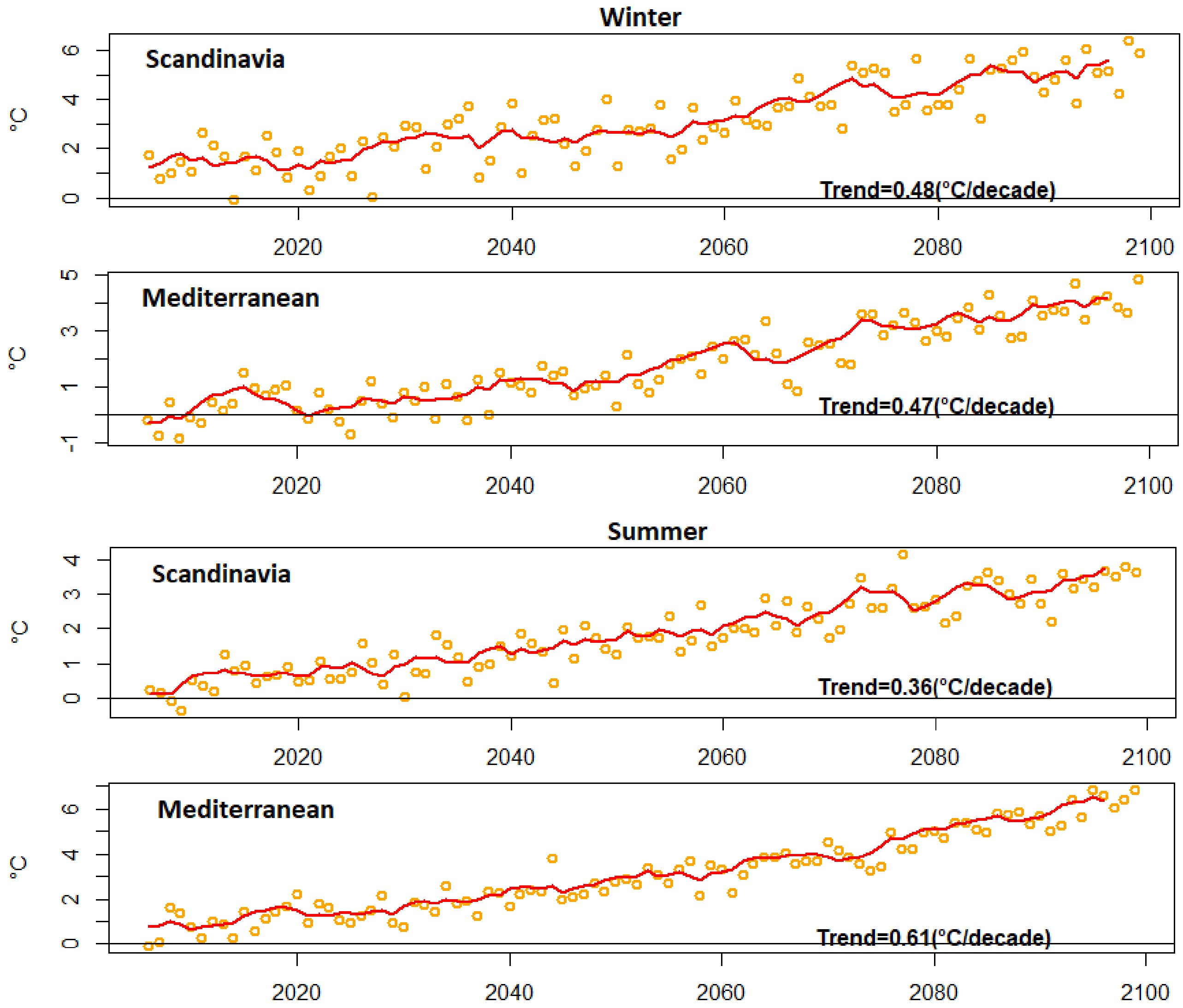


Figure 4: Time series of mean seasonal (winter and summer) temperature anomalies of the period 2006-2100 relative to the reference period (1986–2005) at Scandinavia and Mediterranean regions. The red line shows the 5-year running average.

Table 3: Linear trends (in °C/decade) of the mean seasonal temperature in PRUDENCE sub-areas for the period 2006-2100, relative to the reference period (1986–2005). All trends are statistically significant at 95% level.

Subregions	Temperature Trend (°C/decade)	
	Winter	Summer
AL	**0.45**	**0.59**
IP	**0.34**	**0.65**
BI	**0.26**	**0.39**
FR	**0.35**	**0.58**
EA	**0.53**	**0.46**
ME	**0.39**	**0.47**

In Figure 5 we calculate the differences in mean seasonal temperature between the two future periods (2046-2065 and 2080-2099) and the reference period 1986-2005, where the gradual rise is evident by the end of the century. However, the spatial distribution of temperature changes is different for winter and summer. In winter, there is a gradual increase from southwest to northeast Europe, while in the summer larger differences are projected in the Mediterranean basin and smaller in Northern Europe. This could be attributed to the ability of atmospheric circulation and land surface processes to modulate the European climate. (Wang et al., 2014)

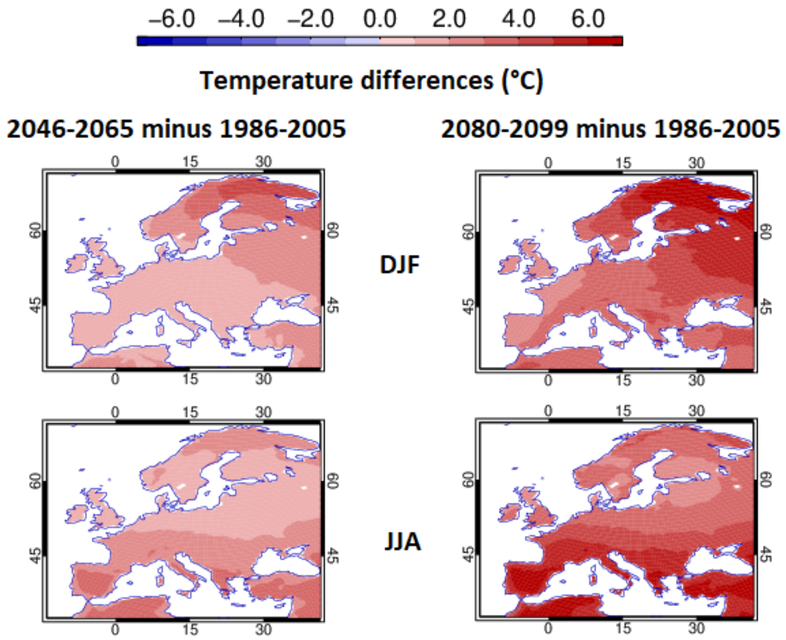


Figure 5: Projected changes of mean seasonal temperature for the period 2046–2065 (left) and 2080-2099 (right), compared to 1986–2005. All changes are statistically significant at 95% confidence level.

4. CONCLUSION

In this work we study the ensemble mean of five regional climate simulations all performed within the Euro-CORDEX framework. The simulations cover the European domain with a resolution of 50 km for the period 1986-2099. All models were driven by different Global Circulation Models (GCMs) and used different configurations. The ensemble mean of models is colder than the EOBS climatology both in summer and winter for the whole domain, with bias to be slightly higher in the summer in most areas. Furthermore, gradual temperature rise is estimated in Europe until the end of the century. Specifically, higher temperature increase is expected in southern regions (Mediterranean, Iberian

Peninsula) in summer season. Our future work will focus on the study of other variables such as soil temperature and precipitation to better interpret climate variation in Europe.

Acknowledgements

The work is supported by EU 7th Framework Programme Marie Curie Actions IRSES project: REQUA (PIRSES-GA-2013-612671). The authors would like to thank Earth System Grid Federation (ESGF) for providing Euro-CORDEX models output. We also acknowledge the technical support of AUTH-Scientific Computing Center for providing scientific software and storage space, making this study possible.

References

1. Neelin D. (2010) "**Climate Change and Climate Modeling**", Cambridge University Press.
2. IPCC (2014) Synthesis Report– **"**Contribution of Working Groups I, II and III to the Fifth Assessment Report of the Intergovernmental Panel on Climate Change", International Panel for Climate Change (IPCC).
3. Hong S.Y. and Kanamitsu M. (2014) 'Dynamical downscaling: Fundamental issues from an NWP point of view and recommendations', **Asia-Pacific Journal of Atmospheric Sciences**, Vol.50, pp.83-104.
4. Laprise R. (2008) 'Regional climate modelling', **Journal of Computational Physics**, Vol. 227, pp. 3641-3666
5. Giorgi F. and Gutowski W. (2015) 'Regional Dynamical Downscaling and the CORDEX Initiative', **Annual Review of Environment and Resources,** Vol.40, pp.467-490
6. Riahi K., Grubler A., Nakicenovic N. (2007) 'Scenarios of long-term socio-economic and environmental development under climate stabilization', **Technological Forecasting and Social Change**, Vol.74, pp.887-935
7. Christensen J. and Christensen O. (2007) 'A summary of the PRUDENCE model projections of changes in European climate by the end of this century', **Climate Change**, Vol.81, pp7-30
8. Mann H. (1945) 'Nonparametric Tests Against Trend', **Econometrica,** Vol.13, pp.245
9. Pavlidis V. (2015) 'Estimation of errors and uncertainties of radiation and cloudiness in regional scale climate simulations', MSc. thesis, Aristotle University, Thessaloniki.
10. Sofiadis I. (2017) 'Study of climate change over Europe for the 21st century using a regional climate simulation driven by the scenario RCP 8.5', MSc. thesis, Aristotle University, Thessaloniki.
11. Boberg F. and Christensen J. (2012) 'Overestimation of Mediterranean summer temperature projections due to model deficiencies', **Nature Climate Change**, Vol. 2, pp.433-436
12. Wang G, Dolman A. Alessandri A. (2011), "A summer climate regime over Europe modulated by the North Atlantic Oscillation", **Hydrology and Earth System Sciences,** Vol. 15, pp.57-64

CLIMATE CHANGE IMPACTS ON THE COASTAL SEA LEVEL EXTREMES OF THE EAST-CENTRAL MEDITERRANEAN SEA

C. Makris*, P. Galiatsatou, Y. Androulidakis, K. Kombiadou, V. Baltikas, Y. Krestenitis and P. Prinos

Division of Hydraulics & Environmental Engineering, Department of Civil Engineering, A.U.Th., GR- 54124, Thessaloniki, Greece

*Corresponding author: e-mail: cmakris@civil.auth.gr, tel: (+30) 2310 995708

Abstract

Extreme events of sea level elevation, due to severe weather conditions, pose great threats to low-land coastal areas by extended inundation hazards. The latter take the form of short- to mid-term flooding due to wave- and storm-induced sea level elevation and run-up on the coast. In this paper, the impact of the combined effect of extreme storm surges and extreme wave set-up in nearshore areas is investigated. The framework is set by future and historic climate change scenarios during a period of 150 years (1951–2100) that affect the occurrence frequency and magnitudes of total (surge- and wave-induced) sea level extremes in the eastern Mediterranean, focusing on the coastal zones of Greece. Inter-annual and multi-decadal patterns, trends and return levels of storm surge and wave set-up extremes are calculated based on non-stationary bivariate statistical analysis with copula functions of the Generalized Extreme Value distribution. The numerical data of storm surge- and wave-induced sea levels are derived from post-processing of simulation results by GreCSS and SWAN models, respectively, in order to transfer validated numerical data from offshore regions towards the shoreline of selected areas prone to coastal flooding. An increase and a consequent attenuation of storminess and inter-annual extremes of total sea level on the coast is estimated during the 1st and 2nd half of the 21st century, respectively. Different morphological characteristics of regional coastal zones in the Aegean Sea are found to influence variability of sea level extremes.

Keywords: Storm surge, Wave set-up, Extremes, Mediterranean Sea, Climate change impact

1. INTRODUCTION

Harsh weather conditions can cause extreme events of sea level elevation (SLE) in the marine environment possibly leading to extended coastal flooding that has severe environmental and societal impacts, such as loss of land and damages to onshore infrastructure, coastal structures and ports. In the framework of a constantly changing climate with extreme SLE events of higher frequency and intensity, both augmented by the estimated mean sea level (MSL) rise, the exposure and vulnerability of society, infrastructure and the environment of coastal areas to severe damages are expected to increase. The effect of climate change on the coastal zones of the Mediterranean and other Seas around Europe has been studied in the past (Benetazzo et al., 2012; Conte and Lionello, 2013; Kvočka et al., 2016; Vousdoukas et al., 2016; Satta et al., 2017; Vibilić et al., 2017), mostly focusing on the variability and long-term trends in the evolution patterns of MSL rise, and the extremes of storm surge events and waves, yet in a separative approach for the several hydraulic features contributing in total SLE.

Our former work has been centered on proper implementation of extremal analysis for hydraulic features in the marine environment (Galiatsatou, 2007; Galiatsatou and Prinos, 2008, 2014, 2015;

Galiatsatou et al., 2016) and validated hydrodynamic modeling of storm surges and waves in coastal zones (Krestenitis et al., 2014, 2015; Androulidakis et al., 2015; Makris et al., 2015, 2016). In the aforementioned studies, the impacts of climate change on the extremes of storm surges and waves have been investigated (taking into account the MSL rise) in selected areas of the Mediterranean, Aegean and Ionian Seas, detecting a considerable increase in the extreme wave/surge climate especially in the 1st half of the 21st century. Yet, former literature has focused on analysis of SLE extremes treating storm surge and severe wave events separately. Only recently Feng et al. (2018) and Galiatsatou et al. (2017, 2018) have made efforts to study storm flood-prone coastal areas based on coupled surge-wave simulations and recent advances in extreme analysis with copula functions (Wahl et al., 2012; Bender et al., 2014), respectively. In the present work, a non-stationary multivariate approach has been developed and implemented to assess design total water levels at the shoreline of selected Greek coastal areas in the Aegean Sea under the effects of climate change.

2. METHODOLOGY

2.1 Methodological approach and topographical characteristics of the study area

The methods and techniques of the present work have been implemented to the annual maxima of random wave characteristics (*i.e.* significant wave height H_s and corresponding peak spectral period T_p) in open seas, nearshore wave-induced sea level η_w, and associated SLE values due to storm surges at selected locations of the east central Mediterranean (Aegean Sea). Three representative high flood-risk study areas (Makris et al., 2016; Galiatsatou et al., 2017, 2018) have been selected (Figure 1); Area 1 in the North Aegean containing the coastal zone of Alexandroupolis and part of the Thracian Sea, Area 2 in the Central Aegean containing the coast of Eresos in southern Lesvos Island, and Area 3 in the South Aegean containing a northern Crete coastal area of Heraklion. The selection of representative group of points was based on proper statistical homogeneity measures for high quantiles of the Hosking and Wallis type (Makris et al. 2016; Galiatsatou et al., 2017, 2018) assessed for annual maxima of H_s and SLE for a control period (1951-2000), related to its counterpart 50-year future periods in 2001-2100. High-wave events exceeding appropriately defined thresholds of H_s (1.5-2 m) were selected at grid points in the study area, for durations >6 hrs, having onshore main wave directions towards respective shorelines. T_p values were associated to the high sea states corresponding to a period of 150 years (1951-2100). The choice of SLE data was based on a 5-day time-window of storm surge-driven sea levels, covering the time of corresponding records of H_s maxima (by 2.5 days bilaterally), indicated in order to estimate the largest possible SLE response to the particular storm events (with maximum duration of 120 hrs in the Mediterranean basin; Conte and Lionello, 2013; Makris et al., 2016).

2.2 Numerical models and data for storm surges and waves

The raw data of marine parameters in the present work are drawn from climatic-type numerical simulations to estimate the (offshore) irregular wave characteristics (H_s, T_p and energy wave spectrum features) from SWAN model implementations (Kapelonis et al., 2015; Makris et al., 2016), and SLE due to storm surges from 2-DH high-resolution simulations with MeCSS and GreCSS hydrodynamic models (Krestenitis et al. 2014; Androulidakis et al. 2015; Makris et al. 2015, 2016). The modelled datasets were validated and bias-corrected by *in situ* measurements, satellite altimetry and modeled forecasts, and covered a 150-year period (1951-2100), using atmospheric forcing of climatic data, produced by a dynamically downscaled simulation with RegCM3 model (Tolika et al., 2015; Vagenas et al., 2017), under 20C3M historical and SRES-A1B future scenarios for green-house gas emissions (Makris et al., 2016; Vagenas et al., 2017).

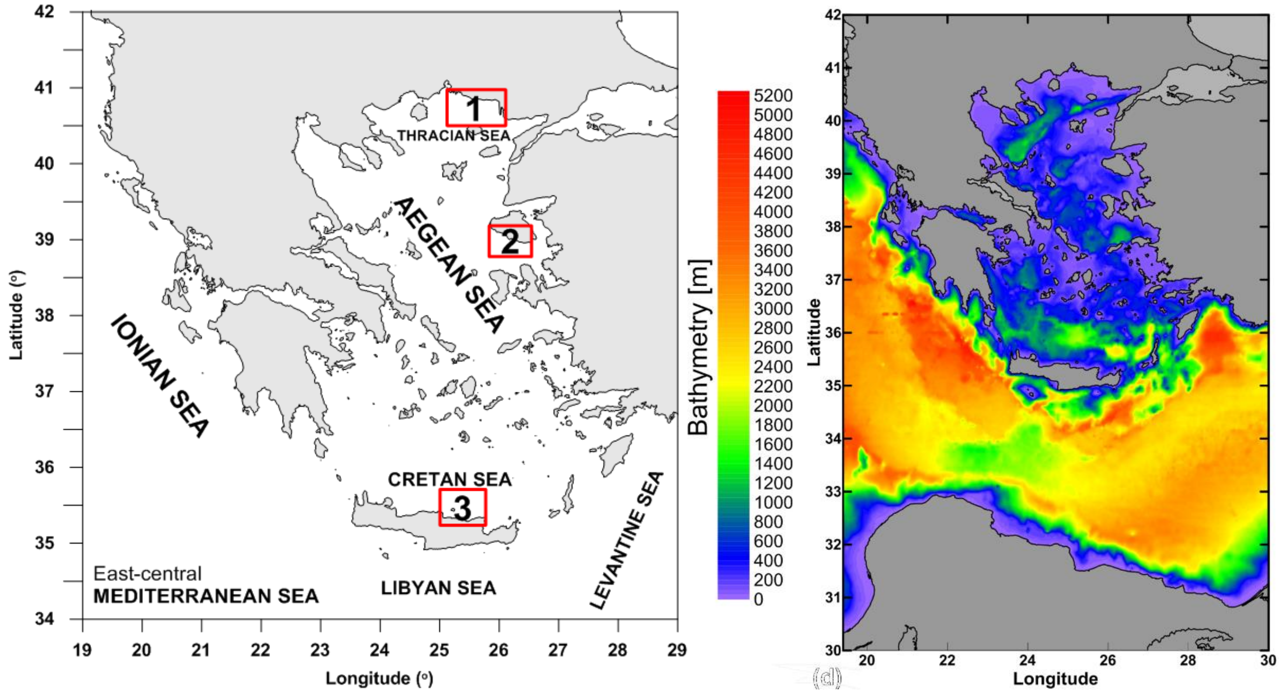


Figure 1: *Left graph*: Selected study areas of the Aegean Sea; 1: Alexandroupolis coastal area in the Thracian Sea (North Aegean), 2: Eresos coastal area in southern Lesvos Island (Central Aegean), 3: Heraklion coastal area in the Cretan Sea (South Aegean). *Right graph*: Marine map of the study area's bathymetry (m) for the 1/20° (~5 Km) resolution computational domain

2.3 Modelling approach for total sea level on the coast

The calculation method of the coastal hazard under investigation, *i.e.* the total (flood) water level at the shoreline and on the coast, is concisely presented in the following (detailed entire approach by Galiatsatou et al., 2018), by implementing a semi-analytic modelling approach for the derivation of the nearshore (surf/swash zone) wave-induced sea levels (Goda, 2000). In order to correctly calculate the total sea level in coastal areas, and specifically inside the surf zone and at the shoreline, we need to transfer the spatially large-scale modelled (wave and storm surge) data from relatively deep (or intermediate) waters in the open sea to nearshore shallow water areas and finally the shoreline boundary. The storm surge is a huge-scale phenomenon (order of several Km) and coastal SLE values were therefore adequately provided by dynamically downscaled numerical simulations in climatic mode (150 years, 1/20° resolution; Makris et al., 2015, 2016). Nevertheless, the wave-induced sea level in nearshore areas and close to the shoreline concerns finer scale effects due to irregular wave breaking. Nonetheless, numerical simulations in climatic mode (150 years) with a 2-DH wave model of very fine spatial resolution is still very arduous in terms of computational resources and available detail in digital bathymetric and terrain models. Therefore, in the present work, we used the offshore SWAN model results of Makris et al. (2016). Consequently we calculated the transformation of extreme random wave characteristics (H_s, T_p, main wave direction) towards the shoreline with a semi-analytical iterative model for irregular wave trains (Makris and Krestenitis, 2009), which takes into account the crude variations of rather simple bathymetries (parallel depth-contours, nearly straight coastlines and uniform slopes) crossing areas of nearshore intermediate to shallow waters and surf zone H_s constraints for irregular wave breaking. Furthermore the wave-induced set-up η_{su} was calculated (Goda 2000), as it represents the short- to mid-term SLE in the coastal zone, due to random wave action in shallow waters and secondary processes due to irregular wave breaking. We also added another smaller component of SLE, *i.e.* the surf beat η_{sb}, associated to wave groups approaching coastal zones in discrete high- and low-frequency bands. Conclusively, we estimated the (potential) total wave-induced sea level η_w=η_{su}+η_{sb} nearshore and on the shoreline, being qualitatively similar to storm surge SLE, rendering it a fitting counterpart in a bivariate analysis of sea level values.

Transformation of random wave characteristics from open seas to shallow coastal waters was based on spectral wave theory and analytic relations of Goda (2000) taking into account irregular wave propagation, refraction, shoaling, and energy dissipation due to breaking and bottom friction. The significant wave height H_s in arbitrary depth d is given by the relation $H_s=k_r{}'\cdot k_s{}'\cdot H_{s,o}$ (where $_o$ index corresponds to deep-water offshore values). For areas with rather parallel depth-contours, the effective spectral refraction and shoaling coefficients, $k_r{}'$ and $k_s{}'$, for irregular waves are given by:

$$k_r' = f\left(k_r, h/L_{o,p}, a_{p,o}, s_{\max}\right),\ \text{from graphs} \qquad k_r' = \sqrt{\left[\sum_{i=1}^{M}\sum_{j=1}^{N}(\Delta E)_{ij}\,(k_r)_{ij}^2\right]},\ \text{analytically} \tag{1}$$

$$k_s' = k_s,\ d_{30} \le d \qquad k_s' = (k_s)_{30}\cdot\left(\frac{d_{30}}{d}\right)^{2/7},\ d_{50} < d < d_{30} \qquad k_s'\cdot\left(\sqrt{k_s'} - B\right) - \Gamma = 0,\ d < d_{50} \tag{2}$$

where $k_r(f,\theta)$ is the linear refraction coefficient of monochromatic wave components with frequency f and propagation direction θ, $(\Delta E)_{ij}$ are the components of relative wave energy with i_{th} discrete frequency and j_{th} angle of incidence for discrete spectral bands, $L_{o,p}$ is the deep water wavelength corresponding to T_p. $H_{s,b}$ (depth-limited breaker height) and the rest parameters are (Goda, 2000):

$$\left(\frac{d_{30}}{L_{o,p}}\right)^2 = \frac{2\pi}{30}\frac{H'_{s,o}}{L_{o,p}}(k_s)_{30},\ \left(\frac{d_{50}}{L_{o,p}}\right)^2 = \frac{2\pi}{50}\frac{H'_{s,o}}{L_{o,p}}(k_s)_{50},\ B = \frac{2\sqrt{3}}{\sqrt{2\pi H'_{s,o}/L_{o,p}}}\frac{d}{L_{o,p}},\ \Gamma = \frac{C_{50}}{\sqrt{2\pi H'_{s,o}/L_{o,p}}}\left(\frac{L_{o,p}}{d}\right)^{3/2}$$

$$C_{50} = (k_s)_{50}\left(\frac{d_{50}}{L_{o,p}}\right)^{3/2}\left[\sqrt{(k_s)_{50}\cdot 2\pi H'_{s,o}/L_{o,p}} - 2\sqrt{3}\frac{d_{50}}{L_{o,p}}\right],\ H_{s,b} = A\cdot L_{o,p}\cdot\left\{1-\exp\left[-1.5\cdot\frac{\pi\cdot d_{s,b}}{L_{o,p}}\left(1+15\cdot m^{4/3}\right)\right]\right\} \tag{3}$$

where A=0.12-0.18 is a shape parameter depending on the position of the broken wave inside the surf zone, $d_{s,b}$ the incipient breaking depth of $H_{s,b}$, and m the bottom slope. Combining iteratively the breaking model with the random wave transformation, we calculated an estimation of the wave set-up evolution in the surf zone transverse to the coast, $d\eta/dx$ (η_{su}, η_{sb} exactly on the shoreline):

$$\frac{d\eta}{dx} = -\frac{1}{(\eta+d)}\cdot\frac{d}{dx}\left[\frac{1}{8}\overline{H_s}^2\left(\frac{1}{2}+\frac{4\pi d/L_p}{\sinh\left(4\pi d/L_p\right)}\right)\right],\quad \eta_{su} = \frac{3\gamma^2/8}{1+3\gamma^2/8}\cdot d_b - \frac{\gamma^2\cdot d_b}{16},\quad \eta_{sb} = \frac{0.01\cdot H'_{s,o}}{\sqrt{\frac{H'_{s,o}}{L_{o,p}}\left(1+\frac{d_{s,b}}{H'_{s,o}}\right)}} \tag{4}$$

where $\gamma=H_{s,b}/d_{s,b}$ is the wave breaking index, L_p the local wavelength corresponding to T_p, and η the local value of the sea level (mean water level) due to the random breaking-induced process of the wave set-up in depth d. The estimation of the total (flood) water level at the shoreline η_t resulted from the summation of all the SLE components: wave run-up $R_{2\%}$ (contains the parameter η_{su}), MSL rise *MSLR* (due to ice melting, steric and mass addition components; Makris et al., 2016) the surf beat η_{sb}, the storm surge-induced SLE, and the highest astronomical tide *HAT* (courtesy of Hellenic Navy Hydrographic Service, https://www.hnhs.gr/en/):

$$\eta_t = R_{2\%} + MSLR + \eta_{sb} + SLH + HAT \tag{5}$$

where the wave run-up at the shoreline was based on the formulation of Stockdon et al. (2006):

$$R_{2\%} = 1.1\left(0.35\tan\beta\left(H_sL_o\right)^{\frac{1}{2}} + \frac{\left(H_sL_o\left(0.563\tan^2\beta+0.004\right)\right)^{\frac{1}{2}}}{2}\right) \quad \text{and} \quad R_{2\%} = 0.043\left(H_sL_o\right)^{\frac{1}{2}},\ for\ Ir < 0.3 \tag{6}$$

with $tan\beta$ the beach face slope and $Ir=m/\sqrt{(H_{s,o}/L_{o,p})}$ the Iribarren number (surf similarity parameter). For dissipative beaches (Ir<0.3) the wave run-up is infragravity dominated.

2.4 Method for extreme value analysis

Extreme value analysis in the present paper is based on the Generalized Extreme Value (GEV) distribution function, which includes location μ, scale σ>0, and shape $\xi \neq 0$ parameters, assessed by Maximum Likelihood Estimation (MLE) or L-moments (LM) procedures (computed from linear combinations of probability weighted moments), providing measures for shape of distributions or data samples, such as location, dispersion, skewness and kurtosis. For data samples of $\{X_1, X_2, \ldots, X_n\}$ arranged in increasing order, the sample probability weighted moments are:

$$b_o = \frac{1}{n}\sum_{j=1}^{n} X_j\ , \quad b_r = \frac{1}{n}\sum_{j=r+1}^{n} \frac{(j-1)(j-2)....(j-r)}{(n-1)(n-2)....(n-r)} X_j \tag{7}$$

Extreme SLE values (*e.g.* 50-year return levels) exhibit non-stationarity, led by natural climatic variability and climate change, *viz.* the El Niño Southern Oscillation (ENSO) or North Atlantic Oscillation (NAO) acting on different time scales. These can have significant impacts on SLE extremes and occurrence frequency of coastal flooding events, thus assuming time-varying μ, σ, ξ:

$$G(x) = \exp\left[-\left\{ 1+\xi(t)\frac{(x-\mu(t))}{\sigma(t)} \right\}^{-1/\xi(t)} \right],\ 1+\xi(t)\frac{(x-\mu(t))}{\sigma(t)} > 0 \tag{8}$$

The return level x_p corresponding to a return period T=1/p is assessed in a non-stationary context as a function of time, representing quantiles of the distribution function of SLE for every year:

$$x_p(t) = \mu(t) - \frac{\sigma(t)}{\xi(t)}\left[1-\left\{ -\log(1-p) \right\}^{-\xi(t)} \right] \tag{9}$$

For the estimation of the parameters of the fitted distribution functions for all sea level variables, a moving time-window of 40-years (Bender et al., 2014) was implemented in the present work, using the LM method for each period. Their length was selected to be large enough to provide a good fit of the marginal distributions of H_s, SLE, etc., as well as of their possible dependence structure. In a multivariate framework (Galiatsatou et al., 2018), the non-stationary marginal distribution functions for wave and storm surge variables has to be followed by a non-stationary joint probability analysis of the dependent variables using bivariate copulas, which model dependence structure of *e.g.* H_s and SLE, independently from their marginal distributions. To estimate the dependence structure of nearshore sea level data within the non-stationarity framework, 40-year moving windows were also applied to the bivariate data (H_s/T_p and H_s/SLE), utilizing Canonical Maximum Likelihood (CML) without first specifying marginal distributions. This way, marginals are first transformed to pseudo-observations with uniform margins $(U_{i1}, U_{i2})^T$ and then the dependence parameter a is estimated as:

$$\hat{a}_{CML} = \mathrm{argmax}_a \sum_{i=1}^{n} \log c(U_{i1}, U_{i2}; a) \tag{10}$$

To select the appropriate copula function among five candidates (*i.e.* Clayton, Frank, Gumbel, Student's t, Gaussian), a parametric bootstrap procedure has been used (Galiatsatou et al., 2017, 2018). The test computes the Cramér – von Mises functional S_n, comparing the empirical copula of the observations with a parametric estimate of the copula derived under the null hypothesis. Approximate p-values for the test have been computed using the parametric bootstrap procedure. Large values of S_n usually result in the rejection of the null hypothesis that the bivariate data result from the tested copula function. After estimating the copula parameters, the statistic S_n and its associated p-value were estimated for all moving windows and all candidate copula functions. For

each bivariate pair, the copula that resulted in *p*-values exceeding the 5% significance level for the entire study period, was selected as the best-fit model and applied for joint exceedance probability estimation. In case more than one of the fitted copulas satisfied the above condition, the selected bivariate model was the one providing the lowest Akaike Information Criterion (AIC) values during the largest part of the studied time interval (Galiatsatou et al., 2017, 2018).

3. RESULTS

3.1 Numerically simulated data

Results for the 50-year patterns of H_s annual maxima in the study area are presented in Figure 2. A projected increase of the Etesian winds at the central part of the Aegean (Tolika et al., 2015; Makris et al., 2016) seems to be responsible for a small but traceable change in $H_{s,max}$ patterns during 2001-2050. Intensification trends are mainly estimated to occur in the northern and central parts of the Aegean Sea, with smaller values in the southern parts of the study area. An increase of $H_{s,max}$ in the Ionian and Libyan Seas during the 1st half of the 21st century and a consequent attenuation towards 2100, follows the climate change patterns of mean sea states (not shown here). During the low-energy seasons, the entire study area reveals a consistent invariance. Figure 3 presents the spatial variability of the averaged (for each of the three periods) values of the Storm Surge Index (SSI), which is a representative annual maximum SLE, *i.e.* yearly mean of three maxima storm surge events (Androulidakis et al., 2015; Makris et al., 2016), over each 50-year period ($SSI_{50\text{-yr}}$). The highest *SSI* values (>0.45 m) can be traced along the northern coasts of the Aegean Sea (coastal zone of Alexandroupolis; Area 1). The SSI decreases from North to South, ranging from 0.32 to 0.38 m for central parts of the Aegean, down to almost 0.3 m in the southern part of the study area (Crete), and below 0.25 m for the northern African coasts. Lower values occur along the entire coastline in the 2nd half of the 21st century, consistent with the estimated storm attenuation towards 2100. The change signals between 2001-2050 and 1951-2000 range from −5.1 to +19.6 % locally. Storm surge-induced SLE is estimated to generally decrease from the current to the future 50-year period, with changes of −17.5 to +1.8 %.

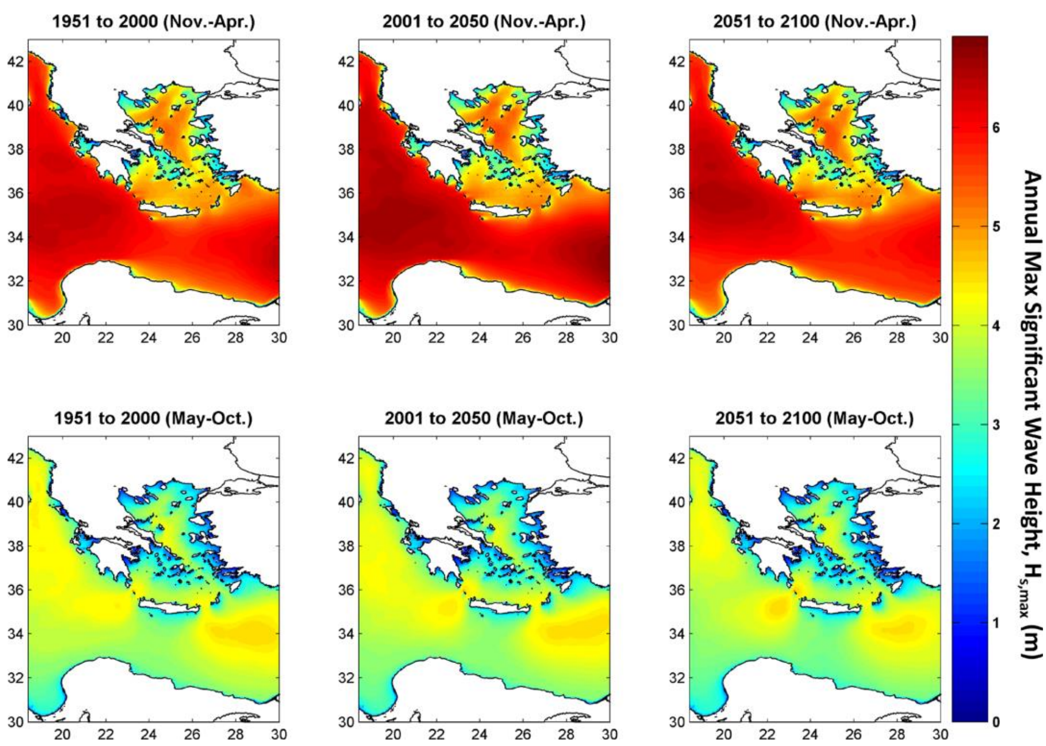


Figure 2: Temporal mean of H_s annual maxima (m) during high- and low-energy (upper and lower graphs, respectively) months over the study area for 50-year reference (left graphs), current (central graphs) and future (right graphs) period time intervals

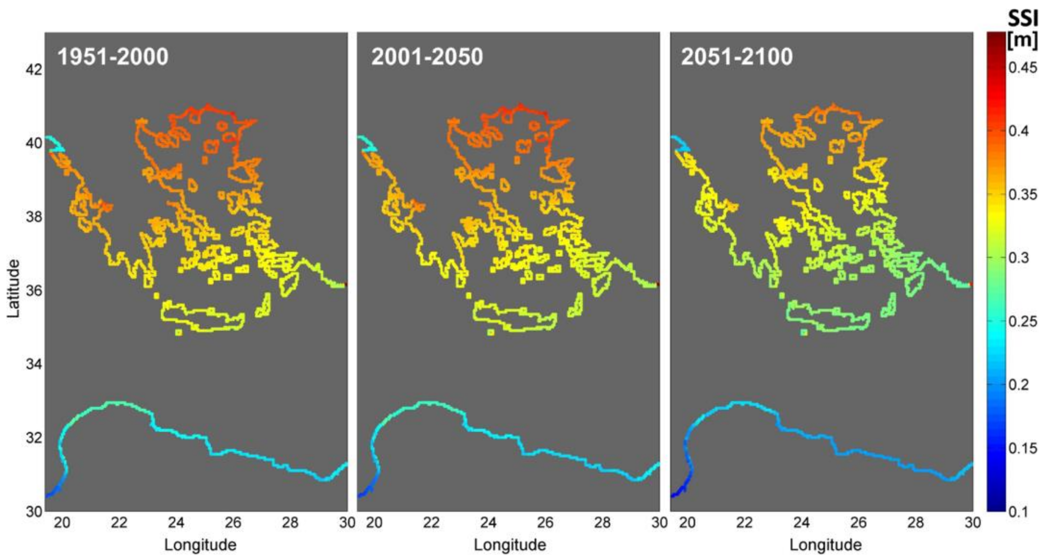


Figure 3: Storm Surge Index SSI (m) along the coastline of the study area, time-averaged over 50-year reference, current and future periods (from left to right)

3.1 Extremes and return values of storm surges, waves, and total sea level on the coast

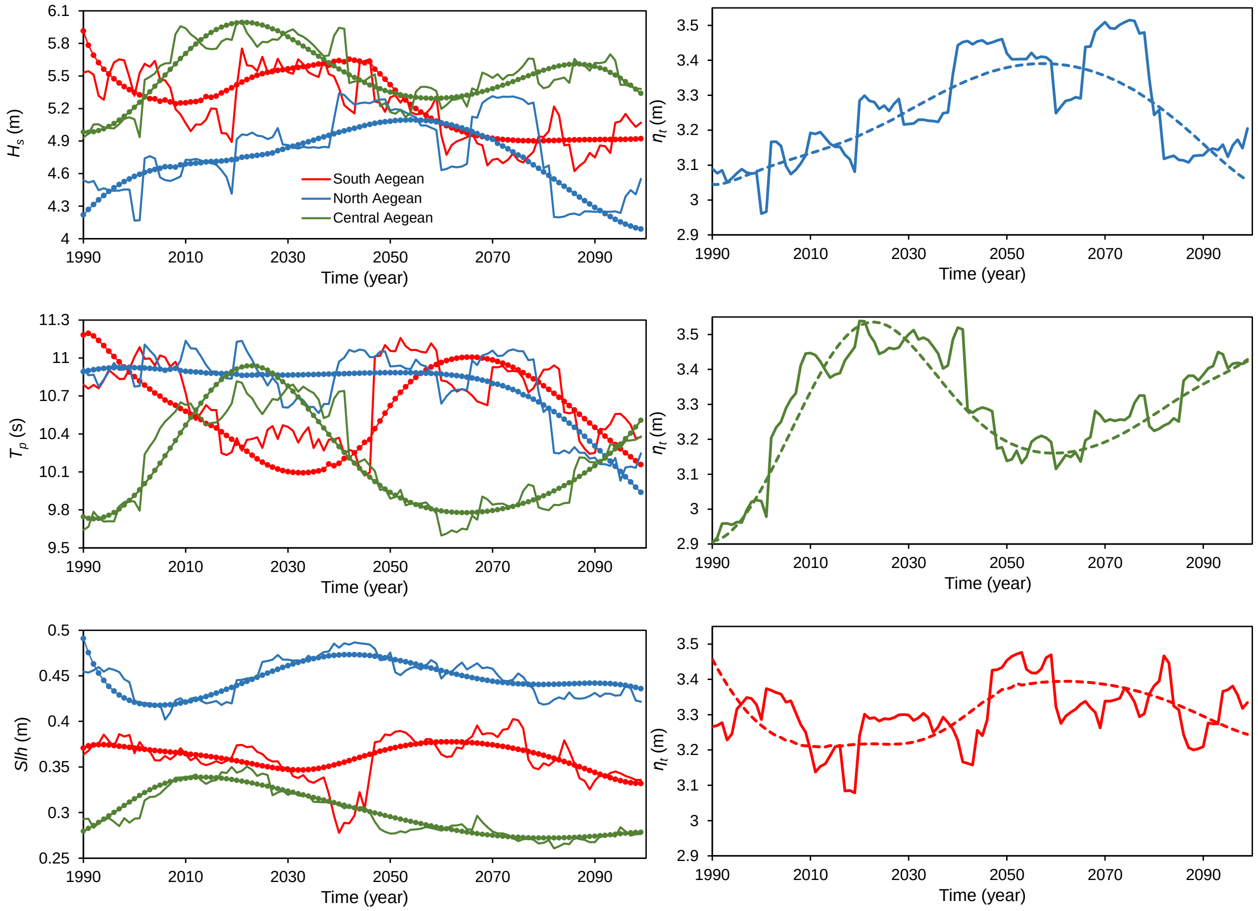


Figure 4: *Left panel:* Time-dependent estimates of MLE wave event of H_s (top graph), T_p (middle graph) and SLE (lower graph) in North Aegean (blue plots), central Aegean (green plots), and South Aegean (red plots). *Right panel:* Time-dependent estimates of total water level at the shoreline η_t at selected profiles in the coastal areas of Alexandroupolis (top), Eresos bay (middle) and Heraklion (bottom). Solid lines represent MLE extracted without parametric trends in marginals and dependence parameter of bivariate data; Dot-lines consider all fitted trends

Figure 4 (left panel graphs) presents the time-dependent most likely design estimates of H_s, T_p and SLE for the three studied areas in the Aegean Sera. In the North Aegean Sea, H_s MLE maxima appeared in the 2nd half of the 21st century, around 2060, when including the parametric trends in the marginal parameters and the dependence structure of the marine variables. Excluding parametric trends, MLE H_s showed a bimodal behavior with pronounced peaks for short periods before and after 2050. MLEs of T_p (thus wave lengths too) are estimated to decrease rapidly during the last 30 years of the 21st century. MLE of storm surge SLE presented more than 16% variations with maxima probably occurring before the middle of the 21st century. In the Central Aegean Sea, MLEs of wave features presented more intense variability (e.g. two distinct peaks for H_s, pronounced around 2020 and towards 2085, with T_p peaking around 2020, too). A progressive decrease of MLEs for storm-induced SLE is obvious after a peak in 2010-2015. In the South Aegean Sea, the most likely design events of H_s, T_p and SLE presented almost 22%, 10% and 37% variations, respectively. Wave heights are estimated to decrease in the 2nd half of the 21st century, while wave periods are expected to increase quite sharply in 2031-2070 and decrease rapidly during 2071-2100. SLE variation followed the T_p trend peaking around 2060.

Figure 4 (right panel graphs) presents η_t in the 1990-2100 interval for three selected coastal profiles having quite similar beach face slopes (7-8%) in each study area. Beach breadths varied from 14 to 40 m with berm heights from 2 to 3.2 m. In Alexandroupolis (Area 1) η_t varied more than 17% in the 21st century with highest values probably occurring in the 2nd half of the 21st century (*i.e.* around 2060 with parametric trends in marginal distributions and dependence structure of marine variables). The variations of total water extremes presented similar trends to those of H_s MLEs. In Eresos (Area 2), η_t variations exceeded 20% in 1990-2100 with maxima of total water level at the shoreline appearing after 2020, presenting similar trends to all marine variables in the area, with wave parameters (especially T_p) having a stronger influence on them. Finally, in the coastal area of Heraklion (Area 3) η_t varies more than 12% in the 21st century, with its maxima around 2060 (or just after 2080 for no parametric trends in marginals and dependence parameter of bivariate data). Total water levels on the coast seem to most likely increase after 2030 maintain quite high values in the 2nd half of the 21st century. Wave periods and storm surges are estimated to heavily influence η_t while high waves appeared less correlated with it compared to central and northern Aegean areas.

4. DISCUSSION AND CONCLUSIONS

In the present study, a novel approach has been developed and applied to selected Greek coastal areas of the Aegean Sea to investigate the changes in the joint probabilities of extreme marine variables (storm surge- and wave-induced sea level elevations) with time. The scope was to properly assess design magnitudes of total (flood) water levels at the shoreline of extended, rather homogenous, coastal areas, under the effect of climate change (based on a rather pessimistic future scenario). The results of coupled, large-scale, numerical simulations of 2-DH hydrodynamic circulation for storm surges and 3rd generation spectral wave transformation, are post-processed and blended with an irregular wave transformation model for wave-induced sea level in nearshore areas and towards the shoreline, leading to a novel, robust, analytic approach for extreme run-up and total flood water levels on the coast (Galiatsatou et al., 2018), modeling dependence structure with the use of copulas. The non-stationary analysis of the marginal distributions of all marine variables revealed statistically significant trends in all parameters of the GEV at the selected areas of the Aegean Sea. Statistically significant polynomial trends were also detected in the dependence structure of both offshore and nearshore bivariate data. Variations in future trends for probable coastal flooding might be attributed to geographical differentiations correlated to climate change signals of weather data (Makris et al., 2016) and variations of marine variable (storm wave and surge characteristics) extremes (Galiatsatou et al., 2017) in the area. The highest values of total water levels on the shoreline were calculated either around 2020 or the middle of the 21st century, while the regime of long wave sea states was correlated (significant influence) on extreme η_t estimates. The spatial differentiations of the patterns of extreme marine variables, based on the intense topographical diversity of the Aegean archipelago, revealed

different results of former studies (Galiatsatou and Prinos, 2014, 2015; Makris et al., 2016), implying the rise of extreme southerly winds in the Aegean Sea towards the middle of the 21^{st} century and beyond (corroborated by Vagenas et al., 2017). In the South Aegean, the Aeolian patterns show a mild rise of northerly extreme winds after the 1^{st} half of the 21^{st} century, which might lead to an increase of extreme peak periods and respective storm surges that are slightly intensified. Nevertheless, due to the complex dense insular formation of the Cyclades, the random wave fields are prone to diffraction, and this seems to cause a slight drop in the significant wave height extremes. These findings (a 20- to 30-year transition of extreme sea level response to climate change on the coastal zone) are different from former studies (Galiatsatou and Prinos, 2014, 2015; Makris et al., 2016), which have shown clear patterns of storminess augmentation in the 1^{st} half, and consequent severe attenuation in the 2^{nd} half of the 21^{st} century. In the Central Aegean, a more coherent pattern of sea level response to climate change signals can be traced, with the shift in the patterns of extreme values of coastal marine parameters following climatic-type changes in northerly and southerly extreme winds, giving rise in sea level extremes around 2020, which is in agreement with relevant previous literature (involving analyses with A1B scenario). Therefore, the proposed novel approach of extreme value calculation (incl. non-stationarity, time-dependence, bivariate analysis of extremes, transferring sea-states from offshore to coastal areas) can produce significant alterations on the patterns of extreme total sea levels on the shoreline, compared to former studies of univariate stationary approaches, providing somewhat safer estimates and thus more reliable risk assessment tools for coastal flooding under the effects of climate change.

References

1. Androulidakis, Y.S. et al. (2015). ‘Storm surges in the Mediterranean Sea: Variability and trends under future climatic conditions’. **Dynamics of Atmospheres and Oceans**, 71, pp. 56-82.
2. Bender, J., Wahl, T. and Jensen, J. (2014). ‘Multivariate design in the presence of non-stationarity’. **Journal of Hydrology**, 514, pp. 123-130.
3. Benetazzo, A. et al. (2012). ‘Wave climate of the Adriatic Sea: a future scenario simulation’. **Natural Hazards and Earth System Sciences**, 12(6), pp. 2065-2076.
4. Conte, D. and Lionello, P. (2013). ‘Characteristics of large positive and negative surges in the Mediterranean Sea and their attenuation in future climate scenarios’. **Global and Planetary Change**, 111, pp. 159–173.
5. Feng, X. et al. (2018). ‘Study of storm surge trends in typhoon-prone coastal areas based on observations and surge-wave coupled simulations’. **International Journal of Applied Earth Observation and Geoinformation**.
6. Galiatsatou, P. (2007). ‘Joint exceedance probabilities of extreme waves and storm surges’. **XXXIII IAHR Congress**, pp. 780.
7. Galiatsatou, P. and Prinos, P. (2008). ‘Non-stationary point process models for extreme storm surges’. **Flood Risk Management: Research and Practice: Proc. Floodrisk 2008**, Oxford, 1045-1054.
8. Galiatsatou, P. and Prinos, P. (2014). ‘Analysing the effects of climate change on wave height extremes in the Greek Seas’. **ICHE 2014**, Hamburg, Lehfeldt & Kopmann (eds), pp. 773-781.
9. Galiatsatou, P. and Prinos, P. (2015). ‘Estimating the effects of climate change on storm surge extremes in the Greek Seas’. **36^{th} IAHR World Congress**, The Hague, The Netherlands.
10. Galiatsatou, P., Anagnostopoulou, C. and Prinos, P. (2016). ‘Modelling nonstationary extreme wave heights in present and future climates of Greek Seas’. **Water Science and Engineering**, 9(1), pp. 21-32.

11. Galiatsatou, P., Makris, C. and Prinos, P. (2017). 'Non-Stationary Joint Probability Analysis of Extreme Marine Variables to Assess Design Water Levels at the Shoreline in a Changing Climate'. **3rd International EVAN Conference**, 5-7 September 2017, Southampton, UK.
12. Galiatsatou, P. et al. (2018). 'Nonstationary joint probability analysis of extreme marine variables to assess design water levels at the shoreline in a changing climate'. **Natural Hazards**, Springer. (*submitted, under review*).
13. Goda Y. (2000). '**Random Sea and Design of Maritime Structures**'. World Scientific.
14. Kapelonis, Z.G., Gavriliadis, P.N. and Athanassoulis, G.A. (2015). 'Extreme value analysis of dynamical wave climate projections in the Mediterranean Sea'. **Procedia Computer Science**, 66, pp. 210-219.
15. Krestenitis, Y. et al. (2014). 'Modeling storm surges in the Mediterranean Sea under the A1B climate scenario'. **12th COMECAP**, Heraklion (Crete), Greece, 28-31 May 2014, pp. 91-95.
16. Krestenitis, Y. et al. (2015). 'Evolution of storm surge extreme events in Greek Seas under climate change scenario'. **11th Pan-Hellenic Symposium on Oceanography and Fisheries**, Mytilene, Lesvos, Greece, 13-17 May 2015, pp. 849-852.
17. Kvočka, D., Falconer, R.A. and Bray, M. (2016). 'Flood hazard assessment for extreme flood events'. **Natural Hazards**, 84(3), pp. 1569–1599.
18. Makris, C.V. et al. (2015). 'Numerical Modelling of Storm Surges in the Mediterranean Sea under Climate Change'. **36th IAHR World Congress**, The Hague, The Netherlands.
19. Makris, C. et al. (2016). 'Climate change effects on the marine characteristics of the Aegean and Ionian Seas'. **Ocean Dynamics**, 66(12), pp. 1603-1635.
20. Makris, C.V. and Krestenitis, Y.N. (2009). 'Free Educational Software on Maritime Hydrodynamics, Coastal Engineering and Oceanography'. **9th Pan-Hellenic Symposium of Oceanography and Fisheries**, Vol.1, pp. 546-551. (*in Greek*)
21. Satta, A. et al. (2017). 'Assessment of coastal risks to climate change related impacts at the regional scale: The case of the Mediterranean region'. **International Journal of Disaster Risk Reduction**, 24, pp. 284-296.
22. Stockdon, H.F. et al. (2006). 'Empirical parameterization of setup, swash, and runup'. **Coastal Engineering**, 53, pp. 573-588.
23. Tolika, K. et al. (2015). 'A comparison of the updated very high resolution model RegCM3_10km with the previous version RegCM3_25km over the complex terrain of Greece: present and future projections'. **Theoretic and Applied Climatology**, pp. 1–12.
24. Wahl, T., Mudersbach, C. and Jensen, J. (2012). 'Assessing the hydrodynamic boundary conditions for risk analyses in coastal areas: a multivariate statistical approach based on copula functions'. **Natural Hazards and Earth System Sciences**, 12, pp. 495-510.
25. Vagenas, C., Anagnostopoulou, C. and Tolika, K. (2017). 'Climatic Study of the Marine Surface Wind Field over the Greek Seas with the Use of a High Resolution RCM Focusing on Extreme Winds'. **Climate**, 5(2), pp. 29.
26. Vibilić, I. et al. (2017). 'The Adriatic Sea: A long-Standing Laboratory for Sea Level Studies'. **Pure and Applied Geophysics**, Sea Level 2017, pp. 1-47.
27. Vousdoukas, M.I. et al. (2016). 'Projections of extreme storm surge levels along Europe'. **Climate Dynamics**, 47(9), pp. 3171-3190.



Protection and restoration of ecosystems

BIOFILM GROWTH IN DRINKING WATER SYSTEMS UNDER STAGNANT CONDITIONS

Erifyli Tsagkari* and William T. Sloan

School of Engineering, College of Science and Engineering, University of Glasgow, G12 8LT, United Kingdom

*Corresponding author: e-mail: Erifyli.Tsagkari@glasgow.ac.uk, tel: +447833637863

Abstract

Safe drinking water is essential for human health and its provision in a changing climate is a global pressing problem. Research communities, governments and drinking water supplying companies are working on improving the quality of drinking water and reducing its cost. Microorganisms colonise the inner surfaces of pipes and form biofilms. In drinking water systems biofilms are problematic as they cause loss of disinfectants, harbour pathogens and affect the aesthetics of drinking water. From the engineering perspective, that leads to corrosion of the pipe's material and reduced life of the existing infrastructure. Thus, it is imperative that we gain a deeper understanding of the growth of biofilms if we are to develop effective strategies for their removal or control.

In this study we focused on the growth of biofilms in drinking water under stagnant conditions, which often occur in parts of drinking water pipes. A bioreactor was used to simulate the service lines of drinking water systems. After 4 weeks, the thickness and density of the biofilms were characterised using gravimetric measurements, and their surface area was determined using fluorescence microscopy. Also, the concentration of cells and microcolonies both in the bulk water and on the reactor surfaces was determined using fluorescence microscopy. Finally, spatial statistics were used to describe the biofilm structures that were formed on the exposed surfaces of the reactor. It was revealed that even under stagnant and oligotrophic conditions, drinking water bacteria moved from the bulk water of the reactor and attached to the available surfaces forming a high number of microcolonies. Biofilms were able to grow on the exposed surfaces of the reactor forming characteristic structures consisting of dense cell clusters. Our results revealed that even under unfavourable conditions biofilms can grow within our drinking water systems.

Keywords: biofilms; drinking water; microscopy; reactor; stagnant

1. INTRODUCTION

Biofilms are found on virtually every wetted surface on earth. Even though the term "biofilm" may not form part of the popular lexicon, most people are familiar with biofilms in one way or another, in particular with those that can be seen by naked eye. The plaque on our teeth is a biofilm, the slime on our contact lenses, the bathroom walls or rotting food is also a biofilm. Similarly, the green of brown coating on rocks, pebbles or sand in a river is a biofilm [Hall-Stoodley et al., 2004]. A biofilm consists of a group of microorganisms, such as bacteria, fungi, viruses and protozoa, which adhere to a surface and are usually housed in a matrix of extracellular polymeric substances (EPS). The EPS are biopolymers including polysaccharides, proteins, nucleic acids and lipids. In most biofilms, the microorganisms may account for less than 10% of the total biofilm dry mass, whereas the EPS matrix may account for over 90% of that. The biofilm matrix has been characterised as a three-dimensional polymer network that interconnects and immobilises the cells that it consists of [Flemming and Wingender, 2010].

It is estimated that 99% of the total population of bacteria in the world are found in the form of a biofilm [Florjanic and Kristl, 2011]. One of the main reasons why bacteria opt for the biofilm, rather than the planktonic mode of life, is the protection that the biofilm offers to them. This might include protection against harsh conditions, such as nutrient deprivation, shear stresses, ultraviolet or acid exposure, metal toxicity, dehydration, salinity, antibiotics and other antimicrobial agents [Hall-Stoodley et al., 2004].

Biofilms can be very useful, especially in the field of bioremediation. Organisms may be used for contaminant removal and for the purification of industrial wastewater. In biofilm filtration systems, the filter medium presents a surface for the microbes to attach to and to feed on the organic material in the water being treated. Such water cleaning systems are biologically more stable and their disinfectant demand is lower than that of conventionally treated systems. Less microorganism induced contamination is likely to occur in water that passes through a biofilm based filter than there is in water that passes through another alternative treatment system [Campos et al., 2002].

On the other hand, biofilms can result in heavy costs for the cleaning and maintenance of the industrial and domestic pipes that they colonise. The environment in which people are mostly exposed to biofilms is the domestic environment [Garrett et al., 2008]. Although drinking water is closely monitored in the developed countries, waterborne disease outbreaks are still being reported. These outbreaks may be associated with pathogenic bacteria and viruses, and biofilms in the water pipe networks are known to create favourable conditions for their survival and growth. In addition, the detachment of biofilms from pipe walls is associated with changes in the water taste, odour and colour. The main challenge of drinking water industries is to deliver water that is microbiologically and chemically safe, aesthetically pleasing and adequate in quantity [Simões, 2012]. Thus, it is crucial to find ways of managing the biofilms that will inevitably form.

Visualising biofilm structures is complicated due to the presence of debris, corrosion products and mineral deposits, which provide new niches for bacteria to colonise [Batté et al., 2003]. Organic and inorganic particles can accumulate in low-flow areas or dead-ends of drinking water systems and enhance microbial activities by providing protection for bacteria against harsh conditions [Simões, 2012, Douterelo et al., 2013]. Biofilms are generally found to form very complex and heterogeneous structures [van Loodsdrecht et al., 1995]. Thicknesses that have been recorded for biofilms in drinking water systems range from a few tens of micrometres [Srinivasan et al., 2008] to a few hundreds of micrometres [Momba et al., 2000]. Biofilms may be formed on the surfaces of drinking water pipes within a few days or months and may reach a cell concentration of 10^7-10^9 cells/cm^2 [Manuel, 2007]. The vast majority of bacteria, estimated at 95% of the total cell population, are attached to the surfaces of the pipes, whereas only 5% are found in the water phase [Flemming et al., 2002].

In drinking water systems under high flow conditions, which are those that are mostly experienced, microorganisms are transported by eddies in the flow [Kumarasamy and Maharaj, 2015]. Under low flow conditions, the transport of bacteria from the bulk water to the exposed surfaces occurs due to Brownian diffusion, sedimentation and cell motility. Stagnant conditions occur regularly in drinking water systems (i.e. during overnight periods or near closed valves and flanges in the system) when the water consumption is low [Manuel et al., 2007]. It is suspected that the biofilm growth characteristics under stagnant conditions would be similar to those in laminar flow, where shear stresses are low and the transport of nutrients and oxygen is driven by diffusion. However, very little is known about biofilm growth under such conditions [Manuel et al., 2007, Liu et al., 2016]. Thus, in this study, the development of biofilms in drinking water was investigated under stagnant conditions after a 4-week period using a bioreactor. A 4-week period is considered a realistic time period of water stagnation in service lines [Zlatanović et al., 2017]. Also, the reactor, which was used, simulated the part of drinking water distribution systems, which is closer to the tap. The exact structure and composition of drinking water biofilms are still unclear and have not been described in detail yet due to difficulties in investigating such a small amount of biomass without disturbing it. Biofilms in drinking water systems are generally thin but these low thicknesses that can be reached

are variable [Wimpenny et al., 2000]. Thus, the goal of this study was to investigate how biofilms were developed under oligotrophic conditions in stagnant water and to characterize them.

2. MATERIALS AND METHODS

2.1 Reactor conditions

Biofilms were grown in a jacketed rotating annular reactor (model 1320 LJ, BioSurface Technologies, US). This reactor presents various advantages such as simple sampling process. Also, the liquid phase of reactor is well mixed, which ensures that there is uniform distribution of bacteria in the bulk liquid [Characklis and Marshall, 1990]. The reactor held 20 new and sterile vertical polycarbonate slides (BST-503-PC) attached to its inner drum. The beveled edges of the slides were dropped into the beveled slots on the reactor inner cylinder and they were removed from it using a sterilized hook. The slides were placed in the inner cylinder in a symmetric way in order to avoid any imbalances. The polycarbonate material of the slides was chosen as one of the plastic materials, which are used in drinking water systems [Szabo et al., 2007, Garny et al., 2008]. The jacket of the reactor allowed the temperature to be maintained in the system via heated water from a bath circulator (Isotemp Bath Circulator, Fisher Scientific, UK). The temperature was chosen at 16^{o}C as the representative temperature of DWDS in the United Kingdom for spring and summer [Douterelo et al., 2013]. The reactor was covered with aluminium foil in order to achieve dark conditions for biofilm growth. The diameter of the pipe, which was simulated using this reactor, was at 30.3 mm. This pipe diameter corresponds to the extremities of drinking water systems where the service lines start [Hall et al., 2009]. The conditions in service lines are generally characterised by longer residence times, higher stagnation periods, reduced flow rates and higher temperatures compared to those in the mains [Zheng et al., 2015].

The medium that the reactor was filled with consisted of 150 ml of nutrient medium and 850 ml of drinking water that was sampled from a domestic tap in Glasgow. The concentrations for mineral salts of the reactor medium were: ammonium sulphate (1.2 mg/l), ammonium chloride (0.9 mg/l), magnesium sulphate heptahydrate (0.3 mg/l), manganese chloride tetrahydrate (0.003 mg/l), copper sulphate pentahydrate (0.002 mg/l), cobalt sulphate heptahydrate (0.001 mg/l), sodium molybdate dehydrate (0.001 mg/l), zinc sulphate heptahydrate (0.01 mg/l), and boric acid (0.75 mg/l) (Milferstedt et al., 2006), and the concentration for glucose of the reactor medium was 1.5 mg/l. These concentrations kept the bulk water conditions in the reactor oligotrophic (Batté et al., 2003). The total organic carbon (TOC) in the bulk water of reactor was determined using a TOC-L analyser (SHIMADZU, Japan) as the difference between the total carbon and the total inorganic carbon. To calculate the TOC 3 samples of 10 ml each were used. The TOC was measured at the onset of the experiment and after 4 weeks. Finally, the concentration of total chlorine of the drinking water, which was sampled from the tap, was measured immediately after its sampling and after 4 weeks. The USEPA DPD Method 8167 [Chamberlain and Adams, 2006] was followed to measure the chlorine concentration using the DR 900 Hach colorimeter (Colorado, US). The measurements were performed for 3 samples of 10 ml each.

2.2 Cells and microcolonies measurements

To calculate the concentration of cells in the bulk water of reactor at the onset of the experiment 3 samples of 5 ml each were used. These samples were filtered through 47 mm Whatman® 0.2 μm membrane filters (Sigma-Aldrich, Irvine, UK) after they were fixed with 0.5 ml of 2% formaldehyde [Kepner and Pratt, 1994]. The membrane filters were then covered with 1 ml of 0.1% Triton X-100 solution in order to evenly disperse the cells. The cells on the membrane filters were then stained with 1 ml of 10 μg/ml (4′,6-diamidino-2-phenylindole) DAPI for 20 minutes in the dark and visualised using fluorescence microscopy (Olympus IX71, Japan) with the oil immersion UPlanFLN objective lens (100X magnification/1.30 numerical aperture). More than 30 images per membrane filter were obtained. The concentration of cells was calculated from [Brunk et al., 1979]:

$$\frac{\text{cells}}{\text{ml}} = \frac{\left(\frac{\Sigma x}{\text{n}} \pm s\right) \text{A}_{\text{memb}} \text{d}}{\text{A}_{\text{field}} \text{V}_{\text{filt}}} \tag{2}$$

where Σx/n is the mean number, s is the standard deviation, A_{memb} is the surface area of the membrane filter, d is the dilution factor, A_{field} is the surface area of the microscope field and V_{filt} is the volume of the liquid sample filtered. The same procedure was used to calculate the concentration of microcolonies in the bulk water of reactor but without using the Triton solution and by using the objective lens with 10X magnification/0.30 numerical aperture instead of the one with 100X magnification/1.30 numerical aperture. The microcolonies visualised had a diameter of approximately 10 μm and consisted of approximately 10 cells.

To calculate the concentration of cells on the reactor slides after the 4 weeks, 3 slides were removed from the reactor. The biomaterial attached to the reactor slides was gently scraped from the slides and diluted in 5 ml distilled water. Then, the 5 ml samples were fixed with 0.5 ml of 2% formaldehyde [Kepner and Pratt, 1994] and filtered on Whatman® 0.2 μm membrane filters. The same procedure described above was followed. The concentration of cells was calculated from [Brunk et al., 1979]:

$$\frac{\text{cells}}{\text{cm}^2} = \frac{\left(\frac{\Sigma x}{\text{n}} \pm s\right) \text{A}_{\text{memb}} \text{d} \text{V}_{\text{susp}}}{\text{A}_{\text{field}} \text{V}_{\text{filt}} \text{A}_{\text{biof}}} \tag{3}$$

where V_{susp} is the total suspension volume and A_{biof} is the area from which the biomaterial was scraped. The same procedure was used to calculate the concentration of microcolonies on the reactor slides. The microcolonies were similar to those described above.

2.3 Biofilm measurements

To calculate the biofilm thickness and density 3 slides were removed from the reactor. Gravimetric measurements were used to characterise the thickness and density of the biofilms attached to the slides [Staudt et al., 2004]. In brief, after the slides were removed from the reactor they were drained for 5 minutes at a vertical position and then they were weighed for the determination of the wet mass. Then, the slides were dried for 24 hours at 65°C in an oven and weighed again. After that, the dried biofilm was washed off the slides with distilled water and laboratory tissues. The clean slides were dried again for 24 hours at 65°C and then weighed again. The dry mass was determined by the weight difference of the slides with and without the dried biofilm. The biofilm thickness, L_F, was determined by:

$$L_F = \frac{m_{WF}}{\rho_{\text{WF}} \text{A}_{\text{F}}} \tag{4}$$

and the volumetric biofilm density, ρ_F, was determined by:

$$\rho_F = \frac{m_{DF}}{\left(\frac{m_{WF}}{\rho_{\text{WF}}}\right)} \tag{5}$$

where m_{WF} and m_{DF} are the wet and dry mass of the biofilm respectively. Also, ρ_{WF} is the density of biofilm, for which there is the assumption that it is equal to that of water at 16°C at 998.946 kg/m^3. Finally, A_F is the surface area of the slide. The areal biofilm density was finally calculated as the product of the biofilm thickness and the volumetric biofilm density.

To visualise the biofilm structures on the reactor slides after the 4 weeks, 3 slides were removed from the reactor. The biofilms on the reactor slides were firstly fixed with 0.5 ml of 4% paraformaldehyde [Chao and Zhang, 2011]. The samples were covered with 1 ml of 10 μg/ml DAPI for 20 minutes in the dark. Biofilm structures were visualised using the objective lens with 100X magnification/1.30 numerical aperture. The surface area of biofilms on the reactor surfaces was then calculated in Matlab by processing more than 30 images obtained from fluorescence microscopy. The original images

were firstly converted to gray-scale images using the Matlab command called “rgb2gray” and then to binary images using the Matlab command called “im2bw” in order to separate the biomaterial from the background of the image. After the surface area of the biofilm was calculated, it was divided to the total surface area of the image in order to finally calculate the percentage of this surface area (%).

2.4 Spatial statistics

Textural entropy was used to characterise the biofilm structures. Entropy is used to describe the randomness of the components of a gray-scale image by comparing the intensity of the image pixels. The higher is the value of the entropy, the more heterogeneous is the biofilm. This means that more complex biofilm structures are demonstrated in the image. Entropy refers to the gray levels, which the individual pixels can adopt. In an 8-bit pixel image, for example, there are 256 such levels [Yang et al., 2000, Beyenal et al., 2004]. The entropy, E, is here defined:

$$E = -\Sigma p \log_2 p \tag{6}$$

where *p* is the pixel intensity associated with the gray level. Entropy was calculated using the Matlab function called “entropy”. To calculate the entropy more than 30 images of the biofilm structures, obtained from fluorescence microscopy, were used.

The semi-variogram was used as another measure to characterise the spatial variance of biofilm structures within gray-scale images and quantify the spatial dependencies in the data sets. Its function relates the semi-variance of the data points to the distance that separates them. Large distance of the data points means more data pairs for the estimation of the semi-variance but less amount of detail in the semi-variogram. In other words, the semi-variogram is a way of graphically capturing the spatial variance of points on a landscape as a function of their distance. All combinations of points at a distance are collated and their variance is determined for all possible separation distances [Carr and de Miranda, 1998]. The semi-variogram was calculated using the Matlab function called “variogram.m”.

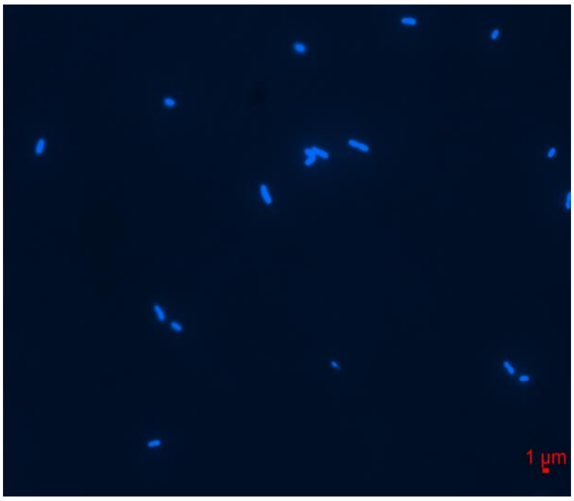
The autocorrelation function (ACF) diagram was used as the last measure to characterise the biofilm structures. The ACF diagram is, in essence, a two-dimensional extension of the semi-variogram. It allows us to assess how the spatial autocorrelation changes with distance. It correlates pixel intensities within gray-scale images and detects the repetitive structures within the image under consideration by combining together all parts of it. The ACF diagram is a real-space image, so that its dimensions have the same meaning as in the original image. Interpretation of the ACF diagram can be understood by imagining the image to be printed on transparency and placed on top of itself but rotated by 180^o. By sliding the top image laterally in any direction, the degree of match with the underlying original image is measured by this function [Heilbronner and Barrett, 2014]. The ACF diagram was calculated using the Matlab function called “autocorr2d.m”.

3. RESULTS AND DISCUSSION

3.1 Reactor medium, cells and microcolonies

The total chlorine of drinking water after it was sampled from the tap was found at 0.36 mg/l and after the 4 weeks it was found at 0 mg/l, as it was expected, since chlorine can decay through its interactions with the material of the slides or with the adhering on them biofilms [Brown et al., 2011]. Also, the TOC of reactor medium at the onset of the experiment was found at (1.95±0.3) mg/l and after the 4 weeks it was found at (0.74±0.1) mg/l. This showed that the TOC was decreased with time probably due to its consumption from the bacteria. The concentration of cells in the bulk water was found at $(5.1 \pm 0.5)*10^5$ cells/ml and the concentration of microcolonies in the bulk water was determined at $(3.6\pm0.2)*10^3$ microcolonies/ml at the onset of the experiment. This showed that cells were formed into microcolonies in the drinking water that was sampled from the tap rather than only being at their own state. The concentration of cells on the reactor slides was determined at $(1.9 \pm 0.3)*10^3$ cells/cm^2 (Figure 1a) after 4 weeks. This indicated that a quite high portion of the bacteria that were in the bulk water at the onset of the experiment were finally transferred to the reactor slides

after the 4-week period. The concentration of microcolonies on the reactor slides after the 4-week period was found at (2.6 ± 0.7)*10^2 microcolonies/cm^2 (Figure 1b). This showed again that a quite high portion of the cells formed microcolonies on the reactor slides after 4 weeks. A microcolony is a form of aggregate, which is the coming together of bacteria in the bulk water that might be transferred finally onto the available surfaces. Thus, it is considered to be an important precursor for the formation of biofilms [Sheng et al., 2010, Saur et al., 2017].

a.


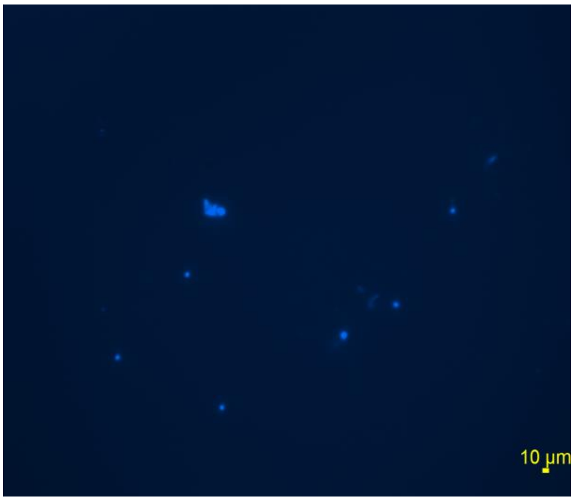
b.


Figure 1 a) Cells of about 1 µm size attached to the reactor slides, b) microcolonies of about 10 µm size attached to the reactor slides as revealed by fluorescense microsocpy.

3.2 Biofilms

Under stagnant conditions, given that bacteria are not transported onto surfaces by flowing water, then one might expect gravity to have an effect; thus, the vertical slides of reactor to be less prone to cell colonisation. Also, the oligotrophic conditions implicate that there is not enough energy given to bacteria to come together to each other and form biofilms. Shear stress conditions have a number of effects on bacteria; they keep them in suspension and increase the probability of bacteria colliding by chance. They also enhance mass transfer processes, oxygen distribution within the bulk water of pipelines and any metabolic reactions between bacteria [Lee et al., 2002, Son et al., 2015]. Thus, it was surprising to find that biofilms did grow in drinking water under stagnant conditions and their percentage of surface area after 4 weeks was found at 19.2%. Also, after 4 weeks the thickness of biofilms was found at 119.54 µm and their density at 9 mg/cm^2. This validated that biofilms did form in drinking water under stagnant conditions. However, the thickness of the biofilm was not high compared to the thicknesses that have been found using the same method under shear stress conditions [Horn et al., 2003, Staudt et al., 2004, Elenter et al., 2007].

3.3 Biofilm structures

Biofilms were found to form patchy structures consisting of rod-shaped bacteria (Figure 2) as revealed by fluorescence microscopy. The hazy part of biofilms in Figure 2 is probably the EPS of biofilms, which surrounded the cells. This patchy structure is also seen in laminar flow conditions where shear stresses are low [Stoodley et al., 1999a]. In turbulent flows biofilms tend to form much different structures such as filamentous structures that are also called streamers [Besemer et al., 2009]. However, streamers have been also identified in rare cases in laminar flow conditions [Rusconi et al., 2010]. Bacteria under low flow conditions tend to form clusters, which are microcolonies that consist of densely packed cells held together by EPS. Thus, the patchy structures consisting of cell clusters, which were identified here, were not a surprising result.

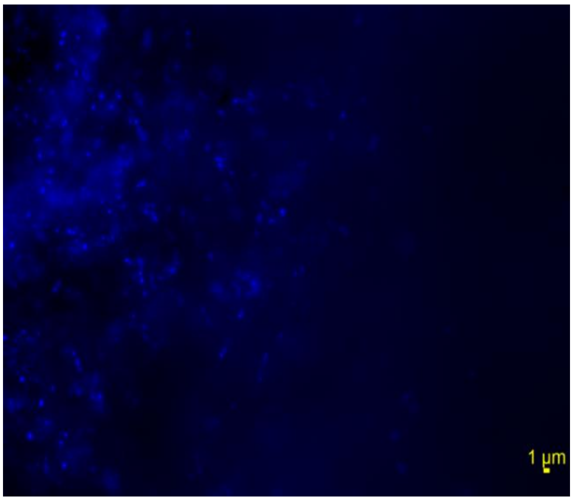
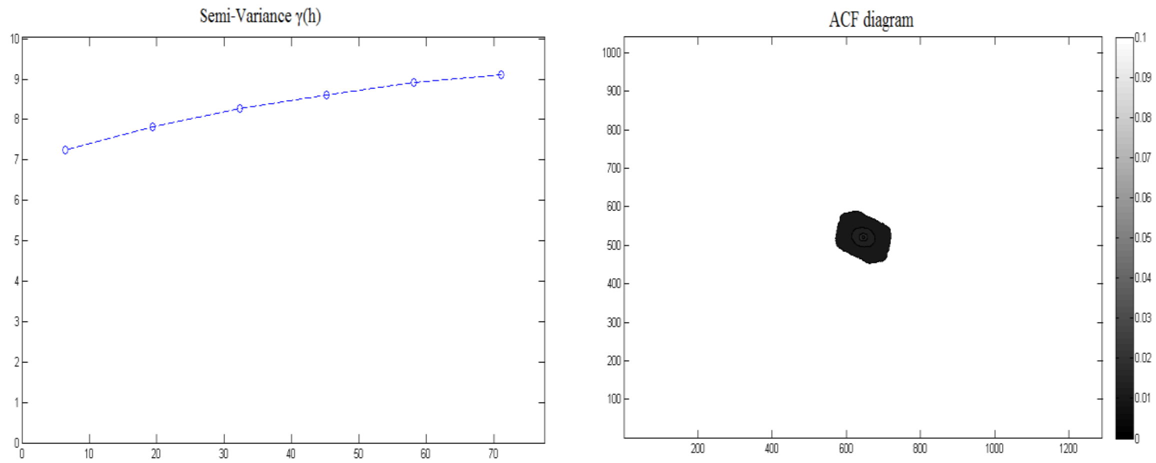


Figure 2 Biofilm structures stained with DAPI as revealed by fluorescence microscopy.

The entropy of biofilms was determined at 1.87. If all of the pixels of the image have the same value, or the image has no structures, or the image is composed of only white pixels or voids, the entropy of the image is 0 showing there is no gray scale variation in the pixels or heterogeneity. Increased numbers of structures in the image increase entropy due to increased gray level variability and heterogeneity in the image [Yang et al., 2000]. Thus, our measurements revealed that since entropy was not 0 or close to 0 this shows that characteristic biofilm structures were actually formed on the reactor surfaces.

The semi-variogram is here demonstrated (Figure 3a). An important part of a semi-variogram is the “origin”, which represents the closest points of the diagram. Another important part of a semi-variogram is the “sill”, which is the variogram upper bound that is equal to the variance of the data set and it also reflects the amount of variability. The sill is usually found at large distances where there is no gradient in the diagram [Cohen et al., 1990, Cressie, 1993]. The lag distance at which the semi-variogram reaches the sill value is the “range”. In total, 12000 points were used for the calculation of the semi-variogram shown in Figure 3a. The gradient in the variance close to the origin was found to be shallow and linear. This indicated that values were co-located as the variance at short distance was found to be low. These measurements showed that the topography of the biofilm was now very heterogeneous, as it was expected for stagnant conditions [Stoodley et al., 1999b]. Finally, the range was found at about 70 μm and the sill was equal to almost 9.

The ACF diagram is here demonstrated as a contour plot (Figure 3b). The almost radially symmetric contours in autocorrelation do not suggest that there was only one spatially-correlated “lump” at the centre of the image. It is the average autocorrelation for all pixels on the image. In the ACF diagram, the central element provides a measure of the size and shape of the basic element that dominates the original image. The rest contour lines reflect the size and shape of the neighbourhood elements of the original image. Finally, the bar on the right side of the ACF diagrams provides a measure of the autocorrelation. The darker is the colour on the bar, the less is the autocorrelation value with its lowest value to be 0 and the highest one to be 1 [Russ, 2011]. In this diagram, the central element was found to be a circular feature, which size and shape corresponded to a cell. The rest contour lines, which were found to surround this main feature, were also circular and corresponded to a microcolony. These measurements suggest that radially symmetrical lumps were the prevalent topographical features, which could be associated with microcolonies. The contour plot in Figure 3b showed that cells align with themselves creating characteristic microcolonies, as it was also indicated in Figure 2.



a. **b.**

Figure 3 a) Semi-variogram; the vertical axis represents the semi-variance and the horizontal one represents the distance in μm, b) ACF diagram; the axes represent the size of the original image in pixels.

Overall, an annular reactor allowed us to grow biofilms in drinking water under stagnant conditions. Understanding the functionality and mechanisms of biofilms during the moderate (weeks) stages of their life will help in the consideration of future design of management strategies to control their growth in real drinking water systems. Our experiments suggest that biofilms were able to form in the reactor even under stagnant and oligotrophic conditions. However, these biofilms were not very thick and dense as it was revealed by gravimetric measurements. Fluorescence microscopy also revealed that biofilms were actually formed on the reactor surfaces creating characteristic patchy structures consisting of cell clusters. Finally, spatial statistics showed that the microcolonies were the most evident feature of the biofilm structures, which were not found to be complex, heterogeneous and irregular. Engineers should not overlook the biofilm-associated problems since a cursory understanding of the biology of the microorganisms that sit at the boundaries of our existing infrastructure will lead to an enhanced functionality of them.

References

1. Batté, M., Appenzeller, B. M. R., Grandjean, D., Fass, S., Gauthier, V., Jorand, F., Mathieu, L., Boualam, M., Saby, S. and Block, J. C. (2003). 'Biofilms in drinking water distribution systems'. **Reviews in Environmental Science and Bio/Technology**, 2**,** pp. 147-168.
2. Besemer, K., Hodl, I., Singer, G. and Battin, T. J. (2009). 'Architectural differentiation reflects bacterial community structure in stream biofilms'. **Isme Journal**, 3**,** pp. 1318-1324.
3. Beyenal, H., Donovan, C., Lewandowski, Z. and Harkin, G. (2004). 'Three-dimensional biofilm structure quantification'. **J Microbiol Methods**, 59**,** pp. 395-413.
4. Brown, D., Bridgeman, J. and West, J. R. (2011). 'Predicting chlorine decay and THM formation in water supply systems'. **Reviews in Environmental Science and Bio-Technology**, 10**,** pp. 79-99.
5. Brunk, C. F., Jones, K. C. and James, T. W. (1979). 'Assay for Nanogram Quantities of DNA in Cellular Homogenates'. **Analytical Biochemistry**, 92**,** pp. 497-500.
6. Campos, L. C., Su, M. F. J., Graham, N. J. D. and Smith, S. R. (2002). 'Biomass development in slow sand filters'. **Water Res**, 36**,** pp. 4543-4551.
7. Carr, J. R. and de Miranda, F. P. (1998). 'The semivariogram in comparison to the co-occurrence matrix for classification of image texture'. **Ieee Transactions on Geoscience and Remote Sensing**, 36**,** pp. 1945-1952.

8. Chamberlain, E. and Adams, C. (2006). 'Oxidation of sulfonamides, macrolides, and carbadox with free chlorine and monochloramine'. **Water Res**, 40**,** pp. 2517-2526.

9. Chao, Y. Q. and Zhang, T. (2011). 'Optimization of fixation methods for observation of bacterial cell morphology and surface ultrastructures by atomic force microscopy'. **Appl Microbiol Biotechnol**, 92**,** pp. 381-392.

10. Characklis, W. G. and Marshall, K. C. 1990. '**Biofilms'**, New York: John Wiley and Sons.

11. Cohen, W. B., Spies, T. A. and Bradshaw, G. A. (1990). 'Semivariograms of Digital Imagery for Analysis of Conifer Canopy Structure '. **Remote Sens. Environ.**, 34**,** pp. 167-178.

12. Cressie, N. 1993. '**Statistics for spatial data, Wiley series in probability and mathematical statistics, Revised Edition'**, New York, Wiley.

13. Douterelo, I., Sharpe, R. L. and Boxall, J. B. (2013). 'Influence of hydraulic regimes on bacterial community structure and composition in an experimental drinking water distribution system'. **Water Res**, 47**,** pp. 503-16.

14. Elenter, D., Milferstedt, K., Zhang, W., Hausner, M. and Morgenroth, E. (2007). 'Influence of detachment on substrate removal and microbial ecology in a heterotrophic/autotrophic biofilm'. **Water Res**, 41**,** pp. 4657-4671.

15. Flemming, H. C., Percival, S. L. and Walker, J. T. (2002). 'Contamination potential of biofilms in water distribution systems'. **Innovations in Conventional and Advanced Water Treatment Processes**, 2**,** pp. 271-280.

16. Flemming, H. C. and Wingender, J. (2010). 'The biofilm matrix'. **Nature Reviews Microbiology**, 8**,** pp. 623-633.

17. Florjanic, M. and Kristl, J. (2011). 'The control of biofilm formation by hydrodynamics of purified water in industrial distribution system'. **International Journal of Pharmaceutics**, 405**,** pp. 16-22.

18. Garny, K., Horn, H. and Neu, T. R. (2008). 'Interaction between biofilm development, structure and detachment in rotating annular reactors'. **Bioprocess Biosyst Eng**, 31**,** pp. 619-629.

19. Garrett, T. R., Bhakoo, M. and Zhang, Z. (2008). 'Bacterial adhesion and biofilms on surfaces'. **Progress in Natural Science**, 18**,** pp. 1049-1056.

20. Hall-Stoodley, L., Costerton, J. W. and Stoodley, P. (2004). 'Bacterial biofilms: from the natural environment to infectious diseases'. **Nat Rev Microbiol**, 2**,** pp. 95-108.

21. Hall, J., Szabo, J., Panguluri, S. and Meiners, G. (2009). 'Distribution System Water Quality Monitoring: Sensor Technology Evaluation Methodology and Results' A Guide for Sensor Manufacturers and Water Utilities. Environmental Protection Agency (EPA), USA.

22. Heilbronner, R. and Barrett, S. (2014). '**Image Analysis in Earth Sciences**', Springer.

23. Horn, H., Reiff, H. and Morgenroth, E. (2003). 'Simulation of growth and detachment in biofilm systems under defined hydrodynamic conditions'. **Biotechnol Bioeng**, 81**,** pp. 607-617.

24. Kepner, R. L. and Pratt, J. R. (1994). 'Use of Fluorochromes for Direct Enumeration of Total Bacteria in Environmental-Samples - Past and Present'. **Microbiological Reviews**, 58**,** pp. 603-615.

25. Kumarasamy, M. V. and Maharaj, P. M. (2015). 'The Effect of Biofilm Growth on Wall Shear Stress in Drinking Water PVC Pipes'. **Polish Journal of Environmental Studies**, 24**,** pp. 2479-2483.

26. Lee, S. H., Lee, S. S. and Kim, C. W. (2002). 'Changes in the cell size of Brevundimonas diminuta using different growth agitation rates'. **PDA J Pharm Sci Technol**, 56**,** pp. 99-108.

27. Liu, S., Gunawan, C., Barraud, N., Rice, S. A., Harry, E. J. and Amal, R. (2016). 'Understanding, Monitoring, and Controlling Biofilm Growth in Drinking Water Distribution Systems'. **Environ Sci Technol**, 50**,** pp. 8954-8976.

28. Manuel, C. M. (2007). '**Biofilm Dynamics and Drinking Water Stability: Effects of Hydrodynamics and Surface Materials**'. Ph.D Thesis, University of Porto, Portugal.

29. Manuel, C. M., Nunes, O. C. and Melo, L. F. (2007). 'Dynamics of drinking water biofilm in flow/non-flow conditions'. **Water Res**, 41**,** pp. 551-562.

30. Momba, M. N. B., Kfir, R., Venter, S. N. and Cloete, T. E. (2000). 'An overview of biofilm formation in distribution systems and its impact on the deterioration of water quality'. **Water SA**, 26**,** pp. 59-66.

31. Rusconi, R., Lecuyer, S., Guglielmini, L. and Stone, H. A. (2010). 'Laminar flow around corners triggers the formation of biofilm streamers'. **Journal of the Royal Society Interface**, 7**,** pp. 1293-1299.

32. Russ, J. C. 2011. '**The image processing handbook, Sixth Edition**', North Carolina State University, Materials Science and Engineering Department, Raleigh, North Carolina, CRC Press.

33. Saur, T., Morin, E., Habouzit, F., Bernet, N. and Escudie, R. (2017). 'Impact of wall shear stress on initial bacterial adhesion in rotating annular reactor'. **PLoS One**, 12**,** https://doi.org/10.1371/journal.pone.0172113

34. Sheng, G. P., Yu, H. Q. and Li, X. Y. (2010). 'Extracellular polymeric substances (EPS) of microbial aggregates in biological wastewater treatment systems: A review'. **Biotechnology Advances**, 28**,** pp. 882-894.

35. Simões, L. C. (2012). '**Biofilms in drinking water**'. Biofilms in drinking water: formation and control. LAMBERT Academic Publishing.

36. Son, K., Brumley, D. R. and Stocker, R. (2015). 'Live from under the lens: exploring microbial motility with dynamic imaging and microfluidics'. **Nature Reviews Microbiology**, 13**,** pp. 761-775.

37. Srinivasan, S., Harrington, G. W., Xagoraraki, I. and Goel, R. (2008). 'Factors affecting bulk to total bacteria ratio in drinking water distribution systems'. **Water Res**, 42**,** pp. 3393-3404.

38. Staudt, C., Horn, H., Hempel, D. C. and Neu, T. R. (2004). 'Volumetric measurements of bacterial cells and extracellular polymeric substance glycoconjugates in biofilms'. **Biotechnol Bioeng**, 88**,** pp. 585-592.

39. Stoodley, P., Boyle, J. D., DeBeer, D. and Lappin-Scott, H. M. (1999a). 'Evolving perspectives of biofilm structure'. **Biofouling**, 14**,** pp. 75-90.

40. Stoodley, P., Dodds, I., Boyle, J. D. and Lappin-Scott, H. M. (1999b). 'Influence of hydrodynamics and nutrients on biofilm structure'. **J Appl Microbiol**, 85**,** pp. 19S-28S.

41. Szabo, J. G., Rice, E. W. and Bishop, P. L. (2007). 'Persistence and decontamination of Bacillus atrophaeus subsp. globigii spores on corroded iron in a model drinking water system'. **Appl Environ Microbiol**, 73**,** pp. 2451-2457.

42. van Loodsdrecht, M. C. M., Eikelboom, D., Gjaltema, A., Tijhuis, L. and Heijnen, J. J. (1995). 'Biofilm structures'. **Water Science and Technology**, 32**,** pp. 35-43.

43. Wimpenny, J., Manz, W. and Szewzyk, U. (2000). 'Heterogeneity in biofilms'. **Fems Microbiology Reviews**, 24**,** pp. 661-671.

44. Yang, X. M., Beyenal, H., Harkin, G. and Lewandowski, Z. (2000). 'Quantifying biofilm structure using image analysis'. **J Microbiol Methods**, 39**,** pp. 109-119.

45. Zheng, M. Z., He, C. G. and He, Q. (2015). 'Fate of free chlorine in drinking water during distribution in premise plumbing'. **Ecotoxicology**, 24**,** pp. 2151-2155.

46. Zlatanović, Lj., van der Hoek, J. P. and Vreeburg, J. H. G. (2017). 'An experimental study on the influence of water stagnation and temperature change on water quality in a full-scale domestic drinking water system'. **Water Res**, 123, pp. 761-772.

RESTORATION OF TWO GREEK LAKES (KASTORIA AND KORONIA): SUCCESS STORIES?

M. Moustaka-Gouni[1*], M. Katsiapi[1,2], N. Stefanidou[1], E. Vardaka, S[3]. Genitsaris[1], K. A. Kormas[4], F. Georgoulis[1]

[1]School of Biology, Aristotle University of Thessaloniki, 541 24 Thessaloniki, Greece
[2]EYATH SA, Thessaloniki Water Treatment Facility, 570 08, Nea Ionia, Thessaloniki, Greece
[3]Department of Nutrition and Dietetics, Alexander Technological Educational Institute of Thessaloniki, 574 00 Sindos, Greece
[4]Department of Ichthyology & Aquatic Environment, School of Agricultural Sciences, University of Thessaly, 384 46 Volos, Greece

*Corresponding author: e-mail: mmustaka@bio.auth.gr

Abstract
Lake Kastoria and Lake Koronia, both shallow (maximum depth 8-9 m) and large lakes (29 and 45 km^2, respectively) of Greece, 50 years ago, have undergone heavy degradation by human activities over the past decades. Since 2002, Koronia became a temporary lake due to a dramatic decrease in surface area and depth owing to unsustainable water management. During the last two decades, efforts have been made for the restoration of both lakes based on programmes of measures. In this work we present the long-term phytoplankton changes in the lakes under restoration aiming to identify a) critical changes in target phytoplankton attributes set for ecological restoration and b) success in ecological water quality improvement. Following 23 years of sewage diversion in Kastoria and the last two years' adjustment of the lake's water level through flushing, all phytoplankton metrics (species composition, phytoplankton biomass, cyanobacterial biomass, *Microcystis* biomass) indicate partial success in community restoration and an obvious water quality improvement. The dominance of several non-harmful and good quality species of the genera *Ceratium*, *Fragillaria*, *Dinobryon*, *Mallomonas*, *Cryptomonas*, *Rhodomonas* and *Nitzschia* indicates species recover, however not complete, opening ecological processes restoration. In particular, after the episode of a heavy toxic cyanobacterial bloom (with *Microcystis* dominating the phytoplankton community) in 2014, the implementation of the flushing tool in 2016 - 2017 resulted in phytoplankton and cyanobacterial biomass decrease and temporal restriction of harmful species. On the other hand, in Lake Koronia, after the metaphyton dominance in the first years following the lake's re-flooding (2010) the phytoplankton "seed-bank" species ruled over. During 2015 -2017, phytoplankton biomass comprised of a mixture of phytoplankton species recruited from the sediment, which dominated in the lake water since 2003. Specifically, in 2015-2017, the composition and species dominance were almost identical with those of the recently re-generated Lake Karla, known for its bad water quality and the recurrent episodes of fish and bird kills. Co-occurrence of the potential toxic, "seed-bank" species *Anabaena aphanizomenoides* /*Aphanizomenon favaloroi*, *Prymnesium parvum*, *Planktothrix* sp., *Anabaenopsis elenkinii*, *Arthrospira fusiformis*, *Cylindrospermopsis raciborskii* and *Pfiesteria piscicida* was recorded in Koronia in 2017. Based on the results of the present study, Lake Kastoria improved to a moderate quality in 2017 while Lake Koronia was characterized by a bad water quality the same year. This study is useful for the decisions involved in water quality management and implementation of the restoration programmes in both lakes.

Keywords: Lakes Kastoria and Koronia, ecological restoration, water quality, phytoplankton

1. INTRODUCTION

The core objective of the Water Framework Directive (WFD) is that all surface waters should be in good or better ecological status by 2015 or at the latest in 2027 (European Commission, 2000). Excess nutrient loading has induced the development of high phytoplankton biomass and harmful algal and cyanobacterial blooms, degrading lake water quality (Vardaka et al, 2005; Michaloudi et al, 2009). During the past century, efforts have been made throughout European countries to reverse eutrophication and improve water quality by implementing various restoration measures. For instance, in Lake Constance, after several decades of eutrophication, a decrease in phosphorus loading over a decade (80' s) led to a partial recovery from eutrophication (Sommer et al, 1993) and finally the lake returned to oligotrophy (Eckmann et al, 2006). However, the eutrophication pressure still represents an important threat to the integrity of lake ecosystems and one of the main causes that 44% of European lakes fail to meet the good ecological status standards (EEA-ETC, 2012). To achieve the good status, the Member States should define and implement the necessary restoration programmes.

Lake Kastoria and Lake Koronia were both shallow and large lakes of Greece 50 years ago. Since then, the lakes have undergone heavy degradation by human activities. During the last two decades, efforts have been made for the restoration of both lakes based on conservation programmes and the implementation of various measures. In Lake Kastoria, a positive phytoplankton response and water quality improvement was observed fifteen years after sewage diversion and nutrient control (Katsiapi et al, 2013). However, a deterioration was evident in 2014 with the appearance of an extended cyanobacterial scum (Figure 1) covering large part of the lake; this intense cyanobacterial incident was responsible for the production of an unpleasant odor affecting the residents of the town of Kastoria, thus even been mentioned in the Greek media. On the other hand, Lake Koronia became a temporary lake since 2002, due to a dramatic decrease in surface area and depth, caused by unsustainable water resource management (Michaloudi et al, 2012). In 2010, dense mats of metaphytic chlorophytes and cyanobacteria appeared in the lake after it was artificially flooded through a channel constructed under the lake's restoration programme (Moustaka-Gouni et al, 2012).

In ecosystem restoration, the assumption is made that with the recovery of species, ecological processes will also be restored (Lake et al, 2007). According to potential degradation - community recovery pathways proposed by Lake et al (2007) and adapted from Sarr (2002), if the disturbance is stopped and the habitat is rebuilt, then recovery will be complete and may be relatively rapid. In many eutrophic lakes, restoration aims at a significant decrease of total phytoplankton biomass with simultaneous shift in species dominance and if nutrients are successfully controlled then the phytoplankton recovery will happen, however, relatively slow (Romo et al, 2005; Katsiapi et al, 2013). In attempts to re-establish populations, knowledge of the species' life-histories is critical. The life history traits contribute to the system's ability to supply recruits and support established species (Palmer et al, 1997). Knowledge of phytoplankton species life-histories is especially decisive for community recovery and restoration success (Moustaka-Gouni et al, 2012) in shallow degraded lakes with long histories of cyanobacterial and other disruptive phytoplankton blooms (e.g. Moustaka-Gouni et al, 2006; Michaloudi et al, 2009). Unsuccessful restoration is usually due to the emphasis paid on restoring the abiotic factors and at the same time ignoring the biotic ones, e.g. phytoplankton species life-histories and their population interactions (Suding et al, 2004). In the present study, we use phytoplankton as a target indicator to identify critical changes for successful ecological restoration and ecological water quality improvement. This selection is based on the double role of phytoplankton as an indicator of ecological water quality and as an impact on ecosystem functioning and services (Katsiapi et al, 2016) due to the formation of disruptive cyanobacterial and algal blooms (Michaloudi et al, 2009; Moustaka-Gouni et al, 2016). Particularly, we combine published information on phytoplankton changes and novel data of recent years from the lakes under restoration, aiming to identify critical changes in phytoplankton indicators for ensuring ecological restoration success. For this, total phytoplankton biomass, phytoplankton species biomass forming harmful and disruptive cyanobacterial and algal blooms, two modified Nygaard's indices and a new index based

on quality group species were estimated according to the innovative phytoplankton community index PhyCoI (Katsiapi et al. 2016). PhyCoI was developed for monitoring ecological status and was validated by using data from Greek lakes (Katsiapi et al, 2016). Ecological water quality was also assessed by using the PhyCoI index. For Lake Koronia, we also focused on species recruitment traits that are critical for their establishment in lake plankton after its drying out (Moustaka-Gouni et al 2012).



Figure 1. View of the water of Lake Kastoria along its shore in the town of Kastoria in September 2014 (cyanobacterial scum) and September 2017 (cyanobacterial bloom).

2. STUDY SITE

Lake Kastoria (40º 83′ 09″ N, 21º 81′ 89″ E) is a polymictic lake with a 30 km^2 surface area, a maximum depth of about 8 m, and an average depth of about 4 m, situated at 625 m above sea level. In Lake Kastoria the presence of toxic cyanobacteria was established in 1987 (Cook et al, 2004). From 1987 until 2014, several toxic cyanobacterial blooms occurred in the lake (Cook et al. 2004; Moustaka-Gouni et al, 2006; Papadimitriou et al, 2010; Katsiapi and Moustaka-Gouni, 2016).

Lake Koronia (40º 40′ 58″ N, 23º 09′ 33″ E) at 75 m above sea level used to be the fourth largest lake in Greece occupying an area of 46 km^2 and having a maximum depth of 8 m in the 1960's. The two lakes in the 1960's had similar basic morphometric attributes for the same lake type (WFD ANNEX II; European Commission, 2000) differing only in their altitude. However, a dramatic decrease in the surface area and depth of Lake Koronia due to anthropogenic effects and enhanced by prolonged drought periods resulted in the drying out of the lake in 2002, 2007, 2009 and in January of 2014 (Michaloudi et al, 2012; Moustaka-Gouni et al, 2012; Moustaka-Gouni et al, unpublished data). However, in 2014 - 2017 heavy rainfalls contributed to a lake maximum depth of about 2 m. In addition to its dramatic size decrease and heavy pollution, Lake Koronia shifted from a freshwater to

a brackish lake. In September - October 2017 although conductivity of the lake water ranged in lower values (5.5 and 6.0 mS cm^{-1}) than previous years (e.g. Michaloudi et al, 2009) , Koronia still remains a very shallow brackish lake, thus a heavily modified water body according to WFD definitions (European Commission, 2000). Regarding the ecological harms in Lake Koronia, in August 1995 (maximum depth 1 m) a massive kill of all fish occurred coinciding with a pH > 10 due to hypertrophic conditions and high photosynthetic rates of high populations of the nanoplanktic phytoplankters *Chlorogonium* and *Oocystis* species (Michaloudi et al, 2012). In 2004, a massive bird and fish kill occurred in the lake coinciding with an extremely dense bloom of the known toxic *Prymnesium parvum* (Genitsaris et al, 2009). In 2007, a mass mortality of flamingos coincided with a dense bloom of known toxic cyanobacteria (Moustaka-Gouni et al, 2007) while a bird kill in August 2015 also coincided with a bloom of known toxic cyanobacteria (this study).

3. METHODS

For the long-term data of this study all the available publications in the scientific literature until January 2018, involving studies on phytoplankton in relation to ecological restoration of Lake Kastoria and Lake Koronia have been used. The most recent data (2014 -2017 for Lake Kastoria and 2015-2017 for Lake Koronia) come from the examination of phytoplankton samples collected from the two lakes respectively.

Phytoplankton sampling was carried out during the warm period of the year in both lakes. In Lake Kastoria samples were collected in August and September 2014, June, July, August and September 2016 and April, May, July, September and October 2017 in one sampling point. In Lake Koronia samples were collected in July, August 2015 (by the National Monitoring Water Network), September 2016 and September and October 2017 in one or two sampling points (in 2017: Analipsi and Anachoma; Figure 2).

Fresh and preserved phytoplankton samples were examined using an inverted microscope with phase-contrast technique (Nikon SE 2000) and species were identified to species level using taxonomic keys and papers (e.g. Hindak and Moustaka, 1988; Moustaka-Gouni et al, 2016. Phytoplankton counts (cells, filaments, colonies) were performed using the Utermöhl method; at least 400 individuals were counted in each sample. The dimensions of 30 individuals (cells, filaments, colonies) were measured and the cell, filament and colony volumes were estimated using appropriate geometric formulae (e.g. Moustaka-Gouni et al, 2014). Both phytoplankton identification and counting were performed in a highly consistent way by two scientists under the supervision of the same expert. Species comprising of more than 10% to the total phytoplankton biomass were considered to be dominant.

The phytoplankton indicator that is used here as a target to identify critical changes for successful ecological restoration and ecological water quality improvement is based on the calculation of the PhyCoI index (Katsiapi et al, 2016). As a target indicator for lake restoration, we adopt here all five metrics of PhyCoI, which are a) the total phytoplankton biovolume / biomass, b) the cyanobacterial biovolume / biomass according to WHO Guidelines for safe water use (Bartram et al, 1999) plus, the biovolume/ biomass of other known ecosystem disruptive algal blooms, c-d) the modified Nygaard Index calculated as two different sub-indices using species richness and biomass, respectively and e) the Quality Group species sub-index using the species richness of certain taxonomic groups that are associated with water quality. Apart of the obvious harm to humans, harmful algal/cyanobacterial blooms may disrupt ecosystem structure and function (e.g. blooms of *Prymnesium parvum*; Michaloudi et al, 2009; Oikonomou et al, 2012) that is important metric in assessing the ecological restoration success of a lake. The sum of their scores is a final indicator value, namely the PhyCoI index, ranging from 0 to 5. This indicator range is subdivided in five classes of ecological quality corresponding to the following levels of impairment: 0-1: bad, >1-2: poor, >2-3: moderate, >3-4: good, >4-5: high/reference. For estimating the score of the metric phytoplankton biovolume / biomass, class boundaries for total phytoplankton biovolume/biomass for Lake Kastoria and Lake

Koronia are those of the preliminary lake types numbered 6 and 8, respectively, by Katsiapi et al (2016).



Figure 2. View of the water of the Analipsi and Anachoma sampling points in Lake Koronia in September 2017.

4. RESULTS AND DISCUSSION

4.1 Phytoplankton long - term changes

The long - term changes of the total phytoplankton biomass scaled up to boundaries of the five classes of ecological classification for the preliminary types of the studied lakes according to Katsiapi et al (2016) are presented in Fig. 3. In Lake Kastoria the high phytoplankton biomass of the period 1994 – 1996, exceeding the poor - bad quality boundary, decreased in 2003 and 2005 indicating a moderate quality; a reverse trend though in 2007 resulted again in a bad lake water quality in 2014. Phytoplankton biomass decreased and water quality improved to a moderate level again in 2016 - 2017. This biomass decline was attributed to a flushing of lake water (Moustaka - Gouni et al, 2017). Particularly, in 2016, water discharge from Lake Kastoria was regulated by ecologically - based water level recessions within critical limits (Moustaka-Gouni et al, 2017). In March 1.27 % of lake water volume was discharged within five days while in May 0.5 % of lake water volume was discharged within two days. A shift of dominance in early summer from toxic cyanobacteria (Katsiapi et al, 2013) to other phytoplankton groups is indicative of an improved water quality (Katsiapi et al. 2016). Species such as the dinoflagellate *Ceratium hirundinella* and the diatom *Fragillaria crotonensis* became dominant in 2016 (Figure 4) while the toxic cyanobacterium *Microcystis* decreased to very low levels. In 2017, the dominance of the chrysophytes *Dinobryon* and *Mallomonas* in April - May, and of the cryptophyte *Cryptomonas* and the diatom *Nitzschia* in October (Figure 4) indicates further improvement of ecological water quality, though within the range of a eutrophic lake. This dinoflagellate, diatom, cryptophyte and chrysophyte dominance from April to October, within the

hottest period that is ideal for cyanobacterial growth, restricted cyanobacteria during July-September, suggesting partial recovery of the phytoplankton community (Katsiapi et al, 2013).

In Lake Koronia, phytoplankton biomass levels were indicative of a moderate water quality after the lake drying out in 2002 and its initial flooding in 2003 (Figure 3). This was due to the initial heterotrophic phase of plankton succession (Michaloudi et al, 2012). Harmful and disruptive blooms contributed to the very high phytoplankton biomass recorded during 2004 - 2011, which was indicative of a bad quality (Moustaka - Gouni et al, 2012). A significant decrease of total phytoplankton biomass with a simultaneous increase of species diversity, indicative of good quality, was recorded in 2015 (Figures 3, 5). However, the low phytoplankton biomass in the summer 2015 was preceded by a heterotrophic phase (until June) when the lake water was dominated by detritus from metaphytic algae and conspicuous heterotrophic bacteria (Moustaka-Gouni et al, unpublished data). In addition to the heterotrophic phase indicating high organic matter, phytoplankton biomass although relatively low was not representative of a good water quality due to the dominance of cyanobacteria (Figure 5). Specifically, in late August, species known to produce cyanotoxins such as *Anabaena aphanizomenoides* re-classified as *Aphanizomenon favaloroi* according to Moustaka-Gouni et al (2016) and *Anabaenopsis elenkinii* (Table 1, Figure 5) comprising half of the total phytoplankton biomass (14.6 mg L^{-1}) coincided with a bird kill in the lake (Action for Wild Life, S. Kalpakis pers. com.). These two cyanobacterial species were also observed in Lake Koronia in 2004 coinciding with a mass bird kill (Michaloudi et al, 2012). It is worth noting that *A. favaloroi*, reported for first time in Europe, formed 100% of the total phytoplankton biomass in the brackish Lake Vistonis in 2014 and was associated with the production of saxitoxins and a massive fish kill in the lake (Moustaka-Gouni et al, 2016). Furthermore, the dominant cyanobacteria *A. favaloroi* and *A. elenkinii* in Lake Koronia in August 2015 also dominated the phytoplankton community of the Greek Lake Karla with a simultaneous cyanotoxins occurrence during the period of pelican mortality in July 2016 (Papadimitriou et al, 2018) and in 2017 (Moustaka-Gouni et al, unpublished data). In 2016 and 2017 despite the increase of water depth an abrupt increase in phytoplankton biomass and a worsening of the water quality (poor in 2016 and bad in 2017) was observed (Figures 3, 5). The dominant species were the known toxin-producing cyanobacteria *A.aphanizomenoides* /*A. favaloroi*, *Cylindrospermopsis raciborskii*, *A. elenkinii* and *Planktothrix* sp. (Figure 5; Table 1). A rare occurrence of the haptophyte *Prymnesium* cf. *parvum* and the dinoflagellate *Pfiesteria piscicida* was also recorded (Table 1). This was the first record of *P. parvum* in the plankton community of Lake Koronia after 13 years of its harmful bloom (Moustaka-Gouni et al. 2012), while this is the first record of *P. piscicida* in the lake. Both species have been also recorded in Lake Karla (Table 1) coinciding with fish kills (e.g. Oikonomou et al. 2012).

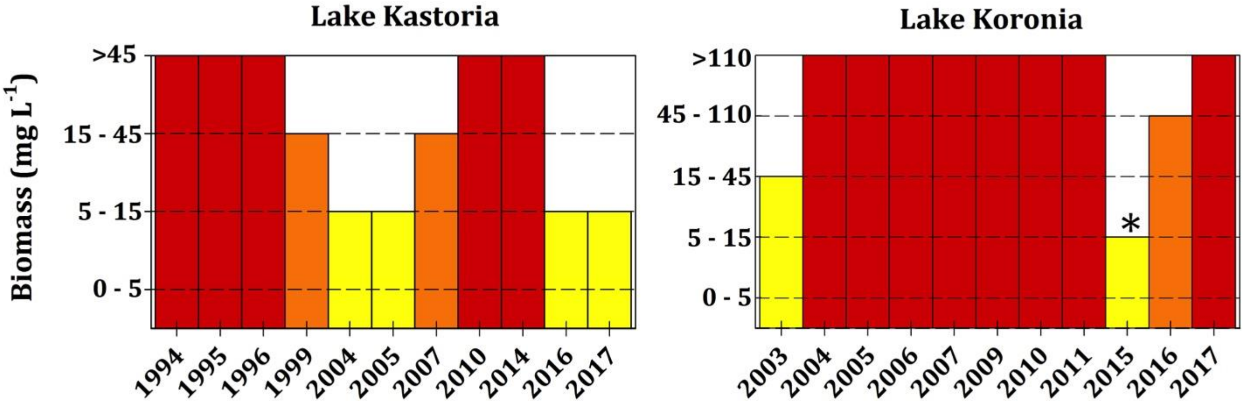


Figure 3. Long-term changes of total phytoplankton biomass scaled up to boundaries of the five classes of ecological classification in lakes Kastoria and Koronia according to Katsiapi et al (2016). Asterisk in Lake Koronia indicates the heterotrophic phase and the cyanobacteria dominance in the relatively low phytoplankton biomass in 2015.

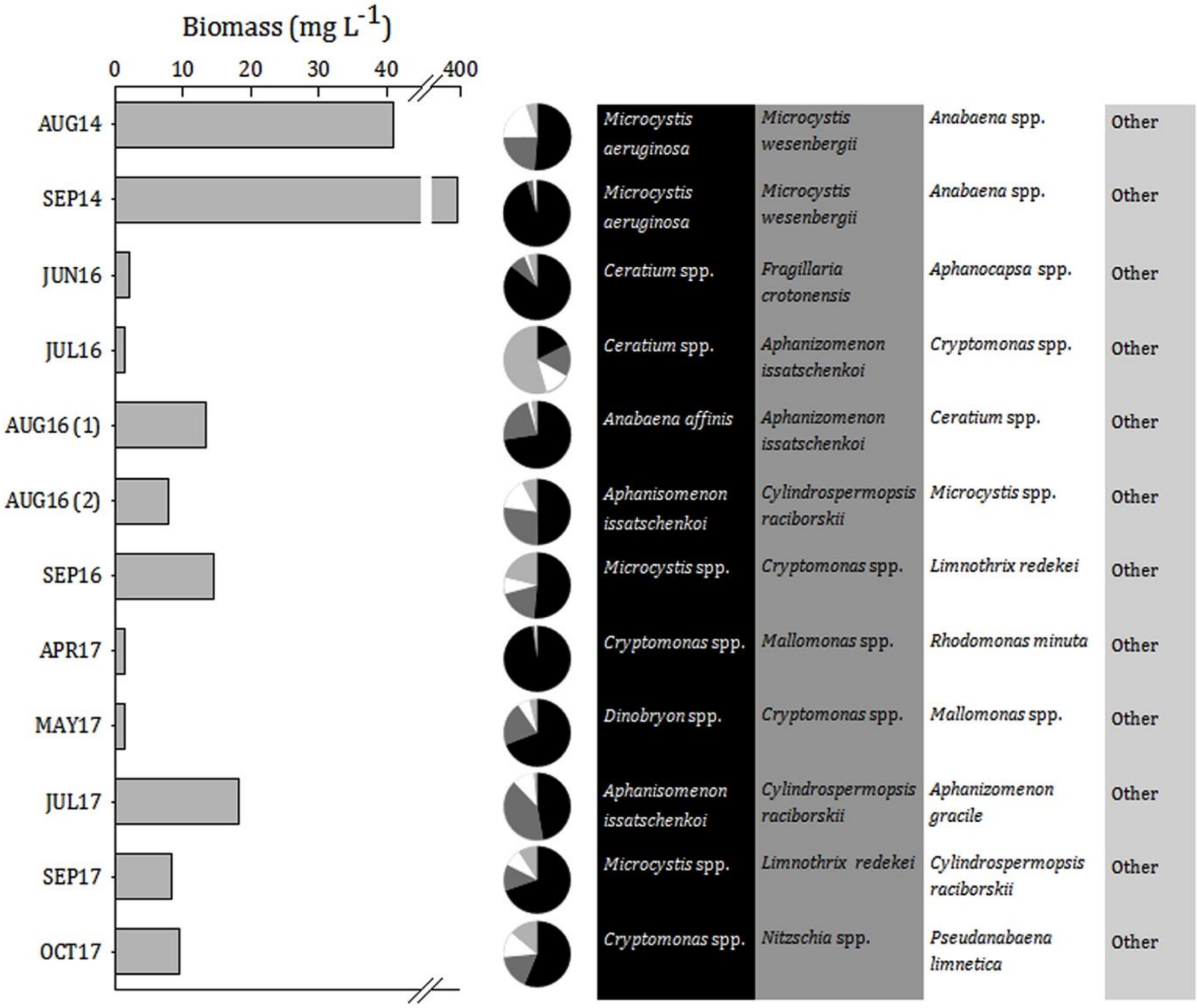


Figure 4. Temporal changes in total phytoplankton biomass and species dominance in Lake Kastoria.

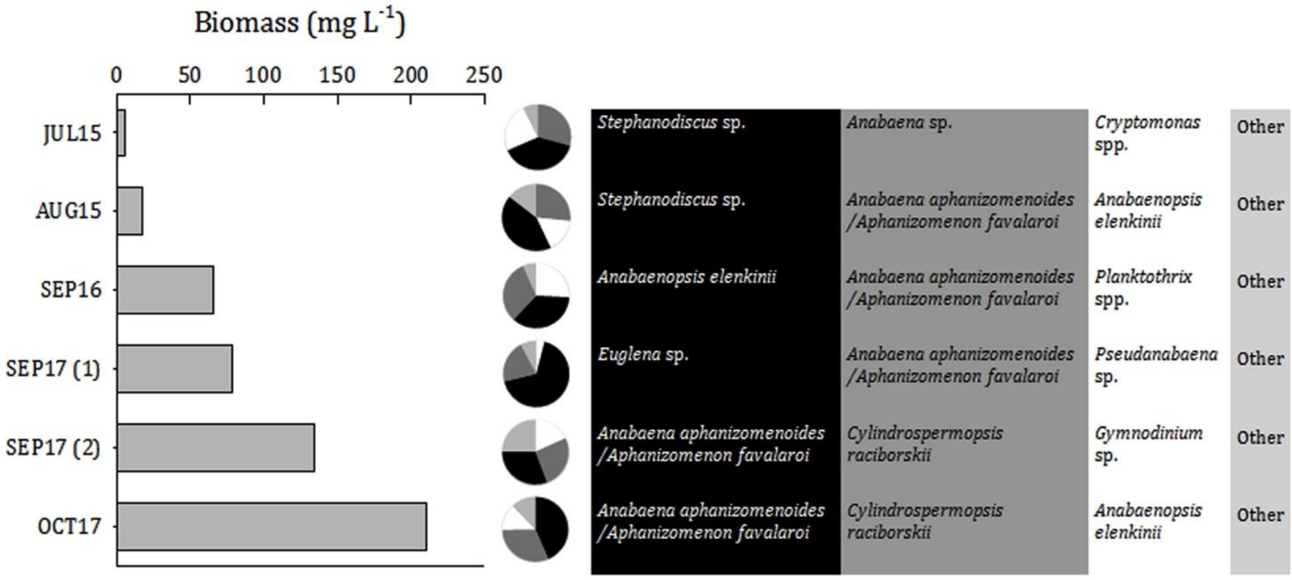


Figure 5. Temporal changes in total phytoplankton biomass and species dominance in Lake Koronia.

Table 1. Known toxin-producing species identified in the phytoplankton of Lake Koronia (this study, 2015-2017) and Lake Karla [according to Oikonomou et al. (2012) and Papadimitriou et al. (2018)].

	Lake Koronia	Lake Karla
Cyanobacteria		
Anabaena aphanizomenoides /*Aphanizomenon favaloroi*	√	√
Anabaenopsis elenkinii	√	√
Arthrospira fusiformis		√
Cylindrospermopsis raciborskii	√	√
Planktothrix sp.	√	√
Prymnesiophyceae		
Prymnesium cf. *parvum*	√	√
Dinophyceae		
Pfiesteria piscicida	√	√

4.2 Phytoplankton indicator for assessing success in ecological restoration

The values of the target indicator (PhyCoI index) of the lakes' restoration success are presented in Figure 6. In Lake Kastoria, a significant decrease of total phytoplankton biomass with a simultaneous decrease of the cyanobacterial biomass and a shift in species dominance from 2014 to 2016 resulted in a sharp increase of the phytoplankton target indicator, reflecting a good water quality. The highest indicator value (4.2) was recorded in April - May 2017 showing a further success in restoration through partial recovery of those phytoplankton species reflecting improvement in ecological water quality. In average, the indicator value was slightly below 3 for the years 2016-2017, the boundary of moderate-good water quality. However, water quality still remains lower than good, while toxicity of the remaining cyanobacteria in the lake water with possible health risks related to the use of lake water for recreational activities has been recorded (Katsiapi and Moustaka-Gouni, 2017). Taking into consideration these results, further effort for restoration should be continued by authorities to eliminate toxic cyanobacteria leading to a complete species recovery.

In contrast to the obvious water quality improvement of Lake Kastoria in 2017 and the ongoing success of ecological restoration (Figure 7), deterioration of water quality was abrupt in Lake Koronia in 2017. The index value decreased from 2.2 (average 2015) and 1.1 (2016) to 0.8 (average 2017) (Figure 6). This deterioration (Figure 7) can be explained by the assumption made by Lake et al (2007) that with the recovery of species, ecological processes will also be restored. In Koronia, phytoplankton species recovery (such as *Stephanodiscus*; Figure 5) was restricted in 2015. In 2016 and 2017, the lake's phytoplankton community (Table 1, Figure 5) was characterized by species dominating degraded lakes with frequent occurrence of harmful cyanobacterial blooms, disruptive

Prymnesium blooms and euglenophytes blooms, characteristic of polluted waterbodies (e.g. Oikonomou et al, 2012; Nikouli et al, 2013; Papadimitriou et al, 2018). Attempts to re-establish populations of good quality species require knowledge of the species' life-histories. In Koronia, when the lake water volume increased in 2015-2017, the phytoplankton life-history traits contributed to the ability of the system to supply recruits (Palmer et al, 1997) and support establishment of the harmful sediment "seed-bank" species, previously established in the degraded lake as invaders and "seed-bank" species (Moustaka-Gouni et al, 2012).

In particular, in 2004, the haptophyte *P. parvum* was considered a successful invader (Moustaka-Gouni et al, 2012) because of its well-known invasive behavior (for review see Roelke et al, 2016) and the favoring habitat conditions in Lake Koronia (brackish water and pollution). *Prymnesium* can survive in a wide range of salinities and it blooms in brackish inland waters worldwide as in the case in the Greek Lake Karla (Oikonomou et al, 2012). It is a heteromorphic haptophyte with flagellate, immotile cells and cysts in its life-cycle, whereas its immotile phase was first described from Lake Koronia (Genitsaris et al, 2009). *A. aphanizomenoides* /*A. favaloroi* and *A. elenkinii* were also recruited from the sediment and overgrew in the lake water. *P. piscicida*, a known harmful dinoflagellate worldwide, reported in Karla Reservoir (Oikonomou et al, 2012) and Ismarida Lake in Greece (Koutrakis et al. 2016) can be considered a new successful invader and a "seed-bank" species for the future. *C. raciborskii* could be a "seed-bank" species due to its trait to form akinetes, as it is known also from the neighboring Lake Volvi (Moustaka-Gouni, 1988). The re-appearance of *Planktothrix* and *Arthrospira* in lake water after several years (Moustaka-Gouni et al, 2007) indicate their recruitment from the sediment. Overall, in the temporary, very shallow Lake Koronia, the phytoplankton community in 2017 was highly determined by the past phytoplankton species pool of the sediment. These results partly explain why phytoplankton community did not recover in Lake Koronia comprising an inherent barrier for successful restoration.

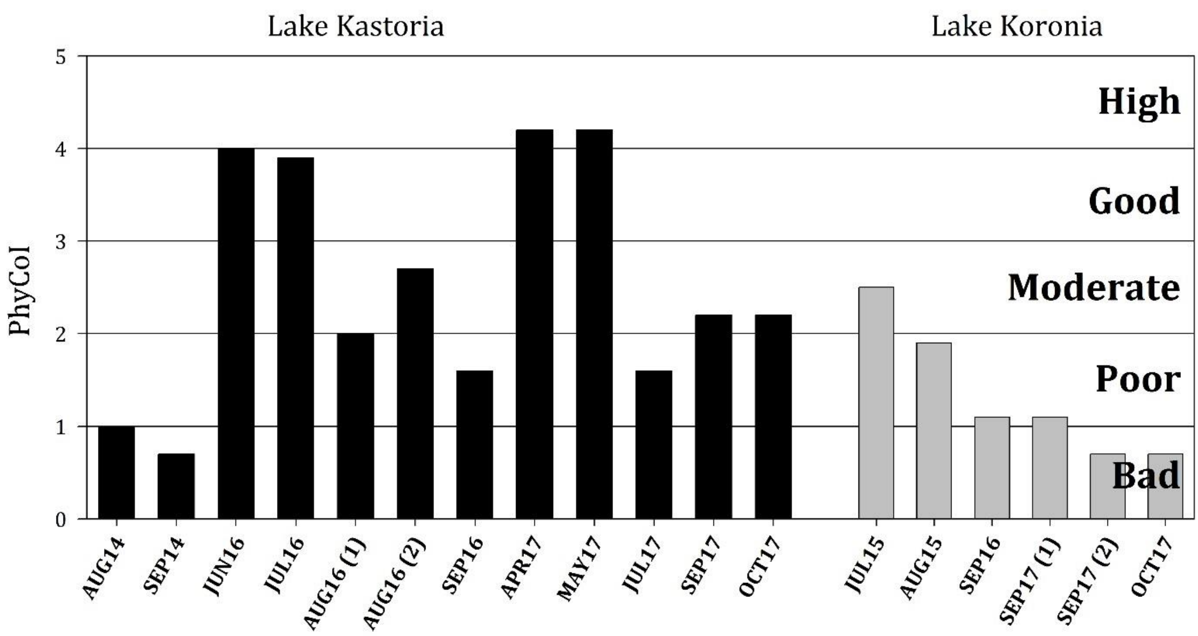


Figure 6. Temporal variations of the values of the target indicator of the lakes' restoration success scaled up to five classes (in the y-axis) of ecological classification according to Katsiapi et al (2016).

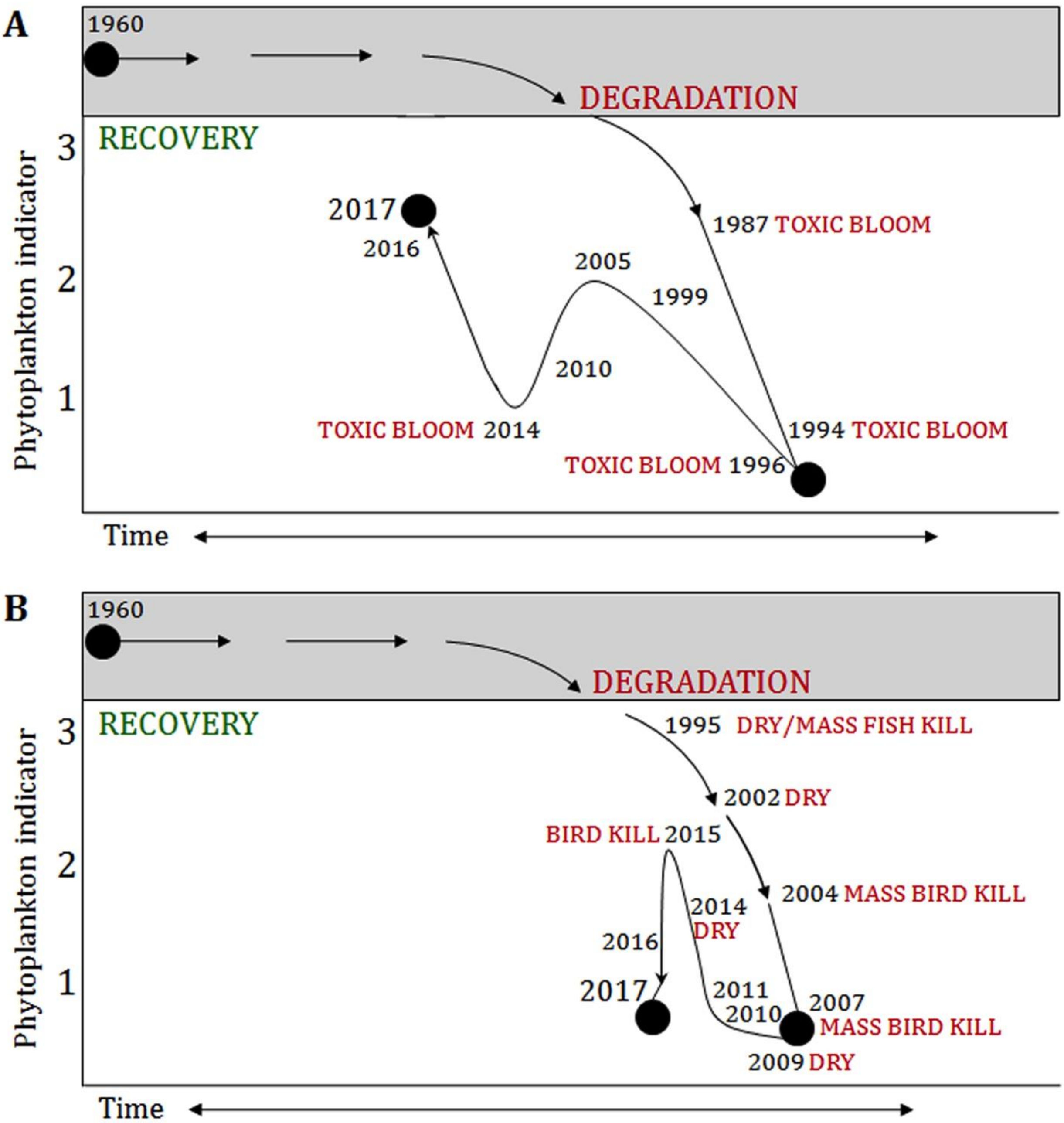


Figure 7. Putative degradation-recovery pathways in Lake Kastoria (A) and Lake Koronia (B) according to the 'shifting target model' as adapted from Sarr (2002) and Lake et al (2007). Phytoplankton indicator in y-axis corresponds to the target indicator of the lakes' restoration success based on PhyCoI (Katsiapi et al, 2016).

References

1. Bartram J., M. Burch, I.R. Falconer, G. Jones and T. Kuiper-Goodman (1999) 'Situation assessment, planning and management'. In: Chorus, I., Bartram, J. (Eds.), '**Toxic Cyanobacteria in Water**', Taylor & Francis, London, New York.

2. Cook C.M., E. Vardaka and T. Lanaras (2004) 'Toxic cyanobacteria in Greek Freshwaters, 1987-2000: Occurrence, toxicity, and impacts in the Mediterranean region', **Acta Hydrochimica et Hydrobiologica**, 32, pp. 107-124.

3. Eckmann R., S. Gerster and A. Kraemer (2006) 'Yields of European perch from Upper Lake Constance from 1910 to present', **Fisheries Management and Ecology,** 13, pp. 381- 390.

4. EEA-ETC (2012) Ecological and chemical status and pressures in European waters. Thematic Assessment for EEA Water 2012, Report, 146. Available at http://icm.eionet.europa.eu.
5. European Community (EC) (2000) 'Directive 2000/60/EC of the European Parliament and of the Council of 23 October 2000 establishing a framework for the Community action in the field of water policy', **Official Journal of the European Communities**, L 327, pp. 1-72.
6. Genitsaris S., K.A. Kormas and M. Moustaka-Gouni (2009) 'Microscopic eukaryotes living in a
7. dying lake (Lake Koronia, Greece)', **FEMS Microbiology Ecology**,69, pp. 75–83.
8. Hindák F. and M. Moustaka (1988) Planktic cyanophytes of Lake Volvi, Greece. Arch. Hydrobiol. Suppl. 80: 497–528
9. Lake P.S., N. Bond and P. Reich (2007) 'Linking ecological theory with stream restoration', **Freshwater Biology**, 52, pp. 597–615.
10. Katsiapi M., E. Michaloudi, M. Moustaka-Gouni and J. Pahissa Lopez (2012) 'First ecological evaluation of the ancient Balkan Lake Megali Prespa based on plankton', **Journal of Biological Research-Thessaloniki**, 17, pp. 51–56.
11. Katsiapi M., M. Moustaka-Gouni, E. Vardaka and K.A. Kormas (2013) 'Different phytoplankton descriptors show diverse changes in a shallow urban lake (L. Kastoria, Greece) after sewage diversion', **Fundamental Applied Limnology,** 182 (3), pp. 219–230.
12. Katsiapi M. and M. Moustaka-Gouni (2016) 'Toxin producing cyanobacteria species identification in aquatic systems'. Technical report In: ARISTEIA operational research program 'Cyanotoxins in Fresh Waters, Advances in Analysis, Occurrence and Treatment - CYANOWATER'.
13. Katsiapi M., M. Moustaka-Gouni and U. Sommer (2016) 'Assessing ecological water quality of freshwaters: PhyCoI—a new phytoplankton community Index', **Ecological Informatics**, 31, pp. 22–29.
14. Koutrakis E.T., G. Emfietzis, G. Sylaios, M. Zoidou, M. Katsiapi and M. Moustaka-Gouni (2016) 'Fish kill in Ismarida lake, Greece: identification of drivers contributing to the event', **Mediterranean Marine Science**, http://dx.doi.org/10.12681/mms.1481.
15. Moustaka M. (1988) The structure and dynamics of the phytoplankton assemblages in Lake Volvi, Greece. I. Phytoplankton composition and abundance during the period March 1984–March 1985. **Archiv fur Hydrobiologie**, 112, pp. 251–264.
16. Moustaka-Gouni, M., E. Vardaka, E. Michaloudi, K.A. Kormas, E. Tryfon, H. Mihalatou, S. Gkelis and Lanaras T. (2006) 'Plankton food web structure in a eutrophic polymictic lake with a history of toxic cyanobacterial blooms', **Limnology and Oceanography**, 51, pp. 715-727.
17. Moustaka-Gouni M., E. Michaloudi, M. Katsiapi and S. Genitsaris (2007) 'The coincidence of an *Arthrospira-Ananaenopsis* bloom and the mass mortality of birds in Lake Koronia', **Harmful Algae News**, 35, pp. 6–7.
18. Michaloudi E., M. Moustaka-Gouni, S. Gkelis and K. Pantelidakis (2009) 'Plankton community structure during an ecosystem disruptive algal bloom of *Prymnesium parvum*', **Journal of Plankton Research**, 31(3), pp. 301–309.
19. Moustaka-Gouni M., E. Michaloudi, K.A. Kormas, **M. Katsiapi**, E. Vardaka and S. Genitsaris (2012) 'Plankton changes as critical processes from restoration plans of lakes Kastoria and Koronia', **European Water**, 40, pp. 43-51.
20. Moustaka-Gouni M., A. Hiskia, S. Genitsaris, M. Katsiapi, K. Manolidi, S. Zervou, C. Christophoridis, T. Triantis, T. Kaloudis and S. Orfanidis (2016) 'First report of *Aphanizomenon*

favaloroi occurrence in Europe associated with saxitoxins and a massive fish kill in Lake Vistonis. Greece', **Marine Freshwater Research**, 67, 1e8.

21. Moustaka-Gouni M., S. Papadopoulos, E. Ampartzaki, S. Gargalas, Th. Mardiris and M. Katsiapi (2017) 'First attempt of using the ecologically based water level management of Lake Kastoria for water quality improvement: Positive results-Zero Cost', **6th Environmental Conference of Macedonia**, Thessaloniki, Greece (in Greek).
22. Moustaka-Gouni M., E. Michaloudi and U. Sommer (2014) 'Modifying the PEG model for Mediterranean lakes—no biological winter and strong fish predation', **Freshwater Biology**, 59, pp. 1136–1144.
23. Nikouli E., K.A. Kormas, P. Berillis, H. Karayanni and M. Moustaka-Gouni (2013) 'Harmful and parasitic unicellular eukaryotes persist in a shallow lake under reconstruction (L. Karla, Greece)', **Hydrobiologia**, 718, 73-83.
24. Oikonomou A., M. Katsiapi, H. Karayanni, M. Moustaka-Gouni and K. Kormas (2012) 'Plankton microorganisms coinciding with two consecutive mass fish kills in a newly reconstructed lake', **Scientific World Journal**, 504135.
25. Palmer M.A., R.F. Ambrose and N.L. Poff (1997) 'Ecological theory and community restoration ecology', **Restoration Ecology**, Vol.5, pp. 291-300.
26. Papadimitriou T., I. Kagalou, V. Bacopoulos and I.D. Leonardos (2010) 'Accumulation of microcystins in water and fish tissues: An estimation of risks associated with microcystins in most of the Greek Lakes', **Environmental Toxicology**, 25, pp. 418-427.
27. Papadimitriou T., M. Katsiapi, K. Vlachopoulos, A. Christopoulos, C. Laspidou, M. Moustaka-Gouni and K. Kormas (2018) 'Cyanotoxins as the "common suspects" for the Dalmatian pelican (*Pelecanus crispus*) deaths in a Mediterranean reconstructed reservoir', **Environmental Pollution,** 234, pp. 779-787.
28. Roelke D.L., A. Barkoh, B.W. Brooks, J.P. Grover, K. D. Hambright, J.W. LaClaire II, P.D.R. Moeller and R. Patino (2016) 'A chronicle of a killer alga in the west: ecology, assessment, and management of Prymnesium parvum blooms', **Hydrobiologia**, 764, 29-50.
29. Romo S., M. J. Villena, M. Sahuquillo, J. M. Soria, M. Giménez, T. Alfonso, E. Vicente and M. R. Miracle (2005) 'Response of a shallow Mediterranean lake to nutrient diversion: Does it follow similar patterns as in northern shallow lakes?', **Freshwater Biology**, 50, pp. 1706-1717.
30. Sarr D.A. (2002) 'Riparian livestock exclosure research in the western United States: a critique and some recommendations', **Environmental Management**, 30, pp. 516–526.
31. Sommer U., U. Gaedke and A. Schweizer (1993) 'The first decade of oligotrophication of Lake Constance', **Oecologia**, 93, pp. 276-284.
32. Suding K.N., K.L. Gross and G.R. Houseman (2004) 'Alternative states and positive feedbacks in restoration ecology', **Trends in ecology and evolution**, 19 (1), pp. 46-53.
33. Vardaka E., M. Moustaka-Gouni, C.M. Cook and T. Lanaras (2005) 'Cyanobacterial blooms and water quality in Greek waterbodies', **Journal of Applied Phycology**, 17, pp. 391–401.

EFFECTS OF CLIMATE CHANGE ON GROUNDWATER NITRATE MODELLING

G. Tziatzios*, P. Sidiropoulos, L. Vasiliades, J. Tzabiras, G. Papaioannou, N. Mylopoulos and A. Loukas

Laboratory of Hydrology and Aquatic Systems Analysis Department of Civil Engineering, UTH, GR 38334 Pedion Areos Volos,Thessalia, Greece

*Corresponding author: email**:** getziatz@uth.gr

Abstract
This paper investigates the impacts of climate change on groundwater quality at the eastern hydrogeological basin of Thessaly in Greece. A modelling system has been applied, consists of General Circulation Model for estimating the precipitation and temperature changes, a surface hydrological model (UTHBAL) for the simulation of the surface hydrological processes and the estimation of the groundwater recharge, a groundwater hydrological model (MODFLOW) for simulation of groundwater flow and finally a transport and dispersion model of examining the nitrate fate and transport under different climate changes. The analysis was conducted for two future periods, a medium term period 2030–2050 and a long term period 2080–2100 examining three different socioeconomic scenarios SRES (A2, A1B and B1). Concerning the results, nitrate concentration in groundwater is likely to increase due to the reduction of groundwater recharge forced by climate change impacts on surface hydrology processes since the agricultural practices does not change.

Keywords: Climate change, water resources management, nitrate contamination, nitrate modelling

1. INTRODUCTION

Water pollution is a top priority for protecting both the quantity and quality of groundwater. Groundwater quality degradation constitutes a common problem in the Mediterranean rural basins because of the multiple pressures in aquifers from excessive pumping and from returning irrigation flow which occurs after intense and extensive use of agrochemicals (Iglesias et al., 2007).

Nowadays, the issue of climate change is crucial to add in the main pressures on groundwater bodies. Climate change is the most important environmental threat that mankind currently faces. Furthermore, it is a fact that climate change and the hydrological cycle are closely linked. The spatial and temporal distribution changes of precipitation; evapotranspiration; temperature as well as the implementation of adaptation strategies in agriculture and ecosystems will have a direct impact on water resources (Stoll et al., 2011).

Mediterranean area is recognized as one of the world regions most affected by climate change. The majority of climatic models and scenarios predict less precipitation, higher mean and maximal temperatures in the Mediterranean during the summer (Pascual et al., 2014). In addition to, changes in the hydrological parameters of precipitation, temperature, evapotranspiration as well as the groundwater recharge bring changes in the quantity and quality assessment of groundwater hydrology (Pulido-Velazquez et al., 2015).

The purpose of this paper targets to the assessment of the impact to climate change on groundwater quality concerning the nitrate pollution in the Lake Karla basin. Nitrogen is the main vital component to enhance the plant growth. Due to this fact, the intensive use of nitrogen-based fertilizers has been

dominated in order to increase the productivity as well as the quality of crops in a large number of rural areas on the world. However, the application of nitrogen-rich fertilizer exceeds the plant demand and the denitrification capacity of the soil. Nitrogen is led to groundwater in the form of nitrate, which is highly mobile with little sorption (Almasri and Kaluarachchi, 2005).

2. KARLA LAKE CATCHMENT STUDY AREA

The basin of Lake Karla is located at the Eastern part of the Larissa plain. It presents a form of closed elongated basin with a maximum length of 52 km and a width of 17-35 km. The basin is surrounded by the river Pinios and the Ossa Mountain in the north, the Mavrovouni mountain and Pelion in the east, the Chalkodonian Mountain and the Megavouni in the south and the Mount Phyllis in the West. It is a rural basin, as the plain is the most productive agricultural area in Greece, without the presence of urban and industrial areas. Cultivations correspond to the 67% of catchment area. The database of CORINE Land Cover 2000 for Greece [EEA, 2007] was used in order to identify land use types of the catchment area. The major crops are cotton, wheat, alfa-alfa, corn, tobacco and orchards (Sidiropoulos et al., 2016).

The average slope of the basin is 11%, the terrain is smooth with less than 5% gradient in the lowlands; while up to 15% slopes in the mountain area. The region of Karla is a tectonic graben formed during the recent geological times (Sidiropoulos et al., 2013).

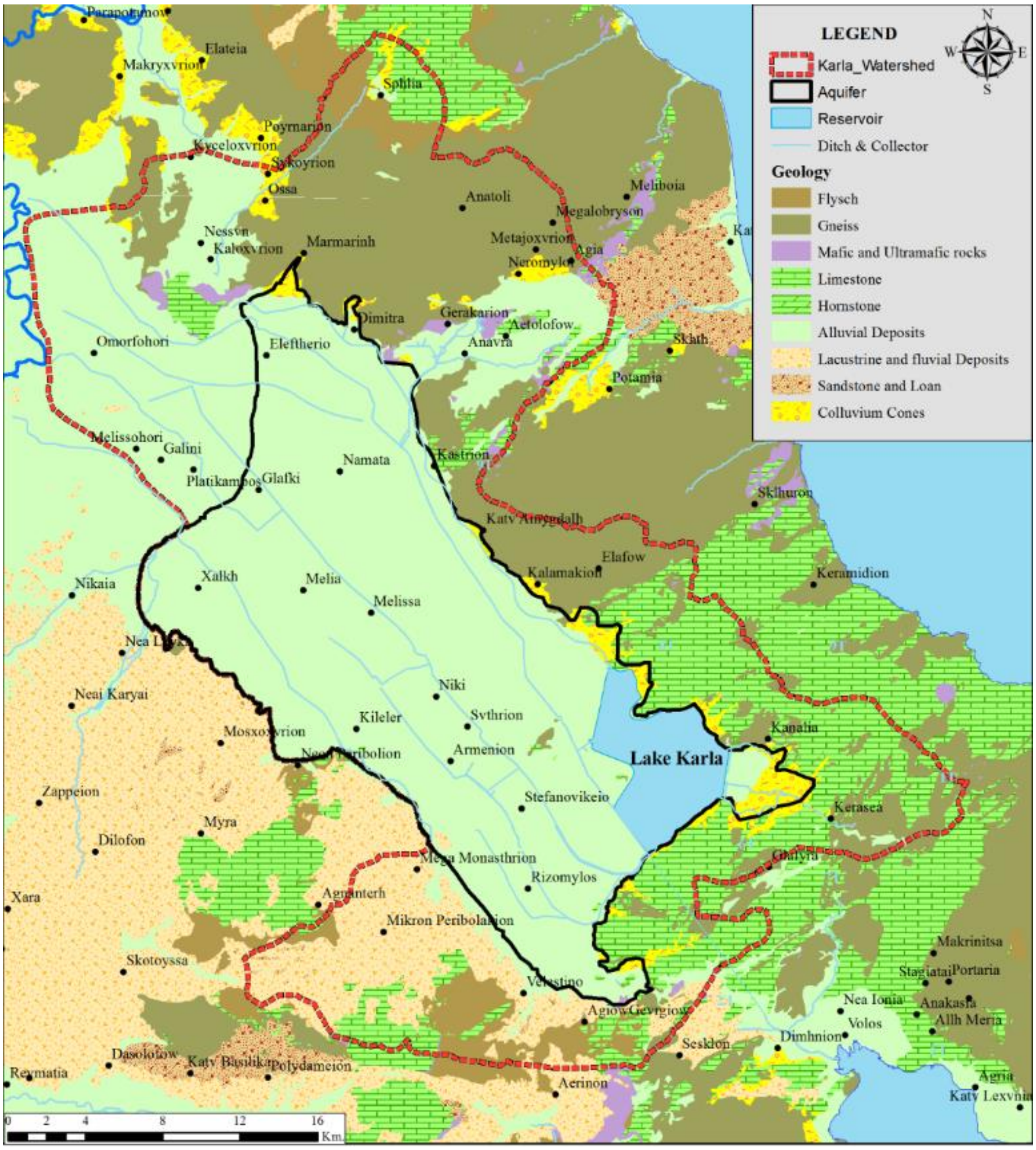
2.1 Climate and Hydrology

The microclimate of the region is classified in the Mediterranean continental climate; characterized by warm and dry summer as well as cold and humid winter. The average annual rainfall in the area is 450 mm. The average temperature is 16-17 ^{o}C, the lowest temperature presented in the winter and the maximum temperature recorded in the summer. Moreover, during the period December-March and rarely during the months of November to April observed frozen days. The mean annual relative humidity is 67- 72 % in the region.

The hydrological basin of Karla presents geomorphological variety with altitude ranges from 40 to 1970 meters and average altitude about 230 m. There are two altitude zones (sub-basins); the mountainous zone (altitude ≥ 200 m.) and the lowland zone (with altitude <200 m). The aquifer of the study area is entirely located in the low altitude zone (Sidiropoulos et al., 2015).

2.2 Geology and Hydrogeological Conditions

Impermeable geological structures cover a 30.6% of the total area of Lake Karla watershed, karstic aquifers cover a 14.5% and permeable structures, which appear mainly in the plain, cover a 54.9%. The studied area of aquifer consists of alluvial deposits (Figure 1). The basement rocks, consisting of impermeable marbles and schist, are located underneath the permeable structures (Mylopoulos and Sidiropoulos, 2014). To the east, there is the Mavrovouni Mountain, which consists mainly of impermeable bedrocks such as schist. The Thessaly plain continues to the west with the Halkodonion Mountain located to the southwest .The underlying aquifer is located in the lower part of the basin, covering an area of 500 km^2. Most of the aquifer's area is plain with an altitude ranging from 45 to 65 m. Only to the southwest the altitude reaches up to 90 m.



Picture 1: Geological map of Lake Karla basin indicating the reservoir and the boundaries of aquifer and of the basin

3. METHODOLOGY – MODELLING SYSTEM

A physically based integrated modelling system was applied and its form presented in Figure 2. The modelling system consists of four computational simulation programs:

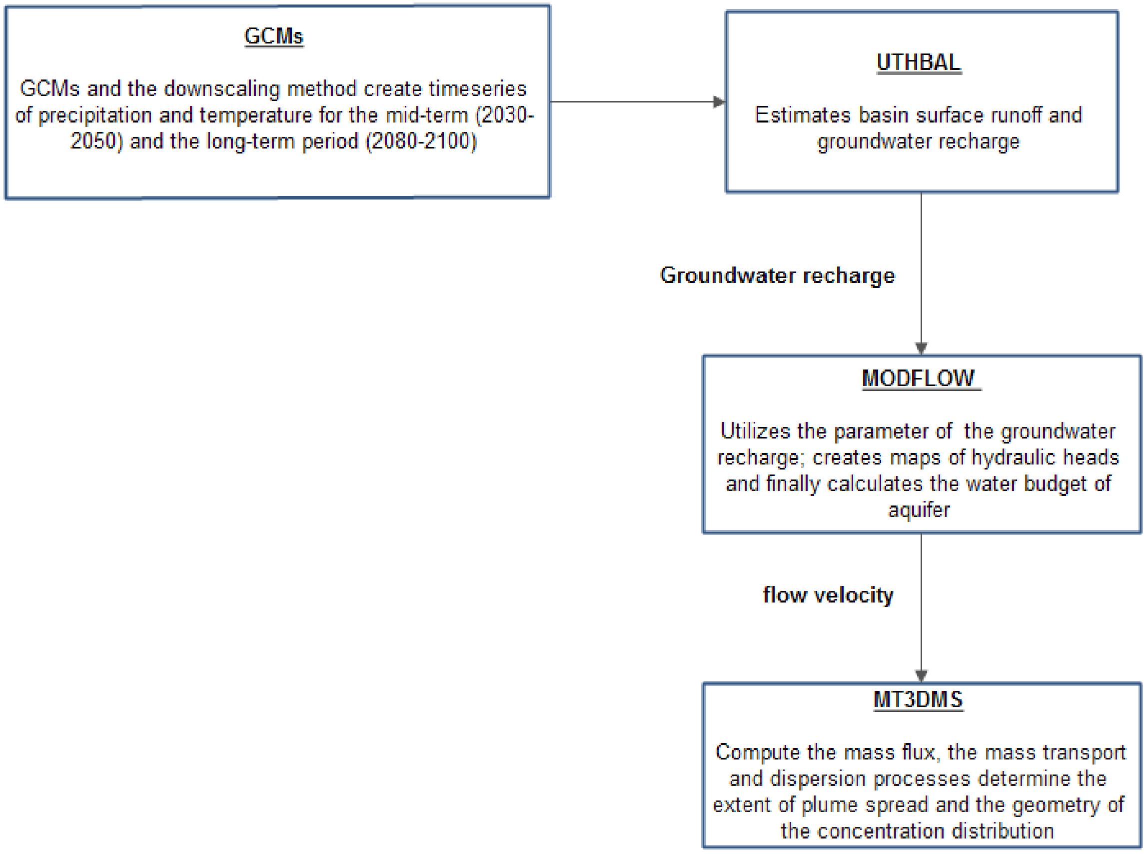
General Circulation Models or global climate models (GCMs)

A Surface Hydrological model (UTHBAL) for the simulation of the surface hydrological processes and the estimation of the groundwater recharge;

A groundwater flow numerical simulator (MODFLOW 2000) and finally

A solute and transport model for the advection and dispersion of nitrates. The evolution of groundwater [NO_3] under climate change was modelled using the MT3DMS code.

Modelling system was applied in a monthly time step from one historical period (06/1995 – 09/2007) and two futures periods (2030 – 2050, 2080 – 2100). Three different socioeconomic scenarios SRES (A2, A1B and B1) were examined for the two future periods, with the application of General Circulation Models. The GCMs did not apply for the historical period.



Picture 2: Flow chart of Nitrate Modelling System

3.1 Global Circulation Models (GCMs)

Climate models are coupled tools for examining local, regional or global climate behavior and variability in relation to altering conditions on the Earth. They are in different forms; ranging from simple climate models (SCMs) of the energy-balance type to Earth-system models of intermediate complexity (EMICs) to comprehensive three-dimensional (atmosphere–ocean) general circulation models or global climate models (GCMs). GCMs are the most sophisticated tools, available to simulate the current global climate and future climate scenario (Green et al.; 2011). GCMs frequently used to develop scenarios of future climate (rainfall; temperature; radiation; etc.) considering different scenarios. The paper analyses three different socioeconomic scenarios, SRESA2, SRESB1 and SRESAB1 for two future periods, one mid-term 2030–2050 and one long-term 2080–2100 (Kløve et al.,2014; Tzabiras et al., 2016).

SRES A2 scenario assumes a strong economic growth, which is regionally oriented, and fragmented technological change with an emphasis on human wealth. The B1 scenario describes a convergent world with the same global population that peaks in mid-century and declines thereafter. SRESA1 indicates a rapid change in economic structures toward a service and information economy, by reducing material and the introduction of clean and resource-efficient technologies. The emphasis is on global solutions to economic, social and environmental sustainability, including improved equity, but without additional climate initiatives. The three A1 categories are distinguished in three subgroups by their technological emphasis: fossil intensive (A1FI), non-fossil energy sources (A1T) and a balance across all sources (A1B) (where the balance is defined as not relying on a heavily one particular energy source, but to the assumption that similar improvement rates apply to all energy supply and end-use technologies) (IPCC, 2007).

3.2 Surface Hydrological Model

According to Loukas et al. (2007) the surface hydrological model has been developed by a network of 12 precipitation stations and 26 meteorological stations in the study area for the estimation of monthly average of surface precipitation; monthly average of evapotranspiration and monthly average of surface temperature for historical period 1995-2007. Subsequently the statistical downscaling method have been applied for the mid-term period (2030-2050) and the long-term period (2080-2100) in the study area (Tzabiras et al., 2016).

3.3 Groundwater Hydrological Model

The groundwater hydrological model has been tested and applied for the study area of the alluvial aquifer by Sidiropoulos et al. (2013). A grid has been formed by 12,500 active cells and dimension of 200 m X 200 m. The inflows into the aquifer are: i) the infiltration due to the rainfall, calculated in a monthly step from UTHBAL, ii) the irrigation return flow, which has been equal to 10% of the irrigation requirements and has been aggregated in the recharge parameter and iii) the moderate hydraulic connection with the adjacent aquifer to the west. The outflows are the extracted groundwater from the wells. Modflow calculates the groundwater movement, the volumetric budget of aquifer and creates maps of hydraulic heads (Sidiropoulos et al., 2015)

3.4 Solute and transport Model

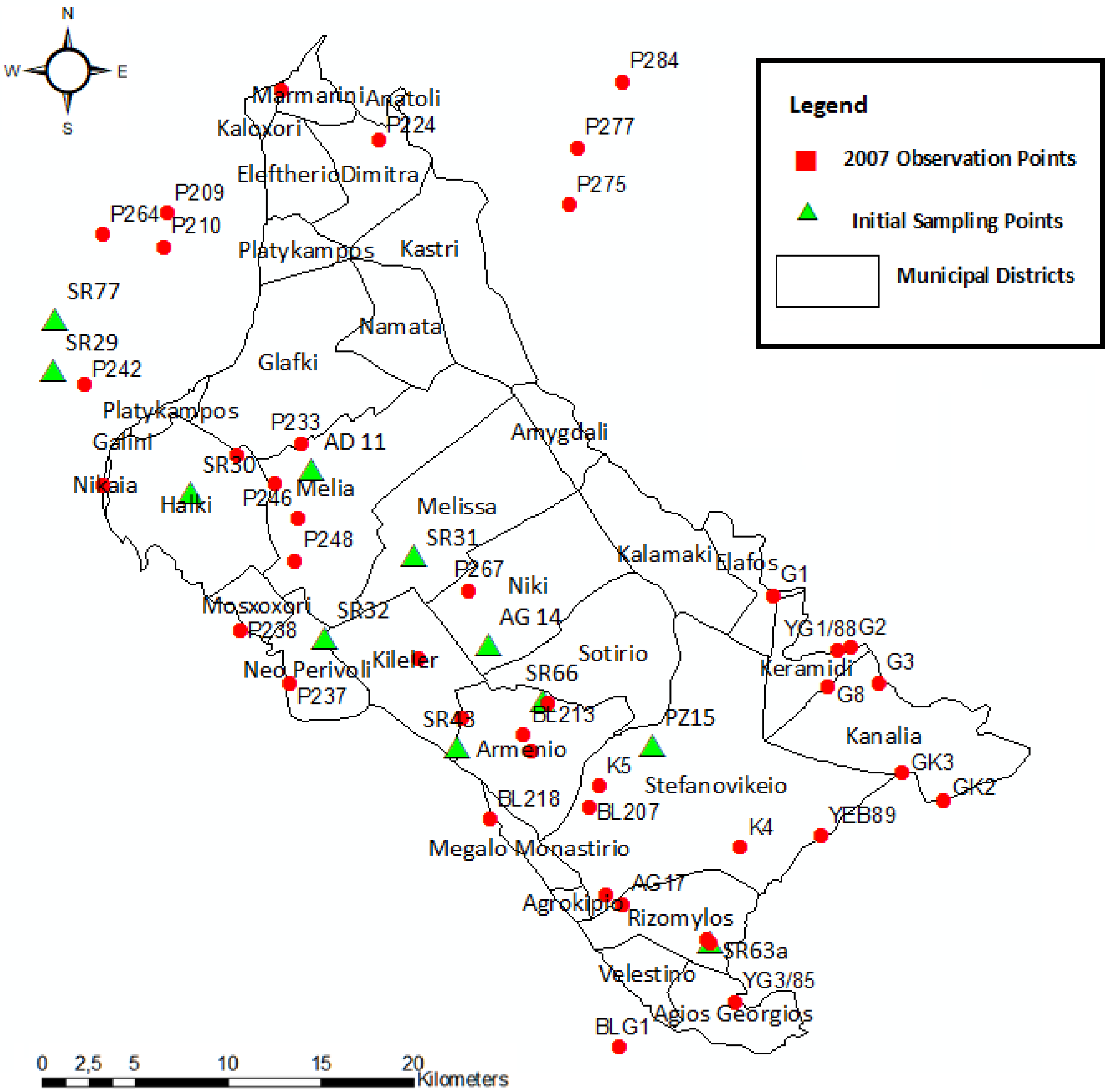
MT3DMS was applied to study the spatial and temporal distribution of nitrate on the groundwater regime for climate change prediction purposes. The spatial distribution of nitrates concentration is defined mainly by the advection and dispersion mechanisms calculating the mass flux at sources/sinks (Sharma et al., 2014). MT3DMS links to MODFLOW, directly. It retrieves the saturated thickness for each cell, fluxes across cell interfaces in all directions, and the locations of flow rates of the various sources and sinks. The nitrate fate and transport model is a three-dimensional areal model, as the groundwater flow model (Almasri and Kaluarachchi, 2005).

Hydrodynamic dispersion coefficients, consist the main parameters of a solute and transport modelling. Longitudinal dispersivity (a_L) symbolizes the local variations in the velocity field of a groundwater solute in the direction of groundwater flow (Schulze-Makuch et al., 2005).

The hydrodynamic dispersion parameters depend on geological characteristics of aquifer. As a result, according to the review paper Gelhar et al. (1992) the longitudinal dispersivity (a_L) was set to 20 m and the transverse dispersivity (a_T) value was equal to 0.1. The parameter of molecular diffusion was considered as neglected. Nitrate leaching was estimated from empirical equation (equation 1) which is based on bibliography data, that is approximately 30% to 50% of the applied nitrogen fertilizer leaches to groundwater in the NO_3 form (Siarkos et al., 2013). Furthermore, the nitrate loading parameter based on data from Wichmann (1992) except from the groundwater recharge, which is calculated by UTHBAL.

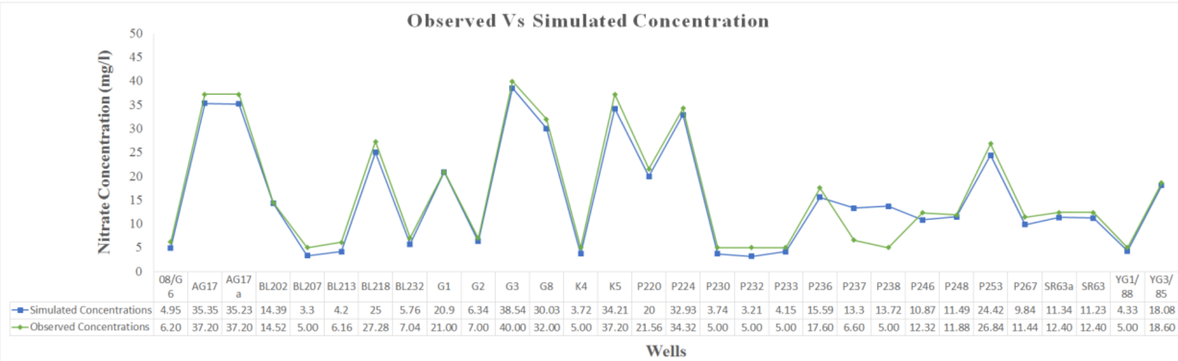
$$\frac{Nitrate\ loading(\frac{Kg}{day})*0.4}{recharge\frac{mm}{365}*cultivated\ area\ (m^2)} \quad (1)$$

Cultivation data have been collected from the Integrated Management System of Cultivated Areas. The spatial reference of cultivations has been done with the use of a Geographical Information System at Municipal District Scale (Figure 3).



Picture 3: Location of Sampling Points

A sensitivity analysis was conducted, in order to determine the parameters which mainly induced the alterations on the simulated nitrate concentrations at the sources/sinks. The sensitivity analysis indicated that the nitrate leaching parameter is the most uncertain parameter. Therefore, the model was calibrated for the nitrate leaching parameter via the trial-and-error approach for the 1995 and 2007. Visual inspection (figure 4) and performance measures as explained by Nash–Sutcliffe model efficiency coefficient (Eff= 0.96) indicate the successful modelling. In this period observed systematic recording of groundwater quality by the Institute of Geological and Mineral Exploration.



Wells	08/G6	AG17	AG17a	BL202	BL207	BL213	BL218	BL232	G1	G2	G3	G8	K4	K5	P220	P224	P230	P232	P233	P236	P237	P238	P246	P248	P253	P267	SR63a	SR63	YG1/88	YG3/85
Simulated Concentrations	4.95	35.35	35.23	14.39	3.3	4.2	25	5.76	20.9	6.34	38.54	30.03	3.72	34.21	20	32.93	3.74	3.21	4.15	15.59	13.3	13.72	10.87	11.49	24.42	9.84	11.34	11.23	4.33	18.08
Observed Concentrations	6.20	37.20	37.20	14.52	5.00	6.16	27.28	7.04	21.00	7.00	40.00	32.00	5.00	37.20	21.56	34.32	5.00	5.00	5.00	17.60	6.60	5.00	12.32	11.88	26.84	11.44	12.40	12.40	5.00	18.60

Picture 4: Observed vs simulated concentration values of calibration process

4. SIMULATIONS – RESULTS

4.1 Surface Hydrological Model

The study indicates that the average annual rainfall will show a decrease in all three socioeconomic climatic scenarios in the medium-term future period 2030-2050. According to the expected trends in all three scenarios, the water budget deficits observed elevated. The climate change impacts are more obvious in the long-term period 2080-2100. As a conclusion should be mentioned the small increase of the average annual temperature in the three scenarios for the medium and long term; simultaneously. The recharge is the parameter which affects mostly the nitrate leaching on aquifer. The recharge was estimated to 81.4 mm for historical period, while it was reached 83.4 mm for SRESB1 scenario in the mid-term period, 81.0 mm for SRESA1B and 78.3 mm for the most intense SRESA2 scenario. Conversely, during the long-term period 2080–2100 the recharge was 80.5 mm for SRESB1, 75.8 mm for SRESA1B and 74.7 mm for SRESA2.

4.2 Groundwater Hydrological Model

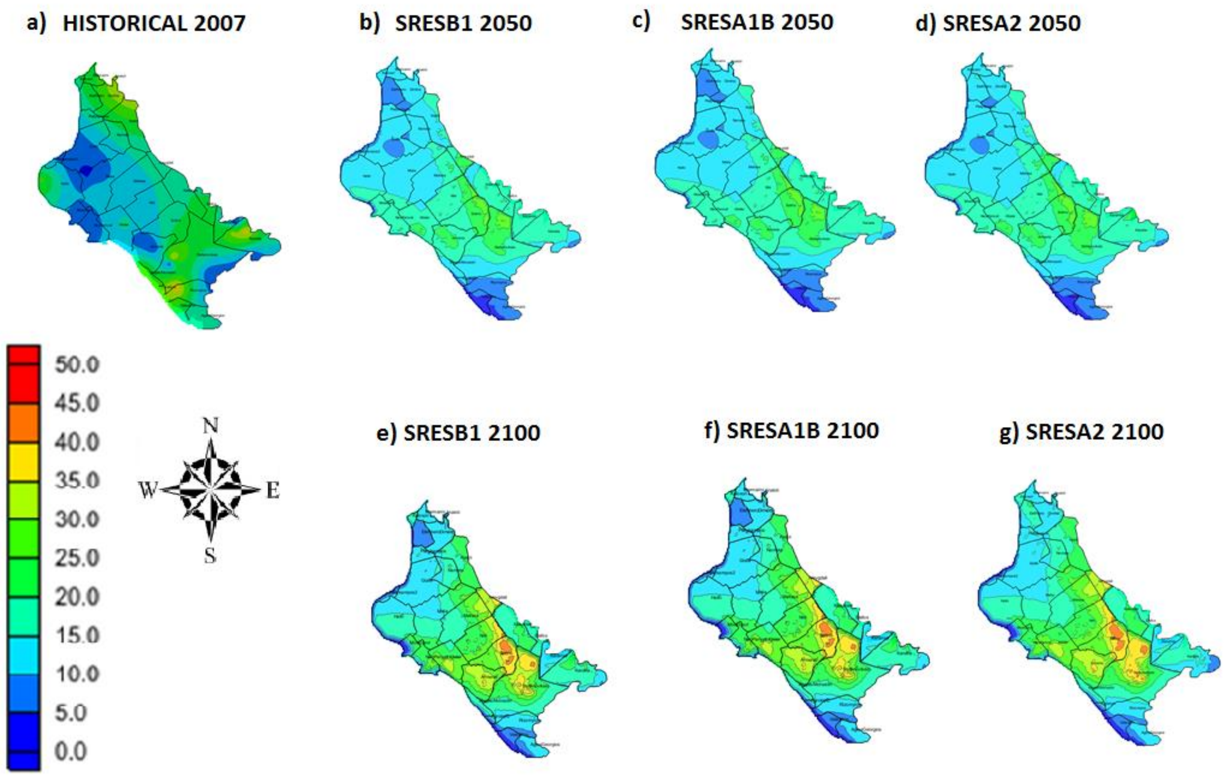
Regarding the historical period 1995–2007, the aquifer's water balance was negative by 143.65 hm^3. For the mid-term period 2030–2050 recorded an increase of water deficit by 1.02 % at 145.11 hm^3 for SRESB1 scenario, 1.62 % at 145.98 hm^3 for SRESAB1 scenario and 1.63 % also at 146 hm^3 for SRESA2 scenario. On the other hand, for the long-term period 2080–2100 groundwater deficit is increased by 4.65 % at 150.33 hm^3 for SRESB1 scenario, by 2.12 % at 146.69 hm^3 for SRESAB1 and by 3.44 % at 148.59 hm^3 for SRESA2 scenario, respectively.

The greatest drawdowns of aquifer are located at its central part for the two future periods. The absolute height of hydraulic heads range from -100 m to 60 m for the medium future period and reach up to -160 m for the long future period. The main feature is that the water demand is increased as a result of climate change and therefore increasing the irrigation requirements.

4.3 Solute and transport Model

All three socioeconomic scenarios present changes in nitrate concentration concerning the historical period. The differences between the three socio-economic scenarios in the medium and the long term period can be characterized as negligible. It is worth noting that there is a slight change in the SRESA2 scenario in the northern part of the study area both in the medium-term (2030-2050) and the long-term (2080-2100). Nitrate concentrations on groundwater range from 0 to 30 - 35 mg /l for the medium term period, while in the long term period range from 0 to 40 - 45 mg/l. The most high nitrate concentrations are recorded on the south eastern part of the study area concerning the medium-term period as well as the long term period.

On the contrary, the nitrate concentrations in the historical period range from 0 - 45 mg/l. The maximum nitrate concentration of 45 mg/l is limited in the historical period on comparison with the nitrate concentration which is recorded extensively on the long period, at the southeastern part. The maximum allowable limit according to directive 98/83/EC is the 50 mg/l. In addition to the maximum limit, the value of 25 mg/l has been also determined as ‘‘indicative value /guidance value’’ by the directive. It is worth to mention the indicative value due to the fact that a large number of water supply wells exist in the studied area, which are utilized for domestic use on the surrounding villages and the Volos city (Sidiropoulos et al., 2015). The differences between the three socio-economic scenarios in comparison with the historical period are ranged from 0 to 10 mg/l in the mid-period and 0 to 15 mg/l in the long period (2080-2100).



Picture 5: Nitrate concentrations maps of: a) Historical Period 2007; b) SRESA1B 2050, SRESA1B 2100 c) SRESB1 2050, SRESB1 2100; d) SRESA2 2050, SRESA2 2100

5. DISCUSSION AND CONCLUSIONS

Climate change and variability will likely have numerous effects on recharge rates and mechanisms. According to Green et al., (2011) a large number of climate change studies have predicted reduced recharge although the effects of climate change on recharge may not necessarily be negative in all aquifers during all the period. The effect of climate variability is responsible for changes in the aquifer. From the groundwater climate change point of view, the optimal groundwater management, the optimum volume of pumped water, the number and the location of pumping wells have to be determined (Sidiropoulos et al., 2013; Tzabiras et al., 2016).

Concerning the groundwater quality, an increase in the concentration of nitrates are observed. This is justified by the fact that nitrates are characterized as water soluble contaminants and the reduction of recharge prevent their dissolution. Antonakos and Lambrakis, (2000), indicated that the areas of increased recharge coincide with the areas of diluted nitrate ion concentration. Therefore, the nitrate concentration in groundwater mainly depends on the recharge

Regarding the implications for nitrate leaching to groundwater as a result of climate change, Stuart and his associates (Stuart et al., 2011) referred to the fact that there is not well enough understanding them yet to make useful predictions without a lot of observed data. The few studies, which address the hydrological cycle, show likely nitrate leaching ranging from limited increases to a possible doubling of aquifer concentrations by 2100, since the current cultivation pattern will not change (Stuart et al., 2011).

Acknowledgements
Georgios Tziatzios has been co-financed -via a programme of State Scholarships Foundation (IKY) - by the European Union (European Social Fund - ESF) and Greek national funds through the action entitled ”Scholarships programme for postgraduates studies -2nd Study Cycle” in the framework of

the Operational Programme ”Human Resources Development Program, Education and Lifelong Learning” of the National Strategic Reference Framework (NSRF) 2014 – 2020.

Dr. Pantelis Sidiropoulos is a post-doctoral scholar of Stavros Niarchos Foundation and the University of Thessaly. Part of the scientific publication was held within the framework of the invitation "Granting of scholarship for Post-Doctoral Research" of the University of Thessaly, which is being implemented by the University of Thessaly and was funded by the Stavros Niarchos Foundation.

References

1. Almasri, M.N., Kaluarachchi, J.J (2007). Modeling Nitrate contamination of groundwater in agricultural watersheds. **Journal of Hydrology**, Vol 343, 211-229.
2. Antonakos A. and Lambrakis N., (2000). Hydrodynamic characteristics and nitrate propagation in Sparta aquifer, **Water Resources Research**, Vol 34, pp. 3977–3986.
3. Gelhar L. W, Welty C.,Rehfeldt K., (1992) ‘A critical review on Data on Field - Scale Dispersion in Aquifers, **Water Resources Research** , Vol 28 , pp. 1955 -1974.
4. Green, T.R., Taniguchi, M., Kooi, H., Gurdak, J.J., Allen, D.M., Hiscock, K.M., Treidel, H., Aureli, A., (2011) ‘Beneath the surface: impacts of climate change on groundwater’, **Journal of Hydrology**, Vol 405, pp. 532–560.
5. Iglesias A., L. Garrote, Fr. Flores, M. Moneo (2007). ‘Challenges to Manage the Risk of Water Scarcity and Climate Change in the Mediterranean, **Water Resources Management**, Vol 21, pp. 775–788.
6. Institute of Geological and Mining Research. Recording and evaluation of the hydrogeological characteristics of the groundwater systems of the country, Basement of the Aquatic Potential of Thessaly, 2010 (WD 08).
7. Intergovernmental Panel on Climate Change IPCC (2007) Climate Change 2007 - The Physical science basis. Contribution of Working Group I to the Fourth Assessment Report of the Intergovernmental Panel on Climate Change (IPCC). Solomon S, Qin D,Manning M, Chen Z, Marquis M, Averyt KB, Tignor M, Miller HL (eds), Cambridge University Press, Cambridge.
8. Kløve, B., Ala-Aho, P., Bertrand, G., Gurdak, J.J., Kupfersberger, H., Kvœrner, J., Muotka, T., Mykrä, H., Preda, E., Rossi, P., Bertacchi Uvo, C., Velasco, E., Wachniew, P., Pulido-Velázquez, M., (2014) ‘Climate change impacts on groundwater and dependent ecosystems’ **Journal of Hydrology**, Vol 518, pp. 250–266
9. Loukas A., Mylopoulos N. and Vasiliades L. (2007) ‘A Modelling System for the Evaluation of Water Resources Management Scenarios in Thessaly, Greece’, **Water Resources Management**, Vol 21, pp. 1673 – 1702.
10. Ministry of Rural Development and Food. Data on the Integrated Management System of Cultivated Areas.
11. Pascual D., Pla E., Lopez-Bustins J.A., Retana J., Terradas J. (2015) ‘Impacts of climate change on water resources in the Mediterranean Basin: a case study in Catalonia, Spain’ **Hydrological Sciences Journal**, Vol 60, pp. 2132-2147.
12. Pulido-Velazquez M., Peña-Haro S., García-Prats A., Mocholi-Almudever A. F., Henriquez-Dole L., Macian-Sorribes H., and Lopez-Nicolas A. (2015) ‘Integrated assessment of the impact of climate and land use changes on groundwater quantity and quality in the Mancha Oriental system (Spain), **Hydrological and Earth System Sciences**, Vol 19, pp.1677-1693.
13. Schulze-Makuch D., (2005). Longitudinal dispersivity data and implications for scaling behaviour. **Groundwater**, Vol 3, 443-456.

14. Sharma MK, Jain CK, Rao GT, Rao VV., (2005) 'Modelling of lindane transport in groundwater of metropolitan city Vadodara, Gujarat, India' **Environmental Monitoring and Assessment** 2015, Vol 187: 295.
15. Siarkos I., Kouvaritaraki D, Charcharidou A. and Theodosiou N., (2013) Modelling the Effect of Agricultural activities on Groundwater Quality in the Aquifer of N. Moudania. Proc. of Int. Conf. **Conference on Environmental Science and Technology XIII**, 5-7 September, Athens.
16. Sidiropoulos P., Mylopoulos N., Loukas A., (2013) 'Optimal management of an overexploited aquifer under climate change: the Lake Karla case, **Water Resources Management**', Vol 27, pp. 1635–1649.
17. Sidiropoulos P., Mylopoulos N., Loukas A., (2015) 'Stochastic simulation and management of an over-exploited aquifer using an integrated modeling system' **Water Resources Management**, Vol 29, pp. 929–943.
18. Sidiropoulos P., Mylopoulos N., Loukas A., (2016). 'Reservoir-aquifer combined optimization for groundwater restoration: The case of Lake Karla watershed, Greece' **Water Utility Journal**, Vol (12), pp. 17-26.
19. Stoll S., Hendricks Franssen H.J., Butts M., and Kinzelbach W. (2011) 'Analysis of the impact of climate change on groundwater related hydrological fluxes: A multi-model approach including different downscaling methods' **Hydrological and Earth System Sciences**, Vol 15, pp. 21–38
20. Tzabiras J., Vasiliades L., Sidiropoulos P, Mylopoulos N, Loukas A (2016) 'Evaluation of Water Resources Management Strategies to Overturn Climate Change Impacts on Lake Karla Watershed' **Water Resources Management**, Vol 30, pp. 5819– 5844.
21. Wichmann W., (1992) '**World Fertilizer Use Manual',** BASF AG, Germany, IFA, France.

AN ASSESSMENT APPROACH TO INVESTIGATE CLIMATE CHANGE IMPACTS IN CHANIA GROUNDWATER SYSTEM

D. Charchousi[1*], K. Spanoudaki[2], A. Karali[3], A. Nanou-Giannarou[4], C. Giannakopoulos[3], M.P. Papadopoulou[1]

[1] Laboratory of Physical Geography and Environmental Impacts, School of Rural and Surveying Engineering, National Technical University of Athens, Athens, Greece,

[2] Institute of Applied and Computational Mathematics, Foundation for Research and Technology-Hellas, Heraklion, Crete, Greece,

[3] Institute for Environmental Research and Sustainable Development, National Observatory of Athens, Athens (Greece),

[4] Laboratory of Applied Hydraulics, Department of Water Resources and Environmental Engineering, School of Civil Engineering, National Technical University of Athens, Athens, Greece

[*]Corresponding author: e-mail: charchousi@gmail.com

Abstract

Prolonged dry periods observed during the past years and intense groundwater abstraction for irrigation purposes have raised awareness on groundwater resources management in many agricultural areas. Climate change is expected to increase the frequency of extreme dry periods and groundwater systems recharge will be seriously affected.

The present study emphasizes on the investigation of climate change impacts on groundwater availability in Chania plain groundwater system. Chania plain is considered one of the most important agricultural regions in Crete, where groundwater is the prime source used for irrigation. Intense irrigation needs put pressure on the groundwater system, especially during the dry period (April-September), when the water table is lowered by around 3.5 m. Groundwater flow simulations for the area, using climatic projections for meteorological variables produced by the RCA4 Regional Climate Model of the Swedish Meteorological and Hydrological Institute (SMHI) driven by the Max Planck Institute for Meteorology model MPI-ESM-LR, forced by the IPCC RCP 4.5 and 8.5 scenarios, have shown an additional decrease of the water table of approximately 4 m, during the dry period of predicted dry years.

Keywords: Groundwater system recharge, IPCC scenarios, MODFLOW, Irrigation water

1. INTRODUCTION

Agriculture is an economic sector vulnerable to climate change, as it is highly dependent on climatic conditions and on the availability of surface and groundwater resources for irrigation purposes. During the last decades, forced by the importance of agricultural sector for the economic sustainability and food security, awareness has been raised on future climate change impacts on irrigation water. In many agricultural regions of the Mediterranean basin, agriculture is already under pressure due to limited irrigation water resources, as Mediterranean countries are already facing extended periods of drought during summer. Additional pressure is expected to be imposed due to water resources vulnerability to future climate change.

Crete is highly dependent on the agriculture sector. The utilised agricultural area (consisting of arable land, permanent crops, pastures - transitional forest/shrubland, pastures - combined

shrubland/herbaceous plants, pastures and heterogeneous agricultural areas) occupies approximately 70% of the total area and amounts to 653,305ha (Hellenic Statistical Authority, 2000/2010). About 42.3% of the cultivated land is irrigated [LIFE ADAPT2CLIMA, 2016].

In the present study, an assessment of groundwater system response to future climate change in Chania Plain, an important agricultural and touristic area of Crete, under the pressure of climate change climatic projections for meteorological variables produced by the RCA4 Regional Climate Model of the Swedish Meteorological and Hydrological Institute (SMHI) driven by the Max Planck Institute for Meteorology model MPI-ESM-LR, forced by the IPCC RCP 4.5 and 8.5 scenarios is presented.

2. CASE STUDY

The Chania Plain is located on the north part of the Chania Prefecture, Crete, Greece (Figure 1). It is mainly an agricultural area, where the main cultivations are olives, avocados, citrus and annual crops such as tomatoes. In the coastal part of the aquifer, tourism zones have been developed.



Figure 1: The Chania Plain aquifer

The pilot aquifer is part of the granular aquifer of Chania, namely GR1300022 and is characterized as satisfying in terms of quality and quantity [Special Secretariat for Water, 2015]. However, the intense agricultural activities in the area impose significanet pressure to the groundwater resources. As shown in Figure 2, the aquifer mainly consists of alluvium deposits, medium permeability rocks and phyllites–quartzites units. A southern part of the aquifer neighbors with high permeability rocks which comprise karstic limestones. In this part of the aquifer, Ayia springs are met, consisting a significant recharge for the groundwater system.

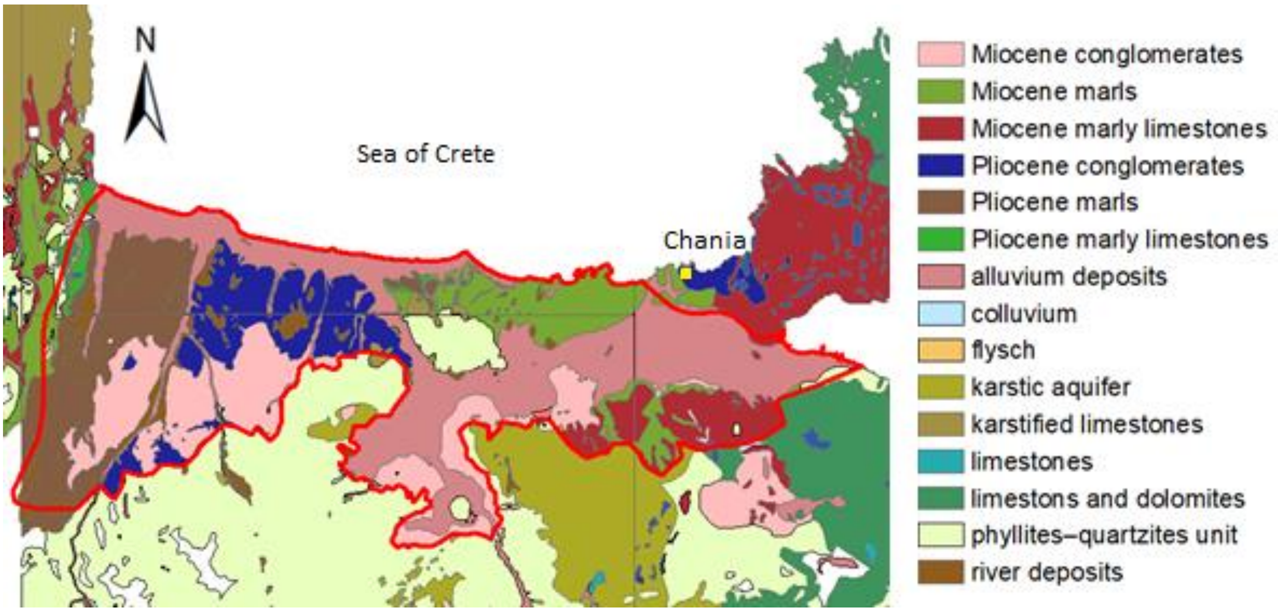


Figure 2: Hydrogeological map of Chania pilot aquifer

3. METHODOLOGICAL APPROACH

A groundwater flow model is developed for Chania Plain aquifer in order to evaluate the impact of future climate change and irrigation practices on groundwater availability. Groundwater flow model calibration and validation is followed by the selection of a characteristic mean hydrological year to approximate the current state with respect to water table. Then, a series of simulation runs were performed in order to estimate changes in groundwater variability under pressure of a foreseen extreme dry hydrological year based on the Regional Climate Models MPI-RCA4, forced by the IPCC RCP 4.5 and 8.5 scenarios. The steps followed to investigate climate change impacts in groundwater system are displayed in Figure 3.

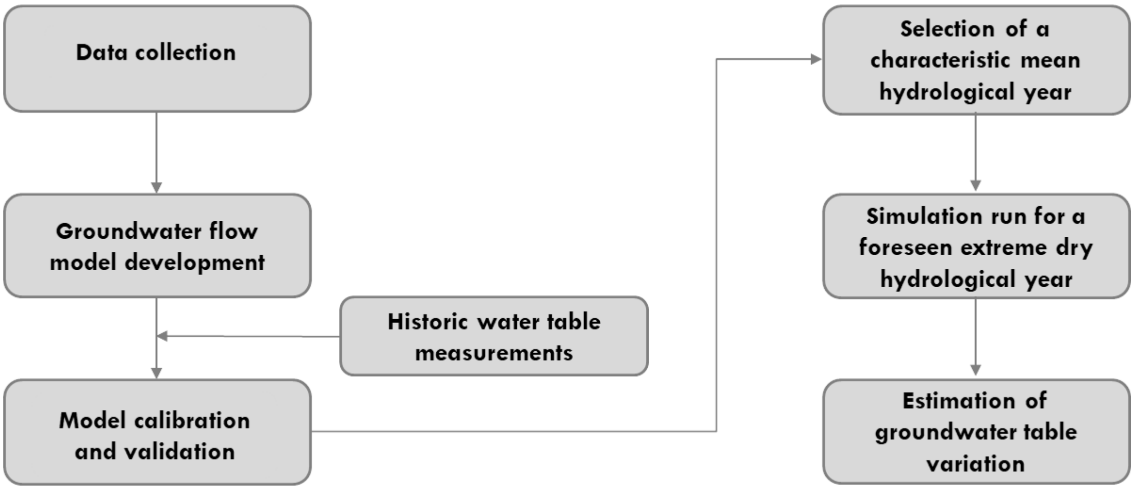


Figure 3: Methodology flow chart

3.1 Groundwater flow model development

The Chania Plain groundwater flow model was developed using US Geological Survey MODFLOW algorithm [McDonald and Harbaugh, 1988], a block-centered finite-difference computer code that solves the groundwater flow equation. Visual MODFLOW Flex [Waterloo Hydrogeologic, 2017] was also used as a pre- and post- processor. The groundwater flow model developed was calibrated on transient conditions for the hydrological years 2004-2008 for the values of hydraulic conductivities and pumping rates obtained from previous reports and the literature using a trial and error approach.

Irrigation return flow during the irrigation season was estimated and included into the model as additional recharge. The groundwater system is also enriched through local river interactions and Ayia springs. Historic hydraulic heads measurements were used to calibrate subsurface flow while pumping rates were estimated based on previous reports and data obtained from communication with local farmers. Since calibration had been completed, the model was validated based on the additional available historic data.

3.2 Climate change projections

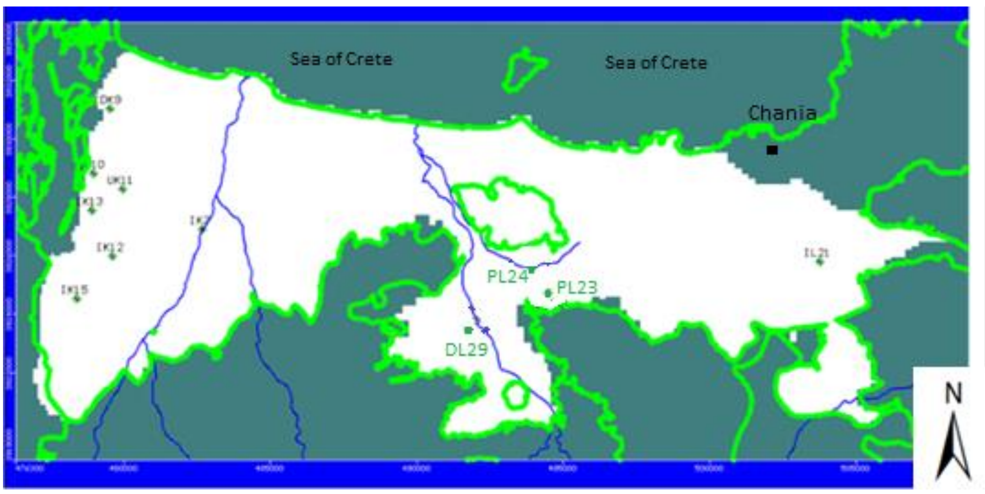
In order to assess climate change impacts on Chania Plain aquifer, future precipitation data derived from sets of Regional Climate Models (RCMs) simulations carried out were used in order to estimate future recharge in the aquifer [LIFE ADAPT2CLIMA, 2017]. Future precipitation data used are based on RCA4 Regional Climate Model of the Swedish Meteorological and Hydrological Institute (SMHI) (Strandberg et al., 2014 and references therein) driven by the Max Planck Institute for Meteorology model MPI-ESM-LR [Popke et al., 2013] hereafter MPI-SMHI. The model has a horizontal resolution of $12km^2$ and was developed within the framework of EURO-CORDEX (Coordinated Downscaling Experiment - European Domain). Future model projections were based on two new IPCC scenarios, namely the RCP4.5 and the RCP8.5.

RCP4.5 is a stabilization scenario where total radiative forcing is stabilized before 2100 by the employment of a range of technologies and strategies for reducing greenhouse gas emissions [Clarke et al., 2007]. Radiative forcing in RCP4.5 peaks at about 4.5 W/m2 (~540 ppm CO_2) in year 2100 (Thomson et al., 2011). RCP4.5 is comparable to the SRES scenario B1 with similar CO_2 concentrations and median temperature increases by 2100 according to Rogelj et al. [2012]. RCP8.5 is characterized by increasing greenhouse gas emissions over time, representative for scenarios in the literature leading to high greenhouse gas concentration levels. RCP8.5 assumes a high rate of radiative forcing increase, peaking at 8.5 W/m^2 (~940 ppm CO_2) in year 2100 (Riahi et al., 2011).

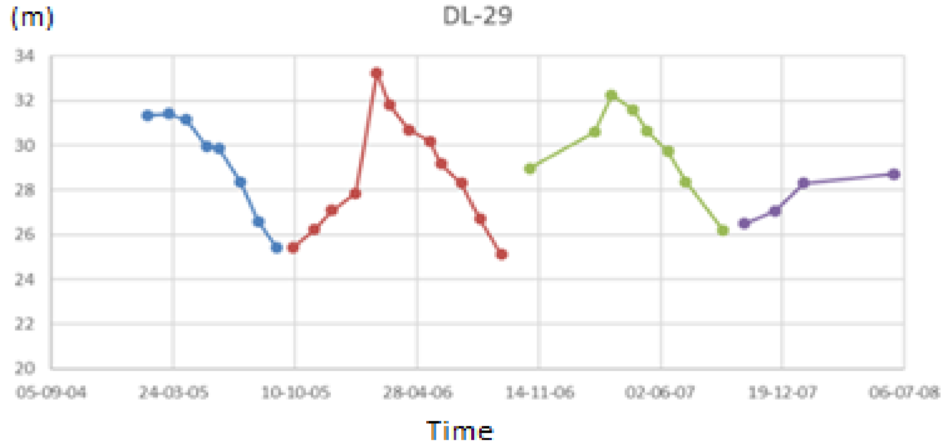
4. RESULTS

4.1 Assessment of the current water resources conditions in Chania Plain aquifer

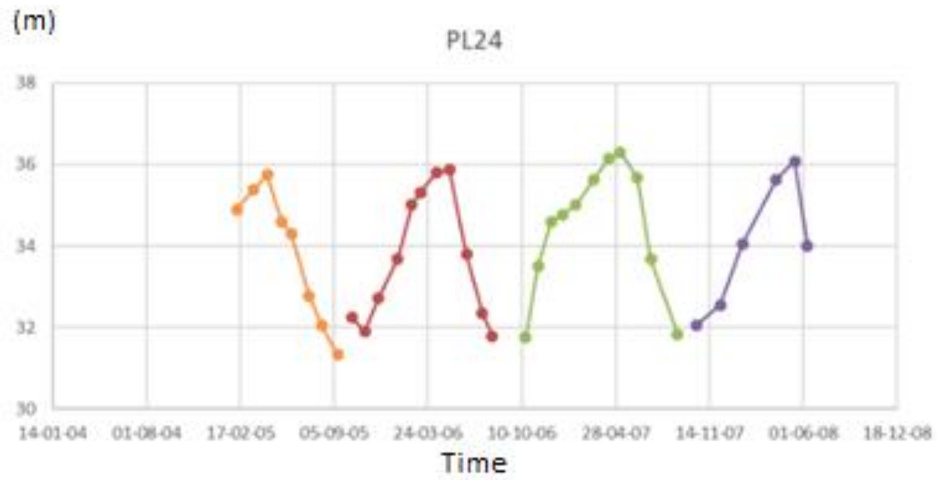
Chania Plain aquifer is characterized as adequate in terms of quantity conditions (Special Secretariat for Water, 2015). Based on available historic head data series, it is observed that there is a balance between groundwater withdrawal and recharge. However, an approximately 3.5 m level difference is observed from dry to wet period (Figure 4).



(a) Wells location in Chania Plain pilot area



(b) Historic hydraulic head measurements – DL29



(c) Historic hydraulic head measurements – PL24

Figure 4: Groundwater level at various observation wells in Chania Plain pilot area

This 3.5 m groundwater level fluctuation between the dry and the wet period is also depicted on the results of the numerical simulations (Figure 5).

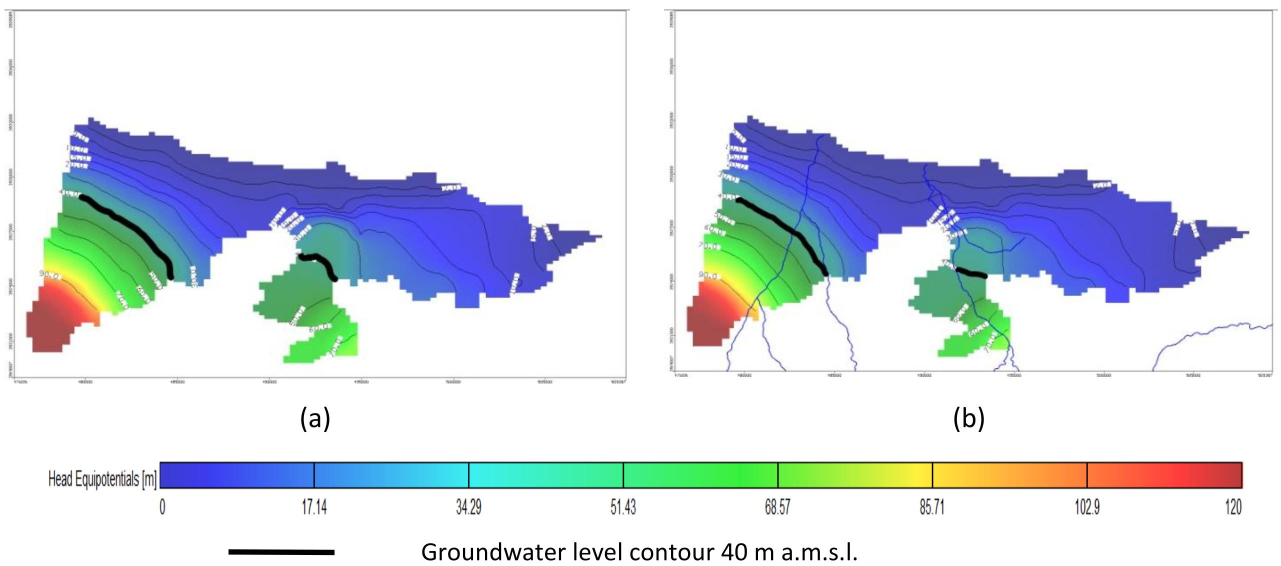


Figure 5: Groundwater level in Chania Plain aquifer for the base hydrological year – (a) end of wet period and (b) end of dry period

4.2 Chania Plain aquifer response to future climate change, under RCP4.5 and RCP8.5

Predicted groundwater level in Chania Plain aquifer for an extreme dry hydrological year, based on the MPI-SMHI model, forced by the IPCC RCP 4.5 and RCP 8.5 scenarios are presented on Figures 6 and 7, respectively.

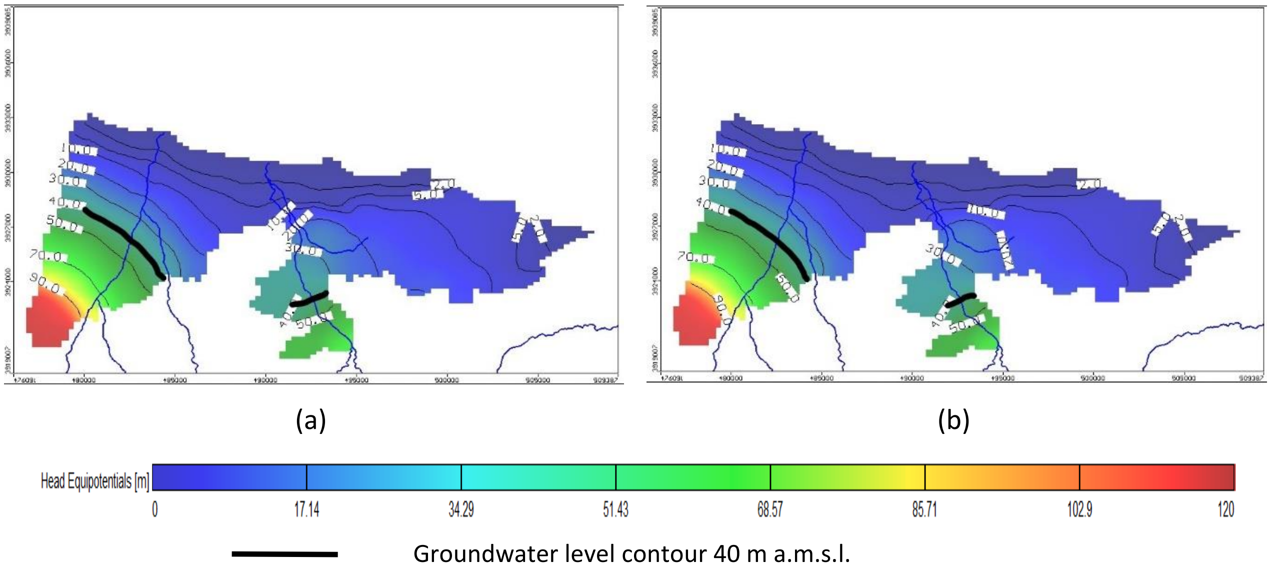


Figure 6: Predicted groundwater level in Chania Plain aquifer for extreme dry hydrological year, based on the MPI-SMHI, under RCP 4.5 – (a) end of wet period and (b) end of dry period

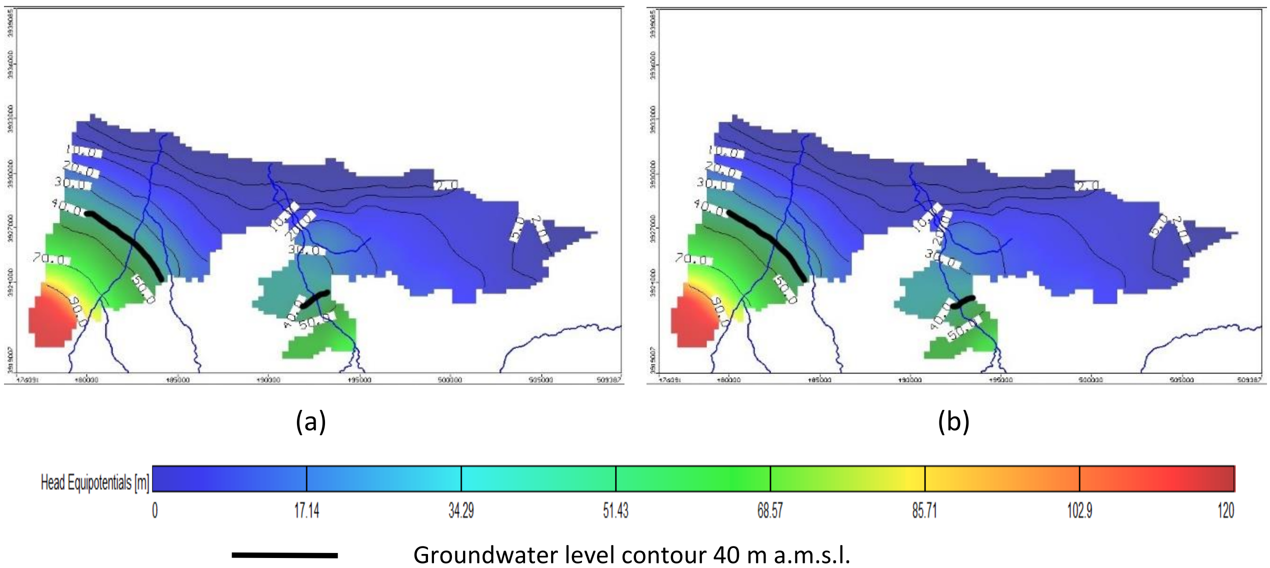


Figure 7: Predicted groundwater level in Chania Plain aquifer for extreme dry hydrological year, based on the MPI-SMHI, under RCP 8.5 – (a) end of wet period and (b) end of dry period

Groundwater flow simulation results for the Chania Plain aquifer, using climatic projections forced by the IPCC RCP 4.5 and 8.5 scenarios, have shown an additional decrease of the water table of approximately 4 m, during the dry period of predicted dry years.

5. DISCUSSION AND CONCLUSIONS

Based on the present analysis Chania Plain aquifer will be subjected to severe climate change impacts, as a mean groundwater level depletion of almost 4 m is foreseen. Especially in Ayia area, 6.5 m depletion of mean groundwater level is estimated. Consequently, the results of the present research underline the need for changes in agricultural practices. At the same time a more direct interpretation of climate change impacts to aquifer sustainability is required. In 2012, Gleeson et al. introduced Groundwater Footprint (GWF) that expresses the area required to sustain groundwater use and groundwater dependent ecosystem services. GWF represents a water balance between aquifer inflows and outflows, focusing on environmental flow requirements. Charchousi et al. [2017] have used the GWF concept to assess groundwater resources sustainability under the current climatic conditions and the existing pumping schemes. The estimated GWF indicates that the groundwater management in the area is sustainable, in accordance to the aquifer characterization by the Special Secretariat for Water [2015] as satisfying in terms of quantity.

The GWF could be proved to be a useful tool for groundwater analysis and policy as it can raise awareness since it is intuitive to the general public. The GWF could also be proved to be useful for identifying groundwater dependent ecosystems vulnerability to future climate change. For these reasons, GWF estimation under the foreseen extreme dry years examined in the present study is ongoing.

Acknowledgements
The authors would like to acknowledge the European financial instrument for the Environment, LIFE, for the financial support in the framework of the ADAPT2CLIMA project LIFE14 CCA/GR/000928.

References

1. Charchousi D., Spanoudaki K. and Papadopoulou M.P. (2017) 'Assessing Groundwater Resources Sustainability Using Groundwater Footprint Concept', **European Geosciences Union General Assembly 2017**, Vienna, Austria.
2. Clarke, L., J. Edmonds, H. Jacoby, H. Pitcher, J. Reilly and R. Richels (2007) '**Scenarios of Greenhouse Gas Emissions and Atmospheric Concentrations'**, Sub-report 2.1A of Synthesis and Assessment Product 2.1 by the U.S. Climate Change Science Program and the Subcommittee on Global Change Research. Department of Energy, Office of Biological & Environmental Research.
3. Gleeson T., Y. Wada, M. F. P. Bierkens and L. P. H. van Beek (2012) 'Water balance of global aquifers revealed by groundwater footprint', **Nature**, 488(7410), pp. 197-200.
4. Hellenic Statistical Authority www.statistics.gr
5. LIFE ADAPT2CLIMA (2016) **'Knowledge capitalization concerning the sectors of agriculture in the regions of Crete, Sicily and Cyprus'**, Deliverable C1.1, project ADAPT2CLIMA LIFE14 CCA/GR/000928. http://adapt2clima.eu/uploads/2017/Del_C1_1.pdf
6. LIFE ADAPT2CLIMA (2017) **'Future projections on climatic indices with particular relevance to agriculture for the three islands (coarse resolution) and for each agricultural pilot area (fine resolution)**', Deliverable C3.1, project ADAPT2CLIMA LIFE14 CCA/GR/000928.
7. McDonald M.G. and A.W. Harbaugh (1988) **'A modular three dimensional finite-difference ground-water flow model**', Techniques of Water-Resources Investigations of the U.S. Geological Survey, Book 6, Chapter A1.

8. Popke D., B. Stevens and A. Voigt (2013) 'Climate and climate change in a radiative-convective equilibrium version of ECHAM6' **Journal of Advances in Modeling Earth Systems**, 5(1), pp. 1–14.
9. Riahi K., S. Rao, V. Krey, C. Cho, V. Chirkov, G. Fischer, G. Kindermann, N. Nakicenovic, and P. Rafaj (2011) 'RCP8.5—A scenario of comparatively high greenhouse gas emissions', **Climatic Change**, 109, pp. 33–57.
10. Rogelj J., M. Meinshausen and R. Knutti (2012) 'Global warming under old and new scenarios using IPCC climate sensitivity range estimates', **Nature Climate Change**, 2, pp. 248–253.
11. Special Secretariat for Water (2015) '**River Basin Management Plan District of Crete'**.
12. Strandberg G., A. Bärring, U.Hansson, C. Jansson, C.Jones and E. Kjellström (2014) '**CORDEX scenarios for Europe from the Rossby Centre regional climate model RCA4**', Reports Meteorology and Climatology, No. 116, SMHI.
13. Thomson A. M., K.V. Calvin, S.J. Smith, G. Page Kyle, A. Volke, P. Patel, S. Delgado-Arias, B. Bond-Lamberty, M.A. Wise, L.E. Clarke and J.A. Edmonds (2011) 'RCP4.5: A pathway for stabilization of radiative forcing by 2100', **Climatic Change**, 109, pp. 77–94.
14. Waterloo Hydrogeologic Inc. (2004) '**Visual MODFLOW Version 3.1.84 Software and Documentation'**, Waterloo Hydrogeologic Inc.

SALINITY EFFECTS ON DIFFERENT VARIETIES OF AMARANTUS SP.

G. Kacienė

Vytautas Magnus University, Dept. of Environmental Sciences, LT-44404 Kaunas, Lithuania

*Corresponding author: e-mail: giedre.kaciene@vdu.lt, tel : +37067245718

Abstract

Amarantus sp. is recognized as a promising plant species due to high nutrition value and resistance to adverse environmental conditions. Due to C4 photosynthetic pathway, amaranth can be grown under elevated salinity or water deficit. As salinity is one of the most serious and continuously increasing limiting agents in agriculture, investigations of resistant, high productivity and nutritional value agricultural crops is of particular importance. The aim of this study was to investigate and to compare the resistance of 3 Lithuanian genotypes of Amaranth (‘Raudonukai’, ‘Rausvukai’ and ‘Geltonukai’) to increased salinity. Pot experiments were conducted in growth chambers, plants were exposed to 50 and 150 mM NaCl levels. Seed germination, shoot growth and photosynthetic rate were investigated. At the earliest growth stage ‘Raudonukai’ demonstrated the highest resistance, germinating 2-3 fold better as compared to other varieties. In contrast, growth of aboveground biomass of ‘Raudonukai’ was the most seriously affected (up to 54% decrease), followed by ‘Geltonukai’ and ‘Rausvukai’. Leaf area decreased similarly in all varieties, slightly higher effect was characteristic for ‘Rausvukai’. The photosynthetic rate declined for all plant species with increasing salinity and exposure time. 50mM salinity level had no impact on photosynthetic performance. The strongest effect for ‘Rausvukai’ and ‘Raudonukai’ was observed after 10 days of exposure to 150 mM (up to 33% and 24% inhibition, respectively), followed by adaptation and recovery to control level after 15 days of exposure. Similar reduction of photosynthetic rate was detected for ‘Geltonukai’, however, photosynthetic adaptation was not observed. Results of this study have shown that Amaranth can be classified as salinity resistant crop species, as vegetative growth and photosynthetic performance were not significantly affected by relatively high (50mM) NaCl concentrations. The negative effects of salinity depended on the growth stage of variety of Amaranth. The most resistant variety at germination growth stage and with respect to photosynthetic performance was ‘Raudonukai’, followed by ‘Rausvukai’ and ‘Geltonukai’.

Keywords: Amarantus sp., Soil salinity, Stress resistance, Germination, Photosynthetic rate

1. INTRODUCTION

Soil salinity is one of the most prevalent soil degradation factor in Earth. In Europe, salt-affected soils are in Hungary, Romania, Greece and Italy. According to the European Commission, there was about had 1-3 million hectares of soils, affected by increased salinity in 2009, in the European Union. More than 800 million hectares of land around the world are affected by salinity. It accounts for over 6% of the world's land area (Munns & Tester, 2008).

Plant growth can be triggered by osmotic and ionic effects of increased soil salinity (Panuccio et al., 2014). The response in plants occurs in two stages: the first one is the osmotic stress phase, the second is the toxic stress induced by salts accumulated in leaves (Munns, 2002). The general effect is necrosis and growth retardation (Omami & Hammes, 2006). One of the strategies to avoid salinity stress is prolonged stomatal closure. It limits transpiration and sustains osmotic balance within plant tissues.

C4 photosynthesis allows the plants to acquire CO_2 during the periods of reduced stomatal conductance, therefore it increases plant resistance not only to drought and heat, but also to increased soil salinity.

One of the C4 plants, characterized by high tolerance to soil salinity is Amaranths (Jeyanthi et al., 2010; Amukali et al., 2016). These plants belong to the dicotyledones class, the caryophyllidae family, the genus Amoranthaceae Juss. Because of the huge variety of genotypes, taxonomic classification of Amaranths is difficult. There are about 60 genotypes of Amaranths in the world, most of which are wild (Stallknecht & Schulz-Schaeffer, 1993). Amaranths are grown mostly for leafs and grains, having high nutritive value (Kauffman & Weber, 1990). The aim of this study was to investigate and to compare the resistance of 3 Lithuanian genotypes of Amaranth ('Raudonukai', 'Rausvukai', 'Geltonukai') to increased salinity at the germination and juvenile growth stages.

2. MATERIALS AND METHODS

Plants were grown in phytotron chambers with the following conditions: photoperiod - 14 h, average day/night temperature - 22° C /16° C, relative humidity - 75 %, light intensity - 150 µmol m-2 s-1. In order to investigate salinity effects on the earliest growth stages of germination of Amaranth plants, seeds were germinated in Petri dishes, 25 seeds in each. Petri dishes were protected from direct light. Seeds were exposed to 0 mM, 50 mM and 150 mM NaCl solutions. Germination was monitored for 7 days.

A pot experiment was carried out to investigate salinity effects on Amaranth's growth and photosynthesis. Ten seeds were planted in plastic pots (volume 3 l), in universal peat substrate, prepared for germination and growing of agricultural plants. Seedlings were rarefied till one plant per pot 1 week after germination. NaCl treatment was started 7 weeks after germination and lasted for 15 days. Plants were watered with equal amounts of 0 mM, 50 mM ir 150 mM NaCl solutions.

At the end of the treatment, photosynthetic rate, dry shoot biomass and leaf area were analyzed. The measurements of gas exchange were performed using a portable closed infrared gas analyzer LI-COR 6400 (LI-COR, Inc., Lincoln, NE, USA) with randomly selected the youngest fully expanded leaf. Leaf area was measured with a scanner (CanoScan 4400F, Canon, USA) and determined using GIMP 2.8 software. All measurements were carried out in three replicates. The data were analysed using STATISTICA 8 and the results were expressed as the mean values and their confidence intervals ($p<0.05$) (±95% CI).

3. RESULTS AND DISCUSSION

3.1 Salinity effect on Amaranth's germination

Salinity effect on Amaranth seed germination highly varied between varieties and NaCl stress intensity (Figure 1). The variety 'Raudonukai' was least affected by increasing salinity: 50 mM NaCl concentration reduced its germination by 18%; 150 mM NaCl concentration induced stronger inhibition, however no statistically significant differences were detected between these two stress levels. The variety 'Rausvukai' was similarly resistant to lower level of salinity, however it was sharply inhibited by stronger NaCl stress. 'Geltonukai' was the most sensitive variety at this growth stage, as germination of these plants were inhibited by approximately 40% and 78% throughout all germinating periods for 50 mM and 150 mM NaCl stress, respectively (Figure 1). Besides inhibition of germination, a delay in it was also observed for all Amaranth's varieties, as it has been already detected in the previous studies (Jeyanthi et al., 2010; Amukali et al., 2016).

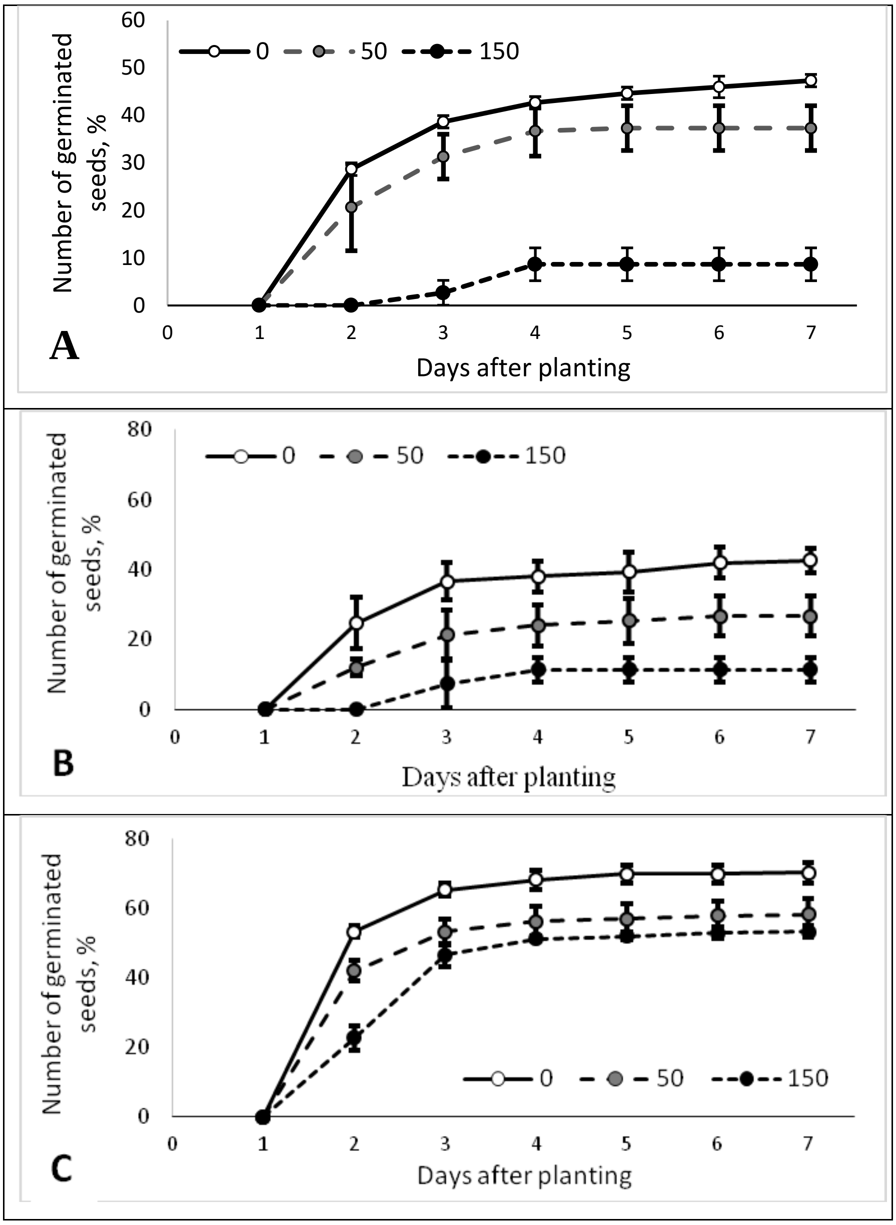


Figure 1. Salinity effects on germination of different varieties of Amaranthus seeds (letters represents different varieties: A-'Rausvukai', B-'Geltonukai', C-'Raudonukai').

3.2 Salinity effects on photosynthesis and plants' growth

Different varieties of Amaranth varied significantly according to the tolerance to increased soil salinity, as was detected by diverse inhibition of growth. 'Rausvukai' was found to be the most tolerant with respect to dry shoot biomass: 150 mM NaCl induced the lowest (15.4%) growth inhibition; about two-fold stronger effect was observed on other investigated varieties. Moreover, 'Raudonukai' was significantly affected by even 50 mM NaCl concentration. Whereas leaf development of different varieties showed an opposite tendency. The treatment with 150 mM NaCl solution reduced leaf area of all varieties of Amaranth plants, but the strongest negative effect was observed for 'Rausvukai': 47% ($p < 0.05$) reduction compared to control was detected. The order of decreasing tolerance to salinity of investigated Amaranth plants with respect to leaf development was as follows: 'Geltonukai', 'Raudonukai' and 'Rausvukai' (Figure 2).

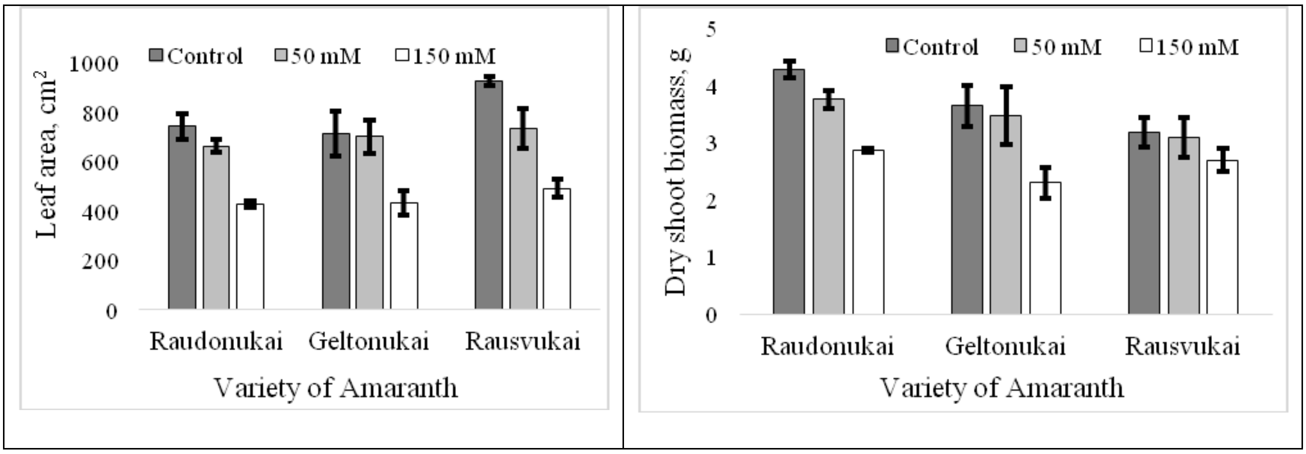


Figure 2. Salinity effects on leaf area and dry shoot biomass of different varieties of Amaranthus.

The photosynthetic response of investigated Amaranth plants was measured 5, 10 and 15 days after the beginning of salinity treatment as well as immediately before the treatment. The negative NaCl effect on photosynthetic carbon assimilation revealed at the10th day of exposure, as photosynthetic rate, measured 5 days after the treatment, did not differ significantly from the values measured before the treatment. The differences between NaCl treated plants and control were also mostly statistically insignificant 5 days after the beginning of the treatment. At the 10th day of the NaCl treatment an effect of 50 mM NaCl level was still negligible for all varieties; however, 150 mM induced significant reduction of photosynthetic rate: ~20% in ‘Raudonukai’ and ‘Geltonukai’ and 31% in ‘Rausvukai’.

The negative effect of lower salinity level was observed at the 15th day of exposure in ‘Geltonukai’ and ‘Rausvukai’, but not in ‘Raudonukai’. Moreover, the photosynthetic rate of the latter variety recovered completely at the 15th day of exposure to 150 mM salinity level. A certain photosynthetic adaptation to high level of salinity was also detected in ‘Rausvukai’ variety. In contrast, “Geltonukai” was not able to adapt to prolonged salinity, as was detected from intensifying impairment of photosynthesis (Table 1).

TABLE 1. Photosynthetic rate (µmols CO_2 m^{-2} s^{-1}) of different varieties of Amaranths exposed to increasing salinity. Values are the means ± SE; letters indicate significant differences between the measurements of particular variety.

Variety	Treatment	Days after beginning of the treatment			
		Before treatment	5 d.	10 d.	15 d.
‘Raudonukai’	Control	2.99 ± 0.13 a	2.77 ± 0.17 ab	2.79 ± 0.09 ab	2.82 ± 0.14 ab
	50 mM		2.79 ± 0.18 ab	2.65 ± 0.05 b	2.74 ± 0.21 ab
	150 mM		2.75 ± 0.23 ab	2.28 ± 0.03 c	2.85 ± 0.08 ab
‘Geltonukai’	Control	2.96 ± 0.10 a	2.68 ± 0.15 ab	2.79 ± 0.07 a	2.92 ± 0.09 a
	50 mM		2.49 ± 0.15 b	3.00 ± 0.07 a	2.41 ± 0.10 bc
	150 mM		2.83 ± 0.13 a	2.26 ± 0.02 c	2.23 ± 0.10 bc
‘Rausvukai’	Control	2.97 ± 0.10 a	2.92 ± 0.26 a	2.85 ± 0.05 a	2.83 ± 0.11 a
	50 mM		2.73 ± 0.22 ab	3.01 ± 0.06 a	2.44 ± 0.12 b
	150 mM		2.70 ± 0.20 ab	2.00 ± 0.03 c	2.69 ± 0.18 ab

4. CONCLUSIONS

Results of this study have shown that Amaranth can be classified as salinity resistant crop species, as vegetative growth and photosynthetic performance were not affected by relatively high (50mM) NaCl concentrations. At the earliest growth stage ‘Raudonukai’ demonstrated the highest resistance, germinating 2-3 fold better as compared to other varieties. In contrast, growth of aboveground biomass of ‘Raudonukai’ was the most seriously affected, followed by ‘Geltonukai’ and ‘Rausvukai’.

In spite of negligible growth inhibition, leaf development of variety 'Rausvukai' was affected stronger than other varieties. Considering the photosynthetic performance, 'Raudonukai' was detected to be the most tolerant variety: carbon assimilation was not affected by lower salinity. Moreover, the negative effect of higher salinity level on this variety was relatively low and completely disappeared after 15 days of the beginning of exposure. In contrast, the strongest inhibition of photosynthetic system was observed in 'Geltonukai'. Summarizing the results of this study it can stated that 'Raudonukai' is the most salinity-tolerant of the three investigated Amaranth varieties, since these plants demonstrated the highest resistance of germination and photosynthetic system. Less tolerant variety is 'Rausvukai', showing the highest resistance with respect to growth of dry shoot biomass, but only moderate resistance of photosynthetic system and high sensitivity of germination. 'Geltonukai', which growth was moderately affected, but germination and photosynthesis was strongly inhibited by NaCl, could be classified as the most salinity-sensitive of investigated Amaranths' varieties.

Acknowledgements
Participation in the conference is funded by the European Social Fund under the No 09.3.3-LMT-K-712 "Development of Competences of Scientists, other Researchers and Students through Practical Research Activities" measure. Many thanks to Giedrė Gelčytė for assistance during the experiment and permission to use her data for this publication.

References

1. Amukali O., B.O. Obadoni and J.K. Mensah (2015) 'Effects of different NaCl concentrations on germination and seedling growth of Amaranthus Hybridus and Celosia argentea', **African Journal of Evironmental Science and Technology**, 9, pp. 301-306.
2. Jeyanthi L.R., Soni D., Dhanalakshmi V. and S. Anbuselvi (2010) 'Effect of exogenous spermidine on salinity tolerance with respect to seed germination', **International Journal of Applied Agricultural Research**, 5, pp. 163-169.
3. Munns R. and M. Tester (2008) 'Mechanisms of salinity tolerance', **Annual Review of Plant Biology**, 59, pp. 651-681.
4. Munns R. (2002) 'Comparative physiology of salt and water stress', **Plant, Cell and Environment**, 25, pp. 239-250.
5. Omami E.N. and P.S. Hammes (2006) 'Interactive effects of salinity and water stress on growth, leaf water relations, and gas exchange in amaranth (Amaranthus spp.)', **New Zealand Journal of Crop and Horticultural Science**, 34, pp.33–44.
6. Stallknecht G.F. and J.R. Schulz-Schaeffer (1993) '**Amaranth rediscovered'**, Wiley.
7. Kauffman C.S. and Weber L.E. (1990) Grain amaranth, **1th National Symposium on New Crops**, pp. 127-139, Indianapolis, Portland.
8. Panuccio M.R., S.E. Jacobsen, S.S. Akhtar and A. Muscolo (2014) 'Effect of saline water on seed germination and early seedling growth of the halophyte quinoa', **AoB Plants**, 6, https://doi.org/10.1093/aobpla/plu047.

"DIRTY" SEA PHENOMENON IN THESSALONIKI BAY: PLANKTON ABETTORS AND PERPETRATORS

S. Genitsaris, N. Stefanidou, M. Moustaka-Gouni*

Department of Botany, School of Biology, Aristotle University of Thessaloniki, 541 24, Thessaloniki, Greece

*Corresponding author: e-mail: mmustaka@bio.auth.gr

Abstract

The "dirty" Sea phenomenon, mentioned also as the mucilage phenomenon in the literature, is caused by the accumulation of gelatinous organic material at and below the water sea surface. The organic material tends to be whitish when young, becoming progressively darker with age. This phenomenon was conspicuous in large extent in Thessaloniki Bay during June 2017. Plankton samples from 3 stations in Thessaloniki Bay were examined before (end of May 2017), during (late June 2017) and after (early July 2017) the phenomenon in order to identify the possible abettors and perpetrators members of plankton. Before the appearance, plankton community consisted of known mucilage producing species such as the autotrophic common diatoms in the Bay *Cylindrotheca closterium, Leptocylindrus minimus, Leptocylindros danicus*, *Skeletonema costatum*, the rare dinoflagellate *Gonyaulax* cf. *fragilis* and the common heterotrophic *Noctiluca scintillans* with its rare relative *Spatulodinium pseudonoctiluca*. These heterotrophic dinoflagellates were responsible for common red tides in the Bay. In May, among the diatoms high abundances were recorded for *Leptocylindros minimus* (26282 cells mL^{-1}), *Dactyliosolen fragilissimus* (866 cells mL^{-1}), and *Cylindrotheca closterium* (168 cells mL^{-1}), while for the heterotrophs high abundance was recorded for the large-sized *Noctiluca scintillans* (0.5 cells mL^{-1}, reaching 5 cells mL^{-1} in the next days). During the phenomenon large mucilage macroaggregates, dead cells of the above mentioned species and alive specimens of the dinoflagellate *Gonyaulax* cf. *fragilis* (68 – 330 cells mL^{-1}) and the diatom *Cylindrotheca closterium* (93 – 393 cells mL^{-1}) were recorded in the "dirty" water. Very abundant mucilage producing species *Skeletonema costatum* (maximum abundance 12454 cells mL^{-1}), *Chaetoceros* spp. (max 10408 cells mL^{-1}), and *Cylindrotheca closterium* (max 1064 cells mL^{-1}) were observed few days later in the "clean" water after the "dirty" Sea phenomenon, which decayed after strong winds, opposed to the rare occurrence of *Gonyaulax* cf. *fragilis* (18 cells mL^{-1}).

Keywords: mucilage, plankton, Thessaloniki Bay, diatoms, *Gonyaulax* cf. *fragilis*, *Noctiluca scintillans*

1. INTRODUCTION

Large aggregates of organic material that are macroscopically visible have been rarely documented in marine waters, mostly in the Marmara Sea, the Tyrrhenian Sea, the Aegean Sea and the Adriatic Sea (Danovaro et al., 2009). Most of these citations concern Northwest Adriatic Sea, along the Emilia-Romagna coast, where the process of eutrophication causes cycles of summer "red tide" events followed by winter and spring large blooms of diatoms, which determine the so-called "dirty waters" (Vollenweider et al., 1992). These structures are considered to be initially produced by mucilage producing diatoms. In particular, the extracellular exudates produced by the in vivo metabolism of the diatoms *Amphora coffeaeformis* and *Cylindrotheca fusiformis* have been identified as the perpetrators of this phenomenon (De Angelis et al., 1993). In addition, Rhinaldi et al. (1995),

also characterized the dinoflagellate *Gonyaulax fragilis* as a possible perpetrator of “dirty sea” phenomena in Adriatic and Tyrrhenian Sea by participating in the mucilage production. A differentiation into five states or stages of the phenomenon was proposed in the case of Adriatic: macroflocs, stringers, clouds, creamy surface layers, and gelatinous surface layers. This classification was based only on size and shape of the macroaggregates, and took into consideration the relative position in the water, stability, behavior, and effect on benthos (Stachowitsch et al., 1990). Although larger aggregates of organic material, caused by mucus (clouds, creamy layers, and gelatinous layers) are less frequent, recurring episodes of the “dirty sea” might lead to anoxia in bottom waters, cause fish kills and other nuisances in fisheries and the regional tourist industry.

Thermaikos Gulf and especially its inner part, Thessaloniki Bay, has been accepting for decades a large volume of domestic and industrial wastes from the city of Thessaloniki. In the 20th century, these wastes were discharged in the Bay without any previous treatment, causing the eutrophication of the system. The past couple of decades, wastewater treatment has been implemented, decreasing the effects of anthropogenic eutrophication (Krestenitis et al., 2012). However, Thessaloniki Bay still remains a nutrient rich environment, in which red tides and episodes of algal blooms frequently occur, with substantial socio-economic impact in the area (Karageorgis et al., 2005). These events might be enhanced by frequently observed in the Bay mucilage producing plankton species, which include *Cylindrotheca closterium*, *Leptocylindrus* sp. and others (see publications by Nikolaides & Moustaka-Gouni, 1990; Friligos et al., 1997; Genitsaris et al., 2011). In Thessaloniki Bay, the “dirty sea” phenomenon appeared on the 22 June 2017, after 24 hours of strong winds (reaching 40 km h^{-1}; data from the Hellenic National Meteorological Service, Thessaloniki Airport Station) in the area, and it lasted for about 10 days. The aim of this paper is to investigate the biological producers of this extensive and unprecedented phenomenon in Thessaloniki Bay, by examining the planktonic community before, during and after the phenomenon, and identifying potential planktonic abettors and perpetrators.

2. MATERIALS AND METHODS

2.1 Sampling

During the last 10 days of June 2017, the coastal front of the city of Thessaloniki was covered in large extend with autochthonous gelatinous organic material which appeared mixed whitish-brownish and became progressively darker with age (Figure 1), causing irritation and unpleasant odor to the citizens of Thessaloniki.



Figure 1. Photographs of the “dirty sea” phenomenon in Thessaloniki Bay, taken about 300 m from the shore, in 28 June 2017.

In total, 7 water samples from the sampling sites shown in Figure 2 were collected before (31 May 2017; 1 sample from site A), during (28 June 2017; 3 samples from sites LM, WT and MG, respectively), and after (7 July 2017; 3 samples from sites LM, WT and MG, respectively) the “dirty sea” phenomenon. The offshore sampling sites were selected based the macroscopic extent of the phenomenon, while the coastal site (WT) was a focal sampling point, on the basis of the recent, frequent red tides formed inshore in Thessaloniki Bay affecting good water quality and aesthetical values for the residents and tourists of the city of Thessaloniki. The samplings in the offshore stations were carried out on board of a ship under the supervision of the Coastal Guard. The water samples were collected from the surface water layer (0-1 m) with a Niskin-type water sampler. Data from samples taken from deeper depths are not included in this paper.

2.2 Microscopy

Fresh and preserved water samples were examined under a light inverted microscope (Nikon SE 2000), and species were identified using appropriate taxonomic keys. Unicellular planktonic organism counts were performed using the sedimentation method of Utermöhl (1958). Briefly, at least 400 plankton individuals were counted in samples, when possible, in sedimentation chambers of 3 mL, 10 mL or 25 mL, depending on the total abundance in each sample. The dimensions of 30 individuals (cells, or colonies) of each dominant species (comprising of ≥ 10 % of the total plankton in terms of abundance and biomass) were measured using the relevant tools of a digital microscope camera (Nikon DS-L1). Mean cell, or colony volume estimates were calculated using appropriate geometric formulae according to Hillebrand et al. (1999).

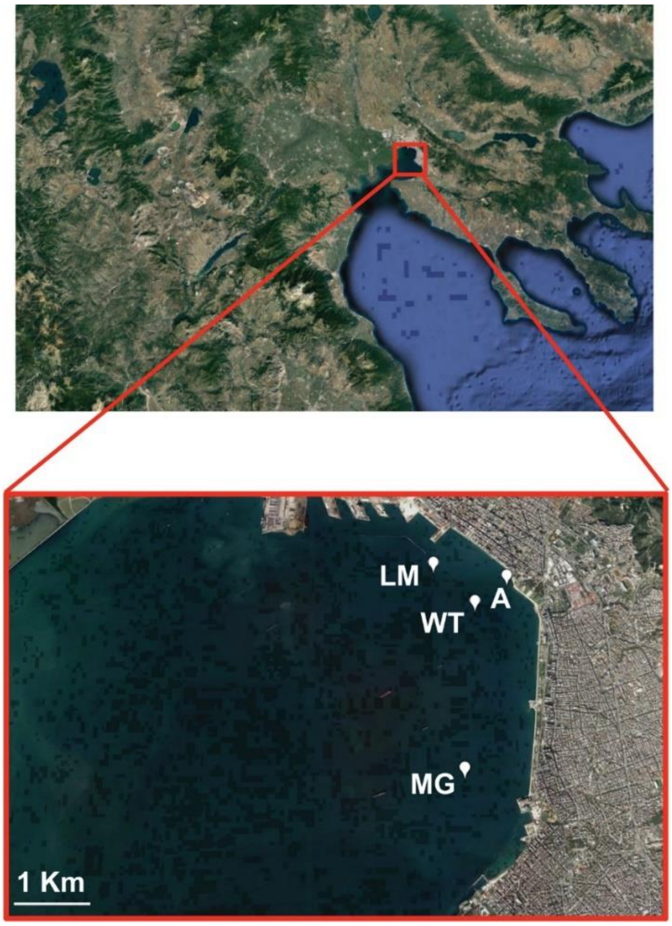


Figure 2. Study area in Thessaloniki Bay, indicating the location of the sampling sites (A: coastal site near the White Tower; LM: about 500 m from the coast near the eastern part of the Port of Thessaloniki; WT: about 500 m from the coast near the White Tower; MG: about 500 m from the coast near Thessaloniki Concert Hall).

3. RESULTS AND DISCUSSION

3.1 Species Composition

Overall, 25 unicellular planktonic taxa were identified in the water samples during the study period in Thessaloniki Bay (Table 1). The highest species number was detected in the sampling of May, in the coastal site A, where 18 taxa were identified. Among the taxa, known mucilage producing species were observed in high abundances, such as the common diatoms in the Bay (Nikolaides & Moustaka-Gouni, 1990; Genitsaris et al., 2011) *Leptocylindros minimus* (26282 cells mL^{-1}), *Dactyliosolen fragilissimus* (866 cells mL^{-1}), and *Cylindrotheca closterium* (168 cells mL^{-1}), and the pelagic dinoflagellate *Gonyaulax* cf. *fragilis* (168 cells mL^{-1}). These species co-occurred with the common heterotrophic dinoflagellate *Noctiluca scintillans* (Figure 3), with its rare relative *Spatulodinium pseudonoctiluca*, which dominated in terms of biomass.

Table 1. List of unicellular planktonic taxa identified in the water samples collected before, during and after the "dirty sea" phenomenon in Thessaloniki Bay. (*) Depicts presence of the organism.

Taxa	Sampling Site (Date)						
	A (May)	LM (June)	WT (June)	MG (June)	LM (July)	WT (July)	MG (July)
Dinophyceae							
Ceratium furca					*	*	*
Gonyaulax cf. fragilis	*	*	*	*	*		
Gymnodinium spp.					*	*	
Gyrodinium spirale	*					*	
Heterocapsa nieii	*						
Karenia sp.	*					*	
Noctiluca scintillans	*	*	*	*			
Prorocentrum micans	*					*	
Protoperidinium spp.					*	*	
Scrippsiella trochoidea						*	
Spatulodinium pseudonoctiluca	*	*	*	*			
Bacillariophyta							
Chaetoceros spp.	*				*	*	*
Cylindrotheca closterium	*	*			*	*	*
Dactyliosolen fragilissimus	*						
Leptocylindrus danicus	*				*	*	
Leptocylindrus minimus	*						
Pseudonitzschia pungens						*	*
Rhizosolenia spp.	*						*
Skeletonema costatum	*				*	*	*
Cryptophyta							
Plagioselmis sp.	*				*	*	
Teleulax acuta	*				*	*	
Haptophyceae							
Chrysochromulina sp.	*				*	*	*
Coccolithales spp.	*				*	*	*
Chlorophyta							
Tetraselmis sp.					*		
Euglenozoa							
Eutreptiella sp.					*	*	

These heterotrophic dinoflagellates, known to especially adapt to a strongly fluctuant environment (Gómes & Souissi, 2007), are characterized as perpetrators in Red Tide events globally (e.g. Uhlig & Sahling, 1990; Hallegraeff, 1993; Huang & Qi, 1997 and many more), and were also responsible for frequent and temporally and spatially extensive red tide events along the front in Thessaloniki Bay during the previous year (Genitsaris et al., unpublished data). The accumulation of autochthonous organic material (dead and alive material) from the repetitive red tides during spring to summer plankton succession (Genitsaris et al., unpublished data), in combination with the hydrodynamic conditions in the Bay and the presence of abundant mucilage producing species before and during the "dirty sea" phenomenon are suggested to lead to the formation of the phenomenon. *N. scintillans* can create a large quantity of mucus (Al Gheilani et al., 2011), observed also in our samples. The mucilage producing species in Thessaloniki Bay were also incriminated for similar phenomena in other marine systems (see Table 2). Moreover, Umani et al. (2007) in a 3 year study on the microbial community of a coastal area in northern Adriatic Sea with frequent reports of "dirty sea" phenomena, showed mucilage formation by plankton species derived from accumulated to slow-to-degrade organic matter, similar to our observations.

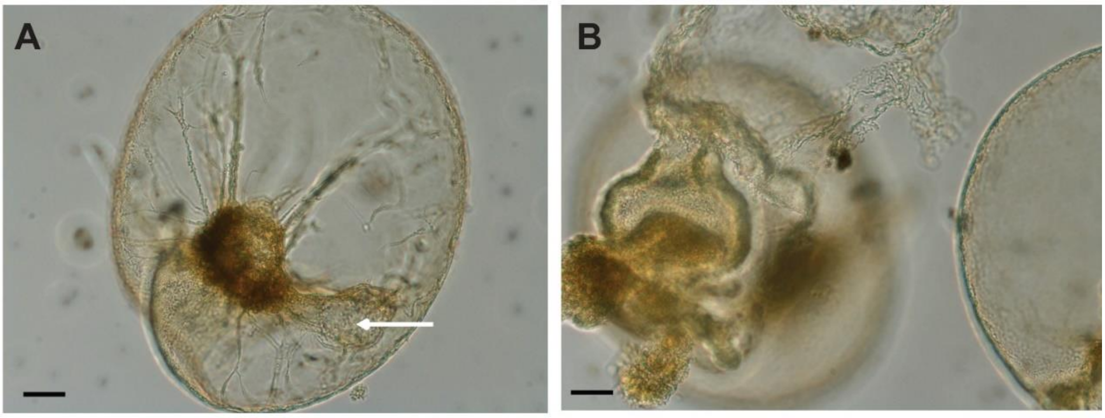


Figure 3. Light micrographs (phase contrast) of preserved samples taken before the "dirty sea" phenomenon (7 June 2017). Water sample indicating (A) the large dinoflagellate *Noctiluca scintillans* (bubble-like), a known red tide forming organism, consuming the dinoflagellate *Gonyaulax* cf. *fragilis* (white arrow); and (B) *Noctiluca scintillans* cells in a stage of degradation and mucus release. Scale bar: 20 µm.

Table 2. List of unicellular planktonic taxa identified as perpetrators and abettors of the "dirty sea" phenomenon in Thessaloniki Bay and in other marine systems.

Planktonic Abettors and Perpetrators in Thessaloniki Bay	Contribution	Other locations of contribution in "dirty sea" phenomena	References
Bacillariophyta			
Chaetoceros spp.	Mucilage formation	Adriatic Sea, Tyrrhenian Sea	Rinaldi et al., 1995
Cylindrotheca closterium	Mucilage formation	Adriatic Sea	De Angelis et al., 1993
Leptocylindrus minimus	Mucilage formation		
Skeletonema costatum	Mucilage formation	Adriatic Sea, Tyrrhenian Sea	Rinaldi et al., 1995
Dinophyceae			
Gonyaulax cf. fragilis	Mucilage formation	Adriatic Sea, Tyrrhenian Sea	Rinaldi et al., 1995
Noctiluca scintillans	Mucus creation, Organic material accumulation	Omani Waters, Adriatic Sea	Al Gheilani et al., 2011; Umani et al., 2004
Spatulodinium pseudonoctiluca	Organic material accumulation	Eastern English Channel	Gómes & Souissi, 2007

During the “dirty sea” phenomenon (June 2017), the diversity, by means of species number, decreased dramatically, and only 4 different taxa were detected, mainly because the samples were characterized by extremely high quantities of dense autochthonous organic material (Figure 4), with remnants of the heterotrophic dinoflagellates previously forming red tides in the area. Also, the thecated dinoflagellate *Gonyaulax* cf. *fragilis* (Figure 4B), a mucilage producing species was occasionally present and identifiable in all three sampling sites. *Cylindrotheca closterium* and *Gonyaulax* cf. *fragilis* were observed to produce mucilage during the phenomenon.

The species number was higher at the end of the phenomenon, reaching 17 identified taxa in the WT site, and 14 taxa in the LM site, in the July sampling. Among these taxa, the identified planktonic abettors and perpetrators of the phenomenon (i.e. the mucilage forming species *Cylindrotheca closterium*, *Leptocylindros danicus*, *Chaetoceros* spp., *Skeletonema costatum*, *Gonyaulax* cf. *fragilis*, and the red tide forming *Noctiluca scintillans* with its rare relative *Spatulodinium pseudonoctiluca*) persisted in the water surface after the “dirty” Sea phenomenon with low numbers. At the same time, plankton bio-indicators of good water quality (species of Coccolithales) also appeared and started increasing in abundance (Table 1).

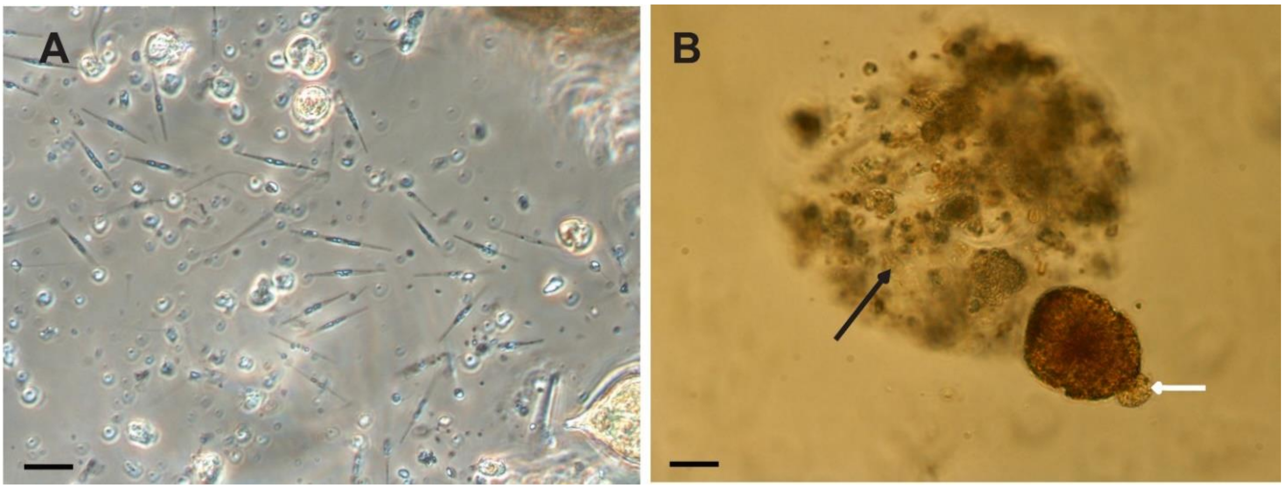


Figure 4. Light micrographs (phase contrast) of preserved samples taken during the “dirty sea” phenomenon. Water sample indicating (A) high numbers of the diatom *Cylindrotheca closterium* (resembling needles) and other planktonic organisms within mucilage below the “dirty” surface; and (B) the dinoflagellate *Gonyaulax* cf. *fragilis* producing mucilage (white arrow) attached in a mucilage aggregate (black arrow). Scale Bar: 20 µm.

3.2 Plankton Abundance and Biomass

Total plankton abundance was higher before and after the “dirty sea” phenomenon, and reached highest values in WT site (> 25 000 cells mL^{-1} in total in both dates), mainly due to the dominance of the diatoms *Leptocylindrus minimus* and *Skeletonema costatum*, respectively (comprising > 50 % of the total plankton abundance). During the phenomenon, the plankton abundance that was recorded was low (<400 cells mL^{-1}; Figure 5A), but in fact the organic matter that covered the surface of the water was extremely high, making it impossible to detect and identify microbial planktoners, except from the thecated *Gonyaulax* dinoflagellate. On the other hand, few days after the phenomenon, in July samplings, the diatoms *Skeletonema costatum* (12454 cells mL^{-1}), *Chaetoceros* spp. (10408 cells mL^{-1}), and *Cylindrotheca closterium* (1064 cells mL^{-1}) prevailed in the water surface, opposite to the rare occurrence of *Gonyaulax* cf. *fragilis* (18 cells mL^{-1}), after decay and dispersal of the micro-aggregates of the phenomenon, due to strong winds (reaching 40 km h^{-1}; data from the Hellenic National Meteorological Service, Thessaloniki Airport Station).

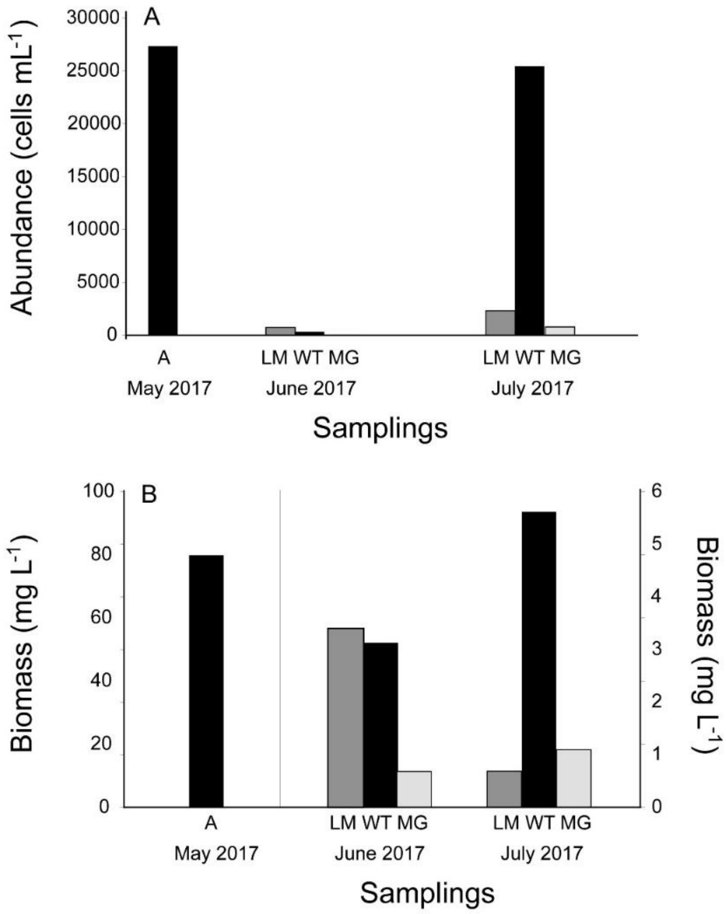


Figure 5. (A) Total plankton abundance (cells mL^{-1}) and (B) biomass (mg L^{-1}) in all samples. In figure (B) primary y-axis corresponds to the biomass of site A, while the secondary y-axis corresponds to the biomass of all other samplings.

On the contrary to abundance data, biomass of alive planktoners was extremely high in the May sampling from the site A (> 75 mg L^{-1}; Figure 5B), due to the high abundance of the large heterotrophic dinoflagellate *Noctiluca scintillans* (0.5 cells mL^{-1}), which made up > 95 % of the total plankton biomass. Its dying is reported to create large quantity of mucus (Al Gheilani et al., 2011). Naturally, the accumulated dead plankton biomass and the produced mucilage making up the autochthonous organic matter of the "dirty sea" was several orders of magnitude higher than that, but it was impossible to calculate with microscopy due to its amorphous mass. The diversity decreased dramatically, and only a few planktonic species were possible to detect. Thus, the abundance and biomass of living plankton appeared extremely low, even though a conspicuous mat of autochthonous organic material produced by plankton covered km^2 along the coastal front. The phenomenon lasted for about 10 days, before strong winds (reaching 40 km h^{-1}; data from the Hellenic National Meteorological Service, Thessaloniki Airport Station) dissolved the mats of mucilagenous material. Mechanical destruction of similar aggregates by wind stress in northern Adriatic Sea, has also been reported (Azam et al., 2007). After the end of the phenomenon, the detected biomass of alive cells dropped dramatically, but still was high for a marine system, especially in WT site (> 5 mg L^{-1}; Figure 5B).

It is generally accepted in the public that the ecological water quality in Thermaikos Gulf has been improved compared to 20 years ago (Mihalatou & Moustaka-Gouni, 2002). However, the "dirty sea" phenomenon, observed in June 2017, in combination with the frequent red tide events in the city front of the Bay recently, sound the alarm and demand continuous monitoring of the biological and abiotic indicators of eutrophication/nutrient pollution and ecological water quality in the Bay. The elimination of the factors contributing to these phenomena, is urgently needed.

Acknoweldgements
This research is implemented through IKY scholarships programme and co-financed by the European Union (European Social Fund - ESF) and Greek national funds through the action entitled “Reinforcement of Postdoctoral Researchers”, in the framework of the Operational Programme “Human Resources Development Program, Education and Lifelong Learning” of the National Strategic Reference Framework (NSRF) 2014 – 2020. We are thankful to the Central Coastal Guard of Thessaloniki and EYATH S.A. for their help in the offshore samplings.

References

1. Al Gheilani H.M., Matsuoka K., Alkindi A.Y., Amer S. and C. Waring (2011) ‘Fish kill incidents and harmful algal blooms in Omani Waters’, **Journal of Agricultural and Marine Sciences**, 16, pp. 23-33.
2. Danovaro R., Umani S.F. and A. Pusceddu (2009) ‘Climate change and the potential spreading of marine mucilage and microbial pathogens in the Mediterranean Sea’, **PLoS ONE**, 4(9), e7006.
3. De Angelis F., Barbaruto M.V., Bruno M., Volterra L. and R. Nicolett (1993) ‘Chemical composition and biological origin of ‘dirty sea’ mucilages’, **Phytochemistry**, 34(2), pp. 393-395.
4. Friligos N., Kondylakis J.C. and R. Psyllidou-Giouranovits (1997) ‘Eutrophication and phytoplankton abundance in the Thermaikos Gulf, Greece’, **Environmental Bulletin**, 6, pp. 27-31.
5. Genitsaris S., Moustaka-Gouni M. and K.A. Kormas (2011) ‘Airborne microeukaryote colonists in experimental water containers: diversity, succession, life histories and established food webs’, **Aquatic Microbial Ecology**, 62(2), pp. 139-152.
6. Gómes F. and S. Souissi (2007) ‘The distribution and life cycle of the dinoflagellate *Spatulodinium pseudonoctiluca* (Dinophyceae, Noctilucales) in the northeastern English Channel’, **Comptes Rendus Biologies**, 330(3), pp. 231-236.
7. Hallegraeff G.M. (1993) ‘A review of harmful algal blooms and their apparent global increase’, **Phycologia**, 32(2), pp. 79-99.
8. Hillebrand H., Dürselen C.-D., Kirschtel D., Pollingher U. and T. Zohary (1999) ‘Biovolume calculation for pelagic and benthic microalgae’, **Journal of Phycology**, 35(2), pp. 403-424.
9. Huang C. and Y. Qi (1997) ‘The abundance cycle and influence factors on red tide phenomena of *Noctiluca scintillans* (Dinophyceae) in Dapeng Bay, the South China Sea’, **Journal of Plankton Research**, 19(3), pp. 308-318.
10. Karageorgis A.P., Skourtos M.S., Kapsimalis V., Kontogianni A.D., Skoulikidis N.Th., Pagou K., Nikolaidis N.P., Drakopoulou P., Zanou B., Karamanos H., Levkov Z. and Ch. Anagnostou (2005) ‘An integrated approach to watershed management within the DPSIR framework: Axios River catchment and Thermaikos Gulf’, **Regional Environmental Change**, 5, pp. 138-160.
11. Krestenitis Y.N., Kombiadou K.D. and Y.S. Androulidakis (2012) ‘Interannual variability of the physical characteristics of North Thermaikos Gulf (NW Aegean Sea)’, **Journal of Marine Systems**, 96-97, pp. 132-151.
12. Mihalatou H.M. and M. Moustaka-Gouni (2002) ‘Pico-, nano-, microplankton abundance and primary productivity in a eutrophic coastal area of the Aegean Sea, Mediterranean’, **International Review of Hydrobiology**, 87(4), pp. 439-456.
13. Nikolaides G. and M. Moustaka-Gouni (1990) ‘The structure and dynamics of phytoplankton assemblages from the inner part of the Thermaikos Gulf, Greece. I. Phytoplankton composition and biomass from May 1988 to April 1989’, **Helgoländer Meeresuntersuchungen**, 44, pp. 487-501.

14. Rinaldi A., Vollenweider R.A., Montanari G., Ferrari C.R. and A. Ghetti (1995) 'Mucilages in Italian seas: the Adriatic and Tyrrhenian Seas, 1988-1991', **The Science of the Total Environment**, 165, pp. 165-183.
15. Stachowitsch M, Fanuko N. and M. Richter (1990) 'Mucus aggregates in the Adriatic Sea: an overview of stages and occurrences', **Marine Ecology**, 11(4), pp. 327-350.
16. Uhlig G. and G. Sahling (1990) 'Long-term studies on *Noctiluca scintillans* in the German Bight population dynamics and red tide phenomena 1968-1988', **Netherlands Journal of Sea Research**, 25(1-2), pp. 101-112.
17. Umani S.F., Beran A., Parlato S., Virgilio D., Zollet T., De Olazabal A., Lazzarini B. and M. Cabrini (2004) '*Noctiluca Scintillans* MACARTNEY in the Northern Adriatic Sea: long-term dynamics, relationships with temperature and eutrophication, and role in the food web', **Journal of Plankton Research**, 26(5), pp. 545-561.
18. Umani S.F., Del Negro P., Larato C., De Vittor C., Cabrini M., Celio M., Falconi C., Tamberlich F. and F. Azam (2007) 'Major inter-annual variations in microbial dynamics in the Gulf of Trieste (northern Adriatic Sea) and their ecosystem applications', **Aquatic Microbial Ecology**, 46, pp. 163-175.
19. Utermöhl H. (1958) 'Zur Vervollkommnung der quantitativen phytoplankton-methodik' **Mitt Int Ver Theor Angew Limnol**, 9, pp. 1-38.
20. Vollenweider R.A., Rinaldi A. and G. Montanari (1992) 'Eutrophication, structure and dynamics of a marine coastal system: results of ten-year monitoring along the Emilia-Romagna coast (Northwest Adriatic Sea)' **International Conference on Marine Coastal Eutrophication'**, pp. 63-106, Bologna, Italy.

MONITORING THE MARINE ENVIRONMENT OF THERMAIKOS GULF

M. Petala[1], V. Tsiridis[1], I. Androulidakis[2], Ch. Makris[2], V. Baltikas[2], A. Stefanidou[3], S. Genitsaris[3], C. Antoniadou[4], D. Rammou[4], M. Moustaka-Gouni[3], C.C. Chintiroglou[4] and E. Darakas[1]*

[1]Laboratory of Environmental Engineering & Planning, Dept. of Civil Engineering,
[2]Laboratory of Maritime Engineering and Maritime Works, Dept. of Civil Engineering,
[3]Laboratory of Botany, School of Biology,
[4]Laboratory of Zoology, School of Biology, Aristotle University of Thessaloniki, 54 124 Thessaloniki, Greece

[*]Corresponding author: e-mail: darakas@civil.auth.gr, tel : +302310995719

Abstract
In this study, the quality of the marine environment of Thermaikos Gulf was appraised by measuring physical, chemical and biological parameters of the water column and the seabed. Water and sediment samples were seasonally collected from three sampling stations located at the inner part of Thermaikos Gulf. Specific physical-chemical characteristics (temperature, salinity, density along with pH and dissolved oxygen) throughout the water column were evaluated by conducting in situ measurements during the sampling campaigns. In situ processing of the water density data enabled the determination of the water column stratification. Afterwards, water samples were collected from the different strata: surface, pycnocline and bottom, to assess relevant variations of the chemical and the biological characteristics of the water masses. The studied chemical parameters included ammonium nitrogen, nitrites, nitrates, phosphates and total phosphorus and the biological ones phytoplankton and protozooplankton species composition, abundance and biomass. Sediment samples were collected with a standard VanVeen grab from each sampling station. Benthic organisms (macro-invertebrates) were sorted, enumerated under major taxa, and identified up to species levels to assess ecological quality status applying the BENTIX biotic index. Sediment composition and organic content were also assessed. The obtained results are discussed with regards to seasonal and spatial variability and water column stratification.

Keywords: Thermaikos Gulf, monitoring, nutrients, phytoplankton, protozooplankton, benthic organisms

1. INTRODUCTION

The European Union Marine Strategy Framework Directive (MSFD) 2008/56/EC establishes an integrated framework for the achievement or maintenance of the good environmental status in the marine systems by the year 2020 the latest. This Directive stipulates detailed procedures for its implementation including the development of marine strategies by Member States, in order to protect and preserve the marine environment. The program of measures shall take into account relevant measures required under the European legislation, in particular the Water Framework Directive (WFD) 2000/60/EC, the Council Directive 91/271/EEC concerning urban waste-water treatment and the Bathing Water Directive (BWD) 2006/7/EC of the European Parliament and of the Council concerning the management of bathing water quality (MSFD, 2008/56/EC). The BWD (Directive 2006/7/EC) aims to protect health and (marine) environment based on scientific knowledge under a

holistic approach that is integrated into all other European measures protecting the quality of all waters through the WFD. WFD introduces the concepts of the ecological and chemical status for the European water bodies. The ecological status is based on biological quality elements supported by hydromorphological and physico-chemical environmental characteristics, and is divided into five classes (‘High’, ‘Good’, ‘Moderate’, ‘Poor’, ‘Bad’). According to the normative guidelines of the WFD, good ecological status is achieved when biological communities present are close to those that would be present with minimal anthropogenic disturbance (2000/60/EC). According to guidelines of the MSFD, qualitative descriptors to be used in assessing the ecological or environmental status include biodiversity, non-indigenous species, exploited fish and shellfish, food webs, human-induced eutrophication, sea-floor integrity, hydrographical conditions, contaminants and contaminants in fish. All in all, the MSFD aims to be based upon an ecosystem-based approach that has a holistic view on the management and protection of marine ecosystems, focusing on ensuring sustainable use of the seas, and providing safe, clean, healthy and productive marine waters (Borja et al., 2008; Borja et al., 2010).

Phytoplankton is the biological element of WFD most closely related to eutrophication and a primary indicator for the assessment of water quality, as it forms the basis of food webs and exhibits high reproduction rates and immediate response to environmental changes. Different phytoplankton attributes are considered essential for the appraisal of ecological status, including species composition, abundance and biomass, as well as frequency and intensity of phytoplankton blooms (WFD, 2000/60/EC). Amongst quality descriptors, phytoplankton biomass, in terms of chlorophyll-α, although it is a gross metric, it is simple and records the responses of phytoplanktonic communities to nutrient enrichments (Tsirtsis and Karydis, 1998; Garmendia et al., 2013). However, chlorophyll-α has been reported as being highly variable, thus also showing higher disagreement with the final classification of the water bodies (Borja et al., 2004). On the other hand, the use of benthic indices has been shown to provide valuable elements for the integrated quality status assessment of water bodies (Borja et al., 2014). Composition and abundance of benthic invertebrate fauna has been proved to be a biological quality element that can be reliably used for the classification of water bodies due to responsiveness to major environmental or anthropogenic changes. Macro-benthic animals are relatively sedentary (they are affected by environmental/ anthropogenic conditions), have relatively long life-spans, consist of different species that demonstrate variable tolerances to chemical stresses and have a substantial role in sediment processes, e.g., enhancing the flow of nutrients and materials between the sediments and the water column, and vice versa, through bioturbation and bioirrigation (Borja et al., 2000). For these reasons macrobenthic communities are listed among quality descriptors for the implementation of MSFD (MSFD, 2008/56/EC). In this context, the classification of ecological status is implemented using indices based on sensitivity/ tolerance of various species. In European waters the most frequently applied indices are AMBI and M-AMBI that have been developed using the data from the coastal marine areas and are mainly used to assess the organic enrichment (Pitacco et al., 2018). However, for the Mediterranean Sea, and especially the eastern basin, the most appropriate index is BENTIX, originally developed in the Aegean Sea (Simboura and Zenetos, 2002), as revealed by the intercalibration procedure of the EU members (Simboura and Reizopoulou, 2008). Accordingly, the BENTIX index, is the official tool for the ecological status assessment in Greece and Cyprus sedimentary bottoms.

In Northern Greece, Thermaikos Gulf is a marine ecosystem of high complexity due to the various activities taking place in the greater area. Thermaikos Gulf is the final receiver of the discharges of Axios, Aliakmon, Loudias and Gallikos Rivers, as well as of the effluents of two municipal wastewater treatment plants of Thessaloniki, with Axios River having the highest contribution of freshwater input into the gulf. However, Thermaikos is not only affected by the discharges of the watersheds of rivers, but also by the discharges of numerous industrial activities located along the coast. The anthropogenic pressures that originate from agricultural, industrial, commercial, marine and aquaculture activities have resulted in elevated concentrations of nutrients in the water column and accumulation of trace elements in sediments (Friligos et al., 1997; Nikolaidis et al., 2006).

Moreover, the exchanges with the open Aegean Sea waters across the southern boundary are an additional factor that affects the stratification, circulation and renewal of the Gulf (Krestenitis et al., 2012). The complexity of Thermaikos Gulf system, the variability of environmental factors and the specific circulation and renewal dynamics of the system require the development of a quality monitoring scheme that takes into account physical, chemical and ecological quality elements (in the context of the European legislation). To this aim, the present study focuses on the quality assessment of the marine environment of Thermaikos Gulf, using physical, chemical and biological/ecological elements of the water column and the seabed.

2. MATERIALS AND METHODS

2.1 Oceanographic surveys

Within the framework of this study, water and sediment samples that were seasonally (July, October and December 2017) collected from three sampling stations located at the inner part Thessaloniki Bay, inner and outer Thermaikos Gulf. The characteristics of the sampling stations (coordinates of each station, corresponding depth and description of the area) are presented in Table 1. As it is shown in Figure 1, the station S1 is located at the discharge point of the Municipal Wastewater Treatment Plant of Thessaloniki (WWTPT) outlet, the station S2 is located at northern Thessaloniki bay, while the station S3 is located at the discharge point of the Municipal Wastewater Treatment Plant of Michaniona-AINEIA.

Table 1. Characteristics of sampling stations

Sampling Station	Longitude	Latitude	Description	Depth (m)
S1	40.55237285	22.8536432	Station at the outlet of the WWTP of Thessaloniki (WWTPT)	25
S2	40.61821578	22.94157171	Inner Thessaloniki bay	13
S3	40.46212649	22.82078561	Station at the outlet of the WWTP of Michaniona (AINEIA)	30

The physical oceanographic parameters were recorded by means of a CTD (SBE 19) profiler. Apart from the standard sensors (conductivity, temperature, pressure), the instrument is equipped with auxiliary sensors for dissolved oxygen and pH. Raw data were properly processed (low-pass filtering, alignment, cell thermal effects removal) and corrected, to assure the accuracy of the derived parameters. The processed data were averaged over depth-bins of 0.25 m. During sampling, in situ processing of the water density data enabled the preliminary determination of the water column stratification. Afterwards, water samples were collected from three levels of the water column (surface, pycnocline and bottom) with a Niskin-type water sampler, in order to investigate the variations of the measured chemical and biological parameters over the water column depth.

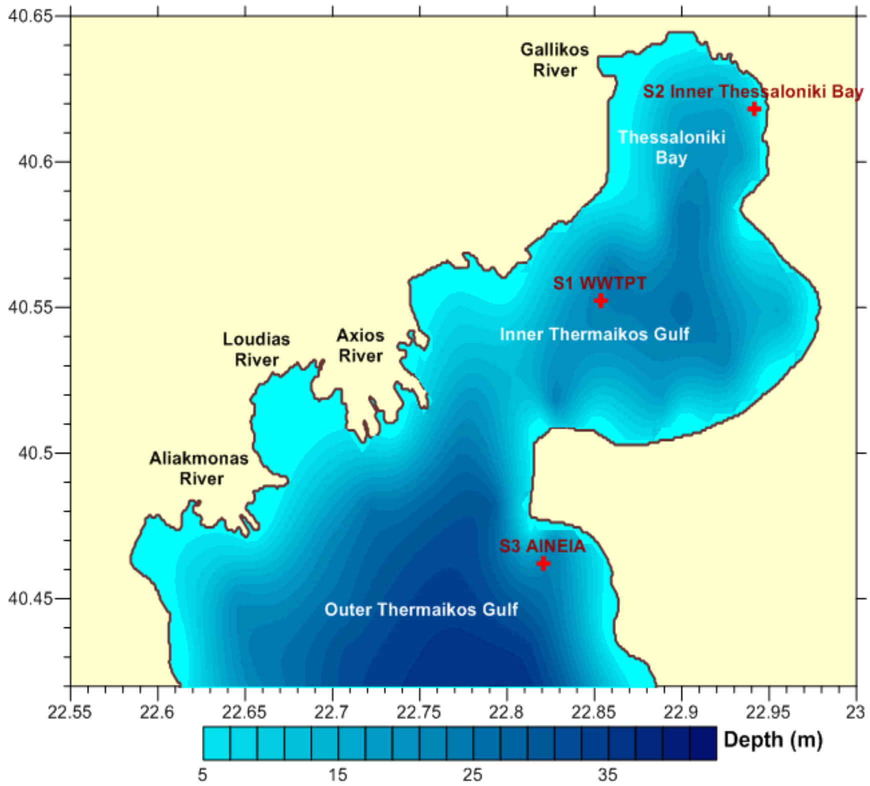


Figure 1. Map of sampling stations, rivers and sub-regions in Thermaikos Gulf.

The chemical status of Thermaikos Gulf was appraised by performing chemical analyses including nitrites (APHA-AWWA-WEF, 1999), nitrates (Grasshoff et al., 1999), ammonium nitrogen (Hach, 2013), phosphates (APHA-AWWA-WEF, 1999), total phosphorus (APHA-AWWA-WEF, 1999) and silica (APHA-AWWA-WEF, 1999; Grasshoff et al., 1999).

2.2 Biological parameters/Phytoplankton and Protozooplankton

Fresh water subsamples (250 ml) were placed at portable refrigerator and subsamples (250 ml) were immediately fixed with Lugol's iodine. Fresh and preserved water samples were examined under a light inverted microscope (Nikon SE 2000), and species were identified using appropriate taxonomic keys. Unicellular planktonic organism counts were performed using the sedimentation method of Utermöhl (1958). Briefly, at least 400 plankton individuals were counted in samples, when possible, in sedimentation chambers of 3 mL, 10 mL or 25 mL, depending on the total abundance in each sample. The dimensions of 30 individuals (cells, or colonies) of each dominant species (comprising of $\geq$ 10 % of the total plankton in terms of abundance and biomass) were measured using the relevant tools of a digital microscope camera (Nikon DS-L1). Mean cell, or colony volume estimates were calculated using appropriate geometric formulae according to Hillebrand et al. (1999).

2.3 Zoobenthos and sediment composition

Two replicate sediment samples were collected with a standard VanVeen grab (0.1 m^2) from each sampling station and period, whereas a third one was collected for sediment composition and organic content analyses. Overall, 18 biological and 9 sediment samples were obtained. Sediment samples were dried out to assess the organic content (H_2O_2 method) and the granulometric composition (siphonometric menthod) applying the Folk's system of sediment classification (Folk et al., 1970). Each biological sample was sieved on board (mesh-opening 1 mm) and preserved in 10% formalin - seawater solution. In the laboratory all living specimens were sorted out from each biological sample under a binocular stereoscope, counted, and identified at species level using relevant identification keys for each major taxa, and a microscope, when appropriate. The species/abundance data matrix was analyzed by standard biocoenotic methods to estimate biodiversity, and by multivariate methods based on Bray-Curtis distances to assess the similarity of zoobenthic communities' structure and

possible spatial or seasonal effects, using the PRIMER software package (Clarke and Gorley, 2006). Also, the BENTIX biotic index was applied to assess the ecological quality status of sampling stations, using the freeware software developed and provided by the National Centre for Marine Research (www. cloudfs.hcmr.gr/index.php).

3. RESULTS

3.1 Physical and Chemical parameters

Very strong stratification, based on both salinity and temperature profiles, was observed in all stations in July, supporting the stability of the water column (Figure 2). The temperature difference between the surface and bottom was around 10°C in the inner Thermaikos Gulf (S1), while the smaller difference was measured in S3 (<3°C). The stations of the inner Gulf (S1 and S2) showed similar distributions in autumn (~21°C) and winter (~13°C). On the contrary, the outer station S3 revealed strong thermocline at 15 m in autumn, where the temperature was reduced by 4°C indicating the possible intrusion of colder waters from the Aegean Sea. This finding agrees with Hyder et al. (2002) and Krestenitis et al. (2012), who showed that this area is the passage of northern Aegean waters supporting the renewal of the Gulf. The same station showed significantly higher temperature values (~16°C) in comparison to the two northern stations (~13°C) in winter. Salinity was very low at the surface of S1 and S2 stations in July (<36). Summer values were lower than winter values in all cases. Moreover, in all cases, salinity was higher in the S3 station, which is usually out of the effect of the riverine waters that are discharged at the western Gulf. Especially in autumn, the salinity distribution of S3 station was not homogenous but increased at 15m from 37 to 39 (Aegean waters). This station is also characterized by warmer and saltier waters along the entire water column during winter.

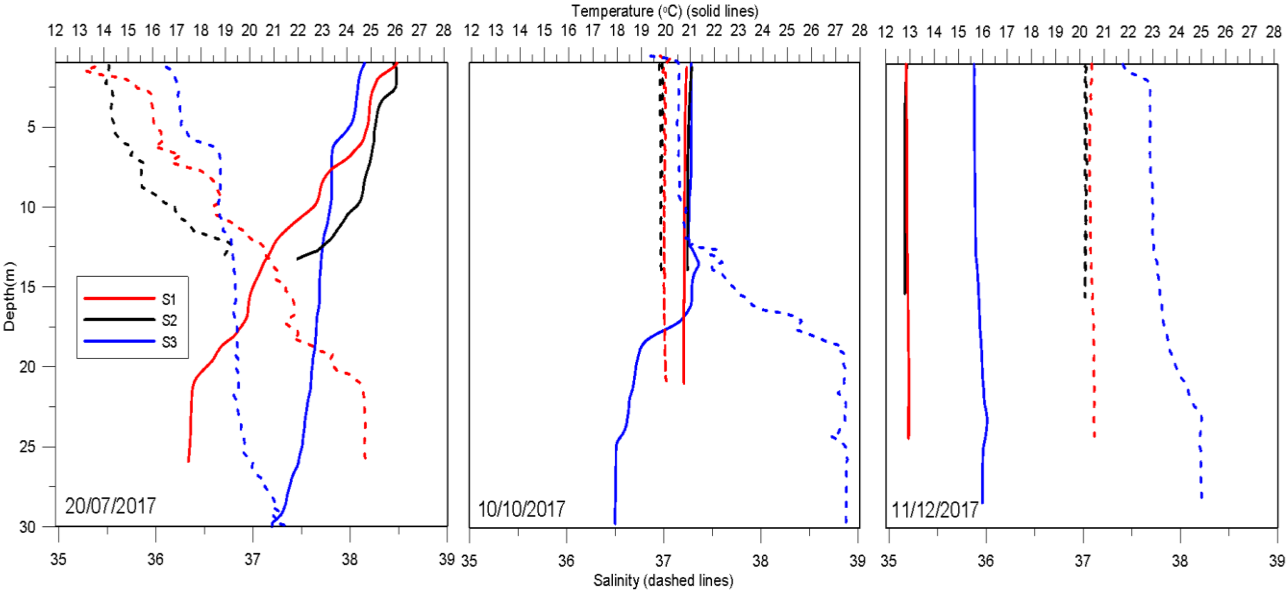


Figure 2. Vertical temperature and salinity profiles of the three Thermaikos stations in July (left), October (middle) and December (right).

The chemical quality of Thermaikos Gulf was mainly based on the seasonal monitoring of nutrients and included the inorganic forms of nitrogen, the orthophosphates and the total phosphorus. The highest concentration of ammonium nitrogen, equal to 1.12 μmol/L NH_4^+, was recorded during the third sampling campaign of December 2017 in the surface sample collected from the sampling station S1 (data not shown). Moreover, relatively high concentration of nitrites, 0.31 μmol/L, was obtained in the same sample, possibly denoting the presence (or the beginning) of reducing conditions in the regional marine environment. The increased concentrations of nitrites were accompanied by a significant reduction of nitrates, as it is shown in Figure 3.

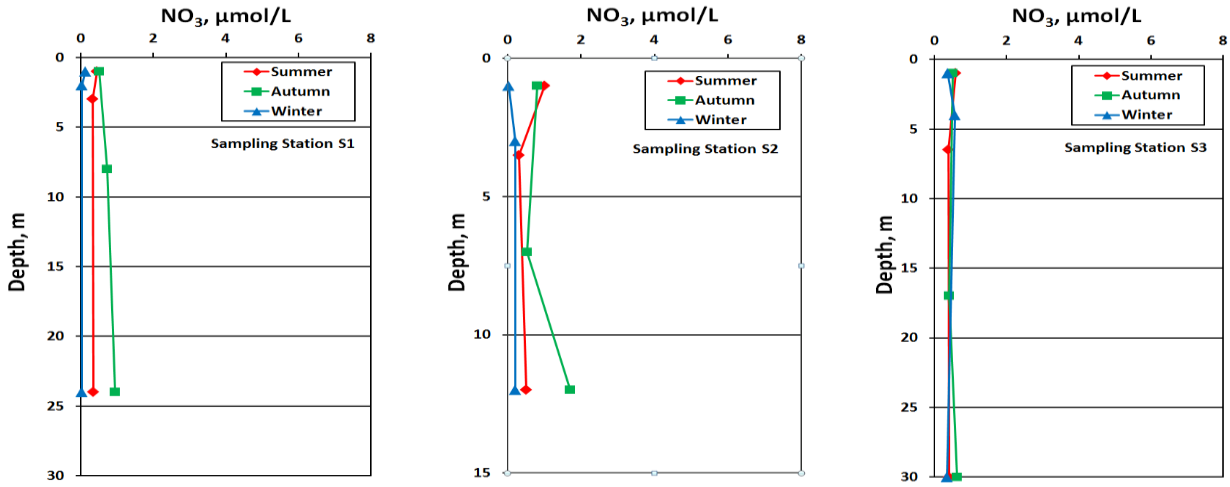


Figure 3. Nitrates concentration results.

The samples collected from the inner part of Thermaikos Gulf indicated rather low concentrations in nutrients of nitrogen and phosphorus. However, during the winter sampling campaign, the red tide phenomenon was observed on the sea surface; the seawater transparency was low, while the total phosphorus concentration was significantly higher compared to the corresponding one measured during the summer period (Figure 4).

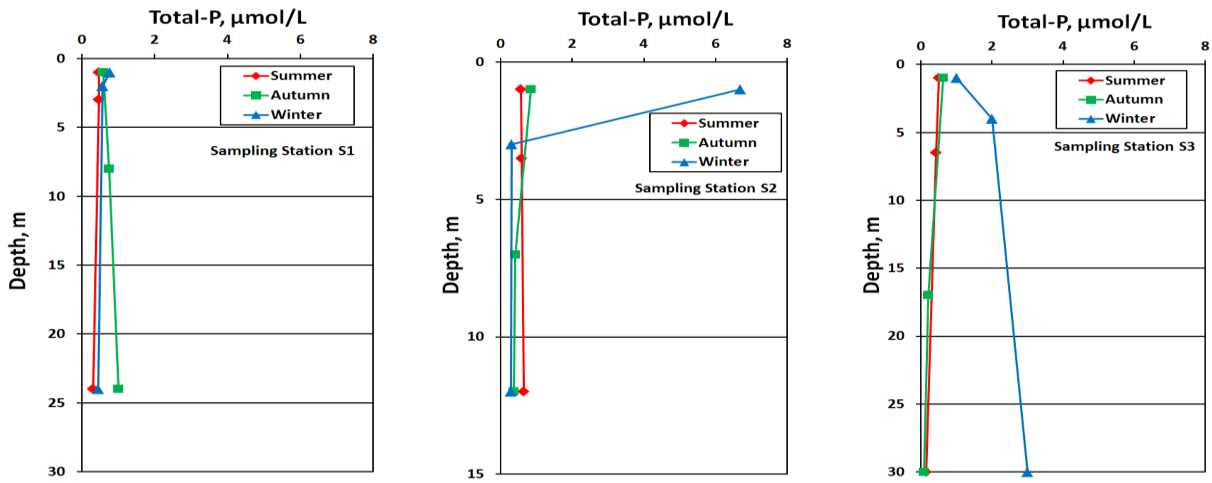


Figure 4. Total phosphorus concentration results.

The results obtained from the third sampling station, at the outer part of Thermaikos Gulf, demonstrated that the concentrations of nutrients were significantly lower compared to the rest sampling stations. However, the concentration of nitrates varied between 0.40 and 0.62 µmol/L, considerably higher compared to the results of 2014 (HCMR, 2015). Still, much higher concentrations, exceeding 2.0 µmol/L, were recorded some years ago (Samanidou et al., 1989). The intensification of sampling and measurements is needed, in order to extract safe conclusions on the quality characteristics of this area.

3.2 Phytoplankton

Species composition

Overall, 87 phytoplankton and 13 protozooplankton taxa were identified in the water samples during the investigation. Within the phytoplankton community, diatoms were recorded with the highest number of species reaching 43 identified taxa, followed by dinophytes (32) and haptophytes (5). For each of the rest phytoplankton taxonomic groups (cryptophytes, chlorophytes, dicthyophytes, euglenophytes, raphidiophytes, xanthophytes) less than 5 representatives were identified. The

protozooplankter *Noctiluca scintillans* (Figure 5d) with its rare relative *Spatulodinium pseudonoctiluca*, responsible for the frequent red tides in Thessaloniki Bay, were recorded in every sample of the inner Gulf (S1 and S2).

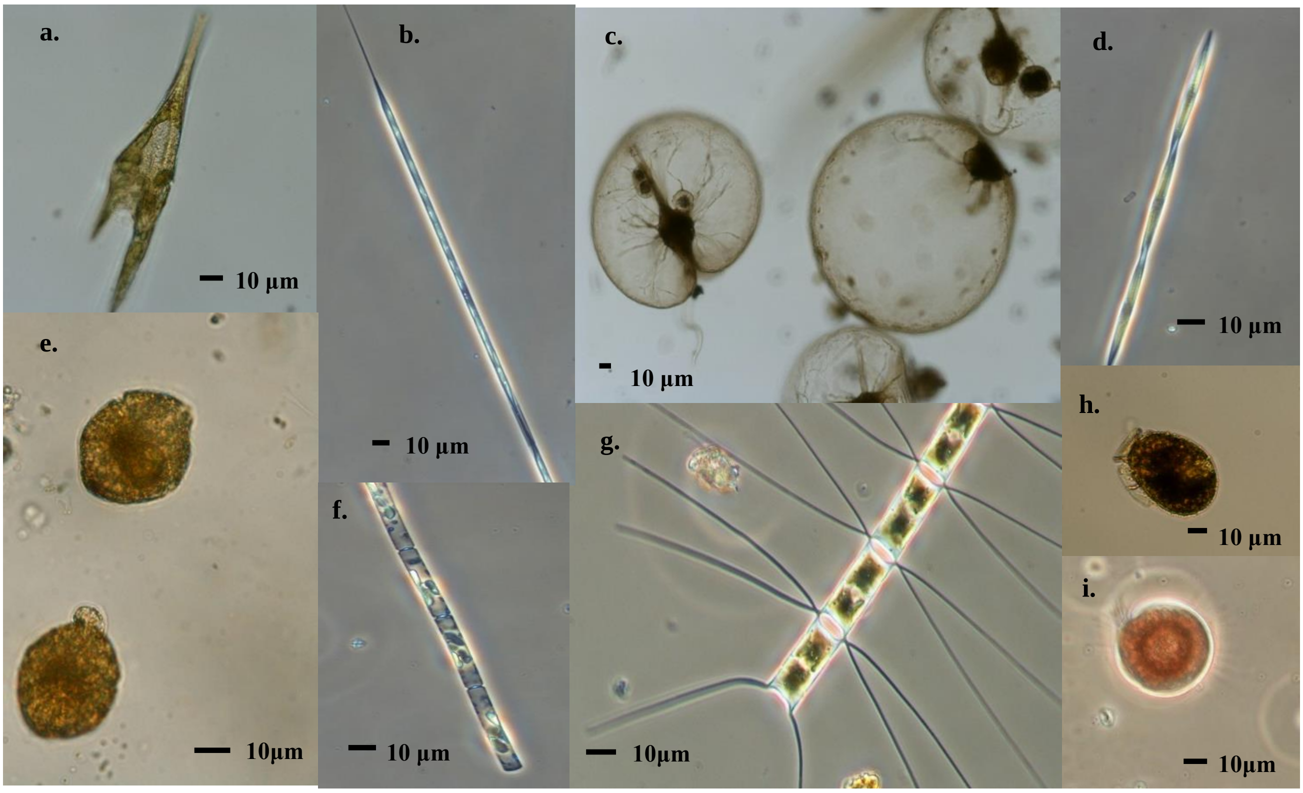


Figure 5. Light micrographs (phase contrast) of phytoplankton and protozooplankton taxa in the water samples from Thermaikos Gulf in June, October and December 2017. a. *Ceratium furca* b. *Rhizosolenia setigera* c. *Noctiluca scintilans* d. *Pseudonitzschia pungens* e. *Gonyaulax* cf. *fragilis* f. *Leptocylindrus danicus* g. *Chaetoceros* sp. h. *Dinophysis* cf. *acuminata* i. *Mesodinium rubrum.*

In July, after the "dirty sea" phenomenon the mucilage forming species *Gonyaulax* cf. *fragilis* and *Chaetoceros* spp. were observed in the samples (Figure 5). During the winter sampling (on December 2017) a large extent red tide was conspicuous in the inner Gulf. The autotrophic ciliate *Mesodinium rubrum* (Figure 5i) was accountable for the phenomenon due to its extremely high abundance (>10000 cell/mL) that was measured in the water samples.

Species number, phytoplankton abundance and biomass

The number of identified species was comparable among the 3 sites following the same trend in terms of increasing depth; higher number of species was observed in the surface samples than the pycnocline and the bottom samples. Diatoms and dinoflagellates were the most diverse taxonomic groups with the first to dominate in richness almost in all samples apart from the occasional dominance of the latter in S1 and S2. The phytoplankton abundance was higher and frequently indicative for bloom formation in the inner gulf (sites S1 and S2) contrary to S3. Characteristically, the maximum measured phytoplankton abundance in S3 was 6 times lower than the maximum in S1 and 12 times lower than in S2. Similarly, the phytoplankton biomass was higher in S1 and S2 than S3 (Figure 6).

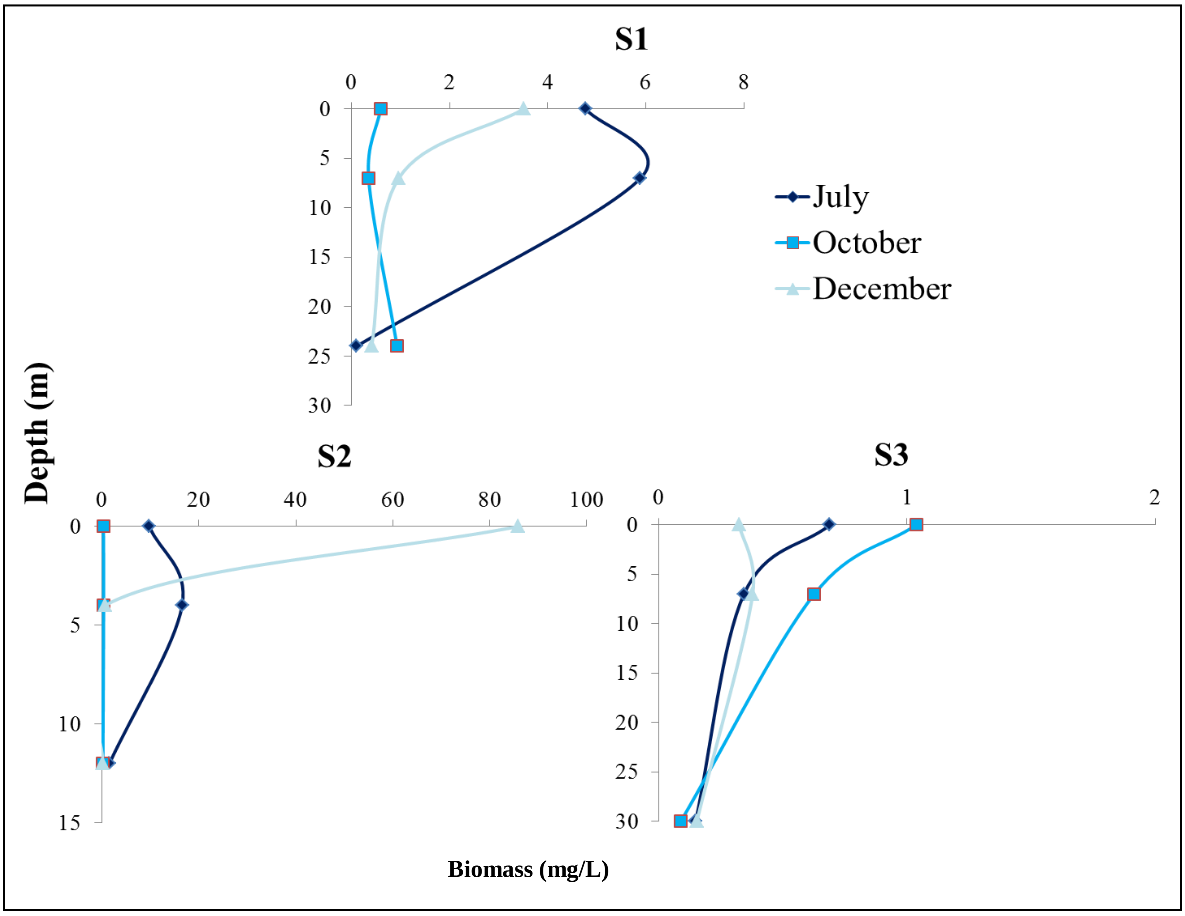


Figure 6. Phytoplankton biomass (mg/L) in each depth and in each site (S1, S2, S3) of Thermaikos Gulf. The dark blue depicts the phytoplankton biomass in July 2017, the ciel blue the biomass in October 2017 and the light ciel blue the biomass in December 2017.

The maximum phytoplankton biomass during the investigation (the extremely high value of 86 mg L^{-1}) was recorded in the surface sample of S2 simultaneously with the extensive red tide in the inner Gulf (on December 2017). The phytoplankton biomass was also high (>5 mg/L) in the surface and pycnocline samples of S1 and S2 on July 2017 (Figure 6). Conversely, the phytoplankton biomass in S3 was typical for oligotrophic marine environments with exception of the surface sample on October 2017 where the measured biomass was 1 mg/L.

3.3 Zoobenthos

According to the granulometric composition, the sediment is characterized as muddy in S1 and S3, and as sandy-mud in S2. The sediment composition was seasonally stable, with the exception of the December period, where the proportion of sand increased in S1 and S3 shifting the characterization of the sea-bottom as sandy-mud, as opposed to S2, where the proportion of clay increased and the sediment became muddy. At the same time, increased amounts of biogenic fragments were also observed in S2. The organic content showed spatial divergences with increased values in S2 (0.1465 ± 0.023) and lower, but inter-se similar, in S1 and S3 (0.1174 ± 0.022 and 0.1104 ± 0.025, respectively). Slight seasonal variations were also detected, but without following a similar trend between stations.

Overall 2,945 macro-invertebrate specimens were collected identified to 207 species. Polychaetes and molluscs were the most speciose groups, followed by crustaceans. The above groups prevailed also in abundance. Zoobenthic diversity and abundance showed significantly ($p<0.01$) higher values in S2 (mean S = 56, mean N = 347/0.1m^2) and decreased ones in S3 (mean S = 29, mean N = 80.33) and S1 (mean S = 16, mean N = 57.66), in particular. The most dominant and frequent species were the polychaetes *Ditrupa arietina*, *Magelona mirabilis*, *Nepthys hystricis*, *Notomastus latericeus*,

Sternaspis scutata, the ophiuran *Amphiura chiajei* and the bivalve *Kurtiella bidentata*. Multivariate analyses discriminated samples primarily according to their geographic origin ($R = 1$ $p < 0.05$) and secondary (within each station group) according to the season of sampling ($R = 0.72$ $p < 0.05$); the latter case mostly due to the divergence of the samples collected in winter (Figure 7). This biotic pattern was mainly correlated with the amount of clay and the organic content of the sediments (Spearman $\rho = 0.625$).

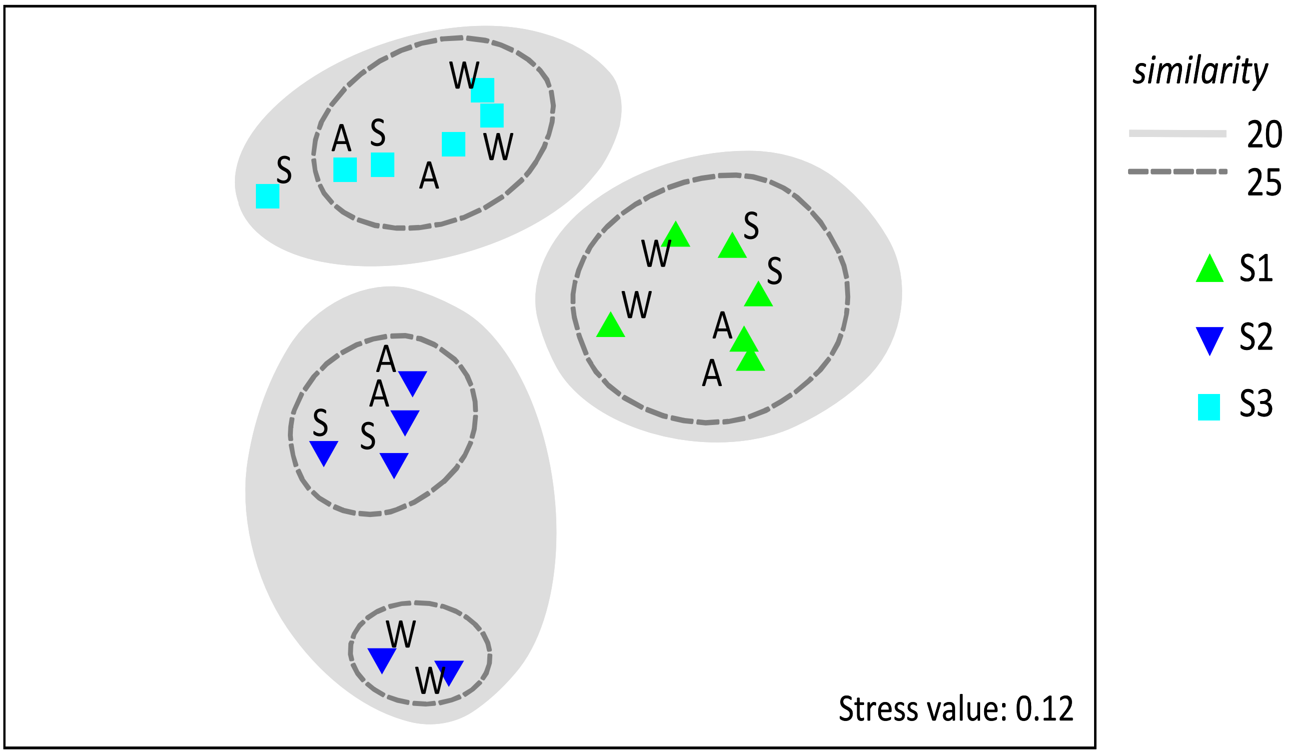


Figure 7. Non-metric multidimensional scaling ordination of zoobenthic samples from Thermaikos Gulf stations (S1-S3), based on Bray-Curtis similarity index calculated from square-root transformed numerical abundance data of macro-invertebrate species. S = summer sampling, A = autumn sampling, W = winter sampling.

The majority of macroinvertebrates were classified into the tolerant category, being positively correlated with organic enrichment, with the exception of S1 in winter, where the sensitive species group prevailed (Table 2). The BENTIX biotic index ranged from 2.51 to 3.66, and accordingly, the ecological quality status of the stations ranged from moderate (S1, S2) to good (S3) (Table 2). The ecological quality status of S1 improved in winter, whereas remained seasonally stable in S2 (moderate) and S3 (good). However, the percentage of species not assigned to any ecological category overpasses 10% in some cases, and so these specific results should be viewed with caution.

4. DISCUSSION AND CONCLUSIONS

Although denser (colder and saltier) waters, possibly originated from the North Aegean, were detected in the outer Gulf during the fall measurements, they were not observed in the northern areas, indicating weak renewal of the inner Gulf. More brackish waters were detected in the drier summer months although the river discharge rates are usually smaller. A possible explanation is the operation of the power generation dams, which exist along the Aliakmonas river, leading to increased outflows toward the sea (Krestenitis et al., 2012). Krestenitis et al. (2012), based on 5 long cruise period (1994-2007) showed a general decrease of Gulf's salinity. On the contrary, the current measurements, almost 10 years later, showed higher salinity values, supporting the inverse of the decreasing trend found in older expeditions.

Table 2. Number of species (S), numerical abundance (N), ecological groups (GS = Sensitive species group, GT = tolerant species group, NA = not assigned species), BENTIX index, and ecological quality (EcoQ) status assessment per seasonal sampling and station (S1 – S3) in Thermaikos Gulf.

Sampling		S	N	Ecological Category			BENTIX	EcoQ
Station	Season			GS	GT	NA		
S1	Summer 2017	18	80	18.75%	71.25%	10.00%	2.55	MODERATE
	Autumn 2017	20	117	15.05%	80.34%	4.62%	2.51	MODERATE
	Winter 2017	30	145	48.97%	35.86%	15.17%	3.66	GOOD
S2	Summer 2017	93	623	32.74%	60.67%	6.58%	3.18	MODERATE
	Autumn 2017	73	635	34.96%	59.53%	5.51%	3.29	MODERATE
	Winter 2017	72	279	30.47%	56.99%	12.54%	2.96	MODERATE
S3	Summer 2017*	48	193	32.12	54.40	13.47	3.02	GOOD
	Autumn 2017*	44	111	33.33	53.15	13.51	3.06	GOOD
	Winter 2017	32	114	39.47	57.01	3.51	3.51	GOOD

* >90% silt limits were used

The chemical status of both the inner and outer part of Thermaikos did not present remarkable variations during summer and autumn, compared to earlier studies (HCMR, 2007; HCMR, 2015). In particular, total phosphorus concentration values were close to those reported earlier for summer and autumn (HCMR, 2007; HCMR, 2015). However, during the winter sampling, extremely high concentrations of phosphates and total phosphorus were recorded in the surface samples, probably related to the observed red tide phenomenon. The measured concentrations were higher than the threshold for the good water quality (Dasenakis et al., 2015). In addition, rather high phosphorus concentration was recorded in the outer part of the Gulf, especially in the sub-surface samples. So far, comparable concentrations were only recorded many years ago (Samanidou et al., 1989), implying the need for consecutive and more extensive monitoring of Thermaikos quality.

The occasional dominance of dinoflagellates in S1 and S2, the frequent phytoplankton blooms concurrently with the high phytoplankton biomass (>0.7 mg/L, Bozatzidou 2013) in all samples of S1 and S2 indicate a less than good water quality according to phytoplankton. Furthermore, the protozooplankton abundance in these sites was indicative of red tide formations. These characteristics demonstrate the eutrophic character of the inner Gulf, which disagrees with the requirement for normal abundance and diversity of marine food webs elements, in order to establish good environmental status (MSFD, 2008/56/EC). On the other hand, the species composition and the phytoplankton abundance and biomass in S3 were indicative for higher than good water quality except for the surface sample on October 2017.

The benthic fauna showed increased abundance but similar diversity values with previous studies (HCMR, 2015). Polychaetes were the most dominant taxon, mainly represented by opportunistic species and thus, indicating the prevalence of slightly disturbed environmental conditions. The structure of zoobenthic communities differed among the three study sites, and especially between the innermost and the outer Thermaikos stations (i.e. S2 vs S3). A typical seasonal pattern, i.e. divergence of winter samples, was assessed in all stations, being more profound in S1 and S2 where colder water

masses occurred compared to the outer Gulf station (S3). The above biotic patterns derived from the combined effect of three main environmental parameters: temperature, clay and sediment's organic content. According to the biological quality element of macro-invertebrates, the water quality status of Thermaikos was assessed as moderate in the inner gulf stations (S1, S2), and as good in the outer station (S3); however, water quality improved in S1 (the station in the intermediated part of the Gulf) during the winter sampling reaching good status. These results are in agreement with the phytoplankton monitoring, and generally conform to previous studies and the national monitoring program (HCMR, 2015).

Acknowledgements
This study was carried under the program "Monitoring of the quality of marine environment of Thermaikos Gulf" funded by Thessaloniki Water Supply & Sewerage Co. S.A (EYATH S.A.). The view expressed herein can in no way be taken to reflect the official opinion of EYATH S.A.

References

1. APHA-AWWA-WEF (1999) 'Standard methods for the examination of water and wastewater', 20th Ed. American Public Health Association: Washington, DC.
2. Borja, A. and D.M. Dauer (2008) 'Assessing the environmental quality status in estuarine and coastal systems: Comparing methodologies and indices', **Ecological Indicators**, Vol. 8, pp 331-337.
3. Borja, Á., F. Franco, V. Valencia, J. Bald and I. Muxica, I. et al. (2004) 'Implementation of the European water framework directive from the Basque country (northern Spain): a methodological approach', **Marine Pollution Bulletin**, Vol. 48 (3-4), pp 209-218.
4. Borja, Á., F. Franco and V. Perez (2000) 'A Marine Biotic Index to Establish the Ecological Quality of Soft-Bottom Benthos Within European Estuarine and Coastal Environments', **Marine Pollution Bulletin**, Vol. 40 (12), pp 1100-1114.
5. Borja, A., T. C. Prins, N. Simboura, J.H. Andersen, T. Berg, J. Marques, . . . and L. Uusitalo (2014) 'Tales from a thousand and one ways to integrate marine ecosystem components when assessing the environmental status', **Frontiers in Marine Science**, Vol. 1, Issue DEC, Article 72.
6. Borja, A. and J.G. Rodríguez (2010) 'Problems associated to the 'one-out, all-out' principle, when using multiple ecosystem components in assessing the ecological status of marine waters', **Marine Pollution Bulletin**, Vol. 60(8), pp 1143-1146.
7. Bozatzidou M. (2013). Assessing the ecological quality of Thermaikos Municipality coastal system (based on phytoplankton). Master Thesis. School of Biology, Aristotle University of Thessaloniki.
8. Clarke K.R. and R.N. Gorley (2006) 'PRIMER v6 user manual and program', PRIMER-E Ltd: Plymouth, UK.
9. Dauer D.M. (1993) 'Biological criteria, environmental health and estuarine macrobenthic community structure', **Marine Pollution Bulletin**, Vol. 26 (5), pp 249-257.
10. Dasenaikis et al. Δασενάκης Μ., Μ. Λαδάκης, Σ. Καραβόλτσος και Β. Παρασκευοπούλου (2015) 'Χημική Ωκεανογραφία', Σύνδεσμος Ελληνικών Ακαδημαϊκών Βιβλιοθηκών- Εθνικό Μετσόβιο Πολυτεχνείο, Αθήνα. ISBN: 978-960-603-234-9.
11. European Commission (EC) (2000) Directive 2000/60/EC of the European Parliament and of the Council of 23 October 2000 establishing a framework for the Community action in the field of water policy. Official Journal of the European Communities L 327: 1-72, European Commission, Brussels.
12. European Commission (EC) (2006) Directive 2006/7/EC of the European Parliament and of the Council of 15 February 2006 Concerning the Management of Bathing Water Quality and

Repealing Directive 76/160/EEC, Official Journal of the European Communities L64: 37-51, European Commission, Brussels.

13. European Commission (EC) (2008) Directive 2008/56/EC of the European Parliament and the Council of 17 June 2008. Establishing a framework for community action in the field of marine environmental policy. Official Journal of the European Communities L164: 19-40, European Commission, Brussels.
14. Friligos N., J.C. Kondylakis and R. Psyllidou-Giouranovits (1997) 'Eutrophication and phytoplankton abundance in the Thermaikos Gulf, Greece', **Fresenius Environmental Bulletin**, Vol. 6, pp 27–31.
15. Folk R.L., P.B. Andrews and D.W. Lewis (1970) 'Detrital sedimentary rock classification and nomenclature for use in New Zealand', **N.Z. Journal of Geology and Geophysics,** Vol. 13, pp 937-968.
16. Garmendia, M., Á. Borja, J. Franco, and M. Revilla (2013) 'Phytoplankton composition indicators for the assessment of eutrophication in marine waters: Present state and challenges within the European directives', **Marine Pollution Bulletin**, 66(1-2), pp. 7-16.
17. Grasshoff K., K. Kremling and M. Ehrhardt (1999) 'Methods of Seawater Analysis, Third, Completely Revised and Extended Edition', WILEY-VCH Verlag.
18. Hach (2013) 'Water Analysis Handbook', Colorado, USA.
19. HCMR (2015) ΕΛΚΕΘΕ (2015) 'Δειγματοληψίες και αναλύσεις για την παρακολούθηση της οικολογικής ποιότητας παρακτίων υδάτων, σύμφωνα με τις απαιτήσεις του Άρθρου 8 της Οδηγίας Πλαίσιο για τα Ύδατα 2000/60/ΕΕ, σε τρεις σταθμούς του Θερμαϊκού κόλπου που ενδιαφέρουν την ΕΥΑΘ' Τεχνική Έκθεση, Αθήνα, Δεκέμβριος 2015.
20. HCMR (2007) ΕΛΚΕΘΕ (2007) 'Παρακολούθηση της ποιότητας του Θαλάσσιου Περιβάλλοντος του κόλπου της Θεσσαλονίκης (ΘΕΡΜΑΪΚΟΣ 2006)' Ενδιάμεση Τεχνική Έκθεση, Αθήνα, Ιούλιος 2007.
21. Hillebrand H., C.-D. Dürselen, D. Kirschtel, U. Pollingher and T. Zohary (1999) 'Biovolume calculation for pelagic and benthic microalgae', **Journal of Phycology**, 35(2), pp. 403-424.
22. Hyder, P., J.H. Simpson, S. Christopoulos, and Y. Krestenitis, (2002) 'The seasonal cycles of stratification and circulation in the Thermaikos Gulf Region of Freshwater Influence (ROFI), north-west Aegean', **Continental Shelf Research**, 22(17), pp.2573-2597.
23. Krestenitis, Y.N., K.D. Kombiadou and Y.S. Androulidakis (2012) 'Interannual variability of the physical characteristics of North Thermaikos Gulf (NW Aegean Sea)' **Journal of Marine Systems**, 96, pp.132-151.
24. Nikolaidis N., A. Karageorgis, V. Kapsimalis, G. Marconis, P. Drakopoulou, H. Kontoyiannis and K. Pagou (2006) 'Circulation and nutrient modelling of Thermaikos Gulf, Greece', **Journal of Marine Systems**, 60, pp 51–62.
25. Pitacco V., M. Mistri and C. Munari (2018) 'Long-term variability of macrobenthic community in a shallow coastal lagoon (Valli di Comacchio, northern Adriatic): Is community resistant to climate changes?' **Marine Environmental Research**, in press.
26. Samanidou V., K. Fytianos and G. Vasilikiotis (1989) 'Distribution of nutrients in the Thermaikos Gulf, Greece', **Toxicological & Environmental Chemistry**, 20-21, pp. 29-37.
27. Simboura, N. and S. Reizopoulou (2008) 'An intercalibration of classification metrics of benthic macroinvertebrates in coastal and transitional ecosystems of the Eastern Mediterranean ecoregion (Greece)', **Marine Pollution Bulletin**, 56, pp. 116-126.

28. Simboura N. and A. Zenetos (2002) 'Benthic indicators to use in ecological quality classification of Mediterranean soft bottom marine ecosystems, including a new Biotic Index', **Mediterranean Marine Science,** 3, pp. 77–111.

29. Tsirtsis G. and M. Karydis (1998) 'Evaluation of phytoplankton community indices for detecting eutrophic trends in the marine environment', **Environmental Monitoring Assessment**, 50, pp. 255-269.

30. Utermöhl H. (1958) 'Zur Vervollkommnung der quantitativen phytoplankton-methodik' **Internationalen Vereinigung fur Theoretische und Angewandte Limnologie**, 9, pp. 1-38.

INVESTIGATION OF QUANTUM DOTS TOXICITY, GENOTOXICITY, CYTOTOXICITY, AND UPTAKE IN RAINBOW TROUT *ONCORHYNCHUS MYKISS* LARVAE

Ž. Jurgelėnė*[1], M. Stankevičiūtė[1], N. Kazlauskienė[1], D. Montvydienė[1], J. Baršienė[1], K. Jokšas[2, 3], A. Markuckas[4]

[1] Institute of Ecology of Nature Research Centre, Akademijos st. 2, LT-08412 Vilnius, Lithuania,
[2]Vilnius University, Faculty of Chemistry and Geosciences, Naugarduko st. 24, LT-03225 Vilnius, Lithuania
[3]Geology and Geography Institute of Nature Research Centre, Akademijos st. 2, LT-08412 Vilnius, Lithuania
[4]Vilnius University, Life Sciences Center, Department of Biochemistry and Molecular Biology, Saulėtekio av. 7, 10223 Vilnius, Lithuania

[*]Corresponding author: e-mail: zivile.jurgelene@gmail.com, tel.: +370 63385183

Abstract
Nanoparticles may be released into the environment and induce harmful effects to the aquatic ecosystem. The aims of the present study were to determine: (1) toxicity, genotoxicity and cytotoxicity to larvae of rainbow trout *Oncorhynchus mykiss* exposed to 4 nmol/L CdSe/ZnS quantum dots (QDs); (2) Cd accumulation; (3) the concentration of metallothionein (MT) in larvae after exposure to QDs; and (4) explain the possible impact mechanism of the QDs to fish larvae. QDs at sublethal concentration was used during the tests. Our findings revealed that heart rate (HR, counts/min) of larvae didn't differ significantly ($p < 0.05$) from the control; gill ventilation frequency (GVF, counts/min) significantly ($p < 0.05$) increased only after 10 days of exposure to QDs compared to the control. Total genotoxicity level (erythroblasts with micronuclei and nuclear buds) in larvae significantly ($p < 0.05$) increased after 4 days of exposure. However, 4 nmol/L QDs did not induce significant cytotoxicity over the concentration applied. QDs induced a significant increase in Cd accumulation in larvae after 4-10 days of exposure in comparison with the control. MT was used as a marker of internal Cd exposure, thus providing indirect information on *in vivo* QDs degradation. The concentration of MT did not change in larvae during treatment. Therefore, QDs were stable during 10 days of exposure. QDs absorption was not found to take place in larvae. Possibly, the effects of QDs to larvae are related to mechanical impact of QDs.

Keywords: quantum dots; fish; accumulation; toxicity, genotoxicity and cytotoxicity; metallothioneins

1. INTRODUCTION

The rapid growth in the nanotechnology industry leads to use of novel nanomaterials like quantum dots (QDs) for biomedical applications, such as diagnostics, drug delivery and nanotherapy. The knowledge regarding the uptake mechanisms of nanoparticles (NPs) and toxicity to organism is not well understood (Murugan et al, 2015). QDs are semiconductor crystals of nanometer dimensions (2–10 nm), containing 200–10000 atoms, and can consist of a cadmium/selenide (CdSe) core with a zinc sulfide (ZnS) shell with some type of surface coating. To their strong fluorescence intensity, their stability, water solubility, small size and flexible surface charge enable QDs suitable agents to study uptake with *in vitro* and *in vivo* studies (Zhang et al, 2011). Nevertheless, little is known about the

environmental risks of exposure to these NPs. Due to their possible large scale of production in future and NPs release in the environment has led to alarming on their potential long-term toxicity related to the fact that these materials contain heavy metals such as Cd, As, Zn, Pb (Libralato et al, 2017).

The question is open about the safety of using QDs for treating patients, as there are not enough reliable studies on their toxicological effects. Oh et al (2016) study showed the need for more in-depth analysis for major QDs types, because QDs toxicity is closely correlated with many specific parameters of QDs, such as surface properties (including shell, ligand and surface modifications), diameter, assay type and exposure time. Two major mechanisms are involved in the toxicity effects of QDs: Cd^{2+} in the structure that could cause interference in DNA repair or increase of oxidative stress and free radical formation. The release of Cd^{2+} from the core of QDs influences toxicity and causing ROS generation (Ji et al, 2015).

Studies undertaken to investigate QDs effect have used a broad range of QDs types and included classical cytotoxicity assays, and have examined the effects of QDs on cellular organelles and gene/protein expression, as well as their behavior and fate in vertebrate and invertebrate models (Oh et al, 2016; Rocha et al, 2017). Fishes or mice are usually employed to evaluate *in vivo* effects of contaminants, but studies with mice are time consuming, present ethical issues and are expensive (Yong et al, 2013). In recent years, the use of fish as an established animal model system for NPs toxicity assay is growing exponentially (Chakraborty et al, 2016; Rocha et al, 2017). Different types of parameters are used to evaluate NPs toxicity such as hatching achievement rate, developmental malformation of organs, damage in gill and skin, abnormal behavior (movement impairment), immunotoxicity, genotoxicity or gene expression, neurotoxicity, endocrine system disruption, reproduction toxicity and finally mortality (Chakraborty et al, 2016).

QDs may be released into the environment and induce harmful effects to humans and the ecosystem (Demir and Castranova 2017). QDs can be transferred from prey to predator in a microbial food chain (Werlin et al, 2011). Lee et al (2015) showed a three-level (from *Astasia longa* (protozoa) to *Moina macrocopa* (cladoceran), and to *Danio rerio* (fish)) transfer of QDs in the aquatic environment. In addition, NPs with certain physicochemical characteristics can readily enter biological membranes (Murugan et al, 2015). NPs may reach the embryo from somatic tissues, in case of their capability to cross species-specific barriers, spanning from embryo protective layers (i.e., chorion membrane for zebrafish and Drosophila) up to the highly structured mammalian placenta (Tortiglione 2011).

Many QDs produced characteristic signs of Cd toxicity that were weakly correlated with metallothionein (MT) expression, indicating that QDs were slightly degraded *in vivo* (King-Heiden et al, 2009). Using MT gene induction as an indicator of Cd^{2+} release, these studies could detect breakdown of QDs after absorption by the organism (King-Heiden et al, 2009). Additionally, the fluorescence emission shifts from red to blue and the excitation fluorescence peak become broader during QDs biodegradation (Alaraby et al, 2015). Furthermore, the QDs degradation could be due to low pH or oxidation of QDs surface (Khalil et al, 2011). The low pH conditions of the gastric tract can contribute to QDs degradation in Drosophila larvae and fish (Alaraby et al, 2015; Duan et al, 2013).

The current knowledge is yet too limited to drawing conclusions about risks of QDs to early development stages. Further investigations are needed for clarify toxic mechanisms of QDs, particularly in early development of organisms. The aims of present study were to assess toxicity, genotoxicity and cytotoxicity to larvae of rainbow trout *Oncorhynchus mykiss* exposed to 4 nmol/L CdSe/ZnS quantum dots (QDs), to determine accumulation of Cd and the concentration of metallothionein (MT) in the whole body of larvae exposed to QDs, and to explain the possible impact mechanism of the QDs to fish larvae.

2. MATERIALS AND METHODS

Exposure of fish was performed at the Laboratory of Ecology and Physiology of Hydrobionts (Nature Research Centre, Lithuania). Embryos of *O. mykiss* in the eyed-egg stage were obtained from Simnas Experimental Hatchery (Alytus District, Lithuania). All studies have been carried out with non-protected life-stages in accordance with Directive 2010/63/EU.

Water-soluble, red emitting semiconductor QDs (Qdot® ITK™, Life Technologies, CA, USA) a size of about 5 - 7 nm as determined by transmission electron microscopy were used at a concentration of 4 x 10^{-9} mol/L. The concentration of QDs was chosen according to the study of Yong et al (2013) who showed that LC_{50} values of CdSe–ZnS to zebrafish are in the range of 0.7 - 4.2 x 10^{-7} mol/L. A volume of 100 μL of a stock dispersion of 8 μmol/L QDs was diluted with deep-well water to achieve final concentrations of 4 x 10^{-9} mol/L in the incubation media. Continuous aeration was used to keep the particles suspended.

The toxicity test was performed in a climate cabinet (Bronson PGC-660, Zaltbommel, the Netherlands) with continuous aeration under static conditions according to ISO 7346-1:1996, without water changing. According to the OECD 210 (OECD 1992), the experiments were carried out in the dark and the larvae were not fed (ISO 10229:1994). The studies were performed in three replicates. Deep-well water used for dilution and as control water had a mean pH of 8.0; the temperature was maintained at 10 ± 0.5 ^{o}C, and the oxygen concentration was 10 mg/L. Dissolved oxygen in the tanks, temperature and pH were measured routinely with a hand-held multi-meter (Multi 340i/SET, WTW, Weilheim, Germany). Heart rate (HR, counts/min) and gill ventilation frequency (GVF, counts/min) of larvae were evaluated using stereomicroscope (RZ Series, Meiji Techno, Saitama, Japan). Samples of larvae were taken upon days 4, 7 and 10 after exposure start.

Induction of micronuclei (MN), nuclear buds (NB), bi-nucleated (BN), fragmented-apoptotic (FA) cells were analysed in erythroblasts of larvae. Total genotoxicity level was assessed as the sum of MN and NB, as well as total cytotoxicity level – as the sum of BN and FA frequencies. Cell smears were prepared from whole larvae (with removed yolk sac) body (gently nipped with tweezers): directly smeared on glass slides and air-dried. Smears were fixed in methanol for 10 min. and later were stained with 10 % Giemsa solution in phosphate buffer pH = 6.8 for 20 - 40 min. The stained slides were analysed under light microscopes Olympus BX51 at final magnification of 1,000×. Micronuclei and other nuclear abnormalities (NAs) were identified following criteria described by Fenech et al (2003). The frequencies of abnormalities were recorded in 1,000 erythroblasts per slide using blind scoring by a single observer.

Experiment of the accumulation of QDs in larvae lasted 10 days: starting from 1-day-old larvae under static conditions according to ISO 7346-1:1996. The Cd accumulation was measured in the whole body of larvae (10 individuals per 3 replicate). Sampled organisms were dried up on absorbent paper, weighted and then stored at −18 °C until Cd analysis. For Cd analysis in larvae, the digestion method was used (Thomas and Mohaideen 2015). The content of Cd in the experimental water and in the whole body of the fish larvae was analyzed by an atomic absorption spectrophotometer SHIMADZU AA-7000 (Japan) with a graphite furnace atomizer GFA-7000 and auto-sampler ASC-7000 (measured wavelength 185 to 900 ± 0.3 nm, high-speed deuterium lamp 185 to 430 nm, heating temperature range 50 to 3000 0C, repeatability 2.5%) according to the analysis method LST EN ISO 15586: 2004. The concentration of Cd standard (Sigma-Aldrich Chemie GmbH, Germany) for atomic absorption spectrophotometer is 1000 mg/L and Cd detection limit is 0.3 μg/L.

MT content determination was assayed according to the method of Peixoto et al (2003). For MT level assays, 7 and 10 days old larvae of rainbow trout were weighted and frozen (-80 °C). The larvae were homogenized with Potter-Elvehjem homogenizer in 4 volumes of 20 mM tris (hydroxymethyl) aminomethane HCl buffer, pH 8.6, containing 0.5 mM phenylmethylsulphonyl fluoride and 0.01% β-mercaptoethanol. The homogenate was then centrifuged at 17,000 × *g* for 30 min at 4 °C. Aliquots of 1 ml of supernatant containing MT were added with 1.05 ml of cold (-20 °C) absolute ethanol and

80 µl chloroform. The samlpes were centrifuged at 6000 × *g* for 10 min at 4 °C. The collected supernatant was combined with three volumes of cold ethanol (-20 °C), maintained at -20 °C for 1 h and centrifuged at 6000 × *g* for 10 min at 4 °C. The metallothionein-containing pellets were then rinsed with 1 ml of 87% ethanol and 1% chloroform mix and centrifuged at 6000 × *g* for 10 min at 4 °C. The MT content in the pellet was evaluated using the colorimetric method with 5,5'-dithio-*bis*(2-nitrobenzoic acid) reagent. The pellet was suspended in 150 µl 0.25 M NaCl and subsequently 150 µl 1 N HCl containing 4 mM ethylendiamintetraacetic acid calcium disodium salt were added to the sample. 4.2 ml 2 M NaCl containing 0.43 mM 5,5'-dithio-*bis*(2-nitrobenzoic acid) buffered with 0.2 M Na-phosphate, pH 8.0 was then added to the sample at room temperature. The sample was centrifuged at 3000 × *g* for 5 min at room temperature. The supernatant absorbance was evaluated at 412 nm. MT concentration was estimated using molar absorption coefficient at 412 nm 14140 $M^{-1}cm^{-1}$ and expressed as micrograms of SH groups per gram of wet weight.

Means and standard deviations or standard errors for each studied parameter were calculated. Differences between the evaluated characteristics studied were tested by two-way ANOVA using Statistica 7.0 software (StatSoft Inc., Tulsa, Oklahoma, USA). Results of nuclear abnormalities assay were analyzed by non-parametric Mann-Whitney test (GraphPad Software Inc., San Diego, CA, USA). Differences were accepted as significant at the 95 % level of confidence ($p < 0.05$).

3. RESULTS

In this investigation, GVF of larvae after 10 days of exposure to QDs significantly ($p < 0.05$) increased as compared to the control (Figure 1 A). Meanwhile, after 4 and 7 days of exposure to QDs GVF of larvae did not differ significantly from the control. Also, HR of larvae throughout the exposure period did not differ significantly from the control, ranging from 101.60 ± 6.73 to 103.73 ± 8.48 counts/min (in control HR was from 101.33 ± 3.90 to 103.20 ± 5.06 counts/min) (Figure 1 B).

Results of total cytotoxicity and total genotoxicity levels in erythroblasts of *O. mykiss* larvae are given in Figure 2. Significant elevation of the total cytotoxicity level was not found after QDs treatment. However, total cytotoxicity level after 4 days of exposure was approximately 5-fold higher compared to the control level. Treatment with QDs significantly increased total genotoxicity level in larvae erythroblasts, which was 2.5-fold higher than the control level.

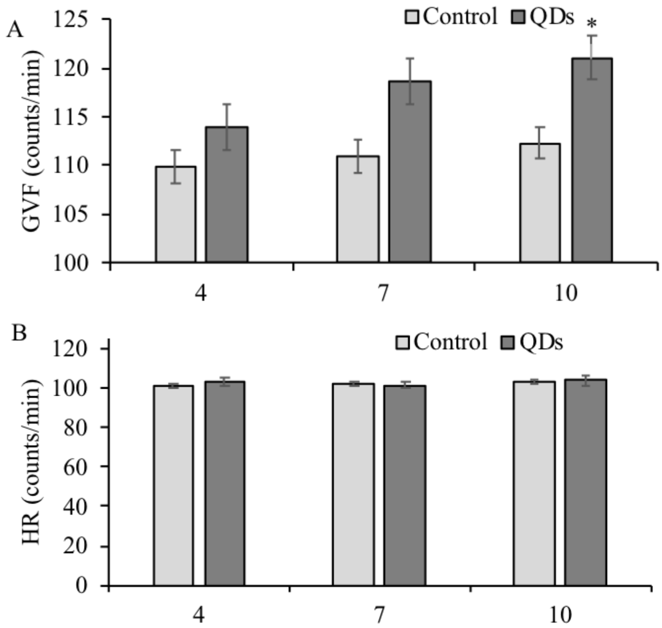


Figure 1. Toxic effect of QDs on biological parameters of *O. mykiss* larvae: (A) GVF (counts/min) and (B) HR (counts/min) (mean ± SEM, N = 15).[*] Significant difference from the control ($p < 0.05$).

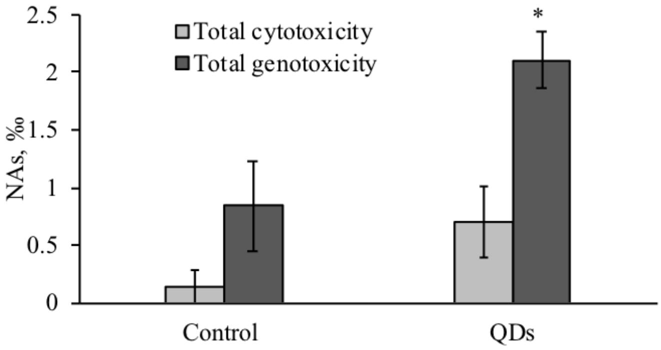


Figure 2. Total cytotoxicity (bi-nucleated (BN)+ fragmented-apoptotic (FA)) and total genotoxicity (micronuclei (MN)+ nuclear buds (NB)) levels (mean ± SEM, N = 7) in erythroblasts of *O. mykiss* larvae in control and QDs exposed groups. Asterisks (*) denote significant differences from control group (p < 0.05)

Changes of Cd concentrations in larvae during experiment are shown in Figure 3. Samples of larvae were taken upon days 4, 7 and 10 after exposure start to determine the accumulation of QDs to rainbow trout larvae depending on the duration of exposure. Cd accumulation in larvae after 4, 7 and 10 days exposures to QDs were significantly ($p < 0.05$) different from the control (Figure 3). The maximum value of accumulated Cd was found in larvae exposed to QDs after 10 days of exposure (1.302 ± 0.272 µg/g). However, accumulation of Cd in larvae did not depend on the duration of exposure.

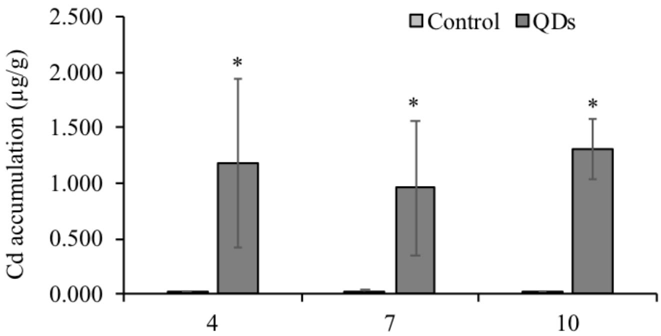


Figure 3. Cd accumulation (wet weight, µg/g) in *O. mykiss* larvae after 4, 7 and 10 days of exposure to QDs.

Measured MT content was used as a marker of internal QDs exposure. However, the MT contents in larvae showed no significant changes after treatment QDs for 7 and 10 days compared to the control (Figure 4).

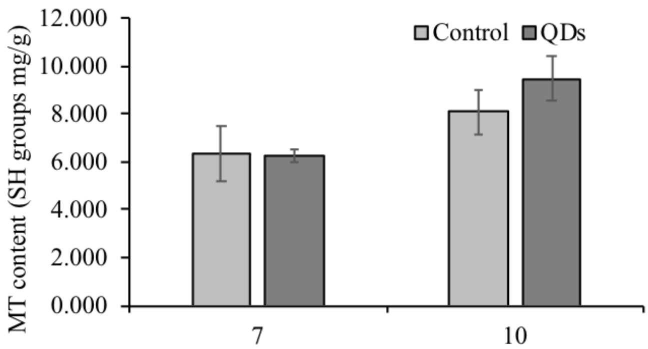


Figure 4. Metallothionein content (SH groups, mg/g) in *O. mykiss* larvae after 7 and 10 days of exposure to QDs.

4. DISCUSSION AND CONCLUSIONS

The toxicity study showed significantly ($p < 0.05$) increased GVF of larvae as compared to the control after 10 days of exposure to QDs, however GVF in larvae showed no significant changes after 4 and 7 days of exposure, and HR in larvae showed no significant changes after 4, and 10 days of exposure to QDs (Figure 1 A and B). One possible explanation for these results is that QDs interfered with breathing due to QDs adhesion in gill. Gill is an important organ for respiration, osmoregulation, acid-base balance and nitrogenous waste excretion (Mansouri et al, 2016). Gills are most important targets of waterborne objects such as NP (Chakraborty et al, 2016). For instance, Cu NPs may damage gills lamellae of zebrafish (Griffitt et al, 2007). It was noticed that gill of larvae forms mucus complex with QDs. Mucus secretion were also observed in the present study and were reported by other authors (Federici et al, 2007; Smith et al, 2007) for rainbow trout exposed to single walled carbon nanotubes and titanium dioxide nanoparticles. In addition, Ag NPs can induce excessive mucus secretion and hyperplasia in gill tissue of zebrafish (Mansouri and Johari 2016). The larvae gradually developed unique systems to protect themselves from the toxicity of chemicals. The number of mucous cells may be an indicator of exposure to stressors (Ostaszewska et al, 2016). An increase in the number of mucous cells secreting sulfated and carboxylated mucins is associated to the increase in mucus viscosity, which improves its protective properties (Kumari et al, 2009). Mucus consists of immunoglobulin, lysosome, and lectin that protect fish against infections. According to Poleksic et al (2010) reduction of mucous cell abundance at the highest AgNPs concentration and a decrease in the number and area of mucous cells in fish exposed to CuNPs show exhaustion of proliferative ability of mucous cells.

The most obvious finding to emerge from the nuclear abnormalities analysis in larvae is that significant increase of total genotoxicity level (as sum of MN and NB frequencies) in QDs exposed larvae eryhtroblasts was determined. Xiao et al (2016) study results revealed that carbon QDs exposure causes significant DNA damage in embryonic cells of Rare Minnow (*Gobiocypris rarus*). Oxidative stress induced DNA damage and the inflammatory response are considered to be the main mechanisms causing toxicity of the NPs (Xiao et al, 2016; Schins and Hei 2006; Schins and Knaapen 2007). Further studies focusing on QDs-induced genotoxicity should be performed using fish erythroblasts/erythrocytes, which, as indicated by the present study, are important targets for *in vivo* QDs toxicity.

As shown in Figure 3, the Cd amount in larvae was significantly ($p < 0.05$) different from the control during the exposure period. QDs potential risk could be caused by the nanomaterial itself or by their free metallic components (Hardman 2006). The determination of chemical concentration in larvae is a challenge since it requires highly sensitive analytical techniques owing to the low sample amount (1 larvae ~ 0.1 g). In this study, larvae do not feed yet, suggesting that one possible way to pass QDs in the larvae are skin-absorption. It is well known that biological barriers play a significant function to determine QDs biodistribution (Chu et al, 2010). A small size of QDs (between 1 and 100 nanometers) permits these NPs to get into the body through cellular barriers and can reach organs and tissues and interact with biological structures, thus impact normal functions in different ways (Maldiney et al, 2011). NPs could accumulate selectively in the head, yolk sac and the tail after NPs enter into the larvae body through swallowing and skin-absorption (Kang et al, 2015). However, QDs could be eliminated in the urine of larvae or degraded into particles and could be removed by lysosome-like vesicles, and then accumulate in the kidney and liver (Lei et al, 2011). In contrast, during normal metabolism, the primary accumulation tissues of heavy metal Cd are the liver and kidneys (Haouem et al, 2007). Lei et al (2011) noted that MAA-QDs were unable to diffuse into the yolk of larvae because of the high content of lipids in the yolk cell.

MT content (an indicator of metal ion exposure) were used to detect toxicity due to Cd^{2+}, however MT contents in larvae did not significantly increase after 7 and 10 days of exposure (Figure 4). Our research data coincides with Fischer et al (2006) data that ZnS shell and surface ligands protect QDs

from degradation *in vivo*. Therefore, QDs were stable during 10 days of exposure and QDs absorption was not in larvae. In contrast with our finding, King-Heiden et al (2009) noticed that QDs degraded at least partially *in vivo*, MT expression correlated with $CdCl_2$ and QDs exposure concentrations.

In summary, this study demonstrates that QDs induced significantly ($p < 0.05$) increased GVF of larvae as compared to the control only after 10 days of exposure to QDs, however QDs did not cause GVF changes in larvae after 4 and 7 days of exposure and HR changes in larvae after 4, 7 and 10 days of exposure (Figure 1 A and B). Furthermore, total genotoxicity level was found to increase significantly after 4 days exposure to QDs (Figure 2). The Cd amount in larvae was significantly ($p < 0.05$) different from the control throughout the exposure period (Figure 3). Our study further demonstrated that the MT levels of larvae were unchanged (Figure 4), which might explain that QDs were stable and QDs absorption was not in larvae. Thus, our findings suggest that exposure to QDs could be due to QDs adhesion in gill, which induced toxicity to larvae. Results of toxicity and genotoxicity studies allow to assuming that the mechanical impact of QDs could be one of the factors induced the changes of physiologic function in fish larvae. However, further investigation must be undertaken to confirm this presumption.

Acknowledgment
Toxicity, accumulation of QDs and MT content assessment was funded by the Research Council of Lithuania, Project No. MIP-108/2015. Genotoxicity and cytotoxicity studies were funded by the Research Council of Lithuania, Project No. S-MIP-17-10.

References

1. Alaraby M., E. Demir, A. Hernández and R. Marcos (2015) 'Assessing potential harmful effects of CdSe quantum dots by using Drosophila melanogaster as *in vivo* model', **Science of the Total Environment,** Vol. 530-531, pp. 66-75.
2. Chakraborty C., A.R. Sharma, G. Sharma and S.-S. Lee (2016) 'Zebrafish: A complete animal model to enumerate the nanoparticle toxicity', **Journal of nanobiotechnology,** Vol. 14: 65.
3. Chu M., Q. Wu, H. Yang, R. Yuan, S. Hou, Y. Yang, Y. Zou, S. Xu, K. Xu, A. Ji and L. Sheng (2010) 'Transfer of quantum dots from pregnant mice to pups across the placental barrier', **Small**, Vol. 6(5), pp. 670-8.
4. Demir E. and V Castranova (2017) 'Evaluation of the Potential Genotoxicity of Quantum Dots. A Review', **Scientific Pages Nanotechnology**, Vol. 1(1), pp. 1-19.
5. Directive 2010/63/EU, of the European Parliament and of the Council of the European Union. On the Protection of Animals Used for Scientific Purposes. Official Journal of the European Union L276, 233-279, 2010.
6. Duan J., Y. Yongbo, L. Yang, Y. Yang, L. Yanbo, H. P, Z. Xianqing, P. Shuangqing and S. Zhiwei (2013) 'Developmental toxicity of CdTe QDs in zebrafish embryos and larvae', **Journal of Nanoparticle Research**, Vol. 15, 1700.
7. Federici G., B.J. Shaw and R.H. Handy (2007) 'Toxicity of titanium dioxide nanoparticles to rainbow trout (*Oncorhynchus mykiss*): gill injury, oxidative stress, and other physiological effects', **Aquatic Toxicology**, Vol. 84, pp. 415-430.
8. Fenech M., W.P. Chang, M. Kirsch-Volders, N. Holland, S. Bonassi and E. Zeiger (2003) 'HUMN project: detailed description of the scoring criteria for the cytokinesis-block micronucleus assay using isolated humanlymphocyte cultures', **Mutation research**, Vol. 534, pp. 65-75.
9. Fischer H.C., L. Liu, K.S. Pang and W.C.W. Chan (2006) 'Pharmacokinetics of nanoscale quantum dots: *In vivo* distribution, sequesteration, and clearance in the rat. **Advanced Functional Materials**, Vol. 16, pp. 1299-1305.

10. Griffitt R.J., R. Weil, K.A. Hyndman, N.D. Denslow, K. Powers, D. Taylor and D.S. Barber (2007) 'Exposure to copper nanoparticles causes gill injury and acute lethality in zebrafish (*Danio rerio*)', **Environmental Science & Technology**, Vol. 41, pp. 8178-8186.

11. Haouem S., N. Hmad, M.F. Najjar, A. El Hani and R. Sakly (2007) 'Accumulation of cadmium and its effects on liver and kidney functions in rats given diet containing cadmium polluted radish bulb', **Experimental and Toxicologic Pathology**, Vol. 59, pp. 77-80.

12. Hardman R. (2006) 'Review A Toxicologic Review of Quantum Dots: Toxicity Depends on Physicochemical and Environmental Factors', **Environmental health perspectives**, Vol. 114, pp. 165-173.

13. ISO 10229: 1994. "Water Quality -- Determination of the Prolonged Toxicity of Substances to Freshwater Fish -- Method for Evaluating the Effects of Substances on the Growth Rate of Rainbow Trout (*Oncorhynchus mykiss* Walbaum (Teleostei, Salmonidae))"

14. ISO 7346-1: 1996. "Water Quality -- Determination of the Acute Lethal Toxicity of Substances to a Freshwater Fish [*Brachydanio rerio* Hamilton-Buchanan (Teleostei, Cyprinidae)]"-- Part 1: Static Method.

15. Ji X., F. Peng, Y. Zhong, Y. Su and Y. He (2014) 'Fluorescent quantum dots: Synthesis, biomedical optical imaging, and biosafety assessment', **Colloids Surf. B Biointerf**, Vol. 124, pp. 132-139.

16. Kang Y.F., Y.H. Li, Y.W. Fang, Y. Xu, X.-M. Wei and X.-B. Yin (2015) 'Carbon Quantum Dots for Zebrafish Fluorescence Imaging', **Scientific Reports**, Vol. 5, 11835, DOI: 10.1038/srep11835.

17. Khalil W.K., E. Girgis, A.N. Emam, M.B. Mohamed and K.V. Rao (2011) 'Genotoxicity evaluation of nanomaterials: DNA damage, micronuclei, and 8-hyroxy-2deoxyguanosine induced by magnetic doped CdSe quantum dots in male mice', **Chemical Research in Toxicology**, Vol. 24, pp. 640-650.

18. King-Heiden T.C., P.N. Wiecinski, A.N. Mangham, K.M. Met, D. Nesbit, J.A. Pedersen, R.J. Hamers, W. Heideman and R.E. Peterson (2009) 'Quantum dot nanotoxicity assessment using the zebrafish embryo', **Environmental Science & Technology**, Vol. 43(5), pp. 1605-1611.

19. Kumari U., M. Yashpal, S. Mittal and A.K. Mitta (2009) 'Histochemical analysis of glycoproteins in the secretory cells in the gill epithelium of a catfish *Rita rita* (*Siluriformes*, *Bagridae*)', **Tissue Cell**, Vol. 41, pp. 271-280.

20. Lee W.M and Y.J. An (2015) 'Evidence of three-level trophic transfer of quantum dots in an aquatic food chain by using bioimaging', **Nanotoxicology**, Vol. 9, pp. 407-412.

21. Lei Y., Q. Xiao, S. Huang, W. Xu, Z. Zhang, Z. He, Y. Liu and F. Deng (2011) 'Impact of CdSe/ZnS quantum dots on the development of zebrafish embryos', **The Journal of Nanoparticle Research**, Vol. 13, pp. 6895-6906.

22. Libralato G., E. Galdiero, A. Falanga, R. Carotenuto, E. de Alteriis and M. Guida (2017) 'Toxicity Effects of Functionalized Quantum Dots, Gold and Polystyrene Nanoparticles on Target Aquatic Biological Models: A Review', **Molecules**, Vol. 22, 1439; doi:10.3390/molecules22091439.

23. LST EN ISO 15586:2004. Vandens kokybė. Mikroelementu nustatymas atominės absorbcijos spektrometrija, naudojant grafitine krosni (ISO 15586:2003).

24. Maldiney T., C. Richard, J. Seguin, N. Wattier, M. Bessodes and D. Scherman (2011) 'Effect of core diameter, surface coating, and PEG chain length on the biodistribution of persistent luminescence nanoparticles in mice', **ACS Nano**, Vol. 5(2), pp. 854-62. doi:10.1021/ nn101937h

25. Mansouri B. and S.A. Johari (2016) 'Effects of short-term exposure to sublethal concentrations of silver nanoparticles on histopathology and electron microscope ultrastructure of zebrafish (*Danio rerio*) gills', **Iranian Journal of Toxicology**, Vol. 10, pp. 15-20.

26. Mansouri B., R. Rahmani, N.A. Azadi and S.A. Johari (2016) 'Combined effects of silver nanoparticles and mercury on gill histopathology of zebrafish (*Danio rerio*)', **Journal of Coastal Life Medicine**, Vol. 4(6), pp. 421-425.

27. Murugan K., Y.E Choonara, P. Kumar, D. Bijukumar, L.C du Toit and V. Pillay (2015) 'Parameters and characteristics governing cellular internalization and trans-barrier trafficking of nanostructures', **International journal of nanomedicine**, Vol. 10, pp. 2191-2206.

28. OECD (Organization for Economic Cooperation and Development). 1992. Guideline for the Testing of Chemicals: Fish, Early-life Stage Toxicity Test, Part 210.

29. Oh E., R. Liu, A. Nel, K.B. Gemill, M. Bilal, Y. Cohen and I.L. Medintz (2016) 'Meta-analysis of cellular toxicity for cadmium-containing quantum dots', **Nature Nanotechnology**, Vol. 11, pp. 479-486.

30. Ostaszewska T., M. Chojnacki, M. Kamaszewski and E. Sawosz-Chwalibóg (2016) 'Histopathological effects of silver and copper nanoparticles on the epidermis, gills, and liver of Siberian sturgeon', **Environmental science and pollution research international**, Vol. 23, pp. 1621-1633.

31. Peixoto N.C., T. Roza, E.M. Flores and M.E. Pereira (2003) 'Effects of zinc and cadmium on HgCl2-delta-ALA-D inhibition and Hg levels in tissues of suckling rats', **Toxicology Letters**, Vol. 46, pp.17-25.

32. Poleksic V., M. Lenhardt, I. Jaric, D. Djordjevic, Z. Gacic, G. Cvijanovic and B. Raskovic (2010) 'Liver, gills, and skin histopathology and heavy metal content of the Danube sterlet (*Acipenser ruthenus* Linnaeus, 1758)', **Environmental toxicology and chemistry**, Vol. 29, pp. 515-521.

33. Rocha T.L., N.C. Mestre, S.M.T. Saboia-Morais and M.J. Bebianno (2017) 'Environmental behaviour and ecotoxicity of quantum dots at various trophic levels: A review', **Environment International**, Vol. 98, pp. 1-17.

34. Schins R.P. and A.M. Knaapen (2007) 'Genotoxicity of poorly soluble particles', **Inhalation Toxicology**, Vol. 19, pp. 189-198.

35. Schins R.P. and T.K. Hei (2006) 'Genotoxic Effects of Particles', In: Donaldson K and Borm P, Particle toxicology. **CRC Press/Taylor & Francis Group**, USA, pp. 285-298.

36. Smith C.J., B.J. Shaw and R.D Handy (2007) 'Toxicity of single walled carbon nanotubes to rainbow trout, (*Oncorhynchus mykiss*): respiratory toxicity, organ pathologies, and other physiological effects', **Aquatic Toxicology**, Vol. 82, pp. 94-109.

37. Thomas S. and J. A. Mohaideen (2015) 'Determination of some heavy metals in fish, water and sediments from Bay of Bengal', **International Journal of Chemical Sciences**, Vol. 13(1), pp. 53-62.

38. Tortiglione C. (2011) 'The heritable effects of nanotoxicity. Review', **Nanomedicine (Lond.)**, Vol. 9(18), pp. 2829-2841.

39. Werlin R., J.H. Priester, R.E. Meilke, S. Krämer, S. Jackson, P.K. Stoimenov, G.D. Stucky, G.N. Cherr, E. Orias and P.A. Holden (2011) 'Biomagnification of cadmium selenide quantum dots in a simple experimental microbial food chain', **Nature Nanotechnology**, Vol. 6, pp. 65-71.

40. Xiao Y., L. Liu, Y. Chen, Y. Zeng, M. Liu and L. Jin (2016) 'Developmental Toxicity of Carbon Quantum Dots to the Embryos/Larvae of Rare Minnow (*Gobiocypris rarus*)', **BioMed Research International**, 11 pages.

41. Yong K.T., W.C. Law, R. Hu, L. Ye, L.W. Liu, M.T. Swihart and P.N. Prasad (2013) ‘Nanotoxicity assessment of quantum dots: from cellular to primate studies’, **Chemical Society Reviews**,42(3), pp. 1236-1250.

42. Zhang L.W, W. Bäumer and N.A Monteiro-Riviere (2011) ‘Cellular uptake mechanisms and toxicity of quantum dots in dendritic cells’, **Nanomedicine (Lond)**, 6(5), pp. 777-791.

ERYTHROCYTIC NUCLEAR ABNORMALITIES, DNA DAMAGE, BIOCONCENTRATION FACTOR AND HEMATOLOGICAL CHANGES INDUCED BY METAL MIXTURE AT ENVIRONMENTALLY RELEVANT CONCENTRATIONS IN *RUTILUS RUTILUS*

M. Stankevičiūtė*[1], G. Sauliutė[1], A. Markuckas[2], T. Virbickas[1], J. Baršienė[1]

[1] Nature Research Centre, Akademijos st. 2, LT-08412 Vilnius, Lithuania
[2]Vilnius University, Life Sciences Center, Department of Biochemistry and Molecular Biology, Saulėtekio av. 7, 10223 Vilnius, Lithuania

[*]Corresponding author: e-mail: milda.stan@gmail.com, tel: +370 60716809

Abstract
The aim of this study was to assess bioconcentration factor (BCF), metallothioneins (MT), genotoxicity, cytotoxicity and changes of haematological parameters in roach *Rutilus rutilus* after 14 days treatment with a six metals mixture (MIX) at environmentally relevant concentrations (Zn – 0.1, Cu – 0.01, Ni – 0.01, Cr – 0.01, Pb – 0.005 and Cd – 0.005 mg/L) and with 6 variants (reduced concentration of single metal while other metals concentration remain constant) of the MIX. Most frequently the highest accumulated amount of metals in tissues (gills, liver, kidneys, muscle) was detected after treatment with variants of MIX. Significantly reduced concentration of accumulated Ni was measured after Cu↓, Cr↓, Pb↓ and Cd↓ treatments (10 times reduced Cu^{2+}, Cr^{6+}, $Pb^{2+}$and Cd^{2+} concentration, respectively) in all tissues (except in liver after Cu↓, Cr↓ and Cd↓ treatments) compared with MIX. Significant *induction* of *MT in liver and kidneys* was *not detected. However, positive correlation* ($r = 0.83$; $p = 0.022$) *was measured between MT and Zn amount in liver.* DNA damage in erythrocytes of roach was examined by comet assay. Additionally, erythrocytic nuclear abnormalities were assessed in erythrocytes of peripheral blood, liver, kidneys and gills. Significant DNA damage was measured after Cr↓, Pb↓ and Zn↓ treatments. Significant elevations in total ENAs were measured after Cr↓ and Ni↓, MIX or Ni↓ treatments in peripheral blood, gills and kidneys erythrocytes, respectively. The frequencies of *separate ENAs* such as micronuclei, enucleus were significantly elevated after Cr↓, Ni↓ treatments in peripheral blood, respectively; apoptotic cells – after MIX treatment in gills and enucleus after Ni↓ treatment in liver compared to control level. Decreased number of *red blood cells*, *haematocrit level*, haemoglobin concentration and increased number of white blood cells in peripheral blood was measured after MIX treatment. However, only decrease in haemoglobin concentration was statistically significant.

Keywords: Genotoxicity; comet assay; cytotoxicity; bioconcentration factor (BCF); *Rutilus rutilus;* metallothioneins

1. INTRODUCTION

Metals in the environment continue to create serious global health concerns, because metals cannot be degraded into non-toxic forms and are persistent pollutants in the ecosystems (Ayangbenro and Babalola, 2017). Metals at certain concentrations are toxic to all life forms. However, contamination of the ecosystems with metals continues to increase and exceed the recommended limit in the environment (Dixit et al, 2015). Several studies showed that metals are toxic to fish even at low

concentrations and are capable of inducing genotoxicity, cytotoxicity, DNA fragmentation and other toxicity endpoints (Zhu et al, 2004; Cavas et al, 2005). Genotoxicity and cytotoxicity of metal mixture at Maximum-Permissible-Concentrations (MPC) previously were evaluated in rainbow trout (*Ochorhyncus mykiss*) (Valskienė et al, 2015) and Atlantic salmon (*Salmo salar*) (Stankevičiūtė et al, 2017). Significant accumulation of metals in *S. salar* tissues also was reported after treatment with metal mixture at MPC (Stankevičiūtė et al, 2017). However, most of the studies evaluating joint metal toxicity are dealing with binary metal mixtures toxicity at high concentrations (Driessnack et at., 2016, 2017; Duran et al, 2015; Winter et al, 2012). Notwithstanding, fish in the environment encounters with complex metal mixtures. Such exposure may lead to higher toxicity and bioaccumulation levels due to interactions of compounds in the metal mixture (Heys et al, 2016; Cedergreen, 2014).

This study was designed to evaluate metal mixture induced genotoxicity, cytotoxicity, changes in haematological parameters, bioaccumulation and metallothioneins content in *R. rutilus* tissues using whole mixture approach. Whole mixture testing is *more similar* to the current *environment exposure, because chemicals in the environment exist in mixtures* and at low concentrations (Heys et al, 2016).

The main objectives of the present study were: 1) to assess bioconcentration factor (BCF) of metals in different tissues (gills, liver, kidneys and muscle) of *Rutilus rutilus* after exposure to metal mixture at a concentration corresponding to Maximum-Permissible-Concentrations (MPC) accepted for the inland waters in EU, 2) to assess DNA damage and nuclear abnormalities in erythrocytes of roach after treatment with metal mixture and variants of this mixture, 3) to evaluate metallothioneins content in liver and kidneys tissue and 4) to assess haematological changes after fish exposure to metal mixture.

2. MATERIALS AND METHODS

2.1 Experimental set-up

The test was conducted on hatchery-reared 3–4 years old juveniles roach (*Rutilus rutilus* Linnaeus, 1758), average total weight 50.9 ± 12.4 g and average total length 160.6 ± 12.2 mm (mean ± SD, N = 56 respectively). The fish was obtained from fish hatchery (Elektrėnai District, Lithuania) and kept for acclimation in holding tanks (1000-L volume) supplied with flow-through aerated deep-well water at least two weeks prior to testing. Fish were kept under a *natural light* cycle and fed commercial fish feed (ALLER PLATINUM) daily in the morning; the total amount was no less than 1% of their wet body mass per day. During the experiment, both water supply and diet were kept as during the acclimation period. Deep-well water was used as the dilution water. Its chemical and physical characteristics have been presented in our previous research (Stankevičiūtė et al, 2017). Reagent grade metal salts («REACHIM» Company, Russia) were used as the toxicants. Stock solution was prepared by dissolving the necessary amount of the salt in distilled water, the final concentration being recalculated according to the amount of metal ion. The experiment was conducted under semi-static rotating water-current conditions on 8 groups of fish (treatment and control, N = 56). Seven *R. rutilus* were put in each *polyethylene* (PE) tank of 35-L total volume filled to a level of 30 L with continuously aerated dilution water (7 treatments), a total of 49 fish in treatment and 7 in control groups. Test fish were exposed for 14 days period to a six metal (Zn, Cu, Ni, Cr, Pb and Cd) mixture (hereinafter referred to as MIX) at a concentration corresponding to Maximum-Permissible-Concentrations (MPC) accepted for the inland waters in EU (Directive 2008/105/EC) (Table 1). Other treatments were performed by reducing MPC of single metal in the mixture (MIX) made of 6 metals by 10-times, while other 5 metals concentrations remain constant (e.g. Zn↓ (metal with reduced concentration in MIX), while Cu, Ni, Cr, Pb, Cd concentrations remain constant (hereinafter referred to as Zn↓) and etc.). Test solutions and clean water were renewed every day, and test fish were transferred into freshly prepared solutions after they were fed.

Table 1. Metals and their test waterborne concentrations (mg/L) in test media.

Metal	Source	Concentration (mg/L)			
		MIX (MPC) nominal	MIX Measured (mean ± SD)	Metal↓ nominal	Metal↓ Measured (mean ± SD)
Zn	$ZnSO_4·7H_2O$	0.1	0.115 ± 0.014	0.01	0.02 ± 0.001
Cu	$CuSO_4·5H_2O$	0.01	0.009 ± 0.001	0.001	0.0018 ± 0.0003
Ni	$NiSO_4·7H_2O$	0.01	0.011 ± 0.002	0.001	< 0.002
Cr	$K_2Cr_2O_7$	0.01	0.012 ± 0.002	0.001	0.0016 ± 0.0002
Pb	$Pb(NO_3)_2$	0.005	0.0045 ± 0.0004	0.0005	< 0.001
Cd	$Cd(CH_3COO)_2·2H_2O$	0.005	0.0052 ± 0.0003	0.0005	0.00042 ± 0.00003

The main physico-chemical parameters of the water were measured routinely with a hand-held multi-meter (WTW Multi 340i/SET, Germany). Designed nominal metal concentrations in the tanks were checked during blank tests (without fish) (N = 4) with an atomic absorption spectrophotometer (SHIMADZU AA-6800, Japan) by graphite furnace technique using proprietary software. Each water sample was acidified with reagent-grade nitric acid (final concentration 0.5% v/v) and analysed in triplicate. Mean measured concentrations are presented in Table 1.

2.2 Metal bioaccumulation analysis

After the testing was completed, fish (of control and metal-exposed groups) were sacrificed. Fish were measured (total body length, mm) and weighed (total body weight, g). Later, they were used in the removal of needed tissues: muscle without skin (~3 g), gills (whole organ), liver (whole organ) and kidneys (whole organ); organs were weighed to an accuracy of ±0.001 g. Fish samples were hot air oven-dried at 85 ºC for 24 hours until reached constant weight, pre-digested tightly in a concentrated ultrapure HNO_3 (60%) and H_2O_2 (30%) (Lach-Ner, Chempur, respectively) at a ratio of 5:1 v/v for eight hours at a room temperature and then microwave-digested quickly (Jia et al 2005). After cooling solutions were filtered through a 0.45 μm glass filter and diluted with deionized water. Metal concentrations were measured by atomic absorption spectrophotometry on Varian Spectr AA 55 (USA) with a graphite furnace technique in accordance with standardized procedure ISO 15586:2003 final concentration being expressed as mg/kg of wet weight. Accuracy of analytical procedure was checked using certified reference material fish homogenate (IAEA–407). Recoveries were in acceptable range (within 10%) of the certified values.

2.3 Bioconcentration factors (BCF) estimations

Tissues with BCF greater than 1,000 are considered high, and less than 250 is low bioaccumulation potential, with those between classified as moderate (Landis et al, 2011). BCF values in this study were calculated as reported by Gobas et al (2009) where bioconcentration factor (BCF) is defined as the ratio of the steady-state metal ions concentrations in the fish vs the concentration in water:

$$BCF = \frac{C_{fish}\,(mg/kg\ wet\ fish)}{C_{water}\,(mg/L)}, \quad (1)$$

2.4 Metallothioneins determination

Metallothionein content determination was assayed according to the method of Peixoto et al (2003). For metallothionein level assays, the liver and kidney were removed, weighted and frozen (-80 °C). The organs were homogenized with Potter-Elvehjem homogenizer in 4 volumes of 20 mM Tris-HCl buffer, pH 8.6, containing 0.5 mM PMSF and 0.01% β-mercaptoethanol. The homogenate was then centrifuged at 17,000 × g for 30 min at 4 °C. Aliquots of 1 ml of supernatant containing metallothioneins were added with 1.05 ml of cold (-20 °C) absolute ethanol and 80 μl chloroform.

The samples were centrifuged at 6000 × *g* for 10 min at 4 °C. The collected supernatant was combined with three volumes of cold ethanol (-20 °C), maintained at -20 °C for 1 h and centrifuged at 6000 × *g* for 10 min at 4 °C. The metallothionein-containing pellets were then rinsed with 1 ml of 87% ethanol and 1% chloroform mix and centrifuged at 6000 × *g* for 10 min at 4 °C. The metallothionein content in the pellet was evaluated using the colorimetric method with DTNB reagent. The pellet was suspended in 150 µl 0.25 M NaCl and subsequently 150 µl 1 N HCl containing 4 mM EDTA was added to the sample. 4.2 ml 2 M NaCl containing 0.43 mM DTNB buffered with 0.2 M Na-phosphate, pH 8.0 was then added to the sample at room temperature. The sample was centrifuged at 3000 × *g* for 5 min at room temperature. The supernatant absorbance was evaluated at 412 nm. Metallothionein concentration was estimated using molar absorption coefficient at 412 nm 14140 $M^{-1}cm^{-1}$ (Eyer et al, 2003) and expressed as micrograms of SH groups per gram of wet weight.

2.5 Erythrocytic nuclear abnormalities (ENAs) analysis in in vivo assay

ENAs analysis was performed in peripheral blood, gills, kidneys and liver erythrocytes. Blood was immediately taken from the caudal vein. A drop of blood was directly smeared on microscopic slides and air-dried. After the sacrifice, small pieces of cephalic kidneys, liver and gills were dissected, softly dragged along clean slide and allowed to dry for 1-2 h. Dried smears were fixed in methanol for 10 min. and were stained with 10% Giemsa solution in phosphate buffer pH = 6.8 for 8 min. (Baršienė et al, 2004). The stained slides were analysed under bright-field microscopes Olympus BX51 (Tokyo, *Japan*) using an immersion objective (1000×) and the photos were taken *with* an Olympus U-CMAD3 (Tokyo, *Japan*) camera. 4,000 erythrocytes with intact cellular and nuclear membrane per fish were evaluated using blind scoring by a single observer. Final results were expressed as the mean value (‰) of sums of analysed individual lesions scored in 1000 erythrocytes per fish sampled from every study group. The formation of micronuclei (MN), binucleated erythrocyte with nucleoplasmic bridge (BNb), nuclear buds (NB), nuclear buds on filament (NBf), 8-shaped nuclei, fragmented (Fr), apoptotic (Ap), binucleated (BN) erythrocytes were identified using criteria described by Fenech et al (2003) and Baršienė et al (2014). Additionally, kidney-shaped, blebbed (BL), vacuolated nuclei (VacNuc), enucleus (EN) erythrocytes were identified (Harabawy and Mosleh 2014).

2.6 Cell isolation and Comet assay

Peripheral blood samples were collected from the caudal vein using an insulin syringe (30G needle, 3.8% *sodium citrate*). Blood was placed in a 15 mL glass bottles containing 10 mL of chilled phosphate buffered saline (PBS). The viability of the erythrocytes was assessed through the Trypan Blue exclusion method (Anderson and Wild, 1994). Only cell suspensions with viability >90% were used. Alkaline comet assay version technique was used as described by Singh et al (1988) with slight modifications (Fatima et al, 2014). The slides were stained with ethidium bromide, placed under a glass cover and analysed by fluorescence microscopy (Olympus BX51, *Olympus U-RFL-T*, Tokyo, *Japan*); the photos were taken *with* an Olympus U-CMAD3 (Tokyo, *Japan*) camera. 50 nuclei of each individual were scored randomly and captured at 40× magnification. Images were analysed using Comet assay IV version 4.2 software and percentage of DNA in the tail (% Tail DNA) was assessed.

2.7 Haematological analysis

Blood was sampled from the caudal vein of fish using an insulin syringe (30G needle, 3.8% *sodium citrate*). Following indices of blood parameters were assessed: erythrocytes (RBC, $10^6 \times mm^{-3}$), haemoglobin concentration (Hb, g/l), haematocrit level (Hct, l/l), leukocyte count (WBC, $10^3 \times mm^{-3}$) were determined using routine methods (Svobodova et al, 1991).

2.8 Data analysis and statistics

Geno- and cytotoxicity data do not follow a normal distribution (Kolmogorov-Smirnov and Shapiro-Wilk normality test). Geno-cytotoxicity data were analysed by the nonparametric Kruskal-Wallis test

followed by Dunns post hoc test (using GraphPad Prism® 5.01 (GraphPad Software Inc., San Diego, CA, USA)). BCF and MT content data follow a normal distribution. Data for BCF in tissues were evaluated by two-way factorial ANOVA followed by Bonferroni post hoc test, MT levels was analysed by a one-way ANOVA followed by Bonferroni post hoc test through STATISTICA 7.0 (StatSoft Inc., Tulsa, Oklahoma, USA) software. Spearman correlation was used to assess the relationship between MT content and metal accumulation in liver and kidneys tissues. The results were expressed as mean ± standard error or standard deviation. The level of significance was established at $p<0.05$.

3. RESULTS

3.1 Bioconcentration factor

According to BCF classification scale (Landis et al 2011), low BCF values of analysed metals were measured in fish tissues, except for Zn [in gills (393.1–613.1)), in liver (170.5–318.8), in kidneys (249.4–476.7)] and Cu (in liver (971.7–1789.8), in kidneys (139.1–561.7)] (Fig. 1). BCF values varied depending on metal, metal mixture treatment and specific tissue. *BCF values* for Zn and Cd in *different tissues* after treatment with metal mixtures followed *the sequence*: gills>kidneys>liver>muscle; Cu – liver>kidneys>gills>muscle; Ni – kidneys>muscle>gills>liver, Cr – liver>gills>muscle>kidneys; Pb – gills>liver>kidneys>muscle.

The highest BCF value for Zn was detected in gills tissue after treatment with Pb↓ mixture, in liver – after Ni↓ and in kidneys – Cu↓ treatment (Fig. 1). Treatments with metal mixtures resulted in the highest Cu BCF values measured in liver tissue. The highest BCF value of Cu was detected in liver after Pb↓ treatment, while in kidneys – after Ni↓ treatment. The lowest BCF values for all analysed metals mostly were detected in muscle tissue after metal mixtures treatment.

BCF of Ni was highly affected by reduction of concentration of all metals (Fig. 1). BCF values for Ni significantly differ after all treatments (with reduced concentrations of single metal) performed in comparison to MIX treatment. The highest Ni amount accumulated in gills and muscle tissues was measured after MIX treatment, in liver – after Cu↓, in kidneys – after Zn↓ treatment. BCF values for Cr in gills and muscle tissues were significantly higher after Ni↓ treatment compared to MIX treatment. While MIX treatment resulted in the highest Cr BCF value in liver tissue, and Cu↓ treatment – in the highest Cr BCF value in kidneys compared to MIX treatment. Significant differences between BCF values for Pb were not detected in kidneys and muscle tissues after all treatments performed. However, the highest Pb accumulation was measured after MIX treatment in gills and liver tissues, followed by Pb↓ treatment in gills tissue. Significant differences between BCF values for Cd were not detected after all treatments performed and in any analysed tissues in comparison to MIX treatment. The highest Cd BCF was measured after Cr↓ treatment in gills and kidneys tissues, while after Zn↓ and Cu↓ treatments in liver tissue.

In summary, 10 times reduction of MPC of certain metal, was not always associated with a significant decrease in the same metal amount accumulated in *R. rutilus* tissues compared to MIX treatment. Furthermore, the highest BCF values for metals were measured mostly after treatments with metal mixtures with reduced metal concentration in comparison to BCF values after MIX treatment.

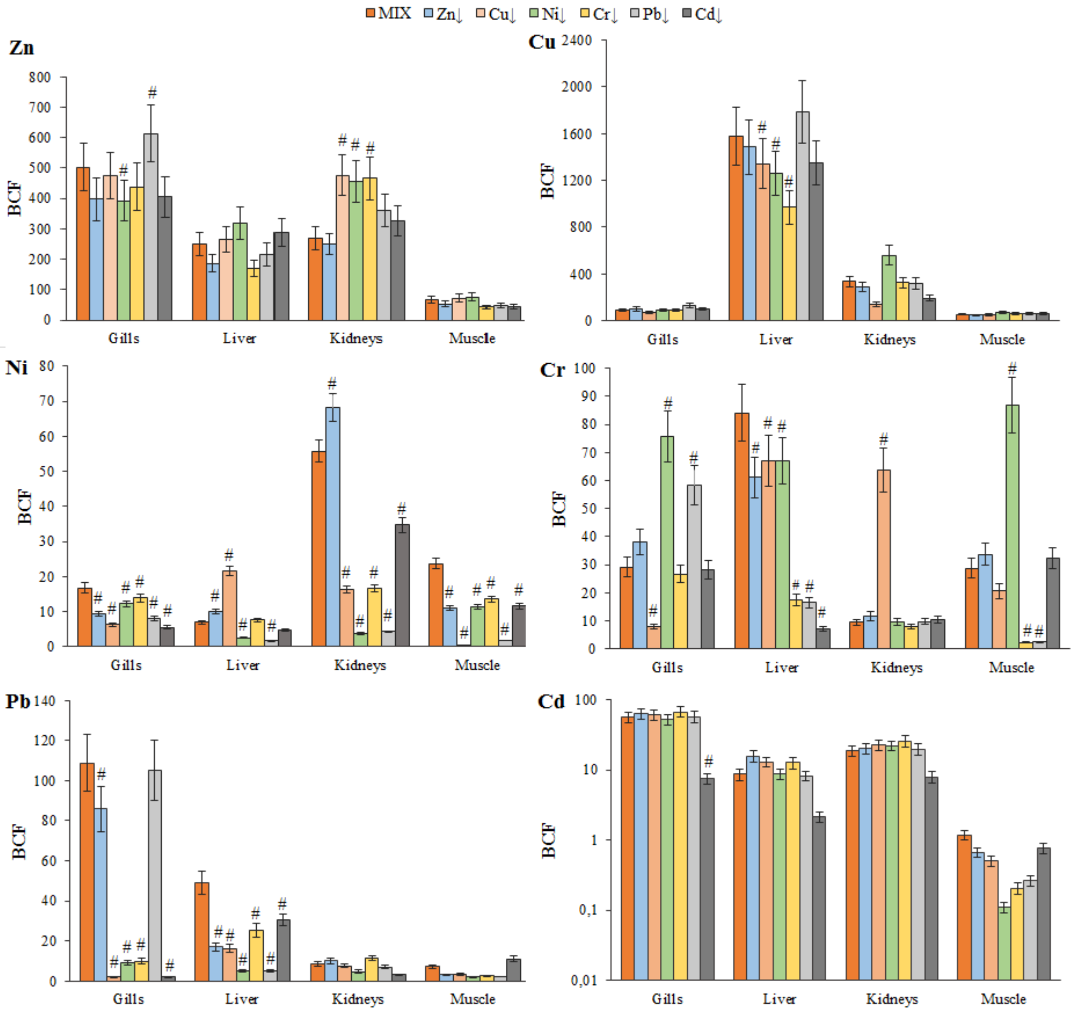


Figure 1. Bioconcentration factor (BCF) in the selected organ tissues exposed to different metal mixture (mean±SD, *N*=7). Grades (#) denote significant differences from MIX treatment groups (p<0.05).

3.2 Erythrocytic nuclear abnormalities

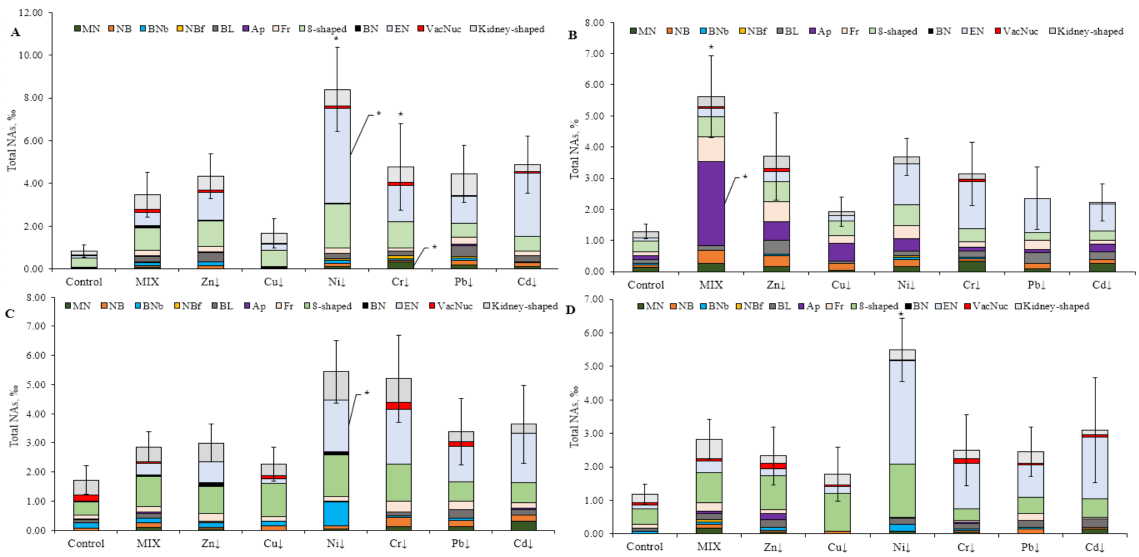


Figure 2. Erythrocyte nuclear abnormalities (ENAs) in (A) peripheral blood, (B) gills, (C) liver and (D) kidneys erythrocytes in control fish and fish treated with metal mixtures (mean±SE, N=7). Asterisks (*) denote significant differences from control group (p<0.05).

14 days treatment with metal mixtures significantly affected micronuclei, enucleus and apoptotic erythrocytes frequencies. The frequencies of *separate ENAs* such as MN, EN were significantly elevated after Cr↓, Ni↓ treatments in peripheral blood erythrocytes, respectively; apoptotic (Ap) cells – after MIX treatment in gills and enucleus after Ni↓ treatment in liver erythrocytes compared to control level. Significant elevations in total ENAs were measured after Cr↓, MIX or Ni↓ treatments in peripheral blood, gills or kidneys erythrocytes (Fig. 2).

3.3 Comet assay

The exposure of fish to Zn↓, Cr↓ and Pb↓ metal mixtures resulted in significant DNA damage compared to those from the control group (Fig. 3). The highest percentage of DNA in the tail (22.59 %) was observed after Cr↓ treatment followed by Pb↓ (16.55 %) and Zn↓ (16.08 %) treatments.

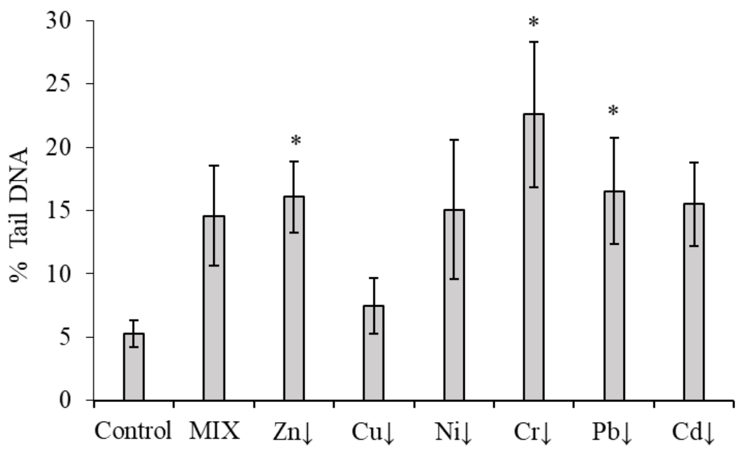


Figure 3. DNA damage (*percentage* of *DNA* in the *tail*) in control fish and fish treated with metal mixtures (mean±SD, *N* = 7). Asterisks (*) denote significant differences from control group (p<0.05).

3.4 Haematological parameters and metallothioneins content

Decreased number of *red blood cells*, *haematocrit* level, haemoglobin concentration and increased number of white blood cells in peripheral blood was measured after MIX treatment (Table 2). However, only decrease in haemoglobin concentration was statistically significant. Metallothionein content in liver and kidneys is presented in Table 2. Liver and kidneys MT level increased 1.22 and 1.25-fold after MIX treatment, respectively, nevertheless, significant differences were not detected. Positive correlation (r = 0.83; *p* = 0.022) was measured between MT and Zn amount in liver.

Table 2. Effects of metal mixture (MIX) on haematological parameters and metallothioneins (MT) content (mean±SD, *N* = 7) in *R. rutilus* liver and kidney.

Treatment	Hb, g/l	Hct, l/l	RBC count, $10^6 \times mm^{-3}$	WBC count, $10^3 \times mm^{-3}$	MT	
					Liver	Kidneys
Control	84.83±11.07	0.328±0.07	1.33±0.12	23.42±9.05	41.7±15.3	12.5±0.969
MIX	64.33±14.88 *	0.233±0.06	1.03±0.33	28.75±11.86	50.8±8.84	15.5±4.31

Asterisks (*) denote significant differences from control group ($p < 0.05$)

4. DISCUSSION AND CONCLUSIONS

The results demonstrated significant DNA damage, elevation in micronucleus, enucleus and apoptotic erythrocytes frequencies depending on analysed tissue and performed treatment. Moreover, the findings of this study revealed that *R. rutilus* exposure to metal mixture and its variants induced

variation in metals BCF values, indicating possible interactions between components of primary metal mixture (MIX) and its variants with 10-times reduced concentration of a single metal. Significant effect of MIX on MT content was not detected. Nevertheless, significant decrease in haemoglobin concentration was noted after MIX treatment.

In the present study, muscle tissue exhibited the lowest and less significant variations in metals BCF values after treatment with MIX variants with 10-time reduced concentration of a single metal, as compared with MIX (except Ni and Cr BCF). The highest values of BCF were detected in metabolic body tissues of *R. rutilus* – gills, liver, kidneys, the least – in muscle. In accordance, Sauliutė et al (2017) study showed similar results of metals BCF values in *S. salar* tissues (Sauliutė et al, 2017). Pb↓ treatment highly affected accumulated amount of Zn and Cr in gill (increased 1.2 and 2.0–fold, respectively) compared to MIX treatment. Zn↓ treatment 1.2-fold increased Ni accumulation in kidneys, meanwhile Ni↓ highly affected accumulated amount of Cr in gill and muscle (increased 2.6 and 3.0–fold, respectively) compared to MIX treatment. The highest amount of Zn, Cr and Ni accumulated was measured after Cu↓ treatment in kidneys and liver, respectively. However, treatments with reduced concentration of a single metal showed the lowest variation in the amount of accumulated Cd in tissues, compared to accumulated amount changes of other metals.

In this study, metal mixtures at MPC induced significant formation of MN, EN and Ap in Cr↓, Ni↓ or MIX treatments depending on analysed tissue. The total level of ENAs was also significantly elevated after Cr↓, Ni↓ or MIX treatments. Gills erythrocytes, considering ENAs induction, were mostly affected by MIX treatment. In peripheral blood erythrocytes, significant changes in single endpoints or total ENAs frequencies were detected after Cr↓ or Ni↓ treatments, in liver and kidneys erythrocytes – after Ni↓ treatment. The potential of metal induced damage to the genetic material using environmentally relevant concentrations has scarcely been investigated. Prior studies, that have evaluated toxicity responses in salmonids after treatment with metal mixture at MCP, also reported significant elevation in geno- and cytotoxicity endpoints after 14 days treatment (Stankevičiūtė et al, 2017, Valskienė et al, 2015). Stankevičiūtė et al (2017) study reported significant genotoxicity induction in kidneys erythrocytes, while significant cytotoxicity was detected in gills erythrocytes of *Salmo salar* after 14-day treatment. Rainbow trout 14 days exposure to metal mixture at MPC also resulted in elevation of genotoxicity endpoints in blood and kidneys erythrocytes, while significant cytotoxicity was detected in all analysed tissues (Valskienė et al, 2015).

In the present study, treatment with MIX resulted in decrease of all analysed haematological parameters, except leukocyte count (WBC). Nevertheless, only decrease in haemoglobin concentration was significant. The results are in accordance with Vosylienė et al (2006) findings, which showed decrease in erythrocyte count, haematocrit level and increase in leukocyte count after rainbow trout exposure to complex metal mixture at various concentrations.

Acknowledgments
This work was funded by the Research Council of Lithuania, Project No. S-MIP-17-10. Metallothioneins determination was funded by the Research Council of Lithuania, Project No. MIP-108/2015.

References

1. Anderson S.L. and G.C. Wild (1994) 'Linking genotoxic responses and reproductive success in ecotoxicology', **Environmental Health Perspectives,** Vol. 102(9-12).
2. Ayangbenro A.S. and O.O. Babalola (2017) 'A New Strategy for Heavy Metal Polluted Environments: A Review of Microbial Biosorbents', **International Journal of Environmental Research and Public Health**, Vol. 14(94).
3. Baršienė J., J. Lazutka, J. Syvokienė, V. Dedonytė, A. Rybakovas, E. Bagdonas, A. Bjornstad, O.K. Andersen (2004) 'Analysis of micronuclei in blue mussels and fish from the Baltic and the North Seas', **Environmental Toxicology,** Vol. 19(4), pp. 365-371.

4. Baršienė J., L. Butrimavičienė, W. Grygiel, T. Lang, A. Michailovas, T. Jackūnas (2014) 'Environmental genotoxicity and cytotoxicity in flounder (*Platichthys flesus*), herring (*Clupea harengus*) and Atlantic cod (*Gadus morhua*) from chemical munitions dumping zones in the southern Baltic Sea', **Marine Environmental Research,** Vol. 96(56-67).

5. Cavas T., N.N. Garanko, V.V. Arkhipchuk (2005) 'Induction of micronuclei and binuclei in blood, gill and liver cells of fishes subchronically exposed to cadmium chloride and copper sulphate', **Food and Chemical Toxicology**, Vol. 43(4), pp. 569-74.

6. Cedergreen N. (2014) 'Quantifying Synergy: A Systematic Review of Mixture Toxicity Studies within Environmental Toxicology', **PLoS ONE,** Vol. 9(5): e96580.

7. Directive 2008/105/EC of the European Parliament and of the Council of 496 16 December 2008 on environmental quality standards in the field of water 497 policy, amending and subsequently repealing Council Directives 82/176/EEC, 498 83/513/EEC, 84/156/EEC, 84/491/EEC, 86/280/EEC and amending Directive 499 2000/60/EC of the European Parliament and of the Council. Official Journal of the European Communities L 500 348, 24/12/2008 p. 0084-0097.

8. Dixit R., D. Malaviya, K. Pandiyan, U.B. Singh, A. Sahu, R. Shukla, B.P. Singh, J.P. Rai, P.K. Sharma, H. Lade (2015) 'Bioremediation of heavy metals from soil and aquatic environment: An overview of principles and criteria of fundamental processes', **Sustainability**, Vol 7, pp. 2189-2212.

9. Driessnack M.K., A.L. Matthews, J.C. Raine, S. Niyogi (2016) 'Interactive effects of chronic waterborne copper and cadmium exposure on tissue-specific metal accumulation and reproduction in fathead minnow (*Pimephales promelas*)', **Comparative Biochemistry and Physiology** – Part C 179 (165-173).

10. Driessnack M.K., A. Jamwal, S. Niyogi (2017) 'Effects of chronic waterborne cadmium and zinc interactions on tissue specific metal accumulation and reproduction in fathead minnow (*Pimephales promelas*)', **Ecotoxicology and Environmental Safety,** Vol. 140, pp. 65-75.

11. Duran S., M. Tunçsoy, B. Yeşilbudak, Ö. Ay, B. Cicik, C. Erdem (2015) 'Metal Accumulation In Various Tissues Of *Clarias Gariepinus* Exposed To Copper, Zinc, Cadmium And Lead Singly And In Mixture', **Fresenius Environmental Bulletin,** Vol. 24(12c).

12. Eyer P., F. Worek, D. Kiderlen, G. Sinko, A. Stuglin, V. Simeon-Rudolf, E. Reiner (2003) 'Molar absorption coefficients for the reduced Ellman reagent: reassessment', **Analytical Biochemistry,** Vol. 312, pp. 224-227.

13. Fatima M., N. Usmani, M.M. Hossain, M.F. Siddiqui, M.F. Zafeer, F. Firdaus, S. Ahmad (2014) 'Assessment of genotoxic induction and deterioration of fish quality in commercial species due to heavy-metal exposure in an urban reservoir', **Archives of Environmental Contamination and Toxicology,** Vol. 67(2), pp. 203-2013.

14. Fenech M., W.P. Chang, M. Kirsch-Volders, N. Holland, S. Bonassi, E. Zeiger (2003) 'HUMN project: detailed description of the scoring criteria for the cytokinesis-block micronucleus assay using isolated human lymphocyte cultures', **Mutation Research,** Vol. 534, pp. 65-75.

15. Gobas F.A.P.C, D. Wolf, W. Burkhard, L.P. Verbruggen, K. Plotzkeet (eds) (2009) 'Revisiting bioaccumulation criteria for POPs and PBT assessments', **Integrated Environmental Assessment and Management,** Vol. 5, pp. 624-637.

16. Harabawy A.S.A. and Y.Y.I Mosleh (2014) 'The role of vitamins A, C, E and selenium as antioxidants against genotoxicity and cytotoxicity of cadmium, copper, lead and zinc on erythrocytes of Nile tilapia, *Oreochromis niloticus*', **Ecotoxicology and Environmental Safety**, Vol. 104, pp. 28-35.

17. Heys K.A., R.F. Shore, M.G. Pereira, K.C. Jones, F.L. Martin (2016) 'Risk assessment of environmental mixture effects', **RSC Advances,** Vol. 6, pp. 47844-47857.

18. ISO 15586:2003. Water quality. Determination of trace elements using atomic absorption spectrometry with graphite furnace. Geneva, International Organization for Standardization.
19. Jia H., H. Ren, S. Satoh, H. Endo, T. Hayashi (2005) ‘Comparison of pre-treatment condition of cadmium in fish sample and diet by microwave digestion method for ICP-AES’, **Journal of the Tokyo University Marine Science and Technology**, Vol. 1, pp. 41-46.
20. Landis W., R. Sofield; M.H Yu, W.G. Landis, R.M. Sofield (2011) ‘Introduction to environmental toxicology: molecular substructures to ecological landscapes’, 4th ed. Boca Raton, Florida: CRC Press.
21. Peixoto N.C., T. Roza, E.M.M. Flores, M.E. Pereira (2003) ‘Effects of zinc and cadmium on $HgCl_2$-ALA-D inhibition and Hg levels in tissues of suckling rats’, **Toxicology Letters**, Vol. 146, pp. 17-25.
22. Sauliutė G., M. Stankevičiūtė, G. Svecevičius, J. Baršienė, R. Valskienė (2017) ‘Assessment of heavy metals bioconcentration factor (BCF) and genotoxicity response induced by metal mixture in *Salmo salar* tissues’, “**Environmental Engineering” 10th International Conference.**
23. Singh N.P., M.T. McCoy, R.R. Tice, E.L. Schneider (1988) ‘A simple technique for quantitationof low levels of DNA damage in individual cells’, **Experimental Cell Research**, Vol. 175, pp. 184-191.
24. Stankevičiūtė M., G. Sauliutė, G. Svecevičius, N. Kazlauskienė, J. Baršienė (2017) ‘Genotoxicity and cytotoxicity response to environmentally relevant complex metal mixture (Zn, Cu, Ni, Cr, Pb, Cd) accumulated in Atlantic salmon (*Salmo salar*). Part I: importance of exposure time and tissue dependence’, **Ecotoxicology**, Vol. 26(8), pp. 1051-1064.
25. Svobodova Z. and B. Vykusova (Eds.) (1991) ‘Diagnostics, Prevention and Therapy of Fish Diseases and Intoxications’ Vodnany: Czechoslovakia.
26. Valskienė R, Stankevičiūtė M, Butrimavičienė L, Greiciūnaitė J, Svecevičius G (2015) ‘Induction of nuclear abnormalities in rainbow trout (*Oncorhynchus mykiss*) after exposure to a model mixture of heavy metals (Zn, Cu, Ni, Cr, Cd, Pb) at maximum permissible concentration‘, **Proceedings of the 18th Conference for Junior Researchers “Science – Future of Lithuania“**, Vol. 15, pp. 100–105.
27. Vosylienė M.Z. and A. Jankaitė (2006) ‘Effect of heavy metal model mixture on rainbow trout biological parameters‘, **Ekologija,** Vol. 4, pp. 12-17.
28. Winter A.R., R.C. Playle, D.G. Dixon, U.W.E. Borgmann, M.P. Wilkie (2012) ‘Interactions of Pb and Cd mixtures in the presence or absence of natural organic matter with the fish gill’, **Ecotoxicology and Environmental Safety**, Vol. 83, pp. 16-24.
29. Zhu Y., J. Wang, Y. Bai, R. Zhang (2004) ‘Cadmium, chromium, and copper induce polychromatocyte micronuclei in carp (*Cyprinus carpio* L.)’, **Bulletin of Environmental Contamination and Toxicology,** Vol. 72(1), pp. 78-86.

GENO-, CYTOTOXICITY AND TOXICITY INDUCED BY *SAPROLEGNIA PARASITICA* AND CADMIUM ALONE AND IN COMBINATION TO *ONCORHYNCHUS MYKISS*

M. Stankevičiūtė*[1], Ž. Jurgelėnė[1], J. Greiciūnaitė[1], S. Markovskaja[1], N. Kazlauskienė[1], J. Baršienė[1]

[1] Nature Research Centre, Akademijos st. 2, LT-08412 Vilnius, Lithuania

*Corresponding author: e-mail: milda.stan@gmail.com, tel: +370 60716809

Abstract
The aims of present study were to determine genotoxicity, cytotoxicity and toxicity induced by *Saprolegnia parasitica* at concentrations 92000, 22400 and 5500 *colony-forming units per milliliter* (cfu/mL) and Cd (2 µg Cd/L as $CdCl_2 \cdot H_2O$) alone and in combination to rainbow trout *Oncorhynchus mykiss* larvae after 8-day treatment. The formations of micronuclei (MN) and nuclear buds (NB) were assessed as genotoxicity, while 8-shaped nuclei and fragmented-apoptotic (FA) erythroblasts were assessed as cytotoxicity endpoints. Significant induction of MN frequency was detected after treatment with the lowest concentration of *S. parasitica* and after co-exposure. In contrast, significant elevation of NB was measured exceptionally after exposure to the highest *S. parasitica* concentration. Total level of genotoxicity endpoints showed significant elevation after the highest, the lowest *S. parasitica* concentrations and co-exposure treatments. Significant changes in cytotoxicity endpoints were not detected after all treatments performed. Surprisingly, exposure to Cd did not induce any significant changes of selected biomarkers. During the treatment, biological parameters such as heart rate (HR, counts/min) and gill ventilation frequency (GVF, counts/min) were assessed. Toxicity study demonstrated that HR of larvae exposed to *S. parasitica* at concentrations 22400 and 5500 cfu/mL, and 5500 cfu/mL+Cd after 8 days was significantly ($p<0.05$) lower as compared to the control. Additionally, *S. parasitica* at 5500 cfu/mL, and 5500 cfu/mL+Cd induced a significant decrease in GVF in larvae at the end of the test.

Keywords: fish; genotoxicity; cytotoxicity; toxicity; *Saprolegnia parasitica*; cadmium

1. INTRODUCTION

The aquatic fungus-like heterotrophs or straminipilous fungi referred also as "water moulds" (traditionally oomycetes) of the order *Saprolegniales* is common and widespread in freshwater environment (Rietmüller, 2000; Dick, 2001). Most of them are saprotrophs decomposing dead organic material, but some species are known to be pathogens and have the ability to infect various aquatic organisms including fish or crustaceans and induce a number of economically important diseases (Willoughby, 1994; Wicker et al, 2001). Fungal disease such as saprolegniosis is known as one of the common salmonids disease (Thoen et al, 2011). Naturally, *Saprolegnia* species are found in all lotic and lentic freshwater basins (Rietmüller, 2000; Markovskaja, 2006). In aquaculture, *Saprolegnia* infection causes severe problem in incubating eggs and newly hatched fry (Hussein et al, 2001; Thoen et al, 2011; Van Den Berg et al, 2013). The lethal impact of saprolegniosis could cause major financial loss in an industry of the global fish industry production (Phillips et al, 2008). According to Bruno et al (2011), over 10% of salmonid eggs become infected with oomycetes in hatcheries each year. Since 2002, when the use of malachite green, an organic dye very efficient at killing the pathogen and previously widely used, was banned due to its toxicity, *Saprolegnia* infection

has reemerged in aquaculture. There are no chemicals now available that provide sufficient protection against the saprolegniosis after hatching (Fornerisa et al, 2003). In order to mitigate *Saprolegnia* infection in aquaculture, the development and testing of general or specific *antifungal agents* has increased (Ali et al, 2014).

Songe et al (2016) emphasized, that *Saprolegnia* infection in salmonids eggs has been scarcely investigated and the role of such infection in fish eggs remains unclear. Moreover, *Saprolegnia parasitica* is thought to be most frequent species of *Saprolegnia* genus infecting fish egg (van West, 2006; Shahbazian et al, 2010). *S. parasitica* causes rapid death of eggs, because of hyphae penetration into the chorion, and consequently failure of osmosis regulation (Songe et al, 2016). In fish, disease is characterized by visible white or grey patches of filamentous mycelium on the body or fins of fish, hyphae penetrate epidermal tissues causing dermal, epidermal damage and cellular necrosis. Furthermore, lethargic behaviour, loss of equilibrium and death are the results of severe infection (Pickering et al, 1982). The parasitic lifecycle of *S. parasitica* has been well described by Andersson and Cerenius (2002), Dieguez-Uribeondo et al (1994), Torto-Alalibo et al (2005), Robertson et al (2009), and van West (2006). The zoospores of this pathogenic oomycete may be transmitted by fish eggs, wild fish, water sources, and equipment (Saha et al, 2016).

It is important to note, that toxins are very important virulence factors for many fungal diseases. Oomycetes are known to secrete toxins, proteinaceous substances or hydrolytic enzymes (Soanes et al, 2007). Torto-Alalibo et al (2005) have exuded and isolated several proteins of *S. parasitica* (CBD proteins, CBEL-like proteins, glycosyl hydrolases, proteases, protease inhibitors) and emphasized that these proteins can have a range of impacts on health. Moreover, *Saprolegnia* infection induce a strong inflammatory response in fish. As concluded by Belmonte et al (2014) *S. parasitica* produces the metabolite prostaglanding E_2 (PGE_2), which increases the inflammatory response in fish leukocytes. Consequently, inflammatory responses may trigger the genotoxicity. Furthermore, joint effects of parasitism and pollution may lead to unexpected toxicity endpoints. Parasites exposed to environmental contaminants is a phenomenon, which is not well understood and, which deserves further investigation (Sures et al, 2017). Additionally, no studies have been conducted to understand the combined impact of the *S. parasitica* infection and sublethal concentration of toxic metal Cd and their geno-, cytotoxicity and toxicity to developing fish. For this reason, the present study has the *following objectives*: a) to identify possible genotoxicity and cytotoxicity potential of *S. parasitica* infection using rainbow trout larvae, b) to assess combined effects of S. *parasitica* infection and Cd exposure on geno- and cytotoxicity endpoints, c) to determine biological effects of *S. parasitica* and Cd alone and in combination.

2. MATERIALS AND METHODS

2.1 Experimental set-up

Rainbow trout *Oncorhynchus mykiss* eggs (at 20 stages, eyed-egg stage embryos (Ballard, 1973)) were obtained from the Simnas hatchery (Lithuania) and risen in bare-bottom tanks supplied with flow-through aerated deep-well water. Studies have been carried out with non-protected life-stages accordance with EU Directive 2010/63/EU. The laboratory treatment was carried out in an environmental chamber (Bronson PGC-660, Zaltbommel, The Netherlands) with continuous aeration under static conditions (static non-renewal experiment) according to ISO 7346-1:1996, without the water being changed. According to the OECD 210 (OECD, 1992), the experiments were carried out in the dark and the larvae were not fed (ISO 10229:1994).

The fungus-like organism *Saprolegnia parasitica* Coker was isolated from naturally infected perch (*Perca fluviatilis*). The identification of *Saprolegnia* isolate was performed at species level, by taxonomic analysis of the sexual structures combined with morphological characterization of its asexual stage under light microscope Nikon eclipse Ci with phases contrast at magnifications x 400

(up to x 1000). The nomenclature of identified species follows Seymour, 1970; Rietmüller, 2000; Dick, 2001; Markovskaja, 2006.

The pure living cultures of *Saprolegnia parasitica* were isolated by the baiting technique (Seymour, 1970). Hemp seeds were used as baits, placed into the vessels with 100 mL of distilled water and hyphae scraped from naturally infected fish. After 5-7 days white hyphae appeared on the hemp seeds with developing asexual and later sexual organs. For the experiments a suspension of *S. parasitica* colony-forming units (cfu - zoospores, oospores, hyphae), prepared from pure living culture with concentration levels of 92000, 22400 and 5500 cfu/mL was used. Additionally, cadmium (2 μg Cd/L) induced geno-, cytotoxicity and toxicity alone and in combination with *S. parasitica* at concentration 5500 cfu/mL were assessed.

Reagent grade cadmium chloride ($CdCl_2 \cdot H_2O$) («REACHIM» Company, Russia) was used as the toxicant and stock solutions were prepared by dissolving a necessary amount of salts in distilled water. The concentration of 2 μg Cd/L was chosen according to the 96 h LC50 for rainbow trout larvae (Cibulskaitė et al, 2015). Nominal metal concentrations in the tanks were checked during blank tests (without larvae) (N = 3) with an atomic absorption spectrophotometer (SHIMADZU AA-6800, Japan). Mean measured concentrations were within 10 – 15% of target.

Experiments were conducted on *O. mykiss* larvae 4 days post hatching. All treatments were carried out with 3 replications and control groups (using glass tanks of 1-L total volume filled to a level of 500 mL with continuously aerated dilution water, a total of 35 larvae per treatment tank and 35 larvae in control tank were used).

2.2 Analytical procedures

The main physico-chemical parameters of the water (temperature, dissolved O_2, pH and conductivity) were measured routinely with a hand-held multi-meter (WTW Multi 340i/SET, Germany). Physico-chemical parameters of the laboratory water (deep-well) were as follows: dissolved oxygen 10±1 mg/L, temperature 10±0.5°C, pH 8.1±0.1. Chemical characteristics of the deep-well water have been presented in our previous research (Stankevičiūtė et al, 2017).

2.3 Nuclear abnormalities (NAs) analysis

Nuclear abnormalities (NAs) analysis was performed in erythroblasts of *O. mykiss* larvae. Blood smears were prepared from larvae body (gently nipped with tweezers): directly smeared on glass slides and air-dried. Smears were fixed in methanol for 10 min. and later were stained with 10% Giemsa solution in phosphate buffer pH = 6.8 for 20 - 40 min. The stained slides were analyzed under light microscope Olympus BX51 (Tokyo, *Japan*) at final magnification of 1,000× and the photos were taken *with* an Olympus U-CMAD3 (Tokyo, *Japan*) camera. Identification of micronuclei, nuclear buds, fragmented-apoptotic and bi-nucleated cells was done using criteria described by Heddle et al (1991) and Fenech et al (2003). The frequencies of abnormalities were recorded in 1,000 erythroblasts per slide using blind scoring. The test was carried out with 10 specimens of larvae in each treatment and control groups for evaluating genotoxicity and cytotoxicity. Genotoxicity [induction of micronuclei (MN) and nuclear buds (NB)] and cytotoxicity [induction of fragmented-apoptotic (FA) and 8-shaped nuclei cells] endpoints were analysed. Considering low frequencies of separate cytotoxicity endpoints, total cytotoxicity level (FA+8-shaped) was assessed as the sum of the frequencies of cytotoxicity endpoints.

2.4 Toxicity assay

Heart rate (HR, counts/min) and gill ventilation frequency (GVF, counts/min) were investigated. Samples of larvae were taken upon days 8 after exposure start. HR and GVF of larvae was measured for each larvae individually, and the mean value for 10 larvae was calculated.

2.5 Data analysis and statistics

The geno- and cytotoxicity data follow a normal distribution (Kolmogorov-Smirnov and Shapiro-Wilk normality test). Geno-cytotoxicity data were analysed by the one-way ANOVA followed by Bonferroni post hoc test (using GraphPad Prism® 5.01 (GraphPad Software Inc., San Diego, CA, USA)) for comparison of differences between groups. Toxicity data (HR and GVF) do not follow a normal distribution (Kolmogorov-Smirnov and Shapiro-Wilk normality test). Differences between the evaluated characteristics studied were tested by nonparametric Kruskal-Wallis test using STATISTICA 7.0 (StatSoft Inc., Tulsa, Oklahoma, USA) software. The results were expressed as mean ± standard error or standard deviation. The level of significance was established at $p<0.05$.

3. RESULTS

Results of micronucleus tests with *O. mykiss* larvae are given in Figure 1. Treatment with the lowest *S. parasitica* concentration (Sap3 – 5500 cfu/mL) significantly increased MN frequencies in erythroblasts of larvae. Cadmium alone did not induce significant MN formation. However, Cd in combination with *S. parasitica* at concentration 5500 cfu/mL significantly increased MN frequencies. Notwithstanding, MN frequencies induced by Cd in combination with the lowest *S. parasitica* concentration (Sap3) did not significantly differ from exposure to *S. parasitica* (Sap3) alone.

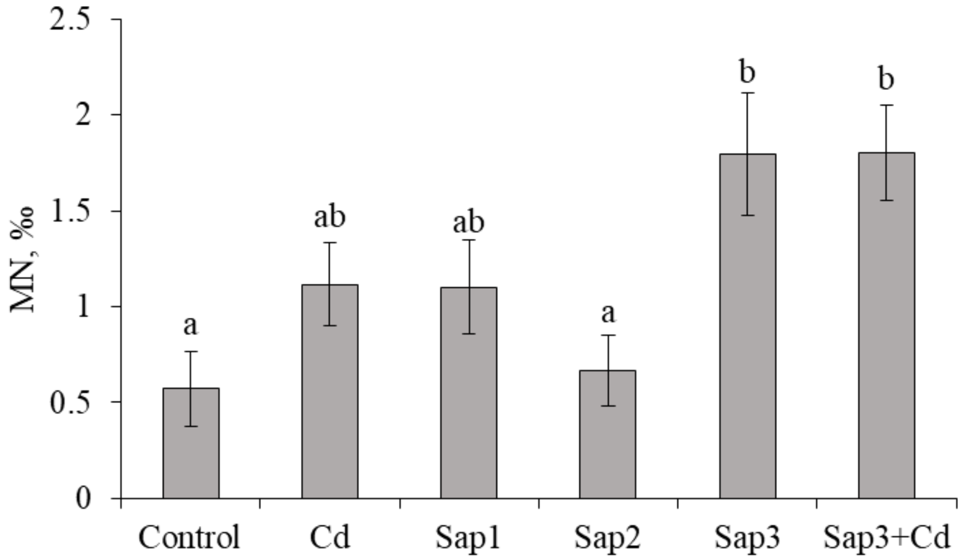


Figure 1. Mean values (mean ± SEM, *N* = 10) of micronuclei (MN) frequencies in erythroblasts of *O. mykiss* larvae treated with cadmium (Cd, 2µg/L), three concentrations of *Saprolegnia parasitica* (Sap1 – 92000, Sap2 – 22400, Sap3 –5500 (cfu/mL)) and Cd in combination with *S. parasitica* (2 µg Cd/L + 5500 cfu/mL). Letters denote significant differences between groups

Analysis of nuclear bud (NB) revealed a significant increase after treatment with the highest *S. parasitica* concentration (Sap1). Exposure to Cd, other *S. parasitica* concentrations and co-exposure did not significantly affect NB responses in erythroblasts of larvae (Figure 2).

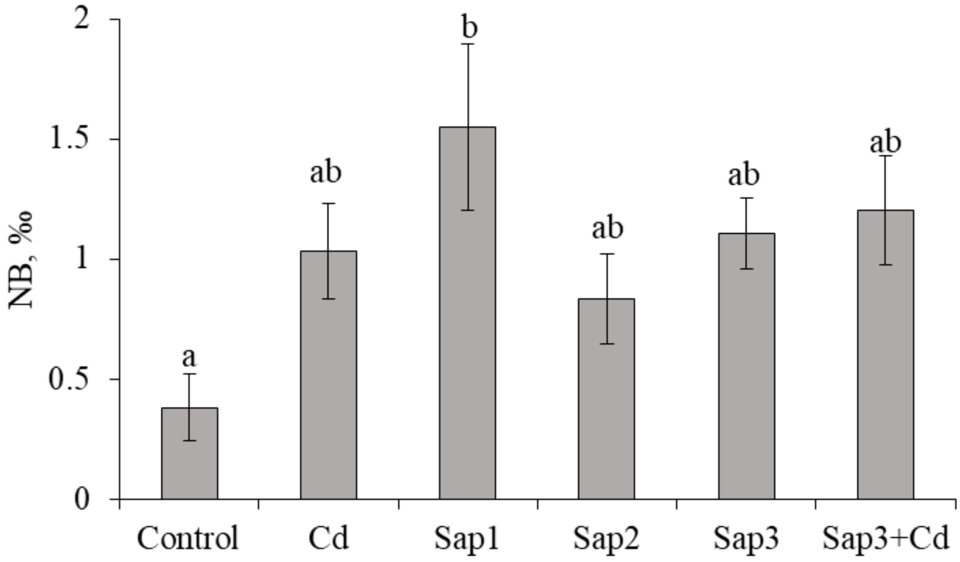


Figure 2. Mean values (mean ± SEM, *N* = 10) of nuclear bud (NB) frequencies in erythroblasts of *O. mykiss* larvae treated with cadmium (Cd, 2µg/L), three concentrations of *Saprolegnia parasitica* (Sap1 – 92000, Sap2 – 22400, Sap3 – 5500 (cfu/mL)) and Cd in combination with *S. parasitica* (2 µg Cd/L + 5500 cfu/mL). Letters denote significant differences between groups

Treatment with all *S. parasitica* concentrations and co-exposure treatment significantly increased total genotoxicity level in larvae erythroblasts, except for the 22400 cfu/mL (Sap2) concentration level.

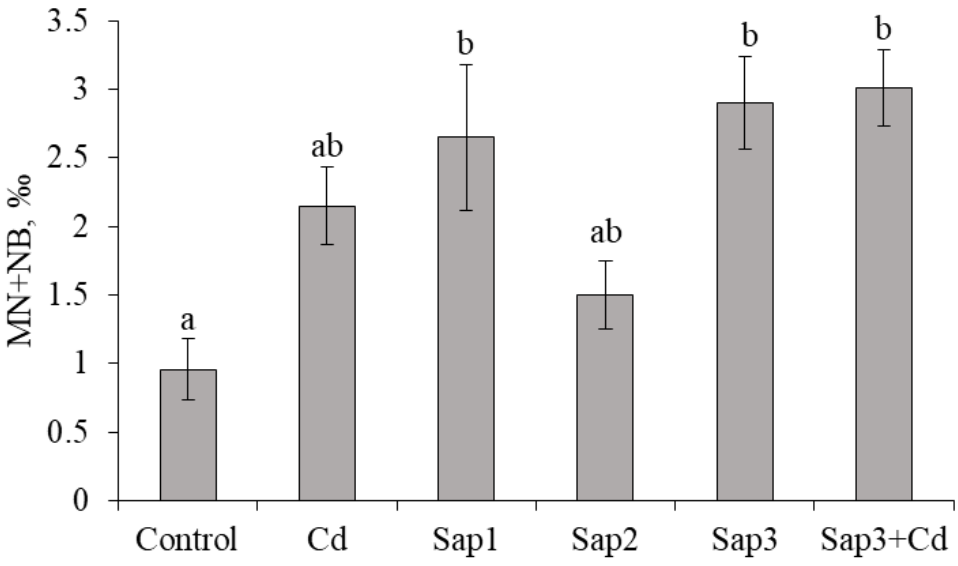


Figure 3. Total genotoxicity (MN+NB) level (mean ± SEM, *N* = 10) in erythroblasts of *O. mykiss* larvae treated with cadmium (Cd, 2µg/L), three concentrations of *Saprolegnia parasitica* (Sap1 – 92000, Sap2 – 22400, Sap3 – 5 500 (cfu/mL)) and Cd in combination with *S. parasitica* (2 µg Cd/L + 5500 cfu/mL). Letters denote significant differences between groups

Significant elevation of total cytotoxicity level was not found after all treatments performed. However, the highest total cytotoxicity level was measured after treatment with the lowest *S. parasitica* concentration (Sap3), followed by Sap3+Cd and Sap2 treatments.

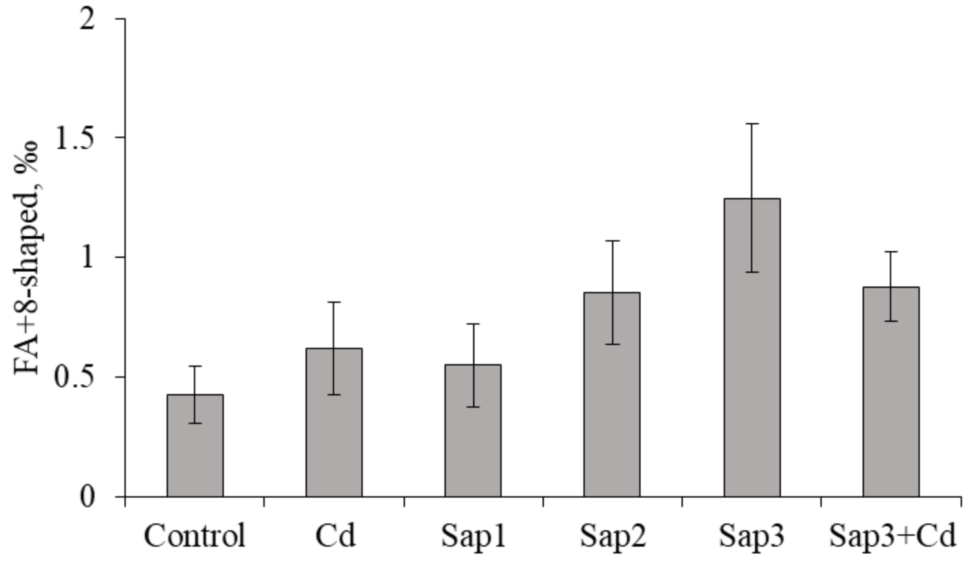
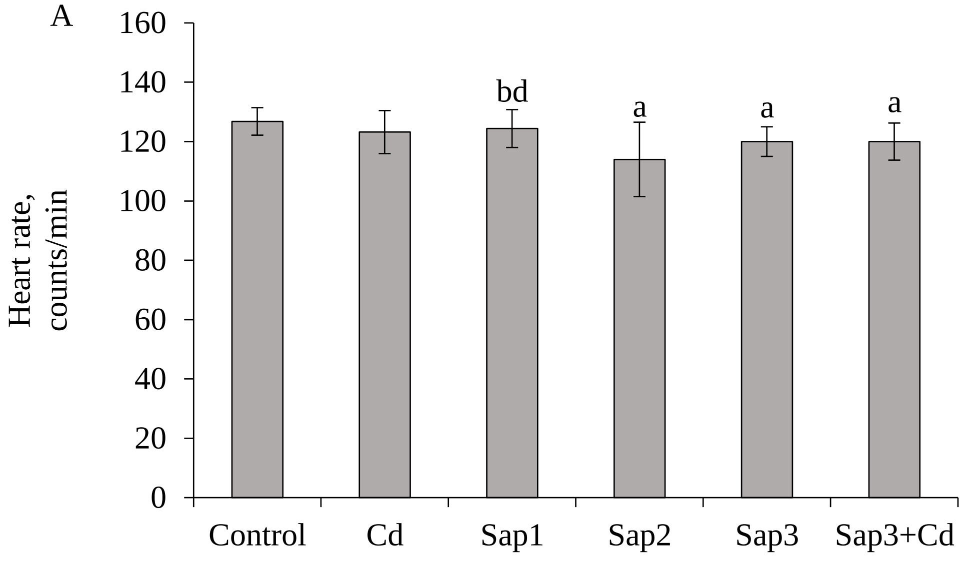


Figure 4. Total cytotoxicity (FA+8-shaped) level (mean ± SEM, *N* = 10) in erythroblasts of *O. mykiss* larvae treated with cadmium (Cd, 2μg/L), three concentrations of *Saprolegnia parasitica* (Sap1 – 92000, Sap2 – 22400, Sap3 –5500 (cfu/mL)) and Cd in combination with *S. parasitica* (2 μg Cd/L + 5500 cfu/mL). Letters denote significant differences between groups

In this investigation, significantly ($p<0.05$) decreased HR of larvae as compared to the control after 8 days of exposure to Sap2 – 22400, Sap3 – 5500 (cfu/mL) and Cd in combination with *S. parasitica* (2 μg Cd/L + 5500 cfu/mL). Meanwhile, in the highest *S. parasitica* treatment (Sap1) HR of larvae did not differ significantly from the control. HR of larvae in the highest *S. parasitica* treatment (Sap1) was significantly ($p<0.05$) different from Sap2 and Sap3+Cd treatments.

The lowest *S. parasitica* concentration (Sap3 – 5500 cfu/mL) and Cd in combination with *S. parasitica* (2 μg Cd/L + 5500 cfu/mL) induced a significant ($p<0.05$) decrease in GVF of larvae. Additionally, GVF of larvae in Cd treatment were significantly ($p<0.05$) different from Sap3 and Sap3+Cd treatment.

A



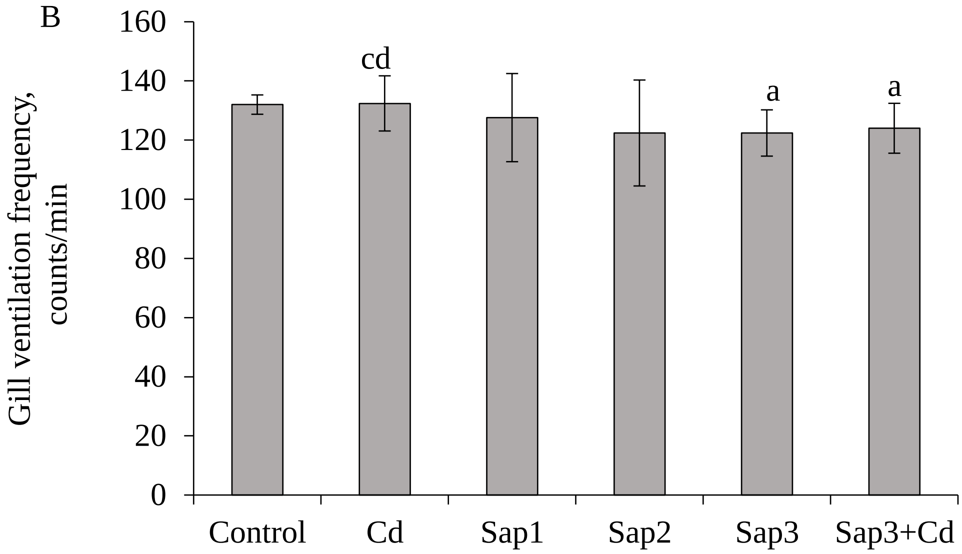


Figure 5. Sub-chronic (8 days of exposure) effect of cadmium (Cd, 2µg/L), three concentrations of *Saprolegnia parasitica* (Sap1 – 92000, Sap2 – 22400, Sap3 –5500 (cfu/mL)) and Cd in combination with *S. parasitica* (2 µg Cd/L + 5500 cfu/mL) on biological parameters of *O. mykiss* larvae: gill ventilation frequency (counts/min) and heart rate (counts/min) (mean ± SD).

[a] Significant difference from the control ($p<0.05$). Significant difference between treatments ($p<0.05$): [b] significant difference from Sap2 treatment; [c] significant difference from Sap3 treatment; [d] significant difference from Sap3+Cd treatment.

4. DISCUSSION AND CONCLUSIONS

This study was designed to identify possible geno- and cytotoxicity potential and to assess biological effects of egg-pathogenic *S. parasitica* infection in rainbow trout larvae. Moreover, the exacerbation of toxicity endpoints of joint parasitism and Cd exposure was assessed. The findings of this study indicated a significant increase of separate genotoxicity endpoints and total genotoxicity depending on exposure concentration of *S. parasitica*. However, genotoxicity endpoints did not show a clear tendency to increase with increasing *S. parasitica* exposure concentration. Belmonte and co-authors (2014) detected the immune suppression in Atlantic salmon before the pathogen infection (establishment) or after early stages of interaction. Moreover, 12 days exposure of fish to *S. parasitica (*10^4 zoospores/cysts liter^{-1}*)* did not cause evidence of infection and no suppression of the antigen, and no induction of proinflammatory genes were detected. These responses might indicate a protection against the oomycetes. In this study, exposure to the highest concentrations of *S. parasitica* did not induce the highest frequencies of all analyzed geno- and cytotoxicity endpoints. These results might indicate the threshold for inhibition of certain geno- and cytotoxicity responses. Further analyses using more frequent sampling and various concentrations of *S. parasitica* are therefore suggested. Scientific literature data related to direct or indirect genotoxic effects induced by *Saprolegnia* do not exist. The genotoxic potential of *Saprolegnia parasitica* in fish has not been investigated at all. This study provides *first* toxicity data that show significantly increased genotoxic activity in rainbow trout after *S. parasitica* exposure. Azimzadeh and Amniattalab (2017) indicated oxidative stress, haematological and histopathological changes in rainbow trout infected with *S. parasitica*. Moreover, parasitic *Saprolegnia* species produces metabolites, which may induce a strong inflammatory response in fish (Belmonte et al, 2014). However, one of the limitations of these findings is that it does not explain which mechanisms (direct or indirect) are responsible for such genotoxicity outcome.

Marcogliese et al (2005) concluded that parasitism in the presence of pollution may further compromise the health by reducing the immunocompetence of the host. Furthermore, exacerbation of toxicity effects may be noted even parasites infestation occurs at low intensities. In agreement with that, the findings of this study, showed the highest total genotoxicity level after joint treatment with the lowest *S. parasitica* concentration and Cd in comparison to other treatments.

In the present study, significant cytotoxicity was not induced by any *S. parasitica* concentration tested, as well as after co-exposure treatment. As emphasized by Schaumburg et al (2006), parasites can induce anti-apoptotic activities in the host.

In addition, during a sub-chronic test, *S. parasitica* induced negative effects on biological parameters (decreased heart rate and gill ventilation frequency) of rainbow trout larvae. Moreover, these effects did not relate to the concentration of *S. parasitica*. However, significant difference between *S. parasitica* treatments was observed only in heart rate measurement. In fish gills serve as a principal organ for respiration, osmoregulation, and excretion (Evans et al, 2005), they also become a potentially important site of penetration by parasites (Mikheev et al, 2014). Therefore, in this study, saprolegniosis seems to have damaged the gill, then gill ventilation frequency decreased in larvae and the deficiency of oxygen induced bradycardia. Furthermore, saprolegniosis-induced hypoxia may be responsible for the significant genotoxicity responses measured in this study. In fish, infection begins on the head, gills, or fins and spreads over the entire surface of the body, for this reason, often osmoregulatory failure results in the death of fish (van West, 2006). On the other hand, in contrast to our study, Mikheev et al (2014) demonstrated that rainbow trout reacted to low oxygen concentration with wider expansion of parasites (*Diplostomum spathaceum*), leading to an increase in gill ventilation frequency. Additionally, physiological or social stressors could produce similar effects on the transmission success of the parasites penetrating fish hosts using the gills.

This study result showed the negative effects of combined parasites and pollutant exposure. Similar results of negative effects were found by Gheorgiu et al (2006), where significantly increased mortality of guppies (*Poecilia reticulata*) exposed to Zn and infected with the monogenean *Gyrodactylus turnbulli* were observed.

Marcogliese et al (2005) noted that cumulative effects of multiple stressors are becoming a major problem in ecotoxicology and many other fields. In conclusion, this study highlights the potential to advance our current understanding of the significance of a biological stressor (pathogen) on geno-, cytotoxicity and toxicity endpoints. Furthermore, the potential to exacerbate toxicity endpoints after fish exposure to multiple environmental stressors (pathogen infection and pollution) is emphasized.

Acknowledgments

This work was funded by the Research Council of Lithuania, Project No. S-MIP-17-10.

References

1. Ali S.E., E. Thoen, Evensen Ø and I. Skaar (2014) 'Boric acid inhibits germination and colonization of Saprolegnia spores in vitro and in vivo', PLoS One, Vol 9, pp. e91878.
2. Andersson M.G. and L. Cerenius (2002) 'Pumilio homologue from *Saprolegnia parasitica* specifically expressed in undifferentiated spore cysts', **Eukaryotic Cell**, Vol 1(1), pp. 105-111.
3. Azimzadeh K. and Amniattalab A. (2017) 'Total Sialic Acid, Oxidative Stress and Histopathological Changes in Rainbow Trout Saprolegniasis (*Oncorhynchus mykiss*)', **Kafkas Universitesi Veteriner Fakultesi Dergisi**, Vol. 23(1), pp. 55-62.
4. Belmonte R., T. Wang, G.J. Duncan, I. Skaar, H. Mélida, V. Bulone, P. van West and C.J. Secombes (2014) 'Role of Pathogen-Derived Cell Wall Carbohydrates and Prostaglandin E_2 in Immune Response and Suppression of Fish Immunity by the Oomycete *Saprolegnia parasitica*', **Infection and Immunity**, Vol 82(11), pp. 4518-4529.

5. Bruno D.W., P. van West and G.W. Beakes (2011) 'Saprolegnia and other oomycetes in: Fish Diseases and Disorders: Viral, Bacterial and Fungal Infections', **CABI International,** Vol 3(2), pp. 669-720.
6. Cibulskaitė Ž., N. Kazlauskienė and V. Kulvietis (2015) 'Sublethal toxicity of quantum dots and heavy metals to rainbow trout (*Oncorhynchus mykiss*) in early ontogenesis. Proceedings of the 18th Conference for Junior Researchers „Science – Future of Lithuania"', **Environmental protection engineering**, pp. 31–37.
7. Dick M.W. (2001) 'Straminipilous Fungi: systematics of the peronosporomycetes, including accounts of the marine straminipilous protists, the plasmodiophorids, and similar organisms', **Kluwer Academic Publishers, Dordrecht.**
8. Dieguez-Uribeondo J., L. Cerenius and K. Soderhall (1994) 'Repeated zoospore emergence in *Saprolegnia parasitica*', **Mycological Research**, Vol 98(7), pp. 810-815.
9. Evans D.H., P.M. Piermarini and K.P. Choe (2005) 'The multifunctional fish gill: dominant site of gas exchange, osmoregulation, acid–base regulation, and excretion of nitrogenous waste', **Physiological Reviews**, Vol. 85(1), pp. 97–177.
10. Fornerisa G., S. Bellardib, G.B. Palmegianoc, M. Sarogliad, B. Sicuroa, L. Gascoe and I. Zoccarato (2003) 'The use of ozone in trout hatchery to reduce saprolegniasis incidence', **Aquaculture**, Vol 221(1-4), pp. 157-166.
11. Gheorgiu C., D.J. Marcogliese and M. Scott (2006) 'Concentration-dependent effects of waterborne zinc on population dynamics of *Gyrodactylus turnbulli* (Monogenea) on isolated guppies (*Poecilia reticulata*)', **Parasitology**, Vol 132(2), pp. 225-32.
12. Hussein M.A., K. Hatai and T. Nomura (2001) 'Saprolegniasis in salmonids and their eggs in Japan', **Journal of Wildlife Diseases,** Vol 37(1), pp. 204-207.
13. ISO (International Organization for Standardization) 10229 (1994) 'Water Quality-Determination of the Prolonged Toxicity of Substances to Freshwater Fish -- Method for Evaluating the Effects of Substances on the Growth Rate of Rainbow Trout (*Oncorhynchus mykiss* Walbaum (Teleostei, Salmonidae))'.
14. ISO (International Organization for Standardization) 7346-1 (1996) 'Water Quality – Determination of the Acute Lethal Toxicity of Substances to a Freshwater Fish [*Brachydanio rerio* Hamilton-Buchanan (Teleostei, Cyprinidae)] -Part 1: Static Method'.
15. Marcogliese D.J., L.G. Brambilla, F. Gagné and A.D. Gendron (2005) 'Joint effects of parasitism and pollution on oxidative stress biomarkers in yellow perch *Perca flavescens*', **Diseases of Aquatic Organisms**, Vol. 63(1), pp. 77-84.
16. Markovskaja S. (2006) 'Saprolegniaceae (Peronosporomycetes) in Lithuania. II. The genus Saprolegnia', **Botanica Lithuanica**, Vol. 12(2), pp. 97-112.
17. Mikheev V.N., A.F. Pasternak, E.T. Valtonen and J.Taskinen (2014) 'Increased ventilation by fish leads to a higher risk of parasitism', **Parasites & Vectors**, Vol 7, pp. 281.
18. OECD (Organization for Economic Cooperation and Development) (1992) 'Guideline for the Testing of Chemicals: Fish, Early-life Stage Toxicity Test', Part 210.
19. Phillips A.J., V.L. Anderson, E.J. Robertson, C.J. Secombes and P. van West (2008) 'New insights into animal pathogenic oomycetes', **Trends in Microbiology**, Vol 16(1), pp. 13–19.
20. Pickering A.D. and L.G. Willoughby (1982) 'Saprolegnia infections of salmonid fish. In: Roberts R.J., editor. Microbial Diseases of Fish', Academic Press, pp. 271-297.
21. Rietmüller A. (2000) 'Morphologie, Ökologie und Phylogenie aquatischer Oomyceten', Bibliotheca Mycologica, Vol.185: 1–344.

22. Robertson E.J., V.L. Anderson, A.J. Phillips, C.J. Secombes, J. Dieguez-Uribeondo and P. van West (2009) 'Saprolegnia – fish interactions. In: Lamour K, Kamoun S, editors. Oomycete genetics and genomics, diversity, interactions and research tools', **Hoboken, NJ, USA: Wiley-Blackwell**, pp. 407-424.

23. Saha H., A.K. Pal, N.P. Sahu and R.K. Saha (2016) 'Feeding pyridoxine prevents Saprolegnia parasitica infection in fish *Labeo rohita*', **Fish and Shellfish Immunology**, Vol 59, pp. 382-388.

24. Seymour R.L. (1970) 'The genus *Saprolegnia*', **Nova Hedwigia**, Vol. 19, pp. 1–124.

25. Schaumburg F., D. Hippe, P. Vutova and C.G. Lüder (2006) 'Pro- and anti-apoptotic activities of protozoan parasites', **Parasitology**, Vol 132(S1), pp. S69–S85.

26. Shahbazian N., H.A. Ebrahimzadeh Mousavi, M. Soltani, A.R. Khosravi, S. Mirzargar and I. Sharifpour (2010) 'Fungal contamination in rainbow trout eggs in Kermanshah province propagations with emphasis on Saprolegniaceae', **Iranian Journal of Fisheries Sciences**, Vol 9(1), pp. 151–160.

27. Soanes D.M., T.A. Richards and N.J. Talbot (2007) 'Insights from sequencing fungal and oomycete genomes: what can we learn about plant disease and the evolution of pathogenicity?', **Plant Cell,** Vol 19(11), pp. 3318-3326.

28. Songe M.M., A. Willems, J. Wiik-Nielsen, E. Thoen, Ø. Evensen, P. van West and I. Skaar (2016) '*Saprolegnia diclina IIIA* and *S. parasitica* employ different infection strategies when colonizing eggs of Atlantic salmon, *Salmo salar* L.', **Journal of Fish Diseases**, Vol. 39(3), pp. 343-352.

29. Sures B., M. Nachev, C. Selbach and D.J. Marcogliese (2017) 'Parasite responses to pollution: what we know and where we go in 'Environmental Parasitology'', **Parasites & Vectors**, Vol 10(1), pp. 65.

30. Thoen E., O. Evensen and I. Skaar (2011) 'Pathogenicity of *Saprolegnia* spp. to Atlantic salmon, *Salmo salar* L., eggs', **Journal of Fish Diseases**, Vol 34(8), pp. 601-608.

31. Torto-Alalibo T., M. Tian, K. Gajendran, M.E. Waugh, P. van West and S. Kamoun (2005) 'Expressed sequence tags from the oomycete fish pathogen *Saprolegnia parasitica* reveal putative virulence factors', **BioMed Central Microbiology**, Vol 5, pp. 46.

32. Van Den Berg A.H., D. McLaggan, J. Dieguez-Uribeondo and P. van West (2013) 'The impact of the water moulds *Saprolegnia diclina* and *Saprolegnia parasitica* on natural ecosystems and the aquaculture industry', **Fungal Biology Reviews**, Vol 27(9), pp. 33-42.

33. Van West P. (2006) '*Saprolegnia parasitica*, an oomycete pathogen with a fishy appetite: New challenges for an old problem', **Mycologist**, Vol 20(3), pp. 99-104.

34. Wicker E., M. Hulle, F. Rouxel (2001) 'Pathogenic characteristics of isolates of *Aphanomyces eusteiches* from pea in France', **Plant Pathology,** Vol 50(4), pp. 433-442.

35. Willoughby L.G. (1994) 'Fungi and fish diseases', **Pisces Press**.

PHYSIOLOGICAL RESPONSE OF BARLEY AND BARNYARD GRASS TO INTERACTIVE EFFECT OF HEAT WAVE AND DROUGHT

A. Dikšaitytė*, G. Juozapaitienė, G. Kacienė, I. Januškaitienė, D. Miškelytė, and J. Žaltauskaitė

Department of Environmental Sciences, Faculty of Natural Sciences, University of Vytautas Magnus, Vileikos str. 8, LT-44404 Kaunas, Lithuania

*Corresponding author: Austra.Diksaityte@vdu.lt

Abstract
The short-term effect of +10 °C heat wave (HW) treatment both as single stressor (in well-watered plants, HWW) and simultaneously with drought (HWD) was tested in growth chambers under control environment using pot grown plants of barley (*Hordeum vulgare* L., var. 'Aura DS') and weed barnyard grass (*Echinochloa crus-galli* L.) that exhibit C_3 and C_4 pathways, accordingly. During the 3-day long HW period, both plants grown under well-watered soil conditions showed significantly increased transpiration rate (*E*) and decreased water use efficiency (WUE). Significant changes of photosynthetic rate (P_r) were detected only for barley plants. On the last day of HW treatment, P_r in well-watered barley plants decreased by 13.8% ($p < 0.05$), compared to the control (CTR) ones. When the HW was imposed simultaneously with drought, at the end of the treatment, before plants were re-watered, *E* and WUE in barley plants were in totally different manner than under the single stressor of HW – by 76.6% ($p < 0.05$) decreased and by 13.0% ($p < 0.05$) increased, accordingly. By contrast, in barnyard grass, under HWD treatment, *E* and WUE were in the same manner as under HWW treatment – by 18.4% ($p < 0.05$) increased and by 19.5% ($p < 0.05$) decreased, accordingly. P_r in HWD-treated barley plants at the end of the treatment was considerably lower by 73.5% ($p < 0.05$) and did not returned to the CTR one's value after one-day recovery. While, in barnyard grass P_r was only 6.3% ($p < 0.05$) reduced, but it fully returned to the CTR one's value after one-day recovery. Therefore, contrary to barley, physiological indices of C_4 weed barnyard grass responded more positive than negative to HWW treatment and demonstrated considerably higher tolerance to drought under high air temperature conditions.

Keywords: heat wave, drought, barley, barnyard grass, photosynthesis, transpiration, water use efficiency

1. INTRODUCTION

Extreme climatic events such as heat waves and drought periods are predicted to increase in frequency and severity in many regions under future climate scenarios (IPCC 2014; Mittal et al., 2014), and in the natural environment these two abiotic stresses often occur simultaneously. In the last century, Europe's climate has become more extreme than previously thought (Della Marta et al., 2007; Toreti et al., 2013) with increasing summer temperature variability (Jones et al., 2008). It has been stated that extreme events occurring during the summer period would have the most dramatic impact on plant productivity (De Boeck et al., 2011). The European summer heat wave and drought with July temperatures up to 6 °C above average and annual precipitation 50 % below average in 2003

demonstrated the profound impact that extreme events may have (Fink et al., 2004). The 2003 European summer heat wave was followed in 2010 by an even more intense and widespread summer heat wave, which scorched enormous areas across Eastern Europe (Barriopedro et al., 2011), including western Russia, Belarus, Estonia, Latvia, and Lithuania (Dole et al., 2011).

Acute heat and drought are perhaps the two most major abiotic stresses for plant vegetation worldwide, and the combination of these stresses causes many physiological changes that affect different plants and crop growth and functioning (Fahad et al., 2017; Sita et al., 2017). Physiological responses of plants to drought stress are complex and vary with plant species and the degree or time of the exposure to drought (Bodner et al., 2015). Moreover, plants respond differently to multiple stresses from how they do to individual stress (Atkinson and Urwin, 2012). The evidence shown that the response of plants to combinations of two or more stress conditions is different from that of single treatment and cannot be directly extrapolated from the response of plants to each of the different stresses applied individually, as the responses to the combined stresses are largely controlled by different, and sometimes opposing, signaling pathways that may interact and inhibit each other (Suzuki et al., 2014). Recent studies that examined plant responses to heat and drought have revealed that when combined with drought stress, heat waves exacerbated the negative effect of drought stress (Dreesen et al., 2012; Rollins et al., 2013; Duan et al., 2017), but the effects caused by the combination of heat and drought were not simply the sum of single heat and drought effects, whereas were mostly larger than the sum of single stresses (De Boeck et al., 2011; Ruehr et al., 2016).

In this study, there were used gas-exchange parameters to compare photosynthetic performance in one of the most important crop, *Hordeum vulagre* (barley, C_3), and one of the most noxious weeds in modern agriculture, *Echinochloa crus-galli* (barnyard grass, C_4), during and after the heat wave both as single stressor and simultaneously with drought, and after one-day recovery, based on the physiological characteristics of these species. Three following specific hypotheses were addressed: (1) HW imposed alone will have a considerably less pronounced negative effect on the C_4 weed than the C_3 crop; (2) drought imposed simultaneously with HW will exacerbate the negative impact of HW with more severe effect for the C_3 crop; (3) post-stress rate of photosynthesis and other gas exchange parameters of C_4 weed after one-day regeneration under control conditions will recover to a larger extent to the control level than the C_3 crop.

2. MATERIALS AND METHODS

2.1 Plant material and growth conditions

Barley (*Hordeum vulgare* L. cv. 'Aura DS') and weed barnyard grass (*Echinochloa crus-galli* L.) seeds were sown in plastic pots (3 l capasity; 10.6 cm diameter) filled with a mixture of field top-soil (taken from Aleksandras Stulginskis University training farm, Kaunas district), perlite and fine sand (5:3:2, by volume) under the monoculture conditions (15 plants per pot). Plants were grown in closed plant growth chamber with volume of 10 m^3 (Vytautas Magnus university, Lithuania) under control environment with a day length of 14 h with lights on at 8:00 h and lights off at 22:00 h, a day/night ambient air temperature of vegetation period of 21/14 °C, ambient CO_2 concentration of 400 μmol mol^{-1}, relative air humidity (RH) of 50±5% during the day and 70±5% at night. A light level of ~270 μmol m^{-2} s^{-1} photosynthetically active radiation (PAR) was provided by a combination of ten natural day-light luminescent lamps (Philips, Waterproof OPK Natural Daylight LF80 Wattage 2×58 W/TL-D 58 W) and one high-pressure sodium lamp (Philips MASTER GreenPower CG T 600 W). Twice during the experiment, plants were fertilized with the complex nutrient (NPK 12-11-18 + microelements) solution to the final N level of 150 kg ha^{-1}. Volumetric soil water content (SWC) was kept at 30% using a Theta Probe ML2x sensor combined with a hand-set HH_2 moisture meter with a depth of 6 cm (Delta-T Devices Ltd., Cambridge, UK). Control (CTR) plants were kept under the conditions mentioned above throughout the experiment.

2.2 Treatments and experimental design

The treatments were imposed when both plants reached the 14 growth stage (Zadoks et al., 1974), i.e. after full expansion of the third true leaf. Half of the seedlings in the CTR growth chamber were randomly assigned to 3 day-long heat wave (HW) treatment and were transferred into HW growth chamber (i.e. 31 ºC for 6.5 h per day and 21 ºC night temperature cycle and an ambient CO_2 of 400 μmol mol^{-1}). The temperature in the heated growth chamber was increased gradually every day from 21 to 31 °C between 9:00-11:00 h, holding the temperature of 31 °C until 17.30 h, and then was gradually decreased from 17:30-19:30 h to 25 °C that was maintained till 22:00 h until the period of night began, when it decreased to 21 °C and was maintained overnight. After 3 day-long HW treatment, at the 4th experimental day plants were moved back to the CTR growth chamber for one-day recovery. In this case, plants in HW were subjected to a 3 day-long of +10 ºC HW treatment for 6.5 h per day. Besides, half of the seedlings in HW treatment were also treated under drought stress (HWD), i.e. were left without additional watering until they were rehydrated to the CTR plants level of 30% SWC at the 4th experimental day (about 15:00 h). Well-watered pots in the HW treatments (HWW), as well as CTR plants, were weighed (in the morning between 11:30 h and 12:00 h) each day to determine gravitational water loss and to maintain target SWC of 30%. Pots within the same growth chamber were rotated every day in order to minimize potential effects of growth chamber on plant performance.

2.3 Leaf gas exchange measurements

Photosynthetic rate (P_r; μmol CO_2 m^{-2} s^{-1}), stomatal conductance (g_s; mol H_2O m^{-2} s^{-1}) and transpiration rate (E; mmol H_2O m^{-2} s^{-1}) were measured with a portable closed infrared gas analyzer LI-COR 6400 (LI-COR, Inc., Lincoln, NE, USA), equipped with a 6 cm^2 leaf chamber. The youngest fully expanded leaves were fixed in the leaf cuvette, and the measurements were recorded 15 min every 10 s when P_r and g_s reached steady state levels. The gas exchange measurements were made at least on one plant of each pot in CTR, HWW and HWD treatments at 10:00 h and 15:00 h, during the 3 day-long HW treatment, after HW and after one-day recovery of HWW and HWD plants in the CTR chamber under unstressed ambient climate conditions. During the measurements, the CO_2 level in the leaf cuvette was set at the same CO_2 level as the plants were growing at (i.e. 400 μmol mol^{-1} CO_2), and a bloc temperature was set according to the plants growing conditions (either 21 or 31 ºC). Air flow rate through the assimilation chamber was maintained at 500 μmol s^{-1}, PAR outside the leaf chamber was 225±1.3 μmol m^{-2} s^{-1}. The air humidity (RH) and vapor pressure deficit (VPD) inside the leaf cuvette were allowed to vary with ambient climate conditions outdoor. During the measurements, RH and VPD in the control plants were, respectively, 23±0.7% and 1.8±0.0 kPa, and 19±1.1% and 3.2±0.1 kPa in the heat-stressed plants (all mean ± SE). Water use efficiency (WUE; μmol CO_2 $mmol^{-1}$ H_2O) was calculated as the ratio of P_r to E. All results were collected from lit leaves of intact plants.

2.4 Statistical analysis

Data shown are mean ± standard error (SE). Statistical analysis was performed using Fisher's Least Significant Difference (LSD) tests ($P < 0.05$) with *STATISTICA 8*. Different lowercase letters in the figure indicated significant difference among treatments within each day.

3. RESULTS AND DISCUSSION

3.1 Effect of heat and drought on photosynthetic rate

Imposed single +10 °C heat wave (HW) treatment decreased photosynthetic rate (P_r) in well-watered (HWW) barley plants by 8.3% ($p < 0.05$) and 13.8% ($p < 0.05$) on the 2th and the 3th days of HW treatment, respectively. However, it returned to the control (CTR) value on day 4, when the HW was released, and did not change from the CTR one's after one-day recovery. No changes of P_r were

found in HWW-treated barnyard grass, moreover, it tended to be even a little bit higher for the entire experimental period (Fig. 1 A and F). It is not very unexpected, as barnyard grass (*Echinochloa crus-galli*) is a weed of warm regions that requires high temperatures for dry matter production and growth (Maun and Bennett, 1986). When the HW was imposed simultaneously with drought (HWD), P_r in barley declined sharply with significant changes from the 2th day and the most pronounced reduction on day 4, before plants were re-watered, when P_r in HWD-treated barley was lower by 73.5% ($p < 0.05$), as compared to the CTR ones. After one-day regeneration under CTR conditions, P_r in HWD-treated barley recovered to a large extent to the CTR one's value, however, was still significant lower (-4.0%, $p < 0.05$). By contrast, P_r in HWD-treated barnyard grass decreased significantly by 6.3% only on day 4, i.e. when the treatment progressed (Fig. 1 A and F). These results reflect that, under the combined impact of HW and drought, the crucial negative factor for both plant P_r was drought, but not heat, what is consistent with the previous studies (Ruehr et al., 2016; Duan et al., 2017). However, barnyard grass showed considerably higher photosynthetic tolerance to drought than did it barley plants, what is also not surprised for the C_4 type plant. Because of these characteristics (being a C_4 weed), barnyard grass has a strong potential for competing with C_3 crops under such extreme climatic events as a periods of heat wave simultaneously with water shortage, that are predicted to increase in frequency and severity in many regions under future climate scenarios (IPCC 2014; Mittal et al., 2014). The evidence already shown that *E. crus-galli* becomes more competitive than agricultural crops and can cause significant yield losses under the conditions of future climate (Awan et al., 2016).

3.2 Effect of heat and drought on stomatal conductance, transpiration and WUE

For the entire experimental period, stomatal conductance (g_s) in HWW-treated barley plants did not differ from the CTR ones, while it tended to decrease and was significantly lower by 23.8% and 11.0% on day 4 and after one-day recovery, respectively, in well-watered barnyard grass (Fig. 1 B and G). Contrary to HWW treatment, g_s in HWD-treated barley decreased sharply from the beginning with the significant changes from the 2th day and the most pronounced reduction of g_s by 83.9% ($p < 0.05$) on day 4, as in the case of P_r. After one-day regeneration under CTR conditions, full recovery of g_s in HWD-treated barley was not observed − it was 20.6% ($p < 0.05$) lower than in the CTR ones. The exacerbated effect of drought on g_s, under HWD treatment, was also found in barnyard grass, as it was also significant lower from the 2th day with the most pronounced reduction by 39.0% ($p < 0.05$) on day 4 and did not returned to CTR value (-12.7%, $p < 0.05$) after one-day recovery (Fig. 1 B and G). It is known that stomatal closures are more closely related to the soil moisture content than leaf water status, and it is mainly controlled by chemical signals such as abscisic acid produced in dehydrating roots (Lisar et al., 2012). Therefore, the results show that g_s of both plants responded more to drought induced stress than to heat, but the changes were considerably higher in barley.

Transpiration rate (*E*), under well-watered soil conditions, during all the HW treatment, was significantly higher by about 80% and 65% in barley and barnyard grass, accordingly, until it got back to the CTR level after the release of HW on day 4 and did not differ from the CTR ones after one-day recovery (Fig. 1 C and H). Contrary to HWW treatment, *E* in HWD-treated barley decreased significantly by 42.0% and 76.6% on the 3th and the 4th days, respectively, as the treatment prolonged (Fig. 1 C). It is shown that heat and drought imposed simultaneously might influence signals that control gas exchange (Prasch and Sonnewald, 2013) that can cause antagonistic responses of plants (Mittler and Blumwald, 2010). For example, during the heat stress, plants can increase transpiration rate to evaporatively reduce their leaf temperature, in order, to avoid overheat and prevent deleterious damages induced by heat stress (Ameye et al., 2012). However, when plants are subjected to heat and drought simultaneously, they often reduce transpiration rate, avoiding unnecessary water loss, at the cost of evaporative cooling, what in turn leads to increased leaf temperature (Barnabas et al., 2008; Ruehr et al., 2016) and the damages on photosynthesis (Duursma et al., 2014; Ruehr et al., 2016), which is thought to be among the most thermosensitive aspects of plant function (Wang et al., 2008). Therefore, the obtained results show that, in the response to the combined impact of HW and drought,

barley plants preferred to reduce their stomata aperture to avoid water loss through transpiration, perhaps at the cost of leaf cooling, once more implying that drought had considerably more negative effect on their leaf physiology than did it HW. These results are consistent with other evidence that water availability has a dominant role in determining plant physiological responses (Carmo-Silva et al., 2012; Ruehr et al., 2016; Duan et al., 2017). However, after one-day regeneration under CTR conditions, *E* in HWD-treated barley fully recovered to the CTR value (Fig. 1 C). In contrast to barley, on the 3^{th} and the 4^{th} days, *E* in HWD-treated barnyard grass was still higher by 25.7% ($p < 0.05$) and 18.3% ($p < 0.05$), respectively, compared to the CTR ones, but also did not differ significantly after one-day recovery (Fig. 1 H). This finding indicates that, under the same conditions with high air temperature and simultaneously the absence of adequate water supply, barley plants, as it was expected to C_3 species, were more susceptible to drought than the C_4 weed barnyard grass, which, with the significant higher *E* under the prolonged HWD treatment, still preferred to employ transpiration cooling to cope with heat instead of reducing transpiration, in order, to save water under drought conditions, even on day 4, when the HW was already released.

During the 3-day long HW treatment, water use efficiency (WUE) in well-watered barley and barnyard grass plants was reduced by 52.7% ($p < 0.05$) and 61.6% ($p < 0.05$) on average, respectively. It returned to the CTR one's level on day 4, after the HW was released, and did not differ after one-day recovery (Fig. 1 D and I). Under the heat wave conditions simultaneously with water shortage, i.e. on the 2^{th} and the 3^{th} days of HWD treatment, WUE in both plants was reduced to a considerably lower extent that under HWW treatment, although was still significantly lower (by 24.4% and 21.9% on average, in barley and barnyard grass, respectively), compared to the CTR ones. However, on day 4, when HW was released, but plants were still not re-watered, WUE in HWD-treated barley increased significantly by 13.0%, compared to the CTR ones. By contrast, in barnyard grass it was continuously lower by 19.5% ($p < 0.05$), already suggesting that barley plants suffered substantially more from drought than did it barnyard grass. Nevertheless, both plants WUE did not differ from CTR ones after one-day recovery (Fig. 1 D and I).

3.3 Effect of heat and drought on intercellular CO_2 concentration

The intercellular CO_2 concentration (C_i) in HWW-treated barley plants did not differ from CTR ones for the entire experimental period. By contrast, it was significantly lower by 12.3% on average on the 3^{th} and the 4^{th} days of treatment in barnyard grass and did not return to the CTR one's value (-6.0%, $p < 0.05$) after one day recovery (Fig. 1 E and J), but it had any influence on P_r (Fig. 1 F). In contrast to HWW treatment, C_i in HWD-treated barley was significantly reduced by 19.6% on average from the 2^{th} day of the treatment. After one-day regeneration under CTR conditions, full recovery of C_i in HWD-treated barley was not achieved (-7.4%, $p < 0.05$) (Fig. 1 E). These results indicate that considerable reduction of P_r in HWD-treated barley to a large extent could be attributed to stomatal closures and consequent reduced intercellular CO_2 concentration. The same assumption was made by Duan et al. (2017), who found that under high soil water availability, despite the initial sharp rise in leaf stomatal conductance and transpiration at the onset of the heat wave, photosynthesis declined gradually in parallel with stomatal conductance as heat wave progressed, maintaining a relatively low leaf level water use efficiency. The exacerbated effect of drought on C_i, under HWD treatment, was also found in barnyard grass, as on the 3^{th} and the 4^{th} days of the treatment it reduced significant more (by about 10%) than under HWW treatment (Fig. 1 J). This also could by in part related to the decrease of P_r in barnyard grass on day 4 under HWD treatment (Fig. 1 F). After one-day recovery, C_i in HWD-treated barnyard grass was also still lower by 6.6% ($p < 0.05$), compared to the CTR ones (Fig. 1 E and J), but it had no influence on photosynthesis.

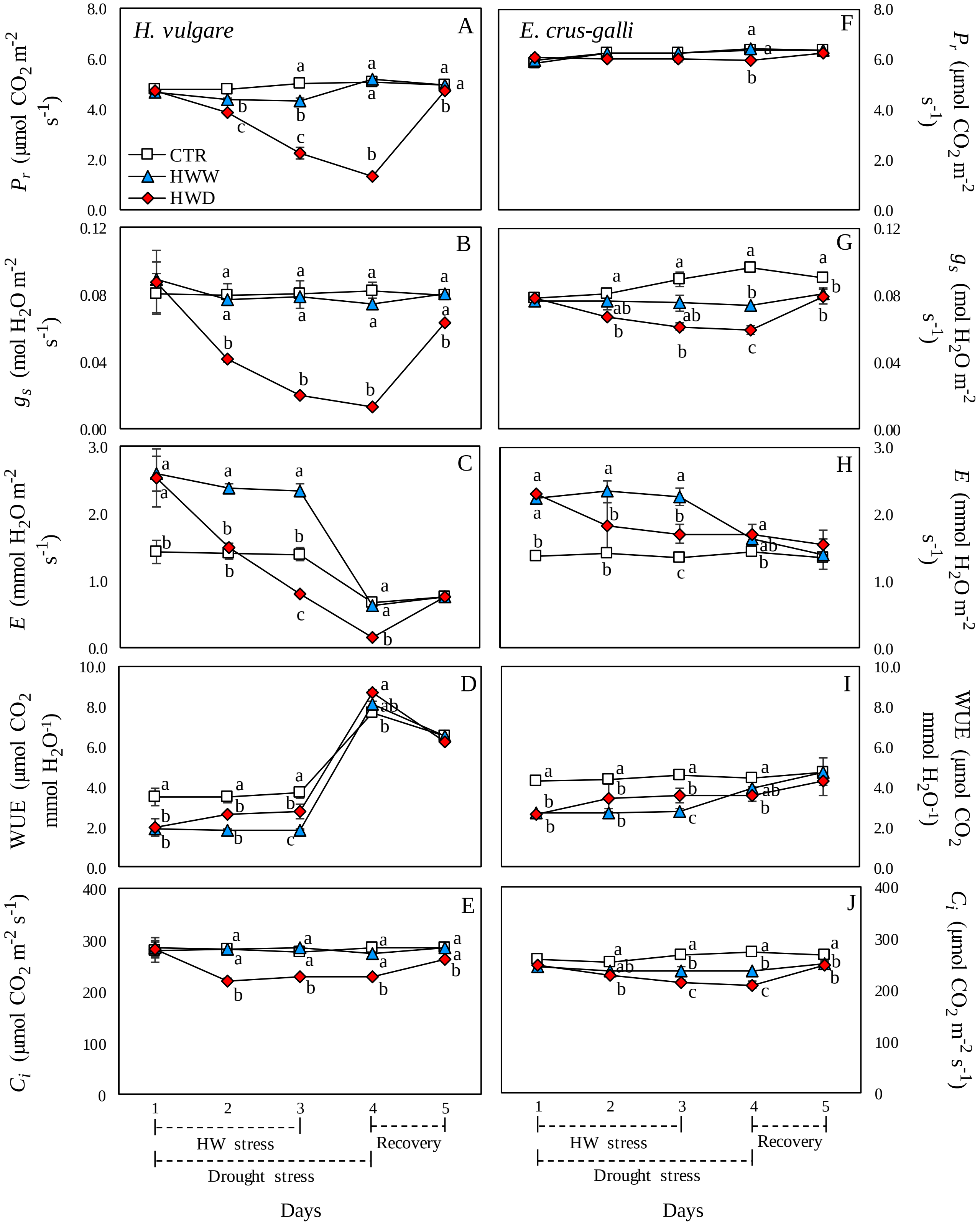


Figure 1. The changes of photosynthetic rate (P_r), stomatal conductance (g_s), transpiration rate (E), water use efficiency (WUE), and intercellular CO_2 concentration (C_i) in *Hordeum vulgare* (barley) (A, B, C, D, E, accordingly) and *Echinochloa crus-galli* (barnyard grass) (F, G, H, I, J, accordingly) during the 3 day-long HW stress (days 1-3), both as single stressor (HWW) and simultaneously with drought (HWD), after the HW (day 4), and after one-day recovery (day 5), compared to the control (CTR) plants. Values are means ± SE for at least three independent replicates. Different lowercase letters indicate significant difference (P < 0.05) among treatments within each day as determined by Fisher LSD test

4. CONCLUSIONS

This study showed a predominant role of soil water availability for barley seedlings even during the short-term heat wave period, as simultaneously impact of HW and water shortage caused far stronger physiological changes in their leaves than the single HW treatment. When the heat stress was accompanied by water stress caused by simultaneously imposed drought, the reductions of P_r, C_i and, especially, g_s in HWD-treated barley were significantly larger, compared to the HWW treatment, with incomplete recovery after one day-long regeneration period under the control one's conditions. By contrast, P_r in HWW-treated barnyard grass tended to be even a little bit higher, and together with the other gas exchange parameters demonstrated considerably higher tolerance to interactive effect of HW and drought with fully or a better recovery to the CTR one's value. Summarizing all the obtained results, it can be concluded that barley, as the C_3 type crop, suffered substantially more from combined impact of HW and drought, while barnyard grass was far less susceptible to HWD treatment. Therefore, being a C_4 type weed, barnyard grass has a strong potential for competing with C_3 crops under such extreme climatic events that are predicted to increase in frequency and severity in many regions under future climate scenarios.

Acknowledgments
This research was funded by the European Social Fund under the No 09.3.3-LMT-K-712 "Development of Competences of Scientists, other Researchers and Students through Practical Research Activities" measure.

References

1. Ameye M., T.M. Wertin, I. Bauweraerts, M.A. McGuire, R.O. Teskey and K. Steppe (2012) 'The effect of induced heat waves on *Pinus taeda* and *Quercus rubra* seedlings in ambient and elevated CO_2 atmospheres', **New Phytologist**, 196, pp. 448-461.
2. Atkinson N.J. and P.E. Urwin (2012) 'The interaction of plant biotic and abiotic stresses: from genes to the field', **Journal of Experimental Botany**, 63, pp. 3523-3543.
3. Awan T.H. and B.S. Chauhan (2016) 'Effect of emergence time, inter- and intra-specific competition on growth and fecundity of Echinochloa crus-galli in dry-seeded rice', **Crop Protection**, 87, pp. 98-107.
4. Barnabas B., K. Jager and A. Feher (2008) 'The effect of drought and heat stress on reproductive processes in cereals', **Plant Cell and Environment**, 31, pp. 11-38. doi: 10.1111/j.1365-3040.2007.01727.x.
5. Barriopedro D., E.M. Fischer, J. Luterbacher, R.M. Trigo and R. García-Herrera (2011) 'The hot summer of 2010: redrawing the temperature record map of Europe', **Science**, 332, pp. 220-224.
6. Bodner G., Nakhforoosh A. and Kaul H.-P. (2015) 'Management of crop water under drought: a review', **Agronomy for Sustainable Development**, 35, pp. 401-442. doi:10.1007/s13593-015-0283-4.
7. Carmo-Silva A.E., M.A. Gore, P. Andrade-Sanchez, A.N. French, D.J. Hunsaker and M.E. Salvucci (2012) 'Decreased CO_2 availability and inactivation of Rubisco limit photosynthesis in cotton plants under heat and drought stress in the field', **Environmental and Experimental Botany**, 83, pp. 1-11.
8. De Boeck H.J., F.E. Dreesen, I.A. Janssens and I. Nijs (2011) 'Whole-system responses of experimental plant communities to climate extremes imposed in different seasons', **New Phytologist**, 189, pp. 806-817.
9. Della-Marta P.M., M.R. Haylock, .J. Luterbacher and H. Wanner (2007) 'Doubled length of western European summer heat waves since 1880', **Journal of Geophysical Research**, 112, pp. 103-113.

10. Dole R., M. Hoerling, J. Perlwitz, J. Eischeid, P. Pegion, T. Zhang, X.-W. Quan, T. Xu and D. Murray (2011) 'Was there a basis for anticipating the 2010 Russian heat wave?' **Geophysical Research Letters**, 38. L06702, doi:10.1029/2010GL046582.
11. Dreesen P.E., H.J. De Boeck, I.A. Janssens and I. Nijs (2012) 'Summer heat and drought extremes trigger unexpected changes in productivity of a temperate annual/biannual plant community', **Environmental and Experimental Botany**, 79, pp. 21-30.
12. Duan H., J. Wu, G. Huang, Sh. Zhou, W. Liu, Y. Liao, X. Yang, Z. Xiao and H. Fan (2017) 'Individual and interactive effects of drought and heat on leaf physiology of seedlings in an economically important crop', **AoB PLANTS**, 9, plw090; 10.1093/aobpla/plw090.
13. Duursma R.A., C.V. Barton, Y.S. Lin, B.E. Medlyn, D. Eamus, D.T. Tissue, D.S. Ellsworth and R.E. McMurtrie (2014) 'The peaked response of transpiration rate to vapour pressure deficit in field conditions can be explained by the temperature optimum of photosynthesis', **Agricultural and Forest Meteorology**, 189, pp. 2-10.
14. Fahad S., A.A. Bajwa, U. Nazir, S.A. Anjum, A. Farooq, A. Zohaib, S. Sadia, W. Nasim, S. Adkins, S. Saud, M.Z. Ihsan, H. Alharby, C. Wu, D. Wang and J. Huang (2017) 'Crop Production under Drought and Heat Stress: Plant Responses and Management Options', **Frontiers in Plant Science**, 8, pp. 1147. doi: 10.3389/fpls.2017.01147.
15. Fink, A.H., T. Brücher, A. Krüger, G.C. Leckebusch, J.G. Pinto and U. Ulbrich (2004) 'The 2003 European summer heat waves and drought – synoptic diagnosis and impacts', **Weather**, 59, pp. 208-216.
16. IPCC (2014) 'Summary for Policymakers' In: *Climate Change 2014: Mitigation of Climate Change. Contribution of Working Group III to the Fifth Assessment Report of the Intergovernmental Panel on Climate Change*. Edenhofer O., Pichs-Madruga R., Sokona Y., Farahani E., Kadner S., Seyboth K., Adler A., Baum I., Brunner S., Eickemeier P., Kriemann B., Savolainen J., Schlömer S., von Stechow C., Zwickel T., Minx J. C. (ed.). Cambridge University Press, Cambridge, United Kingdom and New York, NY, USA, pp. 1-30.
17. Jones G.S., P.A. Stott and N. Christidis (2008) 'Human contribution to rapidly increasing frequency of very warm Northern Hemisphere summers', **Journal of Geophysical Research**, 113, D02109, doi:10.1029/2007JD008914.
18. Lisar S.Y.S., R. Motafakkerazad, M.M. Hossain and I.M.M. Rahman (2012) 'Water stress in plants: causes, effects and responses', **Water Stress**, I.M.M. Rahman (ed.), ISBN: 978-953-307-963-9, InTech, Available from: http://www.intechopen.com/books/water-stress/water-stress-inplants-causes-effects-and-responses.
19. Maun M.A. and S.C.H. Bennett (1986) 'The biology of Canadian weeds. 77. Echinochloa crus-galli (L.) Beauv', **Canadian Journal of Plant Science**, 66, pp. 739-759. doi:10.4141/cjps86-093.
20. Mittal N., A. Mishra, R.Singh and P. Kumar (2014) 'Assessing future changes in seasonal climatic extremes in the Ganges river basin using an ensemble of regional climate models', **Climate Change**, 123, pp. 273–286. doi:10.1007/s10584-014- 1056-9.
21. Mittler R. and E. Blumwald (2010) 'Genetic engineering for modern agriculture: challenges and perspectives', **Annual Review of Plant Biology**, 61, pp. 443-462.
22. Prasch C.M. and U. Sonnewald (2013) 'Simultaneous application of heat, drought, and virus to Arabidopsis plants reveals significant shifts in signaling networks', **Plant Physiology**, 162, pp. 1849-1866.
23. Rollins J.A., E. Habte, S.E. Templer, T. Colby, J. Schmidt and M. von Korff (2013) 'Leaf proteome alterations in the context of physiological and morphological responses to drought and heat stress in barley (*Hordeum vulgare* L.)', **Journal of Experimental Botany**, 64(11), pp. 3201-3212.

24. Ruehr N.K., A. Gast, C. Weber, B. Daub and A. Arneth (2016) ‘Water availability as dominant control of heat stress responses in two contrasting tree species’, **Tree Physiology**, 36, pp. 164-178.

25. Sita K., A. Sehgal, B. HanumanthaRao, R.M. Nair, P.V. Vara Prasad, S. Kumar, P.M. Gaur, M. Farooq, K.H.M. Siddique, R.K. Varshney and H. Nayyar (2017) ‘Food Legumes and Rising Temperatures: Effects, Adaptive Functional Mechanisms Specific to Reproductive Growth Stage and Strategies to Improve Heat Tolerance’, **Frontiers in Plant Science**, 8, pp. 1658. doi: 10.3389/fpls.2017.01658.

26. Suzuki N., R.M. Rivero, V. Shulaev, E. Blumwald and R. Mittler (2014) ‘Abiotic and biotic stress combinations’, **New Phytologist**, 203, pp. 32-43. doi: 10.1111/nph.1279.

27. Toreti A., P. Naveau, M. Zampieri, A. Schindler, E. Scoccimarro, E. Xoplaki et al. (2013) ‘Projections of global changes in precipitation extremes from Coupled Model Intercomparison Project Phase 5 models’, **Geophysical Research Letters**, 40, pp. 4887-4892.

28. Wang D., S.A. Heckathorn, D. Barua, P. Joshi, E.W. Hamilton and J. J. Lacroix (2008) ‘Effects of elevated CO_2 on the tolerance of photosynthesis to acute heat stress in C-3, C-4, and CAM species’, **American Journal of Botany**, 95, pp. 165-176. doi: 10.3732/ajb.95.2.165.

29. Zadoks J.C., T.T. Chang and C.F. Konzak (1974) ‘A decimal code for the growth stages of cereals’, **Weed Research**, 14, pp. 415-421.

SOIL CARBON ACCUMULATION IN BARNYARD GRASS UNDER ELEVATED CO_2 AND SHORT-TERM HEAT WAVES AND DROUGHTS CONDITIONS

Dikšaitytė and G. Juozapaitienė*

Faculty of Natural sciences, Department of Environmental sciences,Vytautas Magnus University
Vileikos 8, Kaunas, LT-44404, Lithuania

[*] Corresponding authors: e-mail: gintare.juozapaitiene@stud.vdu.lt

Abstract
Climate change will increase the frequency of heat waves and droughts. In order of this, such extreme weather events are predicted to impact the terrestrial carbon balance. The aim of this research is to analyze the effect of heat wave as single stressor (in well-watered plants, HWW) and simultaneously with drought (HWD) to soil carbon accumulation in barnyard grass (*Echinochloa crus - galli* L.) soil. For this purpose, plants were grown in a closed growth chambers under conditions of 21°C/400 ppm and 25°C/800 ppm. 3 days long heat waves (21°C/400 ppm vs. 31°C/400 ppm and 25°C/800 ppm vs. 35°C/800 ppm) were applied – single and in combination with drought (i.e. fully and not watered during the heat wave period). The results showed that under drought conditions both heat waves (21°C/400 ppm vs. 31°C/400 ppm and 25°C/800 ppm vs. 35°C/800 ppm) significantly decreased carbon accumulation in barnyard grass soil. Under fully watered conditions only heat wave of 21°C/400 ppm vs. 31°C/400 ppm significantly decreased carbon accumulation in soil. Also, it was estimated, that the heat wave of 25°C/800 ppm vs. 35°C/800 ppm decreased carbon accumulation in soil less than the heat wave of 21°C/400 ppm vs. 31°C/400 ppm. These findings may indicate that elevated CO_2 could mitigate the effects of heat waves and droughts on soil carbon accumulation.

Keywords: heat wave; drought; carbon; soil; barnyard grass

1. INTRODUCTION

Climate change and increasing concentrations of atmospheric greenhouse gases, not only lead to gradual mean global warming but may also change the frequency, the severity and even the nature of extreme events (IPCC, 2013). As a consequence of climate change, the incidence and severity of heatwaves and droughts have substantially increased since the middle of the 20th century (Stocker et al., 2013). Droughts often occur accompanied by severe heatwaves, which together generate combined effects on carbon cycles (Yuan et al., 2016). A synthesis of the direct and indirect impacts of climate extremes on the carbon cycle and the underlying mechanisms is still lacking (Frank, 2015). In a recent broad perspective, Reichstein et al. (2013) highlighted the possibility that climate extremes and their impacts on the global carbon cycle may lead to an amplification of positive climate–carbon cycle feedbacks. Rising atmospheric carbon dioxide (CO2) concentrations are likely to affect several important aspects of grasslands, such as the quantity and quality of the herbage produced, plant species composition, soil fertility and the potential to sequester carbon (C) in the soil, to mitigate the rise in atmospheric CO_2 concentrations (Soussana and Luscher, 2007). Accumulation of C in grassland ecosystems occurs mostly below-ground and changes in soil organic C stocks may result both in land-use changes (e.g. conversion of arable land to grassland) and in grassland management (Soussana et al., 2004). Although C4 plants represent only a small portion of the world´s plant species, accounting for only 3 % of the vascular plants, they contribute about 20% to the global

primary productivity because of highly productive C4 grass-lands (Ehleringer et al., 1997). The conservation of grassland C stocks and the role of grasslands as C sinks will become increasingly difficult to preserve in an altered climate with a high temporal variability and under high atmospheric CO_2 concentrations which may saturate the C sink in soils (Soussana and Luscher, 2007). Despite these difficulties the aim of this research is to analyze the effect of heat wave as single stressor (in well-watered plants, HWW) and simultaneously with drought (HWD) to soil carbon accumulation in barnyard grass (*Echinochloa crus - galli* L.) soil.

2. MATERIAL AND METHODS

The experiment was conducted in a controlled environment chambers located at Vytautas Magnus University. Seeds of weed barnyard grass (*Echinochloa crus-galli* L.) (15 seeds per pot) were planted in 3 L plastic pots containing a growth substrate composed of a mixture of field soil (Luvisols - the soil was taken from ASU Training Farm, Kaunas District), perlite and fine sand (5:3:2, by volume). Plants were grown under control environment with a day length of 14 h, a day/night ambient air temperature of 21/14 °C or elevated of 25/18 °C and ambient CO_2 concentration of 400 μmol mol^{-1} or elevated of 800 μmol mol^{-1}, and relative air humidity (RH) of 50±5% during the day and 70±5% at night. A light level of ~270 μmol m^{-2} s^{-1} photosynthetically active radiation (PAR) was provided by a combination of ten natural day-light luminescent lamps (Philips, Waterproof OPK Natural Daylight LF80 Wattage 2×58 W/TL-D 58 W) and one high-pressure sodium lamp (Philips MASTER GreenPower CG T 600 W). A nutrient supply corresponding to 120 kg N ha^{-1} was used until the beginning of treatment. Additional fertilization with a complex nutrient (NPK 12-11-18 + microelements) solution, increasing the N level until 180 kg N ha^{-1}, was applied one day before the treatment. Volumetric soil water content (SWC) was kept at 30% using a Theta Probe ML2x sensor combined with a hand-set HH_2 moisture meter with a depth of 6 cm (Delta-T Devices Ltd., Cambridge, UK). When plants expanded the third true leaf (BBCH 14 (Meier, 2001)), half of the pots were randomly assigned to 3 day-long heat wave (HW) treatment (i.e. 31 ºC for 6.5 h per day and 21 ºC night temperature cycle and an ambient CO_2 of 400 μmol mol^{-1} and 35 ºC for 6.5 h per day and 25 ºC night temperature cycle and an elevated CO_2 of 800 μmol mol^{-1}). All treatments were run in three replicates. 6.5 h heat cycle was chosen for the purpose to represent natural environment conditions. The temperature in the heated growth chambers was increased gradually every day from 21 to 31 °C and from 25 to 35 °C. Besides, half of the pots in HW treatment were also treated under drought stress - plants were left without additional watering. Well-watered pots in the HW treatments, as well as control plants, were weighed each day to determine gravitational water loss and to maintain target SWC of 30%.

After 3 day-long HW treatment soil samples were taken. The samples were air dried at room temperature and sieved through 2 mm mesh on purpose to remove all visible roots and plant remains. The dried samples of soil were ground to a fine powder with a mill (Retsch HM400, Germany). Organic carbon content was measured with a Shimadzu TOC-V solid sample module SSM-5000A in the laboratory of Vytautas Magnus University. Statistical analyses were carried out using STATISTICA 8 software. Mean values of soil carbon and their standard errors (±SE) were calculated. Mann-Whitney U-test was used to estimate the differences in each parameter. The overall effects of soil carbon and modified climate conditions and their interactions were determined by one-way ANOVA. Spearman's correlation coefficient between watered-drought conditions and soil carbon accumulation was calculated, and the significance of the correlation was tested by the Spearman's test.

3. RESULTS AND DISCUSSION

Changes in climate or altered frequency of extreme events can trigger nonlinear changes in C balance, as new processes become important (Chapin et al., 2009). The results showed that heat wave (21°C/400 ppm vs. 31°C/400 ppm) - single and in combination with drought - significantly decreased carbon accumulation in barnyard grass soil (Figure 1). Under watered heat wave conditions soil

carbon decreased by 9.2% ($p<0.05$). Drought conditions had more negative effect on carbon accumulation in soil. Under heat wave (21°C/400 ppm vs. 31°C/400 ppm) in combination with drought soil carbon decreased by 12.4% ($p<0.05$). According to other authors (Ciais et al., 2005; Saleska et al., 2003), under drier conditions, there are predictions of increased sequestration by suppression of respiration and of net loss of carbon through decreased productivity.

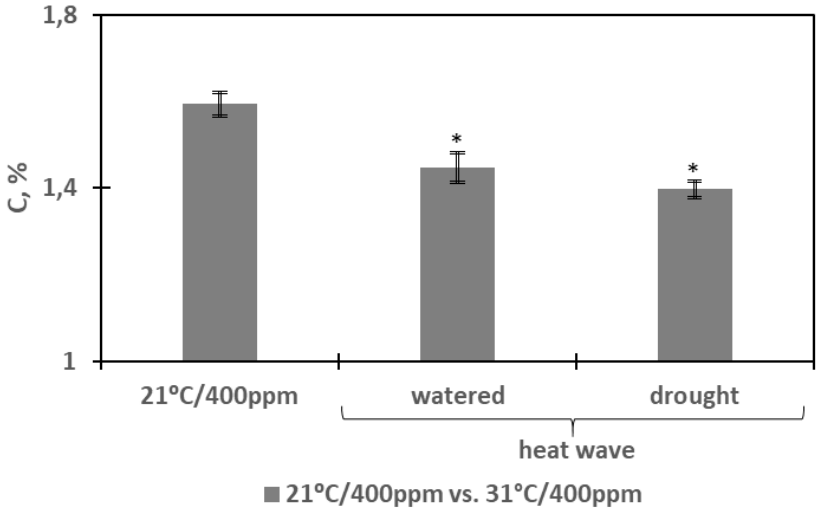


Figure 1. Responses of soil C to heat wave and drought (21°C/400 ppm vs. 31°C/400 ppm) (mean ± SE). Watered: Volumetric soil water content – 30 %, drought: no water irrigation. * - statistically significant difference between 21°C/400 ppm and heat wave of 31°C/400 ppm applied single and in combination with drought at p<0.05.

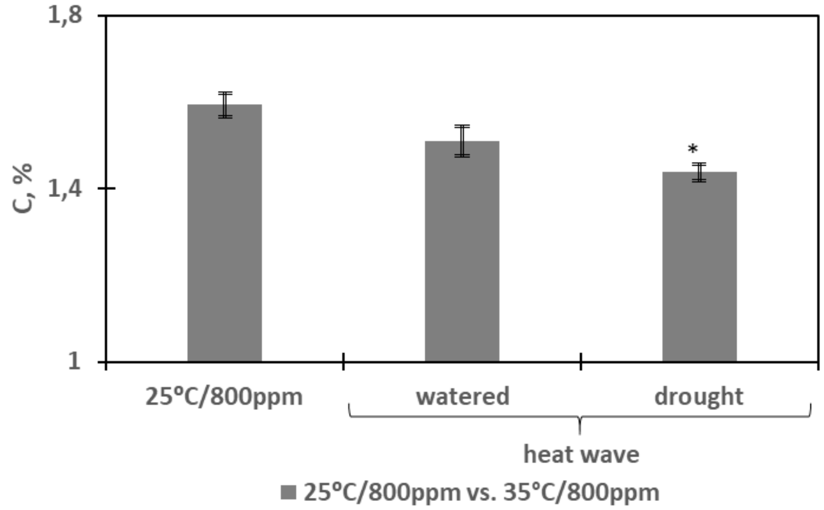


Figure 2. Responses of soil C to heat wave and drought (25°C/800 ppm vs. 35°C/800 ppm) (mean ± SE). Watered: Volumetric soil water content – 30 %, drought: no water irrigation. * - statistically significant difference between 25°C/800 ppm and heat wave of 35°C/800 ppm applied single and in combination with drought at p<0.05.

The heat wave (25°C/800 ppm vs. 35°C/800 ppm) - single and in combination with drought – also decreased carbon accumulation in barnyard grass soil, but the change was not significant under watered conditions (-5.2%, $p>0.05$) (Figure 2). Also, drought conditions had more negative effect on carbon accumulation in soil than watered conditions. Under heat wave (25°C/800 ppm vs. 35°C/800 ppm) in combination with drought soil carbon decreased by 9.7% ($p<0.05$). According to Arnone et al., (2008) one year after an anomalously warm season, soil heterotrophic respiration was enhanced in a grassland, offsetting net ecosystem carbon uptake. The increase in C storage in the particulate soil organic matter with atmospheric CO_2 concentration was found to be non-linear and declining at

above ambient CO_2 concentrations in another research, which may indicate that the soil C sink in grasslands will become saturated in a high atmospheric CO_2 concentration world (Gill et al., 2002). Still, according to some authors (Loiseau and Soussana, 1999a; Gill et al., 2002) due to the large variability in soil C content, significant differences in total soil organic-C content are very hard to detect in individual studies and are usually not significant.

ANOVA analysis showed that modified climate conditions (heat waves (21°C/400 ppm vs. 31°C/400 ppm and 25°C/800 ppm vs. 35°C/800 ppm) – single and in combination with drought) as factor significantly changed soil carbon accumulation in the soil of barnyard grass ($p<0.05$). Also, it was estimated, that there was a significant correlation between watered-drought conditions and soil carbon accumulation. Under drought conditions soil carbon decreased more than under watered conditions ($R=-0.6$, $p<0.05$).

Also, it was estimated, that the heat wave of 25°C/800 ppm vs. 35°C/800 ppm decreased carbon accumulation in soil less than the heat wave of 21°C/400 ppm vs. 31°C/400 ppm. The reason of this may be elevated CO_2 under 25°C/800 ppm vs. 35°C/800 ppm heat wave condition. Recent experimental research confirms that carbon storage in soil organic matter pools is often increased under elevated CO_2, at least in the short term (Allard et al., 2005) and under the predicted near future climate, elevated CO_2 could mitigate the effects of extreme droughts and heat waves on ecosystem net carbon uptake (Roy et al., 2016).

4. CONCLUSIONS

- Under drought conditions both heat waves (21°C/400 ppm vs. 31°C/400 ppm and 25°C/800 ppm vs. 35°C/800 ppm) significantly decreased carbon accumulation in barnyard grass soil.
- The heat wave of 25°C/800 ppm vs. 35°C/800 ppm decreased carbon accumulation in soil less than the heat wave of 21°C/400 ppm vs. 31°C/400 ppm.
- Elevated CO_2 could mitigate the effects of heat waves and droughts on soil carbon accumulation.

Acknowledgments.

This research was funded by the European Social Fund under the No 09.3.3-LMTK-712 “Development of Competences of Scientists, other Researchers and Students through Practical Research Activities” measure.

References

1. Allard V., P. C. D. Newton, L. M. Soussana, R. A. Carran and C. Matthew (2005) **‘**Increased quantity and quality of coarse soil organic matter fraction at elevated CO_2 in a grazed grassland are a consequence of enhanced root growth rate and turnover**’, Plant Soil**, Vol 276, pp. 49–60.
2. Arnone J. A., S. J. Paul, V. D. W. Johnson, J. D. Larsen, R. L. Jasoni, A. J. Lucchesi, C. M. Batts, C. Nagy, W. G. Coulombe, D. E. Schorran, P. E. Buck, B. H. Braswell, J. S. Coleman, R. A. Sherry, L. L. Wallace, Y. Luo and D. S. Schimel (2008) **‘**Prolonged suppression of ecosystem carbon dioxide uptake after an anomalously warm year**’**, **Nature**, Vol 455, pp. 383-386.
3. Chapin F. S. III, J. McFarland, A. D. McGuire, E. S. Euskirchen, R. W. Ruess and K. Kielland (2009) ‘The changing global carbon cycle: linking plant–soil carbon dynamics to global consequences**’**, Vol 97 (5), pp. 840–850.
4. Ciais P., *et al.* (2005) **‘***Europe-wide reduction in primary productivity caused by the heat and drought in 2003***’**, **Nature,** Vol 437, pp. 529–533.
5. Ehleringer J.R., T.E. Cerling and B.R. Helliker (1997) **‘**C4 photosynthesis, atmospheric CO_2 and climate**’**, **Oecologia**, Vol 112, pp. 285-299.
6. Frank D., M. Reichstein , M. Bahn, K. Thonicke, D. Frank, M. D. Mahecha, P. Smith, M. Van Der Velde, S. Vicca, F. Babst, C. Beer, N. Buchmann, J. G. Canadell, P. Ciais, W. Cramer, A.

Ibrom, F. Miglietta, B. Poulter, A. Rammig, S. I . Seneviratne, A. Walz, M. Wattenbach, M. A. Zavala and J. Zscheischler (2015) **'**Effects of climate extremes on the terrestrial carbon cycle: concepts, processes and potential future impacts**'**, **Global Change Biology**, Vol 21, p.2861–2880.

7. Gill R.A., H.W. Polley, H.B. Johnson, L.J. Anderson, H. Maherali and R.B. Jackson (2002) 'Non-linear grassland responses to past and future atmospheric CO_2', **Nature**, Vol 417, pp. 279–282.
8. IPCC (2013) **'**Summary for policymakers. In: Climate Change 2013: The Physical Science Basis**'**. Contribution of Working Group I to the Fifth Assessment Report of the Intergovernmental Panel on Climate Change (eds Stocker TF, Qin D, Plattner G-K, Tignor M, Allen SK, Boschung J, Nauels A, Xia Y, Bex V, Midgley PM), pp. 3–29. **Cambridge University Press**, Cambridge, UK and New York, NY, USA.
9. Loiseau P. and J-F Soussana. (1999) 'Elevated CO_2, temperature increase and nitrogen supply effects on below-ground carbon accumulation in a temperate grassland ecosystem', **Plant and Soil**, Vol 212, pp. 123–134.
10. Meier, U., editor. (2001) 'Growth stages of mono-and dicotyledonous plant's. BBCH monogr. Federal Biological Research Center for Agriculture and Forests, Berlin-Braunschweig, Germany.
11. Reichstein M., M. Bahn, P. Ciais et al. (2013) **'**Climate extremes and the carbon cycle**'**, **Nature**, Vol 500, pp. 287–295.
12. Roya J., C. Picon-Cochardb, A. Augusti, M. Benot, L. Thiery, O. Darsonville, D. Landais, C. Piel, M. Defossez, S. Devidal, C. Escape, O. Ravel, N. Fromin, F. Volaire, A. Milcu, M. Bahn and J. Soussan (2016) **'**Elevated CO_2 maintains grassland net carbon uptake under a future heat and drought extreme**' National Academy of Sciences**.
13. Saleska, S. R. et al. (2003) **'***Carbon in Amazon forests: unexpected seasonal fluxes and disturbance-induced losses***'**, **Science**, Vol 302, pp. 1554–1557.
14. Soussana J-F. and A. Luscher (2007) 'Temperate grasslands and global atmospheric change: a review', **Grass and Forage Science**, Vol 62, pp. 127–134.
15. Soussana J-F., P. Loiseau, N. Vuichard, E. Ceschia, J. Balesdent, T. Chevallier and D. Arrouays (2004) 'Carbon cycling and sequestration opportunities in temperate grasslands', **Soil Use and Management**, Vol 20, pp. 219–230.
16. Stocker T. F. et al. (2013) **'***Technical Summary Climate Change 2013: The Physical Science Basis***'** Contribution of Working Group I to the Fifth Assessment Report of the Intergovernmental Panel on Climate Change ed T.F. Stocker et al. (Cambridge: Cambridge University Press), pp. 33116.
17. Yuan W., W. Cai, Y. Chen, S. Liu, W. Dong, H. Zhang, G. Yu, Z. Chen, H. He, W. Guo, D. Liu, S. Liu, W. Xiang, Z. Xie, Z. Zhao and G. Zhou (2016) **'**Severe summer heatwave and drought strongly reduced carbon uptake in Southern China**', Scientific Reports**, 6.

SHORT-TERM EFFECTS OF ELEVATED AIR TEMPERATURE AND ATMOSPHERIC CO_2 ON BELOW-GROUND CARBON ACCUMULATION IN *HORDEUM VULGARE* AND *PISUM SATIVUM*

G. Juozapaitienė[1*], A. Dikšaitytė[1], J. Aleinikovienė[2]

[1]Department of Environmental Sciences, Faculty of Natural Sciences, Vytautas Magnus University, Vileikos St. 8, Kaunas, Lithuania;

[2] Agroecosystems and soil institute, Aleksandras Stulginskis University, Studentų St. 11, Kaunas district, Lithuania.

*Corresponding author: e-mail: gintare.juozapaitiene@vdu.lt

Abstract

Global changes such as elevated atmospheric CO_2 and air temperature are altering the input rates of carbon to plants and soil. In order to study organic carbon ($C_{org.}$) accumulation in the below-ground and to investigate if there is a dependency between photosynthetic rate and below-ground processes of different crop species under increasing levels of air temperature and atmospheric CO_2, a closed growth chamber experiment was performed with spring barley (*Hordeum vulgare* L.) and pea (*Pisum sativum* L.) in a controlled environment at ambient [21 °C/400 ppm] and elevated [25 °C/800 ppm] temperature and CO_2 conditions. The results showed that after 4 weeks of treatment under elevated air temperature and atmospheric CO_2 conditions barley and pea has accumulated organic carbon in roots and soil by different trends. While organic carbon increased ($p>0.05$) in roots and soil of pea, it decreased ($p>0.05$) in roots and soil of barley under conditions of [25 °C/800 ppm], compared to that under conditions of [21 °C/400 ppm]. Contrary, microbial biomass carbon increased in soil of both plant species - microbial biomass carbon increased by 55% ($p<0.05$) in barley soil and by 40% ($p<0.05$) in pea soil under conditions of [25 °C/800 ppm]. Our results also suggested that there was no significant correlation between photosynthetic rate and below-ground processes.

Keywords: below-ground carbon; closed chamber experiment; spring barley; pea

1. INTRODUCTION

Increase in atmospheric CO_2 concentrations and the rise in temperature will have extreme effects on terrestrial plant growth and productivity in the near future. Carbon dioxide (CO_2) concentration has increased since the pre-industrial period from 280 to 401.62 ppm currently (NOAA, 2016). It is expected that this value could increase to an atmospheric concentration of between 750 and 1300 ppm for the end of the century (IPCC, 2014). Also, emissions of greenhouse gases caused by human activities have augmented 70% from 1970 to 2004. If greenhouse gas emissions continue at high levels, temperature is predicted to increase between 1.8 and 6.0 °C (IPCC, 2014).

A doubling of the CO_2 level initially accelerates carbon fixation in C_3 plants by about 30%, yet after days to weeks of exposure to high CO_2 concentrations, depending on species, carbon fixation declines until it stabilizes at a rate that averages 12% above ambient controls (Curtis, 1996). A change of just 10% in the SOC pool would be equivalent to 30 years of anthropogenic emissions and could dramatically affect concentrations of atmospheric CO_2 (Kirschbaum, 2000). The overall increase in total soil C under elevated CO_2 suggests a potential for soil C sequestration.

While it has long been known that aboveground processes, particularly gross primary production (GPP) and plant community dynamics, strongly control belowground C and nutrient cycling, the specific roles of roots have been less clear (Pendall et al., 2008). The vital role of roots as an interface between the lithosphere and biosphere is necessary to understand plant response to elevated CO_2. Despite the important role roots play, they have been an understudied component of agricultural research since they exist underground (Madhu, Hatfield, 2013). Atmospheric CO_2 is not a factor directly connected to the rhizosphere. Any effect of atmospheric CO_2 enrichment on rhizodeposition is through plant growth, in contrast to factors such as the soil texture or the presence of microorganisms that act more directly on the release of C from roots (Nguyen, 2003). Some research suggests that root inputs to soil represent 5–33% of daily photoassimilate (Jones et al., 2009), also about 40% of photosynthates synthesized in plant parts is lost through the root system into the rhizosphere within an hour and the rate of loss is influenced by several factors, e. g. plant age, different biotic and abiotic stresses, etc. (Kumar, 2006). Also, it is investigated that increased atmospheric CO_2 stimulates photosynthesis (Dijkstra et al., 2005; Hungate et al., 2006) and the release of root exudates, which in turn means more labile carbon available for microbial decomposition and respiration (Hungate et al., 2006; Rayner et al., 2005; Friedlingstein et al., 2006; Ainsworth and Long, 2005; Heath et al., 2005). For this reason, the objective of this paper is to study organic carbon accumulation in the below-ground of different crop species and to investigate if there is a significant correlation between photosynthetic rate and below-ground processes.

2. MATERIALS AND METHODS

The experiment was conducted in a controlled environment chambers located at Vytautas Magnus University in 2017. Seeds of spring barley (*Hordeum vulgare* L. ., var. 'Aura DS') (15 seeds per pot) and pea (*Pisum sativum* L., var. 'Pinochis') (15 seeds per pot) were planted in 3 L plastic pots containing a growth substrate composed of a mixture of field soil (the soil was taken from ASU Training Farm, Kaunas District), perlite and fine sand (5:3:2, by volume). A nutrient supply corresponding to 120 kg N ha^{-1} was used until the beginning of treatment. Additional fertilization with a complex nutrient (NPK 12-11-18 + microelements) solution, increasing the N level until 180 kg N ha^{-1}, was applied one day before the treatments. Elevated atmospheric CO_2 and air temperature (day/night temperature of 25/18 °C and 800 ppm of CO_2) treatment was applied when the seedlings of barley and pea were germinated and lasted for 4 weeks. Until that time all plants were grown in the control chamber under conditions of current climate – an average day/night temperature of 21/14 °C and 400 μmol mol^{-1} of CO_2. The following stable conditions were maintained in all chambers: a photoperiod of 14 h, relative humidity (RH) of 50/60%, and 300 μmol m^{-2} s^{-1} photon flux density of photosynthetically active radiation (PAR). The pots in the chamber were watered sufficiently and regularly. All treatments were run in three replicates.

Photosynthetic rate (Pr, μmol CO_2 m^{-2} s^{-1}) was measured with portable photosynthesis system LI-6400 (LI-COR, USA) equipped with a 6 cm^2 leaf chamber with randomly selected youngest fully expanded intact leaves. Photosynthetic rate were recorded automatically for approximately 5 minutes every 3 s when Pr reached steady state level. During the measurements, leaf chamber conditions were controlled at 400 or 800 μmol mol^{-1} CO_2, and 21 or 25 ºC (bloc temperature), according to the climate treatments. Air flow rate through the assimilation chamber was maintained at 500 μmol s^{-1}. The water vapour concentration of air entering the leaf chamber was not controlled and tracked ambient conditions, relative humidity was 51±0.9 % in ambient and 39±1.6 % in elevated atmospheric CO_2 and air temperature treatment (all mean ± SE). PAR outside the leaf chamber was 226±4.0 μmol m^{-2} s^{-1} on average across all climate treatments.

Measurements of carbon accumulation were carried out at a 28-day period after the treatment. A subsample of plant roots was dried in an electric air-forced oven at 70 °C until a constant dry weight was obtained (at least 72 hours). Soil samples were also taken at a 28-day period after the treatment. The samples were air dried at room temperature and sieved through 2 mm mesh on purpose to remove

all visible roots and plant remains. The dried samples of roots and soil were ground to a fine powder with a mill (Retsch HM400, Germany). Organic carbon content was measured with a Shimadzu TOC-V solid sample module SSM-5000A in the laboratory of Vytautas Magnus University. Microbial biomass carbon was determined by chloroform fumigation direct extraction method (Beck et al., 1997).

Statistical analyses were carried out using STATISTICA 8 software. Mean values of the parameters (plant photosynthetic rate (Pr), carbon of root and soil, microbial biomass carbon) and their standard errors (±SE) were calculated. Mann-Whitney U-test was used to estimate the differences in each parameter. The overall effects of plant species and modified climate conditions and their interactions were determined by two-way ANOVA.

3. RESULTS AND DISCUSSION

Increasing levels of air temperature and atmospheric CO_2 significantly increased ($p<0.05$) barley and pea photosynthetic rate by 48% and 63% respectively under conditions of [25 °C/800 ppm] after 4 weeks of treatment compared to that of the reference treatment (Fig. 1 (A)). For photosynthetic rate, the differences between plant species and modified climate conditions were significant (1 table), but there was no significant correlation between photosynthetic rate and below-ground processes. Isotopic tracer studies have revealed a rapid and close coupling between photosynthesis and belowground C allocation to roots, soil organisms and respiratory processes in forests and grasslands (e.g. Ostle et al., 2000; Johnson et al., 2002). According to Irigoyen (2014) when the atmospheric CO_2 concentration rises suddenly (or in a temporal window up to a few days) from 400 to 700 μmol mol^{-1}, the photosynthetic C fixation of C_3 plants increases. Either an increase in photosynthesis by 25 – 75 % has been detected in many experimental studies on the impact of doubled CO_2 concentration on C3 crops (Urban, 2003; Kirschbaum, 2004).

The results showed that after 4 weeks of treatment under elevated air temperature and atmospheric CO_2 conditions barley and pea has accumulated organic carbon in roots by different trends (Fig. 1 (B)). Roots of barley under conditions of [25 °C/800 ppm] have accumulated less (-2.3%, $p > 0.05$) amount of carbon than under conditions of [21ºC/400 ppm]. Contrary, roots of pea under conditions of [25 °C/800 ppm] after 4 weeks of treatment have accumulated more organic carbon (2.1%), compared to that of the reference treatment, however, the difference was not statistically significant ($p > 0.05$). For carbon in roots, only the interaction between plant species x modified climate conditions were significant ($p<0.1$) (Table 1).

The results of carbon accumulation in plant roots are also inconsistent in other researches. For example, Uprety and Mahalaxmi (2000) have established that elevated CO_2 significantly increased the carbon content of *Brassica juncea* roots, but according to Lu et al. (2016) elevated CO_2 had no effects on the total carbon concentration of wheat root. In general, Wang et al. (2010) noted that biomass C accumulation was greater in winter than in summer crops. CO_2 stimulation of root exudation can speed rhizosphere decomposition, causing soil respiration to respond more strongly to photosynthetic rate than to soil temperature (Craine et al. 1999). Also, plants grown under elevated atmospheric CO_2 concentrations generally increase the partitioning of photosynthates to roots which increases the capacity and/or activity of below-ground C sinks (Soussana and Luscher, 2007).

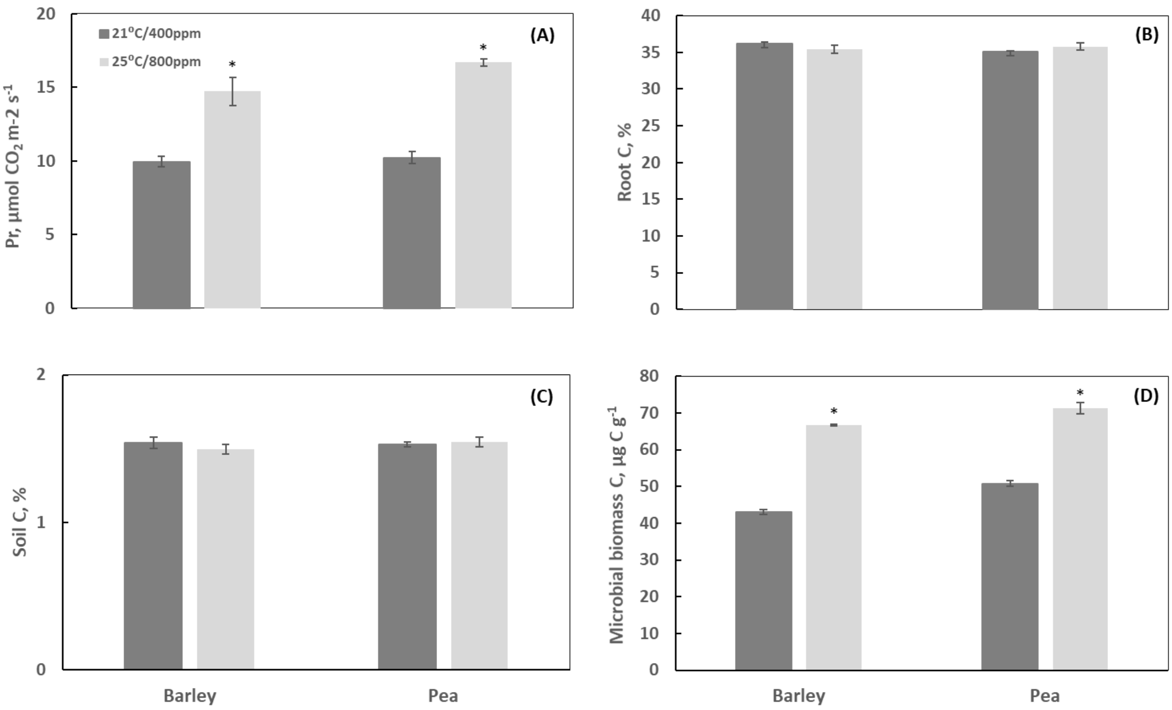


Fig. 1: Responses of photosynthetic rate (A), root C (B), soil C (C) and microbial biomass C (D) to elevated air temperature and atmospheric CO_2 conditions (mean ± SE). * - statistically significant difference between ambient (21ºC/400 ppm) and elevated CO_2 and temperature (25 °C/800 ppm) conditions at p<0.05.

Table 1: Effects (F value) among plant species, modified climate conditions and their interactive effects on photosynthetic rate (Pr), carbon in roots (Croot), carbon in soil (Csoil) and microbial biomass carbon (Cmicrobial). Significance values: * - p<0.05, ** - p<0.1.

	Pr	C_{root}	C_{soil}	$C_{microbial}$
Plant (P)	3.9**	1.04	0.35	42.3*
Modified climate conditions (C)	98.6*	0.02	0.21	543.9*
P x C	2.3	4.11**	0.86	2.85

After 4 weeks of treatment under elevated air temperature and atmospheric CO_2 conditions barley and pea has accumulated organic carbon in soil also by different trends (Fig. 1 (C)). Similarly, as in the case with roots, the amount of organic carbon in barley soil decreased up to 2.8% ($p > 0.05$) under conditions of [25 °C/800 ppm] after 4 weeks of treatment, while it almost has not changed in the soil of pea – only 0.9% ($p > 0.05$) increase under elevated air temperature and atmospheric CO_2 conditions, compared to that of ambient air temperature and atmospheric CO_2 conditions [21 °C/400 ppm]. According to De Graaff et al. (2006) only a small number of experiments reported a significant impact of elevated CO_2 on soil C sequestration, while some studies showed no differences and others found decreases in soil C.

For microbial biomass carbon, the differences between plant species and modified climate conditions were significant (1 table). Microbial biomass carbon increased by 55% (p<0.05) in barley soil and by 40% (p<0.05) in pea soil under conditions of [25 °C/800 ppm] (Fig. 1 (D)). Increasing CO_2 concentrations can lead to enhanced below-ground allocation of labile carbon through roots and root exudates, which can enhance microbial activity and foster decomposition of carbon material that has been deemed stable but was in fact not being attacked because microbes were not active (Heimann and Reichstein, 2008). Microbial activity generally increases with increasing temperature, yet, this simple relationship is confounded by many co-varying factors (Davidson and Janssens 2006), including the temperature sensitivity of different SOM fractions (Fierer et al. 2005, Fang et al. 2005),

soil moisture and aeration (Davidson and Janssens 2006), and allocation of plant C below ground (Högberg et al. 2001).

1. CONCLUSIONS

1. Organic carbon increased ($p>0.05$) in roots and soil of pea, but decreased ($p>0.05$) in roots and soil of barley under conditions of [25 °C/800 ppm], compared to that under conditions of [21 °C/400 ppm].
2. Microbial biomass carbon increased in soil of both plant species - microbial biomass carbon increased by 55% ($p<0.05$) in barley soil and by 40% ($p<0.05$) in pea soil under conditions of [25 °C/800 ppm].
3. Our results also suggested that there was no significant correlation between photosynthetic rate and below-ground processes. Although for photosynthetic rate, the differences between plant species and modified climate conditions were significant.

REFERENCES

1. Ainsworth E. A. and S. P. Long (2005) 'What have we learned from 15 years of free-air CO2 enrichment (FACE)? A meta-analytic review of the responses of photosynthesis, canopy properties and plant production to rising CO_2', **New Phytol,** Vol 165, pp. 351–372.
2. Beck T., R. G. Joergensen, E. Kandeler, F. Makeschin, E. Nuss, H. R. Oberholzer and S. Scheu (1997) 'An inter-laboratory comparison of ten different ways of measuring soil microbial biomass C', **Soil Biol. Biochem**, Vol 29 (7), pp. 1023-1032.
3. Craine J.M., D.A. Wedin and F.S. Chapin III (1999) 'Predominance of ecophysiological over environmental controls over CO_2 flux in a Minnesota grassland', **Plant and Soil**, Vol 207, pp. 77–86.
4. Curtis P. S. (1996) **'**A meta-analysis of leaf gas exchange and nitrogen in trees grown under elevated carbon dioxide**'**, **Plant Cell Environment**, Vol 19, pp. 127–137.
5. Davidson E.A. and I.A. Janssens (2006) 'Temperature sensitivity of soil carbon decomposition and feedbacks to climate change'. **Nature**, 440, 165–173.
6. De Graaff M. A., K. J. Van Groenigen, J. Six, B. Hungate and C. Van Kessel (2006) **'**Interactions between plant growth and soil nutrient cycling under elevated CO_2: a meta-analysis**'**, **Global Change Biology**, Vol 12, pp. 2077–2091.
7. Dijkstra F. A., D. Blumenthal, J. A. Morgan and D. R. LeCain (2010) **'**Elevated CO_2 effects on semi-arid grassland plants in relation to water availability and competition**'**, **Functional Ecology**, Vol 24 (5), pp. 1152–1161.
8. Fang C., P. Smith, J.B. Moncrieff and J.U. Smith (2005) 'Similar response of labile and resistant soil organic matter pools to changes in temperature', **Nature**, Vol 433, pp. 57–59.
9. Fierer N., J.M. Craine, K. McLauchlan and J.P. Schimel (2005) 'Litter quality and the temperature sensitivity of decomposition', **Ecology**, Vol 86, pp. 320–326.
10. Friedlingstein P., P. Cox, R. Betts, L. Bopp, W. von Bloh, V. Brovkin et al. (2006) 'Climate–carbon cycle feedback analysis: results from the C4MIP model intercomparison', **J Clim**, Vol 19, pp. 3337–3353.
11. Heath J., E. Ayres, M. Possell, R. D. Bardgett, H. I. Black and H. Grant et al. (2005) 'Rising atmospheric CO_2 reduces sequestration of root-derived soil carbon', **Science**, Vol 309, pp. 1711–1713.

12. Heimann M. and M. Reichstein (2008) 'Terrestrial ecosystem carbon dynamics and climate feedbacks', **Nature**, Vol 451, pp. 289–292.
13. Hogberg P.A., A. Nordgren, N. Buchmann, A.F.S. Taylor, A. Ekblad and M.N. Hogberg (2001) 'Large-scale forest girdling shows that current photosynthesis drives soil respiration', **Nature**, Vol 411, pp. 789–792.
14. Hungate B.A., E.A. Holland, R.B. Jackson, F.S. Chapin, H.A. Mooney, C.B. Field (1997) 'The fate of carbon in grasslands under carbon dioxide enrichment', **Nature**, Vol 388, pp. 576–579.
15. IPCC (2014) **'**Summary for policymakers**'** In: Climate Change 2014: Impacts, Adaptation, and Vulnerability. Part A: Global and Sectoral Aspects. Contribution of Working Group II to the Fifth Assessment Report of the Intergovernmental Panel on Climate Change. Eds. C. B. Field, V. R. Barros, D. J. Dokken, K. J. Mach,M. D. Mastrandrea, T. E. Bilir, M. Chatterjee, K. L. Ebi, Y. O.Estrada, R. C. Genova, B. Girma, E. S. Kissel, A. N. Levy, S. MacCracken,P. R. Mastrandrea,and L. L.White. Cambridge, United Kingdom:Cambridge University Press.P.1–32.
16. Irigoyena J. J., N. Goicoecheaa, M. C. Antolína, I. Pascual, M. Sánchez-Díaz, J. Aguirreoleaa and F. Morales (2014) 'Growth, photosynthetic acclimation and yield quality in legumes under climate change simulations: An updated survey', **Plant Science**, Vol 226, pp. 22–29.
17. Johnson D., J. R. Leake, N. Ostle, P. Ineson, D. J. Read (2002) 'In situ13CO2 pulse-labelling of upland grassland demonstrates a rapid pathway of carbon flux from arbuscular mycorrhizal mycelia to the soil', **New Phytologist**, Vol 153, pp. 327–334.
18. Jones D. L., C. Nguyen and R. D. Finlay (2009) **'**Carbon flow in the rhizosphere: carbon trading at the soil–root interface**'**, **Plant Soil**, Vol (321), pp. 5–33.
19. Kirschbaum M. U. F. (2000) **'**Will changes in soil organic carbon act as a positive or negative feedback on global warming?**', Biogeochemistry**, Vol (48), pp. 21–51.
20. Kumar R., S. Pandey and A. Pandey (2006) 'Plant roots and carbon sequestration', **Current Science**, Vol 91 (7), pp. 885–890.
21. Lu C., Y. Cao, C. He, X. Bao, R. Fang, Y. Wanf, X. Chen, Y. Shi and Q Li (2016) 'Effects of elevated O_3 and CO_2 on the relative contribution of carbohydrates to soil organic matter in an agricultural soil', **Soil & Tillage Research**, Vol (159), pp. 47–55.
22. Madhu M. and J. L. Hatfield (2013) 'Dynamics of plant root growth under increased atmospheric carbon dioxide**'**, **Agronomy Journal**, Vol 105, pp. 657–669.
23. Nguyen C. (2003) 'Rhizodeposition of organic C by plants: mechanisms and controls**'**, **Agronomie**, EDP Sciences, Vol 23, pp. 375–396.
24. NOAA (2016) 'Up-to-date Weekly Average CO_2 at Mauna Loa**'** http://www.esrl.noaa.gov/gmd/ccgg/trends/weekly.html
25. Ostle N., P. Ineson, D. Benham and D. Sleep (2000) 'Carbon assimilation and turnover in grassland vegetation using an in situ13CO2 pulse labelling system', **Rapid Communications in Mass Spectrometry**, Vol 14, 1345–1350.
26. Pendall E., L. Rustad and J. Schimel (2008) 'Towards a predictive understanding of belowground process responses to climate change: have we moved any closer?', **Functional Ecology**, Vol 22, pp. 937–940.
27. Rayner P. J., M. Scholze, W. Knorr, T. Kaminski, R. Giering and H. Widmann (2005) 'Two decades of terrestrial carbon fluxes from a carbon cycle data assimilation system (CCDAS)', **Global Biogeochem Cycles**, Vol 19.
28. Soussana J-F. and A. Luscher (2007) 'Temperate grasslands and global atmospheric change: a review', **Grass and Forage Science**, Vol 62, pp. 127–134.

29. Uprety D. C. and V. J. Mahalaxmi (2000) 'Effect of elevated CO_2 and nitrogen nutrition on photosynthesis growth and carbon nitrogen balance in Brassica juncea', **Agronomy & Crop Science**, Vol 184, pp. 271–276.

30. Urban O. (2003) 'Physiological impacts of elevated CO_2 concentration ranging from molecular to whole plant responses', **Photosynthetica**, Vol 41, pp. 9–20.

31. Wang Q,Y.Li and A.Alva (2010) 'Growing cover crops to improve biomass accumulation and carbon sequestration:a phytotron study',**Journal of Environmental Protection**,Vol 1,pp. 73–84.

THE USE OF MODERN TECHNOLOGIES IN RECORDING AND MONITORING OF RIPARIAN FORESTRY SPECIES IN GREECE. THE CASE OF CANKER STAIN DISEASE OF PLATANUS ORIENTALIS L.

Grigorios Varras[*1] and Georgios Efthimiou[2]

[1]Department of Agricultural Technology, Unit Floriculture & Landscape Architecture, T.E.I. of Epirus, GR- 47100 Arta, Epirus, Greece.
[2]Department of Forestry and Natural Environment Management, T.E.I of Sterea Hellada, Karpenissi, Central Greece, Greece. gefthi@yahoo.gr

[*]Corresponding author: e-mail: grvarras@gmail.com

Abstract
Modern technologies are a useful tool for recording and monitoring the ecological status of ecosystems. Riparian forests are at risk from intense human activities, pressure and diseases. The *Platanus orientalis* L. is a riparian forestry species that has, for years, withstood human pressure. However, in recent years it is in danger of extinction by *Ceratocystis fimbriata f.sp. platani*. There are records and worrying facts about the spread of the fungus, mainly in western Greece.

Modern technology constitutes a key tool and can be used as an effective way of timely recording and dealing with existing and future interference of the *Platanus* at national level. The system combines innovative basic research into Urban Forestry and urban ecosystems by developing an integrated platform for data collection and decision making to optimally manage and protect the *Platanus* by visualizing and quantifying the problem of the proliferation.

The aim of this paper is to present the electronic database DENDROLOGIO, as well as its first application in the recording of the spread of the post-chromatic ulcer of the *Platanus orientalis* L. in western Greece.

Keywords: Riparian forests, Platanus orientalis L., Dendrologio, Ceratocystis fimbriata f.sp. platani Greece

1. INTRODUCTION

Monitoring of ecological parameters for all natural ecosystems is basic key tool for their rational management and immediate action on probable problem identification. Riparian forest ecosystems, while they are most dynamic ecosystems when operating naturally and unaffected, are at risk of intense human pressures [1, 2].

The use of modern technologies is a useful tool for monitoring the ecological status of riparian forests, identifying problems and pressures (biotic and abiotic), recording the extent of their degradation from human activities or possible disease outbreaks. A serious disease which is threatening to extinction riparian forests of plane tree is the pathogenic fungus *Ceratocystis fimbriata f.sp.platani* which creates the canker stain disease of the plane tree (a new destructive disease) and leads to the total kill of trees or groups of plane trees in rivers and streams of Greek territory [3]. Riparian forests of *Platanus* (habitats 92CO) are protected.

The *Ceratocystis fimbriata f.sp. platani* fungus is considered to be an indigenous species of North America and in the 1930s and 1940s it has taken great proportions in the states of the eastern coast of the USA [4]. In Europe, it was introduced during the Second World War when war material was transferred to plane wood boxes. The first European records of the fungus are made in Italy and France. At first it had observed in Greece in 2003 in Messenia prefecture (southwestern Peloponnese) in natural stands of the oriental plane as well as in ornamental plantings [4, 5]. In 2005 it is already recorded in the prefectures of Arkadia and Ilia [6], in 2010 it is first identified in Epirus [7], while in 2014 it is located in Thessaly [8]. The transmission and spread of the disease is becoming through broken branches and trunks of affected trees transported from river water, with logging remnants which are transported miles away with cars, loggers and pruning tools, if disinfection is not properly disposed of in the outbreak.

Here is coming the decisive role of modern technology to be the management tool for the recording of infected plane trees in order to capture the spread on the map and to take decisive measures to quarantine areas to slow down or even prevent the spread of the destructive fungus in nearby healthy plane forests.

The organization of a sustainable and viable management of canker stain of the plane tree and the pilot application, are expected to provide a good practice for protection against necrosis of the plane trees, caused by the fungus *Ceratocystis fimbriata f.sp. platani* [9]. The pathogen only infects species of the plane tree and completely kills the atoms of the eastern plane tree (*Platanus orientalis*). It is the most destructive disease of the plane tree internationally and since it spreads mainly through contaminated tools, cross border cooperation is essential for the effective management of the disease.

The deterioration of the natural environment will affect the natural as well as the cultural elements of Epirus which are associated with the tradition and history of the plane tree. The phenomena of extensive necrosis are expected to reduce the spread of the disease drastically and directly by creating incentives for protection through awareness campaigns. Similarly, the scientific monitoring/ management/ avoidance of these adverse effects by developing an innovative geographical monitoring system with specialized recording and monitoring methodology, will lead to the upgrade of services for immediate intervention and minimization of the pathogen transmission and spread of the disease. The combination of the above is expected to constitute solutions concerning the sustainability assurance of natural resources, the modernization of the two countries' management with the EU requirements.

2. COMMON PROBLEMS

Common problem is the simultaneous necrosis of thousands of plane trees (*Platanus orientalis*) due to the appearance of the pathogenic and destructive fungus *Ceratocystis fimbriata f.sp. platani*, whose spread is likely to be caused by human activities in the extended plane tree forests of the crossborder region, including the use of contaminated tools and road construction machinery that played an important role in spreading the fungus.

During the last two decades, the transnational cooperation that has taken place in the construction of road projects on the Greek-Albanian border, made it possible for the fungus to be easily transferred from one country to another with tools and road construction machinery, given that the pathogen was first identified in Epirus, in the Region of Ioannina and specifically in the Tiria River area, in a recreational area near the construction site of Egnatia Odos [10], while in Albania it was observed in the Region of Argirokastro, mainly along the highway. The spread of the pathogen is also caused by the transfer of infected wood, used as firewood. The economic crisis played an important role in this task, which has prompted many rural residents as well as urban inhabitants of the two regions, to use firewood for heating, often derived from smuggled logging [7]. In each infestation source, the pathogen is also spread underground from infested trees to adjacent healthy ones by the contact and anastomosis of their roots [11].

This type of disease spread is very common in natural ecosystems of the plane tree along rivers and streams, where trees grow next to each other with their root system in contact. In rivers and streams, the fungus is spread downstream by logs and branches of infested dead trees, which are broken and transferred by the watercourse. Therefore, the spread of the disease from one country to another is given. In June 2014, symptoms and extensive mortality of plane trees was observed in various locations of the prefecture Gjirokastra in southern Albania. It should be recalled that in 2010, the presence of the infestation was reported in Epirus, which is very close to the border with Albania.

Given that plane tree are species of rapid growth not only with great importance in the natural ecosystem, but also from an environmental, economic, social and aesthetic aspect (retention of floods, protection from torrent phenomena and damages due to water overflow, protection of arable riparian land from erosion, protection of riparian settlements and structures such as bridges, warehouses, barn facilities, irrigation networks, dams, fish-farming etc. outstanding beauty in the landscape, landscaping squares and recreational areas of forests). At the same time *Platanus* is creating exceptional environments (on the banks of river basins) and for health and recreation reasons (it is the place where outdoor activities are performed, such as rafting, kayak etc.). It constitutes a priority habitat for conservation in the European Union, since the species occurs only in the southern Balkans in such an extent, forming riparian forests, which in turn make a habitat for various species, such us chickadees, flycatchers, nuthatches, woodpeckers, etc., whose nests are in holes which created by native debranching of the species, which is something that does not happen so often in other types of trees. Plan tree has great historical and social significance since it is inextricably linked to popular tradition, monuments, squares of mountain settlements, thus becoming the most favorites and important species of local communities.

2.1 The importance of the plane tree role in the economies of the Regions

A common feature of both Regions is the significance of the plane tree in areas with tourism (e.g. Ioannina Lake, mountainous settlements, river ecosystems of international repute such as Voidomatis River etc.). Maintaining biodiversity of riparian ecosystems are comparative advantages of the regions that include them**,** and make up their identity, and are the basis for the development and promotion of the country's image, which is an element for tourist development recovery, with respect to the resources on the basis of which it is intended. The protection, conservation and enhancement of the aesthetic landscape are a concern and right of local communities, on the basis of which their identity is constructed. The change from necrosis of the plane trees brings about a deterioration of the historical continuity of the landscape that is now a major political priority, which emerges not only at regional and national level but also (primarily) locally. These elements concerning the pop culture, tradition and natural landscape are today the competitive advantage of local communities for many parts of the world, the pillar of maintaining their identity and their historical character as well as the pillar of the development policies for the utilization of this local resource, in terms of sustainability. The economy of culture and creation is a matter to be studied today in the international economics, while in many regions (both developed and emerging) it is located in the heart of the development of a growth strategy [12, 13].

2.2 Determining the size of the infestation

The approach of the proposal seeks a solution to the phenomenon of the spread of *Ceratocystis fimbriata f.sp. platani*, through an innovative online GIS log open system of infested trees, as well as new recordings, for digital mapping of affected trees, with two quarantine zones under the existing Greek legislation, one within 100 m. (focal strike zone) and another one within 1000 m. (safety-quarantine zone). The maps are automatically posted on an Internet platform, which is combined with an offline field logger, that can be directly utilized for planning, prioritization and implementation of combat measures each year, for monitoring the rate of the pathogen spread, for evaluating the effectiveness of the mitigation measures in previous years with pilot implementation of solutions and for searching response methods and coordinating activities between the two countries. Since the increase in the number of dead plane trees will harm the local economy, we seek in combination, to

implement ways of improving decision-making methods for disease control areas, optimizing the effect by monitoring the progress and evolution of the disease after taking the appropriate measures, monitoring its natural spread rate for scripting the spread with the creation and implementation in practice, of innovative recording tools, monitoring and raising public awareness and services and methods of avoiding proliferation. An innovative approach of the proposal is the achievement of a display system of the recorded plane trees (there will be fields that will be completed, related to the mapping of health or infestation level, for each recording point) as well as the laboratory tests for improvement of the efficiency of the measures. The course or discontinuation of the spread will be monitored (risk management).

2.3 Local population - Services - Synergies

The program benefits the local population since the plane tree is inextricably linked to their history and tradition. A detailed description and recording of historical plane trees and their importance for local communities and areas of outstanding natural beauty filled with plane trees and plane tree forests in Greece. The Forest Services will encourage those responsible for decision-making to minimize forest fires. The building capacity in environmental management supports the reduction of the spread caused by anthropogenic factors that is mainly due to random actions, oversight and lack of disaster risk knowledge. By increasing awareness, joint integrated efforts are maximized.

2.4 Development of an innovative log and recording system of infested trees

The system and especially the web platform, it has to be noted that it consists of three subsystems; 1.The subsystem (A), for storing information that basically constitutes the database of the system proposed. 2. The subsystem (B), for managing stored information, as recorded by the application. Via the subsystem (there are licensing levels), the user is given the opportunity to see the stored information, to process it and to delete it, the exact location, date of sampling, number of trees with symptoms, height and diameter, number of infested trees and possible causes of infestation, geographical coordinates etc. 3.The subsystem (B), or supervisory display subsystem of the recordings, concerning the representation of the recorded information, in text form and by positioning on a map. In subsystem (B) additional features are implemented, such as search, bulk import and export of the recorded information, as well as many other features needed, so as to meet additional requirements. In essence, it has the potential to include other data, according to specific needs (risk management). After the creation of the innovative GIS system that captures and records infested trees, training of those involved takes place as well as the provision of the appropriate hardware for the offline field logger. There is the possibility of changing the background maps (e.g. hydronomic maps, forest maps etc.) for risk management [14].

3. METHODOLOGY

The online Database Support System (DSS), incorporates 3 information sub-systems:

1. IT sub-system for the spatial registration and tree registration,
2. IT sub-system for User Interface Design,
3. IT sub-system for the online development

Some additional functions of the online DSS is the geo-tagging, data search tool and spatial analysis tool. It is an open – source and fully customizable application. For the needs of the pilot version, two (2) zones were defined for each recorded point, that is an infeced tree, the first one of 100 meters, where the risk of attack is intense and the other one of 1000 meters, which also has a risk of spreading the disease, but reduced in comparison with that of 100 meters.

In the first stage, sampling and data collection was performed in site using smart phones or tablets and then a spatial database was developed. The data collected in site were introduced into the database and within a GIS environment in Google maps and in satellite maps. Furthermore, the Main Online

DSS Structure and Info Flow is presented. The online DSS platform is created in Greek language to meet the needs of local Forest Units.

4. RESULTS

Its usage was able to disseminate authenticated information to the forest community about the health of trees in the specific FOREST UNIT that enabled the optimization of forest management with special care to the mitigation of the disease. Therefore, the georeferenced database will be used for integrated management of trees, Local sustainable development, sustainable use of natural resources and environmental protection.

4.1 Main Online DSS Structure and Info Flow

In Figure 1 is mentioned the structure and the flow information of the online DSS. In the home page the user can be informed about the online system and is also given an overview about the fungus that causes the disease of the metachromatic ulcer of the plane tree. There are, also, mentioned the symptoms of the infection of the plane trees and the spread of the disease. Moreover, responding to the disease and "FAQ" about the disease are in home page, too (Figure 2).

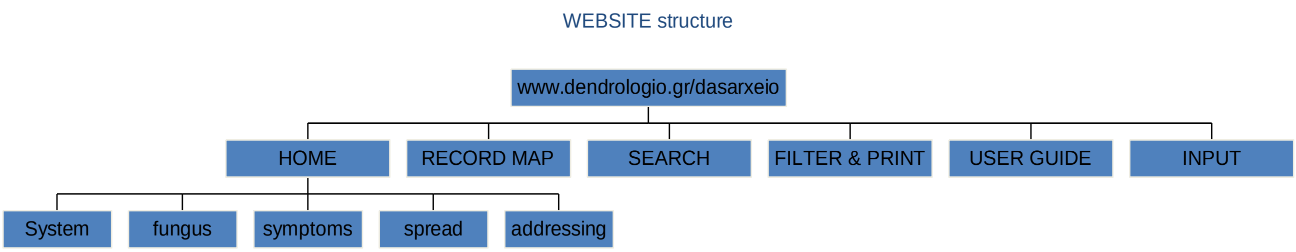


Figure 1: Main Online DSS Structure and Info Flow

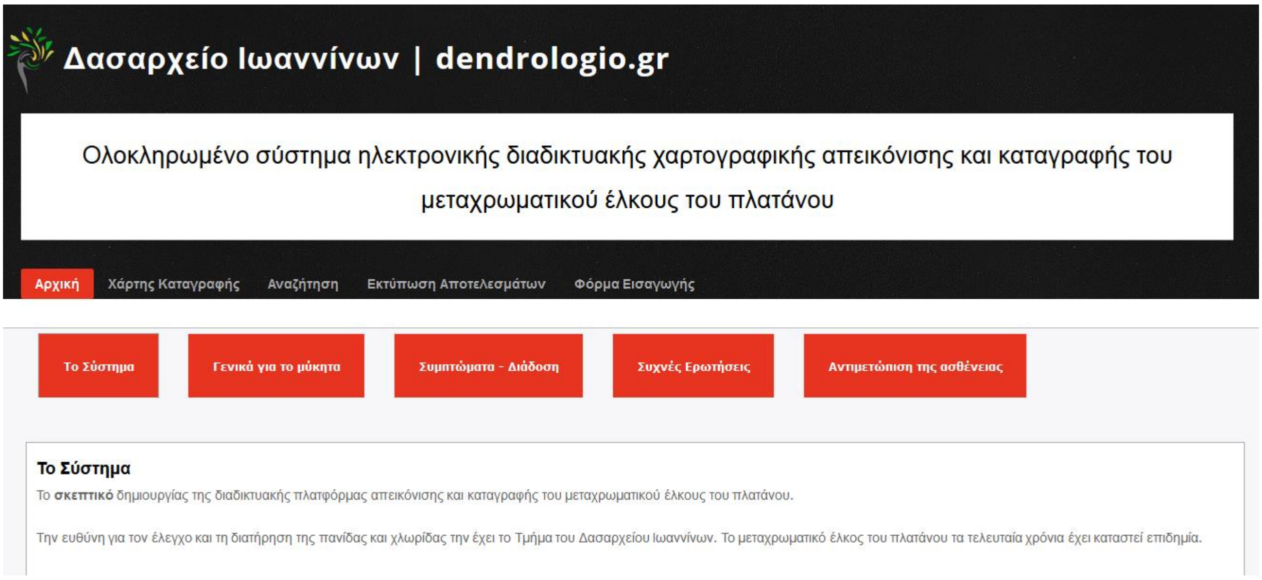


Figure 2: Homepage ain Online DSS Structure and Info Flow

4.2 Record Map

The platform incorporates a RECORD MAP, a visual database with spatial geographic location information, including data on healthy and infected trees in the Forest Unit of Ioannina, in Epirus Region in North-West Greece.

The default is GoogleMap though there is the option of viewing Bing Map, with appropriate color indication that suggests their health. Greek Cadastre maps can also be launched. The quarantine zones are illustrated within a radius of 100m and 1km-with red and yellow color respectively -of the affected plane trees so as to take the appropriate measures to prevent the spread of the disease (Figure 3).

Additional information registered for each tree appears by clicking the left mouse button on the desired tree. With info about sampling and check of the tree, Lab, location, tree type, disease type, results, date, name of employee, sampling protocol no, etc (Figure 4).

4.3 Searching

An infected plane tree of Multiple criteria or combination of them can be used for the online search, such as: Date of sampling, Name of employee, Sampling Protocol no, Type of tree. Moreover, users can even type the entire or part of the search criterion (Figure 5). This results in a view with information and map as in Figure 4.

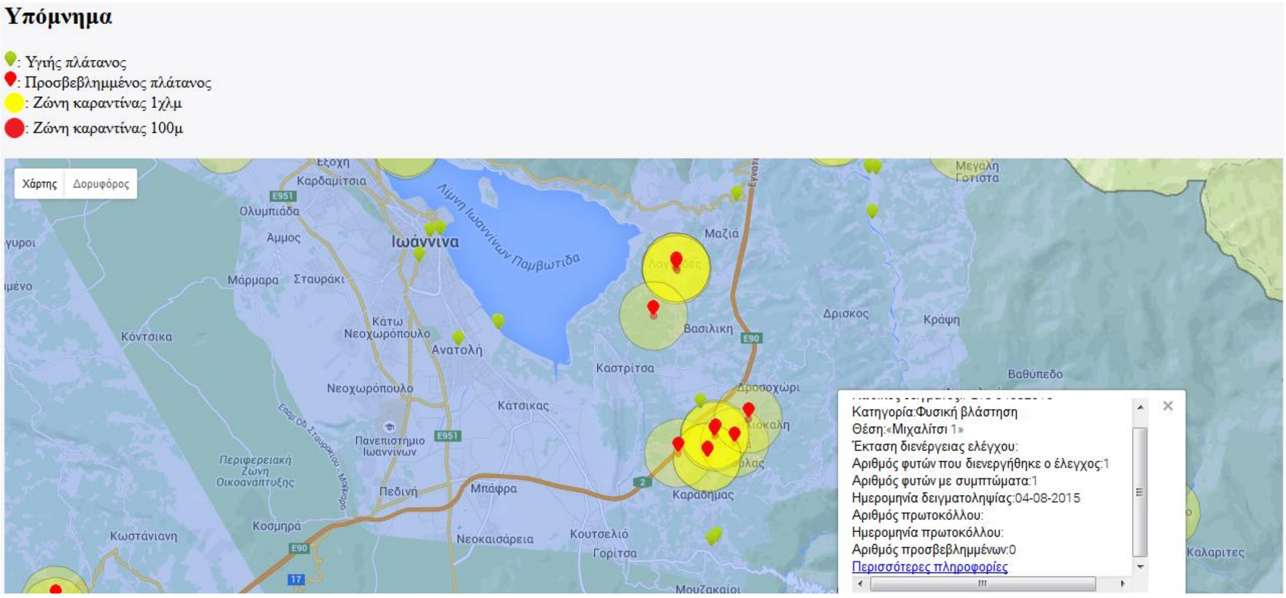


Figure 3: RECORD MAP. Here are mentioned the quarantine zones

4.4 Filtering and Printing

The user can print part of the map or the entire map while the blue dots correspond to the affected plane trees and the yellow zone around them have a radius of 1 km (Figure 6). The user can choose how to view the affected plane trees by setting a specific date (Filter Results), and adjust the brightness of the yellow zone for printing purposes (Select transparency). After that, user decides on the desired print view (e.g. launch Cadastre maps) by pressing the left mouse button on "Print Map", the map is printed on the default printer. Furthermore, the user has the opportunity to save the map in .pdf formation and download the default location. Alternatively, a snapshot of the map can be saved by print screen (PrtSckey).

4.5 Input process and Input Forms

In order to insert a new plane tree in the system, user authentication is required via a Username and Password (Figure 7).

The user fills in the form fields that are presented (Picture 8). If any or some fields remain blank, the plane tree will be accepted by the system. The sampling date is selected by default as the registration date. If the plane tree to be inserted is healthy, the value added in the field "AffectedNumber" is "0".

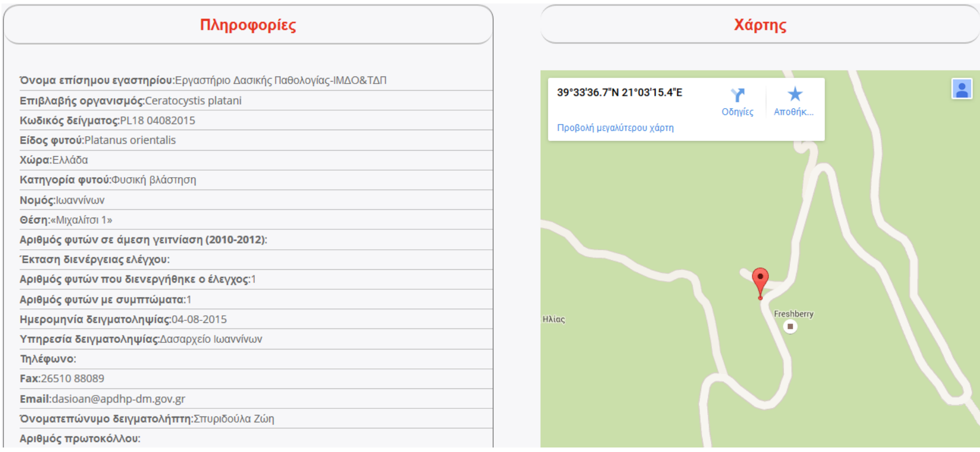


Figure 4: Tree Info window of DENDROLOGIO.gr



Figure 5: Search window

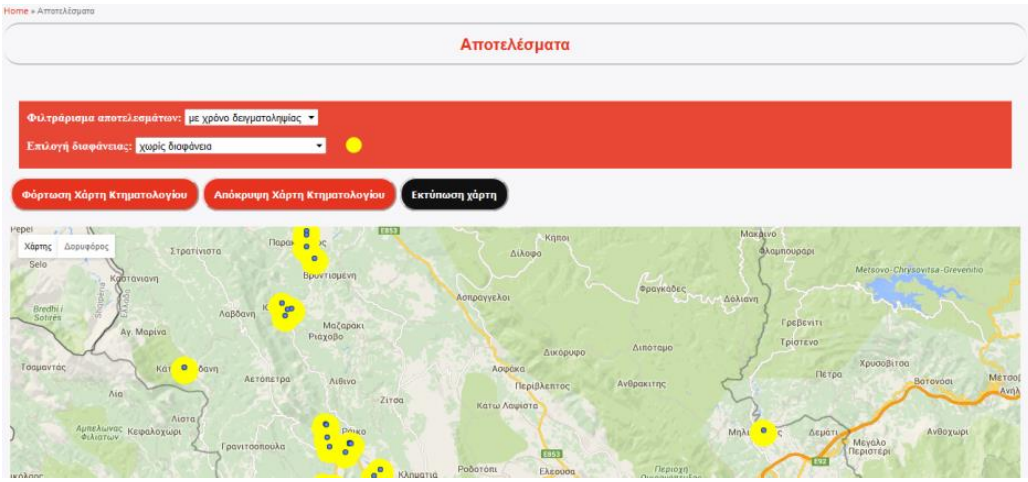


Figure 6: Filtering and Printing Results

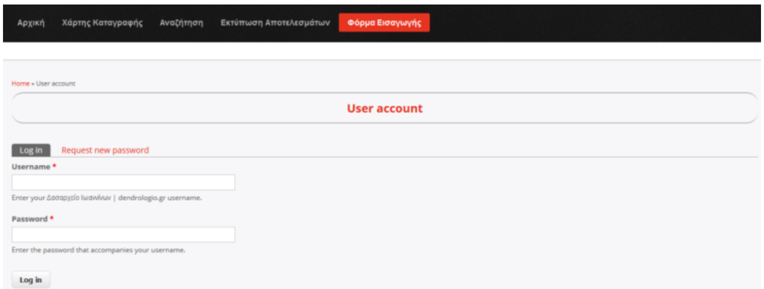


Figure 7: Input process

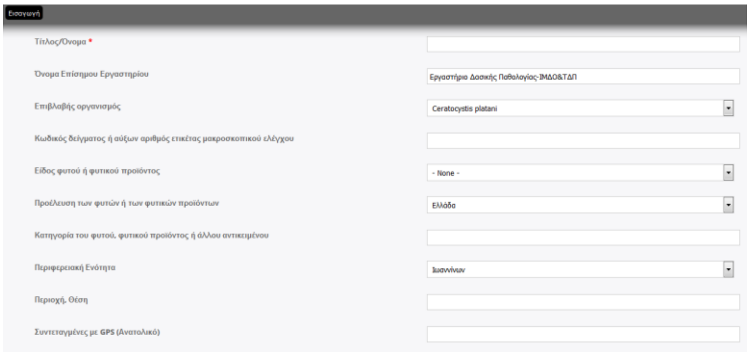


Figure 8: Input Forms

4.6 Placing the trees on the map

Regarding the placement of the new plane tree on the map, it is achieved by pressing the left mouse button on the map point where the plane tree is located, a red indicator is shown at that point while its longitude and latitude are automatically inserted in the corresponding fields of the form. Finally, the new tree is recorded in the system by pressing the left mouse button on the «Save»option (at the bottom left of the form) (Figure 9).

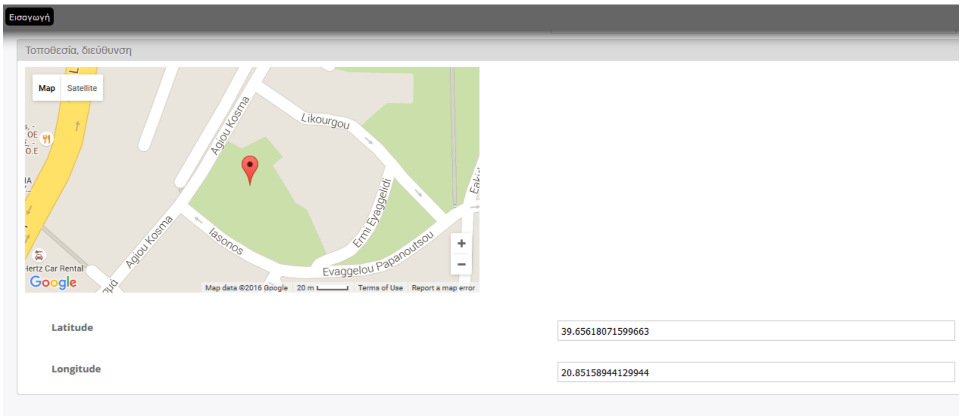


Figure 9: Placing on the Map

References

1. Efthimiou, G. (2000). Structure analysis, dynamic and ecological interpretation of riparian forests of Nestos. PhD thesis, Aristotle University of Thessaloniki, Faculty of Agricultural, Forestry and Natural Environment, Thessaloniki. (in Greek).

2. G. Efthimiou and S. Themelakis. (2017). Riparian Forests and Alien Invasive species. The case of the Riparian Forest of Ardas river (GR1110008), NE Greece. Proc. **18th Panellenic Forest Conference & International Workshop** "Information Technology, Sustainable Development, Scientific Network & Nature Protection" 8-11 October 2017 Edessa Pellas, Greece, (vol 1: 1040-1047), 2017.

3. Tsopelas P. and Soulioti N. (2010). Invasion of the fugus Canker stain Ceratocystis platani in Epirus, Greece: A potential environmental disaster in the natural ecosystems of plane trees. Abst. **15th Hellenic Phytopathological Congr**., Hellenic Phytopathological Society, p. 33. Corfu, Greece. (in Greek).

4. Tsopelas P., and Angelopoulos A. (2004). First report of canker stain disease of plane trees, caused by *Ceratocystis fimbriata f.sp platani* in Greece. **Plant Pathology**, 53(4): 531.

5. Tsopelas P., and Soulioti N. (2013). Canker stain disease: a major threat to natural stands of oriental plane in Greece. Proc. **16th Panhellenic Forestry Conf**. (pp. 175-179). Thessaloniki Greece.

6. Tsopelas P., Angelopoulos A. and N. Soulioti. (2005). Canker stain a new destructive disease of plane in Greece. Proc. **12th Panhellenic Forestry Conf**. (pp. 175-182), Drama, Greece.
7. Tsakiris P., Zoi S., Seli S., Leontaris G. and C. Lagos. (2014). Rapid expansion of canker stain of plane tree (Ceratocystis platani) in Ioannina, Epirus region, NW Greece and the role of economic crisis. Abst. **17th Hellenic Phytopathological Congr.**, Hellenic Phytopathological Society, p. 33. Volos, Greece. (in Greek).
8. Tsopelas P., Soulioti N. and N. Chatzipavlis. (2014). Methods of managing the disease of the post-chromatic ulcer of plane in Greece. Abst. **17th Hellenic Phytopathological Congr.**, Hellenic Phytopathological Society, p. 43. Volos, Greece. (in Greek).
9. EPPO/CABI. (1997). *Ceratocystis fimbriata f. sp. platani*. In: Quarantine Pests for Europe, CAB International, Wallingford (GB). 2nd edn, pp 674-677.
10. Tsakiris P., Zoi S., Seli S., Leontaris G. and C. Lagos. (2014). The most important Europe's plane forests in immediate danger: the rapid the spread of the fungus *Ceratocystis platani* in the region of Ioannina. Abst. **7th PanHellenic Ecology Congr**., p. 163. Mytilini, Greece. (in Greek).
11. Panconesi A. (1999). Canker stain of plain trees: a serious danger to urban plantings in Europe. **Journal of Plant Pathology** Vol. 81, pp 3-15.
12. Tasoulas E., Andreopoulou Z. (2012). Integrated Forest Environments Supporting Proper Management. **Protection and Ecology**, Vol. 13(1), pp 338-344.
13. Tasoulas E, Varras G, Tsirogiannis I, & Myriounis C. (2013). Development of a GIS application for urban forestry management planning, **Procedia Technology**, Vol. 8, pp 70-80.
14. Varras G, Andreopoulou Z, Tasoulas E, Papadimas CH, Tsirogiannis I, Myriounis CH, Koliouska CH. (2016). Multi-purpose Internet-based Information System ‘Urban’. **Urban Tree Database and Climate Impact Evaluation**, Vol. 17(1), pp 380-386.

STABLE ISOTOPE MASS BALANCE TO ASSESS CLIMATE IMPACT IN LAKE SYSTEMS

P. Chantzi* and K. Almpanakis

Laboratory of Physical Geography, Dept. of Physical & Environmental Geography, School of Geology, AUTH GR- 54124 Thessaloniki, Macedonia, Greece

*Corresponding author e-mail : pchantzi@geo.auth.gr, tel : +302310998508

Abstract

Isotope mass balance was performed based on 10 eastern Mediterranean stations from International Atomic Energy Agency - World Meteorological Organization (IAEA-WMO) precipitation network. Theoretical lake water isotope values were calculated and compared with measured lake water isotope values from literature data corresponding to different hydrological types of lake systems in the eastern Mediterranean. It is concluded that isotope limnology theory corresponds well to different lake water systems. $\delta^2H/\delta^{18}O$ ratio is a robust index to monitor the response of lake systems to climate variations. We can estimate the $\delta^2H/\delta^{18}O$ ratio for lake systems with different topographical and hydrological characteristics and compare it with the theoretical values that came up for the eastern Mediterranean lakes resulting in conclusions about the intensification or recession of evaporation process. So, the $\delta^2H/\delta^{18}O$ ratio of measured data in lake systems is a quantitative method to estimate climate change impact to lake systems. Isotope mass balance model unshackles us from the narrow grid-cell station density to satisfy the monitoring goal and facilitates the study of lake systems in a larger spatial scale.

Keywords: Isotope mass balance model, lakes, Mediterranean, climate change

1. INTRODUCTION

It has been well documented that Mediterranean area is strongly affected by climate change (Kelley et al., 2012; Lelieveld et al., 2012). Several climate models end up to higher annual temperatures, lower annual precipitation, sea level rise and intensity of extreme events (Mariotti et al., 2008; Seager et al., 2014). In more detail, according to the IPPC reports 2013, mean temperature increase for the period 2080-2100 is estimated about 2.2-5.1^{o}C, while the decrease in mean annual precipitation is estimated about 4-27%. What we stressed above all is that the most important issue is the increase of interannual variability both for temperature and for precipitation (Giorgi 2006). Water cycle expresses the circulation of water phases (liquid, solid, vapor) in climate system. Consequently, this climate variation, in turn, affects the hydrologic response of Mediterranean basins, where, the seasonality and the complex morphology are principal features (Hoerling et al., 2012). However, the alteration in hydrological balance could have a direct impact both in safe living and economic activities. Extensive droughts or floods increase the risk of extensive disasters. On the other hand, especially in southern Mediterranean countries where their economic base is made up by the two pillars of agriculture and tourism, any disruption to potential evapotranspiration and deficiency in water resources results in several implications on their economic model. This article is focused on lake systems. Well defined lake systems give the opportunity to assess climate variation as 1) they are worldwide representing different climate conditions (temperature, precipitation, moisture), geographic location (north, south), hydrology systems (open, closed, semi-closed), water types (fresh/sea water or mixing processes), 2) the response in long-term intervals including records of hydrologic extremes, 3) they are directly linked to climate variations incorporating the climate-driven episodes of their basins. The question

arises as to whether we can model the lake response to climate variation given the first comment about their diversity in many factors. Water mass balance in lake systems is strongly correlated with several climatic factors such as temperature, evaporation, precipitation and air moisture. Distribution of precipitation, surface and groundwater circulation pattern related to their hydrological type while continental relief define the ratio that a basin is exposed to the wind patterns. As climate change warms the atmosphere and intervenes in water cycle, water mass balance in lake systems give the opportunity to model and quantify the response of large watersheds to climate variation. However, water mass balance requires a narrow grid-cell station density to satisfy the monitoring goal of quantification of lake system responses to climate variation. An excellent tool for this attempt is the combination of water mass balance with isotope hydrology. Stable isotopes of oxygen (^{18}O) and deuterium (^{2}H) in water molecule constitute ideal traces for water cycle in large spatial and temporal scale. Limnological isotope theory (Leng and Marshall, 2004; Roberts et al., 2008) is based on climatic factors and precipitation-evaporation balance (P/E) for the two hydrological conditions of a lake: open and closed systems. In case of hydrological open lakes, the origin of precipitation and temperature oscillations determine the isotopic signature of lake water instant of the precipitation-evaporation balance (P/E) that is the key factor for hydrological closed lakes. The main objective of the study is to compare measured isotope values of different hydrological lake systems with calculated values based on isotope limnology theory aiming to conclude to a tool that will facilitate us to monitor and quantify the response of lake systems in climate variation. This attempt was earthed on east Mediterranean area where Greece belongs.

2. MATERIAL AND METHODS

2.1 Isotope hydrology model for lake systems

The isotopic mass balance (eq. 2) is based on the water mass balance (eq. 1) for a well-mixed lake with constant water density:

$$dV/dt = P + Q_i – E - Q_o \quad (1)$$

$$d(V\delta L)/dt = P\delta_P + Q_i\delta_P – E\delta_E - Q_o\delta_L \quad (2)$$

where: V and t, are the lake volume and unit time. P and E are precipitation and evaporation on lake surface per unit time.

Q factor is calculated by the surface and groundwater budget (Qx=Sx+Gx), where o and i markers correspond to outflow and inflow respectively. The isotope values of precipitation, evaporation and lake water are induced by δ_P, δ_E and δ_L respectively. The results are expressed in standard delta notation (δ) as per mil (‰) deviation from the standard V-SMOW as:

$\delta = ((R_{sample} - R_{standard})/R_{standard}) \times 1000$, where R_{sample} and $R_{standard}$ = $^{2}H/^{1}H$ or $^{18}O/^{16}O$

of sample and standard, respectively. δ_P and δ_L are directly measurable on a water sample however it is not as easy for δ_E. Craig and Gordon (1965) reported an evaporation model that is used to calculate δ_E (eq. 3):

$$\delta_E=(a^*\delta_L-h\delta_A-\varepsilon)/(1-h+\varepsilon_k) \quad (3)$$

where,

h: relative humidity normalized to the saturation vapor pressure at the temperature of the air-water interface

δ_A: the isotopic value of the air-vapor over the lake

ε_k: kinetic fraction factor, for $\delta^{18}O$ with ε_k~14.2(1-h) ‰ (Gonfiantini 1986)

$\varepsilon=\varepsilon^*+ \varepsilon_k$, where $\varepsilon^*=1000(1-\alpha^*)$

α^*: equilibrium isotopic fractionation factor dependent on the temperature at the evaporating surface

^{18}O: $1/a^* = \exp(1137T_L^{-2} – 0.415\ T_L^{-1} – 2.0667*10^{-3}$ (4)
^{2}H: $1/a^* = \exp(24844T_L^{-2} – 76.248\ T_L^{-1} – 52.61*10^{-3}$ (5)

T_L: temperature of the lake surface water in degrees Kelvin (Majoube 1971)

Eq. 5 describes an additional equation for δ_E as proposed by Benson and White (1994) based on the same evaporation theory which has been used in other lake models (Ricketts and Johnson 1996).

$$R_e=[(R_L/a_{eq}) - (RHf_{ad}R_{ad})]/[((1-RH)/a_{kin}) + RH(1-f_{ad})] \quad (6)$$

where,
R_{ad}: isotope ratio of the free atmospheric water vapor with respect to VSMOW,
RH: relative humidity, and
α_{eq}: fractionation factor dependent on equilibrium isotopic fractionation factor with $\alpha_{eq}=(1/\alpha^*)$
α_{kin}: fractionation factor dependent on wind speed where $\alpha_{kin}=0.994$ for wind speeds less than 6.8 $m*s^{-1}$ (Merlivat and Jouzel, 1979)
f_{ad}: fraction of atmospheric water vapor in the boundary layer over the lake where $f_{ad}=0$ in case that all the atmospheric water overlying the lake is derived from evaporation, rather than atmospheric moisture.
Finally, δ_E is calculated by $\delta_i=(R_i-1)10^3$ and $R_i=(R_i/R_{standard})$ where R is the isotope ratio and the standard, in this case, is VSMOW.

2.2 Methodology

The higher precipitation recharge in Greece found in the western part of Greece with the contribution of orographic injections of Pindos Mountains and the mountains of the Peloponnese. Eastern Aegean comes second where the complex topography and the warm Aegean Sea result in a considerable precipitation recharge. These significant precipitation amounts attributed to the depressions of Atlantic or western and central Mediterranean origin that enter Greece on the west during their eastwards route generating south-southwest wind over the Ionian Sea and southern Greece resulting in reduced precipitation recharge in Central Greece. Also, Sahara depression contributes to significant seasonal precipitation amounts (Flocas and Giles, 1991). Literature oxygen and deuterium data from lake water samples in the eastern Mediterranean were collected (**Table 1**). The rule was to cover all the hydrological types of lake systems in a spatial scale. Detailed, Sawa, Koronia and Pikrolimni lakes considered rather closed systems where evaporation process predominates to their isotopic signature contrary to Yliki and Paralimni lakes where key factors are seasonality and precipitation origin. Doirani, Prespa and Ohrid Lakes sit within karstified basins while Ismarida Lake is characterized by fresh-sea water mixing process.

Table 1: Lake sites that correspond to different altitudes and hydrological types

Lake Sites	**$\delta^{18}O_p$‰ VSMOW**	**δ^2H‰ VSMOW**	**Reference**
Mygdonia Basin (Volvi and Koronia Lakes)	-6.6 to -4.8 ‰	-49 to -38.5 ‰	Chantzi et al., 2016
Ismarida Lake	-6.6 to -0.4 ‰	-40 to -8.6 ‰	Gemitzi et al., 2014
Pikrolomni Lake	-7.2 to 4.9 ‰	-52 to 14.7 ‰	Dotsika et al., 2012
Prespa and Ohrid Lakes	-3.8 to -1.7 ‰	-35.4 to -21.4 ‰	Eftimi et al., 2007
Dojran Lake	2 to 2.1 ‰	1.1 to 1.9 ‰	Griggiths et al. 2002a
Kopais Basin (Yliki and Paralimni Lakes)	-7.2 to -5.9 ‰	-49.7 to -38.3 ‰	Griggiths et al. 2002b
Sawa Lake area, southern Iraq	2.5 to 5.9 ‰	28.3 to 29.8 ‰	Ali et al., 2016

The main incoming air flow pattern in Mediterranean area is controlled by the Atlantic Ocean through the Iberian Peninsula or France (for the western Mediterranean) or from the European continent (for the eastern Mediterranean). So, the isotope value of the air-vapor over the lake from advecting air masses could be calculated using the available data from the International Atomic Energy Agency - World Meteorological Organization (IAEA-WMO) precipitation network [IAEA, 2017] for the southern European stations assuming the isotopic equilibrium between precipitation and the air moisture over the continent (Gat et al., 1996). Theoretical isotope values for lake waters that correspond to east Mediterranean area were conducted by 10 stations of the Global Network of Isotopes in Precipitation (GNIP) (IAEA/WMO, 2017). Selected stations distributed in the north-south direction in the eastern Mediterranean area and around it (**Table 2**). The prerequisite to select a station was at least 5-year data for isotope value of precipitation, d-excess, temperature and average vapor pressure. Although Thessaloniki station had available data only for 4 years it was decided to use it, as this station was one of the two available in north Greece with a larger data set than Alexandroupoli station (3 years). In these scenarios, we assume that isotopic signature of waters that enters the lake correspond to that of precipitation stations. Moreover, isotope values for lake waters that correspond to east Mediterranean Sea water were calculated, based on Gat et al, 1996 primarily data, as evaporation process of land-locked Mediterranean Sea participate in isotopic signature of vapors.

Table 2: Selected stations of the Global Network of Isotopes in Precipitation (GNIP) (IAEA/WMO, 2017) for the east Mediterranean

IAEA stations	Time series	Coordinates
Elliniko Athens, Greece	1960; 1962-1968; 1970; 1972; 1974	37º53΄0΄΄N, 23º43΄47.99΄΄E
Pedeli Athens, Greece	2004-2016	38º3΄0.39΄΄N, 23º52΄0.03΄΄E
Thissio Athens, Greece	2000-2016	37º58΄11.99΄΄N, 23º43΄11.99΄΄E
Thessaloniki, Greece	2000-2003	40º40΄12΄΄N, 22º57΄36΄΄E
Irakleio, Greece	1965-1968; 1972-1974	35º19΄47.99΄΄N, 25º10΄47.99΄΄E
Rhodes, Greece	1963-1968; 1972; 1976	36º22΄48΄΄N, 28º6΄0΄΄E
Patra, Greece	2000-2016	36º16΄48΄΄N, 21º47΄23.99΄΄E
Zagreb, Croatia	1980-1995	45º48΄24΄΄N, 15º58΄12΄΄E
Edirne, Turkey	2008-2016	41º40΄41΄΄N, 26º33΄33΄΄E
Ramnicu Valcea, Romania	2012-2016	45º2΄7΄΄N, 24º17΄3΄΄E
Bet Dagan, Israel	1960-1966; 1968-1979	315º59΄50.29΄΄N, 34º48΄58.17΄΄E

Based on monthly data mean hydro-year values were estimated and then the mean values for the given time series for each station (**Table 3**). The calculated mean air temperature corresponded to lake surface temperatures. Relative humidity calculated as p_w/p_{ws} 100% where p_w: vapor partial pressure given by IAEA/WMO, 2017 data, and p_{ws}: saturation vapor partial pressure at the actual dry bulb temperature (Engineering ToolBox, 2004). Both h and RH have the same values % in Eq. 3 and Eq. 6. It is assumed that mean wind spread is less than 6.8 ms^{-1} for the eastern Mediterranean so such that α_{kin} is constant. $\delta_A = \delta_P - \varepsilon^*$ according to Gibson et al. (1999). Evaporation calculated by the proposed equation of Penman (1948) which is simplified by Linacre (1992):

$$E(mm/day) = [0.015 + 4x10^{-4}T_\alpha + 10^{-6}z] \text{ x } [480(T_\alpha + 0.006z)/(84-A) - 40 + 2.3u(T_\alpha - T_d)] \quad (7)$$

where
T_α: air temperature (°C),
z: altitude (m),
A: latitude

Table 3: Summary of average annual hydro-climate factors for the IAEA sites (data from GNIP (IAEA/WMO, 2004)).

	P (mm/yr)	E (mm/yr)	T_{av} (ºC)	$\delta^{18}O_p$‰ VSMOW	δ^2H‰ VSMOW	Altitude (m asl)	RH (%)	Qi=E-P	d-excess
Elliniko Athens	388	1998	18	-6.05	-33.04	19	61	1610	14.96
Pedeli Athens	561	1897	15.2	-7.48	-44.85	451	71	1336	14.98
Thissio Athens	433	2296	18.6	-6.42	-37.18	105	63	1863	14.26
Thessalon iki	335	1949	16	-6.69	-44.48	93	71	1614	9.03
Irakleio	495	1917	18.9	-7.24	-39.20	54	67	1422	18.69
Rhodes	760	2027	18.8	-5.27	-25.70	65	68	1267	14.94
Patra	734	2110	18.1	-5.78	-35.00	112	65	1376	10.99
Zagreb, Croatia	862	1271	11.9	-8.70	-61.15	123	75	409	8.51
Edirne, Turkey	632	1669	15	-8.24	-54.36	80	71	1036	11.58
Ramnicu Valcea, Romania	755	812	11.8	-8.09	-57.72	220	86	57	7.00
Bet Dagan, Israel	536	1792	19.3	-5.15	-23.44	44.9	71	1257	18.64
Sea Water [a]			25.2	-6.42	-43.70	0	46		
Sea Water [a]			16	-12.19	-88.80	0	30		

a: Gat et al., 1996

3. RESULTS AND DISCUSSION

The isotopic signature of Mediterranean lakes presents a high variation as different climatic factors affect them (season, humidity, temperature) in the north-south direction. Their topographical and hydrological regime define the rule under which these climate factors affect lake systems. The character of Mediterranean lakes lies between temperate Europe and North Africa. So, we are witnesses in lakes with fresh water and short residence-time and $\delta^{18}O_L$ values close to those of precipitation and hydrological closed lakes where evaporation process prevails.
In a stable climatic and geomorphological environment, the lake system will be described as constant:

$$d(V\delta_L)/dt = 0 \quad (8)$$
$$dV/dt = 0 \quad (9)$$

In a steady state, there are two border hydrological conditions that correspond to the lake system. The first concerns closed lakes where theoretically there are no outflows. In this case Q_o=0 and according to Eq. 2 and eq.8 the isotope mass balance will be:

$$P\delta_p + Q_i\delta_p = E\delta_E \quad (10)$$

which means that $\delta_E \sim \delta_P$. On the other hand, we have hydrological open lakes where theoretically we have a continuous flow system without evaporation losses E=0:

$P\delta_p + Q_i\delta_p = Q_o\delta_L$ (11)

which means that $\delta_L \sim \delta_P$.

Calculated lake water isotope values δ_L ($\delta^{18}O$ and δ^2H) for hydrological closed lakes presented in **Tables 4 and 5** according to eq.3 and eq.6. Based on (eq.3) $\delta^{18}O_L$ values range from -6.76‰ to -2.17‰ VSMOW and δ^2H_L values from -63.98‰ to -29.51‰ VSMOW. Based on (eq.6) we have two conditions: a) f_{ad}=0 where $\delta^{18}O_L$ values range from 3.17‰ to 6.52‰ VSMOW and δ^2H_L values from -73.12‰ to -43.88‰ VSMOW, b) f_{ad}=1 where $\delta^{18}O_L$ values range from -5.92‰ to 0.07‰ VSMOW and δ^2H_L values from -62.40‰ to -27.77‰ VSMOW. The above equations applied for precipitation data over Mediterranean Sea water stations. For eq.3 mean $\delta^{18}O_L$ and δ^2H_L values were -2.27‰ VSMOW and -56.85‰ VSMOW respectively. For eq.6 mean $\delta^{18}O_L$ and δ^2H_L values were 5.64‰ VSMOW and -50.75‰ VSMOW respectively for f_{ad}=0 while f_{ad}=1 mean $\delta^{18}O_L$ and δ^2H_L values were 1.55‰ VSMOW and -53.03‰ VSMOW respectively. The hydrological status of an open lake is described by $\delta^{18}O_L$ and δ^2H_L data that are equal to precipitation data. In practical terms, that means a range for lake water values from -8.7 to -5.27‰ VSMOW for $\delta^{18}O_L$ and from -61.15 to -25.70‰ VSMOW for δ^2H_L. Mean $\delta^{18}O_L$ and δ^2H_L values from precipitation samples over Mediterranean Sea water were about -9.3‰ VSMOW and -66.25‰ VSMOW respectively for open lake systems.

Table 4: Calculated values of $\delta^{18}O_L$ and δ^2H_L using eq. (10), eq. (3) and eq. (6) for hydrologically closed lakes

	eq. 6								eq. 3	
	f_{ad}=0				f_{ad}=1					
	$\delta^{18}O_E$	$\delta^{18}O_L$	δ^2H_E	δ^2H_L	$\delta^{18}O_A$	$\delta^{18}O_L$	δ^2H_A	δ^2H_L	$\delta^{18}O_L$	δ^2H_L
Elliniko Athens	-6.05	6.2	-33.04	-51.36	-15.91	0.07	-11.37	-38.32	-2.29	-40.7
Pedeli Athens	-7.48	4.4	-44.85	-60.48	-17.59	-2.89	-26.44	-47.6	-4.65	-49.4
Thissio Athens	-6.42	5.66	-37.18	-56.08	-16.24	-0.61	-14.89	-42.29	-2.86	-44.57
Thessaloniki	-6.69	5.16	-44.48	-60.98	-16.73	-2.01	-25.1	-47.53	-3.81	-49.37
Irakleio	-7.24	4.6	-39.2	-58.62	-17.03	-2	-16.52	-43.82	-4.05	-45.89
Rhodes	-5.27	6.52	-25.7	-45.31	-15.08	-0.2	-3.18	-30.36	-2.17	-32.32
Patra	-5.78	6.23	-35	-53.61	-15.63	-0.26	-13.19	-39.7	-2.39	-41.85
Zagreb, Croatia	-8.7	3.22	-61.15	-73.12	-19.12	-4.72	-46.74	-62.4	-6.23	-63.98
Edirne, Turkey	-8.24	3.66	-54.36	-69.62	-18.37	-3.63	-36.19	-56.91	-5.4	-58.74
Ramnicu Valcea, Romania	-8.09	3.17	-57.72	-70.31	-18.51	-5.92	-43.35	-58.07	-6.76	-58.94
Bet Dagan, Israel	-5.15	6.4	-23.44	-43.88	-14.91	-0.61	-0.29	-27.77	-2.38	-29.51
Sea Water [a]	-6.71	5.88	-25.8	-50.6	-15.69	1.76	-14.2	-45.47	-1.58	-48.77
Sea Water [a]	-8.88	5.4	-36.6	-50.89	-22.23	1.34	-69.46	-60.6	-2.96	-64.93
Mean SW		5.64		-50.75		1.55		-53.03	-2.27	-56.85

a: Gat et al., 1996

According to oxygen isotope $\delta^{18}O$ literature data, Ismarida and Pikrolimni lakes (**Table 1**) exhibit the higher variation in isotope values. This range corresponds to eq. 6 for f_{ad}=0, were atmospheric water vapor in the boundary layer over the lake derive by evaporation, for periods with low water-table and eq.3 for periods with high water-table. This observation is totally agreed with the hydrological status of both lakes. Ismarida lake suffers by fresh-seawater mixing process, especially in summer period

where the meteoric load is reduced (Gemitzi et al., 2014). Pikrolimni lake corresponds to a hydrological closed system where the extensive evaporation in summer period defines lake water isotope values (Dotsika et al., 2012). Mygdonia and Kopais basins present lake water isotope values that correspond better to eq.3 and eq.6 for f_{ad}=1 where atmospheric water vapor in the boundary layer over the lake derives from atmospheric moisture. Detailed, in Mygdonia basin, Koronia lake exhibits enrichened $\delta^{18}O$ value (-4.8‰ VSMOW) compared to that of Volvi lake (-6.6‰ VSMOW) (Chantzi et al., 2016). Chantzi (2016) reported that a) groundwaters in Mygdonia basin do not present a long retention time in underground aquifers exhibiting water isotope values close to that of precipitation and b) they are in hydraulic communication with surface lake water. $\delta^{2}H/\delta^{18}O$ ratio for both lakes reflect evaporation processes in their reservoir depending on the seasonality of atmospheric moisture. Regarding, Kopais basin, Yliki and Paralimni lakes sit within a karstified basin. Karst systems are more buffered hydrological and consequently less sensitive to evaporation effect (Roberts et al., 2008). Therefore, it is completely expected that in Kopais basin isotope values of lake waters will be sensitive to atmospheric moisture with respect to seasonality. Indeed, Griggiths et al., 2002b reported the limited degree of evaporative concentration of the modern lake waters in Kopais basin. Moreover, Doirani, Prespa and Ohrid Lakes sit also within karstified basins. Prespa and Ohrid Lakes present oxygen isotope values more enriched than those from Kopais basin though they are also described by eqs. 3 and 6 for f_{ad}=1. Doirani lake exhibits much more enriched oxygen isotope values which meet better eq. 6 for f_{ad}=0. This agrees with the conclusions by Griggiths et al., 2002a for evaporated lake water according to modern precipitation data and the extent aridity in Doirani Lake (Ristevski, 1991). Finally, Sawa lake with oxygen isotope values between 2.5 to 5.9 ‰ VSMOW corresponds better to eq. 6 for f_{ad}=0 confirming its closed hydrological status that suffers by prolonged evaporation losses as Ali et al., 2016 reported. Based on the aforementioned, it seems that eq. 6 for f_{ad}=1 meet better the measured isotope values in east Mediterranean lake waters. On the other hand, eq. 6 for f_{ad}=0 is more realistic for lake systems that suffer by extensive evaporation and/or fresh-seawater mixing processes. It should be emphasized that the f_{ad} fraction of atmospheric water vapor in the boundary layer over the lake with values f_{ad}=0 and f_{ad}=1 reflect the origins of atmospheric water overlying the lake: evaporation and atmospheric moisture respectively. In fact, the actual mechanism over lake surface is a continuous refresh where the air above the lake constantly supplies the evaporation process permitting molecules to pass from the liquid to vapor phase and come away from the lake surface (Tanny and Cohen, 2006). Without this supply, the evaporation would have stopped. The fact that eq. 6 includes the boundary conditions of the above mechanism with f_{ad} factor explains why eq. 6 satisfies the large variations of the measured lake water isotope values according to literature data. As previously reported, the isotopic character of Mediterranean precipitation varies depending on the origin of the air masses and their interaction with the warm Mediterranean. North-east Europe air masses result in depleted water isotopes while the Atlantic Ocean to less depleted (Rindsberger et al., 1983). After their interaction with warmer Mediterranean Sea waters (Gat et al., 1996), the topography in each lake basin determines the extent to which the basin is exposed to the dominant wind patterns. Finally, eq. 3 corresponds better to the period with high water-table as it cannot render accurately the evaporation process.

It is concluded that average values from eq. 3 and eq. 6, for both origins of atmospheric water overlying the lake, are the modeled lake water isotope values for closed hydrological lake systems in the eastern Mediterranean area. Figure 1 displays literature data of measured lake water isotope values in the eastern Mediterranean and the calculated data according to limnological isotope theory. It should be underlined that calculated deuterium isotope data $\delta^{2}H_{L}$ for lake waters do not present large variation with respect to precipitation data (**Table 5**). Ozaydin et al., 2001 reported that deuterium mass balance does not correspond well to sub-basin inflow and outflow load. Gat et al., 1996 reported the constant deuterium sea water values with respect to salinity and oxygen isotopes in measured samples in several Mediterranean Sea stations. He attributed this observation to the mixing process between the isotopically depleted north European precipitation values with enriched Mediterranean vapors. Subsequently, it is evident the large discrimination of d-excess between measured and modeled isotope values (**Figure 1**). This large deuterium excess corresponds to the theoretical static

model for the estimation of lake water isotope values under the evaporation process only in closed lake systems. Greater d-excess attributed to air masses in continental areas, due to extensive seawater evaporation under moisture deficit (Gat and Carmi, 1970; Gat et al., 2003). Actually, d-excess is linked to physical conditions such as moisture, air and sea surface temperature of the oceanic origin and reflect the dominant conditions in interaction and mixing process as sea water air masses move to precipitation site (Merlivat and Jouzel, 1979). It is a parameter that affected by kinetic fractionation process which depends on moisture source areas (oceanic evaporation), cloud (condensation in supersaturation conditions) and sub-cloud layer (re-evaporation of falling raindrops, moisture exchange with ambient air). Detailed, Mediterranean Sea discriminates against open oceans as it is surrounded by continental areas with considerable freshwater run-off. The evaporation process is affected by continental air flow pattern that originates from isotopically depleted north Europe precipitation. This interaction between sea and continental air masses results in the large deuterium excess that characterizes the Mediterranean Sea. Generally, in eastern Mediterranean d-excess has been reported between 15‰ (Gat and Dansgaard, 1972; Bowen and Revenaugh, 2003) and 22‰ (Gat and Carmi, 1970). So, the moisture recycling and mixing during a precipitation event define the isotopic signature of vapor in the cloud and sub-cloud layers mainly throughout a convective event [Bony et al., 2008]. This process covers the distance between measure isotope values from literature data and calculated isotope values for lake waters (**Figure 1**).

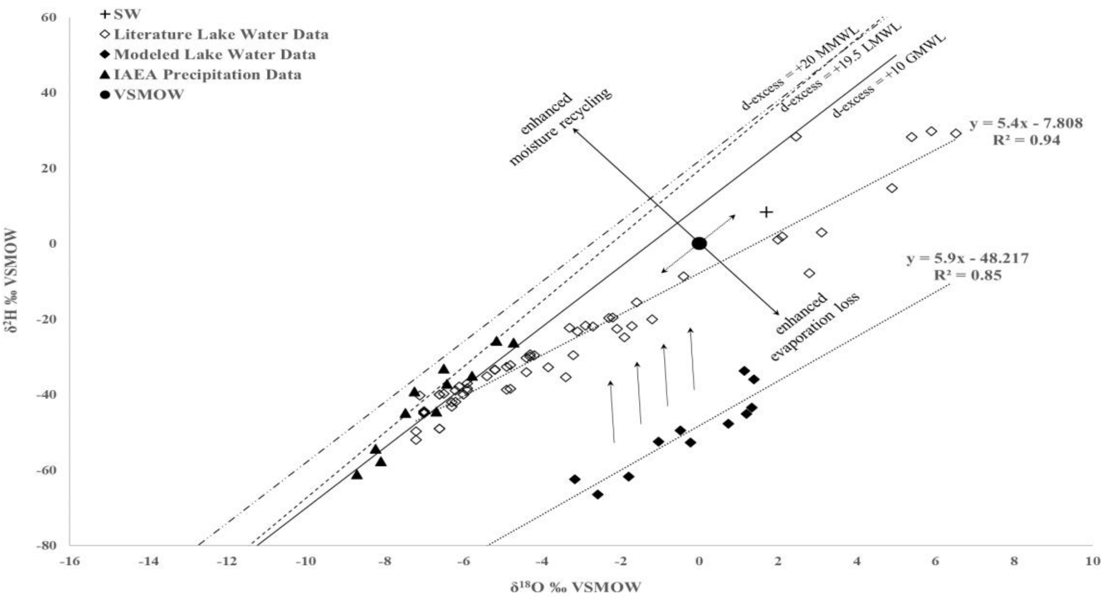


Figure 1. Deuterium (δ^2H‰ VSMOW) and oxygen (δ^{18}O‰ VSMOW) isotope values that correspond to measured values from literature data and calculated values from Global Network of Isotopes in Precipitation (GNIP) (IAEA/WMO, 2017) for the east Mediterranean: Eastern Mediterranean Meteoric Water Line $\delta^2H=8\delta^{18}O+22$ (International Atomic Energy Agency, IAEA, 2001; Bowen and Revenaugh, 2003; Aouad et al., 2004); Local Meteoric Water Line $\delta^2H=8.7\delta^{18}O+19.5$ (Dotsika et al., 2010; Global Meteoric Water Line $\delta^2H=8\delta^{18}O+10$ (Craig,H.,1961).

Lakes with measured isotope data present δ^2H/δ^{18}O ratio about 5.4 while those that their isotope values estimated by isotope mass balance present δ^2H/δ^{18}O ratio about 5.9. Both ratios are similar with strong correlation factor. We should note that δ^2H/δ^{18}O ratio of calculated values describes only hydrological closed lake systems. It is a moderate mean theoretical ratio for closed eastern Mediterranean lake systems considering both equilibrium and kinetic fractionation factors under the evaporation process. However, the δ^2H/δ^{18}O ratio is a key factor for theoretical values. Literature data δ^2H/δ^{18}O ratio is lower than that of calculated data. This is because literature data include Ismarida lake that is characterized by the fresh-seawater process, mainly in summer. Isolating Ismarida lake the δ^2H/δ^{18}O ratio becomes 5.6 closer to the theoretical ratio for continental lake systems.

Furthermore, Gat et al., 1996 performed a large sample collection on shipboard in several Mediterranean Sea stations resulting in water isotope data of Mediterranean Sea water and precipitation in these stations. Using precipitation data, we calculated lake water values that better response to coastal and transitional systems. Considering these calculated values, the theoretical $\delta^2H/\delta^{18}O$ ratio becomes 5.1 closer to measured values when we consider Ismarida lake. Moreover Gat et al., 1996 reported the slope of Local Evaporation Line (MLEL) for the eastern Mediterranean Sea about 4.3. $\delta^2H/\delta^{18}O$ ratio for precipitation data is about 8.0 (Mediterranean Meteoric Water Line to 8.7 (Local Meteoric Water Line). Therefore, we conclude that $\delta^2H/\delta^{18}O$ ratio is a robust index to monitor the response of lake systems to climate events. Based on the topographical and hydrological characteristics of lake systems we can estimate the $\delta^2H/\delta^{18}O$ ratio and compare it with the theoretical values estimated for the eastern Mediterranean lakes resulting in conclusions about the intensification or recession of evaporation process. So, the $\delta^2H/\delta^{18}O$ ratio of measured data in lake systems is a quantitative method to estimate climate change impact to lake systems.

4. CONCLUSIONS

The main objective of present work was to quantify the response of lake systems in climate variation based on isotope mass balance. It is concluded that isotope limnology theory corresponds well to different lake water systems. Eq. 6 for f_{ad}=1 meet better the measured isotope values in east Mediterranean lake waters. On the other hand, eq. 6 for f_{ad}=0 is more realistic for lake systems that suffer by extensive evaporation and/or fresh-seawater mixing process. The different f_{ad}=0,1 fractionation factors characterize the origin of atmospheric water vapor in the boundary layer over the lake (evaporation and atmospheric moisture). In fact, the actual mechanism is a continuous refresh where the air above the lake constantly supplies the evaporation process permitting molecules to pass from the liquid to vapor phase and come away from the lake surface. The fact that eq. 6 includes the above mechanism explains why eq. 6 responds successfully to lake water isotope values covering a large range of eastern Mediterranean lake systems. Moreover eq. 3 corresponds better to the period with high water-table as it cannot render accurately the evaporation process. Lakes with measured isotope data present $\delta^2H/\delta^{18}O$ ratio about 5.4 while those that their isotope values estimated by isotope mass balance present $\delta^2H/\delta^{18}O$ ratio about 5.9. Both ratios are similar with strong correlation factor. The $\delta^2H/\delta^{18}O$ ratio for theoretical values represents hydrological closed systems in the continental eastern Mediterranean area where isotopically depleted north Europe precipitation events and air masses from seawater interact. Measured lake water values present a $\delta^2H/\delta^{18}O$ ratio about 5.4, lower than that of calculated. This is because it includes different hydrological systems. Isolating Ismarida lake as it suffers by fresh-seawater mixing process, then $\delta^2H/\delta^{18}O$ ratio becomes 5.6 closer to the theoretical ratio for continental lake systems. Considering calculated values for lake waters based on precipitation data in several stations in the Mediterranean Sea, the theoretical $\delta^2H/\delta^{18}O$ ratio becomes 5.1 closer to measured values when we consider Ismarida lake. Moreover Gat et al., 1996 reported the slope of Local Evaporation Line (MLEL) for the eastern Mediterranean Sea about 4.3. $\delta^2H/\delta^{18}O$ ratio for precipitation data is about 8.0 (MMWL) to 8.7 (LMWL). Therefore, we conclude that $\delta^2H/\delta^{18}O$ ratio is a robust index to monitor the response of lake systems to climate events. We can estimate the $\delta^2H/\delta^{18}O$ ratio for lake systems with different topographical and hydrological characteristics and compare it with the theoretical values that came up for the eastern Mediterranean lakes resulting in conclusions about the intensification or recession of evaporation process. So, the $\delta^2H/\delta^{18}O$ ratio of measured data in lake systems is a quantitative method to estimate climate change impact to lake systems.

NOTES

This paper is part of first author's PostDoctoral Research entitled "Research of climate impact in the evolution of lake systems using isotope hydrology models" in Geology School of the Aristotle University of Thessaloniki.

References

1. Aouad, A., Travi, Y., Blavoux, B., Job, J.-O., Najem, W., 2004. Isotope study of snow and rain on Mount Lebanon: preliminary results. **Hydrological Sciences Journal** 49 (3), 429-441.
2. Benson, L.V., White, J.W.C., 1994. Stable isotopes of oxygen and hydrogen in the Truckee River Pyramid Lake surface-water system 3. **Source of water-vapour overlying Pyramid Lake. Limnol. Oceanogr**. 39, 1945-1958.
3. Bony, S., C. Risi, and F. Vimeux (2008), Influence of convective processes on the isotopic composition (delta O-18 and delta D) of precipitation and water vapor in the tropics: 1. Radiative-convective equilibrium and Tropical Ocean-Global Atmosphere-Coupled Ocean-Atmosphere Response Experiment (TOGA-COARE) simulations, **J. Geophys**. Res, 113, D19305.
4. Bowen, G.J., Revenaugh, J., 2003. Interpolating the isotopic composition of modern meteoric precipitation. **Water Resources Research** 39, 10 art. no 1299.
5. Chantzi, P., & Dotsika, E., 2016. Mygdonia Basin (N. Greece) in the View of Isotope Geochemistry BT - Energy, Transportation and Global Warming. In P. Grammelis (Ed.), (pp. 677-683). **Cham: Springer International Publishing**.
6. Craig, H., 1961. Isotopic variations in meteoric waters. **Science** 133, 1702-1703.
7. Craig, H., Gordon, L.I., 1965. Deuterium and oxygen-18 variation in the ocean and marine atmosphere. **Stable isotopes in Oceanography Studies and Paleotemperatures. Laboratorio di Geologia Nucleare, Pisa.**
8. Dotsika, E., Lykoudis, S., Poutoukis, D., 2010b. Spatial distribution of the isotopic composition of precipitation and spring water in Greece**. Glob. Planet. Chang**. 71, 141–149.
9. Dotsika E., Tzavidopoulos I., Poutoukis D., Raco B., Maniatis Y., Ignatiadou D., 2012. Isotope contents, Cl/Br ratio and origin of water at Pikrolimni Lake: A natron source in Greece, as archive of past environmental conditions, **Quaternary International**, Volume 266, Pages 74-80
10. Eftimi R., Amataj S., Zoto J., 2007. Groundwater circulation in two transboundary carbonate aquifers of Albania; their vulnerability and protection. **In Selected Papers on Hydrogeology** Vol 11: Taylor & Fracis Group, London, UK, p.p. 199-212.
11. Engineering ToolBox, 2004. Relative Humidity in Air. [online] Available at: https://www.engineeringtoolbox.com/relative-humidity-air-d_687.html
12. Flocas, A.A., Giles, B.D., 1991. Distribution and intensity of frontal rainfall over Greece. **International Journal of Climatology** 11, 429-442.
13. Gat, J.R., Carmi, I., 1970. Evolution of the isotopic composition of the atmospheric water in the Mediterranean Sea area. **Journal of Geophysical Research** 75, 3039-3048.
14. Gat, J.R., Dansgaard, W., 1972. Stable isotope survey of the freshwater occurrences in Israel and the Jordan Rift Valley. **Journal of Hydrology** 16, 177–211.
15. Gat JR, Shemesh A, Tziperman E, Hecht A, Georgopoulos D, Basturk O, 1996. The stable isotope composition of waters of the eastern Mediterranean Sea. **Journal of Geophysical Research-OceansJournal of Geophysical Research-Oceans**, 101, 6441-6451
16. Gat, J.R., Klein, B., Kushnir, Y., Roether, W., Wernli, H., Yam, R., Shemesh, A., 2003. Isotope composition of air moisture over the Mediterranean Sea: an index of the air-sea interaction. Tellus 55B, 959-965.
17. Gemitzi A., Stefanopoulos K., Markantonis M., Richnow H., 2014. Seawater intrusion into groundwater aquifer through a coastal lake - complex interaction characterised by water isotopes ^{2}H and ^{18}O. **Isotopes in Environmental Health Studies**. 50.

18. Gibson, J.J., Edwards, T.W.D., Prowse, T.D., 1999. Pan-derived isotopic composition of atmospheric water vapor and its variability in northern Canada. **J. Hydrol**. 217, 55-74.
19. Giorgi 2006, Climate change hot-spots. **Geophysical Research Letters**, Vol. 33, L08707
20. Gonfiantini, R., 1986. Environmental isotopes in lake studies. In: Fritz, P., Fontes, J.-C. (Eds.), **Handbook of Environmental Isotope Geochemistry Volume 2B**. Elsevier, Amsterdam.
21. Griffiths H.I., Reed J.M., Leng M.J., Ryan S., Petkovski S., 2002a. The recent palaeoecology and conservation status of Balkan Lake Dojran, **Biological Conservation**, Volume 104, Issue 1, Pages 35-49
22. Griffiths S. J., Street-Perrott F. A., Holmes J. A., Leng M. J., Tzedakis C., 2002b. Chemical and isotopic composition of modern water bodies in the Lake Kopais Basin, central Greece: analogues for the interpretation of the lacustrine sedimentary sequence, **Sedimentary Geology**, Volume 148, Issues 1-2, Pages 79-103
23. Hoerling, M., Eischeid, J., Perlwitz, J., Quan, X., Zhang, T., Pegion, P., 2012. On the Increased Frequency of Mediterranean Drought, **J. Climate**, 25, 2146-2161.
24. International Atomic Energy Agency (IAEA), 2001. GNIP Maps and Animations. **International Atomic Energy Agency**, Vienna.
25. IAEA/WMO, 2017. Global Network of Isotopes in Precipitation. The GNIP Database. Accessible at: https://nucleus.iaea.org/wiser
26. IPCC, 2013: Climate Change 2013: The Physical Science Basis. Contribution of Working Group I to the Fifth Assessment Report of the Intergovernmental Panel on Climate Change [Stocker, T.F., D. Qin, G.-K. Plattner, M. Tignor, S.K. Allen, J. Boschung, A. Nauels, Y. Xia, V. Bex and P.M. Midgley (eds.)]. **Cambridge University Press, Cambridge, United Kingdom and New York**, NY, USA, 1535 pp
27. Kelley, C., Ting, M.F., Seager. R. & Kushnir. Y 2012. The relative contributions of radiative forcing and internal climate variability to the late 20th century winter drying of the Mediterranean region**. Climate Dynamics** 38(9-10): 2001-15.
28. Leng, M.J., Marshall, J.D., 2004. Palaeoclimate interpretation of stable isotope data from lake sediment archives. **Quat. Sci. Rev**. 23, 811-831.
29. Lelieveld. J., Hadjinicolaou. P., Kostopoulou. E. et al. 2012. Climate change and impacts in the eastern Mediterranean and the Middle East. **Climatic Change** 1 14(3-4): 667-87.
30. Linacre E., 1992. Climate Data and Resources: A Reference and Guide. Routledge, London, p.366
31. Majoube, F., 1971. Fractionnement en oxygène-18 et un deutérium entre l'eau et sa vapeur. **J. Chim. Phys.** 187, 1423-1436.
32. Mariotti, A., Zeng, N., Yoon, J.-H., Artale, V., Navarra, A., Alpert, P., Li, L. Z. X., 2008. Mediterranean water cycle changes: Transition to drier 21st century conditions in observations and CMIP3 simulations**, Environ. Res. Lett**., 3, 044001.
33. Merlivat, L., Jouzel, J., 1979. Global climatic interpretation of the D-^{18}O relationship for precipitation. **J. Geophys. Res**. 84, 5029-5033.
34. Özaydin V. & Şendil U., Altinbilek D., 2001. Stable isotope mass balance method to find the water budget of a lake. **Turkish Journal of Engin. and Environmental Sciences**. 25. 329-344
35. Penman H.L., 1948. Natural evaporation from open water, bare soil and grass. **Proc. Roy**. Soc. A. 193: 120-145.
36. Ricketts, R.D., Johnson, T.C., 1996. Climate change in the Turkana basin as deduced from a 4000-year long delta O-18 record. **Earth Planet**. Sci. Lett. 142, 7-17.

37. Rindsberge Mr., Jaffe S., Rahamin S., Gat J., 1990. Patterns of the isotopic composition of precipitation in time and space data from Israeli storm collection program, **Tellus**, 42B, 263-271.
38. Ristevski, P., 1991. Areal and time distribution of air temperature and precipitation in the region of Gevgelija and Valandovo. In: Gasevski, M. (Ed.), [Sostojbite i perspectivite za zasˇtita na Dojranskoto ezero. Zbornik na trudovi od sovetvanjeto vo Star Dojran.]. **Dvizˇenje na Ekologistite na Makedonija,** Skopje, pp. 26–35. (in Macedonian with English abstract).
39. Roberts N., Jones M.D., Benkaddour A., Eastwood W.J., Filippi M.L., Frogley M.R., Lamb H.F., Leng M.J., Reed J.M., Stein M., Stevens L., Valero-Garcés B., Zanchetta G., 2008. Stable isotope records of Late Quaternary climate and hydrology from Mediterranean lakes: the ISOMED synthesis, **Quaternary Science Reviews**, Volume 27, Issues 25-26, Pages 2426-2441.
40. Seager. R., Liu. H.B., Henderson. N. et al. 2014. Causes of increasing aridification of the Mediterranean region in response to rising greenhouse gases. **journal of Climate** 27(12): 4655-76.
41. Tanny, J., Cohen, J., 2006. Revisiting the boundary layer structure used in Craig and Gordon's model of isotope fractionation in evaporation, **International Workshop on the Isotope Effects in Evaporation,** Pisa, Italy, pp. 11-21.



Soft and renewable energy sources

A NUMERICAL TOOL FOR THE TIME-DOMAIN ANALYSIS OF FLOATING WAVE ENERGY CONVERTERS

N. Mantadakis* and E. Loukogeorgaki

Division of Hydraulics and Environmental Engineering, Dept. of Civil Engineering, A.U.Th, GR-54124 Thessaloniki, Macedonia, Greece

*Corresponding author: e-mail: mantadaki@civil.auth.gr, tel: +302310995951

Abstract

In the present paper, a computational tool (FloaTWEC tool) is developed for the time-domain analysis of a floating oscillating-body Wave Energy Converter (WEC). Assuming a floating body with six rigid-body modes, the WEC's response is calculated based on the well-known Cummins equation, where fluid memory effects are captured through appropriate convolution terms. The required frequency-dependent excitation loads and hydrodynamic coefficients, as well as the hydrostatic-gravitational coefficients are obtained using a standard hydrodynamics (waves-floating structure interaction) software. The Power-Take-Off (PTO) mechanism can be modeled as a linear or non-linear system, while mooring lines can be considered as additional stiffness forces. The equation of motion is solved using the Newmark implicit time integration scheme, whereas the analysis can be implemented under the action of regular and irregular waves, assuming motion in all or appropriately selected rigid-body modes. FloaTWEC is, initially, validated through comparison of results with numerical and experimental results of other investigators for three different floating structures. Then, it is applied for the case of a heaving WEC with a linear PTO for: (a) assessing its response and its power absorption under the action of regular and irregular waves of different characteristics and (b) investigating the effect of the stiffness of the mooring lines on its performance.

Keywords: wave energy; wave energy converters; time-domain analysis; Cummins equation; absorbed power

1. INTRODUCTION

Wave energy presents an abundant renewable energy source, characterized by higher energy density, compared to other ocean renewable energy forms, limited negative environmental impact in use and larger consistency due to natural seasonal variability (Drew et al., 2009). Its efficient harnessing can contribute to the satisfaction of the European Union's decarbonisation targets, while it can support energy security and long-term economic growth (e.g. Magagna & Uihlein, 2015). The above have fostered, nowadays, the development of the wave energy sector and, so far, a variety of different types of Wave Energy Converters (WECs) exists (Drew et al., 2009; de O Falcão, 2010). Floating oscillating-body devices (e.g. floating heaving WECs), absorbing energy based on the relevant translation or rotational WEC's motion, present a characteristic WEC type that can be deployed in deep waters in order to exploit the corresponding more powerful wave regimes.

The successful design of such WECs requires the development and the application of numerical tools enabling the investigation and the accurate assessment of their performance (hydrodynamic behavior and absorbed power) and, therefore, the efficient handling of existing design challenges. Under this framework, several numerical tools for the hydrodynamic analysis of floating oscillating-body WECs have been and are still being developed (Folley, 2016). Most of these tools are based on the linear wave theory and they enable the implementation of the required analysis in frequency domain by

linearizing the hydrodynamic problem and the floating system (e.g. Babarit, 2010; Schay et al., 2013; Pastor & Liu, 2014). Although frequency-domain numerical tools are characterized by low computational time, they cannot model adequately non-linear effects resulting from different sources (e.g. existence of complex Power-Take-Off (PTO) mechanisms and highly nonlinear relevant control strategies). For overcoming this barrier, time-domain numerical tools should be deployed (e.g. Eriksson et al., 2005; Pastor & Liu, 2014).

Motivated by this, in the present paper a computational tool (FloaTWEC tool) is developed for the time-domain analysis of a floating oscillating-body WEC. Assuming that the floating body is rigid with six Degrees of Freedom (DOFs), the WEC's response is calculated based on the Cummins equation (Cummins, 1962). The required (input to FloaTWEC) frequency-dependent excitation loads (forces and moments) and hydrodynamic coefficients, as well as the hydrostatic-gravitational stiffness coefficients are obtained using a standard hydrodynamics (waves-floating structure interaction) software, which is based on the linear potential theory. The PTO force can be considered in FloaTWEC using either a linear or non-linear model, while mooring lines can be represented as additional stiffness forces. The equation of motion is solved using the Newmark implicit time integration scheme. The analysis can be implemented under the action of regular and irregular waves considering all or appropriately selected DOFs. FloaTWEC is initially validated through comparison of results with numerical and experimental results of other investigators for a variety of floating structures. Then, it is applied for the case of a heaving WEC with a linear PTO in order to: (a) assess its response and its power absorption under the action of regular and irregular waves of different characteristics and (b) examine the effect of the stiffness of the mooring lines on its performance.

2. NUMERICAL FORMULATION

A floating oscillating-body WEC of draft h is placed in an area of constant water depth d, as shown in Figure 1, where indicatively a floating heaving cylindrical WEC of diameter D is considered. In this figure, $OXYZ$ corresponds to the global coordinate system, while the PTO is schematically presented as a damping mechanism.

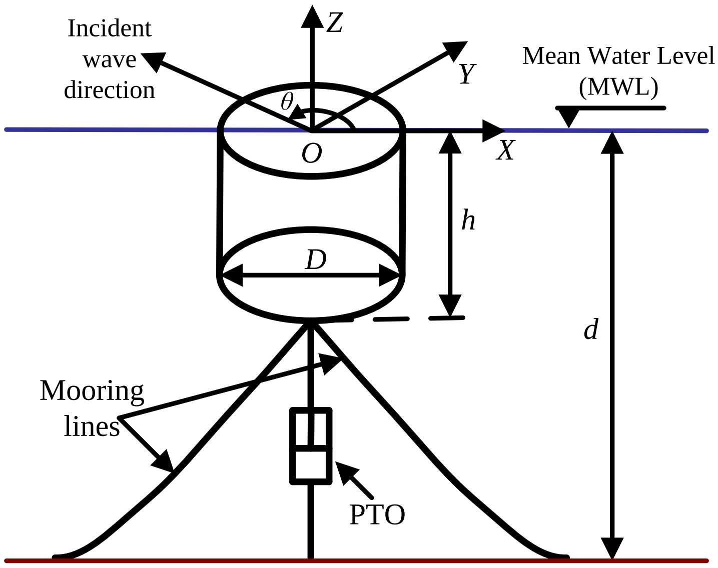


Figure 1. Coordinate system and definition of basic quantities (the cylindrical floating body and mooring lines' position are indicative).

The general procedure applied in the present paper for implementing time-domain analysis of the aforementioned WEC using FloaTWEC is shown in Figure 2. At first, frequency-domain analysis is implemented for calculating the frequency-dependent wave excitation loads and hydrodynamic coefficients (added mass and radiation damping), as well as the hydrostatic-gravitational stiffness

coefficients, which are required as input in FloaTWEC. Next, for given incident wave conditions (regular or irregular waves of direction θ, Figure 1) as well as for specific PTO and mooring lines' characteristics, the equation of motion in time domain is solved and all quantities describing the performance (e.g. response, power absorption etc) of the examined WEC are calculated. In the following sub-sections, a short description of the frequency-domain analysis is, initially, given focusing on the quantities required as input in FloaTWEC, while a detailed description of the time-domain numerical formulation follows. FloaTWEC was developed using Python.

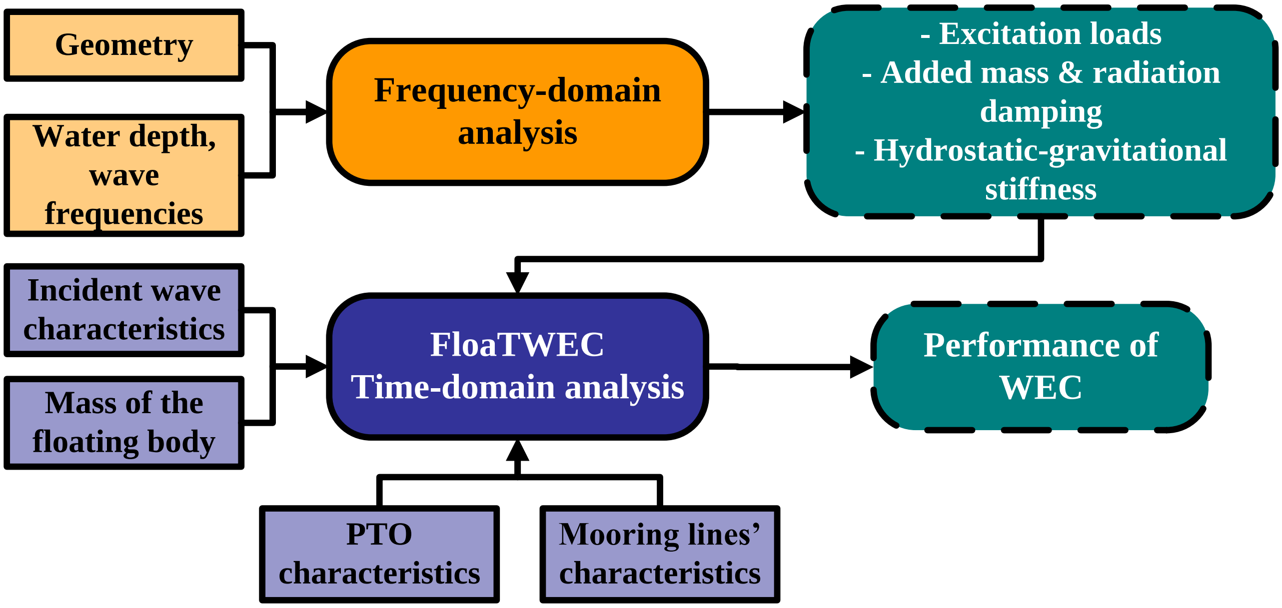


Figure 2. Flowchart for implementing time-domain analysis using FloaTWEC.

2.1 Frequency-domain hydrodynamic analysis

The frequency-domain hydrodynamic analysis of the WEC subjected to incident regular waves is implemented using WAMIT software (Lee, 1995). The analysis is based on a 3D linear wave diffraction theory, where the floating body is also taken to undergo small oscillations in all six DOFs (rigid-body modes), corresponding to three translations (surge, sway and heave) and three rotations (roll, pitch and yaw) along and around X, Y and Z axes respectively. Assuming inviscid and incompressible fluid and irrotational flow, the fluid motion is described in terms of a complex velocity potential, which satisfies the Laplace equation everywhere in the fluid region and consists of three components: the velocity potential of the incident waves, the scattered potential associated with the disturbance of the incident waves by the floating body and the radiation potential related to the waves radiated from the body due to its motions. The solution of the 1st order boundary value problem is based on a direct computational method (3D panel method) utilizing the free-surface Green function and imposing the appropriate boundary conditions on the free surface, the sea bottom and the floating body (Lee, 1995).

Having solved the boundary value problem, the excitation loads, F_i, i=1,…,6 and the added mass and radiation damping coefficients, A_{ij}, B_{ij} i, j=1,…,6 are calculated using the following equations:

$$F_i = -i\omega\rho\zeta_w \iint_{S_B} n_i \phi_D dS \tag{1}$$

$$A_{ij} - i\omega^{-1} B_{ij} = \rho \iint_{S_B} n_i \phi_j dS \tag{2}$$

where ω and ζ_w are the incident wave frequency and the unit wave amplitude respectively, ρ is the mass density of the water, ϕ_D is the diffracted (incident plus scattered) potential, ϕ_j, j=1,..,6 is the

radiation potential of the j^{th} DOF, $(n_1, n_2, n_3)=\mathbf{n}$, with $\mathbf{n}$ the unit vector normal on the body's wetted surface S_B, and $(n_4, n_5, n_6)= \mathbf{x}\times\mathbf{n}$, with $\mathbf{x} = (x, y, z)$.

Finally, it is noted that the hydrostatic-gravitational stiffness coefficients, C_{ij}, i,j=1,…,6 are obtained from WAMIT considering the mean wetted surface of the floating body (Lee, 1995).

2.2 Time-domain analysis

Assuming linear behavior and considering impulses in the components of motion, Cummins (1962) obtained a vector integro-differential equation (known as the Cummins equation) for describing the motion of a floating structure in time domain under the action of waves. In the case of a WEC shown in Figure 1 this equation can be written as follows:

$$\mathbf{M}\cdot\ddot{\xi}(t)=\mathbf{F_{exc}}(t)+\mathbf{F_{rad}}(t)+\mathbf{B^E}\cdot\dot{\xi}(t)-\left(\mathbf{K^E}+\mathbf{C}\right)\cdot\xi(t) \tag{3}$$

where t is time, $\mathbf{M}$ is the 6x6 mass matrix of the floating body, $\mathbf{F_{exc}}$ is the 6x1 matrix of the wave excitation loads, $\mathbf{F_{rad}}$ is the 6x6 matrix of the radiation loads, $\mathbf{B^E}$ is the 6x6 damping matrix caused by an external source (e.g. PTO mechanism), $\mathbf{K^E}$ and $\mathbf{C}$ are the 6x6 stiffness matrices due to an external source (e.g. mooring lines) and due to hydrostatic-gravitational forces respectively, while $\xi, \dot{\xi}$ and $\ddot{\xi}$ are the 6x1 matrices of the floating body's motions, velocities and accelerations respectively.

Considering the action of irregular waves, for a given sea state described by a spectrum with significant wave height H_s, and peak period T_p, $\mathbf{F_{exc}}$ and $\mathbf{F_{rad}}$ (Taghipour et al., 2008) are given by the following equations:

$$\mathbf{F_{exc}}(t)=2\cdot\int_0^{\infty}\left|\mathbf{F}(\omega)\right|\cdot S(\omega)\cdot\cos(\omega t+\varepsilon)d\omega \tag{4}$$

$$\mathbf{F_{rad}}(t)=-\mathbf{A}(\infty)\cdot\ddot{\xi}(t)-\int_{-\infty}^{t}\mathbf{K}(t-\tau)\cdot\dot{\xi}(t)d\tau \tag{5}$$

In Equation 4, $|\mathbf{F}(\omega)|$ is the 6x1 matrix of the amplitude of the complex wave excitation loads as obtained from the frequency domain analysis (Equation 1), $S(\omega)$ is the spectral density of the examined spectrum and $\varepsilon \in [0, 2\pi]$, is the phase of each wave excitation component in the spectrum. In Equation 5, $\mathbf{A}(\infty)$ is the 6x6 added mass matrix corresponding to infinite frequency, with coefficients calculated using Equation 2, τ is an auxiliary (dummy) time variable, while $\mathbf{K}$ is called the "retardation function" and can be calculated as follows (Taghipour et al., 2008):

$$\mathbf{K}(t)=2/\pi\cdot\int_0^{+\infty}\mathbf{B}(\omega)\cdot\cos(\omega t)d\omega \tag{6}$$

where $\mathbf{B}$ is the 6x6 frequency-dependent radiation damping matrix with coefficients calculated using Equation 2. The last term in the right hand side of Equation 5 is the well-known convolution integral, which based on Equation 6 represents the load contribution from the wave radiation damping. This convolution also captures the so-called "fluid memory effects"; namely, the fact that changes in the momentum of the fluid at a particular time affect the motion at the subsequent time.

On the other hand, in the case of an incident regular wave of amplitude A and frequency ω, $\mathbf{F_{exc}}$ and $\mathbf{F_{rad}}$ are simplified as follows:

$$\mathbf{F_{exc}}(t)=A\cdot\left|\mathbf{F}(\omega)\right|\cdot\cos(\omega t) \tag{7}$$

$$\mathbf{F_{rad}}(t)=-\mathbf{A}(\omega)\cdot\ddot{\xi}(t)-\mathbf{B}(\omega)\cdot\dot{\xi}(t) \tag{8}$$

where **A** is the 6x6 frequency-dependent added mass matrix, with coefficients calculated using Equation 2.

The equation of motion in time-domain (Equation 3) is solved in FloaTWEC using the Newmark beta implicit time integration scheme with parameters α and β equal to 1/2 and 1/6 respectively (linear acceleration method), and the response of the WEC (e.g. motions, velocities) are calculated. The power absorbed by the WEC, P, can be, then, obtained depending on the WEC's working direction and the PTO mechanism. For example, in the case of a heaving WEC and a PTO modeled as a linear damping system, with damping coefficient b_{pto}, P is calculated as follows:

$$P(t) = b_{pto} \cdot \left(\dot{\xi}(t)\right)^2 \tag{9}$$

It is noted that the analysis can be implemented considering motion in all DOFs or in specific DOFs (the rest ones are assumed ideally restricted), while in the case of irregular waves a sea state can be described by deploying either the Jonswap or the Pierson-Moskowitz spectrum (DNV-GL, 2017).

Finally, FloaTWEC is capable for calculating the natural period of each i^{th}, i=1,…,6, DOF of the floating body through the following equation:

$$T_{ni} = 2 \cdot \pi \cdot \sqrt{\frac{\left(M_{ii} + A_{ii}(\omega = \omega_{ni})\right)}{C_{ii} + K_{ii}^{E}}} \quad i = 1, ..., 6 \tag{10}$$

3. COMPARISON WITH NUMERICAL AND EXPERIMENTAL RESULTS

The FloaTWEC tool developed in this work is applied for the case of three different floating structures in order to compare results with numerical and experimental results of other investigators.

The first floating structure corresponds to the free heaving cylinder of Watai et al. (2015), which has h=1 m, D=2 m (Figure 1) and mass equal to 3140 kg. The cylinder is placed in an area of infinite water depth, while the action of head (θ=0 deg, Figure 1) regular waves is considered. Indicatively, in Figure 3, part of the time series of the computed heave excitation force, F_{exc3}, and heave displacement, ξ_3, are compared with the corresponding numerical results of Watai et al. (2015) for H=2 m and ω=4.202 rad/sec (Figure 3a), 9.905 rad/sec (Figure 3b) and 2.51 rad/sec (Figure 3c). Moreover, Figure 3d shows the comparison of the computed Response Amplitude Operator in heave, RAO_3, (defined as the ratio of the ξ_3 amplitude to A) with the corresponding results of Watai et al. (2015). In the case of FloaTWEC, RAO_3 has been obtained via the Fast Fourier Transformation (FFT). It can be clearly seen that there is an excellent agreement between the present numerical results and the corresponding ones of Watai et al. (2015).

The second floating structure examined in this work corresponds to the heaving WEC of Eriksson et al. (2005). The WEC consists of a partially submerged cylinder tethered above a linear PTO located on the seafloor. The PTO is connected by a spring of stiffness k_s to the tether and it is modeled as a linear damping system, with damping coefficient b_{pto}. The tether, on the other hand, is modeled as a rigid bar, assuming that the spring force is large enough to keep the tether stretched. Therefore, the spring's stiffness is assumed representative for the stiffness of the WEC's mooring system. In order to compare results, FloaTWEC is applied for the case, where the cylinder has h=1.5 m, D=4 m (Figure 1) and mass equal to 800 kg and it is placed in an area of constant water depth d=23 m. Moreover, based on Eriksson et al. (2005), Equation 3 is solved with K_{33}^E=k_s=3000 N/m and B_{33}^E=b_{pto}=4000 N*sec/m. Considering the action of irregular waves described by the Jonswap spectrum with H_s=1.175 m and T_p=2.228 sec, the time series of ξ_3 computed using FloaTWEC agrees very well with the corresponding one of Eriksson et al. (2005), as shown in Figure 4. The initial small phase-lag observed between the time series of Figure 4 may be attributed to the consideration of different initial conditions in FloaTWEC compared to Eriksson et al. (2005).

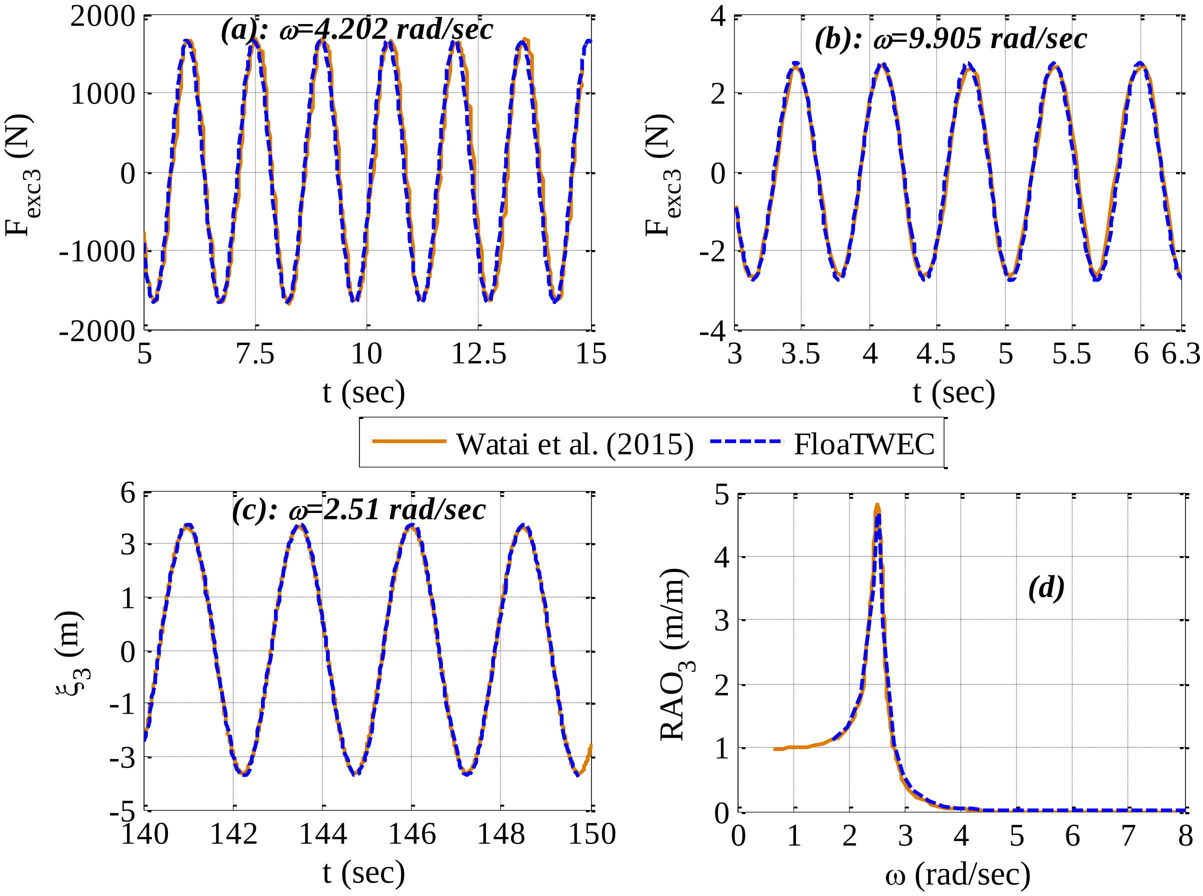


Figure 3. Comparison of F_{exc3} and ξ_3 time series and of RAO_3 with the corresponding results of Watai et al. (2015).

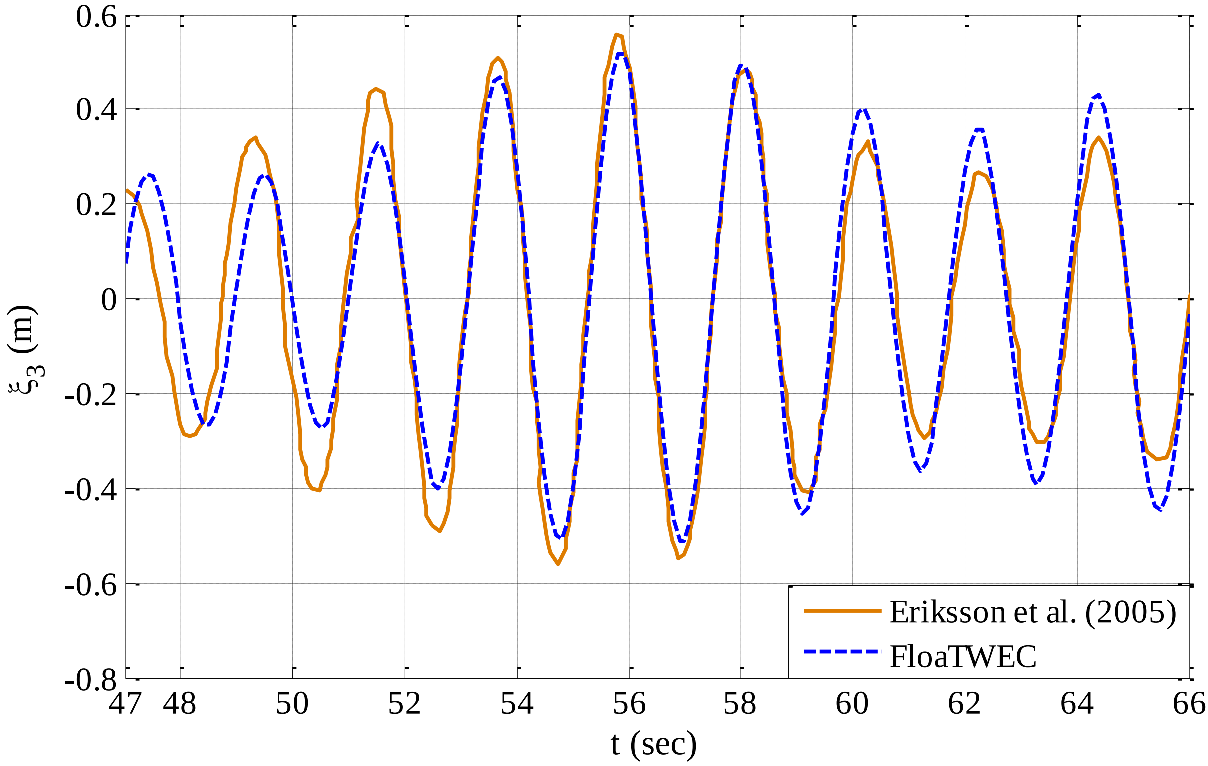


Figure 4. Comparison of ξ_3 time series with the corresponding results of Eriksson et al. (2005) for H_s=1.175 m and T_p=2.228 sec.

Finally, FloaTWEC is applied for the case of a horizontal floating cylindrical WEC in order to compare results with the experimental and the numerical ones of Chen at al. (2016). Considering a geometrical scale 1/10, the cylinder in the physical model has h=0.1 m, D=0.2 m (Figure 1), length and mass equal to 1 m and 25.7 kg respectively, while the PTO corresponds to a linear damping system. The experiments were conducted for d=1 m under the action of regular head waves. It is noted that the numerical model of Chen at al. (2016) is based on the finite element and Volume of Fluid (VOF) methods for incompressible viscous flow. In Figure 5, the time series of ξ_3 computed with FloaTWEC are compared with the corresponding experimental and numerical results of Chen at al. (2016) for the case of ω=4.187 rad/sec and H=0.05 m (Figure 5a), and 0.10 m (Figure 5b) and for B_{33}^E=b_{pto}=100 N*sec/m (Chen at al., 2016). It is clear that the application of FloaTWEC results to ξ_3 values which are very close to the experimental results of Chen at al. (2016). Moreover, the agreement with the experimental results is greatly improved in the case of FloaTWEC compared to the numerical model of Chen at al. (2016), illustrating the accuracy and the efficiency of the tool developed in the present paper.

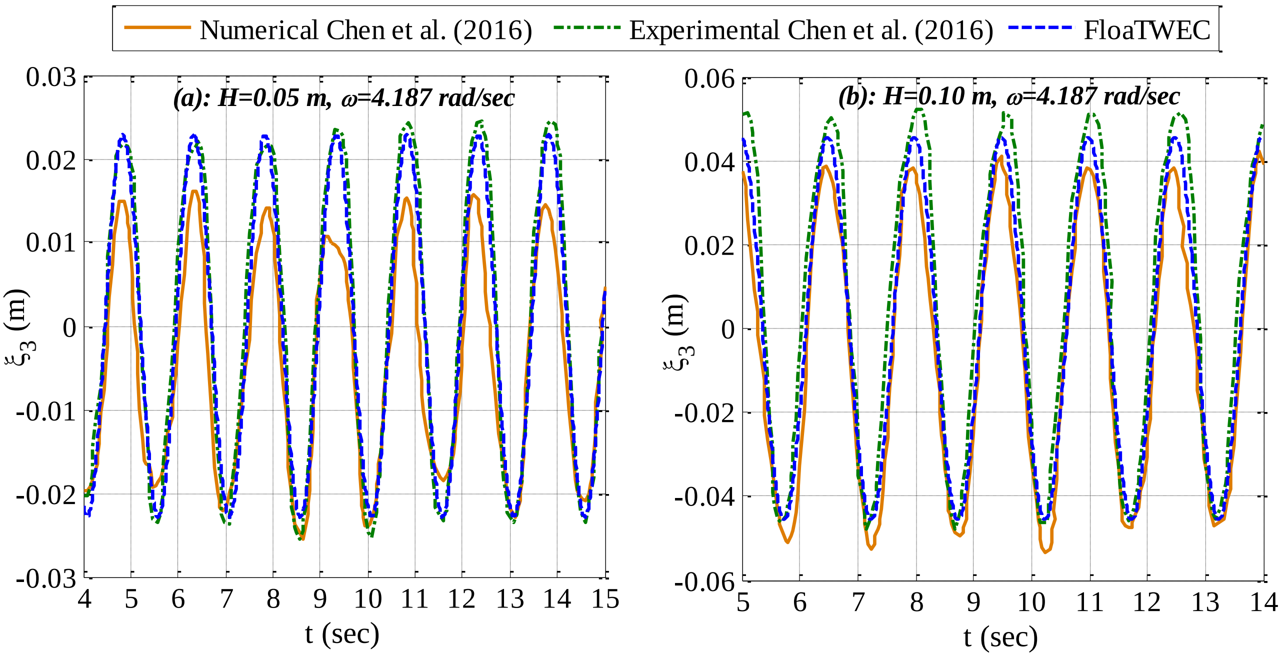


Figure 5. Comparison of ξ_3 time series with the corresponding experimental and numerical results of Chen et al. (2016).

4. FLOATWEC APPLICATION

The developed in the present paper FloaTWEC tool is further applied for the case of the heaving WEC of Eriksson et al. (2005) in order to: (a) assess the response and the power absorption of this WEC under the action of regular and irregular waves of different characteristics and (b) examine the effect of the spring stiffness on the WEC's performance. In all the examined cases, the WEC has the geometric characteristics mentioned in Section 3 and it is placed in an area of constant water depth equal to 23 m. Moreover, based on Eriksson et al. (2005), Equation 3 is solved with B_{33}^E=b_{pto}=4000 N*sec/m assuming all DOFs ideally restricted, except the one corresponding to heave (i.e. the motion along the WEC's working direction). All simulations are performed for 300 sec with a time step of 0.1 sec.

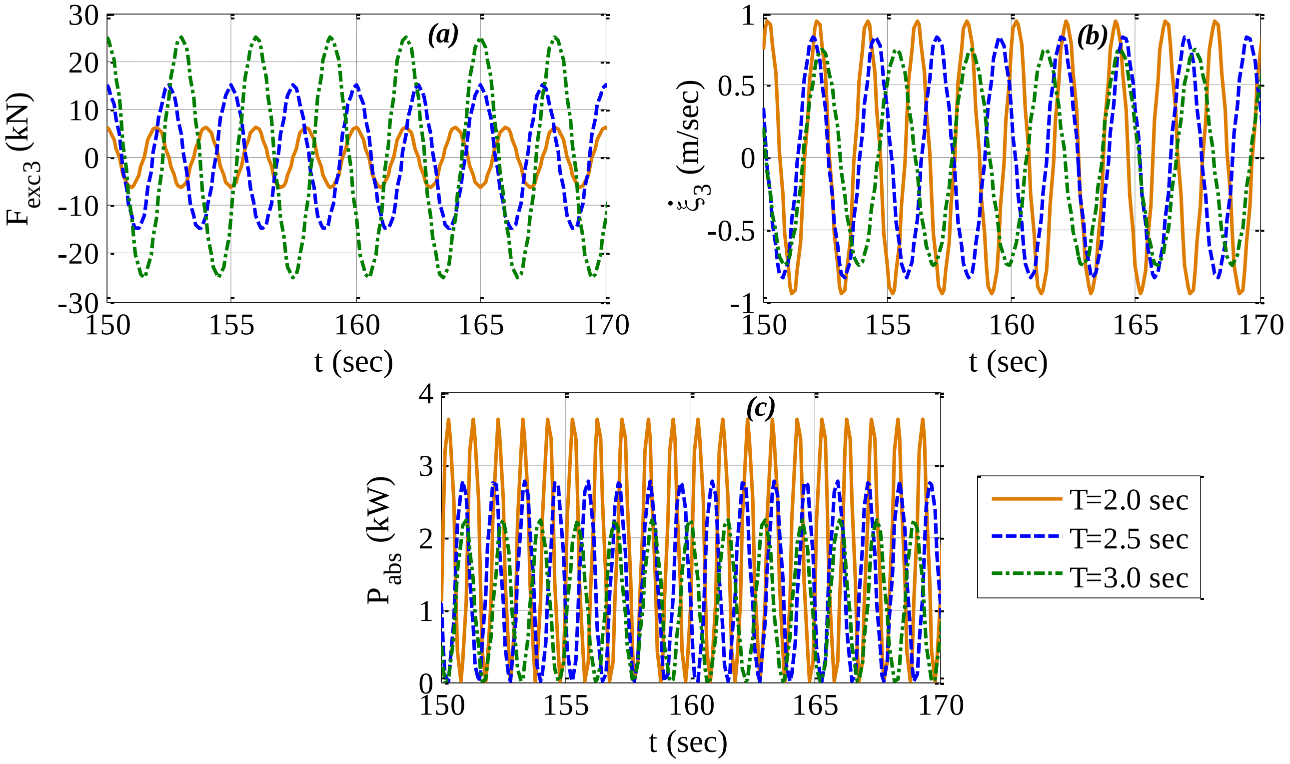


Figure 6. Effect of *T* on F_{exc3}, $\dot{\xi}_3$ and *P* for the case of the examined heaving WEC.

In the case of regular waves, *H* is taken constant and equal to 1.5 m, while three different *T* values are investigated equal to 2.0, 2.5 and 3.0 sec. For these three different *H* and *T* combinations, the equation of motion is solved for K_{33}^E=k_s=3000 N/m. Figure 6 shows the effect of *T* on the heave excitation force, F_{exc3} (Figure 6a), on the heave velocity, $\dot{\xi}_3$ (Figure 6b) and on the power *P* absorbed by the WEC (Figure 6c). Regarding F_{exc3} (Figure 6a), it can be seen that by increasing *T* (i.e. transition to longer waves) larger values of F_{exc3} are observed in consistency with the real physical problem. On the other hand, in the case of the heave velocity (Figure 6b), the largest $\dot{\xi}_3$ values are obtained for *T*=2 sec, while the subsequent increase of *T* leads to a smooth reduction of the WEC's response (12.8% and 21.3% reduction of maximum $\dot{\xi}_3$ values for *T*=2.5 and 3.0 sec respectively with respect to *T*=2.0 sec). This is attributed to the fact that resonance phenomena occur approximately at *T*=2.0 sec, since the natural period of the examined WEC in heave, T_{n3}, (Equation 10) is equal to 2.083 sec. As for the power absorbed by the WEC (Figure 6c), the increase of *T* leads to a reduction of *P* (23.1% and 38% reduction of maximum *P* values for *T*=2.5 and 3.0 sec respectively with respect to *T*=2.0 sec) in absolute accordance with Figure 6b.

Considering the action of irregular waves, focus is given on the effect of T_p and of the mooring lines' stiffness on the WEC's performance. For this purpose, two sea states with H_s=1.175 m and T_p equal to 2.228 sec and 4.0 sec are taken into account, while simulations are performed for three different values of the spring's stiffness, k_s, (representing the stiffness of the WEC's mooring system as mentioned in Section 3). The first value, $k_s^{initial}$, is set equal to 3000 N/m as in Section 3, while the other two values are set equal to 0.25* $k_s^{initial}$=750 N/m and 4*$k_s^{initial}$=12000 N/m.

Regarding the effect of T_p on F_{exc3}, $\dot{\xi}_3$ and *P* (Figure 7), analogous conclusions can be drawn as in the case of regular waves. Specifically, the increase of T_p leads to an increase of F_{exc3} (absolute maximum F_{exc3} values for T_p=2.228 and 4.0 sec are equal to 10 kN and 39.2 kN respectively) and to a more intense variation of this quantity. On the other hand, by increasing T_p a reduction of both $\dot{\xi}_3$ (48.8% reduction of the absolute maximum $\dot{\xi}_3$ value relevant to T_p=2.228 sec) and *P* (73.8% and

63.1% reduction of maximum and mean P values respectively relevant to T_p=2.228 sec) is observed, since resonance phenomena are pronounced in the case of T_p=2.228 sec.

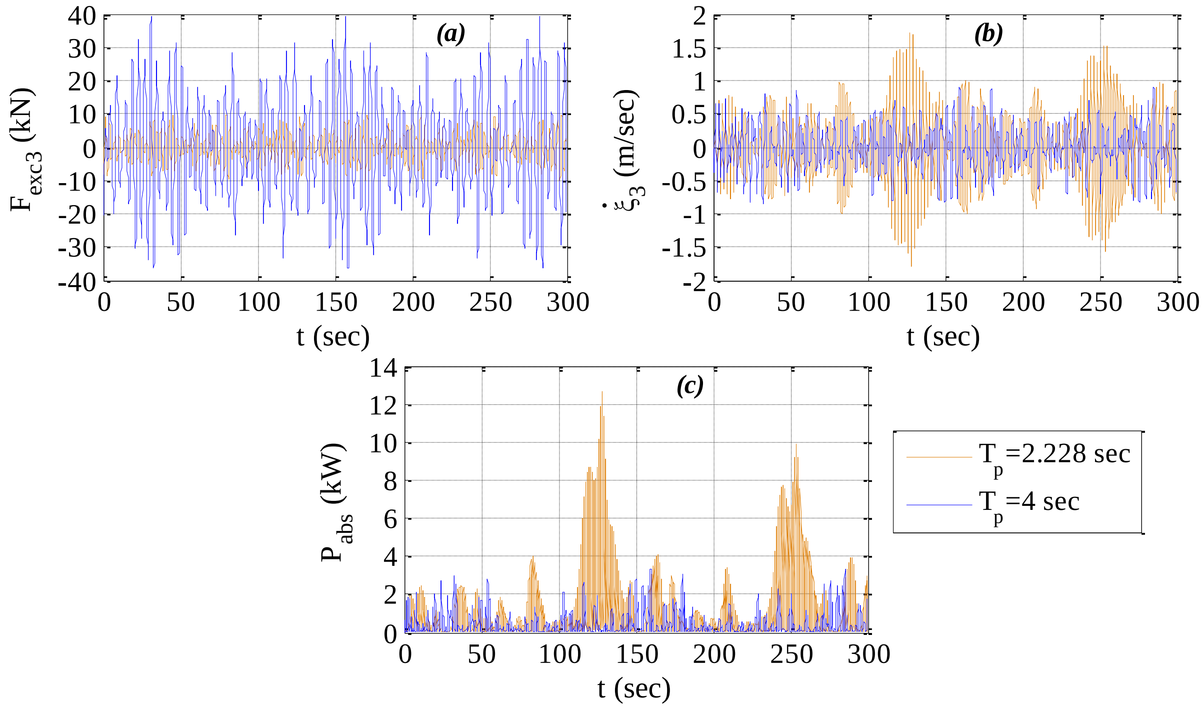


Figure 7. Effect of T_p on F_{exc3}, $\dot{\xi}_3$ and P for the case of the examined heaving WEC with k_s=3000 N/m.

As for the effect of k_s on the performance of the WEC (Figure 8), the time series of $\dot{\xi}_3$ and P for k_s=750 N/m do not show significant differences compared to the corresponding time series for k_s=3000 N/m. Thus, the decrease of k_s from 3000 N/m to 750 N/m has a minor effect on the WEC's performance. This is attributed to the fact that k_s=750 N/m leads to T_{n3}=2.098 sec, which is almost equal to the heave natural period (2.083 sec) obtained for k_s=3000 N/m. The above do not hold true in the case of k_s=12000 N/m, where the decrease of T_{n3} to 2.018 sec leads to smaller $\dot{\xi}_3$ and P values compared to the corresponding values obtained for both k_s=750 N/m and 3000 N/m. For example, by increasing k_s from 3000 N/m to 12000 N/m, a 38.3% reduction of the absolute maximum $\dot{\xi}_3$ value is observed, while the maximum and the mean values of P are reduced by 61.9% and 26% respectively.

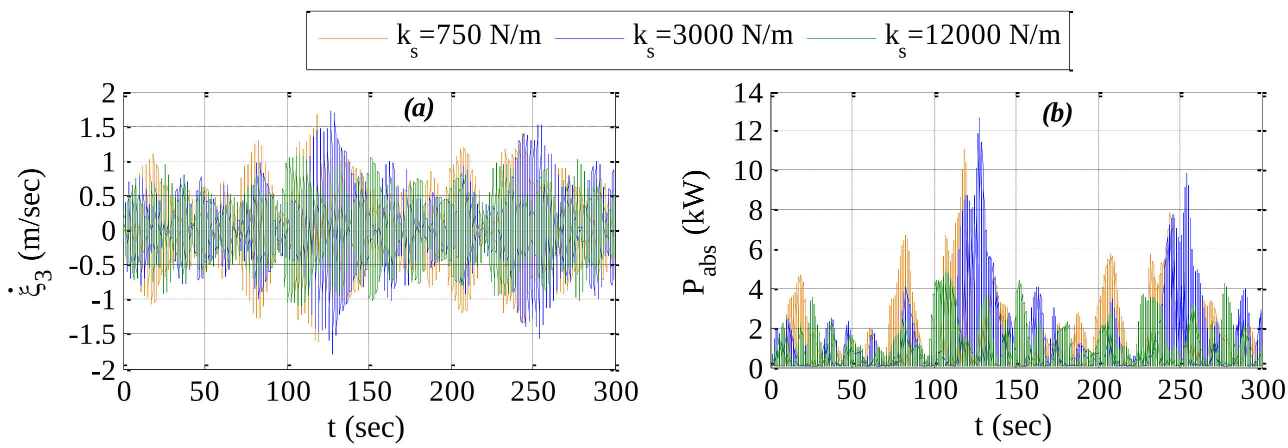


Figure 8. Effect of k_s on $\dot{\xi}_3$ and *P* for the case of the examined heaving WEC under the action of irregular waves with H_s=1.175 m and T_p=2.228 sec.

5. CONCLUSIONS

In the present paper, a computational tool, named FloaTWEC, is developed for the time-domain analysis of a floating oscillating-body WEC. The analysis can be implemented for any geometry under the action of regular and irregular waves assuming motion in all or appropriately selected rigid-body modes. The WEC's response is calculated based on the well-known Cummins equation, while the required frequency-dependent excitation loads and hydrodynamic coefficients, as well as the hydrostatic-gravitational coefficients can be obtained using a standard hydrodynamics (waves-floating structure interaction) software. The PTO mechanism can be modeled as a linear or non-linear system, while mooring lines can be represented as additional stiffness forces.

Initially, the developed tool was applied in order to compare results with numerical and experimental results of other investigators. Excellent agreement of computed results with the aforementioned ones has been observed, which demonstrates the accuracy and the efficiency of FloaTWEC in terms of capturing important aspects of the physical problem.

Finally, the application of FloaTWEC for the case of a heaving WEC with a linear PTO for different incident wave conditions and mooring lines' stiffness has led to the following main conclusions: (a) the increase of the incident wave period increases the heave excitation force in absolute accordance with the real physical problem. At the same time, however, the transition to longer waves conditions leads to a reduction of the response and the power absorbed by the WEC, since resonance phenomena become less significant and (b) for a given sea state the mooring lines' stiffness affect the performance of the WEC only when the change of the stiffness affects directly the intrinsic dynamic characteristics of the WEC (i.e. heave natural period).

The present model can be further applied for the case of a non-linear PTO mechanism, while it can be further extended in order to account for a more accurate modeling of the mooring lines.

References

1. Drew B., A.R. Plummer and M.N. Sahinkaya (2009) 'A review of wave energy converter technology', **Proc. Institution of Mechanical Engineers**, **Part A: Journal of Power and Energy**, Vol. 223(8), pp. 887-902.
2. Magagna D. and A. Uihlein (2015) 'Ocean energy development in Europe: Current status and future perspectives', **International Journal of Marine Energy**, Vol. 11, pp. 84-104.
3. de O Falcão A.F. (2010) 'Wave energy utilization: A review of the technologies', **Renewable and Sustainable Energy Reviews**, Vol. 14(3), pp. 899-918.
4. Folley M. (2016) **'Numerical Modelling of Wave Energy Converters: State-of-the-Art Techniques for Single Devices and Arrays'**, Elsevier.
5. Babarit A. (2010) 'Impact of long separating distances on the energy production of two interacting wave energy converters', **Ocean Engineering**, Vol. 37(8-9), pp.718-729.
6. Schay J., J. Bhattacharjee and C.G. Soares (2013) 'Numerical Modelling of a Heaving Point Absorber in Front of a Vertical Wall', Proc. 32nd Int. Conf. **Ocean, Offshore and Arctic Engineering (OMAE2013)**, Nantes, France, 2013.
7. Pastor J. and Y. Liu (2014) 'Frequency and time domain modeling and power output for a heaving point absorber wave energy converter', **International Journal of Energy and Environmental Engineering**, Vol. 5(2).

8. Eriksson M., J. Isberg and M. Leijon (2005) 'Hydrodynamic modelling of a direct drive wave energy converter', **International Journal of Engineering Science**, Vol. 43, pp.1377-1387.
9. Lee C.H. (1995) '**WAMIT theory manual**', MIT Report 95-2, Department of Ocean Engineering, MIT.
10. Cummins W.E. (1962) '**The impulse response function and ship motions**', Report 1661, Department of the Navy David Taylor Model Basin.
11. Taghipour R., T. Perez and T. Moan (2008) 'Hybrid frequency–time domain models for dynamic response analysis of marine structures', **Ocean Engineering**, No. 35(7), pp. 685–705
12. Det Norske Veritas – Germanischer Lloyds (DNV – GL) (2017) '**Environmental conditions and environmental loads**', Recommended Practice DNVGL-RP-C205.
13. Watai R., F. Ruggeri, C. Sampalo and A. Simos (2015) 'Development of a time domain boundary element method for numerical analysis of floating bodies' responses in waves', **The Brazilian Society of Mechanical Sciences and Engineering**, Vol. 37(5), pp.1569-1589.
14. Chen B., D. Ning, C. Liu, C.A. Greated and H. Kang (2016) 'Wave energy extraction by horizontal floating cylinders perpendicular to wave propagation', **Ocean Engineering**, Vol. 121, pp. 112-122.

OPTIMAL OPERATION SCHEDULING OF MULTIPURPOSE PUMPED STORAGE HYDROPOWER PLANT WITH HIGH PENETRATION OF RENEWABLE ENERGY SOURCES

P.I. Bakanos* and K.L. Katsifarakis

Division of Hydraulics and Environmental Engineering, Dept. of Civil Engineering, A.U.Th, GR-54124 Thessaloniki, Macedonia, Greece

*Corresponding author : e-mail : p.bakanos@civil.auth.gr

Abstract

The high penetration of renewable energy sources, such as solar and wind, into the electricity system requires large-scale, flexible storage and production systems for uninterrupted power supply, to reduce as much as possible the amount of energy discarded. The pumped-storage method through coupled reservoirs has been globally recognized as a mature, competitive and reliable technology for the storage of large quantities of electricity and is suitable for our country, due to its particular geomorphology. Its application may increase the degree of exploitation of hydroelectric projects, without decrease of the availability of water resources. Optimization of renewable energy sources penetration through reversible reservoir systems is a very complex, multi-parameter, non-linear problem, as the reservoirs, besides hydroelectric power generation, serve many other objectives such as water supply, irrigation and flood protection, while their function should observe constraints such as environmental flow.

This paper examines the possibility of optimizing the penetration of wind energy into a pumped-storage multi-reservoir system. The process of simulating and optimizing the system has been implemented through the development of a program in the Microsoft Visual Studio 2015, based on the genetic algorithm (GA) method. Genetic algorithms are a widely used non-linear optimization method that has been successfully implemented to problems of management of large scale complex water and energy systems. The results show that when the operation of the reservoir system is coordinated with the wind farm, the hydroelectricity generation decreases, but the total economical revenue of the system increases by about 7.2% and can achieve high wind energy penetration to the electricity grid.

Keywords: Pumped-storage plant, multi-reservoir systems, renewable energy, optimization, genetic algorithms

1. INTRODUCTION

In recent years, a significant effort has been made in the world to move to a low-carbon society and to achieve energy independence from fossil fuels (e.g. coal, oil and natural gas). In this effort to change the energy paradigm, renewable energy sources such as wind, sun, water, biomass and geothermal heat play a key role. The use of wind and solar energy does not produce toxic pollution or global warming and is one of the cleanest and most sustainable ways to produce abundant and inexhaustible electricity. Renewable energy is the key to long-term efforts to mitigate climate change and will play an increasingly important role in improving overall energy security.

The energy generated from the wind turbines and photovoltaic stations is intermittent, fluctuating and distributed, resulting in instabilities of the electrical system. In order to achieve penetration of

renewable energy sources on a large scale, drastically upgraded flexible and stable systems are required to effectively integrate the volatility and unpredictability of uncontrolled renewable energy and to minimize discarding of produced energy.

In order to ensure the stability of electrical networks, the storage of electricity is of prime importance, in order to match energy production with demand. For this reason, large-scale energy storage techniques attract great interest around the world. Among the alternative energy storage technologies, especially in large-scale applications, the Pumped Hydro Storage (PHS) is the most mature and efficient, in order to increase the penetration of renewable sources, allowing for improved elasticity and efficiency of the energy system [1, 2].

Moreover, it is a suitable technology in autonomous power systems with high levels of renewable generation. The main difference between these plants and normal hydroelectric systems is that, besides producing electricity, they also consume it. The operation of a Pumped Storage Hydro Power Plant (PSHPP) is based on the storage of energy in the form of water pumped from a lower elevation tank to a higher elevation one, using excess of energy produced by green sources (or even by conventional sources), which, without storage, is wasted during low demand hours. These systems are capable of storing and providing significant flexibility in starting, interruptions and demand fluctuations. Pumping-storage facilities also provide ancillary network services, such as network frequency control and reserve creation. This is due to the ability of pumping and storage facilities of the hydroelectric plants, to respond to load changes within a few seconds [3, 4].

2. GENETIC ALGORITHMS

The method of Genetic algorithms (GAs) was developed during the 1960s and 1970s by John Holland and his collaborators [5]. It is a search and optimization technique based on the principles of genetics and natural selection. The method mimics the biological evolution and is based on Darwin's natural selection theory.

The genetic algorithm optimization process begins by coding the values of the decision variables into a string of characters, which in analogy with the biological template, is called chromosome and is an arbitrary solution to the problem under consideration. This is followed by the creation of the initial population, which consists of a number of randomly generated chromosomes. These individuals are evaluated on the basis of mathematically formulated criteria, and each is assigned a fitness value. The fitness function may include penalties, which reduce it when the corresponding solution violates constraints of the problem. Then the next generation of chromosomes is created with the help of three key operators (possibly other additives) that mimic biological processes.

First, the selection operator, according to which the most suitable chromosomes have a higher chance of survival and reproduction, is used. The most popular selection methods are the biased roulette wheel and the tournament. The above methods do not fully guarantee that the best chromosome of one generation will pass to the next one. In order to ensure the "survival" of the fittest chromosome, an additional process, called elitism, is incorporated in many codes [6].

Then the crossover operator is applied, with which descendants are formed from two original chromosomes, exchanging randomly parts thereof. The basic idea is that at least one of the new chromosomes could be better than the two parents, if it includes some of their best features. Finally, the mutation operator, which alters some of the characters that make up the strings of chromosomes, introduces new genetic structures and adds some additional variability and diversity to the population. The mutation helps the algorithm not to be trapped by local optima and to reach the global ones. This process (evaluation of chromosomes - implementation of operators) is repeated for a number of generations, determined from the beginning or resulting from a termination criterion. It is expected that in the last generation the optimal, or at least a very good solution to the problem, will have been found [7].

3. OPTIMAL OPERATION SCHEDULING OF A PSHPP WITH WIND FARM USING GENETIC ALGORITHMS

In this paper we present a tool to design the optimal configuration of a wind farm combined with a pumped storage hydro-plant. The optimal generation scheduling of a hydro pump wind system aims to the utilization of water storage ability to improve wind park operational financial gains and to attenuate the active power output variations due to the intermittence of the wind-energy resource [8]. The short-term hydro-wind scheduling suggests that current market mechanisms are inducing generation companies to generate water flows as large as possible, namely to profit from selling electricity, when prices are higher and to pay for pumping as little as possible when prices are low and the wind is high. At times of low electrical demand and high wind energy generation, electric power is used to pump water into the upper reservoir, so the excess of the wind energy can be stored and not discarded. During periods of high electrical demand, water is released back into the lower reservoir through a turbine, thereby generating electricity. Taking into account the conversion losses of the pumping process and evaporation losses, a maximum of 70% to 85% of the electrical energy used to pump the water into the upstream reservoir can be regained.

3.1 Problem formulation and case study

In the present study we consider an open-loop two-reservoir system with hydropower plants in series into a river, and a wind farm as well, shown in Figure 1. The upstream plant is pump storage, it has three reversible pump turbines and is located at the level of the downstream reservoir. The second hydro power plant has three turbines for electricity generation. The hydropower plants are coordinated and cooperate with the wind park and are connected to the grid. The task is to maximize the financial benefits from operating the system over a 24-hour horizon. The objective function in Equation 1, is to maximize the profit from selling energy or power to the electric grid:

$$MaximizeE_{grid} \Rightarrow MaximizeP_{grid} = \sum_{t=1}^{t=24} c_i \cdot P_{grid,t} \tag{1}$$

The maximization of the objective function of short term pumped storage hydro wind scheduling problem is subject to a number of constraints. The operation constraints are summarized as follows (Equations 2-15):

a) System active power balance

$$P_{grid,t} = P_{w,t} + P_{1,t} + P_{2,t} \tag{2}$$

The output of hourly active power of the system that is injected to the grid is equal to the summation of both the hydro production and the available wind power. If the turbine of hydro plant 1 is in pump mode at time t, the $P_{1,t}$ in Equation 2 can be negative. The hydropower from the two reservoirs is calculated by Equation 3 and the net head is calculated by the following Equation 4:

$$P_{hydro_{i,t}}(MW) = \frac{n_i \cdot \rho \cdot g \cdot Q_{i,t} \cdot H_{net_{i,t}}}{1000} \tag{3}$$

$$Hnet_{i,t} = HF_{i,t} - HT_{i,t} - k_i Q_{i,t}^2 \tag{4}$$

If the turbine is in pump mode the pump power is calculated by Equation 5 and the pump head is calculated by the following Equation 6:

$$P_{1pump,t}(MW) = \frac{g \cdot Q_{i,t} \cdot H_{1pump,t}}{1000 \cdot n_{1pump}} \tag{5}$$

$$H_{1pump,t} = HF_{1,t} - HT_{1,t} + k_i Q_{i,t}^2 \tag{6}$$

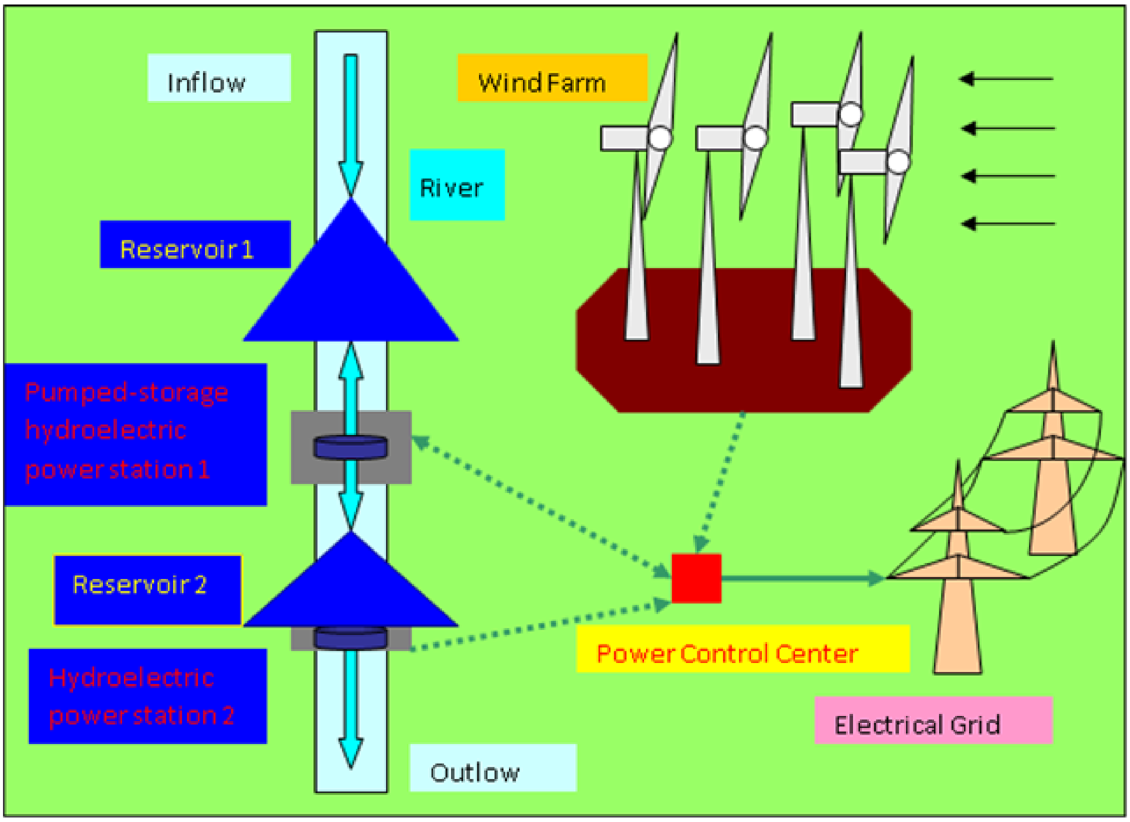


Figure 1: The reservoirs system and the wind Farm (Generated by the authors)

Hydro power plants generation or pumping limits

$$P_{i\ hydro,\ min} \leq P_{i\ hydro,\ t} \leq P_{i\ hydro,\ max} \quad (7)$$

$$P_{1pump,\ min} \leq P_{1pump,\ t} \leq P_{1pump,\ max} \quad (8)$$

Wind power plant generation limit

$$0 \leq P_{w,\ t} \leq P_{w,\ max} \quad (9)$$

The maximum allowable power exchange with the system has a maximum technical power limitation of the transmission line, which is considered as fixed during all 24h periods

$$P_{grid,\ t} \leq 800MW \quad (10)$$

Dynamic water balance in reservoirs or equation of continuity:

$$V_{i,\ t+1} = V_{i,\ t} + I_{i,\ t} - Q_{i,\ t} \quad (11)$$

Maximum and minimum volume levels of reservoirs:

$$V_{i,\ min} \leq V_{i,\ t} \leq V_{i,\ max} \quad (12)$$

Lower and upper discharge limits of the turbines:

$$Q_{i,\ min} \leq Q_i \leq Q_{i,\ max} \quad (13)$$

Lower and upper power limits of the pump mode:

$$Q_{1pump,\ min} \leq Q_{1,\ pump} \leq Q_{1pump,\ max} \quad (14)$$

Initial and final reservoir storage volume:

$$V_{i,12} = V_{i,0} \quad (15)$$

The symbols in Equations 2 to 15 are explained in the following lines:

i: reservoir or hydropower plant index, i = 1,2
t: time interval (h), t = 1; 2; … ;24
E_{grid}: injected energy to network (MWh)
$E_{i,\ t}$: energy output of hydropower plant i (MWh)
$E_{w,\ t}$: available wind energy output of wind farm (MWh)

P_{grid}: injected power to network (MW)
$P_{i,t}$: power output of hydropower plant I at time t (MW)
$P_{w,t}$: available wind power output of wind farm (MW)
c_i: spot electricity price at time t (€/MWh)
$I_{i,t}$: inflow in the reservoir i at time t (m^3/sec)
$V_{i,t}$: water volume of reservoir i at time t (hm^3)
$Q_{i,t}$: discharge from reservoir i through hydro turbine (m^3/sec)
$HF_{i,t}$: Reservoir elevation of the plant at time t (m)
$HT_{i,t}$: Tailrace elevation of the plant at time t (m)
$Hnet_{i,t}$=, Head for the plant at time t for hydropower production (m)
$V_{i,max}$, $V_{i,min}$: max and min volume limits of reservoir i·(hm^3)
$Q_{i,max}$, $Q_{i,min}$: turbine discharge limits for station i; (m^3/sec)
$Q_{1pump,max}$, $Q_{1pump,min}$: pump discharge limits for station 1 (m^3/sec)
$V_{i,0}$: water volume in reservoir i in the first scheduling period(hm^3)
$V_{i,12}$: water volume in reservoir i in the last scheduling period (hm^3)
$n_{i,hydro}$: hydropower generation efficiency factor for hydro plant i
n_{pump}: pumping efficiency for hydro plant 1
k_i: friction coefficients of penstocks (s^2/m^5)
g: gravity acceleration (9.81 m/sec^2)
ρ: water density (1000 kg/m^3)

3.2 Wind power

The wind speed is always fluctuating, and thus the energy content of the wind is always changing. The variation depends both on the weather and on local surface conditions and obstacles. Energy output from a wind turbine will vary as the wind varies, although the most rapid variations will to some extent be compensated for by the inertia of the wind turbine rotor [9]. We consider that the installed capacity of wind farm is $P_{w,max}$ = 1000MW, taking into account the installed capacity of the hydropower plants [8,10]. The wind power forecast (shown in Figure 2) is available for the day-ahead and serves as input. The total energy output of the wind farm in standalone mode is 14300MWh and the profit is 745000.00€.

3.3 Hydropower plants

The technical and operational characteristics of reservoirs and hydropower facilities are summarized in Table 1, while the relationship between elevation and volume is shown in Figure 3. The natural inflow for the first reservoir is $I_{1,t}$ = 0.30hm^3/h (166.67m^3/sec). The second has no natural inflow and $I_{2,t} = Q_{1,t}$

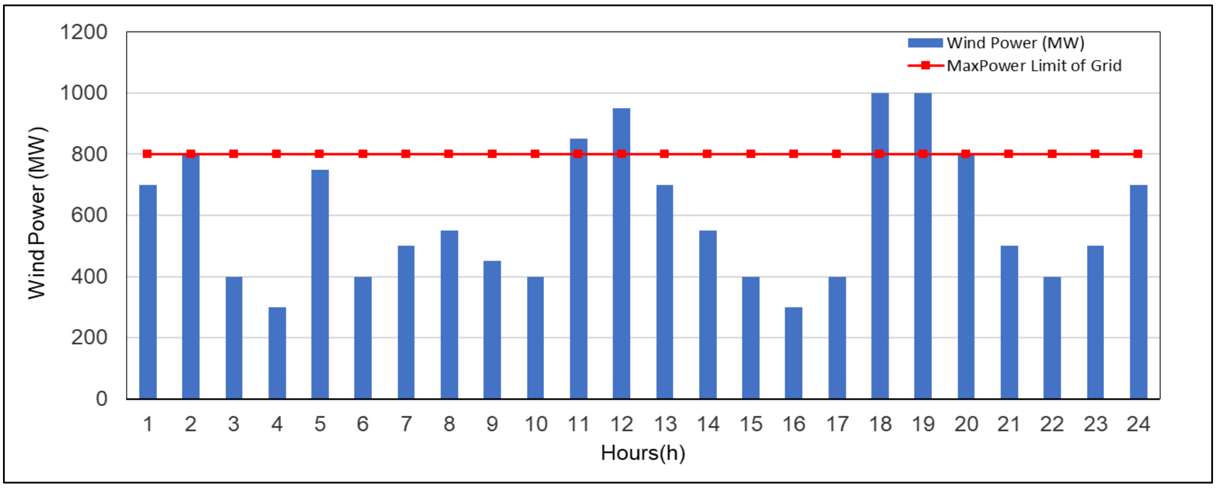


Figure 2: Wind power profile and power limit of the grid

Table 1: Technical and operational characteristics of reservoirs and hydropower facilities

		Reservoir 1	Reservoir 2
Inflow (hm^3/h)		0,30	-
Initial volume (hm^3)		25	21.25
Final volume (hm^3)		25	21.25
Maximum volume operation level (hm^3)		30	25
Minimum volume operation level (hm^3)		20	17.5
Maximum Generation Release (hm^3/h)		1.20	1.20
Minimum Generation Release (hm^3/h)		0.12	0.12
Maximum Pumping Release (hm^3/h)		1.20	-
Minimum Pumping Release (hm^3/h)		0.20	-
Head vs Volume Curve $H_i(m)=a_iV_i^3+b_iV_i^2+c_iV_i+d_i$	a	-0.0071	-0.0052
	b	0.3674	-0.2053
	c	-2.8964	19.651
	d	95.562	-180.81
Maximum Height Level (m)		149.63	100.90
Minimum Height Level (m)		129.79	72.34
Maximum Tailrace level (m)		100.9	20
Minimum Tailrace level (m)		72.34	20
Discharge efficiency		0.88	0.88
Pumping efficiency		0.85	-
Friction coefficients of penstock (sec^2/m^5)		0.00003	0.00007
Generation Capacity Power (MW)		231 (3 x 77)	237 (3 x79)
Capacity Pumping Power (MW)		300 (3 x 100)	-

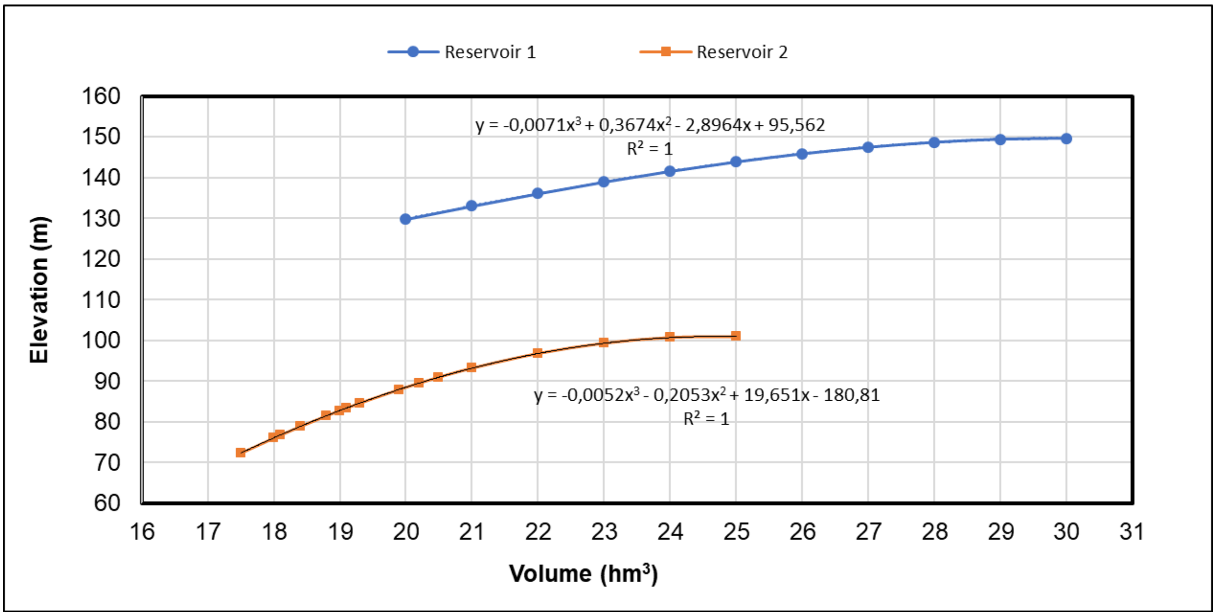


Figure 3: Relationships between reservoirs' water level and volume

3.4 Electricity market price

The 24h day-ahead hourly energy price of the electricity market is shown in Figure 4.

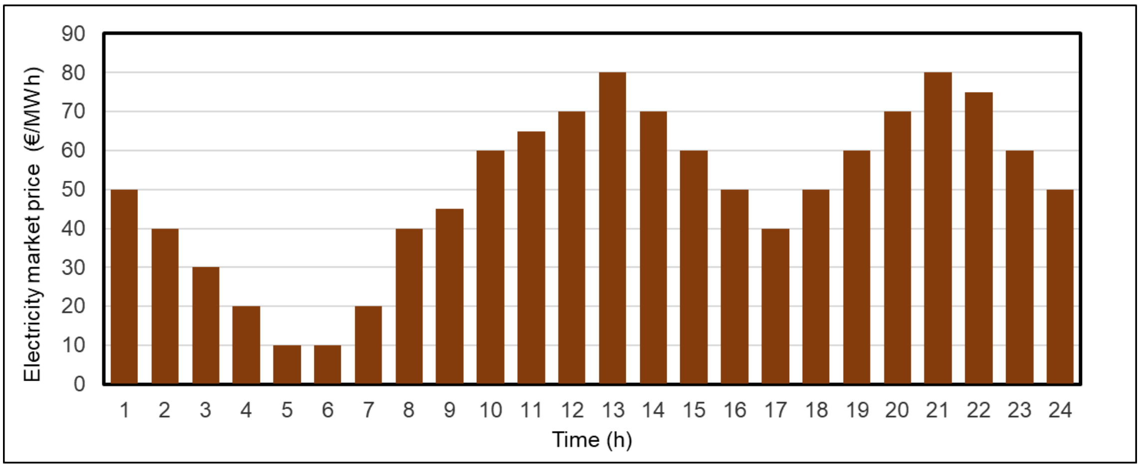


Figure 4: Forecasted market prices of electricity for 24h ahead

4. OPTIMIZATION RESULTS

4.1 Optimization without coordination between wind power and pump storage

In the first case where the reservoir system operates independently of the wind farm, the maximum hydro energy power output, obtained by optimizing the hydrosystem with genetic algorithms is shown in Table 2. The release from the reservoirs and the storage in this case are shown in the diagrams of Figures 5 and 6.

Table 2: Optimization results for case 1

	Pump Storage Hydroplant 1	Hydroplant 2	Total Hydro energy	Wind Farm	System Energy
Energy generation (MWh)	2166.62	2266.10	4432.72	14300.00	18732.72
Energy for pumping (MWh)	-458.50	-	-458.50	-	-458.50
Energy discarded (MWh)	-	-	-	-2456.70	-2456.70
Net energy (MWh)	1.708,12	2.266,10	3974.22	11843.30	15817.52
Economical Revenue	124954,80€	148228,90€	273183.70€	586589.35	859773.05

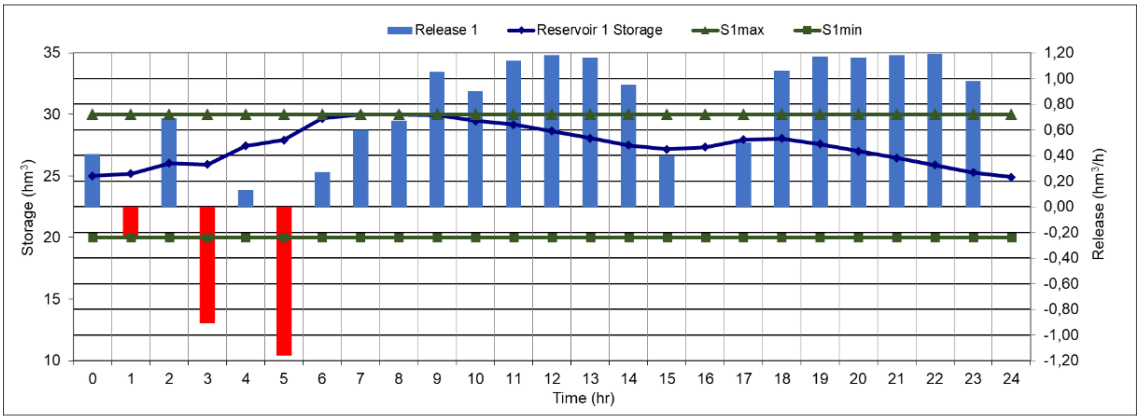


Figure 5: Reservoir 1 storage curve and release profile for case 1

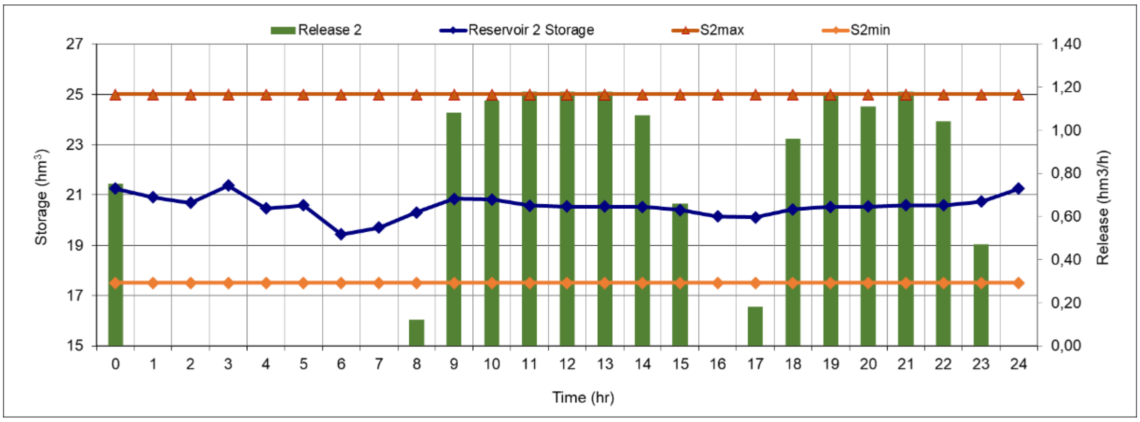


Figure 6: Reservoir 2 storage curve and release profile for case 1

Adding the power of the wind farm to the hydropower the total power exceeds the maximum capacity of the grid and an amount of energy is discarded as shown at diagram fig.7. The wind energy that can be absorbed by the system is 11843.3MWh from the 14300MWh and the discarded energy is 2456.7MWh, which means 83% penetration of wind energy into the grid, as shown in Figure 7. The energy produced from the reservoir system is 3974.22MWh and total energy transferred to the grid is 15817.52MWh. The financial revenue from wind energy is 586589.35€, from hydropower 273183.70€ and the total profit 859773.05€ (Figure 8).

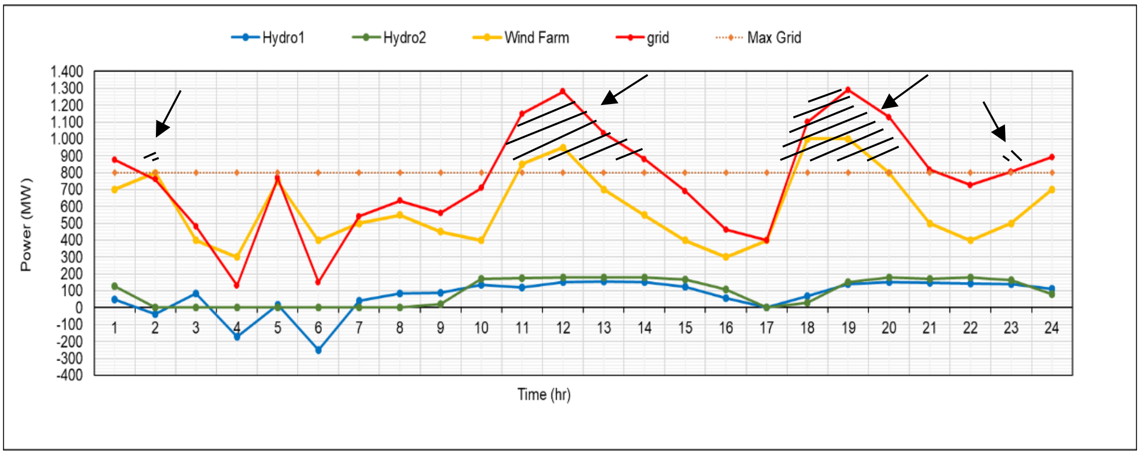


Figure 7: System power output diagram and the energy discarded for case 1

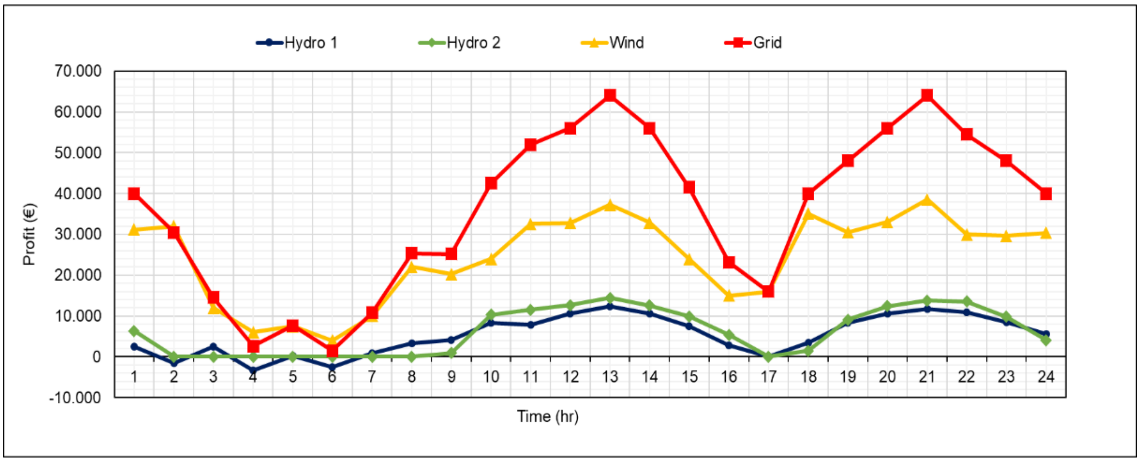


Figure 8: Financial profit diagram for case 1

4.2 Optimization with coordination of wind power and pump storage

Coordinating operation of the reservoir system and the wind farm, the optimization by GAs can balance output of the system and reduce the energy which is discarded to zero, absorbing the excess

power (over 800MW) by pumping water from the downstream reservoir to the upstream one. In this case the maximum hydro energy power output by optimizing the hydro-system with genetic algorithms is shown in Table 3. The release from the reservoirs and the storage in this case are shown in diagrams of Figure 9 and 10.

Table 3: Optimization results for case 2

	Pump Storage Hydroplant 1	Hydroplant 2	Total Hydro energy	Wind Farm	System Energy
Energy generation (MWh)	1923.28	2391.22	4314.50	14300	18614.50
Energy for pumping (MWh)	-601.72	-	-601.72	-	-601.72
Energy discarded (MWh)	-	-	-	0	0
Net energy (MWh)	1321.56	2391.22	3712.78	14300	18012.78
Economical Revenue	60370.40 €	116444.95	176815.35€	745000	921815.35

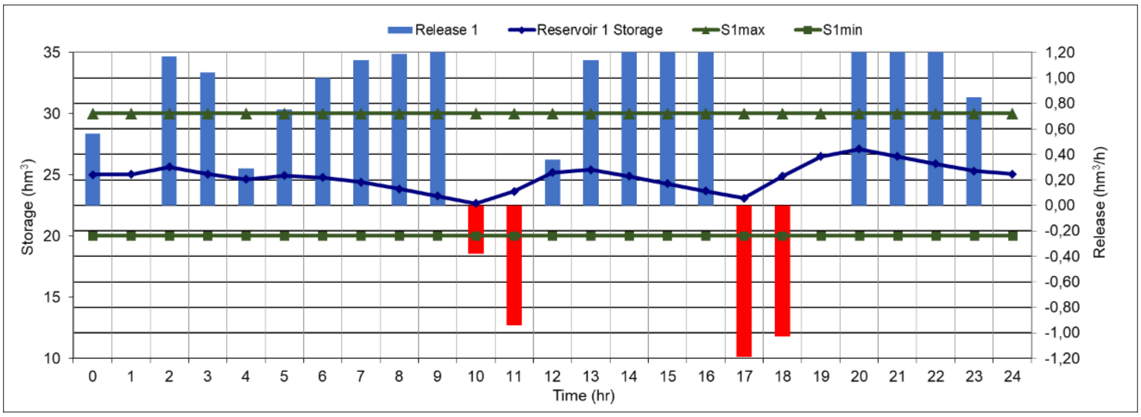


Figure 9: Reservoir 1 storage and release diagram for case 2

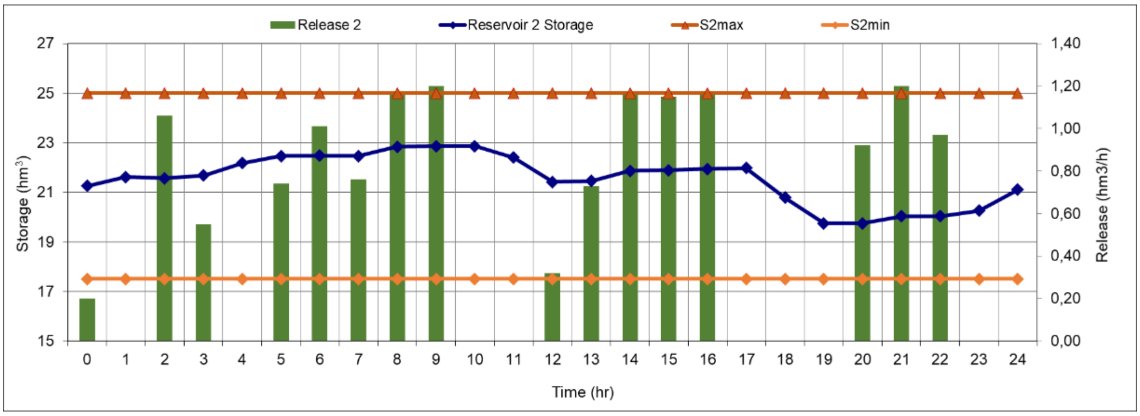


Figure 10: Reservoir 2 storage and release diagram for case 2

The system can absorb all the 14300MWh of wind energy, which is 100% penetration of wind energy. The energy produced from the reservoir system is 3712.78MWh, namely smaller than that of case 1, but the total energy transferred to the grid is 18012.78 MWh, about 14% larger, as shown in Figure 11. The revenue from wind energy in this case is 745000.00€ and from hydropower 176815.35€, summing to a total of 921815.35 €, which means increase 7.2% compared to case 1. The total hydroelectric energy generation and the revenue in the second case are about 7% and 35% smaller respectively, compared to case 1, because in case 1 the reservoir system was optimized taking into account the hydro plant capacity only (Figure 12).

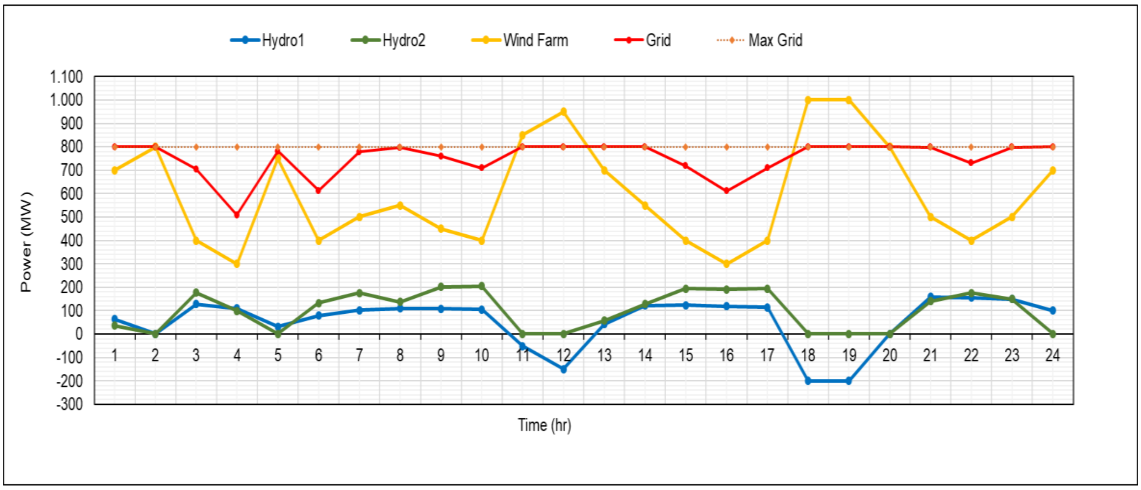


Figure 11: System power output diagram for case 2

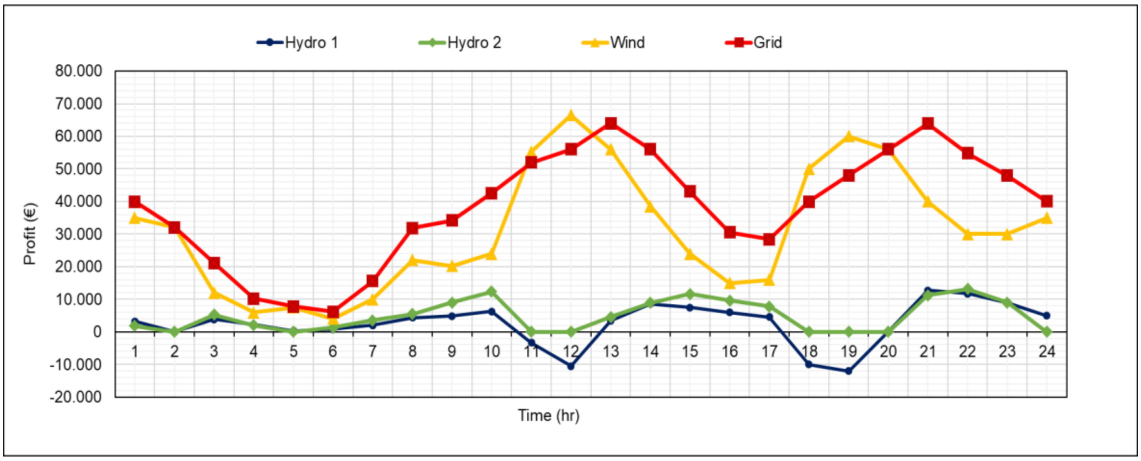


Figure 12: Financial profit diagram for case 2

5. CONCLUSION

In this work, an optimization approach based on genetic algorithms is developed for the optimal scheduling and operation strategy of a cascade two-reservoir system, which has a pumped-storage hydro power plant, a conventional hydro power plant and a wind farm. The aim is to maximize the financial benefits of operating the system over a 24-hour horizon for two cases, with and without coordination. The results show that when the reservoir system is coordinated with the wind farm, the hydroelectricity generation decreases, but the total revenue of the system increases about 7.2% and can achieve high wind energy penetration to the electricity grid.

References

1. E-Storage (2016) World Energy Resources, **World Energy Council**.
2. StoRE (2014) ‘Final Publishable Report’, **Intelligent Energy – Europe** (IEE).
3. Kaldellis J.K. (2010) **‘Stand-Alone and Hybrid Wind Energy Systems’**, Technology, Energy Storage and Applications, Woodhead Publishing.
4. Pérez-Díaz J.I., Chazarra M., García-González J., Cavazzini G. and Stoppato A. (2015) ‘Trends and challenges in the operation of pumped-storage hydropower plants’, **Renewable & Sustainable Energy Reviews**, Vol.44, pp. 767-784.
5. Holland J.H. (1975) ‘**Adaptation in Natural and Artificial Systems**’, University of Michigan Press, Ann Arbor.

6. Katsifarakis K.L. (2012) '**Hydrology, Hydraulics and Water Resources Management: A Heuristic Optimization Approach**', WIT Press.
7. Bakanos P. and K.L. Katsifarakis (2018) 'Development and evaluation of a decision-making system for optimal management of reservoirs in single time horizon', **11th National Conferences on Renewable Energy Sources**, Institute of Solar Technology, Thessaloniki (in Greek).
8. Castruonovo E.D. and Peças Lopes J.A. (2004) 'On the optimization of the daily operation of a wind-hydropower plant', **IEEE Transactions on Power Systems**, 19(3), pp.1599-606.
9. Wagner H.-J. and Mathur J. (2018) '**Introduction to Wind Energy Systems Basics, Technology and Operation',** Springer.
10. Kumar M., Saini P. and Kumar N. (2016) 'Optimization of Wind-Pumped Storage Hydro Power System', **International Journal of Engineering Technology, Management and Applied Sciences**, Vol. 4(4), ISSN 2349-4476.

EVALUATION OF CYPRUS ENERGY RESOURCES IN THE FRAMEWORK OF ENVIRONMENTAL SUSTAINABILITY USING A NOVEL SWOT-PESTEL APPROACH

M. Tsangas* and A.A. Zorpas*

Faculty of Pure and Applied Science, Open University of Cyprus, Environmental Conservation and Management, Laboratory of Chemical Engineering and Engineering Sustainability, Giannou Kranidioti, 33, P.O. Box 12794, 2252, Latsia, Nicosia, Cyprus

*Corresponding author: e-mail: antonis.zorpas@ouc.ac.cy, antoniszorpas@yahoo.com, tsangasm@cytanet.com.cy tel : +357-22411936

Abstract

According to several EU Directives, Cyprus qualifies and is classified as an Emerging Market for Natural Gas and also as Isolated Energy Market. The Country energy natural resources face several contradictions. On one hand, there is not any specific strategy in political level regarding when and how indigenous fossil reserves will be extracted although their commercial exploitation could offer to the Island energy security. Moreover, there are not any oil or gas pipelines as well as no electricity interconnections with other countries. On the other hand, several Sustainability (mainly environmental) targets set by United Nations and the European Commission (either as policies, regulations or directives) must be adopted and therefore fossil fuel use should not be promoted and the contribution of Renewable Energy Sources (RES) must be increased. So, Cyprus needs rather than any other country in the area a holistic sustainable strategy regarding the promotion of RES and to manage its own fossil hydrocarbons reserves. For this a detailed energy resources sustainability strategy analysis is required in order to be able to evaluate the available inputs and to formulate sustainable energy strategic planning. This paper proposes a novel approach to combine PESTEL and SWOT analysis in order to assess the ability to use PESTEL environmental context analysis to categorize and evaluate not only the pillar of externalities, but also the energy resources sustainability internalities. The method is implemented for Cyprus energy resources and emerges not only a number of sustainability opportunities and threats, but also strengths and weakness for the island's future energy resources sustainable development strategy. Furthermore, it is obtained that the proposed novel approach, as it is able to acquire useful results, is promised and suitable for environmental analysis which is a crucial part of the strategic management planning process.

Keywords: PESTEL; SWOT; natural resources; sustainability; energy strategic planning

1. INTRODUCTION

Cyprus has a completely isolated power system and no electricity interconnections (IRENA, 2015). It has also proven natural gas reserves i.e. 141.6 Bcm until 2014 (WEC, 2016) and a renewable energy potential able to provide 25 - 40% of total electricity supply by 2030 as assessed by International Renewable Energy Agency (Lin et al., 2016). It is an insular Country, European Union member since 2004 and according to EU Directives qualifies and is classified as Emerging Market for Natural Gas and as Isolated Energy Market (Directive 2009/72/EC, Directive 2009/73/EC). Although the production of the indigenous natural gas could commence by 2022 (Taliotis et al., 2017) and its exploitation could have considerable impact to the island economic development and energy security (Henderson, 2013), there is not any specific known strategy regarding when and how fossil natural

resources will be extracted. In this framework, there are several energy strategy contradictions. On the one hand, there is the option the natural gas reserves to be exploited and a fossil fuel dominated energy system to be continued with the advantage of the indigenous sources. On the other hand, as required by UN and related EU targets which focus on climate change, reduced hydrocarbon fuels, increased contribution of RES, minimized environmental issues, turn to a low carbon society etc, renewable energy should be promoted and fossil fuel use be mitigated. Therefore, Cyprus needs an efficient energy strategic planning in order to exploit sustainably its energy resources and at the same time conform to global warming mitigation obligations. This paper aims to propose a novel context analysis method, which combines PESTEL and SWOT and is suitable to be used in this process.

2. ENERGY STRATEGIC PLANNING

Due to the crucial importance of sustainable development and climate change mitigation, energy planning optimization has become extremely important (Vazhayil and Balasubramanian, 2012) and moreover not doing rigorous and quantitative energy planning may have high cost (Gómez et al., 2016). Strategic management, initially involves environmental scanning and strategy formulation (i.e strategic planning) and, consequently, strategy implementation, evaluation and control. Environmental scanning requires internal and external factors analysis (Alkhafaji, 2003). Internal and external environmental issues scanning and evaluation is an important step at the preparation of strategic planning (Zorpas et al., 2018). Proper energy planning should be based on an internal and external environment survey and as energy resources availability is key for effective energy planning (Mirjat et al., 2017; Ervural et al., 2018) this paper focuses on such an analysis for Cyprus.

3. ANALYSIS METHOD

3.1 SWOT and PESTEL tools

The PESTLE (Political, Economic, Social, Technical, Legal and Environmental) analysis is an analytical tool for assessing the impact of external contexts on a project or a major operation and also the impact of a project on its external contexts (Basu, 2009). PESTEL (or PESTLE) analysis was originally conceived as ETPS for the economic, technical, political, and social sectors of the environment by Aguilar in 1967. Later in the 1960s, Brown for the Institute of Life Insurance reorganized the analysis as STEP. This macro external environment analysis, or environmental scanning for change, was modified again as so-called STEPE analysis, including also the ecological taxonomy; more recently “L” was also added for legislative or legal concerns (Richardson, 2006). Being a practical business analysis tool (Basu, 2009), PESTEL has been broadly used in environmental research (Fozer et al., 2017; Song et al., 2017; Climent Barba et al., 2016; Zalengera et al., 2014; Shilei and Yong, 2009). As sustainability has social, economic and environmental dimension, it is important in a decision making process to add the institutional dimension (Sharifi and Murayama, 2013). PESTEL provides an essential framework for sustainability analysis and planning.

An important aspect of the strategic planning process is SWOT analysis (Alkhafaji, 2003); that is a strategic analysis tool that combines the study of the strengths and weaknesses of an organization, territory or sector with the study of the opportunities and threats in its environment (Fertel et al., 2013). The name of SWOT analysis is the initials of the words strengths (S), weaknesses (W), opportunities (O), and threats (T). Strengths are positives and weaknesses are negatives related to system internal factors, while opportunities are external factors that have positive interaction with the system and the threats to the system are the negative effects of the system environment (Srdjevic et al., 2012). SWOT analysis is broadly used in energy planning related research (Fertel et al., 2013; Ervural et al., 2018; Khan, 2018).

3.2 SWOT - PESTEL combination novel approach

Prior to the SWOT analysis, the internal and external factors should be well defined (Fertel et al., 2013). As PESTEL refers to external environment factors, it seems suitable for external issues

recognition. The tool may be used for the external environment analysis in order to identify opportunities and threats (Bell and Rochford, 2016). However this paper proposes a novel method, arguing that the PESTEL framework analysis is suitable to spot both external (opportunities and threats) as well internal (strengths and weaknesses) factors.

Although applications conclude to strengths and weaknesses using PESTEL environment analysis are met in the literature (Mayaka and Prasad, 2012; Srdjevic et al., 2012) the issue how the internalities can be provoked by the external environment analysis remains in question. The difficulty to distinguish between internal and external factors may lead to confuse strengths with opportunities or weaknesses with threats (Fertel et al., 2013). To confront this confusion a methodology to discern the internalities from externalities is hereby proposed. In this approach, it is fundamental to define which, concluded by the PESTEL analysis environment factors, may be considered as internal and which as external.

The internal environment involves the resources and capabilities of a company, whereas external environment involves factors beyond the control of a company, but which, nevertheless, are relevant to - and affect the company (Yüksel, 2012). According to Nwagbara (2011) the factors outside the control of the system are external and factors within the control of the system are internal. Outside forces over which management has little or no control, but they affect the organization's development and success compose the external environment (Alkhafaji, 2003).

External environment understanding according to ISO 9001:2015, may be enabled by examining parameters arise by the institutional, technological, cultural, social and financial environment, the competition and the market in international, national, district and local level. In a different approach, according to Bilovaru et al. (2009), referring to a country market characteristics analysis, political, economic, social, technological, environmental and legislative conditions determine country image itself, and, thus, they represent the internal elements of SWOT.

As specified in ISO 9001:2015, internal environment understanding may be enabled by examining parameters connected to organization values, culture, knowledge and performance. Organizations internal environment "is typically described by its organizational structure, resources, climate and culture" (Tang, 1998 cited in Zain and Kassim, 2012). According to literature for SMEs, the categories of internal environmental factors affecting business success are entrepreneur characteristics, SME characteristics, management, products and services, customers and markets, doing business way and cooperation, resources and finance, strategy, company's competitive position, human resources skills, technological capabilities and employees values and backgrounds (Hin et al., 2012). Key internal variables that affect a corporation's strategy formulation are the structure, culture, and resources. Communication processes, work flow, authority and responsibility relationships define structure. Culture is the collection of beliefs, expectations, and values shared by the corporation's members and are transmitted through generations. Corporate resources are the financial, physical, and human resources, organizational systems and technological capabilities (Alkhafaji, 2003).

Based on the internal and external factors outline is derived from the above, two distinguishable sets, referring to energy resources parameters, could be formed. A set including factors classified as internal and a set including factors that are external. So, external or internal factors gleaned by the PESTEL analysis can be distinguished, depending on which set they belong, and they can be classified as S, W, O or T s consequently.

The two sets are the below:

The "Energy resources Internal Factors (IF)" set: IF = {current energy strategy, current production characteristics and resources, energy resources availability}.

The "Energy resources External Factors (EF)" set: EF = {energy demand, economy trend, technology and human resources trends, environmental impacts, legislation, policies, social framework}.

The outline of PESTEL framework can be collected and gleaned by secondary data review as academic literature, government or international organizations websites, factsheets, reports etc. Besides as strengths and opportunities are positives and weaknesses and threats are negatives the methodology sequence proposed to be followed in order to spot them by the SWOT – PESTEL analysis is presented in Figure 1.

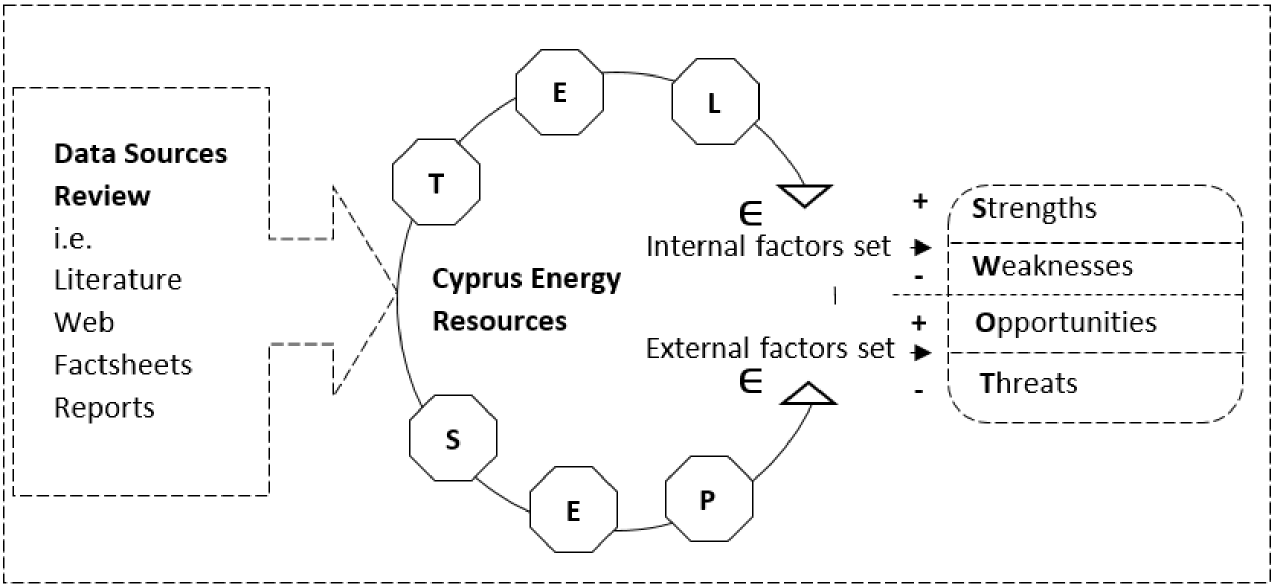


Figure 1. Method

Although sustainability definition is complex and multiply approached, explained and analyzed (Pater and Cristea, 2016; Moldavska and Welo, 2017; Glavic and Lukman, 2007), the results in the proposed method are formulated with a direct approach. Energy resources sustainability strengths, weaknesses, opportunities and threats are either these concern the effort to currently exploit the resources efficiently, or these which are connected to the ability the resources development to be prosperous and not harmful in the long term and for the future generations.

4. CYPRUS ENERGY RESOURCES PESTEL ANALYSIS

4.1 Political Framework

Cyprus is a European Union member since 2004. Its political system is Presidential Republic. On July 1974, Turkey invaded against the Republic of Cyprus and since then 36.2% of the sovereign territory of the country remains under Turkish occupation. This situation is known as the Cyprus problem (PIO, 2017a). Cyprus is geographically and nationally divided into two parts. The south part which is internationally recognized as Republic of Cyprus, and the North part, where there is a self-declared State, recognized only by Turkey. Greek Cypriots live in the southern part and Turkish Cypriots live in the northern part (Laouris and Michaelides, 2017). Hydrocarbon development could potentially be enabler for a Cyprus problem settlement (Gürel and Le Cornu, 2014).

The energy policy of the Government of the Republic of Cyprus has as main axes the market healthy competition ensuring, the energy supply ensuring and the country energy demands satisfaction, with the smallest burden on the national economy and the environment and is fully harmonized with EU energy policy (EAC, 2017a). Cyprus 2020 targets are to reduce 5 % GHG emission limits compared to 2005 greenhouse gas emissions levels, 13% share of energy production by renewable sources and 2.2 Mtoe maximum primary energy consumption (EC, 2018a). Especially for electricity generation and cement and ceramics production the national target set is 21% reduction of GHC emissions by 2020 (DoE, 2017).

So far three hydrocarbons exploration licensing rounds have already held in Cyprus Exclusive Economic Zone (CHC, 2017). According to EU policy, National Governments have control over their oil and gas reserves, but they must follow a set of common EU rules to ensure fair competition during licensing granting for search and production activities (EC, 2018b). Besides, member states must take account the decarbonisation priorities when exploit hydrocarbon reserves (EC, 2014).

Although currently there are no Cyprus pipeline or electric cable interconnections there is such a potential. A 600 kV DC underwater electric cable, currently known as the Euro Asia Interconnector, to connect Israel - Cyprus – Greece transmission networks and a gas pipeline from the East Mediterranean gas reserves to Greece mainland via Crete, currently known as "EastMed Pipeline", have been labelled as Projects of Common Interest (PCI) by European Union (EC, 2017).

4.2 Economic Framework

Cyprus is a eurozone member since 2008 and after financial and economic crisis in 2013 the government required an economic support program funded by EU and IMF which included obligation for a number of reforms as the privatization of state-owned assets, utilities and services (Panayides et al., 2017). The Country has exited the program and fifteen months after the exit Cyprus's economic growth was evaluated as broad-based (IMF, 2017). Country GDP growth rate during the third quarter of 2017 was estimated at + 3.8% comparing to the same quarter of 2016 (MoF, 2017).

Although full liberalization of Cyprus electricity market was formally achieved on 2014, it is not yet implemented in practice. Electricity Authority of Cyprus (EAC) which is semi-public body is presently the only supplier (EC, 2014) and operates three thermal power stations with a total installed capacity of 1478 MW mainly produced with heavy fuel oil (EAC, 2017b). Energy production in Cyprus is mainly depended on imported fuel with 96,4% energy dependence in 2013 amounted 7.1% of the country's GDP, which decreased to 6.7% in 2014 (EY, 2016). Electricity generation of insular systems because of a number of factors are extremely expensive and less secure in the long term (Fokaides and Kyllili, 2014). Cyprus's energy system isolation increases electricity generation costs and imported energy sources dependence (Fokaides et al., 2014).

Cyprus Government supports GHC emissions mitigation targets with renewables and energy efficiency promotion subsidy schemes (Energy Service, 2017), feed in tariffs and net-metering supporting schemes (Poullikas, 2013) and PV projects competitive auctions licensing (Kylili and Fokaides, 2015). Although according to empirical results, renewable energy consumption has positive impact on economic growth, for Cyprus no causality is found (Alper and Oguz, 2016). The natural gas discoveries in Cyprus EEZ are large enough to have considerable impact to the island economic development and energy security (Henderson, 2013) and have the potential within a decade to disengage country energy production from imported oil products and to improve the trade balance in order to reduce the cost of electricity to the economy (Taliotis et al., 2017).

4.3 Social Framework

Cyprus population is estimated at 952100 (PIO, 2017b). In Cyprus there is an ongoing ethnic partition between the Greek Cypriot majority and the sizeable Turkish-Cypriot minority and the island is divided in two ethnically homogenized parts, the Republic of Cyprus in the southern part practically dominated by the Greek-Cypriots, and the 'Turkish Republic of Northern Cyprus', a formation that is recognized only by Turkey occupied by Turkish Cypriots. Although last years there is a relative freedom of movement across the dividing line of the two parts but the partition still remains in place (Zembylas et al., 2016).

Unemployment in Cyprus has a decreasing trend since a peak noted by end of 2015 and in December 2017 was 11.3% decreased, compared to 12.8% in December 2016 (MoF, 2018). Country total employment is forecasted to grow in next years (HRDA, 2017a) and in the same trend new employment needs are also forecasted for electricity supply and natural gas sector (HRDA, 2017b).

4.4 Technical Framework

Energy demand in Cyprus is prospected to rise calculated to be 5% to 44% higher in 2040 than it was in 2010 (Zachariadis and Taibi, 2015). Approved long term forecast of annual total generated electricity upper limit in Cyprus in 2026 according to TSO (2017) is 7215 GWh. Cyprus has significant renewable energy potential with solar potential to be calculated up to 1900 KWh/m^2 per year, total wind potential about 150 and 250 MW (Pilavachi et al., 2009) and annual biodegradable waste biogas generation potential at 242 GWh minimum (Kythreotou et al., 2012). Renewable energy penetration in Cyprus electricity system in 2016 was 8.4% of total generation i.e. 4.7% by wind parks, 3% by PV projects and 0.7% by biomass plants (TSO, 2018).

Cyprus offshore recoverable natural gas quantities are estimated by the Government and foreign energy institutes to may be up to 200 tcf expected to become available in the forthcoming years (Cyprus Institute of Energy, 2012 cited in Fokaides and Kylili, 2014). Proven natural gas reserves until 2014 was 5000.6 bcf (WEC, 2016). Once natural gas becomes available, as a result of provisions made in Vasilikos power station units, generation can switch to this fuel instead of diesel and heavy fuel oil (Taliotis, et al., 2017).

4.5 Environmental Framework

Fossil fuel energy production is connected with many environmental impacts as global warming, ozone layer depletion, abiotic depletion, acidification, eutrophication, fresh water aquatic ecotoxicity, human toxicity, marine aquatic ecotoxicity, photochemical ozone creation and terrestrial ecotoxicity are closely connected with (Atilgan and Azapagicm, 2015). On the other hand producing electricity from RES environmental benefits, including the reduction of GHG emissions, are well known (Serri et al., 2018). However these are also connected with environmental impacts (Zorpas et al., 2017).

Natural gas is a promising transition energy source between higher-carbon fossil fuels and RES in part due to its relatively low GHG emissions and local air pollutants, (Chávez-Rodríguez et al., 2017). On the other hand, offshore hydrocarbon exploration and production as Cyprus case are associated with significant potential impacts to the environment which may include marine pollution and toxicity, benthic disturbance, impacts to wildlife, birds and fish, biological depletion, loss of archaeological heritage, health and safety incidents, atmospheric emissions and drilling fluids, muds and cuttings as well as other solid and fluid waste production (Elbisy, 2016; Speight, 2015). Besides, offshore platforms accidents may result to severe environmental damage (Stout et al., 2017).

4.6 Legal Framework

Several laws and regulations regulate energy activities in Cyprus. Energy infrastructure projects including natural gas and renewable energy projects, with the exception of under 100 kW photovoltaic systems, require Environmental Impact Assessment preparation (Zorpas et al., 2017). Health and Safety issues of energy activities are regulated under Safety and Health at Work Laws of 1996 to 2015 and the related regulations also. Department of Environment strategic plan 2016 - 2018 include activities for appropriate restructure of the institutional framework with respect to the management of the environmental aspects of energy and hydrocarbons (DoE, 2017).

The conditions for granting and using authorizations for the prospection, exploration and production of hydrocarbons are regulated by the Republic of Cyprus legislation harmonized with directive 94/22/EC. The safety of offshore oil and gas operations issues are regulated by legislation harmonized with directive 2013/30/EU which establishes minimum requirements for preventing major accidents in offshore oil and gas operations and limiting the consequences of such accidents.

5. RESULTS

Implementing the methodology presented in Figure 1., the findings that can be classified as internal or external positive or negative effect facts are gleaned by the above PESTEL framework analysis.

So the Cyprus Energy Sources sustainability strengths, weaknesses, opportunities and threats are concluded as follows.

Considering internal factors set members is emerged that, regarding current energy strategy, the lack of a known coherent Country energy strategy is a negative effect fact so it is a weakness. Commencement of hydrocarbons exploitation, interconnections political approval, electricity system legal liberalization and EU membership can be classified as related positives so they are strengths. Regarding energy resources availability, it is positive that the Country has natural gas and renewable energy potential but island energy isolation and imported fuels dependence are negatives. Besides current heavy fuel oil based electricity production has negative effect so it is a weakness referring to production characteristics.

External factors set members consideration emerges that energy demand prospected raise, observed economy growth, GHG emissions reduction targets, solid legal requirements for energy related activities, natural gas and renewables environmental benefits, existing power plants conversion to natural gas potential and natural gas reserves enabled Cyprus problem resolution potential are positive effect facts. These are connected to energy resources external factors set members, so there are opportunities. Relevant negative effect factors, therefore threats, are the Cyprus problem and the existing ethnic partition, electricity system factual liberation delay and the noted unemployment decreasing trend in combination with increased energy sector employment needs.

A Cyprus Energy Sources SWOT matrix containing above results is presented in Figure 2.

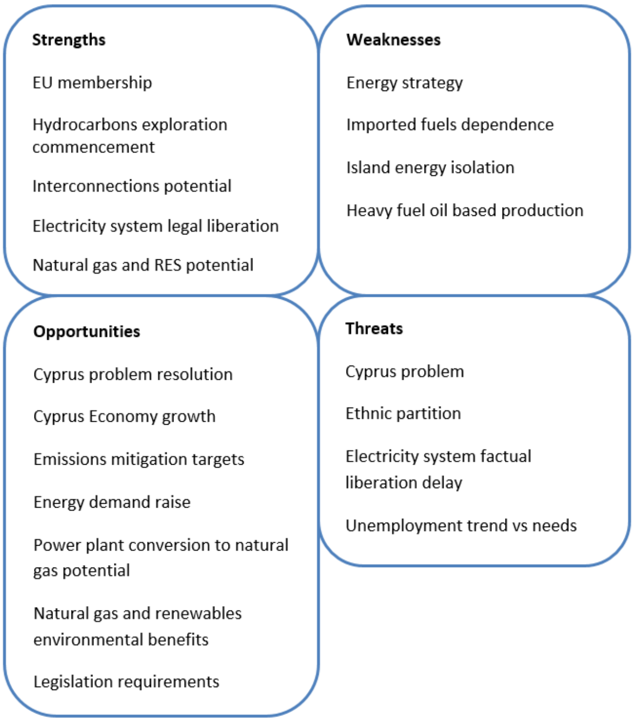


Figure 2. Cyprus Energy Resources SWOT matrix

6. CONCLUSIONS

The proposed SWOT-PESTEL qualitative analysis method implemented, emerged a number of sustainability strengths, weaknesses, opportunities and threats. SWOT analysis typically generates strategic alternatives (Alkhafaji, 2003) and aims to maximize strengths and opportunities potential while minimizing weaknesses and threats effects (Schmoldt and Peterson, 2000 cited in Fertel et al., 2013). So the observations can be used to evaluate the Cyprus energy resources and to formulate energy strategy aiming to maximize strengths, minimize weaknesses, enhance opportunities and confront threats. Therefore, the energy policy of the Country should be more coherent deploying

European Union policies, targets and guidelines. Electricity and pipelines interconnections as well as natural gas reserves exploitation should be sought to in combination with power plants conversion for this fuel use, energy market actual linearization and renewables contribution maximization. Regarding social issues energy sector employment should be taken into consideration and energy planning to be thought as a Cyprus problem solution enabler.

As SWOT analysis, even if it is well structured, it is subjective and it is difficult to reach a consensus about its results (Fertel et al., 2013), the proposed methodology must be connected to the same limitation. But its application shows that it is suitable to overcome the core limitation of effective internal and external factors detection and segregation. It must also be mentioned that limitations of this paper results are that analysis is based on available secondary data and that transportation as well as domestic heating systems energy needs have not been considered.

References

1. Alkhafaji A. F. (2003) '**Strategic Management Formulation, Implementation, and Control in a Dynamic Environment**', The Haworth Press.
2. Alper A. and Oguz O. (2016) 'The role of renewable energy consumption in economic growth: Evidence from asymmetric causality', **Renewable and Sustainable Energy Reviews**, Vol. 60, pp. 953–959.
3. Atilgan B. and Azapagic A. (2015) 'Life cycle environmental impacts of electricity from fossil fuels in Turkey', **Journal of Cleaner Production**, Vol. 06, pp. 555-564.
4. Basu R. (2009) **'Implementing Six Sigma and Lean: A Practical Guide to Tools and Techniques**', Butterworth-Heinemann.
5. Bell G. G. and Rochford L (2016) 'Rediscovering SWOT's integrative nature: A new understanding of an old framework', **The International Journal of Management Education**, Vol. 14, pp. 310-326.
6. Bivolaru E., Andrei R. and Purcăroiu G. V. (2009) 'Branding Romania: A PESTEL Framework Based on a Comparative Analysis of Two Country Brand Indexes', **Management & Marketing,** Vol. 4, No. 4, pp. 101-112.
7. Chávez-Rodríguez M. F. et al (2017) 'Modelling the natural gas dynamics in the Southern Cone of Latin America', **Applied Energy**, Vol. 201, pp. 219–239.
8. CHC (2017), http://chc.com.cy/activities/brief-outline/ (accessed December 27th, 2017)
9. Climent Barba F. et al. (2016) 'A technical evaluation, performance analysis and risk assessment of multiple novel oxy-turbine power cycles with complete CO2 capture', **Journal of Cleaner Production**, Vol. 133, pp. 971-985.
10. **DIRECTIVE 2013/30/EU** of the European Parliament and of the Council of 12 June 2013 on safety of offshore oil and gas operations and amending Directive 2004/35/EC
11. **DIRECTIVE 2009/73/EC** of the European Parliament and of the Council of 13 July 2009 concerning common rules for the internal market in natural gas and repealing Directive 2003/55/EC
12. **DIRECTIVE 2009/72/EC** of the European Parliament and of the Council of 13 July 2009 concerning common rules for the internal market in electricity and repealing Directive 2003/54/EC
13. **DIRECTIVE 94/22/EC** of the European Parliament and of the Council of 30 May 1994 on the conditions for granting and using authorizations for the prospection, exploration and production of hydrocarbons

14. DoE (2017) http://www.moa.gov.cy/moa/environment/environmentnew.nsf/4874C4A6C6CE24F5C2257EF2003365EA/$file/Strategic%20Plan%202016-2018.pdf (accessed December 27th, 2017)

15. EAC (2017a) https://www.eac.com.cy/EN/EAC/Sustainability/Pages/Energiakipolitiki. aspx (accessed December 27th, 2017)

16. EAC (2017b) https://www.eac.com.cy/EN/eac/operations/Pages/Generation.aspx (accessed December 27th, 2017)

17. EC (2018a) https://ec.europa.eu/info/business-economy-euro/economic-and-fiscal-policy-coordination/eu-economic-governance-monitoring-prevention-correction/european-semester/european-semester-your-country/cyprus/europe-2020-targets-statistics-and-indicators-cyprus_en (accessed February 24th, 2018)

18. EC (2018b) https://ec.europa.eu/energy/en/topics/oil-gas-and-coal/oil-and-gas-licensing (accessed February 24th, 2018)

19. EC (2017) 'The Union List of Projects of Common Interest ('Union List')', European Commission.

20. EC (2014), **European Energy Security Strategy**, European Commission.

21. Elbisy M. S. (2016) 'Environmental Management of Offshore Gas Platforms in Abu Qir Bay, Egypt', **KSCE Journal of Civil Engineering**, Vol. 20 (4), pp. 1228–1241.

22. Energy Service (2017) http://www.mcit.gov.cy/mcit/EnergySe.nsf/page11_gr/page11_gr?OpenDocument (accessed December 27th, 2017)

23. EY (2016) **Energy Sector Dynamics**, Ernst & Young.

24. Ervural B. C., Zaim S., Demirel O.F., Aydin Z. and Delen D. (2018) 'An ANP and fuzzy TOPSIS-based SWOT analysis for Turkey's energy planning', **Renewable and Sustainable Energy Reviews**, Vol. 82, Part 1, pp. 1538-1550.

25. Fertel C., Bahn O., Vaillancourt K. and Waaub J-P. (2013) 'Canadian energy and climate policies: A SWOT analysis in search of federal/provincial coherence', **Energy Policy**, Vol. 63, pp. 1139-1150.

26. Fokaides P. A. and Kylili A. (2014) 'Towards grid parity in insular energy systems: The case of photovoltaics (PV) in Cyprus', **Energy Policy**, Vol. 65, pp. 223–228.

27. Fokaides P. A., Miltiadous I.-Ch. , Neophytou M. K.-A. and L.-P. Spyridou (2014) 'Promotion of wind energy in isolated energy systems: the case of the Orites wind farm', **Clean Technologies and Environmental Policy**, Vol. 16 (3), pp 477–488.

28. Fozer D. et al. (2017) 'Life cycle, PESTLE and Multi-Criteria Decision Analysis of CCS process alternatives', **Journal of Cleaner Production**, Vol. 147, pp. 75-85.

29. Glavic P. and Lukman R. (2007) 'Review of sustainability terms and their definitions', **Journal of Cleaner Production**, Vol. 15, pp. 1875-1885.

30. Gómez A., Dopazo, C. and Fueyo N. (2016) 'The "cost of not doing" energy planning: The Spanish energy bubble', **Energy**, Vol 101, pp. 434-446.

31. Gürel A. and Le Cornu L. (2014) 'Can Gas Catalyse Peace in the Eastern Mediterranean?' **The International Spectator**, Vol. 49 (2), pp. 11-33.

32. Henderson S. (2013) '**Natural Gas Export Options for Israel and Cyprus**', The German Marshall Fund of the United States.

33. Hin C. W., Bohari A.M., Isa F. M. and Maddin A. M. (2012) 'Assessing The Model of Wheelen and Hunger (2008) Model of Internal Environmental Scanning And Its Applications to the Small

Medium Enterprise (SME) in Malaysia', **Asian Journal of Business and Management Sciences**, 2 (8), pp.24-33.

34. HRDA (2017a) http://www.anad.org.cy/images/media/assetfile/Forecasts%20of%20Employment%20Needs%20in%20the%20Cyprus%20Economy%202017-2027%20-%20Summary.pdf (accessed December 27th, 2017)
35. HRDA (2017b) http://www.anad.org.cy/images/media/assetfile/D.pdf (accessed December 27th, 2017)
36. IMF (2017) **Country Report No. 17/148**, International Monetary Fund.
37. IRENA (2015) **'Renewable Energy Roadmap for the Republic of Cyprus',** International Renewable Energy Agency.
38. ISO (2015) Quality management systems — Requirements, ISO 9001. ISO, Geneva.
39. Khan M.I. (2018) 'Evaluating the strategies of compressed natural gas industry using an integrated SWOT and MCDM approach', **Journal of Cleaner Production**, Vol. 172, pp. 1035-1052.
40. Kylili A and Fokaides P. A. (2015) 'Competitive auction mechanisms for the promotion renewable energy technologies: The case of the 50 MW photovoltaics projects in Cyprus', **Renewable and Sustainable Energy Reviews**, Vol. 42, pp. 226-233.
41. Kythreotou, N., Tassou, S.A. and Florides, G. (2012) 'An assessment of the biomass potential of Cyprus for energy production', **Energy**, Vol. 47, pp. 253- 261.
42. Laouris Y. and Michaelides M (2017) 'Structured Democratic Dialogue: An application of a mathematical problem structuring method to facilitate reforms with local authorities in Cyprus'. **European Journal of Operational Research**, article in press.
43. Lin J-H., Wu Y-K. and Lin H-J. (2016) 'Successful experience of renewable energy development in several offshore islands', **Energy Procedia**, Vol. 100, pp. 8 – 13.
44. Mayaka. M. A. and Prasad, H. (2012) 'Tourism in Kenya: An analysis of strategic issues and challenges', **Tourism Management Perspectives**, Vol. 1 (1), pp. 48–56.
45. MoF (2017) http://mof.gov.cy/en/economic-indicators/macroeconomics/main-economic-indicators/gdp-growth-rate-2013-q1-2017-q3 (accessed December 27th, 2017)
46. MoF (2018) http://mof.gov.cy/en/economic-indicators/macroeconomics/main-economic-indicators/1-unemployment (accessed February 24th, 2018)
47. Mirjat N. H., Uqaili M. H., Harijan K., Das Valasai G., Shaikh F. and Waris M. (2017) 'A review of energy and power planning and policies of Pakistan', **Renewable and Sustainable Energy Reviews**, Vol. 79, pp. 110-127.
48. Moldavska A. and Welo T. (2017) 'The concept of sustainable manufacturing and its definitions: A content-analysis based literature review', **Journal of Cleaner Production**, Vol. 166, pp. 744-755.
49. Nwagbara U. (2011) 'Waterstone's and the changing bookselling environment in the UK: the journey so far and prospects," **Economic Sciences Series, Petroleum - Gas University of Ploiesti BULLETIN**, Vol. LXII, No. 3, pp. 14-26.
50. Panayides P. M., Lambertides N. and Andreou C. (2017) 'Reforming public port authorities through multiple concession agreements: The case of Cyprus', **Research in Transportation Business & Management**, Vol. 22, pp. 58-66.
51. Pater L. R. and Cristea S. L. (2016), 'Systemic Definitions of Sustainability, Durability and Longevity', **Procedia - Social and Behavioral Sciences**, Vol. 221, pp. 362 – 371.

52. Pilavachi, P.A., Kalampalikas, N.G., Kakouris, M.K., Kakaras, E. and Giannakopoulos, D. (2009) 'The energy policy of the Republic of Cyprus', **Energy**, Vol. 34 pp. 547-554.
53. PIO (2017a) http://www.aspectsofcyprus.com/consequences-of-the-cyprus-problem/ (accessed December 27th, 2017)
54. PIO (2017b) http://www.aspectsofcyprus.com/population/ (accessed December 27th, 2017)
55. Poullikkas A. (2013) 'A comparative assessment of net metering and feed in tariff schemes for residential PV systems', **Sustainable Energy Technologies and Assessments**, Vol. 3, pp. 1-8.
56. Richardson J.V. Jr., (2006) 'The Library and Information Economy in Turkmenistan', **IFLA Journal**, Vol. 32 (2), pp. 131–139.
57. Serri L., Lembo E., Airoldi D., Gelli C. and Beccarello M., (2018) 'Wind energy plants repowering potential in Italy: technical-economic assessment'**, Renewable Energy**, Vol. 115, pp. 382-390.
58. Sharifi A. and Murayama A., (2013) 'A critical review of seven selected neighborhood sustainability assessment tools', **Environmental Impact Assessment Review**, Vol. 38, pp.73–87.
59. Shilei L. and Yong W., (2009) 'Target-oriented obstacle analysis by PESTEL modeling of energy efficiency retrofit for existing residential buildings in China's northern heating region', **Energy Policy**, Vol. 37 (6), pp. 2098-2101.
60. Song J., Sun Y. and Jin L. (2017) 'PESTEL analysis of the development of the waste-to-energy incineration industry in China', **Renewable and Sustainable Energy Reviews**, Vol. 80, pp. 276–289.
61. Speight J. G. (2015) **Handbook of offshore oil and gas operations, First edition**, Elsevier.
62. Srdjevic Z., Bajcetic R. and Srdjevic B., (2012) 'Identifying the Criteria Set for Multicriteria Decision Making Based on SWOT/PESTLE Analysis: A Case Study of Reconstructing AWater Intake Structure', **Water Resour Manage**, Vol. 26, pp. 3379–3393.
63. Stout S. A. et al. (2017) 'Assessing the footprint and volume of oil deposited in deep-sea sediments following the Deepwater Horizon oil spill', **Marine Pollution Bulletin**, Vol. 114 (1), pp. 327-342.
64. Taliotis C., Rogner H., Ressl S., Howells M. and Gardumi F. (2017) 'Natural gas in Cyprus: The need for consolidated planning,' **Energy Policy**, Vol 107, pp. 197–209.
65. The Safety and Health at Work Laws of 1996 to (N. 2) of 2015 (Unofficial Consolidation and Translation of the Law)
66. TSO (2018) http://www.dsm.org.cy/el/cyprus-electrical-system/electrical-energy-generation/energy-generation-records/yearly/res-penetration (accessed February 24th, 2018)
67. TSO (2017) http://www.dsm.org.cy/en/cyprus-electrical-system/electrical-energy-generation/long-term-forecast (accessed December 27th, 2017)
68. Vazhayil J. P. and Balasubramanian R. (2012) **'Hierarchical multi-objective optimization of India's energy strategy portfolios for sustainable development'**, International Journal of Energy Sector Management, Vol. 6, Issue: 3, pp. 301-320.
69. WEC (2016) **'World Energy Resources 2016, 3. Natural Gas'**, World Energy Council.
70. Yüksel I. (2012) 'Developing a Multi-Criteria Decision Making Model for PESTEL Analysis', **International Journal of Business and Manage**ment, Vol. 7 (24) pp. 52-66.

71. Zain M. and Kassim N. M. (2012) 'The Influence of Internal Environment and Continuous Improvements on Firms Competitiveness and Performance', **Procedia - Social and Behavioral Sciences**, 65, pp. 26 – 32.
72. Zachariadis T. and Taibi E. (2015) 'Exploring drivers of energy demand in Cyprus – Scenarios and policy options', **Energy Policy**, Vol. 86, pp. 66–175.
73. Zalengera C. et al. (2014) 'Overview of the Malawi energy situation and A PESTLE analysis for sustainable development of renewable energy', **Renewable and Sustainable Energy Reviews,** Vol. 38, pp. 335–347.
74. Zorpas A. A., Voukkali I. and Pedreno J.N. (2018) 'Tourist area metabolism and its potential to change through a proposed strategic plan in the framework of sustainable development', **Journal of Cleaner Production**, Vol. 172, pp. 3609-3620.
75. Zorpas A., Tsangas M., Jeguirim M., Limousy L. and Pedreno J. N. (2017) 'Evaluation of renewable energy sources (solar, wind, and biogas) established in Cyprus in the framework of sustainable development', **Fresenius Environmental Bulletin**, Vol. 26, pp. 5529-5536.
76. Zembylas M., Charalambous P. Charalalmbous C. and Lesta S, (2016) 'Human rights and the ethno—nationalist problematic through the eyes of Greek-Cypriot teachers' **Education, Citizenship and Social Justice**, Vol. 11 (1), pp. 19 – 33.

BIOCLIMATIC HOUSE DESIGN BY APPLYING PASSIVE SYSTEMS AND GREEN ROOF

[1]S. M. Bagiouk*, [2]S. S. Bagiouk, [2]A. E. Agiou, [1]A. S. Bagiouk

[1]Division of Hydraulics and Environmental Engineering, Dept. of Civil Engineering, Aristotle University of Thessaloniki, 54124 Thessaloniki, Greece

[2]Department of Civil Engineering, Democritus University of Thrace, 67131, Xanthi, Greece

*Corresponding author: [1]E-mail: smpagiou@civil.auth.gr, Tel +30 2310 995893, +30 6944189218

Abstract

A major issue that contemporary society deals with is adopting "sustainability" and "viability" values. The solution to this problem comes through a complex process. In that process the building sector is a vital factor and should not be eliminated. In this paper, it is presented the design and the construction of a house that obeys to the principles of bioclimatic design. In this bioclimatic residence, it is applied passive systems over its building shell. Moreover, one more characteristic which worth to be mentioned is the use of green roof because of the benefits that derives through it. The aim of this paper is the design of a building that exploits natural resources, reduces carbon dioxide emissions and provides thermal comfort to its users. Finally, it is displayed a comparison of the economic and energy benefits between a bioclimatic home and a conventional one.

Keywords: bioclimatic design, green roof, passive systems, energy benefits, natural resources

1. INTRODUCTION

Bioclimatic housing is the environmentally friendly building that utilizes natural factors and climatic data. It is properly adjusted to the topography of the soil and through the right design itis ensured the creation of the appropriate microclimate, providing coolness in the summer and warmth in the winter. It is mainly governed by bioclimatic design which is not a new created design trend as it appears to have been applied since ancient Greece.A characteristic reference is made in the memoirs of Xenophon, as well as in Hippocrates' work ‘’On air waters and places’’, where reference is made to Socrates' Solar House and to the principles of bioclimatic architecture respectively, with the sole aim of ensuring a harmonious relationship between the man and the environment [1]. In modern times, particularly in Europe, where the building sector is responsible for 40% of total energy consumption and 36% of CO2 emissions (European Commission of Energy Efficiency in Buildings) the European Union has been aiming to improve energy efficiency, to reduce greenhouse gas emissions by 20% (compared to 1990), and to increase the amount of RES by 2020[4].In the case of Greece as well as other Mediterranean climate countries, a bioclimatic house can have a 30% energy savings compared to a conventional building.However, this savings can also reach 80% if they are compared to an older one without insulation building[7].Bioclimatic design has the ultimate goal of protecting the environment, saving energy, reducing operating costs and improving the indoor climate of the buildings so as to ensure thermal and visual comfort, as well as offering an overall living quality for users.To achieve this, the correct orientation of the building, the proper layout of the spaces, the proper design of the building shell is chosen, in order to maximize the sunshine during the wintertime and minimize it during the summertime and finally a guiding principle of bioclimatic design is being used, ie the use of passive heating and cooling systems.In the present paper, in the house of which bioclimatic architecture was studied and depicted, the Trombe wall was chosen as a basic passive

system and in addition a planted roof was placed as a passive energy saving technique in order to provide additional environmental and economic benefits.A bioclimatic house in order to approach the standards of the ideal residence should not just provide comfort and energy savings, but it is desirable to offer the user aesthetic satisfaction[2], which in our case is achieved with the planted roof and the features of bioclimatic architecture.The present paper aims to the highlighting of the energy and economic gains generated by the use of passive systems and also at the situating of a planted roof in a hypotheticalhouse designed according to the general principle of bioclimatic design[6].The passive systems[8] as well as the openings were designed and attached to the south face of the study building based on the climatic and environmental conditions of Central Macedonia.In addition, the thermal insulation proposed for the specified house in order to exhibit satisfactory results could display characteristics (thermal conductivity, specific heat capacity, density etc) close to those of graphite expanded polystyrene.Finally, the house under study of this paper has been accepted as being constructed in an open space, remaining unaffected by neighboring buildings.

2. BIOCLIMATIC DESIGN GUIDELINES AND GREEN ROOF

2.1 House shape and orientation

The house has an elongated shape along the east-west axis, creating a larger surface to the south for collecting and utilizing solar heat in the winter months through the openings and passive systems [5]. The ratio of its sides is about = 1/1.5 which makes it very close to the ideal one according to the calculations and the measurements made in various ratios, as with this ratio it is managed to avoid creating dark spaces as there is no part of the house that is not fully illuminated, even partially[9].As far as the orientation is concerned, it follows the Southeastern orientation just like the traditional Greek house[2] as it is considered to be the ideal orientation for the current case and for the geographical position of Greece, in order to exploit the sun and all the environmental benefits.Specifically in the house which is examined, the south side was considered for the living room, the east for the kitchen and the bedrooms and the west side whichis considered most appropriate for the location of a room mainly used in the winter, where sun protection measures were taken in order to avoid overheating of the indoor space in the afternoon hours of the summer.Finally, the north side was considered suitable for warehouses, stairwells and bathrooms which are secondary spaces, as it offers low levels of lighting during all seasons and is characterized by the cold.

2.2 Spaces Layout

The residence that is designed is a two-storey bioclimatic house with a siting of the interior places that utilizes every piece of the house for the intended use [5].More generally, the house meets the general principle of bioclimatic design[6], ie it places the South side for the siting of the most important functions of the building and for use of passive solar heating systems, while the North side is appropriate for maintaining the heat and offering protection against the winds.In particular, in the southern parts of the building are placed the main areas of the house, those rooms in which the tenants spend most of their time such as the living room (Figure 1 and Figure 2).It is considered to be the most suitable choice for these places because during the winter months the sun's rays are low on the horizon and thus they enter deep into the interior by heating and lighting the rooms while during the summer months the rays are high and with the use of a sunblindthe overheating of the interior spaces is prevented.On the contrary, on the northern side there are secondary areas and spaces where the users do not stay for many hours such as a warehouse, bathroom and guesthouse. These spaces are cooler, require more protection from strong winds, act as a buffer zone against cold winds and reduce the heat loss of the main use areas.Also on the eastern side there are placed spaces that need to enjoy the morning sunshine, to warm up in the morning and to cool down at midday hours.Finally in the west there are spaces that are mainly used in the winter and not spaces such as the kitchen since if the heat produced by the cooking added to the heat of the sun, the interior space would be overheated at undesirable levels[16].The need for sun protection of the passive systems and openings to avoid high temperatures during the summer months, can easily beachieved with the installation of special sun

blinds. In this case this role is adopted and implemented by appropriately designed and shaped balconies. In general, the use of sun blinds is not the only option for protection as there is a range of choices.

Another simple and natural way for sun protection of the building ,as well as its passive systems and openings, can be achieved by placing deciduous trees and vegetation in the south orientation, which once again proves that the nature and the environment not only do not oppose the construction but are allies for a much better result.The layout of the places, the relationship between the sides, the openings and the architecture are not the only features that make the building unique since it displays passive systems such as the Trombe wall[8] and the green roof,which besides its energy and economic benefits provides also aesthetic. (Figure 3).

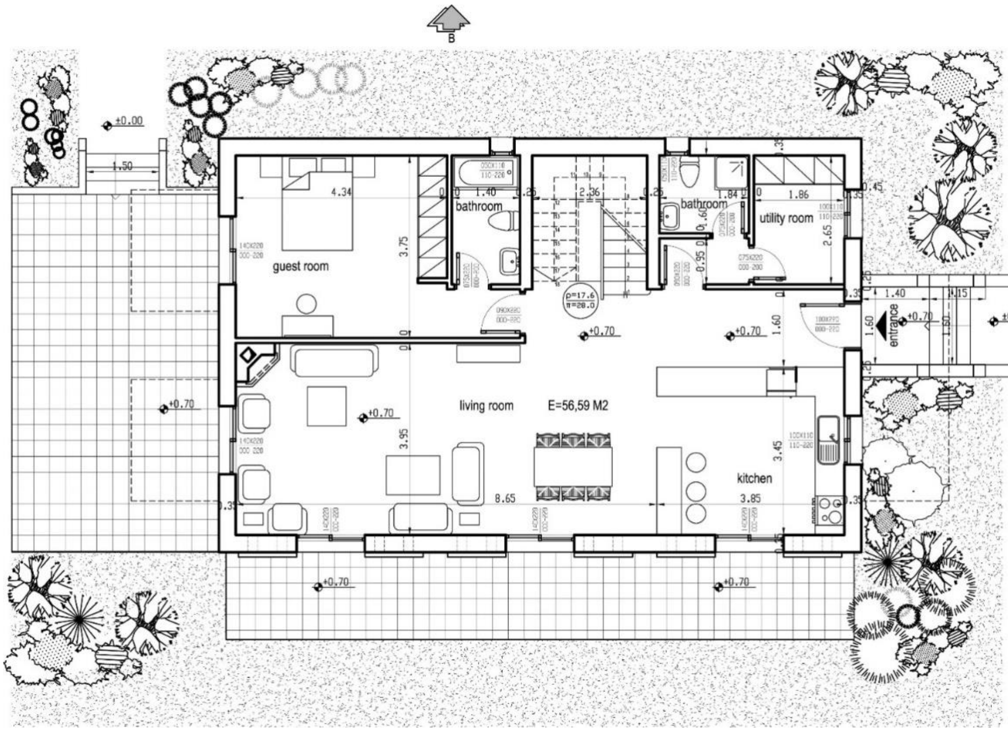


Figure 1. Ground floor plan view

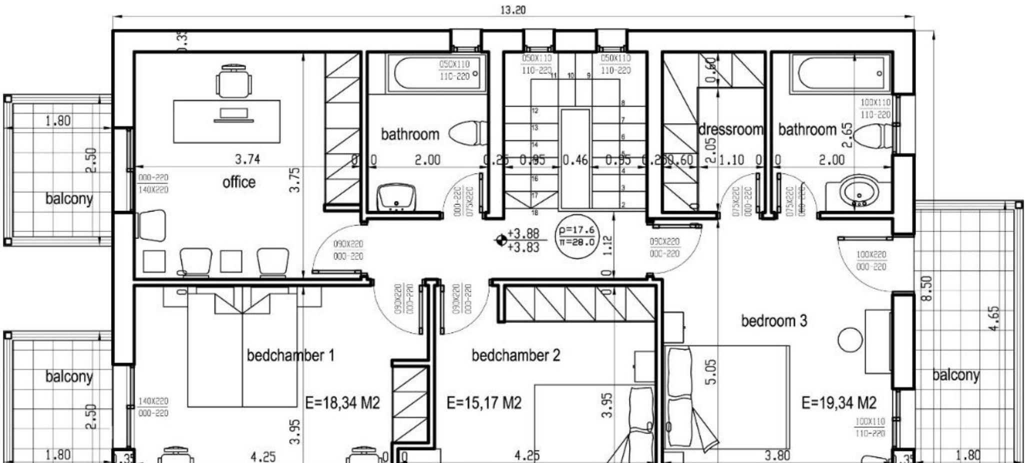


Figure 2. First floor plan view

2.3 Openings

The openings are not designed and manufactured with the same dimensions in all directions but differ as each dimension serves a different purpose. Large size openings are selected to the south, medium size in the east and west, while small openings are selected to the north[12] [6]. The larger openings must be oriented towards the south so as to make the building cool in the summer and warm in the winter, while on the north side of the building there must be placed solid walls and as small as possible openings so that they can function as heat-insulation (thermal losses reduction).However, the northern openings in the house must necessarily exist and not be omitted since they provide adequate natural lighting, cross ventilation and cooling, especially in the north-south direction during the summer months.



Figure 3. South view

2.4 Southern Openings Dimensioning

Considering the relationship between outdoor temperature and openings and knowing the mean outside temperature of the area (4.5 degrees Celsius), a gamut was created within which the area of the openings would range, by multiplying the area of each space by its coefficients.

Using coefficients from semi-empirical formulas [6] [20], the results are as follows:

Area of Living Room, Dining Room, Kitchen= 56,59m^2

Minimum Opening Area of Living Room, Dining Room, Kitchen= 56,59m^{2}x0,13 = 7,36 m^2

Maximum Opening Area of Living Room, Dining Room, Kitchen = 56,59m^{2}x 0,21 = 11,88m^2

7,36<Opening Area <11,88

Minimum Opening Length of Living Room, Dining Room, Kitchen = 7,36/2,20 =3,35

Maximum Opening Length of Living Room, Dining Room, Kitchen=11,88/2,20 =5,40

3,35< Opening Length<5,40

Area of Room 3= 19,34

Minimum Opening Area of Room3= 19,34m^{2}x 0,13 = 2,51m^2

Maximum Opening Area of Room3= 19,34m^{2}x 0,21 = 4,06 m^2

2,51<Opening Area (3,08) <4,06

Minimum Opening Length of Room3= 2,51/2,20 = 1,14

Maximum Opening Length of Room 3= 4,06 /2,20 = 1,85

1,14<Opening Length (1,40) <1,85

Area of Room 2 = 15,17

Minimum Opening Area of Room2= 15,17m^{2}x 0,13 = 1,97 m^2

Maximum Opening Area of Room 2= 13,99m^{2}x 0,21 = 3,18 m^2

1,97<Opening Area (3,08) <3,18

Minimum Opening Length of Room2=1,97/2,20 =0,90

Maximum Opening Length of Room2= 3,18/2,20 =1,45

0,90<Opening Length (1,40) <1,45

Area of Room 1= 18,34

Minimum Opening Area of Room 1= 18,34m^{2}x 0,13 = 2,38m^2

Maximum Opening Area of Room1= 18,34m^{2}x 0,21 = 3,85m^2

2,38<Opening Area (3,08) <3,85

Minimum Opening Length of Room1=2,38/2,20 = 1,08

Maximum Opening Length of Room1= 3,85/2,20 = 1,75

1,08<Opening Length (1,40) < 1,75

Table 1. Relationship between average outdoor winter temperature and openings [6] [20]

Average outdoor temperature(°C)	Openingarea / floorplanunit
1.7	0.16-0.25
4.5	0.13-0.21
7.2	0.11-1.17

2.5 Trombewall pre-dimensioning

The Trombe wall [8] is part of the passive solar design systems and achieves indoor heating by taking advantage of the direct sunlight. It consists of upper and lower opening, glass, gap and high thermal mass wall. The wall is made of materials with high heat capacity and, in our project the wall is made of concrete. The determination of the Trombe wall area results from its relationship to the average outdoor temperature. Using Table 2 [6] [20], combined with the present outdoor temperature of the region (4.5 degrees Celsius), the following results are obtained:

Area of Living Room, Dining Room, Kitchen = 56,59m^2

Minimum TROMBE Wall Area of Living Room, Dining Room, Kitchen= 56,59m^{2}x0,28= 15,85m^2

Maximum TROMBE Wall Area of Living Room, Dining Room, Kitchen= 56,59m^{2}x 0,46 = 26,03m^2

15,85< TROMBE Wall Area <26,03

Minimum TROMBE Wall Length of Living Room, Dining Room, Kitchen=15,85/2,35=6,63

MaximumTROMBE Wall Length of Living Room, Dining Room, Kitchen= 26,03/2,35= 11,08

6,63<TROMBE Wall Length <11,08

Area of Room3 = 19,34

Minimum TROMBE Wall Area of Room3= 19,34m^{2}x 0,28 = 5,42 m^2

Maximum TROMBE Wall Area of Room3 = 19,34m^{2}x 0,46 = 8,90m^2

5,42<TROMBE Wall Area <8,90

Minimum TROMBE Wall Length of Room3= 5,42/2,35=2,31

MaximumTROMBE Wall Length of Room3= 8,90/2,35 = 3,79

2,31<TROMBE Wall Length (2,40) <3,79

Area of Room2 = 15,17

Minimum TROMBE Wall Area of Room2= 15,17m^2x 0,28 = 4,25m^2

Maximum TROMBE Wall Area of Room2= 15,17m^2x 0,46 = 6,98m^2

4,25<TROMBE Wall Area <6,98

Minimum TROMBE Wall Length of Room2= 4,25/2,35 = 1,81

MaximumTROMBE Wall Length of Room2= 6,98/2,35 = 2,97

1,81<TROMBE Wall Length <2,97

Area of Room1 = 18,34

Minimum TROMBE Wall Area of Room1= 18,34m^2x 0,28 = 4,58m^2

Maximum TROMBE Wall Area of Room1= 18,34m^2x 0,46 = 8,43m^2

4,58<TROMBE Wall Area <8,43

Minimum TROMBE Wall Length of Room1= 4,58/2,35 = 1,95

MaximumTROMBE Wall Length of Room1= 8,43/2,35= 3,59

1,95<TROMBE Wall Length <3,59

Table 2. TrombeWall area per indoor area unit 1m2 depending on average winter temperature [6] [20]

Average outdoor temperature(°C)	TROMBE Wall Area/floorplanunit
-1	0.43–0.78
4.5	0.28 – 0.46

2.6 GreenRoofplacement

The Green Roof is not a finding of the recent years as it emerges from the dawn of civilization and the Hanging Gardens of Babylon up to the Modern times, where it plays a leading part in many European cities such as Stuttgart, Germany and the USA as well [14].

For a city to be considered sustainable, according to the European Environment Agency, it should be corresponded 10sq.m. green per inhabitant [3]. In this need, the green roofs of buildings can play a leading role and contribute significantly. They can also provide clean air and cover high oxygen requirements, as only 1.5 square feet of a Green Roof is enough to produce so much oxygen to meet the annual needs of an adult for clean air [3].

The building was not housed with a sloping roof but it was chosen to be placed a planted roof. This option, combined with passive systems [8], appropriate openings' size and orientation, aims at creating a bioclimatic house of great energy potential that, apart from the ecological and economic benefits, it will also achieve an aesthetic result [2]. The type chosen was the extensive type as it was considered the most suitable between the semi-intensive and the intensive type that requires higher planting requirements.

The extensive type [10] is organized on a multi-level stratification with a light growth plant substrate of 10 to 15 cm high, the maintenance of which requires little care. The load ranges from 70 to 140 kg / m and the root system of the plants is superficial. The limited weight does not cause problems and

fear in the static endurance of the building as it will not lead the total load to exceed the calculated load predicted by the static study. Then, while in gradients above 20 ° the additional use of retaining elements of the substrate such as honeycombs are required, in the present construction there is no such thing since the slope placed is the elementary 2% -2.5%. If the slope of the soil does not exceed the 1.5%, water accumulation is likely to occur, which can cause a runoff problem and lead to destruction of the overall structure [13]. In general, care should be taken to avoid stagnant water accumulation, with particular emphasis on the drainage system, as it may create suffocation conditions in the roots of plants, which may lead to the failure of the vegetation installation on the roof. Such cases are avoided when basin planning is in line with national, European legislation and international standards [15] [13].

Ideal plants for this species are low-vegetation plants with a superficial root system that can easily breed, such as vegetal rugs, wildflowers, herbaceous plants, sedum and ground cover plants.

The extensive type roof is not suitable for use and access to humans as opposed to semi-intensive and intensive-type planted roofs [7].

In order to protect the workers who take care of the maintenance of the roof and the electromechanical installations, railings have been installed as safety measures because the roof of the structure is at a height of more than 3 m above the ground [10].

The materials in general that play a leading role in the construction[15] of the planted roofs are: the plant material, the infrastructure materials which are a prerequisite for the vegetation installation and the irrigation system materials, which are necessary for the vegetation maintenance.All materials and components selected are resistant to continuous exposure to water, to the biological action of microorganisms and water-soluble substances, do not contain ingredients that are harmful to plants, do not create air pollution and are compatible with each other according to the International Standards in order to ensure mutual chemical compatibility[10].The stratification of the planted roof is being presented below(Figure 4).

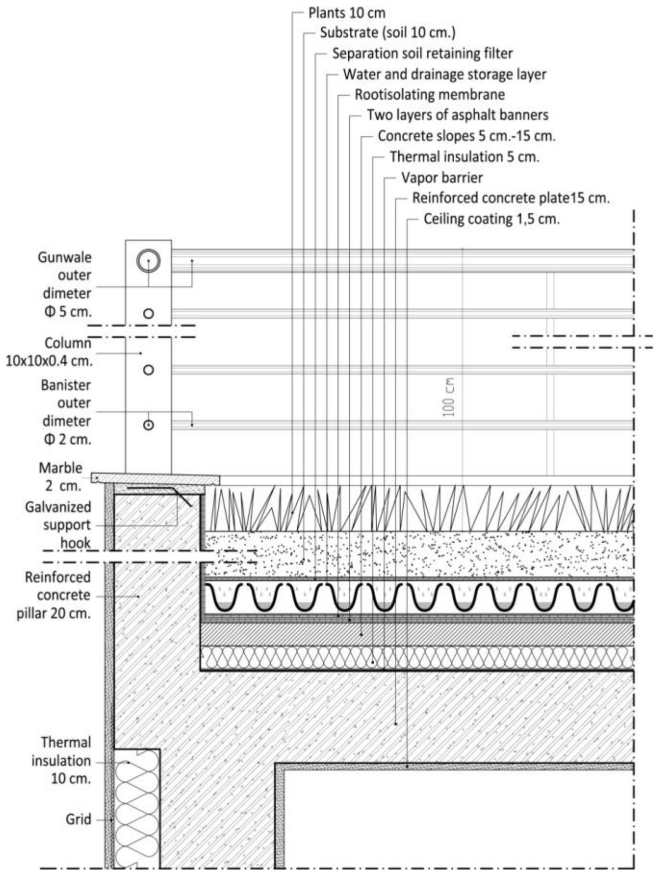


Figure 4. Green Roof section

So the extensive plant roof type will provide an aesthetic result with many energy and economic benefits [13]. It will make possible the existence of an ecological landscape with what that entails with the minimum return, as it offers all the advantages of the Green Roof, requiring a low installation cost and a low to zero maintenance cost. It also, relieves the user of a series of problems in the building endurance since it adds to the total load a minimum weight, compared to other types, intensive and semi-intensive. It also requires minimal care as it does not require daily irrigation-watering of plants from the user. Finally, it provides a high ecological benefit with an immediate depreciation[12], making the choice of a Green Roof placement even more attractive.

2.7 Innovation in the Green Roof.

In the innovation of the planted roof placement, two more proposals that will frame it and make it even more special come to add. These two proposals concern the composting and the water channeling system.Their common denominator is the exploitation of goods that are available but not exploitable posing the nature as an ally and the recycling as a basic principle[5].

Composting [19] is a natural process that converts organic materials into a richly dark substance called compost or soil improver. It is a very direct and important method of recycling and it has been estimated that 35% of household waste can be composted [19]. For the current roof, composting involves the garbage composting so that the rubbish becomes exploitable. In particular, the garbage become a fertilizer which is transported to the roof and to the plants of the green roof. This fertilizer is mainly derived from organic residues and acts as a booster for the growth and healthy preservation of plants. In the present paper, an extensive type for the planted roof has been chosen using plants with a superficial root system that easily germinate like sedum, herbaceous plants, herbs, flowers or lawns a more limited use of compost is made, ie the fertilizer produced. However, in the case of using another type such as semi-intensive or intensive type, it would be beneficial to make a further use of compost-fertilizer to achieve corresponding satisfactory results.

Recycling and the full utilization of every element that is already present and around us is not limited to the use of garbage alone, but extends to the basic and necessary for the plants good, the water. Hence, the next proposal concerns the water channeling system.In particular, it is proposed that the water from the daily use other than sewage and the water coming from the rainwater collection should be concentrated in a reservoir.Then, after the water is set for cleaning (and small treatment) through a filter it is re-used to irrigate the plants of the green roof.Specifically, the collected and treated purified water will be transported with a modern system of drainage water into the roof and by extension on the plants, relieving the user of the house to make additional use of water for watering the plants of the green roof.Finally, this water that has been treated and cleaned can also be used in other cases such as housework, watering of the balcony plants, cleaning of the outdoor areas, etc., offering thereby the residents more possibilities[17] in combination with the economy and a friendlier attitude towards the environment.

3. RESULTS AND DISCUSSION

3.1 Advantages and Benefits of the Green Roof

A bioclimatic home that delivers comfort and energy savings it can also offers the user aesthetic satisfaction, such combination is desirable and brings the construction even closer to the standards of the ideal housing[5].The aesthetics in the present paper, apart from the building architecture, is reinforced and highlighted by the extensive Green Roof type with a variety of plants with a superficial root system that can easily germinate, such as vegetal rugs, wildflowers, herbaceous plants, sedum and ground cover plants.It is capable of adding color, utilizing the free and usually untapped space to create a small oasis and even change not only the image of the construction but also a wider whole such as a city [13]. Besides aesthetic benefits, the planted roof also provides a number of other energy and economic benefits.Specifically, the extensive type [10] chosen in the planted roof is the most

appropriate because it combines all the ecological and economic benefits with zero needs and direct depreciation from the first placement day.Worldwide, it is widely selected but also in the case of Greece it is considered the most efficient as it is combined with its climate, characterized by strong winds, temperature fluctuations and limited water sufficiency. In general, it offers multiple benefits [17] to both their users and the city as well as the whole planet. It improves the air quality as the planted roofs retain the heavy metals and enrich the atmosphere with oxygen. It reduces the external noise by 10 decibel lower, compared to a conventional insulation, resulting in the Green Roof to be seen as an ideal sound-proofing solution [12].The green roof protects the buildings from the fire as it prevents the spread of fire with the use of the planting water retention, which enhances the buildings fire safety and also protects them from electromagnetic radiation to a very high percentage of over 95% [7].The planted roof is not limited to the individual house but extends to the whole city level as it solves the problem of the thermal islands which greatly alters the microclimate of the cities as the planted roofs offer thermal insulation and shade to the buildings by helping them cool and reduce their temperature [12].At the city level, it comes to resolve another problem, the flood defense as it retains and filters over half of the amount of rainwater, providing flood protection in the city[13] and protecting the water from pollution.Another key sector in which the Green Roof benefits, increasing further the value of our construction is the economic one. It provides economic benefits as the green roof of the building is heated and cooled much slower than a typical roof, resulting in the building being air-conditioned easier, more efficiently and at a lower cost. Even in relation to a conventional roof, it reduces the superficial terrace temperature, which can reach 80 ° C to 45 ° C, limiting it thereby even to 35 ° C during the summer days [7] .

Besides the outdoor superficial temperatures reduction, during the summer months it reduces the indoor temperature of the building by up to 10 ° C while in the winter months it reduces the heat loss from inside the building [7].All this result in economical and energy benefits for the construction as the heating and cooling cost of the building is reduced by up to 50% [12].Financial benefits also come from the building maintenance cost reduction, as the Green Roof protects the surface of the roof not only from the weather conditions, but also from the radiation, greatly increasing thereby the shelf life of the roof, which can even reach its doubling[12].The Green Roof building is not only protected from the damage caused by the weather conditions, but also by the strain of the building due to thermal contractions and expansions, as the temperature range of variation of the green roof decreases.Thus, the construction is upgraded because of their high rating in the building energy identity, resulting in increasing its commercial and objective value [13].

The disadvantages they present are much less and in the present construction measures have beentaken for them.

The financial burden, the planted roof's static charge and the continuous care of the garden have been provided and taken into account with the extensive type choice, while the risk of moisture has been addressed by proper waterproofing and drainage of the Green Roof [15][10].Finally, a proposal that can make the green roof even more efficient and provides even more benefits is its combination with photovoltaics[11].In the construction of the paper it would be very simple and feasible as the planted roof is of an extensive type.

The plants remain unaffected and at the same time help to make photovoltaics work more efficiently by relieving them of the problem of overheating [17].

3.2 The Efficiency of Passive Systems and Bioclimatic Architecture.

Passive systems constitute the building elements of the house and belong to the bioclimatic design. Their function is based on the energy exchange with the environment as well as the proper storage and distribution of energy within the premises[8].From thermal analyzes made with the use of software [9][18] (Ecotect Analysis 2011) to houses with passive solar systems (such as the Trombe wall),with proper interior design and seamless southern sunshine, cooling savings of over 28% and heating savings of over 27.5% have been achieved.The thermal needs reduction for cooling and heating becomes more striking, if only the half-day areas and the bedrooms on the southern side

where the total energy savings are up to 45% are considered [9].By creating a bioclimatic home combined with passive systems, the benefits are many not only in the energy, environmental and economic spheres, but also in the level of comfort and living quality[17][5].Specifically, conditions of optical and thermal comfort as well as energy saving for heating and cooling are assured. Sunlight and solar energy and, more generally, renewable sources of energy play a key role in this.In the case of Greece, which is governed by the Mediterranean climate, the buildings can, after being properly designed and built, heated by the sun at 70-80% in the winter and in the summer to be kept cool without air conditioning[6].A fact that makes the need for Bioclimatic Architecture and the use of passive systems even more urgent[8], as Trombe Wall, in our case.Thus, with a small extra construction cost, energy saving can be achieved, large future operating costs can be avoided, the environment can be protected and the houses upgraded to healthy and hospitable buildings [18].But even with passive solar systems and sufficient sunblinds there cannot be 100% energy autonomy throughout the year, yet with the addition of the basic passive system, the Trombe wall, and also with appropriate design based on the climatic characteristics of the area, energy saving for heating 46.6% but also cooling up to 39.5% for southern thermal zones can be achieved[16][18].So when passive technologies are implemented and actualized in a proper and satisfactory way, the difference in the energy balance of the building, which energy technologies are called upon to cover, is very small.Moreover, a Passive Building is profitable to a large extent when it is the result of bioclimatic architecture with the right orientation, proper aspect ratio and optimal spaces layout [16].Furthermore, when it provides high levels of thermal insulation, the desired thermal storage mass that will absorb excess heat per day and attribute it at night, passive technologies such as modern passive systems and glass panes that have characteristics that allow for the necessary solar gain income during the day in winter and limit the thermal losses during the night while not leading to room overheating in the summer [8].Such a passive house reaches the point of using up to 90% less energy for heating and cooling than a conventional building as it interacts with the environment and functions as a living organism that adapts to the local climate and exploits the physical elements [12][16].Although such a building's potentials are increasing to a very large extent, it is still very difficult to achieve energy self-sufficiency and independence. For this reason it is proposed to use RES to meet additional energy needs such as photovoltaic modules[11][18], wind turbines as well as the use and exploitation of *geothermal energy*, which is practically an inexhaustible *source of energy*.Active passive systems such as photovoltaics or wind turbines can also be installed later, which does not bind the manufacturer and the user for their selection and installation during the building construction.Finally, bioclimatic architecture provides many benefits and profits at all levels, making it efficient and appropriate in many cases [17].Even in large urban centers and in densely-built areas where there is a concern about the layout of the buildings on the plot, their orientation and shading from the opposite buildings, there is an answer and such an implementation is possible [6].The answer is not that bioclimatic design cannot be applied or that bioclimatic design is limited to ideal situations but that the way of dealing with it should be changed in such a case that there is no bioclimatic home design but bioclimatic settlement design.

4. CONCLUSIONS

The two-storey bioclimatic house designed and built according to the principles of bioclimatic architecture and the addition of passive systems and Green Roof has presented a plethora of advantages and capabilities that provide the user with a home that covers a large part of its energy needs, which also with the addition of active systems such as photovoltaics will be able to touch energy autonomy [18]. A home that offers comfort and living quality in complete harmony with nature and the environment and multiple economic profits. A number of parameters have been taken, modern technological means have been utilized and an aesthetic result has been presented that provides a healthy, functional and efficient building close to the standards of an ideal home that does not oppose the environment but instead respects, exploits and interacts positively with it.

References

1. Papageorgioy A., 1993. Xenofon the Athenian, Complete Works 1 – Memoir 1.Kaktos, Athens.
2. Tzelepis P., 1997. Greek Folk Architecture.Themelio, Athens.
3. https://www.eea.europa.eu/el(accessed November 6th, 2017)
4. http://eur-lex.europa.eu/legal-content/EN/TXT/?uri=URISERV%3Aen0021(accessedDecember 10th, 2015).
5. Tsipiras K., 1996. The Eco-house. NeaSinora – A. A. Livani, Athens.
6. Axarli K., Giannas S., Evangelinos E., Zaharopoulos E. &Marda N., 2001. Bioclimatic design of buildings and surroundings. VolumeA, GreekOpenUniversity, Patra.
7. Liu, K and Bascaram B., 2003.Thermal performance of green roofs through field evaluation. Greening Rooftops for Sustainable Communities, Proceedings of the First North American Green Roof Conference. Chicago, USA.
8. European Commission, 1998. Energy in architecture, The European Handbook on Passive Solar Buildings. MalliarisPaideia, Athens.
9. Lantitsou K. and Panagiotakis G., 2012. Bioclimatic Design of a Settlement – Based on ECOTECT software. 1st Environmental Conference of Thessaly (eds. A. G. Kungolos, O. Christopoulou, C. Laspidou), September 8–10, Skiathos Island, Greece, 375–382.
10. http://www.cres.gr (accessed September 18th, 2017)
11. Mandalaki M., Papantoniou S. and Tsoutsos T., 2014.Assessment of energy production from photovoltaic modulesintegrated in typical shading devices. Sustainable Cities andSociety, **10**, 222–231.
12. Wines J. 2000.Green Architecture, Koln, Germany.
13. Aravantinos D., Eumoropoulou A., "Planted Roofs", Ktirio Magazine. June 2006, pp. 87-113
14. https://el.wikipedia.org/wiki/(accessed October 9th, 2017)
15. LUCKETT, K. (2009) Green Roof Construction and Maintenance, USA, McGRAW-HILL'S.
16. K. Lantitsou,S. M. Bagiouk, G. D. Panagiotakis, S. S. Bagiouk, 2016. Bioclimatic design in a modern house with Macedonian architecture elements, Proceedings of 13th International Conference on Protection and Restoration of the Environment, Mykonos Island, Greece, July 3–8, 2016, pp 864–870.
17. CHESHIRE, D. G., ZAC; (2007) CIBSE Guide L: Sustainability, U.K., CIBSE.
18. K. Lantitsou,S. M. Bagiouk, S. S. Bagiouk, G. D. Panagiotakis, 2017. Energy upgrade of houses by using Autodesk Revit software Case study: Macedonian building in Northern Greece, Proceedings of Sixth International Conference on Environmental Management,Engineering, Planning and Economics, Thessaloniki, Greece, June 25-30, 2017, pp 739–748.
19. https://el.wikipedia.org/wiki/ (accessed October 13th, 2017)
20. Andreadaki E. (2006) ΄Bioclimatic Design: Environment and Sustainability΄,UNIVERSITY STUDIO PRESS, Thessaloniki

OPTIMIZATION OF SITE SELECTION OF AN ANAEROBIC DIGESTION PLANT FOR TREATMENT AND VALORIZATION OF LIVESTOCK LIQUID MANURE WITH THE AID OF GIS

E.K. Oikonomou*, E. Tekidis and A. Guitonas

Department of Transportation and Hydraulic Engineering, Faculty of Rural & Surveying Engineering, Aristotle University of Thessaloniki, 54124 Thessaloniki, Hellas

*Corresponding author: e-mail: eoikonom@topo.auth.gr, tel: +30 2310 994360

Abstract

Mygdonia Basin is located mostly in north and northeast part of Thessaloniki Regional Department and in a small part of north Halkidiki Regional Department, including two lakes, Koronia and Volvi, the forest of the Macedonian Tembi Valley and many streams forming a dense water network. The whole area of 2,090 km^2 is protected by two Joint Ministerial Decisions, which define all land uses and economic activities that are allowed to be developed in each of its three zones of protection. The area of study involves a "Natura 2000" site – "Special Protected Areas" – as well. The area is characterized for its intense agricultural activities, as well as livestock plants and activities, which demand a great amount of irrigation water; a great number of the 80,722 inhabitants in 80 small towns live from such economic activities. However, most of the livestock farms operate without effective animal wastes management methods, while such wastes involve high organic load.

The present paper investigates the possibility for optimization of site selection of an anaerobic digestion plant for liquid manure treatment in the area of Mygdonia Basin, with the aid of Geographical Information System (GIS). For this reason, legal, social, ecological and economic criteria are set, identified and briefly described. They are related to: the restrictions in land uses and activities permitted by the two joint ministerial decisions for Mygdonia Basin (legal criteria); a minimum necessary distance of the proposed anaerobic digestion plant from current towns (social criteria); the ecological characteristics of the area of study with the "Special Protection Area" and the local wildlife refuges (ecological criteria); and the need for location of the proposed anaerobic digestion plant mostly next to the largest livestock farms (economic criteria). With the appropriate spatial data and spatial analysis within the GIS, the synthesis of all criteria that have been set, is completed successfully and the site for the anaerobic digestion plant location is chosen. The present paper set and selected simple criteria, while the problem of site selection for the anaerobic digestion plant is more complex; however, it is a pilot work showing that there are possibilities to solve problems in this area that has been polluted for more than two decades. Furthermore, a critical comment is made related to the implications of Environmental Impact Assessment Study for such a project, which is strongly affected by land use patterns proposed by General Local Plans.

Keywords: Livestock liquid manure, Anaerobic digestion, Spatial analysis with GIS, Mygdonia Basin

1. INTRODUCTION

Anaerobic digestion is a dynamic biodegradation process: wastes with high organic loading are degraded and stabilized, and thus, converted to biogas methane, carbon dioxide and in less concentration, hydrogen sulfide, hydrogen, nitrogen gas, etc. As a process it may involve biosolids

with low concentration in solids (wet digestion) or with high concentration in solids (dry digestion). Depending on operation temperature, anaerobic digestion is regarded as psychrophilic (10-20^oC), mesophilic (28-38^oC) and thermophilic (50-65^oC). The whole process is divided into three stages: hydrolysis of organic matter, with carbohydrates, proteins and fats being broken down to sugars, amino-acids and fatty acids; acidogenesis, with acidogenic bacteria and hydrogen producing acetogenic bacteria producing acetate, volatile fatty acids, carbon dioxide and hydrogen; and finally, methanogenesis, during which methanogenic bacteria produce methane and carbon dioxide [1]. Problems in the process of anaerobic digestion may be observed in case of accumulation of volatile fatty acids (VFA) during the second stage, when organic loading is high or when hydraulic residence time is short. Specific growth rate of acidogenic bacteria of the second phase is higher than specific growth rate of methanogenic bacteria of the third phase and this is the reason why, not all quantity of volatile fatty acids produced leads to methanization. As a result of this, pH is decreased and anaerobic digestion is blocked. Imbalance appears usually when the operation of digestors starts and until the development of satisfactory methanogenic flora; then the process operates well and appears to be resistant both to changes in substrate as well as any other possible operational accidents, such as high concentration of ammonia nitrogen. Free ammonia levels should be maintained below 80 mg/l, while ammonium ion can generally be tolerated up to 1,500 mg/l as NH_4^+-N [2]. Despite that, it has been found that with acclimatization (usually several months), stable operation can be achieved for ammonia nitrogen concentration up to 8,000 mg/l [3].

Anaerobic digestion, apart from sludge stabilization in Wastewater Treatment Plants (WWTPs), is widely used in high loadings of livestock wastes degradation, producing good quality compost, without pathogens, and producing simultaneously biogas, which may produce thermal and electric power by cogeneration. Consequently, the production of biogas by anaerobic digestion of livestock wastes has many advantages related to: production of renewable energy and reduction of energy deriving from fossil fuels; decrease of imported fossil fuel from Hellas and European Union; contribution to livestock wastes treatment and sanitation, which is a major problem in Hellenic primary sector, causing impacts in water bodies; decrease of greenhouse gas emissions, in terms of CO_2; and finally, positive impacts in creation of new jobs, new economic activities and better operation of livestock farming activities with cost savings to farmers, since the produced residual of digestion may be used as a fertilizer, farms may operate without odors and serious environmental impacts, while their environmental permits may be easier to be obtained [4]. Thus, the process of anaerobic digestion of livestock wastes contributes mostly to the strategic goals of circular economy.

2. THE AREA OF STUDY – MYGDONIA BASIN – CRUCIAL PARAMETERS

Mygdonia Basin, with its 2,090 km^2 surface, is located in the Region of Central Macedonia, east of Thessaloniki (Figure 1), and it comprises two lakes, Koronia and Volvi, and the forest of the Macedonian Tembi Valley with Rihios River (from Lake Volvi to Strymonikos Gulf). Lake Koronia is about 11 km long and 4.5 km wide (surface of 4,600 Ha and max depth of 8 m), and Lake Volvi, the second largest lake in Hellas, is about 19.5 km long and 3.4 km wide (surface of 6,800 Ha and max depth of 21 m). The whole basin is recognized as a region of high ecological importance and it is protected by two Joints Ministerial Decisions 6919/2004 [5] and 39542/2008 [6], which divide it into three zones (Figure 2), with several economic activities being prohibited in its one. A Management Plan o the area is also approved by the Joint Ministerial Decision 58481/2012 [7], which redefines the boundaries of all protected areas within the Mygdonia Basin, redefines all economic activities permitted in these areas and determines all necessary processes for every possible permit and all necessary public authorities that should express their opinion or offer the permits to developers. The wetlands are characterized as "Special Protected Areas" (code GR1220009) and "Site of Community Importance" (codes GR1220001 and GR1220003) the two lakes are protected by Ramsar Convention (code 3GR005) and the Macedonian Tembi Valley belongs to the Network 'Natura 2000'. More than 1,000 different flora species have been identified in forest ecosystems of the basin, 343 different bird species have been recorded (58% of total Greek bird species), 34 mammal

species have been identified (27 of them protected by Hellenic legislation), 35 reptiles and amphibia (17 of them protected by Hellenic legislation) and 29 different fish species can be found in Lake Volvi.

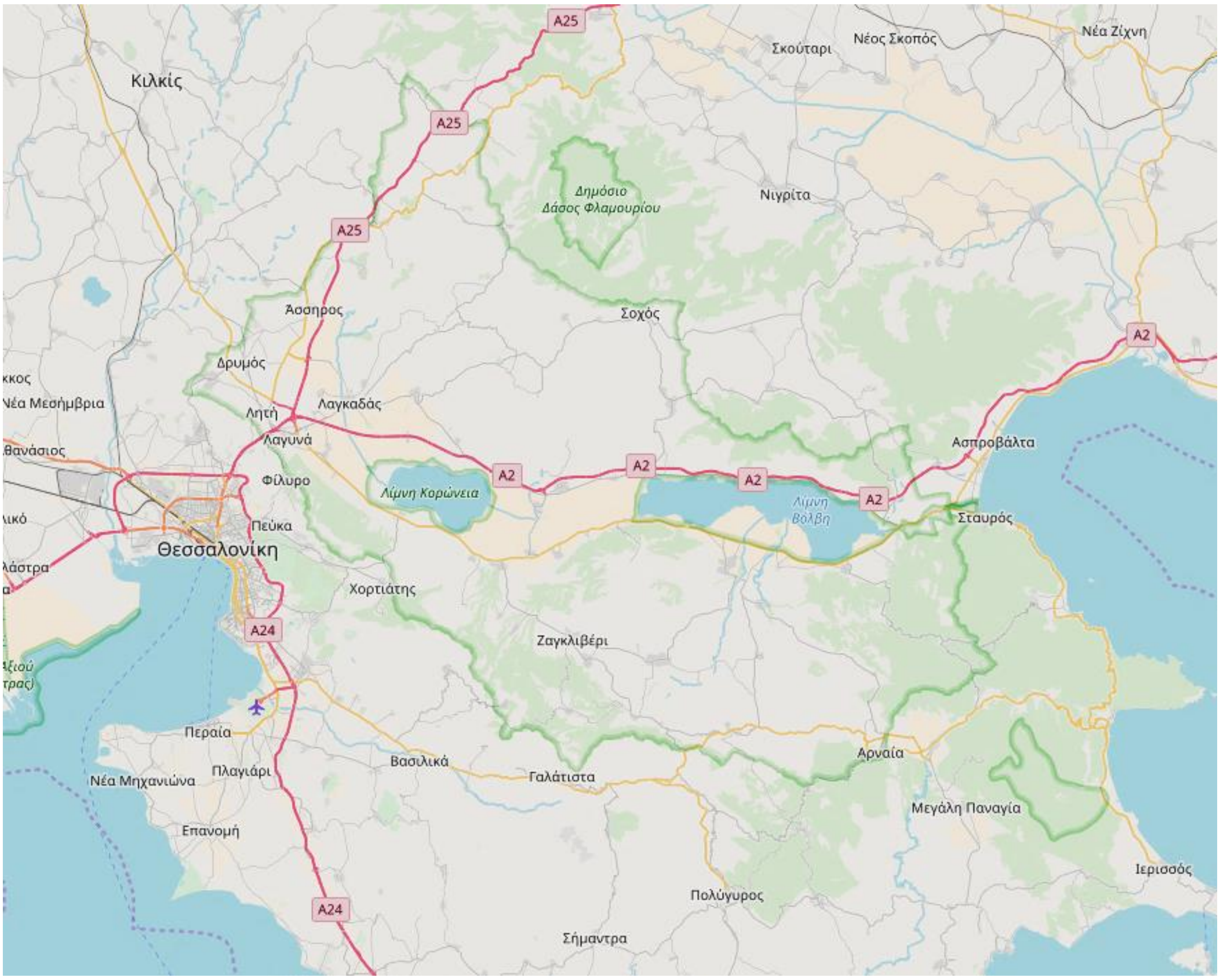


Figure 1: The area of study, Mygdonia Basin with the boundary (in green), the two lakes, Koronia and Volvi, in the middle of the Basin, and Richios River from Lake Volvi to Strymonikos Gulf in the east

The basin includes 80 small towns with a total population of 80,722 inhabitants (census 2011), which are organized in two municipalities and 16 municipal departments (10 of them geographically in the basin). The most popular economic activities involve agriculture, stockbreeding (28,000 cattle and 106,500 sheep and goats, with total 748 livestock farms), fishing (now mostly in lake Volvi) and small industries mostly located in the area of Lagkada city, northwest of Lake Koronia. At this point, it should be underlined that there are many archaeological sites in the basin, as well as many byzantine monuments and traces of villages near the lakes have been found since the Neolithic Era. Macedonian Tembi Valley played always a strategic role in history, being the passage for the communication of Central Macedonia with East Macedonia and Thrace. However, Lake Koronia has been gradually degraded: in 1945 its surface was 4,858 Ha, in 2002 1,925 Ha and in the summer of 2008, there was no water surface. Its depth was diminished from 8.5 m in 1977 to 1 m in 2003 and less than 90 cm in 2004 [8].

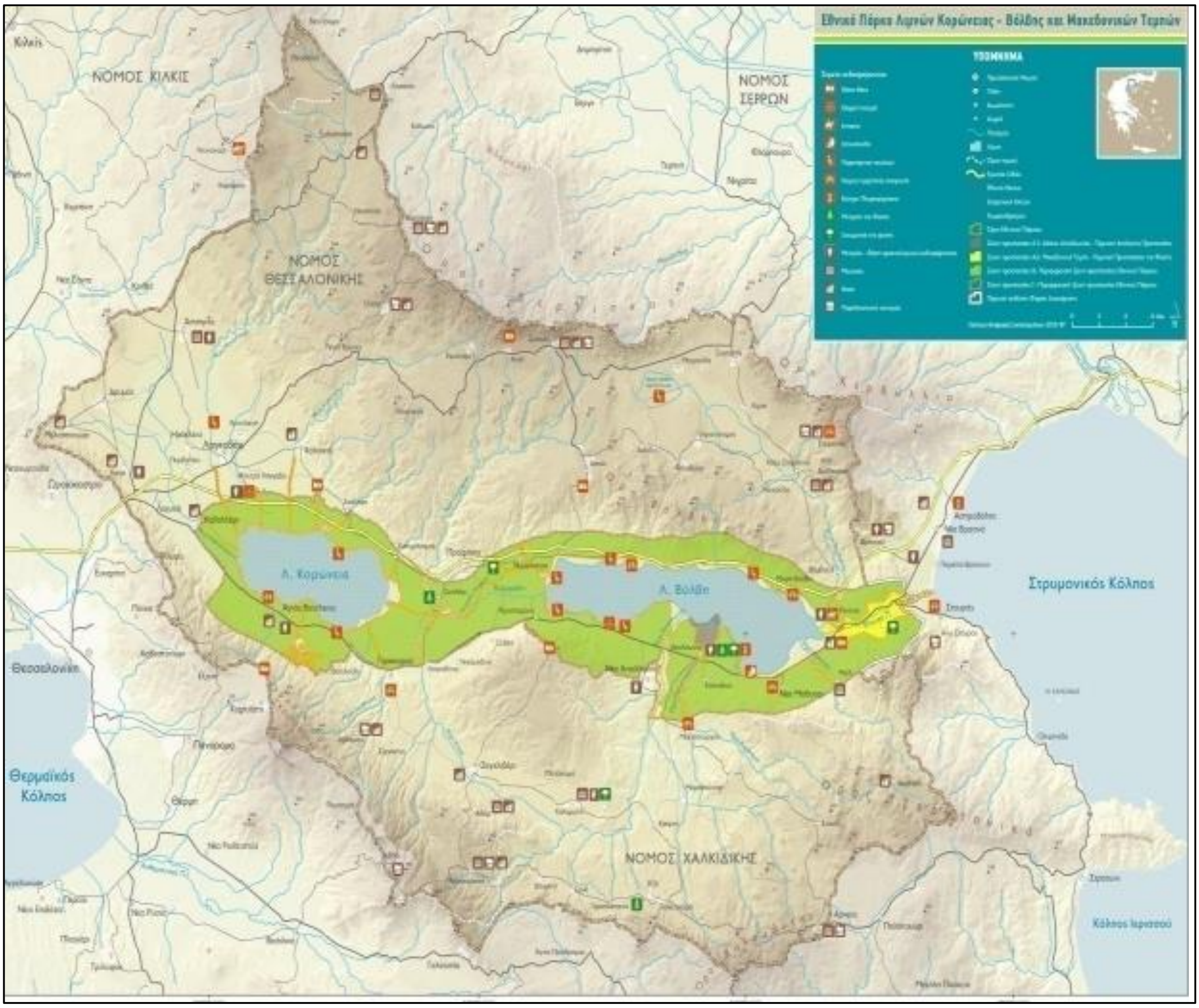
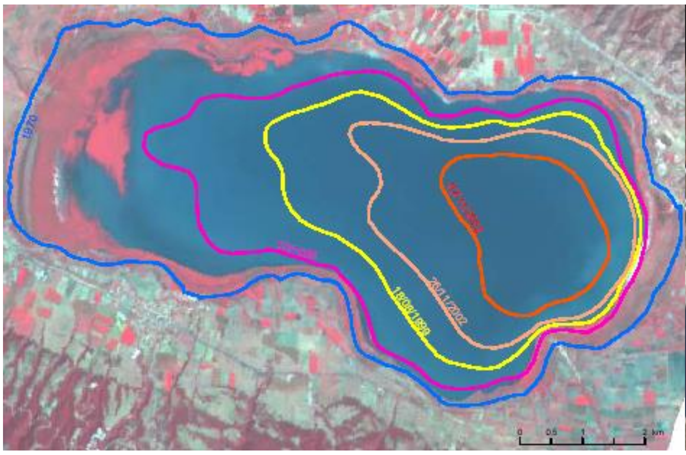
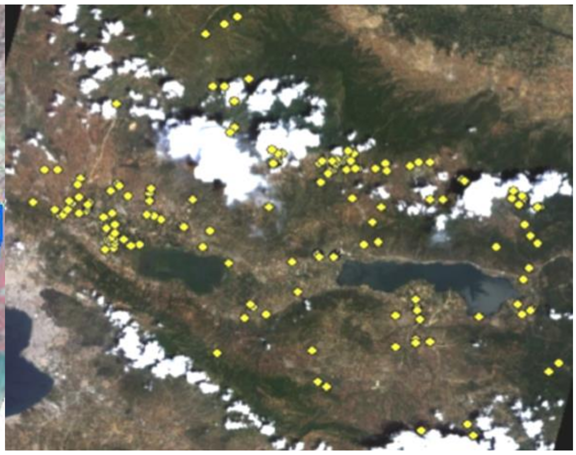


Figure 2: The area of study, Mygdonia Basin with the three subareas: in blue, the area of the two lakes, in green the protected area around the two lakes and Richios River, and in light brown the rest of the protected area





Figures 3 and 4: The evolution of the surface of the Lake Koronia 1945-2002 and the great number of livestock farms, located mostly northwest of the Lake Koronia and north of Lake Volvi

Lake Koronia suffered from severe environmental degradation: total loss of fish stock and loss of wetland birds, due to high concentration of organic and mostly inorganic pollutants. The main reasons

and parameters for such phenomena are summarized as follows: the reduction of rainfall during the period 1988-1993; the existence of around 3,000 irrigation drills in the area, most of them informal; the insufficient irrigation water management, leading to an increase of 23% of water consumption during the period 1996-2001; pollution from agricultural chemicals, inorganic pollution from small industrial plants operating illegally without wastewater treatment facilities and organic pollution from all towns, due to the absence of wastewater treatment plants. It is worth mentioning that pH reached a value of more than 10, concentration of Na^+ was more than 1,200 mg/l, concentration of Cl^- was more than 1,300 mg/l, electric conductivity reached a value of more than 6,000 μS/cm and the ratio of COD to BOD reached a value of more than 20. In September 2004 all fish died and in October of the same year around 30,000 birds also died.

It is worth underlining that the Management Body of Lakes Koronia and Volvi expressed its positive opinion for the operation only of 125 livestock farms out of the total 748 farms, during the process for the renewal of their environmental permits, because the proposed wastes treatment measures were criticized as not adequate. The great majority of the farms treat their wastes by separating solid from liquid, by placing solid wastes in piles, while wastewater is disposed in septic tanks; however, it is impossible to achieve effluent standards of less than 1,200 mg/l BOD and 4,500 mg/l COD, since influent concentration reaches from 15,000 – 35,000 mg/l BOD, depending on the type of livestock. So far, the absence of pollution control measures from public authorities, in combination with the costs of anti-polluting methods in livestock farms, are responsible for the current situation, which seems to be changing towards efforts of sustainable manure waste treatment and management. A possible solution for effective livestock waste treatment in the area of Mygdonia Basin could be anaerobic digestion for the production of biogas, with the aim of producing heat and electricity.

3. SITE SELECTION OF THE BIOGAS PLANT

3.1 The process of licensing a biogas production plant by anaerobic digestion of livestock wastes

The process of licensing a biogas production plant by anaerobic digestion of livestock wastes and other appropriate types of waste involves many steps, as described briefly in the following paragraphs:

- Firstly, a preliminary investigation is needed related to the current land-use patterns in the area or the specific land parcel, the possible existence of forest land or archaeological sites, being obstacles in the process of licensing.
- Secondly, a production permit is needed by the Regulatory Authority for Energy if the electric power produced is more than 1 MW.
- Then the environmental permit is achieved, by conducting an Environmental Impact Assessment Study, either from the Ministry of Environment and Energy or from the Decentralized Administration/Department of Environment and Spatial Planning. The criterion, according to the Ministerial Decision 37674/2016, is the influent annual loading of wastes (more or less than 100,000 t/year for biogas production).
- Then the installation license is needed offered by the Operator of the Electricity Market.
- One more installation license is needed by the Regional Veterinary Department.
- The building permit is needed for the construction of the biogas plant.
- After the plant is constructed, a license for operation is needed by the Operator of the Electricity Market, as well as by the Regional Veterinary Department.

The whole process needs 2-3 years to be accomplished, if it is taken into consideration that only for the environmental permit, 12 – 18 months are needed. Bureaucracy and generally, the operation of the public sector, as well as a framework of land-uses that is 31 years-old (Presidential Decree of

1987), and cadastre and forest cadastre not yet existing in many areas in Hellas, are major parameters that do not aid such investments in renewable energy projects.

3.2 Criteria set for the site selection of the biogas plant

For the site selection for a biogas plant by anaerobic digestion of livestock wastes, spatial, legislative, social, environmental and economic criteria are proposed to be set [9]:

- The spatial criterion is related to the need to select a site as far away from the two lakes as possible.
- Legislative criteria are connected to the joint ministerial decisions already mentioned and the most important commitment is that it is not allowed to choose a land parcel in Protection Zones A and B.
- A social criterion is set that the biogas plant should be located at least 1,000 m away from small towns and villages. The Special Framework of Spatial Planning and Sustainable Development for Renewable Energy Resources [10] defines that Renewable Energy Plants up to 5 MW may be located at no minimum distance from settlements and towns, while for industrial plants a minimum distance of at least 1,000 m away from towns must be kept, according to Hellenic legislation and this was set as a criterion in the case study presented.
- Environmental criteria are related to a commitment that the biogas plant will be located out of areas of the Network “Natura 2000” and out of areas characterized as Wildlife Shelters.

The economic criterion is related to the distance of the proposed biogas plant from livestock farms, according to their livestock capacity, as the more capacity there is an area, the more wastes will be produced and the less distance they will be transported to the biogas plant.

3.3 GIS data setting and processing

After setting the criteria for the site selection of the biogas plant by anaerobic digestion of livestock wastes, the GIS data set is formed and spatial analysis starts:

- The shapefile “NATURA.shp” is formed by the tool “clip”, using the shapefile of all “Natura 2000” areas in Hellas and the latter is ‘cut’ in the area of study. The shapefile of all “Natura 2000” areas can be found in the web GIS “geodata.gov.gr/maps”.
- Then the shapefile “LIVESTOCK_FARMS.shp” is entered using an available Excel file with their coordinates.
- Zones A and B, which involve protected areas and are excluded as possible areas for the site selection of the biogas plant, are introduced by the shapefile “ZONES_A_B_merge.shp”, using the tool “merge”.
- Two existing Wildlife Shelters are also introduced by the shapefile “WS_merge.shp”, using again the tool “merge”.
- All zones that should be excluded from possible areas for the site selection of the biogas plant (Zone A and B of protection areas, “Natura 2000” areas and Wildlife Shelters) are removed from the area of study, the rest of Mygdonia Basin, Zone C, using the tool “erase” and the shapefile “ZONE_FINAL.shp” is formed.
- All towns with their boundaries and with a buffer of 1,000 m around them are introduced by the shapefile “TOWNS_WITH_BUFFER.shp” and again by the tool “erase”, the areas of the towns with their buffer are excluded and a new shapefile is formed, named “ZONE_FINAL_WITHOUT_TOWNS.shp”. The image formed in the GIS is shown in Figure 5.

The economic criterion, as already mentioned, is related to the fact that the biogas plant should be located next to the majority of the livestock farms, as calculated not only by the number of farms, but also by their capacity. For this reason, firstly, the farms in the suitable selected (blue) area are chosen,

then the farms nearby this area and finally, the farms with important capacity and density (forming groups, because of their density). The result is shown in Figure 6.

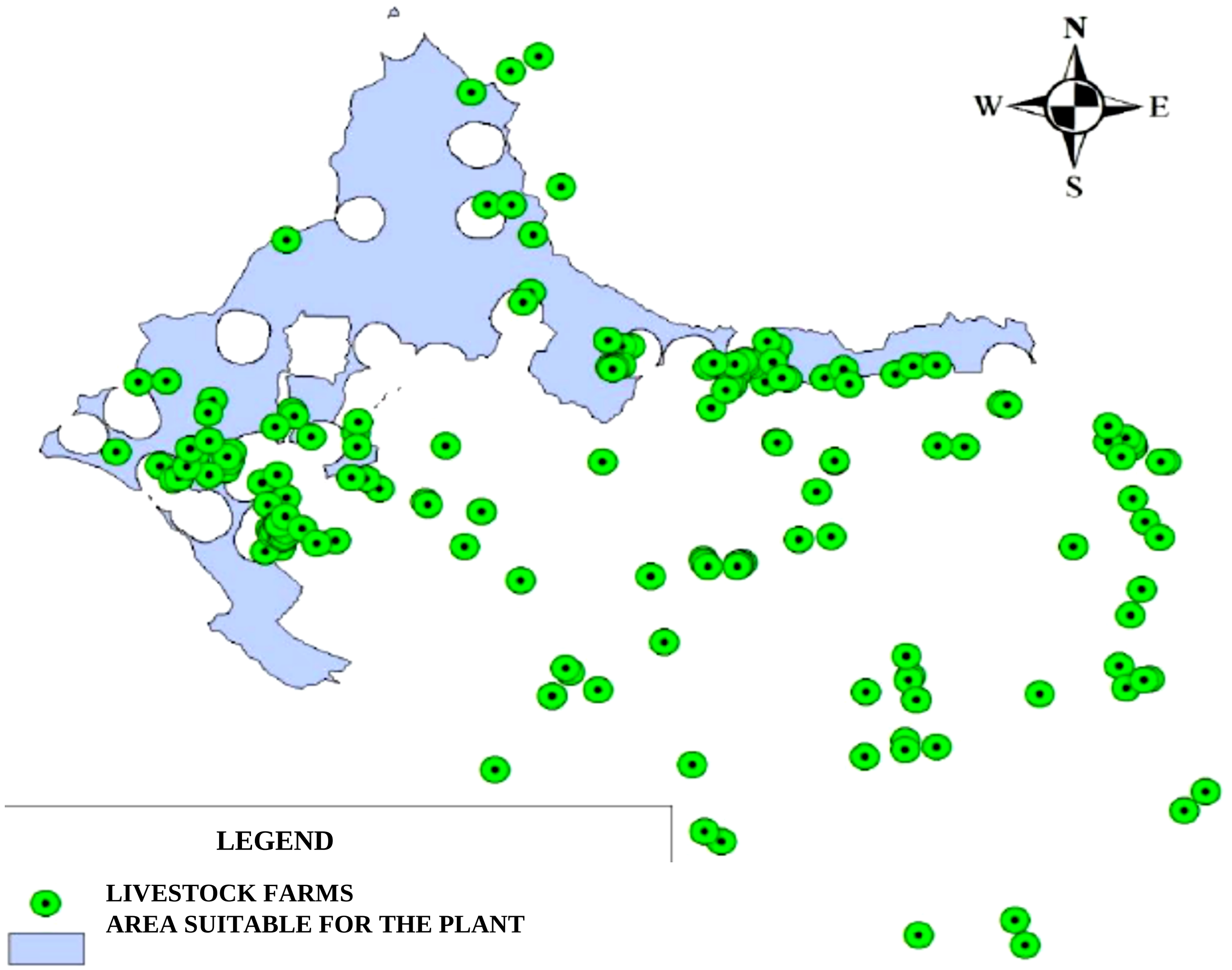


Figure 5: The GIS map, as formed just before the final economic criterion is taken into consideration

- A new shapefile is formed, with the aid of “ExportData”, which is named “LIVESTOCK_FARMS_MAJOR.shp” and by taking data from the attribute table, it is revealed that the 78% of the total capacity of the livestock farms is selected in this process.
- In order to find the best site for the biogas plants, in terms of minimizing total distance travelled, the tool “Median Center” is used in order to measure geographic distributions. Thus, a new shapefile is formed, named “MEDIAN_CENTER.shp”. Consequently, the best site for the construction of the biogas plant, according to the economic criterion implemented, covering the 78% of the total capacity of the livestock farms, is shown in Figure 7.
- As presented in Figure 7, the best site for the biogas plant, “MEDIAN_CENTER”, is located outside the suitable (blue) area, which is the outcome of the implementation of the legislative, social and environmental criteria. As a result of this, with the tool “Near” the point which is the closest to the shapefile “MEDIAN_CENTER.shp”, the exact best site for the biogas plant is found, taking into account all the criteria set, including the economic one. This point is shown in Figure 8.

Finally, the final site for the biogas plant construction, set by all the criteria mentioned before, may be also shown in Google Earth and for this reason, the point is transferred to the system of coordinates

WGS 84, with the aid of the tool "project", in order to change the map projection. At the end, the final shapefile may be transformed to a KML file, by using the tool "LAYER_to_KML.shp".

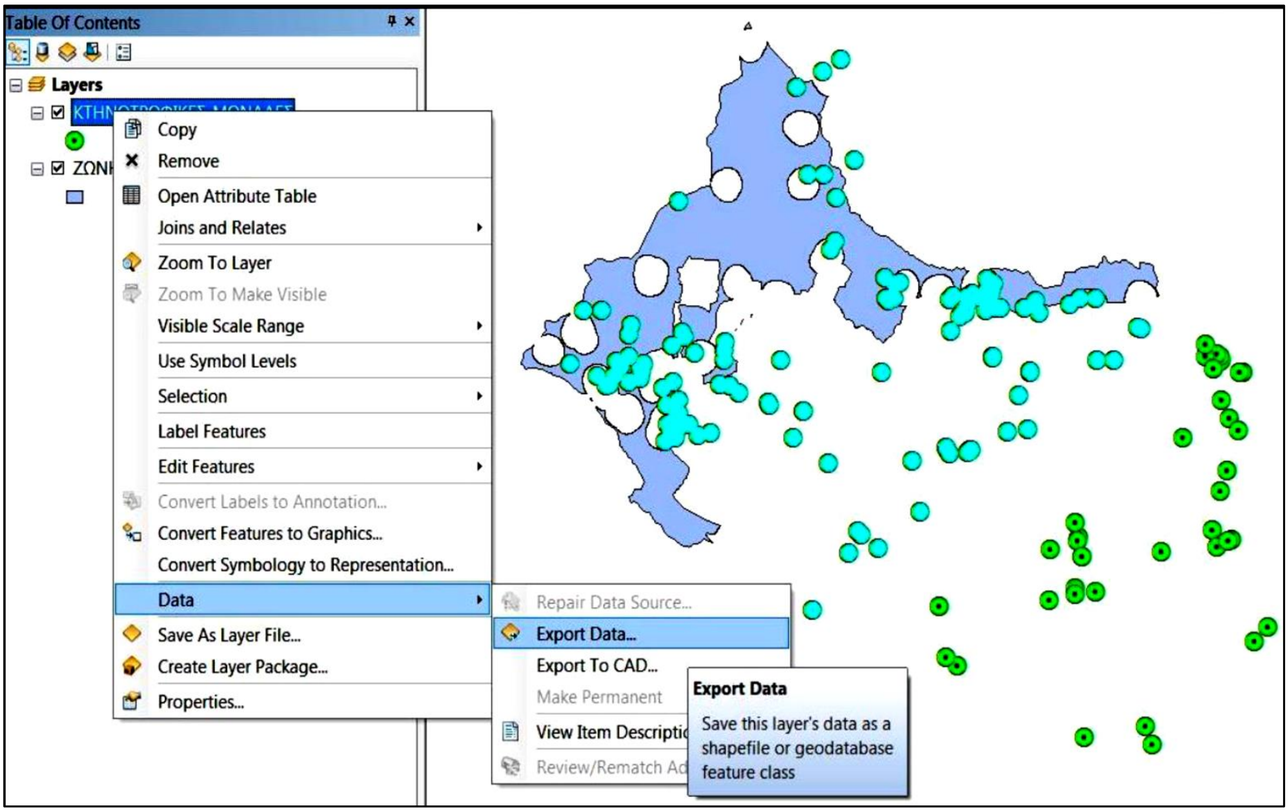


Figure 6: The livestock farms selected, taking into account the economic criterion described

4. DISCUSSION AND CONCLUSIONS

There is an urgent need for Hellas to implement the National Waste Management Plan of 2015, which proposes recycling of organic wastes by composting or efficient use for energy production, which is also considered to be a renewable energy resource, as it derives from biogas produced by anaerobic digestion of the organic wastes. Such methods are important not only because they contribute to valorization of bio-wastes and avoid landfilling of them, but also because the also offer solutions in waste treatment. Especially for livestock farms, this is crucial because many of them have introduced insufficient methods of wastes treatment, with poor results in terms of environmental protection; on the other hand, public authorities are more efficient in environmental inspections and new technologies, such as drones and satellite images offer new opportunities in environmental monitoring, thus, it is much more difficult for livestock farms to support an Environmental Impact Assessment or even ensure their operation license. In the case study of site selection of a biogas production plant by anaerobic digestion of livestock wastes in the ecologically sensitive area of Mygdonia Basin, legislative, social, environmental and economic criteria were set, the data set was introduced in the GIS and the best site was calculated. This methodology is based on the crucial data of the exact position of all livestock farms, as well as their exact capacity.

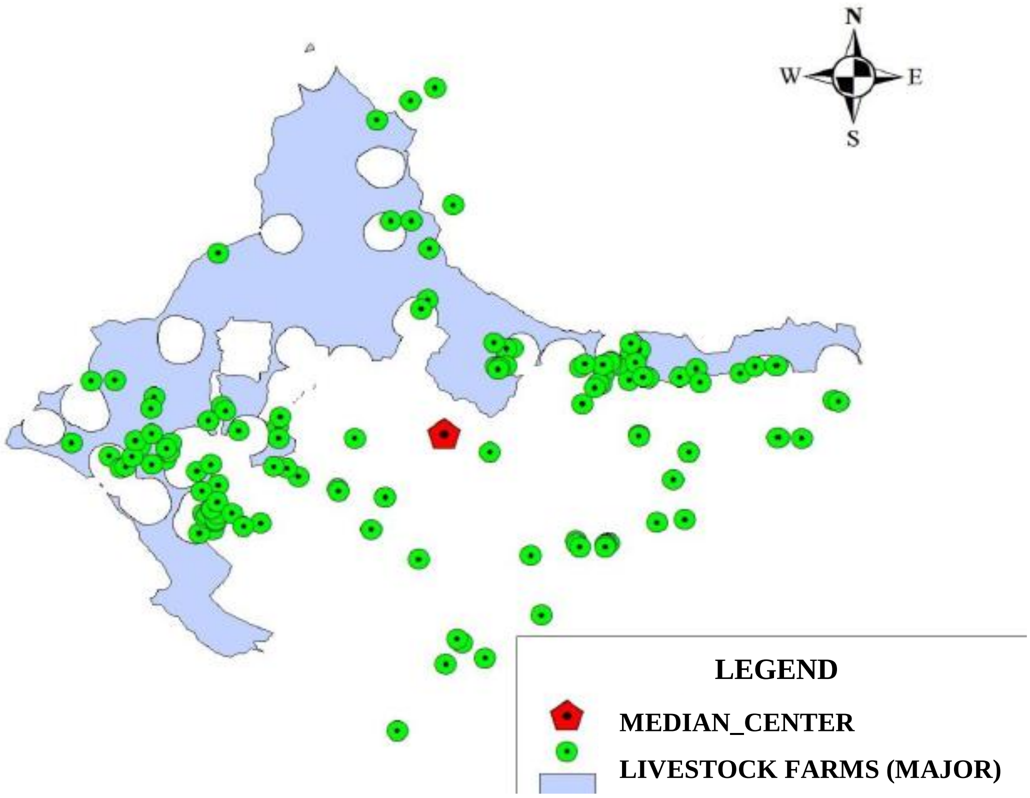


Figure 7: The best site for the biogas plant, "Median Center", according to the economic criterion of travel – distance minimization

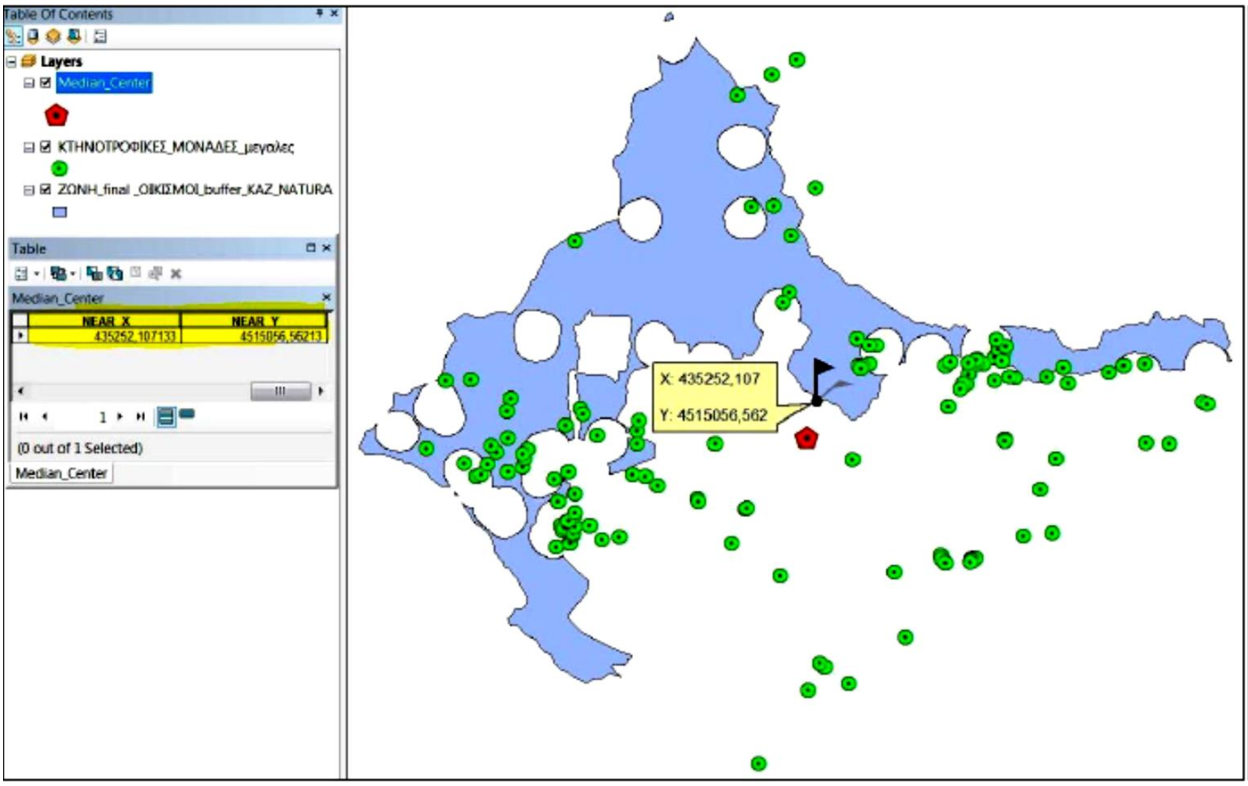


Figure 8: The final site for the biogas plant, taking into account all legislative, social, environmental and economic criteria

The following issues should be also underlined, as crucial factors, towards sustainable bio-wastes management:

- It is not obvious how to choose between anaerobic digestion for biogas production and composting of livestock wastes, with the former producing energy from renewable resources and the latter leading to quality compost, especially in the case of vermicomposting. Although the two different processes seem to be competitive, this is not true for two reasons: firstly, because they can work in synergy e.g. the remaining organic wastes after anaerobic digestion is finished, may be used in a composting or vermicomposting second-phase process, in order to continue wastes treatment, thus producing compost for possible use in agriculture; and secondly, because as Oikonomou et al. (2014) mention [11], there are many small (less than 150 cattle) livestock farms, decentralized, in Hellenic rural and mountainous areas, and in this case composting or vermicomposting in each farm may be a more viable solution for effective wastes treatment. On the contrary, constructing small low-cost effective biogas plants, decentralized in each farm or in a small group of 2-3 farms, might be a more difficult issue to be implemented.
- It is not easy to have an Environmental Impact Assessment study for a biogas plant approved, while the land-use system is based on the well-known presidential decree of 1987, when such environmental systems did not even exist. A new land-use framework is just about to be enacted, however, this is some expectation the last 2-3 years.
- The sustainable model may probably be to construct many biogas production plants, one in every livestock farm, with at least 120 cattle or in a small group of 2-3 farms, as it is better to enhance effective wastes treatment in the source. This seems to be difficult, as farmers may not be willing to invest in such environmental systems or may be difficult to persuade, since environmental legislation is not implemented, while environmental inspections are not so often conducted.
- The recent construction and operation of some biogas production plants show that in the beginning, investors found it difficult to agree with farmers to take their livestock wastes for their plants, as farmers were very suspicious. On the contrary, some other investors offered to buy their livestock wastes, leading to a future competition or "stock exchange" of bio-wastes, with negative impacts on circular economy.

Finally, there is not a framework in Hellas to promote the development of small decentralized biogas production plants, consequently, up until now the most popular investment amongst them seems to be medium-sized biogas plants, leading to the need to transfer bio-wastes from several livestock farms to the biogas plants, thus provoking more negative environmental impacts. It is clear that is investment is based on profit of the investor and not on sustainable treatment and valorization of liquid manure wastes.

References

1. Al Seadi T. (2001). '**Good practice in quality management of AD residues from biogas production.**' Task 24 - Energy from Biological Conversion of Organic Waste. Published by IEA Bioenergy and AEA Technology Environment. Available at: http://www.manuremanagement.cornell.edu/ (accessed February 2nd 2018).
2. FEC SERVICES LTD. (2003). '**Anaerobic digestion, storage, oligolysis, lime, heat and aerobic treatment of livestock manures.'** Final Report / Provision of research and design of pilot schemes to minimize livestock pollution to the water environment in Scotland. Available at: http://educypedia.karadimov.info/library/0002224.pdf (accessed February 2nd 2018).
3. Velsen A.F.M. Van. (1979). 'Anaerobic digestion of wet piggery waste.'. In: **Engineering problems with effluent from livestock**, (ed. J.C. Hawkins), CEC, Luxembourg, pp. 476-489.
4. Al Seadi T. and C. Lukehurst. (2012). '**Quality management of digestate from biogas plants used as fertilizer.**' Task 37- Energy from Biogas. Published by IEA Bioenergy and AEA Technology Environment. Available at: https://www.iea-biogas.net (accessed February 2nd 2018).
5. Joint Ministerial Decision 6919/2004. (2004). '**Characterization of the lake terrestrial and water environment and the wetland system of the lakes Koronia, Volvi and the Macedonian**

Volvi as “National Park” and determination of protection zones and definition of land-uses and restriction of activities and building permits’ Government Gazette D´ 248/2004 (in Greek, available at: www.et.gr).

6. Joint Ministerial Decision 93542/2008. (2008). ‘**Amendment of the Joint Ministerial Decision 6919/2004**’ Government Gazette AAP 441/2008 (in Greek, available at: www.et.gr).
7. Joint Ministerial Decision 58481/2012. (2012). ‘**Approval of the management plan of the National Park of lakes Koronia – Volvi and the Macedonian Tembi**’ Government Gazette B´ 3159/2012 (in Greek, available at: www.et.gr).
8. Michaloudi E., Moustaka-Gouni M., Gkelis S. and K. Pantelidakis. (2008). ‘Plankton community structure during an ecosystem disruptive algal bloom of Prymnesium parvum.”. **Journal of Plankton Research**, vol. 31 (3), pp. 301-309.
9. Ruiz M.C., Romero E., Perez M.A. and I. Fernandez. (2012). ‘Development and application of a multi-criteria spatial decision support system for planning sustainable industrial areas in Northern Spain.’ **Automation in Construction**, vol. 22, pp. 320-333.
10. Joint Ministerial Decision 49828/2008. (2008). ‘**Approval of the Special Framework of Spatial Planning and Sustainable Development for Renewable Energy Resources**’ Government Gazette B´ 2464/2008 (in Greek, available at: www.et.gr).
11. Oikonomou E.K., Guitonas A. and C. Hatzimarianos. (2014). ‘Anaerobic digestion for treatment and valorization of cattle liquid manure.’ **Fresenius Environmental Bulletin**, vol. 23, no. 11, pp. 2707-2711.

DESIGN OF A GROUND SOURCE HEAT PUMP SYSTEM FOR A SCHOOL AND A HOTEL OPERATING IN DIFFERENT SEASONS

S.A. Vlachos*, F. Gaitanis and K.L. Katsifarakis

Division of Hydraulics and Environmental Engineering, Dept. of Civil Engineering, A.U.Th, GR-54124 Thessaloniki, Macedonia, Greece

*Corresponding author: e-mail:sotiris.vlachos@hotmail.com, tel : +306948729855

Abstract

In this paper, we study the design of a ground source heat pump system (GSHP), which serves both a school and an adjacent hotel, to improve the financial performance of the project and minimize the impact on the ground source temperature. For the purposes of this study we assume that the GSHP provides part of the required heating during the school's operating months and part of the required cooling for a five- month- operating period for the hotel.

The paper introduces a simple way to estimate the length of the ground heat exchanger (GHE), minimizing the total cost of the project. The total cost includes the initial cost composed of drilling, excavation, heat pumps and piping network. The operational cost is included to account for the energy consumed for the heating and cooling of the buildings. The peak load for each building is calculated with the commercial software 4M and the monthly & yearly annual load are calculated with both the national calculation tool for building energy performance - TEE KENAK and RETScreen 4. For the calculation of the total length of the GHE, the method proposed by ASHRAE and modified by Philippe is used. We test multiple scenarios for different thermal load inputs, corresponding to different percentages of the heating and cooling demand. The economic viability of the project is determined by calculating the Net Present Value of each of the respective scenarios.

Keywords: Geothermal heat exchanger, Ground Source Heat Pump, RETScreen, Cost optimization

1. INTRODUCTION

Energy is the principal motor of macroeconomic growth and development, prerequisite for meeting basic human needs, but at the same time a source of environmental stress. Therefore, its proper use is a vital component of sustainable development [UNDP, 2002].

During an energy project's lifecycle, environmental impact differs widely. The pollution of the atmosphere is primarily caused by the combustion of fossil fuels in energy conversion devices. The use of nuclear power raises a number of concerns, such as annual generation of 20-30 tons of high-level nuclear waste [Smith et al, 2017]. The use of biomass for energy has to compete with food production. Other renewable energy sources such as solar and wind have implications for land-use [Jenkins, 2015]. Geothermal energy is a renewable energy source which is not bound by the above limitations.

In particular, ground coupled (or ground source) heat pump systems (GSHP) are among the best renewable energy technologies. In 2015, geothermal energy contributed to around 3% of total primary production of renewable energy in the EU-28 countries [Eurostat, 2016]. With regard to other geothermal applications, they have the largest annual energy production and installed capacity worldwide, (55.15% and 70.90% respectively). The installed capacity is 50,258 MWt and the annual energy production is 326,848 TJ/year, with a capacity factor of 0.206 (in the heating mode) [Mac-

Lean et al, 2018]. Although most GSHP systems have been installed in North America, Europe and China, the number of countries using the technology increased from 26 in 2000 to 43 in 2010 and to 48 in 2015 [World Energy Council, 2016]. Additionally, according to the International Energy Agency (IEA) geothermal energy could account for around 3.5% of annual global electricity production and 3.9% of energy for heat (excluding ground source heat pumps) by 2050 [Eurostat, 2016].

The underground heat exchanger of GSHP systems is composed of one or several vertical boreholes, typically 10–15 cm in diameter and 80–200 m long. In each borehole, a U-tube is inserted and connected to the HP (Heat Pump). The fluid circulates in the U-tubes to diffuse heat into the ground in cooling mode or to extract heat from the ground in heating mode. The design of GLHE (Ground-Loop Heat Exchangers) systems requires a forecast of the fluid temperature reached at any time during the exploitation of the system; that temperature is a function of the building variable needs and of the GLHE design and operation. The goal is to ensure that the HP capacity and specifications are neither exceeded nor underexploited.

2. METHODOLOGY

The total cost of the project is obtained by summing the operating costs and the initial capital invested. Every annual money flux is converted into its present value, by means of the pertinent well-known formula.

2.1 Operating cost

The operating cost is the cost of the energy, which is consumed by the heat pump, the heat transfer fluid circulation pump and the backup heating and cooling system. The substantial factor determining the overall behaviour of the shallow geothermal installation is the seasonal heat pump performance. During the heating period, GHP consumes electricity (Q_{HP}) to pump heat from the ground (Q_G). The sum of Q_G and Q_{HP} is delivered to the building. In a similar way, during the cooling period, GHP consumes electricity (Q_{HP}) to pump heat from the interior of the building (Q_B) and to deliver it to the ground (Q_G). The mathematical description for the heating and cooling period respectively takes the form:

$$Q_{Bh} = Q_{Gh} + Q_{HPh} \text{ (kW)} \quad (1)$$

$$Q_{Gc} = Q_{Bc} - Q_{HPc} \text{ (kW)} \quad (2)$$

From its definition, the efficiency coefficient of the heat pump is mathematically described by the relationship:

$$COP = Q_B / Q_{HP} \quad (3)$$

The Coefficient Of Performance (COP) of the heat pump usually results as a function of the fluid inlet temperature of the pump and is provided by the manufacturers.

2.2 Initial cost

The initial cost is the sum of the costs of the heat pump, drilling, excavation and piping:

$$C_{initial} = C_{HP} + C_{drill} + C_{ex} + C_{pipe} \quad (4)$$

The heat pump purchase cost is a function of the maximum heating load that could be delivered to the building by the heat pump. The heat pump cost is evaluated by the following empirical formula:

$$C_{HP} = 0.0443 * Q_{heat}^{\ 2} + 455.63 * Q_{heat} \quad (5)$$

where Q_{heat} is the capacity of the heat pump [kW]. Drilling cost depends on the number of the boreholes and their depth. For our study the cost per meter was assumed 35 €/m with the mathematical description:

$$C_{drill} = 35N_xN_yH \quad (6)$$

N_x equals to the number of boreholes in the x axis, N_y equals to the number of boreholes in the y axis and H is the depth of the borehole.

Excavation is required in order to install the borehole-connectcting pipes. The evaluation of the excavation cost was performed considering that one trench is needed for every row in the x-direction to link the boreholes together. In the present work, we used trench dimensions of 0.6 m width and 1.2 m of depth. So, the excavation cost could be evaluated by:

$$C_{ex} = 9.6[N_y(N_xB) + (N_yB)] \quad (7)$$

Piping cost depends on the length needed. Since the diameter of each pipe might be different, their actual cost per unit length would likely be different. Therefore, the cost for the piping is:

$$C_{pipe} = 2 * 3 * [N_xN_yB + N_yB + N_xN_yH] \quad (8)$$

3. CALCULATION OF THE LENGTH OF A GEOTHERMAL HEAT EXCHANGER

To determine the length of the geothermal heat exchanger we use the equation proposed by ASHRAE and modified by Phillipe and Bernier [ASHRAE, 2009]. This method, based on Kavanaugh and Rafferty's work, requires the peak load, the maximum average monthly load, and the average annual load provided by the geothermal heat exchanger. The peak load of each building was calculated, based on the design study of the existing heating system, following the ASHRAE specifications, while the maximum average monthly load and average annual load were determined by means of the national (Greek) calculation tool for building energy performance TEE-KENAK. To ensure speed in the calculations, according to Kavanaugh and Rafferty - as amended by Bernier - we use the mathematical expression below:

$$L = \frac{q_h R_b + q_y R_{10y} + q_m R_{1m} + q_h R_{6h}}{T_m - (T_g + T_p)} \quad (9)$$

Where L = total drilling length (m), T_m = average fluid temperature in the borehole (°C), T_g = undisturbed ground temperature (°C) and T_p = temperature effect - representing the correction of T_g due to thermal interference between boreholes (°C). Temperatures can be conveniently measured in °C, since temperature differences have the same value in °C and K. Moreover, q_y, q_m and q_h are equal to the annual average ground load, the highest average monthly ground load and the peak hourly ground load, respectively, measured in W. Equation 1 is based on the worst-case scenario represented by three successive thermal pulses with durations corresponding to 10 years, one month, and six hours, as shown in Figure 1 [Philippe et al, 2010].

R_{10y}, R_{1m}, R_{6h} represent soil thermal resistance for soil loads corresponding to 10 years, one month and six hours (m·K/W). They are expressed as follows [Philippe et al, 2010]:

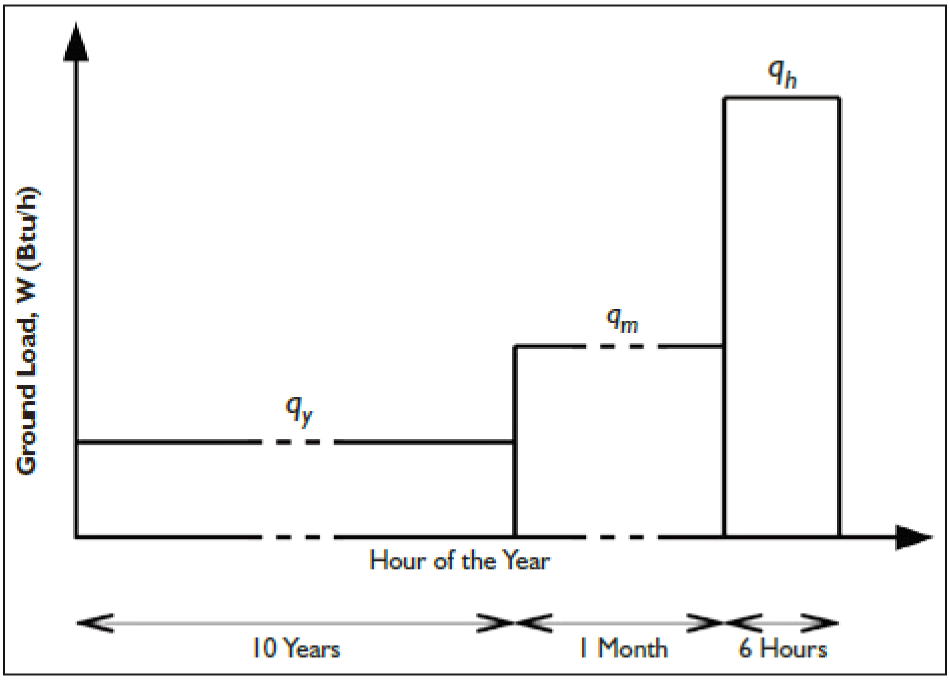


Figure 1: Three consecutive ground load pulses (source: Philippe, 2010)

$$R_{6h} = \frac{1}{k} G\,(\alpha t_{6h} / r^2_{bore}) \tag{10}$$

$$R_{1m} = \frac{1}{k}\ [\,G\,(at_{1m+6h} / r^2_{bore}) - G\,(\alpha t_{6h} / r^2_{bore})\,] \tag{11}$$

$$R_{10y} = \frac{1}{k}\ [\,G\,(\alpha t_{10y+1m+6h} / r^2_{bore}) - G\,(\alpha t_{1m+6h} / r^2_{bore})\,] \tag{12}$$

G-function represents the cylindrical heat source solution, k is the ground thermal conductivity ($W \cdot m^{-1} \cdot K^{-1}$), a is the ground thermal diffusivity ($m^2 \cdot day^{-1}$) and r_{bore} is the borehole radius (m).

The cylindrical heat source solution is strictly valid for one-dimensional (in the radial direction) transient heat transfer. As mentioned by Philippe et al (2010), Eskilson (1987) has shown that axial effects start to be significant, after a time period equivalent to $H^{2/}/(90a)$, where H is the borehole depth. The error introduced when using the cylindrical heat source has been calculated by Philippe et al (2010).

Based on these results, it appears that the axial effects are only significant for the R_{10y} term and that the error remains below 5% for typical values of thermal diffusivities. More accurate solutions, such as the two-dimensional finite line source model could be used [Eskilison, 1987].

The resulting deliverable is the number NB of boreholes that can be constructed in the available area, while the entire calculation procedure follows specific constraints concerning the T_p correlation, which is valid between adjacent boreholes.

The constraints are:

$$-2 \leq \ln\,(t / t_s) \leq 3 \tag{13}$$

$$4 \leq NB \leq 144 \tag{14}$$

$$1 \leq A \leq 9 \tag{15}$$

$$0.05 \leq B / H \leq 0.1 \tag{16}$$

where B is the distance between successive drillings, based on the available ground surface (considered as rectangular) and A the ratio of drillings' numbers along its two dimensions.

3.1 Optimization procedure

With the above methodology, we have determined the length of the geothermal heat exchanger for each building. To deliver the optimal drilling field covering both buildings, we have explored the cost of installing the system to cover different percentages of the peak load (ranging from 10% to100%). We have used the RETScreen 4 software to determine the relationship between power and total energy production for each case, the TEE-KENAK software to calculate the energy demand. The optimization methodology is based on the one presented by Gaitanis et al (2014).

4. CASE STUDY

A school and a hotel nearby were chosen [Vlachos, 2017]. The two-storey school has rectangular shape, with dimensions 33.14 x 12.00 m (Figure 2). The four-storey hotel has square shape with dimensions: 15.55x15.00 m (Figure 3). Both buildings have an inclined tiled roof and the internal height of each floor is 3.00 m. The school building is north to south oriented. Both buildings are located in Paramythia (NW Greece), which belongs to climate zone C. The total area of the structural elements of the buildings in the four main orientations, the heat transfer coefficient of each element as well as the average heat transfer coefficient of the building are presented in Tables 1 and 2.

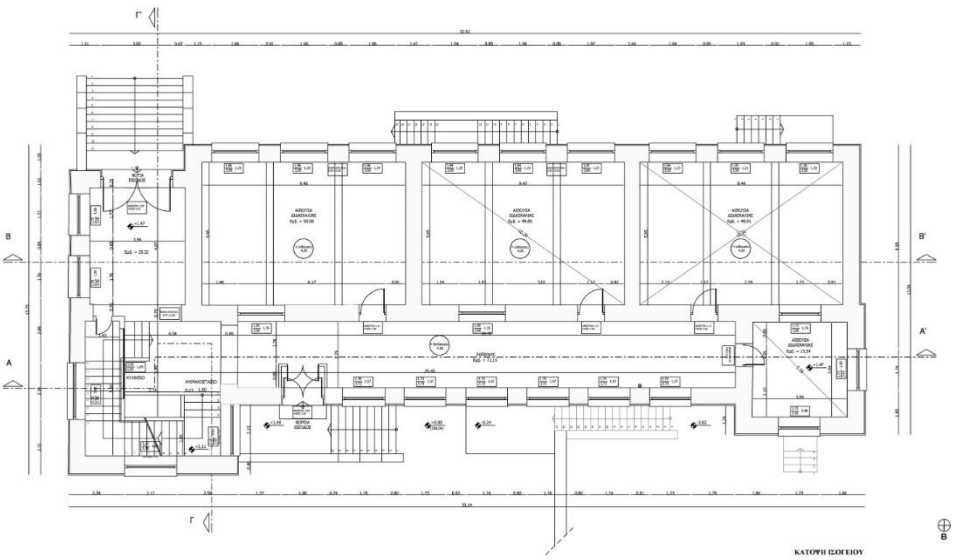


Figure 2: Plan view of the school (Spyropoulos, 2012)

Table 1: Heat transfer coefficients of the School building per structural element and orientation

Structural element	Area (m^2) and orientation of the element				Heat transfer coef. (W/m^2K)
	North	South	East	West	
Masonry walls	201.15	214.51	121.60	121.60	5.20
Reinforced concrete	50.33	74.41	58.02	58.02	4.40
Windows	57.51	98.85	18.82	24.5	4.10
Doors	3.01	8.25	0.00	0.00	5.00
Masonry walls$_{ab}$	53.8	30.22	0.00	0.00	3.10
Reinforced concrete$_{ab}$	21.4	20.11	0.00	0.00	2.80
Floor		1053.64			3.75

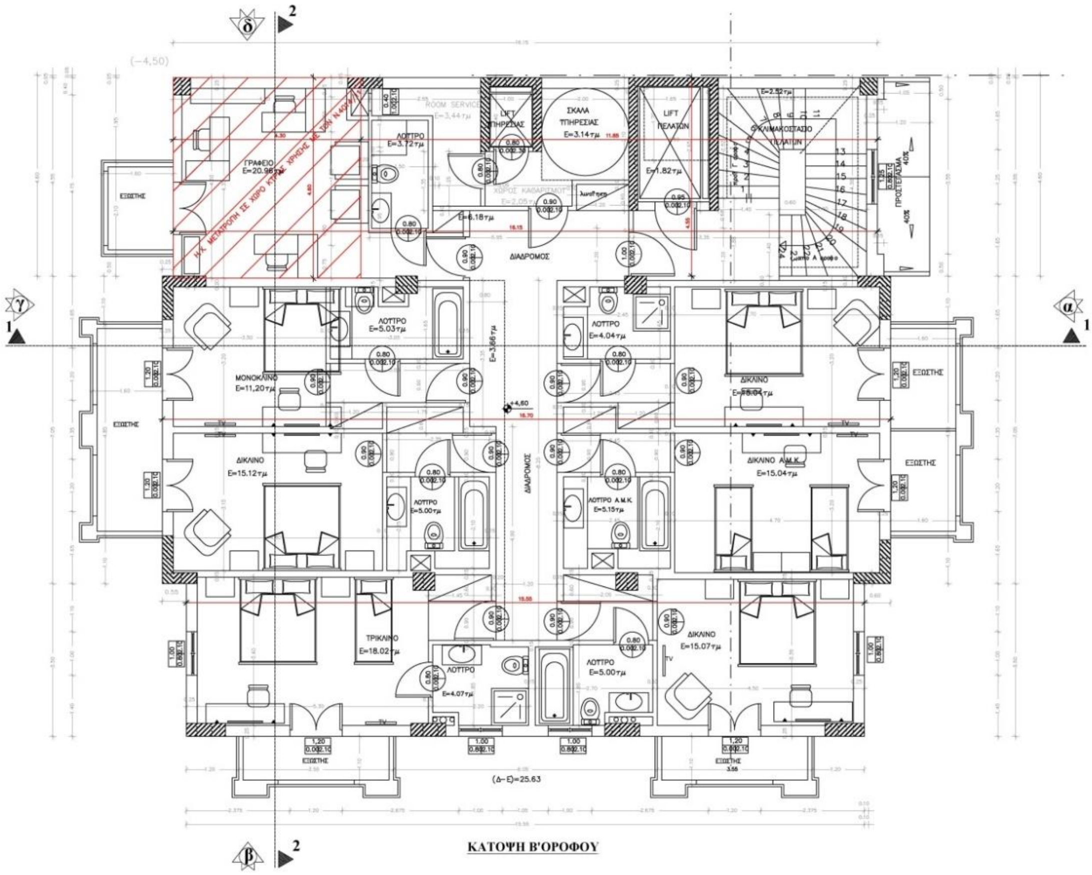


Figure 3: Plan view of the typical floor of the hotel (Spyropoulos, 2012)

Table 2: Heat transfer coefficients of the hotel building per structural element and orientation

Structural element	Area (m^2) and orientation of the element				Heat transfer coef. (W/m^{2}K)
	North	South	East	West	
Brick walls	133.15	134.17	182.34	149.53	0.59
Reinforced concrete	45.21	44.19	81.55	35.61	0.62
Windows	0.00	52.70	50.16	44.55	3.40
Doors	3.01	0.00	3.12	0.00	2.20
Brick walls$_{ab}$	0.00	0.00	0.00	0.00	0.39
Reinforced concrete$_{ab}$	0.00	0.00	0.00	0.00	0.48
Floor	1234				0.54

In Tables 1 and 2, index ab indicates structural element above non-heated space. The large differences in heat transfer coefficients of the two buildings is due to the following reason: The structural elements of the school, which was built in 1937, are not insulated and its windows are single-glazed. On the contrary, the hotel bears insulation and double-glazed windows.

5. RESULTS

First, we checked each building separately. Results regarding the number of required boreholes and the total borehole length appear in the diagrams of Figures 4 and 5. It is clear that the heating requirements are larger.

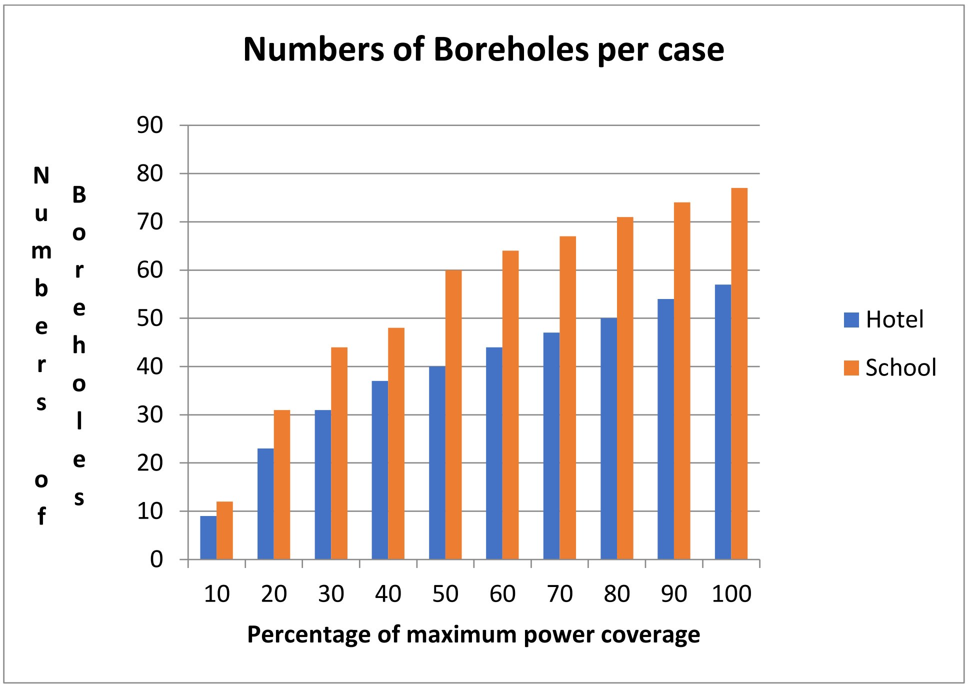


Figure 4: Number of boreholes considering the two buildings separately

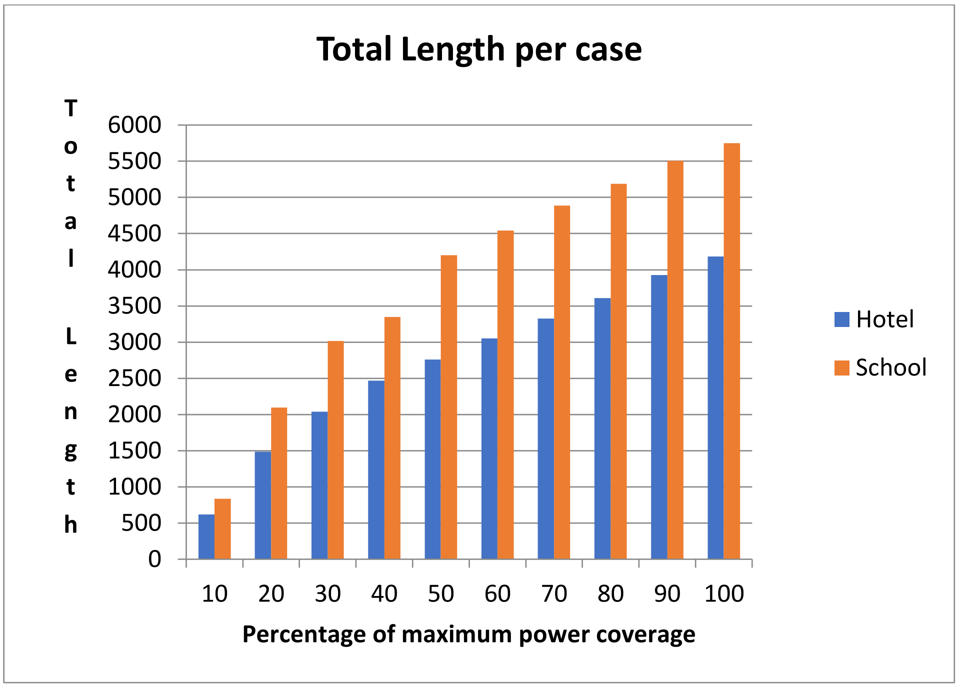


Figure 5: Total drilling length considering the two buildings separately

Then we turned to the combined heating-cooling system and we checked the following combinations in order to select the optimal one (C stands for cooling and H for heating):

- C100 % - H70%   C90% - H70%   C 80% - H 60%   C70% - H50%
- C60%- H40%   C50% - H30%   C40 % - H30%   C30% - H20%

These combinations ensure minimum long-term temperature change of the ground. Among them, we try to find the one with the smallest cost (for a 20-year period), taking into account the auxiliary heating and cooling sources.

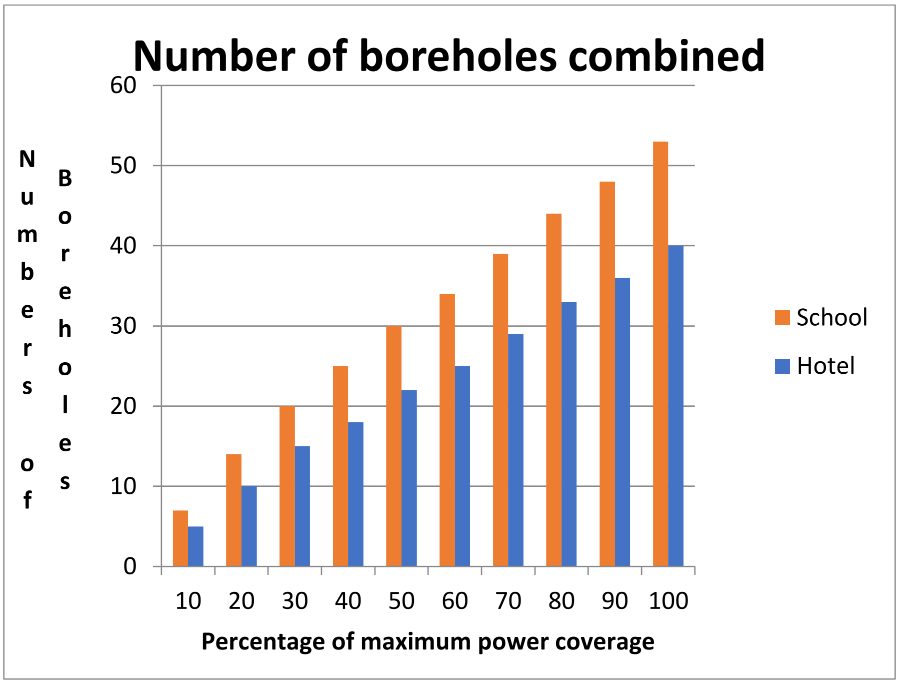


Figure 6: Number of boreholes for the combined heating-cooling system

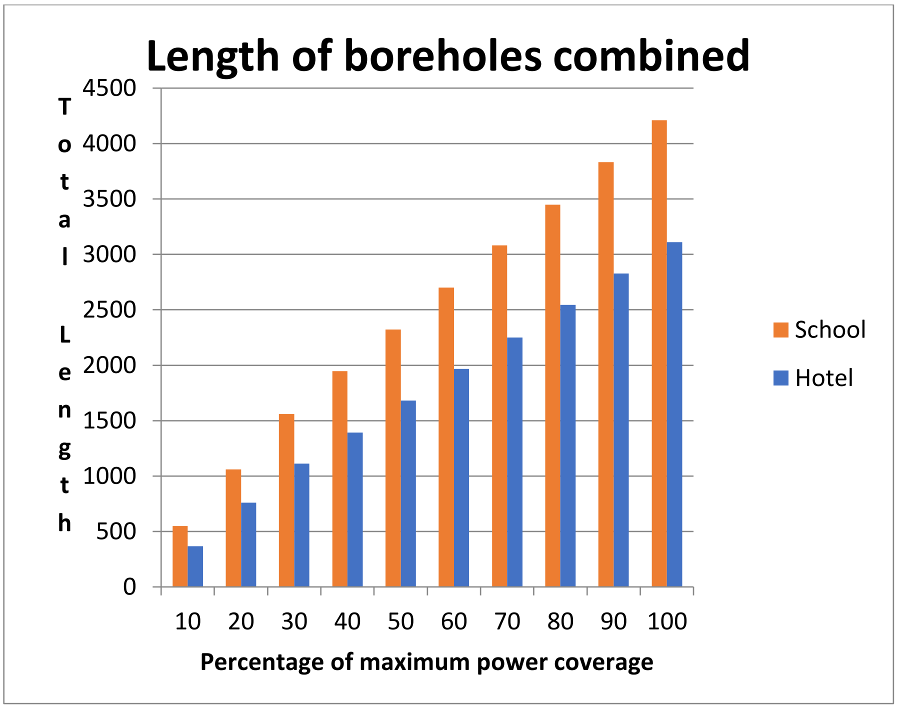


Figure7: Total borehole length for the combined heating-cooling system

In the diagrams of Figures 6 and 7, the required number of boreholes and the total borehole length for the combined heating-cooling system are presented. Comparative results regarding the total cost for the 20 year period appear in Table 3 and in the diagram of Figure 8. It can be concluded that the combination C50-H30 is the optimal one.

Table 3: Aggregated financial results of possible final installation and operating combinations over 20 years

Assumptions	Cost of Drilling	Cost of Excavations	Pipeline Costs	Pump Costs	Hotel's air conditioning unit	Cost Boiler	Operating Cost	Total Cost (€)
C100-H70	110.884	1.708	20.183	112.730		1.405	209.248	456.158
C90-H70	103.761	1.627	18.909	107.379	5.754	1.410	192.209	431.049
C80-H60	90.073	1.423	16.428	93.414	11.518	1.581	196.140	410.575
C70-H50	79.958	1.260	14.586	79.490	17.291	1.727	206.679	400.990
C60-H40	66.731	1.055	12.182	65.609	23.073	1.856	220.038	390.543
C50-H30	56.581	931	10.359	51.769	28.864	1.973	225.202	375.680
C40-H30	55.451	889	10.138	46.477	34.666	1.973	226.392	375.984
C30-H20	40.817	681	7.489	32.691	40.476	2.080	287.696	411.930

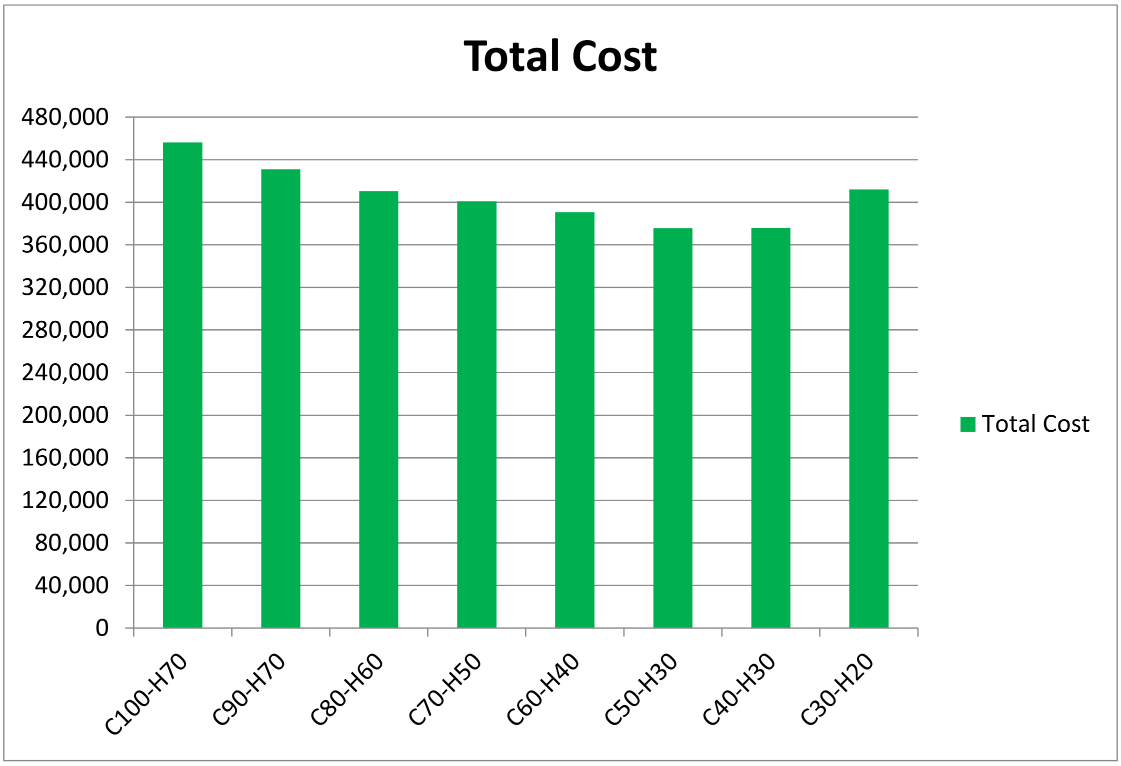


Figure 8: Total cost for the 20-year period

6. CONCLUSIONS

One of the main barriers to the penetration of renewable energy sources, such as GSHP, is the high initial cost, the recovery of which can be achieved in the long run due to the low operating cost. Sharing the initial cost to installations that operate in different periods of the year and in different modes, can improve the GSHP financial performance. In this paper, we have studied a GSHP serving both a school and a hotel, operating during the heating and the cooling period respectively. Our results show that the best financial results are achieved, when the GSHP system is planned to cover 50% of the cooling demand and 30% of the heating demand, with minimum change of the ground temperature. While these results are site-specific, the proposed methodology can be easily applied to other cases with different climate, building and ground features.

References

1. ASHRAE (2011) **'ASHRAE Handbook-HVAC Applications'**.
2. Eskilson P. (1987) '**Thermal Analysis of Heat Extraction Boreholes**', Ph.D. Thesis, University of Lund, Department of Mathematical Physics, Lund, Sweden.
3. Eurostat (2016) http://ec.europa.eu/eurostat/web/environmental-data-centre-on-natural-resources/natural-resources/energy-resources/geothermal-energy (accessed February 1st, 2018).
4. Gaitanis F., Katsifarakis, K.L. and Bikas D. (2014) 'Economic Optimization of Systems Combining Vertical Ground Heat Exchanger with Conventional Heating and Cooling Systems**', 10th National Conference on Renewable Energy Sources,** pp. 1179-1188, Thessaloniki, Greece (in Greek).
5. Jenkins J. (2015) **How Much Land Does Solar, Wind and Nuclear Energy Require?**
6. Kavanaugh S.P. and Rafferty K. (1997) '**Ground-Source Heat Pumps: Design of Geothermal Systems for Commercial and Institutional Buildings**', ASHRAE, Atlanta.
7. Lund, J.W. and Boyd T.L., (2016) '**Direct Utilization of Geothermal Energy 2015 Worldwide Review**,' J. Geothermics, 60, pp. 66-93.
8. Mac-Lean C. (2018) '**Application of low enthalpy geothermal energy: the case of low enthalpy of physical and mathematical sciences at the university of Chile**', Int. J. of Energy Prod. & Mgmt., 3(1), pp. 69-78.
9. Philippe M., Bernier M. and Marchio D. (2010) '**Sizing Calculation Spreadsheet Vertical Geothermal Borefields**,' ASHRAE J., 20, pp. 20-28.
10. Robert F. and Gosselin L. (2014) '**New Methodology to Design Ground Coupled Heat Pump Systems Based on Total Cost Minimization**,' J. App. Ther. Eng. 62, pp. 481-491.
11. Shortall R., Davidsdottir B., and Axelsson G. (2015) '**Geothermal Energy for Sustainable Development: A review of Sustainability Impacts and Assessment Frameworks**', J. Ren. And Sustain. En. Rev., 44, pp. 391-406.
12. Smith S., Clark M., Fairbanks T., Prinzi T., Delgado K. (2017*)* **Nuclear Power – Pros and Cons Thermodynamics**
13. UNDP (2002) **'Energy for Sustainable Development: A Policy Agenda',** United Nations Development Program.
14. Vlachos S. (2017) **'Design of a vertical geothermal heat exchanger system serving a school and a hotel that operate in different periods of time'**, Master thesis, Dept. of Civil Engineering, Aristotle University of Thessaloniki, Greece (in Greek).
15. World Energy Council (2016) **'World Energy Resources'**

FEASIBILITY STUDY OF A FLOATING OFFSHORE WIND FARM IN GREECE

V. Kafritsa* and E. Loukogeorgaki

Division of Hydraulics and Environmental Engineering, Dept. of Civil Engineering, A.U.Th, GR-54124 Thessaloniki, Macedonia, Greece

*Corresponding author: e-mail: vicky.kafritsa@gmail.com, tel: +302310995951

Abstract

Offshore wind energy presents an abundant renewable energy source that can contribute to the satisfaction of the European Union's energy policy targets. Although nowadays large-scale Offshore Wind Farms (OWFs) have been commercially deployed in shallow waters areas, the existence of stronger and more consistent wind fields in offshore areas of deeper waters has triggered the development of floating Offshore Wind Turbines (OWTs) of large capacity and has very recently lead to the installation of the first pilot floating OWF. Greece is a Mediterranean country with a vast wind energy potential at specific marine areas characterized by deep-water conditions. Thus, the potential of deploying floating OWFs should be considered and examined.

Motivated by this, the aim of the present paper is to determine the economic feasibility of a floating OWF in Greece. The proposed OWF is considered to be deployed at a marine location in the north-central Aegean (east of Mykonos island), which satisfies specific sitting criteria, and it is designed to cover the annual energy demands of Mykonos, Delos and Rhenia islands. For the development of the proposed investment, two alternative scenarios are examined, by modifying the number and the rated power of the OWTs, as well as the distances between them. The 1st scenario corresponds to an OWF with 11 floating OWTs (spar buoy floating platform) of 33 MW total rated power, while the 2nd one to an OWF with 7 floating OWTs (spar buoy floating platform) of 35 MW total rated power. The net annual energy production of the two alternative scenarios is estimated considering wake losses, electrical losses and OWTs' availability. Wake effects are estimated using Jensen's model. The selection of the best scenario is based on the comparison of the Levelized Cost of Energy (LCOE) of the two alternatives. The finally selected scenario (1st scenario) is evaluated using the net present value method, the internal rate of return and the payback period of the investment.

The results indicate that the most important parameter affecting LCOE and, therefore, determining the final investment decision between the two proposed alternative scenarios, is the OWF's capacity factor. Moreover, the results of the economic analysis/evaluation of the finally selected scenario clearly illustrate the economic sustainability of the proposed OWF and, therefore, its potential for covering effectively the annual energy demands of the examined islands.

Keywords: Floating offshore wind farm, Levelized cost of energy, Investment evaluation, Net present value, Internal rate of return

1. INTRODUCTION

The recent vast industrialization, the increasing population trends and, therefore, the increasing energy demands have led the governments worldwide to search for renewable energy resources, in order to reduce the dependence on fossil fuel and support environmental sustainability. It is essential for the power generation industry to face the daunting challenge in meeting global energy needs,

which will double globally and triple in developing countries by 2030. The solution to the power generation problem may be given by the exploitation of appropriate wind power generation systems, which have been already used since 1970s (Kaldellis and Za, 2011). Such systems providing not only a wide range of environmental benefits, but constituting an attractive techno-economical solution to the power generation problem are, nowadays, of particular interest.

Wind power generation systems, mostly known as wind farms, are utilized onshore or offshore. Though they have higher capital costs than onshore wind farms, Offshore Wind Farms (OWFs) have attracted great interest recently, as they allow the generation of large amounts of electricity from wind energy (IRENA, 2012). Offshore, average mean wind speeds tend to be higher than onshore; therefore, the electricity output can be increased by 50% compared to onshore wind farms (Li et al., 2010). Additionally, going offshore enables turbines to be installed in plentiful numbers without the planning and space constraints found onshore (Tong, 1998). Ultimately, OWFs will allow a much greater deployment of wind in the longer-term. At the end of 2017, Europe has a total installed offshore wind capacity of 15.78 GW corresponding to 92 OWFs located mainly in the coastal and offshore areas of Northern Europe (EWEA, 2018). Greece, contrary to the northern European countries, has not yet begun to exploit its offshore wind energy potential. In the framework of supporting the future development of Greece's offshore wind policy, a feasibility study of an OWF located in the Greek seas is of significant importance.

A feasibility study aims to uncover objectively and rationally the strengths and weaknesses of a proposed project, the opportunities and threats existing in the natural environment, the resources required to carry through, and ultimately the prospects for success (Georgakellos and Marcis, 2009). In its simplest terms, the two criteria to judge feasibility are cost required and value to be attained (Young, 1970). Many authors have already conducted feasibility studies for offshore wind farms (Pantaleo et al., 2005; Ozerdem et al., 2006; Kim et al., 2013; Satir et al., 2018). Konstantinidis et al. (2014) implemented a viability analysis of an OWF in the Greek sea area based on a techno-economical study. Using the software RETScreen, the annual energy generation was estimated. Followed by the cost estimation, the investment's viability was investigated using the Net Present Value (NPV), the Internal Rate of Return (IRR), the Benefit to Cost Ratio (BCR) and the Cost of Energy (COE).

In the present paper, a techno-economic feasibility analysis of a floating OWF in Greece is presented. The proposed OWF is considered to be deployed at a marine location in the north-central Aegean (east of Mykonos island), which satisfies specific sitting criteria, and it is designed to cover the annual energy demands of Mykonos, Delos and Rhenia islands. For developing the proposed investment, two alternative scenarios, that differ in terms of the number of Offshore Wind Turbines (OWTs), the OWTs' rated power and the distances between OWTs, are proposed and examined. The choice of the best solution is based on the comparison of the Levelised Cost of Energy (LCOE) of the two alternative scenarios. The scenario, finally, selected is financially evaluated using the NPV method, the IRR and the Payback Period (PP) of the investment.

2. SITE SELECTION AND TECHNICAL DESCRIPTION

2.1 Site Selection

In the present paper, the OWF is proposed to be installed at a marine area located in the north-central Aegean and, more specifically, east of the Mykonos island (Figure 1), 42 km from the existing port of Mykonos. The coordinates (based on the Hellenic Geodetic Reference System 1987) of the specific quadrilateral polygon ABCD (Figure 1), where the OWF is proposed to be installed, are shown in Table 1. The proposed area has been selected based on the results of Vasileiou et al. (2017), where a GIS-based multi-criteria decision analysis for the site selection of hybrid offshore wind and wave energy systems in Greece has been implemented. According to that study, the proposed marine area can be considered eligible for the deployment of an OWF, since it does not satisfy a set of exclusion criteria related to: (a) utilization restrictions imposed by human activities and environmental

constraints (e.g. the specific site does not correspond to an area for military operations or hydrocarbons' exploration/exploitation and or to a marine protected area), (b) economic/technical constraints (i.e. mean wind speed is larger than the threshold of 6 m/s, water depth is smaller than the threshold of 500 m) and (c) social implications (i.e. the distance from the shore of the selected area is larger than the threshold of 25 km). Moreover, the selected area is characterized by significant wind speeds (6-8 m/s, 10 m above the mean water level) and water depths (60-200 m) that advocate the deployment of a floating OWF (Vasileiou et al., 2017), while the recent development of electricity transmission infrastructure between Mykonos and mainland, through the Tinos and Andros islands, may contribute to costs' reduction.

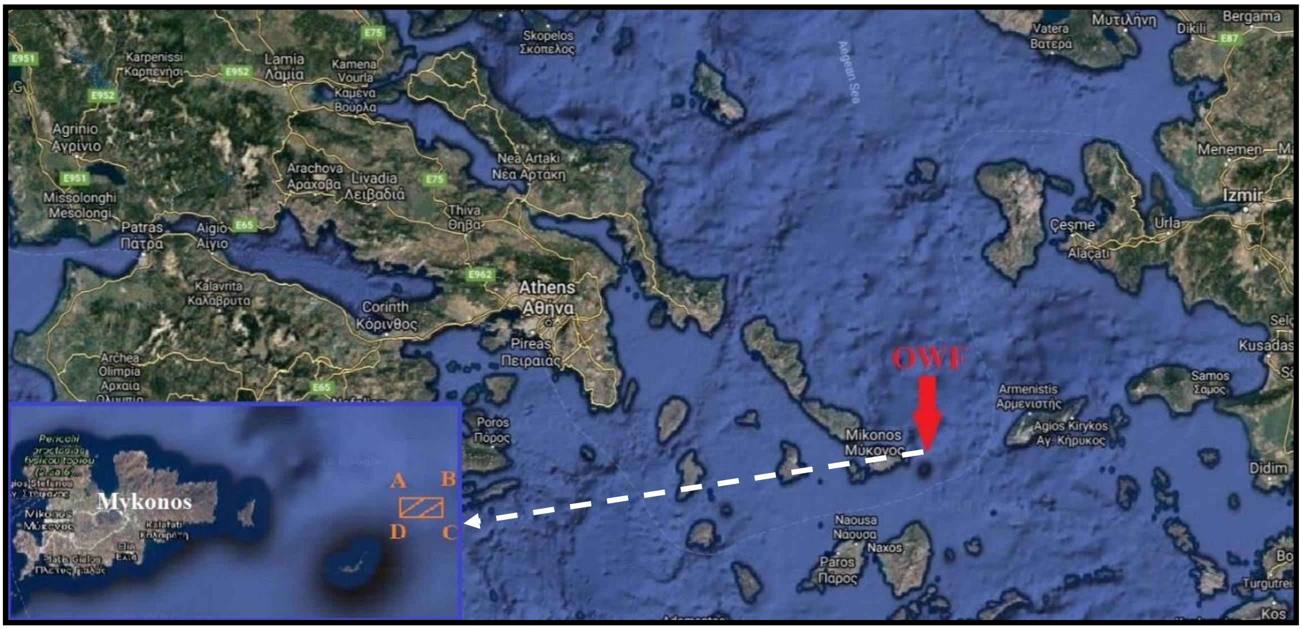


Figure 1: Marine area in the north-central Aegean (red sign) for the deployment of a floating OWF

Table 1: Exact coordinates of the polygon, where the OWF is proposed to be installed

Point	Easting	Northing
A	641680	414974
B	645040	414974
C	645040	413406
D	641680	413406

Wind data, consisting of wind speeds and wind directions, is of significant importance for the Annual Energy Production (AEP) calculations. In the present paper, due to lack of field data for the selected marine area, the required wind data were obtained from the Global Wind Atlas using WaSP software (Mortensen et al., 2011). Based on this data, in the examined marine area winds of northern direction mainly exist, while the average annual wind speed, 100 m above the mean water level, is between 7.4 m/s and 8.5 m/s.

2.2 OWF Scenarios

In the present paper, two alternative scenarios (S1 and S2) of a floating OWF, covering the annual needs of the islands of Mykonos, Rhenia and Delos, are examined. Specifically, based on the wind conditions of the selected marine area, the examined scenarios are formed by deploying two different types of WTs: (a) the WT V112-3 MW (Vestas SA) and the WT G128-5 MW (Gamesa Corp.), which

is suitable for windier sites with an average wind speed at the hub height up to 8.5 m/s. The aformentioned types of turbines have 112 m and 128 m rotor diameter and 3 MW and 5 MW rated power respectively. The hub heights above the mean water level are taken equal to 94 m and 95 m respectively. Considering a mean capacity factor of around 40% (Dodson et al., 2005), the AEP for each WT is estimated equal to 10512 MWh/year and 17520 MWh/year respectively. Based on these values and aiming at covering the annual energy demand of Mykonos, Rhenia and Delos, which for the year 2013 was 113000 MWh (RAE, 2013), the number of WTs required for each examined scenario is, then, defined. The corresponding results are shown in Table 2. It is noted that for both scenarios, a spar-buoy floating platform is seleted as the supporting structure of each OWT.

Table 2: Technical characteristics and AEP of the examined OWF scenarios

Examined scenario	Type of WT	Number of WTs	OWF total rated power (MW)	AEP estimation (MWh/year)
S1	V112-3 MW	11	33	115632
S2	G128-5 MW	7	35	122640

In both scenarios, the WTs are organised into two rows, as shown in Figure 2. As a rule of thumb, the distance of the WTs in an OWF is taken between 5 and 9 rotor diameters along the prevailing wind direction, and between 3 and 5 diameters in the direction perpendicular to the prevailing winds. Based on the above, for each examined scenario the in-between distances of the WTs are taken equal to 7 rotor diameters along the north direction (prevailing wind direction) and 5 rotor diameters in the direction perpendicular to the prevailing winds, as shown in Figure 2. Finally, it is assumed that there is no need for an offshore substation due to the low capacity of the proposed floating OWF.

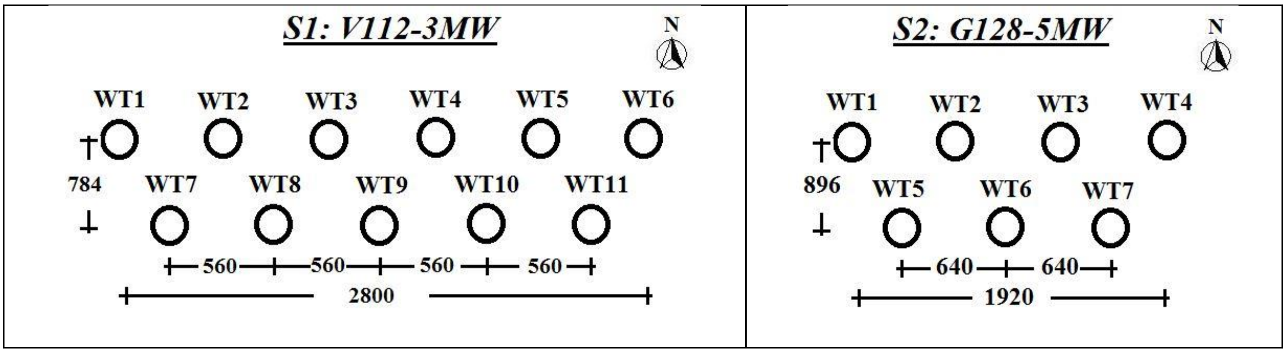


Figure 2: Distances (m) between the WTs for the examined scenarios

2.2 Energy Production

In the present study, gross AEP for each WT is estimated considering the Weibull distribution of the wind obtained by WaSP (Mortensen et al., 2011), along with the power curve of the WT selected for each scenario. As for the net AEP, this quantity is estimated by calculating losses due to wake effects according to Jensen's model (Jensen, 1983), where the frequency of wind direction is taken into account. The corresponding results are presented in Table 3.

It should be mentioned that the wind data obtained from the Global Wind Atlas and used for calculating the net AEP values of Table 3 (111113.60 MWh/y and 104450.56 MWh/y for S1 and S2 respectively) are based on onshore measurements. However, in the marine site, where the OWF is proposed to be installed, obstacles in the prevailing wind direction contrary to an onshore site do not exist. Therefore, the mean wind speed at the examined area is expected to have a bit larger values than the ones obtained from the Global Wind Atlas. This is also confirmed by RAE statistics, where the mean wind speed at the examined area appears to be 10% larger than the mean wind speed obtained from the Global Wind Atlas. Thus, combining all the above, a correction of the net AEP values of Table 3 is required in order to account for larger mean wind speeds. In the light of the above,

a conservative 24% increase of the net AEP is assumed in the present study. Moreover, considering 95% availability of the floating OWF and annual electrical losses equal to 2%, the final net AEP for scenarios S1 and S2 is estimated to reach 128275 MWh/year and 120583 MWh/year respectively. Based on the above, the capacity factor for scenarios S1 and S2 is evaluated to be equal to 44% and 39% respectively, which correspond to quite conservative values.

Table 3: Gross and Net AEP for each floating OWF scenario

<table>
<tr><th colspan="4">Scenario 1 (33 MW)</th><th colspan="4">Scenario 2 (35 MW)</th></tr>
<tr><th>WT No.</th><th>Gross AEP (MWh/y)</th><th>Net AEP (MWh/y)</th><th>Losses (%)</th><th>WT No.</th><th>Gross AEP (MWh/y)</th><th>Net AEP (MWh/y)</th><th>Losses (%)</th></tr>
<tr><td>WT1</td><td rowspan="11">11316.80</td><td>10956.84</td><td>3.18</td><td>WT1</td><td rowspan="7">16543.50</td><td>16007.27</td><td>3.24</td></tr>
<tr><td>WT2</td><td>10415.92</td><td>7.96</td><td>WT2</td><td>15191.38</td><td>8.17</td></tr>
<tr><td>WT3</td><td>10132.66</td><td>10.46</td><td>WT3</td><td>14892.52</td><td>9.98</td></tr>
<tr><td>WT4</td><td>10096.27</td><td>10.79</td><td>WT4</td><td>15100.09</td><td>8.72</td></tr>
<tr><td>WT5</td><td>10147.85</td><td>10.33</td><td>WT5</td><td>14722.82</td><td>11.01</td></tr>
<tr><td>WT6</td><td>10352.57</td><td>8.52</td><td>WT6</td><td>14254.19</td><td>13.84</td></tr>
<tr><td>WT7</td><td>10116.02</td><td>10.61</td><td>WT7</td><td>14282.29</td><td>13.67</td></tr>
<tr><td>WT8</td><td>9768.25</td><td>13.68</td><td colspan="4" rowspan="4"></td></tr>
<tr><td>WT9</td><td>9677.20</td><td>14.49</td></tr>
<tr><td>WT10</td><td>9664.23</td><td>14.60</td></tr>
<tr><td>WT11</td><td>9785.80</td><td>13.53</td></tr>
<tr><td>Total</td><td>124484.83</td><td>111113.60</td><td>10.74</td><td>Total</td><td>115804.50</td><td>104450.56</td><td>9.80</td></tr>
</table>

3. FINANCIAL ANALYSIS/EVALUATION

For realizing an economical sustainable OWF project, the OWF should be capable of producing energy not only in a long-term, but also in a cost-efficient manner. As a result, a financial analysis/evaluation is necessary to illustrate the viability of the proposed OWF, by taking into account the energy production cost as well as the market value of the generated energy (Manwell et al., 2009). In the present study, a financial analysis of the two floating OWF scenarios is implemented to define the most profitable solution by estimating the Levelized Cost of Energy (LCOE) for each scenario. The finally selected scenario is, then, evaluated using the Net Present Value (NPV) method, the Internal Rate of Return (IRR) and the Payback Period (PP) of the investment. The procedure followed is briefly described in Figure 3.

For both scenarios, LCOE is calculated considering Capital Expenditure (CapEx), Operational Expenditure (OpEx) and the Net AEP (Myhr et al., 2014). In the present paper, CapEx including the construction financing, development costs and operational capital besides the investment, is estimated based on Mone et al. (2015) and Heidari (2017). Regarding OpEx, this is rarely reported by developers, so, high amount of uncertainty applies due to lack of empirical data. In this study, investment costs are estimated based on personal communication with a representative from Athens Business Consulting-ABEC LP. In the following paragraphs the results of the economic analysis/evaluation are presented.

3.1 CapEx and OpEx Estimation

CapEx estimation for both floating OWF scenarios is presented in Table 4. The estimated turbine cost includes the tower and the Rotor-Nacelle-Assembly (RNA) cost. Insurance and contingency are considered to be equal to 1% and 9% of the CapEx respectively, according to usual practices.

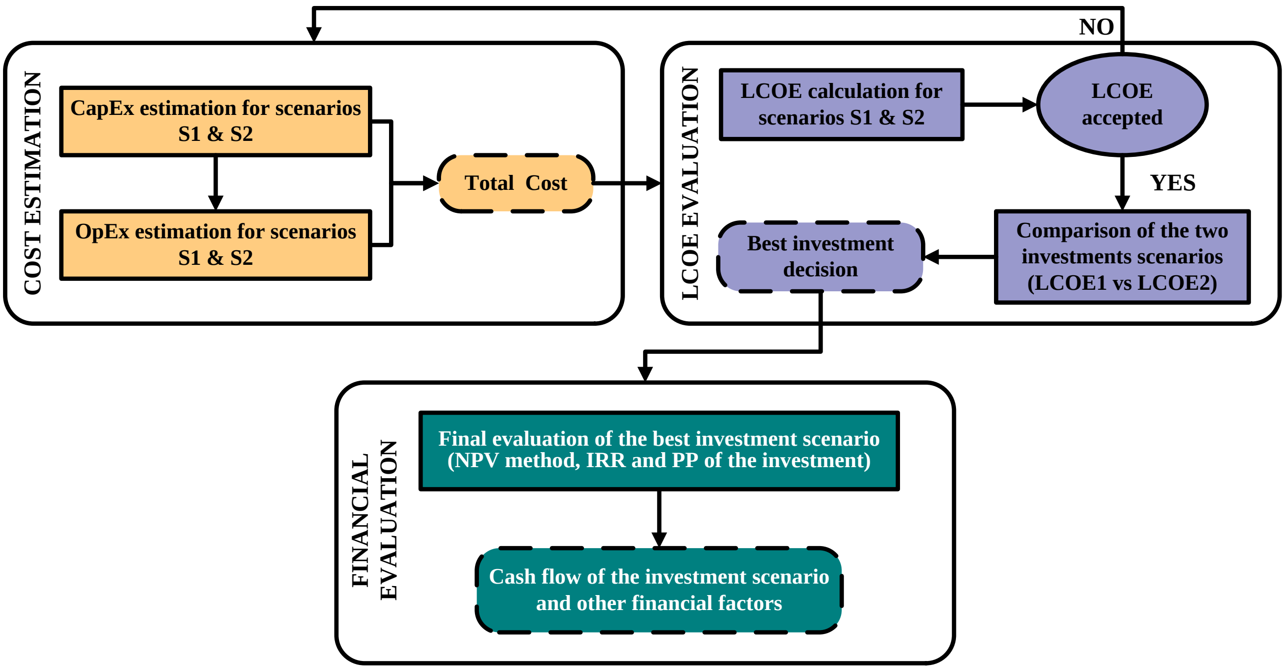


Figure 3: Procedure followed for the financial analysis/evaluation of the examined OWFs

Table 5 presents OpEx estimation for the two proposed scenarios considering maintenance as a percentage of the CapEx assets. Annual transportation costs, personnel costs and overheads are considered similar to both scenarios due to the small difference of the OWF capacity between the two proposed scenarios. Overheads refer to costs related to the incorporated joint venture that will be established for the purposes of the proposed project.

Table 4: CapEx breakdown for both scenarios

CapEx Breakdown	Scenario S1			Scenario S2		
	€/MW	€	Percentage of total CapEx	€/MW	€	Percentage of total CapEx
Project development	74250	2450250	3	72381	2533327	3
Turbine	990000	32670000	40	940950	32933250	39
Substructure	396000	13068000	16	410158	14355519	17
Mooring system	49500	1633500	2	48254	1688885	2
Electrical Interconnector	321750	10617750	13	289523	10133308	12
Installation	396000	13068000	16	410158	14355519	17
Insurance	29700	980100	1	24127	844442	1
Other	0	0	0	0	0	0
Contingency	222750	7350750	9	217142	7599981	9
Total CapEx (€)	**2475000**	**81838350**	100	**2412692**	**84444231**	100

Table 5: OpEx breakdown for both scenarios

OpEx Breakdown	Scenario S1			Scenario S2		
	Asset (€/MW)	Maintenance (% of asset)	Maintenance (€/MW/year)	Asset (€/MW)	Maintenance (% of asset)	Maintenance (€/MW/year)
Project development	74250	0	0	72381	0	0
Turbine	990000	2	19800	940950	2	18819
Substructure	396000	1	3960	410158	1	4102
Mooring system	49500	1	495	48254	1	483
Electrical Interconnector	321750	3	9653	289523	3	8686
Installation	396000	1	3960	410158	1	4102
Insurance	29700	0	0	24127	0	0
Other	0	0	0	0	0	0
Contingency	222750	0	0	217142	0	0
Total Maintenance			37868			36190
Insurance			24750			24127
Transportation			191			191
Personnel			10730			10117
Overheads			1515			1429
TOTAL OpEx (€)			**82560**			**72054**

3.2 Final Investment Decision

The selection of the final investment decision is based on the LCOE calculation for both scenarios for the whole life-cycle of the OWF, which in the present study is taken equal to 25 years (5 years for licensing procedures, design and construction and 20 years for operation). LCOE is calculated considering the sum of lifetime discounted generation costs and the sum of discounted lifetime electricity output, which is the net metered output after all losses. Equity and debt are taken equal to 30% and 70% of the total financing respectively, considering a 5-year grace period for loan repayment. Cost of equity is evaluated using the Capital Asset Pricing Model (CAPM), which estimates the cost of equity by adding the risk-free rate with an additional premium for exposing the investment to systematic risk. In the present study, cost of equity and cost of debt are taken equal to 14.5% and 9% respectively, and the corporate tax rate is considered to be 34% according to the national taxation (2017). Table 6 presents the results of the LCOE for both scenarios.

Comparing LCOE1 with LCOE2, it is obvious that scenario S1 should be selected as the final investment decision; namely, the floating OWF consisting of 11 WT (V112-3 MW) of 33 MW total rated power. The main characteristics of this scenario are summarized in Table 7. The aforementioned result is supported by the fact that the net capacity factor of S1 (44%) is larger than the net capacity factor of S2 (39%), while both scenarios have almost the same costs over lifetime (Tables 4 and 5).

Table 6: LCOE for both scenarios

Scenario S1			Scenario S2		
LCOE Breakdown	**(€/MWh)**	**Percentage of LCOE**	**LCOE Breakdown**	**(€/MWh)**	**Percentage of LCOE**
CapEx	71.78	77.17%	CapEx	78.70	77.35%
OpEx	21.24	22.83%	OpEx	23.04	22.65%
LCOE1 (€/MWh)	**93.02**		**LCOE2 (€/MWh)**	**101.74**	

Table 7: Final investment decision (scenario S1)

Investment Decision	
Type of WT	V112 (Vestas)
Rated Power (MW)	3
Number of WT	11
Total Rated Power (MW)	33
Net AEP (MWh/year)	128271
Capacity Factor (%)	48
CapEx	€ 81838350
OpEx	€ 2724471
LCOE (€/MWh)	93

3.3 Financial Evaluation

Financial evaluation for the final investment decision (Scenario S1, Table 7) is implemented through NPV, IRR and PP, considering 8.51% weighted average cost of capital, 2% inflation rate and 25 years life cycle duration. Revenues are calculated per year considering the electricity price to be 0.185 €/KWh (Feed in Tariff) for an OWF, according to Europe pricing for offshore electricity production. The net cash flow of the investment was calculated per year and it was, then, transformed in present values to calculate the cumulative cash flow presented in Figure 4.

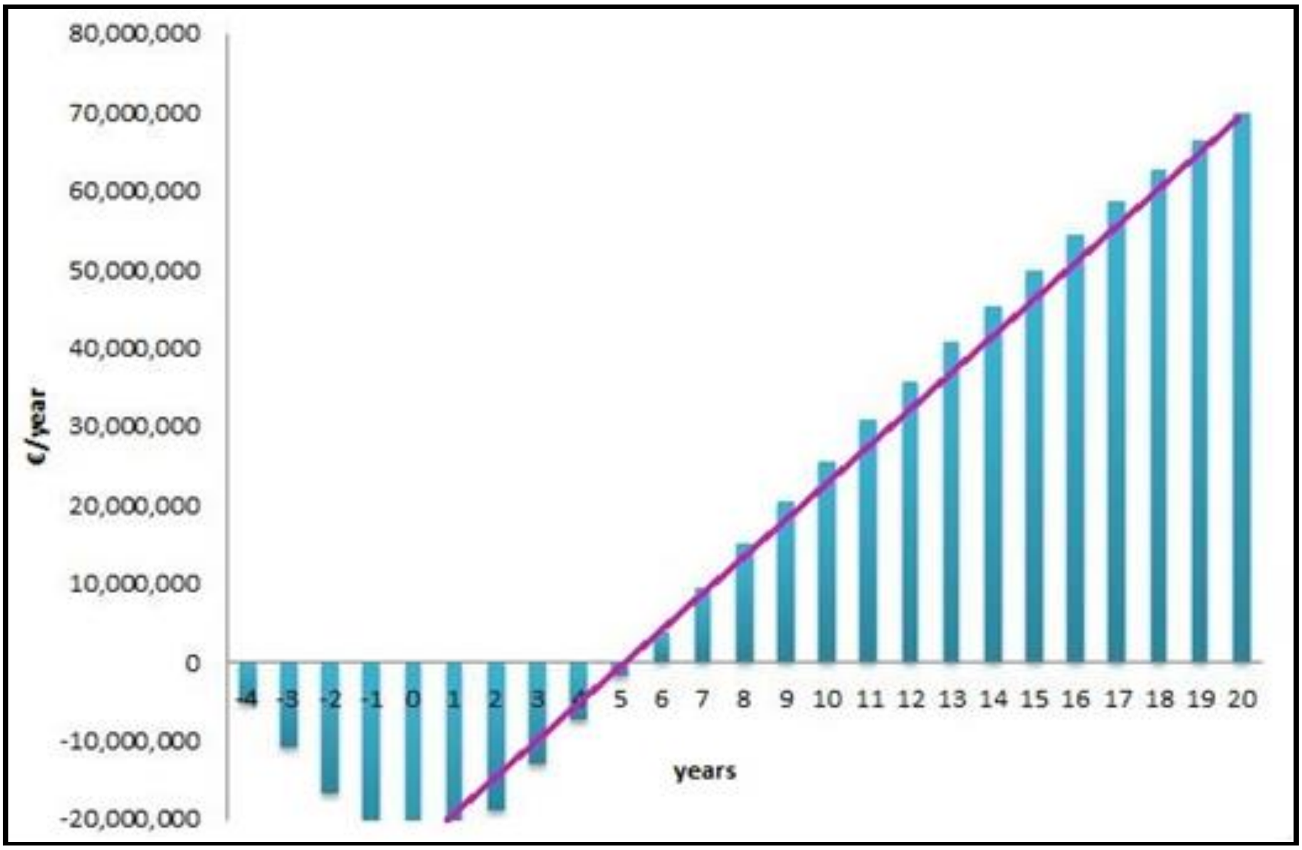


Figure 4: Cumulative cash flow of the final investment decision

As presented in Figure 4, the first 5 years of operation lead to a negative balance resulting in a 5-year PP of the proposed investment. The NPV of the proposed investment is 175878564 € and IRR is 10.1%. The aforementioned results show that the proposed investment is viable since the NPV is

positive and the IRR is larger than the interest rate (8.51%). For Feed in Tariff value less than 0.101 €/KWh the proposed investment is unviable, since such values lead to negative NPV.

4. CONCLUSIONS

In the present study, the economic feasibility of a floating OWF near Mykonos, in the Aegean Sea, in Greece, for electricity production to cover the annual demands of Mykonos, Rhenia and Delos, is implemented. Two alternative scenarios (S1 and S2) are investigated, by modifying the number and the rated power of the OWTs, as well as the distances between them. In the case of scenario S1, the proposed OWF consists of 11 floating OWTs (spar buoy floating platform) of 33 MW total rated power, while scenario S2 corresponds to an OWF with 7 floating OWTs (spar buoy floating platform) of 35 MW total rated power.

Initially, the net AEP for the two alternative scenarios is estimated considering wake losses, electrical losses and OWTs' availability. Specifically, the net AEP of S1 and S2 is estimated to reach 128275 MWh/year and 120583 MWh/year respectively, leading to a net capacity factor equal to 44% (S1) and 39% (S2). The calculation of the CapEx, OpEx and LCOE of the two scenarios follows. In the case of S1, LCOE is equal to 93.02 €/MWh, while for S2 it is 101.74 €/MWh. By comparing the LCOE of the two alterative scenarios, S1 is finally selected to be further financially evaluated using the NPV, the IRR and the PP of the investment. The NPV for this scenario corresponds to a positive number, equal to 175878564 €, indicating the sustainability of the proposed investment. Furthermore, the IRR is 10.1%, which is larger than the weighted average cost of capital (8.51%). Therefore, the viability of the proposed OWF can be demonstrated. Finally, the payback period of the proposed investment corresponds to 5 years.

The results indicate that the capacity factor is the most important parameter affecting LCOE and, therefore, determining the final investment decision. Moreover, the results of the economic analysis/evaluation of the finally selected scenario clearly illustrate the economic sustainability of the proposed OWF and, its ability for covering the annual energy demands of the examined islands.

References

1. Dodson L., K. Busawon and M. Jovanovi (2005). 'Estimation of the power coefficient in a wind conversion system'. **Proc. 44th IEEE Conference on Decision and Control, and the European Control Conference 2005**. Seville, Spain.
2. European Wind Energy Association (EWEA). (2018). '**The European offshore wind industry- Key trends and statistics 2017**'. Wind Europe.
3. Georgakellos D.A. and A.M. Marcis (2009). 'Application of the semantic learning approach in the feasibility studies preparation training process', **Information Systems Management**, Vol. 26, pp. 231-240.
4. Heidari S. (2017). '**Economic modeling of floating offshore wind power**'. Master of Science in industrial economics, Malardalen University: Sweden.
5. International Renewable Energy Agency (IRENA). (2012). '**Renewable energy technologies: Cost analysis series, Wind power**'. IRENA working paper, Bonn, Gernamy.
6. Jensen N.O. (1983). '**A Note on wind generator interaction**'. Technical Report: Riso-M-2411.
7. Kaldellis J. and D. Za. (2011). 'The wind energy (r)evolution: A short review of a long history'. **Renewable Energy**, Vol. 36(7), pp. 1887-1901.
8. Kim J.-Y., K.-Y. Oh, K.-S. Kang and J.-S. Lee. (2013). 'Site selection of offshore wind farms around the Korean Peninsula through economic evaluation'. **Renewable Energy**, Vol. 54, pp. 189-195.

9. Konstantinidis E.I., D.G. Kompolias and P.N. Botsaris. (2014). 'Viability analysis of an offshore wind farm in North Aegean Sea, Greece'. **Journal of Renewable and Sustainable Energy**, Vol. 6, pp. 023116-1-023116-23.

10. Li J., P. Shi, H. Gao, H. Xie, Z. Yiang, W. Tang and L. Ma. (2010). '**2010 China wind power outlook**'. Chinese Renewable Energy Industries Association (CREIA), Global Wind Energy Council and Greenpeace.

11. Manwell J.F., J.G. McGowan and A.L. Rogers. (2009). '**Wind energy explained: Theory, design and application**'. John Wiley & Sons Ltd, UK.

12. Mone C., M. Hand, M. Bolinger, J. Rand, D. Heimiller and J. Ho. (2015). '**2015 Cost of wind energy review**'. National Renewable Energy Laboratory (NREL), Technical Report NREL/TP-6A20-66861, USA.

13. Mortensen N.G., D.N. Heathfield, O. Rathmann and M. Nielsen. (2011). '**Wind atlas analysis and application program: WAsP 10 help facility**'. Roskilde: DTU Wind Energy.

14. Myhr A., C. Bjerkester, A. Agotnes and T.A. Nygaard. (2014). 'Levelized cost of energy for offshore floating wind turbines in a life cycle perspective'. **Renewable Energy,** Vol. 66, pp. 714-728.

15. Ozerdem B., S. Ozer and M. Tosun. (2006). 'Feasibility study of wind farms: A case study for Izmir, Turkey'. **Journal of Wind Engineering and Industrial Aerodynamics**, Vol. 99(10), pp. 725-743.

16. Pantaleo A., A. Pellerano, F. Ruggiero and M. Trovato M. (2005). 'Feasibility study of off-shore wind farms: An application to Puglia region'. **Solar Energy**, Vol. 79(3), pp. 321-331.

17. RAE (2013). http://www.rae.gr/site/el_GR/categories_new/electricity/market/mdn.csp (accessed February 22nd, 2018).

18. Satir M., F. Murphy and K. McDonnell. (2018). 'Feasibility study of an offshore wind farm in the Aegean Sea, Turkey'. **Renewable and Sustainable Energy Reviews**, Vol. 81(Part 2), pp. 2552-2562.

19. Tong K. (1998). 'Technical and economic aspects of a floating offshore wind farm'. **Journal of Wind Engineering and Industrial Aerodynamics**, Vol. 74-76, pp. 399-410.

20. Vasileiou M., E. Loukogeorgaki and D.G. Vagiona .(2017). 'GIS-based multi-criteria decision analysis for site selection of hybrid offshore wind and wave energy systems in Greece'. **Renewable and Sustainable Energy Reviews**, Vol. 73, pp. 745-757.

21. Young G.I.M. (1970). 'Feasibility studies'. **Appraisal Journal**, Vol. 38(3), pp. 376-383.

FLOATING PHOTOVOLTAIC POWER GENERATION SYSTEM DEVELOPMENT IN A LAKE

A. Zamanidou* and E. Loukogeorgaki

Division of Hydraulics and Environmental Engineering, Dept. of Civil Engineering, A.U.Th, GR- 54124 Thessaloniki, Macedonia, Greece

*Corresponding author: e-mail: zamanidou.afroditi@gmail.com, tel: +302310995951

Abstract

Solar energy is practically an inexhaustible, clean source of energy. In order to produce multi-MW electricity from solar energy, large capacity facilities are required, that occupy wide installation areas. Therefore, an important prerequisite at an early stage of the realization of a multi-MW solar energy project is the availability of suitable, large-size, surface areas. In countries, such as Greece, which have quite limited land area, with a significant proportion allocated for agriculture, protected forests and for other land uses, the deployment of floating photovoltaic systems in closed water bodies to harness solar energy presents a potential, attractive, alternative solution.

Motivated by this, the aim of the present paper is to propose, develop and investigate the feasibility of a Floating Photovoltaic power generation System (FPVS) in a lake in Greece. For this purpose, the Polyfytos artificial lake in North Greece is selected, considering environmental/legal restrictions and the available lake's surface size. This selection is further supported by the satisfaction of other site-selection criteria related to economical/technical parameters. The exact installation location of the FPVS in the lake is defined considering, mainly, minimization of visual impacts and shading effects from the surrounding mountains, as well as easy accessibility facilitating maintenance actions. A FPVS of 2 MW power capacity is proposed, so that the electricity demands of the neighboring villages can be met. This FPVS is preliminary designed by defining its geometrical and technical characteristics. For increasing the power production of the proposed FPVS, smart technologies are integrated within its design (i.e. use of tracking system), exploiting the advantage of the FPVS's deployment in a water body. Finally, the economic performance of the proposed FPV power generation system in terms of levelized cost of energy is estimated by calculating and assessing construction, operation and maintenance costs.

The results of the present paper illustrate that the proposed FPVS deployed in the Polyfytos Lake in Greece has the potential to present a viable economic solution for covering effectively the energy demands of the neighboring areas. Moreover, the development of a FPVS over a water reservoir has a significant positive effect (increase) on the electricity production effectiveness compared to a land-based PV power generation system, since in the case of a FPVS smart technologies can be more efficiently applied.

Keywords: Floating photovoltaic power generation system, Greece, Lake, Financial analysis, Levelized cost of energy

1. INTRODUCTION

Solar energy is practically an inexhaustible, clean source of energy. For multi-megawatt scale electricity generation from solar energy, wide installation areas are required, which puts restrictions on land use for agricultural purposes. The main motivation for the deployment of Floating

PhotoVoltaic Systems (FPVSs) was the land premium, especially, for agricultural areas, where the land was more valuable for the growth of the crops (Trapani and Santafé, 2014). FPVSs have been already utilized worldwide, mainly, in closed water bodies within terrestrial areas, such as reservoirs, wetlands, small artificial and natural lakes. A FPVS consists of conventional PV panels installed in the form of PV arrays on a floating structure, which has suitable floaters to balance the structure on the surface of the water. The aforementioned PV arrays avoid the increase of the solar cell's temperature by taking advantage of the surrounding water's existence.

The deployment of a FPVS has numerous advantages compared to onshore PVSs, related mainly to the efficiency of the PV modules and the installation environment (Choi et al., 2013). Specifically, in the case of a FPVS a slight increase in the electrical efficiency of the conventional PV arrays utilized has been observed, which may be related to the cooling provided by the underlying water to the floating PV arrays. Regarding the environment and the ecosystem of the installation area, there are two key benefits: (a) in case of total or partial (at a large percentage) coverage of the reservoir's water surface by the installed FPVS, evaporation of water is reduced significantly, as most of the incident radiation is absorbed by the PV cells, and (b) phytoplankton growth decreases, as the amount of solar radiation reaching the bottom decreases, which in turn reduces the rate of photosynthesis. It is important to note that the aforementioned advantages refer to artificial ponds and reservoirs, where water is used either for irrigation purposes or for water supply. However, the deployment of a FPVS is also characterized by drawbacks and challenges that should be overcome, such as high deployment cost, corrosion risk and difficult access for operation and maintenance.

In general, there are innovative technologies that can be applied to conventional PV arrays in order to increase their efficiency. A solar tracking system can be used to increase PV cell efficiency and, thereby, increase power generation. In this way, the solar rays penetrate perpendicularly to the PV cells, resulting to an increase up to 30% (Choi et al., 2014) of their performance compared to the deployment of a fixed type PV power generation systems. Additionally, the PV panel efficiency is sensitive to the panel temperature and decreases as the temperature of the panel increases. Applying an active cooling technique, the operating temperature of a PV module can be dropped significantly to about 20% and an increase of 9% (Bahaidarah et al., 2014) in the electrical efficiency can be reached. These technology applications for efficiency increase can be implemented either for Onshore PV arrays (OPV) or for FPV arrays. However, in the case of FPV arrays, technologies for increasing efficiency can be realized with simpler structures and they can be applied to a larger number of PV panels.

In light of the above, it is concluded that FPVSs present a novel technology to exploit the most inexhaustible energy source, the sun. Motivated by this, the present paper aims at proposing, developing and investigating the feasibility of a FPVS for power generation in the Polyfytos artificial lake in North Greece. This lake is selected considering environmental/legal restrictions and its available surface size. However, the selected area satisfies additional site-selection criteria related to: (a) the system's production effectiveness, (b) construction and maintenance issues and (c) connectivity with the existing electricity distribution network. The exact installation location of the FPVS is defined in terms of minimizing visual impacts and shading effects from the surrounding mountains, as well as easy accessibility. In order to meet the electricity demands of the neighboring villages, a 2 MW FPVS is proposed and it is preliminary designed, using, also, smart technologies (i.e. tracking system) for increasing the FPVS's power production. Finally, the economic performance of the proposed FPV power generation system in terms of levelized cost of energy is estimated.

2. SELECTION AND MAIN CHARACTISTICS OF THE STUDY AREA

An important prerequisite for the deployment of a FPVS is the determination of a suitable installation area, so that a sustainable system can be realized. According to Choi (2014), as a FPVS corresponds to a floating on the water surface structure, site-selection criteria have to be considered and assessed related to: (a) power generation efficiency, e.g. solar radiation, fog, shade occurrence, etc., (b)

installation and maintenance, e.g. water depth (water level fluctuation), frost, inflow of floating particles, accessibility, interference with dam facilities (water intake tower, waste-way), etc., (c) connectivity with the existing power system, e.g. spare capacity of distribution line, distance to distribution line, distance to load (receptor), etc. and (d) legal restrictions, e.g. special countermeasure area (Framework Act on Environmental Policy), waterfront area (related River Acts), Local Environment Preservation Act, Protection of Wild Fauna and Flora Act, fishing prohibition area, marine leisure activity prohibition area, civil complaints, excessive compensation expense, inducement of environmental problems, etc.

In the case of Greece, all natural lakes and most of existing artificial lakes (created by the Public Power Corporation (PPC) for power generation via hydroelectric power plants) are included in the list of community importance sites of NATURA 2000 network. Therefore, environmental and legislative restrictions lead to a small number of Greek lakes that could be potentially considered for the deployment of a FPVS (Table 1). By taking into account the size of these lakes, Polyfytos artificial lake (Figures 1a~1b) is chosen for the deployment of a FPVS, since it has the largest surface area among the various environmentally eligible candidates. It is noted that the selection of the Polyfytos Lake is further supported by the satisfaction of additional site-selection criteria as described in the following paragraphs.

Table 1: Greek artificial lakes not included in NATURA 2000 list

Name	Location	Surface area (km^2)
Polyfytos Lake	Kozani	74000
Kastraki Lake	Aetolia-Acarnania	26804
Pineios Lake	Elis	19895
Pournari Lake	Arta	8233
Ladona Lake	Arcadia	3048

Lake Polyfytos is an artificial lake of Aliakmonas river, located in North Greece (40.13^o N, 21.58^o E) in the regional unit of Kozani (Figure 1a~1b). The lake was formed in 1973, after the construction of the Polyfytos dam in the river. It is owned by the Greek PPC, but it has been granted to the surrounding residents for fishing and ecotourism exploitation. Briefly, the Polyfytos Lake is used for water supply, irrigation, fishing, power generation, recreation and sports. The lake has a wetland code of 133103000 and does not have any legal status for environmental protection. The lake covers an area of 74 km^2 (flooded) and receives mainly the waters of the Aliakmon River and some torrents from a catchment area of 5630 km^2. The largest area of the lake (about 70%) is located at the territory of the Servia Municipality (Figure 1b). Its maximum length and width are equal to 29.84 km and 4.14 km respectively, while its average depth is equal to 55 m. Changes in water level correspond to about 15 m. The rapid renewal of the lake's water enables rapid removal of polluting loads, resulting in the lake's "mesotrophic" status. Waters mostly flooded the agricultural land after the construction of the dam, and finally artificial lake of Polyfytos was created.

For supporting the adequacy of the Polyfytos Lake for the deployment of a FPVS based on the site-selection criteria mentioned previously in this section, the irradiation of the sun in the study area is, initially, investigated and quantified. This parameter represents the most crucial meteorological parameter affecting the efficiency of the FPVS. For this purpose, climatology maps of the region of Western Macedonia are used (HNSE, 2013). These maps were formed based on simulations using a radiation propagation model, satellite images of cloudiness and satellite assessments of atmospheric suspensions. Considering the map of the regional unit of Kozani, the average annual solar energy per unit area (kWh/m^2) in the area of the Polyfytos Lake is equal to 1485 kWh/m^2, which is the highest average annual solar energy per unit area in the region of Western Macedonia (HNSE, 2013). The aforementioned value has been also verified from (JRC-IET, 2012).

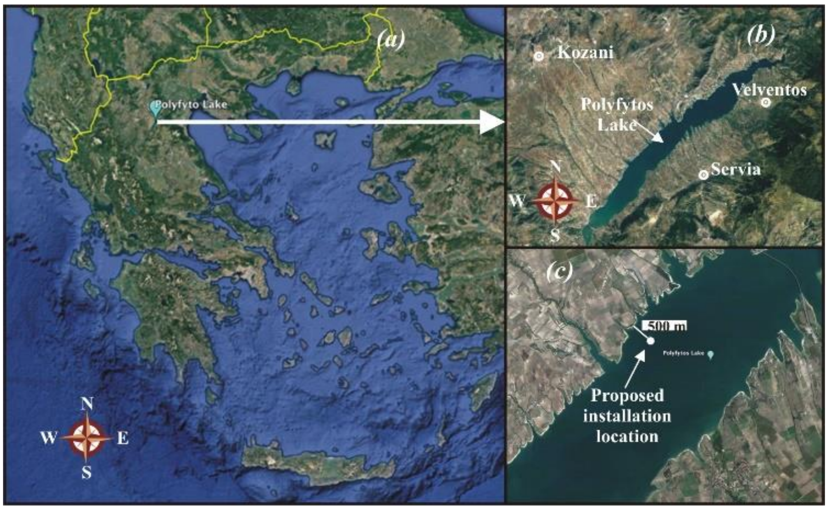


Figure 1: (a)~(b): Study area, (c): FPVS proposed installation location at Polyfytos Lake

Next, the shading percentage of the lake by natural or artificial barriers is investigated. As there are no artificial barriers on the surface of the lake, the shading of the lake by the surrounding mountain masses on December 21, 2015, (winter solstice) is checked, from sunrise until sunset. The natural hurdles are located North, Northeast, East, Southeast and South of the Polyfytos Lake. At several locations on the lake's surface, especially, near the mountains, sunlight is limited.

Furthermore, other weather parameters (i.e. fog, cloudiness, temperature and frost) that affect the PV modules' efficiency and, therefore, the generation performance of a FPVS are taken into account. For this reason, relevant meteorological data of the last 30 years are gathered by the meteorological station in Kozani (National Meteorological Service, 2015) and the following statistical quantities and data are derived and considered for the FPVS's deployment:

- The maximum, monthly average, fog occurs in December (1.32%), while the minimum, monthly average, fog occurs in July and August (0.01%).
- The maximum, monthly average, total cloudiness occurs in December (57.88%), while the minimum, monthly average, total cloudiness occurs in August (27.50%).
- The maximum, monthly average, low cloudiness occurs in December (30.63%), while the minimum, monthly average, low cloudiness occurs in August (14.75%).
- The maximum, monthly average, temperature average appears in August (24.69 °C), while the minimum, monthly average, temperature average appears in January (5.57 °C).
- The maximum, monthly average, temperature minimum appears in July (12.3 °C), while the minimum, monthly average, temperature minimum appears in January (-7.85 °C).
- The maximum, monthly average, temperature maximum appears in July (36.77 °C), while the minimum, monthly average, temperature maximum appears in December (14.9 °C).
- There is no appearance of frost all year round.

Regarding the accessibility and connectivity of the lake with an existing power system, the accessibility of the study area is quite good as the lake is crossed by the national road of the cities of Kozani - Larissa, and there is a network of provincial roads. Additionally, there is large space available for installing a construction site near the lake. The location of the neighboring to the lake villages limits the available FPVS deployment options to the West and Southwest surface of the Polyfytos Lake. This will, to a large extent, prevent, also, the visual disturbance. Finally, around the lake there is an electricity distribution network of PPC, to which the villages around the lake are

connected. Furthermore, there is an electricity transmission line at the Northeastern point of the lake, where the Polyfytos hydroelectric plant is installed.

Additionally to the above, data related to the water depth and the fluctuation levels of the Polyfytos Lake were collected from the Polyfytos Hydroelectric Power Plant (HPP). Water depth presents a parameter which is crucial for defining the FPVS's installation position in the lake, since it has a direct effect on the mooring system's requirements and, therefore, on the construction cost of the FPVS. In the case of the examined lake, the average depth is 55 m, while the maximum depth is located at the position of the dam and is between 75-80 m. On the other hand, the fluctuation of the lake's surface varies between 10 m and 15 m. This fluctuation affects the design requirements of the FPVS's mooring system, which should be selected and designed, so that the FPVS can adequately follow the vertical variations of the free surface in terms of ensuring the continuous and safe operation of the system.

Finally, regarding the water supply and drainage facilities, wastewater from the villages and from irrigation activities dispose after the appropriate treatment into the lake. In addition, part of the lake's water is diverted to the water supply network of Thessaloniki area, when demand is increased. As there is a rapid renewal of the lake water, the inflow and accumulation of floating particles on the lake surface is limited. Thus, the floating structure and the mooring system of the FPVS are not expected to be affected by floating particles.

Table 2: Site-selection criteria and their assessment for the Polyfytos Lake

Criterion		**Value (quantitative or qualitative)**
No	**Description**	
1	Solar Energy	1485 kWh/m^2
2	Shade by surrounding mountains	Only from N, NE, E, SE, S directions
3	Fog-Cloudiness	Medium appearance
4	Temperature	Slight rise in summer
5	Depth	55 m (average)
6	Surface fluctuation	10-15 m
7	Frost	No
8	Inflow of floating matters	No
9	Accessibility	Yes
10	Water supply and drainage facilities	Wastewater inflow
11	Electricity distribution/transmission network	Yes
12	Neighboring villages	Yes (at the N, NW, NE, E, SE and S adjacent sides)
13	Road network	Yes
14	Construction site area	Yes
15	NATURA 2000 restriction	No
16	Restriction zones	No

Table 2 summarizes the above information and provides the site-selection criteria considered for the deployment of a FPVS in Polyfytos Lake. Based on this Table and the aforementioned relevant discussion, it can be concluded that the Polyfytos Lake can be considered suitable for the deployment of a FPVS. Regarding the determination of a specific location in the lake for installing the FPVS, since there are no relevant restrictions in the study area, a specific location is proposed aiming at: (a)

preventing shading during the day, (b) avoiding visual disturbing and (c) ensuring easy access for maintenance. The proposed installation position located in latitude 40°13'10.85" N and longitude 21°56'19.32" E is shown in Figure 1c.

3. PRELIMINARY DESIGN OF THE FPVS

According to the survey on energy consumption in households of the Hellenic Statistical Authority conducted during October 2011 – September 2012, the average annual electricity consumption per household is 3750 kWh (Hellenic Statistical Authority, 2013). Moreover, according to the 2011 Population and Housing Census (Hellenic Statistical Authority, 2014), where the number of households and the number of their members were collected, one person households and two person households constitute 55.2% of the total number of households. Based on the above data and the population (2011 census) of the neighboring to Polyfytos Lake villages, the average annual electricity consumption of the villages is calculated (Table 3), assuming that the households consist of two members.

Table 3: Average annual electricity consumption of villages around Polyfytos Lake

Village	Population	Number of households	Average annual electricity consumption (kWh)
Rymnio	161	81	301875
Goyles	185	93	346875
Kranidia	461	231	864375
Neraida	148	74	277500
Imera	156	78	292500
Avra	56	28	105000
Total	**1167**	**584**	**2188125**

The size of the proposed FPVS is determined in order to meet the energy demands of the villages around the Polyfytos Lake (Table 3). The average annual power production of 1 kW installed in an OPV power plant varies, and for Greece is estimated to be equal to 1300 kWh (obtained from communication with market representatives and verified from JRC-IET, 2012). Thus, the efficiency of an OPV power plant is 14.84%. To produce the annual electrical energy demand of the villages around the Polyfyto Lake (2188125 kWh), a 2 MW OPV power plant, with 2600000 kWh annual energy production, is required. Assuming the same capacity for the proposed FPVS in the examined area, Table 4 shows the FPVS's efficiency estimated for a FPVS: (a) without any smart technologies, (b) with active cooling system and (c) with active cooling system and tracking type system for solar tracking. Based on this Table, it can be easily concluded that the efficiency of the FPVS, where both active cooling and tracking type systems are utilized, is 60.92% higher than the efficiency of an OPV power plant. Moreover, contrary to the OPV power plant, where a 2 MW plant must be installed to meet the annual electricity demands of the villages around the Polyfytos Lake, a FPVS with active cooling and tracking systems of only a 1.1 MW capacity could be utilized to meet the same demand. However, a 2 MW FPVS is, finally, proposed in the present paper assuming that the additional energy generated can be supplied and sold to the central power grid for other use. For the proposed FPVS, Polycrystaline-Silicon (Poly-Si) 250 Wp PV panels (Table 5) are selected to be used considering market availability, lowest possible cost and maximum efficiency. For developing a FPVS of 2 MW capacity and of 4.18 GWh average annual energy production (Table 4), 8000 PV panels (Poly-Si 250 Wp, 60 cells) are required with a total weight of 160000 kg (weight of the PV panels only).

Table 4: Efficiency estimation of a 2 MW FPVS installed at the Polyfytos Lake

Type of PV system (plant)	Nominal capacity (kW)	Average annual energy production (kWh)	Efficiency (%)
OPV power plant	2000	2600000	14.84
FPVS [9]	2000	2885964	16.47
FPVS with active cooling system [3]	2000	3145701	17.95
FPVS with active cooling system and tracking type system [2]	2000	4183783	23.88

Table 5: Technical and geometrical characteristics of Polycrystaline-Silicon 250 Wp PV panel (Poly-Si 250 WP, 60 cells)

Parameter	Value	Parameter	Value
P_{nom} (Wp)	250	Cell Area (m^2)	1.46
Width (m)	0.99	T_{ref} (^{o}C)	25
Length (m)	1.64	Weight (kg)	20
Area (m^2)	1.63		

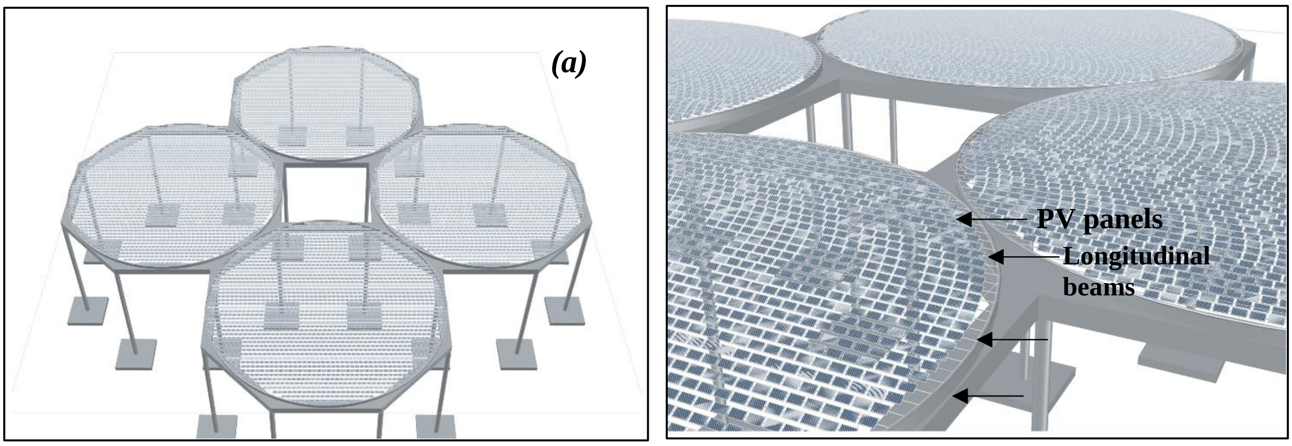


Figure 2: Perspectives of the preliminary design of the proposed FPVS

The design concept of the proposed FPVS as developed in this paper is presented in Figure 2. PV panels are placed in 30^o tilt angle and are arranged in 4 circular grids (Figure 2) of 50 m radius each, in order to prevent shading among the panels and provide adequate distance between them for maintenance accessibility. In each circular grid, the PV arrays are mounted on longitudinal beams, which are supported by a circular ring (Figure 2). All the above are, finally, mounted on a floating polygon (Figure 2). The floating platform of the proposed FPVS consists of 4 polygons (one polygon for each circular grid) with rectangular cross-section of 4 m in width and 3 m in height. Vertical axis tracking system is placed on every floating polygon, while an active cooling system, taking advantage of the surrounding lake water, is deployed for keeping the PV panels' temperature low. Regarding the mooring system, a system that effectively follows the lake's fluctuations is proposed (e.g. Seaflex) (Seaflex, 2018). Based on the above, the total rectangular installation area is estimated equal to 58752 m^2. It is noted that in the present paper the dimensions of the floating platform were preliminary estimated in order to ensure buoyancy. Detailed design and modelling of the hydrodynamic and

structural behavior of the FPVS's floating platform including mooring lines presents items for future investigation.

4. ASSESSMENT OF THE ECONOMIC PERFORMANCE OF THE PROPOSED FPVS

For assessing the economic performance of the proposed FPVS, capital and Operation & Maintenance (O&M) expenditures have to be initially estimated. Starting with the capital expenditures, these costs include the cost of the PV arrays' electromechanical equipment, as well as the construction costs of the floating platform (including the PV panels' mounting configurations and the floaters) and of the mooring system. An estimation of these costs is shown in Table 6.

Table 6: Estimated construction cost of the proposed FPVS

Cost Category	Cost sub-category	Cost (€)
Electromechanical equipment	Main electromechanical equipment (PV panels, inverters, connectors, tracking system, etc.)	2356000.00
	Cables - Tables	165000.00
	Supplementary Systems (Lightning protection, earthing, safety and protection systems)	106000.00
	Subtotal	**2627000.00**
Floating structure and mooring system	Supporting longitudinal beams	450747.00
	Supporting ring	`439000.26
	Floaters	1660479.10
	Mooring system	249071.87
	Subtotal	**2799298.23**
	Total	**5426298.23**

The cost of the electromechanical equipment has been estimated based on relevant costs existing in the case of an OPV power plant (obtained from communication with market representatives) and it includes tracking system for sunlight tracking and cooling system. It is emphasized that the cost estimation of the FPVS's electromechanical equipment is quite conservative, especially with regard to the cost of the tracking and the cooling systems. The latter cost, which is high in OPV installations, can be significantly reduced in the case of a FPVS due to the support structure's simplification. Regarding the cost of the FPVS's platform, this is is estimated using the weight of the steel required for its construction and a unit cost of 0.58 €/kg (average steel cost of 7850 kg/m^3 density in the Greek market). It is mentioned that 4396.95 tn of steel are considered to be required in total (777.15 tn for the longitudinal supporting beams, 756.90 for the circular supporting ring and 2862.90 tn for the floaters) for constructing the FPVS's platform. The above quantities have been defined based on the preliminary design of the FPVS presented in the previous section. As for the mooring system, the Seaflex-type mooring system is proposed (Seaflex, 2018) the cost of which is calculated as a percentage (15%) of the construction cost of the floaters. With regard to the O&M expenditures, these are mainly related to the O&M of the PV panels and are taken equal to 15 €/kW (NREL, 2018). Considering the annual yield of the proposed 2 MW FPVS, the annual O&M cost for the proposed FPVS is calculated equal to 30000 €. Moreover, assuming a 35-year operation period the O&M cost for the proposed FPVS is equal to 1050000 €.

Having estimating capital and O&M expenditures, the Levelized Cost of Energy (*LCOE*) (€/KWh) is used to assess the economic performance and the economic viability of the proposed FPVS. In the present paper, *LCOE* is evaluated based on the methodology described in Said et al. (2015) and

Murphy et al. (2015). Specifically, for a given installation area of a FPVS, the *LCOE* assuming a 35-year operation period Said et al. (2015) is calculated according to the following equation:

$$LCOE = \frac{CCI}{35AEP} \tag{1}$$

where *AEP* is the Annual Energy Production by the FPVS (KWh) and *CCI* is the Capital Cost Indicator of the investment (€), which can be calculated using the following equation:

$$CCI = DCI + 0.3DCI \tag{2}$$

where *DCI* corresponds to the Device Cost Indicator of the FPVS (€). In the present paper, this quantity is calculated as follows:

$$DCI = C_{str}(M_{str} + M_{PV}) + C_{PV}P_{NOM} \tag{3}$$

where C_{str} is the cost per unit weight (€/tn) of the FPVS's floating structure and electromechanical equipment, C_{PV} is the O&M cost per unit power (€/kW) for 35 years related to the nominal power of the PV panels, M_{str} and M_{PV} present the weight (tn) of the floating structure and of the PV panels respectively, while P_{NOM} is the nominal power (KW) of the PV panels. Using the economic and technical data presented previously in the section, C_{str}, C_{PV}, M_{str}, M_{PV}, P_{NOM} and *AEP* are calculated equal to 1234.11 €/tn, 525 €/kW, 4396.94 tn, 160 tn, 2000 kW and 2091888 kWh respectively. Finally, Table 7 shows the *DCI* and *CCI* values (Equations 2~3) and the *LCOE* (Equation 1) of the proposed FPVS. It can be seen that the *LCOE* for the proposed 2 MW FPVS at the Polyfytos Lake corresponds to 0.118 €/kWh; thus, based on the current Greek energy market the proposed FPVS has the potential to be considered as an economic viable solution.

Table 7: Values of quantities for *LCOE* calculation and *LCOE* of the proposed FPVS

Quantity	Value
DCI (€)	6673755.39
CCI (€)	8675882.01
LCOE (€/kWh)	0.118

5. CONCLUSIONS

In the present paper, a 2 MW FPVS is proposed to be installed at the Polyfytos Lake in the North Greece to meet the energy demands of the neighborhood villages. Polyfytos Lake is selected for this installation, as it occupies the largest area compared to other environmentally eligible Greek lakes (not included in the NATURA 2000 network). This selection is further supported by the satisfaction of other site-selection criteria related to economical/technical parameters. The FPVS is proposed to be located at the West side of the lake near its shore, avoiding shading by the surrounding mountains during the day and visual disturbance, and facilitating accessibility for maintenance. For the examined FPVS a 30^o tilt angle to the PV panels is proposed, while a tracking system resulting to a 30% efficiency increase is utilized. Moreover, an active cooling system is deployed, which can keep the temperature of the PV modules closer to the nominal PV cell operation temperature and, thus, it increases the efficiency up to 9%. The two latter smart technologies lead to a FPVS of 60.92% higher efficiency compared to an OPV power plant of the same capacity. The floating platform of the proposed FPVS consists of longitudinal beams and circular rings for supporting the PV arrays, as well as of floating polygons (floaters). Based on this preliminary design, the FPVS's construction cost has been estimated equal to 5.43 M€, while the annual O&M cost corresponds to 30000 €.

Finally, the estimated *LCOE* equal to 0.118 €/kWh, demonstrates the potential of the 2MW FPVS at the Polyfytos Lake to be considered as an economic viable solution.

References

1. Trapani K. and M.R. Santafé. (2014). 'A review of floating photovoltaic installations: 2007-2013'. **Progress in Photovoltaics**, Vol. 23(4), pp. 524-532.
2. Choi Y.K., N.H. Lee and K.J. Kim. (2013). 'Empirical Research on the efficiency of Floating PV systems compared with Overland PV Systems'. **CES-CUBE**, Vol. 25, pp. 284-289.
3. Choi Y.K., N.H. Lee, A.K. Lee and K.J. Kim. (2014). 'A study on major design elements of tracking-type floating photovoltaic systems'. **International Journal of Smart Grid and Clean Energy**, Vol. 3(1), pp. 70-74.
4. Bahaidarah H., A. Subhan, P. Gandhidasan and S. Rehman. (2013). 'Performance evaluation of a PV (photovoltaic) module by back surface water cooling for hot climatic conditions'. **Energy**, Vol. 59, pp. 445-453.
5. Choi Y.K. (2014). 'A case study on suitable area and resource for the development of floating photovoltaic system'. **International Journal of Electrical, Computer, Electronics and Communication Engineering**, Vol. 8(5), pp. 816-820.
6. HNSE. (2013). http://www.helionet.gr/maps/clima_yearly_avg/total/Greece (accessed January 17th, 2018).
7. JRC-IET. (2012). http://re.jrc.ec.europa.eu/pvgis/ (accessed April 23rd, 2018).
8. National Meteorological Service. (2015). Data of Kozani Meteorological Station (station code 16632), period 01/01/1980 - 31/12/2014.
9. Hellenic Statistical Authority. (2013). Press release. Survey on energy consumption in households, 2011-2012.
10. Hellenic Statistical Authority. (2014). Demographic and social characteristics of the Resident Population of Greece according to the 2011 Population - Housing Census revision of 20/3/2014.
11. Seaflex. (2018). http://www.seaflex.net/ (accessed January 17th, 2018).
12. NREL. (2018). https://www.nrel.gov/analysis/tech-cost-om-dg.html (accessed January 17th, 2018).
13. Said M., M. EL-Shimy and M.A. Abdelraheem. (2015). 'Photovoltaics energy: Improved modeling and analysis of the levelized cost of energy (LCOE) and grid parity – Egypt case study'. **Sustainable Energy Technologies and Assessments**, Vol. 9, pp. 37-48.
14. Murphy J., K. Lynch and K. O'Sullivan. (2012). '**MARINA PLATFORM Deliverable D3.3: Methodologies for analysis and assessment of wind-ocean combined concepts**'. Marine Renewable Integrated Application Platform (MARINA PLATFORM) project.

MAXIMIZING THE BUILDING ENERGY PERFORMANCE WITH ADVANCED VENTILATED FAÇADE SYSTEMS ON EXISTING STRUCTURES

D.K. Bikas, K.G. Tsikaloudaki*, T.G. Theodosiou, D.C. Tsirigoti and S.P. Tsoka

Laboratory of Building Construction and building Physics, Division of Structural Engineering, Dept. of Civil Engineering, A.U.Th, GR- 54124 Thessaloniki, Macedonia, Greece

*Corresponding author: e-mail: katgt@civil.auth.gr, tel : +30231099770

Abstract

Within the existing European building stock, a large share is built before 1960, when there were only a few or no requirements for energy efficiency. Given that only a small portion of these buildings have undergone major energy retrofits, it is easily concluded that the oldest part of the building stock contributes greatly to the high energy consumption of the building sector. The most common action for the energy retrofit of the building envelope is the external insulation of the existing walls. Recently, ventilated façade systems were developed to offer thermal insulation together with the protection of buildings against the combined action of rain and wind, offering at the same time high level aesthetic characteristics. However, even if an advanced technological solution is used, such as the ventilated façade one, the poor air quality problems of older buildings are not always addressed, as through the interventions the buildings are made more airtight, and consequently less naturally ventilated. The research project E2VENT, funded within the H2020 program, attempts to address these problems met in existing residential buildings. It concerns merely a cost effective, high energy efficient, low C02 emission, replicable, low intrusive, systemic approach for retrofitting of residential buildings, through the integration of an advanced ventilated façade system, a heat exchanger and a heat storage system.

In this paper the technological solution that is developed within the framework of the research project is described, the possible barriers of its market acceptance are given, and results on its expected performance when installed in typical existing buildings are presented. Emphasis is given on the parameters that are associated with the thermal performance of the E2VENT system, as its main target is to reduce the building energy substantially, supporting the framework of the nZEB concept.

Keywords: Ventilated facade; building energy performance; energy retrofit; existing buildings; thermal insulation

1. INTRODUCTION

Within the existing European stock, a large share (more than 40%) was built before 1960's when there were only few or no requirements for energy efficiency and only a small part of buildings have undergone major energy retrofits [1-2]. That means that the great majority is of low insulation levels and is equipped with old and inefficient systems. For these reasons, the oldest part of the building stock contributes greatly to the energy consumption in the building sector [3-4].

It is now clear that the largest energy saving potential is associated with the older building stock. Moreover, although heating needs in Southern countries such as Portugal and Italy are lower due to milder winters, the energy use in these countries is relatively high, which can be an indication of lack of sufficient thermal envelope insulation in their building stocks [2, 4]. For these countries, where

buildings are usually equipped with air conditioning systems, cooling becomes an important contributor to the overall consumption.

The most common action for the energy retrofit of the building envelope is the thermal insulation and mainly the external insulation of the existing walls. However, the technology used in each case differs with regard to the construction of the existing wall and to the technologies that were applied in every country, according to climate, or special conditions [2, 5, 6]. Recently, ventilated façade systems were developed to offer thermal insulation together with the protection of buildings against the combined action of rain and wind, offering at the same time high level aesthetic characteristics. They constitute of a bearing structure, anchored to the building wall with brackets and anchoring elements, the insulation material and the external cladding, which are separated by the air cavity.

However, even if an advanced technological solution is used, such as the ventilated façade one, the poor air quality problems of older buildings are not addressed. Furthermore, retrofitting strategies usually focus on the reduction of air infiltration, in order to reduce energy demands for heating & cooling. However, as building energy efficiency is improved with insulation and weather-stripping, buildings are being made more airtight, and consequently less naturally ventilated. Since all buildings require air renewal to guarantee acceptable indoor air conditions, the corresponding losses of heat due to the ventilation air are increased.

In this paper, a retrofit solution that improves the energy performance of existing buildings by addressing both ventilation and conductivity losses is presented; such a hybrid solution combines active and passive means and is developed through the research project E2VENT.

2. DESCRIPTION OF E2VENT

The research project E2VENT, funded within the H2020 program (GA 637261), attempts to address these problems met in existing residential buildings. It is merely a cost effective, high energy efficient, low CO2 emission, replicable, low intrusive, systemic approach for retrofitting of residential buildings, through the integration of an advanced ventilated façade system, comprising of various components, described in the following sections.

The research project is run by 13 organizations across Europe (Nobatek, European Aluminium Association, ELVAL, FENIX, FASADA, Pich architects, Tecnalia, Acciona, Cartif, University of Hull, Aristotle University of Thessaloniki, University of Burgos, D’ Appolonia) and coordinated by Nobatek. The project started on January, 2015 and it will last 42 months. Apart from the development of the solution and the necessary preparations for its introduction into the market, the project involves pilot studies, which will demonstrate the capabilities of the system.

The E2VENT system is an external refurbishment solution with external cladding and air cavity that embeds different breakthrough technologies to ensure its high efficiency (Figure 1):

• A Smart Modular Heat Recovery Unit. The heat exchanger is specifically designed for the E2VENT system. It will be aluminium-made, in order to be lighter and with good thermal conductivity. The unit is designed to preheat inlet ventilation air in winter and precool it in summer. Apart from the normal winter and summer modes, it allows heat storage and free cooling modes. The unit is modular, allowing operation in series or parallel, depending on heating/cooling requirements.

• A Latent Heat Thermal Energy Storage Unit. The Latent Heat Thermal Energy Storage Unit (Fig. 2) is based on phase change materials, aiming at providing a heat storage system for the reduction of peak of electricity consumption and/or for cooling in summer.

• A smart management system. Nowadays, Building Energy Management systems (BEMs) are critical elements in the energy retrofitting strategies in buildings, in combination with active and passive solutions. In fact, the BEMs could achieve up to 40% of energy savings by controlling HVAC, lighting and other systems. In E2VENT, a smart management system will control the components on

a real time basis targeting optimal performances. A series of sensors will ensure that the E2VENT system will recognize the predicted weather and communicate with existing systems.

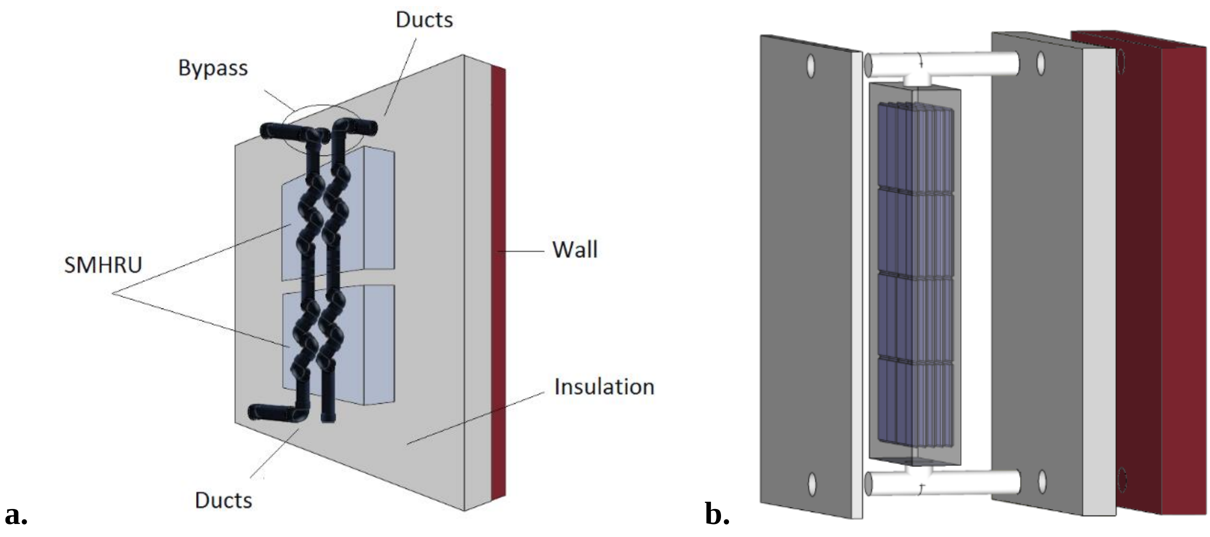


Figure 1. The smart modular heat recovery Unit (a.) and the latent heat thermal energy storage unit (b) of the E2VENT system [7].

• A ventilated façade system. The ventilated façade system is composed of (Fig. 2) the bearing structure, which is made of aluminium and is designed especially for this application, both from a mechanical and a thermal point of view, the thermal protection, offered by thermal insulation positioned on the outer surface of the building and the external cladding, made of composite aluminium panels. Special attention is given to the production of an efficient anchoring system that limits thermal bridges and allows for an easy and durable installation. Load bearing elements made of aluminium, support the ventilated façade. Vertical T-shaped beams bear the outer cladding; each one is supported by an L-shaped bracket, which is anchored on the wall. All bearing elements have been selected in order to comply with the structural requirements and have the necessary bearing capacity for the selected loadings and combination of loadings. Thermal insulation is positioned between the anchors, covering all exterior opaque elements. The structural system selection of building's construction parts involves the choice of the lightest parts of the most economical material, allowing for the most efficient configuration that is appropriate to the anticipated loads [8, 9]. The choice of aluminium as the material of the main supporting system, the anchors and the brackets of the system, is a relatively new but efficient design solution. Wind, seismic, thermal action and any other possible design load imposed on the building according to the limit design states are defined in accordance to Eurocodes. A significant number of analyses of structural models with various cross-section dimensions of the principal structural and connection members has been performed. By this procedure an optimal design by strengthening at specific cases for the system has been attempted.

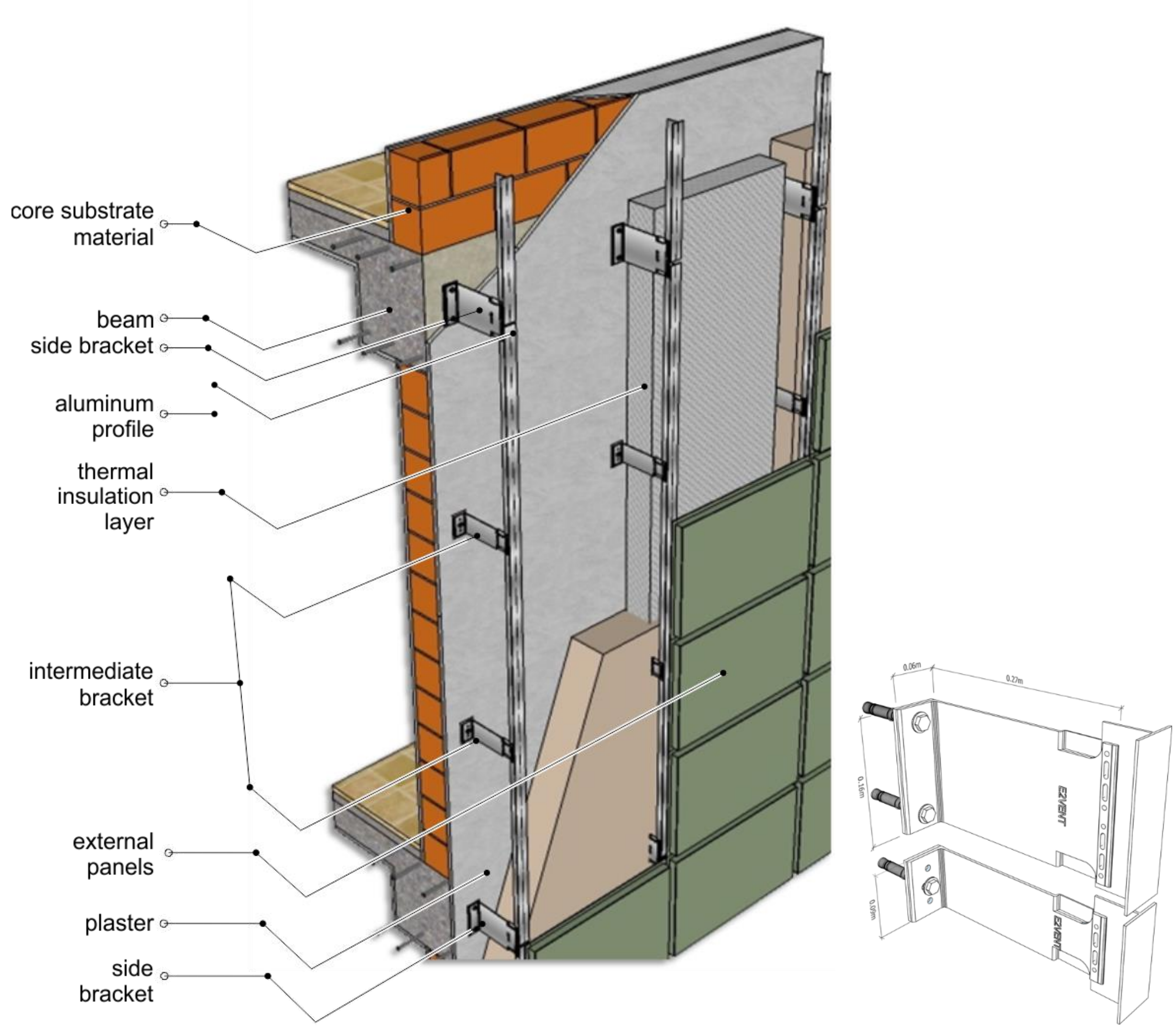


Figure 2. The E2VENT ventilated façade system anchored with full and half height brackets.

3. EXPECTED PERFORMANCE

It is expected that the E2VENT system will lead to significant energy savings and CO2 emissions reduction. This is achieved not only by the thermal protection of the opaque elements, which enhances the thermal behaviour of the building skin, but also by the use of the heat exchanger and the heat storage systems, which contribute to the minimization of heating and cooling loads. Of course, if E2VENT is employed in a major renovation of an existing building, addressing in parallel the glazed components and the HVAC equipment, the building energy performance would be optimized, reaching the nZEB concepts.

The energy behaviour of the system has been assessed with detailed simulations, which showed the capabilities of each component and the system as a whole. Special attention was given in minimizing the thermal break effect occurring at the anchorage points of the cladding. Recent studies have shown that the problem of thermal bridges in cladding systems cannot be neglected since the actual heat flows tend to be significantly higher than the estimated ones when point thermal bridges are not treated properly [10]. Within the framework of this project, the process of developing a thermally efficient anchoring system by proper selection of support system parts, detailed parametric analysis of the characteristics affecting the thermal bridge problem and by integrating advanced modern materials into the final proposed product is presented.

According to EN ISO 20211, a thermal bridge is defined as the “part of the building envelope where the otherwise uniform thermal resistance is significantly changed by full or partial penetration of the

building envelope by materials with a different thermal conductivity, and/or a change in thickness of the fabric, and/or a difference between internal and external areas, such as occur at wall/floor/ceiling junctions" [11].

The three dimensional nature of the thermal bridge effect on cladding systems requires a detailed calculation approach in order to take into account the complex geometry and the great differences in Thermophysical properties of adjacent materials. According to ISO 10211, in order to achieve reliable results regarding the magnitude of thermal bridging in such complicated structures, a detailed finite element analysis is needed. In the case of this study, the calculation platform that was finally selected was ANSYS Workbench.

The conducted multi-parametric showed that the thermal bridge problem is quite complicated and it is strongly related to many factors. Existing technologies like thermal break pads are an established technology that, unfortunately, cannot efficiently minimise the thermal bridge magnitude, especially when the substrate wall is highly thermally conductive like the case of concrete walls. Stability, safety and mechanical requirements are obviously the most important parameters in every construction, and in the case of metal cladding systems, these requirements create limits on the permitted thickness and thermal break layer thermophysical properties.

The type, condition and material of the substrate wall are factors that highly affect the thermal bridge phenomenon. Since the anchors penetrate the insulation material and the thermal break pad in order to be securely fixed within the substrate wall, this part of the support system remains the weakest. The only possibilities for minimising these problems rely on the use of chemical anchors. Although the area of the wall affected by the chemical anchor is limited and can't stop the heat flow, it can provide considerable thermal resistance compared to traditional anchor materials like steel, while at the same time it provides numerous advantages related to the mechanical strength of the system.

The effect of this technology to the overall thermal transmittance of the façade is presented in figure 3. It shows the design U-value (calculated without considering the thermal bridge effect) increment of the building element due to the point thermal bridge effect. It can be seen that, depending on the required thermal insulation protection, the effect can account for more than 50% of the U-value.

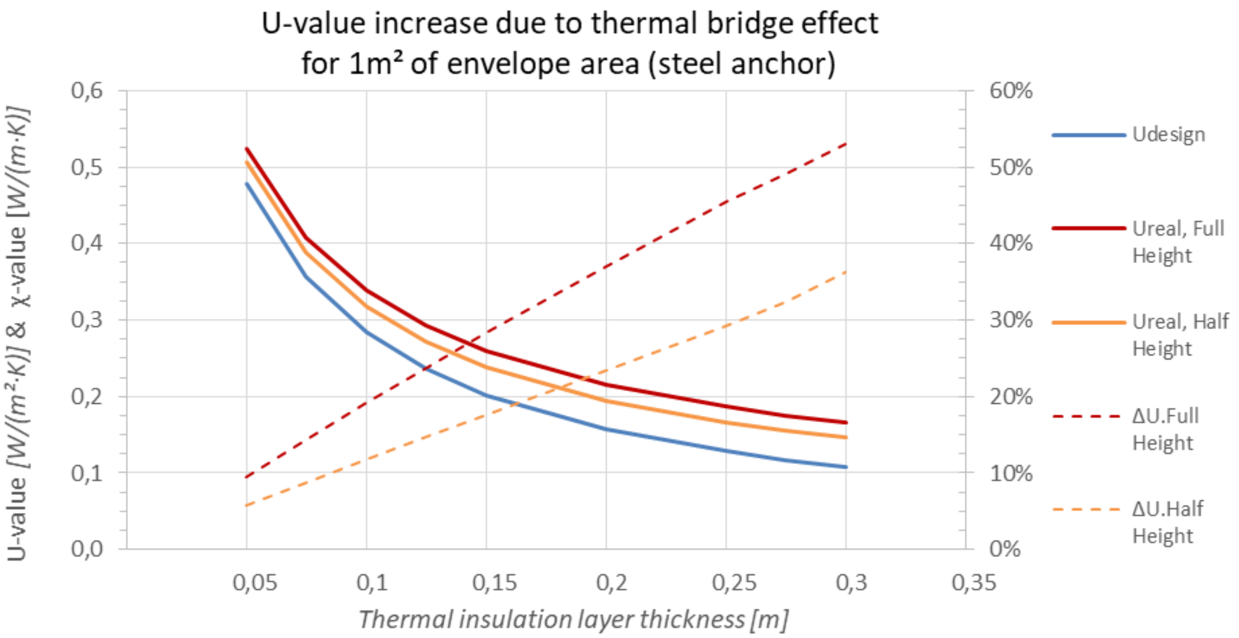


Figure 3. Design and actual thermal transmittance (U-value) of the external envelope for half and full-height steel brackets [10].

4. POSSIBLE BARRIERS

The E2VENT system is designed and developed as a new retrofit solution. In order to ensure its wide acceptance in the European market, it is essential to identify the potential barriers that may come up. These barriers may stem from regulatory and morphological issues, as well as from the façade and the HVAC characteristics of the buildings targeted [12].

Since the implementation of the E2VENT will require additional area coverage, it is essential that the building under a refurbishment study has a leftover of ground surface coverage. E2VENT may meet such problems in densely built areas such as urban centers. A possible solution could be the construction of the system from the first storey and above, which may also be important in cases where shops or other facilities do not allow such interventions. Additionally, buildings under protection of cultural heritage rules may face significant barriers in implementing the E2VENT system. In some cases restrictions permit refurbishment under specific conditions. Finally, a crucial factor is the ownership status of the building. Since a partial implementation of the E2VENT system is not effective or realistic, a single building manager could assist in applying such large-scale actions. On the contrary, the existence of many owners renders the decision of approving the E2VENT system construction very difficult not only on the basis of such a major refurbishment construction, but also to other, minor but still significant decisions like the external color and surface treatment. Although such problems are also present in the case of ETICS, the presence of heat recovery units and thermal storage, adds more complexity to such decisions.

As regards the morphological parameters, the shape of the building is a factor that affects the complexity of the design, the costs and also aesthetics of the building. Box-shaped buildings with flat facades without balconies are preferable. The existence of rooms with overhangs may present some problems, especially in the case where these overhangs do not lay beyond the external panels of the E2VENT. The most significant factor that can hinder the selection of E2VENT may be the presence of balconies. Problems related with balconies are of two types:

Those related to the interruption of the system's continuity on the vertical axis. In this case, the air gap is not continuous; as a result, fastening of the system to existing elements needs some special treatment.

Problems related to the useful width of the balcony after the intervention. In narrow balconies, the presence of the system may cover a relatively large part of the width, leaving a small area that is possibly useless to users since they cannot walk with safety on this. Very narrow balconies may be completely covered by the ventilated façade, altering significantly the architectural view of the building.

Furthermore, the structural system and the materials of the existing façade play an important role in the way the E2VENT system could be applied on a building. Depending on various parameters, not all existing buildings can support such a refurbishment with safety. Buildings with reinforced concrete elements are more likely to support the extra loads. In most cases, anchoring will be mainly fastened on the concrete elements, while secondary or intermediate anchoring could assist load bearing capabilities of a building. In the absence of concrete elements, a higher density of anchors is required complicating the loads study, construction and thermal performance of the ventilated façade.

Façade areas with different colors, shapes and materials will be covered by the panels of the ventilated façade. In such cases, the existing façade pattern could be recreated by the use of panels with different colors. The size, number and shape of doors and windows on the façade affect the construction of E2VENT. Wide glass areas interrupt the façade in a way similar to balconies, but with the additional disadvantage that they decrease further the area available for the ventilation systems installation. In addition, a large number of windows can complicate the construction process, while this is also true in the case of non-orthogonal window layouts. Outgoing elements, small (like window sills and frames) or large (like shading devises), constitute also a factor that needs to be taken into account

since the preservation of smaller architectural elements is impossible, while larger ones may lose their functionality and may need reconstruction.

Among the parameters that should also be taken into account is the existence of air ventilation inlets and exhausts like those usually found at kitchens and bathrooms. During the design process, decisions on how to combine the operation of the E2VENT with existing ventilation strategies should be made. In cases where heating or cooling is provided through individual external units (split-units, external gas boilers, etc.), the design of the façade should take into account the proper integration of these units in order to avoid aesthetic, construction and safety problems.

Apart from the above mentioned technical issues, social barriers may appear, involving mainly the potential users and the technical world (architects, engineers and builders). Both derive from the lack of knowledge or experience in selecting an advanced ventilated façade system as an energy measure for building retrofitting. In order to investigate further the social acceptance of the E2VENT system, a survey was addressed to building professionals and potential users. Given the different background of these two groups, some of the questions are differentiated between the two surveys so as to avoid frustrating and confusing possible end users with specialized technical questions. More than 1000 people answered the two survey forms, providing the E2VENT team with valuable information.

The majority of potential users are owners of an apartment in multifamily buildings in urban centres. According to the obtained results, the improvement of the energy performance of their residence is very significant; however the decision making for implementing an innovative energy efficient technology requires initially their increased awareness on the system's operation. Moreover, thermal insulation efficiency, energy efficiency issues and the risk of water and moisture penetration are the prevailing parameters that influence the users' decision for the refurbishment of the façade of their residence. On the other hand, installation and construction costs along with maintenance frequency, easiness and cost are the most significant restraints that prohibit users from applying such a system. Given that E2VENT solution involves mechanical ventilation, a great number of the respondents seem unwilling to substitute opening of windows and natural ventilation with mechanical means, a fact that can be explained by the increased survey participation of Mediterranean countries. To overpass this obstacle and increase the social acceptance of the system, market managers and other corresponding actors should make efforts to inform the public regarding the advantages of mechanical ventilation such as increased indoor air quality, energy gains etc. Positive end-user opinions appreciated the high thermal insulation efficiency and the energy efficiency of the system as the most important parameters in order to apply it in a retrofit project, but increased cost of acquisition, installation and maintenance were presented as an important obstacle.

In terms of the technical world, the majority of engineers have already experience in retrofit projects but only a few have been implicated in ventilated facades projects. A great number is willing to apply a ventilated façade in a future project but the lack of holistic knowledge may be an important obstacle to face.

5. CONCLUSIONS

This paper presents the main element of a new system developed for building retrofits within the framework of a European Research Project. It comprises advanced technological features, integrated in one modular system, which addresses mainly heat flows through the building skin and heat flows due to ventilation. The system is still under development and its performance has not been validated yet, but it is expected that its impact on the energy and the environmental performance of buildings will be extremely significant.

The improved efficiency of existing buildings represents a high-volume, low-cost approach to reducing energy use and greenhouse gas emissions. Additionally, it not only generates energy savings with attractive levels of return on investment, but it also improves the energy security, creates jobs and makes buildings more liveable.

Acknowledgements
This work has been developed within the project E2VENT: Energy Efficient Ventilated Facades for Optimal Adaptability and Heat Exchange enabling low energy architectural concepts for the refurbishment of existing buildings http://www.e2vent.eu/. The project has received funding from the European Union's Horizon 2020 research and innovation program under grant agreement No 637261.

References

1. Andeweg M. Th., Brunoro S. and Verhoef L.G.W. (2007) COST C16 Improving the Quality of Existing Urban Building Envelopes, state of the art, IOS Publications.
2. Economidou M., Atanasiu B., Despret Ch., Maio J., Nolte I. and Rapf O. (2011) Europe's buildings under the microscope: A country-by-country review of the energy performance of buildings, BPIE.
3. Bragança L., Wetzel Ch., Buhagiar V. and Verhoef L.G.W. (2007) COST C16 Improving the Quality of Existing Urban Building Envelopes, facades and roofs, IOS Publications.
4. Giulio Di R. (2010) COST Action, TU0701 Improving the Quality of Suburban Building Stock, UnifePress.
5. TABULA (2012) "Typology Approach for Building Stock Energy Assessment". Accessed December 2017, http://www.building-typology.eu/.
6. EPISCOPE (2012) Accessed December 2017, http://episcope.eu/building-typology/country/gr/.
7. E2VENT (2015) Accessed December 2017, http://www.e2vent.eu/.
8. Gerhardt H.J. and Janser F. (1994) "Wind Loads on Wind Permeable Facades", Journal of Wind Engineering and Industrial Aerodynamics, Vol. 53, pp. 37-48.
9. Marques da Silva F. and Gomes M.G. (2008) "Gap Inner Pressures in Multi-Storey Double Skin Facades", Energy and Buildings, Vol. 40, pp. 1553-1559.
10. Theodosiou T.G., Tsikaloudaki A.G., Kontoleon K.J and Bikas D.K. (2015) "Thermal bridging analysis on cladding systems for building facades", Energy and Buildings, Vol. 109, pp. 377–384.
11. Anon (2007) BS EN ISO 10211 Thermal bridges in building construction — Heat flows and surface temperatures — Detailed calculations, ISO.
12. Bikas D., Tsikaloudaki K., Kontoleon K.J., Giarma C., Tsoka S., Tsirigoti D. (2017) "Ventilated Facades: Requirements and Specifications Across Europe", Procedia Environmental Sciences vol. 38, pp. 148 – 154.

APPROPRIATE WIND FARM SITTING: THE CASE STUDY OF REGIONAL UNIT OF MAGNESIA

A. Kouroumplis and D.G. Vagiona

Department of Spatial Planning and Development, A.U.Th, GR- 54124 Thessaloniki, Macedonia, Greece

*Corresponding author: e-mail: dimvag@plandevel.auth.gr,

Abstract

Wind energy is one of the most important renewable energy sources, especially in regions where appropriate wind power potential exists, hence, decisions on harvesting such a resource plays an instrumental role in determining the appropriate policies required to achieve energy and climate targets. The appropriate siting of such facilities has become of great concern the last decade and is revealed by the significant growth in onshore wind farm siting applications across different application areas worldwide. Wind velocity, slope, distance from specific areas (protected areas, forests, urban areas, archeological sites) as well as from specific infrastructures (airports, road network, electricity grid) are amongst the prevailing criteria used in defining sustainable sites for wind farm development. The main aim of this paper is to identify appropriate sites for onshore wind farm applications considering the restrictions imposed by the legislative framework of the Special Framework for Spatial Planning and Sustainable Development for renewable energy sources (SFSPSD-RES) (Greek institutional framework for wind farm siting) with the use of Geographical Information Systems (GIS). The application focuses on the Regional Unit of Magnesia. The methodology involves excluding areas and zones defined by the SFSPSD-RES as well as outstanding criteria applied in the international literature review. The results reveal that the appropriate sites for wind farm siting are rather handful mainly due to the low wind potential of the area.

Keywords: Renewable Energy Sources (RES); wind energy; wind farm siting, exclusion criteria

1. INTRODUCTION

Over the past 40 years, there has been a sharp increase in the planet's population, which has a direct result in the exploitation of natural resources. This has influenced the environment negatively leading to its continuous deterioration. Demand for energy in the past years had been mainly covered by conventional forms of energy, such as coal and oil, which burdened the environment even more. In recent years, however, a greater sense of responsibility for environmental issues has been adopted, which has resulted in the development of effective environmental policies. As a result, alternative forms of energy sources, more environmental friendly, have been exploited and developed.

Nowadays, the exploitation of Renewable Energy Sources (RES) help to move to a low-carbon economy, resulting in sustainable development. All the relevant policies aim to adopt environmental friendly sources of energy to cover energy demand and mitigate environmental problems such as air pollution and climate change. The European Union has created a legislative framework for the use of RES so as to curb these emissions and promote cleaner transport but also reduce its dependence on unreliable and volatile fossil fuels markets. The current framework sets the target for all Member States of the European Union, a 20% reduction in greenhouse gas emissions compared to 1990 levels, a 20% penetration of renewable energy in gross final energy consumption and a 20% saving primary energy by 2020.

As far as wind energy is concerned, it is a fast-growing renewable energy technology. It provides a cost-effective and scalable alternative to conventional actions, both in developing and developed countries. No greenhouse gases and other pollutants are emitted, the impact on the environment is almost negligible, and the cost of their construction and operation continues to decline.

Of course, an important prerequisite is that wind farm installations are properly located, since they will mitigate and prevent even more potential impacts on both natural and anthropogenic environment. The most crucial issue of wind farm development is its appropriate sitting. A conventional power plant can be installed almost anywhere, unlike wind farms, which should be located in places where certain wind velocity exists. In addition, specific areas with specific characteristics, either environmental, technical/economic or social, that set the installation of the onshore wind farms unviable, should be excluded from the outset.

In order to avoid the land-based negative impacts of wind farm siting in Greece, minimum and maximum distances and safety limits around specific areas have been recorded in the legislative framework of the Special Framework for Spatial Planning and Sustainable Development for renewable energy sources (SFSPSD-RES) (MEECC, 2008).

In the present paper, the restrictions set by SFSPSD-RES are considered for the appropriate wind farm sitting in the Regional Unit of Magnesia in Greece. It should be noted that in cases where the above-mentioned framework does not provide any specific distances to spatial criteria, values cited in the international literature are considered (eg Baban and Parry, 2001; Tegou et al, 2007; Aydin et al, 2010; Lejeune and Feltz, 2008; Georgiou et al, 2012; Wang et al., 2014; Latinopoulos and Kechagia, 2015; Kazim et al, 2015). The exclusion criteria as well as the minimum safety distances are applied through Geographical Information Systems (GIS). In addition, areas that have been already occupied by wind farms are excluded from the analysis. The paper concludes to appropriate areas for onshore wind farm siting, satisfying environmental criteria as well as technical, economic and social constraints.

2. ONSHORE WIND FARM SITING CRITERIA

2.1 Literature Review on Onshore Wind Farm Siting Criteria

Many environmental, technical, economic and social factors influence decision-making on site selection of onshore wind farm applications, including wind speed, topography and geology of land, network structure, areas with significant natural resources, etc. In order to avoid negative impacts imposed by onshore wind farms, minimum-maximum distances as well as safety limits should be defined around specific areas. The primary siting criteria according to the international literature include: wind velocity, distance from residential areas, distance from areas of environmental interest, distance from networks (road networks, electricity distribution networks, airports, telecommunication infrastructure), distance from tourist activities and points of interest, slope, altitude and land use. The most cited criteria amonsgt them are (Bili and Vagiona, 2017): wind velocity, slope, proximity to residential areas, protected areas and road networks.

1.Wind velocity

Wind velocity is one of the most important factors in determining onshore wind farm siting. The viability of wind energy in a given location depends on the existence of efficient wind velocity at the height at which the turbine is to be installed (Vanek and Albright, 2008). Any wind turbine design option should be based on the average wind speed in the selected wind turbine area (Ucar and Balo, 2009). The criterion of wind velocity is considered as the primary and most important criterion in wind farm siting applications and is incorporated in almost every study.

The proposed wind velocity thresholds found in the literature vary significantly. Argyros (2011) notes that electricity can be generated from a wind turbine even at 2m/s. Baban and Parry (2001) consider the speed limit acceptable at 4-5 m/s, Grammatikogiannis and Stratigea (2009) report that locations

where the wind speed is greater than 7m/s should be selected, while Blankenhorn and Resch (2014) and Latinopoulos and Kechagia (2015) indicate that areas with average wind speed lower than 4.5m/s should not be considered as appropriate. Sunak and Höfer (2015) note that an average annual wind speed below 6 m/s is considered to be no longer economically feasible and, therefore, areas with a wind speed of less than 6 m/s are excluded.

2. Distance from residential areas

Wind farm siting in or close to urban areas is restricted in order to prevent noise and visual impacts, landscape effects and shadow flicker. Moreover, it is not possible to install wind farms in urban areas because of space availability as well as the impact on inhabitants' welfare. The majority of researchers in wind farm siting exclude the developed area itself and a buffer zone around it, apart from Gorsevski et al (2013) and Rodman and Meentemeyer (2006), who solely exclude the developed area.

Buffer zones less than 550 meters from residential areas and 400 meters from mixed land use areas should be excluded according to Höfer et al (2016). Distances from residential areas vary from 500 meters (Yue and Wang, 2006) to 2500 meters (Bennui et al, 2007) in the literature. Ouamni et al (2012) evaluate the feasibility of installing wind turbines in potential areas on the basis of a distance from urban areas greater than 1000m. Gass et al. (2013) applied a GIS buffering to exclude all areas within 1km of distance to settlement areas from technically feasible wind turbine sites. Tsoutsos et al (2015) applied a series of criteria set by SFSPSD-RES and related to the implementation of minimum distances from urban activities. A minimum distance of 1000 m from the settlement boundaries should be considered for towns and settlements with population over 2000 inhabitants and a distance of 1500 m from settlement boundaries of traditional settlements. The minimum distance for the rest settlements as well as monasteries is set to 500 m.

3. Distance from areas of environmental interest

Wind power installations occupy large areas, usually in hills or mountains. The construction of roads to access wind farms, the excavations in construction phase as well as the huge quantities of concrete needed for the bases of turbine towers, change the geomorphology of the area and affect negatively flora and fauna. The proposed distance from areas of environmental distances depends on the regime of environmental protection. For example, Baban and Parry (2001) suggest that the wind farm location should not be located within 1000m of areas of ecological value or special scientific interest. Aydin et al (2010) proposed minimum distances of 1000m from areas of ecological value, of 250m from ecologically sensitive areas, of 500m from wildlife conservation areas and of 300 m from nature reserves to reduce risk to birds. Latinopoulos and Kechagia (2015) propose that wind farms should not be sited on or within 1000m from protected landscapes, in order to preserve the esthetic value of natural environment. According to Tsoutsos et al (2015), a minimum distance from Sites of Community Importance of Natura 2000 should be set to 1500m.

4. Distance from networks (road networks, electricity distribution networks, airports, telecommunication infrastructure)

Wind turbines should be located near existing transmission lines and access roads in order to reduce construction, operational and maintenance costs. However, there is no generally valid definition of a maximum distance from the wind turbines either to the road or to the electricity distribution network. Wakeyama and Ehara (2011) propose a maximum distance of 200 meters from road networks. Bennui et al (2007) and Tegou et al (2010) set the maximum distance to the next road to 2500m, whereas, Baban and Parry (2001) and Gorsevski et al (2013) set it to 9000m and 10000m, respectively. Tsoutsos et al (2015) record a safety distance of 120 meters from all networks, while in Höfer et al areas with a larger distance than 500 m from roads get the lowest value score (the value scores increase with decreasing distance).

5. Distance from tourist activities and points of interest

Tourism, historic, cultural and religious places are considered as restricted areas that are excluded from the total land and the remainder is the land on which it is possible to erect an on-shore wind farm (Ali et al, 2017). To minimize the impact of wind farms on local tourism, Tsoutsos et al (2015) report that wind farms should be at a distance of at least 1000 meters from touristic activities. Xydis et al. (2013) and Latinopoulos and Kechagia (2015) agree with this value in their studies performed in the Greek territory. In order to preserve the cultural heritage, Baban and Parry (2001) claim that wind farms should not be located on or within 1000 m of historic sites and National Trust property. Tsoutsos et al (2015) propose that safety distances of 3000m should be considered from World Heritage, archeological monuments and historical places of high importance, of 500m from the rest archeological sites, cultural monuments, historical sites and of 500m from monasteries.

6. Slope

Soil slope is a very important factor in wind farm siting as it affects the ease of construction and maintenance. Steep slopes may reduce the accessibility of cranes and trucks and increase construction costs. Wakeyama and Ehara (2011) report that the maximum slope ranges from values with a maximum gradient of 20%. Bennui et al (2007) exclude hilling areas steeper than 15% slope, while Haaren and Fthenakis (2011) suggest that the slope should under no circumstances exceed 15%. Höfer et al (2016) assume a maximum slope of 30% that corresponds to the opinions of the regional wind power experts and wind farm planners who participated in a conducted survey. However, very deep slopes (>10%) have been excluded in the majority of wind farm siting studies (eg Baban and Parry, 2001; Haaren and Ftenakis, 2011; Georgiou et al, 2012; Kazim et al., 2015).

7. Altitude

As far as the altitude is concerned, the generated wind energy decreases as the altitude increases, as the air density decreases at higher altitudes. Digital Elevation Models are used to define suitable land based on elevation. Wakeyama and Ehara (2011) select areas with altitudes below 1000m, while Gass et al (2013) and Noorollahi et al (2016) propose 2000m as the cut-off criterion.

8. Land use

Some types of land uses are considered more suitable for onshore wind farm sitting. Areas with sparse vegetation are more suitable for wind farm siting than areas with dense vegetation. Baban and Parry (2001) in their study note that it is forbidden to develop wind energy projects on agricultural land. Land uses such as agricultural land, barren land, grassland and shrubland are considered more appropriate, while forest land less, according to Haaren and Fthenakis (2011). Gorsevski et al (2013) distinguish classes representing different levels of land use suitability. Classes representing cropland, pasture, shrub land, or barren land are considered the most suitable land cover. Grassland and forested land represent moderately suitable land cover. Classes such as low intensity residential areas are considered as the least suitable areas while developed areas, open water, and wetlands are considered constraints. Lozano et al (2014) distinguish nine classes of agrological capacity (suitability of land for agricultural development) that range from 0 (excellent – not suitable to host a wind farm) to 8 (low – very favourable to host wind energy facilities).

2.2 Greek institutional framework for wind farm siting

Article 6 of the Special Framework for SFSPSD-RES (MEECC, 2008) notes that the installation of wind farms is not permitted inside: 1) World Heritage areas, archaeological monuments and historical places of high importance, as well as in archaeological sites of zone A; 2) Areas of absolute protection of the nature; 3) Wetlands RAMSAR; 4) Centre of national forests, nature monuments, aesthetic

forests; 5) Sites of Community Importance of Natura 2000; 6) Inside urban plans and settlement boundaries; 7) Areas of integrated touristic development and organized productive activities of the tertiary sector, thematic parks, touristic ports and beaches; 8) Tourist and residential areas (outside the building plan); 9) Notable coasts and beaches (included in water bathing monitoring program); 10) High-productivity farmland; 11) Quarries and mines; 12) Areas or part of areas that are subject to a specific land-use regime, which forbids wind farm siting.

2.3 Selected criteria and buffer zones for onshore wind farm siting

Several exclusion areas according to criteria recorded in SFSPSD-RES are identified in the Regional Unit of Magnesia. Table 1 lists all the exclusion criteria and incompatible buffer zones for onshore wind farm siting applied in this study. It should be noted that in cases that the SFSPSD-RES does not provide any specific buffer zone, values found in the international literature are considered.

3. ANALYSIS OF THE STUDY AREA

The Regional Unit of Magnesia is one of the 52 Regional Units of Greece and administratively belongs to the region of Thessaly. It has an area of 2637 km^2 and its population population reaches 190010 people according to the 2011 census. The capital of the regional unit of Magnesia is Volos, that counts 144449 inhabitants.

The Regional Unit of Magnesia includes valuable natural and cultural resources as well as remarkable tourist infrastructures. Traditional settlements, facilities of particular architectural interest, historical and archaeological sites, as well as various museums can be found in the area. In addition, there is a railway network, port facilities, an airport, a ski center and numerous tourism paths. The national road network has a total length of 321 km.

Areas that belong to the network of core breeding and resting sites for rare and threatened species, and some rare natural habitat types which are protected in their own right (Natura 2000) include: Oros Pilio (GR 1430008/ 36216.5ha), the area covered by reservoirs of the former Karla lake (GR 1430007/ 12422.9ha), Oros Mavrovouni (GR1420006/ 37146.90ha), Kouri Almyrou-Agios Serafeim (GR1430002/ 100.28ha), Oros Orthys-Vouna Gkouras-farangi Palaiokerasias (GR1430006/ 31093.50ha). In the Regional Unit of Magnesia, several Areas of Outstanding Natural Beauty (AONBs) and Wildlife Refuges can be found.

Figure 1 depicts wind farm applications that are in production license or have already been rejected as well as the wind capacity of the Regional Unit of Magnesia. Wind velocity in the Regional Unit of Magnesia is relatively low, since wind velocity does not exceed 5m/s in most parts of the study area. Nevertheless, in the wider area of Pelion, the wind velocity increases and reaches up to 9m/s. It should also be noted that the highest carrying capacity is measured at Municipal Units of Almyros and Velestinos (> 100).

Table 1: Exclusion Criteria Restrictions

A/A	Exclusion Criteria	Buffer zones SFSPSD-RES (d=85m)	Buffer zones Literature review	Buffer zones Present case study
1	Wind Velocity		5m/s (eg Baban and Parry, 2001; Tegou et al, 2007; Georgiou et al, 2012)	5m/s
2	Distance from areas of environmental interest		1000m (eg Baban and Parry, 2001; Aydin et al, 2010; Wang et al., 2014; Latinopoulos and Kechagia, 2015)	1000m
3	Bathing Waters	1500m		1500m
4	Archaeological monuments and historical places of high importance	595m (7d)		595m
5	Monasteries	500m		500m
6	Distance from residential areas>2000 population	1000m		1000m
7	Distance from residential areas<2000 population	500m		500m
8	Traditional Settlements	1500m		1500m
9	Distance from road networks, electricity distribution networks	127.5m (1.5d)		127.5m
10	Distance from airports		5000 m (Lejeune and Feltz, 2008; Kazim et al, 2015)	5000m
11	High-productivity farmland	127.5m (1.5d)		127.5m
12	Quarries and Mines	500m		500m

* d is the diameter of the wind turbine’s rotor, which is equal to 85 m

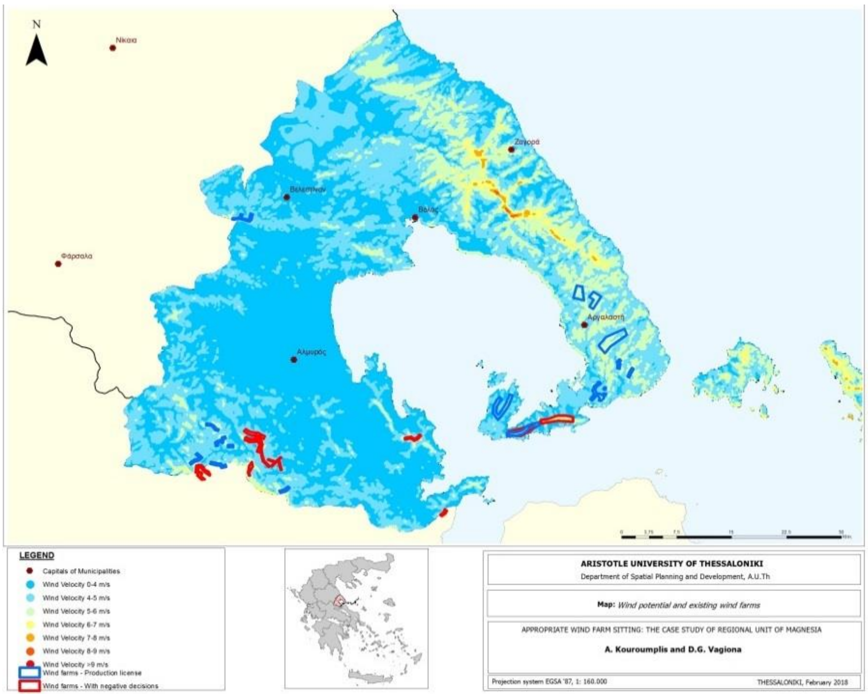


Figure 1: Wind potential and existing wind farms

4. RESULTS AND DISCUSSION

In the present application, areas which are excluded due to incompatibility include ports, the airport, bathing waters, listed cultural monuments, monasteries, telecommunication antennae, the road network and the electricity grid, SCIs and SPAs of the Natura 2000 network, Wildlife Refuges, AONBs, settlements and high-productivity farmland. The excluded areas are presented in Figure 2.

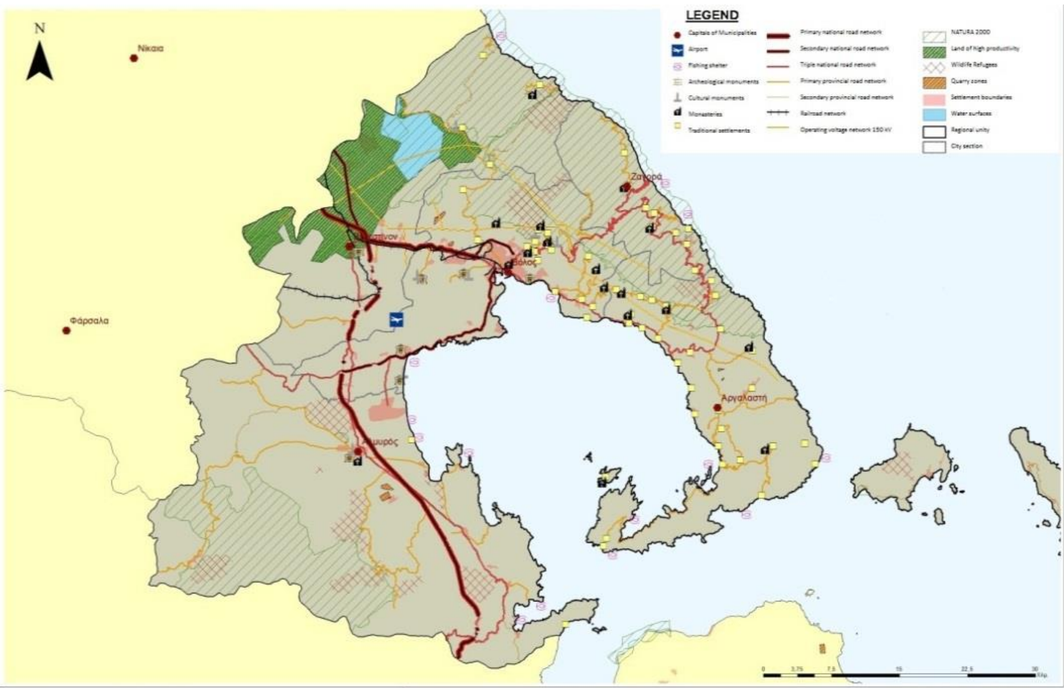
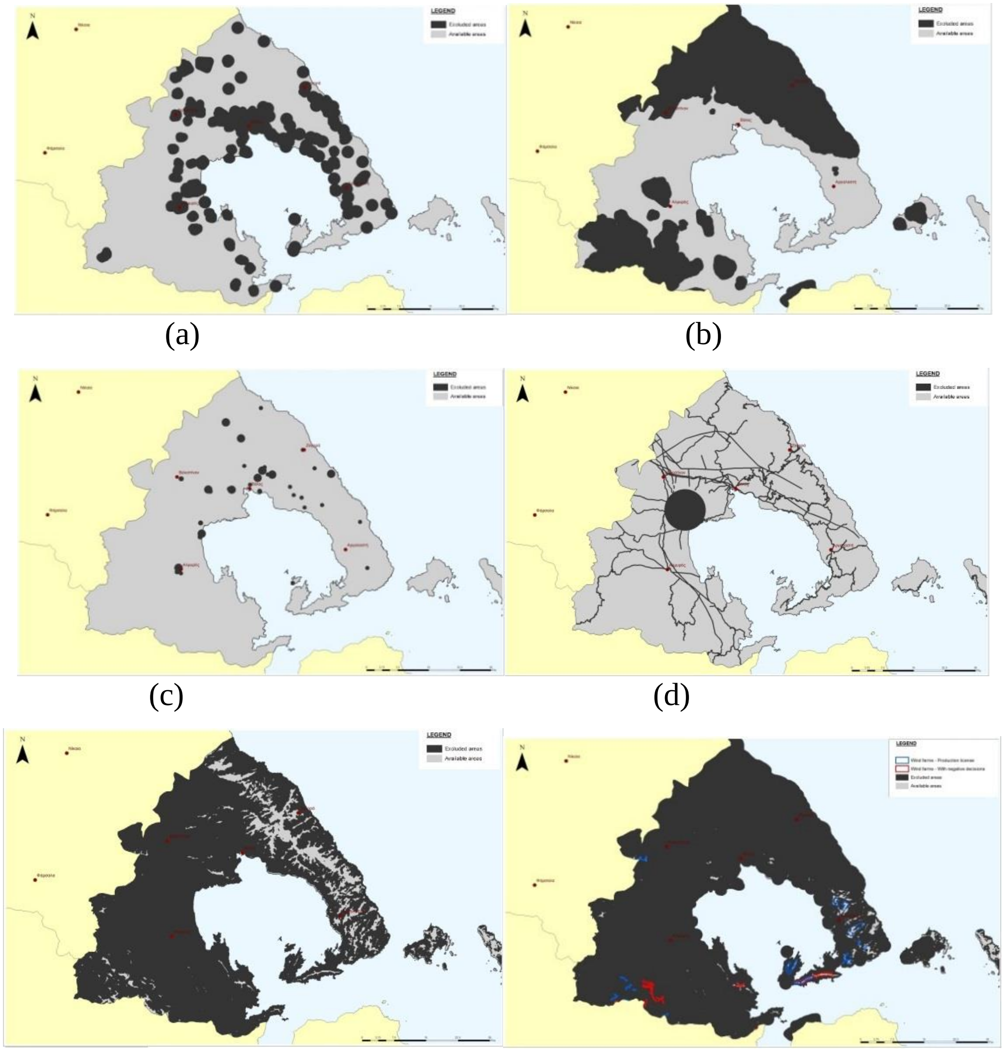


Figure 2: Excluded areas

In addition, the minimum distances presented in Table 1 are applied, leading to the appropriate areas for wind farm siting in the Regional Unit of Magnesia.



(a) (b)

(c) (d)

(e) (f)

Figure 3: (a) Buffer zones from areas of residential areas (b) Buffer zones from areas of environmental interest (c) Buffer zones from cultural interest (d) Buffer zones from infrastructures (e) Areas with wind velocity lower than 5 m/sec and (f) Land suitability areas.

It is obvious that the available areas for wind farm siting in the Regional Unit of Magnesia are really handful due to the special morphology of the area, the prevailing wind (wind velocity below 5m/s) as well as the existing onshore wind farm infrastructures. Compatible areas for wind farm siting can be found mainly on the southern part of Pelion and on the eastern side of the Municipal Unit of Almyros.

The surface of areas that have been already occupied by wind farms in production license covers 0.77% of the total area, while the surface of compatible areas found from the above analysis covers 0.87% of the total area.

5. CONCLUSIONS

In recent years, there has been a constant increase in the share of energy from RES, especially wind energy due to its high potential in final energy consumption. However, wind farm siting is a complex issue, including various technical, socio-economic and environmental factors. Numerous studies investigating onshore wind farm siting can be found in the literature.

A thorough research into the Greek institutional framework, which comprises the Special Framework of Spatial Planning and Sustainable Development for Renewable Energy Sources and an extensive literature review has been performed to formulate the exclusion criteria, which are finally included in

this analysis. The primary objective for selecting the appropriate criteria is the sustainable siting of a wind farm that minimizes or even avoids any impact on physical and anthropogenic environment.

The present research constitutes a mainland application on the Regional Unit of Magnesia, where wind velocity is quite low over a large part of the area. However, it can serve as an ex-ante evaluation of potential new onshore wind farm investments and provide useful directions for policy and decision makers. The criteria selected in this study could be applied in any spatial scale, from local to national contributing to the sustainable onshore wind farm siting.

References

1. Ali S., Lee S.-M., Jang C.-M. (2017) 'Determination of the Most Optimal On-Shore Wind Farm Site Location Using a GIS-MCDM Methodology: Evaluating the Case of South Korea', **Energies**, 10(12), 2072.
2. Argyros N. (2011) **'Econometric study and evaluation of the construction of wind farms in the Greek territory'**, National Technical University of Athens, pp. 54.
3. Aydin N., Kentel E., Duzgun S. (2010) 'GIS-based environmental assessment of wind energy systems for spatial planning: A case study from Western Turkey', **Renewable and Sustainable Energy Reviews**, 14, pp. 364–373.
4. Baban S.M.J. and Parry T. (2001) 'Developing and applying a GIS-assisted approach to locating wind arms in the UK', **Renewable Energy**, 24, 59–71.
5. Bennui A., Rattanamanee P., Puetpaiboon U., Phukpattaranont P., Chetpattananondh K. (2007) Site selection for large wind turbine using GIS, **International Conference on Engineering and Environment (ICEE 2007)**, pp 561-566, Phuket, Thailand.
6. Bili A. and Vagiona D. (2017) Criteria and methodologies for onshore and offshore windfarm site selection: A literature review research, **6th International Conference on Environmental Management, Engineering, Planning and Economics (CEMEPE) and to the SECOTOX Conference**, Thessaloniki, Greece.
7. Blankenhorn V. and Resch B. (2014) 'Determination of Suitable Areas for the Generation of Wind Energy in Germany: Potential Areas of the Present and Future', **ISPRS International Journal of Geo-Information**, pp. 942-967
8. Gass V., Schmidt J., Strauss F., Schmid E. (2013) 'Where the wind blows: Assessing the effect of fixed and premium based feed-in tariffs on the spatial diversification of wind turbines', **Energy Policy**, 53, pp. 323-30.
9. Georgiou A., Polatidis H., Haralambopoulos D. (2012) 'Wind Energy Resource Assessment and Development: Decision Analysis for Site Evaluation and Application', **Energy Sources Part A**, 34, pp. 1759-67.
10. Gorsevski P.V., Cathcart S.C., Mirzaei G., Jamali M.M, Ye X., Gomezdelcampo E. (2013) 'A group-based spatial decision support system for wind farm site selection in Northwest Ohio', **Energy Policy**, 55, pp. 374–85.
11. Grammatikogiannis E. and Stratigea A. (2010) 'Evaluation of Alternative Sites for Wind Park Location: A Methodological Framework', **Technika Chronika** ,3, pp. 85-86.
12. Haaren R. and Fthenakis V. (2011) 'GIS-based wind farm site selection using spatial multi-criteria analysis (SMCA): Evaluating the case for New York State', **Renewable and Sustainable Energy Reviews**, 15, pp. 3332– 3340.
13. Höfer T, Sunak Y, Siddique H, Madlener R. (2016) 'Wind farm siting using a spatial Analytic Hierarchy Process approach: A case study of the Städteregion Aachen', **Applied Energy**, 163, pp. 222–43.

14. Kazim B., Simsek A., Aydin U., Tosun M. (2015) ‘A GIS-based Multiple Criteria Decision Analysis approach for wind power plant site selection’, **Utily Policy**, 37, pp. 86-96.
15. Latinopoulos D. and Kechagia K. (2015) ‘A GIS-Based MultiCriteria Evaluation for Wind Farm Site Selection: A Regional Scale Application in Greece’, **Renewable Energy**, 78, pp. 550-560.
16. Lejeune P., Feltz C. (2008) ‘Development of a decision support system for setting up a wind energy policy across the Walloon Region (southern Belgium)’, **Renewable Energy**, 33, pp. 2416-22.
17. Lozano-Sánchez J.M., García-Cascales M.S., Lamata M.T. (2014) ‘Identification and selection of potential sites for onshore wind farms development in Region of Murcia, Spain’, **Energy**, 73, pp. 311-324.
18. Ministry of Environment, Energy and Climate Change (MEECC). Specific framework for spatial planning and sustainable development for renewable energy sources; 2008. JMD 49828/2008, OGHE B′ 2464/3-12-08.
19. Noorollahi Y., Yousefi H., Mohammadi M. (2016) ‘Multi-criteria decision support system for wind farm site selection using GIS’, **Sustainable Energy Technologies and Assessments**, 13, pp. 38-50.
20. Ouammi A., Ghigliotti V., Robba M., Mimet A. and Sacile R. (2012) ‘A decision support system for the optimal exploitation of wind energy on regional scale’, **Renewable Energy**, 37, pp. 299-309.
21. Rodman L.C., Meentemeyer R.K. (2006) ‘A Geographic Analysis of Wind Turbine Placement in Northern California’, **Energy Policy**, 34, pp. 2137-49.
22. Sunak Y. and Höfer T. (2015) **‘A GIS-based Decision Support System for the Optimal Siting of Wind Farm Projects**’, E.ON Energy Research Center Series.
23. Tegou L.I., Polatidis H., Haralambopoulos D.A.. (2007) Distributed Generation with Renewable Energy Systems: The spatial dimension for an autonomous Grid, **47th conference of the European Regional Science Association ‘Local governance and sustainable development’**, Paris, France.
24. Tegou L.I., Polatidis H., Haralambopoulos D.A. (2010) ‘Environmental management framework for wind farm siting: Methodology and case study’, **Journal of Environmental Management**, 91, pp. 2134–47.
25. Tsoutsos T., Tsitoura I., Kokologos D., Kalaitzakis K. (2015) ‘Sustainable siting process in large wind farms case study in Crete’, **Renewable Energy**,75, pp. 474-480.
26. Vanek F. and Albright L. (2008) ‘Energy Systems Engineering: Evaluation and Implementation’, McGraw-Hill Professional.
27. Ucar A. and Balo F. (2009) ‘Evaluation of Wind Energy Potential and Electricity Generation at Six Locations in Turkey’, **Applied Energy**, 86, pp. 1864-1872.
28. Wakeyama T. and Ehara S. (2011), Estimation of Renewable Energy Potential and Use- A Case Study of Hokkaido, Northern-Tohoku Area and Tokyo Metropolitan, Japan, **World Renewable Energy Congress 2011**, pp 3090-3097, Linkoping, Sweden.
29. Wang Q., Mwirigi M., Kinoshita I. (2014) ‘A GIS-Based Approach in Support of Spatial Planning for Renewable Energy: A Case Study of Fukushima, Japan’, **Sustainability**, 6, pp. 2087-2117.
30. Xydis G. (2013) ‘A techno-economic and spatial analysis for the optimal planning of wind energy in Kythira island, Greece’, **International Journal of Production Economics**, 146, pp. 440-52.
31. Yue C. and Wang S. (2006) ‘GIS-based evaluation of multifarious local renewable energy sources: a case study of the Chigu area of southwestern Taiwan’, **Energy Policy**, 34, pp. 730–42.

HARNESSING THE BLUE RENEWABLE ENERGY SOURCES OF THE COASTAL CEPHALONIA'S PARADOX AND THE EURIPUS STRAIT

A. Stergiopoulou[1], V. Stergiopoulos[2]*, G. Klironomos[2], E. Ververis[2], M. Syrganis[2], K. Papaioannou[2] and M. Theodoridou[2]

[1]Institut für Wasserwirtschaft, Hydrologie und konstruktiven Wasserbau, B.O.K.U. University, Muthgasse 18, 1190 Vienna, Austria
[2]ASPETE, Department of Civil Engineering Educators, ASPETE Campus, Athens 14121, Greece

*Corresponding author : e-mail : bstergiopoulos@aspete.gr

Abstract
The sea represents a huge potential for Blue Renewable Energy Sources (BRES) such as waves, tides and marine currents, including the Euripus Straits and the Cephalonia's Coastal Paradox. The possibility of exploiting the BRES, of zero-head sea and tidal currents, for power generation has given little attention in Europe, in Mediterranean countries and in Greece, despite the fact that such currents, representing a large renewable potential, could be exploited by modern technologies to provide important levels of electric power. The present paper tries to describe simple physical models for the hydraulic explanations of two of the most astonishing marine currents of the world, the Cephalonia's Coastal Paradox (CCP) and the Euripus Strait Current (ESC), continuing to puzzle the scientists for many decades. The CCP is consisting of a mysterious flow of the "through the island" strong underground coastal current, with a continuous seawater inflow in the Livadi Gulf, near Argostoli, reappearing in the other side of the island, in the Gulf of Sami. Passing from the Ionian Sea to the Aegean Sea, the CCP finds its hydraulic flow analogue, in the tidal current of ESC, also among the most famous world coastal phenomena. This is a remarkable exceptional fact in spite that tidal currents in the Mediterranean Sea are in general comparatively weak. Since ancient times many scientists try to cite advanced arguments towards parts of the global "Euripus problem" solution. One of the main aims of the present paper is to propose innovative efficient technical solutions, in order to harness the current potential of the CCP and the ESC, with a series of innovative Horizontal Archimedean Screw Turbines, based on the first in the world Horizontal Archimedean Screw Turbine built and studied at BOKU Vienna University.

Keywords: blue renewable energy sources, coastal Cephalonia's paradox, Euripus strait current, kinetic small hydro plants, Archimedean screw turbines

1. INTRODUCTION

The present paper, part of the research project entitled "Research of Sea Hydraulic Mysteries of Euripus and Cephalonia-Inventory of Blue Hydropotential", examines two special cases of Blue Renewable Energy Sources (BRES) probably unique in the world, Cephalonia and Euripus cases and how harnessing their potential (Figure 1). Both sites are a glance at the sea water current and tidal past and a promising modern look into the future blue renewable hydraulic kinetic energy.

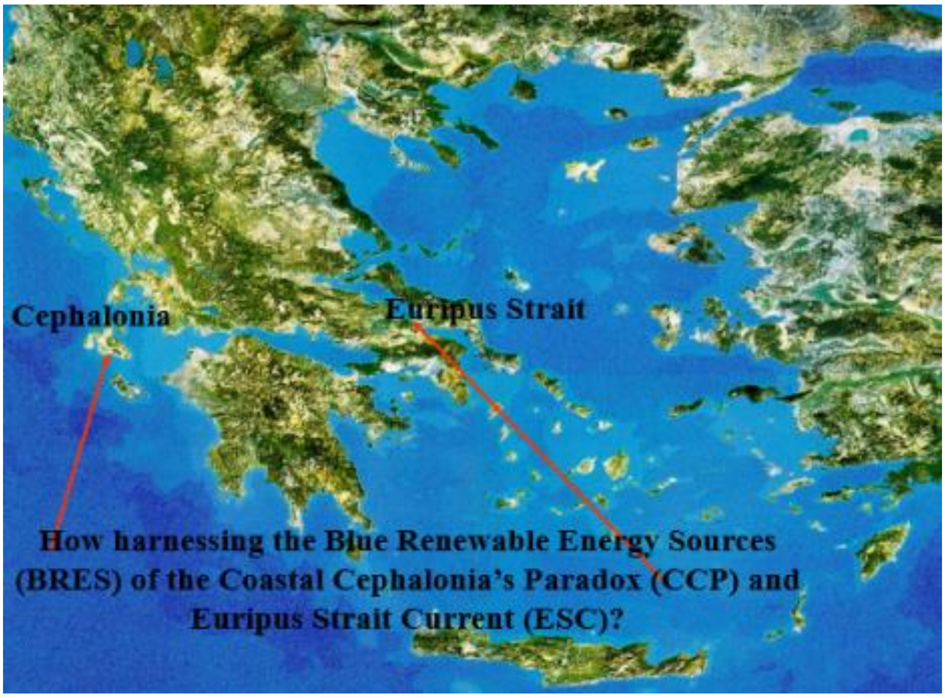


Figure 1: How harnessing the Blue Renewable Energy Sources (BRES) of the Coastal Cephalonia's Paradox (CCP) and Euripus Strait Current (ESC)?

It is well known that the sea represents a huge potential for Blue Renewable Energy Sources such as waves, tides and marine currents, including the Euripus Straits and the Cephalonia's Coastal Paradox**.** The possibility of exploiting the BRES, of zero-head sea and tidal currents, for power generation has given little attention in Europe, in Mediterranean countries and in Greece**,** despite the fact that such currents, representing a large renewable potential, could be exploited by modern technologies to provide important levels of electric power. The particular sea and tidal currents of Cephalonia and Euripus Strait and their living forces were in the past used by sea-mills and tidal mills for cereal exploitation playing an important role to the local society and economy [1,5,6]. The pioneer English Stevenson made important observations of the over the centuries unexplained Thalassomili Katavothres phenomenon and created in 1835 the first cereal productive Argostoli mills exploiting the unknown living forces of sea water penetrated into the local katavothres and disappearing into the porous limestone of the island. According to the geologist Miliaresis [2,3] the 1953's earthquakes made the destruction of the productive Cephalonia sea-mills. Fuller [2] and Crosby [3] made important works about the fundamental role of the slight variations in sea water density introducing sufficient differences in pressure to produce circulation. Koder [4] gives some very valuable information for three existing tidal mills in Negreponte (Chalkis) during the Venetian period. Unfortunately, Cephalonia sea mills and Euripus tidal mills stopped to operate. For the case of Chalkis there are no fingertips of the glorious tidal mill past. For the case of Cephalonia, the sea-mills of nowadays, build in Argostoli during 60's, have only a touristic attraction, without any cereal or electrical productivity.

The island of Cephalonia is the site of one of the most astonishing hydrological phenomena in the world, its coastal cross flow paradox [5]. A strange seawater massive current flows continuously into the karst substratum of the island through sinkholes, in the Livadi Gulf, near Argostoli (Figure 2). The present paper tries to describe some quite simple physical models for the hydraulic explanation of the strange cross-flow Cephalonia's coastal paradox and to find hydraulic correlations with a strong lost and forgotten water near-shore processes memory [6, 7]. This seawater current disappearing in the water channel entrance, in the Livadi Gulf, reappears on the opposite coast of the island at brackish springs, near the town of Sami (Figure 2). This strange "through the island continuous seawater current", seems to be a real world unique sea hydraulic mystery, the so called 'Cephalonia's Coastal Paradox' or 'Cephalonia's Sea-River'.

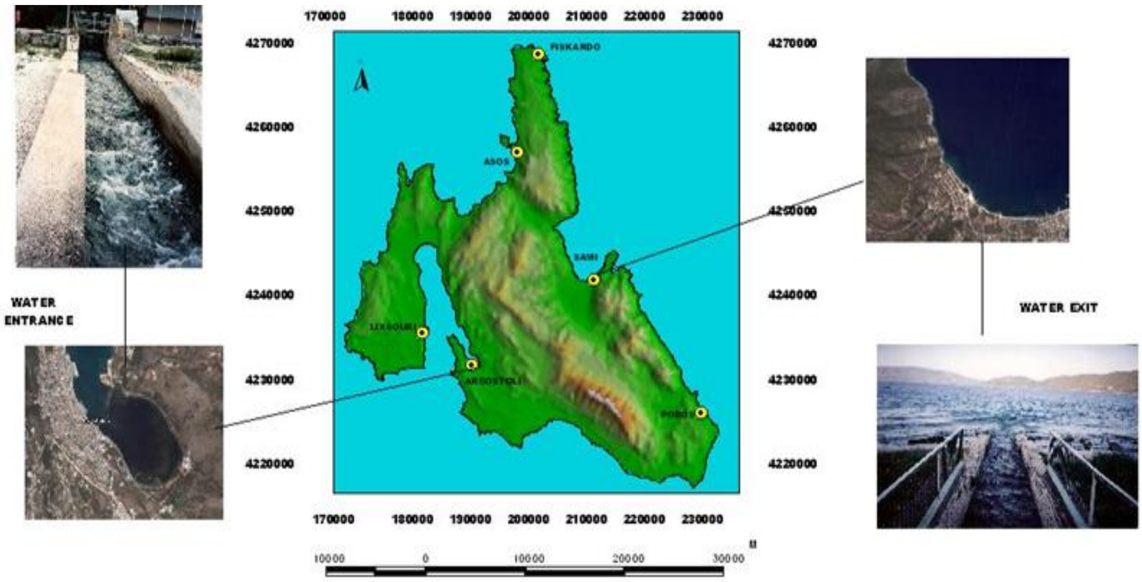


Figure 2: Schematic representation of the most astonishing hydraulic phenomenon in the world.

Passing from the Ionian Sea to the Aegean Sea, the Cephalonian Sea-River finds its hydraulic flow analogue in the tidal current of Euripus Strait, which is also among the most famous coastal phenomena in the world, despite the fact that tidal currents in the Mediterranean Sea are in general comparatively weak. Since ancient times many renowned men of science, Eratosthenes, Strabo, Posidonius, Seleucus, Pliny the Elder and Aristotle among them, cited advanced correct arguments towards parts of the "Euripus problem" concerning the narrow channel of the Euripus, subject to strong tidal currents, which reverse direction approximately four times a day. Between the mid-nineteenth and mid-twentieth centuries, many scientists, among them Eginitis [9] contributed towards the complete solution of the Euripus problem. A recent analysis with simulations of the tidal flows in the North and South Evvoikos Gulfs, separated by the Euripus Strait has been presented by Tsimplis [10].

2. 2. ABOUT THE CEPHALONIA'S COASTAL PARADOX

According to Bonacci's Karst Hydrology the only permanent sea katavothres in the world, is the case of Argostoli [11]. Generally, Cephalonia's katavothres, swallowing sea water permanently, are well-organized fissures in the karst mass through which the water sinks underground and they play an important role, from a hydraulic and hydro-geologic standpoint of view, in the whole water karst flow. This strange strong seawater current is disappearing continuously in the Livadi Gulf through sinkholes, which have formed in fractures in the rock (Triassic, Jurassic, Cretaceous and Cainozoic limestone and dolomite). This seawater current reappears on the opposite coast of the island at brackish springs, near the town of Sami. The underground seawater current route between Argostoli and Sami is about 15Km long (Figure 3). Such inflow-outflow seawater current phenomenon has not been observed in other karst islands in the Mediterranean or in other parts of the world.

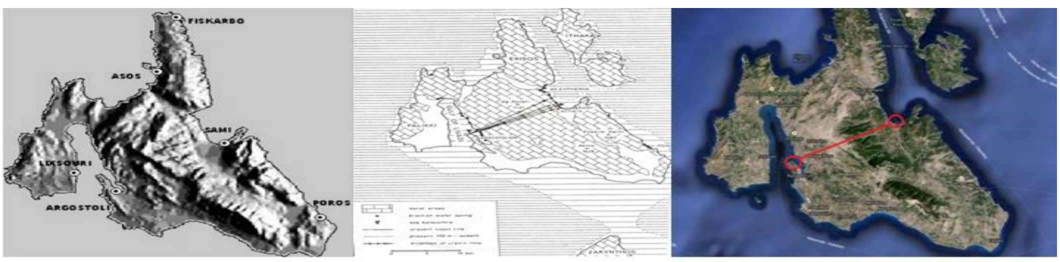


Figure 3: Schematic representation of the Cephalonia paradox.

There must necessarily be a continuous source of energy to cause this hydraulic phenomenon of the continuous inflow of water below sea level, since the latter represents minimum potential for water, in the field of terrestrial gravity. However, it is well known that an important continuous marine current, the Levantine Intermediate Water (LIW), formed in the Levantine Sea, with a Northwards direction follows the Aegean current, which runs round the southern coast of Greece and joins the Adriatic circuit currents, and touches the island of Cephalonia, could probably have a vital driving force importance behind the Cephalonia underground sea. Who maintains the movement of the C.C.P.? Does the presence of a labyrinth of karst conduits play a certain role in the whole throughout current flow? Is it possible to occur simultaneously, various factors, like the energy of the Aegean-Adriatic marine current, the density flow and the presence of karst conduits, for the control of the whole phenomenon? [13, 14]. Which is the role of the Ghyben-Herzberg ratio of fresh and salt-water density to the dynamic interface of this unusual marine current phenomenon? [15, 16]. Many other questions and problems persist. We could probably assume that there is, in the substratum of the island, a kind of strange attractor, a quasi - natural ejector, which works on the principle of the water ram pump jet and that there, is probably operated by infiltration of water [12, 13, 16, 17, 18]. This good hypothesis is nevertheless not very efficient from a hydrodynamic point of view. In addition, it is possible to report that physical conditions of flow through siphons, venturi tubes, and tubular openings in the carbonate rocks could explain the whole phenomenon.

However, judging from the negative head in the sinkholes the velocity of the fresh water appears to be insufficient to operate a ‘natural ram jet pump’ or suggested ‘venturi tubes’. Observing seawater flowing through the entry canal near Argostoli and disappearing in a system of katavothres, they erroneously concluded that it must flow through the interior of the island, where it looses its “earthy” component, thus becoming the pure water that could be observed at the springs in the foothills. The clouds often observed at the relatively high mountainous volume of Ainos further supported this idea (Figure 4). They took this as a clear indication that this water was in fact transformed into clouds when reaching mountaintops, thus closing the hydrological cycle. In the same figure shown is another explanation of the coastal cross-flow current by analogy to a jet pump. According to this analogy high velocity fresh water sucks seawater creates a strong Venturi effect able to power the whole mechanism.

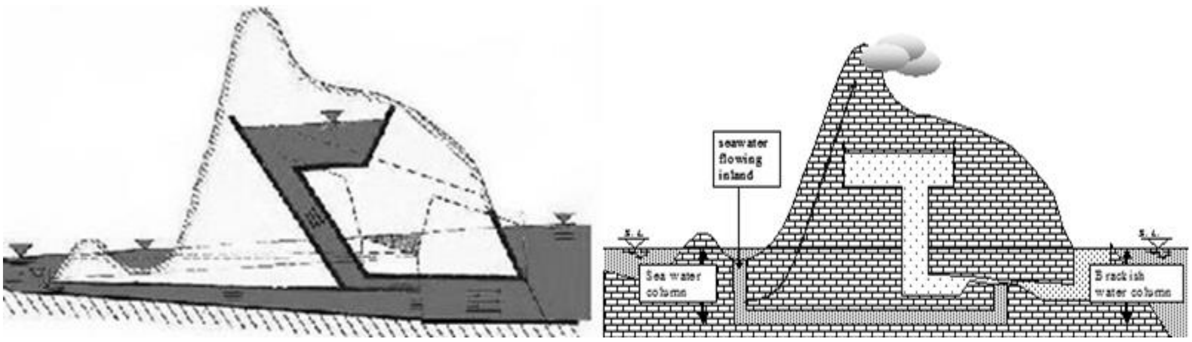


Figure 4: Representations of ‘natural ram jet pump’, ‘venturi tubes’ and other hydraulic hypothesis for the local explanation the CCP.

A quite simple hydrostatic model of three in equilibrium connected vertical tubes (3, 1, 2), filled with sea water, fresh and brackish water, could be used to simulate the Cephalonia Argostoli-Sami sea water flow mechanism (Figure 5). In this three-tube model, H is the unknown depth of mixing zone, ΔH_1 is the karst hydraulic gradient with ρ_1 the density of fresh water, ΔH_2 is the altitude of the exit brackish spring furnishing brackish water having density ρ_2 and ΔH_3 is the input variation of the sea level with a density of sea water ρ_3, with $\rho_1<\rho_2<\rho_3$. According to the principle of communicating vessels the fundamental equation of hydrostatics will give

$$(H+\Delta H_3).\rho_3.g = (H+\Delta H_1).\rho_1.g =(H+\Delta H_2).\rho_2.g$$

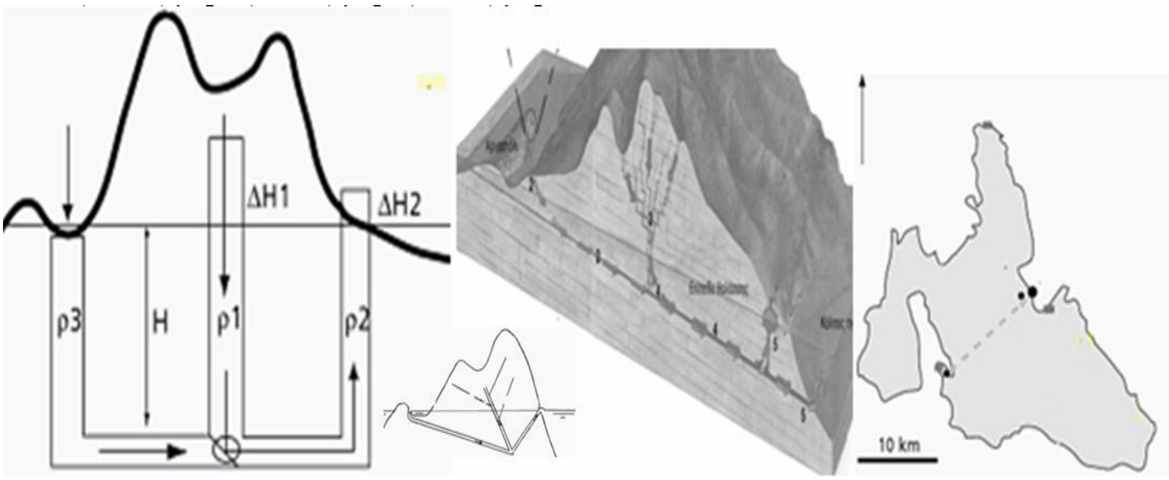


Figure 5: Schematic presentation of the communicating vessels principle with 3 vertical tubes

When fresh water is injected in the fresh water pipe 1, then a current moves towards the brackish pipe 2, where the density is lower than in the sea pipe 3. It is clear that the introduction of fresh water in the brackish pipe provokes a dilution and decreases. After mixing, the brackish water is not as heavy as sea water and, therefore, rises along the interface of the fresh water and salt water to springs. The true causes of the CCP phenomenon have not been elucidated so far. It seems that this throughout Cephalonia current will continue to challenge and to puzzle us continuously.

3. ABOUT THE EURIPUS STRAIT CURRENT

It is well known that gravitational forces between the moon, the sun and the earth cause the rhythmic rising and lowering of ocean waters around the world and the creation of the tide waves. The moon exerts more than twice as great a force on the tides as the sun due to its much closer position to the earth. The development of tidal science began in Antiquity, with the cosmology of Aristotle, who observed that ‘ebbings and risings of the sea always come around with the Moon and upon certain fixed times’. Aristotle used his books “On the Heavens and Physics” to put forward his notion of an ordered universe divided into two distinct parts, the earthly region and the heavens [6, 7]. Other developments in tidal science at this time included those by Pytheas, who travelled through the Strait of Gibraltar to the British Isles and reported the half-monthly variations in the range of the Atlantic Ocean tides, and that the greatest ranges occurred near the new and the full Moons. Many other aspects of the relationship between tides and the Moon are noted in Pliny the Elder’s “Natural History” [6, 7]. Pliny described how the maximum tidal ranges occur a few days after the new or full Moon, and how the tides at the equinoxes in March and September have a larger range than those at the summer solstice in June and winter solstice in December.

Tidal flows are very weak in the Eastern Mediterranean, and the Euripus strait is a remarkable exception. Tidal flow peaks at about 12Km/h, either northwards or southwards, and lesser vessels are often incapable of sailing against it. When nearing flow reversal, sailing is even more precarious because of vortex formation. The whole problem has not yet been given a general and complete solution. Some of the questions associated with this subject have been correctly explained, but not always with completeness and the required scientific proofs, others were given a bad solution or misunderstood, while others have been quite ignored, owing to the lack of the necessary tidal data and some had not been studied at all. The complete solving of the Euripus problem is due to D. Eginitis, who published his conclusions in 1929 [9]. It seems that Eginitis gives the general solution of this famous Euripus tidal problem, with all the proofs provided by the theory and the observations, based on the laws of Hydrodynamics and Celestial Mechanics and the respective rules of Hydraulics, taking into consideration the tide observations made by the Hydrographical Service of the Ministry of Marine.

It seems that the tide observed in the gulf of Euboea is nearly exclusively derivative, and it is produced not only by a local tide of the Aegean Sea as up to this time it was erroneously thought to be, but it comes from the Eastern basin of the Mediterranean Sea which is simultaneously fluctuating with the Western Mediterranean. On this latter there is a slight influence of the tides of the Atlantic Ocean. So the Aegean Sea could be considered as a gulf of the Eastern Mediterranean, through which its tide is transmitted to the gulf of Euboea entering it through its two ends and so reaching Euripus. Without this tide, coming from the Eastern basin of the Mediterranean Sea, the great difference of the times of establishment of the two ports of Chalkis, situated at a distance of a few metres, remains in suspense (left part of the Figure 6). According to Tsimplis et al [10] the reported values for the Euripus Strait tidal currents are as high as 4.4 m/sec, the tidal signal is choked at the strait and consequently very little energy is transferred between the north and the south Evvoikos Gulf. It seems that the sea level of both gulfs oscillates independently of each other and causes significant sea level differences and strong currents across the Euripus Strait. The tide reaches the south part of the north Evvoikos Gulf later than it reaches the northern part of the south Evvoikos Gulf. Moreover, the tidal amplitude is lower at the southern opening of the south Evvoikos Gulf than at the north opening of the north Evvoikos Gulf, due to the standing wave nature of the semi-diurnal tide within the Aegean. The tides are further enhanced while propagating through the canals of Trikeri and Oreoi in the north Evvoikos Gulf. As a result, the north Evvoikos oscillates everywhere with amplitudes which are virtually the same everywhere in the basin. In contrast, the southern Evvoikos Gulf has much smaller tides. Thus the six-hourly variation of currents is produced mainly by the relatively large semi-diurnal tides of the north Evvoikos Gulf, which introduce six- hourly changes in the sign of sea level differences between the two gulfs (left part of the Figure 6). A characteristic optical view of the tidal model of Tsimplis et al [10] concerning the sum of the major tidal components in the Hellenic Seas is given in the right part of the Figure 6**.**

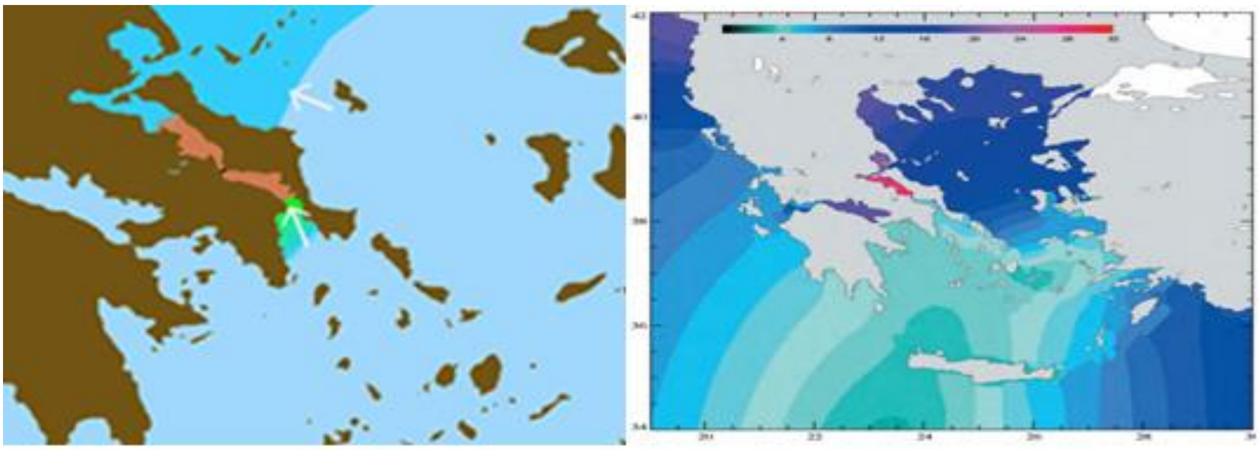


Figure 6: Views of the tidal model of Tsimplis et al [10] for the major tidal components in the Hellenic seas.

The kinetic power P, expressed in W, in sea currents, such as the cases of the Cephalonia's Coastal Paradox (CCP) and the Euripus Strait Current (ESC), is related to the velocity of the water passing through the cross section of a sea channel and is given by the equation $P = (1/2).\rho.\int V^3 \cdot dA$,where ρ is the water density (kg/m^3), A is the cross sectional area of the channel (m^2) and V is the sea current flow velocity (m/s). Figure 7 shows the expected influence of the flow speed on kinetic power density P/A expressed in kW/m^2.

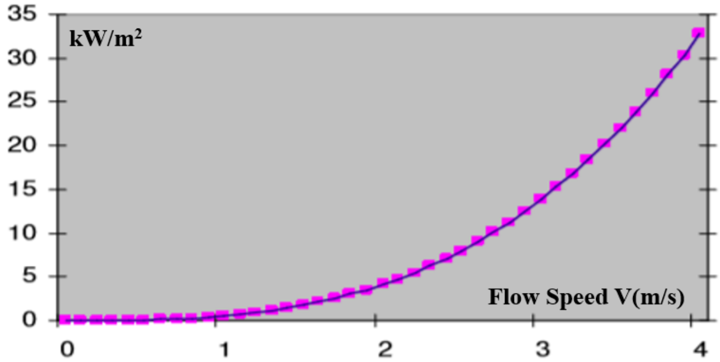


Figure 7: Kinetic power density expressed in kW/m^2.

Figure 7 shows that the kinetic power flux density in a 3m/s current is approximately 15 kW/m2. This suggests that the kinetic power available for conversion in various parts of the world, including those of ESC of Euripus and CCP of Cephalonia, should be very useful blue renewable energy to be exploited by innovative horizontal axis Archimedean screw turbines.

In order to study and to investigate theoretically and experimentally the horizontal screw turbine performances, the first in the world horizontal Archimedean screw turbine has been built and tested at BOKU Vienna University [20]. The basic geometrical characteristics of this innovative screw rotor, that is installed and experimented in the hydraulic channel at the Laboratory of the Institute for Water Management, Hydrology and Hydraulic Engineering, in Vienna, are given in Figure 8. The length L, the diameters (output and input), the pitch S and the number of blades of the screw rotor are L=0.945 m, D_o=200mm, D_i=100mm, S=200mm, S/Do=1 and n=3 (number of blades).

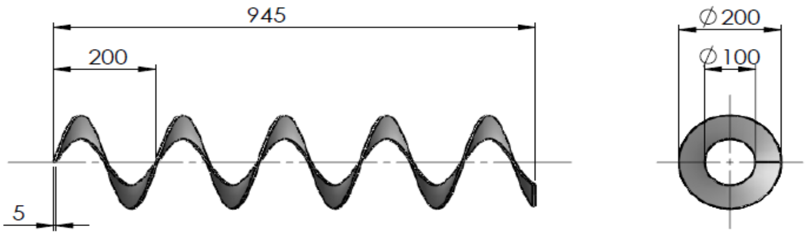


Figure 8: One blade basic design characteristics of the three bladed horizontal screw rotor [20].

The horizontal screw rotor could rotate horizontally and change orientation direction (θ1, θ2, θ3…., with $\Delta\theta=100^o$), forming an upstream maximum value of azimuthal angle of 50^o and a downstream maximum azimuthal angle of 50^o with its initial position, as indicated in Figure 9.



Figure 9: Modalities of horizontal orientation direction changes of the horizontal screw rotor.

Two realistic pictures of the first in the world developed horizontal axis 3-bladed screw turbine, in experimental operation, in the laboratory channel of BOKU Vienna University, with upstream and downstream views, are given in the following Figure 10 [20].

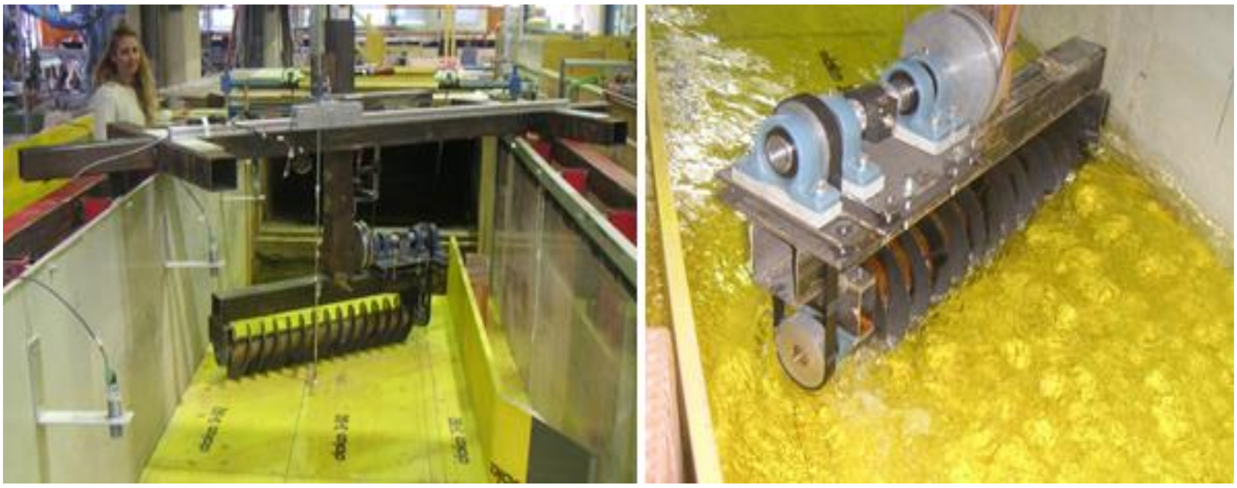


Figure 10: Upstream and downstream views of the horizontal screw rotor in the laboratory channel [20] (*photos: Alkisti Stergiopoulou*).

The hydrodynamic performances estimation of the horizontal screw turbine is based on the idea of the undershot horizontal axis screw waterwheel. Consider the horizontal screw waterwheel, having an effective radius R (m), *a* frontal screw blade wet section A(m^2) and an angular velocity ω(rad/s) rotating in a stream flow of velocity *V* (m/s) (see Figure 11). The available input power P_{in} (W) and the output power produced P_{out}(W) of the horizontal axis Archimedean screw turbine can be determined by the relations P_{in} (W)= (1/2). ρ. V^3.A and P_{out} = T . ω, where ρ=water density (Kg/m^3) and T=torque (N.m). The angular velocity ω is given by ω=2.π.N/60, where N=rotation speed (RPM). The torque T is obtained by the relation T=F_d .R, in function of the drag force exerted on the screw blade F_d =C_d. (1/2).ρ.A.V^2, with C_d the screw blade drag coefficient. The efficiency degree η could be defined by the following relationship $\eta = P_{out} / P_{in}$. A simple schematic representation of the horizontal screw waterwheel rotating in stream flow of velocity V is given in Figure 11.

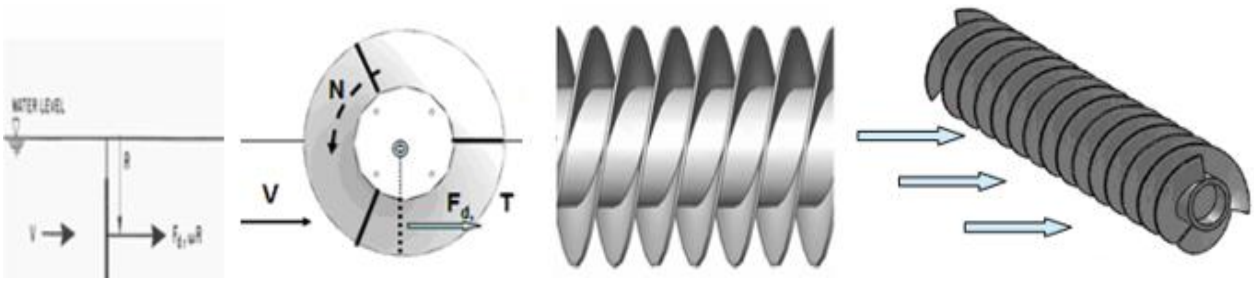


Figure 11: Horizontal screw waterwheel rotating in stream flow of velocity V.

According to the obtained experimental results, the highest value of the experimental efficiency could arrive the level of about 83 %, with an azimuthal angle of 35° at various rotation speeds (e.g. 75 RPM) [20].

4. HARNESSING THE KINETIC POTENTIAL OF THE ESC AND CCP WITH HORIZONTAL ARCHIMEDEAN SCREW TURBINES

According to the two scenarios proposed by Tsimplis [10], concerning the current velocities of the Strait of Euripus, of about 3.4 m/s and 4.4 m/s, the power densities could be $(P/A)_{1,tsimplis}$ = 20.14

KW/m^2 and $(P/A)_{2,tsimplis}$ = 43.66 KW/m^2. Approximate estimations of the theoretical total current power of the strait could be $P_{1,th,tsimplis}$ = 6,45MW and $(P)_{2,th,\ tsimplis}$=13,92MW. By taking into account the Lanchester-Betz limit C_p of about C_p=16/27, the total strait current power could be equal to $P_{1,tsimplis}$ = 3,82MW and $P_{2,tsimplis}$=8,25 MW. For the case of five horizontal axis Archimedean screw turbines to operate in the Euripus Strait, geometrically similar to the first horizontal screw rotor studied in BOKU University, as indicated in Figure 12, with a length 2m and a frontal blade area 2m^2, the maximum installed kinetic power for the set of the five horizontal screw turbines could be $P_{1,5,\ tsimplis}$ =119,37kW and $P_{2,5,\ tsimplis}$ =258,71kW [21].

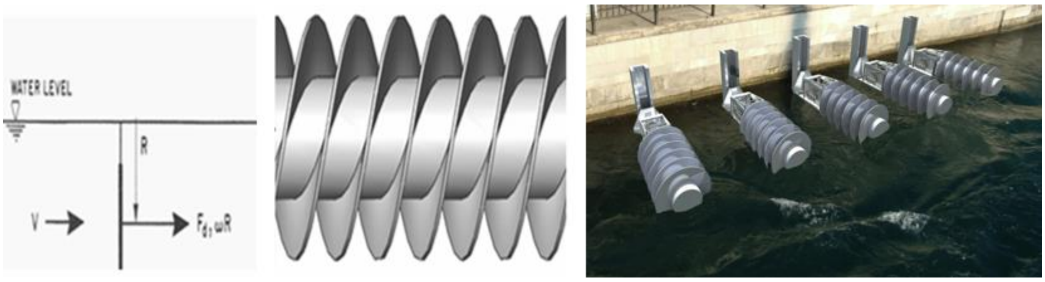


Figure 12: A set of five horizontal axis Archimedean screw turbines to operate in the Euripus Strait (*photo: A. Stergiopoulou*).

For the velocities scenarios of Tsimplis, the approximations made for the installed capacity of a horizontal axis screw turbines park, having 20 similar series of five screw machines, could give $P_{1,park}$=$P_{1,5,20\ tsimplis}$= 2.39 MW and $P_{2,park}$ =$P_{2,5,20\ tsimplis}$ = 5.17 MW. Such future horizontal axis screw turbines parks could be implemented along the coasts or perpendicularly to the main current direction of the Euripus Strait, as indicated in Figure 13.

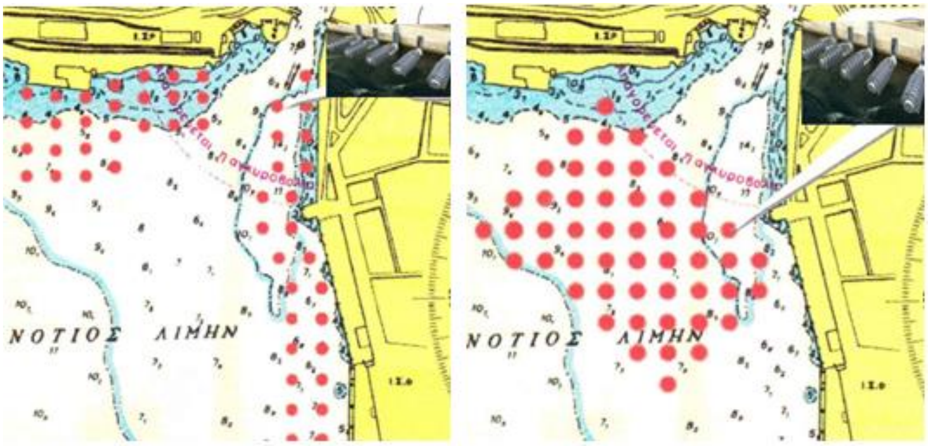


Figure 13: Two future implementation scenario of future horizontal axis screw turbines parks in Euripus.

For the mysterious flow of the Cephalonia's Coastal Paradox (CCP), our mean current velocity measurements, in the input channel of Argostoli, show a mean value of about $V_{1(Argostoli)}$= 0.5 m/s [21]. The measurements of the current velocity in the output channel of Sami show a mean value of about $V_{2(Sami)}$ =1.62 m/s [21]. The input current power density P/A is estimated to be P/A=0.64 kW/m^2. The output current power density P/A is estimated to be P/A=2.18 kW/m^2. For the case of one horizontal axis Archimedean screw turbine to operate in the output channel of Sami, geometrically similar to the first horizontal screw rotor studied in BOKU University, as indicated in the Figure 14, with a length 2m and a frontal blade area 1m^2, the maximum installed kinetic power could be 2kW.

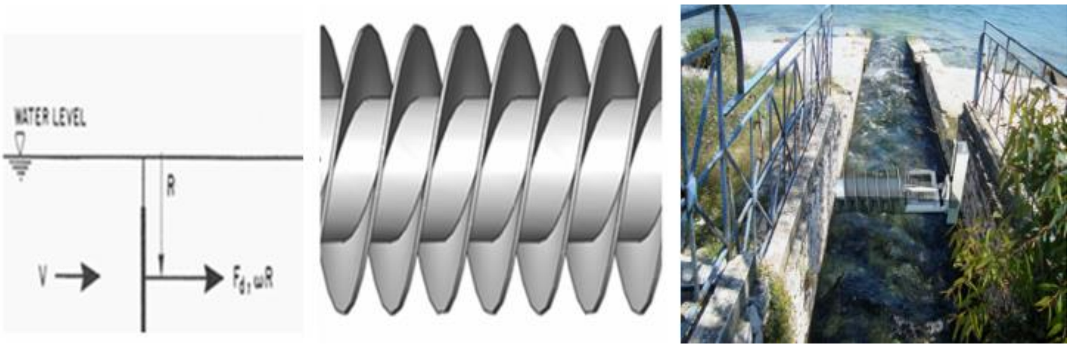


Figure 14: Mechanism of the horizontal axis Archimedean screw turbine to operate in the CCP output channel (photo: A. Stergiopoulou).

A screw hydropower turbines park, with a series of similar 200 horizontal screw turbines, will have an overall installed kinetic power capacity of about 0.4 MW (Figure 15).



Figure 15: Schematic representation of a screw hydropower turbines park in CCP (photo: A. Stergiopoulou).

5. TOWARDS SOME PRELIMINARY CCP AND ESC CONCLUSIONS

Very promising innovative horizontal Archimedean Screw Turbines, based on the first in the world horizontal Archimedean screw turbine built, developed, perfected and studied at BOKU Vienna University, are proposed in the present paper. These horizontal screw turbines could be used in Euripus and in Cephalonia in the future, in the form of Archimedean screw parks, harnessing the kinetic hydropotential of ESC and CCP. Figure 16 gives two artistic views of horizontal axis screw turbines to exploit the blue energy potential of the CCP in the output channel near Sami.



Figure 16: Artistic views of horizontal axis screw turbines in the output channel of the CCP *(photo: A. Stergiopoulou).*

Figure 17 gives a series of artistic views of different horizontal and vertical axis screw turbines in the Strait of Euripus.



Figure 17: Artistic views of horizontal and vertical axis hydrodynamic screws in the ESC. *(photo: A. Stergiopoulou).*

A future aim of the present paper, part of our research project "Research of Sea Hydraulic Mysteries of Euripus and Cephalonia-Inventory of Blue Hydropotential", is to make C.F.D. (Computational Fluid Dynamics) simulations of the very complicated current flows of the CCP and of the ESC, by using the Flow-3D program. To simulate in the present research, the very complex tridimensional flow phenomena of CCP and ESC, in the presence of various rotating horizontal screw turbines, harnessing their important unexploited blue energy potential, a series of modern CFD simulations are required. A first characteristic post-processing view of such a first CFD simulation of the very strange and complicated "through Cephalonia sea river", using the Flow-3D program, is presented in Figure 18.

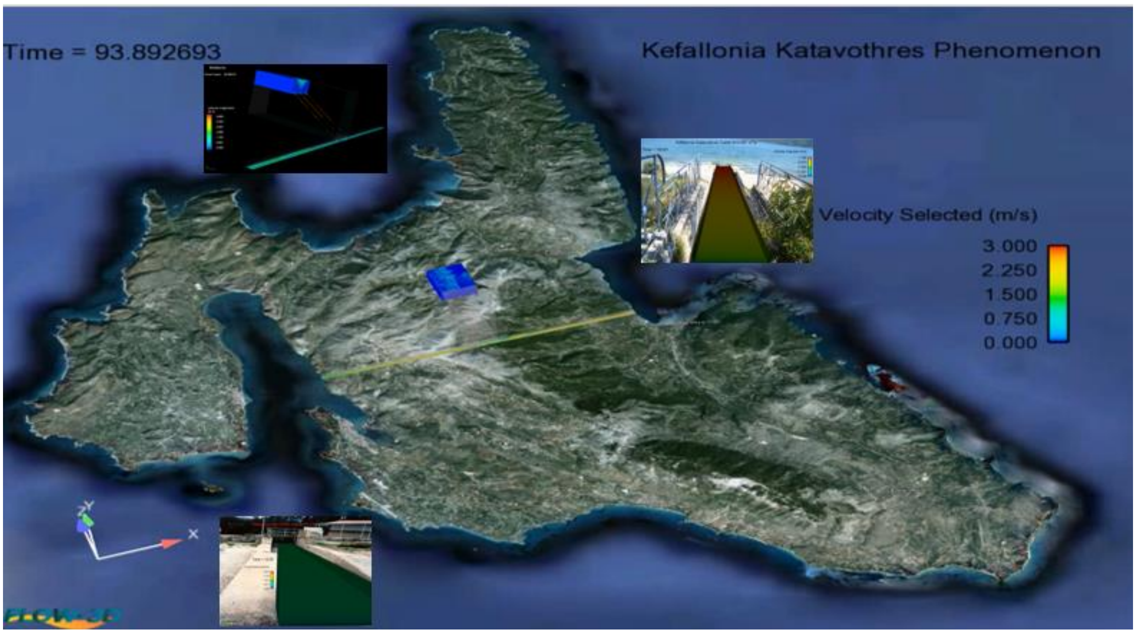


Figure 18: A characteristic C.F.D. post-processing view of the first Flow-3D simulation for the "through Cephalonia sea river".

ACKNOWLEDGMENTS

The research work of the present paper has been financed by the Greek School of Pedagogical and Technological Education through the operational program "Research strengthening in ASPETE"– Project “Aspete’s Coastal Cephalonia’s and Euripus Straits Sea Blue Energy Laboratory” [21].

References

1. Petrochilou A. (1997) ‘About the Sea Mills and the Labyrinth of Cephalonia’ **(personal communication)**

2. Fuller M. L. (1908) ‘Conditions of circulation at the Sea Mills of Cephalonia’, **Bul. Geol, Soc. America**, vol. 18, pp. 221-232.

3. Crosby F.W., Crosby, W.O. (1896) ‘The Sea Mills of Cephalonia’, **Tech. Quart**., vol. 9, pp. 6-23

4. Koder Johannes Negroponte (1973) ‘Untersuchungen zur Topographie und Siedlungsgeschichte der Insel Euboia während der Zeit der Venezianerherrschaft Österreichische Akademie der Wissenschaften Veröffenlichungen der Kommission für die Tabula Imperii Byzantini (Band I), (pp. 77, 80-81, 85) Wien

5. Stergiopoulos V. (2007) ‘About hydraulic paradox of the karst volume of Cephalonia’, **ASPETE Report**, (in Greek).

6. Stergiopoulos V. (1996) ‘Water memory’, **INFORMATION**, Athens.

7. Stergiopoulos V. (1996) ‘The water remembers. You?’, **ASPETE Report**, (in Greek).

8. Stergiopoulos V. (2005) ‘About karst hydrology of Greece”, **ASPETE Report**, (in Greek).

9. Eginitis D. (1929) ‘The problem of the Tide of Euripus’, **Proceedings of the Academy of Athens A**, 49-59 (in Greek).

10. Tsimplis M.N. (1997) ‘Tides and Sea-level Variability at the Strait of Euripus’, **Estuarine, Coastal and Shelf Science**, 44, 91-101

11. Bonacci O. (1987) ‘**Karst hydrology**‘, Springer Verlag, Berlin.

12. Millot C. (2005) ‘Circulation in the Mediterranean Sea: evidences, debates and unanswered questions’, **Scientia Marina**, Consejo Superior de Investigaciones Cientificas.

13. Hamad N., Millot C, Taupier-Letage I. (2006) ‘The surface circulation in the eastern basin of the Mediterranean Sea’, **Scientia Marina**, 70 (3), 457-503.

14. Stergiopoulou, A. and Stergiopoulos, V. (2009) ‘From the old Archimedean Screw Pumps to the new Archimedean Screw Turbines for Hydropower Production in Greece’, Proceedings of **SECOTOX and CEMEPE Conference**, Mykonos.

15. Stergiopoulos V., Stergiopoulos G. and Stergiopoulou A. (2007) ‘The coastal Cephalonia’s paradox: Quo vadis?’, Proceedings of the 1st **International Conference on Environmental Management, Engineering, Planning and Economics - CEMEPE**, Skiathos, 2007.

16. Stergiopoulos V., Stergiopoulou A. (2008) ‘The Coastal Cross-Flow Cephalonia’s Paradox: A Lost Atlantic Attractor’, Proceedings of the **2nd International Conference “The Atlantis Hypothesis: Searching for a Lost Land”**, Athens, 10-11 November 2008.

17. Bauer E.W. (1971) ‘Les secrets du monde souterrain’, **FLAMMARION**, Paris.

18. Drogue C. (1989) ‘Continuous inflow of seawater and outflow of brackish water in the substratum of the karstic island of Cephalonia’, **Journal of Hydrology**, 106.

19. Hydrographical Department of War Navy, (2013) ‘Data for the Tide of Euripus’.

20. Stergiopoulou A. (2017) 'Computational and experimental investigation of the hydrodynamic behavior of screw hydro turbine', **Ph.D. Thesis,** N.T.U.A.
21. Stergiopoulos V., Stergiopoulou A. (2018), 'Research of Sea Hydraulic Mysteries of Euripus and Cephalonia Inventory of Blue Hydropotential', **ACCESS-BEL ASPETE Research Project**.

A PANHELLENIC SURVEY (2017-2018) REGARDING ENERGY NEEDS COMFORT CONDITIONS AND ATTITUDES TOWARDS RENEWABLE ENERGY SOURCES

P. Kosmopoulos[1]*. A. Kantzioura[1], I. Kosmopoulos[1], K. Kleskas[1], A. M. Kosmopoulos[1]

[1]K-eco Projects co, f. Director of the Laboratory of Environmental and Energy Design of Buildings and Settlements, DUTH

*Corresponding author: E-mail: pkosmos@env.duth.gr

Abstract

There is no official estimation regarding the Energy Poverty in Hellas during the recent years. Several studies have been carried out independently, regarding specific areas or social groups, but none has covered the whole of the population.

The main aims of this research study, presented here are how peoples' attitudes and views towards the Energy subjects and the use of Renewable Energy Sources (RES) are affected by the Economic Crisis, and a rather dystopian general future. How serious and important are the environmental issues considered to be when people feel that their everyday life is threatened? This subject is approached through this Panhellenic survey analyzing the data gathered by questionnaires.

A large number of areas and cities have been covered, offering a satisfactory image of the subject.

Conclusions of this research project regard:

a) the comfort conditions in the houses of the participants, and how these conditions have been changed lately. Due to the economic crisis.
b) The attitudes of the people towards Renewable Energy Sources (photovoltaics, wind turbines, etc), the energy saving policy and related devices and how these attitudes have been affected by the economic crisis, the tariff policy and the bureaucracy.
c) The attitudes of the participants towards energy and environmental subjects in our country, and how these attitudes have been affected by the current situations.
The conclusions of the research project are hopefully very important describing the people’s attitudes towards energy needs, fuel consumption and R.E.S. matters during this critical period of the country.

Keywords: Energy needs; social survey; Energy poverty, RES; Economic crisis.

1. INTRODUCTION

The Panhellenic social research presented here, examines the energy consumption, the energy needs, the comfort conditions of the people of today’s Hellas and also their attitudes towards R.E.S.
After an extremely heavy winter (below 0^oC for twenty days, very rare for Greece) and within a framework of an international economic crisis, Hellas has been the first of the European countries that has been badly affected and recently Energy Poverty is a well known fact. But at the same time, according to the E.U. Directives, Hellas has to conform with the regulations regarding the application and the use of Renewable Energy Sources.

It is also interesting to see how environmental matters are faced in general, regarding energy sources, fuels and related costs during this transitory period.

The sensitivity of Hellenic people towards environmental matters is a diachronically acknowledged: the traditional architecture, the antiquities, the natural environment and the related protective legislation, have established a concrete culture, which more or less, nowadays has to be denied. It is obvious that a new environmental aesthetics culture has to be shaped.
But parallel to the above, Hellenic people have to face their household economics, their traditional attitudes towards their environment (both built and natural) and their dependence from imported fuels (oil and gas). Among other research projects, every two years, we conduct a social research regarding the attitudes of Hellenic people towards R.E.S. (see Kosmopoulos 2002; 2004; 2006; 2008; 2011; 2013; 2015; 2017).
This study, adds to the existing literature the recent opinions and attitudes of the participants towards poor comfort conditions, economic crisis, RES and environment aspects.

2. THE RESEARCH PROJECT

The survey has been planned and carried out by members of the K-ecoprojects co. and a large number of students, postgraduates, and PhDs that have attended our lectures.
The questionnaires gathered, have been processed by the staff and the collaborators of K-eco projects. The task has been to extract easily understandable data, in order to help the authorities that might be interested to use the results of our survey. The questionnaire is based upon the Guttman scale (Canter, 1988) but it has been adapted to the well approved and generally accepted 5 point Likert scale, in order to be comparable to all previous relative study (see Kosmopoulos 2002; 2004; 2006; 2008; 2011; 2013; 2015; 2017).

3. THE SURVEY

The research project, regarding the social attitudes towards the environmental subjects during this critical period, has lasted from 1/2017 to 2/2018 (ongoing), all over Hellas (and Cyprus) through the collection of questionnaires, and has covered the following respective number of valid questionnaires:

City	Quest.	City	Quest.
AGRINIO	19	KOZANI	31
ATHINA	219	KOMOTINI	47
ALEXANDROUPOLI	21	KORINTHIA	21
AMYNTAIO	14	KOS	7
VEROIA	21	LARISA	39
VOLOS	43	LEFKADA	7
GIANITSA	14	MYTILINI	17
GREVENA	21	NAFPLIO	13
DIDYMOTEICHO	11	XANTHI	46
DRAMA	23	ORESTIADA	13
EDESSA	21	PATRA	47
IGOUMENITSA	19	PEIRAIAS	33
IRAKLEIO	33	RETHYMNO	17
THESSALONIKI	189	RODOS	13
THIVA	19	SERRES	39
IOANNINA	27	SPARTI	13
KAVALA	29	TRIKALA	11
KALAMATA	19	TRIPOLI	7
KARDITSA	21	TYRNAVOS	8
KASTORIA	29	FLORINA	33
KATERINI	15	CHALKIDA	11
KERKYRA	19	CHANIA	21
KILKIS	12	CYPRUS	47

Map



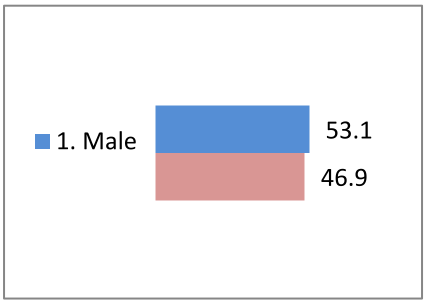
Map source: web.gys.gr and the authors

TOTAL: 1399

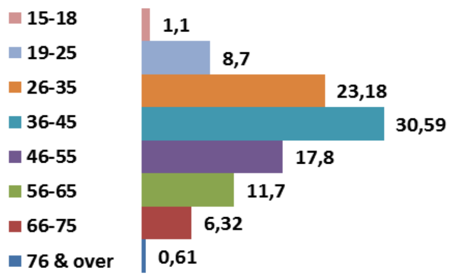
The cities where printed questionnaires have been collected are a) the same with all our previous similar surveys (in order to make analytic comparisons later), and b) they are the home towns of our non-employed collaborators for this -and the previous- surveys. They have been chosen as to cover the different (climatic and economic) areas of Greece.

4. THE SOCIAL SURVEY RESULTS:

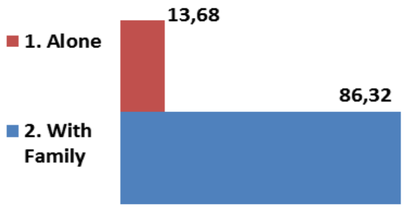
2. Sex



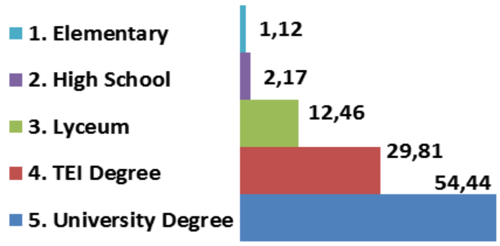
3. Age Groups



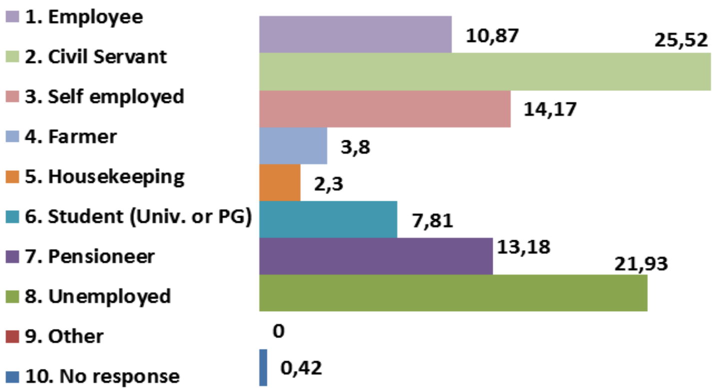
4. I live…



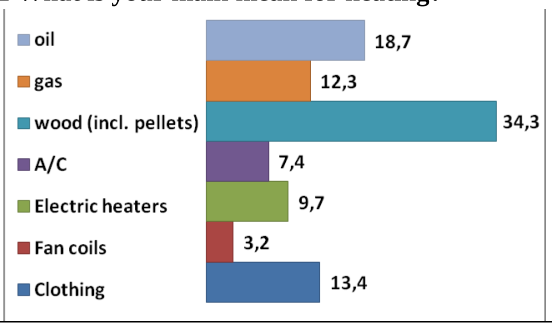
5. Educational level



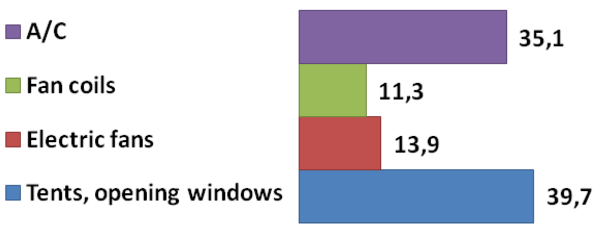
6. Occupation



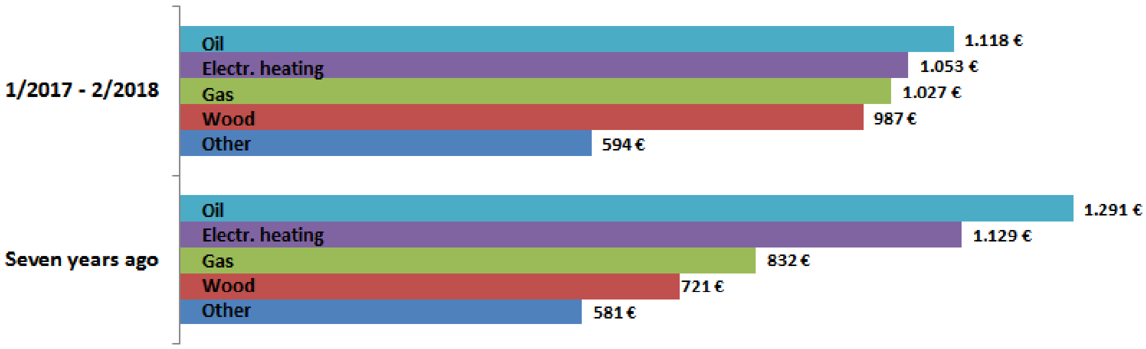
7.1 What is your main mean for heating?



7.2 What is your main mean for cooling?

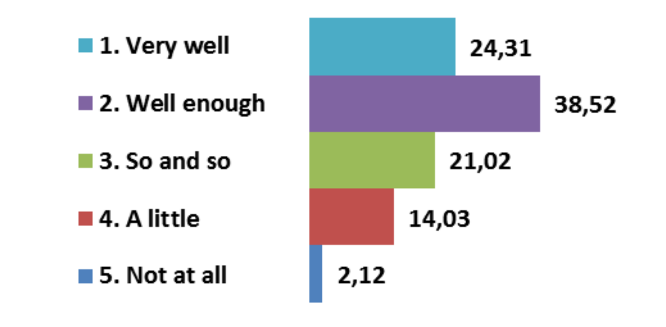


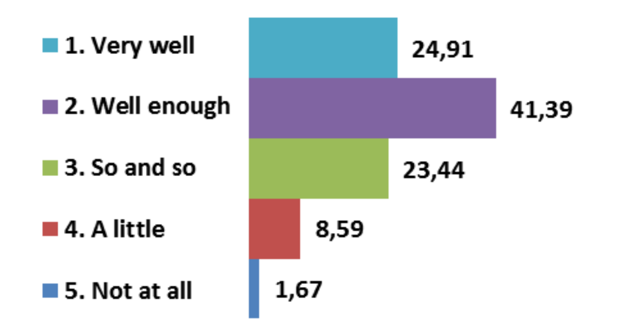
7.3 How much money did you spent annually on various forms of energy, e.g seven years ago and how much this year? (Averages)



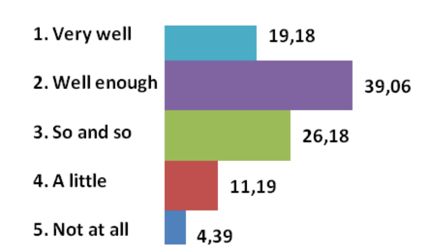
8. Do You know what Renewable Energy Sources are?

9. How well do you know about the following:
9.1 Photovoltaics in buildings:

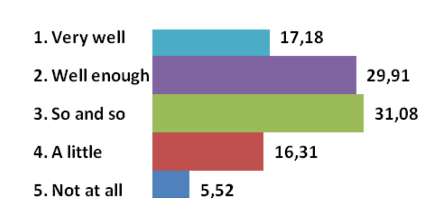




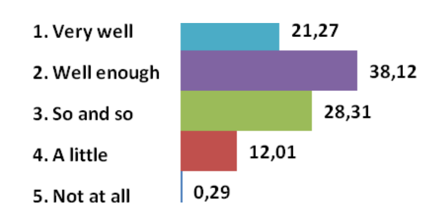
9.2 Photovoltaics in land properties:



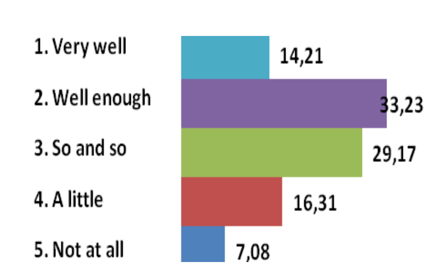
9.3 Photovoltaic Parks:



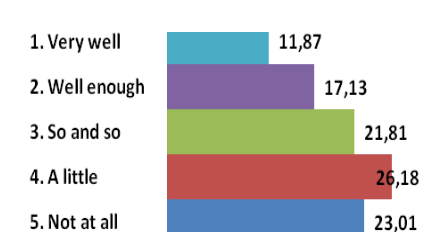
9.4 Wind Generators:



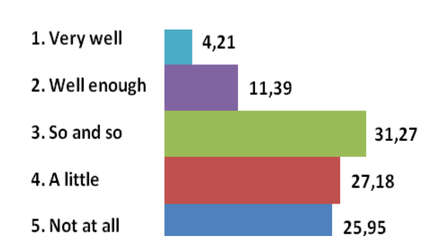
9.5 Wind Generators Parks:



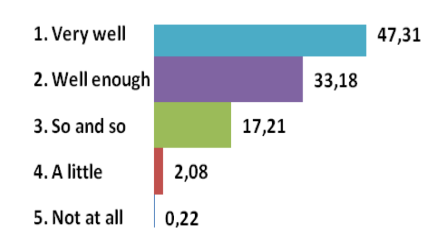
9.6 Geothermy for buildings:



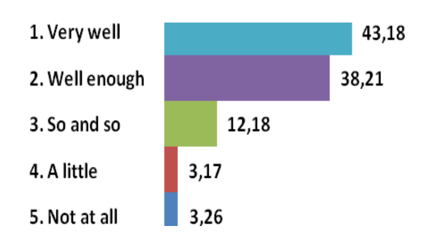
9.7 Geothermy for settlements:



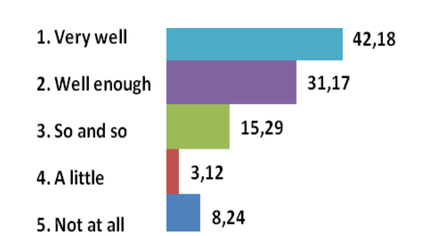
9.8 Biomass (wood blocks and pellets):



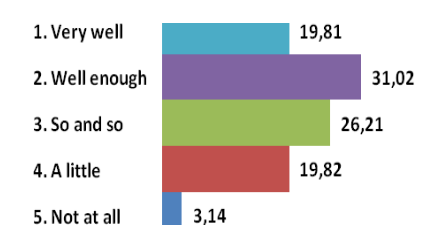
9.9 Double Glazing



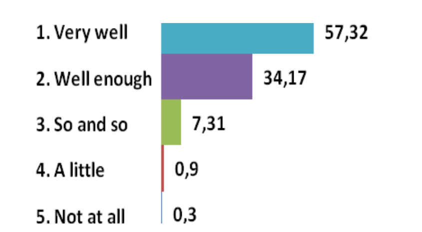
9.10 Insulation in walls



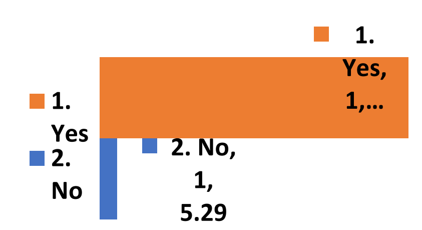
9.11 Glass House:



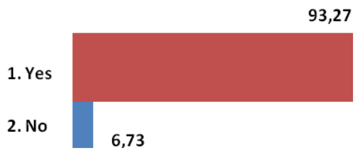
9.12 Fan:



10. Do you know that all of the above can help the family income?



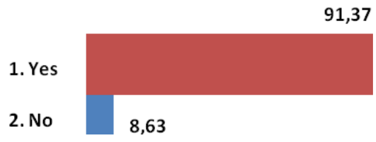
11. Do you know that all of the above can help our national economy to become independent from imported oil and natural gas?



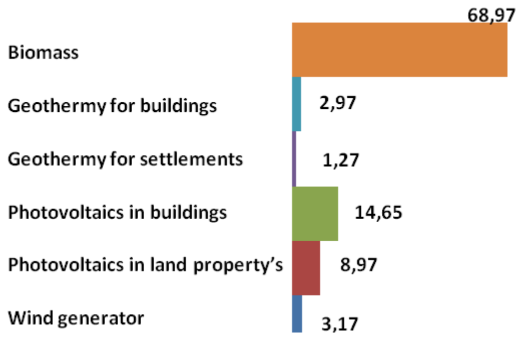
12. Do you know that all of the above can help to reduce environment pollution?



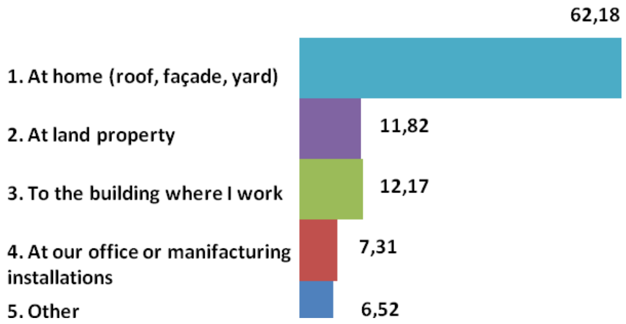
13. Do you already use any of the above?



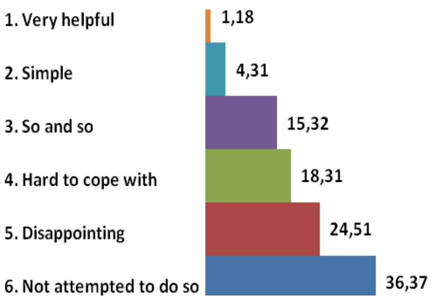
13.1 If yes, which one:



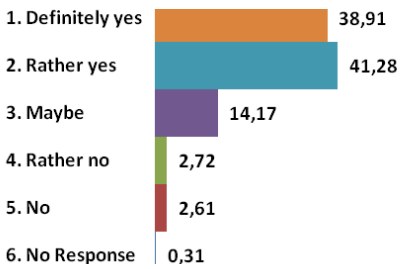
13.2 If no, would you like to install for example P.V.S.?:



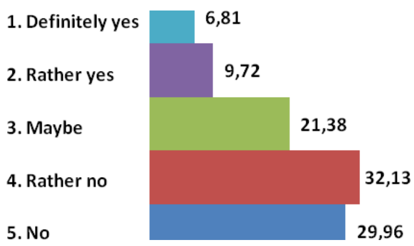
14. If you have already attempted to do so, what is your comment on the necessary beaurocracy?



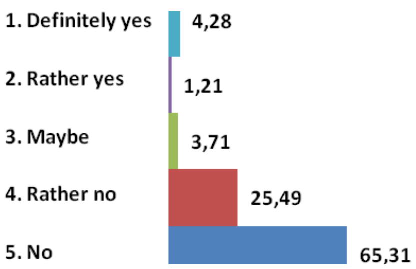
15. If you are reassured from the authorities that you will have definite economic gain, and a simple beaurocratic procedure, would you proceed to install any of the above?



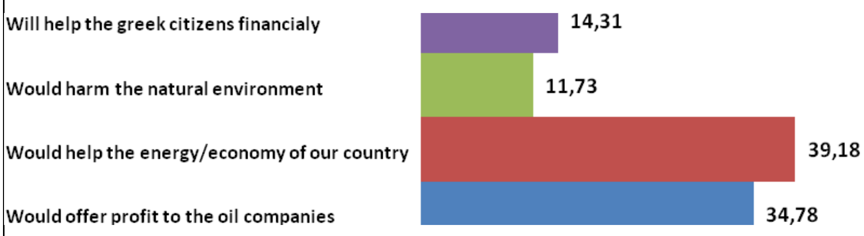
16. Do you think that the installation of P.V.S and W.G.S insult/destroy the aesthetics/natural beauty of buildings and/or the natural environment?



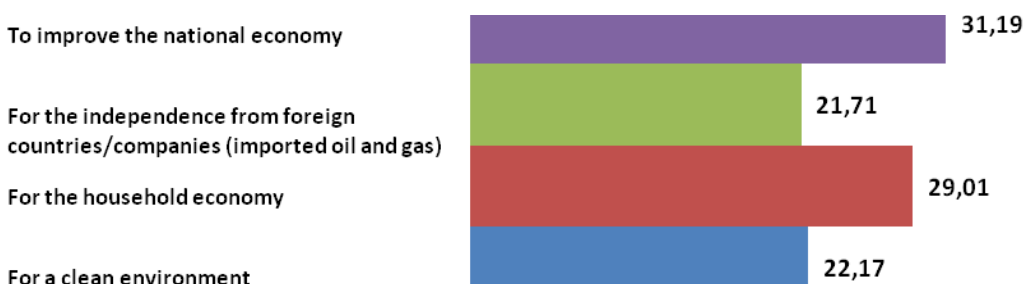
17. Would you accept a nuclear plant in our country?



18. We have learned that there are fossil fuels in our country. Do you think that their exploitation:



19. Finally, would you wish to see a wide use of R.E.S. for the following reasons:



5. DISCUSSION AND CONCLUSIONS

1. Beginning with R.E.S. an important point that has been underlined, is that since August 2012 a new law has decreased the income from the installation of PVs and it seems that this policy will continue. This legislation has a negative effect to the interest towards new installations of PVs. New hopes seem to arise with the Law regarding "Energy Communities" (1/2018).

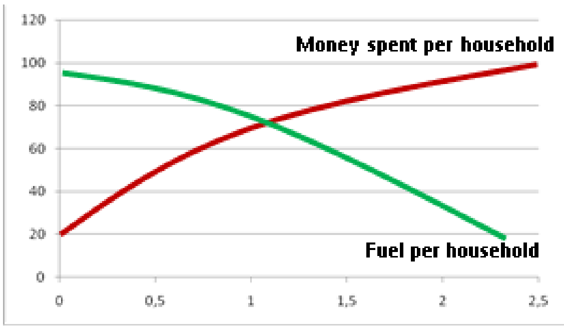
2. Regarding bureaucracy, which seems to be a major problem in Greece, people seem to be disappointed, but in case the state should establish simple and clear rules and also some guaranteed economic gain for the citizens, R.E.S. applications should definitely increase.

3. Another interesting subject, is the change of the attitudes towards the aesthetics of the environment concerning the installation of R.E.S. all over the country. During two previous surveys (e.g. 2007, 2009) people seemed to be firmly against large scale installations, arguing about the natural environment preservation. Nowadays, most people seem to be more interested in installing R.E.S. even in their property, since 55.01% declare not to be disturbed by the PVs and/or W.Gs.

4. Recently, it has been known that in Greece there are large amounts of fossil fuels, oil and gas. Of course people are not precisely informed, but anyway they consider that in case these fuels are exploited, firstly it would help the economy and the energy problem of this country, but also that it would offer profits to the (foreign) oil companies.

5. Regarding the Energy poverty in our country, the average expenses per household, as well as the average consumption of the several fuels, do not fully represent reality: the averages are produced from 0 to X. Thus, as understood, there are families with not at all heating during the winter period. This fact cannot be presented with simple statistics…

6. Recent researches show that especially in large cities (e.g. Athens, Thessaloniki) where apartments have to share the heating expenses, due to the inability of some households to pay the bills, the whole building is without central heating. And moreover, another research (Institute of GSEE 2/2018) shows that 43% of the households in Athens metropolitan area are completely without heating!



The money spent for heating has increased. The quantity of fuel consumed, has decreased. It is completely understood that the decrease of full consumption by the households is in immediate relationship with the decrease of the income of the people (or the lack of it) and of course the increase of the prices of oil and gas…

7. The comfort conditions in the houses, has been differentiated. During the last years, most people say that in their houses, they have to use heavier clothing than in past, because of the lack of heating.

Discussions with older persons lead to the following conclusions:

a. During the 1950's and the 60's people were satisfied with 10^o ~ 12^oC in the mainly used rooms only by burning charcoal and/or wood.

b. During the 1970's, oil has become popular in the houses and multi-storey apartments. It was easy to use and relatively cheap. Therefore, comfort conditions have been altered. For at least three decades, people lived comfortably in their houses with 20^o ~ 25^oC degrees.

c. But during the last decade since 2009, when firstly Hellas has officially been bankrupted, the households' income has decreased dramatically, and prices in general continue to increase. Among the first matters to be affected have been the comfort conditions of the people. Due to the difficulty to pay the costs of heating, many apartments and houses decrease or completely cut the oil burning, and use auxiliary devices for short periods of time. Heavy clothing seems to be again the solution in general… A mean of 17^o ~ 19^oC degrees seems to be very satisfactory in most of the households.

We also have to point out the differentiation between households that have independent means for heating (gas, oil, air-condition, wood burning etc.) and the apartments that have a single and common for all heating system, something very common in the Greek cities; in this case all of the households have to pay their bills, in order for the system to be used for the whole of the apartment building. However, each household has to face independently its own needs, and to invent the most economic combinations for means of heating.

d. Regarding gas, during the last 15 years in several large cities, gas has been distributed and been installed in many households. But since the mean income has decreased and the prices have increased, even gas, seems to be an expensive mean for heating.

e. Prices of electricity tend to put A/C inverters and electric heaters out of question or as a final solution for a short period of time…

f. Now, regarding wood burning. There are the following categories:

Legally bought wood and pellets
Illegally cut wood from the forests
Parts of useless wood furniture (they contain toxic chemicals)

i. We also have to mention newspapers, cardboxes, and paper products with toxic chemicals.

It is a fact that the above heat producing items, are a lot cheaper than oil and gas, not to mention non-organic garbage (even if it is recyclable or toxic) which is completely free.

6. CONCLUDING REMARKS

1. People are interested indeed for the protection of the environment, for the national economy, for the release from imported fuels, and finally for the personal/family economic profit from the application of R.E.S., but they are also disappointed from the new economic policy applied to R.E.S. and the necessary bureaucracy.

2. Now, regarding R.E.S. some 12-15 years ago, after aspiring promises by the state, many people had chosen to install P.V.'s at their houses, buildings or land properties, but their reward has been disappointing. Despite the enthusiasm and the investment, prices per Kwh have dropped down dramatically, and new investors are hard to show up. New hopes seem to rise with the legislation

regarding "Energy Communities", after the well-established and successful example of several E.C. countries. It is a pity that our country is not yet fully exploiting the potential of the sun and the wind.

3. It is completely understood that the decrease of fuel consumption by the households is in immediate relationship with the decrease of the income of the people (or the lack of it) and of course the increase of the prices of oil and gas.

4. Energy poverty in today's Hellas is a fact. Urgent measures have to be applied by the state in order to satisfy the energy needs of the mean households.

5. Finally, I feel ashamed of the fact that when Jeremy Rifkin (The hydrogen economy) visited Greece, said "I wonder how a country with such both sun and wind remains dependant on hydrocarbons". And also recently, Jeffrey Sachs (UN Sustainable Development Network) has stated the same in an interview.

ACKNOWLEDGMENTS

Many thanks are due to the members of K-ecoprojects co. and to all of the students, postgraduates and PhDs who have helped to gather the questionnaires. But most of all to the Greek people that have willingly participated to this research.

References

1. CRES, 2/2018, Observatory for Energy efficiency/poverty, http://www.cres.gr/energy-efficiency/poverty.html
2. Daskalaki, E., Balaras C.A., Droutsa, P., Kontoyannidis, S., Graglia, A. 2007. Datacollection from Energy audits for Hellenic Buildings. In IEE Project. **Data Mine. IEE Project**.
3. E.E. 2008, Commission of the European Communities, Brussels. In Proposal for a directive of the European Parliament on the promotion of the use of energy from Renewable Sources.
4. European Parliament, ITRE Committee, 8/2015, How to end Energy Poverty? (Report)
5. Institute of G.S.E.E., 2018, Report on the economics of Greece
6. Kosmopoulos, P. et al 2011, A Social Survey on how the economic crisis affects peoples' attitudes towards the environmental subjects. **MESAEP.** Ioannina.
7. Kosmopoulos P. et al 2008, Research regarding the R.E.S. applications and attitudes towards the environment, **3rd PERSYMAK** (in Greek)
8. Kosmopoulos, P. et al 2008, Buildings, Energy and the Environment. Thessaloniki: University Studio Press.
9. Kosmopoulos, P. et al 2004, Environmental Psychology. Thessaloniki: University Studio Press.
10. Kosmopoulos, P. et al. 2005, ZED-KIM, a pilot house using renewable energy sources, I.C. MESAEP.
11. Kosmopoulos, P. et al 2005, Social Attitudes about Environmental Design. **I.C.PALENC**. Santorini.
12. Kosmopoulos, P. et al 2006, The use of Renewable Energy Sources in houses. **I.C. PLEA**. Geneva.
13. Kosmopoulos, P., Ioannou, T. 2005, Social Attitudes about Environmental Design and R.E.S..
14. Mihalakakou, G., Santamouris, M., Tsangrassoulis, A. 2002. On the Energy consumption in Residential Buildings. **Energy and Buildings** 34(7, 08):727-36.
15. Panas E., 2012, Research on the Energy Poverty in Greece, T.C.G.

16. The Greek Ombudsman, 2016, The economic crisis should not change to a rejection of the state of justice (Annual report)

17. Tsoutsos, Th. et al. 2009, Photovoltaics in buildings I and II, PURE, I.E., E.C.

18. Papadopoulos, A.. 2002, Strategies for a more efficient integration of Renewable Energy Systems in Urban Buildings**. 33rd Congress on Heating, Refregeration and Air Conditioning**. Belgrade.

19. Renewable Energy Sources and Energy Saving, 2008, www.cres.gr/kape/main.htm. Ed. CRES. Transl. C.R.E.S..

20. Santamouris, M., Asimakopoulos, D., 2013, Energy Saving in Urban Environment Buildings. **Solar Energy and Energy Saving.**

A TWO STEP PROCESS FOR THE ELECTROCHEMICAL CONVERSION OF CO_2 TO METHANOL

A. Schizodimou, I. Kotoulas and G. Kyriacou*

Laboratory of Inorganic Chemistry, Dept. of Chemical Engineering, A.U.Th, GR- 54124 Thessaloniki, Macedonia, Greece

*Corresponding author: e-mail: kyriakou@eng.auth.gr, tel : +302310996238

Abstract

The direct electrochemical conversion of CO_2 to methanol, which is the product of choice, is quite difficult. On the contrary, formic acid is easily formed from CO_2 on various metal electrodes by both high rate and %Current Efficiency (%CE) reaching 90%. This work proposes a two-step process for the electrochemical conversion of formic acid to methanol which includes the conversion of CO_2 to formic acid in the first and the reduction of formic acid to CH_3OH in the second. The work contains experimental results on the reduction of formic acid on chromium and chromium alloys. The main products obtained from the electrochemical reduction of HCOOH on Cr in 85% H_3PO_4, at 80 °C were $HCOOCH_3$ (2.1%), CH_3OH (17.5%) and CH_4 (4.9%). The rate of the reduction increased with the negative potential. The total %CE in some experiments exceeded 100% and this was attributed to the cathodic dissolution of chromium which provided an additional reduction capacity. The reduction on electrodeposited chromium on Pb gave CH_4 (25.7%) and less amounts of CH_3OH and $HCOOCH_3$. On stainless steel cathodes the main products were CH_3OH (%7.2) and $HCOOCH_3$ (23.1%) and smaller amounts of CH_4.

Keywords: Formic acid; electrochemical reduction; chromium

1. INTRODUCTION

Many efforts have been made during the last years aiming to the reduction of the CO_2 emissions through the replacement of fossil fuels by renewable and/or alternative energy sources, like photovoltaics and wind turbines. Given that the energy produced from renewable sources is not constant during time, a stage of electrical energy storage is required. Olah et al. [1], showed that the most efficient way for the storage of the excess of the energy produced by renewable energy sources, is its use for the electrochemical conversion of CO_2 to methanol. Consequently, methanol could be used as a fuel, after minor modifications of the existing internal combustion engines or in fuel cells. Also, methanol could be used as a raw material for the production of other organic compounds of higher added value [2-4]. Therefore, the conversion of CO_2 to methanol is a challenging topic [5, 6]. As it has been proved by literature sources, the direct conversion of CO_2 to methanol is very difficult, because it takes place at extremely low rate for industrial applications. Conversely, CO_2 can be easily converted to formic acid by a %CE near 100% [7]. A different scheme for converting CO_2 to methanol can be a two step process as follows:

In the first stage, CO_2 will be converted electrochemically to HCOOH:

$$CO_2 + 2H^+ + 2e^- \rightarrow HCOOH + H_2O \qquad (1)$$

and in the second stage the produced HCOOH will be converted to CH_3OH

$$HCOOH + 4e^- \rightarrow CH_3OH + H_2O \qquad (2)$$

The conversion of formic acid to methanol according to the reaction (2) is also extremely difficult and, for this reason, this CO_2 reduction scheme was poorly studied in the literature. Prior research from our laboratory showed for the first time that chromium is the most efficient cathode for the reduction of HCOOH. The main products at 85% v/v H_3PO_4 at 80 °C were methyl formate, methanol and small amounts of hydrocarbons with 1-4 carbon atoms. The study was conducted in a narrow range of cathodic potentials from -0.6 V to -0.95 V, where the main products were methyl formate and methanol. The %CEs of methanol and methyl formate displayed a maximum of 37.4% and 166% 37.6% respectively at -0.65 V. The fact that% CE was greater than 100% was attributed to the cathodic dissolution of chromium which gave an additional reduction capacity [8]. The challenge is to find conditions under which Cr dissolution does not take place in order to make a commercially applicable method.

The aim of this present work was to investigate the possibility of avoiding the corrosion of chromium that takes place during the conversion of HCOOH to methanol.

2. MATERIALS AND METHODS

A Teflon cell having a total volume of 24 mL divided in two equal volume compartments by a Nafion 117 (H^+ form) cation exchange membrane was used in all electrolytic experiments. The anode and the cathode were Pt and Cr foils, respectively; having the same geometrical area (7 cm^2).The cell was placed in a thermostated water bath until the required tempera- ture was achieved. The potential was controlled by a Wenking POS 73(Bank Elektronik) potentiostat and the reference was the saturated calomel electrode (SCE). A stream of He having a flow rate of 10 mL min^{-1} was used to withdraw the gaseous products and a part of the produced organic liquids from the cell during the electrolysis. The escaped liquids from the cell by the gaseous stream were collected in three tubes containing cold water. No significant volume loss of the catholyte was observed at the end of electrolysis since the liquid sample was only 1 mL. A gas chromatograph (GC) supplied by a Plot Q 30 m, 0.530 mm and a Molecular Sieve 5A, 30 m, 0.530 mm connected in series by a three way valve and a TCD detector was used for the determination of H_2, CO and CO_2. A second gas chromatograph supplied by a Pora Plot Q 25 m, 0.53 mm column and FID detector was used for the analysis of the low molecular weight organics and hydrocarbons. The detection limit for methane, methyl formate and methanol was 1 ppm and the reproducibility of the experimental results was established to be within 5%.

3. RESULTS AND DISCUSSION

3.1 Reduction of HCOOH on Cr

In this study the reduction was carried out in more negative potentials, where the dissolved chromium which is in the solution mainly in the form Cr(II) could be redeposited on the electrode surface in order to avoid the mass loss of the electrode. The electrodeposition of Cr corresponds to a normal potential of -0.74 V but the deposition in practical applications usually requires a potential more negative than -1.5 V vs. NHE. At so high potential the IR Drop is very high so the measurement of the potential is not reliable. For this reason, our experiments were carried out under galvanostatic conditions.

Table 1 shows the reduction results on an electrolyte consisting of 50/50 v/v of 85% H_3PO_4 and 98% HCOOH.

Table 1: Influence of the current density on the reduction of HCOOH in solutions that made by mixing 85% H_3PO_4 with HCOOH in 50:50 volume proportion at 80 °C. Electrolysis time 90 min

j / mA cm^{-2}	%CE				
	CH_3OH	$HCOOCH_3$	CH_4	H_2	Total
100	2.1	17.5	4.9	174	198.5
150	1.9	16.3	4.5	167	189.7
200	1.6	14.8	5.6	153	175.0
300	0.9	9.2	6.2	111	127.3

The main products of the reduction were CH_3OH, $HCOOCH_3$ and CH_4. The %CEs were significantly lower than that on metallic chromium [8] but the reduction rate was about 1.8 times higher. The % CEs of products, including hydrogen, were higher than 100% in all experiments, and this was attributed to the cathodic corrosion of chromium. In all experiments severe cathode (Cr) corrosion was observed. The corrosion was visible to the naked eye, since the cathodic solution became colored during the time. We conclude that the rate of dissolution of chromium was higher than the rate of deposition of dissolved chromium. Therefore, the electrode corrosion could not be avoided by this way.

3.2 Reduction on electrodeposited chromium on Pb

A further attempt to avoid the problem of the cathodic corrosion of (Cr), was made by reducing HCOOH on electrodeposited Cr on a Pb cathode. In this way we aimed to find conditions under which the amounts of the electrodeposited Cr on the Pb and that of dissolved Cr via cathodic corrosion are equal. The electrodeposition solution contained [9]:

- 50% v/v H_3PO_4 και 50% v/v HCOOH
- $CrCl_3$•$6H_2O$ 100 g/L
- NH_4Cl 80 g/L
- Sodium citrate 95 g/L
- H_3BO_3 40 g/L

The deposition current density was 300 mA/cm^2 and the temperature was 60 °C. The products of the reduction were CH_3OH (0.1%), $HCOOCH_3$ (3.8%) and CH_4 (25.7%). Additional experiments were not carried out in this direction because the main product was CH_4 and not CH_3OH which is the product of choice.

3.3 Reduction of HCOOH on stainless steels

As it was mentioned above, the chromium was dissolved under cathodic conditions resulting in a mass loss of the electrode that makes the method economically inefficient. An additional attempt was made for the reduction of HCOOH on chromium alloys in order to prevent its cathodic corrosion.
The reduction was performed on stainless steel (series 300 according to the American AISI-SAE standards) alloys because they are widely known for their corrosion resistance. The chemical composition of the alloys is shown in Table 2.

Table 2: The chemical composition of austenitic stainless steels

EN	ASTM Standards	C (%)	N (%)	Cr (%)	Ni (%)	Mo (%)	others
1,4301	304	0.04	0.06	18.3	8.7	-	-
1,4541	321	0.04	0.01	17.3	9.2	-	Ti
1,4404	316L	0.02	0.06	17.3	11.0	2.2	-
1.4833	309S	0.06	0.08	22.5	12.5	-	-
1,4845	310S	0.05	0.06	25.0	20.0	-	-

Tables 3 show the products obtained from the reduction of HCOOH on various stainless steels in solutions made by mixing 85% H_3PO_4 with HCOOH in 50:50 volume proportion at 80 °C and potentials of -0.65 V and -0.8 V.

Table 3: %CEs of the reduction products at -0.65V and -0.8 V in solutions made by mixing 85% H_3PO_4 with HCOOH in 50:50 volume proportion at 80 °C. Electrolysis time 90 min

Cathode (ASTM Standards)	**%CE**			
	CH_3OH	**$HCOOCH_3$**	**CH_4**	**H_2**
	-0.65 V			
304	5.5	15.4	0.09	106.8
321	4.6	14.8	0.06	103.5
316L	4.3	14.2	0.08	115.3
309S	6.6	19.3	0.11	120.9
310S	7.2	23.1	0.12	123.2
	-0.80 V			
304	2.5	9.6	0.8	88.2
321	1.9	10.7	0.9	89.5
316L	1.5	8.2	0.5	91.7
309S	2.9	12.2	0.9	102.8
310S	3.5	13.1	1.1	103.5

The % CEs of the products increased with the increase in chromium content of steel since the alloy 310S which contains 25% Cr was the most efficient. The maximum %CEs of CH_3OH, $HCOOCH_3$ were 7.2% and 23.1%, respectively at -0.65 V. The obtained CEs and the reduction rate (8.2 mA/cm^2) were much lower than those reported for the reduction of HCOOH on Cr [8] but the cathodic corrosion of the electrode which is the main problem was significantly lower. It should be mentioned that the reduction potential (-0.65 V) is only 200 mV higher than expected by the thermodynamics. These experiments have shown that chromium alloys can be effective electrocatalysts for the reduction of HCOOH. More efforts should be made in this direction because higher chromium content alloys would give higher %CEs.

4. CONCLUSIONS

The electrochemical reduction of HCOOH on a chromium cathode and 50/50 v/v of 85% H_3PO_4 and 98% HCOOH solution, gave CH_3OH (2.12%), $HCOOCH_3$ (17.5%) and CH_4 (4.9%) as main products. The total %CE in some experiments exceeded 100% and this was attributed to the cathodic dissolution of chromium which provided an additional reduction capacity. The reduction on electrodeposited chromium on Pb, yielded CH_4 (25.7%) and smaller amounts of $HCOOCH_3$ (3.8%) and CH_3OH (0.1%). On stainless steels alloys the main products were CH_3OH and $HCOOCH_3$ with maximum %CEs of 7.2 and 23.1% respectively and less amount of CH_4 (1.1%). The experimental results showed that chromium alloys are promising electrodes for the reduction of HCOOH.

REFERENCES

1. Olah G.A., A. Goeppert and G.K.S. Prakash (2006) **‘Beyond oil and gas: the methanol economy’**, Wiley-VCH Weinheim.
2. Olah G.A., A. Goeppert and G.K.S. Prakash (2009) ‘Chemical Recycling of Carbon Dioxide to Methanol and Dimethyl Ether: From Greenhouse Gas to Renewable, Environmentally Carbon Neutral Fuels and Synthetic Hydrocarbons’, **J. Org. Chem.**, 74, pp. 487-498.
3. G.A. Olah, G.K.S. Prakash, A. Goeppert (2011) ‘Anthropogenic Chemical Carbon Cycle for a Sustainable Future’, **J. Am. Chem. Soc**., 133, pp. 12881-12898.

4. Goeppert A., M. Czaun, J.P. Jones, G.K.S. Prakash and G.A Olah (2014) ‘Recycling of carbon dioxide to methanol and derived products – closing the loop’, **Chem. Soc. Rev.**, 43, pp. 7995-8048.

5. Aresta M. (2010) **‘Carbon Dioxide as Chemical Feedstock’**, Wiley-VCH Verlag GmbH & Co.

6. Faias S., J. Sousa and R. Castro (2009) **‘Embedded Energy Storage Systems in the Power Grid for Renewable Energy Sources Integration’**, in: T. Hammons, Renewable Energy, InTech.

7. Qiao J., Y. Liu and J. Zhang (2016**) ‘Electrochemical Reduction of Carbon Dioxide: Fundamentals and Technologies’**, CRC Press.

8. Kotoulas I. and G. Kyriacou (2017) ‘Conversion of carbon dioxide to methanol through the reduction of formic acid on chromium’, **J. Chem. Technol. Biotechnol**, 92, pp. 1794–1800.

9. P. Benaben (2011) ‘An overview of hard chromium plating using trivalent chromium solutions. Plating and Surface Finishing’, American Electroplaters' Society Inc.

EFFECT OF SUCCESSIVE SMALL HYDROPOWER PLANTS ON WATER QUALITY

G. Kacienė

Department. of Environmental Sciences, Vytautas Magnus University LT-44404 Kaunas, Lithuania

*Corresponding author: e-mail: giedre.kaciene@vdu.lt, tel : +37067245718

Abstract

The aim of this work was to evaluate the influence of two successive small hydropower plants (SHPs) on the water quality of the Vokė river (Lithuania). Two SHPs ('Vokė' and 'Grigiškės') is situated in the 7 km long section of the river, close to Vilnius, the capital and the biggest Lithuanian city. Water samples were taken in the dams above SHPs, in the rapids immediately below SHPs and 2 km below each SHP. The concentrations of nitrates (NO_3^--N), nitrites (NO_2^--N), ammonium (NH_4^+-N) and phosphates (PO_4^{3+}-P), and chemical oxygen demand (COD) were investigated. An increase in N and P compounds was detected in the dams above both SHPs. The highest increases were characteristic for phosphates (~40%, $p < 0.05$) and nitrates (34% and 41%, $p < 0.05$, in the 'Vokė' and 'Grigiškės' dams, respectively). Strong and statistical significant increase in the level of ammonium was observed only in the 'Grigiškės' dam (31%). Contrary to NO_3^--N, NH_4^+-N and PO_4^{3+}-P, concentration of NO_2^--N was lower in the dams of both SHPs. Strong and significant increase in COD (33%, $p < 0.05$) was detected only in the dam of 'Vokė' SHP. Considering the river sections 2 km below the SHPs, water quality changed negligibly. The levels of biogenic N and P compounds tended to decrease; however, sharp increase in PO_4^{3+}-P concentration was detected below 'Vokė' SHP, indicating an impact of subsequent 'Grigiškės' SHP. The levels of nitrates and phosphates were higher in the downstream 'Grigiškės' SHP, as compared to 'Vokė' SHP, both in the dams and in the subsequent rapids. The results of this study have shown that the levels of biogenic and/or organic compounds tend to increase in the dams above SHP. The concentrations of phosphates and nitrates further increase downstream due to the successive SHPs.

Keywords: Small hydropower plants, water quality, biogenic compounds, chemical oxygen demand

1. INTRODUCTION

Hydroelectric power stations are global source of power. Since the first hydroelectric power station, which was built in France in 1880, its size and complexity, due to new stacking technology and market demand, have highly increased. The economic and social benefits of hydropower plants are enormous, due to competitive and universal technology. These include irrigation, water supplies, flood control, recreation (Yuksel, 2010). On the other hand, hydropower plants interfere with environmental integrity. Although hydroelectric power plants are important are important for different sectors of the economy, their adverse environmental effects must be taken into account (Abbasi and Abbasi, 2011).

Hydropower Plants does not consume or purify the water it uses to produce electricity, but disrupts the natural flow of the river and changes the flow distribution in time and space. Since water flow is the main factor promoting the ecological processes of a river, the disruption of natural current drastically affects the status of river ecosystems (Pang et al., 2015). The negative impact on ecosystems, biodiversity, habitats of plants and animals, fish migration is widely investigated (Baxter, 1977; Jansson et al., 2000; Anderson et al., 2006; Santos et al., 2012; Vaikasas et al., 2015). Apart

from this damage, hydropower plants interfere with nutrient cycling (Zhou et al., 2013), the water reservoirs produce large amounts of greenhouse gases (Rosenberg et al., 2000) and pollute water with methylmercury (Pang et al., 2015).

Large hydropower plants are not accepted as a clean, renewable energy source by most ecologists and environmental activists. Therefore small hydropower plants (SHP), which installed power are usually below 10 MW and whose popularity has declined in the middle of XX century, was restored as a substitute for clean energy as alternative for large hydroelectric power plants (Abbasi and Abbasi, 2011; Punys et al., 2015). On a global scale, most political strategies support the idea, that SHP have a minimal impact on the environment or are completely environmentally friendly (Darmawi et al., 2013). However, an increasing number of researches show that SHP interfere with rivers ecosystem stability by reducing the flow rate, increasing accumulation of N and/or phosphorus compounds and changing composition of invertebrates' communities (Zhou et al., 2009; Punys et al., 2015; Vaikasas et al., 2015)

The aim of this study was to evaluate the influence of two successive small hydropower plants (SHP) on the water quality of the Vokė river (Lithuania). Two SHP ('Vokė' and 'Grigiškės') is situated in the 7 km long section of the river, close to Vilnius, the capital and the biggest Lithuanian city.

2. MATERIALS AND METHODS

The investigated river Voke is located 10 km to the Southwest from Lithuania capital Vilnius. It is the left influent of Neris. Total length of Voke is 35.8 km, the capture area 572,7 km², an average discharge 4,9 m³/s. SHP 'Voke' (installed power 300 kW) is located in the southwestern part of Vilnius city. Hydro scheme consists of earth dam with concrete gated overflow spillway. The plant was reconstructed in 2010 from old water mill. The reservoir area is 12.2 ha. SHP 'Grigiskes' (installed power 340 kW) in Grigiškės town, a district of Vilnius city. It was built in 1934 (reconstructed in 2000) sing the existing (since 1922) concrete dam with 5 gates over-flow spillway. The plant is used for electricity production (1,656 GWh), it consists of two turbines. Discharge of one turbine is released into the river Vokė, whereas the second – into short adjacent canal. The reservoir area is 9.7 ha (Lithuanian Hydropower association, Hydropower in Lithuania 1996-2011 http://www.lsta.lt/files/Leidiniai/Lietuvos%20HIDROENERGETIKA/Knyga_Lietuvos%20HIDROENERGETIKA.pdf).

Water samples were taken in six places, in 7 km long section of the Voke river. The following places were chosen: in the reservoirs above SHPs (No 1 and 4), in the rapids immediately below SHPs (No 2 and 5) between the SHPs (No 3) and 2 km below the SHP 'Grigiskes" (6) (Figure 1).

The 1st place is located in the reservoir immediately above SHP 'Vokė". The surroundings of the reservoir have low population density, consists of small forests and meadows.

The 2nd place is below SHP 'Vokė". There is a road network nearby, the river flow is rapid, the bottom predominantly graveled.

The 3rd place is located between the two SHPs: 2,25 km below SHP 'Voke' and 4,25 km above SHP 'Grigiskes'. The shores are forested and winded, the bottom is sandy and intermittently dumbbell.

The 4th place is located in the reservoir immediately above the SHP 'Grigiskes'. The town Grigiskes is situated around the reservoir, there were housing and a highway close to this sampling place. The bottom is covered with deep layer of sludge.

The 5th place is located below the SHP 'Grigiskes'. The river flow is rapid, the bottom predominantly graveled. There is a highway close to the sampling place, the other shore is steep and forested.

The 6th place is located 2 km below the SHP 'Grigiskes' and 1 km above the river inflow. The shores are urbanized.

Water samples were stored at -20 ºC until chemical analysis. The concentrations of nitrates (NO_3^--N), nitrites (NO_2^--N), ammonium (NH_4^+-N) and phosphates (PO_4^{3-}-P) were investigated according to Bartošová *et al.* (2012) with minor changes. Chemical oxygen demand (COD) was analysed using AQUANAL™-professional tube tests and WINLAB® photometer according to manufacturer instructions.

All analysis were performed in three replicates. The data were analysed using *STATISTICA 8* and the results were expressed as the mean values and their confidence intervals (p<0.05) (±95% *CI*).



Figure 1. Sampling points in the river Voke.

3. RESULTS AND DISCUSSION

3.1 Concentrations of nitrogen compounds

The concentrations of inorganic N compounds, such as ammonium, nitrites and nitrates were investigated (Figure 2). Tendentious increases of the levels of ammonium and nitrates are characteristic for water reservoirs above each SHPs. The highest concentration of NH_4^+-N was detected above SHP 'Voke', it gradually decreased until the lowest level between the two SHPs. However, strong and significant increase was observed in the second downstream reservoir above SHP 'Grigiskes': 31% ($p < 0.05$), as compared to the level below this SHP (Figure 2A). Two kilometres below this dam, the level of NH_4^+-N increases again, most possibly due to the impact of diffused pollution from the highway and from the town Grigiškes, situated around the reservoir and

the downstream section of the river. In spite of these fluctuations, the highest concentration of ammonium is characteristic for the first reservoir above the SHP ‘Voke’ and for the rapids immediately below this dam.

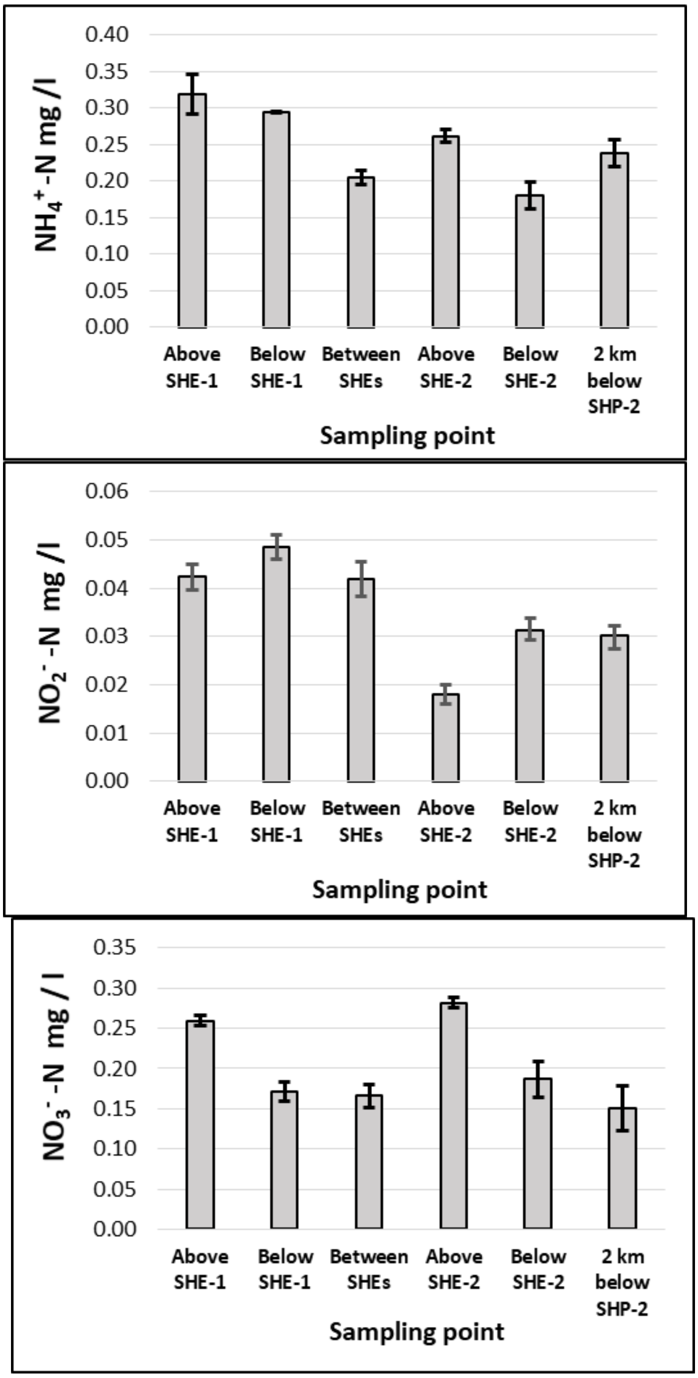


Figure 2. Concentrations of inorganic nitrogen compounds in the section of Voke river, containing two successive SHPs (SHP-1 and SHP-2 are SHP ‘Voke” and SHP ‘Grigiskes”, respectively).

Both SHPs increased the level of nitrates above the dams, inducing even higher increases of NO_3^--N than NH_4^+-N concentrations in the reservoirs. The lowest level of NH_4^+-N varied from 0.166 mg/l in the forested part of the river between the dams till 0,171 mg/l and 0,187 mg/l in the rapids below the dams ‘Voke’ and ‘Grigiskes’, respectively. This level increased till 0,259 mg/l and 0,282 mg/l in the reservoirs above these dams. Therefore, the concentrations of nitrates were higher by 34% and 41% ($p <0.05$) in the ‘Voke’ and ‘Grigiškes’ reservoirs respectively, as compared to the rapids below the

dams. Gradual, but statistically insignificant, decrease of the level of NO_3^--N was observed in the downstream sections of Voke river, several kilometers away from SHPs (Figure 2C).

Contrary to NO_3^--N and NH_4^+-N, concentration of NO_2^--N were lower in the reservoirs of both SHPs (Figure 2B). The lowest concentration of nitrites was found in the reservoir above SHP 'Grigiskes'. The highest level of NO_2-N was characteristic for the rapids below the SHP 'Voke' (0,049 mg/l) and for the sections of the river above and below this dam (0,042 mg/l).

3.2 Phosphate and chemical oxygen demand

Both SHPs increased the level of phosphates in the reservoirs above the dams. The lowest level of PO_4^{3+}-P was detected in the sections of the river immediately below the SHP 'Voke' (0,022 mg/l) and 2 km below SHP 'Grigiskes' (0,021 mg/l) (Figure 3A). The concentrations of PO_4^{3+}-P was higher by ~34% ($p<0.05$) in both reservoirs compared to the rapids below the dams (Figure 3A). An increase of the level of phosphorus compounds is explained by the accumulation of sediments, adsorbing and transporting phosphorus (Mihailova et al., 2013; Zhou et al. 2013). The amount of P sequestration can exceed 80% in big dams, as was detected by Zhou et al. (2013). Phosphorus sequestration in the lower dam (SHP 'Grigiskes') increased PO_4^{3+}-P even several kilometres above the reservoir, in the sampling place between the two dams (Figure 3A). The reservoir 'Grigiskes' was characteristic of the highest concentration of phosphates (0,037 mg/l), this might be influenced by the nearby town Grigiskes and diffused P pollution from uncontrolled point sources in the private sector.

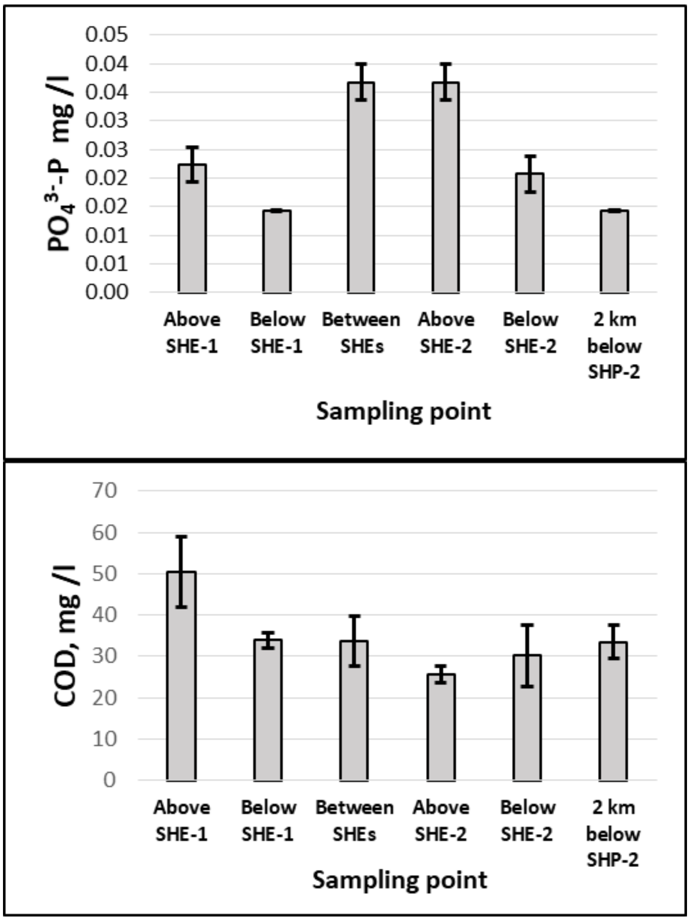


Figure 3. Concentration of phosphates (A) and chemical oxygen demand (B) in the section of Voke river, containing two successive SHPs (SHP-1 and SHP-2 are SHP 'Voke' and SHP 'Grigiskes', respectively).

Water reservoir above SHP 'Voke' was characteristic by the highest value of chemical oxygen demand. COD in this dam (50,4 mg/l) was significantly higher as compared to any other sampling points downstream the Voke river, where COD varied within the range 25,7-33,9 mg/l. The difference

between COD above and below SHP 'Voke' was 33 %. COD was even lower in the downstream reservoir 'Grigiskes' (49 %, $p<0.05$), therefore SHP 'Voke" functions as a trap for organic matter.

4. CONCLUSIONS

Two successive SHPs 'Voke' and 'Grigiskes' changed the levels of biogenic compounds and chemical oxygen demand in the course of the river. The most intensive change was detected for phosphates and nitrates. The level of these substances was approximately one-third higher in the reservoirs above the dams, compared to the rapids below. Both investigated SHP tended to increase NH_4^+-N and to decrease NO_2^--N concentrations in the reservoirs above the dams. The upper SHP 'Voke" seems to function as a trap of organic matter, as COD is sharply higher in the reservoir above this dam as compared to all investigated points in the course of the river below.

Acknowledgements
Participation in the conference is funded by the European Social Fund under the No 09.3.3-LMT-K-712 "Development of Competences of Scientists, other Researchers and Students through Practical Research Activities" measure. Many thanks to Rytis Liasis for assistance during the experiment and permission to use his data for this publication.

References

1. Abbasi T. and S.A. Abbasi (2011) 'Small hydro and the environmental implications of its extensive utilization', **Renewable and Sustainable Energy Reviews**, 15, pp. 2134 –2143.
2. Anderson E.P., M.C.Freeman and C.M. Pringle (2006) 'Ecological consequences of hydropower development in Central America: impacts of small dams and water diversion on neotropical stream fish assemblages', **River research and applications**, 22, pp. 397–411.
3. Bartošová A., A Michalíková, M. Sirotiak and M. Soldan (2012) 'Comparison of two spectrophotometric techniques for nutrients analyses in water samples', **Research Papers Faculty of Materials Science and Technology Slovak University of Technology**, 20(32), pp. 8-19.
4. Baxter R.M. (1977) 'Environemtal effects of dams and impoundments', **Annual Review of Ecology and Systematics**', 8, pp. 255-283.
5. Darmawi, R. Sipahutar, S.M. Bernas and M.S. Imanuddin (2013) 'Renewable energy and hydropower utilization tendency worldwide', **Renewable and Sustainable Energy Reviews**, 17, pp. 213–215.
6. Jansson R., C. Nilsson and B. Renofalt (2000) 'Fragmentation of riparian floras in rivers with multiple dams', **Ecology**, 81, pp. 899-903.
7. Mihailova P., I. Traykov, A. Tosheva and M. Nachev (2013) 'Changes in biological and physicochemical parameters of river water in a small hydropower reservoir cascade', **Bulgarian Journal of Agricultural Science**, 19(2), pp. 286–289.
8. Pang M., L.Zhang, S. Ulgiati and C.Wang (2015) 'Ecological impacts of small hydropower in China: Insights from an emergy analysis of a case plant', **Energy Policy**, 76, pp.112–122.
9. Papadopoulou M.P., E.A. Varouchakis, and G.P. Karatzas (2010), 'Terrain Discontinuities Effects in the Regional Flow of a Complex Karstified Aquifer', **Environmental Modeling and Assessment**, 15(5), pp. 319-328.
10. Punys P., A. Dumbrauskas, E. Kasiulis, G. Vyčienė and L. Šilinis (2015) 'Flow regime changes: from impounding a temperate lowland river to small hydropower operations', **Energies**, 8, pp.7478-7501

11. Rosenberg D.M., P. McCully and C.M. Pringle (2000) ‘Global-Scale environmental effects of hydrological alterations: introduction’, **BioScience**, 50 (9), pp.746-751.
12. Santos J.M., A. Silva, C. Katopodis, P. Pinheiro, A. Pinheiroe, J. Bochechas and M.T. Ferreira (2012) ‘Ecohydraulics of pool-type fishways: Getting past the barriers’, **Ecological Engineering**, 48, pp. 38– 50
13. Vaikasas S., N. Bastiene and V. Pliuraite (2015) ‘Impact of small hydropower plants on physicochemical and biotic environments in flatland riverbeds of Lithuania’, **Journal of Water Security**, 1, pp. 1-13
14. Yuksel I. (2010) ‘Hydropower for sustainable water and energy development’ **Renewable and Sustainable Energy Reviews,** 14, pp. 462–469
15. Zhou A.S., T. Tang, N. Wu, X. Fu, W. Jiang, F. Li and Q. Cai (2009) ‘Impacts of cascaded small hydropower plants on microzooplankton in Xiangxi River, China’, **Acta Ecologica Sinica**, 29, pp. 62–68
16. Zhou J., M. Zhang and P. Lu (2013) ‘The effect of dams on phosphorus in the middle and lower Yangtze river’, **Water resources research**, 49, pp. 3659–3669.
17. http://www.lsta.lt/files/Leidiniai/Lietuvos%20HIDROENERGETIKA/Knyga_Lietuvos%20HIDROENERGETIKA.pdf (accessed March 21st, 2018)



River and open channel hydraulics

DISCHARGE AND SEDIMENT TRANSPORT IN THE NESTOS RIVER BASIN, DOWNSTREAM OF THE DAM OF PLATANOVRISI

G. Paschalidis, I. Iordanidis and P. Anagnostopoulos*

Aristotle University of Thessaloniki, Department of Civil Engineering, Division of Hydraulics and Environmental Engineering, Thessaloniki 54124 Greece

*Corresponding author: E-mail: anagnost@civil.auth.gr, Tel +30 2310 995675, Fax: +30 2310 995680

Abstract

The prediction of the runoff and sediment yield in the basin of the Nestos River, located in Macedonia and Thrace, Northern Greece, is the subject of the present study. The AGNPS software was employed, in order to assess the basin's behavior downstream of the hydroelectric dam of Platanovrisi, which is located approximately at the middle of the river's course inside the Greek territory. The technique used in order to model the impact of the dam, was to modify the study area's digital elevation model and represent the discharge of the dam as a point source of water. Two different simulations were conducted, one for the years 1980-1990 and another for the period 2006-2030. The simulation for the years 1980-1990 was conducted using recorded meteorological data, whereas the simulation for the period 2006-2030 was based on rainfall and climate data generated by two software packages, namely GlimClim and ClimGen.

Keywords: River basin, Discharge, Sediment transport, Dam

1. INTRODUCTION

Watersheds are often subjected to flooding, erosion and sedimentation hazards, leading to environmental, social and economic complications. Thus, proper quantification of soil erosion and runoff in watersheds are essential for effective land use planning. The prediction of the runoff and sediment yield of a watershed has been an ambitious goal for a variety of scientists, such as engineers, hydrologists, geologists and others. In particular, the estimation of sediment yield in various temporal and spatial scales is a vital key point for the assessment and design of major hydraulic systems, such as hydroelectric dams and flood attenuation structures.

Computer modeling is considered to be a cost-effective tool for the prediction of the runoff and sediment yield of a watershed. Several non-point source (NPS) models have been developed for this purpose [1]. The Agricultural Non-Point Source Pollution Model (AGNPS) is a suite of NPS Models, developed as a planning tool for forested or agricultural watersheds [2]. It was developed jointly by the United States Department of Agriculture (USDA) Agricultural Research Service (ARS) and the USDA Natural Resources Conservation Service (NRCS).

In this paper, the Agricultural Non-Point Source Pollution Model (AGNPS) was used to predict runoff and sediment losses from a section of a predominantly forested watershed of Nestos River, in Macedonia and Thrace, Northern Greece. In particular, the study area is the basin downstream of the hydroelectric dam of Platanovrisi, which is located approximately at the middle of the river's course inside the Greek border (Fig. 1). The area of the basin is 884 km2. Runoff and sediment yield were estimated at the location Toxotes, at the outlet of the study area.

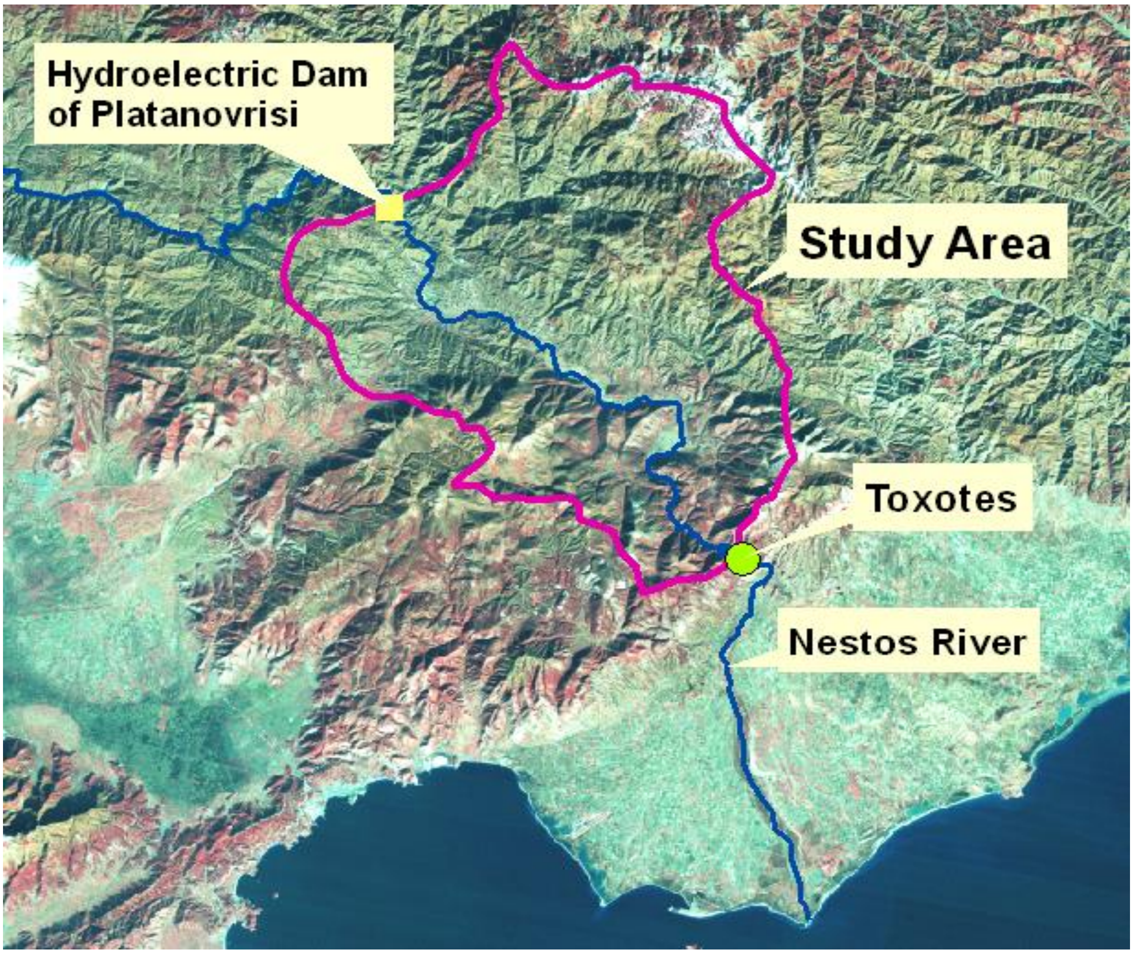


Figure 1. The study area.

AGNPS is a daily time-step, distributed model, which enables the modeling of all different processes and parameters that affect sediment transport, allowing the creation of a detailed model of the study area [3]. Extensive rainfall and climate data, such as wind speed, relative humidity, temperature and solar radiation are also necessary [4]. The use of the model as prediction tool requires its calibration for the conditions in the study area.

Two different simulations were conducted, one for the years 1980-1990 and another for the period 2006-2030. The simulation for the years 1980-1990 was conducted using recorded meteorological data, whereas the simulation for the period 2006-2030 was based on rainfall and climate data generated by two software packages, namely GlimClim and ClimGen.

2. MATERIALS AND METHODS

AGNPS is based on the Revised Universal Soil Loss Equation (RUSLE) combined with a GIS (Geographic Information System) interface for more convenient preparation of input data. RUSLE is a simple empirical model which is based on regression analyses of soil loss rates. It has the following structure, similarly to the USLE [5]:

$$A = R \cdot K \cdot LS \cdot C \cdot P, \tag{1}$$

A is the computed spatial and temporal average soil loss per unit area
R is the rainfall-runoff erosivity factor
K is the soil erodibility factor
LS is the slope length and steepness factor

C is the vegetation cover and management factor
P is the conservation support practices factor

It is widely used because of its relative simplicity, robustness and ability to enable prediction of average annual erosion by multiplying several factors together, such as rainfall erosivity (*R*), soil erodibility (*K*), slope length and steepness (*LS*).

A large amount of input data is necessary for the model setup. AGNPS simulates runoff and sediment transport from land to streams, as a result of storm flow. Runoff is calculated in the model using a variation of the Technical Release 55 (TR-55) method [6]. TR-55 employs simplified procedures to calculate runoff volume in small watersheds. A modified Einstein deposition equation, using the Bagnold suspended sediment formula for the transport capacity by particle size class, was used for the sediment transport in the watershed.

AGNPS uses amorphous cells, each cell being a grouping of individual square grid elements, which collectively represent homogeneous hydrological response units. Using the ArcView interface, the basin is dissected into cells and the attributes of spatial data are allocated to each of the cells. Based on the critical source area (CSA) and minimum source channel length (MSCL) parameter values, the watershed was discretised into 1568 cells and 699 channel reaches.

2.1 Terrain and soil parameters and land use data

The Digital Elevation Drainage Network Model (DEDNM) module of AGNPS performed the terrain parameterization and defined the drainage network. The cell attributes include drainage area, average elevation, average slope, shallow flow slope and length, concentrated flow slope and length, and the *LS*-factor, a basic factor of RUSLE, which computes the effect of slope length and steepness on erosion. The reach attributes include drainage area, contributing cells, receiving reaches, average elevation and channel slope and length

The texture of the soil samples obtained from various locations of the basin were identified and categorized per soil type. Four soil types were identified, the average texture of which was calculated and a specific code number was assigned to each soil type. The average textures, for the four soil types, are shown in Table 1.The AGNPS/ArcView interface was then used to assign the soil type to each cell. The soil properties mentioned before were assigned to each soil code number via the input editor.

Table 1. Average texture of various soil types and corresponding K values

Soil Type	Sand (%)	Clay (%)	Silt (%)	*K* (Mg h)/(MJ mm)
Sandy Clay Loam	55	19	26	0.314
Silty Loam	22	21	57	0.272
Loamy Sand	78	4	18	0.223
Silty Clay Loam	8	39	53	0.285

Land use data were acquired from the European Environmental Agency. This dataset is a raster, geo-referenced, categorized land cover data layer. The raster data were converted into shapefile format using ArcView version 9.3, and the AGNPS/ArcView interface was then used to determine the land use in each cell. According to the existing land use data, the cells within the watershed were classified into groups for more convenient handling and management.

Land uses in AGNPS are classified into two categories:
a) Non-cropland

b) Cropland

There is a total of 16 distinct land uses in the study area. Thirteen of them are "non-cropland uses" and include urban infrastructure, wooded land and other non-cultivated land uses. Annual Rainfall Height, Annual Cover Ratio, Root Mass and Surface Residue Cover were inputted in order to simulate non-cropland uses. Cropland uses consist of crop-related activities such as sowing, harvesting, etc.

Since the study area contains cropland land uses, it is necessary to simulate the effects of agricultural activities such as sowing and harvesting, including their time schedule during a year. The connection of each land use with the above activities was assigned via the input editor and specifically the "Field Data Management" option. Each field data contains one or more events, which are scheduled to take place at a specific time of the year. The time period for sowing and harvesting was determined through the "Management Schedule" option. Furthermore each schedule is associated with the runoff curve number, which corresponds to its own land use.

2.2 Meteorological data

Meteorological (rainfall and climate) data were taken from two meteorological stations inside the basin (Fig. 2). AGNPS requires daily meteorological data for the simulation period, stored in a separate file. The meteorological data contain eight daily parameters: date, precipitation, daily maximum temperature, daily minimum temperature, dew point temperature, sky cover or solar radiation, wind speed and wind direction. These are the minimum information required to calculate surface runoff and other physical processes, which are simulated with AGNPS.

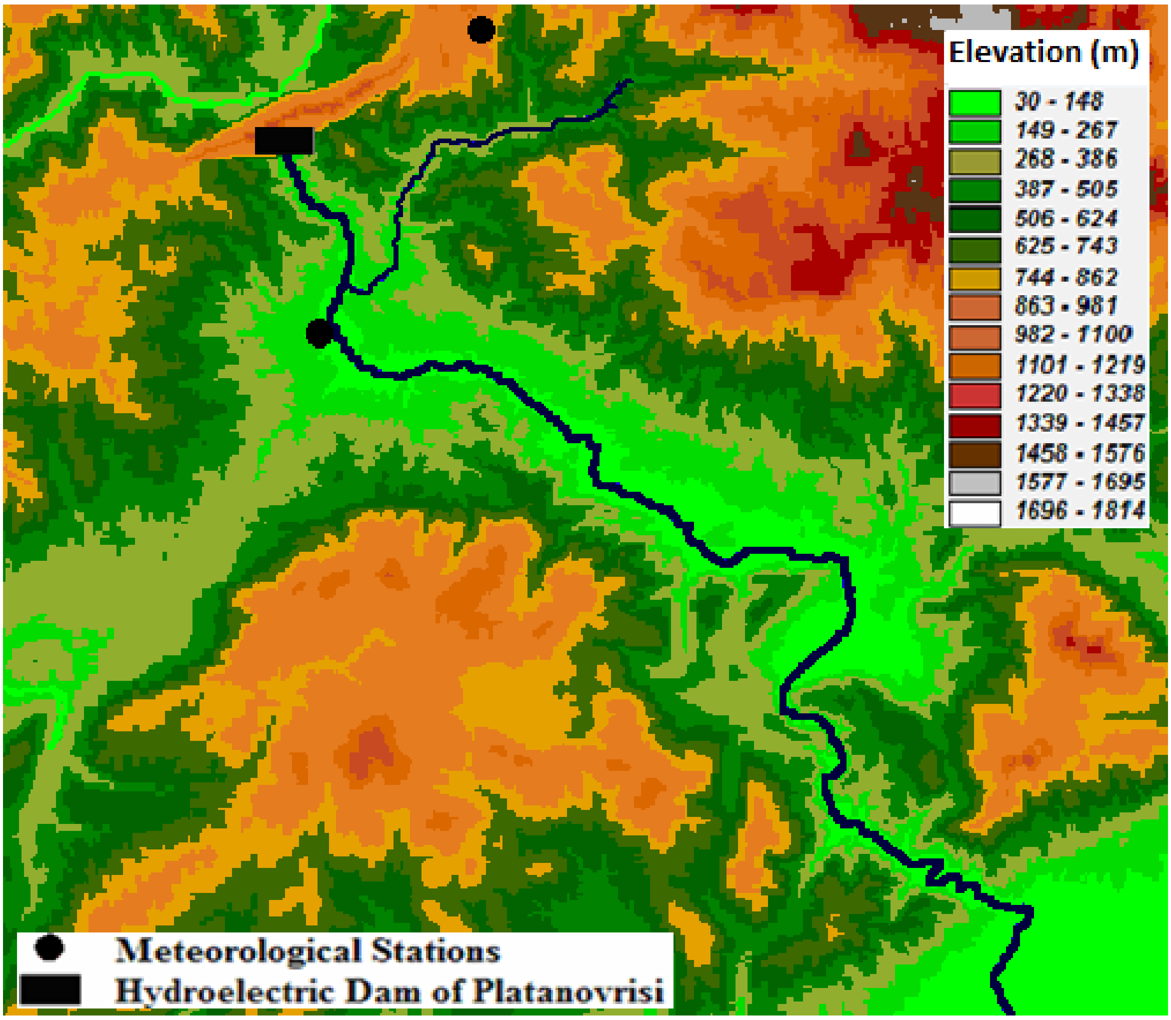


Figure 2. The study area with meteorological stations.

The two meteorological stations mentioned previously contain monthly rainfall and climate data for the period 1964-2009. The complete sets of data on a daily basis suitable for use by AGNPS are confined for the periods 1980-1990 and 2006-2009. Stochastic time-series of the necessary meteorological parameters at a daily time step for the period 2006 to 2030 were generated with the use of two software packages, namely GlimClim and ClimGen. GlimClim was developed by Chandler [7] and ClimGen by the University of Washington in collaboration with the United States Department of Agriculture (U.S.D.A). The rainfall and climate data for the period 2006-2009 were used for the calibration of these two software packages. After the calibration, GlimClim was used to estimate daily rainfall values in the study area for the period 2006-2030 and ClimGen was used to estimate the daily values for all the other meteorological parameters (temperature, relative humidity and wind speed) for the same period.

A large number of simulations was conducted with the use of GlimClim for the period 2006-2030. Since GlimClim is a statistical model; the large number of simulations serves in obtaining an adequate sample of estimated values of rainfall for each day in the simulation period. For all simulations, the rainfall for each day in the interval 2006-2009 was compared with the corresponding recorded value. The simulation which yielded daily estimated rainfall closest to the recorded throughout the interval 2006-2009 was selected as the most reliable.

2.3 Model implementation

AGNPS was employed for the study of sediment transport in the basin of the Nestos River, downstream of the hydroelectric dam of Platanovrisi, which is located approximately at the middle of the river's course inside the Greek territory. An important input parameter for the calibration of runoff is the approximate amount of direct runoff (Curve Number) [6], which provides information on the runoff properties of the soil in the study area. Since runoff is sensitive to changes of the Curve Number, the Curve Numbers must be carefully selected, in order to produce reliable results. Runoff is calculated by

$$Q = \frac{(WI - 0.2\,S)^2}{WI + 0.8\,S}, \quad \text{where} \quad S = 245\left(\frac{100}{CN} - 1\right) \tag{2}$$

where Q is the surface runoff for each cell, WI the water input (precipitation or irrigation), S the retention variable and CN the Curve Number. CN has a range from 30 to 100; lower numbers indicate low runoff potential, whereas larger numbers indicate increased runoff potential. The lower the curve number, the more permeable the soil is. The Curve Number depends on the land use and soil type of each cell, as described by TR-55 [6].

The annual sediment yield, S_y, (tn/km^2) is calculated by

$$S_y = 0.22\,Q^{0.68}\,q_p^{\;0.95}\,K \cdot L \cdot S \cdot C \cdot P \tag{3}$$

where Q the surface runoff, q_p the peak rate of surface runoff and K, L, S, C and P are factors of the Revised Universal Soil Loss Equation (1).

The most important of these factors is the soil erodibility factor, K, which influences the spatial variability of sediment losses. Factor K, which is important for the determination of the sensitivity of soil to erosion, the sediment transportability and runoff rate, is directly related to soil properties. Soil texture, structure and particle composition are the main factors affecting soil erodibility. The values of K range typically from about 0.10 to 0.45 [(Mg h / (MJ mm)]. Similarly to Liu et al. [8], the erodibility factor was calculated using the method in the Erosion Productivity Impact Calculator (EPIC) model, given by the equation

$$K = \{0.2 + 0.3 \exp[-0.256\, S_d\, (1 - S_i\, /100)]\, [S_i\, /(\, C_i + S_i\,)]\}^{0.3}$$
$$\{1.0 - 0.25\, C_0\, /[\, C_0 + \exp(3.72 - 2.95\, C_0\,)]\} \quad (4)$$

where S_d is sand content, S_i is silt content, C_i is clay content and C_0 is soil organic carbon.

The values of *K* for the four soil types of the present study, as calculated using Eq. (4) from the average textures of Table 1, are also listed in Table 1. These values are close to those reported by Liu et al. [8], which lie in the range between 0.278 and 0.344.

Slope length and steepness factors, *LS*, are topographic factors that indicate the terrain impacts on soil erosion. Slope length is evaluated by the model from the change in elevation at a specified distance in the DEM. The steepness factor, which accounts for the effect of slope steepness on soil erosion, is evaluated internally by the model.

The vegetation cover and management factor, *C*, represents the effect of both the natural vegetation cover on reducing soil loss in non-agricultural situations, and of cropping and management practices in agricultural activities. The *C* factor is calculated by the model for all non-water cells in the study area, depending on the land use (cropland or not). For cropland cells AGNPS calculates 24 values of *C* factor for each year, and an average *C* factor for each year for non-cropland cells. For cropland land uses, the effects of agricultural activities, such as sowing and harvesting, and their time schedule during a year, are important for the determination of *C* factor.

The conservation support practice factor, *P*, is the ratio of soil loss under a particular conservation support practice, to soil loss for up and down slope cultivation on the unit plot, with no conservation support [9]. Conservation support practices include cropping along the contour, strip-cropping and terracing. It is evident that the lower the *P* factor value, the better the practice for controlling soil erosion. Similarly to *C* factor, *P* factor is calculated by the model for all non-water cells in the study area. AGNPS calculates sub-factors for contour cropping, strip-cropping and terracing, from which the *P* factor of the corresponding cell for each year is evaluated.

An important requirement of the model application for future predictions is the determination of suitable values of the parameters which influence the sediment yield. The calibration was conducted by modifying the value of each parameter within the limits specified by TR-55 [6]. The selected values of these parameters were those which rendered the difference between estimated and measured values of runoff and sediment yield for a specific year at the location Toxotes minimum. The validation of the calibration was performed using estimated and measured values of runoff and sediment yield at the same location for the following year. The calibration-validation procedure is described in detail by Paschalidis et al. [10].

3. APPLICATION, RESULTS AND DISCUSSION

Two different simulations were performed by AGNPS, one for the period 1980-1990 and another for the period 2006-2030. The purpose of both simulations was the estimation of the runoff and the sediment yield at the outlet of the river Nestos basin, at the location Toxotes. The period 1980-1990 was selected in order to compare the results of AGNPS with those of a study by Hrissanthou [11] at the same location and period of time. The availability of recorded meteorological data throughout this period was expected to increase the accuracy of results. The period 2006-2030 was selected for the future prediction of sediment yield in the study area. The necessary climate and rainfall data required for this simulation, were obtained using the ClimGen and GlimClim.

Table 2 presents the estimated values of sediment yield of the Nestos River for the years 1980-1990 using the AGNPS model, in comparison with results of two different simulation models by Hrissanthou [11] at the same location and period of time. The year average of runoff and sediment yield for the period 1980-1990 are listed in Table 3.

Table 2. Estimated values of sediment yield (*tn/year*)

Year	AGNPS	Hrissanthou [11]	
		Model 1	Model 2
1980	210,182	298,000	278,000
1981	422,646	528,000	588,000
1982	467,195	446,000	426,000
1983	105,124	80,000	73,000
1984	295,626	492,000	494,000
1985	170,985	119,000	131,000
1986	256,752	196,000	198,000
1987	511,482	638,000	673,000
1988	350,203	396,000	383,000
1989	306,669	201,000	207,000
1990	234,517	75,000	64,000

Table 3. Estimated values of mean annual runoff and sediment yield for years 1980-1990

Technique	AGNPS	Hrissanthou [11]	
		Model 1	Model 2
Runoff (m^3/s)	46.3		
Sediment Yield (*tn/year*)	302,852	315,500	319,500

The deviation of the results of the two studies lies within acceptable limits. It is noteworthy, that in spite of the differences in specific years, the mean annual sediment yield for the period 1980-1990 is very close to that obtained by the two models of Hrissanthou [11].

Table 4 presents the estimated values of mean annual runoff and sediment yield at the location Toxotes, for the years 2006-2030 using the AGNPS model. As stated previously, climate and rainfall data for this period were generated by Glimclim and ClimGen. The mean runoff for the period 2006-2030 is lower than that for the period 1980-1990 by less than 5%. The mean sediment yield for the period 2006-2030 is lower than that for the period 1980-1990 by approximately 20%. Therefore, the rainfall and the resulting runoff seem to play a key role for the sediment yield.

Table 4. Estimated values of mean annual runoff and sediment yield using AGNPS for years 2006-2030

Runoff ($m^3/s.$)	44.3
Sediment Yield (*tn/year*)	252,266

4. CONCLUSIONS

The AGNPS software was employed in order to simulate both runoff and sediment yield at the location Toxotes downstream of the hydroelectric dam of Platanovrisi, located in the basin of Nestos River. Two different simulations were performed by AGNPS, one for the period 1980-1990 and another for the period 2006-2030. The mean annual sediment yield for the period 1980-1990 was

very close to that obtained at the same location by Hrissanthou [11], in spite of the differences existing in specific years. Apparently, the good agreement of the mean annual sediment yield reinforces the validity of the present model. The simulation for the period 2006-2030, the necessary climate and rainfall data for which were obtained using the GlimClim and ClimGen software packages, yielded reduced value of the mean runoff by 5% and reduced value of the mean annual sediment yield by 20%, compared to the corresponding values for the period 1980-1990. This constitutes strong evidence, that the rainfall and the runoff play a key role for the sediment yield.

References

1. Binger, R.C., Mutchler, C.K., Murphee, C.E., 1992. Predictive capabilities of erosion models for different storm sizes. **Transactions of American Society of Agricultural Engineering**, 35(2), 505–513.
2. Binger, R.L., Theurer, F.D., 2001. AGNPS98: A suite of water quality models for watershed use. **Proceedings of the Sediment Monitoring, Modeling, and Managing, Seventh Federal Interagency Sedimentation Conference**, March 2001, Reno, NV, USA, 25–29.
3. Binger, R.L., Theurer, F.D., 2005. AnnAGNPS Technical Processes documentation, version 3.2, USDA-ARS, National Sedimentation Laboratory.
4. Iordanidis, I., 2010. Investigation of nitrate pollution in a river basin from rural activities. Ph.D. Thesis, University of Thessaloniki, Department of Civil Engineering, Thessaloniki, Greece (in Greek).
5. Renard, K.G., Foster G.R., Weesies, G.A., McCool, D.K., Yoder D.C., 1997. Predicting soil erosion by water - a guide to conservation planning with the Revised Universal Soil Loss Equation (RUSLE). United States Department of Agriculture, Agricultural Research Service (USDA-ARS) Handbook No. 703. United States Government Printing Office: Washington, DC.
6. Binger, R.L., Darden, R., Herring, G.J., Martz, L.W., 1998. TOPAGNPS User Manual. TR-55 USDA-ARS.
7. Chandler, R., 2002. GLIMCLIM: Generalized linear modelling for daily climate time series (software and user guide), Tech. Rep. 227, Dept. of Stat. Sci., UCL, London.
8. Liu, X., Qi, S., Huang, Y., Chen, Y., Du. P., 2015. Predictive modeling in sediment transportation across multiple spatial scales in the Jialing River Basin of China. **International Journal of Sediment Research**, 30, 250-255.
9. Meyer, D., 1984. Evolution of the universal soil loss equation. **Journal of Soil and Water Conservation**, 39(2), 99–104.
10. Paschalidis, G., Iordanidis, I., Anagnostopoulos, P., 2014. Discharge and sediment transport in a basin with a dam at its upper boundary. **Proceedings of the International Conference on Protection and Restoration of the Environment XII** (eds. A. Liakopoulos, A. Kungolos, C. Christodoulatos, A. Koutsospyros), 29 June-3 July, Skiathos Island, Greece, Vol. II, 1081-1088.
11. Hrissanthou, V., 2002. Comparative application of two erosion models to a basin. **Hydrological Sciences**, 47(2), 279–292.

URBAN STREAMS OF THESSALONIKI (GREECE): SPATIAL AND HYDRAULIC ASPECTS

S. Tsoumalakos* and K.L. Katsifarakis

Division of Hydraulics and Environmental Engineering, Dept. of Civil Engineering, A.U.Th
Thessaloniki, Macedonia, Greece

* Corresponding author: e-mail: tsoustav@yahoo.gr, tsoustav@arch.auth.gr

Abstract

Rapid and poorly planned urban development has resulted in severe deterioration of the environment, in many parts of the world, including Greece. Amongst the environmental elements that have been heavily affected are local streams of small and medium size. Degradation resulted mainly from flaws of the respective legal framework and from trespassing, which was tolerated, more or less, by the pertinent authorities. In other cases, streams were reduced to closed conduits, according to development plans that disregarded environmental components. This behavior towards urban streams had many adverse effects. The most severe is aggravation of flood phenomena, which are further intensified by turning permeable soil into an impermeable surface during the urbanization process.

Today, in contrast to these practices, an attempt is being made to promote streams as key factors in the achievement of sustainable urban development through a more integrated management. Following this approach, we study the possibility of managing the streams that are preserved, at least partly, within the administrative boundaries of the Municipality of Thessaloniki, Greece. Thessaloniki is a very densely built area, within which several streams or stream parts are "hidden". In particular, we analyze and evaluate the spatial and hydraulic characteristics of these streams, together with the pressures they have received from human activities. We round off, this paper, by presenting certain proposals concerning the nexus of streams in the Municipality of Thessaloniki, Greece.

Keywords: urban streams, environmental impact, drainage system, Thessaloniki, Greece

1. INTRODUCTION

Many of the world's cities have been built along rivers or streams. The interaction of their functions with the aquatic element is therefore particularly important and long-lasting. Actually, streams shape the geomorphology and the landscape of the region through which they flow [EEA, 2016], and quite often they influence the way cities develop. In recent decades, they have often been the focus of discussion on the renovation and revival of cities, since, in the past, many streams had been considered a nuisance rather, than a social and environmental asset. Actually, urbanization without proper planning during the second half of the 20th century has led to the deterioration of natural elements, such as streams, in many cities, e.g. in the Mediterranean area [Giannakourou, 2005]. Since the 1980s, though, in many parts of the western and northern Europe, a considerable number of programs and actions for the rehabilitation and reintegration of rivers and streams in urban areas has been developed. They aimed mainly at the creation of new open spaces and the remodeling of the image of the cities, which had largely lost their contact with the natural landscape. For this reason, streams and rivers were the most suitable elements for changing the face of a city and for connecting the artificial with the natural environment [EEA, 2016].

Today, urban streams face a series of important problems. The first problem lies in the quantity of water: surface runoff increases due to extreme weather phenomena and the replacement of natural pervious surfaces with impermeable ones (streets and buildings), resulting in increased flood phenomena. Moreover, the quality of water is also significantly affected by the discharge of polluted surface runoff or even sewage discharge. Urban stream pollution may also affect the downstream areas [American Rivers, 2013]. Another problem results from changes in the structure of urban streams, especially on their banks. The natural banks are replaced by artificial walls, disrupting the connection between the stream and the surrounding area, while, sometimes, the stream is undermined completely [EEA, 2016]. At the same time, such projects remove the riverside vegetation and seriously damage the local flora, while the temperature in the stream and in the surrounding area increases significantly [EEA, 2016].

2. STREAM MANAGEMENT IN THE URBAN AREA: A MODERN CONCEPT

River rehabilitation projects offer an opportunity for future urban planning in the context of sustainable development and quality of life improvement. The concept of restoring streams is related to objectives, measures and actions that have, as their main concern, the improvement of their functions, but also of the environment. In many cases, urban river rehabilitation projects do not begin with the aim of improving aquatic biological systems, but are part of urban regeneration projects, which are closely linked to streams that cross the cities. However, because of the interdependencies created between the ecosystems within and around the streams, it is difficult to bring streams to their initial condition [Simsek, 2012].

In addition to rehabilitation, the practice of stream restoration, which refers to the partial rebuilding of ecosystem functions disturbed by human activities, is very common. This can be achieved by removing, at least partly, the sources of nuisance. The final purpose is the creation and preservation of a natural ecosystem [Simsek, 2012]. Some plans include actual reconstruction of streams, which had been turned into underground pipe systems in previous years. Ideally, such recreated streams should follow their initial course. Such projects, though, are very complex and, in most cases, too expensive.

The improvement of urban streams contributes to the reduction of flood risk. At the same time, creation of new open spaces and enhancement of the greenery network offers access to the natural environment to city inhabitants and supports wildlife. Additionally, another very important asset is the reduction of the urban thermal island phenomenon, by achieving appropriate ventilation conditions.

Moreover, the rehabilitation of streams can have wider socio-economic consequences, as it creates an attractive environment that encourages recreation, enhances the physical and mental health of people, strengthens business investment and tourism locally, and increases the value of real estate. Moreover, management of streams can be integrated with rain water management in urban areas (UN, 2016). Towards this direction, green and blue infrastructure can play a very important role in mitigation flood phenomena, reduction of sewer system operation cost, support of local vegetation and replenishment of local aquifers.

3. THE STREAMS OF THE MUNICIPALITY OF THESSALONIKI, GREECE

The study area, namely the Municipality of Thessaloniki, is shown in Figure 1. Eight streams have been traced and studied. Most of them are characterized by small and intermittent flows. At the time of this survey (summer 2017), water could be seen in 2 stream beds only. This is due to the construction of a flood control channel, a few decades ago, which has cut off the urban stream parts from their mountainous drainage basins. Moreover, rain runoff from the remaining urban parts of drainage basins is partly collected by the sewer system. On the other hand, though, surface runoff increases due to the replacement of natural pervious surfaces with impermeable ones.



Figure 1: (a) Thessaloniki in South-eastern Europe (b) The Municipality of Thessaloniki in the Region of Central Macedonia, Greece. (c) Stream beds in the urban fabric of Thessaloniki Municipality (based on Google maps, processed by the authors)

The visible traces of the studied streams are shown as blue lines in Fig.1(c). Along large parts of their initial course, they have been reduced to underground pipe systems, to spare space for streets or other necessary facilities, such as schools, in poorly planned areas of the urban fabric. Even the preserved stream parts suffer from cross-section reduction, mainly due to trespassing by individuals, motivated by pressing housing demand and encouraged by flaws in the legal system and poor enforcement of the existing one. The construction of the aforementioned flood-control channel (called in Greek Perifereiaki Tafros and literally translated as Circumferential Trench) rendered trespassing on the rest of the steams less risky, from the hydraulic point of view.

Nowadays, within the context of sustainable development, the aforementioned practices are unacceptable. On the contrary, the goal is to regain the natural elements of streams as much as possible and to integrate them in the densely built urban fabric, under given functional and financial

constraints. The task is site-specific, since the characteristics of the preserved stream parts vary widely, even along rather short distances, as testified by the photos of Fig. 2.



Figure 2: Natural elements of streams. (a) In Evangelistrias stream, (b) In Saranta Ekklesies stream. Source: First author's Archive.

4. A COMPARISON OF STREAMS

Our research has identified the types of pressures upon the 8 streams of the specific study area and has classified them in the following way: a) illegal house building, b) road network, c) school building d) athletic facilities and e) broader urban environment. Results regarding each stream are summarized in Table 1.

Table 1: Forms of pressures upon the urban streams of Thessaloniki.

Urban streams of the Municipality of Thessaloniki	Pressures from Illegal House Building	Pressures from the Road Network	Pressures from School Buildings	Pressures from Athletic Centers	Pressures from the Broader Urban Environment
Perifereiaki Tafros (Circumferential Trench)	X		X		X
Regas Feraios Stream		X	X	X	X
Stream of Western Walls	X	X			X
Evangelistria Stream		X		X	X
Saranta Ekklesies Stream	X	X	X	X	X
Doxa Stream	X	X			X
Ortansia Stream	X	X	X	X	X
Nestoros Tipa Stream		X	X		X

Street construction along streams has been one of the main pressures, planned by local or central authorities. The most affected in the study area is the Regas Feraios stream, which has been completely reduced to an underground conduit, to allow mainly for the construction of a street. Its original course can be traced by a longitudinal green space along that street. The streams of Saranta Ekklesies, Doxa, Ortansia and Nestoros Tipa have been partially reduced to underground conduits. Even in the preserved parts, though, their initial stream bed has been partly occupied by streets along them. Moreover, closed conduits have been constructed at the junctions of the streams with transverse streets, as shown in Fig. 3. A notable exception is the Circumferential Trench. Although it has incorporated parts of pre-existing streams, it has not been affected by planned interventions, due to its special role in flood protection. Even when it meets transverse streets, traffic is facilitated via

bridges, without damaging its banks. Typical examples are the bridges of G. Lambrakis Street and of N. Plastira Street (in Municipality of Pylaia - Chortiatis).



Figure 3: Closed conduits at the junctions of streams with transverse streets (a) Doxa stream (b) Ortansia stream. Source: First author's Archive.



Figure 4: Trespassing Illegal house (a) In Doxa stream (b) In Ortansia stream. Source: Author's Archive

The next pressure that affects the streams of the study area stems from illegal private constructions. Within the context of this work, during the field investigation which was conducted, illegal constructions were mainly located at the edges of the urban space and hence in the upper parts of the streams. Trespassers have used stream banks and beds to construct their houses or to extend their properties. Two characteristic examples from Doxa and Ortansia streams are shown in Fig. 4. An important exception is the stream of Evangelistria, where house building has been officially permitted, downstream of its entrance to the urban fabric. Schools and athletic installations are also sources of pressure. We have detected such facilities along the streams of Saranta Ekklesies and Ortansias. Also, part of the bed area of the Regas Feraios stream, which has been reduced to a closed conduit, have served similar purposes.

5. A STRATEGY FOR THE STREAMS OF THE MUNICIPALITY OF THESSALONIKI AND SUSTAINABLE SPATIAL DEVELOPMENT

Table 2: S.W.O.T. analysis

S (Strengths)	W (Weaknesses)	O (Opportunities)	T (Threats)
The existence of parts of the streams whose natural bed has being preserved.	Unregulated urban sprawl and increase of impermeable surfaces.	Connecting urban green spaces with the peri-urban forest.	Increase of flood probability due to increase of impermeable surfaces.
The existence of dense riparian vegetation in several streams.	Reduction of the natural river bed.	Interconnection of green spaces within the urban fabric.	Environmental degradation due to the decline of the natural ecosystem.
The existence of additional non- built areas along some streams.	Partial substitution with closed conduits.	Improvement of soil permeability and the drainage system.	Increase of illegal occupation of the stream bed.
Natural ventilation of the urban area.	Water pollution from surface run-off.		Reducing natural replenicement of shallow aquifers.

Within the framework of this survey, a SWOT analysis has been conducted, summarized in Table 2. This analysis forms the basis for building an integrated strategy for the streams, following the three pillars of sustainable development: society - economy - environment. A basic concept of a modern strategy is that streams are free spaces and as such they must remain. Based on this reasoning, the basic principles of designing and management of the streams of Thessaloniki are organized. This is done for the protection of their surviving parts, and of the vegetation that accompanies them. The overall objectives set, at a strategy level, for the streams of the area under study, are summarized as follows:

- Maintenance of the natural stream bed and its banks where feasible.
- Reduction of the use of impermeable materials to delimit the streams.
- Preservation and even upgrading of the role of streams as drainage systems, using ecological rain water management techniques (e.g. Katsifarakis et al, 2015).
- Reduction of the pressures on the streams, caused by external interventions and trespassing.
- Introduction of a participatory process by inviting the citizens of Thessaloniki to actively participate in the effective management of streams.

The main purpose of these general objectives is the creation of networks of green spaces where their main trunk will be the streams themselves. Moreover, as the streams of Saranta Ekklesies and Ortansia (and the Circumferential Trench as well) extend up to the peri-urban forest of Thessaloniki, they can serve for the connection of the urban fabric with the forest area. Conservation of currently not built spaces close to the preserved stream beds, and their incorporation within the green space network, would greatly increase its value.

The management of these natural aquatic elements within the urban fabric can be accomplished by creating a multifunctional project plan. The aim of this project should therefore be to balance the issues related to the three main pillars of sustainable urban development, with a particular emphasis on the hydraulic and environmental role of the streams. Their hydraulic role can be upgraded in connection with ecological rain management techniques. Construction of rain gardens in parts of the beds of the Saranta Ekklesies, Doxa and Ortansia streams [Basdeki et al, 2017, Katsifarakis et al, 2015] would increase their role in mitigation of local flood phenomena and would contribute to the replenishment of the local shallow aquifer. Regarding the environmental role of streams, it is extremely important to strengthen local biodiversity and to improve the connection amongst the preserved parts of the streams, which are fragmented.

Sustainable development (society - economy - environment), with regard to the streams, should be sought, taking into account the context in which its three main pillars are accomplished. For this reason, it is proposed - at a social level - to create public spaces that are the links of the areas previously separated by these natural aquatic elements. Therefore, there is talk of upgrading the quality of life at, primarily, a local level, as well as setting up a network of recreational activities or even commuting at a daily basis. The economic sector concerning the streams under scrutiny, may develop as a natural consequence of a wider urban regeneration, but it is not the primary focus in the present work. However, it is worth noting that the creation of some urban cultivation on the banks and slopes of streams can contribute to the achievement of specific economic benefits (either individually or collectively). Regarding the environmental field, which is probably the most important part of stream management, we propose creation of urban habitats or at least strengthening of existing ones. These biotopes enhance urban biodiversity while at the same time improve microclimate conditions locally. In this way, streams can contribute to the achievement of urban resilience against extreme climate change.

However, the streams of the area under scrutiny, as already mentioned, are facing a number of pressures. The two main ones are street networks and trespassing. Regarding the street networks, it is proposed that we redefine the importance and the role of the car as well as the occupation of land so as to serve its needs, in the fringes of the stream areas. This can be achieved by taking into account both the principles of sustainable urban mobility and the impact of the presence of cars on both sides of the streets. Regarding trespassing, demolition of illegal constructions, currently in use, is not recommended in the current framework of financial crisis, which has led to an increased number of homeless people. On the contrary, abandoned installations should be demolished right away. Moreover, further trespassing should be discouraged, with an appropriate surveillance of the stream areas and by explicitly denying any possibility of “legalizing” illegal constructions in the future. Finally, integration of schools and sport facilities, which have been constructed in streams, should be sought, as they can contribute to the smooth reintegration of streams into the urban fabric.

6. CONCLUDING REMARKS

The main purpose of this work is to contribute to the protection and restoration of streams that are preserved within the administrative boundaries of the Municipality of Thessaloniki, Greece. Within its framework, the basic pressures that have been exerted upon the streams, are identified and classified. These pressures are tightly connected to the built environment, and are the main obstacles to achieving environmental balance, even around preserved stream parts.

Today, although these water elements are fragmented, they are still an important mechanism for ventilating a densely populated urban environment, such as that of Thessaloniki. The existence of streams in the urban tissue can make a significant contribution to improving the microclimate of the area through which they pass. Moreover, although their hydraulic role has been greatly reduced (with the exception of the Circumferential Trench), they are still important points of reference, especially during the periods of rainfall, when the city's sewer network fails to cope. At the same time, they can serve for the replenishment of local aquifers, especially in a city where impermeable surfaces dominate. Apart from the city's ventilation and the hydraulic role of streams, it is particularly important to use these elements for recreational purposes. Although the city of Thessaloniki has a wide and fully-fledged coastal urban front, which is a point of reference and recreation for its citizens, at a neighboring level, even in the inner part of the city, it lacks significantly in spatial amenities. This spatial inequality can be reduced by restoring the streams of the study area.

References

1. American Rivers (2013) Daylighting Streams: Breathing Life into Urban Streams & Communities At: http://americanrivers.org/wpcontent/uploads/2016/05/AmericanRivers_daylighting-streams-report.pdf (accessed November 25, 2017).
2. Basdeki A., L. Katsifarakis and K.L. Katsifarakis (2017) "Design, calculations and performance evaluation of rain gardens in an urban neighborhood of Thessaloniki, Greece", **Desalination and Water Treatment,** 99, pp. 4-7
3. European Environment Agency (EEA) (2016). Rivers and lakes in European cities. Past and future challenges. Luxembourg: Publications Office of the European Union (26).
4. Giannakourou, G. (2005). Transforming Spatial Planning Policy in Mediterranean Countries: Europeanization and Domestic Change. European Planning Studies. 13(2).
5. IPCC (2012). Summary for Policymakers: In Managing the Risks of Extreme Events and Disasters to Advance Climate Change Adaptation. Special Report of Working Group I and II of the Intergovernmental Panel on Climate Change. UK. Cambridge: Cambridge University Press. At: https://www.ipcc.ch/pdf/special-reports/srex/SREX_Full_Report.pdf (Accessed: December 12, 2017).
6. Katsifarakis K.L, M. Vafeiadis and N. Theodossiou (2015) "Sustainable Drainage and Urban Landscape Upgrading Using rain gardens. Site Selection in Thessaloniki, Greece**", Agriculture and Agricultural Science Procedia** 4, pp. 338-347
7. Simsek, G. (2012). Urban River Rehabilitation as an Integrative Part of Sustainable Urban Water Systems. 48th ISOCARP Congress. http://www.isocarp.net/Data/case_studies/2239.pdf (accessed November 14, 2017).
8. Special Service for Public Works of Thessaloniki (2003) General Regulatory Plan for Flood Protection and Sewerage of the Rainy Regions of Thessaloniki. (December 2003). Athens: Ministry of Environment, Urban Planning and Public Works. General Secretariat for Public Works. Special Service of Public Works for Water Supply, Sewage and Wastewater Treatment of Thessaloniki. (in Greek).
9. United Nations (UN) (2016). River Restoration. A strategic approach to planning and management. Paris: United Nations Educational, Scientific and Cultural Organization. At: http://unesdoc.unesco.org/images/0024/002456/245644e.pdf (accessed December 20, 2017).

ON THE USE OF THE INTEGRAL MOMENTUM-BALANCE TO CALCULATE DRAG ON A SQUARE CYLINDER IN A COMPOUND-CHANNEL FLOW

M. Gymnopoulos[1*], P. Prinos[2], E. Alves[3] and R. M.L. Ferreira[4]

[1] Instituto Superior Técnico, Universidade de Lisboa, PT- 1049-001 Lisboa, Portugal
[2] Division of Hydraulics and Environmental Engineering, Dept. of Civil Engineering, Aristotle University of Thessaloniki, GR- 54124 Thessaloniki, Greece
[3] Laboratório Nacional de Engenharia Civil, PT- 1700-066 Lisboa, Portugal
[4] CERIS, Instituto Superior Técnico, Universidade de Lisboa, PT- 1049-001 Lisboa, Portugal

[*]Corresponding author: e-mail: miltos.msn@hotmail.com, tel : +306979284007

Abstract
River flooding, threatens nearby infrastructure, as overbank flow occupies the adjacent berms (floodplains) and poses significant drag loads on the existing structures. The drag coefficient of such structures is possible to be influenced by the strong shear-layer formed at the interface of the main channel and the floodplain. Herein, this assumption is investigated in an experimental configuration involving the placement of an emergent cylinder at the main-channel/floodplain interface. The drag force on the cylinder at a certain distance from the floodplain bed is assessed through the application of the momentum-balance equation, in its integral form. The method is based on local measurements of the mean flow and turbulence characteristics. Drag is expressed as counteraction to the force on the flow in a control volume and is estimated as the residual in the momentum-balance equation.

The experiment was conducted in the straight compound-channel facility of Laboratório Nacional de Engenharia Civil (LNEC), Lisbon. Uniform-flow conditions were set in the channel for a relative flow-depth $h_r=h_{fp}/h_{mc}=0.31$ (h_{fp} is the floodplain flow-depth and h_{mc} is the main-channel flow-depth). A square cylinder was placed in one of the floodplains right next to the main-channel/floodplain interface. An Acoustic Doppler Velocimeter (ADV) was used for measuring the three-component instantaneous velocities at sequential positions on the surfaces of a fluid control-volume.

The terms of the momentum-balance equation were estimated. Then the drag coefficient emerged from the respective drag force and the characteristic velocity U_0 that accounts for the existence of the compound-channel-flow shear layer. The same calculations were applied to the case in which a cylinder is found in flow with uniform upstream velocities. This reference case is represented by placement of the cylinder in the middle of the floodplain in the same facility. The effect of the shear flow is assessed through comparison of the corresponding terms of the momentum-balance equation and the drag coefficients.

Keywords: Drag, Momentum balance, Square cylinder, Compound channel, Velocity measurements

1. INTRODUCTION

Bluff bodies in open-channel flows are commonly met in the form of vegetation elements and infrastructure e.g buildings and bridge piers. During flood events, cylindrical structures, found at close proximity to river banks, obstruct the overbank flow, and are subjected to the relevant drag loads. In this work the drag force on such an obstacle in an open-channel flow is assessed experimentally. In particular, the study considers a compound-channel flow, where a square cylinder

is placed on the floodplain, near the main-channel/floodplain (mc/fp) interface. In such a case, the cylinder faces a strong shear-layer that is typical in compound channels and is formed at the interface. This region is characterized by strong streamwise-velocity gradients in the lateral direction (Prinos et al., 1985) and the presence of secondary currents and vortices (Nezu & Nakayama, 1997; Shiono & Knight, 1991) travelling along the interface. Consequently, the wake of the obstacle is influenced by these processes.

The objective of the current study is to determine the effect of the shear layer of the compound-channel flow on the cylinder-wake processes and the value of the drag coefficient. The drag effect on the flow is estimated considering momentum balance, as proposed by Hinze (1975). The relevant equation is applied in its integral form in a fluid control-volume encompassing the cylinder. Mean-velocity and flow-depth measurements within the control volume are fed into the equation for extracting the mean drag force at a certain distance from the channel bed. The main contributions to drag in the momentum-balance equation are presented and discussed. Then, the drag coefficient is estimated based on a velocity that characterizes the flow in the interfacial shear layer. The relevant estimated value is compared to the one of a cylinder in flow with uniformly-distributed velocities found by the authors and those mentioned by previous studies.

2. THEORETICAL CONSIDERATIONS

Conservation of time-averaged momentum is considered in a fluid control-volume, encompassing the wake of an emergent cylinder. The relevant equation writes as:

$$\int_{S_c\backslash S^{(0)}} \rho U_i (U_j n_j)\mathrm{d}S = \int_{S_c\backslash S^{(0)}} -Pn_i \mathrm{d}S + \int_{V_c} \rho g_i \mathrm{d}V + \int_{S_c\backslash S^{(0)}} -\rho \overline{u_i' u_j'} n_j \mathrm{d}S + \int_{S_c\backslash S^{(0)}} T_{ij} n_j \mathrm{d}S + \left(\int_{S^{(0)}} -Pn_i \mathrm{d}S + \int_{S^{(0)}} T_{ij} n_j \mathrm{d}S \right) \tag{1}$$

where n_i is the outward pointing normal unit-vector, U_i is the time-averaged velocity vector, P is the time-averaged pressure, T_{ij} is the time-averaged viscous-stress tensor, $-\rho\overline{u_i' u_j'}$ the Reynolds-stress tensor, g_i the acceleration of gravity, ρ the fluid density, V_c the control volume, S_c the total surface of the control volume and $S^{(0)}$ the part of S_c that is bounded by the cylinder wall. The last two terms in the right-hand part of Eq. (1) compose the acting force on the flow by the cylinder, so that

$$L|R_i| = \left| \int_{S^{(0)}} -Pn_i \mathrm{d}S + \int_{S^{(0)}} T_{ij} n_j \mathrm{d}S \right| \tag{2}$$

where L is the wet length of the cylinder, $\int_{S_0} -\mathrm{P}n_i \mathrm{dS}$ is the pressure component and $\int_{S_0} \mathrm{T}_{ij} n_j \mathrm{dS}$ is the viscous component of the average force R_i on the cylinder per unit length.

Applying Eq. (1) to a prismatic control volume with height h (Figure 1a) and assuming negligible viscous stresses we get:

$$R_i h = \int_{V_c} \rho g_i \mathrm{d}V + \sum_{k=1\ldots6} \left\{ -\int_{S^{(k)}} \rho U_i^{(k)} \left(U_j^{(k)} n_j^{(k)} \right) \mathrm{d}S + \int_{S^{(k)}} -P^{(k)} n_i^{(k)} \mathrm{d}S + \int_{S^{(k)}} -\rho \overline{u_i' u_j'}^{(k)} n_j^{(k)} \mathrm{d}S \right\} \tag{3a}$$

with $n^{(1)}$=[-1,0,0], $n^{(2)}$=[0,+1,0], $n^{(3)}$=[+1,0,0], $n^{(4)}$=[0,-1,0], $n^{(5)}$=[0,0,+1], $n^{(6)}$=[0,0,-1].

After converting the integral components to summations of discrete values, for the streamwise direction x we get:

$$R_x h = \rho g \sin(\theta) V_c + \rho \sum_{k=1\ldots6} -\left[U_x^{(k)} \left(U_j^{(k)} n_j^{(k)} \right) \right] S^{(k)} + \sum_{k=1\ldots6} \left[-P^{(k)} n_x^{(k)} \right] S^{(k)} + \rho \sum_{k=1\ldots6} \left[-\overline{u_x' u_j'}^{(k)} n_j^{(k)} \right] S^{(k)} \tag{3b}$$

where tan(θ) is the channel slope. Brackets denote surface averaging.

In this paper, sum $\rho \sum_{k=1\ldots6} -\left[U_x^{(k)}\left(U_j^{(k)} n_j^{(k)}\right)\right] S^{(k)}$ is referred as "net momentum-transport term", $\sum_{k=1\ldots6}\left[-P^{(k)} n_x^{(k)}\right] S^{(k)}$ as "pressure-difference term" and $\rho \sum_{k=1\ldots6}\left[-\overline{u'_x u'_j}^{(k)} n_j^{(k)}\right] S^{(k)}$ as "net stress term".

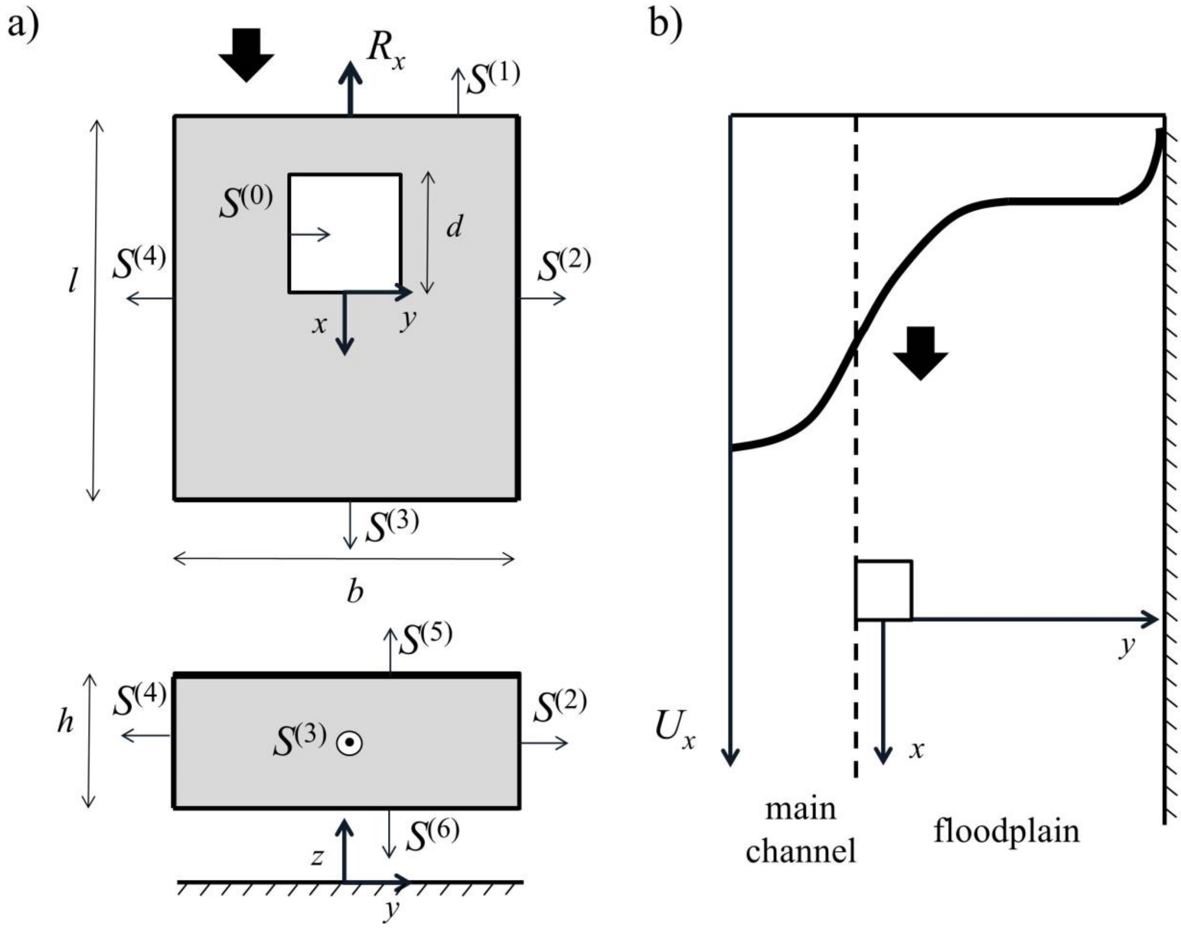


Figure 1: a) General depiction of the control volume in the x-y and y-z planes b) velocity profile across the symmetric part of a compound channel

The drag coefficient per unit wet length of an isolated square cylinder is estimated as:

$$C_d = \frac{2R_x}{\rho U_0^2 d} \tag{4}$$

where d is the width of the cylinder and U_0 the streamwise velocity of the upstream flow laterally averaged within the limits of the cylinder's frontal area.

3. EXPERIMENTAL FACILITY, EQUIPMENT AND PROCEDURE

3.1 Experimental facility

Experiments were conducted in the 10m-long straight symmetrical compound channel of the National Laboratory for Civil Engineering in Portugal (LNEC). The trapezoidal section of the main channel rests in the middle of the compound channel with side slope 1:1. The floodplain consists of two adjacent sections bounded with vertical walls, as shown in Figure 2, where the main geometric features of the channel are presented. The longitudinal bed-slope is 0.0011. The bottom of the main channel is hydraulically smooth (polished concrete) while that of the floodplain is artificially roughened by a layer of synthetic grass, the detailed characteristics of which are described in

Fernandes, Leal, and Cardoso (2014). The inlet of the main channel is separated from the inlet of the floodplain, improving the efficiency in establishing uniform-flow conditions. Adjustable tailgates are placed at the outlet for defining uniform-flow depth for a given total discharge. Water depth is measured by point gauges at 1 m and 8 m downstream the channel entrance. The two independent inflow rates (main channel and floodplain) are monitored by electromagnetic flowmeters. A more detailed description of the facility can be found in Fernandes (2013).

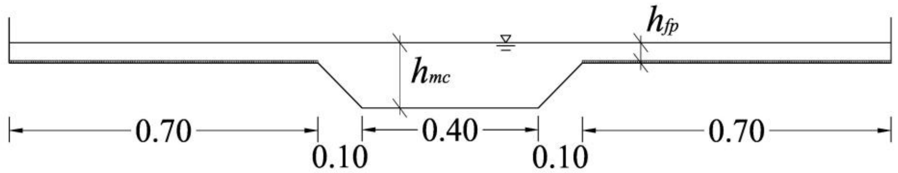


Figure 2: Channel cross-section

3.2 Experimental configuration

A square cylinder was placed initially in the middle of the floodplain, in order to obtain drag in flow with uniform velocities-distribution. Then the cylinder was placed at the mc/fp interface, as shown in Figure 1b. The two experiments will be referred as S0 and S1 respectively. Uniform-flow conditions were established in the compound channel, under which the cylinder was emergent in both tests. Total discharge Q_{tot} was distributed in the main channel and the floodplains as shown in Table 1. The relative flow-depth h_r, defined as the ratio between the floodplain flow-depth, h_{fp}, and the main-channel flow-depth, h_{mc}, was fixed at 0.31. Under these flow conditions the cylinder is emergent. A summary of the main parameters including the Reynolds number based on the cylinder width ($Re_d=U_0d/v$) is given in Table 1.

Table 1: Experimental flow-conditions and parameters

Experiments	Re_d (-)	h_r (-)	h_{fp} (m)	Q_{tot} (ls^{-1})	Q_{mc} (ls^{-1})	Q_{fp} (ls^{-1})	d (m)
S0	8365	0.31	0.045	58.9	42.3	16.6	0.045
S1	12032	0.31	0.045	58.9	42.3	16.6	0.045

3.3 Velocity and depth recordings

The three dimensional (3-D) instantaneous-velocity field was acquired with a side-looking Nortek-Vectrino Acoustic Doppler Velocimeter (ADV) at a rate of 200 Hz. The duration of measurements was set at three minutes. The grid shown in Figure 3 was applied at two elevations from the floodplain bed, z=0.015 m ($h_{fp}/3$) and z=0.012 m. Despiking of the velocity time-series was achieved by applying the phase-space filter, proposed by Goring and Nikora (2002). Measurements of the free-surface elevation were conducted with ultrasound recorders. The recordings had duration of two minutes and were performed at a rate of 10 Hz.

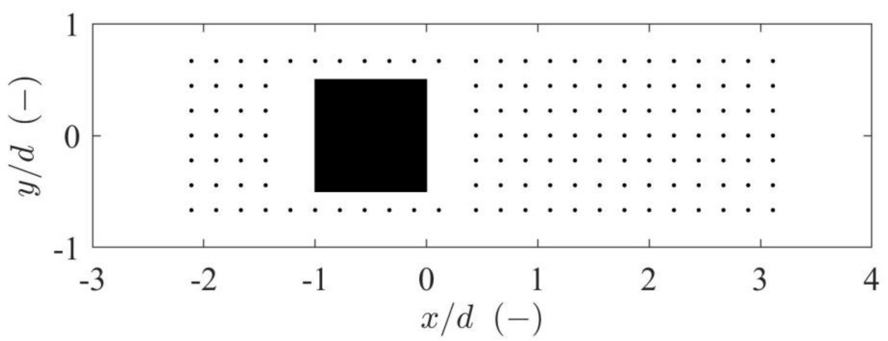


Figure 3: The grid of the measuring points, applied at two elevations for both S0 and S1. The flow is from left to right

4. RESULTS

4.1 Contributions to drag

The drag force was estimated by Eq. (3b) for a variety of control volumes with the same width b=1.33d and height h=3 mm, and various lengths l (Figure 1a). For each calculation, inlet surface $S^{(1)}$ was set at a fixed distance of x/d=2.11 (Figure 3),while the position of the outlet surface $S^{(3)}$ varied within the range 0.89 <x/d<3.11. For each case of the assumed control volume, estimation of the drag force R_x, involved evaluation of the terms of Eq. (3b). Each term in Eq. (3b) corresponds to a particular hydrodynamic process in the wake flow. The contribution of a term to drag expresses the magnitude of the related process relatively to that of the others occurring in the wake region. Therefore, considering multiple cases of positioning of $S^{(3)}$ of the control volume, besides the fact that someone can obtain drag assuming different control-volume geometries, it is also possible to observe the nature and behavior of these processes along the flow direction.

In general, an obstacle in a flow causes pressure drop and momentum loss of the fluid at the downstream shaded region. Then, longitudinal momentum is laterally drawn into the area of the maximum pressure-drop, restoring it partially. Since the lateral faces of the examined control volumes are found close to the cylinder's walls, the shaded region is encompassed and the relevant processes are evident though the values of the contributions to Eq. (3b). Herein, these contributions are discussed. The ones referring to the sheared wake (S1) are compared to those referring to the symmetrical wake produced by the cylinder in flow with uniformly-distributed velocities (S0). The presented terms of Eq. (3b) represent momentum-transport processes, fluid pressure and turbulent stresses. Fluid pressure is considered to follow hydrostatic distribution along depth. In Figures 4a and 4b, the three main contributing terms are examined for different distances of $S^{(3)}$ downstream the cylinder for cases S0 and S1. The terms are normalized with the quantity $C= \rho U_0^2 dh/2$.

As it may be observed in Figures 4a and 4b, all processes in S1, including the turbulent stresses, have similar tendencies with those occurring in S0. In particular, significant pressure differences are observed at small distances downstream the cylinder (S1). These differences gradually decrease, while momentum influxes in the near-wake field and generation of turbulence become stronger. However, the gradients of all terms are more intense than those corresponding to S0 test. This may be attributed to the higher Reynolds number of the flow in the main channel, next to the mc/fp interface of the compound channel, which distorts the geometry of the wake, suppressing its boundaries at smaller distance downstream the cylinder. Higher Reynolds number though, cannot explain the differences that the patterns of the particular terms exhibit, in comparison with those of the symmetrical wake.

The main difference is the increased contribution of the net transport term at the expense of the net stress term and the pressure-difference term. Moreover, the gradient of the curve that the relevant values form is positive throughout the entire examined downstream length, which contrasts to the findings referring to S0, where the contribution of this term decreases up to distance x/d~1.2. Analysis of results, not presented in this paper, demonstrated that this distance coincides with the wake-formation length.

Higher positive values of the net momentum-transport term in Eq. (3b) imply net influx to the control volume. The responsible underlying mechanisms are better understood if the behavior of the particular transport terms is investigated. Figure 5 presents the net contribution of the flux imbalance at the control surfaces a) in the streamwise direction and b) in the lateral direction. Higher positive values of the flux imbalance between $S^{(1)}$ and $S^{(3)}$ denote significant momentum loss in the main-flow direction downstream the obstacle. On the other hand, positive values of the flux imbalance between $S^{(2)}$ and $S^{(4)}$ imply net momentum-influx from the lateral control-volume faces. According to Figure 5a, momentum loss due to streamwise-velocity deficits downstream the obstacle is more intense in

the symmetrical-wake case. At the same time, integral momentum transfer at the lateral control surfaces $S^{(2)}$ and $S^{(4)}$ (Figure 5b) is directed outwards the low-pressure region. This means that flow deflection upstream the cylinder is so intense that fluxes from $S^{(2)}$ and $S^{(4)}$ downstream the cylinder do not compensate for the lost momentum of the deflected flow. When the wake is sheared, instead, integral lateral fluxes have values close to zero, meaning that flow deflection upstream the cylinder is balanced with flow attraction downstream. At this point, it can be assumed that this balance derives rather from limited flow deflection than intense flow attraction, since the S1 curve (Figure 5b) is found well above the S0 curve, and at the same time, both curves have similar gradients.

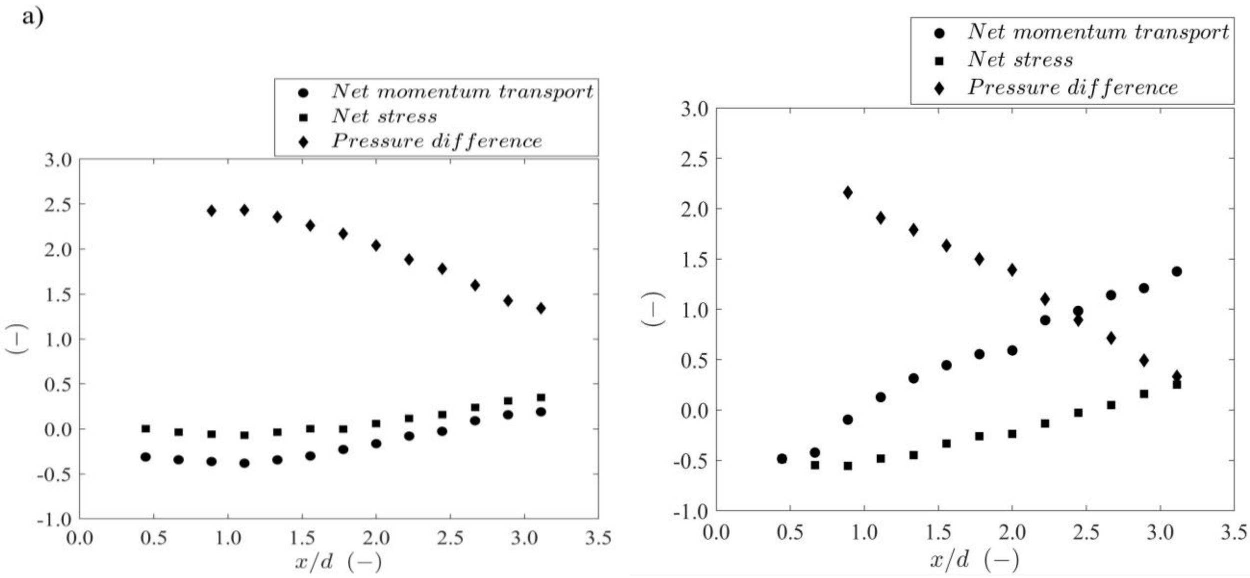


Figure 4: Contributions of the terms of Eq. (3b) for different positions of the outlet surface $S^{(3)}$ of the control volume for a) S0 and b) S1

In order to investigate the source of this flux balance on $S^{(2)}$ and $S^{(4)}$ for the S1 case, the relevant longitudinal flux-imbalance-distribution is examined in Figure 6. Negative fluxes upstream and at the sides of the cylinder (x/d<0) are due to the flow-deflection process described above. It is well seen in Figure 6 that these fluxes for S0 are higher than those for S1. Therefore, the assumption made in the previous paragraph can be considered valid.

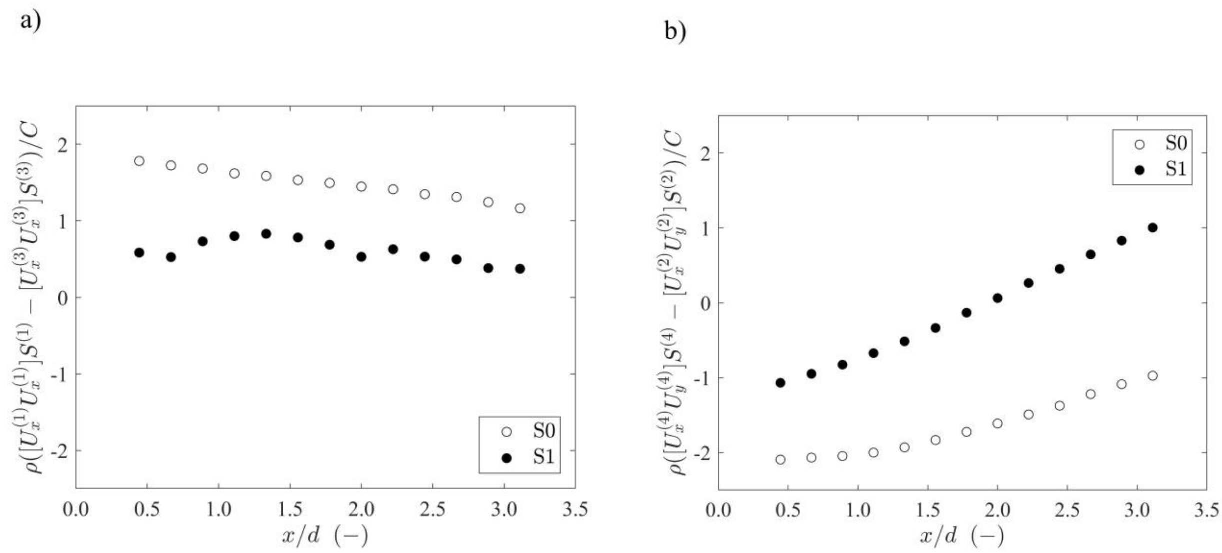


Figure 5: Contribution of the transport-terms imbalance on a) $S^{(1)}$, $S^{(3)}$ and b) $S^{(2)}$, $S^{(4)}$

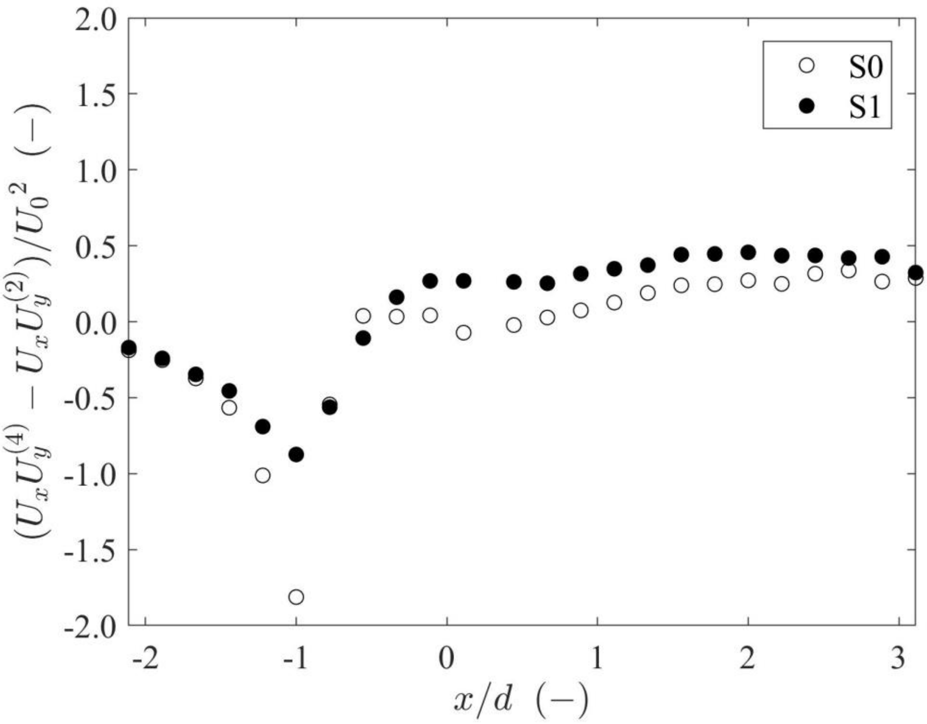


Figure 6: Flux-imbalance distribution on $S^{(2)}$ and $S^{(4)}$

Distribution of the net-stress (turbulent) contributions of S1 has similar gradients to that of S0 (Figure 4). However, the relevant values are decreased to such a level, so that they are significantly outweighed by those of the net momentum-transport. This decrease is more evident for x/d>1.2, where the corresponding values for S0 become positive. Someone would expect that the turbulent contributions for S1 would exceed those for S0, due to the existence of the shear layer which leads to stronger shear stress in the region next to the mc/fp interface. It appears though, that the aforementioned momentum transfer from the sides of the shaded region includes fluxes from the high-velocity fluid of the main channel, enriching the wake with streamwise momentum and prohibiting the formation of high streamwise-velocity gradients in the lateral direction. Therefore, relatively mild velocity gradients do not generate significant shear stresses on $S^{(2)}$ and $S^{(4)}$, and in turn, high stress contributions to drag.

4.2 Drag coefficient

The drag coefficient of the cylinder subjected to the shear flow was estimated for the elevation of reference $z=h_{fp}/3$. Its value is compared to that of the cylinder in flow with uniform velocities distribution (experiment S0). Table 2 summarizes the results and presents the values produced by other studies regarding similar Re_d numbers for symmetrical wakes.

The C_d of the cylinder at the interface seems to be lower than that of the cylinder in S0 experiment. This difference is better evaluated by comparing it with the range of values of the symmetrical-wake C_d of the previous studies. This range is bigger but is formed with values concerning also air flows. The coefficient referring to a closed water-channel (Lyn et al., 1995), as well as that produced in an open-channel flow for several Re_d numbers (Robertson, 2016) are higher than those of S0. The relevant difference is significant, and of the same magnitude with the difference between C_d of S0 and S1. Therefore, the reference test S0 is considered to be necessary for assessing the drag coefficient of the cylinder in the shear layer, since otherwise it would be further underestimated accounting for the existing studies. As a conclusion, in any case and given that the bed friction effect is not felt at the elevation of calculation of the drag force, drag coefficient C_d of the cylinder decreases when it is subjected to the shear layer of the compound channel.

Table 2: Drag coefficient of isolated square cylinder

Studies	Re_d (-)	C_d (-)
Current, S0	8365	2.06
Current, S1	12032	2.00
Yen and Yang, 2011	6300	1.86
Norberg, 1993	13000	2.15
Yen and Liu, 2011	21000	2.06
Lyn et al., 1995	21400	2.10
Robertson, 2016	10000-22000	2.11

5. CONCLUSIONS

This study demonstrated how the shear layer of a compound channel affects drag on an emergent square cylinder located at the interface between the main channel and the floodplain. The momentum-balance equation was applied in its integral form in an assumed control volume for the estimation of the drag force at a certain elevation from the floodplain bed. The wake processes were also identified through determination of the terms engaged in the momentum-balance equation and they were compared to the ones related to the symmetrical wake produced by a cylinder in a flow with uniform velocities distribution.

The main deviations that emerged through this comparison are:

- the lower streamwise-momentum deficits in the shaded region donwstream the cylinder,
- the limited flow deflection upstream the obstacle,
- the lower net shear from the flow at the sides of the cylinder wake.

Regarding the drag coefficient C_d, a small decrease was observed comparatively to that yielded by the cylinder with the symmetrical wake. The assessed value is found within the range of values mentioned in previous studies and it approximates rather the lower estimations.

References

1. Fernandes J.N. (2013). ‘Compound channel uniform and non-uniform flows with and without vegetation in the floodplain’. Ph.D thesis, Univ. of Lisbon, Portugal.
2. Fernandes J.N., J.B Leal and A.H. Cardoso. (2014). ‘Improvement of the lateral distribution method based on the mixing layer theory’. **Advances in Water Resources**, Vol. 69, pp. 159-167.
3. Goring D.G. and V.I. Nikora. (2002). ‘Despiking acoustic doppler velocimeter data’. **Journal of Hydraulic Engineering**, Vol 128(1), pp. 117-126.
4. Hinze J.O. (1975). ‘Turbulence’. McGraw-Hill.
5. Lyn D.A., S. Einav, W. Rodi and J.H. Park. (1995). ‘A laser-Doppler velocimetry study of ensemble-averaged characteristics of the turbulent near wake of a square cylinder’. **Journal of Fluid Mechanics**, Vol. 304, pp. 285-319.
6. Nezu I. and T. Nakayama. (1997). ‘Space-time correlation structures of horizontal coherent vortices in compound channel flows by using particle-tracking velocimetry’. **Journal of Hydraulic Research**, Vol. 35(2), pp. 191-208.
7. Norberg C. (1993). ‘Flow around rectangular cylinders: pressure forces and wake frequencies’. **Journal of Wind Engineering and Industrial Aerodynamics**, Vol. 49, pp. 187-196.

8. Prinos P., R. Townsend and S. Tavoularis. (1985). ‘Structure of turbulence in compound channel flows’. **Journal of Hydraulic Engineering**, Vol. 111(9), pp. 1246-1261.
9. Robertson F.H. (2016). ‘An experimental investigation of the drag on idealised rigid, emergent vegetation and other obstacles in turbulent free-surface flows’. Ph.D thesis, Univ. of Manchester, UK.
10. Shiono K. and D.W. Knight. (1991). ‘Turbulent open channel flows with variable depth across the channel’. **Journal of Fluid Mechanics**, Vol. 222, pp. 617-646.
11. Yen S.C. and J.H. Liu. (2011). ‘Wake flow behind two side-by-side square cylinders’. **International Journal of Heat and Fluid Flow**, Vol. 32, pp. 41-51.
12. Yen S.C. and C.W. Yang. (2011). ‘Flow patterns and vortex shedding behavior behind a square cylinder’. **Journal of Wind Engineering and Industrial Aerodynamics**, Vol. 99(8), pp. 868-878.

A FUZZY MULTICRITERIA DECISION APPROACH TO SELECT THE OPTIMAL TYPE OF SPILLWAY AT A SPECIFIC DAM

V. Balioti*, C. Tzimopoulos and C. Evangelides

Division of Transportation and Hydraulic Engineering, Dept. of Rural & Surveying Engineering, A.U.Th, GR- 54124 Thessaloniki, Macedonia, Greece

*Corresponding author: e-mail: vasilikimpalioti@hotmail.com , tel : +306939320723

Abstract

The selection of the optimal type of a spillway is considered as one of the most important parameters for the dam construction. The objective of this research is to develop a multi-criteria decision making model (MCDM) based on fuzzy set theory. For this purpose 5 alternative types of spillways were selected with nine criteria. Since most information available in this stage is not numerical and uncertain, fuzzy set theory and linguistic variables, parameterized by triangular fuzzy numbers (TFN), are used to represent the evaluation ratings of candidate items. The developed model, which is a combination of both methods TOPSIS (Technique for Order Preference by Similarity to Ideal Solution) and AHP (Analytic Hierarchy Process), ranks candidate items and assists decision makers in selecting the most proper type of spillway. An example of selecting the optimal spillway is used to illustrate the concept developed.

Keywords: Optimal spillway, Linguistic variables, MCDM, TFN, Fuzzy, TOPSIS method, AHP

1. INTRODUCTION

Multi-criteria decision making methods (MCDM) in a fuzzy environment can deal with problems which are too complex or ill-defined. In other words, a MCDM method is the process of finding the optimal alternative among all feasible alternatives (Tecle et al. 1988; Weng et al. 2010). Several techniques are available such as the Compromise Programming (Zeleny, 1974), the Analytic Hierarchy Process (Saaty, 1980), the Cooperative Game Theory (Nash, 1953; Szidarovszky et al., 1984), the Composite Programming (Bardossy et al., 1985) etc. Among those techniques we selected TOPSIS method into fuzzy environment, using a linguistic scaling and a part of the AHP to assign weights to the data of the problem.

The optimal type of a spillway is one of the most complex issues in water management including considerable uncertainty due to the existence of qualitative criteria. The main criteria were determined using extensive library studies and experts' opinion. The institutes that were found to give special recommendations for the spillway type selection are the Indian Standards Institute (Bureau of Indian Standards, 1982) and U.S. Bureau of Reclamation (Reclamation, 2014). Finally, nine criteria have been chosen: a) C_1= construction costs, b) C_2= maintenance costs, c) C_3= foundation, d) C_4= reservoir capacity, e) C_5= static/ construction difficulty, f) C_6= discharge capacity, g) C_7= physical space, h) C_8= conveyance feature (costs and construction difficulty) and i) C_9= aesthetic, to evaluate the five alternatives (types of spillway): a) X_1= ogee or overfall spillway, b) X_2= shaft or morning glory spillway, c) X_3= side channel spillway, d) X_4= siphon spillway and e) X_5= gated spillway.

2. TOPSIS (TECHNIQUE FOR ORDER PREFERENCE BY SIMILARITY TO IDEAL SOLUTION) METHOD

TOPSIS (Technique for Order Preference by Similarity to Ideal Solution) method was first developed at 1981 by Yoon and Hwang (Yoon and Hwang, 1981). Its basic concept is that the chosen alternative should have the shortest distance from the ideal solution and the farthest from the negative-ideal solution. In the last two decades TOPSIS and Fuzzy TOPSIS have been employed in many fields; fuel buses selection (Vahdani et al., 2011), bridge scheme selection (Mousavi, 2008), inter-company comparison (Deng et al., 2000), risk identification (Ebrahimnejad et al., 2010), robotics (Chu and Lin, 2003), supply chain management (Chen et al., 2006), temporary storage design in industrial plants (Heydar et al., 2008) etc. For hydraulic and water management issues in particular, it has been used in selecting dam site (Tzimopoulos et al., 2013), irrigation networks (Tzimopoulos et al., 2012, Tzimopoulos, 2012), risk assessment of dam removal (Qi, 2010) etc.

There have been several approaches for Fuzzy TOPSIS. The chosen one for this application is Chen's approach (Chen, 2000). According to this theory, the attributes are expressed in TFNs, the normalization method is linear and vertex method is proposed for the calculation of the distance measurements for the final ranking. The procedure of fuzzy TOPSIS is similar to the classic one and can be expressed in a series of steps:

a) Construct the normalized decision matrix.

– In the fuzzy environment, in order to avoid the complicated normalization formula used in classical TOPSIS, the linear scale transformation is used to transform the various criteria scales into a comparable scale.

$$\tilde{r}_{ij} = \left(\frac{a_{ij}}{c_j^*}, \frac{b_{ij}}{c_j^*}, \frac{c_{ij}}{c_j^*} \right), \; c_j^* = \max_i c_{ij} \tag{1}$$

where $\tilde{x}_{ij} = (a_{ij}, b_{ij}, c_{ij})$ are the elements of the decision matrix.

b) Construct the weighted normalized decision matrix.

$$\tilde{v}_{ij} = \tilde{w}_j \cdot \tilde{r}_{ij}, \qquad j=1,2,\dots m\,,\; i=1,2,\dots n \tag{2}$$

c) Determine the fuzzy ideal and fuzzy negative-ideal solutions.

$$A^+ = \{\tilde{v}_1^+, \tilde{v}_2^+, \dots \tilde{v}_m^+\} \tag{3}$$

$$A^- = \{\tilde{v}_1^-, \tilde{v}_2^-, \dots \tilde{v}_m^-\} \tag{4}$$

where $\tilde{v}_j^+$=(1,1,1) and $\tilde{v}_j^-$=(0,0,0), j=1,2,…m.

d) Calculate the separation measure:

– Ideal separation

$$S_i^+ = \sum_{j=1}^{m} d(\tilde{v}_{ij}, \tilde{v}_j^+) \qquad i=1,2,\dots n \tag{5}$$

– Negative-ideal separation

$$S_i^- = \sum_{j=1}^{m} d(\tilde{v}_{ij}, \tilde{v}_j^-) \qquad i=1,2,\dots n \tag{6}$$

where $d(\tilde{v}_{ij}, \tilde{v}_j^+)$ and $d(\tilde{v}_{ij}, \tilde{v}_j^-)$ are distance measurements calculated with the vertex method:

$$d(\tilde{x}_{ij}, \tilde{y}_{ij}) = \sqrt{\frac{1}{3}\left[\left(x_{ij}^1 - y_{ij}^1\right)^2 + \left(x_{ij}^2 - y_{ij}^2\right)^2 + \left(x_{ij}^3 - y_{ij}^3\right)^2\right]}, \quad (7)$$

$$\tilde{x}_{ij} = \left(x_{ij}^1, x_{ij}^2, x_{ij}^3\right),\ \tilde{y}_{ij} = \left(y_{ij}^1, y_{ij}^2, y_{ij}^3\right)$$

e) Calculate the relative closeness to the Ideal Solution.

$$c_i^* = \frac{S_i^-}{(S_i^+ + S_i^-)}, \qquad 0 < c_i^* < 1, \quad i=1,2,\ldots,n \quad (8)$$

$c_i^* = 1$ if $A_i = A^+$

$c_i^* = 0$ if $A_i = A^-$

f) Rank the preference order.

– A set of alternatives can now be preference ranked according to the descending order of c_i^*

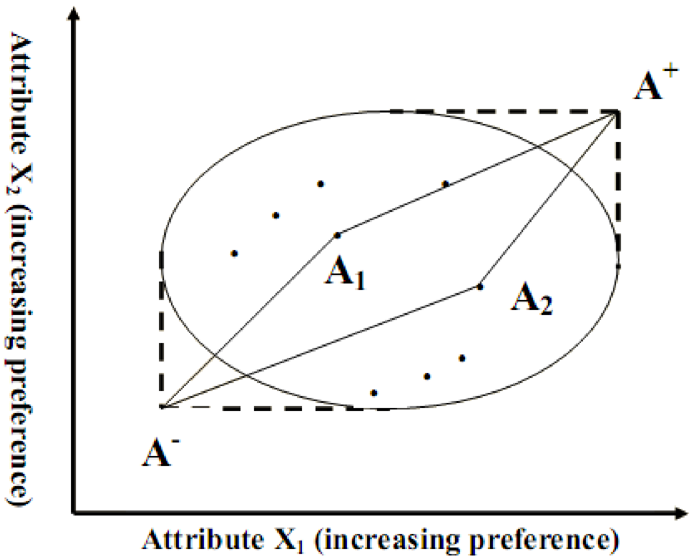


Figure 1: Basic concept of TOPSIS method (A^+: Ideal point, A^-: Negative -Ideal Point)

The method presupposes that:

a. Each criterion in the decision matrix takes monotonically either increasing or decreasing utility.

b. A decision matrix of n alternatives and m criteria and a set of weights for the criteria are required.

c. Any outcome which is expressed in a non-numerical way should be quantified through the appropriate scaling technique.

3. LINGUISTIC VARIABLES EXPRESSED IN TFN (TRIANGULAR FUZZY NUMBERS)

The extension of TOPSIS method in the fuzzy environment can be achieved by expressing the weights of criteria and ratings as linguistic variables. A linguistic variable is a variable whose values are linguistic terms. The concept of linguistic variable is very useful in dealing with situations which are too complex or too ill-defined to be reasonably described in conventional quantitative expressions

(Zadeh, 1975). According to many authors, the linguistic variables can be expressed in positive triangular fuzzy numbers as shown in Tables 1 and 2 (Chen, 2010).

Table 1: Linguistic variables for the importance weight of each criterion

Very low (VL)	(0.1,0,0)
Low (L)	(0.3,0.1,0.1)
Medium low (ML)	(0.5,0.3,0.3)
Medium (M)	(0.7,0.5,0.5)
Medium high (MH)	(0.9,0.7,0.7)
High (H)	(1,0.9,0.9)
Very high (VH)	(1,1,1)

Table 2: Linguistic variables for the ratings

Very poor (VP)	(1,0,0)
Poor (P)	(3,1,1)
Medium poor (MP)	(5,3,3)
Fair (F)	(7,5,5)
Medium good (MG)	(9,7,7)
Good (G)	(10,9,9)
Very good (VG)	(10,10,10)

4. TRIANGULAR FUZZY NUMBERS (TFN)

We define a fuzzy number $\tilde{M}$ on R^+ to be a triangular fuzzy number in case its membership function

$$\mu_{\tilde{M}}(x): R \rightarrow [0, 1] \text{ is equal to } \mu_{\tilde{M}}(x) = \begin{cases} \dfrac{x}{c-\ell} - \dfrac{\ell}{c-\ell}, & x \in [\ell, c], \\ \dfrac{x}{c-u} - \dfrac{u}{c-u}, & x \in [c, u], \\ 0, & \text{otherwise} \end{cases} \tag{9}$$

where $\ell \leq c \leq u$. The triangular fuzzy number $\tilde{M}$ can be denoted by (ℓ, c, u).

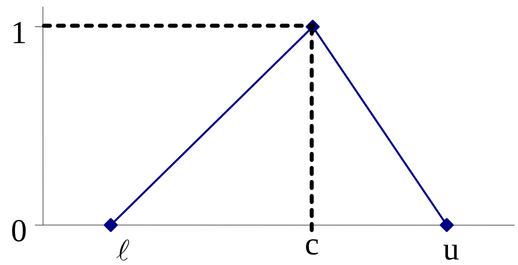


Figure 2: A triangular fuzzy number $\tilde{M}$

Consider two triangular fuzzy nucbers $\tilde{M}_1$ and $\tilde{M}_2$, $\tilde{M}_1 = (\ell_1, c_1, u_1)$ and $\tilde{M}_2 = (\ell_2, c_2, u_2)$.

1. $(\ell_1, c_1, u_1) + (\ell_2, c_2, u_2) = (\ell_1 + \ell_2, c_1 + c_2, u_1 + u_2)$ (10)

2. $(\ell_1, c_1, u_1) \times (\ell_2, c_2, u_2) = (\ell_1 \times \ell_2, c_1 \times c_2, u_1 \times u_2)$ (11)

3. $(\lambda, \lambda, \lambda) \times (\ell_1, c_1, u_1) = (\lambda \ell_1, \lambda c_1, \lambda u_1)$, $\lambda>0$, $\lambda \varepsilon R$ (12)

4. $(\ell_1, c_1, u_1)^{-1} = (1/u_1, 1/c_1, 1/\ell_1)$ (13)

5. ANALYTIC HIERARCHY PROCESS (AHP) SCALING

The analytic hierarchy process (AHP) (Saaty, 1980) is based on decomposing a complex MCDM problem into a system of hierarchies. There is a fundamental scale of absolute numbers from 1 to 9 shown in Table 3, in order to design the hierarchy.

When we estimate dominance in making comparisons, particularly when the criterion of the comparisons is intangible, instead of using two numbers w_i and w_j from a scale (rather than interpreting the significance of their ratio w_i/w_j) we assign a single number drawn from the fundamental scale 1 to 9 of absolute numbers shown in Table 3 to represent the ratio $(w_i/w_j)/1$. It is a nearest integer approximation to the ratio w_i/w_j. The derived scale will reveal what the w_i and w_j are. This is the main fact about the relative measurement approach and the need for a fundamental scale.

Table 3: Fundamental Scale of Absolute Numbers

Intensity of Importance	Definition	Explanation
1	Equal Importance	Two activities contribute equally to the objective
2	Weak or slight	
3	Moderate importance	Experience and judgment slightly favor one activity over another
4	Moderate plus	
5	Strong importance	Experience and judgment strongly favor one activity over another
6	Strong plus	
7	Very strong or demonstrated importance	An activity is favored very strongly over another; its dominance demonstrated in practice
8	Very, very strong	
9	Extreme importance	The evidence favoring one activity over another is of the highest possible order of affirmation
Reciprocals of above	If activity i has one of the above nonzero numbers assigned to it when compared with activity j, then j has the reciprocal value when compared with i	A logical assumption

6. ILLUSTRATIVE APPLICATION

The chosen dam is named “Pigi Dam” by “Kotza- Dere” river, which is located in Northern Greece. It is considered as a large dam (GCOLD, 2013) and was constructed on 1999. It is a rockfill dam with the upstream face made of concrete (impervious zone) constructed for irrigation. The dam is 38 m tall, 159 m long and its volume is calculated at 139×10^3 m^3. Its reservoir capacity and surface are 2,750 $\times10^3$ m^3 and 265 $\times10^3$ m^2 respectively and the discharge capacity of its spillway is 884 m^3/s.

In order to define the optimal type of this dam’s spillway, the calculation steps that need to be made are described below. Firstly, the decision maker computes the weights for the different criteria (Table 5) and the decision matrix by creating pairwise comparison matrices according to AHP. It is important to mention that in all cases, C.R. (Consistency Ratio) is less than 0.1 and the judgments are acceptable.

Table 4: Comparison matrix for the weights

	C^1	C^2	C^3	C^4	C^5	C^6	C^7	C^8	C^9
C^1	1	1	4	4	4	5	7	3	9
C^2	1	1	4	4	4	5	7	3	9
C^3	0.25	0.25	1	0.2	1	4	6	0.25	6
C^4	0.25	0.25	5	1	5	6	5	0.25	7
C^5	0.25	0.25	1	0.2	1	5	5	0.25	6
C^6	0.20	0.20	0.25	0.17	0.20	1	3	0.2	4
C^7	0.14	0.14	0.17	0.20	0.20	0.33	1	0.14	5
C^8	0.33	0.33	4	4	4	5	7	1	8
C^9	0.11	0.11	0.17	0.14	0.17	0.25	0.20	0.13	1

Table 5: Criteria’s weights

C^1	C^2	C^3	C^4	C^5	C^6	C^7	C^8	C^9
0.235	0.235	0.074	0.133	0.075	0.039	0.029	0.164	0.015

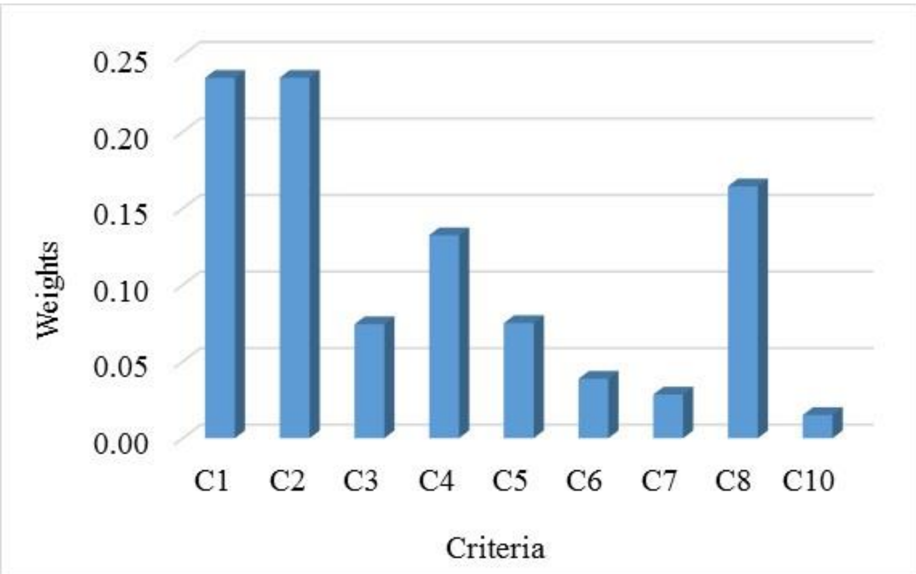


Figure 3: Importance of each criterion after AHP evaluation

Table 6: Decision matrix after AHP evaluation

	C^1	C^2	C^3	C^4	C^5	C^6	C^7	C^8	C^9
X_1	0.22	0.50	0.29	0.08	0.36	0.06	0.13	0.11	0.28
X_2	0.47	0.13	0.06	0.08	0.04	0.52	0.34	0.04	0.52
X_3	0.22	0.26	0.06	0.08	0.08	0.06	0.13	0.28	0.06
X_4	0.05	0.07	0.29	0.08	0.16	0.28	0.34	0.28	0.06
X_5	0.03	0.03	0.29	0.67	0.36	0.06	0.06	0.28	0.06

At the second step fuzziness is introduced to the process so as to confront the uncertainties of judgments or calculations of the previous step. After normalizing the decision matrix and the weights' matrix for the criteria by dividing each element with the maximum value per criterion, the decision maker reconstructs these matrices using linguistic variables. Finally, he applies the linguistic variables to the TFNs proposed by Chen in Tables 1 and 2.

Table 7: Linguistic and fuzzy weights

C^1	C^2	C^3	C^4	C^5	C^6	C^7	C^8	C^9
VH	VH	ML	M	ML	L	L	MH	L
(0.9,1,1)	(0.9,1,1)	(0.1,0.3,0.5)	(0.3,0.5,0.7)	(0.1,0.3,0.5)	(0,0.1,0.3)	(0,0.1,0.3)	(0.5,0.7,0.9)	(0,0.1,0.3)

Table 8: Decision matrix in linguistic terms

	C^1	C^2	C^3	C^4	C^5	C^6	C^7	C^8	C^9
X_1	F	VG	VG	P	VG	P	MP	F	F
X_2	VG	MP	P	P	P	VG	VG	P	VG
X_3	F	F	P	P	MP	P	MP	VG	P
X_4	P	P	VG	P	F	F	VG	VG	P
X_5	P	P	VG	VG	VG	P	MP	VG	P

Table 9: Fuzzy decision matrix

	C^1	C^2	C^3	C^4	C^5	C^6	C^7	C^8	C^9
X_1	(3,5,7)	(9,10,10)	(9,10,10)	(0,1,3)	(9,10,10)	(0,1,3)	(1,3,5)	(3,5,7)	(3,5,7)
X_2	(9,10,10)	(1,3,5)	(0,1,3)	(0,1,3)	(0,1,3)	(9,10,10)	(9,10,10)	(0,1,3)	(9,10,10)
X_3	(3,5,7)	(3,5,7)	(0,1,3)	(0,1,3)	(1,3,5)	(0,1,3)	(1,3,5)	(9,10,10)	(0,1,3)
X_4	(0,1,3)	(0,1,3)	(9,10,10)	(0,1,3)	(3,5,7)	(3,5,7)	(9,10,10)	(9,10,10)	(0,1,3)
X_5	(0,1,3)	(0,1,3)	(9,10,10)	(9,10,10)	(9,10,10)	(0,1,3)	(1,3,5)	(9,10,10)	(0,1,3)

The procedure continues with the TOPSIS' calculations (Equations 1-8).

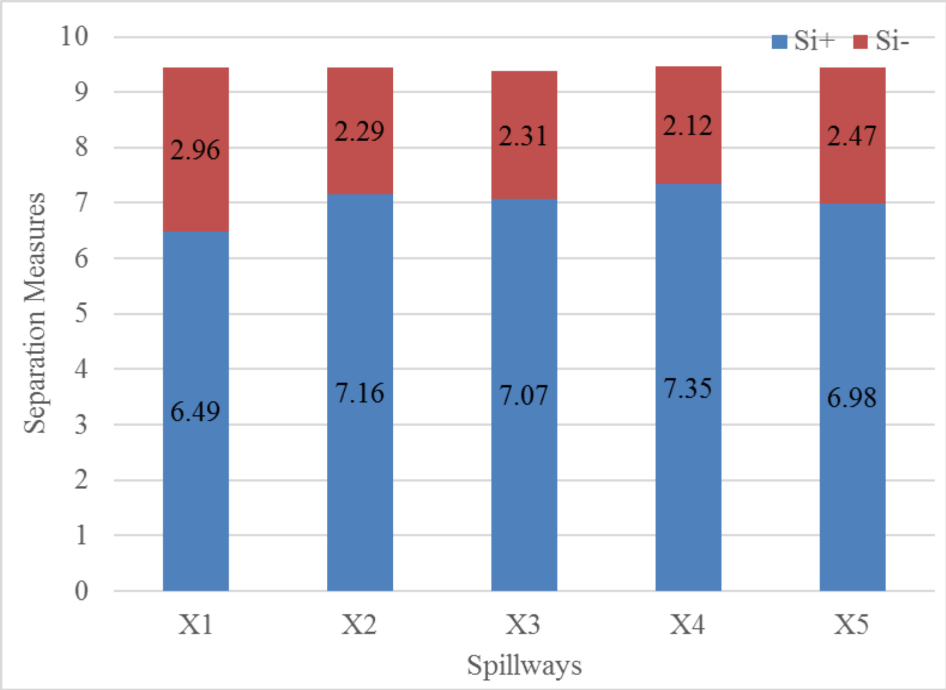


Figure 4: Separation measures; Ideal separation, Negative-ideal separation

Finally, we obtain the ranking between the alternatives by calculating the relative closeness.

X_1 (0.313) >X_5(0.261) > X_3(0.246) > X_2(0.243) > X_4(0.224)

X_1= ogee spillway > X_5= gated spillway > X_3= side channel spillway > X_2= shaft spillway > X_4= siphon spillway

7. DISCUSSION AND CONCLUSIONS

This paper presents the first application of the combination of the proposed MCDM methods with fuzzy logic to solve the problem of selecting the optimal type of a spillway in all types and sizes of dams.

Although a spillway is an important chapter in hydraulics, little guidelines on how to select its type can be found in literature. As a result, in most cases, the selection derives from a techno-economic and feasibility analysis. Our study proves that more parameters rather than technical feasibility and low construction costs should be taken into consideration. X_2 (shaft or morning glory spillway) spillway has the highest evaluation for C^1 (construction costs) criterion (Table 8), which means that it is the most cost-efficient alternative. Nevertheless, in the presented approach, X_2 would be the fourth choice out of the five.

Finally, it is suggested that engineering problems involving decision making could be better dealt with MCDM methods and fuzzy logic. It helps the decision maker not only to get the optimal solution, but also have a ranking order. The aforementioned process could also be implemented in various engineering problems.

References

1. Bardossy, A., I. Bogardi and L. Duckstein. (1985). ‘Composite Programming as an Extension of Compromise Programming’. **Mathematics of Mulitobjective Organization**, ed. P. Serafine, pp. 375-408, Springer-Verlag, New York.
2. Bureau of Indian Standards. (1982). ‘IS 10137: Guidelines for selection of spillways and energy dissipators’. New Delhi.

3. Chen, C. T. (2000). ‘Extensions of the TOPSIS for group decision-making under fuzzy environment’. **Fuzzy sets and systems**, Vol 114(1), pp. 1-9.
4. Chen, C. T., C. T. Lin and S. F. Huang. (2006). ‘A fuzzy approach for supplier evaluation and selection in supply chain management’. **International journal of production economics**, Vol 102(2), pp. 289-301.
5. Chu, T. C. and Y. C. Lin. (2003). ‘A fuzzy TOPSIS method for robot selection’. **The International Journal of Advanced Manufacturing Technology**, Vol 21(4), pp. 284-290.
6. Deng, H., C. H. Yeh and R. J. Willis. (2000). ‘Inter-company comparison using modified TOPSIS with objective weights.’ **Computers & Operations Research**, Vol 27(10), pp. 963-973.
7. Ebrahimnejad S., S. M. Mousavi, and H. Seyrafianpour. (2010). ‘Risk identification and assessment for build–operate–transfer projects: A fuzzy multi attribute decision making model’. **Expert systems with Applications**, Vol 37(1), pp. 575-586.
8. GCOLD (Greek Committee on large dams). (2013). ‘The dams of Greece’. Proc. Nat. Conf. **2nd National Conference on Dams.** Athens, Greece.
9. Heydar, M., R. Tavakkoli-Moghaddam, S. M. Mousavi and S. M. H. Mojtahedi. (2008). ‘Fuzzy multi criteria decision making method for temporary storage design in industrial plants.’. **In Industrial Engineering and Engineering Management, 2008. IEEM 2008. IEEE International Conference** on pp. 1154-1158.
10. Mousavi, S. M., H. Malekly, H. Hashemi, and S. M. H. Mojtahedi. (2008). ‘A two-phase fuzzy decision making methodology for bridge scheme selection.’. **In Industrial Engineering and Engineering Management, 2008. IEEM 2008. IEEE International Conference** on, pp. 415-419.
11. Nash J. F. (1953). ‘Two-Person Cooperative Games’. **Econometrica** Vol. 21, pp. 128-140.
12. Qi, C. Q. (2010). ‘Research on risk assessment of dam removal.’. **Future Information Technology and Management Engineering (FITME), 2010 International Conference** on, Vol. 2, pp. 185-188. IEEE.
13. Reclamation, U. B. O. (2014). ‘General Spillway Design Considerations.’ Design Standards No. 14 Chapter 3: Final: Phase 4.
14. Saaty T. L. (1980). ‘The Analytic Hierarchy Process: Planning, Priority Setting, and Resources Allocation’, McGraw-Hill.
15. Szidarovsky, F., L. Duckstein and I. Bogardi. (1984). ‘Multiobjective Management of Mining under Water Hazard by Game Theory’. **European Journal of Operations Research** Vol. 15, pp. 251-258.
16. Tecle A., M. Fogel and L. Duckstein. (1988). ‘Multicriterion selection of wastewater management alternatives’. **Journal of Water Resources Planning and Management**, Vol 114(4), pp. 383-398.
17. Tzimopoulos, C., V. Balioti and C. Evangelides. (2012). ‘Multi- criteria decision making using TOPSIS method. Application in irrigation networks.’ **Proc. Int. Conf. XI Protection and Restoration of the Environment**, (PRE XI). Thessaloniki, Greece.
18. Tzimopoulos, C. (2012). ‘Application of the TOPSIS method in the irrigation networks of GOEV-Thessaloniki.’. **Proc. Nat. Conf. 2nd National Joint Conference HHA-EEDYP**, Patras, Greece.
19. Tzimopoulos, C., V. Balioti and C. Evangelides. (2013). ‘Fuzzy multi- criteria decision making method for dam selection’. **Proc. Int. Conf. 13th International Conference on Environmental Science and Technology (CEST 2013)**, Athens, Greece.

20. Vahdani, B., M. Zandieh and R. Tavakkoli-Moghaddam. (2011). ‘Two novel FMCDM methods for alternative-fuel buses selection’. **Applied Mathematical Modelling**, Vol 35(3), pp. 1396-1412.
21. Weng S. Q., G. H. Huang and Y. P. Li. (2010). ‘An integrated scenario-based multi-criteria decision support system for water resources management and planning–A case study in the Haihe River Basin’. **Expert Systems with Applications**, Vol 37(12), pp. 8242-8254.
22. Zadeh, L. A. (1975). ‘The concept of a linguistic variable and its application to approximate reasoning—I’. **Information sciences**, Vol 8(3), pp. 199-249.
23. Zeleny M. (1974). ‘A Concept of Compromise Solutions and the Method of the Displaced Ideal’. **Computers and Operations Research** Vol. 1, pp. 479-496.

MODELLING ENVIRONMENTAL FLOWS WITH LAGRANGIAN PARTICLE MESH-FREE METHODS

A. Liakopoulos*, F. Sofos, T. Karakasidis

Hydromechanics and Environmental Engineering Laboratory,
Dept. of Civil Engineering, University of Thessaly,
Pedion Areos, GR-38334, Volos, Greece

*Corresponding author: e-mail: aliakop@civ.uth.gr

Abstract

Particle methods are computational techniques in which material particles move under the action of forces obtained from the discretization of the governing partial differential equation (e.g. the Navier-Stokes equations in fluids). A large group of recently proposed particle methods are meshless, i.e they do not require an associated mesh or grid in order to track the motion of the particles. As such, particle methods are very well suited for modelling and simulating flows with interfaces undergoing large deformations. In this paper we present a brief review of particle methods with emphasis on the method of Smoothed Particle Hydrodynamics (SPH). Basic concepts of the SPH method such as the integral interpolation method, the discretization of partial differential equations (PDEs) based on distributed nodal points (particles), and the choice of interpolation kernel functions are reviewed. We describe recent work on corrections applied to the original SPH method, the implementation of the method in LAMMPS and on validation of computer codes based on test cases.

Keywords: Particle Methods, Smoothed Particle Hydrodynamics (SPH), LAMMPS, Environmental flows

1. INTRODUCTION

The methods of conventional Computational Fluid Dynamics and Computational Hydraulics are based on Partial Differential Equations (PDEs) derived in the conceptual framework introduced by Euler. These methods have reached a very good level of maturity nowadays. However, at the same time, the weaknesses of these methods have been exposed and the limits of their applicability are now fairly well understood. For example, these methods fail in cases of large deformation of free surfaces or, more generally, interfaces. In contrast, Lagrangian methods, based on the concept of describing the flow by following the motion of fluid particles appear to have the capability to overcome the problems associated with large deformations. In addition, Lagrangian particle-based methods offer a unified framework for overcoming the difficulties associated with multi-scale modeling and simulation.

A number of particle methods have been proposed over the past three decades, e.g. Smoothed Particle Hydromechanics, Moving Particle Semi-implicit, Element–free Galerkin method, Material Point Method, among many others. These particle methods do not require a mesh (grid) for their implementation. It should be noted that there are particle methods that require grid such as the Particle in Cell (PIC) method. These methods are not in the category of numerical methods discussed in this work.

Among the particle methods, Smoothed Particle Hydrodynamics has become very popular with researchers in coastal engineering, computational hydraulics and wave/structure interaction. SPH was originally proposed as a method for the solution of problems in astrophysics (Lucy, 1977, Gringold & Monaghan 1977) for the solution of Newtonian non-viscous compressible flow. For approximately fifteen years the method was exclusively at the hands of astrophysicists. Monaghan (Monaghan, 1994) proposed the application of SPH to free-surface flow simulation. The original formulation assumed a weakly compressible fluid. Monaghan's paper kicked off a period of great interest in SPH which lead to significant improvements and extensions of the method. SPH is a purely Lagrangian method. Its success depends on the use of appropriate interpolation kernels (smoothing kernels), i.e. functions that interpolate the unknowns based on their values at irregularly spaced points (i.e., at the positions of particles). Some subtle points of the method include the topics of consistency, stability and convergence. SPH offers a number of important computational and modeling advantages over traditional CFD methods. SPH momentum equation does not contain the nonlinear advection terms that create a lot of difficulties in the computation of momentum dominated flows. Consequently, SPH does not require upwinding schemes. The method follows easily free surfaces in liquid flows without the need of special techniques, such as Volume of Fluid (VOF) or level-set methods to track the free-surface. Furthermore, SPH incorporates easily solid boundaries of complex geometry and serves as an approximate Large Eddy Simulation (LES) method in fluid flow simulation (for another view see Cleary and Prakash 2004). In addition, SPH can easily incorporate models of processes, such as heat transfer, solidification, solute transport, sediment transport, etc. to the basic fluid flow SPH equations. Generally, mesh-free particle methods are better suited for adaptive refinement procedures and for multi-scale computations (Li and Liu 2002, 2004).

2. THE METHOD OF SMOOTHED PARTICLE HYDRODYNAMICS

The central idea in SPH is the subdivision of the system under study to a number of moving particles ("chunks" or blobs of matter) (Monaghan, 1988 and 1992). The conservation laws of continuum fluid dynamics, in the form of partial differential equations, are transformed into their particle forms by integral equations through the use of an interpolation function that gives the kernel estimate of the field variables at a point. Information is extracted only at discrete points (the particles) and the integrals are evaluated as sums over neighboring particles. Each particle has a constant mass and time-dependent velocity, density, pressure, dynamic viscosity, temperature (as needed by the problem under study). In the SPH framework the governing PDEs describing the system in motion are transformed to a number of ordinary differential equations (ODEs). For example, a possible form of SPH formulation of conservation of momentum and mass PDEs leads to a set of ODEs for the velocities and densities of the particles which can be integrated by a numerical method of integration of ODEs (e.g. Verlet, Euler, Runge-Kutta, etc). The positions of the particles are then calculated by integrating the velocity. Detailed work on SPH can be found in (Gingold and Monaghan, 1977; Koumoutsakos, 2005; Shao, 2009; Bouscasse et al. 2013; Hieber and Koumoutsakos, 2008).

3. THE MATHEMATICS OF SMOOTHED PARTICLE HYDRODYNAMICS

In this section we briefly review the basic steps in developing an SPH formulation for a given partial differential equation. The case of Navier-Stokes equations and the energy equation for a Newtonian fluid is treated in some detail.

3.1 Integral approximation of functions and their derivatives

The starting point of an SPH formulation is an integral approximation of a function $f(\mathbf{x})$. In its ideal form the approximation has the form of the identity

$$f(\mathbf{x}) = \int_{\Omega} f(\mathbf{x}')\,\delta(\mathbf{x}-\mathbf{x}')\,\mathrm{d}\mathbf{x}' \qquad (1)$$

where $\mathbf{x}$ is the position vector and $\delta(\mathbf{x}-\mathbf{x}')$ is the Dirac's delta function defined as

$$\delta(\mathbf{x}-\mathbf{x}') = \begin{cases} 1 & \text{όταν} \quad \mathbf{x} = \mathbf{x}' \\ 0 & \text{όταν} \quad \mathbf{x} \neq \mathbf{x}' \end{cases}$$

In section 3 boldface characters denote vectors or tensors. Dirac's delta function is a generalized function (distribution) of point support that has the important property (1).

In order to be able to use the integral representation given by eq. (1) in a discrete computational scheme one has to replace the delta function by another function, say $\mathrm{W}(\mathbf{x}-\mathbf{x}';\mathrm{h})$ with finite support. This function is called kernel of the integral approximation and plays the role of a smoothing function over a spatial neighbourhood of dimension h.

$$f(\mathbf{x}) \approx \int_{\Omega} f(\mathbf{x}')\,\mathrm{W}(\mathbf{x}-\mathbf{x}';\mathrm{h})\,\mathrm{d}\mathbf{x}' \tag{2}$$

As expected the kernel (smoothing function) has to satisfy a number of conditions (Monaghan 1992). Equally important for the success of the SPH method is that the spatial derivatives can be computed by formulas of the form

$$\nabla \cdot f(\mathbf{x}) \approx -\int_{\Omega} f(\mathbf{x}') \cdot \nabla \mathrm{W}(\mathbf{x}-\mathbf{x}';\mathrm{h})\,\mathrm{d}\mathbf{x}' \tag{3}$$

It is clear that the choice of the kernel is important for the success of the method. Furthermore, the smoothing length h has to be chosen judicially.

3.2 Discretization using a set of particles

The second step in developing an SPH formulation is the discretization of the problem domain by a set of point masses (particles). The smoothing kernels (also known as interpolation kernels) are centered at the point masses. The value of a field variable and its derivative at particle i are calculate by the discete forms of equations (2) & (3). For a variable $f(\mathbf{x})$, we calculate its value at $\mathbf{x}_i$ by

$$f(\mathbf{x}_i) = \sum_{j=1}^{\mathrm{N}} \mathrm{m}_j \frac{f_j}{\rho_j} \mathrm{W}(\mathbf{x}_i - \mathbf{x}_j) \tag{4}$$

and the gradient at position $\mathbf{x}_i$ by

$$\nabla f(\mathbf{x}_i) = \nabla \sum_{j=1}^{\mathrm{N}} \mathrm{m}_j \frac{f_j}{\rho_j} \mathrm{W}_{ij} = \sum_{j=1}^{\mathrm{N}} \mathrm{m}_j \frac{f_j}{\rho_j} \nabla_{\mathrm{j}} \mathrm{W}_{ij} \tag{5}$$

Since W is radially symmetric

$$\nabla_j \mathrm{W}_{ij} = \frac{\mathbf{x}_{ij}}{\left\|\mathbf{x}_{ij}\right\|} \frac{\mathrm{dW}_{ij}}{\mathrm{dr}_{ij}} \tag{6}$$

where $\mathbf{x}_{ij} = \mathbf{x}_i - \mathbf{x}_j$, $\quad x_{ij} = \left\|\mathbf{x}_{ij}\right\|$, $\quad \mathrm{W}(\mathbf{x}_i - \mathbf{x}_j) = \mathrm{W}(x_{ij})$

3.3 An SPH formulation of the Navier-Stokes equations

Starting point of the procedure is the general continuum form of the conservation equations for a general fluid. In rectangular Cartesian coordinates (x^1, x^2, x^3) the conservation equations for mass, momentum and energy are written in indicial notation as

$$\frac{\mathrm{D}\rho}{\mathrm{Dt}} = -\rho \frac{\partial \upsilon^{\beta}}{\partial x^{\beta}} \tag{7}$$

$$\frac{\mathrm{D}\upsilon^{a}}{\mathrm{Dt}} = \frac{1}{\rho}\frac{\partial \sigma^{\alpha\beta}}{\partial x^{\beta}} + \mathrm{b}^{a} \tag{8}$$

$$\frac{\mathrm{De}}{\mathrm{Dt}} = \frac{1}{\rho}\sigma^{\alpha\beta}\frac{\partial \upsilon^{a}}{\partial x^{\beta}} - \frac{\partial q^{a}}{\partial x^{a}} \tag{9}$$

where ρ is the fluid density, $\left(\upsilon^{1},\upsilon^{2},\upsilon^{3}\right)$ are the components of the velocity vector, $\sigma^{\alpha\beta}$ the components of the total stress tensor, $\left(q^{1},q^{2},q^{3}\right)$ is the heat flux vector, $\left(\mathrm{b}^{1},\mathrm{b}^{2},\mathrm{b}^{3}\right)$ is the body force per unit mass, $a = 1,2,3$ and $\beta = 1,2,3$. Here, repeated indices imply summation from 1 to 3. The symbol $\frac{\mathrm{D}}{\mathrm{Dt}}$ denotes the material (substantial) derivative. Incorporating the constitutive equations for Newtonian fluids we obtain the well known Navier-Stokes equations. Incorporating the SPH particle approximation for the dependent variables and their derivatives (eqs. 4 and 5) we obtain the SPH equations for the Navier-Stokes, continuity and energy equations as follows:

$$\frac{\mathrm{D}\rho_{i}}{\mathrm{Dt}} = \sum_{j=1}^{\mathrm{N}} \mathrm{m}_{j}\upsilon_{ij}^{\beta}\frac{\partial \mathrm{W}_{ij}}{\partial x_{i}^{\beta}} \tag{10}$$

$$\frac{\mathrm{D}\upsilon_{i}^{a}}{\mathrm{Dt}} = -\sum_{j=1}^{\mathrm{N}} \mathrm{m}_{j}\left(\frac{\sigma_{i}^{\alpha\beta}}{\rho_{i}^{2}} + \frac{\sigma_{j}^{\alpha\beta}}{\rho_{j}^{2}}\right)\frac{\partial \mathrm{W}_{ij}}{\partial x_{i}^{\beta}} + \mathrm{b}_{i}^{a} \tag{11}$$

$$\frac{\mathrm{De}_{i}}{\mathrm{Dt}} = \frac{1}{2}\sum_{j=1}^{\mathrm{N}} \mathrm{m}_{j}\left(\frac{\mathrm{p}_{i}}{\rho_{i}^{2}} + \frac{\mathrm{p}_{j}}{\rho_{j}^{2}}\right)\upsilon_{ij}^{\beta}\frac{\partial \mathrm{W}_{ij}}{\partial x_{i}^{\beta}} + \frac{\mu_{i}}{2\rho_{i}}\varepsilon_{i}^{\alpha\beta}\varepsilon_{i}^{\alpha\beta} \tag{12}$$

where $\upsilon_{ij} = \upsilon_{i} - \upsilon_{j}$ and

$$\varepsilon^{\alpha\beta} = \frac{\partial \upsilon^{\beta}}{\partial x^{a}} + \frac{\partial \upsilon^{a}}{\partial x^{\beta}} - \frac{2}{3}\left(\nabla \cdot \vec{\mathrm{V}}\right)\delta^{\alpha\beta}$$

$$\sigma^{\alpha\beta} = -\mathrm{p}\delta^{\alpha\beta} + \tau^{\alpha\beta}$$

where $\tau^{\alpha\beta}$ are the components of the stress deviator, m_{j} is the mass of the jth particle, ρ_{i} is the density of the ith particle, p_{i} is the pressure of the ith particle, $\left(\upsilon_{i}^{1},\upsilon_{i}^{2},\upsilon_{i}^{3}\right)$ the velocity of the ith particle, and μ_{i} the dynamic viscosity coefficient of ith particle.

3.4 The choice of the smoothing function

It is obvious that the choice of the smoothing function W and the smoothing length, h, is very important and can lead to success or failure of the method. A smoothing function must have a number of properties such as the "property of unity", compact support (i.e, local support), positivity, decay, smoothness, symmetry, as well as the "Delta function property". Among these seven desirable properties, two of them are indispensable:

$$\int_{\Omega} \mathrm{W}\left(\mathbf{x} - \mathbf{x}';\mathrm{h}\right)\mathrm{d}\mathbf{x}' = 1 \qquad \text{("unity" property)} \tag{13}$$

and

$$\lim_{\mathrm{h}\to 0} \mathrm{W}\left(\mathbf{x} - \mathbf{x}';\mathrm{h}\right) = \delta\left(\mathbf{x} - \mathbf{x}'\right) \qquad \text{("Delta function" property)} \tag{14}$$

A number of smoothing function have been proposed over the years (see Liu & Liu 2010). Here we list the most important of them. Let $R = \dfrac{|\mathbf{x}-\mathbf{x}'|}{h}$. Then, three useful smoothing functions are:

Gaussian kernel (Gingold & Monaghan, 1977)

$$W(R, h) = a_d e^{-R^2} \tag{15}$$

where

$$a_d = \frac{1}{h\sqrt{\pi}} \quad \text{for 1-D,} \quad a_d = \frac{5}{h^2\pi} \quad \text{for 2-D,} \quad a_d = \frac{105}{h^3\pi^{3/2}} \quad \text{for 3-D problems.}$$

Cubic B-Spline

$$W(R, h) = a_d \times \begin{cases} \frac{2}{3} - R^2 + \frac{1}{2}R^3, & 0 \le R < 1 \\ \frac{1}{6}\left(2 - R^3\right), & 1 \le R < 2 \\ 0, & R \ge 2 \end{cases} \tag{16}$$

	1-D	2-D	3-D
a_d	$1/h$	$15/7\pi h^2$	$3/2\pi h^3$

Quintic spline

$$W(R, h) = a_d \times \begin{cases} (3-R)^5 - 6(2-R)^5 + 15(1-R)^5, & 0 \le R < 1, \\ (3-R)^5 - 6(2-R)^5, & 0.5 \le R < 2, \\ (3-R)^5, & 2 \le R < 3, \\ 0, & R > 3 \end{cases} \tag{17}$$

	1-D	2-D	3-D
a_d	$120/h$	$7/478\pi h^2$	$3/359\pi h^3$

3.5 SPH equations as solved in LAMMPS

In the LAMMPS implementation the field variables are $\{\rho, \mathbf{v}, e, P, Q\}$ that is density, velocity, internal energy, the stress tensor, and the heat flux vector. The descritized equations are:

Local density for particle i

$$\rho_i = \sum_{j=1}^{N} m_j \frac{\rho_j}{\rho_j} W_{ij} = \sum_{j=1}^{N} m_j W_{ij} \tag{18}$$

This is frequently referred in the mathematical literature as “partition of unity”.

Momentum equation for particle i

$$\frac{d\mathbf{v}_i}{dt} = -\frac{P_i}{\rho_i^2} \cdot \sum_{j=1}^{N} m_j \nabla_j W_{ij} - \sum_{j=1}^{N} m_j \frac{P_j}{\rho_j^2} \nabla_j W_{ij} \tag{19}$$

where P is the stress (pressure) tensor. Note that the pair-wise forces are

$$\mathbf{f}_i = m_i \frac{d\mathbf{v}_i}{dt} = -\sum_{j=1}^{N} m_i m_j \left(\frac{P_i}{\rho_i^2} + \frac{P_j}{\rho_j^2} \right) \nabla_j W_{ij} \tag{20}$$

Continuity equation

$$\frac{d\rho_i}{dt} = -\sum_{j=1}^{N} m_j \mathbf{v}_j \nabla_j W_{ij} - \mathbf{v}_i \sum_{j=1}^{N} m_j \nabla_j W_{ij} - \sum_{j=1}^{N} m_j \mathbf{v}_{ij} \nabla_j W_{ij} \tag{21}$$

Energy equation

$$m_i \frac{de_i}{dt} = -\frac{1}{2} \sum_{j=1}^{N} m_i m_j \left(\frac{P_i}{\rho_i^2} + \frac{P_j}{\rho_j^2} \right) : \mathbf{v}_{ij} \nabla_j W_{ij} - \sum_{j=1}^{N} \frac{m_i m_j}{\rho_i \rho_j} \frac{\left(\kappa_i + \kappa_j\right)\left(T_i - T_j\right)}{r_{ij}^2} \mathbf{r}_{ij} \cdot \nabla_j W_{ij} \tag{22}$$

Newman-Richter type artificial viscosity

Monaghan has introduced an artificial viscosity term in order to avoid instabilities in this SPH formulation of the N-S equations. It is adopted in the LAMMPS formulation so that the pair-wise forces are modified and take the form

$$\mathbf{f}_i = m_i \frac{d\mathbf{v}_i}{dt} = -\sum_{j=1}^{N} m_i m_j \left(\frac{P_i}{\rho_i^2} + \frac{P_j}{\rho_j^2} + \Pi_{ij} \right) \nabla_j W_{ij} \tag{23}$$

With

$$\Pi_{ij} = -\alpha\, h \frac{c_i + c_j}{\rho_i + \rho_j} \frac{\mathbf{v}_{ij} \cdot \mathbf{r}_{ij}}{r_{ij}^2 + \varepsilon h^2} \tag{24}$$

where $c_i =$ speed of sound of particle i, $c_j =$ speed of sound of particle j, $\alpha =$ auxiliary factor for control of dissipation, $\varepsilon =$ auxiliary factor used to avoid singularities when $r_{ij} \to 0$. As a rule of thump $\varepsilon \approx 0.01$. The energy equation has to be also modified.

3.6 Some remarks about SPH formulations for fluids

In relation to the application of the SPH method in fluid dynamical problems we should mention that the treatment of pressure for incompressible flow can be carried out either through an equation of state or by enforcing the incompressibility condition via a Poisson equation for pressure. Another important issue in viscous water flows is the treatment of viscosity, which is a key quantity in determining water transport. In addition, the computational enforcement of boundary conditions (especially inlet-outlet boundary conditions) requires further development (Lykov et al., 2015 Lei et al., 2011). Collision detection at impermeable solid boundaries is also very important.

4. RESULTS

We applied the SPH simulation method on a software platform that has been widely used for research, primarily for Molecular Dynamics simulations of atomistic systems, LAMMPS-Large-scale Atomic/Molecular Massively Parallel Simulator (Plimpton, 1995). Due to its particle nature, SPH is directly compatible with the existing code architecture and data structures present in LAMMPS for MD (Sofos et al., 2009, 2010, 2013, Liakopoulos, 2016) and Dissipative Particle Dynamics (DPD) (Kasiteropoulou, 2012). Furthermore, its parallel nature offers a boost in all simulations that could be

executed in parallel tasks (Herault et al., 2010, Verma et al., 2017, Wu et al., 2017). Here we investigate two SPH test cases, the development of an unsteady (transient) Couette flow, and the well-documented, water column collapse example. Model screenshots are created with Ovito [Stukowski, 2010].

4.1 Transient Couette flow

A 3-D rectangular simulation box is created for unsteady Couette flow, as shown in Fig. 1. The dimensions in x-, y- and z-directions are L_x^*=20, L_y^*=10, L_z^*=10. The asterisc denotes values scaled to Lennard-Jones values. Wall and fluid particles are set on fcc sites in the beginning of the simulation and remain on their initial position until the upper rigid plate moves. The upper wall is given a constant velocity, v_x^* =3.0, in the x-direction and drives the flow due to friction. There are 2000 wall particles and 6000 liquid particles in the simulation. The nominal density is constant ρ^*=1. Periodic conditions are enforced in the x and z directions. The simulation runs with a timestep of Δt^*=0.001 for $2x10^6$ timesteps.

4.2 Water column collapse in a tank with obstacles

In this example we present the collapse of a water column in a rectangular tank with obstacles (Gomez-Gestheira et al. 2010). Walls remain stationary. Simulation for $5x10^4$ timesteps (or, 7.5 sec) can reveal the full evolution of the phenomenon (Fig. 3) and agrees with documented results.

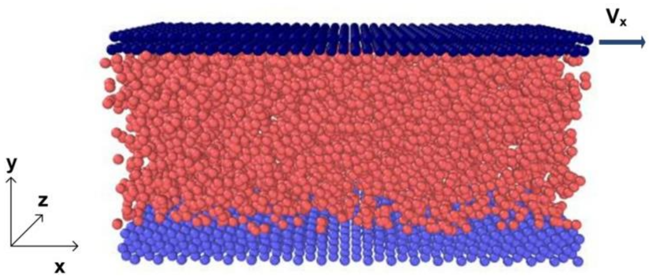


Figure 1: A Couette flow model (L_x^*=20, L_y^*=10, L_z^*=10)

The velocity profiles extracted at various times are shown in Fig. 2. Velocity profiles tend to reach a linear velocity distribution across the y-direction at steady state, as expected from the Navier-Stokes theory.

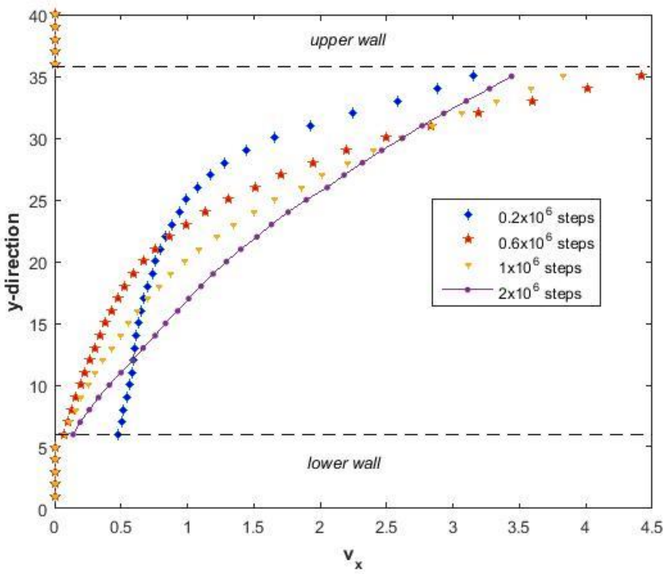


Figure 2: Couette flow: x-Velocity profile across the y-direction.

5. CONCLUSIONS

We have shown that the SPH method, as a purely particle method, has many similarities to Molecular Dynamics, the well-documented atomistic simulation method, as well as to mesoscopic methods such as Dissipative Particle Dynamics (DPD). We have also reviewed some of the most basic concepts in the SPH formulation for solving partial differential equations with emphasis on the particular method for the N-S equations implemented in LAMMPS. SPH is well suited for flows of liquids with free surface such as wave propagation, wave/structure interaction, wave/ship interaction, sloshing to mention a few. Furthermore, SPH is very useful in applications in soil mechanics, geotechnical engineering, and water resources engineering such as: flood wave propagation modeling, floodplain inundation predictions, open channel hydraulics etc. Finally, we would like to address the practical problem of reducing the required CPU time for SPH and more generally for particle methods. Parallel processing and hardware innovations offer the best hope for improvements. The high-performance parallel architecture provided by CUDA-enabled GPUs is ideal for SPH models. The use of graphic cards and CUDA has allowed much finer details to be revealed, due to the ability to run computations with hundreds of times more particles in far shorter times than required for similar code runs on a single CPU or even on many clusters.

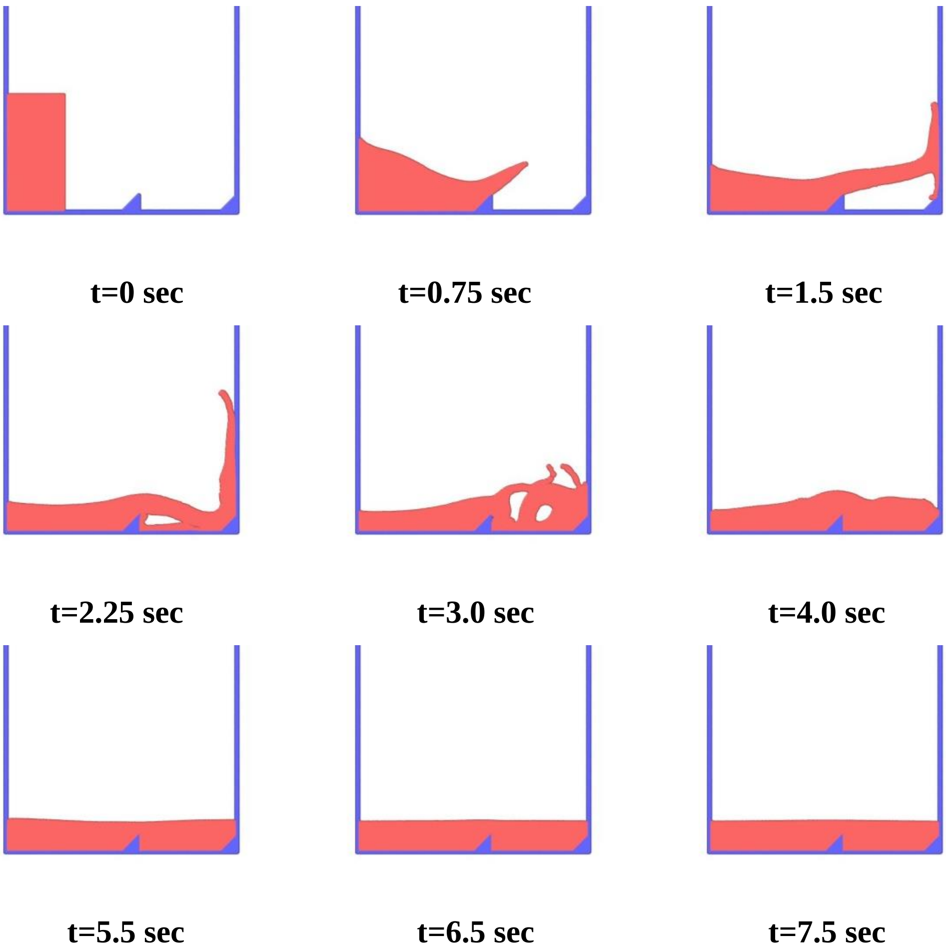


Figure 3:Water column collapse in a tank with obstacles

References

1. Bouscasse B., Calagrossi A., Marrone S., Antuono M. (2013) ‘Non linear water interaction with floating bodies in SPH’, **J. Fluids Struct.** 42, 112-129.
2. Cleary P.W., Prakash M. (2004) ‘Discrete–element modelling and smoothed particle hydrodynamics: potential in the environmental sciences’, **Phil. Trans. R. Soc. Lond.** A 2004 362 2003-2030; DOI: 10.1098/rsta.2004.1428.
3. Gingold R.A., J.J. Monaghan (1977) ‘Smoothed particle hydrodynamics: theory and application to non-spherical stars’, **Mon. Not. R. Astron. Soc.** 181, 375–389.
4. Gomez-Gesteira M., Rogers B.D., Dalrymple R.A., Crespo A.J.C. (2010) ‘State-of-the-art of classical SPH for free-surface flows’, **Journal of Hydraulic Research**, 48(extra):6, 27.
5. Hérault Alexis, Bilotta Giuseppe, Dalrymple A. Robert (2010) “SPH on GPU with CUDA”, **Journal of Hydraulic Research**, Vol. 48 Extra Issu, e pp. 74–79, doi:10.3826/jhr.2010.0005.
6. Hieber S.E., Koumoutsakos P. (2008) ‘An immersed boundary method for smoothed particle hydrodynamics of self-propelled swimmers’, **J. Comput. Phys.**, 227, 8636–8654.
7. Kasiteropoulou D., Karakasidis T.E., and Liakopoulos A., (2012) ‘A Dissipative Particle Dynamics study of flow in periodically grooved nanochannels’, **International Journal for Numerical Methods in Fluids**, v. 68, Issue 9, pp. 1156–1172.
8. Koumoutsakos P. (2005) ‘Multiscale flow simulations using particles’, **Annu. Rev. Fluid Mech.** 37, 457–487.
9. Lei Huan, Fedosov Dmitry A., Karniadakis George Em. (2011) ‘Time-dependent and outflow boundary conditions for Dissipative Particle Dynamics’, **Journal of Computational Physics** 230 3765–3779.
10. Li S., Liu W.K. (2002) ‘Meshfree and particle methods and their applications’, **Appl. Mech. Rev** 55(1), 1-34. doi:10.1115/1.1431547.
11. Li S., Liu W.K. (2004) ‘**Meshfree Particle Methods**’, Springer.
12. Liakopoulos A., Sofos F., Karakasidis T.E. (2016) ‘Friction factor in nanochannel flows’, **Microfluidics Nanofluidics**, Vol. 20, Issue 1, pp. 1-7.
13. Liu M.B., Liu G.R. (2010) ‘Smoothed Particle Hydrodynamics (SPH): an Overview and Recent Developments’, **Arch of Comput Methods in Eng.**, 17:25-76.
14. Lucy L.B. (1977) ‘A numerical approach to the testing the fission hypothesis’, **Astron. J.** 82, pp.1013–1024.
15. Lykov K., Li X., Lei H., Pivkin I.V., Karniadakis G.E. (2015) ‘Inflow/Outflow Boundary Conditions for Particle-Based Blood Flow Simulations: Application to Arterial Bifurcations and Trees’, **PLoS Comput Biol** 11(8).
16. Monaghan, J. J. (1988) ‘An introduction to SPH’, **Computer Physics Communications** 48, pp. 89–96.
17. Monaghan, J. J. (1992) ‘Smoothed Particle Hydrodynamics’, **Annual Review of Astronomy and Astrophysics** 30, pp. 543–574.
18. Monaghan, J. J. (1994) ‘Simulating free surface flows with SPH’, J**. Comput. Phys.** Vol. 110, 399 406.
19. Plimpton S. (1995) ‘Fast Parallel Algorithms for Short-Range Molecular Dynamics’, J**. Comp. Phys.** 117, 1-19.
20. Shao S. (2009) ‘Incompressible SPH simulation of water entry of a free-falling object’, **Int. J. Numer. Methods Fluids** 59, 91–115.

21. Sofos F., Karakasidis T.E. and Liakopoulos A. (2009) ‘Transport properties of liquid argon in krypton nanochannels: Anisotropy and non-homogeneity introduced by the solid walls’, **Int. J. Heat Mass Transf.**, 52 735-743.

22. Sofos F., Karakasidis T.E., Liakopoulos A. (2010) ‘Effect of wall roughness on shear viscosity and diffusion in nanochannels’, **Int J Heat Mass Tran** 53: 3839–3846.

23. Sofos F., Karakasidis T.E., Liakopoulos A. (2013) ‘Parameters affecting slip length at the nanoscale’, **Journal of Computational & Theoretical Nanoscience**, Vol. 10, pp.1-3.

24. Stukowski A. (2010) ‘Visualization and analysis of atomistic simulation data with OVITO - the Open Visualization Tool’, **Modelling Simul. Mater. Sci. Eng.** 18, 015012.

24. Verma K., Szewc K. and Wille R. (2017) Advanced load balancing for SPH simulations on multi-GPU architectures, **IEEE High Performance Extreme Computing Conference (HPEC)**, Waltham, MA, pp. 1-7.

25. Wu W., Li H., Su T., Liu H., Lv Z. (2017) ‘GPU-accelerated SPH fluids surface reconstruction using two-level spatial uniform grids’, **The Visual Computer** 33, 1429-1442.



Environmental law and economics

SPATIAL MULTI-CRITERIA DECISION MAKING MODEL FOR SUSTAINABLE COASTAL LAND-USE AND DEVELOPMENT. THE CASE STUDY OF KALAMARIA-PILEA SEAFRONT IN THESSALONIKI, GREECE.

S. Anastasiadis*, A. S. Partsinevelou and Z. Mallios

*Corresponding author: e-mail: stavrosanastasiadis@yahoo.gr, tel: +302313302679
Division of Urban Planning and Urban Development,
Dept. of Urban Planning, Municipality of Pilea-Chortiatis,
GR- 55535 Thessaloniki, Macedonia, Greece

Abstract

In the last decade, applications of the Multi-Criteria Decision Making (MCDM) techniques in GIS-based land suitability procedures have been increased, especially at a regional-scale planning processes. Through these procedures, conflicts between urban growth and ecological conservation have been brought to the forefront, especially in developing coastal areas, while potential ecological environmental risks have been emerged as a result of land-use changes (e.g. urbanization). An optimized land-use planning and development could reduce this risk at a regional scale. Modern planning theories encourage approaches with Multi-Criteria Decision Making (MCDM) techniques, combined with GIS, as they have been applied successfully in a number of land suitability analysis and environmental planning and management scenarios.

This study aims to present a realistic and detailed set of criteria and a group decision making, by using MCDM techniques and Analytical Hierarchy Procedure (AHP - Fuzzy AHP), in order to define the most preferred option to secure a sustainable coastal land-use and development at the Pilea-Kalamaria seafront in Thessaloniki, Greece, where no land-use is configured in its largest part. In order to built the MCDM model, the study was organized into four principal stages: (i) defining the land suitability criteria of the model, (ii) ranking the importance of each criterion, (iii) generating land suitability maps for each criterion, and (iv) generating a final map with the suitable land-uses of the study area accompanied by a detailed analysis of the results of the MCDM model and a comparison of the results with the most recently approved General Urban Plan of the study area.

Keywords: MCDM model; land-use planning; coastal area; urban development; spatial optimization

1. INTRODUCTION

Urban land-use suitability can be influenced by the large numbers of environmental, economic and social factors, such as ecological health, population growth and economic development. As cities expand physically, the frontiers between urban and rural activity are distorted and merged, presenting opportunities for beneficial linkages (Phua & Minowa, 2005).

Over the past years, many tools based on Geographic Information Systems (GIS) and Remote Sensing (RS) techniques have proved useful for land management. The incorporation of multi-criteria evaluation methods into GIS has emerged as a promising research area by creating a modular hierarchical system of the land suitability index, which will aim at delivering a strategic environmental assessment of developmental land-uses for regional planning (Marull et al., 2007). However, the limitation of most existing multi-criteria evaluation models and land-use allocation models is that the uncertainties about the future distribution of land-uses are not explicitly taken into

account (Verdoodt & Ranst, 2006). There are many important factors associated with environmental quality, construction investment, soil resources and population density during the evaluation process. These factors can be sorted into different indicators, but the complicated interrelationships among them cannot be simply expressed by the restrictive equalities or inequalities in the conventional evaluation models (Mosadeghi, 2013, Langemeyer et al., 2016).

For the creation of a realistic Multi Criteria Decision Model (MCDM), the Analytic Hierarchy Process (AHP) is proved as a useful systematic analysis tool for handling multi-criteria decision-making process. It enables the consideration of social and economic objectives, which are recognized to be of the same importance as the ecological and environmental ones (Xu et al., 2006, Zeng et l., 2007). However, it depends excessively on the subjective weight of each performance indicator from experience, while the interrelationships among multiple indicators are ignored (Yang et al., 2008).

This study proposes a spatial analysis system for urban land-use management integrating environmental assessment tools with multi-criteria land resources information system, in order to define the most preferred option to secure a sustainable coastal land-use and development. The MCDM model was created using AHP analysis in order to rank correctly the importance of each criterion used. An integrated land suitability evaluation model based on GIS is proposed and applied in Kalamaria-Pilea seafront as a case study.

The great needs in the area of Thessaloniki, which is densely populated around of its historical center, highlight the fact that its urban and metropolitan area must be redefined. Therefore, in the region of Thessaloniki, the reconstruction and development of the seafronts of Kalamaria and Pilea will help to create a connection with the historical center of the city, thus achieving new dynamics in the transformation of the city. Similar examples of expansion of metropolitan areas with the simultaneous development of new recreational areas, cultural sites and green spaces, could be seen in many European cities, such as in London and in Barcelona (Organization of Thessaloniki, 2001). The construction and redevelopment of Kalamaria-Pilea seafront will upgrade the wider urban landscape and the offer of high quality of life, which is general considered as a first priority (Anastasiadis, 2015).

2. THE STUDY AREA

The Kalamaria-Pilea seafront is bordered southeast by the coastal front of Thermi, in which most of the facilities of Thessaloniki International Airport ‘Macedonia’ are extended, while at northeast is bordered by the urban area of Kalamaria Municipality. Also in the extended area of Kalamaria-Pilea seafront, a part of the farm of the Aristotle University of Thessaloniki is included (Figure 1).

The Kalamaria-Pilea seafront was used for many years as an open beach, with the beach of Dalianon to be widely known. This situation changed radically after the apparent contamination of Thermaikos Gulf, when it stopped being a pole of attraction for the residents' summer baths (Anastasiadis, 2015).

The total length of the Kalamaria-Pilea seafront is approximately 3.5 km. Characteristic features of this area are its key location, where there is access to central public transport facilities, as well as the existence of large free spaces that allow the further urban development of the seafront. Road network along the coastline does not exist and the beach is accessible to pedestrians only from the shopping center ‘Apollonia Politia’ up to the farm of the University of Thessaloniki.

Despite the very good features of the area, the Kalamaria-Pilea seafront is a neglected area with strong signs of abandonment and contamination from the existing land uses (small shipbuilding zones, etc.). However, according to the approved General Urban Plans of the Municipality of Kalamaria and the Municipality of Pilea-Chortiatis, an urban planning is proposed for the seafront, which aims in the sustainable development of the area.



Figure 1: The extended study area of the Kalamaria-Pilea seafront in Thessaloniki.

3. METHODOLOGY

This study aims to present a realistic and detailed set of criteria and a group decision making, by using MCDM techniques and Analytical Hierarchy Procedure (AHP), in order to define the most preferred option to secure a sustainable coastal land-use and development at the Pilea-Kalamaria seafront in Thessaloniki, Greece.

Before building the MCDM model for the study area, it was necessary to map the land cover at the Kalamaria-Pilea seafront. For this purpose, a cloud-free Sentinel-2A image was downloaded for the 28th of June 2017 and orthorectified. This imagery was selected in order the peak of the vegetative season to be captured, thereby enhancing the detection of green spaces, which are the free spaces of the study area (Lefebvre et al., 2016).

In order to proceed with the MCDM model of the Kalamaria-Pilea seafront, it was necessary to know the opinion of the inhabitants about the development of the area, as the approved Urban Plans were not put to public consultation. This problem was solved by conducting an in-depth research, using a well-formatted questionnaire, through personal interviews and via the internet (electronic survey), where the results were included in the criteria used for the model.

Finally, in order to built the MCDM model, the study was organized into four principal stages: (i) defining the land suitability criteria of the model, (ii) ranking the importance of each criterion, (iii)

generating land suitability maps for each criterion, and (iv) generating a final map with the suitable land-uses of the study area accompanied by a detailed analysis of the results of the MCDM model and a comparison of the results with the most recently approved General Urban Plan of the study area.

3.1 Mapping the land cover of the area using Sentinel-2A imagery

For mapping the current unexploited space in the study area, the orthorectified Sentinel-2A on the Hellenic Geodetic Reference System (GGRS'87) was used, which has accuracy up to 10 m. Specifically, the bands 12, 11 and 4 were selected using the ENVI software, in order to map the urban area and the free space in each municipality in the Kalamaria-Pilea seafront, as the combination of these 3 bands results an enhancement of the urban area shown with purple color, while the free space is designated with green or/and white color (Figure 2). Here it should be noted that the farm of the University of Thessaloniki was not taken into account, as it cannot be exploited further.

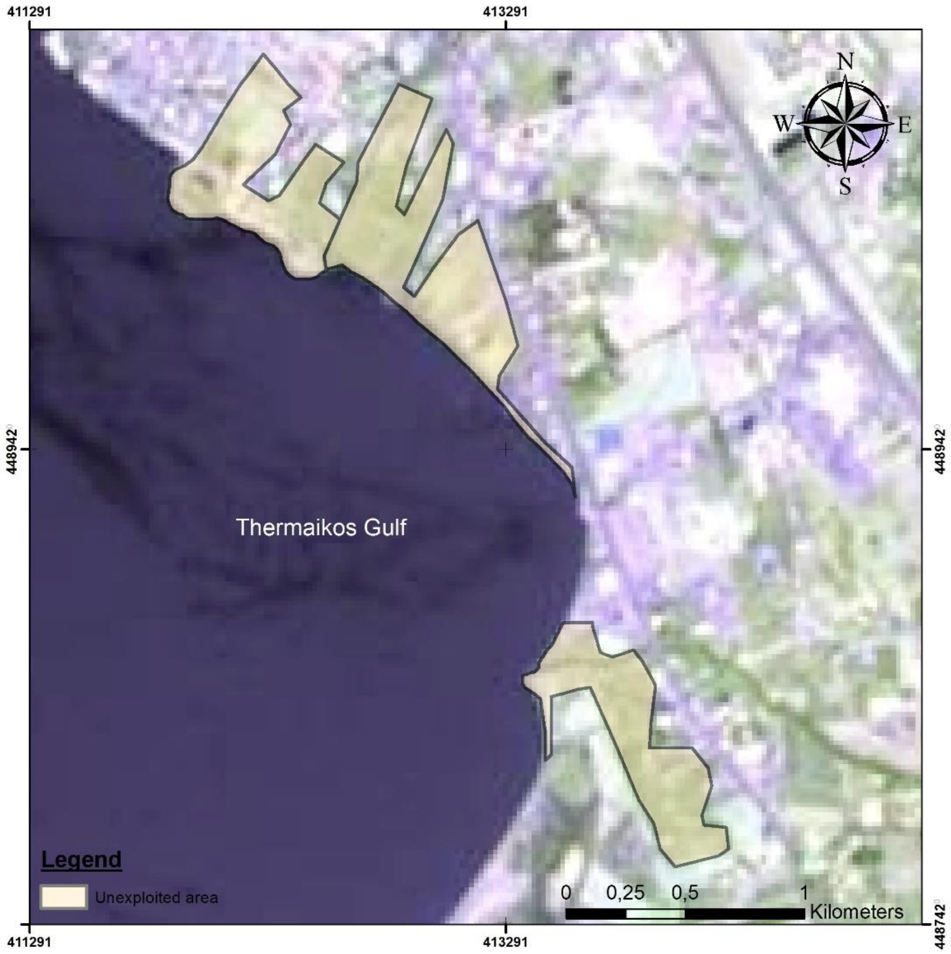


Figure 2: Unexploited area of the Kalamaria-Pilea seafront in Thessaloniki.

3.2 Defining the land suitability criteria

Significant steps have been taken recently around the world to harmonize land use with natural terrain conditions, as well as to assess the relative degree of intolerance of the terrain with regard to proposed land use alterations (Collin & Melloul, 2012). In this study, in order to secure an environmental friendly and sustainable coastal land-use and development at the Pilea-Kalamaria seafront in Thessaloniki, areas which are environmentally unsuitable for exploitation must be first excluded.

For this purpose, some basic environmental criteria have been applied in the unexploited areas, such us the morphology, the hydrology and the distance from the coastline (Table 1 & Table 2). Thus, areas that are in a distance less than 50 m from the coastline, have a high morphological slope (>20%) based on the Digital Elevation Model of the area and are in a distance less than 100 m from a stream

are considered unsuitable for further exploitation and have been excluded (Figure 3). The environmental factors of soils and vegetation were not used for this study area, as the geology of the unexploited space is characterized by the presence of undivided Holocene deposits and a sandstone-marl series (Antoniades & Ioannidis, 1970), which are partly impermeable soils, while at the same time there is no tree cover in the same areas.

At this point it should be noted that while in the General Urban Plan of the Municipality of Kalamaria the areas that should not be used for the protection of the environment have not been included in the general urban plan of the Municipality of Pilea-Chortiatis, environmental criteria have not been included and the areas that are designated to be developed are different.

In order to proceed with the definition of the final criteria which will determine the final land uses of the study area, the results of a well-formatted questionnaire were used, which constitute the socio-economical criteria. The results of the analysis this questionnaire indicate that the inhabitants of both municipalities (Kalamaria and Pilea-Chortiatis), prefer the construction of specific activities, with low cost and high economic benefit (Anastasiadis, 2015). These results, according to each answer's percentage, were weighted in order to show the preferences of the public (Table 3).

Table 1: Land usage categories and intensities for various environmental factors (modified from Melloul and Collin, 2001).

Environmental Factor	Ranking Criteria		Recommended Land-Use Intensity								
			Conservation	Recreation		Agricultural		Residential Settlement		Commercial & Industrial	
				High Intensity	Low Intensity	Field Crops	Orchards	High Intensity	Low Intensity	High Intensity	Low Intensity
Morphology	High slope	>20%	1	1	1	1	1	1	1	1	1
	Low slope	<20%		3	2	4	2	4	3	5	4
Hydrology	Distance from hydrological network	<100m	1	1	1	1	1	1	1	1	1
		>100m		3	2	4	2	4	3	5	4
Soils	Permeable		1	1	1	1	1	1	1	1	1
	Impermeable			3	2	4	2	4	3	5	4
Vegetation	Tree cover		1	3	2	4	2	4	3	4	4
	Other cover			3	3	4	3	4	3	5	4

Table 2: The environmental criteria used in the MCDM model.

Environmental Factor	Ranking Criteria		Recommended Land-Use
Morphology	High slope	>20%	None
	Low slope	<20%	Commercial & Industrial
Hydrology	Distance from hydrological network	<100 m	None
		>100 m	Residential Settlement
Distance from the coastline	<50 m		None
	>50 m		Commercial & Industrial Residential Settlement Agricultural Recreation

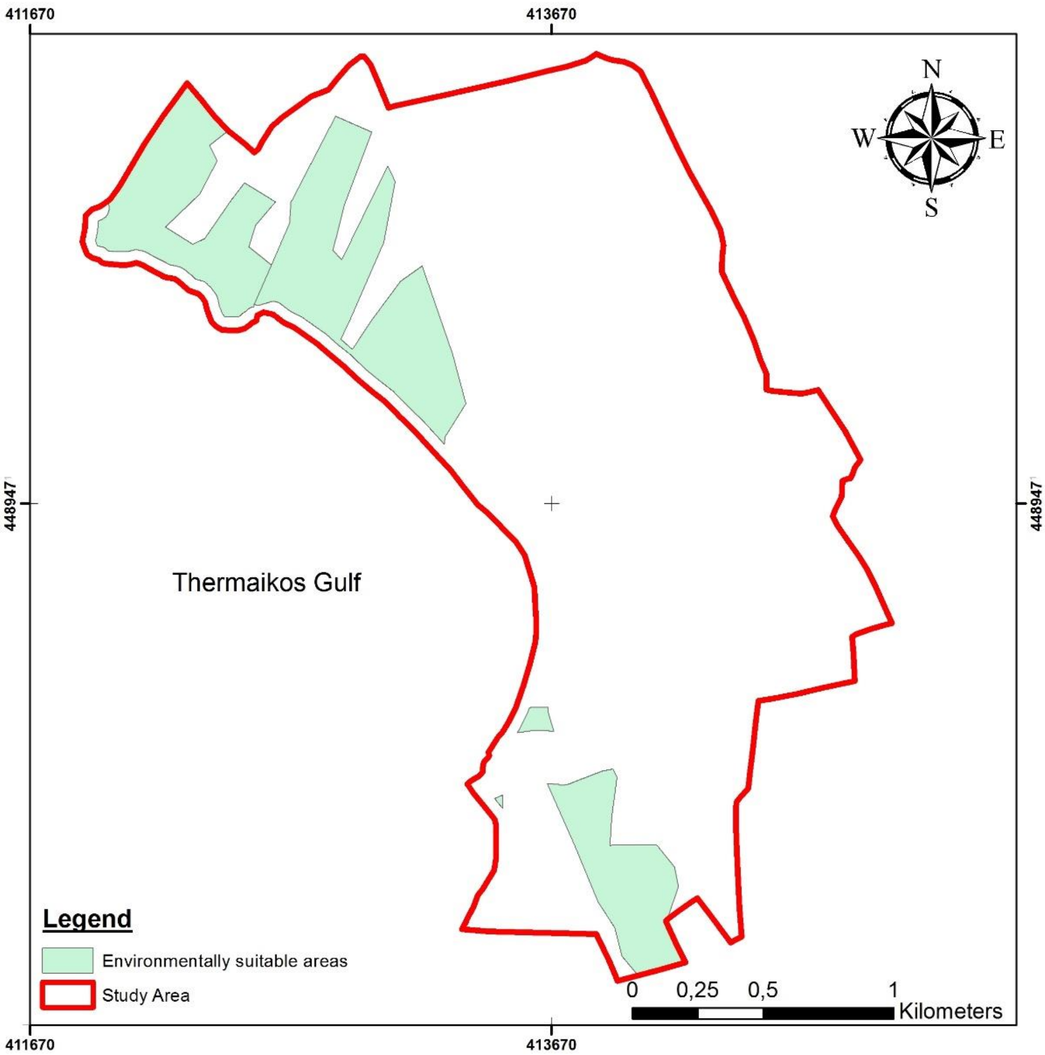


Figure 3: Environmentally suitable areas for sustainable land use development.

Table 3: The socio-economical criteria used in the MCDM model

Socio-economical Factor	Ranking Criteria	Weights resulting by questionnaires
Activities	Sports, etc.	4
	Shopping Malls	3
	Cultural Sites	2
	Tourist Facilities	1
Cost	Low	3
	Medium	2
	High	1
Economic Benefit	Low	1
	Medium	2
	High	3

As a result, the main criteria that have been used in order to finalize the MCDM model are:

- The type of the facility that is going to be constructed, which is related with the environmental impact. For example, sport facilities that are related to nature (such as swimming) are more

environmental friendly than shopping malls and tourist facilities that would completely change the present landscape.

- The cost of the facility.
- The economic benefit.

3.3 Ranking the importance of each criterion – AHP Analysis

The selection of the criteria mentioned was based on the preferences of the public and the environmental impact that would have in today's landscape. These criteria were weighed according to Analytical Hierarchy Process (AHP) proposed by Saaty (1977). The Analytical Hierarchy Process is a well-known and excellent method of calculating criteria of gravity ratios, which helps to obtain subjective and objective evaluation measures. It is a very useful tool for checking the correctness of these measures and the alternatives proposed, significantly reducing the error rate.

This process involves pairing comparisons and creates a list of reasons. It takes inputs as pair wise comparisons and generates relative weights (gravity coefficients). In particular, the weights are determined by normalizing the eigenvector associated with the maximum value of the inverse ratio.

The relationship of each criterion is expressed by numerical values given as in Table 4. These values are not arbitrary, they follow a certain scale of sizes. This price comparison scale was proposed by Saaty (1977) and Saaty & Vargas (1984) and ranges from 1 to 9. The value 1 expresses criteria of equal importance, while at the other end of the scale, value 9 represents criteria which are of great importance compared to those that are compared each time.

Table 4: The fundamental scale of AHP (Saaty & Vargas, 2001).

Intensity of Importance	Definitions	Explanation
1	Equal importance	Two activities contribute equally to the objective
2	Weak importance	Experience and judgement slightly favour one activity over another
3	Moderate importance	
4	Moderate plus importance	Experience and judgement strongly favour one activity over another
5	Strong importance	
6	Strong plus importance	An activity is favoured very strongly over another; its dominance demonstrated in practice
7	Very strong or demonstrated importance	
8	Very, very strong importance	The evidence favouring one activity over another is of the highest possible order of affirmation
9	Extreme importance	

After the correlation of the criteria has been made, the values are processed in order to weight the criteria. In order to reduce any chance of error, Saaty (1977) proposed a numerical index to check the correctness of the matrix comparison matrix, the so-called CR (consistency ratio). This index is equal to the fraction of the consistency index CI and an average consistency index RI. The RI value is the average consistency value of random squares of different classes (Saaty, 1977), while for $CR \geq 0.1$, Saaty & Vargas (1984) proposed a re-examination of the original table.

Final results of the AHP analysis are shown in Table 5. From this analysis the Land Use Sustainability (LUS), can be calculated by the following equation:

$$LUS=0.48*E+0.41*B+0,11*C$$

Where:

E, the Environmental friendly facility
B, the economic Benefit
C, the Cost of the construction and the conservation of the facility

Table 5: Weights of paired factors concerning the MCDM model for the Kalamaria-Pilea seafront.

CRITERIA
ENVIRONMENT = E
COST = C
ECONOMIC BENEFIT = B

In general
C<B<E

	Step 1: Pair wise comparison		
Factor	E	B	C
E	1,00	1,00	5,00
B	1,00	1,00	3,00
C	0,20	0,33	1,00
Total	2,20	2,33	9,00

LUS = Land Use Suitability
LUS = 0,48*E + 0,41*B +0,11*C

	Step 2: Normalization				
Factor	E	B	C	Total	Average
E	0,45	0,43	0,56	1,44	0,48
B	0,45	0,43	0,33	1,22	0,41
C	0,09	0,14	0,11	0,34	0,11
Total	1,00	1,00	1,00	-	1,00

	Step 3: Consistency analysis					
Factor	E	C	B	Total	Average	Consistency Measure
E	0,45	0,43	0,56	1,44	0,48	3,04
C	0,45	0,43	0,33	1,22	0,41	3,03
B	0,09	0,14	0,11	0,34	0,11	3,01
Total	1,00	1,00	1,00			CI= 0,01
						RI= 0,58
						CR= 0,03

3.4 Land suitability maps generation

According to the LUS equation the land suitability map of the study area is generated, where from the environmentally suitable areas, 48% must be an environmental friendly facility, 41% must be a facility which will provide a sufficient economic benefit, while the 11% will be not developed in order to keep the cost low.

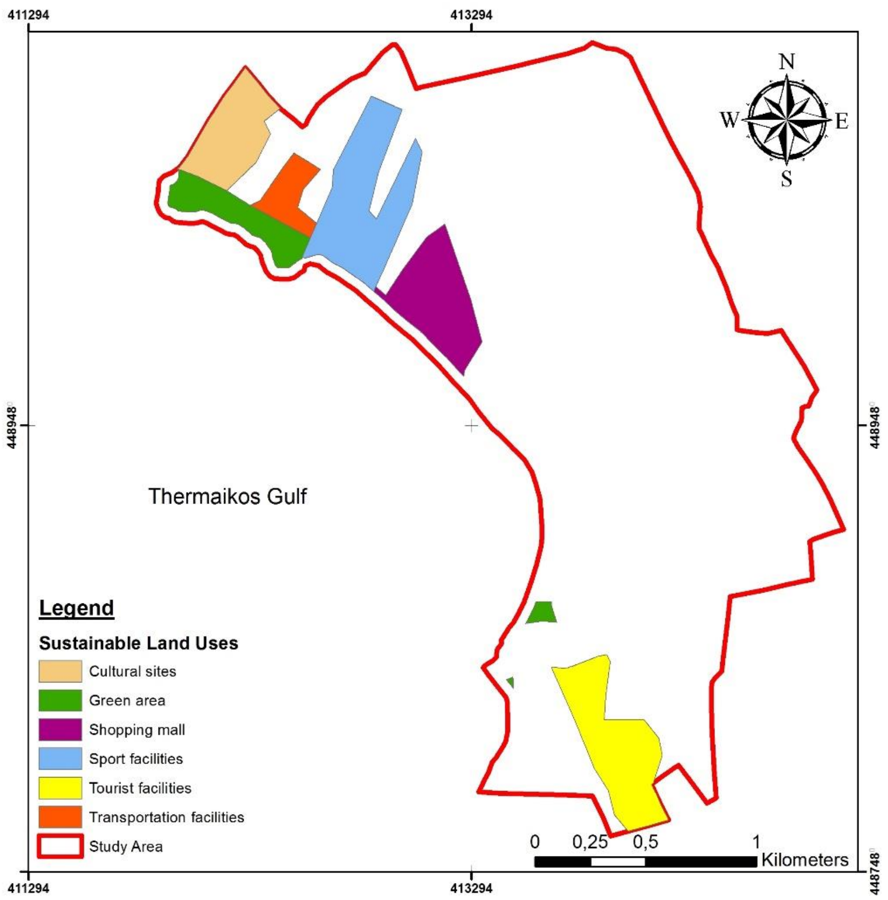


Figure 4: Final sustainable land uses in the Kalamaria-Pilea seafront.

For the areas selected in the Kalamaria-Pilea seafront 32,5% belongs to Kalamaria Municipality, while the rest 67,5% belongs to Pilea-Chortiatis Municipality. This means that this area must have land uses within the municipality borders, as it is very difficult to have multiple land uses using area from both municipalities.

According to the above criteria, the final land use sustainable development map has been created, with the use of ArcGIS 10.5 software and the Raster Calculator tool (Figure 4).

4. RESULTS OF THE MCDM MODEL

By applying the MDCM model and the AHP analysis in the study area, the sustainable land uses of the Kalamaria-Pilea seafront were selected according to Figure 4. Transportation facilities were selected in a key area, where most of the facilities would be accessible to the public. Small green areas were selected, in order to keep the cost low, while tourist facilities were selected to be developed at the southern part of the study area, as in a small distance the marina of Pilea will be constructed, according to the General Urban Plan of Municipality of Pilea-Chortiatis. Furthermore, sport facilities and shopping malls were selected to be constructed as they were chosen by the public through the questionnaire. Finally, the area of each sustainable land use is presented in Table 6.

Table 6: Type and total area of each selected sustainable land use for the Kalamaria-Pilea seafront.

Sustainable Land Use	Area (km^2)
Cultural sites	0,12
Green areas	0,09
Shopping malls	0,15
Sport facilities	0,22
Tourist facilities	0,18
Transportation facilities	0,05

5. DISCUSSION AND CONCLUSIONS

Multi-Criteria Decision Making (MCDM) techniques in GIS-based land suitability procedures have been increased, especially at a regional-scale planning processes. By selecting basic environmental criteria and socio-economical criteria based on the public’s opinion, which could be easily given through a well-formatted questionnaire, the sustainable land uses for any area with no land cover can be extracted and be added to a General Urban Plan of any Greek Municipality.

The MDCM model, which has been presented in the current study, is enhanced by using the AHP analysis in order to minimize the errors in selecting the suitable land use. In addition, Remote Sensing Methods have been proved necessary in order to map the study area in its current situation.

Finally, it should be noted that the selection of land uses must be focused both on the environment and the economic development of each municipality, as it has been observed from the current study that the General Urban Plan of Municipality of Kalamaria had both designated green areas, several facilities and zones of environmental protection (coastal zone), while the General Urban Plan of Municipality of Pilea-Chortiatis has focused only for the economical development of the municipality, without concerning about the environmental protection of the coastal zone. This had the result that the sustainable land uses which were selected for the Municipality of Kalamaria were close enough to its General Urban Plan, while the sustainable land uses which were selected for the

Municipality of Pilea-Chortiatis differ from its General Urban Plan, demonstrating that this General Urban Plan should be furthermore studied.

References

1. Anastasiadis S. (2015) **'Investigation of the possible development of Kalamaria-Pilea Seafront'**, Master of Science Thesis, Aristotle University of Thessaloniki.
2. Antoniades P. and Ioannides K. (1970) **'Geological map of Thessaloniki'**, Institute of Geological and Mining Research, Greece.
3. Collin M.L, Melloul A.J. (2012) **'Land-Use Planning Guidelines for Optimal Coastal Environmental Management'**, Journal of Environmental Protection, 3, pp 485-501.
4. Langemeyer J., Gomez Baggethum E., Haase D., Scheuer S., Elmqvist T. (2016) **'Bridging the gap between ecosystem service assessments and land use planning through Multi-Criteria Decision Analysis'**, Environmental Science and Policy, 62, pp 45-56.
5. Lefebvre A., Sannier C., Corpetti T. (2016) **'Monitoring Urban Areas with Sentinel-2A Data: Application to the update of the Copernicus High Resolution Layer Imperviousness Degree'**, Remote Sensing, 8, 606.
6. Marull J., Pino J., Mallarach J., et al. (2007) **'Land suitability index for strategic environmental assessment in metropolitan areas'**, Landscape Urban Plan, 81(3), pp 200-12.
7. Melloul A. J. and Collin M. L. (2001) **'A Hierarchy of Ground- Water Management, Land-Use, and Social Needs Integrated for Sustainable Resource Development'**, Environment, Development and Sustainability Journal, Vol. 3, pp 45-59.
8. Mosadeghi R. (2013) **'A spatial multi-criteria decision making model for coastal land use planning'**, PhD Thesis, Griffith University.
9. Organization of Thessaloniki (2001) **'Transformations of the urban landscape. Architectural studies and works of the European Capital of Culture Organization Thessaloniki 1997'**, Livani Publishing House SA, Thessaloniki.
10. Phua M.H., Minowa M. (2005) **'A GIS-based multi-criteria decision making approach to forest conservation planning at a landscape scale: a case study in the Kinabalu Area, Sabah, Malaysia'**, Landscape Urban Plan, 71 (2-4), pp 207-222.
11. Saaty T.L. (1977) **'A scaling method for priorities in hierarchical structures'**, Journal of Mathematical Psychology, Vol. 15, pp 234 – 281.
12. Saaty T.L., Vargas L. (1984) **'Inconsistency and Rank Preservation'**, Journal of Mathematical Psychology, 28, pp 205-214.
13. Verdoodt A. & Ranst E.V. (2006) **'Environmental assessment tools for multiscale land resources information systems: a case study of Rwanda'**, Agric Ecosyst Environ, 114(2-4), pp 170-84.
14. Xu M., Zeng G.M., Xu X.Y., et al. (2006) **'Application of Bayesian regularized BP neural network model for trend analysis, acidity and chemical composition of precipitation in north Carolina'**, Water Air Soil Pollut, 172(1/4), pp 167-84.
15. Yang F., Zeng G., Du C., Tang L., Zhou J., Li Z. (2008) **'Spatial analyzing system for urban land-use management based on GIS and multi-criteria assessment modeling'**, Progress in Natural Science, 18, pp 1279-1284.
16. Zeng G.M., Jiang R., Huang G.H., et al. (2007) **'Optimization of wastewater treatment alternative selection by hierarchy grey relational analysis'**, J Environ Manage, 82(2), pp 250-89.

APPLYING THE CONTINGENT VALUATION METHOD TO ESTIMATE THE ECONOMIC VALUE OF THE THESSALONIKI SUBURBAN SEICH-SOU FOREST AMENITIES

E.K. Oikonomou* and A. Guitonas

Department of Transportation and Hydraulic Engineering, Faculty of Rural & Surveying Engineering, Aristotle University of Thessaloniki, 54124 Thessaloniki, Hellas

*Corresponding author: e-mail: eoikonom@topo.auth.gr, tel: +30 2310 994360

Abstract

Environmental economic valuation of natural public goods and resources is focused on how to place a monetary value on goods and bads, arising from changes that take place within the natural environment and affect environmental quality or the available stocks of some natural resources. The economic techniques available for economic valuation can be divided into three groups: conventional market approaches; constructed market approaches; and implicit market approaches. In constructed market, the most widely approach used is the contingent valuation method (CVM), which uses a direct approach – some form of questionnaire – in order to ask people what they are willing to pay (WTP) for an environmental benefit or willing to accept (WTA) in compensation for a loss. The popularity of the method may be attributed mainly to two factors: firstly, it does not require any great amount of data that is usually necessary for other techniques; and secondly, it can be applied in a great variety of goods and services, including use and non-use values.

In the present paper the results of a questionnaire survey are presented, in an effort to investigate on people's WTP for better eco-management and protection of the important for Thessaloniki suburban forest of Seich-Sou. The current situation of the forest is characterized by abandonment and low quality of green space and tree flora, as a result of the ten-year on-going Greek economic crisis. However, the forest is regarded as of vital importance, because of its contribution to the quality of urban life: the micro-climate of the Thessaloniki's urban area is strongly and positively affected by the forest; it contributes to flood protection; it offers recreational activities; it offers a pleasant landscape, etc. The paper describes how the questionnaire has been formed in order to seek for reliable answers; how the survey has been organized, designed and implemented; and how the results have been critically assessed, in order to reach to safer conclusions on the WTP answer. General conclusions may be reached on the successfulness of organizing WTP surveys during the Greek economic crisis, by comparing the results of a similar survey conducted some years before this crisis.

Keywords: Contingent valuation method, Seich-Sou suburban forest, Willingness to pay, Questionnaire survey

1. INTRODUCTION

Suburban forest areas are of vital importance, since they strongly affect positively many parameters of the quality of life of urban areas inhabitants: they are close to urban areas, contributing, thus, to enlarge the surface of green space in the built environment; they are visited by many inhabitants, usually for walking, and other purposes related to sports and light recreation activities, covering such needs and offering a better quality for their body and mind; they may decrease levels of atmospheric pollution, noise pollution and they create better micro-climate conditions for the near-by urban area;

they have an educational role, offering the opportunity for schools excursions and students visits; they contribute positively to better relations between different groups and stakeholders in urban societies; and in some cases, they enhance touristic activities, thus, offering opportunities for income increase of local people. Suburban forests usually form better urban landscapes and affect real estate and housing prices in areas next to green spaces. The contribution of suburban forests to the quality of life in urban areas should also be taken into consideration under the parameter that by 2025, around 3 billion people will be living in cities, while in Hellas, more than 60% of total population already lives in cities and towns of more than 10,000 inhabitants, according to the population census of 2011 of the Hellenic Statistical Authority. In several USA cities relevant research has estimated in monetary expression the economic costs of measures to decrease atmospheric pollution that are not implemented, due to the existence of such forest areas or economic benefits or the economic benefits from measures that are not needed, in order to prevent soil erosion or the economic benefits that are gained in energy consumption for heating and cooling, due to better micro-climate conditions, etc. [1]. In this paper the results of a questionnaire survey are presented, which was conducted by using the Contingent Valuation Method, in order to investigate on the economic value of the suburban forest of Thessaloniki, Seich-Sou. The paper includes a brief description of the most important characteristics of the area of study, some details on the questionnaire survey design and implementation, and finally, the results of the survey with useful comments on the quality and reliability of the survey and its results.

2. ENVIRONMENTAL VALUATION BY ECONOMIC TECHNIQUES

Environmental valuation by economists is focused on how to place a monetary value on goods and bads arising from changes that take place within the natural environment and affect environmental quality or the available stocks of some natural resources, which impact on the utility or well-being of individuals. The total value of a change in environmental goods is considered to be the sum of the values of its effects on individuals, while different kinds of impact can be compared and some quantity of money can always act as a substitute for some quantity of an environmental good; and finally, environmental goods of equal value can be substituted for each other with no loss of welfare. In order to determine the Total Economic Value (TEV) of a resource, use values and non-use values need to be captured by valuation techniques [2]. Use values may be subdivided to actual use values and option values, with the former reflecting the benefits that result from the direct contact with the natural resource and the latter expressing a preference, ‘a willingness to pay’, for the preservation of an environmental asset against the probability that the individual will make use of it. On the contrary, non-use values or else existence values, correspond to those benefits that do not imply direct contact between the consumers and the good, and they derive from the knowledge that a particular good exists [3], [4]. Finally, the TEV of an environmental asset is obtained by summing up actual use value, option value and existence value. The economic techniques available for environmental valuation can be divided into three groups: conventional market approaches; constructed market approaches; and implicit market approaches. These groups are subdivided into actual behavior-based techniques, potential behavior-based techniques and other techniques. Conventional market approaches seek to establish a link between an environmental impact and some other good that already has a market value. Implicit market techniques assume that the behavior of individuals reveals implicit valuations of features of the environment: wages accepted to work in locations with different levels of environmental quality, prices or rents paid for properties that have particular levels of environmental amenities or costs associated with specific activities, such as recreational trips. In constructed market, the most widely approach used is the contingent valuation method (CVM), which uses a direct approach – some form of questionnaire – in order to ask people what they are willing to pay (WTP) for an environmental benefit or willing to accept (WTA) in compensation for a loss [5].

The CVM, used in the research presented in this paper, is especially used in environmental cost-benefit (CBA) and impact assessment (EIA). However, it is suggested that WTP is better than WTA and it should be used in CV studies, although in developing countries, EIA Studies deal with the

negative environmental effects of a proposed project and thus, WTA compensation is considered a more appropriate measure [6]. The popularity of the method may be attributed mainly to two factors: firstly, it does not require any great amount of data that is usually necessary for other techniques; and secondly, it can be applied in a great variety of goods and services, including use and non-use values. However, the CVM is not a panacea: the questionnaire response is not appropriate to the respondents who are ignorant of the object of preservation interest; respondents may not imagine the same product as questioners think they are offering; the scenario suggested for paying for the product (the 'payment vehicle') may not be believable; and finally, there may not be incentives for respondents to answer truthfully [7]. Thus, Carson et al. believe that the CVM survey results should not draw attention to the final economic result, by a direct economic interpretation, unless the environmental good that is valued, is clearly explained to the respondents, its delivery to the public is acceptable and a realistic scenario of payment is created [8]. Since the 1990s, the CVM has been widely implemented as a valuation tool for environmental goods and services e.g. the World Bank has commissioned CVM studies through its WASH (Water for Sanitation and Health) program to measure people's WTP for water projects in developing countries. Valuations of benefits from air quality improvements have also been estimated using CVM; some argue that the CVM is particularly useful for valuing visibility improvements at national parks or assessing ecological benefits, such as preserving endangered species, where existence value is likely to be significant [4].

The accuracy of the CVM is not easy to define and a number of problems, known as systematic biases, appear leading to unreliable or inaccurate bids or responses [6]:

- WTP seems to be the most appropriate measure for gainers and WTA the proper measure for losers, assuming that it is easy to identify gainers and losers, and consequently.
- Strategic bias appears when the respondents on purpose misrepresent their true WTP or WTA, in order to manipulate the results of the survey, for example to generate high values. Several studies conclude that strategic bias is not a significant problem because it can be ameliorated by proper survey design. Sometimes respondents are not WTP for goods because they anticipate enjoying them without payment (the free-rider problem).
- The final value obtained in a survey is strongly influenced by the form of questioning (design bias). The question posed could be a single closed-format question or it could be an iterative bidding process or a continuous open-ended bid. The final value is also influenced by the starting point bias when the interviewer suggests some amount of money.
- The 'vehicle' or instrument of payment bias is referred to the form or method of payment by which the bids offered by respondents will be collected (e.g. changes in taxes, entrance fees, extra charges on bills, higher prices on goods, etc.). Studies show that WTP may be higher with payroll taxes compared with increased entrance fees.
- The information bias refers to the level of information about the environmental good under evaluation, which is given to the respondents. Studies, such as Hoehn and Randall, reveal the strong relation between resource quality information and contingent values [9].

3. IMPLEMENTATION OF THE CVM IN SEICH-SOU ENVIRONMENTAL VALUATION

3.1 The area of study

The Seich-Sou suburban forest of Thessaloniki is located in the northeast of the city, sometimes adjacent to the urban limit (Figure 1), and it took its current form, as an artificial forest, in the 1930s, when a major reforestation project took place, mostly with pine trees, in an area of 3.000 hectares. Historical sources mention that from the establishment of Thessaloniki around the year 315 b.C. by Kassandros, king of Macedonia after Alexander the Great, rich forest areas existed all around today's urban area; however, during the Byzantine Empire and the Ottoman Empire, the forest areas gradually

disappeared, as wood was needed for several purposes. And since the hilly area northeast of Thessaloniki includes many springs and streams, the reforestation project that started in the 1930s contributed also to the protection of the urban area from flooding. During the period of 1931-1953, around two million of small trees (90% of them were pine trees) were used for the reforestation project; simultaneously, the first flood defense projects were constructed. In 1973, by the Prefectural Decision 2193/9-10-1973, the area of Seich-Sou was declared as forest protection area. In the summer of 1997 a fire destroyed almost 55% of the total forest area, but nowadays, the signs show that the forest is recovering, while some more flood defense projects were constructed, in order to avoid soil erosion in the parts of the forest that were affected by the fire. The natural environment of the forest involves 277 species of flora, 18 species of fauna, 95 bird species and 21 species of reptiles. The surface water network comprises 17 small streams, with basins from 0.4 to 5.6 km^2 and mean slope of the basins from 8% to 16%.

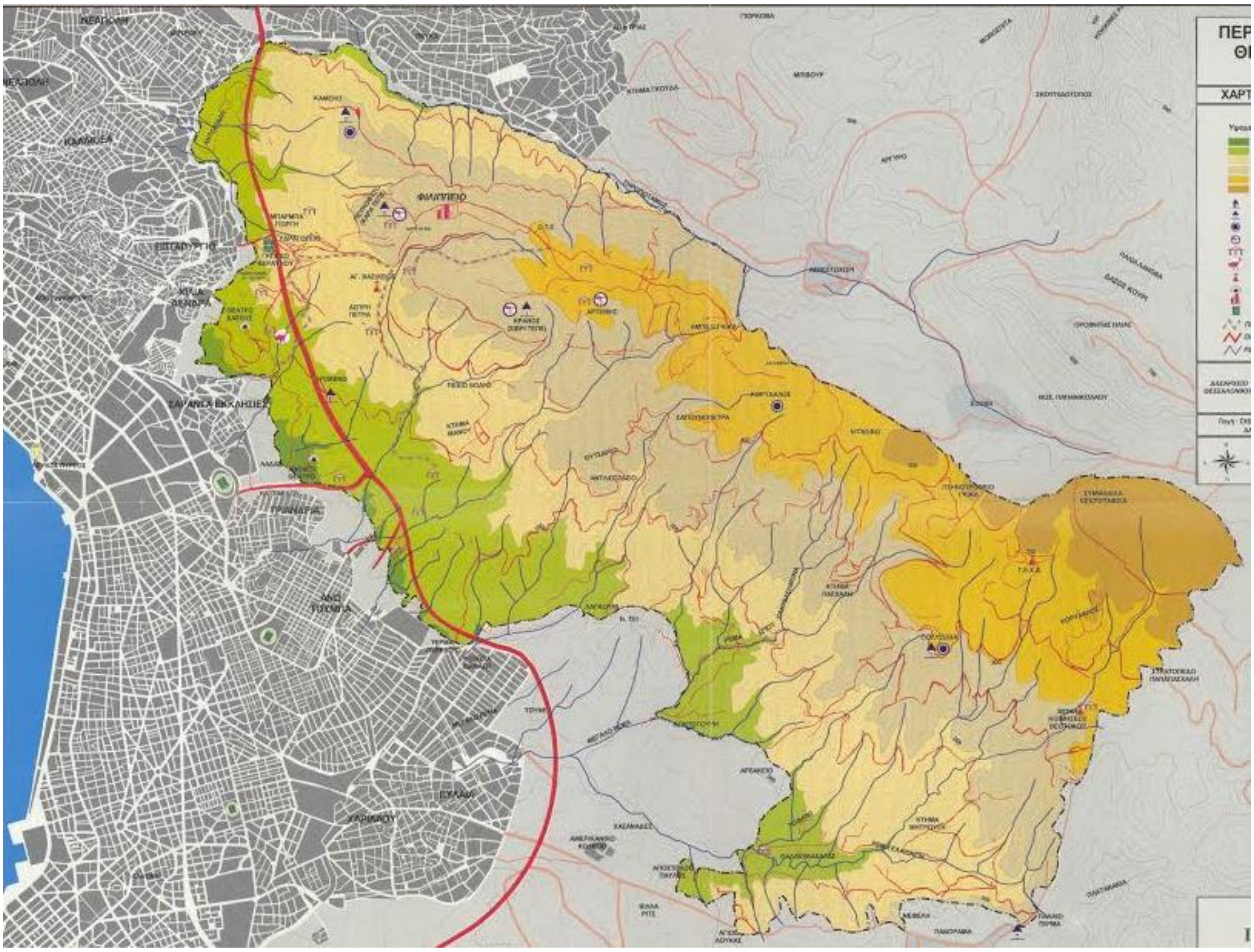


Figure 1: The Seich-Sou is next to the city border, while part of the city by-pass was constructed inside the forest area (green and yellow colors express levels of altitude)

The last 10 years, in the period of Hellenic economic crisis, many problems arose for the condition of the Seich-Sou suburban forest: increased possibility for fire, mostly due to many wastes, disposed all-round the forest area by irresponsible visitors, while wastes collection services were weakened; illegal wastewater disposal in few streams; illegal wood cutting for heating purposes; and finally, pine processionary caterpillars reflect a great danger for trees, as they form many nests, while there is almost no funding, in order to spray with appropriate airplanes. Therefore, there is an urgent need to find the necessary funds, so as to implement a program towards forest restoration and protection. As all these parameters are well-known to many citizens of Thessaloniki, it was an opportunity to conduct surveys and investigate on their WTP, in order to ameliorate the Seich-Sou and thus, relate this WTP to the value of the forest.

3.2 Questionnaire survey planning, design and implementation

In order to conduct a questionnaire survey, there is a need to: define the aims of the survey and how the results will be used; design the necessary research methods and techniques; develop the survey instrument; select people to be approached (target groups); assemble the questionnaire package (how the survey questions look, the sections of the questionnaire and type of questions); conduct the survey; and, finally, process and report the survey results [10]. While constructing the questionnaire used in the survey, the following elements were considered: the shorter the questionnaire is, the higher the response rate; specific questions are better than general ones; and closed questions force people to choose among offered alternatives, instead of answering in their own words, but they are more specific and therefore, more apt to communicate the same frame of reference to all respondents. The contingent valuation scenario should be also short, realistic and simple. As mentioned by Converse and Presser, the two main advantages of specificity are a more precise communication of question intent and an aid for the respondent to recall [11]. To sum up with, closed questions produce answers that can be meaningfully compared as well as less variable answers, they are easier to be answered and finally, they produce answers that are easier to computerize, analyse and process. However, closed questions may also produce problems associated with recording responses, as the interviewer may record answers inaccurately or even neglect to read all of the response options [12]. The order of question sequence is also very important: the questionnaire must be attractive to the respondent, avoid putting ideas into the respondent's mind early in the interview and the first questions seem to be crucial in order to "hook" the respondent into answering the survey. Apparently, the first questions should be intriguing (perhaps asking for an opinion on an interesting topic), easy to answer, general and impersonal [11, 13].

200 hundred interviews were conducted in June 2014, with 120 respondents that were visitors and were found and interviewed in the forest, and 80 respondents, inhabitants of Pefka, which is a suburb of Thessaloniki, a town of 13,000 inhabitants, the closest community to the Seich-Sou. The reason to conduct the survey also in Pefka was the available information that although this suburb is adjacent to the forest, the interaction between the forest and the urban area is poor. The respondents were asked questions related to their relation with the forest (how often they visit it, for which reasons, how much time they spend, their knowledge about the degradation problems facing the forest), their WTP in order to raise funding to support forest protection and restoration, and finally, some personal information, related to their annual income, their education level, their age, their profession, etc. The questionnaire involved 18 questions, all of them closed and semi-closed.

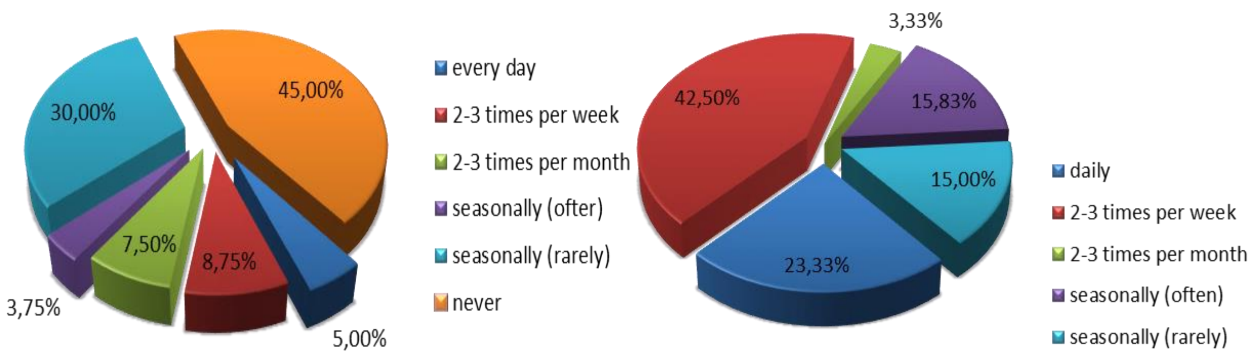
3.3 The results of the survey

The results of the CVM survey are presented in the following paragraphs, separately for visitors interviewed in the forest and inhabitants of Pefka suburban town:

- 25% of Pefka inhabitants visit often the forest (more than seasonally often), while for the Seich-Sou visitors this percentage is more than triple, 85%. In total, 61% of all respondents visit the forest often. The main reasons for Pefka inhabitants for not visiting the forest often are "lack of free time" (27%), "forest degradation" (27%), "other choices" (25%) and "no combination to other activities" (10%).
- The main reasons for visiting the forest by Pefka inhabitants are "recreational activities" (36%), "sports/cycling" (30%) and "walking" (28.3%), while for visitors interviewed in the forest the results reflect 28.3%, 13.3% and 41.7% respectively (in total 30.7%,18.5% and 37.6% respectively).
- The two target groups of the questionnaire survey responded to the most important problems that the forest was facing, leading to its degradation and the respondents replied "the absence of organized sites for recreation" (26% – 27%), "safety of the forest" (22% – 30%), "no maintenance of paths" (17% – 18%), "no organized sports facilities" (14% – 10%) and

"accessibility problems" (13% – 10%) – the first percentage in every parenthesis reflects results from Pefka residents and the second from visitors in the forest.

- The forest area is accessible to all respondents "on foot" (57%), "in car" (30%), "by bicycle" (8.4%), "by bike" (2.6) and "by bus" (2%), showing that many visitors live nearby the forest and when they live in a more distance, they travel in car, because there no buses serving effectively the several entrances to the forest. This is why 65% of total visitors of the forest travel up to 10 minutes to arrive to the forest, either on foot or in car.
- The average time spent in the forest is, for the inhabitants of Pefka, "less than an hour" (59%) or "2 – 3 hours" (41%), while for the visitors interviewed in the forest, "2 – 3 hours" (67.5%), "more than 3 hours" (20%) and "less than an hour" (12.5%).



Figures 4 & 5: The frequency of visit to the forest, by Pefka inhabitants and visitors of Seich-Sou

- The respondents were also asked to evaluate the benefits of Seich-Sou for Thessaloniki and its inhabitants. Pefka inhabitants recognize the following benefits from the most important to the less important: "flood protection", "source of oxygen", "better micro-climate", "recreation/sports", "landscape", "tourism" and "educational/scientific benefits". For the visitors interviewed in the forest, "source of oxygen", "recreation/sports", "flood protection", "landscape", "better micro-climate", "educational/scientific benefits" and "tourism".
- The respondents were asked to comment on the necessary projects for the forest protection and restoration. For the Pefka inhabitants from the most important to the less important, the projects are: "new recreation infrastructure", "lighting", "ensure safety", "restoration of paths", "construction of WC", "wastes collection", "provision of freshwater and electricity", "more garbage bins" and "new sites for view appreciation". For the respondents interviewed in the forest, "more garbage bins", "restoration of paths", "construction of WC", "new recreation infrastructure", "new sites for view appreciation", "provision of freshwater and electricity", "ensure safety", "wastes collection" and "lighting".
- Results for socioeconomic characteristics of total respondents are presented in Tables 2 and 3:

Table 2: Age of the respondents

	The age of the respondents						Total
Classification of age	18-24	25-34	35-44	45-55	56-65	66 +	
Number of responses	20	51	37	38	23	31	200
Percentage	10,0%	25,5%	18,5%	19,0%	11,5%	15,5%	100%

Table 3: Main profession of the respondents

	Main profession						Total
Type of profession	Employee in the private sector	Employee in the public sector	Self-employed	Retired	Student	Other	
Number of responses	60	23	46	41	14	16	200
Percentage	30,0%	11,5%	23,0%	20,5%	7,0%	8,0%	100%

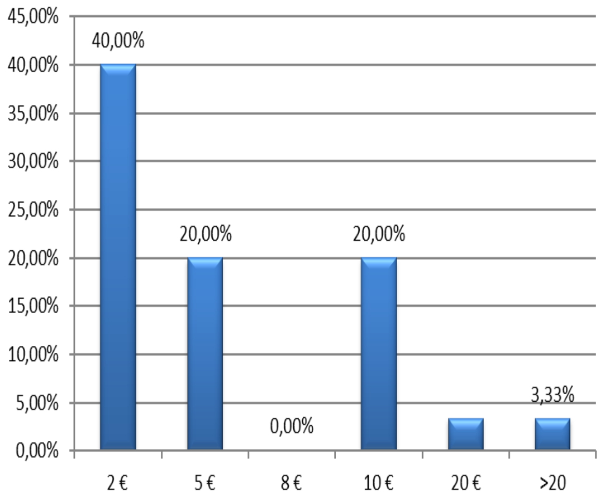
Table 4: Family annual income of the respondents

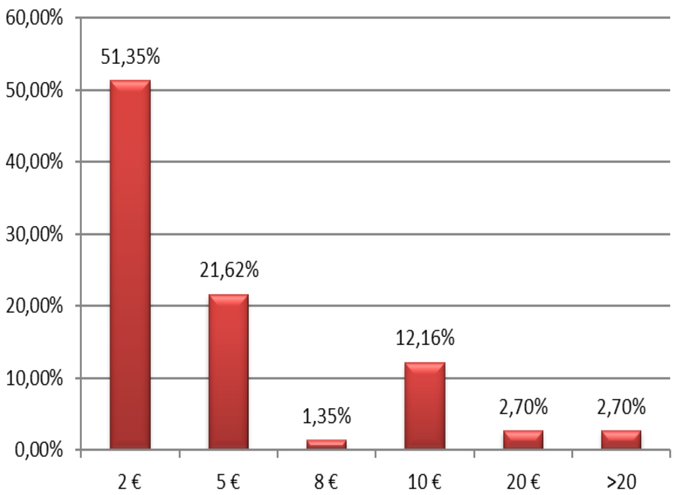
	Annual family income						Total
Classification of income	<8.000€	8.001-16.000€	16.001-24.000€	24.001-32.000€	32.001-40.000€	>40.000€	
Number of responses	42	60	50	28	12	8	200
Percentage	21,0%	30,0%	25,0%	14,0%	6,0%	4,0%	100%

The final and crucial question in the research was related to the WTP of the respondents, in order to enhance protection and restoration of the Seich-Sou forest. Out of the 200 respondents in total, 104 were positive in financial contribution (52%), which is a typical percentage of positive response in many CVM studies. However, the positive response percentage is much different between Pefka inhabitants (37.5% - 30 positive answers out of 80 respondents) and respondents interviewed in the forest (61.7% - 74 positive answers out of 120 respondents), which was expected, since as already shown, Pefka inhabitants do not often visit the forest, do not spend so much time when they visit the forest, etc. The average WTP was calculated to 5.07 € for the 104 total positive respondents, with the average being 5.27 € for positive Pefka inhabitants and 4.99 € for positive respondents interviewed in the forest. The answers to the willingness-to-pay question are presented in the following Table 5 and Figures 6 and 7:

Table 5: The WTP bids for positive Pefka inhabitants, respondents interviewed in the forest and total respondents

	Willingness-to-pay bids							Total
Bids in €	2 €	5 €	8 €	10 €	20 €	>20 €	other	
Number of responses (Pefka)	12	6	0	6	1	1	4	30
Percentage	40.0%	20.0%	0%	20.0%	3.33%	3.33%	13.33%	100%
Number of responses (forest)	38	16	1	9	2	2	6	74
Percentage	51.4%	21.6%	1.4%	12.2%	2.7%	2.7%	8.0%	100%
Total number of (positive) responses	50	22	1	15	3	3	10	104
Percentage	48.1%	21.2%	0.9%	14.4%	2.9%	2.9%	9.6%	100%





Figures 6 and 7: The WTP bids for positive Pefka inhabitants and respondents interviewed in the forest

Furthermore, to those who were negative in WTP, responded for their reason of their denial: for Pefka inhabitants 53% of the respondents mentioned that public authorities / the state should protect the forest with economic funding from people's taxes; 27.5% replied that they cannot afford it; and 17.7% do not trust public authorities with financial management and they are suspicious of using the money in the proper way for the forest protection and restoration. On the other hand, for respondents that were interviewed in the forest, 43.4% replied that public authorities / the state should protect the forest with economic funding from people's taxes; 37.8% are suspicious on the effective financial management for the protection of the forest; and 17% replied that they cannot afford it. Finally, to those who were positive in WTP (total respondents), there was one more question about the appropriate vehicle of payment and they replied that the best would be if all Thessaloniki inhabitants become members of an environmental organization and pay a subscription there (64%), 20% believe that they should pay an extra amount to the local municipality, 10.7% by a new environmental tax and 4.9% of the respondents believe that people should buy tickets in the entrances of the forest.

3.4 Discussion

It is always a challenge in a WTP survey and research to conclude from the WTP bids that the results and answers are reliable or not and exclude unreliable questionnaires from the final results of the survey. Statistical analyses are not always the correct methodology, in order to investigate the issue of reliability and research on the biases mentioned in paragraph 2 of the current paper. Such biases are successfully dealt with the aid of some questions in the survey that are related on to each other; consequently, their results can be examined together and compared for their reliability. For this reason, in the present CVM survey, after the first results, further analysis was made, comparing results of WTP with other answers e.g. in socioeconomic and other questions.

The WTP results are strongly correlated with the annual family income of the respondents. 30% of the respondents replied that their annual family income was 8,001 – 16,000 €, 25% was 16,001 – 24,000 €, 14% was 24,001 – 32,000 €, etc. or 45% of the respondents replied 16,001 – 40,000 €, as seen in Figure 8. Calculating the WTP of each group of family annual income, one would expect that there is a certain ration between them, meaning that the more annual income is, the more could be the WTP bid. The results are shown in Figure 9, but since there were only four respondents with more than 40,000 € annual family income, these four questionnaires may be excluded from WTP results and then Figure 10 can show better the relation between WTP and family annual income. From Figure 10 it may be concluded either that the average of 5 € for respondents with family annual income of 16,001 – 24,000 € is higher than 'expected' (4.50 € approximately) or the average of 4.80 € for respondents with family income of 24,001 – 32,000 € is lower than 'expected' (5.40 € approximately).

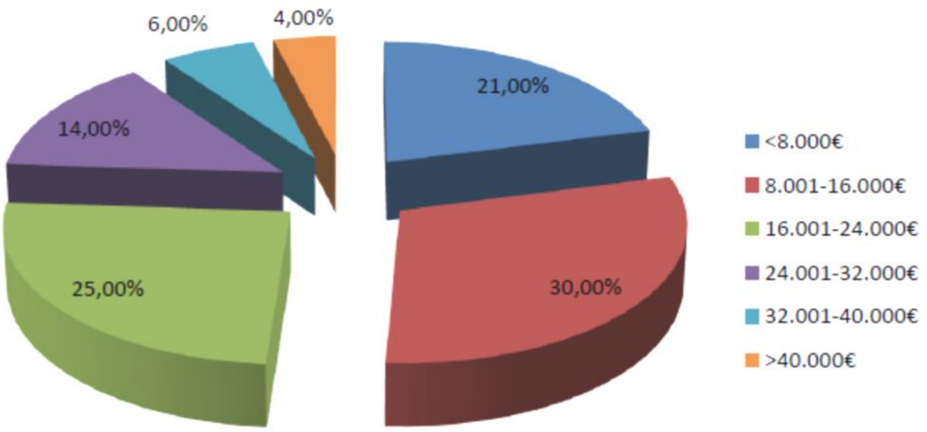
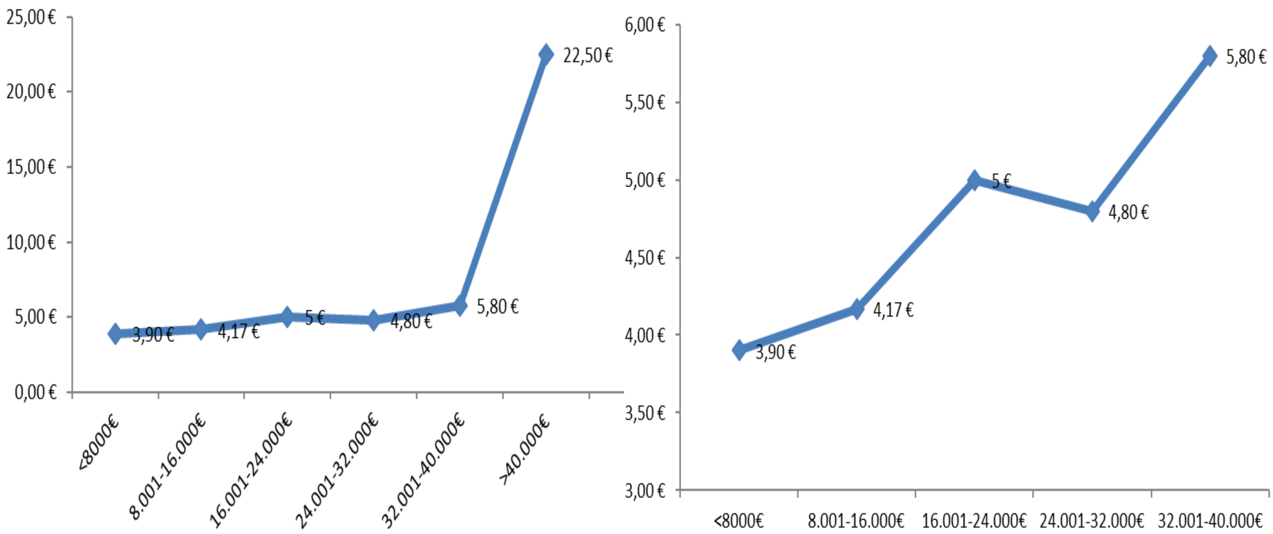


Figure 8: The annual family income of the respondents

Further analysis, as shown in Figure 11, reveals that WTP results, according to family annual income of the respondents, are different for Pefka inhabitants than respondents interviewed in the forest. For Pefka inhabitants it seems that WTP results are quite reliable, as it is shown that there is a certain 'rational' ratio between family annual income and WTP bids, except for respondents with annual income of 16,000 – 24,000 € (2.85 € WTP, while the 'proper' would be around 5.30 €). On the contrary, for respondents interviewed in the forest, it seems that WTP results may not correlate with family annual income, since all averages were calculated between 4.10 € and 4.60 €, while the average of 5.75 € for respondents with family annual income 16,001 – 24,000 € may be unreliable. Another possible explanation could be that replies of respondents interviewed in the forest, with family annual income of less than 16,000 € were more optimistic in WTP bids, as they are visitors of the forest, they really need to help financially with forest protection and restoration, and they also realize that the whole questionnaire survey is just theory and the WTP question is completely hypothetical. All these comments are based on the assumption that respondents are honest while answering about their family annual income.



Figures 9 and 10: The WTP results, according to the family annual income (FAI) of the respondents, and again the results, after excluding the four respondents with FAI of more than 40,000 €

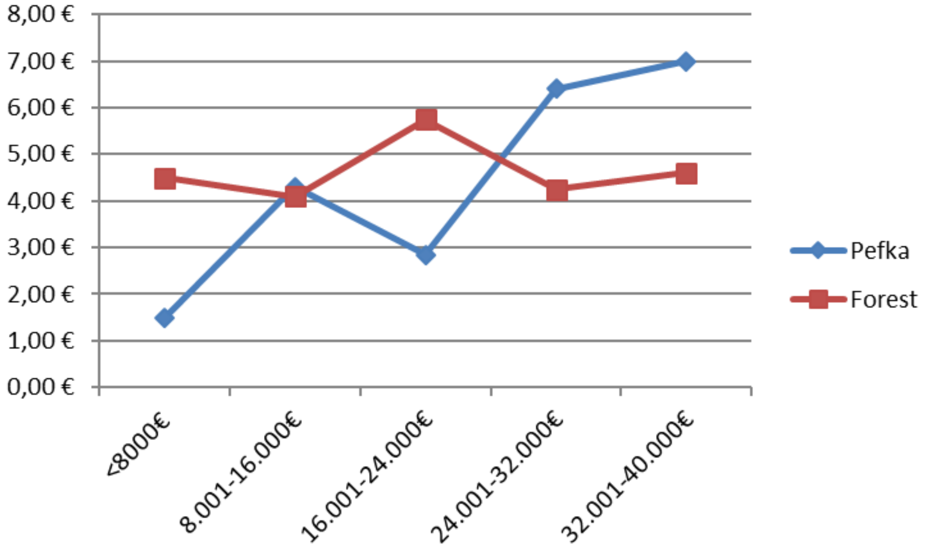


Figure 11: The WTP results, according to the family annual income of the respondents of Pefka inhabitants and respondents interviewed in the forest

Comparing WTP averages, according to the educational status of the respondents, it seems that the more educated they are, the bigger is the WTP bid, which seems reasonable, since it could be generally stated that people with better educational status may have a bigger family annual income or they can realize better the usefulness of the Seich-Sou. Results are shown in Figure 12: the relation between WTP and education seems 'linear' for the first three groups, while WTP results become much higher for the respondents with postgraduate studies.

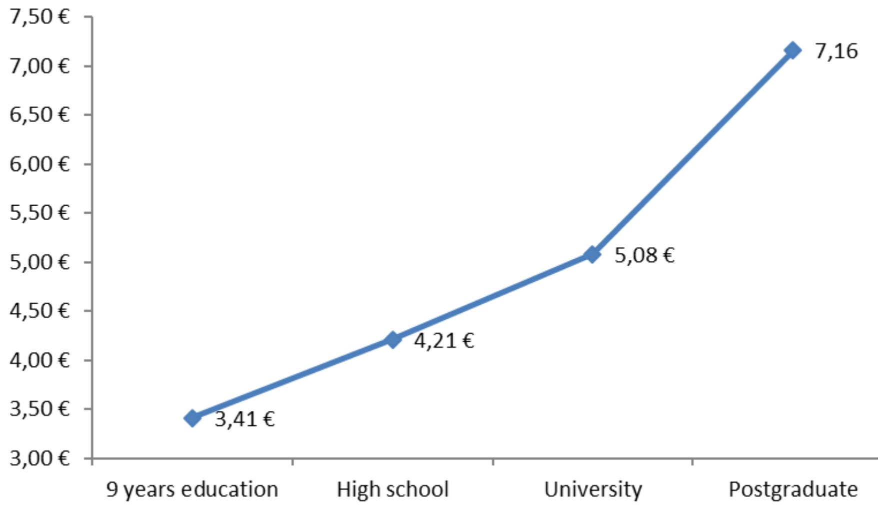
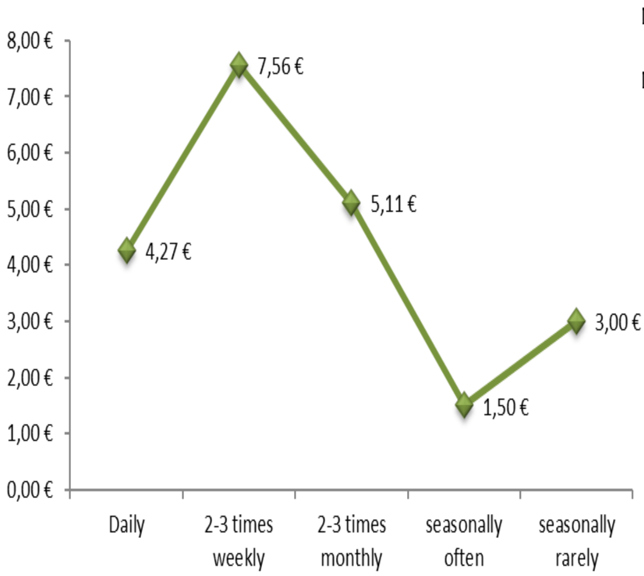
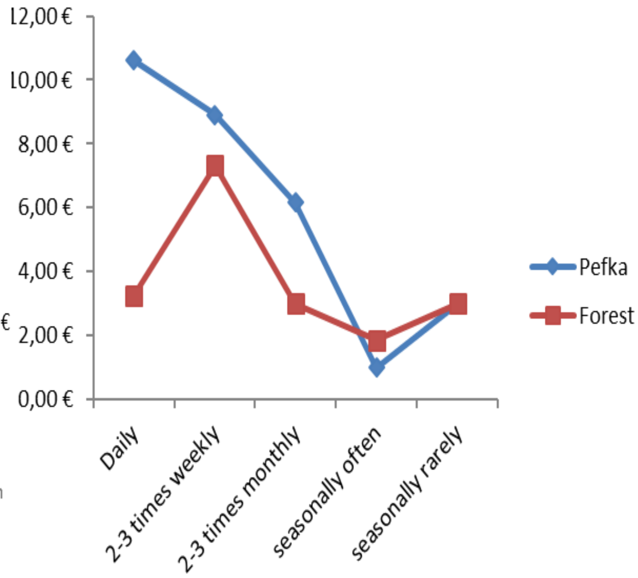


Figure 12: The WTP results, according to the educational status of the respondents

Finally, the WTP results were correlated with the frequency of visits of the respondents, while it would be expected that the more often they visit the forest, the higher would be the WTP bid. In Figure 13 results are presented for all the respondents and it could be concluded that for daily visitors and seasonally often visitors one would expect higher WTP bids than the averages calculated.

Looking at WTP results for Pefka inhabitants and the respondents interviewed in the forest, as presented in Figure 14, it seems that for Pefka inhabitants' replies are more reliable, with the only exception of the average of 'seasonally often' visitors. On the other hand, WTP averages of the respondents interviewed in the forest seem that they are not in a linear relation with visit frequency. If it is assumed that often visitors were more honest, then the average of seasonally rarely visitors is higher than expected and the average of daily visitors is much lower than expected.





Figures 13 and 14: The WTP results, according to the visit frequency of all respondents, and again the results, separately for Pefka inhabitants and respondents interviewed in the forest.

4. CONCLUSIONS

The WTP questionnaire survey for the suburban forest of Thessaloniki – Seich-Sou – was a pilot survey, addressed to 200 respondents in total, 80 Pefka inhabitants and 120 respondents interviewed in the forest. WTP results were calculated and further analysis was made, correlating WTP averages with other parameters and more specifically, with the annual income of the respondents, the educational status and the visit frequency. In some cases, some WTP averages seem to lack reliability, but generally, the WTP survey overall could be characterized by success and reliability, especially if it is taken into consideration that the interviews were conducted with the aid of a postgraduate student of the Aristotle University of Thessaloniki who has none experience in surveys and the project was not funded. To summarize, the following comments may interpret some of the results of the survey:

- The WTP question was quite vague, because it did not clarify if the WTP bid was monthly, yearly or just once, because of an emergency situation, related to lack of funding by the Region of Central Macedonia, in order to support protection and restoration of the forest Seich-Sou. A vague WTP question may lead to higher WTP bids and higher averages. On the other hand, this might be one reason why daily and seasonally often visitors are willing to pay less than other categories of respondents, because they may have understood that they would pay every time they visit the forest.
- The WTP question did not mention any specific ‘vehicle of payment’ e.g. an increase in the municipal taxes paid through the electricity power bill, and this absence make the interviewers think of the WTP question as completely hypothetical and so for this reason again, their answers may result in higher WTP bids than they were really willing to pay.
- Pefka inhabitants were not so positive to support financially the forest for its protection and restoration, because as it had been already known, the access from the town of Pefka to the forest was very difficult and still is, consequently, they are not so often visitors and this is why the positive response percentage for WTP was 37.5% for them and 61.7% for respondents interviewed in the forest.
- The WTP survey was conducted in the middle of 2014, with Hellas being for the fifth year in economic crisis, with many families losing even more than 50% of their annual income, and with a high percentage of unemployment, almost 30%, rising to 50% for young people at the age of 25 – 35 years old.

- Finally, if the WTP survey was to be repeated, it would be better to focus only on respondents interviewed in the forest and not to any Pefka inhabitants, as they seem not to have a strong relation to the forest, which is adjacent to the suburban town, but with not an easy access. And the WTP question would be more specific referring to the 'vehicle of payment' and the frequency of payment e.g. monthly, yearly, occasionally, etc.

ACKNOWLEDGEMENTS

The authors are grateful for the assistance given by Mrs E. Zoura, Forester AUTh, MSc in Water Resources, particularly with her assistance in the interviews of the survey.

References

1. Kalavrytinos N. and D. Damigos. (2006). 'The economic value of urban green spaces in Attica Basin.' **Technika Chronika Scientific Journal of the Technical Chamber of Greece**, vol. II, no. 1-2, pp. 7-21 (in Hellenic with extended summary in English).
2. Edwards-Jones G., Davies, B. and S. Hussain. (2000). **'Ecological Economics-An Introduction.'** Blackwell Science Ltd.
3. Pearce D.W. and R.K. Turner. (1990). **'Economics of natural resources and the environment.'** Harvester Wheatsheaf.
4. Callan S.J. and J.M. Thomas. (1996). **'Environmental Economics and Management-Theory. Policy and Applications.'** Irwin.
5. Munasinghe M.C. (1993). **'Environmental Economics and Sustainable Development.'** World Bank Environment Paper No 3, The World Bank, Washington DC.
6. Venkatachalam L. (2004). 'The contingent valuation method: a review.' **Environmental Impact Assessment Review**, vol. 24, pp. 89-124.
7. Price C. (2000). 'Valuation of unpriced products: contingent valuation, cost-benefit analysis and participatory democracy.' **Land Use Policy**, vol. 17, pp. 187-196.
8. Carson R.T., Flores N.E. and N.F. Meade. (2001). 'Contingent valuation: controversies and evidence.' **Environmental and Resource Economics**, vol. 19, pp. 173-210.
9. Hoehn J.P. and A. Randall. (2002). 'The effect of resource quality information on resource injury perceptions and contingent values.' **Resource and Energy Economics**, vol. 24, pp. 13-31.
10. Oppenheim A.N. (1966). **'Questionnaire Design and Attitude Measurement.'** First ed., Heinemann, London.
11. Converse J. and S. Presser. (1986). **'Survey Questions – Handcrafting the Standardized Questionnaire.'** SAGE Publications.
12. Foddy W. (1993). **'Constructing Questions for Interviews and Questionnaires – Theory and Practice in Social Research.'** First ed., Cambridge University Press.
13. Suckie L.A. (1992). **'Questionnaire Survey Research: What Works.'** Association for Institutional Research, Florida.

APPLYING A CONTINGENT VALUATION METHOD (CVM) FOR THE PRESERVATION /RESTORATION OF THREE LAKES IN NORTHERN GREECE

Odysseas N. Kopsidas*

Department of Industrial Management & Technology, University of Piraeus, 80 Karaoli & Dimitriou, GR 18534 Piraeus, Greece,

*Corresponding author: e-mail: odykopsi@yahoo.gr, +30 6974964415

Abstract

The preservation/restoration of natural environment is usually entailing high cost mostly paid by citizens through taxes. The effect of these taxes is double. The direct effect is the obvious additional income for the State, and the indirect effect is an additional income for the citizen, due to increasing tourism. Since the evaluation of this good cannot be in market terms, we apply a modified Contingent Valuation Method (CVM), which is part of Experimental Economics, in order to find out the order of concern that people have about natural environment. We also, try to investigate their willingness to pay (WTP) for supporting activities for preservation/restoration of three lakes in Northern Greece, in particular, lake of Ioannina, lake of Florina and lake of Kastoria. For the purpose of this research, we use parametric and non-parametric approaches, as well as Linear Regression and Logic Models.

Keywords: Valuation Method (CVM), Natural Environment, Willingness to pay (WTP), Logit Model, Linear Regression, Parametric and Non-Parametric Approaches.

1. INTRODUCTION

Wetlands –and especially lakes– are the most productive ecosystems in the world. They support plenty of ecological activities and important natural habitats. These ecological activities translate strictly into economic functions and services such as flood protection, water supply, improved water quality, commercial and recreational fishing and hunting (Barbier et al., 1997; Woodward and Wui, 2001; Brouwer et al., 1999; Brander et al., 2006).Although, it is a common knowledge that the multiple role of wetlands is usually biased towards the economics benefit from commercial use and exploitation. Usually, the natural benefits of wetlands are underestimated, and the order of exploitation is so high that leads to the extensive degradation (Fog &Lampio, 1982). Despite the uncertainty in total area of wetlands around the world, there are some figures indicating the importance of the problem. In Europe, 50% to 60% of wetlands have been lost in past century due to the human intervention, while the United States have lost 54% of its original wetlands (Barbier et al., 1997). The accelerated rate of wetlands loss was a great alarm for many countries and scientists around the world to take care of the situation. In 1971, more than100 countries created the Ramsar Convention of Wetlands of International Importance, providing the first step for a greater international cooperation about the protection and the “wise use” of wetlands and their resources (Ramsar, 1996). The increasing number of valuation studies on environmental sector contributes evidence about the importance of wetlands. Kazmierczak (2001) and Boyer and Polasky (2004) provide a variety of studies which include many valuation methods, such as Contingent Valuation Method (CVM), replacement value method etc. Woodward and Wui (2001) use 39 wetlands valuation studies to create a meta-analysis using CV method. Brouwer et al. (1999) also created a

meta-analysis of 30 CV applications. A few years later, Brander et al. (2006) made a meta-analysis using 190 wetlands valuation studies.

Despite the fact that there is a great international scientific concern about the restoration and protection of wetlands, in Greece there are only a few studies. Kontogianni et al. (2001) used CVM to evaluate stakeholders' preferences among four possible hypothetical scenarios for a wetland in Lesvos Island. Another CV research by Psychoudakis et al. (2005) estimates the use values of ecological functions of Zazari-Cheimadidita wetland. In present study, we are using CVM to valuate three wetlands in Greece. In particular, we are investigating the willingness to pay (WTP) of local citizens to preservation/restoration of three lakes in Northern Greece, lake of Ioannina (lake Pamvotida), lake of Kastoria (lake Orestiada) and lake of Florina (lake Cheimaditida). This research is organized in five sections. The first section is the introduction and previous relative works. In section 2, we present some information about each lake, which leads us to this research. In section 3, we present the data and the empirical analysis of the research. Last but not least, in section 4 there are the conclusions, while the bibliography takes place in section 5.

2. KNOWING THE LAKES

2.1 Lake of Florina (Lake Cheimaditida)

Cheimaditida is a lake of northern Greece, located 40km south of the prefecture of Florina. It is one of the lakes formed among the mountains of Verno, Voras, Askio and Vermio. Among these mountains, there are some more wetlands, like Lake Vegoritida, Lake Zazari etc. Cheimaditida's surface is around 10.8 squared km, its maximum length is 6.3km and it is located in an altitude of 593m. Its average depth is 1 meter and the maximum is 2.5m. The water quality of Lake Cheimaditida is affected by household waste of the adjacent nine communities. Apart from this pollution, the quality of lake water is affected by livestock waste from animals, which are breeding around. However, the critical pollution factor is the excessive use of fertilizers and pesticides in crops, which end up in lake through ground dismantling. The level of Lake Cheimaditida has been dramatically reduced in recent decades, mainly due to irrigation, with adverse effects on the flora and fauna of the area. The Greek Biotope-Wetlands Center investigated the concern of local citizens (farmers, fishermen and local authorities) about the problem. The results declared the willingness of the citizens to pay for the restoration of the lake.

2.2 Lake of Kastoria (Lake Orestiada)

Lake of Kastoria, Orestiada, is located in Western Macedonia in western part of Kastoria Prefecture, northeast, east and southeast of the town of Kastoria and between the aerias of Verno, Aschi, Korissos and Vigla. Orestiada's surface is around 28 squared km and located at an altitude of 630m. Orestiada's average depth is around 3.5 meters and the maximum depth is 9.5 meters. The coast length is about 31km. The water of the lake comes mainly from streams. In the area, there are nine streams leading to the lake. The largest of these is the stream of Xiropotamos. In addition to streams, rain water and snowfall, Lake Orestiada is also fed by many lush springs. Orestiada is an urban lake with intense human activity over the last decades, due to the threat of ecological balance of the area which is polluted by urban waste water, sewage effluents, fertilizers and solid waste. In Orestiada, the eutrophication phenomenon is intense, with all its negative effects on the quality of its water. The water of the lake, as the ultimate recipient of all natural processes, as well as the human activities, is constantly receiving loads of nutrients and other components and, in particular, phosphorus charges. According to results of a study which took place in lake of Kastoria (Mantzafleri et al., 2009), when the lake freezes perhaps every year, there is a decrease in oxygen and in the summer an increase in pollution due to agricultural activities.

2.3 Lake of Ioannina (Lake Pamvotida)

Lake of Ioannina, Lake Pamvotida, is located in the north-western part of Greece at an altitude of 470 meters above the sea level and is perhaps one of the rare cases, where a lake has been connected

so much to the history and like of a city, Ioannina. The lake is 7.5km long, $1{,}5-5$ km wide, has average depth $4-5$meters, maximum depth 11 meters and surface around 22.8 squared km. It is surrounded by the Mitsikeli and Tomaros mountains and it is formed by water of three main springs. The drainage of the water takes place through the Lapista ditch and flows from the river Kalamas. The pollution of the natural environment of Lake Pamvotida and mainly of the lake's waterderives from human activities related to the city of Ioannina, small and large communities and residential areas located around, as well as the industrial output. The main source of pollution of the lake is urban and industrial waste water, as well as the waste of a large number of poultry farms, pig farms and cheese dairies in the area, many of which are illegal. Around 75%of the output of these farms is transferred indirectly to the lake resulting a crucial pollution to the water.

3. DATA AND EMPIRICAL RESULTS

3.1 Data

In order to investigate the willingness to pay (WTP) of the citizens around each lake, we collected three random samples from each town (Ioannina, Florina, Kastoria) and we asked them to complete some questionnaires. We collected 60 questionnaires from citizens of Florina, 90 questionnaires from citizens of Ioannina and 80 questionnaires from citizens of Kastoria. The main question we asked on each interviewee is the amount of money that he/she is willing to pay per month in order to restore the lake of his/her town. We also asked their opinion about the lake and their living distance from the lake. A list of variables which were tested is the following.

Table 1: List of Variables

$\boldsymbol{X_1}$:	Visiting the lake
$\boldsymbol{X_2}$:	Way of information about the lake condition
$\boldsymbol{X_3}$:	Ecological condition of the lake
$\boldsymbol{X_4}$:	Main problem of the lake
$\boldsymbol{X_5}$:	Reason of the ecological problem
$\boldsymbol{X_6}$:	Authorities' concern about the lake
$\boldsymbol{X_7}$:	Membership of an ecological organization
$\boldsymbol{X_8}$:	Local authorities participation every 100 euro
$\boldsymbol{X_9}$:	People participation every 100 euro
$\boldsymbol{X_{10}}$:	What do you wish to be done?
$\boldsymbol{X_{11}}$:	Willingness to pay for the restoration (WTP)
$\boldsymbol{X_{12}}$:	Willingness to pay for the restoration if you were living next to the lake (WTP1)
$\boldsymbol{X_{13}}$:	What do you want to restore first?
$\boldsymbol{X_{14}}$:	Amount of money that you would accept in order not to restore the lake (WTA)
$\boldsymbol{X_{15}}$:	Industries
$\boldsymbol{X_{16}}$:	Gender
$\boldsymbol{X_{17}}$:	Age
$\boldsymbol{X_{18}}$:	Living
$\boldsymbol{X_{19}}$:	Heritage close to the lake
$\boldsymbol{X_{20}}$:	Working around the lake
$\boldsymbol{X_{21}}$:	Distance from the lake
$\boldsymbol{X_{22}}$:	Working condition
$\boldsymbol{X_{23}}$:	Work relative to the lake
$\boldsymbol{X_{24}}$:	Marital status
$\boldsymbol{X_{25}}$:	Members of the family
$\boldsymbol{X_{26}}$:	Education level
$\boldsymbol{X_{27}}$:	Income according to citizen in Northern Greece
$\boldsymbol{X_{28}}$:	Income according to citizen of the town

The above table shows the variables of the model. In this model, the WTA is the dependent variable and the others are independent variables. So, the WTA is estimated as a function of all these variables.

3.2 Empirical Results

In the first part of the analysis we present some descriptive statistics about citizens' willing to pay in each town. In Table1, we present the descriptive statistics for WTP.

Table 2: Descriptive Statistic for WTP of the citizens of each town

	Mean	Standard Deviation	Range	Min	Max
Ioannina	1.99	0.772			
Kastoria	13.16	11.221	50		
Florina	8.22	12.356	50		

On the one hand, descriptive statistics provide evidence that citizens of Kastoria are willing to pay more for the restoration of the lake. On the other hand, citizens of Ioannina are willing to pay far less for the restoration of their lake.

In the next part of the analysis we estimate a linear regression model with dependent variable X_{11} (WTP). One of the main supposes of linear regression is the absence of multi-collinearity between the independent variables. In order to examine the existence or absence of multi-collinearity we estimate a Variance Inflation Factor (VIF) test in SPSS. From this test we observe that X_{17} and X_{22}have VIF-value higher than. In order to solve this problem, we choose to exclude X_{17} from the model. Then we estimate the linear model with remain variables for each lake and the results can be observed in Table 3.

Table 3: Linear Regression Model for each lake

Town	Linear Regression Model
Ioannina	$X_{11} = 0.195 * X_4 + 0.349 * X_6 - 0.174 * X_{10} - 0.595 * X_{12}$
Kastoria	$X_{11} = 1.164 - 0.279 * X_9 + 0.82 * X_{12} - 0.147 * X_{14} - 0.173 * X_{19} + 0.113 * X_{28}$
Florina	$X_{11} = 0.743 + 0.222 * X_7 - 0.322 * X_9 + 0.581 * X_{12} - 0.174 * X_{19}$

Note 1: The coefficients which were not statistically significant are excluded from the models.
Note 2: Coefficients were examined in 5% level of significance.

Table 3 provides evidence that only few variables can affect the WTP of the local citizens. Some variable were found statistical significant in every model and some variables only in one model. This happens because every area in Greece has its own particularities. In the next step of the analysis, we made a Variance analysis (ANOVA) of each model, in order to examine if there is a good adaptation of the theoretical model. The results of each model are presented in Table 4 below.

Table 4: ANOVA for every model of each town

Town	Model	Sum of Squares	Df	Mean Square	F statistic	Sig
Kastoria	Regression	36.408	19	1.916	19.851	0.000*
	Residual	5.792	60	0.097		
	Total	42.200	79			
Ioannina	Regression	39.670	25	1.587	7.625	0.000*
	Residual	13.319	64	0.208		
	Total	52.989	89			
Florina	Regression	39.421	19	2.075	4.762	0.000*
	Residual	17.429	40	0.436		
	Total	56.850	59			

As it is observed in the last column of table 4 the p −value of F −statistic in each model in lower than 0.05, which means that all models have good adaptation to the theoretical model. This is powerful evidence that our research is steady and our results are valid. The R^2 factors for Kastoria, Ioannina and Florina are 0.863, 0.789 and 0.765 respectively.

In the last step of analysis is the estimation of a logit model for every model (one for each lake). First, we estimate the fitting of each model by the logit fitting information test, the results of which are presented in Table.

Table 5: Logit Model Fitting Information

Town	Model	−2Log Likelihood	Chi-square	Df	Sig
Kastoria	Intercept Only	175.04			
	Final	0.000	175.049	19	0.000*
Ioannina	Intercept Only	199.351			
	Final	76.177	123.174	24	0.000*
Florina	Intercept Only	152.153			
	Final	78.925	73.228	19	0.000*

As it is observed in the last column of the table 5 the fit of the models are statistically significant while the p −value of all three tests is lower than 0.05, which means that the results of the logit estimation will be valid. In any case the binary dependent variable is WTA.

In Table 6 below, we can see the results of the logit model (we show only the statistically significant variables). The provided model is a function of nonlinear regression analysis. Especially it is used the Logit model which is located in logistic models of regression analysis. In this model the dependent variable is the WTA and all the others are independent.

Table 6: Logit estimation result

Town	Variable affect WTP (sign)
Kastoria	$X_{12}(+), X_{13}(+), X_{14}(-), X_{19}(+)$
Ioannina	$X_1(-), X_4(+), X_6(+), X_{10}(-), X_{12}(+), X_{15}(+)$
Florina	$X_{10}(-), X_{12}(+), X_{24}(-)$

According to Table 6, we can say for example for Kastoria, that if the citizens live next to the lake(X_{12}), the possibility to pay is higher, while the same possibility is also higher if the citizens have heritage next to the lake (X_{19}). On the other hand, the possibility to pay is lower if a good amount of money is offered to them in order to ignore the degradation of the lake (X_{14}). Similar results are excluded for each town.

4. CONCLUSION

According to the results of the empirical analysis we can separate the conclusion in three different sections, each for every lake. About the lake of Kastoria, Orestiada, we found that the citizens are able to play higher amount of money for the restoration of the lake, while they believe that the protection of the lake is a crucial subject. The same willingness to pay is increased if the citizen lives close to the lake, if the amount of money that would get as compensation is decreased, if he/she has heritage next to the lake and if his/her income is higher than the average of the local community.

About the lake of Ioannina, Pamvotida, we found that a citizen's willingness to pay is increased if he/she visits the lake very often, if he/she believes that the appearance of the lake is awful, if he/she thinks that the local authorities are not able to take care of the problem and if he/she lives close to the lake.

Finally, about the lake of Florina, Cheimaditida, we also found that a citizen's volition to pay for the preservation/restoration of the lake is increased, while the ecological condition of the lake is really bad. The same willingness to pay is also increased if the citizen lives close to the lake and if the citizen is married.

According to the results above, we cannot ignore the fact that those three important wetlands of Greece are degraded. Citizens who live next to those lakes declare to pay higher in order to restore the lake. This is evidence about the condition around these lakes. It is important to mention that there are different parameters that affect the citizens' willingness to pay in every town. This is a normal fact because of the very different situation and living conditions in every town resulting to different requirements of local people. Last but not least, is the social dimension which appears in Florina, because if the citizen declares "married", is willing to pay higher in order to restore the lake. It is probably a future concern because he/she wants his/her children to grow up in more healthy and beautiful environment. This study is about three big wetlands of Greece. It should be a part of a greater project about environmental protection which has to be supported by every single citizen and all authorities because the environmental pollution may lead to the human extinction.

References

1. Barbier, E. B., Acreman, M. C. and Knowler, D. (1997). **'Economic valuation of wetlands'**: A guide for policy makers and planners. *Ramsar Convention Bureau, Gland, Switzerland.*
2. Boyer, T. and Polasky, S. (2004). **'Valuing urban wetlands'**: A review of non-market valuation studies.*Wetlands*, 24(4), pp.744-755.
3. Brander, L., Florax, R. and Vermaat, J. (2006). **'The Empirics of Wetland Valuation'**: A Comprehensive Summary and a Meta-Analysis of the Literature. *Environmental & Resource Economics*, 33(2), pp.223-250.
4. Brouwer, R., Langford, I., Bateman, I. and Turner, R. (1999). **'A meta-analysis of wetland contingent valuation studies'**. *Regional Environmental Change*, 1(1), pp.47-57.
5. Fog, J., Lampio, T., Rooth, J. and Smart, M. (1982). **'Managing Wetlands and Their Birds'**. *International waterfowl Research Bureau, Slimbridge, England.*
6. Kazmierczak, R.F. (2001). **'Economic linkages between coastal wetlands and hunting and fishing'**: a review of value estimates reported in the published literature. *Louisiana State University Agricultural Center*, Baton Rouge, Staff Paper 2001-03.
7. Kontogianni, A., Skourtos, M., Langford, I., Bateman, I. and Georgiou, S. (2001). **'Integrating stakeholder analysis in non-market valuation of environmental assets'**. *Ecological Economics*, 37(1), pp.123-138.
8. Mantzafleri, N., Psilovikos, A. and Blanta, A. (2009). **'Water Quality Monitoring and Modeling in Lake Kastoria, Using GIS'**. Assessment and Management of Pollution Sources.*Water Resources Management*, 23(15), pp.3221-3254.
9. Psychoudakis, A., Ragkos, A. andSeferlis, M. (2005). **'An assessment of wetland management scenarios'**: the case of Zazari–Cheimaditida, Greece. *Water Supply* 5(6), pp.115–123.
10. Ramsar, (1996). **'Wetlands, Biodiversity and the Ramsar Convention'**: IUCN Publications Services Unit, 219c Huntingdon Road Cambridge CB3 0DL UK. 196 pp. 1996.
11. Woodward, R. T., and Wui, Y. S. (2001). **'The economic value of wetland services: A meta-analysis'**. *Ecological Economics*, 37(2), pp.257–270.

EXAMINATION OF THE PROPOSAL FOR THE CONSTRUCTION OF A PIER AT NEW WATERFRONT OF THESSALONIKI

E. I. K. Koutsovili*, A. D. Kosta, Z. Mallios and T. Karambas

Department of Civil Engineering, Aristotle University of Thessaloniki, 54124, Thessaloniki, Greece

*Corresponding authors: e-mail: koutsovil@civil.auth.gr, kostaalexa@civil.auth.gr

Abstract

The waterfront of Thessaloniki in northern Greece is one of the essential features of the city and consists of two parts the old and the new waterfront. It is a reference point for the city and the residents' favorite leisure area, especially during the summer months. In this paper is presented an estimation of the social benefits derived from the potential construction of a pier at the waterfront of Thessaloniki, by the Contingent Valuation Method (CVM). According to the CVM framework, personal interviews were conducted on a representative sample of Thessaloniki residents. The questionnaires included questions about the demographics of the respondents and their opinion about the proposed project, while the citizens' willingness to pay for the maintenance of the project was extracted through a dichotomous choice question. Finally, the statistical analysis of the sample data and the reduction of the results in the overall population lead to an estimate of the total value of the project and its contribution to the welfare of the city residents. Finally, a cost-benefit analysis was carried out to highlight the importance of the project to the welfare of the residents of Thessaloniki.

Keywords: Contingent Valuation method, Cost benefit analysis, Thessaloniki

1. INTRODUCTION

Thessaloniki is a city of around 1,000,000 inhabitants, which is located in northern Greece and is the second largest Greek city. One of the essential features of the city is the waterfront, which consists of two parts the old, and the new waterfront. It is a reference point for the city and its inhabitants, and a place where most of the city residents prefer as a recreational area, especially during the summer months. The waterfront of Thessaloniki is one of the largest urban waterfronts worldwide that can be accessed throughout its length by feet.

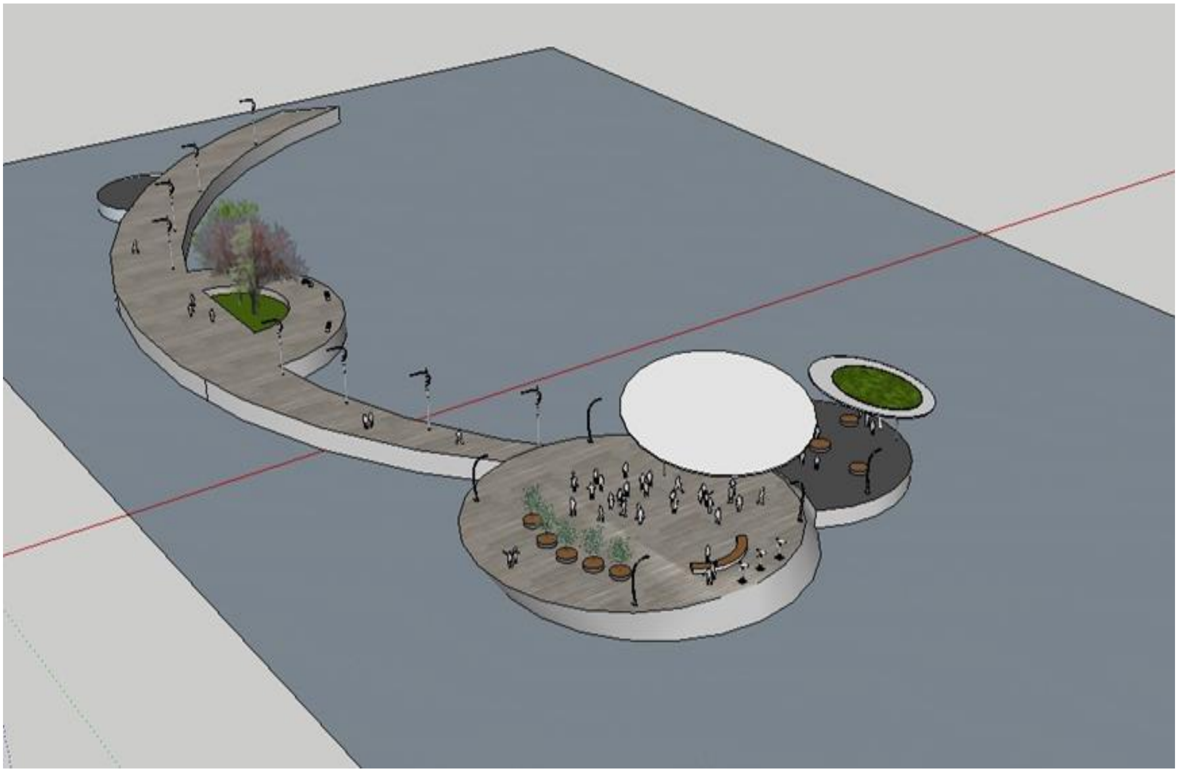
The recent reconstruction projects on Thessaloniki's coastal front have made it even more attractive, offering city residents who visit it many leisure opportunities. Visitors of the waterfront can either enjoy the sun and the sea in one of the thematic parks along the shore or spend time with activities such as walking, running and cycling. However, there are many who claim that the form of the waterfront keeps the man away from the sea. So, additions, which bring the visitors of the waterfront closer to the sea, should be made. With this reasoning, the present study examines whether the citizens of Thessaloniki agree with this idea, and then assesses the social benefit that will derive from the addition of a pier to the coastal front. The purpose of the new pier would be to give visitors of the coastal front the opportunity to walk on it and thus get closer to the sea. The assessment of the social benefit expected from the construction of the pier is achieved by carrying out a contingent valuation survey.

Contingent valuation is a well-known method that is used for the valuation of goods that are not subject to financial transactions (Mitchell and Carson, 1989). Such goods are water, air quality, etc. On the other hand, examples of implementation of the method to projects concerning the quality of the urban environment as the one discussed in this paper can be found in works such as those in Jim and Chen (2011) and Latinopoulos et. al. (2016). To close, the evaluation of the project is accomplished, with a cost - benefit analysis, which compares the social benefit resulting from the contingent valuation method with the indicative construction budget. In particular, cost benefit analysis is carried out in terms of economic analysis. The economic analysis appraises the project contribution to the welfare of the region or the country. It is made on behalf of the whole society (region or country) instead of just the owner of the infrastructure like in the financial analysis.

2. MATERIALS AND METHODS

2.1 General description of the pier

The proposed pier will be extended 80m from the coast and it will reach 5.5m in depth. This will consist of a vertical bent curve front 50m in length and 8m in width, two “fins” left and right of the platform 4m and 7m respectively and two rounded squares at the end of the platform 20m and 30m in diameter. The squares will be constructed at different levels with slope 10% and will have vegetation, benches, metal sunshades and equipment as shown in picture 1.



Picture 1: The proposed Pier - View from above

2.2 The survey questionnaire

The Contingent Valuation Method (CVM) is a well-known and very popular valuation technique. It is used to elicit the value people ascribe to non-marketable environmental goods and services (Mitchell and Carson, 1989). The method is applied by conducting a questionnaire survey. The questionnaire describes a hypothetical market where the environmental goods under consideration are being traded. In the context of the survey, a random sample of people are asked to state their maximum willingness to pay (WTP) (or their maximum willingness to accept compensation - WTA) for a hypothetical change in the level of supply of the environmental goods or services being studied. The analysis of the data obtained from the survey sample leads to the assessment of the value of this change (Carson et al., 2003; Mitchell and Carson, 1989).

Following the CVM framework the questionnaire formed for the survey presented here, consists of twenty questions in total, divided into three sections. The first section, consisting of seven questions related to the respondents demographic characteristics (sex, age, education level, etc.). The second section consists of nine questions and concerns the respondent's attitude about the environment good in question, e.g. the activities the respondents prefer when they visit the waterfront (biking, walking, etc.) and their opinion about the proposed project on the waterfront of Thessaloniki, in general. Following the above two sections, respondents were introduced all information regarding the proposed project about the construction of a pier at the waterfront of Thessaloniki. Then, each respondent had to answer the questions of the third section. At first, the respondents were asked if they find the proposal useful and if they agree with this project. If their answer was negative, they had to explain their refusal, but if their answer was positive, they were explained that to allow the construction and the maintenance of the pier, there should be an increase in municipal taxes they already pay. This kind of question is introduced here in order to identify those who have indifference for the project and therefore a zero WTP. According to the scenario of the hypothetical market, respondents should express agreement or disagreement about the proposed increase in taxes, which will be paid through the electricity bill every two months. This issue was described as payment principle by Kontogianni et al. (2001). Negative respondents to the payment principle question were next asked to explain their attitude. On the other hand, those who agreed with the tax increase were asked a dichotomous choice question (or a close-ended format question). The question was if they were willing to pay or not a certain amount (bid) of increase on the taxes per electricity bill, for the construction and the maintenance of the proposed project. This particular elicitation format (payment vehicle) was chosen because, as it is suggested by the CVM literature (Arrow et al., 1993; Bateman and Turner, 1993), it has to be a realistic way of payment, familiar and acceptable by the respondents. The initial bid values were randomly selected from the following five bid levels, €1, €2, €5, €7 and €10 per bill, and they were almost uniformly distributed across the sample.

This structure of the questionnaire, and especially the precedence given to the question about respondents agreement with the project and, the payment principle question, was chosen to face the frequent problem of biases introduced in the estimation of central tendency measures of WTP (Kontogianni et al., 2001). These biases are mainly related to a large proportion of respondents in the sample who give a negative response when answering dichotomous valuation choice questions. The reasons leading to such answers can be one or more of the following: aversion or indifference to the good, inclination for a free riding access to it, inability to pay the proposed or any amount at all, disagreement with the proposed institutional setting, adverse reaction to the interview in general, or in particular to the payment vehicle adopted etc. (Kontogianni et al., 2001). In our case, we expected that some respondents could express indifference, since it is possible that many people will not find useful and will not agree with the construction of the proposed pier and its maintenance. The question that arises at this point is on how to confront this issue. In the literature, there is a big debate and there have been many different approaches such as those proposed by Haab and McConnell (1997), Kristrom (1997), and Reiser and Shechter (1999). All approaches aim to recognize the two different categories of people who do not accept the payment principle question. In any case, researches try to identify protest respondents and exclude them from the sample; this is why debriefing questions exist in all CVM questionnaires. In this paper, we follow the approach of Reiser and Shechter (1999) because of its simplicity. We examine how the mean and the median WTP are affected by the different treatment of those who gave a negative answer to the payment principle question.

2.3 Logistic Regression

In most CVM surveys, the dichotomous choice format is used for the elicitation of the respondents WTP. The expressed WTP in this case is not a monetary value but a "yes" or "no" to a proposed "bid". Consequently, this type of responses form a binary depended variable and, the WTP value can be obtained by introducing a statistical model that links the dependent variable to the monetary amounts which people are asked to pay in the survey (the "bid" values). Notably the most commonly used distribution function in the analysis of a binary dependent variable is the logistic distribution

(Hosmer and Lemeshow, 2000). Logistic regression is used in this case in order to form a model that describes the relation between the dependent binary variable and all other independent variables. The logistic function that is implemented to perform such an analysis is:

$$\pi(x_i) = \frac{e^{g(x_i)}}{1+e^{g(x_i)}} = \frac{1}{1+e^{g(x_i)}} \tag{1}$$

where $\pi(x_i)$ is the expected value of the outcome variable, given a set of k explanatory variables x_i. The logistic function is useful because it can take an input with any value from negative to positive infinity, whereas the output always takes values between zero and one and hence is interpretable as a probability. As in our case $k > 1$ (i.e. more than one explanatory variables) the above relation describes a multiple logistic function, the inverse of the logistic function or logit transformation is defined as:

$$g(x_i) = \ln\left[\frac{\pi(x_i)}{1-\pi(x_i)}\right] = B_0 + B_1 x_1 + B_2 x_2 + \ldots + B_k x_k \tag{2}$$

The logit, $g(x_i)$, is linear in its parameters and continuous. Fitting the logistic regression model to a set of data - like those obtained from CVM surveys - requires the estimation of the values of the unknown coefficients B_0 which is the constant term, B_1 which is the coefficient of the "bid" variable and the rest of B_i's, which relate to the corresponding specific variables of the model. The application of the maximum likelihood method is the best approach to yield the values of the unknown parameters (Hosmer and Lemeshow, 2000). The corresponding likelihood function of the logit transformation is:

$$\prod_{1}^{n} \pi(x_i)^{y_i} \left[1-\pi(x_i)\right]^{1-y_i} \tag{3}$$

where y_i is the response of the i-th individual to the valuation question. After estimating the unknown coefficients, the logistic regression model can be utilized for the estimation of the central tendency measures of WTP. In the subsequent analysis we have used the following formulas to estimate the mean and the median WTP (Ekstrand and Loomis, 1998; Hanemann, 1984).

$$MeanWTP = \frac{\ln\left[1+e^{(B_0)}\right]}{|B_1|} \tag{4}$$

$$MedianWTP = \frac{B_0}{|B_1|} \tag{5}$$

For the current analysis, B_1 is the estimate of the bid amount coefficient and B_0 is the sum of the estimated constant plus the sum of the products of the mean of each variable in the model times their coefficients.

On the other hand, Reiser and Shechter (1999) assumed that the population of interest could be considered to be composed of two sub-populations. One sub-population is simply not willing to pay at all for the good in question, while the other sub-population is willing to pay and has a continuous WTP distribution. In this case, the corresponding likelihood function for the analysis takes the following form (Reiser and Shechter, 1999):

$$\prod_{1}^{n} p^{(1-S_i)} [1-p]^{S_i} \prod_{1, S_i=1}^{n} \pi(x_i)^{y_i} [1-\pi(x_i)]^{(1-y_i)} \tag{6}$$

where p denotes the probability that an individual chosen at random has zero WTP and S_i is the response of the i-th individual to the payment principle question, $\pi(x_i)$ is the expected value of the outcome variable, given a set of k explanatory variables x_i, and y_i is the response of the i-th individual to the valuation question. The likelihood function of equation 6 breaks up into two separate parts:

$$\prod_{1}^{n} p^{(1-S_i)} [1-p]^{S_i} \tag{7a}$$

$$\prod_{1,S_i=1}^{n} \pi(x_i)^{y_i} \left[1-\pi(x_i)\right]^{(1-y_i)} \tag{7b}$$

Equations 7a and 7b are actually two logistic regression models, so the mean value of eq.7a can be estimated by the following equations:

$$Logit\ \ p_i = a_0 + a_1 x_1 + ... + a_n x_n \tag{8a}$$

$$\hat{p} = \frac{n - \sum_{i=1}^{n} S_i}{n} \tag{8b}$$

Equation 8b is actually the mean value of the payment principle question. In other words, it is the observed percentage of respondents, who refused to pay anything for the construction of the proposed pier. It follows that the mean and median WTP for this setting is the product of (1 – p) times the outcomes of equations 4 and 5 respectively.

2.4 Cost Benefit Analysis

Cost benefit analysis is defined as a systematic process for calculating and comparing benefits and costs of a decision, a policy or a project in general. A cost benefit analysis aims at a conclusion about the liability of a proposed investment, by examining the values of three major indicators, Net Present Value (NPV), Internal Rate of Return (IRR) and the Benefit - Cost Ratio (European Commission, 2014). In this study due to lack of space, the analysis is limited to the assessment of one of these indicators, the net present value.

Net present value is the difference between the present value of the projects' cash inflows and the present value of the projects' cash outflows as they are estimated for the needs of the analysis. NPV is one of the measures used in capital budgeting to analyze the profitability of an investment. NPV compares the values of a monetary unit received or spend today to the value of that same monetary unit received or spend in the future, taking inflation and returns into account. The net present value of an investment is given by the following equation:

$$NPV = -C_0 + \sum_{t=1}^{N} \frac{NB_t}{(1+r)^t} \tag{9}$$

Where, C_0, is the construction cost of the project in question, NB_t, is the net benefits of the year t, r, is the discount rate, and N, is the project's life cycle in years. Positive NPVs indicate feasible investments, while negative ones imply non-acceptable investments. For projects related to the government policy as the one described in the current study, net benefits for year t are given as:

$$NB_t = SB_t + B_t - OM_t \tag{10}$$

where, SB_t, is the estimated social benefit of year t, B_t, is the income of the year t, OM_t, is the operation and maintenance cost of the year t. According to the European Commissions', guide to Cost-Benefit analysis of investment projects the discount rate and the project life cycle of such projects are defined to 6% and 30 years respectively (European Commission, 2014).

3. RESULTS AND DISCUSSION

3.1 Survey design and data

The survey was conducted in the spring of 2017 in the city of Thessaloniki. Using the random sampling method 350 questionnaires were filled in by in-person contingent valuation interviews. Of all the questions that respondents had to answer during the interview, a set of explanatory variables was formed and used for the estimation of the logistic regression models. Table 1 presents the

variables that turned out to be significant in any of the models presented below, plus their descriptive statistics, which were calculated for the whole sample of 350 respondents. Of all the respondents, 336 (96%) agreed with the construction of the pier and only 14 (4%) denied. In addition, 203 respondents (58%) answered "yes" to the payment principle question, meaning that most of the respondents are willing to accept higher taxes for the construction and the maintenance of the project. On the other hand, the remaining 133 (38%) respondents that agreed with the proposal, refused to accept higher taxes for this purpose. They justified their response as follows: a) 45 (33.8%) because they are not able to pay more taxes; b) 66 (49.6%) because they believe that the construction and the maintenance of the pier is a state's obligation; c) 4 (3.0%) because they are not willing to pay if they do not use the pier; d) 18 (13.5%) because they believe that the taxes that they already pay are enough for the construction and the maintenance of the project.

In Table 1, the descriptive statistics of the variables reveal some interesting information about the sample. First, it is impressive that the great majority (96%) of the respondents agree with the proposed project, but those who are willing to pay something for the project are much less. Most of the respondents believe that the proposed project will be a significant aesthetic upgrade for the waterfront of Thessaloniki, and it will offer new recreational activities to its visitors. Most of the respondents were between 21-30 years old while most of them were university graduates. The average value of the "Income" variable is 2.37 meaning that the respondents average monthly income is between 400 and 600 €/month.

Table 1: Variables description and descriptive statistics

Variable name	Variable description	Mean	Std. Dev.
WTP	Willingness to pay a certain amount (0 = no, 1 = yes)	0.41	0.49
Construction	Agreement to the construction of the pier (0=no, 1=yes)	0.96	0.20
Bid	Proposed bid (1€, 2€, 5€, 7€, 10€)	5.00	3.29
P.Princ	Payment principle question (0 = no, 1 = yes)	0.58	0.49
Income	Respondents monthly family income: **1** = <400 €/mon, **2** = 401 - 600 €/mon, **3** = 601 - 800 €/mon, **4** = 801 - 1000 €/mon, **5** = 1001 - 2000 €/mon, **6** = >2001 €/mon	2.37	1.73
Winter	Frequency of respondents visits to the waterfront in winter	4.68	5.01
New activities	Rating of the contribution of the pier in new activities (0-5)	3.69	1.10
Aesthetic upgrade	Rating of the contribution of the pier in aesthetic upgrade of the waterfront (0-5)	3.93	1.12
Age group	Age of respondents in year groups (1 = 16-20, 2 = 21-30, 3 = 31-40, 4 = 41-50, 5 = 51-60, 6= >60)	2.74	1.35
Walk	Frequency of the respondents walking during a week	2.54	2.06
Tourism	Rating of the contribution of the pier in the development of tourism	3.79	1.07
Education	Education Level (1=primary school, 2= secondary school, etc.)	3.77	0.73

It worth to mention that the pretty big percentage of younger ages in combination of the economic crisis that our country is suffering from, is the main reason for the very low average income of the participants. Finally, the high participation rate of younger ages is due to their greater desire to participate in the survey in relation to older ages.

3.2 Models and results

Three separate models were estimated for the analysis of the data collected from the questionnaire survey. The first model examines the relation between the answer that the 350 respondents gave to the payment principle question and their personal characteristics. Table 2 presents the results of the logistic regression for this model. The variables that turned out to be significant and included in the model are presented together with the values of the estimated coefficients, the relevant standard errors, the Wald statistic and the corresponding significance level. Parameters that assess the performance of the models are also included in the table. The performance statistics of this model indicate that the goodness of fit of this model is quite low. The obvious explanation for this result is that the agreement or not of the respondents to the imposition of the proposed tax depends on a parameter that was not detected and was not included in this survey.

Table 2: Estimated parameters of the model for the payment principle question

Variable name	B	S.E.	Wald	Sig.	Exp(B)
Education	0.303	0.157	3.726	0.054	1.353
Income	0.113	0.068	2.793	0.095	1.120
Winter	0.055	0.025	4.801	0.028	1.057
New activities	0.273	0.109	6.262	0.012	1.314
Aesthetic upgrade	0.279	0.107	6.824	0.009	1.322
Constant	-3.418	0.795	18.468	0	0.033
-2 Log Likelihood	445.124				
Nagelkerke R Square	0.114				
Cox and Snell R Square	0.085				
Overall Percentage	61.7				
N	350				

For the estimation of the second model, is assumed that all the respondents expressed their WTP. Meaning that those who did not agree with the tax increase in the first place would be negative to any bid, in case they were offered one, if the payment principle question were not posed to them at all. On the other hand, for the estimation of the third model, the answers of 262 of the respondents are analyzed. This group includes those who agreed with the tax increase and answered the bid question (203), those who answered "no" to the construction of the pier (14) and those who invoke disability to pay (45). It is accepted that those who have a financial burden have stated true zero WTP because they want to contribute but they cannot. In addition, people who did not agreed with the construction of the proposed pier are included to this analysis because they do not find any utility to the project and therefore they state a true zero WTP.

The results from the application of the logistic regression for the two models formed for the estimation of respondents WTP are shown in Tables 3 and 4. In each table, the variables that turned out to be significant and included in each model are presented together with the values of the estimated coefficients, the relevant standard errors, the Wald statistic and the corresponding significance level. Like before, the parameters that assess the performance of the models are also included in each table. Finally, the values of the mean and median WTP for both models are also shown in tables 3 and 4, which were estimated by equations 4 and 5 respectively. All variables used for forming these models and described in detail in Table 1 were more or less expected to be included in the analysis. The coefficients of all models mostly in terms of their signs but also and in terms of their values are reasonable and explain the attitude of the respondents.

Table 3: Estimated parameters for the valuation question and all respondents

Variable name	B	S.E.	Wald	Sig.	Exp(B)
Age group	-0.320	0.120	7.153	0.070	0.726
Income	0.387	0.092	17.679	0.000	1.472
Winter	0.079	0.024	11.019	0.001	1.082
New activities	0.225	0.117	3.691	0.055	1.252
Aesthetic upgrade	0.338	0.119	8.046	0.005	1.402
Amount	-0.140	0.038	13.853	0.000	0.869
Constant	-2.271	0.649	12.245	0.000	0.103
-2 Log Likelihood	419.929				
Nagelkerke R Square	0.196				
Cox and Snell R Square	0.145				
Mean WTP	€6.10				
Median WTP	€2.14				
Overall Percentage	67.7				
N	350				

Table 4: Estimated parameters for the valuation question for 262 respondents

Variable name	B	S.E.	Wald	Sig.	Exp(B)
Education	0.476	0.198	5.578	0.016	1.609
Income	0.315	0.089	12.403	0.000	1.370
Walk	0.135	0.072	3.522	0.061	1.144
Winter	0.090	0.033	7.528	0.006	1.094
Tourism	0.495	0.143	11.978	0.001	1.641
Amount	-0.140	0.044	10.316	0.001	0.869
Constant	-4.218	1.062	15.572	0.000	0.015
-2 Log Likelihood	301.523				
Nagelkerke R Square	0.269				
Cox and Snell R Square	0.201				
Mean WTP	€9.32				
Median WTP	€7.07				
Overall Percentage	70.2				
N	262				

The significantly large difference between the estimated values of mean and median WTP for the model of Table 3 is explained by the fact that the analysis included all responses. Consequently, as shown in Table 1, there was a large negative response rate to the valuation question leading to this outcome. On the other hand comparing the estimated values of WTP shown in Tables 3 and 4, the

estimated values for the mean WTP from the two models are €6.10 and €9.32 respectively, whereas the same values for the median are €2.14 and €7.07. This significantly large difference between the estimated values of the mean and the median WTP derived from the two models, is explained by the fact, that in the model of table 3 were included the data collected from all respondents, while in the model of table 4 most of the negative answers to the valuation question were not taken into account.

Following the approach of Reiser and Shechter (1999) described above, two more values for mean and median WTP are estimated respectively, by multiplying the (1-*p*) value of the first model with the mean and the median WTP of the third model. The estimated mean and the median WTP following this approach are €5.47 and €4.15 respectively. This last estimate of the mean WTP is very close and comparable to the estimate of the mean WTP of the second model. The advantage of this approach is that using the whole sample leads to more symmetric values of mean and median WTP. This result also indicates that we cannot say which one is the true estimate of the WTP, but it is safer to say that WTP ranges between €5.47 and €9.32.

3.3 Cost - Benefit analysis

The cost-benefit analysis presented here is carried out in terms of economic analysis and not in terms of financial analysis, as there is no direct income for the city from the pier itself. Therefore, to carry out the cost-benefit analysis for the construction project of the pier, it is claimed that the project will be completed in two years and the time horizon of the analysis will be thirty years. Specifically, the costs to be considered are the construction cost of the project for the first two years, which was estimated at €1,211,490.55, and the annual operating cost, which was estimated at €35,920. As for the construction cost, it is the sum of costs in the first and the second year. In particular, the first year is assumed that will be completed the 60% of the construction, meaning the cost will be €726,872.49 and the second year, the cost will be €484,618.06 as it will be completed the remaining 40%. The next years, there are no more construction costs as the construction of the project will have been completed. Regarding the annual operating costs, they start from the third year and consist of maintenance and electricity costs and clean-up cost and they were estimated at €34.000 and €1.920 respectively. In particular, an indicative amount of maintenance cost per year is estimated to be around €4000. The electricity cost is estimated about €30000 per year, as it is considered that, the pier will have 20 luminaires operating for 12 hours per day. Operating costs are increased by 12% to take account of unforeseen costs. Finally, the clean-up cost is estimated to be €1920, based on the assumption that 480 work hours are required per year, with remuneration 4€ per hour.

On the other hand, the benefit in the analysis is the estimated social benefit, which according to welfare theory equates to the willingness of citizens to pay, which was estimated in the previous section. In particular, the annual value of the project for the citizens of Thessaloniki is estimated by the reduction of the samples' mean willingness to pay, which was estimated by the logistic regression models, in the total population of the city. So, by accepting the most conservative estimate of the willingness to pay which is €5,47 according to the approach of Reiser and Shechter (1999), the annual value of the project for the residents of Thessaloniki equals to the product of the mean WTP (€5.47) times the number of households that exist in the city (332848 households) and times the number of bills paid by every household in a year (6 bills). The amount resulting from this reduction is €10,924,071.36. So, the net benefit required for the cost benefit analysis is:

$$NB_t = SB_t - OM_t = €10{,}924{,}071.36 - €31{,}920 = €10{,}892{,}151.36 \qquad (10)$$

The NPV for the project under study is estimated for thirty years, as follows:

$$NPV = -C_0 + \sum_{t=1}^{N} \frac{NB_t}{(1+r)^t} = -€1{,}211{,}454.16 + \sum_{t=1}^{30} \frac{€10{,}892{,}151.36}{(1+0.05)^t} = €153{,}356{,}974.17 \qquad (11)$$

The NPV value estimated by equation 11 is particularly high, even by the most conservative estimates. This value is significantly higher from corresponding NPV value of about €95,000,000 estimated by Kaitsis and Mallios (2015) in a similar analysis for the reformation project of the new

waterfront of Thessaloniki. The conclusion drawn from the comparison of these two estimates is we can assume that when the respondents stated their WTP for the construction of the pier, they subconsciously stated their WTP for the entire waterfront of Thessaloniki. Therefore, we can assume that the actual social benefit that will derive from the upgrade of the coastal front of the city due to the addition of the proposed pier is the value resulting from the difference between these two estimates. In any case, the estimates highlight the importance of the waterfront for the city of Thessaloniki; indicate that the construction of a pier at the Waterfront of Thessaloniki is a project with a positive influence for the welfare of the local society.

4. CONCLUSIONS

The application of the contingent valuation method for the estimation of the social benefits that will derive from the construction of pier at the waterfront of Thessaloniki and the cost-benefit analysis that followed highlight the following useful conclusions concerning the city of Thessaloniki but also some technical issues of the method. As for the city of Thessaloniki, it is proved that the residents of the city recognize the need for more amenities in the city, give high priority and bring into this need a significantly high value. On the other hand, the conclusions of the different values of the WTP estimated above are summarized as follows: a) the payment principle question is useful but not able to identify free riders or protest responses even with the combination of the debriefing questions; b) questions like the one about the agreement of the respondents for the proposed project, which was introduced in this study for the first time, are proved useful for the identification of true zero bids and similar questions should be incorporated in all CVM studies; c) it is safer to report a range for the WTP instead of a single value. Finally, the application of the cost-benefit analysis leads on the conclusion that a project can be considered unprofitable in financial terms, but it can become necessary because of its social and environmental scope. After all, when the state chooses to build a project, its primary objective is to use and meet various needs and, secondarily, to profit from it.

References

1. Arrow, K., Solow, R., Portney, P. R., Leamer, E. E., Radner, R., and Schuman, H. (1993). Report of the NOAA Panel on Contingent Valuation. **Federal Register**, 58(10), pp. 4601–4614.
2. Bateman, I. J., and Turner, R. K. (1993). Valuation of the environment, methods and techniques: the contingent valuation method. **Sustainable Environmental Economics and Management: Principles and Practice, Belhaven Press, London**, pp. 120–191.
3. Carson, R. T., Mitchell, R. C., Hanemann, M., Kopp, R. J., Presser, S., and Ruud, P. A. (2003). Contingent valuation and lost passive use: Damages from the Exxon Valdez oil spill. **Environmental and Resource Economics**, 25(3), pp. 257–286.
4. Chen, W. Y., and Jim, C. Y. (2011). Resident valuation and expectation of the urban greening project in Zhuhai, China. **Journal of Environmental Planning and Management**, 54(7), pp. 851–869.
5. Ekstrand, E. R., and Loomis, J. (1998). Incorporating respondent uncertainty when estimating willingness to pay for protecting critical habitat for threatened and endangered fish. **Water Resources Research**, 34(11), pp. 3149.
6. European Commission. (2014). **Guide to Cost-Benefit analysis of investment projects**. Brussels.
7. Haab, T. C., and McConnell, K. E. (1997). Referendum Models and Negative Willingness to Pay: Alternative Solutions. **Journal of Environmental Economics and Management**, 32(2), pp. 251–270.
8. Hanemann, M. W. (1984). Welfare Evaluations in Contingent Valuation Experiments with Discrete Responses. **American Journal of Agricultural Economics**, 66(3), pp. 332.
9. Hosmer, D. W., and Lemeshow, S. (2000). **Applied logistic regression**. N. York: J Wiley & Sons.
10. Kaitsis, A., and Mallios, Z. (2015). Valuation of the "New Waterfront" of the city Thessaloniki in Greece with the Contingent Valuation Method. In **Fifth International Conference on**

Environmental Management, Engineering, Planning & Economics pp. 525–532. Mykonos Greece.

11. Kontogianni, A., Skourtos, M. S., Langford, I. H., Bateman, I. J., and Georgiou, S. (2001). Integrating stakeholder analysis in non-market valuation of environmental assets. **Ecological Economics**, 37(1), pp. 123–138.
12. Kristrom, B. (1997). Spike Models in Contingent Valuation. **American Journal of Agricultural Economics**, 79(3), pp. 1013–1023.
13. Latinopoulos, D., Mallios, Z., and Latinopoulos, P. (2016). Valuing the benefits of an urban park project: A contingent valuation study in Thessaloniki, Greece. **Land Use Policy**, 55, pp. 130–141.
14. Mitchell, R. C., and Carson, R. T. (1989). **Using Surveys to Value Public Goods: The Contingent Valuation Method**. Washington DC: Resources for the Future.
15. Reiser, B., and Shechter, M. (1999). Incorporating zero values in the economic valuation of environmental program benefits. **Environmetrics**, 10(1), pp. 87–101.

DRONES AND ENVIRONMENTAL PROTECTION LAW IN GERMANY AND GREECE

A.K. Douka

Lawyer, PhD Candidate, Aristotle University of Thessaloniki,
GR - 55131 Thessaloniki, Macedonia, Greece

*Corresponding authors: e-mail: anastdouka@law.auth.gr

Abstract
Unmanned aircrafts, subsumed under the term "drones", have become in recent years due to their number and wide application a mass phenomenon. Despite the overall contribution of drones to the environmental protection, they may also have negative effects on the environment. There are fears that birds, seals or other animals are disturbed, that the drone controllers enter protected areas or that the landscape is affected. At EU level, the development of special drone rules is at a draft stage. The aviation Regulation (EC) No 216/2008 provides technical safety requirements, the airfields and controllers of unmanned aircrafts, but for a drone weight above 150 kg. Those below that weight are to be regulated by each Member State as they see appropriate. In Germany, the new Drone Regulation entered into force on 7 April 2017. It integrated nature conservation aspects of drone operations into the existing aviation legislation. However, the German nature conservation legislation lacks explicit provisions regulating drone flights as a permissive intervention to protected areas. In Greece, the Regulation of Flights of Unmanned Aircraft Systems (drones) entered into force on 1 January 2017 (Off. Gaz. B 3152/30-9-2016). This Regulation specifies the terms, conditions and the way for obtaining the license of a drone operator, instructor and examiner, but does not contain any specific nature conservation standards regarding the use of drones. The aim of the present paper is to examine: a) the new general legislative framework for drones and b) the legal conflicts arising out of the use of drones in protected areas in Germany and Greece.

Keywords: drones, environmental protection, legal conflicts, protected areas

1. INTRODUCTION

1.1 Current state of the drone use

Drones, known in the colloquial speech as aircrafts, which are operated with no pilot on board (Juul, 2015), can be generally used for scientific, commercial, military, police and private purposes (Brahms and Maslaton, 2016). The field of application for military purposes ranges from simple reconnaissance tasks to complex surveillance scenarios using armed systems (Müllenstedt, 2015). Although drones were initially developed for military and defense purposes, they are increasingly used for various civil purposes, including photography, rescue operations, infrastructure monitoring, forest fire monitoring, farming and aerial mapping (House of Lords and European Union Committee, 2015). The provision of Internet access and the transport of goods by drones are in test operation (Brahms and Maslaton, 2016). Nevertheless, there is criticism about the use of drones over demonstrations, major events or in general over densely populated areas due to the danger of falling (Sattler and Regh, 2011).

Remarkable is that the progressive integration of drones into airspace poses various risks. In some cases drones have narrowly missed commercial manned aircrafts, flown over or landed on the residences of public figures, nuclear power stations, embassies and tourist attractions, obstructed

firefighting and injured people (Juul, 2015). Because of the fact that drones usually carry video cameras to allow the remote pilot to fly them, they may record images and include technologies such as high-power zoom, microphones and a multitude of sensors as well as GPS systems recording the location of persons filmed (Juul, 2015). As a result, concerns are expressed about the increasing use of drones in respect of data protection and privacy (House of Lords and European Union Committee, 2015).

The use of drones can also have negative effects on the natural environment. Irresponsible drone use could cause harm to birds including disrupting nests by reducing the breeding success of sensitive bird populations, provoking attacks, scattering leks, interrupting feeding and midair collisions (Mayntz, 2017).

1.2 The European regulatory framework

Under the EU Aviation Law, drones are referred to as unmanned aircrafts (Annex II (i) of the Aviation Regulation 206/2008). Both the German and the Greek Aviation Law draw a distinction between model aircrafts and unmanned aerial systems according to the purpose of the use of drone. Drones used for the purpose of sport or for recreational activities are classified as model aircrafts (§ 1 para. 2 no. 9 of the German Air Traffic Act (Luftverkehrsgesetz, hereinafter: LuftVG) and art. 3 of the Greek Regulation of Flights of Unmanned Aircraft Systems), whereas drones operated for any other purpose, such as for commercial visual recordings for commercial purposes, are called unmanned aerial systems (§ 1 para. 2 of the German LuftVG and art. 3 of the Greek Regulation of Flights of Unmanned Aircraft Systems).

At EU level, the Aviation Regulation (EC) No 216/2008 provides technical safety requirements, the airfields and controllers of unmanned aircrafts, but for a drone weight above 150 kg (art. 4 § 4 in conjunction with Annex II (i) of the Aviation Regulation (EC) No 216/2008). Those below that weight are to be regulated by each Member State as they see appropriate.

The EU proposed a change to the Aviation Regulation (EC) No 216/2008 (European Commission, 2015). Following the so - called Riga Declaration (Riga Declaration on remotely piloted aircrafts (drones), 2015), the European Aviation Safety Agency (EASA), on behalf of the European Commission, made initial proposals for the establishment of a single legislative framework for the use of drones of all weight classes. Based on the risk the operation is posing to third parties (persons and property), drones are divided into three categories: ‘Open category’ (low-risk), ‘Specific category’ (medium-risk) and ‘Certified category’ (high-risk). The safety should be provided, among other things, by operational limitations, especially by "geo-fencing". Geo-fencing is the concept of restricting drone access by designating specific areas where the drone’s software and/or hardware is designed not to enter, even if the pilot, without intent, instructs the drone to go (European Aviation Safety Agency (EASA), 2015). The proposed changes are based on the regulatory approach, to develop the potentials of drone technology and thereby to ensure the security of their operation (Schrader, 2017). The Riga Declaration introduced the cause of noise by the use of drones as an environmental issue, which needs to be addressed at the local level (Riga Declaration on remotely piloted aircrafts (drones), 2015). However, it is noted that the proposed European framework about drones lacks in nature conservation issues, as geo-fencing does not contain nature conservation areas (Schrader, 2017).

2. GERMAN LAW

2.1 The new Drone Regulation

The former German Aviation Law contained different levels of regulation for model aircrafts and for unmanned aerial systems. The rise of aircraft models below 5 kg was possible for people of all ages without prior knowledge and without any air traffic permission (§ 20 para. 1 no. 1 a) of the Regulation relating to air events, Luftverkehrsverordnung, hereinafter: LuftVO). The rise of unmanned aerial systems was subject to authorization (§ 20 para. 1 no. 7 LuftVO). An authorization was issued if their

use did not pose a risk to the aviation safety or public safety or order and there was no violation of data protection rules (§ 20 para. 4 LuftVO).

The Federal Ministry of Transport adopted the new Drone Regulation, which introduced amendments to Air Traffic Licensing Order (Luftverkehrs-Zulassungs-Ordnung, hereinafter: LuftVZO) and to LuftVO and which entered into force, with minor exceptions, on 7.4.2017. According to the new legislative framework, drones up to 250g are not subject to any specific restrictions. Drones weighing over 250g must have the name and address of the controller attached (§ 19 para. 3 LuftVZO). For unmanned aerial systems and model aircrafts with a take-off mass above 5 kg there is an authorization requirement (§ 21a para. 1 no. 1 LuftVO). The authorization is granted when the intended operation does not pose a danger to the aviation safety or public safety or order and there is no violation of data protection and nature conservation rules (§ 21a para. 3 no. 1 LuftVO). However, there is an exception from the authorization requirement, if the drone operation is necessary for the fulfillment of official tasks (§ 21a para. 2 no. 1 LuftVO).

2.2 Nature conservation aspects

Nature conservation aspects, which are not limited to the protection of certain areas, but, for example, may include species protection aspects, are expressly mentioned in the terms of the new authorization procedure (Schrader, 2017). According to § 21a para. 6 LuftVO, protection regulations, such the Federal Nature Conservation Act (Bundesnaturschutzgesetz, hereinafter: BNatSchG), which have been issued under this Act or continued to apply, as well as the nature conservation laws of the countries, remain unaffected. Moreover, in accordance with § 21b para.1 no. 6 LuftVO, general operating bans exist in environmentally sensitive areas, such as nature reserves, national parks and Natura 2000 sites, as far as the operation of unmanned aircrafts in these areas are not otherwise regulated by the national provisions. In this regard, the new German Aviation Law recognizes further protective provisions of the nature conservation law, whereas it does not contain any regulations on geo-fencing (Schrader, 2017).

Legal conflicts can most likely arise in nature reserves (Schrader, 2017). Drones can be beneficial for nature conservation law. They can be used for nature photography or for the rescue of wild animals from an agricultural mowing (Thaysen, 2016). Furthermore, drones can be used as monitoring aids for the observation of nature and landscape (§ 6 BNatSchG). In the field of landscape planning, drones can be used to determine the existing state of nature and landscape. At local level, they can collect information for landscape and green order plans (§ 11 BNatSchG) and determine soil and water parameters in addition to vegetation, landscape features, larger animals and impairments (Schrader, 2017).

Moreover, drones can be used for carrying out and securing the compensation measures. The competent authority has to carry out appropriately compensation and replacement measures, including any necessary maintenance measures (§ 17 para. 7 BNatSchG). For this purpose, it may require the polluter to submit a report. Drones can contribute to these controls (Schrader, 2017).

In addition, drones can play an important role in the protection of nature, landscape and species. Drones in a monitoring program could contribute to the examination of the achievement of the protective purpose in many protected areas, especially outside the Natura 2000 network. As far as the observation of invasive species is concerned (§ 40 para. 2 BNatSchG), recorders on drones, programmed for the giant hogweed or the Himalayan balsam, can more effectively identify the spread than inspections (Schrader, 2017).

On the other hand, it is noted that the German Air Traffic Act (LuftVO), applying to a federal level, lacks in explicit provisions with regard to the protection of the nature reserves. All acts, leading to destruction, damage or change of territories or its constituents or to lasting disruption, are prohibited (§ 23 para. 2 BNatSchG). This absolute prohibition on change also applies to the national parks (§ 24 para. 3 BNatSchG). However, § 21 b para.1 no. 6 LuftVO on general operating bans for unmanned aircrafts in environmentally sensitive areas does not refer to national parks, national natural

monuments and natural monuments mentioned in §§ 24 para.4, 28 para. 2 BNatSchG, which are also like nature reserves protected, so that there is no air traffic operating ban over them (Schrader, 2017).

At the legislation level of the individual German states, drones had for the first time in 2016 an effect on a state nature conservation law.§ 13 para. 3 no. 3 of the National Nature Conservation Act of Schleswig-Holstein prohibits in nature reserves the rise and landing of model aircrafts and unmanned aerial systems. Forbidden is, however, the rise and landing in only one nature reserve, but not close to it. This prohibition is narrower than the prohibition on change of § 23 para 2 BNatSchG (Schrader, 2017), which also includes activities outside of one nature reserve (Landmann, Rohmer and Gellermann,2017).

Moreover, National Nature Conservation Act of Schleswig-Holstein does not regulate the overflight and does not make clear, whether the prohibition 'in nature reserves' applies also to types of areas equal to nature reserves. The remaining legislative gaps regarding overflight, rise and landing in areas close to nature reserves or in areas equal to nature reserves may be filled by the individual protection statement of the respective area (Schrader, 2017).

As mentioned above, drones can disturb birds. Drones could violate the general prohibition of deliberate disturbance of wildlife (§ 39 para. 1 no. 1 BNatSchG) as well as the special prohibition of disturbance of wildlife of protected species and European species of birds during certain time - periods (§ 44 para. 1 no. 2 BNatSchG). A disturbance, according to § 44 para. 1 no. 2 BNatSchG, presupposes the detrimental effects of actions on the psychological well-being of a protected animal and its externally recognizable fear, escape or startle reactions (Landmann, Rohmer and Gellermann, 2017). Externally recognizable reactions have to be considerable for the conservation status of the local population. A deliberate disturbance presupposes positively the intent of the disturbance and negatively the absence of any justifying, apologizing or otherwise objectively comprehensible reason (Giesberts L., Reinhardt M. and Gläß, 2017). In this context, the disturbance for a simple private photography or without any justification would be deliberate, whereas a scientific animal photography not. An expertise is required in order to be able to fulfill the requirements of a prohibited state in individual cases prove by drones. A professional expertise is needed in order to prove in individual cases the fulfillment of the requirements of the above mentioned prohibitions (Schrader, 2017).

3. GREEK LAW

3.1 The Drone Regulation

In Greece, the first Drone Regulation, issued by the Civil Aviation Authority (hereinafter: CAA), entered into force on 01.01.2017 (Off. Gaz. B 3152/30-9-2016). The Regulation applies only to Unmanned Aerial Systems (Art. 2§1 of the Regulation). Aeromodels, unmanned aircrafts used for military or other state purposes by the respective state bodies (armed forces, security forces, etc.) as well as tethered or free balloons are excluded from the scope of the Regulation (Art. 2§2 of the Regulation).

The Regulation defines the whole procedure regarding Unmanned Aerial Systems, including safety, privacy, data protection, civil liability and environmental protection issues. The structure of the Regulation is formulated within the framework of the principles of the European Aviation Safety Agency (EASA) in such a way as to enable the full integration of the relevant European regulations in the future.

According to the Regulation, drones are classified into three categories: open, specialized and certified. All drones flying more than 50 meters away from their operator, regardless of the reasons for their use, should be recorded in a register of the Civil Aviation Authority (Art. 10§1 of the Regulation). Upon request by the interested parties, drones are categorized in the open or special category and are included in the special register of unmanned aircrafts of the CAA. Drones,

categorized by the CAA in the certified category, are entered in the register of Greek civil aircrafts and they receive nationality and registration marks (Art. 10§1 of the Regulation).

Drones of the open category have a take-off mass below 25 kg, fly in less than 500 meters away from the operator and the maximum allowable flight height is 400 feet. The operator has direct view of the drone. Flights of drones of this category are forbidden above concentrations of persons, unless they have a commercial license and meet specific safety requirements (Art. 6§1 of the Regulation).

For drones belonging to the special category, an operating permission is required. This is granted under the condition that the person concerned provides a security risk assessment plan, a flight operation's manual and an insurance contract (Art. 8§1 of the Regulation). In case of commercial use of the drones belonging to this category, a registration of the drones in a special register and the obtaining of a special license through a fee payment are also required (Art. 8§2 of the Regulation).

For drones of the certified category, a registration of the aircraft in a special register and the issue of a special certificate of airworthiness are required (Art. 9 of the Regulation).Furthermore, the operator of this category is obliged to have a special training, the content of which and the exams required will be determined by a decision of the CAA operation commander (Art. 9§3 of the Regulation).

For the commercial exploitation of unmanned aircraft of any category, a special license provided by the CAA is required (Art. 13§1 of the Regulation), which has a twelve-month validity and is renewed after re-control and a new fee payment (Art. 13§4 of the Regulation). A prerequisite for the granting of the license is, among others, a certification that the operator of drones has obtained basic knowledge of air traffic rules after the attendance of certain relevant courses (Art. 13§2 of the Regulation).

The Regulation contains specific rules for air traffic and the conduct of unmanned aircraft flights. Among others, it provides that drone flights are generally allowed in airspace segregated from the airspace used by manned aircraft. In particular, Unmanned Aerial Systems are allowed to fly: a) below the permitted limits for the operation of manned aircrafts in accordance with Instrument Flight Rules (IFR) and/or Visual Flight Rules (VFR) or at a maximum altitude of 400 feet above ground or sea surface; b) above the upper limits of the controlled airspace for the operation of manned aircraft (flight level: 460-46.000 feet); c) within temporary segregated areas for drone flights, which are determined by the air traffic services of CAA and d) at defined traces and heights specified by special authorizations of the air traffic services of CAA (Art. 5§1 of the Regulation).

On the contrary, drone flights are generally prohibited in airspace: a) in which flights of manned aircrafts take place in accordance with Instrument Flight Rules (IFR) and/or Visual Flight Rules (VFR); b) within the airport operations zones and, in any event, in a distance less than 8 km from the aerodrome perimeter and from landing/ take-off paths from/to the airport; c) in prohibited areas for unmanned aircraft systems as defined by the competent bodies and published by a decision of CAA and d) in areas, defined by air traffic services as prohibited and restricted, in which the flights of manned aircrafts are not allowed (Art. 5§2 of the Regulation). However, in special cases and upon request to the CAA, it is possible to allow the flight in airspace concerned (Art. 5§3 of the Regulation).

Finally, the Regulation provides that unmanned aircrafts belonging to special, certified category or to the open category with a take-off mass between 4 kg - 25 kg as well as unmanned aircrafts for professional use of any category/subcategory require an insurance coverage for damage to third parties (up to 150.000 € for third party material damages and up to 1,000,000 € for personal injuries, Art. 14 of the Regulation). The Regulation also refers to privacy issues. In particular, it provides that any possible processing of personal data during air transport operations of drones has to comply with the relevant legislation in force (Art. 15 of the Regulation).

3.2 Nature conservation aspects

Similar problems with those arising under German law are also found here. The only nature conservation aspect of the Greek Drone Regulation is the general ban on the operation of drones over

environmental protection areas. According to Art.19§3 of the Regulation, the operation of drones over these areas is subject to special authorization by the Ministry of Environment, Energy and Climate Change.

Pursuant to Art. 19 of Law 1650/1986, as amended by Art. 5 of Law 3937/2011, environmental protection areas are strict nature reserves (areas with extremely sensitive ecosystems), nature reserves (areas of high ecological or biological value, in which any activity or operation changing or altering the physical condition, composition or development of the natural environment is prohibited), natural parks (terrestrial, maritime areas or areas of a mixed character of particular value and interest because of the quality and variety of their natural and cultural features), and Natura 2000 sites.

This general ban does not contain any specific nature conservation standards for the use of drones. It does not specifically define to which of the above-mentioned environmental protection areas the general ban on drone flights applies, if there are any exceptions from this general ban and, if so, on the basis of which criteria and at which height are drone flights allowed over an environmental protection area. On the other hand, a basic lack of this general provision is that it does not prohibit drone flights close to environmental protection areas, and in particular close to Natura 2000 sites.

This provision seems at first sight to protect the environment against the operation of drones. However, this general prohibition of drone flights over environmental protection areas may also run counter to the environmental protection. The general requirement for a special authorization for the operation of unmanned aircrafts over all the above-mentioned environmental protection areas, even if it works for the benefit of the environment (e.g. forest fire monitoring etc.), may eventually become fatal.

Furthermore, a special provision for the protection of birds against the noise caused by the drones is not detected in the Regulation. According to the general provision of Art.11 of the Common Ministerial Decision No 33318/3028/11.12.1998 (Off. Gaz. B 1289/28-12-1998) implementing Directive 92/43/EC, only the deliberate disturbance of wildlife during their reproduction season, during the period in which the pups are dependent on the mother, during hibernation and migration is prohibited. It is therefore necessary to prove the drone operator's intention to disturb the bird. This is extremely difficult to prove in case of the use of drone for both recreational and professional purposes given their general contribution to the environmental protection.

4. CONCLUSIONS

It follows from the above that there is a paradox with the use of drones. While they generally contribute to the protection of the environment, they run the risk of disturbing birds. The environmental factors that should be taken into account by the legislator for the operation of drones over environmental protection areas are abstract and general in both German and Greek law. There is therefore a need for a common European Regulation that will introduce clear restrictions on the drone flights over sensitive ecosystems such as nature reserves and the Natura sites. The restrictions in order to be clear and efficient, should provide for the permissible distance between the operator and the drone and prohibit on the basis or numerical criteria low flights of drones over the above-mentioned areas. Geo-fencing technology (software program incorporated in the drone to define geographical boundaries) could be especially helpful for the achievement of this goal.

References

1. Brahms F. and Maslaton M. (2016) ‘Die gewerbliche Nutzung von Drohnen im Lichte der geplanten Novelle der LuftVO’, **Neue Zeitschrift für Verwaltungsrecht**, Vol. 16, pp. 1125 – 1130.
2. Juul M. (2015) ‘Briefing of the European Parliamentary Research Service, Civil drones in the European

Union'http://www.europarl.europa.eu/RegData/etudes/BRIE/2015/571305/EPRS_BRI%282015%29571305_EN.pdf (accessed February 28th, 2018).

3. Müllenstedt D. (2015) ***'Technische Grundlagen des Einsatzes von unbemannten Flugsystemen***,http://docplayer.org/19747107-Technische-grundlagen-des-einsatzes-von-unbemannten-flugsystemen.html (accessed February 28th, 2018).

4. House of Lords *and European Union* Committee (2015) '7th Report of Session 2014-15. *Civilian Use of Drones in the EU'*, https://publications.parliament.uk/pa/ld201415/ldselect-/ldeucom/122/122.pdf (accessed February 28th, 2018).

5. *Sattler Y. and Regh T. (2011)* 'Unbemannte Flugsysteme im zivilen Krisenmanagement. Echte Perspektive oder technische Spielerei? 'https://www.bbk.bund.de/SharedDocs/Downloads/-BBK/DE/Publikationen/Publ_magazin/bsmag_1_11.pdf?__blob=publicationFile (accessed February 28th, 2018).

6. Mayntz M. (2017) 'Birds and Drones. Drones - Helpful or Harmful to Birds?' https://www.thespruce.com/birds-and-drones-3571688 (accessed February 28th, 2018).

7. European Commission (2015) 'Proposal for a Regulation on the European Parliament and of the Council on common rules in the field of civil aviation and establishing a European Union Aviation Safety Agency, and repealing Regulation (EC) No 216/2008 of the European Parliament and of the Council', http://eur-lex.europa.eu/resource.html?uri=cellar:da8dfec1-9ce9-11e5-8781-01aa75ed71a1.0001.02/DOC_1&format=PDF (accessed February 28th, 2018).

8. Riga Declaration on remotely piloted aircraft (drones) (2015) 'Framing the future of aviation', https://ec.europa.eu/transport/sites/transport/files/modes/air/news/doc/2015-03-06-drones/2015-03-06-riga-declaration-drones.pdf (accessed February 28th, 2018).

9. European Aviation Safety Agency (EASA) (2015) 'Proposal to create common rules for operating drones in Europe', https://www.easa.europa.eu/system/files/dfu/205933-01-EASA_Summary-%20of%20the%20ANPA.pdf (accessed February 28th, 2018).

10. Schrader C. (2017) 'Drohnen und Naturschutzrecht', **Natur und Recht**, Vol. 39, pp. 378 – 385.

11. Thaysen J. (2016) 'Mehr Wildrettung bei der Mahd', https://www.lksh.de/fileadmin/-dokumente/Bauernblatt/PDF_Toepper_2016/BB_16_23.04/44-45_Thaysen.pdf (accessed February 28th, 2018).

12. Landmann R., Rohmer G. and *Gellermann M.* (2017) **'Umweltrecht, Kommentar'**, § 23 BNatSchG, recital 19, C.H. Beck, Munich.

13. Landmann R., Rohmer G. and *Gellermann* M. (2017) **'Umweltrecht, Kommentar'**, § 44 BNatSchG, recital 10, C.H. Beck, Munich.

14. Giesberts L., Reinhardt M., *Gläß A. – C.* (2017) '**BeckOK Umweltrecht**', § 39 BNatSchG, recital 3, C.H. Beck, Munich.

Protection and Restoration of the Environment XIV

Water and wastewater treatment and management

FROM WASTE TO ENERGY: OPTIMIZING GROWTH OF MICROALGAE *SCENEDESMUS OBLIQUUS* IN UNTREATED ENERGETIC-LADEN WASTEWATER STREAMS FROM AN AMMUNITION FACILITY FOR BIOENERGY PRODUCTION

A. RoyChowdhury[1], J. Abraham[1], T. Abimbola[1], Y. Lin[1], C. Christodoulatos[1], A. Lawal[1], P. Arienti[2], B. Smolinski[2], and W. Braida[1]*

[1]Stevens Institute of Technology [2]RDECOM-ARDEC, Picatinny Arsenal

*Corresponding Author: email: wbraida@stevens.edu, Tel: +1 516 567 4835

Abstract

Wastewaters from industrial ammunition facilities often contain enough nutrients to support microalgae growth. Initial studies showed promising results on sustaining growth of a freshwater microalgae *Scenedesmus obliquus* under a blend of untreated energetic-laden wastewater from an industrial ammunition facility. Initial laboratory studies were scaled up to 100L open raceway reactors for growing *S. obliquus* in the same untreated wastewater mixture. The raceway reactors were set-up up as follows: 50 rpm paddle-mixer speed, 14:10 hours light:dark photoperiod, and 68-95 μmol/m^2/s of light intensity. Continuous monitoring of pH and temperature of the growth medium, periodic analysis of cell density and dry weight of microalgae, and analysis of the media's nutrient contents were performed. Biomass harvesting from the raceway reactors was conducted on a weekly basis and the harvested algal biomass was tested for its oil content. Different conditions such as light penetration, nutrient availability, and retention times were evaluated in order to optimize the biomass growth as well as the oil content of *S. obliquus* in a semi-continuous setting. The results showed that only nitrogen starvation increased the lipid production from 13% to 29% of oil based on the dry weight of biomass, whereas no increment in oil or biomass production was noticed with the increase of light penetration in the two different retention times tested. This study provided significant information towards microalgae growth in energetic-laden wastewater streams. This study also showed that wastewaters from industrial ammunition facilities can be reused for culturing microalgae, which can be utilized for renewable energy production.

Keywords: microalgae, energetic-laden wastewater, renewable energy

1. INTRODUCTION

The manufacturing of energetic compounds at industrial ammunitions facilities generates large variety of wastewater streams containing organic pollutants (e.g., solvents, energetic materials residues, reagents) which are also rich in nutrients, mainly nitrogen. These streams are subject to regulatory discharge permits and require different levels of treatment (e.g., physical-chemical, biological) prior to disposal into adjacent water bodies. Previous studies have shown (Abraham et al., 2016, 2018; RoyChowdhury et al., 2017) that many of these streams can support algae growth without or with minimal treatment. For this study, 10 different untreated wastewater samples were obtained from an industrial ammunition plant. Laboratory based toxicity studies showed that several of these untreated wastewater samples could be used to grow microalgae *Scenedesmus obliquus* at appropriate dilution levels. Thus, 100L open raceway reactors were set-up for culturing *Scenedesmus obliquus* in ammunition-laden untreated wastewater streams with the objective of assess biomass and

oil productivity depending upon reactor operation conditions (nutrient level, hydraulic retention time, and light penetration).

2. MATERIALS AND METHODS

Based on the results of our previous laboratory studies a mixture of wastewaters was prepared by mixing 55% of wastewater#2, 40% of wastewater# 4, and 5 % of wastewater#1 diluted 1000 times in wastewater#3 to use it as culture media of *Scenedesmus obliquus*. The characteristic of the individual wastewater samples along with the mixture are presented in Table 1.

Table 1. Characterization of selected untreated waste streams and their mixture.

Waste Streams	pH	TN (ppm)	N-NH_3 (ppm)	N-NO_3^- (ppm)	N-NO_2^- (ppm)	TP (ppm)	TOC (ppm)	Energetic Compound Identified
1	5.12	287,000	82,400	124,645	B.D.L.	B.D.L.	192	-
2	6.75	33.70	0.53	1.21	1.41	0.04	57.1	RDX
3	4.61	16.30	28.30	B.D.L.	B.D.L.	0.04	175	-
4	6.59	221	12.70	2.84	70.86	0.12	2132	RDX, NTO, NQ
Mixture	7.06	87	4.45	19.8	B.D.L.	77.5	1042	RDX

TN: total nitrogen, TP: total phosphorus, TOC: total organic carbon, B.D.L. = below method detection limit.

2.1 Setting-up 100L Raceway Reactor for Algal Culture Using Untreated Wastewater

Initially, one 100L raceway reactor (R1) was filled up with 90L mixed wastewater, then the chemicals present in commercial BG-11 media were added to it with exception of all nitrogen sources as it is presented in Table 2. Then reactor was inoculated with 10L of *Scenedesmus obliquus* inoculum. The reactor was operated under a 14:10 hour light:dark period, 68-95 μmol photons/m^2/s light intensity (using a HydroFarm FLP46, fluorescent grow light fixture), and 50 rpm speed of the rotating wheel. Every week a 10L volume was removed (harvested) from the reactor and was processed for oil extraction as described below. DI water was added in the raceway reactor (~1-1.5L/day) every day to make-up the natural evaporation of water from the raceway reactor and to maintain the 100L working volume. The raceway reactor was equipped with a continuous monitoring systems of pH and temperature and these data was logged in and saved for recording purposes. Samples were periodically collected and analyzed for cell density (by measuring fluorescence at 685 nm using a Synergy mx Biotek microplate reader), dry weight (following standard USEPA protocol), change in nutrient concentrations (using a Dionex IC with IonPac 4 mm×250 mm AS16 column equipped with a IonPac 4 mm×50 mm AG16 guard column), and RDX concentration change over time (using Agilent HPLC). The 100L raceway reactor, R1 was operated for a period of 37 days.

2.2 Culture of *Scenedesmus obliquus* in Raceway Reactors using untreated wastewater and 50L working volume

It has been shown that light penetration plays an important role in algae growth. Over time, it was observed that the liquor in R1 was getting darker as a result of algae growth which was potentially inhibiting light penetration and uniform light distribution throughout the reactor. In order to assess light penetration, the entire 100L content of the R1 reactor was divided into two aliquots and two new raceway reactors with a working volume of 50L each were set-up and were labelled as R2 and R3. It was hypothesized that by lowering the total volume inside the reactor from 100L to 50L the light penetration pathway will be reduced allowing a better light distribution throughout the whole reactor

volume. Both raceway reactors were kept under the same operating condition as of raceway reactor R1. This study was also designed to analyze the impact of different retention time on algae growth. In order to assess this, 10L working volume was harvested from R2 and 4L working volume was harvested from R3 on a weekly basis. The harvested liquor was processed for oil extraction and the equivalent amount of wastewater mix was added to each of the reactors after harvesting. Natural evaporation from the reactors was compensated as described in section 2.1. As before, continuous monitoring of pH and temperature of the culture media was performed for both reactors. Periodically, samples were collected from both reactors and were analyzed for cell density, dry weight, change in nutrient concentrations, and RDX concentration over time following the previously mentioned analytical procedures. Both reactors were operated for 77 days.

Table 2. Composition of media used for *Scenedesmus obliquus* culture in 100L raceway reactor. This media was prepared by modifying Sigma Aldrich's C3061- BG-11 medium.

	Composition	mg/L
1	Magnesium sulfate. $7H_2O$	75
2	Potassium phosphate dibasic	40
3	Calcium Chloride dihydrate	36
4	Sodium carbonate	20
5	Citric acid	6
6	Ferric ammonium citrate	6
7	Boric acid	2.86
8	Manganese chloride. $4H_2O$	1.81
9	EDTA disodium magnesium	1
10	Sodium molybdate. $2H_2O$	0.39
11	Zinc sulfate. 7 H_2O	0.222
12	Cupric sulfate. $5H_2O$	0.079
13	Colbat nitrate. $6H_2O$	0.0494

2.3 Harvesting of Algae

Algae slurry/liquor removed from the raceway reactors was first subjected to gravity settling for 24h after which the supernatant was decanted. The biomass rich slurry after gravity settling was further dewatered using an EXD explosion-proof centrifuge purchased from Thermo-Electron Corporation. The centrifuge has a maximum capacity of 6L (1L in each of the 6 centrifuge cups) with a working volume of 4.8L (800mL in each of the 6 centrifuge cups). The slurry samples to be centrifuged were collected in 1000mL Nalgene™ PPCO centrifuge bottles. The centrifuge was run at 2900rpm for 15 minutes. After the removal of water, the final concentrated slurry from each of the bottles were added together to make one sample slurry. The final slurry was further homogenously mixed on the shaker before the dry weight was determined.

2.4 Dry Weight Determination of Algae Slurry and Paste

A CO_2 Resistant Shaker operating at 120rpm was used to mix the slurry for 10 minutes before dry weight determinations. Then, 2mL of the sample slurry was collected in each of 3 tared sample tubes. Whatman glass microfiber filter purchased from Fisher Scientific with a pore size of 0.7micron were first rinsed with de-ionized water by placing a stack (minimum of 2) on a filter funnel and then deionized water was made to flow through with the aid of a vacuum pump. The filter were ashed in

a furnace at 550°C for 20 minutes. The 2mL samples collected were then vacuum filtered and all solids in the sample were retained on the glass microfiber filter. The three sample residues obtained from the filtration step were collected in an aluminum pan and placed in an oven at 105°C for 16 hours to completely dry the sample. The dry weight percent was calculated as shown below:

$$\text{Dry weight (\%)} = \frac{\text{mass of (dry biomass + filter paper) (g)-mass of ashed filter paper (g)}}{\text{mass of the 2mL sample (g)}} \times 100 \qquad (1)$$

2.5 Extraction of Oil from Algae and Quantification of Extractables

A Soxhlet extractor equipped with Whatman cellulose thimbles of pore size 10µm and dimensions 27mm X 80mm (external diameter x external length) (Fisher Scientific) was used for oil extraction using ethanol (Reagent Grade) as solvent. The biomass to solvent ratio used was 1:25 and the heating mantle was set to 150°C. The time taken for complete extraction varies between 6 and 10 hours. The boiling flask with the wet extracted lipids was placed in an oven at 105°C for 16 hours for complete dryness. After drying, the dried lipid was weighed relative to the tared boiling flask and recorded. The weight percent of the lipid extract was calculated as shown below:

$$\text{\% wt of extractables (lipids) in dry biomass} = \frac{\text{dry mass of lipids (g)}}{\text{dry mass of biomass, m (g)}} \times 100 \qquad (2)$$

3. RESULTS AND DISCUSSION

3.1 Culture of Scenedesmus obliquus in 100L Raceway Reactor (R1)

Over the 37 days of the experiment, the average pH of the media in R1 was 8.6 ± 0.16, and the average temperature was 19.9°C ± 0.6. pH values were within the optimum algae growth range (pH 7-9) throughout the study. Although the raceway reactor was open and maintained under laboratory condition, the temperature was always within optimum algae growth range, 18-25°C.

Figure 1 represents the changes in cell density and dry weight for the algal culture over time. At the end of the study (day 37), cell density in the reactor was 2.49×10^7 cells/mL. The fluctuation in the cell density observed in Figure 1 was due to the harvesting process. The gradual increase in the dry weight in R1 can also be seen in Figure 1. The highest dry weight was obtained in the raceway reactor at day 35 and was 0.4± 0.1 g/L. Both, cell density and dry weight increases, were indicative of algal growth in R1 and showed that *Scenedesmus obliquus* can grow in untreated ammunition-laden wastewater without showing any toxic impact. No external nitrogen source (in form of nitrogen containing salts) was added into the system during this study assuming that all necessary nitrogen sources would be provided by the wastewater streams. After each week's harvesting and addition of 10L of wastewater mixture to compensate for the volume harvested, total nitrogen concentration of the system always increased (data not shown). Concentrations of nitrate and sulfate (data not shown) indicates that suitable nutrient sources were present in the media for sustaining algae growth throughout the experiment. Figure 2 shows the change in color in R1 as result of algae growth.

3.2 Culture of *Scenedesmus obliquus* in 50L Raceway Reactors R2 and R3

The daily change in pH and temperature in reactors R2 and R3 were logged in through their respective probes and data acquisition system. The average pH of R2 and R3 were 8.45± 0.33 and 8.58± 0.31,respectively, both values within the 7-9 optimum pH range. The average temperature of R2 and R3 were 17.36°C ± 1.19 and 17.03°C ± 1.08, respectively.

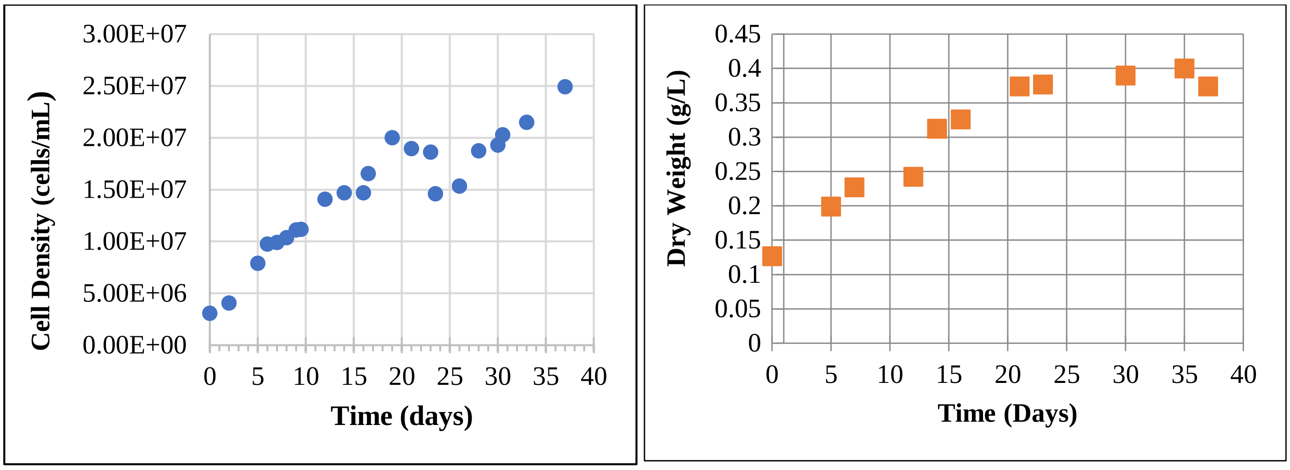


Figure 1. Change in *S. obliquus* cell density (left) and dry weight (right) in the 100L raceway reactor, R1 over time.

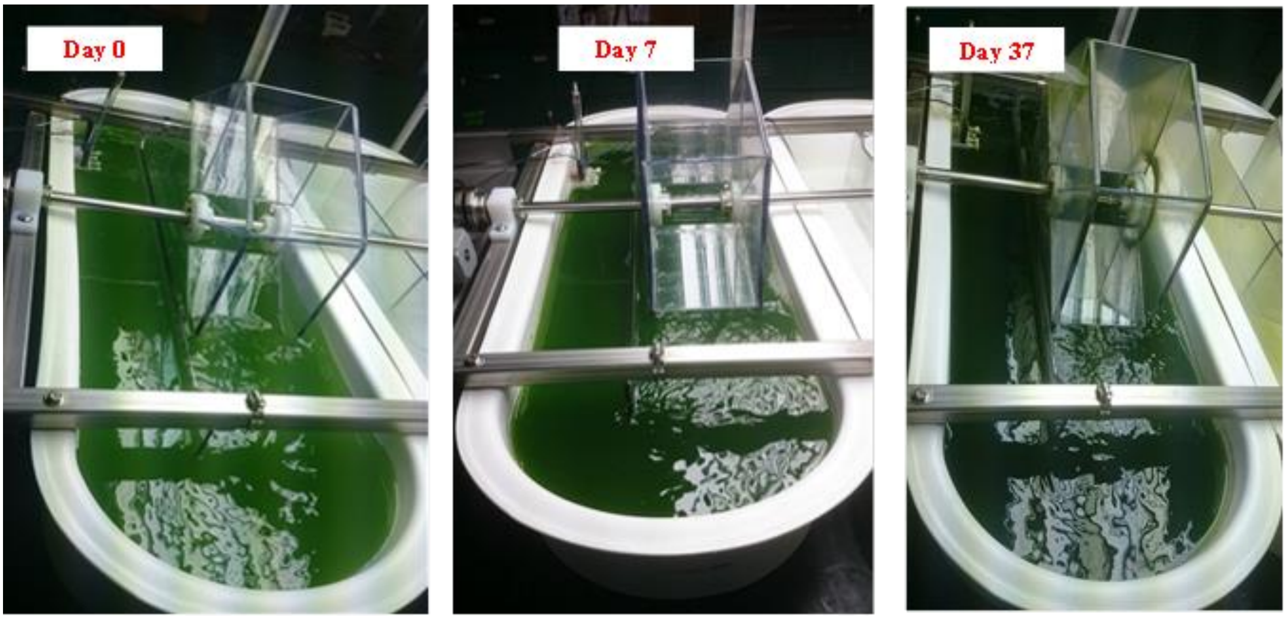
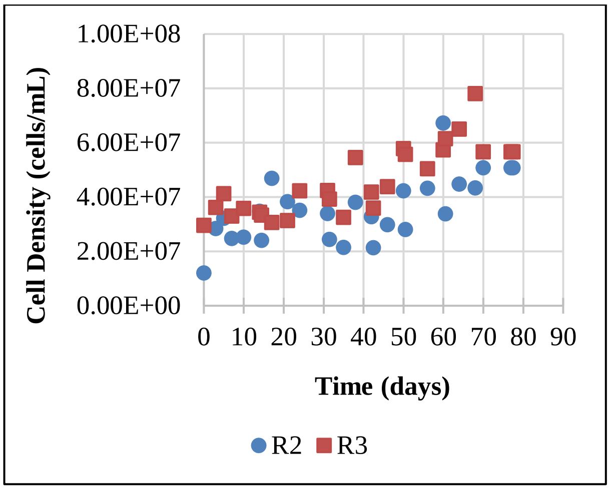


Figure 2. R1 color evolution as a result of algae growth.

Figure 3 presents the changes in cell density of the algae culture for R2 and R3 over time. In both reactors cell density gradually increased over time. No significant difference in cell density was found between R2 and R3 throughout the study. Also, no major difference in cell density was observed between R1, R2 and R3 on equivalent time point throughout the study. For example on day 37 of study the measured cell density of R1, R2 and R3 were 2.49×10^7, 2.15×10^7, and 3.26×10^7 cells/mL, respectively. This result showed that different light penetration paths (changing depths) did not made any significant change in algal growth for the system tested. It was found that at day 77, cell density in R2 and R3 were 5.08×10^7 and 5.67×10^7 cells/mL, respectively. Figure 3 also presents the change of dry weight in algal culture in R2 and R3 over time. A steady increase in dry weight was noticed in both reactors during the study. A dry weight of 0.88± 0.15 and 1.31± 0.23 g/L was found in R2 and R3 respectively on day 77. At the beginning of this study, nitrate and phosphate salts (sodium nitrate and sodium phosphate monobasic) were added to both reactors at a N:P ratio of 15:1 (150 mg/L of nitrate and 10 mg/L of phosphate) to ensure that the media in both reactors contained enough nutrient to support algae growth. Due to the depletion of nutrient levels inside the reactors, a second addition of nitrogen and phosphate salts at the 15:1 ratio was made to both reactors on day 31. All throughout the study a steady decrease in nitrate concentration was observed in both reactors which correlates with the steady increase of algae biomass (data not shown).



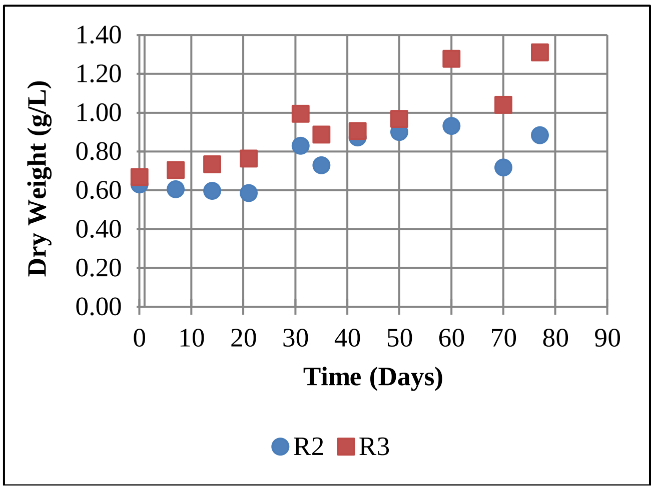


Figure 3. Change in *S. obliquus* cell density (left) and dry weight (right) in the 50L raceway reactor, R2 and R3, over time.

3.3 Effect of Phosphorus and Nitrogen Concentration on the Amount of Algae Oil Recovered

Oil extraction was carried out on a weekly basis (7 days interval) by implementing the protocols presented in sections 2.3, 2.4 and 2.5. Table 3 shows the amount of oil extracted along with the concentrations of nutrients in the reactor at the time of harvesting *S. obliquus* (R1). Prior to the weekly oil extraction, triplicate concentrated algae slurry samples were prepared from the 10L of liquor harvested from the raceways by dewatering the sample to about 5wt% total solid, following the procedure presented in section 2.3. At the end of the experiment, the oil content of *S. obliquus* was recorded as a percentage of the dry weight of the algae slurry sample extracted. The maximum deviation of oil content from average oil content recorded was 0.5%. The trends in the variation of algae oil content with nutrient are shown in Figures 4(a.) and 4(c.) while oil productivity changes with nutrient are shown in Figures 4(b.) and 4(d.). Oil productivity is presented in (gal/acre year) to compare with baseline values used to measure the performance of algae cultivation on large scale.

Table 3. Biomass productivity, oil content and oil Productivity of *S. obliquus* grown in the munitions-laden wastewater.

Day	Dry weight (g/L)	Biomass Productivity (g/m^2d)[1]	Nitrates (mg/L)	Phosphorous (mg/L)	Oil content %	g oil/m^2 d	Oil productivity (gallons/acre year)[2]
7	0.227	2.903	31.75	10.9	13.0	0.3774	170.44
16	0.326	2.507	29.11	5.8	17.1	0.4321	195.16
23	0.377	2.206	22.1	6.05	14.9	0.3287	148.45
30	0.390	1.781	16.27	2.8	25.6	0.4559	205.91
37	0.374	1.356	14.26	4.7	26.5	0.3593	162.29

1. Biomass productivity calculated by converting the dry weight (g/L) to (g/m^3), dividing by the time interval (days) and then multiplying by the pond depth (8inches = 0.2032m).
2. Oil productivity was calculated by multiplying the oil content with the biomass productivity and an appropriate conversion factor (451.63) to convert from g/m^2/day to gallons/acre/year.

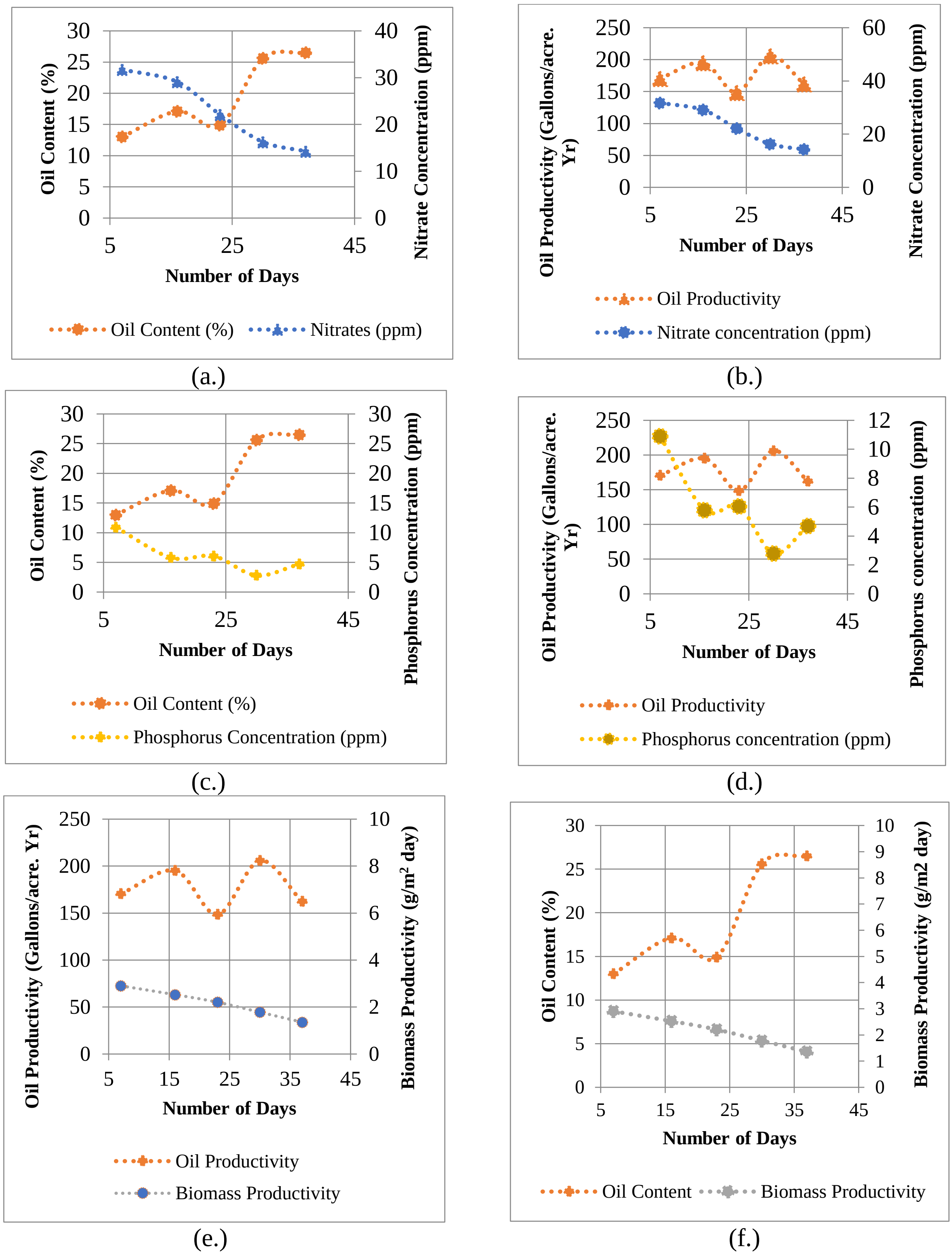


Figure 4. Variation of oil content and oil productivity of *S. obliquus* with nutrient concentration over the period of algae cultivation: (a.) Plot of oil content and nitrate concentration versus time of cultivation; (b.) Plot of oil productivity and nitrate concentration versus time of cultivation; (c.) Plot of oil content and phosphorus concentration versus time of cultivation; (d) Plot of oil productivity and phosphorus concentration versus time of cultivation; (e.) Plot of oil productivity and biomass productivity versus time of cultivation; (f.) Plot of oil content and biomass productivity versus time of cultivation.

These baseline values are set at 13g/m^2 of biomass a day at 25 wt% oil content which is equivalent to an oil productivity of 1300 gal/acre year. (Davis et al, 2012). As it was pointed out, the sole source

of nitrate used in algae cultivation in the R1 experiment was the wastewater. After every weekly harvest, 10L of fresh wastewater were used to make up the reactor volume and replenish the consumed nitrates, nevertheless nitrates and phosphorus might have been the limiting substrate for algae growth during the first experiment.

The oil content of *S. obliquus* increased as the concentration of nitrate decreased. According to previous research on the effect of nutrients availability on the accumulation of lipid in algae, nitrogen starvation is one most critical processes enhancing lipid metabolism in algae (Darzins et al, 2008). The observed increase in the oil content of algae was a confirmation of this established mechanism for improving oil content. However, in the third week of the experiment, the oil content dropped and this was suggested to be the result of the increase in the concentration of phosphorus in the third week. Figure 4(f.) shows the variation in the oil content and biomass productivity at a given time points over the growth period while Figure 4(e.) presents the variation of oil productivity and biomass productivity at given time points during the period of growth. Biomass productivity decreased as a result of depriving algae of nutrient while the oil content increased (from 13% to 26.5%). On the other hand, the trend in oil productivity only showed that an optimum exist while the increase in the concentration of phosphorus in the third week explains the drop in oil productivity during that week. The variation in the concentrations of nutrients was observed to affect the oil productivity indirectly through changes in the oil content of algae. Oil productivity can improve if one of the two parameters (biomass productivity and oil content) is kept fairly constant and the other is increased by using any of the available mechanisms to achieve this purpose. For example nutrient starvation mechanism can be implemented to improve the rate of lipid synthesis in algae while other growth parameters such as light intensity and rate of mixing can be enhanced to keep high biomass productivity. Batch operations using high nutrient concentration during the exponential growth phase and nutrient starvation before harvesting could be an alternative approach to maximize oil productivity.

3.4 Effect of Retention Time and Light Penetration on the Amount of Algae Oil Recovered

In this study, *S. obliquus* liquor cultivated in R1 was divided into two reactors (R2 and R3) to reduce the depth of algae in the raceways thereby reducing light intensity attenuation. Similarly, weekly harvest was carried out by removing 10L of algae slurry from R2 while 4L slurry was harvested from R3. Thus, R2 has shorter retention time compared to R3. These two factors were investigated over a growth period of 77 days. In the first two weeks, a mix of slurry from the two reactors was dewatered and used for extraction due to the limited amount of biomass produced. The oil content of algae in the first and second week of the experiment does not change significantly from the last oil content obtained in the previous experiment, (26.5±0.2)%. Table 4 shows the oil content of *S. obliquus* recovered over the growth period while Figure 5 provides a graphical representation of the oil recovery trends.

Based on the oil content data obtained for R3 and R2, it was observed that the recovered oil content from algae in R3 was higher than those in R2 (see Figures 5 and 6). Apart from nutrient-depleted and harsh environmental conditions to which algae respond by biosynthesizing lipids to store carbon and energy as an adaptive feature, aging of algal culture can also affect triacylglycerol and fatty acid composition of algae (Darzins et al, 2008). This explains why the values of oil content of algal slurry samples from R3 are higher than those from R2. Thus the age of the algae culture (based on the hydraulic retention time) adds to the effect of nutrient concentrations (nitrogen and phosphorus) on algae's oil content. In agreement with the outcome of the previous experiment, oil content of algae increased with decrease in the concentration of nitrate in both R3 and R2. The effect of nutrient was evident especially on the 36th day of the experiment (see Figure 5). The maximum deviation from the average oil content recorded was ±1.65%. In the 5th week, maximum oil content was achieved in R3 (29.5±0.34) % while the maximum oil content obtained in R2 was (27.93±0.15) % in the 10th week.

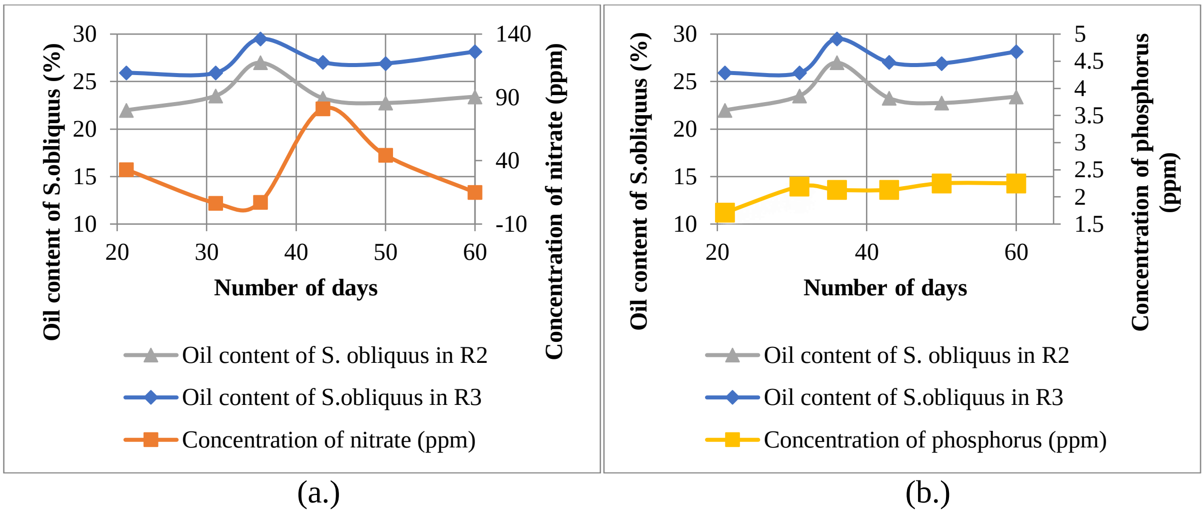


Figure 5. Variation of oil content of *S. obliquus* with nutrient concentration in R2 and R3 for the first 60 days: (a.) Variation with nitrate concentration (b.) Variation with phosphorus concentration.

Table 4. *S. obliquus* oil content as a function of retention time.

Day	Oil Content R3 (4 L sample) %	Oil Content R2 (10L sample) %	Oil Content R2/R3 mixture
7	-	-	26.73
14	-	-	26.97
21	25.92	21.97	-
31	25.92	23.50	-
36	29.50	26.99	-
43	27.03	23.25	-
50	26.91	22.75	-
60	28.16	23.41	-
70	26.53	24.83	-
77	28.15	27.93	-

4. CONCLUSIONS

The current research assessed the feasibility of growing microalgae, specifically *S. obliquus*, using untreated or minimally treated (e.g. dilution) munitions-laden industrial wastewater with minimum addition of external sources of nutrients. Nevertheless, extensive optimization work is necessary in order to bring up biomass yields to accepted industry standards. The influence of light penetration, hydraulic retention time, and nutrient content was also preliminarily assessed. Light penetration did not have a major role on algae biomass yield and oil content in the raceway setup using in this study perhaps due the particular high mixing rate that can be achieved allowing all biomass to be exposed to light in a fairly constant fashion. Older biomass (higher retention time) appears to favor higher oil content, although clear trends could not be developed. Nutrient starvation shows the stronger correlation with algae oil content underlying the need of perform an optimization process using the engineering variables at hand (nutrient profile, retention time, mixing rate, CO_2 uptake, etc.) in order

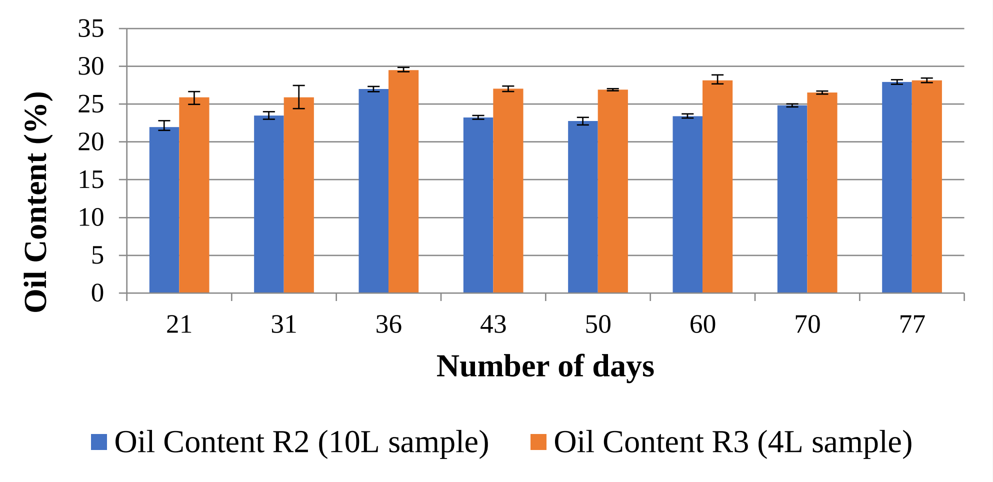


Figure 6. Changes on oil content of *S. obliquus* in R2 and R3 over the entire growth period.

to maximize the algae oil yield which is the product of the algae biomass yield times the algae's oil content. Lastly, the fate of the energetic materials during algae growth is not discussed as it was outside the scope of the current study.

Acknowledgment
This work was supported by the Consortium for Energy, Environment and Demilitarization (CEED) contract number SINIT-15-0013.

References

1. Abraham J., A. RoyChowdhury, C. Christodoulatos, Y. Lin P. Arienti, B. Smolinski, and W. Braida (2016) 'The cycle of nutrients at industrial plants: valorization of energetic-laden wastewater streams using microalgae *Scenedesmus obliquus* to produce bioenergy', 2nd RCN Conference on Pan American Biofuels & Bioenergy Sustainability, Buenos Aires, Argentina, September 13-16, 2016.
2. Abraham J., Y. Lin, A. RoyChowdhury, C. Christodoulatos, P. Arienti, B. Smolinski, and W. Braida (2018) 'From Waste to Energy: Algae Toxicological Assessment and Valorization of Energetic-laden Wastewater Streams Using *Scenedesmus obliquus*', **Journal of Cleaner Production** (submitted, under review).
3. Davis R., D. Fishman, E.D. Frank, M.S. Wigmosta, A. Aden, A.A. Coleman, P.T. Pienkos, R.J. Skaggs, E.R. Venteris, and M.Q. Wang, M.Q. (2012). Renewable Diesel from Algal Lipids: An Integrated Baseline for Cost, Emissions, and Resource Potential from a Harmonized Model. http://www.nrel.gov/docs/fy12osti/55431.pdf.
4. Darzins A., Q. Hu, M. Sommerfeld, E. Jarvis, M. Ghirardi, M. Posewitz, and M. Seibert, (2008). Microalgal triacylglycerols as feedstocks for biofuel production: perspectives and advances, **The Plant Journal**. 54, 621-639.
5. RoyChowdhury, A., J. Abraham, C. Christodoulatos, Y. Lin, P. Arienti, B. Smolinski, and W. Braida (2017) Generation of bioenergy from energetic-compounds-contaminated wastewater streams using microalgae *Scenedesmus obliquus*. 33rd Annual International Conference on Soils, Sediments, Water, and Energy. Amherst, Massachusetts October 16-19, 2017.

ELUTION HISTORY OF BASIC OXYGEN FURNACE SLAG TO PRODUCE AKLALINE WATER FOR REAGENT PURPOSES

A. Caicedo-Ramirez[1], M.T. Hernandez[1], D.G. Grubb[2],*

[1]Department of Civil, Environmental, and Architectural Engineering, University of Colorado Boulder, ECOT 441 UCB 428, Boulder, CO 80309-0428, USA
[2]Phoenix Services LLC, 148 W. State Street, Suite 301, Kennett Square, PA 19348 USA

*Corresponding Author: email: dennis.grubb@phxslag.com, tel: +12155272786

Abstract
This paper summarizes the elution history of packed BOF slag fines (< 10 mm diameter) after a running liquid:solid (L/S) ratio of 1573 L/kg (13111 pore volumes or PV) with an empty bed contact time (EBCT) of 15 min. High alkalinity (>1000 mg $CaCO_3$/L) was obtained up to a L/S 63 L/Kg (526 PV). pH >12 persisted to about L/S <77 L/Kg (580 PV), then monotonically decreased to approximately 11 at 150 L/Kg (1245 PV) when it appears the residual lime/portlandite content was exhausted, which triggered the dissolution of calcium silicates, most prominently, larnite. The pH plateaued thereafter, likely due to buffering effect of silicic acid ($pKa_{1(H4SiO4)} \approx 9.8$) from the larnite. Thereafter, calcium concentration approached background levels of the influent tap water (~12.10 mg/L) whereas the dissolved silicon increased and remained steady between 1 and 10 mg/L. The mass loss of BOF slag fines measured at the end of the experiment was 19.4 wt%. Based on the QXRD data, the sequential dissolution of lime/portlandite and larnite appear to be the dominant processes driving changes in alkalinity, pH, and aqueous elemental composition. Aluminum hydroxide [$Al(OH)_3$] also dissolved, further adding to the amorphous content. The Toxicity Characteristic Leaching Procedure (TCLP) and de-ionized water leaching data suggest that the BOF slag fines are non-hazardous, and exceptionally clean from an environmental perspective and compare very well with the TCLP data of other US BOF slags [Proctor et al 2000], in either the virgin or exhausted form.

Keywords: BOF slag, leaching, XRD, calcium, silicon, pH buffering,

1. INTRODUCTION

Prior research conducted at the Stevens Institute of Technology [Jagupilla et al 2012a,b; Grubb et al 2016a,b] revealed that the leaching of a ~0.3 m long, 10.2 cm diameter packed column of <10 mm basic oxygen furnace (BOF) steel slag aggregate particles by tap water and acidic metals-laden solutions at typical groundwater velocities (~1 m/day) did not reduce the effluent pH of the BOF slag packed column below its natural pH of approximately 12.5 for over a 100 pore volumes (PV). This was due, in part, to the very strong alkaline buffering capacity of the BOF slag. Grubb et al [Grubb et al 2011] showed that the 10 mm minus fraction (BOF slag fines) took 7.5 equivalents of HNO_3 to achieve a neutral pH at a liquid:solid (L/S) ratio of 20:1. The BOF slag was found to contain approximately 10-15 wt% lime/portlandite as well as several other Ca, Fe and Mg silicates and oxides that produced alkalinity. Since there is anecdotal evidence BOF slag excavated from the internal cores of historical dumps and stockpiles dating back to the 1800s and impacted ground water have pH values close to its natural pH of 12.0 to 12.5 [e.g. Roadcap et al 2005], this naturally lead to the question as to when the pH would significantly drop by water leaching. Accordingly, a study was undertaken to intentionally leach a BOF slag sample in attempt to lower its pH near neutrality. This

is the first step in an assessment of the potential value of using BOF slag eluate as a possible reagent substitute for conventional lime-water or for irrigation purposes, as silicic acid (H_4SiO_4) is an essential source of silica for plant growth and health to improve the blight, pest and drought resistance of plants [Datnoff et al 2011].

2. MATERIALS & METHODS

2.1 BOF Slag media

Freshly crushed, screened, and de-metallized BOF slag fines (< 10 mm diameter) produced at the Indiana Harbor East (IHE) Steel Mill in East Chicago, IN, were randomly collected and stored in a sealable clean plastic bucket at their natural moisture content. These materials were used as-is for column testing. The total and leaching behavior of the BOF slag media is described elsewhere [Grubb et al submitted].

2.2 Column Experiment

Two clear PVC columns, end caps and all tubing were fabricated to study the elution history of the BOF slag fines in parallel. The column diameter and length were set at 8.5 cm (3.35 in) and 10.4 cm (4.09 in), respectively. A schematic and photo of the packed column is shown in Figure 1. Preliminary determination of the pore volume (PV) of the packed column was as follows: 500 g of BOF slag fines was added to the elution column in a vertical orientation. Next, tap water was slowly added and the water-slag slurry was mixed until saturation. The column was then gently tamped until all visibly entrapped air bubbles were removed. The volume of water added to reach saturation was defined as the PV (60 mL).

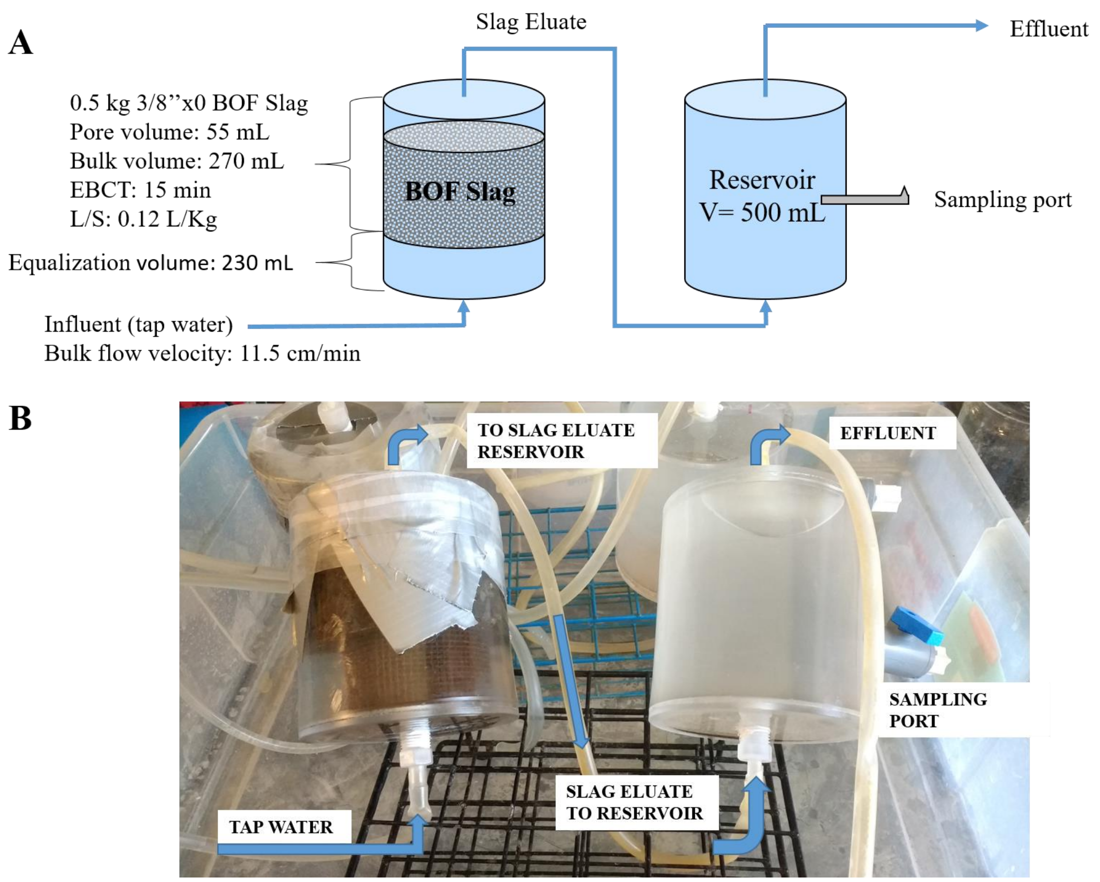


Figure 1. A) Elution system diagram with relevant design parameters. B) Photograph of the elution system (front view). Flow direction indicated with blue arrows.

A palladium circular screen (mesh size 2 mm) was inserted at 4.05 cm from the bottom of the empty elution column to facilitate the uniform egress and flow of the tap water into the packed column. Prior slag addition, a filter paper (No.1 Whatman) was placed completely covering the mesh in order to avoid solid fines from settling at the bottom. Leak-proof grease and paraffin film were used to secure the end caps to the column. The columns were packed with 500 g of pre-wetted BOF slag fines on top of the filter paper to facilitate workability and densification. Based on the aspect ratio (H/L) considerations, the compacted height of the BOF slag media in the column was 4.76 cm (1.87 in).

The elution process was conducted in a continuous up-flow mode through use of a peristaltic pump (Masterflex® L/STM 7520-10, Cole-Parmer). The eluate from the columns was directed to the bottom of equally-sized cylindrical PVC reservoirs. Effluent samples were taken at half the height of the reservoir by means of a septum sampling port. An Empty Bed Contact Time (EBCT) of 15 minutes was used to reliably achieve a target effluent construction of approximately 1000 mg/L Ca and pH~12.5 consistent with the equilibrium concentration of Ca from prior column and EPA 1313 testing [Jagupilla et al 2012b; Grubb et al submitted].

Eluate samples (25 mL) were taken at different PV intervals from both packed columns and were analyzed for pH, alkalinity, conductivity, and elemental composition (Ca, Si, Al, Fe, Mg, Mn, Na, K). pH and conductivity were measured by using a calibrated pH meter (SympHony SP70P, VWR), and conductivity meter (FiveGoTM F3, Mettler Toledo). Alkalinity was measured by titration of aliquots with 0.1 N H_2SO_4 to a final pH of 4.5. Elemental composition of the eluate was determined by inductively coupled plasma optical emission spectrometer (ICP-OES), on a calibrated ARL 3410+. An analytical blank, along with three standards that were made by accurately diluting certified standards, were used for calibration.

3. RESULTS

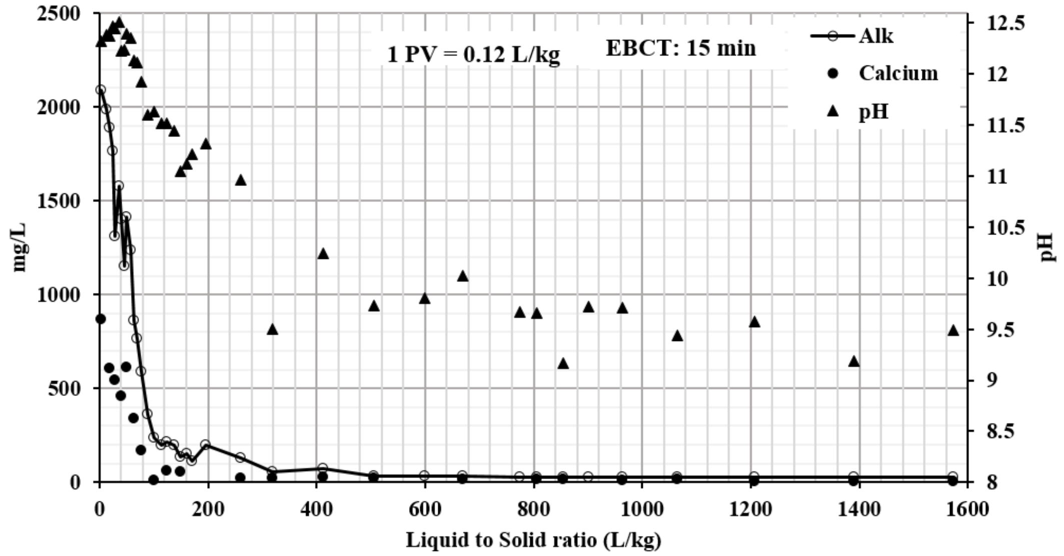
The elution history for the two parallel elution systems was recorded for a total running L/S of approximately 1573 L/kg (13111 PV) and reported as the averages, as shown in Figure 2. Influent tap water elemental concentrations were monitored for the duration of the experiment and used as background control, as provided in Table 1.

Alkalinity changes were described by an initial sharp decreasing profile. High alkalinity (>1000 mg $CaCO_3$/L) was obtained up to 63 L/kg (526 PV). After 318 L/kg (2650 PV), a plateau was reached and minimum changes occur thereafter. A similar trend was observed for dissolved calcium, which rapidly decreased from ~870 mg/L to the background level of the influent water (~12.1 mg/L) after L/S 150 L/kg (1245 PV). pH decreased from ~12.5 to ~9.7 after 505 L/kg (4212 PV) and stabilized at ~9.7 for the duration of the experiment.

The BOF slag elution history suggests that most of the alkalinity was initially provided by dissolution of readily available calcium compounds (e.g. lime and portlandite). Lime (CaO) readily hydrates to portlandite [$Ca(OH)_2$] which further dissociates producing the initially very elevated pH (~12.5) and Ca concentration observed in Figure 2. As the lime and portlandite are exhausted, this triggers the dissolution of many other minerals in the BOF slag, including larnite [$Ca_2(SiO_4)$]. Larnite, a major constituent of BOF slag (see Table 2), initially hydrates to produce portlandite and the ultimate end-products of the dissolution process are OH^-, Ca and dissolved silicates such as silicic acid, or $H_4(SiO_4)$ [Roadcap et al 2005; Huijgen and Comans, 2006; de Windt et al 2001; van Zomeren et al 2011], the latter of which has a pKa on the order of 9.7 to 9.9.

This explanation is reinforced by the observed changes in elemental Si concentrations in the BOF slag eluate. Silicon concentrations increased then fluctuated between 1 and 10 mg/L after 260 L/Kg (2160 PV). Aluminum concentration was observed at ~ 0.1 mg/L until L/S 260 L/Kg (2160 PV). A slightly decreasing profile occurred thereafter. All other analyzed elements (except for aluminum) were found within, or below, the concentration range of the influent water for the duration of the experiment (see Table 1).

Split samples of the BOF slag fines in their "as-received" (virgin) and "exhausted" (exhausted) condition after L/S 1575 L/kg (13100 PV) leaching were analyzed by quantitative x-ray powder diffraction (QXRD) using the Rietveld (1969) method, the Toxicity Characteristic Leaching Procedure (TCLP; EPA Method 1311) and De-ionized water (DIW) leaching by ASTM D3987. The raw QXRD results based on the analysis of two replicates are shown in Table 2. The exhausted BOF slag fines results may somewhat reflect that the inner core of the larger BOF slag particles (10 mm top size) may still resemble its initial composition because it was occluded from the pore solution during the extended leaching test. Nevertheless, comparison of the two samples still reveals several significant differences in the mineralogy of the virgin and exhausted BOF slag fines by the Student t-test with $p<0.05$. The mineralogical trends suggest that the sequential dissolution of lime/portlandite and larnite resulted in the increased formation of amorphous and calcite/vaterite (both $CaCO_3$). Aluminum hydroxide [$Al(OH)_3$] also dissolves, further adding to the amorphous content.



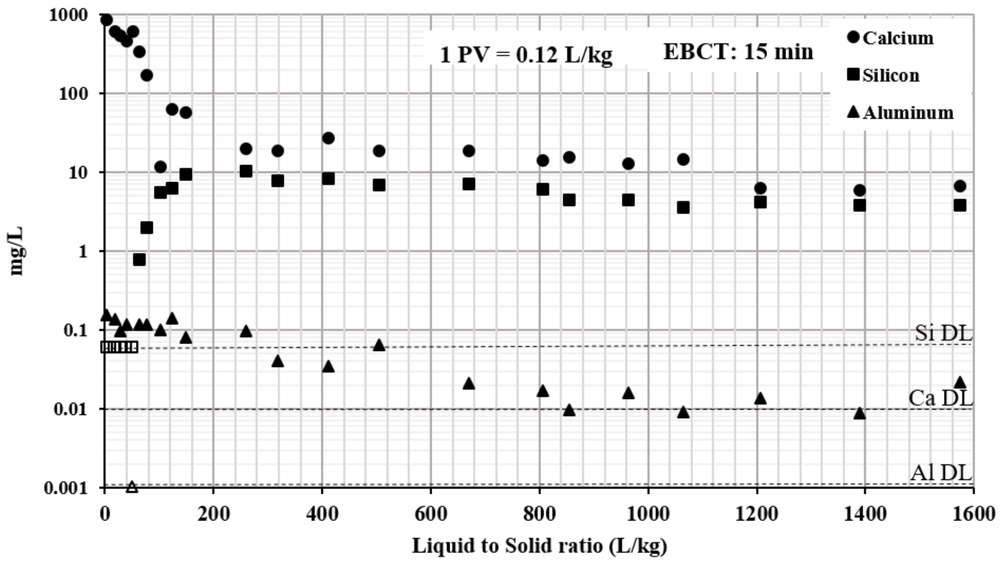


Figure 2. (TOP) Average alkalinity (Alk), dissolved calcium and pH of BOF slag eluate with increasing L/S ratio. (BOTTOM) Average concentrations of major elements (Ca, Si, Al) of BOF slag eluate with increasing L/S ratio. Dotted lines indicate the detection limit (DL) for each element.

Table 1. Average **influent tap water concentrations of major elements (mg/L) and total alkalinity (mg CaCO3/L) (n=4).**

	Ca	Si	Mg	Na	K	Mn	Al	Fe	Alk
Average	12.10	1.86	1.64	3.33	0.28	<0.001	<0.007	<0.06	25.2
St. Dev.	6.62	0.28	0.6	1.69	0.48	-	-	-	9.3

The mineralogical change correlates well with the dissolved elemental concentration history previously presented in Figure 2. Due to the extended elution duration, a significant portion of the initial BOF slag was lost. Figure 3 shows the normalized weight percentages of the key minerals corrected for the 19.4 wt% mass loss between virgin and exhausted BOF slag fines. To make the trends clear in Figure 3, the lime and portlandite contents have been paired because of their linkage by direct hydration. Also paired are the calcium carbonates (calcite and vaterite) as these are polymorphs and constitute the end-products of the carbonation of slag by atmospheric CO_2. The loss of the residual lime content and carbonation of the BOF slag are unmistakable, as is the loss of larnite, very likely by the aforementioned hydration reactions that produce the silicate concentrations observed in the Figure 2 and Table 3.

Table 2 Average QXRD results of virgin and exhausted <10 mm BOF Slag fines (n=2).

Compounds		**Virgin BOF Slag Fines**		**Exhausted BOF Slag Fines**		**Significant Difference**
		Average	**SD**	**Average**	**SD**	
Mineral Name	**Formula**	**wt%**		**wt%**		**(*t*-test, *p*<0.05)**
Amorphous Material		40.7	1.8	47.3	0.6	Yes
Srebrodolskite	Ca2Fe2O5	13.4	0.6	14.5	0.1	No
Larnite	Ca2SiO4	10.9	0.1	7.8	0.0	Yes
Portlandite	Ca(OH)2	6.0	0.0	0.6	0.0	Yes
Wuestite	FeO	5.5	0.1	6.1	0.4	No
Magnesioferrite	MgFe2O4	5.6	0.3	6.4	0.0	No
Calcite	CaCO3	4.2	0.1	7.1	0.4	Yes
Nordstrandite/Gibbsite	Al(OH)3	4.2	0.4	1.2	0.1	Yes
Akermanite	Ca2(Mg0.75Al0.25)(Si1.75Al0.25O7)	2.9	0.1	3.1	0.8	No
Magnesium Iron Oxide	Fe0.23Mg0.77O	2.2	0.1	2.6	0.1	Yes
Vaterite	CaCO3	1.7	0.1	1.6	0.0	No
Lime	CaO	1.3	0.1	1.1	0.0	No
Periclase	MgO	1.2	0.4	0.5	0.1	No
Hydrotalcite	Mg6Al2(CO3)(OH)16-4(H2O)	0.5	0.2	0.2	0.3	No
Quartz	SiO2	0.3	0.1	0.3	0.1	No
	Sum	100.2	0.1	100.2	0.1	

Notes: wt% = percent by dry weight based on averages.

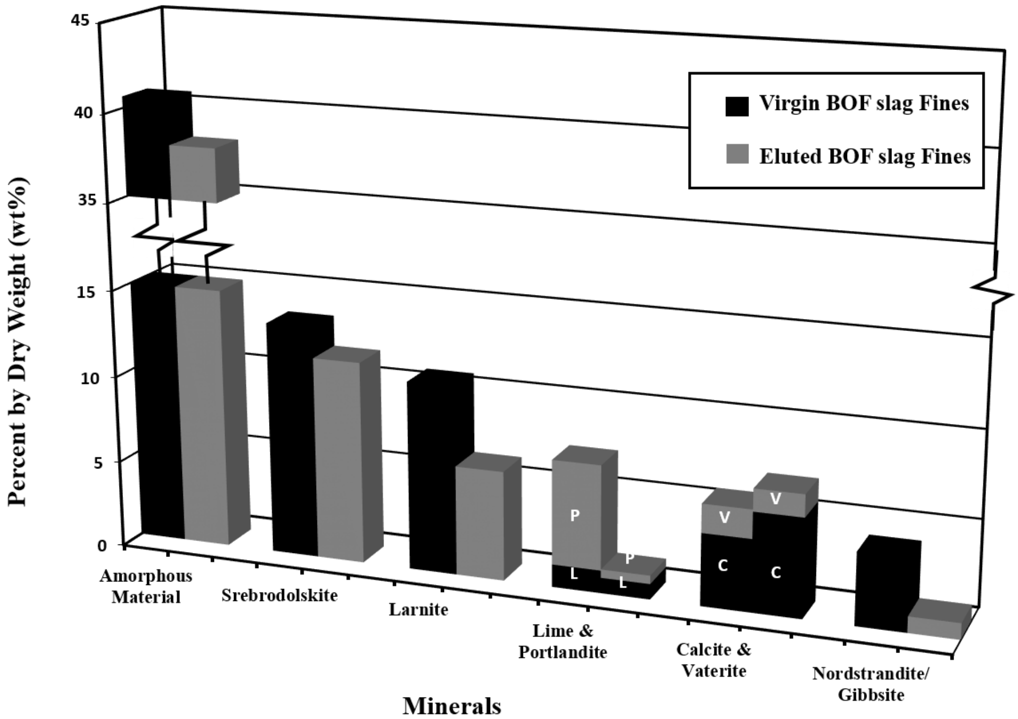


Figure 3 Mineralogical comparison of virgin and exhausted BOF slag fines (<10mm fraction) after a running L/S of 1575 L/kg (13100 PV) of water flow, corrected for mass loss (19.4 wt%). P = Portlandite, L = Lime, V = Vaterite, C = Calcite.

Table 3 shows the TCLP for the virgin and exhausted BOF slag fines samples as well as the DIW leaching of the exhausted BOF slag fines by ASTM D3987 for the EPA Target Analyte List (TAL) metals, less mercury (Hg), as it typically occurs at <0.5 mg/kg in BOF slag [Proctor et al 2000]. The RCRA metals limits are shown for comparison to illustrate the both the virgin and exhausted BOF slag fines are non-hazardous. The TCLP data suggest that the BOF slag fines are exceptionally clean from an environmental perspective and compare very well with the TCLP data of other US BOF slag [Proctor et al 2000], in either the virgin or exhausted form.

Table 3 Leaching comparison of virgin and exhausted <10 mm BOF slag fines after approximately 13100 PV tap water leaching (L/S ~ 1575).

Constituent	Symbol	RCRA (mg/L)	Virgin BOF Slag Fines (TCLP) Replicate 1		Replicate 2		Average		Exhausted BOF Slag Fines (TCLP) Replicate 1		Replicate 2		Average		Exhausted BOF Slag Fines (ASTM DI Water) Replicate 1		Replicate 2		Average	
post-extraction pH (SU)	**-**	**12**	**12.6**		**12.7**		**12.7**		**10.7**		**10.8**		**10.8**		**10.7**		**10.9**		**10.8**	
Metals (mg/L)																				
Aluminum	Al		0.90	J	0.46	J	0.68	J	0.79	J	0.48	J	0.64	J	0.17	J	0.17	J	0.17	J
Antimony	Sb		0.0014	J	0.0011	U	0.0013	J	0.0011	U	0.0011	U	0.0011	U	0.00080	UJ	0.00080	U	0.00080	UJ
Arsenic	As	5	0.0027	U	0.0027	U	0.0027	U	0.0027	U	0.0027	U	0.0027	U	0.00040	U	0.00040	U	0.00040	U
Barium	Ba	100	0.13		0.56		0.35		0.045		0.93		0.49		0.0046	B	0.0074	B	0.0060	B
Beryllium	Be		0.00043	U	0.00043	F1F2	0.00043	U	0.00043	U	0.00043	U	0.00043	U	0.00010	U	0.00010	U	0.00010	U
Cadmium	Cd	1	0.0010	U	0.0010	U	0.0010	U	0.0010	U	0.0010	U	0.0010	U	0.00010	U	0.00010	U	0.00010	U
Calcium	Ca		1300		1500		1400		680		750		715		68		75	F1	72	
Chromium	Cr	5	0.0099		0.0077		0.0088		0.038		0.034		0.036		0.050	B	0.046	B	0.048	B
Cobalt	Co		0.00032	U	0.00032	U	0.00032	U	0.00032	U	0.00032	U	0.00032	U	0.00010	U	0.00010	U	0.00010	U
Copper	Cu		0.0060	U	0.0060	U	0.0060	U	0.021		0.011	J	0.016	J	0.028	B	0.026	B	0.027	B
Iron	Fe		0.12	J	0.12	U	0.12	J	0.31	J	0.12	U	0.22	J	0.12	U	0.12	U	0.12	U
Lead	Pb	5	0.0022	J	0.0037	J	0.0030	J	0.0034	J	0.0021	J	0.0028	J	0.00010	U	0.00012	J B	0.00011	J
Magnesium	Mg		1.3		0.38	J	0.84	J	3.7		3.0		3.4		0.13	U	0.13	U	0.13	U
Manganese	Mn		0.0077	J	0.0046	U	0.0062	J	0.055		0.038		0.047		0.0035	BJ	0.0020	J B	0.0028	JB
Nickel	Ni		0.0011	U	0.0011	U	0.0011	U	0.0011	U	0.0011	U	0.0011	U	0.00050	U	0.00050	U	0.00050	U
Potassium	K		4.2	B*	3.8	B	4.0	B*	2.7	JB*	2.8	JB	2.8	JB	0.41	U*	0.41	UF1*	0.41	U*
Selenium	Se	1	0.021	U	0.021	U	0.021	U	0.021	U	0.021	U	0.021	U	0.0019	JB	0.0021	B	0.0020	JJB
Silicon	Si		1.3		1.1		1.2		39		38		39		20		18	F1	19	
Silver	Ag	5	0.00043	U	0.00043	U	0.00043	U	0.00043	U	0.00043	U	0.00043	U	0.00080	U	0.00080	U	0.00080	U
Thallium	Tl		0.0012	J	0.00068	J	0.00094	J	0.00065	U	0.00065	U	0.00065	U	0.00080	U	0.00080	U	0.00080	U
Zinc	Zn		0.019	J	0.21		0.11	J	0.029	J	0.49		0.26	J	0.0052	U	0.0052	U	0.0052	U

TCLP = Toxicity Characteristic Leaching Procedure, EPA 1311. , RCRA = Resource Conservation and Recovery Act. , "B" flag = Compound was found in the blank and sample. , "F1" flag = MS and/or MSD Recovery is outside acceptable limits. , "F2" flag = MS/MSD RPD exceeds control limits, "J" flag = Result is less than the RL but greater than or equal to the MDL and the concentration is an approximate value. , "U" flagged = The analyte was analyzed for, but was not detected above the reported sample quantitation limit. * = LCS or LCSD is outside acceptance limits.

Numerically, the TCLP results of the exhausted BOF slag sample are very similar to the virgin sample except for the lower pH (~2 units), dissolved Ca (50% less), dissolved Cr and Mg (~4x more) and dissolved Si (30x more). The DIW water extraction results on the exhausted sample show much less dissolved Ca, Mg and Si but slightly more Cr than the TCLP results for essentially the same pH. Compared to the virgin sample, many of the dissolved concentrations of the amphoteric metals (e.g. Cd, Pb, Zn) and oxyanions (e.g. As, Se) are significantly less than the virgin sample TCLP results due to pH solubility-controlled behavior.

4. CONCLUSIONS

This paper summarizes the elution history of packed BOF slag fines (<10 mm diameter) after a running L/S of 1573 L/kg (13111 PV) and an EBCT of 15 min. pH >12 persisted to about L/S <77 L/Kg (580 PV), then monotonically decreased until residual portlandite/lime was leached out. pH plateaued thereafter, likely due to buffering effect of silicic acid ($pKa_{1(H4SiO4)} \approx 9.8$). High alkalinity (>1000 mg $CaCO_3$/L) was obtained up to a L/S 63 L/Kg (PV 526). Minor changes occurred after 318 L/kg (2650 PV), with values approaching that of the influent tap water (~25.2 mg $CaCO_3$/L). Calcium leaching trend followed pH and alkalinity profiles. After L/S 150 L/Kg (1245 PV), calcium concentration approached the background level of the influent tap water (~12.10 mg/L).

Dissolved silicon increased and remained steady between 1 and 10 mg/L after 150 L/Kg (1245 PV). Silicon concentrations after L/S 260 L/Kg (2160 PV) were likely governed by silicic acid, since pH ~ Pka_1 ~ 9.8. Aluminum concentrations were observed at ~ 0.1 mg/L until L/S 260 L/Kg (2160 PV). A slightly decreasing profile occurred thereafter. No other analyzed element was detected at relevant levels. The mass loss of BOF slag fines after the experiment resulted in 19.4 wt%. Based on the QXRD data, the sequential dissolution of lime/portlandite and larnite are suggested to be the dominant processes driving changes in alkalinity, pH, and aqueous elemental composition. Aluminum hydroxide [$Al(OH)_3$] also dissolved, further adding to the amorphous content. The TCLP data suggest that the BOF slag fines are exceptionally clean from an environmental perspective. Compared to the virgin fraction, the exhausted BOF slag fines leached significantly less amphoteric metals and oxyanions, due to pH solubility-controlled behavior.

The fact that neutral pH was not achieved at the end of the experiment indicates the remarkable capacity of BOF slag fines in generating high-pH, environmentally clean eluate for extended liquid:solid ratios. These properties make BOF slag eluates an attractive alternate for lime water solutions.

Acknowledgments

The mineralogical evaluations shown in **Table 2** were completed by Pittsburgh Mineral and Environmental Technology Inc. (New Brighton, PA). The TCLP and ASTM D3987 testing on shown in **Table 3** was completed by the former CH2M Applied Sciences Laboratory (Corvallis, OR).

References

1. Datnoff, L.E., Snyder, G.H. and Korndörfer, G.H. eds., 2001. **Silicon in agriculture (Vol. 8). Elsevier.**
2. De Windt, L. Chaurand, P., and J. Rose (2011) "Kinetics of steel slag leaching: batch test and modeling." **Waste Management 31**, 225-235.
3. Grubb, D.G., Jagupilla, S.C., and Wazne, M., 2016a. Immobilization of Copper (Cu), Nickel (Ni) and Lead (Pb) using Steel Slag Fines," ***Geo-Chicago 2016: Sustainable Waste Management and Remediation*, Geotechnical Special Publication 273**, N. Yesiller, D. Zekkos, A. Farvid, A. De and K.R. Reddy (eds.), pp. 70-78.
4. Grubb, D.G., Jagupilla, S.C., and Wazne, M., 2016b. Immobilization of Cadmium (Cd) and Zinc (Zn) using Steel Slag Fines," **Geo-Chicago 2016: Sustainable Waste Management and**

Remediation, Geotechnical Special Publication 273, N. Yesiller, D. Zekkos, A. Farvid, A. De and K.R. Reddy (eds.), pp. 513-521.

5. Grubb, D.G., Wazne, M, Jagupilla, S.C., and Malasavage, N.E., 2011. The beneficial use of steel slag fines to immobilize arsenite and arsenate: Slag characterization and metal thresholding studies, **J. Hazard. Toxic Radioact. Waste 15(3)** 130-150.
6. Grubb, D.G., Berggren, D.R.V., and A.C. Garrabrants (submitted). "Metals Leaching from Basic Oxygen Furnace (BOF) Slag Fines: USEPA Method 1311, 1312, 1313, 1315 and 1316 results". **J. Hazard. Toxic Radioact. Waste**, submitted.
7. Huijgen, W.J.J., and R.B. Comans (2006). "Carbonation od steel slag for CO2 sequestration: Leaching of Products and Reaction Mechanisms." **Environ. Sci. Technol.**, 40(8), 2790-2796.
8. Jagupilla, S.C., Grubb D.G., and Wazne, M., 2012a. "Immobilization of Sb(III) and Sb(V) using Steel Slag Fines," **GeoCongress 2012:State of the Art and Practice in Geotechnical Engineering**, Geotechnical Special Publication 225, R. Hryciw, A. Athanosopoulos-Zekkos, and N. Yesiller (eds.), pp. 3988-3994.
9. Jagupilla, S.C., Grubb D.G., and Wazne, M., 2012b. "Immobilization of Se(IV) and Se(VI) using Steel Slag Fines," **GeoCongress 2012:State of the Art and Practice in Geotechnical Engineering**, Geotechnical Special Publication 225, R. Hryciw, A. Athanosopoulos-Zekkos, and N. Yesiller (eds.), pp. 4033-4041.
10. Rietveld, H. M. (1969). "A profile refinement method for nuclear and magnetic structures." ***J. Appl. Crystallogr.***, 2, 65–71.
11. Roadcap, G.S., Kelly, W.R., and C.M. Bethke, (2005). "Geochemistry of extremely alkaline (pH>12) ground water is slag-fill aquifers." ***Ground Water*** **43**(6), December, 806-816
12. Proctor, D. M., and et al. (2000). "Physical and chemical characteristics of blast furnace, basic oxygen furnace, and electric arc furnace steel industry slags." **Environ. Sci. Technol.**, 34(8), 1576–1582.
13. van Zomeren, A., van der Laan S.R., Kobeson, H.B.A, Huijgen, W.J.J., and R.B. Comans (2011). "Changes in mineralogical and leaching properties of converter steel slag resulting from accelerated carbonation at low CO2 pressure," **Waste Management 31**, 2236-2244.

PHOSPHATE REMOVAL USING A REACTIVE GEOCOMPOSITE MAT PROTOTYPE

D.G. Grubb[1*], A.S. Filshill[2], D.R.V. Berggren[3]

[1] Phoenix Services LLC, 148 West State Street, Suite 301, Kennett Square, PA 19348, USA;
[2] INOVA Geosynthetics,1500 Chester Pike, Eddystone, PA 19022, USA;
[3] Jacobs, 1100 NE Circle Blvd., Suite 300, Corvallis, OR 97330, USA

[*]corresponding author: dennis.grubb@phxslag.com; +12155272786

Abstract

This paper reports on the development and prototype testing of a *Reactive Geocomposite Mat* or RGM that allows for passive treatment of impacted water is both the cross-plane and in-plane directions. The RGM was fabricated of and Enkadrain™ core and reactive media sandwiched between two non-woven geotextiles. For illustrative purposes, a testing program was carried out to evaluate the potential removal of orthophosphate at typical stormwater concentrations (1 mg/L) using a proprietary phosphorus removal media (PRM-1). As-received PRM-1 was tested in the RGM configuration to assess the response in PO_4 removal, total dissolved solids (TDS) and total suspended solids (TSS) as a function of the hydraulic residence time (HRT). Overall, the PRM-1 was able to achieve greater than 90% removal of dissolved PO_4 concentrations at HRTs greater than 30 seconds. Total PO_4 removal was greatest (near 55%) at an HRT of 60 seconds. It was hypothesized that a majority of the dissolved PO_4 transforms to a colloidal form at HRTs ≥30 seconds, but are kinetically or physically limited from precipitating out of solution. Below a 30-second HRT, the RGM was overwhelmed and PO_4 removal significantly decreased, with an increasing percentage of the total PO_4 found in the dissolved form. TDS concentrations remained under secondary drinking water criteria (500 mg/L) while TSS was below 14 mg/L throughout the test.

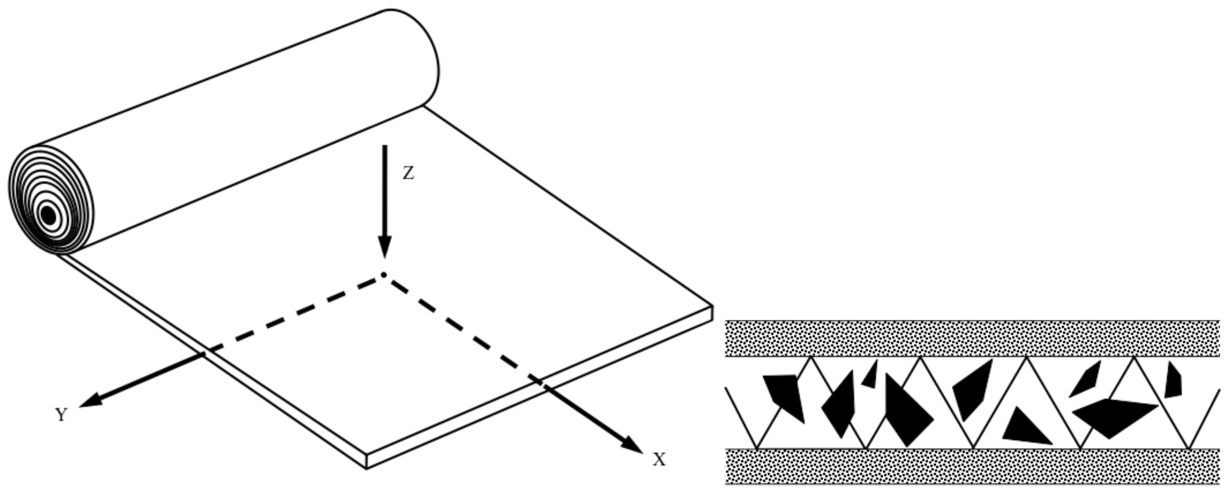
Keywords: Passive treatment, geocomposites, mats, water treatment, phosphorus removal

1. INTRODUCTION

About 15 years ago, CETCO (www.cetco.com) introduced their Reactive Core Mat (RCM™) product line which primarily features the use of granulated organoclay (about 1 lb/ft^2) between two needle-punched nonwoven geotextiles (NWGTs) as a flexible mat for use in sediment capping applications to eliminate the migration of hydrocarbons (including free product) perpendicular to the roll direction of the mat (cross plane direction). The RCM base technology enabled other (relatively soft) reactive media to be placed between the NWGTs prior to needle punching such as granular activated carbon (GAC) and apatite, the latter of which was intended to immobilize heavy metals. These thin layered mats are less than 25 mm (1-inch) in thickness, meaning they *de facto* treat water in only the cross-plane direction, or Z direction shown in **Figure 1a**. However, a major fabrication limitation of needle-punching is that hard, granular media cannot be incorporated into the RCM platform because the needle boards would require frequent change out due to the breakage and dulling of needles.

A second major technology platform for reactive treatment and sediment capping applications is currently offered by Aquablok (www.aquablok.com). Aquablok uses a composite particle approach without geosynthetics for treating impacted and upwelling waters into streams, rivers, estuaries, etc. The composite particles typically have a hard, quarried aggregate core serving as ballast (to prevent erosion) coated by either high swelling clays (Aquablok; for permeability reduction) or reactive

coatings (Aquagate; for water treatment as a granular media) whose chemistries can be tailored to the remedial challenge. In many cases, Aquagate is placed directly on the sediment surface by itself to treat water in the cross-plane direction. However, this can lead to large treatment layer thicknesses depending on the mass loading of contaminants, necessary reaction times, etc. However, thin drainage blankets of Aquagate (typically 5 to 15 cm) with long flow paths can be created by placing an upper layer of Aquablok above the Aquagate except for intentionally day-lighted sections at the offshore edges of the application area to enable treated water to enter the water column and to dissipate upwelling water pressures. However, while it enables in-plane flow (X and Y-directions, **Figure 1a**), the Aquablok system does not incorporate geosynthetics whatsoever, but the layering approach is typical for the creation of horizontal and sloped reactive lenses of porous media in remedial engineering. The authors are not aware of another pre-fabricated geocomposite system akin to the RCM that can enable in-plane flow.



a) b)

Figure 1. a) Reactive geocomposite mat (RGM) design showing cross-plane (Z) and in-plane (X,Y) flow directions. b) Cross section showing reactive media (black polygons) embedded in Enkadrain core heat bonded to outer geotextiles.

This paper reports on a new generation of thin layer mats for treating impacted waters which may be placed in a variety of settings. The *Reactive Geocomposite Mat* or RGM is a US patent pending technology that is comprised of an Enkadrain™ core heat-bonded to opposing woven or nonwoven geotextiles with opening sizes selected based on the reactive aggregates used. Intermingled on both sides of the Enkadrain are single or various granular, porous reactive media that are trapped in place due to the irregular 3D waffle-board or egg-carton like mesh of the Enkadrain, see **Figure 1b** for cross-section. The incorporation of the Enkadrain™ in the RGM imparts two major engineering advantages over the current offering of pre-fabricated geosynthetic mats: 1) it enables in-plane flow in the X,Y directions as shown in **Figure 1a**; and, 2) its particle entrapment enables the RGM to be used in both sloped and vertical orientations without risk of the reactive media moving or slumping within the RGM to the bottom of the profile. Moreover, depending on the challenge, one (or both) of the geotextiles may be switched to a geomembrane to redirect cross-plane (Z) water flow to in-plane (X,Y) flow.

Photos of an RGM prototype are shown in **Figure 2a** wherein a hard aggregate material (grey) with a top size of 9.5 mm (3/8-inches) is nested on both sides of a 20-mm thick Enkadrain™ core (white) sitting atop a lower 4-ounce non-woven geotextile (NWGT) (black). **Figure 2b** shows the final prototype after heating bonding of a second, upper NWGT to the topmost asperities of the Enkadrain™ core.

One potential application for the RGM would be to use it as a thin layer mat to aid in the rapid removal of phosphorus from agricultural runoff and stormwater sources, and/or roof gardens etc. According, to demonstrate the potential efficacy and use of the RGM, a RGM profile containing phosphorus removal media (PRM-1) was tested in the cross-plane direction, as this would be the shortest flow path for prototype testing.



Figure 2. Photo showing PRM-1 aggregates nested within Enkadrain core atop 4 ounce polypropylene nonwoven geotextile (NWGT) (left). Final prototype after heat bonding of top NWGT (right).

2. MATERIALS & METHODS

2.1 Materials Characterization

PRM-1 is a mixture of Ca-Mg-Fe silicates and oxides (including lime) comprised primarily of hard sand-sized particles. A photograph of the as-received PRM-1 (Figure 3) provides an indication of the grain size and consistency of the material.

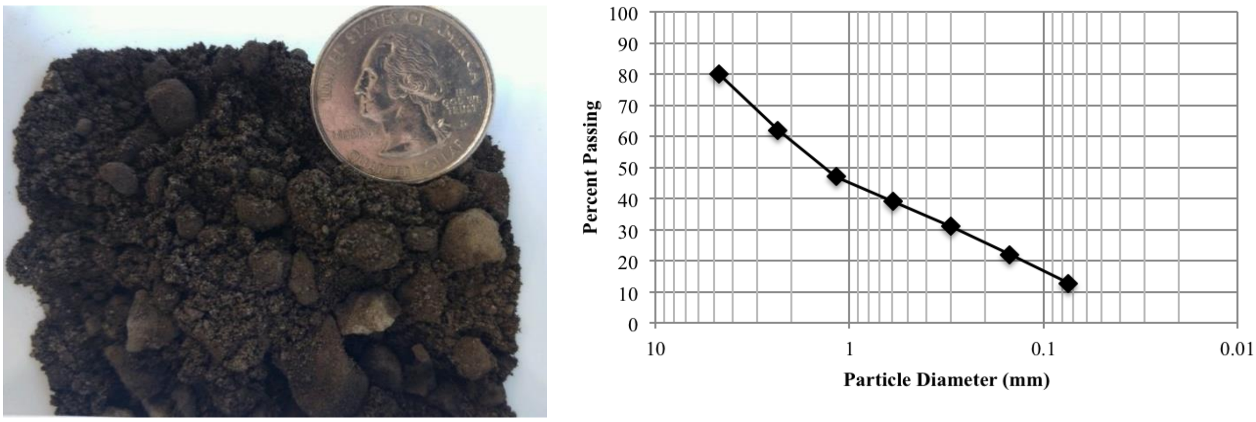


Figure 3. Photo (left) of PRM-1 aggregate and grain size (right).

The PRM-1 was homogenized and a subsample having a representative particle-size distribution was collected for analysis of moisture content and loss on ignition (LOI) by ASTM D2974. A moisture content of 6.33% and LOI of 2.39% were measured for the PRM-1 media. A 1 mg/L phosphate solution was made in 75-L batches using dechlorinated tap water and sodium phosphate dibasic heptahydrate ($Na_2HPO_4 \cdot 7H_2O$, ACS grade). The PO_4 solution was analyzed for total PO_4 and ortho-PO_4 prior to contact with PRM-1.

2.2 RGM Column Testing

The test column consists of a 25 cm (10-inch) diameter PVC column with a single end cap and central drain to release PO_4-impacted water sprayed over the RGM. The RGM was composed of PRM-1 deployed within a 20-mm Enkadrain core and confined by 4-ounce NWGT. PRM-1 was inserted at a density of 4 pounds per square foot (lb/ft^2) or approximately 19.5 kg/m^2. As shown in the **Figure 4**,

the RGM was supported by a two-dimensional geogrid and addition drainage support, and weighed down with a 1-inch layer of polypropylene beads, which also promoted an even distribution of flow. The individual layers are shown as an exploded view in **Figure 5**. To mitigate the potential for channeling, the effluent discharge was raised to a height equal to that of the upper RGM, maintaining saturated conditions within the mat.

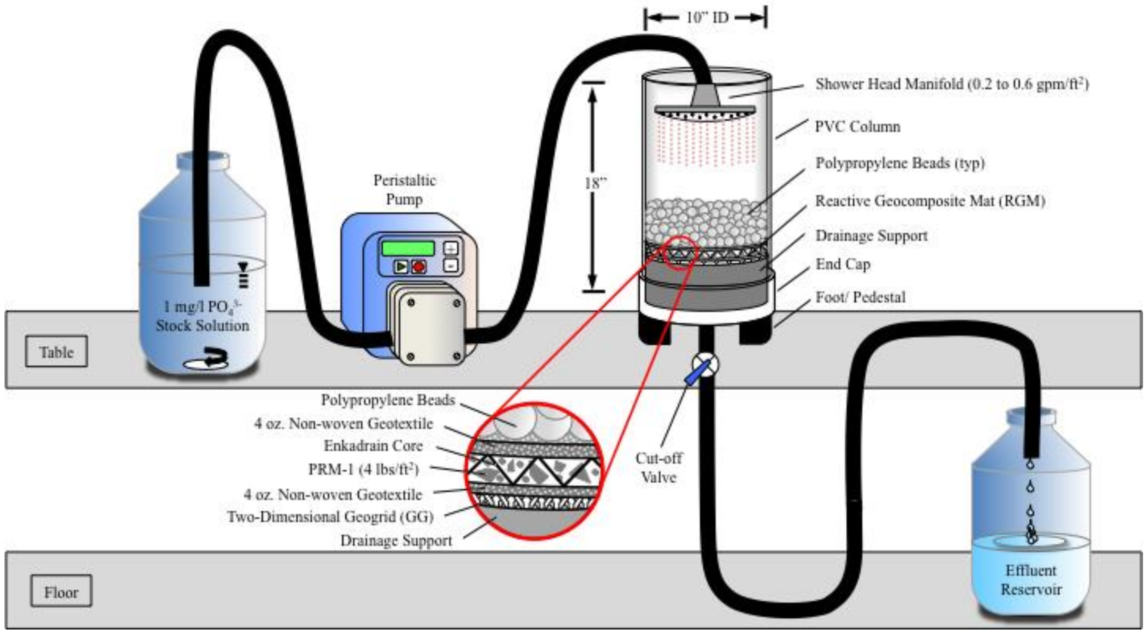


Figure 4. Schematic of High Flow Reactive Geocomposite Mat (RGM) Testing Device.



Figure 5. Exploded view of RGM layers shown in Figure 4. From left to right: Drainage support (white), geogrid support (black), lower 4-oz NWGT (black), Enkadrain (white), upper 4-oz NWGT (black) and sample tray with plastic beads (white) and PRM-1 (grey).

A total of 225 L of fluids were delivered to the top of the RGM through a rain-shower head during testing. The first 25 L was tap water to set a baseline, while the remaining fluid was the PO_4-impacted water (1 mg/L PO_4). The fluids were delivered at various HRTs, including 30 seconds (25 L of tap water followed by 50 L of impacted water), 60 seconds (100 L impacted water), and 20 seconds (50 L impacted water), which correspond to flow rates of 0.8, 0.4, and 1.2 L/minute, respectively. Effluent samples (500 milliliters) were collected for every 5 L of effluent, then submitted for analysis of pH, dissolved (ortho-) PO_4, total PO_4, TDS, and TSS.

2.3 Chemical Analysis

pH, total PO_4, TSS, and TDS measurements were not filtered prior to submission for analysis, while ortho-PO_4 samples were filtered through a 0.45 μm syringe filter. pH was measured immediately after collection using a Thermo Scientific Orion 3 Star pH benchtop meter. Total PO_4 and ortho-PO_4 were analyzed via USEPA methods 365.4 and 365.1 respectively. TSS and TDS were measured following Standard Method 2540 D and C, respectively. Standard analytical quality assurance/quality control

(QA/QC) procedures were followed for all chemical analyses, which includes analysis of method and analytical blanks, evaluation of initial and continuing calibration standards, and assessment of mass recovery from spiked analytical samples.

3. RESULTS & DISCUSSION

Effluent pH is plotted in Figure 6. pH was the highest (12.0) in the first effluent tap water sample, and gradually decreased to a pH of 11.5 over the first 75 L of effluent (equivalent to 188 pore volumes, or 81.4 liquid-to-solid (L/S) ratios. The pH then increased to 11.9 when the HRT was increased to 60 seconds, and gradually decreased with increasing L/S. When the HRT was decreased from 60 seconds to 20 seconds at an L/S of 190, the pH decreased from 11.5 to 11.0 within one 5-L sample interval, then continued to decline for the remainder of the test. The final effluent pH was 10.7.

The effluent ortho-PO_4 concentration and removal trends are shown in Figure 7 and Figure 8, respectively. Ortho-PO_4 removal was greater than 93 percent at HRTs of 30 and 60 seconds, but rapidly decreased at an HRT of 20 seconds, as the flow rate likely overwhelmed the treatment kinetics. Total PO_4 removal (Figure 9 and Figure 10) also increased with increasing HRT, however, overall removal was much lower than dissolved PO_4. An average total PO_4 removal of 36%, 55%, and 24% was measured at HRTs of 30, 60, and 20 seconds, respectively. Total PO_4 was not detected (<0.153 mg/L) in the tap water flushes at the initiation of column testing, and therefore, was not being released from the PRM-1. These results suggest that at HRTs of 30 seconds or greater, dissolved PO_4 partially transformed to colloidal PO_4 and remained suspended in the effluent flow, while the remainder precipitated out of solution. The steady increase of ortho-PO_4 concentrations under the 20-second HRT while total PO_4 was nearly constant indicates that the total mass of PO_4 that precipitates out of solution is primarily a function of the HRT, but the ratio of dissolved to colloidal PO_4 is not fixed under a single HRT.

Trends in TDS are presented in Figure 11. Immediately after initiation of flow with tap water, TDS values were near 550 mg/L, and rapidly decreased below the secondary drinking water standard (500 mg/L) within an L/S of 10. Concentrations continued to decrease until an L/S of 40 was reached. Here, the TDS appeared to stabilize at a concentration of 250 mg/L until the HRT was increased to 60 seconds. It is not clear why the TDS values initially rebounded when the HRT was doubled from 30 to 60 seconds, but the system gradually stabilized to 250 mg/L again. The 20 second HRT data suggests that water was passing through the RGM without significant reaction. Although an increase in TDS was associated with the longer HRT (60 seconds), concentrations at all points were below the secondary drinking water criteria after a short-lived initial flush.

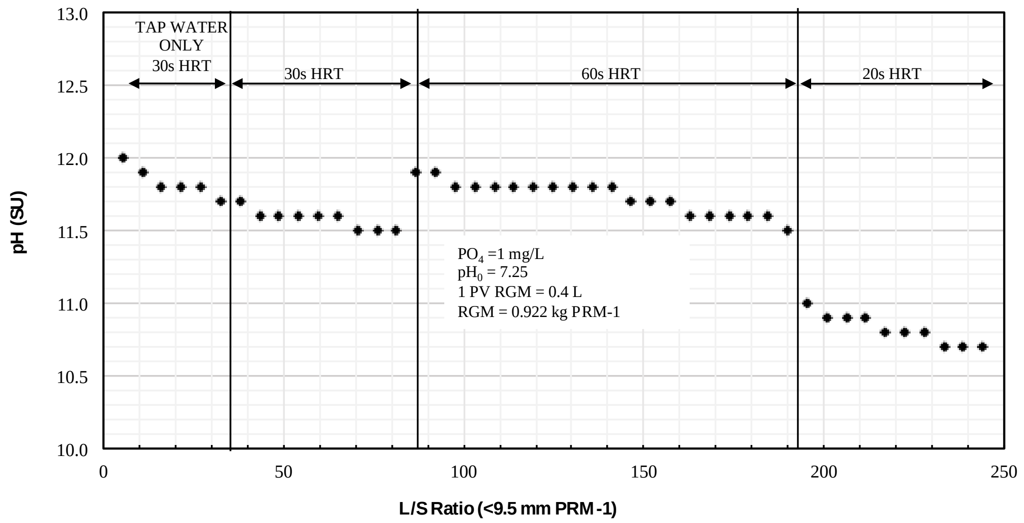


Figure 6. Effluent pH from RGM in Vertical Cross-Plane Flow Format for Different Hydraulic Residence Times (HRTs).

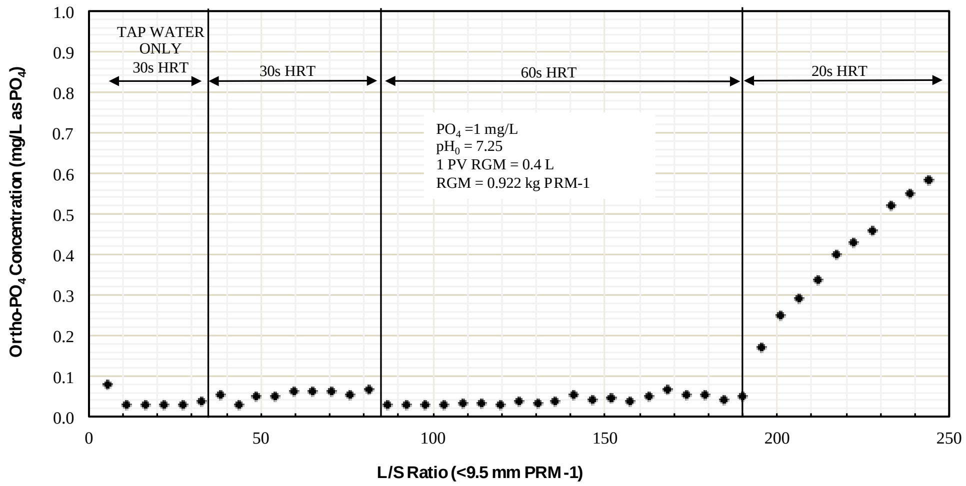


Figure 7. Effluent Ortho-PO4 (Dissolved) Concentrations from RGM in Response to Simulated Rain Event.

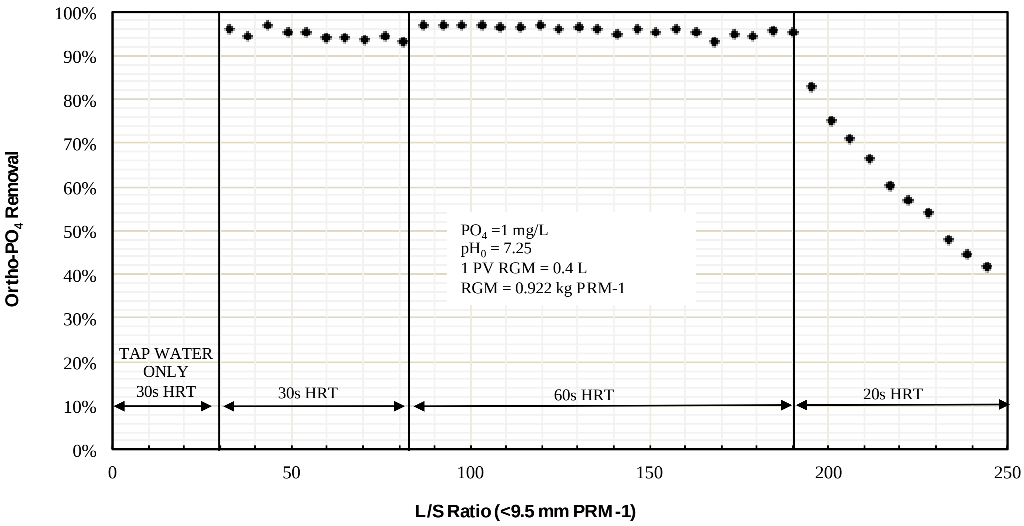


Figure 8. Removal of Ortho-PO4 by RGM in Response to Simulated Rain Event.

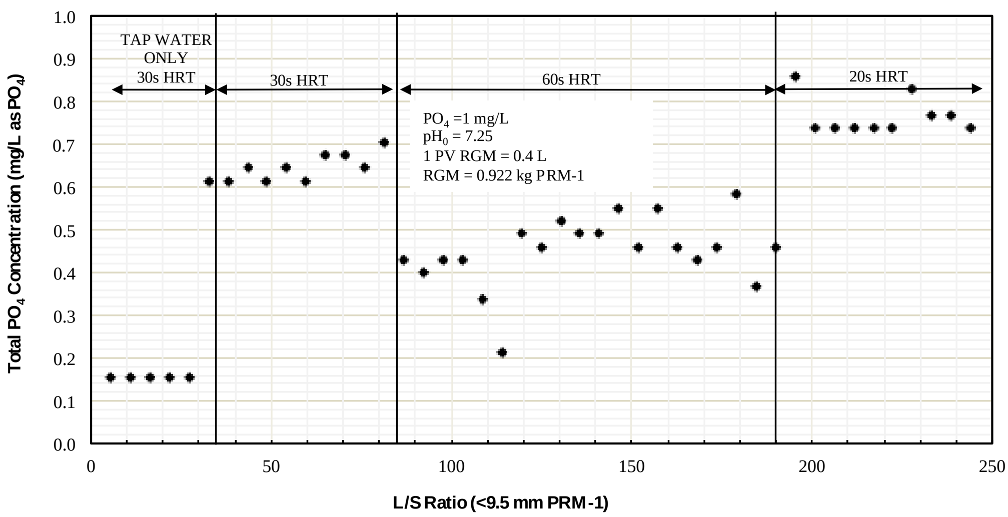


Figure 9. Effluent Total PO4 Concentrations from RGM in Response to Simulated Rain Event.

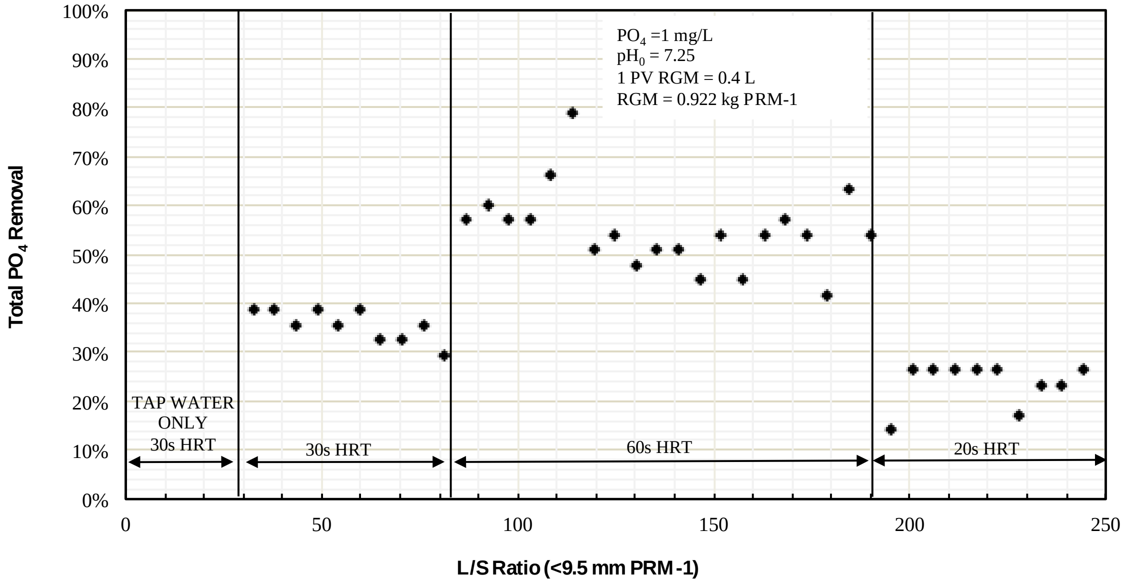


Figure 10. Removal of Total PO4 by RGM in Response to Simulated Rain Event.

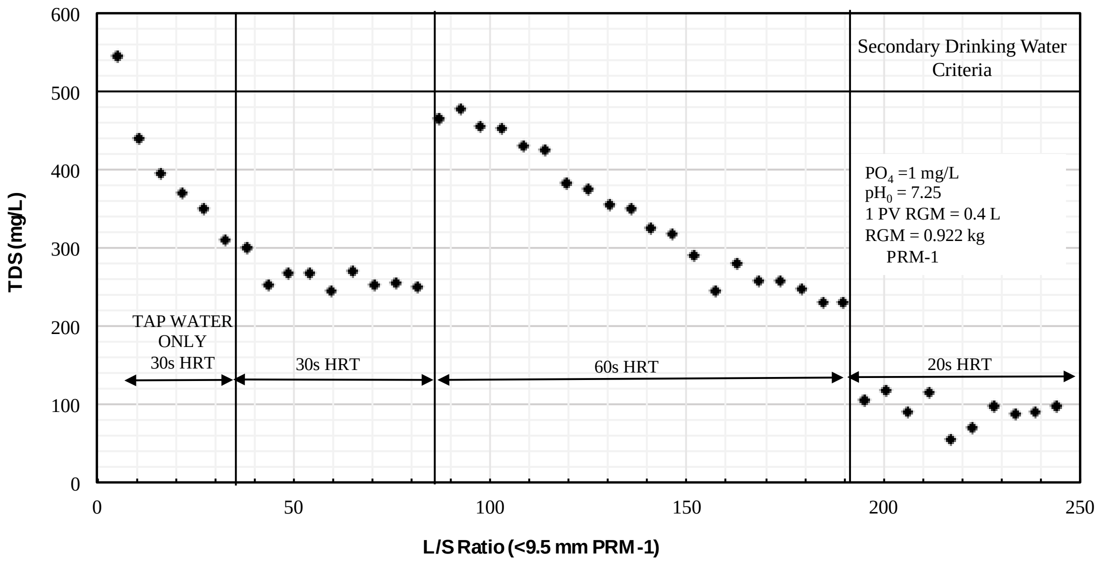


Figure 11. Effluent Total Dissolved Solids (TDS) Concentration from RGM in Response to Simulated Rain Event.

TSS trends are presented in **Figure 12**. The TSS concentration was scattered, but many samples had a concentration below the reporting limit of 6.3 mg/L. On average, the samples collected at a 30s HRT were near 1.8 mg/L greater than those at the 60s HRT, while all samples under the 20s HRT were below the reporting limit. These trends match the PO_4 data well, with total PO_4 (believed to be predominantly in colloidal form at HRTs $\geq$ 30 seconds) at 30 seconds being slightly greater than at 60 seconds, and an overall decrease of colloidal PO_4 under an HRT of 20 seconds.

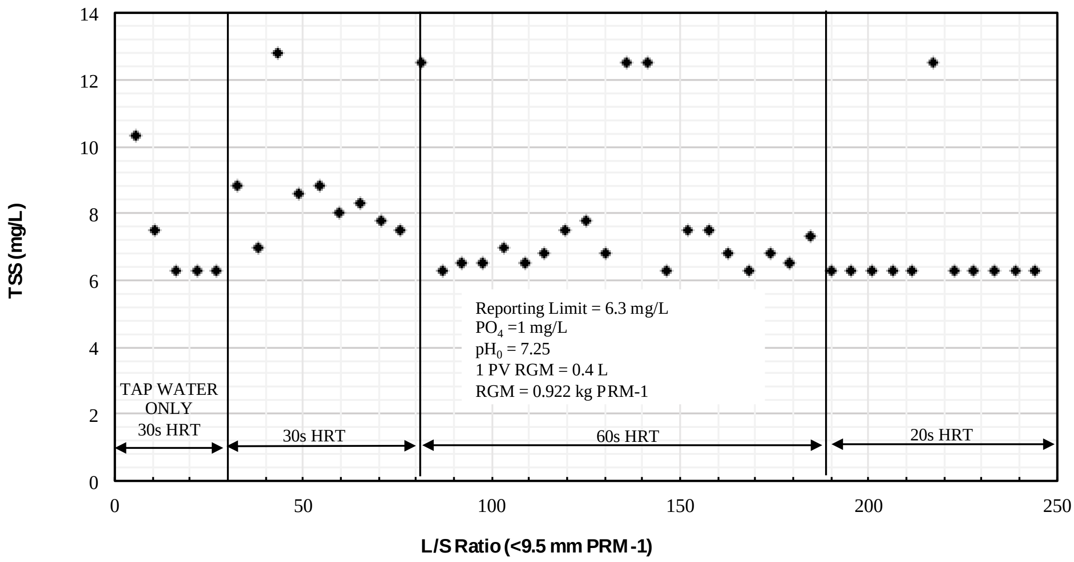


Figure 12. Effluent Total Suspended Solids (TSS) Concentration from RGM in Response to Simulated Rain Event.

4. CONCLUDING REMARKS

This testing program was carried out to evaluate potential enhancements offered by the preferential use of PRM-1 in an RGM. As-received PRM-1 was tested in the RGM configuration to assess the response in PO_4 removal and other pertinent parameters (TDS and TSS) when HRT changes.

Overall, the PRM-1 was able to achieve greater than 90 percent removal of dissolved PO_4 concentrations at HRTs greater than 30 seconds. Total PO_4 removal was greatest (near 55%) at an HRT of 60 seconds. It is hypothesized that a majority of the ortho-PO_4 transforms to a colloidal form at HRTs ≥30 seconds, but are kinetically or physically limited from precipitating out of solution. Below a 30-second HRT, the RGM was overwhelmed and PO_4 removal significantly decreased, with an increasing percentage of the total PO_4 found in the dissolved form. TDS concentrations remained under secondary drinking water criteria (500 mg/L) while TSS was below 14 mg/L throughout the test.

Ongoing research with the RGM is being conducted at the Arizona State University Center for Bio-mediated and Bio-inspired Geotechnics (ASU-CBBG) where PRM-1 is being paired with biologically active organic media to enable the joint removal of phosphorus and nitrogen in an effort to develop an RGM that can aid in the rapid removal of nutrients to streams, rivers and estuaries to prevent bacterial and algal blooms. The organic media will also aid in pH buffering.

Acknowledgements
Thanks to Ryan Church of Phoenix Services LLC for constructing the flow-through test apparatus.

UTILIZATION AND DESIGN OF FIRE SAFETY SYSTEMS WITH THE USE OF TREATED WASTEWATER

M. G. Zerva and I. K. Kalavrouziotis

School of Science and Technology,
Hellenic Open University,
Tsamadou 13-15 & Saint Andrea, GR- 26222 Patras, Greece

*Corresponding author: e-mail: ikalabro@eap.gr

Abstract

Over the past few years, a number of natural phenomena such as earthquakes, greenhouse effect, floods and fires have been taking place, for which reference is made in the present work. Due to the fact that fires can often be catastrophic, various techniques are being applied for their control, which usually are based on the evolution of technology. Thus, the present work examines and designs fire protection plans using treated wastewater originating from the Wastewater Treatment Plant of Patras. By means of this system, the negative effects of the fire are significantly reduced and at the same time the environment is adequately protected and the ecosystem are not subjected to the adverse and harmful effects of the sea and lake, water use, which is used to extinguish the fires. In fact, in the present study, the area that studied was the Industrial Park of Glafkos Patra, where the fire hydrants were fed with the treated water with the assumptions that were made on the basis of the design of the fire safety system. The relevant results and the various computational methods used for the completion of this study were listed accordingly.

Keywords: Fire; fire safety systems; fire detection; Fire brigade; fire hydrants.

1. INTRODUCTION

Fire is one of the most important inventions of humanity which plays an important role in today's scientific successes. On the other hand, it can be so damaging to the extent that it can wipe out an entire ecosystem.

To deal with the above phenomenon, man devised various techniques and constructed various modern means of extinguishing. As time goes by, this phenomenon shows signs of becoming worse and due to the fact of the constant evolution of technology and accumulation of thermal load goods, the risk of fires are increasing. For this reason, the prevention and suppression of fires is assigned to certain services (Bento-Gonçalves et al., 2012) as shown in Figures 1 and 2.In Figure 1 below, the fire categories and in Figure2, the mission of the Fire Brigade are reported.

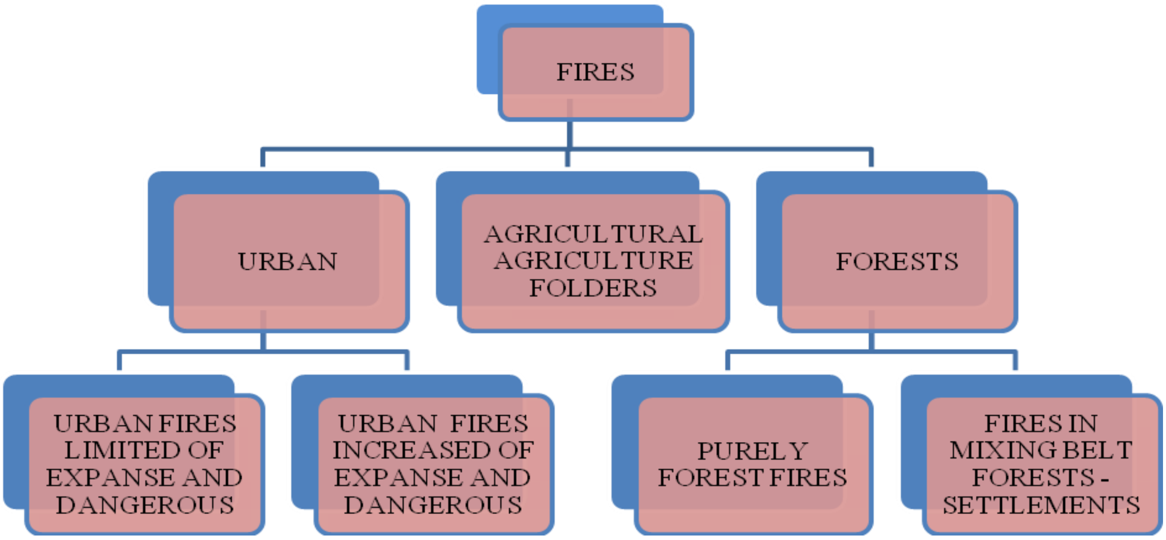


Figure 1: Fire categories (Fire- fighting side), (Panagiotidis K. G., 2011).

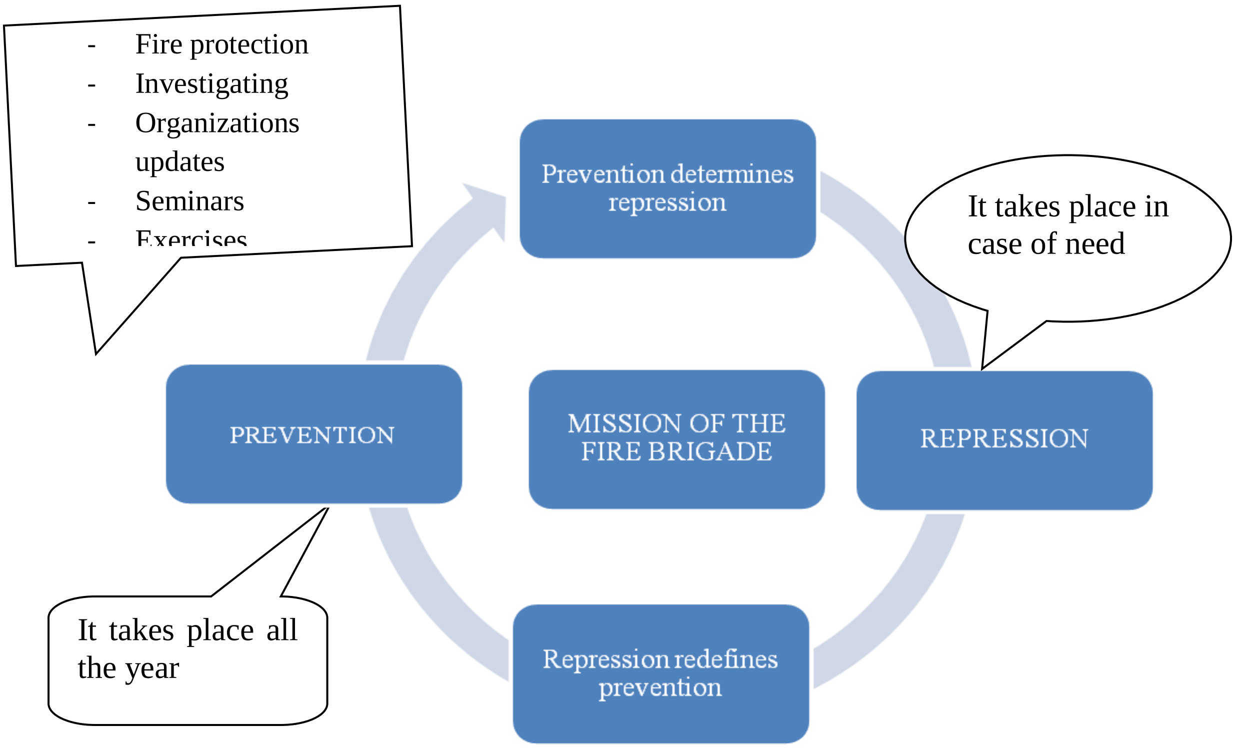


Figure 2: Mission of the Fire Brigade. Relationship between Prevention and Repression, (Panagiotidis K. G., 2011).

The severity of the fire delineates how ecosystems respond to fire and it is commonly used to describe the effects of fire on soil, the flora and fauna, water, the atmosphere, and even on the society. The severity of burning can be categorized as light/-low-, medium- or high-intensity, as it is considered a product of fire intensity and duration. It is difficult to determine the relationship between the intensity and the severity of the fire, because of some problems that arose by relative research (Hungerford et al., 1990). For the treatment of these problems, DeBano et al. (1998) setup the following criteria:

- Low fire severity: - <2% is burned severely, <15% is burned moderately and the rest is burned with low severity or does not burn at all.
- Moderate fire severity: <10% is burned severely,>15%is burned moderately and the rest is burned with low severity or does not burn.

- High fire severity: >10% there are areas that are burned with high severity, >80% is burned moderately and the rest is burned with low severity.

A product that can be used as an indicator of the severity of a fire is ash, as it is the material which biomass is burned with. Essentially, the ash is the residue a fire leaves.

Thus, taking into consideration the negative effects of the phenomenon of fire, there is an urgent need to find various fire safety and fire extinguishing systems so as, with proper prevention, to achieve their complete extinguishing. In Table 1 below, the intensity of fire as a function of temperature is given.

Table 1: Intensity of fire as a function of temperature (Panagiotidis K. G., 2011).

Intensity of fire	Temperature (°C)
Low	up to 800
Medium	800-1000
High	1000-1200

The purpose of fire protection systems is to reduce the risk of fires. Applying the most appropriate method or technique, we can create conditions for more effective prevention and suppression of fires, always based on the rules of fire protection.

The present study aims at designing fire protection systems for the Industrial Park of Glafkos Patra, which will use the treated wastewater originating from the Wastewater Treatment Plant of Patras. This water will be, at the same time, an innovative means for fire- fighting, with the prerequisite that it will be utilized properly in fire safety systems for the elimination of fires.

2. MATERIALS AND METHODS

2.1 Description of Wastewater Treatment Plant of Patras

The facilities of Wastewater Treatment Plant (WTP) of Patras are located in «Kokkinos Mylos», in the southwestern edge of the Municipality of Patras, a plot of about 80.000square meters (50.000 square meters' constructions, 15.000square meters of lawn, 200 trees, 2000 shrubs) and are one of the most modern wastewater treatment plants in Greece. It boasts the latest and the most modern technology and it has been in operation since 2001. This plant covers the needs of people residing in the Municipalities of Patras, Rio, Parallax, Vrachnaika and Messatida. This particular plant solely processes urban wastewater (Municipal Corporation Water Supply of Patras).

The disinfected wastewater is driven to the loading shaft of the underwater pipeline, out falling through a1000-mm-diameter HDPE, where an average initial dilution of 100 is made for the most difficult conditions, and then the wastewater is driven out to the sea. The treated wastewater is disposed of in the Patraikos Gulf, at the «Kokkinos Mylos" site. In particular, the treated sewage is discharged into the sea at a depth of approximately 35 m with a disposal pipeline of, about 215 m long on the earth and about 975 m under the water. It's important to note that the wastewater treatment pipeline from the plant outlet shaft to the recipient shaft is located underground. Also, a part of the treated water feeds the industrial water production plant, with the ultimate goal of saving water for the operation and irrigation of the plant. Therefore, it covers almost all the plant's requirements in industrial water, such as for scrub washing, as well as for the irrigation of the outside area of the facility (Municipal Corporation Water Supply of Patras).



Figure 3: Location of WTP Patras from a close view (maps.google.com).

2.2 Purpose of the study

The purpose of this study is the design and develop fire safety systems so as to enable proper use of treated water and prevent its disposal in the Patraikos Gulf or in landfills. Ultimately, treated water will be used for irrigation, agriculture, fires extinguishing, etc., producing many environmental benefits.

2.3 Installation sites of fire protection systems

In the context of our study, an installation will be set up, where the treated water will be stored next to the Sewage Treatment Plant in "Kokkinos Mylos", in Patra. In this facility reservoir will be built to store a part of the treated water from the Wastewater Treatment Plant and the stored water will then be fed to the fire hydrants which will be located in the Industrial Park of Glafkos Patras. In Figure 4 below, the hydrants network located in the Industrial Park of Glafkos Patras is given, which consists of 28 fire hydrants.

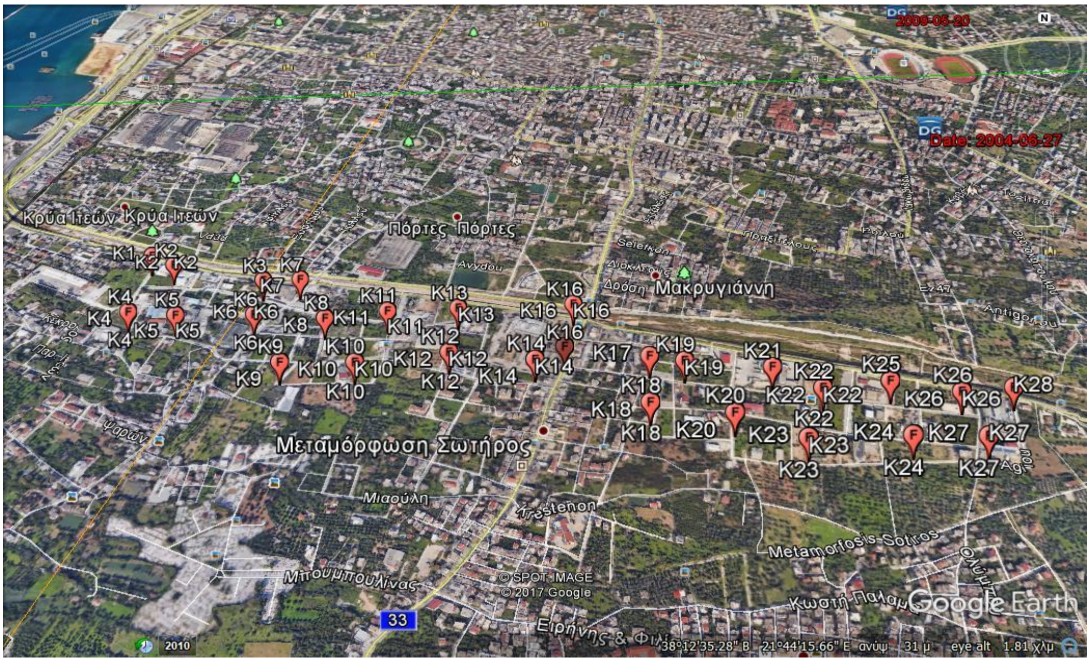


Figure 4: Hydrants network in the area of the Industrial Park of Glafkos Patras (Google Earth).

2.4 Characteristics of the treated water storage reservoir

The capacity of the reservoir to be built next to the WTP facilities should cover the operation of the 28 fire hydrants. Therefore, a concrete reservoir will be constructed in an adjacent site in the Wastewater Treatment Plant, with dimensions of 9m x 6m x 4m and a total capacity of 216m^3, as calculated below. The reservoir will be fed with a 2"pip.

The reservoir will be accompanied by all the required filling and level control instruments, as well as the emergency stop instruments including the inspection port for maintenance and cleaning.



Figure 5: Reservoir site in the Wastewater Treatment Plant (Google Earth).

In Figure 5 the reservoir where, the treated water from the Wastewater Treatment Plant will be stored to be transferred afterwards to the fire hydrants, shown with a blue square shape, with the help of the "red line", which represents the path from the reservoir until the desired height where the hydrants are located, the treated water will be transported through pipelines (made of polyethylene). In Figure 6 below, the path (red line) of the water flow until the fire hydrants is seen.



Figure 6.: Pipe transfer route of the treated wastewater from the reservoir to the fire hydrants (Google Earth).

3. SIMULATIONS – RESULTS

For the design of the fire safety system it was assumed that at an event of a fire, 3 fire hydrants will be opened manually. If a hydrant produces water for two hours with a rate of 10lt/ sec, then the three hydrants will produce water with a rate of 30 lt / sec.

As mentioned above, the pipes to be used for the hydrant network will be made of third generation polyethylene for water systems. Assuming that the operating pressure is 16 bar and the outer diameter of the tubes is Φ225 then the wall thickness will be 20.5 (unit). Then, the internal diameter of the tubes can be calculated as follows:

$$d_{inter.} = 225 - 2*20{,}5 = 184 \text{ mm} = 0{,}184 \text{ m}$$

The provision of m^3/ h units to find the water supply speed that comes out of the reservoir can then be converted as shown below:

$$Q= 30\frac{lt}{sec} = 30\ \frac{lt * 3.600 sec * 1m^3}{sec * 1hr * 10^3 lt} = 108\ \frac{m^3}{hr}$$

Therefore, the water supply speed is:

$$u= \frac{Q}{A} = \frac{108\frac{m^3}{hr}}{\frac{\pi * D^2}{4}} = \frac{108\frac{m^3}{hr}}{\frac{3{,}14 * 0{,}184^2}{4}} = \frac{432}{0{,}106}\frac{m}{hr} \Rightarrow u = 4.075{,}47\ \frac{m}{hr} \Rightarrow u \approx\ 1{,}13\frac{m}{sec}$$

Also the volume of the reservoir for duration t = 2hr is calculated as follow:

$$V= Q * t= 30\ \frac{lt}{sec} * 2hr \Rightarrow V= 30\ \frac{lt}{sec} * 7200 \cancel{sec} \Rightarrow V= 216.000 \text{ lt} \Rightarrow V_{res.}= 216\ m^3$$

According to the above calculations, the dimensions of the reservoir will be 9m x 6m x 4m. and the length of the water transfer path to the hydrants is L = 2,102 m (Google Earth). Therefore, it is necessary to measure the Pump Manometric, which is indicated below:

Manometric =Hgeod. + H_{losses}+ Hf

- Hgeod. altitude difference between the reservoir and the fire hydrant at the highest point, which is 52-2 = 50 m.
- H_{losses} are 44 m (1 atm = 10m, 4 atm= 40m, 40m * 1.1 [local losses] = 44m.
- As to the calculation of the permanent energy losses in the circular cross-section (linear losses), the following Darcy-Weisbach equation has been taken into consideration:

$$H_f= f * \frac{L}{D} * \frac{u^2}{2g} \quad (1),$$

Where → f: coefficient of friction
L: cylindrical pipeline length
D:cylindricalpipeline diameter
g: 9.81 m/sec^2

The coefficient of friction f is given by: $f = a + bR^{-c}$ (2) (Brater E.F.)

where, $a = 0{,}094 * \left(\frac{\varepsilon}{D}\right)^{0{,}225} + 0{,}53\left(\frac{\varepsilon}{D}\right)$

$b = 88{,}0\left(\frac{\varepsilon}{D}\right)^{0{,}44}$

$c = 1{,}62\left(\frac{\varepsilon}{D}\right)^{0{,}134}$

The Flow Loss Factor f is given by the Moody diagram, as a function of the Reynolds flow number and the relative roughness of the pipe:

$F = F\left(Re, \frac{\varepsilon}{D}\right)$ Re=

where, ε = absolute roughness (mm)

ε/ D= relative roughness

V= kinematic coherence (KatsaprakakisD.Al.)

From the tables presenting the properties of water, we find the kinematic consistency equal to V = 1.15×10^{-6} m^2/ sec.

Then the Reynolds flow number is calculated:

$$Re = \frac{u * D}{V} \Rightarrow Re = \frac{1{,}13\,\frac{m}{sec} * 0{,}184\,m}{1{,}15\,x10^{-6}\,\frac{m^2}{sec}} = 1{,}808 \times 10^5$$

Also, the absolute roughness of polyethylene (PE) is ε = 0.005cm. So, the relative roughness is calculated as:

$$\frac{\varepsilon}{D} = \frac{0{,}005\ mm}{184\ mm} = 2{,}72x10^{-5}$$

Substituting the relative roughness for the constants a, b and c, we have:

$a = 0{,}094 * \left(\frac{\varepsilon}{D}\right)^{0{,}225} + 0{,}53 * \left(\frac{\varepsilon}{D}\right)$

$= 0{,}094 * (2{,}72 \mathbf{X}\ 10^{-5})^{0{,}225} + 0{,}53 * (2{,}72 \mathbf{X}\ 10^{-5})$

$= 8{,}83 \times 10^{-3} + 1{,}44 \times 10^{-5} \Rightarrow$ $a = 8{,}84 \times 10^{-3}$

$b = 88{,}0\left(\frac{\varepsilon}{D}\right)^{0{,}44} = 88{,}0 * (2{,}72 \mathbf{X}\ 10^{-5})^{0{,}44} = 88 * 9{,}8 \times 10^{-3} \Rightarrow$ $b = 0{,}86$

$c = 1{,}62\left(\frac{\varepsilon}{D}\right)^{0{,}134} = 1{,}62 * (2{,}72 \mathbf{X}\ 10^{-5})^{0{,}134} \Rightarrow$ $c = 0{,}40$

So, by replacing the equation (2) we have $\Rightarrow$ $f = a + bR^{-c} \Rightarrow$

$f = 8{,}84x10^{-3} + 0{,}86 * (1{,}808\ x10^5)^{-0{,}40} = (8{,}84 + 7{,}89)\ x10^{-3} \Rightarrow$

$f = 0{,}0156$

So the equation (1) becomes:

$$H_f = f * \frac{L}{D} * \frac{u^2}{2g} = 0{,}0156 * \frac{2.102\ \mathbf{m}}{0,184\ \mathbf{m}} * \frac{\left(1,13\ \frac{\mathbf{m}}{\mathrm{sec}}\right)^2}{2 * 9,81 \frac{\mathbf{m}}{\mathrm{sec}^2}} = \frac{41{,}94\ m}{3{,}61} \Rightarrow H_f = 11{,}62\mathrm{m}$$

Therefore, Manometric $=H_{geod.} + H_{losses} + H_f = 50\mathrm{m} + 44\mathrm{m} + 12\ \mathrm{m} = 106\ \mathrm{m}$

Consequently, the total height losses are 106 m. Essentially, the required manometric height of the pump (energy difference) is the sum of the height difference (= static height difference) and the loss of pressure (loss height) in the pipes and fittings.

In fact, the total manometric is the total pressure produced by the pump to transfer the treated water from the reservoir that is too low (with a flow rate of 108 m^3/ hr) and to raise it to a height of 106 meters (where the fire hydrants are located), in order to provide the needed kinetic energy or pressure. That is, the pump creates a vacuum which absorbs water and transfers it to the network.

Thus, the manometric attempts to overcome the altitude differences and the flow of water through the pipe (linear and local losses) and operates at a pressure of 4 atm.

In fact, the pump system is so important because it can transport water through a piping network even at very high heights, and in particular, for this study, it's enabled through an installation which is located to the Wastewater Treatment to launch so much water that it can supply 28 fire hydrants located in the area of our case study, the Industrial Park of Glafkos Patras.

In brief, our findings are reported in the table below.

Table 2: Summary of the study results.

DESCRIPTION	VALUE
Operating pressure	16 bar
Outer tube diameter	Φ225
Wall thickness of pipes	20,5(units)
Inner tube diameter	0,184 m
Provision (Q)	108 m^3/hr
Water supply speed (u)	1,13 m/sec
Reservoir volume ($V_{res.}$)	216 m^3
Path length (L)	2.102 m
Reynolds number	1,808 x 10^5
Relative roughness	2,72 x10^{-5}
Total manometric	106 m

4. DISCUSSION AND CONCLUSIONS

For everything we mention above and for the proper management of water, the innovation of this work is evident. With the design of fire protection systems, wastewater treatment is being utilized to, extinguish fires, without inexorably use of water in the network and the sea. Thus, the treated waste water originating from the Wastewater Treatment of Patras can be used to extinguish fires and not being disposed of in Patraikos Gulf or in landfills. Therefore, many environmental and economic benefits are generated, as water scarcity is one of the most important environmental problems for many countries in the world.

Concluding, it should have mentioned that prevention is a profound concept, which relieves us of moral, criminal or even administrative responsibilities. For this reason, as the ultimate aim is the suppressing of fires, the necessary actions to be taken are as follows:

- Cleaning of the premises.
- Appropriate ventilation of the premises.

- Storage of flammable materials in separate rooms.
- Prohibition of open flame in areas of production.
- Ban on smoking in hazardous areas.
- Detailed maintenance of electrical installations.
- Defining safety zones and access roads within production areas, warehouses, forests, etc.
- Fully inform the public about any appropriate measures.
- Signaling and flags with special symbols or colors.
- Instructions (eg. signs with recommendations for the handling of dangerous articles.
- Communication, alarm, intercom, fire announcement and dehumidification systems.

Because of the originality of this paper, comparing the results with corresponding results from other researches is not easy, but we believe that this will be the trigger for further studies.

References

1. Bento-Gonçalves A., Vieira A., Úbeda X., Martin D., (2012). ‘Fire and soils: Key concepts and recent advances’, **Geoderma** 191 (2012) 3-13.
2. Brater F. Ernest. ‘Horage Williams King’, Late Professor of Hydraulic Engineering University of Michigan, Sixth Edition, Handbook of Hydraulics for the Solution of Hydraulic Engineering Problems, McGraw – Hill Book Company.
3. DeBano, L.F., Neary, D.G., Ffolliott, P.F., (1998). ‘Fire’s Effects on Ecosystems’, John Wiley & Sons, New York.
4. Hungerford, R.D., Harrington, M.G., Frandsen, W.H., Ryan, R.C., Niehoff, J.G., (1990). ‘Influence of fire on factors that affect site productivity’, In: Harvey, A.E., Neuenschwander, L.F. (Eds.), Symposium on Management and Productivity of Western-Montana Forest Soils. Boise, Idaho, USA, pp. 32–51.
5. Katsaprakakis D. Al. 'Pipes', Hydrodynamic Machines, Wind Energy Laboratory, T.E.I. of Crete.
6. Municipal Corporation Water Supply of Patras. ‘Facilities of Wastewater Treatment Plant of Patras, Protection of the sea - Respect for the environment'.
7. Panagiotidis K.G., (2011). ‘Investigation of the experience of permanent and seasonal firemen in Forest Fire Management aiming at the formulation of an integrated Forest Fire Management System: The case of the Fire Service of Rhodes’, University of Aegean, Faculty of Humanities, Department of Preschool Education and Educational Design, Environmental Education, Postgraduate Diploma, Rhodes.

CARBON NANOTUBES APPLICATION FOR HEXAVALENT CHROMIUM ADSORPTION FROM CONTAMINATED GROUNDWATER

Thanasis Mpouras*, Angeliki Polydera, Dimitris Dermatas

School of Civil Engineering, Department of Water Resources and Environmental Engineering, National Technical University of Athens, Iroon Polytechniou 9, 157 80 Zografou, Athens, Greece

***Corresponding author:** e-mail: th.mpouras@gmail.com, tel.: +30 210 772 2835

Abstract

In recent years, nanomaterials have attracted increasing concern in the sector of water treatment. The present study investigates the removal of hexavalent chromium from groundwater using multi-walled carbon nanotubes as adsorbent. In order to determine the adsorption efficiency of carbon nanotubes batch and column experiments were conducted using groundwater sampled in a heavily polluted area in Asopos river basin, Viotia, Greece. Batch experiments were used for investigating the effect of pH, the concentration of the adsorbent and contact time on the sorption process. Afterwards, by using up-flow column experiments the adsorption capacity of carbon nanotubes for hexavalent chromium was determined. Hexavalent chromium desorption from the nanotubes was also tested in order to check the reversibility of the process and thus to estimate the potential reusability of the nanomaterial. According to the results, the adsorption was found to be a fast process and adsorption capacity was increased with decreasing pH values and increasing the adsorbent's concentration. The desorption efficiency of the nanomaterial indicated that carbon nanotubes have promising potential for environmental remediation as adsorbing materials.

Keywords: Multi wall carbon nanotubes, hexavalent chromium, adsorption, groundwater

1. INTRODUCTION

Chromium, a heavy metal that naturally occurs in the Earth's crust, can be found in the environment in several oxidation states. The trivalent (Cr(III)) and hexavalent (Cr(VI)) are the most common states in groundwater. Cr(III) is an indispensable element for the human beings and seems to be much less hazardous than Cr(VI), which is reported to cause serious health problems (dermatitis, diarrhea, nausea, bronchitis, internal hemorrhage etc) and act as carcinogenic agent (Dehghani et al., 2016). Additionally, Cr(VI), which usually occurs as an oxyanion in the form of CrO^{4-} and $Cr_2O_7^{2-}$, is soluble in almost the whole pH range and more mobile than Cr(III) (Zeng et al., 2010).

Groundwater contamination with Cr(VI) can be either of geogenic or anthropogenic origin. However, significantly high concentrations of Cr(VI) in groundwater, even in the range of mg/L, are attributed exclusively to anthropogenic activities (Dermatas et al., 2015; Dermatas et al., 2016). Mining, electroplating, textile dyeing and leather tanning are some indicative industrial activities which lead to accidental or uncontrolled release of chromium to the environment. More specifically, chromium concentration may range from 0.5 to 270 mg/l in industrial wastewater and, as a result, high levels of Cr(VI) concentrations can be found in groundwater (Saha et al., 2011; Dermatas et al., 2016).

In recent years, several methods have been applied for the removal of Cr(VI) from wastewater or groundwater, including ion exchange, reduction of Cr(VI) to Cr(III) prior to precipitation using reducing agents, coagulation, solvent extraction, membrane technologies, chemical precipitation and

adsorption on natural or synthetic materials (Qureshi et al., 2017; Jung et al., 2013). Among the aforementioned techniques, adsorption seems to have many advantages, such as operation simplicity, low cost, high removal efficiency, as well as the potential regeneration of the adsorbent (Borna et al., 2016). The use of nanomaterials as adsorbents results in even higher performance of the process, due to their fast kinetics, high reactivity and large specific area (Zhang et al., 2016).

Carbon nanotubes (CNTs) are a relatively new form of carbon materials that were discovered by Iijima (Iijima, 1991). They are allotropes of carbon with a cylindrical structure and can be manufactured as single-walled (SWCNTs) or multi-walled (MWCNTs), depending on their number of graphite layers (Jung et al., 2013). Their potential for regeneration and reuse is their main advantage comparing to common activated carbon and other nanomaterials (Matlochová et al., 2013; Gehrke et al., 2015). This property in combination with their high surface area makes CNTs very attracting adsorbents. Consequently, CNTs are of the most common and efficient nanomaterials employed for removal of heavy metals from polluted water.

The present study aims at investigating the Cr(VI) removal capacity of MWCNTs from heavily contaminated groundwater. The effect of pH, the adsorbent's concentration and the contact time for achieving equilibrium, on Cr(VI) adsorption were tested by carrying out batch experiments. In addition, column experiments were performed in order to investigate the potential of using CNTs at up scaling applications for the treatment of such Cr(VI) contaminated groundwater.

2. MATERIALS AND METHODS

2.1 Multi-walled carbon nanotubes (MWCNTs) characterisation

The MWCNTs used in the present study were provided by Glonatech S.A. (Greece). They are produced by the chemical vapor deposition (CVD) method. The morphology of MWCNTs was analyzed by scanning electron microscopy (SEM) (JEOL FEG 7401F). A thermogravimetric analysis (TGA) was also performed using a Perkin Elmer 4000 instrument, in order to estimate the purity and the thermal stability of the material. Finally, for the determination of point of zero charge (PZC) different amounts of MWCNTs (0.01, 0.1, 1, 5, 10, 20 % wt) were suspended in 0.1 M NaCl solution and the solution pH was measured after 24hr of contact time.

2.2 Batch experiments

Batch experiments were performed to investigate Cr(VI) sorption behavior on MWCNTs using Cr(VI) contaminated groundwater sampled from Inofyta area, Greece. Cr(VI) concentration in groundwater was equal to 11 ppm. All batch experiments were conducted at room temperature (23^{o}C). The samples were placed in an orbital shaker at 200 rpm and after equilibrium they were filtered through a 0.45μm pore membrane filter (Whatman No 45) and analyzed for Cr(VI) applying the 7196A (diphenylcarbazide) EPA method. All the experiments were performed in duplicates and mean values are reported.

The effect of pH, adsorbent's concentration and contact time were investigated. The effect of pH on the sorption process was tested in the range of 3-9. pH adjustment was achieved by using HCl and NaOH solutions of 0.01M. In this case the contact time was 24 hours and MWCNTs concentration was equal to 25g/l. In order to assess the effect of MWCNTs concentration, dosages in the range of 10 to 50g/l, were used. Two series of experiments using these dosages and different pH values 7 and 8 were carried out while contact time was kept constant at 24hr. For investigating the effect of contact time, Cr(VI) concentration was measured in the range of 15 to 120min. Three series of experiments at pH values 7, 8.3 and 9 were carried out. The concentration of the adsorbent was constant at 25g/l.

The percentage sorption of Cr(VI) was calculated according to the following equation:

$$A(\%) = \frac{C_o - C_f}{C_o} * 100 \tag{1}$$

where C_o ($mg \cdot L^{-1}$) is the Cr(VI) initial concentration and C_f ($mg \cdot L^{-1}$) the final Cr(VI) concentration in the equilibrium solution

2.3 Column experiments

Despite the fact that batch experiments provide important information regarding the adsorption of Cr(VI), column experiments are useful for the practical application of this process for the treatment of polluted water (Goel et al., 2005). For this reason, three up-flow column experiments were conducted by using a column of 135 ml total volume (diameter=3cm, height=19cm) and a peristaltic pump for achieving the proper contact time. In the inlet and outlet of the column 0.45 μm pore membrane filters (Whatman No 45) were placed for filtering groundwater and to avoid leakage of the adsorbent. The column was continuously fed with the heavily contaminated groundwater (11ppm Cr(VI) concentration) while the pH of the groundwater was adjusted at 4, 7 and 8.3 (three series of column experiments). The pH value of 8.3 refers to the pH value of groundwater as measured after sampling. For the adjustment of the two other pH values HCl 0.01M was used. The pH value 7 aimed at investigating Cr(VI) adsorption capacity of MWCNTs in the case of treating groundwater with lower pH, while the pH value 4 at investigating the adsorption capacity of MWCNTs towards wastewater that would simulate the physicochemical properties of groundwater. Parameters like contact time, flow rate and MWCNTs concentration were constant at all series of experiments and equal to 1hr, 0.3ml/min and 40g/L, respectively.

Finally, in order to check the reversibility of the process column experiments were performed aiming at Cr(VI) desorption. The column was continuously fed with NaOH solution 0.1M in order to increase the pH of the solution at value around 12. This would cause the desorption of Cr(VI) from the carbonaceous material.

3. RESULTS AND DISCUSSION

3.1 Characterisation of CNTs

SEM analysis provides useful information regarding the shape, size and orientation of MWCNTs. Figure 1 illustrates that MWCNTs are randomly oriented, significantly tangled and curved. Their diameter ranges from 26 to 82 nm. TGA analysis showed that the tested MWCNTs are oxidized between 550 and 670 °C in air conditions (Figure 1). The residual verified purity higher than 94%. The high thermal stability under oxidative environment is a unique characteristic of MWCNTs comparatively with other carbonaceous materials. Regarding pH_{PZC}, it was estimated at 6.32, which is in agreement with values reported in other studies (Ai et al., 2011; Pourfadakari et al., 2016).

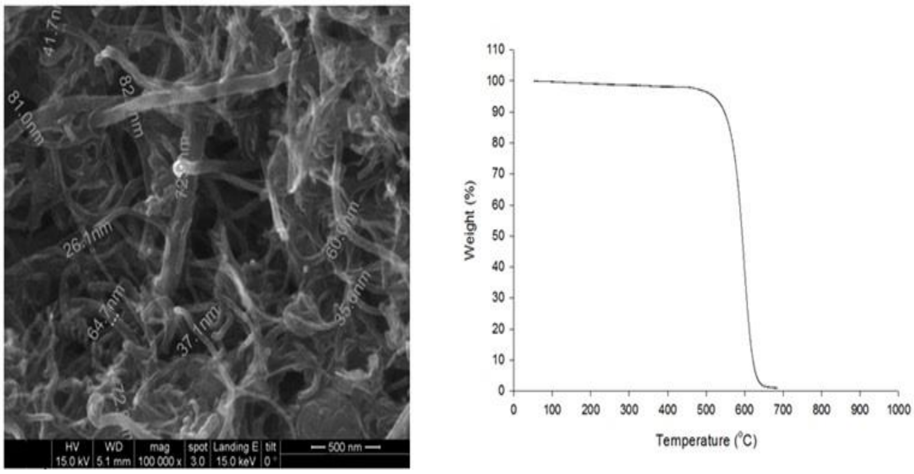


Figure 1. SEM image (left) and TGA analysis (right) of the tested MWCNTs.

3.2 Results of batch experiments

3.2.1 Effect of pH on Cr(VI) adsorption

In this series of experiments the effect of pH on Cr(VI) adsorption from groundwater was investigated using 25 g/L MWCNTs and equilibrium time equal to 24 h. Adsorption efficiency of Cr(VI) maximized (100%) for pH values up to 6.3 and decreased sharply for higher pH values reaching almost 20% at pH equal to 9 (Figure 2). In the tested pH range (3-9), Cr(VI) exists as hydrogen chromates ($HCrO_4^-$) at low pH values and chromates (CrO_4^{2-}) at higher pH values. Cr(VI) adsorption is generally attributed to electrostatic forces between Cr(VI) ions and the surface of MWCNTs. It is known that functional groups such as –OH and –COOH exist on the MWCNTs surface. For pH values lower than the PZC point these groups are protonated causing attraction to the chromium anions and thus, enhancing adsorption capacity of the solid surface. In addition, at low pH values possible reduction phenomena of Cr(VI) by the functional groups have been reported. On the contrary, for pH values higher than the PZC point the surface is negatively charged due to the deprotonation of the functional groups causing electrostatic repulsions with chromates, reducing thus the adsorption phenomena (Hu et al., 2009; Qureshi et al., 2017; Di et al., 2004).

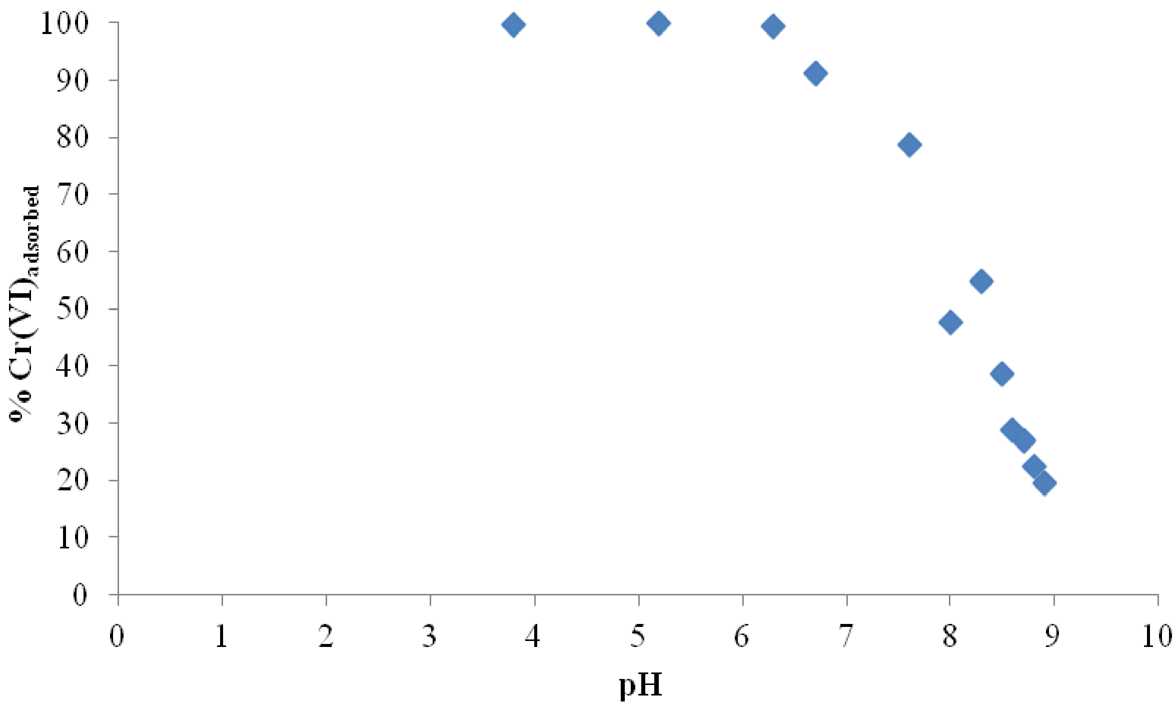


Figure 2. Effect of pH on Cr(VI) adsorption ($[Cr(VI)]_0$=11mg/L, C_{MWNTs}=25g/L, t=24h)

3.2.2 Effect of adsorbent's concentration on Cr(VI) adsorption

The effect of adsorbent dosage on Cr(VI) adsorption was investigated for two different pH values, 7 and 8, in the range 10 to 50 g/L (Figure 3). Results showed that adsorption efficiency increased with increasing the MWCNTs concentration, independently the pH values. This phenomenon is attributed to the higher number of available sites for Cr(VI) sorption with increasing the mass of MWCNTs. However, the pH value of the groundwater affected significantly Cr(VI) adsorption since the increase was found to be higher for the lower pH value. This can possibly be attributed to the presence of enhanced electrostatic attractions at pH 7 than for pH value 8, indicating that the parameter of pH plays an important role on Cr(VI) adsorption. More specifically, adsorption increased from 40% to 100% at pH equal to 7, and from 40% to 88% at pH 8.

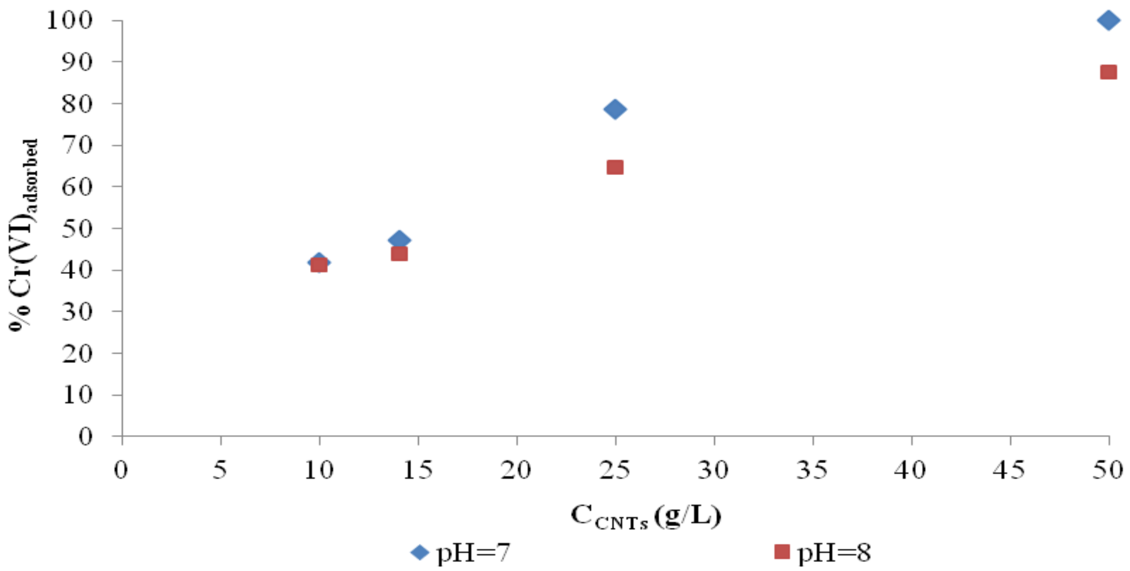


Figure 3. Effect of adsorbent's concentration on Cr(VI) adsorption for two pH values ($[Cr(VI)]_0$=11mg/l, t=24hr)

3.2.3 Effect of contact time on Cr(VI) adsorption

Figure 4 presents the effect of contact time on Cr(VI) adsorption for three different pH values (7, 8.3 and 9) in the range of 15-120 min. The results showed that for pH equal to 7 equilibrium is reached in almost 15 minutes, while for pH equal to 8.3 and 9 equilibrium in almost 60 minutes. The decrease of pH caused a slight decrease at the time needed for achieving equilibrium. However, at all cases the time required for equilibrium was much lower than the 24 h used in this study. These low values of time required for achieving equilibrium indicate that adsorption mainly occurs only on the surface of MWCNTs and probably not to sorption phenomena in the structure of MWCNTs which would demand more contact time (Di et al., 2004). In addition, as shown from Figure 4, the effect of pH is more significant than the contact time since the adsorption efficiency was found to be controlled by pH value.

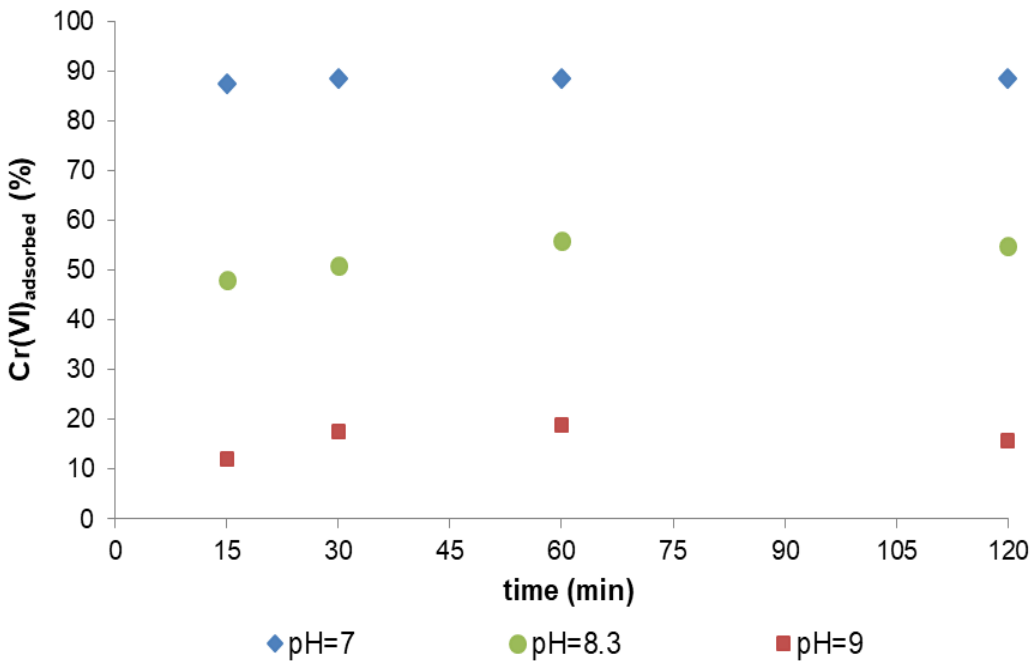


Figure 4. Effect of contact time on Cr(VI) adsorption for three pH values ($[Cr(VI)]_0$=11mg/l, C_{MWNTs}=25g/l)

3.3 Results of column experiments

3.3.1 Effect of pH on Cr(VI) adsorption

The column experiments were conducted using MWCNTs/groundwater (g/L) ratio equal to 40, contact time equal to 1 hr and initial Cr(VI) concentration equal to 11 mg/L. Three series of column experiments were carried out testing different pH values 4, 7 and 8.3 (Figure 5). The operation of each column ended when removal percentage reached almost 10%. At all cases, as operation time increased, Cr(VI) removal was gradually decreased indicating the saturation of the MWCNTs regarding Cr(VI) removal capacity. At the pH values tested, the total volume of groundwater passed through the column was 3.5, 1.1 and 0.6 L, respectively. The corresponding total amount of Cr(VI) removed at these cases was 36, 4.7 and 0.7 mg. It is clear that the pH of groundwater plays a crucial role regarding the removal capacity of MWCNTs.

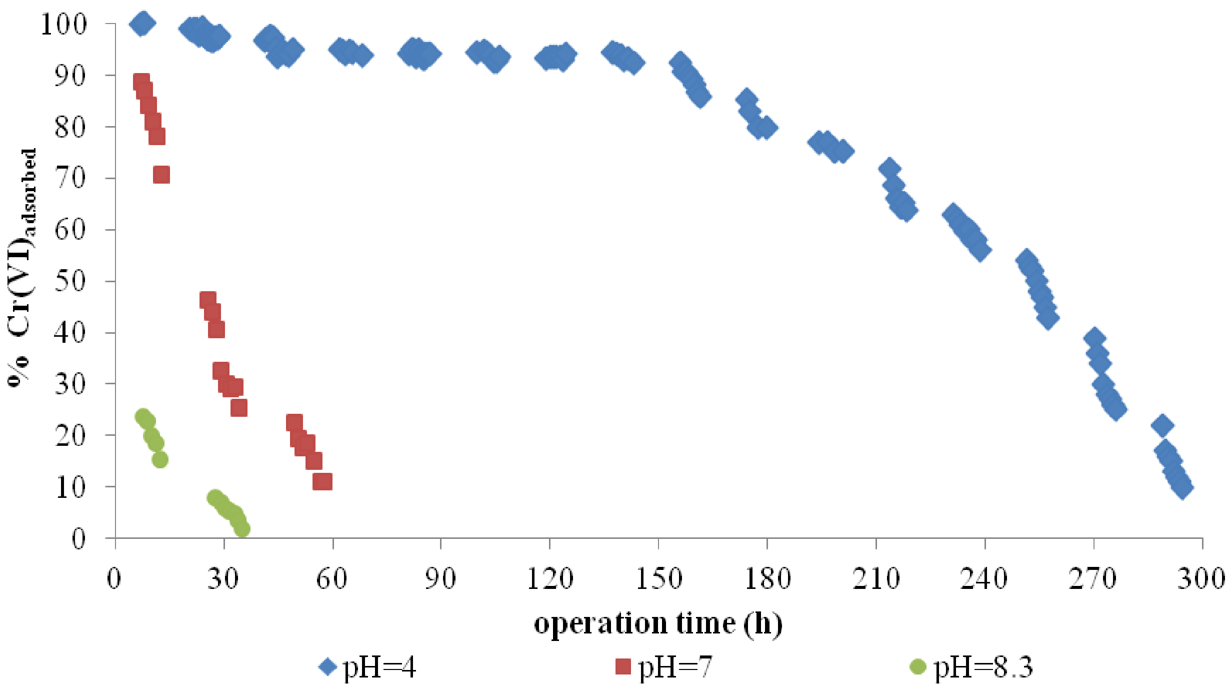


Figure 5. Cr(VI) adsorption capacity over operation time during column experiment for three different pH values ($[Cr(VI)]_0$=11ppm, contact time=1hr, C_{MWNTs}=40g/l).

3.3.2 Regeneration of MWCNTs

In order to verify the reversibility of the adsorption process, column experiments were performed aiming at Cr(VI) desorption (Figure 6). The columns were loaded with the material used in each case described in paragraph 3.3.1 and were continuously fed with NaOH solution 0.1M which created an effluent with pH about 12. This would cause the desorption of Cr(VI) from MWCNTs. The operation of the column was stopped since Cr(VI) concentration in the effluent was measured lower than 20 μg/L. The amount of the base solution used in each case for initial pH 4, 7 and 8.3 was equal to 1.5, 0.6 and 0.5 L, respectively. The difference of the amount adsorbed in the first step and of the desorbed amount of Cr(VI) indicates that the removal mechanism can be attributed to irreversible adsorption mechanisms like chemisorption or to possible Cr(VI) reduction after adsorption. Reduction can be attributed to the surface functional groups or to the residual catalyst that used in the synthesis process. Thus, further investigation is needed in order to determine the exact removal mechanism and determine the reusability of MWCNTs for decontamination of Cr(VI) contaminated groundwater.

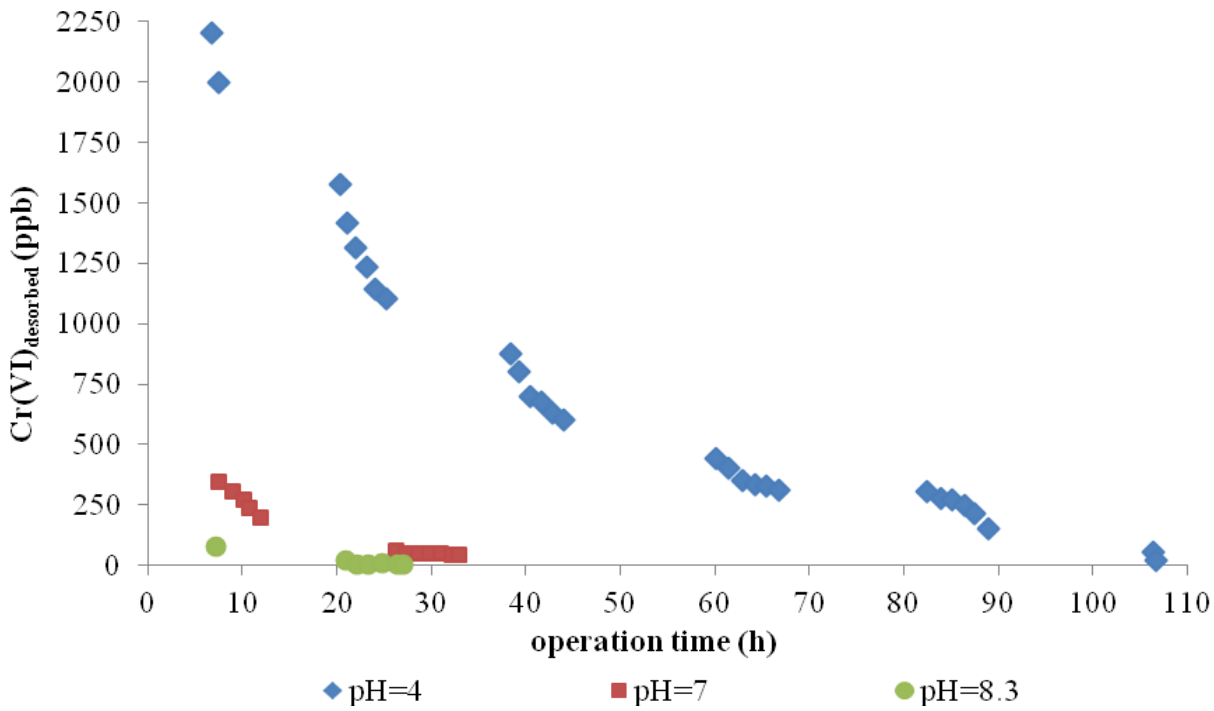


Figure 6. Cr(VI) desorption over operation time for the three tested pH values (contact time=1h, C_{MWCNTs}=40g/l)

4. CONCLUSIONS

The MWCNTs exhibited high adsorption capacity for Cr(VI). Depending on solution pH, MWCNTs concentration and contact time, Cr(VI) removal could even reach 100%. The pH estimated as a crucial factor on adsorption, since Cr(VI) was maximized for pH values lower than pHPZC and was sharply decreased for higher pH values. Increase in MWCNTs concentration led to higher removal percentage while the short contact time required for adsorption indicates that MWCNTs are effective adsorbents that can be used in practical applications. The crucial role of pH was also verified when performing column experiments, since MWCNTs with pH solution equal to 4 adsorbed almost 8 and 50 times higher amount of Cr(VI) than MWCNTs with pH equal to 7 and 8.3, respectively. Finally, desorption column experiments indicated that only a very small amount of the adsorbed Cr(VI) can be desorbed back to the aqueous solution. This phenomenon is possibly due to irreversible adsorption mechanisms or reduction of Cr(VI) to Cr(III). As a result, more investigation is necessary for the determination of the exact removal mechanism and the potential reusability of MWCNTs for water treatment applications.

AKNOWLEDGEMENTS

The authors gratefully acknowledge the company Glonatech SA (www.glonatech.com) for supplying the multi-walled carbon nanotubes.

References

1. Ai L., Zhang C., Liao F., Wang Y., Li M., Meng L. and Jiang J. (2011) ‘Removal of methylene blue from aqueous solution with magnetite loaded multi-wall carbon nanotube: Kinetic, isotherm and mechanism analysis’, **Journal of Hazardous Materials**, 198, pp. 282–290.

2. Borna M.O., Pirsaheb M., Niri M.V., Mashizie R.K., Kakavandi B., Zare M.R. and Asadi A. (2016) ‘Batch and column studies for the adsorption of chromium(VI) on low-cost Hibiscus Cannabinus kenaf, a green adsorbent’, **Journal of the Taiwan Institute of Chemical Engineers**, 68, pp. 80–89.

3. Dehghani M.H., Heibati B., Asadi A., Tyagi I., Agarwal S. and Gupta V.K. (2016) 'Reduction of noxious Cr(VI) ion to Cr(III) ion in aqueous solutions using H_2O_2 and UV/H_2O_2 systems.", **Journal of Industrial and Engineering Chemistry** ,33, pp. 197–200.
4. Dermatas D., Mpouras T., Chrysochoou M., Panagiotakis I., Vatseris C., Linardos N., Theologou E., Boboti N., Xenidis A., Papassiopi N. and Sakellariou L. (2015) 'Origin and concentration profile of chromium in a Greek aquifer', **Journal of Hazardous Materials**, 281, pp. 35-46.
5. Dermatas D., Panagiotakis I., Mpouras T. and Tettas K. (2016) 'The origin of Hevalent Chromium as a Critical Parameter for Remediation of Contaminated Aquifers', **Bulletin of Environmental Contamination and Toxicology**, 98, pp. 331–337.
6. Di Z.C., Li Y.H., Luan Z.K. and Liang J. (2004) 'Adsorption of Chromium(VI) Ions from Water by Carbon Nanotubes', **Adsorption Science & Technology**, 22, 6, pp. 467-474.
7. Gehrke I., Geiser A. and Somborn-Schulz A. (2015) 'Innovations in nanotechnology for water treatment', **Nanotechnology, Science and Applications**, 8, pp. 1–17.
8. Goel J., Kadirvelu K., Rajagopal C. and Garg V.K. (2005) 'Removal of lead(II) by adsorption using treated granular activatedcarbon: Batch and column studies', **Journal of Hazardous Materials**, B125, pp. 211–220.
9. Hu J., Wang S.W., Shao D.D., Dong Y.H., Li J.X. and. Wang X.K (2009) 'Adsorption and Reduction of Chromium(VI) from Aqueous Solution by Multiwalled Carbon Nanotubes', **The Open Environmental Pollution & Toxicology Journal**, 2, pp. 66-73.
10. Iijima S. (1991) 'Helical microtubules of graphitic carbon', **Nature**, 354, pp. 56-58.
11. Jung C., Heo J., Han J., Her N., Lee S.-J., Oh J., Ryu J. and Yoon Y. (2013) 'Hexavalent chromium removal by various adsorbents: Powered activated carbon, chitosan, and single/multi-walled carbon nanotubes', **Separation and Purification Technology**, 106, pp. 63-71.
12. Matlochová A., Plachá D. and Rapantová N. (2013) 'The Application of Nanoscale Materials in Groundwater Remediation', **Polish Journal of Environmental Studies**, 22, pp. 1401-1410.
13. Pourfadakari S., Yousefi N. and Mahvi A.H. (2016) "Removal of Reactive Red 198 from aqueous solution by combined method multi-walled carbon nanotubes and zero-valent iron: Equilibrium, kinetics, and thermodynamic", **Chinese Journal of Chemical Engineering**, 24, pp. 1448–1455.
14. Qureshi M.I., Patel F., Al-Baghli N., Abussaud B., Tawabini B.S. and Laoui T. (2017) 'A Comparative Study of Raw and Metal Oxide Impregnated Carbon Nanotubes for the Adsorption of Hexavalent Chromium from Aqueous Solution', **Bioinorganic Chemistry and Applications**, Article ID 1624243, 10 pages.
15. Saha R., Nandi R. and Saha B. (2011) 'Sources and toxicity of hexavalent chromium', **Journal of Coordination Chemistry**, 64, pp. 1782–1806.
16. Zeng Y., Woo H., Lee G. and Park J. (2010) 'Adsorption of Cr(VI) on hexadecylpyridinium bromide (HDPB) modified natural zeolites', **Microporous and Mesoporous Materials**, 130, pp. 83–91.
17. Zhang Y., Wu B., Xu H., Liu H., Wang M., He Y. and Pan B. (2016) 'Nanomaterials-enabled water and wastewater treatment', **Nano Impact**, 3–4, pp. 22–39.

THE USE OF NANOCRYSTALLINE TITANIUM DIOXIDE IN REMOVING HEAVY METALS FROM WATER: A HISTORICAL PERSPECTIVE OF SCIENTIFIC ADVANCEMENTS

G. P. Korfiatis*, X. Meng and Q. Shi

Center for Environmental Systems, Stevens Institute of Technology, Hoboken, New Jersey 07030, United States

*Corresponding author: e-mail: gkorfiat@stevens.edu, tel.: +12012165348

Abstract

In early 2000, a research group at Stevens Institute of Technology discovered that nanocrystalline TiO_2 (anatase) with a particle size of about 7 nm had very high adsorption capacity for arsenic, lead, and other heavy metals. When the particle size increased from 7 to 30 nm, the adsorption capacity decreased dramatically. A patent application was filed in 2002 and a U.S. patent was granted in 2005 for the invention. This patented nano-crystalline TiO_2 shows high performance for heavy metal removal in water and consists of anatase with crystalline diameter of 7 nm and specific surface area of 330 m^2/g. It exhibited much higher arsenic removal ability than other commercial TiO_2 materials (Degussa P25 and Hombikat UV100, 3.5-22.5 mg/g) (Dutta et al., 2004; Pena et al., 2005a), and was effective in removing other heavy metals such as lead, copper, uranium, mercury, chromium, and cadmium. This invention became the catalyst for systematic studies of the adsorption mechanisms of many heavy metals leading to significant increases in publications on the subject. Before 2003, most of researchers used commercial TiO_2 (Degussa P25) as photocatalyst for oxidation of organic compounds and very few researchers studied its adsorption properties. Degussa P25 is a mixture of anatase and rutile with a particle size of 30 nm and a specific surface area of 55 m^2/g, compared to a specific surface of 330 m^2/g for nanocrystalline TiO_2 (anatase, 7 nm). It has much lower adsorption capacity than nanocrystalline TiO_2. From 2003 to 2017, the annual publication rate on heavy metal removal by TiO_2 has increased from less than 10/yr to more than 90/yr while the annual rate of citations of the related papers have increased from 150/yr to about 1900/yr. A commercial entity was launched in 2005 to market the nanocrystalline TiO_2 product for treatment of arsenic and heavy metals in water. The annual sales of the adsorbent have reached $7M in 2017. This paper addresses the historical scientific developments of nanocrystalline TiO_2 that have taken place over the past 15 years and the impact these developments have had on water treatment.

Keywords: nanocrystalline TiO_2; heavy metal; arsenic; adsorption; oxidation; water treatment

1. INTRODUCTION

TiO_2 had been recognized as an effective photocatalyst for treatment of organic compounds for many years before it was used as adsorbent for heavy metal removal from water in the research around 2000. In 1998, studies regarding the Pb^{2+} and Cr(VI) adsorption ability of TiO_2 were reported (Hongxiang et al., 1998; Vohra and Davis, 1998). A material consisting of calcium oxalate-coated with TiO_2 layer was tested for Pb^{2+} and Hg^{2+} extraction from aqueous solutions (Fu et al., 1998). Lee and Choi (2002) reported oxidation of As(III) to As(V) in TiO_2 suspension.

In 2001, a research group at Stevens Institute of Technology synthesized the nano-crystalline TiO_2, which showed high performance for heavy metal (such as arsenic, lead, and selenium) removal in

water. This work led to a patent (Meng et al., 2005) and a 14 publications (Bang et al., 2005; Jing et al., 2005a; Jing et al., 2005b; Pena et al., 2005b; Pena et al., 2006; Wazne et al., 2006; Choy et al., 2008; Jing et al., 2008; Liu et al., 2008; Xu et al., 2008; Jing et al., 2009; Xu and Meng, 2009a; Bang et al., 2011; Guan et al., 2012). According to Google Scholar, those publications have been cited by other researchers in about 70 countries more than 1650 times. Our study regarding nanocrystalline TiO_2 and the historical perspective of scientific advancements after our work are reviewed in this paper.

2. DEVELOPMENT AND ADSOPRTION PROPERTIES OF THE NANOCRYSTALLINE TITANIUM DIOXIDE

The nanocrystalline TiO_2 was synthesized through hydrolysis of titanium solutions under controlled temperature (Meng et al., 2005). The transmission electron microcopy (TEM) image in Figure 1 shows the morphology and size of the primary TiO_2 particles. The X-ray diffraction (Figure 2) analysis determined that the precipitates were anatase and the average size of the primary crystalline particles was about 6.6 nm. The specific surface area of the material was 330 m^2/g. It showed significantly higher As(III) (37.5 mg/g) and As(V) (59.9 mg/g) removal ability than other commercial TiO_2 materials (Degussa P25 and Hombikat UV100, 3.5-22.5 mg/g) (Dutta et al., 2004; Pena et al., 2005a). The nanocrystalline TiO_2 could also be used for the removal of other heavy metals, such as lead, copper, uranium, mercury, cadmium, chromium, and arsenic (Meng et al., 2005). The mechanisms of arsenic adsorption by the nanocrystalline TiO_2 was investigated with electrophoretic mobility (EM) measurements, Fourier transform infrared (FTIR) spectroscopy, extended X-ray absorption fine structure (EXAFS) spectroscopy, and surface complexation modeling (Pena et al., 2006). Both As(V) and As(III) formed bidentate binuclear surface complexes with an average Ti-As(V) bond distance of 3.30 Å and Ti-As(III) bond distance of 3.35 Å.

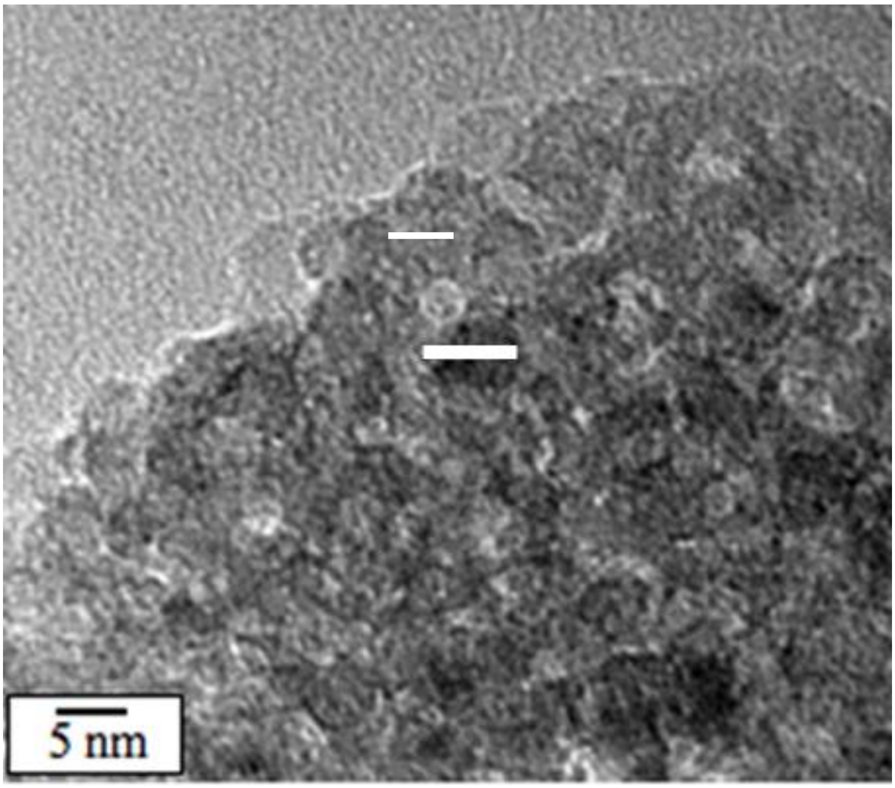


Figure 1. Transmission electron microscopy image of nanocrystalline TiO_2.

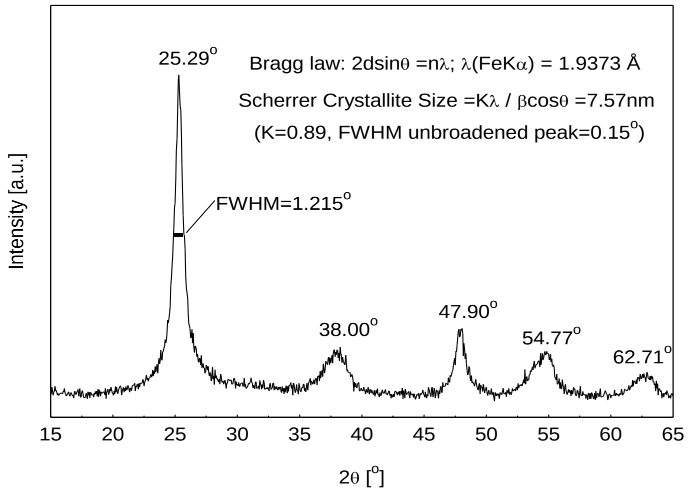


Figure 2. X-ray diffraction spectra of nanocrystalline TiO_2.

Further research was performed to study and effect of the nanocrystalline TiO_2 size on the adsorption properties (Xu and Meng, 2009b). The anatase TiO_2 samples with crystallite size of 7.0, 10.5, 14.8 and 30.1 nm were prepared by calcining the 6.6 nm TiO_2 at 200, 350, 500, and 700 °C for 3 h. The crystalline size the nano TiO_2 had significant effect on the As(III) and As(V) removal. With increasing size, the specific surface area, pore volume and surface –OH density decreased, and the average pore diameter increased. The As(III) and As(V) removal ability of TiO_2 decreased significantly with the increase of crystalline size (Figure 3). The amount of adsorbed As(V) decreased from 26.5 to 1.7 mg-As/g when the crystalline size of TiO_2 increased from 6.6 to 30.1 nm. The size effect was mainly attributed to the reduced specific surface area and surface –OH density.

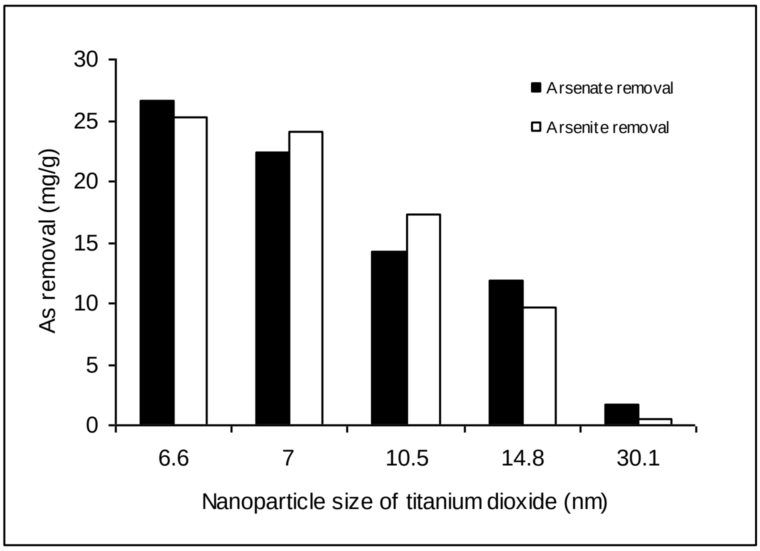


Figure 3. Size effects of nanocrystalline TiO_2 on As(V) and As(III) removal, 1g/L TiO_2 in tap water, 50 mg-As/L, mixed for 1 hour, pH=7.0 ± 0.1.

3. PROGRESS IN TITANIUM DIOXIDE RESEARCH

Since the Stevens group reported the effective removal of arsenic by nanocrystalline TiO_2 in early 2000s, many researchers have made significant progress, such as development of TiO_2 composite adsorbent, treatment of other heavy metals with TiO_2, and synthesis of TiO_2 with specific facets and high adsorption capacities.

3.1 Treatment of other heavy metals using TiO_2

The application of nanocrystalline TiO_2 was extended from arsenic and uranium to other heavy metal removal (Table 1). For example, Engates and and Shipley (2011) synthesized TiO_2 nanoparticles with the specific surface area of 185.5 m^2/g. They further compared the performance of heavy metal removal by nano and bulk TiO_2 (size of 329.8 nm, and surface area of 9.5 m^2/g). The results indicated much higher lead (Pb^{2+}, 83.1 mg/g), zinc (Zn^{2+}, 15.3 mg/g), and nickel (Ni^{2+}, 6.8 mg/g) removal by nano TiO_2 than bulk TiO_2 (64.7, 6.2, and 3.7 mg/g for Pb^{2+}, Zn^{2+}, and Ni^{2+}, respectively).

Moreover, a commercial nanostructured TiO_2 (10-15 nm) from was proved to be able to remove selenite (Se(IV) and selenite (Se(VI) effectively at pH 2-6 (Zhang et al., 2009). Zhao et al. (2009) synthesized nanohybrid WO_3/TiO_2 by a sol-gel method with titanium alkoxide and phosphotungstic acid ($H_3PW_{12}O_{40}$) as precursors. The WO_3/TiO_2 consists of WO_3 clusters on nano TiO_2 (15-20 nm) and performed well for silver (Ag^+) removal. Additionally, different nanocrystalline TiO_2 with a size range from 40-150 nm was synthesized and successfully used for antimony (Sb) removal (Song et al., 2017; Yan et al., 2017).

Table 1. Nanocrystalline TiO_2 used for other heavy metals removal.

Crystalline size of TiO_2 (nm)	Heavy metals	Published year	Reference
8.3	Ni^{2+}, Zn^{2+}	2011	(Engates and Shipley, 2011)
10-15	Se(IV), Se(VI)	2009	(Zhang et al., 2009)
40-150	Sb(VI) and Sb(III)	2017	(Song et al., 2017; Yan et al., 2017)
15-20	Ag^+	2009	(Zhao et al., 2009)

3.2 Nanocrystalline TiO_2 based composite adsorbents

After the good performance of TiO_2 for heavy metal removal was reported, numerous studies were reported regarding composite materials by doping nanocrystalline TiO_2 on other well-known adsorbents. Widely used composites are TiO_2-coated carbon-based materials, including graphene (Wang et al., 2017), graphene oxide (Lee and Yang, 2012), carbon nanotube (Doong and Chiang, 2008), and chitosan (Tao et al., 2009; Samadi et al., 2014). The synthesized composite materials showed good removal performance for Zn^{2+}, Cd^{2+}, Pb^{2+}, Hg^{2+}, Fe^{2+}, Cr(VI), As(V), and As(III). Moreover, TiO_2 was also composited with other metal oxides for heavy metal removal. Slag-iron oxide and WO_3 were synthesized in the presence of Ti(IV) solution, and tested for removal of Ag^+, Cr(VI), Hg^{2+}, and As(V) removal (Zhang and Itoh, 2006; Zhao et al., 2009).

Table 2. Composited adsorbents based on nanocrystalline TiO_2 for heavy metal removal

Adsorbents	Heavy metals	Published year	Reference
TiO_2-Fe_2O_3	As(III)	2006	(Zhang and Itoh, 2006)
TiO_2-carbon nanotube	Cu^{2+}	2008	(Doong and Chiang, 2008)
TiO_2-chitosan	Pb^{2+}	2009	(Tao et al., 2009)
TiO_2-WO_3	Cr(VI), Hg^{2+}, Ag^+	2009	(Zhao et al., 2009)
TiO_2-graphene oxide	Zn^{2+}, Cd^{2+}, Pb^{2+}	2012	(Lee and Yang, 2012)
TiO_2/Cu-chitosan	Pb^{2+}, Cr(VI)	2014	(Samadi et al., 2014)
TiO_2-graphene	Cr(VI)	2017	(Wang et al., 2017)

3.3 Effect of crystalline facets

As a nanostructured metal oxide with good crystalline quality, significant structural differences occurred on different crystalline facets of TiO_2, which obviously affects the heavy metal removal ability. The effects of crystalline facets on As(V) and As(III) removal were revealed by Yan et al. (in 2016). The {001} facets on TiO_2 showed higher performance for As(V) and As(III) removal than {101} surfaces. Moreover, the crystal facets also determine the adsorption of Sb(III) on nanocrystalline TiO_2 (Song et al., 2017; Yan et al., 2017). Nanocrystalline TiO_2 with a high index crystalline facet of {201} showed better Sb(III) removal than that with a crystalline facet (e.g. {001} and {101}), although the former had a lower surface area. This difference was attributed to the higher surface energy (γ = 1.72 J m^{-2}) of {201} facets calculated by density functional theory (DFT).

4. CONCLUSIONS

A historical progress in the development of TiO_2-based adsorbents for treatment of heavy metals is summarized in Figures 4 and 5. After the discovery of high adsorption property of nanocrystalline TiO_2 with crystalline size within a range of about 1 – 30 nm, the application of TiO_2 has expanded from photo-catalysis to adsorption of heavy metals. Various TiO_2-based composite adsorbents and TiO_2 with specific crystalline facets have been developed.

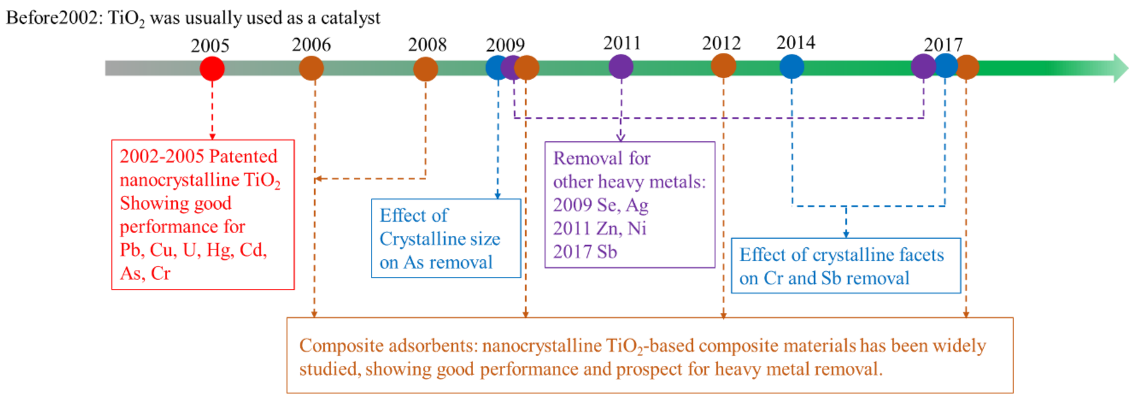


Figure 4. Progress of heavy metal removal by nanocrystalline TiO_2.

Figure 5 shows that the number of papers on heavy metal removal by TiO_2 has increased exponentially from a few per year before 2003 to about 90 per year after 2014. Meanwhile the citation of related publications has increased from less than 150 per year before 2003 to about 1900 per year since 2016.

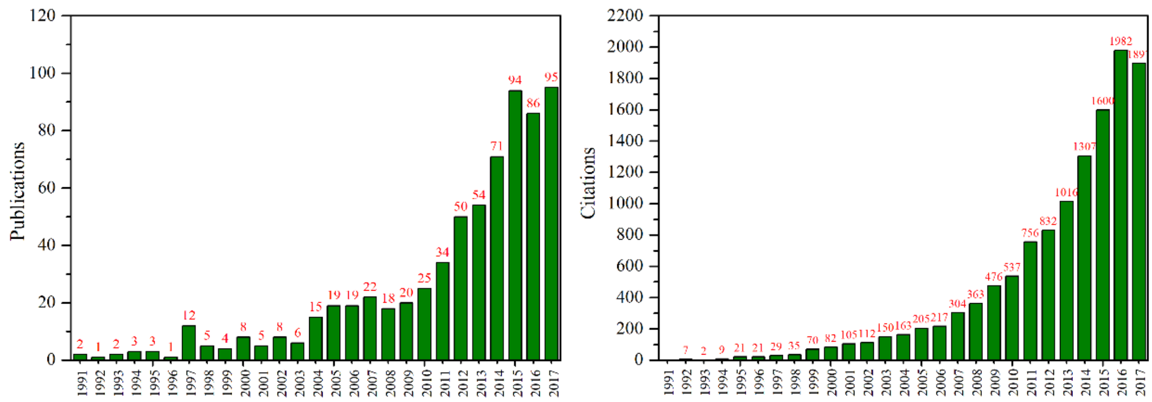


Figure 5. The number of publications (left) and citations (right) on heavy metal removal using TiO_2 from 1991 to 2017, through the Web of Science™ Core Collection. The keywords for searching are “heavy metal” and “TiO_2.”

References

1. Dutta, P.K., Ray, A.K., Sharma, V.K., Millero, F.J. (2004) 'Adsorption of arsenate and arsenite on titanium dioxide suspensions', **Journal of Colloid and Interface Science** Vol 278(2), pp. 270-275.
2. Pena, M.E., Korfiatis, G.P., Patel, M., Lippincott, L., Meng, X.G. (2005a) 'Adsorption of As(V) and As(III) by nanocrystalline titanium dioxide', **Water Research** Vol 39(11), pp. 2327-2337.
3. Hongxiang, F., Gongxuan, L., Shuben, L. (1998) 'Adsorption of Chromium(VI) Ions on to TiO2 from Aqueous Solution', **Adsorption Science & Technology** Vol 16(2), pp. 117-126.
4. Vohra, M.S., Davis, A.P. (1998) 'Adsorption of Pb(II), EDTA, and Pb(II)-EDTA onto TiO2', **Journal of Colloid and Interface Science** Vol 198(1), pp. 18-26.
5. Fu, H.X., Lu, G.X., Li, S.B. (1998) 'Adsorption of chromium(VI) ions on to TiO2 from aqueous solution', **Adsorption Science & Technology** Vol 16(2), pp. 117-126.
6. Lee, H., Choi, W. (2002) 'Photocatalytic Oxidation of Arsenite in TiO2 Suspension: Kinetics and Mechanisms', **Environmental Science & Technology** Vol 36(17), pp. 3872-3878.
7. Meng, X., Dadachov, M., Korfiatis, G.P., Christodoulatos, C. (2005) Methods of preparing a surface-activated titanium oxide product and of using same in water treatment processes. US Patent: 6,919,029.
8. Bang, S., Patel, M., Lippincott, L., Meng, X. (2005) 'Removal of arsenic from groundwater by granular titanium dioxide adsorbent', **Chemosphere** Vol 60(3), pp. 389-397.
9. Jing, C., Liu, S., Patel, M., Meng, X. (2005a) 'Arsenic leachability in water treatment adsorbents', **Environmental science & technology** Vol 39(14), pp. 5481-5487.
10. Jing, C., Meng, X., Liu, S., Baidas, S., Patraju, R., Christodoulatos, C., Korfiatis, G.P. (2005b) 'Surface complexation of organic arsenic on nanocrystalline titanium oxide', **Journal of Colloid and Interface Science** Vol 290(1), pp. 14-21.
11. Pena, M.E., Korfiatis, G.P., Patel, M., Lippincott, L., Meng, X. (2005b) 'Adsorption of As (V) and As (III) by nanocrystalline titanium dioxide', **Water Research** Vol 39(11), pp. 2327-2337.
12. Pena, M., Meng, X., Korfiatis, G.P., Jing, C. (2006) 'Adsorption mechanism of arsenic on nanocrystalline titanium dioxide', **Environmental Science & Technology** Vol 40(4), pp. 1257-1262.
13. Wazne, M., Meng, X., Korfiatis, G.P., Christodoulatos, C. (2006) 'Carbonate effects on hexavalent uranium removal from water by nanocrystalline titanium dioxide', **Journal of Hazardous Materials** Vol 136(1), pp. 47-52.
14. Choy, C.C., Wazne, M., Meng, X. (2008) 'Application of an empirical transport model to simulate retention of nanocrystalline titanium dioxide in sand columns', **Chemosphere** Vol 71(9), pp. 1794-1801.
15. Jing, C., Liu, S., Meng, X. (2008) 'Arsenic remobilization in water treatment adsorbents under reducing conditions: Part I. Incubation study', **Science of the Total Environment** Vol 389(1), pp. 188-194.
16. Liu, S., Jing, C., Meng, X. (2008) 'Arsenic re-mobilization in water treatment adsorbents under reducing conditions: Part II. XAS and modeling study', **Science of the Total Environment** Vol 392(1), pp. 137-144.
17. Xu, Z., Jing, C., Li, F., Meng, X. (2008) 'Mechanisms of photocatalytical degradation of monomethylarsonic and dimethylarsinic acids using nanocrystalline titanium dioxide', **Environmental Science & Technology** Vol 42(7), pp. 2349-2354.

18. Jing, C., Meng, X., Calvache, E., Jiang, G. (2009) 'Remediation of organic and inorganic arsenic contaminated groundwater using a nanocrystalline TiO 2-based adsorbent', **Environmental Pollution** Vol 157(8), pp. 2514-2519.

19. Xu, Z., Meng, X. (2009a) 'Size effects of nanocrystalline TiO 2 on As (V) and As (III) adsorption and As (III) photooxidation', **Journal of Hazardous Materials** Vol 168(2), pp. 747-752.

20. Bang, S., Pena, M.E., Patel, M., Lippincott, L., Meng, X., Kim, K.-W. (2011) 'Removal of arsenate from water by adsorbents: a comparative case study', **Environmental Geochemistry and Health** Vol 33(1), pp. 133-141.

21. Guan, X., Du, J., Meng, X., Sun, Y., Sun, B., Hu, Q. (2012) 'Application of titanium dioxide in arsenic removal from water: a review', **Journal of Hazardous Materials** Vol 215(pp. 1-16.

22. Xu, Z., Meng, X. (2009b) 'Size effects of nanocrystalline TiO2 on As(V) and As(III) adsorption and As(III) photooxidation', **Journal of Hazardous Materials** Vol 168(2), pp. 747-752.

23. Engates, K.E., Shipley, H.J. (2011) 'Adsorption of Pb, Cd, Cu, Zn, and Ni to titanium dioxide nanoparticles: effect of particle size, solid concentration, and exhaustion', **Environmental Science and Pollution Research** Vol 18(3), pp. 386-395.

24. Zhang, L., Liu, N., Yang, L., Lin, Q. (2009) 'Sorption behavior of nano-TiO2 for the removal of selenium ions from aqueous solution', **Journal of Hazardous Materials** Vol 170(2), pp. 1197-1203.

25. Zhao, D., Chen, C., Yu, C., Ma, W., Zhao, J. (2009) 'Photoinduced Electron Storage in WO3/TiO2 Nanohybrid Material in the Presence of Oxygen and Postirradiated Reduction of Heavy Metal Ions', **The Journal of Physical Chemistry C** Vol 113(30), pp. 13160-13165.

26. Song, J., Yan, L., Duan, J., Jing, C. (2017) 'TiO2 crystal facet-dependent antimony adsorption and photocatalytic oxidation', **Journal of Colloid and Interface Science** Vol 496(Supplement C), pp. 522-530.

27. Yan, L., Song, J., Chan, T., Jing, C. (2017) 'Insights into Antimony Adsorption on {001} TiO2: XAFS and DFT Study', **Environmental Science & Technology** Vol 51(11), pp. 6335-6341.

28. Wang, W.L., Wang, Z.F., Liu, J.J., Zhang, Z.G., Sun, L.Y. (2017) 'Single-step One-pot Synthesis of Graphene Foam/TiO2 Nanosheet Hybrids for Effective Water Treatment', **Scientific Reports** Vol 7, pp. 8.

29. Lee, Y.-C., Yang, J.-W. (2012) 'Self-assembled flower-like TiO2 on exfoliated graphite oxide for heavy metal removal', **Journal of Industrial and Engineering Chemistry** Vol 18(3), pp. 1178-1185.

30. Doong, R.-A., Chiang, L.-F. (2008) 'Coupled removal of organic compounds and heavy metals by titanate/carbon nanotube composites', **Water Science and Technology** Vol 58(10), pp. 1985-1992.

31. Tao, Y., Ye, L., Pan, J., Wang, Y., Tang, B. (2009) 'Removal of Pb(II) from aqueous solution on chitosan/TiO2 hybrid film', **Journal of Hazardous Materials** Vol 161(2), pp. 718-722.

32. Samadi, S., Khalilian, F., Tabatabaee, A. (2014) 'Synthesis, characterization and application of Cu–TiO2/chitosan nanocomposite thin film for the removal of some heavy metals from aquatic media', **Journal of Nanostructure in Chemistry** Vol 4(1), pp. 84.

33. Zhang, F.-S., Itoh, H. (2006) 'Photocatalytic oxidation and removal of arsenite from water using slag-iron oxide-TiO2 adsorbent', **Chemosphere** Vol 65(1), pp. 125-131.

34. Yan, L., Du, J., Jing, C. (2016) 'How TiO2 facets determine arsenic adsorption and photooxidation: spectroscopic and DFT studies', **Catalysis Science & Technology** Vol 6(7), pp. 2419-2426.

DEGRADATION OF 2,4-DINITROANISOLE (DNAN) IN AQUEOUS SOLUTIONS BY MG-BASED BIMETALS

A. Mai[1], P. Karanam[2], E. Hadnagy[2], S. Menacherry[3], W. Braida[1], C. Christodoulatos[1], A. Koutsospyros[2*], T. S. Su[1]

[1]Center for Environmental Systems, Stevens Institute of Technology,Hoboken, NJ 07030, USA
[2]Department of Civil and Environmental Engineering, University of New Haven
[3]Department of Chemistry and Chemical Engineering, University of New Haven, West Haven, CT 06516, USA

[*]Corresponding author: e-mail: akoutsospyros@newhaven.edu, tel : +012039327398

Abstract
The industrial production of munition 2,4-dinitroanisole (DNAN) generates waste streams that require treatment. Treatment of DNAN has been attempted previously using zero-valent iron (ZVI) and Fe-based bimetals. Use of Mg-based bimetals maybe advantageous to Fe in terms of potential higher reactivity and relative insensitivity to pH conditions. This work reports results on the degradation of DNAN by three Mg-based bimetals: Mg/Cu, Mg/Ni, and Mg/Zn. Kinetic data obtained in benchtop-scale batch reactors were modelled according to a pseudo-first-order expression. Parametric studies were conducted to assess the effect of type of bimetal pair and initial pH on DNAN degradation. Pseudo-first order kinetic constants were 0.119, 0.102, 0.018, and 0.009 min^{-1} for Mg/Cu, Mg/Zn, Mg/Ni, and ZVMg, respectively (unadjusted initial pH, 0.5% S/L, 10:1 Mg: catalytic metal). Initial acidification with acetic acid (pH range 3.3-4.0) improved significantly the reaction rate by all of the attempted bimetal formulations and ZVMg producing DNAN degradation half-lives in the range of 0.9-1.4 minutes. Constant temperature experiments at 20, 26, 32, 36 and 45^{0}C, using the most effective bimetal pair under normal pH conditions (Mg/Cu), were conducted under identical conditions of solids loading (0.5% S/L) and base to secondary metal ratio (10:1). The activation energy for the reductive degradation of DNAN by Mg/Cu bimetal was determined to be 8.18 kJ/mol.

Keywords: 2,4-dinitroanisole, DNAN, insensitive munition, magnesium bimetal, reductive degradation

1. INTRODUCTION

The search for safer explosives that reduce the risk of accidental detonation has led to development of new energetic compounds. The nitro-aromatic compound DNAN is an explosive of decreased sensitivity often incorporated into various munitions formulations. The production of DNAN generates contaminated wastewater streams that, if untreated, may pose environmental risk [Olivares *et al.*, 2016]. Several researchers currently work on elucidating the fate and transport of DNAN and its transformed products [Olivares *et al.*, 2016; Hawari *et al.*, 2015; Taylor *et al.*, 2017; Arthur *et al.*, 2017], however, more work is needed for complete characterization. Meanwhile, various treatment methods have been tested for the removal and/or degradation of DNAN.

Known treatment methods of DNAN include biotic (using various strains of bacteria) and abiotic (photochemical degradation, chemical oxidation/reduction) technologies. One type of abiotic process involves treatment using zero-valent metals (e.g. zero-valent iron, ZVI) or bimetal combinations

(typically iron- or magnesium-based) to degrade DNAN via a reductive pathway. ZVI and iron-based bimetals have been most commonly used for the degradation of DNAN [Liu *et al.*, 2015; Ahn *et al.*, 2011; Shen *et al.*, 2013; Koutsospyros *et al.*, 2012; Kitcher *et al.*, 2017]. However, recent advances in bimetal technology indicate that magnesium-based bimetals can successfully degrade various types of organic [Ghauch & Tuqan, 2009; DeVor *et al.*, 2008] and inorganic [Ramavandi *et al.*, 2011] contaminants and offer a promising more effective alternative to Fe-based treatment [Morales *et al.*, 2002].

Previously, treatment of DNAN by Fe-based bimetals have been studied [Koutsospyros *et al.*, 2012; Kitcher *et al.*, 2017]. Koutsopyros *et al.* (2012) used Fe/Cu to remove DNAN and other explosive and energetic compounds from industrial pinkwater and reported short treatment times in the span of minutes. Kitcher *et al.* (2017) treated DNAN both in insensitive munition explosive (IMX) wastewater and pure solutions with Fe/Cu bimetal under acidic pH conditions (2.3-2.9). The major variables studied in Kitcher's work included: matrix effects, activation energy, effect of pH and acid type, impact of solid vs. dissolved base metal (i.e. Fe), and impact of type of bimetal contact (i.e. physical mixture of Fe^0/Cu^0 vs. Cu-coated Fe^0). Both of these studies investigated DNAN removal in acidic media (i.e. pH <3) since Fe-based bimetals have been shown to be the most effective in degrading organic contaminants at acidic pH levels [Khalil *et al.*, 2016; Rivero-Huguet & Marshall, 2009; Tian *et al.*, 2009]. Mg-based bimetals, on the other hand, may be less sensitive to pH conditions [Patel & Suresh, 2008], thus providing a potential alternative for DNAN treatment for situations when additional pH adjustment in the treatment system is undesired. The treatment of DNAN with Mg-based bimetals has not yet been researched, nor have subsequent parametric studies been established.

In the present work, parametric studies were conducted to investigate the reaction kinetics of DNAN degradation by various Mg-based bimetals. This work reports on the impact of secondary metal type (namely Cu, Ni, and Zn), initial pH adjustment, and temperature.

2. MATERIALS AND METHODS

2.1 Chemicals and materials

Solid magnesium particles (20-230 mesh, reagent grade, 98% purity), copper (II) chloride (99%), nickel (II) chloride (98% purity), zinc chloride (98% purity) and glacial acetic acid (99 %+) were all purchased from Sigma Aldrich (St. Louis, MO). Syringe filters (0.45 micron, nylon) were purchased from Achemtek (Worcester, MA). DNAN solids and DNAN standard dissolved in acetonitrile were obtained from an industrial munitions facility. Catalytic metal chloride solutions (i.e. $CuCl_2$, $ZnCl_2$, $NiCl_2$) were prepared in DI water such that addition of a fixed volume, i.e. 1 mL, to the reactor delivered a 10:1 ratio of Mg base metal to secondary metal (i.e. Ni, Cu, or Zn).

2.2 Kinetic experiments

All batch experiments were carried out in 40 mL Volatile Organic Analyte (VOA) vials containing 24 mL reaction solution with 0.5 % solids-to-liquids (S/L) ratio and 10:1 Mg to secondary metal (i.e. Cu, Ni, and Zn) ratio in both the absence and presence of 4.35 N acetic acid. First, 0.12 g of Mg granules was placed in the reactor vial and 12 mL of water was added and mixed fully. Next, to synthesize the bimetal reagent, 1 mL of the catalytic metal solution was added and mixed for 5 minutes. The reaction was initiated by adding 10 mL of DNAN solution of 250 ppm. In the unadjusted initial pH experiments, 1 mL of water was added and in the lowered initial pH experiments, 1 mL of 4.35N acetic acid was added to the reaction mixture. Experiments were conducted in duplicate. Venting was provided for the hydrogen gas generated by capping the reactor with punctured aluminum foil. The initial and the final pH of the solution were measured. At the end of the reaction, an aliquot of the reaction solution was taken using a 0.45 μm nylon syringe filter and subsequently samples were stored in amber glass vials.

Sacrificial sampling was used to determine the rates and extent of degradation of DNAN, as opposed to semi-continuous sampling from one large batch reactor. Separate identical batch reactors were

prepared and were removed for sampling at the prescribed times of 5, 10, 15, 30, 60, 90, 120 and 150 minutes.

2.3 Temperature controlled experiments

Degradation of DNAN by Mg/Cu was tested at different temperatures (i.e. 20°C, 26°C, 32°C, 36°C and 45°C) to evaluate the impact of temperature and to determine the activation energy of the reaction. The experimental conditions were the same as in previous experiments, i.e. 0.5% S/L ratio and 10:1 base metal to catalyst ratio. The initial pH was not adjusted. A temperature control chamber was used to maintain constant temperature during the reaction. The reaction solution was equilibrated to the specified temperature prior to the start of the reaction. The temperature was measured using a thermometer placed in water to remove bias from the digital controller of the constant temperature chamber. Samples were taken at 5, 10, 15, 20, and 30 minutes. All experiments were conducted in duplicate.

2.4 Analytical methods

DNAN concentrations were analyzed by reversed-phase high pressure liquid chromatography (HPLC) on an Agilent 1260 instrument (Santa Clara, CA) equipped with a Grace Alltech Adsorbosphere HS C-18 (5μm, 150x4.6mm) and a DAD detector. The mobile phase was an isocratic mixture of methanol: water at 70:30 (v/v), pumped at 1 mL/min; the injection volume was 10 μL of sample; the analytical wavelength was 254 nm. At these conditions, DNAN eluted at 4.1 min. Blank samples and known concentration standards were periodically run for QA/QC purposes.

3. RESULTS AND DISCUSSION

In this work, the impacts of catalytic metal type, initial pH, and temperature on DNAN degradation by Mg-based bimetals are reported.

3.1 Influence of the catalytic metal

The kinetics of DNAN degradation in aqueous solutions was investigated using three bimetallic systems, namely Mg/Cu, Mg/Ni and Mg/Zn, and treatment effectiveness was compared to that with zero-valent magnesium (ZVMg) without the addition of a catalytic metal. Kinetic experiments were conducted to establish time-concentration profiles and a pseudo-first-order reaction rate constant, k was determined by fitting and exponential decay model via nonlinear regression.

Time-concentration profiles for ZVMg and the three bimetallic systems (i.e. Mg/Cu, Mg/Ni, Mg/Zn), shown in Figure 1, indicate a fast DNAN degradation reaction for the first 30 minutes, which tends to taper off thereafter. DNAN degradation by ZVMg alone (i.e. without a catalytic metal), was the least effective with 34% DNAN removal in 150 minutes (Figure 1a). On the other hand, treatment with Mg/Cu removed 99% of DNAN in 30 minutes (Figure 1b), while 99% removal by Mg/Zn was achieved after 120 minutes (Figure 1d). Treatment with Mg/Ni was slower with 93% of DNAN degradation in 150 minutes (Figure 1c). These results proved that the presence of a catalytic metal increased both the rate and the extent of DNAN degradation. In addition, the extent to which DNAN removal efficiency was improved depended on the catalyst type, generally Cu being the most effective, followed by Zn, and then by Ni.

The pH of each bimetal system was initially in the neutral range of 6.8-7.8 and increased to a final pH of 9.7-10.3 (Figure 1). Conversely, for ZVMg treatment, the system pH was generally slightly higher with an initial pH of 11.4 and final pH of 10.9. The initial pH (measured at time 0) was determined immediately after the addition of the DNAN solution to the synthesized bimetal.

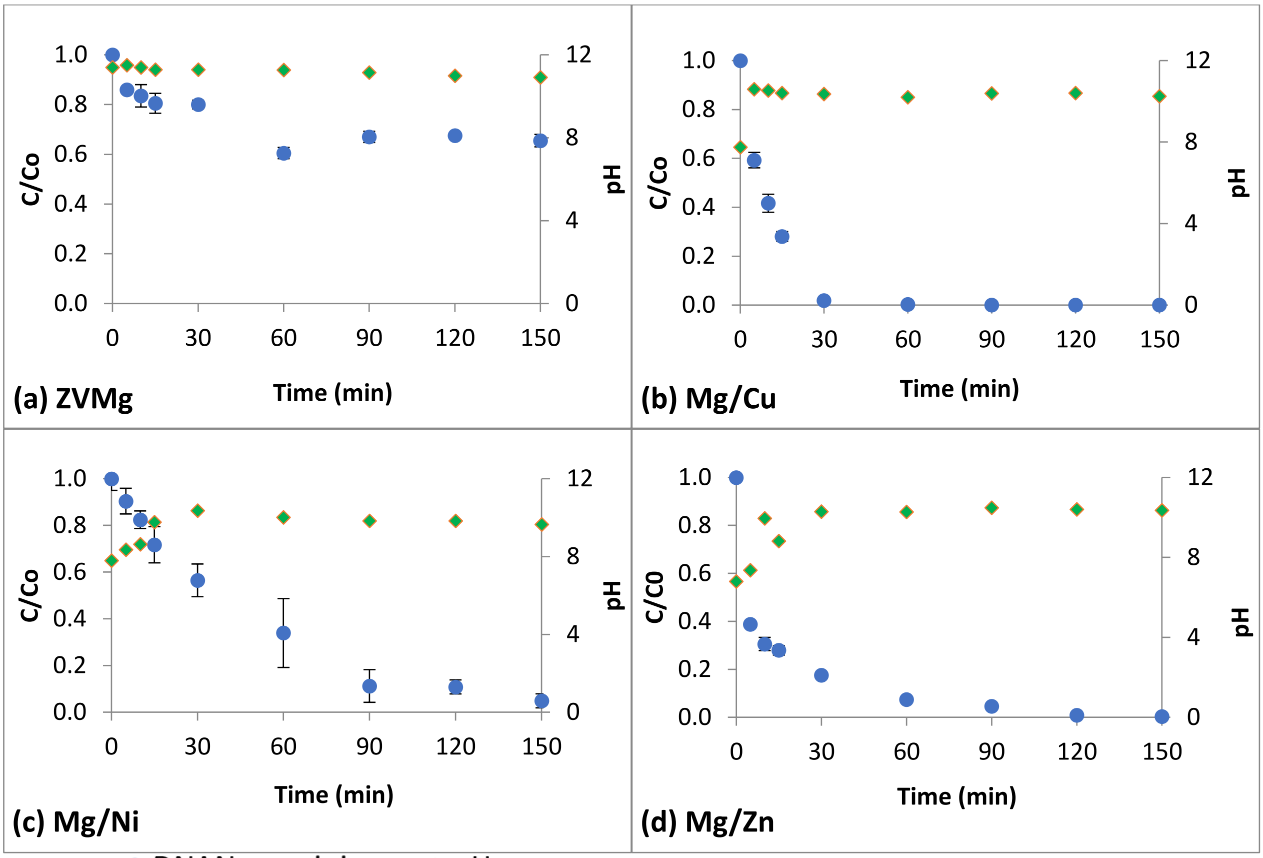


Figure 1: DNAN degradation and pH over time by: (a) zero-valent magnesium (ZVMg), (b) Mg/Cu, (c) Mg/Ni, and (d) Mg/Zn (0.5% S/L, 10:1 Mg to catalyst ratio)

The time-concentration profiles were used for the determination of reaction rate constants. The reaction was evaluated by applying a pseudo-first-order kinetic expression (Equation 1) to the initial nonlinear portion of the C/C_0 vs. time (t, min) curve and the reaction rate constants were determined by nonlinear regression analysis:

$$\frac{C}{C_0} = exp(-kt) \quad (1)$$

Where: C = Contaminant concentration at time t (mg/L)

C_o = Initial contaminant concentration (mg/L)

k = Pseudo-first-order reaction rate constant (min^{-1})

t = Reaction time (min)

DNAN degradation was the slowest using ZVMg with a reaction rate constant of 0.009 min^{-1} (Table 1). The fastest reaction rate constant (0.119 min^{-1}) was achieved with Mg/Cu and was 13.6 times faster than that of ZVMg. Treatment by Mg/Ni and Mg/Zn gave reaction rate constants of 0.018 and 0.102 min^{-1} (5 and 10 times faster than ZVMg), respectively. Half-lives were determined from Equation 1 for the C/C_0 = 0.5 and the determined reaction rate constants. The determined half-lives for the three bimetal formulations are in the range 5.8-37.7 minutes and are much shorter than the half-life of ZVMg which is longer than 1 hour.

Table 1: Reaction rate constants of DNAN degradation

Treatment System	k (min^{-1})	R^2	k/k_{ZVMg}*	Half-Life, min
ZVMg	0.009	0.781	1	78.8
Mg/Cu	0.119	0.946	13.6	5.8
Mg/Ni	0.018	0.995	2.1	37.7
Mg/Zn	0.102	0.726	11.6	6.8

*Reaction rate constants are normalized with respect to ZVMg

3.2 Influence of lowered initial pH

DNAN degradation kinetic experiments using low initial pH conditions were also performed and results of these experiments were compared to the initial unadjusted pH runs. The initial pH of the reaction solution was lowered by addition of 4.35N acetic acid. The experimental conditions were kept the same as in the unadjusted pH experiments at 0.5% S/L ratio and 10:1 base metal to catalyst ratio. The lowered adjusted initial pH for all treatment systems was between 3.3 and 4.0. No subsequent pH adjustments were made and the reaction pH was measured at each sampling time. In a low pH medium, any oxidized layer of the metal surface is dissolved, typically resulting in increased reactivity of the bimetal surface [Liu *et al.*, 2015; Guan *et al.*, 2015].

ZVMg alone removed 98% of DNAN in just 10 minutes under acidic conditions, showing excellent treatment efficiencies superior to those obtained in the unadjusted pH runs (Figure 3). In addition, treatment with ZVMg at the lowered initial pH resulted in at least 5 times faster DNAN degradation than treatment without pH adjustment by any bimetal system. Mg/Zn effectively removed 99% of DNAN in 10 minutes and exhibited the fastest reaction kinetics compared to ZVMg and the other two bimetals (i.e. Mg/Cu and Mg/Ni, Figure 4d). Treatment with Mg/Cu and Mg/Ni exhibited slightly slower reaction kinetics with 93% DNAN removal within 10 min (Figure 4b, 4c).

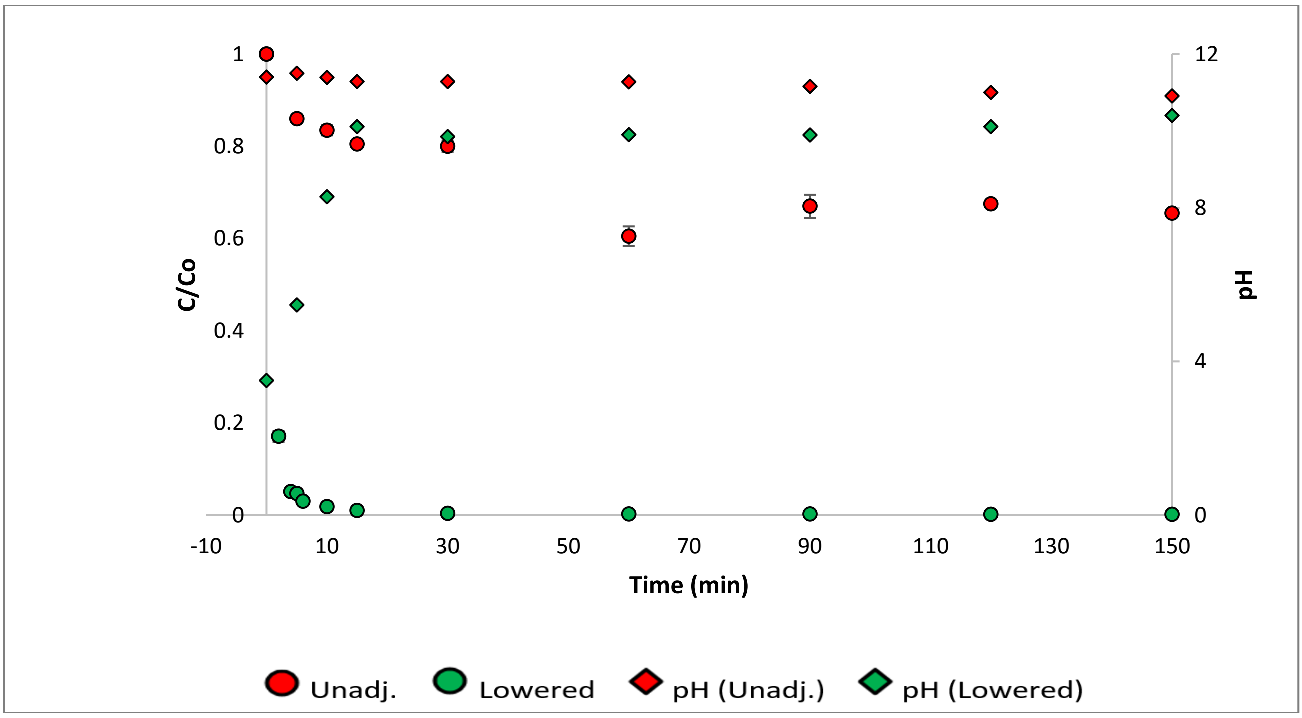


Figure 2: Comparison of DNAN degradation kinetics and pH for unadjusted and lowered initial pH conditions in the ZVMg treatment system

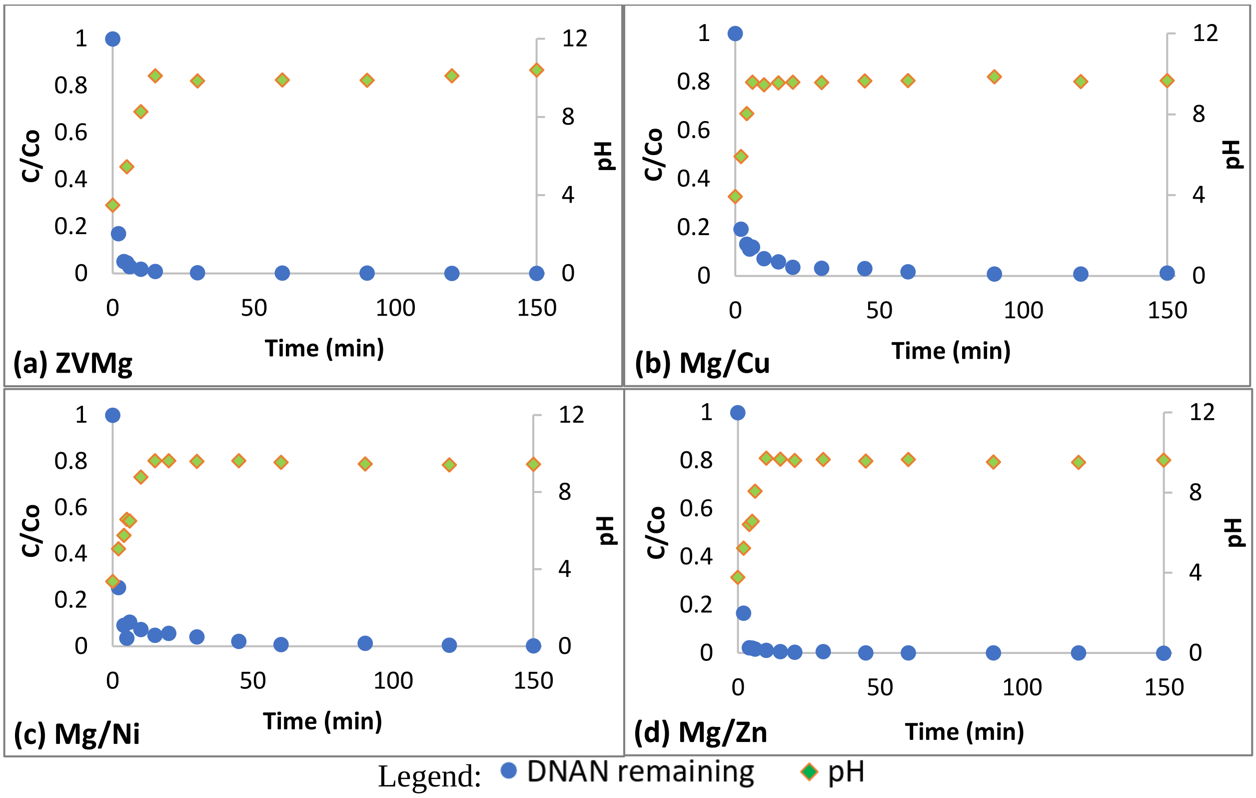


Figure 3: DNAN removal and pH over time with lowered initial pH: (a) ZVMg, (b) Mg/Cu, (c) Mg/Ni, and (d) Mg/Zn (0.5% S/L, 10:1 Mg to catalyst ratio)

Despite differences in degradation rates, all treatment systems exhibited ultimately the same DNAN removal efficiency of over 99.7% in 150 min. Furthermore, pH measurements showed that within 30 min, the pH equilibrated to approximately 9.6 where it remained for the rest of the reaction for all systems. For ZVMg, the pH equilibrated slightly higher at approximately 10.

A visual examination of the concentration-time curves reveals a rapid reaction period within the first 10 min producing near zero values thereafter. This behavior is consistent with reported literature [Rivero-Huguet and Marshall, 2009] for other bimetal systems. Accordingly, the rapid target compound depletion is dominated by the reduction reaction whereas passivation phenomena control the final period. Viewed under this prism, the pseudo-first order model describes adequately the initial reaction period but falls short of producing a good fit for the final period data. Thus, kinetic constants reported herein, are obtained using the initial slope method for reaction times of 2,4,5,6, and 10 min. The nonlinear regression analysis produced fair to very good quality curve fitting with correlation coefficients (R^2 values) in the range of 0.765-0.934 (Table 2). Data variability is attributed to challenges associated with sampling and quenching a rapid heterogeneous reaction rather than to model inadequacies. The reported values of the determined pseudo-first order constants vary within the same order of magnitude (0.5 - 0.8 min^{-1}), show a much smaller variability than the unadjusted respective values, and mark comparable treatment effectiveness for all ZVMg and bimetal systems (DNAN half-lives 0.9-1.4 min).

In comparison to the bimetal systems, ZVMg was affected drastically by the lowered pH, showing a 73-fold increase of the rate constant. Mg/Ni and Mg/Zn were fairly affected by the lowered pH showing increases of *k* by 29 and 8-fold, whereas Mg/Cu was less affected with an increase of *k* by 4-fold. Interestingly, although the DNAN degradation performance of Mg/Cu was superior to the other bimetals (Mg/Zn and Mg/Ni) in the unadjusted initial pH experiments, this was reversed when the initial pH was lowered. This performance reversal may be associated to reaction mechanisms elicited by the lowered pH. Under lowered initial pH, corrosion of the bimetal (and thus the subsequent production of electrons) as well as dissolution of passivating oxide layers may be dominant. Conversely, under normal initial pH conditions, electron release may be dominated by the

galvanic potential of the bimetal pair. Thus, corrosion and dissolution appear to dominate DNAN degradation rates for all systems (ZVMg, bimetals) for lowered initial pH, while the galvanic potential difference (highest for Mg/Cu) controls the unadjusted pH conditions. Further work is required to test and validate this hypothesis.

Table 2: Reaction rate constants (k) with lowered initial pH

Treatment System	k (min^{-1})	R^2	$k_{adj\ pH}$/ $k_{unadj\ pH}$	Half-Life, min
ZVMg	0.641	0.934	72.8	1.1
Mg/Cu	0.497	0.831	4.2	1.4
Mg/Ni	0.525	0.765	29.2	1.3
Mg/Zn	0.776	0.930	7.6	0.9

3.3 Impact of temperature and activation energy

The impact of temperature on DNAN degradation kinetics was evaluated for the most effective bimetal pair (Mg/Cu) under normal pH conditions, at temperature values of 20^{0}C, 26^{0}C, 32^{0}C, 36^{0}C and 45^{0}C. The experimental conditions were the same as in previous tests, i.e. 0.5% S/L ratio and 10:1 base metal to catalyst ratio with unadjusted initial pH. As expected, as the temperature increased, reaction rates also increased. The activation energy (E_a) of the reaction was determined by the Arrhenius equation (Equation 2, Arrhenius S.A., 1889):

$$k = A * exp\left(-\frac{E_a}{RT}\right) \quad (2)$$

Where: E_a = Activation energy (kJ/mol)

k = Reaction rate constant (s^{-1})

A = Pre-exponential Factor (s^{-1})

T = Temperature (^{0}K)

R = Universal gas constant (8.31×10^{-3} kJ/mol·K)

The slope of the fitted line is obtained by regression analysis of the linearized form of Equation 2:

$$lnk = lnA - \frac{E_a}{RT} \quad (3)$$

The activation energy for DNAN degradation by Mg/Cu was determined to be 8.18 kJ/mol (Figure 4). For DNAN degradation by Fe/Cu bimetallic systems, the activation energies were reported as 121.8 kJ/mol and 30.57 kJ/mol in Koutsospyros et al. (2012) and Kitcher et al. (2017), respectively. However, several differences must be noted between those and the present study including the type of bimetal pair (Fe/Cu vs. Mg/Cu), preparation of the bimetal matrices (contacted primary and catalytic metal surfaces vs. primary metal coated with the catalytic metal) as well initial pH of the reaction (acidified at pH 3.0 vs. normal unadjusted pH).

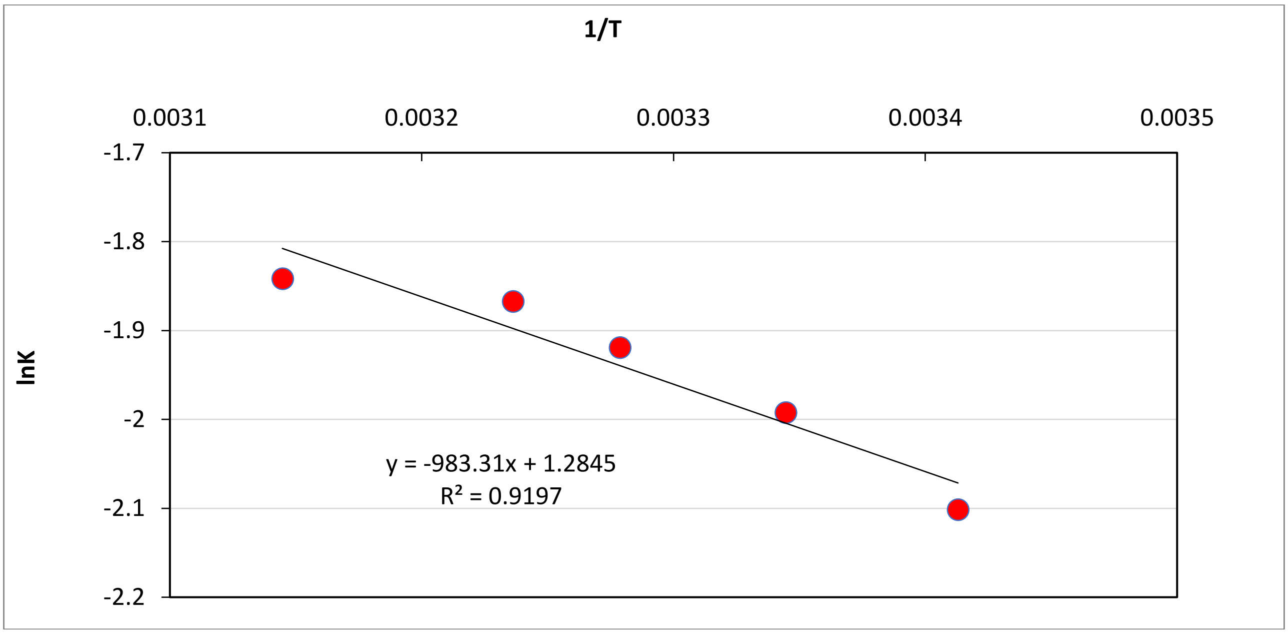


Figure 4: Natural logarithm of the degradation rate constant plotted as a function of inverse temperature for DNAN removal using Mg/Cu (0.5% S/L, 10:1 Mg to catalyst ratio)

This indicates that the Mg/Cu technology is a potentially more viable option, since generally a lower activation energy indicates less energy needed for a compound to undergo reactions. Furthermore, determination of the activation energy allows extrapolation of kinetics constant at another temperature in a similar range, again using Equation 2.

4. CONCLUSIONS

The addition of a catalytic metal to zero-valent magnesium created an effective means for removal of DNAN, while ZVMg, without any catalytic metal, was only effective in low pH media. At neutral pH, Mg/Cu was the most effective and removed 98% of DNAN in 30 minutes, whereas the same extent of removal by Mg/Zn was achieved at 120 min. The largest extent of removal for Mg/Ni was 95% at the end of the tested 150 min. ZVMg, without any catalytic metal, was not as effective and resulted in only 33% DNAN removal after 150 min. These findings may help determining an appropriate technology for the treatment of certain waste materials, e.g. in acidic mediums, only ZVMg may be necessary, whereas in neutral pH media, use of bimetals may be necessary.

Furthermore, the kinetics of the DNAN degradation reaction followed a pseudo first order model. Parametric studies of the reaction kinetics showed that the addition of Cu, Ni and Zn increased the kinetic constant by 14, 2, and 12 times, respectively, compared to that of ZVMg alone. In addition, the lowering of the initial pH of the reaction solution had a significant impact on DNAN degradation. Under acidic initial pH conditions, all three bimetallic systems as well as ZVMg were very effective; almost complete removal of DNAN was achieved using Mg/Zn and ZVMg within 10 min and approximately 90% degradation was observed by Mg/Cu and Mg/Ni in only 15 min. Further work may be done on investigating the roles of acidic pH and the galvanic potential simultaneously on the bimetal configuration. The activation energy of DNAN degradation by the Mg/Cu bimetallic system was calculated as 8.18 kJ/mol. Overall, the magnesium-based bimetallic treatment system was shown to be a promising method for DNAN degradation in aqueous solutions.

References

1. C.I. Olivares, L. Abrell, R. Khatiwada, J. Chorover, R. Sierra-alvarez, J.A. Field, (Bio) transformation of 2 , 4-dinitroanisole (DNAN) in soils, **Journal of Hazardous Materials**. 304 (2016) 214–221.

2. J. Hawari, F. Monteil-Rivera, N.N. Perreault, A. Halasz, L. Paquet, Z. Radovic-Hrapovic, S. Deschamps, S. Thiboutot, G. Ampleman, Environmental fate of 2,4-dinitroanisole (DNAN) and its reduced products, **Chemosphere**. 119 (2015) 16–23.
3. S. Taylor, M.E. Walsh, J.B. Becher, D.B. Ringelberg, P.Z. Mannes, G.W. Gribble, Photo-degradation of 2,4-dinitroanisole (DNAN): An emerging munitions compound, **Chemosphere**. 167 (2017) 193–203.
4. J.D. Arthur, N.W. Mark, S. Taylor, J. Šimunek, M.L. Brusseau, K.M. Dontsova, Batch soil adsorption and column transport studies of 2,4-dinitroanisole (DNAN) in soils, **Journal of Contaminant Hydrology**. 199 (2017) 14–23.
5. J. Liu, C. Ou, W. Han, Faheem, J. Shen, H. Bi, S. Xiuyun, J. Li, L. Wang, Selective removal of nitroaromatic compounds from wastewater in an integrated zero valent iron (ZVI) reduction and ZVI/H2O2 oxidation process, **RSC Advances**. 5 (2015) 57444–57452.
6. S.C. Ahn, D.K. Cha, B.J. Kim, S.Y. Oh, Detoxification of PAX-21 ammunitions wastewater by zero-valent iron for microbial reduction of perchlorate, **Journal of Hazardous Materials**. 192 (2011) 909–914.
7. J. Shen, C. Ou, Z. Zhou, J. Chen, K. Fang, X. Sun, J. Li, L. Zhou, L. Wang, Pretreatment of 2 , 4-dinitroanisole (DNAN) producing wastewater using a combined zero-valent iron (ZVI) reduction and Fenton oxidation process, **Journal of Hazardous Materials**. 260 (2013) 993–1000..
8. A. Koutsospyros, J. Pavlov, J. Fawcett, D. Strickland, B. Smolinski, W. Braida, Degradation of high energetic and insensitive munitions compounds by Fe/Cu bimetal reduction, **Journal of Hazardous Materials**. 219–220 (2012) 75–81.
9. E. Kitcher, W. Braida, A. Koutsospyros, J. Pavlov, T.-L. Su, Characteristics and products of the reductive degradation of 3-nitro-1,2,4-triazol-5-one (NTO) and 2,4-dinitroanisole (DNAN) in a Fe-Cu bimetal system, **Environmental Science and Pollution Research**. 24 (2017) 2744–2753.
10. A. Ghauch, A. Tuqan, Reductive destruction and decontamination of aqueous solutions of chlorinated antimicrobial agent using bimetallic systems, **Journal of Hazardous Materials**. 164 (2009) 665–674.
11. R. DeVor, K. Carvalho-Knighton, B. Aitken, P. Maloney, E. Holland, L. Talalaj, R. Fidler, S. Elsheimer, C.A. Clausen, C.L. Geiger, Dechlorination comparison of mono-substituted PCBs with Mg/Pd in different solvent systems, **Chemosphere**. 73 (2008) 896–900.
12. B. Ramavandi, S.B. Mortazavi, G. Moussavi, A. Khoshgard, M. Jahangiri, Experimental investigation of the chemical reduction of nitrate ion in aqueous solution by Mg/Cu bimetallic particles, **Reaction Kinetics, Mechanisms and Catalysis**. 102 (2011) 313–329.
13. J. Morales, R. Hutcheson, C. Noradoun, I.F. Cheng, Hydrogenation of Phenol by the Pd/Mg and Pd/Fe Bimetallic Systems under Mild Reaction Conditions, **Industrial & Engineering Chemistry Research**. 41 (2002) 3071–3074.
14. A.M.E. Khalil, O. Eljamal, S. Jribi, N. Matsunaga, Promoting nitrate reduction kinetics by nanoscale zero valent iron in water via copper salt addition, **Chemical Engineering Journal**. 287 (2016) 367–380.
15. M. Rivero-Huguet, W.D. Marshall, Reduction of hexavalent chromium mediated by micro- and nano-sized mixed metallic particles, **Journal of Hazardous Materials**. 169 (2009) 1081–1087.
16. H. Tian, J. Li, Z. Mu, L. Li, Z. Hao, Effect of pH on DDT degradation in aqueous solution using bimetallic Ni/Fe nanoparticles, **Separation and Purification Technology**. 66 (2009)

84–89.

17. U.D. Patel, S. Suresh, Effects of solvent, pH, salts and resin fatty acids on the dechlorination of pentachlorophenol using magnesium-silver and magnesium-palladium bimetallic systems, **Journal of Hazardous Materials**. 156 (2008) 308–316..

18. X. Guan, Y. Sun, H. Qin, J. Li, I.M.C. Lo, D. He, H. Dong, The limitations of applying zero-valent iron technology in contaminants sequestration and the corresponding countermeasures: The development in zero-valent iron technology in the last two decades (1994-2014), **Water Research**. 75 (2015) 224–248.

POTABLE WATER DISINFECTION WITH SILVER IONS DURING SPACE MISSIONS: THE ROLE OF WATER TANK AND WATER SUPPLY MATERIALS

V. Tsiridis[1], M. Petala[1*], I. Mintsouli[2],N. Pliatsikas[3], S. Sotiropoulos[2], M. Kostoglou[4], E. Darakas[1], T. Karapantsios[4]

[1]Laboratory of Environmental Engineering & Planning, Dept. of Civil Engineering,
[2]Laboratory of Physical Chemistry, Dept. of Chemistry,
[3]Division of Solid State Physics, Dept. of Physics,
[4]Laboratory of Chemical and Environmental Technology, Dept. of Chemistry, Aristotle University of Thessaloniki, 54 124 Thessaloniki, Greece

*Corresponding Author: e-mail: petala@civil.auth.gr, tel: +302310 996208

Abstract
The availability of potable water, both in terms of quality and quantity is essential for the International Space Station (ISS) crew. Potable water is produced on ground and is transported to the ISS. During each launching campaign, water quality complies either to Russian or US standards. The disinfection agent is silver for the Russian type of water and iodine for the US type of water. So far, fluctuations of silver concentration in water have been confirmed and thus, health issues arise concerning the safe storage of potable water supplies in future (long term) missions.

The aim of this study is a) to evaluate the behavior of the disinfectant agent, silver, with various metallic and polymeric wetted materials used throughout the process of water preparation and storage, and b) to examine the phenomena responsible for silver concentration fluctuations in water systems for crew usage. Silver ions were added into Russian type water electrolytically, so as to reach either a silver ions' concentration equal to 10 or 0.5 mg Ag^{+}/L. Afterwards, water was brought in contact with various surfaces at surface (S) to volume (V) ratio equal to 5.0 cm^{-1} and temperature 30^{o}C, and was stored either for 7d (water with high Ag concentration) or 28 d (water containing low Ag concentration). At the end of the storage period all surfaces were leached, in order to examine the deposition of Ag onto the surfaces. Moreover, solid surfaces were further analyzed (using SEM and/or XPS), in order to elucidate the underlined deposition phenomena.

Silver losses from water containing 10 mg Ag^{+}/L varied from 7.4% up to 96.8%, while silver losses from water containing 0.5 mg Ag^{+}/L varied between 62.5% and 100%. Leaching of wetted materials verified the deposition of silver onto their surface. The phenomena that were responsible for silver deposition are discussed thoroughly, with respect to the type of wetted surface material.

Keywords: Silver deposition, Potable water, Disinfection, International Space Station

1. INTRODUCTION

Orion Multi-Purpose Crew Vehicle (MPCV) has been designed by National Aeronautics and Space Administration (NASA) for exploration missions beyond low-Earth orbit. Orion MPCV will carry the Orion service module, which is provided by the European Space Agency (ESA) and is designed for the storage of water, nitrogen and oxygen, among other duties [Jones, 2012]. Potable water is, after oxygen, the second consumable needed by crew members to live aboard a spacecraft and by far, the most critical with regards to mass. In the context of manned long term spaceflight missions, long

shelf life for potable water is required. To this regard, prevention of water contamination within the water systems is essential, in order to prevent potential crew health risks. Currently, control of potable water contamination is ensured by the addition of adequate amounts of biocidal agents at production sites [Rebeyre, 2012]. There are two water quality standards defined for water consumption by the ISS crew: the US potable water and the Russian potable water. The major differences between the two types of water are summarized as follows: the disinfection agent is silver for the Russian type of water and iodine for the US type of water, the TOC maximum acceptable levels are significantly higher according to the Russian water quality standards, Russian standards enable more minerals than the US ones and the maximum allowable total chromium level is significantly higher in the Russian type of water compared to the US type of water. So far, the European Space Agency (ESA) has successfully delivered potable water using ionic silver as biocide [Rebeyre, 2012] aboard by the Automated Transfer Vehicle (ATV). For future long term missions, ionic silver has been identified as the biocide agent of potable water (Wallace et al., 2016). Ionic silver has been acknowledged as an efficient disinfectant agent and can be safely consumed by humans, unless it is consumed at high concentrations for a long period of time [Wadher and Fung, 2005]. Besides NASA's plans to use ionic silver in future long term missions, ionic silver is currently used as the disinfectant agent for potable water aboard the Russian segment of the International Space Station (ISS). However, during the launch campaigns a fluctuation of silver was observed by performing water quality analyses at different steps of the water process during each campaign, implying possible water quality degradation [Wallace et al., 2016; (Rebeyre, 2012b].

The main type of wetted surface of water storage tanks from the Ground Support Equipment (GSE) used for water transportation and loading has been Stainless Steel (SS). Indeed, there are few relevant studies found in literature, which show that silver depletion from bulk water might occur on SS depending on various factors, such as the wetted surface area to water volume ratio (S/V), type of wetted surface, etc [Callahan et al. 2007; Roberts et al. 2007; Petala et al. 2017; Petala et al. 2016]. However, other types of materials –part of the water systems– may come in contact with water and contribute to the silver ions' concentration variation. The understanding of the underlying phenomena may contribute to optimize water systems used aboard. Besides, such systems are also used in terrestrial applications, such as portable water purification (employed by military personnel, survivalists, and others for water purification when they need to obtain drinking water from untreated sources) [Shamsuddin et al. 2016] or drinking water disinfection for unprivileged societies [Parr and Kim 2016].

This work is part of a project supported by ESA (European Space Agency) to examine the phenomena responsible for biocide concentration fluctuations in water systems for space crew usage. The scope of this work is to investigate the decrease of biocidal Ag+ concentration in water exposed to different types of materials and assess the chemical state of deposited Ag on these materials. To this aim, specific objectives of the work are: (i) to investigate the types of materials that may cause silver depletion from water, (ii) to verify silver deposition on the surfaces and (iii) to examine the materials' surfaces after exposure to water with high silver ions' concentration.

2. MATERIALS AND METHODS

Potable water for the Russian ISS crew originates from Regina Margherita ground water in Torino. Raw ground water complies with the water quality requirements without any pre-treatment, whereas the quality is rather stable over years, regarding both chemical and microbiological parameters [Lobascio et al. 2004]. The treatment steps for the Russian water preparation are [Lobascio et al. 2004] : a) addition of sodium fluoride solution, prepared directly in the source water, to the raw water in the reaction tank, b) mixing and further treatment using a silver ionization cell, in order to dissolve silver ions, c) microfiltration for the removal of the readily produced insoluble silver chloride, d) ionization treatment for the achievement of the target final concentration of silver in the water, which is 10 mg/L for disinfection water and 0.5 mg/L for the flight potable water and e) final step of

microfiltration prior to the transfer to the Water Gas Liquid Unit (WGLU). Afterwards, the WGLU is transferred to the launch site, where the potable water is loaded into the ATV water tanks. The loading procedure includes an initial step of soaking with high silver concentration (10 mg/L) water for 24 h, then draining and flushing with high silver concentration (10 mg/L) water, and finally draining and filling with low silver concentration (0.5 mg/L) water [Grizzaffi et al. 2008]. In this study, both types of water were examined, in order to better elucidate the underlying phenomena related to silver ions concentration fluctuations.

2.1 Water preparation

Water was produced in the lab according to the Russian water standards containing either 0.5 mg Ag/L or 10 mg Ag/L. The produced water complied with the quality determined during ATV missions (Lobascio et al. 2004). Water was freshly prepared, before each experiment, in 1 L volumetric flasks. The basis for either type of water was ultrapure water (Direct-Q 3 UV, Millipore). Adequate quantities from stock solutions of various salts were introduced to ultrapure water, so as to comply with the water quality standards. Next, silver ions were added using a silver ionization unit (CSG-1, UK) equipped with silver electrodes of high silver purity (99.99%). Water was filtered through a 0.2 μm filter (Pall Corporations, USA) after the addition of silver ions and silver concentration was measured spectrophotometrically (LCK354, Hach Lange). The chemical characteristics of the produced water are presented in Table 1. All hardware items (glassware, plastic ware, etc) were sterilized prior to use, in order to avoid microbial contamination.

2.2 Types of tested surfaces

Flat strip coupons of solid materials (Length x Width x Depth: 76 x 12.7 x 1.6 mm) were obtained from Metal Samples (Alabama, USA). The types of tested coupons included: Teflon FEP 500L (polymeric), Teflon PTFE (polymeric), EPR Parker (rubber), SS 316L (stainless steel), SS 15-5 pH (heat and air passivated stainless steel), SS 316L/ WW (stainless steel with welding), SS 316L/ P (acid passivated stainless steel), SS 316L/ P&E (acid passivated and electropolished stainless steel) and Ti Alloy 6Al4V (titanium alloy).

Table 1: Composition of high (10 mg Ag/L) and low (0.5 mg Ag/L) silver concentration water

Parameter	Concentration		Parameter	Concentration	
	High Ag conc. water	*Low Ag conc. water*		*High Ag conc. water*	*Low Ag conc. water*
Silver (mg/L)	**10**	**0.5**	TOC (mg/L)	0.5	0.5
pH	8.14	8.10	TDS (mg/L)	235	235
Conductivity (μS/cm)	338	310	Ammonium (mg/L)	<0.05	<0.05
Calcium (mg/L)	41.8	42.7	Color (Pt-Co)	0.0	0.0
Magnesium (mg/L)	12.5	12.8	Chromium (μg/L)	6.0	6.0
Turbidity (NTU)	0.23	0.10	Nickel (μg/L)	3.0	3.0
Nitrate (mg/L)	13.4	18	Barium (μg/L)	6.0	6.0
Chloride (mg/L)	<0.05	0.8	Zinc (μg/L)	3.0	3.0
Fluoride (mg/L)	1.0	1.0	Total coliforms (CFU)	0	0

Prior to experiments (about 24h before) coupons were meticulously cleaned, according to JRP5322.1G (NASA) and ASTM G1 protocols (JSC, 2008; ASTM, 1999). After cleaning, all coupons were dried and stored under nitrogen atmosphere until the performance of the experiments.

Verification of their cleanliness was performed not only by visual inspection under UV light (Figure 1a), but also by measuring the dynamic surface tension of MilliQ water after contact with the cleaned coupons for more than 3 hours. Dynamic surface tension is determined using the maximum bubble pressure technique. In all cases, the surface tension of water was practically the same with that of MilliQ water (about 71-72 mN/m), as shown in Figure 1b.

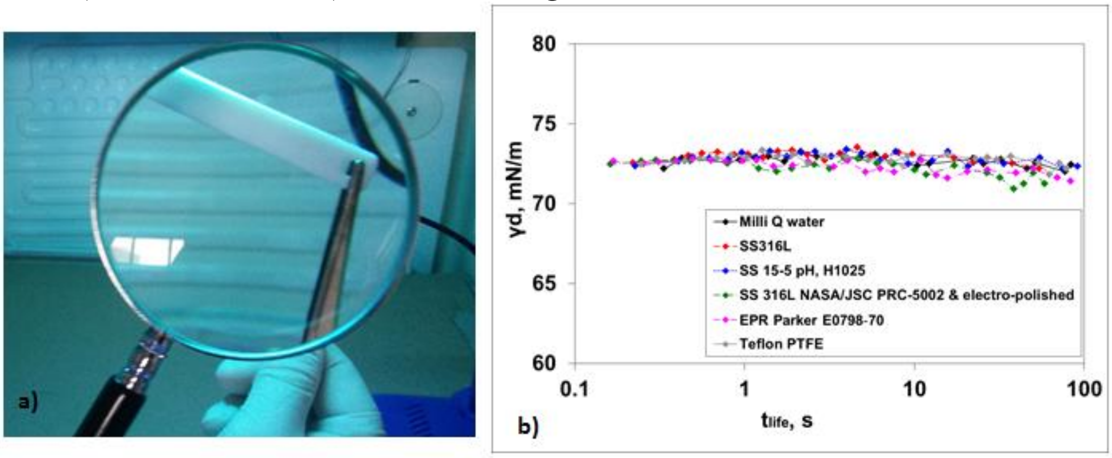


Figure 1: Verification of coupons' cleanliness: a) inspection under UV light, b) results obtained from dynamic surface tension measurements

2.3 Testing procedures

Exposure of various types of surfaces to water disinfected with silver ions took place inside polypropylene containers (HJ-Bioanalytik, Germany), as described elsewhere [Petala et al. 2016]. Tests were implemented in triplicate, while in each series of tests, there was also a blank sample (without exposed metal) in order to examine possible deposition of silver on the polypropylene (PP) walls of the experimental container (multiwell plate). Testing conditions were based on a worst case scenario that is high surface to volume ratio (S/V=5 cm^{-1}), high temperature (30°C) and exposure

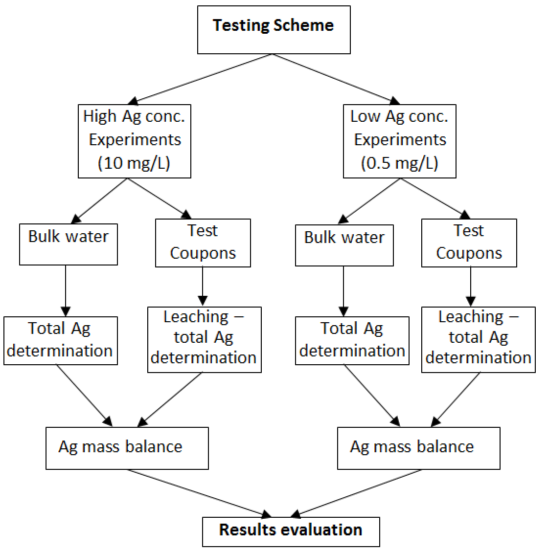


Figure 2: Testing methodology for the evaluation of silver deposition

time of 14 d and 28 d for the low silver concentration water, and 7 d for the high silver concentration water. These conditions were chosen, in order to intensify the phenomena and verify the deposition of silver on the surfaces. After the exposure periods, both liquid and solid samples were analyzed

regarding the concentration of silver (Figure 2) using the methodology described in detail elsewhere [Petala et al. 2016]. Silver mass balance was calculated for each material, while the surfaces that were prone to silver deposition were further analyzed using X-ray photoelectron spectroscopy (XPS).

3. RESULTS AND DISCUSSION

Initial experiments included the exposure of all types of materials to water with high silver ions concentration (10 mg/L) for 7 d at temperature 30°C and S/V ratio equal to 5.0 cm^{-1}. The initial Ag concentration in the bulk water was 10 mg/L, while the final Ag concentration in the bulk water after contact with each solid material is presented in Table 1. Solid materials caused removal of silver from the disinfection water bulk in the order: Teflon PTFE(7.4%)< Teflon FEP 500L (14.7)<SS 316L / P&E (21%)< EPR Parker (63.2%)<SS 15-5 pH (78.4%) < 316L/ WW (84.2%) < SS316L/ P (94.7%) < SS316L (96.8%) ~ Ti Alloy 6AL-4V(96.8%).

Afterwards, all solid materials were exposed to potable water (0.5 mg/L Ag) for 14d and for 28d at temperature 30°C and S/V ratio equal to 5.0 cm^{-1}. Solid materials after 14d of exposure to potable water caused removal of silver from the bulk water in the order: Teflon FEP 500L (41.8%)<Teflon PTFE (45.2%)< SS316L (97.9%)< EPR Parker (98.5%)< SS 15-5 pH (99%)< 316L/ WW(100%)~ SS316L/ P ~ SS 316L/ P&E ~Ti Alloy 6AL-4V. Solid materials after 28d of exposure to potable water caused removal of silver from the bulk water in the order: Teflon PTFE (62.5%)< Teflon FEP(65.3%)< SS316L(100%)~ EPR Parker~ SS 15-5 pH~ 316L/ WW~ SS316L/ P~ SS 316L/ P&E~ Ti Alloy 6AL-4V.

Leaching of coupons was performed after each batch of experiments in order to realize whether the silver was deposited on the solid materials or the PP walls of the multiwell plate. Indeed, significant amount of silver was recovered in the leachates and silver mass balance closed reasonably well (>90%). Therefore, leaching of coupons showed that in all cases silver was deposited on the surface of the solid materials [Petala et al. 2016]. The surfaces that were more prone to silver deposition were identified after calculating the concentration of deposited silver per materials surface unit, for the case of high silver concentration water. The results that are shown in Figure 3, demonstrate that the metallic surfaces favor the deposition of silver.

Table 2: Silver concentration in bulk water after contact with the solid materials for 7d at 30°C and S/V ratio equal to 5.0 cm^{-1}

Type of surface	Silver concentration after 7d (mg/L) (Initial Ag conc. 10 mg/L)	Silver concentration after 14d (mg/L) (Initial Ag conc. 0.5 mg/L)	Silver concentration after 28d (mg/L) (Initial Ag conc. 0.5 mg/L)
Blank	9.5	0.482	0.479
Teflon FEP 500L	8.1	0.279	0.166
EPR Parker	3.5	0.007	0.006
SS 316L	0.3	0.010	0.004
SS 15-5 pH	2.05	0.004	0.000
Ti Alloy 6AL-4V	0.3	0.000	0.000
SS 316L/ WW	1.5	0.001	0.000
SS 316L/ P	0.5	0.001	0.000
SS 316L/ P&E	7.5	0.001	0.000
Teflon PTFE	8.8	0.263	0.180

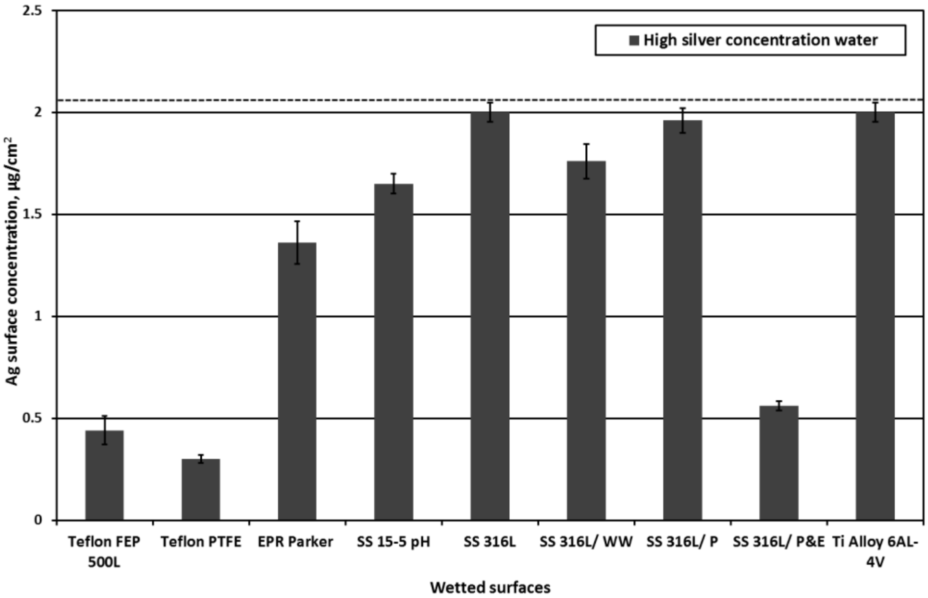


Figure 3: Surface concentration of silver considering the silver mass in the leachates and the wetted surface area of each material. The dashed line refers to the maximum silver concentration if all silver from the bulk water (with initial silver concentration 10 mg/L) was deposited on the wetted surface

The maximum concentration of silver was calculated equal to 2 μg/ cm^2 on the SS and titanium alloy surfaces. Remarkably, the treatment of SS surface by acid passivation and electro polishing resulted in much less silver deposition, slightly above 0.5 μg Ag/cm^2 of wetted surface. This value was comparable to those obtained for Teflon materials that presented the lowest silver surface concentration after their contact with the high silver concentration water. The presence of silver was also verified by using XPS analysis. Figure 4 shows the atomic concentration of depth profiles obtained by XPS spectroscopy data for SS 316L. The very high carbon atomic concentration obtained in the case of not-sputtered sample indicates surface contamination. The carbon concentration was dramatically reduced between 0 and 20 sec that is after 1 nm of Ar sputter – etching. Due to carbon contamination, significant Fe, Cr and Ni concentrations (characteristics of a SS substrate) only appear after sputtering/cleaning of the surface. At 20 sec the surface is almost clean from carbon contamination, allowing the appearance of Fe, Cr and Ni peaks. The Ag concentration slightly increases and then remains almost stable.

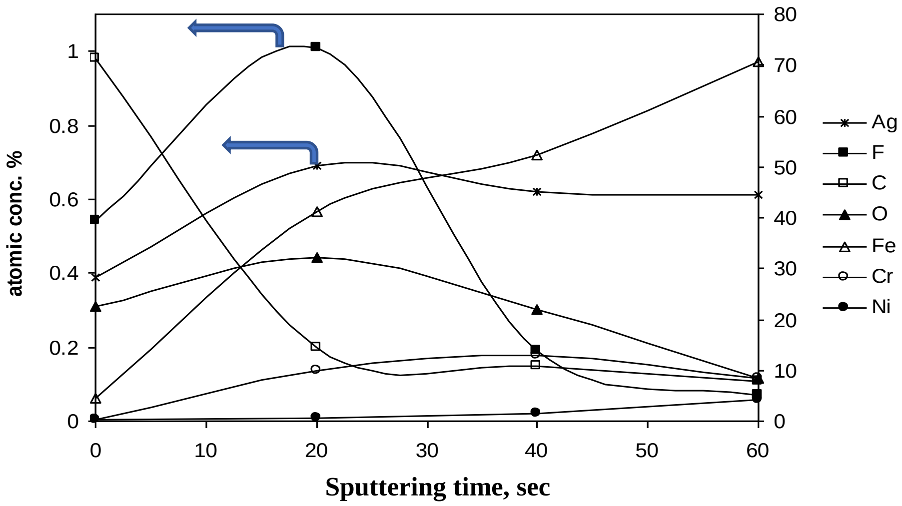


Figure 4: Atomic concentration depth profiles obtained by XPS spectroscopy data for the SS 316L coupon

Moreover, XPS analysis data revealed that silver was in its metallic form on the SS surface, in line with a galvanic deposition mechanism [Petala et al. 2016, Petala et al. 2017]. According to this, silver is reduced on the surface of the samples while components of the underlying metal are oxidized. As regards titanium, XPS spectroscopy confirmed the presence of Ag on its top surface layers, too (Figure 5). This was observed in the wide XPS spectra (data not shown) before and after sputtering, as in the case of SS316L. After sputtering, the carbon atomic concentration was diminished indicating almost total removal of surface contamination. Therefore, the concentrations of the other constituents of the tested coupon (Ti, Al and V) significantly increased.

However, the results of XPS analysis showed that, unlike stainless steel substrates, silver is present in its oxidized forms Ag^{+} and Ag^{+++} on Ti Alloy 6Al-4V. Thus, it is either deposited in ionic form (possibly bound on O-containing surface groups-see also below) or originally deposited as metallic silver (via a galvanic deposition mechanism that involves silver ion reduction and substrate oxide growth) and subsequently transformed to Ag_2O and Ag_2O_3 oxides by oxygen spillover from oxygen-rich Ti, Al and V [14]. The ionic form of silver on the coupon could be explained by an ion-exchange mechanism, whereby positively charged Ag ions are bound by the negatively charged native oxide surface of TiO_2 at the pH>7 values of the experiment [Mintsouli et al. 2018].

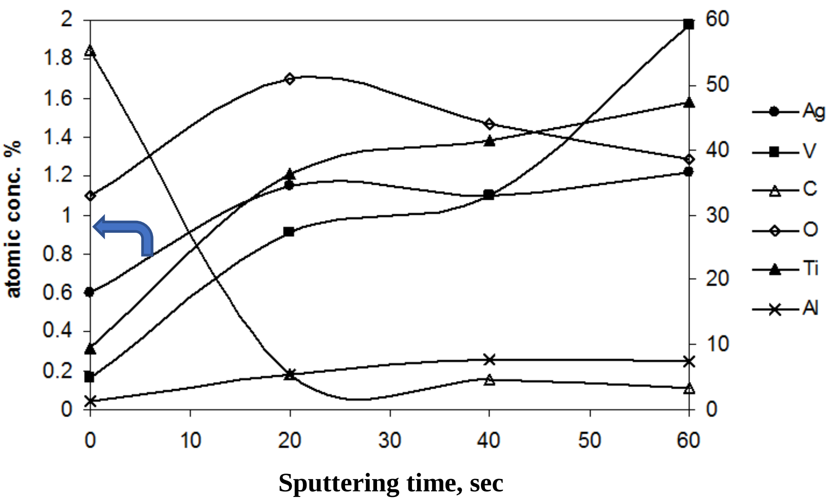


Figure 5: Atomic concentration depth profiles obtained by XPS spectroscopy data for the Ti alloy 6Al-4V coupon

4. CONCLUSIONS

The results of this study demonstrated that silver contained in water interacts with the solid materials of the ATV water system. Silver was almost fully depleted from water bulk after a 7-day exposure period of metallic surfaces to potable water. On the other hand, exposure of surfaces to conditioning water revealed that non-passivated metallic surfaces along with rubber surface led to significantly higher silver removal from the water bulk compared to the rest of the materials. Best performance – less silver removal- was observed for SS electropolished and Teflon materials. Analysis of leachates from the exposed surfaces allowed to close the total silver mass balance reasonably well proving that silver was deposited on the surfaces. Detailed XPS analysis indicated the chemical state of deposited silver on the examined surfaces.

Spectroscopic analysis confirmed that the thickness of the deposited silver layer on SS surface was thicker than 3 nm, as shown by the repeated sputter-etching process applied to different spots of the SS coupons and the resulting near constancy of Ag composition as determined by XPS. The chemical state of silver was identified by high resolution XPS analysis. Results verified that both metallic Ag and Ag oxides exist on the surface layers of silver deposits. Silver oxides are found on the outer surface of the deposits (in depth less than 1 nm), while interior to the deposits, Ag is in its metallic

form. Therefore, silver is deposited in its metallic form on all SS surfaces, in line with a galvanic deposition mechanism.

On the other hand, on the Ti6Al4V alloy surface, Ag is found only in its oxidized form (as AgO, a mixture of Ag_2O and Ag_2O_3). The above does not exclude the possibility of galvanic replacement mechanism also for the Ti alloy. This would be the case, if the initially deposited metallic silver was transformed to oxides by oxygen spillover from the O-rich moieties of the surface oxides of the Ti, V and Al components of the Ti alloy, whereby surface oxygen species are replenished by water dissociation. Alternatively, an ion-exchange mechanism might hold in the case of the Ti alloy, whereby Ag ions are bound by the negatively charged native Ti surface oxides/hydroxides (acidic dissociation of OH surface groups at pH values higher than the TiO_2 isoelectric point of pH<7).

References

1. Callahan M.R., N.K. Adam, M.S. Roberts, J.L. Garland, J.C. Sager and K.D. Pickering (2007) ‘Assessment of Silver Based Disinfection Technology for CEV and Future US Spacecraft: Microbial Efficacy’**, SAE International Technical Paper Series**, 01- 3258.
2. Grizzaffi, L., C. Lobascio, G. Bruno and A. Saverino (2008) ‘ATV Water Preparation Campaign’ Proc. of Int. Conf. **International Conference on Environmental Systems**, ICES 2008-01-2192.
3. Jones T.D. (2012) ‘The view from here: Moving beyond earth: NASA's steps through 2020’, **Aerospace America**, Vol. 50(3), 16-19.
4. Lobascio, C., G. Bruno, L. Grizzaffi, L. Meucci, M. Fungi and D. Giacosa (2004) ‘Quality of ATV Potable Water for ISS Crew Consumption’ **Proc. of Int. Conf. International Conference on Environmental Systems**, ICES 2004-01-2491.
5. Mintsouli I., V. Tsiridis, M. Petala, N. Pliatsikas, P. Rebeyre, E. Darakas, M. Kostoglou, S. Sotiropoulos and Th. Karapantsios (2018) ‘Behavior of Ti-6Al-4 V surfaces after exposure to water disinfected with ionic silver’, **Applied Surface Science**, Vol. 427, pp 763-770.
6. Parr J.M.P. and Y. Kim (2016) ‘Electrochemical silver dissolution and recovery as a potential method to disinfect drinking water for underprivileged societies’, **Environmental Science and Water Research Technology**, 2, pp 304-311.
7. Petala M., V. Tsiridis, E. Darakas, I. Mintsouli, S. Sotiropoulos, M. Kostoglou, Th. Karapantsios and P. Rebeyre (2016) ‘Silver deposition on wetted materials used in the potable water systems of the International Space Station’, **Proc. of Int. Conf. 46th International Conference on Environmental Systems**, 10-14 July, Vienna, Austria, ICES-2016-445, pp 1-12.
8. Petala M., V. Tsiridis, I. Mintsouli, N. Pliatsikas, T. Spanos, P. Rebeyre, E. Darakas, P. Patsalas, G. Vourlias, M. Kostoglou, S. Sotiropoulos and T. Karapantsios (2017) ‘Silver deposition on stainless steel container surfaces in contact with disinfectant silver aqueous solutions’, **Applied Surface Science,** 396, pp 1067-1075.
9. Rebeyre P. (2012) ‘ATV Water Quality: ATV1 and ATV3 Water Quality Overview’, **TEC-MMG/2012/324.**
10. Rebeyre P. (2012b) ‘ATV Water Process Overview – ATV Water Delivery System, Water Production and transportation to Launch Site, **Water Quality Control’ TEC-MMG/2010/29**.
11. Roberts M.S., M.E. Hummerick, S.L. Edney, P.A. Bisbee, M.R. Callahan, S. Loucks, K.D. Pickering and J.C. Sager (2007) ‘Assessment of Silver Based Disinfection Technology for CEV and Future US Spacecraft: Microbial Efficacy’, **SAE International Technical Paper Series**, 01-3142.
12. Shamsuddin N., D.B. Das and V.M. Starov (2016) ‘Membrane-Based Point-Of-Use Water Treatment (PoUWT) System in Emergency Situations’, **Separation and Purification Reviews**, 45(1), pp 50-67.

13. Wadhera A. and M. Fung (2005) 'Systemic argyria associated with ingestion of colloidal silver', **Dermatology Online Journal**, Vol. 11 (1), pp 12.
14. Wallace W.T., S.L. Castro-Wallace, C.K. Mike Kuo, L.J. Loh, E. Hudson, D.B. Gazda, J.F. Lewis (2016) 'Effects of Material Choice on Biocide Loss in Orion Water Storage Tanks', **Proc. of Int. Conf. 46th International Conference on Environmental Systems**, 10-14 July, Vienna, Austria, pp 1-10.

DETERMINATION OF AMMONIUM IN RECYCLED AND POTABLE WATER SAMPLES FOR SPACE APPLICATIONS

G. Giakisikli, V. Trikas, Th. Karapantsios*, G. Zachariadis, A. Anthemidis

Department of Chemistry, Aristotle University of Thessaloniki, GR - 54124 Thessaloniki, Macedonia, Greece

*Corresponding Author: e-mail: karapant@chem.auth.gr, tel: +302310997772

Abstract

In terms of crew survival, water is the second most consumable needed in manned space missions, after the air, and by far, the most critical with respect to mass. There is a great need for water recycling systems, which are being developed by the European Space Agency (ESA), the Russian Federal Space Agency (ROSCOS-MOS) and the National Aeronautics and Space Administration (NASA), to minimize the water supplied from the ground. So far, water recycling is limited to water recovery from cabin condensate and urine. Ammonium ion is considered as one of the critical chemical components in the waste water stream to recycle as it is the product of urea decomposition. For this reason, there is a need for continuous monitoring of ammonium ion in different stages of recycling process. There are numerous analytical methods, including automated or batch ones, available in the literature for reliable NH_4^+ determination in recycled waters. However, in space, the analytical procedure differs significantly from the one on earth. Sequential injection analysis (SIA) coupled with a fluorimetric detector is a potential candidate for such purpose and has the advantage of not only performing automated analysis, but also improving sensitivity with the possibility of further miniaturization.

Keywords: Trade-off methodology, Sequential injection analysis, Ammonium determination; Fluorimetry, Microgravity, International space station

1. INTRODUCTION

The International Space Station (ISS) is a microgravity research laboratory in low Earth orbit, suited for the testing of spacecraft systems and equipment required for long-lasting manned space missions. Water is provided to the crew from appropriate water storage/transfer systems. It would be impractical to stock the ISS with water for long periods of time, or continuously supplying it from the Earth, so the development of water recycling systems is critical [H.W. Jones and M.H. Kliss (2010)]. The recycling system developed by ESA is designed to produce hygiene and potable water either from cabin condensate or grey water (waste hygiene water) or even urine, by physical/chemical processes in order to remove contaminants, as well as different filtration steps and heat sterilization to ensure the water quality. The produced water requires a high level of quality control, which until now, it involves its transportation to Earth, resulting in questionable measurements due to the time lapse between the sample collection and ground analysis. Thus, there is a need for in-flight analytical measurements.

In the ISS, there are some requirements of ESA that should be fulfilled, in order an analyzer to properly operate in space. The requirements concern the analytical performance characteristics of the method (limit of detection/quantification, dynamic range, selectivity, precision, accuracy), and the space adaptation characteristics (mass/volume of the analyzer, power consumption, voltage/current intensity) due to limitations in space and energy availability [W. T. Wallace, D. B. Gazda, T. F.

Limero, J. M. Minton, A. V. Macatangay, P. Dwivedi and F. M. Fernandez (2015)]. Thus, an analyzer must be microgravity compatible, operating in a fully automated mode for long periods. The low consumption of sample/reagent solutions is important, considering the limited space in the ISS and the weight. Special care should be taken to a totally closed system to avoid any leaking of fluids or release of gases into the isolated station's environment. Finally, the use of low toxicity reagents and minimum flammable materials is important to ensure the safety of the crew and the station.

A factor that affects the quality of the water is the concentration of the ammonium ion/ammonia; thus, its continuous on-line monitoring is crucial. In water, both toxic unionized ammonia (NH_3) and the relatively non-toxic ionized ammonium ion (NH_4^+) exist. Each form is converted to the other depending on the pH, salinity and temperature. NH_4^+ is predominant when the pH is below 9.0, while NH_3 exists at higher values. Several automated analytical techniques have been developed for the quantitative determination of the two species with various detectors (spectrophotometric, fluorimetric, conductimetric), but there are only few that meet the requirements for proper operation in space. The automated flow analyzers, based on the flow injection analysis (FIA) and sequential injection analysis (SIA) techniques, work in a totally "closed loop" mode and offer automatic on-line liquid manipulation using low volumes of sample/reagents solutions, resulting in minimum waste production.

The aim of this work is to perform a trade-off analysis of the automated flow methods for NH_4^+ determination, reported in the literature, based on critical operational parameters under space conditions and to select the top ranked one for evaluation. For this purpose, a SI analyzer with a fluorimetric detector was employed and tested. A fully automated method has been developed to meet the requirements for possible use in manned space missions. The derivatization reaction between ammonia and o-phthaldialdehyde in the presence of sulfite in alkaline media (pH ca. 11) results in the formation of a fluorescent product (isoindol-1-sulfonate), which is then quantified at 425 nm. The chemical, flow and space factors affecting the operation of the system were optimized, to enhance the effectiveness of the proposed method. The accuracy and precision of the method were estimated by analyzing a standard reference material (SRM) as well as using the Certified Method (phenate). The method was applied to hygiene and potable water samples.

2. EXPERIMENTAL

2.1 Instrumentation

A miniSIA flow analyzer with an acrylic Chem-on-Valve™ monolithic manifold (https://www.globalfia.com) was used throughout the experiments for the ammonium determination. The device is equipped with a bi-directional milliGAT™ pump coupled to a thermostated holding coil and a multi-position valve (MPV) modified in such a way in order to accept the Chem-on-Valve (COV) manifold. This configuration facilitates the fluid manipulation in a microfluidic way inside the closed system. Two fiber optic cables are used for the emission and excitation light as well as a fluorescence flow cell which is directly mounted on the COV. A monochrome white LED is used as an excitation light source (365 nm). A fluorimetric spectrometer (Ocean Optics USB-4000) is used as a detection system. The monochromator has been set at 425 nm emission wavelength. The recorded fluorescence intensity is given as arbitrary units (AU). The FloZF 5.2 software (https://www.globalfia.com) is used for the device control and data acquisition. The tubing is made from PEEK or PTFE. Polyethylene bottles were used as solution containers.

A Varian DMS 100S UV Visible Spectrophotometer with a 1.0 cm × 1.0 cm absorption cell was used for ammonium determination by employing the reference method (indophenol blue). The analytical wavelength was set at 640 nm. A Sartorius analytical balance has been employed for mass measurements. An Orion EA940 pH-meter has been used for pH measurements.

2.2 Reagents and samples

All chemicals were of analytical reagent grade and provided by Merck (Darmstadt, Germany, http://www.merck.de). All ammonium standard solutions were prepared by appropriate stepwise dilution of 1000 mg L^{-1} NH_4^+. A 10.0 mmol L^{-1} o-phthaldialdehyde (OPA, $C_8H_6O_2$) solution was prepared by dissolving 268.0 mg of solid in 50.0 mL methanol and filling the volumetric flask to 200.0 mL with double deionized water (DDW). Phosphate buffer was prepared by dissolving 26.81g Na_2HP0_4 in 900 mL of DDW, adjusting the pH to 11.0 with 2.0 mol L^{-1} NaOH and filling the volumetric flask to 1000 mL (0.1 mol L^{-1}). A 1000 mL solution of 3.0 mmol L^{-1} Na_2SO_3 was prepared by dissolving 378.0 mg of solid Na_2SO_3 in phosphate buffer. The reagent solutions are light sensitive, so they were kept in dark bottles in the fridge remaining stable for at least 5 weeks. A 20% m/v alkaline citrate solution was prepared by dissolving 50.0g trisodium citrate and 2.5g NaOH in 250 mL of DDW. A 5% m/v sodium hypochlorite solution was prepared by dissolving 5.0g sodium hypochlorite (NaClO) in 100.0 mL of DDW. A 0.5% m/v sodium nitroprusside solution was prepared by dissolving 1.25g sodium nitroprusside ($Na_2Fe(CN)_5NO$) in 250.0 mL of DDW. A 1% m/v sodium hypochlorite solution in 16% m/v citrates was prepared by mixing 80.0 mL of 20% m/v alkaline citrate solution and 20.0 mL of 5% m/v sodium hypochlorite solution. A 11.1% v/v phenol (C_6H_6O) solution in ethanol was prepared.

An ammonium standard reference solution from NIST (National Institute of Standards and Technology, Gaithersburg, MD, USA) NH_4Cl in H_2O 1000 mg L^{-1} NH_4^+ CertiPUR® was analyzed to investigate accuracy. Three different potable artificial water samples (PAW) at 0.0, 0.4 and 0.8 mg L^{-1} concentration level of NH_4^+ and three different hygiene artificial water samples (HAW) at 0.0, 1.0 and 5.0 mg L^{-1} concentration level of NH_4^+ were prepared. The chemical composition of each artificial water sample is given in Table 1. Laboratory glassware was treated with freshly prepared 10% (v/v) nitric acid solution for at least 24 hours and finally rinsed with ultra-pure deionized water before use to avoid contamination factors as much as possible.

Table 1: Chemical composition of artificial potable (PAW) and hygiene (HAW) water samples. Concentrations are given in mg L^{-1}. All solutions are slightly acidic (6.0-6.5)

Parameter	PAW1	PAW2	PAW3	HAW1	HAW2	HAW3
Ammonium	-	0.4	0.8	-	1.0	5.0
Chloride	100	100	200	125	125	250
$P\text{-}PO_4$	2.5	2.5	5.0	25	25	50
Nitrate	12.5	12.5	25	25	25	50
Sodium	75	75	150	140	140	280
Potassium	1.5	1.5	3.0	3.0	3.0	6.0
Magnesium	25	25	50	25	25	50
Calcium	50	50	100	50	50	100
Fluoride	0.5	0.5	1.0	5.0	5.0	10
Iron	0.15	0.15	0.30	1.5	1.5	3.0
Copper	0.5	0.5	1.0	1.5	1.5	3.0
Zinc	2.5	2.5	5.0	2.5	2.5	5.0
Cadmium	0.0025	0.0025	0.005	0.025	0.025	0.050
Nickel	0.025	0.025	0.050	0.250	0.250	0.500
Lead	0.025	0.025	0.050	0.250	0.250	0.500
Chromium	0.025	0.025	0.050	0.250	0.250	0.500
Manganese	0.025	0.025	0.050	0.250	0.250	0.500
Arsenic	0.005	0.0050	0.010	0.050	0.050	0.100
Mercury	0.001	0.001	0.002	0.010	0.010	0.020

2.3 Analytical procedure

The manifold of the flow system is schematically presented in Figure 1. The analysis of ammonium using the miniSIA is based on the OPA method. Three operational sequences have been used during the experiments. At the beginning, the analyzer runs the "startup" sequence in order to prepare the device (filling of the tubes, heating of the holding coil) for the analysis. Then, the "analytical cycle" sequence begins, during which appropriate portions of sample/standard solution (40.0 μL), OPA (40.0 μL) and sodium sulfite (20.0 μL) solutions are sequentially aspirated with a flow rate of 10.0 μL s^{-1}, into the thermostated holding coil in a sandwich type format by means of the milliGAT pump in order to produce a fluorescent product (isoindol-1-sulfonate) which can be directly quantified. The chemical reaction between ammonia and o-phthaldialdehyde in the presence of sulfite takes place in alkaline media (pH ca. 11). The fluorescent product, is time and temperature affected, thus, after a 2-min stop in the thermostated holding coil at 70 ^{o}C, it is delivered into the flow-cell where it is quantified at 425 nm (excitation wavelength, 365 nm). Finally, the analyzer runs the "shutdown" sequence in order to clean the entire system (rinsing of the tubing, holding coil and flow-cell).

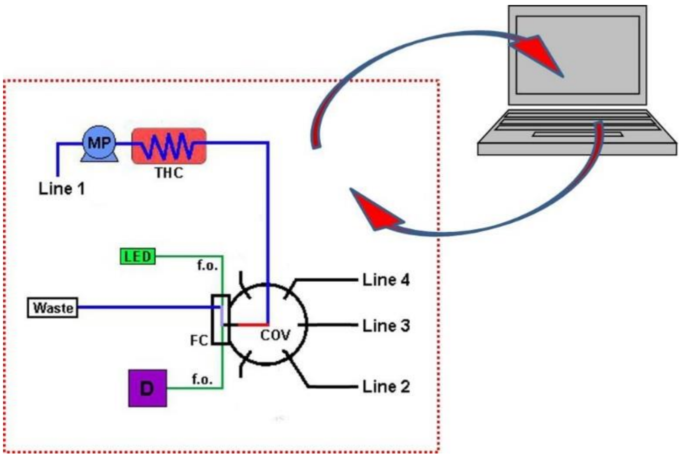


Figure 1: Schematic diagram of the miniSIA Flow Analyzer. MP, milliGAT^{TM} pump; D, detector; THC, thermostated holding coil; FC, flow cell; COV, Chem-on-Valve; f.o., fiber optics; LED, led excitation light source; Line 1, DDW; Line 2, Std sol./sample; Line 3, OPA sol.; Line 4, sulfate sol

3. RESULTS AND DISCUSSION

3.1 Trade-off methodology

There are many published automated flow methods for ammonium/ammonia determination in the literature. The flow systems, which are commonly used for ammonium determination, are categorized as follows: segmented flow analysis (SFA), flow injection analysis (FIA) [N. Amornthammarong and J.-Z. Zhang (2008), Y. Zhu, D. Yuan, Y. Huang, J. Ma, S. Feng and K. Lin (2014)], sequential injection analysis (SIA) [R. A. Segundo, R. B. R. Mesquita, M. T. S. O. B. Ferreira, C. F. C. P. Teixeira, A. A. Bordalo and A. O. S. S. Rangel (2011)], multisyringe flow injection analysis (MSFIA) [C. Henrıquez, B. Horstkotte and V. Cerdà (2013)], multiCommutated flow injection analysis (MCFIA) [S. M. Oliveira, T. I. M. S. Lopes, I. V. Toth and A. O. S. S. Rangel (2009)] and multipumping flow injection analysis (MPFIA) [C. Henríquez, B. Horstkotte and V. Cerdà (2014)] with or without a gas diffusion (GD) unit. Among them, only few meet the requirements for proper operation in space conditions.

In accordance with the ESA standard procedures, trade-off studies shall evaluate the candidate concepts for a mission candidate technique. Therefore, to evaluate and select the most appropriate of them, a trade-off methodology has been developed taking into account the detection / quantification requirements (LOD, LOQ, accuracy, repeatability, etc.) and critical items regarding the adaptation to space (microgravity applicability, volume/mass of the analyzer, solutions consumption, wastes production) as well as safety criteria (use of hazardous materials/reagents, pressure, heating, flameability). Every criterion was scored, based on defined scale/levels of each one with a specific

weighting factor (WF). Each particular weighting factor has been attributed to every criterion taking into consideration the significance of the specific parameter. For instance, parameters that could affect the crews' wellbeing, such as maintenance and safety issues, were evaluated as of higher importance (x10 WF) compared with others that are subject to design adaptation and could be optimized, like volume of the analyzer (x5 WF) and power consumption (x4 WF). In addition, since the concept of the WF refers mainly to the criteria, in order to distinguish between the examined methods, a scale was required to be established for each criterion in order to provide a reliable assigned value for each one. The scale of the criteria is based on numeric features. The score of each criterion for every method was given as the result of a value (into the range of scale) x weighting factor.

The requirements for the developed method are the following: working range, 0.1 mg L^{-1} - 50 mg L^{-1} NH_4^+, limit of detection, 0.05 mg L^{-1} NH_4^+; limit of quantification, 0.1 mg L^{-1} NH_4^+, precision, at a value of standard deviation of ± 0.05 mg L^{-1}; accuracy, at an error level of 0.05 mg L^{-1}. The space adaptation criteria are the following: volume of the on-line ammonium analyzer, lower than 516×440×253 mm^3 (based on the ISS Locker); mass of the on-line ammonium analyzer, lower than 27 Kg; minimal consumed sample volume and waste generation during analysis; safe disposal; power consumption, lower than 300W; current intensity, 116-126V DC. Finally, special attention should be focus on the safety. The Table 2 presents the examined parameters together with the score of each one as well as the total score of each analytical flow method.

The SIA fluorimetric methods [N. Amornthammarong and J.-Z. Zhang (2008), C. Frank, F. Schroeder, R. Ebinghaus, W. Ruck, (2006)] were top ranked compared to the others, according to the trade-off methodology. Among the commercially available SIA systems coupled with a fluorimetric detector, the miniSIA analyzer seemed to be more promising and selected for further evaluation. The miniSIA analyzer is an automated and miniaturized integrated system with a low volume and mass (size: 200 mm × 300 mm × 250 mm; weight: 7.5 Kg, power: 110-250VAC, 2.5A). It is an easy-to-use system which allows for an automatic handling of the solutions without any human intervention, avoiding any potential errors, regarding overpressure or overheating of the system. In addition, it uses low volumes of sample/reagents solutions resulting in low production of wastes, considering not only the restricted space inside the ISS, but also the weight. Finally, the operation of the whole procedure in a totally "closed loop" makes it microgravity applicable and prevents problems like leakage or gas elimination, which could create harmful environment inside the limited and isolated space station.

Table 2: Trade off methodology of the examined flow methods

Trade off criteria		Scale	Weighting factor	A	B	C	D	E	F	G
Analytical Performance	Limit of Detection	0-5	10	50	50	50	50	50	50	50
	Limit of Quantitation	0-5	9	45	45	45	45	45	45	45
	Working range	0-5	3	12	15	12	12	12	6	9
	Selectivity / interferences	0-2	5	0	0	10	10	10	0	0
	Precision	0-10	4	36	28	40	40	20	28	32
	Accuracy	0-5	6	18	18	30	30	24	18	30
Adaption Characteristics	Volume of analyzer	0-5	5	25	25	25	25	25	25	25
	Mass of the analyzer	0-5	5	25	25	25	25	25	25	25
	Sample volume	0-5	5	25	25	25	25	25	20	25
	Wastes Volume	0-5	5	20	25	25	25	25	20	25
	Power consumption	0-3	4	12	12	12	12	12	12	12
	Maintenance	0-5	10	0	0	30	30	30	0	0
Safety Criteria	Hazardous Reagents / Wastes	0-5	10	40	40	30	30	20	40	30
	Heating	0-2	10	20	20	0	0	0	20	20
	Total score			328	328	359	359	303	314	328

*A, MPFIA-GD-Conductimetric [8]; B, MSFIA-GD-Conductimetric [6], C, FIA-OPA-SULFITE-Fluorimetric [3]; D, SIA-OPA-SULFITE-Fluorimetric [9]; E, FIA-INDOPHENOL-UV-Vis [4]; F, SIA-GD-INDICATOR-UV-Vis [5]; G, MCFIA-GD-INDICATOR-UV-Vis [7].

3.2 Chemical and flow parameters optimization

All chemical and flow parameters of the proposed system considering the requirements for space adaptation and safety criteria were thoroughly studied.

Effect of temperature: The chemical reaction which takes place in the OPA method is depended on the temperature of the mixture inside the holding coil, affecting the formation of the fluorescent product. The effect of temperature was studied from 30 to 80 ºC. The experimental results showed that the increase of the temperature was effective in accelerating the desired reaction in the studied region, as it increased the fluorescence intensity (Figure 2). However, 70 ºC were selected in order to avoid any possible bubbles formation inside the closed system.

Effect sample aspiration order: In SIA methods, the aspiration order of the solutions into the holding coil is a key factor to the formation of the fluorescent product. Six reagents/standard aspiration order combinations have been studied. The results showed that the highest sensitivity was achieved by consecutive aspiration of 20 μL of 15.0 mmol L^{-1} OPA solution, 20.0 μL of 2.0 mg L^{-1} NH_4^+ standard and 20.0 μL of 3.0 mmol L^{-1} sodium sulfite solution, as given in Figure 3. Thus, the aspiration order of OPA-Standard/Sample-Sulfite was adopted.

Effect of concentration and volume of OPA solution: The concentration of OPA solution and its aspirated volume inside the holding coil are of high significance to its complexation with ammonia, affecting the efficient formation of the fluorescent product. The effect of OPA concentration was studied at concentrations between 0.5 and 50.0 mmol L^{-1}, while the effect of the volume was studied at the range of 20.0 - 50 μL. The concentrations of NH_4^+ standard and sulfite solutions were 2.0 mg L^{-1} and 3.0 mmol L^{-1}, respectively. The fluorescent intensity increased as the concentration of the reagent increased up to 3.0 mmol L^{-1} and, then, remained practically stable. Regarding the aspirated volume of OPA solution, the results showed an increase in the intensity by increasing the volume up to 40.0 μL, while at higher values a slight decrease was observed. Hence, a volume of 40.0 μL of OPA solution at a concentration level of 3.0 mmol L^{-1} was chosen as optimum.

Effect of sample volume: In on-line flow systems, sample volume plays a significant role affecting the sensitivity of the method. In order to evaluate the influence of the sample volume on the intensity, a standard solution of NH_4^+ at a 2.0 mg L^{-1} concentration level was used, varying the aspirated volume within the range 5.0 - 60.0 μL. The experimental results showed a positive correlation of the analytical signal with the sample volume up to 40.0 μL, leveling off at 50.0 μL, while at higher volumes, a slight decrease of the signal was observed (Figure 4). Therefore, a sample volume of 40.0 μL of was adopted for further studies.

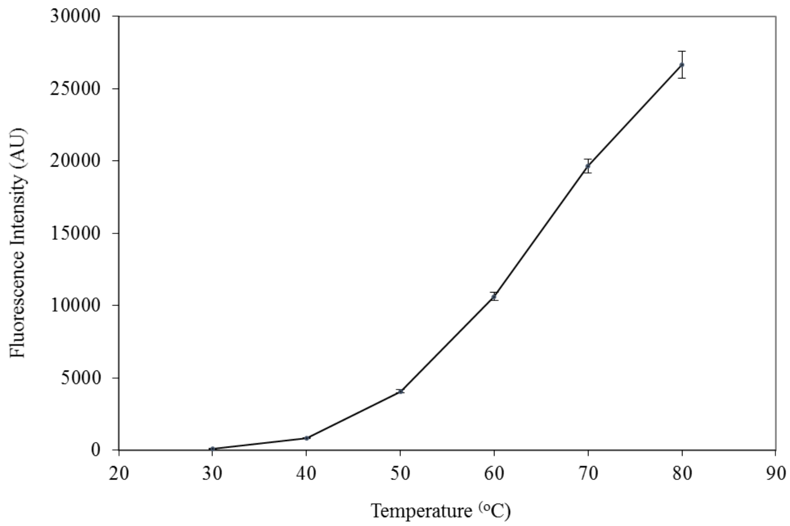


Figure 2: Effect of temperature on the fluorescence intensity of 2.0 mg L^{-1} NH_4^+. Heating time: 90 s. Error bars were calculated based on standard deviation values (±1s)

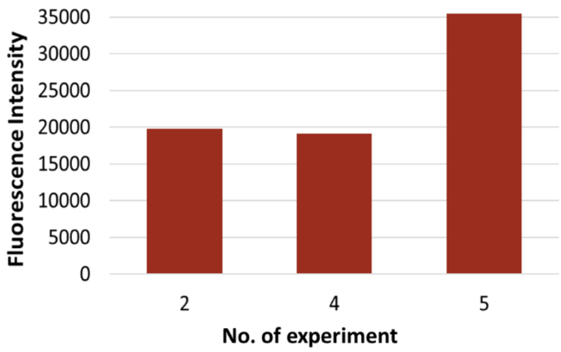


Figure 3: Effect of reagents/standard (or sample) aspiration order on the fluorescence intensity of 2.0 mg L^{-1} NH_4^+

Effect of concentration and volume of sodium sulfite solution: The presence of sodium sulfite as a reducing agent enhances the sensitivity and the specificity of the reaction between OPA and ammonium ion, by eliminating possible interferences of dissolved amino acids and primary amines [Z. Genfa and P. K. Dasgupta (1989)]. Experiments using different concentrations of sodium sulfite solution showed that at 3.0 mmol L^{-1} concentration level the fluorescent reaction was maximum and, thus, it was employed for the study of the effect of its volume on the fluorescence intensity. The aspirated volume of sulfite solution was studied in the range between 5.0 and 25.0 μL. An increase of the analytical signal was observed by increasing the sulfite volume up to 20.0 μL, while then it was leveled off. Consequently, a volume of 20.0 μL was used as optimum.

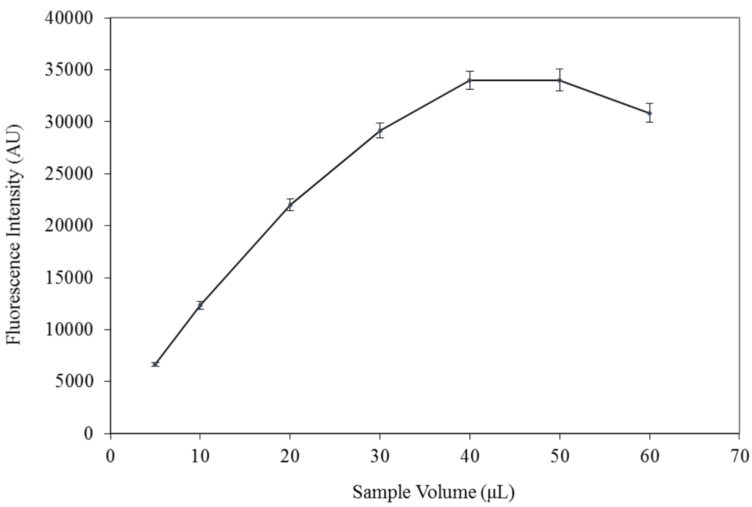


Figure 4: Effect of sample volume on the fluorescence intensity of 2.0 mg L^{-1} NH_4^+. Error bars were calculated based on standard deviation values (±1s)

Interferences: The water system in ISS recycles cabin condensate, hygiene waters and urine. Thus, primary amines are a potential interference, which has been studied at concentrations up to 0.40 mg L^{-1} CH_3NH_2 for interfering in 0.50 mg L^{-1} NH_4^+ determination using the optimized method. Higher concentrations of methylamine are not expected, according to the Reference Documents of ESA for the quality of the recycled water in ISS. Another compound that could act as interference is the silver ion which is used as a disinfectant in the ISS water system [M. P. Arena, M. D. Porter and J. S. Fritz (2003)]. Experimental results revealed that CH_3NH_2 and Ag(I) can be tolerated at least up to 0.40 and 1.0 mg L^{-1} (Table 3).

Table 3: Potential interferences in 0.50 mg L^{-1} NH_4^+ determination with the miniSIA method

Interferences	Concentration (mg L^{-1})	Deviation (%)*
CH_3NH_2	0.10	-0.4
	0.20	2.0
	0.40	9.9
Ag(I)	1.00	0.8

3.3 Chemical and flow parameters optimization

The analytical performance characteristics of the miniSIA method for NH_4^+ determination under the optimal conditions were calculated and presented below. With a total analysis time of 174 s, the proposed method was linear from 0.06 mg L^{-1} up to 4.00 mg L^{-1} NH_4^+, while the sensitivity, S (slope of calibration curve) was S = 13218 L mg^{-1}. The detection limit, based on 3s criterion, was found to be 0.018 mg L^{-1}, while the quantification limit, based on 10s criterion, was found to be 0.06 mg L^{-1}, according to IUPAC [International Union of Pure and Applied Chemistry (IUPAC)]. The "intra-day precision" was calculated to be 2.30 % (at 0.50 mg L^{-1}, 5-subsequent times), while the "inter-day precision" was calculated to be 2.40 % (at 0.50 mg L^{-1}, 5-times 5-subsequent days).

In order to validate the accuracy of the proposed method, an NTRM reference material was analyzed using the miniSIA Flow Analyzer under the proposed method. The reference material was an ammonium standard solution traceable to SRM from NIST NH_4Cl in H_2O 1000 mg L^{-1} NH_4^+ CertiPUR®. The relative error was calculated to be 2.52%. The accuracy of the method was also tested using the certified method (indophenol blue) for ammonium determination [Standard Methods for the Examination of Water and Wastewater]. For this purpose, three potable artificial water samples (PAW) as well as three hygiene artificial water samples (HAW) at different concentrations of ammonium were prepared and analyzed with both the miniSIA method and the certified method. The results are presented in Table 4. The overall relative errors were 3.39% and 2.33% for PAW and HAW samples respectively.

Table 4: Accuracy of the miniSIA method comparing with the Certified Method

Sample	True value (mg L^{-1})	Certified Method Actual value (mg L^{-1})	miniSIA method Actual value (mg L^{-1})	Relative Error (%)
PAW1	0.00	0.00	0.00	0.00
PAW2	0.40	0.33	0.32	3.03
PAW3	0.80	0.7	0.75	7.14
Overall relative error				3.39
HAW1	0.00	0.0	0.0	0.00
HAW2	1.00	1.05	1.08	2.86
HAW3	5.00*	5.72	5.38	5.94
Overall relative error				2.93

*, after 1:1 dilution

The volume of the consumed solutions and produced wastes during the analytical cycle is also an issue to be considered in case of an analyzer for possible operation in a space shuttle. These volumes were calculated during an analytical cycle using the miniSIA ammonium analyzer and are presented in Table 5. The very small amounts of sample and reagents solutions as well as the wastes have been considered as acceptable to be used in space missions, allowing the miniSIA analyzer' s operation in a green-friendly manner.

Table 5: Volume of consumed solutions and produced wastes during the analytical cycle

Solutions	Volumes of consumed solutions (μL)	Volumes of produced wastes (μL)
Sample/std solution	40.0	40.0
OPA solution	40.0	40.0
Sodium sulfite solution	20.0	20.0
Carrier solution	390.0	390.0
Total volume	490.0	490.0

The developed method was applied to the determination of ammonium in real water effluents produced by the Water Treatment Unit Breadboard (WTUB) located in the Antarctic Concordia research station. Concordia is a selected place from ESA to test the water recycling system, similar to that in ISS, as it is a realistic simulation for some aspects of human spaceflight. Three different types of water samples were provided by ESA: 1 (urine and shower water), 2 (shower water) and 3 (grey water). These water samples have similar chemical composition as the ones of the recycled water on board the ISS. The water samples were analyzed with the miniSIA and the certified method and the results were compared (Table 6).

Table 6: Results of the analysis of WTUB water samples by CM and miniSIA

Sample	CM (mg L^{-1})	miniSIA (mg L^{-1})	Standard error (%)
1 (urine+shower)	3.55	3.28	-7.6
2 (shower)	0.34	0.32	-5.9
3 (grey water)	18.66	19.02	+1.9

The results of ammonium determination in WTUB water samples ranged between 0.30 up to 19.00 mg L^{-1}. Regarding the comparison of miniSIA with the CM method, good agreement was observed, and the percentage error ranged from -7.6% up to +1.9%, which complies with the space flight requirement for accuracy.

4. CONCLUSIONS

A trade off methodology has been developed for the evaluation of the published flow methods for ammonium/ammonia determination in terms of the ISS requirements for proper operation in space conditions. The miniSIA analyzer coupled with a fluorimetric detector was selected among other flow systems and evaluated with a view to a possible use for water quality monitoring in recycled potable and hygiene water samples in a microgravity environment. The analyzer is adaptable to space flight requirements considering that its volume and mass are suitable for the limited room-space inside the ISS. In addition, it allows for automatic handling of the solutions as well as the use of minimum sample and reagents volumes, resulting in low waste generation per analytical cycle. It is an integrated system which performs the analysis principle and measurements in a closed flow system without any crew involvement avoiding any possibility for fluid or gas discharges Thus, it conforms to the safety requirements not only for the crew, but also for the ISS environment.

References

1. H.W. Jones and M.H. Kliss (2010) ‘Exploration life support technology challenges for the crew exploration vehicle and future human missions’, **Adv. Space Res.** Vol 45, pp. 917–928.
2. W. T. Wallace, D. B. Gazda, T. F. Limero, J. M. Minton, A. V. Macatangay, P. Dwivedi and F. M. Fernandez (2015) ‘Electrothermal vaporization sample introduction for spaceflight water quality monitoring via gas chromatography-differential mobility spectrometry’, **Anal.Chem**. Vol. 87, pp. 5981–5988.

3. N. Amornthammarong and J.-Z. Zhang (2008) 'Shipboard fluorometric flow analyzer for high-resolution underway measurement of ammonium in seawater', **Anal. Chem**. Vol. 80, pp.1019-1026.
4. Y. Zhu, D. Yuan, Y. Huang, J. Ma, S. Feng and K. Lin (2014) 'A modified method for on-line determination of trace ammonium in seawater with a long-path liquid waveguide capillary cell and spectrophotometric detection', **Marine Chemistry** Vol. 162, pp. 114–121.
5. R. A. Segundo, R. B. R. Mesquita, M. T. S. O. B. Ferreira, C. F. C. P. Teixeira, A. A. Bordalo and A. O. S. S. Rangel (2011) 'Development of a sequential injection gas diffusion system for the determination of ammonium in transitional and coastal waters', **Anal. Methods** Vol. 3, pp. 2049-2055.
6. C. Henrıquez, B. Horstkotte and V. Cerdà (2013) 'Conductometric determination of ammonium by a multisyringe flow injection system applying gas diffusion', **Intern. J. Environ**. Anal. Chem. Vol. 93, pp. 1236-1252.
7. S. M. Oliveira, T. I. M. S. Lopes, I. V. Toth and A. O. S. S. Rangel (2009) 'Determination of ammonium in marine waters using a gas diffusion multicommuted flow injection system with in-line prevention of metal hydroxides precipitation', **J. Environ. Monit**. Vol. 11, pp. 228–234.
8. C. Henríquez, B. Horstkotte and V. Cerdà (2014) 'A highly reproducible solenoid micropump system for the analysis of total inorganic carbon and ammonium using gas-diffusion with conductimetric detection', **Talanta** Vol. 118, pp. 186–194.
9. C. Frank, F. Schroeder, R. Ebinghaus, W. Ruck, (2006) 'A Fast Sequential Injection Analysis System for the Simultaneous Determination of Ammonia and Phosphate' **Microchim Acta Vol. 154, pp. 31–38.**
10. Z. Genfa and P. K. Dasgupta (1989) 'Fluorometric Measurement of Aqueous Ammonium Ion in a Flow Injection System', **Anal. Chem**. Vol. 61, pp. 408-412.
11. M. P. Arena, M. D. Porter and J. S. Fritz (2003) 'Rapid, low level determination of silver(I) in drinking water by colorimetric–solid-phase extraction', **Anal. Chim**. Acta Vol. 482, pp. 197–207.
12. International Union of Pure and Applied Chemistry (IUPAC), Compendium of Analytical Nomenclature, Definitive Rules 1997, 3 rd ed.Blackwell, Oxford, 1998.
13. Standard Methods for the Examination of Water and Wastewater, © Copyright 1999 by American Public Health Association, American Water Works Association, Water Environment Federation

Acknowledgements
The authors would like to thank ESA for its financial support through the project "On-Line Ammonium Analyzer for water recycling systems, Contract No: 4000113078/14/NL/SFe".

GIS' CONTRIBUTION IN BIOLOGICAL PROCESSING OF WASTE WATERS IN SMALL SETTLEMENTS. CASE STUDY BY USING AN ARTIFICIAL WETLAND SYSTEM.

S. Kariotis, E. Giannakopoulos and I.K. Kalavrouziotis*

School of Science and Technology, Hellenic Open University, Tsamadou 13-15 & Saint Andrea, 26222 Patras, Greece

*Corresponding author e-mail: *ikalabro@eap.gr*, Tel +302610 367546, Fax: +302610 367528

Abstract

The construction of natural waste processing systems should take into account a wide range of territorial and legal factors in order to reduce negative impacts on the environment. This article describes the contribution of Geographical Information Systems (GIS) technology to generate spatial data for site assessment in small settlements, for the construction of natural waste processing systems by using artificial wetlands (AWL's) method. The site suitability is assessed on a scale based on territorial indexes that measure the risk of contamination of the following environmental components: surface water, groundwater, atmosphere, soil and human health. The GIS technology described in this article has been used to evaluate an area for the construction of an AWL in the settlement Orinis of Municipality Serres in Greece, with fewer than 2000 people, where there isn't a waste processing system. The results showed that the use of GIS technology is a base tool to analyse and make decisions for the finding of areas for construction of natural waste processing systems that constitute the optimal solution to protect the environment for small settlements according to the European Union waste management program.

Keywords: artificial wetland system; geographical information systems (GIS); waste waters

1. INTRODUCTION

Landfill siting is a complex process involving social, environmental and technical parameters as well as government regulations. As such, it evidently requires the processing of a massive amount of spatial data. Various landfill siting techniques have been developed for this purpose. Some of them use Geographic Information Systems (GIS) to find suitable locations for such installations (Zamorano et.al., 2008; Kontos, D, Th. et al., 2003; Siddiqui M., 1996). For example, in the past, Lin and Kado (1998) developed a mixed-integer spatial optimization model based on vector-based data to help decision makers find a suitable site within a certain geographic area (Lin and Kado, 1998), while recently Heidi et.al. are described the contribution of Geographical Information Systems (GIS) technology to generate spatial data for site assessment in small settlements, for the construction of natural waste processing systems by using AWL's method (Heidi et.al., 2016). According to Alemany et al. these systems constitute the optimal solution to protect the environment of small settlements (Alemany et.al., 2005) and the site suitability must is assessed on a scale based on territorial indexes that measure the risk of contamination of the following environmental components: surface water, groundwater, atmosphere, soil and human health (Dai et. Al., 2016). This article describes the contribution of Geographical Information Systems (GIS) technology to generate spatial data for site assessment in small settlements, with fewer than 2000 people, for the construction of natural waste processing systems by using artificial wetlands method. The GIS technology described in this article has been used to evaluate an area for the construction of an AWL in the settlement Orinis of

Municipality Serres in Greece, with fewer than 2000 people, where there isn't a waste processing system.

2. METHODOLOGY

2.1 Phase 1: Plotting artificial wetlands plants (AWL's) with GIS Tool

The current map projection system in Greece is the Transverse Mercator Projection 6° (TM_87) and Datum, GGRS_87 with GRS_80 ellipsoid (Kariotis and Panagiotopoulos, 2013). HMGS' schematic maps on a scale of 1:5,000 were used for the vectorization of the road and hydrographic network. The 1:5,000 scale allows for accuracy of about 1.25 m during the vectorization (resolution ¼ mm in relation to the scale).HMGS' schematic maps are in azimuthal projection (HATT) with Bessel as a reference ellipsoid. Greece has been divided in large 1:100,000 mapsheets, each of which has its own Cartesian coordinate system. The 1:5,000 HMGS maps refer to 1:100,000 mapsheets where the mapsheet centre distance is per 30' (large mapsheets). HATT was converted to TM_87 (GGRS_87). Simultaneous, the Orthophotomaps of the National Cadastre and Mapping Agencywere used to locate forest areas so that siting in said areas could be avoided. For this aim, ArcGIS program and EGSA projection system_87 were used with 421,501 points in X, Y, Z format. The points were input in such a way that a simple data file can be converted to usable information, exportable to shape file.

2.2 Phase 2: Parameterization of the model

The eligible sites must fall within the boundaries of the study area, which are also the administrative boundaries of the settlement. An additional criterion is for the site to be in such a position that allows for the transport of the waste through gravity alone (minimizing operational cost). Therefore, the desirable altitude of the unit should be lower than that of the lowest part of the designated boundaries of the settlement, according to the prefectural planning decisions which demarcate the settlement. Spatial queries were submitted so that the information returned fulfil the requirements above. The queries were submitted so that there is a circumferential safety margin in the rendering of the terrain (i.e. there will be no gaps in the terrain).

3. APPLICATION OF THE METHODOLOGY: RESULTS AND DISCUSSION

3.1 Point selection

According to criterions of point selection (see methodology), discern that there are 1,413 sites within the settlement boundaries. Classified by altitude, it ensures that the site with the highest altitude is Z=899.64m and the lowest is Z= 711.71m. Thus, a second query was submitted to the system, which deals with the selection of sites with an altitude lower than 711.71m (select by Attributes) from the total number of the areas introduced in the system. The sites were then limited to the south side of the settlement. This area fulfills the requirements above.

Upon this result, the third spatial query was introduced to choose the areas that are included within the study area that is the administrative boundaries of the settlement. Selection of areas within a 50m radius of the administrative boundaries of the settlement is recommended (and applied in this study) to ensure that the relief of the terrain corresponds to the boundaries of the area and there are no gaps. The result is the highlighted blue area in Figure 1. With the procedure mentioned above, the initial 421,501 points have been limited to 25,854. The Attribute table shows that the altitude variation ranges between 711.70 and 348.68 m.

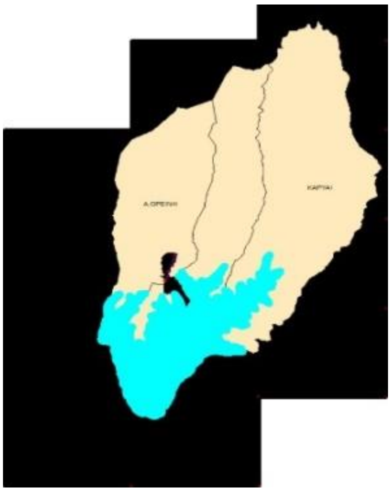


Figure 1: Result Select by Location

3.2 TIN (triangulated irregular network) creation

The Delaunay triangulation is fundamental in computational geometry and is used for terrain modelling. TIN creation aims for the digital rendering of the terrain and contributes to spatial selection as it calculates the slope of the terrain. Therefore, with a similar query, polygons with less than 10% ground gradient can be chosen and the researcher can limit their research in alternative positions that will emerge (Astaras et.al., 2011) (Figure 2). The application of the algorithm shows that 51,676 triangles have been created covering the area, the slope of each has been calculated and expressed as a percentage (%) and the orientation is also calculated. The result of Figure 2 includes triangles whose size is bigger than 200 m^2 (gray areas). Provided the primary points were distributed in grid data per 20m in X and Y, the triangles created will have a maximum area of 200m^2. Any larger triangle is located circumferentially of the area in question and contains incorrect information. With the fourth query, only triangles with an area ≤200m^2 are requested. Out of 52,676 triangles, 50,609 were selected, which have an area of ≤200 m^2, which means that the gray areas in Figure 2 were removed. Figure 3 shows the area without such errors. The next selection criterion is the slope that was defined at ≤10% to save up on earthworks. The next task is to integrate adjacent triangles so that there is a single polygon from which the area will initially be assessed.

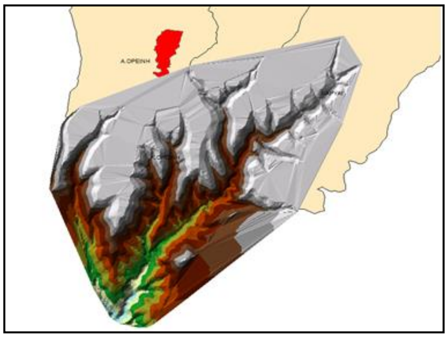


Figure 2 Colour gradation of altitude result

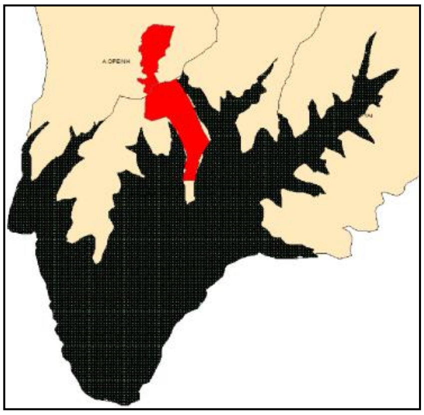


Figure 3: TIN debugging

After the integration, 551 polygons were created out of the original 1,023 triangles. Sorting the table by AREA and descending order it is discernible that there are only 6 integrated locations with an area > 3,000 m^2. In this point, the research will focus on locations: far (1st alternative) and next to (2nd alternative) from final recipient stream, Figure 4.

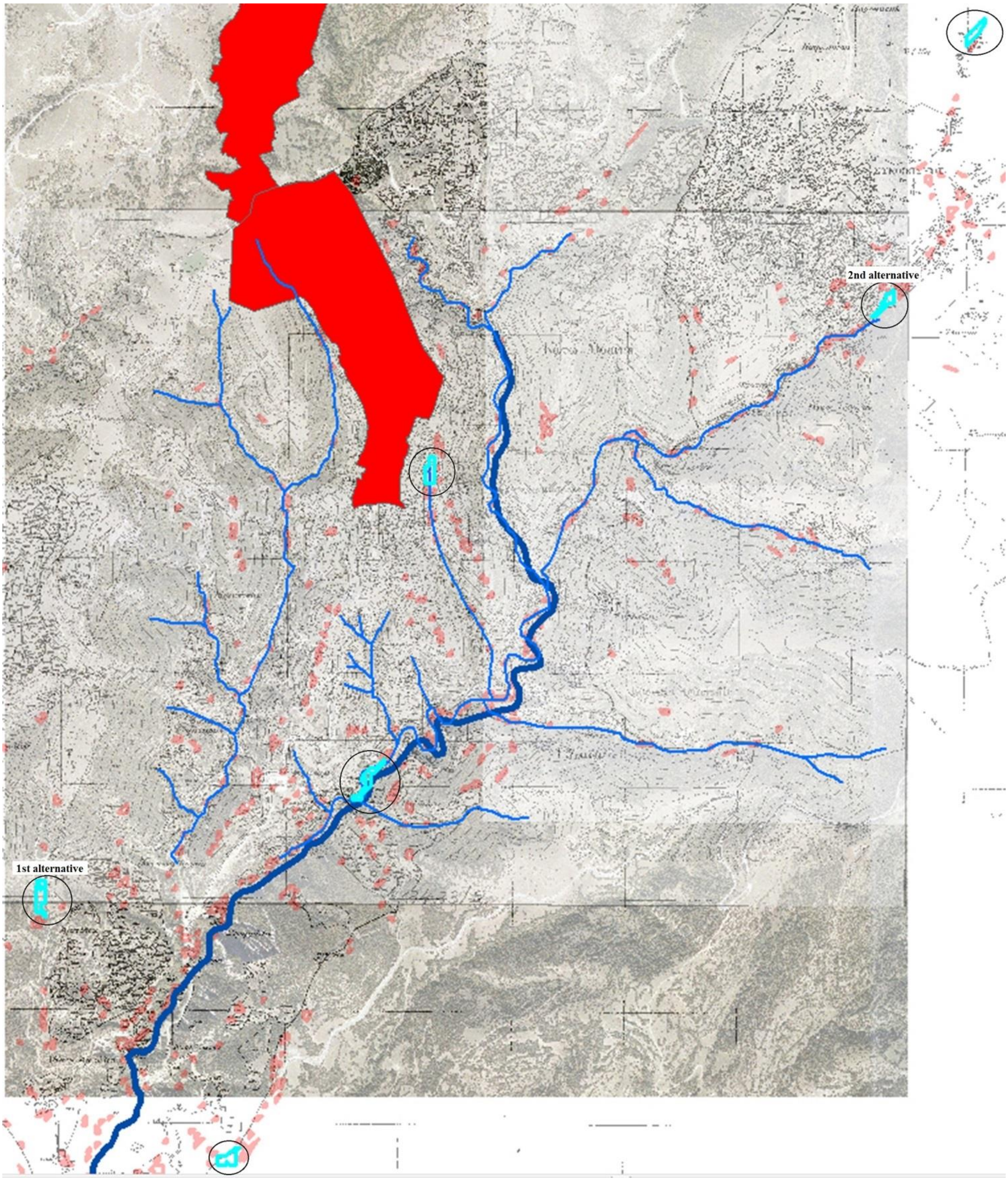


Figure 4: Six locations with an area > 3,000 m²

Through geodata.gov.gr, we can reject additional areas downstream by uploading the hydrographic network and importing the shape file in the working environment. When georeferenced pictures of MinAgric are imported, from which information about the ownership status is obtained, Figure 5 occurs.

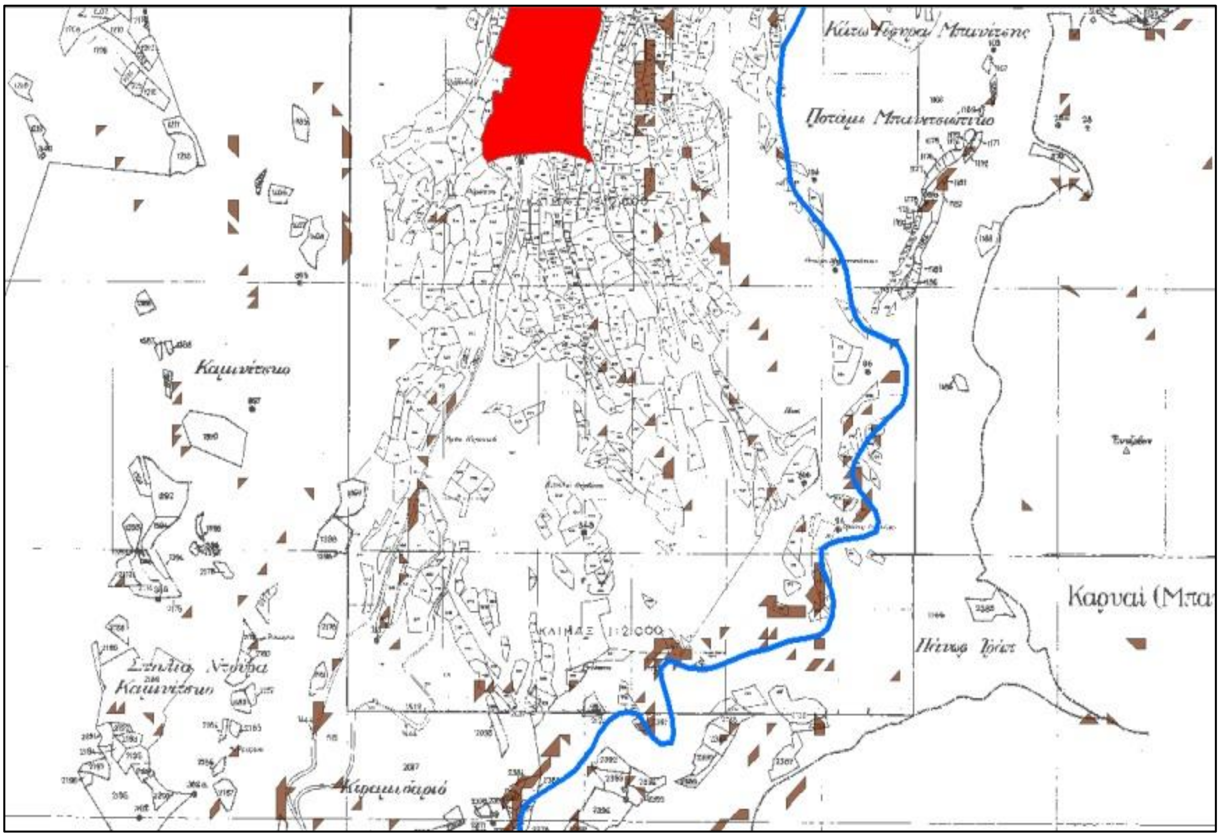


Figure 5: Hydrographic network and MinAgric schematic map (ownership)

1st alternative: A=4,800 m^2, distance from settlement boundaries 2,200 m. The Figure 6 shows long distance from settlement (2,200 m) without expropriation required, away from final recipient stream/

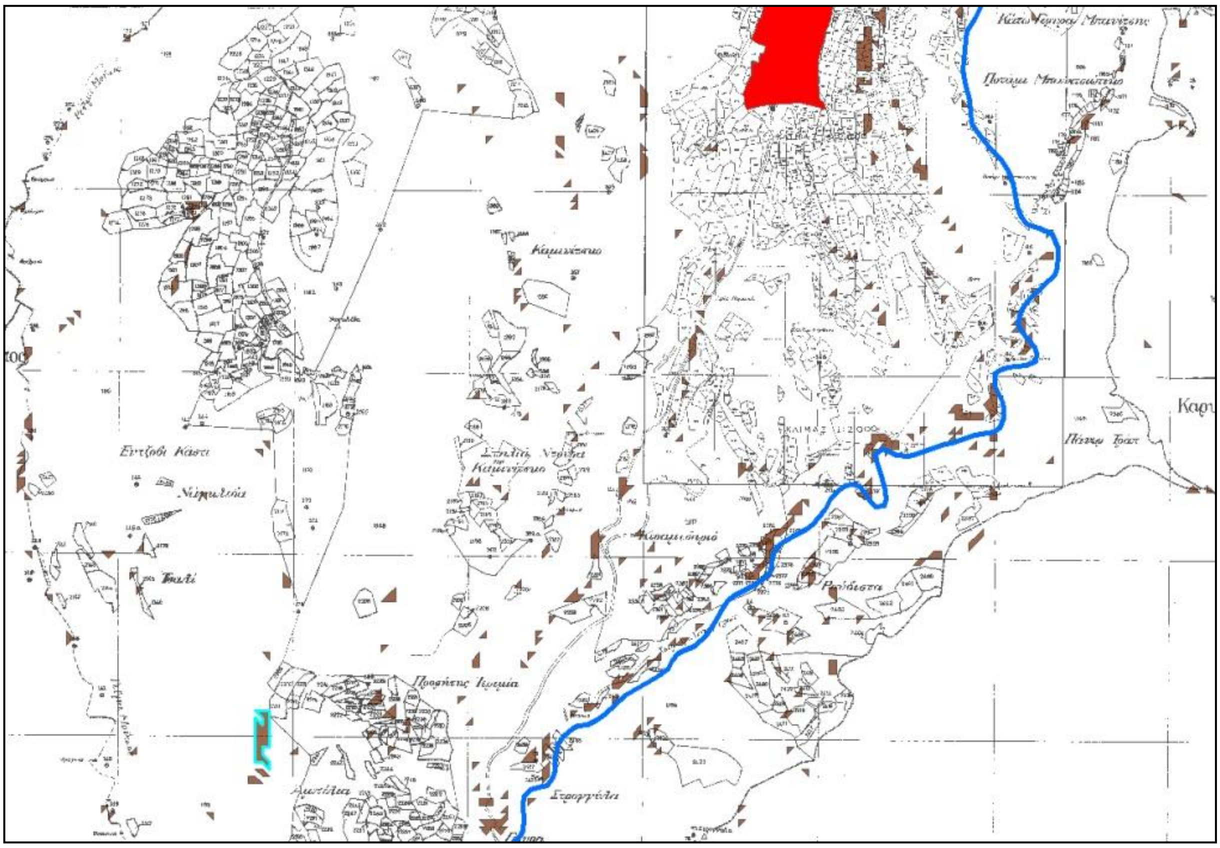


Figure 6: 1st alternative

2nd alternative: A=3,200 m^2, distance from settlement boundaries 2,000 m. This alternative rejected, because it is downstream from the final recipient (Figure 7).

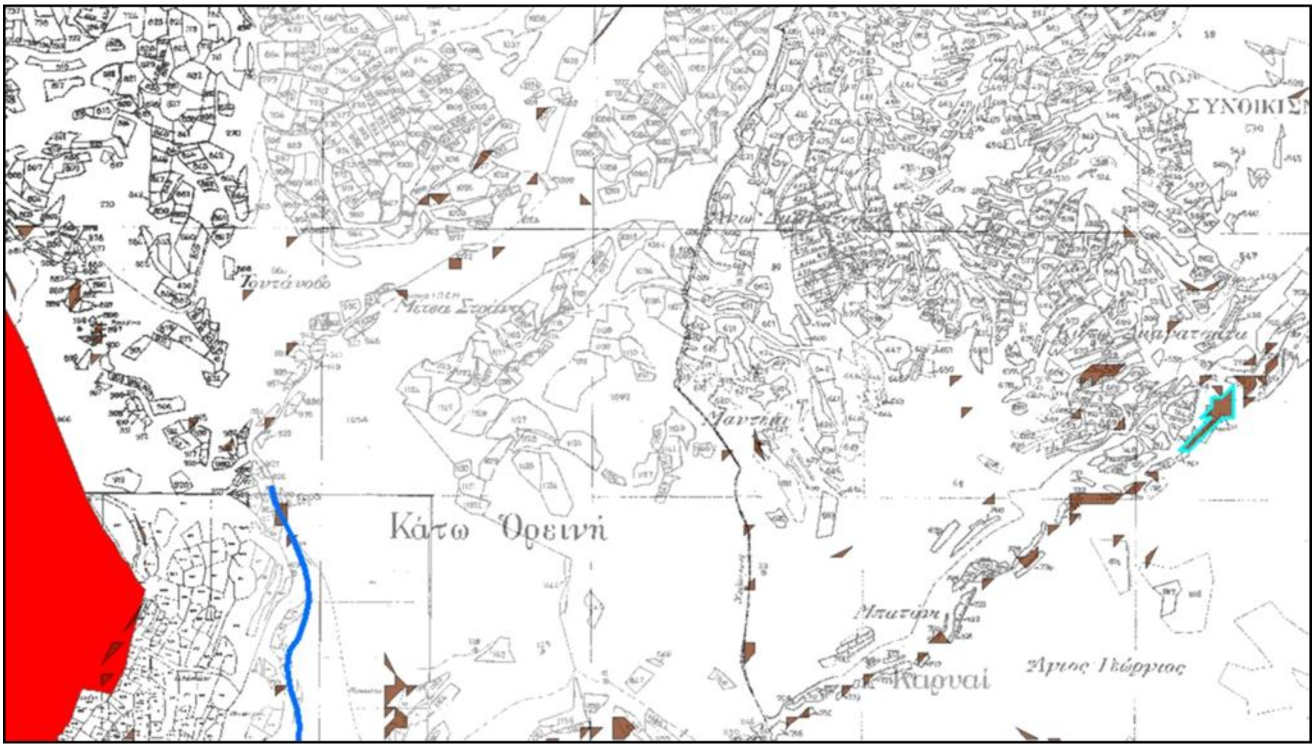


Figure 7: 2nd alternative

If the area query is expanded to include areas under 3,000 m^2, two more interesting alternatives come up, which are not only adjacent to the final recipient but also connected to neighbouring areas, therefore eligible for the location of the unit.

4. CONCLUSION

Environmental management is, to a large degree, a spatial procedure. The data used for the placement study require the clear definition of the criteria and characteristics these places should govern. Therefore, combinational, multi-parameter and multi-level interpretation of map data is required to reject or accept alternate site locations. The proposed criteria are financial and concern the minimization of construction and operating cost of the unit. In the placement study, alternative sites that fulfil the criteria are selected and eventually the most appropriate one is chosen. The slope of the land, the distance from the settlement (which also affects the anthropogenic factor) and the possible expropriation required for the construction play a major role in the construction cost. The use of GIS deals with spatial and descriptive issues without substituting the researcher but minimizing the alternate site research time and giving results that fulfil the required criteria. Therefore, an interaction between the researcher and the software develops in which the researcher defines the criteria and the software in essence carries out the repetitive process of testing to reach one or more optimal results. The results showed that the use of GIS technology is a base tool to analyse and make decisions for the finding of areas for construction of natural waste processing systems such as AWL's that constitute the optimal solution to protect the environment for small settlements according to the European Union waste management program

References

1. Alemy J., Comas J., Turon C., Balaguer M.D., Poch M., Puig M.A., Bou J., (2005) **‘**Evaluating the application of a decision support system in identifying adequate wastewater treatment for small communities. A case study: the Fluvia River Basin’, **Water Science & Technology**, Vol.51, pp.179-186
2. Dai C., Guo H.H., Tan Q., Ren W., (2016) ‘Development of a constructed wetland network for mitigating nonpoint source pollution through a GIS-based watershed-scale inexact optimization approach’, **Ecological Engineering**, Vol.96, pp.94-108
3. Heidi van Deventer, Jeanne Nel, Namhla Mbona, Nancy Job, Justine Ewart-Smith, Kate Snaddon, Ashton Maherry, (2015) ‘Desktop classification of inland wetlands for systematic conservation planning in data-scarce countries: mapping wetland ecosystem types, disturbance indices and threatened species associations at country-wide scale’, **Aquatic Conservation**, 57-75
4. Zamorano Montserrat, Molero Emilio, Hurtado Alvaro, Grindlay Alejandro, Ramos Angel, (2008) ‘Evaluation of a municipal landfill site in Southern Spain with GIS-aided methodology’, **Journal of Hazardous Materials,** Vol.160, pp.473-481.
5. Kariotis S. and Panagiotopoulos, **Applied Surveying, Tome A, Disigma**, 137, 2013
6. Kontos, D, Th., D.P. Komilis, P,D., HalvadakisP, C., (2003), SitingMSW landfills in Lesvos Island with a GIS-based methodology,**Waste Management and Research** 21(3) 262–327.
7. Lin, Y, H., Kado J, J., (1998) A vector-based spatial model for landfill siting, **Journal of Hazardous Materials** 58, 3–14.
8. Siddiqui, Z, M.,(1996), Landfill siting using Geographic Information Systemes: a demonstration, **Journal of Environmental Engineering** 122 (6) 515–523.

PERFORMANCE EVALUATION OF FE-MN BIMETAL MODIFIED KAOLIN CLAY MINERAL IN AS(III) REMOVAL FROM GROUNDWATER

R Mudzielwana[1*], W.M Gitari[1] and P Ndungu[2]

[1]Department of Ecology and Resource Management, University of Venda, Thohoyandou, South Africa, +27 (0) 15 962 8572,
[2]Department of Applied Chemistry, University of Johannesburg, South Africa, +27 (0) 11 559 6180.

*Corresponding author's email address: mudzrabe@gmail.com

Abstract
In this study Fe-Mn bimetal modified kaolin clay mineral was synthesized and its performance for As(III) removal from groundwater was evaluated. The adsorbent was characterized using XRF, FTIR and SEM. The adsorbent contains SiO_2 (39.39%), AlO_3 (9.89%), FeO (16.66%) and MnO (4.02%) as main chemical constituents. Its morphology appears more porous and granulated. Effect of contact time, initial pH, initial concentration and co-existing ions on As(III) removal by Fe-Mn bimetal modified kaolin were evaluated using batch experiments. The results showed that the % As(III) removal was above 80% at initial pH range of 2-10 from initial As(III) concentration of 5 mg/L, contact time of 60 min at 250 rpm shaking speed, adsorbent dosage of 0.4 g/100 mL. The adsorbent was successfully regenerated for up to 4 adsorption-desorption cycles. The adsorption of As(III) in presence of co-existing anions can be summarized in a decreasing order of Cl^-> F^-> NO_3^->SO_4^{2-} >CO_3^{2-}. The adsorption data fitted better to pseudo second order reaction kinetic model indicating that adsorption occurred through chemisorption. Furthermore, isotherm data was described by Langmuir adsorption isotherm model. These results proved that Fe-Mn bimetal modified kaolin clay mineral is a promising adsorbent for As(III) remediation from groundwater.

Keywords: Adsorption; Characterization; kaolinite; Pseudo second-order; Langmuir adsorption isotherm.

1. INTRODUCTION

Clean and drinkable water is a necessity for human wellbeing. Nowadays there is reduction in clean water due contamination of water bodies by geochemical factors and industrial activities. Arsenic is one of the contaminants of that poses threat to living organisms, in particular human beings. It is linked to development of various types of cancer, skin thickening and neurological disorder diseases (Tiwari and Lee, 2012). Evidence of these diseases and their link to arsenic has been reported in countries such as India, China, Mexico, Bangladesh, Chile and United States (Naujokas et al., 2013; Rahman et al., 2018).
Due to increasing incident rate of arsenic related diseases, the World Health Organization (WHO) reduced the standard of arsenic in water for human consumption to 0.01 mg/L from 0.05 mg/L in 1993 (WHO, 1993; Smith and Smith, 2004). This standard has been accepted by several countries including South Africa (Kempster et al., 2006). As such in areas where there is no alternative source of clean water, efforts need to be directed towards removal of arsenic to a permissible limit of 0.01 mg/L. Adsorption is often considered as a sustainable and flexible method for arsenic removal and other contaminants due to its simplicity in design. Several adsorbents such as iron coated cement

(Kundu and Gupta, 2007), Fe/Al bimetallic (Cheng et al., 2016), lepidocrocite (Wang and Giammar, 2015), modified montmorillonite (Ren et al., 2014), surfactant modified bentonite clay (Su et al., 2011), hydrous ferric oxide (Wilkie and Hering).
Iron oxides have shown higher adsorption efficiency in wide range of pH towards arsenic species mainly As(V) than As(III) which is highly toxic. As such pre-oxidation of As(III) to As(V) is widely preferred to enhance its removal by iron oxides based sorbents. Manganese oxide is a known to be a good oxidizing agent for As(III). For this reason, several studies has been conducted on synthesis of Fe-Mn binary sorbent for arsenic removal from water (Li et al., 2012; Zhang et al., 2012; Cui et al., 2014; Qi et al., 2015). Although clay modified with iron oxides and manganese oxides has been evaluated for arsenic removal (Mishra and Mahato, 2016), little has been done in synthesis of clay based Fe-Mn binary sorbents. Therefore, this present study aims at 1) to synthesize Fe-Mn binary coated clay adsorbent for As(III) removal, 2) to optimize the conditions for As(III) removal using synthesized adsorbent, 3) to elucidate As(III) removal mechanism.

2. MATERIAL AND METHODS

2.1 Materials

Locally available kaolin clay soils containing quartz and kaolinite as main minerals was collected from Dzamba Village, Limpopo Province South Africa. All chemical reagents were purchased from Rochelle Chemicals & Lab Equipment CC, South Africa Ltd and were of analytical grade and they were used without further purification. Stock solutions containing 1000 mg/L As(III) was prepared by dissolving 0.1733 g $AsNaO_2$ respectively, in a 100 mL flask using Milli-Q water (18.2 MΩ/cm). The solution was preserved by adding few drops of 3 M HNO_3. Working solutions were prepared by appropriate dilutions.

2.2 Synthesis of Fe-Mn bimetal modified kaolin rich mineral

To synthesize Fe-Mn binary modified kaolin clay (FMK), solutions of Fe and Mn were mixed together at a volume ratio of 7.5 mL: 2.5 mL (Fe: Mn) in a 250 mL plastic bottle to make up a final volume of 10 mL. To this, 1 g of clay was added and the mixture was agitated for 10 min to ensure proper soaking. This was followed by addition of 20 mL of 2 M NaOH to the mixture to precipitate Fe and Mn into their respective oxides. The mixture was agitated for further 60 min and then aged for 48 hours for further precipitation. Thereafter, the mixture was centrifuged at 3000 rpm. And the residues were washed with Milli-Q water to remove excess supernatants till the pH was close to neutral and then oven dried for 12 hours at 110 ^{O}C. Modified clay was then milled to pass through 250 µm sieve and then stored in a zip lock plastic bag.

2.3 Physicochemical characterization of the modified clay

Elemental composition of the modified clay were examined using S1 titan hand held XRF (Bruker, Germany). Functional groups were determined using ATR Diamond FTIR (Bruker, Germany). The morphological characteristics determined using scanning electron microscopy (SEM) (Leo1450 SEM, Voltage 10 kV, working distance 14 mm).

2.4 Batch adsorption experiments

The efficiency of Fe-Mn bimetal modified kaolinite clay mineral in As(III) removal was evaluated using batch experiments. Parameters such as contact time, adsorbent dosage, adsorbate concentration and initial solution pH were evaluated. To evaluate the effect of contact time, 100 mL solution contain 5 mg/L As(III) was pipetted onto 250 mL plastic bottle and 0.1 g of the modified clay was added. Mixtures were agitated for various contact times ranging from 10 to 120 min on a Stuart Reciprocator Table Shaker. To evaluate the effect of adsorbent dosage, the clay mass was varied from 0.05 to 0.5 g. For the effect of adsorbate concentration, the concentration was varied from 1 to 30 mg/L and to evaluate the effect of pH the initial solution pH was adjusted from 2 to 12 using 0.1 M NaOH and 0.1 M HCl. The effect of co-existing anions was carried out in the presence of 5 mg/L of Cl^-, F^-, NO_3^-,

CO_3^{2-}, SO_4^{2-}. After agitation, samples were filtered using 0.45 μm pore filter membrane using a vacuum pump. The solution pH was measured using JENWAY 3510 pH meter. The residual As(III) concentration was measured using ScTRACE Gold electrode attached to 884 professional VA Polaography (Metrohm, SA). A composite solution containing 1 mol/L sulfamic acid, 0.5 mol/L citrilc acid and 0.45 mol/L KCl was used an electrolyte. All experiments were carried out in triplicate and the mean values were reported. Equation 1 and 2 were used to compute the percentage of removal and the adsorption capacity respectively.

$$\% \, removal = \left(\frac{C_i - C_e}{C_i}\right) \times 100\% \quad (1)$$

$$q_e = \left(\frac{C_i - C_e}{m}\right) \times v \quad (2)$$

Where C_i and C_e represent the initial and equilibrium As(III) concentration (mg/L) respectively and m represent mass of the dry adsorbent (g). V is the volume (L) and q_e is the adsorption capacity (mg/g).

2.5 Adsorbent regeneration and reuse

To evaluate the reusability of the adsorbents, 4 repetitive adsorption cycles were conducted as follows: 100 mL of solution containing 5 mg/L of As(III) was pipetted into 250 mL and 0.4 g of the clay soils was added to make adsorbent dosage of 0.4 g/100 mL. Mixtures were agitated for 60 min at 250 rpm. After agitation samples were filtered through 0.45 μm filter membranes. Residues were rinsed with Milli-Q water to remove free As(III) ions and then oven dried at 105 ◦C and reused for adsorption. For regeneration, residues were treated with 100 mL of 0.01 M Na_2CO_3 for 30 min to desorb the adsorbed ions thereafter samples were filtered to through 0.45 μm filter membrane and then washed gently with Milli-Q water. The regenerated adsorbent was then used for As(III) adsorption. The procedure was repeated up to 4th adsorption cycles.

3. RESULTS AND DISCUSSION

3.1 Physicochemical characterization

3.1.1 Bulk chemical composition

Table 1 presents major and minor chemical composition of raw kaolinite and Fe-Mn modified kaolinite clay. From the results it is observed that SiO_2 and AlO_3 are the major chemical oxides of the clay. After modification an increase in Fe_2O_3 and MnO was observed which shows that the material was successfully coated. Furthermore, a decrease was observed in the percentage composition of other oxides. This could be attributed to ion exchange, dilution and dialumination during modification.

Table 1: chemical composition of raw and modified clay.

Oxides(%w/w)	SiO_2	Al_2O_3	Fe_2O_3	MnO	MgO	CaO	K_2O	TiO_2
Raw	56.06	22.05	3.88	0.01	0.57	0.95	0.16	1.76
Modified	39.39	10.08	16.66	4.02	LOD	0.55	0.13	1.31

3.1.2 Morphological analysis

Figure 1A and B presents SEM micrographs of raw and modified kaolin clay soils, respectively. The morphology of the raw clay appears spongier with some irregular shaped agglomerates. After modification, the surface appears more porous with irregular shaped agglomerates. The EDS spectrum for the modified clay confirmed the presence of Mn and Fe on the surface of the clay. Which shows that the surface of the clay has been modified successfully.

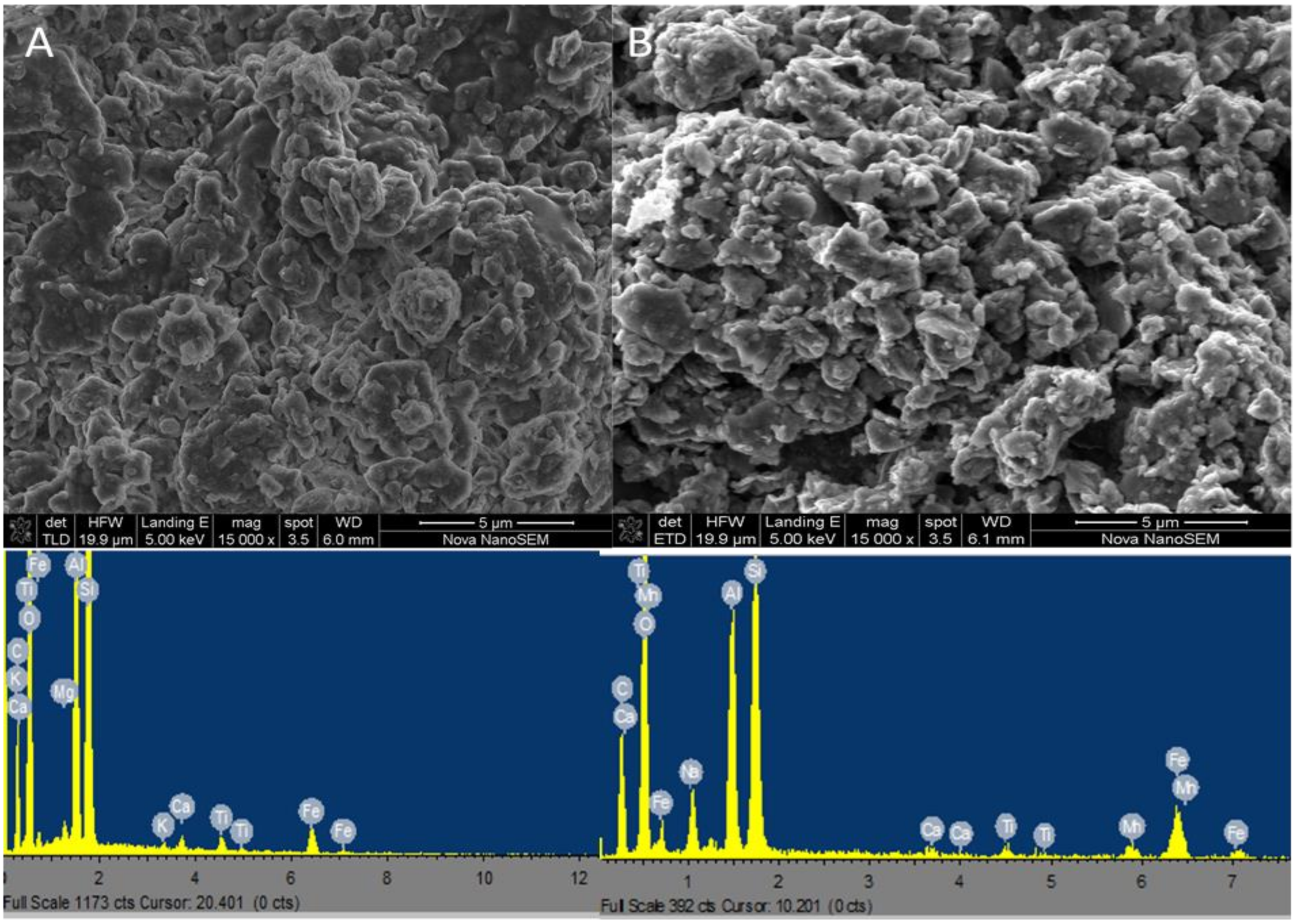


Figure 1: Micrographs of raw and modified kaolin clay soil.

3.1.3 FTIR analysis

The FTIR spectra of raw and modified kaolin clay recorded is presented in Figure 2. The spectra showed major band at 3619.36 cm^{-1} showing the vibration of structural -OH group of the clay material. The bands observed at 3633 and 1601 cm^{-1} could be attributed to vibration of hydroxyl groups in due to physiosorbed water and the hydroxyl groups located between the octahedral and tetrahedral sheets of the clay.

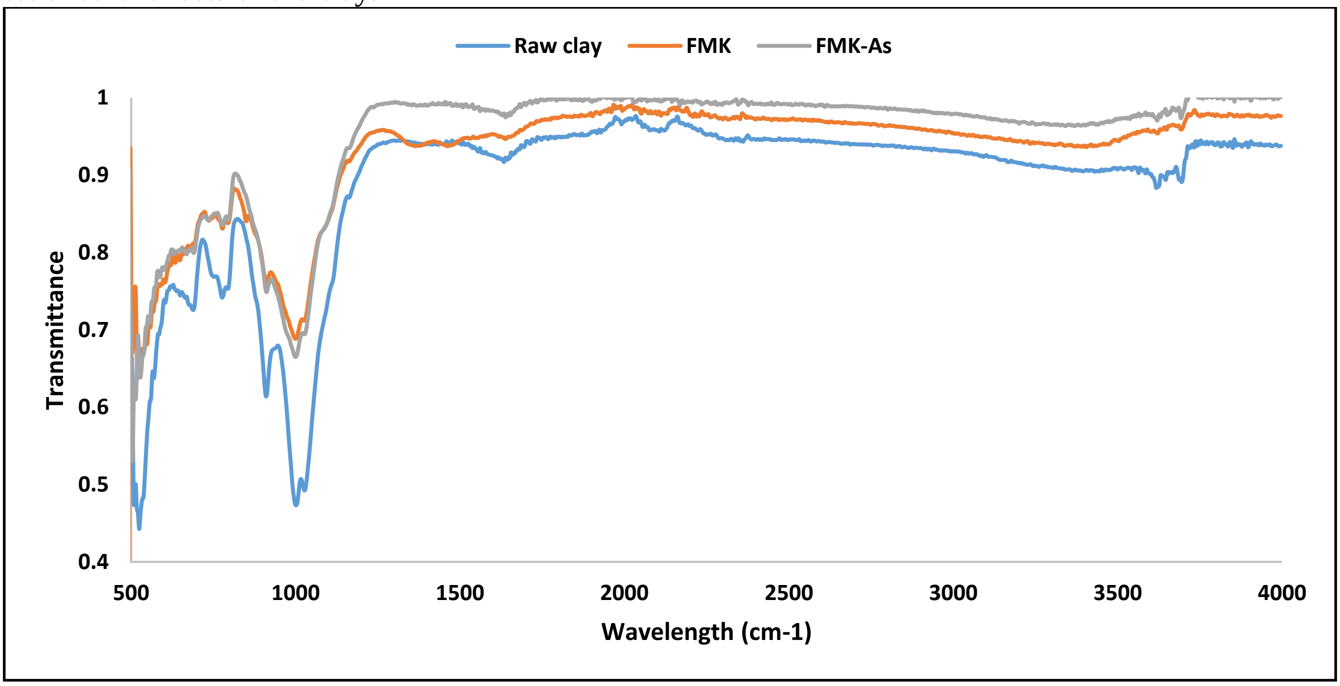


Figure 2: FTIR spectra of raw, modified clay (FKM) and after As(III) adsorption (FKM-As)

The band at 1020 cm^{-1} could be associated with the vibration of Si-O. The bands at 918, 762.96, 665 and 532 cm^{-1} could be ascribed to the vibration of Al-OH-Al, Al-O-Si. After modification, a decrease in the transmittance intensity of major bands at 1020, 918, 762. 96, 665 and 532 cm-1 was observed. This could be ascribed to loss of silica and alumina during modification of the clay with Fe-Mn oxides. A slight increase in these band was observed in the spectra recorded after As(III) adsorption.

3.2 Batch experiments

3.2.1 Effect of contact time and adsorption kinetics

The effect of contact time on As(III) adsorption capacity by Fe-Mn modified clay is depicted in Figure 3. It is observed that the adsorption capacity increased with increasing contact time reaching a maximum of 5.68 mg/g at 120 min. The increase in sorption capacity could be attributed to availability of more active sites in the adsorbent. The system reached equilibrium within 60 min and it was therefor used as optimum contact time for subsequent experiment. To further illustrate the rate limiting steps and possible reaction mechanism, linear equations of pseudo first order and pseudo second order reaction models (Eq. 3 and 4) together with the intra-particle model of Weber Morris (Eq. 5) were used (Tran et al., 2017; Weber and Morris, 1963).

$$\log(q_e - q_t) = -\frac{K_1 t}{2.303} + \log q_e \quad (3)$$

$$\frac{t}{q_t} = \left(\frac{1}{q_e}\right) t + \frac{1}{K_2 q_e^2} \quad (4)$$

$$q_t = K_{id} t^{1/2} + C_i \quad (5)$$

Where q_e and q_t (mg/g) are the adsorption capacities of As(III) on the adsorbents at the equilibrium and at time t (min), K_1 (min^{-1}) and K_2 (mg/g. min^{-1}) are the rate constants of the pseudo first order equation and pseudo second order equation, respectively. K_{id} (mg/g. $min^{1/2}$) is the intra-particle diffusion rate constant and C_i is the intercept.

The adsorption data was described better by pseudo second order model as shown by the plot in Figure 4 as compared to pseudo first order model (figure not presented). This suggests that As(III) adsorption occurred via chemisorption. This was further confirmed by the models constant values as presented in Table 2. The intra-particle diffusion plot showed three different phases (Figure 5). The first linear plot indicate adsorption of As(III) on the external surface of the adsorbent, second plot indicate the film transport of As(III) into the pores of the adsorbent and lastly the third one indicate the intra-particle diffusion at equilibrium. The K_{id} value phase 1 was higher compared to K_{id} values at phase 2 and 3 indicating that adsorption on the external surface was much faster compared to other phases. This could be attributed to increasing mass transfer resistance as confirmed by increasing boundary layer thickness constant (C_i) value from phase 1 to 3.

Table 2: Constant values for Pseudo first order and second order reaction kinetics models.

Pseudo first order			Pseudo second order		
K1 (min^{-1})	q_e (mg/g)	R^2	K^2(g/mg.min^{-1})	q_e (mg/g)	R^2
0.027	1.76	0.89	0.028	6.0	0.99

Table 3: Constant values for Intra-particle diffusion model.

K_{id1} (mg/g. $min^{-0.5}$)	C_{i1}	K_{id2} (mg/g. $min^{-0.5}$)	C_{i2}	K_{id3} (mg/g. $min^{-0.5}$)	C_{i3}
0.724	1.22	0.241	3.77	0.05	5.10

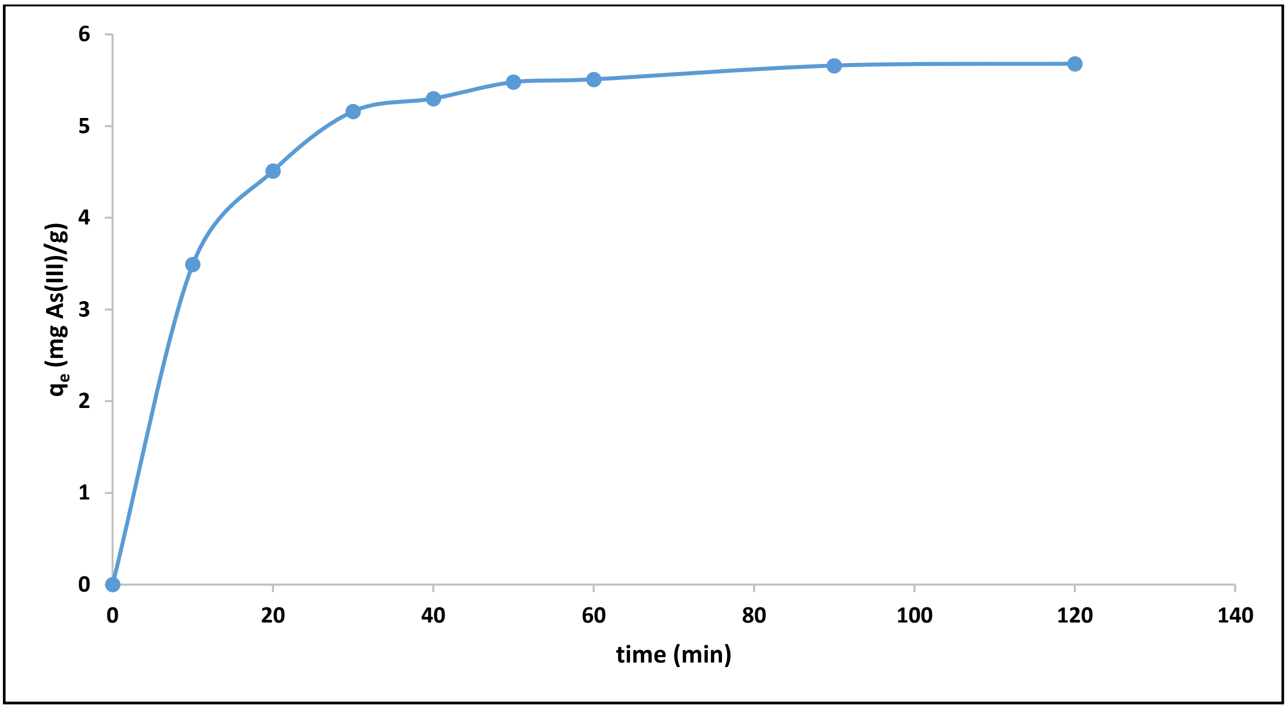


Figure 3: Effect of contact time on As(III) adsorption capacity (0.1g /100 mL adsorbent dosage, 5 mg/L adsorbate concentration, 6.4 solution pH and 250 rpm shaking speed).

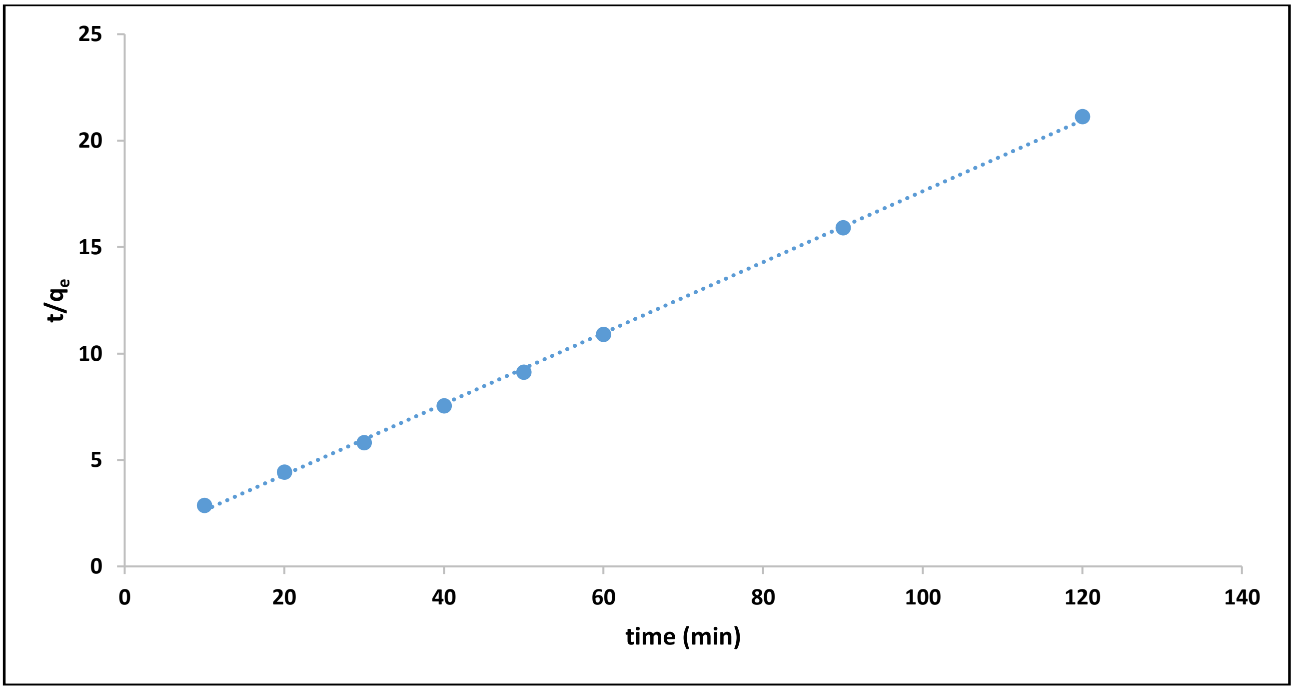


Figure 4: Linear plot for pseudo second order.

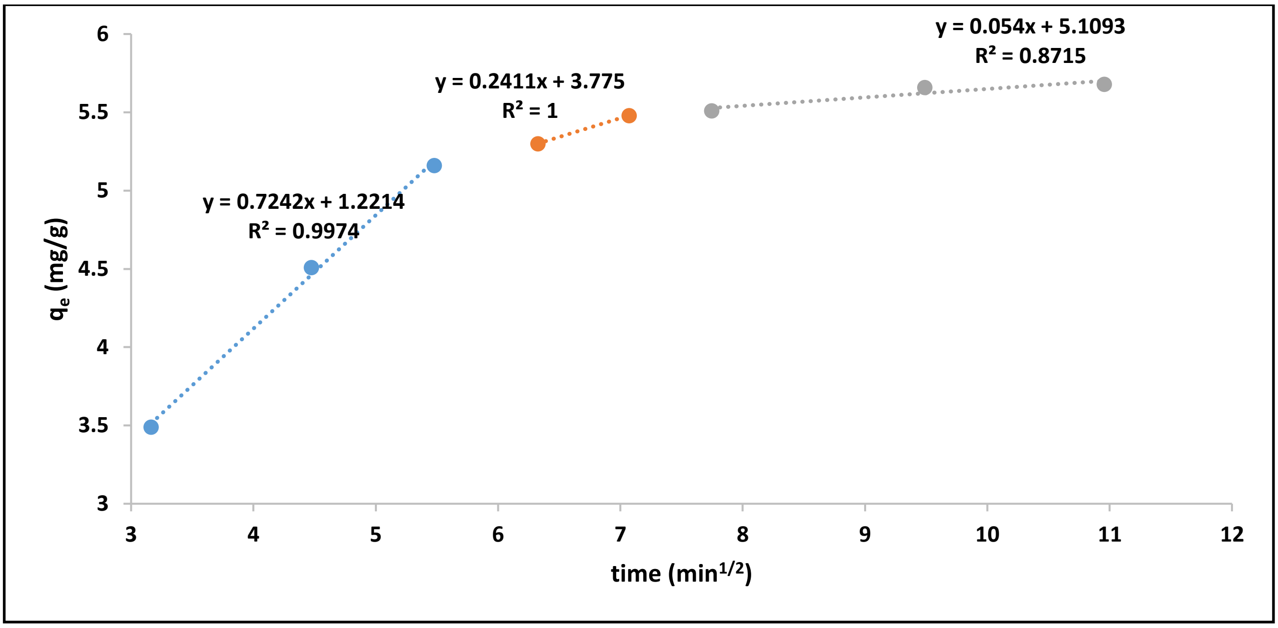


Figure 5: Intra-particle diffusion plot.

3.2.2 Effect of adsorbent dosage

Figure 6 presents the effect of adsorbent dosage on As(III) percentage removal and also on the q_e (mg/g) adsorption capacity. The results showed that the percentage As(III) removal increased with increasing adsorbent dosage up to 0.4 g/100 mL thereafter, no further increase was observed. Conversely, the adsorption capacity decreased with increasing adsorbent dosage. The trend is linked to increasing active adsorption sites for a limited As(III) ions available in the solution as the adsorbent dosage increases. Therefore, 0.4 g/100 mL was chosen as the optimum adsorbent dosage for subsequent experiments.

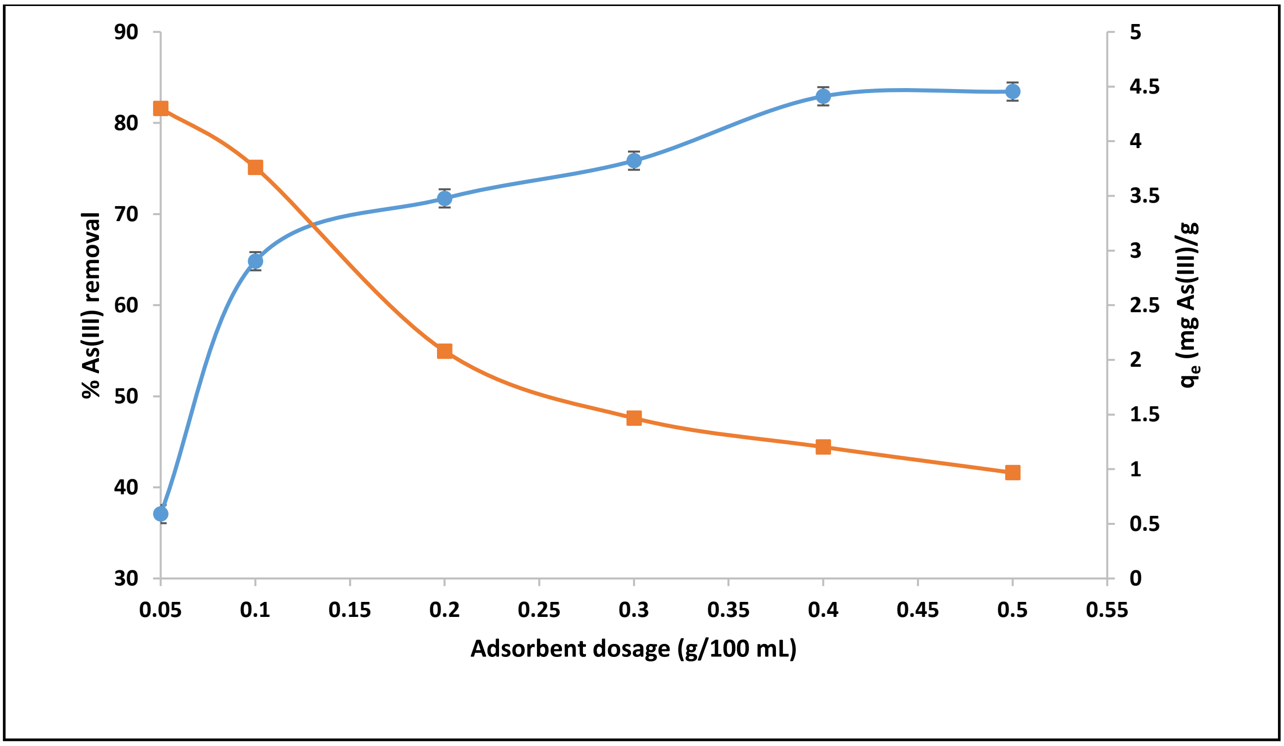


Figure 6: Effect of adsorbent dosage onto % As(III) removal and As(III) adsorption capacity (Adsorbate concentration 5 mg/L; pH 6.32 and contact time of 60 mins at 250 rpm).

3.2.3 Effect of adsorbate concentration and adsorption isotherms

Figure 7 depicts the effect of adsorbate concentration on % As(III) removal and As(III) adsorption capacity. It is evident that the percentage As(III) removal decreases with increasing adsorbate concentration while the adsorption capacity increases as the initial concentration. This could be attributed to increasing ratio between the active adsorption sites and the adsorbate molecules as the concentration increases. At lower concentration, the ratio of active sites is to As(III) ions is higher resulting in sufficient interaction of ions with the active sites for efficient As(III) removal.

To further illustrate the relationship between the adsorbate concentration and the adsorbent the linear equations for Langmuir (Eq. 6) and Freundlich (Eq. 7) isotherm model were used (Langmuir, 1918; Tran et al., 2017).

$$\frac{C_e}{q_e} = \left(\frac{1}{Q_{max}}\right) C_e + \frac{1}{Q_{max} K_L} \quad (6)$$

$$\log q_e = n \log C_e + \log K_F \quad (7)$$

Where C_e (mg/L) is the As(III) concentration at equilibrium, q_e (mg/g) is the adsorption capacity at equilibrium, Q_{max} (mg/g) is the maximum saturated monolayer adsorption capacity, K_L (L/mg) is the constant related to the affinity between adsorbent and adsorbate, K_F (mg/g) is the Freundlich constant related to adsorption capacity and n is the Freundlich intensity parameter which indicate the magnitude of the adsorption driving force or the surface heterogeneity. The value of Q_{max} and K_L are determined from the slope and intercept of C_e/q_e Vs C_e while the value of K_f and n are determined from the slope and intercept of log q_e Vs log C_e. The data for adsorption of As(III) by Fe-Mn modified clay fitted better to Langmuir adsorption isotherm as compared to Freundlich isotherm model. Figure 8 shows the plot for Langmuir isotherm model while Table 4 presents the constant values for both isotherm models. The better fitting to Langmuir isotherm model suggests monolayer uniform adsorption on the surface of the adsorbent.

Table 4: constant values for Langmuir and Freundlich adsorption isotherms.

Langmuir adsorption isotherm			Freundlich adsorption isotherm		
q_m (mg/g)	K_L (L/mg)	R^2	K_f (mg/g)	n	R^2
2.07	0.64	0.99	1.54	0.44	0.90

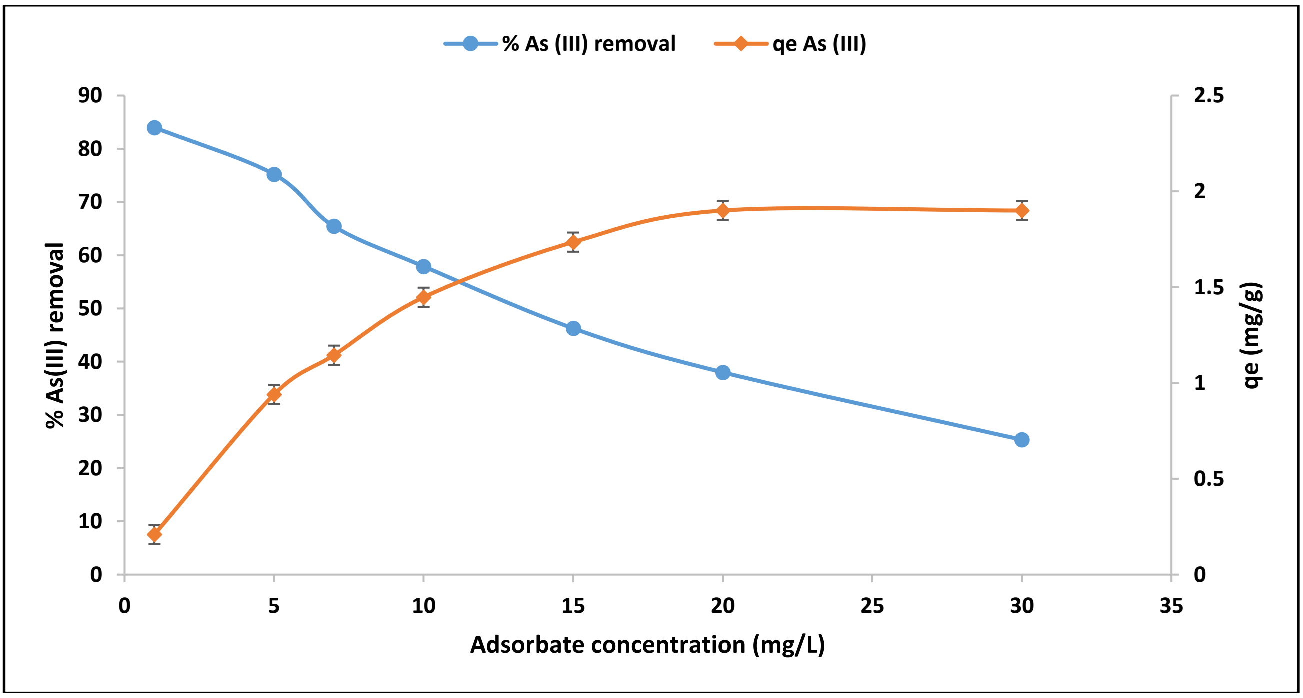


Figure 7: Effect of adsorbate concentration on As(III) removal and adsorption capacity (0.4 g adsorbent dosage, 6.33 pH, 60 min contact time at 250 rpm)

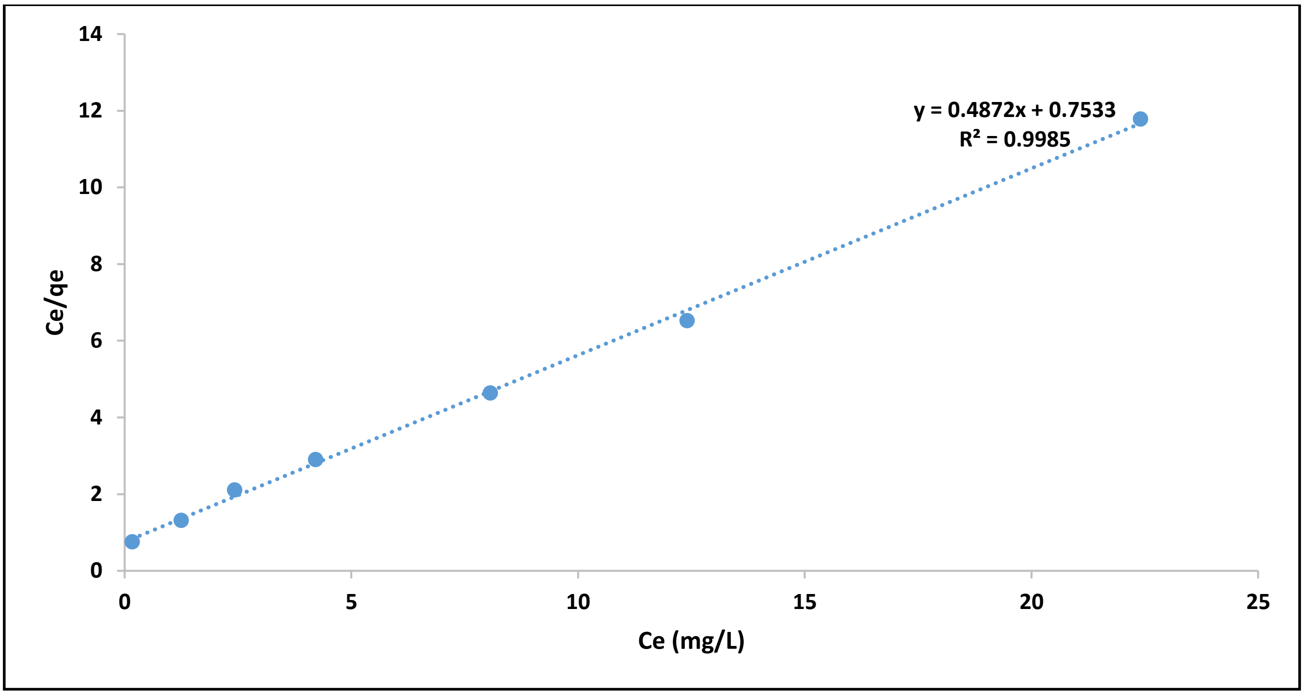


Figure 8: Linear plot for Langumuir adsorption isotherm.

3.3.4 Effect of pH

Figure 9 shows the effect of pH on adsorption of As(III) removal. It is evident that the percentage As(III) removal remained above 80 % from the initial pH of 2-8 and then decrease drastically at pH above 8. This trend can be attributed to As(III) speciation at different pH values. At pH <9 the most dominant species of As(III) is neutrally charged H_3AsO_3 whereas at pH>9 the dominant species is negatively charged $H_2AsO_3^-$. The decrease in As(III) removal could be attributed to electrostatic repulsion between the OH- in the adsorbent surface and also the competition between the abundant OH- in the solution and $H_2AsO_3^-$.

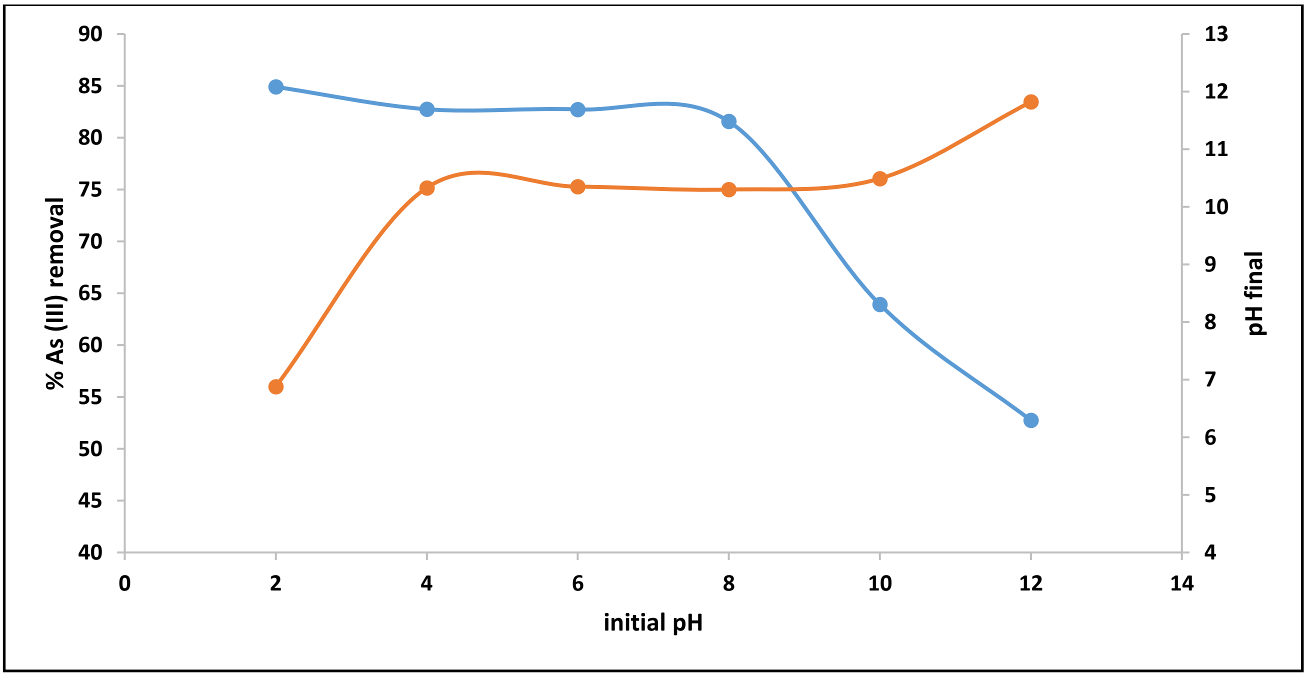


Figure 9: Effect of initial pH on % As(III) removal (5 mg/L adsorbate concentration, 0.4 g/100 mL adsorbent dosage and 60 min contact time).

3.3.5 Effect of competing anions

The effect of co-existing anions is presented in Figure 10. The presence of fluoride, nitrate, carbonate and sulphate ions showed inhibition of As(III) by FMK by about 1% while chloride showed greater influence by about 2.5%. Although the As(III) removal decreased in the presence of other anions, the overall % of removal was still beyond 90 %. As such FMK synthesized in this study can still be used to treat groundwater containing all these ions. The effect of co-existing anions on As(III) removal can be summarized in the decreasing order of Cl^{-}> F^{-}> NO_3^{-}>SO_4^{2-}>CO_3^{2-}.

3.3.6 Regeneration and reuse

For the adsorbent to be considered economically viable for use in water it must be able to be reused and regenerated effectively. To evaluate the regeneration potential, Na_2CO_3 was used as a regenerant solution. After each adsorption cycle, adsorbent was treated with 100 mL deionized water, oven dried and reused for As(II) removal. Figure 11 shows the results for four adsorption- reuse cycles. The value for fresh denotes the percentage As(III) removal observed from freshly prepared sorbent. The results showed that the % As(III) removal with the first two cycles was almost equal to the one that was archived by fresh adsorbent. The percentage removal showed significant decrease going to 3rd and 4th adsorption cycles. This could be attributed to two possible factors 1) inadequate regeneration of the adsorbent and 2) dissolution of major chemical oxides from the adsorbent due to treatment by alkaline solution. The same trend was observed after treating used sorbent with Milli-Q water. This result signifies that FMK is a possible candidate for As(III) removal from groundwater.

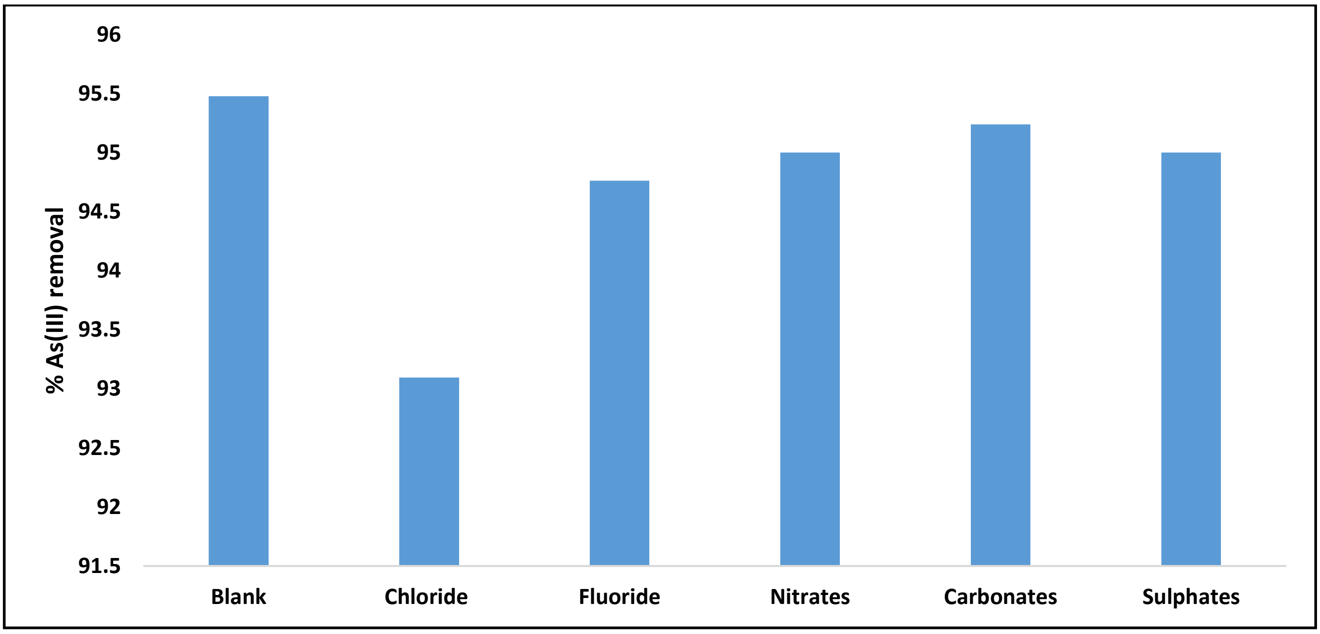


Figure 10: Effects of co-existing anions in As(III) removal by FMK (5 mg/L As(III) initial concentration, 5 mg/L of each co-existing ions, 0.4 g/100 mL adsorbent dosage, 6.7 initial pH and 60 min agitation time at 250 rpm)

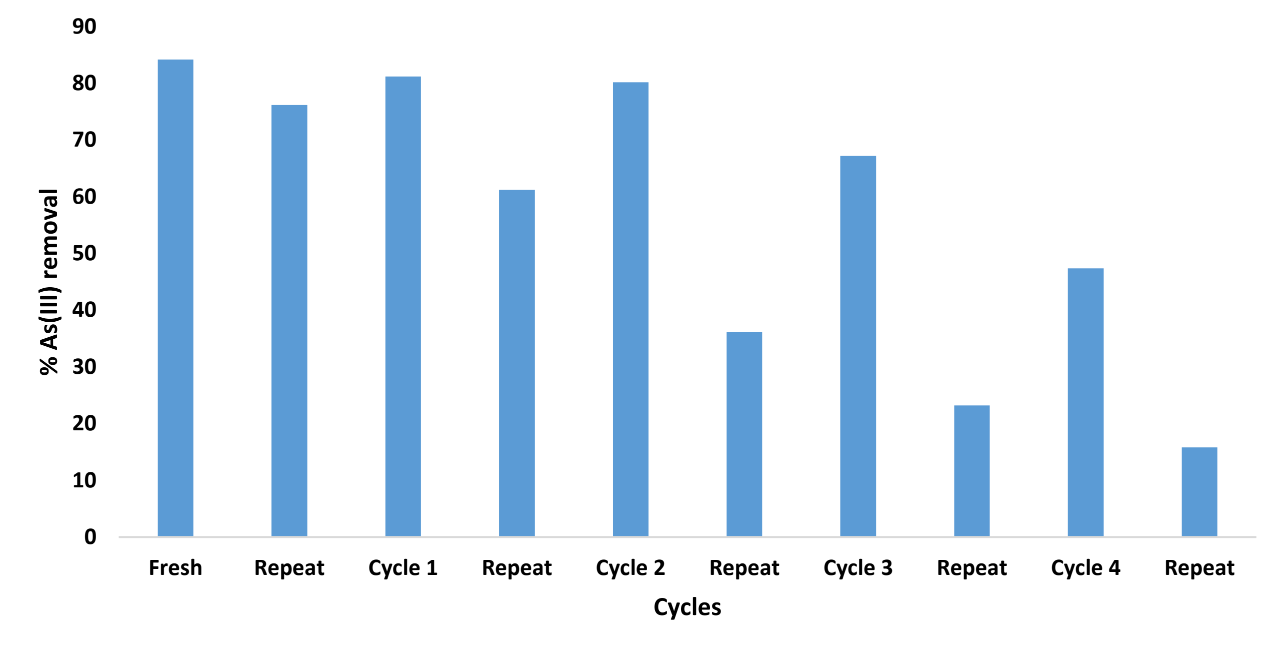


Figure 11: Variation of % As(III) removal as a function of regeneration and repeat cycles (6 mg/L As(III), 0.4 g/100 mL adsorbent dosage, 60 min contact time at 250 rpm shaking speed).

4. CONCLUSIONS

The Fe-Mn bimetallic modified kaolin clay was successfully synthesized. The prepared FMK proved to be effective for As(III) removal from water. The percentage of removal was found to be above 80% at pH range between 2 and 8 from the initial As(III) concentration of 5 mg/L using 0.4 g/100 mL adsorbate concentration after 60 min of contact time. As(III) removal was observed to be low at alkaline pH levels. The adsorption kinetics data fitted well to pseudo second order of reaction indicating that As(III) adsorption occurred via chemisorption. Furthermore, the data also fitted well to Langmuir adsorption isotherm indicating monolayer adsorption of As(III) on the surface of adsorbent. The adsorption of As(III) in presence of co-existing anions can be summarized in a decreasing order of Cl^{-}> F^{-}> NO_3^{-}>SO_4^{2-}>CO_3^{2-}. The adsorbent was effectively regenerated and reused for 4 consecutive cycles although a decrease in As(III) removal was noted after the 2nd regeneration cycle. The obtained results suggest that FMK developed in this study is a possible candidate for As(III) removal from groundwater.

Acknowledgement
Authors would like to acknowledge financial assistance from National Research Foundation, SaiF and University of Venda (RPC).

References

1. Cheng, Z. Fu, F. Dionysiou, D.D. Tang, B. 2016. Adsorption, oxidation, and reduction behavior of arsenic in the removal of aqueous As(III) by mesoporous Fe/Al bimetallic particles. **Water Research**, 96, pp. 22-31.

2. Cui, H.J. Cai, J.K. Zhao, H. Yuan, B. Ai, C.L. Fu, M.L., 2014. Fabrication of magnetic porous Fe–Mn binary oxide nanowires with superior capability for removal of As(III) from water. **Journal of Hazardous Materials**, 279, pp. 26–31.

3. Kempster, P.L. Silberbauer, M. Kuhn, A., 2007. Interpretation of drinking water quality guidelines – The case of arsenic. **Water SA,** 33(1), pp. 95-100.

4. Kundu, S. Gupta, A.K., 2007. Adsorption characteristics of As(III) from aqueous solution on iron oxide coated cement (IOCC). **Journal of Hazardous Materials**, 142, pp. 97–104.

5. Langmuir, I., 1918. The adsorption of gases on plane surfaces of glass, mica and platinum. **Journal of the American Chemical Society,** 40 (9), pp. 1361-1403.
6. Li, X. He, K. Pan, B. Zhang, S. Lu, L. Zhang, W., 2012. Efficient As(III) removal by macroporous anion exchanger-supported Fe–Mn binary oxide: Behavior and mechanism. **Chemical Engineering Journal,** 193(194); 131–138.
7. Mishra, T. Mahato, D.K. 2016. A comparative study on enhanced arsenic(V) and arsenic(III) removal by iron oxide and manganese oxide pillared clays from ground water. **Journal of Environmental Chemical Engineering,** 4, pp. 1224–1230.
8. Naujokas, M.F. Anderson, B. Ahsan, H. Aposhian H.V. Graziano, J.H. Thompson, C. Suk, W.A., 2013. The Broad Scope of Health Effects from Chronic Arsenic Exposure: Update on a Worldwide Public Health Problem. **Environmental Health Perspectives,** 121(3), pp. 295-302.
9. Qi, J. Zhang, G. Li, H., 2015. Efficient removal of arsenic from water using a granular adsorbent: Fe–Mn binary oxide impregnated chitosan bead. **Bioresource Technology,** 193, pp. 243–249.
10. Rahman, M.A. Rahman, A. Khan, M.Z.K. Renzaho, A.M.N., 2018. Human health risks and socio-economic perspectives of arsenic exposure in Bangladesh: A scoping review. **Ecotoxicology and Environmental Safety**, 150, pp. 335–343.
11. Ren, H. Zhang, Z. Luo, H. Hu, B. Dang, Z. Yang, C. Li, L, 2014. Adsorption of arsenic on modified montmorillonite. **Applied Clay Science**, 97–98, pp. 17–23.
12. Smith, A.H. Smith M.M.H., 2004. Arsenic drinking water regulations in developing countries with extensive exposure. **Toxicology.** 198, pp. 39–44.
13. Su, J. Huang, H.G. Jin, X.Y. Lu, ZQ. Chen, Z.L., 2011. Synthesis, characterization and kinetic of a surfactant-modified bentonite used to remove As(III) and As(V) from aqueous solution. **Journal of Hazardous Materials,** 185, pp, 63–70.
14. Tiwari, D. Lee, S.M., 2012. Novel hybrid materials in the remediation of ground waters contaminated with As(III) and As(V). **Chemical Engineering Journal**, 204–206, pp. 23–31.
15. Tran, H.N. You, S.J. Bandegharaei, A.H. Chao, H.P. 2017. Mistakes and inconsistencies regarding adsorption of contaminants from aqueous solutions: A critical review. **Water Research,** 120, pp. 88-116.
16. Wang, L. Giammar. D.E., 2015. Effects of pH, dissolved oxygen, and aqueous ferrous iron on the adsorption of arsenic to lepidocrocite. **Journal of Colloid and Interface Science**, 448, pp. 331–338.
17. Weber, W.J. Morris, J.C., 1963. Kinetics of adsorption on carbon from solution. **Journal of the Sanitary Engineering Division,** 89(2), pp. 31-60.
18. WHO, 1993. Guidelines for Drinking Water Quality: Recommendations, Vol. 1. World Health Organization, Geneva.
19. Wilkie, J.A. Hering, J.G., 1996. Adsorption of arsenic onto hydrous ferric oxide: effects of adsorbate/adsorbent ratios and co-occurring solutes. **Colloids and Surfaces A: Physicochemical and Engineering Aspects**, 107, pp. 97-110.
20. Zhang, G. Liu, H. Qu, J. Jefferson, W., 2012. Arsenate uptake and arsenite simultaneous sorption and oxidation by Fe–Mn binary oxides: Influence of Mn/Fe ratio, pH, Ca^{2+}, and humic acid. **Journal of Colloid and Interface Science,** 366, pp. 141–146.

REUSE POTENTIAL OF CATAPHORESIS WASTEWATERS IN AUTOMOTIVE INDUSTRY

P. Karacal[1], C. Aliyazicioglu Ozdemir[2], E. Erdim[2] and F. Germirli Babuna*[1]

[1]Environmental Engineering Department, Istanbul Technical University, Maslak 34469, Istanbul, Turkey

[2]Environmental Engineering Department, Marmara University, School of Engineering, Goztepe, Kadikoy 34722, Istanbul, Turkey

*Corresponding author: e-mail: germirliba@itu.edu.tr, tel: +905324090355

Abstract

Extensive amount of water input together with various chemicals are required by automotive industry. The cataphoresis process is composed of two main sub-processes: pretreatment and electrodeposion (ED) coating. The retreatment or surface preparation process consists of a series of operations, which includes the hot water rinsing, degreasing, rinsing, surface activation and phosphate coating followed by several rinsing steps. After these operations, electrodeposition coating takes place. As a result, of the cataphoresis process, a metal surface resistant to corrosion and ready to further surface applications is obtained. Recycling and reuse of wastewater in this process is of great importance for sustainability studies as substantial amounts of water is consumed and wastewater is generated out of it. On the other hand, there is limited information in the literature on the reuse of wastewaters produced from cataphoresis rinse pools. The wastewater originating from the cataphoresis process contains heavy metal ions. In order to remove heavy metal ions from these effluents various treatment methods ie. chemical precipitation, adsorption, oxidation-reduction, electrochemical treatment, membrane technologies etc. can be used. The economic and technical limitations resulting from applying the mentioned methods trigger research activities to focus on promising emerging technologies such as removal with nanoparticles. In this context the objective of this study is to evaluate the widely used cataphoresis process of automotive industry in terms of its water consumption and pollution loads, and to investigate the reclamation and reuse potential of segregated effluents arising from this process. The results indicate that 43 % of the continuous effluents arising from cataphoresis process is reusable in nature. The amount of reusable wastewater streams can also be elevated by adding discharges from cooling system and boiler to the mentioned segregated wastewaters. By doing so 20 % of the whole wastewaters can be designated as reusable effluents after being subjected to an appropriate treatment.

Keywords: industrial pollution; wastewater reuse; cataphoresis; automotive manufacturing; segregated effluents.

1. INTRODUCTION

The depletion and pollution of the water resources can be considered as one of the most important environmental problems in the world. Due to industrialization and the increase in the consumption, water resources are declining and getting more polluted every day. Over the last decade water reclamation and reuse applications have increased as they represent effective approaches for conserving limited, high-quality fresh water supplies. To meet the future needs of domestic and industrial water requirements and to protect the quality of water resources, methods should be developed to reduce water usage and water-wastewater management strategies need to be improved.

Therefore, studies on re-use and recovery of wastewater in industrial sectors gain more and more significance.

Effluents from industrial process and operations, such as metal finishing, electroplating and mining contain heavy metals. Heavy metals, such as mercury, lead, cadmium, nickel generates toxic wastewaters.

According to the data of 2016, the automotive sector corresponds to about 5 % of the world's economy. As a result, the sector is placed as the fourth largest economy with a share of 4 trillion dollars (IDBT, 2017). The automotive industry in Turkey plays an important role in the manufacturing sector of the Turkish economy. In 2017, Turkey produced more than 1 million motor vehicles (AMA, 2017). With a cluster of car makers and parts suppliers, the Turkish automotive sector has become an integral part of the global automotive manufacturers network, exporting nearly 28.4 billion dollar worth of motor vehicles and components (AMA, 2017).

Quite a high amount of water with various chemical additives are consumed by automotive industry. It is stated in the literature that approximately a water usage ranging from 2.31 to 8 m^3/vehicle is required for car assembly and production (Tejeda et al, 2012). The wastewaters generated from the mentioned sector in turn are treated by means of many different technologies; such as micro filtration (Zhang et al, 2006), oxidation (Zhu et al, 2017), coagulation-flocculation (Bakar and Halim, 2017), advanced oxidation (Consejo et al, 2005; Mudliar et al, 2009). Moreover, biological treatment can also be applied for removing pollutants from these effluents (Sarioglu and Gokcek, 2016; Mackulac et al, 2016).

The cataphoresis process, composed of two main sub-processes, pretreatment and electrodeposion (ED) coating, is an important operation in automotive industry. The pretreatment or surface preparation process consists of a series of operations which include the hot water rinsing, degreasing, rinsing, surface activation and phosphate coating followed by several rinsing steps (US EPA, 1994). After these operations electrodeposition coating takes place. As a result, the cataphoresis process, a metal surface resistant to corrosion and ready to further surface applications is obtained (US EPA, 1994). Recycling and reuse of wastewater in this process is of great importance from a sustainability standpoint as substantial amounts of water is consumed and wastewater is generated out of it. On the other hand, there is limited information in the literature on the reuse of wastewaters produced from cataphoresis rinse pools. The wastewater originating from the cataphoresis process contains heavy metal ions. In order to remove heavy metal ions from these effluents various treatment methods ie. chemical precipitation, adsorption, oxidation-reduction, electrochemical treatment, membrane technologies etc. can be used.

In this context the objective of this study is to evaluate the widely used cataphoresis process of automotive industry in terms of its water consumption and pollution loads, and to investigate the wastewater reclamation and reuse potential of segregated effluents generated from the mentioned process.

2. MATERIALS AND METHODS

The study covers and provides the necessary information on the technical steps required for a comprehensive survey, involving detailed process profile, water demand, wastewater generation, wastewater segregation for optimum treatment, water balance and conceptual basis of wastewater recycling potential. All wastewater samples collected (once every 2 months) from the processes on a regular basis, were analyzed directly. The wastewater samples were characterized in terms of chemical oxygen demand (COD), pH, suspended solids, ammonium nitrogen (NH4-N). All analyses were carried out according to the Standard Methods (APHA, 1998). The analytical methods adopted are given in Table 1.

Table 1: Adopted wastewater characterization methods

Parameter	Method
pH	Electrometric Method
COD	Closed Reflux-Colorimetric
Suspended Solids	Gravimetric Method
NH_4-N	Nesslerization (SM 4500-NH_3 C)

3. DESCRIPTION OF THE INDUSTRY AND PRODUCTION PROCESSES

In the automotive industry, production processes are basically divided into four main production lines. These four main production lines are: pressing, welding, painting and assembly.

The production of vehicles starts with the press process. The parts forming the body of the vehicles are shaped on the press lines. Chassis and some body parts of trucks and busses are compressed in the pressing area. Pressing takes place in three steps. In the first stage, industrial flat plate sheets that come as plate get in first form. Then by means of the second press stage, the edges and the inner parts the segment which has been shaped in the previous step are cut out. In addition, cutting and drilling operations required to achieve the final shape of the part is performed in this stage. During the third stage of the press process holes are opened at the required points and the edges of the part are curled.

Spot welding is the most commonly used welding process for automotive and sheet metal works. At car body parts assembling line, sheet bodies are linked with spot welding machines. Then iin the 'carrossery' section of the production line; vehicle cabin, front side panel engine cover parts integration are performed. Annually, the production capacity of the assembly line is 12,500 vehicles.

The aim of painting is to form a coating film on the surface of an object in order to protect the object and give a fine appearance. Painting may also have other special functions. There are various types of coating methods. Spray painting and cataphoresis are currently used in many types of industrial painting. First, the vehicle bodies will undergo surface preparation and pre-paint treatment. This preparation involves thorough washing and wipe-cleaning. The pre-paint treatment process causes a chemical crystallization to occur on the vehicle surface that provides improved paint adhesion and anti-corrosion protection. The vehicle bodies are then conveyed directly from this phosphate pre-paint treatment process to the electro-coating process, which is typically a full immersion process. The vehicle bodies are immersed in the electro-coating bath, which causes electro-deposion on the vehicle bodies. That is, opposite charges are applied to the material and the vehicle, which causes the material to readily adhere to the surface of the vehicle. After applying the electro-coating, the vehicle bodies are conveyed to a curing oven (bake oven) where the coating is cured and dried prior to being conveyed to the prime-coat spray booth. As the vehicle moves toward and into the prime-coat spray booth, sealers and other protective coatings, such as antichip, are applied.

The assembly department is the last stage in the production process. The components of the car such as the seat, steering wheel, tires, headlights, mirrors, interior wardrobe, instrument panel, electrical system, doors and mechanics parts such as engine, gearbox etc. produced in the factory are installed to the car.

The processes investigated in this study are from a real car body-assembling factory. Process water is supplied from well water and then it is passes through disinfection, sand filter, activated carbon, ion-exchange, RO treatment and DI if necessary to used up different processes. The majority of this water (%41) is used for paint shop operations. 17 per cent are used for irrigation and fire systems and 83 percent is allocated for sanitary purposes, cooling tower and other purposes. The wastewater from the production plant is treated onsite with standard physical-chemical treatment before discharge. The annual amount of wastewater generation is 23,000 m^3.

4. WATER CONSUMPTION AND QUALITY REQUIREMENTS FOR VARIOUS WATER USES

Throughout the plant water is used not only for the production process and domestic purposes (water supply for workers and personnel), but also for irrigation and in the fire suppression system. Figure 1 presents the total water consumption of the plant. The total daily water requirement is calculated as approximately 134 $m^3\ d^{-1}$.

The appropriate quality criteria for water consumption in industrial applications changes according to the specific demands of the manufacturer. Apart from irrigation, three different water quality requirements are set by the manufacturer i.e., for fresh cooling water inputs and for process waters (either deionized (RO/DI) or soft). The relevant quality requirements for different type of water uses in the installation are classified as well water, soft water, potable water and reverse osmosis (RO) treated or deionized DI water. As may be noted from the Table 2, conductivity and pH level is the sole quality parameter considered for the production lines. The specified conductivity level varies in a wide range from 2 to 1080 $\mu S\ cm^{-1}$, depending on the particular use. Process water requirement is divided into soft water, deionized (DI) water / reverse osmosis (RO) as given in Table 2.

Table 2: Water quality requirements

	Well Water	Potable Water	Soft Water	RO/DI Water
pH	7.95	7.86	8.07	7.3-9.5
Conductivity (µS/cm)	1080	397	210	2.12-16.19

The amount of either continuous or intermittent water requirements within the whole plant are presented in Figure 1. Water requiring spots in the premise together with their amounts are given in Table 3.

Table 3: Water consumption

Input purpose	Amount m^3/d	Type	Quality
Irrigation	20.80	Intermittent	Well
Fire System	1.72	Intermittent	Well
Domestic	51.29	Continuous	Potable
Non-process			
Boiler	1.61	Intermittent	Well
Cooling	17.10	Intermittent	Soft
Cooling	1.61	Intermittent	Well
Process			
1	22.20	Intermittent	Soft
2	17.2	Intermittent	DI/RO

5. WASTEWATER GENERATION AND TREATMENT

Process wastewaters together with domestic effluents and non-process discharges are produced in the premise. Both continuous as well as intermittent wastewater discharges are generated from the production processes. The flowrates of segregated process wastewaters are outlined in Table 4. As can be seen from the table process effluents are 37 % of the total amount.

Table 4: Wastewater generation

Wastewater source	**Amount m^3/d**
Domestic	34.83
Non-process	
Boiler	1.10
Cooling	9.87
Process	
Bus Paintshop	9.86
Truck Paintshop	14.00
TOTAL	65.51

Domestic wastewater is treated by sequencing batch reactors after passing from drum screens. In Table 5 raw wastewater characterization together with the effluent of treatment plant are listed.

Table 5: Wastewater characterization

Parameter	**Raw wastewater**	**Effluent of treatment**
Chemical Oxygen Demand (COD mg/L)	551	53
Suspended solids (SS mg/L)	205	20
Oil and Grease (mg/L)	7.49	0.34
Ammonium nitrogen (NH_4-N mg/L)	0.57	33.7
Nitrite Nitrogen (NO_2-N mg/L)	<0.03	0.84
Total Chromium (T.Cr mg/L)	0.005	0.006
Chromium (Cr^{+6} mg/L)	<0,01	<0,01
Iron (Fe mg/L)	1.196	0.47
Aluminum (Al mg/L)	1.234	0.309
Lead (Pb mg/L)	0.003	0.0027
Copper (Cu mg/L)	0.017	0.013
Zinc (Zn mg/L)	2.727	0.297
Mercury (Hg mg/L)	<0.00013	<0.00013
Fluoride (F^- mg/L)	14.7	1.82
pH	6.45	7.33

6. REUSE POTENTIAL OF CATAPHORESIS EFFLUENTS

Approximately 59 % of the process wastewaters are generated from truck paint shop where cataphoresis process takes place. Cataphoresis process operates with 10 baths totally, in two stages, of Pretreatment (PT) and Electrodeposition (ED). In the Pretreatment (PT) line the metal car body pass through the subsequent baths of hot water rinsing (bath 1), degreasing (bath 2), rinsing I (bath 3), surface activating (bath 4), phosphate (bath 5), rinsing II (bath 6), DI water rinsing (bath 7). Besides, in the Electrodeposition (ED) line, the metal car body pass through cataphoresis painting (bath 8), UF rinsing (bath 9), DI water rinsing (bath 10) baths. Both continuous and intermittent discharges arise from these baths. Water requirement and wastewater generation of cataphoresis process are given in Table 6 and 7, respectively.

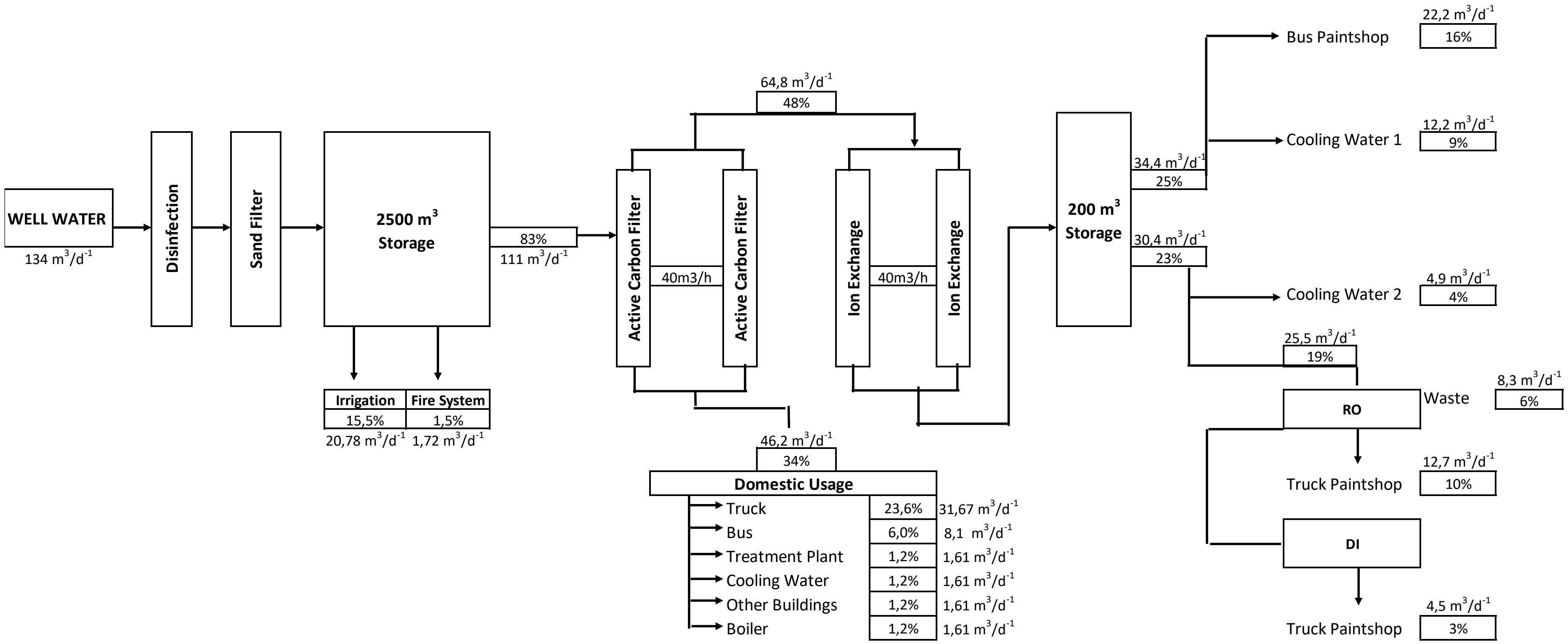


Figure 1. The total water usage of the plant

Table 6: Water requirement and frequency of Cataphoresis process baths

Name of the bath (Bath Number)	DI/RO Water Requirement and frequency(m3)		Total DI/RO water requirement (m^3 /year)
	Continuous	Intermittent	
Hot water rinse (1)	1 m^3 /day	100 m^3 /year	340
Degreasing (2)	1 m^3 /day	50 m^3 /year	290
Water rinse tank-1 (3)	1 m^3 /day	700 m^3 /year	940
Surface activation (4)	1 m^3 /day	200 m^3 /year	440
Phosphating (5)	0.4 m^3 /day	-	96
Water rinse tank-2 (6)	1 m^3 /day	700 m^3 /year	940
DI Water rinse tank (7)	1 m^3 /day	500 m^3 /year	740
ED Coating (8)	-	-	-
UF Rinse (9)	-	-	-
DI Water Rinse (10)	1 m^3 /day	100 m^3 /year	340

Table 7: Wastewater generation in Cataphoresis process baths and frequency of discharges

Name of the bath (Bath Number)	Wastewater Generation and frequency		Total Wastewater Generation (m^3/year)
	Continuous	Intermittent	
Hot water rinse (1)	0.6 m^3 /day	100 m^3 /year	244
Degreasing (2)	0.6 m^3 /day	50 m^3 /year	194
Water rinse tank-1 (3)	0.6 m^3 /day	700 m^3 /year	844
Surface activation (4)	0.6 m^3 /day	200 m^3 /year	344
Phosphating (5)	-	-	*negligible*
Water rinse tank-2 (6)	0.6 m^3 /day	700 m^3 /year	844
DI Water rinse tank (7)	0.6 m^3 /day	500 m^3 /year	644
ED Coating (8)	-	-	*negligible*
UF Rinse (9)	-	-	*negligible*
DI Water Rinse (10)	0.6 m^3 /day	100 m^3 /year	244
TOTAL	4.2 m^3 /day	2350 m^3 /year	3358

The results of the characterization study performed on the mentioned bath discharges are tabulated in Table 8. As baths 8 and 9 are operated as a closed loop system, characterization of it is not given in the mentioned table.

Table 8: Wastewater characterization of Cataphoresis process baths

Parameter	**Bath Number**							
	1	**2**	**3**	**4**	**5**	**6**	**7**	**10**
pH	11	12.6	10.6	10.3	3	6	6	5
Conductivity (µS/cm)	2005	27800	1226	1430	1608	342	27	59
Zinc (mg/l)	0.176	ND	ND	ND	ND	ND	ND	ND
Nickel (mg/l)	0.027	ND	ND	ND	ND	ND	ND	ND
Manganese (mg/l)	0.03	ND	ND	ND	ND	ND	ND	ND
Phosphate (mg/l)	7.817	109	5	163	16331	127	<0.15	<0.15
Nitrite (mg/l)	2.449	8.34	<0.2	<0.2	28.8	<0.8	<0.2	0.3
Nitrate (mg/l)	2.074	925	<0.2	<0.2	839	78	<0.2	13
Sulphate (mg/l)	3.0175	11	0.8	1.4	118	2	0,3	3
Chloride (mg/l)	4.519	8.34	1.1	1.3	20.4	0.6	0.5	<0.2
Iron (mg/l)	0.24	ND	ND	ND	ND	ND	ND	ND

As can be seen from Table 8, conductivity levels together with other pollutant parameters of continuous effluents arising from baths 6, 7 and 10 are relatively low. Therefore, these baths are

chosen as the reusable wastewater streams. By doing so 43 % of the continuous effluents can be reused.

Apart from the mentioned reusable effluents of cataphoresis process, discharges generated from boilers and cooling system can also be recovered and reused. As a result 20 % of the whole wastewaters can be quoted as reusable effluents.

7. DISCUSSION AND CONCLUSIONS

Reuse potential of cataphoresis wastewaters in an automotive industry is investigated. The results of the study indicate that around 43 % of the continuous effluents generated from cataphoresis operations are reusable after passing through an appropriate treatment. Besides when discharges from cooling system and boiler are added to the mentioned reusable process effluents, 20 % of the whole wastewaters can be quoted as reusable in nature.

Therefore, the reuse of segregated cataphoresis wastewaters together with discharges of cooling system and boiler could contribute to sustainable production once a cost-effective treatment process is addressed.

References

1. Bakar A. F. and Halim A. A. (2013) "Treatment of automotive wastewater by coagulation-flocculation using poly-aluminum chloride (PAC), ferric chloride (FeCl3) and aluminum sulfate (alum)", **AIP Conference Proceedings**, 1571, 524.
2. Cosejo C., Ormad M. P., Sarasa J. and Ovelleiro L. J. (2005) "Treatment of wastewater coming from painting process: Application of conventional and advanced oxidation technologies" **Ozone Science and Engineering,** 27, 279.
3. Sarioglu M. and Gokcek O. B. (2016) "Treatment of automotive industry wastewater using anaerobic batch reactors: the influence of substrate/inoculum and molasses/wastewater" **Process Safety and Environmental Protection,** 102, 648.
4. IDBT (2017) Turkey Automotive Competitiveness and Internal Market Prospects Demand Dynamic Perspective in 2020, Industrial Development Bank of Turkey, January 2017.
5. Mackulak T., Bodik I., Smolinska M. Takacova A, Drtil M., Gal M. and Faberova M. (2016) "Automotive industry wastewater treatment by mixture of enzymes" **Monatsh Chem**, 147, 159.
6. Mudliar R., Umare S. S., Ramteke D. S. and Wate S. R. (2009) "Energy efficient-advanced oxidation process for treatment of cyanide containing automobile industry wastewater" **Journal of Hazardous Waste,** 164, 1474.
7. AMA (2017) Automotive Industry Monthly Report, Automotive Manufacturers Association, November 2017
8. Tejada F., Zullo J., Yen J., Guldberg T. and Bras B. (2012) "Quantifying the life cycle water consumption of a passenger vehicle" **Proceedings of 2012 SAE World Congress, Conference and Exposition.** SAE International, Troy.
9. U.S. EPA (1994) Emission Standards Division, Automobile Assembly Plant Spray Booth Cleaning Emission Reduction Technology Review, EPA-453/R-94-029, Research Triangle Park, North Carolina, March 1994.
10. Zhang J., Sun Y., Chang Q., Liu X. and Meng G. (2006) "Improvement of crossflow microfiltration performances for treatment of phosphorus-containing wastewater" **Desalination,** 194, 182.

11. Zhu Y., Zhu T., Groetzbach M., Han H. and Ma Y. (2017) “Multi-level contact oxidation process performance when treating automobile painting wastewater: Pollutant removal efficiency and microbial community structures” **Water,** 9, 881.

SPONSORS

Faculty of Engineering, Aristotle University of Thessaloniki	Research Committee, Aristotle University of Thessaloniki	Regional Association of Solid Waste Management Agencies of Central Macedonia

Thessaloniki Water Supply & Sewerage Co S.A.	ATTIKO METRO S.A.	Greek National Tourism Organization

Ydrofili T.S.A.	Manolesakis G. and CO	Haitoglou Bros S.A.

PROTECTION
AND
RESTORATION
OF THE
ENVIRONMENT
XIV